CUMULATIVE INDEX

Volumes 16–20

NUCLEAR SCIENCE ABSTRACTS

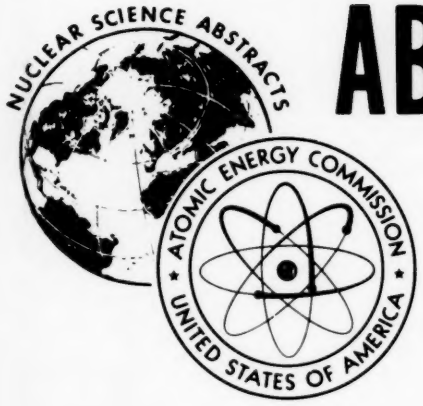

Volumes 16 through 20

1962 – 1966

SUBJECTS (M)

UNITED STATES ATOMIC ENERGY COMMISSION
Division of Technical Information

USAEC DEPOSITORY LIBRARIES

Collections of USAEC reports are maintained in the libraries of the organizations listed below for reference use by the general public. Facilities for making photocopies are available. The USAEC also makes available through these libraries atomic energy reports of countries other than the U. S. that are abstracted in *Nuclear Science Abstracts*.

ALABAMA
Auburn, Auburn University
ALASKA
College, University of Alaska
ARIZONA
Tucson, University of Arizona
ARKANSAS
Fayetteville, University of Arkansas
CALIFORNIA
Berkeley, University of California
Davis, University of California
Los Angeles, University of California
San Diego, Public Library
Stanford, Stanford University
COLORADO
Boulder, University of Colorado
Denver, Public Library
CONNECTICUT
New Haven, Yale University
DELAWARE
Newark, University of Delaware
DISTRICT OF COLUMBIA
Washington, Library of Congress
FLORIDA
Coral Gables, University of Miami
Gainesville, University of Florida
Tallahassee, The Florida State University
GEORGIA
Atlanta, Georgia Institute of Technology
HAWAII
Honolulu, University of Hawaii
IDAHO
Pocatello, Idaho State University
ILLINOIS
Chicago, John Crerar Library
Chicago, University of Chicago
Evanston, Northwestern University
Urbana, University of Illinois
INDIANA
Bloomington, Indiana University
Lafayette, Purdue University
IOWA
Ames, Iowa State University
KANSAS
Manhattan, Kansas State University
KENTUCKY
Lexington, University of Kentucky
Louisville, University of Louisville
LOUISIANA
Baton Rouge, Louisiana State University
New Orleans, Tulane University
MARYLAND
Baltimore, Johns Hopkins University
College Park, University of Maryland
MASSACHUSETTS
Cambridge, Harvard University
Cambridge, Massachusetts Institute of Technology
MICHIGAN
Ann Arbor, University of Michigan
Detroit, Public Library
East Lansing, Michigan State University
MINNESOTA
Minneapolis, University of Minnesota
MISSISSIPPI
State College, Mississippi State University
MISSOURI
Kansas City, Linda Hall Library
Rolla, University of Missouri School of Mines and Metallurgy
St. Louis, Washington University
MONTANA
Bozeman, Montana State College
NEVADA
Las Vegas, Nevada Southern University
Reno, University of Nevada
NEW JERSEY
Princeton, Princeton University
Teaneck, Fairleigh Dickinson University
NEW MEXICO
Albuquerque, University of New Mexico
NEW YORK
Albany, The University of the State of New York
Buffalo, State University of New York at Buffalo
Ithaca, Cornell University
New York, Atomic Industrial Forum, Inc.
New York, Columbia University
New York, New York University
Rochester, University of Rochester
Schenectady, Union College
Syracuse, Syracuse University
Troy, Rensselaer Polytechnic Institute
NORTH CAROLINA
Charlotte, Public Library of Charlotte and Mecklenburg County
Durham, Duke University
Raleigh, North Carolina State College
NORTH DAKOTA
Grand Forks, University of North Dakota
OHIO
Cincinnati, University of Cincinnati
Cleveland, Public Library
Columbus, Ohio State University
Toledo, University of Toledo
Youngstown, Youngstown University
OKLAHOMA
Norman, University of Oklahoma
Stillwater, Oklahoma State University
OREGON
Corvallis, Oregon State University
Portland, Reed College
PENNSYLVANIA
Philadelphia, University of Pennsylvania
Pittsburgh, Carnegie Library
University Park, Pennsylvania State University
PUERTO RICO
Rio Piedras, University of Puerto Rico
RHODE ISLAND
Providence, Brown University
SOUTH CAROLINA
Columbia, University of South Carolina
TENNESSEE
Knoxville, University of Tennessee
Memphis, Public Library
Nashville, Joint University Libraries
Oak Ridge, Oak Ridge Associated Universities
TEXAS
Austin, University of Texas
College Station, Texas A & M University
Dallas, Southern Methodist University
Houston, Rice University
Lubbock, Texas Technological College
San Antonio, Public Library
UTAH
Salt Lake City, University of Utah
VIRGINIA
Blacksburg, Virginia Polytechnic Institute
Charlottesville, University of Virginia
Norfolk, Old Dominion College
WASHINGTON
Pullman, Washington State University
Seattle, University of Washington
WEST VIRGINIA
Morgantown, West Virginia University
WISCONSIN
Madison, University of Wisconsin
Milwaukee, Public Library
WYOMING
Laramie, University of Wyoming

UNITED STATES ATOMIC ENERGY COMMISSION

NUCLEAR SCIENCE ABSTRACTS

Cumulative Index

Volumes 16 through 20

1962 - 1966

SUBJECTS (M)

Division of Technical Information

This eleven-volume set is for sale by the
Superintendent of Documents, U. S. Government Printing Office
Washington, D. C. 20402 Price $36.00

STAFF OF NUCLEAR SCIENCE ABSTRACTS

John W. Norris
Managing Editor

Donald D. Davis
Assistant Managing Editor

David E. Bost
Production Manager

Robert E. Upchurch
Subject Heading Specialist

J. Paul Meredith
Descriptive Cataloging Specialist

Clara L. Fox
Corporate Author Specialist

Mary H. Newman
Reports Evaluator

Brainard L. Patton
Scheduling and Publishing Coordinator

Section Editors

Everett J. Hoffman
Chemistry

Robert C. Kelly
Engineering; Earth Sciences

Lee M. Thompson
General Physics

Charles E. Stuber
High Energy Physics

Hugh E. Voress
Life Sciences

Lawrence T. Whitehead
Nuclear Data

James M. Jacobs
Reactor Technology; Metals and Ceramics

Abstractors

F. S. Armstrong*
Mary M. Brown
Jane G. Buchanan
D. Lamar Cason
Bennie G. Di Bona
Helen G. Donald
James R. Dulaney
Wells L. Green
Bernard O. Griggs
Harry G. Grisham
Mary C. Grissom
Miriam P. Guthrie
Fernando Hamilton
Phyllis C. Hansen
Thomas F. Heagerty
Carolyn D. Houston
Rose V. Jermain
Sidney F. Lanier
Betty L. McDowell
William D. Matheny
John H. Mitchell
Dora H. Moneyhun
Luther Norene
Carol Oen
Jean F. Peckham
Henry D. Raleigh
Mona H. Raridon
Julia S. Redford
Ned W. Rizzardi
Francis L. Sachs
Lila B. Smith
Polly C. Summers
Anne G. Ward
Helen L. Ward
David C. West
Milton O. Whitson
Juanita Wilson

*Atomic Energy of Canada, Ltd.

Acknowledgments

Agreements between the United States Atomic Energy Commission and the following organizations with regard to providing continuing services and specific literature coverage for *Nuclear Science Abstracts* are gratefully acknowledged:

American Institute of Physics; Atomic Energy of Canada Limited; Atomic Energy Research Establishment, United Kingdom; Aktiebolaget Atomenergi, Sweden; European Atomic Energy Community (EURATOM); Gmelin Institute, International Atomic Energy Agency; Japan Atomic Energy Bureau—Japan Atomic Energy Research Institute; Netherlands Patent Office; Reactor Centrum Nederland.

Communication concerning the editorial policy and content of *NSA* should be addressed to the Managing Editor, *Nuclear Science Abstracts*, AEC Division of Technical Information Extension, P. O. Box 62, Oak Ridge, Tennessee 37830.

Use of funds for printing this publication approved by the Director of the Bureau of the Budget, June 28, 1966.

Cumulative Index
Volumes 16-20, Subjects, 1962-1966

NUCLEAR SCIENCE ABSTRACTS

A semimonthly publication of the USAEC Division of Technical Information, Edward J. Brunenkant, Director. Published by the USAEC Division of Technical Information Extension, Robert L. Shannon, Extension Manager.

Nuclear Science Abstracts provides the only comprehensive abstracting and indexing coverage of the international literature on nuclear science and technology. *NSA* covers scientific and technical reports of the U. S. Atomic Energy Commission and its contractors, those of other U. S. Government agencies, and those of other governments, universities, industrial, and research organizations. It also covers patents, books, and journal literature on a worldwide basis. A list of the journals scanned appears in Issues 1 and 13 of each volume. Nearly 400,000 abstracts have appeared in *NSA* through Volume 20. The subject matter covered in *NSA* is described in Issue 1 of each volume and in TID-4552, *Subject Scope of Nuclear Science Abstracts*. The latter is available free from the U. S. Atomic Energy Commission, Division of Technical Information Extension, P. O. Box 62, Oak Ridge, Tennessee 37830.

Abstracts are arranged according to subject categories which are defined in Issue 1 of each volume. If the language of the original item is not English, the language is indicated. Translations are not abstracted if an abstract of the original item has appeared in *NSA*.

AVAILABILITY OF PUBLICATIONS ABSTRACTED

The public availability of all U. S. Atomic Energy Commission reports is indicated in the report number indexes. The availability of other reports, when known, is also indicated. The availability of some unnumbered reports is given in the abstract.

Dissertations abstracted in *Dissertation Abstracts* and included in *NSA* are available from University Microfilms, Inc., 315 N. First Street, Ann Arbor, Michigan 48103.

Information on the availability of the published literature and unpublished conference papers abstracted in *NSA* may be obtained from the Division of Technical Information Extension, P. O. Box 62, Oak Ridge, Tennessee 37830.

HOW TO OBTAIN NUCLEAR SCIENCE ABSTRACTS

NSA is available to the general public on a subscription basis from the Superintendent of Documents, U. S. Government Printing Office, Washington, D. C. 20402, as follows:

For the 24 regular issues, $30.00 domestic, $37.00 foreign. A single issue costs $1.75, plus 25 percent for foreign mailing. Domestic rates apply to the United States, Canada, Mexico, and Central and South American countries except Argentina, Brazil, Guyana, French Guiana, Surinam, and British Honduras. Foreign rates apply to the countries excepted above and to all other countries throughout the world.

For the quarterly, semiannual, and annual indexes, $22.00 domestic, $25.00 foreign.

Multivolume subject and author indexes are available as follows:

Vols. 1-4 (1948-1950). Johnson Reprint Corporation, 111 Fifth Avenue, New York, N. Y. 10003, $30.00.

Vols. 5-10 (1951-1956). Superintendent of Documents, U. S. Government Printing Office, Washington, D. C. 20402, $5.25.

Vols. 11-15, Subjects. Superintendent of Documents, U. S. Government Printing Office, Washington, D. C. 20402, $19.00.

Vols. 11-15, Personal Authors. Superintendent of Documents, U. S. Government Printing Office, Washington, D. C. 20402, $14.25.

Vols. 11-15, Corporate Authors. Superintendent of Documents, U. S. Government Printing Office, Washington, D. C. 20402, $2.50.

Vols. 16-20. (To be issued in 1967.)

Cumulative Report Number Index, Vols. 1—15 Revised, is available from the Superintendent of Documents, U. S. Government Printing Office, Washington, D. C. 20402, $4.00.

Cumulative Report Number Index, Vols. 16—20, is available from the Superintendent of Documents, U. S. Government Printing Office, Washington, D. C. 20402, $4.25.

Annual indexes are available separately from the Superintendent of Documents, U. S. Government Printing Office, Washington, D. C. 20402, as follows:

Vol. 16, Subjects and Authors, $9.75.
Vol. 17, Subjects and Authors, $12.25.
Vol. 18, Subjects and Authors, $12.50.
Vol. 19, Subjects and Authors, $12.50.

Annual indexes for Vol. 20 were not issued since they are a part of the cumulation for Vols. 16–20.

NSA is available on an exchange basis to universities, research institutions, industrial firms, and publishers of scientific information. Inquiries should be directed to the U. S. Atomic Energy Commission, Division of Technical Information Extension, P. O. Box 62, Oak Ridge, Tennessee 37830.

Government agencies may obtain *NSA* free of charge.

INTRODUCTION

Subject entries in this index are generally specific materials, things, and processes. These are followed by modifiers that describe the properties of, and processes applied to, the entries.

The number preceding the colon is the *NSA* volume number, and the number following is the abstract number. The designation (R) following the abstract number indicates that the abstract is of a progress report; (P) indicates a patent; and (T) indicates a translation. Abstracts for reports other than progress reports carry no letter designation. References to report numbers, where appropriate, are included after the abstract number of the citation. Published literature (journal article or book) is identifiable by the absence of a report number.

Special characters are added to modifiers in the field of physics; if the modifier does not establish the experimental or theoretical character of a reference, a symbol (E), (T), or (E/T) is placed immediately after the modifying phrase and before the journal reference number. The value of this identification has been established by the American Institute of Physics.

The user should bear in mind that the ideas presented in the original literature, rather than key words, have been indexed. The indexers have tried to select what seemed the most probable and logical place to look for typical information. Since it is not possible to anticipate where a user would look for information, numerous cross references are included.

Experience in using an index of this type will be the best guide in obtaining the desired information, and a consideration of synonymous or closely related terms as well as recent developments in scientific terminology will prove valuable.

Information must be so indexed as to be of the greatest use to the greatest number of users. This requires that a topic be indexed to headings that most specifically describe it and not ordinarily to the headings that describe its ultimate use, nor to the general class headings that include the specific headings. For example, information on the treatment of thyroid disease with I-131 would be indexed under Thyroid Gland and under Iodine Isotopes I-131, but not necessarily under Radiotherapy. A study of the effects of x radiation on hair would be indexed under both X Radiation and Hair.

The broad, general class headings are used only for general information or for comprehensive reports or articles.

Subject Heading Styles

Generally, the direct form of subject entry is used rather than inverted headings, e.g., Amino Acids rather than Acids, Amino; Helium Isotopes He-4 rather than Helium—isotopes He-4 or Helium—He-4 isotopes. Note, however, that in some cases parenthetic modifying terms or inverted headings of the form Neutrons, Fast are used in preference to a direct entry that would result in the scattering of information. Organic compounds are usually entered in the index in the inverted form so that substituted compounds can be listed near the parent compound; e.g., Benzene, Bromo- rather than Bromobenzene. Subject headings were chosen from TID-5001(5th Rev.) "Subject Headings used by the USAEC Division of Technical Information."

Alphabetization

Subject headings are alphabetized word-by-word. A parenthetic qualifier following a subject heading is disregarded in alphabetizing unless there are two or more headings identical except for the parenthetic qualifier, in which case the qualifier determines the order. Headings involving Greek letters are arranged as if the names of the letters were spelled out.

Examples:

M-Capture
see Electron Capture
Magnesium
Magnesium Alloys
Manganese Fluorides
Manganese(II) Fluorides
Mesons
Mesons (π)
Mesons (ρ)
3-Pentanol, 2,4-Dimethyl-
2-Pentanol, 2-Methyl-
2-Pentanol, 4-Methyl-

Nomenclature of Inorganic Compounds

Inorganic compounds are indexed in the direct form, listing cations in the order of increasing valence in the case of polycationic salts of varying valence and in alphabetic order for polycationic salts in which all cations have the same valence; e.g., Sodium Aluminum Silicates and Potassium Sodium Sulfates.

Multicomponent Alloys and Other Systems

Multicomponent alloys, except well-known trade names, are indexed under a heading in the form "element alloy" for each element in the alloy. The modifier begins with element symbols for each component arranged alphabetically as if the English name for the element were spelled out.

Example: Copper–Gold Alloy is indexed
Copper Alloys
Cu–Au . . .
Gold Alloys
Cu–Au . . .

Well-known alloys such as Zircaloy-2 are indexed directly to the trade name; cross references referring from each component of the alloy to the entry for the trade name are included.

Multicomponent systems of nonmetallic elements are indexed in a manner similar to alloys except the main heading used contains the word "Systems" in place of "Alloys."

Example: Silicon–Tungsten Systems are indexed
Silicon Systems
Si–W . . .
Tungsten Systems
Si–W . . .

Multicompound systems and mixtures of compounds are indexed under the main heading for each component compound; the modifiers begin with an alphabetical listing of compound formulas.

Example: Lead Titanate–Lead Zirconate is indexed
Lead Titanates
$PbTiO_3$–$PbZrO_3$ . . .
Lead Zirconates
$PbTiO_3$–$PbZrO_3$ . . .

A mixed system of compounds and elements is indexed using a combined form of the above conventions, e.g., a dispersion of copper and alumina would be indexed

Aluminum Oxides
Al_2O_3–Cu . . .
Copper Systems
Al_2O_3–Cu . . .

Physical States and Configurations of Materials

Specification of the physical state, if other than normal, or geometric configuration of the material is included in the modifying phrase, i.e., liquid metals would be indexed to the metal with "liquid" in the modifier, and carbon crucibles would be indexed to Carbon with "crucibles" appropriately placed in the modifier and also to Crucibles if appropriate.

Modifying Phrases

The modifiers appearing under a subject heading are written specifically to describe the relation of the item being indexed to that heading. Effort is exerted to begin the modifier with the word judged to be of greatest use to the greatest number of users: this, however, does not obviate the need to consider all modifiers under the main heading(s) of interest.

Modifiers are usually intended to form a meaningful phrase when combined with the main heading. Some are intended to be read following the main heading, e.g., the entry Hydrogen—sorption by charcoal is read "hydrogen sorption by charcoal"; however, as a result of placing the important word first, many modifiers must be arranged for smooth reading, e.g., Formaldehyde—yields in radiolysis of ethyl ether, effects of deuterium on is read "effects of deuterium on formaldehyde yields in radiolysis of ethyl ether" and Uranium—crystal structure of, effect of cooling rate on allotropic transformations in is read "effect of cooling rate on allotropic transformations in crystal structure of uranium." Prepositions are sometimes omitted if no ambiguity results.

SUBJECTS (M)

M

M-257
see SAP

M-Capture
see Electron Capture

McKelveyite
see Mckelveyite

MACHINE TOOLS
(Including hydraulic presses, lathes, mills, etc.)
see also Dies
see also Drills
see also Molds
analysis of numerically controlled, computer program for, 20: 35184 (Y-1400(Rev.1))
book: *Reasoned Technology of Manufacturing Tube-Drawing Machinery (Chap. III)*, 16: 13188(T) (FTD-TT-61-333)
clamp for positioning graphite rods and blocks for machining, 17: 1598(P)
construction, use of radioisotopes in, 16: 13415(T) (AEC-tr-4492(p.1-5))
control and operation of Gorton lathes, 20: 46144(R) (HW-67765)
control of, computer program for automatic, 20: 31478 (K-1670)
control of, computer program for automatic, 20: 31327 (K-1671)
control of, feasibility of computer positioning, 20: 10477 (SCL-DC-65-130)
control of, using isotopes and radiations, 20: 43789
control system acceleration switching valve for, 19: 48106 (Y-1488)
cutting properties and machinability of sintered carbide, use of radioisotopes for testing, 18: 7099
description of copying lathe for radioactive materials in hot cell, 19: 30716(P)
description of hydrostatic boring bar and spindle for lathe, 19: 44170 (Y-DA-921)
description of Soviet vertical lathe, for pressure vessel of Czechoslovakian nuclear power plant, 19: 11331(T) (ORNL-tr-409)
design and operation of hydraulic press for low-level radioactive solid waste, 17: 29135(R) (UCRL-7254(p.34-9))
design and operation of, for machining spheres to submicron tolerances, 20: 46146 (Y-KE-204(Rev.))
design for flange maintenance in Hanford-N reactor, 20: 36509
design for machining interior of torus sectors, 17: 1594(P)
design for radioactive materials, 20: 4126
design for remote cutting of process tube joints in sodium–graphite reactors, 19: 40125 (NAA-SR-9821)
design for remote grinding by ultrasonic methods, 20: 9472
design of chuck for sectioning diffusion samples, 17: 8296
design of multiple-shaft tool head for simultaneous expansion of ferruled tubes, 16: 33464(P)
design of remote-control, for fuel rod processing, 18: 31705(P)
design of turning tool for beryllium, 17: 6620
design of, computer programs for, 20: 16154 (Y-1420(Rev.1))
development for underwater refurbishing of fuel assemblies, 20: 10269 (BNWL-174)
development for very high-pressure pressing, 18: 8775 (Y-DA-470)
development of, for irradiated fuel elements, 20: 4128
diameter gage for, 20: 39032
drive system evaluation for machining round parts, 19: 46461 (RFP-562)
feed rate checks of numerically controlled, 19: 44642 (RFP-570)
for forming fins on tubes, 16: 7873(P)
inspection of, interferometry uses for, 20: 27122 (Y-KE-194)
interferometer gage for, 20: 45847
lathe part programming, graphical computer system for, 19: 40293 (SCL-DC-65-86)
measuring device for, single-transducer differential, 20: 31333 (Y-1541)
mimic setter for single point tool bits on two-axis numerical control turning, 20: 41079 (RFP-666)
operation of, uses of radioisotopes in controlling, 20: 19128
performance of duplicator lathe with hydrostatic bearing slides and electrohydraulic control system, 20: 9098 (Y-1498)
performance optimization of numerically controlled, 20: 5220 (UCRL-13185)
position monitoring devices for, 20: 20989 (Y-1506)
power requirements of, for uranium, 20: 39027 (Y-DA-1287)
programming of numerically controlled, training manual for APT system for, 19: 5582 (SCL-DC-64-100(Vol.I))
programming of numerically controlled, training manual for APT system for, 19: 5588 (SCL-DC-64-100(Vol.II))
programming of numerically controlled, reference material for APT system for, 19: 5584 (SCL-DC-64-100(Vol.III))
programming of numerically controlled, STRESS postprocessor for, 20: 12546 (SC-RR-65-548)
programming of numerically controlled, APT post processor for, 20: 45238 (K-1675)
slide bearing material for, use of teflon as, 20: 35610 (Y-1547)
spindle design, 19: 48093 (RFP-654)
spindle expansion effects on lathe-type, 16: 16473 (HW-71980)
testing of tape control, for effects of spindle expansion, 17: 14421 (RFP-302)
tracer lathe control without cams, plate device for, 18: 40977 (LA-DC-6017)
use of, for embossing fuel element cladding, 20: 35879(P)
use with gages, for fabrication and inspection, 20: 3627 (RFP-670)
wear of shearing dies and punches, radiological measurements, 16: 16067
wear of, measurement by activation analysis, 18: 16165 (TID-7689(p.137-42))

MACHINING
see also Grinding
bibliography on electron beam, 1957 to 1961, 16: 22566 (NP-11777)
book: *Machining Difficult Alloys*, 17: 6608
computer program for, 17: 27509 (TID-18844)
contour specification in, computer program in, 18: 13372 (SCL-TM-64-26)
control in automatic sheet stamping, radiometric, 16: 33355
coolants for Hastelloy-C, refrigerated, 18: 17977(R) (ORNL-TM-793)
design of equipment for electrical-discharge, of metallographic specimens, 20: 16951 (ORNL-TM-1161, pp 159-81)
development of Bridgeport milling machine for remote control, 17: 4334(R) (IDO-16805(p.36-43))
development, state-of-the-art in aerospace areas, 16: 25501 (MAB-139-M(M5))
developments in close tolerance, 20: 6690 (Y-NA-14)
dimension control using radiation sources, slot method for, 16: 27346
drilling of uranium castings, 17: 39502 (NLCO-886)
effect on mechanical properties of metals, 19: 28776 (DMIC-213)
effects of temperature on operations in, 20: 6688 (Y-DA-1014)
end milling of U-500 alloy, performance of high-speed steels in, 17: 6614
equipment for finned-tube, automatic, 19: 44655(P)
equipment for spent fuel element, 20: 16598(P)
equipment using electron beams for, 17: 511 (DMIC-174)
expansion of cutting tools in, measurement of, 20: 47093 (UCRL-50116)
fabrication of nuclear submarine components, tracer-controlled equipment

for, 16: 4262
gaging device for oval-bore, 20: 41436(P)
gaging equipment for cylindrical pellet, 20: 43474(P)
gaging in, use of optical projectors for functional, 20: 35601 (SC-R-66-914)
gripping device design for, 16: 309(P)
inspection gage for average radius, 20: 29668 (Y-NA-18)
inspection of, numerically controlled, 19: 4285 (Y-KE-162)
interferometer design for, 20: 39031
method for micro-, by sputtering through mask of contamination, 19: 39136
method for rapid fabrication of prototype circuit boards from drawing, 18: 43119 (SC-R-64-137)
method of electron-beam, 20: 9482(P)
methods development for reactor materials, 18: 32119
methods development for reactor materials, 18: 41987
methods for remote disassembly and sampling of irradiated components, 19: 34292 (BNWL-SA-76)
methods for unfamiliar materials, 20: 43864 (Y-1550)
methods of, for refractory materials, 17: 34358(R) (ASD-TDR-63-581)
methods of, for fabrication of space-age hardware, 19: 6286
milling of high-strength steels and heat-resisting alloys, 17: 6612
performance evaluation system for personnel, 18: 21731 (Y-1461)
plant for graphite components for Trawsfynydd Nuclear Power Station, 18: 39867
radius generation in vibratory deburring, graphs of running time vs., 20: 43847 (BDX-613-85)
surface finishes produced on high-temperature alloys by electrochemical, 19: 28776 (DMIC-213)
surface finishing by single-point tool techniques, 18: 33205 (Y-1463)
swarf collector design for decontamination of small lathes, 18: 12607
temperature effects on accuracies in, 20: 39009 (UCRL-14944)
tracer plate for, engineering drawings of, 20: 25531
turning of rare metals, 19: 30696 (RDB(C)TM-278)
use of electrical-discharge, in core drilling beryllides, 16: 33446 (DC-60-3-173)

Magnesia
see Magnesium Oxides

MAGNESITES
see also Magnesium Carbonates
emanation of inhomogeneously labeled, apparatus for, 18: 5694

MAGNESIUM
see also Alkaline Earth Metals
abrasion of, friction, wear, and work-hardening during, 18: 18363
abundance in primary cosmic radiation, 17: 22403 (AD-282243)
abundance in 3 Centauri A, 16: 4659
abundance variations in A, Ap, and B stars, 18: 24274
acoustic properties, 18: 31842(R) (NYO-2910-4)
alloying effects of uranium on, 16: 5719 (NP-11169)
alloying effects on solubility of bismuth–uranium–zirconium, 16: 2251
alloying effects on aluminum crystallization, 16: 6730
alloying effects on solubility of uranium in cadmium and zinc, 16: 28555 (TID-7623(p.105-21))
alloying effects on aluminum corrosion, 17: 1881
alloying effects on physical properties of cerium, 17: 14824 (LADC-5615)
alloying effects of, on strain hardening of aluminum polycrystals, 17: 23969 (UCRL-10365)
alloying effects of, on hydrogen agglomeration in aluminum, 17: 24000
alloying effects on ignition temperature of plutonium in air and oxygen, 17: 36860(R) (ANL-6648)
alloying effects on titanium corrosion by mercury at 538°C, 17: 36861(R) (ANL-6764)
alloying effects on corrosion of aluminum–nickel–silicon systems, 17: 37005(R) (KR-49)
alpha elastic scattering at 24.7 Mev, relative cross sections for, 18: 34902
alpha elastic scattering by, distorted-wave model in, (E/T), 20: 1238
alpha elastic scattering at 24.7 Mev, optical-model analysis of, (E/T), 20: 30413
alpha reactions (α,Li^6) with, 18: 16951(R) (TID-20311)
alpha reactions (α,n) at 2 to 5.4 Mev, neutron yields in, 19: 45301
alpha reactions (α, beryllium-7) at 42 Mev, cross sections and yields for, 16: 33814
alpha reactions (α,n) with, neutron yields from, 17: 33017
alpha reactions (α,n) with, neutron yields from, 17: 33018
alpha reactions, neutron yields from, 16: 33803
alpha scattering at 13 to 30 Mev, differential cross section for, 17: 29577 (UCRL-7063)
alpha scattering at 25 Mev by, differential cross section for elastic (E), 19: 1234 (PAN-347)
alpha scattering at 28 Mev, distorted-wave and optical model analysis of, (T), 19: 29294
analysis and determination, 20: 14500
analysis for aluminum, absorptiometric, 17: 7958 (PG-Report-348)
analysis for boron, absorptiometric method for, 17: 15881 (PG-Report-409)
analysis for boron using curcumin, 17: 25118 (PG-Report-251)
analysis for boron, spectrographic method using copper fluoride carrier distillation, 17: 28779(R) (MCW-1480)
analysis for boron, cadmium, manganese, silicon, and zinc, spectrochemical, 18: 11967(R) (MCW-1482(p.37-46))
analysis for cadmium, spectrophotometric, 20: 7011 (NLCO-964)
analysis for copper, activation, 19: 10985(T) (AEC-tr-6227/3(p.193-200))
analysis for hafnium or zirconium using catechol violet, colorimetric, 19: 19780
analysis for iron, spectrophotometric, 18: 11967(R) (MCW-1482(p.37-46))
analysis for oxide, 16: 32880(R) (MCW-1475)
analysis for oxygen, methods for, 20: 3878 (LYCEN-6524)
analysis for oxygen, activation, 20: 24977 (NLCO-973)
analysis for oxygen by neutron activation, 20: 33154 (NLCO-979)
analysis for scandium after solvent extraction using diantipyrilmethane, 18: 13702
analysis for sodium, effects of threshold reactions on activation, 19: 4085
analysis for titanium, colorimetric, 16: 5293
analysis for trace amounts of zinc using 1-(2-thiazolylazo)-2-naphthol, spectrophotometric, 19: 19814
analysis of, mass spectrometric, 17: 25668
analysis of target foils of, methods for, 20: 8855
analysis of, review on methods for, 19: 22107
analysis of, use of activation methods for, 18: 29577
analytical chemistry of, review on, 17: 19948
anodized coatings, spectral reflectance, 16: 8434 (ASD-TR-61-147)
argon ion reactions with, atom ejection patterns for, 17: 34553(R) (ORNL-3480(p.72-5))
atomic structure of, correlation effects in, 18: 7427
atomic structure, random-phase approximations for calculation of, 17: 8954 (UCRL-10510)
bibliography, 16: 19248 (NP-11628)
bibliography on, 17: 6521 (NP-12417)
bibliography on, Defense Metals Information Center selected accessions, January 1963, 17: 14739 (NP-12525)
bibliography on, DMIC selected accessions, Sept. 1962, 17: 419 (NP-12170)
bibliography on, DMIC accessions, May 1963, 17: 29246 (AD-407822)
binding by lipoproteins in blood serum and cell membranes, 20: 42743 (UCRL-14631)
body level determinations, comparison of direct and isotope dilution methods, 16: 7384(R) (TID-14565)
boiling burnout and heat transfer in liquid, test of, 20: 47034
bonding to aluminum, hot-press, 19: 40949 (ISC-640)
bonding to cobalt, iron, nickel, palladium, or platinum, method of measuring quality of, 20: 8503(P)
bonding to uranium using intermediate layers of aluminum, copper, nickel, and zirconium, diffusion, 18: 37652 (A/CONF.28/P/526)
bonding to zirconium, 18: 30107 (AERE-R-4594)
book: *The Role of Magnesium in Biologic Processes*, 17: 27052
bremsstrahlung emission by incident electrons on, intensity variation with target voltage, 17: 39741
bremsstrahlung reactions (γ,n) to 30 Mev, total cross sections for, (E), 19: 37833 (R) (TID-21940(Paper II))
bremsstrahlung reactions (γ,π^0) at 166 Mev, angular distributions from, (E), 4898
bremsstrahlung reactions (γ,p) at 31 Mev, spectra from, (E), 20: 6399
calibration as neutron-threshold detector, effects of boron-10 shields, 16: 3181 (NDL-TR-9)
casting, 17: 4910(R) (MAB-139-M(C7))
catalytic effects on decomposition of tritium-labeled compounds, 19: 7491
chelation of, development of agents for, 18: 8393(R) (TID-19989)
cleaning by ionic bombardment at medium and low energies, 18: 28107
coating with titanium esters and polymers, 17: 3436(P)
combustion in fluorine, calorimetry of, 17: 14118(R) (ANL-6596 (p.164-74))
combustion in oxygen, luminous energy of, 19: 42887
combustion of coatings of, in air, 17: 8832
combustion of, in fluorine, calorimetry of, 16: 28641(R) (ANL-6543)
combustion of, powders for extinguishing, 20: 46007(P)
combustion with fluorine, products and yields from, 20: 5523(R) (ANL-6925, pp 175-85)
compatibility of coatings of, with plutonium, thorium, and uranium,

17: 8843
compatibility with lead telluride, 16: 24161 (NAA-SR-Memo-7172)
content and distribution in acid igneous rocks of Africa, 18: 37358
content and distribution in dolomites and limestones, 19: 9400
content and ionization in solar chromosphere at height of 1000 km, 20: 2771(T)
content in calf intestine, effects of diet on, 20: 32908(R) (ORO-648, pp 71-90)
content in distilled beryllium, calculation and determination of, 19: 22104 (UCRL-12253)
content in fallout from Chinese atomic test, Oct. 1964, 20: 39110
content in high-purity beryllium, 19: 13216
content in high-velocity A stars, 18: 36135
content in human diet, effects of magnesium content in sea foods and water supplies on, 19: 42669
content in human erythrocytes and serum, 17: 10148
content in mammalian cells, effects of cell cycle stage on, 20: 18204(R) (LA-3432, pp 130-77)
content in Mediterranean Sea, effects of season, temperature, and Nile River flooding on, 20: 43508(R) (NP-16179)
content in *Mytilus* shell, ecological effects on, 19: 26251
content in open-ocean silts, 20: 12540(R) (NYO-2882-8)
content in organs and tissues of humans outside continental U. S., 19: 21831
content in rat kidney mitochondria, effects of vitamin D on, 20: 8559
content in schlieren granite segregations, 19: 24699
content in skeletal carbonates of marine organisms, 20: 24851
content in stellar atmospheres, (T), 19: 4785
contents in meteorites, 18: 34398
corrosion, 16: 27589 (BM-RI-5990)
corrosion and mechanical properties, effects of aluminum, copper, and zinc on, 16: 17990
corrosion by aluminum–silicon and water of coatings of, on uranium, 19: 40949 (ISC-640)
corrosion by chloride ions, electrochemistry of pitting, 20: 11231 (CEA-R-2815)
corrosion by chlorine trifluoride–urania reaction-gas mixtures, 20: 12925(R) (EURAEC-1446)
corrosion by gas–oil, hydrogenated terphenyl, and monoisopropylbiphenyl at 330 to 400°C, 20: 25492(T) (AECL-2330, pp 196-217)
corrosion by humid air at 350°C, 17: 3420 (BLG-124)
corrosion by impure Santowax, 17: 23891 (NAA-SR-7755)
corrosion by in-pile OMRE coolant, effects on properties, 18: 35937 (NAA-SR-9796)
corrosion by moist air, carbon dioxide, nitrogen, and oxygen at 350 to 600°C, 18: 2179 (CEA-2280)
corrosion by polyphenyls at 330 to 400°C, 16: 22547
corrosion by reactor coolant, 16: 491(T) (CEA-tr-A-979)
corrosion by sea water, sodium chloride, and sodium hydroxide, galvanic, 20: 11230 (BM-RI-6715)
corrosion by terphenyls, 16: 22551
corrosion by terphenyls at 400 to 450°C, 17: 37478 (EUR-379.e)
corrosion by water or water vapor in radiation environment, 19: 7870
corrosion by water in spent fuel cooling pond, effects of contact with dissimilar metals, pH, and temperature on, 19: 11694
corrosion in water-cooled reactors, 18: 11373
corrosion of, by demineralized water, effects of chlorides, fluorides, and purity on, 17: 20424
corrosion of coatings of, by humid air at high temperatures, effects of hydrofluoric acid on, 17: 1886(P)
corrosion of sintered, by carbon dioxide, 17: 25738
corrosion of, book, 18: 22451
corrosion of, effects of cobalt and gallium on, 18: 20482
corrosion of, research programs on aqueous, 19: 4627
corrosion of, review, 19: 7868
corrosion protection of uranium by flame-sprayed deposits, 19: 13922
corrosion resistance to mercury at 900°F, 20: 2264
cosmic-ray reactions with, in stony meteorites, production of helium-3 and neon-21 by, 18: 20204
creep cavities in, nucleation of, 19: 41063
creep of, cavitation along grain boundaries during, 19: 41057
creep of, effects of aluminum and zirconium on, 20: 11313
crystal dislocations in, anisotropy effects on, 16: 33604
crystal lattice dynamics of, (E/T), 19: 42891
crystal lattice dynamics, 17: 36428 (NP-13020(p.340-5))
crystal lattice vibrations of, spectra of, 18: 16891(R) (GA-4881)
crystal lattice vibrational spectra, 18: 24168
crystal structure of, internal friction and dislocation studies of, 19: 1958 (NYO-2471-3)
crystal structure of, effect of high pressure on, (E), 20: 13316
crystal structure, effects of alloying additions of other metals on, 20: 2399
crystallization and strength of, effects of thorium and zinc on, 18: 4267
crystallization following deformation and annealing, effects of cadmium, lanthanum, and tin on, 19: 28831
crystallization of, effects of cadmium, lanthanum, and tin on, 20: 19240
deficiency in rats, effects on magnesium-28 uptake by, 18: 29204
deformation and flow of polycrystalline, effects of pressure on, 19: 37048 (WVT-6431)
deformation of crystalline, 18: 37682(R) (MIT-1310-1)
deformation of, effects of lithium on, 19: 43997(R) (UCRL-11889)
deposition in bones of 30- to 630-day-old white rats, 16: 9913
deposition of films of, on uranium metal, 18: 25911(P)
deposition on plutonium dioxide and/or uranium dioxide pellets, 18: 41989(P)
deposition on uranium, uses of copper and nickel for interlayers in, 19: 4143
deposition on uranium, hot dip, 19: 40949 (ISC-640)
detection limit and sorption characteristics of, use of hollow cathode tube for study of, 17: 24080
determination as impurity in and volatilization from tungsten, semi-quantitative spectrographic, 16: 4131 (BM-RI-5903)
determination as impurity in bismuth, spectrographic, 17: 27309
determination as trace impurity in plutonium–thorium–uranium and thorium–uranium alloys, 19: 17798
determination by atomic absorption spectroscopy using induction-coupled plasmas, 20: 40796(R) (IS-1500(Sect.C))
determination by chromatography and flame spectrophotometry, 17: 14178
determination by charged-particle reactions at 2 Mev, 20: 43097
determination by double-activation methods, 19: 13249
determination by flame photometry, effects of ions on, 19: 7274(R) (IDO-14636)
determination by flame photometry, 19: 44122
determination by flame photometry, 20: 4053
determination by isotope dilution, 19: 7289
determination by neutron activation, 16: 18827
determination by plasma spectroscopy, limits for, 17: 40427(R) (NYO-10063(p.1-6))
determination by potentiometric titrations, 18: 1489(R) (IS-700(Sect.C))
determination by radiometric titration, 20: 16386
determination by spectroscopy using high-frequency plasma flames, 18: 10020
determination by spectroscopy using plasma jet, 20: 14492
determination by thermal-neutron activation methods, sensitivity for, 19: 9071
determination by titration, suitability of tetrathylenepentaminehepta-acetic acid for, 19: 19813
determination by x-ray spectrometry using electron-beam excitation, 17: 15908
determination by x-ray fluorescence, equipment for, 19: 5826
determination by x-ray fluorescence analysis, 19: 22154
determination in artificial graphite, 18: 9584
determination in aluminum and zinc alloys and calcium minerals, photometric, 18: 13645(T) (AEC-tr-6346)
determination in aluminum ingots, x-ray fluorescence, 20: 8828 (K-1638)
determination in aluminum by x-ray spectrography using direct electron excitation, 20: 26755
determination in aqueous solutions, design of oxyacetylene burner for measuring sensitivity of spectrophotometric, 20: 29083(R) (UCRL-14767)
determination in aluminum by neutron activation methods, 20: 38804
determination in americium and plutonium by spark-source mass spectrography, 20: 40816 (RFP-699)
determination in beryl ores, gravimetric, 16: 12954 (PG-Report-267)
determination in beryllium, 16: 26912
determination in beryllium oxide, spectrophotometric, 18: 3694
determination in biological materials, activation, 18: 23418
determination in beryllium oxide, device for quantitative, 19: 11007
determination in biological tissues, activation, 19: 15333 (AE-168)
determination in blood serum, spectrometric, 19: 33692(R) (NYO-1397-1)
determination in biological materials by EDTA-titration, 19: 35893(R) (NYO-3234-1)
determination in beryllium oxide, spectrographic comparison of standards on, 20: 6998 (AAEC/TM-294)
determination in blood serum and ores, activation, 20: 16336(R) (NYO-10175)
determination in blood and hair of man, activation, 20: 36728
determination in biological materials, radiochemical separation methods for activation, 20: 38842
determination in biological materials, use of automated gamma spectrometers in activation, 20: 38843

determination in clams by activation, 17: 26963 (EUR-128.i)
determination in corn leaves, method for, 18: 39067
determination in cerium, erbium, and lutetium, mass spectrographic, 19: 2232
determination in calcium, polarographic, 20: 16406
determination in cement raw materials by x-ray emission method using alpha and x-ray sources, 20: 23568
determination in europium oxide, spectrographic, 17: 2931
determination in erythrocytes and plasma in human blood, activation, 20: 38852
determination in fossil foraminiferal carbonates from deep ocean cores, 16: 29187 (TID-16359)
determination in fluorine, combustion, 17: 1359(R) (ANL-6569)
determination in gallium arsenide, activation, 17: 32004
determination in geological samples, activation, 19: 36243(R) (X64-17610)
determination in graphite and basalts by neutron activation methods, 20: 29140
determination in high-purity tantalum by spectrography using d-c arc method, 20: 20608
determination in iron and nickel base alloys, spectrographic, 16: 11539
determination in industrial solutions, quantometric and spectrographic, 18: 19910
determination in its binary alloys, 19: 32055(R) (ANL-7020(p.231-7))
determination in iron and rare earths, complexometric, 20: 25008
determination in igneous and metamorphic apatites, spectrographic, 20: 26787
determination in lake water, thermal neutron activation, 18: 5220
determination in lithium fluoride–magnesium fluoride–yttrium fluoride, 20: 4999(R) (ORNL-2599)
determination in lanthanum oxide, spectrographic, 20: 22895
determination in meteorites and terrestrial rocks, activation, 17: 33851
determination in minerals, chromatographic and flame spectrophotometric, 17: 40745
determination in molybdenum and its compounds, spectrographic, 18: 17766
determination in muscle tissue, activation, 18: 39054 (AE-151)
determination in mixed oxides with rare earths, complexonometric, 18: 39139
determination in meteorites, activation, 19: 7349
determination in molybdenum and tungsten, spectrographic, 19: 30143
determination in magnesium alloys, electrographic, 20: 267
determination in mineral and natural waters, flame photometric, 20: 38798 (NIJS-R-465)
determination in neptunium by ion exchange and spectrography, 17: 15896
determination in niobium, chemico-spectrographic method for, 17: 40758
determination in nodular cast iron by activation using 12-Mev deuterons, 19: 321
determination in nuclear grade uranium, flame photometric, 19: 42418 (NIJS-R-448)
determination in nuclear grade uranium by flame photometry, 20: 26811
determination in ore by activation analysis, 16: 689
determination in ocean-bottom cores by activation analysis, 17: 15886 (TID-18125)
determination in ocean-bottom core samples by activation analysis, engineering drawings of equipment for, 17: 35667
determination in organic reactor coolants, spectrographic, 18: 184
determination in presence of alkaline earth metals by paper chromatography and flame spectrophotometry, 16: 11549
determination in powdered samples by spectrochemical methods, 19: 22120
determination in plutonium fluorides and peroxides, review on spectrographic, 20: 14464 (RFP-599)
determination in plutonium by carrier distillation methods, spectrographic, 20: 40814 (RFP-664)
determination in powder samples by spectrographic methods, semiquantitative, 20: 43104
determination in rare earth oxides, spectrographic method for, 16: 20327
determination in recent carbonate sediments of northern Florida Keys area, 16: 27456
determination in rare earths at 1 to 1000 ppm level, 17: 1377 (BM-RI-6097)
determination in rare earth oxides by atomic absorption spectrophotometry, 20: 33151 (IS-T-88)
determination in salt solutions by spectrophotometric titration using 1,3-dimethylvioluric acid, 16: 12968
determination in stratospheric aerosols, 16: 25609 (AFCRL-62-299)
determination in silicate rocks, x-ray fluorescence spectrographic, 16: 30353
determination in silicate rocks, quantometric and spectrographic, 18: 19910
determination in silicon, activation, 19: 2240
determination in solids by spark source mass spectrometry, quantitative, 19: 13247
determination in silicates, spectrographic, 19: 13266
determination in spleen tissue and RNA, neutron activation, 19: 13206 (SGAE-BL-13/1964)
determination in simulated high-altitude atmospheric samples, flame photometric and gravimetric, 19: 13203(R) (NYO-3276-8)
determination in sea water and silts, spectroscopic, 19: 36315
determination in sintered and zone refined boron-10, spectrographic, 20: 43090(R) (TID-23342)
determination in rat brain and tumors by neutron activation and fast radiochemical isolation, 20: 33182(T) (AEC-tr-6639, pp 108-13)
determination in serum, activation, 20: 16347
determination in silicates, activation, 20: 26782
determination in tissue, after neutron activation, 17: 31813 (AERE-R-4309)
determination in tantalum by d-c arc method, spectrographic, 18: 19894
determination in tantalum by anion exchange in hydrofluoric–nitric acid mixtures, 18: 35455
determination in trace amounts in aluminum by x-ray spectrography, 19: 38571
determination in uranium concentrates, spectrophotometric, 16: 11775(R) (NLCO-790)
determination in uranium, spectrophotometric, 16: 12979
determination in uranium leach solutions, 16: 14668
determination in uranium compounds by reversed-phase partition chromatography, 16: 23636 (TID-7629(p.276-84))
determination in uranium(IV-VI) oxide by carrier distillation excitation, effects of graphite electrode grade on, 17: 10538 (TID-16295)
determination in uranium-233-labeled uranium dioxide, spectrographic, 18: 9980
determination in uranium and its compounds and alloys, methods for, 19: 19823
determination in uranium by atomic absorption spectrophotometry, 20: 1753
determination in uranium, spectrophotometric, 20: 7011 (NLCO-964)
determination in vanadium, chemico-spectrographic, 18: 13708
determination in water, silver-spark spectrographic, 17: 1381 (IDO-14591)
determination in water produced in nuclear reactors for marine propulsion, methods for, 17: 33789 (EUR-224.i)
determination in yttrium, methods for, 20: 4299(R) (ORNL-2711)
determination in zirconium alloys, 17: 6020
determination in Zircaloy-2, spectrographic, 20: 29113
determination of, in residues by iron flux method, spectrographic, 17: 19942 (PG-Report-157)
determination of, in erythrocytes and blood serum, radiometric, 17: 40477
determination of low concentrations of, spectrographic, 17: 28803(T) (AEC-tr-5867)
determination of microgram concentration, radiometric, 16: 4144
determination of, method for, 17: 28801 (IDO-14316(Suppl.4))
determination of trace amounts in rare earth compounds, spectrographic, 16: 28869 (JEN-107-DQ/I-33)
determination of traces of, in presence of calcium, spectrophotometric, 18: 9970 (IS-777)
determination of trace, spectrophotometric, 19: 9046(R) (IS-900(Sect.C))
determination of traces in cobalt oxide, spectrographic, 19: 15336 (AEET/Spec./3)
determination of trace amounts of, in beryllium by spectrography, 20: 16352
determination of trace amounts of, by reactor neutron activation methods, 20: 26760
determination of, re-activation, 18: 12019
determination of, radiometric titration, 18: 27311
determination of, by alpha scattering methods, 20: 22964
determination of, evaluation of titrimetric EDTA method with visual indicator end points for, 20: 43067(R) (IDO-14679, pp 6-46)
determination of, in nickel base alloy by deuteron activation methods, 20: 40812 (ORO-2980-14)
determination using titanium yellow and EDTA, 19: 19779
determination, use of pulsed neutrons in activation, 19: 36323
deuteron differential elastic scattering cross sections at 14.7 to 18.1 Mev, 16: 12426 (INSJ-44)
deuteron elastic scattering at 11.8 Mev, angular distributions, 16: 3637
deuteron elastic scattering at 1 to 20 Mev, 16: 12514
deuteron elastic scattering at 12.8 Mev, cross sections for, 17: 9507 (PAN-203)
deuteron elastic scattering at 6.5 Mev, polarization in, 17: 38157
deuteron elastic scattering by, energy dependence of angular distributions from, 18: 1052

deuteron elastic scattering by, nuclear tensor potentials from, 18: 17041
deuteron elastic scattering at 26 Mev, angular distributions from, 18: 28634
deuteron elastic scattering at 26 Mev, optical model analysis of, (E/T), 20: 3053
deuteron elastic scattering at 27.5 Mev, angular distribution for, (E/T), 20: 3057
deuteron reactions at 19.6 Mev, optical model parameters for, 18: 1051
deuteron scattering at 8.7 to 12 Mev, angular distributions, 16: 13953 (JÜL-30-KP)
deuteron scattering at 13 Mev, angular distributions from elastic, 16: 21566
deuteron scattering at 3 to 30 Mev, optical model analysis of, 17: 11676
deuteron scattering at 10.1 Mev, optical potentials for distorted wave analyses of, 17: 38184
deuteron scattering at 26.5 Mev, total cross sections for, (E), 19: 5164
deuteron scattering by, cross sections for, (T), 20: 3026
development and properties for fuel element cladding, review, 16: 16661
diffusion in gamma–cerium, electro-, 19: 34722
diffusion in gamma-cerium, gamma-uranium, and epsilon-plutonium, electro-, 20: 23734
diffusion in superimposed films of superconducting indium and normal, 17: 34594
diffusion in zirconium at 623°C, electron-probe microanalysis of, 19: 14016
diffusion into zirconium, 18: 30107 (AERE-R-4594)
diffusion of argon and helium in, tracer studies of, 20: 7095
diffusion of beryllium to surface of, on heating at 300 to 500°C, 19: 47071
diffusion of beryllium at 500 to 600°C in, spectral analysis of, 20: 25019
diffusion of cerium and neodymium in, 16: 22619
diffusion of cerium and lanthanum in, 20: 17038
diffusion of plutonium and uranium in, 17: 41452
diffusion of plutonium in, coefficient of, 18: 36017
diffusion of plutonium in, coefficients for, 19: 40961
diffusion of plutonium in, at 420 to 500°C, 19: 47066
diffusion of plutonium in, at 420, 460, and 500°C, 20: 5848
diffusion of silver-110 in, 17: 22200(T)
dislocation interactions and mobility in crystalline, 19: 32048(R) (NP-15073)
dislocations in, electron microscopic studies, 17: 11182 (AROD-3394.1)
dispersion in graphite, optimum pressure and temperature for liquid, 20: 39355 (EUR-2988.f)
dissolution by acids, 16: 33431(R) (TID-16833)
dissolution in magnesium chloride, mechanism of, 17: 19723 (BNL-759 (p.14-38))
dissolution in magnesium chloride, chronopotentiometric study of, 17: 31795(R) (BNL-782(p.18-43))
dissolution in molten bismuth, development for LMFRE, 16: 9672 (TID-14879)
dissolution of irradiated, equipment and methods for, 18: 25610 (SGAE-CH-4/1964)
dissolution of, media for, 18: 26903
distribution among cellular fractions of dog kidney, 20: 35224
distribution coefficient between fused bismuth and fused salt eutectic, 17: 21683
distribution in soils at Eurochemic site in Belgium, 16: 34144(T,R) (EURAEC-275)
ductility of, pressure effects on, 19: 46983 (AD-612159)
effects of dietary, on strontium-89 content of rat skeleton, 19: 21845
effects of dietary, on strontium-89 excretion by rats, 19: 31757
effects of, on enzyme activity in erythrocyte membranes, 18: 29342
effects of, with calcium on manganese sorption by barley roots, 20: 16174(R) (RLO-1547-3)
effects of, with ferric and ferrous iron on manganese sorption by barley roots, 20: 16174(R) (RLO-1547-3)
effects on calcium-to-strontium-90 ratios in barley and oat culture media and tissues, 20: 42766
effects on cellular aggregation in sponges, 18: 29207
effects on cesium sorption by marine sediments, 19: 43964
effects on cobalt radiation emission spectroscopy, 20: 14444(R) (MLM-1268)
effects on contraction of smooth muscles of rabbit aorta, 19: 25851
effects on corrosion of titanium by mercury at 371°C, 16: 12649(R) (ANL-6485)
effects on corrosion properties of niobium-zirconium alloys in boiling mercury, 19: 15991(R) (BNL-841(p.63-101))
effects on corrosion resistance of beryllium, 19: 22913(P)
effects on corrosion of container materials by liquid bismuth alloys, 18: 4193 (BNL-811)
effects on crystallization of graphite in nodular cast iron, tracer studies, 17: 557
effects on determination of lithium in uranium by flame photometry, 20: 25014
effects on discontinuous precipitation in beryllium–copper alloys, 20: 37253
effects on electric resistivity changes during age-hardening of aluminum–zinc alloys, 19: 9612(T) (AI-Trans-68)
effects on elimination of strontium-89 from rats, 16: 9834
effects on elimination of strontium-89 from bone, 16: 33316(R) (TID-16769)
effects on fluorescence of salicylate, 17: 33879
effects on fluorescence of uranium in sodium carbonate–sodium fluoride melts, 18: 33506
effects on fracture mechanisms in beryllium single crystals, 20: 23714
effects on growth of beryllium oxide crystals, 17: 30511 (NAA-SR-8235)
effects on heterometric determination of vanadium, 19: 36289
effects on heterometric determination of vanadium using 5, 7-diiodo-8-hydroxyquinoline, 20: 257
effects on high-temperature properties of eutectic alloys, 20: 17108
effects on *in vitro* calcification, 20: 5237(R) (UR-668, pp 55-109)
effects on inotropic action of fluoride in rat ventricle, 20: 36567
effects on magnetic susceptibility of vanadium oxide, 16: 15126(R) (NP-11584)
effects on mechanical properties of aluminum, 17: 18707
effects on mechanical properties and microstructure of cobalt and nickel alloys, 20: 27550
effects on neutron-activation determination of lithium, 19: 36253
effects on optical absorption of color centers of lithium fluoride, 17: 15960 (TID-18146)
effects on optical properties of x-irradiated lithium fluorides, 19: 19998
effects on performance of lithium fluoride as thermoluminescent dosimeter material, 18: 35773(R) (UCRL-7811)
effects on phase transformations in gallium–plutonium alloy and plutonium, differential thermal analysis of, 20: 41452 (MLM-1172)
effects on plasticity of nickel, 20: 46213
effects on polarographic determination of zirconium, 19: 34122
effects on precipitation of uranium as α-nitroso-β-naphtholate, 19: 13302
effects on radiochemical determination of strontium in animal or vegetable samples, 20: 22906
effects on radioinduced color centers in lithium fluorides, (E), 20: 42563
effects on radiosensitivity of plants, 20: 42915
effects on reaction of alumina with nickel, 20: 35834(R) (BMI-1767)
effects on separation of uranium from chloride solutions by solvent extraction using trioctylamine, 18: 27627
effects on separation of uranium from sulfate solutions by solvent extraction using trioctylamine, 18: 27626
effects on sintering of beryllia powder, 20: 35857 (AAEC-TM-311)
effects on sorption of europium on red clay from Pacific, 19: 42600(R) (NP-15342)
effects on spectra of nitrogen-15 in ATP, 20: 29083(R) (UCRL-14767)
effects on spectrophotometric determination of aluminum, 19: 13226
effects on spectrophotometric determination of thorium, 19: 24408
effects on strontium-90 uptake by algae, 17: 40531 (TID-7664(p.231-46))
effects on strontium uptake by Chlorella, 18: 35299
effects on strontium uptake and retention, 18: 41063
effects on strontium-89 uptake by freshwater fish, 19: 8757
effects on strontium-90 uptake by rats, 19: 27948
effects on thermoluminescence of doped lithium fluorides, 18: 23828(R) (UCRL-7637)
effects on urinary excretion of skeletal calcium-45 and phosphorus-32 from intact and parathyroidectomized rats, 16: 7401
electric conductivity of, effects of lattice vacancies on, 17: 11231
electric conductivity of, effects of temperature and pressure on, 17: 36494
electric conductivity, 19: 4687
electric discharge in, ion concentration and spectral broadening in, 17: 9060
electric double layer capacity in molten salt systems, 17: 8092
electric mobility in bismuth (liquid) at 500°C, 17: 4946
electric mobility in liquid bismuth alloys, 18: 546 (IP-488)
electrodiffusion in solid bismuth, 19: 32677 (BNWL-67)
electron attenuation and diffraction by crystals of, 17: 620
electron backscattering at 1 to 3.5 Mev, 16: 12344
electron beam attenuation in thin films of, 20: 41621 (ORNL-TM-1565)
electron binding energies of, L_I, (E), 19: 18707
electron energy levels of, lifetime of first-excited ^1P_u, 18: 42729
electron energy loss in films of, 17: 20791
electron magnetic elastic scattering at 41.5 Mev, 17: 7222
electron pair production in screened nuclear field in, (T), 19: 43280
electron reactions at 10.5 ev, bulk and surface plasma oscillations in,

18: 38175
electron reactions with, ionization cross sections for, (T), 20: 19400
electron reactions with, photon emission from, 18: 16670
electron scattering by, study of nuclear magnetic transitions by inelastic, 17: 19078
electron spectra of, Auger, (E), 20: 25745
electron transmission through thin foils of, plasmon excitation in, (E), 20: 15951
electron-pair momentum distribution in, (T), 19: 23464(T)
electronic structure, 17: 32659
energy levels, 17: 41873 (WASH-1044)
energy levels of ionic, Hartree-Fock wave functions for, (T), 20: 25716 (AD-631601)
exchange reactions with calcium, potassium, and sodium on ion exchange resin, equilibrium constant for, 17: 27038
exchangeable mass in alcoholics and control subjects, 16: 7384(R) (TID-14565)
excretion in rabbits, tracer study, 17: 49
excretion in urine, development of chelating agents for enhancing, 16: 5130 (TID-14373)
explosibility of powders of, 19: 36698 (BM-RI-6516)
explosion of wires of, in nitrogen, x-ray analysis of aerosol composition and size produced by, 18: 41381
extrusion by hydrostatic methods, 19: 18436
extrusion by hydrostatic methods, 19: 44651
fabrication and properties of, as reactor fuel canning materials, 18: 557
fluorescence self-absorption of, K, 18: 18919
fluorescence yields in proportional and scintillation detectors, 18: 3796
forging of, effects of beryllium, hydrogen, manganese, thorium, and zirconium on, 19: 7886(P)
gamma absorption at 11 to 30 Mev, cross sections for, (E), 19: 43297
gamma absorption coefficient, 16: 6655
gamma and neutron heating of, in experimental channels of FRJ-2 reactor, 20: 5202
gamma attenuation of liquids, 16: 9226
gamma attenuation coefficient of, temperature dependence of cobalt-60, (E), 19: 5391
gamma attenuation coefficients at 0.03 to 10 Mev, 19: 35569
gamma attenuation coefficients at 0.01 to 100 Mev, 20: 36350
gamma backscattering at 662 kev, (E), 19: 13789
gamma heating, calorimetric measurements, 16: 6821(R) (ORNL-3213 (p.95-102))
gamma reactions (γ,n) from threshold to 80 Mev, cross sections for, 18: 11209 (LNF-63/47(p.194-8))
gamma reactions (γ,p), cross section for, 18: 22897
gamma reactions (γ,n) to 30 Mev, cross sections for, (E), 19: 10332
gamma reactions (γ,n) at 11 to 30 Mev, cross sections for, (E), 20: 4849(R) (UCRL-14360, pp 1-50)
gamma reactions (γ,α) at 31 Mev, alpha spectra from, (E), 20: 38037
gamma reactions (γ,n) at 0 to 80 Mev, 17: 40095
gamma resonance scattering, pulse-height spectra, 16: 8225
gamma spectra from 14-Mev neutron activation, determination by, 19: 26241
grain boundaries in high-purity, small-angle tilt motion in, 20: 31714(R) (UCRL-16658, pp 99-103)
grain boundary cavitation in, effects of moist carbon dioxide on, 17: 32584
grain size of, effects of barium, beryllium, calcium, and strontium on, 18: 39947
grain-boundary cavities in, effects of substructure on nucleation of, 18: 26021
Hartree-Fock potential of neutral atoms of, analytical expressions for, 18: 16656
heat of fusion, 20: 41412(R) (IS-1500(Sect. M))
heat of solution in hydrochloric acid, 16: 3013
heat transfer to pool-boiling, 19: 46550
helium ion reactions at 25 to 50 kev, K x-ray production cross sections from, (E), 20: 29936
helium-3 reactions with, production of short-lived radioisotopes in, 17: 26633
helium-3 scattering at 26–33 Mev, cross sections for elastic, 17: 21090
helium-3 elastic scattering by, optical model analysis of, 18: 40638
hydrogen ion reactions at 25 to 50 kev, K x-ray production cross sections from, (E), 20: 29936
ignition in carbon dioxide, effects of air, oxygen, and water vapor on, 19: 7849 (CEA-R-2494)
ignition in flame, 18: 25328(R) (SC-DC-64-864)
influence of, content of soils on wheat and barley growth variations, 20: 40532(R) (COO-1097-17)
internal friction in cold-worked, 16: 29397
internal friction at low temperature, 19: 11727 (NYO-2471-4)
internal friction in crystals of, at 4.2 to 300°K and 4 to 40 kc, 16: 2199 (TID-14140)
internal friction of lithium-doped single crystals of, 20: 33883 (NYO-2471-19)
ion exchange behavior in hydrochloric acid–organic solvent media, 18: 39124
ion exchange in concentrated hydrochloric and perchloric acids, distribution coefficients for, 18: 17759
ion exchange on Bio-chelex 100, activation energy and diffusion coefficients for, 18: 1641
ion exchange on phosphate glass electrode, 18: 3780
ion exchange paper chromatography of, 18: 17785
ionization by collisions with nitrogen and oxygen molecules, 18: 755
ionization equilibria in sun, (T), 20: 19338
ionization on rhenium surfaces, (E), 19: 27733
iron-57 Mössbauer spectra in, 20: 30766
laser bombardment on, mass spectra of vapor ejected from, 18: 22049
light emission from, at 50°C in 0.25 to 27 μ wavelength region, 17: 15953 (NASA-TN-D-1523)
luminescence effects in lithium fluoride crystals, 18: 17892
luminescent effects of, on uranium, 17: 15928
magnetic breakdown in crystals of, de Haas-van Alphen effect in, 17: 27870
magnetic properties, de Haas–van Alphen oscillations up to 190 kgauss, 16: 15447
melting temperature of, equations for calculating, 18: 25990
mercury ion reactions with, ion emission in, (E), 19: 39374
meson (μ⁻) transitions in mesic atoms of, energy of, 20: 4825(R) (ANL-7081, pp 81-93)
meson (μ) range up to 10^8 Bev in, (T), 19: 4897 (LNF-64/38)
meson (π⁻) reactions (π⁻,nγ) with, energy spectra from, (E), 19: 21315
meson (μ) capture, Fermi interactions in, 16: 15590
meson (μ⁻) capture by, x-ray spectra from, 17: 26578
meson (μ⁻) magnetic moment in mesic, 16: 13865 (NEVIS-101)
meson (μ⁻) reactions, polarization retention measurements, 16: 8230
meson (μ⁻) reactions, capture-rate measurements, 16: 8231
metabolic effects on strontium in rats, 16: 27468 (NP-11941(p.30-1))
metabolism, 19: 63
metabolism and physiological role of, in man, 18: 7993 (CONF-355-2)
metabolism and toxic effects in Habrobracon, 19: 10741 (TID-21559)
metabolism by virus, 19: 33782
metabolism in cattle, effects on calcium metabolism, 19: 31756
metabolism in chickens, effects of dietary calcium and phosphorus levels, tracer study, 17: 23027
metabolism in corn plants, genetic control of, 18: 6596(R) (TID-19842)
metabolism in dogs, tracer study, 17: 27022
metabolism in human fetuses, 19: 43701
metabolism in intestinal tract of rats, tracer study, 19: 14985
metabolism in lobsters, tracer study of, 19: 33761
metabolism in man, tracer study, 19: 42243 (TID-21163)
metabolism in rats, tracer study, 19: 14984
metabolism in rats, tracer study, 19: 29848 (ACRH-103(p.62-75))
metallurgical effects on beta phase stability in plutonium, 16: 19352 (HW-SA-2560)
metallurgical effects on corrosion resistance of Hastelloy C, 16: 22636
mining of, use of nuclear explosions in, 20: 9093(R) (ORNL-3830, pp 271-4)
Mössbauer effect of gold-197 in, relation between chemical shift and electronegativity in, 20: 7055 (UCRL-16436)
neutron absorption by, measurements for $E_0 \leq 30$ Mev, 20: 24575 (LNF-66/7)
neutron absorption cross section in pitchblende, thermal, 20: 37994
neutron activation at 14.3 Mev, (E), 20: 19809 (CEA-R-2900)
neutron capture by, 18: 9317(R) (PR-P-59(p.37-45))
neutron capture cross sections, 16: 26509
neutron capture cross sections for, pile oscillator method for thermal (E), 19: 1546 (CEA-R-2485)
neutron coherent scattering length, 17: 34841
neutron coherent scattering amplitude and cross sections for, 18: 7679 (CONF-346-6)
neutron cross sections, library of 40-group BPG and spectral "B" codes, 16: 12422 (BAW-158)
neutron cross sections at 0.025 ev to 18 Mev, 16: 24796 (UNC-5002)
neutron cross sections at 1.44 ev (E), 19: 3288
neutron cross section at 2200 m/s, (E), 19: 35378(R) (EANDC(E)-57(U))
neutron diffraction at high pressures, 20: 14059(R) (IDO-17104)
neutron diffraction properties of, 20: 26396(R) (IDO-17140)
neutron elastic and inelastic scattering at 14 Mev, cross sections for, 17: 28276
neutron elastic scattering at 2.8 Mev, polarizations in, 16: 11026
neutron elastic scattering and polarization by, at 2.8 Mev, 17: 17294

neutron elastic scattering at 0.3 Mev, angular distributions for, 18: 17090
neutron elastic scattering at 0.8 Mev, angular distributions of, (T), 19: 37884
neutron elastic scattering at 0.8 Mev, cross sections for, (T), 20: 15770
neutron flux and spectrum measurements on foils of, 20: 21427(R) (NASA-CR-54904)
neutron inelastic scattering by, collective nuclear energy levels from fast, 17: 848
neutron inelastic scattering at 14 Mev, collective-state excitation by, (E/T), 19: 23697
neutron inelastic scattering by, gamma yields from, (E), 19: 35406(T) (ANL-Trans-177)
neutron inelastic scattering at 14.1 Mev, gamma yields from, (E), 19: 35417
neutron inelastic scattering in single crystals of, phonon dispersion relations from thermal, 16: 32370
neutron inelastic scattering at 14.1 Mev, spectra for, (E), 20: 28268 (FEI-30)
neutron inelastic scattering by, frequencies of normal modes from thermal, (E), 20: 34810 (BNL-940, pp 78-82)
neutron inelastic scattering by, frequency of normal lattice modes from, 20: 38397
neutron radiative capture cross sections at 30 and 65 kev, 18: 34274(R) (NIRS-2(p.3-15))
neutron reactions (n,γ), gamma spectra at 14 Mev, 16: 2502(T) (AEC-tr-4718)
neutron reactions at 0.1 to 100 Mev, total cross sections for, 16: 11021
neutron reactions (n,p) at 14 Mev, angular distributions and spectra from, 16: 11028
neutron reactions at high energies, table of radioisotopes produced in, 17: 794 (CERN-62-22)
neutron reactions with, production of short-lived radioisotopes in, 17: 26633
neutron reactions (n,γ) with, gamma spectra from fast, 18: 44807
neutron reactions (n,p) with, for photoneutron spectra measurements, 19: 31304
neutron reactions at 14 Mev, gamma emission in, (E), 19: 37890
neutron reactions (n,n′γ) at 3.0 to 4.5 Mev, gamma angular distributions from, (E/T), 19: 47589(R) (TID-22012, pp 53-66)
neutron reactions (n,n′γ) at 14 Mev, elemental analysis by, 20: 27170 (UCRL-14654-T)
neutron resonance absorption integrals for, (E), 20: 15691 (CEA-R-2840)
neutron scattering angular distribution, 16: 12419 (ANL-5567(Rev.))
neutron scattering at 2.0 to 5.0 Mev, angular distributions from, 16: 15686
neutron scattering at 0.1 to 2.4 Mev, polarization asymmetries, 16: 17091
neutron scattering at 14 Mev, optical-model analysis, 16: 23089
neutron scattering by, differential cross section and polarization for, 17: 41528(R) (ANL-6720(p.16-28))
neutron scattering at 0.4 to 1.2 Mev, cross sections for, 18: 9331
neutron scattering by, cross sections for, 18: 15476
neutron scattering at 2.5 Mev, cross sections for inelastic, 18: 14851
neutron scattering cross sections at 0.5 to 0.8 Mev, 18: 26571
neutron scattering at 0.24 Mev, polarization effects on, (T), 19: 19108
neutron scattering total cross sections at 12 to 14 Mev, (E), 20: 11949 (AD-625747)
neutron separation energy, (E), 20: 24329(R) (ANL-7108, pp 1-4)
neutron total cross sections at 28.4 Mev, 16: 5969
neutron total cross section, 17: 15272
neutron total cross section of, fast, 17: 20982 (HW-SA-2875)
neutron total cross section for, 17: 22568 (WASH-1041)
neutron total cross sections at 2.8 to 5.2 Mev, 18: 6210
neutron total cross sections at 0.3 to 2.7 Mev, resonance structure in, 18: 13066
neutron total cross sections at 28 Mev, 18: 44711
neutron total cross sections at 0.5 to 2.2 Mev, (E), 19: 19095 (WASH-1053)
neutron total cross sections of, (E), 19: 41723
neutron total cross section at 4 to 12 Mev, (E), 20: 19805(R) (ANL-7110, pp 1-28)
neutron total cross sections at 12 to 16 Mev, (E), 20: 28396
neutron total cross sections at high energies, fluctuations in, 20: 38173
nuclear resonance fluorescence in, (E), 19: 41828
nutritional needs and toxic effects of, in man, 19: 21990
oxidation and squeeze energy principle, 16: 16696
oxidation at low pressures at 77 to 304°K, 16: 25716 (NP-11876)
oxidation by carbon dioxide and helium, 16: 12694
oxidation in damp carbon dioxide at high temperatures, kinetics of, 17: 29287
oxidation in gas-cooled reactors, 18: 11372
oxidation inhibition in, by beryllium, 17: 25715
oxidation kinetics in water-saturated oxygen at 350 to 600°C, 16: 16348
oxidation kinetics in air, nitrogen, and oxygen, 17: 6577
oxidation of surface of single crystals of, kinetics of, 17: 35701 (TID-17487)
oxidation protection at high temperatures, 18: 12590(P)
oxidation-reduction reactions with niobium oxides, 17: 12678
oxidation, tracer studies of mechanism of, 19: 9098 (UCRL-7631-T)
oxide film formation on crystals of, structure and orientation of, 17: 35704 (TID-17807)
oxygen-16 scattering by, elastic, 17: 31507
particle-density radial distribution in arc plasma of, (E), 20: 8241
partition coefficients and reciprocal ionic radii, 17: 27562 (INSJ-54)
performance as reactor coolant, evaluation of, 18: 20192
performance for removing chlorine from organic reactor coolants, 19: 18047 (CRCE-1188)
phase transformations in, relation of c/a ratio and elastic moduli temperature dependence with, 19: 44676(R) (ANL-7000, pp 176-82)
phonon dispersion relations for crystals of, 16: 27835
phonon dispersion relations in crystals of, determination of neutron spectrometric, 17: 20971
photoionization of, cross sections for, 17: 10681(R) (TID-17743)
photon albedo spectra for, 18: 30939
photon elastic scattering at particle threshold energy, cross sections for, 17: 17153
photon reactions with Coulomb field of, pair production total cross sections for high-energy, (T), 20: 17754
photon scattering, resonant, 16: 2334
plastic deformation, 18: 39835
Poisson's ratio measurements, 19: 26823 (TID-21843)
polarography of, in acetone solution, 17: 14253
positron annihilation in, band structure from, 17: 3624
positron annihilation with core electrons in, momentum distributions for, (T), 20: 37821
positron emission by, after alpha irradiation, 17: 36671(T) (AEC-tr-5976)
precipitation and recrystallization of, effects of aging and plastic deformation on, 17: 34446
precipitation using dimethylbenzenearsonic acid, 19: 9136
precipitation using trichlorobenzenearsonic acid, 19: 9137
preparation as radiation target materials, methods development for, 18: 27815(R) (ORNL-TM-718)
preparation by reduction of magnesium sulfate using catalytic nascent hydrogen, 19: 46253(T) (ORNL-tr-803)
preparation of crystals of, by Bridgman method, 16: 91 (PAN-244/1-B)
preparation of isotopic bulk materials and foils of, from oxide, 20: 13216 (ORNL-P-1899)
preparation, properties and uses of, chemical process monograph on, 19: 18407
prismatic slip in single crystals of, effects of lithium on, 18: 34134 (UCRL-11417)
processing deuteron-irradiated, for separation of sodium-22, 19: 40637(T) (ORNL-tr-625)
production and fabrication for use in reactors, industrial problems created by, 18: 14389
production by fusion electrolysis, 18: 25913(P)
production by fusion electrolysis, 20: 25214(P)
production by reaction of calcium carbide with magnesium fluoride slag, 16: 11775(R) (NLCO-790)
production by salt electrolysis, 19: 28752(P)
production by vacuum distillation, 18: 34051 (ORNL-TM-749)
production by vaporization and condensation, retort cover for, 16: 16673(P)
properties, 17: 25820
properties and structure, effects of alloying elements on, 17: 29349
properties as canning material for uranium fuel elements, 18: 1253 (NP-13218)
properties as reactor material, 16: 18050
properties for reduction of zirconium tetrachloride, 16: 12087 (BM-RI-5933)
properties for use as reactor material, 16: 4994
properties for use as canning and structural material for reactors, 17: 35111
properties for use as reactor material, 19: 13907
properties for use as fuel element can, effects of manganin and zirconium on, 19: 20610(P)
properties for use as fuel-element cladding, 19: 22884
properties for use in nuclear reactors, 20: 21382
properties of liquid, 16: 19370 (TIM-65)
properties of, for use in electric discharge machining of SAP, 20: 33851
proton elastic scattering, polarization effects, 16: 4791
proton elastic scattering at 4.5 Mev, polarization in, (E), 19: 47692

proton inelastic scattering at 15 to 1900 kev, x-ray yields from, (E), 19: 39881
proton reactions (p,n) at 18.5 Mev, angular distributions of quasielastic, 18: 40587
proton reactions at 150 Mev, gamma spectra from, 16: 31088
proton reactions at 540 Mev, cross section for production of rare gases from, 17: 19255
proton reactions at 130 to 400 Mev, production cross sections for isotopes in, 17: 28943(R) (TID-18961)
proton reactions at 660 Mev, 17: 41884
proton reactions at 97 Mev, delayed emission in, 18: 6189
proton reactions at 60 to 500 kev, K-shell x-ray production in, 18: 7775
proton reactions at 130 to 400 Mev, isotope formation cross sections for, 18: 22881
proton reactions at 30 to 150 kev, K x-ray emission following, 18: 30322(T) (UCRL-Trans-1056(L))
proton reactions at 0.5 to 3 Mev, formation cross sections for nuclides from, 18: 43601(R) (TID-21007)
proton reactions at 25 to 100 kev, K x-ray production in, (E), 19: 30946 (UCRL-7700)
proton reactions at 0.05 to 2.9 Bev, induced activity data and cross sections for spallation, 20: 32549
proton reactions (p,beryllium-7) at 27 to 31.5 Mev, cross sections, 16: 29851
proton reactions with, rare gas and tritium production cross sections for, 18: 15189 (CERN-64-12)
proton reactions with, production of delayed proton emitters in, (E), 19: 14546
proton reactions with atoms of, production of highly excited hydrogen atoms by charge-exchange, (E), 20: 11471(T)
proton reactions with, ionization cross sections for, (T), 20: 19400
proton reactions with neutral ground state of, formation of excited hydrogen atoms in, (T), 20: 41634
proton scattering asymmetries in inelastic, 16: 3628
proton scattering, polarization effects, 16: 4794
proton total cross sections at 16.4 Mev, (E), 20: 1208
proton total reaction cross section at 16.6 Mev, measurement of, 18: 1086
quantum defect for ^3S state, 17: 20736
radiation effects on fatigue properties of, neutron, 17: 461
radiation effects on content of, in yeast nucleic acids, 17: 35540
radiation effects on rate of reactions of powdered, with oxygen, 18: 41530
radiation effects on internal friction of, neutron, 18: 44240(T) (AEC-tr-6475)
radiation effects on content of, in blood serum, 19: 8880
radiation effects on content in dog tissues, 19: 19540
radiation effects on corrosion by Santowax OM at 500 to 700°F, fast-neutron, 20: 5846
radiation effects on tensile properties of, neutron, 20: 7639
radiation effects on content of, in milk after mammary gland exposure in cattle and goats, gamma and x, 20: 22594
radiation effects on soil content of, effects of soil type on gamma, 20: 40637(R) (ORO-2754-7)
radiation effects on content in liver, 16: 9860(T)
radioinduced growth of, 17: 470
radioinduced heating, design of calorimeter for measuring gamma and neutron, 16: 26502
radioinduced production of helium and hydrogen in, neutron, 19: 26901
radioinduced thermoluminescence of lithium fluoride doped with, effects of pre-irradiation annealing on, 20: 45008
radiosensitivity effects on plants, 19: 42369
reaction with hafnium and zirconium tetrachlorides in alkali metal halide melt, 18: 27878(P)
reactions at 8 to 13 Mev, gamma and neutron yields in, 18: 44775
reactions in gaseous mixtures, combustion, 20: 29641(R) (SC-DC-65-1691)
reactions of fused, with water, 18: 44922(R) (ANL-6800(p.326-402))
reactions of gaseous, with rare earth chlorides, thermodynamics of, 20: 43222
reactions of liquid, with thorium fluorides in presence of lithium fluorides, 18: 31543(P)
reactions of vaporous, with oxygen, 17: 3574(R) (NP-12212)
reactions with air, carbon dioxide, and water in reactor environment, 18: 1258 (NP-13223)
reactions with ammonium nitrate and oxalate and potassium and sodium sulfates, precipitation, 17: 10621
reactions with autoprothrombin C, complexing in, 19: 32190
reactions with benzophenone, spin distributions in, 17: 4535
reactions with carbon dioxide to 450°C, 19: 22997 (TRG-Report-842)
reactions with crucibles of refractory compounds with boron, carbon, and nitrogen at 400 to 1500°C, 19: 37112
reactions with graphite–bismuth–uranium systems at 500 to 1100°C, 16: 13585 (TID-14950)
reactions with hafnium and zirconium halides to prepare hafnium and zirconium metal, 18: 31544(P)
reactions with hydrogen at −195°C, 16: 112
reactions with hydrochloric acid, heat of, 17: 27323 (UCRL-7325-T)
reactions with materials used in graphite moderated reactors in carbon dioxide and *in vacuo*, 19: 22997 (TRG-Report-842)
reactions with molten salts, 17: 179
reactions with silver nitrate in nonaqueous solvents, 16: 5311(R) (TID-14361)
reactions with thorium halides, 18: 12571(P)
reactions with U_3O_8 to produce UO_2, 20: 23592
reactions with uranium tetrafluoride in briquettes, 16: 15121 (NLCO-841)
reactions with uranium tetrafluoride, semicontinuous, 19: 24919 (NLCO-922)
reactions with uranium tetrafluoride, design of belt furnace for, 19: 37019(P)
reactions with uranium tetrafluoride for uranium metal production, reduction, 20: 749(R) (NLCO-965, pp 1.1-5)
reactions with uranium tetrafluoride, 20: 761(P)
reactions with uranium tetrafluoride, determination of uranium in waste from, 20: 3906
reactions with uranium fluorides, 20: 5870(P)
reactions with uranium(VI) fluoride to prepare uranium metal, 20: 8949
reactions with uranium tetrafluoride to prepare uranium metal, 20: 25530
reactions with uranium tetrafluoride to prepare uranium, 20: 25549(P)
reactions with water at high temperatures during core meltdown, (E/T), 19: 47960(T) (ORNL-tr-694)
reactions with yttrium chloride in fused salt bath, 19: 18437
reactions with zirconium chlorides in fused salts, 19: 22950
reactions, with gelatin, potentiometric studies on binding, 18: 41423
recrystallization of, alloying effects of cerium on, 19: 44710(T) (JPRS-24761, pp 29–40)
reduction of hafnium and zirconium chlorides by liquid, 17: 40826(P)
reduction of scandium fluoride using, 19: 7495
reduction of thorium tetrachloride by, preparation of thorium by, 18: 44070
reduction of uranium tetrafluoride, design of bell furnace for, 19: 39113(R)
reduction of uranium tetrafluoride to metal by, comparison of electrolytic and ferrosilicon-process, 20: 15050(R) (NLCO-970, pp 3.1-4)
reduction of uranium(IV) fluoride, process for, 20: 39342(P)
reduction of zirconium tetrachloride using, preparation of zirconium by, 17: 16615
refining by vacuum distillation, 20: 27417(T) (UCRL-Trans-10036)
separation by anion exchange in acetic acid–nitric acid medium, 18: 16131
separation by anion exchange in acid-organic solvent media, 18: 23707(R) (TID-20609)
separation by anion exchange in mixed aqueous and non-aqueous systems, 19: 2243
separation by reversed-phase chromatography on D2EHPA treated paper, 18: 16141
separation by reversed-phase chromatography using paper treated with di-(2-ethylhexyl) orthophosphoric acid, 18: 39096
separation from alkaline earth elements, aluminum, and iron by cation exchange, 18: 17959
separation from aqueous solutions by solvent extraction using diphenylarsinic acid, 17: 21787
separation from aqueous solutions by solvent extraction using bis(2-ethylhexyl) phosphate, 20: 9049(R) (ORNL-3830, pp 193-221)
separation from barium, calcium, and strontium by paper electrophoresis, 17: 21786
separation from barium, calcium, and strontium by cation exchange, 18: 17958
separation from beryllium using arsonic acids, 16: 8685(T) (AWRE/TRANS/25)
separation from bismuth by ion exchange, 17: 32195(T) (KFK-tr-130)
separation from calcium, 16: 11584(T) (CEA-tr-R-1421)
separation from calcium and strontium by anion exchange, 18: 16132
separation from calcium, strontium, and yttrium by reversed-phase partition chromatography, 18: 39078
separation from calcium and strontium by ion exchange, 19: 9046(R) (IS-900(Sect.C))
separation from calcium and strontium by ion exchange on zirconium molybdate crystals, 19: 13218
separation from calcium, potassium, sodium, and strontium by ion exchange, 19: 44122
separation from cerium by ion exchange chromatography, 19: 26480
separation from chloride solutions by ion exchange, 20: 4053

separation from cobalt, nickel, and zinc by complex formation and solvent extraction, 19: 19833 (CEA-R-2628)
separation from curium by precipitation with arsenazo and crystal violet, 20: 25021
separation from graphite above 1750°C in inert gases, 19: 38762
separation from halide salt baths, effects of calcium and zinc additions on, 17: 36860(R) (ANL-6648)
separation from hafnium by electron-beam melting, 19: 4582 (BM-RI-6560)
separation from hydrochloric acid solutions by solvent extraction using 2-ethylhexanol, 19: 36252
separation from large amounts of uranium, anion-exchange, 19: 7620(R) (TID-21411)
separation from lead by anion exchange in nitric acid-tetrahydrofuran media, 18: 31446
separation from lithium hydroxide by solvent extraction, 17: 32193 (ORNL-TM-637)
separation from lithium by ion exchange chromatography, 18: 21975
separation from lithium fluoride by zone refining, 18: 22019(R) (ORNL-3591(p.231-40))
separation from low-level wastes by precipitation, 16: 25036 (ORNL-TM-260)
separation from manganese by cation exchange, 19: 13535
separation from metallic mixture by ion exchange chromatography, 17: 5991
separation from mercury, 19: 15332(R) (BNL-841(p.52-62))
separation from nitrate solutions by solvent extraction using di(2-ethylhexyl)phosphoric acid, 17: 17949(R) (ORNL-TM-449)
separation from nitric or sulfuric acid solutions, ion exchange selectivity scales for, 19: 9257
separation from other materials by electrolytic extraction, 19: 46454
separation from other inorganic ions by paper chromatography, 20: 12939
separation from perchloric acid solutions by solvent extraction using bis(di-*n*-hexylphosphinyl)methane, 18: 9970 (IS-777)
separation from perchloric acid solutions by ion exchange materials, 20: 20823
separation from pure metals using thionalide, 16: 18835
separation from pyridine, 16: 2504(T) (JPRS-11068)
separation from rare earths by ion exchange in isopropyl alcohol, 18: 20104
separation from rare earths by extraction using fused chlorides, 20: 4297(R) (IS-1200(Sect.M))
separation from rhenium by anion exchange chromatography, 19: 24433
separation from scandium by ion exchange chromatography, 20: 16574
separation from scandium by ion exchange chromatography, 20: 20821
separation from sea water by sorption on ferric hydroxide gel, 18: 37083
separation from silver by partition chromatography, 20: 4054
separation from sodium by solvent extraction using ethanol, 19: 40686
separation from strontium by hydroxide precipitation, 19: 24604 (BNWL-46)
separation from thorium and uranium by paper chromatography, 18: 33505
separation from thorium by ion exchange in nitric acid solution, 20: 20624
separation from titanium by cation exchange chromatography, 17: 32054
separation from titanium, vanadium, and zirconium by zone melting, 18: 8456
separation from trivalent rare earths by cation exchange, 17: 10734 (IS-508)
separation from uranium by hydraulic separator, 16: 11775(R) (NLCO-790)
separation from uranium using 8-hydroxyquinolate, gravimetric, 18: 21995
separation from uranium by ion exchange and elution with ascorbic acid, 18: 25611(T) (AEC-tr-6227/1(p.1-8))
separation from uranium by ion exchange, 19: 7641
separation from uranium by cation exchange chromatography, 19: 13245
separation from uranium by ion exchange, 19: 44119
separation from uranium by partition chromatography on silica-gel column, 20: 9073
separation from uranium by combined ion exchange-solvent extraction using nitric acid–tetrahydrofuran solutions, 20: 20811
separation from waste solutions by sodium carbonate–hydroxide precipitation, 17: 12366(R) (RAI-104)
separation from waste solutions by combined sodium carbonate-hydroxide precipitation and foam process, 17: 28584(R) (RAI-113)
separation from zirconium by ion exchange on pyrocatechol-*O,O*-diacetic acid, 18: 33508
separation of protactinium from, by sorption on activated charcoal, 20: 43148
separation of rare earths from, by pyrometallurgy, 19: 9604(R) (IS-900(Sect.M))
separation of rare earths from, by precipitation using ammonium cinnamate, 20: 45611
separation of scandium from, by ion exchange chromatography, 19: 533
separation of trace elements from, by precipitation ion exchange, 20: 1958
separation using α-hydroxyisobutyric acid, chromatographic, 18: 16142
shear stress of, effect of lithium content on critical resolved, 19: 30808
Slater-Condon parameters of, determined from spectral data, 17: 31118
soaps of, preparation and properties of, 20: 35931
sodium-22 separation from deuteron-irradiated targets of, 19: 44100
solubility in bismuth (liquid) at 500°C, 16: 13137
solubility in cerium, 17: 14824 (LADC-5615)
solubility in lanthanide metals, solid, 20: 17016 (IS-1175)
solubility in liquid sodium, effects of free energy gradient on, 18: 22488 (NAA-SR-8381)
solubility in liquid zinc, 20: 22966 (ANL-7083)
solubility in molten magnesium chloride, anodic chronopotentiometric studies of, 17: 7991 (BNL-6583)
solubility in rare earths, 19: 9604(R) (IS-900(Sect.M))
solvent extraction by di(2-ethylhexyl) phosphate–tributyl phosphate, 19: 24604 (BNWL-46)
solvent partition in tributyl phosphate–hydrochloric acid or –nitric acid systems, 18: 33685
solvent properties for zirconium, 16: 19395
solvent properties for thorium, 17: 28465 (TID-7650(p.436-53))
solvent properties of liquid and solid, for niobium and vanadium, 18: 28002
solvent properties for barium-140 and lanthanum-140 from irradiated chromium–uranium droplets, 20: 292 (UCRL-16173)
solvent properties of liquid, for barium and lanthanum, 20: 31320 (UCRL-16108)
sorption and exchange in peat, 18: 23806
sorption and excretion in breast fed babies, effects of phosphates on, 18: 29219
sorption by coal from acetic and perchloric acid solutions, 17: 25371
sorption by gastrointestinal tract of sheep, tracer study, 17: 5737
sorption by intestine in rats, effects of calcium and strontium on, 18: 8092
sorption by nuclear sulfonic acid resin, 17: 28855
sorption by rat intestines, effects on intestinal mucosa, 19: 8775
sorption of phosphorus-32 from magnesium sulfate solutions by, conditions for, 17: 14236
sound propagation in solid-rod, 16: 23972 (ANL-6515(p.133-61))
spectra in reaction zone of acetylene air flame, excitation of atomic, 17: 27371(T)
spectra of, arc, 18: 6358
spectra of, electric discharge, 17: 34642
spectra of, infrared, 17: 32739
spectra of, K x-ray, 17: 30484
spectra of minerals, effects of temperature on infrared, 17: 33880
spectra of, spin-orbit coupling in band structure, 17: 16845
spectra of, muonic K x-ray, 18: 42626(R) (ANL-6879(p.69-87))
spectra of, wavelengths of Lyman lines in, 20: 25731
spectral line oscillator strengths, 16: 18224(T)
stress-strain distribution in lap-jointed thin shells of, 18: 18355 (UCRL-7304)
structural properties and uses in reactors, survey, 16: 16036
structure of, co-extruded with magnesium–zirconium alloy, 18: 14503
superconducting transition temperature in, 16: 15334
surface binding of, by marine bacteria, 18: 19520(R) (TID-20499)
surface properties and volume of, relation between, 17: 41476(T)
swaging powders of, in aluminum cans, 19: 26785 (INR-557/XIV)
temperature effects on mechanical properties of, cryogenic, 17: 6542
temperature of plasma of, spectroscopic determination of, 20: 26275
temperature of transient discharge plasma of, determination using Stark broadening, (T), 20: 34736
tensile properties of, effects of zirconium on, 19: 11682
tensile testing of single crystals of, dislocation motion in, 20: 27548
thermal capacity at 50 to 750°K, 18: 16891(R) (GA-4881)
thermal conductivity, 19: 4687
thermal expansion down to 1.5°K, 18: 18837
thermal expansion at 1.5 to 12°K, 18: 37716
thermodynamic properties of liquid and solid, 20: 7555 (CONF-650559-8)
thermodynamics in potassium chloride (liquid), oxygen equilibrium potential diagram for, 16: 20426
thermoelectric properties, (E), 19: 16439(R) (AD-604997)
thermoluminescence effects on sapphire and sodium borate glass, 16: 13060
tracer applications survey, 16: 1359
ultraviolet absorption, effects on valence electrons, 16: 10947 (AROD-2810.4)
ultraviolet emission from electron-bombarded foils of, 20: 14004
uptake by corn plants, effects of soil fertility on, 20: 40735 (NYO-2744-

37)
uptake by plants, effects of beryllium on, 19: 45802
uptake by woody plants, regularities in, 19: 6964
use as activator in lithium fluoride crystals, 20: 46940 (AD-640317)
use as filling layer in sheathed fuel elements, 19: 25718(P)
use as lining in electron beam apparatus, 20: 11418(P)
use as threshold detector for fast neutrons, (E), 19: 39007
use for reduction of uranium oxides in preparation of intermetallic uranium–zinc, 19: 32769(P)
use in coolant-flow rotameters for water-cooled reactors, 16: 27393(P)
use in fast-neutron activation dosimetry, 17: 34288
use in metallothermal reduction of titanium and zirconium oxides, 20: 7100
use in production of uranium, methods of shortening heating cycles in thermite bomb reactors, 16: 7614 (MCW-1452)
use in reactors, 19: 17183
use in reduction of yttrium fluorides, 16: 2992 (IS-374)
use of kryptonated, for determining acidity of aqueous hydrochloric acid solutions, 19: 36267
use of liquid, in separation of thorium and uranium, 16: 8810 (NAA-SR-6666)
uses in preparation of beryllium, 19: 412(P)
uses in reactor fuel elements for high-temperature applications, 19: 3607(P)
vapor pressure at 223 to 385°C, 19: 20556 (NASA-TN-D-2723)
vaporization in space vehicle reentry, 20: 33884(R) (SC-CR-66-2029)
vaporization rates of, 20: 33884(R) (SC-CR-66-2029)
viscosity of liquid, based on atomic parameters, 20: 20656 (UCRL-11930)
viscosity of, relation of atomic mobility to, 17: 4945
welding by friction, 17: 1908
welding of sintered, flash butt, 18: 2195 (CEA-2295)
welding of, characteristics of electron beam, 18: 34112
wetting effects on outside of chromium alloy tubes during mercury-pool boiling heat transfer, 19: 11367
with 2,4-pentanedione, heat of combustion of, 16: 11609
x-ray emission at 80 to 180Å, 16: 8129
x-ray spectra of, plasmon satellites in, 17: 13424
x-ray spectrum from mesic (μ), 17: 22264(R) (ANL-6679)
x-ray absorption, effects on valence electrons, 16: 10947 (AROD-2810.4)
x-ray emission spectra from solar, isothermal quiet-corona model for line intensities in soft, 20: 19338
x-ray mass absorption coefficients at 7 to 17 Å, (E), 19: 6394
x-ray self-absorption of, K, 18: 18919
x-ray spectra from μ-mesic atoms of, nuclear charge distribution from, 19: 27518
x-ray spectra of μ- and π-mesic atoms of, (E), 20: 34103
x-ray total cross sections at 15 to 30 Mev, (E), 19: 12573

MAGNESIUM ACETATES
preparation and crystal structure of ammoniated, 19: 40507

MAGNESIUM ALLOYS
see also Magnox Alloys
analysis for cerium by potentiometric titration using vanadium(II) salts, 20: 274
analysis for hafnium and zirconium by EDTA titration, 18: 1556
analysis for hydrogen, 17: 21622
analysis for insoluble and soluble forms of zirconium, 16: 12977
analysis for rare earths by successive potentiometric titration, 20: 38830
analysis for rare earths and zirconium, quantometric, 20: 43112
analysis for thorium and zirconium using xylenol orange, 17: 15921
analysis for zirconium using morin, photocolorimetric, 16: 149
analysis for zirconium using Arsenazo III, spectrophotometric, 18: 31413
analysis for zirconium, photometric, 18: 33512
analysis of Magnox ZR55 and Magzan, for thorium, spectrographic, 19: 36233 (PG-Report-615)
analytical chemistry of, review on, 17: 19948
bibliography on high-temperature, 18: 32067(T) (JPRS-25069(p.32-53))
bonding with epoxy adhesives, effects of surface preparations on, 19: 36995 (BDX-613-68)
casting of, effects of beryllium on, 18: 22513
coating of, review of techniques for protective, 19: 4605
coating with titanium esters and polymers, 17: 3436(P)
compatibility with carbon dioxide in gas-cooled reactors, 20: 13199
composition for uranium fuel canning with improved grain growth resistance, 19: 4705(P)
corrosion, 17: 6572 (OTS-61-31480)
corrosion by carbon dioxide and water, 16: 32083(T) (CEA-tr-A-1148)
corrosion by chloride ions, electrochemistry of pitting, 20: 11231 (CEA-R-2815)
corrosion by gas–oil, hydrogenated terphenyl, and monoisopropylbiphenyl at 330 to 400°C, 20: 25492(T) (AECL-2330, pp 196-217)
corrosion by impure Santowax, 17: 23891 (NAA-SR-7755)
corrosion by water, electrochemical, 16: 12055
corrosion by water or water vapor in radiation environment, 19: 7870
corrosion of, by mineralized water, effects of chlorides, fluorides, and purity on, 17: 20424
corrosion of, book, 18: 22451
corrosion of, review, 19: 7868
corrosion of, translations on, 19: 6271(T) (JPRS-27451)
creep behavior of heat-treated, 16: 21076
creep, cavitation and cracking during, 16: 2231
creep cavities, methods for metallographic examination of intergranular, 16: 25790
development as reactor material, 18: 44075
diffusion of plutonium in, at 420 to 500°C, 19: 47066
electric conductivity, 19: 4687
electric strength of, effects of grain size and porosity on pulse, 20: 25574 (SC-DC-66-1509)
extrusion by hydrostatic methods, 19: 18436
extrusion by hydrostatic methods, 19: 44651
fabrication for use in reactors, 19: 37008
fabrication of reactor components of, 20: 801(P)
fabrication of tubes of, 19: 24967(P)
fabrication of, for use as element cladding, 19: 30713(P)
fatigue under strain-controlled low-cycle conditions, 16: 16767
grain growth reduction by addition of manganese, 18: 32211(P)
ignition and corrosion of, at high temperatures, 17: 16598
ignition in reactors, temperature calculations for, 19: 25708 (TRG-Report-848)
interactions with gas flow in MHD generators, 20: 41738
magnetic susceptibility of semiconducting, 18: 2163(R) (IS-700(Sect.M))
mechanical properties of ultrahigh-strength, 17: 14874
mechanical properties for use as fuel canning material, 17: 30927
oxidation and squeeze energy principle of Magnox A 12, 16: 16696
oxidation inhibition in, by beryllium, 17: 25715
oxidation protection at high temperatures, 18: 12590(P)
phase diagrams of rare-earth-containing, types, 19: 23004(T) (JPRS-28849(p.148-57))
pressing coating of, on reactor fuel, grain-size control in, 20: 5871(P)
pressing coatings of, on fuel elements for operation at 140 to 350°C, 20: 5872(P)
processing of high-temperature, 18: 32066(T) (JPRS-25069)
properties, 17: 25820
properties as canning material for uranium fuel elements, 18: 1253 (NP-13218)
properties as fuel-element cladding, 20: 39443(P)
properties for use as fuel-element cladding, 19: 22884
properties for use as fuel cladding material in reactors, 19: 39206
properties for use in nuclear reactors, 20: 21382
properties of commercial, review, 19: 6245 (DMIC-206)
properties of, effects of uranium on, 17: 418 (NP-12164)
properties of, handbook on, 18: 10535 (N63-18835)
protective coatings, development for use on components of airborne vehicles, 16: 10454(R) (NP-11312)
radiation effects on mechanical properties, fast neutron, 16: 572 (REIC-20)
reactions of liquid, with water, 16: 31614
reactions with uranium to 450°C, 19: 22997 (TRG-Report-842)
separation from praseodymium by fused chloride extraction, 20: 5594(R) (ANL-6925, pp 21-106)
structural properties and uses in reactors, survey, 16: 16036
tensile properties, 16: 22586 (DMIC-Memo-150)
thermal conductivity from uranium to, 16: 13223
thermal conductivity, 19: 4687
thermodynamic properties of thermal energy-storage binary, partial molar, 20: 37722(R) (N-65-30843)
thermophysical properties of, 17: 6549
use as filling layer in sheathed fuel elements, 19: 25718(P)
uses as fuel element cladding, 17: 34445
uses in separation of americium and curium, 18: 43727(P)
vaporization rates of AZ31 and HM31A, 20: 33884(R) (SC-CR-66-2029)
welding of Magnox, prevention of contamination from electrodes in resistance, 16: 19326(P)
welding of Magnox, resistance, 16: 30768(P)
welding technology of, review on, 17: 22146
Al–Be–Mg, analysis for beryllium, colorimetric, 20: 29111
Al–Be–Mg, beryllium distribution and grain size in cast, 17: 31002
Al–Be–Mg, cavitation and creep properties at 20 to 500°C, 16: 16762
Al–Be–Mg, diffusion of beryllium to surface of, on heating at 300 to 500°C, 19: 47071
Al–Be–Mg, directional diffusion creep in, 18: 12699
Al–Be–Mg, effects of heat on beryllium distribution in, 19: 30769

Al–Be–Mg, mechanical properties, 17: 34445
Al–Be–Mg, oxidation by carbon dioxide–carbon monoxide mixtures at 500 to 700°C, 17: 25739
Al–Be–Mg, structural changes during creep deformation of, 17: 466
Al–Ce–Mg, hydridation, 17: 36329
Al–Cr–Mg, erosion by water of rotating disks of, 19: 44625 (TIM-894)
Al–Cu–Mg, degassing, 17: 12601
Al–Cu–Mg, mechanical properties, review, 16: 13617
Al–Cu–Mg, thermal capacity and conductivity at −180 to +200°C, 17: 11200 (USNRDL-TR-599)
Al–Cu–Mg–Mn, erosion by water of rotating disks of, 19: 44625 (TIM-894)
Al–Cu–Mg–Mn, proton reactions at 660 Mev, 17: 41884
Al–Cu–Mg–Mn, sputtering by 2-kev mercury ions, energy distributions of particles from, 18: 14625
Al–Cu–Mg–Zn, corrosion resistance of, effects of age hardening, chromium, and silver on stress, 18: 25946(T) (RSIC-177)
Al–Cu–Mg–Zn, mechanical and structural properties of type 7075, effects of zirconium additions on, 16: 9222
Al–Cu–Mg–Zn, mechanical properties, review, 16: 13617
Al–Cu–Mg–Zn, tensile properties of welded, 16: 6697 (NP-11227)
Al–Fe–Mg–Mn, microstructure of 214X, electron microscopic studies using ultramicrotome, 18: 7206 (GAT-T-1121)
Al–In–Mg, corrosion, 19: 6271(T) (JPRS-27451)
Al–Li–Mg, bonding of LA141, surface preparation and epoxy adhesive for, 19: 36995 (BDX-613-68)
Al–Li–Mg, phase transitions and tensile properties, 16: 24164 (NP-11778)
Al–Li–Mg–Th, preparation and properties at high temperatures, 19: 37153(P)
Al–Li–Mg–Y, preparation and properties at high temperatures, 19: 37154(P)
Al–Mg, alloying effects of uranium on, 16: 5719 (NP-11169)
Al–Mg, analysis for beryllium, spectrophotometric, 18: 29573
Al–Mg, analysis for magnesium, electrographic, 20: 267
Al–Mg, analysis of, for antimony, 17: 5960 (PG-Report-337)
Al–Mg, analysis of, for cobalt, 17: 5960 (PG-Report-337)
Al–Mg, annealing neutron-irradiated, 17: 39693
Al–Mg, anodization of, determination of optimum conditions for, 17: 34412 (ORNL-TM-641)
Al–Mg, casting 10% aluminum, effect of beryllium additions on, 16: 9247
Al–Mg, clustered vacancy annihilation and precipitation in, 18: 7244
Al–Mg, corrosion of, electrochemical, 18: 14404(R) (EURAEC-95)
Al–Mg, corrosion by water, effects of heat flux on, 18: 14408 (ORNL-3541)
Al–Mg, corrosion of, effects of indium on, 18: 20482
Al–Mg, corrosion by heavy water, 18: 37637 (A/CONF.28/P/591)
Al–Mg, creep at high temperatures, effects of recovery treatment on, 19: 43997(R) (UCRL-11889)
Al–Mg, creep behavior of heat-treated, 17: 14851 (TRG-Report-420)
Al–Mg, creep cavities in, nucleation of, 19: 41063
Al–Mg, crystal structure of Mg_2Al_3in, 19: 46984(R) (AD-612275)
Al–Mg, crystal structure, 20: 2399
Al–Mg, decomposition reactions of solid solutions of, effects of vacancies on, 18: 34135(T) (AI-Trans-53)
Al–Mg, defect clusters in irradiated, 16: 13649
Al–Mg, deformation stacking after cold-working, 16: 10594
Al–Mg, deformation of, piezoelectric pulse measurements during, 17: 11250
Al–Mg, development of prismatic dislocation loops from quenched-in vacancies in, 17: 37592
Al–Mg, diffusion of plutonium at 420 to 500°C in, 19: 47066
Al–Mg, diffusion of beryllium to surface of, on heating at 300 to 500°C, 19: 47071
Al–Mg, dislocations in, vacancy climb rate of prismatic, 17: 1953 (UCRL-10441)
Al–Mg, dislocation loops in, negative climb of prismatic, 19: 2806 (UCRL-11239)
Al–Mg, dislocation climb in quenched, kinetics of, 19: 39169 (UCRL-16090)
Al–Mg, dislocation loop climb in, negative, 19: 43997(R) (UCRL-11889)
Al–Mg, distribution of rare earths between magnesium chloride–potassium chloride–sodium chloride and, at 550 to 600°C, 19: 32279(R) (ANL-7020(p.3-99))
Al–Mg, effects of lanthanum and neodymium on secondary electron emission properties of activated, 17: 37545(T)
Al–Mg, effects of barium, beryllium, calcium, and strontium on grain size of, 18: 39947
Al–Mg, electron characteristic energy loss in, 17: 22300
Al–Mg, explosibility of powders of, 19: 36698 (BM-RI-6516)
Al–Mg, fatigue of Magnox Al80, plastic strain range at 350 to 500°C, 20: 39419
Al–Mg, fatigue properties at 200 to 500°C, 17: 27847
Al–Mg, fatigue test values of, 17: 11245
Al–Mg, gamma attenuation, 16: 9226
Al–Mg, grain-boundary sliding, 16: 21024 (ASD-TR-61-383)
Al–Mg, heat resistance, mechanical properties, and recrystallization of, 18: 16496
Al–Mg, kinetics of anodic attack on, effect of thermal and mechanical treatment on, 17: 18022
Al–Mg, magnetization of superconducting, (E), 20: 37935 (CEA-R-2906)
Al–Mg, mechanical properties of 6061, 18: 12653 (ORNL-3557)
Al–Mg, microstructure of, electron microscopic studies using ultramicrotome, 18: 7206 (GAT-T-1121)
Al–Mg, performance of Magnox AL80 as reactor components, 18: 37667 (A/CONF.28/P/146)
Al–Mg, performance as reactor material, 18: 44183
Al–Mg, plasticity, method for determination, 16: 10587
Al–Mg, Portevin-Le Chatelier effect in, contribution of vacancies to, 16: 27667
Al–Mg, precipitation and recrystallization of, 17: 34446
Al–Mg, preparation of, method for obtaining fine grain size and incorporating zirconium in, 16: 27577(P)
Al–Mg, preparation of, method for obtaining finer grain size and incorporating zirconium in, 16: 27578(P)
Al–Mg, preparation and properties of metastable solid solutions in, 18: 9781 (TID-20021)
Al–Mg, properties for cryogenic applications, 19: 23070
Al–Mg, quench-aging of vacancies in, 18: 2233 (UCRL-10879)
Al–Mg, radiation damage to, basic mechanism study of, 16: 13643 (TID-14667)
Al–Mg, radiation effects, studies by transmission electron microscopy, 16: 21101
Al–Mg, radiation effects on aging and resistivity of, 18: 34244
Al–Mg, radiation effects on, mechanisms of recovery from electron, 19: 27735(R) (NAA-SR-10850)
Al–Mg, radiation effects on, annealing electron, 19: 40286(R) (NAA-SR-11200)
Al–Mg, radiation effects on corrosion and mechanical properties of, neutron, 19: 44752 (CEA-tr-A-1818)
Al–Mg, radiation effects on tensile properties of AL80, neutron, 20: 7639
Al–Mg, radioinduced dislocation loops in, effects of magnesium concentration on fission-fragment, (E), 20: 15145
Al–Mg, reactions of 6061 alloy with steam, 18: 26824(R) (ANL-6885)
Al–Mg, reactions of hydrogen with calcium, cerium, lanthanum, thorium, and yttrium in liquid, 18: 35548
Al–Mg, reactions with steam at 800 to 1300°C, 19: 11682
Al–Mg, reactions with steam at 1200 to 1600°C, 19: 17174(R) (ANL-6900(p.232-303))
Al–Mg, rupture behavior at temperatures up to 150°C, 16: 10586
Al–Mg, separation of lanthanum from, by fused chloride extraction, 20: 5594(R) (ANL-6925, pp 21-106)
Al–Mg, solvent properties for rare earths, 19: 14765(R) (ANL-6977)
Al–Mg, solvent properties for rare earths in halides, 19: 17176(R) (ANL-6965(p.1-41))
Al–Mg, solvent properties for rare-earth fission products, 19: 24064(R) (ANL-6997)
Al–Mg, solvent properties for rare earths at 550 and 600°C, 19: 32279(R) (ANL-7020(p.3-99))
Al–Mg, solvent properties for rare earth elements in molten chloride salts, 20: 3865 (ANL-7064)
Al–Mg, solvent properties of liquid, for praseodymium, 20: 20802(R) (ANL-7055, pp 21-98)
Al–Mg, stacking-fault energies of, 20: 31715(R) (UCRL-16658, pp 105-20)
Al–Mg, structure evolution through annealing, 16: 19386
Al–Mg, surface structure and brightness of pure, 16: 10588
Al–Mg, swaging powders of, in aluminum cans, 19: 26785 (INR-557/XIV)
Al–Mg, tensile properties of welded, 16: 6697 (NP-11227)
Al–Mg, thermal stability at 150 to 300°C, 17: 34461
Al–Mg, thermodynamic properties of, partial molar, 20: 37722(R) (N-65-30843)
Al–Mg, use in preparation of uranous chloride by reduction of uranyl chloride, 19: 38662
Al–Mg, vacancy aggregation in, from quenching, 19: 997(R) (NYO-2994-1)
Al–Mg, vacancy binding energy of magnesium in, 17: 35264(R) (UCRL-10706(p.111-203))
Al–Mg–Mn, creep properties at high temperatures, 18: 26066(P)
Al–Mg–Mn–Zn, corrosion, 19: 6271(T) (JPRS-27451)

Al–Mg–Mn–Zn, plastic anisotropy of AZ31B sheet, 19: 39149 (AD-425880)
Al–Mg–Zn, aging sequence in, 17: 1976
Al–Mg–Zn, bonding of AZ31, surface preparation and epoxy adhesive for, 19: 36995 (BDX-613-68)
Al–Mg–Zn, deformation stacking after cold-working, 16: 10594
Al–Mg–Zn, dispersion hardening of, effect of pre-aging on, 16: 10598
Al–Mg–Zn, effects of polarization on stress corrosion of, 17: 32530
Al–Mg–Zn, fatigue at low endurance, during strain and stress, 16: 13615
Al–Mg–Zn, mechanical properties, review, 16: 13617
Al–Mg–Zn, precipitation in vicinity of grain boundaries, 16: 19420
Al–Mg–Zn, stress corrosion under constant tensile and bend stress, 16: 10468
Al–Mg–Zn, stress-corrosion cracking of, effect of corrosion conditions on, 17: 22124
Al–Mg–Zn, temperature dependence in stress corrosion, 17: 11139
Al–Mg–Zn, tensile properties of welded, 16: 6697 (NP-11227)
Al–Mg–Zr, creep rates, 20: 11313
Al–Mg–Zr, phase studies on intermetallic compounds in extruded and heat-treated, 18: 35985 (BM-RI-6498)
Au–Mg, electron transfer in dilute, 17: 37189
Au–Mg, radiation effects at 80°K on, resistivity recovery from proton, 20: 21445
Ba–Mg, crystal structure of Ba_2Mg_{17} in, 17: 29334
Ba–Mg, elastic constants of, relation to cohesion and stability of intermetallic phases, 18: 44228
Ba–Mg, heat resistance, mechanical properties, and recrystallization of, 18: 16496
Ba–Mg, structure of intermetallic compounds in, 17: 23964(R) (TID-18619)
Be–Ca–Mg, diffusion of beryllium to surface of, on heating at 300 to 500°C, 19: 47071
Be–Ca–Mg, effects of heat on beryllium distribution in, 19: 30769
Be–La–Mg, diffusion of beryllium to surface of, on heating at 300 to 500°C, 19: 47071
Be–La–Mg, effects of heat on beryllium distribution in, 19: 30769
Be–Mg, analysis, methods of spectral, 16: 22037
Be–Mg, compatibility with carbon dioxide, 20: 11225
Be–Mg, corrosion resistance, 19: 22913(P)
Be–Mg, corrosion in moist carbon dioxide at 650-750°C, 20: 2277(P)
Be–Mg, crystal structure of intermetallic compound $MgBe_{13}$ in, 16: 12121
Be–Mg, development for heat-resistant cladding, 18: 37608 (A/CONF. 28/P/340)
Be–Mg, diffusion of beryllium to surface of, on heating at 300 to 500°C, 19: 47071
Be–Mg, fabrication of super heat-resistant, 17: 32553
Be–Mg, fabrication and properties of, effects of magnesia on, 19: 42830
Be–Mg, oxidation of, at 470, 520, and 580°C, 17: 14861(T) (AERE-Trans-913)
Be–Mg, preparation of, by powder-metallurgical methods, 16: 5697
Be–Mg, preparation and properties of, 19: 30795
Be–Mg–Mn–Zr, fabrication and properties, 19: 36970(P)
Be–Mg–Th, diffusion of beryllium to surface of, on heating at 300 to 500°C, 19: 47071
Be–Mg–Th, effects of heat on beryllium distribution in, 19: 30769
Be–Mg–Zn, diffusion of beryllium to surface of, on heating at 300 to 500°C, 19: 47071
Be–Mg–Zn, effects of heat on beryllium distribution in, 19: 30769
Bi–Ca–Mg, phase studies, 16: 29430
Bi–Mg, electric mobility of magnesium in liquid, 18: 546 (IP-488)
Bi–Mg, phase studies, 19: 37072
Bi–Mg, superconductivity, 20: 44554
Bi–Mg, thermoelectric properties of, (E), 19: 16439(R) (AD-604997)
Bi–Mg–Sn, phase studies, 16: 29431
Ca–Mg, diffusion of beryllium to surface of, on heating at 300 to 500°C, 19: 47071
Ca–Mg, elastic constants of, relation to cohesion and stability of intermetallic phases, 18: 44228
Ca–Mg, heat capacity at high temperatures, 19: 9604(R) (IS-900 (Sect.M))
Ca–Mg, heat capacity of intermetallic compound, at 4 to 287°K, 20: 41412(R) (IS-1500(Sect. M))
Ca–Mg, heat of fusion of intermetallic compound, 20: 41412(R) (IS-1500(Sect. M))
Ca–Mg, heat resistance, mechanical properties, and recrystallization of, 18: 16496
Ca–Mg, heats of formation and fusion of intermetallic compound $CaMg_2$ in, 19: 19838 (IS-1070)
Ca–Mg, properties for use as getter for deoxidation of tantalum, 18: 12552 (LAMS-3022)
Ca–Mg, properties of intermetallic compounds in, 19: 39177
Ca–Mg, reactions with hydrogen at 450 to 637°C, 18: 35549
Ca–Mg, thermal stability at 150 to 300°C, 17: 34461
Ca–Mg, thermodynamics of compound formation in, from vapor pressure measurements, 16: 19353 (IS-440)
Ca–Mg, thermodynamics of intermetallic compounds in, 18: 35549
Cd–Mg, additive effects on reduction of plutonium, uranium, and zirconium in halide salt–metal systems, 17: 36860(R) (ANL-6648)
Cd–Mg, corrosive effects on carbon steel and stainless steel at 750°C, 20: 2265
Cd–Mg, crystal structure of, effect of high pressure on, (E), 20: 13316
Cd–Mg, crystallization following deformation and annealing, 19: 28831
Cd–Mg, crystallization, 20: 19240
Cd–Mg, distribution of praseodymium between magnesium chloride–potassium chloride–sodium chloride and, at 600°C, 19: 32279(R) (ANL-7020(p.3-99))
Cd–Mg, mechanical properties of intermetallic compound single-crystal, 20: 31714(R) (UCRL-16658, pp 99-103)
Cd–Mg, ordering effects on diffusion of cadmium in, 17: 37537
Cd–Mg, separation of uranium from, by fused chloride extraction, 20: 5594(R) (ANL-6925, pp 21-106)
Cd–Mg, solvent properties for rare earth elements in molten chloride salts, 20: 3865 (ANL-7064)
Cd–Mg, solvent properties for uranium, 20: 5594(R) (ANL-6925, pp 21-106)
Cd–Mg, vapor pressure, 17: 12672(T) (AEC-tr-5626)
Cd–Mg–Pu–Zn, stability in mild steel and stainless steel containers at 600°C, 20: 5594(R) (ANL-6925, pp 21-106)
Cd–Mg–U, thermodynamic properties of liquid and solid, 20: 7555 (CONF-650559-8)
Cd–Mg–U–Zn, corrosive effects on ferrous alloys in presence of chloride flux, at 600 and 650°C, 19: 32279(R) (ANL-7020(p.3-99))
Cd–Mg–U–Zn, corrosive effects with chloride flux on carbon steel, Croloy, and stainless steel at 600 to 650°C, 20: 5594(R) (ANL-6925, pp 21-106)
Cd–Mg–U–Zn, corrosive effects in fused chloride mixtures, on stainless steel, 20: 20802(R) (ANL-7055, pp 21-98)
Cd–Mg–U–Zn, phase studies, 20: 5594(R) (ANL-6925, pp 21-106)
Cd–Mg–U–Zn, precipitation of U_2Zn_{17} from, cadmium and magnesium substitution in, 19: 32279(R) (ANL-7020(p.3-99))
Cd–Mg–Zn, corrosive effects on carbon steel, stainless steel, and tantalum at 500, 750 and 850°C, 20: 2265
Cd–Mg–Zn, creep properties, 17: 11179 (AERE-M-1149)
Cd–Mg–Zn, distribution of praseodymium between magnesium chloride–potassium chloride–sodium chloride and, at 600°C, 19: 32279(R) (ANL-7020(p.3-99))
Cd–Mg–Zn, solubility of praseodymium and uranium in, 18: 33678(R) (ANL-6875)
Cd–Mg–Zn, solvent properties for uranium, 17: 37001(R) (ANL-6780)
Cd–Mg–Zn, solvent properties for uranium at 600°C, 17: 40422(R) (ANL-6784)
Cd–Mg–Zn, solvent properties for uranium at 600 and 700°C, 18: 15426(R) (ANL-6810)
Cd–Mg–Zn, solvent properties for uranium at 600 and 650°C, 18: 15663(R) (ANL-6808)
Cd–Mg–Zn, solvent properties for praseodymium, 18: 24952(R) (ANL-6880(p.6-48))
Cd–Mg–Zn, solvent properties of liquid, for uranium, 18: 43359(R) (ANL-6800(p.43-196)
Cd–Mg–Zn, solvent properties of liquid, for plutonium and uranium, 19: 15662(R) (ANL-6900(p.45-142))
Cd–Mg–Zn, solvent properties for fissium–plutonium–uranium fuel pins, 19: 23991(R) (ANL-7003)
Cd–Mg–Zn, solvent properties for plutonium at 350 to 700°C, 19: 32279(R) (ANL-7020(p.3-99))
Cd–Mg–Zn, solvent properties of melts of, for plutonium and uranium, 20: 447
Ce–Mg, analysis of, for cerium, x-ray-fluorescence, 16: 5283
Ce–Mg, annealing effects on properties and recrystallization of, 18: 28001
Ce–Mg, crystal structure of Ce_2Mg_{17}, 17: 37539(T)
Ce–Mg, crystal structure of $CeMg_3$, 18: 14509
Ce–Mg, crystal structure of magnesium-rich phases in, 18: 39961(T)
Ce–Mg, crystal structure, 20: 2399
Ce–Mg, heat resistance, mechanical properties, and recrystallization of, 18: 16496
Ce–Mg, hydridation, 16: 6399
Ce–Mg, hydrogen absorption, 17: 32643
Ce–Mg, mechanical properties at 100 to 300°C, 17: 1920 (BM-RI-6078)
Ce–Mg, oxidation by moist nitrogen at 475 to 600°C, 19: 20485
Ce–Mg, phase studies on, 18: 14506
Ce–Mg, phase studies, 19: 9721
Ce–Mg, phase studies, 19: 41011 (IS-T-15)

Ce–Mg, phase studies, 19: 47059
Ce–Mg, phase studies, 20: 9531
Ce–Mg, preparation and properties, 17: 14747(T) (AEC-tr-5677)
Ce–Mg, preparation and phase diagram of, 17: 23973(T) (UCRL-Trans-930(L))
Ce–Mg, spectrophotometric analysis for cerium using sulfanilic acid, 20: 16398
Ce–Mg, structure of intermetallic compounds in, 19: 23008(T) (JPRS-28849(p.191-4))
Ce–Mg, thermal stability at 150 to 300°C, 17: 34461
Ce–Mg, thermodynamics of formation of intermetallic compounds, 20: 41412(R) (IS-1500(Sect. M))
Ce–Mg–Mn, welding of vacuum-tight joints in, by seam process, 19: 22945(T)
Ce–Mg–V, mechanical properties at 100 to 300°C, 17: 1920 (BM-RI-6078)
Ce–Mg–Zn–Zr, ultrasonic wave attenuation and delay in, 19: 32761
Ce–Mg–Zr, mechanical properties at 100 to 300°C, 17: 1920 (BM-RI-6078)
Ce–Mg–Zr, ultrasonic wave attenuation and delay in, 19: 32761
Co–Mg, elastic constants of, relation to cohesion and stability of intermetallic phases, 18: 44228
Co–Mg, phase studies and thermodynamics of formation of $MgCo_2$, 18: 32167
Co–Mg, phase studies, 19: 9604(R) (IS-900(Sect.M))
Co–Mg, thermodynamic properties, 18: 2163(R) (IS-700(Sect.M))
Co–Mg–Nd, corrosion, 19: 6271(T) (JPRS-27451)
Cu–In–Mg, crystal structure of intermetallic compound $MgInCu_4$ in, 16: 3488
Cu–Mg, bonding to aluminum, hot-press, 19: 40949 (ISC-640)
Cu–Mg, corrosion by aluminum–silicon and water of coatings of, on uranium, 19: 40949 (ISC-640)
Cu–Mg, deposition on uranium, hot dip, 19: 40949 (ISC-640)
Cu–Mg, distribution of plutonium, praseodymium, and uranium between potassium chloride–magnesium chloride–sodium chloride and, at 600 to 800°C, 19: 32279(R) (ANL-7020(p.3-99))
Cu–Mg, elastic constants of, relation to cohesion and stability of intermetallic phases, 18: 44228
Cu–Mg, nuclear magnetic resonance of copper-63 in, 18: 44229
Cu–Mg, precipitation cell growth in, effects of deformation on, 17: 34421(T) (AEC-tr-5964)
Cu–Mg, separation of praseodymium from, by extraction using halides, 19: 17176(R) (ANL-6965(p.1-41))
Cu–Mg, solvent properties for rare earth elements in molten chloride salts, 20: 3865 (ANL-7064)
Cu–Mg, solvent properties of liquid, for plutonium, praseodymium, and uranium, 20: 20802(R) (ANL-7055, pp 21-98)
Cu–Mg, solvent properties of, for iron, 20: 31314(R) (ANL-7175, pp 1-41)
Cu–Mg, thermodynamics of compound formation in, from vapor pressure measurements, 16: 19353
Cu–Mg, uranium distribution between liquid, and fused magnesium chloride, (E), 20: 14007(R) (ANL-7122, pp 1-41)
Cu–Mg, uses in processing of impure uranium, 19: 7648(P)
Cu–Mg, uses in purification of uranium, 19: 4265(P)
Cu–Mg–Zn, liquid miscibility of, at high temperatures, 20: 31314(R) (ANL-7175, pp 1-41)
Cu–Mg–Zn, thermal capacity, 20: 27494(R) (NYO-3454-6)
Dy–Mg, crystal structure of Dy_5Mg_{24} in, 17: 20469
Dy–Mg, high-temperature allotropy and phase studies on, 18: 24176
Dy–Mg, phase studies, 19: 41011 (IS-T-15)
Dy–Mg, phase studies, 20: 9531
Dy–Mg, structure of intermetallic compounds in, 19: 23008(T) (JPRS-28849(p.191-4))
Dy–Mg, thermodynamic properties, 19: 41013 (IS-T-25)
Dy–Mg, thermodynamics of formation of intermetallic compounds, 20: 41412(R) (IS-1500(Sect. M))
Er–Mg, crystal structure of Er_5Mg_{24} in, 17: 20469
Er–Mg, hexagonal crystal structure in $ErMg_3$, 18: 44181
Er–Mg, high-temperature allotropy and phase studies on, 18: 24176
Er–Mg, phase studies, 19: 4676
Er–Mg, preparation and properties, 16: 30811(T) (AEC-tr-5296)
Er–Mg, structure of intermetallic compounds in, 19: 23008(T) (JPRS-28849(p.191-4))
Er–Mg, thermodynamic properties, 19: 41013 (IS-T-25)
Er–Mg, thermodynamics of formation of intermetallic compounds, 20: 41412(R) (IS-1500(Sect. M))
Eu–Mg, hexagonal crystal structure in $EuMg_3$, 18: 44181
Eu–Mg, phase studies, 19: 4676
Eu–Mg, properties of intermetallic compounds in, 19: 39177
Eu–Mg, structure of intermetallic compounds in, 19: 23008(T) (JPRS-28849(p.191-4))
Fe–Mg, crystal structure of nitrogen-containing, 16: 2259
Ga–Mg, corrosion, 19: 6271(T) (JPRS-27451)
Ga–Mg, crystallographic parameters, 17: 18822
Ga–Mg–Nd, corrosion, 19: 6271(T) (JPRS-27451)
Gd–Mg, crystal structure of intermetallic phases in, 17: 37541(T)
Gd–Mg, electric conductivity of dilute, 18: 7245
Gd–Mg, electric conductivity at low temperatures in magnetic fields, 20: 9530
Gd–Mg, high-temperature allotropy and phase studies on, 18: 24176
Gd–Mg, magnetic properties of, 20: 31758
Gd–Mg, phase diagram and properties, 16: 561
Gd–Mg, phase diagram, 19: 23004(T) (JPRS-28849(p.148-57))
Gd–Mg, phase studies and properties, 17: 39581
Gd–Mg, phase studies, 19: 41011 (IS-T-15)
Gd–Mg, phase studies, 20: 9531
Gd–Mg, structure of intermetallic compounds in, 19: 23008(T) (JPRS-28849(p.191-4))
Gd–Mg, thermodynamic properties, 19: 41013 (IS-T-25)
Gd–Mg, thermodynamics of formation of intermetallic compounds, 20: 41412(R) (IS-1500(Sect. M))
Ge–Mg, electric, spectral, and thermal properties, 19: 9767(R) (IS-900(Sect.P))
Ge–Mg, electron spin resonance, 19: 9767(R) (IS-900(Sect.P))
Ge–Mg, partial molar properties of, 20: 25572(R) (NASA-CR-67221)
Ge–Mg, refractive index of, method for determining, 17: 18057
Ge–Mg, semiconductor properties of Mg_2Ge, 18: 2401(R) (IS-700(Sect.P))
Ge–Mg, sound velocities in intermetallic compound, (E/T), 20: 4476(R) (IS-1200(Sect.P))
Ge–Mg, spectrum of Mg_2Ge, infrared absorption, 19: 43630 (IS-T-17)
Ge–Mg, thermal capacity of intermetallic compound in, 20: 3863(R) (IS-1200(Sect. C))
Ge–Mg, thermodynamic properties, 20: 15056(R) (NYO-2916-10)
Ho–Mg, high-temperature allotropy and phase studies on, 18: 24176
Ho–Mg, thermodynamic properties, 19: 41013 (IS-T-25)
Ho–Mg, thermodynamics of formation of intermetallic compounds, 20: 41412(R) (IS-1500(Sect. M))
In–Mg, corrosion, 19: 6271(T) (JPRS-27451)
In–Mg, crystal structure of, effect of high pressure on, (E), 20: 13316
In–Mg, crystallographic parameters, 17: 18822
In–Mg, positron annihilation in, temperature dependence of, 20: 11678
In–Mg, superconductivity of dilute primary solid solutions of, 17: 39789
In–Mg–Ni, crystal structure of $MgNi_3In$ in, 17: 20468
In–Mg–Zn, corrosion, 19: 6271(T) (JPRS-27451)
La–Mg, analysis of, for magnesium, x-ray fluorescence, 16: 5283
La–Mg, crystal structure of La_2Mg_{17}, 17: 37539(T)
La–Mg, crystallization following deformation and annealing, 19: 28831
La–Mg, crystallization, 20: 19240
La–Mg, diffusion of beryllium to surface of, on heating at 300 to 500°C, 19: 47071
La–Mg, phase studies, 19: 41011 (IS-T-15)
La–Mg, phase studies, 20: 9531
La–Mg, structure of intermetallic compounds in, 19: 23008(T) (JPRS-28849(p.191-4))
La–Mg, thermodynamics of formation of intermetallic compounds, 20: 41412(R) (IS-1500(Sect. M))
Li–Mg, aging and tensile properties of, effects of silicon on, 18: 30211
Li–Mg, casting and melting technique for, 16: 30720 (NP-12047)
Li–Mg, creep in, 17: 35264(R) (UCRL-10706(p.111-203))
Li–Mg, creep of intermetallic compound single-crystal, 20: 31714(R) (UCRL-16658, pp 99-103)
Li–Mg, deformation of single crystals of, 17: 36307
Li–Mg, development of, review of, 16: 10521 (DMIC-Memo-146)
Li–Mg, elastic constants of single crystals of, 16: 5733
Li–Mg, electric conductivity of dilute, effects of martensitic transformation on, 16: 6733
Li–Mg, electron concentration in polycrystalline, 18: 12788
Li–Mg, electron penetration of spacecraft shielding of, (E), 20: 42520
Li–Mg, machining procedures for, 20: 43864 (Y-1550)
Li–Mg, martensitic transformation in, correlation of, with elastic anisotropy, 16: 33488
Li–Mg, neutron induced (t,p) reactions in, 19: 33285
Li–Mg, nuclear spin absorption spectra of, at 0 to 50 kc, 16: 13795
Li–Mg, nuclear spin relaxation times of lithium-7 in, 18: 2401(R) (IS-700(Sect.P))
Li–Mg, phase transitions and tensile properties, 16: 24164 (NP-11778)
Li–Mg, prismatic slip in single crystals of, effect of lithium content on, 19: 30808
Li–Mg, prismatic slip in, dislocation mechanisms for, 19: 30808
Li–Mg, protective coatings for, anodic, 20: 29366(R) (TID-22970, pp 375-91)
Li–Mg, solvent properties for zirconium, 17: 31000

Li–Mg, thermoelectric power of, at 0.1 to 1.2°K, 16: 9239
Li–Mg, use as reductant for green salt, 17: 1556(R) (NLCO-860)
Li–Mg–Th, preparation and properties at high temperatures, 19: 37153(P)
Li–Mg–Th–Y, preparation and properties at high temperatures, 19: 37154(P)
Li–Mg–Th–Zn, preparation and properties at high temperatures, 19: 37153(P)
Li–Mg–Th–Zr, preparation and properties at high temperatures, 19: 37153(P)
Li–Mg–Tl, preparation, properties, and structure of intermetallic compound $LiMg_2Tl$ in, 20: 11282 (UCRL-12119-T)
Li–Mg–Y, preparation and properties at high temperatures, 19: 37154(P)
Li–Mg–Zn, phase transitions and tensile properties, 16: 24164 (NP-11778)
Lu–Mg, high-temperature allotropy and phase studies on, 18: 24176
Lu–Mg, phase studies, 19: 41011 (IS-T-15)
Lu–Mg, phase studies, 20: 9531
Lu–Mg, thermodynamic properties, 19: 41013 (IS-T-25)
Lu–Mg, thermodynamics of formation of intermetallic compounds, 20: 41412(R) (IS-1500(Sect. M))
Mg–Ag, annealing behavior of internally oxidized, at low temperatures, 17: 34418 (UCRL-10816)
Mg–Ag, annealing of cold-worked, effects of internal oxidation on, 17: 35264(R) (UCRL-10706(p.111-203))
Mg–Ag, annealing of deformed AgMg, 19: 39168(R) (TID-22015)
Mg–Ag, crystal structure of, effect of high pressure on, (E), 20: 13316
Mg–Ag, crystal structure of silver-rich, disorder-order transformations of, 20: 33870(R) (MIT-1002-1)
Mg–Ag, deformation of single crystals of, at 77 to 300°K, 19: 43997(R) (UCRL-11889)
Mg–Ag, deformation of intermetallic compound in, effects of annealing on, 20: 33870(R) (MIT-1002-1)
Mg–Ag, deformation of silver-rich, effects of, on electric conductivity and tensile properties, 20: 33870(R) (MIT-1002-1)
Mg–Ag, entropy of formation of AgMg ordered phase, (T), 20: 2349 (UCRL-16320)
Mg–Ag, heat of formation at 0°C, 17: 29328(R) (TID-19007)
Mg–Ag, heats of formation of silver-rich solid solutions, 19: 39168(R) (TID-22015)
Mg–Ag, heats of formation of silver-rich, 20: 33870(R) (MIT-1002-1)
Mg–Ag, lithium reactions at 20 to 60 kev, secondary electron emission from, (E), 20: 19363
Mg–Ag, mechanical properties of intermetallic compounds in, effects of composition and structure on, 17: 541 (WADD-TR-60-184(Pt.III))
Mg–Ag, mechanical properties of internally oxidized, 20: 3639 (UCRL-11194)
Mg–Ag, oxidation, 17: 3569 (ASD-TDR-62-707)
Mg–Ag, performance as dynodes, effects of cesium on, 18: 23865
Mg–Ag, performance as photomultiplier dynodes, 18: 35841(R) (TID-20422)
Mg–Ag, performance as photomultiplier dynodes, 18: 35844(R) (TID-20425)
Mg–Ag, performance as dynodes in high-speed photomultipliers, (E), 19: 15875(R) (TID-21213)
Mg–Ag, photosensitivity of, 20: 17984
Mg–Ag, properties of, effects of physical parameters on, 16: 5724 (WADD-TR-60-184(Pt.II))
Mg–Ag, self-diffusion of silver-110 in, 18: 26051
Mg–Ag, slip in AgMg at low temperature, mechanism of, 18: 33201 (UCRL-10916)
Mg–Ag, solvent properties of, for chromium–uranium alloy fuels, 16: 16464
Mg–Ag, stoichiometry and temperature effects on pest degradation in AgMg in, 18: 42055
Mg–Ag, use of, in separation of thorium and uranium, 16: 8810 (NAA-SR-6666)
Mg–Hg, corrosive effects on niobium–zirconium alloy at 315 to 870°C, 18: 4160(R) (BNL-799(p.74-100))
Mg–Hg, heat transfer by bubble boiling of, effects of pressure on, 19: 24682
Mg–Hg, superconducting transition temperature of intermetallic compounds in, 20: 31757
Mg–Hg–Ni, corrosive effects on titanium of mercury-based, 19: 44616(R) (ANL-7000, pp 122-37)
Mg–Hg–Zr, corrosive effects on titanium of mercury-based, 19: 44616(R) (ANL-7000, pp 122-37)
Mg–mischmetal, mechanical properties at 100 to 300°F, 17: 1920 (BM-RI-6078)
Mg–misch metal–Zn, plastic anisotropy of ZE10A sheet, 19: 39149 (AD-425880)
Mg–Mn, analysis of, for nickel, spectrophotometric, 16: 18817 (PG-Report-295)
Mg–Mn, analysis of, for antimony, 17: 5960 (PG-Report-337)
Mg–Mn, analysis of, for cobalt, 17: 5960 (PG-Report-337)
Mg–Mn, cavitation and creep properties of, at 20 to 500°C, 16: 16762
Mg–Mn, creep behavior of, effects of heat treatment on, 16: 552
Mg–Mn, creep in, diffusion, 20: 13309
Mg–Mn, crystal structure of nitrogen-containing, 16: 2259
Mg–Mn, effects of grain size on compressive creep and tensile deformation at 450°C, 18: 42059
Mg–Mn, fatigue of, effects of high-frequency vibrations on, 20: 43957
Mg–Mn, heat resistance, mechanical properties, and recrystallization of, 18: 16496
Mg–Mn, oxidation of, by carbon dioxide–carbon monoxide mixtures at 500 to 700°C, 17: 25739
Mg–Mn, performance as reactor components, 18: 37667 (A/CONF.28/P/146)
Mg–Mn, thermal stability at 150 to 300°C, 17: 34461
Mg–Mn, thermophysical properties, 18: 10552
Mg–Mn–Nd, effects of plastic deformation on properties and structure of, 18: 16495
Mg–Mn–Nd, phase studies, 17: 18848
Mg–Mn–Nd–Ni, effects of plastic deformation on properties and structure of, 18: 16495
Mg–Mn–Th, bonding of HM21, surface preparation and epoxy adhesive for, 19: 36995 (BDX-613-68)
Mg–Mn–Th, corrosion, 19: 6271(T) (JPRS-27451)
Mg–Mn–Th, effects of alloying agents on mechanical properties of, 17: 32595
Mg–Mn–Th, mechanical properties of, alloying effects on, 18: 32156(T) (JPRS-25069(p.1-31))
Mg–Mn–Th, phase studies, 18: 32156(T) (JPRS-25069(p.1-31))
Mg–Mn–Zr, cavitation and creep properties of, at 20 to 500°C, 16: 16762
Mg–Mn–Zr, design for fuel element canning, 17: 16730(P)
Mg–Mn–Zr, diffusion of plutonium in MAGZAN-II and ZR55, at 420, 460, and 500°C, 20: 5848
Mg–Mn–Zr, ignition in carbon dioxide, effects of air, oxygen, and water vapor on, 19: 7849 (CEA-R-2494)
Mg–Mn–Zr, performance as reactor components, 18: 37667 (A/CONF.28/P/146)
Mg–Nb, phase diagrams, 18: 28002
Mg–Nd, alloying effects on composition and mechanical properties of, 18: 28000
Mg–Nd, analysis of, for neodymium, x-ray fluorescence, 16: 5283
Mg–Nd, corrosion of, effects of cobalt and gallium on, 18: 20482
Mg–Nd, crystal structure of $NdMg_{12}$, 17: 37539(T)
Mg–Nd, crystal structure of magnesium-rich phases in, 18: 39961(T)
Mg–Nd, crystal structure, 20: 2399
Mg–Nd, decomposition of supersaturated neodymium-rich solid solution in, 17: 32594
Mg–Nd, effects of plastic deformation on properties and structure of, 18: 16495
Mg–Nd, effects of plastic deformation on properties and structure of, 18: 34148
Mg–Nd, electric conductivity anomalies below 273°K in dilute, 16: 10734
Mg–Nd, electric conductivity of, 17: 4951
Mg–Nd, electric conductivity of dilute, 18: 7245
Mg–Nd, electric conductivity at low temperatures in magnetic fields, 20: 9530
Mg–Nd, heat resistance, mechanical properties, and recrystallization of, 18: 16496
Mg–Nd, mechanical properties of, effects of alloying elements on, 19: 44709(T) (JPRS-24761, pp 17–28)
Mg–Nd, microstructure of, effects of heat treatments on, 20: 7615
Mg–Nd, phase studies, 16: 20372(T) (AEC-tr-4457(p.197-204))
Mg–Nd, phase studies and properties, 17: 39581
Mg–Nd, phase studies on, 18: 14506
Mg–Nd, phase studies, 19: 9721
Mg–Nd, phase studies, 19: 41011 (IS-T-15)
Mg–Nd, phase studies, 20: 9531
Mg–Nd, properties and structure of, 20: 17110
Mg–Nd, structure of intermetallic compounds in, 19: 23008(T) (JPRS-28849(p.191-4))
Mg–Nd, thermal stability at 150 to 300°C, 17: 34461
Mg–Nd, thermodynamics of formation of intermetallic compounds, 20: 41412(R) (IS-1500(Sect. M))
Mg–Ni, analysis for magnesium, electrographic, 20: 267
Mg–Ni, crystal structure of nitrogen-containing, 16: 2259
Mg–Ni, distribution of praseodymium between magnesium chloride–potassium chloride–sodium chloride and, at 600°C, 19: 32279(R) (ANL-7020(p.3-99))
Mg–Ni, elastic constants of, relation to cohesion and stability of

intermetallic phases, 18: 44228
Mg–Ni, heat resistance, mechanical properties, and recrystallization of, 18: 16496
Mg–Ni, production of splatcooled, 19: 41021(R) (NMI-8002.1)
Mg–Ni, solvent properties for rare earth elements in molten chloride salts, 20: 3865 (ANL-7064)
Mg–Ni, thermodynamics of compound formation in, from vapor pressure measurements, 16: 19353 (IS-440)
Mg–Pr, analysis of, for praseodymium, x-ray fluorescence, 16: 5283
Mg–Pr, crystal structure of intermetallic compound $PrMg_{12}$ in, 19: 16143(T)
Mg–Pr, phase studies, 19: 41011 (IS-T-15)
Mg–Pr, phase studies, 20: 9531
Mg–Pr, thermodynamics of formation of intermetallic compounds, 20: 41412(R) (IS-1500(Sect. M))
Mg–Pu, density and phases of plutonium-base, 20: 46144(R) (HW-67765)
Mg–Pu, diffusion of plutonium at 420 to 500°C, 19: 47066
Mg–Pu, liquid miscibility gap in phase diagram of, 19: 32279(R) (ANL-7020(p.3-99))
Mg–Pu, melting points of, effects of composition on, 20: 5594(R) (ANL-6925, pp 21-106)
Mg–Pu, phase diagram, 17: 4984
Mg–Pu, phase studies and properties of, bibliographic study of, 16: 32115 (KFK-105)
Mg–Pu, phase studies, 19: 17176(R) (ANL-6965(p.1-41))
Mg–Pu, phase studies, 20: 31314(R) (ANL-7175, pp 1-41)
Mg–Pu, preparation, 17: 16568
Mg–Pu, structure of intermetallic compounds in, 17: 3536
Mg–Pu, thermodynamic properties of, 18: 44224
Mg–Pu, thermodynamics of dilute-plutonium liquid, 20: 43819
Mg–Pu–U–Zn, corrosive effects on type 405 stainless steel, 20: 20802(R) (ANL-7055, pp 21-98)
Mg–Pu–Zn, liquid miscibility of, at high temperatures, 20: 31314(R) (ANL-7175, pp 1-41)
Mg–rare earth, crystal structure and properties, 19: 11744
Mg–rare earths, crystal structure of intermetallic compounds in, 19: 41040
Mg–rare earths–Zn–Zr, crystal structure, 20: 2399
Mg–rare earths–Zr, crystal structure, 20: 2399
Mg–rare earth, phase studies, 19: 41011 (IS-T-15)
Mg–rare earth, phase studies and solid solubilities of, 20: 4297(R) (IS-1200(Sect.M))
Mg–rare earth, preparation by magnesium salt reduction of halides, 19: 40955
Mg–rare earth–Zn, preparation and properties, 19: 4709(P)
Mg–Sc, crystal structure of AB type compound in, 19: 37063
Mg–Sc, phase diagrams, 20: 41412(R) (IS-1500(Sect. M))
Mg–Sc, phase studies, 19: 7495
Mg–Sc, structure of intermetallic compounds of, 19: 32755
Mg–Sm, phase studies at 400 to 1100°C, 17: 34330(R) (USBM-U-1057)
Mg–Sm, phase studies, 18: 2174(R) (USBM-U-1082)
Mg–Sm, thermodynamic properties, 19: 41013 (IS-T-25)
Mg–Sm, thermodynamics of formation of intermetallic compounds, 20: 41412(R) (IS-1500(Sect. M))
Mg–Sn, chemical shift and electronegativity of tin-119 in, 20: 7055 (UCRL-16436)
Mg–Sn, crystal structure of, effect of high pressure on, (E), 20: 13316
Mg–Sn, crystallization following deformation and annealing, 19: 28831
Mg–Sn, crystallization, 20: 19240
Mg–Sn, evaluation of, as coating for vanadium alloys, 16: 2168(R) (ARF-2227-2)
Mg–Sn, infrared reflectivity of, effects of temperature on, 20: 14227(R) (TID-22419)
Mg–Sn, Moessbauer measurements in, 20: 41637
Mg–Sn, preparation and properties of single-crystal, (E), 20: 4476(R) (IS-1200(Sect.P))
Mg–Sn, preparation of single-crystal, 20: 15056(R) (NYO-2916-10)
Mg–Sn, refractive index of, method for determining, 17: 18057
Mg–Sn, studies of equilibration in monocrystals of, 20: 15056(R) (NYO-2916-10)
Mg–Sn, tin-119 gamma resonance absorption in, 18: 19117
Mg–Sn, tin-119 Mössbauer effect in, 20: 12285
Mg–Sr, crystal structure of Sr_2Mg_{17} in, 17: 29334
Mg–Sr, crystal structures of intermetallic compounds of, 20: 41455(R) (NYO-2731-7)
Mg–Sr, elastic constants of, relation to cohesion and stability of intermetallic phases, 18: 44228
Mg–Sr, phase studies, 16: 13010(R) (TID-15150)
Mg–Sr, properties of intermetallic compounds in, 19: 39177
Mg–Sr, structure of intermetallic compounds in, 17: 23964(R) (TID-18619)
Mg–Tb, high-temperature allotropy and phase studies on, 18: 24176
Mg–Tb, phase studies, 19: 4676
Mg–Tb, structure of intermetallic compounds in, 19: 23008(T) (JPRS-28849(p.191-4))
Mg–Tb, thermodynamic properties, 19: 41013 (IS-T-25)
Mg–Tb, thermodynamics of formation of intermetallic compounds, 20: 41412(R) (IS-1500(Sect. M))
Mg–Th, analysis of, for thorium, x-ray fluorescence, 16: 5283
Mg–Th, crystal structure of stoichiometric, 19: 9604(R) (IS-900(Sect.M))
Mg–Th, decontamination of, pyrometallurgical method for, 19: 5999
Mg–Th, diffusion of beryllium to surface of, at 300 to 500°C, 19: 47071
Mg–Th, ductility in, mechanisms of, 20: 11301
Mg–Th, elastic constants of, relation to cohesion and stability of intermetallic phases, 18: 44228
Mg–Th, electric conductivity of liquid and solid, 16: 25754 (IS-437)
Mg–Th, electric conductivity of, 17: 4446 (IS-500(Sect.E))
Mg–Th, extrusion strengthening by manganese additions in, 19: 9680
Mg–Th, fabrication of rolled articles, 17: 20440(P)
Mg–Th, free energy of formation of $ThMg_2$, 17: 35686 (IS-589)
Mg–Th, heat resistance, mechanical properties, and recrystallization of, 18: 16496
Mg–Th, hexagonal crystal structure in $ThMg_2$, 18: 44181
Mg–Th, phase studies, 16: 30877
Mg–Th, phase studies, 18: 2163(R) (IS-700(Sect.M))
Mg–Th, phase studies, 18: 32156(T) (JPRS-25069(p.1-31))
Mg–Th, precipitation and recrystallization of, 17: 34446
Mg–Th, preparation and properties, 16: 19255
Mg–Th, preparation, 17: 18692(P)
Mg–Th, preparation, 17: 21609(P)
Mg–Th, preparation by reaction of liquid magnesium with thorium fluoride, 18: 31543(P)
Mg–Th, processing for fission product separation using molten salts, 18: 10204(P)
Mg–Th, production of, by reduction of thorium tetrafluoride, 16: 12048(P)
Mg–Th, production of, from fused chlorides, 16: 3404(P)
Mg–Th, properties of, effects of aluminum, calcium, cerium, manganese, zinc, and zirconium on, 16: 9246
Mg–Th, properties and structure of, alloying effects of manganese and zirconium on, 17: 32596
Mg–Th, purification by transfer to liquid magnesium–zinc alloy in fused salt, 19: 20066
Mg–Th, radiation effects on crystal structure and tensile properties of, 16: 7929 (DC-59-10-116)
Mg–Th, separation of thorium from, by lithium extraction, 16: 33068 (NAA-SR-6405)
Mg–Th, separation of rare earths from, by solvent extraction, 18: 2163(R) (IS-700(Sect.M))
Mg–Th, separation of thorium from, using liquid lithium, 18: 25904
Mg–Th, separation of thorium from, by precipitation using lithium, 19: 6004(P)
Mg–Th, separation of cesium from, using pyrometallurgy, 19: 9604(R) (IS-900(Sect.M))
Mg–Th, thermal stability at 150 to 300°C, 17: 34461
Mg–Th, thermodynamics of formation of $ThMg_2$, 18: 5792
Mg–Th, thermodynamic properties of, 18: 44224
Mg–Th, thorium production from sponge, using electron-beam melting, 20: 41412(R) (IS-1500(Sect. M))
Mg–Th, uses in fuel element end caps to, reduce creep, 18: 42102(P)
Mg–Th–Zn–Zr, corrosion, 19: 6271(T) (JPRS-27451)
Mg–Th–Zn–Zr, mechanical properties of, at high temperatures, 16: 27688(P)
Mg–Th–Zr, age hardening mechanism in, 19: 4685
Mg–Th–Zr, bonding of HK31, surface preparation and epoxy adhesive for, 19: 36995 (BDX-613-68)
Mg–Th–Zr, corrosion, 19: 6271(T) (JPRS-27451)
Mg–Th–Zr, mechanical properties at 205 to 565°C, 19: 4684
Mg–Th–Zr, plastic anisotropy of HK31A sheet, 19: 39149 (AD-425880)
Mg–Ti, wetting effects on outside of chromium alloy tubes during mercury-pool boiling heat transfer, 19: 11367
Mg–Tm, high-temperature allotropy and phase studies on, 18: 24176
Mg–Tm, thermodynamic properties, 19: 41013 (IS-T-25)
Mg–Tm, thermodynamics of formation of intermetallic compounds, 20: 41412(R) (IS-1500(Sect. M))
Mg–U, phase studies, 17: 29255 (ZFK-WF-13)
Mg–U, properties as fuel element material, 18: 1247 (NP-13212)
Mg–U, thermodynamic properties of, 18: 44224
Mg–U–Zn, corrosive effects on refractory metals in presence of molten chlorides, 20: 2266
Mg–U–Zn, corrosive effects with fused chlorides, on carbon and zirconium boride, 20: 20802(R) (ANL-7055, pp 21-98)
Mg–U–Zn, stability of, effects of impurities on, 18: 17921(R) (ANL-6725(p.31-88))

Mg–V, phase diagrams, 18: 28002
Mg–Y, aging behavior and mechanical properties of, 20: 23669
Mg–Y, analysis for oxygen, 20: 4299(R) (ORNL-2711)
Mg–Y, atomic number effects correction in electron probe microanalysis of, 17: 27268
Mg–Y, crystal structure of Y_5Mg_{24} in, 17: 20469
Mg–Y, crystal structure, 19: 9604(R) (IS-900(Sect.M))
Mg–Y, enthalpies of formation and vapor pressures of, 20: 4297(R) (IS-1200(Sect.M))
Mg–Y, enthalpy of formation, 19: 9604(R) (IS-900(Sect.M))
Mg–Y, hexagonal crystal structure in YMg_{12}, 18: 44181
Mg–Y, magnetic susceptibility and specific heat of superconducting binary complex phases of, 18: 37715
Mg–Y, phase diagram, 19: 23005(T) (JPRS-28849(p.158-65))
Mg–Y, phase diagrams, 20: 4297(R) (IS-1200(Sect.M))
Mg–Y, phase studies and properties, 17: 39581
Mg–Y, phase studies, 18: 2163(R) (IS-700(Sect.M))
Mg–Y, preparation by reduction of yttrium chloride by magnesium in fused salt bath, 19: 18437
Mg–Y, preparation by magnesium salt reduction of halides, 19: 40955
Mg–Y, structure of intermetallic compounds in, 19: 23008(T) (JPRS-28849(p.191-4))
Mg–Y, thermodynamics of compound formation in, determination of, from vapor pressure measurements, 16: 19353 (IS-440)
Mg–Y, thermodynamics of formation of intermediate phases in, 19: 37069
Mg–Yb, hexagonal crystal structure in $YbMg_{12}$, 18: 44181
Mg–Yb, phase studies, 19: 25016
Mg–Yb, phase studies, 20: 4297(R) (IS-1200(Sect.M))
Mg–Yb, structure of intermetallic compounds in, 19: 23008(T) (JPRS-28849(p.191-4))
Mg–Zn, alloying effects of uranium on, 16: 5719 (NP-11169)
Mg–Zn, analysis for ruthenium using 1-nitroso-2-naphthol, spectrophotometric, 20: 12788
Mg–Zn, analysis of, for zinc, x-ray fluorescence, 16: 5283
Mg–Zn, corrosion of, effects of indium on, 18: 20482
Mg–Zn, crystal structure, 20: 2399
Mg–Zn, diffusion of beryllium to surface of, on heating at 300 to 500°C, 19: 47071
Mg–Zn, direct reduction of thorium dioxide by, 17: 3872
Mg–Zn, distillation, 17: 36860(R) (ANL-6648)
Mg–Zn, distillation of, apparatus for, 18: 43359(R) (ANL-6800(p.43-196))
Mg–Zn, distribution of elements between molten magnesium chloride and, 17: 40421(R) (ANL-6766)
Mg–Zn, distribution of praseodymium between magnesium chloride–potassium chloride–sodium chloride and, at 600°C, 19: 32279(R) (ANL-7020(p.3-99))
Mg–Zn, effects on thorium dioxide reduction in liquid halide salts, 19: 9618(P)
Mg–Zn, elastic constants of, relation to cohesion and stability of intermetallic phases, 18: 44228
Mg–Zn, enthalpy of formation of intermetallic compounds MgZn, $MgZn_2$, and Mg_2Zn_{11} in, 16: 4581
Mg–Zn, evaluation of, as coating for vanadium alloys, 16: 2168(R) (ARF-2227-2)
Mg–Zn, exchange of plutonium in liquid systems with chlorides, thermodynamics of, 20: 43819
Mg–Zn, heat of fusion of intermetallic compound, 20: 41412(R) (IS-1500(Sect. M))
Mg–Zn, heats of formation and fusion of intermetallic compound $MgZn_2$ in, 19: 19838 (IS-1070)
Mg–Zn, phase separation in, x-ray studies of, 17: 8861
Mg–Zn, phase separation of, supernatant solutions from uranium, 17: 36860(R) (ANL-6648)
Mg–Zn, precipitation and recrystallization of, 17: 34446
Mg–Zn, reactions with uranium oxides, 18: 17922(R) (ANL-6725 (p.88-99))
Mg–Zn, reactions of hydrogen with calcium, cerium, lanthanum, thorium, and yttrium in liquid, 18: 35548
Mg–Zn, reactions with uranium oxide, 20: 741 (ANL-7057)
Mg–Zn, reactions with thorium dioxide, 20: 742 (ANL-7058)
Mg–Zn, reactions with plutonium dioxide, 20: 2220 (ANL-7059)
Mg–Zn, reduction of plutonium, thorium, and uranium oxides using, 16: 828
Mg–Zn, separation of uranium from liquid, by hydridation, 19: 17176(R) (ANL-6965(p.1-41))
Mg–Zn, separation of plutonium from, by fused chloride extraction, 20: 5594(R) (ANL-6925, pp 21-106)
Mg–Zn, separation of californium and yttrium from, by fused chloride extraction, 20: 5594(R) (ANL-6925, pp 21-106)
Mg–Zn, solvent properties for plutonium and uranium, 17: 1359(R) (ANL-6569)
Mg–Zn, solvent properties of liquid, for zirconium, 17: 1359(R) (ANL-6569)
Mg–Zn, solvent properties for zirconium at 482 to 758°C, 17: 14116(R) (ANL-6596(p.29-118))
Mg–Zn, solvent properties for thorium at 750 to 850°C, 17: 36860(R) (ANL-6648)
Mg–Zn, solvent properties for uranium at 500 to 900°C, 17: 36860(R) (ANL-6648)
Mg–Zn, solvent properties for thorium, 17: 40421(R) (ANL-6766)
Mg–Zn, solvent properties of liquid, for transuranic elements, 19: 36553
Mg–Zn, solvent properties for rare earth elements in molten chloride salts, 20: 3865 (ANL-7064)
Mg–Zn, solvent properties of, for chromium, iron, niobium, and zirconium, 20: 31314(R) (ANL-7175, pp 1-41)
Mg–Zn, sorption of impurities in magnesium–thorium alloy by liquid, in fused salt, 19: 20066
Mg–Zn, sorptive properties for curium in presence of americium, 18: 43733(P)
Mg–Zn, thermal stability at 150 to 300°C, 17: 34461
Mg–Zn, thermodynamic properties, 18: 2163(R) (IS-700(Sect.M))
Mg–Zn, thermodynamic properties, 19: 9604(R) (IS-900(Sect.M))
Mg–Zn, vapor pressure, 17: 12672(T) (AEC-tr-5626)
Mg–Zn–Zr, bonding of ZK60, surface preparation and epoxy adhesive for, 19: 36995 (BDX-613-68)
Mg–Zn–Zr, casting, 18: 14452(P)
Mg–Zn–Zr, corrosion resistance of, to carbon dioxide and air at 500°C, alloying effects of beryllium and manganese on, 16: 30892(P)
Mg–Zn–Zr, corrosion, 19: 6271(T) (JPRS-27451)
Mg–Zn–Zr, creep properties of, for use as fuel element can, 16: 15236(P)
Mg–Zn–Zr, hot brittleness of, 19: 37092
Mg–Zn–Zr, oxidation by carbon dioxide–carbon monoxide mixtures at 500 to 700°C, 17: 25739
Mg–Zn–Zr, preparation for casting, 18: 22469(P)
Mg–Zn–Zr, structure, 18: 2258
Mg–Zn–Zr, thermal stress in Z.W. 1, 16: 20811(P)
Mg–Zn–Zr, ultrasonic wave attenuation and delay in, 19: 32761
Mg–Zr, analysis for bonding and inclusions in, by x-ray emission in electron microscopy, 20: 20593
Mg–Zr, analysis of, for zirconium, x-ray fluorescence, 16: 5283
Mg–Zr, corrosion resistance of, to carbon dioxide and air at 500°C, alloying effects of beryllium and manganese on, 16: 30892(P)
Mg–Zr, corrosion by humid air at 350°C, 17: 3420 (BLG-124)
Mg–Zr, corrosion by carbon dioxide at 450 to 550°C, 17: 25737
Mg–Zr, creep behavior of, effects of heat treatment on, 16:552
Mg–Zr, creep behavior and stress rupture of, in carbon dioxide at 400 and 450 and 200°C, 18: 42058
Mg–Zr, crystal structure, 20: 2399
Mg–Zr, development and fabrication of EdF2, for fuel cans, 20: 15018
Mg–Zr, diffusion of plutonium in, at 420 to 500°C, 19: 47066
Mg–Zr, dissolution using sulfuric acid, flowsheet for, 20: 4048(R) (NP-15406)
Mg–Zr, fabrication and mechanical properties, 17: 25751
Mg–Zr, fatigue of, effects of high-frequency vibrations on, 20: 43957
Mg–Zr, fatigue properties at 200 to 500°C, 17: 27847
Mg–Zr, fine-grain structure in co-extruded, 18: 14503
Mg–Zr, fine-grained structure in magnesium extruded, 18: 34182
Mg–Zr, forging, 19: 7886(P)
Mg–Zr, formation of zirconium hydride in, 18: 5797
Mg–Zr, formation of zirconium hydride in homogenized, 19: 2815
Mg–Zr, grain-boundary denuded zones in, 17: 25796
Mg–Zr, grain-boundary cracking and mode of creep failure in, 18: 26032
Mg–Zr, heat resistance, mechanical properties, and recrystallization of, 18: 16496
Mg–Zr, heat treatment of, effects on creep strength, 18: 42054
Mg–Zr, heat-treatment process for, 20: 4456(P)
Mg–Zr, ignition in carbon dioxide, effects of air, oxygen, and water vapor on, 19: 7849 (CEA-R-2494)
Mg–Zr, mechanical properties, 17: 30925
Mg–Zr, metallurgical properties of, methods for improving, 18: 2290(P)
Mg–Zr, nondestructive method for testing cladding of, 20: 14711
Mg–Zr, oxidation by carbon dioxide–carbon monoxide mixtures at 500 to 700°C, 17: 25739
Mg–Zr, oxidation at 400 to 600°C in damp oxygen, 18: 22449
Mg–Zr, performance of Magnox ZA as reactor components, 18: 37667 (A/CONF.28/P/146)
Mg–Zr, phase diagram, liquidus curve of, 20: 812 (BM-RI-6673)
Mg–Zr, phase study of zirconium-rich phases, 16: 21044(T) (AEC-tr-5127)
Mg–Zr, phase studies, 17: 1920 (BM-RI-6078)
Mg–Zr, phase studies on, 18: 32185
Mg–Zr, preparation and properties, 16: 19255

Mg–Zr, preparation of hafnium-free, 17: 36207
Mg–Zr, production for use as fuel element canning, 19: 30662(P)
Mg–Zr, properties of, for use in canning fuel elements, 17: 25793
Mg–Zr, properties of, for use in canning fuel elements, 17: 25794
Mg–Zr, properties as cladding material in gas-cooled graphite-moderated reactors, 18: 15496(T) (AEC-tr-6329)
Mg–Zr, properties for use as fuel element can, effects of manganin on, 19: 20610(P)
Mg–Zr, recrystallization grain growth of, effects of hydration on, 20: 37252
Mg–Zr, thermophysical properties, 18: 10552
Mg–Zr, ultrasonic wave attenuation and delay in, 19: 32761
Mg–Zr, use for natural-uranium cladding, 18: 37645 (A/CONF.28/P/57)
Pb–Li–Mg, atomic structure of Li_2MgPb, 17: 35805
Pb–Mg, corrosive effects on Croloy 2¼, 18: 4193 (BNL-811)
Pb–Mg, distribution of praseodymium between magnesium chloride–potassium chloride–sodium chloride and, at 600°C, 19: 32279(R) (ANL-7020(p.3-99))
Pb–Mg, mass transfer of iron to cold zone in liquid, inhibition of, 16: 19029(P)
Pb–Mg, phase separation in, x-ray studies of, 17: 8861
Pb–Mg, solvent properties for rare earth elements in molten chloride salts, 20: 3865 (ANL-7064)
Sb–Mg, distribution of praseodymium between magnesium chloride–potassium chloride–sodium chloride and, at 600°C, 19: 32279(R) (ANL-7020(p.3-99))
Sb–Mg, preparation, 16: 13676(R) (AD-260368)
Sb–Mg, solvent properties for rare earth elements in molten chloride salts, 20: 3865 (ANL-7064)
Sb–Mg, thermoelectric properties of, (E), 19: 16439(R) (AD-604997)
Sb–Mg, thermoelectric properties of intermetallic compound Mg_3Sb_2 in, 16: 18017(R) (AD-266019)

MAGNESIUM ALUMINATES
effects on oxidation resistance and strength of chromium–magnesia composites, 19: 41022(R) (NP-15292)
emissivity, 17: 6675(R) (PWA-2128)
fabrication and properties of spray-dried and hot-pressed, 19: 13898(R) (RFP-490)
point defect sites in crystals of, internal friction peak from symmetry splitting of equivalent, 17: 32607
preparation of single crystals, 16: 22114
properties of flame-sprayed coatings of, for use in space technology, 18: 16521
thermal expansion in air, 17: 3478 (JPL-TR-32-297)
$LaAlO_3$–$MgAl_2O_4$, phase studies and structure of, 18: 41449
$MgAl_2O_4$–$NdAlO_3$, constitution diagram and thermal properties, 17: 20016
$MgAl_2O_4$–$NdAlO_3$, phase diagram, 17: 27335

MAGNESIUM ALUMINUM SILICATES
structural properties of $Mg_2Al_4Si_5O_{18}$, 17: 14210 (NBS-MON-25(Sect.1))

MAGNESIUM BORATES
boron-11 nuclear magnetic resonance in colemanite, inderite, and lesserite, 16: 18884
spectra of, infrared, 17: 18048

MAGNESIUM BORIDES
chemical properties, 16: 17694
effects on thermoelectric properties of MCC 50, 19: 12129(R) (ASD-TDR-62-896(Pt.II))
stability and structure of, 17: 8083

MAGNESIUM BROMATES
molecular structure, 19: 9046(R) (IS-900(Sect.C))
radiolysis of anhydrous, 18: 1725(R) (ORNL-3488(p.42-54))
radiolysis of, gamma, 20: 23115
radiolysis products from, gamma, 19: 46332(R) (ORNL-3832, pp 50-65)
thermal decomposition of, search for perbromate in, 19: 36402

MAGNESIUM BROMIDES
binding energy of gaseous, 16: 28964
bromine-81 quadrupole bonding and resonance in solid layer type, 16: 7538
butyl-, reactions with water-t to produce tritiobutane, 17: 8176
corrosive effects on stainless steels under stress, mechanism of, 16: 30733 (ARF-2181-12)
crystal lattice energy of, relation of self energy of gaseous ions to, 18: 16017
dissociation energy of gaseous, 18: 32153(R) (UCRL-11317(p.176-97))
enthalpy and lattice energies of, calculation of, 19: 17901
polymerization of, spectra of, 17: 4530
sorptive properties of, for cadmium-115, indium, mercury, and zinc-65, 17: 15992
vaporization of, 17: 2956 (UCRL-9840)
vinyl-, uses in preparation of carbon-14-labeled acrylic and glyceric acids and glycerol, 19: 46310
LiBr–$MgBr_2$, phase diagrams, 20: 36788 (YALE-2723(Vol.2))
$MgBr_2$–KBr, phase diagrams, 20: 36788 (YALE-2723(Vol.2))
$MgBr_2$–NaBr, phase diagrams, 20: 36788 (YALE-2723(Vol.2))

MAGNESIUM CARBIDES
preparation, 18: 26824(R) (ANL-6885)
solubility in lithium chloride–magnesium chloride system at 600°C, 17: 36861(R) (ANL-6764)

MAGNESIUM CARBONATES
see also Magnesites
additive effects on densification of thorium oxide–uranium oxide pellets, 16: 7874 (ANL-6375)
calcination to oxide for sintering, 19: 16005(T) (AEC-tr-6537)
calcining, 16: 10536(R) (NP-11356)
content of, in sediments of Bay of Roquebrune, 20: 36553
decomposition of basic, thermal, 17: 27313(R) (ASD-TDR-62-843)
irradiation for production of sodium-24, neutron, 18: 32000(T) (ORNL-tr-230)
reactions with rare earth oxides, ionic field strengths as criteria for compound formation in, 19: 46246(R) (TID-22207, Paper F)
sorptive properties for low concentrations of iodine, 17: 18171 (AERE-R-4219)
spectrum at low temperatures, infrared, 16: 33002
thermoluminescence properties of, for use as radiation dosimeter, 20: 36913
$CaCO_3$–$MgCO_3$, precipitation with magnesium from aqueous solutions at high temperatures, 20: 18631 (NYO-2266-1)

MAGNESIUM CERIUM NITRATES
cerium nucleus alignment in, 16: 31097
cerium ordered state in, effects on nuclear orientation in, 18: 35522
cerium-137 nuclear orientation in, temperature scale from, 20: 1338
cerium-139 nuclear alignment in, intermediate state reorientation in, 19: 41840
cobalt-60 gamma anisotropy in, 18: 35522
cobalt-60 nuclear alignment in, gamma anisotropy in, 19: 33257
crystal structure of hydrated, 18: 3754
crystalline field splittings in, 18: 2478
gamma anisotropy from cobalt-60 aligned in, 19: 35467
magnetic susceptibility at 1.5 to 36°K, 18: 2478
nuclear alignment of cerium-141 in, 16: 26224 (NP-11865)
nuclear demagnetization in, cooling effects, 18: 4494
nuclear orientation of chromium-51 in, 17: 34882 (NP-13051)
nuclear polarization in magnesium-cerium-lanthanum double nitrate, magnetic-field effects, 16: 15443
promethium isotope alignment in, coupling constants and magnetic moments determined by, 17: 19351
proton polarization and spin relaxation rates in, at low temperatures, (E/T), 20: 3143
rare earth ion orientation in, quadrupole coupling constants from, (E), 20: 20146
rare earth ion quadrupole coupling in lattices of, 19: 47883 (UCRL-16279)
specific heat at 2 to 25°K, anomalous contribution from ground-state transition, 18: 16574
specific heat of, low-temperature, (E), 20: 30283
spectra of cerium ions in, line widths of emission, 16: 21205
spectra of, infrared, 18: 235
spin-lattice relaxation at 1 to 5°K, in fields up to 1 kOe, 16: 24313
spin-lattice relaxation time, 17: 33857 (AFCRL-63-192)
use as low-temperature scale, correlation for, 19: 21162(R) (UCRL-11828(p.199-201))
use for liquid helium-3 nuclear cooling, 20: 4780
use for low-temperature thermometry with liquid helium-4, 20: 32336
use in mutual inductance system for temperature measurement, 17: 41194 (TID-19533)
use in mutual inductance system for measuring low temperatures, 18: 18159
He-3–$MgCe(NO_3)_5$, thermal relaxation time at low temperatures, (E), 20: 11922

MAGNESIUM CHLORATES
radioinduced defects in, electron paramagnetic resonance study of x, 19: 24568(T)

MAGNESIUM CHLORIDES
binding energy of gaseous, 16: 28964
chloride ion mobilities in liquid, 16: 157 (IS-344)
corrosive effects on stainless steels under stress, mechanism of, 16: 30733 (ARF-2181-12)
corrosive effects on stainless steel (304), 17: 3419 (ARF-2152-18)
corrosive effects on nickel alloys and stainless steels at high temperatures, 17: 36928(R) (GEAP-4126)
corrosive effects on stainless steel, 18: 4761(R) (GEAP-4383)
corrosive effects of boiling, on cladding materials, 18: 4796(R)

(GEAP-4153)
corrosive effects on type 304 stainless steel, 18: 14415
corrosive effects on 18/10 and type 304 stainless steel at 154°C, 18: 18318(T,R) (EURAEC-836)
corrosive effects on stainless steel, 18: 32063(T,R) (EURAEC-1060)
corrosive effects on Incoloy 800 and stainless steel type 304 at 142°C, 19: 16020
corrosive effects on austenitic stainless steel, 19: 22893 (DP-957)
corrosive effects on stainless steel, 19: 26766(R) (EURAEC-1309)
corrosive effects on high purity stainless steel, 19: 40947(R) (EURAEC-1403)
corrosive effects on stainless steels, effects of silicon on, 19: 42803(R) (EURAEC-1397)
corrosive effects on titanium alloys at 650°F, 19: 44621 (CONF-651006-1)
corrosive effects on austenitic and austeno-ferritic stainless steels, stress, 20: 2256(R) (EURAEC-1449)
corrosive effects on failure of Incoloy 800 and stainless steel under stress, 20: 4328 (WCAP-3269-50)
corrosive effects on iron- and nickel-base alloys at 154°C, stress-, 20: 9408 (BNWL-154)
corrosive effects of, on iron-base alloys, mechanisms of stress-, 20: 16968 (COO-1319-33)
corrosive effects on chromium–iron–nickel alloys, effects of surface preparation on, 20: 23598(R) (COO-1319-34)
corrosive effects on chromium–iron–nickel-base alloys, effects of composition and microstructure on, 20: 23599 (COO-1319-36)
corrosive effects on high-purity stainless steels, effects of steel composition on stress-, 20: 27482(R) (EURAEC-1453)
corrosive effects on austenitic and austeno-ferritic stainless steels, stress-, 20: 29639(R) (EURAEC-1578)
crystal lattice energy of, relation of self energy of gaseous ions to, 18: 16017
crystallization with rare earths, 16: 26995
density of solutions of, uses of radioisotopes in measuring, 19: 24896
diffusion of water in, coefficients of, 20: 1865
dissociation energy of gaseous, 18: 32153(R) (UCRL-11317(p.176-97))
distribution of elements between molten magnesium–zinc alloy and, 17: 40421(R) (ANL-6766)
effects of, on excretion of strontium-90 from mice, 20: 32922
effects on cesium displacement and sorption by soils, 17: 39072
effects on formation of corrosion-resistant films on titanium and zirconium oxides, 18: 20481
effects on radioinduced changes in proteins, 20: 49
effects on self-diffusion of water at 23°C, 19: 32159
effects on stress corrosion cracking of chromium–iron–nickel alloy, 20: 31676(R) (COO-1319-39)
effects on strontium-85 elution from mouse bones, 19: 43706
effects on strontium-90 excretion by mice, 20: 8563
electric conductivity of melts, temperature coefficients for, 18: 23456(T) (AI-Trans-46)
electrolytic properties in mixtures with strontium chlorides, 18: 5275
enthalpy and lattice energies of, calculation of, 19: 17901
equivalent conductance in water, effect of transference number, 16: 3010
free energy of formation at 400 to 600°C, 16: 25392
free energy of formation at 400 to 500°C, 17: 7989 (BNL-6059)
polarography in mixture of lithium and potassium chlorides, 16: 2953
polymerization of, spectra of, 17: 4530
positron annihilation in, origin of second lifetime component from, (E), 20: 19486
precipitation of uranium(VI) with, in presence of sodium carbonate, 19: 19870
properties of solutions of, in dimethyl sulfoxide, 20: 293 (UCRL-16330)
radiation effects on corrosive effects of, on stainless steels, 19: 47079 (AERE-R-5014)
radiosensitivity effect on barley seeds, 18: 33409
reaction to, of irradiated mitochondria, 17: 30354
reactions in dioxane–water solutions, nuclear magnetic resonance spectra of, 17: 40800
reactions with thorium chlorides in melts, tensiometric and thermal analyses, 16: 4169
reactions with yttrium chloride, 19: 7502
reduction by high-frequency hydrogen discharge to dihalide and metal, 19: 39180
separation of americium and rare earths from, by solvent extraction using triisooctylamine, 20: 18562(R) (EUR-2640.e)
solvent partition in amine systems, 18: 37275 (A/CONF.28/P/755)
solvent properties for magnesium, anodic chronopotentiometric studies of, 17: 7991 (BNL-6583)
solvent properties for magnesium, chronopotentiometric study of, 17: 31795(R) (BNL-782(p.18-43))
solvent properties of aqueous solutions of, for radium and uranium, 18: 16133
solvent properties of molten, for transuranium elements, 19: 36553
Soret coefficients and transport heats at 25°C, 16: 11666
sorptive properties of, for cadmium-115, indium, mercury, and zinc-65, 17: 15992
spectra of dysprosium, europium, samarium, and terbium ions in calcination products of, luminescence, 18: 6803
spectra of liquid, Raman, 20: 38871(R) (NYO-1769-54)
spectra of, doublet system in emission, 18: 29624
thermal decomposition of, factors affecting, 20: 2520(R) (IA-920)
thermodynamic properties of, 18: 25360
thermodynamics of titanium in, oxygen equilibrium potential diagram for, 16: 20426
thermodynamics of, in anhydrous *N,N*-dimethylformamide and *N*-methylformamide at 25°C, 20: 3926 (TID-22374)
uranium distribution between fused, and liquid copper–magnesium alloy, (E), 20: 14007(R) (ANL-7122, pp 1-41)
uses in purification of yttrium, 18: 43732(P)
vapor pressure of, bell method measurements of, 19: 9151
vaporization of, 17: 2956 (UCRL-9840)
Al–Mg–$MgCl_2$–KCl–NaCl, corrosive effects on steels and tantalum at 500 to 800°C, (E), 20: 14007(R) (ANL-7122, pp 1-41)
$BaCl_2$–$MgCl_2$, phase diagrams, 20: 36787 (YALE-2723(Vol.1))
$BeCl_2$–$MgCl_2$, phase diagrams, 20: 36787 (YALE-2723(Vol.1))
$CaCl_2$–CaF_2–Mg–$MgCl_2$–Zn, corrosive effects on silicon carbide at high temperatures, 19: 17176(R) (ANL-6965(p.1-41))
$CaCl_2$–$MgCl_2$, phase diagrams, 20: 36787 (YALE-2723(Vol.1))
$CaCl_2$–Mg–$MgCl_2$–MgF_2–U–Zn, reactions with alumina crucibles at 800°C, 17: 36860(R) (ANL-6648)
$CaCl_2$–$MgCl_2$, solvent properties for magnesium fluorides at 610 to 830°C, 18: 19456(R) (ANL-6840)
$CaCl_2$–$MgCl_2$, reactions with cerium–fissium–uranium–zirconium alloys at 1200°C, 19: 17176(R) (ANL-6965(p.1-41))
$CaCl_2$–$MgCl_2$, solvent properties for californium–yttrium alloys, 19: 17176(R) (ANL-6965(p.1-41))
$CaCl_2$–$MgCl_2$, solvent properties for magnesium fluorides, 19: 15662(R) (ANL-6900(p.45-142))
$CdCl_2$–$MgCl_2$, phase diagrams, 20: 36787 (YALE-2723(Vol.1))
Cd–LiCl–Mg–$MgCl_2$–NaCl–U–Zn, corrosive effects on reactor materials, 18: 36751 (ANL-6912)
Cd–Mg–$MgCl_2$–Pu–KCl–NaCl, corrosive effects on SS 304, 18: 36751 (ANL-6912)
CsCl–$MgCl_2$, phase diagrams, 20: 36788 (YALE-2723(Vol.2))
CuCl–$MgCl_2$, phase diagrams, 20: 36788 (YALE-2723(Vol.2))
Cu–$MgCl_2$, corrosive effects on steels, 20: 31314(R) (ANL-7175, pp 1-41)
Cu–$MgCl_2$–KCl–NaCl, corrosive effects on ferrous alloys, 20: 31314(R) (ANL-7175, pp 1-41)
Cu–Mg–$MgCl_2$–KCl–NaCl–U, chemical compatibility with vitreous carbon containers at 800°C, (E), 20: 14007(R) (ANL-7122, pp 1-41)
LiCl–$MgCl_2$–MgF_2–Zn–$ZnCl_2$, corrosive effects on tungsten alloys at 800°C, 17: 36860(R) (ANL-6648)
LiCl–$MgCl_2$–NaCl, effects on corrosion of ferrous alloys by cadmium–magnesium–uranium–zinc at 600 and 650°C, 19: 32279(R) (ANL-7020(p.3-99))
LiCl–$MgCl_2$–NaCl, liquidus lines at 450 to 600°C, 18: 35060(R) (ANL-6904)
LiCl–$MgCl_2$–NaCl, liquidus temperatures, 19: 32279(R) (ANL-7020 (p.3-99))
LiCl–$MgCl_2$–KCl, liquidus temperatures, 19: 32279(R) (ANL-7020 (p.3-99))
LiCl–$MgCl_2$–NaCl, melting points of, effects of composition on, 20: 5594(R) (ANL-6925, pp 21-106)
LiCl–$MgCl_2$–KCl, melting points of, effects of composition on, 20: 5594(R) (ANL-6925, pp 21-106)
LiCl–$MgCl_2$, phase diagrams, 20: 36788 (YALE-2723(Vol.2))
LiCl–$MgCl_2$, phase studies, 17: 14116(R) (ANL-6596(p.29-118))
LiCl–$MgCl_2$, phase studies at 575 to 725°C, 17: 40421(R) (ANL-6766)
LiCl–$MgCl_2$–NaCl, phase studies on, 18: 24813(R) (ANL-6880 (p.49-67))
LiCl–$MgCl_2$–KCl, phase studies on, 18: 24813(R) (ANL-6880(p.49-67))
LiCl–$MgCl_2$–KCl, phase studies on, 18: 36751 (ANL-6912)
LiCl–$MgCl_2$–NaCl, phase studies, 19: 15662(R) (ANL-6900(p.45-142))
LiCl–$MgCl_2$, solvent properties for magnesium sesquicarbide at 600°C, 17: 36861(R) (ANL-6764)
LiCl–$MgCl_2$–KCl, solvent properties of liquid, for rare earths, 20: 4297(R) (IS-1200(Sect. M))
LiCl–$MgCl_2$, solvent properties for californium and yttrium, 20: 5594(R) (ANL-6925, pp 21-106)
LiCl–$MgCl_2$, structure of liquid, 19: 2278(T) (ANL-Trans-117)

$LiCl–Mg–MgCl_2–MgF_2–Zn–ZnCl_2$, corrosive effects on anodized beryllium at 800°C, 17: 36860(R) (ANL-6648)
$LiCl–Mg–MgCl_2–NaCl–Zn$, corrosive effects on reactor materials, 18: 36751 (ANL-6912)
$MgCl_2–AgCl$, phase diagrams, 20: 36787 (YALE-2723(Vol.1))
$MgCl_2–KCl–NaCl$, corrosive effects with cadmium alloys, on stainless steel, 20: 20802(R) (ANL-7055, pp 21-98)
$MgCl_2–KCl–NaCl–UO_2Cl_2$, electrolysis of molten, at 500 to 600°C, 20: 43266(P)
$MgCl_2–KCl–NaCl$, exchange of plutonium in liquid systems with magnesium–zinc alloys, thermodynamics of, 20: 43819
$MgCl_2–KCl$, phase diagrams, 20: 36788 (YALE-2723(Vol.2))
$MgCl_2–KCl–NaCl$, separation of rare earth fission products from, by extraction using magnesium alloys, 20: 3865 (ANL-7064)
$MgCl_2–KCl–NaCl$, solvent properties for lanthanum, plutonium, and praseodymium, 20: 5594(R) (ANL-6925, pp 21-106)
$MgCl_2–KCl–NaCl$, solvent properties for uranium, 20: 5594(R) (ANL-6925, pp 21-106)
$MgCl_2–KCl–NaCl$, solvent properties of liquid, for praseodymium, 20: 20802(R) (ANL-7055, pp 21-98)
$MgCl_2–KCl$, spectra of liquid, Raman, 20: 38871(R) (NYO-1769-54)
$MgCl_2–KCl$, stability of zirconium dichloride in, 20: 1822(T) (ANL-Trans-233)
$MgCl_2–KCl$, thermodynamic properties at 725°C, 20: 24971(R) (BNL-954, pp 50-83)
$MgCl_2–NaCl$, corrosive effects on titanium-base alloys at 550 to 600°F, stress, 20: 11227
$MgCl_2–NaCl$, phase diagrams, 20: 36788 (YALE-2723(Vol.2))
$MgCl_2–NaCl$, stability of zirconium dichloride in, 20: 1822(T) (ANL-Trans-233)
$MgCl_2–Na_2CO_3–UO_2(NO_3)_2$, uranium precipitation in, mechanism of, 20: 38928
$MgCl_2–NCl–NaCl$, rate processes in packed column during bismuth extraction from, 17: 27492 (BNL-791)
$MgCl_2–NiCl_2$, spectra of nickel(II) in melts of, absorption, 20: 3921(R) (ORNL-3870, pp 56-60)
$MgCl_2–RbCl$, phase diagrams, 20: 36788 (YALE-2723(Vol.2))
$MgCl_2–SnCl_2$, phase diagrams, 20: 36788 (YALE-2723(Vol.2))
$MgCl_2–SrCl_2$, phase diagrams, 20: 36788 (YALE-2723(Vol.2))
$MgCl_2–TlCl$, phase diagrams, 20: 36788 (YALE-2723(Vol.2))
$MgCl_2–ZnCl_2$, phase diagrams, 20: 36788 (YALE-2723(Vol.2))
$Mg–MgCl_2$, free energy of solution of, 19: 11103
$Mg–MgCl_2$, kinetics of dissolution in, 17: 2461(R) (BNL-731(p.18-46))
$Mg–MgCl_2–Ag$, thermodynamic properties, 18: 3671(R) (BNL-799 (p.26-54))
$Mg–MgCl_2–Zn$, distribution studies in, 17: 3871
$Mg–MgCl_2–Zn$, solvent properties for californium and einsteinium at high temperatures, 19: 15662(R) (ANL-6900(p.45-142))
$MgCl_2–KCl$, free energy of formation of $KMgCl_3$ at 450°C, 19: 38575 (BNL-9343)
$MgCl_2–KCl–NaCl$, distribution of rare earths, plutonium, and uranium between magnesium alloys and, 19: 32279(R) (ANL-7020(p.3-99))
$MgCl_2–KCl–NaCl$, electrolysis of uranyl chloride in, preparation of uranium dioxide by, 18: 2206
$MgCl_2–KCl–NaCl$, exchange of barium ions between potassium hexatitanate and molten, 19: 32279(R) (ANL-7020(p.3-99))
$MgCl_2–KCL–NaCl$, rate processes in packed column during bismuth extraction from, 17: 27492 (BNL-791)
$MgCl_2–KCl–NaCl$, separation of rare earths from, by extraction using aluminum–magnesium alloys, 19: 17176(R) (ANL-6965(p.1-41))
$MgCl_2–KCl–NaCl$, solvent properties for cerium and uranium from bismuth–magnesium alloy at 500°C, 17: 10581 (BNL-639)
$MgCl_2–KCl–NaCl$, solvent properties for praseodymium, 18: 24952(R) (ANL-6880(p.6-48))
$MgCl_2–KCl–NaCl$, use as bath in electrolytic production of uranium dioxide crystals, 19: 34199(P)
$MgCl_2–KCl–ThCl_4$, phase studies of thorium chloride–eutectic mixtures, 19: 2280(T) (IS-Trans-7)
$MgCl_2–NaCl$, corrosive effects on stainless steels, effects of pH on, 19: 42803(R) (EURAEC-1397)
$MgCl_2–NaCl$, solvent properties for niobium, 18: 16032
$MgCl_2–NaCl$, thermodynamic properties of fused, 16: 20042(R) (BNL-696)
$MgCl_2–NaCl$, thermodynamic properties of fused, 17: 7992 (BNL-6589)
$MgCl_2–PuCl_3$, phase studies, 16: 6419
$(NH_4)_2CO_3–MgCl_2–SiO_2–UO_2(NO_3)_2$, reactions in, silicate formation in, 20: 36797
$PbCl_2–MgCl_2$, phase diagrams, 20: 36788 (YALE-2723(Vol.2))

MAGNESIUM CHROMATES
Szilard-Chalmers reaction in, magnesium isotope effects in, 17: 40891

MAGNESIUM CHROMITES
crystal structure of $MgCr_2O_4$, neutron diffraction study of, 19: 2274 (PAN-536/II)

MAGNESIUM COMPLEXES
chlorophyllin, radiosensitivity effects in mice, gamma, 20: 1692
formation, optimum conditions for, 19: 13374
with [(1,2-dimethylethylene)dinitrilo]- and (propylenedinitrilo)-tetraacetic acids, stability of, 20: 12594(R) (NP-15679)
with adenosine triphosphate, infrared spectra of, in heavy water, 19: 5936
with adenosine triphosphate, stability constants of, 16: 7556
with adenosinephosphoric acids, stability constants of, 16: 28948
with aminoacetone-*N,N*-diacetic acid, dissociation and stability constants of, 18: 19946
with condensed phosphates, stability constants, 17: 2962
with cupferron, thermal dissociation, 19: 7366
with diacetamide, properties and spectra of, 20: 8494 (TID-22449)
with mercaptosuccinic acid and 2,3-dimercaptosuccinic acid, formation and properties of, 18: 8394 (TID-20013)
with methanol, isotopic dilution studies on, 17: 2948(R) (TID-17216)
with *N*-(2-pyridylmethyl)iminodiacetic acid, stability of, 17: 15993
with polyaminocarboxylic acids, stability of, 17: 40840
with solochrome violet RS, polarography of, 20: 16406
with substituted 2-(pyridyl)- and 2-(quinolyl)-1,3-indanediones, acid dissociation and formation constants of, 18: 25457
with tetracycline, stability, 17: 23052
with triethylenetetraaminehexaacetic acid, formation constants of, 18: 8396 (TID-20015)
with 2-methyl-4,6-heptanedione, stability constants of, 19: 11056(T) (AEC-tr-6227/3(p.183-92))
with 2,6-pyridinedicarboxylic acid, ion exchange properties of, 20: 18685
with 8-quinolinol, stability at high temperatures, 16: 10009
with 8-quinolinol derivatives, electronic absorption spectra, 19: 43989 (MIT-905-20)

MAGNESIUM COMPOUNDS
see also Grignard Reagents
crystal structure and homogeneity ranges of, with rare earth selenides, sulfides, and tellurides, 19: 37052
crystallography of, with perovskite-like structure, 19: 25014
effects of dietary, on strontium-90 metabolism in animals, 19: 40342
effects on radiolysis of water, 20: 8981 (CEA-R-2794)
electric conductivity of m-benzenedisulfonate in water, 17: 14268
electric conductivity in nonaqueous solvents, 18: 41472
preparation and crystal structure of scandates, 19: 13364
properties for moderator use, survey, 16: 5655 (NEPA-947)
reactions of molten, with rare earth halides, 19: 40955
structure of phenylmagnesium bromide dietherate, 17: 23239
thermodynamic properties, 19: 16202

MAGNESIUM COUPLES
graphite/Mg, corrosion pitting by chloride ions, 20: 11231 (CEA-R-2815)
Mg/Pt, corrosion pitting by chloride ions, 20: 11231 (CEA-R-2815)
Mg/stainless steel, corrosion pitting by chloride ions, 20: 11231 (CEA-R-2815)

MAGNESIUM DEUTERIDES
spectra of, ultraviolet, 18: 1654
spectra, parameters for $A^2\pi \rightarrow X^2\Sigma$ transitions in, 16: 27840
structure of, neutron-diffraction study of, 17: 23309

MAGNESIUM, DIMETHYL-
spectra of hydrogen and lithium-7 in ether solutions of methyllithium complexes with, NMR, 20: 43393

MAGNESIUM ERBIUM SELENIDES
preparation, (E), 19: 13297

MAGNESIUM FERRATES(III)
magnetic fields in, Mössbauer study of effective, 19: 38026 (INP-407/PL)

MAGNESIUM FLUORIDES
see also Potassium Magnesium Fluorides
binding energy of gaseous, 16: 28964
crystal lattice energy of, relation of self energy of gaseous ions to, 18: 16017
deposition of films of, on quartz for ultraviolet optics, 17: 23606 (MATT-187)
determination in beryllium, 16: 26912
dissociation energy of gaseous, 18: 32153(R) (UCRL-11317(p.176-97))
electron penetration depths at 1 to 30 kev, 18: 44476
enthalpy and lattice energies of, calculation of, 19: 17901
fluorine replacement by chlorine in, 16: 26992
growth and structure of vapor-deposited crystalline, 16: 32909(T) (AEC-tr-5393)
growth of crystalline, preferred orientation of, 16: 33486(T) (AEC-tr-5391)
growth of crystalline, orientation phenomena in, 16: 32908(T) (AEC-tr-5392)
growth of highly perfect single crystals of, for use in lasers, 17: 37744

hardness of crystalline divalent, 16: 10728
heat of formation, 17: 40421(R) (ANL-6766)
heat of formation, 19: 32118(R) (ANL-7020(p.165-74))
heat of reaction of, with aluminum, 17: 35800
heat of sublimation and vapor pressure of, 20: 26874
heats of ionization and sublimation and polymerization for, 17: 16770(R) (ANL-6666)
hydrolysis at 745 to 825°C and 1 to 20 mm mercury, mechanisms and thermodynamics of, 18: 22021 (UCRL-11103)
hydrolysis by water vapor at high temperatures, kinetics of, 19: 15418 (UCRL-9821(Rev.))
hydrolysis by water vapor at high temperatures, mechanism of, 19: 15419 (UCRL-11103(Rev.1))
hydrolysis of, kinetics of, 17: 35264(R) (UCRL-10706(p.111-203))
hydrolysis of, at high temperatures, 20: 31719(R) (UCRL-16658, pp 155-69)
ion penetration depths at 1 to 30 keV, 18: 44476
ion range-energy relations for, (T), 19: 30967
melting of, volume change in, 20: 25572(R) (NASA-CR-67221)
particle size analysis, comparison of methods for, 17: 12065(R) (NLCO-865(p.43-51))
particle size analysis of, comparison of methods for, 19: 2576 (NLCO-925)
polymerization of, spectra of, 17: 4530
preparation of pure single crystals of, 17: 8013 (UCRL-10105)
production by hydrofluorination of magnesium oxide, 20: 4999(R) (ORNL-2599)
radiation effects on absorption spectra of, x, 18: 17898
radioinduced color centers in rutile crystals of, 19: 20618 (NBS-8614)
radioinduced defect clusters in, electron microscopy of, 20: 42554
separation from uranium, 16: 3065(R) (MCW-1469)
separation from uranium by hydraulic separator, 16: 11775(R) (NLCO-790)
separation of uranium from, 18: 12038 (ORNL-3544)
solubility in calcium chloride–magnesium chloride system at 610 to 830°C, 18: 19456(R) (ANL-6840)
solubility in calcium chloride–magnesium chloride at 600 to 800°C, 19: 15662(R) (ANL-6900(p.45-142))
sorptive properties for technetium, 17: 18181 (TID-18290)
sorptive properties for uranium hexafluoride, 18: 12038 (ORNL-3544)
sorptive properties for americium in presence of curium, 18: 43733(P)
sorptive properties of solid, for volatile fluorides in uranium hexafluoride, 20: 27038 (K-1666)
sorptive properties for plutonium hexafluoride, 20: 45789(R) (ORNL-3945, pp 48-71)
spectra of vaporized, 19: 46982(R) (AD-611856)
spectra of, infrared reflection and transmission, 18: 15711(R) (TID-20256)
thermodynamic properties of, 18: 25360
thermodynamic properties of gaseous, mass spectrometric studies of, 18: 27356 (CONF-74-27)
thermodynamic properties in *N,N*-dimethylformamide and *N*-methylformamide solutions, 20: 3924 (TID-22366)
use in photocathode processing, 17: 18543(R) (TID-14035)
use of gels of, in preparation of reactor fuels, 18: 43535(P)
uses in separating volatile fluoride impurities from uranium hexafluoride, 19: 13553(P)
uses in separation of americium and curium, 18: 43727(P)
vaporization of, 17: 2956 (UCRL-9840)
Al_2O_3–MgF_2, phase studies, 20: 37722(R) (N-65-30843)
BaF_2–MgF_2, solvent properties for uranium dioxide at 1150°C, 19: 11050 (MCW-1490)
BeF_2–MgF_2, phase diagrams, 20: 36787 (YALE-2723(Vol.1))
$CaCl_2$–Mg–$MgCl_2$–MgF_2–U–Zn, reactions with alumina crucibles at 800°C, 17: 36860(R) (ANL-6648)
CaF_2–MgF_2, phase diagrams, 20: 36787 (YALE-2723(Vol.1))
CaO–MgF_2, phase studies, 20: 37722(R) (N-65-30843)
LiCl–$MgCl_2$–MgF_2–Zn–$ZnCl_2$, corrosive effects on tungsten alloys at 800°C, 17: 36860(R) (ANL-6648)
LiCl–Mg–$MgCl_2$–MgF_2–Zn–$ZnCl_2$, corrosive effects on anodized beryllium at 800°C, 17: 36860(R) (ANL-6648)
LiF–MgF_2, phase diagrams, 20: 36788 (YALE-2723(Vol.2))
LiF–MgF_2–YF_3, analysis for magnesium and yttrium, 20: 4999(R) (ORNL-2599)
LiF–MgF_2–YF_3, analysis for oxygen, 20: 4299(R) (ORNL-2711)
MgF_2–KF, phase diagrams, 20: 36788 (YALE-2723(Vol.2))
MgF_2–MgO, phase studies, 20: 37722(R) (N-65-30843)
MgF_2–MgO, phase studies of melts of, 20: 45647
MgF_2–NaF, phase diagrams, 20: 36788 (YALE-2723(Vol.2))
MgF_2–RbF, phase diagrams, 20: 36788 (YALE-2723(Vol.2))
MgF_2–ScF_3, phase diagram, 17: 23321
MgF_2–UF_4, preparation of double fluoride, 17: 8230(P)
MgF_2–UO_2, phase studies of melts of, 20: 45647

MAGNESIUM HOLMIUM SELENIDES
preparation, (E), 19: 13297

MAGNESIUM HYDRIDES
properties of diatomic ions of, use of Platt electrostatic model for calculation of, 18: 12074
spectra of, ultraviolet, 18: 1654
spectra, parameters for $A^1\pi \rightarrow X^1\Sigma$ transitions in, 16: 27840

MAGNESIUM HYDROXIDES
calcination to oxide for sintering, 19: 16005(T) (AEC-tr-6537)
decomposition, effects of water vapor, 17: 18070
dehydration, emanation during, 16: 31661
electron energy levels in, neutron inelastic scattering studies of, 17: 29445
formation of double, in nitrate solutions, 16: 22142
free energy of formation at 1650 to 2000°K, 17: 23864(R) (BMI-1619(Del.))
neutron inelastic scattering spectra of deuterated and normal, vibrational modes in, (E), 19: 45482
neutron scattering by lattice of, spectra from inelastic, 18: 39154 (EUR-1643.e(p.174-80))
radiation effects on rate of decomposition of, beta and gamma, 20: 38955
sorption of carbon dioxide on, isotopic exchange in, 19: 26344
thermal decomposition of single crystals, 16: 1731 (AERE-R-3801)
$Al(OH_3)$–$Mg(OH)_2$, crystalline in dialyzed medium, composition and structure of, 17: 10619

MAGNESIUM HYPOPHOSPHITES
radiation effects on ESR in single crystals of, 20: 414

MAGNESIUM IODIDES
binding energy of gaseous, 16: 28964
crystal lattice energy of, relation of self energy of gaseous ions to, 18: 16017
dissociation energy of gaseous, 18: 32153(R) (UCRL-11317(p.176-97))
enthalpy and lattice energies of, calculation of, 19: 17901
iodine-127 quadrupole bonding and resonance in solid layer type, 16: 7538
polymerization of, spectra of, 17: 4530
sorptive properties of, for cadmium-115, indium, mercury, and zinc-65, 17: 15992
stability and thermodynamic properties, 18: 1675
vaporization of, 17: 2956 (UCRL-9840)
MgI_2–KI, phase diagrams, 20: 36788 (YALE-2723(Vol.2))
MgI_2–NaI, phase diagrams, 20: 36788 (YALE-2723(Vol.2))

MAGNESIUM IONS
activity coefficient function in perchlorate solutions, 18: 10035 (CONF-387-1)
content in Matsesta mineral water, 19: 655
determination in perchloric acid solutions by Donnan membrane equilibrium, 18: 43403
displacement in soils by beryllium, 19: 45802
distribution coefficient in zone melting of lithium fluoride, 19: 34144 (ORNL-3658)
effect on salt filtration properties of cellophane, 20: 35495
effects on adsorption of europium on barium sulfates, 19: 32306
effects on copper determination, 20: 36726
effects on diffusion current and half-wave potentials of uranyl ions in l-ascorbic acid electrolytes, 16: 28856
effects on electrochemical reduction of aqueous hydrogen ions, 17: 20051
effects on electrolytic precipitation of cerium oxide, 19: 34223
effects on formation of single-crystal beryllium oxide, 20: 36814
effects on hydrogen yields in radiolysis of 2-propanol in water, 18: 13885
effects on hydrogen yields from radiolysis of water, 19: 26397
effects on oxygen and strontium uptake by rat liver mitochondria, 19: 14972
effects on strontium uptake by rat liver mitochondria, mechanism of, 19: 14970
effects on structure of ribonucleic acid, 19: 9157(R) (NYO-2567-1)
effects on uptake of rubidium by barley sprouts, 17: 17741
electron affinities of, relativistic and nonrelativistic, 17: 27996
energies in high-speed plasma beams in vacuum arcs, 18: 40708
energy levels and wave functions for, (T), 19: 16370 (UCRL-7943-T)
energy levels of, (T), 20: 11450 (UCRL-7842-T)
energy levels of, 20-parameter eigenfunctions and energies of 2^1S states of, 17: 11751
energy loss in gases and solids, 16: 12295
entropy and heat of formation in aqueous solution, equation for calculation of, 18: 22066
exchange of methanol between solvent and solvated, 17: 12258
hydration numbers, 17: 30544
precipitation with calcite and calcium carbonate–magnesium carbonate

system from aqueous solutions, 20: 18631 (NYO-2266-1)
production using laser light, 18: 34297
radioinduced reduction of divalent, gamma, 18: 17905
radioprotective effects in mice, 18: 13567
radiosensitivity effects on DNA, 17: 33726
radiosensitivity effects on bacteria, x, 19: 26123
range-energy relations in aluminum, (E), 19: 9893 (NAS-NRC-PUB-1133 (p.173-86))
reactions of, with methanol, isotopic dilution studies on, 17: 2948(R) (TID-17216)
reactions with atoms and ions at 0.4 to 2 kev, radiation emission from, 18: 36145
reactions with copper at 30 kev, x-ray diffraction studies of precipitates from, 17: 1964
reactions with nitrogen at 0.4 to 2 kev, charge exchange and excitation in, 18: 32449
salting out effects in thorium nitrate–TBP systems, 18: 13944
separation by thin-layer ionophoresis, 18: 10185
separation from cesium by nitrobenzene, 17: 21720
separation from lithium and sodium by ion exchange, 16: 17768
solvent extraction from molten nitrate by liquid silicone–TBP at 150°C, 19: 19833 (CEA-R-2628)
sorption by aminodiacetate resin Dowex A-1, 20: 16358
sorption of divalent, by phosphorus-containing ion exchangers, from acetic acid–sodium acetate solutions, 20: 35593
sorption on zirconium phosphates, tracer studies of, 19: 32293
spectra in Scylla plasma, x-ray, 17: 13639
spectra of, with σ-semiquinones, electron spin resonance, 18: 39190
spectral line intensities of lithium-like, 18: 17185
spin hamiltonian parameters of, in axially symmetric and cubic crystals, 17: 33857 (AFCRL-63-192)
thermodynamic equilibrium in chromosphere, departures from, 16: 16898
toxicity of, in mouse, determination by LD_{50} on thirtieth day of, 17: 17719
uptake by barley roots, uranyl effects on selective inhibition in, 20: 20402
use for exchange in clay mineral studies, comparison with calcium and strontium, 18: 16200
van der Waals radii of, relation of hydration energy to, 18: 16016

MAGNESIUM ISOTOPES
content in natural samples, ratio variation in, (E), 20: 18908
distribution in dolomites, 16: 27448
effects on retention in Szilard-Chalmers reaction in magnesium chromate, 17: 40891
enrichment by ion migration in molten halides, 16: 464
gamma reactions on, cross sections for, 19: 12496
nuclear energy levels and properties, survey, 16: 18483
preparation, determination, and properties of radioactive, 16: 1349
preparation of accelerator targets of, 19: 38658
proton decay, 18: 18876 (KFK-185)
proton reactions on, sodium-22 yields from, 17: 8153
proton scattering by, optical-model analysis of, (T), 19: 10259 (UCRL-7666)
separation by amalgam exchange, calculation of coefficients for, 19: 18373
separation by isotopic exchange, 19: 18369
separation from isotopes of other elements, summary of, 20: 13345(R) (NP-15772)
separation in calutrons, 18: 34005(R) (ORNL-TM-879)
separation in calutrons, 18: 34007(R) (ORNL-TM-890)
separation of stable, in calutrons, 18: 34005(R) (ORNL-TM-879)
separation of, performance of separator for, 20: 16928(R) (INSJ-92)

MAGNESIUM ISOTOPES Mg-21
beta decay of, delayed proton emission in, 18: 40523
beta decay of, log ft values for superallowed transitions in, (E), 20: 24407
decay of, delayed proton emission in, (E), 19: 14546
decay of, delayed proton emission in, (E), 19: 47613
decay of, log ft values for, (T), 19: 21379
decay scheme, 18: 6189
production and properties of, (E), 19: 14546
proton decay, (E), 19: 21271(T) (KFK-tr-161)

MAGNESIUM ISOTOPES Mg-22
alpha reactions (α,γ) at 1.6 to 3.2 Mev, angular correlations and distributions from (E), 19: 1677
beta decay energies, 16: 7061
energy levels, 16: 7097

MAGNESIUM ISOTOPES Mg-23
beta decay of, model for relative period of, 17: 29632
electron scattering by, 18: 9344
energy level distributions, (T), 19: 45313
energy levels, 18: 18881 (NP-13784)
energy levels and gamma spectra, 16: 31088
gamma spectra, 20: 44634(R) (IDO-17188)

MAGNESIUM ISOTOPES Mg-24
alpha capture and scattering by, 18: 24625 (WASH-1046)
alpha diffraction scattering, 16: 31115
alpha diffraction scattering by, nuclear surface diffuseness effect on, (T), 19: 10289
alpha elastic and inelastic scattering at 22.5 Mev, differential cross sections for, 17: 33101
alpha elastic and inelastic scattering by, at 18 to 21.4 Mev, 18: 26550(R) (ORNL-3582(p.101-2))
alpha elastic scattering at 3.2 to 4.5 Mev, silicon-28 energy level parameters from, 18: 9389
alpha elastic scattering at 28.5 Mev, optical potentials in, (E/T), 20: 4859
alpha elastic scattering at 8 to 19 Mev, (E), 20: 34572
alpha inelastic scattering at 22.5 Mev, magnetic substates population from, 17: 33099
alpha inelastic scattering by, angular correlations in, 18: 16928 (ANL-6848(p.153-8))
alpha inelastic scattering by, polarization effects in, 18: 42669
alpha inelastic scattering by, levels from, (T), 19: 14489 (ANL-6878 (p.143-73))
alpha inelastic scattering at 28.5 Mev, excitation of unnatural parity 3^+ state in, (T), 19: 45318
alpha inelastic scattering at 42 Mev, alpha-gamma coincidences in, 20: 3141
alpha inelastic scattering at 28.4 Mev, collective enhancement of 3^- state in, (T), 20: 22107
alpha reactions (α,γ) at 3.21–4.35 Mev, equipment for, 18: 7729
alpha reactions (α,d) with, $(d_{5/2})^2$ and $(f_{7/2})^2$ levels from, 18: 16933 (ANL-6848(p.182-7))
alpha reactions (α,Be^8) at 42 Mev, 18: 16951(R) (TID-20311)
alpha reactions (α,d) at 45 to 50 Mev, highly populated levels in, 18: 34779 (UCRL-11341)
alpha reactions (α,γ) with, distributions from, (E), 19: 14517 (CONF-640301(p.109-42))
alpha reactions (α,γ) at 8.0 to 10.5 Mev, gamma spectra from, (E), 19: 19095 (WASH-1053)
alpha reactions (α,p), Q value for, (E), 19: 43303
alpha reactions (α,d) at 42 to 53 Mev, deuteron energy spectra from, (E), 20: 12061
alpha reactions (α,d) at 42 to 53 Mev, energy spectra from, (E), 20: 24358(R) (UCRL-16580, pp 1-93)
alpha reactions $(\alpha,Be\text{-}7)$ at 35 to 65 Mev, angular-momentum effects in, (E), 20: 32507
alpha reactions (α,p) with, testing T-invariance by, (E), 20: 44793
alpha reactions (α,γ), gamma spectrum and excitation function, 16: 2504(T) (JPRS-11068)
alpha reactions (α,γ) on, energy levels from, 17: 7262
alpha reactions (α,γ) at 1.5 to 3.5 Mev, 17: 10240(R) (NP-12208)
alpha reactions, (α,γ) resonance in, 17: 16916
alpha reactions (α,γ), resonances, 17: 19253
alpha reactions (α,p) at 22 Mev, angular distributions from, 17: 28288
alpha reactions (α,γ) at 3.2 to 4.5 Mev, silicon-28 energy level parameters from, 18: 9389
alpha reactions with, angular distributions for, 18: 7696(R) (ORNL-TM-761)
alpha scattering at 13-30 Mev, differential cross sections for, 17: 26526
alpha scattering at 13 to 30 Mev, differential cross section for, 17: 29577 (UCRL-7063)
alpha scattering at 42 Mev, 18: 16951(R) (TID-20311)
alpha scattering at 24.3 Mev, excitation of 5.22-Mev (3^+) level by, 18: 19076
alpha scattering at 28.5 Mev by, cross sections for elastic and inelastic, (E), 19: 23642
alpha scattering at 28.5 Mev, (E), 19: 31262
alpha scattering at 18 to 21.4 Mev, silicon-28 energy levels from, (T), 20: 3069
alpha scattering by, differential cross sections of fourth excited state, 17: 9589
alpha scattering by, compound-nucleus mechanisms in, (T), 19: 17013
alpha scattering cross sections at 18 to 21 Mev, 18: 24620(R) (ORNL-TM-874)
bremsstrahlung reactions (γ,p) at 24 Mev, cross sections for, 17: 17155
bremsstrahlung reactions (γ,p) at 20.5 to 40 Mev, angular and energy distributions for, 18: 32787
bremsstrahlung reactions (γ,p) at 23 to 26.5 Mev, angular and energy distributions for, 18: 32788
bremsstrahlung reactions (γ,p) at 25.5 Mev, energy spectra from, (E),

19: 47699
bremsstrahlung reactions (γ,p) at 31 Mev, spectra from, (E), 20: 6399
Coulomb excitation of, reorientation effects in, 17: 17140
decay, 18: 32329
decay schemes of excited states, 16: 11000
deuteron diffraction scattering at 19.6 and 21 Mev, (T), 19: 21427
deuteron elastic scattering at 10 Mev, angular distributions from, 16: 23080
deuteron elastic scattering at 0.8 to 2.2 Mev, excitation functions for, (E), 19: 35450
deuteron elastic scattering at 7.8 Mev by, cross sections for, (E), 20: 12095
deuteron inelastic scattering at 8.7 to 12 Mev, angular distributions, 16: 13953 (JÜL-30-KP)
deuteron inelastic scattering by, 17: 13602
deuteron inelastic scattering at 11.8 Mev, differential cross sections for excitation of first excited state in, 17: 38277
deuteron reactions (d,p) at 10.1 Mev, analysis, 16: 12482
deuteron reactions (d,p) at 10 Mev, angular distributions from, 16: 21592
deuteron reactions (d,p) at 15 Mev, angular dependence of proton polarization in, 16: 21597
deuteron reactions (d,p) at 10 Mev, angular distributions from, 16: 23080
deuteron reactions (d,p) at 15 Mev, proton polarization in, 17: 838
deuteron reactions (d,p) on, knock-out mechanism in, 17: 17168
deuteron reactions (d,p), angular distributions in, 17: 31077(R) (CU(PNPL)-228)
deuteron reactions (d,p), proton polarization from, 17: 36716
deuteron reactions (d,p) at 3 to 5 Mev, angular distributions for, 17: 36669 (WASH-1042)
deuteron reactions (d,p) at 15 Mev, angular dependence of polarization and differential cross sections for, 17: 38248
deuteron reactions (d,p) with, gamma angular correlations in direct, 17: 38258
deuteron reactions (d,p) with, compound nucleus formation effects in, 17: 38222
deuteron reactions (d,n) with, angular distribution for, 17: 41873 (WASH-1044)
deuteron reactions (d,p) with, distorted-wave calculations of angular distributions from, 17: 26588
deuteron reactions (d,n) at 3 Mev, emission spectra of, 18: 12453 (CONF-340-15)
deuteron reactions (d,p) at 15 Mev, polarization angular distributions from, 18: 13104
deuteron reactions (d,α), sodium-22 energy levels from, 18: 17055
deuteron reactions (d,d' γ) with, gamma-deuteron correlation in, 18: 16922 (ANL-6848(p.123-4))
deuteron reactions (d,t) with, angular distributions and spectra from, 18: 18881 (NP-13784)
deuteron reactions (d,p) at 10.1 Mev, finite range effects in, 18: 24686
deuteron reactions (d,p) at 1 to 2 Mev, 18: 32772
deuteron reactions (d,p) with, spectra from, 18: 42679
deuteron reactions (d,p) at 700 to 1500 kev, 18: 44823
deuteron reactions (d,p) at 15 Mev (E), 19: 3340
deuteron reactions (d,p) with, spins of states from, (E), 19: 14495 (ANL-6878(p.279-301))
deuteron reactions (d,n) at 7.0 Mev, (E), 19: 14765(R) (ANL-6977)
deuteron reactions (d,α) at 5 to 20 Mev, (T), 19: 14556
deuteron reactions (d,p) with, high partial waves in, (T), 19: 16933
deuteron reactions (d,p) at 9 and 11 Mev, angular distributions from, (E), 19: 19095 (WASH-1053)
deuteron reactions (d,p) at 10 Mev, cross sections for, 19: 33302
deuteron reactions (d,α) at 11.45 to 12.10 Mev, (E), 20: 6369
deuteron reactions (d,p) at 10.1 Mev, angular distributions for, (T), 20: 17692 (ORNL-TM-1414)
deuteron reactions (d,n) at 7.0 to 10.0 Mev, (E), 20: 19805(R) (ANL-7110, pp 1-28)
deuteron reactions (d,α) at 11.45 to 12.1 Mev, angular distributions from, 20: 40065(R) (BMwF-FB-K-66-01)
deuteron reactions (d,p) with, mechanism of, (T), 20: 42394
deuteron reactions (d,α) with, mechanism of, (T), 20: 42394
deuteron reactions (d,p) at 2.8 to 6.1 Mev, cross-section fluctuations in, (E), 20: 44738
deuteron reactions (d,α) at 4.5 to 10 Mev, excitation function of, (E), 20: 44768
deuteron reactions (d,p) at 10 Mev, testing T invariance by, (E), 20: 44805
deuteron reactions (d,p) at 5 and 6 Mev, (E), 20: 44737
effects on magnesium oxide crystal lattice constants, 19: 4158
electron inelastic scattering at 40 to 70 Mev, M1 transitions following, 18: 24675
electron inelastic scattering at 55 Mev, cross sections for, 18: 32781
electron scattering shape parameters, 16: 11007
electron scattering by, excitation of rotational levels in, 18: 11288
electron scattering by, collective excitations in, 18: 13047 (JINR-P-1495)
electron-pair annihilation in, internal pair production coefficients from, (E), 19: 43330
energy level distributions, (T), 19: 45313
energy level excitation by 14-Mev neutrons, cross section for first, 18: 6264
energy level lifetimes, from resonance scattering of bremsstrahlung, 16: 26275
energy level spacings, 16: 6018
energy level spectrum of, L-S coupling for, 17: 21072
energy levels, 16: 32424
energy levels, 17: 32723(R) (PR-P-57(p.5-20))
energy levels, 17: 40033
energy levels, 18: 18910
energy levels, 18: 21306
energy levels, 18: 38169
energy levels, 18: 42755
energy levels, (E), 19: 41828
energy levels, (T), 20: 1227
energy levels, (T), 20: 19984
energy levels, 18: 15173 (BNL-7800)
energy levels, (E), 19: 23355(R) (BNL-867(p.1-117))
energy levels, 18: 18881 (NP-13784)
energy levels, 19: 37823(R) (ORNL-3800(p.1-49))
energy levels and gamma spectra, 16: 12486
energy levels at 7.5 to 10 Mev, 19: 1053(R) (PR-P-62)
energy levels from carbon-12 (O-16,α) reactions, parity and spin of, (E), 20: 32556
energy levels from carbon-12 (O-16,α) reactions, 20: 38008(R) (AECL-2595)
energy levels of, excited by alpha inelastic scattering, 18: 1082
energy levels of, parity and spin of 7.35 Mev, 17: 24447
energy levels of, parity and spin for, 17: 28324
energy levels of, parities and spins of, 18: 8917(R) (PR-P-59(p.4-20))
energy levels of, spin assignments for, 17: 33012
energy levels of, parity and spin of 11.933-Mev, 18: 11275
energy levels of, parity and spin of, 18: 13074
energy levels of, properties of rotational, 18: 13115
energy levels of, T = 2, 18: 28705
energy levels of, anomalous ordering of, 18: 36651
energy levels of, parameters for, 18: 40585
energy levels of, Hartree-Fock theory for, 18: 42737
energy levels of, models for collective, (T), 19: 14518 (CONF-640301 (p.143-64))
energy levels of, rotational, (E), 19: 23805
energy levels of, 0+, (T), 19: 25548
energy levels of, mean life of 4.12-Mev, 19: 27563
energy levels of, 8.44 and 9.52 Mev doublet, 19: 26922(R) (PR-P-64)
energy levels of, parity and spin for, (E), 19: 43358
energy levels of, parity and spin of, (E/T), 19: 47589(R) (TID-22012, pp 53-66)
energy levels of, parity and spin, 20: 5928(R) (PR-P-66)
energy levels of, gamma branching in, (E/T), 20: 6295 (NP-15647)
energy levels of, E1-giant resonances in, (T), 20: 8134
energy levels of, review of collective vibrations in, (T), 20: 10079
energy levels of, asymmetric-rotator model for rotational, (T), 20: 13849
energy levels of, electromagnetic properties of giant dipole resonances in s-d, 20: 26165
energy levels of, excited by alpha particles, 20: 42347
energy levels, rotational, 19: 9771(R) (PR-P-63)
energy spectrum of, SU3 shell-model classification for, 17: 19347
excitation functions in aluminum-27 (p,α) reactions at 6 to 10 Mev, (E), 19: 12537
excited state spectrum, first, 16: 17108
E1 resonance in, calculations of ground-state correlation effects, 16: 21524
gamma cascades at 6 to 8 Mev from proton capture by sodium-23, 16: 9458
gamma decay, 18: 18949
gamma E-2 transitions in, 17: 41965
gamma reactions (γ,p) with, cross sections, (E/T), 19: 14528 (LAL-1120)
gamma reactions (γ,n) at 11 to 30 Mev, cross sections for, (E), 20: 4849(R) (UCRL-14360, pp 1-50)
gamma reactions (γ,n) and (γ,p) at 10 to 27 Mev, cross sections, 16: 23057
gamma reactions (γ,p), proton energy distribution from, 17: 17152
gamma resonance scattering by, level lifetimes from, (E), 20: 28334

gamma resonant scattering at 1.38 Mev, (E/T), 19: 33391
gamma spectra, 17: 32435
gamma transition energies in, determination of, (E), 19: 6664
giant E1 resonance in, analysis by random-phase approximation, 16: 26253
ground state energy of truncated Hamiltonian for, B.C.S. method for, 17: 40064
helium-3 reactions (He^3,α) at 26 to 33 Mev, differential cross sections and angular dependences of, 18: 6262
helium-3 elastic scattering at 12 Mev, 18: 38144
helium-3 reactions (He-3,n) with, Q-value for, (E), 19: 31320
helium-3 reactions (He-3,n) at 5.5 Mev, silicon-26 levels from, (E), 19: 45355
helium-3 reactions (He-3,d) at 24.4 Mev, momentum spectra from, (E), 20: 13345(R) (NP-15772)
helium-3 reactions (He-3,t) at 37.8 to 40.1 Mev, aluminum-24 levels and mass from, (E), 20: 32473
mass difference from aluminum-27, 17: 19253
neutron activation of foils of, fast, 17: 36347(R) (NARF-62-18P)
neutron capture by, resonances from, (E), 19: 45356
neutron capture, spectra of resonance and thermal, (E), 19: 35399 (ORNL-P-1307)
neutron elastic and inelastic scattering at 2.8 Mev, polarization in, 18: 24694
neutron elastic and inelastic scattering at 14.1 Mev, 18: 26600
neutron elastic and inelastic scattering at 0.5 to 3 Mev, 18: 30835
neutron inelastic scattering by nonspherical, 17: 17248
neutron inelastic scattering at 3.5 Mev, gamma angular correlations in, 17: 38275
neutron inelastic scattering at 14 Mev, cross section for excitation of first level in, 18: 6264
neutron inelastic scattering by, gamma angular distributions from, 18: 19015
neutron inelastic scattering at 14 Mev, gamma emission in, 18: 44794
neutron inelastic scattering at 14 Mev, (E), 19: 43373
neutron inelastic scattering at 3 to 4.5 Mev, angular distributions and energy levels from, (E/T), 19: 47638
neutron inelastic scattering at 14 Mev, angular distributions for, 20: 1219
neutron inelastic scattering at 2.8 Mev, gamma spectra from, (E), 20: 8085 (USNRDL-TR-916)
neutron inelastic scattering at 3.3 and 3.5 Mev, angular correlations for, (E), 20: 26131
neutron reactions (n,p), cross sections, 16: 6539 (NDL-TR-15)
neutron reactions (n,n'γ), n'-γ correlation at 3.25 Mev, 16: 15651
neutron reactions (n,α), cross section and threshold energies, 16: 17730
neutron reactions (n,p) at 12 to 18 Mev, cross sections for, 17: 853
neutron reactions (n,p) at 5 to 20 Mev, cross sections for, 17: 13497
neutron reactions (n,nγ) with, 1.37-Mev gamma angular distribution from, 17: 20564(R) (TID-18442)
neutron reactions (n,p) with, product half life for, 17: 25857(R) (PR-P-56(p.4-18))
neutron reactions (n,p) at threshold, cross sections for, 17: 26421 (EUR-10.e)
neutron reactions (n,p) with, cross sections for fast, 17: 31056
neutron reactions (n,p), production of sodium-24 by, 17: 30165
neutron reactions (n,p) at 12.5 to 21.0 Mev with, cross sections for, 17: 40049
neutron reactions (n,n'γ) with, angular distributions from, 18: 11187 (ANL-6797(p.389-92))
neutron reactions (n,p) with, use for production of carrier-free sodium-24, 18: 12523 (SGAE-1963/3B)
neutron reactions at 12.5 to 21 Mev, cross sections for, 18: 16970
neutron reactions (n,γ) with, spectra from resonant, 18: 26542(R) (ORNL-3582(p.71-5))
neutron reactions (n,p) at 14 Mev, cross section fluctuations in, 18: 28682
neutron reactions (n,n'γ) at 3.0 to 4.35 Mev, angular distributions from, 18: 30736(R) (TID-20658)
neutron reactions (n,p) with, use in production of sodium-24, 18: 31999(T) (ORNL-tr-191)
neutron reactions (n,p) with, production of carrier-free sodium-24 by, 18: 43675
neutron reactions (n,p) with, calculated cross sections, 19: 1053(R) (PR-P-62)
neutron reactions (n,p), production of sodium-24 by, 19: 2701
neutron reactions (n,p) with, cross sections for, (E), 19: 5230
neutron reactions with, sodium-24 preparation by, 19: 15610
neutron reactions (n,p), thermal, 19: 22801
neutron reactions (n,p), cross section for, (E), 19: 35378(R) (EANDC(E)-57(U))
neutron reactions (n,p) at 12.6 to 19.6 Mev, cross sections for, (E), 20: 9990
neutron reactions (n,2n) at 12 to 18 Mev, cross sections for, (E), 20: 15863
neutron reactions (n,p) with, sensitivity of, for activation analysis, 20: 16332 (GA-6691)
neutron reactions (n,p), threshold cross section and energy for, 20: 16335(R) (NBS-TN-276)
neutron reactions (n,p) at 0 to 20 Mev, cross sections for, 20: 19810 (EUR-119.e(Vol.2))
neutron reactions (n,p) at 6.3 Mev, cross section and threshold energy for, 20: 21427(R) (NASA-CR-54904)
neutron scattering at 2.9 Mev, gamma production cross sections for, 16: 7095
neutron scattering at 1 to 4 Mev, cross sections for energy level excitation in, 18: 21217
neutron scattering at 14 Mev, cross sections for, (T), 19: 33359
nitrogen nucleus reactions (N^{14},N^{13}), angular distribution and ranges of nitrogen-13, 16: 21416
nitrogen-14 nucleus reactions at 28 Mev, nucleon transfer in, 16: 21575
nitrogen-14 reactions (N-14, N-13) with, particle transfer model for, 20: 4851
nuclear charge density of, model for, 17: 29633
nuclear deformation in, stability of axially asymmetric, 17: 40113
nuclear dipole resonance in, 18: 40556
nuclear structure of, α-particle model of, 17: 5374
nuclear structure of, geometric position of alpha clusters in, 18: 18943
nuclear structure calculations for, 18: 34781 (UCRL-11376)
nucleon binding energies, 16: 11007
nucleon inelastic scattering by, models for, 18: 2403(R) (PR-P-58)
nucleon inelastic scattering by, angular correlations for, 18: 7780
nucleon spatial correlations in, 19: 19152
pairing energies of, Hartree-Fock model for, 17: 40064
photofission of, binary, 17: 21052
photon absorption giant resonance, dipole, 16: 17109
photon reactions (γ,n) at 15 to 30 Mev, cross sections for, (E/T), 19: 35375 (CEA-R-2736)
photoproton emission and angular distributions, 16: 7079
preparation as radiation target material, 18: 27811(R) (ORNL-TM-198)
preparation for radiation targets, from magnesium oxide, 20: 44717
preparation of bulk materials and foils of, from oxide, 20: 13216 (ORNL-P-1899)
preparation of thin self-supporting foils of, by rolling, 20: 25520 (AERE-R-5097, Paper 22)
production by cyclotron-produced and cosmic mesons (μ), 20: 43550(R) (NYO-844-67)
production in (γ,α) reactions in silicon surface barrier detectors, pulse height defect for, 19: 30561
proton elastic and inelastic scattering at 6.9 Mev, angular distribution from, 17: 11743
proton elastic and inelastic scattering at 5.8 Mev, polarization in, (E), 19: 47697
proton elastic and inelastic scattering at 5.8 Mev, polarization in, (E), 20: 15806
proton elastic scattering at 22.2 Mev, angular distributions and cross sections, 16: 9462
proton elastic scattering at 5.45 Mev, 17: 2314
proton elastic scattering cross sections, 17: 17261
proton inelastic scattering, angular correlations from, 16: 32427
proton inelastic scattering at low energies, reaction mechanism in, 17: 4084
proton inelastic scattering at 10.3 Mev, 18: 21252
proton inelastic scattering at 2.015 to 4.20 Mev, differential cross sections for, (E), 19: 21426
proton inelastic scattering at 40 Mev, (T), 19: 37862
proton inelastic scattering at small angles, (E), 20: 12003(T)
proton inelastic scattering at 3.2 Mev, recoil-nuclei slowing down from, (E), 20: 28334
proton reactions (p,t) with, $T = T_z + 2$ states from, 18: 16923 (ANL-6848(p.125-9))
proton reactions (p,2p) at 185 Mev, 18: 26567
proton reactions (p,γ) at 3 Mev, spectra of, 18: 27793
proton reactions (p,n), aluminum-24 ground-state mass from, 18: 38140
proton reactions (p,n) at 25 Mev, aluminum-24 isomeric state from, (E), 20: 28424
proton reactions (p,α) at 40 Mev, spectra from, (E), 20: 36176(R) (TID-22971, pp 41-140)
proton reactions (p,γ) at 0.3 to 2.1 Mev, resonance strengths for, (E), 20: 42182
proton reactions (p,n) with, aluminum-24 mass from threshold energy for, (E), 20: 44812
proton reactions at 150 Mev, gamma spectra from, 16: 31088

proton reactions (p,γ) at 1.49 Mev, aluminum-25 3.70-Mev level spin from, 17: 28266
proton reactions (p,γ) with, aluminum-25 excited-state lifetime from, 17: 34943
proton reactions (p,γ) with, gamma spectra for, 17: 38588 (CU(PNPL)-227(p.35-48))
proton reactions (p,d) with, nuclear structure studies using, 18: 1088
proton scattering at 10.7 Mev, angular correlations in inelastic, 16: 21561
proton scattering at high-energies, spin-flip, 18: 38125
quasimolecular states in, partial widths and spins of, 17: 19356
scattering by carbon, electronic stopping cross sections in, 17: 37670
superfluidity effects in, 18: 2951
triton elastic scattering at 10 Mev, optical model analysis of, (E/T), 19: 25518
triton elastic scattering at 12 Mev, angular distributions from, (E), 20: 28325
triton reactions (t,p) at 10 and 11 Mev, angular distributions from, (E), 19: 21311
triton reactions (t,p) at 10 and 11 Mev, DWBA analysis of angular distributions for, (E/T), 20: 28326
triton reactions (t,d), reduced widths of rotational states in, 16: 33841
wave function of quasimolecular state of, 18: 38170

MAGNESIUM ISOTOPES Mg-25

alpha inelastic scattering by, levels from, (T), 19: 14489 (ANL-6878 (p.143-73))
alpha reactions (α,nγ) with, silicon-28 levels from, (E), 20: 34678
alpha reactions (α,γ), gamma spectrum and excitation function, 16: 2504(T) (JPRS-11068)
alpha reactions (α,αp), production of sodium-24 in, 16: 33814
alpha scattering at 42 Mev, 18: 16951(R) (TID-20311)
concentration using electrical mass filter, 16: 9092(T) (AEC-tr-4987)
deuteron elastic scattering at 10 Mev, angular distributions for, 18: 26561
deuteron elastic scattering at 0.8 to 2.2 Mev, excitation functions for, (E), 19: 35450
deuteron elastic scattering at 7.8 Mev by, cross sections for, (E), 20: 12095
deuteron reactions, energy level from, 16: 2546
deuteron reactions (d,p) at 15 Mev, proton polarization in, 16: 11017
deuteron reactions (d,p) at 10.8 Mev, polarization in, 16: 21581
deuteron reactions (d,p), proton angular distribution, 17: 2051(R) (CU(PNPL)-219)
deuteron reactions (d,n) on, distributions from, 17: 2251
deuteron reactions (d,t) with, geometric correction for, 17: 22555 (JINR-P-1214)
deuteron reactions with, method for analyzing, 17: 36669 (WASH-1042)
deuteron reactions (d,p) at 3.0 to 5.2 Mev, 18: 9409
deuteron reactions (d,α) at 3.35 to 7.7 Mev, total cross sections for, 18: 13068
deuteron reactions (d,α) at 3 to 8 Mev, cross section correlation with spin of states for (2I + 1) rule, 18: 19033
deuteron reactions (d,t) with, angular distributions and spectra from, 18: 18881 (NP-13784)
deuteron reactions (d,t) with, geometric effects in, 18: 18910
deuteron reactions (d,α) at 1.5 to 2.5 Mev, spectra from, (E), 19: 5166
deuteron reactions (d,p) at 9 Mev, angular distributions from, (E), 19: 19095 (WASH-1053)
deuteron reactions (d,p) at 10 and 11 Mev, angular distributions from, (E), 19: 21311
deuteron reactions (d,α) with, aluminum-27 lifetime in, (E), 19: 23637
deuteron reactions (d,p) at 10 Mev, magnesium-27 deformation and energy levels from, 19: 33302
deuteron reactions (d,α) at 1.5 to 2.5 Mev, differential cross section fluctuations in, (T), 19: 47659
deuteron reactions (d,p) at 7 and 8 Mev, (E), 20: 4849(R) (UCRL-14360, pp 1-50)
deuteron reactions (d,α) at 11.45 to 12.10 Mev, (E), 20: 6369
deuteron reactions (d,pγ) at 3.00 and 5.22 Mev, angular correlations in, (E), 20: 6410
deuteron reactions (d,n) with, aluminum-26 spectroscopic factors from, 20: 30481
deuteron reactions (d,α) at 11.45 to 12.1 Mev, angular distributions from, 20: 40065(R) (BMwF-FB-K-66-01)
deuteron reactions (d,α) at 3 and 5.5 Mev, aluminum-26 energy levels from, (E), 20: 44601(R) (ANL-7218)
deuteron reactions (d,p) at 8.0 Mev, magnesium-26 energy levels from, (E), 20: 44725
energy level lifetimes, from resonance scattering of bremsstrahlung, 16: 26275
energy level lifetime, first, 17: 19355
energy level properties, 16: 21413
energy level spacings, 16: 6018
energy level transitions in, 17: 11660
energy level transitions in, probability for two-quantum (E), 19: 3323
energy levels, 16: 26306
energy levels, 18: 19033
energy levels, (E), 19: 14559
energy levels, (E), 19: 16901
energy levels, (T), 20: 12002
energy levels (E), 19: 3340
energy levels, (T), 19: 14489 (ANL-6878(p.143-73))
energy levels, 18: 18881 (NP-13784)
energy levels, asymmetric-core collective model for, 16: 21459
energy levels from deuteron beam reactions with light nuclei, 16: 11040
energy levels from magnesium-24 (d,p), 16: 12482
energy levels from silicon-28 (n,α) reactions at 14.6 Mev, 16: 17076
energy levels from (n,α) reactions with silicon-28, 16: 23130
energy levels from silicon-28 (n,α) reactions, 17: 9556
energy levels from (n,α) reactions on silicon-28 at 13.4 and 13.8 Mev, 17: 17145
energy levels from reactions (n,α) with silicon-28 at 14.55 Mev, 18: 38069 (NP-14111)
energy levels, hyperfine structure of metastable ^2P, 16: 24849
energy levels of, detection of high-angular-momentum, 17: 19218 (LADC-5391)
energy levels of single-particle states, unified model, 16: 1083
energy levels of, rotational motion in, 18: 22915
energy levels of, models for collective, (T), 19: 14518 (CONF-640301 (p.143-64))
energy levels of, energy and spin of, (T), 19: 14575
energy levels of, spin of, (E/T), 19: 23754
energy levels of, parity and spin of, (E), 19: 29274
energy levels of, excited by alpha particles, 20: 42347
enrichment using electrical mass filter, 16: 6680
excitation functions from aluminum-27 (d,α) reactions at 2 Mev, (E/T), 19: 37848
excited states of, cross sections for transitions to, 17: 9567
fabrication as radiation target, 18: 27813(R) (ORNL-TM-428)
gamma reactions (γ,p) with, cross sections, (E/T), 19: 14528 (LAL-1120)
gamma reactions (γ,p) at 10 to 27 Mev, cross sections, 16: 23057
gamma reactions (γ,p), proton energy distribution from, 17: 17152
gamma spectra, 20: 44634(R) (IDO-17188)
helium nucleus reactions (helium-3,t), spectra from, 17: 5391
helium-3 reactions (He-3,α) at 5.5 Mev, cross sections for, (E/T), 19: 37849
helium-3 reactions (He-3,d), aluminum-26 spectroscopic factors from, 20: 30481
helium-3 reactions (He-3,d) at 17 and 22 Mev, aluminum-26 energy levels from, (E), 20: 44601(R) (ANL-7218)
magnetic octupole moments, 16: 8226
neutron inelastic scattering at 2.8 Mev, gamma spectra from, (E), 20: 8085 (USNRDL-TR-916)
neutron reactions (n,p), cross sections for, 19: 29228(R) (AEET/NP/10)
neutron reactions (n,p) at 14.8 Mev, cross sections for, (E), 20: 36212
neutron scattering at 1 to 4 Mev, cross sections for energy level excitation in, 18: 21217
neutron separation energy for, (E), 19: 39862
nitrogen-14 reactions (N-14,N-13), indirect interaction theory for, 17: 20991 (TID-18507)
nuclear structure, 18: 19031
nucleon inelastic scattering by, models for, 18: 2403(R) (PR-P-58)
performance as solar neutrino detector, 20: 37793
photon absorption giant resonance, dipole, 16: 17109
production in (n,α) reactions with silicon, 18: 16971
production in silicon-28 (n,α) reactions, fluctuations in excitation function for, 17: 28295
proton capture (p,γ) at 0.95 to 1.80 Mev, gamma spectra from, 16: 17103
proton elastic and inelastic scattering at 5 and 6 Mev, (E), 20: 44737
proton elastic and inelastic scattering at 4.5 to 6.1 Mev, cross-section fluctuations in, (E), 20: 44738
proton elastic scattering at 5.45 Mev, 17: 2314
proton inelastic scattering parameters of, 18: 34752(R) (CU(PNPL)-234)
proton inelastic scattering at 17.5 Mev, coupling effects in, (E), 20: 1192
proton inelastic scattering at 1.96 Mev, mean lifetime of first excited state from, (E), 20: 15780
proton reactions (p,α) at 9 Mev, 18: 34821
proton reactions (p,γ) at 956 to 1716 kev, resonances in, 18: 42630 (COO-1120-24)
proton reactions (p,2p2n) at 15 to 155 Mev, excitation functions for, 18: 44770

proton reactions (p,γ) at 1 to 2 Mev, level parameters from, (E), 19: 5142
proton reactions (p,2p) at 300 to 400 Mev, cross sections for, 19: 37835(R) (TID-22024)
proton reactions (p,n) at 8.0 to 14 Mev, (E/T), 20: 4849(R) (UCRL-14360, pp 1-50)
proton reactions (p,γ) at 920 kev to 1.8 Mev, energy spectra from, (E), 20: 6438
proton reactions (p,n) with, cross sections for, (E), 20: 19838 (UCRL-14760-T)
proton reactions (p,γ) at 0.956 to 1.716 Mev, gamma angular correlations from, (E), 20: 30528
proton reactions (p,d) at 39.8 Mev, cross sections for, (E), 20: 36176(R) (TID-22971, pp 41-140)
proton reactions (p,γ) at 0.3 to 2.1 Mev, resonance strengths for, (E), 20: 42182
proton reactions (p,d) at 15 Mev, testing T invariance by, (E), 20: 44805
proton reactions (p,γ) with, aluminum-26 excited-state lifetime from, 17: 34943
proton reactions (p,d) with, nuclear structure studies using, 18: 1088
proton scattering, cross sections for, 16: 33838
proton scattering at 17 Mev by, cross sections for, 16: 33902
proton scattering at 6 to 7.5 Mev by, cross sections for elastic and inelastic, (E), 19: 23641
recoil from silicon-28 (n,α) reactions in silicon, ionization defects from, (E), 20: 13989
spin-orbit interactions, 18: 18942
triton elastic scattering at 12 Mev, angular distributions from, (E), 20: 28325
triton reactions (t,α) with, excitation functions for, 18: 12521(R) (BNL-823(p.57-65))
triton reactions (t,α) with, 18: 24625 (WASH-1046)
triton reactions (t,α) with, excitation functions for, 19: 15332(R) (BNL-841(p.52-62))
triton reactions (t,p) at 12 Mev, magnesium-27 deformation and energy levels from, 19: 33302
triton reactions (t,α) with, excitation functions for, (E), 19: 36452(R) (BNL-900(p.105-20))
triton reactions, energy level from, 16: 2546

MAGNESIUM ISOTOPES Mg-26

alpha inelastic scattering by, levels from, (T), 19: 14489 (ANL-6878 (p.143-73))
alpha reactions (α,He-6) at 40 Mev, 18: 15173 (BNL-7800)
alpha reactions (α,d) at 42 to 53 Mev, deuteron energy spectra from, (E), 20: 12061
alpha reactions (α,He-8) at 80.0 Mev, helium-8 mass from, (E), 20: 17794
alpha reactions (α,d) at 42 to 53 Mev, energy spectra from, (E), 20: 24358(R) (UCRL-16580, pp 1-93)
alpha reactions (α,γ), gamma spectrum and excitation function, 16: 2504(T) (JPRS-11068)
alpha reactions (α,n), 16: 31108
alpha reactions (α,2p) at 42 Mev, excitation functions for, 16: 33814
alpha scattering at 42 Mev, 18: 16951(R) (TID-20311)
concentration using electrical mass filter, 16: 9092(T) (AEC-tr-4987)
deuteron elastic scattering at 0.8 to 2.2 Mev, excitation functions for, (E), 19: 35450
deuteron elastic scattering at 7.8 Mev by, cross sections for, (E), 20: 12095
deuteron inelastic scattering at 12 Mev, angular distributions from, (E), 19: 21311
deuteron reactions, energy level from, 16: 2546
deuteron reactions (d,p) and (d,pγ) with, 17: 41873 (WASH-1044)
deuteron reactions (d,p) at 6 and 10 Mev, 18: 16918 (ANL-6848(p.104-5))
deuteron reactions (d,t) with, angular distributions and spectra from, 18: 18881 (NP-13784)
deuteron reactions (d,p) at 1 to 2 Mev, 18: 32772
deuteron reactions (d,p) at 2.8 Mev, proton-gamma coincidences for, 18: 32833
deuteron reactions (d,p) with, spectra from, 18: 42679
deuteron reactions (d,p) with, models for, (E/T), 19: 6702
deuteron reactions (d,n) at 2.9 Mev, isobaric analog states in, (E), 19: 10316
deuteron reactions (d,p) at 5 to 20 Mev, (T), 19: 14556
deuteron reactions (d,p) at 9 and 11 Mev, angular distributions from, (E), 19: 19095 (WASH-1053)
deuteron reactions (d,d′) and (d,p), at 10 Mev, DWBA constant from angular distributions from, (E/T), 20: 10041
deuteron reactions (d,pγ) at 4.28 Mev, angular correlations in, (E), 20: 13768 (CONF-650410-40)
deuteron reactions (d,pγ) at 3.0 to 4.8 Mev, magnesium-27 level spins and deformation parameter from, (E), 20: 22099
deuteron reactions (d,pγ) at 1.8 Mev, magnesium-27 energy levels from γ-p angular correlation measurements on, (E), 20: 38187
deuteron reactions (d,α), 20: 46580(R) (BMwF-FBK-66-05)
effects on magnesium oxide crystal lattice constants, 19: 4158
energy level of, existence of 0⁺ first, 17: 5376
energy level spacings, 16: 6018
energy level transitions in, 20: 21984 (BNL-948, pp 751-6)
energy levels, 16: 26306
energy levels, 17: 11299(R) (ANL-6612)
energy levels, 17: 15275
energy levels, (E), 19: 41828
energy levels (E), 19: 3340
energy levels and gamma spectra, 16: 31088
energy levels and gamma spectra, 17: 41289
energy levels and gamma spectra, 18: 30717(R) (COO-605-6)
energy levels, evidence for first-excited state at 1.33 ± 0.02 Mev, 16: 21527
energy levels from deuteron beam reactions with light nuclei, 16: 11040
energy levels from deuteron reactions (d, helium-3) with aluminum-27 at 12.8 Mev, 16: 26313
energy levels from deuteron reactions (d,He³) on aluminum-27, 17: 9508 (PAN-207)
energy levels from (n,α) reactions on silicon-29 at 13.4 and 13.8 Mev, 17: 17145
energy levels from magnesium-25 (d,p) reactions at 8.0 Mev, (E), 20: 44725
energy levels of, 17: 38091(R) (TID-19350)
energy levels of, existence of 1.33-Mev, 18: 2947
energy levels of, from aluminum-26 decay, 17: 31534
energy levels of, spin assignments for, 17: 33012
energy levels of, 1.33-Mev spin-zero, 17: 22565 (TID-15266)
energy levels of, reduced widths and strength functions of, (E), 19: 17009
energy levels of, parity and spin of, (E), 19: 21311
energy levels of, parity and spin of, (E), 20: 6410
energy levels of, excited by alpha particles, 20: 42347
enrichment using electrical mass filter, 16: 6680
fabrication as radiation target, 18: 27813(R) (ORNL-TM-428)
gamma reactions (γ,p) at 10 to 27 Mev, cross sections, 16: 23057
gamma reactions (γ,p), proton energy distribution from, 17: 17152
helium ion reactions (He-4, He-6) with, 18: 42755
helium nucleus reactions (helium-3,t), spectra from, 17: 5391
helium-3 reactions (He-3,α) on, energy levels from, 17: 19218 (LADC-5391)
helium-3 reactions (He-3,t) at 25 Mev, 18: 26596
helium-3 reactions (He-3,α) at 5.5 Mev, cross sections for, (E/T), 19: 37849
helium-3 reactions (He-3,p) at 12 Mev, Q value for, 20: 16331 (GA-6568)
neutron inelastic scattering at 3 to 4.5 Mev, angular distributions and energy levels from, (E/T), 19: 47638
neutron inelastic scattering at 2.8 Mev, gamma spectra from, (E), 20: 8085 (USNRDL-TR-916)
neutron reactions (n,helium-3) at 14.5 Mev, cross-section upper limits, 16: 8219
neutron reactions (n,α) at 14.8 Mev, cross sections for, (E), 20: 36212
neutron scattering at 1 to 4 Mev, cross sections for energy level excitation in, 18: 21217
neutron separation energy for, (E), 19: 39862
nucleon inelastic scattering by, models for, 18: 2403(R) (PR-P-58)
performance as solar neutrino detector, 20: 37793
preparation as radiation target material, 18: 27811(R) (ORNL-TM-198)
preparation by electromagnetic separation, 18: 28608
production in (n,α) reactions with silicon, 18: 16971
proton (p,α) reactions at 20-Mev, angular distribution from, (E/T), 19: 12552
proton elastic scattering at 5.45 Mev, 17: 2314
proton elastic scattering, 17: 31077(R) (CU(PNPL)-228)
proton elastic scattering at 0.85 to 4.58 Mev, 18: 42623(R) (ANL-6879 (p.21-34))
proton inelastic scattering parameters of, 18: 34752(R) (CU(PNPL)-234)
proton inelastic scattering at 2.3 to 3.3 Mev, resonances in, 19: 3263
proton inelastic scattering at 5.67 to 6.46 Mev, angular correlations and distribution in, (E/T), 19: 41693
proton inelastic scattering at 17.5 Mev, (E), 20: 1192
proton reactions (p,γ) at 292 kev, angular distributions from, 18: 11275
proton reactions (p,t) at 28 Mev, 18: 15173 (BNL-7800)
proton reactions (p,t) at 38.7 Mev, 18: 28705
proton reactions (p,γ) at 1.967 Mev, aluminum-27 energy levels from, 18: 28607
proton reactions (p,γ) at 2 to 2.3 Mev, aluminum-27 energy levels from, 18: 28608
proton reactions (p,γ) at 2.3 to 2.9 Mev, resonances in, 19: 3263

proton reactions (p,n) at 5 to 10 Mev, thresholds for, (E), 19: 14607
proton reactions (p,2pn) at 300 to 400 Mev, cross sections for, 19: 37835(R) (TID-22024)
proton reactions (p,α) at 9 to 13 Mev, modulated fluctuations in, (E/T), 19: 43334
proton reactions (p,p′γ) at 5.67 to 6.46 Mev, angular distributions and excitation functions for, (E), 20: 3092
proton reactions (p,n) at 8.0 to 14 Mev, (E/T), 20: 4849(R) (UCRL-14360, pp 1-50)
proton reactions (p,γ) and (p,p′γ) at 2.298 Mev, gamma spectra from, (E), 20: 15761
proton reactions (p,n) with, cross sections for, (E), 20: 19838 (UCRL-14760-T)
proton reactions (p,αγ) at 9.3 to 10.5 Mev, sodium-23 levels from, (E), 20: 32509
proton reactions (p,αγ) at 8.5 to 10.5 Mev, sodium-23 gamma multipole mixing ratios and spins from, (E), 20: 32567
proton reactions (p,α) at 9.0 to 13.26 Mev, cross section fluctuations in, (E/T), 20: 34589
proton reactions (p,d) at 39.8 Mev, cross sections for, (E), 20: 36176(R) (TID-22971, pp 41-140)
proton reactions (p,t) at 39.8 Mev, (E), 20: 36176(R) (TID-22971, pp 41-140)
proton reactions (p,p) at 8.34 and 14 Mev, statistical fluctuations in cross section for, 20: 40065(R) (BMwF-FB-K-66-01)
proton reactions (p,α) at 11 and 13.26 Mev, statistical fluctuations in cross sections for, 20: 40065(R) (BMwF-FB-K-66-01)
proton reactions (p,γ) at 0.3 to 2.1 Mev, resonance strengths for, (E), 20: 42182
proton reactions (p,γ) at 1.966 Mev, resonance strength for, (E), 20: 42198
proton reactions (p,He-3) at 50 Mev, sodium-24 isobaric analogue states from, (E), 20: 44758
proton reactions (p,α), statistical fluctuations in, 20: 46580(R) (BMwF-FBK-66-05)
proton reactions (p,γ) below 1 Mev, resonances in, 16: 13989
proton reactions (p,n), Q-value measurement for, 16: 21615
proton reactions (p,α) at 9.90 Mev, sodium-23 energy levels from, 16: 26310
proton reactions (p,γ), 661-kev resonance spectra from, 17: 11680
proton reactions (p,γ) at 2.81 Mev, 17: 11686
proton reactions (p,α) on, distributions from, 17: 31466
proton reactions (p,γ) at 0.2 to 3.0 Mev, resonances in, 18: 2941
proton reactions (p,γ), at 1.8 to 2 Mev, resonance levels for, 18: 9342
proton scattering, cross sections for, 16: 33838
proton scattering at 17 Mev by, cross sections for, 16: 33902
proton scattering by, 17: 36669 (WASH-1042)
proton scattering by, mechanisms for, (E/T), 19: 5193
trition reactions (t,p) with, use for production of magnesium-28, 19: 2693 (BNL-3138)
triton elastic scattering at 12 Mev, angular distributions from, (E), 20: 28325
triton reactions (t,p) with, excitation functions for, 18: 12521(R) (BNL-823(p.57-65))
triton reactions (t,d) at 6 and 10 Mev, 18: 16918 (ANL-6848(p.104-5))
triton reactions (t,p) at 10 Mev, angular distributions from, 18: 19021
triton reactions (t,p) with, 18: 24625 (WASH-1046)
triton reactions (t,p) with, excitation functions for, 19: 15332(R) (BNL-841(p.52-62))
triton reactions (t,p), excitation function, 19: 30627 (BNL-9166)
triton reactions (t,p) excitation functions for, (E), 19: 36452(R) (BNL-900(p.105-20))
triton reactions (t,d) at 10 Mev, triton internal wave function for absolute cross section prediction for, (E/T), 20: 10041
triton reactions, energy level from, 16: 2546
triton reactions (t,α) at 5.75 and 5.96 Mev, energy levels from, 16: 17092
triton reactions (t,p), 17: 19725 (BNL-759(p.47-53))
triton reactions (t,p) at 2.7 Mev, cross section for, 17: 31797(R) (BNL-782(p.51-9))

MAGNESIUM ISOTOPES Mg-27

beta decay scheme of, 17: 13505
decay, 17: 40097
decay half life, from aluminum-27 (n,p) reactions, (E), 19: 31244 (ZfK-RN-23)
decay of, energy levels in aluminum-27 below 2.21 Mev from, 18: 9377
decay scheme, 18: 42763
decay scheme, discrepancies in, 16: 2545
determination in aluminum by beta counting, self-absorption coefficients for, 18: 13669
determination in IRL Reactor pool by gamma spectrometry, 17: 40702 (TID-7655(p.107-18))
deuteron reactions, energy level from, 16: 2546
energy level radiative decay of, low-lying, 18: 32833
energy levels (E), 19: 3340
energy levels, 18: 16918 (ANL-6848(p.104-5))
energy levels, 20: 13768 (CONF-650410-40)
energy levels and gamma spectra of, 19: 1589
energy levels and deformation of, spins of low-lying, 19: 33302
energy levels and nuclear deformation from deuteron reactions (d,pγ) with magnesium-26, 20: 22099
energy levels from deuteron beam reactions with light nuclei, 16: 11040
energy levels, gross-structure properties of, 16: 23123
energy-level quantum numbers and transitions, (E), 20: 38187
formation from proton spallation of aluminum at 28 Bev, cross sections, 16: 29842 (BNL-6034)
gamma dose constants for, 20: 46617
gamma spectra, 17: 9549
gamma spectra, 17: 34966
gamma spectra, 18: 1050
gamma spectra of neutron-irradiated, 20: 16336(R) (NYO-10175)
neutron separation energy for, (E), 19: 39862
production in alpha and proton reactions with aluminum at 500 to 700 Mev, cross sections for, 18: 32849
production yields in carbon-12 reactions with aluminum-27 at 3.0 to 126.0 Mev, 16: 9460
production yields in nitrogen-14 reactions with aluminum-27 at 8.0 to 147.0 Mev, 16: 9460
production yields in oxygen-16 reactions with aluminum-27 at 8.0 to 168.0 Mev, 16: 9460
proton reactions (p,γ) at 1966, 1548, and 1249 kev, gamma-gamma angular correlations in, 18: 7776
recoil in neutron reactions (n,p) with aluminum-27 at 14.8 Mev, ranges for, 18: 2859
recoil range of, from (n,p) reactions on aluminum-27, 17: 2299
recoil range of, from (n,α) and (n,p) reactions with aluminum-27, 18: 44765
separation from manganese-56 by solvent extraction using diethyl-dithiocarbamic acid, 20: 16336(R) (NYO-10175)
separation from neutron-irradiated biological materials, use of Szilard-Chalmers effect in, 20: 18583
triton reactions, energy level from, 16: 2546

MAGNESIUM ISOTOPES Mg-28

decay of, half life of excited levels from, (E), 20: 28473
determination in kidney and muscle tissues in rats by EDTA titration and scintillation counting, 18: 39069
deuteron reactions, energy level from, 16: 2546
distribution in tissues of cow, calf, and fetus, 20: 45293
energy levels, 18: 19021
exchange with chlorophyll a, 16: 25155
half life, 18: 2836 (BNL-6887)
half life, 19: 2693 (BNL-3138)
preparation, 18: 12521 (BNL-823(p.57-65))
preparation of carrier-free, 17: 19725 (BNL-759(p.47-53))
preparation of high-specific activity, 19: 15332(R) (BNL-841(p.52-62))
preparation of, survey of methods for, 17: 8124 (BNL-6607)
production by magnesium-26(t,p) reaction, 19: 30627 (BNL-9166)
production by secondary nuclear reactions, 19: 30267
production by triton reactions (t,p), in-pile, 19: 33285
production in bremsstrahlung reactions (γ,2p) with silicon-30 at 51.4 Mev, cross sections and yield curves for, (E), 20: 12094
production in helium ion and proton reactions with copper, gold, silver, and uranium, 16: 2498 (UCRL-9683)
production in helium ion and proton reactions with copper, gold, silver, and uranium at 320 to 880 Mev, 17: 31525
production in magnesium-26(t,p) reactions in reactors, 19: 36892
production in proton reaction on heavy nuclei at 660 Mev, 16: 29864
production in reactors, 17: 3022 (BNL-6407)
production in thermal-neutron fission of uranium-235, (E), 20: 42298
production of high specific activity, 17: 31797(R) (BNL-782(p.51-9))
production of ultrahigh specific activity, by recoil techniques, 18: 3672(R) (BNL-799(p.64-73))
production of, process for, 19: 2693 (BNL-3138)
production of, techniques for, 18: 41892 (BNL-864)
production, review, 19: 2700
properties and uses of, produced at Brookhaven, 19: 22853 (ORNL-TM-1047(p.113-16))
sorption and distribution in chicks, effects of vitamin D, 17: 23024
transfer rate across isolated pericardium, 16: 31456
triton reactions, energy level from, 16: 2546
uptake by organs in magnesium-deficient rats, 19: 27933
uptake by rat tissues as affected by magnesium deficiency, 18: 29204
use in hematology and radiodiagnosis, 18: 17695

use in tracer studies in biology, 19: 58
yields in proton spallation of copper at 24 Bev, 16: 24859

MAGNESIUM LANTHANUM NITRATES
deuterium NMR and polarization in, at 1.4°K, (E/T), 20: 8288(T) (BNL-tr-4)
deuteron polarization in crystals of, dynamics of, 19: 23627 (JINR-P-2007)
deuteron polarization in crystals of, by solid-effect method, 19: 35425(T)
electron spin relaxation time of cerium, neodymium, and praseodymium trivalent ions in, temperature dependence from spin echo studies of, 17: 37787
field gradient and antishielding factor at nucleus of, measurement of, 17: 12278
ion spin lattice relaxation at 1.2 to 5°K, rare earth, (E), 20: 28644
manganese spectra in, satellite lines in, (E), 19: 17934
neodymium spin-lattice relaxation in, magnetic field dependence of (E), 19: 2335
neodymium-143 hyperfine spin lattice relaxation in neodymium-doped, (E), 20: 28644
nuclear polarization in magnesium-cerium-lanthanum double nitrate, magnetic-field effects, 16: 15443
nuclear polarization in, by rotation, 17: 21057
nuclear polarization in neodymium-doped, transient effect in, 20: 24446
paramagnetic resonance linewidths of trivalent rare-earth ions in, (E), 19: 5891
properties of neodymium-doped, for r-f amplification, 19: 33710(P)
proton dynamic polarization in cerium-doped, (E/T), 19: 17932
proton dynamic polarization in $(Nd,La)_2Mg_3(NO_3)_{12}\cdot 24\ H_2O$, 19: 26355
proton dynamic polarization in rotating crystals of, (E), 20: 3311
proton dynamic polarization in $(Nd, La)_2Mg_3(NO_3)_{12}\cdot 24H_2O$, 20: 20166
proton polarization in hydrated, 16: 4776
proton polarizations in single crystals of, 17: 4100
proton polarization in, at 0.5°K, 17: 37984
proton polarization in, effects of cerium on, 17: 37228(T)
proton polarization in single crystals of, effects of neodymium-142 on, 18: 23444 (JINR-P-1626)
proton polarization in neodymium-142-doped, in magnetic fields, (E), 19: 9884 (JINR-P-1868)
proton polarization and spin relaxation rates in, at low temperatures, (E/T), 20: 3143
proton polarization in cerium-doped crystalline, dynamic, (E), 20: 5021
proton polarization in, liquid helium uses for, 20: 36121 (LA-DC-7794)
proton polarization in dysprosium-doped, (E), 20: 45004
rare-earth ion spin-lattice relaxation in, (E), 20: 12300
specific heat at 2 to 25°K, 18: 16574
spectra of cerium and neodymium ions in, line widths of emission, 16: 21205
spectra of hydrated, at 20 to 290°K, infrared, 20: 16429
spin-lattice and spin-spin relaxations in, 16: 10722
spin-lattice relaxation of rare earth ions in, 16: 27813
spin-lattice relaxation of trivalent cerium and neodymium ions, 16: 27814
spin-lattice relaxation of rare earth ions in, from paramagnetic resonance transient recovery, 18: 2484
spin-lattice relaxation of rare earth ions in, phonon spin-heating in, 18: 2485
structural properties of $La_2Mg_3(NO_3)_{12}\cdot 24H_2O$, 17: 14210 (NBS-MON-25 (Sect.1))
use in polarized-proton radiation targets, 18: 37819 (UCRL-11438)
use of oriented, neutron target, 19: 1538

MAGNESIUM LUTETIUM SELENIDES
preparation, (E), 19: 13297

MAGNESIUM MANGANESE FERRATES
magnetic properties of, effects of rare earth oxides on, 17: 16019

MAGNESIUM MOLYBDATES
formation, thermodynamic properties, 16: 11672
preparation and structure of, 19: 43991 (N64-26433)
stability of gaseous, 20: 25091

MAGNESIUM NEODYMIUM NITRATES
magnetic and thermal properties at 0.1 to 3°K, 16: 20438
neodymium spin-lattice relaxation in, magnetic field dependence of, 19: 5921
proton dynamic polarization in $(Nd,La)_2Mg_3(NO_3)_{12}\cdot 24\ H_2O$, 19: 26355
proton dynamic polarization in $(Nd,La)_2Mg_3(NO_3)_{12}\cdot 24H_2O$, 20: 20166
spin-lattice relaxation at 1 to 5°K, in fields up to 1 kOe, 16: 24313

MAGNESIUM NIOBATES
crystal structure, 16: 11650
crystallographic and magnetic structure, 16: 7532
luminescence of, self-activated, 18: 20060

MAGNESIUM NITRATES
see also Magnesium Cerium Nitrates
see also Magnesium Lanthanum Nitrates
see also Magnesium Neodymium Nitrates
analytical use for ion exchange separation of americium, curium, and rare earths, 20: 18562(R) (EUR-2640.e)
crystallization with cerium-group nitrates, 16: 27148
effects on sorption of dyes by labeled barium sulfate, 18: 39305
effects on thorium nitrate complex with triisobutyl phosphate, 20: 6891
effects on uranium and plutonium activity coefficients in nitric acid solutions, 20: 1967
nuclear polarization of hydrated, 18: 39578
reactions of, with dinitrogen tetroxide and spectra of anhydrous, 17: 15995
salting-out properties in uranyl nitrate extraction from aqueous solutions, 17: 10770
separation of rare earths from solutions of, by anion exchange chromatography, 19: 40659
separation of trivalent americium, californium, and curium ions from, by solvent extraction using tertiary and quaternary amines, 20: 45804
solvent properties for uranyl nitrate, 17: 3007
sorptive properties for silver-110m in nitric acid solutions, 17: 23384 (SCR-593)
spectra in TBP solutions, infrared and uv absorption, 19: 24439
spectra in tributyl phosphate, infrared, 16: 31610 (AERE-R-3031)
spectra of dysprosium, europium, samarium, and terbium ions in calcination products of, luminescence, 18: 6803
$Mg(NO_3)_2$–$Th(NO_3)_4$, crystal structure of octahydrates, 19: 19852
$Mg(NO_3)_2$–$UO_2(NO_3)_2$–H_2O, activity coefficients of, at 25°C, 20: 29196
$Mg(NO_3)_2$–$UO_2(NO_3)_2$–H_2O, chemical potential of water in, at 25°C, 18: 3776

MAGNESIUM NITRIDES
vaporization kinetics, 20: 31718(R) (UCRL-16658, pp 149-54)
vaporization of, kinetics, 19: 30750 (UCRL-16018)

MAGNESIUM OXALATES
pyrolysis of, carbon-13 isotope effects on, 19: 17912

MAGNESIUM OXIDES
additive effects on sintering of thorium oxide–uranium oxide pellets, 16: 17996(R) (EURAEC-4)
additive effects on uranium oxide sintering properties, 17: 12637
additive effects on pulse height of quartz phosphors, 17: 27701
additive effects on creep, hardening, and strength of uranium alloys, 17: 32657
additive effects on mechanical and thermal properties of zirconium oxide ceramics, 17: 41469
additive effects on thermal properties of zirconia, 18: 593 (ARL-63-170)
additive effects on creep, recrystallization, and sintering of beryllium oxide, 18: 7187
analysis for boron, spectrographic method using copper fluoride carrier distillation, 17: 28779(R) (MCW-1480)
analysis for bromine, activation, 19: 26917(R) (IA-984)
analysis for silicon, spectrographic, 19: 283 (AERE-R-4420)
analysis for zirconium by neutron activation, 20: 35386 (AERE-R-5108)
behavior at high rates of heat transfer, 18: 37700
bending and crystal structure of high-density compacts of, at high temperatures, 17: 3485(R) (RAD-SR-62-219)
bonding and chemical reactions with fluophosphoric acid, mechanism of, 20: 29145 (NP-16047)
bonding to nickel, 17: 34365 (LADC-5598)
brittle behavior and mechanical properties, 16: 13566(R) (ARF-8203-17)
brittle behavior and fracture mechanics of, 17: 25770(R) (ARF-B6012-1)
brittle behavior and fracture mechanism of, 17: 39537(R) (IITRI-B6012-2)
catalytic activity for decomposing nitrous oxide, 17: 41333(R) (ANL-6677)
catalytic effects on radioinduced isomerization of 2-butene, 18: 23667
catalytic properties for hydrogen-deuterium exchange, radiation effects, 17: 6086
chromium ESR in, isotopic shift in absorption spectra of, 19: 387
chromium spectra in, isotope shift in R lines of, 18: 42193
chromium-51 recoil reactions with, from irradiated chromates on, 19: 13452
cleaning surfaces of, by heating and sputtering, 18: 30166(R) (AD-439716)
coating fuel particles using, 17: 3379(R) (BMI-1596(Del.))
coating with molybdenum or tungsten by chloride and oxide processes, evaluation of, 19: 40986
coating with molybdenum or tungsten by chloride and oxide processes, 20: 29631
compaction by gas pressures, method for isostatic, 19: 941
compatibility with graphite in argon and vacuum environments at 900 to 1500°C, 17: 25685(R) (BMI-1624(Del.))
compatibility with carbon-plutonia systems at 1550 to 1750°C, 19: 909(R) (UNC-5096)
compatibility with refractory metals at high temperatures, 19: 7851

(CNLM-5942)
compatibility with urania, 20: 11224
compatibility with refractory metals and alloys, 20: 17022 (N-65-18933)
content in thalenites from Japan, 20: 29399
content in zircon from Kyoto Prefecture, Japan, 19: 36296
corrosion by cerium–cobalt–plutonium alloy at 750°C, 16: 22549
corrosion by manganese–plutonium–uranium alloy at 900°C, 16: 22549
corrosion by molten magnesium fluoride in uranium fluoride reduction, 16: 11774(R) (NLCO-685)
cracks in single-crystals, nucleation of, 20: 29624(R) (TID-22970, pp 257-329)
creep and deformation of, lattice diffusion-controlled mechanisms in, 20: 27527
creep in single-crystal, at 1450 to 1700°C, steady-state, 19: 47009 (NP-15514(Vol.2))
creep of single-crystal, 20: 31719(R) (UCRL-16658, pp 155-69)
creep-rupture deformation of, role of grain boundaries in, 17: 37504(R) (ASD-TDR-62-225)
crystal growth of, by sintering, 20: 25536
crystal lattice constants of, isotope effects on, 19: 4158
crystal size distribution of, from x-ray line broadening, 20: 34858
crystal structure, 17: 39537(R) (IITRI-B6012-2)
deformation and grain boundaries in, 17: 32584
deformation of crystalline, strain-stress curves for, 20: 31719(R) (UCRL-16658, pp 155-69)
deformation of, dislocation substructures formed during plastic, 20: 29711 (UCRL-11996)
deformation of, x-ray line broadening studies of introduction and removal of, 19: 9693
deformation properties and hardness of, at high temperatures, 20: 33920
density and moisture absorption rates of, determination at high temperature, 17: 12626(R) (AD-275787)
density of hot pressed and sintered compacts of, 16: 12696
density of powders of, effects of sintering temperature and atmosphere on, 16: 3480 (WADD-TR-61-262)
density of powders of, method for determination of bulk, 17: 34462
deposition of coatings of, on ceramic fuel particles, 17: 25694 (TID-7654(p.10-70))
deposition of coatings of, on sodium iodide crystals, 17: 6491(P)
deposition of coatings of, on uranium(IV) oxide pellets, 16: 17966(R) (BMI-1541(Del.))
deposition on plutonium dioxide and/or uranium dioxide pellets, 18: 41989(P)
deposition on uranium fuel particles, 17: 3378(R) (BMI-1583(Del.))
determination by measurement of x radiation intensity by non-dispersive spectrometry, 17: 38948
determination in clay, acetic acid leachates, sand, and silt, spectrochemical, 16: 4379
determination in cement raw mixes, design of spectrometer for, 19: 6170
determination in magnesium metal, 16: 32880(R) (MCW-1475)
determination in Moldavites by mass spectrometry and x-ray fluorescence, 20: 16711(R) (MIT-1381-13)
determination in silicate rocks, x-ray fluorescence spectrographic, 16: 30353
development of coatings of, for thermoelectric elements, 17: 23861(R) (AD-282505)
development of compacts of, 16: 2182 (NP-10936)
dielectric constants and losses, 18: 7214 (NP-13431)
dielectric losses in, frequency and temperature dependences of, 19: 19851(T) (ORNL-tr-491)
diffusion into iron oxide at 1300 to 1400°C, 20: 43813(R) (COO-1122-3)
diffusion of cobalt and ferrous oxide in, 16: 20395
diffusion of ferrous oxide in, 17: 421(R) (TID-17007)
diffusion of fission products in, 18: 14522
diffusion of iodine and rare gases in, 18: 16424(R) (GEMP-270A)
diffusion of iron into single crystals of, 18: 8801 (UCRL-11073)
diffusion of nickel oxide into single crystals of, 19: 43997(R) (UCRL-11889)
diffusion of oxygen and oxide inclusions in, activation method for studying, 18: 42044
diffusion of oxygen in surface defects in, tracer-activation study of, 19: 18467 (UCRL-7938)
diffusion of oxygen in grain boundaries of, effects of iron on, 20: 830 (UCRL-14215)
diffusion of xenon-133 in, 17: 3378(R) (BMI-1583(Del.))
dislocation dipoles in crystalline, mechanisms of, 20: 31713(R) (UCRL-16658, pp 93-8)
dislocation loops in, electron microscopic determinations of, 18: 20546
dislocations in deformed, 19: 43997(R) (UCRL-11889)
dissociation energy of, mass spectrometric determination of, 18: 23455 (WADD-TR-60-782(Pt.XXII))
dissociation energy of, atomic model for calculation of, 18: 31496
dissociation energy, (E), 19: 8105
dissociation of films of, by low-energy-electron-bombardment, 17: 20537 (ASD-TDR-63-175)
ductile properties of single crystals of, at room temperatures, 17: 18735 (AD-283585)
effects as reflector on resolving power of lithium glass phosphors, 19: 2622
effects of additives of, on modulus of rupture of beryllia, 19: 44599(R) (GEMP-50A)
effects of coatings of, on thermionic emission of lead on rhenium and tungsten, 17: 41471
effects on chromium-51 recoil processes in potassium chromate, 19: 13499
effects on crystallization and sintering of mullite, 19: 13973
effects on crystal structure of hafnium and zirconium oxides, 19: 26359
effects on densification during sintering of beryllium oxide, 19: 24963
effects on electron emission ratio enhancement from iron oxides, 19: 41124(R) (NP-15108)
effects on fritting of beryllium oxide, 18: 22500(T) (UCRL-Trans-1042(L))
effects on grain boundary hardening in sintered beryllium oxide, 20: 846
effects on grain growth in alumina coatings on uranium dioxide particles, 19: 15990 (BMI-1708)
effects on hydrofluorination kinetics of urania, 20: 23612
effects on ion-exchange properties of aluminum silicates, 20: 43449
effects on oxidation of copper at 800°C, 20: 23686
effects on polymorphism of zirconium oxide, 20: 3953
effects on properties of beryllium oxides, 16: 2732 (GA-2262)
effects on properties and sinterability of zirconium oxide, 18: 34155
effects on properties of zirconia at high temperatures, 20: 5851
effects on radioinduced polymerization of acrylonitrile and methylmethacrylate, 18: 12171
effects on radioinduced polymerization of acrylonitrile with methylmethacrylate, 19: 11183
effects on radioinduced polymerization of diphenylvinylphosphine oxide, 20: 408
effects on sintering of alumina, 19: 20461 (NP-14893)
effects on sintering behavior of urania powders, 20: 37202
effects on strontium-85 metabolism by rats, 20: 12606
effects on structure and properties of sintered alumina bodies, 19: 32740(T) (NP-tr-1239)
effects on thermal stability of zirconium oxide, 19: 20585
effects on thermoelectric properties of molybdenum, tantalum, and tungsten at 1500°C, 18: 622
effects on thermoelectric properties of MCC 50, 19: 12129(R) (ASD-TDR-62-896(Pt.II))
elastic moduli of single-crystal, at 298 to 1600°K, 19: 32048(R) (NP-15073)
elastic properties at high temperatures, 16: 7921
elastic properties of, method for calculating isotropic, 20: 33899
electric charge storage and trapping in cable insulation of, 18: 22197 (AEEW-R-205)
electric conductivity, 16: 30901(R) (GACD-3178)
electric conductivity at 900 to 1300°C, 17: 172(T)
electric conductivity of, for use as insulation in thermocouples, 17: 32644
electric conductivity of, radiation effects on, 17: 3577(R) (TID-17067)
electric conductivity at 1500 to 1800°C, effects of air ionization in furnace on, 19: 25035
electric conductivity at 1100 to 1600°C, 20: 17022 (N-65-18933)
electric properties at high temperatures, 16: 15126(R) (NP-11584)
electric properties, 18: 17370(T) (SC-T-64-44)
electric properties of, effects of lattice energy and temperature on, 19: 21601(T) (ORNL-tr-490)
electron absorption coefficient at 0.2 to 7.3 ev, 16: 12254
electron absorption coefficients at 100 to 1200 kv, (E), 20: 13967
electron absorption coefficients in, up to 1000 kev, 20: 45014
electron attenuation and diffraction by, 17: 620
electron bombardment, 17: 3569 (ASD-TDR-62-707)
electron bombardment of, emission spectra from, 18: 18562
electron diffraction at 100–300 kev, mean inner potential from relativistic formula for, 17: 37793
electron diffraction pattern of surface of, 17: 41553(R) (NP-13160)
electron diffraction by films of, 17: 20537 (ASD-TDR-63-175)
electron emission by superconducting vanadium films on, 18: 30166(R) (AD-439716)
electron emission by films of, secondary, 17: 3569 (ASD-TDR-62-707)
electron emission by films of, coefficient for secondary, 17: 41553(R) (NP-13160)
electron escape mechanism in polar, secondary, 17: 667
electron reactions with films of, ion desorption in, 17: 41553(R) (NP-

13160)
electron secondary emission and scattering distributions by coatings of, 16: 24335
electron spin resonance spectra of iron group ions in, 18: 2469
electron spin resonance spectra of spin-1 ions in, Jahn-Teller effects in, 20: 12294
electronegativity and ion radii of, prediction of phases in binary systems with other oxides from, 19: 23061
electronic properties of films of, 18: 30166(R) (AD-439716)
electronic structure of single crystals of, electron bombardment study of, 18: 14474 (TID-20264)
electronic structure, 18: 37115 (ANL-6856)
emissivity of, comparison of calculated and measured, 19: 6292 (ASD-TDR-62-719(Pt.II))
energy levels of, 20: 6532 (CALT-221-13)
erbium EPR in crystals of, 20: 10264
europium sulfide epitaxial growth on crystals of, 19: 11079
evaporation at 1800 to 2300°K, rates of polycrystalline, 20: 31669
evaporation in vacuum at 1864 to 2333°K, 19: 29468(R) (ANL-7017)
evaporation rates at 1790 to 2300°K, 19: 43985(R) (ANL-7000, pp 85-110)
examination of sintered, x-ray, 17: 3501
extrusion, analysis of plasticizer and vehicle requirements for ultrasonic, 16: 12072 (NYO-10006)
extrusion at high temperatures, 17: 39537(R) (IITRI-B6012-2)
fabrication and properties of spray-dried and hot-pressed, 19: 13898(R) (RFP-490)
fabrication and properties of pure high-density fine-grained ceramics of, 19: 24979 (AROD-2884.4)
fabrication by hot pressing, 17: 39518
fabrication by hot-pressing, effects of lithium fluoride on, 20: 15010 (UCRL-16534)
fabrication by semicontinuous pressure sintering, 20: 46160(R) (AD-638453)
fabrication of large dense bodies of, 19: 28795(P)
fabrication of stirrers of, by isostatic-pressing, 19: 34657(R) (RFP-518)
fission fragment recoil in, expansion induced by, 19: 18547
fission-fragment damage in, (E), 19: 39245
fracture and slip properties of as-cleaved crystals of, 17: 12699
fracture of, Petch equation for grain size effect in, 20: 5903
friction between surfaces of, at high temperatures in vacuum, argon, helium, and nitrogen atmospheres, 19: 28826
grain-boundary sliding in, 16: 30791 (MRC-182)
grinding slabs of, technique for diamond, 17: 37498
growth and properties of crystals of, 20: 22311(R) (AD-622068)
growth of crystals of, in supercritical water systems, 18: 4171(R) (ORNL-3470(p.3-5))
growth of films of, on magnesium crystals, kinetics of, 17: 35701 (TID-17487)
hardness, 16: 10728
heat capacity of powders of, at low temperatures, 16: 6724 (UCRL-9880)
hot-pressing of, design of equipment for, 18: 7175
hot pressing of high density, apparatus for, 16: 19267
incorporation into uranium dioxide lattice, 17: 27487
interactions of particles of, with ionized argon, 18: 6309 (NP-13402)
internal friction and Young's modulus of polycrystalline, 16: 9188(R) (AROD-2891.1)
ion reactions at 40 kev, lattice disorders from krypton and xenon, (E), 20: 27595
iron-57 Mössbauer spectra in, hyperfine structure of, 17: 13235
irradiation for production of sodium-24, neutron, 18: 31999(T) (ORNL-tr-191)
lattice parameters and thermal expansion of, x-ray diffraction study of, 18: 26109 (LA-2687)
luminescence properties of manganese-activated, correlation to electron spin resonance spectra, 18: 2487
luminescence spectra of, effects of samarium and dysprosium on, 20: 7098
manganese EPR in, spectra of, 18: 29960
manganese-ion exchange interactions in, biquadratic, 18: 14632
mechanical and thermal properties, 16: 29398
mechanical properties of, effects of grain size and temperature on, 17: 12669(R) (RAD-SR-63-29)
mechanical properties of single crystals of, at high temperatures, 18: 16472 (HR-64-253)
mechanical properties at room temperature to 1000°C, effects of dislocation impurity interactions on, 18: 22483 (HR-64-258)
mechanical properties, 19: 11682
mechanical properties of, grain boundary and surface effects on, 19: 16199
mechanical properties of polycrystals and single crystals of, at room temperature to 2000°C, 19: 20607
mechanical properties, effects of grain parameters on, 19: 32048(R) (NP-15073)
mechanical properties of, effects of grain boundaries on, 20: 11227
mechanical properties of single-crystal, alloying effects of manganese and nickel oxides on, 17: 41425 (HR-63-274)
melting temperature, evaluation for space technology, 18: 16521
meson (μ^+) depolarization in, (E), 19: 12167 (NEVIS-124)
microcrack growth in ascleaved single-crystal, 16: 20436
microstructure of powders of, effects of sintering time, temperature, and atmosphere on, 16: 3480 (WADD-TR-61-262)
moisture control in agglomeration mixtures of, using neutron probe, 20: 13156
neutron cross sections at 1.44 ev (E), 19: 3288
neutron production above 1 Mev of F-centers in, (E), 20: 37998
neutron resonance absorption integral of, (E), 20: 14008(R) (ANL-7122, pp 42-69)
neutron scattering by paramagnetic, 19: 29228(R) (AEET/NP/10)
neutron spectra at 14 Mev, 19: 10983(R) (TEES-2671-3)
neutron transmission in crystalline, 18: 42579 (BLG-260)
niobium film epitaxial growth on, 19: 7860
nuclear magnetic resonance of oxygen-17 in solid, 17: 22339
optical absorption and thermoluminescence in single crystals of, 18: 37220
optical absorption at 650 to 1200°C, 16: 3458(R) (NP-11055)
optical spectra, ESR of excited ^2E level of chromium and vanadium ions in, 20: 46942 (NYO-2150-18)
oxygen exchange with water at 50 and 100°C, 17: 27313(R) (ASD-TDR-62-843)
performance as gaseous core reactor tube, 20: 20301 (NP-15906)
performance as magnetohydrodynamic electric insulation, 18: 12859 (NP-13516)
performance as melting-point temperature sensors up to 6000°F, (E), 19: 30489 (SC-DC-65-1237)
phase studies and properties of, bibliography on, 16: 33480 (UCRL-6262 (Pt.2))
photoelectron emission in, numerical analysis, 17: 22380
physical properties at 1700 to 2000°K, effects of heat treatments, 16: 16726(R) (NP-11311)
physical properties of, bibliography on, 20: 43911 (UCRL-6262(Pt.1))
plastic deformation at 1000 to 1600°C of single crystals of, stress-strain measurements, 18: 34132 (UCRL-11323)
plastic deformation of single crystals of, at 1000 to 1600°C, (E), 19: 28813 (UCRL-10316)
plastic deformation of single crystals of, 19: 43997(R) (UCRL-11889)
plastic flow initiation in single crystals of, effects of dislocation configurations on, 18: 34123 (HR-64-269)
point defect sites in, internal friction peak from symmetry splitting of equivalent, 17: 32607
positron annihilation in, angular correlations from, 18: 33605
positron three-quantum decay in, 18: 44559
positronium lifetime in, (E), 20: 37819
preparation and properties of high-porosity, 18: 39951
preparation and properties of sintered compacts of, 16: 10536(R) (NP-11356)
preparation and properties of coatings of, 16: 26476 (TID-7622(p.57-73))
preparation by thermal decomposition of basic carbonate, 17: 27313(R) (ASD-TDR-62-843)
preparation of crystals of, 16: 17582(R) (ORNL-3262(p.187-94))
preparation of high-purity, for growing single crystals, 16: 28918 (ORNL-TM-302)
preparation of polycrystalline, 20: 31719(R) (UCRL-16658, pp 155-69)
preparation of porous low-thermal-conductivity ceramic of, 18: 41955(P)
preparation of pure, 17: 15859(R) (ORNL-3397(p.112-13))
preparation of single-crystal, 17: 25092(R) (ORNL-3417(p.285-300))
preparation of slip casting slurries of, method for, 18: 4236(P)
preparation, properties, and uses of high-temperature, 17: 18678(T) (AEC-tr-5711)
properties as fuel particle coating, 18: 39949
properties as magnetohydrodynamic insulation, 18: 7458 (PWA-2125)
properties for high-temperature insulation of thermocouples, 20: 41461(R) (UCRL-7361(Pt.3))
properties for magnetohydrodynamic cell insulators, 17: 31012
properties for use as insulator-seal combination in thermionic cells, 17: 1916(R) (ARF-2215-6)
properties for use in vacuum electrothermics, 19: 11733
properties for use as fuel-propellant partition in gaseous fuel rocket reactors, 19: 40229 (LA-3229, pp 116-36)
properties, mechanical and physical, 16: 30853
properties of explosively shocked crystalline, 19: 32048(R) (NP-15073)
properties of, for coating uranium oxide fuel powders, 17: 13876(R) (BMI-1603(Del.))
properties of hot-pressed, 18: 7175
properties of, mechanical and thermal, 17: 41469
properties of sintered, 17: 25795

properties, ion exchange and sorptive, 19: 348(R) (ORNL-3679(p.117-26))
protective effects of coatings of, against oxidation of uranium(IV) oxide powders, 17: 20401 (BMI-1625)
radiation and doping effects on catalytic activity of, on thermal decomposition of potassium perchlorate, 19: 26414
radiation damage, neutron, 19: 26883 (LA-3285)
radiation effects on defect clusters in, 16: 25865
radiation effects on, 16: 30717(R) (ANL-6516)
radiation effects on chemisorption of hydrogen and oxygen by, fast neutron, 17: 3558
radiation effects on catalytic activity, 17: 10672 (BNL-6097)
radiation effects on magnetic properties, 17: 12737
radiation effects on catalytic activity in hydrogen-deuterium exchange, 17: 18125
radiation effects on curvature of, fission-fragment, 17: 23864(R) (BMI-1619(Del.))
radiation effects on, 17: 36367
radiation effects on dislocation behavior and yield stress in, fast neutron, 17: 37583
radiation effects on, 17: 41333(R) (ANL-6677)
radiation effects on electron emission by, transient proton, 18: 2337
radiation effects on electric conductivity of single crystals of, electron, 18: 4330(R) (TID-19744)
radiation effects on, 18: 18307
radiation effects on strength of, fast neutron, 18: 20595
radiation effects on macroscopic growth of, neutron, 18: 20597
radiation effects on chemisorption and surface defects in, 18: 22140
radiation effects on crystalline, deuteron and fission-fragment, 18: 25893(R) (ANL-6868(p.355-72))
radiation effects on crystal structure and mechanical properties of sintered, neutron, 18: 30261
radiation effects on, neutron, 19: 25053(R) (ORNL-3731(p.207-28))
radiation effects on, fast neutron, 19: 30828(R) (ORNL-3789(p.230-8))
radiation effects on trapped hole centers in, ESR studies of x, 19: 34231
radiation effects on fine structure of optical absorption bands in, neutron, 19: 40632
radiation effects on electric conductivity of, electron, 19: 42545
radiation effects on catalytic properties for decomposition of, nitrous oxide, neutron, 19: 44680(R) (ANL-7000, pp 227-32)
radiation effects on crystal structure of, mechanism of beta, 20: 2426 (LA-3387)
radiation effects on, x-ray line broadening in fast neutron, (E), 20: 2445
radiation effects on gas bubble formation in, fast-neutron, 20: 4387(R) (ORNL-3870, pp 38-43)
radiation effects on structure of, neutron, 20: 17148
radiation effects on oxygen chemisorption by, fast-neutron and gamma, 20: 18787
radiation effects on, fast-neutron, 20: 23774(R) (ORNL-3913, pp 75-109)
radiation effects on dimensions and electric resistivity of, fast- and thermal-neutron, 20: 27588 (LA-DC-6822)
radiation effects on mechanical properties of, 20: 27612
radiation effects on sintered compacts of, at 100 to 1100°C, fast-neutron, 20: 27613
radiation effects on, 20: 29623(R) (TID-22970, pp 121-256)
radiation effects on thermoluminescence of nickel-doped and pure, uv and x, 20: 34828
radiation effects on, electron, neutron, and x ray, 16: 33399
radiation effects on electron spin-lattice relaxation in, neutron, 17: 8901
radiation effects, 17: 22222 (MMPP-NPC-1-3)
radiation effects on curvature of poly and single, fission-fragment, 17: 23864(R) (BMI-1619(Del.))
radiation effects on optical properties and point defects of, 17: 35791
radiation effects on structure of single, neutron, 17: 39692
radiation stability of, effects of heat treatment on, 19: 25063
radioinduced blistering of, ion, (E), 20: 29816
radioinduced catalytic activity in, EPR spectra of ultraviolet, 18: 30293
radioinduced color center formation in crystals of, review on, 19: 11240
radioinduced color centers in, symmetry of neutron, (E), 20: 32717
radioinduced defects in single-crystal, 20: 35932 (LA-3501)
radioinduced displacements in, electron spin resonance study of, 16: 13657
radioinduced exchange-coupled F-center pairs in, neutron, 20: 34821
radioinduced grafting of methyl methacrylate to surface of powders of, 18: 320
radioinduced growth of neutron, 19: 34759
radioinduced impurity centers, effects on coloration, 16: 13661
radioinduced lattice defects in, electron microscopic observations of, 19: 11812
radioinduced luminescence of, energy variation of ion, 20: 5573
radioinduced phonon infrared absorption spectrum in, neutron, 19: 41106
radioinduced sorptive properties for gases, 17: 18152
radioinduced stresses in, from fission fragment bombardment, 17: 27888 (BMI-1635)
radioinduced swelling of, fission fragment, 20: 11227
radioinduced thermoluminescent reduction of chromium ions in, 19: 40631
radioinduced transmutations in, calculation of gas volume from neutron, 20: 31799
radioinduced trapped hole center containing fluorine in crystalline, 19: 38729
radioinduced zero-phonon transition spectra in single crystals of, neutron, (E), 20: 9585
radiolysis of azoethane adsorbed on, 18: 39316
radiolysis of azoethane adsorbed on, energy transfer in gamma, 20: 23116
reactions of crucibles of, with nickel-base alloys at high temperatures in vacuum, 16: 6756
reactions of sintered, with beryllium to 600°C *in vacuo*, 19: 22997 (TRG-Report-842)
reactions with aluminum oxides and lanthanum or neodymium oxides at 1400 to 1500°C, 20: 16482
reactions with barium, potassium, and sodium chlorides, 20: 26816 (HW-72369)
reactions with carbon, molybdenum, and molybdenum–rhenium at 2450°C, 19: 44598(R) (GEMP-49A)
reactions with copper and nickel mattes, slags, molten salts, and refractory metals, 20: 14989
reactions with glass, 16: 31376
reactions with graphite, mechanism for, 17: 27344
reactions with Magnox alloy to 500°C, compatibility of, 19: 22997 (TRG-Report-842)
reactions with Magnox alloy to 500°C, 19: 22997 (TRG-Report-842)
reactions with metal borides, carbides, and nitrides at 1800 to 2000°C, 18: 43463
reactions with molybdenum, niobium, and tungsten at 1600 to 2100°C, 16: 4555(T) (FTD-TT-61-74)
reactions with neptunium dioxide, 17: 23359
reactions with organic matrix materials in ice-water system, 18: 15722 (TID-20332)
reactions with sodium vapor at 940°C, 16: 25318 (RAD-TM-60-44)
reactions with uranium(IV-VI) oxide at high pressure and temperature, 16: 17966(R) (BMI-1541(Del.))
reactions with uranium oxides at high pressure and 900 to 1200°C, 16: 25302 (BMI-1585)
reactions with uranium(IV-VI) oxide, formation of uranate in, 19: 15451(T) (ANL-Trans-33(p.224-7))
reactions with uranium to 500°C, 19: 22997 (TRG-Report-842)
separation of zirconium oxide from, as function of SO_4–ZrO_2 ratio, 17: 32077
sintering effects on cerium oxide, 17: 18836
sintering mechanisms of, 20: 41064(R) (IS-1500(Sect.E))
sintering of high-purity active, for high densities, 19: 16005(T) (AEC-tr-6537)
sintering of, mechanism of first stage in, 18: 4217(T) (AEC-tr-6159)
sintering of powders of, 17: 3501
sintering of powders of, evaluation of procedures in, 17: 6590 (ASD-TDR-62-700)
sintering of pure and doped compacts of, isothermal shrinkage in, 16: 31364
sintering of, effects of hafnium dioxide on, 19: 32709
sintering properties of, effects of hafnia additions on, 20: 31669
solubility in vanadium oxide at 685°C, enthalpy for, 20: 7072
sorption of carbon dioxide on, isotopic exchange in, 19: 26344
sorption of carbon dioxide at 300 to 900°C by, effects of calcination on, 17: 27313(R) (ASD-TDR-62-843)
sorptive properties of activated, for ruthenium, 17: 38578(R) (HW-78188)
sorptive properties of particles of, for radioiodine, 20: 216 (CONF-650407, pp 242-75)
specific heat at 500 to 1300°C, measurement of mean, 18: 13779
spectra at 0.2 to 9.5 μ, optical absorption, 18: 30113(R) (HW-76304(p.2.1-43))
spectra at 90 and 320°K, cathodoluminescence, 17: 6089
spectra, Franck-Condon factor arrays for band, 16: 22129
spectra in low frequency region, infrared, 18: 23549
spectra, infrared absorption, at 2 to 22μ, 16: 18859(T) (UCRL-Trans-795(L))
spectra of chromium and vanadium ions in, effects of perturbations on optical, 18: 42155 (ML-1190)
spectra of chromium and vanadium ions in, perturbation effects on, 19: 32048(R) (NP-15073)
spectra of, in 300 to 1000 mμ region, reflectance, 17: 15970
spectra of neutron-irradiated, stress effects on, 20: 45025
spectra of suspensions of, in thin polyethylene films, infrared transmission, 19: 19917
spectra of, vibrational analysis of, 18: 24316
spheroidization of powders of, by induction-coupled plasma torch

method, 16: 5698
sputtering by uranium-ion bombardment, measurement of, 20: 46309(T)
stabilization of zirconium oxides with, effects of iron oxide on, 16: 24203
strength of crystals of, 18: 2286
strength of hot-pressed, effects of process variables on, 20: 31669
strength of polycrystalline, effects of compressive surface layers on, 20: 33860 (AD-634361)
strength of sintered, effects of grain size on, 19: 22952
strength properties, effects of slow cooling on, 16: 3458(R) (NP-11055)
structure and orientation of films of, formed on magnesium single crystals, 17: 35704 (TID-17807)
structure effects on beryllium oxides, 16: 5689 (ORNL-TM-94)
structure of explosively shocked single crystals of, 19: 16060 (AROD-4434:2)
sublimation at 1780 to 2010°K, free energy of, 17: 35251(R) (BMI-1632 (Del.))
surface energy, 17: 37505 (ASD-TDR-63-605(Pt.I))
tensile properties of, effects of dislocations on, 17: 18787 (AD-297058)
tensile properties of single crystals of, at 1000 to 2000°C, 19: 11682
tensile properties, 20: 27525
tensile strength for machining, effects of PVA binders on, 20: 11277 (RFP-659)
thermal capacity and conductivity at −180 to +200°C, 17: 11200 (USNRDL-TR-599)
thermal conductivity of, at 200 to 2500°C, 16: 33146 (ASD-TDR-62-348)
thermal conductivity at 400, 600, and 800°C, 17: 29331(T) (AEC-tr-5872)
thermal conductivity of sintered, at 450 to 720°C, 17: 40791
thermal conductivity at 200 to 1500°F, 18: 6537(R) (ORNL-TM-603)
thermal conductivity of foams of, for use above 3000°F, 18: 16520
thermal conductivity of partially reduced, 19: 18448 (AECL-2169)
thermal conductivity of powders of, 17: 27368
thermal conductivity of powders of, at 100 to 850°C, 20: 12854
thermal conductivity of powders of, at 100 to 850°C, (T), 20: 12855
thermal conductivity of powders of, in air at 200 to 1500°F, 20: 23652 (ORNL-3510)
thermal conductivity of powders of, under compressive stress, 20: 45056
thermal diffusivity at high temperatures, transient measurement of, 20: 37722(R) (N-65-30843)
thermal energy storage in, in solar-thermionic power supplies, 17: 9113
thermal expansion in air and argon, 17: 3478 (JPL-TR-32-297)
thermal expansion, x-ray studies, 17: 16668
thermal expansion of compacts of, at −200 to 0°C, 16: 21057
thermal properties at high temperatures, 16: 4551 (WADD-TR-60-904)
thermal properties to 5000°F, 16: 18938
thermal properties of, at 500 to 5000°F, 17: 16636 (ASD-TDR-62-765)
thermal stress properties of coatings, 19: 24076(R) (GA-4966)
thermodynamic properties at 298 to 1200°K, 17: 32086
titration in bentonites in salt solutions, double-hydroxide formation in, 16: 22142
use as a diathermanous substance in thermal reactors, 19: 42065(P)
use as phosphor for accelerator beam spot observations, 20: 46242(R) (TID-23239)
use for neutron dosimetry at high temperatures, 19: 24841 (FZK-208)
use in metal-ceramic structural composite materials, 19: 9609(R) (ML-TDR-64-83)
use in MHD duct walls, preparation and testing for, (E), 20: 41718
use of, in nuclear rockets, 17: 8710 (TID-16315(Del.))
uses in refining of irradiated uranium, 19: 30346(P)
vaporization in magnetohydrodynamic generators, 17: 36334
vaporization in magnetohydrodynamic cells, 18: 7456 (ASD-TDR-63-4019)
vaporization of, thermodynamics, 19: 36649 (AD-614997)
vaporization of, to 2300°C, 20: 13265(T) (AD-623208)
vaporization of, thermodynamics of, 20: 36841
wave functions for F centers in, 17: 37856
xenon-133 release from, 18: 8712 (BMI-1651)
xenon-133 diffusion in, thermal release study of fission-recoil, 18: 18373
Al_2O_3–BaO–CaO–MgO–SiO_2, presintering of compositions in, 19: 20461 (NP-14893)
Al_2O_3–BeO–MgO, coating of, for beryllium oxide–calcium aluminate crucibles, 19: 28801(P)
Al_2O_3–BeO–MgO, compatibility with molybdenum, molybdenum-rhenium alloy, rhenium, rhenium-tungsten alloy, and tungsten at 1866 to 2200°K, 17: 41354 (NP-13158)
Al_2O_3–BeO–MgO, heat storage for solar-thermionic power supplies in, 17: 9113
Al_2O_3–BeO–MgO, properties, 17: 41354 (NP-13158)
Al_2O_3–BeO–MgO, properties as reactor fuel matrix material, 18: 37724
Al_2O_3–BeO–MgO, properties of molten, for fuel matrix for homogeneous 20: 31726
Al_2O_3–BeO–MgO, radiation effects on, in-pile, (E), 20: 5115(R) (GA-4967)
Al_2O_3–CaO–MgO, coating of, for beryllium oxide–calcium aluminate crucibles, 19: 28801(P)
Al_2O_3–CaO–MgO, heat storage for solar-thermionic power supplies in, 17: 9113
Al_2O_3–CaO–MgO–ZrO_2, phase studies on, 18: 16490
Al_2O_3–Cr_2O_3–MgO, effects of coatings of, on strength of ceramic materials, 20: 33860 (AD-634361)
Al_2O_3–Cr_2O_3–MgO–SiO_2–TiO_2–ZrO_2, phase diagrams, 20: 8932
Al_2O_3–Cr_2O_3–MgO–SiO_2, preparation for glass seals, 20: 46181(P)
Al_2O_3–Fe_2O_3–MgO–MnO_2 neutron radiation effects on magnetic properties of, 17: 2042
Al_2O_3–Fe_2O_3–MgO–SiO_2, neutron spectra at 14 Mev, 19: 10983(R) (TEES-2671-3)
Al_2O_3–MgO, development of low-temperature sintering process for, 17: 12626(R) (AD-275787)
Al_2O_3–MgO, formation of delta-phase spinel, 19: 4664(T) (UCRL-Trans-1130)
Al_2O_3–MgO, grain boundary precipitation in, 20: 31738
Al_2O_3–MgO, preparation, properties, and aerospace applications, 19: 37142
Al_2O_3–MgO, radiation damage, neutron, 19: 26883 (LA-3285)
Al_2O_3–MgO, radiation effects on dimensions and electric resistivity of, fast- and thermal-neutron, 20: 27588 (LA-DC-6822)
Al_2O_3–MgO, thermal conductivity and total emissivity of coatings of, 19: 23076
Al_2O_3–MgO–SiO_2, devitrification, 19: 20461 (NP-14893)
Al_2O_3–MgO–SiO_2, spectra of, gamma radiation effects on, 19: 34754
Al_2O_3–MgO–SiO_2, vibratory compaction formation of pellets of, ultrasonic, 16: 7867 (NYO-10005)
Al_2O_3–MgO–TiO_2, heat storage for solar-thermionic power supplies in, 17: 9113
Al_2O_3–MgO–UO_2, phase studies, properties, and structures of, 20: 21359 (WAPD-T-1581)
Al_2O_3–MgO–ZrO_2, melting diagram, 18: 30188
Al_2O_3–MgO–ZrO_2, phase studies, 20: 7621
Be–Mg–MgO, fabrication and properties, 19: 42830
Be–MgO, properties of, summary of mechanical and physical, 18: 2159(R) (GEMP-28A)
BeO–Li_2O–MgO, properties as reactor fuel matrix material, 18: 37724
BeO–MgO, compatibility with rhenium, rhenium-tungsten alloy, and tungsten at 2085 to 2200°K, 17: 41354 (NP-13158)
BeO–MgO, density of hot-pressed and sintered, 16: 12696
BeO–MgO, effects of tungsten filler on specific weight of, in solar thermionic power system, 20: 25764 (N-65-32965)
BeO–MgO, fabrication, 16: 25734 (NAA-SR-7293)
BeO–MgO, heat storage for solar-thermionic power supplies in, 17: 9113
BeO–MgO, performance in solar thermal storage system, (E), 19: 12150
BeO–MgO, phase studies, 17: 27833
BeO–MgO, phase studies, 18: 20577
BeO–MgO, phase studies, 20: 5181(R) (ORNL-3029)
BeO–MgO, properties of irradiated and unirradiated, 17: 25688(R) (GEMP-177A)
BeO–MgO, properties, 17: 41354 (NP-13158)
BeO–MgO, properties as reactor fuel matrix material, 18: 37724
BeO–MgO, radiation effects on mechanical and physical properties, 16: 4586(R) (GEMP-6A)
BeO–MgO, radiation effects on, fast-neutron, 17: 36345(R) (GEMP-26A)
BeO–MgO, radiation effects on, 19: 5473(R) (GA-4622)
BeO–MgO, radiation effects at high temperatures, 19: 30646(R) (GEMP-46A)
BeO–MgO, radiation effects on thermal diffusivity of, fast neutron, 19: 44599(R) (GEMP-50A)
BeO–MgO, radiation effects on, in-pile, (E), 20: 5115(R) (GA-4967)
BeO–MgO–ZrO_2, heat storage for solar-thermionic power supplies in, 17: 9113
BeO–MgO–ZrO_2, melting temperatures, 17: 14740 (TID-11295(2nd Ed.))
BeO–MgO–ZrO_2, phase studies, 17: 27833
BeO–MgO–ZrO_2, properties of molten, for fuel matrix for homogeneous thermal nuclear reactors, 20: 31726
B_2O_3–MgO, emission spectra of cerium- and samarium-activated phosphors of, 19: 40494(T)
B_2O_3–MgO, heat storage for solar-thermionic power supplies in, 17: 9113
CaF_2–MgO, mechanical properties, 18: 1834(R) (IS-700(Sect.E))
CaO–MgO, diffusion in, 20: 31719(R) (UCRL-16658, pp 155-69)
CaO–MgO, grain boundary precipitation in, 20: 31738
CaO–MgO–SiO_2–ZrO_2, properties of, for use as refractory material, 16: 21067
CaO–MgO–ZrO_2, phase studies, 17: 32653
CeO_2–HfO_2–MgO–Mo, composites of, process development for macrolaminate particle, 19: 36958(R) (NP-15139)
CeO_2–HfO_2–MgO–Mo, development of macrolaminate particle composite materials of, 19: 13894(R) (NP-14677)
CeO_2–HfO_2–MgO, preparation and properties as paint, 18: 35923(R)

(AD-602215)
CeO_2–HfO_2–MgO–Mo, preparation and properties as macrolaminate particle composites, 18: 35923(R) (AD-602215)
CeO_2–HfO_2–MgO, properties of sintered, using argon, hydrogen, and vacuum environments, 18: 41930(R) (NP-14294)
CeO_2–HfO_2–MgO–Mo, preparation and properties of laminated sheets of, 18: 41930(R) (NP-14294)
CeO_2–HfO_2–MgO–Mo, preparation and properties of macrolaminate particle composites of, 19: 20558(R) (NP-14888)
CeO_2–MgO, transport numbers in, 19: 32737(T) (NP-tr-1236(p.74-8))
CoO–MgO, catalytic effects on decomposition of nitrous oxide, 19: 44680(R) (ANL-7000, pp 227-32)
Co_3O_4–MgO, ordering in solid solutions of, effects of heat on, 16: 2924 (ASD-TR-61-92)
CoO–MgO, phase studies at 800 to 1400°C, 20: 338
Cr–MgO, development of ductile composites of, with improved strength and oxidation resistance, 19: 41022(R) (NP-15292)
Cr–MgO, fabrication and mechanical properties at high temperatures, 17: 25684(R) (ASD-TDR-63-297)
Cr–MgO, mechanical and oxidation properties of composites of, 17: 41431(R) (NP-13157)
Cr–MgO, oxidation by air, effects of impurities on, 18: 35982(R) (AD-603124)
Cr–MgO, preparation and properties, 17: 30914(R) (NP-12973)
Cr–MgO, properties at high temperatures, 18: 14391
Cr_2O_3–MgO, formation of refractories of, 19: 40997(P)
Cr_2O_3–MgO–O, phase studies on, 20: 13260(R) (NP-15852)
Cr_2O_3–MgO–ZrO_2, phase studies of, use of chemical analysis in, 20: 35527
FeO–Fe_2O_3–MgO, phase studies, 18: 26058
Fe_2O_3–MgO, Mössbauer effect in, 16: 13777
Fe_2O_3–MgO, phase studies in, effects of heat on ordering in solid solutions in, 16: 2924 (ASD-TR-61-92)
FeO–MgO, phase studies at 800 to 1400°C, 20: 338
FeO–MgO system, electric conductivity of, 17: 421(R) (TID-17007)
Fe_2O_3–MgO–MnO, neutron radiation effects on magnetic properties of, 17: 2042
FeO–MgO–SiO_2, phase studies and thermodynamic properties, 18: 13727(R) (TID-20232)
FeO–MgO–SiO_2, solid solutions in, 19: 13280(R) (TID-21569)
GeO_2–MgO, glass formation limits in, calculation of upper, 19: 44016
graphite–MgO, protective effects against oxidation of uranium dioxide compacts coated with, 17: 37477 (BMI-1647)
HfO_2–MgO, stability of solid solutions in, 16: 15219
La_2O_3–MgO, phase diagram, 19: 23012(T) (JPRS-28849(p.201-6))
La_2O_3–MgO, phase studies, 18: 7239
LiF–MgO, fabrication by semicontinuous pressure sintering, 20: 46160(R) (AD-638453)
MgF_2–MgO, phase studies, 20: 37722(R) (N-65-30843)
MgF_2–MgO, phase studies of melts of, 20: 45647
Mg–MgO, fabrication and properties, 17: 25752
Mg–MgO, fabrication of super heat-resistant, 17: 32553
Mg–MgO, fabrication and properties of, 19: 42830
Mg–MgO, preparation and properties of powdered, 19: 30795
Mg–MgO, welding of composite, flash butt, 18: 2195 (CEA-2295)
Mg–Mn, ordering in solid solutions of, effects of heat on, 16: 2924 (ASD-TR-61-92)
MgO–Ag, annealing effects on structure of dispersion-hardened, 20: 2325 (HW-SA-3767)
MgO–Ag, structure of deformed, 20: 2324 (HW-SA-3765)
MgO–Ag, studies of surfaces of, 19: 36338(R) (NP–15160)
MgO–Mg_2TiO_4, properties as electrolytic cells for winning and refining of plutonium, 20: 21239 (RL-SEP-824)
MgO–MnO, ammonia decomposition on solid solutions of, 19: 24530
MgO–MnO, ordering in solid solutions of, effects of heat on, 16: 2924 (ASD-TR-61-92)
MgO–MnO, preparation and plastic properties of single crystals of, 17: 41425 (HR-63-274)
MgO–Mo, stability and strength at 1650 to 2210°C, 19: 26853
MgO–NiO, ordering in solid solutions of, effects of heat on, 16: 2924 (ASD-TR-61-92)
MgO–NiO, phase studies at 800 to 1400°C, 20: 338
MgO–NiO, preparation and plastic properties of single crystals of, 17: 41425 (HR-63-274)
MgO–paraffin–polyethylene–TiO_2, dosage determination of x radiation absorption in Grenz-ray region, 19: 24784
MgO–Pd–Ag, preparation and properties of magnesia-base cermets of, 20: 37209
MgO–PuO_2, compact powder welding to aluminum, stainless steel, and zirconium alloys, 18: 44120
MgO–PuO_2, dissolution in 1.7*M* sulfamic acid, 18: 9646(R) (HW-78388 (p.11.1-15))
MgO–PuO_2, fabrication and testing, 17: 7547(R) (HW-74761(p.3.1-39))
MgO–PuO_2, fabrication into pellets, 18: 14436(T,R) (EURAEC-908)
MgO–PuO_2, irradiation testing, 18: 29001(R) (HW-79280(p.5.1-25))
MgO–PuO_2, pellet welding to aluminum, stainless steel, and zirconium alloys, 18: 44120
MgO–PuO_2, phase diagrams, 19: 20589
MgO–PuO_2, phase studies, 17: 23866(R) (HW-76300)
MgO–PuO_2, phase studies, 17: 31681(R) (HW-76559)
MgO–PuO_2, phase studies, 17: 36196(R) (HW-76301(Paper 1))
MgO–PuO_2, phase studies, 17: 37003(R) (HW-78118)
MgO–PuO_2, phase studies, 18: 12643(R) (HW-76303(p.2.1-35))
MgO–PuO_2, phase studies, 19: 9691
MgO–PuO_2, phase studies, 19: 40958
MgO–PuO_2, radiation effects on, 17: 23866(R) (HW-76300)
MgO–PuO_2, radiation effects, 17: 36198(R) (HW-76301(Paper 3))
MgO–PuO_2, radiation stability of, 18: 2359
MgO–PuO_2, radiation effects on, 18: 2161(R) (HW-76302)
MgO–PuO_2, radiation effects, 18: 8721(R) (HW-78388(p.5.1-22))
MgO–PuO_2, radiation effects on, 18: 12724(R) (HW-76303(p.4.1-43))
MgO–PuO_2, radiation effects on, 18: 12725 (HW-SA-3127)
MgO–ReO_2, compound formation in, at 860 to 1300°C, 20: 26340(R) (AD-631987)
MgO–Sc_2O_3, electric properties of solid solutions, 19: 36338(R) (NP–15160)
MgO–Sc_2O_3, phase studies, 18: 7239
MgO–Sc_2O_3, phase studies on, 18: 23529
MgO–SiO_2, fabrication and properties of lightweight, 16: 27597 (BM-RI-6025)
MgO–SiO_2, glass formation and structure in, 19: 44015
MgO–SiO_2, preparation, properties, and aerospace applications, 19: 37142
MgO–SiO_2, radiation effects of 1.2-Mev gammas on, at 70 to 400°F, 16: 24244 (TID-15981)
MgO–SiO_2, radiation effects on, fission-fragment, 18: 2352
MgO–SiO_2, radiation effects on forsterite, neutron, 19: 30828(R) (ORNL-3789(p.230-8))
MgO–SiO_2, sorptive properties for cesium, 17: 36997(R) (TID-19189)
MgO–SiO_2, strength of polycrystalline forsterite and steatite, effects of compressive surface layers on, 20: 33860 (AD-634361)
MgO–SnO_2, radiation damage effects on tin-119 Mössbauer effect in, neutron, 20: 3065
MgO–Ta_2O_5, phase studies, 17: 27834
MgO–ThO_2, electric conductivity at 300 to 1000°C, 19: 9715
MgO–TiO_2, development of, for encapsulation of thermoelectric materials, 16: 13676(R) (AD-260368)
MgO–TiO_2, heat storage for solar-thermionic power supplies in, 17: 9113
MgO–TiO_2, reactions with molten barium, potassium, and sodium chlorides, 20: 26816 (HW-72369)
MgO–TiO_2, use as container material in continuous electrowinning of plutonium, 19: 18397 (RL-SEP-30)
MgO–U_3O_8, crystal structure and phase studies on, 18: 12658
MgO–UO_2, differential thermal analysis, 16: 23652
MgO–UO_2, diffusion of gaseous fission products from, 17: 35115
MgO–UO_2, fabrication, properties, and radiation stability of, 17: 33262
MgO–UO_2, fabrication, properties, and radiation stability of, 17: 34508
MgO–UO_2, phase studies, 16: 27642(T) (FTD-TT-62-505)
MgO–UO_2, phase studies of, at 1200°C and 6×10^4 atm, 16: 4450(R) (BMI-1546(Del.))
MgO–UO_2, phase studies, 17: 37536
MgO–UO_2, preparation for irradiation tests, 17: 6536(T,R) (EURAEC-230)
MgO–UO_2, properties as reactor fuel, 18: 31005
MgO–W, development of oxidation-resistant, 20: 19193
MgO–Y_2O_3, phase studies, 18: 7239
MgO–Y_2O_3, phase studies, 18: 18396
MgO–Y_2O_3, thermal expansion to above 2000°C, 18: 25355
MgO–Y_2O_3–ZrO_2, phase studies of, on annealing and cooling, 20: 3953
MgO–ZrO_2, analysis, chemical, 16: 23599 (ARL-180)
MgO–ZrO_2, corrosion by barium vapor at 800 to 1000°C, 18: 44498(R) (MND-2812-3)
MgO–ZrO_2, grain boundary precipitation in, 20: 31738
MgO–ZrO_2, heat storage for solar-thermionic power supplies in, 17: 9113
MgO–ZrO_2, phase boundaries of cubic solid solutions of, 17: 15974
MgO–ZrO_2, phase boundaries of cubic solid solutions at 1400 to 2285°C, 17: 15975
MgO–ZrO_2, phase studies, 17: 27833
MgO–ZrO_2, phase studies, 17: 32653
MgO–ZrO_2, phase studies, 19: 34708
MgO–ZrO_2, preparation, properties, and aerospace applications, 19: 37142
MgO–ZrO_2, radiation effects, 17: 13678(R) (HW-75914)
MgO–ZrO_2, stability of solid solutions in, 16: 15219
MgO–ZrO_2, stability of solid solutions in, 19: 34701

MAGNESIUM PERCHLORATES
hydrolysis of uranyl ion in, complexes in, 18: 13734

hydrolysis of uranyl ion in, equilibria in, 18: 13737
radioinduced decomposition, 19: 13453
radioinduced decomposition of, mechanism for, 19: 13454
radiolysis of, mechanism and products of, 18: 3860
reactions with dioxane, structure of addition compound formed in, 17: 4452

MAGNESIUM PHOSPHATES
crystal structure of, x-ray diffraction study of, 20: 232(R) (NYO-901-37, pp 80-4)
sorption effects on thorium in ethanol-nitric acid solutions, 16: 17606
use of ortho-, as multi-threshold neutron detector, 18: 12479
$Mg_3(PO_4)_2$–$Sr_3(PO_4)_2$, phase equilibria and tin-activated luminescence in, 16: 3009

MAGNESIUM PHOSPHITES
hyperfine interactions in irradiated single crystals of hexahydrate, 16: 18090

MAGNESIUM PHTHALOCYANINE
spectrum of, evidence of hydrogen bonding to uranyl nitrate hexahydrate from luminescence, 18: 16043(T)
magnesium phthalocyanine–$UO_2(NO_3)_2$, photoinduced luminescence in, 18: 10150

MAGNESIUM SCANDIUM SELENIDES
preparation, (E), 19: 13297

MAGNESIUM SELENIDES
electron spin resonance spectra of transition metal ions in, 18: 2469
preparation of magnesium rare earth selenides, (E), 19: 13297
radioinduced displacements in, electron spin resonance study of, 16: 13657

MAGNESIUM SILICATES
see also Magnesium Aluminum Silicates
development for removal of pesticides from food extracts, 17: 18333(R) (SAN-1022)
dielectric constants and losses, 18: 7214 (NP-13431)
formation of, in silica solution, effect of insoluble uranyl ions on, 20: 36797
melting temperature, evaluation for space technology, 18: 16521
performance as substrate for niobium stannide films (E), 19: 984
radioinduced luminescence in meteorites, proton, 18: 36148
sorptive properties for cesium, 17: 36997(R) (TID-19189)
sorptive properties for organic compounds, 18: 25032(T) (SC-T-64-618)
$FeSiO_3$–$MgSiO_3$, phase studies at 800 to 1400°C, 20: 338

MAGNESIUM SILICIDES
crystal structure of, determination of electronic structure from, (E/T), 20: 4476(R) (IS-1200(Sect.P))
effects on creep deformation and grain-size stability of aluminum–magnesium–silicon system, 18: 42061
electron band structure of, self-consistent calculations of, 20: 8284 (IS-T-49)
electron spin resonance, 19: 9767(R) (IS-900(Sect.P))
electron spin resonance of Mn^{2+} in, (E/T), 20: 4476(R) (IS-1200(Sect.P))
Hall and Seebeck coefficients at 7 to 1000°K, 16: 4582
piezoresistance of n-type Mg_2Si, 18: 42154 (IS-811)
properties of, partial molar, 20: 25572(R) (NASA-CR-67221)
properties, electric and thermal, 19: 9767(R) (IS-900(Sect.P))
refractive index of, method for determining, 17: 18057
semiconductor properties, 18: 2401(R) (IS-700(Sect.P))
thermal capacity, 20: 3863(R) (IS-1200(Sect. C))

MAGNESIUM STRONTIUM COBALT LANTHANUM OXIDES
crystal structure, 20: 12865

MAGNESIUM SULFATES
see also Ammonium Magnesium Sulfates
acoustic properties of aqueous, 18: 31842(R) (NYO-2910-4)
analysis for molybdenum and tin using 8-quinolinol, spectrophotometric, 16: 16314
catalytic activity, effects of sulfur-35 and x radiation, 16: 227
catalytic activity of, effects of sulfur-35 labeling on, 18: 12188
catalytic effects on conversion of cyclohexanol to cyclohexene, effects of impurities on, 17: 39191(R) (ORNL-3452(p.210))
catalytic effects of sulfur-35-labeled, on polarization of alcohols, 19: 28433
catalytic properties for cyclohexanol dehydration, radiation effects, 16: 27099
catalytic use in dehydration of dodecyl alcohol, tracer study, 16: 4127
corrosive effects on A238 aluminum alloy, 18: 25920(R) (ANL-6868 (p.338-54))
crystal structure and hydrogen bonding of hexahydrate, 18: 25020 (UCRL-10832)
crystal structure of hydrated, 18: 32159
crystal structure of tetrahydrate of, 18: 36871 (BNL-7281)
dehydration effects, functions of bisulfate stage, 16: 14696 (TID-15420)
dehydration of monosulfate, bisulfate formation in, 16: 5313 (TID-14384)
dehydration of monohydrate to anhydrate of, bisulfate formation in, infrared studies of, 17: 16028
effects on gamma-induced polymerization of acrylonitrile in aqueous solution, 18: 29716(T,R) (AEC-tr-6231(p.175-85))
effects on strontium-85 uptake by rats, 19: 6959
effects on strontium-85 metabolism in rats, 19: 33743
effects on strontium-90 metabolism in dogs, rabbits, and rats, 19: 42254
effects on strontium-90 excretion by mice, 20: 8563
efficiency in removing strontium-89 and -90 from mouse skeleton, 19: 29999
neutron reactions with, preparation of carrier-free phosphorus-32 in, 18: 32002
osmotic coefficients as function of concentration at high temperatures, 16: 14735
osmotic coefficient at 140°C, 17: 40805
osmotic coefficients of aqueous, at 165°C, 19: 30151(R) (ORNL-3789 (p.139-63))
osmotic properties at 152°C, 18: 22014(R) (ORNL-3591(p.84-101))
performance as fast-neutron threshold detector, (E), 19: 22695 (IEA-83)
phosphorus-32 sorption from solutions of, by magnesium, 17: 14236
polymerization effects on acrylonitrile in aqueous solution, 16: 30455
properties as catalyst in dehydration of cyclohexanol in vapor phase, effects of external and incorporated radiation on, 17: 12742
properties as catalysts in dehydration of cyclohexanol, effects of alpha particles from protactinium-231 on, 18: 23672
protective effects against radiation effects on amino acid content in wheat sprouts, 18: 33398
protective effects against radiation damage to rat fetuses *in utero*, 19: 7216
radiation effects of sulfur-35 on surface, 16: 580
radiation effects on catalytic dehydration of cyclohexanol by, 17: 37263
radiation effects on specific surface of radioactive catalysts of, 18: 41308(T) (ORNL-tr-259)
radiation effects on catalytic activity, 19: 5969
radioinduced catalytic effects of, on conversion of cyclohexanol to cyclohexene, 16: 32896(R) (ORNL-3314(p.184-6))
radioinduced phosphorus in, oxidation states of, 20: 33341
radiolysis of hydrated, yields in, 19: 40610
radiolysis of hydrated, gamma, 20: 36903
reactions with cristobalite, 17: 15986
reduction by hydrogen, 17: 10246(R) (ORNL-TM-403)
reduction by hydrogen, 18: 33529 (ORNL-3334(Pt.II))
self-diffusion effects of, on water at 25°C, 17: 10613
shock wave effects on, 16: 22051 (ORNL-TM-256)
solubility and stability in aqueous sulfuric acid at 200 to 350°C, 19: 30151(R) (ORNL-3789(p.139-63))
solubility and stability in heavy-water solutions of deuterosulfuric acid at 200 to 350°C, 19: 30151(R) (ORNL-3789(p.139-63))
Soret coefficients and transport heats at 25°C, 16: 11666
spectra of dysprosium, europium, samarium, and terbium ions in calcination products of, luminescence, 18: 6803
transfer between heavy and light water, ionic hydration in, 17: 6096
transition temperature of cobalt or zinc in, 20: 18677
$MgSO_4$–K_2SO_4, solvent properties for silver sulfate, 17: 2989
$MgSO_4$–Na_2SO_4, catalytic effects on conversion of cyclohexanol to cyclohexene, effects of impurities on, 17: 39191(R) (ORNL-3452 (p.210))
$MgSO_4$–Na_2SO_4, effects of sulfur-35 on exchange reactions in, 20: 10936(T) (CEA-tr-A-1855)
$MgSO_4$–Na_2SO_4, radiation effects on catalytic dehydration of cyclohexanol in vapor phase, 17: 12742
$MgSO_4$–Na_2SO_4, radiation effects on catalytic dehydration of cyclohexanol by, 17: 37263
$MgSO_4$–Na_2SO_4, specific surface of radioactive catalysts of, 18: 41308(T) (ORNL-tr-259)
$MgSO_4$–Na_2SO_4, surface area and radioactivity of sulfur-35-labeled, 19: 20013

MAGNESIUM SULFIDES
determination in Pesyance meteorites, spectrographic, 16: 17893
hardness of crystalline, 16: 10728
luminescence properties for gamma dosimetry, infrared-stimulated, 19: 40879 (UCRL-12371)
performance as luminescent dosimeter material, 18: 35773(R) (UCRL-7811)
preparation for luminescence dosimeters, 20: 5742(R) (UCRL-14351)
radioinduced displacements in, electron spin resonance study of, 16: 13657
reactions with yttrium sulfide, 16: 18864
transition metal ion ESR in, 18: 2469
MgS–rare earth sulfides, crystal structure of solid solutions in, 20: 332

MAGNESIUM SYSTEMS
Al–Cr–Mg–Si, corrosion by aqueous sodium chloride at 150°C, 20: 22857(R) (ORNL-3913, pp 111-32)
Al–Fe–Mg–Ni–Si–Ti–Zr, coating with aluminum–nickel layers by

chemical deposition, 19: 39143(P)
Al–Fe–Mg–Ni–Si, corrosion by water and steam, 20: 763 (BNWL-125)
Al–Fe–Mg–Ni–Si, performance as fuel element cladding, 20: 8439(R) (KR-97)
Al–Fe–Mg–Si, corrosion by water and steam, 20: 763 (BNWL-125)
Al–Li–Mg–silicate, preparation as phosphor for neutron detection, 19: 15927
Al–Mg–$MgCl_2$–KCl–NaCl, corrosive effects on steels and tantalum at 500 to 800°C, (E), 20: 14007(R) (ANL-7122, pp 1-41)
Al–Mg–Ni–Si, fatigue properties of IFA-3 aluminum-base, 20: 7566 (KR-99)
Al–Mg–Ni–Si, fatigue properties at 250 to 350°C, low-cycle, 20: 13308
Al–Mg–Ni–Si, properties for use as fuel element canning material, 17: 14735 (KR-31)
Al–Mg–Si, additive effects of beryllium on, 17: 39561
Al–Mg–Si, aging and quenching characteristics of, electron transmission microscopy studies of, 16: 24194
Al–Mg–Si, dispersion hardening of, effect of pre-aging on, 16: 10598
Al–Mg–Si, effect of homogenization on, 17: 12701
Al–Mg–Si, effects of magnesium silicide particles on creep deformation and grain-size stability of, 18: 42061
Al–Mg–Si, fabrication of cylinders of Anticorodal, using magnetic fields, 20: 19199 (RT/EL-(65)9)
Al–Mg–Si, hardening behavior of, effects of annealing and quenching conditions on, 17: 22182
Al–Mg–Si, mechanical properties and part strength of, effects of beryllium on, 19: 4702
Al–Mg–Si, origin and development of cup and cone defects in, at room temperature, 18: 27933
Be–Mg–MgO, fabrication and properties, 19: 42830
$CaCl_2$–CaF_2–Mg–$MgCl_2$–Zn, corrosive effects on silicon carbide at high temperatures, 19: 17176(R) (ANL-6965(p.1-41))
$CaCl_2$–Mg–$MgCl_2$–MgF_2–U–Zn, reactions with alumina crucibles at 800°C, 17: 36860(R) (ANL-6648)
C–Co–Mg, phase studies of, atomic size effects in, 19: 23111
C–Mg–Ni, phase studies of, atomic size effects in, 19: 23111
Cd–LiCl–Mg–$MgCl_2$–NaCl–U–Zn, corrosive effects on reactor materials, 18: 36751 (ANL-6912)
Cd–Mg–$MgCl_2$–Pu–KCl–NaCl, corrosive effects on SS 304, 18: 36751 (ANL-6912)
Cd–Mg–UCl_4–Zn, corrosive effects of, on stainless steel at 650°C, 20: 31314(R) (ANL-7175, pp 1-41)
Ce–Mg–TiO_3, mechanical properties at 100 to 300°C, 17: 1920 (BM-RI-6078)
Co–Mg–N, crystal structure, 16: 2259
Co–Mg–Si, thermal capacity at 1.5 to 4°K, 20: 27494(R) (NYO-3454-6)
Cu–Mg–$MgCl_2$–KCl–NaCl–U, chemical compatibility with vitreous carbon containers at 800°C, (E), 20: 14007(R) (ANL-7122, pp 1-41)
Cu–Mg–Si, electronic specific heats at 1.5 to 4°K, 19: 30743(R) (NYO-3454-1)
Ge–Mg–Si, radiation effects on electric properties of $Mg_2Ge_{0.8}Si_{0.2}$, 20: 2502
LiCl–Mg–$MgCl_2$–MgF_2–Zn–$ZnCl_2$, corrosive effects on anodized beryllium at 800°C, 17: 36860(R) (ANL-6648)
LiCl–Mg–$MgCl_2$–NaCl–Zn, corrosive effects on reactor materials, 18: 36751 (ANL-6912)
Li–Mg–Si, fabrication and properties of cast, 20: 15007 (NP-15881)
Mg–$MgCl_2$, free energy of solution of, 19: 11103
Mg–$MgCl_2$, kinetics of dissolution in, 17: 2461(R) (BNL-731(p.18-46))
Mg–$MgCl_2$–Ag, thermodynamic properties, 18: 3671(R) (BNL-799 (p.26-54))
Mg–$MgCl_2$–Zn, distribution studies in, 17: 3871
Mg–MgO, fabrication and properties, 17: 25752
Mg–MgO, fabrication of super heat-resistant, 17: 32553
Mg–MgO, fabrication and properties of, 19: 42830
Mg–MgO, preparation and properties of powdered, 19: 30795
Mg–MgO, welding of composite, flash butt, 18: 2195 (CEA-2295)
Mg–Mn–O, phase studies of, 19: 20573
Mg–Ni–Si, corrosion by steam and water at high temperatures, 19: 30669(R) (HW-84573(p.5.1-22))
Mg–O–Ag, internal friction in, 17: 35264(R) (UCRL-10706(p.111-203))
Mg–Si, corrosion by steam and water at high temperatures, 19: 30669(R) (HW-84573(p.5.1-22))
Mg–Si, electric conductivity, Hall coefficients and mobility, and Seebeck coefficients at 7 to 1000°K of p- and n-type Mg_2Si single, 16: 25799 (IS-362)
Mg–UF_4, homogeneity of compacted pellets of, apparatus for testing, 16: 30655(P)
Mg–UO_2, fission product diffusion from, 18: 14514
Mg–UO_2, properties in dispersion type fuel elements, 20: 6684
Mg–UO_2, swaging powders of, in aluminum cans, 19: 26785 (INR-557/XIV)
Mg–ZrH_4, production for use as fuel element canning, 19: 30662(P)

MAGNESIUM TANTALATES
crystal structure, 16: 11650
crystallographic and magnetic structure, 16: 7532

MAGNESIUM THULIUM SELENIDES
preparation, (E), 19: 13297

MAGNESIUM TITANATES
heat of formation, 16: 22613
radiation effects on electric conductivity, slow-neutron, 16: 24266
reactions with zirconium titanates at high temperatures, 16: 5352
MgO–Mg_2TiO_4, properties as electrolytic cells for winning and refining of plutonium, 20: 21239 (RL-SEP-824)

MAGNESIUM TUNGSTATES
luminescence decay after excitation with uv light and electrons, 16: 19539
stability of gaseous, 20: 25091

MAGNESIUM URANATES
conversion into fluorides, 16: 18980(P)
decomposition and phase studies, 16: 22046 (DC-61-6-13)
formation and structure of, from reactions of magnesium oxide with uranium oxide, 19: 15451(T) (ANL-Trans-33(p.224-7))
preparation and properties, 19: 42462
preparation, properties, and spectra of, 20: 40901
reduction to uranium, 18: 25618
thermal stability of, under high oxygen pressure, 17: 37174 (UCRL-7044)

MAGNESIUM YTTERBIUM SELENIDES
preparation, (E), 19: 13297

MAGNESIUM YTTRIUM SELENIDES
preparation, (E), 19: 13297

MAGNESIUM ZIRCONATES
coating of uranium rods by, effects of, on nonmetallic impurities in uranium, 20: 9455
deposition and oxidation of coatings of, on graphite, 19: 6270(R) (WADD-TR-61-72(Vol.XXXIV))
reactions with molten barium, potassium, and sodium chlorides, 20: 26816 (HW-72369)

MAGNET COILS
see also Solenoids
analysis of axisymmetric, computer programs for, (E/T), 19: 23162 (ORNL-3575)
analysis of force-free-coil force-bearing-shell systems, computer methods, 16: 15399
analysis of mirror, for producing imploding spherical shock wave, 18: 26151
cables for superconducting, use of multiwire, 20: 9914
calculations for superconducting, for production of high uniform fields, 19: 6025 (CEA-R-2606)
conference on, Chicago, April 27-29, 1964, 19: 2736
construction of trim, for Berkeley 88-in. cyclotron, 17: 7407
cooling system for, design of water, 20: 10128 (CONF-650512, pp 177-81)
cooling system for superconducting, design of cryostat for, 20: 19731
critical currents in superconducting, temperature cycling effects on, 18: 42553
critical currents in high-field superconducting, (E), 19: 16797
cryogenic, materials and cost calculations for, 16: 31881
current degradation in Nb–Zr superconducting, mechanism of, 20: 8004
current density distributions in, calculation of, 17: 4784
current distribution in superconducting, optimum, (T), 20: 37971
current setting for Analogue II cyclotron, 17: 7400
degradation of large superconducting niobium–zirconium, (E), 19: 25444
description of force-free and force-reduced toroidal, 16: 15400
description of sensor for measuring control rod release and drop times, 16: 10246
design and development, 16: 32492(R) (ORNL-3315(p.72-8))
design and fabrication for 4-Bev electron synchrotron, 20: 17199 (CONF-650922, pp 686-99)
design and fabrication of cryogenic, with integral coolant passages, 20: 17874 (CONF-650922, pp 630-42)
design and performance of sodium cryogenic, 17: 35965 (UCRL-7401)
design and performance of Astron, 18: 15344 (UCRL-7549-T)
design and performance of superconducting Helmholtz, 19: 25443
design and performance for Cambridge electron accelerator, 19: 37306
design and performance for plasma engines, 19: 40762 (N64-31010)
design and performance of sodium cryogenic, 20: 9888 (CONF-650512, pp 152-5)
design and performance of superconducting, for alternators, 20: 34458
design and performance of superconducting, for MHD power generation, 20: 39643
design and technology of, for experimental plasma physics, 19: 25582
design data for calculation of flux density of, 17: 9072
design economy optimization of, for controlled fusion research, 20: 34708 (NASA-TM-X-1251)

design for accelerator beam deflection, 17: 2357
design for electromagnetic metal forming, 20: 40490 (Y-1483)
design for generating a plasma-confining field, 17: 1599(P)
design for high-gradient cusp geometry for plasma containment, 20: 15928(P)
design for magnetic mirror machines, engineering drawings for, 20: 6514
design for plasma containment, 19: 19248 (MPI-PAE/P1/1/65)
design for plasma containment, 20: 4995(P)
design for production of strong pulsed fields, 19: 38935
design for pulsed strong fields, 18: 5447 (CERN-63-36)
design for use in high-energy physics, (T), 20: 17175 (CONF-650922, pp 1-26)
design for water-cooled d-c magnets, 20: 16585 (CONF-650922, pp 349-55)
design for 100-kgauss mirror magnets for Phoenix machine, 16: 15423
design for 80-inch bubble chamber, 18: 7034 (BNL-7491)
design of air-core betatron, 20: 5961
design of baseball seam, 20: 44867 (UCRL-70026)
design of coaxial-cylinder, for inductive pinch devices, (E), 19: 14661 (IPP-1/9)
design of coreless, for FFAG accelerators, 17: 21106 (CEA-2227)
design of correcting, for Harwell Variable Energy Cyclotron, 17: 31554 (NIRL/R/28)
design of cryogenic, for energy storage, 20: 17597 (CONF-650922, pp 625-9)
design of eighth-order power optimized, analysis of, (E), 20: 2522 (ORNL-P-1516)
design of field coils for magnetohydrodynamic generators, 16: 12224 (NP-11436)
design of force-free, using superconductors, 16: 12249
design of force-free toroidal, 18: 32271 (MATT-208)
design of helical-ribbon, for 60-kgauss steady-field magnets, 16: 15439
design of helical, for intense magnetic fields, 18: 12433(P)
design of helical, for Astron tank, 20: 46825 (UCID-15022)
design of high-field, for magnetohydrodynamic generators, 17: 9076
design of high-field superconducting, 20: 17598 (CONF-650922, pp 745-52)
design of interleaved fractional-turn, for high fields with short rise times, 19: 44136 (LA-3234)
design of interleaved fractional-turn, for pinch devices, 20: 10126 (CONF-650512, pp 162-7)
design of multilayer pure-copper, for cryogenic 300-kgauss pulsed-field magnet, 16: 15421
design of multipolar windings, 20: 10123 (CONF-650512, pp 128-30)
design of precooled, for production of multisecond pulses up to 75 kgauss, 16: 15419
design of pulsed-air type for betatrons, 16: 14103 (AFCRL-62-249)
design of pulsed, for high fields, 17: 3603
design of spiral-ribbon aluminum, for cryogenic 100-kgauss magnet, 16: 15407
design of spiral-ribbon aluminum, for cryogenic 200-kgauss magnet, 16: 15408
design of superconducting, for 25-kgauss iron-core magnet, 16: 15430
design of superconducting, preliminary results on, 17: 14939 (LNF-62/58)
design of superconducting Helmholtz, 19: 745
design of superconducting, for plasma research, 19: 47533
design of superconducting Helmholtz, 20: 17586 (CONF-650922, pp 509-16)
design of superconducting, for, 20: 40169 (NASA-TN-D-3595)
design of water-cooled, 18: 13008(R) (ORNL-3564(p.100-25))
design of 30 kG superconducting, 20: 19736
design of, B_o/B_{max} ratio tables for, 20: 36979 (ORNL-3972)
design of, determination from specified magnetic fields, (T), 19: 47121 (UCRL-16080)
design of, electrolytic tank analog for, 20: 38189 (AD-636095)
design optimization of high-field, 16: 15405
development and stress analysis of, for cryogenic magnets, 19: 12428(R) (NBS-8481)
development at ORNL, 16: 32485(R) (ORNL-3315)
development for GVL-2 magnetic trap, 18: 17116 (NP-13711)
development for ultrahigh fields, 20: 32337
development of cryogenic, for high fields, 16: 15403
development of cryogenically cooled and superconducting, 20: 17592 (CONF-650922, pp 574-87)
development of helix- and disk-type, for high axial fields and gradients, 16: 15398
development of pulsed and superconducting, in Italy, 17: 23713
development of pulsed, for superconductor studies, 20: 44512
development of superconductor, at ORNL, 17: 17336(R) (ORNL-3392 (p.66-85))
development of superconducting, for magnetic mirror system, 19: 33276
development of superconducting, 20: 40014(R) (ORNL-3989, pp 109-27)
development of tape-wound, 19: 18604
development of 200-kgauss, review, 18: 11108
development, properties, and uses of superconducting, 18: 13010
dielectric measurements on ring, device for, 17: 19423 (TID-18301)
dislocation calculations for, 16: 9510(R) (ORNL-3239(p.79-84))
economics and properties of superconducting, 19: 12453
efficiency for magnetic susceptibility measurements, 18: 18482
electric currents in inductively coupled system of, computer program for, 18: 36724 (UCRL-7864)
energy losses from superconducting, (E), 20: 17630
energy storage in superconducting, 18: 15038 (IDA/HQ-63-1412(Vol.I) (p.53-75))
energy storage in superconducting, (T), 19: 27366 (IPP-4/13)
energy storage in, superconducting power switches for, 18: 26493
fabrication, 20: 16988 (CONF-650922, pp 305-12)
fabrication for Argonne Synchrotron, 20: 17186 (CONF-650922, pp 356-65)
fabrication of large copper, x radiography of brazed joints in, 19: 46965 (UCRL-16383)
fabrication of niobium-tin superconducting, 20: 9897
fabrication of ZGS ring, prestressing techniques in, 20: 17201 (CONF-650922, pp 733-44)
fabrication of 28.5-kgauss superconducting niobium-tin, 16: 15429
field configuration from axially symmetric air-core, program for, 19: 34774 (PPAD-524-E)
field contours for perfectly conducting, 16: 15414
field distribution in single-turn, 16: 2307(T) (AEC-tr-4721)
field distributions from, 19: 9308 (IPP-4/8)
field distribution, heating, and stresses in pulsed, calculation of, 19: 37256(T) (SLAC-Trans-16)
field distribution in, for 70-Bev accelerator, (E), 19: 37423
field distribution along axis of superconducting, (E), 19: 38933
field energy removal from superconducting, methods for, 18: 34690
field intensity along axes of circular, 16: 15268 (NASA-TN-D-1013)
field properties of large-volume, (E), 20: 17600(R) (ORNL-3908, pp 114-48)
flux accumulation in superconducting, development of pumping method for, 17: 16174 (LADC-5418)
flux path through sets of, adjustment by coil tilting, 16: 15401
Hall effect measurements on superconducting niobium–zirconium, 20: 17600(R) (ORNL-3908, pp 114-48)
heating effects on properties of superconducting, (E/T), 20: 13675
inductance of toroidal, 17: 29401(T) (NP-tr-1039)
insulation for, charged-particle effects on, 19: 32830 (SLAC-40)
insulation for, development of, 18: 33717
Lorentz force measurements on, system for, 19: 15918
materials for superconducting, testing of, 20: 13666 (IPP-4/22)
motion of conducting body in cylindrical, (T), 19: 37236
performance and protection of superconducting, 19: 25442
performance of cryogenic, superconducting, and water-cooled, for industrial MHD generator, (T), 19: 16462
performance of large superconducting, 20: 46546
performance of niobium–tin superconducting, in superfluid helium, (E), 20: 24268
performance of niobium–zirconium superconducting, 20: 40015(R) (ORNL-TM-1598)
performance of small superconducting, 19: 43233
performance of stabilized superconducting, (E/T), 19: 27370 (NP-14995)
performance of superconducting, in magnetic mirror systems, (E), 19: 10449
performance of superconducting-iron-winding, for MAD generator, (E/T), 19: 16461
performance of superconducting, (E/T), 19: 45192 (ORNL-TM-1266)
performance of superconducting, 20: 17590 (CONF-650922, pp 550-9)
performance of, effects of insulation structure on, 20: 11387 (CONF-650922-28)
performance of, with superconducting cables, 20: 17591 (CONF-650922, pp 560-7)
plasma production in single turn conical, 17: 9749
power supplies for superconducting, use of flux pumps as, (E/T), 20: 17596 (CONF-650922, pp 615-24)
power supplies for, design of capacitor, 20: 36982
power supplies for, design of economical, 20: 45839 (UCRL-70020)
power transfers from r-f, to ion cyclotron waves in cold plasma, (T), 20: 20013 (NASA-TN-D-3361)
production of force-free, using analog-model methods, 16: 15418
production of helical-ribbon and concentric-helix, for fields around 100 kgauss, 16: 15434
properties of air-core, 17: 3095
properties of relativistic electron, for plasma containment, 20: 38210 (UCRL-12455(Rev.1))
properties of superconducting niobium–tin, 17: 29386 (CEA-2239)

protection of superconducting, against overheating, 17: 20764
protection of superconducting, during transition, 17: 27942 (NIRL/R/32)
protection of superconducting, dynamic, (E), 20: 46548
quenching characteristics of square superconducting, 16: 15396
radiation effects on ferrite cores, pulsed, 16: 10229
radiation effects on, pulsed, 18: 10580 (USAELRDL-TR-2299)
shunt resistor for paralleling large, design of variable, 20: 11388 (CONF-650922-29)
size limitations on large superconducting, 17: 39721 (NP-13148)
stress analysis of tape-wound, (T), 20: 1264 (NBS-8843)
stresses in, calculation of mechanical, 20: 46243(T) (AERE-Trans-1056)
superconducting, use for magnetohydrodynamic power generation, 17: 9071
testing of large superconducting, facility for, 20: 40049
thermal switches for coolant system for, response of, 17: 33158(R) (ORNL-3472(p.84-106))
threading digital computer, 18: 11556(P)
training effect in multilayer superconducting, (E), 20: 11895
use as measuring element in fast high-current gas discharges, 20: 32571 (IPP-1/2)
use of cryogenic, for strong bubble chamber fields, 18: 14204 (CEA-2362)
use of high-purity aluminum at −423°F in, 20: 46547
use of niobium–zirconium superconducting, in double Helmholtz arrangement, 20: 5614
use of superconducting, in magnetic mirror machines, 20: 26249 (N-65-36897)

Magnetic Bremsstrahlung
see Cyclotron Radiation

MAGNETIC CLUTCHES
design, 18: 17989(P)
design with contact-indicating means, 17: 13743(P)
electric characteristics of magnetohydrodynamic, 17: 3591

MAGNETIC FIELDS
see also Electric Fields
see also Electromagnetic Fields
see also Fluxmeters
see also Geomagnetic Fields
acceleration of conducting gas by moving, 16: 33941
acceleration of superconducting solenoids in traveling, 20: 41554
acoustic wave interactions with, plasma kinetic correlations with, (T), 19: 47732
action integral for charged particles trapped in, invariance of, 18: 34293
adiabatic invariants of gyrating particles in, (T), 20: 15623 (MPI-PAE/P1.15/65)
air ionization coefficients in crossed electric and, 19: 23828(R) (TID-21499)
Alfven wave propagation in rotational, 17: 34645
Alfvén wave propagation in dipole, 18: 30324
Alfven waves in, extenuation of, 18: 15359
alkaline-atom and electron-beam polarization in dipole, 20: 27635
amplification device for, 19: 30989(P)
amplification within sunspot groups, (T), 19: 27060
amplitude and phase of, from electromagnetic-wave propagation in stratified flat conductor, (T), 19: 33121
amplitude and phase of wake, from pulsed charges moving in conducting pipes, (T), 20: 44052
analysis by zonal harmonic series, 16: 15397
analysis of analog, electrolytic tank design for, 20: 38189 (AD-636095)
analysis of axisymmetric, computer programs for, (E/T), 19: 23162 (ORNL-3575)
analysis of high-field limits on, in Brookhaven AGS, (T), 19: 44858 (BNL-9480)
analysis of spiral, 16: 26371 (JINR-P-930)
analysis of straight-axis and toroidal vacuum, (T), 20: 28494(R) (MATT-Q-22, pp 215-319)
analysis of surfaces in, stellarator perturbations, 16: 3790
analysis of "wells" in, in plasma, 17: 42068
analysis of, computer programs for, 18: 34266 (CLM-R-31)
analysis of, using TRIM code, (E), 20: 940 (UCRL-16382)
annihilation and reconnection of, in solar flares, 17: 32859
annihilation at boundary between two plasmas, (T), 19: 23824 (NP-14890)
annihilation at plasma-plasma interface, rate of, 18: 7830
arc discharge extinction by transverse, 16: 9534
atomic energy level crossings in, 18: 30406
atomic energy level transitions in rotating, 18: 40143
atomic energy level mixing in external fields, interference phenomena in, 19: 45270 (JINR-P-2248)
attenuation by superconductor films, 16: 9308
auroral effects of interplanetary, 17: 12881
behavior of solar, during flares, 18: 44384
bias effects on plasma production, 16: 6043 (JÜL-19-PP)
bibliography, 17: 27937 (AID-62-155)
bibliography on interplanetary, 19: 34833 (N64-21485)
bibliography on production and use of strong pulsed, 17: 11442
biological and chemical effects, 16: 1308(R) (LAMS-2627(p.94-8))
biological effects on Drosophila, 18: 9803 (AD-404251)
Bloch electron symmetry transforms in, 18: 9184
Bloch particle energy band decoupling in, 16: 15323
book: *Analysis and Computation of Electric and Magnetic Field Problems*, 19: 39311
book: *Biological Effects of Magnetic Fields*, 19: 24235
book: *High Magnetic Fields*, 16: 15395
book: *Lectures on Magnetoionic Theory*, 18: 42548
book: *Mathematical Models for Computing Electric and Magnetic Fields*, 20: 17161
book: *Physics and Techniques of Strong Magnetic Fields*, 20: 4486
book: *Stellar and Solar Magnetic Fields*, 19: 44932
boson-system response to, Green's function for, 18: 22786 (NP-13893)
boundaries in wedge-type magnetic spectrometer, impulse calculation of, 18: 12420 (SLAC-24)
boundary from line currents in streaming plasma, (T), 20: 44912
boundary layer between rarefied plasma and, structure of, (T), 19: 41905
calculation for baseball seam conductors, 20: 10127 (CONF-650512, pp 168-72)
calculation for pulsed controlled-thermonuclear fusion experiments, 20: 32596
calculation for right-circular conical current sheets using Legendre polynomials, 18: 34273 (NASA-TN-D-2400)
calculation for synchrocyclotrons, computer program for, 20: 39537
calculation for uniform-field bending magnets, 19: 39317 (NRL-6248)
calculation in gaps of iron-core magnets, 16: 15409
calculation in planar air–iron-conductor geometries, 19: 9774 (UCRL-7784)
calculation of even Ioffe bar, (T), 20: 15878 (IPP-6/42)
calculation of minimum-B, method using Laplace equation for, 20: 28537
calculation of nonlinear, method for, 19: 44876 (UCRL-16287)
calculation of pulsed, methods of, (T), 19: 12637(R) (LA-3202-MS)
calculation of rapidly pulsed, method for, (T), 20: 26246 (LA-3416)
calculation of triple focusing, 16: 3226
calculation of, computer program for, 19: 1059
calculations for AGS magnets, computer, 19: 37316
calculations for bubble chamber magnets, (T), 19: 26663 (MURA-708)
calculations for FFAG accelerators using relaxation methods, (E), 19: 20729 (MURA-706)
calculations for 100-Mev FFAG accelerators, 20: 11391 (NP-15274)
calculations of poleshoe cross section in magnetic quadrupole lens, 16: 4886 (DESY-A2.78)
calculations of, method for, 19: 44811 (UCRL-7784-T(Rev.1))
calibration and measurement, 17: 16790 (TID-18216)
cancellation of external, use of combination of cylindrical current sheets for, 20: 37313 (BNL-10143)
characteristics in strong-focusing annular accelerator, 16: 6040
characteristics of interplanetary, 16: 10400 (ASD-TR-61-322(p.1-7))
characteristics of magnetohydrodynamic, 17: 11365
charge transport in strong, perturbation theory for transverse, 18: 42511
charged particle acceleration in modulated, 16: 32205
charged particle acceleration by oscillating, 17: 22685
charged-particle behavior in plasma-free, 16: 1115 (NYO-9495)
charged particle Brownian diffusion in, 16: 11083
charged-particle behavior in static asymmetric magnetic mirror geometry, 17: 7465
charged-particle behavior in static axially symmetric magnetic mirror and cusp geometries, 17: 7466
charged particle behavior in, kinetic theory of, 17: 21156
charged-particle behavior in variable, adiabatic approximation for spin 1 and ½, 18: 6079
charged particle behavior in variable, 18: 14772
charged particle collisions in, integral for, 16: 27917(T) (FTD-TT-62-378)
charged-particle collection by Langmuir probe in strong, mechanisms for, 18: 7803
charged-particle Coulomb scattering by plasma in, cyclotron radiation line profile from, 18: 7817
charged particle capture in dipole, (T), 19: 4746(T) (FTD-TT-64-1077(p.191-9))
charged particle deflection by, 17: 4212
charged particle diffusion across, in plasma, 17: 13656
charged particle diffusion in strong, 17: 22756
charged-particle diffusion across, in plasma of finite length, 18: 9515
charged particle distribution in, 18: 16731(T) (FTD-TT-64-90(p.110-27))
charged particle distribution in varying, variation of, 18: 28276
charged-particle diffusion across, equations for, 20: 30714
charged particle focusing by spiral, 16: 31848
charged particle focusing in cylindrically symmetric r^{-4}, 17: 16387

charged particle focusing in azimuthal asymmetric, for synchrocyclotron, 17: 42024
charged particle focusing in crossed electric and, 18: 24262
charged particle focusing by, 19: 15925
charged particle focusing in azimuth-dependent, (T), 19: 34510
charged particle focusing by symmetric, nonlinear, (T), 20: 27652
charged particle injection in axially symmetric, parameters for gyromagnetic radiation production in, 17: 37719
charged-particle injection into strong, theory of, 18: 1097(R) (AFCRL-62-717)
charged particle motion under conditions of time reversal, 16: 3616 (TID-14188)
charged particle motion in dipole, 16: 8112
charged particle motion in inhomogeneous, 16: 17197
charged particle motion in, 16: 23208
charged particle motion in dipole, 16: 33712
charged particle motion in, adiabatic approximation for, 17: 2374
charged particle motion in crossed electric and, 17: 2119
charged particle motions in spiral ridge, 17: 5424
charged-particle motion in, canonical formalism of, 17: 20557 (IPPJ-5)
charged particle motion in time-varying axial, 17: 20738
charged-particle motion in, non-adiabatic, 17: 22719 (IPPJ-8)
charged particle motion in inhomogeneous, 17: 24549
charged particle motion in helically invariant, 17: 31595
charged particle motion in dipole, 17: 32878
charged-particle movements in, computer solution for, 17: 36768
charged particle motion in helical, 17: 42051 (NP-13104)
charged-particle motion in, 17: 42072
charged-particle motion in undulated, 18: 1127 (NP-13109)
charged particle motion in spiral, stability of, 18: 1165
charged-particle motion in corrugated, 18: 4646
charged particle motion in cusped, 18: 4654
charged-particle motion in cylindrically symmetric, relativistic, 18: 5889
charged-particle motion through plasma in, electromagnetic radiation from, 18: 7829
charged-particle motion in rectangularly pulsed, 18: 9220
charged-particle motion in magnetic field, Feynman histories for, 18: 9240
charged particle motion in transverse, 18: 15395
charged particle motion in axisymmetric barriers, 18: 15417
charged particle motion in, in circular accelerators, 18: 16612
charged particle motion in, 18: 16553(T) (FTD-TT-64-90(p.80-109))
charged particle motion in, 18: 16554(T) (FTD-TT-64-90(p.128-62))
charged particle movement in, energy dissipation in, 18: 26128
charged particle motion in, equations for nonrelativistic, 18: 26147
charged particle motion in axisymmetric, 18: 30626
charged particle motion in stationary-non-uniform, adiabatic invariants of, 19: 1249
charged particle motion in inhomogeneous (T), 19: 3128
charged particle motion in homogeneous, high-frequency quasipotential for, (T), 19: 5368
charged particle motion in inhomogeneous, mean drift of, (T), 19: 10134
charged particle movement in, allowed regions of, 19: 10185
charged particle motion in perpendicular, and rotating electric fields, (T), 19: 14367
charged particle motion in inhomogeneous, (T), 19: 16248 (AD-603602)
charged particle motion in monopole, Alfven invariant of, (T), 19: 18594
charged particle motion in time-varying, (T), 19: 18764
charged particle motion in nonuniform weak, non-adiabatic, (T), 19: 23193
charged particle motion in, in gravitational field, (T), 19: 26926
charged particle motion in, effects of fringing fields on, (T), 19: 41139
charged particle motion in, zone for, (E/T), 20: 25847
charged-particle motion in constant longitudinal and rotating transverse, 20: 30693
charged particle motion in simple force-free, (T), 20: 31812
charged-particle magnetic moment in, second-order, (T), 20: 38208 (PPL-AF-4)
charged particle motion in non-resonant h-f and, 20: 40193
charged particle motion in, radiation deceleration effects on, (T), 20: 42431
charged particle motion in axially symmetric nonstationary, (T), 20: 41558
charged particle orbit in, 16: 607
charged particle orbits in spiral, stability of, 17: 21107 (MURA-661)
charged particle orbits in Heliotron, (T), 19: 41885
charged particle precession in nonuniform, elliptic functions for, 18: 44312
charged particle resonances in time-dependent, spin ½, (T), 20: 4648
charged particle scattering in homogeneous, with central potential, 16: 12342
charged-particle systems in constant, radiation damping of relativistic, 18: 7821
charged particle scattering in, 19: 25071(R) (TID-21667)
charged particle trajectories in homogeneous, with linear time dependence, 16: 12301
charged particle trajectories in, 16: 19532
charged particle trajectories in, 17: 9057
charged particle trajectories in cusped, analysis of, 17: 26708
charged particle trajectories in, 17: 36516
charged-particle trajectories in nonhomogenous, 17: 37673
charged-particle track curvature in, momentum determination from, 18: 855 (PAN-386/VI)
charged-particle trajectories in cusped, 18: 915
charged-particle transport matrix in quadrupole, 18: 2442
charged particles in, magnetic moment of gyrating, (T), 20: 40229
charged-particle acceleration in stellar, processes for, 18: 32354
charged-particle acceleration in, 18: 32924
charged-particle adiabatic motion in varying, (T), 20: 28133
charged-particle acceleration by, with alternating phase velocities, (T), 20: 34724
charged-particle betatron oscillations in constant, 18: 30347 (NP-13983)
charged-particle beam bending in, space-charge effects on, (T), 20: 11378 (AD-626633)
charged-particle beam emission from plane in homogeneous, in diodes and electron tubes, (T), 20: 25640
charged-particle beam focusing in alternating-gradient, chromatic aberrations in, (T), 20: 13360 (CERN-65-42)
charged-particle beam aberration and displacement in prism fringe, (T), 20: 21484
charged-particle Brownian motion in fluids in crossed electric and, (T), 20: 11802
charged-particle beam focusing in helical, 20: 37334
charged-particle beam parameters in channels of, effects of channel errors on, 20: 41538 (LNF-66/29)
charged-particle confinement and motion in perturbed, 18: 42831
charged-particle charge and energy flows in strong, nonequilibrium system of, (T), 20: 17487
charged-particle containment and motion in static, (T), 20: 6459 (CNIE-PE-1)
charged-particle distributions in dipole, 18: 42867 (MTP-RP-64-1)
charged-particle density fluctuations in plasma in, (T), 20: 34735
charged-particle focusing in quadrupole, aberrations in (T), 19: 770 (INSJ-78)
charged-particle focusing in, (T), 19: 14145(T) (CEA-tr-R-1799)
charged-particle injection and trapping in static, 18: 22556
charged-particle interactions with turbulent plasma in, 19: 37975
charged-particle kinetics in uniform, equations for, 18: 36400
charged-particle motion in axisymmetric, nonadiabatic, 18: 17169
charged-particle motion in axisymmetric, 18: 20645
charged-particle motion in dipole, glow discharge experiments on area of, 18: 26117(T) (JPRS-23767(p.57-61))
charged-particle motion in, Alfvén's theory for, 18: 30648 (AFCRL-64-226)
charged-particle motion in, space-charge compensation in, 18: 36082(T) (FTD-TT-64-619)
charged-particle motion in interplanetary, cosmic-ray anisotropy theories from, 18: 36179 (NASA-TN-D-2404)
charged-particle motion in, 18: 37811
charged-particle motion in changing, with nonadiabatic intervals, 18: 40401
charged-particle motion in homopolar, effects of friction of, 18: 40688
charged-particle motion in "corkscrew," stability of, 18: 42216
charged-particle motion at cyclotron frequency in, 18: 44854 (ML-1215)
charged-particle motion across discontinuities in, Fermi acceleration in, (T), 19: 5023
charged-particle motion in, allowed regions of, (T), 19: 6585
charged-particle motion in dipole, theorems on, 19: 27112 (P-2496 (RAND))
charged-particle motion across shock fronts in, (T), 19: 30971
charged-particle motion in cusped, nonadiabatic, (T), 19: 31361
charged-particle motion in dipole, (T), 19: 33155
charged-particle motion in electromagnetic waves in static, Dirac and Klein-Gordon equations for, 19: 35205
charged-particle magnetic moments in axially symmetric, (T), 19: 37232
charged-particle motion in, (T), 19: 41142
charged-particle motion in constant, difference equations for, 19: 41145
charged-particle motion in helical, (T), 19: 41187(T)
charged-particle motion in, cylindrical functions for, 19: 42956
charged-particle momentum in, conic reprojection of photographs for calculating, 20: 2728
charged-particle momentum in, determination of, (T), 20: 4583 (JINR-P-2371)
charged-particle momentum in, effects of field nonhomogeneity on photographic analysis of, 20: 2729
charged-particle motion in crossed electric and, (T), 20: 1266 (NP-15450)

charged-particle motion in dipole, in external homogeneous magnetic field, (T), 20: 29829
charged-particle motion in static, first order correction to magnetic moment for, (T), 20: 32669
charged-particle motion in, bibliography on, 20: 34780 (N-66-13563)
charged-particle motion in combined mirror-multipole cusp, (T), 20: 10212
charged-particle motion in cusped, adiabatic invariance of, 20: 8214
charged-particle motion in helical toroidal, nonlinear theory of fast, 20: 13371
charged-particle motion in, computer for determining, 20: 17906
charged-particle motion in, in magnetic analyzers, (T), 20: 13091
charged-particle motion in time-dependent axially symmetric, (T), 20: 20023
charged-particle motion in, (T), 20: 21454
charged-particle motion in, effect of field gradient on polarization of spin-½, (T), 20: 21481
charged-particle motion in quadrupole, equations for, 20: 39484 (CERN-66-21, pp 1-30)
charged-particle motion in crossed electric and, (T), 20: 40243
charged-particle motion in spatially periodic, 20: 42501
charged-particle motion in, cyclotron radiation in, 20: 44913
charged-particle motion in matter in, maximum likelihood analysis of, 20: 46812 (JINR-P-2829)
charged-particle motion in, adiabatic invariance properties of, 20: 46817 (JUL-384-PP)
charged-particle nonadiabatic losses from multipolar, (E/T), 20: 10145 (NASA-TN-D-3164)
charged-particle optics in, dispersive effects in, 18: 18519
charged-particle orbits in Heliotron (E/T), 19: 1700 (IPPJ-21)
charged-particle orbits in axisymmetric, computer program for, 19: 37672 (ORNL-TM-1172)
charged-particle orbits in, measurement using current-carrying wire, 20: 16771 (CONF-650922, pp 467-71)
charged-particle scattering by cosmic, (T), 19: 28980
charged-particle shielding by nonaxially symmetric, 20: 28594
charged-particle trajectories in, three-dimensional, (T), 19: 27299
charged-particle trajectories in, measurement using current-carrying wire, (E/T), 20: 17196 (CONF-650922, pp 497-504)
charged-particle trapping in, method for, 20: 32642(P)
charged-powder motion in, (T), 19: 6397
Cherenkov emission from charged particles in circular orbit in external, 16: 17033
compression between two semi-infinite slabs of constant conductivity, Joule heating effects on, 18: 14612
compression by collapsing metallic shell, 17: 9755
compression by collapsing liners, (T), 19: 18564 (LGI-63/25)
compression by condenser discharging, crowbar system for, 20: 10117 (CONF-650512, pp 57-62)
compression by exploding foils, (E), 19: 20717
compression by explosives, energy conversion efficiency in, 20: 41086
compression devices for, noncylindrical explosive, 20: 41091
compression devices for, using explosives, 20: 41094
compression devices for, design of explosive, 20: 41095
compression in apertures in semiconductive devices, 19: 14458(P)
compression in apertures in superconducting solenoids, 19: 14459(P)
compression in cylindrical liners, limitations of, 20: 41083
compression in explosion geometry, 20: 41093
compression in high field superconductive device, 19: 33184(P)
compression of cylindrical, limitations of, 20: 41085
compression of cylindrical, diffusion limitations of, 20: 41089
compression of deuterium plasma by, 17: 9734
compression of, devices for, 20: 41096
compression of, diffusion limitations of, 20: 41082
compression of, diffusion and surface instabilities in, (T), 20: 41090
compression of, mathematical models for, 20: 2523 (SC-RR-65-449)
compression of, properties of, 20: 41081
compression properties of, calculation of implosive, 20: 41088
compression techniques for metallic particle acceleration, development of, 20: 41084
conducting layer in traveling, higher-space-field harmonic effects on, (T), 20: 29830
conduction maximum variation principle for, 16: 25988
configuration for thermonuclear plasma containment, octupole, 17: 40163(R) (TID-19431)
configuration for stellarators, (T), 19: 6801
configuration for near-ideal neutrino horn, finger, (T), 19: 30877 (BNL-9062)
configuration from axially symmetric air-core solenoids, program for, 19: 34774 (PPAD-524-E)
configuration in plasma-filled waveguide, bifurcation, (T), 20: 6481
configuration in polytropic stars, equilibrium, (T), 20: 19343
configuration of dipole-interplanetary transition-region, effects of polar disturbances on, (E), 20: 11827
configuration of, from elliptic loops, 17: 36521
configuration of intense discharge in, 17: 9718
configuration of interplanetary, effects on polar cap absorption and Forbush decreases, (T), 19: 37716
configuration of interplanetary, from propagation of protons from solar flares, (T), 20: 23851
configuration of rotating, in polyphase system with skew pole pieces, (T), 19: 41152
configuration of surfaces of, in helical stellarator, (T), 19: 31351
configuration of, from cylindrical coil, 18: 44301
configuration of, from surface currents on tori, (T), 19: 5372
configuration of, determination of geometry and current of coils for producing specified, (T), 19: 47121 (UCRL-16080)
configurations for bubble chambers, 18: 7030 (BNL-7480)
configurations for minimum-B plasma containment, 18: 13008(R) (ORNL-3564(p.100-25))
configurations in proton synchrotron x-blocks, 17: 935
configurations in high-current toroidal discharge, 17: 9745
control and measurement of spectrometer, by Hall probe, 18: 8649(R) (TID-19940(p.77-118))
control and measurement of, NMR system for, 18: 27782
control and measurement of, in beta spectrometers, 18: 31968
control and measurement at 1 to 13 kG, proton magnetic resonance system for, 19: 11481
control by proton resonance of variable, 17: 3283
control in beta spectrometers, circuit for, 19: 4524
control of flux path through sets of coils by coil tilting, 16: 15401
control of, design of variable-mode magnet-cycle timer for Brookhaven AGS, (E), 19: 28935 (BNL-8971)
convection and dissipation effects in viscous fluid flow, 16: 5472
cooling rate of mercury in, equation for, 16: 1775
coordinates of hydromagnetic equilibria, 17: 9712
correction of 7-Bev proton synchrotron, system for, 17: 925
corrections and measurements for 30-Mev betatron, 19: 8051
corrections of low-induction, in proton synchrotrons, 17: 937
cosmic particle motion in interstellar, 18: 30435 (CONF-320-3)
cosmic particle scattering by galactic, energy spectra effects from, 18: 9057(T)
cosmic particle scattering by interplanetary, 18: 22702
cosmic radiation modulation by interplanetary, 19: 20889
cosmic-ray deceleration in, 17: 12991
cosmic ray modulation by interplanetary, 19: 25201
cosmic-ray acceleration by magnetic pumping in, 18: 20823
cosmic-ray modulation by interplanetary, 19: 25212
cosmic-ray modulation by interplanetary, solar-activity effects on, 19: 25215
Coulomb interaction in plasma in, uniform, 17: 11869
creation in space, 16: 21234
critical behavior of, in thin superconductors, 17: 25928
critical current strengths of two-component diffusion layers on niobium in, 18: 30217
current flux function for axi-symmetric, 17: 11355
current loop motion in, 16: 9521(T) (AEC-tr-4727)
currents in two-dimensional, forces on, 20: 37316 (BNL-10324)
cusped configuration of, asymptotic formulas for, 18: 21387 (NYO-10435)
cyclotron radiation from boundary with plasma, 17: 9710
cyclotron radiation from electrons in homogeneous, (T), 19: 41393(T)
cyclotron radiation emission from intense, (T), 20: 44061
cyclotron wave production and coupling in electron beams, 16: 10656 (AD-259848)
deflection of electron beams by, equations for, 18: 8925
deformation by Joule heating windings in toroidal plasma device, corrections for, 18: 11321
deformation in MHD shock-front interior, during propagation in electro-neutral media, (T), 20: 21806
deformation of moving, in conductive medium, 17: 6811(T) (FTD-TT-62-981)
description of helical-symmetry, having potential wells, 19: 47154
description of solar, 18: 10730
design for Analogue II cyclotron, 17: 7399
design for isotopic beam separation, 20: 41405
design for large ion pumps, 18: 20158
design for ORIC, computer programs for, 17: 7385
design for particle beam control, relations for, 18: 30343 (CERN-64-24)
design for plasma research, 17: 4195
design for trapping colliding beams, 16: 22933
design for Univ. of Colorado cyclotron, 17: 7372
design for use in swimming pool reactor irradiations, 16: 26615 (CEA-2134)
design for 450-Mev spiral ridge cyclotron, 17: 7397
design of axially-symmetric, numerical method for, 17: 4784
design of axially symmetric, with minimum field strength region,

18: 22944 (MATT-256)
design of caulked cusp, calculations for, (T), 19: 33410(R) (LA-3320 (p.35-44))
design of current regulators for magnetic lenses, 19: 2568 (AECL-2061)
design of high-order double focusing, for beta spectrometers, 20: 16868
design of linear electromagnetic brake, (E), 19: 40724
design of plasma-containment apparatus using annular, 20: 15927(P)
destruction by occurrence of solar flares, 17: 3910(T) (FTD-TT-62-99)
detection and measurement in solar atmosphere, 16: 16897
detection and measurmenets of interplanetary, (E), 20: 31883
detection of small, circuit for, 20: 19771
determination for axially symmetric coils, computer programs for, 16: 8242 (PPAD-395-D)
determination for relativistic cyclotron with fixed frequency, 17: 36726
determination for magnetic lenses, (T), 20: 39011
determination in parallel-disk resonator (T), 19: 2579 (UCRL-7610)
determination in theta-pinch plasmas using lasers, (E), 20: 12164 (ARL-65-129)
determination of critical, in superconducting cylinder, (T), 19: 19037
determination of, from thin layer and envelopes, 17: 36522
detonation wave propagation in conducting fluids in, 18: 34329
development for caulked cusp devices, (E/T), 19: 12637(R) (LA-3202-MS)
development of a-c, for beam storage in betatrons, 17: 26652
development of azimuthally varying, for beta spectrometry, 20: 23427(R) (UCRL-16580, pp 219-50)
development of Crab Nebula, theory for, 18: 8995(T)
development of nonadiabatic, for trapping thermonuclear plasma, (E/T), 20: 13925(R) (TID-22419, pp 99-147)
dielectric breakdown mechanisms in, time lags of, 16: 33584 (TID-16718)
diffusion in metals, Joule heating effects on, 20: 41087
diffusion in moving conductors, (T), 19: 11827 (LGI-64/4)
diffusion in plasma, nonlinear, 16: 31143 (UCRL-6114)
diffusion in shock wave interactions with electromagnetic fields, 18: 34333
diffusion of charged particles from plasma decay in, 18: 17227
diffusion of cosmic particles in interstellar, 17: 608(T) (JPRS-15740 (p.92-102))
diffusion of isothermal plasma in, (T), 19: 5329
diffusion of plasma in, effects of Coulomb collisions on, 17: 24573
diffusion of plasma in, effects of drift waves on, 17: 35039
diffusion of plasma perpendicular to, leakage flux from, 17: 42101
diffusion of plasma across, Boltzmann moment equations for, 18: 17226
diffusion of plasma across, 18: 36708(R) (AFCRL-64-277)
diffusion of plasma across, 18: 40426
diffusion of plasma in, effects of friction tensor on, 19: 8502 (IPP-6/17)
diffusion of stellarator plasma across, mechanisms for enhanced, (T), 19: 19240 (IPP-2/31)
discharges in transverse, breakdown characteristics of electrodeless, 17: 20751
dispersion of sector, with double-focusing beam, (T), 19: 41194
distortion by flow in shock tube, 16: 5796
distortion by flow of conducting fluid past cylindrical obstacle, 16: 11069 (AFOSR-1551)
distortions in helical, compensation of, (E/T), 20: 20080
distribution along axis of superconducting coils, (E), 19: 38933
distribution and intensity of solar corona, correlation with coronal polar rays, 19: 25132
distribution and strength of galactic, (E), 20: 37368
distribution around cylindrical conductors, helically symmetric, 17: 32797
distribution around coils, 19: 9308 (IPP-4/8)
distribution in coils for 70-Bev accelerator, (E), 19: 37423
distribution in current-carrying layer of magnetoactive plasma, (T), 19: 41882
distribution in cyclotrons, correction of radial, 20: 17187 (CONF-650922, pp 377-89)
distribution in finite helical solenoid, 17: 41551 (NASA-TN-D-1993)
distribution in focusing nuclear instruments, 17: 14631
distribution in intergalactic and interstellar space, 20: 23854
distribution in isochronous cyclotron, (E), 19: 23212
distribution in plasma, 18: 17104 (ARL-250(Pt.II))
distribution in plasma waveguides, 18: 26778
distribution in rotating plasma at thermodynamic equilibrium, 18: 26717
distribution in theta pinch, 17: 7477
distribution in toroidal pinch, 18: 38210
distributions and properties in interplanetary space, 17: 7678
distributions and structure in outer atmosphere of sun, 17: 31245 (D1-82-0216)
distributions in beam-analyzing magnets of Frascati synchrotron, (E), 19: 11864 (LNF-63/82)
distributions in caulked, stuffed cusps, (T), 19: 33405(R) (LA-3320 (p.6-13))
distributions in caulked, stuffed cusps, (E), 19: 33406(R) (LA-3320 (p.14-18))
distributions in laminar wall flow jet, (T), 19: 4748
distributions in stabilized z-pinch discharge, 17: 9737
distributions in theta-pinch devices, (T), 19: 19238 (IPP-1/31)
distributions of, computer calculations using triangle meshes, (E), 19: 7838 (UCRL-7880)
disturbances around body moving in plasma, 18: 44873
disturbances in geophysical, at high latitudes, 16: 29487 (UAG-C-23)
disturbances in interplanetary, from cosmic-ray Forbush data, 19: 25241
disturbances in interplanetary, by solar flares, (T), 20: 44098
disturbances of helical, (T), 19: 5374
dynamics of Bloch electrons in, (T), 20: 30735(R) (TID-22970, pp 331-73)
dynamics of degenerate electron gas in, 18: 15383
dynamics of interplanetary, 18: 5911
dynamics of system of self-gravitating particles in collisionless gases in, 20: 42041
effect of h-f, on plasma, paramagnetic, (E), 20: 38220
effect of helical, on stellarator plasma, 18: 2981(R) (MATT-Q-20)
effect of helical, on ohmic heating of discharge plasma, (E), 20: 4937 (IAE-907)
effect of interplanetary, on earth bow shock stand-off distance, (T), 19: 6438
effect of magnetic screening on, in Helmholtz configuration, 18: 39577
effect of trapped, on plasma characteristics, 17: 9732
effect on binding energy of charged particles, 19: 47143
effect on breakdown time lag of low pressure neon discharge, 20: 2835
effect on cathode jets in impulse discharge of transverse, (E), 20: 40232
effect on convective heat transfer in turbulent flow of conducting fluid in tube, (T), 19: 32389(T)
effect on dupolasmatron discharge, 18: 28776
effect on electric conductivity of graphite, 18: 30210(T)
effect on electric current in cesium thermionic cell, (E/T), 19: 16450
effect on energy gap in type II superconductors, 18: 11114
effect on free convection heat transfer in laminar boundary-layer flow, 16: 7667
effect on microwave surface impedance of superconductors, (T), 19: 16786
effect on nuclear magnetic field, in paramagnetic materials, 18: 30863
effect on operation of MHD parallel-plate slider bearing, (T), 19: 18089
effect on oscillations in electron gas, 19: 44849
effect on performance of positive ion sources, 18: 43910
effect on stability of gravitating plasma column, (T), 19: 17088
effect on stability of turbulent flows of conducting fluid, 19: 44835
effect on stability of Penning discharge, (E), 19: 47780
effect on 21-cm hydrogen line splitting of galactic, 17: 6910
effects and properties of stellar, review of theories on, 19: 34834 (N64-21684)
effects in fluid flow boundary layer separation, (T), 19: 41114 (AD-617258)
effects of amplitude and polarity on plasma compression, 17: 9740
effects of arbitrarily oriented, on fluid flow in rectangular ducts, 20: 28045
effects of axial and radial, on spectra of gas discharges, 17: 35055
effects of constant axial, on plasma stability, 18: 9541
effects of convection on solar, 18: 44351
effects of coplanar, on conducting gas channel flow stability, (T), 20: 6174
effects of corotating structure in interplanetary, on cosmic radiation and geomagnetic activity, (E), 20: 5972
effects of crossed electric and, on electrons, 19: 39270(R) (TID-21894)
effects of crossed, on gaseous Townsend discharge, (T), 19: 47127
effects of crossed electric and, on plasma, (E), 20: 17943
effects of curved, on cesium plasma, (E), 19: 27609 (MPI-PA-12(64))
effects of direction and magnitude on magnetoresistance of thallium at 1 and 4.2°K, 20: 2329 (IS-T-35)
effects of earth-polar, on charged particles, 16: 18290 (AFCRL-1015)
effects of external, on ion beam focusing in electromagnetic fields, (T), 20: 9616
effects of external, an oblique plasma-wave propagation, 20: 24550
effects of external, on low-frequency oscillations in inhomogeneous plasma, (T), 20: 26327
effects of helical, on plasma heating in S-1 pinch device, (E), 20: 34723
effects of hexapole, on plasma drift in theta pinch, 18: 7816
effects of high, on nuclear emulsion measurements, 17: 18529 (CERN-63-3(p.297-314))
effects of high pulsating, on electric conductivity of antimony-indium intermetallic compounds, (E), 20: 26386
effects of imperfections on orbit stability in cyclotrons, 17: 7383
effects of inclined interplanetary, on solar corona and supercorona shape, (T), 20: 7689

effects of inhomogeneities of, on flow in Hall-type MHD generators, (T), 20: 39692
effects of internal, on thermal conductivity of degenerate stellar cores, (T), 19: 37436
effects of interplanetary, on cosmic-ray intensity in space, 17: 12973
effects of interplanetary, on solar particle propagation, 17: 12988
effects of interplanetary, on solar wind interactions with geomagnetic field, 17: 27574
effects of interplanetary, on solar cosmic particles, 18: 7443
effects of interplanetary, on cosmic radiation, 18: 16735
effects of interplanetary, on solar wind, 18: 18545
effects of interplanetary, on solar particles from chromospheric flares (E/T), 19: 2959
effects of interplanetary, on solar wind, (E/T), 19: 8060
effects of interplanetary, on galactic cosmic radiation, (T), 19: 16430
effects of interplanetary, on cosmic-ray intensity, (E), 19: 27121
effects of interplanetary, on galactic cosmic radiation, (E/T), 19: 29021
effects of interplanetary, on solar proton propagation, (T), 19: 41228
effects of interplanetary, on geomagnetic fields, (E), 20: 19642 (N-65-23066)
effects of interplanetary, on solar neutron-decay protons, 20: 21495
effects of interplanetary, on cosmic ray Forbush decrease, (E), 20: 37534
effects of interstellar, on ionization front in HII region, 18: 14711
effects of longitudinal, on meson (μ^+) depolarization quenching in targets, (E/T), 19: 45079
effects of longitudinal, on h-f discharge initiation in rare gases, (E/T), 20: 11780
effects of longitudinal inhomogeneity of transverse, on MHD mercury flow in square channel, (E), 20: 21807
effects of longitudinal, on critical fields of superconducting plane films, (T), 20: 28191
effects of magnetic traps on carrier lifetimes in indium antimonides, 18: 30305 (D1-82-0340)
effects of megagauss, on Faraday rotation in glass and quartz, 20: 41515
effects of minimum, on plasma stability, (T), 20: 32623
effects of multipole, on hydromagnetic eigenmodes in plasma, (T), 20: 6492
effects of nonuniform, on mass spectrometer performance, 18: 12422
effects of nonvarying axial, on plasma stability, 17: 7428 (NP-12342)
effects of nuclear, second-order, 17: 11617 (BNL-6205)
effects of, on space periodicity in plasma of gaseous discharge, 17: 31622
effects of pulsed, on performance of spark detectors, 17: 12569
effects of quadrupole, on plasma stability in indium antimonides, 18: 42839
effects of r-f, on nuclear spin system, (T), 19: 23660
effects of rotating transverse, on electron density distribution in plasma, (T), 19: 43422
effects of self-induced, on toroidal plasmas, (E), 20: 22175 (AD-624081)
effects of shock-tube plasma, 18: 19240
effects of solar wind, diurnal variations of cosmic rays from, 20: 7755(T) (NASA-TT-F-91, pp 127-50)
effects of solar, on flare emission, 18: 42254 (TID-21105)
effects of solar, on flare phenomena, 18: 44383
effects of stability of infinite cylinders of conducting fluids, 18: 18779
effects of strength of, on magnetization of gadolinium at 298°K, 17: 32646
effects of strong, on magnetohydrodynamic stability of plasma, 17: 19470(T) (MATT-Trans-3)
effects of strong d-c, on niobium–zirconium superconducting properties, 20: 37950
effects of time-dependent, on motion of charged particles in, 16: 10810 (AFCRL-636)
effects of transverse, on conducting turbulent flow in rectangular tubes, 17: 21893
effects of transverse, on toroidal discharge, 18: 19131 (NP-13613)
effects of transverse, on vertical two-phase flow, 18: 30300 (ANL-6854)
effects of transverse, on electric conductivity of plasma in thermionic cells, (T), 19: 21580
effects of transverse, on low-voltage cesium arcs, (E), 19: 37988
effects of transverse, on resonance peaks of hot asymmetric plasma, (T), 19: 47746
effects of transverse, on one-dimensional ionized gas flow, (T), 20: 4717
effects of transverse, on electric discharge in vacuum, (E), 20: 11769 (LGI-65/30)
effects of transverse, on forced convection liquid mercury heat transfer, 20: 27112
effects of transverse, on flow of visco-elastic fluid between non-conducting plates, (T), 20: 37871
effects of transverse, on boundary layer of conducting fluids, (T), 20: 46428
effects of transverse, on toroidal-confined plasmas, 20: 46880
effects of trapped, on theta pinch plasmas (E), 19: 1775
effects of traveling, on conducting bodies, (T), 20: 17162
effects of uniform transverse, on fluid flow in rectangular ducts, (T), 20: 9843
effects of uniform increasing, on ionization of hydrogen and nitrogen, (E), 20: 11768 (JUL-327-PP)
effects of uniform, magnetohydrodynamic viscous fluid flow in spherical envelope, (T), 20: 11777
effects of uniform, on laser-produced plasma expansion, (E), 20: 20045
effects of variably curved, on cesium plasma, (E/T), 20: 28493(R) (MATT-Q-22, 113-214)
effects of weak, on beta radioactivity, 18: 28724
effects of weak, on viscous fluid flow, (T), 20: 11776
effects of, combined with x radiation on barley seeds, 20: 18387
effects of, combined with x radiation on plant germination and seedling development, 20: 18388
effects of, combined with gamma radiation on Drosophila behavior, 20: 18410
effects on absorption spectra of erbium ethylsulfate, 19: 11085
effects on acceleration of irradiation in chemical reactions, 19: 4223
effects on angular correlations of nuclear radiation, 17: 11386
effects on angular correlation of nuclear radiation, dipole, 17: 31428
effects on argon and nitrogen plasmas, 16: 9506(R) (ORNL-3239(p.16-46))
effects on argon plasma in linear discharge, 18: 30884 (JEN-129-DF/I-40)
effects on atomic and nuclear quantum levels, 18: 11198 (JINR-P-1222)
effects on autoelectron emission, 18: 32667
effects on biological systems, 19: 5598(R) (NYO-3291-1)
effects on biological radiation effects, 18: 5006(R) (UCRL-11033(p.55-8))
effects on boundary layer in conductive gas flow, 18: 2975 (AD-283026)
effects on buoyancy and surface tension in cellular convection of electrically conducting liquids, (T), 20: 25980
effects on cesium thermionic-converter current, (E/T), 20: 25770
effects on channel flow of electrically conducting gas, (T), 19: 24680
effects on characteristics of microwave gas-discharge duplexers, (E), 19: 42678 (AD-609658)
effects on charged-particle escape from plasma, 19: 37947(T) (NASA-TT-F-169)
effects on charged particle beam propagation in cold plasma, wave excitation from, (T), 20: 22286
effects on coaxial plasma gun, longitudinal, (E), 20: 46905
effects on compressible flow of gas with infinite conductivity, 18: 32295
effects on conductivity in laminar fluid flow around plates, (E/T), 19: 14146(T) (FTD-TT-64-803)
effects on conducting turbulent fluid flow, coefficient of hydraulic friction from, (E/T), 20: 9841
effects on convection heat transfer, 17: 14464
effects on convective heat transfer in turbulent conducting fluid flow in channels, 20: 11793
effects on cosmic gas flow, (T), 19: 9879
effects on counter-streaming ion beams, harmonic generation from, (T), 20: 9846
effects on critical currents in superconductors, 18: 22833
effects on critical currents in superconducting films, (E), 20: 6232
effects on critical currents in superconducting tin films, 20: 15662
effects on current density in plasma, 17: 28397
effects on current-voltage characteristics of superconducting rings having insulating junctions, 20: 19770
effects on cylindrical plasma layer, 18: 30911
effects on density measurements of neutral gases in rotating plasma device, 18: 27778
effects on diffusion in cylindrical discharges, 19: 23164(R) (SU-SEL-64-103)
effects on diffusion in argon plasma, (E), 19: 27604 (JPL-TR-32-695)
effects on diffusion losses in thermal alkali-metal plasmas, 19: 33422 (NYO-2813-30)
effects on diffusion in r-f discharges, (E/T), 19: 39269(R) (SU-SEL-64-133)
effects on diffusion in plasma, 20: 4479(R) (TID-22179, pp 1-83)
effects on dipole oscillation in hot cathode discharge tube, 18: 9489
effects on dipole resonance spectrum of plasma waves in hot nonuniform column, (E), 19: 41932
effects on directional distribution of photons from two-quantum positron annihilation in titanium, 19: 1253
effects on Drosophila during solar flare activity, 16: 31409
effects on Drosophila behavior, 20: 18410
effects on electric conductivity, 18: 16660
effects on electric conductivity of semiconductors, device for measuring, 18: 20307
effects on electric current density and energy gap for superconductors,

18: 30680
effects on electric arcs in annular gap of concentric electrodes, shaping (T), 19: 1710 (NASA-TN-D-2155)
effects on electric conductivity of semiconductors, (T), 19: 8013(T) (UCRL-Trans-1088(L))
effects on electric discharges, (T), 19: 12709
effects on electric currents of cesium thermionic cells, (E/T), 19: 25252
effects on electric conductors, Joule loss in, 19: 43637 (TID-21171)
effects on electric conductivity of plasma, (T), 19: 43424
effects on electric probes in plasma, (T), 20: 8256
effects on electric arcs, induced gas flow from, (E), 20: 28060
effects on electric arc in transverse argon flow, 20: 28087
effects on electron-beam wave propagation, 16: 8154
effects on electron distribution function in ionized gases, 16: 12215 (JPL-TR-32-102)
effects on electromagnetic radiation from sources in magnetoplasma, 17: 21197
effects on electroconductivity of gases, 17: 32814
effects on electromagnetic transition angular correlations in atomic energy levels, 17: 41650
effects on electron and ion velocity distribution in plasma, 17: 42100
effects on electromagnetic forces in conducting liquids, 19: 1058
effects on electron probe currents, (E/T), 19: 6785
effects on electron tunneling, 19: 12865(R) (NAA-SR-10501)
effects on electron tunneling in metallic films, 19: 27735(R) (NAA-SR-10850)
effects on electromagnetic wave scattering by plasma column, (T), 19: 33463
effects on electromagnetic wave scattering by plasma column, (T), 19: 33464
effects on electron probe saturation currents in plasma, 19: 43408 (IPPJ-33)
effects on electromagnetic wave propagation through plasma, 19: 45387 (D1-82-0442)
effects on electron and ion emission from electrode materials for cesium ion engines, 19: 46571 (HRL-5249-S)
effects on electron transport phenomena in tin at liquid helium temperatures, 19: 47534
effects on electrostatic oscillations in collisionless electron plasma, (T), 20: 15879 (IPP-6/43)
effects on electromagnetic oscillations in plasma, (T), 20: 30677
effects on electromagnetic wave propagation in plasma, (T), 20: 30678
effects on energy degeneracy of electrons, 17: 29557
effects on energy gain in electron beam-plasma ion interactions, 17: 33194
effects on energy gap in superconducting thin films, 18: 6110
effects on energy gap in superconducting films, 18: 16885
effects on energy gap and microwave absorption in superconducting films, 18: 40452
effects on energy gaps in superconductors, (T), 19: 8368
effects on energy gap and microwave absorption in superconducting films, 19: 10210
effects on enhanced pulses in silicon semiconductor detectors, (E), 19: 24847
effects on entropy, internal energy, and thermal capacity of manganese chlorides at 0 to 4.2°K, 19: 11080
effects on erbium single crystals from 10 to 300°K, (E), 20: 6547
effects on etching of quartz, 18: 16535
effects on excited gadolinium-155 γ--γ angular correlations, (E), 20: 13763 (CONF-233(Vol.4), pp 710-19)
effects on external bremsstrahlung circular polarization from ferromagnetic materials, 20: 7718 (KFK-329)
effects on flow of electrically conducting media in flat channels with various boundary conditions, 16: 7966(T) (FTD-TT-61-228(p.12-20))
effects on flow of hydromagnetic fluid around rotating spheroid, 18: 32297
effects on flow of conducting fluids around insulated bodies, 19: 9339
effects on flow of jet of conducting liquid, 20: 39934
effects on fluid flow and heat transfer in toroidal channel, 16: 30559 (UCRL-9574)
effects on fluid flow, 20: 25976
effects on fluid MHD turbulence, 19: 1063
effects on fluid magnetic moment motion in, statistical theory for spin relaxation, (T), 20: 27762
effects on formation time of uhf pulse discharge in air, (E), 19: 30860
effects on galactic spiral structure, 18: 10736
effects on gamma-gamma angular correlations, 17: 26475
effects on gas discharges between coaxial cylinders, 20: 3202
effects on gas kinetic equations, 16: 18140 (AD-266087)
effects on glow discharge expansion in, (E), 20: 25847
effects on gravitational collapse of interstellar gas cloud, 20: 31862
effects on h-f discharge plasma, (E), 20: 32634
effects on heart function in frogs, 19: 21776 (UCRL-12389)
effects on heat conduction by high-pressure arc, 19: 3436
effects on heat transfer and laminar magnetohydrodynamic flow in vertical channels, 16: 13272
effects on heat transfer and flow of plasma in channel, 16: 18569
effects on heat transfer by electrolytes, 19: 9338
effects on heat transfer by liquid mercury, 19: 46547
effects on high-energy galactic cosmic radiation, (E), 20: 31884
effects on high-frequency conductivity of plasma in quasi-equilibrium, 19: 43447
effects on hydrodynamic wave reflection and refraction at fluid interfaces, 17: 25423
effects on hydrogen plasma flowing transversely, 18: 17174
effects on hydromagnetic waves in toroidal plasma, (E), 19: 47742
effects on hydromagnetic flow against rotating disks, 20: 11778
effects on immune reactions, 17: 37037
effects on impure sodium, 19: 40409(R) (MSAR-65-95)
effects on indium antimonide photoconductivity, 19: 17079(R) (TID-21380(p.45-61))
effects on infrared absorption by superconducting lead films, (E), 20: 40044
effects on interactions of quantum gas, generalized Boltzmann equation for, 19: 32801
effects on internal fields in gamma-irradiated triglycine sulfate crystals, 20: 46947
effects on interplanetary gas, 17: 12984
effects on interplanetary, on cosmic ray daily intensity variations, 20: 9689
effects on ion gage operation, 16: 31749 (MATT-80)
effects on ion mobility and vortex ring formation in helium II, (E), 19: 12451
effects on ion source performance in mass spectrometers, 18: 31859
effects on ionization of xenon in shock tube MHD generator, 19: 31321(R) (AD-609273)
effects on ionized gas flow between plates, 17: 13659
effects on ionized gases, hydrodynamic turbulence in, (T), 19: 41114 (AD-617258)
effects on jet-driven vortex flow of electrolytic conductor, 19: 23200
effects on kinetics of susceptibility of low-pressure gases, (T), 20: 25977
effects on laminar and turbulent MHD free jet, perturbation solution for, (T), 20: 6175
effects on light propagation, 17: 16974
effects on magnetic surfaces in Etude Stellarator, 18: 17178
effects on magnetic properties of irradiated iron, 18: 39994 (EURAEC-1157)
effects on magnetohydrodynamic turbulence in presence of Hall effect, (T), 20: 19634
effects on man, 16: 12848
effects on man, 17: 28
effects on matter, 18: 44315
effects on mercury column falling under gravity, 16: 4610(R) (TID-14435)
effects on MHD shock wave propagation, radiative energy flux from, (T), 20: 21788
effects on microwave electric conductivity of semiconductors, (T), 19: 8014(T) (UCRL-Trans-1089(L))
effects on microwave-plasma interactions, perturbation theory for, (T), 19: 10415
effects on microwave absorption by superconducting aluminum, (E), 19: 14450
effects on microwave absorption by superconducting aluminum, (E), 19: 14456
effects on microwave surface impedance of superconducting aluminum, (E), 19: 14457
effects on mitotic division of cells in tissue culture, 18: 19495(T) (UCRL-Trans-1027(L))
effects on Neidigh pressure gradient arcs, 16: 9515 (ORO-500(p.25-39))
effects on neutralized ion beams, electrostatic wave dispersion relations for, (T), 20: 9845
effects on neutrons, (T), 20: 30734(R) (TID-22970, pp 1-63)
effects on noise fluctuations in electron beams, (T), 20: 17505
effects on nonuniform solar wind velocity on interplanetary (T), 19: 2957
effects on nuclear resonance absorption of gamma rays, 16: 15618(R) (ARF-1166-15)
effects on nuclear quadrupole relaxation time, 18: 17814
effects on nuclear spin-lattice relaxation, (T), 19: 39880
effects on nuclei in samarium compounds, temperature dependence of, 20: 2520(R) (IA-920)
effects on complex permeability and conductivity of metals, 19: 22998 (UCRL-11251)
effects on optical properties of color centers, (T), 19: 10670 (COO-1198-223)
effects on parallel fluid flow, (T), 20: 39943

effects on parameters of h-f discharge plasmas, (E), 20: 20087
effects on particle stopping power of plasmas, 17: 19493
effects on particle beam radius in synchrocyclotrons, measurement of, 17: 42025
effects on performance of hydrogen thyratrons, 20: 35966 (SLAC-PUB-193)
effects on photon frequencies, 16: 29682
effects on Pippard superconductors, gauge-invariant nonlocal theory for, 20: 19740
effects on plant germination and seedling development, 20: 18388
effects on plasma in krypton discharge, 17: 5460
effects on plasma containment in theta pinch, hexapole, 17: 26712
effects on plasma decay, 17: 42132
effects on plasma macroscopic stability, 18: 16773
effects on plasma wave collision damping, (T), 19: 8524
effects on plasma heat transfer, 19: 17141
effects on plasma flow, (E), 19: 41936
effects on polarization of radiation from electron-helium collisions, (E), 19: 6646
effects on positive column of low-pressure arc discharges in mercury, 18: 17142
effects on positive column of hot-cathode mercury discharge, (E), 20: 44917
effects on pressure in cylinder-symmetric electric arc column, 18: 7822
effects on propagation of UHF telemetry signals through ionized medium, 16: 10660 (AFCRL-337)
effects on properties of superconducting films, (T), 20: 9937
effects on radio-wave transmission through plasma sheath, (T), 20: 42426
effects on radioinduced luminescence of diamonds, 19: 7569
effects on radioinduced polymerization of formaldehyde at −196°C, 19: 9180
effects on radioinduced chromosomal aberrations, 20: 10672
effects on radioinduced defects in iron, 20: 37288
effects on rare earth electric conductivity, (E/T), 20: 4476(R) (IS-1200(Sect.P))
effects on resistors for inverter applications, 19: 40845(R) (N64-33676)
effects on resonances of surface waves propagating along cylindrical plasma column, (T), 20: 13941
effects on rotating fluids, 17: 32874
effects on rotation of electric arc in annular gap (E/T), 19: 1699 (ARC-CP-743)
effects on saturation electron current of electrostatic probes, (E), 19: 14695
effects on scintillation counter operation, 20: 5736 (NP-15597)
effects on separation of laminar boundary layer from surface of circular cylinder, 19: 18595
effects on separation of MHD boundary layers, (E/T), 19: 32788(T) (FTD-TT-65-27)
effects on shielding properties of superconducting surface sheaths, (E), 20: 42127
effects on shock propagation in conical tubes, 17: 36519
effects on shock wave propagation in ionized gases, 16: 11064 (AD-259452)
effects on shock wave dissipation, damping, 18: 7387
effects on shock wave structure in helium, 18: 19224
effects on shock-produced argon plasma, double probe technique, 18: 19242
effects on shock-wave heating of solar corona, (T), 19: 23252
effects on single crystals of terbium, 20: 9528
effects on small pulsed dipole-induced oscillations in collisionless plasma, (T), 20: 6498
effects on small-amplitude wave propagation in hot plasma, (T), 20: 6500
effects on solar corona, (T), 19: 41241
effects on solar proton intensity and energy, 17: 12942
effects on spark chamber performance, 17: 23714
effects on spark mixing in spark chambers, (E), 20: 7371(T) (BNL-tr-17)
effects on specific heats of spin systems, 19: 1172
effects on spectral lines from shock-ionized gases, 18: 30908
effects on spin orientation of spin-½ particles with pseudoscalar charge density, 18: 20946
effects on spinning superconductor, supporting (E/T), 19: 3175 (NASA-CR-108)
effects on stability of laminar and turbulent fluid flow, 18: 10246
effects on stability of Couette flow between rotating cylinders, 18: 20191
effects on stability of fluid flow down inclined plane, 19: 18117 (NP-14816)
effects on stability of channel flows, (T), 19: 18577
effects on stability of dilute gases, (T), 20: 2573
effects on stability of electrically conducting liquid layer, 20: 2820 (AD-614645)
effects on Stark broadening of Balmer lines in hydrogen plasma, (E), 20: 10208
effects on stationary corona discharge, 18: 28164
effects on sub-Alfvenic flow in ducts, (T), 20: 24182 (JPL-TR-32-871)
effects on superconductors, 17: 8959
effects on superconductor energy gap, 17: 9035
effects on superconductor energy gaps at finite temperatures, 18: 7650
effects on superconductor energy gaps and thermal conductivity, 18: 22838
effects on superconding rod with anchored filament structure, 18: 24552
effects on superconductor electrodynamics, nonlinear, 18: 34721
effects on superconducting films, theory of, 18: 38024
effects on superconductors (T), 19: 1480 (NP-14406)
effects on superconductivity of ferromagnetic materials, theory of, 19: 10209
effects on superconductivity of thin films, 19: 14449
effects on superconductors, (E), 19: 31175
effects on superconducting spheres, force calculations for, (T), 20: 26023 (JPL-TR-32-806)
effects on superconducting transitions and low temperature cooling by adiabatic demagnetization, 20: 28174
effects on superconducting spheres, suspending, (E), 20: 19728
effects on surface wave in a conducting liquid, 16: 23184
effects on surface superconductivity, (T), 20: 11891 (COO-264-224)
effects on surface wave propagation along annular mercury plasma column, (E), 20: 30574
effects on temperature in type II superconductors, (E), 19: 5105
effects on the light characteristics of a pulsed discharge in argon, 17: 7486
effects on thermal conductivity of superconductors, 18: 30679
effects on thermal instability of spherical gases, (T), 20: 15876 (IPP-6/33)
effects on thermal convection in conducting fluid, 20: 39939
effects on thermionic power generation, 16: 9307
effects on thermionic converter performance, (E/T), 19: 23349
effects on thermocouple voltages, 17: 30828
effects on thermodynamic equilibria and rate processes, 19: 7358 (MATT-235)
effects on thin-film superconductors, theories of, 17: 22343
effects on thin films, parallel and perpendicular anisotropy, (T), 20: 28604 (IFA-FT-57)
effects on thin superconducting films, 18: 34682(R) (NBS-8407)
effects on thin-film superconductors, 19: 31331(R) (NBS-8797)
effects on transport properties of gaseous diatomic molecules, 20: 7118
effects on travelling-wave plasma jets, Lorentz forces in, (T), 20: 10183
effects on trypsin, spectra of, 18: 27203
effects on turbulence propagation in conducting gas, 17: 36531
effects on turbulent mercury flow at various Reynolds numbers, 19: 26509
effects on two-dimensional conducting fluid flow, 17: 20185
effects on type-I superconductors in, mechanical forces, (E), 20: 42134
effects on type-II superconductors, eddy currents from, 20: 30262
effects on type-II superconductors in superconducting sheath state, (E/T), 20: 42125
effects on ultrasonic attenuation in metals, 17: 36487
effects on ultrasonic attenuation in superconducting niobium, (E), 19: 10192
effects on ultrasonic wave propagation in niobium–zirconium alloys, 20: 863
effects on ultrasonic attenuation by superconductors, (E/T), 20: 30735(R) (TID-22970, pp 331-73)
effects on velocity distribution in turbulent liquid flow, (E), 19: 23176
effects on wave propagation in rarefied plasma, (T), 20: 42489
effects on x-irradiated barley seeds, 20: 18387
Einstein-Maxwell equations for dipole, exact solution of, 20: 15155
electric arc motion in, 18: 1119 (ARL-63-151(p.478-94))
electric arc motion in transverse, 18: 1120 (ARL-63-151(p.495-541))
electric beam motion in, cyclotron and plasma wave interactions in two-stream, (E/T), 19: 12660
electric breakdown in crossed electric and, 18: 20153
electric charge motion in nonhomogeneous static, nonadiabatic approximation for, 20: 27661
electric conductivity of nonhomogeneous plasma in, (T), 20: 41768
electric discharge breakdown in, with perpendicular electric field, 17: 6821
electric discharge in, helical instability in positive-column, 17: 17352
electric discharge stabilization in, hot-cathode partially ionized-gas, 17: 29406
electric discharge in plasma in strong, resonance phenomena of cyclotron radiation from, 17: 38385
electric discharge in crossed electric and, plasma rotation in, 18: 21501
electric discharge propagation in crossed electric and, gaseous, 18: 40062
electric discharge in transverse, breakdown in h-f electrodeless, (T), 19: 11833

electric discharge in argon flow in, (E), 20: 41770
electric drift current in ionized low-density gases in axially symmetric, 17: 25922
electric-arc stability in minimum-B, (E), 19: 10428
electric, thermal, and thermoelectric transport in, quantum theory of, 19: 6413
electromagnetic conversion processes at high energies in, (T), 20: 44061
electromagnetic fields of moving dipole, (T), 19: 31114
electromagnetic interactions in uniform static, 16: 23175 (AD-269379)
electromagnetic wave guiding by, in plasma, 17: 9709
electromagnetic wave propagation in plasma in alternating, 17: 22286(T) (JPRS-18823(p.159-74))
electromagnetic wave propagation through plasma slabs in, 17: 33218
electromagnetic wave propagation in plasma in, nonlinear, 18: 6316
electromagnetic wave propagation by plasma in, 18: 6371
electromagnetic wave interactions with ionizing shock waves in d-c, 18: 26125
electromagnetic wave propagation in plasma in strong, 18: 26784
electromagnetic wave propagation in metals in, 18: 28160
electromagnetic wave propagation in bismuth plates in, 18: 28161
electromagnetic wave absorption in electron-phonon systems in, relaxation in, 18: 28178
electromagnetic wave interactions with plasma layer in static, 18: 28803
electromagnetic wave interactions with plasma layer in static, 18: 28804
electromagnetic wave propagation through inhomogeneous plasma in (T), 19: 1795
electromagnetic wave absorption and emission by charged particles in, (T), 19: 12332
electromagnetic wave propagation in plasma in, cyclotron resonance harmonics for, (T), 20: 8237
electromagnetic wave reflection and refraction by plasma in, plane, (T), 20: 17915
electron acceleration in longitudinal, by plane electromagnetic wave propagation, (T), 20: 21485
electron and ion beams in, natural coordinate system for studying, 20: 938 (SLAC-46)
electron attenuation in, quantum and classical theory of radiative, 18: 6041
electron beam compression by, 18: 7348
electron beam diocotron instability in crossed electric and, (T), 20: 3252 (NP-15578)
electron beam focalization using magnetic shell around accelerating cavity, 18: 8964
electron beam focusing in symmetric growing, vertical, 18: 20704
electron beam focusing by axial, transverse wave propagation in, (E/T), 19: 11844
electron beam focusing by axially symmetric, (T), 19: 37412
electron beam focusing by, self-consistent problem in, (T), 20: 27650 (NP-16013)
electron beam focusing and stability in periodic, (T), 20: 27663
electron beam focusing in, outer electron trajectories in, 20: 41551
electron beam focusing in, outer electron trajectories in, 20: 41552
electron beam interactions with plasma in, modes of instability excited by, 17: 42104
electron beam interactions with plasma in, instabilities from, 17: 42112
electron beam interactions with plasma in azimuthally varying, wave propagation in, 18: 1141
electron beam interactions with plasma in, (E/T), 19: 6758
electron beam motion in perturbed, in betatrons, 18: 24256
electron beam nonadiabatic trapping in toroidal, (T), 20: 28497(R) (TID-22956, pp 55-147)
electron beam perturbations in, 17: 3587
electron beam quantum depolarization in storage ring, high-energy, (T), 20: 17689 (NP-15783)
electron beam reflection by high-frequency, 16: 2323
electron beam stability in periodic, (T), 19: 4780
electron beam stability in periodic and uniform, (E/T), 19: 14184
electron beam trajectories in, 16: 32280 (ORO-538)
electron beam trajectories in, method for calculation of, 20: 27668
electron beam transmission in crossed electric and, cyclotron wave and noise propagation in, (T), 19: 6401
electron containment in cusped, adiabatic region in, 18: 28891
electron Coulomb interactions in, 17: 11538
electron cyclotron radiation emission in, absorption coefficient and intensity of, 17: 26303
electron cyclotron harmonics in nonrelativistic plasma in, (T), 19: 47749
electron density and energy in helium afterglow plasma in toroidal, (E/T), 20: 30710
electron depolarization in, relativistic, 17: 41840
electron depolarization in constant, relativistic, 19: 27217
electron detachment from 20-Mev deuterium ions by, probability of, 17: 36499
electron diffraction at flux lines of, (T), 20: 34833
electron diffusion in plasma in, coefficients for, (E), 19: 19233 (GA-6106)
electron diffusion in crossed electric and, (T), 19: 43439
electron drag by traveling, in plasma, (E/T), 19: 27680
electron focusing in accelerating, (T), 20: 11399 (UCRL-7566(Rev.1))
electron gas in, ground state of, 20: 921
electron gas instability in, quantum helicon dispersion relation for, 18: 42188
electron gas transport properties in, (T), 20: 40183
electron injection into plasma in strong, 18: 32937
electron interactions with electromagnetic waves in, analysis of, 18: 28396
electron loss mechanism in, 17: 12903
electron loss mechanism in, with mirror geometry, 19: 44823
electron magnetic moment in strong, conducting, (T), 19: 11850
electron magnetic susceptibility in uniform, 20: 41635
electron mobility in, (T), 19: 18588
electron motion in, quantum fluctuation effects on, 16: 9385
electron motion in modulated, 17: 36505
electron motion in helical, 17: 42137
electron motion in, polarization of radiation from, 18: 18736
electron motion in crossed electric and magnetic, 18: 40077
electron motion in crossed electric and spatially modulated, (E/T), 19: 6765
electron motion in, quantum operators for, (T), 19: 10133
electron motion in, (T), 19: 11828 (NP-14645)
electron motion in, effects of synchrotron emission on spin orientation in, (T), 19: 12244
electron motion in constant homogeneous, relativistic oriented-spin, (T), 19: 14152
electron motion in constant homogeneous, polarized, (T), 19: 14153
electron motion in nonuniform, equations for, (T), 19: 16684
electron motion in, diochotron and negative mass instabilities in, 19: 41180
electron motion in Faraday-cup, secondary, (E), 20: 13382
electron motion in uniform, self-consistent hydrodynamic approximation for relativistic, 20: 22287
electron motion on flux surfaces of, in hard-core and stabilized pinch discharges, 17: 42097
electron motions in, Bloch, 16: 24318
electron orbits in focusing, 19: 47186
electron oscillations in nonuniform plasma in, longitudinal, 18: 9523
electron oscillations in, random-phase approximation for self-consistent field of (T), 19: 3394 (AD-602039)
electron pair single-photon annihilation in, spin orientation effects on polarized, (T), 20: 25852
electron polarization in inhomogeneous, 18: 28409
electron quantum gas oscillations in uniform, (T), 19: 19291
electron radiative polarization in, (T), 20: 15638
electron relativistic motion in external, (T), 20: 15640
electron resonance motion in helical, 19: 33102
electron scattering by, in impenetrable torus, 17: 29588
electron scattering by shielded, Aharonov-Bohm effect in, (T), 19: 27315
electron scattering by, Aharonov-Bohm effect for bound states in, (T), 19: 27316
electron temperature distributions in plasma in, 18: 21468
electron trajectories in crossed electric and space-modulated, 17: 39802
electron trajectories in static, calculation of nearly circular, (T), 19: 29112(R) (AD-611161(App.I))
electron trajectories in focused, pressure effects on lifetime of, (E/T), 20: 21482
electron transfer and thermal flow in, quantum theory of, 18: 18783
electron translation in, Bloch, 18: 24504
electron translation in, irreducible representations for Bloch, 18: 24505
electron transport in, kinetic coefficients, 16: 6808(R) (ORNL-3213 (p.9-10))
electron transport mechanisms across, below 10^{-9} mm mercury, 16: 22760
electron transport in media in, quantum theory of, 18: 44639
electron transport in, quantum theory of, 19: 8318
electron transport in, equations for, 19: 47799
electron transport properties in, 20: 37866
electron trapping in bumpy toroidal, 18: 2985(R) (UCRL-10852)
electron velocity distribution in slightly ionized gas in crossed electric and, 17: 18960
electron velocity distribution in argon in, (E/T), 19: 37214
electron wave propagation in plasma in, collision effects on, 18: 7818
electron-beam focusing by, 20: 7665
electron-beam stability and wave amplification in spatially periodic, (T), 19: 33437
electron-optical properties of two-dimensional electric and, 18: 14185
elementary particle motion in, equations for, 18: 12904 (JINR-P-1491)
elementary particle polarization in, equations for, 19: 25294

energy and inductance in two-dimensional, stored, 20: 37315 (BNL-10323)
energy balance of cylindrically symmetric hydrogen arc in, 19: 25596
energy dissipation in solar atmosphere, 18: 44409
energy dissipation from solar, flare production in, 18: 44413
energy dissipation to charged particles near zero field lines in plasma, (T), 20: 30676
energy in, hamiltonians for, 20: 25646
energy of, transformation from plasma energy by standing magnetohydrodynamic waves, 18: 7830
energy storage and dissipation in solar, 18: 44410
energy storage systems for, design of inductive, (T), 19: 33411(R) (LA-3320(p.45-9))
energy transfer from moving bodies to, 16: 13724
equation of magnetic surfaces in, solution by perturbation method, 20: 44028 (IAE-1150)
equilibrium of parallel lines of, particle orbits in, 19: 41208 (ORNL-3827)
evaluation of helical-resonant, for trapping electron beams, 16: 4610(R) (TID-14435)
evidence for galactic, 18: 28202
evidence for interplanetary, from solar-particle propagation effects, 16: 18302
evolution of solar, (T), 20: 15223
example of toroidal, destitute of magnetic surfaces, 16: 23185
excitation in cylinder with coaxial shield, by electric pulse, (T), 20: 21456
excitation in motion of highly conducting fluid, self-, (T), 19: 4764
existence in solar prominences, 17: 13285(T)
existence of galactic (M82), 18: 20718
expansion about uniform axial, for closed-line average minimum-B configuration, 20: 42455
Fermi gas thermal conductivity in quantizing, 18: 42483
ferromagnetic spin system response to, quantum theory for, 18: 22786 (NP-13893)
filamentary structure of force-free, 16: 29500
flow in constant, momentum integral approximation for compressible magnetogasdynamic boundary-layer, 17: 28010
flow in, Malkus theory of turbulent channel, 20: 38240
flow of ionized gas through, for power generation, 16: 31701
flow of mercury in transverse, hydraulics of, (E), 20: 41774
flow past nonconducting flat plate in transverse, 16: 25913 (NP-11892)
fluctuations in high-current toroidal discharges, 17: 42090
fluctuations in undisturbed photosphere, 19: 41221
fluctuations in, determination from curvature of 13.8-Bev/c proton tracks in photographic emulsion, 18: 30538
fluid flow boundary layers in crossed, 20: 37869
fluid flow in aligned, compressible conducting inviscid, 18: 10241
fluid flow in axial, laminar, (T), 19: 26940
fluid flow in, circulation and vorticity in compressible viscous, 16: 8891
fluid flow in presence of, 18: 32294
fluid flow in transverse, oscillation in conducting incompressible, 17: 20187
fluid flow in transverse, hydromagnetic stability of Couette, 18: 34317
fluid flow in transverse, heat transfer in, 18: 34359
fluid flow in transverse, turbulent, (T), 19: 6396
fluid flow in, laminar compressible boundary layers in, 19: 20122
fluid flow in, magnetic energy production and dissipation in, 18: 34327
fluid flow in, oscillations of conducting, 18: 43764
fluid flow in, theory of channel, 18: 26718
fluid flow past insulated plate in, viscous conducting, 18: 34316
fluid flow past porous flat plate under transverse, (T), 20: 39929
fluid stability in horizontal, viscous electrically conducting, 17: 34587
fluid stability in, transfer-function method for determining, 20: 24196
fluid stability in, variational methods for Rayleigh-Taylor, (T), 20: 30172
fluid velocity in parallel, instability of surface of discontinuity of, 17: 28013
flux amplification of, development of multi-stage explosive, 17: 41537 (ASD-TDR-63-38)
flux compression by explosives, review of, 20: 3166 (LA-DC-7252)
flux compression by cylindrical liners, (T), 20: 17157 (EUR-2620.i)
flux compression in hard superconductors, 18: 28509
flux compression in, cylindrical explosive systems for, 20: 4477 (LA-DC-7289)
flux configuration of interplanetary, 19: 25212
flux conservation by superconducting thin film rings, 18: 34698
flux density in contained plasma, Ohm's law for, 18: 40693
flux density of solar, (T), 20: 4524
flux explosion of by eddies, (T), 20: 39567
flux flow in type-II superconductors, viscous drag coefficient in, (T), 19: 8357
flux flow resistance in type-II superconductors, (T), 19: 35338
flux intensifications in plasma, 19: 37934 (N64-33632)
flux line motion in superconductors, quantized, (T), 19: 8352
flux line motion in type-II superconductors, dissipative mechanism in, (E/T), 19: 8355
flux line motion in mixed state of type-II superconductors, (T), 20: 26040(T)
flux lines in type-II superconductors, motion of quantized, (T), 20: 24281
flux loss in theta pinch, antiparallel bias, 20: 36304
flux movement through bulk superconductors, energy losses from, (E), 19: 6618
flux penetration in superconductors, (T), 19: 39712
flux penetration in thin-walled superconducting cylinders, (T), 20: 24265 (N-65-15147)
flux pinning in superconductors, quantized, 18: 32698
flux quantization in superconductors, quasiparticle transformation for, 18: 6116
flux quantization in superconducting cylinders, (T), 19: 10205
flux quantization in superconductors, 19: 12444
flux quantization in superconducting rings with Josephson tunneling, (E), 19: 23592
flux quantization in superconducting cylinders, (T), 20: 4784
flux, theory of quantized, 16: 5781 (UCRL-6630-T(Rev.))
flux transport by shock-produced plasma, 18: 35007
flux trapping and compression in superconductors, (E), 19: 6605
flux trapping by superconducting toroids, 16: 19535
flux trapping in superconducting ring, time-reversal invariance in, 16: 12210(R) (ANL-6488)
flux trapping in, effects on r-f losses in superconductors, 20: 40042
flux trapping with adiabatically invariant quantum numbers by superconductors, temperature variation of, 18: 15058
flux variations in conducting fluid flow, lines-of-force compression, 20: 21790
flux variations in, of sunspots and faculae, 20: 39561(T)
focusing properties of homogeneous sector, in spectrograph, 16: 19137
focusing properties of homogeneous, with straight-line boundary, 17: 5157
focusing properties of long lenses with zero field at source, 17: 24244
focusing properties of long lenses with nonzero field at source, 17: 24145
focusing properties of rotational, 17: 36506
focusing properties for charged-particle beams, 18: 2403(R) (PR-P-58)
focusing properties of sextupole, for neutral particles, 18: 34369 (JINR-P-1681)
focusing properties of alternating, (T), 19: 37411
focusing properties of inhomogeneous, for mass separators, 20: 19163
focusing properties of azimuthally invariant vector-type, 20: 27392 (ORNL-TM-1475)
force effects of high-frequency, on plasma, 19: 1742
force line distribution in, 16: 26402 (JINR-P-929)
force lines of, from vortex currents flowing over surface of torus, 17: 29679
force-free, determination of, from value for field strength, 19: 1746
forces exerted on plasma, 16: 23182
formation in symmetrical magnet gap, 16: 10670 (JINR-P-836)
free nuclear induction in, effects of reaction of receiving circuit, 16: 27752(T) (JPRS-14515(p.220-45))
frequency stabilization circuit for, automatic tuning of, 19: 36776
galactic, cosmic radiation and radio emissivity in open model of, 16: 15482
gamma intensity modulation by, 17: 15087 (TID-17670)
gas discharge in transverse, ion motion in, 18: 21488
gas flow in transverse, profile correction for sustaining, (T), 20: 4716
gas flow in tranverse, by piston movement, 19: 34799
gas flow in, partially ionized, 18: 43763
gas flow in, theory of, 18: 35035
gas flow in, transverse momentum transport in viscous diatomic, (E), 20: 28073
gas flow into homogeneous, end effects on compressed, (T), 19: 36624
gas flow stability in, Rayleigh-Taylor, 18: 18478
gas rotation in, stability of, 18: 18480
gas rotation in, stability of rarefied gravitational, (T), 19: 11847
gas stability in, ionized (T), 19: 2912
gaseous discharge stability in, without longitudinal current, 17: 42071
gradients in quadrupole and hexapole, oscillating coil measurements of, 18: 42164 (UJV-944/63)
gravitation properties of axisymmetric, 19: 41544
gravity waves in conducting fluid in, 17: 5476
gravity waves in horizontal, effects of electric conductivity on, 19: 23850
growth in turbulent conducting fluid, 17: 25912
Hall coefficient measurement in a-c, method for, 19: 2891 (PAN-518/II)
Hall effect in inhomogeneous, normal component of, 17: 25871(T) (AEC-tr-5827)
heat exchange in transverse homogeneous, 19: 44202
heat transfer effects, 17: 29073 (TID-17162)
heat transfer from plasma flows in, 18: .1121 (ARL-63-151(p.542-56))

heat transfer in metals in strong, (T), 19: 16179
heating effects in theta pinch, 16: 24886 (CLM-R-19)
helium-3 superfluidity in, destruction of, (T), 19: 23586
homogeneity in axially symmetric improvement of, (E/T), 19: 10392(R) (MATT-Q-21)
hydrogen-ion injection at 100 kv into, by crossed electric fields, 16: 23188
hydrogen ionization in, by Lorentz force, (E), 19: 33467
hydromagnetic flow in transverse, 16: 21117 (AD-269326)
hydromagnetic wave propagation through ionized gas in, 17: 7472
hydromagnetic wave propagation in inhomogeneous, linear approximation for, 17: 27995
hydromagnetic wave propagation in, inhomogeneous Alfvén, 18: 20651
hydromagnetic wave propagation in dipole, Alfven, 18: 28483
hydromagnetic wave propagation in inhomogeneous, in nonviscous perfectly conducting fluid, 18: 30893 (PAN-501/VII)
hydromagnetic wave propagation in rarefied plasma in strong, Alfvén, (T), 20: 26318
hydromagnetic wave propagation along, in cold, collision-free plasma, (T), 20: 28538
hydromagnetic wave propagation in transverse, 20: 44941
ideal polar surfaces required for weak or strong focusing in nuclear apparatus, 17: 28350
image characteristics of sector for ion beams, 16: 29068(T) (AEC-tr-5279)
in hollow explosive-driven cylindrical conductor, (T), 19: 47120 (UCRL-14349)
index, determination by potential network method, 16: 14105 (IFA-M-24)
index determination, accuracy of equipotential method, 16: 14106 (IFA-M-25)
index of d-c, instrument for measuring, 20: 21006
induction in cylinder with rotating internal field, 18: 28162
induction in superconducting cylinders by rotation, 20: 13690
induction lines in radially symmetric, 17: 20540 (CEA-2254)
inhomogeneities in, detection with charged particles, (T), 20: 44038
intensity along axes of circular cylindrical coils, 16: 15268 (NASA-TN-D-1013)
intensity and polarities of sunspots during IGY, 20: 2563
intensity in cosmic radio sources, (T), 19: 14281
intensity in ionospheric sporadic-E layers, correlation with electron density, (T), 20: 44468
intensity in solar corona, estimation from radio burst measurements, 20: 19355
intensity of interplanetary, solar flare effects on, (E), 20: 4527
intensity of pulsed, in multiturn coils, (E/T), 19: 6398
intensity of, ferromagnetic resonance method for measurement of, 18: 14193(P)
intensity reduction in expandable superconducting enclosure, 19: 39742
intensity variations of, in Compton Spectrometer, design of control system for, 17: 6438 (TID-15530)
intensity variations in sun spot groups, (T), 20: 39559
interaction of oscillating, with Couette fluid flow, 18: 36085
interaction of shock waves with, 17: 5459
interaction of solar wind with solar, (T), 20: 37349
interaction of solar wind with sun's, (T), 20: 39573
interaction with plasma in cavity resonator, 17: 9750
interaction with shock-produced moving plasma, 16: 3769 (WADD-TR-60-836)
interactions in chromosphere, review on, 18: 14712
interactions of barrier, with neutralized electron–ion beams, 18: 19237
interactions of dipole, with supersonic plasma stream, 18: 15407
interactions of dipole, with moving plasma, (E), 19: 5338
interactions of dipole, with neutral ion streams, (T), 19: 6381 (AFCRL-63-723)
interactions of dipole, with neutral plasma streams, (T), 19: 8550
interactions of dipole, with streaming plasma, (T), 19: 43438
interactions of dipole, with plasma, (E), 20: 17551
interactions of external, with plasma clusters, 18: 1163
interactions of galactic, with solar wind, theoretical study of interface in, 18: 19246
interactions of high, with electronic and nuclear magnetic moments in solids, 16: 15448
interactions of interplanetary, with solar wind (T), 19: 2950
interactions of inhomogeneous, with plasma streams, (E/T), 19: 5333
interactions of interplanetary, with comet tails and solar wind, (T), 19: 23235 (SC-RR-64-967)
interactions of interplanetary, with plasma flux, 19: 37435
interactions of Ioffe, with plasma, 18: 40658 (IPPJ-26)
interactions of multipole, with hydrogen plasma, (T), 19: 27052
interactions of spatial-periodic, with plasma, 16: 28304
interactions of space-periodic, with plasmoids (T), 19: 3443
interactions of spatially modulated, with plasmoids, (T), 19: 41901
interactions of transverse, with fluid in couette flow, 17: 17339 (R63SD16)
interactions of transverse, with plasma, energy spectra of, 19: 3423
interactions of very high pulsed fields with conductors, dynamic and skin effects, 16: 15414
interactions with gamma radiation, Zeeman line splitting by r-f, 16: 5887
interactions with moving plasma, 16: 29955
interactions with charged particles in plasma, 16: 32508
interactions with shock-heated air plasma, 17: 7491
interactions with superconductors, 17: 6784 (CERN-62-30)
interactions with free-surface waves on liquid metals, 17: 16784 (NASA-TR-R-161)
interactions with high-density plasmoids, 17: 35037
interactions with moving plasma clusters, 18: 6376
interactions with charged particles, microwave amplification by, 18: 18454 (NP-13778)
interactions with channel-constrained magnetoplasma flow, 18: 19241
interactions with plasma sources, interface geometry in, 18: 19246
interactions with expanding plasma cylinder, 18: 21427
interactions with plasma in parametric MHD generator, effects of, 18: 22711 (RTD-TDR-63-4132)
interactions with plasma, review on, 18: 24746 (ARL-64-34)
interactions with flowing plasma, 18: 36704(R) (AD-434097)
interactions with a-c traveling wave plasma, 19: 12721
interactions with high-density hydrogen plasmas, (E), 19: 19286
interactions with plasma bunches, research on, 19: 39955 (IAE-663)
interactions with turbulence in conducting fluid, (T), 19: 42943
interactions with ionized gas flow, self-excitation in, 19: 44839
interactions with solar wind, 20: 4529
interactions with plasma of infinite conductivity, (T), 20: 6444 (AD-617553)
interactions with moving conducting rings, induced voltage from, (E/T), 20: 8202
interactions with electrons, phonon production in, (E/T), 20: 13925(R) (TID-22419, pp 99-147)
interactions with shock waves, 20: 15882(R) (NP-15868)
interactions with conducting fluid flow, effect of busbars on, (T), 20: 25964
interactions with fast plasmoids, (E), 20: 28551
interactions with argon electric arcs, emission coefficient of atomic spectral line from, 20: 36084 (AD-631672)
interactions with conducting fluids, MHD properties of, (T), 20: 37867
interactions with plasma, particle trajectories in, (T), 20: 40283
interactions with plasma cooled by solid walls, (T), 20: 44905
interactions with plasmoids, properties of acute-angled, 20: 44975
interactions with plasma, h-f, (T), 20: 30624
interplanetary and solar, evolution of, 19: 23537
interplanetary, effects of, on comet tails, 17: 36556
interplanetary, cosmic-ray determination of, 18: 24330
interplanetary, connection of geomagnetic tail lines to, 20: 39986
interplanetary, effects on magnetosphere, 18: 22811
introduction into type-II superconducting cylinders, (E/T), 19: 41612
ion beam focusing by, effects of fringing on, 18: 14695
ion beam focusing by azimuthally invariant, 20: 7477
ion beam focusing by linear stationary, peculiarities in, 20: 46258 (NP-16312)
ion beam focusing in current-carrying ring, 20: 42512
ion beam motion in, space charge effects in, 18: 30633
ion beam neutralization by electron injection in, 18: 24301(T) (FTD-TT-64-176)
ion beam space charge compensation by electrons in, 18: 44307
ion motion in three-dimensional, focusing effects on, 18: 2492
ion optics in rotational symmetry, 18: 22790
ion optics of combined radial electric fields and inhomogeneous, 17: 36419 (NP-13020(p.265-70))
ion orbit stability in eccentric, (T), 20: 19306 (ZfK-PhA-2)
ion rotation in, spectral splitting due to, (T), 20: 44967
ion trapping in, device design and method for, 16: 14195(P)
ionization diffusion in dipole, equation for ambipolar, 17: 24113
light propagation in homogeneous, theory of, 18: 28433
limits of, in hard superconductors at low temperatures, 17: 3635
line-of-force reconnection for geo- and interplanetary, mechanism for, 20: 32277
lines of force, 16: 28267
liquid flow in, visco-elastic electrically conducting, 17: 24164
liquid rotation in uniform transverse, conducting, (T), 19: 23198
loss in charged-particle accelerators, device for measuring index of, 20: 5959
magnetic dipole quantum containment by, 17: 25992
magnetic materials in two-dimensional, interface theorem for analysis of, 20: 46251 (BNL-10587)
magnetic moment invariance for low-frequency electrostatic instabilities, 18: 9453 (GA-4843)
magnetic moment of cylindrical tin superconductors in transverse,

18: 11105
magnetic potential of axially symmetric, (T), 19: 16271
magnetic surfaces in toroidal helical, 17: 29475
magnetization of iron, by step-increased magnetic fields, (T), 19: 25625(T) (AI-Trans-84)
magnetoacoustic wave excitation in plasma in, 18: 9483
magnetohydrodynamic stability in circular, 16: 27793
magnetohydrodynamic flow along wavy walls parallel to external, 17: 20641
magnetohydrodynamic waves in rotating liquids in presence of, 17: 20186
magnetohydrodynamic flow in, at low Reynolds number, 17: 23485
magnetohydrodynamic flow past body of revolution in uniform, singular perturbation method for, 17: 24169
magnetohydrodynamics in, harmonic-disturbance subjected, 17: 23487
magnetohydrodynamic flow past semi-infinite plate in, boundary layer for two dimensional, 17: 27554
magnetohydrodynamic flow past semi-infinite plate in, boundary layer for two-dimensional, 17: 27555
magnetohydrodynamic flow past semi-infinite plate in, pressure gradient effects on two-dimensional, 17: 27556
magnetohydrodynamic flow past rigid bodies in aligned, 18: 26126
magnetohydrodynamic flow in uniform, stagnation-point, 18: 34319
magnetohydrodynamic shock in interplanetary, 18: 34393
magnetohydrodynamic flows induced by, (E), 19: 8034
magnitude and orientation of solar, (E/T), 19: 12046
mapping axially symmetric, method for, 17: 22726(R) (SIT-P91)
measurement and correction of MURA accelerator, methods for, 18: 42227
measurement and production of strong, 18: 44315
measurement and regulation using Hall probes, 17: 8536 (TID-17610)
measurement and stabilization of, devices for, 19: 44352 (UJV-1339/65)
measurement and stabilization at 0.1G to 20KG, NMR system for, 20: 27241
measurement at nuclei of gold-197 dissolved in cobalt, iron, and nickel, 17: 24750(R) (UCRL-10624)
measurement by ferromagnetic resonance magnetometers, 20: 2104 (MATT-362)
measurement by nuclear magnetometer, accuracy of, 19: 28612(T) (FTD-TT-64-1104)
measurement, design of Hall-effect gaussmeter for, 16: 8898 (ASD-TR-61-273)
measurement, design and characteristics of instrument for, 17: 14634
measurement for planets and satellites, 17: 32879
measurement in a-c accelerators, design of electron tube for, 18: 16626
measurement in beam transport systems, semiautomatic system for, 20: 17192 (CONF-650922, pp 456-66)
measurement in bubble chambers using antiproton trajectories, 20: 35769
measurement in cyclotron acceleration gap, 17: 931
measurement in cyclotrons, automatic data logging and processing system for, 20: 17188 (CONF-650922, pp 415-20)
measurement in cyclotrons, using Hall effect, 20: 17189 (CONF-650922, pp 421-7)
measurement in electromagnetic shock tube using large area probes, 20: 10205
measurement in high-temperature plasma, Zeeman effect for distortions in, 17: 26719
measurement in inhomogeneous field separator project, 18: 27812(R) (ORNL-TM-415)
measurement in interplanetary space, 16: 30993
measurement in interstellar clouds, 17: 9157
measurement in isochronous cyclotron acceleration gap, 19: 12028
measurement in linear pinch devices, probes for, 20: 6507
measurement in Milky Way galaxy, 18: 2514
measurement in optical system of 5-Gev antiproton beam, (E), 19: 20723 (JINR-P-1945)
measurement in plasma, probe for, 17: 21986
measurement in plasma using Zeeman effect, 18: 19190
measurement in small space at low temperatures, probe for, 17: 18581
measurement in solar prominences, 18: 44348
measurement in space, U. S. program for, 18: 21090
measurement in spiral-ridge cyclotrons, 16: 17165
measurement in strong-focusing synchrotron, (E), 19: 30901
measurement in superconducting solenoids, probe for, 19: 9460
measurement in synchrotrons, induction apparatus for, 17: 30817
measurement in 7-Bev proton synchrotron, equipment for, 17: 909
measurement, literature survey of methods, 17: 14628
measurement methods up to 1000 kgauss, review, 16: 15402
measurement of ambient, using helium-3 quantum resonance magnetometer, 20: 642(P)
measurement of center plane and radial components of, in cyclotron, 19: 41195
measurement of changing, equipment for, 17: 939
measurement of Cosmotron, 20: 932 (BNL-9557)
measurement of critical, for bulk high-field superconductors, 20: 46514
measurement of, design of isofield chart tracer for, 16: 33253
measurement of, design of Hall probe assembly for, 17: 7350 (UCRL-10085)
measurement of earth, by magnetic resonance, 16: 27412(P)
measurement of force-free, in solar chromosphere, 18: 28221
measurement of galactic, direct method, 17: 15048
measurement of galactic, using Zeeman effect, 18: 4386
measurement of galactic, using Zeeman effect, 18: 4387
measurement of galactic, using Zeeman effect, 18: 4388
measurement of galatic, 19: 37449
measurement of gradients in, design of instrument for, 16: 33179
measurement of gradients in, design of super-regenerative circuit for, 16: 33177
measurement of gradient, using Hall effect, 20: 17194 (CONF-650922, pp 483-6)
measurement of harmonic content in beam transport systems, search coils for, 20: 17195 (CONF-650922, pp 487-96)
measurement of high pulsed, 17: 23604 (LNF-63/3)
measurement of high gradient time variant, digital system for, 20: 5682 (MURA-716)
measurement of indices of inhomogeneous, 19: 11480
measurement of inhomogeneous, using nuclear resonance, 19: 4440
measurement of inhomogeneous, effect of nuclear nutation in NMR, (E/T), 19: 26933
measurement of inhomogeneous, using nuclear resonance, (E/T), 19: 40851
measurement of inhomogeneous, using proton resonance, 19: 44353(T) (SLAC-Trans-22)
measurement of interstellar, from intensity relations of cosmic x rays and cosmic γ rays, 18: 9050
measurement of interplanetary, 18: 28225
measurement of interplanetary, 19: 43226
measurement of internal, in solids, 20: 40342
measurement of ionospheric, equipment for vlf, (E), 20: 6180 (AD-619250)
measurement of lunar, 18: 5959
measurement of multipole, (E/T), 20: 13365 (SLAC-39(Rev.))
measurement of MURA accelerator, equipment for, 18: 42228
measurement of nonlinear, in quadrupole electron lenses, 17: 38372
measurement of oscillating, properties of peaking strip probes for, 18: 29958
measurement of planetary and interplanetary, 19: 18658
measurement of, probe for, 16: 33593
measurement of pulsed alternating, 17: 930
measurement of quadrupole, method for, 20: 17190 (CONF-650922, pp 431-46)
measurement of rapidly pulsed, method for, 19: 44805 (CEA-R-2769)
measurement of rapidly varying megagauss, using Zeeman effect, 20: 27244
measurement of residual, using galvanometers and flip coils, 20: 20806(R) (MLM-1274)
measurement of solar, method for, 18: 44367(T)
measurement of solar, at flare positions, 18: 44385
measurement of solar, 20: 29910
measurement of strength of, by alignment of metastable helium atoms, 18: 12840(P)
measurement of strong d-c, single-pickup NMR, 18: 37478(T) (AEC-tr-6398(p.311-13))
measurement of superconductor, device for, 18: 30683
measurement of synchrotron, 17: 938
measurement of terrestrial, using nuclear-resonance filter, 18: 26458
measurement of time-varying, 17: 5425
measurement of time-varying, using Zeeman effect, (E), 19: 20257 (IPP-1/19)
measurement of transient, application of Faraday magneto-optical effect for diagnostic, 16: 4920
measurement of, using nuclear magnetic resonance, 17: 8562(P)
measurement of Venusian, by Mariner II, 17: 15051
measurement of Venusian, by Mariner II, 17: 15154
measurement of weak, by magnetic resonance, 16: 27411(P)
measurement of weak, using nuclear induction, 18: 4068(P)
measurement of weak inhomogeneous, NMR techniques for, 18: 37477(T) (AEC-tr-6398(p.306-10))
measurement of 0.01 to 20 G, instrument for, 20: 15160 (LNF-65/44)
measurement of, double-coil method for, (E), 19: 46731(T) (SLAC-Trans-21)
measurement of, equipment for, 20: 15882(R) (NP-15868)
measurement of, NMR device for, 20: 16770 (CONF-650922, pp 428-30)
measurement of, nuclear spin alignment by nutation in NMR, (E/T), 19: 26935
measurement of, performance of scanning and recording systems for, (E), 20: 2105 (UCRL-16357(Rev.))
measurement of, techniques for, (E), 20: 627 (UCRL-16357)

measurement of, use of NMR signals for, 19: 26938
measurement of, using gamma resonant absorption, 19: 38966(P)
measurement of, using NMR field probes, (E), 20: 2112
measurement of, using backscattering of beta particles, 20: 25370(P)
measurement, performance of Hall probes, 16: 328 (BNL-5750)
measurement techniques for multipole, in Stanford linac, 19: 34813 (SLAC-39)
measurement using EMR, 18: 22315 (SLAC-26)
measurement using Hall generators, 18: 41713 (JINR-P-1689)
measurement using superconductor quantizer, 18: 42552 (SEL-63-128)
measurement using flow probe, NMR-line width in, 19: 26934
measurement using NMR continuous-flow transducer, 20: 7351
measurement using Hall effect, 20: 17191 (CONF-650922, pp 447-55)
measurement using Hall effect, method of, 20: 17193 (CONF-650922, pp 472-5)
measurements by Mössbauer resonance of gamma rays, 16: 32000 (ARF-1166-22)
measurements for AERE spiral ridge cyclotron, 17: 7374
measurements for ORIC, 17: 7375
measurements for 48 synchrotron magnets, 16: 8247 (TID-13720)
measurements in orthogonal pinch device, 17: 9743
measurements, methods using coil and integrator, 16: 14104 (DESY-A2.84)
measurements of, for Berkeley cyclotron, 17: 7373
measurements of solar, review on, 19: 47208
measurements of, using Zeeman effect, 19: 3434
measurements on alternating and static, 17: 21981(T) (AERE-Trans-903)
measurements on interplanetary, 18: 42292
measurements using Hall generators, 16: 22332 (USNRDL-TR-559)
measurements with Explorer X, 17: 12985
meson (μ^+) and (π^+) decay in longitudinal, angular distributions for, 18: 36309
meson (μ) depolarization in weak, 16: 5892
meson (π) and proton curvature in, measurement of, 17: 18524 (CERN-63-3(p.211-19))
microwave emission from plasmas in, 18: 22963
microwave generation from 100-kev bunched electron beams in circular orbit in, (E), 19: 29111(R) (AD-611161)
microwave propagation in plasma with sheared, (T), 19: 8523
microwave propagation from bunched electron beams in circular orbits in, (T), 19: 29113(R) (AD-611161(App.II))
microwaves in cylindrical beam-plasma systems in longitudinal, (T), 20: 8227
model for interplanetary, 17: 37914
model for interplanetary, 18: 18598
model for quiet interplanetary, 20: 39575
model for studying, analog, 20: 17181 (CONF-650922, pp 126-40)
model of, in interplanetary space, 16: 32249 (AFCRL-62-225)
model of solar, (T), 19: 27047
models of interplanetary, 17: 12995
modulation combined with frequency in electron paramagnetic resonance spectrograph, 18: 25762
modulation of cosmic radiation intensity by interplanetary, 17: 12993
modulation of spinning search coil signal by time-variant, 17: 16389
motion in planetary radiation belts, mirror-point, 18: 42162(R) (TID-20963)
motion of conducting body in inhomogeneous, (T), 19: 37236
motion of gravitating cosmic gaseous masses in (T), 19: 1161
motion of plasma across, 16: 26414 (UCRL-6294)
movement, 16: 6840
neutron polarization direction change in rotating, 18: 11150
neutron yield effects in deuterium plasmas, 17: 9766
nuclear energy level mixing in external fields, interference phenomena in, 19: 45270 (JINR-P-2248)
nuclear polarization boundaries in, from nuclear relaxation dispersion, 19: 23786
observations of stellar and solar, (E/T), 20: 41616
optical properties for photons and particles, 16: 15478
optimization of, computer program for, 18: 10622 (CERN-64-3)
origin and theory of, 18: 7389
origin of interplanetary, solar, 18: 44359
origin of stellar, MGD theory for, 18: 22650(T) (JPRS-24435(p.274-304))
oscillation in orthogonal pinch discharge, 17: 9742
Overhauser effect in low, 17: 13192
paramagnetic spin-spin relaxation in strong, 18: 16046
parameters in air gap of electromagnet, 17: 15330
parameters of helical, equations for, 16: 6053
particle arrangement in lines-of-force pattern by, 18: 5848 (SC-TM-40-59(51))
particle dynamics in longitudinally varying, adiabatic approximation for, 17: 11795 (SLAC-4)
particle-focusing properties of cylindrically symmetric, 17: 10935
particle focusing by prolate spheroidal, superposed spheroidal, and uniform, 17: 20754
particle gyrations in mirror, 17: 9760
particle injection into mirror-cusp, high-energy neutral, (T), 20: 38277
particle interaction with low-frequency plasma oscillations in arbitrary constant, 17: 21177
particle motion in cusped, slightly non-adiabatic, 16: 23218
particle motion in, 17: 40171
particle motion in planetary-nebula, (T), 19: 23241
particle nonadiabatic scattering in, (T), 20: 28497(R) (TID-22956, pp 55-147)
particle orbit in stellarator, 16: 6054
particle precession in nonuniform, spinning, 18: 9239
particle trajectory in, recordings by spark chambers, 16: 374
particle trajectories in time-dependent, 16: 32463 (58-RL-2070)
particle trajectories in slowly varying, approximations for, 17: 28017
particle trajectories in rapidly varying, 18: 21449
penetration by electron-neutralized proton beams, transverse, 18: 19238
penetration depth in superconducting niobium, temperature dependence of, (E), 19: 14435(R) (NP-14676)
penetration depth in superconducting niobium, (E/T), 19: 39726
penetration in cylindrical conductors, calculation of skin effect, 20: 45827 (LA-3500)
penetration in plasma, skin effect in, 18: 24800
penetration in superconductors, noise propagation from, 17: 39746
penetration in type II superconductors, surface superconductivity breakdown from, (T), 20: 2900
penetration in Type-II superconducting plates, (E), 20: 42132
penetration into electron gases, (T), 20: 34339
penetration into plasma, finite ion gyro-radius effect on, 18: 44882
penetration into plasma with Hall effect, (T), 19: 21527
penetration into superconducting alloys, depth of, 18: 36436
penetration into superconducting indium disks, (E), 19: 33157
penetration into thin-walled metallic cylinder, 20: 23813
penetration of, into superconducting sphere, transient effects of, 17: 16816
penetration of mixed state phase boundary in superconducting type-II niobium–zirconium alloy, velocity of, (T), 20: 8011
penetration of pulsed longitudinal, into cylindrical shield, (T), 19: 32817
penetration of r-f, into plasma sheath, 18: 1143
penetration of solar photospheric, into interplanetary space, (E), 20: 15215
penetration of superconductors by, 18: 9262(R) (NP-13492)
penetration of superconducting indium, (E), 19: 23564
performance of crossed electrostatic–magnetic, for plasma acceleration, 18: 41599
performance of quadrupole, in mass separator, 16: 9106
perturbation of helical, compensation of, (E), 19: 41116 (IAE-668)
perturbations in MURA accelerator, effects and tolerances of, 18: 42226
perturbations in toroidal plasma-confining, 16: 32502 (GA-2925)
photon reactions with interstellar, Doppler shift from, 18: 24289
plasma acceleration by pulsed, 17: 9770
plasma acceleration by traveling, 17: 16771(R) (ASD-TDR-62-1105)
plasma acceleration by momentum transfer through, neutral, 17: 21138 (NP-12154(Rev.))
plasma acceleration by high-frequency, 17: 42138
plasma acceleration by gradients of, 18: 26742
plasma acceleration from pulsing, analysis of, 19: 46575 (NASA-TN-D-3006)
plasma acceleration by, turbulence in current sheet in, 20: 6450(R) (AD-619527)
plasma acceleration in external, resonance conditions for, (T), 20: 12196
plasma acceleration in external, resonance conditions for, (T), 20: 12197
plasma acceleration by self-induced, Hall current effects on flow distribution during, (T), 20: 26306
plasma acceleration and reflection by h-f and static, at electron cyclotron resonance, 20: 30646
plasma acceleration in external, induction effects on, (T), 20: 40192
plasma acceleration in, theory of supersonic, (T), 20: 40240
plasma acceleration in r-f and static, (E/T), 20: 40268
plasma Alfven wave dissipation in inhomogeneous, 17: 42163
plasma angular momentum relations in, 16: 23199
plasma arc stability in axial, (E/T), 20: 20008 (N-65-22329)
plasma behavior, 17: 17360
plasma binary correlation function in uniform, (T), 19: 14679
plasma boundary layer with, structure of, 18: 10912
plasma boundary layer with, calculation of shape of, 18: 17165
plasma boundary with, turbulence instabilities at, (E/T), 19: 23913
plasma bubble expansion in weak, 16: 22712(R) (AFSWC-TDR-62-12 (Vol.II)(Chap.2))
plasma bubble expansion in strong, 16: 22713(R) (AFSWC-TDR-62-12 (Vol.II)(Chap.3))

plasma bubble expansion in weak, 16: 22714(R) (AFSWC-TDR-62-12 (Vol.II)(Chap.4))
plasma bubble expansion in, in vacuum, 16: 22715(R) (AFSWC-TDR-62-12(Vol.II)(Chap.5))
plasma bubble expansion in, Taylor instability of, 16: 22718(R) (AFSWC-TDR-62-12(Vol.II)(Chap.8))
plasma bubble expansion in, Taylor instability of, 16: 22719(R) (AFSWC-TDR-62-12(Vol.II)(Chap.9))
plasma bunch in axially symmetric, magnetic moment of, (T), 19: 37995
plasma bunch interactions with axially symmetric, 18: 32891 (NP-14071)
plasma bunch motion in toroidal, 18: 17113 (NP-13698)
plasma collapse in, instabilities of cylindrical shell, 17: 4198
plasma collisions in transverse, depolarization and heating in, (T), 19: 21537
plasma column expansion in longitudinal, (T), 20: 40237
plasma column instability in axial, 18: 38219
plasma column stability in longitudinal, (T), 19: 14702
plasma column, stability in longitudinal, (T), 19: 45386 (D1-82-0439)
plasma compression by, theory of cylindrical, 16: 1113 (NP-10852)
plasma compression and containment by longitudinal, 16: 32499
plasma compression experiments, 17: 9735
plasma compression experiments, 17: 9739
plasma compression by cylindrical multipolar cusp, adiabatic, 17: 21166
plasma compression by, initial condition effects on adiabatic, 17: 26693
plasma compression by, with charge separation, (T), 19: 14705
plasma compressional heating by, effect of frequency on, (T), 19: 39991
plasma compression by explosively produced, (E), 20: 4941 (LA-DC-7290)
plasma compression by cusp, electron density and temperature in shock-heated, (E), 20: 6495
plasma compression in toroidal, adiabatic, (E), 20: 30660
plasma compression, confinement, and stability in cusped, (E), 20: 36306
plasma confinement, transition-region analysis, 16: 7214
plasma confinement in cusped static, 16: 15742
plasma confinement by cusped-geometry, research on, 17: 22726(R) (SIT-P91)
plasma confinement by rotating, stability of, 18: 15330 (LRP-12-64)
plasma confinement in, at high pressures, 18: 26762
plasma confinement in toroidal, Chew-Goldberger-Low theory at higher order for, 20: 38271
plasma confinement by multipole, calculations for, 17: 2114(R) (TID-18503)
plasma containment by external and internal, 16: 1153
plasma containment by periodic, 16: 21677
plasma containment by d-c, with external forces, 16: 21678
plasma containment by toroidal, 16: 31160
plasma containment in cusped, mirror, and uniform, 16: 32503
plasma containment in Heliotron, 17: 5475
plasma containment by, apparatus for, 17: 17390(P)
plasma containment by d-c, steady state theory of, 17: 26671 (NP-12808)
plasma containment in, topology for, 17: 26689
plasma containment by static, 17: 26692
plasma containment in, parameters for high-temperature, 17: 29691
plasma containment and heating by alternating, 17: 36750 (LRP-3-63)
plasma containment by increasing, 17: 36821
plasma containment in, geometry for, 17: 42106
plasma containment by, apparatus for, 17: 42136
plasma containment by cusp, 18: 1164
plasma containment and heating by alternating, 18: 6312 (SSD-TDR-63-312)
plasma containment by cusped, 18: 6386
plasma containment by picket fence geometries, 18: 6395
plasma containment by traveling, theory, 18: 9494
plasma containment by rotating, 18: 9496
plasma containment in cusp-like, 18: 9518
plasma containment by cusped and mirror, cold, 18: 13138(R) (ORNL-3564(p.44-62))
plasma containment in configurations with multipole stabilization, 18: 21414
plasma containment by, plasma duplexer performance with, 18: 24740(R) (AD-426769)
plasma containment in, configurations for, 18: 24755 (NP-13895)
plasma containment in, theory of, 18: 26718
plasma containment in cusped geometry, 18: 26783
plasma containment by, boundary layer structure in Maxwellian, 18: 30872 (AFCRL-63-376)
plasma containment in cusped, 18: 36743
plasma containment in, particle content in sheath for, 18: 40657 (CONF-471-34)
plasma containment in quadrupole and mirror (E), 19: 1759
plasma containment in resonant h-f, 19: 1760
plasma containment in multiply periodic interconnected, (T), 19: 5335
plasma containment in toroidal, having rotational transforms, (T), 19: 5336
plasma containment in crossed electric and, (E), 19: 6764
plasma containment by rapidly growing, (E), 19: 6767
plasma containment in toroidal, (T), 19: 6769
plasma containment in helical, behavior of force lines in, (T), 19: 6770
plasma containment by, microinstabilities in, (T), 19: 12710
plasma containment by, equilibrium and stability conditions for toroidal, (T), 19: 12713
plasma containment in variable curvature, losses in, (E), 19: 14665 (MATT-310)
plasma containment in, minimum B configuration for, (T), 19: 14693
plasma containment by, geometries for, 19: 14723
plasma containment by, equilibrium conditions for, 19: 14724
plasma containment and heating in toroidal, 19: 17154(P)
plasma containment by combined d-c and r-f, 19: 17155(P)
plasma containment by rotating, 19: 21508
plasma containment in, configuration singularities for, 19: 21534
plasma containment by three-cusp, (E), 19: 21568
plasma containment by, research on, 19: 23163(R) (ORNL-3650(p.111-86))
plasma containment by, (E), 19: 23899
plasma containment in toroidal, (E), 19: 29418
plasma containment in h-f quadrupole, 19: 31347
plasma containment by, research at UKAEA Culham laboratory, 19: 33446
plasma containment by, for space applications, (E/T), 19: 33400 (AD-608379)
plasma containment and stability in, (E/T), 19: 33402(R) (AFCRL-65-315)
plasma containment in longitudinal stationary, (T), 19: 35531
plasma containment in multipole, (E), 19: 39954(R) (COO-1233-20)
plasma containment in, electrostatic instabilities in, (T), 19: 41866 (UCRL-12052)
plasma containment by toroidal rotating, 19: 41950(P)
plasma containment by, magnetic shear effects on stability of, (E), 19: 45415 (UCRL-14137)
plasma containment in galaxies by, bridge mechanism for, (T), 19: 44926(T)
plasma containment in toroidal, low-β, (T), 19: 47819
plasma containment in toroidal, (T), 19: 47820
plasma containment in magnetic wells, (T), 19: 47822
plasma containment in rotating crossed electric and, (E/T), 20: 1266 (NP-15450)
plasma containment in minimum-B and saddle, (E), 20: 3184 (UCRL-14310)
plasma containment in helical, apparatus for stable, 20: 4995(P)
plasma containment in static parabolic, efficiency of, 20: 8195
plasma containment in toroidal, 20: 10140 (MATT-391)
plasma containment in toroidal octopole, (E), 20: 6460 (GA-6594)
plasma containment in trap of, increasing on all sides, (T), 20: 10158
plasma containment in sustained theta pinch, (E), 20: 12161 (65RL-3940E)
plasma containment and stability in toroidal, 20: 12174 (MPI-PAE/P1.6/65)
plasma containment in permanent dipole, stable, (E), 20: 12202
plasma containment by dipole, (T), 20: 13928(T) (AD-625070)
plasma containment by, research progress on, 20: 15882(R) (NP-15868)
plasma containment and heating by, (T), 20: 17927
plasma containment and heating by, (E), 20: 17928
plasma containment and motion in toroidal octupole, (E), 20: 26287
plasma containment and trapping by, deuterium, (E), 20: 26319
plasma containment in closed minimum-B, analysis of, 20: 30609
plasma containment by longitudinal, h-f discharge, (E), 20: 34752
plasma containment in, curvature effects on, (E/T), 20: 38326
plasma containment in spherical cavity, (T), 20: 40277
plasma containment and heating in low-frequency rotating, (E/T), 20: 40279
plasma containment in closed mixed electric and, 20: 40280
plasma containment in megagauss, 20: 42434
plasma containment properties of, book on, 20: 44985(T)
plasma containment by, 17: 9761
plasma cyclotron instability in, inhomogeneous, 17: 21176
plasma cyclotron instability in, wave amplification from, 18: 24790
plasma cylinder containment in uniform, by rotating electromagnetic field, 20: 22288
plasma cylinder rotation in longitudinal, 18: 32935
plasma decay in, 18: 15399
plasma decay in strong, 17: 35054
plasma decay in, mechanisms for, (E), 19: 6779
plasma decay rates in, 18: 44911
plasma density fluctuations and rotation in longitudinal, 18: 21504
plasma density in stationary, 17: 9715
plasma density variations in nonuniform, (E/T), 20: 8240
plasma diagnostics in, radio-wave, (T), 19: 5284(T) (AEC-tr-6518(p.112-

17))
plasma diffusion across, stability at low pressures, 16: 7213
plasma diffusion across, 16: 17175 (AFCRL-1028)
plasma diffusion across, 16: 23179 (NYO-7989)
plasma diffusion across, fully-ionized, 17: 31580(T) (AERE-Trans-934)
plasma diffusion and thermal conduction across, unified theory of, 17: 35042
plasma diffusion across, 18: 3003
plasma diffusion across, turbulent, 18: 15711(R) (TID-20256)
plasma diffusion across, 18: 21389 (TID-20509)
plasma diffusion across, experiments on, 18: 40677
plasma diffusion and heat transfer in, 18: 44899
plasma diffusion across, in arc discharge halo, 18: 44856 (ORNL-P-456)
plasma diffusion across, in Q-1 device at high column currents (E/T), 19: 1704 (MATT-291)
plasma diffusion and fluctuations in, bounds on, (T), 19: 19293
plasma diffusion and fluctuations in, microscopic, (T), 19: 19295
plasma diffusion across, (E/T), 19: 19306
plasma diffusion across, (E), 19: 21475 (LA-DC-6383)
plasma diffusion across, 19: 25570
plasma diffusion and oscillations in, (E), 19: 31369
plasma diffusion across, 19: 33153
plasma diffusion across axial, cylindrical discharge, (E/T), 19: 37940(R) (TID-21845)
plasma diffusion and stability in, (E/T), 19: 45380(R) (AD-426192)
plasma diffusion across, (T), 19: 47838
plasma diffusion across, in r-f discharges, (E), 20: 17954
plasma diffusion across, effects of microinstabilities on, (E), 20: 20017(R) (NYO-2813-36)
plasma diffusion across, (T), 20: 22189(R) (TID-22809)
plasma diffusion and thermalization in, turbulent, (T), 20: 30620
plasma diffusion across, equations for, 20: 30714
plasma diffusion across longitudinal, (E/T), 20: 30596
plasma diffusion across, relation to decay along field, (E/T), 20: 32647
plasma diffusion across spatially periodic, 20: 44973
plasma diffusion across spatially modulated, resonance in, 20: 44974
plasma diffusion across, computer simulation of, 20: 46875
plasma diffusion coefficients in, estimation methods for, (T), 19: 8555
plasma diffusion in uniform one-dimensional, 16: 17198
plasma diffusion in, 17: 11881
plasma diffusion in, 17: 11890
plasma diffusion in, recombination emission in, 18: 6380
plasma diffusion in, 18: 26768
plasma diffusion in, 18: 26772
plasma diffusion in cylindrical configuration, transverse, (T), 19: 5308
plasma diffusion in, (T), 19: 6778
plasma diffusion in, mechanisms of, 19: 17078(R) (TID-21380(p.31-6))
plasma diffusion in, ambipolar, (T), 19: 31396
plasma diffusion in, stability criteria for, 19: 39968 (ORNL-P-1338)
plasma diffusion in, 19: 45410(R) (TID-22183)
plasma diffusion in, measurement and theory of, 20: 24508 (N-66-15390)
plasma diffusion in, from hard-core and pinch discharges, (E), 20: 30639
plasma diffusion in, properties of, 20: 38249
plasma diffusion in, computer simulation of anomalous, 20: 38328
plasma diffusion in toroidal traps in, effects of disturbances on, 20: 44875(T) (MATT-Trans-37)
plasma dipole interactions in strong-field geometries, 18: 1100(R) (AFCRL-1118)
plasma dipole resonance frequency in axial d-c, 17: 24590
plasma discharge distribution in, 16: 33945
plasma discharge in longitudinal, turbulent convection in, 17: 42098
plasma discharge in, hysteresis in, 18: 21403
plasma discharges in, fast-programming of toroidal, 17: 26709
plasma dissipative tensors in, 19: 1754
plasma distribution in, transport coefficient of, 18: 44900
plasma drift across toroidal, 20: 10171
plasma drift and losses in curved, (T), 20: 36298
plasma drift in curved, analysis of, 18: 15336 (NP-13631)
plasma drift in curved, (T), 19: 8521
plasma drift instability in, nonlinear theory of inhomogeneous, 17: 42129
plasma drift instability in, 20: 34731
plasma drift velocity across, 16: 2617
plasma drift wave propagation transverse to external, stability of, (T), 20: 22282
plasma dynamics in, 16: 1118 (SIT-P30)
plasma dynamics in rotating, 18: 40689
plasma electric conductivity in, high-frequency, 17: 26706
plasma electric conductivity in, third Chapman-Enskog approximation to fully ionized, (T), 20: 8238
plasma electric conductivity in, partially ionized, (T), 20: 26309
plasma electric field distribution in mirror, 18: 3011
plasma electron-density perturbations in, from rapidly moving body, 17: 24568(T)
plasma electron energy and lifetime in radially increasing, increases in 18: 21499
plasma electron heating by h-f, adiabatically confined, (E), 20: 30663
plasma electrostatic instability in, 18: 26732
plasma entry into axial, mechanism of, (E/T), 20: 22224
plasma equilibria in minimum-B, pressure effects on, 20: 46878
plasma equilibrium configuration in theta discharges with reversed trapped, 16: 2610
plasma equilibrium in, current-carrying toroidal, 17: 28392
plasma equilibrium in space-periodic, 18: 21434
plasma equilibrium in toroidal, (T), 19: 47809
plasma equilibrium in uniform, homogeneous, (T), 20: 38343
plasma expansion in nonuniform, dynamics of, 19: 29412
plasma flow across, equations for, 17: 36757 (PIBMRI-1001-62)
plasma flow across azimuthal, 18: 26773
plasma flow across, nonequilibrium processes in, (T), 19: 10444
plasma flow across, one-dimensional, (T), 20: 30597
plasma flow and injection in axial guide, 18: 19243
plasma flow and losses in, 16: 29935
plasma flow around dipole, (E), 19: 40009
plasma flow in, 18: 9473
plasma flow in aligned, equations for collisionless, 20: 32649
plasma flow in axial, velocity of, 18: 21484
plasma flow in crossed electric and, one-dimensional, (T), 20: 1294
plasma flow in electric and, stress tensor for, 18: 26734
plasma flow in perpendicular, 17: 31571 (GA-4285)
plasma flow in transverse, velocity of, 18: 21485
plasma flow in transverse, Monte Carlo analysis of, 19: 1712 (NASA-TN-D-2211)
plasma flow in, free-streaming pulsed, (E), 20: 12235
plasma flow in, Legendre transformations and potential equations for, (T), 19: 14688
plasma flow over conducting surfaces in, boundary conditions for, 18: 35005
plasma flow perpendicular to, stability of nonuniform, 18: 19251
plasma fluctuations and pumpout in toroidal wells, (T), 20: 38266
plasma gravitational resistive instabilities in, 18: 7806
plasma heating and stabilization by, (E), 19: 27601 (IAE-674)
plasma heating by oscillating, (T), 19: 47767
plasma heating by h-f, resonant, (E), 20: 13946(T)
plasma heating in, by magnetic pumping, 18: 4683(P)
plasma helical instability in high, suppression of, 18: 28799
plasma in curved, low-frequency hydromagnetic waves in, 18: 9524
plasma in, electron cyclotron resonance in, 18: 2980 (IPPJ-15)
plasma in inhomogeneous, Alfvén wave damping in collisionless, (T), 19: 23936
plasma injection and pinching in, electron-optical observation of, (E), 19: 5276(T) (AEC-tr-6518(p.10-19))
plasma injection and trapping in, transverse, (E), 19: 37994
plasma injection and compression in cusped, (E), 20: 30644
plasma injection into, emission light separation during, 17: 11854
plasma injection into, coaxial gun for, 17: 19453(R) (LAMS-2874)
plasma injection into cusped, 17: 22712 (AD-283078)
plasma injection into solenoidal, 18: 30932
plasma injection into, (E), 19: 31348
plasma injection into multipole, axial, (E), 19: 31391
plasma injection into cusped, (E), 19: 47858
plasma injection into, effects of toroidal drift on transverse, (E), 20: 3205(T)
plasma injection into curvilinear, deuterium, (E), 20: 36294
plasma injection in multipole, transverse, (E), 20: 40254
plasma instabilities in, microscopic, 17: 9728
plasma instabilities in sheared configurations of, current-driven, (T), 20: 8233
plasma instabilities in dipole, 20: 10193
plasma instabilities from pinch discharges in rotating, (T), 20: 26253 (NP-15974)
plasma instabilities due to longitudinal, (T), 20: 40239
plasma instability in, Rayleigh-Taylor, 17: 4197
plasma instability in crossed electric and, 17: 17356
plasma instability in heterogeneous external, 17: 36814
plasma instability in crossed electric and, 18: 1155
plasma instability in, at low pressures, (T), 19: 17132
plasma instability in longitudinal, electron-hole, 19: 29424
plasma instability in, critical correlations associated with helical, (T), 19: 31395
plasma instability in, collision-induced, (T), 20: 38253
plasma interactions with wave disturbances in, density, axial drift, and temperature for, 17: 26676 (UCRL-7253)
plasma interactions with three-dimensional dipole, characteristics of, 17: 28381
plasma interactions in transverse, 18: 17115 (NP-13706)
plasma interactions with d-c, 18: 26775

plasma interaction with three-dimensional dipole, (E), 19: 14707
plasma interactions with, in outer space, (T), 19: 19266(T) (FTD-TT-64-1316(p.948-51))
plasma interaction with dipole, (E), 19: 29399
plasma interactions in quadrupole, polarized, (E), 19: 31392
plasma interactions in, counterstreaming, (E), 19: 41926
plasma interactions with cylindrical, (T), 20: 17956
plasma interactions with, power generation by, (E/T), 20: 23990(R) (AD-625575)
plasma interactions with line current, analysis of, (T), 20: 42453
plasma ion acoustic wave excitation in uniform, (T), 19: 10417
plasma jet configuration and particle losses in curved, 18: 35023
plasma jet diffusion across, (T), 20: 44963
plasma jet interactions with, produced by straight wire, 16: 20619
plasma jet interaction with, (T), 20: 40231
plasma jet motion in, 18: 21486
plasma jet motion in, in air, 18: 21487
plasma kinetic equation in strong static, 17: 5447
plasma kinetics in weak, 17: 5446
plasma kinetics in, equations for, 18: 17199
plasma kinetics in, radiative transfer in, 18: 28788
plasma kinetics in, book on, 18: 35028
plasma kinetics in rotating, Lorentz, 18: 40687
plasma kinetics in high, Vlasov equation for, (T), 19: 47753
plasma kinetics in rotating, 20: 6479
plasma kinetics in strong electric and, 20: 40249
plasma loop motion in, 17: 11892
plasma loss rates in toroidal minimum-B, alkali, (E/T), 20: 30656
plasma magnetohydrodynamic flow at right angles to, wall friction in one-dimensional, 17: 26702
plasma motion across, processes for, 17: 26690
plasma motion across, heat transfer in nonisothermal, 18: 35026
plasma motion in asymmetry, theta-pinch, (E), 19: 40010
plasma motion in curved, 16: 3782
plasma motion in cusped, 18: 26741
plasma motion in external, 17: 26724
plasma motion in external, 18: 44908
plasma motion in nonuniform, equations for, 19: 29413
plasma motion in rotating, Langevin equation for, 18: 40686
plasma motion in strong, survey of turbulent, 17: 26685(T)
plasma motion in strong, 18: 35027
plasma motion in solar, (T), 19: 27048
plasma motion in, transverse, 17: 9751
plasma motion in transverse, velocity probe for, (E), 19: 12655
plasma motion in toroidal octupole, (E), 19: 41896
plasma motion in toroidal octupole, (E), 20: 30708
plasma motion in toroidal octupole, equipotential surfaces of, 20: 38192 (COO-1233-32)
plasma motion in, with crossed electric field, 16: 9533
plasma motion in, with crossed electric field, 16: 11080(T) (FTD-TT-62-43)
plasma motion in, transverse, (E), 19: 33414(R) (LA-3320(p.71-6))
plasma motion in, of toroidal solenoids, (T), 19: 37996
plasma motion near zeros of, 19: 47847
plasma motion transverse to, stability criterion for, 17: 9782
plasma moving striation in longitudinal, (E), 19: 41888
plasma noise of h-f discharges in, (T), 19: 12654
plasma oscillations in uniform axial, longitudinal, 16: 3783
plasma oscillations in static external, initial value problem, 16: 18568
plasma oscillations in non-uniform, 17: 11847
plasma oscillations in constant, 17: 36816
plasma oscillations in, spin effects on electron, 18: 6347
plasma oscillations in, stable longitudinal, 18: 6348
plasma oscillations in uniform axial, anharmonic and harmonic, 18: 6353
plasma oscillations in uniform, dispersion relations for longitudinal, 18: 9520
plasma oscillations in uniform, quantum, 18: 13145
plasma oscillations in strong, high-frequency, 18: 17109 (NP-13612)
plasma oscillations in, stability of, 18: 24787
plasma oscillations in, 18: 26777
plasma oscillations in, spin effects of long-wavelength, 18: 42842
plasma oscillations in, h-f, (E), 19: 6749
plasma oscillations in, (T), 19: 17113
plasma oscillations in external, homogeneous collisionless, (T), 19: 17115
plasma oscillations in, 19: 19284
plasma oscillations in, low-frequency, (E), 19: 23833(T) (AEC-tr-6527 (p.169-82))
plasma oscillations in weakly inhomogeneous, 19: 23849
plasma oscillations in, (T), 19: 31367
plasma oscillations in, electrostatic, (T), 19: 37968
plasma oscillations in, initial-value problem for, (T), 20: 20004 (N-65-16489)
plasma particle energy gains by reflection from r-f, 18: 21520
plasma particle orbits in d-c, 18: 21521
plasma particle trapping in, heavy, 19: 17090
plasma penetration by, 17: 36754 (PIBMRI-929-61)
plasma penetration and flow in local concentrated, (T), 20: 46498
plasma penetration of longitudinal, nonlinear effects in resonance, 18: 6365
plasma pinch by, gamma emission in, 16: 31165
plasma pinch stability in, 17: 2392
plasma pinch stability in, 17: 17376
plasma polarization in curved, (E), 19: 47797
plasma polarization in toroidal, triple-helical field effects on, (E), 20: 22275
plasma polarization in toroidal, (E), 20: 22276
plasma polarization in opposite-curved toroidal, (E), 20: 22277
plasma positive column diffusion in, 17: 38378(T) (AEC-tr-5985)
plasma positive column diffusion in, 18: 4656
plasma pressure variations and thermal conductivity in, 18: 21483
plasma processes in longitudinal, toroidal, 17: 9756
plasma production in trap of, by action of light on dense matter or particle beams, 18: 22972
plasma production in, 19: 23828(R) (TID-21499)
plasma production by laser beam ionization of gases in, (E), 19: 35542(T)
plasma production by injection in cusp, dense, (E), 20: 30643
plasma production in crossed electric and, (E), 20: 3177 (NP-15570)
plasma propagation velocity, 16: 2593(T) (AEC-tr-4722)
plasma propagation in, analysis of axially symmetric hard magnetic piston for, 17: 4172 (NP-12203)
plasma puff expansion in longitudinal, 18: 19244
plasma puffs in longitudinal, hydromagnetic model for, 20: 30715
plasma pumping by constricting, for energy extraction, 20: 34777(P)
plasma resonance interaction with spatially rotating static, 17: 21161
plasma resonance probe in, theory of, 18: 36734
plasma resonances in, local, (T), 19: 17147
plasma resonances in, (E/T), 19: 35540
plasma resonances in dipole, toroidal-mode, (T), 20: 15592
plasma ring dynamics in, (T), 19: 27596 (ARL-65-12)
plasma ring motion in coaxial, 16: 1274 (NASA-TR-R-121)
plasma ring motion in coaxial, (T), 19: 23900
plasma rotation in, ion, (T), 19: 23873
plasma rotation in, from coaxial guns, (E), 19: 47849
plasma rotation in crossed electric and, 20: 26252(R) (NASA-CR-67221, pp 2.2-21)
plasma rotational motion in, momentum balance of, 17: 31585
plasma sheaths in, models for, 18: 7805
plasma space and velocity distribution in perturbed, 17: 19488
plasma stability in homogeneous, 16: 17193
plasma stability in, from atomic bomb debris, 16: 22710(R) (AFSWC-TDR-62-12(Vol.II))
plasma stability in inhomogeneous, 17: 9693
plasma stability in, effects of viscosity, 17: 9722
plasma stability in homogeneous, without longitudinal current, 17: 11889
plasma stability in, inhomogeneous, 17: 21175
plasma stability in, transverse wave growth effects in electron-positron, 17: 24570
plasma stability in strong, positive column, 17: 24585
plasma stability in, finite resistivity effects on gravitational, 17: 26713
plasma stability in uniform, h-f electrostatic, 17: 33195
plasma stability in longitudinal, 17: 36818
plasma stability in homogeneous external, 17: 40177
plasma stability in, 18: 4653
plasma stability in, pressure effects on, 18: 6368
plasma stability in high-frequency, 18: 6379
plasma stability in, equation for, 18: 7800
plasma stability in varying longitudinal, 18: 19170
plasma stability in strong, effects of conductivity on, 18: 21430
plasma stability in crossed electric and, 18: 21505
plasma stability in, heterogeneous, 18: 26767
plasma stability in minimum-B geometries, 18: 40663 (SIT-131-A)
plasma stability in d-c, 18: 40676
plasma stability in, hydromagnetic, (T), 19: 14725
plasma stability in minimum-B configurations of, potential effects on, (T), 19: 19303
plasma stability in transverse, (E), 19: 21577
plasma stability in nonuniform, (T), 19: 27649
plasma stability in axisymmetric, (T), 19: 29416
plasma stability in strong, current-carrying cylindrical, (T), 19: 33491
plasma stability in, (T), 19: 43446
plasma stability in spatially varying, (T), 19: 47840
plasma stability in, effects of "line-tying" on, (T), 20: 1280 (UCRL-16055)
plasma stability in, negative V'' on general axis for, (T), 20: 8235

plasma stability in, collision effects on, 20: 10133 (CONF-650562-2)
plasma stability in axial uniform, (T), 20: 10152 (TID-22463)
plasma stability in toroidal discharges, (T), 20: 13929(T) (NP-tr-1340)
plasma stability in Heliotron, 20: 26278
plasma stability in toroidal discharges, (T), 20: 30617
plasma stability in toroidal, (E), 20: 30640
plasma stability in, flute, 20: 40217(T)
plasma stability in toroidal, with longitudinal fields, 20: 42402 (IAE-1149)
plasma stability in toroidal, 20: 42403 (IAE-1151)
plasma stability in, ion diffusion effects on, (T), 20: 44923(T)
plasma stationary containment by, at anisotropic pressure, 18: 6321
plasma stream interactions with dipole, cavity formation in, 18: 17149
plasma stream intersections with transverse, stability of, 18: 28894
plasma streaming in inhomogeneous, 18: 19247
plasma streaming through dipole, 17: 26697
plasma structure and behavior in, 18: 1095(R) (AFCRL-62-184)
plasma torus equilibrium in, 17: 13630
plasma transient processes in, (T), 19: 12695
plasma transmission through 90° bend in, mass and energy analysis of, 17: 15347 (MATT-135)
plasma transport equations for, 18: 35018
plasma transport in d-c and h-f, (T), 19: 6742
plasma transport phenomena in strong, 18: 6372
plasma turbulence from ionization instability in, 18: 19252
plasma turbulent convection in, 16: 23198
plasma turbulent diffusion in, amplitude damping of stationary oscillations during, 18: 6364
plasma two-stream instability in strong, 18: 42823
plasma universal instability in, 18: 9527
plasma universal instability in complex, (T), 19: 40018
plasma vorticity in, kinematics of, 18: 44871
plasma wave damping in inhomogeneous, 18: 15400
plasma wave damping in weak, calculation of, 18: 32923
plasma wave propagation in, dispersion curves for l-f, 17: 28375
plasma wave propagation in inhomogeneous, heating by anomalous dissipation of Alfvén, 18: 4644
plasma wave propagation in "spoke-wheel", 18: 17150
plasma wave propagation in, structure of, 18: 19184
plasma wave propagation in weak, collisional damping of, 18: 21404
plasma wave propagation in, collision-free, 18: 26746
plasma wave propagation in, two-component, 18: 32916
plasma wave propagation along (T), 19: 3441
plasma wave propagation in, dispersion relation for transverse, 19: 19287
plasma wave propagation across, (T), 19: 21521
plasma wave propagation in, non-linear constant profile, 19: 37935 (N64-33635)
plasma wave propagation in cylindrical, (T), 20: 1288
plasma wave propagation in, cyclotron harmonic, (E), 20: 22226
plasma-jet interaction with crossed magnetic and, (E/T), 19: 25563
plasma-jet motion in toroidal, (E), 19: 27683
plasmas confined by, structure boundary layers of, 17: 19449 (CEA-2245)
plasmas in inhomogeneous, longitudinal waves in interface, 17: 21143
plasmoid deformation in, 16: 2596(T) (AEC-tr-4726)
plasmoid heating and oscillation in axisymmetric, (T), 20: 30559 (FTI-114/P-044)
plasmoid motion in, deuterium, (E/T), 20: 28486 (IAE-1016)
plasmoid motion in curvilinear, (E/T), 20: 30647
plasmoids in, theory of force-free, 18: 26751
polarity distribution of interplanetary, variations in, 20: 31860
polarity reversal of solar, with prominence filament motion, (E), 19: 16334
pole surfaces for strong- and weak-focusing, 17: 32791
positron focusing in accelerating, (T), 20: 11399 (UCRL-7566(Rev.1))
positron reactions at 0.4 to 24 Mev, depolarization in, (E), 19: 8166
potential functions for, three-dimensional, 20: 17177 (CONF-650922, pp 89-95)
power for fast-rising, development of ultra-low-inductance capacitor banks for, 17: 31568 (CONF-24-12)
production and properties of, 18: 32275(R) (ORNL-3652(p.105-31))
production and research uses of 100-kgauss, facility for, 16: 15436
production and research uses of 125-kgauss, facility for, 16: 15433
production and research uses of 100-kgauss, facility for, 16: 15434
production and research uses of 57-kgauss, facility for, 16: 15435
production and use of very high, continuous, 16: 2343
production and use of high, 16: 31879
production and uses of strong (E), 19: 2897
production by current source in partly ionized gas, (T), 19: 19279
production by cylindrical current arrays, 20: 37314 (BNL-10148)
production by elliptical current sheets, 20: 37318 (BNL-10436)
production by hydrodynamic self-excitation in toroidal vortexes, (T), 20: 46431(T)
production by linear current in ideally conducting cylinder with longitudinal cut, 16: 11081(T) (NSF-62-35(3))
production by motion of geomagnetically trapped particles, 16: 29634 (CRSR-117)
production by rotating superconductor, 18: 15057
production by solenoid containing cylindrical conductor, (T), 19: 18571(T) (ORNL-tr-460(p.1-19))
production by spreading electric currents, 17: 36515
production by superconductors, 17: 27936 (AERE-M-1207)
production by superconductor solenoid, 19: 23938(P)
production by "tennis ball seam" single-loop conductor, 18: 44850 (CLM-R37)
production by thick solenoids of finite length, axial and radial components in, 17: 25850 (NASA-TR-R-170)
production during gravitational collapse, (T), 19: 12346
production for MHD generator, economics of, (T), 19: 16462
production for plasma containment and heating, 18: 24804(P)
production for theta-pinch experiments, system for, 18: 9446 (63-RL-3254E(Rev.))
production for thermonuclear research, review of, 20: 22302
production for 700-Mev relativistic proton cyclotron, 19: 1095 (JINR-P-1738)
production in solar photosphere, kinetic theory of, 17: 32854
production in sunspots, processes for, 18: 4391(T)
production in toroidal Heliotron, 20: 30595
production in Van Allen belt, 19: 37709 (N64-33627)
production of axially symmetrical, in ferromagnetic system, (T), 19: 14151
production of axially symmetrical, of specified shape, 19: 23177
production of axially symmetric, air-core magnet for, 19: 44165 (CERN-65-29)
production of azimuthally symmetric force-free, 16: 33641
production of, by flux compression in superconductors, 17: 621
production of circular homogeneous, 18: 2440
production of closed minimum-B, (T), 20: 13930(T) (NP-tr-1343)
production of constant, shaped, 17: 24172
production of constant-gradient, use of elliptical current sheets for, 20: 37317 (BNL-10341)
production of, current-density calculations for, 17: 11440
production of curved, using straight coil systems, (E/T), 20: 28495(R) (MATT-Q-22, pp 321-85)
production of, design of device for, 17: 4209(P)
production of fast-pulsed, using thyratrons, 18: 42208 (DESY-64/7)
production of h-f rotating, on surface of cylindrical hydrogen plasma column, 20: 36281 (LRP-26/66)
production of helical, coil shape for, (T), 20: 30703
production of helical minimum-B configuration, (T), 20: 38219
production of hexapolar, design equations for, 19: 26485
production of high, cryogenic-magnet facility for, 16: 15440
production of high, using helix- and disk-type coils, 16: 15398
production of high, by magnetohydrodynamic flux concentrator, 16: 15416
production of high, review, 16: 16828
production of highly homogeneous, by pole-face shaping, 16: 22776
production of high pulsed, in small areas, 16: 31867
production of high large-volume, by cryogenic coils, 16: 31881
production of high pulsed, 17: 12743 (AD-277626)
production of high, by flux compression in superconductors, 17: 13868
production of high-intensity, using purified aluminum solenoid at low temperatures, 17: 30651(P)
production of high, superconducting magnets for, 17: 41592
production of high-intensity, for plasma confinement, 18: 9553(P)
production of high, review of magnets for, 18: 10657
production of high, by flux compression in superconductors, 18: 36521
production of high, by superconducting solenoids, 18: 36520
production of high quasi-stationary, equipment for, 18: 44308
production of high pulsed microsecond, using condenser discharge, 18: 43745(T) (NP-tr-1183)
production of high pulsed, exploding mercury coil for, (E), 19: 11843
production of high, Soviet research on, (E/T), 19: 15700 (ATD-P-64-46)
production of high, superconductors for, 19: 16792
production of high, methods for, 19: 37210
production of high pulsed, explosion devices for, 20: 25633
production of high-intensity toroidal, coil design procedure for, 18: 32271 (MATT-208)
production of homogeneous, superconducting cylinders for, 18: 22831
production of homogeneous, in superconducting solenoids, 17: 41200
production of inhomogeneous, shimming of pile pieces for, 17: 41207
production of intense, design of helical coils for, 18: 12433(P)
production of intense fast-rising pulsed, 19: 7776
production of intense, from electron beam injection in rotating, 20: 40282
production of large-area, by air-core coils, 17: 3095
production of large, cylindrical explosive system for, 20: 4477 (LA-DC-

7289)
production of large-volume, by explosive generators, 20: 9598 (CONF-650512, pp 156-61)
production of large, by capacitive discharges in magnet coils, 20: 36982
production of large, pulse transformers for, 20: 41092
production of large, using capacitor-bank discharges, 20: 41080 (UCRL-14831)
production of magnetoacoustic wave in electric conductor, 18: 9519
production of megagauss, by explosive-driven flux compression system, 18: 5846 (LADC-5915)
production of megagauss, for containment of plasma, 18: 9554(P)
production of megagauss, by flux compression, 18: 22574
production of megagauss, by explosive flux compression, 19: 39300
production of megagauss, for plasma confinement, 20: 6515(P)
production of megagauss, by imploding metallic foils, (E), 20: 44031
production of minimum B, caulked cusp machine for, 20: 8181(R) (LA-3434)
production of minimum-B configuration, for plasma containment, 20: 10127 (CONF-650512, pp 168-72)
production of multipole, device for, 17: 38399
production of profiles of, by model solenoid, 19: 26488 (AD-610579)
production of pulsed and steady high, facility for, 16: 15438
production of pulsed, design of solenoids for, 17: 3086 (NIRL/R/19)
production of pulsed, for charged-particle beam deflection, 18: 2509
production of pulsed, effects of circuitry on, 18: 2510
production of pulsed, magnets for, 18: 9457 (NP-13514)
production of pulsating, using superconductor gates, 19: 19057
production of pulsed strong, flux concentrator for, 19: 38934
production of pulsed, design of apparatus for, 19: 44861 (IAE-795)
production of pulsed, power supply for, 19: 44449 (IAE-704)
production of quadrupole, conductor design for, 20: 8181(R) (LA-3434)
production of r^{-1}, 17: 16387
production of solar, from plasma thermal currents, 18: 4392(T)
production of square-wave alternating, 17: 4794
production of steady high-intensity, survey of methods and applications of, 18: 8922
production of strong, technology and methods for, 17: 28006
production of strong, transformer coils for, 18: 5447 (CERN-63-36)
production of strong, design and operation of 650-kev solenoid for, 18: 17972
production of strong, by flux compression, (T), 19: 20678
production of strong, survey on, 19: 20701
production of strong, by implosion of conducting shells, (T), 19: 37228
production of toroidal, with negative V″, 19: 31394
production of traveling, for magnetic induction plasma engine, 17: 12758(R) (N62-11118)
production of turbulent, in plasma flow over magnetic dipole, (E), 19: 33425 (SIT-P144)
production of ultrahigh, methods for, 20: 32337
production of uniform, in superconducting cylindrical shells, 16: 22752
production of uniform kOe, solenoid design for, 18: 41597(T) (SLAC-Trans-7)
production of, using superconductive coils, 17: 34438
production of v-h-f pulsed, power supplies for, 18: 5583
production of very strong, cryogenic coils for, 18: 14204 (CEA-2362)
production of very strong, 18: 28498
production of 101-kgauss, with niobium–tin superconducting solenoid, 18: 958
production of 10^4 to 10^6 gauss, review, 17: 24539
production of 120-kG, by condenser bank, 20: 46815 (JUL-374-PP)
production of 300-kgauss, by implosive flux concentrator, 16: 15417
production of 330-kgauss 0.1-sec-pulsed, 16: 15420
production of 36-kgauss, facility for, 16: 15441
production of 450-kgauss pulsed, using a flux concentrator, 16: 15415
production of 50- to 60-kgauss steady, facility for, 16: 15439
production of, design of multipolar windings for, 20: 10123 (CONF-650512, pp 128-30)
production of, design of 625-kJ capacitor battery for, 20: 43457
production of, performance of 625-kJ capacitor battery for, 20: 43458
production of, strip conductor design for, 18: 27645
production using superconducting Nb_3Sn, 18: 44682
propagation by accelerated electric dipole, 18: 7585
propagation of solar particles through interplanetary, 17: 12989
properties and structure of interplanetary, 20: 4529
properties and theory of planetary, review of, 20: 34390
properties and variations of interplanetary (T), 19: 2948
properties as momentum-defining slit for electron linear accelerator, 17: 23632
properties in discharge positive column, 17: 42047 (D1-82-0283)
properties in moving, conducting medium, 19: 1748
properties in space, 18: 6088
properties of, along axes of electromagnetic lenses, 16: 27807
properties of contracting gas cloud, 20: 41602
properties of crossed electric and, for beta and mass spectroscopy, 20: 14882
properties of, from helical coils, 17: 11879
properties of galactic and interplanetary, 18: 32504
properties of galactic, 19: 1150
properties of interplanetary, from solar flare cosmic ray observations, 16: 10784
properties of interplanetary, 16: 15515
properties of interplanetary and solar, 18: 30671
properties of interplanetary, 18: 32357
properties of interstellar, 18: 32354
properties of interplanetary, model for (T), 19: 1154
properties of interplanetary, review of, 20: 7990
properties of interplanetary, review of, 20: 15232
properties of interplanetary, (E), 20: 31887
properties of interstellar, Petschek's mechanism for dissipating, 20: 41595
properties of interstellar, 20: 44881
properties of ionospheric frozen-in, (E/T), 19: 8335
properties of semi-stable quadrupole–octupole periodic, (T), 19: 7998 (64-RL-3778E)
properties of small-scale solar, kinematical hydromagnetic model for, 20: 21503
properties of solar, 16: 15516
properties of solar chromospheric, 18: 44415
properties of solar, review of, 19: 14221
properties of solar, fine-structure in, (T), 19: 44918(T)
properties of stellar, during collapse, 18: 37833
properties of stellar, (T), 20: 7712
properties of, studies by electron beam interactions, 16: 33657
properties of, effects of flow of incompressible, viscous, electrically conducting fluid on, 19: 593
protective effects of pre-treatment of mice with, against radiation mortality, 18: 1453
proton motion in, beta and meson (π) emission in, (T), 19: 12267
proton optics of deflecting, floating-wire method in study of, 16: 10689
proton reactions with emulsions in pulsed, determination of mean-free-path for, 17: 22438
quantization in superconducting cylinders, 16: 12298
quantization in superconducting cylinders, 16: 19536
quantization in superconductors, microscopic theory of, 19: 14439
quantization of flux in superconducting cylinders, 17: 2134
quantization of flux in multiply connected superconductors, 18: 6112
quantization of flux of, in superconducting cylinders, 18: 6121
quantization of flux of, in superconducting films, 18: 11134
quantization of, in association with electric currents, 17: 6804 (UCRL-6630-T)
radiation from charged particles in dipole, cyclotron, (T), 19: 35043
radiation from fluid-mechanical sources in electron plasma in, 18: 36726
radiation of atomic electrons in alternating, 17: 20705(T)
radiofrequency skin depth in d-c, nonresonant changes in, (E/T), 20: 30734(R) (TID-22970, pp 1-63)
ray tracing in magnetic lens system, IBM 7090 program for, 18: 36110 (BNL-8213)
reduction of fringing, in particle-analyzing magnets, 18: 20644
research progress on mirror geometries, 18: 6302(R) (LAMS-3004)
reversal by decelerating relativistic electrons, 16: 23187
review on interplanetary, 18: 2513(T) (FTD-TT-63-968(p.89-171))
rotational motion of electrically conducting fluid between coaxial cylinders in, 17: 22385
rotational transforms in Stellarator-type vacuum, 16: 7216
rotational transform changes in stellarator, 18: 32942
rotor suspension in, 19: 6060
saturation effects in, system for self-correction of, 17: 42023
scanning in mass spectrometers, automatic device for, 17: 37411
scattering effects of, Compton, 18: 13141(R) (ORNL-3564(p.80-99))
sector boundaries in homogeneous exact focusing, 16: 17170
sector boundary calculation, 16: 3582
separation of oppositely directed, by plasma sheaths, 16: 15739
shape in air-coil betatron, 16: 23161(R) (SIT-P54)
shape measurements for AVF cyclotrons, 17: 7387
shaping by superconducting surfaces, 18: 16604 (BNL-7534(p.449-77))
shaping for cone in Berkeley cyclotron, 17: 7390
shaping for Univ. of Manitoba cyclotron, 17: 7368
shielding against d-c, demagnetization of materials for, 18: 30940
shielding from, by rotating superconducting cylinder, 18: 2768
shielding of space vehicles with, 20: 40292
shielding properties of, for space vehicle, 17: 18389 (TID-7652(p.808-18))
shielding properties, 17: 31633 (ASD-TDR-63-194)
shimming of sector-focused isochronous cyclotrons, 17: 7362
shock propagation in transverse, solutions for, 18: 14599
shock propagation in gases in, evolution of trans-Alfvenic, 18: 26122

shock propagation in nonuniform, 20: 6158(R) (AD-619999)
shock wave attenuation in ionized gas in transverse, 18: 26802
shock wave decay in, magnetohydrodynamic piston-produced, 18: 7410
shock wave interactions with, MHD supported, 19: 41120 (N64-30509)
shock wave propagation in fluid containing uniform transverse, cylindrical, 17: 24108
shock wave propagation in plasmas in, effects on collisionless, 17: 26687(T)
shock wave propagation in plasma in, radiation smoothing of, 18: 3005
shock wave propagation in plasma in transverse, analysis of, 18: 26752
shock wave propagation in conducting gas in weak (T), 19: 2911
shock wave structure in plasma in, 18: 28808
solar activity effects on interplanetary, 17: 24212
solar, generation of flares by varying, 17: 13273(T)
solar, patterns in sunspots, 17: 39827
solar, relation to solar flare intensity, 17: 39826
solar, variations during solar flares, 17: 13181(T)
solar wind interaction with, in comets, (T), 19: 14220(T)
sound absorption in liquid metals in d-c, measurement of, 18: 26131
sound wave propagation in, wavelength dependence in, 18: 20643
sound wave reactions with metals in, nonextremal Fermi-surface orbits from resonances in, 18: 32070
space charge effect on transitions of, toward plasma regime, (T), 20: 2856
space propulsion by magnetic field-dipole interaction, (T), 19: 9790
space-charge propagation along electron beam in infinite, 18: 42177
sphere gravitational stability in, gaseous, (T), 20: 25701
sphere motion through conducting fluid in transverse, non-conducting, 17: 32783
sphere motion through conducting fluid in transverse, conducting and non-conducting, 17: 32784
stability effects of longitudinal external, on plasma, 16: 31167
stability effects on conducting fluid sphere, 16: 881
stability in plasma at finite pressure, 18: 32934
stability in solar flare region, 18: 44414
stability in 7-Bev proton synchrotron, 17: 920
stability of, 18: 9541
stability of electron-hole plasmas in longitudinal, 16: 29902 (D1-82-0182)
stability of flexible conductor in longitudinal, (T), 20: 46448
stability of force-free, 17: 3619
stability of orbits in corkscrew, 17: 35260(R) (TID-19135)
stability of periodic, hydromagnetic, (T), 19: 43435
stability of plasma column in longitudinal, (E/T), 19: 17101
stability of rotating plasma in twisted, (T), 19: 33436
stability of shearing, in incompressible plasma, (T), 19: 43433
stability regions in, magnetic axis form effects on, 17: 42044 (CEA-2319)
stabilization in accelerator beam deflection system, 18: 22592 (PAN-477/1A)
stabilization, in beta spectrometer, 16: 357
stabilization in electromagnets, design of servosystem for, 17: 26253(P)
stabilization of d-c, by superconducting solenoids, 17: 18977
stabilization of electromagnet, apparatus, 16: 19144(P)
stabilization of inhomogeneous, equipment for EPR, 19: 26931
stabilization of longitudinal, in beta spectrometer, 16: 1965
stabilization of magnetic mirror, MHD, 20: 24549
stabilization of weak inhomogeneous, NMR for, 19: 26930
stabilization of, using Hall-effect control systems, (E), 19: 44173
stabilization of, equipment for, 20: 7350
stabilization using broadband EPR transducer, (E), 19: 26918 (JINR-P-1990)
stabilization using broadband EPR field sensor, 20: 31813
stabilization with superconducting tubes, 18: 11111
stabilizer for, spin-oscillator-type, 19: 26932
star formation in rotating, (T), 20: 39568
strength in circular cylinder, ferromagnetic material effects on, (T), 20: 29835
strength in solar loop prominence systems, 18: 42275
strength in solar corona above active regions, (T), 20: 34069(T)
strength of circular-current-induced, computer analysis of, 17: 3357 (MSUCP-8)
strength variation during current onset in linear pulse discharge, 17: 9746
structure in interplanetary, sector, (E), 19: 32883
structure in interplanetary space, review of, 20: 37898
structure in plasma jet with intrinsic current, 18: 40712
structure in solar convection zone, (T), 19: 25120
structure in solar photosphere, (E), 20: 31892
structure of axisymmetric force-free, in dissipative plasma, (T), 19: 40049
structure of external, for toroidal plasma, (T), 19: 27670
structure of force-free, in solar corpuscular streams, (T), 20: 23855
structure of helical, in cylindrical chamber, 16: 28299
structure of helical, effects of perturbations on, 16: 28300
structure of, in cosmic sources of synchrotron radiation, 17: 13333(T)
structure of interplanetary, from cosmic ray asymmetry, 19: 25243
structure of interplanetary, 19: 39364
structure of interplanetary, quasi-stationary corotating, 20: 5972
structure of interplanetary, correlations with solar flare proton flux, (E), 20: 11852
structure of interplanetary, 20: 34046
structure of interplanetary, (E), 20: 34047
structure of interplanetary, temporal independence of small-scale irregularities in, (T), 20: 34059
structure of interplanetary, filamentary, (E), 20: 34131
structure of solar corona, arch, (T), 19: 12047
structure of solar and interplanetary, relations between, 20: 23867
structure of solar, reconnection and annihilation in, (T), 20: 31895
structure of solar, solution of MHD equation for, 20: 34035
structure of solar, flare effects on, 20: 39557
structure of solar, flare effects on, 20: 39558
structure of sunspots above flare regions, 19: 37445
structure of sunspot, (T), 20: 27712
structure of synchrotron, 16: 17164
structure of toroidal, having no magnetic surfaces, 17: 22309
structure of toroidal, 18: 5878
structure of unsymmetric toroidal, (T), 19: 47144
structure regularity in outer solar corona, 17: 2067(T) (JPRS-15517 (p.423-30))
superconducting resistance states induced by, 18: 22826
superconducting-sphere suspension in, 18: 30677
superconducting transitions of transition metal alloys in high, 17: 25938
superconductivity in strong, surface, 18: 40462
superconductor behavior in, theory of local, 17: 39769
superconductor critical fields and magnetic moments in homogeneous, 17: 31227
superconductor electric current density and energy gap equation in slowly varying static, 17: 39766
superconductor phase transitions induced by, cylindrical, 17: 37681
superconductor suspension in, force calculations for spherical, 20: 42130
superconductors in strong, small, (T), 19: 16799
supernova explosion into interstellar, model for early stages of, (T), 20: 2569
supernova explosion into interstellar, weak-field limit for, (T), 20: 2570
supernovae, influence of cosmic rays on character of, 17: 13330(T)
surface wave generation in mercury by, time-varying, 17: 12748 (AFOSR-2956)
surfaces, effects of crimped field on, 16: 3791
surfaces in, mathematical analysis of, 16: 30987
switching intense, fractional nsec, 19: 7776
synchrotron radiation from turbulent, in superstars, 19: 25133
theory and evidence of interplanetary, 19: 16359
theory of neutron star, 19: 18670
theory of plasma in strong, interrelated with hydromagnetics, 16: 2380
theory of thermal generation in stars, 16: 2387 (ML-837)
theory of two-dimensional, as functions of complex variables, 19: 16252 (BNL-8888)
thermomagnetic phenomena in metals in strong, (T), 19: 16178
tolerances on stray, in Stanford linear accelerator, 18: 8957 (SLAC-20)
topological characteristics for plasma containment, 20: 42461
topology, 16: 19871
transport coefficients in, 16: 15727
transport in shock-produced plasma, (E/T), 20: 36290 (TID-23144)
transport of solar, from spot and bipolar regions, (T), 20: 29906(T)
transport of trapped, in shock-produced plasma, 19: 14718
transport on sun, (T), 19: 9839
transport properties of plasma in uniform, effect of neutral particles, 16: 3776
trapping by finite volume flux surfaces, 18: 15369
trapping by niobium–tin superconducting hollow cylinders, temperature dependence of, (E), 20: 32316
trapping by theta-pinch plasma, end losses and contraction-wave collection rate from, (E), 20: 20060
trapping in hollow soft superconducting cylinders, length dependence of, 17: 36468
trapping in pinch devices, 17: 9733
trapping in superconductors, multiple-level memory cells from quantization of, 17: 37721
trapping in superconducting ring, 18: 21097 (UCRL-7308-T)
trapping in superconductors, r-f, 20: 11926
trapping in theta-pinch device, 17: 9719
trim-coil currents for cyclotron, computer programs for, 17: 7386
turbulence level in tubular pinch discharge, ion energy correlation to, 17: 42102
turbulent flow of mercury in transverse, skin friction coefficients for, 17: 16229 (NP-12631)

ultrasonic attenuation in metals in longitudinal, giant quantum oscillations in, (T), 19: 9794
ultrasonic attenuation in superconductors in strong, (E), 19: 21188
use as cosmic-particle shields for space vehicles, 16: 15432
use for charged-particle shielding, Liouville theorem for, (T), 19: 23945
use for curving high-energy particles in nuclear emulsions, 16: 16966 (NP-11592(Vol.I)(p.301-5))
use for space vehicle shielding, 17: 22769
use in acoustic wave generation at microwave frequencies in dysprosium films, 20: 14003
use in arc welding equipment, 19: 34307(P)
use in focusing neutrino beams, 16: 31926
use in motion sensing systems, 20: 41224 (EGG-1183-2078)
use in proton spin generators, 19: 26645
use in skin dose reduction during radiotherapy, 18: 39018
use of crossed, for accelerating conducting fluids, 16: 7965(T) (FTD-TT-61-228(p.1-11))
use of dipole, in shielding space vehicles, 18: 42867 (MTP-RP-64-1)
use of dipole, in shielding of space vehicles against charged particles, simulation of, 20: 24578
use of high, in solid state research, 20: 2519(R) (AD-615152)
use of large pulsed, in solid state research, 20: 42526
use of multipole, in plasma injection control, 20: 30579
use of pulsed, in devices with trochoidal electron beams, 20: 5929
use of pulsed, in superconductivity research, 20: 32312(R) (UCRL-16658, pp 133-43)
use of 200-kgauss pulsed, for magnetization measurements on solids, 16: 15456
use of 200-kilogauss pulsed, for momentum measurements of high-energy particles in nuclear emulsions, 16: 19502
uses for dynamic stabilization of plasma, (E), 19: 47842
uses in studies of properties of solids, 16: 15442
uses of axially symmetric, for plasma containment, 19: 19327(P)
uses of high, 16: 31880
uses of saw-toothed time-varying, in plasma heating, 17: 5442 (UCRL-6355)
uses with nuclear emulsions, for track analysis, 18: 23946
vacuum chamber effects on, in proton synchrotrons, 17: 936
variation in bubble chambers, correction for, 17: 23705
variation with time in sunspots, (T), 20: 25690
variations in interplanetary, (E), 20: 39575
variations in sector-focused cyclotrons, measurement using induction coils, 19: 37418
variations of lunar, 18: 30395
variations of solar, during flares, 18: 44386
Vector equation for varying, generalization of Ohm's law for, 16: 28294
wave propagation across, theory of nonlinear, (T), 20: 40235
wave propagation in, geometrical solutions for, 17: 8987
Zeeman effect in alternating, 17: 28034(T)

MAGNETIC FILTERS

ion motion in quadrupole-field, 19: 13201(R) (MLM-1217)
performance of quadrupole mass, 18: 31853

MAGNETIC INDUCTION

use for measurement of surface temperature of metals, 18: 12416 (HW-79621)

Magnetic Lenses

see Electromagnetic Lenses

MAGNETIC MATERIALS

see also Ferromagnetic Materials
see also Paramagnetic Materials
analysis of axisymmetric, computer programs for, (E/T), 19: 23162 (ORNL-3575)
analysis using Lamb-Moessbauer effect and neutron scattering, 19: 43484
atomic structure of, usefulness of neutron scattering for determining, 20: 25717 (BNL-946)
book: *Magnetic Neutronography*, 20: 36370
book: *Magnetism and Magnetic Materials*, 20: 32738
book: *Metals Reference Book.*, Vol. I and II, 3rd edition, 18: 32080
book: *Methods of Quantum Theory of Magnetism*, 20: 34864
book: *Nuclear Resonance in Magnetic Materials*, 18: 44843
chemical bonding in, analysis of effects of covalent, 19: 2269 (BNL-8514)
classification of, review on, 19: 11745
conference, 20: 24638
development and evaluation for space electric power systems, 18: 41928(R) (NASA-CR-54089)
development and testing for space power systems, 18: 34036(R) (NASA-CR-54041)
development for high-temperature operation, 20: 43815(R) (NASA-CR-54356)
diffusion in, departure of temperature dependence from Arrhenius relation, 19: 968 (UCRL-12029-T)
domain wall dynamics, 16: 15126(R) (NP-11584)
effects of small amounts of, on ultrasonic attenuation by superconductors (T), 19: 3179
effects on superconducting films, 18: 15102
electric conductivity of metallic, effects of Coulomb reactions on, 19: 26922(R) (PR-P-64)
electrodynamic field equations for magneto-electric, 17: 5126
electron interactions in, correction terms for hyperfine, 17: 37773
electron spin wave interactions in, at finite temperatures, (T), 20: 26342 (CEA-R-2821)
energy-level ordering in ferri-, 16: 32202
induction heating of, simplified calculation of, 17: 8276 (HW-SA-2270)
interactions of, imbedded in metals, 18: 42076
magnetic exchange interactions in transition metal compounds, lectures on, 19: 27710 (KR-93)
magnetic field interface with, theorem for, 20: 46251 (BNL-10587)
magnetic structure of, application of coupling rules to analysis of, 18: 42160 (ORNL-P-295)
magnetic transitions in ferri-, 16: 4655(T)
magnetic transitions in, Heisenberg and Ising models for, 18: 44217
magnon properties in, lectures on, 17: 13194
model of, (T), 19: 28842
Moessbauer effect in, hyperfine structure splitting in, (T), 19: 43384
neutron diffraction, 16: 22633
neutron diffraction by, covalency effects in (E/T), 19: 2269 (BNL-8514)
neutron diffraction analysis of, instrumentation for, (E), 19: 4449 (ANL-6920)
neutron elastic scattering by complex, slow, 17: 28236(T)
neutron inelastic scattering in franklinite, 16: 32369
neutron inelastic scattering by, magnetism studies from cold, 18: 32713 (CEA-R-2412)
neutron inelastic scattering by, 18: 38570 (A/CONF.28/P/12)
neutron inelastic scattering by, survey on, 20: 19797
neutron scattering in, effect of spin-spin interaction on, 17: 7072(T)
neutron scattering by, thermal, 17: 32987
neutron scattering research on, conference, 17: 37814
neutron scattering by spin waves in, 18: 7853(R) (KR-58)
neutron scattering by, at and near Curie point, theory of, 19: 12467
neutron scattering at Curie temperature, angular resolution for cold and thermal, 20: 22325
neutron scattering by, cold, 20: 28256
nuclear magnetic resonance linewidth in, correlation effect on, 17: 31206
nuclear magnetic resonance of ferri- and ferro-, 18: 30303 (CEA-R-2336)
paramagnetic g-value shifts in, by exchange interactions, 18: 709
phase transitions in, review on, (E/T), 20: 24199
photon interactions with spin waves in, (T), 20: 32735
plasma axial oscillations in, (T), 20: 46862
polarization of nuclei in, 17: 7267(T)
properties at 600 to 1400°F for use in space electric power systems, 20: 4379 (NASA-CR-54091)
properties, determination by microwaves, 16: 21010(R) (AD-264878)
properties for electromagnetic pumps, 19: 38781(R) (N64-25903)
properties of linear chains of spins, dynamic, (T), 20: 25630
properties of metals, survey, (T), 19: 40074 (CONF-796(Paper 3))
properties of square-loop, 19: 23164(R) (SU-SEL-64-103)
properties of square-loop, 19: 39269(R) (SU-SEL-64-133)
properties of submicron cobalt and iron particle compacts, 17: 41334 (ASD-TDR-63-423)
properties of, theory, 17: 13199
properties, review, 16: 16827
radiation and temperature effects on permanent, 16: 7944
radiation damage in Permalloy films, 19: 14113
radiation effects on soft, 16: 19397
radiation effects of charged particles and neutrons on, review of, 17: 31050
radiation effects on, 18: 658 (REIC-32)
radiation effects on, 18: 10346(R) (X64-11113)
radiation effects on, neutron, 18: 10346(R) (X64-11113)
radiation effects on, neutron, 18: 30290
radiation effects on performance of, in telemetry electronics, 18: 33839 (RTD-TDR-63-4287(Vol.II))
radiation effects on thin films of, coating effects on, (E), 19: 28881
radiation effects on hard and soft, electron, neutron, and proton, 19: 37179
radiation effects on, review of, 20: 16911
rare earth ion spectra in, optical absorption, 20: 22311(R) (AD-622068)
relaxation phenomena near critical points, 20: 30780
screw-spin structures in, magnetization properties of, 17: 13173
space groups in, special positions in, 17: 37797
spin ordering in dilute alloys of, 17: 20495
spin systems in, neutron magnetic scattering studies on, 17: 38027(T) (AEC-tr-5734(p.140-52))
spin-wave scattering by defects in, 17: 34657
spin waves in exchange-coupled crystalline, 16: 15326

spin-wave excitation in, by neutron inelastic scattering, 19: 41987
spin-wave theory for, formulation of, 20: 27500
structure, neutron diffraction analysis, 16: 3508
structure of, magnetic coupling mechanisms in, 18: 42161 (ORNL-P-297)
structure of, neutron diffraction studies of, 18: 44419 (BNL-7311)
structures of, use of Faraday and Kerr effects to obtain pictures of, 19: 34427(T) (NP-tr-1232)
surface properties, 17: 41421 (ASD-TDR-63-424)
survey of hyperfine fields in, 16: 10672 (MRL-110)
susceptibilities in Bloch-electron theory, 16: 21176
theory and uses of, conference on, 17: 37685
theory of magnetothermomechanics, 17: 6859
theory of NMR modes in, 17: 11379
thermoelectric power of dilute-alloy, 19: 16198
variant effects in ordered crystals of, magnetic symmetry and, 17: 24150

MAGNETIC MIRROR MACHINES
bibliography, 17: 28361 (NP-12921)
bibliography on, 18: 40656 (CLM-Bib-5)
book: *Controlled Thermonuclear Reactions*, 19: 19320
bremsstrahlung spectra from, 18: 13137(R) (ORNL-3564(p.28-43))
bremsstrahlung spectra from, 19: 21482(R) (ORNL-3760(p.23-9))
capacitor bank operation for Scylla IV, performance of, 20: 8181(R) (LA-3434)
charged-particle energy distribution in, (E), 20: 36329
charged-particle injection into, longitudinal, 18: 21370 (CEA-R-2410)
charged-particle motion in non-adiabatic, stochastic, 20: 38246
charged-particle trajectories in, analog computer techniques for determining, 20: 17906
charged-particle trapping in, lifetime of, 20: 44855 (IAE-1078)
components development for, 20: 8181(R) (LA-3434)
compression facility development for, 19: 31335(R) (UCRL-12303)
compression in multipole, longitudinal, (T), 19: 21516
containment circuit, 16: 4940(P)
data acquisition system for Alice, tape recorder, 20: 43638 (UCRL-70018)
description and performance of Russian Ogrenok, 16: 23237
description of Phoenix neutral-injection machine, 16: 23236
design, 16: 6071(P)
design and operation of Alice, 17: 4181(R) (UCRL-10294)
design and operation of, for producing counterrotating plasma, 17: 31630(P)
design and operation of MACETIE I and II Machines, 20: 46819 (NP-16293)
design and operation of VGL-2, 20: 46841
design and performance of Elmo, 16: 9506(R) (ORNL-3239(p.16-46))
design and performance for electron containment, 19: 41858 (NP-15217)
design economy optimization of, for controlled fusion research, 20: 34708 (NASA-TM-X-1251)
design for confinement of electrons for long periods, (E), 20: 3225
design for improved confinement of charged particles, 16: 2618(P)
design for plasma electron heating, 20: 8180 (IAE-912)
design for thermonuclear reactions, 16: 14192(P)
design for use as plasma injection chamber, 19: 33505(P)
design of, 20: 38325
design of cryogenic VGL-2, 20: 30655
design of ELMO, 19: 21482(R) (ORNL-3760(p.23-9))
design of Heliotron C, 20: 3174(R) (NP-15562, pp 30-7)
design of pyrotron for improved particle reflection at mirrors, 16: 6066(P)
design of Pyrotron, 19: 19327(P)
design of Q device, 20: 20018(R) (TID-22785)
design of Q-1 quiescent plasma source, 18: 9528
design of traveling-wave pyrotron, 17: 26740(P)
design using quadrupole fields, 20: 12163(R) (AD-625424)
design using superconducting coils, 20: 26249 (N-65-36897)
development, 17: 960 (NP-12171)
development, 17: 19453(R) (LAMS-2874)
development, 17: 19456 (NP-12651)
development, 17: 19465(R) (UCRL-10607)
development, 17: 29656(R) (LAMS-2916)
development, 18: 24763(R) (UCRL-11172)
development, 19: 19260(R) (UCRL-12028)
development, 19: 19261(R) (UCRL-12028(p.5-40))
development, 19: 31335(R) (UCRL-12303)
development during 1958 to 1960, 18: 6387
development in Pyrotron program, 19: 19265(R) (UCRL-12028(p.121-36))
development of MACETIE, 20: 3173(R) (NP-15562, pp 20-9)
development of OGRA, 18: 6388
development of PQ, in Japan, 17: 21139 (NP-12712)
development of QP machine, 20: 3172(R) (NP-15562, pp 4-19)
development of Scylla, 16: 15719(R) (LAMS-2682)
development of Scylla, 16: 29904(R) (LAMS-2721)
development of Scylla, 16: 33927(R) (LAMS-2754)
development of Scylla IV, 17: 11831(R) (LAMS-2816)
development of Scyllac, 19: 43413 (LA-3253(Rev.))
development of toroidal Scylla theta-pinch, (E/T), 19: 25553 (LA-3289)
development of Toy Top III, 16: 4907(R) (UCRL-9777)
development status of 2X and Scylla IV, 20: 20365
development using superconducting coils, 19: 33276
developments at ORNL, 17: 33151(R) (ORNL-3472(p.1-8))
diagnostics and plasma density of Table Top, 16: 4907(R) (UCRL-9777)
diagnostics of ALICE, 16: 4907(R) (UCRL-9777)
diffusion of cesium plasma in, ion loss effects on, 18: 13165
electron cyclotron resonance instability in, 18: 35008
electron cyclotron heating in, (T), 20: 12163(R) (AD-625424)
electron heating in, by electric field oscillations, 18: 15346(T) (AEC-tr-5474)
electron heating in, h-f, (T), 19: 8522
electron motion in, 17: 19450 (IPPJ-2)
electron trapping in French CAPEL, 18: 24747 (CEA-R-2417)
electron velocity distribution from, system for measuring, 20: 12163(R) (AD-625424)
electron-beam injection, (E), 20: 36327
electron-beam injection into constant-field, pulsed, (E), 20: 36328
electron containment in CAPEL-A, 5-kev, 18: 32930
electrostatic and magnetic field calculation for, (T), 20: 26246 (LA-3416)
end closures for, solenoid arrangement for, 17: 33221(P)
energy and velocity of plasma rotation in Ixion III, 16: 8273
energy balance and self-sustaining thermonuclear reaction in, (T), 20: 10159
energy spectra of plasma electrons in, 16: 8282
energy storage and delivery systems performance in Scylla IV, (E), 19: 21474 (LA-3189)
energy storage system for 3.5-megajoule Scylla IV, 16: 14151
equipment for Scylla IV, engineering drawings of Zeus transmission system coaxial header, 17: 19503
gas pressure in, anisotropy of radial, (E), 20: 13907 (IPP-2/42)
hydrogen arc for DCX, 18: 2998
hydrogen atom and molecular ion accumulation and injection in, high-energy, 17: 33187
hydrogen atom ionization in, Lorentz neutral, 17: 19465(R) (UCRL-10607)
hydromagnetic characteristics of Ixion III, 16: 8272
impurity atoms in, pumping-out requirements for neutral, 16: 23240
injection components for Phoenix II, 20: 36279 (CLM-R-59)
injection in, ion density relations with time for neutral, 17: 9689 (UCRL-7033)
injection into, possibilities of very high-energy, 17: 33160(R) (ORNL-3472(p.119-20))
injection method for, 18: 24767(T) (KFK-tr-141)
injection of high-energy molecular ions into, 16: 4906 (UCRL-5827)
injection of 20-kev neutral hydrogen atoms into electron-cyclotron plasma in, (E), 19: 47837
instabilities in, analysis of, 16: 31144 (UCRL-6705-T)
instrumentation for DCX-1, 16: 1985
ion density limit for, fast, 18: 13135(R) (ORNL-3564(p.1-13))
ion heating in, using alternating electric fields, (E), 19: 29430
ion source for Ogra, for production and injection of hydrogen ions, 18: 19220
ion trapping in, ion-cyclotron, 17: 38379(T) (NP-tr-1057)
loop currents in Toy Top coils, computer program for, 18: 36724 (UCRL-7864)
magnet coil design for, cryogenic, 20: 17874 (CONF-650922, pp 630-42)
magnet coil system of Toy Top, re-design of pulsed-field, 17: 4181(R) (UCRL-10294)
magnet sectors for Scylla IV, curved, 20: 8181(R) (LA-3434)
magnetic coils for ALICE, engineering drawings of trapping, 20: 6514
magnetic field disturbances in, local, 17: 9696
magnetic field in Scylla 1, external probe measurement of, 17: 19456 (NP-12651)
magnetic field production in toroidal Heliotron, 20: 30595
magnetic fields for, production of circular homogeneous, 18: 2440
magnetic fields in, IBM 7090 program for calculating, 17: 19465(R) (UCRL-10607)
magnetohydrodynamic stabilization in, 20: 24549
microwave excitation in P-3 "Puffatron" at electron cyclotron frequency (E), 19: 3401 (UCRL-12057-T)
mirror inserts for Scylla IV, single-turn, 20: 8181(R) (LA-3434)
mirror magnet design for Phoenix, 100-kgauss, 16: 15423
operation and electron temperature measurements, 16: 6547 (ONR-9 (Vol.I)(p.323-7))
operation of Scylla IV, 20: 8181(R) (LA-3434)
operation of steady-state deuterium, economic aspects of, 16: 32466 (61-RL-2725E)
operational analysis of P-4 steady-state plasma system, 16: 4907(R)

(UCRL-9777)
operations of Scylla IV, (E), 19: 33415(R) (LA-3320(p.78-82))
parameters and properties, status, 16: 9540
particle containment and injection in, 18: 4643(T) (AEC-tr-6131)
particle injection system for Phoenix II, neutral, 20: 36279 (CLM-R-59)
particle injection through cusp configuration of, properties of, 20: 44971
particle losses by scattering, 16: 15734
particle motions in, equations for, 17: 33165
plasma behavior in Orekh, pulsed, 16: 23221
plasma behavior in, research on, 17: 19456 (NP-12651)
plasma behavior in Scylla I, fast θ-pinch, 17: 31574 (LAMS-2911)
plasma behavior in OGRA, 18: 15347(T) (AEC-tr-5804)
plasma bunch interactions in, 19: 27599 (EUR-CEA-FC-273)
plasma capture by, (E/T), 19: 47839
plasma column end effects in Q-1 device, (T), 20: 12236
plasma compression in, boundary condition effects in, (E), 20: 12238
plasma compression in, adiabatic, 20: 30636
plasma confinement in Table Top, stable and unstable modes of, 17: 4181(R) (UCRL-10294)
plasma confinement and heating in DECA-2, 20: 6469(T) (UCRL-Trans-1256(L))
plasma confinement in FII, critical voltage for, 20: 46867
plasma containment and instabilities in, 16: 15473
plasma containment and properties in Ogra, 16: 23229
plasma containment in, geometry for, 17: 42106
plasma containment geometries in, 18: 36743
plasma containment in, research on, 18: 38200 (A/CONF.28/P/297)
plasma containment in DECA 1, 18: 42836
plasma containment in, with nonadiabatic field perturbation, (T), 19: 17073 (IPP-6)
plasma containment in, (T), 19: 17074 (IPP-9)
plasma containment in, magnetic shear effects on, (E), 19: 45415 (UCRL-14137)
plasma containment in PR-5, 19: 47857
plasma containment in, effects of mirror losses by collisions on, (T), 20: 24538
plasma containment in, hot-electron, (E), 20: 24540
plasma containment and heating in DECA II, 20: 30607
plasma containment in Probkatron, properties of, 20: 40194
plasma containment in, pulse-injected, 20: 44972
plasma containment in, nonadiabatic analysis for, 20: 44977
plasma cyclotron and thermal radiation emission in Ogra, 16: 23230
plasma decay in, hot-electron, (T), 20: 24185(R) (TID-22735, pp 109-52)
plasma density and velocity in DECA II, 17: 26666
plasma density distribution in, using Lorentz trapping, (E/T), 19: 23917
plasma density in Q-3, effect of current heating on, (E), 19: 21541
plasma density in Scylla IV during preionization, (E), 19: 33416(R) (LA-3320(p.83-7))
plasma diagnostics of high-compression and neutral injection experiments, 16: 1984
plasma diamagnetism in Scylla I, theta-pinch, 17: 42050 (LADC-5601)
plasma diffusion across magnetic fields in Q-3, (E), 19: 19246 (MATT-328)
plasma diffusion and instabilities in Q-type, (E/T), 20: 38324
plasma diffusion in, 18: 28796
plasma diffusion in, classical and enhanced, 18: 28795
plasma diffusion in Q-1 (E/T), 19: 1704 (MATT-291)
plasma diffusion in Q-1 device, Bohm, (T), 19: 40014
plasma diffusion in Q, enhanced, 20: 6466 (SIT-2813-33)
plasma diffusion in Q devices, end plate effects on, (T), 20: 32611
plasma diffusion in Q-type, (T), 20: 38203 (NP-16237)
plasma diffusion in, properties of, 20: 38313
plasma drifts and losses in Q-type, with curved fields, (T), 20: 36298
plasma electron and ion density distribution in, (T), 20: 32609
plasma electron cyclotron heating in ELMO, 20: 40173(R) (ORNL-3989, pp 31-42)
plasma energy escape from, calorimetric studies, 16: 33934 (UCRL-13045)
plasma flute instability in, (T), 19: 12661
plasma flute instability in, (E), 19: 25583
plasma flute instability at ion gyrofrequency in, (T), 20: 8229
plasma flute instability in, (T), 20: 10168
plasma flute instability in, effects of density on, (T), 20: 30707
plasma form in Table Top III, rotating, 17: 19465(R) (UCRL-10607)
plasma free-streaming experiments in Q device, (E), 20: 12235
plasma heating and stability in Scylla, 17: 9730
plasma heating and stability in Scylla III, effect of bias and preionization fields on, 17: 29655 (LADC-5531)
plasma heating and containment in, (E), 20: 24546(T)
plasma heating by excitation at electron-cyclotron frequencies, 16: 23242
plasma heating by electron beams, mirror ratio effect on, (E), 20: 13947(T)
plasma heating in, 16: 32488(R) (ORNL-3315(p.21-44))
plasma heating in QP, ion cyclotron resonance, (T), 20: 10135 (IPPJ-37)
plasma heating in, (E/T), 20: 13908 (IPP-2/44)
plasma heating in QP, ion cyclotron resonance, 20: 40260
plasma heating in, properties of electron cyclotron, (E/T), 20: 17888(R) (ORNL-3908, pp 32-51)
plasma heating in, electron cyclotron, 20: 24497(R) (AD-628004)
plasma heating under electron beam instability conditions, (E), 20: 30659
plasma in P-4 (steady-state) system, compression and confinement in, 17: 19465(R) (UCRL-10607)
plasma injection, 16: 1151
plasma injection and trapping in, by cyclotron-resonance energy transfer, 16: 23238
plasma injection at high β, 16: 8274
plasma injection into Scylla, by coaxial guns, 16: 8277
plasma injection into GVL-2, 18: 17108 (NP-13609)
plasma injection using theta-pinch device, properties of, 20: 42504
plasma instabilities in, 17: 7448
plasma instabilities in Scylla III, stabilization of flute, 17: 29654 (LADC-5530)
plasma instabilities in Table Top III, 17: 42114
plasma instabilities in, critical length determination for convective-loss-cone, (T), 20: 12233
plasma instabilities in, electron-cyclotron, (E), 20: 38274
plasma instability inherent to loss-cone particle distribution in, h-f electrostatic, (T), 19: 19304
plasma instability in, dissipative, (T), 19: 43445
plasma instability in, nonlinear mechanics of, (T), 20: 13905 (CONF-651056-1)
plasma interchange modes in, stability against, 18: 1142
plasma ion cyclotron heating in Heliotron-B, 20: 38258
plasma ion cyclotron resonance heating in QP, 20: 46819(R) (NP-16293)
plasma ion loss in Q, electric field effects on, (T), 20: 26242 (IPP-2/46)
plasma ion losses through charge exchange in, 20: 30584
plasma jet configuration and particle losses in curved fields of, 18: 35023
plasma kinetics in, 17: 19465(R) (UCRL-10607)
plasma kinetics in ALICE, 17: 19465(R) (UCRL-10607)
plasma loss from Q-3, (E), 20: 28493(R) (MATT-Q-22, pp 113-214)
plasma losses from, through mirrors, 17: 35056
plasma losses from Orekh, bolometer measurement of, (E), 19: 5301(T) (AEC-tr-6518(p.248-51))
plasma magnetic field measurements in Scylla I theta pinch, 17: 33178
plasma oscillations in PIG source in QP, 20: 46819(R) (NP-16293)
plasma production in, high-density proton, 17: 17338(R) (ORNL-3392 (p.89-93))
plasma production and properties in EPA, 18: 30892 (ORNL-P-3)
plasma production in, hot, dense, 18: 30916
plasma production for DCX-type, 18: 32920
plasma production in Scylla IV, properties of, 18: 32921
plasma production in, high-temperature, 18: 32947(P)
plasma production in, by electron beam injection, 18: 42162(R) (TID-20963)
plasma production in Bille-en-Tete "A", 19: 27600 (EUR-CEA-FC-274)
plasma production in, by fast particle injection, 19: 27622(T) (CLM-Trans-6)
plasma production and properties in two-stage, 20: 17953
plasma production by molecular hydrogen ion injection in, (E), 20: 30634
plasma production in, hot-electron, 20: 38211(T) (AEC-tr-6782)
plasma properties and stabilization in, 17: 33152(R) (ORNL-3472 (p.9-23))
plasma properties in Scylla IV theta pinch, (E), 19: 47722 (LA-DC-7039)
plasma properties in, (E), 20: 1272(R) (ORNL-3836, pp 36-66)
plasma properties in, relativistic electron, (T), 20: 30638
plasma radial distribution in, (E/T), 20: 46861
plasma rotation in, (E/T), 19: 12690
plasma spectra in Scylla, x-ray, 17: 13639
plasma stability, effects of transverse conducting planes on, 16: 23241
plasma stability in, 16: 23224
plasma stability in, kinetic theory of flute, 18: 21371 (CLM-R-33)
plasma stability in high-energy neutral injection, 18: 28794
plasma stability in, analysis of, 18: 34979 (UCRL-11077)
plasma stability in, 18: 42788 (CLM-R-38)
plasma stability in, theory of, 18: 44884
plasma stability in, ion-cyclotron resonance (E/T), 19: 1719 (ORNL-3696)
plasma stability in, effects of stabilizing rods on, (T), 19: 47835
plasma stability in negative V, (T), 20: 3167 (MATT-374)
plasma stability in, (T), 20: 30635
plasma stability in, flute, (E/T), 20: 38323
plasma stability in, flute, 20: 40217(T)
plasma stable oscillations in ALICE, 17: 26720

plasma x-ray spectra in Scylla, 16: 29908 (TID-12518)
positron containment in, 16: 4907(R) (UCRL-9777)
properties of Scylla I, 20: 8181(R) (LA-3434)
research progress on, 18: 2985(R) (UCRL-10852)
research progress on, 18: 6302(R) (LAMS-3004)
scattering losses from, 16: 18571
spark gap design for, 50 to 80 kv, 17: 17387
spectra of impurities in Scylla, 17: 5515
spectrometer design for use in DCX-2, (E), 20: 3178 (ORNL-P-1513)
stability of, theory of, 17: 9687(R) (TID-17475)
surface bombardment studies for, 17: 19465(R) (UCRL-10607)
switch design for high-current circuit in, 16: 17219(P)
synchrotron radiation from hot-electron plasma in pulsed, 18: 42837
uses of Scylla I for simulation of solar iron-ion spectra, (E), 19: 32854(R) (LA-3320(p.100-3))
vacuum system for Ogra-1, ultrahigh, 20: 30701
vacuum system gate valves for ALICE, engineering drawings of, 20: 6513
vacuum systems, 16: 29928
x-ray production in Scylla I, 17: 11831(R) (LAMS-2816)
Zeeman effect measurement in Scylla I, 17: 11831(R) (LAMS-2816)

MAGNETIC MIRRORS

charged particle adiabatic containment by multipole cusp, (T), 20: 6496
charged particle behavior in static asymmetric, 17: 7465
charged particle behavior in static axially symmetric, 17: 7466
charged particle containment and motion in, (T), 19: 16248 (AD-603602)
charged particle distribution in, 18: 16731(T) (FTD-TT-64-90(p.110-27))
charged particle escape from plasma in magnetic bottle, 18: 26799
charged particle motion in, adiabatic approximation for, 17: 2374
charged particle motions in, 17: 19450 (IPPJ-2)
charged particle motion in, 17: 36769
charged-particle motion in, with secondary electromagnetic fields, 18: 6320
charged particle motion in, at small pitch angles, 18: 7798
charged particle motion in axisymmetric, 18: 15417
charged particle motion in, 18: 17125
charged particle nonadiabatic losses from axisymmetric, (E/T), 20: 10145 (NASA-TN-D-3164)
charged particle scattering in, nonadiabatic, 20: 4948(R) (TID-22179, pp 85-175)
charged particle trajectories in, 16: 32281 (ORO-569)
charged particle trapping in, 17: 4176 (TID-17197)
charged-particle trapping in, nonadiabatic injection, 17: 42115
charged particle trapping and containment in nonadiabatic, statistical theory for, (T), 20: 6494
charged particle trajectories in composite, intermingling in, (T), 20: 22274
charged-particle containment in, (T), 20: 22229
charged-particle injection into, 18: 32924
charged-particle injection into trap of, through acute-angle trap, (T), 20: 10147 (NP-15795)
charged-particle injection into, (E/T), 20: 24570
charged-particle losses in axisymmetric and multipolar, 20: 32545
charged-particle motion in, 18: 26702(T) (AEC-tr-5589(p.637-77))
charged-particle motion in nonadiabatic, (T), 19: 47748
charged-particle motion in, correction to second adiabatic invariant of, (T), 20: 38275
charged-particle reactions with, (T), 19: 47821
charged-particle temporary capture in static, (T), 20: 32582
containment of slow ions in, in a plasma with positive potential, (T), 20: 3227
cyclotron instability of electron beams in, theory of two-stream, 20: 44894
design, 18: 15419(P)
design economy optimization of, for controlled fusion research, 20: 34708 (NASA-TM-X-1251)
design for Alice, 20: 10124 (CONF-650512, pp 131-7)
design for plasma compression, 17: 9809(P)
design for plasma containment using particle-velocity-vector polarization, 18: 11357(P)
design of achromatic deflecting, for ion beams, 17: 20767
design of caulked cusp, calculations for, (T), 19: 33410(R) (LA-3320 (p.35-44))
design of superconducting, 20: 46544
design using cusps for plasma containment, 20: 24489(R) (AD-624486)
design with radially increasing field, (T), 19: 5313
dissociation of molecular hydrogen ions by Lorentz force in, (E), 20: 46863
effects on carrier lifetimes of indium antimonides, 18: 30305 (D1-82-0340)
effects on plasmas, 16: 9506(R) (ORNL-3239(p.16-46))
electromagnetic fields in caulked, stuffed cusps, (T), 19: 33405(R) (LA-3320(p.6-13))
electron acceleration and capture in, during electric breakdown of plasma, (E), 20: 28582
electron cyclotron resonance in, (T), 19: 5370
electron heating in, turbulent, (E), 20: 12206(T)
electron leakage from, correlations with electron precipitation in auroral-zone ionosphere, (E), 20: 21836
electron loss from, with superimposed helical magnetic field, 19: 47145
electron motion and loss mechanisms from, with bottle geometry, (E), 19: 10422
electron trapping in, 18: 15396
electron trapping at 1.8 kev by periodic electrostatic perturbations, 18: 24747 (CEA-R-2417)
energy storage systems for, design of inductive, (T), 19: 33411(R) (LA-3320(p.45-9))
feasibility of toroidal caulked cusps for thermonuclear containment, (T), 19: 33409(R) (LA-3320(p.33-4))
field design for, 18: 22944 (MATT-256)
field distributions in caulked, stuffed cusps, (E), 19: 33406(R) (LA-3320(p.14-18))
gas discharge experiments in, three-phase, 17: 26737
ion angular and velocity distributions in long, 16: 8264 (UCRL-6554)
ion escape from, due to instability connected with loss cone, (T),
ion distribution in long, approximate asymptotic equation for, 16: 3785 20: 3229
ion flow in, due to turbulent diffusion, (T), 20: 40236
ion injection in HX apparatus, r-f electric field effects on molecular hydrogen, (E), 20: 22207
ion trajectories in, 16: 29925
ion trajectories in, 17: 2388
magnet design for, 18: 17116 (NP-13711)
magnetic fields for, superconducting coils for, (E), 19: 10449
molecular ion injection and trapping in, use of r-f field for, 20: 30580
neutron polarization angle adjustment in, 16: 14233(R) (KR-16)
particle energy distribution in, 17: 36807
particle injection into, high-energy neutral, (T), 20: 38277
particle trajectories in rapidly varying, 18: 21449
plasma behavior in, computer programs for analysis of, 18: 34266 (CLM-R-31)
plasma bunch containment in, effects of h-f fields on, (E), 19: 14676(T) (UCRL-Trans-1163(L))
plasma configuration in, rarefied, (T), 20: 42458
plasma confinement by injection and trapping, 17: 2379
plasma confinement in, at high pressures, 18: 26762
plasma containment lifetimes in, 16: 23222
plasma containment in cusp, 17: 4200
plasma containment by, 18: 1164
plasma containment in, with hexapole stabilizing fields, 18: 40695
plasma containment in, charged, 18: 40726
plasma containment in, with superposed quadrupole fields (E), 19: 1759
plasma containment by combined-field, (E), 19: 10405
plasma containment in radial, with minimum B configuration, (T), 19: 14693
plasma containment by, (E), 19: 23829(R) (TID-21548)
plasma containment by, cooperative effects in tenuous energetic, (E), 19: 40017
plasma containment by, high-temperature, 19: 40045
plasma containment in, 19: 40046
plasma containment in, (E), 19: 47848
plasma containment by, stability of infinite uniform, (T), 20: 4981
plasma containment and motion in, (T), 20: 6459 (CNIE-PE-1)
plasma containment in trap, with field increasing on all sides, (T), 20: 10158
plasma containment and properties in, (E/T), 20: 12163(R) (AD-625424)
plasma containment in, (E), 20: 26288
plasma containment by, first order correction to first adiabatic invariant for, (T), 20: 32669
plasma containment in, hydrogen, (E), 20: 36327
plasma containment by constant-field, using pulsed electron-beam injection, 20: 36328
plasma containment by, superconducting magnetic coils for, 20: 40169 (NASA-TN-D-3595)
plasma containment in, laser-produced, 20: 42415 (TID-22928)
plasma containment in, properties of cesium, 20: 46877
plasma deformation and drift from inhomogeneity in, 18: 21402
plasma diagnostics in, mass-spectrographic escaping, (E), 19: 5290(T) (AEC-tr-6518(p.163-70))
plasma diagnostics in, using microwaves, (T), 19: 5334
plasma diffusion across, (E), 19: 21475 (LA-DC-6383)
plasma electron cyclotron instability in, (E/T), 20: 22197
plasma electron cyclotron heating in, (T), 20: 26259(R) (TID-22881)
plasma end loss in slow theta pinch, (E), 20: 38256
plasma equilibrium in, hydromagnetic equations for two-fluid bounded, 16: 18565
plasma heating by shock waves in, (T), 19: 23826(T) (UCRL-Trans-1185(L))

plasma heating by E X B mechanism in, (E), 19: 33406(R) (LA-3320 (p.14-18))
plasma heating in, electron cyclotron, (E), 20: 46903
plasma in, containment of hot-electron, (E), 20: 3184 (UCRL-14310)
plasma injection, 16: 28304
plasma injection in Deca, use of ion detector in studies of, 17: 21130 (CEA-2252)
plasma injection into, 18: 17110 (NP-13623)
plasma injection in, (E), 20: 26288
plasma injection into, rotating source for, 20: 26289
plasma instability in, low-frequency flute, (T), 19: 31364
plasma instability in, ion diffusion into loss cone from, (T), 20: 8187(T) (UCRL-Trans-1275(L))
plasma interactions with walls of, 17: 9752
plasma ion energies in, 18: 26701(T) (AEC-tr-5589(p.626-36))
plasma ion escape from, energy of recharged, 20: 44976
plasma ion losses from, analysis of, (T), 20: 30618
plasma ion velocity in composite, (T), 20: 22274
plasma jet polarization interactions in countercurrent, (E), 20: 22273
plasma loss through apertures in, with field increasing toward the periphery, 17: 11841(T) (AEC-tr-5620)
plasma losses by cross-field diffusion in, 18: 44856 (ORNL-P-456)
plasma negative-mass instability in, hot proton, (E), 20: 12247
plasma particle motion in, 17: 42057
plasma potential in, 16: 2609
plasma production by neutral atom injection in, 17: 5473
plasma production in, physics of, 17: 17332(R) (ORNL-3392(p.28-46))
plasma production in, at 0.03 to 3 torr, (E), 19: 8504 (SC-RR-64-988)
plasma production in, (E), 19: 12637(R) (LA-3202-MS)
plasma production in, hot thermonuclear, 19: 41852 (IAE-676)
plasma production by neutral hydrogen injection in well geometry of, (E), 20: 30632
plasma properties in Heliotron and TP, 20: 46819 (NP-16293)
plasma recombination at ends of, (T), 19: 27611 (MPI-PA-14/64)
plasma reflection by, 18: 14848
plasma stability in spindle cusp, 17: 42113
plasma stability in, 18: 26695(T) (AEC-tr-5589(p.83-96))
plasma stability in, 18: 26744
plasma stability in, (E), 19: 12671
plasma stability in, maximum pressure for, (T), 19: 14701
plasma stability in pulsed, (E), 19: 45388 (GA-6432)
plasma stability in, effect of relativistic electrons on, (T), 20: 4950(T) (UCRL-Trans-1261(L))
plasma stability in, hot electron, (E), 20: 8236
plasma stability in, (E), 20: 10174
plasma stability in, relation to toroidal confined, 20: 42402 (IAE-1149)
plasma temperatures in, with axial current, 18: 28816
plasma transport properties in, one-dimensional macroscopic, 18: 9512
plasma transverse diffusion in, (T), 19: 5308
plasma trapping in, by ion acceleration, 18: 6360
plasma wave damping at ion cyclotron resonance in, (E/T), 19: 5272 (UCRL-11619)
plasmoid motion in adiabatic trap with, 17: 26680
scattering losses from, ambipolar, 18: 44886
shock wave propagation in, effects of, (E), 20: 13921(R) (NP-15703, pp 52-63)
theory of nonadiabatic, 16: 2594(T) (AEC-tr-4724)
use in high-temperature plasma research, 19: 27586 (AD-428606)
use of two-stage, in production of hot plasma, (E), 20: 26248 (N-65-33300)
with cusped fields, 16: 3772

MAGNETIC MOMENTS

see also Nuclear Magnetic Moments
calculation for strange baryons, (T), 20: 34207
calculation of electron anomalous, field theory, 19: 37635
Cherenkov emission from, in transparent uniaxial ferroelectric, 18: 885(T)
corrections for nucleon interactions, mathematical analysis, 16: 18318 (AFOSR-1568)
dipole, dissipation in 2-level systems, 18: 21046
electromagnetic radiation from moving point multipoles, 18: 28094(R) (TID-20607)
hyperfine interaction with S electron of displaced nucleus, 16: 7122
interactions between electronic and nuclear, dynamic polarization effects in, 16: 28046
interactions of electronic and nuclear, with high magnetic fields in solids, 16: 15448
interactions of electronic and nuclear, hyperfine, 16: 32408
interactions of point dipoles with dipole layers, 18: 28094(R) (TID-20607)
measurement of, by Mossbauer scattering, 17: 40435(R) (NYO-10063 (p.99-104))
measurement of planetary, by auroral zone x-ray emission, (T), 19: 12409(T)
measurement of, produced by rotating superconductors, 20: 19771
molecular-beam uses in study of, 19: 41143
of excited nuclei, review, 17: 15278
of radioactive nuclei, measurement of, by optical pumping techniques, 17: 34640
of small superconductors, formulas for calculation of, 18: 18834
plasma interaction with two-dimensional dipole, 17: 5477
production in SNAP-10A, analysis of, (T), 20: 1528 (NAA-SR-11207)
radiation from waveguide accelerated dipole, 18: 40340
source system structure for multipole, 18: 28429
space propulsion by magnetic field-dipole interaction, (T), 19: 9790
transition probability for multipoles, $\Delta S = \pm 1$, 18: 20751

MAGNETIC MONOPOLES

action principle for, 20: 33978
behavior of Dirac, in cosmic space, expectance study of, 18: 8992
detection and measurement of Dirac, using superconducting cylinders, (E), 19: 41391
detection of fast, using Cherenkov emission and ionization loss, (T), 19: 45149
effects on elementary particle structure, (T), 19: 35103
existence of ferromagnetically trapped, of cosmic-ray origin, negative results, 17: 37867
existence of, forbidden by parity conservation, 17: 17399
existence of, forbidden by parity conservation, 17: 40242
existence of parity-violating, 18: 21062
existence of, Dirac, 17: 26420 (CERN-63-13)
field theory of Dirac, impossibility of Lorentz-invariant, 20: 1069
interactions of, angular momentum in weak, (T), 19: 18579
interactions with electromagnetic fields, quantum theory, 16: 24927
interactions with electric charge, spin angular momentum in, (T), 20: 4684
motion in dipole field of earth, (T), 20: 23965
motion through permeable media, Cherenkov emission and energy losses in, 19: 18950
production by protons at 30 Bev, search for, 17: 13439
production in cosmic radiation, (E/T), 20: 41676
production in nucleon-nucleon interactions, cross sections, 16: 9375
production of Dirac, by cosmic radiation, 18: 18603
production of Dirac, 18: 40067
properties of Dirac, 20: 35948 (AD-635253)
properties of, pseudoscalar, (T), 19: 35042(T)
signs of, 18: 34291
work function of, calculation of, 17: 35260(R) (TID-19135)

MAGNETIC PARTICLE INSPECTION

development of, for coating–metal bonds, 18: 39465(R) (IITRI-N213-20)
improvement of method by addition of radioactive material to particles, 17: 30678(P)
uses on pressure vessel weldments, 19: 13999(R) (SWRI-1228-43)

MAGNETIC PROBES

analysis of induction coil, for fast high-current gas discharges, 20: 32571 (IPP-1/2)
bibliography, 17: 28361 (NP-12921)
design and frequency response of multi-coil, 17: 30808
design and performance of Hall-generator, for accelerator measurements, 16: 22332 (USNRDL-TR-559)
design and performance for diagnosis of beam-plasma discharge, 17: 35260(R) (TID-19135)
design and performance of cesium NMR, for use with Varian fluxmeter at low temperatures, 20: 37972
design for electric discharges (E/T), 19: 1721 (RT/F1(64)-8)
design for field measurements in plasma, 17: 21986
design for field measurements in linear pinch devices, 20: 6507
design for plasma diagnostics, 18: 32275(R) (ORNL-3652(p.105-31))
design for studying gasdynamics of current sheath, 19: 1708(R) (NASA-CR-53229(p.23-30))
design for use in cyclotron-resonance plasma accelerators, 19: 42630(R) (NP-15333)
design of high frequency, for electric conductivity measurements in arc plasma jets, 19: 12716
design of wideband integrator, 16: 20661
design, performance, and use of inductive loop, for plasma diagnostics, (T), 20: 8255
development, 19: 44223(R) (NP-15438)
development for magnetohydrodynamic turbulence research, 17: 42048 (DCAS-TDR-62-167)
development of external, 17: 19453(R) (LAMS-2874)
development of NMR, for flux density measurements, 19: 9460
diagnostic use for plasma, 19: 40059
diagnostic use in azimuthal pinch discharges, 18: 26735
effects of, in plasma, 17: 42050 (LADC-5601)
effects on magnetic field diffusion in theta pinch, (E/T), 19: 21524
effects on plasma, 18: 28094(R) (TID-20607)

fabrication and performance of magnetoresistance, for magnetic field measurements, 17: 18581
performance for plasma diagnostics, 19: 47817
performance of large area, in electromagnetic shock tubes, 20: 10205
plasma diagnostics with, dense, 17: 42038 (ARL-63-105)
plasma instability detection using, 18: 13137(R) (ORNL-3564(p.28-43))
plasma measurements using, boundary errors in, (E), 19: 23902
plasma structure observation by, 18: 1095(R) (AFCRL-62-184)
properties for measuring transient electromagnetic fields in air and conducting media, 18: 19474 (SC-R-740)
resolution for plasma diagnostics, 18: 42847
response of, method for measuring, 19: 20293
signal sampling equipment for multi-coil, design of, 20: 19998 (CLM-R-50)
use for plasma measurements in electric discharges, (E), 20: 13639 (JUL-281-PP)
use in plasma acceleration measurements, 19: 29410
use in plasma conductivity measurements, errors in, 17: 9796
use in plasma temperature measurement, (E/T), 19: 10392(R) (MATT-Q-21)
use in study of MHD turbulence, 17: 40213
use of Hall, for regulating magnetic fields, 17: 8536 (TID-17610)

MAGNETIC PROPERTIES

approximation of spontaneous magnetization, magnetic susceptibility by Ising model, 16: 3805
bibliography on rare earth, 18: 24178
book: *High-Temperature Materials.* No. 2, *Properties Index*, 18: 26064(T)
book: *Magnetic Transitions*, 16: 4655(T)
calculation of diamagnetic nuclear shielding constant from x-ray scattering, 17: 18940
de Haas-van Alphen effect in crystals, sample orienting device for studies of, 17: 20332
determination from electron and neutron diffraction, conference on, 17: 37790
electrodynamic field equations for magneto-electric media, 17: 5126
hysteresis loops using pulsed fields, distortions in, 17: 8550
magnetization characteristics of screw-spin structures, 17: 13173
measurement at high pressures, device for, 20: 21357 (UCRL-16299)
measurement in solids using high magnetic fields, 16: 15442
measurement in transition-metal carbides, borides, and nitrides, design and operation of potentiometer for, 19: 47009 (NP-15514(Vol.2))
measurement of, equipment for, 17: 39382(T,R) (EURAEC-700)
measurement of magnetizations, ring balance for, 16: 9185 (AD-261209)
measurement of, of crystals, 17: 22382
measurement of saturation magnetization of iron alloys by force method, apparatus for, 19: 44678(R) (ANL-7000, pp 186-200)
measurement of, using backscattering of beta particles, 20: 25370(P)
measurement technique for Hall coefficients, 17: 8852
model for, in hard-superconductors, 17: 619
models for magnetic breakdown of solids, (T), 19: 6383 (NASA-TN-D-2554)
neutron diffraction studies of, review of techniques for, 19: 25029
nuclear magnetization in liquids due to Overhauser effect, 16: 21357 (RADC-TR-61-132)
of current systems, computer programs using zonal harmonics for, 17: 3358 (ORNL-3318)
of heavy rare earths, relations with dilution and temperature, 18: 39883 (AFCRL-64-199)
of metals, survey, (T), 19: 40074 (CONF-796(Paper 3))
of rare earth nitrate solutions, 19: 26917(R) (IA-984)
of solids, 17: 41420(R) (AD-292905)
physical effects of, description of, 17: 3370 (AD-276381)
review, 16: 16827
similarities analysis, 16: 17174 (AD-266636)
temperature dependence of, in superconductors, 17: 11369
theory of galvano-, for anisotropic semiconductors, 16: 24331
theory of, in solids, 17: 13199
theory of magnetothermomechanics, 17: 6859
theory of, review, 17: 13174
use of 200-kgauss pulsed magnetic fields for magnetization measurements on solids, 16: 15456

Magnetic Pumps
see Electromagnetic Pumps

MAGNETIC RECORDING SYSTEMS

bibliography, 16: 6683
circuit design and performance of four-channel, for medical studies, 16: 10231
criteria for neutron time-of-flight analysis, 16: 14093
data collection with high storage density, stepping motor for, 19: 36780
data display from multiparameter, uses in nuclear spectroscopy, 18: 43938 (ORNL-P-437)
data entry into multichannel analyzer memory using keyboard, 19: 722 (HW-68302)
data maintenance, 18: 13382 (WAPD-TM-402)
description for automatic recording of information from spectrograms, 18: 32281(R) (UCRL-11213(p.139-53))
description of Harwell tape, 18: 25747 (NAS-NRC-Pub-1184(p.296-304))
description of instrumentation for tape, for multiparameter nuclear experiments, 19: 20255 (EUR-2119.e)
description of Micro Tape and magnetic drum, 18: 25881 (NAS-NRC-Pub-1184(p.266-8))
design and instrumentation of Harwell, 16: 14091
design and method for digital data storage and display, 17: 30798 (CREL-1145)
design and performance of two-dimensional, 16: 27367
design and performance of 65,000-channel, 17: 38591 (CU(PNPL)-227 (p.69-73))
design and properties of, 17: 38595 (CU(PNPL)-227(p.84-9))
design and use of analog, 16: 27371
design for multichannel pulse analyzers, 18: 5655
design for use with seismometer array, 19: 34377 (AD-609851)
design of digital readout circuits for wire spark chambers (E), 19: 2600 (BNL-8519)
design of five-channel, for recording and reproduction of cosmic ray data, 16: 8030 (NP-11232(p.54-56A))
design of, for use with juke-box sample changer, 17: 23600 (LADC-5476)
design of gamma intensity time recorder, 19: 20397
design of multichannel, for digital storage of three parameter nuclear events, 16: 13341
design of multichannel pulse analyzer, 19: 34444
design of reactor period meter, 18: 7866(T) (AERE-Trans-969)
design of tape storage, for low count rate multichannel analysis, 19: 13768
design of 900-channel magnetic-core, 16: 27373
design of, incorporated in radioisotope scanner, 19: 13795
development and operation of multiparameter pulse-height, 17: 32343 (UCRL-10874)
development for nuclear data processing, 19: 36779
development of carrier-erase, 19: 26636 (SCL-DR-64-131)
development of data acquisition, for Alice, 20: 43638 (UCRL-70018)
development of, for neutron time-of-flight analyzers, 17: 356 (CREL-1073)
development of magnetic-tape type for neutron time-of-flight analysis, 16: 1937 (CREL-1036)
development of multiparameter pulse-height, 17: 24750(R) (UCRL-10624)
development of SHLOG program for data retrieval, 18: 6566 (WAPD-TM-370)
development of thin-film fast magnetic memories, 18: 23862
for strain gages, 17: 6405 (SCTM-364-61(73))
for two modes of pulse recording on tape, 18: 20276 (AAEC/TM-227)
improvement of information capabilities of drums, studies of possible, 18: 33191 (SC-RR-64-512)
information on digital tape, used at Harwell, 19: 717 (AERE-M-1472)
logic for tracing of multiple-generation structures, 19: 33695 (SC-DC-65-1426)
magnetic pulse generator to drive magnetic logic, 17: 23609 (SCTM-76-63(24))
multitrack recording in, 16: 27372
performance, for measuring effects of atomic explosions, 16: 11356 (WT-1)
performance for spark chamber track recording, 19: 18321
performance of magnetic-tape multidimensional analyzers using recording check and memory check, 18: 24012
processing of data from, design of tape-to-card converter for, 16: 8826 (AERE-R-3346)
properties of content-addressable stores for pulse analyzers, 18: 41756 (AERE-R-4677)
radiation effects on performance of, in telemetry electronics, 18: 33838 (RTD-TDR-63-4287(Vol.I))
tape for, radioinduced curing of, 18: 5706(P)
tape recorders for slow data handling, 19: 36793
tape recording and reading unit with parity detection for, 18: 23853
tape recording at random time intervals, transistorized buffer memory for regularization of data flow for, 18: 23854
tape recording standards for seismic data recording in Vela-Uniform projects, 18: 6989 (AD-289031)
triggering system for, negative-time and transient, 19: 26629 (ECOM-2519)
use for direct recording of spark chamber events, 18: 31900 (CERN-64-30(p.345-9))
use in spark chamber experiments, 19: 36855
use of closed-loop system for recording events with erratic time distribution, 18: 24001
use of ferrite core matrix for scattering experiment in sonic spark chamber, 18: 24000
use of intermediate memory in analyzers under pulse conditions, 18: 24011
use of two-channel tape, for data from scintillation scanning of radio-

isotopes in body organs, 17: 32351
use of two-dimensional, for thermal neutron spectra measurements, 19: 37776

MAGNETIC RESONANCE
see also Nuclear Magnetic Resonance
acoustic, excitation in plasma, 18: 15364
book: *Atlas of Electron Spin Resonance Spectra. Theoretically Calculated Multicomponent Symmetrical Spectra*, 18: 8948(T)
book: *Electron Spin Resonance in Biology*, 18: 33227
book: *Free Radicals as Studied by Electron Spin Resonance*, 17: 1508
book: *Magnetic Resonance at High Pressure*, 18: 22584
book: *Nuclear Magnetic Resonance and Electron Spin Resonance Spectra. Index for 1958–1963*, 20: 30510
book: *Principles of Magnetic Resonance*, 18: 40080
book: *Quantum Radiofrequency Physics*, 20: 925(T)
book: *Solid State Physics. XIII.*, 16: 21221
book: *Topics in Radiofrequency Spectroscopy*, 17: 8093
calculation of best fit of hyperfine-structure parameters to data of atomic, computer program for, 20: 46139 (PUC-937-175)
conference on electron paramagnetic resonance, 18: 2463
conference on electronic magnetic resonance and solid dielectrics, Bordeaux, Sept. 17 to 21, 1963, 19: 9798
conference on magnetic and electric resonance and relaxation, Eindhoven, July 1962, 18: 18492
conference on use of, to determine biological effects of radiation, 20: 40592
cross relaxation in non-Zeeman spin systems, 18: 6780 (AD-299997)
crystal lattice effects in electron para-, (T), 20: 12274(R) (COO-578-18)
deoxyribonucleic acid studies using, after irradiation, 20: 40594
detection and measurement using pulsed fields up to 700 kgauss, 16: 15446
detection of spin, using bolometers, (E/T), 20: 45007
double-resonance effects and saturation in electron, of dilute free radical solutions, (T), 19: 42490
effects of uv radiation on, in squid melanin, 20: 26648
electron paramagnetic resonance apparatus operating at liquid helium-3 temperatures, 16: 19133
electron spectra of irradiated biological materials, 17: 24982
electron spin resonance, use for identifying radiochemical species, 16: 2984
electron spin resonance spectra of organic radicals, second-order structure, 16: 7580(R) (RRL-71)
electron spin resonance spectra of irradiated high polymers, 16: 22235
electron spin resonance studies of radioinduced defects in metal oxides and azides, 19: 13424(R) (NYO-2047-30)
electron spin spectra of irradiated polymers, output saturation in, 18: 23617(T,R) (AEC-tr-6316(p.310-13))
electron spin spectra of transition metal ion complexes, 19: 40465 (UCRL-16175)
enzyme inactivation studies using, 20: 40596
equipment for double-resonance experiments, 20: 38402
expectation values for low-field, Bloch equations for, 17: 9004
ferro-, design and construction of recording spectrometer for measurement of, 17: 41197
free radical studies by, in radiation biology, 20: 40597
g-shifts in electron, of F-centers, 18: 29784
hyperfine interactions of paramagnetic ions, 18: 11294
in biological systems, 18: 33283(R) (TID-20889)
in rare earths, theory, 16: 27815
in spiral spin structures, effects of applied magnetic fields on, 17: 31184
integration of chart-recorded data on, semiautomatic machine for, 19: 280(R) (ORNL-3679(p.94-116))
magnetometer design for measurement of proton, (E), 19: 40857
measurement for free radicals, equipment for, 18: 3708(P)
measurement in boreholes, method and apparatus for, 20: 9159(P)
measurement in irradiated substances, design of hyperfrequency spectrograph for, 17: 29178
measurement in rare earth ethyl sulfates, equipment for, 20: 15991
measurement of, design of atomic beam apparatus for, 17: 18893 (BNL-6277)
measurement of double, spectrometer for, 19: 26644
measurement of electron spin, cryostat for, 18: 29663
measurement of electron para-, resonator for, 18: 29955
measurement of electron para-, in plasma, (E), 20: 38220
measurement of ENDOR of F centers in potassium chloride, 20: 42566)T)
measurement of EPR of radioinduced defects in germanium dioxide glass, 18: 28049 (ORNL-3635)
measurement of ESR difference spectra at 77°K, 18: 43611
measurement of para-, noise effects in, 18: 33855
measurement of, data recorder pen recentering circuit for, 18: 18158
measurement of, superconducting solenoid for, 20: 9231
method for determining free radical yield in x-irradiated DNA of various molecular weights, 20: 420
modifications in irradiated biological systems, 16: 7438
molecular-beam uses in study of, 19: 41143
nucleic acid studies using, qualitative and quantitative results, 20: 40593
observation of electron, quarter-wave coaxial resonator for, 18: 18133 (JINR-P-1554)
of biological materials, 18: 29169
of electrons in electrolytes, free radicals, and ionic crystals, 16: 3539(T) (AEC-tr-3973(Pt.II and Add)(p.721-81))
of electrons in metals, 16: 32244
of fluids and solids, research on, 19: 25071(R) (TID-21667)
of irradiated frozen aqueous solutions, 18: 39344
of organic solutions, 19: 33922
of radicals trapped in irradiated alkyl halides, 17: 3053
of S-state ions in metals, 16: 21192
para-, line shape of electron, method of calculating, 19: 340(R) (HW-81746(p.3.120-3))
photoinduced during photosynthesis, 18: 17409(R) (UCRL-11046 (p.101-15))
photoinduced, in organic solutions of chloranil, 18: 17852(R) (UCRL-11046(p.90-100))
plasma dipole, theory for splitting, 17: 42077
propagation in cylindrical and spherical earth-ionosphere, micropulsations of, (T), 20: 4728 (AD-618118)
properties of, atomic-beam determination of, 17: 20997 (UCRL-10609)
properties of magnetoplasma, in metals, 17: 16841
protein studies using, after irradiation, 20: 40595
proton orbit effects in cyclotrons, 17: 4152 (TID-17246)
quantum statistical theory for, 17: 19172
quantum transitions in large-angular-momentum molecular, 18: 26422
radiation effects on, of organic compounds, 18: 1777
radiation effects on protein, gamma, 18: 23289
radiation effects on, of collagen solutions, light, uv, and x, 20: 36585
radioinduced, in amylose, gamma, 17: 35905
radioinduced in crystalline trypsin, γ and uv, 20: 14273
radioinduced in lettuce seeds, effects of hydration on, 20: 40631(R) (ORNL-3922, pp 161-6)
radiosensitivity determination in nucleosides and nucleotides using, 19: 31825
relaxation in liquids, effects of molecular shapes on, 17: 18077
relaxation of ionic, effects on relaxation of nuclear, 16: 33013
relaxation of spin-lattice in paramagnetic salts, 17: 16839
relaxation, temperature effects on spin-lattice, 16: 25995
saturation effects in electron spin spectra of free radicals in irradiated polymers, 18: 24220(T,R) (AEC-tr-6316(p.603-8))
spectra of electron, of F-centers in potassium chloride at 4°K, (E), 19: 8001(R) (IITRI-1184-15)
spectra of electron, in polystyrene, 20: 4479(R) (TID-22179, pp 1-83)
spectra of electron, of irradiated silicate glasses, 20: 42538
spectra of ESR, analog system for integrating, 20: 19039 (RISO-M-233)
spectra of ESR, computer programs for calculating, 20: 27718 (AD-632523)
spectra of F centers, saturation, 19: 33514(R) (COO-587-17)
spectra of F-centers in gamma-irradiated sodium cyanide at 300°K, 20: 43350
spectra of lithium aluminum hydride and lithium hydride, 16: 26977
spectra recording of EPR, magnetic-field pulse modulation method for, 20: 43657
spectral line broadening in EPR, effect of crystal lattice thermal oscillations on, (T), 20: 13976
spectrometer for electron para-, sensitivity of, (E), 19: 32510
spectrometer for electron para-, 19: 32515
spectrometer for irradiating wet biological systems, 18: 20293
spectrometers for electron para-, development of, 18: 29960
spectroscopy of electron para-, instruments for, (E), 19: 22654 (CEA-R-2506)
spin in external static and oscillating fields and heat bath, quantum statistical theory of, 17: 2049 (AD-274740)
spin induction in electron, 17: 32754
spin relaxation in, statistical theory of, 19: 16288
spin resonance line shapes, effect of probes on, (T), 19: 20839
spin temperature formalism for analysis of, (T), 20: 2864 (COO-1198-300)
studies of magnetic exchange interactions in transition metal compounds, 19: 27710 (KR-93)
techniques for radiation-produced radicals, 20: 42433
theory of combined, in crystals, 19: 11124
theory of double, 18: 44295
theory of ENDOR, of F-centers in sodium chloride type crystals, 19: 19920
theory of multiple spectra of, 18: 42307
theory of para-, 17: 33929
theory of spin-spin coupling due to substituent molecular groups, 19: 32048(R) (NP-15073)

theory of, use in organic chemistry, 19: 9046(R) (IS-900(Sect.C))
ultrasonic cw spectrometer for studying electron spin-phonon interactions in solids, 16: 23950
use in biochemistry, review of, 20: 33267
use in radiation chemistry in solid state, 20: 20729 (PB-181506, pp 85-103)
use in radioprotective compound studies, 20: 40598
use in radiosensitizing compound studies, 20: 40598
use in study of ultra-slow atomic motions, 19: 9919
use of atomic, for nuclear half-life measurement, 19: 798
use of electron para-, for studying free radicals, 16: 6545 (ONR-9 (Vol.I)(p.220-33))
use of electron paramagnetic, to identify free radicals, 16: 14472(T) (JPRS-12465(p.30-3))
use of electron spin, in biological studies, 17: 15547
use of electron spin, in studies of radiation damage in solids, 19: 20620(R) (NYO-2024-8)
use of electron spin, in studies of fast neutron damage to silicon, 20: 43986 (AD-637937)
use of electronic and nuclear, in crystallography, 19: 34707
use of EPR for magnetic-field stabilization, equipment for, 19: 26931
use of para-, on irradiated crystals and transition elements, 18: 43459
use to measure earth's magnetic field, 16: 27412(P)
use to measure weak magnetic fields, 16: 27411(P)
uses of electron, in inorganic and organic chemistry, 16: 9970

Magnetic Resonance Accelerators
see Cyclotrons

MAGNETIC SEPARATORS
design of double-focusing for mass-number identification of product nuclei, 20: 31484
design of momentum analyzing slit device for particle beams, 19: 38967(P)
design of, with small magnetic field volume for isotope separation, 17: 22071(T) (AERE-Trans-918)
design of, for separating electrically conducting fluids, 18: 22192(P)
development and performance for isotope separation, 18: 27831(R) (ORNL-3606)
ion source for isotopic, 19: 2698 (NP-14370)
voltage stabilizer in isotope, static characteristics of, 20: 4281 (IAE-926)

Magnetic Storms
see Geomagnetic Storms

MAGNETIC SUSCEPTIBILITY
bibliography and review on analytical applications and instrumentation, 16: 14652
detection and measurement in fields up to 310 kgauss, 16: 15455
determination in strong fields, (T), 19: 11850
measurement as function of pressure, method for, 19: 43997(R) (UCRL-11889)
measurement by Faraday method, superconducting magnet design for, 20: 3919(R) (ORNL-3870, pp 3-6)
measurement by mutual inductance method, efficiency of coil system for, 18: 18482
measurement device, design, 16: 16513 (AE-64)
measurement device for, design and construction of, 17: 16380 (AERE-R-4186)
measurement for paramagnetic compounds in dilute solution, 17: 6884
measurement in intermetallic compounds and solid solutions, 18: 26522(R) (ANL-6868(p.326-30))
measurement in rare earth oxides, apparatus for, 20: 3318
measurement of de Haas–Van Alphen effects in ferromagnetic metals, lead, and tungsten, (E), 20: 4476(R) (IS-1200(Sect.P))
measurement of deHaas-van Alphen effect in single-crystal beryllium, 19: 16133
measurement of, design of balance for, 17: 6385 (CEA-2187)
measurement of low-temperature, design of apparatus for, 18: 36444
measurement of metal, methods for, 20: 41455(R) (NYO-2731-7)
radiation effects on, in inorganic solids, 17: 37575(T) (FTD-TT-63-424)
relaxation and recovery in nickel, effects of deformation, quenching, and radiation on, 18: 14571
theory of, in molecules, 17: 36437 (NP-13020(p.451-3))
theory of transverse complex, 20: 25638

Magnetic Waves
see Electromagnetic Waves

MAGNETISM
see also Electromagnetism
behavior in superconductors, theory, 17: 13197
book: *Magnetism and Magnetic Materials*, 20: 32738
book: *Methods of Quantum Theory of Magnetism*, 20: 34864
book: *The Collected Papers of Lord Rutherford.* I., 16: 15351
conference, 20: 24638
conference at Phoenix, Ariz., November 1961, 16: 16827
conference on, 17: 37769
conference on, 19: 38037
energy matrix and overlap of many-electron systems, theory, 16: 18601
Green's function method for antiferromagnetism, (T), 20: 44029 (IS-T-99)
Heisenberg model of, high-temperature series expansions for spin-½, (T), 19: 9793
measurements in ferromagnetic materials, pulsed-field, 16: 25882 (ASD-TR-61-630)
Mössbauer studies of, review of advances in, 20: 22327
research in Japan on low-temperature, 19: 23550
research programs on, at low temperatures, 20: 30735(R) (TID-22970, pp 331-73)
spin screw structure, anisotropy energy and magnetic field effects on, 16: 16829
theory and uses of, conference on, 17: 37685
theory for earth and stellar, test for dynamo, 17: 25449
theory for, temperature renormalization of free spin-wave, 17: 39750
theory of ferro- and antiferro-, in cubic clusters of spins, 17: 5027 (AD-273950)
theory of, in solids, 17: 13199
theory of, low-temperature effects in, 18: 9281
theory of, review, 17: 13174
theory of spin couplings in, Heitler-London method of calculation, 17: 11420
theory of, validity of unrestricted Hartree-Fock method in, 17: 37773
theory of, Green function formulation of, 19: 28842
theory of, Green's function in quantum-statistical, 19: 5018 (KFKI-64-1)
thermal cycling effects on, 16: 32636
transport along superconducting films, radiation-induced, 17: 9020

MAGNETITE CONCRETES
composition and properties of scrap-iron-aggregate, 20: 27478 (CEA-R-2941)
economics and technology for shielding, 16: 24230
gamma attenuation in, accuracy of calculations for, 19: 43464
gamma attenuation in laminated, 19: 3450 (AE-157)
gamma buildup factors for, 0.5- to 10-Mev, 18: 26814(T) (ORNL-tr-80)
gamma dose buildup factors for (T), 19: 3456(T) (ORNL-tr-349)
gamma dose buildup factors for, (T), 20: 1311 (RT/PIMA(65)2)
gamma scattering by duct in, streaming in, (T), 20: 6530
gamma shielding by, nomograms for determining thicknesses for, 19: 21598
neutron attenuation in, mechanisms for, 19: 29455
neutron attenuation in laminated, 19: 3450 (AE-157)
neutron attenuation in, accuracy of calculations for, 19: 43464
neutron spectra in reactor shield, foil-activation measurement of (E/T), 19: 3771 (AE-155)
performance as reactor shielding, (E/T), 19: 14754
performance as reactor shielding, (E/T), 19: 14755
preparation and properties of steel-aggregate, for shielding, 16: 24231
shielding properties, 17: 2743
shielding properties of, tests on, 17: 11218
shielding properties of, effects of barium and cadmium salts on, 17: 27930
C–Fe–Magnetite, neutron attenuation by, 17: 3805

MAGNETITES
see also Iron Oxides
see also Magnetite Concretes
age estimation by analysis for helium from thorium and uranium decay in, 18: 14067(R) (NYO-7243)
age estimation from helium content of, 20: 16714
age estimation methods for, radiometric, 18: 31048(R) (COO-689-42)
age of Cornwall, Pa., 16: 16577 (TID-14861(Vols.I&II))
analysis for plutonium by sublimation *in vacuo*, 16: 18833
analysis for uranium, polarographic, 18: 1572
argon and helium content of, origin of, 20: 16714
diffraction patterns of powdered, neutron, 20: 12545(R) (PAEC(A)AR651)
formation in underground nuclear explosion in halite, 20: 7253
iron-57 magnetic resonance in, 16: 18481
iron-59 exchange between ferrous chloride and, in solution, 17: 33875(T) (AEC-tr-5937)
iron-57 nuclear magnetic relaxation in, spin echo studies of, 19: 22259
magnetic coupling in, temperature dependence of, 17: 11222
magnetic susceptibility of grout mixtures of, effects of explosive shock on, 18: 34284 (UCRL-13088)
magnon spectra of, temperature effects on, (E), 20: 30765
neutron beam polarization by magnetized single crystals of, thermal, 17: 18537 (KR-37)
neutron collisions in, critical removal angles for, (E), 19: 38020
neutron scattering by, measurements of acoustical and optical spin waves from, 16: 31582 (AECL-1575)
neutron scattering by acoustic spin waves in, polarized, 16: 32366
neutron scattering in, spin-wave, 17: 22271 (MMPP-NPC-1-4)
neutron spin wave scattering by, polarized, 17: 39065
nuclear magnetic resonance of iron-57 in, 17: 5113

nuclear magnetic resonance of iron-57 in, temperature dependence of, 17: 13153
nuclear spin-wave properties in, 16: 25979
oxidation of cylinders of, to hematite in water vapor, mechanism of, 19: 12882 (TID-21573)
oxygen isotope fractionation between quartz, calcite and, for geothermometry, 18: 33785
oxygen-16/-18 ration in, from iron formations in Quebec, 20: 37013
performance as cold neutron monochromator, · 20: 21949
preparation and properties of superfine, 16: 13064
properties for purification of PWR coolants, 16: 17559(R) (ORNL-3262(p.55))
solubility in hydrochloric acid, 18: 22012(R) (ORNL-3591(p.67-9))
solubility in water at 164 to 260°C, effects of hydrogen on, 19: 30150(R) (ORNL-3789(p.113-21))
solubility in water at high temperatures, 20: 17158(R) (ORNL-3900, pp 82-149)
solubility in water at high temperatures, 20: 23602(R) (ORNL-3913, pp 53-73)
sorptive properties for pressurized-water loop corrosion products, 19: 30150(R) (ORNL-3789(p.113-21))
spin-wave dispersion curves for ordered, 17: 8074
spin waves in, temperature behavior of, 17: 37829

MAGNETO-OPTICAL ROTATION

in vicinity of iron-57 gamma absorption line, 18: 13089
induction in type II superconductors, Faraday unipolar, 20: 40016
measurement in plasma, microwave-cavity, 17: 33198
measurement of gamma-ray, using Mössbauer effect, 18: 9133
mechanisms of, in rare-earth(III) phosphate glasses, 18: 7428
of biological polymers, · 19: 48104 (UCRL-16278)
of halides at fusion, 19: 11115
properties in crown glass and quartz, in megagauss fields, 20: 41515
theory, 18: 1325(R) (UCRL-10934)
theory of, in anisotropic plasma, 20: 20020
use for ionospheric electron density measurements, 18: 42535
use in measurements of transient magnetic fields, 16: 4920
use of Faraday and Kerr effects to obtain pictures of magnetization structures, 19: 34427(T) (NP-tr-1232)
use of laser beam, for determination of plasma magnetic fields, (E), 20: 12164 (ARL-65-129)
use to measure plasma densities, 16: 19585
use to measure plasma magnetic fields, (E), 19: 10426

Magnetofluiddynamics
see Magnetohydrodynamics

Magnetogasdynamics
see Magnetohydrodynamics

MAGNETOHYDRODYNAMIC CELLS

acceleration of fluids in two-phase nozzle in two-fluid, analytical and experimental study, 19: 4874 (ORNL-3605(Vol.2)(p.353-70))
air preheater for power plants, high-temperature regenerative, (E), 20: 39725
air preheating for open-cycle, (T), 20: 39653
alkali metal gaseous compounds for, spectrometry of, 20: 39724
alkali metal vapor non-equilibrium ionization in, 18: 32522
analyses for a-c power generation, 18: 36241
analysis and performance of vortex, 18: 12859 (NP-13516)
analysis for a-c power generation, (T), · 19: 23352
analysis of crossed-field plasma accelerators, 18: 36717 (NSL-62-113-10 (Pt.II))
analysis of d-c, (T), 19: 9986
analysis of laminar-flow induction, 19: 39270(R) (TID-21894)
analysis of linear, 18: 42351
analysis of liquid-metal cycle, for commercial power systems, 19: 25254
analysis of nonequilibrium ionization in, 16: 32467 (62-RL-2922E)
analysis of parametric (T), 19: 1222
analysis of, using gas with suspended dust, 18: 42350
bibliography, 17: 11322 (NP-12429)
bibliography, 20: 17326 (AED-C-15-10)
bibliography, Direct Energy Conversion Literature Abstracts, 16: 9288 (NP-11302)
bibliography, Direct Energy Conversion Literature Abstracts, · 16: 15269 (NP-11455)
bibliography on, 18: 819 (NP-13277)
bibliography on direct energy conversion by, 16: 16808 (NP-11472)
book: *Energy Conversion*, 18: 12866
book: *Physical Processes in Magnetohydrodynamic Generators*, 20: 29979
channel geometries for, using nonferrous magnets, (T), 19: 10004
characteristics and power balance of, 17: 6817
characteristics, graphical method for study of, 17: 27997
characteristics of MPD, as electric generators, (T), 19: 14290(R) (EDR-3965)
characteristics of closed-cycle, for reactor power conversion, (T), 20: 39682
characteristics of sub-atmospheric, (E), 20: 39709
characteristics of linear and turbulent, (T), 20: 39707
combustion chamber linings for, design of, 19: 34636(P)
condensing ejectors for liquid-metal, test facility for, 20: 4948(R) (TID-22179, pp 85-175)
condensor test facility for, steam–water, 20: 7775(R) (AD-622945)
conductivity of helium-3 plasma in, neutron-induced, 20: 39683
conductivity of potassium-seeded argon plasma in, nonequilibrium, (T), 20: 39684
conference, 18: 26257
conference on, 18: 12867
conference on, 19: 14299
construction of closed-cycle potassium-seeded argon, 20: 41678 (IPP-3/40)
conversion factor and electric yield of, in open-cycle generator, 19: 12153
corrosion and seed recovery in, 19: 14302
cross sections and transport in seeded inert-gas, (E/T), 19: 9942
current and potentials for segmented electrode, calculation of, (T), 20: 11539 (65RL-3888E)
current and voltage distributions in MGD, effects of electrode geometry on, 19: 32928
current density distribution in, with segmented electrodes, 20: 44165 (IPP-3/41)
current distribution in, with segmented electrodes, (E/T), 20: 39718
current exchange between electrodes and working fluid, (E/T), 19: 14298
description of channel-flow apparatus, for analyses of, 16: 29957
description of cyclic-combustion vortex-flow, 18: 830
description of, for uses in space vehicles, 16: 28633
description of liquid-metal-vortex, 18: 7462
description of, to control and use dissipated energy from space-vehicle re-entry, 19: 35000 (NP-15086)
design, 16: 22802
design, 17: 28103(P)
design, 18: 9079(P)
design, 19: 25262(P)
design, 19: 32933(P)
design, 19: 44991(P)
design, 20: 31979(P)
design, 20: 41696
design, 19: 31461(R) (ANL-7010(p.235-87))
design and analysis of, for d-c power generation, 17: 9083
design and characteristics of, with series-connected electrodes, 17: 9085
design and construction of large-scale, 17: 9075
design and construction of closed-cycle, 17: 9089
design and construction of closed-loop, using cesium-seeded helium, 17: 9091
design and construction of closed-loop, 17: 20534(R) (AD-293438)
design and development of vortex, for electric power generation, 17: 2363(R) (NP-12191)
design and development of, review, 17: 25391
design and development of self-excited, 18: 20835(R) (NP-13814)
design and development of long-life closed-loop (E/T), 19: 1205(R) (AD-605365)
design and development of open-cycle d-c, (E/T), 19: 10001
design and development of nonequilibrium, (E/T), 19: 9959(R) (AD-421896)
design and development of linear and radial explosive-driven, (E/T), 19: 9965(R) (MHD-660)
design and development of liquid-metal, 20: 20177(R) (BNL-929, pp 83-105)
design and development of vortex, 17: 2363(R) (NP-12191)
design and efficiency of open-cycle fossil-fuel, 17: 9078
design and operation of a-c liquid potassium–sodium flashing-cycle, 18: 19456(R) (ANL-6840)
design and operation of closed-loop, 18: 20830(R) (AD-432464)
design and operation principles, 18: 28807
design and operation of gas-fired, (E), 19: 6491
design and operation of gas-fired, (E), 19: 9981
design and operation of cold-cathode, 19: 14305(P)
design and performance of hydromagnetic d-c converter, 16: 18146 (ASD-TR-61-102)
design and performance of two-fluid system, 16: 21151
design and performance for generator-motor loop, 18: 7456 (ASD-TDR-63-4019)
design and performance of Mark I, 18: 9076
design and performance for 250- and 1000-Mw generators, 18: 18622 (PWA-2170)
design and performance of, with channel constant cross section, 18: 44506
design and performance of high-power, (T), 19: 20910

design and performance, 20: 7778
design and performance of inductively coupled a-c, 20: 17330
design and performance of self-excited, (E), 20: 31976
design and status of long-life closed-loop, 17: 18890(R) (AD-284753)
design and testing of vortex type, 16: 32475 (ASD-TDR-62-459)
design and testing of NaK and potassium, 20: 41733
design and theoretical performance of, using potassium vapor, 17: 24028(R) (AD-286278)
design and uses of plasma diode in, 18: 10836
design criteria of a-c, 16: 2326
design description of 300-Mw(e) coal-burning plant, 16: 33102
design eliminating undesirable Hall effects, (E), 19: 4883(P)
design feasibility for 1000-Mw, 16: 3767 (PWA-1940)
design for a-c current production, 20: 31978(P)
design for direct a-c generation with inductance extraction, 18: 12885(P)
design for direct power generation, 19: 16465(P)
design for direct power generation, 20: 25775(P)
design for high-power, short-interval output, 18: 14781 (IDA/HQ-63-1412 (Vol.I)(p.125-31))
design for nuclear reactors, 20: 47024
design for plasma acceleration and/or compression, 19: 33509(P)
design for plasma production and purification, 20: 38339(P)
design for power generation, 17: 5629
design for power production, (T), 19: 9989
design for power reactors, 20: 24769(P)
design for producing a-c power, 19: 39449(P)
design for reducing short-circuit end effects, 19: 29037(P)
design for space propulsion power systems, 20: 20874(P)
design for wall and electrode experiments, 17: 9092
design of a-c, 17: 37674
design of a-c, 18: 5982(P)
design of a-c, 18: 18632(P)
design of a-c, 18: 20890(P)
design of a-c, 19: 20914
design of a-c, 19: 32934(P)
design of a-c, 20: 6026(P)
design of a-c, 20: 13439(P)
design of a-c, 20: 13440(P)
design of a-c, 20: 13443(P)
design of a-c rotating machine, 20: 41749
design of a-c, using fissionable material in fluid flow, 19: 35012(P)
design of a-c, with rotating magnetic field, 19: 39447(P)
design of acoustically resonant Stirling engine for, 18: 24364 (ANL-6802(p.166-9))
design of ARGAS closed-loop, 20: 39680
design of closed-Brayton-cycle, 19: 21690(R) (LA-3244)
design of closed-cycle, 18: 10838(P)
design of closed-cycle, 19: 12155
design of closed-loop test apparatus, 19: 37516(R) (NP-15120)
design of coil system for induction-type, 20: 4948(R) (TID-22179, pp 85-175)
design of conduction-type, 18: 32527(P)
design of E.T.L. Mark II, 20: 41714
design of fluid-metal, (T), 19: 9992
design of fossile fueled, thermal ionization effects on, 18: 12871
design of generator using gas flow, 19: 3021(P)
design of Hall-current, 17: 29479(P)
design of high efficiency, using coal burned in oxygen to produce plasma, 20: 39043(P)
design of high-efficiency a-c, 20: 6028(P)
design of high-power, using rocket engines, 18: 14782 (IDA/HQ-63-1412 (Vol.I)(p.132-64))
design of induction-type, (E/T), 19: 9993
design of large combustion-fired generator, 20: 39654
design of large scale, 20: 29984(P)
design of large-scale, for easy assembly and servicing, 20: 9705(P)
design of liquid-metal Faraday-type, review, 16: 33658
design of liquid-metal conduction, 19: 16448(R) (TID-21380(p.85-111))
design of miniature, for production of short high-energy pulses, 20: 11550(P)
design of multi-stage, with reheat means, 20: 6029(P)
design of nuclear, 17: 28551(P)
design of nuclear electric generator, 18: 32525(P)
design of nuclear electric generator, 18: 32526(P)
design of nuclear, for a-c power production, 18: 20889(P)
design of open-cycle, with high preheat temperature of air, 20: 39689
design of pebble-bed inert-gas, 20: 41736
design of permanent insulating duct walls for, 17: 6849
design of pulse a-c type for direct conversion of kinetic to electric energy, 16: 27167
design of reactor-powered liquid metal, (T), 19: 9991
design of segmented-electrode amplidyne, 20: 41720
design of self-excited explosive-driven, 20: 27791
design of self-excited Faraday-type, 20: 41709
design of two-fluid system for thermal-electric power conversion, 19: 14303(P)
design of two-phase liquid metal, 20: 41734
design of U- and T-duct, (T), 20: 41767
design of walls and electrodes for, 20: 41726
design of 1-Mw open-cycle, 19: 20912
design of 250- and 1000-Mw generators, 18: 5976 (PWA-2164)
design of, cross-connection effects on, (T), 19: 9988
design of, gas property considerations in, (T), 19: 6508
design of, use of incompletely burned fuel gases in, (T), 19: 9995
design of, with minimum short-circuit losses, 20: 46449(P)
design of, with provision for removing sulfur dioxide from exhaust gas, 20: 29982(P)
design optimization of generating duct for, 20: 34135
design optimization of power plants using, (T), 20: 41765
design study of fissile gas-fueled reactor system, 17: 2600
design to eliminate flow interference and charge leakage, 20: 9703(P)
design to eliminate pressure gradient changes with lead changes, 20: 41690(P)
design to reduce short circuit end effects, 19: 35010(P)
design using cesium ore as seeding material, 19: 29036(P)
design using cesium minerals for plasma seeding, 20: 6030(P)
design using electrode temperature differential, 19: 35009(P)
design using helical gas flow, 20: 6027(P)
design using liquid metal vortex in radial magnetic field, 19: 1212
design using mercury, 18: 12875
design using spiral flow path, 20: 9706(P)
design with acoustic resonator for bunching particles in conducting fluid, 19: 47297(P)
design with continuous reheating of the working fluid, 19: 44990(P)
design with duct cross section increasing in direction of flow, 19: 35011(P)
design with fissionable materials in working fluid, 20: 34143(P)
design with gas-cooled walls, 19: 30985(P)
design with radial configuration, 19: 32935(P)
design with semi-open operating cycle, 20: 29983(P)
development, 16: 18142(R) (AD-266553)
development, 16: 18148 (ASD-TR-61-704)
development, 16: 19476(R) (TID-15642)
development, 16: 19508
development, 16: 21847 (AFOSR-2352)
development, 16: 21850(T) (AD-266765)
development, 17: 20536 (ASD-TDR-62-320)
development, 17: 21401(R) (TID-18585)
development, 18: 3038(R) (ANL-6801)
development, 18: 24374
development, 18: 26824(R) (ANL-6885)
development, 18: 28094(R) (TID-20607)
development, 18: 36244
development, 18: 36751 (ANL-6912)
development, 18: 45080(R) (ANL-6936(p.73-6))
development (E/T), 19: 1215
development, (E), 19: 4885(P)
development, (E), 19: 4887(P)
development, (E), 19: 4888(P)
development, 19: 6874(R) (ANL-6944(p.77-81))
development, 19: 17083
development, 19: 24064(R) (ANL-6997)
development, 19: 31462 (ANL-7028)
development, (E), 19: 35008
development, 19: 35606(R) (ANL-7045(p.49-59))
development, 19: 37202(R) (BNL-900(p.1-28))
development, 20: 15300
development, 20: 32633
development, 20: 34140
development, 20: 34445
development, 20: 44169
development and closed-loop operation, 17: 6772(R) (AD-276597)
development and component testing of closed-loop, 17: 25844(R) (AD-402124)
development and economics of, 18: 40216
development and feasibility, 18: 4425
development and future potentials of, review, (E), 19: 8132 (NP-14492)
development and lifetime-prolongation studies on, 18: 4424(R) (AD-299699)
development and operation principles, 16: 18132(T) (FTD-TT-61-310)
development and operation of cesium–helium, (E), 19: 12131 (IRD-64-36(Pt.1))
development and operation of, book on, 20: 7784
development and performance, 16: 24884 (ASD-TDR-62-259)
development and performance of variable-area potassium–sodium alloy, 17: 36861(R) (ANL-6764)

development and performance of oil-fired, (E/T), 19: 9999
development and possibilities, 20: 44166
development and testing of vortex, 16: 29109(R) (NP-11954)
development and testing of jet pump cycle, 18: 19456(R) (ANL-6840)
development and testing, 18: 21698(R) (ANL-6860)
development and testing of liquid metal pistos, 19: 17179(R) (BNL-841 (p.I-17))
development and theory of laminar-vortex, 17: 15023
development and thermodynamic performance in space power systems, 17: 38577 (R62SD83)
development and uses of, 18: 40219
development at Brookhaven, 17: 31794(R) (BNL-782(p.1-17))
development, comparison and review, 16: 15389
development for AARR, 20: 6665(R) (ANL-7105, pp 59-71)
development for commercial power production, 17: 15019
development for conversion of nuclear energy from fission of uranium-235 into electric energy, (E), 19: 4884(P)
development for direct conversion of heat to electricity, 19: 47286
development for electric power systems, review of, 19: 6500
development for gas-cooled reactors, 18: 38498 (A/CONF.28/P/693)
development for generation of alternating current, (E), 19: 4886(P)
development for large-scale power production, economics of, 19: 12135
development for power generation, 17: 35078(R) (ANL-6739)
development for power generation, 17: 35079(R) (ANL-6749)
development for power generation for space vehicles, 17: 42411
development for power generation, 18: 12863
development for power generation, 18: 15426(R) (ANL-6810)
development for power generation, 18: 15663(R) (ANL-6808)
development for power reactors, 19: 12797
development for power generation, review on, 19: 41320
development for power reactors, 20: 23998
development for reactors, 18: 45044
development for space power systems, status of, 18: 34001
development for space vehicle re-entry control (T), 19: 1224
development for space power, 20: 7782
development for use as electric power sources, 18: 24375
development in U. S., review of, 18: 12878
development in USSR, 16: 6872
development in USSR, 16: 9297(T) (FTD-TT-61-226)
development of alkali-metal-vapor, 19: 4873 (ORNL-3605(Vol.2)(p.316-52))
development of Brayton cycle, 20: 7775(R) (AD-622945)
development of Brayton cycle, (E), 20: 13432(R) (TID-22419, pp 149-76)
development of cesium--helium, (E), 19: 12132 (IRD-64-36(Pt.2))
development of closed-loop, summary, 18: 18614(R) (AD-428194)
development of closed-cycle, 18: 20834(R) (NP-13803)
development of closed-cycle magnetoplasmadynamic, for reactors, 18: 36245
development of closed-cycle MPD, 20: 31977
development of commercial, 17: 15021
development of combustion-fired, shock tube studies of, 20: 44167
development of d-c sodium-potassium, 20: 27790
development of electrodeless, 17: 15024
development of electrodeless, using nonequilibrium ionization, 18: 42347 (AI-64-48)
development of electrodeless-induction-chamber, for high-voltage a-c currents, (T), 20: 25772
development of explosive-driven power generator, 19: 8130(R) (MHD-655)
development of fossil-fueled, (E), 19: 10002
development of hypersonic-plasma, (E), 19: 6489 (SC-RR-64-979)
development of liquid-metal, 18: 14776 (CONF-414-1)
development of liquid-metal, 18: 36227(R) (AD-603235)
development of liquid-metal, 19: 27132(R) (NP-14819)
development of liquid-metal, 20: 4573
development of liquid-metal, 20: 7776(R) (AD-624736)
development of liquid-metal-slug, 20: 26533(R) (BNL-954, pp 16-49)
development of liquid-metal a-c, 20: 31973
development of long-life closed-loop magnetohydrodynamic generator, 17: 18890(R) (AD-284753)
development of long-life closed-loop, 18: 36226(R) (AD-601255)
development of low-power, 16: 18133(T) (FTD-TT-62-120)
development of magnetoplasmadynamic, 18: 12874
development of MPD, nonequilibrium ionization studies for, 20: 31963
development of nonequilibrium, 18: 30473(R) (AD-427870)
development of nonequilibrium, 18: 36223(R) (AD-434574)
development of nonequilibrium a-c linear induction (E/T), 19: 1219
development of nuclear, 17: 37001(R) (ANL-6780)
development of nuclear-, 18: 37870 (A/CONF.28/P/133)
development of pressure jet tube, 19: 32929
development of pulsed fission plasma and reciprocating liquid metal piston, 18: 4688(R) (BNL-799(p.1-25))
development of, review, 17: 15018
development of, review of, 17: 25975
development of, review of recent, 18: 826
development of vortex, 17: 12757(R) (N62-10970)
development of vortex, 17: 13623(R) (NP-12523)
development of vortex, for electric power generation, 17: 24045(R) (NP-12790)
development of vortex, for closed-cycle power conversion system, 17: 37645(R) (DCAS-TDR-62-171)
development of 15-kw solar, 17: 9110
development of 300-Mw(e) coal-burning plant, 16: 33103
development of, C.N.E.N. program for, 20: 13431 (RT/FI(65)31)
development of, reasons for, 18: 14777 (CONF-414-2)
development of, review of, 18: 24359 (ANL-6802(p.101-9))
development of, review of, 18: 34499
development of, review of, 18: 36243
development of, recent progress in, 19: 4877
development of, review of, 20: 45184
development of, with nonequilibrium ionization, 18: 30480(R) (MND-3127)
development on national basis, requirements for, 18: 12879
development problems in direct-current, (T), 19: 9967
development progress, 16: 10759
developments for space applications, 17: 6551
developments in, 19: 47285
developments in vortex, 17: 12759(R) (N62-11129)
diagnostics and operation of closed-loop, (E/T), 19: 9990
diagnostics and operation of closed-loop, 19: 47728
diagnostics and operation of closed-loop plasma, 20: 31975
dimensions of induction, reduction by skin heating of, (T), 20: 39693
duct configurations for, optimum, 18: 36246
duct design for, (T), 19: 41316
duct design for, (T), 19: 43031
duct design for, conditions for minimum volume, (T), 20: 39664
duct design for, elongated generating, 20: 44171(P)
duct equations for, method of integrating constant Mach number, 18: 20839
duct materials for, testing of, 19: 9627
duct volume minimization in, 20: 39703
duct wall design for, 20: 44172(P)
ducts for 1000 kw, design of, 19: 6494
dynamic properties of, 17: 634
economics of power generation by, 17: 9075
economics of power production by, 17: 9077
economics of power plant (T), 19: 1216
economics of reactors and, for commercial power, 20: 2670 (LA-DC-7330)
efficiencies of Brayton-cycle, using cesium--noble-gas mixtures, (T), 19: 16447 (NASA-TN-D-2651)
efficiency, 17: 20784
efficiency, 18: 9529
efficiency, (T), 19: 41316
efficiency and current output of, with segmented electrodes and nonuniform velocity, 17: 9096
efficiency and stability of large inert-gas, (T), 20: 41703
efficiency and thermodynamic, parameters for closed-loop, (T), 20: 39720
efficiency and velocity profiles with segmented electrodes, 16: 11338 (R61SD150)
efficiency of, 17: 41654
efficiency of closed-loop, using thermal nonequilibrium ionization, (T), 19: 6512
efficiency of close-cycle nuclear, (T), 20: 39728
efficiency of closed-loop, with thermal nonequilibrium ionization, (T), 20: 41742
efficiency of constant-temperature, duct length effects on, 18: 12873
efficiency of, effects of channel profiling on, 17: 6812(T) (FTD-TT-62-1181)
efficiency of gas and steam cycles for nuclear, 18: 26258
efficiency of liquid-metal, (E), 20: 39716
efficiency of liquid-metal injector, (T), 20: 41778
efficiency of low-temperature, combined with steam power plant, 19: 12138
efficiency of natural gas-powered, (T), 19: 10000
efficiency of power generation for conducting liquid axial flow in radial field, (T), 20: 25965
efficiency of power plants with, (T), 20: 39732
efficiency of power stations using, effect of various parameters on, (T), 20: 39705
efficiency of Rankine-cycle, using "perfect thermodynamic vapor", 20: 42045
efficiency of striated-layer, (T), 19: 9971
efficiency of thermal cycle in, (T), 20: 31962
efficiency of two-phase liquid-metal, (T), 20: 39634 (JPL-32-946)
efficiency of, length and temperature effects on, 18: 36242
efficiency of, search for optimum Mach number for entrance velocity for

gases to improve, 18: 14788
efficiency of, with sodium as fluid, 20: 25769
electric and hydraulic properties of oil-fired, (E), 20: 41780
electric arc rotation in annular (T), 19: 1699 (ARC-CP-743)
electric arc rotation in annular (T), 19: 1710 (NASA-TN-D-2155)
electric characteristics and efficiency of, calculation of, 17: 9079
electric characteristics of conducting steady flow in, 17: 34578
electric characteristics of, calculation by conformal mapping, (T), 19: 9977
electric characteristics, (T), 20: 41748
electric characteristics of JAERI, (E), 20: 41781
electric conductivity in, methods of increasing, 17: 9093
electric conductivity of seeded air combustion products in, 18: 18623
electric conductivity of seeded combustion products in channel flow in (E/T), 19: 1218
electric conductivity in magnetoplasmadynamic, (E), 19: 4879
electric conductivity of seeded combustion products in, (E), 19: 20909
electric conductivity of closed-loop cesium-seeded helium, using auxiliary ionization, (E), 20: 24186
electric conductivity of two-phase potassium mixture for, (E), 20: 39742
electric conductivity in seeded argon plasma in, (E), 20: 39727
electric conductivity of nitrogen with suspended powder in, (T), 20: 41713
electric conductivity in plasmas of, scalar and tensor, (E), 20: 41737
electric conductivity of helium–cesium plasma in, wall-radiation effects on, (T), 20: 41754
electric conductivity of combustion gas in, (E), 20: 41758
electric current and field distributions in, analysis of, 18: 42358
electric current and potential distributions in, fringe effects from, 19: 44840
electric current distribution in Faraday-type, (T), 20: 41700
electric current distribution in Faraday-type segmented-electrode, (T), 20: 41759
electric current density distribution in segmented-electrode, (T), 20: 41763
electric current generation during plasma flow through a pipe, 16: 24902
electric d-c states of opposite-stream diode, 19: 38007
electric discharge in, boundary layer effects on, 18: 15354
electric discharge in, properties of (E/T), 19: 1214
electric discharges in closed-cycle, properties of, (E/T), 20: 11541 (AERE-R-5107)
electric end losses in variable-area MHD channels, (T), 19: 34772 (ANL-6963)
electric generation in explosion-driven, 18: 14784 (IDA/HQ-63-1412 (Vol.I)(p.171-3))
electric glow discharges in argon seeded with cesium or potassium, low-voltage, 17: 37748
electric impedance calculations for, 17: 9077
electric impedance of, 18: 7460
electric impedance of, (E/T), 19: 35006
electric insulation for, water-cooled, 18: 14794
electric loss mechanisms in linear, operating at large Hall parameters, 20: 41787
electric parameters of synchronous, (T), 20: 39676
electric potential distribution in diode, 18: 15397
electric potential drop near electrode surfaces in, for power generation, 18: 44503
electric potentials in, with nonequilibrium ionization, (T), 19: 25250
electric potential drop in, analysis of, (T), 20: 29976 (IPP-3/38)
electric potential and current at cathode of, (E), 20: 41756
electric power generation by, 16: 2840
electric power generation by, 16: 3580
electric power generation by, 20: 37724
electric power production by explosive-driven, pulsed, 18: 16743 (MHD-646)
electric properties of d-c, two-dimensional analysis of, (T), 20: 25762 (INR-654/XVIII/PP)
electric properties of linear Hall- and Faraday-type, 20: 39640
electric properties of supersonic, with arc-heated argon plasma, 20: 39646
electric properties of plasma in, (E), 20: 41708
electrical characteristics of combustion, under open-flame conditions, 20: 41755
electrical energy generation by, preliminary studies of, 17: 5527
electrical equivalent circuits of, (T), 20: 39696
electrical insulation of, high-alumina concrete for, (E), 20: 39698
electrode arrangement for, optimum, 20: 27792
electrode construction and testing for, auxiliary-arc, (E), 20: 41745
electrode design for, (E), 19: 4889(P)
electrode design for, 20: 2677(P)
electrode design for, consumable, 20: 9707(P)
electrode development for hypersonic plasma generator, (E), 19: 20905 (SC-RR-65-54)
electrode development for Renardieres 8-Mw, 20: 41725
electrode effects on electrical parameters of, (T), 20: 39697
electrode fabrication for, 16: 10492
electrode geometries for, performance analysis of, 17: 41558 (R63SD62)
electrode losses in segmented-electrode, (T), 19: 23345 (NP-14891)
electrode losses in, with nonequilibrium ionization, 18: 26252 (BSD-TDR-64-35)
electrode materials for, testing of, 19: 16196
electrode materials for, electrochemical properties of, (E), 20: 39723
electrode performance in, high-melting, (E), 20: 39736
electrode potential distributions in, 20: 46325
electrode protection method for, 20: 41689(P)
electrode structure for, design, 19: 32936(P)
electrodes and generating walls in fossile-fueled, performance of, 18: 12877
electrodes for, design of, 19: 43033(P)
electrodes for, fabrication and properties of boride, 19: 6495
electrodes for, material testing for, (T), 20: 39708
electrodes for, oxidation protection for, 19: 43034(P)
electrodynamic fringing field in a-c, equations for (T), 19: 1220
electrodynamic response of inductive, 17: 41645
electromagnetic properties of dense plasma in variable field, (E), 20: 39739
electron and gas temperature in argon–potassium, (E/T), 19: 6505
electron density and distribution function in gases of, 19: 44982
electron emission in, using seeded plasma, (T), 19: 6501
electron heating in Hall fields of, 17: 9098
electron-ion recombination in, 17: 9097
electron temperature elevation and gas conductivity in, 17: 9095
electron temperature in linear, (T), 19: 20907
electron temperature increases in plasma of, (T), 19: 39437
electron temperatures in plasma of, spectroscopic measurement of, 20: 24517
electron temperature and density in, relaxation lengths of, (T), 20: 39674
electron-ion recombination mechanisms in inert-gas-alkali metal vapor, 18: 40215 (NRC-62-90)
end effects in induction, (T), 20: 39717
end losses in, (T), 20: 41776
end losses in liquid-metal variable cross section, reduction of, (T), 20: 41716
end losses in magnetohydrodynamic channels with tensor electric conductivity and segmented electrodes, 16: 28621 (R62SD35)
energy conversion in, using traveling magnetic waves, 18: 44877
energy conversion in, direct, 19: 32930
energy conversion in, use of ducts of disk geometry for, (T), 20: 39663
energy losses in, ohmic and viscous, (T), 20: 25961
energy sources for, parameters of explosive, 18: 24365(R) (ASD-TDR-63-37)
engineering aspects, 16: 31706
entropy production and performance of, for space systems, 17: 32824
equations for a-c generators with rotating fields, 16: 15284(T) (FTD-TT-62-90)
exhaust of, separation of potassium from, (T), 19: 9983
exhaust velocity, analysis of optimum, 16: 14362
explosive-driven, effects of curved duct on, (E), 20: 39694
feasibility for use in nuclear power plants, 20: 14132 (LA-3368)
feasibility of large fuel-burning MHD-steam, 18: 40218
feasibility studies of liquid metal, 19: 48053(R) (ANL-7090, pp 55-68)
field coils for, 16: 12224 (NP-11436)
field variables in segmented-wall, method for analysis of, 17: 6796 (NP-12332)
flame temperature in, spectroscopic measurement of, (E), 20: 2673
flame temperatures in, optical measurements of, (E), 19: 6492
flame temperatures in infrared region, measurement of, (E), 19: 6496
flow conversion in, effects of instability and turbulence on inhomogeneous, (E), 20: 39704
flow in ducts of, boundary-layer and impact-wave theory of, 20: 41735
flow in Hall-type, effects of field inhomogeneities on, (T), 20: 39692
flow in induction, striated, (T), 20: 41711
flow in, analysis of two-dimensional channel, 20: 41696
flow in, hydraulic approximation for, (T), 20: 41704
flow of conductivity fluid in Hall-type, (T), 20: 39685
flow processes in, efficiency of striated-, (T), 20: 39737
flow turbulence of mercury in, (E), 20: 41707
flow velocity optimization in channel with argon–potassium oxide plasma, (T), 20: 13436
fluid dynamics in, 18: 12865
fluid dynamics in large, (T), 20: 39729
fluid dynamics of d-c, 18: 37873 (AERE-R-3757)
fluid electron density elevation by thermal emission from suspended dust particles, (T), 19: 6493
fluid flow in a-c induction, magnetic Reynolds number criterion for, (T), 19: 23348

fluid flow in channels of, electrical measurements on (E), 19: 1217
fluid flow in duct of series-flow, (T), 20: 41698
fluid flow in, variational analysis of, 20: 13437
fluid flow instability in striated layer, Rayleigh-Taylor, (T), 19: 44984
fluid mechanics of, (E), 19: 9997
fluid performance in nonequilibrium, (T), 19: 4875
fluid switching in, (T), 20: 41724
fuel combustion with ionizing additives for, composition and thermodynamic properties of products in, (T), 20: 41785
fuel for, thermodynamic properties of oil combustion products for, 20: 39938
fuels for, 19: 23350
gas as working fluid in, properties of seeded combustion, 20: 39636
gas braking processes in, 18: 12868
gas conductivity tensor for, 18: 36248
gas flames in, aerodynamics of, (T), 19: 41144
gas flow at duct outlet, recovery of residual enthalpy in, (T), 20: 39658
gas flow in, (T), 20: 24193
gas flow in, boundary layer calculations for, (T), 20: 41779
gas flow in, effects of Hall effect, ion slip and viscosity on, (T), 20: 21574
gas flow stability in, 18: 9062 (63-RL-3506E)
gas flow stability in, linearized perturbation analysis of, 18: 30482 (R64SD-5)
gas flows in, shock relations in nonaligned, (T), 20: 32118 (NYO-1480-29)
gas superheating in, use of shock waves for, (T), 20: 39686
gas suspensions for, electric conductivity enhancement by thermionic emission from, 20: 21575
gas velocity in d-c, optimum, 18: 12872
Hall current flow in, control of, 19: 31421(P)
Hall effect and end loop losses of, 17: 9087
Hall effect and induced ionization in, 19: 47290
Hall effect and nonequilibrium in, using segmented electrodes, 19: 12154
Hall effect and Ohm's law applications for, 19: 1749
Hall phenomena in combustion-product plasma in, (E), 20: 39740
heat exchanger for, design of, 19: 40752(P)
heat loss in open cycle, conditions for recovery of, 19: 12146
heat transfer characteristics of, 18: 2490
heat transfer in channel flow in, wall electric conductivity effects on, (T), 19: 12137
heating of electrons in, induced by electric fields, 16: 27761
induction-coupled MPD channel flow, 18: 19241
injection of liquid metals in, 20: 39669
internal resistance of staggered-electrode, 20: 44164 (IPP-3/39)
ion slippage effects in, (T), 20: 46910
ionization effects on low-temperature operation of closed-loop, nonequilibrium, (E), 20: 41747
ionization from metastable molecular states excited by fission fragments in, (T), 20: 41732
ionization in, alkali metal vapor nonequilibrium, 18: 812(R) (AD-293420)
ionization in, analysis of nonequilibrium of, 17: 9668 (62-RL-3113E)
ionization in combustion chamber of, (E), 20: 41710
ionization in magnetoplasmadynamic cells, non-equilibrium, 18: 32520
ionization in, nonequilibrium, 17: 5479
ionization in reaction zone of, chemical, (T), 20: 41730
ionization in, effects of excited atoms on nonequilibrium, (E), 20: 41757
ionization in, magnetically induced nonequilibrium, (E), 19: 9985
ionization in, magnetically induced nonequilibrium, (E), 20: 41715
ionization in, magnetically induced, (E), , 20: 41786
ionization in, method for producing extra-thermal, (T), 19: 6506
ionization in, nonequilibrium, (E), 19: 32931
ionization in, nonequilibrium, (T), 20: 21573
ionization in, non-equilibrium, 16: 19844 (R62SD13)
ionization in, nonequilibrium, 17: 34630
ionization in, parameters for nonthermal, 18: 42785(R) (AD-600531)
ionization in, use of electron beam, 19: 47289
ionization relaxation processes in, (E), 20: 41789
jet compressor development for closed-cycle magnetoplasmadynamic, 19: 32921(R) (AD-610151)
kinetic energy transformation into electrical energy by isothermal damping in a transverse magnetic field, 16: 24901
life of, development of nonthermal ionization ionization for prolonged, 18: 5977 (RTD-TDR-63-4071(Pt.I))
lifetime of gas- and vapor-cycle, prolongation of, 18: 12853(R) (AD-409905)
liquid-metal cycles in, properties of, 20: 39726
liquid-metal emulsions for, (T), 20: 39678
Lorentz force measurements in, system for, 19: 15918
losses near walls in, effects of ionization saturation and geometry on, (E), 20: 39673
magnet design, (T), 19: 10003
magnet design for, superconducting, 18: 10829(R) (AD-405829)
magnet design for, cryogenically cooled, 20: 41727
magnet design optimization for MHD generators, 20: 39668
magnet parameters for, optimalizing, (T), 20: 41746
magnet system designs for, 20: 11548
magnet system optimization for, superconducting, (T), 20: 25771
magnetic circuit for MAD, superconducting-iron-winding, (E/T), 19: 16461
magnetic-field production for, 17: 9076
magnetic saturation of iron in travelling-wave, (T), 19: 35004
magnetic-field production for industrial, (T), 19: 16462
magnetoacoustic waves in Hall-type, growth rate of, (T), 20: 46323
magnetoplasmadynamics of rotary-arc, 18: 4677
magnets for, superconducting, 17: 9071
magnets for superconducting, 18: 7459 (RTD-TDR-63-4170)
magnets for, design and performance of superconducting, 20: 39643
magnets for, design of, 20: 41688
materials and structures for 200-kw, testing of, 20: 41784
materials development, 16: 17314(R) (AD-266439)
materials development, 17: 5639(R) (DCAS-TDR-62-32)
materials evaluation and requirements for, 17: 31012
materials for electrodes and insulators for, 17: 9073
materials for open-cycle, structure and testing of, 19: 16460
materials for walls and electrodes, production and testing of, 20: 39690
materials for walls and electrodes, preparation and testing of, (E), 20: 41718
materials for, long-duration testing of refractory, 19: 16197
materials for, properties and testing of ceramic, 19: 9724
materials for, thermal conductivity of, 19: 16195
materials interaction with gas flow in, (E), 20: 41738
materials limitations in induction, (T), 20: 39731
microwave power production by, device for, 17: 36447 (RADC-TDR-62-464(Vol.2))
model of slender-channel, 18: 36233
model of, one-dimensional, 16: 19860
model tests of, use of electrolyte in, 17: 37649 (MIT-DSR-8535)
motion of conducting gas in, 16: 4623(T) (FTD-TT-61-104)
nozzle pumping characteristics, 18: 35060(R) (ANL-6904)
operating principles, 19: 4876
operation, (T), 19: 47288
operation and theory of a-c, (T), 19: 9980
operation at large Hall parameters and Mach numbers, 20: 39667
operation at part load in power plants, (T), 20: 41775
operation in nonequilibrium mode without seeding, (E), 20: 39679
operation mechanisms, (T), 19: 9964 (IPP-3/19)
operation of closed-cycle MPD generator with nonequilibrium ionization, 18: 30472 (AD-427774)
operation of closed-cycle, at constant Mach number, (T), 19: 27131 (IRD-64-36(Pt.3))
operation of closed-loop, at International Research and Development Co., Ltd., 20: 39687
operation of CNEN blow-down loop, 20: 39675
operation of constant-efficiency and constant-field, optimum dynamic regimes of, (T), 20: 25773
operation of, for conversion of nuclear energy to electrical energy, principles for, 17: 20681
operation of liquid-metal, using condensing ejectors, (T), 19: 9978
operation of liquid metal, with large magnetic Reynolds numbers, (T), 20: 27796
operation of nonequilibrium, with nonseeded argon, (T), 20: 41721
operation of open-cycle kerosene-burning, (E), 20: 39688
operation of 100-kw model, 20: 39672
operation of, optimal, (T), 20: 2674
operation of, power plants with, (T), 20: 39741
operation principles of, (T), 19: 12133(T) (FTD-TT-64-103)
operation with jet compressors of closed-cycle, (E/T), 20: 41753
operation with potassium-seeded fossil fuel, 20: 39695
operation with potassium vapor, 20: 46320(R) (AD-628187)
operation with two-phase liquid metal flows, 20: 41728
optimization, (T), 19: 9996
optimization of open-cycle power plants, (T), 20: 39719
optimization of small commercial-size, 17: 15022
oscillation of plasma diodes in, initiation threshold and characteristics of, 17: 4177 (UCRL-6572)
parameters of constant-Mach-number, 17: 20684
particle dynamics in, 18: 11308
performance, 18: 34501
performance, (E/T), 19: 41315
performance, 16: 5788
performance analysis of, for combustion of hydrocarbons and air, 16: 33590
performance and properties of, using burning gases as heat sources, 16: 29505
performance and theory of closed-cycle, using nonequilibrium ionization in

pure alkali metal vapor systems, 17: 25862 (R62SD94)
performance and theory of a-c electrodeless, 17: 37643(R) (ASD-TDR-62-411(Pt.I))
performance and uses of, status report, (E), 19: 23346 (NP-14919)
performance as generator and accelerator, graphical presentation of, 19: 47296
performance as rockets, 17: 15011
performance at large Hall numbers, (T), 20: 17332
performance calculations for finite-length inductive, (E/T), 19: 9960(R) (AD-607784)
performance calculation of idealized, with nonequilibrium electron heating, 20: 39647
performance characteristics of liquid-metal and liquid metal-gas, 19: 1207 (ANL-6870)
performance evaluation of Mark V self-excited rocket driven, 19: 35001 (NP-15088)
performance for electric power generation, 18: 40217(T)
performance for linear induction, (T), 19: 39432 (JUL-256-TP)
performance for pulsed power production, 19: 16446(R) (MHD-666)
performance for space propulsion, 16: 28632
performance for space uses, using superconducting magnets, 17: 32224
performance for space vehicles, 19: 39442
performance in combination with internal combustion electric generator for production of a-c current, 20: 37728(P)
performance in nuclear propulsion systems, 16: 28624
performance in power plants, (E), 20: 41769
performance in rocket reactors for fuel-propellant energy exchange, 19: 40238 (LA-3229, pp 286-312)
performance of, (T), 20: 46327
performance of a-c, 17: 12828
performance of a-c, 18: 12876
performance of a-c induction, 17: 13662
performance of a-c induction, 17: 13662
performance of burning-gas-heated, 16: 29505
performance of cesium–helium (E), 19: 1221
performance of chemically fueled, for space uses, 17: 9124
performance of chemically fueled, 18: 34296
performance of closed-cycle, for use with jet compression of working fluid, (T), 19: 6510
performance of closed-cycle, using cesium-seeded helium at high temperatures, (E), 19: 6513
performance of closed-loop, (E), 20: 41741
performance of continuous-flow vortex, 17: 20562(R) (NP-12717)
performance of crossed-field, for rocket propulsion, 16: 16013
performance of cylindrical induction-type, (T), 20: 41694
performance of diagonal-wall, (E), 20: 39702
performance of electrohydrodynamic, for space uses, 17: 9122
performance of electrohydrodynamic, model for, 17: 34652
performance of electric power generating, 19: 25071(R) (TID-21667)
performance of electrodeless travelling-wave, (T), 19: 35003
performance of, experimental and theoretical, 17: 15020
performance of explosive-driven, parametric studies of, (E/T), 19: 9974
performance of explosive-driven, (T), 19: 9975
performance of Faraday-type, with series-connected electrodes, (E), 20: 6025
performance of Faraday-type, 20: 39645
performance of finite- and infinite-length, (T), 19: 23343 (AE-175)
performance of Hall-current, at constant electron temperature, (E), 20: 21572
performance of Hall-type, (E), 20: 41761
performance of ideal, minimum-entropy-increase formalism for, (T), 19: 9972
performance of inductive, 17: 15025
performance of induction, prediction of, 19: 27132(R) (NP-14819)
performance of inductive multiphase, finite width effects on, 20: 36017
performance of induction synchronous, with modulated conductivity, 20: 41683
performance of ionized-vapor-jet systems, 16: 19623
performance of, ionization nonequilibrium contribution to, 17: 31098
performance of large, experimental and analytical evaluation of, 18: 18620 (NP-13768)
performance of liquid-metal-piston, for Rankine cycles, 19: 3019
performance of liquid-metal, (E/T), 19: 4870 (BNL-8199)
performance of liquid-metal condensing ejector, 19: 25071(R) (TID-21667)
performance of liquid metal slug, 19: 41314 (BNL-9329)
performance of Mark II, fluid mechanical studies of, 17: 33212
performance of, model for, 18: 2404(R) (TID-19651)
performance of modulated conductivity induction synchronous, 19: 47293
performance of noble gas, (E/T), 19: 9968
performance of nuclear, for space power, 17: 31768
performance of nuclear, with thermal equilibrium and magnetically induced nonthermal ionization, (T), 19: 6511
performance of open-cycle, facility for evaluating, 20: 39667
performance of parametric, analysis of, 18: 22711 (RTD-TDR-63-4132)
performance of plasma jet-driven, (E), 19: 9979
performance of plasma-jet driven, (E), 20: 13435
performance of Polish, 16: 5788
performance of potassium-vapor, 19: 44981(R) (NP-15435)
performance of radial-flow Hall current, 19: 43029 (NASA-TN-D-2973)
performance of Rankine-cycle, in space power systems, (E/T), 20: 28497(R) (TID-22956, pp 55-147)
performance of segmented electrode, for various electrode-insulator length ratios, 19: 30980
performance of segmented-electrode, effect of wall conductance on, (T), 20: 39712
performance of self-excited, 20: 21564 (AD-627037)
performance of separated liquid-driven-vortex concept for, 18: 32518
performance of spatially constant B/ρ-type, with energy losses, (T), 20: 41722
performance of Stanford, effects of wall leakage on, (E/T), 20: 41739
performance of two-phase liquid–vapor, (E/T), 19: 14289 (CONF-640701-113)
performance of two-dimensional segmented-electrode, (T), 19: 23344 (IPP-3/26)
performance of, under nonuniform and time-varying load, 17: 20561 (NP-12715)
performance of, using alkali-metal-seeded flames, 17: 15027
performance of, using non-equilibrium ionization in alkali metal vapors and seeded gas systems, 17: 32817
performance of, wall friction and heat transfer effects on, 18: 817(R) (NP-13265)
performance of, analysis of, 18: 13131 (NASA-TN-D-2118)
performance of, effects of Hall effect, ion-slip, and viscosity on, (T), 19: 9973
performance of, effect of electrode size on, (T), 20: 21571
performance of, effects of ion slip and electrode segmentation on, (T), 20: 39713
performance of, electrode current saturation effects on, (E), 20: 39660
performance of, gas dynamics for, 20: 46326
performance of, Hall effects and induced ionization in, (E), 20: 2671
performance of, magnetic field strength dependence of, (T), 19: 6509
performance of, nonlinear effects of fluctuations on, (T), 19: 47294
performance of, review, 18: 22712
performance of, role of Hall effect in, 18: 36248
performance of, using liquid metal flow, 18: 18616 (ASD-TDR-63-700)
performance of, using air plasma jet, (E/T), 19: 23351
performance of, using shock-heated argon, 20: 37882
performance of, viscous Hall and ion-slip effects on, (T), 19: 9976
performance of, with segmented electrodes, 18: 16741 (BSD-TDR-63-248)
performance of, with electrodes of finite length and segmentation, (T), 20: 39661
performance using potassium-seeded combustion gases, (E), 19: 6503
performance using liquid-metal power cycles, (T), 20: 9694 (ANL-6954)
performance using inert gases, 20: 17328
performance using liquid metals, 20: 20201(R) (ANL-7110, pp 311-401)
performance using magnetoactive cold plasma with ambipolar potential, (E), 20: 29978
performance using oxygen enrichment, (T), 20: 41744
performance with non-equilibrium ionization, analysis of, (T), 19: 6507
performance with wire electrodes, 18: 2571 (BSD-TDR-63-196)
photoionization in, ultra-violet, (T), 19: 8136
plasma acceleration in, analysis of Hall-current produced, (T), 20: 32573 (N-65-12780)
plasma conductivity and diffusion in, 18: 7790 (PWA-2133)
plasma conductivity in, (E), 19: 6741
plasma conductivity measurements in, methods for, 20: 15897
plasma current distribution in linear Hall, (T), 20: 13428 (JAERI-1093)
plasma diagnostics in MPD, using spectroscopy, 18: 32521
plasma diagnostics in, theory for inert, 20: 21569 (IPP-3/29)
plasma diagnostics in, microwave interferometry for, (E), 20: 41717
plasma dynamics in Hall-type, (T), 20: 39735
plasma electric conductivity and power density in, (T), 19: 14294 (IPP-3/18)
plasma electric conductivity in, slightly ionized nonequilibrium, (T), 20: 19417(R) (N-65-21774)
plasma electric conductivity in, seeded, 20: 23995 (N-66-16138)
plasma electric conductivity enhancement for, optimum seed determination for, (T), 20: 26256 (R-66SD19)
plasma electron heating by electric fields in, argon-cesium, (T), 19: 23861(T)
plasma flow between electrodes in, boundary layer in, (E), 20: 2672
plasma flow in, boundary layer in, (T), 19: 14714
plasma flow in, boundary layer on insulator walls for, (T), 20: 39933
plasma flow in, kinetic equations for non-equilibrium, (E/T), 19: 39440
plasma flow in, optimum Mach number for, (T), 20: 39691
plasma flow processes in, cesium–helium, (T), 19: 27131 (IRD-64-

36(Pt.3))
plasma flow properties in, (E/T), 20: 21561(R) (AD-623096)
plasma fluctuations effects on performance of, 20: 41692
plasma instability in vertical field, gravitational, (T), 20: 11538 (65SRL-3814E(Rev.))
plasma ionization in, nonequilibrium, (T), 19: 39438
plasma ionization in, using electron beams and electric fields, (E), 20: 23994 (N-65-14601)
plasma jets for, development of, 18: 44507
plasma jets for, electron density and temperature measurements in, 19: 29417
plasma oscillations in low-pressure, 18: 6304 (NP-13334)
plasma oscillations in, 18: 20840
plasma production from flames in, 18: 36247
plasma properties in, measurement of, 19: 37513(R) (AD-608638)
plasma properties in explosive-driven, 20: 41686
plasma properties and flow in circular, (T), 20: 41697
plasma stability and transition to turbulence in, effects of crossed electric and magnetic fields on, 19: 12719
plasma stream of arc, effects of polarity on, 17: 17385
plasma supersonic flow in, (E/T), 19: 9969
plasma transport in, 18: 26771
plasma velocity in channels of (E), 19: 1213
plasma wave growth and interactions in, 19: 47295
plasmas for, electric conductivity of, 18: 32892 (NP-14077)
potential drop near electrode surfaces in, 18: 44503
power cycles for nuclear power plants using liquid-metal, 20: 29980
power density in non-steady modulated, (T), 20: 39730
power density of nonequilibrium, effects of carrier gas seeding on, 19: 14301
power density of, effect of degree of ionized-gas expansion in nozzle on, (T), 20: 25774
power efficiency of a-c, with electrodes, 20: 27799
power generation behavior of, with electrons much hotter than ions, 16: 27838
power generation by, fundamental advantages of, 16: 33616
power generation by, efficiency of, 17: 5628
power generation by, optimization study of, 17: 9072
power generation by open-cycle, 17: 9082
power generation by, graphical analysis method for, 17: 9084
power generation by, review of, 17: 22298
power generation by, conditions for maximum efficiency of, 17: 24137
power generation by liquid metal slugs, feasibility of a-c, 17: 40422(R) (ANL-6784)
power generation by a-c electrodeless, 18: 2570 (ASD-TDR-62-411 (Pt.II))
power generation by, no-load voltages in argon plasma for, 18: 9072
power generation by, effects of boundary layer on, 18: 9073
power generation by, effects of plasma relaxation on, 18: 9074
power generation by, time variations in plasma electron density in, 18: 9075
power generation by, analysis of combined conventional-MHD plant for, 18: 10837
power generation by liquid stream acceleration by vapor stream in, 19: 14297
power generation by, status of, 19: 25257
power generation by combustion oscillations in propulsion systems, 19: 36633 (AD-608206)
power generation by large-scale open loop, efficiency of, 19: 47291
power generation by liquid-metal, evaluation for central-station, 20: 29974(R) (ANL-7190, pp 167-75)
power generation by, viscosity and nonequilibrium ionization effects on, 20: 41783
power generation by, future potentials of, 18: 20838
power generation in, from supersonic rocket exhaust, 17: 41664
power generation in, with microwave generators, 18: 821(R) (RADC-TDR-62-464(Vol.3))
power generation in, conditions for maximum, 18: 20836 (R61SD066)
power generation using plasma flow, research progress on, (E/T), 20: 25766(R) (N-65-35576)
power generator efficiency, effects of tensor conductivity and viscosity, 16: 10675 (R61SD100)
power levels, 16: 17314(R) (AD-266439)
power output calculations for, 20: 27786 (IPP-3/37)
power output of Hall effect, (T), 20: 17521
power production by, use of natural gas in, 19: 9987
production of by-product fixed nitrogen in, (T), 19: 9982
properties, 18: 26255
properties and performance for power generation, 18: 4426
properties and prospective electric-power uses, review, 16: 25089
properties and uses, review, 20: 44175
properties in direct conversion of nuclear energy, 16: 27789
properties of electrodeless, self-excitation, (T), 20: 13429 (N64-32348)
properties of explosive, 18: 14783 (IDA/HQ-63-1412(Vol.I)(p.165-70))
properties of explosive-driven, (E), 20: 41685
properties of high-density plasma working fluid, (T), 20: 39656
properties of inductive, for space vehicle re-entry, 17: 33441
properties of jet-driven, measurements of, 19: 29034
properties of lightweight high-power, 16: 27741 (NP-11716)
properties of linear, with one or more loads, (T), 20: 19414 (AE-214)
properties of magnetically loaded, explosive-driven, 20: 41687
properties of, review of, 18: 2564 (DL-55)
properties of, with nonequilibrium ionization, 18: 14787
radiative losses in closed-cycle 300-Mw, 20: 39681
radioinduced ionization of linear constant-Mach number, neutron, (T), 19: 29031 (AE-173)
recent progress in, 17: 39733
recombination in cesium-seed argon plasma, conductivity effects of three-body collisional, 18: 44500 (NASA-TN-D-2004)
relaxation phenomena in, (T), 20: 39700
relaxation processes in nonequilibrium plasma of, (T), 20: 41766
research in closed-cycle, 18: 22714
research on, 17: 21401(R) (TID-18585)
research on fission-fragment powered, 20: 26533(R) (BNL-954, pp 16-49)
research on, with auxiliary ionization, 17: 24041(R) (MND-2866-1)
research on, CEA, 20: 13433
research program in United Kingdom, review on, 19: 20908
research programs on, at Siemens-Schuckertwerke laboratories, Erlangen, Germany, 19: 42228
research programs on liquid-metal, 20: 23997(R) (TID-22735, pp 153-7)
research progress on, 18: 15711(R) (TID-20256)
research progress on, using liquid metals, 18: 22710(R) (NP-13881)
research progress at MIT, 19: 34994(R) (AD-612710)
research progress, 19: 34995(R) (AD-612901)
research progress on liquid-metal, 19: 44981(R) (NP-15435)
research progress, 20: 15882(R) (NP-15868)
research progress, (E/T), 20: 23990(R) (AD-625575)
review, 17: 1721
review, 18: 36089
review, 18: 36240
review of energy conversion by, 17: 31229
review on, with nonequilibrium ionization, (E/T), 19: 25248
seed fraction optimization in cesium–helium plasma, (T), 19: 27131 (IRD-64-36(Pt.3))
seeding criterion for nonequilibrium, (T), 19: 34999 (NASA-TN-D-2873)
self-excitation of a-c, (T), 19: 9984
stability in, linear theory for a-c fluctuations for, 20: 9699
status and uses, 19: 27135
studies, 19: 8133(R) (NP-14538)
studies of closed-cycle, 18: 37868 (A/CONF.28/P/45)
superconducting magnet for, (E), 20: 39733
survey of coal-fired d-c generators, 18: 9078
tensor conductivity effects on and currents in crossed field, having skewed electrodes, 16: 17188
test facility for, closed-loop, (E), 19: 9998
testing of d-c, liquid metal, 19: 47292
testing of ion engines, techniques for flight-simulation, 18: 34261 (AEDC-TDR-64-127)
theory of, 18: 12869
theory of acoustically excited, (E), 19: 10447
theory of choking performance in, 17: 9080
theory of electric ionization in operation of, 17: 8922 (JAERI-1037)
theory of electrodeless a-c, 20: 13430 (N64-32349)
theory of end effects in a-c induction, (T), 19: 9994
theory of liquid-metal induction, 20: 41701
theory of plasma fluctuations in, (T), 19: 6387 (NP-14569)
theory of vortex generator, 17: 39804
theory of, with rotating field, 17: 18913(T) (FTD-TT-62-1797)
thermal efficiency of gas–steam cycle in reactor-coupled, 20: 38488 (AERE-R-5031)
thermal insulation design for, 20: 9704(P)
thermal loss to walls in oil-fired, by radiation, (E), 20: 41777
thermal radiation flux from potassium-seeded flames, (E), 20: 39710
thermodynamic analysis of thermal system of, 17: 41567(T) (FTD-TT-62-1326)
thermodynamic analysis of, 20: 12421
thermodynamic cycles in nuclear power plants, 17: 40350(T) (JPRS-21241)
thermodynamic scheme of open-cycle, 18: 9070
thermodynamics of high-temperature open-cycle, (T), 20: 41752
thermodynamics of, analysis of, 19: 30981
use as d-c voltage converters, 17: 15026
use for power production in conjunction with nuclear reactor and radioisotope heating, 20: 36016 (RISO-M-399)
use in control system for rocket re-entry vehicle, 17: 9081

use in electric power stations, 19: 48013
use in large power plants, 19: 16464
use in MHD transformers, 19: 39448(P)
use in mobile power units, evaluation and survey, 16: 13682 (ANL-6483)
use in power plants, (T), 20: 41693
use in Rankine-cycle space power systems, (T), 20: 41719
use in reactor power plants, optimization of parameters for, (T), 20: 41740
use in single-loop MHD Brayton cycle power plants, (T), 20: 41706
use in steady-flow separation of uranium-235 from hydrogen moderator of gaseous-core rocket reactors, 18: 17323
use in steam power plants, (T), 20: 41743
use of cesium–neon mixtures for working substances in, 16: 18134(T,P) (FTD-TT-62-227)
use of electrodeless, in space power systems, 20: 19423 (N-65-27044)
use of nonequilibrium r-f plasma in, 17: 9090
use of nonthermal ionization in, 17: 16188
use of shock-wave, with high-temperature gas-cooled reactor for power source, 20: 39639
use of thermoacoustic oscillators in, 19: 16459
use with conventional nuclear power plants, 18: 828
use with gas-cooled reactors, 17: 28548
use with gaseous fuel reactors, 19: 45540(P)
use with nuclear reactors, problems of, 18: 5979
viscosity effects, 16: 1126
viscous effects in, 17: 9094
vortex flow in arc heaters, 18: 21393
vortex power generation in, 16: 2785 (AD-256797)
wall effects, 17: 9074
wall structure for, 19: 14304(P)
wall structure for, anisotropic, 20: 24001(P)
wall vaporization in, 17: 36334
wave amplification in, method for, 19: 31420(P)
xenon ionization in, magnetic, 19: 31321(R) (AD-609273)

MAGNETOHYDRODYNAMICS

see also Electrodynamics
see also Electrohydrodynamics
see also Hydromagnetic Waves

acceleration of conducting gas by moving magnetic field, 16: 33941
acceleration of ions by momentum transfer through electric fields in a nonthermal plasma, 18: 4354
acceleration of plasma in intersecting electric and magnetic fields, 16: 19864
adiabatic curve analysis, 16: 5833
adiabatic invariants in, asymptotic behavior of, 16: 26422
adiabatic two-fluid equations in steady state, discontinuous solution for, 16: 8262 (NYO-9763)
Alfvén flow of incompressible electrically conducting fluids, (T), 19: 26928
Alfven solutions of linearized equations of, in inhomogeneous fields, 18: 15359
Alfvén wave attenuation in relativistic, 19: 1753
Alfvén wave stability, 18: 22956
Alfvén waves in liquid, generation and resonance properties of, 18: 44299
alternating fields in, 16: 11088
analog studies of aligned-field flows, 18: 12766 (NP-13566)
analysis of boundary layer problems in, 16: 7966(T) (FTD-TT-61-228 (p.12-20))
analysis of Hall and ion slip effects in nonuniform gases, 16: 21119 (AFBSD-TR-61-80)
analysis of ionizing fronts in, 17: 7433 (UCRL-9971)
analysis of journal bearing with conducting lubricant, 16: 33106
analysis of liquid-metal bearings, 16: 30521
analysis of liquid-metal cycle, for commercial power systems, 19: 25254
analysis of traveling wave pump, 17: 36825
analytic methods and approximations for problems in, 16: 19036 (AFSWC-TN-61-29(Pt.I)(p.20-45))
anisotropic conducting flow between parallel plates (T), 19: 2913
applicability of perfect-fluid, to magnetic channel flow, 19: 16270
approximations for properties of working fluids for, (T), 19: 9799
azimuthal magnetic field in the conical theta pinch, 17: 36784
bibliography, 16: 14190
bibliography, 17: 28361 (NP-12921)
bibliography, 18: 9449 (AD-405732)
bibliography, 19: 47280 (AD-613358)
bibliography of Russian literature on, 17: 41557 (R62SD90)
bibliography on, 16: 32517 (SB-426(Suppl.1))
bibliography on, 18: 20621 (AFCRL-62-1075)
bibliography on, 19: 5265 (JUL-Bibl-6)
bibliography on research on, 16: 29942 (ST1/PUB/21/7)
bibliography, 1953 to 1962, 16: 21660 (AD-271170)
bidimensional flow with nonaligned field in, 17: 22735
book: *A Textbook of Magnetohydrodynamics*, 20: 28088
book: *An Introduction to Plasma Physics*, 18: 17192
book: *Electromagnetics and Fluid Dynamics of Gaseous Plasma*, 16: 29944
book: *Electromagnetodynamics of Fluids*, 20: 37884
book: *Elementary Plasma Physics*, 17: 40201
book: *Elements of Magnetogasdynamics*, 19: 14165
book: *Engineering Magnetohydrodynamics*, 19: 39306
book: *Field-Coupled Surface Waves*, 18: 42202
book: *Fluid Mechanics and Magnetohydrodynamics*, 17: 5519
book: *Fundamental Topics in Relativistic Fluid Mechanics and Magnetohydrodynamics*, 19: 19325
book: *Hydrodynamic and Hydromagnetic Stability*, 16: 3795
book: *Linearized Analysis of One-Dimensional Magnetohydrodynamic Flows*, 19: 28516
book: *Liquid Metal in An Electromagnetic Field*, 18: 42166(T) (JPRS-26459)
book: *Magnetogasdynamics and Plasma Dynamics*, 16: 29941
book: *Magnetohydrodynamics*, 17: 28070
book: *Magnetohydrodynamic Shock Waves*, 18: 34360
book: *Magnetohydrodynamics*, 20: 7975(T)
book: *Non-linear Wave Propagation*, 19: 19319
book: *Physical Gas-Dynamics. Gases at High Temperatures*, 19: 19318
book: *Plasma Hydromagnetics*, 17: 9785
book: *Plasma Physics and Magnetofluidmechanics*, 17: 31626
book: *Plasma Waves*, 18: 11353(T)
book: *Problems in Magnetogasdynamics*, 18: 35028
book: *Problems in Magnetohydrodynamics. Vol. IV*, 19: 27688
book: *Problems in Plasma Theory. No. 4*, 19: 5385
book: *Problems of Magnetogasdynamics. Part I*, 18: 26807
book: *Theory of Ion Flow Dynamics*, 16: 30988
book: *Wave and Oscillation Effects in Super-High Frequency Electron Fluxes*, 17: 17388
boundary conditions in channel flow, 17: 9088
boundary condition for closed magnetopause, 19: 23538
boundary-layer behavior at low magnetic Reynolds number in anisotropically conducting medium, 17: 15367
boundary layer behavior in, influence of Hall effects on, 20: 17534
boundary layer discontinuity equation for, 17: 22366
boundary layer effects on electrostatic probe performance, (T), 20: 5689
boundary-layer equations for conducting fluid in homogeneous magnetic field, 16: 29593
boundary layer equations in, similarity solutions of, 19: 17124
boundary layer flow of incompressible conducting fluid past magnetized flat plate, 16: 16512
boundary layer flow with parallel, 17: 12834
boundary-layer formation during abrupt motion of solid, (T), 20: 28084
boundary layer friction and heat exchange in, 18: 26787
boundary layer mechanisms and problems in, review of, 17: 956 (NP-12150)
boundary layer of conducting vortex flow over disk with axial magnetic field, 17: 9679 (NP-12372)
boundary layer on plane in anisotropic, 18: 20642
boundary layer on electrically conducting wall, equation for, 20: 44408
boundary layer problem for conducting fluid in magnetic field, solution of turbulent free-convection, 17: 20176
boundary layer separation from surface of cylinder in, 19: 18595
boundary layers in, magnetic-field effects on separation of, (E/T), 19: 32788(T) (FTD-TT-65-27)
boundary problem in, of incompressible fluid, 17: 2104
boundary problem of stationary, classical solution of, 17: 36794
boundary problem of conducting viscous flow in plane channels, 17: 39806
boundary problem solutions, 16: 3789
boundary problem solution for conducting fluid subjected to harmonic disturbances and magnetic field, 17: 23487
boundary-layer flow in, effect of magnetic fields and temperatures on free laminar, 20: 42039
boundary-layer flow equations, 20: 44406
boundary-layer problems in, modified Pohlhausen velocity profile for, (T), 20: 34335
calculations of linear z-pinch discharge, 17: 9737
channel entrance flows in, analysis of, 18: 36084
channel flow in, effects of electric conducting walls on, 17: 23490
channel flow in presence of heat transfer in, effects of wall conductance on steady incompressible, 18: 21392
channel flow of electrically conducting fluid, 18: 23777
channel flow under time-dependent pressure gradient, 16: 3778
channel flow velocity profiles and entry lengths, (T), 20: 13432(R) (TID-22419, pp 149-76)
channel flow with extra-thermal ionization, analysis of, (T), 19: 6506
channel flow with nonuniform conductivity, variational solution for, 20: 46427
channel flow, propagation of small amplitude waves in steady,

18: 26805
characteristic locus in polar coordinates, 16: 18239
collisionless shock in two-fluid system, 17: 9698
combustion and detonation in, 16: 22814
combustion in, 16: 865
combustion of gases in, 17: 4193
conducting flow in rectangular channel in transverse fields, 17: 32813
conducting flow in plane channels, 18: 20659
conducting flow through rectangular tubes, 16: 11837
conducting fluid disturbance in magnetic field (T), 19: 2910
conducting gas flow between coaxial permeable cylinders in magnetic field, 18: 42349(T) (NASA-TT-F-240)
conducting incompressible flow at low Reynolds numbers, 18: 34359
conducting laminar flow in flat duct with traveling magnetic field, 17: 13193
conducting one-dimensional flow in tubes, mathematical analysis of, 17: 2404
conducting viscous flow in nonuniform fields, 18: 8495
conduction processes in rectangular ducts with controlled electric fields, (E), 19: 9804
conductivity and Hall effects on flow stability, 19: 39270(R) (TID-21894)
conductivity of cesium plasma, effect of gaseous impurities on, (E), 20: 39659
conference, 17: 19468(T) (FTD-TT-62-1301)
conference, 20: 34350
conference, Evanston, Ill., Aug. 23 to 25, 1961, 16: 15376
conference on, 19: 47153
conference on, 19: 37241
conference on engineering aspects of, 19: 1089
conference on MHD propagation and instabilities in plasmas, Palo Alto, California, December 14 and 15, 1962, 18: 7831
conference on radiation and waves in plasmas, 16: 4930
confinement of partially ionized gases in periodic magnetic fields, 16: 19835 (AFCRL-62-222)
conservation equations for nonequilibrium plasma, (T), 19: 19280
continuum theory of, for moving media, 16: 29948
convection from vertical plates, analysis, 17: 16247
convection in conducting flow in magnetic fields, 19: 9780
convection in, theory of turbulent, 18: 28156(T)
convection of ionized fluids in, 17: 3593
convective heat transfer between flowing fluid and boundary surface, 16: 20607
conversion of thermal energy into electricity with magneto-gas-dynamics, review, 17: 18930
correspondence between fluid magnetodynamic flow and ordinary gas flow, 17: 4678
cosmic, 16: 26051
couette flow behavior with oscillating transverse magnetic field, 17: 17339 (R63SD16)
Couette flow between relatively moving non-porous and porous walls, 16: 15288
Couette flow stability of conducting fluids, 17: 25913
Couette motion, flow formation in, 16: 13768
covariant treatment of linearized, 17: 26733
current distribution in conducting media, 18: 8944
current-layer diffusion in one-dimensional pinch, 17: 5474
current-voltage curves for moving argon plasma, (E), 20: 39655
damping of linearized magnetoacoustic waves, resonant ohmic, 20: 17946
description of liquid metal flywheel for inertial navigation, 20: 27074
description of mercury test loop for study of laminar and turbulent discharge at University of Grenoble, 17: 29674
design equations for constant enthalpy accelerator, 18: 5849 (SSC-TDR-63-270)
design equations for minimum-length crossed-field accelerators, 19: 33434
detonation and ionization shock waves, 16: 1149
detonation in shock waves, 19: 44837
detonation-wave structures in conducting gases, 16: 19640
development of, using nonthermal ionization for use in nuclear power plants, 17: 12002
developments in liquid metal, 19: 23353
developments in, review of principles for, 18: 28807
differential equations of, solutions, 16: 27776
differential equations for, solutions, 17: 14480 (RM-3386-PR)
differential equations in, applications of partial, 20: 2530
discontinuities in, endo- and exothermal, 18: 1158
discontinuities in conducting inviscid fluid, (T), 19: 41157
discontinuities in solar wind, 20: 37387
dispersion relation for relativistic streams, 19: 27621 (UCRL-12207)
distortion of weak magnetic field by flow of conducting fluid past cylindrical obstacle, 16: 11069 (AFOSR-1551)
disturbances propagating from solar flares, model for, 20: 46273 (AD-640661)
drag and heat transfer in electrically conducting fluid flow, 20: 28058
drag and search coil response in moving magnetized plasma, 17: 17345
dynamic equations for partially ionized gases in, 18: 30870 (AD-428797)
eddy production in turbulent flows in, (T), 19: 18557 (AD-424952)
effect of transverse magnetic field on separation in, 18: 19149
effects of external short-circuit ring on cylindrically converging shock waves in, 18: 11326
effects of magnetic fields on flowing plasma, 18: 36704(R) (AD-434097)
effects of transverse magnetic field on vertical two-phase flow in, 18: 30300 (ANL-6854)
effects of wall conductance in Couette flow, 18: 39447
effects on plasma flow in open channels, 19: 33432
ejection of spheres from conducting fluid, 17: 24170
electric characteristics of magnetic viscous couplers in, 17: 3591
electric conductivity of cold plasma at high current densities, 16: 26412
electric conductivity in, finite, (T), 20: 6157 (AD-617898)
electric conductivity of nonequilibrium plasma, seeding for, 20: 38288
electric current density in quasi-one-dimensional, (T), 20: 41723
electric discharge in conducting jet of viscous fluid, (T), 20: 40241
electric discharge experiments on alkali metal-seeded inert gases, (E), 20: 39715
electric end losses in variable-area MHD channels, (T), 19: 34772 (ANL-6963)
electric nonequilibrium conductivity in, theory, 17: 15028
electric power generation by, a-c, 17: 966
electric power generation by, closed-cycle, 18: 28308
electric properties of seeded flames for use in, 17: 9099
electric properties of gas-electrode contacts in, 19: 12152
electric-field distribution in flow of isotropic fluid with alternating conductivity, (T), 20: 11803
electrical insulators for MHD flow, (E), 20: 39657
electroconducting liquid in laminar or turbulent motion in presence of transverse magnetic field, 17: 29675
electromagnetic energy flow in, Poynting vector for, (T), 19: 25118
electromagnetic field distribution in conducting slab, effect of toothed inductor on, (T), 20: 39937
electromagnetic phenomena in motion of bodies in conducting fluid in a magnetic field, 17: 2396
electromagnetic properties of high-temperature ionized flames, 16: 14135 (AFOSR-990)
electromagnetic r-f emission from cylindrical plasma, theory, 16: 14138 (NP-11369)
electromagnetic radiation from plane turbid layers, 16: 26425
electromagnetic wave creation, detection, and propagation in partially ionized gases, 18: 30876 (AFCRL-63-782(Vol.I))
electromagnetic wave creation, detection, and propagation in partially ionized gases, 18: 30877 (AFCRL-63-782(Vol.II))
electromagnetic wave reflection from magneto-ionic medium, 19: 27594 (AFCRL-64-610)
electron density and temperature of cesium-seeded helium plasma, (E), 20: 39665
electron density in one-dimensional channel flow, non-equilibrium excitation effects on, (T), 20: 39714
electron distribution function and state populations in non-equilibrium, (T), 20: 39711
ellipsoid motion in fluid in transverse magnetic fluid, 17: 36441 (NP-13071)
emission by elastic conductor and fluid in isotropic magnetic field, 19: 2906
energy balance in, equation for, 20: 2823
energy conversion in inhomogeneous flow, 17: 33219
energy conversion from capacitor discharges, 20: 9607
energy flow in conducting fluid motion with magnetic field generation, 18: 14600
engineering aspects of, conference, 17: 15009
entropy gradients in, relation of, to vortex strength, 17: 36763
entry problem in electrohydrodynamic fluid flow in plane and annular channels, 17: 37842
equation derivation in anisotropic, 17: 15369
equations, analysis of intrinsic, 16: 17174 (AD-266636)
equations and hypotheses of, 17: 5522
equations for, analogy to electrohydrodynamics, 16: 18233
equations for conducting fluid in constant dipole magnetic field, 16: 22796
equations for conducting, incompressible flow in uniform magnetic field, 18: 14651
equations for nonequilibrium plasma systems, 18: 40705
equations for nonstationary, Riemann wave analog in, 18: 36728
equations for one-dimensional unstable flow in strong fields, 17: 32755
equations for plane-symmetrical fields in, exact solutions of, 18: 34295
equations for plasma containment, 16: 618
equations for plasma systems with large currents, generalized, 16: 33943

equations for plasma pinch equilibria, 17: 21182
equations for plasma with anisotropic velocity distribution, (T), 19: 27695
equations for plasma waves in inhomogeneous medium, 20: 6511
equations for quasi-two-dimensional flow, 17: 2087
equations for quasineutral plasma, (T), 20: 3159 (AD-618138)
equations for relativistic compressible hydromagnetic flows, intrinsic, 17: 31104
equations for relativistic plasma stability in, 17: 36815
equations for self-gravitating and radiating gaseous systems, virial tensor, 19: 28976 (D1-82-0366)
equations for, in anisotropic media, 18: 24768
equations for, solutions of, 19: 28922
equations governing, 16: 7973
equations in anisotropic media, derivation of fundamental, 19: 1066
equations in, proof of exclusion in magnitudes for incompressible, 17: 38408
equations of, 17: 16788 (R58AGT967)
equations of, 17: 40161 (NP-13153)
equations of, absolute space-time form, 17: 34639
equations of flow, 17: 36541
equations of motion for compressible-fluid flow in, force-free field effects on, 19: 37951
equations of relativistic, derivation of, 17: 6829
equations of relativistic, mathematical study of, 19: 34778
equations of stability, Lagrangian formulation of, 17: 9725
equations of, geophysical uses of, 19: 26508
equations of, uses in geophysics, (T), 20: 6212
equilibria in, properties of coordinate systems, 17: 9712
equilibria in toroidal magnetic surfaces, 18: 6340
equilibria stability criterion, 16: 18580
equilibria with finite pressure in minimum-B systems, 19: 19264(R) (UCRL-12028(p.81-120))
equilibria with finite pressure in minimum-B systems, 19: 31335(R) (UCRL-12303)
equilibrium and stability in, 17: 4199
equilibrium in, axisymmetric meridional, (T), 20: 42409 (IPP-6/50)
equilibrium of circular jets, 16: 15743
equilibrium of spherical gravitating gaseous mass in non-uniform rotation, 16: 27764
evolutionality conditions in, (T), 19: 6762
exchange invariance in, 19: 19264(R) (UCRL-12028(p.81-120))
facility design for studying sodium (liquid), 16: 13220
Fermi acceleration of charged particles by hydromagnetic shocks in magnetic fields, 17: 15097
field mode concept in, 17: 11365
fields in magnetohydrostatics, equations for force-free, 20: 21792
flow about a magnetized sphere, first-order, 17: 3104 (AD-275462)
flow about blunt bodies, 16: 25874 (AFOSR-2714)
flow acceleration through sonic velocity, channel, 18: 10623 (D1-82-0239)
flow along wavy walls parallel to external magnetic field, 17: 20641
flow around magnetized spheres, viscous, 18: 40049 (NP-14232)
flow between parallel planes, Hartmann, (T), 20: 38281
flow between two concentric rotating cylinders in radial magnetic field, incompressible, 16: 3563
flow control and generation with, vortex, 17: 22725 (ORNL-TM-479)
flow equations for, 18: 1099 (AFCRL-62-1112)
flow equations for Faraday generators, solution of one-dimensional, (T), 19: 14296
flow equations for chemically reacting plasma, 19: 29396 (R65SD-7)
flow evolution, 16: 18561(T) (FTD-TT-62-338(p.1-9))
flow evolution prerequisites, 16: 19862
flow, exact solutions to class of linearized problems in, 16: 16806 (BSD-TDR-62-42)
flow, formulation of quasi one-dimensional, 17: 5523
flow from large reservoirs, analysis of, 16: 27766
flow in channels, skin friction and heat transfer in, (T), 19: 41119 (MIT-36-P)
flow in circular and rectangular channels, effects of wall conductance on, 20: 34331 (N-66-13027)
flow in crossed electric and magnetic fields, quasi-one-dimensional, 17: 22760
flow in, entropy perturbations in one-dimensional, 17: 23481
flow in flat ducts, heat transfer in, 18: 39448
flow in liquid metal MHD channels, 18: 22710(R) (NP-13881)
flow in magnetic field of intermediate strength, 19: 29384 (AD-607846)
flow in magneto-gas dynamic generator, analysis of radial field vortex, 17: 24163
flow in magnetogasdynamic source, 17: 11830 (D1-82-0166)
flow in, momentum integral approximation for compressible boundary-layer, 17: 28010
flow in planar-magnetic and gravitational fields, nonuniform rotational, 20: 6172
flow in rectangular tubes, turbulent, 17: 21893
flow in rectangular ducts, conducting wall effects on electric current patterns in, 17: 24078
flow in shock tubes, boundary layer, 20: 42037 (UTIAS-115)
flow in strong fields, unstable plane parallel partially ionized, 18: 43763
flow in, transpiration cooling in stagnation-point, 16: 33131
flow in transverse electric and magnetic fields, 17: 39808
flow in viscous, conducting, axially-symmetric systems, 17: 11438
flow in viscous conducting fluid, jet-vortex, (T), 20: 37878
flow in, calculations for boundary layer for, 20: 46447
flow in, Hartmann-Poiseuille, (T), 20: 46425(R) (AD-828181)
flow in, Malkus theory of turbulent channel, 20: 38240
flow in, numerical method of characteristics for, (T), 20: 38241
flow induction by applied electric and magnetic fields, (E), 19: 8034
flow of anisotropically conducting liquid in alternating magnetic field, (T), 19: 41149
flow of axisymmetric free jet, Hall potentials and perturbations in, 19: 9797
flow of compressible electrically conducting gas, stability of, (T), 19: 25585
flow of conducting fluid in electromagnetic fields, classical, 16: 15377
flow of conducting gas through heated plane tube in magnetic field, 16: 27202(T) (FTD-TT-62-333)
flow of conducting viscous fluid in transverse fields, 17: 2106
flow of conducting non-Newtonian fluid in annulus with radial magnetic field, 17: 12431
flow of conducting fluid, linear equations, 17: 14460
flow of conducting compressible fluid in magnetic field with helical symmetry, equations for, 17: 24579
flow of conducting fluid, viscous free-jet, 17: 25914
flow of conducting gas in presence of thin profiles, 17: 28371
flow of conducting incompressible fluid over plate in magnetic field, 17: 32781
flow of conducting fluids, equations for, 17: 36527
flow of conducting liquid past semi-infinite plate, boundary layer for two-dimensional, 17: 27555
flow of conducting fluid over body in the presence of parallel applied magnetic field, upstream wake from, 18: 7838
flow of conducting compressible fluid across magnetic field, symmetric, 18: 19150
flow of conducting viscous fluid between parallel plates, 18: 20660
flow of conducting fluid in alternating magnetic field, conductivity distribution in, 18: 34358
flow of conducting liquids in magnetic fields between coaxial cylinders, 19: 592
flow of conducting viscous fluid in transverse magnetic field, (T), 19: 4766
flow of conducting fluid through transverse magnetic field, analysis of unsteady, 19: 18558 (ANL-6937)
flow of conducting liquid, forced oscillations in, (E), 19: 23171
flow of conducting incompressible fluids, isotropic turbulence in, (T), 19: 24678
flow of conducting liquid between conducting walls, convective, (T), 19: 24679
flow of conducting gas in channel with transverse magnetic field, (T), 19: 24680
flow of conducting fluid in rectangular duct, (T), 19: 26503
flow of conducting fluid near stagnation point, (T), 19: 30385
flow of conducting gas, longitudinal oscillations in one-dimensional, (T), 19: 33449(T)
flow of conducting media in electromagnetic field, equations for one-dimensional, 19: 37239
flow of conducting gas in crossed fields, laminar boundary layer of, (T), 19: 40044
flow of conducting fluid in receptacle with conducting walls, (T), 19: 41154
flow of conducting viscous fluid, momentum source in, (T), 19: 42945
flow of conducting viscous fluid in boundary layers, effect of pressure gradient on, 19: 47140
flow of conducting incompressible fluid, oscillating dielectric sphere induced, (T), 20: 6161 (NP-15630)
flow of cylindrical conducting gas column in longitudinal magnetic field, 20: 40237
flow of electrically conducting gas in a channel with a traveling magnetic field, 16: 9527(T) (FTD-TT-61-113)
flow of electrically conducting fluid along channel in magnetic field, 18: 26140
flow of electrically conducting incompressible fluid between plane walls, (T), 19: 4750
flow of fluid annulus between two cylinders, 17: 2409
flow of imperfectly conducting fluid with quasi-aligned field, (T), 19: 23170
flow of incompressible fluids about spheres moving toward magnetic

fields, analysis, 16: 12613 (NP-11383)
flow of incompressible conducting fluid in axisymmetric tubes, 16: 16854
flow of incompressible electrically conducting gases, effects of magnetic field of current loop, 16: 16812 (SCR-439)
flow of incompressible conducting fluids in annuli in, 17: 4682
flow of incompressible viscous fluid in rectangular channel, laminar, 17: 4683
flow of incompressible viscous fluid about spherical magnetic quadrupoles, (T), 20: 4725
flow of incompressible infinitely conducting fluid in, large-amplitude, (T), 20: 4718
flow of incompressible viscous fluid about electrically conducting obstacle, (T), 20: 44405
flow of infinitely conducting gas in magnetic fields, two-dimensional (T), 19: 3017
flow of inviscid compressible fluid past slender body in magnetic field, 16: 15392
flow of inviscid compressible conducting fluid in crossed electric and magnetic fields, quasi-one-dimensional equations for, 16: 15393
flow of inviscid conducting fluid in a channel, heat dissipation in, 17: 9067
flow of inviscid conducting fluid in oblique magnetic field, equations for one-dimensional unsteady, 17: 14459
flow of inviscid compressible conducting fluid, nonisentropic one-dimensional, 17: 23482
flow of inviscid uniformly conducting fluid at low magnetic Reynolds number, two-dimensional, 17: 23485
flow of ionized gas through magnetic field for power generation, 16: 31701
flow of ionized gas with thermal radiation effects in transverse electromagnetic field, plane couette, 18: 19239
flow of ionized gas in magnetic field, 19: 23207
flow of ionized viscous gas, effects of anisotropic conductivity on, 17: 36514
flow of liquid gallium in test loops, 19: 40727
flow of liquid metal in electromagnetic field, convection in, (T), 19: 26510
flow of medium with finite conductivity, in presence of mass forces, 20: 6171
flow of mercury in transverse magnetic field, (E), 19: 24683
flow of mercury, hydraulics of, (E), 20: 41774
flow of nonequilibrium plasma, (T), 20: 42454
flow of partially ionized gas, transport equations, 16: 21682
flow of partially ionized medium along plane channel, viscous drag and heat transfer in, (T), 19: 41147
flow of perfectly conducting fluid with aligned magnetic field, 17: 31153
flow of plasma in, vector equations for, 18: 42797 (SCTM-93-63(71)(p.13-22))
flow of polytropic gases, singular surfaces in, (T), 19: 25251
flow of rotating weakly ionized plasma, (E), 19: 21570
flow of sodium in rectangular duct, (E), 20: 39706
flow of thermally-conducting gas, reciprocal relations for rotational, 18: 23778
flow of visco-elastic fluid between non-conducting plates, (T), 20: 37871
flow of viscous conducting fluid past fixed obstacle, 16: 5473
flow of viscous compressible fluid past flat plates and wedges, 16: 15390
flow of viscous conducting liquid over surface of half-space, boundary layer in, (T), 19: 41146
flow of viscous electrically conducting fluid past semi-infinite plate, (T), 20: 39945
flow of viscous liquids between parallel planes, 16: 11092
flow of viscous liquid past semi-infinite plate against pressure gradient, boundary layer for two-dimensional, 17: 27554
flow of viscous liquid past semi-infinite plate against pressure gradient, boundary layer for two-dimensional, 17: 27556
flow of weakly conducting fluid between parallel plates, (T), 19: 26511
flow of weakly dissipative fluids, 17: 28005
flow over porous surfaces, 18: 10240
flow over wedge, hypersonic, 17: 16855
flow over wedges in, (T), 20: 38242
flow past a body of revolution in uniform magnetic field singular perturbation method for, 17: 24169
flow past a thin airfoil, 17: 20630
flow past a wedge with a perpendicular magnetic field, shock-wave formation in supersonic, 17: 41576
flow past blunt axisymmetric bodies, 16: 15391
flow past nonconducting flat plate in transverse magnetic field, 16: 25913 (NP-11892)
flow past semi-infinite plate, transverse, 17: 5485
flow pattern properties at small magnetic Reynolds number, 18: 16579
flow problems, solutions for two-dimensional, 16: 15714 (AFBSD-TN-61-31)
flow processes in MPD generators, parameter analyses for, 19: 9328 (IRD-63-82)
flow stability between rotating cylinders in circular magnetic fields, 16: 27793
flow stability between concentric cylinders with circular magnetic field, 18: 31722 (MTI-64TR-25)
flow stability in rapidly alternating field, 16: 12302
flow studies, 19: 28493 (ARL-65-18)
flow through cylindrical channel, electrical effects of, 18: 23773
flow, turbulence and charge loss in transverse magnetic field, 17: 5525
flow velocity in, analysis of, 17: 9086
flows in, equations for one-dimensional unsteady, 18: 4636 (NP-13296)
flows in, equations for two-dimensional, 18: 4638 (NP-13298)
flows in plasma, high-velocity (T), 19: 3444
flows of conducting fluids in, laminar one-dimensional, 18: 2491
flows of electrically conducting liquids in, instabilities in, 17: 4681
flows past wedges in, analysis of inviscid supersonic, 17: 6898
fluctuation in, theory of, 17: 20788
fluctuations in, spectral distributions of correlation functions for, 17: 24071(T) (JPRS-19316(p.125-46))
fluid convection between heated walls, free, 18: 39449
fluid flow and extra-thermal ionization in, 20: 44402(R) (AD-628065)
fluid flow and heat transfer about rotating disk, 16: 13739
fluid flow around plane plates in, incompressible, viscous, conducting, 16: 24894
fluid flow around blunt bodies in, hypersonic, 17: 15016
fluid flow around magnets, field-aligned, (T), 20: 17509 (D-1-82-0469)
fluid flow behind spheres, wakes from (E/T), 19: 3016 (BSD-TDR-64-107)
fluid flow between flat parallel plates in, electrically conducting, 17: 30669
fluid flow between coaxial cylinders, instability of, (T), 19: 18606
fluid flow between flat plates in transverse fields, conducting viscous, (T), 19: 30861
fluid flow between nonconducting plates in, incompressible, (T), 19: 41135
fluid flow between coaxial tubes, incompressible, 20: 25968
fluid flow between moving plane porous walls in, (T), 20: 37876
fluid flow between coaxial cylinders, (T), 20: 46439
fluid flow boundary layer between parallel streams in magnetic fields, (T), 20: 15570 (N65-21084)
fluid flow boundary layer around body in magnetic fields, 20: 39935
fluid flow boundary layer over stationary base, rotational, 20: 39936
fluid flow characteristics in, 18: 28094(R) (TID-20607)
fluid flow discontinuity in, stability of Kelvin-Helmholtz, 17: 32774
fluid flow disturbances in, propagation of weak, (T), 20: 6170
fluid flow equations for entry in rectangular divergent channels, 20: 46440
fluid flow generated by oscillating solid boundaries in, linear and nonlinear, 18: 44297
fluid flow in aligned magnetic field, compressible conducting inviscid, 18: 10241
fluid flow in, angle indicator for, 17: 32388
fluid flow in annular channel, steady state laminar, 18: 2443
fluid flow in annular circular cylindrical induction compressor, (T), 19: 8016
fluid flow in annular channel with radial fields, laminar, (T), 19: 20663
fluid flow in annular channel with radial magnetic field, transient, (T), 19: 41137
fluid flow in annular channel in magnetic fields, viscous electric-conducting, (T), 20: 9842
fluid flow in annular channel, incompressible electrically conducting, (T), 20: 39942
fluid flow in, at entrances to annular channels, 17: 638
fluid flow in channel, boundary-layer equations for compressible, 18: 1870
fluid flow in channels, formalism for, 18: 10243
fluid flow in channel entrance section, heat transfer in, 18: 44316
fluid flow in channel with electrically conducting walls, heat transfer in, (T), 19: 4747
fluid flow in channel entrance, (T), 19: 8017
fluid flow in channel in transverse electromagnetic fields, (T), 20: 13635 (ARL-63-175(Pt.3))
fluid flow in channels, self-induced magnetic field in, (T), 20: 28065
fluid flow in channels with external magnetic fields, (T), 20: 46446
fluid flow in channels, turbulence effects on, 20: 46445
fluid flow in closed regions with axial symmetry, perturbational technique for, (T), 20: 13643
fluid flow in conducting tube with magnetic field, influence of Hall effect on stability of incompressible conducting, 17: 42087
fluid flow in conference, (E/T), 19: 16294
fluid flow in convective channel, (T), 19: 41115 (ANL-6967)
fluid flow in convergence channels, two-dimensional, laminar, (T),

20: 25956
fluid flow in crossed magnetic fields, 20: 37869
fluid flow in ducts in, analysis of transient, (T), 19: 18568 (WAPD-T-1655)
fluid flow in ducts, unsteady, convective, (T), 20: 28051
fluid flow in, effects of very high magnetic fields, 16: 15470
fluid flow in, effect of wall conductance on energy conversion in laminar, 17: 39727
fluid flow in electromagnetic field, action principle for, 18: 5467
fluid flow in entrance region of flat rectangular duct, finite difference analysis of laminar, 18: 7346
fluid flow in entrance region of flat duct, analysis of laminar, (T), 19: 30843 (AD-608860)
fluid flow in entrance region of parallel-plate channel, (T), 20: 4709
fluid flow in entrance region of flat channel with parabolic velocity, (T), 20: 32226
fluid flow in entrance region of flat duct, laminar, 20: 34347
fluid flow in, exact solutions for incompressible inviscid, 17: 37838
fluid flow in insulating cylinders with axial magnetic fields, (T), 20: 34334
fluid flow in jets, effects of extremities and nonuniform conductivity on, (T), 20: 28053
fluid flow in, magnetic-field loops in, 17: 37841
fluid flow in magnetic fields, equations for, 18: 20677
fluid flow in magnetic field, natural and forced thermal convective, (T), 20: 39930
fluid flow in, nonisentropic perturbations of, 17: 16510
fluid flow in nonuniform field, two-dimensional channel, (T), 20: 4715
fluid flow in open channels, variable conductivity effects on, (T), 20: 21780 (AD-622036)
fluid flow in pipe and channels in, laminar, (T), 19: 44824
fluid flow in plane channels in, conducting, 19: 34792
fluid flow in progressive magnetic field, two-dimensional nonstationary, (E), 20: 19624
fluid flow in rectangular tubes, laminar, 16: 7204
fluid flow in rectangular channel, current distribution in, (T), 19: 41148
fluid flow in rectangular channel, Hall effect in conducting, (T), 20: 7974
fluid flow in rectangular channel at high Hartmann number, 20: 44413
fluid flow in rocket motor nozzles, steady-state, 18: 1871
fluid flow in rough pipes, friction coefficients for, 20: 46441
fluid flow in semibounded channel, (T), 20: 28068
fluid flow in spherical envelope, equations for, (T), 20: 11776
fluid flow in spherical envelope in, (T), 20: 11777
fluid flow in, stability of inviscid swirling, 17: 3128
fluid flow in steady magnetic field, equations for viscous, 20: 25976
fluid flow in straight channel inlet region, (T), 20: 21801
fluid flow in, theory of compressible, inviscid, transonic, 17: 637
fluid flow in transverse magnetic fields in, stability of Couette, 18: 34317
fluid flow in transverse field, turbulent, (T), 19: 6396
fluid flow in, analysis of unsteady convective, 18: 42861
fluid flow in, analysis of conducting incompressible, 20: 42036 (SC-RR-66-356)
fluid flow in, axisymmetric incompressible, (T), 20: 9852
fluid flow in, boundary layer effects in turbulent, 18: 28165
fluid flow in, boundary-layer compatibility conditions for, (T), 19: 39277
fluid flow in, boundary-layer analysis of turbulent channel, 20: 4948(R) (TID-22179, pp 85-175)
fluid flow in, boundary layer for plane laminar, 20: 42044
fluid flow in, combined forced and free convection channel, 19: 33433
fluid flow in, compressible dissipative, (T), 20: 15585
fluid flow in, Couette, (T), 19: 16291
fluid flow in, damping of homogeneous turbulence in, (T), 20: 11804
fluid flow in, effects of extremities on electromagnetic and velocity fields in, (T), 20: 28052
fluid flow in, electric conductivity effects on stability of parallel, (T), 20: 7961 (NASA-TN-D-3144)
fluid flow in, electric and magnetic field effects on boundary layers in, (T), 20: 46428
fluid flow in, entry length and velocity profiles for channel, (E), 20: 7775(R) (AD-622945)
fluid flow in, equations solutions for, 19: 20764
fluid flow in, equations for two-dimensional vortex, (T), 20: 7963
fluid flow in, existence principle for stationary, (T), 20: 1093
fluid flow in, expansion methods for, 19: 1064
fluid flow in, field effects on turbulence in, 19: 1063
fluid flow in, generalized Helmholtz and Larmor theorems for, 20: 34333 (N-66-17261)
fluid flow in, heat transfer in transient, (T), 20: 6176
fluid flow in, incompressible, 18: 10242
fluid flow in, inertial-range spectra of turbulent, (T), 19: 39292
fluid flow in, influence of relative roughness on friction coefficient, 19: 44826
fluid flow in, instability of laminar, 20: 36087
fluid flow in, integral methods for, 20: 11792
fluid flow in, Kelvin-Helmholtz problem with finite conductivity in, 19: 32795
fluid flow in, laminar compressible boundary layers in, 19: 20122
fluid flow in, limit theorem for, 20: 4719
fluid flow in, limit theorem for, (T), 20: 4720
fluid flow in, localism hypothesis for turbulence in conducting, 19: 44836
fluid flow in, magnetic flux concentration in, 18: 10630
fluid flow in, magnetic energy production and dissipation in, 18: 34327
fluid flow in, multifluid theory of, 20: 34326 (AD-634521)
fluid flow in, numerical integration of equations of motion of viscous, 20: 44404(R) (AD-628179)
fluid flow in, plane, (T), 20: 11791
fluid flow in, properties and problems of, 20: 6156 (AD-617562)
fluid flow in, properties of, (T), 20: 37867
fluid flow in, Rayleigh's problem in, (T), 20: 15578
fluid flow in, rotating, (T), 20: 24181 (AD-627919)
fluid flow in, solutions for laminar heated and MGD jet problems in, 19: 25084
fluid flow in, stability and turbulence in, 18: 10246
fluid flow in, stagnation-point, 18: 34319
fluid flow in, stability of Couette, 18: 40068
fluid flow in, stability of nondissipative incompressible, (T), 19: 6389
fluid flow in, stability of dissipative incompressible, (T), 19: 6390
fluid flow in, statistical theory for homogeneous turbulence in, 19: 41127 (SUDAER-233)
fluid flow in, stabilizing effect of magnetic field on turbulent, 19: 44835
fluid flow in, stability of incompressible nonconducting, (T), 20: 25958
fluid flow in, stability of conducting free surface in, (T), 20: 37874
fluid flow in, steady disturbances in laminar boundary layer, 20: 4098 (AD-614633)
fluid flow in, survey on, 18: 34264 (ARL-63-175(Pt.II))
fluid flow in, symmetric motions of incompressible viscous, 19: 44816
fluid flow in, thermal boundary-layer equations in, (T), 19: 39276
fluid flow in, theory of laminar boundary layer in, 20: 11790
fluid flow in, thermal stability of confined, 20: 20854 (AD-621523)
fluid flow in, theorems for highly conducting viscous, 20: 39932
fluid flow in, theory of plane laminar, 20: 41773
fluid flow in, transverse magnetic field in Prandtl-Meyer, (T), 20: 21776 (AD-621429)
fluid flow in, variational principles for equations of incompressible viscous, 20: 37877
fluid flow in, with aligned velocity and magnetic fields, (T), 20: 24180 (AD-627885)
fluid flow induced by rotating disk in, equations for viscous conducting, 20: 25962
fluid flow interactions with traveling magnetic field, (T), 20: 25964
fluid flow model for, entrance, (T), 20: 46426 (SC-RR-66-357)
fluid flow near stagnation point, two-dimensional inviscid, (T), 20: 11795
fluid flow of conducting compressed liquid, equations for, 18: 42850
fluid flow on stationary infinite disks in, rotating, 18: 42185
fluid flow over flat plate, viscous incompressible (T), 19: 577 (AFOSR-64-0719)
fluid flow over flat plate, equations for, 20: 28040 (AD-609534)
fluid flow over flat porous plate in transverse field, (T), 20: 30180
fluid flow past a slender body, axially symmetric, 20: 37870
fluid flow past circular cylinders in, viscous, (T), 19: 44825
fluid flow past cylindrical body, boundary layer and heat transfer in, 17: 34105
fluid flow past flat plate, effect of standing sound field on, 20: 25978
fluid flow past insulated flat plate in, viscous conducting, 18: 34316
fluid flow past nonconducting walls in, 18: 20650
fluid flow past porous flat plate under transverse field, (T), 20: 39929
fluid flow past rigid bodies in aligned fields, analysis of, 18: 26126
fluid flow past thin bodies, two- and three-dimensional inviscid, 18: 10244
fluid flow problems in, solution using von Karman-Pohlhausen method, 20: 9851
fluid flow stability in channels in aligned fields, 18: 34267 (D1-82-0331)
fluid flow through duct with applied magnetic field, 16: 7195 (ARL-34)
fluid flow turbulence in, in presence of Hall effect, (T), 20: 19534
fluid flow up vertical plate in, analysis of, 18: 26124
fluid flow velocity in, use of Pitot and Prandtl tubes for measuring, (E/T), 20: 25963
fluid flow with field variations in, 20: 21790
fluid flow with Hall effect, similarity rules for, 19: 23167
fluid flow with heat additions, quasi-one-dimensional, 17: 30671
fluid flow with heat addition in, quasi-one-dimensional, (T), 19: 39302
fluid flow with heat transfer in, effects of channel wall electric conductivity on, (T), 20: 4703 (AD-619101)
fluid flow with ignorable coordinate, steady incompressible viscous, (T),

19: 39301
fluid flow with temperature-dependent electric conductivity, channel, (T), 20: 2824
fluid flow-magnetic field interactions in, hypersonic, 19: 41120 (N64-30509)
fluid flows in, closed-form analytic solutions for laminar channel entrance, (T), 19: 39278
fluid instability near magnetic neutral line, 17: 14467
fluid instability in Bénard problem in, with large Hartmann numbers, 20: 28081
fluid interactions in Lagrangian formalism for, (T), 19: 18560 (CEA-R-2608)
fluid motion in, quasirigid stationary, (T), 20: 21787
fluid motion influenced by Coriolis forces, calculation of Lorentz field strength for turbulent, (T), 20: 32235
fluid rotation in, magnetic field effects on behavior of, 17: 32874
fluid sphere in magnetic fields, equilibrium configuration and oscillations of, 17: 14962
fluid stability in magnetic field in, transfer-function method for, (T), 20: 24196
forces on bodies in conducting liquids in, 19: 1058
formulation of, Lorentz invariance and momentum-energy tensors in, (T), 20: 24178 (AD-625268)
free oscillating movement between two infinite, parallel, vertical planes of electroconducting fluid, 17: 19479
free oscillations of electroconductive liquid in uniform magnetic field, experimental study of, 17: 22731
friction factor measurements for liquid-metal channel flows, 19: 39270(R) (TID-21894)
fully-developed, non-Newtonian, 17: 30673
gas deflagration and detonation waves with ionization in electromagnetic field, 17: 28014
gas flow along insulating plane in magnetic fields, Hall effect in two-dimensional, (T), 20: 15568 (AD-620324)
gas flow around bodies, (T), 20: 17525
gas flow around profiles, subsonic, (T), 20: 46433
gas flow around slender bodies in, (T), 20: 24179 (AD-625938)
gas flow at channel entrance, electromagnetic field effects on supersonic, 20: 9849
gas flow boundary layer on thermally insulated semi-infinite flat plate, compressibility effects on, (T), 20: 19632
gas flow by piston movement in transverse field, conducting, 19: 34799
gas flow classification in, nonstationary axially symmetric, 20: 34351
gas flow dynamics in, (T), 20: 4702 (AD-619094)
gas flow in canal with crossed electric and magnetic fields, effects of anisotropic conductivity, 16: 28294
gas flow in channels with axial magnetic fields, (T), 20: 46436
gas flow in coaxial channel in, quasi-one-dimensional approximation of steady, 19: 44830
gas flow in coplanar channel, effect of viscosity anisotropy on ionized, (T), 20: 7973
gas flow in diverging channel with transverse magnetic field, (T), 20: 46435
gas flow in exit region of transverse magnetic field, (T), 20: 24193
gas flow in homogeneous fields, compressed, (T), 19: 36624
gas flow in linear channels in, electrode current distributions in, 20: 34332 (N-66-16250)
gas flow in magnetic fields, electrically and thermally conducting, 20: 30185
gas flow in nonequilibrium, plane steady, (T), 20: 17515
gas flow in nozzles, patterns of, (T), 19: 14135 (NP-14785)
gas flow in transverse fields, method for sustaining, (T), 20: 4716
gas flow in transverse field, equations for conducting, 20: 25959
gas flow in tubes, one-dimensional, (T), 19: 14138 (NP-14789)
gas flow in, book on radiative, 20: 32238
gas flow in, deflagrations and properties of ideal, 20: 2821 (AD-618296)
gas flow in, description of channel, 20: 46434
gas flow in, determination of currents and fields in two-dimensional, (T), 20: 24192
gas flow in, electric conductivity of vortex, 20: 44412
gas flow in, electrode-induced potentials in, 20: 46325
gas flow in, equations for, (T), 19: 37212
gas flow in, Hall effect in axial-symmetric, (T), 20: 17521
gas flow in, heat transfer in, 20: 9848
gas flow in, hysteresis phenomena in, 20: 44411
gas flow in, magnetic field effects on stability of channel, (T), 20: 6174
gas flow in, nonequilibrium ionization in channel, 20: 46443
gas flow in, one-dimensional ionizing, (T), 20: 4717
gas flow in, one-dimensional, (T), 20: 21777 (AD-621442)
gas flow in, optimum conditions for Hall effect in channel, 19: 44832
gas flow in, potential equations and vortex theorems for, (T), 19: 14137 (NP-14788)
gas flow in, properties of small magnetic Reynolds number, (T), 20: 21781 (AD-622568)
gas flow in, reduction of three-dimensional compressible, 19: 44850
gas flow in, stationary rotational, (T), 19: 9879
gas flow in, swirling motion due to Hall effect in, 19: 1065
gas flow in, theory of, 18: 35035
gas flow in, theory of two-dimensional, 18: 34321
gas flow in, thermodynamic equilibrium diagrams for, 20: 34330 (N-66-10545)
gas flow in, two-dimensional, ideal variable-conductivity, (T), 20: 25986
gas flow in, ultrasonic, (T), 20: 17513
gas flow in, variational methods for two-dimensional, (T), 19: 14139 (NP-14790)
gas flow induced by moving plate, boundary-layer solutions of Rayleigh's problem, (T), 19: 26920 (NP-14938)
gas flow near channel angle, axially symmetric, (T), 19: 32816
gas flow near flat plate in magnetic field, conducting, (T), 20: 25957
gas flow past blunt or nonblunt body in hypersonic, 18: 34272 (NASA-CR-88)
gas flow past cylinders, variational methods for, (T), 19: 14134 (NP-14784)
gas flow past solid objects, 18: 37815
gas flow past wedge, shock wave stability in, (T), 20: 19631
gas flow theory for, one-dimensional, 20: 46432
gas flow through channels in, hydraulic approximation for, 20: 44407
gas flow through nozzles, sonic line of, (T), 19: 8018
gas flow with Hall effect in, Rayleigh problem in, (T), 20: 17512
gas flow with orthogonal magnetic and velocity field distributions, (T), 20: 17532
gas flow with tensor conductivity, two-dimensional, (T), 20: 13634 (AE-210)
gas flows around hypersonic blunt bodies in, 17: 15017
gas flows in, effects of channel and electrode properties on (E), 19: 2887 (BSD-TDR-64-20)
gas flows in, properties of small Reynolds number, (T), 20: 21782 (AD-623812)
gas ionization under closed-cycle MPD generator conditions, magnetically induced nonequilibrium, 18: 30472 (AD-427774)
gas rotation in magnetic field, stability of rarefied gravitational, (T), 19: 11847
geophysical-field effects on plasma in magnetosphere, 17: 14506
gravitational stability of infinite cylinders of fluids in magnetic fields, 18: 18779
gravitational stellar collapse in relativistic, 20: 28153
gravity waves of a conducting fluid in a horizontal magnetic field, 17: 5476
Hall effect in, calculation of, 17: 20631
Hall effect in liquid flow in traveling magnetic field, (T), 19: 14149
Hamiltonian and Lagrangian methods in, 17: 7430 (UCRL-6387)
heat transfer and laminar skin friction variations with flow velocity in presence of magnetic field, 18: 32294
heat transfer and charge losses in counter-current flow, (E), 19: 26502
heat transfer by flows in, 18: 817(R) (NP-13265)
heat transfer in, 18: 22233
heat transfer in channel, effects of wall conductance, 17: 8349
heat transfer in incompressible fluid flow, (T), 20: 24204
heat transfer in liquid flows in conducting channels in, 18: 2490
heat-transfer rates from plasmas in regions of high magnetic-field strength, 17: 42143
heat transfer to MHD fluid, 20: 41105
heater for, description of graphite inert-gas, 17: 39715 (BSD-TDR-63-109)
heaters for, development of graphite, 18: 29832
heating of multicomponent plasma, ohmic, 17: 2380
heating of solar corona, 17: 13658(T)
helical flow of strong electrolytes, effects of magnetic field, 16: 30551 (MIT-AL-TR-23)
Helmholtz instability in, 16: 10737
hydrodynamic approximation for charged particle motion in plasma, 16: 29932
hydromagnetic discontinuity in gases in, combustible adiabatic for, (T), 20: 30177
hydromagnetic equilibria and stability, 18: 6341
hydromagnetic flow, exact solutions for two-dimensional, 16: 24887 (D1-82-0170)
hydromagnetic flow characterized by large magnetic Reynolds numbers, 17: 36757 (PIBMRI-1001-62)
hydromagnetic flow against a rotating disk, equations for, 20: 11778
hydromagnetic stability of hard-core pinches, 16: 28288
hydromagnetic stability at a fluid velocity discontinuity between compressible fluids, 18: 16564
hydromagnetic stability, 19: 27614 (NASA-TN-D-2791)
hydromagnetic swirl development in "crowbarred" plasma, 16: 33947

hydromagnetic wave motion from oscillating boundary in, 18: 28141
hydromagnetic wave propagation by oscillating conducting boundary, 18: 34328
hypersonic shock layer support in, 17: 6783 (BSD-TDR-62-337)
incompressible conducting flow, effects of uniform vorticity on, 16: 15287
incompressible flow in, general characteristics of two-dimensional, 17: 5483
incompressible flow in two-dimensional field, 17: 12835
incompressible flows in, nonlinear effects in, 18: 19143
incompressible jets in, free, plane, laminar, 18: 14607
incompressible viscous flow in transverse magnetic field, analysis of, 18: 8498
induction-coupled MPD channel flow, 18: 19241
industrial applications of, review of, 17: 5526
instabilities of conducting fluids in magnetic fields, 16: 23207
instability of a surface of discontinuity of velocity in a parallel uniform magnetic field, 17: 28013
instability of Alfvén waves in, 17: 9704
instability of compressed fluid in, 17: 32812
instability of interfaces between dissimilar, incompressible, accelerated plasmas, 16: 28266
interaction of conducting fluid stream with traveling wave of magnetic field, 17: 37674
interaction of cylindrical shock wave with magnetic field in a conducting fluid, 17: 5459
interaction of electromagnetic waves with nonuniform plasma flows, analysis, 17: 9685 (R62SD14)
interaction of shock waves with magnetic fields and basic laws of, 16: 12604 (AFCRL-62-240)
ion pressures, gravitational stabilization factors from, 16: 13803
ionization in high-pressure cesium-helium transient discharge, nonequilibrium in, 17: 9669 (62-RL-3122E)
ionization nonequilibrium in expanding quasi one-dimensional airflows, 16: 10686
ionization of hydrocarbon combustion products, (T), 20: 41731
jets confined by transverse magnetic field, evolution of, (E), 20: 19625
Joule dissipation in channels (T), 19: 2914
kinetic formulation of rotational flow, 16: 3759 (AD-257441)
kinetic theory of hydromagnetic fields, 17: 32854
kinetics in stellar atmospheres, 18: 18533 (AFCRL-63-674)
Kutta-Joukowski condition in, 18: 18481
laminar boundary layers of cylindrical bodies in, (T), 19: 10446
laminar flow at entrance of flat duct, equations for, 16: 13738
laminar flow in, entry problem equations error and stability for, 17: 25422
laminar flow in plane channels, 16: 18234
laminar flow in porous wall annulus, 17: 5467
laminar jet against wall in transverse field, (T), 19: 4748
laminar plane free jet of incompressible fluid in presence of transverse magnetic field, 17: 22732
laminar plane free jet of incompressible fluid in presence of transverse magnetic field, 17: 29673
lectures, 18: 22549 (AD-436274)
lectures, 18: 22929 (AFCRL-63-907)
lectures on, 17: 4179 (UCRL-6879)
lectures on, 18: 42795 (SCTM-93-63(71))
liquid flow in annulus, radial magnetic field effects on finitely conducting, unsteady, (T), 20: 21789
liquid flow in annular ducts in, in circular and radial magnetic fields, (T), 20: 25981
liquid flow in annular channel with porous walls, axial and radial pressure variations for steady, (T), 20: 32222
liquid flow in channels, one-dimensional conducting-metal, (T), 20: 25954
liquid flow in channels with finite wall conductivity, viscous conducting, (T), 20: 25961
liquid flow in channel with porous walls, steady, (T), 20: 32221
liquid flow in circular tubes, (E), 20: 28064
liquid flow in curved pipe, (T), 20: 39931
liquid flow in radial field, power generation in conducting, (T), 20: 25965
liquid flow in rectangular channels, effects of transverse magnetic field mercury, (E), 20: 28070
liquid flow in, boundary-layer equations for, (T), 20: 28044
liquid flow in, discontinuities in inviscid, (T), 19: 4759
liquid flow in, exponential velocity distribution of, (T), 20: 28069
liquid flow in, forced oscillations of heavy, viscous electroconductive, (E), 19: 39281
liquid flow in, Hartmann layer effects on, (E/T), 20: 2831
liquid flow in, non-Newtonian, 20: 28067
liquid flow in, square-channel, (E), 20: 21807
liquid flow in, structure of electrically conducting, 20: 37868
liquid flow near stagnation point, axisymmetric, viscous, (T), 20: 28083
liquid flow, resistance and flow-profile studies, 16: 12239(T) (FTD-TT-61-281)
liquid flow transition regimes in channels, (T), 20: 25960
liquid laminar flow in, drag and heat exchange in, (T), 20: 24190
liquid metal drop motion in dielectric medium, effects on, (T), 20: 28066
liquid metal flow between coaxial cylinder conductors, 19: 23172
liquid metal flow resistance in circular channels, (T), 20: 30183
liquid motion in coaxial cylinders, 20: 37879
liquid rotation in uniform transverse magnetic fields, rotations of conducting, 19: 23198
liquid trans flow in stationary, conducting, (T), 20: 25966
lubrication flow between parallel rotating disks, 16: 19055
lubrication theory in, 16: 16855
magnetic-field and velocity distributions in fluid flows in, 17: 11352
magnetic field effects on gas flow in horizontal tube with heat difference, 16: 1129
magnetic-field effects on gravity propagation in electrically conducting fluids, 16: 16899
magnetic field effects on gravitating spheres, 16: 18116 (NP-11463 (Pt.3)(p.447-55))
magnetic field effects on surface wave in conducting liquid, 16: 23184
magnetic field effects on gas flow in anisotropic, 17: 13659
magnetic field interactions with surface waves, 17: 16784 (NASA-TR-R-161)
magnetic field reversal in collisionless plasma, 16: 6048 (TID-14082)
magnetic field scattering in conducting fluid, 18: 32906
magnetic fields in, properties of semistable quadrupole–octupole periodic, (T), 19: 7998 (64-RL-3778E)
magnetic flux interchange instabilities in, (T), 20: 13638 (IPP-6/39)
magnetic moment of gyrating charged particle, 17: 9760
magneto-acoustic wave in nonuniform field, anisotropic properties of, 16: 15378
magneto-gravitational instability of stratified media, 16: 12242
magnetoacoustic resonances in plasma, 16: 29931
magnetoacoustic wave properties in non-dissipative fluids, 16: 28282 (UCRL-10161)
magnetoacoustic wave propagation in cylindrical plasma, 16: 29933
magnetogasdynamic flow, substitution principle for steady, 17: 20640
magnetohydrodynamic, entropy perturbations in one-dimensional, 17: 23481
magnetoplasmadynamics of rotary arc plasma generator, 18: 4677
magnetosonic waves in "aligned-fields" compressible flows, 16: 29959
magnetostatic models for rotating conducting liquid spheres, 16: 15483
mathematical analysis of pressurized journal bearing, using liquid metal lubricant, 16: 20570
mathematical problems in, 17: 39457
mathematical problems in, (T), 19: 16251 (AFOSR-64-1647)
mean value theorem derived from generalized virial theorem of fluid mass of infinite conductivity exposed to self-gravitation, 18: 14602
mechanics, 16: 603
microwave absorption and reflection by nonuniform stratified media, 17: 15030
microwave diagnostics of a partly ionized flow in a magnetic field, 17; 40211
microwave propagation in magneto-ionic ducts, 18: 30878(R) (AFCRL-64-219)
model applications in, one- and two-fluid, 17: 29477
moment equations for gases in, 17: 5129
Monte Carlo analysis of plasma flow in transverse magnetic field, 19: 1712 (NASA-TN-D-2211)
motion in, mathematical analysis of unsteady, 16: 2321
motion of a conducting viscous gas in magnetic and electric fields, 16: 19861
motion of conducting compressible fluid around thin fins with magnetic field perpendicular to the flow direction, 17: 24575
motion of electrically conducting spherical fluid mass with circumferential current lines in parallel planes, 17: 41584
motion of gravitating cosmic plasma in magnetic fields (T), 19: 1161
motion of incompressible viscous fluid around axis, (T), 19: 42933
motion of plasma in a channel with external magnetic field, 16: 19866
motion of viscous incompressible weakly conductive fluid outside magnetized sphere, 17: 28368
motion of viscous hydromagnetic fluid between rotating coaxial cylinders of finite length, unsteady, 17: 22385
motions in many-component, nonstationary spiral, 16: 19863
movement in space of perfectly conducting compressible fluid, 17: 22734
nozzle flow in presence of magnetic field with three transitions, 16: 11074 (NYO-9600)
of chaotic turbulent media, 18: 11327
of compressible flow of gas with infinite conductivity, 18: 32295
of conducting incompressible flow in tubes, 16: 11841
of cylindrical flow, direction of onset of instability in, (E/T), 19: 8526
of detonation waves, 16: 7196 (ARL-69)
of flow of incompressible, viscous, electrically conducting fluid, 19: 593
of fluid flow around rotating spheroid in coaxial magnetic field,

18: 32297
of fluid flow in rectangular tube at high Hartmann number, 17: 28015
of gas-solid suspensions, 17: 24027 (AD-282604)
of incompressible viscous liquid, stationary currents in, (T), 19: 30387
of induction devices, study, 16: 11070 (AFOSR-1864)
of jet-driven, confined vortex-type flow, 19: 23200
of oscillating sphere, 18: 30309 (NP-14087)
of partially ionized gases, 16: 5086(R) (NP-11057)
of partially ionized gases, research in Project Squid on, 18: 1094(R) (AD-420576)
of plane interface between vacuum and electrically conducting fluid, 19: 23850
of spherical conductors, 18: 16547 (AD-416626)
of sunspot processes, 19: 2938
of system of collisionless gas with self-gravitating particles in magnetic fields, 20: 42041
of turbulence, spectral and fluctuation theories of, 19: 1751
Ohm's law for, nonlinear terms in generalized, (T), 20: 21778 (AD-621943)
oscillations between parallel planes in, 18: 12769
oscillations in conducting incompressible flow in transverse magnetic field, 17: 20187
oscillations in electrically conducting gaseous atmosphere exposed to gravitation, 16: 27763
oscillations in relativistic plasma, linear, 16: 1108 (ARL-TR-60-274 (Pt.II))
oscillations in rotating ellipsoidal fluid mass, (T), 19: 18587
oscillations of a capillary jet of finite conductivity in a uniform axial magnetic field, 17: 41612
oscillations of conducting fluid in magnetic field, 17: 32782
oscillations of convective unstable conducting fluid, 18: 43764
oscillations of infinitely long cylinders, radial, 16: 15337
oscillations of mercury in a magnetic field, 16: 11093
oscillations of planes in, solutions for torsional, 18: 42173
oscillations of self-gravitating fluids, 16: 16900
oscillations of viscous liquid sphere in rotation, equations of torsional, 17: 33184
oscillations of viscous conducting liquid in magnetic field, forced, (T), 19: 27635
particular solutions of hydrodynamic equations of a rarefied plasma in the case of axially symmetric motion, 16: 19870
performance for separating electrically conducting fluids, 18: 22192(P)
performance of crossed-field magneto-aerodynamic accelerators, 18: 41599
performance of long-lived ducts, 19: 9292
performance of re-entry vehicle channel, 16: 31148
periodic boundary-layer flow in, 16: 27210
perturbations due to oscillating dipoles, (T), 20: 37875
perturbations of equipartition state in, tensor virial approximation for, 17: 14963
phase and group velocities of magnetosonic waves, relation to hyperbolicity of equations, 16: 15341
pipe flow in, at high Hartmann numbers, 16: 27209
pipe flow in, solution of, 16: 27208
plane flows in, general results on theory of, 17: 5524
plane piston motion in conducting media, equations for, 17: 2108
plasma acceleration and heating in electric discharges, 17: 990
plasma acceleration by traveling magnetic field, 18: 4664
plasma acceleration by momentum transfer through magnetic fields, 18: 4665
plasma beam generation and ejection by, device for, 19: 28532(P)
plasma blob motion in non-homogeneous magnetic field, 16: 15725(T) (AEC-tr-4932)
plasma channel flow with Hall currents, 17: 42039 (ARL-63-145)
plasma characteristics in, virial theorem for, 17: 17372
plasma characteristics in Hall propulsor, 18: 21391
plasma collective properties in, review of, 17: 7490
plasma compression experiments, 17: 9741
plasma configuration stability in, 17: 40154 (AERE-M-1213(Pt.III))
plasma containment, applications of integral theorems, 16: 17330
plasma containment by periodic magnetic field, device for, 18: 1098 (AFCRL-62-858)
plasma containment and stability in cusped fields, 18: 44867
plasma cylinder stability in magnetic field, 17: 21183
plasma cylinder stability in magnetic fields, 17: 42139
plasma diagnostics using noise analysis, 20: 15569 (INR-626/IX/R)
plasma dipole resonances in magnetic fields, 17: 42077
plasma dynamics in, 16: 29935
plasma dynamics in, model and numerical technique for, 20: 13960
plasma dynamics, semiclassical variational principle for, 16: 29953
plasma equations, 16: 26420
plasma equilibria at high pressures, 18: 26762
plasma flow across azimuthal magnetic field, (T), 19: 17117
plasma flow around cylinders in weak magnetic field, shock structure in, (T), 20: 25951 (N-65-35269)
plasma flow at right angles to magnetic field, wall friction in one-dimensional, 17: 26702
plasma flow equations in, 18: 4637 (NP-13297)
plasma flow in channels, energy conversion with Hall currents in, 18: 21410
plasma flow in crossed electric and magnetic fields, (T), 19: 5359
plasma flow in cylinders, analysis of, 18: 24769
plasma flow in cylinders, equations for finite conductivity, 19: 30866
plasma flow in insulated channels, boundary layer effects on, 17: 33201
plasma flow in magnetic field, current sheath and oscillations in, 18: 15333 (N63-20250)
plasma flow in magnetic fields, similarity analysis of, (T), 20: 17910
plasma flow in one dimension with heat transfer, 18: 17172
plasma flow in shallow channel, temperature distribution in, (T), 19: 17118
plasma flow in, Joule heating effects on, 20: 28585
plasma flow in, methods for analyzing one-dimensional time-dependent, (T), 19: 23862(T)
plasma flow in, nonstationary axisymmetric, (T), 20: 32231
plasma flow in, one-dimensional unsteady, (T), 19: 4872 (NP-14505)
plasma flow in, single fluid theory of, 20: 3233
plasma flow in, turbulence in, (T), 19: 14664 (JHU-23-P)
plasma flow over biased body, analysis of, 18: 22945 (NP-13798)
plasma flow over conducting surface, boundary conditions for, 18: 15335 (NP-13624)
plasma flow over conducting surfaces, boundary conditions for, 18: 35005
plasma flow past magnetic dipole, 17: 40160 (NP-13136)
plasma flow past thin airfoil, 16: 15394
plasma flow patterns in, two-dimensional, (T), 20: 25982
plasma flow through uniform transverse magnetic field in duct, ion slip, 16: 19851
plasma flow through nozzles, containment properties of, (E), 20: 20300 (NP-15904)
plasma flow through nozzles, containment properties of, (T), 20: 20299 (NP-15903)
plasma flow with axial symmetry, magnetic channeling effect in one-dimensional, 18: 19147
plasma flows in, model for nonlaminar, axial, quasi-Brillouin, 17: 967
plasma generation by combustion and premodulation, 19: 12148
plasma in perpendicular electric and magnetic fields, current density in, (T), 19: 33433
plasma instabilities in, effects on solar flare production, 17: 33166
plasma instability due to finite resistivity, 17: 26675 (UCRL-7107)
plasma interactions with electron beams in, 16: 26424
plasma jet flow-field perturbations and Hall potentials in, axisymmetric, (E/T), 20: 30176
plasma jet velocity profiles in, affinity of excess, (E), 20: 19626
plasma kinetics in, MGD equations for, 18: 35034
plasma longitudinal oscillations in, stability criteria for, 16: 32505
plasma motion in magnetic fields, transverse, 17: 9751
plasma one-dimensional acceleration in, 17: 973
plasma one-dimensional unsteady flow in, (T), 20: 30570
plasma oscillations in, long-wavelength modes for, 17: 972
plasma oscillations, longitudinal, 17: 2382
plasma penetration into vacuum in magnetic field, 18: 26711(T) (FTD-TT-64-400)
plasma physics of unidimensional flow of conducting fluids, 18: 2993
plasma pinch discharges in, similarity solutions for transient, 18: 34997
plasma Poiseuille flow in, 17: 5494
plasma potential and energy distributions in injection devices, 17: 2379
plasma probe theory for, 20: 41782
plasma propagation in, analysis of axially symmetric hard magnetic piston for, 17: 4172 (NP-12203)
plasma properties in, nonisothermal, 16: 12637
plasma properties, calculation of nonequilibrium monatomic, 17: 33208
plasma properties in, 19: 1769
plasma radial oscillations in pulsed electrodeless discharge, 17: 11892
plasma radiation losses behind strong shock waves, 17: 2389
plasma research programs at MIT on, 17: 35260(R) (TID-19135)
plasma rotation in, 18: 21443
plasma stability conditions in, 16: 1114 (NP-10876)
plasma stability criteria in, near magnetic axis of revolution symmetry, 17: 26667 (CEA-2269)
plasma stability in, sufficient conditions for, 17: 2381
plasma stability in, integral of energy for toroidal, 17: 26691
plasma stability in, resistivity effects on multipolar, 17: 33175
plasma stability in strong magnetic fields, 17: 33188
plasma stability in, in cylindrical geometry, 17: 42067
plasma stability in a magnetic field, 17: 42082
plasma stability in, effects of collisions and gyrations on, 18: 42833

plasma stability in time-dependent magnetic field, (T), 20: 46860
plasma stability theory in, 16: 29949
plasma stability theory in, (T), 20: 40239
plasma stability with finite conductivity or current-carrier mass, (T), 19: 12711
plasma thermodynamics in, infinite-conducting, (T), 19: 45417
plasma turbulence in, effects of drift instability on inhomogeneous, (T), 20: 28547
plasma waveguide excitation by coaxial waveguide, 20: 12208
plasma-analysis techniques in, (T), 19: 38010
potential streaming in, 17: 36765
power extraction probes for shock-heated plasma, effects of magnetic field on, 18: 19242
power generation and propulsion developments, review, 16: 15389
power generation by, review of theory for, 17: 8962
power generation by, from supersonic rocket exhaust, 17: 41664
power generation by, economics of central, 19: 12157
power generation by, a-c, (T), 19: 23352
power generation efficiency of Carnot-cycle magnetoplasmadynamic generators, 17: 5088
power generation for marine vessels, 18: 4359
power generation in flowing plasma—external circuit interaction for one-dimensional channel flow, optimization of, 18: 7837
power generation principles, (T), 20: 41693
problems concerning the fixed convection flow in vertical channels, 16: 19868
processes in ionized gas, irreversible, 17: 31106
processes in, theory of irreversible, 16: 26415
production of magnetoacoustic waves, 18: 9519
progress in, 17: 39733
propagation of elliptically polarized monochromatic waves in, (T), 19: 6412
properties in analogy to plasma physics, 17: 5520
properties of, (T), 20: 37867
properties of liquid metals, (T), 20: 11771(T) (NP-tr-1346)
propulsion and power generation by, 18: 22928(R) (AD-435879)
propulsion, review of developments, 16: 6247
propulsion system, description of closed-cycle MHD-nuclear, 16: 9706 (AFBSD-TR-61-58)
pulse propagation in relativistic medium in, dispersion relations for, (T), 20: 25985
radial flow of an electroconducting gas in a moving magnetic field, 16: 1128
radiative equilibrium of electroconductive spherical gaseous mass uniformly rotating and gravitating, 18: 14601
Rayleigh problem in, operational calculus for, (T), 19: 20665
Rayleigh problems, effects of conductivity and viscosity on incompressible flow, 16: 14160
Rayleigh-Taylor problem of two superposed fluids in magnetic field, effects of electric conductivity on, 17: 28012
Rayleigh-Taylor instability under electromagnetic forces, 18: 19248
Rayleigh-Taylor instabilities in, in mercury flow, 19: 37964
Rayleigh's problem in, 17: 37888
Rayleigh's problem in, Hall effect in, 18: 36716 (NP-14209)
relation to aerodynamics, 17: 13862
relativistic, interpretation of shock relations in, 18: 24227
research by Soviet and Latvian scientists, 20: 42042
research on, development of closed-loop unit for, 17: 34541(R) (NP-13063)
research on plasmas, 17: 21401(R) (TID-18585)
research programs for re-entry information, 16: 6253 (ARGMA-TN-2H1N-30)
research programs on plasma, 16: 11078 (USCEC-79-101)
research programs on, 16: 30172(R) (TID-16489)
research programs on, 17: 13879(R) (TID-17943)
research programs on, 20: 1534(R) (LA-3370)
research programs on, 20: 28864(R) (NP-15976)
research progress on, 18: 2975 (AD-283026)
research progress on, 18: 2404(R) (TID-19651)
research progress on, 18: 15711(R) (TID-20256)
research progress, 19: 14667(R) (NP-14571)
research progress on, 19: 25071(R) (TID-21667)
research, review, 17: 20648
response of spectrum of isotropic turbulence to suddenly applied magnetic field, 17: 36776
review, lecture notes, 16: 4895 (D1-82-0024)
Reynold's number in, calculation of, 20: 32700
rocket thrust vectoring by, 17: 5641 (NP-12264)
scaling laws for a perfect gas, 17: 36789
seeding of gases for power generation at relatively low temperatures, 17: 2079
shock behavior in T-shaped tubes, 18: 8924
shock discontinuities in perfectly conducting gas flow, (T), 20: 37872
shock equations of classical and relativistic, 20: 19627
shock-front instabilities in rarefied plasma, 16: 29962
shock fronts in gas, 19: 18585
shock growth and propagation in magnetogasdynamic flow, 18: 16560
shock ionization of gases, densities in (E/T), 19: 3395 (AD-606894)
shock motion in ducts, evolutionary, 17: 9068
shock propagation along plasma column, 17: 2384
shock propagation in conical chambers, effects of magnetic fields on, 17: 36519
shock propagation in, conditions for, 18: 10245
shock propagation in, similarity rules for hypercritical and trans-Alfvénic, 18: 28142
shock propagation in plasma, 18: 35006
shock propagation in perpendicular magnetic field, radiative energy flux from one-dimensional plane, (T), 20: 21788
shock propagation in argon–hydrogen mixtures, (E), 20: 32217 (N-65-33713)
shock propagation in computer program for, 20: 36086 (UCRL-14931)
shock relations for, 16: 22716(R) (AFSWC-TDR-62-12(Vol.II)(Chap.6))
shock strength vs. area variations in channels, 17: 32742
shock structure in slightly ionized gas, Hall current effects on, (T), 20: 25967
shock structure without collisions, 17: 5487
shock wave attenuation in ionized gas in transverse magnetic field, 18: 26802
shock wave decay in, piston-produced, 18: 7410
shock wave endothermic and exothermic processes in, 17: 2103
shock wave evolution and stability in low-density plasma, (T), 19: 27690
shock wave excitation in fluid with ideal conductivity, resonance, 17: 22392
shock-wave formation by nonuniform expansion of a piston into an ionized medium with a weak magnetic field, 17: 36774
shock wave position in conical flow, 17: 36766
shock wave propagation in, 17: 2375
shock wave propagation in conducting gas in weak magnetic field (T), 19: 2911
shock wave propagation in inhomogeneous magnetic field, (T), 19: 12693
shock wave propagation in gases, (T), 19: 27689
shock wave propagation from explosions, (T), 19: 27692
shock wave propagation in pinch plasma, (T), 19: 27693
shock wave propagation in conducting media, ionizing, 19: 39267 (NP-15157)
shock wave propagation in ducts, effects of non-uniformities in piston motion on, 19: 42932
shock wave propagation in conducting incompressible fluids in magnetic fields, (T), 20: 1092
shock wave propagation in electroneutral media in, magnetic field deformation and electric structure in wave-front interior, (T), 20: 21806
shock wave propagation and attenuation in gases, (T), 20: 24191
shock wave properties in, (E), 19: 6386 (NP-14546)
shock wave scheme in, 17: 9699
shock wave stability in, 16: 22721(R) (AFSWC-TDR-62-12(Vol.II) (Chap.11))
shock wave structure in, 16: 21206
shock wave structure in, 16: 21662 (AFSWC-TDR-62-42)
shock wave structure in gas with anisotropic conductivity, 16: 33957
shock-wave structure, theoretical model of, 17: 22761
shock wave structure in, effects of electron inertia on, 18: 26149
shock wave structure in plasma, radiative (T), 19: 1718 (NP-14442)
shock wave structure and solitary waves in, collisionless, (T), 19: 29132 (NYO-1480-12)
shock wave structure in, effects of electron temperature and Hall currents on, 20: 30191
shock waves, evolutionarity, 16: 2590(T) (AEC-tr-4703)
shock waves in, 16: 9530(T) (JPRS-11725)
shock waves in, driven by time-varying magnetic fields, 16: 33614
shock waves in, flow behind, 17: 3612
shock waves in fully ionized perfect gas, properties of plane perpendicular, 18: 26693 (RISO-76)
shock waves in gases, production of space-charge separation by, 16: 29943
shock waves in ionized hydrogen, 17: 39707 (AD-414622)
shock waves in magnetogasdynamic flow, 17: 20714
shock waves in MGD, dissipative model for steady-state, 20: 34352
shock waves in non-uniform ducts, perturbation from, 17: 24168
shock waves in nonaligned flow in perfect gases, (T), 20: 15576
shock waves in relativistic, (T), 20: 19623
shock waves in stability and structure of trans-Alfvénic, 19: 23180
shock waves in steady, two-dimensional flows, properties of oblique, 16: 29960
shock waves in, theory of electromagnetically driven, 16: 29958
shock waves in, ionizing, (T), 19: 18566 (NP-14858)

shock waves in, oblique, (T), 19: 4767
shock waves, research program, 16: 15715(R) (AFCRL-62-230)
shock waves with finite electric conductivity in, 20: 39944
shock-wave production and propagation, 18: 44284 (AD-603951)
shock-wave propagation in cold and preheated gas in inverse-pinch shock tube, 18: 11338
shock-wave propagation in electromagnetic tube, 18: 44288 (NP-14347)
shock-wave seeding with alkali metals, inert-gas, (E/T), 19: 35526 (NRC-7884)
similarity rules in, based on multi-fluid theory, (T), 19: 41156
simple waves and shocks in, 17: 5489
simplified theory of isotropic turbulence in, 17: 39740
sinusoidal forced oscillations of electroconductive liquid in presence of transverse magnetic field, 18: 15362
skin effect in traveling-wave devices, 17: 32775
skin friction in turbulent channel flow, 17: 16229 (NP-12631)
solar atmospheric properties in, 17: 9786
solar-flare disturbance propagation in interplanetary space, 16: 30996
solution for arbitrary flow discontinuity in transverse fields, 16: 11838
solutions for boundary-layer equations in, 18: 42174
solutions for magnetogasdynamics problems in three dimensions, 18: 19172
source current motion along magnetic fields, 17: 32708 (D1-82-0254)
space propulsion system based on, research on, 17: 28362 (NP-12935)
sphere rotation in conducting viscous fluid in, 18: 20664
stabilities of sheet pinch, finite-resistivity, 17: 21158
stability and surface waves of interface of hydrodynamic systems, 16: 3777
stability conditions, equilibrium tests of, 16: 18207
stability conditions for ideally conducting fluid, 16: 28293
stability criterion for arbitrary equilibria, 16: 4921
stability in circular fields, 16: 18235
stability in finite conductivity, analog computation for, 20: 2836
stability in non-viscous, incompressible fluid, 16: 19486
stability in, two-stream, 17: 5441 (TID-17370)
stability in, effect of finite Larmor radius on, 19: 27607 (LA-3260)
stability in, effect of ion gyration radius on gravitational, 20: 2885
stability in, effect of energy dissipation and temperature dependence of transfer coefficients on, (T), 20: 11794
stability in, variational properties of, 18: 34326
stability of a heterogeneous shear layer in a magnetic field, 17: 5484
stability of axial current fluid, effect of surrounding neutral medium, 16: 602
stability of axially symmetric motions in, 17: 11887
stability of axially symmetric, conducting, vortex flow between coaxial cylinders, 17: 11439
stability of channel flows, (T), 19: 18577
stability of cosmic plasma in, against gravitational forces (T), 19: 1147
stability of curved viscous flows, 16: 8261 (NP-11269)
stability of cylindrical plasma in, 16: 15729
stability of dissipative vortex flow, (T), 19: 13592
stability of electrical conducting inviscid fluid in axial current, coaxial conducting cylinder, and longitudinal magnetic field, 16: 600
stability of electrical conducting inviscid fluid slab in homogeneous magnetic field, 16: 601
stability of extraordinary wave in collisionless plasma, 18: 9545
stability of flexible conductor in longitudinal magnetic field, (T), 20: 46448
stability of fluid flow down inclined plane in magnetic field, analysis, 19: 18117 (NP-14816)
stability of gravitational fluid layer with decreasing density, 16: 11840
stability of gravitating cylinder in magnetic field, 18: 30920
stability of hydromagnetic systems, effects of electric and thermal conductivity and viscosity on, 17: 21134 (MATT-143)
stability of ideally conducting fluid in longitudinal field, 17: 22313
stability of inviscid vortex flow with finite conductivity, 18: 34363
stability of ionized gas in magnetic field (T), 19: 2912
stability of liquid layers, 20: 2820 (AD-614645)
stability of liquid metal flow in, gravitational, 20: 34133
stability of magnetically confined plasma, 18: 11304 (SIT-110)
stability of plasma in static equilibrium, 16: 1111 (NP-10848)
stability of plasma tori, 18: 11311
stability of shocks attached to point of dihedral in, 17: 36767
stability of sound in nonhomogeneous plasma, (T), 20: 41764
stability of static systems, 16: 14161
stability of static systems, Kruskal and Oberman energy principle, 16: 14162
stability of stationary systems in, with anisotropic pressure, (T), 19: 17152
stability of stellar atmospheres in, (T), 19: 10160 (NASA-TN-D-2218)
stability of supermassive stars, effects of magnetoturbulent energy on, 19: 47200
stability of system equilibria in, solution using an energy principle, 17: 5521
stability of tangential discontinuity in compressible fluid in intense magnetic field, (T), 19: 30871
stability of toroidal equilibria in multipolar fields, 16: 28279 (MATT-116)
stability of toroidal plasma, 17: 9763
stability of toroidal plasma structure, 17: 42053 (PIBMRI-1025-62)
stability of toroidal plasma, (T), 19: 6799
stability of uniformly rotating cylindrical plasma, 17: 9711
stability of viscous flow in a curved channel in presence of a magnetic field, 16: 1930
stability of viscous flow between cylinders in magnetic fields, 16: 11068 (AFCRL-635)
stability of viscous conducting fluids in magnetic fields, 18: 44300
stability of viscous conducting fluid in uniform rotational motion, (T), 19: 42953
stability of vortex flow, nondissipative and incompressible analysis, 17: 4661 (ORNL-TM-402)
stability of vortex sheets in fluid flows in, (T), 19: 4757
stability of, nonuniform current and field distribution effects on, 20: 42040
stability, axisymmetric equilibrium, (T), 20: 44858 (IPP-6/48)
stagnation-point flow for small magnetic Reynolds number, 16: 12609 (AROD-2311:6)
stagnation point in, axisymmetric, 16: 5786
stationary currents in infinitely conducting gas, properties of axially symmetric and plane, 17: 15368
stationary equations for compressible ideal fluid of infinite conductivity in rotating frame of reference, 17: 13274(T)
stationary supersonic flow over wedge, automodel solution for, 17: 2105
stationary turbulence in magnetic fields, (T), 19: 4768
streaming in cylindrical tube, exact solution, 16: 859
streaming of electrically conducting gases in magnetic fields (E/T), 19: 1085
structure of ionizing shocks, 16: 19850
structure of slow shock in two-fluid system with dissipation, 18: 24226
studies of explosive, 19: 8130(R) (MHD-655)
superconducting magnet applications in, 18: 13010
survey, 18: 679 (ARL-63-175(Pt.I))
Taylor-Proudman theorem in, 16: 27772
technology and uses, 16: 8018
temperature distribution scaling parameters, 16: 18240
temperature field stability in plane-electric-discharge channel in, wall effects on, (T), 20: 28085
temperature instability in, 17: 20752
temperatures and velocities in laminar conducting flow, equations for, 16: 32190
theorem in, Chapman-Jouget, 19: 44837
theoretical aspects of, review of work in United Kingdom on, 18: 7835
theory, 18: 17107 (JÜL-145-TP)
theory, differential solutions for pressure-compensated fields, 16: 16638
theory, eikonal method for analysis of disturbances, 16: 18556 (AFOSR-1546)
theory for channel flow and magnetic containment, 18: 26718
theory for cosmogony, 18: 22650(T) (JPRS-24435(p.274-304))
theory for electron density fluctuations in plasma, 17: 42078
theory for ideal conductors, general relativistic, 20: 11772
theory for interactions of conductors with very high pulsed magnetic fields, 16: 15414
theory for magnetospheric boundary stability, validity of, 20: 32254
theory for plasma interactions with high-frequency field, 20: 3207
theory for space applications, 19: 1163
theory for stability of toroidal pinch discharge, 17: 42086
theory for toroidal vortexes, field generation, 20: 46431(T)
theory, generalization of Oseen's solutions, 16: 1116 (PLR-75)
theory in investigations of plasma, 16: 9519(T) (AEC-tr-4704)
theory, linearized three-component, 16: 23180 (NYO-9189)
theory of, 17: 37872
theory of choking performance in, 17: 9080
theory of deflagration and detonations in, 18: 36715(R) (NAVWEPS-8132)
theory of dynamos in, 19: 1067
theory of entrance flows in constant-area channels, (T), 19: 8037
theory of hydromagnetic magnetic-flux concentrator, 16: 15416
theory of hydromagnetic dynamo, 20: 25984
theory of isentropic flow in, in aligned fields, 16: 29469 (AFOSR-2715)
theory of planar traveling waves on free surface of inviscid liquid, 18: 21445
theory of plasma fluctuations in MHD channels, (T), 19: 6387 (NP-14569)
theory of radiation, 16: 21124 (AFOSR-2674)
theory of relativistic, 19: 39279

theory of, review, 17: 9138
theory of thin flanges in, 17: 4664
theory of thin flanges in, with orthogonal magnetic field, 17: 5077
theory of two-dimensional, in transverse fields, 16: 18216
thermal conductivity and flux in, 17: 36525
thermal radiation emission by fluid in Couette flow in magnetic field, 18: 31734
thermal stability of completely confined fluids in, (T), 20: 17535
thermodynamic vapor, properties of "perfect", (T), 20: 42045
thermodynamics of, with vapor-fluid injector, (T), 20: 13438
thermonuclear uses, 18: 24763(R) (UCRL-11172)
three-dimensional jet vortex in viscous conducting fluid, 18: 37813
transient flow in channels, 17: 18920
transition regimes in fluid flow, elliptical-hyperbolic, 17: 40172
transverse diffusion in quasi-static positive column, 16: 4901 (D1-82-0118)
turbulence, 17: 3574(R) (NP-12212)
turbulence damping, final state and energy spectra of, 16: 28261
turbulence in, (T), 19: 17145
turbulence in conducting fluid, (T), 19: 42943
turbulence in, energy spectrum of isotropic, 17: 31623
turbulence in, energy exchange and vorticity production in, 17: 41560 (SSD-TDR-62-121)
turbulence in, review, 17: 7492
turbulence in structure of small-scale, 18: 14051
turbulence in weakly conducting incompressible liquid in homogeneous magnetic field, (T), 19: 42937
turbulence, orders of magnitude, 16: 19487
turbulence propagation in conducting gas, analysis of, 17: 36531
turbulence studies in, 17: 5435(R) (DCAS-TDR-62-45)
turbulence studies in a linear pinch, 17: 40213
turbulence with a uniform imposed magnetic field, 17: 36775
turbulences in, 17: 42048 (DCAS-TDR-62-167)
turbulent flow of electroconductive liquid in presence of magnetic field, 17: 7442
two-dimensional incompressible flow in nonuniform fields, 16: 18215
two-dimensional motion in magnetogasdynamics, 16: 11839
two-fluid, equation development for, 20: 2838
uniqueness of solutions of equations of, 16: 19490
uniqueness theorem, 16: 11089
use for external propulsion of submarines, field configuration for, 19: 12139
use for increasing load capacity of bearings, 20: 40216
use for power production in fast breeder reactors, 18: 35166(T) (ANL-Trans-38)
use for space flight control, (T), 19: 10421
use in analysis of stellar explosions, 16: 32251
use in explanation of existence of magnetic fields of earth and stars, 17: 26255
use in explanation of existence of magnetic fields of earth and stars, 17: 26256
use in heavy water concentration, 19: 44578(P)
use in space engines, 18: 4353
use in supersonic air and space travel, theory of, 18: 2993
use of crossed magnetic fields for accelerating conducting fluids, 16: 7965(T) (FTD-TT-61-228(p.1-11))
uses and limitations, 18: 42798 (SCTM-93-63(71)(p.23-43))
uses in high-velocity flight and plasma production and propulsion, 16: 7193 (AFOSR-1782)
uses of, for control and utilization of dissipated energy from space vehicle re-entry, 19: 35000 (NP-15086)
variational principles in, 20: 28063
velocity distribution in channel flow with variable conductivity, (T), 20: 24177 (AD-624667)
viscoelectric fluid flow analogy in, 18: 14661
viscous shock layer in hypersonic flow, 18: 30936
vortex flow in, 18: 8496
vortex rings near walls, behavior of quantized, (T), 19: 8346
vortex structure in dense, inviscid plasma, 17: 978
vortices in, theory, 17: 15023
vortices in viscous conducting fluid, (T), 19: 33399 (AD-607999)
wakes from three-dimensional conducting flow, current and motion relations for, 17: 20181
wall effects in ducts, 17: 9074
wave damping in plasma, (T), 19: 27696
wave excitation by plasma interactions with point alternating-current sources, 16: 29952
wave experiments in, 18: 32883 (AFCRL-63-782(Vol.III))
wave fronts in, (T), 19: 23846
wave growth and stability in slightly ionized plasma in magnetic field, 18: 26689 (BSD-TDR-64-34)
wave motion in collision-free plasma, finite-amplitude compression, 18: 21386 (NYO-10434)
wave motion in, finite, 16: 3590
wave motion in infinite cylindrical plasma confined by magnetic field, 18: 9544
wave motion in steady two-dimensional flow, oblique shock and simple, 18: 20630 (NYO-10436)
wave motion of compressible fluid, nonisentropic perturbation in, 17: 950 (AD-273247)
wave phenomena in a magnetoplasma, 16: 1109 (BSR-455)
wave propagation from discontinuities in perfect gases, (T), 19: 27691
wave propagation in horizontally stratified ionosphere at oblique angle, 16: 12607 (AFCRL-566)
wave propagation in infinite uniform plasma, 16: 24880 (AFCRL-896(Pt.II))
wave propagation in collisionless plasma, linear theory for, 16: 29946
wave propagation in plasma, 16: 33944
wave propagation in partly ionized gases, 17: 5468
wave propagation in partially ionized gases, 17: 27540(R) (NP-12767(p.65–7))
wave propagation in fully ionized plasma, quasi-one-fluid theory of, 17: 38383
wave propagation in, book on field-coupled surface, 18: 42202
wave propagation in ionospheric plasma at extremely low frequency, 18: 44848 (AFCRL-64-280)
wave propagation in relativistic, Riemann, (T), 19: 20668
wave propagation in, one-dimensional, (T), 19: 32803
wave propagation in conducting compressible fluid in nonuniform ducts, (T), 20: 1091
wave propagation in rotating liquids, effect of Hall current on, 20: 4711
wave propagation in ideal perfectly conducting liquid in, particular cylindrical solutions for radial, 20: 21791
wave propagation in, simple-, (T), 20: 25979
wave propagation in nonrelativistic, Riemann, 20: 28062
wave propagation in stratified incompressible fluid in, Alfven, 20: 36088
wave propagation in compressible perfect fluid of infinite conductivity, relativistic, 20: 44409
wave propagation theory in, (T), 19: 5332
wave properties in relativistic anisotropic, 17: 28066
wave properties in, 18: 22558
wave surface in fluid with polar magnetic field, (T), 19: 18584
wave transformation in, 19: 45432
waves in inhomogeneous hydromagnetic medium and geomagnetic micropulsations, extremely low-frequency, 17: 5433 (D1-82-0150)
waves in magneto-ionic mediums, polarization of, 16: 11067 (AFCRL-621)
Zemplen theorem in, 17: 6827

MAGNETOMETERS

see also Fluxmeters

book: *Geophysics and Space Data Bulletin No. 3*, 19: 47447 (AD-612083)
calibration for synchrotron magnet measurements, 20: 19291 (CALT-68-67)
description of, for geomagnetic field mapping, 17: 32862
description of NMR, 20: 34650
design, 16: 6612
design, 17: 938
design, 18: 14167(T) (JPRS-23408)
design, 18: 42164 (UJV-944/63)
design and operation for DASA Project 6.5A for Johnston Island tests, 18: 29915 (AFCRL-63-939(3))
design and operation of search-coil, for satellite measurements of geomagnetic fields, 20: 30236
design and performance of Hall, 16: 17835
design and performance of precision rotating-coil, 16: 31948
design and performance of proton precession, 17: 18290 (NADC-AW-6226)
design and performance for alternating and static fields, 17: 21981(T) (AERE-Trans-903)
design and performance of nuclear, 19: 28612(T) (FTD-TT-64-1104)
design and performance of transistor, for FIAN accelerator field measurements, 19: 32843
design and performance of ferromagnetic resonance, 20: 2104 (MATT-362)
design and performance of helium, for low temperatures, 20: 13046
design and performance of transistorized autodyne, 20: 41247
design and theory of helium, 16: 11854 (NP-11366)
design for d-c field index measurement, 20: 21006
design for heterogeneous fields, 20: 31487
design for indices of inhomogeneous magnetic fields, 19: 11480
design for inhomogeneous fields, 19: 22679
design for inhomogeneous fields, 19: 40851
design for ionospheric use, 20: 6180 (AD-619250)
design for measuring field changes, 17: 939
design for measuring weak fields, 18: 35828(P)
design for measuring superconducting samples, 19: 21486(R) (ORNL-3760(p.77-93))
design for measuring ambient fields, 20: 642(P)

design for orientation device for cosmic-ray measurements, 19: 25192
design for particle spectrometers, 19: 44352 (UJV-1339/65)
design for plasma diagnostics, 18: 32275(R) (ORNL-3652(p.105-31))
design for pulsed alternating fields, 17: 930
design for small fields, 18: 22316 (TID-20537)
design for superconductivity measurements, using Hall effect, 18: 32275(R) (ORNL-3652(p.105-31))
design for superconducting materials, 20: 41228(R) (ORNL-3875, pp 15-20)
design for type II superconductivity measurements, 18: 954 (NP-13274(p.40-6))
design for use in proton-resonance measurements, (E), 19: 40857
design for weak fields, 16: 7742(P)
design for weak fields using Overhauser effect, 17: 32745
design for weak fields, 19: 34442
design for 0.01- to 20-G measurements, 20: 15160 (LNF-65/44)
design for 7-Bev proton synchrotron, 17: 909
design for 7-Bev synchotron field measurements, 18: 18502 (AERE-A/R-2538)
design of automatic torque, 17: 1941(R) (NP-12214)
design of automatic scanning, 17: 37411
design of cesium-vapor, having 0.1- to 1.0-γ sensitivity, 17: 341
design of differential NMR, 18: 29935
design of electron spin resonance, for alternating magnetic fields, 16: 23947
design of free-precession nuclear, 16: 16519 (CEA-1931)
design of Hall-effect gaussmeter, 16: 8898 (ASD-TR-61-273)
design of Hall effect, 16: 30634(P)
design of Hall-effect, for fields up to 30,000 oersted, 17: 39386
design of helium, for space uses, 17: 16874
design of high-stability Hall-effect, 20: 14822(R) (RHEL/R-112, pp 99-128)
design of induction, 17: 30817
design of induction, for geomagnetic field measurements, 19: 19006
design of magnetic resonance, for weak fields, 17: 27678(P)
design of NMR, 20: 16791
design of NMR, 19: 718 (CEA-R-2383)
design of NMR, for homogeneous and inhomogeneous fields, (E), 20: 2112
design of NMR, using flowing liquid samples, 20: 16770 (CONF-650922, pp 428-30)
design of nuclear precession, 16: 17869(P)
design of nuclear induction, 18: 4070(P)
design of nuclear induction, for weak fields, 18: 23869(P)
design of nuclear precession, 19: 22678
design of nuclear-induction, for weak fields, 18: 33870(P)
design of nuclear, for measuring inhomogeneous fields, 18: 12417 (JINR-P-1475)
design of optically pumped nuclear, for measuring total earth's field, 18: 5589
design of proton magnetic resonance, for inhomogeneous fields, 19: 44353(T) (SLAC-Trans-22)
design of recording, for measurement of hysteresis curves of superconductors, (E), 20: 2913
design of self-oscillating rubidium, for earth's field, 18: 20294
design of transistorized, with proton source, 17: 41220
design of vibrating coil, for temperatures below 0.3°K, 20: 46550
design of, engineering drawings for, 20: 14831
design of, for geomagnetic field intensity measurements, 18: 20288
design, operation and theory of rocket-borne, 16: 23836 (AFSWC-TDR-62-25)
design with film Hall probe for measurements on superconductors, 20: 24269
development for cyclotron inhomogeneous fields, 19: 12000
development for fields up to 1000 kgauss, review, 16: 15402
development for high fields at low temperatures, 18: 33865
development for high-gradient time-variant fields, 20: 5682 (MURA-716)
development for superconducting magnets, 18: 30683
development of double-coil proton magnetic resonance, 19: 46731(T) (SLAC-Trans-21)
development of low-temperature micro-, 17: 33158(R) (ORNL-3472 (p.84-106))
development of NMR spectrometer as, 19: 9460
development of NMR continuous-flow transducer, 20: 7351
development of NMR, 20: 27241
development using Zeeman effect, 20: 27244
performance and use in geomagnetic fields, 16: 27860(T) (JPRS-13505)
performance for hydromagnetic wave detection, frequency modulation in, (T), 20: 914 (NASA-TN-D-2950)
performance of scanning, review, (E), 20: 2105 (UCRL-16357(Rev.))
performance of spinning search coil, 17: 16389
performance of zero reading, for mas spectrometer, 19: 34556
performance of, review, (E), 20: 627 (UCRL-16357)
properties of chemical, 18: 22315 (SLAC-26)
proton resonance type, frequency of oscillator in, 17: 3283
review of satellite, 17: 20222
sensing coil signal-to-noise ratios in nuclear, 16: 20682
signal analysis of free nuclear precession, for geomagnetic field measurements, 20: 11817(T)
use in archeology, 16: 15012
use in detecting ionospheric currents, (E), 19: 8333
use of polycrystalline bismuth wire, for high fields at low temperatures, 17: 6424

MAGNETOSPHERE
bibliography on, 20: 35985 (NASA-SP-7026)
boundary and plasma density profile of, review on, 19: 19009
boundary between radiation belts and, influence of geomagnetic field variations on, (E), 20: 46487
boundary compression, of solar plasma flux correlation with, 19: 41580
boundary formation in, mechanisms for particle trapping from, (T), 20: 28128
boundary layer measurements by satellite, 19: 16762
boundary layers of, shape of, 20: 46925
boundary motion of, correlation to magnetic activity on earth surface, 17: 41683
boundary of extended tail of, 20: 34358 (N-66-16697)
boundary of outer, 17: 28123
boundary of, determination of, (T), 19: 27348
boundary of, effects of geomagnetic storm on, 19: 35276
boundary of, magnetic-field component perpendicular to, 20: 42068
boundary of, magnetic structure on attitude of, 20: 42068
boundary of, motion of outer, (E), 20: 17541 (N-65-19719)
boundary of, observations on, 18: 24749 (CONF-521-2)
boundary of, outer, 18: 15026
boundary of, relation between solar wind parameters and geomagnetic activity from, 20: 24220
boundary of, solar wind discontinuity effects on, (T), 19: 21148
boundary shape of, under solar wind pressure, (T), 19: 6431
boundary stability, (T), 19: 40000
boundary with solar wind, model for broad disordered transition region in, 18: 18798
boundary with solar wind, stability of, (T), 19: 16745
boundary with solar wind of closed, magnetogasdynamic solution to, 19: 23538
boundary with solar wind effects of space charge convection on, (T), 20: 2856
boundary with solar wind, 20: 17249
charged particle acceleration in, 19: 14426
charged particle fluxes in near-earth, (E), 19: 9946 (ASE-546)
charged particle mirrors points in, electric field effects on, (T), 19: 33128
charged particle motion in, model for auroral, (T), 19: 41583
charged particle measurements in, from Vela Project, 19: 47450 (LA-DC-7365)
charged particle trapping in, magnetic coordinates for analyzing, 20: 39989
charged particles in, angular distribution, energy, and intensity of trapped, 19: 47444 (AD-611629)
charged-particle acceleration by electromagnetic fields in, 19: 31153
charged-particle acceleration by electromagnetic fields in, (T), 20: 11837
charged-particle acceleration and transport in, (T), 20: 28099(T)
charged-particle acceleration in neutral sheet in tail of, models for, 20: 37901
charged-particle energy in, relation with disturbance field near earth, (T), 20: 34373
charged-particle flux in, 18: 15026
charged-particle geomagnetic cut-off rigidities in, 20: 39988
charged-particle interactions with fields of, (T), 20: 11849
charged-particle inflation of inner, during magnetic storm, (E), 20: 44445
charged-particle motion during magnetic storms, (T), 19: 21128(T)
charged-particle motion in, adiabatic, (T), 20: 19640 (N-65-21332)
charged-particle mirror points in, (T), 20: 24212
charged-particle motion in deformed, trapped-region asymmetrical configuration determination from, (T), 20: 30224
charged-particle motion in, trapped, (T), 20: 32279
charged-particle penetration processes in, 20: 30205(T) (NASA-TT-F-389, pp 386-425)
charged-particle streams in, effects of geomagnetic field variations on, 19: 21126
charged-particle trajectories in current-sheet model of, (T), 19: 29130 (AFCRL-64-726)
charged-particle transport in outer, computation of trapped, 20: 21831
charged-particle trajectories in tail models of, 20: 34361 (N-66-17233)
cosmic-particle penetration through and trapping in, 18: 42540
cyclotron instabilities in, 20: 21825
effects of compression and expansion of, on cosmic ray cutoff rigidities and impact zones, (T), 20: 37598

effects of magnetopause on cosmic particle trajectories, (T), 20: 37597
effects of tail of, on cosmic-ray cutoffs, (T), 19: 41307
effects on auroral and geomagnetic storms, 19: 47481
effects on cosmic ray cutoff rigidities, compression, (T), 20: 27771(T)
effects on electron intensity variations in outer radiation belt, (E), 20: 34367
effects on ionospheric electron and ion temperatures, 20: 19648
effects on solar wind, 18: 18545
electric currents in (E/T), 19: 3172
electric currents in, effects on N-S asymmetry of S_q, (E/T), 20: 44438
electric field distribution in, model for, 20: 19674
electric field effects on electrons trapped in, dynamo-, (T), 19: 47453
electric field in, theory of, 20: 32287
electric fields in, effects on trapped particles, 19: 10169
electrodynamics of, 18: 21078
electromagnetic and hydromagnetic waves in, properties of, 20: 13645 (AWRE-O-9/66)
electromagnetic radiations from electrons in, ulf, 19: 33140
electromagnetic wave propagation in, at hydromagnetic and whistler frequencies, (T), 20: 44469
electron acceleration near bow shock in outer, (E/T), 19: 8336
electron acceleration in, during magnetic storms, 19: 35293
electron acceleration in, auroral, (T), 19: 37721
electron acceleration near bow shock of, 20: 23912
electron and ion density and temperature in, 18: 15024
electron and proton flux in, 17: 22413
electron and proton density in outer, at≅40 kev, 17: 28123
electron and protons in, energy spectra and angular distribution of, 19: 35303
electron and proton intensities in, satellite measurements of, 19: 35304
electron and proton reactions with electromagnetic waves in, gyroresonance radiation from, (T), 20: 4747
electron and proton stable trapping in, limiting fluxes of, (T), 20: 11820
electron and proton drift in, formation of Van Allen belts from, 20: 30207 (NASA-TT-F-389, pp 442-53)
electron and proton energy spectra in tail of, 20: 32252
electron and proton flux distribution in, determination of, 20: 32674 (NP-15697(Vol.3))
electron burst in tail of, auroral absorption event correlation with energetic, (E/T), 20: 34384
electron content and density near ionization knee of, (E), 20: 19668
electron content in tail of, 40-kev, (E), 19: 47458
electron density and geomagnetic field strength in remote, whistler measurements for, 17: 28020
electron density and energy distributions at boundary of, 18: 22808
electron density and temperature profiles in, 20: 39978
electron density distribution in, height dependence of, 18: 2734
electron density distribution in, measurement using hydromagnetic whistlers, 20: 32290
electron density in, whistler measurements of, 18: 38015
electron density measurements using whistlers, 19: 12426
electron diffusion and convection behind bow shock of, energy spectra variations for, (T), 20: 34378
electron distributions in, evaluation of models for, 17: 41666 (D1-82-0245)
electron distribution in, hydromagnetic wave dispersion characteristics for, (T), 20: 6202
electron distribution in, spatial and temporal, 20: 34354 (N-66-11230)
electron flux at 0 to 10 kev, structure of, (E), 20: 37904
electron flux distribution in, (E), 19: 18976
electron flux in, 18: 28488
electron flux in boundary region of, 18: 28290
electron flux in distant zone of, periodic modulations of, 20: 23911
electron high-energy pulses near bow shock of, spectra of, (E), 20: 37900
electron intensities in outer, 18: 28487
electron intensity beyond boundary of, with energies >30 kev, 18: 34680
electron intensity near boundary of, high-energy, (E), 19: 6481
electron interaction frequency and lifetime in, (T), 19: 47453
electron motion at 10 to 900 kev in spherically confined, correlations with inner radiation belt structure, (T), 20: 34393
electron motion in, positron tracers for trapped, 18: 7606
electron plasma oscillation fields in, ambient, (T), 19: 47477
electron plasma oscillations in, (E/T), 20: 19644 (N-65-23933)
electron precipitation by vlf waves in, 18: 18800
electron scattering in outer, effects of electrostatic plasma oscillations on, 20: 32262
electron trajectories in presence of whistler-mode waves in, (T), 19: 21099
electron trapping in dark, low-energy, 20: 11823
electron velocity spectra in, from cyclotron absorption of whistler power, (E), 19: 47463
electron velocity distribution in, determination from whistler attenuation, (T), 20: 17558
electron velocity distribution in, cyclotron wave generation effects on, 20: 34355 (N-66-14637)
electron, proton, and ion energy, spatial, and temporal distribution in, 20: 30220(T) (NASA-TT-F-389, pp 633-52)
electrons and protons in, distributions of trapped, 19: 16763
electrons in, effects of dynamo-electric field on, (T), 19: 5078
electrostatic field propagation into ionosphere, effects of, (T), 19: 33142
energy transfer to, from force-free magnetic fields in solar plasma streams, (T), 20: 23855
fluctuations of isothermal, magnetohydrodynamic equations for, 20: 46470(T)
fluctuations of, plasma concentration from toroidal, (T), 20: 46471(T)
gas motions in, ionospheric damping of, 17: 24124
geomagnetic storm effects on, 20: 9870
geomagnetic storm effects on tail of, 20: 32253
geomagnetic storms in, solar-wind flux interpretations for, 17: 28116
geomagnetic storms in, mechanism for, 19: 35277
geomagnetic variations in, classification of diurnal, 20: 4742
hydrodynamic wave propagation in, low-frequency, 20: 40224
hydromagnetic motions in, (T), 19: 6603
hydromagnetic oscillations in, geomagnetic pulsations from, 18: 18826
hydromagnetic oscillations in nonuniform, coupling resonance of, (T), 20: 19692
hydromagnetic wave propagation in, from high-altitude explosions, 17: 23532
hydromagnetic wave propagation to earth from, 18: 15030
hydromagnetic wave emission by, 18: 30653
hydromagnetic wave emission by, 18: 30654
hydromagnetic wave propagation in, 18: 32357
hydromagnetic wave propagation in (T), 19: 2951
hydromagnetic wave propagation in, geomagnetic sudden commencements from, (T), 19: 5075
hydromagnetic wave propagation in, whistler mode of, (T), 19: 18979
hydromagnetic wave excitation in, by solar wind, (T), 19: 29137
hydromagnetic waves in, low frequency, 19: 35263
hydromagnetic wave propagation in, (T), 19: 43217 (NASA-CR-281)
hydromagnetic wave, transmission in impulse response in, (T), 19: 47467
hydromagnetic wave propagation in, (T), 20: 1100
hydromagnetic wave amplification in, by cyclotron instability process, (T), 20: 19666
hydromagnetic waves in uniform cold, properties of three-dimensional, (T), 20: 19693
hydromagnetic wave propagation in boundary of, excitation mechanism for, 20: 25991
hydromagnetic wave emission in, (T), 20: 28505
hydromagnetic wave propagation in, detection of, 20: 44431
interaction of solar corpuscular streams with, magnetic field effects on, 20: 39963(T)
interaction with solar plasma, 18: 44670
interaction with solar plasma, (T), 20: 15593
interaction with solar wind, field perturbation from simulated, (E), 20: 17546
interactions with solar wind (E), 19: 3152
interactions with moving bodies, 20: 17537 (JPLAI/LS-641)
interface of solar wind and, stability of, 19: 9861
ion currents in, from ionospheric dynamo theory, 20: 17553
ion distributions in, helium and hydrogen, (E), 20: 6198
ion flux in, 18: 28488
ion oscillations in, electrostatic, (E), 19: 37720
ionization density of, whistler determination of knee position in, (E), 20: 19667
ionization depletion in outer, during magnetic disturbances, 18: 40426
ionization interchange with ionosphere, anomalies from, 18: 30664
kinetics of, geomagnetic micropulsation correlations with, (E), 20: 28103(T)
magnetic disturbance indicators in, use of auroral rays for, 17: 24215
magnetic field at magnetopause, (E), 20: 32281
magnetic field configuration in tail of, effects on auroral current systems, (T), 19: 47469
magnetic field line reconnection in, mechanism for geo- and interplanetary, 20: 32277
magnetic field measurements in, 20: 37917
magnetic line configuration in, 18: 18796
magnetic sudden impulses in, 18: 18758
magnetic toroidal resonances and vibrating field lines in, 20: 24217
model, (T), 20: 15587 (AD-620244)
model of, (T), 19: 33147
models for antisolar tail of, (T), 19: 18966 (NP-14436(Rev.))
origin, 18: 28458
oscillations in, hydromagnetic, 19: 19003
oscillations in, theory for Dst main phase, 20: 36100 (NBS-8815, pp 20.1-3)

oscillations of, effects on ionospheric PCA, 18: 28206
particle acceleration in, mechanisms for trapped, 17: 26266 (AFSWC-TDR-62-133)
particle scattering in, nonadiabatic, 20: 4948(R) (TID-22179, pp 85-175)
particles in, bibliography and review on energetic, 17: 36565
penetration by quadrupole component of earth's magnetic field, cosmic-ray longitudinal effect from, 18: 30650
plasma circulation in, geomagnetic disturbances from, (T), 19: 5077
plasma density and flow in tail of, 20: 21828
plasma density in, 20: 34362 (N-66-17243)
plasma density in, micropulsation whistlers for diagnostics of, (T), 19: 41596
plasma flow around, second standing shock wave in, 20: 21821
plasma injection in, mechanism for solar, 18: 18830
plasma instabilities in, wave generation from, 18: 11079
plasma instabilities in, 19: 45186
plasma instability in, auroral charged-particle precipitation mechanism from, 17: 41679
plasma interaction with simulated, (E), 19: 14707
plasma motion in, effects of ionospheric electrostatic fields on, (T), 19: 41593
plasma motions of, ionosphere dynamo production of, (T), 19: 10178
plasma sheet in tail of, (E), 20: 9864
plasma trapping in, simulated, 18: 34984
plasma waves in, survey of low-frequency, 20: 21812 (AD-622223)
propagation of sudden impulses in, 19: 33116 (N64-18475)
properties of, determination from geomagnetic pulsations, 20: 36105 (NBS-8815, pp 34.1-4)
properties of, interplanetary magnetic field effects on, 18: 22811
properties of, measurements of, (T), 19: 47484
properties of, review of, 19: 14431
properties of, review of, 20: 7990
properties of, review of, 20: 15232
properties of, review of, 20: 37911
proton cutoff in, at 1.5 Mev over polar regions, 18: 14766
proton distribution at 1.1 to 63 Mev in inner, (E), 19: 45189
proton flow, 20: 4479(R) (TID-22179, pp 1-83)
proton injection into, mechanism for low-energy, 19: 33152
proton interactions with rotations, geomagnetic field disturbances from trapped, 18: 7602
proton motion at 10 to 710 Mev in spherically confined, correlations with inner radiation belt structure, (T), 20: 34393
protons in, Mariner 4 measurements of low-energy, 20: 44455
radiation effects on outer, solar corpuscular, 18: 20722
radio wave propagation along plasma slab in, whistler, (T), 19: 29144
ring current belts in, asymmetrical particle trapping in, 19: 43230
shape of, effects of interaction of solar wind with geomagnetic cavity on, 18: 15036
shock wave interactions with, (T), 19: 25426(T)
shock wave propagation in, hydromagnetic, (T), 19: 19008
solar corpuscular radiation interactions with, energy transfer in, 18: 28494
solar corpuscular radiation effects on, analysis of, 18: 28495
solar corpuscular stream effects on, properties of, 18: 44646
solar energy transmission to, scheme for, 20: 36099 (NBS-8815, pp 19.1-3)
solar plasma interactions in, geomagnetic storm sudden commencements from, 18: 7603
solar plasma motion in, diamagnetic ring current, (T), 19: 33146
solar plasma reactions with, shock structure from, (T), 19: 29132 (NYO-1480-12)
solar wind effects on, 18: 15034
solar wind effects on field lines and plasma in outer, (T), 19: 45162
solar wind effects on threshold for plasma instability in transition region of, (T), 19: 47460
solar wind effects on boundary on, (T), 20: 11838
solar wind flow over, 18: 16629 (AD-430410)
solar wind frictional interactions with, storm production by, 18: 18824
solar wind interactions with, hydromagnetic coupling in, 18: 18831
solar wind interactions with, simulation of, (E), 19: 5056
solar wind interaction with, geomagnetic cavity from, (T), 19: 21146
solar wind interaction with, frictional, (T), 19: 23529
solar wind interaction with, (E), 19: 29399
solar wind interactions with, MHD shock propagation from, (T), 19: 45165
solar wind interaction with, 20: 1098
solar wind interactions with, (T), 20: 17232
solar wind interaction with, (T), 20: 24224
solar wind interactions with, effect of Earth's rotation on, (T), 20: 24209 (N-65-33285)
solar wind interactions with, 20: 30210(T) (NASA-TT-F-389, pp 499-517)
solar wind interactions with, fluid dynamics of, (T), 20: 32275
solar wind interactions with, particle aspects of, (T), 20: 32276
solar wind interactions with, shock wave from, (E/T), 20: 32281
solar wind interactions with, simulation of, 20: 32284
solar wind interaction with, (E), 20: 32286
solar wind interactions with, models of, 20: 34076
solar wind interactions with, proton velocity distributions in, (T), 20: 36116
solar wind interactions with, discontinuities in, 20: 37387
solar wind interactions with, boundary, tail, and ring current effects on, (T), 20: 46493
solar wind interface with, hydromagnetic stability of, 18: 30390
solar wind particle penetration into, (T), 20: 42069
solar wind penetration in, mechanism for, (T), 20: 24227
solar wind reactions with, neutral-point expansion of, 18: 22810
solar wind reactions with, (E/T), 19: 8060
solar-wind effects on rotating, (T), 19: 31156
stability of boundary of, validity of hydromagnetic approach to determining, 20: 32254
stability of tail-like region of, (T), 20: 34388
stability of, hydromagnetic, 18: 15023
stability of, solar wind effects on, (T), 19: 18977
structure, 20: 39957(T)
structure of lunar, (T), 20: 31899
structure of, auroral storm effects on internal, (T), 20: 34391
structure of, effects on auroral storms and geomagnetic fields, 20: 19688
structure of, hydromagnetic wave effects on, 18: 42526
structure of, linear stability in, (T), 20: 32278
structure of, Newtonian theory for, 20: 32282
structure of, nightside, (E/T), 19: 37718
structure of, PCA events from tail-like, (T), 19: 45172
structure of, relation to auroral storm occurrence, 20: 34357 (N-66-16393)
structure of, review of measurements of, 20: 37898
structure of, tail-like (E/T), 19: 1467 (NP-14436)
structure of, tail-like, (E), 19: 37717
structure of, time variation of, 20: 28132
sudden impulses in, observations on, 18: 26447
tail of, length and structure of, 20: 32258
transition zone of, particle flux in, (E), 20: 32280
variations in tail of, correlations with radiation-belt changes during magnetic storms, (E), 20: 11831
viscous interaction with the solar wind, 18: 15032
wave propagation in, low-frequency micropulsation, (T), 19: 41595
wave propagation in, (T), 19: 29143
whistler echo phenomena in, 19: 25429

Magnetrons
see Microwave Oscillators

MAGNETS
(Usually electromagnets is intended)
aberration properties of systems of octopole and quadrupole, computer program for third-order, 20: 17220
aberrations and quadrupoles for paraxial rays in bending, 17: 6782 (ANL-6611)
aberrations of quadrupole, 19: 20252 (CONF-640204(p.82-92))
alignment in accelerators, effects on equilibrium orbits, 17: 4131 (BNL-6512(p.50-6))
alignment method for 300-Bev synchrotron, 17: 11786 (CTSL-36)
analysis of axisymmetric, computer programs for, (E/T), 19: 23162 (ORNL-3575)
analysis of high-field limits on, in Brookhaven AGS, (T), 19: 44858 (BNL-9480)
analysis of superconducting, for magnetohydrodynamic cells, 18: 7459 (RTD-TDR-63-4170)
analysis of superconducting, for FFAG accelerators, 19: 28960 (MURA-709)
armature release in, detection device for, 20: 42583(T) (WAPD-Trans-34)
assembly and positioning for 1-Bev electron synchrotron, 16: 9472 (INSJ-46)
beam focusing by quadrupole, 17: 28357 (BNL-7120)
beam handling for Berkeley cyclotron, 17: 7409
behavior of superconducting, 16: 30170(R) (ORNL-3313(p.179-208))
bibliography on cryogenic, 17: 14931 (CLM-Bib-3)
book: *Particle Accelerators*, 16: 11063
book: *Physics and Techniques of Strong Magnetic Fields*, 20: 4486
calculations for superconducting, for production of high uniform fields, 19: 6025 (CEA-R-2606)
calculations of poleshoe cross section in magnetic quadrupole lens, 16: 4886 (DESY-A2.78)
calibration and compensation for proton synchrotron, 17: 929
calibration in beam transport system of Stanford Linear Accelerator, 20: 17206 (CONF-650922, pp 823-34)
calibration of, assembly for, 17: 928

calibration of superconducting, using NMR, 19: 29156 (NYO-2150-4)
calibration of synchrotron, assembly for, 17: 927
calibration of uncorrected superconducting, 20: 44993 (NYO-2150-19)
characteristics for DCX-2, 16: 9505(R) (ORNL-3239(p.10-15))
characteristics of 7-Bev proton synchrotron, method for determining, 17: 934
characteristics of CERN pulsed, 17: 18529 (CERN-63-3(p.297-314))
charged particle beam deflection by uniform-field circular-pole, (T), 19: 14195
charged-particle beam deflection by, compensation of dispersion in, (T), 20: 7672 (JINR-P-2408)
charged-particle beam transport in deflecting systems of, symmetry properties for, (T), 20: 11411
charged-particle focusing by quadrupole, aberrations in (T), 19: 770 (INSJ-78)
charging circuit and transformer for, design of superconducting, 18: 37310 (AERE-M-1397)
comparison of distributed and lumped inflector, 17: 19410 (BNL-6880)
construction and assembly for Cambridge Electron Accelerator, 16: 9477 (TID-13716)
construction and calibration of inhomogeneous deflecting, for use in magnetic analysis, 17: 14953 (UCRL-10526)
construction of multilimb core for betatron, method for, 16: 28235
construction of 60-gauss, for nuclear magnetic measurements, 17: 2255
control system for electro-, using proton resonance, 18: 29944
control systems for stabilizing coil currents in, design, 18: 31920
control systems for, design of Hall-effect, (E), 19: 44173
coolant system cleaning method for water-cooled, (E), 20: 1992
cooling by liquid gases for magnetohydrodynamic cells, 19: 10000
cooling of normal-superconducting junctions in, fins for, 17: 12830
cooling system for cryogenic, design and performance of, 19: 42613
cooling system for superconducting, for bubble chambers, 20: 17595 (CONF-650922, pp 611-14)
cost analysis for accelerator systems of, 19: 47170 (UCRL-16384)
cost analysis for, for 200-Bev alternating-gradient synchrotron, (T), 19: 20734 (UCRL-11800)
cost estimation of accelerator, computer program for, 20: 2545 (UCRL-16386)
cost factors, 20: 16584 (CONF-650922, pp 271-80)
current control systems for, in Brookhaven AGS, (E), 19: 20094 (BNL-8969)
current control system for NMR spectrometer, 19: 44356
current density reduction in superconducting, 17: 25873
current regulator, design of transistorized, 16: 25566 (NP-11883)
current regulators for Princeton Synchrotron, design of, 20: 17205 (CONF-650922, pp 817-22)
current shim for cyclotron, 20: 17187 (CONF-650922, pp 377-89)
current shunt for, design of solid-state, 16: 1877 (BNL-5662)
current stabilization of a-c electro-, with nonlinear impedance, 17: 16202(P)
current stabilization in electro-, design of servosystem for, 17: 26253(P)
current stabilization in synchrotron electro-, 19: 12035
current stabilization system for, design and performance analysis of, 20: 25344 (INR-639/III/E)
current transfer to superconducting, contact analysis of, 18: 44675 (BSD-TDR-64-110)
current-carrying capacity of superconducting, degradation of, 18: 30308 (NASA-TN-D-2345)
currents in superconducting foil, flux pump for generation of high, 17: 24152
demagnetizing ferro-, design of device for, 17: 16402(P)
description, in Figure-8 and Model C stellarators, 16: 15472
description of a-c sextupole, for proton polarization, 16: 4777
description of, for production of force-free fields, 16: 33641
description of, for compensating geomagnetic field in magnetic spectrometers, 17: 34251
description of high-field, hard-superconductor, 17: 619
description of minimum-B, using iron quadrupoles, 18: 32275(R) (ORNL-3652(p.105-31))
description of standard CERN, 17: 18516 (CERN-63-3(p.81-93))
description of superconducting 100-kOe, 18: 30227
description of 9.5-kOe, for production of nuclear orientation, 20: 5715 (AEET-227)
design and construction for beam transport systems, 16: 17160
design and construction of air-core, 17: 4195
design and construction of 100 kgauss d-c, 18: 26167 (CERN-64-23)
design and construction for beam bunching for nanosecond pulses, 18: 37818 (NP-14168)
design and construction for variable-energy cyclotrons, 19: 20753(P)
design and construction of superconducting, for corpuscular ionography, 20: 21876
design and construction of superconducting, 20: 37934 (BNL-10380)
design and development of high-vacuum encapsulated, 20: 504(R) (ORNL-3836, pp 120-9)
design and fabrication of niobium–zirconium superconducting, 20: 5614
design and operation of single-turn inflector, for quenching beam oscillations, (E/T), 19: 34821
design and performance of compression, 16: 4883 (AWRE-NR/P-5/61)
design and performance of pulsed 200-kilogauss, 16: 11812 (CERN-62-7)
design and performance of pulsed 60- and 200-kgauss, for nuclear particle studies, 16: 15480
design and performance of air-core electro-, for plasma research, 16: 26403 (PAN-301/XVIII)
design and performance of high-field superconducting, 17: 28074
design and performance of Brookhaven Alternating-Gradient Synchrotron, 17: 40139 (BNL-7229)
design and performance of long-wire superconducting, fed by flux pump, 18: 6108
design and performance of 10-kgauss superconducting, 18: 9266
design and performance of beam-focusing, for Princeton Synchrotron, 18: 42211 (PPAD-503-E)
design and performance of superconducting quadrupole, (E/T), 19: 25441
design and performance of superconductivity, 19: 37742
design and performance of niobium–tin superconducting, 19: 47526
design and performance of aluminum cryogenic, 20: 1264 (NBS-8843)
design and performance of cryogenic, 20: 9888 (CONF-650512, pp 152-5)
design and performance of septum, for fast and slow particle ejection from CERN proton synchrotron, 20: 13359 (CERN-65-36)
design and placement for neutron-proton differential cross section measurements, 20: 44632 (CONF-660303, pp 1084-91)
design and properties of, for extraction of secondary particles from CERN synchrotron, 17: 9644 (CERN-62-24)
design and properties of saturable-fin, for synchrotron, 17: 31555 (NIRL/R/33)
design and testing for 7-Bev accelerator, 17: 11762 (BNL-767(p.1-31))
design and testing of, for Stanford linear accelerator, 17: 17317(R) (SLAC-8)
design and testing of superconducting, 19: 39741
design and testing of iron-core, for plasma containment, 20: 26274
design and uses of superconducting, 19: 19021
design calculations for synchrotron, 18: 10706
design features for spiral ridge cyclotrons, 17: 7355
design for accelerator beam bending, 17: 40144 (NP-13152)
design for accelerator beam deflection, 18: 26185(P)
design for accelerators, 19: 32851(P)
design for accelerators, review of, 20: 2533 (BNL-9536)
design for accelerators, computer program for, 20: 2546 (UCRL-16389)
design for AGS, parameters of, (T), 20: 930 (BNL-9553)
design for beam transport system for 0.5-Bev/c pions, 19: 2928 (UCRL-11086)
design for beam transport systems of CERN proton synchrotron, 20: 17183 (CONF-650922, pp 218-38)
design for betatrons, 20: 23844(P)
design for Cambridge Synchrotron, 18: 34367 (CEAL-1000)
design for CEA beam bypass system, 20: 11383 (CEAL-TM-152)
design for cesium ion rocket motors, 19: 38834(R) (N64-29495)
design for cyclotron beam extraction, 17: 7403
design for d-c MHD generators, (T), 20: 41746
design for deflecting charged-particle beams, 17: 36741(P)
design for deflection of Van de Graaff beams, 18: 2505
design for diffusion chambers, 17: 23605 (LNF-63/4)
design for experimental plasma physics, review on, (T), 19: 25582
design for extraction of external proton beam from Bevatron, (E), 19: 25101 (UCRL-11812)
design for FFAG accelerators, 17: 33115 (CONF-125-5)
design for Figure-8 and Model C stellarators, 16: 15472
design for gamma-ray circular polarization measurements on aluminum-24, engineering drawings for, 19: 30873
design for Hamburg Electron Synchrotron, 20: 17213(T) (UCRL-Trans-1312)
design for large bubble chambers, 20: 16810 (CONF-650922, pp 366-76)
design for large isochronous cyclotron, 17: 7396
design for linear accelerators, 17: 15323 (TID-15917)
design for magnetohydrodynamic generators, 20: 11548
design for MHD cells, 20: 41688
design for Michigan State University 50-Mev Cyclotron, 17: 38350 (CERN-63-19(p.270-8))
design for momentum measurements in 80-in. hydrogen bubble chamber, 18: 7029 (BNL-7479)
design for MURA accelerator, 18: 42224
design for nuclear magnetic resonance detectors, 16: 14987(P)
design for producing axially symmetrical fields of specified shape, 19: 23177
design for production of high quasi-stationary fields, 18: 44308
design for pulsed fields, 18: 9457 (NP-13514)
design for pulsed-field production, 19: 44861 (IAE-795)

design for shielding, 17: 28410
design for space vehicle shielding, 20: 40291
design for spark chambers, using tape-wound coils, 20: 16809 (CONF-650922, pp 253-61)
design for spiral sector FFAG accelerators, 16: 28229 (TID-7636 (p.476-8))
design for Stanford linac, 18: 36111 (SLAC-28)
design for Stanford linac switchyard, (E), 19: 4774 (SLAC-PUB-53)
design for Stellarator stabilization, (E/T), 20: 28495(R) (MATT-Q-22, pp 321-85)
design for synchrocyclotrons, analytic method for, 18: 34376
design for synchrotrons, computer codes for, 19: 28965 (UCRL-11798)
design for transmitted electron beam disposal, 18: 10694(R) (NP-13571 (p.14-17))
design for transverse focusing, 19: 34794
design for UCLA spiral-ridge cyclotron, 17: 7353
design for Univ. of Mich. cyclotron, 17: 7365
design for Univ. of Mich. cyclotron beam handling system, 17: 7367
design for Univ. of Milan AVF cyclotron, 17: 7361
design for use in high-energy physics, (T), 20: 17175 (CONF-650922, pp 1-26)
design for variable-length focusing, 17: 17310 (BNL-6844)
design for velocity spectrometer, 20: 39502
design for 7-Bev proton synchrotrons, 17: 896
design for 7-Bev proton synchrotrons, 17: 897
design for 7-Bev proton synchrotron, 17: 924
design for 700-Mev cyclotron, 17: 7398
design for 700-Mev relativistic proton cyclotron, 19: 11943
design for 800-Mev separated-orbit cyclotron, (E), 19: 25096 (ORNL-P-1135)
design for 90°bending of 100-Mev electron beams, 20: 17200 (CONF-650922, pp 715-22)
design of air-cooled, wet-cell-powered 10-kOe, 17: 40196
design of air-core, for production of axially symmetric fields, 19: 44165 (CERN-65-29)
design of analyzing, for particle interaction products, 16: 25910(R) (NP-11749)
design of belt, for measuring ion beams, 16: 11897
design of bending, with nonsaturating shims for homogeneous field, 18: 8956 (SLAC-19)
design of betatron, 20: 13392(P)
design of coincidence, for reactor safety systems, 18: 28946
design of compact inhomogeneous-field, for mass spectrometer, 19: 43997(R) (UCRL-11889)
design of conical, with field varying as 1/r, 17: 41207
design of cryogenic 300-kgauss pulsed-field, 16: 15421
design of cryogenic 100-k gauss, 17: 22400(P)
design of cryogenic and superconducting, 20: 1120(R) (ORNL-3836, pp 90-110)
design of cryogenic, for energy storage, 20: 17597 (CONF-650922, pp 625-9)
design of electrical coil for efficient cooling, 16: 3233(P)
design of focusing, for Stanford klystrons, 17: 39381(R) (TID-19482)
design of focusing quadrupole, relations for, 17: 42014 (NP-13185)
design of focusing, for proton linear accelerator, 18: 20681 (TID-20457)
design of force-free toroidal, (E/T), 19: 10392(R) (MATT-Q-21)
design of fringing shims for poles, 16: 12585 (NIRL/R/6)
design of high-energy, 17: 19409 (BNL-772)
design of high-field cryogenic, 16: 15440
design of high-current-density septum, for accelerators, 20: 2544 (UCRL-16309)
design of high-field electro-, 19: 6029
design of high-field, for alternating-gradient synchrotron, 19: 30875 (BNL-8905)
design of high-field superconducting, 20: 17598 (CONF-650922, pp 745-52)
design of high-field superconducting split coil, with forced liquid helium cooling, 20: 36125 (SLAC-PUB-182)
design of high-field liquid-neon-cooled, 20: 46543
design of linear accelerator, 20: 2521 (LNF-65/28)
design of linear electromagnetic brake, (E), 19: 40724
design of liquid-hydrogen-cooled 100-kgauss, 16: 15407
design of liquid-neon-cooled 200-kgauss, 16: 15408
design of megagauss, using capacitor discharges, 20: 16587 (CONF-650922, pp 680-3)
design of minimum-B superconducting, for plasma use, (E), 20: 1279 (UCRL-14233)
design of momentum-analyzing, for magnetic spectrometer, 20: 14822(R) (RHEL/R-112, pp 99-128)
design of multipolar winding, 20: 10123 (CONF-650512, pp 128-30)
design of nested-solenoid superconducting 70-kG, (E), 19: 22474 (ANL-7002)
design of Nimrod, apparatus and methods used in, 17: 28349 (NIRL/R/4)
design of nsec ferrite-core, for synchrotron-beam switching, (E), 20: 939 (UCRL-16364)
design of permanent, for duoplasmatron ion sources, 19: 25088(P)
design of phasotron, 17: 36732
design of Philips AVF cyclotron, 17: 7363
design of precooled, for production of multisecond pulses up to 75 kgauss, 16: 15419
design of pulsed step, for Bevatron beam control, 20: 39508
design of pulsed 200-kOe, for analysis of reactions in emulsion, 16: 27785
design of pulsed, for bubble chambers, 20: 16811 (CONF-650922, pp 663-79)
design of quadrupole type with non-circular aperture and linearized end fringing field, 16: 2561 (DESY-A2.81)
design of quadrupole, analog computer for, 17: 7346 (TID-17429)
design of quadrupole, effects of modifications on, 17: 19413 (CEAL-1001)
design of quadrupole, for 88-in. cyclotron, 17: 36738
design of quadrupole and sextupole, for 200-Bev proton synchrotron, 19: 44878 (UCRL-16375)
design of quadrupole, for Alice, 20: 10124 (CONF-650512, pp 131-7)
design of septum, for beam extraction from Brookhaven AGS, (E), 19: 47158 (BNL-910)
design of six-field compensating pole windings of, for U-7 ITEP proton synchrotron, (E/T), 19: 32829 (NP-15056)
design of six-pole, equations for, 19: 26485
design of square-wave field-reversal, for gamma circular polarization analyzer, 18: 8622
design of stabilized superconducting, (E), 19: 14437
design of strong focussing synchrotron, 16: 6031 (DESY-A2.82)
design of strong focusing, pole profile, 17: 15318 (DESY-A-2.95)
design of superconducting solenoid with reduced winding space using Helmholtz coils, 18: 9268
design of superconducting, for magnetohydrodynamic cells, 18: 10829(R) (AD-405829)
design of superconducting, with inductive excitation, 18: 16880
design of superconducting, 18: 21118
design of superconducting, 18: 24547
design of superconducting, for variable bandwidth traveling wave masers, 19: 41638
design of superconducting, for shielding of space vehicles, 19: 42615
design of superconducting, for measurement of hyperon (Ξ^-) magnetic moment, (E), 20: 990 (BNL-9490)
design of superconducting, 20: 13667 (JINR-P-2533)
design of superconducting, for traveling-wave masers, 20: 17626
design of superconducting, for 90° deflection of 30-Mev protons, 20: 17197 (CONF-650922, pp 536-40)
design of superconducting, for polarized proton targets, 20: 17586 (CONF-650922, pp 509-16)
design of superconducting, for magneto-optical studies, 20: 17588 (CONF-650922, pp 525-9)
design of superconducting, 20: 17594 (CONF-650922, pp 604-10)
design of superconducting, 20: 20365
design of superconducting, for magnetic bottle, 20: 40169 (NASA-TN-D-3595)
design of superconducting bottle, 20: 46544
design of system of, for polarization of neutron beams, 17: 9149(P)
design of system of, for beam transport from Stanford linac, (E/T), 19: 4775 (SLAC-PUB-57)
design of uniform-field wedge, for linear accelerators, 19: 37309
design of variable induction, for synchrotrons, 17: 263(P)
design of water-cooled, 16: 13191
design of water-cooled d-c, 20: 16585 (CONF-650922, pp 349-55)
design of watertight electro-, for pool-type reactor control-rod drives, 16: 28484(P)
design of watertight electro-, for pool-type reactor control rod handling, 17: 31703(P)
design of weight-optimized superconducting, 17: 32224
design of 10-kOe, with stepped pole pieces, 18: 2441
design of 100-kgauss mirror, for Phoenix machine, 16: 15423
design of 120-kgauss, using electromagnet-solenoid combination, 16: 15411
design of 150-kgauss transverse-field pulsed, 17: 23710
design of 150-kOe cryogenic pulsed, 20: 1991
design of 180° deflection, for absolute determination of particle energies, 16: 6574
design of 20-KG, for precessing polarization of fast neutrons, 19: 37242 (AE-189)
design of 200-kgauss pulsed, for emulsion experiments, 17: 23711
design of 25-kgauss iron-core superconductor-coil, 16: 15430
design of 30-kgauss superconducting solenoidal, 16: 15431
design of 300-kgauss implosive flux-concentrator, 16: 15417
design of 300-kgauss pulsed, for bubble chamber use, 16: 15422
design of 36-kgauss d-c, 16: 15441

design of 40,000-gauss superconducting, 20: 40018
design of 400-kgauss pulsed and 120-kgauss steady-field type, 16: 15438
design of 450-kgauss pulsed flux-concentrator-type, 16: 15415
design of 50- to 60-kgauss steady-field, 16: 15439
design of 55-kgauss superconducting niobium-zirconium, 16: 15427
design of 60-kOe superconducting permanent, 18: 30687
design of, computer program for, 20: 27078 (SLAC-56)
design of, for electron storage ring, 19: 30874(R) (AD-609057)
design of, for isochronous cyclotrons, 19: 12026
design of, for magnetohydrodynamic cells, (T), 19: 10003
design of, for NMR spectroscopy, 19: 15837
design of, three-dimensional potential functions for, 20: 17177 (CONF-650922, pp 89-95)
design of, use of conformal transformation in, 20: 17179 (CONF-650922, pp 104-110)
design optimization for MHD generators, 20: 39668
design parameters of, for 25-Mev betatron, 17: 35009
design with optimum field-homogeneity and power characteristics, 18: 32275(R) (ORNL-3652(p.105-31))
design with uniform induction, 20: 17184 (CONF-650922, pp 239-47)
design, fabrication, and performance of cryogenic aluminum, 19: 12428(R) (NBS-8481)
design, fabrication, and testing for Argonne synchrotron, 19: 37308
development, 16: 4904(R) (NBS-7207)
development, 16: 12612(R) (NBS-7218)
development, 18: 2985(R) (UCRL-10852)
development, 18: 22552(R) (LAL-1090)
development, 19: 46643(R) (LAL-1136)
development, 18: 13008(R) (ORNL-3564(p.100-25))
development and evaluation of ceramic-insulated magnet wire for use in high-temperature and radiation environments, 16: 10624 (XDC-59-4-6)
development and performance of superconducting aluminum, 17: 33149(R) (NBS-7919)
development for Argonne ZGS, 16: 4882(R) (ANL-6427)
development for Bevatron, 18: 14685(R) (UCRL-10626)
development for generation of 100,000-gauss fields, 16: 16828
development for high-energy accelerators, 18: 14694
development for ion engines, 20: 39093
development for magnetohydrodynamic cells, (E), 19: 10001
development for particle accelerators, 20: 17222
development for radiation-detection instruments, 19: 9491(R) (TID-21335(p.108-50))
development for research reactor, 16: 20029
development for Stanford linear accelerator, 17: 29643(R) (SLAC-16)
development for Stanford Linear Accelerator, 17: 35000(R) (SLAC-10)
development for Stanford linear accelerator, 17: 42015(R) (SLAC-18)
development for Stanford linear accelerator, 18: 8958(R) (SLAC-23)
development for Stanford linear accelerator, 18: 22593(R) (SLAC-27)
development for storage rings for 100-Mev electron beams, 18: 30355(T) (AEC-tr-6392(p.1-20))
development for Stanford Linear Accelerator, 20: 13366(R) (SLAC-53)
development of adaptive, 19: 23164(R) (SU-SEL-64-103)
development of alternating-gradient accelerator, 20: 34003(P)
development of aluminum, 18: 13133(R) (NBS-8212)
development of cryogenic, 16: 13177(R) (NP-11413)
development of cryogenic, 18: 34682(R) (NBS-8407)
development of cryogenically cooled and superconducting, 20: 17592 (CONF-650922, pp 574-87)
development of, for cyclotrons, 17: 602(R) (CU(PNPL)-218)
development of, for synchrotrons, 17: 4124 (BNL-6512(p.24-8))
development of high-field, in USSR, (E/T), 19: 15700 (ATD-P-64-46)
development of high-field, 19: 44357
development of high-field, 20: 30735(R) (TID-22970, pp 331-73)
development of large-volume superconducting, (E), 19: 10189 (RLE-TR-427)
development of magnetoplumbite, review, 17: 37699
development of modified strontium ferrite, 17: 37699
development of pulsed, with fields up to 15 k gauss, 19: 44888
development of stainless steel for NRU Reactor, 16: 14221 (CRE-1062)
development of superconducting high-field, 16: 16830
development of superconducting, review, 16: 28209 (TID-7636(p.299-308))
development of superconducting, 17: 2339 (TID-16867)
development of superconducting, 17: 24053(R) (ORNL-3432)
development of superconducting, for magnetohydrodynamic cells, 17: 31012
development of superconducting, 17: 34549(R) (ORNL-3480(p.41-5))
development of superconducting, for bubble chambers, 18: 862(R) (TID-19590)
development of superconducting, 18: 13012
development of superconducting, 18: 34715
development of superconducting, for MHD cells, 18: 36243
development of superconductive, book, 18: 36438
development of superconducting, 18: 42554
development of superconducting permanent, from Nb,Sn wires at 14°K, 18: 44682
development of superconducting, 19: 1487
development of superconducting, (E/T), 19: 6607
development of superconducting, for thermonuclear research, 19: 12436
development of superconducting, at RCA, 19: 27135
development of superconducting, 19: 33161
development of superconductive, 19: 45212
development of superconductors for high-field, 20: 19724 (N-65-25286)
development of superconducting, 20: 34422
development of 112 kgauss superconducting, 19: 19058
development of 200-kgauss, review, 18: 11108
development of 83-inch cyclotron analyzer, 17: 22667(R) (TID-18578)
development using superconducting stripe, 20: 26024 (N-65-35356)
development, properties, and uses of superconducting, 18: 13010
distribution in 7-Bev proton synchrotron, 17: 932
economics and properties of superconducting, 19: 12453
economics of normal and superconducting, in fusion power plants, 17: 15036
economics of superconducting, for high-energy physics, 18: 11104 (NIRL/R/53)
economics of superconducting, 19: 1069
efficiency criterion for iron-core, 16: 15410
efficiency of deflection systems of, for defocusing and focusing atomic beams, (T), 20: 9622
elastic properties of hcp, strain effects on, 19: 43483
electric current pulses in, low-inductance shunt for measuring, 18: 39588
electric current supplies for superconducting, review on, 19: 37749
electric resistance of synchrotron, effects on field asymmetry, 17: 926
electro-, design for producing high-intensity magnetic fields using purified aluminum solenoid at low temperatures, 17: 30651(P)
electro-, properties of nonsuperconducting, 16: 28208 (TID-7636 (p.294-8))
electro-, proton resonance field regulator for, 17: 14620
electro-, design for BSR-II, engineering drawings of, 18: 13343
electro-, design for rod lifting in swimming pool reactor, 19: 5555(P)
electro-, field-controlled power supply for, 18: 25642
electromagnetic forces in superconducting, device for measuring, 19: 10208
excitation method for delay-type, short-pulse, 20: 15157 (CERN-66-1)
excitation of accelerator, stabilization of, 17: 19434
fabrication and performance of superconducting, 20: 28176
fabrication of contoured poles for FFAG accelerator, 20: 17185 (CONF-650922, pp 248-52)
fabrication of superconducting, 17: 20438
fabrication of superconducting, development of epoxy molding technique for, 18: 20134(R) (ORNL-TM-792)
fabrication of 28.5-kgauss superconducting niobium-tin, 16: 15429
fabrication of 59-kgauss superconducting niobium-zirconium, 16: 15428
fabrication of, using superconducting wire, 19: 22947
facility for high-field cryogenic, description, 16: 15406
feasibility of superconducting, for fields over 100 kgauss, 16: 15460
feasibility of superconducting thin-septum, for accelerators, 19: 44877 (UCRL-16346)
field analysis for, TRIM code for, (E), 20: 940 (UCRL-16382)
field calculations in gaps of iron-core, 16: 15409
field calculations for bubble chamber, (T), 19: 26663 (MURA-708)
field calculations for AGS, computer program for, 19: 37316
field calculations for accelerator beam bending, 19: 39317 (NRL-6248)
field control in Princeton-Pennsylvania 3-Bev Proton Synchrotron, 16: 17157 (PPAD-442D)
field dispersion of sector, with double-focusing beam, (T), 19: 41194
field distributions from, 19: 9308 (IPP-4/8)
field distribution of 2-meter spark chamber, model for calculating, 20: 19041 (SLAC-57)
field distribution in unsaturated O-shaped double-winding, for MHD machines, (T), 20: 25635
field formation in symmetrical gap, 16: 10670 (JINR-P-836)
field fringing in analyzing, reduction of, 18: 20644
field fringing in uniform-field wedge, calculations for, 19: 37310
field inhomogeneities in betatron H-, 17: 9655
field intensity of superconducting, devices for measuring, 18: 30683
field measurement for hexapole and quadrupole, 18: 42164 (UJV-944/63)
field measurement techniques for multipole, in Stanford linac, 19: 34813 (SLAC-39)
field measurement and spectroscopy for multipole, 19: 37313
field measurements in multipole, (E/T), 20: 13365 (SLAC-39(Rev.))
field parameters for charged-particle beam deflection, 18: 2509
field quality in quadrupole, method of calculating, 20: 17182 (CONF-650922, pp 208-17)
field stability and sweep using drift-free amplifier, 20: 7350

field stabilization using broadband EPR transducer, (E), 19: 26918 (JINR-P-1990)
field stabilization in EPR spectrometer, 19: 32519
field uniformity of, use of conformal mapping for improving, 20: 44064
flux density of hexapolar lenses, variations in, 20: 44063
focusing effects of four- and six-pole, for atomic hydrogen beams, (T), 20: 4559
focusing properties of 45°, for beam deflection, 17: 2354
heat transfer in cryogenic aluminum, (T), 20: 1264 (NBS-8843)
hydrogen atomic beam focusing by six-pole, (T), 19: 20302
inductance and resistance of solid-core, model for, 19: 37307
inductive behavior of superconducting, 17: 41596
inductors for, design and performance of, 20: 27076
installation in 7-Bev proton synchrotron, 17: 904
insulation for pulsed-coil, development of, 18: 33717
insulator design for superconducting, 18: 30684
intensity in, two-dimensional equations for long coil measurements of, 17: 15315 (BNL-6808)
interactions with charged particle beams in AGS, computer analysis of, (T), 19: 28932 (BNL-8677)
ion beam focusing by, effects of fringing on, 18: 14695
klystron focusing with permanent, 18: 2500(R) (TID-19422)
magnetic center of, equipment for measuring, 20: 39503
magnetic flux accumulation in high-current superconducting, 18: 43755(P)
magnetic flux jumping and trapping in superconducting, 18: 42560
magnetic forces in, computer program for calculating, 20: 33430 (UCRL-14917)
magnetic properties of electro-, design and characteristics of instruments for measurement, 17: 14634
magnetic properties of steels for use in, 20: 17009 (CONF-650922, pp 287-96)
magnetic properties of steels for use in gradient, 20: 17010 (CONF-650922, pp 297-304)
magnetic-field readout for superconducting, inverse, (E), 20: 28215
magnetoresistance of steady-state, 17: 4171(R) (NBS-7280)
materials for 50-225 KG, 20: 41097
measurements on Argonne BM-102 bending, magnetic, 17: 11804 (TID-17693)
measurements on beam quadrupole, 18: 10678 (BNL-7700)
modification of Brookhaven AGS, computer analysis of effects of, (T), 19: 28937 (BNL-9057)
Mössbauer effects in, (E/T), 20: 30735(R) (TID-22970, pp 331-73)
motion of proton-synchrotron, by geophysical forces, 19: 37255(T) (AEC-tr-6581)
neutron depolarization effects in precession, fast, 19: 21209
operation of mass spectrometer electro-, 17: 4554
operation of sodium, 19: 31335(R) (UCRL-12303)
operation of superconducting, 16: 29481(R) (NP-11989)
optical properties of quadrupole doublets, 17: 32703 (BNL-795)
optics of midplane of uniform-field wedge, first- and second-order matrix equations for, 18: 18529
optimization in beam transport systems, computer program for, 17: 23636
particle trajectories for rectangular, with uniform field, 17: 12753 (BNL-6717)
performance in 1-Bev synchrotron, 17: 883 (INSJ-50)
performance of AGS, 20: 19285(R) (BNL-929, pp 44-57)
performance of central region of variable energy cyclotron, 19: 44869 (NIRL/R/87)
performance of cyclotron-beam, method for measuring, 18: 732(R) (TID-19561)
performance of high-field, 19: 37210
performance of iron-core, in pulsed operation, 16: 25969
performance of large homopolar, at Canberra, 16: 24877
performance of solid iron, in cosmic meson (μ) spectrograph, 19: 34972
performance of superconducting, 18: 11100 (LNF-63/67)
performance of superconducting, using niobium stannide ribbon (E), 19: 571
performance of superconducting, rocket engine vibration effects on, (E), 19: 8337
performance of superconducting, for Mössbauer-effect studies, (E), 19: 14507 (BNL-8745)
performance of superconducting niobium–zirconium, 19: 31335(R) (UCRL-12303)
performance of superconducting, for bubble chambers, 19: 40869 (CONF-650510-14)
performance of superconducting, as space-vehicle dynamic radiation shield, (T), 20: 3241 (NASA-SP-71, pp 199-209)
performance of superconducting, for space power systems, 20: 19424 (NASA-TN-D-3345)
performance of superconducting, using aluminum stranded cables, (E/T), 20: 28218
performance of superconducting, for MHD generators, (E), 20: 39733
pole face computation for focusing nuclear instruments, ideal, 17: 14632
pole-face shaping for homogeneous fields, 16: 22776
pole face windings, 16: 26370 (DESY-A1.9)
pole faces for nuclear instruments, 16: 13291 (IFA-M-26)
pole-piece-surface calculations, for spectrometer, 16: 5538
pole profile calculations using method of equivalent currents, 20: 17178 (CONF-650922, pp 96-103)
pole profiles in, 16: 6035 (JINR-P-808)
pole shoe assembly design for, 20: 11423(P)
pole surfaces for strong- and weak-focusing, 17: 32791
poles for alternating gradients, 17: 15314 (BNL-6794)
potential measurements of aluminum, at cryogenic temperatures, 18: 24544(R) (NBS-8253)
potting compounds for, 20: 29366(R) (TID-22970, pp 375-91)
power supplies, design of low-ripple motor-generator for, 16: 15437
power supplies for pulsed, energy storage and transfer properties, 16: 15424
power supplies for 7-Bev proton synchrotron, 17: 899
power supplies for spectrometer, 17: 18557 (Y-1414)
power supplies for experimental, 17: 18216 (CEAL-TM-102)
power supplies for MURA accelerator, 18: 42225
power supplies for mass spectrometer, 19: 15830
power supplies for Bevatron, design, (E), 19: 25103 (UCRL-11952)
power supplies for Brookhaven AGS focusing, design of pulsed, (E), 19: 28936 (BNL-8983)
power supplies for, survey of, 20: 17202 (CONF-650922, pp 755-68)
power supplies for ZGS, design of, (E), 20: 17204 (CONF-650922, pp 808-16)
power supplies for pulsed, use of acyclic generators as, 20: 16772 (CONF-650922, pp 769-75)
power supplies for, status of solid-state, 20: 16773 (CONF-650922, pp 779-87)
power supplies for synchrotron, flat topping of, 20: 19303 (PPAD-581D)
power supplies, transistorized current regulators for, 16: 13352
power supply and support for mobile electro-, design, 20: 3353(P)
power supply characteristics for intermittent uses, 16: 15425
power supply conversion of Brookhaven AGS, for beam intensity increasing, 20: 928 (BNL-9500)
power supply for accelerator, ripple filter for, 17: 19412 (BNL-6922)
power supply for BSB synchrotron, design of, 20: 27648 (NP-16009)
power supply for magnet model VI, 16: 11817 (NIRL/R/3)
power supply for MURA FFAG magnet modeling program, design of, 20: 17203 (CONF-650922, pp 776-8)
power supply for synchrotron, use of ion inversion transformer as, 19: 37425
power supply for Stanford linac beam switching, pulsed, 19: 37320
power supply for, using silicon rectifiers, 17: 23633
power supply for ZGS ring, design of, 20: 17227
power supply for ZGS, analog computer representation of, 20: 21488
power supply for 100-kgauss 1.5-Mw, use of homopolar generator for, 16: 15412
power supply for 20-kgauss, homopolar generator for, 16: 15413
power supply for 88-in. cyclotron, 17: 7412
power supply for, design of 300-kw modular, 20: 45838 (UCRL-70017)
power supply instability effect on, 17: 940
power supply rectifier phase control for ring, 17: 13615 (TID-17835)
power-supply systems for external proton-beam, for bevatron, 19: 37317
preparation of superconducting, review of, 20: 23253 (LNF-66/13)
production from submicron cobalt and iron particles, 17: 41334 (ASD-TDR-63-423)
production of high-field superconducting, 18: 15045
production of superconducting wire, 18: 42563
properties and feasibility of superconducting high-field, 19: 16792
properties and uses of superconducting, survey, 16: 25881 (ASD-TN-61-160)
properties for super-high-energy accelerator beam separation, r-f, 20: 27642 (BNL-10222)
properties of beam deflecting systems of, reflection, 18: 42239
properties of beam-analyzing, at Frascati synchrotron, (E), 19: 11864 (LNF-63/82)
properties of beam-analyzing, at Princeton synchrotron, 19: 44871 (PPAD-2137-556)
properties of Brookhaven AGS experimental, 17: 9642 (BNL-6435)
properties of high-field superconducting, (E), 19: 19018 (ORNL-TM-1083)
properties of high-field superconducting, review of, 20: 28172 (BNL-10147)
properties of large-volume, highly uniform, at ORNL, 20: 44030 (ORNL-P-2492)
properties of magnetohydrodynamic flux-concentrator-type, 16: 15416
properties of permanent, for AGS injection beam focusing, (T), 19: 47160 (BNL-9482)
properties of sector, for 50-Mev separated-orbit cyclotron, 19: 47167 (ORNL-P-1619)
properties of strong-focusing, 20: 39494 (LNF-66/15)

properties of superconductors as permanent, 17: 5084
properties of superconducting niobium–zirconium alloy, 17: 22365
properties of superconducting, 17: 32712 (LNF-63/26)
properties of superconducting, for high magnetic fields, 17: 41592
properties of superconducting alloy, 18: 40458
properties of superconducting, 19: 6616
properties of superconducting, 19: 23163(R) (ORNL-3650(p.111-86))
properties of superconducting quadrupole, for lens systems, 20: 31815 (BNL-10144)
properties of superconducting, (T), 20: 42135
properties of symmetric quadrupole triplets, (T), 20: 2539 (SLAC-47)
properties of two-dimensional, computer program for solving mathematical models for, 20: 39499 (UCRL-16959)
properties of, for Adone accelerator, (E), 19: 14174 (LNF-64/34)
properties of, for cyclotron beam extraction, 19: 47166 (ORNL-P-1605)
pulser for beam switching, for Stanford linear accelerator, 19: 27025 (SLAC-36)
pulser for, development hydrogen thyratron, 18: 30339 (BNL-8033)
pulsing equipment for accelerator, 17: 24518 (DESY-A-2.98)
radially-magnetized permanent, for proton-accelerator injectors, 17: 19426(T) (FTD-TT-63-68)
radiation effects, 16: 19441
radiation effects on superconducting, 20: 36124 (RHEL-R-118)
radiation effects on film-insulated wires for, gamma, 20: 41503
refrigeration development for cryogenic, 20: 1265 (NBS-3346)
refrigeration for cryogenic, 18: 21095(R) (NBS-8239)
refrigeration for cryogenic, 19: 31331(R) (NBS-8797)
refrigeration systems for thermonuclear reactor, performance of pulsed, 20: 1263 (NBS-8817)
regulators for ORIC, 17: 7376
remanent induction of permanent, temperature effects on, 17: 41538 (ASD-TDR-63-500)
research on superconductivity, 17: 21388(R) (LNF-63/11)
review of high-field types, 18: 10657
review on high-field superconducting, 19: 21165
saturation effects in, system for self-correction of, 17: 42023
stabilization of superconducting, by incorporation of channels for liquid helium flow, 20: 36122 (LA-DC-7801)
status of Argonne synchrotron, 18: 12806 (TID-7686(p.9-12))
status of superconducting, 18: 44689
superconducting and cryogenic, NASA research on, 17: 13861
superconducting, feasibility, 16: 15426
superconducting, performance as space-vehicle power supplies, 17: 9112
superconducting, review of materials and causes of current degradation for, 18: 4492
superconducting, uses of, 17: 4647
superconducting, use for magnetohydrodynamic power generation, 17: 9071
superconducting, methods for evaluation of materials for use as, 18: 44683
superconducting, model solenoid for, 19: 26488 (AD-610579)
superconducting, nuclear magnetic resonance spectroscopy of, 18: 43920
superconducting, transition processes in, (E), 20: 41760
superconductivity degradation in ribbon-wound niobium stannide, (E), 19: 1515
superconductors for, 18: 26478
support for electron synchrotron, design of pneumatic, 19: 23219
survey of conventional and superconducting, 18: 8922
survey on high-field, 19: 20701
switches for, design of fast and slow Mjoule, 17: 15038
system design for achromatic translation of charged-particle beams, 18: 22637
technology of, conference on, 20: 17156 (CONF-650922)
technology of, for high-energy physics, 20: 17176 (CONF-650922, pp 27-55)
testing of high-field superconducting, 19: 37736(R) (ORNL-TM-1173)
theory of force-free toroidal electro-, with external force-bearing current loops, 16: 32479 (MATT-127)
time dispersion in double-focusing bunching, 16: 4883 (AWRE-NR/P-5/61)
triggering parallel ion inverters for synchrotron, 19: 37424
use in achromatic translation system for charged-particle beams, 17: 31274 (CONF-46-38)
use in debunching and momentum analyzing linac beam, 16: 8244 (TID-13717)
use in deflection of accelerator electron beam, 20: 25674(P)
use in positioning reactor control rods, 19: 40140(P)
use in systems for transport of secondary charged particle beams, 17: 11790 (PPAD-459F)
use of nonferrous in magnetohydrodynamic cells, channel geometry for, (T), 19: 10004
use of permanent, in ion rocket, 17: 42407
use of quadrupole triplet, as momentum spectrometer, 19: 807
use of quadrupole and box, for focusing and steering particle beams, 20: 44065
use of quadrupole, for beam focusing in long straight sections of alternating-gradient synchrotrons, 19: 18649(P)
use of sectored toroidal, in gamma spectrometer, 17: 25629
use of standard, with spark chambers, optical system for, 17: 23659
use of superconducting, in ESR studies, 18: 23524
use of superconducting, in thermonuclear propulsion systems (T), 19: 1810
use of superconductivity, for space vehicle shielding, (E/T), 19: 8560
use of superconducting, for MHD generators, (T), 20: 25771
use of 200-kgauss pulsed, for high-energy particle analysis, 16: 15479
use, in ionizing-radiation detectors, 18: 10428(P)
uses for bending beams of charged particles, 18: 16627(P)
uses in apparatus for scanning surface with beam of charged particles, 18: 16628(P)
uses in manipulation of reactor control rods, helical springs for suspending and supplying electricity for, 19: 1829(P)
uses in neutron generators for deflection of ion beam to stabilize output, 18: 39581
uses of iron transmission, for circular-polarization measurements on gamma radiation, 20: 5764
uses to stir solutions in diffusion cells, engineering drawings of apparatus for, 20: 221

Magnons (Scattering centers in magnetic materials, analogous to phonons)
see Magnetic Materials

MAGNOX ALLOYS

alloying effects of bismuth, zinc, or zirconium on properties of, for use as canning material, 18: 27999
alloying effects of beryllium and calcium on properties of, for use as canning material, 18: 27999
analysis for aluminum, beryllium, calcium, iron, silicon, and zinc, spectrochemical, 19: 42414 (JEN-146-DQ/I-47)
analysis for diffused titanium using electron microprobe, 19: 30077 (EUR-1819.e(p.27-36))
analysis for elements, spectrographic, 18: 3682
analysis for impurities, spectrochemical, 17: 40734
analysis for iron in MN 70, absorptiometric, 17: 23256 (PG-Report-437)
analysis of AL-80 and ZR-55, for iron, spectrophotometric, 17: 27236 (PG-Report-453)
analysis of AL-80, for aluminum, volumetric, 17: 27237 (PG-Report-454)
analysis of Magnox MN 70 for iron, spectrophotometric, 17: 27234 (PG-Report-437)
analysis of MN70 for aluminum and calcium, spectrographic, 17: 17969 (PG-Report-347)
analysis of type-Al-80, for hydrogen, 20: 29100
analysis of type-Zr-55, for hydrogen, 20: 29100
analysis of ZR55 for thorium, spectrographic, 19: 36233 (PG-Report-615)
bonding to uranium through titanium spacer, 18: 37618 (A/CONF.28/P/864)
chemical composition and properties of, for use as reactor materials, 18: 34176
corrosion by carbon dioxide, effects of gas impurities, pressure, and temperature on, 20: 7524
corrosion by water in spent fuel cooling pond, effects of contact with dissimilar metals, pH, and temperature on, 19: 11694
corrosion in reactors, 19: 20488
corrosion of Al 80, by carbon dioxide at high temperatures, 20: 25494
creep behavior of ZA, at 400 and 450°C in carbon dioxide and water, 17: 27849
creep buckling of AL80, at 295°C, 20: 9519
creep cavitation in A12, 17: 32613
creep deformation of AL 80, grain boundary migration in, 20: 13311
creep ductility of ZA, effects of heat treatment in hydrogen at 500°C before working on, 17: 27848
creep ductility of AL80 under reactor conditions, 19: 18497
deformation of, as fuel element cladding, 19: 39220
development for advanced GCR, review of, 20: 6612 (INR-622/IX/R)
development for fuel elements, 18: 37614 (A/CONF.28/P/560)
diffusion of fission products and plutonium in cans of, from irradiated fuel elements, 20: 25582
expansion of tubular, equipment for measuring, 20: 43960
fabrication and properties as fuel element material, 18: 20463
fatigue of Al80, plastic strain range at 350 to 500°C, 20: 39419
fatigue of, effects of high-frequency vibrations on, 20: 43957
grain growth and hydrogen pickup of Zr 55 at 475 and 600°C, effects of heat treatment atmosphere on, 17: 27846
ignition of A12, in carbon dioxide, effects of air, oxygen, and water vapor on, 19: 7849 (CEA-R-2494)
mechanical properties for use as fuel canning material, 17: 30927
performance as canning material in Berkeley and Bradwell Reactors, 19: 43539
performance as fuel element cladding, 18: 45067

properties as canning material for uranium fuel elements, 18: 1253 (NP-13218)
properties for use in reactor fuel elements, 19: 10524
properties of A12 and ZA for use as canning materials, comparison of, 18: 26025
properties of welded sheaths, sheets, and tubes of, 18: 7172
radiation effects on fuel elements using, 18: 20463
radiation effects on mechanical properties of, 18: 37617 (A/CONF.28/P/857)
radiation effects on, 18: 45060
radiation effects on tensile properties of AL80, neutron, 20: 7639
radiation effects on fatigue properties of AL80, neutron, 20: 9580
reactions with carbon dioxide to 600°C, 19: 22997 (TRG-Report-842)
reactions with materials used in graphite moderated reactors in carbon dioxide and *in vacuo*, 19: 22997 (TRG-Report-842)
reactions with uranium to 475°C in argon, 19: 22997 (TRG-Report-842)
recrystallization in, secondary, 17: 27845
recrystallization properties of type AL80, 20: 23705
removal from uranium fuel elements at Windscale, 18: 37254 (A/CONF.28/P/160)
sealing stainless steel-sheathed thermocouple into end cap of, 19: 2770
stress relaxation in polycrystalline AL80, high-temperature, 19: 14045
tensile properties of AL80 cans from irradiated fuel elements, 18: 12736 (TRG-Report-611(p.11))
tensile properties of AL80, grain-size effects on, (E), 20: 4437
thermal capacity of A12, at 0 to 600°C, 19: 13987 (IGR-TM/C-0176)
thermal fatigue behavior under constraint, 18: 37672 (A/CONF.28/P/431)
thermal fatigue properties, 18: 32192
uses in canning uranium fuel rods, (E), 19: 10521
welding sheaths, sheets, and tubes of, techniques for, 18: 7172
Magnox–Ti–U, inter-diffusion in, electron beam analysis of, 18: 39058 (EUR-1643.e(p.275-300))
Magnox–U, radiation effects on heat transfer and structural properties, 19: 19401

MAINE

fallout monitoring in, methods for, 17: 21461
monitoring water supplies in, 17: 18424
radiation effects on congenital malformations in infants in, natural background, 19: 33853
radioactivity from natural sources, 17: 27629
radioactivity in ground waters, 1959 and 1960, 16: 22403 (NP-11638)
radioactivity in ground water in, 20: 37006

MAIZE

(Indian corn; Zea mays)

agronomic performance of hybrids and inbreds of, for 1962 field studies, 18: 8016(R) (TID-19851)
ammonium sulfate uptake by, tracer studies of, 19: 31696
analysis for elements in leaves of, method for, 18: 39067
auxin transport in, 18: 9787(T) (AEC-tr-6261)
calcium metabolism in seedlings, replacement of calcium by strontium, 17: 28653
calcium metabolism by hybrids of, effects of genotype, environment, and nitrogen fertilizer on, 19: 33740(R) (NYO-2744-26)
calcium transport in primary root, 20: 45270 (AD-639836)
calcium–strontium accumulation in, genetic analysis of, 19: 41
calcium-45 transport in paired root segments of, method for determining wounding response in, 20: 16170 (AD-628805)
carbon-14 distribution in leaves of, 18: 38749
cerium-144 uptake by, effects of humus and lime on, 16: 14451
cesium-137 transfer from soils to, for dairy cattle feed, 20: 37038
cesium-137 transport in, 19: 12911 (NP-14752)
cesium-137 uptake by, effects of soil temperature on, 20: 3668
deuterium effects on root morphogenesis in, 18: 29213
differential element accumulation in, genetic factors, 17: 7751(R) (TID-17552)
effects of blood serum and gastric juices from irradiated animals on growth of, 18: 41125
effects of deuterium on root development in, 18: 19662
effects of epoxybutane and methanesulfonate on, genetic, 20: 40708
effects of ethyl methanesulfonate on, genetic, 20: 8664
effects of ethyl methanesulfonate in, genetic, 20: 18334
effects of gases at 3 to 45°C on seed of, biological, 20: 14216 (BNL-9859)
fallout monitoring in Swedish, 1962, 18: 23790 (NP-13828)
fertilizer utilization by, radioisotope study of nitrogen and phosphorus, 20: 9(R) (STI/DOC/10/42, pp 61-9)
gamma attenuation coefficients for, (E/T), 20: 716
genetic control of accumulation of strontium and other elements in, 18: 8016(R) (TID-19851)
genetic effects of heavy cosmic-ray particles on seeds of, 18: 3474 (BNL-6857)
genetics of, effects of pollen irradiation on, 19: 42331
gibberellic acid effects on subsequent growth of irradiated, 19: 33968
iron absorption by roots and movement along xylem in, 17: 40495(R) (TID-19389)
iron-59 absorption by leaves of, effects of pH on, 16: 28720
leucine uptake by etiolated, 19: 31681(R) (ORNL-3768(p.164-76))
lipoxidase activity in seedlings of, 18: 15704 (TID-18662)
metabolic control in embronic, 19: 31795(R) (ORNL-3768(p.181-6))
metabolism of calcium, strontium, and other elements by, effects of environment on, 18: 3453 (TID-19757)
metabolism of calcium, magnesium, phosphorus, potassium, and strontium by, genetic control of, 18: 6596(R) (TID-19842)
metabolism of cations by hybrids of, effects of genotype, environment, and nitrogen fertilizer on, 19: 33740(R) (NYO-2744-26)
metabolism of corn roots, effects of 2,4-D and sugars, 16: 28 (ORO-470)
metabolism of minerals in, genetic control of, 20: 40735 (NYO-2744-37)
metabolism of tritiated water in roots of *Zea mays*, 19: 43702
mineral metabolism in, genetic control of, 18: 3454(R) (TID-19786)
mutations, analysis, 17: 28765
mutations, effects of extragenic factors, 16: 31509
mutations in irradiated and nonirradiated, variations in polygenic, 16: 28766 (RT/BIO(62)49)
mutations in, natural and artificially induced, 18: 3499 (TID-19787)
mutations in, comparisons of radiation- and chemical-induced, 20: 45361 (TID-22622)
mutations in, effects of ethyl methanesulfonate on, 20: 18184(R) (BNL-929, pp 115-25)
mutations induced in endosperm and seedlings by diepoxybutane and x irradiation, 16: 1602
mutations induced in seeds of, differences and frequency in chemical and radioinduced, 17: 38690
mutations of *Zea mays*, chemically induced, 19: 15010 (BNL-7815)
mutations of, induced by ethyl methanesulfonate, 20: 1656
nucleic acid synthesis in seedlings of, 18: 27011(R) (ORNL-3601 (p.188-206))
oxidative phosphorylation by root and shoot mitochondria in seedlings of, temperature effects on, 19: 6920
phenylalanine uptake by etiolated, 19: 31681(R) (ORNL-3768(p.164-76))
phosphorus absorption by roots and movement along xylem in, 17: 40495(R) (TID-19389)
phosphorus-32 absorption by leaves of, effects of pH on, 16: 28720
phosphorus-32 uptake by roots of, effects of placement in soil on, 17: 38724
phototropism in, biochemical effects of, 18: 17365(T) (AEC-tr-6362)
radiation effects on metabolic reactions, 16: 1492(T) (JPRS-10170 (p.405-17))
radiation effects on seeds and seedlings, 16: 26682 (BNL-5899)
radiation effects on *Zea mays* seedling roots, 17: 1321
radiation effects on nucleic acid distribution and metabolism in seedling of, from *Zea mays*, 17: 1322
radiation effects on ribonuclease activity in *Zea mays* seedlings, 17: 1323
radiation effects on growth and development of, seed, 17: 3260
radiation effects on, neutron and x-ray seed exposure, 17: 10380
radiation effects on growth, 17: 17806
radiation effects on stored kernels, 17: 28716
radiation effects on genetic variability in, 17: 30301
radiation effects on peroxidase activity in seedlings of, gamma, 17: 30357
radiation effects on seeds of, from satellite flights, 17: 31947
radiation effects on growth and development of, repeated and single, 17: 38844
radiation effects in, genetic, 18: 1374 (BNL-7367)
radiation effects on growing of, 18: 2120
radiation effects on root meristems of, x, 18: 5016
radiation effects on root morphogenesis in, tritium and x, 18: 11780
radiation effects on B^a chromosome in TB-3a in, use of A-B translocations in mutation studies on, 18: 19513
radiation effects on hydroponically grown, gamma, 18: 33997
radiation effects on pollen of, genetic, 18: 36967
radiation effects on development of seeds of, gamma and neutron, 18: 38942
radiation effects on germination and yield of, uv, 18: 41209
radiation effects on respiration intensity in, gamma, 18: 41126
radiation effects in *Zea mays*, meson (μ^-) and (π^-), 18: 41157
radiation effects on chemical composition of plants cultivated in different climates, 19: 2109
radiation effects on, meson and x, 19: 5696
radiation effects on nucleic acid metabolism in seeds and seedlings of, 19: 12959 (TID-21460)
radiation effects on genetic mutability increase in, 19: 15113
radiation effects on geotropism in, protective effects of auxins against gamma, 19: 15164
radiation effects on seedlings of, gamma, 19: 15178

radiation effects on growth, mutations, and yields of, 19: 17569
radiation effects on genetic, 19: 19527
radiation effects on germination of seeds of, 19: 19528
radiation effects on development of seeds of, 19: 21870
radiation effects on germination and seedlings of, small-dose, 19: 25931
radiation effects on yields of, seed-irradiation, 19: 36008
radiation effects in seeds of, physiological, 19: 45836
radiation effects on seedling growth of, from irradiated seeds, 20: 109
radiation effects on growth of seedlings of, in contaminated soil, β, 20: 5305
radiation effects on, gamma, 20: 6876
radiation effects on, γ, 20: 8664
radiation effects on growth and pH in seedlings of, effects of dose on β, 20: 10683
radiation effects on genetic variability in, 20: 10603(R) (IAEA-2466-11)
radiation effects on development and growth of, by seed exposure to gamma, uv, and x rays, 20: 10613(T) (NP-tr-1344)
radiation effects on genetic variability in, 20: 12641 (TID-22582)
radiation effects on root growth in seedlings of, from tritiated water and tritiated thymidine, 20: 16227(R) (NYO-3561-2)
radiation effects in, genetic uv and x, 20: 18334
radiation effects on, mutagenic, 20: 18409
radiation effects on, following seed soaking in phosphorus-32 solutions, 20: 18442
radiation effects on x-ray diffraction spectra of amidones in, γ, 20: 29255
radiation effects on mutations of, x, 20: 31109
radiation effects on water content of leaves of, γ, 20: 31110
radiation effects on development of, γ, 20: 31113
radiation effects on seeds of, genetic fast-neutrons and x, 20: 31092
radiation effects on carbohydrates, proteins, and seed sprouting in, 20: 35250
radiation effects on, uv and x, 20: 38617
radiation effects on genetics of, neutron, 20: 40618(R) (NYO-2740-3, pp 166-215)
radiation effects on, x, 20: 40708
radiation effects on seed of, fast-neutron and x, 20: 42843 (BNL-10358)
radiation effects on, effects of nutrient medium on γ, 20: 42915
radiation effects on yield and food value of, following seed irradiation, 20: 45455
radiation effects, genetic, 19: 21918
radioactivity of, from Iasi, Rumania, beta, 20: 25292
radioinduced endosperm mutations in, frequency of γ, light, and uv, 20: 18392
radioinduced mutagenesis in, use of interchanges involving A and B chromosomes, 16: 1597
radioinduced mutations, 16: 28828
radioinduced mutations, 16: 32735(R) (TID-16979)
radioinduced mutations, 17: 2834(R) (TID-17287)
radioinduced mutations, 17: 7880
radioinduced mutations in, 17: 15626 (BNL-6027)
radioinduced mutations, 17: 24894(R) (TID-18673)
radioinduced mutations, 17: 28711
radioinduced mutations in seedlings of, rate of artificial, 17: 38694
radioinduced mutations in, acute vs. chronic gamma, 18: 11731
radioinduced mutations of, 18: 11649 (TID-20031)
radioinduced mutations of, 18: 13453(R) (TID-20220)
radioinduced mutations of, yield from, 18: 33279(R) (TID-20823)
radioinduced mutations of, 18: 38777(R) (TID-21068)
radioinduced mutations in, gamma, 18: 41097
radioinduced mutations of *Zea mays*, 19: 15010 (BNL-7815)
radioinduced mutations in, 19: 21861(R) (NP-14937(p.116-25))
radioinduced mutations in, meson, neutron, proton, and x, 19: 43712 (BNL-9383)
radioinduced mutations of, x, 20: 1656
radioinduced mutations in, effects of dose on γ, 20: 8692
radioinduced mutations in pollen mother cells of, γ, 20: 18335
radioinduced mutations in, gamma and neutron, 20: 22661
radioinduced somatic mutations in seedlings of, effects of temperature on, 16: 28765 (RT/BIO(62)44)
radioinduced somatic mutations in, effects of temperature on, 17: 10394
radioinduced sterility in pollen of, γ, 19: 43767
radiosensitivity of hybrids and inbreds, differences in, 16: 1606
radiosensitivity of chromosomes in seed during germination, 17: 15650
radiosensitivity of hybrid forms of, 18: 19746
radiosensitivity of chromosomes in seeds of, 19: 2062 (BNL-8462)
radiosensitivity of, fast neutrons and gamma, 19: 3964
radiosensitivity of, effects of genetic makeup on, 19: 17569
radiosensitivity of sprouting seed of, effects of 2,4-dinitrophenol on fast neutron and gamma, 19: 19582
radiosterilization of, dietary effects on dogs, 16: 32004(R) (NP-12064)
radiosterilization of sweet corn, effects on flavor and storage time, 17: 15675
reproduction of, tracer studies of effects of fertilizers on, 20: 31109
reversion frequency in, effects of ploidy on, 20: 40509 (TID-22965)
root and foliar absorption of strontium and cesium by young plants of, tracer study of, 18: 31088
root development in, effects of absorbed tritiated thymidine on, 17: 35444 (BNL-6548)
rubidium uptake by roots of, 16: 32699
rubidium-86 uptake by, effects of diffusion on, 18: 15801
rubidium-86 uptake by roots of, effects of placement in soil on, 17: 38724
ruthenium-106 uptake by, effects of humus and lime on, 16: 14451
sex expression in, 18: 23127 (BNL-805(p.109-25))
strontium absorption, effects of aluminum and calcium in substrate, 17: 7751(R) (TID-17552)
strontium metabolism by hybrids of, effects of genotype, environment, and nitrogen fertilizer on, 19: 33740(R) (NYO-2744-26)
strontium substitution for calcium in, 18: 21784
strontium transport in primary root, 20: 45270 (AD-639836)
strontium uptake by roots, 17: 15610
strontium-85 translocation from leaves of, 19: 5623
strontium-85 transport in isolated root segments, 20: 45269 (AD-639699)
strontium-89 absorption by leaves of, effects of pH, 16: 28720
strontium-89 transport in, effects of chloranilic, malic, oxalic, and tartaric acids on, 20: 26621
strontium-89 transport in, 19: 12911 (NP-14752)
strontium-89 uptake by, effects of humus and lime on, 16: 14451
strontium-90 content of German Democratic Republic, 1963 and 1964, 20: 45964 (SZS-7/66)
strontium-90 uptake by, effects of soil temperature on, 20: 3668
strontium-90 uptake by, effects of liming and soil types on, 20: 6745
uptake of calcium, magnesium, phosphorus, strontium, and zinc by hybrids of, effects of soil fertility on, 20: 40735 (NYO-2744-37)
uptake of cerium, iron, and manganese, effects of soil colloids on, 20: 22547 (TID-21702)
use as radiation dosimeter during space flight, 20: 18964
variations in, gametophyte dependence of, 18: 19507 (TID-20402)
water content of, determination of, using neutron thermalization, 20: 37154
zirconium-95 uptake by, effects of soil temperature on, 20: 3668

MAKROFOL
ion tracks in, registration mechanisms of heavy, 20: 5755
performance as heavy ion detector, 20: 5756
performance for heavy ion detection, 20: 5756

MALATES
effects on pH of dialyzed zirconyl chloride, 17: 35718
metabolism by *Staphylococcus aureus* and its radioinduced mutant, 17: 5790(T)
polonium-210 binding by, in blood, 19: 2042
radiation effects on, ESR studies of bond breakage of hydroxyl groups in, 19: 22326
radiation effects on oxidation of, in *Vibrio cholerae*, 20: 16198

MALATHION
labeling with phosphorus-32 and sulfur-35, 20: 38931
labeling with phosphorus-32, 20: 43397

MALAYA
fallout monitoring, 1961 and 1962, 18: 25698

Maleates
see Maleic Acid, Derivatives

MALEIC ACID
catalytic effects on uranium(IV)–thallium(III) reaction, 16: 9981 (TID-15019)
catalytic effects on oxidation of uranium(IV) by thallium(IV) in perchloric acid, 16: 28858
complexes of, with alkali metals, evidence for, 16: 32999
complexes with europium, formation and stability constants, 17: 25367
complexes with uranyl ion, formation constants for, 20: 8880 (COO-1020-10)
determination by xenon trioxide oxidation, titrimetric, 20: 31196
effects on exchange between tetravalent and hexavalent uranium, 20: 23038
effects on gamma sensitivity of spores of food-spoilage fungi and yeasts, 20: 43784
effects on radioinduced isomerization of α-phenylcinnamic acid, 20: 14596
effects on radioinduced graft polymerization of polypropene to acrylonitrile, 2-methyl-5-vinylpyridine, and styrene, 18: 25505(T) (AEC-tr-6372(p.363-9))
effects on radiosensitivity of fruit-spoilage fungi, 20: 13137 (NP-15360)
effects on rate of reaction between uranium(IV) and thallium(III), 19: 46277
effects on uranium(IV)–(VI) exchange reactions, 18: 12043 (TID-20147)
effects on uranium(IV)-(VI) exchange reactions, 19: 7506

labeling with tritium, effects of support on exchange, 19: 42522
mechanisms of Diels-Alder, 19: 23355(R) (BNL-867(p.1-117))
production by thermal oxidation of phenol at 100 to 200°C, 18: 43460
radiation effects on properties of coatings of copolymers with vinyl chloride, 17: 36362
radioinduced cis-trans isomerization to fumaric acid, 16: 14490
radioinduced crosslinking in resin with phytic acid and propylene glycol, hardening in, 18: 25527(T) (AEC-tr-6372(p.533-8))
radiolysis of, ESR studies of free radicals in gamma, 19: 15641
radiosensitivity effects on mitosis in MTK sarcomas in mice, 16: 8604
radiosensitivity effects on *Pseudomonas*, 16: 17509
reactions of, with zirconyl chloride, 17: 20014
reactions with aqueous beryllium nitrate solutions, 16: 4126(T) (AAEC/Trans-8)
thermal oxidation at 100 to 200°C, decomposition products of, 18: 43460
maleic acid–2-propanol, radiolysis yields in, 20: 18730 (UJV-1468)

MALEIC ACID, DERIVATIVES
cellulose, graft-copolymerization of, with vinyl monomers, 20: 36906(P)
chloro-, cell parameters and space groups of cesium, potassium, and rubidium, 16: 1741
chloro-, potassium salt, crystal structure, 19: 36437
dibutyltin dimaleate, Mössbauer spectra of, in polyethylene, 19: 7580
effects on pH of dialyzed zirconyl chloride, 17: 35718
excretory effects on cesium-137 in rats, 17: 4391
potassium hydrogen chloromaleate, structure from neutron diffraction data, 19: 280(R) (ORNL-3679(p.94-116))
potassium hydrogen chloromoleate, molecular structure by neutron diffraction, 19: 46161(R) (ORNL-3832, pp 116-50)
radiation effects on potassium hydrogen maleate, electron magnetic, resonance spectra of, 17: 8158
radioinduced formation of dimethyl maleate from dimethyl fumarate, gamma-, 19: 42554
radioinduced radical formations in potassium hydrogen maleate, electron spin resonance study of, 18: 13833 (CONF-403-1)
radiosensitivity effects of N-ethylmaleamic acid on *Pseudomonas*, 16: 17509

MALEIC ACID, DIALLYL ESTER
effects on radioinduced crosslinking of polymers, 18: 8407 (RAI-329)
radioinduced cross linking with, 18: 27531

MALEIC ACID, DIBUTYL ESTER
radioinduced polymerization of, 19: 46377

MALEIC ACID, DIETHYL ESTER
radioinduced polymerization with styrene, 17: 32177
radioinduced polymerization, 18: 25491(T) (AEC-tr-6372(p.207-12))
radioinduced polymerization of, properties of polymer obtained in, 19: 46377
radioinduced polymerization of, infrared studies of gamma, 20: 9010

MALEIC ACID, DIHYDROXY-
analytical uses for determination of rare earths, 19: 46216
uses in determination of ytterbium, 20: 14490
uses in separation of rare earths from iron, manganese, and uranium, 19: 46452

MALEIC ACID, DIMETHYL ESTER
radioinduced isomerization of, effects of alkali metal bromides on, 20: 14596
radioinduced reactions with iron carbonyls, 20: 33381

MALEIC ACID, DIOCTYL ESTER
radioinduced polymerization of, 19: 46377

MALEIC ACID, HYDRAZIDES
chromatid aberrations induced in Vicia by, effect of DNA on, 18: 8158
effects on *Vicia faba* seeds, 16: 1595
effects with water-d_2 on growth of peppermint, 19: 35920
penetration of carbon-14-labeled, through cuticular membranes, 20: 16146 (COO-588-39)

MALEIC ANHYDRIDE
decomposition of Diels-Alder adduct with 2-methylfuran, mechanism of, 17: 25283
dimethyl-, radiation effects on C_4-cyclodimerization of, 18: 8423
effects of irradiated, on polymerization of isobutyl vinyl ether and *N*-vinylcarbazole, 20: 23148
effects on initiation of polymerization of cyclic ethers by benzoyl peroxide and radiation, 20: 23147
effects on polymerization of cyclic ethers in liquid state, 19: 26375
effects on polymerization of cyclic ethers, mechanism of, 19: 26425
effects on polymerization of *N*-vinylcarbazole, ESR studies of, 20: 23058
effects on radioinduced polymerization of *N*-vinylsuccinimide, 18: 37236
effects on radioinduced polymerization of 3,3-bis(chloromethyl)oxetane and trioxane, 19: 15618
effects on radioinduced polymerization of cyclic ethers, 19: 26424
effects on radioinduced polymerization of cyclic ethers, 20: 38953
radioinduced codimerization of methallyl chloride with, 20: 40971
radioinduced decomposition in presence of iron carbonyls in benzene, 18: 35635
radioinduced graft polymerization to polypropylene, 19: 17999
radioinduced polymerization of unsaturated esters of, with styrene, 17: 32177
radioinduced polymerization, 18: 25491(T) (AEC-tr-6372(p.207-12))
radioinduced polymerization with polymers and woods, properties of products of, 18: 37190 (BNL-874(p.37-8))
radioinduced polymerization with acenaphthylene, solid-state, 19: 15617
radioinduced polymerization with styrene, 19: 22349
radioinduced polymerization with α-methylstyrene, 19: 22350
radioinduced polymerization with acenaphthylene in solid state, 19: 28401
radioinduced polymerization with α-methylstyrene, 19: 36489
radioinduced reactions with iron carbonyls, 20: 33381
radioinduced solid-state polymerization with acenaphthylene, gamma, 20: 29274
radiolysis of, in benzene solution, products of gamma, 20: 33345
radiosensitivity effects on *Pseudomonas*, 16: 17509
reaction with 2-methylfuran, deuterium isotope effect in Diels-Alder, 17: 4568
reactions with anthracene, butadiene, and cyclopentadiene, deuterium isotope effects in, 18: 35527
reactions with cyclopentadiene, secondary deuterium isotope effect in, 17: 6122
reactions with 2-methylfuran, deuterium isotope effects on mechanism of Diels-Alder, 19: 22267
use as catalyst in graphite fabrication, 19: 32710(P)
maleic anhydride–styrene, properties of polymers in radioinduced graft polymerization of polypropylene to, 18: 27574
maleic anhydride–styrene, radioinduced graft polymerization to polypropylene, 18: 27573
maleic anhydride–styrene, radioinduced polymerization on polypropylene, 18: 27575
maleic anhydride–styrene–vinyl acetate, radioinduced graft polymerization of polypropylene, 18: 27576
maleic anhydride–vinyl acetate, radioinduced graft polymerization on polypropylene, 18: 27575

MALEIMIDE
dioxime of, analytical uses and reactions of, 20: 43095
N-(*N*-acetyl-4-sulfamoyl)-, reactions between cysteine and sulfur-35-labeled, 20: 10937(T) (NP-tr-1323)
radioinduced polymerization of liquid and solid, gamma, 20: 26973
sensitizing effects on radioinduced polymerization of rubbers, 17: 29165
substituted, preparation of sulfur-35-labeled, 20: 10937(T) (NP-tr-1323)
toxic effects in HeLa cells in culture, 20: 26622

MALEIMIDE, *N,N′*,4,4′-BIPHENYLYLENEDI-
radioinduced polymerization of, 20: 1930

MALEIMIDE, *N*-ETHYL-
effect on radiosensitivity of *Micrococcus radiodurans*, 17: 33732
effects on anoxic radiosensitivity of *Shigella sonnei*, 16: 21959
effects on lethal radiation effects on *E. coli*, 18: 125
effects on mercury-203 uptake by rabbit kidney tissues, 17: 35430
effects on radiosensitivity of rabbit erythrocytes, 19: 17550
effects on radiosensitivity of fruit-spoilage fungi, 20: 13137 (NP-15360)
effects on radiosensitivity of bacteria, spores, and yeasts, 20: 37144
protective effects against radiation damage to ribonuclease, 17: 13926
radiosensitivity effects on bacteria, 16: 12923
radiosensitivity effects on *Pseudomonas*, 16: 17509
radiosensitivity effects on bacteria, 17: 35482
radiosensitivity effects of, in *E. coli*, 18: 126
radiosensitivity effects in Drosophila, x, 18: 36987
radiosensitivity effects on bacteria, 19: 44552 (BLG-327)
radiosensitivity effects on sodium uptake by human erythrocytes, γ, 20: 8610
radiosensitivity effects on chromosomes in Vicia roots, 20: 10624
radiosensitivity effects on HeLa cells in culture, x, 20: 31130
radiosensitivity effects on *Thiobacillus thiooxidans*, x, 20: 31139
sensitizing effects on radioinduced polymerization of rubbers, 17: 29165

MALEIMIDE, *N*-PHENYL-
effects on radioinduced vulcanization of saturated polymers and synthetic rubbers, 17: 32167

MALEIMIDE, *N,N′*-PHENYLENEDI-
effects on radioinduced vulcanization of saturated polymers and synthetic rubbers, 17: 32167
radioinduced polymerization of, yields in, 20: 1930
radiosensitivity effects on *Pseudomonas*, 16: 17509

MALIBU POWER REACTOR
containment and site, 18: 40882
engineered safeguards of, effects on distance requirements, 19: 33594 (CONF-650201(p.98-101))
fuel scheduling for, using IBM 1620, 18: 35187
hazards summary, 18: 43031 (NP-14290(Pt.B))
hazards summary, 18: 45026 (NP-14290(Pt.A))

operation and safeguards of, regulatory actions relative to, 19: 12795
radioisotope production in, economic and technical feasibility of, 19: 28723

MALIC ACID
catalytic effects on oxidation of uranium(IV) by thallium(IV) in perchloric acid, 16: 28858
determination by xenon trioxide oxidation, titrimetric, 20: 31196
diethyl ester, synthesis of deuterated, 18: 1713
effects of light on content of, in Lemna, 20: 45255
effects on exchange between tetravalent and hexavalent uranium, 20: 23038
effects on rate of reaction between uranium(IV) and thallium(III), 19: 46277
effects on strontium-89 transport in bean and corn plants, 20: 26621
effects on uranium(IV)–(VI) exchange reactions, 18: 12043 (TID-20147)
effects on uranium(IV)-(VI) exchange reactions, 19: 7506
labeling with tritium by enzymatic reactions in tritiated water, 18: 31120
labeling with tritium by enzyme reactions and Wilzbach method, 18: 43574
metabolism of, by *Saccharomyces cerevisiae*, radio-gas chromatographic studies of, 20: 45580
production in gamma radiolysis of aqueous fumaric acid, 20: 10875
radiation effects on metabolism in apples, 16: 8582
radiation effects on Tetrahymena, uv and x, 19: 43856
reactions of, with zirconyl chloride, precipitate formation in, 17: 20014
stability constants of chelate compounds of, with uranyl ion, 16: 17666
$LaCl_3$–malic acid–KOH, compound formation in, 20: 35517
malic acid–TBP, viscosity, 19: 13196 (TID-20400)

MALIC ACID COMPLEXES
with alkali metal cations, formation constants of, 17: 28788
with hafnium and zirconium, equilibrium and stability constants of, 18: 27414
with lanthanum and ytterbium, formation and properties of, 17: 18082
with rare earths, stability constants for, 18: 41451
with thorium, 17: 14366
with thorium, infrared spectra of, 19: 11058
with uranium, structure of, 17: 23249
with uranyl ion, polarography at 15°C, 20: 295
with uranyl ion, reactions and structures of, at dropping mercury electrode, 19: 379
with uranyl ions, formation constants of, 18: 8397 (TID-20018)
with uranyl ions, spectra of, infrared, 19: 19911

Malic Acid, 2-Thio-
see Succinic Acid, Mercapto-

MALIC ENZYMES
deuterium effects on diphosphopyridine nucleotide reactions in dehydrogenase, 16: 31395(R) (ANL-6535(p.96-9))
radiation effects on activity of rat, protective effects of torantil, trasylol, and trioxyethylrutin against, 17: 28754
radiation effects on activity of, 17: 28706

MALONALDEHYDE
radiation effects on binding of, with heme proteins, 20: 42799(R) (UCB-34P95-1)
radioinduced in amino acids, effects of impurities, 20: 42799(R) (UCB-34P95-1)
reactions of uv-induced, in linoleic and linolenic acids, with peroxidase and thiobarbituric acids, 20: 35543
yields in gamma radiolysis of galactose, effects of sodium borate on, 20: 35540

MALONAMIDE
complexes with thorium and uranium tetrachlorides and uranyl chloride, 20: 33294
N,N'-dimethylmethyl-, yields in uv-radioinduced oxidation of dimethylthymine in aqueous solutions, 20: 23158
radiation effects on ESR spectra of, anisotropic hyperfine structure in gamma, 19: 7554

Malonates
see Malonic Acid, Derivatives

MALONIC ACID
carbon-14 incorporation in C_3O_2 by exchange with carbon dioxide in radiation field, 16: 15085
catalytic effects on oxidation of uranium(IV) by thallium(IV) in perchloric acid, 16: 28858
complexes of, with beryllium, physico-chemical properties of, 16: 22153
complexes with europium, formation and stability constants, 17: 25367
complexes with thorium, formation constants and stability, 17: 21729
complexes with zirconium, 16: 11676
decarboxylation of, theory of carbon isotope effects in, 18: 3802
decarboxylation of, carbon isotope effects in, 18: 35578
decarboxylation of, carbon-13 isotope effects in, 20: 8970
decomposition of, uranyl sensitized photo-, 17: 10697
determination by xenon trioxide oxidation, titrimetric, 20: 31196
effects on exchange between tetravalent and hexavalent uranium, 20: 23038
effects on ion-exchange separation of uranium from rare earths and thorium in aqueous media, 18: 20114
effects on radioinduced redox processes in ammonium iron sulfate, 18: 13878
effects on rate of reaction between uranium(IV) and thallium(III), 19: 46277
effects on uranium(IV) –(VI) exchange reactions, 18: 12043 (TID-20147)
effects on uranium(IV)-(VI) exchange reactions, 19: 7506
electron spin resonance of gamma irradiated, 16: 232
electron spin resonance of x-ray-irradiated single crystals of potassium hydrogen salt of, 16: 234
ethyl-, electron spin resonance of free radicals in gamma-irradiated, 16: 115
ionization constants of substituted, deuterium isotope effects, 18: 27490
oxidation by cerium in sulfuric acid, mechanism of, 18: 41424
paramagnetic resonance line widths in irradiated crystals, 16: 5231
polarography of uranyl ion in, 18: 31485
precipitation of cerium and lanthanum using, 18: 25351
radiation effects on, recombination of free radicals following, 19: 13465
radiation effects on, at 77°K, ESR study of free radicals from x, 20: 45755
reactions of, with zirconyl chloride, precipitate formation in, 17: 20014
reactions with aqueous beryllium nitrate solutions, 16: 4126(T) (AAEC/Trans-8)
spectra of irradiated, zero-field electron magnetic resonance, 17: 33899
thermal decomposition of, deuterium isotope effects on, 19: 17947

MALONIC ACID, BUTYL-
radiation effects on, at 77°K, ESR study of free radicals from x, 20: 45755

MALONIC ACID, DERIVATIVES
diethylbenzylacetamidomalonate, labeling with tritium by exposure to tritium gas, 19: 2366
effects on pH of dialyzed zirconyl chloride, 17: 35718
oxidative effects of inorganic, on metabolism of *Staphylococcus aureus* and its radioinduced mutant, 17: 5790(T)
properties of malonate as bridging group for electron transfer, 16: 1659

MALONIC ACID, DIETHYL ESTER
analysis for active hydrogen by NMR spectroscopy, 18: 33475
tritium exchange in aqueous solutions of, 18: 10136
tritium exchange in aqueous solutions of, 18: 10136
tritium exchange with hydrocarbons, effects of catalysts on, 20: 16492

MALONIC ACID, DIMETHYL-
paramagnetic resonance line widths in irradiated crystals, 16: 5231

MALONIC ACID, ESTERS
bromination of, deuterium isotope effects on, 19: 38692
ionization constants of substituted, deuterium isotope effects, 18: 27490
labeling with carbon-14, side reactions in, 19: 13408
methyl, synthesis of carbon-14-labeled, 19: 13408
reactions with iodomethane, 19: 13408

MALONIC ACID, ETHYL-
radiation effects on, temperature dependence of hyperfine couplings of radicals from, 20: 33375
radiation effects on, at 77°K, ESR study of free radicals from x, 20: 45755

Malonic Acid, Hydroxy-
see Tartronic Acid

MALONIC ACID, *n*-PROPYL-
radiation effects on, temperature dependence of hyperfine couplings of radicals from, 20: 33375
radiation effects on, at 77°K, ESR study of free radicals from x, 20: 45755

MALONIC ACID, THIO-
protective effects of, against radiation damage in bovine serum albumin, 17: 28757

MALONIC ACID, URANYL SALTS
stability and composition, 19: 40482

MALONIC ACID, YTTERBIUM SALTS
dissociation constants of, electrolytic, 20: 36830

MALONONITRILE
(2,5-cyclohexadiene-1,4-diylidene) di-, isotope effects on exciton resonance in morpholinium and methyltriphenylarsonium complexes of, (E), 20: 1841
dimethyl-, thermodynamic properties of, 19: 48090 (COO-1149-53)
protective effects against radiation mortality in mice, 16: 4000(R) (NP-11020(p.65-77))
protective effects against radiation injuries, 16: 8635(T) (JPRS-11942)
protective effects against radiation injuries and nitrogen mustard in *E. coli*, 16: 16297
protective effects of, against toxicity of 2,2'-dichloro-*N*-methyldiethylamine, 17: 27030
radiolysis and photolysis of, at 77°K, 20: 35551
radioprotective activity in *E. coli*, method of determining, 17: 35409

radiosensitivity effects of, in *E. coli* and Streptomyces, 17: 38770
MALTONIC ACID
yields in radiolysis of oxygenated solutions of maltose, 18: 13866
MALTOSE
biochemical effects of malt extract on blood of athletes, comparison with glucose, 16: 26666(T) (JPRS-13555)
cesium-137 content in, used for brewing, 20: 45957 (NYO-3364-23)
oxidation by bromine, tritium isotope effects in, 18: 20031
radiation effects on, electron spin resonance investigations of gamma, 17: 27454
radiation effects on cyanohydrin reaction, background, 17: 33981
radiation effects on anhydrous, electron spin resonance studies of gamma, 19: 19994
radioinduced free radicals in, gamma, 18: 23651(T,R) (AEC-tr-6316 (p.573-86))
radiolysis, 17: 21740
radiolysis of aqueous solutions of, acid formation in, 20: 31304
radiolysis of oxygenated solutions of, yields in, 18: 13866
radiosensitivity effects on streptomycin-sensitive strains of *Proteus mirabilis*, uv, 20: 22758
use in gamma and neutron dosimetry, 19: 22774
MAMMALS
(See also specific mammals.)
see also Animals
see also Rodents
see also Whales
aging of, review on mutation and radiation effects on, 20: 6771 (BNL-9653)
analysis for radioactivity, whole-body counting, 16: 27288
blast effects, 16: 21870(R) (DASA-1271)
blood circulation in, tracer studies of, 18: 43165
blood picture in wild mice, rats, and muskrats, 17: 2786(R) (ORNL-3347 (p.47-72))
blood, chemical composition of, 17: 19787 (AERE-R-4196)
body water volume and turnover in seven species, tracer study, 16: 17420
book: *Mammalian Radiation Lethality*, 20: 5405
calcium metabolism in, applications of chelation in studies of, 18: 11616
calcium metabolism, tracer studies, 17: 23028
carcinogenesis in, role of somatic mutations in, 18: 19505 (BNL-7912)
cells of, life cycle analysis, 17: 35484
cesium metabolism, tracer study of, 17: 23028
cesium-137 content in Alaskan caribou, 20: 12983
cesium-137 content in whales,, 20: 38560
characteristics and care of chimpanzees, 17: 7927
cytogenetics of, review on, 17: 24839
cytology of genetics of, 17: 24836
differentiation and proliferation of bone marrow cells in, effects of blood loss, transfusion, and irradiation on, 20: 45480
ecological study of marine, in Cape Thompson region in Alaska, 19: 31636 (PNE-400)
ecology of large, at Savannah River Plant site, 18: 11568 (TID-19562)
ecology of pocket gopher, ground squirrel, and chipmunk under natural environments, 18: 6591(R) (TID-19895)
ecology of small herbivorous, in waste disposal area, 16: 9824
ecology of small, on radioactive bed of drained White Oak Lake, 16: 17374
ecology of small, at Nevada Proving Grounds, effects of underground nuclear explosion on, 18: 11567 (PNE-226F)
ecology of, at Nevada Proving Grounds, 1963, 18: 11569(R) (UCLA-520 (p.81-108))
ecology of, at Savannah River Plant, 19: 35887 (TID-21713)
ecology of, Cape Thompson area, Alaska, 19: 25785 (PNE-420)
ecology of, of Nevada Test site, 19: 33702 (TID-21941)
effects of chemical radioprotective compounds on, effects of biological and chemical factors on, 20: 18472
effects of deuterium in, 18: 31081
effects of manganese in, 18: 21700 (BNL-7855)
fallout content in caribou and reindeer tissues, 1964, 19: 22552
fallout in lungs of deer, 18: 25693
fission product metabolism in, research program at Hanford Lab., 1956 to 1964, 19: 12893(R) (HW-83613)
fission product uptake by small, after rocket reactor test, 16: 32693 (TID-16835)
genetic code for hemoglobin synthesis in, 19: 40296 (TID-21856)
genetics of, in medicine, 17: 13912
hematological studies of small, micro-techniques for, 19: 27896 (ORNL-3806)
hematology of, in White Oak Lake area, 19: 6931(R) (ORNL-3697(p.65-84))
impact effects on mice, rats, guinea pigs, and rabbits, 16: 18731(R) (DASA-1245)
inventory of small, at Nevada Test Site, 20: 45264(R) (UCLA-12-595, pp 72-89)
iodine-131 metabolism in small vertebrates, 18: 6591(R) (TID-19895)
iodine-131 uptake by thyroid gland of, effects of diet on, 20: 38549 (UCLA-12-592)
leukocytes of, method for cultivation and preparation of, 18: 15682 (LADC-5746)
manganese-54 content in whales, 20: 38560
marine, of northwest Alaska, 1961, 19: 33694 (PNE-466)
mercury metabolism and chelation in, effects of various chelating agents on, 19: 25844
photoreactivation of ultraviolet damage in hamsters and mice, 20: 42869
protection against radiation, review of chemical, 16: 17545
protection of, against radiation injuries, theory of, 17: 19881
protein synthesis in pancreas of, 19: 3812(R) (TID-21287)
radiation damage in, extrapolation number for, 17: 33712
radiation dosage from internally deposited radioisotopes, 17: 24880 (CEA-2282)
radiation dose, from ingested radionuclides, 17: 33551
radiation dose response relations for, 20: 6803
radiation dose to, from internally deposited radioisotopes, computer calculation of, 20: 31441 (BNWL-SA-40)
radiation doses to populations in White Oak Lake bed, 16: 2060(R) (ORNL-3189(p.81-104))
radiation effects on cells of, in culture, 16: 21897 (AECL-1510)
radiation effects on, research on genetic, 17: 92
radiation effects on DNA incorporation in, 17: 12164
radiation effects on, chemical protection against, 17: 25033
radiation effects on late pathological, 17: 27146
radiation effects on, from underground explosions, 17: 33507
radiation effects on populations, 17: 33581
radiation effects on eyes in, bibliography on, 17: 35447 (TID-3912)
radiation effects on, therapeutic effects of bone marrow transplantation on, 17: 37119
radiation effects on blood serum glucose content in, 17: 38885 (SAM-TDR-63-40)
radiation effects on sterility in mink, x, 18: 83
radiation effects on, of heavy charged particles, 18: 15826
radiation effects on cells of, protective effects of natural substances against, 18: 15897
radiation effects on, RBE of fast neutron, 18: 17499
radiation effects on tumor cells of, 18: 19572
radiation effects on myoglobins in tuna yellowfish, gamma, 18: 21825 (TID-7684(p.110-12))
radiation effects on blood vessels in, 18: 27062(R) (NYO-1680-1)
radiation effects on morphology of cells of, x, 18: 29377
radiation effects on life spans of, model for, 18: 29411
radiation effects on malignant and normal cells of, 18: 29518
radiation effects on eyes of, index to literature survey on, 18: 35318 (TID-3912(Index))
radiation effects on ovaries of, 18: 35322(R) (TID-20941)
radiation effects on whale liver vitamin A, 18: 35374
radiation effects on, bibliography on, 18: 36948 (AD-438177)
radiation effects on, bibliography on, 18: 36949 (AD-438178)
radiation effects on, survey of, 18: 36985
radiation effects on metabolism in mitochondria of cells of nervous system in, 18: 38952
radiation effects on immune reactions in, 18: 38956
radiation effects on mitosis in, fast-neutron, 18: 41229
radiation effects on nucleic acid synthesis in, 18: 43276
radiation effects on leukopoiesis in, 19: 2064 (BNL-8486)
radiation effects on, prediction of lethal, 19: 8784 (CONF-813-1)
radiation effects on central nervous systems of, 19: 8950
radiation effects on developing embryos, 19: 19466
radiation effects on, high-energy particle, 19: 21817(R) (BNL-867(p.119-50))
radiation effects on cells of, model for recovery from x, 19: 26072
radiation effects on, protective effects of serotonin against, 19: 28125
radiation effects on, gamma and neutron, 19: 29890(R) (ANL-6971 (p.117-19))
radiation effects on liver of, beta, 19: 36000
radiation effects on cell nuclei in bone marrow, synergistic effects of vibration on, 19: 38358 (AD-612660)
radiation effects on cardiac metabolism, 19: 40357(T) (FTD-TT-65-48, pp 552–3)
radiation effects on, protective effects of thiolic compounds against, 19: 46010
radiation effects in, acute pathological, 19: 45981
radiation effects combined with nonradiation factors on, mechanism of response for, 19: 45824(T) (NASA-TT-F-354)
radiation effects on, delayed pathological, x, 20: 1716
radiation effects on adaptive responses of, x, 20: 5319
radiation effects on embryos of, 20: 8659
radiation effects on, review of genetic, 20: 10688

radiation effects on, gamma, 20: 12667
radiation effects on retina in, review of laser, 20: 22629
radiation effects on immune reactions in chimeras, 20: 26691
radiation effects on bone marrow cells in different phases of cell cycle in, x, 20: 32997
radiation effects on response to tapeworm infestations, x, 20: 36607(R) (TID-23114)
radiation effects on nitrogen metabolism, comparison with frogs, 20: 42787
radiation effects on aging of, 20: 45411
radiation effects on large, fast-neutron, 19: 8783 (BNL-8571)
radiation effects on free-living populations, neutron and gamma, 17: 33582
radiation effects, pathological, 19: 12970
radiation effects, pathological, 19: 31809
radiation effects, genetic, 19: 33838
radiation injuries, effects of dose rate and duration on repair rate, 17: 13987 (UR-621)
radiation injuries in, chemical protection against, 18: 1459
radiation injuries in, recovery from, 18: 19762
radiation injuries of, pathogenesis of acute whole-body, 18: 37017
radiation injuries in, role of spleen in, 19: 7024
radiation injuries, protective effects of chemical agents, 19: 19643
radiation injuries of testis of, delayed, 20: 12686
radiation injuries of, effects of physiological condition on recovery from, 20: 22694
radiation injuries in, biological model for, 20: 22613(R) (NIRS-4, pp 21-8)
radiation injury and recovery in, 19: 2063 (BNL-8469)
radiation injury and repair in tissues of, 20: 31045
radiation injury repair rate in normal and neoplastic tissues of, 18: 59
radiation protection in, review, 18: 13573
radiation recovery response of tumor cells, 20: 45409
radiation response of organs and tissues in, proton, 19: 19812 (BNL-6966)
radiation sensitivity of, effects of chemicals on, 17: 15753
radiation syndrome in, lethal studies of acute, 18: 29319
radiation syndrome in, pathological aspects of acute, 18: 29320
radio-ecology of eastern chipmunk, *Tamias striatus*, in Pennsylvania, 17: 7797(R) (TID-17502)
radio-ecology of northern pocket gopher, *Thomomys talpoides*, in Wyoming, 17: 7797(R) (TID-17502)
radioinduced anomalies in, following prenatal exposure, 20: 22756
radioinduced carcinogenesis in, 18: 31189
radioinduced chromosomal aberrations in tissue cultures from, x, 19: 178
radioinduced congenital malformations in, 19: 134
radioinduced lethal mutations in, 18: 1442
radioinduced lung tumors in, 19: 45808(R) (NYO-901-36)
radioinduced mutations in, 19: 33957
radioinduced mutations in, neutron, 20: 16159(R) (ORNL-3900, pp 150-81)
radioinduced tumors in, reaction mechanisms for, 17: 40642
radioinduced tumors in, etiology of, 19: 45859
radioisotope accumulation by small herbivorous, in areas contaminated by waste disposal, 16: 9824
radioisotope assimilation by granivorous and herbivorous, comparison, 20: 45264(R) (UCLA-12-595, pp 72-89)
radioisotope content of fin whale off Oregon coast, gamma-emitting, 19: 6936
radiosensitivity of, effects of adenosine and adenosinephosphoric acids on, 16: 31527
radiosensitivity of, role of catalase in, 17: 12129 (TID-16249)
radiosensitivity of, protective effects of organic compounds against, 17: 30396
radiosensitivity of cells of, 17: 35371
radiosensitivity of hematopoietic system in, effects of species on, 17: 40659 (BNL-7207)
radiosensitivity of cells of, 18: 58
radiosensitivity of erythropoiesis in, 18: 38870
radiosensitivity of germ cells in, 19: 7057
radiosensitivity of immune reactions in, 19: 13068
radiosensitivity of tissues of, 19: 33934
radiosensitivity of gonads of, 19: 43756
radiosensitivity of, cyclic variations in, 20: 5336
radiosensitivity of intestinal cells of hedgehog, *Erinaceus europaeus*, effects of hibernation on x, 20: 5377
radiosensitivity of hematopoietic system, 20: 22704
radiosensitivity to x rays, 16: 1486(T) (JPRS-10170(p.279-312))
sodium-22 content in muscles of Canadian, 20: 4161
strontium metabolism, tracer study of, 17: 23028
strontium saturation of skeleton, 16: 20108
strontium-90 metabolism in, effects of calcium, phosphates, and stable strontium on, 19: 38335 (NP-14926)
strontium-90 uptake by skeleton of, effects of diet on, 18: 19533
study in eastern Chukchi Sea, 19: 25812 (PNE-479)
study of marine, in Cape Thompson region in Alaska, 19: 31637 (PNE-401)
study of marine, in Cape Thompson region in Alaska, 19: 31639 (PNE-405)
sulfur-35 distribution in tissues of, 18: 31168
thyroxine secretion rates of opossum and other, 18: 45164 (CONF-722-1)
toxic effects of plutonium-239 in, 18: 15786(T) (FTD-TT-63-559)
toxicity of tritiated thymidine in, 18: 17424
zinc-65 metabolism in small vertebrates, 18: 6591(R) (TID-19895)
zinc-65 content in whales, 20: 38560

MAMMARY GLAND
see also Breasts
amino acid synthesis in cows, tracer study, 17: 23029
calcium transport in, 18: 11621
cancers of, prognostic indications for, 20: 60(R) (NYO-901-37, pp 33-68)
carcinoma of, repair of thoracic wall after resection and radiotherapy of, 19: 4027
carcinomas of, induced by x radiation or hydrocarbons, hormone dependence of, 18: 1427
cell DNA synthesis in mouse, 19: 21817(R) (BNL-867(p.119-50))
cell generative cycle in neoplasms of mouse, 18: 21701 (BNL-7925)
desoxyribonucleic acid synthesis in cells of mouse, effects of ovarian hormones on, 19: 24240 (BNL-8053)
iodine-131 uptake and accumulation by lactating, in rat, 17: 24851
irradiation of cow and goat, design and performance of facility for, 20: 23242
neoplastic lesions in mouse, chemically induced, 20: 20502
neutron exposure, immediate detection, 17: 18323 (HW-73891(Rev.))
pathology of tumors in, 20: 24829(R) (NEIC-RR-17)
permeability to sodium-24, potassium-42, chlorine-36, and iodine-131, 16: 5142
phosphorus-32 uptake and distribution in healthy human, 19: 14993
radiation and hormone effects on structure of, rat electron microscopy of, 19: 15034
radiation dose effects on tumor growth in F_1 hybrid mouse, 19: 38403
radiation dose to tumors of mouse, determination of, 19: 26077
radiation effects on development, 16: 20170
radiation effects on tumor incidence in rat, whole-body, effects of injected tumor fluid on, 16: 20253
radiation effects on lymphatic bed, 16: 32749(T) (JPRS-15018(p.135-43))
radiation effects on sub-cellular structure and ATPase activity in tumors of mouse, x, 18: 3534
radiation effects on carcinomas of, preoperative histological effects of, 18: 11720
radiation effects on autotransplants of adenocarcinoma in mouse, 19: 7041
radiation effects on development of, in pregnant mice, 19: 17617
radiation effects on carcinoma of mouse, 19: 26076
radiation effects on activity of, 19: 40353(T) (FTD-TT-65-48, pp 16–17)
radiation effects on lactation in dairy cows, 19: 43800
radiation effects on cow and goat, gamma and x, 20: 22594
radiation effects combined with urethan on tumor induction in mouse, 20: 42873
radiation injuries of, in children treated for hemangiomas by radium, 20: 38787
radiodiagnosis of tumors of, using bremsstrahlung produced by radiophosphorus in paraffin, 20: 20540
radioinduced adenocarcinomas in mouse, fast-neutron, γ, or combined fast-neutron and γ, 20: 45417
radioinduced carcinogenesis in epithelium of rat, relation of DNA synthesis to x, 20: 42840(R) (ANL-7136, pp 164-90)
radioinduced neoplasia in rats, 17: 13965 (BNL-6704)
radioinduced neoplastic lesions in mouse, x, 20: 20502
radioinduced tumors in rats, hormonal factors, 16: 32791
radioinduced tumors of rat, morphology of niobium-95, 18: 13462(T) (JPRS-23559(Del.)(p.28-35))
radioinduced tumors in rat, effects of dose and energy on proton beam, 20: 6885
radioinduced tumors in rat, effects of exposure fractionation and protraction on gamma, 20: 18319
radiosensitivity of, 19: 46090
radiosensitivity of skin of, of guinea pigs, 19: 45869
radiotherapy, effects on cardiac muscle, 16: 61
radiotherapy of carcinomas of, injuries from, 18: 41286
radiotherapy of cancers of, 19: 9027
radiotherapy of carcinomas in, effects of irradiation technique on efficiency of gamma, 19: 30038
radiotherapy of carcinomas of, effects of 5-fluorouracil on, 19: 40394
radiotherapy of carcinomas of, using cobalt-60 or iridium-192 wire applicator, 19: 46047
radiotherapy of carcinoma of, pathological effects on lungs, 19: 46063
radiotherapy of carcinomas of, dosimetry in γ, electron, and x, 20: 18545

radiotherapy of carcinomas of, effects on hematopoiesis, 20: 18552
radiotherapy of cancer of, effects on lungs, 20: 22725
radiotherapy of carcinomas of, supplementary treatment in, 20: 22838
radiotherapy of carcinomas of, surgery and combined gamma and x, 20: 22839
radiotherapy of carcinomas of, using yttrium-90, 20: 31153
radiotherapy of carcinomas of, development of metastases in gamma and x, 20: 36697
radiotherapy of, effects on skin, 18: 3644
radiotherapy of melanoma of, using iridium-192 wire applicator, 19: 46047
radiotherapy of milk-duct carcinomas in, method for assessing preoperative x, 19: 36187
radiotherapy of neoplasia in human, development of pericarditis from, 19: 10945
radiotherapy of skin metastases arising from neoplasms of, 20: 43039
radiotherapy of tumors of, 19: 28212
radiotherapy of tumors of, pathological effects on heart, 20: 213
radiotherapy of, complications in, 18: 11903
radiotherapy of, effects on leukocyte count of x, 20: 24940
radiotherapy of, using internal implants of cobalt-60 wire, 19: 32006
radiotherapy using palladium-103, 20: 20542
strontium transport in, 18: 11621
strontium-90 excretion by, after chronic ingestion by milk cows, 19: 40332
synthesis of DNA in alveolar cells of mouse, effects of 17-β-estradiol and progesterone on, 19: 6924
therapy of cancer of, using radiation hypophysectomy, 19: 26207
therapy of carcinomas of, by yttrium-90 pituitary destruction, 20: 10752
tumor growth in rat, 19: 43649 (UCRL-16177)
tumorigenic effects of irradiated plasma in rat, 18: 38775(R) (ORO-624)

MAN
see also Medical Personnel
actinium-227 distribution in, 20: 38554
actinium-228 content in lungs of, determination of, 20: 9198
activation of, by radiation exposure, 19: 27989
adrenaline metabolism, 16: 17406
aerosol deposition in lungs of, method for determining, 19: 3850
aerosol deposition, clearance, and retention in lungs of, biological processes in, 19: 3851
age changes in bone structure and mineralization, 16: 31447
age estimation of bones and tools of prehistoric, by carbon-14 method, 20: 18937
age of Nevada mummy using radiocarbon, estimation of, 19: 30428
age-related changes in erythrocyte agglutinability in bomb survivors, 16: 7436
albumin metabolism in carcinomatous, 19: 31671(R) (NIRS-3(p.57-63))
aldosterone secretory rates in, effects of isotope fractionation in isotope dilution analysis of, 19: 7344
alkaline earth metabolism in, tracer studies of, 19: 27941
allergic reaction in aerial dispersal of radiosterilized screwworm flies, 19: 43652
alpha radioactivity in, techniques for studies of, 18: 35271
alpha-emitters in bones and teeth of, 18: 19532
altitude effects on, 17: 35286(T) (FTD-MT-62-78(p.564-75))
altitude effects on neonatal death rate, 19: 29829(R) (ANL-6971(p.89))
americium content in lungs of, design of chest phantom for determining, 19: 30473
analysis after neutron activation, radiometric, 19: 40800(R) (AERE-PR/HPW-7)
analysis by whole-body counting, 16: 19075 (TID-15659)
analysis by whole-body counting, 19: 6126(R) (HW-83605)
analysis for americium-241 and plutonium-239 in, using whole-body counter, 19: 38545(R) (RFP-552)
analysis for arsenic in finger nails and hair of, activation, 18: 10029
analysis for arsenic in teeth of, activation, 19: 7318
analysis for barium-140 in radioisotope mixture in, 20: 6923
analysis for beryllium in tissue and urine samples of, 20: 43108
analysis for body composition, radioisotope dilution method, 19: 15006
analysis for cesium-137, whole-body counting, 16: 18738
analysis for cesium-137, whole-body counting, 16: 26712
analysis for cesium, 16: 32703
analysis for cesium-137, whole-body counting, 17: 24848 (TID-18713)
analysis for cesium-137 by whole-body counting, 17: 33527
analysis for cesium-132 and potassium-40, whole-body counter for, 18: 14260
analysis for cesium-134 by whole-body counting or analysis of urine, 18: 33265
analysis for cesium-137 by whole-body counting or analysis of urine, 18: 33265
analysis for cesium-137, lead-210, platinum-195, radium-226, and rhenium-186 by whole-body counting, 18: 43184(R) (MIT-952-1(p.150-62))
analysis for cesium-137 content, whole-body radiometric, 19: 623 (HW-SA-3689)
analysis for cesium-137 and potassium-40, 19: 4503
analysis for chlorine-38 and sodium-24 by neutron activation, 19: 22137
analysis for copper and zinc in lung tissue of, by neutron activation methods, 19: 40452
analysis for deposited plutonium, whole-body counting, 17: 13882 (HW-SA-2653)
analysis for deposited radium and thorium, radiometric, 18: 35301
analysis for deposited radionuclides, whole-body, 18: 35760 (HW-67245(Rev.))
analysis for deposited radioisotopes, direct and indirect methods for, 18: 37106
analysis for deposited radionuclides, whole-body radiometric, 19: 12910 (DPSPU-64-30-7B)
analysis for deposited radiation in, whole-body counting, 19: 22635
analysis for fallout particles in lungs of, 18: 13688
analysis for gamma radioactivity, design of whole-body counting facility, 16: 8532(R) (ACRH-16(p.126-35))
analysis for gamma-emitting isotopes, computer program for processing data from, 16: 27465(R) (NP-11928)
analysis for gamma radioactivity, whole-body counting, 17: 1175(R) (HW-70050(p.31-77))
analysis for gamma-emitting radioisotopes, whole-body counting, 17: 21563
analysis for gamma radiation, whole-body counting, 17: 35340(R) (UCLA-515(p.55-73))
analysis for gamma-emitting radionuclides, whole-body spectrographic, 18: 17721 (BNL-7885)
analysis for gamma radioactivity, whole-body, 18: 20337 (NYO-2553-1)
analysis for gamma radioactivity in, whole-body, 19: 13637
analysis for inhaled radioisotopes, whole-body gamma spectrographic, 17: 24853
analysis for internally deposited gamma radiation, 16: 16144
analysis for internally deposited radioactivity, whole-body counting, 16: 16145
analysis for internally deposited radium and thorium, whole-body counting, 16: 16146
analysis for internally or externally deposited radioactivity, whole-body counting, 16: 16150
analysis for internally deposited tracer elements, whole-body counting, 16: 16155
analysis for internally deposited radioactivity, whole-body counting, 16: 16133
analysis for internally deposited gamma radiation, whole-body counting, 16: 16143
analysis for internally deposited radioisotopes, 16: 16158
analysis for internally deposited radioactivity by whole-body counting, 16: 19172(R) (AD-266007)
analysis for internally deposited radium-226 and strontium-90, 18: 37466
analysis for internal gamma contaminants, whole-body, 18: 43318 (IDO-12038)
analysis for internal contamination, methods for, 19: 26279
analysis for lanthanum-140 in radioisotope mixture in, 20: 6923
analysis for mixed radioisotopes in, γ spectrometric, 20: 6923
analysis for muscle electrolytes, neutron activation, 17: 37051
analysis for natural radioactivity, whole-body counting, 16: 16134
analysis for naturally occurring potassium-40, whole-body counting, 17: 2799 (LADC-5446)
analysis for naturally occurring radium-226, polonium-210, and lead-210, 17: 2801 (TID-17191)
analysis for neptunium-237, protactinium-233, cobalt-60, zirconium-95, and niobium-95 in, by whole-body counting, 17: 5704 (TID-12790)
analysis for niobium-95 in radioisotope mixture in, 20: 6923
analysis for phosphorus-32 distribution, radiometric, 17: 31876
analysis for plutonium-239, partial-body counting, 16: 16148
analysis for plutonium and uranium, design of counter for, 20: 11107 (RFP-462)
analysis for plutonium, review on, 20: 14239 (JUL-312-ST)
analysis for potassium, lean body mass, and total fat content by whole-body counting methods employing potassium-40 and tritiated water, 16: 16151
analysis for potassium, 16: 32703
analysis for potassium by whole-body counting of potassium-40, 17: 19795
analysis for potassium-40 by whole-body counting, *in vivo* determination of lean body mass from, 18: 33487
analysis for potassium-40, whole-body radiometric, 19: 56
analysis for radioactivity by whole-body counting, characteristics of phosphors for, 16: 8950
analysis for radioactivity, whole-body counting, 16: 16136
analysis for radioactivity, whole-body counting, 16: 16137

analysis for radioactivity, whole-body counting, 16: 16139
analysis for radioactivity, whole-body counting, 16: 16140
analysis for radioactivity, whole-body counting, 16: 16141
analysis for radioactivity, whole-body counting, 16: 16142
analysis for radioactivity, whole-body counting, 16: 27348 (HASL-100)
analysis for radioactivity, whole-body counting, 16: 30575 (HW-SA-1917)
analysis for radioisotopes deposited internally, 16: 31451
analysis for radioactive contaminants, whole-body gamma spectrographic, 17: 2789(R) (ORNL-3347(p.142-54))
analysis for radioactivity, whole-body counting, 17: 28626
analysis for radioactivity, from natural and artificial sources, whole-body counting, 17: 30287(R) (NP-12977)
analysis for radioactive contaminants, whole-body, 18: 6717
analysis for radioactivity in France, 18: 16204(R) (SCPRI(RM)-XII-1963)
analysis for radium, whole-body counting, 16: 16147
analysis for radium, whole-body counting, 16: 16171
analysis for radium, 16: 19181 (NP-11641)
analysis for radium-226 and radium-228, whole-body counting, 16: 32691(R) (TID-16765)
analysis for radium-224, whole-body, 18: 36943
analysis for radium-226 and radium-228, whole-body, 18: 43222(R) (MIT-952-1(p.1-112))
analysis for rhenium-186, whole-body, 18: 43184(R) (MIT-952-1(p.150-62))
analysis for rhodium-103 in radioisotope mixtures in, 20: 6923
analysis for rubidium, 16: 32703
analysis for ruthenium-103 in radioisotope mixture in, 20: 6923
analysis for sodium-22, whole-body counting, 16: 16156
analysis for sodium-24, calibration of whole-body monitor for, 18: 29875 (AEEW-M-334)
analysis for strontium-90, radiometric, 16: 10329
analysis for thorium(IV) oxide daughters after thorotrast injection, alpha spectrometric, 18: 17699
analysis for thorium-232 by whole-body counting, 18: 33269
analysis for trace elements, activation, 19: 7319
analysis for trace elements in diseases in, activation, 20: 38847
analysis for tritium, use of urine for, 20: 22546 (CONF-640413, pp 132-6))
analysis for uranium, 17: 33512
analysis for zirconium-95 in radioisotope mixture in, 20: 6923
analysis for 23 elements in various tissues, spectrographic, 17: 2788(R) (ORNL-3347(p.101-41))
analysis of blood and hair of, activation, 20: 36728
analysis of bones of, for strontium-90, 18: 10000
analysis of Eskimos for cesium-137, whole-body counting, 17: 2798 (HW-SA-2764)
analysis of Eskimos, for cesium-137, 18: 2021(R) (HW-77609(Sect.2))
analysis of excreta of, for deposited radioisotopes, 19: 30460
analysis of, for cesium-137 content, whole-body, 17: 36019 (AE-119)
analysis of, for cesium-137 content, whole-body, 17: 36085
analysis of, for deposited radium-224 and radium-226, 17: 37008(R) (NYO-9505(p.1-39))
analysis of, for radioisotopes, whole-body, 17: 37009(R) (NYO-9505 (p.40-51))
analysis of lung mineral content in chronic berylliosis, 17: 28647
analysis of lungs of, for antimony deposits, x-ray-absorption, 20: 6955
analysis of newborns, infants, and children, for gamma-emitting radioisotopes, whole-body, 17: 35432
analysis of residents of northern Alaska for cesium-137 content, whole-body counting, 17: 35329(R) (HW-76000(p.239-43))
analysis of, shielded room for whole-body radiometric, 17: 33643
analysis of, shielded room for whole-body radiometric, 17: 33644
analysis of tissues for trace elements, emission spectrography, 17: 17720
analysis of tissues from, for radioisotope contamination, radiometric, 17: 37023(T) (JPRS-20988)
analysis of urine of, for cesium-137, method for, 18: 13667
analysis of, design of whole-body counter for, radiometric, 19: 22802
analysis of, for trace elements in organs and tissues of, outside continental U. S., 19: 21831
analysis of, for whole-body content of cesium-137, iodine-131, and potassium-40, 18: 29975(R) (COO-119-229(p.186-98))
analysis of, radiometric, 19: 2707 (BNL-8432)
analysis of, whole-body radiometric, 19: 9501
anatomical characteristics affecting geometries in whole-body counting, 16: 16138
anomalies of, role of genetic factors in congenital, 20: 6841
anomalies of, role of radiation in congenital, 20: 6841
antigenicity of cell-free spleen extracts from, 20: 45483
arsenic-72 dosimetry in, calculation of, 17: 5735
atomic-bomb effects on, latent, 19: 10846
barium content in bones and diet, 16: 23370 (AERE-R-4035)
barium-133 metabolism in, 20: 18226
benign tumor of, after administration of thorotrast, 17: 28604
beryllium content in postmortem lungs of, 17: 33513
beryllium disease in, diagnosis and symptomatology of, 17: 38730
beryllium toxicity in, clinical picture of, 17: 10313
biochemical changes in athletes from malt extract, 16: 26666(T) (JPRS-13555)
biogenesis and metabolism of aldosterone in elderly, tracer study on, 20: 38547(R) (NYO-918-15)
biological effects of magnetic fields, 17: 28
biological effects of radiation on, 18: 8233
biological factors affecting maximum permissible body burdens of radioisotopes in, 18: 15908
biological half life of cesium in acute and chronic exposure in, calculation of, 18: 31
bismuth nephrotoxicity in, 17: 38720
blood circulation in lungs and heart in, tracer studies of, 18: 11848(R) (UCLA-520(p.53-74))
blood circulation in, effects of anesthesia on, tracer study, 19: 36160
blood circulation in, measurement using nuclear image amplifier with technetium-99m and xenon-133, 20: 3802 (ORNL-IIC-5, pp 239-42)
blood flow measurements in, tracer measurement of, 18: 38768
blood irradiation, extracorporeal method for, 18: 29459
blood platelets of, method for preserving, 19: 43638(R) (TID-22130)
blood serum complement fixation by *Paramecium caudatum* cultures used as antigen, 19: 27973
blood volume distribution in, tracer study, 20: 6987
blood, chemical composition of, 17: 19787 (AERE-R-4196)
body burden from rare earths in, method based on excreta measurements for determining, 19: 26617
body burden of radioisotopes in, conference on evaluation of, 19: 46
body composition chronologic change in, analysis by potassium content, 19: 6976
body composition in, use of radioisotopes in determining, 19: 25891
body composition of, determined by whole-body counting of potassium-40, 19: 56
body fluids measurements in, tracer methods, 19: 43898
body mass of, potassium-40 measurement of lean, 20: 6694(R) (MIT-952-2)
body water content of, determination by tritium tracer method, 18: 1351
body water measurements using tritium, 19: 19480
body weight and organ weight of, in India, 19: 42229 (AEET/HP/Th-21)
body weight norms in Indian, use in establishing standards for radiation dosimetry, 20: 20374
body weight relative to motor aptitude in, use of liquid scintillation counting in, 18: 31078
bone marrow content measurements, tracer method, 16: 16107
bone marrow distribution in, effects of erythropoietic stimulation on, tracer study using radioiron, 18: 21766(R) (UCRL-11184(p.6-19))
bone marrow regeneration in, 18: 33216
bone marrow regeneration in, cytology of, 20: 3789
bone marrow proliferation in, time parameters of, 20: 42705 (BNL-10405)
bone marrow transplantation in, method for irradiation of lymph system for preparation of, 17: 21480
bone marrow transplants in, therapy for radiation sickness, 18: 17667
bone marrow transplants in, effectiveness against leukemia of, 19: 13141
bone marrow transplantation in identical twin, 19: 21802
bone marrow transplants in, therapeutic use of, 20: 8525
bone marrow transplants in, effects of immunosuppressive agents on, 20: 8525
bone marrow viability in, poststorage techniques for preserving, 18: 19526
book: *Background Irradiation of the Human Body*, 16: 17442(T) (JPRS-13288)
book: *Effects of Atomic Explosions on Man*, in German, 16: 5124
book: *Radiation and Health*, 17: 5906
book: *Radiation Hygiene. Vol. II. Public Health*, 18: 16252
book: *Radiation Protection Practice. Part I. Fundamentals*, in German, 18: 20274
book: *Radioactive Fallout, Soils, Plants, Foods, Man*, 19: 26619
boron metabolism in, 19: 24245
brain tumor radiotherapy in, using proton beam Bragg peak, 18: 3668
breath analysis for carbon-14, design of equipment for, 19: 32041
bromide space and body fluids in, determination after intravenous administration of bromine-82, 18: 1356
bronchial asthma in, tracer study of, 17: 33497
cadmium metabolism, physiological effects, and biological specificity in, 17: 38704 (BNL-7252)
calcium absorption by intestine of, tracer study, 19: 12935
calcium content in urine of, evidence for existence of nonexchangeable, 19: 14996
calcium content of bone of, 19: 40781(R) (NP-15179)
calcium excretion in urine of, relation to calcium/strontium ratio in diet, 19: 52
calcium levels in, metabolic factors in, 18: 38752

calcium metabolism in bone, tracer study, 17: 5742
calcium metabolism, relation of strontium metabolism, tracer study, 17: 30262
calcium metabolism in, during radiotherapy for cancer, 17: 40502
calcium metabolism in, 18: 11576(T) (AEC-tr-6331)
calcium metabolism in, 18: 29215
calcium metabolism in, tracer studies of, 18: 33277 (ST1/DOC/10/28 (p.21-38))
calcium metabolism in, tracer study on effects of exercise on, 19: 25862
calcium metabolism in, tracer studies, 19: 31701(R) (COO-587-2)
calcium metabolism in, double tracer method for analyzing, 19: 46138
calcium metabolism in, effects of strontium-85 injection on, 20: 32
calcium metabolism in, 20: 24829(R) (NEIC-RR-17)
calcium metabolism by, tracer studies of effects of thyroid disorders on, 20: 31142
calcium metabolism in bones of, using radioisotope tracers and whole-body counters, 20: 42764
calcium metabolism in, mathematical model for, 20: 5260
calcium metabolism kinetics, computer study, 17: 23032 (BNL-6208)
calcium retention by infant, 17: 23063
calcium sorption by kidneys of, discrimination in, 17: 19760
calcium sorption from gastrointestinal tract in, isotopic method for measuring, 19: 35901
calcium–strontium metabolic relations in, 17: 35426
calcium turnover in, method for measuring, 18: 13416 (CONF-355-4)
calcium-40 and -47 metabolism in, 19: 35911
calcium-45 metabolism by bones, effects of disease on, 19: 13149
calcium-45 metabolism in, 18: 25
calcium-45 secretion in saliva of, 19: 17479
calcium-45 sorption in, method for determining, 18: 4978
calcium-45 turnover time and excretion by, 18: 29214
calcium-45 uptake by respiratory tract in, combined thallium-204 and, 20: 10546
calcium-47 content in blood serum and saliva after intravenous administration, 19: 21846
calcium-47 metabolism in, whole-body counters for measuring, 19: 15295
calcium-47 metabolism in, kinetics of, 20: 5260
calcium-47 metabolism in, 20: 18226
calcium-47 sorption in, effects of vitamin D on, 19: 10757
calcium-47 uptake by, liquid scintillation measurement of, 18: 23226
cancer in, radiological and clinical statistics for, 19: 45921
cancer susceptibility as function of age, epidemiology of, 19: 38364
carbohydrate metabolism in, computer analysis of tracer results, 19: 5603 (BNL-8641)
carbon-14 content in, following atmospheric atomic explosions, (E), 19: 24709
carbon-14 content in blood of Norwegian, 19: 32483
carbon-14 distribution in plasma lipids of, 19: 27936
carbon-14 uptake from atmosphere by tissues of, 19: 3882
carbon-14-labeled diethylstilbenediol metabolism in, 19: 45797
carcinogenesis susceptibility, age differences in, 16: 7430
carcinogenic effects of thorium dioxide in, 17: 17873
carcinogenic effects of radiation in, mechanism of, 19: 7226
carcinoma and sarcoma development in, with radiodermatitis, 19: 167
carcinoma development in mastoid and paranasal sinuses in radium-bearing, 19: 7035
carcinoma development following radiotherapy of laryngeal papillomatosis in juvenile, 20: 43023
carcinoma of cervix of, radiation response as therapeutic indicator in stage I of, 19: 9043
carcinoma of liver induced by Thorotrast in, 19: 24266
carcinoma radioinduction in, 20: 41207
cesium and rubidium content in tissues of, determination of, by activation analysis, 20: 46030(R) (AERE-PR-HPM-9, pp 6-17)
cesium content in, 19: 40781(R) (NP-15179)
cesium content in bone, muscle, and soft tissue of, 17: 15603
cesium metabolism, 16: 25157
cesium metabolism, 18: 11588
cesium metabolism in, 18: 35300
cesium metabolism by, tracer studies of, 18: 43176(R) (LA-3132-MS (p.49-58))
cesium metabolism in, tracer study, 20: 23808(R) (NIRS-4, pp 3-12)
cesium metabolism in, comparison with other mammals, 20: 42768
cesium metabolism by, effects of age on, 20: 6719(R) (ORNL-3849, pp 183-213)
cesium retention, 16: 1319(R) (LAMS-2627(p.163-74))
cesium uptake and release by erythrocytes in, 18: 27043
cesium-134 occurrence in Finnish and Swedish Lapps, 16: 31469
cesium-134 uptake by Alaskan, 17: 41067
cesium-137 content in New Mexico from 1956 to 1961, 16: 1328(R) (LAMS-2627(p.223-5))
cesium-137 content from 1956 to 1961, 16: 2861(R) (ANL-6398(p.41-2))
cesium-137 content in 1958 to 1961 in England, 16: 10330
cesium-137 content in Negro and white, Nashville, Tennessee, 16: 27465(R) (NP-11928)
cesium-137 content in urine from, estimation of body burden from, 17: 16343
cesium-137 content in Alaskan, 17: 41066
cesium-137 content in muscles in, in Tokyo, Dec. 1961 to Nov. 1962, 18: 4983
cesium-137 excretion and retention by, 17: 24857
cesium-137 levels in, 18: 3614
cesium-137 retention in bones of adults and children, 17: 40503
cesium-137 uptake by, under natural conditions, 17: 16304
cesium-137 uptake and excretion by, 18: 3473
cesium-137 uptake by, route of, 18: 3613
cesium-131 metabolism in, 19: 38502
cesium-131 metabolism in, 19: 38503
cesium-131 secretion in saliva of, as compared to potassium-39, 19: 19486
cesium-132 distribution in, 19: 27(R) (HW-81746(p.2.16-18))
cesium-132 distribution and excretion, 20: 30988
cesium-132 retention in, after intravenous administration, 18: 15764(R) (LAMS-3034(p.21-33))
cesium-132 retention in, whole-body, 18: 29198 (LADC-5937)
cesium-133, cesium-137, and potassium contents in brain and muscle tissues, 18: 21790
cesium-134 and -137 content in, 19: 20225
cesium-134 and sodium-22 content in, 20: 8980(R) (BNWL-36, pp 3.1-122)
cesium-134 content in, in Alaska and Washington, 1962–63, 19: 22535 (HW-SA-3487)
cesium-137 and strontium-90 contents of bones and tissues in, in Finland, 20: 31142
cesium-137 biological half life in, 18: 15774(R) (LAMS-3034(p.184-6))
cesium-137 body burdens in Oslo, Norway, 1963 and 1964, effects of milk consumption on, 19: 6980
cesium-137 body burden of, in Toronto, 20: 5671
cesium-137 body burden in Norwegian school children, 20: 35708
cesium-137 body burden of Eskimos, 20: 37042
cesium-137 body burden, relation to dietary intake and excretion, 20: 42794
cesium-137 body burdens in Alaskan Eskimo, 1965, 20: 45314
cesium-137 contamination in, body burdens for accidental, 19: 25899
cesium-137 contamination of, accidental, 19: 26604
cesium-137 contamination in diet of, 20: 521(R) (HASL-164)
cesium-137 content in Finnish Lapps, 1961, effects of diet on, 18: 14149
cesium-137 content of, in southern Finland, 1961 to 1964, 18: 25687 (NP-13981)
cesium-137 content in Finnish Lapps, 1964, 18: 25710 (NP-13984)
cesium-137 content of muscles in, 18: 31316
cesium-137 content of urine in, 18: 33805(R) (NIRS-2(p.57-67))
cesium-137 content from fallout in, 1962 to 1964, 18: 37457
cesium-137 content in, at Hanford, 18: 36920 (HW-82409)
cesium-137 content in Eskimos, 1964, 18: 43799 (HW-SA-3688)
cesium-137 content of, New Mexico, 1963 and 1964, 18: 43833(R) (LA-3132-MS(p.153-69))
cesium-137 content of Arctic, 18: 43329
cesium-137 content of, in Germany, 1963, 19: 2036
cesium-137 content and half life in, after accidental exposure, 19: 3857
cesium-137 content in Canadian Eskimos, 1964, 19: 11417 (NP-14670)
cesium-137 content in Alaskan natives, 19: 13625 (HW-SA-3392)
cesium-137 content in, 1960–1964, 19: 15806
cesium-137 content in, 1955 to 1964, 19: 22533(R) (ANL-6839(p.79-84))
cesium-137 content in Alaskan Eskimo hair, relation of body burden to, 19: 22619
cesium-137 content in, from fallout, 19: 26604
cesium-137 content in normal German, 19: 26606
cesium-137 content from accidental exposure and fallout in Italian, whole-body measurements on, 19: 26607
cesium-137 content from fallout in Swedish, from 1961–1963, 19: 26608
cesium-137 content of, whole-body liquid-scintillation measurement of, 19: 28600
cesium-137 content of, 19: 34372
cesium-137 content in, from fallout in West Cumberland, England, 19: 34418
cesium-137 content in, indirect determination of, 19: 35922
cesium-137 content in, in Norway, 1963 and 1964, 19: 36652 (NYO-3364-3)
cesium-137 content in blood of, method for determining, 19: 38349
cesium-137 content of Alaskan, whole-body, 19: 40780 (BNWL-SA-242)
cesium-137 content of, relation to blood content, 19: 40781(R) (NP-15179)
cesium-137 content in, blood analysis determination of, 19: 40309(R) (NP-15180)
cesium-137 content in, in Switzerland, 1963, 19: 44269
cesium-137 content of, whole-body, 19: 46612

cesium-137 content in, in Ottawa, Canada, April 1965, 20: 7308 (NP-15642, pp 3-12)
cesium-137 content in Alaskan, seasonal variations in, 20: 9166(R) (BNWL-36, pp 2.1-58)
cesium-137 content in hair of, 20: 8506 (CONF-727, pp 21-4)
cesium-137 content in urine of, in northern Canada, 1965, 20: 9175 (NP-15763, pp 3-12)
cesium-137 content in Eskimo, measurement using unshielded body counters, 20: 9266
cesium-137 content in, from fallout, 20: 6714
cesium-137 content in, in South Australia, 20: 6754
cesium-137 content in Alaskan, whole-body, 1965, 20: 10723
cesium-137 content in Alaskan, 20: 12983
cesium-137 content of, in Norway, 20: 14739 (TID-22655)
cesium-137 content in urine of, Japan, 1964, 20: 16731 (NP-15883)
cesium-137 content of, whole-body, 20: 16303(R) (AD-626384)
cesium-137 content in, September 1962 to August 1963, 20: 18961
cesium-137 content in U. S., 1965, 20: 18973
cesium-137 content in, 1956 to 1965 whole-body, 20: 18203(R) (LA-3432, pp 21-55)
cesium-137 content in, 20: 18220
cesium-137 content in, effects of age and diet on, 20: 18233
cesium-137 content in, effects of diet on, 20: 18234
cesium-137 content in, in Alaska, whole-body, 1964, 20: 10718(R) (BNWL-122, pp 172-5)
cesium-137 content in Alaskan Eskimos, effects of diet on, 20: 23283 (BNWL-SA-556)
cesium-137 content in Canadian, 1960 to 1964, 20: 23390
cesium-137 content in Japanese, 20: 25321 (NP-16036)
cesium-137 content in Alaskan, Finnish, and Russian, 1962–1965, 20: 26599(R) (NP-16002, Paper 3)
cesium-137 content in Finnish, 1962, 20: 26605(R) (NP-16002, Paper 9)
cesium-137 content in Norwegian, 1962 through 1965, 20: 29432
cesium-137 content in Finnish Lapps, 1966, 20: 31444 (CONF-660405-15)
cesium-137 content in, effects of diet on, 20: 31442 (BNWL-SA-661)
cesium-137 content in Japanese, 1964, 20: 33574
cesium-137 content in, effects of diet on, 20: 33587
cesium-137 content in Alaskan Eskimos, 1965, 20: 33593
cesium-137 content in, Saclay Center of Nuclear Studies, France, March 1962 to February 1966, 20: 35348
cesium-137 content in India, 1962 through 1965, 20: 39154
cesium-137 content in Sweden, correlation with content in reindeer meat, 20: 42736
cesium-137 content in bones in, Moscow, 1961 to 1964, 20: 42741 (NP-16265)
cesium-137 content in Chicago, Ill., 1965, 20: 43512(R) (ANL-7136, pp 315-27)
cesium-137 content, whole-body counting of, 17: 5672(R) (LAMS-2780(p.130-80))
cesium-137 content in, spectrometric determination of, 19: 18270
cesium-137 content of, in England, 16: 28736
cesium-137 content in, correlation with fallout rate and ground deposition, 19: 11426
cesium-137 distribution and excretion in, 18: 43213
cesium-137 distribution in tissues of, 20: 24845
cesium-137 distribution in, 20: 31142
cesium-137 excretion by, effects of Prussian Blue on biological half life, 20: 38557
cesium-137 excretion, effects of potassium intake, 16: 16152
cesium-137 fallout content in adults, children, and pregnant women, 20: 46031(R) (AERE-PR-HPM-9, pp 17-26)
cesium-137 half life in, 20: 521(R) (HASL-164)
cesium-137 metabolism by, 19: 8737 (BNL-8657)
cesium-137 metabolism in, 19: 15223
cesium-137 metabolism in dystrophic, normal, and pregnant, enriched uranium oxides, 20: 45284 (K-C-822)
cesium-137 pathological effects in, deposited, 19: 35945 (NP-15184)
cesium-137 retention in, as function of time, 19: 8755
cesium-137 retention and excretion in accidentally exposed, 19: 25896
cesium-137 retention and distribution in, half life for, 19: 25897
cesium-137 uptake from eating reindeer meat, 19: 19(R) (HW-81746 (p.2.4-5))
cesium-137 uptake by, from reindeer, 20: 12578
cesium-137 uptake by, hazards from, 20: 22795
cesium-137 uptake and distribution from ingested marine animals, 20: 35682
cesium-137 uptake from fallout by lungs of, 19: 3856
cesium-137 uptake, distribution, gross metabolism, and transfer in, 19: 25894
chemical composition of, 19: 63
chest x rays of, modification of film size for, 17: 27610
chromium content in organs and tissues of, 19: 14955 (CEA-R-2585)
chromium-51 metabolism and fecal excretion by, after oral administration, 20: 12612
chromosomal diseases in, role of heredity and radiation exposure in, 18: 33336
chromosome aberrations in, relation between pathological conditions and, 16: 25181(R) (TID-16317)
chromosome analysis of thyroid tumors in, 19: 21903
chromosome analysis in, 19: 29884 (ACRH-103(p.37-47))
chromosome analysis using computer, 19: 38302(R) (TID-21641)
chromosome anomalies in, relation to mongolism and leukemia, 17: 40634
chromosome constrictions in secondary, 18: 1330
chromosome cytology of, review on, 17: 24835
chromosome morphology in leukemia patients, 19: 33806
chromosome patterns in mongols, 19: 45915
chromosome patterns in leukemia, 19: 45915
chromosome patterns of, 20: 94
chromosome preparation from, semi-automatic system for, analysis, 20: 40497(R) (NYO-3400-1)
chromosome replication in females, tracer study, 19: 15150
chronic radiodermatitis in, induction of, by low-level soft x radiation exposure, 18: 27151
circulatory diseases, effects of vasoconstrictor drugs in, 19: 26164
compatibility with spacecraft materials, 20: 4312
congenital malformations in children born in Alberta, 1961, 19: 21895
contamination by accidental exposure to sulfur-35, body-burden and treatment in, 17: 36053
contamination by polonium-210, monitoring case of internal, 18: 8583
contamination by plutonium, medical treatment for, 19: 36129
contamination by strontium-90 titanate, body burden for internal, 19: 26613
contamination with polonium-210, 19: 705
content of cesium-137 in, 20: 7335
content of cesium-137 in normal, 20: 6694(R) (MIT-952-2)
content of cesium-137, iodine-131, strontium-89, and strontium-90 in U. S., 1965, 20: 38743
content of orally injested radium and thorium in, 20: 6694(R) (MIT-952-2)
content of thorium-232 daughters in Thorotrast-injected, 20: 5237(R) (UR-668, pp 55-109)
contents and distribution of 24 trace elements in tissues, 17: 17721
copper metabolism in, 18: 35280 (TID-7678(p.581-606))
copper metabolism in, effects of Wilson's disease, tracer study, 19: 33754
cortical bone, composition of, 17: 7763
cosmic radiation effects on, in high-altitude aircraft, 20: 2657 (NASA-SP-71, pp 287-99)
counting one, two, and three γ-emitting isotopes in, 20: 22933
cystinuria etiology in, 19: 10696 (TID-20342)
cytology of blood formation in bone marrow, 20: 35200
dental survey of children of Hiroshima and Nagasaki, 19: 24228
deposition of inhaled cobalt-60 oxide particles in, determined by whole-body counting, 20: 7332
deposition of particles in lungs of, tracer study, 20: 46031(R) (AERE-PR-HPM-9, pp 17-26)
determination of daughter products of radon and thoron in, following alpha radiotherapy, 20: 38775
diabetes in, tracer methods for diagnosis and evaluation of, 18: 35424 (TID-7678(p.473-95))
diabetes incidence in Hiroshima and Nagasaki, 19: 15199
diamine oxidase content of tissue during pregnancy, 19: 35950(R) (TID-22047)
diiodotyrosine and triiodothyronine metabolism by, tracer studies of, 20: 30965
diseases and life processes in, radiation in study of, 17: 19743 (TID-18468(p.1-126))
diseases in, role of trace elements in degenerative, 18: 23199 (BNL-828)
distribution of radium-226, radium-228, lead-210 and thorium-228 in radium painters, 20: 40621 (NYO-3086-5)
DNA-ase activity in urine of, 19: 28005
dosimeters for radiological, design and use of film-badge, 20: 45998
dust inhalation and recovery from lungs of, comparison of, 19: 3853
ecological effects of nuclear warfare on, 19: 19504 (RM-2801-PR)
ecology of, effects of nuclear warfare on, 19: 20199 (HI-388-RR(Pt.III))
effects of age on bone composition in, 18: 33276(R) (NYO-910-7)
effects of atomic bomb exposure on eyes of Japanese, 19: 13039
effects of beryllium on, 20: 42751
effects of beryllium on, 20: 42752
effects of beryllium on, 20: 42753
effects of biological stress on phosphatide content of blood plasma, 20: 36606(R) (NYO-1864-23)
effects of blast on, pathological, 20: 2083 (CEX-65.4)
effects of cell-free spleen extracts on immune reactions to skin grafts, 20: 45483
effects of cesium-137 on, after single exposure, 18: 6687
effects of deposited radium-226 in, pathological, 19: 21813(R) (ANL-6839

(p.7-11))
effects of diabetes mellitus on blood vessels in retina and kidneys of, 18: 36924(R) (UCRL-11387(p.105-13))
effects of erythropoietin on hematopoietic system, 17: 28689(R) (UCRL-10683(p.44-53))
effects of fallout on, pathological, 20: 29407(T) (AEC-tr-6666)
effects of fish content in diet on content of cesium-137 in, 20: 45507
effects of individual differences on levels of stable elements resulting from environmental contamination, 17: 2788(R) (ORNL-3347(p.101-41))
effects of injected Thorotrast in, pathological, 19: 43738
effects of isogenic marrow infusion on recovery from idiopathic bone marrow failure, 19: 21803
effects of leukemia on metabolism of children, 20: 10545
effects of microwaves on, thermal, 20: 16235
effects of nuclear warfare on sociological behavior in, 20: 40738
effects of radiation, review, 17: 7884
effects of radioactivity in diet on carcinoma incidence in, 20: 38739
effects of radiodermatitis on content of cobalt, copper, nickel, and zinc in blood and skin, 20: 45309
effects of radioisotopes on, review on, 17: 14028
effects of radiosterilized food on, 20: 39302
effects of radium exposure on life span of, 18: 19551 (NYO-2762)
effects of radium deposited in, pathological, 19: 43830
effects of radium-226 on bone and joint changes in, long-term, 19: 17470
effects of shelter-centered civilian defense program on, 18: 39545
effects of space flight in, bibliography on biological, 19: 43718 (NASA-SP-7011(12))
effects of space flight in, bibliography on biological, 19: 43719 (NASA-SP-7011(13))
effects of space flight on, problems of environmental, 19: 45746
effects of space flight on, bibliography, 20: 56 (NASA-SP-7011(15))
effects of space flight on, 20: 16231 (UCRL-16377)
effects of space flight on, medical and physiological, 20: 32893 (AD-627686, pp 357-84)
effects of stress on monoamine dioxidase activity in blood, 18: 25086(R) (TID-20636)
effects of Thorotrast in, pathological, 20: 6735
effects of thyroid disease on calcium metabolism, tracer study, 19: 10748
effects of tritium in, 19: 33781
effects of tropical environment, 16: 14415
effects of work in betatron and cyclotron labs on blood picture of, 19: 20237
effects on space flight on, conference on environmental, 20: 24828
efficiency of preserved bone marrow transplants in stimulating blood formation in, 20: 36546
elimination of deposited radioactive materials from, treatment methods, 19: 15005
endocrine function in atomic bomb survivors, 20: 45254
environmental effects on, in spacecraft, 17: 36559
environmental requirements in space, 16: 20237
epidemiological studies of, 19: 29829(R) (ANL-6971(p.89))
epidemiological studies of, 20: 42700(R) (ANL-7136, pp 162-3)
epidemiology of leukemia in, review on, 19: 28034
epidemiology of New Jersey radium cases, 20: 20387(R) (NYO-2181-3)
error rate prediction for, in man-machine system, 18: 17358 (SC-R-685)
estrogen effects on liver function in, 19: 31668(R) (ACRH-23(p.158-69))
etiology of leukemia in children, 19: 33854
etiology of leukemia in, review of, 20: 45250
etiology of leukemia in, 20: 45367
excretion of β-aminoisobutyric acid, 20: 12545(R) (PAEC(A)AR651)
excretion of copper by, effects of diseases on, 20: 8568
excretion of manganese by, effects of diseases on, 20: 8568
excretion of urine by, use of creatinine as index of rate of, 20: 30983
explosion effects on, display system for studying atomic, 20: 1987 (UCRL-13139)
exposure to atmospheric tritium, formula for calculating maximum permissible, 20: 23371 (CONF-640413, pp 124-7)
eye burn damage from exoatmospheric nuclear explosion, calculation of, 18: 21875
fallout content in diet and excreta of Japanese, 19: 38894
fallout content in, from atomic explosions, 20: 9170 (CONF-765)
fallout decontamination by remote medical facilities of, 18: 29183
fallout distribution in tissues of, tracer study, 20: 46031(R) (AERE-PR-HPM-9, pp 17-26)
fallout effects on, 18: 37040
fallout hazards to, 17: 39345
fallout hazards to, from food, 18: 3605
fallout hazards to, 18: 3625
fallout hazards to, prediction of, 20: 16160 (UCRL-14739(Pt.2))
fallout metabolism in, 19: 15747 (ACRH-102)
fallout monitoring in, in England, 19: 24783
fallout particle retention by, estimation of, 19: 24726
fallout uptake, 18: 35260(R) (AERE-PR/HPM-5)
fallout uptake by, 18: 25693
fallout uptake by, real and simulated, 20: 20466
fat content of, measurement using krypton-85 as tracer, 19: 10775
fatty acid absorption from intestine of, tracer study, 19: 12916
fatty hydroperoxides in diet of, relation to atherosclerosis of aorta, 19: 26413
fission product aerosol concentrations for maximum permissible, 19: 689 (HW-SA-3550)
fission product deposition in lungs and pulmonary lymph nodes, 19: 9367 (IAEA-R-1)
fission product deposition in lungs and pulmonary lymph nodes of, 20: 31142
fission product metabolism, 8-year survey of Marshall Islanders exposed to local fallout, 17: 5699 (BNL-6503)
fission product permissible limits, 16: 25643 (CEA-2163)
fission product retention after inhalation of irradiated uranium, 19: 10749
fission product uptake and metabolism by, 19: 3834
flashblindness in, caused by nuclear weapons explosions, 19: 8806
fluorine-18 distribution in skeletons of living, positron camera determination of, 19: 31708(R) (UCRL-11833(p.100-11))
fluorine-18 metabolism in blood, bones, tissues, and urine in, 20: 27032
formulae for assessing body content of radiostrontium in adult, 20: 42779
gamma absorbed doses in, measurement of, 20: 26660(T) (JPRS-35011, pp 25-35)
gamma dose to, from fallout, 19: 38891
gamma doses from teletherapy, 16: 23399
gamma emission from chromium-51 and iron-54 in, method for measurement of, 17: 10271
gamma radiation dose from internally deposited radioisotopes in, 18: 13452(R) (TID-20219)
gamma spectrum from, computer code for analyzing, 20: 23335 (AD-621120)
gamma-globulin metabolism in, tracer study, 20: 10571
gamma-globulin metabolism in agammaglobulinemic, tracer study, 20: 10572
gastrointestinal transit time in, for ceramic spheres containing manganese-54 or uranium carbide particles, 20: 42740 (LA-DC-7764)
genetic data on, computer analysis, 19: 42653 (AECL-2222)
genetic effects of radiation, 16: 16225
genetic effects of atomic-bomb radiation on, in Japan, 17: 4381
genetic effects of small radiation doses on, 17: 19908
genetic factors, 17: 33459(R) (ANL-6723(p.140-1))
genetic factors affecting normal variation, 16: 11441(R) (ANL-6464 (p.75-6))
genetic factors associated with diseases of, 19: 33957
genetic factors in, 18: 8046(R) (NP-13507)
genetic factors in, identification of, 20: 12565
genetic studies of, 19: 38328
genetic studies on selected population of, 20: 26655(R) (NP-15975)
genetic study of hereditary defects in, 19: 10719 (AECL-2107)
glomerular filtration rate in, use of iodine-131-labeled Hypaque for determining, 19: 46071
glucose kinetics in, carbon-14 tracer technique for determining, 19: 31706(R) (UCRL-11833(p.34-49))
glyceride synthesis in obese and diabetic, 18: 31076
glycosuria incidence in Hiroshima and Nagasaki, 19: 15199
gold (colloidal) content in tissues of, 17: 33501
gold determination in serum and urine of, neutron activation method for, 18: 29598
gold-198 uptake by bone marrow in, whole-body counting and scanning of, 19: 19718
gold-198 uptake by lymph system, in lymphography of, 19: 19719
granulocytopoiesis time parameters for, 19: 17402 (BNL-7955)
gross body composition of, whole-body tracer study of effects of age on, 20: 22800(R) (NIRS-4, pp 73-7)
growth of pulmonary metastatic tumors in, 20: 43033
hazards from radioactive contamination of food and water, 16: 10340
hazards of dental radiography to, 17: 36077
hazards to, from eating fish contaminated with radioisotopes, 20: 29405 (NP-14694)
hazards to, from radioactive waste disposal, 20: 45942 (AECL-2478)
hazards to, from use of radioisotopes in aerospace and traditional contexts, 20: 46003
heart disease incidence in, relation of serum lipid and lipoprotein content to atherosclerosis and ischemic, 20: 20370 (UCRL-14658)
hematopoiesis in, tracer study, 19: 17404 (BNL-8819)
heme synthesis in aspirated bone marrow from, 19: 10774
Hodgkin's disease in, following Thorotrast administration, 17: 33750
human errors in man-machine systems, reduction of, 18: 21719 (SC-R-748)
hydrogen content in, neutron capture measurement of, 20: 30993
hydrogen content of, determined by whole-body counting, 20: 46031(R) (AERE-PR-HPM-9, 17-26)

hypertension in, effects of excess salt ingestion on, 18: 15668 (BNL-7787)
hypertension in, review on, 20: 10451 (BNL-8671)
hypertension induction in, effects of excess salt ingestion and genetic factors on, 18: 21702 (BNL-7971)
hyperthyroidism in, therapy in children, 20: 10738
immune reaction to radiation, 19: 8800(T) (NP-tr-1204)
immune reactions to kidney transplantation in, effects of immunosuppression with whole-body x radiation or chemicals, 18: 27019(R) (TID-20719)
immune reactions to bone marrow transplants in, 19: 8785 (EUR-1607.e)
immune reactions to rabbit papilloma virus in, 20: 6700(R) (ORNL-3853, pp 183-207)
immune reactions to transplanted bone marrow in, 20: 8522
impact effects, 16: 18731(R) (DASA-1245)
incidence and mechanism of autoimmunity in, following radiotherapy, 20: 33119
induction of aseptic meningitis in, subarachnoid injection of iodine-131-labeled human serum albumin, 20: 3843
injuries from atomic explosions, medical aspects of, 19: 13130
insulin metabolism in diabetic and normal, tracer study, 20: 20383 (CNEA-185)
intoxication by radioisotopes, problems in analysis of, 18: 8097
iodine isotopes in body and thyroid of, radiation exposure from, 19: 8756
iodine metabolism in adults and children, 17: 35405 (LADC-5794)
iodine metabolism in adults and children, 18: 15775(R) (LAMS-3034 (p.187-200))
iodine metabolism in, book, 18: 41295
iodine metabolism in thyroid during pregnancy, effects of sporadic goiter and thyrotoxicosis on, 19: 14959
iodine metabolism by, seasonal variations in, 19: 27922
iodine metabolism in, tracer study, 19: 45754 (CEA-R-2787)
iodine metabolism in children, 19: 45784
iodine metabolism in thyroid gland of, tracer study, 19: 45792
iodine metabolism in, tracer studies, 20: 3844
iodine metabolism in, mathematical model of, 20: 14249
iodine metabolism in, tracer study, 20: 14249
iodine metabolism in, mathematical model of, 20: 14250
iodine metabolism by, effects of age on, 20: 6719(R) (ORNL-3849, pp 183-213)
iodine-131 absorption by thyroid of, effects of exercise on, 18: 8081(T)
iodine-131 contamination through food chain, methods for preventing, 18: 8240
iodine-131 content in thyroid, 1958 to 1962, 16: 11401(R) (TID-15155)
iodine-131 content in, in Utah from 1962 fallout, 17: 31848
iodine-131 content in thyroid in adults, children, and fetuses in Michigan, 1959 to 1963, 17: 34145 (CONF-66-6)
iodine-131 deposition and behavior in environment of, 18: 8066
iodine-131 effects on chromosome anomalies of circulating leukocytes in, 17: 5836
iodine-131 excretion by, after therapeutic dose, 18: 3464
iodine-131 ingestion and inhalation by, comparison of doses from, 18: 8237
iodine-131 retention, 16: 1325(R) (LAMS-2627(p.204-12))
iodine-131 retention, 16: 1333(R) (LAMS-2627(p.270-9))
iodine-131 uptake, errors in whole-body counting techniques, 16: 1336(R) (LAMS-2627(p.291-7))
iodine-131 uptake and transfer in pregnant women, 17: 38703 (BNL-7177)
iodine-131 uptake by thyroid gland of, effects of physiological factors on, 18: 8083
iodine-131 uptake by, effects of sodium iodide on, 18: 8087
iodine-131 uptake and elimination, 18: 8088
iodine-125 and -131 metabolism in adults and children after ingestion, 18: 17456
iodine-125, -131, and -132 uptake by organs and whole-body in children, dose levels for, 19: 8779
iodine-131 concentration in breasts of lactating woman, 19: 36141
iodine-131 content of thyroid gland of, May 1962 to Jan. 1963, 18: 17454
iodine-131 content in skin and hair of, 18: 23207(T) (JPRS-24704 (p.6-11))
iodine-131 content in ovary and fetuses, after oral administration to pregnant women, 19: 10758
iodine-131 content in thyroid gland of children, effects of milk content on, 19: 22014 (HW-SA-3338)
iodine-131 content in, from fallout, 20: 6714
iodine-131 content of thyroid gland of, effects of age, diet, and environmental factors on, 20: 6748
iodine-131 content in thyroid gland and urine of, Japan, 1964, 20: 16730 (NP-15882)
iodine-131 content in thyroid in, activation studies on, 20: 38564
iodine-131 content, contribution of fallout to, 18: 18110
iodine-131 distribution in ovaries of, 18: 25120
iodine-131 distributions in, analog-computer analysis of, (E), 19: 13859 (HW-84448-10)
iodine-131 distribution in plasma lipids of, 19: 27936
iodine-131 metabolism by thyroid in, effects of adrenaline, 19: 21833
iodine-131 metabolism in, model for, 19: 24474
iodine-131 metabolism in thyroid of, effects of iodide depletion on, 19: 31726
iodine-131 metabolism following chronic ingestion, 19: 35905
iodine-131 metabolism in goiterous, age effects on, 19: 43691
iodine-131 metabolism in, effects of climatic temperature, 19: 45779
iodine-131 metabolism in fetuses of, 20: 1600
iodine-131 metabolism in thyroid of, measurements of, 20: 3660 (NP-15528)
iodine-131 metabolism in thyroid of, effects of 4-aminosalicylic acid on, 20: 32911
iodine-131 uptake by thyroid in, hypothermia effects on, 19: 12944
iodine-131 uptake and distribution in blood plasma, salivary-gastric secretions, thyroid, and urine in, effects of gastrointestinal cycle on, 19: 14983
iodine-131 uptake by blood plasma and saliva in, ratio of, in thyroid disease, 19: 14973
iodine-131 uptake by blood, blood plasma, and ovaries in, beta activity from, 19: 19483
iodine-131 uptake by thyroid in, Japanese survey on, 19: 22036
iodine-131 uptake by, 19: 24782
iodine-131 uptake by thyroid in, effects of thermal stress on, 19: 31721
iodine-131 uptake by thyroid in, from milk, 20: 8555(R) (TID-22448)
iodine-131 uptake by thyroid gland of, from milk, 20: 10530(R) (BNWL-122, pp 113-17)
iodine-131 uptake by, effects of food contamination on, 20: 18211(R) (UCLA-12-S76, pp 88-111)
iodine-131 uptake by thyroid gland of, effects of environmental contamination on, 20: 18941(R) (IDO-12047)
iodine-131 uptake by thyroid in, effects of potassium iodide on, 20: 40564
iodine-131 uptake from ingested milk by, 20: 5237(R) (UR-668, pp 55-109)
iodine-131 whole-body incorporation and retention in, inhibition of, 20: 10543
iodine-131-labeled insulin uptake by, 18: 17436
iodine-131-labeled growth hormone of, techniques for rapidly producing, 18: 23225
iodine-131-labeled somatotropic hormone metabolism in, with liver cirrhosis, 19: 6960
iodine-131-labeled iodide distribution in, 19: 10756
iodine-131-labeled haptoglobin excretion in urine of, 19: 39
iodine-131-labeled triiodothyronine uptake by, 19: 27934
iodine-131-labeled pharmaceuticals in, stability of, 19: 22022
iodine-131-uptake by thyroid of, fifteen minute test for, 18: 43203
iodine-131, -133, and -135 content in, after accidental exposure to fission product gases, 19: 4415
iodine-137 uptake by thyroid gland in adolescent and adult, 20: 38553
iodobenzoic acid metabolism in, tracer study, 20: 22557
ionic composition of intracellular medium in, determined by activation analysis, 20: 28871(R) (EUR-2636.f,i)
iron absorption by, tracer studies of effects of anemia and gastrectomy on, 18: 29223
iron metabolism by, tracer studies of, 18: 27044
iron metabolism in, tracer study using whole-body counting, 18: 36904 (UCRL-11019)
iron metabolism in, tracer studies using iron-59 and whole-body counting, 20: 169
iron metabolism in, tracer study of, 20: 6995
iron metabolism, tracer study, 17: 28687(R) (UCRL-10683(p.19-31))
iron metabolism, tracer study, 17: 28688(R) (UCRL-10683(p.32-7))
iron-59 absorption by, determination of, by whole-body counting, 17: 38702 (BNL-6822)
iron-59 uptake by, 16: 27465(R) (NP-11928)
iron-52 distribution in bone marrow in, use of positron scintillation camera for determining, 18: 29230
iron-55 content in blood of, 20: 153(R) (NYO-3086-1 Pt.X)
iron-55 content in, 20: 9166(R) (BNWL-36, pp 2.1-58)
iron-55 content in, in Alaska and Richland, Washington, 20: 9171 (CONF-650616-27)
iron-55 content of, effects of diet on, 19: 33778
iron-59 intestinal absorption, comparison of methods for measuring, 18: 25072
iron-59 uptake by bone marrow cells of, effects of anoxia on *in vitro*, 19: 14961
iron-59 uptake by gastrointestinal tract in, method for whole-body counting, 20: 35206
karyotype abnormalities in, genetic explanation of, 18: 27004(R) (ORNL-3601(p.47-59))

karyotype analysis of, automatic equipment and computer calculations for, 19: 24206 (LADC-6449)
karyotype of lymphocytes from, in tissue culture, 18: 36914(R) (UCRL-11387(p.165))
kidney transplantation in, 19: 19463
kidney transplantation in, clinical evaluation, 19: 19520
kidney transplantation from non-twin donors, case studies of, 18: 8130
kidney transplants from cadaver in, renograms of, 19: 5733
kidney transplants in, radioisotope function studies in, 19: 10947
krypton-85 and nitrous oxide uptake by brain of, 18: 19522
latent injuries in, surviving atomic bomb, 20: 45420
sarcoma, 18: 29229
lead-210 content in bones of, radiation dose rates from, 20: 14353
lead-210 content in bones of, with osteogenic sarcoma, 18: 29229
lead-210 excretion by, effect of EDTA on urinary, 17: 39317 (TID-19436)
lead-210/strontium-90 correlations in bones, 20: 42781
lead-212 content in lungs of, determination of, 20: 9198
lean body mass and total fat determinations for males and females at various ages, 18: 36940
leukemia development in, in Hiroshima and Nagasaki, 1946 to 1964, 20: 36645
leukemia etiology in, 19: 28067
leukemia etiology in, 19: 43828
leukemia etiology and treatment in, 19: 43840
leukemia in, frequency distribution of, 19: 24230
leukemia incidence in, exposed to radiation, 16: 26749
leukemia incidence and origin in, twin study of, 18: 29497
leukemia incidence in children, relation to diagnostic radiographic exposure, 18: 31125 (CEA-R-2320)
leukemia initiation in, 19: 24231
leukemia radioinduction in, 20: 41207
leukemia radiotherapy in, induced complications from, 17: 35397
leukemia treatment in, use of whole-body x irradiation and bone marrow transplants for, 20: 1700
leukemia treatment in, use of whole-body x irradiation and hematopoietic tissue transplants for, 20: 1701
leukocyte number in blood of, factors affecting, 20: 40612 (EUR-2711.f)
leukocytes of, method for preserving, 19: 43638(R) (TID-22130)
life span and disease incidence in children of Hiroshima exposed to radiation from atomic bomb, 18: 98
lipid content of brain in, effects of aging on, 18: 11574(R) (UCLA-520 (p.15-25))
lipid metabolism in leukocytes of, 19: 17429 (TID-20520)
lipid transfer in serum of, effects of low-density lipoproteins on, 19: 31710(R) (UCRL-11833(p.145-53))
lipid-lipoprotein content in serum of, sex differences in, 19: 31709(R) (UCRL-11833(p.134-44))
liver cirrhosis induced by Thorotrast in, 19: 19560
liver function in, effects of allergies on, tracer study, 19: 42379
lung cancer in, etiology of, review, 20: 45397
magnesium metabolism in, 18: 7993 (CONF-355-2)
magnesium metabolism in, tracer study, 19: 42243 (TID-21163)
magnetic field tolerance, 16: 12848
manganese metabolism and tissue distribution by, 18: 21763 (BNL-7940)
manganese metabolism, physiological effects, and biological specificity in, 17: 38704 (BNL-7252)
manganese-54 content in liver of, dietary route of, 19: 25859
mediastinal teratoma in atomic bomb survivor, 20: 33086
medical care of contaminated injured, after nuclear disaster, 17: 41020 (HW-SA-2859)
medical management of contaminated, after radiation accident, 19: 22637
mercury determination in blood of, activation analysis method for, 19: 31728
mercury-203 uptake by kidneys of, as localization technique, 18: 17692
mercury-203-Neohydrin metabolism in, 19: 13171
metabolism in skin of, 19: 29848 (ACRH-103(p.62-75))
metabolism in, carbon-14 tracer studies of, 19: 31776
metabolism in, tracer studies of, 18: 41021 (BNL-857)
metabolism of iodine-131-labeled triiodothyronine in thyroid in, factors affecting, 20: 36573
metabolism of iodine-131-labeled triolein in, as affected by age, 20: 42782
metabolism of isotopic drugs in, digital computer analysis of, 18: 36935
metabolism of radioiodine by, review of, 20: 45294
metabolism studies in, 19: 6948(R) (ORNL-3697(p.178-92))
metal content of brain of, relation to degenerative diseases, 17: 35419
microwave effects on, pathological, 20: 38622
microwave effects on blood serum proteins of, 20: 42876
microwave exposure criteria for, 19: 46706
mineral content of bones of, use of iodine-125 for measuring, 18: 31406
mineral content of, calcium, potassium, and strontium, 19: 13122(T) (JPRS-27535)
mineral content of teeth, effects of gold prosthetics on, 19: 43634 (NYO-3481-6)
mission in space, 17: 18354 (TID-7652(p.vii-xvii))
molecular weight determination of blood factors VIII and IX in, using electron irradiation, 18: 29233
molybdenum-99 content in blood, feces, and urine of, 18: 21800
mongolism in, as related to parents' history of radiation exposure, 20: 35196
monitoring for alpha sources, 18: 33819
monitoring for deposited radioactive materials, 16: 3189 (Y-1363)
monitoring of, for gamma radiation, design, construction, and performance of Winfrith whole-body monitor for, 17: 23543 (AEEW-R-215)
movement coordination system response in Parkinson syndrome patients, 16: 4610(R) (TID-14435)
mutagenesis in, 19: 43642(R) (NYO-2280-8)
mutations in, 19: 28062
mutations, chemically induced, 19: 36085
myxedema in, following x radiotherapy of laryngeal cancer, 20: 40780
natural selection rates in, effects of family planning on, 19: 31684(R) (UCRL-11833(p.29-33))
nerve grafts in, effects of radiation processing of graft material on take, 18: 9869
neutron dosages to, in supersonic flight in upper atmosphere, 18: 30399
neutron dose estimations in, fast, 18: 1487(R) (HW-77609(Sect.3))
neutron dose linear energy transfer in phantoms simulating, 18: 38725
reaction in hair for, 19: 18195 (LA-DC-6646)
neutron doses to, during criticality accident, use of sulfur-32 (n,p)
neutron dosimetry in, effects of tissue absorption, scattering, and moderation of, 20: 24946
neutron radiography of, 19: 22018 (BNL-8165)
neutron spectra in phantoms of, 19: 18269 (UCRL-11599(Rev.))
neutron tissue dose at large distances from source, 17: 23093 (UCRL-10559)
niobium content of, 19: 33724
niobium-95 uptake from fallout by lungs of, 19: 3856
nutrient absorption by intestine of, effects of hookworm infection on, 18: 21724(R) (TID-20404)
nutrition of, effects of vitamin A in foods on, 19: 17641
nutritional need and toxic effects of inorganic trace elements in, 19: 21990
nutritional requirements of diet for occupants of fallout shelters, 18: 27739
nutritional requirements of, whole-body tracer studies on, 18: 36940
offspring of Hiroshima bomb survivors, congenital abnormalities in, 16: 28837
oral cavity malignancies in, treatment with radiotherapy and surgery, 20: 45561
organ weight in, effects of age on, 19: 45755 (CEA-R-2809)
osteoid content of vertebral bones of, effects of age on, 20: 5233(R) (COO-119-232, pp 99-121)
osteomyelitis of jaws after radiotherapy of oral tumors, 18: 15860
osteoradionecrosis of lower jaw of, following radiotherapy in head region, 20: 45555
oxygen balance in, effects of cystamine and *S*-β-aminoethylisothiuronium on, 17: 31833
oxygen tension in tumors of, polarographic method for determining, 19: 27902
ozone effects on x-irradiated erythrocytes in, 18: 19538
parasitology research in, use of radioisotopes for, 18: 3437 (CEA-Bib-31)
parathyroid gland function in, with thyroid disease, effects of therapeutic doses of iodine-131 on, 18: 15926
pathological effects of radium dial paints on, epidemiological follow-up of, 17: 16342
pathological effects of deposited radium-226 and radium-228 in bones of, 18: 17474 (NYO-10604)
pathological effects of deposited radium in, 18: 19550 (NYO-2181-1)
pathological effects of injected Thorotrast in, delayed, 18: 25147
pathological effects of injected Thorotrast in, delayed, 18: 31208
pathological effects of deposited radium in, 19: 30013 (ACRH-103 (p.104-20))
pathological effects of deposited Thorotrast in, 19: 29913
pathological effects of gamma radiation in, 19: 31838
pathological effects of thermonuclear explosions on, 19: 33872
pathological effects of Thorotrast pyelography in, 19: 36086
pathological effects of Thorotrast in, 19: 45980
pathology of berylliosis in, 20: 11038
pathology of diabetes in, relation of content of chemical elements in blood serum to, 18: 15728 (UCRL-10873)
percutaneous absorption in, clinical significance of, 18: 33224
phosphatase content of leukocytes in, 19: 43829
phosphatide content and composition in blood, 20: 36606(R) (NYO-1864-23)
phospholipid analysis in tissues of, method for, 18: 17763

phosphorus retention in infant, 17: 23063
phosphorus-32 uptake and incorporation by erythrocytes in adults and erythroblastic and normal infants, 16: 12864
phosphorus-32 uptake by femoral head and trochanter in, 18: 5192
phosphorus-32 content of, coincidence arrangement of proportional counter and scintillator for *in vivo* determination, 19: 26(R) (HW-81746(p.2.12-16))
phosphorus-32 passage through blood-brain barrier in, during cerebral concussion of contusion, 18: 35293
phosphorus-32 uptake by erythrocytes of, *in vitro* studies of, 18: 43205
phosphorus-32 uptake and distribution in healthy mammary gland, 19: 14993
phosphorus-32 uptake by, from Columbia River fish, 20: 30969 (BNWL-SA-45)
photosensitivity of skin of, effects of furocoumarins on, 20: 18466
physiological age tests for, 20: 1587
physiology of, computer analysis of gamma spectroscopic data on, 19: 45771
physiology of, in space environment, research studies on, 19: 21812 (AEDC-TDR-63-256)
physiology, body composition, metabolism, and endocrinology in, 18: 27019(R) (TID-20719)
pituitary gland destruction in, use of yttrium-90 for, 19: 19660
placental site localization by isotopic placentography, 18: 29170
plastic clothing on, for physiological effects of, 19: 15778 (AECL-2123)
plutonium body burden assessment in, 18: 23825 (LADC-6104)
plutonium content in lungs of, design of chest phantom for determining, 19: 30473
plutonium distribution from fallout, 16: 25171
plutonium elimination by, effects of DTPA on, 18: 31109
plutonium excretion following skin contamination, 17: 37044
plutonium exposures of, evaluation of, 18: 132 (BNL-7041)
plutonium maximum permissible body burden for, 18: 432 (HW-67197)
plutonium metabolism in, mathematical models for, 18: 33267
plutonium metabolism and properties in, review on, 20: 14239 (JUL-312-ST)
plutonium poisoning in, evaluation and treatment of, 19: 26579 (RFP-446)
plutonium-239 content in, at Hanford, 18: 36920 (HW-82409)
plutonium-239 content in lungs of, proportional counters for determining, 19: 30584
plutonium-239 excretion by, effects of Pentacene on urinary, 18: 13431
plutonium-239 inhalation by, maximum permissible concentrations for bone, liver, and lungs from, 20: 26708 (AHSB(RP)R-69)
plutonium-239 metabolism by, after exposure by inhalation, 19: 3854
plutonium-239 retention and uptake by, computer study of, 19: 7209(R) (ORNL-3697(p.207-9))
plutonium-239 retention by, inhaled, 18: 33260
polonium contamination in, biological half life of, 20: 8539 (CONF-727, pp 32-8)
polonium-210 content in urine of, with and without exposure to radon-222, 18: 35289
polonium-210 content of, methods of measurement, 18: 43199
polonium-210 content in, (E), 20: 8572
polonium-210 content in urine of normal, 20: 31187
polonium-210 distribution and excretion by, 19: 2052
polonium-210 in cigarette smokers, evaluation of, 18: 41066
potassium content of human body, 17: 2799 (LADC-5446)
potassium content, total, 17: 17722
potassium content in, determination by whole-body counting for diagnosis, 18: 17709
potassium content of, determined by whole-body counting of potassium-40 in, 18: 27031 (AEEW-M-391)
potassium content and distribution in, 18: 43193
potassium content of, measurement by whole-body counting and isotope dilution, 19: 21816(R) (ANL-6839(p.63-78))
potassium content in, determined by whole-body counting of potassium-40, 20: 6743
potassium content of, based on whole-body counting of potassium-40, clinical applications of, 20: 6988
potassium content of, effects on incidence of muscular dystrophy and myotonia atrophica, 20: 6989
potassium content of, relation to age and sex, 20: 6749
potassium content of, effects of body composition on, 20: 6751
potassium content of, based on whole-body counting of potassium-40, 20: 6754
potassium content in Finnish Lapps, 1966, 20: 31444 (CONF-660405-15)
potassium content in bone, muscle, and soft tissue of, 17: 15603
potassium metabolism in, comparison with other mammals, 20: 42768
potassium uptake and release by erythrocytes in, 18: 27043
potassium-40 content in, whole-body water-shielded counter for, 18: 10427
potassium-40 content in, determination using liquid scintillation counters, 18: 31948
potassium-40 content in, whole-body counting, 19: 22533(R) (ANL-6839 (p.79-84))
potassium-40 content as basis for calculation of body cell mass in, 19: 29877
potassium-40 content in, relation to age and sex, 20: 6749
potassium-40 content of, effects of low-potassium diet, 20: 6752
potassium-40 content in, September 1962 to August 1963, 20: 18961
potassium-40 content in tissues of, internal radiation dose from, 20: 42940
potassium-40 content, whole-body counting of, 17: 5672(R) (LAMS-2780(p.130-80))
potassium-40 levels in, spectrometric measurement for, 19: 18270
potassium-40 uptake from fallout by lungs of, 19: 3856
potassium-42 distribution in, factors affecting, 18: 33238
potassium-42 measurement in, for calibrating potassium-40 gamma detection efficiency of whole-body counter, 20: 42739(R) (COO-1339-3)
proton beam dosimetry for, 19: 22593 (JINR-P-2008)
proton dosage to, in supersonic flight in upper atmosphere, 18: 30399
psychiatric behavior, relation to geophysical parameters, 19: 21942
pulmonary air-cleansing mechanisms for inhaled particles, 19: 3826
pulmonary deposition and clearance of particles, tracer study using whole-body counting, 16: 16149
pyretic effects of steroids in, 19: 31667(R) (ACRH-23(p.143-57))
radiant energy dose to, from radiodiagnosis, 20: 33099
radiation absorption by tissues of, gamma and x, 19: 13188
radiation absorption by, during diagnostic radiography, x, 20: 3816
radiation absorption by retina and choroid of eyes of, light, 20: 45401
radiation and alkylating agent effects on immunologic disorders in, hypothesis in, 19: 17507
radiation and heat therapy for cancer in, 17: 35363
radiation and skin diseases, solar, review of, 20: 40696
radiation and toxic chemical effects on alkaline phosphatase activity in granulocytes in, 19: 19570
radiation body burdens in, from fallout, 18: 31083 (HASL-147)
radiation burden from fallout and natural radioactivity, in Germany, 3rd quarter 1962, 18: 12357
radiation burden from iodine-131 in, effects of thyroid function on, 20: 36675
radiation burden from fallout, in West Germany, 20: 40570
radiation burden from fallout, in West Germany, 20: 43626
radiation burden to, from radioactive materials in environment, Federal Republic of Germany, 4th quarter, 1962, 18: 11898
radiation burden to, in Federal Republic of Germany, 3rd quarter, 1962, 18: 14091
radiation burden to, from radium-226 and strontium-90, 19: 26612
radiation burden to intestine of, from implanted radium, comparison of measurement methods for, 20: 45566
radiation contamination of diet of, fallout, 19: 2186
radiation counting, whole-body, 17: 1173(R) (HW-70050)
radiation damage, reliability of sex-ratio method for estimating, 16: 5218 (A/AC.82/G/L.671)
radiation damage to myocardium of, by lung tumor-therapy, 17: 28720
radiation death from accidental critical excursion, at Los Alamos, 17: 10874
radiation dosage for permissible internal, 16: 29251(T) (FTD-TT-62-668)
radiation dosage in diagnostic radiology, reduction of, 19: 46037
radiation dosage to, problems in reduction of diagnostic, 19: 46146
radiation dose absorbed by, during diagnostic radiography, x, 20: 5440
radiation dose appreciation in, methods of, 17: 37111
radiation dose arising from medical procedures, 16: 20211
radiation dose calculations for, from exposure to contaminated atmosphere, 18: 43331
radiation dose calculations for internally deposited gamma-emitting isotopes in, 19: 36161
radiation dose curves for various depths of tissue during radiotherapy, 20: 45564
radiation dose determinations in, following injections of iodine-131-labeled polyvinylpyrrolidone, 20: 3675
radiation dose estimations for internally-deposited radioisotopes in, 19: 22637
radiation dose for, maximum-permissible, 19: 24761
radiation dose for, maximum permissible, 18: 31828
radiation dose from internally-deposited radioisotopes, 16: 9822
radiation dose from radon-enriched air and water, 16: 30688
radiation dose from solar particle storms to shielded astronauts, 16: 14366
radiation dose from radiologic examinations for congenital heart disease, 16: 20890
radiation dose from inhaled radon, 17: 315
radiation dose from diagnostic radiology, 17: 6348
radiation dose from consumption of fallout-contaminated milk, 18: 6973

(NP-13432)
radiation dose from diagnostic radiography, effects of altering physical roentgenographic factors on, 19: 13155
radiation dose from fallout to, relation of nutrition to, 19: 18200
radiation dose from injestion of Clinch River fish and water, calculation of, 19: 31617(R) (ORNL-TM-1081)
radiation dose from neutrons, depth variation in, 19: 36035
radiation dose from fallout, 1954 to 1963, 19: 38861
radiation dose from nuclear rocket debris, external and internal, 19: 45655 (NUS-229)
radiation dose from diagnostic radiography, 19: 46112
radiation dose from chest x ray using portable equipment, 20: 8796
radiation dose from internally deposited strontium-90 in, effects on clinical findings, 20: 38623
radiation dose from internally deposited radium-226 in, effects on clinical findings, 20: 38623
radiation dose from inhaled or ingested iodine-131-methyl iodide in, 20: 41192(R) (IDO-12053)
radiation dose from ingested iodine-131 in milk by children, effects of season on, 20: 41192(R) (IDO-12053)
radiation dose from inhaled iodine-131 in, 20: 41192(R) (IDO-12053)
radiation dose from individual radionuclides in fallout, method of calculating, 20: 45891 (UCRL-14922)
radiation dose measurements following exposure to neutrons and gamma radiation from critical assembly, 16: 8653
radiation dose measurements for, during therapeutic radiography, 18: 17702
radiation dose measurements for, from diagnostic radiography, 20: 1703
radiation dose of adults and children from fallout, 1963, 18: 31771
radiation dose of, from external and internal contamination, 19: 22627
radiation dose of, from cosmic radiation, 20: 3731
radiation dose rates in Scotland localities, environmental gamma, 18: 35750
radiation dose to various parts of body from exposure to radioactive aerosol released in big reactor accident, 16: 22481
radiation dose to, during radiography, 17: 34159
radiation dose to gonads of, from radiology, 17: 36083
radiation dose to thyroid in, from passage of iodine-131 from contaminated forage through milk, 17: 35297(R) (HW-76000(p.60-2))
radiation dose to intestinal tract of, from ingested nonabsorbed beta particles, 18: 1968
radiation dose to, from ingested radioisotopes, 18: 6993 (OCD-OS-62-135)
radiation dose to children from radioisotope diagnostics, 18: 39006
radiation dose to various argons of, from reactor fission products, computer analysis of, 19: 3887 (CONF-642-8)
radiation dose to organs in, from iodine-131 incorporated in Tolpovidone, 19: 14987
radiation dose to skeleton of, from deposited radium-226, 19: 21814(R) (ANL-6839(p.18-39))
radiation dose to astronauts in space, computer codes for evaluation of absorbed, 19: 38014 (N64-29363)
radiation dose to organs in, formulas and methods for calculating, 19: 43853
radiation dose to gonads of children, during diagnostic radiography, 20: 3854
radiation dose to children, from radiographic diagnosis of congenital heart disease, 20: 5455
radiation dose to skeleton of, time variation of strontium-90, 20: 5429
radiation dose to gonads in, from benign tumor therapy during childhood, 20: 13013
radiation dose to thyroid of, from accidental iodine-131 release at nuclear facilities, 20: 18983
radiation dose to skeleton in, from strontium-90 content in river water, 20: 30943(R) (ORNL-TM-1465)
radiation dose to bones of, from strontium-90, maximum permissible body burden for, 20: 33100
radiation dose to children from diagnostics, reduction of, 20: 35683
radiation dose to skeleton of, from strontium isotopes, 20: 43605
radiation dose to respiratory tract of, from radon-220 and -222 decay products, 19: 4012
radiation dose to, from inhaled fission products, 19: 42670
radiation dose to, from ingested fission products, 19: 45755 (CEA-R-2809)
radiation dose to, from ingestion of water contaminated by fallout, 19: 46633 (AD-276187)
radiation dose to, from natural radioactivity, 19: 46688
radiation dose to, from contaminated foods, 20: 13000(R) (EUR-2520.f)
radiation dose to, from ingested radioactive materials, 20: 14794
radiation dose to, from ingested radioactive materials, 20: 14795
radiation dose to, from radionuclides released to Clinch River, 20: 22514 (ORNL-P-2021)
radiation dose to, during diagnostic radiography, x, 20: 22845
radiation dose to, from fluoroscope examinations, 20: 43050
radiation dose to, USSR maximum permissible, 16: 3280(T) (JPRS-9706(p.8-15))
radiation dose to, USSR maximum permissible, 16: 3281(T) (JPRS-9706(p.16-20))
radiation doses during diagnosis of, integral-absorbed, 19: 36135
radiation doses inside spacecraft, from solar-flare protons, 16: 30992
radiation doses to Mexican family exposed to unshielded 5-C cobalt-60 source for 4 months, 18: 18080
radiation doses to, from artificial and natural sources, (E), 19: 22015
radiation doses to, 1951 to 1960, evaluation of, 20: 11015
radiation doses to astronauts during ninth Mercury-Atlas mission, 20: 18942 (N-65-17115)
radiation doses to, from natural radioactivity, 20: 25335
radiation doses to, from cesium-137 deposition in Tokyo, 20: 35676
radiation doses to Eskimos ingesting cesium-137, 20: 43622
radiation doses to gonads of, from diagnostic radiography, calculation procedure for, 20: 43026
radiation dosimetry and scattering in, 16: 24026
radiation dosimetry of body tissues during space flight, 17: 14086
radiation dosimetry in, geometrical analysis of seated body for, 17: 35511
radiation dosimetry of Thorotrast cases, 18: 20340(R) (TID-20525)
radiation dosimetry in, analysis and sampling methods for assessing, 19: 30474
radiation dosimetry for, performance of cadmium sulfide detectors for intracavitary, 19: 36195
radiation dosimetry by beryllium-7 measurements in tissues of, proton, 19: 44327
radiation dosimetry in, using angle of incidence measurements, 20: 4207
radiation dosimetry in tissues in, use of stable isotopes in estimating, 20: 6725 (ORNL-P-1836)
radiation dosimetry of pelvic region, combined cobalt-60 teletherapy and radium γ, 20: 45515
radiation effects, 16: 5621
radiation effects combined with hematoporphyrin on glycolysis in cancer tissue on, 16: 25234
radiation effects of atomic explosion on growth of Hiroshima children, 16: 8544 (TID-14848)
radiation effects of nonionizing radiation, 16: 32727 (NP-12127)
radiation effects on heredity, investigations of areas of high natural radiation, 16: 2912
radiation effects on infant thyroids, from iodine-131 in milk, 16: 30691
radiation effects on, theory, 16: 30259
radiation effects, repeated low-level, 16: 2890 (AF-SAM-61-93)
radiation effects, high-level whole-body, 16: 8657
radiation effects, high-level whole-body, 16: 8659
radiation effects, 16: 6664
radiation effects on population from radioactive areas on small island, 16: 16173
radiation effects, calculation of LD_{50} from Hiroshima and Nagasaki data, 16: 17435 (A/AC.82/G/L.750)
radiation effects on chromosome aberrations in, whole-body fission neutron and gamma, 16: 17493
radiation effects on children, 16: 18798
radiation effects, review, 16: 20181
radiation effects, review, 16: 20261
radiation effects, 16: 22489
radiation effects on reproductive function of women, lower abdominal, 16: 20265
radiation effects on, genetic, 16: 23461
radiation effects on blood plasma proteins, 16: 23412 (CEA-2132)
radiation effects, 17: 12058(R) (BNL-742(p.87-120))
radiation effects, 17: 12134(T) (FRL-TN-90)
radiation effects, 17: 18369 (TID-7652(p.269-74))
radiation effects, biological, 17: 1667
radiation effects, biological, 17: 1681
radiation effects, biological, 17: 1279
radiation effects from radiological warfare, 17: 1673
radiation effects from whole-body exposure to doses of 400 to 450 rads in 8 hours, 17: 5874
radiation effects, genetic, 17: 39352
radiation effects of microwaves on, 17: 18449
radiation effects on, 17: 14066
radiation effects on, 17: 27151
radiation effects on amnion cells from, gamma, 17: 35574
radiation effects on blood serum of, 17: 2856
radiation effects on blood serum content of glucuronic acid in, 17: 7869
radiation effects on blood coagulation in, occupational, 17: 10446
radiation effects on blood vessels in kidneys in, 17: 23132
radiation effects on blood picture after mixed gamma and neutron exposure, 17: 23175
radiation effects on bone marrow cells in atomic bomb survivors,

17: 5785
radiation effects on brain in, electroencephalography of, 17: 35494
radiation effects on cerebral content of ATP, ADP, and AMP in, x, 17: 35563
radiation effects on cells of, protective effects of nucleosides against uv and x, 17: 40613
radiation effects on, chronic internal, 17: 27150
radiation effects on, cosmic, 17: 27196
radiation effects on developing nervous system, 17: 15638 (TID-18139)
radiation effects on deoxycytidine content in urine in, 17: 40681
radiation effects on, diagnosis and therapy of, 17: 4754
radiation effects on ear in, 17: 5834
radiation effects on embryos of, from radiography of pregnant females, 17: 35544
radiation effects on epitheliomas in, effects of cyclohexanol on recovery from, 17: 37132
radiation effects on erythrocytes in, 17: 27166
radiation effects on esophagitis in, therapeutic, 17: 10269
radiation effects on, exposed *in utero*, 17: 10875
radiation effects on fibrinolytic activity in lungs of, therapeutic, 17: 19854
radiation effects on, from fallout, 17: 28636
radiation effects on, from diagnostic and therapeutic application of radioisotopes, 17: 37121
radiation effects on, galactic, 17: 41712 (RM-3043-PR)
radiation effects on genetics in, 17: 20271
radiation effects on, genetic, 17: 39350
radiation effects on genetics of, 17: 38806
radiation effects on hair of, x, 17: 38791
radiation effects on, hereditary, 17: 14068
radiation effects on histology of intestines in, therapeutic, 17: 21560
radiation effects on, in space, 17: 5868
radiation effects on incidence of leukemia in, 17: 27210
radiation effects on iron metabolism in blood plasma and hemoglobin in, therapeutic, 17: 7870
radiation effects on kidney function in, early, 17: 27077
radiation effects on, late, 17: 18370 (TID-7652(p.275-90))
radiation effects on leukemia incidence in, 17: 15834
radiation effects on leukemia incidence in, diagnostic and therapeutic, 17: 21584
radiation effects on leukocyte chromosomes in, x, 17: 38792
radiation effects on liver function in, 17: 10464
radiation effects on, long-term somatic, 17: 14067
radiation effects on lung tissues, gamma, 17: 33692
radiation effects on metaphase/prophase ratio in, 17: 10411
radiation effects on microscopic structures of intestinal mucosa in, 17: 24990
radiation effects on motility of leukocytes in, during therapy, 17: 10445
radiation effects on mutations and somatic anomalies in, relation of dose to, 17: 15665
radiation effects on mucopolysaccharides in aortic wall in, 17: 24904
radiation effects on nephritis in, therapeutic, 17: 10440
radiation effects on osmotic resistance of leukocytes in, x, 17: 35584
radiation effects on, pathology of whole body, 17: 35573
radiation effects on peripheral blood in, therapeutic, 17: 7874
radiation effects on performance of, acute, 17: 18372 (TID-7652(p.343-74))
radiation effects on properdin level in, 17: 7818
radiation effects on, problems in diagnosis and treatment of, 17: 41062
radiation effects on, research on genetic, 17: 92
radiation effects on receptor apparatus of cutaneous and visual analyzers in, 17: 5851
radiation effects on, recording of statistics on somatic, 17: 12090
radiation effects on, review on, 17: 12159
radiation effects on rubidium-86 and sodium-22 excretion in, therapeutic, 17: 21445
radiation effects on secondary response to tetanus toxoid in, x, 17: 35530
radiation effects on serum complement in, x, 17: 37126
radiation effects on skin of, case study of beta, 17: 13904
radiation effects on skin of, energy dependence of x, 17: 37109
radiation effects on sodium metabolism in, gamma, 17: 33696
radiation effects on, statistics on dosage in, 17: 12092
radiation effects on thyroid gland cancer in children, therapeutic, 17: 10262
radiation effects on uranium miners and millers, mortality patterns in, 17: 41150
radiation effects, review, 17: 3196
radiation effects, review, 17: 15634 (TID-15964)
radiation effects, somatic, 17: 19870
radiation effects, somatic, 17: 23214 (TID-16981)
radiation effects therapy in, use of hemopoietic replacement for, 17: 35370
radiation effects on, analysis of, 17: 37107
radiation effects on skin and tumors of, combined actinomycin D and, 17: 28741
radiation effects on, space-flight, 17: 27115
radiation effects from atomic explosion on rate of stillbirths for pregnant women in Hiroshima, 18: 102
radiation effects from atomic explosion on rate of stillbirths for pregnant women in Hiroshima, 18: 103
radiation effects on brain of, after scalp epilation, x, 18: 136
radiation effects on, gamma, 18: 137
radiation effects on erythrocyte metabolism in, 18: 1419
radiation effects in, effects of dose rate on, 18: 1445
radiation effects on, review, 18: 3516
radiation effects on femoral neck bones in, 18: 3535
radiation effects on congenital anomalies in, theorem for, 18: 3506
radiation effects on, review, 18: 3632
radiation effects on morphology of bone marrow in, therapeutic dose, 18: 3656
radiation effects on hematological system in, long-term whole-body, 18: 6640
radiation effects on thyroid of, iodine-131 and x, 18: 8163
radiation effects on dermis, epidermis, scales, and serum proteins of skin of, uv, 18: 8168
radiation effects on, biological and genetic, 18: 8194
radiation effects on bone growth in children, therapeutic dose, 18: 8218
radiation effects on electric resistance of erythrocytes in, 18: 9874
radiation effects on reactivity of organs in, conference on, 18: 9882
radiation effects on blood pressure and pulse, occupational, 18: 9883
radiation effects on, 18: 9952
radiation effects on euploid cells in bone marrow of, radium-226 and strontium-90, 18: 11715
radiation effects on children, fallout vs. natural, 18: 11892
radiation effects on, from fallout radioisotopes, 18: 13396
radiation effects on blood clotting in, x, 18: 13486
radiation effects of fallout in, 18: 14133(T) (JPRS-23284)
radiation effects on leukocyte chromosomes in, x, 18: 15840
radiation effects on sodium ion flux in erythrocytes of, x, 18: 15873
radiation effects on embryos of, 18: 17542
radiation effects on functional changes of small intestine in, tracer studies of, 18: 17562
radiation effects of cosmic particles on, 18: 17596
radiation effects on, protective effects of Synkavite against, x, 18: 17687
radiation effects on lipid metabolism in bone marrow and white blood cells in, 18: 19552(R) (NYO-2769-1)
radiation effects on fertility of, after accidental exposure, 18: 19648
radiation effects on oral membranes in, x, 18: 19624
radiation effects on populations of, low-dose, 18: 19625
radiation effects on hematological response in, homogeneous *vs.* inhomogeneous, 18: 19584
radiation effects on bone marrow repopulation in, x, 18: 19592
radiation effects on bone marrow cytology in, gamma and neutron, 18: 19602
radiation effects on, therapy for, 18: 19763
radiation effects on, protective effects of bone marrow transplants against, 18: 19764
radiation effects on cells nuclei in, relative γ and x, 18: 19685
radiation effects on, protective effects of bone marrow against gamma, 18: 19769
radiation effects on somatic cells in, 18: 22297
radiation effects on, during space flights, 18: 21829(T) (FTD-TT-64-33)
radiation effects on lymphocytes of, x, 18: 23294
radiation effects on erythrocytes in, effects of monomer solutions on, 18: 23381
radiation effects on adrenal activity in, 18: 25104
radiation effects on skin of, 18: 25080 (AHSB(RP)R-39(p.11-19))
radiation effects on, 18: 25144
radiation effects on, physical aspects of, 18: 25145
radiation effects on blood picture in, 18: 25174
radiation effects on kidney transplant rejection in, 18: 27249
radiation effects on hematopoietic system in, 18: 27076
radiation effects on burns in, 18: 29404
radiation effects on, protective effects of bone marrow transplants against, gamma and x, 18: 29407
radiation effects on malignant cells of, protective effects of photoreactivation against, uv, 18: 29428
radiation effects on liver of, gamma, 18: 29540
radiation effects on spermatogenesis in, design of irradiation facility for study of neutron, 18: 29245 (TID-20783)
radiation effects on oxygen uptake by skin of, uv and x, 18: 29269
radiation effects on nervous system of, electroencephalographic study, 18: 29302
radiation effects on vision in, 18: 29323

radiation effects on behavior in, 18: 29324
radiation effects on blood coagulation in, 18: 31152
radiation effects on developing embryos and fetuses of, 18: 31217
radiation effects on kidney transplantation in, gamma, 18: 31226
radiation effects on electrophoretic distribution of blood serum proteins, 18: 33353
radiation effects on population of Niue Island in South Pacific, 18: 35382
radiation effects on, bibliography on, 18: 36948 (AD-438177)
radiation effects on, bibliography on, 18: 36949 (AD-438178)
radiation effects on, survey of, 18: 36985
radiation effects on nervous response to conditioned reflexes of, 18: 37016
radiation effects on genetics in, 18: 38818
radiation effects on bone marrow in, 18: 38823
radiation effects on developing nervous system in, review on, 18: 38845
radiation effects on liver and spleen in, Thorotrast, 18: 38846
radiation effects on brain of, 18: 38850
radiation effects on eyes of, x, 18: 41196
radiation effects on genetics of, 18: 41267
radiation effects on permeability of intestinal wall of, tracer study of, 18: 41151
radiation effects on iron absorption by intestine of, tracer study of, 18: 41152
radiation effects on, from chronic external radium exposure, 18: 43222(R) (MIT-952-1(p.1-112))
radiation effects on genetics of, medical, 19: 226
radiation effects on intestine in, 19: 137
radiation effects in, good and bad, 19: 2189
radiation effects on, in space vehicles, 19: 2190
radiation effects on, physiological, 19: 3894(R) (ORO-625(p.56-63))
radiation effects on chromosomes of embryonic fibroblasts from, gamma, 19: 3960
radiation effects on mitotic activity in fibroblasts of, gamma, 19: 3962
radiation effects on intestinal absorption of vitamin B_{12} in, 19: 5639
radiation effects on stomach function in, x, 19: 5715
radiation effects on cerebral cortex and protein metabolism in, 19: 2123
radiation effects on cytogenetics of, 19: 2067(R) (EUR-1893.i)
radiation effects on eosinophils in, x, 19: 2137
radiation effects on, epilation dose, 19: 2124
radiation effects on, mechanisms of, 19: 2084
radiation effects on, Thorotrast, 19: 2120
radiation effects on life span, calculation of, 19: 7207(R) (ORNL-3697 (p.199-202))
radiation effects on immune reactions in, 19: 7009 (AD-600299)
radiation effects on genetics of, review on, 19: 7050
radiation effects on, hematologic manifestations of, 19: 7136
radiation effects on sternal marrow regeneration in, dosage, 19: 7141
radiation effects on, review on background and occupational, 19: 7161
radiation effects on white blood cell count and tumor development in, small dose, 19: 7042
radiation effects on magnesium content of blood serum, 19: 8880
radiation effects on proliferation of stem-cells developed from lymphocytes in, 19: 8890
radiation effects on skin of, following breast radiotherapy, beta and x, 19: 8901
radiation effects on intracutaneous and intramuscular resorption of gold-198 and iodine-131 by, 19: 8918
radiation effects on lungs of, in mining and processing rare metal ores, 19: 8984
radiation effects on cytoplasmic budding in lymphocytes in, 19: 8821
radiation effects on peripheral blood in, occupational, 19: 8990
radiation effects on gonads in, 19: 8993
radiation effects on genetics of, diagnostic and therapeutic, 19: 8993
radiation effects on cancer development in, review on, 19: 10806
radiation effects on blood flow in skin of, telangiectasis development as repair sign in, 19: 10827
radiation effects on brain, pathological, 19: 10857
radiation effects on survival of cell cultures from, pulsed x, 19: 10876
radiation effects on aberrations in chromosomes of, diagnostic, 19: 10893
radiation effects on, effects of bone marrow transplants on, 19: 10901
radiation effects on genetics in, maximum permissible level for protection against, 19: 10927
radiation effects on metabolism in, whole-body gamma, 19: 12952 (DASA-1422)
radiation effects in, low-dose, 19: 12984
radiation effects on development and course of osteonecrosis of cranial vault in, long-term, 19: 12995
radiation effects on survival of transplanted kidney in, 19: 13034
radiation effects on degeneration in pelvic ganglia, cyclotron, 19: 13043
radiation effects on blood picture in, testing by parameters alpha and beta, 19: 13046
radiation effects on development of antibiotic-resistant intestinal bacteria in, 19: 13047
radiation effects on development of lung fibrosis and pneumonitis in, symptoms and treatment of, 19: 13050
radiation effects on, protective effects of bone marrow transplants against lethal, 19: 13095
radiation effects on urinary excretion of β-aminoisobutyric acid by, 19: 13007
radiation effects on absorption of iodine-131-labeled triolein in, x, 19: 15111
radiation effects on immune response to homologous bone marrow transfusions in, 19: 15114
radiation effects with 6-mercaptopurine on kidney transplants between unrelated persons, 19: 15147
radiation effects on urinary amino acid excretion by, accidental partial-body electron, 19: 15181
radiation effects in, whole-body exposure, 19: 15209
radiation effects on thyroid cancer development in, 19: 15065
radiation effects on brain in, following pituitary therapy, necrotic gamma, 19: 15071
radiation effects on life span of, review on, 19: 17514
radiation effects on nuclei in embryo cell cultures of, low dose, 19: 17611
radiation effects on proliferative capacity of cultured cells of, LET effects on RBE of alpha, 19: 17560
radiation effects on phagocytic activity of leukocytes in, 19: 19507(R) (TID-21712)
radiation effects on developing embryos, 19: 19466
radiation effects on genetics of, exposed as infants, 19: 19568
radiation effects on mechanical resistance of erythrocytes in, 19: 19595
radiation effects on healthy lung tissue in, after therapy of tumor, 19: 19683
radiation effects in, genetic and somatic, 19: 22071
radiation effects on electrical activity of, 19: 24293
radiation effects on gamma-globulins in, gamma and x, 19: 24355
radiation effects in, genetic and somatic, 19: 24757
radiation effects on, review, 19: 24366
radiation effects on, biological, 19: 25906(R) (ORINS-49(p.9-39))
radiation effects on intestinal bacteria in, alpha and gamma, 19: 26012
radiation effects on frontal white matter in brain of, gamma, 19: 26079
radiation effects on kidney cell cultures of, oxygen effects on alpha and x, 19: 26151
radiation effects on development of extraskeletal osteogenic sarcoma in, therapeutic, 19: 26169
radiation effects from radium-226 and -228 on, relation between biological response and internal dose, 19: 25900
radiation effects on electroretinographic response to partial retinal stimulation in, 19: 25915
radiation effects on ploidy in colchicine-treated leukocytes of, 19: 25953
radiation effects on eyes of, ultraviolet, 19: 25972
radiation effects on, research program of WHO on, 19: 25978
radiation effects on kidney cells from, sensitivity effects of heavy ions and iododeoxyuridine on x, 19: 26125
radiation effects on blood lysozyme activity, 19: 28101
radiation effects on brain functions and structure in prenatally irradiated, 19: 28109
radiation effects on, 19: 28110
radiation effects on heart blood circulation in angina pectoris patients, 19: 28180
radiation effects on gastric acid secretion in ulcer patients, 19: 27957
radiation effects on gastric acid secretion in ulcer patients, 19: 27958
radiation effects in, carcinogenic, 19: 27975
radiation effects on reproductive capabilities of women, 19: 27986
radiation effects on immune reactions to kidney transplants in, 19: 27987
radiation effects on mitosis in leukocytes of, beta, 19: 27993
radiation effects on immune reactions to kidney transplants, 19: 28012
radiation effects on ischemia-induced damage to kidney of, x, 19: 28064
radiation effects from yttrium-90 intracellular implantation on pituitary function in, 19: 30029
radiation effects on neonatal death rate, environmental, 19: 29829(R) (ANL-6971(p.89))
radiation effects from fallout exposure, 19: 29895 (BNL-908)
radiation effects on vertebral growth in, 19: 29920
radiation effects on antibody production in, 19: 29981
radiation effects on, pathological, 19: 29989
radiation effects on leukocyte chromosomes in, aberrant x, 19: 31792(R) (ORNL-3768(p.94-8))
radiation effects in, pathological, 19: 31865
radiation effects on genetics of, review on, 19: 31868
radiation effects from iodine-131 on leukocyte chromosome patterns, 19: 31884
radiation effects on immune reactions to kidney transplant, 19: 31956
radiation effects in, pathological, 19: 31962
radiation effects on immune reactions to organ transplants in, 19: 32026

radiation effects on leukocyte chromosomes in, aberrant Thorotrast, 19: 31671(R) (NIRS-3(p.57-63))
radiation effects in, review of late pathological, 19: 31804
radiation effects on life span of, 19: 33784 (ABCC-15-63)
radiation effects on leukocyte chromosomes in, x, 19: 33875
radiation effects on immune reactions to renal heterotransplants in, 19: 33808
radiation effects on chromosomes in, frequency and etiology of, 19: 33823
radiation effects on immune reactions to kidney transplants, 19: 33828
radiation effects on congenital malformations of infants, natural background, 19: 33853
radiation effects in, genetic, 19: 33867
radiation effects on respiratory tract of, from radon-220 and -222 inhalation, 19: 35979
radiation effects on Brazilian, background, 19: 36004
radiation effects on blood circulation in skin of, uv, 19: 36032
radiation effects on patch tests in, uv, 19: 36033
radiation effects on sexual behavior in, effects of dose on, 19: 36041
radiation effects on vestibular analyzers in occupationally exposed, x, 19: 36042
radiation effects on, effects of pyridoxal-5'-phosphate on, 19: 38461
radiation effects on nervous system of, 19: 40349 (BNL-9345)
radiation effects on immune reactions in, infrared, 19: 42283
radiation effects on thyroid in, latent x, 19: 42286
radiation effects on reticuloendothelial cells in, 19: 42296
radiation effects on cells of, from clinical and occupational exposures, 19: 42353
radiation effects on, chronic, x, 19: 42667
radiation effects on, correlation of animal studies with, 19: 43843
radiation effects on metabolites, use in exposure diagnosis, 19: 43852
radiation effects at low doses, review on, 19: 43752
radiation effects on, protective effects of erythropoiesis-stimulating preparation against, 19: 43872
radiation effects on, in space flight, 19: 46001
radiation effects in, genetic, 19: 45967
radiation effects in, genetic, 19: 45973
radiation effects on immune response to transplanted kidneys in, 19: 45888
radiation effects in skin of, ultraviolet, 19: 45907
radiation effects on granular and transitional cell layers in skin of, 19: 45913
radiation effects on intestine in, review, 19: 45922
radiation effects in, genetic, 19: 46695
radiation effects on chromosome pattern, 19: 45808(R) (NYO-901-36)
radiation effects on lifetime health and mortality patterns of, employed in nuclear energy installations, 19: 45810(R) (NYO-3394-2(Rev.))
radiation effects on, physiological, 19: 45815(R) (ORO-631, pp 67-76)
radiation effects on creatine excretion by, use as damage indicator, 19: 45864
radiation effects on central nervous system in, after radiotherapy of nasal cavity, 19: 45983
radiation effects on, diagnostic use of blood picture for determining, 20: 116
radiation effects in skin of, toxic effects of ultraviolet, 20: 74
radiation effects on vertebral column of, following childhood radiotherapy, 20: 1702
radiation effects on herpes zoster inflammations in, x, 20: 3836
radiation effects on chromosomes in, 20: 3705(R) (AD-617601)
radiation effects on, low-dose, x, 20: 3779
radiation effects on development of jaw bones, in children, 20: 3808
radiation effects in, low-level, 20: 3770
radiation effects on white blood cells during space flight, 20: 5297 (ORNL-P-1734)
radiation effects from internally deposited radioisotopes on, biological, 20: 6904
radiation effects on immune reactions to baboon kidney transplants in, 20: 6813
radiation effects on melanocyte populations in skin of, uv, 20: 6840
radiation effects on, pathological, 20: 6846
radiation effects on leukemia in, after extracorporeal exposure of blood and lymph, 20: 6926 (BNL-9726)
radiation effects on children, carcinogenic, 20: 8767
radiation effects on taste sensitivity of, x, 20: 8789
radiation effects on organs and tissues of, dose relations for x, 20: 8808
radiation effects on sodium uptake by erythrocytes from, factors affecting γ, 20: 8610
radiation effects on metabolism in skin, uv, 20: 8678
radiation effects on children, review, 20: 8680
radiation effects on chromosomes in genetically abnormal, x, 20: 8707
radiation effects on, environmental, 20: 8711
radiation effects on, from thermonuclear explosions, 20: 10701
radiation effects on creatine excretion by, 20: 12545(R) (PAEC(A)AR651)
radiation effects on blood picture in, 20: 10660
radiation effects on, 20: 12699
radiation effects on respiratory center of, x, 20: 12702
radiation effects on, leukemogenic, 20: 12707
radiation effects on, review, 20: 12708
radiation effects on growth of children of Marshall Islands exposed to fallout in 1954, 20: 13011
radiation effects on tooth structure, 20: 14323
radiation effects on, low-dose γ and x, 20: 14331
radiation effects on, at very low dose rates, 20: 14352
radiation effects on immune reaction to *Treponema pallidum* in, γ, 20: 14308
radiation effects on Japanese, medical survey of 10-year fallout, 20: 16226 (NP-15891)
radiation effects on morphology of erythrocytes in, x, 20: 16250
radiation effects on skin pigments in, uv, 20: 16261
radiation effects on bone marrow and granulocyte blood picture of, x, 20: 18381
radiation effects on, review, 20: 20367
radiation effects on DNA synthesis in embryonic cells from, x, 20: 18264
radiation effects on development of fetuses and babies of, diagnostic-radiography, 20: 18536
radiation effects on incidence of mongolism in children after parental exposure, 20: 20454
radiation effects on melanin patterns in, solar, 20: 20458
radiation effects on blood picture in Japanese, gamma and neutron, 20: 20481
radiation effects on testicular functions of, x, 20: 22617(R) (RLO-1780-1)
radiation effects on immune reactions to bone marrow transplants, 20: 22695
radiation effects on chromosome pattern of leukocytes of, 20: 22800(R) (NIRS-4, pp 73-7)
radiation effects on bone-marrow chromosomes of, 20: 22582
radiation effects on eyes of, laser, 20: 22628
radiation effects on fetal, 20: 22681
radiation effects on catheptic activity of leukocytes in, after low-dose exposure, 20: 24869
radiation effects on hematopoietic system of, pathological, 20: 26653 (EUR-2634.d)
radiation effects on, pathological x, 20: 26668
radiation effects on, 10-Mev electron, 20: 28929 (CONF-651109, pp 574-98)
radiation effects on blood picture in, nuclear explosion, 20: 28876
radiation effects on, from criticality accidents, γ and neutron, 20: 28970
radiation effects on, physiological, 20: 28974
radiation effects on blood coagulation in, review, 20: 28985
radiation effects on, review, 20: 29478
radiation effects on gonadal and gonadotropic hormones in, 20: 31034(R) (RLO-1780-7)
radiation effects on function and hormones in gonads of, 20: 31035(R) (RLO-1780-8)
radiation effects on tissue cultures from, protective effects of AET, serotonin, and streptomycin against gamma, 20: 31121
radiation effects on proliferation of leukocytes of, in culture, x, 20: 31067
radiation effects on live births among atomic bomb survivors, 20: 31091
radiation effects on creatine metabolism in, gamma and x, 20: 32931
radiation effects on skin of, variations of, with anatomic location and time, 20: 32971
radiation effects on pigment mosaics in skin on, cellular survival curve test for, 20: 32981
radiation effects on retinal blood vessels of, laser, 20: 35258
radiation effects on, review on protective effects of bone marrow grafts against whole-body, 20: 35325
radiation effects on brain function in, dose effects in, 20: 36651
radiation effects on thymine metabolism in, 20: 37025(R) (PG-Report-705)
radiation effects on function of basic cerebral nervous processes in, uv, 20: 36626
radiation effects on, protection against, 20: 38718
radiation effects on spermatogonia in, x, 20: 40627(R) (ORNL-3922, pp 84-8)
radiation effects on leukocytes from, uv, 20: 40581(R) (ORNL-3922, pp 50-1)
radiation effects on, following therapy, 20: 40659
radiation effects on pituitary function in, following nasopharyngeal carcinoma therapy, x, 20: 40660
radiation effects on genetics of, review, 20: 40662
radiation effects on, from supersonic transport environment, 20: 40525
radiation effects on thyroid in, β and x, 20: 42857(R) (TID-23228)
radiation effects on proliferative activity of lymphocytes from, x, 20: 42872

radiation effects on mitosis in erythroblasts of, chronic low-level, 20: 42884
radiation effects on transformation of blood lymphocytes to blast cells in, x, 20: 42903
radiation effects on, dynamics of lethal x, 20: 42934
radiation effects on development of children given therapy for enlarged thymus, x, 20: 45433
radiation effects on nitrogen balance following x radiotherapy, 20: 45447
radiation effects on, radiobiological basis of, 20: 45450
radiation effects on metabolism in, effects of bone marrow transplants on, 20: 45485
radiation effects on blood and liver enzyme activity in, with secondary syndrome after bone marrow grafting, 20: 45486
radiation effects on dental tissues of, laser, 20: 45404
radiation effects on chromosomes in bone marrow and leukocytes of, whole-body mixed γ and neutron, 20: 45405
radiation effects on, genetic, 20: 45406
radiation effects on aging of, 20: 45411
radiation effects on, during space flight, 17: 22957
radiation effects, chronic low-level, 18: 13459(T) (JPRS-23224)
radiation effects, ultraviolet, 19: 13000
radiation effects, low-level, 19: 21990
radiation effects, biological, 19: 24268
radiation effects, biological, 19: 25907(R) (ORINS-49(p.127-31))
radiation effects, somatic, 19: 43838
radiation effects, genetic, 19: 43823
radiation exposure of, protective measures against, 17: 16348
radiation exposure of, background *vs.* radiological, 17: 33660
radiation exposure of, survey of available information sources concerning, 17: 37113
radiation exposures of, permissible doses and biomedical considerations in iodine-131, 18: 8241
radiation exposure in, background, 18: 43838
radiation exposure of, ICRP recommendations for, 19: 11439
radiation exposure of, environmental, 19: 15814
radiation exposure to, from consumption of seafoods, 19: 24759
radiation exposure of, maximum permissible emergency, 19: 24762
radiation exposure to populations of, measurement of environmental, 19: 28593
radiation exposure of, living in areas of high natural radioactivity, 20: 12988
radiation exposure, determination of LET in manned space vehicles, 20: 39158
radiation from natural sources in Alps mountains as possible cause of foehn sickness, 20: 45461
radiation hazard from diagnostic radiography of pregnant women, 20: 214
radiation hazards from milk and water supplies contaminated by fall-out, 16: 24014 (NP-11715)
radiation hazards from internally deposited radioisotopes, 17: 2821 (HW-SA-2800)
radiation hazards to, medical problems in, 17: 12501
radiation hazards to, from food and milk contaminated by fallout, 17: 12503
radiation hazards from diagnostic radiography, 17: 20254
radiation hazards from environmental exposure, genetic, 17: 23211
radiation hazards to, from radium watch dials, 17: 25500
radiation hazards to, 17: 34169
radiation hazards to, from environmental contamination by iodine-131 produced by thermonuclear explosions, 17: 34144 (CONF-66-5)
radiation hazards to, from nuclear testing and fallout, 17: 36069
radiation hazards to, a review, 17: 36074
radiation hazards to, during space flight, 17: 35277(T) (FTD-MT-62-78 (p.37-148))
radiation hazards to fetuses and embryos of, diagnostic, 17: 35523
radiation hazards to, from Nevada test site, 18: 4043
radiation hazards to, from iodine-131, 18: 4044
radiation hazards in, 18: 9935
radiation hazards to, diagnostic, 18: 13574
radiation hazards to, from industrial exposure, 18: 19597
radiation hazards to, evaluation of, 18: 22296
radiation hazards to, comparison with other hazards, 18: 22298
radiation hazards to, 18: 29389
radiation hazards to, during space flight, 18: 29908
radiation hazards to, from radioactive contamination of food chain, 18: 31082 (EUR-1612.f)
radiation hazards from diagnostic radiography to, 18: 31809
radiation hazards from fallout fission products, 18: 31816
radiation hazards to, during space flight, 18: 31824
radiation hazards to, computer analyses of space-flight, 18: 35048 (AMRL-TDR-64-11)
radiation hazards to, from nuclear explosions, 18: 35769 (TID-7695 (p.161-8))
radiation hazards to gonads of children from radiotherapy of angiomas, 18: 41261
radiation hazards from waste disposal, 19: 1947
radiation hazards to, during manned space flight, 19: 2184 (LA-DC-6681)
radiation hazards to, from environmental iodine-131, 19: 5725 (UR-653)
radiation hazards to, 19: 10872
radiation hazards to female, from radiography, 19: 10976
radiation hazards in radiodiagnosis of, explanation of, 19: 15311
radiation hazards from nuclear explosions to, genetic and somatic, 19: 15241
radiation hazards in space flight, physiological foundations of, 19: 18198
radiation hazards to children, evaluation of, 19: 17700
radiation hazards from low-voltage sources for, 19: 28014
radiation hazards from diagnostic radiographic examinations of children, 19: 31985
radiation hazards from diagnostic radiography, 19: 32012
radiation hazards from diagnosis, problems in evaluating, 19: 36128
radiation hazards of diagnostic radiography in, 19: 43914
radiation hazards of diagnostic radiography of pregnant women, 19: 46062
radiation hazards of diagnostic radiography during pregnancy, 20: 195
radiation hazards from uranium carbide fuel particles, 20: 1694
radiation hazards of diagnostic radiography during pregnancy, 20: 5476
radiation hazards to, from cosmic and gamma activities in building materials, soils, and water, 20: 7324(T) (CEA-tr-R-1850)
radiation hazards to, in space flight, 20: 10719(T) (NASA-TT-F-353, pp 3-20)
radiation hazards to, from inhalation of radioiodines, 20: 16734 (TID-22693)
radiation hazards to, program for control of, 20: 16160 (UCRL-14739 (Pt.2))
radiation hazards to, in atmosphere, 20: 16732 (NP-15898)
radiation hazards to fetal, from placental transfer of fission products, 20: 16301
radiation hazards to, in space flight, 20: 29058
radiation hazards to skin of, uv, 20: 32970
radiation injuries, review, 16: 6667
radiation injuries following whole-body exposure, 16: 6669
radiation injuries, assessment of acute, 16: 8647
radiation injuries, diagnosis and treatment of acute, 16: 8645
radiation injuries, diagnosis and treatment of acute, 16: 8654
radiation injuries, late pathological effects, 16: 8650
radiation injuries, pathology of acute, 16: 8648
radiation injuries, pathology of acute, 16: 8651
radiation injuries, treatment, 16: 8649
radiation injuries, pathology and treatment of acute, 16: 6668
radiation injuries, pathology and treatment of acute, 16: 6359
radiation injuries to fetuses of, 18: 5020
radiation injuries in, diagnosis and treatment, 18: 11769
radiation injuries from thermonuclear war in, 18: 22293
radiation injuries of, pathogenesis of acute whole-body, 18: 37017
radiation injuries in, effects of bone marrow injections, 19: 213
radiation injuries of urinary tract from radiotherapy of female genital carcinomas, 19: 131
radiation injuries of, diagnosis, 19: 8782 (BNL-7790)
radiation injuries in, treatment with bone marrow transplants of, 19: 10907
radiation injuries of, protective effects of isogenic bone marrow infusions against, 19: 10913
radiation injuries from Thorotrast in kidneys of, after pyelography, 19: 13132
radiation injuries following acute whole-body exposure, diagnosis and therapy of, 19: 15211
radiation injuries in, problems in surgery of, 19: 15236
radiation injuries from accidental exposures, symptoms, 19: 15045
radiation injuries in infants from diagnoses, protective measures for, 19: 19677
radiation injuries in, pathology of proton-induced, 19: 24260(R) (NASA-CR-53780)
radiation injuries in, induced by whole-body subacute gamma exposure, 19: 26026
radiation injuries in, diagnosis of, 19: 27989
radiation injuries in, therapy of acute, 19: 27990
radiation injuries in, medical management of, 19: 27992
radiation injuries of, induced by radiotherapy of ankylosing spondylitis, 19: 32017
radiation injuries of, treatment of nuclear explosion, 19: 32492
radiation injuries to, clinical picture of accidental and therapeutic, 19: 31827
radiation injuries of, after high-level exposure, 19: 45997
radiation injuries in, diagnosis by lymphocyte chromosome studies, 19: 45916
radiation injuries in, diagnosis by lymphocyte chromosome studies,

19: 45917
radiation injuries of thyroid gland from internally deposited iodine-131, 19: 36089
radiation injuries in, diagnosis using of blood pictures, 20: 64 (SZS-5 (1965))
radiation injuries of, diagnosis by morphological study of lymphocyte nuclei, 20: 1612 (EUR-2505.e)
radiation injuries in, biological methods for detecting, 20: 3770
radiation injuries to, protective effects of bone marrow grafts against, 20: 5420
radiation injuries to, from barium-140 deposited in aortic walls, chemical protection against, 20: 31142
radiation injuries to, as result of atomic explosions, 20: 35706
radiation injuries of, diagnosis using leukocyte chromosome aberration analysis, 20: 38593 (ORNL-P-2175)
radiation injuries due to chronic low doses, 20: 42865
radiation injuries to fetuses of, review of, 20: 45449
radiation injuries in, diagnosis of, 19: 33958 (ORNL-P-1446)
radiation injuries of skin of, therapeutic effects of peloidin on, 19: 2173
radiation injury after nuclear accident involving uranium-235, 19: 31858
radiation injury in children treated for hemangiomas by radium, 20: 38787
radiation injury on eyes of, following therapy of canthus and eyelid carcinomas, 20: 40689
radiation injury prophylaxis and therapy, 16: 20242
radiation injury recovery rate, relation with metabolic rate, 16: 17542
radiation injury therapy with bone marrow transplantations, 16: 14595
radiation injury to, from thermonuclear detonations, 17: 23225
radiation injury therapy using bone marrow transfusions in, 20: 45520
radiation monitoring of, Leishman-stained blood films, technique for, 17: 28717
radiation monitoring, instrument sensitivities for, 18: 14196 (AEEW-M-335)
radiation monitoring of farmers near Hanford, 19: 22617
radiation monitoring, whole-body gamma counter for, 19: 22705
radiation monitoring in Alaskan, shadow-shielding whole-body counter for, 20: 659
radiation protection of, admissible doses in, 17: 8472
radiation protection in, review of chemical, 18: 8203
radiation protection problems for, in space flight, 18: 12390
radiation protection of, significance of relative biological effectiveness in, 19: 17698
radiation protection during radiographic examinations, 19: 20229
radiation protection during diagnostic radiography, 19: 30034
radiation protection of abdominal region during pelvic radiology of, shield design for, 19: 30007
radiation protection during long-duration space flights, 19: 31803(T) (UCRL-Trans-1225)
radiation protection during space flight, 19: 31810
radiation protection of, effects of body's absorption and scattering on dosimetry for, 19: 34410
radiation protection on space stations, shielding requirements for, 19: 40063 (NP-15125)
radiation protection of, in contaminated environments, 20: 11039
radiation protection of patients during diagnostic and therapeutic radiography, 20: 40733 (ISS-66/16)
radiation protection of, role of free radicals in chemical, 17: 14550
radiation protection in x-ray testing of steel tube welding seams, regulations for, 17: 32307
radiation recovery in, evaluation of predictive techniques for, 18: 29386
radiation response and sensitization in, with cervical carcinoma, 19: 45830
radiation scanning of, effects on gamma-sources, beta bremsstrahlung, 19: 30582
radiation sickness in, symptoms of, 17: 7915
radiation sickness in, effects of meclizine and pyridoxine on nausea and vomiting in, 17: 10489
radiation sickness in, case history of ophthalmological changes in acute, 17: 31978
radiation sickness in, therapeutic effects of bone marrow transfusions on, 18: 13570
radiation sickness from radium bromide ingestion, treatment of, 18: 17650
radiation sickness in, protective effects of bone marrow hemopoietic cell transplantations against, 18: 33403
radiation sickness in, medical supportive treatment of, 18: 43304
radiation sickness sequelae in, 19: 7160
radiation sickness in, review on treatment of, 19: 7186
radiation sickness in, suggested treatment for, 19: 7199
radiation sickness in, acute, 19: 8946
radiation sickness in, protective effects of phenothiazine derivative against, 19: 13111
radiation sickness in, protective effects of Marophen against, 19: 15235
radiation sickness in, diagnosis, syndrome, and treatment of, 19: 19553
radiation sickness in, development, symptoms, and treatment of, 19: 38471(T)
radiation sickness from accidental and therapeutic exposure, nursing care of, 19: 45912
radiation sickness in, pathology of, 20: 26659(T) (JPRS-35011, pp 2-24)
radiation sickness in, protective effects of bone marrow transplants against, 20: 36669
radiation sickness diagnosis and therapy in, 20: 38774
radiation sickness in, case history of acute, 18: 1379(T) (FTD-TT-63-558)
radiation sickness of, clinical recovery from acute, 19: 17497(T) (JPRS-28780(p.24-8))
radiation sickness in, diagnosis of chronic, 18: 25153
radiation sickness in Hiroshima and Nagasaki, late effects of acute, 18: 37018
radiation studies on, review on, 19: 2086
radiation syndrome in, survey of symptomatology, 17: 37120
radiation syndrome in, 18: 27117
radiation syndrome following accidental exposure to cobalt-60 source, acute, 16: 12942
radiation tolerance criteria in space flight, 16: 20882
radiation tolerance dose to ovaries in, 17: 15594
radiation tolerance of spinal cord of, 20: 45441
radiation toxicity in, drug standard for prevention and treatment of, 18: 11862
radioactive contamination of organs in, from fallout, 17: 16346
radioactive contamination of, gastrointestinal analysis of, 18: 14105 (EUR-489.f)
radioactive contamination of, large-surface methane flow counter for detecting, 19: 7743
radioactive contamination of, through atmosphere and water supplies, 19: 24758
radioactive contamination of food chain of, 19: 24760
radioactive contamination of, diagnosis and therapy of external and internal, 19: 27991
radioactive contamination of, by fallout in meat, 19: 30401 (CEA-R-2738)
radioactive contamination of Alaskan, whole-body measurement of, 19: 44289 (HW-SA-3750)
radioactivity, 16: 10331
radioactivity assessment in, conference on, 19: 29842
radioactivity content in, from fallout, 20: 8979(R) (BNWL-36)
radioactivity counters for, directory of whole-body, 1964, 18: 37551
radioactivity distribution in, equipment for pictorial reproduction of, 19: 847(P)
radioactivity distribution in, whole-body scintillation scanning of, 19: 30580
radioactivity due to plutonium-239 in, measurement of, 20: 7456
radioactivity due to potassium-40 in, measurement of, 20: 7456
radioactivity due to cesium-137 in, measurement of, 20: 7456
radioactivity due to uranium-235 in lungs, measurement of, 20: 7456
radioactivity from diagnosis in, whole-body counting of, 19: 15284
radioactivity from radium-226, strontium-90, and thorium-228 in body and excreta of, from chronic exposure, 19: 26610
radioactivity in Alaskan, 1962-1964, 20: 9166(R) (BNWL-36, pp 2.1-58)
radioactivity in Alaskan, 20: 26626
radioactivity in diet of, effects of cesium-137, iodine-131, and strontium-90 in milk on, 20: 39157
radioactivity in foods of, factors affecting, 20: 12979 (EUR-2287.d)
radioactivity in organs, characteristics of body cross-section scan phantom for external detection, 16: 9063
radioactivity in, survey of whole-body monitors for determination of, 17: 36159
radioactivity in teen-age diet in U. S., 1963, 18: 37446 (TID-21081)
radioactivity in, development of portable gamma spectrometer for, whole-body counting of, 19: 18258 (HW-84250)
radioactivity in, carbon-14 and tritium, 19: 22616
radioactivity in, conference on assessment of, 19: 26603
radioactivity in, measurement of, 19: 30470
radioactivity in, Los Angeles, 1960 to 1964, 19: 32485
radioactivity in, whole-body counters for measuring, 19: 32787(R) (NIRS-3(1-17))
radioactivity in, detection and measurement, 19: 34053
radioactivity in, detection and measurement of, 19: 34068
radioactivity in, detection and measurement of, 19: 34099
radioactivity in, whole-body counting of, 19: 38890
radioactivity in, whole-body counting of, 19: 46656
radioactivity in, computer program for analyzing whole-body data on, 19: 46658
radioactivity in, performance of large liquid scintillation detector for whole-body measurement of, 19: 46775
radioactivity in, calibration of whole-body counting instruments, 20: 5426
radioactivity in, whole-body counting of, 20: 5427

radioactivity in, design of mobile whole-body counter for measurement of, 20: 7455
radioactivity in, from deposited Thorotrast, whole-body, 20: 6752
radioactivity in, effects of cesium-137 content of diet on, 20: 7334
radioactivity in, calibration of instruments for measuring of, 20: 6694(R) (MIT-952-2)
radioactivity in, facility for whole-body counting of, 20: 7325
radioactivity in, effects on diet on Eskimo, 20: 27194 (CONF-660405-14)
radioactivity in, effects of diet on Lapp, 20: 27206(R) (NYO-3446-5)
radioactivity in, performance of sodium iodide counters for detecting, 20: 31443 (CONF-650673-1)
radioactivity in, from food chain in Sweden, 1961 to 1965, 20: 35705
radioactivity in, whole-body counting, 20: 35357
radioactivity in, effects of iodine isotopes released during nuclear explosions on, 20: 43574 (CONF-660538-1)
radioactivity induced in, during high-energy radiotherapy, 19: 40392 (NYO-3364-6)
radioactivity induced in, by exposure to high-energy betatron beams, 19: 40392 (NYO-3364-6)
radioactivity monitoring, 18: 39634
radioactivity of Arctic, effects of fallout fission products on, 18: 25055 (NP-13985)
radioactivity of Alaskan, effects of diet on, 19: 40780 (BNWL-SA-242)
radioactivity of bones in, with leukemia, beta and gamma, 20: 36559
radioactivity of Lapps, whole-body, 19: 46587(R) (NYO-3446-3)
radioactivity of, spectroscopy of gamma, 18: 1942 (CEA-2231)
radioactivity of, water-shielded room for whole-body counting, 18: 10427
radioactivity of, native to northern Alaska, effects of diet and age on, 18: 41646(R) (HW-80500(p.191-4))
radioactivity of, in Brazil, 18: 41649 (TID-20955)
radioactivity of, origin of natural, 18: 43210
radioactivity of, calculation of natural, 19: 4408
radioactivity of, due to fallout fission products, 1964, 19: 9370 (NP-14556(p.11-80))
radioactivity of, whole-body, 19: 26162(R) (ORINS-49(p.98-110))
radioactivity of, whole-body, 19: 26667(R) (ORINS-49(p.111-26))
radioactivity of, in Argentina, 19: 30402 (NP-14904)
radioactivity of, whole-body counting, 19: 33990
radioactivity of, whole-body counting of tracer, 19: 46137
radioactivity of, whole-body counting, 20: 1710
radioactivity of, undergoing radioisotope therapy, 20: 38790
radioactivity uptake by thyroids in children, following nuclear weapons test in Nevada, 20: 43590 (UCRL-14707)
radioactivity, detection and measurement of, 19: 34052
radiobiological effects of atomic explosions on, 17: 7705
radiocardiography of hemodynamic characteristics of left heart and pulmonary circulation in, 20: 10478 (TID-22492)
radiodermatitis in, effects on trace element content of blood, 18: 33285(T) (JPRS-25502)
radiodermatitis in, effects on blood serum protein fractions, 19: 19598
radiodiagnosis and therapy of thyroid disease in, using iodine-131, 19: 13160
radiodiagnosis effects on genetic mutations and leukemogenesis in, 17: 8439
radiodiagnosis hazards to, 20: 202
radiodiagnosis in, effects on chromosome aberrations in, 17: 5846
radiodiagnosis in, protective housing for x-ray tube for, 20: 33132
radiodiagnosis in, hazards from, 18: 37039
radiodiagnosis of parathyroid tumors in, using photoscanning techniques, 19: 5744
radiodiagnosis of myocardial lesions in, cesium-131 scanning for, 19: 5747
radiodiagnosis of myocardial infarcts in, cesium-131, 19: 15253
radiodiagnosis of brain tumors in, using iodine-131-labeled serum albumin and mercury-203-labeled neohydrin, 19: 15255
radiodiagnosis of hyperthyroidism remission in, by iodine-131 uptake by thyroid, 19: 15269
radiodiagnosis of female genital lymph system by lymphography, 19: 17708
radiodiagnosis of lead poisoning in, using lead-210, 19: 17711
radiodiagnosis of pulmonary embolism in, by photoscanning using chromium-51 or iodine-131, 19: 19724
radiodiagnosis of anemia in, 19: 26167
radiodiagnosis of neoplastic recurrence and post-radiation sclerosis in, 19: 26189
radiodiagnosis of diseases of, relation between excretory urography and radioisotope renography in, 19: 38520
radiodiagnosis of elderly, use and abuse of, 19: 46116
radiodiagnosis of kidney diseases in children, 20: 6947
radiodiagnosis of amniotic fluid in pregnant, by isotope dilution and scanning, 20: 45527
radiodiagnosis of, bone marrow dosage from, 19: 15326
radiodiagnostic procedures for, 17: 27208
radiogenic keratoacanthosis in, 17: 35587
radiography of children, diagnostic, 19: 31989
radiography of pelvic dysplasia in infants, radiation hazards of, 19: 19678
radiography of, using gamma transmission, 19: 46750 (AECL-2270)
radioinduced aberrations in lymphocyte chromatids of, x, 19: 2130
radioinduced ablation of pituitary in, use of Bragg peak of proton beam for, 19: 26210
radioinduced aging in, 20: 12644
radioinduced aging in Japanese, γ and neutron, 20: 20480
radioinduced and natural carcinogenesis in, theory of initiation, 19: 24325
radioinduced arcus senilis in eyes of, 18: 27134
radioinduced atherosclerosis in, 18: 33277 (STI/DOC/10/28(p.21-38))
radioinduced autoimmunity following x radiotherapy, 20: 43027
radioinduced autonomic dystonias in nervous system of, symptoms and treatment of, 20: 6791(T) (JPRS-33039, pp 1-8)
radioinduced bone sarcomas in, from therapy, 17: 21538
radioinduced bone tumors in, 20: 20460
radioinduced brain lesion of, 19: 45995
radioinduced cancer in, mechanisms for, 20: 6851
radioinduced carcinogenesis in, gamma and x, 17: 35582
radioinduced carcinomas in, Thorotrast, 18: 43235
radioinduced carcinogenesis in, effects of age on, 19: 15146
radioinduced carcinoma in, 19: 22020
radioinduced carcinoma of thyroid in, 19: 24284
radioinduced carcinogenesis in, theory of initiation, 19: 24326
radioinduced carcinogenesis in, etiology of, 20: 6769 (AD-624917)
radioinduced carcinoma in children following radium therapy of hemangioma, 20: 38788
radioinduced carcinogenesis in, 20: 40659
radioinduced cardiac fibrosis in, 18: 3508
radioinduced cataracts in, effect of dose fractionation on, 18: 25200
radioinduced cataracts in following atomic-bomb exposure, 19: 10845
radioinduced cataracts in children of Hiroshima, 19: 10858
radioinduced changes in amnion cells, gamma, 17: 28766
radioinduced chromosome aberrations in, 17: 25014
radioinduced chromosomic anomalies in, after whole-body irradiation, 17: 28725
radioinduced chromosomal aberrations in leukocytes of, x, 18: 1394
radioinduced chromosomal aberrations in, gamma and neutron, 18: 19582
radioinduced chromosomal abnormalities in, beta and x, 18: 19583
radioinduced chromosomal aberrations in chromosomes of, x, 18: 21856
radioinduced chromosome aberrations in leukocytes of, 18: 29354
radioinduced chromosome aberrations in leukocytes of, 18: 38798
radioinduced chromosome aberrations in human somatic cells, 18: 43227 (ORNL-P-419)
radioinduced chromosome aberrations in, 18: 43284
radioinduced chromosomal aberrations in tissue cultures from, 19: 3961
radioinduced chromosome aberrations in, 19: 10815
radioinduced chromosome damage in, effects of time in culture on *in vivo*, 19: 17559
radioinduced chromosome doubling in leukocytes of cancer patients, 19: 28040
radioinduced chromosome aberrations in, 19: 28054
radioinduced chromosomal aberrations in, alpha, 19: 31792(R) (ORNL-3768(p.94-8))
radioinduced chromosome aberrations in, 19: 43834
radioinduced chromosome aberrations in, 20: 60(R) (NYO-901-37, pp 33-68)
radioinduced chromosome aberrations in, effects of dose on, 20: 16230(R) (TID-22644)
radioinduced chromosome aberrations in leukocytes of, *in vitro* and *in vivo*, 20: 22581
radioinduced chromosome aberrations in, following cancer therapy, 20: 42931
radioinduced congenital malformations in, 19: 134
radioinduced cytologic changes in salivary glands of, following cobalt-60 radiotherapy, 20: 40644
radioinduced dermatitis in, surgical treatment of therapeutic, 17: 21479
radioinduced dermatitis in, effects of irradiation on lymph vessels in, x, 18: 19604
radioinduced effects on cell nuclei in, 17: 30358
radioinduced enteropathy of small bowel, 18: 43246
radioinduced epidermal cysts in, x, 18: 21857
radioinduced epilation in, x, 18: 29394
radioinduced epilation in, effects on hair color of, 18: 38857
radioinduced epilation in, development of late carcinoma after, 19: 112
radioinduced erythema in, dose determinations for uv, 19: 45881
radioinduced erythema in, uv, 20: 14310
radioinduced erythema in, differences in 250- and 300-nm uv, 20: 22722
radioinduced gastrointestinal injury of, from radium therapy, 17: 28703
radioinduced gastric hyalinization in, 20: 8515

radioinduced genetic damage in, by pelvic diagnostic radiography of females, 18: 27073
radioinduced hemolysis of erythrocytes in patient with protoporphyrinemia, 19: 28033
radioinduced hemolysis and swelling in erythrocytes of, γ, 20: 8980(R) (BNWL-36, pp 3.1-122)
radioinduced hypocoagulability in, x, 17: 35474
radioinduced inactivation of hormones in, methods for assaying, 18: 41144
radioinduced infections after whole-body exposure to suppress immune reactions to kidney transplants, 19: 27987
radioinduced injuries in, surgical treatment of, 17: 35384
radioinduced injuries from thorotrast, 18: 17512
radioinduced injuries to eyes of, from nuclear explosions, 20: 45451
radioinduced intestinal ileus in, from pelvic radiotherapy, 17: 27078
radioinduced kidney carcinomas in, Thorotrast, 18: 41208
radioinduced lesions in, therapy and prognosis of, 18: 9927
radioinduced leukemia in, after radiation therapy and diagnosis, 17: 33695
radioinduced leukemia in, 17: 36084
radioinduced leukemia following iodine-131 therapy in, 17: 35566
radioinduced leukemia in, from health examinations, 17: 35493
radioinduced leukemia in, 17: 39351
radioinduced leukemia in, 17: 40626
radioinduced leukemia in, 18: 19579
radioinduced leukemia in, evidence for, 18: 27124
radioinduced leukemia in, dose effects on development of, 18: 38827
radioinduced leukemia in infant, x, 19: 3946
radioinduced leukemia in, 19: 12985
radioinduced leukemia in, 19: 21958
radioinduced leukemia in, 19: 24277
radioinduced leukemia in, 19: 24295
radioinduced leukemia in, chromosome analysis of, 19: 25924
radioinduced leukemia in, incidence of, 19: 28108
radioinduced leukemia in, review, 19: 28046
radioinduced leukemia in, 19: 28067
radioinduced leukemia in Japanese, incidence of, 19: 42294
radioinduced leukemia in, etiology of, 19: 43827
radioinduced leukemia in, dose relations, 20: 161
radioinduced leukemia in, statistical study of etiology of, 20: 5307
radioinduced leukopenia in, protective effects of adenine against, 16: 17484
radioinduced leukopenia in, prognostic significance, 17: 15819
radioinduced leukopenia in, therapy using batyl alcohol, 20: 45489
radioinduced liver tumors of, incidence of thorotrast, 17: 28600
radioinduced liver tumors in, Thorotrast, 18: 25205
radioinduced liver carcinomas in, Thorotrast, 18: 27126
radioinduced lung cancer in uranium miners, 19: 28581
radioinduced lung injuries following radiotherapy of cancer, γ, 20: 43030
radioinduced malignant hemangioblastoma in, 17: 21571
radioinduced malignant tumors in, Thorotrast, 19: 8940
radioinduced menopause in, complications from, 18: 29474
radioinduced menopause in women, 19: 28036
radioinduced mutation in Japanese, 18: 17555
radioinduced mutations in, cosmic, 18: 21900
radioinduced mutations, 19: 36085
radioinduced mutations, 19: 36093
radioinduced myelitis in, x, 20: 3771
radioinduced neoplasms in, survey, 17: 14037
radioinduced neoplasms in, 19: 8791 (NP-14556(p.81-110))
radioinduced nephritis in, 18: 33332
radioinduced nephritis in, after radiotherapy, 18: 38791
radioinduced nephritis following radiotherapy in, 19: 24303
radioinduced nutritional diseases in, 20: 3251
radioinduced osteogenic sarcoma in, 19: 31846
radioinduced pigmentation of, synergistic effects of dimethylchlortetracycline on, 19: 12971
radioinduced pulmonary fibrosis in, gamma *vs* x, 17: 38828
radioinduced rectal carcinoma following cancer therapy in, 17: 35550
radioinduced renal hypertension in, effects of nephrectomy on, 19: 8973
radioinduced sarcoma in, 19: 12986
radioinduced sarcomas in, 19: 28038
radioinduced scar carcinomas in, 17: 38754
radioinduced secondary amenorrhea in, therapeutic use of hormones for, 18: 3641
radioinduced sister chromatid exchanges in leukocytes of, x, 20: 40628(R) (ORNL-3922, pp 89-93)
radioinduced skin carcinomas in, histopathology of x, 17: 35513
radioinduced skin sarcomas on, from therapy of lupus vulgaris, 19: 15066
radioinduced skin cancer on, prevention and treatment of, 19: 17631
radioinduced skin lesions on, use of fresh blood autofibrin films for treatment of, 19: 19642
radioinduced skin cancers in, 19: 45945
radioinduced spinal cord injuries, pathogenesis of, 20: 45440
radioinduced thyroid carcinomas in, review, 18: 29467
radioinduced thyroid cancers in residents of Hiroshima, 20: 22693
radioinduced trisomy 17-18 in, 19: 31844
radioinduced tumors in, reaction mechanisms for, 17: 40642
radioinduced tumors in, from deposited radium or thorotrast, 18: 8116 (TID-20008)
radioinduced tumors in Thorotrast, 18: 38787
radioinduced tumors in neck of, thorotrast, 19: 24319
radioinduced tumors in, 19: 29965
radioinduced tumors of thyroid, in children, 19: 29948
radioinduced tumors in, 19: 45942
radioinduced tumor in, after injection of Thorotrast, 19: 46092
radioinduced tumors in, statistical study of etiology of, 20: 5307
radioiodine uptake in infants, 17: 15600
radioiodine uptake from milk by, method for predicting, 20: 30980
radioiodine uptake from milk by, use of countermeasures in predicting, 20: 30981
radioisotope body-burden estimations in Brazil, 20: 40522(R) (NYO-3273-7)
radioisotope contents in children, newborn infants, and stillborns, gamma, 17: 27013 (TID-18878)
radioisotope contents in total teen-age diet in U. S., 1963, 19: 9416
radioisotope content in diet of, 19: 24248
radioisotope content in urine of, method for determining, 19: 30140
radioisotope content of, whole-body techniques for counting, 20: 35189
radioisotope contents in Arctic, 20: 43005
radioisotope distribution in, measurement of, 17: 30084
radioisotope distribution in, computer simulation of, 19: 40282 (BNWL-SA-171)
radioisotope distribution and dose in, method for external measuring of, 20: 31158
radioisotope hazards, identification, and removal, 17: 1183
radioisotope incorporation and excretion by, 17: 41
radioisotope injection in, technique for intravenous, 19: 28184
radioisotope metabolism in, 18: 11589
radioisotope metabolism in, maximum permissible levels for, 19: 5610
radioisotope metabolism in, 19: 29879
radioisotope removal from, by chelation, 19: 24238 (AWRE-O-4/65)
radioisotope removal from, developments in chelation therapy for, 19: 46017
radioisotope renography in children, 19: 46109
radioisotope retention data on, computer code for analyzing, 20: 23336 (AD-621270)
radioisotope secretion by, survey of decorporation methods for, 19: 3881
radioisotope tolerance levels in, review, 18: 3623
radioisotope transfer mechanisms in placentas of, effects of inactive carriers on, 20: 31142
radioisotope uptake, maximum permissible levels of, 16: 30689
radioisotope uptake by, countermeasures for, 18: 3607
radioisotope uptake by, following accidental exposure, 20: 9199
radioisotope uptake from Clinch and Tennessee rivers, 20: 8479(R) (ORNL-3849, pp 1-42)
radioisotopes in urine of, interpretation of analytical results for, 20: 8542 (CONF-727, pp 85-101)
radioisotopes in, whole-body measurements of deposited gamma-emitting, 18: 31061(R) (NP-14125)
radioisotopes incorporated in, counter for determining, 18: 16244
radiological effects on pregnancy in, 18: 9947
radiology in, protective measures for pediatric, 19: 36204
radiometric analysis of, whole-body spectroscopic, 18: 9977
radiometric analysis of, for cesium-137 and potassium-40, use of Humco II whole-body counter for, 18: 16300(R) (LAMS-3034(p.143-51))
radiometric analysis of, for potassium-40 distribution, whole-body, 18: 27050
radionuclide contamination of milk from, in Boston and Chicago, 19: 28601
radionuclide uptake by, 19: 28597
radionuclide urinary excretion rates, 18: 33518
radionuclides in, dosimetry of internally administered, 19: 15314
radioscanning of brain of, effects of age on arsenic-74, 18: 13589
radioscanning of, techniques for, 19: 30012 (ACRH-103(p.76-103))
radiosensitivity, comparison of sensitivity of chromosomes in *in vitro* cells, 16: 28781
radiosensitivity effects of chemicals in, effectiveness of, 19: 33985
radiosensitivity of, correlated with radiotherapy results, 17: 35351
radiosensitivity of individuals, effects of body constitution on differences in, 18: 11706
radiosensitivity of leukemic and normal leukocytes in, 19: 7037
radiosensitivity of tumor cells in, effects of 5-bromodeoxyuridine on, 19: 7039
radiosensitivity of hematopoietic system in, 19: 15210

radiosensitivity of developing fetuses, 19: 15213
radiosensitivity of skin of, 19: 19605
radiosensitivity of lymphocytes in, hypothesis for, 19: 24347
radiosensitivity of eyes of, 19: 24386
radiosensitivity of tumors of, factors affecting alpha and x, 19: 26075
radiosensitivity of lymphocytes in peripheral blood from, 19: 25945
radiosensitivity of embryo of, 19: 29987
radiosensitivity of brain of, 19: 31869
radiosensitivity of developing fetuses of, 19: 31840
radiosensitivity of gonads, 19: 31976
radiosensitivity of developing fetuses, 19: 33797
radiosensitivity of heart, kidneys, and liver in, implications for radiology, 19: 36058
radiosensitivity of gonads in children, 19: 43893
radiosensitivity of, effects of age, 19: 43915
radiosensitivity of skin of, 19: 43819
radiosensitivity of brain and central nervous system of, 19: 45892
radiosensitivity of eyes of, 19: 46655
radiosensitivity of chromosomes in leukocytes in, 20: 5304(T) (JPRS-32985, pp 45-50)
radiosensitivity of tumors in, effects of actinomycin on, 20: 10700
radiosensitivity of spinal cord of, x, 20: 16251
radiosensitivity of tissues of, 20: 16322
radiosensitivity of, effects of pyridine diphosphate nucleotides on, 20: 18535
radiosensitivity of chromosomes from embryonic fibroblasts of, x, 20: 22668
radiosensitivity of chromosomes in cultured blood leukocytes from, with Down's syndrome and normal blood, 20: 35273
radiosurgery of brain in, 18: 13580
radiotherapy and surgery of cervical carcinomas in, urologic complications in, 19: 17722
radiotherapy and surgery combined for malignancies in, review of, 20: 45547
radiotherapy effects on incidence of cancer of larynx in, 17: 21488
radiotherapy effects on urinary excretion of 17-ketosteroids in, 17: 35585
radiotherapy effects on, protective effects of cobalt, copper, and iron against, 17: 38758
radiotherapy effects on course of pulmonary tuberculosis in, esophageal cancer, 18: 31180
radiotherapy effects on development of maliga struma in, 19: 7031
radiotherapy effects on chromosomes in, 19: 7072
radiotherapy effects on mucous membrane in, protective effects of trihydroxyethylrutoside against megavoltage, 19: 8977
radiotherapy effects on development of hepatitis in, 19: 9008
radiotherapy effects on osmotic exchange of leukocytes in, with malignant tumors, 19: 13055
radiotherapy effects on vaginal smear in cervical cancer patients, use as prognostic index, 19: 15254
radiotherapy effects on development of myocardial and pulmonary fibrosis in, 19: 17552
radiotherapy effects on gliomas in, 19: 22035
radiotherapy for malignant tumors in, effects of dose fractionation on, 18: 3654
radiotherapy for skull base metastases in, 20: 45562
radiotherapy for, review on hazards and possibilities of radioisotopes for, 20: 35369
radiotherapy for, use of data processing installations for planning of, 20: 45565
radiotherapy in, effects on blood of, 18: 38826
radiotherapy in, skin lesions induced by, 18: 38842
radiotherapy of abdominal-pelvic region in, effects on intestinal absorption by D-xylose, 19: 17725
radiotherapy of abdomeno-pelvic region, effects on vitamin B_{12} sorption by intestines, 19: 28198
radiotherapy of acne in, evaluation, 17: 35364
radiotherapy of angiomas in children, gonad dose in van der Plaat, 19: 13147
radiotherapy of benign and malignant diseases in children, sequelae to, 19: 15037
radiotherapy of benign tumors in children, late pathological effects, 19: 27956
radiotherapy of benign neck lesions in, incidence of thyroid cancer from, 19: 31971
radiotherapy of bladder carcinoma in, linear accelerator supervoltage, 19: 9004
radiotherapy of bones in, effects on bone sarcoma development, 19: 26168
radiotherapy of bronchogenic carcinoma, case study of leukemia development from, 19: 7072
radiotherapy of brain of, late radiolesions from, 19: 26187
radiotherapy of brain tumors in, comparison of high-voltage and conventional methods, 20: 45560
radiotherapy of burns on, effectiveness of x-ray, 18: 13594
radiotherapy of cancers in, problems in neutron, 17: 12082
radiotherapy of cancer in, chromosomal patterns during, 19: 6972
radiotherapy of carcinoma of cervix, fever as complication in, 19: 9002
radiotherapy of cancer in, effects on liver function, 19: 19684
radiotherapy of cancer of gastrointestinal tract in, with and without 5-fluorouracil, 19: 26195
radiotherapy of cancer in children, 19: 28143
radiotherapy of cavernous hemangiomas in, effectiveness of, 19: 30015
radiotherapy of cancers in, effects on immune reactions, 19: 32009
radiotherapy of carcinoma of vocal cord in, effects on larynx from radium, 19: 38519
radiotherapy of cerebral astrocytomata in, effects of whole-body hypothermia on, 17: 10438
radiotherapy of cervical cancer in, techniques of, 17: 35350
radiotherapy of cervical carcinomas in, complications from, 18: 3652
radiotherapy of cervical carcinoma in, complications from, 19: 8999
radiotherapy of cervical cancer, late effects on life span as function of regional dose, 19: 17718
radiotherapy of cervical carcinomas, effects on glucose-6-phosphate-dehydrogenase activity in vaginal secretions, 19: 17735
radiotherapy of chest tumors in, effects on heart of, 17: 17786
radiotherapy of diffuse reticulum cell sarcomas in, gold-198, 18: 3669
radiotherapy of euthyroid goiters in, using iodine-131, 19: 19685
radiotherapy of female carcinomas, effects on blood serum protein fractions, 19: 9041
radiotherapy of, gastrointestinal disturbances after, 17: 38850
radiotherapy of glomus jugulare tumor in, exodontia after, 19: 28169
radiotherapy of gynecological cancer in, late effects from, 17: 10372
radiotherapy of gynecologic cancer in radionecrosis of femoral neck from, 19: 9040
radiotherapy of gynecological carcinomas in, effects on blood coagulation, 19: 15293
radiotherapy of head and neck tumors in, effects of, on ears, 17: 7813
radiotherapy of hemangioma in, cobalt-60, 18: 9958
radiotherapy of hemangiomas in children, 20: 5443
radiotherapy of hemangiomas in children, x radiation dose to gonads from, 20: 31156
radiotherapy of hemangioma in, late effects on skin from, 20: 35381
radiotherapy of head and neck tumors in, performance of γ and x, 20: 45556
radiotherapy of head and neck malignancies in, review of electron, 20: 45557
radiotherapy of hyperthyroidism in, development of acute myelosis from, 18: 9876
radiotherapy of hyperthyroidism using iodine-131, development of acute myelomonocytic leukemia from, 19: 31837
radiotherapy of hyperthyroidism using iodine-131, effects on cytoplasmic and thyroglobulin antibodies, 19: 43902
radiotherapy of hyperthyroidism in, analysis of 348 cases of iodine-131, 20: 45548
radiotherapy of larynx, oral cavity, and pharynx in, protective effects of Tanderil against burns and sickness from, 19: 13110
radiotherapy of leukoplakia of urethra using phosphorus-32 chromic phosphate implantation, 18: 15935
radiotherapy of leukemia in, using tritiated thymidine injections, 20: 40743 (BNL-9374)
radiotherapy of leukemia in, combined with hematopoietic tissue grafts, 20: 45550
radiotherapy of liver in, development of veno-occlusive disease in, 20: 33106
radiotherapy of lung carcinoma in, effects of, on respiratory function, 17: 23197
radiotherapy of lung cancer in, gamma, 17: 37122
radiotherapy of lung and pelvic cancer in, using yttrium-90 suspensions, 17: 38783
radiotherapy of lung carcinomas of, comparison of cobalt-60 tele- and orthovoltage, 19: 15279
radiotherapy of malignant neoplasms in, effects on peripheral blood picture in, 17: 5850
radiotherapy of malignant tumors in, effects on blood serum proteins, 17: 7873
radiotherapy of malignant tumors, protective effects of essential amino acid on blood in, 17: 7879
radiotherapy of malignant tumors in, effects of adrenal steroid therapy on symptoms from, 17: 10268
radiotherapy of malignancies in, effects of, on lymphocyte polysaccharides and serum glycoproteins in, 17: 14007
radiotherapy of malignant tumors in, using gamma unit, 18: 25254
radiotherapy of malignant nasopharynx tumor in, 19: 9000
radiotherapy of malignant tumors in, using yttrium-90 microspheres, 19: 10938
radiotherapy of mammary neoplasia in, development of pericarditis from, 19: 10945

radiotherapy of malignancies in, evaluation of four years' experience with whole-body, 19: 15305
radiotherapy of malignant tumors in, effects on glycide metabolism, 19: 22024
radiotherapy of mammary carcinoma in, development of acute hemorrhagic purpura from, 19: 26204
radiotherapy of malignant tumors in children, effects on pelvic bones and spine, 19: 26205
radiotherapy of malignant hemangioendothelioma in, palliation in, 19: 28206
radiotherapy of malignant diseases in children, effectiveness of, 20: 16306
radiotherapy of malignant tumors in, occurrence of herpes zoster in, 20: 35380
radiotherapy of malignant tumors of, using laser beams, 20: 38780
radiotherapy of, method for yttrium-90, 18: 3638
radiotherapy of mediastinal gland in, development of radiation pneumonitis after, 19: 22027
radiotherapy of milk-duct carcinoma in, method for assessing preoperative, 19: 36187
radiotherapy of myelosis in, effects of myleran administration with, 19: 13170
radiotherapy of myositis in, electromyographic changes from, 20: 35354
radiotherapy of nasopharyngeal tumor in, cervical myelitis from, 18: 3661
radiotherapy of neoplasms in, use of Pyrexal for assay of granulocyte reserve in, 19: 15259
radiotherapy of non-malignant diseases of neck and pharynx, cancer induction in, 16: 25201
radiotherapy of pituitary region in, with diabetic retinopathy, 19: 15312
radiotherapy of pituitary gland in, developments in methods for, 19: 26209
radiotherapy of postoperative parotitis in, γ and x, 20: 45535
radiotherapy of retinoblastoma in, effects of triethylenemelamine on, 19: 13146
radiotherapy of reticuloses in, review of, 20: 45537
radiotherapy of reticulum cell sarcoma of skin using laser and x radiation combined, 20: 45568
radiotherapy of salivary glands in, clinical study of short term effects from, 19: 28140
radiotherapy of sarcoma in limbs of, production of anoxia prior to, 20: 45517
radiotherapy of seminal carcinoma in, fathering of normal baby after, 19: 15278
radiotherapy of skin carcinomas in, 17: 35356
radiotherapy of skin diseases in, histological changes from, 18: 29470
radiotherapy of skin tumors of, 20: 6975
radiotherapy of stomach of, effects of glycerol-guaiacol-ether on gastric changes after, 18: 9923
radiotherapy of superior mediastinal obstruction combined with demecolcine, effectiveness of, 19: 28156
radiotherapy of testicular seminomas and teratomas, survey of, 19: 31958
radiotherapy of thorax in, dosimetry of pneumonitis development in, 17: 14004
radiotherapy of thyroid gland in, histological method for evaluating, 18: 21937
radiotherapy of thymus as children, effects on development of thyroid neoplasia in adulthood, 19: 7034
radiotherapy of thyrocardiac disease in, using iodine-131, 19: 15299
radiotherapy of thyrotoxicosis using Iodine-131 in, development of hypoparathyroidism from, 19: 17706
radiotherapy of thyrotoxicosis using iodine-131, development of hypothyroidism from, 19: 28188
radiotherapy of thyroid diseases in children, 19: 28196
radiotherapy of thyroid tumors in children using iodine-131, 19: 32025
radiotherapy of tumors in, effects of heat treatment on, 17: 35355
radiotherapy of tumors in, effects of preoperative, 18: 29454
radiotherapy of tumors in children, 19: 249
radiotherapy of tumors in, effects on urinary 17-ketosteroids, 19: 5714
radiotherapy of tumors in, anabolic effects of steroids in, 19: 19669
radiotherapy of tumors in, dosimetry in epithermal-neutron, 20: 14421
radiotherapy of tumors in ear, nose, and throat region with fast electrons, 20: 45554
radiotherapy of upper jaw and orbital tumors, dosimetry for, 20: 45563
radiotherapy of, using microspheres containing scandium-46 and yttrium-90, 17: 10288
radiotherapy of uterine cervix carcinoma in, protective effects of adenine on hematopoiesis in, 17: 7835
radiotherapy of uterine cervix carcinomas in, morphology of lymph nodes after, 19: 17709
radiotherapy of uterine carcinomas in, histopathological analysis of, 19: 36173
radiotherapy of uterine carcinoma in, complicated by psoriasis, γ and radium, 20: 45532
radiotherapy of uterine cancer in, effects on leukocyte count and mucosa of bladder and rectum following x, 20: 45540
radiotherapy of vagina of, cytological changes from, 17: 28707
radiotherapy of, atlas of single-field dose distributions in, 20: 8749 (STI/PUB/96(Vol. I))
radiotherapy of, detection of Philadelphia chromosome following, 19: 34039
radiotherapy of, effects on isoenzymes and lactate dehydrogenase in melanoma ascites, serum, and tumor homogenates, 19: 46124
radiotherapy of, prevention and reduction of generalised and local reactions in, 19: 13109
radiotherapy of, use of heavy particles with high energy for, 19: 17728
radiotherapy using gold-198, hazards from, 18: 1466
radiotherapy with high-voltage electrons, effectiveness and kinetics of, 20: 45567
radiotherapy with the betatron of malignancies of head and neck region, results of, 20: 45559
radium and strontium-90 metabolism by, 20: 31142
radium body burden in British luminous dial workers, 17: 12093
radium content in teeth in luminous dial painters, 17: 13925
radium deposition in skeleton of, effects of, 17: 25042
radium deposits in, analysis of breath for determination of, 18: 33262
radium distribution in bone, 16: 2858(R) (ANL-6398(p.5-23))
radium distribution in, determined by whole-body counting, 17: 10300(R) (COO-226(p.71-77))
radium poisoning in, research study review, 19: 43672(R) (TID-22131)
radium poisoning of, survey of cases of, 18: 43222(R) (MIT-952-1 (p.1-112))
radium uptake by, data analysis for, 20: 6694(R) (MIT-952-2)
radium uptake, retention, and excretion by, 17: 28628
radium-224 uptake by melanomas in, 18: 3489(R) (COO-228(p.127-31))
radium-226 content from natural environmental radioactivity, 17: 21443
radium-226 uptake and fecal excretion by, dietary effects on, 17: 28629
radium-224 metabolism in, 18: 43183(R) (MIT-952-1(p.113-49))
radium-226 and -228 content in bones of, with osteogenic sarcoma, 18: 29229
radium-226 body burden of, method for determining, 18: 33821
radium-226 burden to bone tissue in, method for calculation of, 19: 26609
radium-226 content of bone and diet of, in Puerto Rico, 19: 2033
radium-226 content in placenta and fetal skeleton in, 19: 20216
radium-226 content of, whole-body counting, 19: 22685(R) (ANL-6839 (p.12-17))
radium-226 content of blood cells and plasma after intravenous injection, 19: 29866
radium-226 content in, determination from radon-222 in expired air, 19: 46677
radium-226 content in body and bones of, 20: 603
radium-226 content in, Bombay and Kerala, India, 20: 16747
radium-226 content in, estimation from radon exhalation, 20: 43604
radium-226 content in deciduous teeth of, as indicator of exposure from drinking water, 20: 45505
radium-226 content in, natural, 18: 36944
radium-226 dosimetry and metabolism in tissues in, 20: 32919
radium-228 excretion by, method for determining rate of, 20: 24840
radium-228 in diet of, 20: 148(R) (NYO-3086-1 Pt.IV)
radium-233 metabolism in, 20: 18226
radon exposure of, maximum permissible concentrations for, 18: 31084 (UR-648)
radon metabolism in, effects of silicosis on, 19: 31732
rare earth pharmacology and toxicology, 19: 35916
respiration and oxygen stores in, oxygen-18 isotopic dilution studies on, 20: 38941 (RRL-2310-182)
response of, to sound from ultrasonic devices, 18: 21704 (HW-SA-3028)
rubidium content in bone, muscles, and soft tissues in, 17: 15603
rubidium-86 uptake by erythrocytes of, 18: 27048
salmonellosis epidemiology in, relation to food transmission, 18: 13397
scandium-46 decontamination in, DTPA and EDTA for, 20: 31
scandium-46 metabolism by, 19: 43692
scandium-47 metabolism and fecal administration by, after oral administration, 20: 12612
screening for neutron exposure after radiation accident, 17: 5775 (TID-14529)
skin tumors induced by ultraviolet radiation in, 18: 27127
sodium metabolism, tracer study, 17: 23068
sodium metabolism in, tracer study, 18: 38754
sodium-22 content in, study by coincidence gamma spectra, 18: 43372 (HW-SA-3680)
sodium-22 content in Alaskan, 20: 4161
sodium-22 content in, 20: 9166(R) (BNWL-36, pp 2.1-58)
sodium-22 content in, residing in Alaska and Washington, 1962 and 1963, 19: 22535 (HW-SA-3487)
sodium-22 content in, 19: 20225
sodium-24 clearance from gastrocnemius muscle of, 19: 8770

sodium-24 content in, at Hanford, 18: 36920 (HW-82409)
sorption and excretion of strontium in breast-fed babies, 18: 29219
sorption of orally administered zinc-65, effects of dietary zinc on, 16: 17417
sorption properties for cobalt-60-labeled cobalt chloride, 18: 8091
space flight effects on, 18: 13392
space flight effects on astronauts, 19: 25820 (AD-608798)
space flight effects on, review of USSR data on, 19: 42232(T) (ANL-Trans-209)
space flight environment of, bibliography on, 18: 6587 (NP-13406)
space flight medical problems in, 18: 25045
space travel by, bibliography on biological and medical aspects of, 19: 42231 (NASA-SP-7011(11))
spectra from neutron-exposed, gamma, 20: 6694(R) (MIT-952-2)
spermatogenesis in, timing of, 20: 22617(R) (RLO-1780-1)
spermatogenesis rate in, tracer study of, 18: 23176
spleen transplantation in, 19: 19522
stable element metabolism by, 16: 1428(R) (ORNL-3189(p.197-210))
steroid hormone synthesis in placenta of, tracer study, 19: 31670(R) (NIRS-3(p.19-56))
steroid metabolism in, 19: 29854(R) (TID-21859)
strain and stress relations of heat in, physiological indexes, 16: 23376 (TID-7616(p.61-8))
stresses in space flight, methods for improving tolerance to, 19: 43842
strontium biological half life in skeleton of, 18: 13436
strontium content in human, 19: 6948(R) (ORNL-3697(p.178-92))
strontium content of bones of, effects of age, 19: 33750
strontium content of bone of, 19: 40781(R) (NP-15179)
strontium content in ribs of, spectrographic method for determining, 19: 40309(R) (NP-15180)
strontium content in bones and diet, 16: 23370 (AERE-R-4035)
strontium infusion in, comparison of calcium tolerance test with effects of, 17: 21430
strontium levels in, metabolic effects on, 18: 38752
strontium metabolism, tracer study, 17: 27049
strontium metabolism in, during radiotherapy for cancer, 17: 40502
strontium metabolism in newborn, 19: 29865
strontium metabolism in, effects of steroid hormones, age, and sex on, 19: 45805
strontium metabolism by, effects of age on, 20: 6719(R) (ORNL-3849, pp 183-213)
strontium metabolism in, bibliography on, 17: 5747
strontium metabolism kinetics, computer study, 17: 23032 (BNL-6208)
strontium metabolism in, bibliography on, 17: 5747
strontium movement in skeleton of, 17: 5712
strontium retention by infant, 17: 23063
strontium-85 excretion, effects of calcium gluconate and ammonium chloride, 16: 6283
strontium-85 excretion in, effects of calcium salts of bis-2-aminoethyl ether tetraacetate and gluconate on, 16: 9828
strontium-85 excretion by, 17: 24855
strontium-85 excretion by, effects of calcium, chelates, and strontium on, 17: 28633
strontium-85 metabolism in bones of, after tumor surgery, 18: 21
strontium-85 movement in, 17: 17718
strontium-85 retention by, 17: 24858
strontium-85 uptake, retention, and excretion by, 17: 28631
strontium-89 and -90 content in breast milk in, 17: 21943
strontium-90 balances in, 17: 35421
strontium-90 content in children and infants bones and testicular tissues, Germany,1958 to 1960, 16: 11984
strontium-90 content in British population, 1961, 17: 2805
strontium-90 content in bones in, effects of age on, 17: 5714
strontium-90 content, 1962, 17: 7773 (NYO-9934(Vol. I))
strontium-90 content in blood plasma and urine in, on low-calcium diet, 18: 1362
strontium-90 content in bones of, in Poland in 1960 and 1961, 18: 4990
strontium-90 content in long bones of, in Western Germany, 18: 5152
strontium-90 distribution in, data tabulation, 16: 14448 (NYO-9934 (Vol.II))
strontium-90 excretion in young adults, 16: 31457
strontium-90 excretion, 17: 2789(R) (ORNL-3347(p.142-54))
strontium-90 levels in Eskimos, 1959 to 1962, 16: 15040
strontium-90 metabolism in bones in, 17: 5715
strontium-90 uptake by, effects of barium sulfate and calcium phosphate on, 17: 28632
strontium-90 uptake from foods by, 1961, 17: 31846
strontium-90 uptake by, control and therapy, 17: 35434
strontium-85 and -90 availability to, from flour and milk, 19: 36733
strontium-85 and -90 uptake and retention in, 20: 42762
strontium-85 content following intravenous injection in, 20: 32
strontium-85 metabolism in, 19: 22019(R) (UCLA-12-541(p.51-91))
strontium-85 metabolism and excretion in, 19: 21828
strontium-85 metabolism in, 20: 18226
strontium-85 secretion in saliva of, 19: 17479
strontium-85 sorption by kidneys in, discrimination in, 17: 19760
strontium-85 sorption in, method for determining, 18: 4978
strontium-85 uptake by axial skeleton of, 19: 9035
strontium-85 uptake from gastrointestinal tract of, effects of sodium alginate on, 20: 16173 (PG-Report-686)
strontium-85 uptake from gastrointestinal tract in, effects of sodium alginate on, 20: 24941
strontium-85, -89, and -90 occupational exposure, maximum permissible, 18: 15907
strontium-89 and -90 uptake from airborne particles by infants, 19: 3855
strontium-89 and -90 pathological effects in, deposited, 19: 35945 (NP-15184)
strontium-89 and -90 inhalation accepted limits for, 16: 9054
strontium-90 and stable element uptake, excretion, and retention by infants on normal diet, 19: 25901
strontium-90 biological half-life in, 19: 35 (TID-7696(p.120-39))
strontium-90 body burden and urinary excretion in, measurement of, 19: 25902
strontium-90 body burdens in, review of methods for estimating, 20: 32
strontium-90 content in children's bones in Denmark, 1961–1962, 18: 12351
strontium-90 content in urine of, effects of diet on, 18: 13823
strontium-90 content of bones and tissues of German, 18: 17432
strontium-90 content in skeleton of, determined by accumulation in teeth, 18: 31110
strontium-90 content in diet of estimation from excreta analysis, 19: 2018
strontium-90 content in bones of, in Osaka, Japan, 1957–1959, 19: 11426
strontium-90 content of teeth in, 19: 15239
strontium-90 content in bone tissues in, 19: 15001
strontium-90 content in bones and diet of Argentine children, 19: 20165(R) (TID-21711)
strontium-90 content in bones of Japanese, 19: 31672(R) (NIRS-3 (p.65-77))
strontium-90 content of bones of, effects of age, 19: 33750
strontium-90 content of bones of children, 19: 34370
strontium-90 content of, 19: 34372
strontium-90 content in diet of infant, 20: 521(R) (HASL-164)
strontium-90 content in, from fallout, 20: 6714
strontium-90 content as function of age of, model for estimating, 20: 6724 (ORNL-P-1830)
strontium-90 content in bones of children in U. S., 1965, 20: 16662(R) (HASL-165)
strontium-90 content in primary teeth of children in New Jersey, 20: 16763
strontium-90 content of, whole-body, 20: 16303(R) (AD-626384)
strontium-90 content in Canadian, 1960 to 1964, 20: 23390
strontium-90 content in, effects of diet on, 20: 31442 (BNWL-SA-661)
strontium-90 content in children's teeth, regional variations in, 20: 32913
strontium-90 content in bones of, as related to content in milk, 20: 45886 (NP-16262)
strontium-90 content in bones of, determined from extracted teeth, 20: 45956 (NP-16257)
strontium-90 content in bones of, in Poland, 1962–1964, 20: 45313
strontium-90 content in, correlation with fallout rate and ground deposition, 19: 11426
strontium-90 content, contribution of fallout to, 18: 18110
strontium-90 content of bones of, 17: 8463
strontium-90 excretion in urine of, relation to calcium/strontium-90 ratio in diet, 19: 52
strontium-90 in bones from food contamination in New York City, Poland, and Great Britain, 20: 43619
strontium-90 ingestion or inhalation by, method for estimating amount of, 19: 25883
strontium-90 maximum permissible body burden for, 19: 46634 (AD-423463)
strontium-90 metabolism kinetics in, 18: 20235 (NP-13868)
strontium-90 metabolism in, 18: 35290
strontium-90 metabolism in, effects of starvation on, 18: 35291
strontium-90 metabolism in, theoretical analysis of, 18: 38738
strontium-90 metabolism by, 19: 8737 (BNL-8657)
strontium-90 metabolism in, 1961 to 1965, 19: 42638 (HASL-163)
strontium-90 metabolism by, 19: 45793
strontium-90 metabolism by, 19: 46634 (AD-423463)
strontium-90 metabolism in, 18: 25
strontium-90 uptake by bones of, dependence on age, 18: 13435
strontium-90 uptake by, significance of, 18: 37364 (A/CONF.28/P/769)
strontium-90 uptake from diet, absorption coefficient for, 19: 8758
strontium-90 uptake by London infant, 19: 14991
strontium-90 uptake and distribution from ingested marine animals, 20: 35682
strontium-90 uptake by, factors affecting, 20: 41142

strontium-90 urinary excretion in, effects of intravenous calcium and oral ammonium chloride on, 19: 42252
subdivided populations of, equations for inbreeding frequency in, 19: 31670(R) (NIRS-3(p.19-56))
sulfur content in tissues in, estimation of, 20: 30982
sulfur-35 content in blood of, after intravenous or intraperitoneal injection, 19: 27942
sunlight effects on thickness of skin in negroid and white, 18: 8167
taste radiosensitivity in, 19: 45825(T) (NSJ-tr-32)
technetium metabolism in, tracer study of, 20: 3663 (TID-22318)
technetium-95 and technetium-96 metabolism in, 20: 45297
thallium-204 uptake by respiratory tract in, combined calcium-45 and, 20: 10546
therapeutic effects of semicarbazide-cadmium on malignant tumors in, 18: 25054
therapeutic effects of bone marrow in, exposed to whole-body irradiation, 19: 194
therapy for elimination of radioactive and toxic materials, 19: 13097
therapy for internally deposited radioisotopes in, 18: 1461
therapy of brain tumors in, effects of boron compounds for neutron capture, 17: 10282
therapy of Ewing's sarcoma in, effectiveness of chemo- and radio-, 20: 33111
therapy of heart disease in, using iodine-131 for thyroid suppression, 19: 13179
therapy of malignancies in, using autologous bone marrow transfusion following nitrogen mustard, 19: 12896
therapy of melanoma in, using radium-226, case history, 18: 29435(R) (COO-119-229(p.74-9))
therapy of polycythemia in, phosphorus-32, 17: 33491
therapy of radiation injuries in, 19: 33958 (ORNL-P-1446)
therapy of thrombocytopenia in, with stored platelets, 18: 33215(R) (TID-20824)
therapy of thrombocytopenia using infusions of frozen blood platelets, 20: 40496(R) (NYO-1753-3)
therapy of, using radioisotope deposition, 17: 27208
thermal radiation temperature measurements in skin of, 20: 614
thorium dioxide effects on sarcoma development in liver in, 17: 27081
thorium distribution in, following thorotrast injection, 17: 19907
thorium effects on, 19: 29991
thorium isotopic content in, 20: 30989
thorium-228 content in, natural, 18: 36944
thorium-232 decay products in tissue of Thorotrast-injected, 19: 19497(R) (ANL-6938(p.127-39))
thorium-234 metabolism in, 18: 43183(R) (MIT-952-1(p.113-49))
Thorotrast and decay products in, toxic effects and tissue distribution of, 20: 23380(R) (TID-22841)
Thorotrast deposits in organs in, effects of, 17: 4414
Thorotrast metabolism in, 20: 1596
Thorotrast metabolism in, 20: 6822
thorotrastosis in, clinical considerations of, 18: 35360
thymidine metabolism in, tracer method for measurement of, 18: 27049
thyroid disease in, effects of geography on incidence of, 17: 40442 (NP-13175)
thyroid function studies in infants, using iodine-131 and whole-body counting, 19: 26162(R) (ORINS-49(p.98-110))
thyroid gland weights in, 17: 40493(R) (TID-18790(App.I))
thyroid gland weights in, 17: 40494(R) (TID-18790(App.II))
thyroid hormone metabolism in children, 18: 15782 (TID-7689(p.22-5))
thyroid pathology and physiology in, 20: 31162
thyroid studies in, uses of radioiodine for, review of, 20: 45294
thyroid tumors in Nagasaki bomb survivors, 16: 32843
thyroidectomy of, iodine-131 dose determination in, 17: 35396
thyroxine deiodination in, 18: 9752 (IA-900)
thyroxine metabolism in, effects of thyroid diseases on, 19: 31768
tissue cultures of leukocytes, 17: 5676 (SAM-TDR-62-99)
tissue distribution and expiration of injected tritium-labeled water, 16: 9823
tissue transplantation in, survey of problems in, 18: 31311
tolerance to hyperbaric oxygen, 19: 38500
trace element adsorption and elution on hair of, tracer study, 20: 38543
trace element content in saliva of, neutron activation analysis method for, 19: 33765
trace elements in heart of, neutron-activation determination of, 18: 33457 (AE-146)
treatment of leukemia, using bone marrow transplants and irradiation, 19: 10901
treatment of pernicious anemia in, body retention of hydroxocobalamin and cyanocobalamin in, 18: 15666 (BNL-6942)
treatment of polycythemia vera using phosphorus-32, leukemia incidence from, 19: 28189
treatment of radiation injuries from high dose level exposures, 16: 25184(T) (SCL-T-424)
triiodothyronine metabolism in, tracer study using whole-body counting, 19: 28177
tritium assimilation at Savannah River Plant, biological half life of, 17: 33785 (DP-831(p.38-45))
tritium biological half life in, 19: 10740 (DPSPU-64-30-9)
tritium biological half life in, 19: 15343 (DPSPU-63-30-37)
tritium content in, maximum permissible, 20: 23370 (CONF-640413, pp 117-23)
tritium excretion following uptake of water-t, 19: 7206(R) (ORNL-3697 (p.173-7))
tritium metabolism in, 20: 23370 (CONF-640413, pp 117-23)
tritium metabolism, 19: 38355
tritium-labeled compounds in feces of, determination of, 18: 12009
tumor development in, from Thorotrast deposition near kidney, 17: 21525
tumor development in carotid artery in, from thorium dioxide injections, 17: 23201
tumor development in, effects of Thorotrast on, 17: 38760
tumor diagnosis and pathology in, relation of Kaposis visceral sarcoma to, 19: 15046
tumor diagnosis in, using internally deposited phosphorus-32, 17: 28645
tumor formation in bone marrow of, after phosphorus-32 treatment of myeloleukemia, 18: 9905
tumor induction in liver in, by thorium dioxide, 20: 123
tumor localization in, use of iodine-131-labeled compounds for, 17: 26992
tumor treatment in, using bone marrow transplants, 20: 22534
uptake and retention of calcium-47 and strontium-85, 19: 35893(R) (NYO-3234-1)
uptake of iodine-131- and mercury-203-labeled compounds by tumors in, in oxygen environment, 20: 36576
uranium carbide microsphere gastrointestinal passage by, 19: 42258 (LA-3365)
uranium concentrations for, maximum permissible, 19: 21830
uranium contamination in, measurement by analysis of urine, 20: 43000
uranium content in urine in, interpretation of data on, 16: 31983 (AHSB(RP)-R-15)
uranium content in, effects of content in food, soil, and water supplies on, 19: 19490
uranium content in urine of, background and occupational, 19: 36718
uranium content of bones and organs of, 18: 1344(T) (AEC-tr-6137)
uranium dust inhalation by, excretion and retention after, 19: 26615
uranium excretion and retention by, after inhalation of uranium-235-, 20: 45282(R) (COO-119-234, pp 297-318)
uranium metabolism in, 19: 36 (TID-7696(p.166-80))
uranium oxide deposition in lungs of, effects of chemical composition and particle size on, 20: 41204 (Y-1544-A)
uranium uptake by, permissible limits of, 19: 7208(R) (ORNL-3697 (p.202-6))
uranium uptake in, dietary, 20: 8740 (CONF-727, pp 136-41)
ureter strictures in carcinomatous, isotope-renogram method for diagnosing, 19: 31671(R) (NIRS-3(p.57-63))
urinary content of tritium-labeled estrogens and ketosteroids after labeled testosterone injection, 20: 18230
use of bone marrow injections for treatment of leukemia in, 20: 8793
use of radioisotope kidney function tests in paraplegic, 20: 6963
use of whole-body irradiation and bone marrow transfusions for therapy of leukemia in, 20: 45520
vanadium metabolism in enamel of teeth of, 19: 35896
vitamin B_{12} metabolism in, tracer study of, 20: 6990
vitamin B_{12} metabolism in, tracer study of, 20: 6991
vitamin B_{12} metabolism in, effects of cyanocobalamin on, 19: 31624 (BNL-8132)
vitamin B_{12} distribution in, 18: 3450 (BNL-6913)
vitamin B_{12} retention, comparison with ill patient, 16: 1334(R) (LAMS-2627(p.280-3))
yttrium content of bones of, 17: 8463
zinc metabolism in cirrhotic and normal liver of, tracer study, 20: 18222
zinc metabolism, physiological effects, and biological specificity in, 17: 38704 (BNL-7252)
zinc-65 constant in, effects of chelates on, 20: 20397
zinc-65 content in, at Hanford, 18: 36920 (HW-82409)
zinc-65 content of hair of, 19: 3873
zinc-65 content of, from consumption of Pacific Ocean oysters, 20: 553 (BNWL-SA-293)
zinc-65 metabolism in, 19: 17480
zinc-65 metabolism in, effects of dietary calcium on, 19: 45787
zinc-65 uptake and distribution in normal and tumor tissue in, 19: 43699
zinc-65 uptake by, from Columbia River fish, 20: 30969 (BNWL-SA-45)
zirconium-95 content in lungs of, from fallout inhalation, 19: 11434
zirconium-95 contents of, in England, 16: 28736
zirconium-95 uptake from fallout by lungs of, 19: 3856

MAN (STANDARD)

anatomical data of West European, from birth to adult age, 17: 33479

(EUR-147.f)
blood content and weight of Japanese, 19: 40781(R) (NP-15179)
bone and tissue composition in, 17: 39312(R) (ORNL-3492(p.176-82))
chemical composition of organs and tissues, 20: 10698
gastrointestinal tract food retention time and mass of, 20: 14794
radiation dose to intestinal tract of, from ingested nonabsorbed beta particles, 18: 1968
radiation interactions, heavy primary cosmic, 16: 20239
radiation interactions, proton, 17: 28686(R) (UCRL-10683(p.1-14))
radioisotope excretion analysis, estimation of body burden from, 16: 8516
radioisotope toxicity classification for, 17: 34189
tissue composition in bone and striated muscle, 18: 5109

MANDELIC ACID
analytical use for differential spectrophotometric determination of hafnium in presence of zirconium, 17: 12221
analytical use in determination of hafnium in aluminum alloys, 18: 5210 (CONF-157-5)
analytical uses for volumetric determination of zirconium, 18: 177
complexes with lanthanum, rare earths, and yttrium, formation and stability constants of, 20: 12817 (IS-1311)
complexes with neptunium, thorium, and zirconium, solvent extraction studies on formation of, 20: 20561 (JAERI-1099)
complexes with rare earths, stability of, 20: 40902
complexes with thorium, stability constants of, 17: 30490
complexes with thorium, infrared spectra of, 19: 11058
compound formation with samarium, gadolinium, and erbium, 19: 44028
labeling with tritium at α-carbon atom, 19: 46306
mandelic acid–uranyl acetate–water, complexes in, 17: 1518
metabolism in Pseudomonas mutants, 20: 20376
metabolism in Pseudomonas mutants, 20: 20470
preparation of deuterated, reactions in catalytic, 19: 36449
radiolysis of aqueous solutions of DL-, gamma, 20: 25149
radiolysis of DL-, products formed in, 18: 6859
radiolysis of oxygenated solutions of, product yields from gamma, 20: 20759
solvent properties for scandium, 16: 12988
use in determination of zirconium, 20: 35413
use in hafnium and zirconium determination, 19: 46224
1,8-dihydroxy-3,6-disulfo-2-naphthylazo-, preparation from diazotized amino mandelic acids and chromotropic acid, 19: 34209
mandelic acid–uranyl acetate–water, complexes in, 17: 1518

MANDELIC ACID, *p*-BROMO-
analytical uses for determination and separation of europium and holmium, 19: 336
compound formation with samarium, gadolinium, and erbium, 19: 44028
reactions with dysprosium, 20: 43140
use in determination of rare earths in presence of uranium(VI), 20: 43141
use in separation of uranium from zirconium alloys, 18: 25283
uses in determination of ytterbium, 20: 14490

MANDELIC ACID, CHLORO-
analytical uses for determination and separation of europium and holmium, 19: 336
reactions with dysprosium, 20: 43140
use in determination of rare earths in presence of uranium(VI), 20: 43141
uses in determination of ytterbium, 20: 14490

MANDELIC ACID, HAFNIUM SALTS
thermal decomposition, 18: 41382

Mandelic Acid, Hexahydro-
see Cyclohexaneglycolic Acid

MANDELIC ACID, 4-HYDROXY-3-METHOXY-
radiation effects on excretion of, x, 18: 21898

MANDELIC ACID, α-METHYL-
complexes with rare earths, stability of, 20: 40902

MANDELIC ACID, ZIRCONIUM SALTS
thermal decomposition, 18: 41382

MANGANATE IONS
radiation effects on oxidation and reduction of, electrochemical processes in, 18: 29793
radiolysis of aqueous solutions of, pulse, 19: 38728

MANGANATES
see also Erbium Manganates
see also Holmium Manganates
see also Lanthanum Manganates
see also Lutetium Manganates
see also Niobium Manganates
see also Permanganates
see also Plutonium Manganates
see also Potassium Manganates
see also Potassium Permanganates
see also Scandium Manganates
see also Thulium Manganates
see also Ytterbium Manganates
see also Yttrium Manganates
electrochemical reactions of, kinetics of, 17: 28877
magnetic susceptibilities, 16: 25882 (ASD-TR-61-630)
radioinduced reduction in potassium hydroxide solutions, 16: 33029
radioinduced reduction in alkaline solutions, 18: 37170 (A/CONF.28/P/113)

MANGANESE
see also Transition Metals
abundance in 3 Centauri A, 17: 32851
addition of trace amounts to chromium–nickel steel, method for, 20: 41418(R) (GEAP-5150)
alloying characteristics with rare earths, 18: 41924(R) (IITRI-578P19-13)
alloying effects on hot workability of Type 304 stainless steel containing boron, 16: 2144 (ANL-6393)
alloying effects on properties of magnesium–thorium alloys, 16: 9246
alloying effects on properties of rare earths, 16: 3474(R) (USBM-U-863)
alloying effects on corrosion of Zircaloy-3 by steam and water, 16: 486 (BM-RI-5865)
alloying effects on retention of alpha phase nuclei in beta uranium, 16: 4576
alloying effects on zirconium corrosion in hydrochloric acid at 150 to 250°C, 16: 13533
alloying effects on corrosion resistance of magnesium–zinc–zirconium alloys to carbon dioxide at 500°C, 16: 30892(P)
alloying effects on oxidation of niobium–zirconium alloys in air and steam, 16: 32078 (AERE-R-4134)
alloying effects on aluminum corrosion, 17: 1881
alloying effects on delta-prime phase of plutonium, 17: 3535
alloying effects on titanium, 17: 16580(P)
alloying effects on mechanical properties of vanadium, 17: 25771 (ASD-TDR-62-667)
alloying effects on properties and structure of magnesium–thorium alloys, 17: 32596
alloying effects on ignition temperature of plutonium in air and oxygen, 17: 36860(R) (ANL-6648)
alloying effects on hardness of chromium, 17: 37548
alloying effects on ductility and electric conductivity of hardened steel, 17: 39545(T,R) (EURAEC-599)
alloying effects on grain-refinement and beta to alpha transformation in uranium, 17: 41468
alloying effects on critical temperature of aluminum, 18: 2287
alloying effects on stainless steel as reactor material, 18: 8838
alloying effects on corrosion resistance of zirconium in carbon dioxide, 18: 12576 (GEAP-4089(Vol.I)(Paper 3))
alloying effects on iron–nickel alloys, 18: 24161
alloying effects on composition and mechanical properties of magnesium–neodymium alloys, 18: 28000
alloying effects on magnesium-base alloys, 18: 32211(P)
alpha elastic scattering at 24.7 Mev, relative cross sections for, 18: 34902
alpha scattering at 25 Mev by, differential cross sections for elastic (E), 19: 1234 (PAN-347)
analysis and determination, 20: 14500
analysis by photoneutron emission, 18: 37070 (A/CONF.28/P/825)
analysis for copper and iron by x-ray fluorescent spectroscopy, 17: 2913
analysis for impurities, methods of spectrochemical, 16: 22038
analysis for scandium after solvent extraction using dientipyrilmethane, 18: 13702
atomic Slater-Condon parameters for, 17: 2426
behavior in fused lithium chloride–potassium chloride eutectic, chromatographic and electrophoretic, 18: 43479
bonding to uranium by catalyst and solid state diffusion, 17: 25786 (UCRL-13075)
bremsstrahlung emission by incident electrons on, intensity variation with target voltage, 17: 39741
bremsstrahlung reactions with, isomer production in, (E), 20: 46733
compatibility with plutonium, thorium, and uranium, 17: 8843
concentration by marine organisms, 17: 12112
content and deposition in open-ocean silts, 20: 12540(R) (NYO-2882-8)
content and distribution in acid igneous rocks of Africa, 18: 37358
content and distribution in shallow marine environments, 20: 18895 (NYO-3450-1, pp 217-76)
content in calcites in Providencia area, Zacatecas, Mexico, 20: 18631 (NYO-2266-1)
content in Columbia River, seasonal changes in, 19: 2540
content in distilled beryllium, calculation and determination of, 19: 22104 (UCRL-12253)
content in high-purity depleted uranium metal, 19: 24481 (GAT-T-1141)
content in human brain, 17: 35419
content in human erythrocytes and serum, 17: 10148
content in human saliva, neutron activation analysis method for, 19: 33765

content in mammalian cells, effects of cell cycle stage on, 20: 18204(R) (LA-3432, pp 130-77)
content in man, effects of administration of manganese sulfate on, 20: 24998
content in meteoritic chondrules, (E), 19: 28536
content in normal and leukemic leukocytes, activation analysis of, 18: 33517
content in organs and tissues of humans outside continental U. S., 19: 21831
content in ORR pressurized-water corrosion loop, 19: 30150(R) (ORNL-3789(p.113-21))
content in pulmonary tissue relative to beryllium, 17: 28647
content in red giant stars, theory for, 18: 16634
content in red-colored Paleozoic deposits in Northern Tien Shan, 20: 14780(T) (AEC-tr-6579)
content in river waters, 17: 30687
content in rocks, effects of clay content on, 20: 29417
content in schlieren granite segregations, 19: 24699
content in sea water from Indian Ocean, uptake by marine organisms, 20: 40572
content in sun, deviations from thermodynamic equilibrium in, 18: 30387
content in total diet of Japanese people, 19: 9419
content in Van Arkel-refined zirconium, comparison with Knoll-refined, 17: 33819
contents in meteorites, 18: 34398
contents in meteoritic and terrestrial matter, 19: 37428(R) (N64-32896)
corrosion resistance to mercury at 900°F, 20: 2264
critical temperature of, alloying effects of aluminum and zinc on, 18: 2287
crystallization with thionalid, tracer study of co-, 16: 12961 (USNRDL-TR-551)
cycle in nature, tracer study, 17: 33602
density of states in superconducting lead doped with, (E), 19: 8349
determination as impurity in and volatilization from tungsten, semi-quantitative spectrographic, 16: 4131 (BM-RI-5903)
determination as impurity in natural fluorites by activation methods, 19: 17835
determination as trace in standard rocks G-1 and W-1, spectrographic, 16: 20831
determination as trace impurity in uranium, 18: 29591
determination as trace impurity in plutonium–thorium–uranium and thorium–uranium alloys, 19: 17798
determination by activation methods, 19: 19806
determination by calculation of weight from activities and neutron fluxes measured after irradiation, 18: 27297
determination by charged-particle reactions at 2 Mev, 20: 43097
determination by precipitation as diliturate, thermogravimetric, 18: 35467
determination by precipitation as diliturate, 19: 19824
determination by potentiometric titration of acid liberated by complex formation, 19: 46205
determination by solvent extraction and spectrophotometry using 1-(2-pyridylazo)-2-naphthol, 16: 139
determination by spectroscopy using high-frequency plasma flames, 18: 10020
determination by spectrochemical methods, voltage-fluctuation patterns in, 19: 40416
determination by thermal-neutron activation methods, sensitivity for, 19: 9071
determination by titration, suitability of tetraethylenepentaminehepta-acetic acid for, 19: 19813
determination in aluminum, activation and colorimetric, 16: 1710
determination in aluminum, activation, 16: 25288
determination in aluminum and uranium using 8-quinolinol, spectrophotometric, 16: 12970
determination in aluminum, x-ray spectroscopic, 17: 10571
determination in aluminum by activation methods, 17: 21635
determination in Armco iron, use of radioisotopes for, 17: 33822
determination in aluminum by activation and gamma spectrometry, 18: 31391
determination in aerosols, activation, 19: 19771(R) (TEES-2671-4 (Chap.9))
determination in aluminum, activation, 19: 28224 (SGAE-CH-13/1964)
determination in aluminum, activation, 19: 46207
determination in algae, neutron activation, 19: 45775
determination in aluminum ingots, x-ray fluorescence, 20: 8828 (K-1638)
determination in automobile lubricants, activation, 20: 14439(R) (GA-5556)
determination in automobile tire rubber, activation, 20: 14439(R) (GA-5556)
determination in automobile paint, activation, 20: 14439(R) (GA-5556)
determination in asbestos using ion exchange, activation, 20: 16336(R) (NYO-10175)
determination in aluminum, activation, 20: 22896
determination in aluminum by neutron activation, 20: 33164(T) (AEC-tr-6639, pp 28-31)
determination in americium and plutonium by spark-source mass spectrography, 20: 40816 (RFP-699)
determination in biological material, activation, 16: 7385
determination in biological materials, 16: 18823
determination in biological materials, activation, 16: 23403
determination in beryl ores, volumetric, 16: 11517 (PG-Report-266)
determination in beryllium, activation, 17: 25123
determination in blood and tissues, activation, 17: 39012
determination in bismuth, spectographic, 17: 27309
determination in beryllium oxide, spectrophotometric, 18: 3694
determination in bismuth, activation, 18: 13682
determination in boron, x-ray-fluorescence, 18: 29564(R) (NBL-210 (p.41-7))
determination in biological materials, activation, 18: 43399
determination in beryllium oxide, device for quantitative, 19: 11007
determination in biological tissues, activation, 19: 15333 (AE-168)
determination in beryllium by activation, 19: 24415
determination in beryllium oxide, spectrographic comparison of standards on, 20: 6998 (AAEC/TM-294)
determination in beryllium, spectrophotometric, 20: 16361
determination in botanical materials, activation, 20: 18602
determination in bone, activation, 20: 24983
determination in blood and serum, neutron activation, 20: 24998
determination in boron by neutron activation, 20: 33173(T) (AEC-tr-6639, pp 67-9)
determination in blood in arthritic and healthy patients, activation, 20: 38845
determination in clay, acetic acid leachates, sand, and silt, spectrochemical, 16: 4379
determination in chicken, neutron activation, 16: 20337
determination in complex minerals by combination of neutron activation and paper chromatography, 16: 27436
determination in carbonatites, spectrographic, 17: 27228 (EUR-32.f)
determination in cerebrospinal fluid and serum, activation, 18: 37086
determination in corn leaves, method for, 18: 39067
determination in clays, rocks, and sands, activation, 18: 43401
determination in cerium, erbium, and lutetium, mass spectrographic, 19: 2232
determination in cobalt, activation, 19: 5829
determination in copper by activation, 19: 40422
determination in cigarette tobacco, activation, 20: 14439(R) (GA-5556)
determination in commercial plastics, activation, 20: 14439(R) (GA-5556)
determination in calcium carbonate, chalk, and potassium hydroxide, substoichiometric activation, 20: 16403
determination in cerium, cobalt, and plutonium alloys by ion exchange separation and potentiometric titration, 20: 36713 (LA-3402)
determination in diabase W-1 and granite G-1, spectrographic, 16: 17895
determination in drugs, activation, 19: 24400 (KR-91)
determination in drugs, hair, oils, river silts, and tobacco, activation, 20: 1739(R) (GA-4297)
determination in deep-sea nodules and sediments, activation, 20: 12976
determination in europium oxide, spectrographic, 17: 2931
determination in enamel of teeth, neutron activation, 19: 38562
determination in erythrocytes and plasma in human blood, activation, 20: 38852
determination in fossil foraminiferal carbonates from deep ocean cores, 16: 29187 (TID-16359)
determination in fluid inclusions from fluorite and quartz, activation, 17: 25134
determination in fuel element descaling solutions, spectrophotometric, 19: 7274(R) (IDO-14636)
determination in fuel descaling make-up solutions, 19: 32059(R) (IDO-14655)
determination in gelatin by neutron activation, 19: 26262
determination in ginseng by activation methods, 19: 42446
determination in greases and soils, activation, 20: 1738(R) (GA-4041)
determination in gasoline by activation analysis, 20: 33168(T) (AEC-tr-6639, pp 46-9)
determination in human teeth by gamma spectrometry, 16: 8671 (AE-61)
determination in human mandibular articular disc by gamma spectrometry and neutron activation, 17: 28811
determination in human whole blood, activation, 17: 40739
determination in hair by activation methods for identification of individuals, 19: 17824
determination in human blood serum, activation, 20: 1586
determination in hair and paint in criminal cases, activation, 20: 8827(R) (GA-6152)
determination in hair samples in criminal cases, activation, 20: 14439(R) (GA-5556)
determination in high-purity tantalum by spectrography using d-c arc

method, 20: 20608
determination in iron, spectrographic, 17: 2907 (WAL-TR-823.5/1)
determination in industrial solutions, quantometric and spectrographic, 18: 19910
determination in iron, activation, 19: 10980 (EURAEC-1273)
determination in iron by activation methods, 20: 5514
determination in igneous and metamorphic apatites, spectrographic, 20: 26787
determination in Korean Schinseng roots by activation, 17: 30121
determination in lactose, activation, 18: 180
determination in lanthanum oxide, spectrographic, 20: 22895
determination in lanthanum oxide, spectrographic, 20: 22945
determination in meteorites and terrestrial rocks, activation, 17: 33851
determination in magnesium, spectrochemical, 18: 11967(R) (MCW-1482 (p.37-46))
determination in molybdenum and its compounds, spectrographic, 18: 17766
determination in minerals, activation, 18: 21991
determination in mixture with uranium using potassium dichromate, titrimetric, 18: 33496
determination in marble samples from Aegean Islands, Greece, and Turkey, activation, 19: 5830
determination in minerals and rocks by activation, use of paper chromatography and computers in, 19: 7338
determination in meteorites, activation, 19: 7349
determination in manganese–plutonium–uranium alloys, x-ray fluorescence spectrometric, 19: 9061 (LA-3160)
determination in manganese–plutonium–uranium alloys, x-ray-fluorescent, 19: 21690(R) (LA-3244)
determination in minerals by neutron activation, 19: 30424
determination in marine plants and animals, spectroscopic, 19: 36314
determination in mollusks from Lake Maggiore, activation, 19: 45788
determination in mixtures by x-ray fluorescence using promethium-147/aluminum and tritium/zirconium sources, 20: 3883 (ORNL-IIC-5, pp 154-81)
determination in multielement mixtures by x-ray fluorescence methods, 20: 20644
determination in minerals and rocks using paper chromatography, 20: 35389 (CEA-R-2791)
determination in mosaic virus and nucleic acids in tobacco plants, 20: 38846
determination in natural water, quantitative spectrographic, 16: 17597
determination in nuclear steels, neutron activation, 16: 20330
determination in niobium by radioactivation analysis, 16: 23633 (TID-7629(p.239-44))
determination in nickel steel and electro-etch residues, activation, 17: 5984
determination in neptunium by ion exchange and spectrography, 17: 15896
determination in natural diamonds, activation, 17: 31995
determination in niobium, chemico-spectrographic method for, 17: 40758
determination in nucleic acids, activation, 18: 19892
determination in niobium and tantalum by activation, 19: 24416
determination in nickel, photometric, 19: 36297
determination in ore by activation analysis, 16: 689
determination in oxidized stainless steel, radiometric, 16: 12668 (WAPD-BT-24(p.89-98))
determination in organic reactor coolants, spectrographic, 18: 184
determination in old Damascus steel sword, activation, 19: 15346 (IS-1105)
determination in oils and silts in water, activation, 20: 14439(R) (GA-5556)
determination in pure phosphorus, activation, 17: 10562
determination in polyphenyls by activation analysis, 17: 38945
determination in petroleum and its products, activation, 18: 15968
determination in polyphenyls, x-ray-spectrographic, 18: 19844 (ISPRA-455)
determination in pharmaceuticals, activation, 19: 13268
determination in pure water by extraction photometry, 19: 15388
determination in pure niobium, activation, 19: 17785 (SGAE-CH-11/1964)
determination in pure aluminum, activation, 19: 19775(R) (UCRL-11828(p.197-9))
determination in presence of nickel by activation methods, 19: 19796
determination in ppm range by d-c arc excitation, spectrochemical, 19: 19827
determination in powdered samples by spectrochemical methods, 19: 22120
determination in plants, activation, 19: 26917(R) (IA-984)
determination in protactinium-233–thorium dioxide–manganese dioxide, 19: 32059(R) (IDO-14655)
determination in pure aluminum by neutron activation methods, 19: 36251
determination in plants, activation, 20: 3901
determination in potassium chloride and sodium chloride single crystals, activation, 20: 12805
determination in plutonium fluorides and peroxides, review on spectrographic, 20: 14464 (RFP-599)
determination in paper samples in criminal cases, activation, 20: 14439(R) (GA-5556)
determination in plutonium–uranium–zirconium alloy by anion exchange-partition chromatography and spectrography, 20: 26764
determination in plutonium by carrier distillation methods, spectrographic, 20: 40814 (RFP-664)
determination in plant materials, activation, 20: 43060 (CEA-R-2967)
determination in powder samples by spectrographic methods, semi-quantitative, 20: 43104
determination in quartz crystals from Providencia area, Zacatecas, Mexico, activation, 20: 18631 (NYO-2266-1)
determination in rare earth oxides, spectrographic method for, 16: 20327
determination in rocks and soils in Norway, activation, 19: 308
determination in reactor-grade uranium oxide, activation, 19: 5827
determination in rocks, activation, 20: 20646
determination in rocks by resonance and thermal neutron capture cross sections, 20: 22962
determination in sea water in Chesapeake Bay area, 16: 14998(R) (NYO-8100)
determination in stratospheric aerosols, 16: 25609 (AFCRL-62-299)
determination in sea water, activation, 17: 4469
determination in Santowax OMP by spectrographic methods, 17: 7959 (RT/CHI(62)13)
determination in SAP, x-ray spectrographic, 17: 27226 (EUR-21.f)
determination in siliceous rocks, activation, 18: 5514
determination in silicon, activation, 18: 6773
determination in silicate rocks, quantometric and spectrographic, 18: 19910
determination in silicon, activation, 18: 33502
determination in surface waters by activation analysis, 18: 37072 (A/CONF.28/P/854)
determination in solar corona, 18: 40109
determination in silicon, activation, 19: 2240
determination in stainless steel, radiochemical, 19: 7274(R) (IDO-14636)
determination in solids by spark source mass spectrometry, quantitative, 19: 13247
determination in silicates, spectrographic, 19: 13266
determination in sea water by quantitative solvent extraction and spectrography, 19: 28253
determination in sea water and silts, spectroscopic, 19: 36315
determination in sodium loop transfer samples, methods for, 20: 12766 (GEAP-4178)
determination in soils, activation, 20: 14439(R) (GA-5556)
determination in stainless steel, activation, 20: 16338 (RT/CHI-(65)36)
determination in serum, activation, 20: 16347
determination in sea water, activation, 20: 18576(R) (TID-22660)
determination in silicon dioxide, activation, 20: 20634
determination in sulfide ores by neutron activation methods, 20: 26759
determination in seawater, activation, 20: 43085(T) (TID-23295, Sect. 2)
determination in sintered and zone refined boron-10, spectrographic, 20: 43090(R) (TID-23342)
determination in terphenyls and plastics, neutron activation, 17: 23273
determination in terphenyls, activation, 17: 28813
determination in tissue, after neutron activation, 17: 31813 (AERE-R-4309)
determination in tantalum by d-c arc method, spectrographic, 18: 19894
determination in trace amounts in uranium and uranium compounds, 18: 25272 (VDDIT-90)
determination in tantalum by anion exchange in hydrofluoric–nitric acid mixtures, 18: 35455
determination in terphenyls, use of computers in activation, 19: 7335
determination in tissues, spectrochemical method for, 20: 5251(R) (UR-668, pp 123-49)
determination in thumbnail clippings, activation, 20: 14493(R) (GA-5556)
determination in tissues using neutron activation analysis, 20: 33226
determination in uranium compounds, spectrographic, 16: 32932
determination in uranium leach solutions, 16: 14668
determination in uranium compounds, spectrographic, 16: 16304 (CNEN-96)
determination in uranium compounds by reversed-phase partition chromatography, 16: 23636 (TID-7629(p.276-84))
determination in uranium(IV-VI) oxide by carrier distillation excitation, effects of graphite electrode grade on, 17: 10538 (TID-16295)
determination in uranium tetrafluoride, spectrographic, 18: 170 (RT/CHI(63)-21)
determination in uranium-233-labeled uranium dioxide, spectrographic, 18: 9980
determination in uranium, methods for, 18: 9991
determination in uranium by ion exchange and square-wave polarography, 18: 17735

determination in uranium solutions, activation, 19: 329
determination in uranium, activation, 19: 5832
determination in uranium and its compounds and alloys, methods for, 19: 19823
determination in urine, neutron activation, 19: 32082
determination in urine, activation, 20: 8568
determination in uranium tetrafluoride, spectrographic, 20: 14473
determination in uranium by carrier distillation, spectrographic, 20: 18563 (EUR-2647.f)
determination in uranium–zirconium alloy by anion exchange-partition chromatography and spectrography, 20: 26764
determination in vanadium, chemico-spectrographic, 18: 13708
determination in water, silver-spark spectrographic, 17: 1381 (IDO-14591)
determination in white lead for age determination of paintings, activation, 19: 5820
determination in wood in criminal cases, activation, 20: 14439(R) (GA-5556)
determination in zone-refined aluminum, activation, 17: 35663
determination in zone-melted aluminum, activation, 18: 27293
determination in zirconium by activation, 19: 24418
determination in Zircaloy-2, spectrographic, 20: 29113
determination in zinc sulfate and sulfide, interfering reactions in activation, 20: 36755
determination in zinc sulfate and sulfide using ion exchange chromatography and activation methods, 20: 36757
determination of, in ores, x-ray spectrum, 17: 15900
determination of, in presence of alkali metals, chemical spectrographic, 17: 15923
determination of, in residues by iron flux method, spectrographic, 17: 19942 (PG-Report-157)
determination of, in uranium concentrates and ores, spectrographic, 17: 23254 (PG-Report-220)
determination of, in erythrocytes and blood serum, radiometric, 17: 40477
determination of, method for, 17: 28801 (IDO-14316(Suppl.4))
determination of microtraces of, in hydrochloric and nitric acids, activation, 18: 5228
determination of microgram quantities of, 18: 11968 (NP-13501)
determination of protein-bound in blood serum, activation, 16: 2882
determination of radioactive, in fission product–corrosion product mixtures, 16: 31559
determination of trace amounts in rare earth compounds, spectrographic, 16: 28869 (JEN-107-DQ/I-33)
determination of traces in beryllium, photometric, 17: 19963
determination of traces of, using oxycellulose, 17: 35656
determination of traces of, in biological samples, activation, 18: 13414 (BNL-7362)
determination of traces of, in water by atomic absorption spectrometry, 18: 33461 (DP-879)
determination of traces of, in polyphenyls, 19: 302 (RT/CHI(64)-11)
determination of traces in cobalt oxide, spectrographic, 19: 15336 (AEET/Spec./3)
determination of trace amounts in uranium compounds, activation, 20: 1784
determination of trace amounts of, in iron, activation, 20: 14471
determination of trace amounts of, in beryllium by spectrography, 20: 16352
determination of trace amounts of, by reactor neutron activation methods, 20: 26760
determination of trace amounts of, in tungsten and molybdenum by atomic absorption spectrophotometry, 20: 43154
determination of, properties of formaldoxime for spectrophotometric, 18: 39085
determination of, neutron activation, 20: 2520(R) (IA-920)
determination of, by paper chromatography and precipitation using phosphorus-32-labeled phosphate, 20: 35409
determination of, in uranium, by activation analysis, 20: 36715
determination of, in carbazole by neutron activation methods, 20: 43116
determination of, in standard rocks by neutron activation and gamma spectrometric methods, 20: 45587
determination using wall-stabilized arc discharge, 17: 25124
determination using thenoyltrifluoroacetone, spectrophotometric, 18: 43418
determination using sodium perxenate, spectrophotometric, 20: 16351
determination, use of photoneutron counting in activation, 19: 36322
deuteron elastic scattering at 6.5 Mev, polarization in, 17: 38157
deuteron reactions (d,t) at 21.6 Mev, 17: 6780(R) (ANL-6603(p.52-5))
diffusion in gamma uranium, 17: 41333(R) (ANL-6677)
diffusion in gamma uranium, 18: 25969(R) (ANL-6868(p.287-302))
diffusion in gamma uranium, 18: 44208
diffusion in gamma cerium, electro-, 19: 34722
diffusion in gamma-phase uranium, 20: 19175 (ANL-6568)
diffusion in gamma-cerium, gamma-uranium, and epsilon-plutonium, electro-, 20: 23734
diffusion in titanium at 900 to 1650°C, 17: 34454
diffusion into alkaline earth fluoride lattices, 16: 11653
dissociation energy of gaseous and heat of vaporization of solid, correlation of, 17: 6095
distribution and metabolism in man and animals, tracer study of, 19: 21817(R) (BNL-867(p.119-50))
distribution coefficient in hydrochloric acid and ion exchange resins, 16: 7503
distribution coefficient between fused bismuth and fused salt eutectic, 17: 21683
distribution, excretion, and metabolism, tracer studies, 16: 1401
distribution in deep-sea silts and sea water, 20: 18892 (NYO-3450-1, pp 41-89)
distribution in mollusk tissues, 19: 45788
distribution in tissues, effects of hepatic damage, tracer study, 16: 14440
distribution of, in tissues of rats and man, 18: 23199 (BNL-828)
distributions in hot-pressed tantalum carbide, 17: 37558
effect on determination of oxygen in steel by isotope dilution method, 19: 43946
effect on properties of low-alloy steels for reactor pressure vessels, 20: 39444(P)
effects of nitrogen mustard on content of, in spleen in rats, 17: 40547(R) (NYO-10569)
effects of, on potentiometric-acidimetric determination of zirconium, 17: 23288
effects of, on superconducting properties of vanadium silicides, 16: 30821
effects of traces of, on corrosion of chromium–nickel steel, 20: 41418(R) (GEAP-5150)
effects on activation determination of arsenic in ores and rocks, 20: 16364
effects on alpha-induced luminescence of zinc-cadmium sulfides, 19: 448
effects on chlorine determination in paper pulp by activation methods, 20: 8854
effects on complexometric determination of zirconium using stilbazogall II, 19: 30138
effects on corrosion of Zircaloy-2 by steam and water at 750 and 680°F, 16: 10463
effects on corrosion resistance of beryllium, 19: 22913(P)
effects on density of states in superconductors, 19: 47535
effects on dislocation properties in iron, 19: 16070 (EURAEC-1075)
effects on distribution of strontium-90 in water-bearing strata by ground waters, 19: 46602
effects on ductility of iodide chromium, 18: 32189
effects on expansion of cerium–cobalt–plutonium alloys on freezing, 19: 39161 (LA-DC-6956)
effects on extrusion strengthening of magnesium–thorium alloys, 19: 9680
effects on fluorescence of uranium in sodium carbonate–sodium fluoride melts, 18: 33506
effects on forging of magnesium, 19: 7886(P)
effects on fracture mechanisms in beryllium single crystals, 20: 23714
effects on gamma-induced color centers in glass, 16: 19451(T)
effects on growth of beryllium oxide crystals, 17: 30511 (NAA-SR-8235)
effects on impact strength of weld metal of arc welding electrode, 19: 14051
effects on indium superconductivity, 18: 40450
effects on luminescence of copper-activated zinc sulfide, 17: 11228(T)
effects on magnetic susceptibility of hafnium, titanium, and zirconium, 19: 28840
effects on mammals, 18: 21700 (BNL-7855)
effects on mechanical properties of aluminum–copper–iron–tin–titanium–vanadium alloys, 19: 46985 (AD-613651)
effects on Néel temperature of chromium, (E), 19: 4741 (IS-1033)
effects on oxidation of graphite, 19: 22911
effects on oxidation resistance and strength of chromium–magnesia composites, 19: 41022(R) (NP-15292)
effects on phase transformations in steel, 18: 24152(T,R) (EURAEC-1001)
effects on phase transformations in gallium–plutonium alloy and plutonium, differential thermal analysis of, 20: 41452 (MLM-1172)
effects on photometric determination of cerium in cast iron and steels, 20: 43143
effects on preparation of uranium carbide by carbothermic reduction of oxide, 20: 33841 (NAA-SR-10624)
effects on properties of Zircaloy-2, 18: 44031 (BM-RI-6536)
effects on properties of boron steel, 20: 39426
effects on properties of magnesium-base alloys for fuel-element cladding, 20: 39443(P)
effects on radiation effects from phosphorus-32 on metabolism in wheat plants, 20: 35226
effects on radioinduced luminescence of zinc silicates, 20: 5573
effects on reconstitution of blastocyst formation in rabbits, 19: 25864

effects on silicide coatings for tantalum-base alloys, 17: 23945(R) (ASD-TDR-63-232)
effects on spectrophotometric determination of aluminum, 19: 13226
effects on spectrophotometric determination of zinc using 1-(2-thiazolylazo)-2-naphthol, 19: 19814
effects on spectrophotometric determination of thorium, 19: 24408
effects on spectrophotometric determination of cerium, 19: 32075
effects on superconducting transition temperature of vanadium silicide, 19: 39196
effects on thermal conductivity of selenium, 20: 46211
effects on x-irradiation coloration of sodium chloride crystals, 16: 13661
electron paramagnetic resonance in strontium chloride crystals, spectra of, 18: 13780(T)
electron reactions with, K x-ray emission in, (E), 19: 16377
electron spectra from, KLL-Auger, (E), 20: 15243 (CONF-233(Vol.3), pp 480-6)
electron spin resonance in gallium arsenide, 17: 12277
energy level transitions in, Coster-Kronig, (T), 20: 15238 (CONF-233 (Vol.3), pp 398-418)
energy level widths for, K, (T), 20: 15239 (CONF-233(Vol.3), pp 419-39)
energy levels of mesic (μ) atoms of, quadrupolar effects on, (T), 19: 39368 (NP-15089)
evaluation as detector for fast neutron flux in reactors, 16: 12801(R) (IA-685)
excretion in feces and urine in colostomized pullets, 19: 43693
excretion in urine of man, effects of diseases on, 20: 8568
explosibility of powders of, 19: 36698 (BM-RI-6516)
fluorescence, K-shell yields, 16: 26000
fluorescence yields in proportional and scintillation detectors, 18: 3796
gamma attenuation at 0.1 to 10 Mev, coefficients for, 18: 35058
gamma reactions (γ,n) with, neutron angular distribution from, 18: 34935
gamma spectra from 14-Mev neutron activation, determination by, 19: 26241
Hartree-Fock potential of neutral atoms of, analytical expressions for, 18: 16656
heat capacity of superconducting gamma, at 0.066 to 4.2°K, 18: 31433(R) (UCRL-11317(p.18-31))
hyperfine structure of, relativistic quadrupole interaction in, (E/T), 20: 15265
inflammability of powdered, at 180 to 1100°C, 18: 44211
influence of, content of soils on wheat and barley growth variations, 20: 40532(R) (COO-1097-17)
ion exchange behavior in hydrochloric acid–organic solvent media, 18: 39124
ion exchange in concentrated hydrochloric and perchloric acids, distribution coefficients for, 18: 17759
ion exchange on resins, effects of boric acid and potassium hydroxide on, 17: 27493 (WCAP-3716)
ion exchange paper chromatography of, 18: 17785
isotopic exchange in soils, 17: 15581
laser beam reactions with, uv spectra from plasma produced from, (E), 20: 38300
luminescent effects of, on uranium, 17: 15928
machining procedures for, 20: 43864 (Y-1550)
magnetic fields of, internal effective, (E), 19: 4700
magnetic susceptibility of, pressure effects on, (E), 20: 13312(T)
manganese-55 NMR linewidth in beta, (E), 19: 21366
melting temperature of, equations for calculating, 18: 25990
meson (μ^-) capture by, x rays from, 18: 19044
meson (μ^-) capture by, probability for, (T), 20: 28456
meson (μ) decay in, measurement of bound-to-free rates of, 18: 12964
meson (μ) capture, Fermi interactions in, 16: 15590
meson (μ) cascades in, x-ray emission from, 16: 15692
meson (μ) scattering, x-ray emission in, 16: 19705
metabolism and distribution in animals and man, tracer studies of, 18: 21763 (BNL-7940)
metabolism and toxic effects of, in man, 18: 7989 (BNL-7394)
metabolism by snails, 19: 10731(R) (NP-14669)
metabolism, effects of adrenocorticosteroid hormones, 16: 5136
metabolism in body, clinical and biological studies of, 18: 13414 (BNL-7362)
metabolism in chickens, tracer study, 20: 29
metabolism in man, 16: 7359
metabolism, physiological effects, and biological specificity of, in man, 17: 38704 (BNL-7252)
motion of particulate, on graphite surfaces, 18: 27872
neutron absorption cross sections, 2200 m/sec, 17: 29576 (PAN-410/IX)
neutron absorption by, resonance, 19: 32058(R) (GA-5978)
neutron absorption cross sections for, reactivity method for measuring, 20: 38414
neutron absorption cross section in pitchblende, thermal, 20: 37994
neutron activation and photon-producing cross sections, tabulation, 16: 23008 (XDC-60-8-81)
neutron activation of, measurement of neutron flux density by, 17: 25601 (PAN-408/IX)
neutron activation cross sections of, thermal, 17: 26466 (PAN-407/IX)
neutron activation in beryllium oxide moderated cores containing hydrogen, 18: 23011 (GAMD-2871)
neutron activation of, absolute measurement of efficiency of neutron sources by, 18: 26504
neutron cadmium ratio determinations in JEN-1 reflector, 16: 11324
neutron capture by, average level widths of compound nucleus from, (E), 20: 32424
neutron capture by, energy resolution of gamma spectra from, 20: 29078(R) (AD-633252)
neutron capture by, gamma spectra from thermal, (E), 19: 6695
neutron capture by, gamma spectra from, (E), 19: 19095 (WASH-1053)
neutron capture by, use for absolute calibration of neutron sources, 19: 33188 (AAEC/TM-288)
neutron capture by, gamma spectra from resonance, (E), 20: 15731(R) (RPI-328-49)
neutron capture by, gamma spectra from, (E), 20: 28287(R) (TID-22844, pp 36-53)
neutron capture cross sections at 30 and 65 kev, 16: 33792(R) (ORNL-TM-383)
neutron capture cross sections at 4 to 220 kev, total, 18: 42650 (TID-21144)
neutron capture cross sections, 19: 29468(R) (ANL-7017)
neutron capture cross sections in fast reactors, 20: 34950
neutron capture gamma spectra, 16: 19745(R) (ARF-1193-9)
neutron capture gamma spectrum, 16: 28024(R) (ARF-1193-12)
neutron capture gamma spectra, 17: 17255
neutron capture in, resonance and thermal, (E), 19: 16972
neutron capture rate in, iterative five-group analysis of, 18: 27841 (AEEW-M-424)
neutron cross sections, library of 40-group BPG and spectral "B" codes, 16: 12422 (BAW-158)
neutron cross sections, corrections, 16: 24796 (UNC-5002)
neutron cross sections for, nine and sixteen group, 17: 22789 (GEMP-173)
neutron cross sections for, 9- and 16-group, 20: 4829 (GEMP-173(Suppl.1))
neutron elastic scattering at 0.68 to 1.25 Mev, (E/T), 20: 19805(R) (ANL-7110, pp 1-28)
neutron elastic scattering at 3.2 Mev, (E/T), 20: 46644
neutron form factors and spin density distributions for, comparison with Hartree-Fock calculations, 17: 6646 (BNL-5674)
neutron inelastic scattering by, 18: 11195(R) (EANDC(E)-49(L))
neutron inelastic scattering at 14.1 Mev, gamma yields from, (E), 19: 35417
neutron inelastic scattering to 14 Mev, energy spectra of, (E), 20: 31566
neutron radiative capture cross sections at 30 and 65 kev, 18: 34274(R) (NIRS-2(p.3-15))
neutron reaction rate in foil of, thermal-spectrum, 18: 7026 (AEEW-R 217)
neutron reactions, cross sections, 16: 2774(R) (IDO-16710)
neutron reactions (n,t), cross section, 16: 7048
neutron reactions at high energies, table of radioisotopes produced in, 17: 794 (CERN-62-22)
neutron reactions (n,t), cross sections for, 17: 2242 (TID-16949)
neutron reactions (n,t) with, cross sections for, 17: 9619
neutron reactions (n,γ) with, recoil atom charge from, 17: 28969
neutron reactions (n,t) on, cross sections for, 17: 31434
neutron reactions (n,γ) with, gamma spectra of fast and thermal, 18: 24699
neutron reactions at 4 to 5 Mev, compound-nucleus level widths from, 18: 36645
neutron reactions with, cross sections for in-pile, (E/T), 19: 10643 (EURAEC-1198)
neutron reactions (n,γ) with, spectra of thermal, (E), 19: 35439
neutron reactions at 50 to 260 kev, total cross sections for, (E), 20: 40069(R) (EANDC(E)-66(U))
neutron resonance integral, 16: 9653 (KAPL-2000-16)
neutron resonance integrals for, 18: 24625 (WASH-1046)
neutron resonance absorption and scattering by foils of, self-shielding factors for, 20: 8053
neutron resonances, 16: 3208
neutron scattering by, 18: 24625 (WASH-1046)
neutron scattering by, differential cross sections for, (E), 19: 8469
neutron scattering by, angular distributions of, 19: 31252
neutron scattering cross sections at 700 to 1200 kev, (E), 20: 30360 (WASH-1068)
neutron total cross sections at 28.4 Mev, 16: 5969
neutron total cross section at 200 ev to 1 Mev, 17: 36669 (WASH-1042)
neutron total cross section at 0.8–1.2 Mev, effective, 18: 11195(R) (EANDC(E)-49(L))

neutron total cross section at 0.01 ev to 50 kev, 18: 24678
nuclear polarization in, method for, 17: 7267(T)
nuclear properties for use as neutron detector, 18: 30695
nutritional needs and toxic effects of, in man, 19: 21990
performance as electrode in contact ion engines, 19: 13613
photon reactions up to 80 Mev, neutron emission in, 18: 38152
photoneutron activation in potassium permanganate solution, method for, 17: 9490
precipitation using dimethylbenzenearsonic acid, 19: 9136
precipitation using trichlorobenzenearsonic acid, 19: 9137
precipitation with calcite at 90 to 325°C, 16: 25319 (TID-16128)
preparation of kryptonated, by diffusion, 20: 18570(R) (NYO-2757-5)
preparation of pure, 18: 25912(P)
preparation of self-supporting radiation targets of, 20: 17218
preparation of thin layers of, for use as cyclotron irradiation target, 19: 28966
production in supernova interiors, rapid nuclear processes for, 17: 39835
properties as absolute neutron flux monitor, 16: 27334
properties as neutron threshold detector, 18: 13242
properties as reactor control material, 16: 32120 (TID-16597)
properties as spiked-poison in neutron capture studies of boron, 18: 2798
properties for use as oxidation-resistant coating for uranium, 19: 13925
properties of films of, as neutron-measuring probes, 16: 336 (NP-10851)
properties of films of, as neutron-measuring probes, 16: 14927(T) (CEA-tr-A-1090)
properties of foils of, as neutron flux monitor, comparison of, with aluminum–cobalt wires, 17: 4333(R) (IDO-16805(p.7-35))
properties of tetravalent, as phosphor activator, 17: 12822
protective effects of dietary, against radiation injuries in rats, 17: 19872
protective effects against nucleic acid decomposition by nuclease, 18: 25085 (SGAE-BL-5/1964)
proton elastic scattering at 9–22 Mev, optical-model analysis of, 17: 28316
proton inelastic scattering by, effects of E1 resonances on, 16: 33906
proton reactions at high energies, table of radioisotopes produced in, 17: 794 (CERN-62-22)
proton reactions at 0.05 to 2.9 Bev, induced activity data and cross sections for spallation, (E/T), 20: 32549
proton reactions (p,pn) at 20 to 150 Mev, excitation functions for, 16: 28042
proton reactions with, rare gas and tritium production cross sections for, 18: 15189 (CERN-64-12)
radiation effects on availability in soils, 16: 16176 (NP-11578)
radiation effects on tissue content in dogs, guinea pigs, and rabbits, beta and x, 18: 38872
radiation effects on content of, in blood, liver, and spleen in dogs, 19: 17537
radiation effects on electric conductivity of alkali halides doped with, x, (E), 19: 26386
radiation effects on color stability of glass of, dosimetry relation to, 17: 23787
radiation effects on content of, in spleen in rats, 17: 40547(R) (NYO-10569)
radiation effects on metabolism of, in rats, 19: 43852
radiation effects at low temperatures on resistance of alpha-, proton, 20: 19269
radiation effects on optical absorption of, in alkali borate glass, 20: 36887
radioinduced heating of, gamma, 18: 10346(R) (X64-11113)
radioinduced production of helium and hydrogen in, neutron, 19: 26901
radiolysis of aqueous solutions of, spectra of abnormal valency states in, 17: 35909
radiosterilization effects on content of, in strawberries, gamma, 20: 13143(R) (UCD-34P80-3, pp 55-7)
reactions of liquid, with thorium dioxide, 17: 28828(R) (TID-18951)
reactions with benzenearsonic acid and its derivatives in acid media, precipitation, 17: 12198
reactions with beryllium to 600°C *in vacuo*, 19: 22997 (TRG-Report-842)
reactions with boron nitride at high temperatures, 18: 41373(R) (TID-20951)
reactions with crucibles of refractory compounds with boron, carbon, and nitrogen at 400 to 1500°C, 19: 37112
reactions with fast neutrons, helium and hydrogen production in type 347 stainless steel in, 20: 7490(R) (BMI-1745, Sect.A)
reactions with graphite, composition and structure of carbides formed in, 20: 17030(T) (LA-tr-66-1)
reactions with magnesium to 650°C, 19: 22997 (TRG-Report-842)
reactions with silver nitrate in nonaqueous solvents, 16: 5311(R) (TID-14361)
reactions with thorium oxides, 17: 25164 (TID-18684)
role in enzyme systems by which RNA is synthesized, 20: 16160 (UCRL-14739(Pt.2))
role of, in etiology of degenerative diseases in man, 18: 23199 (BNL-828)
sedimentation in open ocean, mechanisms for, 18: 36897(R) (TID-20887)
separation by anion exchange in acetic acid–nitric acid medium, 18: 16131
separation by anion exchange in acid-organic solvent media, 18: 23707(R) (TID-20609)
separation by anion exchange in mixed aqueous and non-aqueous systems, 19: 2243
separation by cation exchange, 19: 13535
separation by reversed-phase column chromatography, 17: 1401
separation by solvent extraction using mono-octyl ester of α-aniline benzylphosphonic acid, 16: 13157
separation from actinide transition elements by ion exchange, 19: 24449
separation from aluminum and iron by column and electrochromatography in molten sulfates, 20: 35430
separation from aqueous solutions by solvent extraction using 8-hydroxyquinoline-N-oxide, tracer studies of, 17: 21783
separation from aqueous solutions by solvent extraction using diphenylarsinic acid, 17: 21787
separation from aqueous sulfuric acid solutions by solvent extraction using *N*-octylanilinobenzylphosphonate, 18: 27330
separation from cadmium, tracer studies, 16: 3305 (BMI-1553)
separation from cerium, chromium, and vanadium, 17: 12213
separation from cerium by ion exchange chromatography, 19: 26480
separation from chloride solutions by solvent extraction using amines, 17: 17949(R) (ORNL-TM-449)
separation from chromium, cobalt, and iron by ion exchange, 18: 11536(T) (AEC-tr-6305)
separation from chromium, nickel, rare earths, and silver by ion exchange chromatography, 20: 20634
separation from chromium, cobalt, and iron by paper chromatography, 20: 26786
separation from cobalt by ion exchange, 17: 31797(R) (BNL-782(p.51-9))
separation from cobalt, copper, iron, and zinc by anion exchange using tartaric acid, 17: 40917 (AD-288767)
separation from cobalt and sodium by electrophoretic focusing, 18: 35466
separation from cobalt by solvent extraction, 20: 5602
separation from Hanford wastes by solvent extraction, 20: 16329 (BNWL-187)
separation from hydrochloric acid solutions by solvent extraction using 2-ethylhexanol, 19: 36252
separation from iron by reversed-phase chromatography, 16: 11734
separation from iron by thin-layer chromatography, 19: 9266
separation from iron by precipitation of iron with pyridine, 19: 22312
separation from iron by extraction-chromatography using tetrabutyl hypophosphate–tetrabutyl pyrophosphate mixture, 19: 42439
separation from iron by ion exchange, 20: 33402
separation from lithium fluoride by zone refining, 18: 22019(R) (ORNL-3591(p.231-40))
separation from metal ionic mixtures, electrochromatographic, 17: 10753
separation from metal mixtures by thin layer chromatography, 20: 36753
separation from niobium in fluoride solutions by solvent extraction using pyrogallol, 18: 10189
separation from nitric or sulfuric acid solutions, ion exchange selectivity scales for, 19: 9257
separation from nickel by solvent extraction using TBP, 19: 36297
separation from other metals by ion exchange chromatography in tartrate medium, tracer studies of, 19: 7627
separation from other metal ions on silica columns treated with dinonyl naphthalenesulfonic acid, 19: 15691
separation from other metals by ion exchange, 19: 15692
separation from other metals by reversed-phase chromatography, 19: 30331
separation from other metals by partition chromatography of chloride solutions, tracer studies of, 19: 32288
separation from other inorganic ions by paper chromatography, 20: 12939
separation from other elements by ion exchange using triisooctylamine, 20: 43439
separation from plutonium by anion exchange, 17: 4629
separation from protactinium by solvent extraction, 18: 20105
separation from protactinium by solvent extraction, 19: 30337
separation from pure metals using thionalide, 16: 18835
separation from rare earths by ion exchange in isopropyl alcohol, 18: 20104
separation from rare earths by precipitation using dihydroxymaleic acid, 19: 46452
separation from rare earths, solvent extraction method for, 20: 16329 (BNWL-187)
separation from rare earths by ion exchange chromatography, 20: 18827
separation from rhenium by anion exchange chromatography, 19: 24433

separation from salts by solvent extraction using 8-mercaptoquinoline in chloroform, 20: 10759 (INP-427/C)
separation from scandium by precipitation using cinnamic acid, 18: 43426
separation from scandium sulfate by solvent extraction using sulfuric acid, 19: 30196
separation from scandium by ion exchange chromatography, 20: 16574
separation from scandium by ion exchange chromatography, 20: 20821
separation from silver by partition chromatography, 20: 4054
separation from solutions of bone, milk, and teeth ash by solvent extraction using sodium diethyldithiocarbamate, tracer studies of, 20: 10950
separation from thorium, titanium, and zirconium using ammonium cinnamate, 16: 28900
separation from thorium by ion exchange in nitric acid solution, 20: 20624
separation from titanium by cation exchange chromatography, 17: 32054
separation from titanium using benzoylphenylhydroxylamine, direct weight gravimetric, 17: 38940
separation from titanium and zirconium by zone melting, 18: 8456
separation from uranium, photolytic, 16: 7620
separation from uranium ores, 16: 22259(R) (ACCO-20)
separation from uranium by ion exchange and elution with ascorbic acid, 18: 25611(T) (AEC-tr-6227/1(p.1-8))
separation from uranium by cation exchange chromatography, 19: 13245
separation from uranium by chromatography on cellulose columns, tracer studies of, 19: 40687
separation from uranium by ion exchange, 19: 44119
separation from uranium by combined ion exchange–solvent extraction using nitric acid–tetrahydrofuran solutions, 20: 20811
separation from zinc in aqueous solution by solvent extraction using dithizone–chloroform, 19: 26471
separation of, from indium and gallium using cinnamic acid, 17: 15924
separation of, from thiocyanate solutions by solvent extraction using 4-methyl-2-pentanone, 17: 20122
separation of protactinium from, by sorption on activated charcoal, 20: 43148
separation of rare earths from, by precipitation using ammonium cinnamate, 20: 45611
separation of scandium from, by ion exchange chromatography, 19: 533
separation of scandium from, by precipitation using ammonium cinnamate, 20: 25012
separation of thorium-230 from, by ion exchange, 20: 38834
separation of trace amounts of, from alkali metals, alkaline earths, and rare earths, 20: 1958
separation of traces of, from iron by paper chromatography, tracer studies of, 20: 29342
separation of, from thallium by ion-exchange chromatography, 20: 36935
separation of, from thorium in sulfuric acid solutions by ion exchange, 20: 43147
separation of, from zinc, in hydrochloric acid solutions by ion-exchange chromatography, 20: 45809
Slater-Condon parameters of, determined from spectral data, 17: 31118
solubility in bismuth (liquid) at 500°C, 16: 13137
solubility in liquid cadmium, 17: 1985
solubility in liquid cadmium, 17: 7655(R) (ANL-6600)
solubility in liquid zinc at 750°C, 17: 35078(R) (ANL-6739)
solubility in liquid zinc, 20: 22966 (ANL-7083)
solubility in manganese chloride (liquid), 17: 35687 (IS-596)
solubility in mercury, 17: 28906
solvent partition in aqueous bromide–TBP systems, 18: 25382
solvent partition in tributyl phosphate–hydrochloric acid or –nitric acid systems, 18: 33685
sorption by barley roots, effects of polyvalent cations on, 20: 16174(R) (RLO-1547-3)
sorption by soil colloids, 20: 19
sorption from nitric acid by ion exchange paper, 19: 24435
sorption from sulfuric acid by anion exchange resins, 18: 31680
sorption of trace amounts of, by glass, tracer studies of, 20: 31245
sorption on anion exchange papers in hydrobromic and hydrochloric acids and lithium chloride, 18: 25374
sorptive properties of evaporated films of, for carbon monoxide at 0°C, 20: 21388
spark patterns produced by grinding of, 18: 19493(T) (SC-T-64-47)
spectra in lithium chloride–potassium chloride, crystal field, 16: 30371 (TID-16693)
spectra in reaction zone of acetylene air flame, excitation of atomic, 17: 27371(T)
spectra of, arc, 18: 6358
spectra of, correlation of dissociation energies and excitation potentials in flame, 17: 14234
spectra of, electric discharge, 17: 34642
spectra of, infrared, 17: 32739
spectra of low-energy x rays from target, effects of electrons in 80 to 180A region, 16: 23032
spectra of minerals, effects of temperature on infrared, 17: 33880
spectra of, in zeta pinch, 19: 25564
spin density in ferrimagnetic antimony–manganese alloys, aspherical, 17: 37695
spin density in ferrimagnetic manganese–platinum alloys, radial, 17: 37696
sputtering by noble-gas ions at 100 to 600 ev, yields from, 16: 22753
superconductivity of lead and tin in superimposed layers with, 18: 32704
surface tension of liquid, 19: 32048(R) (NP-15073)
thermal activation of bare and cadmium-clad foils of, 17: 36347(R) (NARF-62-18P)
thermal capacity of gamma, electronic and hyperfine, 18: 28006
thermal capacity of alpha, at 1.75 to 4.2°K, 19: 34716
thermal capacity of gamma, magnetic hyperfine, 20: 832 (UCRL-16180)
tracer applications survey, 16: 1359
tracer applications, 16: 6446
transition probabilities of forbidden lines of, calculation of, 18: 14736
uptake by corn plants, effects of soil colloids on, 20: 22547 (TID-21702)
uptake by Japanese, effects of environment on, 19: 6970
uptake by plants, 20: 19
uptake by rice, effects of irrigation on, 20: 40574
use as tracer for activation analysis of cotton, 17: 27634(R) (NCSC-2477-4)
use in determination of neutron spectra, 16: 7252
use in measurement of epithermal neutron spectra, 16: 4336
use in neutron flux detector utilizing calorimetric conversion, 18: 14290(P)
use in pyrotechnic delay mixtures, 17: 36448 (SC-4790(RR))
valence in brass from magnetic measurements, 17: 11297 (AE-95)
vapor pressure, 20: 331
voltammetry in phosphoric acid–sulfuric acid or sulfuric acid using pyrolytic graphite electrode, 18: 19967
wire activations in thin clean critical slab, analysis by transport approximations, 16: 18631
x-ray absorption at room temperature and –180°C, 17: 39798
x-ray emission at 80 to 180Å, 16: 8129

MANGANESE ALLOY COUPLES

Chromel/constantan, thermocouple tables, smoothed, 19: 20268 (ORNL-3649(Vol.2)(Sect.2.6))
constantan/Cu, thermocouple tables, smoothed, 19: 20267 (ORNL-3649(Vol.2)(Sect.2.5))
constantan/Fe, thermocouple tables, smoothed, 19: 20266 (ORNL-3649(Vol.2)(Sect.2.4))
Invar/Ni, tensile properties of, testing, (E), 19: 20554 (LA-3161)
Alumel/Chromel, radiation effects on thermoelectric properties of, (E), 19: 24014 (CONF-640607(Vol.II)(Paper D-4))
Constantan/Cr, radiation effects on thermoelectric properties of, (E), 19: 24014 (CONF-640607(Vol.II)(Paper D-4))
Constantan/Fe, radiation effects on thermoelectric properties of, (E), 19: 24014 (CONF-640607(Vol.II)(Paper D-4))
constantan/Fe, thermocouple tables for cryogenic JN/JP, smoothed, 19: 20275 (ORNL-3649(Vol.2)(Sect.2.13))
constantan/Fe, thermocouple tables for cryogenic YN/YP, smoothed, 19: 20276 (ORNL-3649(Vol.2)(Sect.2.14))
constantan/Cu, thermocouple tables for cryogenic, smoothed, 19: 20273 (ORNL-3649(Vol.2)(Sect.2.11))
Cr/Cu–Mn–Ni, neutron radiation effects on, 18: 44261
Cu–Mn–Ni/Fe, neutron radiation effects on, 18: 44261

MANGANESE ALLOYS

see also A-286 Alloy

phase diagrams of rare-earth-containing, types, 19: 23004(T) (JPRS-28849(p.148-57))
preparation of oxidation-resistant, 19: 24929(P)
properties and structures of intermetallic compounds with lanthanides, 16: 1687
Al–Be–Mn, determination of $AlMnBe_4$ in commercially pure beryllium, 17: 27856
Al–Ce–Cu–Mn, structure of intermetallic compounds in, 19: 23010(T) (JPRS-28849(p.197-8))
Al–Ce–Mn, crystal structure of compounds in, 17: 14883(T)
Al–Ce–Mn, phase studies and structure, 17: 36326
Al–Cu–Mg–Mn, erosion by water of rotating disks of, 19: 44625 (TIM-894)
Al–Cu–Mg–Mn, proton reactions at 660 Mev, 17: 41884
Al–Cu–Mg–Mn, sputtering by 2-kev mercury ions, energy distributions of particles from, 18: 14625
Al–Cu–Mn, neutron diffraction study of κ magnetic phase of, 17: 16702
Al–Cu–Mn, paramagnetism and valency in, 17: 32561 (AE-111)
Al–Dy–Mn, phase studies, Laves, 16: 25798
Al–Fe–Mg–Mn, microstructure of 214X, electron microscopic studies using ultramicrotome, 18: 7206 (GAT-T-1121)
Al–Fe–Mn–U, intermetallic compounds of, phase diagrams, 20: 43980
Al–Ho–Mn, phase studies, Laves, 16: 25798

Al–Mg–Mn, creep properties at high temperatures, 18: 26066(P)
Al–Mg–Mn–Zn, corrosion, 19: 6271(T) (JPRS-27451)
Al–Mg–Mn–Zn, plastic anisotropy of AZ31B sheet, 19: 39149 (AD-425880)
Al–Mn, analysis for magnesium, activation and colorimetric, 16: 1710
Al–Mn, annealing neutron-irradiated, 17: 39693
Al–Mn, critical temperature of superconducting, 17: 29457
Al–Mn, crystal structure of nitrogen-containing, 16: 2259
Al–Mn, crystal structure of the tetragonal ferromagnetic phase of, 17: 34422
Al–Mn, magnetic moments of manganese atoms in, neutron-diffraction analysis of, 16: 31571 (RCN-8)
Al–Mn, microstructure of, electron microscopic studies using ultramicrotome, 18: 7206 (GAT-T-1121)
Al–Mn, preparation by levitation melting, 20: 25521 (AERE-R-5097, Paper 23)
Al–Mn, solidification and structure of, effects of high cooling rate on, 19: 9673(T) (SC-T-64-2011)
Al–Mn, superconducting transition in, (E), 20: 9915
Al–Mn, superconducting critical temperature of, transition-metal impurity effects on depression of, (E), 20: 37955
Al–Mn, surface investigations on, 17: 41421 (ASD-TDR-63-424)
Al–Mn, work-softening of, effects of second phase on, 17: 24002
Al–Mn–Ag, ferromagnetism, 16: 22638
Al–Mn–Ag, phase studies, 16: 22637
Al–Mn–Ni, composition of X phase in, 17: 11249
Al–Mn–Ni–Ti, corrosion by halide volatility separation process gases and liquids, 20: 33413(R) (K-1669)
Al–Mn–Tb, phase studies, Laves, 16: 15798
Al–Mn–Th, phase studies of $ThAl_2$–$ThMn_2$, 18: 20554
Al–Mn–Ti, corrosion by mercury, 18: 10492
Al–Mn–Ti–V, properties of aged, 20: 4360(R) (AD-619399)
Al–Mn–U, crystal structure of UAlMn phase in, 18: 39978
Al–Mn–U, electric and thermal properties of Laves phases of intermetallic compounds in, 20: 873
Al–Mn–U, phase studies of pseudo-binary system UMn_2–UAl_2 in, 18: 39979
Al–Mn–Y, crystal structure of intermetallic compounds in, 20: 39414
Al–Mn–Y, magnetic susceptibility at 4 to 300°K, 19: 30743(R) (NYO-3454-1)
Au–Mn, atomic number effects correction in electron probe microanalysis of, 17: 27268
Au–Mn, crystal spin-screw structure of, magnetic field effects on, 16: 16829
Au–Mn, crystal structure of Au_3Mn, 20: 17066
Au–Mn, electron diffraction diagrams of antiphases with non-integral periods, 17: 22179
Au–Mn, heat capacities of intermetallic compound in, at 0.14 to 1.18°K, 20: 39470(R) (ORNL-3924)
20: 32684(R) (UCRL-16658, pp 21-38)
Au–Mn, hyperfine structure of intermetallic compound in, 20: 22859(R) (UCRL-16580, pp 149-205)
Au–Mn, magnetic structure of, neutron diffraction study of, 16: 7986
Au–Mn, magnetic structure of, near 50:50 composition, 16: 21213
Au–Mn, magnetic susceptibilities, 16: 25882 (ASD-TR-61-630)
Au–Mn, magnetic structure of, neutron diffraction studies of effects of pressure on, 20: 31756
Au–Mn, neutron diffraction patterns of, 17: 37795
Au–Mn, neutron reaction rates in foils of, 18: 7026 (AEEW-R-217)
Au–Mn, neutron scattering, 16: 18444
Au–Mn, radiation and heat-treatment effects on electric and magnetic properties, 18: 24210
Au–Mn, radioinduced coloration in glass sheets of, 18: 36060
Au–Mn, structure of, 17: 578
Au–Mn, thermal capacity of, magnetic hyperfine, 20: 832 (UCRL-16180)
Au–Mn, thermal capacity below 1°K, 20: 29791
Au–Mn, thermoelectric properties of, with less than 0.2% manganese, magnetic field effects on, 16: 15449
Be–Co–Mn, phase studies, ternary laves, 16: 3489
Be–Mg–Mn–Zr, fabrication and properties, 19: 36970(P)
Be–Mg–Mn–Zr, improving metallurgical properties of, 18: 2290(P)
Be–Mn, beryllium-9 NMR in intermetallic compounds of, Knight shift in, (E), 20: 28625
Be–Mn, corrosion resistance, 19: 22913(P)
Be–Mn, ductility at high temperatures, 19: 4639(P)
Be–Mn, phase studies, 16: 2180 (NMI-1252)
Bi–Mn, phase studies, 19: 37072
Bi–Mn, surface investigations on, 17: 41421 (ASD-TDR-63-424)
Ce–Co–Mn–Pu, analysis for cerium and manganese by ion exchange separation and potentiometric titration, 20: 36713 (LA-3402)
Ce–Co–Mn–Pu, phase studies, 19: 13886(R) (LA-3208-MS)
Ce–Mg–Mn, welding of vacuum-tight joints in, by seam process, 19: 22945(T)
Ce–Mn, density and expansion coefficients at 25 to 800°C, 19: 37032 (LA-DC-6580)
Ce–Mn, phase studies, 17: 40342(R) (LAMS-2973)
Ce–Mn, phase studies, 18: 18360(T) (AEC-tr-6387)
Ce–Mn, phase studies at 500 to 800°C, 19: 2818
Ce–Mn, phase studies at 500 to 800°C of cerium-rich, 20: 5851
Ce–Mn–Pu, phase studies, 18: 7125(R) (LAMS-3021)
Ce–Mn–U, phase studies of, eutectic temperature and composition from, 16: 17297(R) (LAMS-2681)
Co–Cu–Mn–Ni, corrosion by liquid sodium at 700 and 1200°F, 20: 9422 (NAA-SR-11326)
Co–Fe–Mn–Ni, mechanical properties at 70 to 2000°F, 17: 18758 (NAA-SR-Memo-8052)
Co–Fe–Mn–U, crystal structure and intermetallic phases, 17: 37559
Co–Mn, atomic and magnetic ordering in, 16: 30717(R) (ANL-6516)
Co–Mn, chemical ordering in, 20: 36355 (ANL-7182)
Co–Mn, ferromagnetic nuclear resonance and saturation magnetization in, 18: 36032
Co–Mn–U, crystal structure and intermetallic phases, 17: 37559
Co–Mn–U, phase diagrams, intermetallic compounds in, 20: 874
Co–Mn–U, phase studies on, eutectic temperature and composition from, 16: 17297(R) (LAMS-2681)
Cr–Co–Fe–Mn–Mo, corrosion by mercury at high temperatures, 18: 7152
Cr–Co–Fe–Mn–Ni, corrosion by mercury at high temperatures, 18: 7152
Cr–Co–Fe–Mn–Ni–W, corrosion by mercury at high temperatures, 18: 7152
Cr–Co–Fe–Mn–Mo–Ni–W, corrosion of Raonel, by coal gasification products at high temperatures, 19: 42127(R) (TID-22009)
Cr–Co–Fe–Mn–Mo–Ni, corrosion of Vitallium, by boiling hydrofluoric acid–nitric acid solutions, 20: 37169(R) (BMI-1774)
Cr–Co–Fe–Mn–Mo–Ni–Ti, corrosion of Hanford 22, by boiling hydrofluoric acid–nitric acid solutions, 20: 37169(R) (BMI-1774)
Cr–Co–Fe–Mn–Mo–Ni–Ti, corrosion of Hanford 23 and 24, by boiling hydrofluoric acid–nitric acid solutions, 20: 37169(R) (BMI-1774)
Cr–Co–Fe–Mn–Mo–Ni–W, mechanical properties at high temperatures, 17: 14811 (ASD-TDR-61-529)
Cr–Co–Fe–Mn–Ni–W, tensile properties of L-605, effects of cold deformation on, 20: 39399 (NASA-TN-D-3528)
Cr–Cu–Fe–Mn–Ni–Ti, corrosion of Corronel-230, by FTW-65 Purex wastes, 19: 31617(R) (ORNL-TM-1081)
Cr–Cu–Fe–Mn–Mo–Ni–Ti, corrosion of Hanford 21, by boiling hydrofluoric acid–nitric acid solutions, 20: 37169(R) (BMI-1774)
Cr–Cu–Fe–Mn–Mo–Ni, corrosion of Illium R, by boiling hydrofluoric acid–nitric acid solutions, 20: 37169(R) (BMI-1774)
Cr–Cu–Fe–Mn–Ni, effects of ammonium fluoride–formic acid–nitric acid anodic solutions against corrosion of, 18: 35959
Cr–Fe–Mn–Mo–Ni–W, corrosion and metallurgical changes in, caused by steam at 1200 to 1500°F, 16: 24126
Cr–Fe–Mn–Mo–Ni–Ti, corrosion of Hanford 20, by boiling hydrofluoric acid–nitric acid solutions, 20: 37169(R) (BMI-1774)
Cr–Fe–Mn–Mo–Ni–Ti, corrosion of Hanford 17, by boiling hydrofluoric acid–nitric acid solutions, 20: 37169(R) (BMI-1774)
Cr–Fe–Mn–Mo–Ni, specification for type 355 plate, sheet, and strip for irradiation testing, 17: 41347 (HW-75208)
Cr–Fe–Mn–Ni, corrosion of, by water in pressurized water reactors, 16: 7855
Cr–Fe–Mn–Ni, corrosion of, effects of carbon, nitrogen, niobium, and titanium on, 16: 13536
Cr–Fe–Mn–Ni, corrosion by superheated steam, cycle tests of, 17: 21229 (TID-7658(p.20-6))
Cr–Fe–Mn–Ni, corrosion of Incoloy, by superheated steam, 17: 38465 (TID-7674(p.11-16))
Cr–Fe–Mn–Ni, corrosion of Incoloy by oxygenated steam at 500°C and 3000 psi, 17: 38466 (TID-7674(p.16))
Cr–Fe–Mn–Ni, corrosion of Incoloy-800 by ferric chloride and superheated steam, 18: 1241(R) (GEAP-4332)
Cr–Fe–Mn–Ni, corrosion by boiling magnesium chloride, 18: 4796(R) (GEAP-4153)
Cr–Fe–Mn–Ni, corrosion by copper chloride at high temperatures, 18: 4796(R) (GEAP-4153)
Cr–Fe–Mn–Ni, corrosion by superheated steam at 1020°F, 18: 7957(R) (GEMP-257)
Cr–Fe–Mn–Ni, corrosion of aluminum-modified Incoloy 800, by steam at 650°C, 18: 19456(R) (ANL-6840)
Cr–Fe–Mn–Ni, corrosion of Incoloy 800 by superheated steam, 18: 27909
Cr–Fe–Mn–Ni, corrosion by mercury at 600 to 1000°F, 18: 27913
Cr–Fe–Mn–Ni, corrosion of Incoloy, by superheated steam at 550°C, 18: 32139(R) (HW-81269(p.5.1-23))
Cr–Fe–Mn–Ni, corrosion of Corronel 230, by boiling hydrofluoric acid–nitric acid solutions, 20: 37168(R) (BMI-1771)
Cr–Fe–Mn–Ni, corrosion of Corronel 230, by boiling hydrofluoric acid–nitric acid solutions, 20: 37169(R) (BMI-1774)

Cr–Fe–Mn–Ni, descaling by sodium carbonate–sodium hydroxide solutions, 18: 22441 (HW-79048)
Cr–Fe–Mn–Ni, fabrication and property specifications for fuel element tubes of Incoloy-800, 18: 1241(R) (GEAP-4332)
Cr–Fe–Mn–Ni, mechanical properties at high temperatures, 17: 14811 (ASD-TDR-62-529)
Cr–Fe–Mn–Ni, mechanical properties of, effects of steam at 1050°F on, 18: 4795(R) (GEAP-3924)
Cr–Fe–Mn–Ni, mechanical properties at high temperatures, 18: 4796(R) (GEAP-4153)
Cr–Fe–Mn–Ni, oxidation of Incoloy-800 by helium–steam at 1700°F, 18: 32043(R) (HW-81269(p.4.1-64))
Cr–Fe–Mn–Ni, phase diagrams of, effects of additive on, 16: 30822
Cr–Fe–Mn–Ni, properties as fuel element cladding material, 17: 36928(R) (GEAP-4126)
Cr–Fe–Mn–Ni, properties as fuel element cladding material, 17: 36929(R) (GEAP-4243)
Cr–Fe–Mn–Ni, radiation effects on, in superheated steam, 17: 21235 (TID-7658(p.59-77))
Cr–Fe–Mn–Ni, thermal-stress-fatigue properties of Incoloy, 18: 596(R) (ATL-A-139)
Cr–Fe–Mn–Ni, thermal stress fatigue tests of Incoloy 800, 19: 13980(R) (ATL-A-144)
Cr–Mn, antiferromagnetism of, at 95 to 300°K, 19: 40077 (IS-T-18)
Cr–Mn, crystal structure of dilute, 18: 25979(R) (ORNL-3582(p.7-8))
Cr–Mn, electric conductivity and thermoelectric power of, at 4.2 to 450°K, 19: 40077 (IS-T-18)
Cr–Mn, magnetic properties, 19: 23057
Cr–Mn, magnetic structure, 18: 37142
Cr–Mn, paramagnetic susceptibility, 16: 10576
Cr–Mn, properties of, at high temperatures, 16: 30779 (BMI-1277)
Cr–Mn, segregation in, 17: 8810 (NP-12451)
Cr–Mn–Mo–Ni, properties for use in liquid-hydrogen bubble chamber, 19: 42808
Cr–Mn–Ni, properties for use in liquid-hydrogen bubble chamber, 19: 42808
Cr–Mn–U, melting point, 16: 6104(R) (LAMS-2647)
Cr–Mn–V, cryogenic properties, 19: 9767(R) (IS-900(Sect.P))
Cu–Ge–Mn, paramagnetism and valency in, 17: 32561 (AE-111)
Cu–Mn, copper-63 nuclear spin echoes in, (E/T), 19: 41988
Cu–Mn, crystal structure of, acoustic attenuation study of friction on fast moving dislocations in, 18: 34276 (NP-14129)
Cu–Mn, heat capacity of manganin at 0.2 to 4.2°K, 17: 35263(R) (UCRL-10706(p.1-110))
Cu–Mn, heat capacity of superconducting, below 1°K, 18: 31433(R) (UCRL-11317(p.18-31))
Cu–Mn, heat capacities at <0.15°K, 20: 32684(R) (UCRL-16658, pp 21-38)
Cu–Mn, iron-57 hyperfine magnetic field in, (E), 19: 39212
Cu–Mn, magnetic interactions in and antiferromagnetic properties of, 17: 18778(T) (AEC-tr-5726)
Cu–Mn, spin ordering of paramagnetic states in superconducting, 20: 2918
Cu–Mn, thermal capacity below 1°K, 20: 832 (UCRL-16180)
Cu–Mn, thermal capacity below 1°K, 20: 29791
Cu–Mn–Ni, corrosion by nitric acid, 17: 6192(T,R) (EURAEC-382)
Cu–Mn–Ni, corrosion by liquid sodium at 700 and 1200°F, 20: 9422 (NAA-SR-11326)
Cu–Mn–Ni, electric conductivity of constantan as function of temperature, 19: 11475 (NAA-SR-Memo-10366)
Cu–Mn–Sn, structure and magnetic properties of, alloying effects on, 16: 9185 (AD-261209)
Cu–Mn–Zn, diffusion in solid, mechanisms of, 19: 42843(R) (COO-359-10)
Cu–Mn–Zn, effects on properties of magnesium and magnesium–zirconium alloy for use as fuel element can, 19: 20610(P)
Cu–Mn–Zn, paramagnetism and valency in, 17: 32561 (AE-111)
Cu–Mn–Zr, analysis for bonding and inclusions in, by x-ray emission in electron microscopy, 20: 20593
Dy–Fe–Mn, phase studies in, Laves, 16: 25798
Dy–Ho–Mn, phase studies in, Laves, 16: 25798
Dy–Mn, crystal structure of intermetallic compound Dy_6Mn_{23} in, size-factor limitation in, 19: 23079
Dy–Mn, crystal structure of Dy_6Mn_{23} in, 20: 17096(T)
Dy–Mn, crystal structures of intermetallic compounds of, 20: 21403
Dy–Mn, crystal structure of intermetallic compound, 20: 43918
Dy–Mn, dysprosium hyperfine magnetic field in intermetallic compounds of, (E), 20: 22330
Dy–Mn, existence of Dy_xMn_y compound in, 19: 14074
Dy–Mn, magnetic moments of intermetallic compound Dy_6Mn_{23} in, 19: 23109
Dy–Mn, magnetic properties of $DyMn_x$, 17: 37709
Dy–Mn, phase diagram, 20: 21403
Dy–Mn, phase studies by differential thermal, thermomagnetic, and x-ray analysis of, 19: 46989 (AD-614466)
Dy–Mn, preparation by sinter process using mercury, 19: 46908 (AD-614464)
Dy–Mn, preparation and structure, 20: 15110
Dy–Mn–Tm, phase studies in, Laves, 16: 25798
Er–Fe–Mn, erbium-166 Mössbauer spectra in, hyperfine structure of, 18: 21272
Er–Mn, crystal structure of intermetallic compound Er_6Mn_{23} in, size-factor limitation in, 19: 23079
Er–Mn, crystal structure of Er_6Mn_{23} in, 20: 17096(T)
Er–Mn, crystal structures of intermetallic compounds of, 20: 21403
Er–Mn, crystal structure of intermetallic compound, 20: 43918
Er–Mn, existence of Er_xMn_y compound in, 19: 14074
Er–Mn, magnetic moments of intermetallic compound Er_6Mn_{23} in, 19: 23109
Er–Mn, magnetic structure of intermetallic compound $ErMn_2$ in, 20: 18556(R) (BNL-929, pp 66-82)
Er–Mn, phase studies by differential thermal, thermomagnetic, and x-ray analysis of, 19: 46989 (AD-614466)
Er–Mn, preparation by sinter process using mercury, 19: 46908 (AD-614464)
Er–Mn, preparation and structure, 20: 15110
Er–Mn–Pr, magnetic properties and structure of $ErMn_2$–$PrMn_2$ in, 20: 27494(R) (NYO-3454-6)
Fe–Mn, antiferromagnetism in f.c.c. and h.c.p., 17: 37688
Fe–Mn, brittle fracture in, relation between twinning and, 19: 26815 (EURAEC-1195)
Fe–Mn, deformation behavior, effects of interstitials on, 19: 43997(R) (UCRL-11889)
Fe–Mn, diffusion of manganese in, at 1300 to 1500°K, 18: 32153(R) (UCRL-11317(p.176-97))
Fe–Mn, dislocation twins in, etch-pit studies of, 18: 16471 (EURAEC-978)
Fe–Mn, dislocation mechanisms in, effects of interstitial impurities, strain rate, and temperature on, 20: 33887 (UCRL-16770)
Fe–Mn, effects of strain rate, structure, and temperature on flow stress at 77 to 370°K, 20: 3641 (UCRL-11512(Rev.))
Fe–Mn, electric conductivity of, effect of composition on, 19: 34675(R) (EURAEC-1394)
Fe–Mn, electronic specific heat, 17: 16698
Fe–Mn, flow stress at room temperature, relations with stress, 18: 18413(R) (EURAEC-975)
Fe–Mn, hyperfine structure of iron-57 spectra in, 17: 13236
Fe–Mn, iron-57 gamma absorption in, s-electron density from isomer shifts in spectra of, 17: 37777
Fe–Mn, magnetic hyperfine field and electric quadrupole coupling in, (E), 20: 28657
Fe–Mn, mechanical properties of, 19: 34675(R) (EURAEC-1394)
Fe–Mn, Mossbauer effect in, 17: 29627
Fe–Mn, radiation effects on mechanical properties, 17: 18852 (BNL-6249)
Fe–Mn, radiation effects of neutrons on ductile-brittle transitions in, 18: 36045(R) (EURAEC-1100)
Fe–Mn, radioinduced embrittlement at low temperatures, neutron, 18: 30229 (BNL-8015)
Fe–Mn, thermal neutron magnetic scattering at high temperatures, 18: 16506
Fe–Mn, thermodynamic properties from vapor pressure measurements, 19: 2276 (UCRL-11575)
Fe–Mn, thermodynamic functions of, formed by neutron irradiation of natural iron, 19: 30755
Fe–Mn, thermodynamic properties at 1450°K, 19: 43997(R) (UCRL-11889)
Fe–Mn–Mo, crystal structure of, neutron diffraction studies of atom ordering in, 19: 9676
Fe–Mn–Nb–Ta–Ti, analysis of, methods for, 19: 28242
Fe–Mn–Ni, martensitic reaction nucleation rate in, 20: 29623(R) (TID-22970, pp 121-256)
Fe–Mn–Ni, phase studies of, martensite transformation characteristics in, 16: 6750
Fe–Mn–Ni, preparation and tensile properties, 19: 17443(P)
Fe–Mn–Ni, structure of antiferromagnetic, 17: 22186
Fe–Mn–rare earth, magnetic properties at 1.4 to 300°K, 18: 12683
Fe–Mn–U, crystal structure and intermetallic phases, 17: 37559
Fe–Mn–U, magnetic properties of UFe_x–UMn_x system in, 17: 23872(R) (TID-18626)
Fe–Mn–U, melting points in, 16: 6104(R) (LAMS-2647)
Fe–Mn–W, properties as metalizing paint for metal-to-ceramic seals, 20: 27401(R) (AD-632362)
Fe–Mn–Zn, spin wave dispersion in, 17: 38031(T) (AEC-tr-5734(p.188-92))
Ga–Mn, phase studies of nitrogen-containing, 16: 16768
Gd–Mn, analysis by x-ray fluorescence, 18: 27340

Gd–Mn, atomic radii and interatomic distances in intermetallic compounds in, 18: 28029
Gd–Mn, crystal structure of intermetallic compound Gd_6Mn_{23} in, 18: 32162
Gd–Mn, crystal structure of intermetallic compound Gd_6Mn_{23} in, size-factor limitation in, 19: 23079
Gd–Mn, crystal structure of Gd_6Mn_{23} in, 20: 17096(T)
Gd–Mn, crystal structure and magnetic properties of intermetallic compounds of, 20: 21403
Gd–Mn, crystal structure of intermetallic compound, 20: 43918
Gd–Mn, existence of Gd_6Mn_{23} compound in, 19: 14074
Gd–Mn, magnetic moments of intermetallic compound Gd_6Mn_{23} in, 19: 23109
Gd–Mn, magnetic properties of $GdMn_2$, 17: 37709
Gd–Mn, magnetic properties of, 19: 46988 (AD-614465)
Gd–Mn, magnetic properties of intermetallic compound $GdMn_5$ in, at 80 to 1400°K, 20: 7610
Gd–Mn, phase diagram, 20: 21403
Gd–Mn, phase studies, 19: 46908 (AD-614464)
Gd–Mn, phase studies by differential thermal, thermomagnetic, and x-ray analysis of, 19: 46989 (AD-614466)
Gd–Mn, preparation, phase studies, and properties of, 19: 46987 (AD-614462)
Gd–Mn, preparation by sinter process using mercury, 19: 46908 (AD-614464)
Gd–Mn, preparation and structure, 20: 15110
Gd–Mn, structure of $GdMn_2$, 18: 34026 (AD-428771)
Ge–Mn, manganese-55 nuclear magnetic resonance in Mn_5Ge_3 at 1.6, 4.2, and 77.0°K, 17: 39599
Ge–Mn, neutron diffraction by Mn_5Ge_3, (E), 19: 8469
Ge–Mn, phase studies of nitrogen-containing, 16: 16768
Ge–Mn–Th, crystal structure of intermetallic compound $ThMn_2Ge_2$ in, 19: 23037
Hf–Mn, magnetic properties at 1.1 to 4.2°K and 30 kOe, 20: 10272(R) (NAA-SR-9339)
Hf–Mn, structure of intermetallic compound $HfMn_2$ in, 16: 2253
Ho–Fe–Mn, phase studies in, Laves, 16: 25798
Ho–Mn, crystal structure of intermetallic compound Ho_6Mn_{23} in, size-factor limitation in, 19: 23079
Ho–Mn, crystal structure of Ho_6Mn_{23} in, 20: 17096(T)
Ho–Mn, crystal structure and magnetic properties of intermetallic compounds of, 20: 21403
Ho–Mn, crystal structure of intermetallic compound, 20: 43918
Ho–Mn, existence of Ho_6Mn_{23} compound in, 19: 14074
Ho–Mn, magnetic moments of intermetallic compound Ho_6Mn_{23} in, 19: 23109
Ho–Mn, magnetic properties of $HoMn_2$, 17: 37709
Ho–Mn, magnetic properties of intermetallic compound $HoMn_5$ in, at 80 to 1400°K, 20: 7610
Ho–Mn, phase diagram, 20: 21403
Ho–Mn, phase studies by differential thermal, thermomagnetic, and x-ray analysis of, 19: 46989 (AD-614466)
Ho–Mn, preparation by sinter process using mercury, 19: 46908 (AD-614464)
Ho–Mn, preparation and structure, 20: 15110
In–Mn, critical temperature of superconducting, transition metal impurity effects on depression of, (E), 20: 37955
In–Mn, electric conductivity and superconducting transition temperature of, (E), 19: 19046
In–Mn, magnetorestrictive properties of superconducting, (E), 19: 10197
In–Mn, phase studies of nitrogen-containing, 16: 16768
In–Pb–Mn, critical temperature of superconducting, transition metal-impurity effects on depression of, (E), 20: 37955
Lu–Mn, crystal structure of intermetallic compound Lu_6Mn_{23} in, size-factor limitation in, 19: 23079
Lu–Mn, crystal structure of Lu_6Mn_{23} in, 20: 17096(T)
Lu–Mn, crystal structure of intermetallic compound, 20: 43918
Lu–Mn, existence of Lu_6Mn_{23} compound in, 19: 14074
Lu–Mn, magnetic moments of intermetallic compound Lu_6Mn_{23} in, 19: 23109
Lu–Mn, neutron reaction rates in foils of, 18: 7026 (AEEW-R-217)
Lu–Mn, preparation and structure, 20: 15110
Mg–Mn, analysis of, for nickel, spectrophotometric, 16: 18817 (PG-Report-295)
Mg–Mn, analysis of, for antimony, 17: 5960 (PG-Report-337)
Mg–Mn, analysis of, for cobalt, 17: 5960 (PG-Report-337)
Mg–Mn, cavitation and creep properties of, at 20 to 500°C, 16: 16762
Mg–Mn, creep behavior of, effects of heat treatment on, 16: 552
Mg–Mn, creep in, diffusion, 20: 13309
Mg–Mn, crystal structure of nitrogen-containing, 16: 2259
Mg–Mn, effects of grain size on compressive creep and tensile deformation at 450°C, 18: 42059
Mg–Mn, fatigue of, effects of high-frequency vibrations on, 20: 43957
Mg–Mn, heat resistance, mechanical properties, and recrystallization of, 18: 16496
Mg–Mn, ordering in solid solutions of, effects of heat on, 16: 2924 (ASD-TR-61-92)
Mg–Mn, oxidation of, by carbon dioxide–carbon monoxide mixtures at 500 to 700°C, 17: 25739
Mg–Mn, performance as reactor components, 18: 37667 (A/CONF.28/P/146)
Mg–Mn, thermal stability at 150 to 300°C, 17: 34461
Mg–Mn, thermophysical properties, 18: 10552
Mg–Mn–Nd, effects of plastic deformation on properties and structure of, 18: 16495
Mg–Mn–Nd, phase studies, 17: 18848
Mg–Mn–Nd–Ni, effects of plastic deformation on properties and structure of, 18: 16495
Mg–Mn–Th, bonding of HM21, surface preparation and epoxy adhesive for, 19: 36995 (BDX-613-68)
Mg–Mn–Th, corrosion, 19: 6271(T) (JPRS-27451)
Mg–Mn–Th, effects of alloying agents on mechanical properties of, 17: 32595
Mg–Mn–Th, mechanical properties of, alloying effects on, 18: 32156(T) (JPRS-25069(p.1-31))
Mg–Mn–Th, phase studies, 18: 32156(T) (JPRS-25069(p.1-31))
Mg–Mn–Zr, cavitation and creep properties of, at 20 to 500°C, 16: 16762
Mg–Mn–Zr, design for fuel element canning, 17: 16730(P)
Mg–Mn–Zr, diffusion of plutonium in MAGZAN-II and Zr55, at 420, 460, and 500°C, 20: 5848
Mg–Mn–Zr, ignition in carbon dioxide, effects of air, oxygen, and water vapor on, 19: 7849 (CEA-R-2494)
Mg–Mn–Zr, performance as reactor components, 18: 37667 (A/CONF.28/P/146)
Mg–Zn, phase studies by neutron diffraction, 20: 12545(R) (PAEC(A)AR651)
Mn–Ag, thermal capacity below 1°K, 20: 29791
Mn–Hg, crystal structure of, neutron-diffraction-analysis of, 19: 18464 (PAN-599/VI)
Mn–Hg, magnetic structure of, 18: 9317(R) (PR-P-59(p.37-45))
Mn–Hg, magnetic structure of, 19: 9703
Mn–Hg, vapor pressures of intermetallic compounds in, 19: 23091
Mn–Hg–Sm, preparation, 18: 34027 (AD-428772)
Mn–Hg–Y, preparation, 18: 34026 (AD-428771)
Mn–Hg–Y, preparation, 18: 34027 (AD-428772)
Mn–Mo, magnetic susceptibility and specific heat of superconducting binary complex phases of, 18: 37715
Mn–Mo–Ti, stability of beta phase, effects of aluminum on, 20: 9512
Mn–Nd, crystal structure of intermetallic compound Nd_6Mn_{23} in, size-factor limitation in, 19: 23079
Mn–Nd, existence of Nd_6Mn_{23} compound in, 19: 14074
Mn–Nd, magnetic moments of intermetallic compound Nd_6Mn_{23} in, 19: 23109
Mn–Nd, preparation and structure, 20: 15110
Mn–Ni, conduction electron momentum in, electron–positron annihilation studies, 17: 11275
Mn–Ni, crystal structure of, neutron diffraction studies on, 20: 39407(T) (ANL-Trans-344)
Mn–Ni, electron-positron annihilation contribution to electric conductivity of, 17: 29368
Mn–Ni, electronic specific heat, 17: 16698
Mn–Ni, fabrication of sintered foils of, for neutron dosimetry, 18: 41980 (PAN-496/XIV)
Mn–Ni, magnetic moment distributions in dilute, 17: 37694
Mn–Ni, magnetic structure from polarized neutron diffraction, 18: 37710
Mn–Ni, magnetic structure of, from polarized neutron scattering, 20: 20335
Mn–Ni, neutron elastic scattering by, cross sections for, (E/T), 20: 26346 (NP-16010, pp 1-41)
Mn–Ni, order-disorder transformations in, 17: 18824
Mn–Ni, phase studies, 20: 39407(T) (ANL-Trans-344)
Mn–Ni, phase transformations in, 17: 25783 (UCRL-7210)
Mn–Ni, polarized neutron diffraction for ferromagnetic moment per atom of $MnNi_3$, 17: 37527
Mn–Ni, radiation effects on atomic mobility and electric conductivity of, gamma, 18: 42138
Mn–Ni–Pd, use for braze bonding stainless steel cans to stainless steel–uranium dioxide cermets, 19: 4635
Mn–Ni–Sc, crystal structure of Laves phases in, 20: 41412(R) (IS-1500 (Sect. M))
Mn–Ni–U, eutectic temperature and composition of, 16: 17297(R) (LAMS-2681)
Mn–Pd, antiferromagnetism of the antiphase domain structure of the intermetallic compound $MnPd_3$ in, 17: 3620
Mn–Pd, magnetic properties at 90 to 1100°K, 20: 7585(T) (ANL-Trans-251)

Mn–Pd, magnetic properties of Mn_3Pd_3, 20: 20360(R) (PRNC-73)
Mn–Pd, magnetic structure of zeta–Pd_3Mn_2, 20: 28610(R) (PRNC-84)
Mn–Pd, neutron magnetic scattering by fcc, (E/T), 19: 37118
Mn–Pd, thermoelectric powers at 700°C, 18: 25970(R) (ANL-6868 (p.303-25))
Mn–Pd–Ag, use for braze bonding stainless steel cans to stainless steel–uranium dioxide cermets, 19: 4635
Mn–Pd–Pt, magnetic properties of 1- and 3 Pd_xMn–Pt_xMn, 17: 26456(R) (ORNL-3425(p.120-3))
Mn–Pr, preparation and structure, 20: 15110
Mn–Pt, activity coefficient of manganese in, 19: 13280(R) (TID-21569)
Mn–Pt, atomic magnetic moment of platinum in, 16: 16838
Mn–Pt, chemical ordering in, 20: 36355 (ANL-7182)
Mn–Pt, crystal and magnetic structure of $PtMn_x$, 18: 25971(R) (ANL-6868(p.331-7))
Mn–Pt, crystal structure of $PtMn_3$, chemical order-disorder in, 19: 44679(R) (ANL-7000, pp 205-12)
Mn–Pt, crystal structure of intermetallic compound $PtMn_3$ in, neutron diffraction studies of disorder in, 19: 47028
Mn–Pt, magnetic ordering in, 19: 34711
Mn–Pt, magnetic structure in $PtMn_3$, 19: 44679(R) (ANL-7000, pp 205-12)
Mn–Pt, manganese radial spin density in ferrimagnetic $MnPt_3$, 17: 37696
Mn–Pt, neutron diffraction by ordered, at 26 and 250°C, 20: 5912
Mn–Pt, phase studies at 800 to 1400°C, 20: 338
Mn–Pu, ignition temperatures in air and oxygen, 17: 35078(R) (ANL-6739)
Mn–Pu, phase diagram, 17: 4984
Mn–Pu, phase diagram, 17: 16567
Mn–Pu, phase studies and properties of, bibliographic study of, 16: 32115 (KFK-105)
Mn–Pu, structure of intermetallic compounds in, 17: 3536
Mn–Pu–U, analysis for manganese, x-ray fluorescence spectrometric, 19: 9061 (LA-3160)
Mn–Pu–U, analysis for manganese, x-ray-fluorescent, 19: 21690(R) (LA-3244)
Mn–Pu–U, analysis for plutonium, 19: 24402 (LA-3258)
Mn–Pu–U, analysis for plutonium, x-ray fluorescence spectrometric, 19: 40408 (LA-3333)
Mn–Pu–U, corrosive effects of, on ceramic materials at 900 to 1000°C, 16: 17297(R) (LAMS-2681)
Mn–Pu–U, corrosive effects of, on container materials at 850 to 900°C, 16: 22549
Mn–Pu–U, corrosive effects on yttrium at 900°C, 18: 30975(R) (LAMS-3096)
Mn–Pu–U, reactions with yttrium, 17: 22855(R) (LAMS-2875)
Mn–rare earths, magnetic moments of intermetallic compound in, 19: 23109
Mn–rare earth, phase studies of, at 75 to 90 at.% manganese, 16: 16744
Mn–rare earth, preparation of amalgams for studies of, 18: 34028 (AD-430037)
Mn–rare earths, preparation and structure, 20: 15110
Mn–rare earth, preparation by amalgam process, 20: 21403
Mn–rare earth, preparation and properties, 18: 5350(P)
Mn–rare earths, properties of, equipment for measuring, 19: 46988 (AD-614465)
Mn–Re, intermetallic compounds in, 17: 8727
Mn–Re, phase studies, 16: 559
Mn–Rh–Ti, superconductivity, 18: 21112
Mn–Ru–U, eutectic temperature and composition in, 16: 17297(R) (LAMS-2681)
Mn–Sc, crystal structure of, 18: 24157
Mn–Sc, crystal structure of intermetallic compounds of, 18: 39927
Mn–Sc, structure of intermetallic compounds in, 19: 23011(T) (JPRS-28849(p.199-200))
Mn–Sm, amalgam studies, 18: 34026 (AD-428771)
Mn–Sm, analysis by x-ray fluorescence, 18: 27340
Mn–Sm, crystal structure of intermetallic compound Sm_6Mn_{23} in, size-factor limitation in, 19: 23079
Mn–Sm, crystal structure of Sm_6Mn_{23} in, 20: 17096(T)
Mn–Sm, crystal structure and magnetic properties of intermetallic compounds of, 20: 21403
Mn–Sm, existence of Sm_xMn_{23} compound in, 19: 14074
Mn–Sm, magnetic moments of intermetallic compound Sm_6Mn_{23} in, 19: 23109
Mn–Sm, magnetic properties of intermetallic compound $SmMn_2$ in, at 80 to 1400°K, 20: 7610
Mn–Sm, phase studies by differential thermal, thermomagnetic, and x-ray analysis of, 19: 46989 (AD-614466)
Mn–Sm, preparation, phase studies, and properties of, 19: 46987 (AD-614462)
Mn–Sm, preparation by sinter process using mercury, 19: 46908 (AD-614464)
Mn–Sn, preparation and structure, 20: 15110
Mn–Sn, critical temperature of superconducting, transition metal impurity effects on depression of, (E), 20: 37955
Mn–Sn, hyperfine structure of tin-119 Mössbauer spectra in, 17: 13245
Mn–Sn, magnetic fields at tin nuclei in, 17: 13245
Mn–Sn, magnetic structure and transitions in, 17: 39714 (BNL-7325)
Mn–Sn, pressure-volume variations below 300°K, (E), 19: 23054
Mn–Sn, spin ordering of paramagnetic states in superconducting, 20: 2918
Mn–Sn, superconducting properties, 16: 22631
Mn–Tb, atomic radii and interatomic distances in intermetallic compounds in, 18: 28029
Mn–Tb, crystal structure of intermetallic compound Tb_6Mn_{23} in, size-factor limitation in, 19: 23079
Mn–Tb, crystal structure of Tb_6Mn_{23} in, 20: 17096(T)
Mn–Tb, crystal structure of intermetallic compound, 20: 43918
Mn–Tb, existence of Tb_xMn_{23} compound in, 19: 14074
Mn–Tb, magnetic moments of intermetallic compound Tb_6Mn_{23} in, 19: 23109
Mn–Tb, magnetic properties of $TbMn_2$, 17: 37709
Mn–Tb, magnetic structure of $TbMn_2$, neutron diffraction studies of, 18: 8787 (BNL-7510)
Mn–Tb, magnetic structure of intermetallic compound $TbMn_2$ in, 20: 18556(R) (BNL-929, pp 66-82)
Mn–Tb, preparation and structure, 20: 15110
Mn–Tc, phase studies on, 17: 11220
Mn–Th, atomic radii and interatomic distances in intermetallic compounds in, 18: 28029
Mn–Th, preparation by electrolysis of oxides in fluoride melts, 20: 27402 (BM-RI-6789)
Mn–Ti, combustibility temperature of, 19: 37093
Mn–Ti, corrosion of nitrided, by mercury to 538°C, effects of inhibitors on, 17: 41333(R) (ANL-6677)
Mn–Ti, corrosion by mercury, 18: 10492
Mn–Ti, electric conductivity of, at 1.1 to 35°K, maxima in, 16: 27818
Mn–Ti, localized magnetic states and superconductivity in, 17: 32706 (CONF-23-19)
Mn–Ti, magnetic moments and superconductivity of, 18: 34700
Mn–Ti, magnetic resistivity of, at 1.1 to 4.2°K, negative values in, 16: 27818
Mn–Ti, superconducting properties, 18: 967
Mn–Ti, superconducting transition anomalies in, (E), 19: 10214
Mn–Ti, tensile properties at room temperature, 18: 18380
Mn–Ti, thermal properties of, at high temperatures, 16: 4551 (WADD-TR-60-904)
Mn–Ti–Zr, magnetic moments and superconductivity of, 18: 34700
Mn–Ti–Zr, tensile properties at room temperature, 18: 18380
Mn–Tm, crystal structure of intermetallic compound Tm_6Mn_{23} in, size-factor limitation in, 19: 23079
Mn–Tm, crystal structure of Tm_6Mn_{23} in, 20: 17096(T)
Mn–Tm, crystal structure of intermetallic compound, 20: 43918
Mn–Tm, existence of Tm_xMn_{23} compound in, 19: 14074
Mn–Tm, magnetic moments of intermetallic compound Tm_6Mn_{23} in, 19: 23109
Mn–Tm, magnetic structure of intermetallic compound Mn_2Tm in, 20: 18556(R) (BNL-929, pp 66-82)
Mn–Tm, preparation and structure, 20: 15110
Mn–U, corrosive effects of, on ceramic materials at 900 to 1000°C, 16: 17297(R) (LAMS-2681)
Mn–U, corrosive effects of, on container materials at 850 to 950°C, 16: 22549
Mn–U, corrosive effects on carbide crucibles at 1100°C, 17: 7658(R) (LAMS-2815)
Mn–U, corrosive effects of liquid, on tantalum and yttrium, 20: 4077(R) (IS-1200(Sect. E))
Mn–U, corrosive effects of liquid, on tantalum and yttrium, 20: 41064(R) (IS-1500(Sect.E))
Mn–U, crystal structure and intermetallic phases, 17: 37559
Mn–U, electric and thermal properties of Laves phases of intermetallic compounds in, 20: 873
Mn–U, electric conductivity, 16: 13616
Mn–U, melting point of, effects of impurities on eutectic, 20: 4077(R) (IS-1200(Sect. E))
Mn–U, melting point of, effects of impurities on eutectic, 20: 41064(R) (IS-1500(Sect.E))
Mn–U, metallographic tests on arc melted, 20: 29775
Mn–U, phase diagram, 17: 25786 (UCRL-13075)
Mn–U, phase studies, 16: 17297(R) (LAMS-2681)
Mn–U, phase studies, 17: 29255 (ZFK-WF-13)
Mn–U, phase transformation and grain refinement, 17: 27862
Mn–V, crystal structure and phase studies, 18: 25970(R) (ANL-6868 (p.303-25))
Mn–W, ductility at low temperatures, 18: 28028
Mn–Y, analysis by x-ray fluorescence, 18: 27340
Mn–Y, atomic radii and interatomic distances in intermetallic compounds

in, 18: 28029
Mn–Y, crystal structure of intermetallic compound Y_6Mn_{23} in, size-factor limitation in, 19: 23079
Mn–Y, crystal structure of Y_6Mn_{23} in, 20: 17096(T)
Mn–Y, crystal structure and magnetic properties of intermetallic compounds of, 20: 21403
Mn–Y, existence of Y_6Mn_{23} compound in, 19: 14074
Mn–Y, magnetic properties of intermetallic compound YMn_5 in, at 80 to 1400°K, 20: 7610
Mn–Y, phase diagram, 17: 14740 (TID-11295(2nd Ed.))
Mn–Y, phase studies, 16: 13633
Mn–Y, phase studies of, at 75 to 90 at.% manganese, 16: 16744
Mn–Y, phase studies by differential thermal, thermomagnetic, and x-ray analysis of, 19: 46989 (AD-614466)
Mn–Y, preparation, phase studies, and properties of, 19: 46987 (AD-614462)
Mn–Y, preparation and structure, 20: 15110
Mn–Y, structure of YMn_2 and YMn_4, 18: 34026 (AD-428771)
Mn–Y, structure of Laves phase YMn_2, 18: 34027 (AD-428772)
Mn–Zn, analysis for beryllium, spectrophotometric, 19: 5789
Mn–Zn, crystal and magnetic structure of, 19: 9704
Mn–Zn, crystal structure of nitrogen-containing, 16: 2259
Mn–Zn, crystal structure, 18: 2403(R) (PR-P-58)
Mn–Zn, de Haas-van Alphen effect in, exhibiting a resistance minimum, 17: 13155
Mn–Zn, magnetic structure of, 18: 9317(R) (PR-P-59(p.37-45))
Mn–Zn, phase studies of nitrogen-containing, 16: 16768
Mn–Zn, spin scattering in superconducting, (E), 20: 34464
Mn–Zn, superconductivity in, effects of s-d exchange interactions in, 18: 24555
Mn–Zn, superconducting critical temperature of, transition metal impurity effects on depression of, (E), 20: 37955
Pb–Mn, spin ordering of paramagnetic states in superconducting, 20: 2918
Sb–Cr–Mn, magnetic structures in, 17: 32622
Sb–Cr–Mn, magnetic structures in, 19: 38060
Sb–Mn, magnetic structures of chromium-modified Mn_2Sb, 17: 31205
Sb–Mn, manganese aspherical spin density in ferrimagnetic Mn_2Sb, 17: 37695
Sb–Mn, pyrophoricity, 17: 6693(T) (AEC-tr-5544)
Sb–Mn–Ni, antimony-121 and -123 NMR in ferromagnetic, (E/T), 19: 23663

MANGANESE ALUMINATES
neutron magnetic inelastic scattering by, filter-cutoff method for, 20: 32706

Manganese Ammonium Fluorides
see Ammonium Manganese Fluorides

MANGANESE ARSENIDES
phase transitions in single-crystal, magnetic field effects on ferromagnetic-paramagnetic, 16: 15459

MANGANESE, BISCYCLOPENTADIENYL-
preparation by reaction of manganese chloride with magnesium cyclopentadienide, 20: 35493

MANGANESE BORATES
polymorphism, x-ray analysis, 16: 162

MANGANESE BORIDES
electric conductivity, 16: 23662 (AE-76)
electronic structure, 16: 23662 (AE-76)
preparation by carbon reduction of oxide with boric oxide, 20: 19702
stability and structure of, 17: 8083

MANGANESE BROMIDES
bromine-81 quadrupole bonding and resonance in solid layer type, 16: 7538
electron energy losses in, and mechanisms of, 17: 13165
magnetic properties of crystalline, 19: 21759(R) (NYO-3402-1)
preparation of high-purity crystalline, 19: 21759(R) (NYO-3402-1)
preparation of high purity crystalline, 20: 17978(R) (NYO-3402-2)
spectra of aqueous solutions of, ESR, 20: 43184 (UCRL-17064)
spectra of tetra, arrangement of bromide ions, 16: 92(R) (TID-13601)
thermal conductivity at cryogenic temperatures, 19: 21759(R) (NYO-3402-1)
vaporization of, 17: 2956 (UCRL-9840)

MANGANESE CARBIDES
preparation, composition, and structure of, 20: 17030(T) (LA-tr-66-1)
reactions of, with water and various organic compounds, 17: 1363(T) (AEC-tr-5515)
MnC–UC, thermodynamic properties, 18: 2222 (LADC-5907)

MANGANESE CARBONATES
magnetic properties, 20: 35841(R) (NAA-SR-11900)
magnetic susceptibility at 100 to 300 kgauss, 16: 15455
neutron elastic and inelastic scattering by, cross sections and polarization of, 18: 42320(T)
radiation effects on thermal decomposition at 170 to 290°C, gamma, 19: 13434

radiation effects on thermal decomposition of, gamma, 20: 25171
reactions with rare earth oxides, ionic field strengths as criteria for compound formation in, 19: 46246(R) (TID-22207, Paper F)
spectrum at low temperatures, infrared, 16: 33002

MANGANESE CARBONYL, CYCLOPENTADIENYL-
crystal structure, 20: 3863(R) (IS-1200(Sect.C))
preparation by reactions of manganese chloride with carbon monoxide and magnesium cyclopentadienide, 20: 35493

MANGANESE CARBONYL HYDRIDES
spectra of, stretching absorptions in infrared, 18: 31469

MANGANESE CARBONYLS
see also Manganese Carbonyl Hydrides
crystal structures of, comparison with rhenium and technetium carbonyls, 19: 36367
cyclopentadienyl complexes of, reactions of recoil manganese-56 with, 20: 23095
decomposition in ion source of mass spectrometer, mechanism of, 20: 14584(R) (TID-22444)
effects on radioinduced reactions of carbon monoxide and olefins, 18: 1731 (TID-19671)
preparation and properties of *tetra-*, 18: 37162
radioinduced ionization of, by electron impact, 19: 26401
with cyclopentadienyliron, crystal structure, 20: 3863(R) (IS-1200 (Sect. C))

Manganese Cesium Fluorides
see Cesium Manganese Fluorides

MANGANESE CHLORIDES
chlorine-35 quadrupole bonding and resonance in solid layer type, 16: 7538
crystal structure of tetrahydrate of di-, 18: 31361(R) (UCRL-11213 (p.87-138))
effects of injections on protein fractions in serum of irradiated rabbits, 20: 42870
electron energy losses in, and mechanisms of, 17: 13165
electron spin resonances at 25 to 500°C, 16: 13018 (UCRL-9944)
entropy, internal energy, and thermal capacity at 0 to 4.2°K, effects of magnetic field on, 19: 11080
separation by reversed-phase partition chromatography using organophosphorus compounds, 18: 25614
separation from aqueous solutions by extraction using n-butanol, 16: 14820(R) (TID-15379)
separation from salts by extraction chromatography using organic phosphorus compounds, 20: 10759 (INP-427/C)
solvent properties for manganese, 17: 35687 (IS-596)
specific heat of crystals of, at low temperatures in applied magnetic fields, 17: 655
spectra of aqueous solutions of, ESR, 20: 43184 (UCRL-17064)
spectra of tetra, arrangement of chloride ions, 16: 92(R) (TID-13601)
uptake of manganese-54-labeled, by Amphiuma hepatocytes, 20: 8573
vaporization of, 17: 2956 (UCRL-9840)
$MnCl_2$–NaCl, radioinduced color center formation and impurity distribution, 18: 5862(T)
Mn–$MnCl_2$, free energy of solution of, 19: 11103

MANGANESE CHROMITES
magnetic structure at 4.2 to 300°K, 16: 18067
magnetic structure of, 17: 37823

MANGANESE CHROMIUM FERRATES
magnetic susceptibilities, 16: 25882 (ASD-TR-61-630)

Manganese Cobalt Oxides
see Cobalt Lanthanum Oxides

MANGANESE COMPLEXES
chlorophyllin, radiosensitivity effects in mice, gamma, 20: 1692
fluorescence of, in region of thermal extinction, relationship between lifetime and intensity of, 17: 12242
formation of, thermodynamics and kinetics of, 18: 17717(R) (TID-20438)
protective effects against radiation sickness in mice, 18: 9931
reactions of hematoporphyrin, with water, 17: 4561(R) (UCRL-10350)
with acetylacetone, cobalt-60 recoil effects following (n,γ) reactions with cobalt acetylacetonate in, 19: 30313
with adenosine triphosphate, stability constants of, 16: 7556
with adenosinephosphoric acids, stability constants of, 16: 28948
with carbamic acid, synthesis, 16: 6425
with chloride and sulfate ions in perchlorate solutions, paramagnetic resonance studies of, 18: 21730 (UCRL-10446)
with citric acid enzyme, dissociation constant of, 20: 10479 (UCRL-12140)
with cupferron, thermal dissociation, 19: 7366
with cyanide in molten salts, stability of, 19: 32122(R) (NYO-2747-3)
with diacetamide, properties and spectra of, 20: 8494 (TID-22449)
with EDTA, bonding and structure of, 17: 33896
with ethylenediaminetetraacetic acid, radioprotective effects of, in mice, 18: 13567

with ethylenediaminetetraacetic acid, radioprotective effects in mice, 18: 13567
with hexamethylphosphoramide, NMR contact shifts in, 20: 12828 (TID-21587)
with mercaptohydroquinone and 4-mercaptoresorcinol, stability of, 19: 26237
with mercaptosuccinic acid and 2,3-dimercaptosuccinic acid, formation and properties of, 18: 8394 (TID-20013)
with methylenephosphonic acid derivatives, preparation and properties of, 20: 12533 (COO-1020-6)
with *N*-(2-pyridylmethyl)iminodiacetic acid, stability of, 17: 15993
with phthalocyanato and pyridine ligands, structure of, 20: 22859(R) (UCRL-16580, pp 149-205)
with porphyrin, preparation and photochemistry of, 18: 17408(R) (UCRL-11046(p.87-9))
with solochrome violet RS, polarography of, 20: 16406
with substituted 2-(pyridyl)- and 2-(quinolyl)-1,3-indanediones, acid dissociation and formation constants of, 18: 25457
with thiodibenzoylmethane, stability of, 20: 20693
with 1-(2-pyridylazo)-2-naphthol, formation constants and distribution equilibria of, 17: 14381
with 2-methyl-4,6-heptanedione, stability constants of, 19: 11056(T) (AEC-tr-6227/3(p.183-92))
with 8-quinolinols, luminescence yields of, 20: 10456 (COO-773-3)

MANGANESE COMPOUNDS
crystallography of, with perovskite-like structure, 19: 25014
cyclopentadienyl, covalent radii and length of metal-metal bonds in, 19: 17922
neutron total cross sections of, temperature effects of magnetic order on, 18: 36034
preparation of plutonate, with perovskite structure, 18: 23521(P)
solubility and thermolysis of dilliturate, 19: 19824
with lanthanide elements, preparation and properties, 18: 5350(P)

MANGANESE COUPLES
Mn–Sn, electric and thermal conductivity in superconducting, (E), 20: 15656

MANGANESE DEPOSITS
age determination from radium and thorium-230 content in, in Indian and Pacific Oceans, 17: 34127
analysis for manganese content by activation determination of manganese-56, 19: 9086
occurrence of radioactive, in lower Rio Itapicuru Valley, Bahia, Brazil, 16: 3242 (TEM-567)

MANGANESE DYSPROSIUM SELENIDES
preparation and crystal structure, 20: 38884

MANGANESE FERRATES
see also Magnesium Manganese Ferrates
see also Manganese Chromium Ferrates
magnetic susceptibilities, 16: 25882 (ASD-TR-61-630)
Moessbauer spectrum of, at 4.2, 78, and 300°K, 20: 36817
Mössbauer absorption spectra of iron-57 in, temperature dependence of, 17: 33926
neutron scattering by, 17: 38047(T) (AEC-tr-5734(p.275-8))
preparation and magnetic properties, 16: 13567 (ARL-66)
preparation of crystals of, by zone melting at 2320 to 3800°K, 17: 32590
radiation effects on magnetic properties of, neutron, 18: 7330

MANGANESE FERRITES
inversion degree and oxygen parameter of, 17: 37827
magnetic fields in, Mössbauer study of effective, 19: 38026 (INP-407/PL)
magnetic properties of, effects of rare earth oxides on, 17: 14880
magnetic properties of, effects of rare earth oxides on, 17: 16019

MANGANESE FLUORIDES
see also Ammonium Manganese Fluorides
see also Cesium Manganese Fluorides
see also Manganese Silicon Fluorides
see also Potassium Manganese Fluorides
see also Rubidium Manganese Fluorides
see also Sodium Manganese Fluorides
analysis by potentiometric titration with sodium methylate in methanol, 16: 7530
atomic structure of, usefulness of neutron scattering for determining, 20: 25717 (BNL-946)
effects on fluorine-19 spin-lattice relaxation in calcium fluorides, 18: 32879
effects on freezing point depressions in sodium fluoride, 17: 37213
fluorine-19 nuclear magnetic relaxation in, 17: 5402
fluorine-19 NMR in, critical fluctuations in, (E), 20: 1347
heat of sublimation and vapor pressure of, 20: 26874
magnetic properties of, 17: 11222
magnetic susceptibilities, 16: 25882 (ASD-TR-61-630)
magnetization and specific heat of antiferromagnetic, spin-wave theory of, 18: 5870
magnetization of, random phase approximation in sub-lattice, 18: 40120 (TID-21083)
neutron magnetic inelastic scattering by, filter-cutoff method for, 20: 32706
neutron magnetic scattering in single crystals of, 19: 38038
neutron scattering by paramagnetic, thermal, 17: 20978
nuclear magnetic resonance of fluorine-19 in, pressure effects, 17: 2738
nuclear magnetic resonance in, 17: 33857 (AFCRL-63-192)
preparation of crystals of, by Czochralski method, 16: 1754
spin-flopping in MnF_2, induced by high pulsed magnetic fields, 16: 25882 (ASD-TR-61-630)
spin-wave dispersion at 4.2°K in single-crystal, from inelastic neutron scattering, 18: 11135
spin-wave dispersion in, (E/T), 19: 11768
vaporization of, 17: 2956 (UCRL-9840)

MANGANESE(II) FLUORIDES
neutron scattering on, covalent spin distributions from polarized thermal, 17: 37692
spectra of aqueous solutions of, ESR, 20: 43184 (UCRL-17064)
spin wave dispersion at 4.2 to 70°K, 18: 10091
thermal capacity of antiferromagnetic, at 1.0–4.2°K, 17: 37789

MANGANESE FORMATES
heat of dissociation, 16: 100(T) (AEC-tr-4847)
magnetic susceptibility of tetrahydrate of, at liquid helium temperatures, 18: 12062

MANGANESE HYDROXIDES
sorptive properties for strontium, 16: 27058
sorptive properties for trace amounts of cerium and yttrium, 16: 27059
sorptive properties for ruthenium, uranium, and zirconium ions, 17: 40792
sorptive properties for fission products, 18: 39303

MANGANESE IODIDES
iodine-127 quadrupole bonding and resonance in solid layer type, 16: 7538
spectra of aqueous solutions of, ESR, 20: 43184 (UCRL-17064)
vaporization of, 17: 2956 (UCRL-9840)

MANGANESE IONS
antishielding factors for, perturbed wave functions for, 17: 37644 (BNL-6681)
catalytic effects on reactions of hydrogen peroxide with uranium(VI) ions, 16: 111
catalytic effects on corrosion of stainless steel by nitric acid, 16: 13534
catalytic properties of, for use in cerium(IV) oxidimetry, 17: 176
chromatography on acetylated filter paper, 16: 6379
crystalline field splitting of ^6S ground state of, 17: 33857 (AFCRL-63-192)
determination by nuclear magnetic relaxation, 18: 6771
determination of, in pyruvate carboxylase, 20: 42773
distribution coefficient in zone melting of lithium fluoride, 19: 34144 (ORNL-3658)
effects on catalytic properties of rare earth oxides, 19: 5902
effects on copper determination, 20: 36726
effects on dephosphorylation of cocarboxylase, riboflavin-5-phosphate, and pyridoxal phosphate, 20: 20375
effects on electron spin resonance spectra of irradiated silicate glasses, 20: 42538
effects on formation of single-crystal beryllium oxide, 20: 36814
effects on hydrogen yields in radiolysis of 2-propanol in water, 18: 13885
effects on hydrolysis of α-D-glucose 1-phosphate, 20: 16421
effects on nuclear magnetic resonance spectrum of lithium fluoride, 17: 20048
effects on radiation damage in ribonuclease and trypsin, 20: 32939
effects on spectrophotometric determination of erbium, holmium, and neodymium, 20: 43100
effects on structure of ribonucleic acid, 19: 9157(R) (NYO-2567-1)
electron pammagnetic spectrum of, 17: 20048
electron paramagnetic resonance of bivalent, in undercooled borate glass, 17: 23364
electron paramagnetic resonance and optical absorption of tetravalent, in strontium titanate, 18: 2464
electron paramagnetic resonance spectrum of divalent, in calcium oxide single crystals, 18: 2468
electron paramagnetic resonance in magnesium oxides, spectra of, 18: 29960
electron spin resonance properties, 16: 13017 (UCRL-9873)
electron spin resonance of divalent, in oxides and sulfides of calcium, magnesium, and strontium and in calcium selenide, 18: 2469
electron spin resonance spectra correlation to luminescence properties of phosphors activated by, 18: 2487
electron spin resonance in zeolites, 18: 34268 (IFA-IS-27)
electron spin resonance of divalent, in strontium fluoride, 19: 7511
electron spin resonance spectrum in borate glass, 19: 20620(R) (NYO-2024-8)
electron spin resonance of divalent, 20: 5533
electronic g factors of low-lying levels of singly ionized, (E), 19: 47240

exchange interactions of divalent, in magnesium oxide, biquadratic, 18: 14632
magnetic behavior of divalent, exchange polarization mechanism for paired-electron contributions to, 17: 37772
magnetic moments of configuration in rare earth manganates, 18: 24128 (CONF-405-34)
oxidation-reduction kinetics, 18: 35494 (BNL-7289)
paramagnetic resonance in calcium tungstate crystals, lattice sites from, 17: 35712
precipitation with calcite at 40 to 325°C from aqueous solutions, 20: 18631 (NYO-2266-1)
proton relaxation times of aqueous solutions of, effects of heavy water on, 19: 2350
quadrupole antishielding factor of divalent, 17: 22607
radioinduced divalent, in strawberries, γ, 20: 25461
radioinduced oxidation and reduction in acetone solutions, 17: 28958
radioinduced reduction of, in irradiated aqueous sulfate glasses at 77°K, 20: 33378
radiolysis of aqueous solutions of, pulse, 19: 38728
radioprotective effects in mice, 18: 13567
radiosensitivity effects on catalase, x, 19: 11218
reactions of, with membrane ligands in yeasts, 17: 13931
reflectance effects on zirconium oxide, 18: 14722(R) (TID-20233)
separation from metal ions by extraction using 8-quinolinethiol, 17: 10768
separation from titanium using vanillin, 19: 333
Slater-Condon parameters of, determined from spectral data, 17: 31118
sorption by aminodiacetate resin Dowex A-1, 20: 16358
sorption from perchloric acid solutions by cellulose and resin sulfonic acid exchangers, 18: 35473
sorption of divalent, by phosphorus-containing ion exchangers, from acetic acid–sodium acetate solution, 20: 35593
spectra in magnesium lanthanum nitrates, satellite lines in, (E), 19: 17934
spectra in maple leaves and pine needles, EPR, 19: 25892
spectra in rutile, ESR, 18: 25411
spectra in strontium oxide crystals, paramagnetic resonance, 18: 37136
spectra of aqueous solutions of, ESR, 20: 43184 (UCRL-17064)
spectra of zero-field splitting in, 17: 37754
spin correlations in manganese oxides, 18: 39237
stability constants and structure, effects of ligand fields, 17: 28911
toxicity of, in mouse, determination by LD_{50} on thirtieth day of, 17: 17719
uptake by barley roots, uranyl effects on selective inhibition in, 20: 20402

MANGANESE ISOTOPES
abundance of, mass spectrographic determination of, 18: 8298
analysis of terrestrial, for manganese-53, 17: 696
binding energies and spectra of, from residual two-body interaction theory, 18: 4605
composition in terrestrial samples, 18: 18027
distribution and natural carriers of, in sea water, 20: 31422
distribution in nature, 17: 33602
gamma reactions on, cross sections for, 19: 12496
half lives, 17: 33602
nuclear potentials, evidence for distortion, 16: 21565
preparation, determination, and properties of radioactive, 16: 1349
production and uses of, 19: 24909
production by neutron reactions (n,γ) at 15 Mev, 17: 30159
production by proton reactions in iron, 16: 1808(R) (TID-12849)
proton reactions on, iron-55 yields from, 17: 8153
separation of, radiochemical, 17: 6128 (ORNL-TM-438)

MANGANESE ISOTOPES Mn-50
beta decay of, conserved vector current hypothesis and ft values for, (E/T), 19: 39859
beta decay, energy spectra, and magnetic moment of, $f_{7/2}$ model for, 20: 22131
decay scheme, 17: 7138 (PUC-1962-61)
energy levels, inversion of lowest T = 0,1 states in, 16: 13997
energy levels of, isotope shifts of isobaric-analog, (E), 20: 22095
energy levels of, model for, 20: 22131
half life of isomeric, 17: 9626
positron decay, 17: 5325 (PUC-1962-62)

MANGANESE ISOTOPES Mn-51
beta and gamma spectra and energy levels, 16: 17148
beta decay of, log ft values for, (T), 20: 19932
beta decay of, positron branching in, 18: 38098
energy level spacings in, 19: 21446
energy levels, 18: 24660
energy levels, 18: 34793
energy levels and mass from iron-54 (p,α) reactions at 12 Mev, (E), 20: 10018
energy levels from proton reactions (p,γ) with chromium-50, (E), 20: 26110
energy levels from iron-54 (p,α) reactions, (E), 20: 34639
energy levels in, resonance, 16: 26235
half life, 20: 16331 (GA-6568)
yields in proton spallation of copper at 24 Bev, 16: 24859

MANGANESE ISOTOPES Mn-52
beta decay, beta-gamma circular-polarization correlation parameters in, 16: 15683
beta decay of, beta-gamma circular polarization correlation in, 16: 31102
beta decay of, asymmetry parameters and isotopic spin impurity coefficients for, (E), 19: 8447
beta decay of, charge dependence of nuclear forces in $\Delta T = \pm 1$, 18: 19024
beta decay of, chromium-52 level structure from, (E), 20: 30458
beta decay of, circular polarization of gamma radiation following, 18: 21309
beta decay of, Coulomb matrix elements and impurity coefficients in, 18: 28665
beta decay of, Fermi matrix elements for, (T), 19: 35389 (KFK-313)
beta decay of, log ft values for, (T), 20: 19932
beta decay of, matrix elements from β-γ correlations from, (E), 20: 32506
beta emission from, hindrance phenomena in, 16: 23073
decay, beta-gamma circular-polarization correlation and isospin conservation in, 16: 21616
decay of isomeric, 18: 15209 (UCOL-521)
decay of, ratio of electron capture to positron emission in, 18: 2886
decay of, K-capture to positron ratios for, (E), 20: 15711 (CONF-233 (Vol.2), pp 345-58)
decay schemes for, 17: 22563 (NP-12663)
energy levels, 16: 3753(R) (UCOL-P-508)
energy levels, (E), 20: 38053
energy levels of, isotope shifts of isobaric-analog, (E), 20: 22095
energy levels of, spin and magnetic moment of ground-state, (E), 20: 26109
gamma spectra, 20: 44634(R) (IDO-17188)
half life measurements from 440-Mev proton reactions with stone meteorites, 17: 28943(R) (TID-18961)
hyperfine structure and magnetic moment of isomeric, (E), 20: 1204
metabolism in chickens, 20: 29
nuclear magnetic dipole moments for, (T), 20: 19932
nuclear polarization in, dynamic methods for, 17: 13592
photoproduction of isomeric, yield ratios for, (E/T), 20: 1246
photoproduction of isomeric, (E), 20: 46733
positron emission from polarized, asymmetry of, 18: 4582 (NP-13378)
preparation and mouse metabolism of, 18: 17452
preparation for use in foundry research, 19: 32660
production by deuteron reactions (d,2n) with chromium in cyclotron, 19: 32660
production by proton reactions in thick iron targets, cross sections for, 18: 26583
production in proton reactions with iron and nickel at 130 to 400 Mev, cross sections for, 18: 22881
production in proton reactions with iron at 400 Mev, Monte Carlo calculation of, 20: 22035
production in proton reactions with iron at 400 Mev, (T), 20: 32560
production in proton bombardment of iron and stone meteorites, cross sections for, 17: 28943(R) (TID-18961)
production in 100-Mev to 1-Bev proton reactions with iron, 17: 28943(R) (TID-18961)
production of carrier-free, in ORNL cyclotron, 19: 22851 (ORNL-TM-1047 (p.72-6))
separation from chromium-51, vanadium-48, and zinc-65, method for, 19: 46210
uptake by brain tumors, 18: 1471
uptake by mice, effects of age on, 18: 17453
yield in alpha and proton reactions with copper, 20: 30531
yield in proton reactions with yttrium, 20: 30531
yields in proton spallation of copper at 24 Bev, 16: 24859
yields of metastable, in proton spallation of copper at 24 Bev, 16: 24859

MANGANESE ISOTOPES Mn-53
abundance in stone meteorites, 19: 8052 (NYO-8924)
activity measurements in iron meteorites, 17: 28943(R) (TID-18961)
activity measurements in stone meteorites, 17: 28943(R) (TID-18961)
content in Bondoc meteorite, cosmogenic, 19: 32884
content in iron meteorites, (E), 20: 41614
determination in stone meteorites, 18: 43601(R) (TID-21007)
determination on earth and in meteorites, 17: 696
energy level at 377 kev, half life of, (E), 20: 38030
energy level density from (p,α) reactions, 16: 18477
energy levels, 16: 28099
energy levels, 18: 24660
energy levels, 18: 34855
energy levels, 18: 34797

energy levels, (E), 20: 38053
energy levels from iron-56 (p,α) reactions at 12 Mev, (E), 20: 10018
energy levels from proton reactions (p,γ) with chromium-52, (E), 20: 26110
energy levels from proton reactions (p,γ) with chromium-52 at 1.36 to 2.26 Mev, (E), 20: 32446
energy levels from iron-56 (p,α) reactions, (E), 20: 34639
energy levels from chromium-53 (p,n) reaction, (E), 20: 38034
energy levels in, resonance, 16: 26235
energy levels of, gamma decay of, (E), 20: 42381
half life, 17: 28943(R) (TID-18961)
half life, 19: 12605
half life of, from meteorite observations, 19: 47627
production in proton reactions with iron targets, 18: 43601(R) (TID-21007)
production in reactions of cosmic rays with meteorites, 16: 1808(R) (TID-12849)
production in thermal neutron reactions with iron, cross sections for, 19: 12605

MANGANESE ISOTOPES Mn-54

activity and half life of, (E), 20: 5928(R) (PR-P-66)
activity measurements in fragment of Sputnik IV, 17: 28943(R) (TID-18961)
activity of, method for determining gamma, 20: 9196
beta activity measurements in France, 20: 41189 (CEA-R-3020)
binding energy, magnetic moment, and spin of ground-state, effective neutron-proton interaction for, 18: 6231
content and motion in soil, 19: 36661
content from fallout in mollusks, relation of, to age, 17: 31847
content in air and rain, up to 1964, 19: 7696 (AERE-R-4687)
content in air from Chinese detonations in 1964, 20: 8980(R) (BNWL-36, pp 3.1-122)
content in air samples collected at Richland, Wash., 1962, 1963, and 1964, 19: 2541
content in airborne particles in Cincinnati, May 1962 to Dec. 1963, 19: 4367
content in animals of California coast, 19: 38895
content in animals, birds, fish, and plants in region of Cape Thompson, Alaska, 1959 to 1962, 20: 7319 (PNE-480)
content in atmosphere in 1962, 18: 1975
content in atmosphere and drinking water, Moncloa Station, Spain, 1964, 19: 46597
content in atmosphere, 1962 through mid-1964, 20: 8980(R) (BNWL-36, pp 3.1-122)
content in atmospheric dust and rain water, 1964–65, 20: 16660 (AERE-R-4997)
content in barley, rye, tea leaves, and wheat, 20: 16167
content in Bogou iron meteorite, 20: 16674
content in bovine and human lives, dietary route of, 19: 25859
content in Canadian biota, 20: 4161
content in dusts and rainwater, June to Dec., 1963, in Germany, 20: 27167
content in fallout, increase between 1962 and 1963, 17: 41055
content in fallout, 19: 32430
content in fallout, 1964, 20: 11018
content in fallout over Black Sea, 1964, 20: 14741
content in fish in Barents Sea, 19: 24724
content in fish in Northeast Pacific Ocean, 20: 40523(R) (RLO-1750-8 (Vol.1))
content in freshwater clams, 20: 29462
content in iron meteorites, gamma spectrometric study of, 18: 2516
content in juniper trees in Georgia, 20: 29410
content in marine organisms near Columbia River mouth, interspecies differences in, 17: 24866
content in marine organisms off southern California coast, 18: 32
content in marine organisms, 19: 31696
content in mollusks in Lake Maggiore, Italy, 20: 16185
content in nekton and macroplankton in Pacific Ocean off Oregon coast, 18: 1341(R) (TID-19608)
content in Netherlands diet, 1964, 20: 33575
content in northern stratosphere, 1962-63, 19: 40785 (TID-21224)
content in organisms and water in Gulf of Mexico, 20: 18200 (NYO-3450-1, pp 109-29)
content in plankton in Tyrrhenian Sea, 19: 29845
content in plants after Russian nuclear tests, 17: 17739
content in plants before and after Salmon Event, 20: 16743 (VUF-1021)
content in Po Valley rice, effects of crop irrigation on, 20: 12986
content in rainwater at Ispra during 1963 and 1964, 19: 34373
content in rainwater at Milan following Chinese nuclear explosions, 19: 42643
content in salmon in northeast Pacific Ocean, 20: 45961(R) (RLO-1750-8(Vol.3), (Paper 2))
content in sedge from Chariot site environment, 19: 25798 (PNE-447)
content in silt in Escaut River, Belgium, control of, 20: 22515(T) (ORNL-tr-965)
content in soils, 20: 33519
content in Sputnik 4 fragment, 17: 37922
content in Sputnik 4 fragment, 18: 13666
content in Sputnik 4 fragment, 18: 26127
content in stone meteorites, gamma spectrometric study of, 18: 2515
content in stratospheric and tropospheric air filter samples collected in 1961 and 1962, 19: 9755 (HASL-153)
content in stratosphere, 19: 20657(R) (DASA-1309)
content in stratospheric and tropospheric samples in Project Star Dust, 1963, 20: 16727(R) (HASL-168)
content in stratospheric and tropospheric samples in Project Star Dust, 1964, 20: 16728(R) (HASL-169)
content in surface air, 18: 37380
content in tissues of fin whale captured off Oregon coast, 19: 6936
content in unio mussels, comparison with fallout and lake water, 19: 10762
content in vegetation in Northern Alaska from fallout, 17: 27053 (HW-SA-3050)
content in water supply in Germany from fallout, 19: 15792
content in whales, 20: 38560
content in wheat and other foods, 20: 23300
content of, in marine organisms, 19: 10732
content of, in tuna from Western Pacific, 1962, 18: 27703 (UWFL-90)
content on air filters at Hanford, methods of gamma spectrometry for monitoring, 19: 620(R) (HW-81746(p.3.51-5))
contents in air in Hanford Works Area, 19: 13626 (HW-SA-3742)
contents in animals, plants, rain water, and soils from Chariot site environment, 19: 25797 (PNE-446)
contents in animals and plants from Chariot site environment, 19: 25799(R) (PNE-448)
decay of, L/K ratio for electron capture, 17: 28325
decay of, calibration of ionization chamber for particles from, 19: 6194
decay of, gamma transitions in, (E), 19: 39866
decay of, K conversion coefficients from, (E/T), 20: 8080 (ORNL-P-1700)
decay of, K/L ratio for electron-capture, (E/T), 20: 15713 (CONF-233 (Vol.2), pp 365-8)
decay of, x-ray emission rates for electron-capture, (E), 20: 15242 (CONF-233(Vol.3), pp 465-79)
deposition in precipitation at Westwood, New Jersey, 19: 7701 (NYO-2415-12)
deposition on platinum anode, effects of hydrogen ion concentration on, 20: 18676
deposition, computer program for evaluating radiochemical data on, 19: 40636 (WAPD-TM-516)
detection and measurement in plant samples, 20: 9144
determination in Alaskan vegetation, gamma spectrometric, 19: 9366 (HW-SA-3316)
determination in atmospheric and precipitation samples, methods for radiochemical, 20: 14430 (AD-620219)
determination in Bruderheim chondrite, 16: 917
determination in Bogou iron meteorite, nondestructive, 18: 27707
determination in bovine feces, forage, and grain, gamma spectrometric, 19: 32101
determination in biological materials by paper chromatography and radiography, 20: 26786
determination in Columbia River, 20: 8980(R) (BNWL-36, pp 3.1-122)
determination in crushed oil shales, activation, 20: 23236(R) (ORNL-TM-1496)
determination in Columbia River plume at sea, techniques for, 20: 25282 (RLO-1750-4)
determination in decontamination solutions, 19: 32059(R) (IDO-14655)
determination in drinking and rain water, 20: 7021
determination in fallout, gamma spectrometric, 18: 12349
determination in fallout, 1962, gamma spectrometric, 18: 41360
determination in irradiated polyphenyls, 16: 7496
determination in iron meteorite, spectrometric, 18: 15985
determination in irradiated stainless steel by group separation and gamma spectrometry, 18: 41325
determination in irradiated steel by ion-exchange separation and gamma spectrometry, 19: 46195
determination in meteorites, 17: 12452 (LA-2765)
determination in mass transfer samples, methods for, 20: 12766 (GEAP-4178)
determination in presence of chromium-54, iron-59, and tungsten-181, radiometric, 16: 11553
determination in presence of cesium-137, integral gamma spectrum for, 20: 33212
determination in simulated high-altitude radionuclide samples, radiometric, 19: 13203(R) (NYO-3276-8)
determination in sectioned soil cores, autoradiographic, 19: 32106
determination of, in stratosphere, 17: 6271(R) (NYO-10464)

determination on filter papers, 19: 42424(R) (NYO-3276-10)
diffusion in aluminum at 450 and 650°C, 16: 22623
distribution coefficients between bis(2-chloroethyl) ether and hydrochloric acid solutions, 19: 26718 (ORNL-3802)
distribution in atmosphere of Northern Hemisphere, Jan. to April 1963, Star Dust program measurements of, 18: 41642(R) (DASA-1308)
distribution in ground-level aerosols, 19: 13687
distribution in mollusk tissues, 19: 45788
distribution in mollusks of Columbia River estuary, 20:40523(R) (RLO-1750-8(Vol.1))
distribution of injected, in rat tissues, 20: 18203(R) (LA-3432, pp 21-55)
distributions in stratosphere, 18: 35715(R) (DASA-1307)
electron capture decay, K-shell fractions, 16: 26336
electron capture decay of, 18: 11195(R) (EANDC(E)-49(L))
electron capture ratios of, 17: 13533
electron capture radiation from, measurement of absolute activity of, 18: 6187
electron capture ratios, M/L, 20: 40153
electron (K) capture fractions, 16: 7732
electron-capture decay of, absolute activity determination of, 20: 3034
elution during isolation of rat liver nuclei, 18: 41051
energy level density from (α,n) reactions, 16: 18477
energy levels, (T), 20: 26139
energy levels in, resonance, 16: 26235
energy levels of, spins and parities of, 18: 21208 (NP-13841)
energy levels of, isotope shifts of isobaric-analog, (E), 20: 22095
energy-level structure of, calculations using shell model with configuration mixing, (T), 20: 42201
excretion by mice, effects of temperature on, 18: 43173(R) (LA-3132-MS(p.32-6))
fallout in India, 19: 36650 (AEET-208)
gamma angular distribution of, oriented in antiferromagnetic $CoCl_2 \cdot 6H_2O$, 17: 4509
gamma dose constants for, 20: 46617
gamma dose rate from, 20: 45949 (CLOR-49/D)
gamma spectra, 16: 12265
gamma spectra, 17: 34967
gamma spectra, 20: 44634(R) (IDO-17188)
gamma spectra of, dependence of shape on measuring conditions of scintillation, 18: 18232
gamma spectra of, least-squares analysis of, 18: 33926
gamma spectra of, in stratospheric fallout, 19: 22544
gamma spectrum, 18: 18174 (BRL-1230)
gamma spectrum of, 17: 22008 (LADC-5609)
gamma transition at 835.0 kev, (E), 20: 3043
gastrointestinal transit of ceramic spheres containing, in animals and man, 20: 42740 (LA-DC-7764)
half life, 16: 2541
half life, 18: 34885
half life, 20: 8076 (NP-15663)
half life measurements from 440-Mev proton reactions with stone meteorites, 17: 28943(R) (TID-18961)
hyperfine field of, in nickel, 17: 40087
measurement in fallout, 20: 25288
metabolism by dogs, mice, monkeys, and rats, retention functions for, 20: 45296
metabolism by snails, 19: 11391(R) (NP-14658)
metabolism in aquatic organisms, 20: 16160 (UCRL-14739(Pt.2))
metabolism in chickens, 20: 29
metabolism in dogs, mice, monkeys, and rats, 18: 43172(R) (LA-3132-MS(p.25-31))
metabolism in dogs, monkeys, mice, and rats, 20: 36554 (LA-DC-7305)
metabolism in mice, radiation effects, 16: 9882
metabolism in rats and mice, 18: 15767(R) (LAMS-3034(p.49-52))
metabolism in scorbutic guinea pigs, 19: 43697
monitoring in food, surface water, and vegetation in Savannah River Plant area, July through Dec. 1965, 20: 27195(R) (DPST-66-30-1)
neutron activation cross section for, thermal, 18: 40474 (IDO-16977 (p.23-43))
neutron reactions (n,p), use in determining neutron spectra in steel, 19: 7992
nuclear orientation in manganese silicon fluoride crystals, 17: 4510
nuclear orientation in copper, gold, and silver, gamma-ray anisotropy from, (E), 20: 22097
nuclear polarization in, dynamic methods for, 17: 13992
nuclear polarization in iron, hyperfine field, magnetic resonance, and specific heat contributions from, 17: 26553
nucleon interactions in, properties from effective, (T), 20: 17735
orientation in ammonium manganese sulfates, 18: 42558
preparation, 18: 17452
preparation by neutron irradiation of iron, 19: 22312
preparation of carrier-free, from iron irradiated in Rossendorf cyclotron, 17: 19268
preparation of, by neutron irradiation of iron, 20: 33402
production and detection in stainless steel loop coolant, 16: 11957(R) (JAERI-5003(p.112-14))
production and separation of, method for, 17: 10676 (NP-12231)
production at ORNL, 19: 26718 (ORNL-3802)
production by cyclotron irradiations, 20: 46613
production by gamma reactions (γ,n) at 20 Mev, 17: 30161
production by proton reactions in thick iron targets, cross sections for, 18: 26583
production in atomic explosions, 20: 23314
production in cyclotrons, yields, 16: 12590
production in lithium-6 reactions with iron-54 at 21 to 63 Mev, excitation functions for, 18: 9398
production in lithium-6 reactions with iron-54 at 21 to 63 Mev, statistical analysis of, 18: 9399
production in ORR pressurized-water corrosion loop, calculations on, 19: 30150(R) (ORNL-3789(p.113-21))
production in proton reactions with iron and nickel at 130 to 400 Mev, cross sections for, 18: 22881
production in proton reactions with iron targets, 18: 43601(R) (TID-21007)
production in proton reactions with iron at 400 Mev, Monte Carlo calculation of, 20: 22035
production in proton reactions with iron at 400 Mev, (T), 20: 32560
production in proton bombardment of iron and stone meteorites, cross sections for, 17: 28943(R) (TID-18961)
production in reactor by neutron reactions (n,p), 17: 24508
production in stainless steel by cosmic protons, 17: 3938
production in thick iron targets by protons at 3 Bev, 17: 5336
production in 100-Mev to 1-Bev proton reactions with iron, 17: 28943(R) (TID-18961)
production in 20-Mev linear electron accelerator, purity and yield in, 19: 32836
production of carrier-free, by in-pile irradiation of iron, 18: 37063 (EUR-1641.i)
production of carrier-free, from natural iron in LITR and ORR, 20: 9030
production of carrier-free, 20: 43398
radioactivity of, absolute measurement of, 20: 15690 (CEA-R-2813)
separation from cobalt-60 and iron-59 by ion exchange, 20: 14433(R) (BAW-298)
separation from copper-64 and zinc-65 in sea water, method for, 20: 18576(R) (TID-22660)
separation from iron-59 by preferential evaporation, 19: 15381
separation from iron in hydrochloric acid by solvent extraction using methyl isobutyl ketone, 20: 22874 (ORNL-TM-1481)
solvent distribution between bis(2-chloroethyl) ether and hydrochloric acid, coefficient of, 20: 18571 (ORNL-TM-1420)
sorption by mud in sea water, 19: 33668
sorption from sea water by montmorillonite clay, 20: 18576(R) (TID-22660)
sorption on sediments in Columbia River, 19: 15784(R) (HW-83614)
transport in Columbia River, 20: 25290
uptake and concentration in female mice, 18: 20
uptake by crustacea, mollusks, and plankton in Bay of Venice, 20: 20386(R) (NP-15916)
uptake by marine and terrestrial mollusks, 20: 24844
uptake by marine mollusks, 20: 40528
uptake by mollusks, determination of, 19: 2058
uptake by plants in Georgia piedmont, 20: 12985
uptake by rat hair, 20: 1695
uptake by scallops, 19: 43663
uptake by swine blood cells in vitro, effects of dietary calcium, zinc, and corn oil on, 20: 40556
uptake of chloride-incorporated, by Amphiuma melanocytes, 20: 8573
use in pyruvate carboxylase activity studies, 20: 42773
yields in iron-54 (n,p) reaction, 17: 39980 (ORNL-TM-666)
yields in proton spallation of copper at 24 Bev, 16: 24859

MANGANESE ISOTOPES Mn-55

alpha elastic scattering on, deformation magnitude and sign from, 17: 31471
alpha inelastic scattering at 43 Mev, (E), 19: 41760
alpha reactions (α,n) at 14 to 20 Mev, evaporation spectra of, 18: 32800
alpha reactions (α,n), model of isomeric ratios in, 19: 22282(R) (NYO-1930-40)
alpha reactions (α,n) at 14 and 17 Mev, angular distributions from, (E), 19: 33240 (IFA-CRD-30)
alpha reactions (α,n) to 42 Mev, isomeric ratios from, (E), 19: 41695
alpha reactions (α,n), statistical model for isomeric ratios in, 19: 41696
alpha reactions (α,n) at 14 and 17 Mev, angular distributions from, (E), 20: 10000
alpha reactions (α,n) at 6.4 to 13.2 Mev, isomeric cross section ratios for, (E), 20: 28352
alpha reactions (α,n) at 17 Mev, level density parameters from, (E),

20: 38115
alpha reactions (α,n) on, cross sections for, 16: 33845
alpha reactions (α,p) at 22 Mev, angular distributions from, 17: 28288
binding energy, magnetic moment, and spin of ground-state, effective neutron-proton interaction for, 18: 6231
bremsstrahlung reactions at 1 Bev, equivalent-quantum cross sections for spallation, (E), 20: 24433
charged-particle reactions, cross sections for, 18: 40515 (ORNL-CPX-1)
deuteron reactions (d,p) and (d,2n) at 3 to 11.6 Mev, absolute cross sections and excitation functions for, 17: 31520
deuteron reactions (d,p) with, compound nucleus formation effects in, 17: 38222
deuteron reactions (d,α) and (d,p) at 3 to 4.3 Mev, energy levels from, 18: 19046
electron energy levels of, g-factors and hyperfine-interaction constants for, (E), 20: 9962(R) (ANL-7029, pp 9-12)
electron (K) fluorescence yields, 16: 7732
energy levels excited by 6.6-Mev protons, 16: 17146
energy levels from iron-58 (p,α) reactions, (E), 20: 34639
energy levels in, resonance, 16: 26235
energy levels of, first, 17: 4095
energy levels of, parity and spin assignments for excited, 17: 24487
fluorine isotope reactions (F^{19},F^{18}) up to 43 Mev, 16: 21428
gamma absorption cross section, (T), 19: 45366
gamma radiation from, measurement of, 18: 180
gamma reactions (γ,p) with, cross sections, (E/T), 19: 14528 (LAL-1120)
helium-3 reactions (He-3,2p) at 12 Mev, Q value for, 20: 16331 (GA-6568)
hyperfine structure of, analysis by exchange polarization, 19: 27580
ion reactions with, neutron-transfer mechanisms in, (E), 19: 37823(R) (ORNL-3800(p.1-49))
ion reactions with, copper recoil ions from heavy, (E), 20: 12085
neutron absorption by, in heavy water, 18: 7885 (AEEW-M-363)
neutron absorption by, in pressure tube reactors, 18: 7888 (AEEW-R-186)
neutron absorption by, resonance integral determination in, 19: 23657
neutron activation cross sections, 16: 18484
neutron activation cross sections at 24 kev, (E), 19: 16935
neutron capture and scattering cross sections, 18: 2969
neutron capture at 14 Mev, gamma spectra from, (E), 20: 19829 (NIJS-R-455)
neutron capture by, rates of, in ZEEP cell tests, 17: 2468 (CRRP-985-E)
neutron capture by, cross sections for, 17: 31758
neutron capture by, gamma-gamma cascades in thermal, (E), 19: 14561
neutron capture cross section at 14.7 Mev, (E), 20: 46614
neutron capture, rate measurements, 16: 17233 (CRRP-985-D)
neutron elastic scattering at 0.3 to 14 Mev, spin-spin interactions in, 18: 24645
neutron elastic scattering on, deformation magnitude and sign from, 17: 31471
neutron evaporation spectra from, angular momentum effects in, 18: 28628
neutron potential scattering cross sections, 18: 2849
neutron radiative capture cross section from 1.0 to 19.5 Mev, (E), 20: 42332
neutron reactions (n,p) at 14 Mev, direct and evaporation mechanisms, 16: 4850
neutron reactions (n,He^3) at 14.5 Mev, cross-section upper limits, 16: 8219
neutron reactions (n,γ) at fission energies, 16: 18429
neutron reactions (n,α) at 12 to 18 Mev, cross sections for, 17: 853
neutron reactions (n,pγ) at 14 Mev, cross sections for, 17: 2242 (TID-16949)
neutron reactions (n,2p) at 14.8 Mev, cross section limit, product half life, and Q value for, 17: 2242 (TID-16949)
neutron reactions (n,α) at 14.8 Mev, cross sections for, 17: 2242 (TID-16949)
neutron reactions (n,p) at 14.8 Mev, separation energies for, 17: 2242 (TID-16949)
neutron reactions (n,αγ), (n,αn), (n,pn), and (n,2n) at 14.8 Mev, cross sections for, 17: 2242 (TID-16949)
neutron reactions (n,helium-3) at 14.8 Mev, cross section limit, product half life, and Q value for, 17: 2242 (TID-16949)
neutron reactions at 14 Mev on, alpha distributions from, 17: 13511
neutron reactions (n,2n) at 14 Mev, cross sections for, 17: 26551
neutron reactions (n,2n) with, cross sections for fast, 17: 31056
neutron reactions (n,d) at 14 Mev, cross sections for ground-state transitions in, 17: 34920
neutron reactions (n,2p) at 14.7 Mev, cross-section limits for, 17: 36707
neutron reactions (n,2p) at 14.8 Mev, cross-section limits for, 18: 1077
neutron reactions (n,He^3) at 14.8 Mev, cross-section limits for, 18: 1077
neutron reactions (n,2n) with, 18: 11195(R) (EANDC(E)-49(L))
neutron reactions (n,γ), cross sections for, 18: 16947 (NP-13661)
neutron reactions (n,α) at 14 Mev, nuclear shell effects in cross sections for, 18: 18977
neutron reactions (n,α) at 12.5 to 19.6 Mev, cross sections for, 18: 24602 (NP-13930(p.43-9))
neutron reactions (n,n^2γ) at 1.0 and 4.0 Mev, cross sections and spectra for, 18: 30736(R) (TID-20658)
neutron reactions (n,γ) with, backscattering from, 19: 3347
neutron reactions (n,α) at 12.6 to 19.6 Mev, excitation functions for, (E), 19: 6669
neutron reactions (n,2n) at 14 Mev, shell effects in, (T), 19: 12536
neutron reactions (n,α) at 14.8 Mev, cross section for, (E), 19: 14615
neutron reactions (n,He-3) at 14.8 Mev, cross section for, (E), 19: 14615
neutron reactions (n,α) at 14 Mev, excitation cross sections for, (E), 19: 16951
neutron reactions (n,α) at 14.8 Mev, cross sections for, (E), 19: 27516
neutron reactions (n,2n) with, fission-averaged cross sections, 19: 29319
neutron reactions (n,α) at 12.5 to 19.6 Mev, cross sections for, (E), 19: 35378(R) (EANDC(E)-57(U))
neutron reactions (n,γ), spectra from, (E), 19: 35378(R) (EANDC(E)-57(U))
neutron reactions (n,γ) with, rates for, (E/T), 19: 45522 (AE-195)
neutron reactions (n,γ) in soil, activity induced by, 19: 47569 (CEX-62-50)
neutron reactions (n,2n) at 12.6 to 19.6 Mev, excitation function for, (E/T), 19: 47571 (EUR-2456.e)
neutron reactions (n,γ) to 10 kev, cross sections for, (E/T), 19: 47634
neutron reactions (n,γ), cross sections for resonance and thermal, (E), 20: 3031
neutron reactions (n,2n) at 12.6 to 19.6 Mev, cross sections for, (E), 20: 9990
neutron reactions (n,γ) at 200 to 525 ev, multiple scattering in, (T), 20: 11967 (JINR-P-2455)
neutron reactions (n,He-3) at 14.8 Mev, effective cross sections for, (E), 20: 15739
neutron reactions (n,γ) with, gamma spectra from thermal, (E), 20: 22064
neutron reactions (n,γ) with, cross sections for, (E), 20: 30360 (WASH-1068)
neutron reactions (n,γ) at 0.1 to 14 Mev, cross sections for, (T), 20: 30378
neutron reactions (n,γ) with, resonance activation integral cross sections for, (E), 20: 40069(R) (EANDC(E)-66(U))
neutron reactions (n,2n) at 3 Mev above threshold, cross section for, (E), 20: 46614
neutron resonance integral for, 17: 22566 (TID-18590)
neutron resonance absorption integrals of, activation measurements of, 17: 26423 (GA-3125)
neutron scattering at 2.9 Mev, gamma production cross sections for, 16: 7095
neutron scattering cross section for, multilevel effects in, 18: 7702 (WAPD-T-1630)
neutron scattering at 0.4 to 1.2 Mev, cross sections for, 18: 9331
neutron scattering at 3 to 650 kev, cross sections, phase shifts, and strength functions for, (E), 19: 10319
neutron total cross section, 18: 42622(R) (ANL-6879(p.2-20))
nitrogen ion scattering at 11 Mev, Coulomb excitation in, 18: 38128
nitrogen-14 reactions with, excitation functions for one-neutron-transfer, (E/T), 19: 47586 (ORNL-TM-1218)
nitrogen-14 reactions at 20 to 42 Mev, excitation functions for, (E), 19: 47667
nuclear magnetic resonance in potassium manganese fluorides, excitation of, 17: 37689
nuclear magnetic resonance in germanium–manganese alloys at 1.6, 4.2, and 77.0°K, 17: 39599
nuclear magnetic resonance in manganese nitrides, hyperfine fields and moments from, 18: 19979
nuclear magnetic resonance in cesium manganese fluoride, 18: 26159
nuclear magnetic resonance in potassium manganese fluorides, mode mixing in, 18: 35559
nuclear magnetic resonance linewidth in beta manganese, (E), 19: 21366
nuclear magnetic resonance in manganese selenide, coupling constants from zero-field, (E), 20: 3295
nuclear properties of, shell model calculation of, 17: 7240
nuclear properties of, semiatomic model for, 17: 22629
nuclear quadrupole moment, 17: 7275
nuclear resonance in antiferromagnetic potassium manganese fluorides, 16: 616
nuclear resonance fluorescence at 126 kev, 16: 21443
nuclear resonance excitation, 16: 29146
nuclear resonance excitation of first excited level of, 17: 23624
nuclear structure of, shell-model calculations for, 17: 7145 (UCRL-6404)
nucleon interactions in, properties from effective, (T), 20: 17735
nucleus reactions on, mechanisms for carbon-12, nitrogen-14, and oxygen-16, 16: 33891
performance of activation detectors of, for neutron flux measurements, 20: 33636
photon reactions at 300-Mev peak, isomer production in, (E/T), 20: 1246

proton elastic scattering at 22.2 Mev, angular distributions and cross sections, 16: 9462
proton elastic scattering, isotopic, isotonic, and shell closure effects on polarized, 17: 19360
proton elastic scattering at 5 and 14 Mev, spin-spin interactions in, 18: 24645
proton elastic scattering on, deformation magnitude and sign from, 17: 31471
proton inelastic scattering at 6.6 Mev, 16: 17146
proton inelastic scattering at 3 to 4.3 Mev, energy levels from, 18: 19046
proton reaction with, cross section fluctuations in, 18: 32848
proton reactions (p,d) at 17 to 18.5 Mev, neutron shell configuration studies from, 18: 21291
proton reactions (p,α) at 11 to 12.5 Mev, 18: 34855
proton reactions (p,n) with, thresholds for, (E), 19: 6704
proton reactions (p,n) at 4.5 and 5.9 Mev, excited levels from, (E), 19: 19214
proton reactions (p,n) at 3.5 to 6.75 Mev, total cross sections for, (E), 19: 23682
proton reactions (p,α) and (p,p) at 6.75, cross sections for, (E), 19: 23682
proton reactions (p,n) at 3.315 and 3.525 Mev, iron-55 energy levels from, (E), 19: 47696
proton reactions (p,n) at 14.2 Mev, angular distributions, Q values, and spectra from, 20: 13345(R) (NP-15772)
proton reactions (p,n) at 14.2 Mev, Q-values and differential cross sections for, (E/T), 20: 34520 (INSJ-97)
proton reactions (p,pn) with, manganese-54 production by, (E), 20: 46613
proton reactions (p,n), 16: 2492(R) (TID-14186)
proton reactions (p,n), neutron yield resonances, 16: 2495(R) (TID-14256)
proton reactions (p,α) at 7.6 to 12.9 Mev, cross sections, 16: 6005
proton reactions (p,pn), excitation functions, 16: 5963
proton reactions (p,pn) at 20 to 155 Mev, excitation functions for, 16: 21484
proton reactions (p,α) at 18 Mev, seniority wave function effects on angular distributions and cross sections, 16: 21578
proton reactions (p,pn) at 370 Mev, cross sections for, 17: 796 (NEVIS-109)
proton reactions (p,n), cross section relations with energy, 17: 7144 (TID-17357(Pt.III))
proton reactions (p,n) at 6.75 Mev with, cross section for, 17: 22618
proton reactions (p,n) with, fluctuation in excitation function for iron-55 states from, 17: 31484
proton reactions (p,t) at 40 Mev, angular distributions and energy spectra for, 17: 38232
proton reactions (p,n) with, excitation function fluctuation in, 17: 41873 (WASH-1044)
proton scattering spectra, 16: 2492(R) (TID-14186)
proton scattering at 6.6 Mev, energy levels from, 16: 19816
proton scattering at 9.4–22.2 Mev, local optical potentials for, 17: 38185
spectra, hyperfine structure splitting of ground state, 16: 19544
spectra of, measurement of Kα x, (E), 19: 20323(R) (NYO-3246-4)
use in neutron detection by resonance activation, 20: 19018(R) (ANL-7110, pp 231-310)
x-ray emission from, Kα, 20: 40294
x-ray fluorescence coefficient of, L-shell, (E), 19: 27492

MANGANESE ISOTOPES Mn-56

activity of, method for determining gamma, 20: 9196
backscattering in iron from (n,p) and (n,γ) reactions, 19: 3347
beta decay, beta-gamma correlation, 16: 17144
beta decay of, β-γ asymmetry in 2.86-Mev, (E/T), 19: 31240 (TID-21815)
beta decay of, circular polarization of gamma radiation following, 18: 21309
beta decay of, gamma spectra for, 18: 34840
beta decay of, higher-order effects in allowed, (E), 20: 26176
beta decay of, transitions to vibrational levels in, 18: 36625
beta decay of, 1.65-Mev transition in, (E), 19: 31239 (TID-21804)
beta decay rate of, measurement by β-γ coincidence method, 18: 14259
beta emission from, hindrance phenomena in, 16: 23073
beta spectrum, 17: 5387
content in Hanford reactor effluent, 19: 685(R) (HW-81746(p.3.33-6))
content in reactor effluent water, effects of sodium silicate addition on, 18: 36752 (HW-75782)
decay for long periods, hidden-variable nonexistence in, 16: 23121
decay of, calibration of ionization chamber for particles from, 19: 6194
decay, polarization of electrons in beta, 16: 21614
decay scheme, 16: 4810
decay scheme, 17: 19259
detection of, coincidence system for, 18: 35880
determination by photoneutron production in heavy water by gamma decay, 19: 19806
determination in atmospheric aerosols by activation analysis, 18: 29566(R) (NP-14096(p.17-22))
determination in aqueous solutions by Cherenkov counting, 19: 42581
determination in boreholes, activation, 19: 9086
determination in copra and desiccated-coconut oils, activation, 20: 14463 (PAEC(D)CH-652)
determination in heavy-water moderator by sequential analysis, 18: 27287 (DP-886)
determination in IRL Reactor pool by gamma spectrometry, 17: 40702 (TID-7655(p.107-18))
determination in manganese sulfate solutions, coincidence counters for, 17: 41239 (ANL-6760)
determination in neutron-irradiated clays and soils, 20: 43607
determination in organic reactor coolant, 18: 21553 (NAA-SR-Memo-7771)
determination in phantoms, whole-body counter for, 18: 14260
determination in river water, activation, 17: 30185
distribution in neutron irradiated potassium permanganate, 17: 39137
distribution in soils exposed to nuclear detonations, 16: 12814 (WT-1117)
dosimetry of, equation for internal, 20: 18955
energy level structure, (E), 19: 35439
energy levels, 16: 14041
energy levels from thermal neutron reactions (n,γ) with manganese 56, (E), 20: 22064
energy levels of, reduced widths and strength functions of, (E), 19: 17009
energy-level spectra, (E), 19: 11558
equipment for research on, 17: 6170
gamma dose constants for, 20: 46617
gamma specific emission coefficient, 17: 6431 (CEA-2036)
gamma spectra, 17: 34966
gamma spectra, (E), 20: 28461
gamma spectra, 19: 4474 (TID-7705(p.113-23))
gamma spectra, 19: 28639 (TID-21830)
gamma spectra and energy levels, 16: 18431
gamma spectra of, computer program for determination of, 19: 18387
half life, 19: 33350
half life, 20: 16331 (GA-6568)
half life of, (E), 19: 21290
neutron reactions (n,α) at 14 Mev, nuclear shell effects in cross sections for, 18: 18977
nuclear moments and spins, 17: 22222 (MMPP-NPC-1-3)
preparation and properties of, for use as neutron sources, 18: 16379
preparation of high-specific-activity, using Szilard-Chalmers effects of 8-hydroxyquinolates, 16: 27043(T) (CEA-tr-X-444)
production by iron-56 (n,p) reaction, 17: 22645
production by neutron reactions (n,γ), 18: 37592
production by Osaka Radiation Center linear accelerator, 17: 35006
production in atmosphere by neutron activation of airborne dust, inhalation hazard from, 19: 26589
production in soil by neutron reactions (n,γ) on manganese-55, activity from, 19: 47569 (CEX-62-50)
production in Szilard-Chalmers reactions with potassium nitrosylopentacyanomanganate, 17: 32168
reactions of recoil, with cyclopentadienyl manganese tricarbonyl, 20: 23095
recoil chemistry in neutron-irradiated manganese oxides and permanganates, Moessbauer effect studies on, 19: 42573
retention of recoil, in neutron irradiated potassium permanganate at low temperatures, 16: 16423
separation from magnesium-27 by solvent extraction using diethyldithiocarbamic acid, 20: 16336(R) (NYO-10175)
separation from neutron-irradiated aluminum, radiochemical, 20: 33164(T) (AEC-tr-6639, pp 28-31)
separation of ionic, at submicromolar concentrations by paper electrophoresis, 16: 17710
sorption by Columbia River particulate material, 18: 35761 (HW-79279)
sorption from reactor effluent by particles in Columbia River, 19: 215(R) (HW-81746(p.3.81))
tracer applications in industry, 17: 6372
use in calibration of neutron sources, 20: 3321(R) (ANL-7082, pp 29-53)
use in neutron-source calibration, 19: 15877
yields in proton spallation of copper at 24 Bev, 16: 24859

MANGANESE ISOTOPES Mn-57

beta spectra, 18: 6280

MANGANESE LUTETIUM SELENIDES

preparation, (E), 19: 13297

Manganese Magnesium Ferrates

see Magnesium Manganese Ferrates

MANGANESE MOLYBDATES

preparation and structure of, 19: 43991(N64-26433)
preparation, crystal structure, and magnetic susceptibility of, 20: 26864

MANGANESE NIOBATES

crystal structure, 16: 11650
crystallographic and magnetic structure, 16: 7532

MANGANESE NITRATES
analytical use for ion exchange separation of americium, curium, and rare earths, 20: 18562(R) (EUR-2640.e)
nitrogen-14 NMR in, (E), 20: 12325
separation by reversed-phase partition chromatography using organophosphorus compounds, 18: 25614
$Mn(NO_3)_2$–$Th(NO_3)_4$, crystal structure of octahydrates, 19: 19852
MANGANESE NITRIDES
ferromagnetic properties of, and its mixed crystals, 20: 4402(T) (ANL-Trans-230)
magnetic structure, 16: 15221
manganese-55 NMR in, hyperfine fields and moments from, 18: 19979
MANGANESE ORES
geochemical survey, in San Jose Co., Utah, 16: 27437
radium, thorium, and uranium abundance ratios in, 20: 29425
MANGANESE OXALATES
pyrolysis of, carbon-13 isotope effects in, 18: 1728 (TID-19650)
radiation effects on dehydration of dihydrate, 16: 17720
radioinduced crystallization of anhydrous, 18: 16096
MANGANESE OXIDES
see also Cobalt Manganese Oxides
analysis for oxygen-18, mass spectrometric, 20: 8852
analytical use for precipitation of strontium-90 in seawater, 20: 24973 (AD-632528)
analytical use in scavenging radioisotopes in sea water, 17: 40748
analytical use of colloidal, in foam chromatography separation of radioisotopes in aqueous solutions, 20: 20628
beta backscattering, 16: 9409
catalytic effects on decomposition of tritium-labeled compounds, 19: 7491
catalytic properties of, isotopic exchange studies of, 18: 13739
content in thalenites from Japan, 20: 29399
content in zircon from Kyoto Prefecture, Japan, 19: 36296
corrosive effects on reactor cooling systems, evaluation of, 19: 36984
crystal lattice distortions from magnetic ordering at low temperatures, 19: 11078
crystal structure of, vacancy interaction energies in, 17: 35781
crystal structure at 4.2 and 290°K, 17: 39400
crystal structure of alpha-, neutronographic studies of, 18: 8847
determination by measurement of x radiation intensity by non-dispersive spectrometry, 17: 38948
determination using sulfatoceric acid, 18: 41355
effects on fritting of beryllium oxide, 18: 22500(T) (UCRL-Trans-1042(L))
effects on radioinduced coloration of glass, 19: 32607(P)
effects on radioinduced reactions of isobutane and olefins, 18: 13836(R) (NYO-10025)
effects on radiolysis of ammonium perchlorate, 19: 7573
effects on sintering of alumina, 20: 43813(R) (COO-1122-3)
effects on sulfuric acid leaching of uranium from ore, 16: 33059
effects on superconducting transition temperature of lead, (E), 20: 2916
electron energy losses in, and mechanisms of, 17: 13165
electronic properties of single-crystal, effects of ion-bombardment on, 20: 17151
emissivity of, measurements of, 17: 16787(R) (PWA-2163)
free energy of formation at 1100°F, 17: 32571(R) (MSAR-63-105)
hardness of crystalline, 16: 10728
hardness of crystalline tetravalent, 16: 10728
machining procedures for single crystals of, 20: 43864 (Y-1550)
magnetic properties of, determination of, by neutron diffraction, 20: 20360(R) (PRNC-73)
magnetic spin correlations in, near Neel temperature, 18: 16894(R) (MIT-3031-1)
magnetic structure of, long-range, (E), 20: 13993
magnetic susceptibility at 100 to 300 kgauss, 16: 15455
magnetic susceptibilities, 16: 25882 (ASD-TR-61-630)
manganese ion spin correlations in, 18: 39237
$MnZn(Fe_2O_4)_2$, neutron total cross section at 11.5 Å, 18: 34752(R) (CU(PNPL)-234)
neutron diffraction by, covalency effects in (E), 19: 2269 (BNL-8514)
neutron inelastic scattering by, measurement of magnetic, (E), 19: 8375 (BNL-7645)
neutron magnetic scattering by, (E), 19: 43486
neutron resonance absorption integral of, (E), 20: 14008(R) (ANL-7122, pp 42-69)
neutron scattering by, magnetic, 17: 38027(T) (AEC-tr-5734(p.140-52))
neutron scattering by paramagnetic, energy spectra in, 19: 38063
neutron total cross section at 11.5 Å, 18: 34752(R) (CU(PNPL)-234)
non-stoichiometry in, evaluation of, 18: 29673
nuclear magnetic resonance of oxygen-17 in, 18: 11193 (CONF-250-18)
oxidation of ferrous ions by, 16: 27023
oxidative effects on aqueous uranium(IV), tracer study, 16: 11602
oxygen isotope exchange reactions in, temperature effects on rate of, 19: 44104
polarography in lithium and lithium sodium metaphosphates at 750 and 730°C, 18: 1516
preparation for controlled sorptive properties, methods for, 20: 40476(R) (BNWL-267)
preparation of single crystals, 16: 22114
preparation, properties, and aerospace applications, 19: 37142
proton reactions at 660 Mev, 17: 41884
radiation effects on catalytic activity, pile, 16: 11769
radiation effects on films of, on glass, 16: 21108
radiation effects on magnetic properties, 17: 12737
radiation effects on catalytic properties of, fast neutron, gamma, and proton, 19: 4225
radiation effects on sorptive properties of, for hydrogen, 20: 8985
radiation effects on catalytic activity of, in decomposition of hydrogen peroxide, 20: 43364
radioinduced transition radiation from, fast electron, 18: 12747
radiolysis in hydroxide solutions, mechanisms and yields in, 18: 10144
reactions with uranium dioxide, effects of halides on, 18: 19943
reactions with uranium dioxide in sulfuric acid, effects of iron(II) on, 19: 4260
recoil chemistry of manganese-56 in neutron-irradiated, Moessbauer effect studies on, 19: 42573
separation of by-product, from Rand barren solutions, 16: 22262 (ACCO-23)
sorptive properties for strontium, 16: 11735
sorptive properties in aqueous solutions, 16: 16389
sorptive properties for protactinium, 16: 16396
sorptive properties for strontium, 16: 27015
sorptive properties for strontium, effects of ethanol on, 16: 31629
sorptive properties for strontium, 17: 30604
sorptive properties for protactinium, 18: 20105
sorptive properties for radium in liquid wastes, 19: 34269
sorptive properties of hydrous, for radionuclides in waste solutions, 20: 5206
sorptive properties for chloride and potassium ions, effects of pH on, 20: 14651
sorptive properties for radiocolloids of ruthenium-106, effects of pH on, 20: 18847
sorptive properties of activated, for cerium, 20: 26847
sorptive properties of, effects of competing ions on, 20: 40476(R) (BNWL-267)
spectra in low frequency region, infrared, 18: 23549
spectra of, in 300 to 1000 mμ region, reflectance, 17: 15970
thermal energy storage in, in solar-thermionic power supplies, 17: 9113
thermodynamics of nonsubstitutional solid solutions of, statistical model for, 18: 25421
use in determination of cerium-144, cesium-137, cobalt-60, plutonium-244, and strontium-90 in sea water, 20: 35405
use in head-end step in Thorex Process, 19: 40649 (DP-982)
use in separation of protactinium-233 from irradiated thoria, 19: 40644 (BNWL-78)
Al_2O_3–Fe_2O_3–MgO–MnO, neutron radiation effects on magnetic properties of, 17: 2042
$BaCO_3$–MnO_2, effects on production of boron nitride by reaction of boron oxide with ammonia or nitrogen, catalytic, 19: 36430(P)
Co_3O_4–Mn_3O_4, phase studies at 800 to 1400°C, 20: 338
CoO–MnO, phase studies at 800 to 1400°C, 20: 338
CoO–MnO–SiO_2, phase studies and thermodynamic properties, 18: 13727(R) (TID-20232)
CoO–MnO–SiO_2, solid solutions in, 19: 13280(R) (TID-21569)
Fe_2O_3–MgO–MnO, neutron radiation effects on magnetic properties of, 17: 2042
FeO–MnO, phase studies at 800 to 1400°C, 20: 338
Fe_3O_4–Mn_3O_4, phase studies at 800 to 1400°C, 20: 338
Fe_2O_3–MnO_2, sorptive properties for fission products, 20: 40476(R) (BNWL-267)
FeO–MnO–SiO_2, activities at 1150°C, ternary diagram, 19: 13280(R) (TID-21569)
Fe_2O_3–MnO_2–Sc_2O_3, phase studies of solid solutions in, 20: 36839
Fe_2O_3–MnO_2–WO_3, properties as metalizing paint for metal-to-ceramic seals, 20: 27401(R) (AD-632362)
Fe_2O_3–MnO–ZnO, neutron magnetic inelastic cross section of, 17: 36669 (WASH-1042)
Fe_2O_3–MnO–ZnO, neutron radiation effects on magnetic properties of, 17: 2042
MgO–MnO, ammonia decomposition on solid solutions of, 19: 24530
MgO–MnO, ordering in solid solutions of, effects of heat on, 16: 2924 (ASD-TR-61-92)
MgO–MnO, preparation and plastic properties of single crystals of, 17: 41425 (HR-63-274)
MnO_2–MoO_3, properties as metalizing paint for metal-to-ceramic seals, 20: 27401(R) (AD-632362)

MnO–NiO, phase studies at 800 to 1400°C, 20: 338
MnO–rare earth oxides, preparation and magnetic properties, 19: 42463
Mn_2O_3–Sc_2O_3, magnetic susceptibility, 20: 29168
Mn_2O_3–Sc_2O_3, phase studies, 20: 29168
MnO–Sc_2O_3, phase studies, 20: 29168
MnO_2–SiO_2, chemical effects of, on radiolysis of propene and 2-methylpropene, 16: 30447(R) (NYO-10024)
MnO_2–SiO_2, phase studies, 16: 24148(R) (ASD-TR-61-676)

MANGANESE PERCHLORATES
separation by reversed-phase partition chromatography using organophosphorus compounds, 18: 25614

Manganese Potassium Fluorides
see Potassium Manganese Fluorides

Manganese Rubidium Fluorides
see Rubidium Manganese Fluorides

MANGANESE SCANDIUM SELENIDES
preparation, (E), 19: 13297

MANGANESE SELENIDES
magnetic structure and transitions in, 17: 39714 (BNL-7325)
manganese-55 NMR in, coupling constants from zero-field, (E), 20: 3295
preparation of manganese rare earth selenides, (E), 19: 13297

MANGANESE SILICATES
free energy of formation of MnSiO, and Mn_2SiO_4, 19: 13280(R) (TID-21569)
$FeSiO_3$–$MnSiO_3$, phase studies at 800 to 1400°C, 20: 338
Fe_2SiO_4–Mn_2SiO_4, phase studies at 800 to 1400°C, 20: 338

MANGANESE SILICIDES
crystal lattice parameters, 19: 44679(R) (ANL-7000, pp 205-12)
electron structure and physical properties of crystals of, 17: 27875
thermoelectric properties, 17: 6771 (AD-276005)

MANGANESE SILICON FLUORIDES
structure of crystalline hexahydrated, 17: 4510

Manganese Sodium Fluorides
see Sodium Manganese Fluorides

MANGANESE STEEL
austenite content, effects of aging conditions, 16: 30837
brittle fracture behavior of, temperature effects on, 17: 23972(T,R) (EURAEC-521)
cavitation by bismuth, lead, and mercury, 16: 13537
cavitation by bismuth, lead, and mercury, 16: 33434(T) (AEC-tr-5382)
ductility of SOUDOTENAX-56, 17: 11171(T,R) (EURAEC-330)
ductility of, measurement, 18: 35987(R) (EURAEC-1019)
fabrication and properties, 18: 15565
flame cutting of 200-mm-thick sheets of, 17: 23928(T) (EURAEC-511)
grain growth and transformations in austenized Ammo, effects of temperature on, 20: 33865 (EURAEC-1623)
heat treatments at 900°C, austenizing effects on PM 24, 20: 43891 (EURAEC-1686)
magnetic properties of irradiated, 16: 33570
mechanical properties of, effects of boron and rare earth alloying on, 17: 39582
performance for ionization chamber construction, 20: 5716 (AEEW-M-470)
properties of low-carbon, 20: 13186 (TRG-Report-840)
radiation effects on strain-aged pressure vessel, 16: 16773 (AE-65)
radiation effects at 60 to 400°C, 17: 24014(T,R) (EURAEC-530)
radiation effects on impact and tensile properties of, 17: 36359
radiation effects on pressure vessels of, fast-neutron, 20: 21228 (AE-221)
radiation effects on tensile properties of type T-450, irradiated at 30°R, fast-neutron, 20: 27589(R) (NASA-CR-54881)
radiation effects on SA 302 B, 20: 30788(R) (ANL-7190, pp 176-88)
radiation effects on fatigue of A302B, neutron, 20: 39406 (WAPD-T-1864)
solubility of niobium carbides in, 17: 20471
tensile properties of T-450, evaluation, 18: 30238(R) (NP-14102)
welding of plates of, deformation and temperatures in electroslag, 17: 23929(T) (EURAEC-593)
welding of, residual stresses in, 17: 1900(T,R) (EURAEC-331)
welding procedures for, electro-slag, 20: 2281(R) (EURAEC-1408)
B–C–Cr–Mn–Mo–Ni–Nb–V, precipitation of niobium carbide in, 18: 37726
C–Cr–Co–Mn–Mo–Ni, mechanical properties of welded, 19: 22863(R) (AD-606809)
C–Cr–Mn, radiation effects on mechanical properties of, 20: 2438
C–Cr–Mn–Mo–Ni, mechanical properties of welded, 19: 22863(R) (AD-606809)
C–Cr–Mn–Mo–Ni–Si, strength and toughness of dynamically strain-aged, 20: 7584 (UCRL-16363)
C–Cr–Mn–Mo–Ni–Si–V, strength and toughness of dynamically strain-aged, 20: 7584 (UCRL-16363)
C–Mn, brittle fracture of welded plates of, 17: 39469(T) (EURAEC-602)
Cr–Mn, austenite content of, effects of aging conditions on, 16: 30837
Cr–Mn, creep-rupture properties, 17: 39531(R) (EURAEC-689)
Cr–Mn–Mo–Ni, development of high-strength weldable low-alloy, 20: 27481(R) (EURAEC-1419 and App.)
Cr–Mn–Mo–Ni, ductility of low-alloy, effects of alloying additions on, 20: 27481(R) (EURAEC-1419 and App.)
Cr–Mn–Mo–Ni, welding of very thick plates of, process development for, 20: 23621(R) (EURAEC-1548)
Cr–Mn–Mo–V, reactions with carbon dioxide to 400°C, 19: 22997 (TRG-Report-842)
Cr–Mn–Ni, mechanical properties of austenitic cast, at 2.5 to 4.5°K, 20: 19232
Cr–Mn–Si, corrosion by mercury and sodium amalgam at 200 to 500°C, 18: 18312(T) (CEA-tr-A-1455)
Cr–Ni, corrosion by mercury and sodium amalgam at 200 to 500°C, 18: 18312(T) (CEA-tr-A-1455)
Mn–Mo, addition of metallic aluminum and aluminum nitride to, for improved mechanical properties, 19: 41085(P)
Mn–Mo, brittle fracture of welded plates of, 17: 39469(T) (EURAEC-602)
Mn–Mo, embrittlement during stress-relief annealing after welding, 17: 12638
Mn–Mo, embrittlement by stress-relief annealing after welding operations, 18: 8807(T) (EURAEC-431)
Mn–Mo, embrittlement by plastic fatigue of A302B, 20: 15039 (EURAEC-1475)
Mn–Mo, embrittlement by plastic deformations at 20 to 400°C, 20: 23718
Mn–Mo, fatigue strength of A302B, effects of weld defects on, 20: 15059(R) (SWRI-1228-1-20)
Mn–Mo, fracture toughness of ASTM A302 B, 20: 10487 (WERL-8844-9)
Mn–Mo, heat treatment to improve notch toughness of, 20: 23724
Mn–Mo, mechanical properties of weld in, 17: 39512(T) (EURAEC-667)
Mn–Mo, mechanical properties of electroslag welds in, effects of oxidation on, 18: 8731(T) (EURAEC-510)
Mn–Mo, mechanical properties of A302-B, effects of cold-working and heat treatments on, 20: 19205(R) (GA-6923)
Mn–Mo, mechanical properties of ASTM A302B, effects of fabrication on, 20: 27449 (SWRI-1228-4-17)
Mn–Mo, properties of 200 mm thick plate, effects of sample position on, 19: 42846(R) (EURAEC-1399)
Mn–Mo, properties of type 302B, effects of fabrication and heating on, 20: 41451(R) (GA-7101)
Mn–Mo, radiation effects on embrittlement of, 16: 33569
Mn–Mo, radiation effects on embrittlement of, neutron, 16: 22700
Mn–Mo, radiation effects on embrittlement and hardening of neutron, 17: 31063
Mn–Mo, radiation effects on tensile properties of, effects of irradiation temperature on fast neutron, 18: 8877(T) (EURAEC-816)
Mn–Mo, radiation effects on mechanical properties of, fast-neutron, 18: 30263
Mn–Mo, radiation effects on embrittlement of, 18: 37749 (A/CONF.28/P/420)
Mn–Mo, radiation effects on deformation properties of A302B, neutron, 20: 2436 (WERL-8844-4)
Mn–Mo, radiation effects on mechanical properties of A302B and AMMO2, fast-neutron, 20: 5846
Mn–Mo, radiation hardening of A302B, effects of irradiation temperature on fast-neutron, 20: 11342 (EURAEC-1502)
Mn–Mo, radiation effects on impact strength of A-302B, combined stress and fast neutron, 20: 11227
Mn–Mo, radiation effects on mechanical properties of SA302B, fast-neutron, 20: 19178(R) (IDO-17154)
Mn–Mo, radiation effects on pressure vessels of, fast-neutron, 20: 21228 (AE-221)
Mn–Mo, radiation effects on A302B at 450 to 480°F, neutron, 20: 37289
Mn–Mo, radioinduced embrittlement of, neutron, 20: 27610
Mn–Mo, specification for A302 Grade B plate specimens for irradiation testing, 17: 41344 (HW-74939)
Mn–Mo, tempering behavior of pressure-vessel, 19: 26817 (KAPL-3092)
Mn–Mo, tensile properties of 200-mm-thick plate, effects of heat treatment and cooling rate on, 20: 33909
Mn–Mo, thermal stress fatigue of A-302B, 20: 11227
Mn–Mo, weld bead deposition on sheet specimens of, for bending tests, 17: 41390(T,R) (EURAEC-768)
Mn–Mo, weld bead deposition and properties on sheet specimens of, 18: 32115(T,R) (EURAEC-1018)
Mn–Mo, weld zone fracture toughness of A302B, 20: 9488(R) (BNWL-166, pp 4.8-11)
Mn–Mo, welding of, inspection and testing of sheets for, 17: 520(T,R) (EURAEC-351)
Mn–Mo, welding of thick plates of, by submerged-arc techniques, 19: 11691(R) (EURAEC-1221)
Mn–Mo, welding procedures for A302B, electro-slag, 20: 2281(R) (EURAEC-1408)
Mn–Mo, welding techniques for pressure-vessel, 18: 23074
Mn–Mo, welding thick plates of LMS2V, cracking and hardness changes from, 20: 15000 (EURAEC-1517)
Mn–Mo–Ni, stress rupture properties at 500 and 600°C of stainless-clad,

18: 10567
Mn–Mo–Ni–Nb, radiation effects on mechanical properties of low-alloy, neutron, 20: 19258 (UJV-1470/65)
Mn–Mo–Ni–V, welding procedures for, electro-slag, 20: 2281(R) (EURAEC-1408)
Mn–Mo–V, properties of Ammo, variations in samples of, 20: 41447(R) (EURAEC-1669)
Mn–Mo–V, transformation curves for continuous cooling of, from 1100°C, 20: 46184 (EURAEC-1677)
Mn–Ni, grain size and transformation of sustenized Wel-Manix, 20: 33866 (EURAEC-1649)
Mn–Si, radiation effects on plastic deformation of, 17: 32684
Mn–Si, review on radiation effects on crystal lattice of, 18: 14565
MANGANESE STRONTIUM LANTHANUM OXIDES
crystal structure, 20: 12865
MANGANESE SULFATES
see also Ammonium Manganese Sulfates
analysis for manganese-56, coincidence counters for activation, 17: 41239 (ANL-6760)
content in baths for neutron source calibration, determination of, (E/T), 19: 47552
effects on acrylonitrile polymerization in aqueous solution, 16: 30455
effects on gamma-induced polymerization of acrylonitrile in aqueous solution, 18: 29716(T,R) (AEC-tr-6231(p.175-85))
magnetic and crystal structure, 16: 18445
magnetic structure, (E), 20: 6546
magnetic susceptibility at 100 to 300 kgauss, 16: 15455
neutron absorption in, use in calibration of NBS-I photoneutron source, 17: 41849
neutron absorption in, use for calibration of photoneutron source, 19: 35358
neutron capture with charged-particle emission in, determination for source calibration, (E), 19: 45232
neutron escape from baths of, calibration of neutron sources from, 20: 24310
neutron leakage from baths of, 16: 24432
nuclear magnetic resonance in, uses for magnetic field measurements, (E), 20: 2112
performance for absolute calibration of neutron sources, 19: 33188 (AAEC/TM-288)
radiolysis of hydrated, yields in, 19: 40610
radiolysis of hydrated, gamma, 20: 36903
separation from iron and uranium by solvent extraction using alkyl phosphoric acids, 18: 13936
sound sorption at 25°C, 19: 32048(R) (NP-15073)
spectra of aqueous solutions of, ESR, 20: 43184 (UCRL-17064)
use in absolute calibration of neutron sources, 20: 36144 (ZFK-RN-33)
use in neutron-source calibration, 18: 22853
MANGANESE SULFIDES
anisotropic superexchange in beta, 16: 22786
explosibility of powders of ores of, 19: 36698 (BM-RI-6516)
hardness of crystalline, 16: 10728
reactions with yttrium sulfide, 16: 18864
spin arrangements in beta, relation to anisotropic superexchange interactions, 16: 22785
CrS–MnS, magnetic ordering in face-centered, (E), 20: 24646
MnS–rare earth sulfides, crystal structure of solid solutions in, 20: 332
MANGANESE SYSTEMS
Al–C–Mn, phase studies of, atomic size effects in, 19: 23111
Al–C–Mn–Nb, phase studies, 20: 15103
Al–C–Mn–Ta, phase studies, 20: 15103
Al–Cr–Fe–Mn–Mo–Ni–Si, machining characteristics, 17: 14778(R) (ASD-TR-7-532a(IX))
Al–Cu–Fe–Mn–Ni–Si–Ti, corrosion by molten fluoride mixture at 650°C, 17: 34345 (BMI-X-247)
Al–Mn–Ni–Si, air and helium effects on voltage drifts in thermocouples of, 17: 30829
Al–Mn–Ni–Si, behavior of Alumel thermocouple wire in carbon dioxide–carbon monoxide, 19: 22664 (ORNL-P-1070)
Al–Mn–Ni–Si, magnetic field effects on thermocouple wires of, 17: 30828
Al–Mn–Ni–Si, neutron-induced composition changes in, 17: 30826
Al–Mn–Ni–Si, radiation effects on thermoelectric properties, 18: 32237
Al–Mn–Ni–Si, reactions with beryllium to 600°C in carbon dioxide and *in vacuo*, 19: 22997 (TRG-Report-842)
Al–Mn–Ni–Si, reactions with Magnox alloy to 550°C in argon and carbon dioxide, 19: 22997 (TRG-Report-842)
Al–Mn–Si, phase studies, 19: 14060
B–Cu–Mn, crystal structure, 20: 14532
Be–Mn–O, phase studies of, 19: 20573
C–Co–Mn, crystal structure studies, 19: 44679(R) (ANL-7000, pp 205-12)
C–Cr–Co–Fe–Mn–Mo–Ni–W, corrosion by mercury at high temperatures, 18: 7152
C–Cr–Fe–Mn–Mo–Si–Ti, corrosion of 5 Croloy Ti by steam and chloride salt at high temperatures, 18: 4161 (GEAP-4351)
C–Cr–Fe–Mn–Mo–Si, corrosion of Croloy 1¼ and 5Si by liquid bismuth alloys, 18: 4193 (BNL-811)
C–Cr–Fe–Mn–Mo, corrosion of Croloy 2¼ and 9M by liquid bismuth alloys, 18: 4193 (BNL-811)
C–Cr–Fe–Mn–Mo–Si, corrosion of Croloy 1¼ by liquid lead alloys, 18: 4193 (BNL-811)
C–Cr–Fe–Mn–Mo, corrosion of Croloy 2¼ by liquid lead alloys, 18: 4193 (BNL-811)
C–Cr–Fe–Mn–Mo, corrosion of 2¼ Croloy by steam and chloride salt at high temperatures, 18: 4161 (GEAP-4351)
C–Cr–Fe–Mn–Ni, performance of Incoloy in nuclear superheated steam environments, 18: 4161 (GEAP-4351)
C–Cr–Fe–Mn–Si, radiation effects on thermal decomposition of, 18: 30259
C–Cr–Mn–Ni, corrosion by steam, 18: 30143
C–Cr–Mn–Si, galling tests of Aircolite for HTGR valve seats, 19: 11304 (GAMD-3058)
C–Cu–Fe–Mn–Ni, magnetic field effects on thermocouple wires of, 17: 30828
C–Cu–Fe–Mn–Ni, neutron-induced composition changes in, 17: 30826
C–Fe–Mn, explosibility of powders of, 19: 36698 (BM-RI-6516)
C–Fe–Mn–Ni, preparation and tensile properties, 19: 17443(P)
C–Fe–Mn–Ni, tensile properties of Invar sheet at cryogenic temperatures, 19: 13989 (LA-3192)
C–Ge–Mn, crystal structure and phase studies on, 18: 10561
C–Mn–Ni–Si, use for braze bonding stainless steel cans to stainless steel–uranium dioxide cermets, 19: 4635
C–Mn–P–Si–S, crack growth testing of, 20: 28694(R) (GEAP-4964)
C–Mn–Si, crystal structure and phase studies on, 18: 10561
C–Mn–Sn, phase studies of, atomic size effects in, 19: 23111
C–Mn–Zn, magnetic properties of Mn_3ZnC in, 20: 22312(R) (AD-622796)
C–Mn–Zn, phase studies of, atomic size effects in, 19: 23111
Cr–Co–Fe–Mn–Ni–Si–W, bonding of, controlling factors in diffusion, 19: 24964
Cr–Cu–Fe–Mn–Ni–Si, corrosion of Incoloy 800 by superheated steam, 18: 21668(R) (GEMP-274)
Cr–Cu–Fe–Mn–Ni–Si, corrosion of Incoloy 800 by superheated steam containing chloride, 18: 30129 (GEAP-4450)
Cr–Cu–Fe–Mn–Ni–Si, corrosion of Incoloy 800 by superheated steam, 18: 30130 (GEAP-4495)
Cr–Cu–Fe–Mn–Ni–Si, fabrication of Incoloy 800 tubes for use as fuel cladding, 18: 32101 (GEAP-4557)
Cr–Cu–Fe–Mn–Ni–Si, performance of Incoloy 800 as fuel cladding for supercritical-water reactors, 18: 35691(R) (WCAP-3374-1)
Cr–Cu–Fe–Mn–Ni–Si, properties of Incoloy 800 as fuel sheaths in nuclear superheat reactors, 18: 44033 (GEAP-4633)
Cr–Cu–Fe–Mn–Ni–Si, strain cycle tests of Incoloy 800 tubes, 18: 39813 (GEAP-4462)
Cr–Fe–Mn–Mo–Ni–Si, corrosion and metallurgical changes in, caused by steam at 1200 to 1500°F, 16: 24126
Cr–Fe–Mn–Mo–Si, corrosion of Sicromo by cesium, 17: 30944
Cr–Mn–Ni–Si, mechanical properties of, effects of steam at 1050°F on, 18: 4795(R) (GEAP-3924)
Mg–Mn–O, phase studies of, 19: 20573
Mn–$MnCl_2$, free energy of solution of, 19: 11103
Mn–Na–Te, thermoelectric properties at high temperatures, 17: 29854(R) (MND-2584-4)
Mn–O–V, magnetic structures in, 19: 38061
Mn–O–Y, magnetic structure, 19: 38057
Mn–Si, development of, for tantalum alloy and metal protection, 16: 24148(R) (ASD-TR-61-676)
Mn–Si, thermal expansion coefficients of, x-ray diffraction studies of, 16: 33489 (ASD-TR-61-676)
Mn–Si–Th, crystal structure of compound in, 19: 20568
Mn–Si–Ti, phase studies, 19: 14060
Mn–Si–U, eutectic temperature and composition in, 16: 17297(R) (LAMS-2681)
Mn–Si–U, melting point, 16: 6104(R) (LAMS-2647)
Mn–Si–U, phase studies and crystal structures of compounds in, 19: 18503
Mn–Si–U, preparation and crystal structure of compounds in, 19: 19871
Mn–ZnS, electroluminescence in magnetic field of thin film of, 18: 1126(R) (NBS-7973)
MANGANESE TANTALATES
crystal structure, 16: 11650
crystallographic and magnetic structure, 16: 7532
MANGANESE TELLURIDES
radiation effects on thermoelectric properties at 50 to 200°C, 16: 27696 (WCAP-1680)
structure, effects of magnetic moments on, 18: 37115 (ANL-6856)
tellurium-125 gamma absorption in, spectrum hyperfine structure from

recoilless resonant, 17: 34908
tellurium-125 Mössbauer effect in, (E), 20: 20148
MANGANESE TUNGSTATES
magnetic susceptibility and reflectance spectra of, 20: 26864
MANGANESE URANATES
crystal structure of, 17: 37826
crystal structure and density of, 20: 2400
preparation and structure of, 18: 12047
properties and structure, 17: 10633
MANGANESE YTTERBIUM SELENIDES
preparation, (E), 19: 13297
MANGANESE YTTRATES
magnetic properties and structure, 18: 3772
magnetic structure, 17: 28891
MANGANESE ZINC FERRATES
cation distribution in, 20: 24791 (IKF-16)
magnetic properties, 18: 26058
magnetic structure of, neutron diffraction for, 17: 28899(T)
neutron inelastic scattering by, measurement of magnetic, (E), 19: 8375 (BNL-7645)
neutron total cross sections at 78 to 507°K, 17: 31077(R) (CU(PNPL)-228)
neutron total cross section at 11.5 A, 18: 34752(R) (CU(PNPL)-234)
spin waves in, 17: 37832
MANGANITES
hydrogen position in, from neutron diffraction, 17: 37810
preparation and properties, 19: 42463
Manipulators
see Remote-Control Equipment
MANITOBA
age of early Precambrian rocks from southeastern, 16: 29206
age of uranium minerals in Huron Claim, 16: 29197
MANNITOL
analysis for oxygen, activation, 18: 37092
effect on titration of aqueous boric acid using sodium hydroxide, 18: 23412 (UCRL-7756)
effects on renal transport of calcium and strontium in dogs, osmotic-diuresis, 20: 30
effects on reproductive capacity of HeLa and L cells, 18: 43306
formation of kinase and dehydrogenase of, in *E. coli*, 20: 6729 (TID-22375)
radiolysis of aqueous oxygenated solutions of, 17: 12342
radiolysis of solid, yields in, 18: 310
tritium isotope effects on oxidation in *Acetobacter suboxydans*, 16: 17383
uptake in corn roots, 16: 28 (ORO-470)
volatilization effects on boron in hydrochloric and nitric acids and water, 16: 2972
1,6-bis[(2-chloroethyl)amino]-1,6-dideoxy-, labeling with carbon-14, 19: 34207
MANNOSE
decomposition of carbon-14-labeled, in storage, 17: 4599
effects on cesium-137 uptake by wheat roots, 19: 50
formation of, in irradiation of D-glucal, 17: 20068
metabolism of deuteriated, by ascites tumor cells, 18: 38763
oxidation by bromine, tritium isotope effects in, 18: 20031
oxidation by iodine, isotope effects and water-t yield in, 18: 5359
oxidation by sodium chlorite, tritium kinetic isotope effects in, 18: 25459
preparation of carbon-14-labeled, by use of yeast, 18: 38746
radiation effects on, electron spin resonance investigations of gamma, 17: 27454
radiation effects on serum, x, 18: 38901
radiolysis of aqueous solutions of, effects of dose rate and concentration on gamma, 19: 24579
radiolysis of, mechanism and products formed in, 17: 23411
radiolysis of solution *in vacuo*, tracer and paper-chromatographic studies of products from, 16: 25439
radiolysis products, 16: 15075
radiotherapy effects on serum levels of genital-tumor, gamma, 18: 38800
reactions with carbonyl reagents, carbon-14 and tritium isotope effects, 16: 23577
recrystallization of D-mannose-1-t phenylhydrazone, isotope effects in, 17: 6118
separation of protium and deuterium forms of, by gas chromatography, 19: 36546
uptake by corn roots, 16: 28 (ORO-470)
MANOMETERS
see also Pressure Gages
see also Vacuum Gages
description of electronics of differential micro-, 19: 9450 (UCRL-11218(Pt.I))
design and fabrication of, using plutonium-240 source, 20: 13045
design and operation of differential micro-, 19: 38315 (UCRL-16073)
design for leveling beam focusing lenses, 18: 10341(R) (NP-13571 (p.24-5))
design for measuring level of liquid metal, engineering drawings for, 19: 4292
design of bakeable Bourdon-type, for ultra-high vacuum systems, 17: 21994
design of electro-pneumatic constant-volume, 17: 32337 (K-1577)
design of floating-cup differential, 20: 9049(R) (ORNL-3830, pp 193-221)
design of magnetic-ionization-type, 18: 20198
design of small-displacement self-balancing liquid servo-, for fast response to pressure changes, 18: 41724 (WAPD-T-1708)
development of alpha-ionization type, 16: 13474(T) (AEC-tr-4492(p.322-8))
development of differential micro-, 19: 46726 (UCRL-11218(Pt.II))
development of micro-, for low pressure measurement, 19: 20142
operation of thermistor, 18: 7289(R) (GEMP-30A)
performance of ionization, for pulse plasma jet pressure measurements, 20: 44978
properties of Newtonian-oscillating, time-dependent, 17: 27654 (LADC-5535)
radiation effects on oil adsorbed on surfaces of, 18: 27599
temperature distributions in molten sodium in, 18: 1834(R) (IS-700(Sect.E))
temperature distribution in hollow cylindrical column, 18: 37475 (IS-805)
temperature distribution in hollow cylindrical, 19: 9281(R) (IS-900 (Sect.E))
Manuals
see Handbooks and Manuals
MARBLE
analysis for manganese and sodium, activation, 19: 5830
diffusion of radioisotopes in melted, 19: 37085
gamma attenuation in, 17: 35065
manganese and sodium content in, from Aegean Islands, Greece, and Turkey, 19: 5830
MARCOULE REACTORS
accident at site of, radiation protection methods in, 17: 41054
cooling system of, development of gas-bearing compressors for, 16: 28407 (TID-7631(p.292-306))
design and development, 17: 26877
development and operation, 18: 4811
environs monitoring, 17: 41048
environs monitoring, 1961 and 1962, 18: 20209 (CEA-2397)
fuel element development, 18: 9695
fuel element fabrication for, 17: 12642
fuel-element failure detection systems, 16: 14281 (CEA-2051)
fuel element processing at, performance of TBP in, 18: 13960
fuel loading programs for, use of punched card system in, 17: 38628
iodine-131 release to atmosphere from, control of, 18: 43875
kinetics and operations of, 18: 38296 (A/CONF.28/P/75)
loading of, programming for operational, 18: 9696
metal passivation for use in, 19: 26771
operation and testing, 16: 26460 (CEA-2158)
performance of, review of, 20: 1482
radiation control in environment of, 17: 42424
radiation protection at, evolution of, 17: 41042
safety, 18: 38401 (A/CONF.28/P/81)
safety and personnel protection at, 17: 41045
stack-disposal fall-out patterns, normal and accidental, 16: 395 (CEA-1924)
waste disposal from, in Rhone River, 17: 42423
waste disposal from, in Rhone River, 17: 42423
waste processing, chimney baffle model studies, 16: 4367 (CEA-2004)
waste processing of low-level solid matter from, 17: 26938
waste release to atmosphere from, control of, 17: 41048
wastes from, process for fixation in glass of, 20: 45231
MARCOULE REACTORS (G-1)
construction and design, 16: 30111
coolant activation, formation of argon-41 in, 19: 29716 (CEA-R-2764)
coolant flow rate adjustment in, 19: 3612 (CEA-R-2345)
coolant processing for, secondary, 18: 12667
design and operation of, review of, 17: 40355
fuel element combustion incident, analysis, 16: 23293
fuel element rupture detection in, 17: 9869
graphite for use in, annealing of radioinduced defects in, 20: 35939
introduction of output of, into national electric complex, problems and solutions connected with, 17: 40360
moderator for, preparation of artificial-graphite, 18: 9584
radiation protection at, methods of, 17: 41043
Wigner effect in, annealing of, 17: 37639
MARCOULE REACTORS (G-2)
caisson design and engineering for, 17: 26890(T) (AEC-tr-5828)

characteristics of, summary of, 17: 13796
construction and design, 16: 30111
construction of, review of phases in, 17: 40358
control data processing using numerical units for, 18: 24828
control rod calibrations for, 19: 29622 (CEA-R-2719)
coolant activation, formation of argon-41 in, 19: 29716 (CEA-R-2764)
coolant activity, analysis, and leaks, 20: 18120
coolant flow rate adjustment in, 19: 3612 (CEA-R-2345)
coolant processing for, secondary, 18: 12296
coolant properties in, analysis of, 20: 20232 (CEA-R-2847)
design and characteristics of, review of, 17: 40356
design and construction of prestressed concrete pressure vessel, 17: 13720
design of, using prestressed concrete for vessels, 18: 4812
fuel elements for, 18: 15496(T) (AEC-tr-6329)
fuel elements for, residual power of, 20: 36459 (CEA-R-3004)
fuel elements from, radiography of, 19: 46558(T) (ORNL-tr-748)
fuel-handling equipment for, 17: 13716
heat exchangers for, radioprotection during work on, 20: 20233 (CEA-R-2870)
information processing for, equipment descriptions for, 18: 33098 (CEA-R-2433)
loading and unloading system for fuel rods in, 17: 40357
moderator for, preparation of artificial-graphite, 18: 9584
neutron physics studies with, 18: 9682
operation, 17: 22903 (CEA-2258)
performance, 18: 38548 (A/CONF.28/P/35)
performance of, assessment of, in four years' operation, 17: 40359
personnel instruction and organization, 18: 9681
power control and measurement systems for, 20: 18119
power from, introduction into national electric complex, 17: 40360
pressure vessel design and construction, 16: 3912(T)
pressure vessel for, construction and performance of concrete, 18: 9688
pressure vessel for, prestressed concrete, 18: 35196
pressure vessel for, design of prestressed concrete, 20: 47018(T) (ORNL-tr-1282)
pressure vessels of, reduced-scale resistance models for, 20: 35027(T) (ORNL-tr-1226)
prestressed concrete vessel testing, 20: 47019(T) (ORNL-tr-1284)
radiation measurements near, (E), 19: 12801 (CEA-R-2599)
radiation protection at, methods of, 17: 41043
safety and shutdown systems of, 18: 9689
temperature control system for, automatic, 18: 9680
tritium production in cooling system of, 17: 9833 (CEA-2205)

MARCOULE REACTORS (G-3)

caisson design and engineering for, 17: 26890(T) (AEC-tr-5828)
construction of, review of phases in, 17: 40358
control data processing using numerical units for, 18: 24828
control rod calibrations for, 19: 29622 (CEA-R-2719)
coolant activation, formation of argon-41 in, 19: 29716 (CEA-R-2764)
coolant activity, analysis, and leaks, 20: 18120
coolant processing for, secondary, 18: 12296
coolant properties in, analysis of, 20: 20232 (CEA-R-2847)
design and characteristics of, review of, 17: 40356
design and construction of prestressed concrete pressure vessel, 17: 13720
design of, using prestressed concrete for vessels, 18: 4812
fuel element failure in, radioprotection and decontamination operations for, 19: 45565 (CEA-R-2781)
fuel element rupture detection in, 18: 9679
fuel element rupture detection in, 19: 29715 (CEA-R-2710)
fuel element rupture in, detection system for, 20: 10288 (CEA-R-2784)
fuel elements for, 18: 15496(T) (AEC-tr-6329)
fuel elements for, residual power of, 20: 36459 (CEA-R-3004)
fuel handling equipment for, 17: 13716
heat exchangers for, radioprotection during work on, 20: 20233 (CEA-R-2870)
information processing for, equipment descriptions for, 18: 33098 (CEA-R-2433)
loading and unloading system for fuel rods in, 17: 40357
moderator for, preparation of artificial-graphite, 18: 9584
neutron physics studies with, 18: 9682
operation, 17: 22903 (CEA-2258)
performance, 18: 38548 (A/CONF.28/P/35)
performance of, assessment of, in four years' operation, 17: 40359
personnel instruction and organization, 18: 9681
power control and measurement systems for, 20: 18119
pressure vessel design and construction, 16: 3912(T)
pressure vessel for, construction and performance of concrete, 18: 9688
pressure vessel for, prestressed concrete, 18: 35196
pressure vessel for, design of prestressed concrete, 20: 47018(T) (ORNL-tr-1282)
pressure vessels of, reduced-scale resistance models for, 20: 35027(T) (ORNL-tr-1226)
prestressed concrete vessel testing, 20: 47019(T) (ORNL-tr-1284)
radiation dose rates in pressure vessel of, 19: 45566 (CEA-R-2785)
radiation measurements near, (E), 19: 12801 (CEA-R-2599)
radiation protection at, methods of, 17: 41043
safety and shutdown systems of, 18: 9689
temperature control system for, automatic, 18: 9680
tritium production in cooling system of, 17: 9833 (CEA-2205)

MARIA

see Maritime Nuclear Steam Generator

Marine Products Development Irradiator

see Irradiation Facilities

MARITIME GAS COOLED REACTOR

see also Beryllium Oxide Reactor Experiment
beryllium oxide tube fabrication for, 16: 2732 (GA-2262)
containment and safety systems, review, 16: 1250(R) (NDA-2159-2)
control system transient analysis, 17: 21313 (GAMD-2970(and Add.1,2, &3))
cooling system leaks, fission product plateout from, 16: 29369 (GA-1934)
core design of, thermal aspects of, 17: 1117 (GAMD-1542)
core support structure of, design of, 17: 1118 (GAMD-1652)
design and development, review, 16: 11298
design objectives for land-based, 16: 26592 (GAMD-1722)
design status, July 1, 1960, 16: 5017 (GA-1612(Vol.I))
development, 16: 6212(R) (GA-1532)
development, 16: 6213(R) (GA-1738)
development, 16: 9642(R) (GA-1954)
development, 17: 24676(R) (GA-2568)
development, 17: 38431(R) (GA-2372)
development, Jan.-Mar. 1961, 18: 3175(R) (GA-2178)
development, Oct.-Dec. 1961, 18: 3294(R) (GA-2847)
development of, status report on, 17: 19613(R) (GA-3128)
development of turbomachinery for, 16: 28394 (TID-7631(p.104-15))
development review, 16: 8360 (GA-2603)
fuel development for, 17: 14727(R) (BMI-1600(Del.))
fuel development, radiation-effects studies, 16: 9190(R) (BMI-1549 (Del.))
fuel element fabrication and non-nuclear testing for, HDR-3, 19: 1877 (GAMD-2251)
fuel element testing in, EBOR HDR-3, 19: 1878 (GAMD-3611)
fuel elements for, radiation-effects studies, 17: 3378(R) (BMI-1583(Del.))
fuel elements for, performance of sheaths on, 17: 22091 (GAMD-1130)
fuel elements, irradiation testing, 16: 5759 (HW-69403)
fuel elements of, radiation effects on, 16: 28642(R) (BMI-1581(Del.))
fuel materials for, radiation-effects study of candidate, 17: 2(R) (BMI-1589(Del.))
fuel materials, radiation-effects studies on candidate, 16: 12650(R) (BMI-1561(Del.))
fuel materials, radiation effects, 16: 14375(R) (BMI-1557(Del.))
fuel materials, radiation-effects studies of candidate, 16: 17229(R) (BMI-1565(Del.))
fuel materials radiation effects studies, 16: 20041(R) (BMI-1574(Del.))
heat exchanger design and testing, 18: 3295(R) (GA-3005)
pressure vessel and thermal shields, design analysis, 16: 5018 (GAMD-1572)
safety review, 16: 31278 (UNC-5029)
thermal design considerations for, 18: 33084 (A/CONF.28/P/226)
turbine materials for, development of high-temperature, 17: 22852(R) (GA-2696)

MARITIME NUCLEAR STEAM GENERATOR

blower design feasibility study for 630 A, 19: 42142 (R62FPD-252)
boiler design for Mark III, 19: 42133 (GEMP-340)
boiler design selection for 630A, 19: 35831 (GEMP-353)
control system development for 630A, use of once-through two-tube boiler in, 19: 35827 (GEMP-338)
criticality studies of 630A, 17: 35137 (CONF-39-48)
criticality studies of 630A, 19: 35830 (GEMP-344)
criticality studies, 17: 35137 (CONF-39-48)
design, 17: 26098
design, 19: 3753
design, 16: 28531 (GEMP-108)
design and development of 630A, Apr.-May 1964, 18: 33127(R) (GEMP-295)
design and development of 630A, June-July 1964, 18: 40925(R) (GEMP-304)
design and development of CNSG, 20: 26528
design and development of Mark IV, 20: 36520
design and development, Aug.-Nov., 1963, 18: 7957(R) (GEMP-257)
design and development, 18: 13315(R) (GEMP-231)
design and development, Apr.-May, 1964, 18: 33127(R) (GEMP-295)
design and development, 17: 7599(R) (GEMP-160)
design and development, 17: 33312(R) (GEMP-215)

design and development of 10,000-SHP 630A, 17: 38544 (GEMP-239)
design and optimization studies on Mark V configuration, (E), 19: 38231 (GEMP-359)
design and performance of 19-cell 630, 17: 35141 (GEMP-232)
design of, 19: 12820
design of CNSG I, II, and III, 18: 40906
design of CNSG III, 19: 3749
design of Consolidated Nuclear Steam Generator II, 18: 21667 (BAW-1280)
design of Mark IV, bibliography for, 19: 35828 (GEMP-341)
design of 630-A, 19: 3753
design of, related to other maritime reactors, 17: 33335
design, operation, and performance of 630A, 19: 29733 (CONF-640810-1)
development, 18: 24939(R) (GEMP-285)
development of CNSG III, 20: 3552
development of 27,300-SHP, 17: 11982(R) (GEMP-175)
development of 630A, 18: 21668(R) (GEMP-274)
development of 630A Mark IV, 19: 8653(R) (GEMP-318)
development of 630 A, Dec. 1964, 19: 31593(R) (GEMP-328)
development of 630A Mark V, 19: 35829 (GEMP-342)
development of 630A Mark IV, 20: 3546 (GE-TM-64-12-12)
economic analysis of, for 47,000-DWT tanker, 19: 45657 (TID-22088)
performance of 630A Mark V, 19: 42132 (GE-TM-65-3-6)
status of CNSG, 19: 25757
uses, 18: 40802
uses of General Electric 630A, 18: 40802

MARITIME ORGANIC MODERATED REACTOR
(Atomics International)
safety analysis for coolant flow and pressure loss, 16: 22471

MARITIME PRESSURIZED WATER REACTOR
accident analysis for, 17: 35135 (BAW-1164(Vol.VII))
accident analysis for, postulated, 17: 35135 (BAW-1164(Vol.VII))
accident analysis for, fission product release in maximum credible, 17: 42350 (ORNL-3361)
accident in, fission product release from maximum credible, 17: 42350 (ORNL-3361)
accidents in, performance of iodine-vapor-adsorption systems during, (E), 19: 17349 (ORNL-3726)
bibliography on, 19: 35838 (TID-3582)
containment for, safety of double, 18: 40757 (ORNL-3657)
containment leak rate testing, 20: 12473 (TID-22459)
containment leak-rate testing, 19: 38250
containment of, safety of double, 18: 40757 (ORNL-3657)
containment systems for, siting effects of, 17: 41092
containment vessel for, leak-testing of, 18: 29116
containment vessel leak rate tests on N.S *Savannah*, 19: 3752
containment vessel leak rate tests on N.S. *Savannah*, 20: 3551 (TID-22316)
control rod drive analysis, 16: 32534 (DANATOM-06-61)
control rod drive system of NS *Savannah*, hazards analysis and modifications, 17: 26844 (BAW-1249(Vol.II))
control rod drives for N.S. *Savannah*, design of, 20: 35109 (BAW-1249 (Vol.1))
control rod handling in N. S. *Savannah* heterogeneous core, 16: 14296 (MND-C-2487(p.131-45))
control system of, study of possible improvements in, 18: 15596 (NYO-8590)
coolant monitoring system for, 18: 45077
coolant system testing for, effects of wet chloride-bearing thermal insulation on austenitic steel piping, 18: 27904 (ORNL-TM-14)
cooling of NS *Savannah* core during refueling, 17: 26845 (BAW-1277)
cooling system radioactivities in N.S. *Savannah* during startup and early operation, 18: 17320 (NSEC-72)
core lifetime analyses, 17: 19629 (ORNL-3261(Suppl.))
core lifetime studies, 18: 43063 (ORNL-TM-716)
core performance of, 18: 9723
core structures for, characteristics of Zircaloy, (E), 19: 40218
critical assembly study of Core II loading, analysis, 19: 21716 (GEAP-3514)
criticality studies on 4%-enriched uranium dioxide cores, 16: 21257 (BAW-1216)
criticality studies for zero-power test, 16: 34062 (BAW-1202)
description of core and fuel of, for Core II, (E), 19: 14873 (GEAP-3246 (Rev.2))
design, 19: 42143
design and operation data, 19: 33704
design for N. S. *Savannah*, review, 16: 11294
design of CNSG I, II, and III, 18: 40906
design summary, 17: 12015
design summary, 17: 12015
design, construction, and operation, 18: 7963
design, construction, and operation, 18: 7963
development, 16: 8347(R) (BAW-1145)
development and operation of, 17: 19631(R) (ORNL-3416)
development and operation, 19: 27811(R) (ORNL-3775)
development and operation, 19: 27811(R) (ORNL-3775)
development of N. S. *Savannah*, 16: 14312(R) (ORNL-3238)
economic aspects of NS *Savannah* and NMSR program, 18: 29104 (BAW-1263)
electric system, 16: 34083
electric system, 16: 34083
fission-gas storage unit for, design, 17: 13
fission product release in accidents, adsorption systems for iodine in, 17: 25087(R) (ORNL-3417(p.260-6))
fission product retention by confinement system, 18: 23002(R) (ORNL-3591(p.191-8))
fuel and pressure vessel materials testing, design of in-pile loop for, 17: 9852 (ORNL-3188)
fuel assembly for Core II, compression-tensile tests of prototype, 19: 10615 (GEAP-3445)
fuel assembly for Core II, analysis of mechanical characteristics of, 19: 12810 (GEAP-3375(Rev.1))
fuel assembly for, mechanical behavior of prototype replacement, 19: 10610 (GEAP-3249)
fuel assembly prototype, pressure drop tests, 19: 10606 (GEAP-3174)
fuel assembly prototype, thermal shock tests in heat transfer facility, 19: 10607 (GEAP-3194 & Add.)
fuel assembly testing, fabrication and preirradiation data for, 19: 10508 (GEAP-3376)
fuel assembly testing, modification in, 19: 10509 (GEAP-3376(Add.))
fuel assembly testing for Core II, (E), 19: 14874 (GEAP-3446)
fuel assembly top tie leaf spring tests for Core II, (E), 19: 17338 (GEAP-3455)
fuel burnout analysis for Core II, 19: 10611 (GEAP-3329(Rev.1))
fuel-cycle cost savings from changes in N.S. *Savannah*, potential, 16: 15915 (ORNL-TM-144)
fuel element containers, comparison of stainless steel and Zircaloy for, 16: 18661 (ORNL-3261)
fuel element design criteria for, (E), 19: 12806 (GEAP-3250)
fuel element handling and loading characteristics for, (E), 19: 12807 (GEAP-3252)
fuel element internal pressure from fission gas release in Core II, calculations, 19: 10614 (GEAP-3381(Rev.1))
fuel element irradiation testing, 16: 7934(R) (GEAP-3808)
fuel element irradiation testing for, nonsintered uranium dioxide (E), 19: 3727 (ORNL-TM-921)
fuel element irradiation characteristics for Core II, (E), 19: 12805 (GEAP-3248)
fuel element radiation stability, 16: 19434 (BAW-1247)
fuel element shipping from NS *Savannah* for reprocessing, safety analysis of, 18: 440 (NP-13235)
fuel element testing for, 18: 6512 (BAW-170)
fuel element testing in in-pile loop, water chemistry after SISBM, 18: 32964 (GEAP-4291)
fuel element testing for Core I, 16: 32537(R) (GEAP-3956)
fuel element testing for Core I, 16: 32537(R) (GEAP-3956)
fuel elements for, development of, 16: 30166(R) (ORNL-3313(p.1-18))
fuel elements for, radiation effects on, 17: 25078(R) (ORNL-3417(p.189-206))
fuel elements for, effects of substitution of Zircaloy for stainless steel in, 18: 1286 (ORNL-3476)
fuel elements for, irradiation characteristics of core-2, (E), 19: 12811 (GEAP-3559)
fuel elements for, zero power testing of Core II, 20: 40445 (BAW-1225)
fuel for Core II, thermo-hydraulic steady-state analysis of, 19: 10609 (GEAP-3244)
fuel for, evaluation of nonsintered uranium dioxide for use as, 18: 22492 (ORNL-TM-818)
fuel irradiation program, 16: 22649(R) (GEAP-3905)
fuel irradiation testing for N.S. *Savannah* I, 16: 7934(R) (GEAP-3808)
fuel rod assembly for Core I, post-irradiation examination of, 18: 10574 (GEAP-4359)
fuel rod cladding stress analysis for Core II, 19: 10613 (GEAP-3339)
fuel rod test assembly for Core I, post-irradiation examination of, 18: 10574 (GEAP-4359)
fuel rods for, vibration testing of, (E), 19: 17339 (GEAP-3583)
fuel time constants and control element slot coolant flow for Cores I and II, 19: 10608 (GEAP-3224)
hazards analysis for dockside operation, 18: 40933 (TID-21054)
hazards evaluation of NS *Savannah*, 17: 35155 (TID-17885)
health physics program for N. S. *Savannah*, 16: 9057
kinetics of, for first and second fuel loadings, (T), 19: 12804 (GEAP-3152)
kinetics of, for second fuel loading, (T), 19: 12808 (GEAP-3303)
legal aspects of operation of Savannah, in foreign ports, 20: 2088

licensing activities for, 18: 1267
materials, 16: 25760 (ORNL-3281)
monitoring of, for shielding leakage, 16: 31275 (ORNL-3336)
operation and safeguards of, regulatory actions relative to, 19: 12795
operation, hazard evaluation of accidental release at Camden, N. J., 16: 14311 (ORNL-2867(Rev.))
operation of N.S. *Savannah*, May 1963 to Aug. 1964, 19: 25755
operation of, summary of initial, 17: 19637 (TID-18390)
operation, May–Aug. 1964, 20: 12474(R) (TID-22460)
operations summary for May 1962 to March 1963, 18: 33131 (TODD/SML-NSS-6)
performance, 20: 26528
performance of N.S. *Savannah* Core II, 17: 28527 (GEAP-3828)
piping of, ultrasonic inspection for damage to, 17: 42340 (BAW-1269)
pressure losses and flow rates in fuel assemblies in, 19: 10612 (GEAP-3330)
pressure vessel cyclic loading tests for N. S. *Savannah*, 16: 14310 (NYO-9614)
pressure vessel for N. S. *Savannah*, radioinduced changes in brittle-fracture properties, 16: 13642 (ORNL-TM-132)
pressures vessel stress analysis, 16: 4246 (NYO-2856)
reactivity manual on NS *Savannah*, 18: 40924 (BAW-1187)
reactivity noise analysis, (E), 19: 40164
reactivity transients in, spectra of, 18: 15583
reactivity transients in, computer analysis of, 17: 9830 (BAW-1260)
safety, 16: 11295
safety criteria, 16: 11295
safety criteria for, 18: 15600
safety criteria for docking sites, 17: 13727
safety criteria, survey, 18: 15600
safety during operation at 80 Mw, 18: 13313 (BAW-1264)
safety evaluation, 18: 31018 (EUR-1621.e)
safety evaluation for, 19: 1924 (EUR-1621.e(Vol.II))
safety evaluation of N. S. *Savannah*, 20: 28817 (EUR-1621.e(Vol.3))
safety evaluations, 19: 27811(R) (ORNL-3775)
safety evaluations, 19: 27811(R) (ORNL-3775)
safety hazards analysis of, for second fuel loading, (T), 19: 12809 (GEAP-3367)
site criteria for, 17: 13727
stability on N. S. Savannah, measurement by noise analysis, 16: 24539
startup and operation of, initial, 18: 1288
testing and initial operation of, 17: 10105
testing of, program summary, 17: 21319 (TID-18467)
testing of, summary of prefueling program, 17: 19636 (TID-18325)
thermal operating performance of NS *Savannah*, 18: 15434 (TID-7669)
ventilation system filter tests for, 18: 36844 (TID-20426)

MARITIME REACTORS
see also Naval Reactors
bibliography on, 19: 12803 (AED-C-22-03)
bibliography on, 20: 26516 (AED-C-22-05)
bibliography on, 20: 40444 (AED-C-22-06)
boiler design, 16: 8852(P)
book: *Biological Shielding for Maritime Reactors*, 20: 26529
book: *Nuclear Energy Propulsion for Merchant Vessels. 3rd Yearbook of the Research Society for Development of Nuclear Energy Utilization in Shipbuilding and Ship Transport*, in German, 19: 3744
book: *Nuclear Propulsion for Merchant Ships*, 16: 23327
characteristics of gas-cooled, 16: 11299
circuits for saturated steam processes with organic-moderated, 16: 11290
collision barriers, effectiveness of, 20: 47061
collision protection for, 19: 3768
comparison, 16: 11283
comparison, 16: 11285
comparison of types, 16: 15934
components testing for, rolling stand for, 17: 40264 (EUR-375.d)
concepts for British nuclear ship, 17: 17581
conference proceedings, 16: 11281
considerations for small experimental nuclear ship, 16: 11296
construction of, quality control and testing in, 18: 35206
construction rules for nuclear-powered merchant vessels, 18: 17321 (RTI/ING(63)-5)
containers, vapor suppression in, 16: 8412
containment and installation of German advanced pressurized-water, on ore-carrier ship, 18: 38554 (A/CONF.28/P/540)
containment and restraint devices for, design, 17: 17487(P)
containment vessel design for, factors in, 19: 12829
control of pressurized-water cooled, heavy-water moderated, 17: 13803(P)
control of steam-cooled, analysis of, 17: 10985
control rod drive for, with means for holding rods in shutdown position, 16: 21773(P)
control rod drive mechanism specifications for pressurized-water, 17: 42353 (TID-19425)
control rod drive mechanism for gas-cooled, 18: 13229(P)
control rod latch system for, 20: 18041(P)
control system for pressurized-water, design of, 19: 29774(P)
control systems evaluation for, (E), 19: 17355
coolant flow in boiling-water, two-phase, 18: 38558 (A/CONF.28/P/801)
coolant pumps, comparison of electric and steam driven, 16: 26584 (CEND-150(Pt.IV))
coolant treatment for fission product separation in air-cooled, 18: 15597 (TID-7677(p.545-52))
core and fuel assembly design and testing for Vulcain, 18: 38553 (A/CONF.28/P/515)
core and fuel element design for, 17: 32236(P)
core design and fuel elements in organic moderated, 16: 11293
criticality studies of 630A, 17: 35137 (CONF-39-48)
description for propulsion of ore transports (E), 19: 3734
description of advanced pressurized water, for *Otto Hahn*, 19: 33659
description of British Marine Reactor Project, 17: 22892
description of German (E), 19: 3731
description of Lenin, 16: 25008
description of *Lenin*, Nero, *Otto Hahn*, and Vulcain, (E), 19: 43590
description of, in Euratom countries, 19: 29470 (EUR-2271.f)
design, 16: 3929(P)
design, 19: 24159
design and development of NERO, 16: 30088(R) (NP-11909)
design and development, 16: 34068(R) (GEMP-144)
design and development of 630 A, 17: 7599(R) (GEMP-160)
design and development of 630A, summary of, 17: 33312(R) (GEMP-215)
design and development of Rock'n Roll Project for studying stability of boiling water, 17: 35157(T) (AEC-tr-3874)
design and development of 10,000 SHP 630A, 17: 38544 (GEMP-239)
design and development of 630A, Aug. 15-Nov. 15, 1963, 18: 7957(R) (GEMP-257)
design and development of 630A, 18: 13315(R) (GEMP-231)
design and development of 630A, Apr.–May 1964, 18: 33127(R) (GEMP-295)
design and development of Vulcain, 18: 38555 (A/CONF.28/P/565)
design and economic evaluation of automatic control of T7 tanker boiling water reactor propulsion system, 16: 11222 (GEAP-3528 (Rev.1))
design and economic evaluation, 17: 21326
design and operation of, effects of oscillations of ship on, 17: 15406 (NP-12558)
design and operation of, effects of vibration studies on, 17: 15407 (NP-12559)
design and operation, 20: 36521
design and performance, 16: 20011
design and performance characteristics of 19-cell 630, 17: 35141 (GEMP-232)
design and performance, 18: 11462
design concept description of pressurized-water, 17: 12020
design features of Belgian, pressurized-water VULCAIN reactor, 16: 11280
design for easy refueling, 17: 29816(P)
design for easy servicing and re-fueling, 19: 5536(P)
design for German ships, 19: 48051
design for heat and power production, cost structure, 16: 11302
design for once-through steam generation, 20: 30931(P)
design for radio-controlled towing craft, 20: 42666(P)
design for 70,000 ton tanker, 16: 32590
design in Japan, 19: 38249
design modifications for water circulation system for, 18: 19419(P)
design of advanced pressurized-water, 18: 40936
design of boiling water, 16: 5006(P)
design of boiling, 16: 21836(P)
design of boiling, 16: 23308(P)
design of boiling-water, 18: 1289
design of boiling water, with steam jet propulsion system, 19: 40255(P)
design of boiling-water, 18: 35217(P)
design of CNSG I, II, and III, 18: 40906
design of Consolidated Nuclear Steam Generator II, 18: 21667 (BAW-1280)
design of Consolidated Nuclear Steam Generator III, 19: 25757
design of Consolidated Nuclear Steam Generator, 19: 33661
design of Danish Alpha II and American Consolidated Nuclear Steam Generator, 17: 33335
design of direct-cycle boiling-water, for propulsion of a tanker, 17: 15403 (NP-12555)
design of, effects of acceleration due to oscillation and vibration of ship on, 17: 15411 (NP-12564)
design of, for merchant ship uses, 17: 13775 (BAW-1243)
design of forced-circulation, pressurized-water, 20: 18126 (EUR-2629.i(Vol.1))

design of gas cooled graphite or beryllium oxide moderated, 16: 11297
design of gas-cooled high-temperature, 16: 21826
design of gas-cooled, with biological shield for access and fueling operations, 18: 19422(P)
design of gas-cooled high-temperature, 19: 12823
design of German pressurized-water, 20: 12463 (CONF-640810, pp 138-55)
design of high-temperature, 16: 6230
design of Integral BR and Vulcain, critical evaluation of, 17: 29813
design of Japanese, 20: 12462 (CONF-640810, pp 122-37)
design of organic cooled and moderated, 16: 11289
design of pressure vessel and shielding arrangement for, 17: 28559(P)
design of pressurized water, 16: 3928(P)
design of pressurized-water, 17: 2603(P)
design of pressurized-water, 17: 38560
design of pressurized-water, for research ships (E), 19: 3733
design of pressurized-water, 19: 47923
design of steam-cooled light-water-moderated, 17: 12006
design of steam-cooled, water-moderated, 18: 38565
design of superheat, for passenger liner, 17: 40333 (ACNP-6125 (Suppl.1))
design of three-pass light-water, 16: 28593(P)
design of unified modular, 18: 19406 (CEND-169)
design of Unified Modular Plant, 19: 24158
design of UNIMOD, 18: 19406 (CEND-169)
design of water-cooled and -moderated, 18: 24946(P)
design of 630-A boiling-water, 19: 3753
design of 630A, 16: 28531 (GEMP-108)
design of, review of, 20: 1422
design of, special requirements in, 19: 3764
design principles of gas-cooled, 17: 29807(T) (TRG-Inf-Ser-314)
design studies of indirect cycle, 16: 28527 (CEND-150(Pt.II))
design studies of, in Norway, 17: 22875
design using water as primary and secondary coolants, 18: 43072(P)
design with emergency core cooling by convection, 16: 31319(P)
development, 16: 20012
development, 16: 30124
development, 17: 1045(R) (NP-12101)
development, 19: 1929
development, 20: 35038
development, 20: 8439(R) (KR-97)
development, 20: 10276(R) (NP-15580)
development and economic aspects of Alpha II, 17: 2575 (DANATOM-04-62)
development and economics of, review of, 20: 32854
development and legal aspects of, 17: 2599
development at Petten research centers, Netherlands, 19: 42227
development for merchant ships, world survey of, 19: 33657
development for merchant ships, EURATOM program for, 19: 33658
development for merchant vessels, 20: 26522
development for merchant vessels, feasibility of, 20: 26523
development for merchant vessels, economic advantages of, 20: 26524
development for naval vessels, 20: 28824
development for U.S. Merchant Marine, 18: 35203 (NP-14139)
development in France, 20: 14176
development in Germany, 16: 11284
development in Germany, 17: 24696
development in Great Britain, review, 17: 17580
development in Italy, 18: 43071
development in Japan, 18: 40937
development in Norway, 16: 11288
development of Belgian Vulcain, review of, 20: 10422
development of, bibliography on, 18: 6511 (AED-C-22-01)
development of Dutch, role of critical experiments in, 20: 47057
development of NERO, 18: 38556 (A/CONF.28/P/588)
development of NERO, 19: 29736(R) (EUR-2180.e)
development of NERO, 20: 12490
development of NERO, 20: 11355
development of PWR, for German tanker, 18: 23092
development of PWR, in Italy, 19: 33660
development of PWR, 19: 40251
development of PWR, for oceanographic research ship, 20: 18129
development of Vulcain, 18: 43044
development of Vulcain, 19: 5533
development of Vulcain, review of, 20: 10493
development of, with auxiliary heat exchanger system, 17: 35168(P)
development of 27,300-SHP power plant, 17: 11982(R) (GEMP-175)
development of 630A steam generator for, 16: 30068(R) (GEMP-130)
development of, EURATOM program on, 18: 43066
development of, Euratom program for, 19: 21724
development of, Joint Committee hearing on, 20: 30930
development program for, status of Netherlands, 18: 43069
development status and perspective, 20: 35133
development survey, 19: 1931
dynamics of boiling, effects of ship motion, 17: 17578
dynamics of natural-circulation boiling, 18: 43068
dynamics of pressurized-water, 18: 19411 (RT/ING(63)-19)
economic and legal problems of insurance for, 19: 3761
economic and nuclear analyses of NERO, 20: 5176 (EUR-2468.e)
economic competitiveness, 16: 32584
economic factors, comparison with oil fired ship power plants, 16: 24971 (CEND-150(Pt.I))
economic feasibility of, for tankers, Danish studies on, 17: 22872
economics, 19: 3759
economics, 19: 3760
economics, 20: 12459 (CONF-640810, pp 1-6)
economics and prospects of, 18: 9720
economics and safety of, review of, 18: 4837
economics of, 20: 36511 (CEA-R-3022)
electric power system for Lenin icebreaker, 16: 11240(T) (JPRS-12183(p.35-54))
emergency cooling system for shutdown, 16: 14264(P)
engineering drawings for gas-cooled, with reciprocating engine, 18: 40938
evaluation of types, 16: 8379
evaluation of types, 16: 15933
external force acting on, as result of ship motion in rough sea, 16: 11303
fabrication problems for (E), 19: 3732
feasibility of barge-mounted, 18: 36801 (AD-437833)
feasibility studies for boiling-water, 19: 12835
flooding device for, 17: 29770(P)
forces on from sea water, measurements, 16: 8415
fuel and cladding materials for, analysis, 20: 10354
fuel assembly mounting device for pressurized-water, 19: 29775(P)
fuel charging aboard ship, 17: 40402(P)
fuel charging and discharging system, 16: 21774(P)
fuel element burnup in, for icebreaker *Lenin*, gamma spectrometric measurements of, 20: 45863
fuel element fabrication and testing for, 20: 12397(R) (EURAEC-1506)
fuel element locking arrangement for boiling, 17: 2609(P)
fuel element mounting device for pressurized-water, 18: 26961(P)
fuel element securing device for, 19: 45550(P)
fuel element support design for, 17: 38515(P)
fuel-element-support design for, 17: 38529(P)
fuel element testing for Vulcain, (E), 20: 12396(R) (EURAEC-1505)
fuel element testing for Vulcain, 20: 47006(R) (EURAEC-1666)
fuel elements for NERO, testing in Petten critical facility, 20: 46231
fuel insurance, factors affecting, 16: 11309
fuel rods for NERO, local-cooling-absence effects on cladding temperature at support location on, (T), 20: 24758
fuel rods for NERO, influence of local absence of cooling on cladding temperature of, (T), 20: 24758
hazards evaluation for, 17: 1091
heat exchanger design for removing shutdown heat in gas-cooled, 18: 19421(P)
heat transfer and hydraulic characteristics of water-cooled, 20: 8449
installation and testing of, safety procedure, 19: 14879(T) (JPRS-28656)
instrumentation for, transistorized, 19: 10630
instrumentation for Belgian Vulcain pressurized-water, (E), 19: 24006 (CONF-640607(Vol.I)(Paper A-2))
instrumentation for BR3/Vulcain experiments, (E), 19: 24167 (CONF-640607(Vol.I)(Paper B-2))
instrumentation problems, survey, 16: 11308
insurance coverage for the *Otto Hahn*, problems of, 20: 24824
kinetic analysis of, computer programs for, 19: 14767(R) (KR-86)
kinetics of boiling-water, effects of ship's motion on, 18: 7962
kinetics of boiling water, 18: 38557 (A/CONF.28/P/748)
leak detection and measurement in, 18: 35207
lubricants for, development and properties of, 17: 4957
moderator flow-control device for, 17: 33293(P)
neutron penetration in shielding, theoretical predictions, 16: 8410
nozzle design for pressurized water, stress analysis for, (T), 20: 30928
operating cost reductions of organic moderated, 16: 11291
operating experience of *Lenin* icebreaker from 1959 to 1963, 18: 38552 (A/CONF.28/P/313)
operation of nuclear icebreaker Lenin, 19: 5535
operation of Vulcain, annual summary for 1961, 18: 6554(R) (NP-13387)
organic coolant for organic moderated, 16: 11292
performance of Lenin during first voyage, 16: 25009
performance of simulated 1300- and 2100- psi self-pressurized, 16: 12730 (CEND-150(Pt.III))
performance of T7 boiling, effects of ship motion on, 16: 9646 (GEAP-3567)
port surveys of nuclear ships, 18: 43852
power system for Lenin icebreaker, 16: 11239(T) (JPRS-12183(p.11-34))

pressure vessel design for, effects on hull construction of, 17: 15401 (NP-12553)
radioactivity inventories and decay heat of, effects of operating condition on, 20: 47060
reactivity control in pressurized-water, by water density variation, (T), 19: 12824
research, 20: 12461 (CONF-640810, pp 105-6)
research and development status in EURATOM, 18: 43059(R) (EUR-1850.e(p.173-8))
review, 19: 12830
review of design of pressurized-water, 17: 19643
review of gas-cooled and pressurized-water, 18: 3309
review of U. S., 18: 43052
rolling effects on boiling-water, 18: 19414
safety, 16: 9026 (NP-11306)
safety, 18: 35209
safety, 19: 5534
safety acceptance of, standardization of international law for, 19: 2565
safety analysis methods for steam-cooled, 16: 8402
safety aspects, 16: 3302
safety aspects, 16: 8395
safety aspects of advanced gas-cooled, 16: 8403
safety measures for Lenin icebreaker, 16: 11238(T) (JPRS-12183 (p.1-10))
safety measures for, 17: 15404 (NP-12556)
secondary shield design for pressurized water, 16: 11305
servicing, ship design for easy, 16: 31315(P)
shield optimization for organic-moderated, (E), 19: 5521 (EUR-1888.d)
shielding for boiling, 19: 24152
shielding for, development of lead-clad steel, 18: 32952
shielding for, lead slab structure as gamma, 19: 27706
shielding of, testing of secondary, 18: 26958 (NP-12562)
shielding, review of requirements, 16: 8409
ship design using, passenger, 18: 38566
shutdown of gas-cooled, heat exchanger for fuel element cooling, 16: 6151(P)
startup sequence for, automation of, 20: 18130
status of CNSG, 19: 25757
steam generator development and testing for NERO, 19: 40250
steam generator improvements for, 17: 9964(P)
steam generator of NERO, heat transfer in, 19: 28495 (EUR-2183.e)
structural components, testing under simulated shipboard conditions, 16: 8416
support in ship, 16: 20019(P)
testing of structural members, rolling stand for, 17: 21896
testing under simulated operating conditions, facility for, 19: 27816
thermal insulation tests for Consolidated Nuclear Steam Generator, 19: 25751 (TID-21212)
use in commercial tanker, 16: 11287
use in surface-effect ships, 18: 35215
use of water-filled containment in, rupture tests on, 17: 38538 (BAW-1258)
utilization of pressurized water, review of British developments, 16: 11300
vibration of, on ships, 17: 15410 (NP-12563)
water produced in evaporators of, determination of impurities in, 17: 33789 (EUR-224.i)

MARIUS

see Fontenay-aux-Roses Reactors

MARSHALL ISLANDS

book: *Effects of Atomic Explosions on Man*, in German, 16: 5124
effects of fallout on people on Rongelap Island, medical survey 11 years after exposure, 20: 7296 (BNL-9698)
fall-out effects on population, 1961 survey, 16: 21901 (BNL-727)
fallout effects on population of, acute and residual pathological, 17: 33757 (BNL-7145)
fallout effects on residents of, 18: 17491
fallout effects on residents of, 19: 21817(R) (BNL-867(p.119-50))
fallout effects on residents of, 19: 29895 (BNL-908)
fission product contamination of 1963 food on Rongelap, resulting from 1954 fallout, 19: 8737 (BNL-8657)
medical survey of natives exposed to local fallout, eight-year summary, 17: 5699 (BNL-6503)
medical survey of population exposed to fallout from thermonuclear device in 1954, 17: 25473 (BNL-780)
pathological effects of fallout in population of, ten years post-exposure, 20: 90
population of, fallout effects on skin of, 19: 177
radiation effects from fallout on intraoral condition of population of, 18: 15843
radiation effects on growth of children of, 1954 fallout, 20: 13011
radiation monitoring population of, whole-body, 17: 3202 (BNL-5974)
radioactive contamination decay, distribution, and uptake in Rongelap Atoll, 18: 9817
soils of Rongelap Atoll, study, 19: 9363 (TID-21432)

MARTENSITES

burst transformation, 17: 3496 (UCRL-10415)
corrosion by steam at 546°F, 16: 15145 (NP-11552)
crystal structure and strength of, effects of carbon pairs on, 18: 32150(R) (UCRL-11317(p.150-8))
crystallography, 18: 20537(T,R) (EURAEC-977)
determination in stainless steel, method for, 19: 40947(R) (EURAEC-1403)
formation and mechanical properties of nitrogenous, in austenite monocrystals, 18: 32150(R) (UCRL-11317(p.150-8))
fracture of, effects of atomic displacements on, 20: 29623(R) (TID-22970, pp 121-256)
hardness of deformed and thermal cycled, 18: 32150(R) (UCRL-11317 (p.150-8))
phase transformations in, dilation parameters in, 16: 25763 (TID-16191)
properties of low-carbon, 18: 10546(T,R) (EURAEC-432)
radioinduced in 304 and 348 stainless steels, effects of annealing and cold work on, neutron, 20: 46225 (BNWL-238)
strengthening of, by strain tempering, 20: 29623(R) (TID-22970, pp 121-256)
structure in, fine, 19: 40283 (COO-1198-237)
thermal stability in niobium–tin–zirconium alloys at 400 to 700°C at times to 2000 hr, 19: 14041

MARYLAND

aerial surveying for environmental levels of gamma radiation, 1961, 18: 1946 (CEX-61.6.3)
aerosol size distribution in Baltimore, 19: 4394 (CONF-555-7)
areal geology and aeroradioactivity surveying of, 20: 20928 (CEX-59.4.17)
cesium-137 and strontium-90 uptake by animals and plants in, coefficients of variance for, 19: 1997
cosmic ray measurements, 1956, 16: 10803
gamma aeroradioactivity at 500 ft over, mapping of, 19: 46614
radiological monitoring in Sharpsburg, Washington County, 17: 41135

MASERS

analysis of possibility of nuclear gamma-ray, 17: 34986
applications and theory of, conference on, 18: 20316
book: *Quantum Radiofrequency Physics*, 20: 925(T)
book: *Topics in Radiofrequency Spectroscopy*, 17: 8093
bremsstrahlung, using stimulated emission by electrons, 17: 9213
conference, 18: 26435
design and construction of nuclear magnetic resonance, 18: 18141
design and performance of hydrogen, (E/T), 19: 23289
design of nonresonant nutation, for NMR magnetic-field measurement, 19: 26935
design of nuclear magnetic, for frequencies below 50 Mc, 17: 16908(P)
design with superconductive magnetic field, 17: 16909(P)
development, 17: 1941(R) (NP-12214)
development, 17: 8928(R) (NP-12325)
development, 18: 29925(R) (MDL-Q3)
development and feasibility of gamma, 16: 32007(R) (NYO-10142)
development and uses, review of, 19: 41143
development of ammonia, with separated cavities, 18: 28094(R) (TID-20607)
development of ammonia, using separated oscillating fields, 18: 42162(R) (TID-20963)
development of ammonia two-cavity, for molecular clocks, 19: 25071(R) (TID-21667)
electron cyclotron, 18: 22862
energy exchange processes in, 18: 2719
frequency control in, 18: 24516(T) (JPRS-24633)
gain mechanism in cyclotron, quantum mechanical properties of, 20: 19462
gain of rubidium-87, buffer gas and optical pumping effects on, 18: 42175
hazards from, 18: 15685 (LADC-5764)
infrared, plasma diagnostics with, 18: 35013
magnet design for variable bandwidth traveling wave, superconducting, 19: 41638
measurements using two-cavity, 20: 14227(R) (TID-22419)
noise propagation in amplifying, 18: 922
operation of three-level, effects of Stokes shift on, 18: 34280(R) (NYO-2680-1)
performance as atomic clock, 18: 43921
performance for hyperfine separation of ground-state atomic hydrogen, 18: 796
performance in time measurements, relativistic effects on, (T), 20: 21866
properties of electron and induction, 16: 32458(R) (LAL-1035)
properties of hydrogen, 17: 34569
properties of solid-state, 16: 32246
radiative transport in, Kubo response functions for, (T), 19: 4752

radio wave amplification by, 19: 33710(P)
resonant modes for, quantum electrodynamics in theory of, 20: 11878
review, 19: 1083
saturation of cyclotron radiation, 17: 36386 (LADC-5797)
superconducting magnets for traveling-wave, 20: 17626
theory of gamma, using nuclear reactions, 17: 36614
theory of hydrogen, 16: 18265
transitions in ammonia, 3-2, 18: 15711(R) (TID-20256)
use in plasma heating, 19: 43460(P)
use of ammonia as, for pre-amplifier in electron-spin-resonance spectrometer, 17: 34215
use of infrared and optical, in spectrometers, 17: 14926(R) (AD-296893)
use of infrared, in plasma diagnostics, 18: 32905

MASERS (OPTICAL)
activation of, using light from nuclear reactor, 19: 21710
amplification of, krypton–mercury system optical properties for, 17: 26458(R) (ORNL-3425(p.128-30))
analysis for chromium in ruby, activation, 18: 178
applications and theory of, conference on, 18: 20316
atom-electron collision processes in, 18: 32484
beam absorption by plasma, effects from, 20: 17531
beam clashing experiments with, photon energy increase for, 17: 37661(R) (TID-19415)
beam effects on atomic energy level shifts, (T), 19: 47233
beam effects on eyes, damage from, 20: 33050
beam effects on materials in the Woodbury-Raman shifted mode, 19: 32048(R) (NP-15073)
beam effects on nucleation in freon bubble chambers, 20: 13084
beam effects on prebreakdown and breakdown in cloud chambers, 20: 41375
beam effects on solids, elastic explosions from, (T), 20: 30740
beam effects on tellurium-125, method for observing two-photon photoeffect from, (T), 20: 34539
beam effects on transparent dielectrics, breakdown from, 20: 34860
beam emission by ruby, processes in, 19: 32048(R) (NP-15073)
beam fluctuations and mixing, (T), 19: 23184
beam focusing in air, plasma production by, (E), 20: 17908
beam heating of metal, for metal-water reactions, 19: 17178(R) (ANL-6965(p.91-8))
beam intensity calculation from multiphoton processes, (T), 20: 19356 (CEA-R-2888)
beam intensity of, probability distributions of, (T), 19: 37223
beam interactions with atomic electrons, 18: 34458
beam interactions from, detection of photon-photon, (E), 19: 39264 (CONF-796(Paper 14))
beam interactions with electron beams, Compton scattering in, (E), 19: 41328 (IS-1187)
beam interactions with θ-pinch plasma, Faraday effect in He–Ne, 19: 41947
beam interactions with plasma, 19: 47234
beam interactions in air, spark discharge from, (E), 19: 47781
beam interactions with electron beams, monochromatic gamma beam production in, (E/T), 20: 936 (SLAC-41)
beam interactions with electrons, energy spectra and polarization from Compton, (T), 20: 11667
beam interactions in plasma, quantum theory for, (T), 20: 12246
beam interactions in helium plasma, (E/T), 20: 28497(R) (TID-22956, pp 55-147)
beam interactions with electron beams, production of polarized photon beams by, 20: 27960
beam interactions with atomic xenon and molecular hydrogen, ionization from, (E/T), 20: 27721(T) (NP-tr-1380)
beam of, plasma breakdown by absorption of, 18: 32931
beam reaction with solid particles, plasma production by, (E), 19: 23923
beam reactions in gases, plasma production from, (T), 20: 10181
beam reactions in nitrogen gas, induced discharges from, (E), 20: 9844
beam reactions in air, plasma production in, (T), 20: 12190
beam reactions on tungsten surface, ion generation by, (E), 19: 41943
beam reactions on beryllium surfaces, momentum transfer by giant-pulsed, (E), 20: 31810
beam reactions on carbon surfaces, momentum transfer by giant-pulsed, (E), 20: 31810
beam reactions on aluminum surfaces, momentum transfer by giant-pulsed, (E), 20: 31810
beam reactions on zinc surfaces, momentum transfer by giant-pulsed, (E), 20: 31810
beam reactions on silver surfaces, momentum transfer by giant-pulsed, (E), 20: 31810
beam reactions on tungsten surfaces, momentum transfer by giant-pulsed, (E), 20: 31810
beam reactions with foils, plasma production in, 18: 2412
beam reactions with foils, plasma production in, 18: 35039
beam reactions with molecules, dissociation in, 18: 35632
beam reactions with noble gases, ionization and dielectric breakdown in, (E), 19: 20847
beam reactions with sodium uranyl acetate crystals, luminescence from, 19: 20010
beam reactions with aluminum, plasma production in, 19: 31333 (TID-21824)
beam reactions with iodine ions, two-quantum photodetachment of electrons in, (E), 19: 32898
beam reactions with gases in magnetic fields, ionization in, (E), 19: 35542(T)
beam reactions with titanium hydrides, low-voltage discharges from, (E), 19: 41133
beam reactions with solids, production of hot plasma by pulsed, (E), 19: 45409 (TID-22132)
beam reactions with graphite, molecular emission spectra in jets from, (E), 19: 44803(R) (ANL-6877, pp 21-7)
beam reactions with plasma, perturbation induced in, (E), 19: 47777
beam reactions with plasma, heating effects of, (T), 20: 3185(T) (TT-1193)
beam reactions with lithium hydride, plasma production in, (E), 20: 10148(R) (NYO-3578-2)
beam reactions with metals, energy and intensity of ions from, (E), 20: 11463
beam reactions with hydrogen and rare gases, cross sections for multi-phonon ionization, (T), 20: 15276
beam reactions with gases, breakdown and heating in focused, 20: 17531
beam reactions with gases, plasma production from, (E), 20: 20045
beam reactions with plasma, imploding shock waves driven by, 20: 22245
beam reactions with plasma, (E/T), 20: 23809(R) (TID-22735)
beam reactions with metal, production of dense plasma bursts by, 20: 24528
beam reactions with lithium hydrides, plasma production in, (E/T), 20: 26254(R) (NYO-3578-3)
beam reactions with beryllium, carbon, and molybdenum, ionization in, (E), 20: 27728
beam reactions with deuterium, plasma production in, 20: 30665
beam reactions with air, high-temperature plasma production from spike-mode, (E), 20: 30590(T)
beam reactions with argon gas at low pressure, ionization in, (E), 20: 32665
beam reactions with gases and solids, plasma production by, 20: 32666
beam reactions with plasma, electron temperature measurement from, 20: 36324
beam reactions with argon gas, carbon, and metals, plasma production from, (E), 20: 38300
beam reactions with tungsten, ion emission from, 20: 37298
beam reactions with aluminum targets, magnetic mirror containment of plasma from, 20: 42415 (TID-22928)
beam rectification in crystals, (E/T), 19: 31647 (TID-21807)
beam rotation in plasma, 18: 17103 (ARL-64-6)
beam scattering by plasma, 18: 34348
beam scattering by plasma, spectrum from, 18: 44846 (AD-603950)
beam scattering by plasma, nonlinear resonant mixing by, (T), 19: 21546
beam scattering by plasma, (E), 20: 10202
beam scattering by plasma, cooperative effects in, (E), 20: 15911
beam scattering by dense theta-pinch plasma, electron density and temperature measurement from, (E), 20: 20043
beam scattering by plasma, nonlinear, (T), 20: 26290
beam scattering by electrons in plasma, (T), 20: 28554
beam scattering by hot electron plasma, relativistic theory of, 20: 30716
beam scattering from, line-profile effects in stimulated, (T), 20: 17464
beam scattering on plasma thermal density fluctuations, review of, 20: 38336
bibliography, 16: 18122 (UCRL-6769)
bibliography on materials for, 17: 18669 (ASD-TDR-62-1026)
biological hazards from, 18: 31796 (SC-DC-64-879)
bombardment of boron, graphite, and magnesium by, mass spectra of vapor ejected from, 18: 22049
book: *Quantum Optics and Electronics*, 19: 23473
charged particle beam acceleration by focused, 19: 31042
chromium-50 and -52 emission spectra in ruby, (E), 20: 3283
coherent emission at 1.047 μ by praseodymium ions in calcium tungstate crystals, 16: 29512
conference, 18: 26435
conference on, 18: 14658
conference on photographic and spectroscopic optics, 20: 21458
coupling to photodiodes, 18: 14350(R) (TID-20257)
cryogenic aspects, 18: 22844
crystals for, growth of doped lanthanum trifluoride as, 18: 12776
crystals for, preparation of europium–β-diketone chelate, 20: 31232
crystals for, review of spectroscopic properties of activated, 19: 20849
design and performance of interferometers of, for repetitively pulsed plasma, 19: 47730

design and use for plasma production, 20: 26245 (LA-3369)
design of helium-neon, for plasma electron density measurements, 17: 28367
design of helium-neon, 19: 32048(R) (NP-15073)
design of instrument for retinal coagulation using, 20: 40791
design of Michelson laser interferometer, (E), 20: 626 (SCL-DC-65-92)
design of pulsed, 19: 36773
design of 10-Gw ruby, 20: 27249
development, 17: 8928(R) (NP-12325)
development, 18: 685(R) (MDL-Q1)
development and use in plasma diagnostics, 20: 15873 (IPP-1/42)
development for Mach-Zehnder interferometers, for plasma diagnostics, 20: 17875 (IPP-1/35)
development for power generation, review of, 18: 34499
development from Scylla I, 20: 8181(R) (LA-3434)
development of continuous-wave, 19: 25071(R) (TID-21667)
development of giant, 17: 19453(R) (LAMS-2874)
development of, optical pumping techniques in, 17: 34640
development of rare-earth-doped, 17: 34655
development of rare-earth glass, 19: 32048(R) (NP-15073)
development of rotating-prism, 18: 26992
development of ruby, 16: 33927(R) (LAMS-2754)
development using highly ionized plasma, 20: 12209
developments at Columbia Radiation Laboratory, 17: 36442(R) (NP-13084)
diagnostic use for plasma refractivity studies, 18: 24783
diagnostic use for plasma density measurements, (E/T), 19: 6783
diagnostic use for plasma electron density and temperature measurements, (E/T), 19: 10424
diagnostic use for plasma electron density and velocity distributions, 19: 27640
diagnostic use for plasma electron density, 19: 31323(R) (AD-610846)
diagnostic use for plasma electron densities, (E), 19: 39978
diagnostic use for plasma electron density measurements, (E), 19: 39979
diagnostic use for plasma, 19: 40059
diagnostic use for plasma electron densities, 20: 4948(R) (TID-22179, pp 85-175)
diagnostic use to measure plasma magnetic fields by means of Faraday effect, (E), 19: 10426
effects of giant pulsed, on solid targets, 20: 17531
effects of neodymium-glass and ruby, on rabbit eyes, 20: 22628
effects on body tissues, prevention of, 20: 26673
effects on chemotaxis in Euglena and leukocytes, 20: 5396
effects on coagulation of eye retina of cats, monkeys, and rabbits, 20: 45370
effects on erythrocytes, 20: 3741
effects on eye retina, 20: 45368
effects on eyes, radiation protection criteria for, 18: 35773(R) (UCRL-7811)
effects on eyes, radiation protection criteria for, 19: 11423(R) (UCRL-12004)
effects on growth of tissue culture carcinoma cells, effects of γ radiation on, 20: 45568
effects on hard dental tissues of man, 20: 45404
effects on leukocytes, effects of various vital stains on, 20: 35337
effects on mammalian retina, review, 20: 22629
effects on nuclear decay processes, (E/T), 20: 12102
effects on oral mucosa and teeth in hamsters, 20: 22717
effects on oxygenated and reduced hemoglobin, spectral absorption curves of, 20: 3741
effects on plasma resonance in argon and nitrogen, (E/T), 20: 13942
effects on rabbit eyes, 20: 40692
effects on rabbit eyes, 20: 40791
effects on reticulum cell sarcoma of skin, alone and combined with x radiation, therapeutic, 20: 45568
effects on retinal blood vessels in man, monkeys, and rabbits, 20: 35258
effects on superconductivity in pure undoped semiconductors, (T), 20: 8026(T)
effects on tumors, use in radiotherapy, 20: 38780
electric discharges in helium–neon, current-voltage characteristics of h-f, 20: 21808
electric discharge dynamics in large diameter magnetically confined ion gas, 20: 44410
electric fields from radiation of, use in particle acceleration, 17: 19420 (SLAC-12)
electromagnetic, thermal, and ultrasonic effects on eyes from, 20: 36612
electron and ion emissions induced in titanium and deuterated titanium surfaces by, 19: 1171
electron emission induced in targets by, 17: 25954
electron interactions with field of, nonrelativistic quantum theory for, 20: 44486
electron scattering by beams from, nonlinear, (E), 20: 1003
electron temperatures of, soft x-ray emission determination of, (E), 20: 42475
emission by europium benzoylacetonate, effects of inorganic ions on shift of, (E), 19: 6455
emission by pinch plasma, (E), 20: 17924(T)
emission processes in rare earth chelate, 18: 24229
emissions from europium chelate, 19: 15606
emissions in neodymium glass, time behavior of stimulated, 17: 41610(T)
energy exchange processes in, 18: 2719
energy transfer in crystalline, 18: 26119
energy transfer in silicate glass, 19: 14240
engineering uses for cutting and welding, 18: 20120
europium diketone chelate use in liquid, 20: 26866
excitation by nuclear heat, 18: 18624
excitation of Raman spectra of molten salts, method for, 20: 38872(R) (NYO-1769-68)
fabrication of giant-pulse, 19: 32048(R) (NP-15073)
feasibility of radiation pumped, 16: 32007(R) (NYO-10142)
fluorescence in anthracene crystals induced by, triplet excitons in delayed, 17: 25307
fluorescence in ruby rods, 20: 4949(R) (UCRL-14360, pp 85-94)
fluorescent lifetimes of ruby rods with population inversion, calculations, 19: 27887 (UCRL-7765-T(Rev.1))
frequency mixing in, photoelectric, 19: 39269(R) (SU-SEL-64-133)
frequency variations in helium-neon, 18: 30328
fringe counting system for interferometer, 18: 15695 (SC-TM-162-63-81)
gain characteristics of rubidium, 18: 5847(R) (NP-13401)
gas breakdown by giant light pulses, (E), 19: 23922
gas breakdown by light pulses from, 18: 34350
gas breakdown by light from, time evolution of, 19: 44821
gas discharges in helium-neon, 18: 28175
gas ionization by light pulses from ruby, 19: 34769(R) (AD-612498)
growth of highly perfect fluoride single crystals for use in, 17: 37744
hazards evaluation of, in industry and research, 20: 29480
hazards from, 18: 15685 (LADC-5764)
hazards to eyes of range finder operators, 20: 22628
hosts for, crystal growth and properties of cerium and thorium dioxides as, 20: 2312 (AD-619197)
infrared emission from ytterbium-activated silicate glass, 17: 34572
intensity of discharge in air, space-time distribution of, 20: 32224
intensity of, high-order correlation functions of, 17: 35260(R) (TID-19135)
interference of light from two, quantum theory of, 18: 26425
ion generation by ruby laser beam on tungsten wire, 19: 11825 (CAL-RM-1863-E)
ion photoproduction with, 18: 34297
ionization of gases by intense, (E), 20: 40190
light from ruby, absorption by fully ionized plasma, (T), 19: 10390 (IPP-6/27)
light from, Compton scattering by 6-Bev electrons, (E), 19: 27137 (CEAL-1014)
light from, production of sideband, 19: 39269(R) (SU-SEL-64-133)
light production by, coherent, 19: 31019
light scattering by plasma from, diagnostic uses of, (E), 20: 38259
light scattering from, Brillouin, 19: 39273(R) (UCRL-12204, pp 60-5)
light sources for, triggering systems for xenon flash tubes, (E), 19: 38292 (BNL-9257)
materials for, research on, 17: 25843(R) (AD-282296)
materials for, spectral properties of solid-state, 17: 34571
materials for, evaluation of rare earth ions excited by energy transfer from excited organic compounds for, 19: 11083
materials for, evaluation of europium chelates as, 19: 11088
materials for, gamma radiation effects on, 20: 37280 (NYO-3330-11)
mirror coatings for, effects of nitrobenzene immersion on damage resistance of dielectric, (E), 20: 31787
molecular collisions in, resonant excitation transfer in, 18: 32491
monitoring in industry and research, 20: 28936
multiphoton processes in ruby, calculation of order of magnitude of, (E), 19: 4831
noise in, analysis of oscillator, 18: 15711(R) (TID-20256)
noise in, analysis of nonlinear, (T), 19: 31336(R) (UCRL-12473 (p.72-9))
noise measurement in, 19: 25071(R) (TID-21667)
noise measurements on, 18: 42162(R) (TID-20963)
noise propagation in amplifiers of, sources for, 18: 922
nonlinear effects on metals, 17: 35260(R) (TID-19135)
nuclear pumping of gas, optimum design for, (T), 20: 2591 (ANL-7030)
operation of, detection of pure axial-mode, 17: 29461
operation of dysprosium-doped calcium fluoride, under continuous pumping, 20: 33974
operation of ruby pulse, using triggerable passive Q-switch, 20: 34698 (IPP-4/34)

operation of ruby, 20: 37174
operation of xenon, 5d-6p transitions from pulsed, (E), 19: 39394
operation of, eye protection during, 19: 28576(R) (UCRL-12167)
optical pumping of, use of plasma pinch light source for, 18: 42153 (AROD-3323:4)
optical pumping of, use of plasma pinch for, (E), 19: 4838
optical pumping transients in rubidium-87 gas, 20: 2596 (UCRL-16241)
oscillation in helium–neon, satellite, 19: 27065 (ORNL-P-116)
oscillation in rubidium-87, under optical pumping, 18: 30408
oscillations in single and multiple element, conditions and linewidth for steady, 18: 5856
oscillations of coupled-mode, (T), 19: 27711 (UCRL-7497)
oscillators for, noise modulation of, 18: 2404(R) (TID-19651)
output photon statistics, 17: 21401(R) (TID-18585)
performance as heat sources for metal–water reaction studies, 20: 6552(R) (ANL-6925, pp 187-233)
performance for magnetic field determination in theta-pinch plasma, (E), 20: 12164 (ARL-65-129)
performance for plasma diagnostics, (E), 19: 12629 (AFOSR-64-1143)
performance in detecting particles in gas streams, 20: 9053(R) (ORNL-3830, pp 252-60)
performance in interferometric measurements of plasma electron density, 19: 41924
performance of barium glass, containing neodymium and uranyl ions, (E), 19: 14239
performance of carbon dioxide, Fermi resonance and isotope shift effects on, (E), 20: 19937
performance of europium chelate, deuterium isotope effects on, 20: 16781
performance of, h-f, as interferometer in plasma diagnostics, (E/T), 19: 39993
performance for theta-pinch plasma diagnostics, (E/T), 19: 10387 (IPP-1/30)
performance using samarium-doped strontium fluoride crystals, 16: 27827
photoelectric effect induction by, in borosilicate glass and quartz, 17: 29397 (TID-18984)
photon correlations in laser interferometers, effect of high-velocity translation on, 20: 4223 (UCRL-14345)
photon echo resonance in ruby, 18: 5847(R) (NP-13401)
photon echo resonance in ruby, (E), 19: 14230(R) (AD-608160)
photon processes in, (T), 20: 19356 (CEA-R-2888)
physical properties of significance as a hazard to personnel, 20: 40691
plasma compression using giant-pulse, (T), 19: 33468
plasma density measurements using helium–neon, (E), 19: 17120
plasma density measurement using helium–neon, 19: 47759
plasma diagnostics from polarization of light from ruby, 18: 19201
plasma heating by pulsed beams from, (T), 19: 37973
plasma production by, 18: 28793
plasma production by, (E/T), 19: 10392(R) (MATT-Q-21)
plasma production by, (E), 19: 23829(R) (TID-21548)
plasma production by ruby temperature determination in carbon, 19: 25581
plasma production by high-power, ion energies in, 20: 44932
plasma refractive index from phase measurements of, 17: 38381
power for, description of direct nuclear-to-beam conversion systems for, 18: 28312
power of ruby, determination of giant-transient, 19: 9777(T) (JPRS-27372)
power transmission to, development of thermal radiation focusing guide for, 17: 3573(R) (NP-12206)
preparation and properties of sodium-rare earth molybdate monocrystals for, 20: 7064
preparation of rare-earth-activated alkaline earth halofluoride, 19: 24537(P)
probe measurements in h-f plasma, multiple, 18: 6323
production from magnetic pinch in indium antimonides, 20: 26240 (D-1-82-0502)
production in fluorinated europium acetonates in acetonitrile, 19: 9785
production in indium arsenide by electron bombardment, 19: 16238
properties of cesium–nitrogen, 17: 9019
properties of europium benzoylacetonate, 17: 37668
properties of europium benzoylacetonate, 18: 33561
properties of neptunium for use in, 19: 22205
properties of rare-earth activated, 17: 37177
properties of rare earth-doped zinc sulfide, 19: 23164(R) (SU-SEL-64-103)
properties of 3- and 4-level, 17: 32804
properties of, coherence, (T), 19: 28998
properties of, photomixing studies on, 19: 23164(R) (SU-SEL-64-103)
properties of, with two active centers, 18: 30333
protection from, eye, 18: 10308(R) (UCRL-7571)
pulse reflection from ionospheric sporadic E-layer, (E), 19: 27346
pumping of, using diode lasers, 18: 9003
pumping of, efficiency of nuclear, 20: 20201(R) (ANL-7110, pp 311-401)
pumping of, nuclear, (T), 19: 8116
pumping of, use of plasma theta pinch for, 20: 26273
pumping of, using theta pinch, 19: 4444
pumping of, using intense discharges in z pinch geometry, (E), 20: 24187
pumping of, using nuclear radiation, 20: 32740
pumping solid-state, using theta pinch, 19: 4442
quantum electronics of, conference on, 20: 27251
quantum theory of coherence and noise in, 19: 20843
radiation damage by Compton scattering of gamma and x rays used in pumping, 18: 20625 (N63-21469)
radiation effects on ruby, gamma, 17: 39695
radiation effects on oxidation of, 18: 37761 (BNL-874(p.26))
radiation effects on energy output of ruby, gamma, 19: 11609
radiation effects on properties of ruby, (E/T), 19: 46873 (N64-32322)
radiation effects on gallium arsenide diode, gamma, 20: 11178
radiation effects on, 20: 16505 (BNL-949)
radiation effects on ruby, x, 20: 20110 (NASA-TN-D-3379)
radiation effects of, pathological, 20: 28936
radiation effects of, pathological, 20: 29457
radiation emission in gaseous, electron inversions and populations in, 18: 22211
radiation emission in gaseous, (T), 19: 32524
radiation emission from gaseous, interactions with matter, 20: 11470
radiation field from, nonlinear effects of, 19: 47123(T) (JPRS-31032, pp 1-14)
radiation from gas, third order perturbation theory for, 20: 21522
radiation from polygonal-cross section, 17: 28063
radiation from ruby, resonance effects on ruby targets, 18: 30298(R) (AD-439695)
radiation from ruby scattering by plasma, 19: 17080(R) (TID-21380 (p.63-84))
radiation from, infinite model for pulsed, 20: 24593
radiation from, Thompson-scattering by particle beams, (E/T), 20: 13925(R) (TID-22419, pp 99-147)
reactions with surfaces, production of neutral particles in, (E), 20: 46314
relaxation in ruby, cross, 18: 15711(R) (TID-20256)
research programs of U. S. Army on, 1962 summary, 17: 33413(R) (NP-12967)
research programs on emission, excitation, and modulation of, 19: 32048(R) (NP-15073)
research progress on rubidium and ruby, 18: 20627(R) (NP-13815)
resonator modes in argon–bromine, (E/T), 19: 47219 (AD-614253)
safety hazards in use of, 17: 29131(R) (UCRL-7254(p.6-16))
scattering of light from, by θ-pinch plasma, 17: 31600
scattering of light from, by plasma, 19: 37963
spectra in rare-gas, emission, 18: 26114(R) (ORNL-3582(p.36-7))
spectra of chelate, ligand-field, 18: 33565
spectra of deuterium oxide and water vapor, (E), 19: 9792
spectra of rare earth-doped zinc sulfide, emission, 19: 39269(R) (SU-SEL-64-133)
spectra of, Einstein relations for absorption and broadband emission (T), 19: 1076
spectral line width and intensity variations in, 20: 4949(R) (UCRL-14360, pp 85-94)
theory of, 18: 24309
theory of laser oscillators, 19: 31336(R) (UCRL-12473(p.72-9))
thermionic emission induced in tungsten by, 17: 25872
threshold effects of uranium doping on, scattering extinction coefficient for, 17: 22305
ultrasonic wave generation from, effects of, on neurological and retinal changes, 20: 28951
use as plasma diagnostic probe, feasibility of, 18: 36707 (AFCRL-64-254)
use as strain seismograph, feasibility of, 20: 25304 (BNWL-241)
use for accelerating charged particles, drift tubes for, (T), 19: 20709
use for argon arc plasma diagnostics, (E), 20: 32599
use for determining electron density and velocity behind shock waves, (E), 20: 6490
use for electron temperature measurement in theta-pinch plasma, (E), 20: 10198
use for gas breakdown studies, 18: 21513
use for high energy gamma production in electron accelerators, 17: 21125
use for induction of metal–water reactions, 20: 20925(R) (ANL-7055, pp 177-212)
use for interferometer measurement of plasma density in transverse mode, 19: 47745
use for ionization of gases, (T), 19: 16280
use for particle acceleration, (T), 19: 6418
use for plasma diagnostics, 18: 24745 (ANL-6802(p.120-5))
use for plasma diagnostics, (E), 19: 12631 (AROD-4832.2)
use for plasma diagnostics, 20: 24497(R) (AD-628004)
use for plasma diagnostics, 20: 30556(R) (AD-631993)

use for plasma diagnostics, 20: 32598
use for plasma electron density measurements, (E), 20: 12165 (ARL-65-135)
use for plasma electron density measurements, review on, 20: 22295
use for plasma electron density determination, 20: 42432
use for plasma heating, 18: 19179
use for plasma production, 18: 19165
use for plasma production (T), 19: 3396 (MATT-222)
use for plasma-flow velocity profile measurements, 20: 38238
use for propulsion of interstellar vehicles, (T), 20: 36997
use for remote opening of metal containers, 20: 5669
use for remote opening of metal containers, 20: 9105
use for stimulated Compton scattering of electrons by standing waves of light, 17: 34757
use for theta-pinch plasma diagnostics, 20: 32621
use in bubble chamber illumination and photography, 20: 16841
use in cancer research and radiotherapy, review, 20: 40776
use in coagulation in ocular fundus of human and rabbit eyes, 20: 45401
use in communications systems for space vehicles, 17: 21372
use in cytological research, 20: 3741
use in determining electron time-of-flight in photomultiplier tubes, 20: 11071
use in electron density measurements in plasma, 19: 12647
use in electron density measurement in plasma, 20: 3234
use in electron density measurement in plasmas, 20: 46848
use in emission spectrography, 19: 13233
use in high-energy physics, 19: 1388
use in infrared interferometers, 19: 17079(R) (TID-21380(p.95-61))
use in interferometric measurement of plasma electron densities, (E), 20: 13923(R) (TID-22419, pp 77-84)
use in investigating the second postulate of special relativity, 19: 14416
use in length-measuring interferometer, 18: 39574 (Y-1466)
use in measurement of electron density in plasma, 19: 43453
use in motion detection, 20: 41224 (EGG-1183-2078)
use in plasma diagnostics, 17: 19456 (NP-12651)
use in plasma diagnostics, 18: 19140(T) (ORNL-tr-58)
use in plasma diagnostics, feasibility of, 18: 28771 (UCRL-7712)
use in plasma diagnostics, (E), 19: 12637(R) (LA-3202-MS)
use in plasma diagnostics, 19: 19311
use in plasma diagnostics, 20: 3232
use in plasma diagnostics, (E), 20: 12163(R) (AD-625424)
use in plasma diagnostics and heating, 20: 15882(R) (NP-15868)
use in plasma diagnostics, 20: 42445
use in plasma electron diagnostics, (E), 19: 5278(T) (AEC-tr-6518(p.33-8))
use in plasma electron density measurement, 20: 40226
use in plasma production, 18: 28896
use in plasma research, review, 20: 24530
use in production of polarized photons, 20: 15306(R) (CEAL-1026)
use in production of electrons, 20: 19283
use in production of ion and electron beams, 20: 46887
use in pulse measurements of thermal conductivity at high temperatures, 20: 823 (LA-DC-7456)
use in quenching of metastable hydrogen, 17: 37866
use in radiotherapy of eye lesions, 20: 36682
use in radiotherapy of recurrent toxoplasmic retinochoroiditis, 20: 36683
use in study of reactions of fused reactor fuels with water, 18: 44922(R) (ANL-6800(p.326-402))
use of europium benzoylacetonate as, 17: 20723
use of helium-neon, for high density shocked plasma, 20: 8216
use of hydrogen, for determining hyperfine separation of deuterium, (E), 20: 11481
use of infrared, in spectral slit-width studies, 18: 4325 (CONF-76-7)
use of infrared, for testing space isotropy and special relativity, 18: 11016
use of infrared, for plasma diagnostics, 20: 4992
use of infrared, in plasma diagnostics, 20: 8268
use of moving mirror laser interferometer for plasma diagnostics, (E), 19: 12686
use of pulsed ruby, in schlieren photography, 18: 19200
use of pulsed ruby lidar for detection of nuclear explosions, 20: 25307 (UCRL-13204)
use of ruby, for theta-pinch plasma diagnostics, 18: 19202
use studies on, 19: 39269(R) (SU-SEL-64-133)
use to induce reactions of aluminum foil with water, 19: 32447(R) (ANL-7020(p.175-97))
use with interferometers for plasma density measurements, 20: 6471
uses for plasma diagnostics, (E/T), 19: 8500 (IPP/6/9)
uses in optical-maser-homodyne spectrometers, 18: 30298(R) (AD-439695)
uses in welding, 20: 11260
uses of gas, for plasma diagnostics, (E), 20: 17508 (ARL-65-246)
uses of i-r, for simulating transient radiation effects on semiconductors, (E), 19: 32778 (SC-DC-65-1421)
uses of ruby, for vaporization of lithium hydride plasma, (E), 19: 47846
uses of, development of new, 19: 23164(R) (SU-SEL-64-103)
wave pulses from, behavior and shape of, 18: 32290

Masks
see Gas Masks

MASONITE
sorption of x radiation in Grenz-ray region, dosage determination of, 19: 24784

Masonite (Wood Product)
see Building Materials

MASS LAW
analysis, 18: 2438
calculation of, statistical problems in, 19: 29351
for nuclides, (T), 20: 12090
formula for, development of semiempirical, 17: 24750(R) (UCRL-10624)
use of, in determining equilibria between binary alloys and slag, 16: 28928(T) (AEC-tr-5268)

Mass Spectrographic Analysis
see Mass Spectrography

MASS SPECTROGRAPHY
absolute characteristic curves of photographic materials used in, for positive ions, 17: 20596(T) (AEC-tr-5767)
analysis by isotope dilution, calculation of optimal conditions for, 19: 17773 (EUR-2219.e)
analysis for trace impurities by spark-source, absolute, 19: 26226 (CEA-R-2721)
analysis of elements for isotopes, ORNL procedures for, 18: 6746 (ORNL-3528)
analysis of gases for trace impurities, blending of gas mixture standards for, 19: 24643 (TRG-Report-270)
analysis of iron- and nickel-base alloys, spark-source method for, 19: 34114 (WAPD-T-1662)
analysis of metals and alloys for trace elements, using isotope dilution, 19: 15405
analysis of nuclear materials by, survey, 18: 13615 (CONF-433-1)
analysis of reactor materials by, review, 19: 5810
analysis of solids by, detectors and ion sources for, 16: 30352
analysis of solids by, ion source for, 17: 32389
analysis of solids by, 17: 10943
analysis of solids by, errors using high-frequency sparks in, 18: 8034(T) (SC-T-531)
analysis of solids by spark-source, 19: 42411 (CEA-R-2757)
analysis of uranium for isotopes, 19: 42412 (GAT-T-1224)
analytical uses at ORNL, 20: 14428(R) (ORNL-3889)
appearance potential determination by critical slope method, 16: 25320 (TID-16157)
background and optimum counting times for, counting statistics theory for variance in, 18: 19878
background effects in spark-source, reduction of, 20: 31203
bibliography and review, 16: 14647
bibliography on, 20: 36712 (IS-1335)
book: *Advances in Analytical Chemistry and Instrumentation*, Vol. III, 18: 43437
book: *Mass Spectrometry of Organic Ions*, 18: 10025
book: *Methods and Uses of Mass Spectroscopy*, 17: 3276(T) (AEC-tr-5080)
cell design for gas, 19: 22101 (RFP-456)
conference on advances in, Oxford, Sept. 1961, 17: 38970
data processing by computer, 19: 42409 (AWRE-O-37/65)
development and use in reactor technology, 16: 23625 (TID-7629 (p.142-50))
development at ANL, 17: 41534(R) (ANL-6720(p.77-89))
development for burnup determination in reactor fuels, 18: 3139 (WAPD-T-1499)
development for gas analysis using photographic-plate ion detection, 17: 10537 (TID-15724)
development for transplutonic elements and uranium, 20: 14458(R) (ORNL-3889, pp 39-43)
development for use in fuel depletion studies, 18: 3140 (WAPD-T-1615)
development of, for use in reactor fuel burnup analysis, 16: 32538(R) (GEAP-4053-1)
development of spark-source, for boron in nickel alloys and steels, 20: 33158 (Y-1543)
development of, for ruthenium isotope yield analysis in uranium burnup, 20: 29080(R) (IDO-14676)
developments at ANL, November and December, 1961, 16: 9277(R) (ANL-6455)
developments in, for analytical uses, 20: 22894
developments in, review of, 18: 19861
double-oven methods for lithium halide vapor properties, 16: 18885
electron-extraction methods in, for analysis of solids, 17: 33834
emulsion blackening curves for cation, 16: 11916

emulsions for use in, properties of ion-sensitive, 19: 43979
equipment and methods in, review, 17: 17649
equipment and methods in, at New Zealand's Institute of Nuclear Sciences, 18: 1317(R) (NP-13210)
equipment and methods for, in determination of trace impurities in inorganic solids, 19: 43978
equipment for, of photoionization, 18: 35555
errors in isotopic-dilution analysis, 17: 12204
errors in uranium isotopic ratio measurements due to impurities, 18: 11965 (K-1400)
excess-kinetic-energy ions in organic mass spectra, 18: 20026
excitation effects in, review, 17: 36538
fragment masses in high-molecular-weight, 16: 17729
interference in, caused by hydrogen accumulations, 17: 2727
interpretation of plates in, computer program for quantitative, 19: 11495
ion counting and intensity measurements in, application of Allen multiplier and commercial counter installation to, 17: 22387
ion currents in secondary electron amplifiers, analysis, 16: 2003
ion decay in, metastable, 18: 12013
ion energies in, spark-source, 19: 7778
ion optics for, transfer matrices in, 19: 22674
ion source for analysis of low-vapor-pressure materials by, 20: 31204
ion sources for, description of vacuum-arc, 17: 12536
ion sources for, design and performance of triggered low-voltage positive, 18: 18164
isotopic analysis by surface ionization, internal standard technique for, 17: 27279
isotopic peak height calculations in, 20: 20610
lines of elements, tables of, 18: 4328 (NP-13361)
measurement of high-energy ions by, 18: 31512
measurements of, effects of temperature on, 17: 38984
method for determining boron isotopes in boron trifluoride, 19: 38541 (K-L-6057)
method of, for radiolysis yield analysis, 18: 10155
methods and uses, 19: 2245
methods for analysis of solids by, review of, 20: 31201
methods for determining uranium isotopes in uranium, 19: 11014
methods for tranuranic elements, 20: 20365
methods for, for refractory materials at high temperatures, 18: 39149
methods for, review, 17: 7986
methods for, using crossed electric and magnetic fields, 20: 14882
methods of, for ultra-pure substances, review of, 20: 45590
nuclear emulsions for, properties of, 18: 39148
of gaseous ions in glow discharges, 19: 6479
of gaseous reactions, problems in continuous, 19: 7518
of mixtures of amino acids, 17: 17986
of smallest quantities of matter in nuclear physics, 19: 14214
performance for accurate determination of reactor-fuel burnup, (E), 19: 21667(R) (GEAP-4776)
performance for measuring isotopic yields in nuclear reactions, (E), 20: 8105
photographic emulsion for, 18: 21960 (SC-TM-64-534)
photometric evaluation in, validity of reciprocity law in, 18: 1998
physics and technology of gas analysis, 16: 5292
research programs on, at Marie Curie Sklodowska University, Poland, 18: 21989
resolution in, effects of ionization energy on, 17: 2728
review of techniques for solids, 17: 27278
sample bonding to surface ionization filaments for, development of improved, 16: 29316 (IDO-14590)
sample preparation for uranium, 17: 2926
sensitivity and techniques, 16: 5294
sensitivity for trace elements, extension of, 18: 5242
spark-source, evaluation of photographic plate emulsion uniformity for, 17: 30835
spark source methods of, efficiency of, 20: 40796(R) (IS-1500(Sect.C))
summary of problems and equipment, 17: 10942
surface ionization studies with tungsten crystals, 17: 24750(R) (UCRL-10624)
techniques, theory, and uses of field ion, review on, 20: 31199
temperature effects in, 17: 10240(R) (NP-12208)
theory, 17: 26769 (PWAC-393)
theory and use of surface ionization, 17: 27225 (AERE-R-4295)
theory and uses of, conference on, 20: 31197
thermal ionization, internal standard technique for precise isotopic abundance measurements in, 16: 16317
use at ORNL, summary on, 19: 17781(R) (ORNL-3750)
use for analysis of chemisorption and exchange of gases on surfaces, 17: 40825
use for analysis of solids by spectra excitation with d-c spark in vacuum, 17: 40755
use for analysis of liquids and solids, review on, 18: 14188
use for ion-component measurements on plasma, 19: 19289
use for isotope analysis, ion production technique in, 20: 31207
use for isotopic analysis of water ionized in strong electrical field, 20: 1829
use for lead isotope determination, 20: 7287
use for measurement of relative ionization cross sections, 16: 5782(T) (AD-257713)
use for moisture determinations, review, 17: 4465
use in burnup determination in reactor fuels, 19: 28225 (SGAE-PH-11/1964)
use in determination of impurities in solids, review, 17: 7986
use in determination of ionization cross sections and partial vapor pressure of molecules, 17: 33891
use in determination of impurities in solids, relative sensitivity coefficient for, 19: 13247
use in isotope abundance measurements, review of, 20: 31399
use in isotopic analysis of sulfur, 20: 16379
use in nuclear studies, review, 17: 17649
use in plasma diagnostics, ion sampling in, 20: 46852
use in reactor fuel burnup analysis, 20: 16046
use of, for study of homolytic reactions in deuterated compounds having phenyl radicals, 16: 28934(T) (SCL-T-431)
use of graphite-coated tungsten filament for uranium isotopic analysis, 17: 25122
use of, in mass determinations, sources of error in, 17: 10614
use of photographic emulsions as ion detectors in, 19: 9463
use of spark-source, for analysis of elements for undiscovered isotopes, 18: 8298
use of spark source, for geochemical analyses, 19: 11406
use of spark-source, for quantitative analysis, 20: 31202
use of, in study of composition and thermodynamic properties of nonstoichiometric compounds, 20: 31723
uses, 19: 41243(T) (FTD-TT-64-1368)
uses for determination of isotope abundances of trace amounts of lead, 19: 18151
uses for isotopic analysis, computer program and recorder chart-to-punched card converter in, 20: 26794
uses for study of metallogeny of Middle Europe, 19: 13644
uses in determination of enthalpy-composition functios of nonstoichiometric binary compounds, 19: 22197
uses in nuclear science, 19: 38925
uses in studies of ion-molecule collisions, 17: 12829
uses of spark source, for analysis in atomic energy programs, 19: 19830
vaporization of metals in, calculations, 19: 46943(T) (FTD-TT-65-611)

MASS SPECTROMETERS

see also Apotrons
see also Calutrons
see also Cyclorators
see also Electromagnetic Separation
see also Ion Sources
see also Isotrons
see also Line Recorders
see also Trochotrons

adaptation of Consolidated Model 21-611-1, in analysis of uranium for hydrogen, 16: 261(R) (MCW-1465)
amplifier for use with, design of, 20: 25358
analyzer designs for r-f, with two and three drift spaces, 19: 30500
angle of incidence instrument for, 20: 39029
applications, characteristics, and problems of Uppsala, 16: 9123
applications of Orsay double-deflection, in nuclear physics, 16: 9124
automation of, for isotopic analysis of reactor materials, 19: 46181 (WAPD-T-1769)
background and peak optimum counting times in, 18: 39082
beam analyzer for, design of double-acting, 17: 39397
beam focusing device for, 20: 19013(P)
beam focusing in, electrostatic system for, 19: 36852
beam focusing in, by electric and magnetic sector fields, (T), 19: 36854
beam focusing in, inhomogeneous magnetic fields for, 20: 19163
beam focusing on analyzer of, line-type, 18: 12439(P)
bibliography on, covering Jan. 1958 to Dec. 1960, 17: 38993
book: *Dynamic Mass Spectrometers*, 20: 36777(T)
book: *Mass Spectrometry. Part I. Physics and Apparatus Fundamentals. Part II. Applications*, in German, 18: 39143
calculation of oxygen isotope abundance ratios in, 17: 41586
calibration and instrumentation of tandem-90°, 19: 30081(R) (NBL-216)
calibration of magnetic deflection, 19: 903(R) (SRIA-128)
cathode selection for omegatron, 18: 37483(T) (NASA-TT-F-141(p.96-107))
characteristics of C.E.C. 21-103C, using boron trifluoride, 16: 30613
charged-particle detector for magnetic analyzers, 17: 32428
circuits for, review of, 20: 2100 (IS-1193)
cleaning sample valves in, systems for, 18: 25269(R) (NLCO-905)
collection efficiency of, tracer technique for determining, 20: 19150
collector contamination in, tracer determination of, 20: 19149

collector design for adsorption studies using, 20: 18994 (SGAE-PH-31/1965)
collector system for, 17: 25560
collector systems for radiation source preparation, 16: 9117
conference on, 20: 19141
connection of, to getter-ion pump, 17: 8565(P)
construction and characteristics, 17: 25558
construction and performance for isotopic ratio measurements on uranium hexafluoride, 16: 14943
construction and properties of Dresden, 17: 2695
construction of double-beam, 17: 1398
construction of double-focusing alternate-gradient, 17: 3280
construction, operation, and performance, of omegatron type, 16: 10201
contamination in, effect of gas scattering on, 20: 19146
control unit for, construction of electronic, 18: 18021(R) (TID-20411)
corrections for tailing in lead isotope analyses, 16: 20843
data accumulator for, description of, 17: 24750(R) (UCRL-10624)
data display system for fast-scanning, 19: 39022
data recording for, oscillographic camera for time-resolved, 17: 36119 (SCDC-3041)
data recording systems for time-of-flight, design of photographic, 19: 747
data recording system for, design of digital, 19: 39023
data recording system for isotopic, development of, 20: 5584 (WAPD-T-1770)
description, 19: 38925
description and analytical use of spark-source, at Y-12 plant, 18: 43898 (Y-KG-24)
description and characteristics of Russian, 19: 20261 (JINR-P-1949)
description and characteristics of 100-in. radius, at Argonne, 19: 22822 (ORNL-TM-1047(p.93-7))
description and performance of time-of-flight, for studying free radicals, 16: 5244
description and performance, at Stockholm, 16: 9109
description and performance of Tokyo sector-type double-focusing, 18: 31839 (INSJ-637
description and performance of electrostatic time-of-flight, 19: 7772 (SGAE-PH-9/1964)
description and uses of, review, 17: 10942
description and uses of coincidence, 17: 29935
description and uses of LNR-JINR, 20: 19156
description for controlling and measuring high vacuum processes, 16: 19279
description of, 20: 41261(P)
description of CERN "missing-mass spectrometer" for unstable boson detection, 18: 31873 (CERN-64-30(p.49-56))
description of fission-recoil, 19: 29382
description of getter-ion type pump for use in, 16: 4333
description of pulsed, 17: 20669
description of tandem-magnetic-analyzer, 17: 35668
description of, at installations in India, 20: 5715 (AEET-227)
description of, for analyzing sodium-ion beams, 18: 30166(R) (AD-439716)
design, 16: 27390(P)
design, 19: 1940
design, 20: 36779(P)
design, 20: 29709(R) (TID-22970, pp 65-119)
design adaptation of time-of-flight, for studying charge transfer, ion dissociation, and photoionization, 18: 8626
design and construction of quadrupole-field, 16: 14916 (NP-11459)
design and construction of high-frequency, 16: 23954
design and construction of modulated molecular beam, for investigation of reactive gas-surface interactions, 18: 4065
design and construction, 18: 10026
design and construction for determination of deuterium in hydrogen, 18: 12421
design and construction of time-of-flight, for neutron scattering studies, 20: 1144 (AD-614451)
design and construction of time-of-flight, 20: 11072
design and development for selected area analysis, 19: 44354
design and operation of Colutron, 17: 27714 (UCOL-P-516)
design and operation of two-dimensional magnetic prism, 16: 376
design and operation of drift tube, for studying low-energy ion-molecule reactions, 16: 8952
design and operation of r-f, for measuring ion composition of upper atmosphere, 16: 22335(T) (JPLAI-tr-27)
design and operation of automatic, for relative measurements of uranium isotopes, 17: 23597 (K-1444)
design and operation of Colutron Mark II velocity-filter, 20: 19162
design and operation of electron-bombardment, 20: 31488
design and performance of high resolving power, 16: 355(T) (NP-tr-791)
design and performance of h-f, for isotope separation on small scale, 16: 3373(T) (UCRL-Trans-732(L))
design and performance of two-stage, 16: 5536
design and performance of 60° sector-type, 16: 10251
design and performance of perfect focusing, 16: 17849
design and performance in measuring deuteron and proton angular distributions, 16: 23080
design and performance for isotope ratio analyses, 16: 31842
design and performance of high-resolution, 16: 31863
design and performance of double-magnet, 16: 31864
design and performance of perfect-focusing, 17: 34214
design and performance of quadrupole, 17: 36133
design and performance of mass filter molecular beam, 17: 35263(R) (UCRL-10706(p.1-110))
design and performance of Argonne 100-in.-radius double-focusing, 17: 38979
design and performance of 360° tandem, 17: 10912 (TID-16312)
design and performance of high resolving power two-stage, 17: 10932
design and performance of time-of-flight circuit for particle analysis, 17: 23715
design and performance of sector-type magnetic, for analyzing ion beams, 17: 30812
design and performance of all-metal, for isotopic analysis of hydrogen, 17: 23279
design and performance of two-step, 18: 3700
design and performance of double-focusing counter-tube, for determination of mass spectra and trace analysis, 18: 10357
design and performance for multiatomic ion beams with 0.1 to 10⁷ coul/kg, 18: 18165
design and performance of quadrupole, 18: 23433
design and performance of magnetron type, 18: 31407
design and performance of small, 18: 41731
design and performance of high-sensitivity, for isotope geochemistry, 19: 32090
design and performance of dynamic-functioning, 19: 32535(P)
design and performance for heavy ion acceleration, 19: 34829
design and performance of spark-source, 20: 14458(R) (ORNL-3889, pp 39-43)
design and performance of 255° double-focusing, 20: 19160
design and performance of magnetless dynamic, (E/T), 20: 20991
design and performance of, for reactor fuel burnup determinations, 20: 22405
design and performance of, with large mass dispersion, 20: 23442
design and performance of r-f, for satellite measurements of atmospheric composition, 20: 29545
design and performance of tandem, for isotopic analysis, 20: 31206
design and performance of sector-type double-focusing, 20: 31208
design and performance of electrostatic time-of-flight, 20: 31209
design and performance of low-resolution, 20: 31169 (D-1-82-0508)
design and performance of magnetic heavy-particle, 19: 15878
design and use of high-pressure, for studying chemical reactions, 17: 1728
design and use of electric-quadrupole-focusing, in charge/mass determinations of liquid droplets, 18: 4351
design and uses of cascade, 17: 10909 (TID-15951)
design and uses of time-of-flight, 20: 10790
design and uses of time-of-flight, 20: 10791
design and uses, review, 16: 11554
design at Aldermaston, England, 16: 9102
design at Uppsala, 16: 9104
design at Vienna, 16: 9103
design changes for M1-1305, 20: 16798
design, characteristics, and performance of, constructed at the Laboratoire de Géologie et Géochimie Nucléaires, 17: 16385 (NP-12457)
design, construction, and properties, for trace analysis, 16: 14969
design, construction, and performance of quadrupole, 17: 14598 (NP-12593)
design conversion from single to double focusing, 16: 28868 (IS-504)
design for analyses of ultra-high vacuum systems, 16: 31755
design for analysis of fission product beams, 18: 20311
design for argon and potassium, 19: 28420(R) (NP-14825)
design for argon determination in potassium–argon age estimation, 19: 7315
design for assay of lithium isotopes, 20: 25472
design for chemical reaction observations, 17: 32360
design for detection of free radicals in gases, 16: 338 (NP-10899)
design for determination of argon-40 in minerals, 19: 4444
design for determining molecular beam intensity distribution, 20: 43658
design for evaluating ion sources, 16: 26390(T) (FTD-TT-61-242 (p.162-6))
design for fission fragments, 19: 34458
design for gas analysis using modulated beam, 17: 37410
design for gas analysis and leak detection, 19: 30111
design for gaseous uranium hexafluoride samples, 16: 25600(P)
design for heavy particles, 18: 692 (TID-18275)

design for increased resolution using electrostatic mirrors, 16: 25576(T,P) (FTD-TT-62-369)
design for ions from alpha irradiation of organic gases at near atmospheric pressures, 17: 37260
design for irradiation of organic compounds using carbon ions, 16: 11743
design for isotope separation, 18: 39584
design for isotope separation, 19: 34614
design for isotopic analysis of uranium hexafluoride, 20: 20588
design for leak detection, 19: 15851(P)
design for measurement of partial pressures in vacuum systems, 19: 24476
design for particle identification, 19: 28962(R) (NIRL/R/81)
design for plasma analysis, 19: 31418(P)
design for positive ions in ionosphere, 19: 35231 (AD-613042)
design for preparation of isotopic sources, 19: 34457
design for rapid analysis of solid-state samples, 16: 14981(P)
design for use in geochemistry, 19: 22567(R) (NYO-1669-10)
design for use with refractory materials at high temperatures, 18: 39149
design for vacuum fusion equipment, 20: 3863(R) (IS-1200(Sect. C))
design improvement of double focusing, 16: 29120(T) (AEC-tr-5314)
design magnetron-type, 19: 32529(P)
design modifications of Argonne, 20: 19159
design of all-metal, double collector type, for isotopic analysis of hydrogen, 17: 14175
design of alpha-particle ionization, 20: 31270
design of analyzer tube assemblies for, 16: 23857 (Y-1393)
design of automatic, for continuous operation, 16: 3165(P)
design of automatic recording, for monitoring uranium isotope concentrations, 17: 8528 (K-1445)
design of automatic scanning, 17: 10933
design of bakeable, 17: 2061(R) (TID-16592)
design of coincidence, 16: 26643(R) (JLI-650-8-8)
design of coincidence, 18: 41506(R) (ML-TDR-64-169)
design of, combined with gas chromatograph, 17: 10558
design of delayed warm-up filament power supply for, 20: 641(P)
design of Dempster-type, for separation of uranium-236, 16: 27534 (ORNL-1169)
design of double-deflection, for production of high-purity isotopes, 16: 9107
design of double-focusing, focusing properties of nonhomogenous magnetic fields in, 17: 37673
design of double-magnetic-stage-type, 17: 23720
design of double-stage, at Aldermaston, 17: 38980
design of double-focusing, for use as ion counter, 19: 28622
design of drift-tube, 20: 17298
design of electric quadrupole, 16: 22389
design of electrostatic, for plasma ion densities, 19: 23856
design of electrostatic, 20: 18995 (SGAE-PH-39/1966)
design of, for analysis of particles of high kinetic energy, 17: 38978
design of, for determination of critical ionization potentials by electron impact, 17: 38991
design of, for high transmission, dispersion, and resolution, 17: 25660(P)
design of, for measurement of uranium-235/uranium-238 isotopic ratio in uranium hexafluoride, 17: 38981
design of fringe-field-free, 19: 18247
design of h-f, 17: 41232(P)
design of high-pressure, for studying ion processes, 18: 8617
design of high-resolution, for trace impurity and molecular weight determinations, 16: 10197 (WADC-TR-59-107(Pt.III))
design of high-vacuum, 18: 8638(P)
design of high-frequency, 19: 4098(P)
design of high-frequency, 19: 4099(P)
design of high-frequency, 20: 29126
design of high-resolution, 20: 26812
design of ion collecting apparatus for, to prevent secondary emission effects, 18: 16289(P)
design of isotope-separating, (E), 20: 5826
design of large double-focusing, 17: 38977
design of Mattauch-Herzog type, with two-stage electrostatic field, 20: 23441
design of monopole-electric-field, 17: 12541
design of multi-stage, 19: 46725(R) (TID-22141, pp 101-10)
design of multiple-dispersion, with ion mirror, 17: 18563
design of multiple-dispersion, 18: 16291(P)
design of omegatron, for improved sensitivity, 17: 1734(P)
design of omegatron-type, 17: 20339(P)
design of omegatron-type, for improved sensitivity in gas analysis at low pressures, 17: 20340(P)
design of omegatron, for vacuum systems, 18: 29950
design of oscillating-ion type, for gas analysis in vacuum, 17: 15935(P)
design of panoramic rapid scanning-sector, for following gas reactions, 16: 13356
design of quadrupole, for energetic particle measurements, 19: 4445
design of r-f quadrupole, 17: 36452(R) (TID-19303)
design of radiofrequency, 17: 29171 (NP-12947)
design of radiofrequency, for studies of light hydrocarbons, 17: 38987
design of rapid-scanning radiofrequency, 16: 31752
design of second-order double-focusing, 18: 5593
design of sector-type double-focusing, 19: 16852(R) (NP-14647)
design of selecting, with high resolving power, 18: 25772(P)
design of SGAE, in Seibersdorf Reactor Center, 17: 10923
design of small bakeable, 17: 6379 (61-RL-2501G(Rev.))
design of spark-source, 17: 10943
design of surface ionization source for, with vacuum lock, 17: 18558 (Y-1415)
design of time-of-flight, for eliminating stray ions, 17: 1732(P)
design of time-of-flight, for studies of ion-molecule interactions, 17: 38989
design of time-of-flight, for positive-ion mobilities and concentrations, 18: 37795(T) (NASA-TT-F-141(p.143-51))
design of time-of-flight, with high duty cycle, 18: 39601
design of two-stage magnetic, 18: 20306
design of wide angle, for analyses of molybdenum-uranium hexafluoride mixtures, 16: 25313 (K-1433)
design of, with heterogeneous electrostatic field, 16: 30623
design of 360°-deflection, (T), 20: 18998
design of 6-in.-radius, single-focusing, 16: 14616(R) (NBL-177)
design of 6-inch, for isotopic analysis of gases, liquids, or solids, 17: 20308 (NBL-191)
design of 94-channel, for analysis of pulsed ion beams, (E), 20: 5698
design of, for simultaneous collection of positive and negative ions, 20: 40796(R) (IS-1500(Sect.C))
design of, phase space representations for charged-particle motion for, 20: 41567
design of, using twin crucibles, 19: 5919
design perspectives for, 20: 19155
design producing fluctuating component in ion stream, 19: 38958(P)
design using photoionization, 20: 23420(R) (ANL-7108, pp 57-60)
design utilizing combined electric and magnetic fields, 16: 27401(R)
design with built-in system for automatic processing of output data, 16: 20670
design with field variations, 19: 42679 (JINR-P-2160)
design with magnetic sector field, 19: 11043(P)
design without magnetic fields, 16: 3375(P)
design without magnetic fields, 17: 14617(T) (AEC-tr-5670)
detection of metastable-ion dissociation in double-focusing, (T), 19: 4842
detectors for, design of semiconductor electron multipliers for, 18: 18198
deuterium–hydrogen exchange in, 17: 35706(R) (TID-19307)
deuterium-hydrogen isotopic exchange on filaments of, 18: 18021(R) (TID-20411)
development, 20: 26095 (SGAE-PH-34/1965)
development and evaluation of 18-stage radiofrequency, 16: 22344
development and testing of double-focusing, with inhomogeneous magnetic field, 17: 21995
development and uses of, review of, 17: 32350
development and uses of, survey of, 18: 27318
development and use of two-stage, 19: 280(R) (ORNL-3679(p.94-116))
development for determining ion and neutral content of ionosphere, 20: 43648
development for high-temperature vaporization studies, 17: 30512 (NLCO-880)
development for thermochemical studies, 17: 25269
development of auxiliary equipment for, 17: 35253(R) (IA-775)
development of Consolidated–Nier, for automatic monitoring of gas streams in tritium production, 17: 14596 (KAPL-902)
development of flight-type, 18: 37480(T) (NASA-TT-F-141(p.22-47))
development of, for analysis of 10^{-14}- to 10^{-18}-cm^3 samples of noble gases at STP, 16: 31754
development of, for continuous automatic determination of gaseous impurities in uranium hexafluoride, 17: 38976
development of, for reduction of analysis time, 17: 38982
development of high-sensitivity, 18: 29861(R) (WERL-9)
development of high-sensitivity medium-resolution, 19: 43633(R) (NP-15354)
development of Lissajous, 17: 10898(R) (N62-10115)
development of molecular beam electric resonance, 17: 36442(R) (NP-13084)
development of multi-ion source, for isotope separation, 20: 19140
development of pulsed-molecular-beam, 17: 10910 (TID-16209)
development of quadrupole, for atmospheric studies, 19: 6168
development of r-f, 18: 20618(R) (NP-13799)
development of, for use in crossed molecular beam studies, 20: 43288(R) (CALT-532-1)
development with automatic range switching, 18: 29952
developments in, for chemical analysis, 19: 32059(R) (IDO-14655)
developments in, since 1926, 20: 31808

device for evaporating high-melting solids in, 17: 21987
dissociation of metastable ions in, lifetimes for, 19: 4188
double focusing, calibration of channel sensitivity, 16: 11910
double-focusing, use in organic chemistry, 17: 35643
dry box system for, engineering drawings of, 18: 31702
effect of formation of directed ion beam in triple-plate source, 16: 11874
electric field generation for omegatron, sweep oscillator for, 18: 37484(T) (NASA-TT-F-141(p.108-18))
electrode system design for omegatron, 20: 9234
electromagnetic lenses in isotope separator, spherical aberration effects in, 19: 34615
electromagnetic lenses for, focusing properties of, 20: 9613 (SGAE-G-3/1965)
electron beam location and geometry for flight, 20: 46025
electron gun design for, 20: 40796(R) (IS-1500(Sect.C))
electron multiplier detectors in, isotopic discriminations by, 16: 5513
electron multiplier tube for time-of-flight, design of magnetic-focusing, 17: 41217
electron multiplier for, 18: 13358(R) (MLM-1151)
electron multiplier for, characteristics of resistance-strip, 19: 6203
electron multiplier spectra in converted, comparison with electrometer spectra, 19: 11492
electron multiplier design for, 19: 11494
electron multiplier system for, improvement in peak shape from, 20: 9233
electron optical system, design, 16: 19139
electrostatic analysis design for, 19: 38963(P)
electrostatic quadrupole lens pair design for, 16: 29160
emission regulator circuit for radiofrequency, 18: 14166 (TID-20301)
engineering drawings of single-direction focusing, for carbon-14 separation, 18: 17986
evaporation system for, design and performance of, 20: 45594
features and performance of electric quadrupole, 16: 9106
filament assemblies for, equipment for loading boron, plutonium, and uranium in, 20: 18568(R) (NBL-230)
filament current controller for MS5, circuit design and performance for, 16: 19093
filament design for simultaneous analysis of two samples, 16: 9962
filament preparation for, engineering drawings of vacuum chamber for, 19: 34454
filter for, solid-state circuit for monopole, 18: 31858
flash lamp synchronization for fast reaction studies, 19: 36756 (SC-RR-65-185)
focusing in axially symmetric, two-directional, 16: 22390
focusing properties for inhomogeneous-field, 20: 27392 (ORNL-TM-1475)
for measuring heat of formation of metal monomers and dimers, 16: 15294
head attachment design for use in ultra-high vacuum leak detector, 20: 29496
imaging properties of magnetic heavy-particle, 19: 13710
ion acceleration apparatus for coincidence, 19: 24837(P)
ion beam current measurement, apparatus, 16: 7741(P)
ion beam double focusing in, with inhomogeneous magnetic field, 20: 29493
ion beam formation in Pretoria isotope, 19: 34613
ion beam formation in sector-type, 20: 19144
ion beam intensity measurement, device for, 18: 35823(P)
ion beam reactions with materials in, 20: 21219
ion beam scattering in double-direction focusing, (E), 19: 42692
ion beam transmission efficiency for, (T), 20: 29490
ion charge distribution in, measurement using Mylar films, (E), 19: 38940
ion collector assembly for, 19: 15831
ion collector design with a secondary particle collecting electrode for, 19: 38962(P)
ion collector for nitrogen and oxygen isotopes, 16: 6611
ion converter detector with gate connections for, 20: 13047
ion current in, device for measuring, 17: 12535(T,P) (FTD-TT-62-1529)
ion detection in, using electron multiplier tubes, 20: 5706
ion detection in, amplifier design for, 20: 21039 (KAPL-3122)
ion detector design, 16: 22393(P)
ion detector design for, 17: 1731(P)
ion dissociation processes in drift tube of time-of-flight, effect of potential barrier on, 18: 8625
ion focusing and generating system for, design, 17: 29186(P)
ion focusing in, double deflection system for, 19: 42705(P)
ion lens system for, design, 17: 29187(P)
ion mass discrimination in, kinetic energy from, 18: 35815
ion-molecule reactions in ionization chambers of, 17: 31219
ion-optical considerations on, 16: 9105
ion-optical properties of magnetic-field, 17: 4796
ion optics for, 19: 22674
ion optics for, (T), 20: 29489
ion optics in, computer analysis, 19: 9474 (ANL-6903)
ion optics of combined radial electric and inhomogeneous magnetic fields in, 17: 36419 (NP-13020(p.265-70))
ion production for, by disruptive vacuum spark, 18: 8040(T) (SC-T-537)
ion pump protect circuit for filament and accelerating-voltage, 18: 8611(R) (NBL-204(p.29-32))
ion pumps for surface ionization in, 20: 43068(R) (IDO-14679, pp 47-50)
ion resonances in omegatrons, 17: 20653
ion retarding system for, 20: 25473
ion scattering in, 18: 12423
ion source and multiplier modifications for time-of-flight, to increase sensitivity, 17: 36175
ion-source assembly design for, 17: 37328(P)
ion source design for short-lived isotopes, 16: 9110
ion source design for short-lived isotopes, 16: 9112
ion source design for time-of-flight, 16: 30615
ion source design for, 17: 10567
ion source design for high-pressure, 17: 33901
ion source design for, 18: 23406 (CONF-512-4)
ion source design for reduced memory effect in isotopic analysis of uranium hexafluoride, 18: 35824(P)
ion source design for, 20: 13051(P)
ion source development for, 19: 18166
ion source development for, 19: 26917(R) (IA-984)
ion source for, 20: 8875(P)
ion source for, energy distributions of ions formed in pulsed r-f, 18: 8623
ion source for magnetic-deflection, design of pulsed, 19: 15474
ion source for Orsay, performance of thermal, 20: 19142
ion source for time-of-flight, for continuous operation, 18: 5590
ion source for, using low- and high-vapor-pressure samples, 18: 7024(P)
ion source for, current-voltage characteristics of Penning, 20: 11077
ion source for, design of thermal, 18: 31382
ion source for, design of Penning, 19: 6166
ion source for, design for three-stage analysis, 19: 22680
ion source for, design of tritium, 19: 42481
ion source for, performance with auxiliary source magnet, 18: 31859
ion source for, use of sputtering for, 18: 39057 (CONF-520-1)
ion source for, using piezoelectric vacuum vibrator, 19: 20292
ion source for, with adjustable electron gun and no magnetic field, 19: 32538(P)
ion source performance, parallel-filament lateral-arc, 16: 9113
ion source pressure measurement at very high pressures in, 17: 32387
ion-source shielding from stray magnetic fields, 16: 14124
ion source temperature stabilizer for, 16: 27329
ion sources design for, electron-bombardment, 20: 8842
ion sources for, description of r-f, 17: 41602
ion sources for, improvement of ion transmission in, 17: 37404
ion sources for Orsay, design and performance of, 20: 19143
ion sources for, preparation of tungsten filaments as, 17: 8570(P)
ion sources for, design of cold electron sources for, 18: 22210
ion sources for, design of cold-cathode electron-collision, 20: 13053(P)
ion sources for, design and performance of high-temperature hollow-cathode, 20: 19002
ion sources for, performance of cold-electron, 18: 39600
ion sources for, plasma-compression, 20: 19001
ion sources for, uranium ion production in, 18: 18148
ion sources for, using quadrupole lenses, 19: 36853
ion sources, initial velocity discrimination effects in crossed-field, 16: 16846
ion sources, molecular secondary processes in, 16: 8915(T) (CEA-tr-R-1409)
ion sources of, design of vacuum locks for, 18: 14178
ion trajectories in monopole, (T), 20: 20994
ionization-curve recording, device for automatic, 18: 43916
Knudsen cell, use and operation of, 17: 12747(R) (AFCRL-62-373)
loading of plutonium samples in glove box on filaments of, design of flip-flop unit for, 18: 29927(R) (NBL-210(p.35-7))
M/e positions for, measurement of, 17: 21976 (NBL-194)
magnet current stabilizer for heavy-particle, 17: 34264
magnet power supply for, design, fabrication, and performance of, 17: 18557 (Y-1414)
magnet power supplies for, 19: 15830
magnetic analyzer calculations for Russian, 19: 20260 (JINR-P-1948)
magnetic analyzers of, calculations for, 20: 31484
magnetic fields of, automatic scanning device for, 17: 37411
magnetic scanning in omegatron, residual gas analysis by, 18: 2005
magnetometers with zero reading for, performance of, 19: 34556
mass discrimination in, detection and determination of, 16: 29153
matrix treatment of ion focusing in Browne-Buechner, 17: 32362
measurement of ionization potentials using, magnetic field effect in, 18: 25345
measurement of two ion currents by pulse counting in, simultaneous, 17: 10908 (TID-15865)
measuring circuit in, 17: 8583(P)
operation and optimization of, with reduced magnetic field volume, 20: 19158

operation and performance of Zeutheo, 17: 2697
operation at low pressures, mass peaks from adsorbed gases in, 17: 32345
operation difficulties of HERMES, 16: 9108
operation for optimum resolution and performance, 16: 4266(P)
operation of Dempster-type, metastable ion peaks in, 20: 22859(R) (UCRL-16580, pp 149-205)
operation of double-magnetic-deflection, 19: 17781(R) (ORNL-3750)
operation of double-magnetic-deflection, 20: 17158(R) (ORNL-3900, pp 82-149)
operation of, formation of deuterium and hydrogen ions in, 16: 31758
operation of omegatron, analysis for optimum, 19: 34447
operation of radiofrequency, with parabolic potential, 17: 6416
operation of, interactions in sample gas mixtures in, 18: 37482(T) (NASA-TT-F-141(p.66-95))
operation under fast scanning conditions, peak distortion in, 20: 25353
oscillation amplitudes in, calculation of, 17: 2724
output reading for Dual 12-in., step-scan programmer for, 20: 27354
peaks produced by exposure to hydrochloric acid--water in cycloidal focusing, metastable, 19: 36751 (NASA-TM-X-1111)
performance, 19: 28420(R) (NP-14825)
performance and uses in nuclear and radiochemistry, 20: 25181
performance at CERN synchrotron, with on-line Mercury computer, (E), 19: 26968 (CERN-65-5)
performance at 10^{-3} to 10^{-11} Torr, 16: 31751
performance errors in precision determination of isotopic composition of elements, 19: 36310
performance evaluation of inverted magnetron-type, for space probe use, 17: 30837
performance for analysis of fission product beams, 18: 20312
performance for argon isotope determinations, 20: 7252
performance for ionization studies in impure shock-heated argon, 20: 43123
performance for isotope separation, 20: 19145
performance for measuring isotopic yields in nuclear reactions, (E), 20: 8105
performance for preparation of beta sources, beam retarding techniques for, 19: 34616
performance for preparation of nuclear reaction targets, 20: 19167
performance for study of outgassing of elastomers and plastics, 19: 32417
performance in analysis of uranium standards, 19: 30081(R) (NBL-216)
performance in DCX-2 for recording vacuum conditions, 20: 22857(R) (ORNL-3913, pp 111-32)
performance of Argonne, 20: 9366
performance of double-focusing, magnetic field nonuniformity effects on, 18: 12422
performance of double-focusing, 19: 15925
performance of Karlsruhe, for lead and antimony isotopes, 20: 19147
performance of multiphase, 20: 11192 (SGAE-PH-30/1965)
performance of omegatron, radio-frequency absorption in, 19: 9464
performance of r-f, for space applications, 18: 2015
performance of r-f Bennett-type, at high pressures, 18: 4055 (NP-13372)
performance of r-f, (E), 19: 38926
performance of semiautomatic radiofrequency, 19: 46772
performance of ultrahigh vacuum, under high argon pressures, 20: 31390
performance of 12-in., single-focusing, surface ionization type, 16: 12949 (K-1463)
performance of 255° modified-calutron, for separating heavy isotopes, 19: 11640 (ORNL-P-744)
performance of 255° inhomogeneous-field, for isotopic separation, (E), 19: 35510
performance of, using razor blades as field ionization sources, 20: 31198
physics research with, 20: 4215(R) (ANL-7081, pp 134-49)
power supplies for, design for use as accelerating potentials, 17: 18545 (TID-16632)
power supply for double-focusing, design of, 20: 14830
power supply for electron gun of, 18: 9752 (IA-900)
problems and uses of spark-source, 17: 33850
properties, 20: 35720
pulse amplifier-discriminator for surface-ionization, 19: 28618
pulse generator design for time-of-flight, 18: 14180
quadrupole mass filter as analyzer in, operation, 17: 10945
reactions in, secondary, 16: 15296
resolution and sensitivity of double-focusing, 19: 9466
resolution improvements in, for atomic mass determinations at Z = 32 to 42, 18: 1056
resolution of, for separation of fission products, 20: 434 (JUL-248-NP)
resolving power multiplier for, design and performance, 16: 8954
resolving power of velocity modulation type, effects of space charge, 17: 3295
response of MS-7, for impurity determinations, 19: 26226 (CEA-R-2721)
review of Harwell, 18: 25740 (EANDC(UK)-25L)
sample changer for, description of, 20: 14829
sample introduction in, design of system for, 19: 9046(R) (IS-900(Sect.C))
sampling by, through pinhole in the adiabatic flow region, 17: 32361
scanning circuits for, 17: 20320
separating power characterization, 16: 9100
sluice design for, fast-acting, vacuum, 16: 6595
source handling systems for, design of vacuum seals and valves for, (E), 20: 2159
source leak valve design for, 20: 4230(P)
source valve design for, 19: 4448(P)
spectra in, Aston bands in, 18: 18267
stabilization of isotope-separating, 19: 4573
testing, 18: 24300(R) (NP-13953)
theory and performance of farvitron, 16: 14968
theory and uses of, 17: 31103
theory and uses of quadrupole, review on, 19: 20300
theory of omegatron, 18: 37481(T) (NASA-TT-F-141(p.48-65))
theory of, review of statistical, 17: 38983
use as a chromatographic detector, 17: 12326 (TID-17508)
use as effusiometer, 18: 33867
use as leak detector in vacuum systems, 18: 27777
use as sampling probe for discharge plasma, 20: 15915
use as vacuum gage at 10^{-13} torr, 20: 45874 (NASA-TM-X-1268)
use for analysis of liquids and solids, review on, 18: 14188
use for analysis of vapor species over solid inorganic materials, bibliography on, 19: 32123 (ORNL-TM-989)
use for isotope dilution analysis, 19: 11008
use for isotope separations at Princeton-Pennsylvania accelerator, 20: 19889
use for low oxygen pressure measurements, 19: 32413(R) (WERL-2823-17)
use for measurement of isotopic composition of samples, elimination of errors in, 20: 10793
use for measuring kinetic energy of fragment ions, 18: 25763
use for measuring relative abundances of isotopes, 20: 1774
use for plasma analysis in magnetic trap, (E), 19: 5290(T) (AEC-tr-6518(p.163-70))
use for preparation of radiation targets, 20: 19151
use for speed measurements on sputter ion pumps, 19: 40777
use for study of ion reactions with chemical compounds, 20: 18780
use for study of secondary processes after ion acceleration in time-of-flight, 19: 7391
use for studying corrosion films on Inconel and stainless steel, 19: 22665 (WERL-1114-1)
use in activation analysis, 20: 35457
use in analysis of 10^{-9} gram samples using sputtering, 18: 39057 (CONF-520-1)
use in atmospheric studies, conference on, 18: 37793(T) (NASA-TT-F-141)
use in atomic mass determinations, 20: 15853
use in detection of molecular beams, 20: 31492
use in electron-induced surface ionization studies, (E), 19: 9941
use in high-energy sputtering studies, 20: 31905
use in isotopic analysis of gaseous substances, effects of gas flow conditions on accuracy of, 18: 1997
use in isotopic analysis, 19: 7274(R) (IDO-14636)
use in kinetic analyses of transient chemical reactions, 19: 42461 (SC-R-65-956)
use in lithium isotope abundance measurements, 20: 31205
use in measuring ion concentrations quantities in ionosphere, 20: 44457
use in nuclear reaction analyses, 18: 38085(T) (AEC-tr-6398(p.288-95))
use in plasma composition analysis, (E), 19: 5288(T) (AEC-tr-6518 (p.146-53))
use in plasma source condensations analyses, (E), 19: 5289(T) (AEC-tr-6518(p.154-62))
use in preparation of radioactive samples, 20: 19166
use in rubidium/strontium determination, 18: 3678(R) (NYO-10517 (p.135-41))
use in studies of residual gases, 19: 29812(R) (SRIA-425-4)
use of double focusing, for gas determinations, 19: 38546(R) (RFP-552)
use of ion pump for evacuating, 17: 1738(P)
use of multi-ion source, 20: 19157
use of omegatron, in gas-mixture analyses, 18: 37483(T) (NASA-TT-F-141(p.96-107))
use of r-f, for measuring kinetic energy of fragment ions, 19: 42506
use of r-f, in measurement of fragment-ion kinetic energies, (E/T), 19: 38927
use of Seibersdorf, in nuclear physics, 20: 19164
use of spark-source, for analysis of extremely small zones in metallic samples, 17: 30838

use of spark-source, for analysis of insulating powders, 18: 1597
use of spark-source, in analysis of alloys and elements, 20: 235 (Y-KG-28)
use of time-of-flight, for retarding potential difference studies of appearance potentials, 18: 21703 (CONF-296-4)
use of time-of-flight, for atmospheric density, 18: 37487(T) (NASA-TT-F-141(p.132-42))
use of, in study of atomic impact phenomena on metal surfaces, 20: 31907
use of, in study of ion–molecule reactions, 20: 31224
use on-line for lithium-8 and -9 detection in proton reactions with carbon, 20: 19886
use on-line for separation of krypton and xenon isotopes, 20: 19887
use on-line with CERN synchrocyclotron for nuclear decay studies, 20: 19885
uses for analyzing nuclide yields from uranium-235 thermal fission, (E), 19: 45260(R) (IDO-14660)
uses in isotopic dilution analysis, 19: 9074
uses in nuclear physics, (E), 19: 9781
uses in studying properties of excess-kinetic-energy ions in organic mass spectra, 18: 25019 (UCRL-10823)
uses of double focusing, in studies of secondary processes, 16: 22370
uses of omegatron, for isotopic analysis of argon, 19: 17839
utilization of, in corrosion study, 17: 22120
vacuum in, liquid nitrogen systems for, 18: 29954
vacuum lock design for, 19: 30505(P)
vacuum lock for sample changing in, 20: 43068(R) (IDO-14679, pp 47-50)
vacuum lock for, description of alumina sliding-shaft, 19: 34424 (BNWL-SA-62)
vacuum pump for, characteristics of all-metal-exhaust, 20: 43068(R) (IDO-14679, pp 47-50)
vacuum seal for, design of electrical pass-through, 16: 29103 (IS-212)
vacuum system design for, 18: 37486(T) (NASA-TT-F-141(p.123-31))
vacuum systems for, use of titanium–ion pumps in, 17: 25576
vacuum systems for, use of ion pumps in, 17: 35630(R) (NBL-195)

MASS SYNCHROMETERS

see also Mass Spectrometers

MASS TRANSFER

across interface of suddenly pressurized, liquid-vapor system, 19: 22499
analysis of thermodynamic systems in, computer program for, 19: 7682 (NAA-SR-Memo-9851)
analysis of, design of equipment for, 20: 39050 (UCRL-16535)
between confined plasma jets and gas coolants, 20: 15584
between tube wall and fluid streams at Reynolds numbers from 10^3 to 10^5, 17: 10790 (AERE-R-4197)
between two fluid phases, validity of addition-of-resistances equation for, 18: 31362(R) (UCRL-11213(p.154-61))
bibliography on, 19: 18121(T) (FTD-TT-64-395)
bibliography on, international, 17: 12430
book: *Advances In Heat Transfer, Vol. III*, 20: 29381
book: *Heat and Mass Transfer.* Vol. III. *Heat and Mass Transfer in Phase Transformations*, 20: 25264
book: *Radiative Contributions to Energy and Momentum Transport in a Gas*, 20: 7976
book: *Recent Advances in Heat and Mass Transfer*, 16: 8893
boundary conditions and equations for, in zone melting, 17: 23874 (UCRL-10433)
by particles in air flow through vertical conduits, 19: 342(R) (HW-81746(p.4.67-71))
conference, June, 1961, Minsk, Russia, 16: 4280(T) (NP-tr-827)
conference, Minsk, USSR, June 1961, 16: 25527 (RM-2852-PR)
description of extraction process, mathematical, 18: 37258 (A/CONF.28/P/346)
design of equipment for study of, between liquid metals and solids, 20: 14975 (ANL-7091)
determination of rates of, profilometric, 17: 6236
diffusion in solution, survey of optical techniques for studying, 19: 1975 (UCRL-11542)
eddy diffusivity in turbulent water flow in pipe, radial variation of, 18: 31721 (IS-830)
equations of simultaneous heat and, computer program for solving partial differential, 20: 4103 (NAA-SR-Memo-11099)
flow structure effects on, in heterogeneous processes, 16: 4299(T) (NP-tr-827(p.84-6))
fractionating effects of, in vapor condensation, 19: 22484(R) (NYO-2765-1)
from cylinder surface to incompressible laminar flow, theoretical and experimental studies, 19: 7683(R) (NP-14544)
from rigid surface in laminar flow, effects of physical properties of liquid, 16: 27207
from submerged surfaces to fluidized beds, computer program for, 17: 12390 (ANL-SL-SL-2342)
Heat and Mass Transfer. Vol. II. *Heat and Mass Transfer in Interactions of Bodies with Liquid and Gas Streams*, 20: 24203
in a turbine contactor, 18: 10179 (DP-847)
in boundary-layer flows, Blasius series for, 20: 31220(R) (UCRL-16658, pp 39-72)
in concurrent gas-liquid flow, 18: 39438 (UCRL-11570)
in fixed and fluidized beds, 17: 6232
in forced-circulation, poly-metallic loops, 16: 15146 (PWAC-203)
in gaseous systems, 18: 1834(R) (IS-700(Sect.E))
in gases, interfacial rates for large gradients of concentration and temperature, 16: 23822 (NP-11818)
in immiscible systems, 17: 39082(R) (TID-19451)
in laminar flow, equipment for determining, 20: 23217(R) (UCRL-16580, pp 251-4)
in packed beds, design equations for estimating, 16: 19043 (DC-54-1-75)
in stirred vessel extractor, hydrodynamic model, 17: 16241
in turbulent flow in pipes, correlation of, 18: 14037 (UCRL-10556)
in turbulent flows, studies of gas-phase, 19: 589 (UCRL-11629)
in turbulent liquid streams, 17: 23476 (IS-419)
in turbulent pipe flow, 17: 34090 (EUR-293.e)
in turbulent systems, spectroscopic studies of, 18: 22222 (IS-738)
interfacial phenomena in, design of viscometer for studying, 16: 11503(R) (ORNL-TM-34)
liquid-phase, in packed columns at low flow rates, 18: 35656 (IS-817)
measurement of, equipment for, 17: 27967
measurement of mutual diffusion coefficients of gases, optical system for, (E), 19: 4111(T) (ORNL-tr-316)
mechanisms of gas-bubble, 18: 20189
of AGR fuel rods on dimple brace configurations, 20: 41109
of forced convection through laminar boundary layers on flat plate, effects of wires near outer edge on, 19: 40746
plasma discharge cooling at axisymmetric stagnation points by, 16: 13261
processes of, in solids subjected to temperature gradient, 19: 38678
research programs of U. S. Army on, 1962 summary, 17: 33413(R) (NP-12967)
resistance to, in diaphragm diffusion cell, 17: 30503 (CONF-14-5)
solution of equations for combined chemical reaction associated and molecular diffusion, 16: 2990 (AERE-R-3853)
studies using thermodynamics of irreversible processes, 16: 4162(T) (AEC-tr-4902)
theory of, equations for, 17: 2064(T) (FTD-TT-62-65)
through fixed and fluidized beds, 16: 25532
to gas-fluidized bed of particles, studies of mechanism of, 18: 35682 (ANL-6807)
unsteady, in rotating disc–revolving fluid system, 16: 30565

MASSACHUSETTS

aerial gamma monitoring of, correlation with areal geology, 18: 43798 (CEX-59.4.14)
civilian defense training program for medical personnel in, 18: 31810
Dedham, age of granites in, 18: 3987(R) (NYO-10517(p.53-4))
geologic dating of granites, quartzites, and slates in, use of rubidium–strontium and strontium-87/-86 methods for, 20: 16711(R) (MIT-1381-13)
macroscopic benthic fauna off Cape Cod, 18: 17363 (TID-20363)
radionuclide contamination of milk in Boston, 19: 28599
radionuclide contamination of human milk in Boston, 19: 28601

Massachusetts Institute of Technology Reactor

see MIT Research Reactor

Masurium

see Technetium

Materials Accounting

see SF Materials Accounting

Materials of Construction

see Building Materials

MATERIALS TESTING

(See also the specific material or equipment concerned or properties being tested; see also specific testing procedures, e.g., Sonic Inspection, Fluorescent Penetrant Inspection, and Magnetic Particle Inspection.)
see also Fatigue
see also Fracture Tests
see also Mechanics
see also Metallurgy
see also Photoelasticity
ablation testing device for re-entering bodies, (E), 19: 47117(R) (SC-DC-65-1698)
activation analysis for, 16: 23964 (ANL-6515(p.9-27))
alternating thermal stress resistance of metals, 16: 22643
apparatus for metals at 10^{-6} to 760 mm Hg, 16: 13564 (AFOSR-2139)
automatic machine design for fuel element cladding, 17: 14469 (HW-SA-1821)
automatic processing of tensile test data, 17: 39264 (HW-71570)
betatron for nondestructive, portable, 18: 25677

bibliography on, 18: 18015 (SB-411(Suppl.1))
bibliography on Soviet technology, 16: 6262 (XDC-60-4-61)
bonded joint, correlation of heat transfer and ultrasonic transmission properties for, 20: 29386 (ANL-7074)
book: *Corrosion. Vol. II. Corrosion Control*, 19: 7869
book: *Elevated-Temperature Testing of Metals*, 20: 7245(T)
book: *Gammagraphy, A Method for Nondestructive Materials Testing*, 19: 28521
book: *Metals Reference Book.*, Vol. I and II, 3rd edition, 18: 32080
book: *Nondestructive Testing*, 2nd Ed., 20: 23263
book: *Nuclear Technology in Construction*, 19: 38828
book: *Proceedings of the Fifth Annual Symposium on Nondestructive Evaluation of Aerospace and Weapons Systems Components and Materials*, 20: 45868
brazed joints, comparison of methods for nondestructive, 19: 44207(R) (ANL-7000, pp 146-52)
brittle failure, uncertainty in Robertson tests for, 19: 42627 (EURAEC-1406)
brittle fracture testing, energy release rate determination for biaxial specimen in, 19: 9668 (WERL-8844-2)
brittleness test for powder metallurgy materials, 17: 30974 (LAMS-2906)
buildings and facilities for environmental, 20: 9125
calibration of Charpy impact test machine, 19: 1004(R) (ORNL-3676 (p.125-56))
cavitation damage to impellers, coatings for indicating, 19: 44212 (TIM-878)
color radiography for, photographic methods in, 20: 20863
comparison of drop weight and crack arrest tests for measuring the brittle fracture transition temperature, 17: 22203
compressed gas gun for transient stress, 18: 33756
conference on, 17: 34114
conference on nondestructive, Osaka and Tokyo, March 1960, 16: 6617
conference on nondestructive, San Antonio, Oct. 1963, 18: 10254
conference on nondestructive, London, Sept. 9 to 13, 1963, 19: 40754
conference on nondestructive, 20: 14701 (STI/PUB/105(Vol.1))
controlled impacts, performance of high-velocity propellant gun for, 16: 1884 (SC-4652(RR))
crack detection by gamma defectoscopy, 16: 19152
crack testing machine design, 4000-ton, 16: 8979
creep and fatigue criteria for high-temperature turbocompressor loop materials, 18: 27684 (MTI-63TM8)
creep resistance and hot hardness, apparatus for measurement of, 19: 30393 (HW-80723)
creep-rupture properties of refractory metals, equipment and techniques for, 20: 29710 (TID-22986)
cryogenic in-pile loop for, 17: 1628
cryostat for tensile, at 4 to 300°K, 19: 23581
data from mechanical, computer processing of, 18: 8502 (HW-SA-3108)
data processing in, computer system for, 18: 8503 (SC-4944(RR))
data recording system for in-pile fatigue testing, 20: 14059(R) (IDO-17104)
defectoscopy by fast neutrons for, 20: 25454
defectoscopy of components and materials of First Czechoslovakian Atomic Power Station, (E), 20: 6633(T) (AECL-2286)
defectoscopy with gamma and x rays, parameters, 16: 29180
defectoscopy, design of automatic gamma detector for, 19: 36770(T,P) (FTD-TT-64-1381)
design and fabrication of liquid metal temperature-controlled irradiation capsule, 20: 23770 (BNWL-SA-604)
design of dynamic torsion machine for producing square microsecond torsion pulses, 18: 13375 (TID-20172)
design of high-temperature high-vacuum equipment for, 20: 21350 (ORNL-TM-1426)
design of hyperfrequency spectrometer for study of irradiated substances, 17: 29178
design of machine and specimens for creep tests, 17: 20400 (AGN-8062)
design of pulsed reactor for studies on electronic equipment, 16: 30913
design of remote hardness tester, 17: 35998 (LADC-5760)
design of rolling stand for testing maritime reactor components, 17: 40264 (EUR-375.d)
determination of defect geometry by ultrasonic pulse analysis testing, 16: 8876 (WAL-TR-830.5/3)
determination of emissivity and thermal properties by electron beam heating, 16: 11929 (WADD-TR-60-190)
determination of elastic properties of perforated materials, 16: 33485 (WAPD-DLE-319)
determination of materials behavior from true stress-strain relations, 16: 20806 (NAA-SR-6376)
determination of radiation effects on metals and alloys at cryogenic temperatures, 17: 16742(R) (NP-12628)
development for reactor materials, review of, 17: 11123
development of centrifugal testing equipment, 16: 7743(R) (AGN-8045)
development of diametral-compression test, 16: 2182 (NP-10936)
development of eddy current, radiography, and ultrasonic techniques for, 17: 41333(R) (ANL-6677)
development of in-pile creep testing machine, 16: 8972 (CRRL-1054)
development of infrared and electromagnetic methods for use in, 17: 13678(R) (HW-75914)
development of irradiation techniques for, 17: 4249(R) (NAA-SR-7400 (Sect.VII))
development of Lamb waves for, 16: 14988(R) (ANL-6329)
development of method for determining ductile-brittle transition temperature, 17: 11187(R) (EURAEC-447)
development of nondestructive methods for, 16: 31197(R) (ANL-6597)
development of nondestructive techniques for, 16: 30717(R) (ANL-6516)
development of nondestructive methods for, 16: 30167 (ORNL-3313 (p.19-64))
development of nondestructive techniques for, 17: 4225(R) (ANL-6635 (p.28-50))
development of nondestructive methods for, 17: 19720 (ANL-6698)
development of nondestructive methods for, 17: 27560 (WAPD-T-1530)
development of nondestructive techniques for reactor component, 17: 35079(R) (ANL-6749)
development of nondestructive techniques for reactor components, 18: 15663(R) (ANL-6808)
development of nondestructive techniques for reactor components, 18: 19456(R) (ANL-6840)
development of nondestructive methods using gamma radiography for, of pipe welds, 19: 597
development of nondestructive, for reactor materials, 19: 22660(R) (HW-83298(p.7.1-30))
development of nondestructive, 19: 34425(R) (HW-84384(p.7.1-27))
development of nondestructive methods for, 20: 4110(R) (ORNL-3870, pp 146-54)
development of nondestructive methods for, 20: 19178(R) (IDO-17154)
development of radiographic techniques for inspection of uranium tubular shapes, 16: 7745 (WAL-TR-142.1/1)
development of radiometric techniques for, 17: 2050 (ARF-1209-6)
development of scintillation spectrometry for, 16: 31956 (HW-SA-2728)
development of ultrasonic methods for, 17: 1901(T,R) (EURAEC-375)
development of ultrasonic and radiometric methods for, 17: 15385(R) (ANL-6683)
development of vacuum facilities for, at 2000 to 6000°F, 17: 250(R) (NP-12147)
development of vacuum facilities for, at 2000 to 6000°F, 17: 251(R) (NP-12148)
developments and predictions for nondestructive, 19: 22510 (SC-DC-65-1123)
developments and uses of eddy-current, 20: 2025 (BNWL-SA-349)
device for creep testing in reactors, 17: 20190(P)
device for nuclear fuel clad tubing inspection, design of double frequency eddy current, 18: 41628
device for producing acceleration pulses for, 17: 27947 (TID-18816)
device for tensile testing in liquid hydrogen, 17: 25
eddy current and electromagnetic methods for, development of, 16: 33273(R) (ANL-6414)
eddy-current equipment and techniques for, 17: 7555(R) (HW-74761 (p.11.1-14))
eddy-current, for finned APM tubing, 17: 35999 (NAA-SR-Memo-7769)
eddy-current methods for fuel elements, 16: 6619
eddy-current methods for, 16: 30651
eddy-current methods of signal analysis for broadband electromagnetic, 17: 8381 (HW-67639)
eddy-current methods, 17: 34115
eddy-current methods for, theory and use of pulsed, 17: 37347 (ANL-FGF-394)
eddy current methods for tubing of N-Reactor, 18: 27750(R) (HW-79280 (p.7.1-22))
eddy current methods for hydride detection and process tubing flaws, 19: 13702(R) (HW-81984(p.7.1-26))
eddy current probe design for measuring plate spacing in fuel elements, 18: 19280 (ORNL-3580)
eddy current technique for measuring tube-to-tube annulus, 17: 4689
eddy-current coil development, 18: 43773(R) (ORNL-3670(p.122-8))
eddy-current diffusion in flat thick metals, 18: 31736 (HW-79844)
eddy-current methods of, for hot sodium bonding in stainless steel-clad uranium carbide, 19: 20531
eddy-current methods for, of finned fuel cladding, 20: 14703
eddy-current methods for multi-parameter, of structural components, 20: 14708
eddy-current methods for, of reactor tubes during processing and production, 20: 14720
eddy-current nondestructive, engineering drawings for phase-sensitive concentrate for, 19: 20132
eddy-current techniques for, review of, 17: 10815 (TID-16062)
eddy-current, for reactor components, 19: 27740 (UJV-1176/64)

eddy-current, impedance of coils, for, 18: 10249 (CONF-310-3)
elastic body reactions to shocks, spectra for, 17: 21809 (UCRL-7291)
electromagnetic examination of small bores in metal surfaces, 19: 4341 (ACF-3)
electromagnetic inspection of thin-walled tubing, pulsed system for, 18: 25674 (ANL-6728)
encapsulation of uranium in potassium–sodium alloys for, 20: 33940 (DP-MS-66-1)
engineering drawings for stress-strain, of brittle materials, 18: 16187
environment for, process with controlled flowing atmosphere to provide high-purity, 19: 18408
environmental, procedures and standards for, 20: 33475 (SC-4452D(M))
equipment and experiment design for in-pile, 16: 10635
equipment and method for testing thick plates for brittle fracture, 16: 8980
equipment and methods for mechanical evaluation of refractory materials at 4000°F, 16: 16572 (ASD-TR-61-74)
equipment and method for hole detection in sheet materials, 18: 22236(P)
equipment and methods for electron-acoustic and radiometric, 18: 31739
equipment and methods for space electric power systems, 18: 34046(R) (NASA-CR-54041)
equipment and methods for ultrasonic, 19: 13602
equipment and methods for nondestructive, of reactor control fuel, and target elements, 19: 20126 (DPSPU-65-30-11)
equipment and methods for nondestructive, of finned SAP tubing, 20: 14712
equipment and method for, of Zircaloy-2 canning tubes by ultrasonics, 20: 14714
equipment and methods for, of irradiated reactor components, 20: 14719
equipment and methods for comparison of neutron effects on steels, 20: 41504
equipment and optical problems in strain measurement of brittle material, 17: 23963(R) (TID-18612)
equipment and techniques for radiometric, in Japan, 20: 20867
equipment and techniques for, in the USA, 20: 45865
equipment design and development for 6000-ton testing, 18: 8504(T,R) (EURAEC-605)
equipment design for brittle, 16: 12109(R) (ORO-518)
equipment design for bending refractory materials, 17: 3485(R) (RAD-SR-62-219)
equipment design for ultra-short-time creep rupture, 17: 3498 (WADC-TR-59-762(Pt.IV))
equipment design for creep and strain-aging, 17: 30962(R) (ASD-TDR-63-238)
equipment development and evaluation for nondestructive, of coextruded fuel elements, 16: 8974 (HW-64788)
equipment development for eddy-current, 19: 24689 (HW-81780)
equipment for drop-weight bulge testing of high-strength materials, 19: 20462(R) (NRL-6258)
equipment for eddy-current, 17: 34107 (CONF-112-3)
equipment for eddy-current, 19: 33713(P)
equipment for electromagnetic inspection of thin-wall refractory-metal tubing, 19: 20454 (CONF-650212-1)
equipment for evaluating mechanical properties of niobium and niobium alloys, 20: 4299(R) (ORNL-2711)
equipment for experiments on in-reactor mechanical properties, 20: 31785 (ORNL-P-2162)
equipment for fatigue testing, 16: 25606 (TID-15356)
equipment for fuel element thermal shock measurements, 19: 27772 (ACNP-64010)
equipment for gaging of rod-like objects, radiometric, 20: 25371(P)
equipment for hardness measurements at elevated temperatures, 17: 30675 (ORNL-3448)
equipment for high-speed fatigue testing, 17: 29322 (HW-74677)
equipment for high-speed studies of strain rate effects, 19: 9657 (HW-SA-3770)
equipment for high-speed impact tests, explosive, 19: 13600(T) (AWRE-Trans-49)
equipment for high-temperature wires, 19: 44213
equipment for high-temperature tensile, 20: 30875(R) (ANL-7190, pp 143-55)
equipment for hot hardness testing, 19: 18390(R) (GEMP-43A)
equipment for hydrodynamic and thermodynamic, 19: 22494
equipment for impact-shock, 20: 41113
equipment for in-cell measurement of elasticity modulus of irradiated materials, 17: 40987 (UCRL-7173)
equipment for in-reactor, 18: 43778(P)
equipment for inspecting specimens of irradiated pressure vessel steel, 17: 34112 (TRG-Report-170)
equipment for irradiated specimen testing, 16: 10263 (NSF-62-35(5))
equipment for irradiation of stressed steel specimens, 19: 11378(P)
equipment for mapping data from heat-transfer testing of fuel elements, 17: 3290
equipment for measuring thermal stresses, 16: 20811(P)
equipment for measuring physical properties at high temperatures, 17: 29318 (GA-3559)
equipment for measuring tensile properties of brittle materials, 17: 34396 (ASD-TDR-63-245)
equipment for measuring tensile properties, design of medium-speed, 18: 27685
equipment for measuring stress-strain properties of brittle materials at high temperatures, 19: 7909 (TID-21430)
equipment for nondestructively mapping fuel core to cladding heat transfer, 16: 11932
equipment for nondestructive testing of Zircaloy-clad reactor fuel for cladding defects, 18: 14054 (DP-851)
equipment for NPR pipe seam weld evaluation, 18: 22234 (HW-77831)
equipment for radiography of circumferential welds in small-diameter tubes, 20: 7242 (LA-DC-6977)
equipment for radiometric, safety device for, 20: 29515(P)
equipment for reactor fuel core, data recording, 19: 45500 (HW-65756)
equipment for refractory-alloy, 19: 24916(R) (GEMP-334A)
equipment for remote, for hardness, 20: 9126
equipment for tensile testing of irradiated structural materials at high temperatures, 20: 2031
equipment for tensile testing of irradiated materials at low temperatures, 20: 2032
equipment for thermodynamic and hydrodynamic, 19: 22493
equipment for thermodynamic, auxiliary systems for, 19: 22495
equipment for thermodynamic and hydrodynamic, 19: 22496
equipment for thermodynamic, measuring and control systems in, 19: 22513
equipment for tube-leakage, 17: 12449(P)
equipment for, in combined cryogenic and radiation environment, 20: 9122
equipment, rolling stand for testing maritime reactor components, 17: 21896
ether–nitrogen and ether–air explosions in gloved box, 20: 41203 (UCRL-16259)
facilities for, at Riso metallurgical laboratory, 17: 11121
facilities for compression-tensile-shear and irradiation testing at 30° to 540°R, 17: 24
facilities for nondestructive, at Lawrence Radiation Laboratory, 16: 6621
facilities for nondestructive, of irradiated fuel elements, 20: 4118
facilities for pressure-tube, 17: 16740 (HW-76158)
facilities for radiation effects, 17: 18364 (TID-7652(p.201-20))
facilities for 5000°F brittle, 16: 3462 (ORO-461)
facility design for collector targets, 20: 41122
facility for cryogenic in-pile irradiation, 18: 28048 (NP-13980)
facility for in-pile, in 20-Mw swimming-pool reactor, 17: 14909
facility, for reactor control systems, 16: 30037
facility for, for components and materials of sodium-cooled reactors, 19: 13599 (SAN-8002(p.151-75))
facility for, operation of, for sodium-cooled reactor components, 20: 22520(R) (NAA-SR-11805)
fatigue properties of heat-resisting alloys, methods for plastic, 20: 9378(R) (GEMP-54A)
fatigue properties of heat-resistant alloys, experimental procedures for, 20: 27486(R) (GEMP-400A, pp 185-201)
flaw detection using gamma rays, nomogram for, 17: 25521
flaw detection using radioactive magnetic test particles, 17: 30678(P)
flow detection, evaluation of gamma sources for, 17: 327
for nuclear space power systems, 18: 9713 (CONF-375-3)
for nuclear-powered spacecraft, 18: 34247
for satellite applications, use of vacuum chambers in, 16: 31782
for space vehicles, 20: 11520
for Tokai nuclear power station, 18: 37617 (A/CONF.28/P/857)
fracture toughness of irradiated materials, evaluation of double cantilever beam method for, 20: 889(R) (BNWL-120, pp 4.1-59)
fracture toughness of ceramics and metals, effects of geometry on, 20: 12555 (WAPD-T-1828)
fracture toughness of metals, double cantilever beam specimen for, 20: 12972 (BNWL-168)
fracture toughness of low-strength, moderate-toughness steels, method for, 20: 23661 (WERL-8844-11)
fracture toughness testing, use of DCB specimens in, 20: 27576(R) (BNWL-207, pp 4.44-55)
fracture toughness of reactor pressure vessel steels, methods development for, 20: 29700(R) (COO-1477-4)
gamma scanning of hot-rolled ingots before cutting, 20: 43870
gamma sources for, 17: 10818
gas tunnel for, for components of gas-cooled power reactors, 19: 22492
Hall effect devices for metals, 16: 19149 (NP-11650)
hardness, equipment for testing beryllium by impact, 20: 39436
high-rotational-speed techniques for, 16: 24166 (NP-11854)
impact tests on scale model of cask, 17: 36000 (ORNL-TM-629)

in-cell fabrication and testing of irradiated fuel element cladding tensile specimens, 17: 3714
infrared techniques for, 16: 23973 (ANL-6515(p.163-86))
infrared thermal method for nondestructive, 19: 15727 (HW-SA-3379)
inspection of CVTR pressure tubes and thermal baffles during refueling, 18: 15517 (CVNA-199)
instrumentation for in-pile, (E), 19: 11471 (HW-75132)
loops for design of inpile, 19: 45676 (IDO-16871-4)
machining methods in, for fuel elements, 20: 4128
measurement error in nondestructive, program for estimating, 17: 3134 (HW-SA-2801)
measurement of grain size in outer annular region of metal bars by ultrasonics, 17: 32263(P)
measurement of stress-strain properties of brittle materials, development of facility for, 18: 5782(R) (TID-19812)
measurement of Young's modulus, method for, 18: 16186 (WADD-TR-61-72 (Vol.XXIII))
metallography in nondescructive, 19: 46556 (NMI-4997, pp 1-21)
method for magnetic-particle, using radioactive iron oxide paste, 20: 14721(P)
method for measuring fracture toughness of mild steel, development of double cantilever beam, 20: 7241(R) (COO-1477-2)
method for measuring hardness of a fast-traveling metallic workpiece, radiation-reflection, 20: 13054(P)
method for nondestructive, of irradiated fuel elements, 19: 22505(R) (NP-14968)
method for pressure vessel steel, 20: 41444(R) (COO-1477-5)
method for railway sleepers using gamma radiation, nondestructive, 19: 9467(P)
method for residual stress measurement in heavy steel weldments, 19: 42819 (DF65SL-205)
method for shock testing on shakers, 18: 35700 (NAA-SR-Memo-8162(Rev.))
method of, for installed carbon beds, 20: 39017(R) (DP-1053)
method using gamma radiation, nondestructive, 19: 9468(P)
methods and equipment for inspecting sodium bonds in EBR-II fuel elements, 17: 37488 (ANL-6724)
methods development for reactor materials, 18: 32119
methods development for reactor materials, 18: 41987
methods for, combined gamma radiographic and ultrasonic, 16: 30654
methods for crack arrest, 16: 8978
methods for determining radiation effects on reactor pressure vessels, nondestructive, 18: 23780(R) (SWRI-1243-11)
methods for evaluating coated refractory metal sheet, 18: 41926 (MAB-201-M)
methods for explosive cartridges, radiographic, 20: 39334
methods for fatigue crack propagation in high-strength alloys, 20: 33858(R) (AD-634094)
methods for fuel-element, 18: 37353 (A/CONF.28/P/429)
methods for heat-resisting materials, 20: 46207
methods for honeycomb sandwich structures at high temperatures, 20: 9537
methods for irradiated materials, nondestructive, 19: 22507 (ORNL-P-1109)
methods for measuring shift in nil ductility transition temperature, 17: 23496(R) (EURAEC-652)
methods for measuring fracture-toughness of high-strength alloys, 19: 7893 (DMIC-207)
methods for nondestructive, development of, 18: 27751(R) (HW-80284 (p.7.1-18))
methods for nondestructive, of coating-metal bonds, 19: 20127(R) (IITRI-N213-23)
methods for nondestructive, of limits of fault detection of boilers, 20: 23260
methods for pressure vessel steel welds, evaluation of, 18: 16459(T,R) (EURAEC-962)
methods for pressure vessels and welds, 19: 24090(R) (SWRI-1228-56)
methods for pressure vessels, 20: 29389
methods for process control and research, nondestructive, 19: 22508 (ORNL-P-1188)
methods for radiographic flaw detection, 19: 46564
methods for reactor components, nondestructive, 17: 17448
methods for reactor applications, 18: 11376
methods for reactor components, eddy-current, 19: 23996(R) (ORNL-3650(p.1-110))
methods for testing hardened ducts for cables, 18: 33181 (EGG-1183-1019)
methods for tubing, nondestructive pulsed electromagnetic field and radiography, 19: 44587(R) (ANL-7000, pp 3-63)
methods for, development of nondestructive, 19: 35605(R) (ANL-7045 (p.24-48))
methods for, development of nondestructive, 19: 38080(R) (HW-84609)
methods for, development of nondestructive, 19: 36749(R) (HW-84609 (p.7.1-17))
methods for, development of nondestructive, 20: 31670
methods in metallurgy, neutron activation, 19: 36258
methods in neutron radiography, 16: 19148(R) (ANL-6279)
methods of characterizing materials above 1500°C, 19: 9349
methods of eddy-current, development and uses of, 19: 40757
methods of, for determining effects of space environment, evaluation of, 17: 29271
methods of, for refractory metal sheets, 17: 22095 (MAB-192-M)
methods of nondestructive, 17: 1626 (LADC-5354)
methods of nondestructive, 18: 9636 (ANL-6632)
methods of nondestructive, gamma and x-ray attenuation, 19: 42071
methods of, for irradiated ceramic fuel elements, 20: 4130
methods research and development programs of Department of Defense, committee reports 1961 and 1962, 17: 18286 (MAB-187-M(Vol.II))
methods used in environmental tests at Sandia Corporation, standard, 18: 31056 (SC-4452(M))
methods using gamma radiation, 17: 1629
methods using reflected fields, development of pulsed eddy current system for, 16: 31953 (ANL-FGF-353)
mobile unit for nondestructive, design of, 16: 30649 (UCRL-6243)
moduli at high temperatures, ultrasonic method for obtaining dynamic, 17: 34416 (UCRL-7326(Rev.I))
Mössbauer effect in nondestructive, 18: 12326
neutron image intensification system for, development of, 19: 44207(R) (ANL-7000, pp 146-52)
neutron radiographic inspection techniques for, 17: 8380 (ANL-FGF-386)
neutron radiography for, development of fast, 17: 10189 (AD-275297 (p.112-15))
neutron radiography, review of techniques for field use, 17: 30677
neutron radiography for, fundamentals of, 17: 30147
neutron radiography procedure for, 20: 11005(P)
non-destructive, summary of research and development in, 17: 31681(R) (HW-76559)
non-destructive, use of betatrons in, 17: 294
non-destructive, use of cesium-137 in, 17: 10817
nondestructive, amplification effects of lead foils for film exposure to gamma sources in, 18: 8696
nondestructive, characteristics of 15-Mev betatron for, 17: 36001
nondestructive, conference on, 16: 23963 (ANL-6515)
nondestructive, design and operation of 31-Mev betatron for, 17: 32609
nondestructive, design and characteristics of 18-Mev betatron for, 17: 32610
nondestructive, development of techniques, 16: 7306
nondestructive, development of automatic methods for reactor fuel elements, 16: 31321 (HW-65761)
nondestructive, development of, 17: 10184 (AD-275297)
nondestructive, development for reactor materials, 17: 14740 (TID-11295(2nd Ed.))
nondestructive, development of radioisotope techniques for, 17: 10186 (AD-275297(p.29-34))
nondestructive, development of eddy-current, electromagnetic, and ultrasonic methods for, 18: 8606(R) (HW-78388(p.7.1-10))
nondestructive eddy-current, radiographic, and ultrasonic, development in, 17: 10187 (AD-275297(p.51-65))
nondestructive electromagnetic and magnetic methods of, for reactor components, 18: 25678
nondestructive equipment and techniques for measuring nil ductility transition temperature of pressure vessel steels, 18: 10250(R) (SWRI-1296-6-8)
nondestructive equipment for irradiated specimens from Grenoble reactors, 19: 46559(T) (ORNL-tr-749)
nondestructive, evaluation of methods for coating-metal bonds, 16: 29311 (ARF-1213-2)
nondestructive evaluation of metal fatigue, 19: 39151 (AFOSR-65-0981)
nondestructive flaw detection using backscattered radiation, 19: 44214(P)
nondestructive gamma scanning methods of, for irradiated fuel elements, 20: 5093
nondestructive heat transfer, infrared radiometer design for, 17: 14595 (HW-SA-2856)
nondestructive, instrumentation for, for measuring nil ductility transition temperature of irradiated material, 18: 410 (SWRI-1296-6-5)
nondestructive, magnetic tester performance for measuring interlayer air-gaps between steel reinforcing bands of pressure vessels, 16: 2017
nondestructive magnetic permeability methods of measuring thickness of nickel on uranium fuel cores, 20: 25271
nondestructive, measurement of dielectric adequacy, 17: 18771 (TID-18387)
nondestructive measurement of residual stresses in metals and metal structures, 19: 44643 (RSIC-410)
nondestructive methods for fuel elements, 16: 2016
nondestructive methods for reactor tubes, 16: 6618
nondestructive methods for reactor components, 16: 6620

nondestructive method for detecting inhomogeneities in alloys, 16: 17870(P)
nondestructive method for locating inhomogeneities in alloys, 16: 17879(P)
nondestructive methods development for evaluation of ceramic-metal bonds, 17: 6509(R) (ARF-1213-5)
nondestructive method for bulk density measurement in bricks using gamma ray transmission, 17: 12448
nondestructive methods for fuel elements, 17: 22927 (TID-7642 (p.337-59))
nondestructive methods for measuring fuel content in reactor fuel elements, review of, 17: 34106 (CONF-80-4)
nondestructive method for measuring thickness of rolled fuel elements, 17: 34110 (NP-13030)
nondestructive methods for determining nil ductility transition temperature of pressure vessel steels, 17: 34111(R) (SWRI-1296-6-2)
nondestructive methods of, 17: 33426 (TID-7660(p.72-90))
nondestructive methods for crack propagation in pressure vessels subjected to low-cycle fatigue, 17: 37515 (SWRI-5-1276-7-2)
nondestructive, methods for, 18: 3298(R) (ORNL-2221(Pts.1-5)(Del.))
nondestructive, methods development for, 18: 3969(R) (ORNL-3470 (p.94-7))
nondestructive method for bridgewire welds, 18: 9761 (SC-DR-251-63)
nondestructive methods of, technical progress review on, 18: 18338
nondestructive methods of, 18: 21698(R) (ANL-6860)
nondestructive methods for nuclear fuels, review, 18: 23036
nondestructive methods for, 18: 25675(R) (ANL-6868(p.219-28))
nondestructive methods for fast reactor fuel elements, 18: 26893(R) (ANL-6868(p.11-108))
nondestructive methods for reactor components, review, 18: 32976 (A/CONF.28/P/245)
nondestructive methods for reactor fuel elements, 18: 35060(R) (ANL-6904)
nondestructive methods, review, 19: 598
nondestructive methods, development at Hanford, 19: 2526 (HW-SA-3578)
nondestructive methods of, review of development of, 19: 11711
nondestructive methods of, for determining composition of fuel plates, 19: 17378
nondestructive method for reactor fuel elements, 19: 20135(P)
nondestructive methods of, using low-energy gamma and x radiation, 19: 22152
nondestructive methods of, use of americium-241 in, 19: 24901
nondestructive methods for isotope heat sources, 19: 24902 (BNWL-51)
nondestructive method for pipes in hot blooms using gammascope, 19: 28519
nondestructive methods, principles, 19: 36630 (CONF-650517-1)
nondestructive methods for thin-walled tubing and automatic fuel inspection, 19: 38823 (BNWL-SA-97)
nondestructive methods for, development of, 19: 40113(R) (ANL-7071)
nondestructive methods, summary of new developments in, 19: 40989
nondestructive methods for small-diameter refractory-alloy tubing, 19: 44211 (ORNL-P-1543)
nondestructive methods of, development of, 19: 44207(R) (ANL-7000, pp 146-52)
nondestructive method for density determination using gamma sources, 19: 46892(P)
nondestructive methods of, for Kiwi reactor fuel elements, 19: 42146
nondestructive methods of, at Harwell, 20: 4119
nondestructive methods of, for fuels, at Dounreay, 20: 4120
nondestructive methods of, for fuel elements, 20: 4121
nondestructive methods of, for highly radioactive materials, 20: 4122
nondestructive methods of, for fuel rods, 20: 4123
nondestructive methods of, for irradiated fuel, 20: 4124
nondestructive methods for SAP tubing, 20: 5630 (NAA-SR-Memo-11562)
nondestructive methods used at NRTS, 20: 14197
nondestructive methods plutonium-enriched fuel rods, 20: 14707
nondestructive methods for, of reactor pressure vessel, 20: 14709
nondestructive methods for, of pressure vessels during fabrication, 20: 14710
nondestructive methods for, 20: 14711
nondestructive methods for, of thin-walled tubes, 20: 14713
nondestructive methods development at ORNL, 20: 18020(R) (ORNL-3900, pp 2-81)
nondestructive methods of, for pressure vessels, 20: 16617
nondestructive methods for nuclear fuels, 20: 23261
nondestructive method for reactor fuel element burnup determination, development of Compton γ spectrometer for, 20: 35633(R) (NP-16149)
nondestructive methods of, for reactor fuels, 20: 41112 (IITRI-578P11-54)
nondestructive method for surface, neutron device for, 20: 41115(P)
nondestructive methods of, facilities and equipment for, 20: 45867
nondestructive methods for plastic fatigue of pressure vessels, 20: 5894 (SWRI-1228-3-3)
nondestructive methods for reactor fuel elements, 20: 20865
nondestructive methods for, development of, 20: 11260
nondestructive methods for pressure vessels, 20: 1366
nondestructive methods for, photoelastic, 20: 2026 (UCRL-13188)
nondestructive, neutron and ultrasonic-imaging methods of, 18: 3038(R) (ANL-6801)
nondestructive, of reactor pipes, pumps, and valves, 16: 31709
nondestructive, properties of beta-excited x-ray sources for, 18: 518 (IITRI-1209-9)
nondestructive radiometric methods of, for sandwich-type fuel plates, 19: 22511
nondestructive radiological methods of, book, 19: 38829
nondestructive radiometric, method of gage compensation for, 20: 5712(P)
nondestructive remote methods development for Elk River Reactor pressure vessel, 20: 42636(R) (SWRI-1228-4-22)
nondestructive, review of radioisotope uses in, 16: 32014
nondestructive, stray and scattered radiation intensity and energy distributions from 15-Mev betatron in, 18: 8506
nondestructive techniques assessing radiation damage to pressure vessels, 16: 16791
nondestructive techniques for, 16: 4365(T) (TG-230-T256)
nondestructive techniques for detecting metallurgical defects in APM products, 18: 22487 (NAA-SR-8262)
nondestructive testing of fuel elements at Hanford measurement error program for, 19: 9347 (HW-SA-3400)
nondestructive, uses of particle accelerators in, 16: 17162
nondestructive, using 15-Mev betatron, stray and scattered radiation intensity and distributions in, 18: 7366
nondestructive, conference on, 20: 14017 (STI/PUB/105(Vol.2))
nondestructive, development for reactor components and materials, 18: 41933 (TID-11295(3rd Ed.))
nondestructive, development for evaluation of reactor components and materials, 18: 43773(R) (ORNL-3670(p.122-8))
nondestructive, design of portable equipment for neutron radiographic, 20: 7243
nondestructive, development of alpha counter, gamma spectrometer, and x-ray fluorescence method for, 20: 27120 (BNWL-SA-646)
nondestructive, design of gage for, of thin coatings, 20: 45864
nondestructive, electromagnetic pulse method for metal sheet, 19: 28523(P)
nondestructive, gamma-ray image converter for, 19: 24691(P)
nondestructive, methods for radiography in presence of background radiation, 19: 11376
nondestructive, methods for leak-testing reactor fuel elements, 20: 42610(T) (AI-Trans-206)
nondestructive, of HFFR fuel element homogeneity, 18: 17977(R) (ORNL-TM-793)
nondestructive, of welds, 20: 25268 (ORNL-P-2107)
nondestructive, preparation of radiation sources for, 18: 18016
nondestructive, protective measures, 18: 39472
nondestructive, radioactive paramagnetic powder for use in, 19: 15730(P)
nondestructive, review of Hanford programs of, 19: 7690(R) (HW-83608)
nondestructive, summary for ANP program of, 16: 28646(R) (ORNL-2247(Pts.1-5))
nondestructive, use in design development programs, 18: 45183 (SC-R-64-175)
nondestructive, using x-ray-sensitive vidicon, 20: 4999(R) (ORNL-2599)
nondestructive, use of gammagraphy in, 20: 27121 (NP-15961)
nondestructive, using gamma radiography, 20: 46115
of plutonium-base fuel elements, research program, 17: 10249(T,R) (EURAEC-301)
parameter identification in eddy-current, 18: 14055 (HW-79553)
penetration tests of high-strength materials, equipment and method for, 20: 14702 (Y-1490)
photogrammetric techniques for measuring surface contours of irradiated samples, 20: 9123
Poisson's ratio and shear property measurement for brittle materials at high temperatures, 19: 7909 (TID-21430)
precision of nondestructive, of thermoelectric materials, 17: 36477
properties of ultrasonic, 18: 35208
puncture-resistance, of hot-rolled and stainless steels, 20: 43492 (ORNL-TM-1312(Vol.2))
radiation effects on mechanical properties of reactor materials, nondestructive methods development for, 20: 27580(R) (GA-6996)
radiation effects, use of reactor as radiation source in, 19: 12852
radiation, for space applications, 17: 8910
radiation hazards from welding, 20: 606
radiation protection in nondestructive, 17: 14574
radiation protection in, 18: 34223
radiation protection of personnel in gamma and x-ray defectoscopy, evaluation of dosimeters for, 20: 31464
radiation sources in, low-energy gamma and x-ray, 20: 4111 (ORNL-IIC-5)

radiographic and ultrasonic techniques for pressure vessels, 18: 20457(R) (SWRI-1228-19)
radiographic and ultrasonic techniques for steel welds, 18: 39463(R) (EURAEC-663)
radiographic and ultrasonic techniques for steel welds, 18: 39464(R) (EURAEC-762)
radiographic equipment for testing reactor fuel elements, 17: 296(P)
radiographic method for continuously following structural changes in materials, 17: 25429(P)
radiographic methods of on-stream, economics of, 20: 23262
radiographic techniques, 16: 10270
radiographic techniques for heavy welds, betatron, 16: 19151
radiographic techniques in, color, 16: 23975 (ANL-6515(p.203-17))
radiographic techniques for, 16: 30653
radiographic techniques using electron linear accelerator, 16: 6622
radiographic techniques using 8-Mev linear accelerator, 16: 10271
radiographic techniques in, 18: 8507
radiographic techniques for steel welds, 19: 595(R) (EURAEC-1151)
radiographic, design of image intensifier tubes for, 18: 43958
radiographic, using cesium-137 and cobalt-60, 19: 32395
radioisotope techniques, 16: 12042
radioisotope uses review, 16: 13192
radioisotope uses in, 18: 26992
radioisotope uses in, 18: 39721(T) (AEC-tr-6390(p.1-3))
radioisotope uses in, in Switzerland, 18: 41889
radiological, parameters for dynamic methods of, 17: 8384
radiometric coin identification, apparatus for, 19: 38956(P)
radiometric methods of, in textile industry, 19: 30613
radiometric methods of, review of, 19: 42629
reactor design for, selection of Japanese, 19: 24183
reactor design for, 19: 43596
reactor irradiation studies at 4°K, 16: 33571
reactor simulation of radiation and vacuum environments for nuclear-powered space vehicles, 18: 10262
red-heat method for detecting metallurgical bonding defects in stainless steel-clad fuel sheets, 16: 6616 (APEX-143)
reference gage for radiographic inspection of tubing, 17: 25428(P)
reference notches for, use of electrical discharge machining for producing, 20: 4110(R) (ORNL-3870, pp 146-54)
research and development programs at Materials Central, Wright-Patterson AFB, 16: 1292 (WADC-TR-53-373(Suppl.7))
research and development on, 17: 6532 (WADC-TR-53-373(Suppl.9))
research on, review of, 17: 3390(R) (WADC-TR-53-373(Suppl.8))
research program on cryotemperature, radiation, and vacuum effects, 18: 652(R) (FZK-163)
research programs of U. S. Army on, 1962 summary, 17: 33413(R) (NP-12967)
research programs on, 1964 Army Dept. summary, 19: 32048(R) (NP-15073)
scintillation gamma flaw detection for, 18: 39729(T) (AEC-tr-6390 (p.57-65))
shock, computer program for calculating responses of structures mounted on Navy shock machines, 18: 9756 (KAPL-M-LD-9)
shock testing facility, design of pulsed five-million-pound, 19: 45720 (UCRL-12055-T)
shock-testing methods, 18: 4911 (SC-TM-172A-62(73))
shock, uniformity control by shock spectra analysis, 16: 8975 (SCR-267)
shock, control of pulse rise times in explosive-gas, 20: 1566 (SC-DC-65-1545)
space-simulated reactor operation, problems in, 18: 13326
spacing measurements by eddy-current techniques, 16: 13370 (ORNL-TM-129)
specifications for piping and pressure vessels, fabrication and materials, 18: 10258
spectrometer for nondestructive, 19: 26515(R) (NP-14992)
standardization of requirements for nuclear bomb warhead test conditions, 18: 12325
standards for nuclear industry, 16: 21742
statistical analysis of, in brittle materials, (T), 19: 24991 (UCRL-12405)
statistical evaluation of measurements, 17: 8383 (TID-17656)
steel samples for research on brittle fracture of weldments, 20: 41447(R) (EURAEC-1669)
steel welds, evaluation of variables of radiographic, 19: 40753(R) (EURAEC-1378)
strain fatigue in biaxially stressed tubes, method for, 20: 23658 (WCAP-3269-42A)
strength properties of ceramic materials, diametral strength test for, 20: 27409(R) (GEMP-58A)
stress properties of brittle materials to 5200°F, design of facility for determining, 16: 7895 (ORO-461(Rev.))
stress-rupture tests, extrapolation, 16: 8976(T) (CRGM-1034)
stress states in transversely impacted beams, determination using spark cinematography, 16: 4364(T) (SCL-T-390)
surface coating measurements in, preparation of irradiated materials for, 20: 33474 (BNWL-SA-594)
surface crack detection using diamond stylus and strain gage, 19: 44210 (KAPL-M-6484)
survey of nondestructive methods in the U. S., 16: 33274
system for, theory of radiological, 16: 31954 (D2-9518)
temperature measurements on irradiated materials, magnetic method for, 20: 29387
temperature verification systems for, engineering drawings of, 19: 20133
tensile, on alloys irradiated by fast neutrons at low temperatures, 18: 30238(R) (NP-14102)
tensile, on fast-neutron-irradiated alloys, 19: 6364(R) (NP-14443)
theory and techniques of environmental, 17: 29084 (SC-4799(M))
thermostat design for in-pile and out-of-pile, 18: 39567 (IDO-16977 (p.44-54))
ultrasonic apparatus for inspection of tube welds, 16: 2018(P)
ultrasonic apparatus using immersion, 17: 297(P)
ultrasonic apparatus for echo testing of refractory metal discs, 18: 1883(T) (NP-tr-1076)
ultrasonic determination of elastic moduli of high-temperature materials, 19: 44207(R) (ANL-7000, pp 146-52)
ultrasonic equipment for heat-exchanger, engineering drawings for, 18: 27687
ultrasonic imaging equipment and techniques, 17: 30676 (TID-19009)
ultrasonic imaging methods for, review of, 17: 37346 (ANL-6680)
ultrasonic imaging system for, use of television camera tube in, 18: 31738
ultrasonic inspection of NS *Savannah* primary piping for damage, 17: 42340 (BAW-1269)
ultrasonic inspection of tubes for use in fast reactors, 17: 40422(R) (ANL-6784)
ultrasonic inspection of thick steel welds, 18: 43771(R) (EURAEC-882)
ultrasonic inspection, survey of, 19: 18131 (ACF-4)
ultrasonic inspection, properties of, 19: 40989
ultrasonic inspection of steel welds, use of dynamic screen images for, 19: 44209(R) (EURAEC-1422)
ultrasonic method for fuel element cladding, 16: 28542(R) (SRO-68)
ultrasonic method for thickness measurement using Lamb waves, 18: 11551(P)
ultrasonic methods for fatigue testing, 17: 32262 (HW-SA-2927)
ultrasonic radiation images, system for television presentation of, 19: 44207(R) (ANL-7000, pp 146-52)
ultrasonic research and developments at Hanford, 18: 14056 (HW-SA-3307)
ultrasonic system for testing pipes, 17: 3140(P)
ultrasonic techniques for, development of, 17: 11130
ultrasonic techniques for steel welds, 19: 596(R) (EURAEC-1152)
ultrasonic tester for inspecting closures of Hanford fuel elements, 17: 34109 (HW-74625)
ultrasonic testing of thin-wall tubing, performance of equipment for, 18: 41626 (HW-81957)
ultrasonic wave propagation in nondestructive, 18: 45169 (HW-SA-3697)
ultrasonic, of thin-wall tubing, 18: 35699 (HW-81956)
use of accelerators in, for missile and space programs, 17: 10193 (AD-275297(p. 278-85))
use of acoustic emission for, of overstress in reactor pressure systems, 20: 11001 (BNWL-SA-438)
use of activation analysis in nondestructive, 18: 10024
use of bremsstrahlung in flaw detection, 20: 23259(T) (AEC-tr-6466/1, pp 131-4)
use of eddy currents for spacing measurements, 17: 14740 (TID-11295 (2nd Ed.))
use of gamma spectrometry for reactor fuel element testing, 17: 29085 (TID-17097)
use of Lamb waves in nondestructive, 17: 20189 (ANL-6630)
use of Mössbauer effect in nondestructive, 18: 10255
use of Mössbauer effect in nondestructive, 18: 10256
use of neutron radiography in nondestructive, review of, 20: 29627
use of pinch-type electric discharge for, 16: 8829 (ARGMA-TR-2H2R)
use of radiation backscattering in nondestructive, 18: 10257
use of strain gages in, 20: 18880 (Y-RD-5)
use of ultrasonics for detecting nonbond areas, 17: 14740 (TID-11295 (2nd Ed.))
use of, neutron radiography for, of irradiated fuel elements, 19: 11377
vaporization of magnetohydrodynamic materials, 18: 7456 (ASD-TDR-63-4019)
vibration method for measuring elastic constants of small plates, 18: 25679
welded materials, double cantilever beam method for, 20: 9488(R) (BNWL-166, pp 4.8-11)
x-ray equipment for, design of high-energy, 17: 10192 (AD-275297 (p.173-91))
x-ray methods for stress analysis of ultra-high-strength materials,

19: 22515
MATERIALS TESTING ACCELERATOR TARGETS
fabrication of bismuth, for polonium-208 production in Mark I, 18: 20486 (MTA-15)
MATERIALS TESTING ACCELERATORS (MARK III)
feasibility study, 18: 30345 (NAA-SR-130(Del.))
MATERIALS TESTING REACTOR
(Oak Ridge National Laboratory—Reactor Test Station, Arco.)
analyzer for velocity selector, design of 4096-channel, 16: 8904 (IDO-16688)
beryllium damage in, 18: 3379
bibliography on operation and characteristics of, 18: 7971 (VDIT-80)
capsule experiments on thermal conductivity of oxide fuels, in A31SE facility, 18: 45109 (TID-7697(p.2.13.1-29))
coolant maintenance, 18: 38290
core design for Phoenix fuel experiments in, 19: 38081(R) (HW-84609 (p.3.1-16))
cores in Cycle 108 of, kinetics of, (E), 19: 38266(R) (HW-84608(p.31-53))
design and operation of, manual for, 18: 21682 (IDO-16871-2)
development, 16: 2774(R) (IDO-16710)
development, 17: 4331(R) (IDO-16805)
development progress July 1 to September 30, 1961, 16: 9696(R) (IDO-16733)
engineering capabilities of in-pile irradiation facilities, 16: 11314 (APEX-716)
engineering capabilities and procedures for capsule-type irradiations in, 17: 19579 (IDO-16428(Rev.1))
experimental facilities for fissiochemical production of hydrazine, 17: 40850(R) (AGN-AN-1013)
experimental facilities, capsule design and characteristics, 18: 45122 (TID-7697(p.3.5.1-17))
experimental facilities for, fuel irradiation, 20: 42581(R) (ORNL-3875, pp 125-50)
fissiochemical production of hydrazine in loop in, 19: 42525(R) (AGN-8137(Vol.II))
fuel assembly failures in, mechanical, 17: 40406 (IDO-16862)
fuel burnup determination using gamma spectrometry, 20: 21050
fuel element burnup in, ceramic and metallic, 20: 6558(R) (ANL-7115, pp 42-67)
fuel element criticality, 19: 33704
fuel element design and performance, review, 16: 16669
fuel element fabrication for, 17: 4918
fuel element fission break in, 19: 27821 (IDO-17064)
fuel element testing in, 18: 26893(R) (ANL-6868(p.11-108))
fuel element testing in, 18: 36792(R) (HW-81600(p.4.1-28))
fuel element testing in, 19: 10513(R) (HW-81601(p.4.1-30))
fuel element testing for, 20: 14059(R) (IDO-17104)
fuel elements for, cladding with aluminum–boron carbide-clad, (E), 19: 31465 (IDO-17042(p.1-10))
fuel elements of, ultrasonic water-gap measurements in, 20: 14195
fuel irradiation in, irradiation properties of plutonium, (E), 19: 10514 (HW-83431)
fuel irradiation testing in, 20: 2429 (ORNL-3837)
fuel loading schedule for, 18: 40753 (IDO-16977(p.1-20))
fuel recovery, 16: 27534 (ORNL-1169)
fuel recovery by Eurex process using amine solvents, 17: 23436 (RT/CHI(63)-3)
fuel rod rejuvenation, 18: 2161(R) (HW-76302)
fuel test 1T1 for comparison of bare vs. capped thermocouples, 16: 10615 (DC-60-4-84)
fuel testing for ANP development in, 16: 10625 (XDCL-60-6-710)
fuel testing in, calculations for Phoenix, 19: 35612(R) (HW-84384 (p.3.1-11))
graphite pebble bed in, radiation damage to, 19: 32059(R) (IDO-14655)
in-pile loops for, installation and maintenance of pressurized-water, 18: 3339 (TID-7663(p.715-37))
in-pile loop operation in, ANL-2 pressurized-water, 18: 43075 (ANL-6821)
irradiation of capsules at fuel specimen temperatures above 2000°F, 18: 45113 (TID-7697(p.2.17.1-7))
loading analysis (E), 19: 3571
loading, calculation procedure, 16: 12776 (IDO-16661)
materials irradiation testing in, handbook for, 20: 18135 (IDO-17135)
moderator stored energy, 17: 5014
neutron beams from, intensity measurements on, (E), 19: 31217 (IDO-17042(p.11-47))
neutron cross section measurements at, 17: 4036
neutron dosimetry program at, fast, 17: 31056
neutron flux in beam hole with velocity selector, (E), 19: 12849
neutron flux in, measurement of fast, during cycle 146, 16: 18687 (IDO-16678)
neutron flux in the HT-2 beam port of, 17: 14308(R) (AGN-AN-847)
nuclear design characteristics of, with high-exposure (Hx) plutonium fuel, (T), 19: 31605 (HW-84575)
operating and safety experience, 18: 9725 (HN-172(Vols.I&II))
operation, 17: 4330(R) (IDO-16781)
operation and safety experience, 17: 26076
operation, Jan. 1–Mar. 31, 1963, 17: 35254(R) (IDO-16898)
operation of, administrative controls in, 18: 3333 (TID-7663(p.336-52))
operation of, training of personnel for, 18: 3335 (TID-7663(p.386-402))
operation, 9-yr experience, 16: 14341
operation, Oct. 1-Dec. 31, 1963, 18: 40944(R) (IDO-16977)
rabbit facility of, organic capsule irradiations in, 17: 22220 (IDO-16850)
reactivity of, poisoning effects of gadolinium oxide-bearing capsules on, 18: 42913(R) (ACNP-64586)
reactivity perturbations, calculation of localized absorber effects, 16: 3827 (IDO-16029)
reflector damage, 18: 8906
reflector of, beryllium damage in, 17: 36970 (IDO-16899)
shim rod calibrations, 16: 3829 (IDO-16712)
shutdown of, scheduling projects and use of manpower in, 16: 19912 (IDO-16738)
use for Phoenix-fuel power demonstrations, feasibility of, (T), 20: 10350(R) (BNWL-152)
use in neutron physics research, 16: 18424
Materials Testing Reactor Mockup
see Low Intensity Test Reactor
MATERIALS TESTING REACTOR MOCKUP
administration of organization for, 16: 30144 (ORNL-TM-276)
contamination and radiation alarm systems for, 20: 23463 (ORNL-TM-1460)
control rod calibration for, by rod-drop method, 17: 33374 (ORNL-TM-605)
coolant-loss testing during 1951, 52, and 53, 18: 35222 (ORNL-TM-632)
design and utilization of, 16: 30145 (ORNL-TM-279)
design of in-pile loop for thoria-urania slurry tests, 16: 10621 (ORNL-3222)
engineering capabilities of in-pile irradiation facilities, 16: 11314 (APEX-716)
experiments in, general standards guide for, 16: 28602 (ORNL-TM-281)
facilities for, engineering drawings of irradiation, 19: 31615
fuel cycles and loading programming for, 16: 26620 (ORNL-TM-277)
fuel irradiation in, 19: 23996(R) (ORNL-3650(p.1-110))
instrumentation and control systems of, design of, 19: 45680 (ORNL-TM-1190)
instrumentation, design of safety, 16: 4326 (ORNL-TM-77)
neutron flux densities in, 19: 45681 (RCN-36)
neutron flux in, fast, 19: 22818(R) (ORNL-3650(p.221-38))
neutron flux measurements in (E), 19: 996(R) (NRL-Memo-1351)
neutron flux measurements in, fast and thermal, (E), 20: 12501 (ORNL-TM-1163)
operation, 19: 23163(R) (ORNL-3650(p.111-86))
operation of, administration of, 18: 3332 (TID-7663(p.287-335))
operation, safety precautions, and training program, 18: 15645
MATHEMATICAL TABLES
see also Mathematics
arcsin, arccos, and d(arcsin)/dx, 19: 30640 (SC-R-64-1386)
book: *Handbook of Statistical Tables*, 16: 27557
Brillouin functions for half-integer and integer values from 1/2 through 5, 16: 7825 (BNL-702)
Clebsch-Gordan coefficients, 16: 21348 (IFA/FT-40)
Clebsch-Gordan coefficients of SU_3, 19: 16722
conversions between binary shaft position encoder outputs and degree and radian measure, (T), 19: 44580 (AERE-R-4964)
decompositions of even numbers below 2×10^4 into sums of two lucky numbers, 19: 9580 (LA-3106(Vol.II))
definite integrals with modified Bessel functions, 19: 9574 (CERN-64-51)
distribution of the coefficient of coherence for stationary bivariate Gaussian processes, 17: 22082 (SCR-483)
doppler integrals for one-dimensional heat-flow equation, (T), 19: 15983 (TID-21304)
of Bessel functions, 18: 41908 (ORNL-P-310)
of eigenvalues and eigenvectors of Hamiltonian, 17: 605 (TID-15749)
of incomplete gamma function for use in radiobiological problems, 16: 2859(R) (ANL-6398(p.24-35))
of Riemann Zeta function of incomplete mode, (T), 19: 21228 (ANL-6970)
one-sided tolerance limits and variable sampling plans, 17: 23849 (SCR-607)
Racah and Z coefficients, table, 17: 24392 (LAMS-1739)
Racah 12-j coefficients, tables of, 17: 13481 (BLG-142)
roots of 10,000 integers, 17: 20395 (SCR-501)
secant integrals of first and second kinds, 17: 4881
$\sin^2\theta$ vs θ and 2θ in 0.005 degree increments, 18: 24990 (IS-842)
values of Calabro kappa-square reliability statistic, 19: 9583 (UCRL-7920(Rev.I))
Whittaker functions and logarithmic derivatives, 17: 24459
MATHEMATICS

(See also specific problem for application of mathematics; also specific mathematical methods, e.g., Monte Carlo Method, Stochastic Methods, etc.)
see also Bessel Functions
see also Biometry
see also Computers
see also Constants and Conversion Factors
see also Differential Equations
see also Fourier Transforms
see also Games Theory
see also Harmonic Analysis
see also Mathematical Tables
see also Monte Carlo Method
see also Perturbation Theory
see also Racah Coefficients
see also Statistics
see also Topology
Abrikosov's periodic solution for Ginzburg-Landau equations for superconductors, 18: 32706
accumulation functions in, theory and uses of, 18: 36865 (BNL-7192)
addition theorems for spherical wave functions, 16: 20946
adiabatic two-fluid equations in steady state, discontinuous solution for, 16: 8262 (NYO-9763)
algebra of charged systems, 18: 20981
algebra of field operators, reduction of, 17: 19521
algebra of four-state safety devices, 16: 33361 (HW-74100)
algebra of quasilocal observables, representation of symmetry groups on, 20: 7915
algebra of reliability of four-state safety devices, 17: 8696 (HW-SA-2304)
algebraic structures and differential topology, 17: 4878 (TID-17355)
algebraic structure of n-body problem, (T), 19: 41122 (N64-31207)
algebraic systems, partially lattice-ordered groups in, 19: 9576 (IFA-EC/7)
algebras of local observables in quantum field theory, von Neumann, 18: 7570
algorithm for $Av = \lambda Bv$, 20: 43805 (ORNL-3980)
algorithm for calculating elementary symmetrical polynomial, 18: 12533 (JINR-P-1497)
algorithm for inverse matrices, 19: 15981(R) (ORNL-3714(Vol.I)(p.70-7))
algorithm for matrix eigenvalue calculations, convergence of QR, 18: 21713 (NYO-10437)
algorithms for least squares solutions, comparison of, 18: 5723(R) (ORNL-3499(Vol.I)(p.173-6))
amplitudes and subgroups of Lorentz group, relativistic, (T), 19: 36910
analog and digital iterative solution of linear equations, 19: 13863(R) (TID-21413)
analog to digital conversion, errors and precisions in, 17: 32408
analysis of ergodic mechanical systems, 17: 2070(T) (UCRL-Trans-874(L))
analysis of field in space by, 18: 15687 (LAMS-3027)
analysis of hypergeometric functions and values, 19: 9767(R) (IS-900(Sect.P))
analysis of linear systems by calculation of the time domain, computer program for, 17: 32476 (UCRL-10927)
analysis of quadded logic, 19: 20439(R) (COO-614-31)
analysis of time-dependent system failure rates, use of tree diagrams in, 19: 12874 (SC-R-64-1376)
analysis of Visconti integral equations for physical systems, 16: 2630
analysis of wave propagation in inhomogeneous media by invariant bedding, 16: 10676 (SC-4669(RR))
analysis of $x^n dx$ data distributions, method for, 19: 39087
analytic continuation problems in general Jordan domains, 19: 33684 (BNL-8110)
analytic solution of the Percus-Yevick equation of statistical mechanics, 18: 21029
angular momentum transformation matrix elements for crystalline electric field, 18: 14979
antisymmetric multidimensional functions analysis by Slater determinants, 16: 22771
approximation-theory lectures, 19: 9582 (TID-21390)
arithmetic recoding with applications in multiplication and division, 17: 8702 (TID-16821)
asymptotic behavior of Green functions, 17: 28178
asymptotic properties of systems having nonzero total mass, 16: 22793
automorphic functions in, theory for non-compact case, 19: 877
Banach spaces in, Hilbert-Schmidt and nuclear power applications in, 20: 2215
bases for irreducible representations of the unitary group, 17: 36841
Bernstein-polynomial approximation of two-variable functions, 18: 25887
Bessel functions in, calculation of integrals for, 20: 19170 (CEA-R-2927)
Bethe-Salpeter equation for general-mass case, invariant solutions of exact, 17: 24262 (BNL-6324)
biharmonic equations, computer program for solving, 18: 18273 (WAPD-TM-346)
binary additive number theory in, tables of decompositions for, 19: 873 (LA-3106(Vol.I))
binomial distribution, asymptotic covariances for maximum likelihood estimators of parameters of negative, 19: 36901 (K-1643)
block iterative methods for two-cycle matrix equations, 16: 25691 (WAPD-TM-327)
Boltzman equation for hard-sphere gas molecules, differential formalization of, 18: 8932
Boltzmann equation solutions for determination of one-particle velocity distribution functions for dilute gas, 16: 19481 (WIS-OOR-31)
Boltzmann equation in derivation of density of neutral exosphere, 16: 19154 (AFCRL-1038)
Boltzmann equation in, kinetic integral solutions of, 17: 39455
Boltzmann equation, asymptotic theory of, 17: 39456
Boltzmann equation for stationary problems, explicit solution of one-velocity multi-dimensional, 19: 3195
Boltzmann transport equation solution for periodic lattices, 17: 26400
Boltzmann-Vlasov equation in one-dimensional case, existence proof for, 18: 536 (JÜL-126-MA)
Boltzmann's equation solution from inversion by Wild's formula, 18: 16419
Bondi-Metzner group in, representations of generalized, 20: 43807
book: *Applications of Nonlinear Partial Differential Equations in Mathematical Physics*, 20: 2530
book: *Conclusions of Mathematical Sciences*, Vol. 37, 20: 924
book: *Dictionary of Nuclear Science and Techniques* (E/T), 19: 1985
book: *Direct Methods of Qualitative Spectral Analysis of Singular Differential Operators*, 20: 29615
book: *Elements of Hamiltonian Mechanics*, 16: 13836
book: *Elements of Numerical Analysis and Mathematical Processing of Experimental Results*, 17: 27726
book: *Group Theory*, 16: 16639
book: *Group Theory; The Application to Quantum Mechanics*, 18: 11024
book: *Irreducible Representations of the Space Groups*, 19: 32673
book: *Iterative Solution of Elliptic Systems and Applications to the Neutron Diffusion Equations of Reactor Physics*, 20: 22400
book: *Lectures on Lie Group Theory*, 20: 13169
book: *Lie Groups for Physicists*, 20: 14955
book: *Mathematical Methods of Physics*, 18: 32303
book: *Mathematical Models for Computing Electric and Magnetic Fields*, 20: 17161
book: *Matrix Mechanics*, 19: 41568
book: *Methods in Computational Physics. Vol. 2. Quantum Mechanics*, 18: 30645
book: *Non-linear Wave Propagation*, 19: 19319
book: *Nuclear Glossary. English-French, French-English* (E/T), 19: 1984
book: *Numerical Methods of Reactor Analysis*, (E/T), 19: 6849
book: *Physicomathematical Aspects of Biology*, 16: 32687
book: *Symmetry. An Introduction to Group Theory and Its Applications*, 18: 39803
book: *The Optimal Design of Chemical Reactors. A Study in Dynamic Programming*, 16: 13507
book: *The Principles and Applications of Variational Methods* (T), 19: 2713
book: *The Theory of Incomplete Cylindrical Functions and Their Uses*, 19: 42956
Boolean algebra processing for automatic drafting, 19: 8712(R) (SCL-DC-64-130)
Boolean logic combinatorial switching in, duality theorem for, (T), 20: 11198(R) (COO-614-34, Sect. IIIB)
boundary conditions for even-order spherical harmonics method, 17: 26003
boundary conditions for P_N approximation in, variational vacuum, 20: 30116
boundary curves for 4-point function, equations for intersections of, 16: 22894
boundary layer problems, method for solution of, 19: 12714
boundary terms in time-dependent synthesis techniques, 19: 33207
boundary value problems in, singularity of solutions of, 18: 44976
boundary value problems in, convergence of discrete approximations for, (T), 20: 7481 (LA-3386)
bounds on generalized Fourier coefficients, 18: 34020
bounds on matrix elements of bounded operators, 18: 34021
calculating roots by logarithmic and Newton methods, 17: 22080 (ISS-63/2)
calculation of ϵ or $1/\epsilon$, rapidly converging, 18: 30537
calculation of ground-state properties of many-particle systems using reduced density matrices, 17: 33227 (NYO-10431)
calculation of Laplace transforms, numerical, 20: 20201(R) (ANL-7110, pp 311-401)

calculation of least squares, computer program for, 17: 18658 (HW-61265)
calculation of ψ, ϕ, and their derivatives, 20: 5829 (CEA-R-2824)
calculation of thermal stresses, analytical and numerical, 20: 45828 (UCRL-14737)
calculations for stochastic theory of mortality, 17: 33454(R) (ANL-6723 (p.65-6))
calculus in quantum electrodynamics, functional, 20: 24258
calculus of variations in, control optimization by, 18: 35921 (HW-SA-3190)
canonical and Hamiltonian formalism applied to Sturm-Liouville equation, 16: 20942
canonical invariance in Markovian relaxation processes, 18: 16417
Cartesian tensors in spaces with indefinite metric for relativity theory, 20: 11879
Case's solutions for Boltzmann equations applied to half-space problems, 19: 29184
Chamber's solution of the Boltzmann equation, 16: 27555
Chebyshev approximation for nonfulfilled Haar condition, 19: 34617 (HMI-B-40)
Chebyshev polynomial representation of power series, 18: 27853
Chebyshev quadrature on infinite intervals, 17: 7655(R) (ANL-6600)
Christoffel symbols in tensor calculus, computer program for calculating, 19: 36909 (UCRL-14177)
classification of non-compact real simple Lie groups, 20: 738
classroom method for calculation of P_N approximations, 17: 26233
Clebsch-Gordon coefficients in, calculation of, 18: 18756
Clebsch-Gordon coefficients of group D_4, 18: 18757
closed extension of the Laplace operator, 16: 30716 (UCRL-6272)
cluster and product properties of sequences of symmetric functions, 18: 34313
coding objects for self-organization, feasibility of, 17: 16506 (SCTM-251-62(24))
coherence of functions in, (T), 19: 5038
column extractor separating chamber calculations, 17: 17955(T) (TRG-Inf-Ser-278)
combination of probability and relativity in applied, 17: 18921
commutation relations in quantum field theory, normal representation by von Neumann algebras of canonical, 18: 926
compactification of homogeneous spaces and contraction of Lie groups, 18: 16420
complex bucklings in three-group-theory solutions for diffusion equations, 19: 5118
complex Riemannian geometry, used to linearize electron wave equation, 17: 13460
compound decision problems, asymptotic solutions to, 18: 19455 (ANL-6820)
computer method for representing three-dimensional arrays as equations, 18: 35922 (SC-RR-64-546)
computer program for least-squares or rational approximation of decay-type functions, 16: 24086 (ARL-229)
computer program for random matrix generation and diagonalization, 17: 8694 (BNL-760)
computer program for minimization of functions in, 18: 41910(T) (ANL-Trans-60)
computer program for stepwise regression analysis, 20: 23577 (AD-625328)
computer program to fit functions of one variable, 17: 3356 (KAPL-M-WBJ-1)
computer uses in, outline, 19: 46902 (ANL-7050, pp 207-13)
conference on applied, Karlsruhe, Germany, April 16 to 20, 1963, 18: 33209
conformal invariance in, 17: 5572
conjugate straight line method of many-variable function minimization, 17: 23843 (JINR-P-1228)
contraction of Lie groups, 19: 11666
convergence of Balayage method in Hilbert space, 18: 32016 (HMI-B-32)
convergence rates of variational calculations, 18: 30104
convex sets in, applications of, 19: 39082 (TID-22032)
coördinate conditions from variational principles, 16: 24315
coordinate systems for, null flat-space, 18: 2152
coordinate systems in, development for vector problems, 20: 938 (SLAC-46)
coordinates for charged particle trapping in geomagnetic fields, magnetic, 20: 39989
Coulomb Green Function, integral representation for, 17: 4884
Coulomb Green's function for nonrelativistic Schroedinger equation in closed form, 18: 28453
cross sections in P_1-age approximation of transport equation, 20: 2520(R) (IA-920)
crossing symmetry in S-matrix theory, 17: 17034
crystal algebra studies, 17: 1941(R) (NP-12214)
cubic spline curve fitting technique, computer program for, 17: 18665 (Y-1400)
cumulants in statistical, 16: 7230
curve fitting in, computer program for, 20: 35184 (Y-1400(Rev.1))
curve fitting in, Gaussian iterative least square techniques for, 20: 39327 (LA-3362)
curve fitting, integration and interpolation programs for Philco 2000, 18: 24993 (KAPL-M-6139)
data analysis, computer programs for statistical, 17: 8704 (WAPD-R (WB)-1)
data fitting to empirical and semiempirical formulas, computer program for, 20: 9372 (NP-15717)
data smoothing, principles of circuits for, 17: 6505 (TID-17315)
definite integral of product of functions, evaluation method for, 17: 41329 (UCRL-7148-T)
definition of S-matrix for stochastic field theory, 17: 13394
density matrix representations, 17: 5051
derivation of matrix equation from differentiated Schroedinger equation, evaluation of infinite sum by, 17: 12839
derivation of Sommerfeld solution for diffraction of plane, scalar wave by half-plane, 16: 20944
derivation of tracer balance equation for flow measurements, 18: 37349
determination of components of the spin affine connection, 16: 24924
determination of the analytical region, 16: 15761 (JINR-P-225)
determination of the minima-of-functions coordinates by linearization, 16: 16634 (JINR-D-810)
developments at ORNL, 16: 15112(R) (ORNL-3264)
developments at ORNL, 17: 20394(R) (ORNL-3423)
dielectric formulation of many-body problems, 17: 17075
difference algorithm in, convergence of, 20: 16935
difference methods for hydrodynamic equations, 17: 14952 (UCRL-6719-T)
difference schemes in, von Neumann stability criterion for Godunov and Ryabenkii, 19: 874 (NYO-1480-4)
differential equations in, numerical solution to initial valve, (T), 20: 12529 (BNL-8798)
differentials and gradients of functionals, 16: 477 (T) (UCRL-Trans-170)
diffusion functions for small argument, 17: 4883
diffusion problems, condition for reality of eigenvalues for one-group multiregion two-dimensional, 16: 4740 (ORNL-TM-73)
diffusion theory boundary conditions, 19: 5124
dimensional analysis of radioinduced temperature fields in materials, 20: 46230
diophantine inequalities in, generating functions for solving, (T), 20: 12528 (BNL-8694)
Dirichlet series and Toeplitz forms, 18: 16415
discontinuities in integral-transform solutions, 16: 20947
discovery of Mersenne prime M_{9689}, 17: 23851(R) (TID-18629)
discrimination of curves, method of experiment planning for, 19: 39088
dispersion relations, geometrical method of investigating, 17: 18944
dispersion relations for causal transform in, correspondence with one-dimensional dynamical system, 20: 25727
displacements in Lobachevsky space and on the sphere, accidental, 17: 37449 (JINR-P-1281)
distance properties of tree codes, 17: 35260(R) (TID-19135)
distribution of superconducting current, theorem for exterior-interior problem associated with, 17: 12867
distribution theory development and solutions, 18: 4155 (HMI-B-30)
distributions and spaces of sequences in, 17: 9047
distributions and spaces of sequences in, 17: 9048
divergences in unrenormalized theories, 16: 26079 (JINR-P-964)
dose calculations in interstitial radium therapy, 20: 43616
double dispersion approach to Bethe-Salpeter equation, 17: 36567 (BNL-6406)
dynamic linear systems approximation, 19: 23164(R) (SU-SEL-64-103)
dynamic programming and invariant imbedding methods in, 17: 8705
eigenfunction expansions for self-adjoint operators, 19: 26746 (BNL-7963)
eigenfunction expansions and group representations in, 20: 19172 (IC-66/12)
eigenfunctions and values of linear operators, analogies between higher-order analytical and numerical perturbation-iteration determination of, 18: 7118
eigenvalue density for random matrices, relation of zeros of classical polynomials to, 19: 7840
eigenvalue distribution in statistical matrix ensembles, 19: 15984
eigenvalue problem $Tu - \lambda Su = 0$ with nonsymmetric and unbounded operators, 17: 24050 (NYO-10425)
eigenvalues of a matrix, methods for computing, 17: 33226 (NYO-10429)
eigenvalues of random real symmetric matrices, isolated, 18: 34023
eigenvalues of self-adjoint operators, methods for lower bounds to, 19: 7841
eigenvalues of Wilkin's equation, 17: 31386
elementary properties of the Lyapunov mapping $X \to AX + XA^*$, 16: 4431

(ANL-6456)
elliptic equations in, alternating-direction iteration theory for, 19: 29167 (CONF-650505-2)
elliptic integrals of first and second kinds, normal, 18: 17354 (IS-639)
elliptic integrals, tables for evaluation using R function, 19: 38296 (IS-T-14)
elliptic integrals evaluation and reduction, 20: 4476(R) (IS-1200(Sect.P))
elliptic-type integral, evaluation of generalized, 17: 14721
elliptical partial differential equations, approximation method for solution of, 18: 2143 (HMI-B 31)
embedding class two, empty space-times of, 20: 21849
embedding of general-relativistic plane-wave space-times, in pseudo-Euclidean space, 19: 12349
embedding of relativistic Riemannian spaces in pseudo-Euclidean spaces, 19: 11662
embedding of Riemannian manifolds into Euclidean spaces, isometric, 19: 11661
ensemble for random matrices, exponential, (T), 19: 14557
enumeration of linear and connected linear graphs for up to 18 points, 18: 36885 (LADC-5995)
equation for determination of rupture-time curves of metals, 20: 41495(R) (EURAEC-1621)
equation systems in, solutions of nonlinear, 19: 38298 (SC-DC-65-1428)
equation variation by time-independent techniques in, 18: 30101
equations for beam-generated plasma sheaths, 20: 28497(R) (TID-22956, pp 55-147)
equations for branching stochastic processes, 17: 10520(T) (NP-tr-946)
equations for conversion relations, of partially ionized gases, 17: 6786 (DCAS-TDR-62-133)
equations for degenerate fields with twisting rays, 19: 21120
equations for fallout isoconcentration line determination, 20: 16664(R) (UCRL-14534, pp 19-22)
equations for fully ionized two-particle, methods for treating Boltzmann-Maxwell, (T), 19: 41931
equations for nonstationary magnetohydrodynamics problems, Riemann wave analog in, 18: 36728
equations for prediction of particle deposition on ground from elevated source, 20: 41188(R) (BNWL-235-1)
equations for reduction of Feynman diagrams in, 20: 7917
equations in, computer program for complex zeros of arbitrary, 20: 19997 (CLM-R-48)
equations in, computer program for solving real polynomial, 20: 24816 (ANL-6987)
equations in, method for finding extrema of, (T), 20: 734 (JINR-P-1988)
equations in, multiple regression computer program for solving polynomial, 20: 29613 (TRG-Report-1198)
equations in, reduction of minimization of quadratic, (T), 19: 20441 (JINR-P-1958)
equations involving chronological variables, constitutive, (T), 20: 10481 (UCRL-12228)
equations of serial linear systems in, algorithm for, 18: 38712 (SC-R-64-190)
ergodic transformations and convergence theorem for measures, 17: 11068 (TID-15948)
error control in polynomial procedures, 19: 18383(R) (TID-21595)
error determination in one-parameter systems, 19: 42225 (UCRL-12050)
error integrals on real axis, method for calculating, (T), 19: 13867
error propagation in recurrence relations, 18: 8709(R) (TID-19993)
Eulerian variance analysis of turbulence dissipation, 19: 20654(R) (ANL-6938(p.242-51))
evaluations of functions by Chebyshev polynomials, 19: 31461(R) (ANL-7010(p.235-87))
existence of quasi-ergodic systems, proof of, 17: 12584(T) (UCRL-Trans-891(L))
expansion of delta and Green's functions, three-dimensional, 19: 9590
expansion of Fourier-type integrals, 19: 9767(R) (IS-900(Sect.P))
expansion of functions in terms of Chebyshev polynomials, 20: 5828 (AAEC/TM-293)
expansion of integral sine and integral cosine functions, 19: 40944
expansion of positive kernel into bilinear series, theorems for, 18: 8037(T) (SC-T-534)
expansions of Coulomb wave functions in terms of Bessel functions, 16: 29972
exponential moments for radiation propagation calculations, 18: 2142 (EUR-462.f)
expressions for 3-j symbols, 17: 16957 (ORNL-TM-514)
Fano X-coefficients and A-functions for nuclear spectroscopy, 18: 39795 (NASA-TN-D-2454)
Feynman diagram majorization, 16: 10826
Feynman graph calculations, numerical method for, 16: 17959 (JINR-D-821)
Fibonacci sequence in, nonexistence of squares in, 19: 27885 (UCRL-7623)
Fibonacci spaces in, 19: 34619 (LA-DC-6544)
finite difference scheme for Dirichlet and Neumann problems, 17: 8701 (NYO-9760)
finite-part integrals in, generalization of Hadamard's definition of, 18: 11007
flattening procedure for empty cylindrical cavities, 16: 2559 (BNL-5753)
Fock representation of Duffin-Kemmer algebra, 16: 17963
Fokker-Planck equation solution, 17: 29242 (CEA-2275)
for stereoscopic projection of points, 19: 35861 (LA-DC-6520)
form-sheet calculations, computer program for, 19: 36903 (KAPL-M-6456)
formalism for expansion methods in mathematical physics, (T), 19: 16274
formalism for radical of hemiring, 19: 38297 (ORNL-3655)
formalism for treatment of lattice vibrations, 17: 12863
formalism of eigenvalue problems for unitary operator, 18: 7569
formula for Dirichlet L-functions, asymptotic, (T), 19: 20450
formula for fallout distribution calculations, 20: 29407(T) (AEC-tr-6666)
formulas for calculation of rate of particle rainout from nuclear device cloud, 20: 39107 (UCRL-14700)
formulas for three-dimensional pure rotation group, 18: 16421
formulation of disposition-analysis techniques within multivariate analysis, 19: 6237 (SC-R-64-1359)
foundation for empirical science, 20: 39998 (KAPL-3147)
Fourier integrals in, asymptotic expansion of, 18: 26280
Fourier series of Gegenbauer's function, 20: 4476(R) (IS-1200(Sect.P))
Fredholm equation with Green's function kernel, Born approximation technique for determinatal solution of, 18: 2688
frequency response of non-linear systems, 16: 4370 (ONR-9(Vol.3))
function approximations for editing and fitting two-dimensional data, linear computations of, 17: 25678 (UCRL-10734)
function of, approximate reconstruction of one-dimensional, from its moments, 20: 31658 (NAA-SR-Memo-11653)
functional optimization in several dimensions, computer program for, (T), 19: 24911 (KAPL-M-6174)
functions generalization, 16: 18120 (NP-11463(Pt.3)(p.489-500))
functions in, asymptotic representation of spheroidal, 20: 21223 (JINR-P-2564)
functions in, computer programs for special, 20: 31646 (AECL-1744)
functions in, computer programs for special, 20: 31647 (AECL-1744 (Pt.A)(ADD.1))
functions of noncommuting operators, expansions of exponential, 20: 11209
functions related to Doppler coefficients, 17: 1044 (NDA-2014-162)
gauge coordinate group of physical theory, 20: 4656
gauge invariance and correlated boson fields, 17: 6969
gauge invariance of Hartree-Fock approximation, 19: 23275
Gauss-Hermite numerical integration formulas, generalization, 16: 15101 (CDRP-182-103)
Gegenbauer polynomials, sum formula for, 17: 41332
general computational methods of Chebyshev approximation, 16: 22526(T) (AEC-tr-4491)
generalization of Wigner-Racah angular momentum calculus, 17: 13144
generalization of algorithm for interpolation functions, 17: 35079(R) (ANL-6749)
generalization of two-compartment model with random variable flows, 19: 6949(R) (ORNL-3697(p.193-8))
generalization of complex spherical function to four dimensions, 20: 16941
generalized asymptotic series in, derivations of Dirac's function for, 17: 18666
generalized cumulant expansion in, 17: 3365
generalized discrete-continuum radial integrals with Coulomb functions, 20: 41633
generalized oscillator operators, irreducible representations of, 17: 12762 (NYO-10253)
generalized overrelaxation method for operator equations, 17: 8700 (NYO-9192)
generalized path variable method, Boltzmann equations in, 17: 16511
generalized recursive interpolation, 19: 31461(R) (ANL-7010(p.235-87))
generation of analytic complex functions, from values at given points, 16: 33738
generation of biorthogonal polynomials by third-order differential equations, 16: 17964
geodesic correspondence transformation, field interactions from, 18: 32631
geometry of hypercubes, theorems on, 18: 9765 (SC-TM-356-63(91))
Goldstone perturbation expansion, corrections to, 17: 6497 (NP-12304)
graphical method for calculating radiation dose to man from individual radionuclides in fallout, 20: 45891 (UCRL-14922)
Green functions in, relations between, 19: 28728 (IC/65/35)
Green functions, theory and applications of, 18: 34648
Green's distributions for the iterated Klein–Gordon operator, 16: 22764
Green's function for the linearized Vlasov equation, 16: 13502 (NYO-9601)
Green's function in, derivation of biharmonic, 17: 6846

Green's function, decoupling procedure in, 18: 36083
Green's function, representations for nonrelativistic Coulomb, 18: 16416
Green's functions for external fields, 18: 26386 (NP-13958)
Green's functions for related two-point boundary value problems, 19: 44582 (ORNL-3646)
group representation generalization, 16: 15339
group representation in, invariants for the unimodular unitary semisimple Lie, 17: 22084
group theory and modern analysis, 17: 41328 (TID-19502)
group theory in, Clebsch-Gordan series in, 20: 44322
group theory in, symmetry properties of 3j-symbols in, 20: 21730
groups in, algebra of projective representations at finite, 19: 39085
groups in, Casimir operators for U(n) and SU(n), 20: 30147
groups in, combination of internal-symmetry and Lorentz-invariant, 19: 20449
groups in, physical state vector-space representations of noncompact, 20: 31663
groups in, space-time and Galileic, 20: 33768
groups in, unitary representations of pseudo-orthogonal, 20: 14951
Hamiltonian formulation of classical mechanics, treating time as a dynamical variable, 16: 28337
Hankel functions of imaginary argument, tables of spherical, 20: 735 (NRL-6288)
Hankel transforms in, theorem for generalized, 17: 34316
Hausdorff summability methods, theorems, 17: 20398
heat equation solution, continuation in space variable, 19: 14898 (BNL-7850)
Heisenberg nonlinear theory in 5-dimensional space, 16: 15764
Helmholtz wave equation in, solution of, 19: 15988
Hilbert space integrals in, reduction of multiple, 20: 23580
Hilbert spaces in, elementary properties of nested, 20: 26001
Hilbert spaces of generalized functions, type-S, 19: 9585
Hilbert spaces of analytic functions, 20: 736
Hilbert transforms and singular integrals in, method of symmetric pairing for, 19: 26745 (ANL-6988)
hydrodynamics of classical system with Coulomb particle interactions, statistical derivation of, 17: 41611
hypergeometric functions inequalities, 20: 4476(R) (IS-1200(Sect.P))
hypergeometric mean values in, definition of, 20: 4476(R) (IS-1200 (Sect.P))
implicit finite difference schemes for hyperbolic systems, 17: 27722 (NYO-10426)
implicit, numerical solution for 2-dimensional, time-dependent diffusion, 16: 8015
input-output solution of optimal control problems, 20: 4948(R) (TID-22179, pp 85-175)
integer linear programming in combinatorial analysis, (T), 19: 45709 (SC-R-65-963)
integer programming problems in, decomposition of, 20: 14950(R) (COO-614-41)
integral equation representation of multi-compartment system, 17: 38912
integral equations and inequalities for correlation functions in classical fluids, 18: 2432
integral equations and boundary value problems, approximate methods for solving, 19: 34621 (WAPD-T-1764)
integral equations in, iterative methods of resolution of, (T), 20: 4764
integral equations in, numerical solution of singular, 20: 16936
integral inequality of potential theory, 18: 32025
integral of spherical harmonics, tabulation of, 18: 2147 (NP-13311)
integral representation for four-point function, Bergman-Weil-like, 20: 27984
integral transforms in, method for quadrature for Euler, 20: 16937
integrals involving products of G-function and Gauss's hypergeometric function in, 18: 39801
integrals of triple products of associated Legendre functions, 18: 39802
integration of differential equations method for, 19: 45703 (LA-DC-6667)
integration of Egelstaff S-functions, 17: 31681(R) (HW-76559)
integration over a triangle, FORTRAN II for IBM 7090 for, 18: 20090 (CERN-64-32)
integration over function spaces, theories of, 20: 23579
integration rules for rational functions, geometric mean, 18: 19456(R) (ANL-6840)
interpolation procedure for analysis of tabulated data, progressive four-point, 19: 10704 (UCRL-7681)
invariant imbedding of Lorentz algebra in semisimple algebra, 19: 25342
inversion of cyclic matrices, 18: 34019
inversion of large symmetric positive definite matrices, comparison of methods for, 17: 23847 (ORNL-3430)
irreducible representation in a direct product of irreducible representations of SU(3), multiplicity of, 17: 16512
irreducible representations of SU(3), direct product decomposition in, 17: 19527
iteration, calculation of optimum parameters in alternating-direction-implicit, 17: 4880
iteration methods for n space variables in, alternating direction, 18: 539
iterative method for integration and differentiation of multivariable functions, 17: 8703 (TID-17654)
iterative methods for solution of diffusion problems in r-θ geometry, 18: 42609 (TID-20165)
iterative methods for inversion of linear operators and matrices, 19: 26747(R) (COO-614-23)
Kemmer algebra, review, 17: 20953
kinematics of relativistic two-particle system, 17: 713 (NYO-10247)
kinetic equations and integrability condition in many-time formalism, 18: 42156 (MPI/PA/7/64)
Krook equation with electric forces, Green's function for linearized one-dimensional, 17: 21159
Lagrange multiplier problems in, numerical solutions for, (T), 20: 12544 (ORNL-3846)
Lagrangian hydrodynamic equations, numerical solution of one-dimensional, 16: 30557 (UCRL-6267)
Laplace equation in, graphical method for solution of multi-dimensional, 20: 7951
Laplace transform of product of two Whittaker functions, (T), 20: 4293
Laplace's equation, numerical solution of, 17: 39454
least squares analysis, computer program for, 17: 807 (TID-16989)
least squares fit including estimate of error in parameters, computer program for, 16: 10389 (DC-60-1-159)
least squares fitting of planes, method for, 17: 36185 (LADC-5581)
least squares solutions of linear and nonlinear equations in, variational method for, 18: 32020 (MLM-1186)
least-squares computer programs for complicated functions, 18: 39793 (IDO-16977(p.55-72))
Lie-algebra in perturbation theory, 16: 22528
Lie-algebra in reduction of triple product of octets, 17: 14713 (IA-777)
Lie algebra in, special functions for, 20: 19174
Lie algebra of generalized Poincare groups, (T), 19: 43063
Lie algebra representations for mass and momentum operators in combined invariance theories, 20: 7923
Lie algebras in, branching rules and Clebsch-Gordan series for, 20: 2216
Lie algebras, invariants of semisimple compact, 19: 7842
Lie group dynamical formalism, 16: 22805
Lie group representations, explicit constructive determinations for unitary groups SU_n, 18: 2151
Lie group representations, explicit conjugation operation for SU_n, (T), 19: 8263
Lie group representations, canonical classification for tensor operators in SU_n, (T), 19: 8264
Lie group representations, 19: 28731 (NP-14824)
Lie groups, 19: 11665
Lie groups in elementary-particle physics, Casimir operators of, (T), 20: 11609
Lie groups in, canonical realizations of, 20: 16939
Lie groups in, direct products of irreducible representations of SU(n), 20: 15458
Lie groups in, invariants of simple (T), 19: 1410 (NP-14404(p.23-35))
Lie groups in, invariants of semi-simple, 20: 9371 (IC/65/86)
Lie groups in, representations of semisimple, 20: 11721
Lie groups in, structure of Clebsch-Gordan series for semisimple, 20: 32158
Lie groups in, theorem on contraction of, 20: 21227
Lie groups in, unitary irreducible representations of L(1,4), 20: 25801
Lie groups, singular actions of, 16: 29308
Lie groups, power and exponential maps of, 18: 12535
linear matrix equations solutions, 16: 12263
linear velocity-gradient term in time-dependent pair distribution function, 17: 31655
Liouville theorem for variational analysis, general forms of, 20: 5830 (CERN-65-38)
location of Fourier map maxima, computer program for, 17: 36183 (ANL-6699)
logic primitives in, properties of complete sets of, 19: 10702 (UCRL-7652-T)
Lorentz-covariant functions in, analytic continuation of holomorphic, 20: 24162
Low equations in, solution of nonregularized, 18: 11199 (JINR-P-1445)
lower bounds to eigenvalues of self-adjoint operators, truncations in method of intermediate problems for, 16: 3378 (AD-257717)
Mach reflection calculation progress, 16: 9290(R) (NYO-9764)
magnetogasdynamic constant Mach number duct equations, 18: 20839
manipulation via time-shared computer display systems, 17: 26021
many-body problems in, 17: 11482 (NP-12435(Pt.II))
many-body systems in, approach to equilibrium, 18: 22583
mapping function at corners, development of, 19: 45702 (LA-DC-6556)
Markov processes and the H-theorem in, 17: 21203

master equation for ergodic problem, 16: 27556
matrices and vectors in, computer program package for processing, 18: 44019 (K-DP-364)
matrices in, exponential representation of complex Lorentz, 18: 2155
matrices in, normal forms of complex square, 17: 2452
matrices in, algorithms for characteristic roots and vectors of normalizable, 19: 2710
matrices in, combinatorial problems of totally unimodular, 18: 30092 (EUR-1632.f)
matrices in, computer program for inversion of nonsingular square, 18: 34016 (JEN-122-DF/I-38)
matrices in, computer program for manipulation of, 18: 24060 (KAPL-M-6148)
matrices in, correlation functions for eigenvalues of real quaternian, 20: 16938
matrices in, Monte Carlo--Hotelling computer inversion of, 18: 36883 (HW-SA-3193)
matrices in, multiplication of Boolean, 18: 36882 (HW-SA-3170)
matrices in, theory for tensorial, 19: 44584
matrices with non-commutative elements, Hamilton-Cayley theorem for, 20: 24167
matrix decomposition, inherent error analysis in, 19: 39080 (LA-DC-7192)
matrix diagonalization in, numerical computations for random, 17: 32480
matrix element of space group operators, 19: 34623
matrix elements in, invariance hypothesis for hamiltonian, 18: 32026
matrix elements of generators of U_n, normalization coefficients for, 19: 44585
matrix theory applications in reactor physics calculations, 20: 45058
matrix theory, vector products in skew-symmetric, 17: 25676 (TID-18703)
Maxwell's equations involving creation of charge, comparison of generalizations of, 18: 701
Mayer's fugacity series for particle systems with two-body interactions, 18: 2431
mean square discretization error estimation, 17: 3364 (WAPD-T-1531)
mean square error of non-linear function, formula for, 18: 8032(T) (AEC-tr-6246)
measures in dual space of nuclear space, rotationally invariant, 18: 40555
method for constructing solvable Schroedinger potentials, 18: 9237
method for selecting tests, 18: 30093 (EUR-1824.i)
method of calculation of dispersion and induction energies at finite internuclear distances, 16: 9322
methods development for evaluation of functions, 20: 20201(R) (ANL-7110, pp 311-401)
methods development for reactor analysis, synthesis, 20: 46967
methods for inverting large symmetric positive definite matrices, 19: 347(R) (ORNL-3679(p.60-83))
methods for numerical analysis, 19: 26750(R) (NYO-1480-16)
methods for radiological target analysis, 20: 18938 (AD-629784)
methods for reduction of control and programming problems to Bolza problems in the calculus of variations, 17: 18662 (RM-2888-PR)
methods for reduction of crystal texture data to inverse pole figures, 20: 39402 (ORNL-3979)
methods in equation development, 20: 17160
methods of defining limits of uncertainty for complex systems, 18: 2146 (IDO-16925(p.87-93))
methods of least squares, application of, 20: 41408
Milne problem for non-absorbing medium with linearly anisotropic, 16: 31006 (BNL-5151)
Minkowski spaces in, relation between isoberic and, 20: 13615
models for computation of transients in packed tubular chemical reactors, 19: 19734 (UCRL-11757)
models for distribution of radionuclides in organs and tissues, 20: 6719(R) (ORNL-3849, pp 183-213)
models in physical sciences, conference on, 17: 36187
models of linear dynamic systems, 19: 39269(R) (SU-SEL-64-133)
moment of inertia of cladded triflute plane area, 16: 7952 (DC-60-12-141)
moment problem in, theory for, 20: 8487 (ORNL-3694)
moments of sequential decoding computation, 17: 35260(R) (TID-19135)
momentum-space vertex function analyticity properties, 16: 20937
Monte Carlo integration of the Schroedinger equation, 18: 22800
motion of non-conducting sphere through conducting fluid in presence of magnetic field, 16: 30706 (AROD-407:59)
multiple integral evaluation in, saddle-point method for, 18: 44431
non-Abelian gauge fields and Lorentz gauge formulation, 17: 16513
number generators for, Fourier analysis of random, 20: 5833 (ORNL-3866)
number sequences in, generation and testing of random, 19: 26749 (IS-1128)
number theory, theorems for elementary, 19: 42224 (UCRL-12041-T)
numbers in, distribution properties of prime, 18: 32023
numerical approximation to solution of parabolic equations in one space variable, 17: 3363 (WAPD-T-1211)
numerical calculation of Bickley functions, 18: 5722 (KR-55)
numerical computation of temporal development of currents in gas discharge, 17: 14978
numerical estimation of Laplace transforms, 19: 24064(R) (ANL-6997)
numerical integration methods, 19: 31461(R) (ANL-7010(p.235-87))
numerical solution of coupled integro-differential equations, 16: 27553
numerical solutions and uses of the fold integral, 16: 33362 (LA-2729)
numerical solution of coupled partial differential equations, 17: 1808 (KAPL-M-EPS-2)
of isobaric spin space, 17: 40233
of obtaining the infinitesimal operators in the homogeneous Lorentz group, 16: 29306 (PAN-298/VII)
one-center expansion of Meijer's G-function, 18: 40407
operator equations in, extension and solution of nonlinear, (T), 20: 11197(R) (COO-614-34, Sect. IIIA)
operator representation of Lie algebra in, three-dimensional homogeneous rotation group for, 17: 32478
operators in Banach spaces, uses in fixed-point theorems, 20: 14950(R) (COO-614-41)
operators in Banach space, nonlinear P-compact, 20: 35829(R) (COO-614-45)
operators in Hilbert space, 20: 737
operators in quantum field theory, functional differential calculus of, 18: 12534
operators in, formalism of multiplicative, 20: 13165 (JINR-E-2542)
operators in, nonsymmetric linear and unbounded, 19: 20446
operators in, relation between three-dimensional isotropic harmonic oscillator and SU(3) group, 19: 21083
operators in, self-adjointness of, 20: 23581
optimization of finite difference operators, method for, 18: 14349(R) (TID-20238(Paper 2))
orthant probabilities for equicorrelated variables, 17: 14720
orthogonal polynomial angular expansion of the Boltzmann equation, 17: 39961
orthogonality relations between functions and their adjoints, 17: 25680
oscillations of solutions of a nonlinear differential equation, 17: 36186
Padé approximation method, theory of, 19: 34618 (LA-DC-6526)
pairing-force hamiltonian, restricted class of eigenstates of, 17: 15146
parameter search strategy on analog computer, for fitting data to mathematical model, 19: 28735 (TID-21546)
particle-and-force models for calculations in fluid dynamics, 17: 11310 (LA-2806)
peripheral model for inelastic processes, formulation of, 17: 13373
perturbation approach to electrostatic problem for irregularly shaped conductors, technique for complicated boundary-value problems in, 18: 2433
perturbation expansion of Green's functions, 16: 19887 (ANL-6527)
perturbation expansion for Klein-Gordon equation, 19: 8266
phase-space integral evaluation, 18: 10927
photoeffect evaluations by hypergeometric functions F_1 and Φ_1 in two variables, 18: 538
PIC finite difference equations for motion of compressible fluids, effects of nonlinearity on stability properties of, 17: 18262 (LA-2414)
P_N calculations for the classroom, 18: 6151
Poisson equation, solution of two-dimensional, 17: 1156 (NASA-TN-D-1323)
Poisson integral, boundary values of partial derivatives, 16: 4446
polynomial approximation to confluent hypergeometric function, 19: 40943
polynomial equations with coefficients equal to their roots, 19: 27850 (LADC-6477)
polynomial equations in, solutions for, 20: 43806 (ORNL-4008)
polynomial regression, IBM 650 Routine VIII, 16: 7831 (DP-664)
polynomial root-finding techniques in, using computers, 19: 42798 (LA-3355)
polynomials in spacing distribution functions, 17: 11063 (BNL-757)
positive semi-groups on n-dimensional torus, 17: 20392 (JUL-101-PP)
potential equations in, solution of boundary value using boundary coverings, 20: 11200 (HMI-B-41)
potential theory, discrete, 16: 3391
potential theory in, for compact set of continuous functions in Euclidean m-space, 17: 23859
potential theory in, Bergman's integral operator in generalized axially symmetric, 18: 30102
potentials for denumerable Markov chains, 16: 12019
power function for body retention of radionuclides, 20: 6719(R) (ORNL-3849, pp 183-213)
power series in, coefficients in powers of, 19: 14927 (UCRL-7588)
probability in, informational model of, 18: 19512
processing of counting data, 20: 33629 (NAS-NS-3109)
program for evaluation of exponential integral, 16: 10382 (DC-57-1-19)
program models of, for diet selection to minimize weighted radioisotope intake, 17: 39346
projection methods application to calculation of electromagnetic

transitions in nuclei, 18: 13085
properties of nonlinear transformations, 18: 3402 (LADC-5688)
pseudo-random sequences, properties, 16: 4436 (CNEN-88)
quadrature formulas for singular integrals, 18: 534 (JINR-P-1317)
quadrupole moments in static, axially symmetric metrics, 16: 18187
quaternion products and rotation-matrix products in, correspondences between, 20: 7482 (SC-DC-65-1898)
random-walk solutions of partial difference equations for lattices, 17: 16509
random walks on plane net containing internal traps and trapping boundaries, 17: 11907 (TID-15885)
random-matrix theory in, eigenvalue distributions from ensembles in (T), 19: 1054 (PUC-1964-153)
rational approximations for the error function, 16: 4447
recurrence relations for Appell functions in, calculation of matrix elements in angular momentum representation, 17: 16962
recurrence relations algorithms, 19: 18383(R) (TID-21595)
recurrence relations for integrals involving products of Legendre functions, 20: 4294
recursion formulas in, 19: 871 (JINR-P-1739)
reduced matrix element of an irreducible spherical tensor operator for, derivation of, 20: 1329
reduction formula for the five-point function, 17: 20397
refraction arrival amplitude calculations by Zvolinskii's near-front approximation, 17: 11337 (UCRL-7146)
Regge plane, canceling cuts in, 17: 19119
Regge 6-j symbols, recursion relations and simplified expressions for, 17: 22436 (ORNL-3440)
regression analysis on power and exponential functions, computer calculations for, 18: 44026
regula falsi for complex variables, 17: 23845 (LADC-5465)
regula falsi for two variables, convergence of, 17: 23844 (LADC-5460)
relations between N-dimensional Lagrange and Taylor operators, 18: 8708 (SLAC-22)
relativistic Coulomb Green's functions in closed form, 17: 42179
relativistic formulations of Maxwell's equations, 17: 40228
representation of non-compact groups in, using rigged Hilbert spaces, 19: 21081 (ICTP-64/9)
representation theory for nonunitary groups, 17: 37451
representation theory of Lie groups, 19: 15979 (COO-427-44)
representations of homogeneous Lorentz group, irreducible unitary, 19: 16682
representations of G_2 algebra, irreducible, (T), 19: 39594
representations of special unitary group, reduction of, (T), 19: 43074
representations of 2 + 1 Lorentz group, 20: 739
representations of continuous groups, 20: 740
representations of inhomogeneous Lorentz group using contraction of (1 + 4) de Sitter group, 20: 14954
representations of Lorentz group, contraction to representations of Euclidean group, 20: 14953
representations of SL(n,C) groups in, homogeneous functions for unitary, 20: 24137
representations of noncompact rotation group in, generalized spherical functions for, 20: 29614
research, 20: 21224(R) (ORNL-3919)
research in progress under Army Research Office, 20: 40485(R) (AD-63609[A])
research on phase space, 20: 24326 (AD-626056)
research on, Air Force, 19: 48087 (AD-613537)
research program in, AEC, 18: 16413 (TID-4005(Pts.3&4, Rev.2))
research programs, Bureau of Standards annual summary, 16: 13835
research programs, summary for AEC in 1961, 16: 12825
research programs at Hahn-Meitner Institute for Nuclear Research, 1961, 16: 25083 (HMI-B-22)
research programs of U. S. Army on, 1962 summary, 17: 33413(R) (NP-12967)
research programs on, at Hahn-Meitner Institute for Nuclear Research, 17: 37002(R) (HMI-B-26)
research programs at BNL on, July 1962 to July 1963, 18: 7987(R) (BNL-806(p.3-90))
research programs on, Hahn-Meitner Institute for Kernforschung, 1963, 18: 33182(R) (HMI-B-34)
research programs at BNL, July 1963 to July 1964, 19: 23355(R) (BNL-867(p.1-117))
research programs at ORNL, 1964, 19: 22859(R) (ORNL-3766)
research programs on, 1964 Army Dept. summary, 19: 32048(R) (NP-15073)
research programs on, 19: 40396(R) (HMI-B-39)
research programs at ORNL on, 20: 16159(R) (ORNL-3900, pp 150-81)
research programs at BNL on, 20: 19169(R) (BNL-929, pp 106-11)
research programs on, 20: 31165(R) (HMI-B-46)
research programs in India on, 1965–1966, 20: 36539(R) (NP-16171)
research programs on, 20: 41406(R) (IS-1500(Sect. M and C))
research progress in applied, 16: 4430(R) (ANL-6453)
research progress under U. S. Army auspices, 1961, 16: 20043(R) (NP-11537)
research progress at Argonne National Lab., 1961, 17: 7655(R) (ANL-6600)
research progress in, 18: 11550
research progress at ORNL, 18: 14347(R) (ORNL-3567)
restricted three-body problem, asymptotic matching in, 20: 17584
review on invariant imbedding techniques, 19: 15985
Riemann metrics of the plane three-body problem, curvature of, 17: 14966
Riemannian spaces of N dimensions containing Fermi subspaces of $N - 1$ dimensions, 17: 20755
rings of, computer programming from linear ordered, 20: 5831 (EUR-1919.f)
role of Newton's polygon in present development of, 16: 25692(T) (AEC-tr-5139)
roots of n-degree polynomials, IBM-610 program for calculating, 17: 16425 (ISS-62/11)
rotation group in four dimensions, Racah algebra for, 19: 15986
rotation group, Euler theorem for irreducible representations of, 20: 9374
rotation groups in, (n+1)-dimensional Lorentz group from n-dimensional inhomogeneous, 19: 37684
rotation transforms, particle symmetries from 4- and 8-, 18: 30543
rotational system in Lie algebras, scalar invariants of, 19: 9586
S-matrix for one-dimensional Schrödinger equation, 16: 2483 (JINR-D-690)
Schroedinger equation solution, computer program for, 19: 8109
Schroedinger operators in three-dimensional Euclidian space, (T), 20: 1111
second order, formally self-adjoint uniformly elliptic differential operators, closed extensions of, 17: 11072 (UCRL-6648-T)
self-avoiding walks on integral points in Euclidean space, number of, 18: 34312
separability of subsets of a monoid, 19: 15980 (EUR-2186.e)
separation of the rotational coordinates from the N-particle Schroedinger equation, 17: 9818 (WIS-NSF-19)
series analysis, generalization of Schuster test for autocorrelated, 16: 3390(T) (SCL-T-388)
series expansion of determinants and solution of secular equation, 20: 13168
series expansions for Bessel and Legendre functions, asymptotic, 18: 27854
simplification of two-body unitarity relations, 16: 2625 (AFOSR-1176)
singularities of solutions of nonlinear hyperbolic partial differential equations, 18: 20441
solution of Bethe-Salpeter equations, 17: 13340 (JINR-E-1114)
solution of Boltzmann transport equation, 17: 5539
solution of Boolean equation, computer program for, 18: 7117 (EUR-211.f)
solution of diffusion coefficient by diffusion equation and solution for sphere, 17: 12662 (CRRP-1124)
solution of dispersion-type nonlinear integral equations, numerical, 19: 20445
solution of elasticity problems in cylindrical coordinates, 19: 31461(R) (ANL-7010(p.235-87))
solution of exterior boundary value problems for the wave equation, 17: 6503 (TID-14920)
solution of flexure problem of thin plates, 16: 7830 (DC-58-5-47)
solution of hyperbolic equations with constant coefficients, 16: 20943
solution of integral equations, 18: 862(R) (TID-19590)
solution of integral equations, 18: 44027
solution of Laplacian for progressive substitution method, 18: 41911
solution of linear differential equations, use of linear programming in, 16: 20932 (UCRL-10110)
solution of linear integral equations using Padé approximates of perturbation series solution, 18: 2153
solution of linear equations using three-dimensional alternating direction iterative methods, 18: 8710 (WAPD-BT-29(p.81-5))
solution of linear equations with unbounded operators, 19: 20439(R) (COO-614-31)
solution of linear equations with unbounded operators, 19: 26747(R) (COO-614-23)
solution of matrix and operator equations, 19: 13863(R) (TID-21413)
solution of Maxwell's equations for magneto-ionic media with sources, 17: 5530 (AFCRL-62-247)
solution of Milne integral equation for line profiles by power series expansion, 18: 39800
solution of one-group diffusion equation with variable coefficients, 17: 11590 (NP-12368)
solution of Poisson's equation using Fourier analysis, 18: 39805
solution of singular equations, convergence of accelerated iterative method in, 20: 35829(R) (COO-614-45)
solution of time-dependent differential equations, variational formalism for, 20: 41409

solution of transcendental equations by series reversion, 19: 29468(R) (ANL-7017)
solution to nonlinear diffusion equations for semi-infinite media, 16: 13932 (UCRL-6721)
solution to relativistic dispersion relations for photoproduction by Omnès method, 19: 21461
solution to transport equation, 16: 21130(R) (NP-11643)
solutions for coefficients in expansions of powers of power series, (T), 19: 18384 (UCRL-7779)
solutions for empty-space metrics containing geodesic rays, 18: 722
solutions for five-step, three-dimensional random walks, 16: 13086(R) (TID-15262)
solutions for limiting cases in applied systems in, asymptotology for, (T), 19: 47150
solutions for Riccati equations arising in one-dimensional diffusion problems, 16: 27549 (SCR-499)
solutions of Dirichlet problem for mixed-type equation with discontinuous coefficient, 17: 39451 (BNL-6829)
solutions of inexact integral equations, analytic approximation techniques in, 18: 7119
solutions of modified Dirac equation, 16: 21261 (AFOSR-TR-60-172)
solutions of simultaneous linear equations, using MATQ subroutine, 19: 17419 (ORNL-TM-1037)
solutions of the Boltzmann equation, generalized normal, 17: 37453
solutions to Dirac equation with Yukawa potential, 17: 16990
solutions to one-constraint Lagrange-multiplier problem, (T), 19: 18382 (ORNL-3742)
solutions to three-dimensional equation of radiative transport, Fourier techniques for, 17: 712 (NRL-5838)
solvable potentials for dispersion relations, 16: 22728 (NYO-10134)
space and time synthesis by variational method, 17: 9863 (WAPD-T-1534)
spaces in, description of Brouwer, 19: 21078 (AFOSR-64-1380)
spaces of valve functions in semi-norm linear space, 20: 33767
spectral theory of closed operators in Hilbert space determined by Laplace operator and boundary conditions, 16: 30714 (UCRL-6226)
spectrum of Dirichlet singular second order elliptic operators, discreteness criteria for, 17: 23853 (UCRL-10744)
spin-component analysis of single-determinant wave functions, 17: 36842
spin matrix analytic function expansion, method for, 20: 4476(R) (IS-1200(Sect.P))
spinor space equivalence to 4-dimensional Euclidean complex space, 16: 9302
spinors in, intrinsic theory of two-component, 19: 44583
splitting of the Riemann tensor, 17: 5568
stability by Liapunov's direct method, 16: 20948
stability test for sampled data systems, 19: 13863(R) (TID-21413)
stationary Markov processes, 16: 13501 (JÜL-25-PP)
statistical mechanics of moderately dense fluids in, theory of irreversible, 18: 20633 (TID-20512)
statistical theory of electronic energies, computations using, 17: 19227 (TID-18340)
statistical thermodynamics of nonuniform fluids, 17: 12864
studies of equilibrium and nonequilibrium processes, 16: 9558 (NP-11225)
Sturm-Liouville problem, sublinear, 16: 18206
SU(6) symmetry, invariant derivation of, 19: 20448
successive over relaxation factor estimation, 19: 34620 (WAPD-T-1712)
symmetric representation for 3-body problems, 17: 9194 (NP-12384)
symmetrical matrix of 6j symbols, definition, 16: 12350
symmetry groups in, Clebsch-Gordan coefficients of SU_n, 19: 16722
symmetry groups in, Gelfand states and irreducible representations of, 20: 21734
symmetry properties of matrices of summability theory, 20: 3629 (SC-DC-64-288)
symmetry relation in relaxation dispersions, 18: 16567
synthetic method applications to slab geometry problems, 17: 5303 (TID-15405)
synthetic method solution of transport equation, 17: 5302 (TID-15404)
systems of compartments, metric properties of, 18: 22410(R) (UCRL-11184(p.141-9))
Talmi formation and unitary symmetry of oscillators, 19: 10130
Talmi transformation and related formulas in, 20: 21226
techniques in nuclear spectroscopy, 17: 4108
theorem for stochastic methods, limiting, 18: 21734(T) (ORNL-tr-42)
theorem in switching theory, 20: 14950(R) (COO-614-41)
theorems for eigenvalue problems with sublinear operators, 18: 15686 (LADC-5774)
theorems for multicomponent diffusion systems, 16: 3392
theorems for unitary operator construction, 17: 32717(R) (NP-12996(p.29-35))
theory of deterministic and stochastic equations, 19: 11664
theory of dimensional analysis and model testing, 16: 303(T) (AEC-tr-4850)
theory of distributions, 16: 18120 (NP-11463(Pt.3)(p.489-500))
theory of group-theoretical cones, 19: 33697 (SC-R-65-870)
theory of inverse moments, 17: 36182 (AFOSR-62-72)
theory of irreducible representations of simple groups, 18: 39799
theory of irreversible processes in many-particle systems, new method of, 17: 11832 (MATT-106)
theory of irreversible processes, 17: 14951 (TID-18050)
theory of Lie groups, 17: 19525
theory of nearly periodic systems, asymptotic, 16: 32204 (MATT-86)
theory of numbers, use in studies of polymer degradation, 16: 18109 (NP-11463(Pt.2)(p.289-312))
theory of operational equations, variational principles in, 16: 476(T) (UCRL-Trans-169)
theory of transformation matrices, 20: 2604
thin-region integral method discrete quadrature parameters for thin binary slab cells, tables, 17: 398 (ANL-6613)
trace problem, 16: 2119
transfer function synthesis as a ratio of two complex polynomials, 17: 30900 (ANL-6716)
transfer functions, properties of certain classes, 16: 21219
transformational properties of β-matrices, 17: 19164
transformations in curved space-time, generalized covariance for, 19: 11663
transformations of two-dimensional data, 17: 3359 (PPAD-473E)
transport equations, incorporation of error function absorption coefficient in, 16: 21328
transport theory, generalized variational method for neutron, 19: 8383
trinomial expansions in, computer program for calculating, 20: 41407 (ORNL-4004)
two-group diffusion equations for stationary systems, computer numerical solution, 16: 21341
uniqueness of solutions to Boltzmann equation, 17: 25682
unnormalized, computer study of, 20: 11196(TR) (COO-614-34, Sect. IIB)
unrestricted Hartree-Fock method, 18: 5916
use for determination of normalized response of two coupled mass spring systems, 16: 589 (SCR-408)
use of abstract algebra in physics, 19: 34784
use of even approximations in the spherical method, 16: 14244(T) (FTD-TT-61-124)
use of Gaussian function in statistical and quantum mechanical calculations, 18: 30646
use of group theory in nuclear theory, 20: 1236
use of K-factors for reliability evaluation of test programs, 20: 40447 (NAA-SR-11913)
use of Lyapunov's second method for design of adaptive and nonlinear controllers, 16: 3386 (PIBMRI-937-61)
use of method of weighted residuals in solution of neutron diffusion equations, (T), 20: 24302 (GA-6273)
use of Poisson collections in particle diffusion calculations, 18: 20442
uses in radiochemistry, 19: 18038 (CEA-R-2620)
validity of Baker-Hausdorff and Magnus theorems, global, 17: 37452
variant of Bethe-Goldstone wave equation, 16: 31012 (TID-11120)
variational method of solving double exponential by least squares, 19: 14911(R) (MLM-1216)
variational principles for problems in hydrodynamic and hydromagnetic stability, 16: 20945
variational procedure for calculating fast few-group constants, 17: 5298 (KAPL-2220)
vector integral equations, theory, 16: 4438 (D1-82-0051)
vectorial subdivision for spatial integration of cubic-symmetric functions, 19: 18379 (LA-DC-6351)
velocity potential of surface waves on sloping beach, 19: 10708 (UCRL-12185)
vibrations of nonlinear continuous strings in, 17: 2450
virial equations for stability of rotating configurations, higher order, 20: 4295
Vlasov equation integration, 17: 19488
von Karman equations for bending of rectangular plates, iterative solutions of, 18: 28089 (IMM-NYU-322)
von Neumann algebras of local observables in quantum field theory, 18: 2687
vorticity transport equation, solutions, 16: 317 (SC-4640(RR))
wave equations in, hyperspherical harmonics and tensors from three-dimensional, 18: 7579
wave equations, stroboscopic-perturbation technique for nonlinear, 18: 11001
wave function description using S-matrix theory, 16: 9566
wave function expansion by Neumann series, S-matrix representation from, 18: 14985
wave (Laplace) equation, radiation field of pulse solutions of, 16: 29984
weakly positive matrices, 18: 24062
weighted residuals in, choosing weighting functions for, 17: 26006

weighting functions in weighted residual method, selection rule for, 18: 20440 (WAPD-T-1576(Rev.))
Wightman function analyticity, 16: 5650
Wigner distribution function in, application to second virial coefficients, 18: 14986
Yvon approximation method for solution of the Boltzmann equation. root distribution of characteristic polynomials in, 17: 30904
3-spinor applications and properties, 16: 18205

MATING

radiation effects on, of Drosophila, x, 20: 10644
radiation effects on male eye gnat competitiveness in, 20: 38632
radiation effects on screw-worm fly, compared with effects of chemosterilants, 20: 42724
radiation effects on patterns of, in *Ips confusus*, y, 20: 42883
radiation effects on the competitiveness of male *Trogoderma glabrum* during, y, 20: 40673
survey on fertility and assortative, use of, in quantitative genetic studies on human populations, 17: 12097

Matrices

see Reactor Matrices

MATTER

(Theoretical studies only)
alpha-clustering in nuclear, at low density, 17: 34962
alpha clustering in nuclear, (T), 20: 32542
alpha scattering by, energy-loss spectra from, 18: 5994 (NYO-10716)
atomic-beam range-energy relations in, (T), 19: 6822 (HMI-B-37)
behavior at high temperatures and pressures, Thomas-Fermi treatment, (T), 19: 27286 (CEA-R-2603)
beta reactions in, isotope effect in, 18: 32773
binding energy and equilibrium density of nuclear, perturbation theory for, 18: 2878
binding energy of nuclear, corrections to ground-state, 18: 42685
binding energy of nuclear, 18: 42686
binding energy of nuclear, effects of short-range repulsion on, 18: 42687
binding energy of nuclear, (T), 20: 19983
binding energy of nuclear, saturation, 20: 30434
binding energy of nuclear, D-, P-, and S-wave, 20: 42281
binding energy of, two-nuclear potential and, (T), 19: 10365
book: *Antimatter*, 20: 44282
book: *Passage of Charged Particles Through Matter*, 17: 28071
book: *Structure of Matter*, 19: 41829(T)
charged particle absorption by, (E/T), 19: 9886 (NAS-NRC-PUB-1133)
charged particle energy losses in, computer analysis of, (E), 19: 8009 (TID-21338(p.146-67))
charged particle energy losses and ranges in, tables, (E), 19: 8005 (NASA-SP-3013)
charged particle energy losses in, (T), 19: 18902
charged-particle multiple scattering in, 17: 32931
charged particle range-energy relations in, 16: 29592
charged particle reactions with, dE/dx and range energy graphs for, 20: 46601 (UCRL-2426(Vol.2)(1966 Rev.))
charged particle slowing down in, similarity analysis of, (T), 19: 9887 (NAS-NRC-PUB-1133(p.1-16))
charged particle stopping by, (E/T), 19: 9889 (NAS-NRC-PUB-1133 (p.39-47))
charged particle stopping by, shell corrections to, (T), 19: 9890 (NAS-NRC-PUB-1133(p.49-67))
charged particle stopping by, effects of excitation energy on, (E), 19: 9892 (NAS-NRC-PUB-1133(p.99-101))
charged particle slowing down in, problems, (E/T), 19: 9896 (NAS-NRC-PUB-1133(p.281-4))
charged-particle energy losses in, (E), 20: 46312
charged-particle energy losses in thin layers, (T), 20: 46313
charged-particle penetration in, review, 18: 10636
charged-particle range-energy relations in, (E), 19: 9888 (NAS-NRC-PUB-1133(p.17-37))
charged-particle stopping by, computer program for calculations of, 19: 41954 (NP-15338)
composition in a steady universe, relation to energy production, 17: 41687
composition of, and antimatter in universe, 18: 18535 (NP-13715)
compressibility and polarizability of nuclear, (T), 19: 33374
compression of nuclear, neutrino spectra from neutron production in, (T), 20: 8097
conservation principles and structure of, 20: 1039(T)
content of anti-, in vicinity of Tunguska meteor of 1908, 19: 30929
cosmological existence of superdense states of, (T), 19: 12040(T) (UCRL-Trans-1114(L))
creation by gravitational waves, (T), 19: 47136
creation from radio-source and quasi-stellar stars, 20: 23864
creation in the universe, Mach's principle in, 17: 22377
creation of antimatter and, in stars, 16: 9333(T) (FTD-TT-61-314)
creation of primordial, in steady-state universe, 20: 37361
creation rate in universe, Heisenberg uncertainty principle for, 19: 41227
critical point of nuclear, (T), 19: 14217
density matrix for, approximation to Dirac, 18: 10791
density of cosmic, in oscillating world model, 20: 34032
density of, along trajectories of cosmic nuclei, (E), 19: 34927
detection of anti-, optical method for, 19: 20774(T)
dielectric susceptibility of, in states with population inversion, 17: 17374
diffusion coefficients in ternary mixtures, thermal, 17: 31220
diffusion in, iterative analysis of, (T), 19: 12459 (TID-21110)
distribution functions of charged particle systems in equilibrium, 18: 34415
distribution in oscillating universe, (T), 20: 34057
distribution in space of dustlike, cosmological energy equation, (T), 20: 37352
distribution in universe, 20: 27685
distributions of, dynamics and stability of spherically symmetric, 20: 11889
dynamic response of half-infinite bodies of, to explosions in spherical cavities, (T), 19: 6384 (NP-14508)
Einstein equations for electromagnetic fields and incoherent, homogeneous solutions of, 19: 39648
elastic properties of, relativistic theory for, 17: 15003
electric conductivity of strongly compressed, 18: 10568
electric currents in anisotropic, electromagnetic fields from, 18: 40164
electrodynamic properties of magneto-electric, 17: 5126
electrodynamics of moving polarizable media, 18: 28094(R) (TID-20607)
electromagnetic-signal propagation through, distortion effects, 17: 16890
electromagnetic wave scattering by plane layers of turbid, 17: 9014(T)
electromagnetic wave interactions with, review on, (T), 19: 16498
electromagnetic-wave propagation in time-varying medium with square-wave modulation of permittivity, (T), 19: 37206 (SC-R-64-1378)
electron depolarization in infinite, 18: 36275
electron emission by, theory for secondary, 17: 6832
electron energy-loss spectra in, below 2 Mev, 17: 29992
electron inelastic scattering by nuclear, linear response to, (T), 19: 21393
electron range-energy relation in, semi-empirical, 18: 20929
electron range-energy relations in, tables, (E), 19: 8004 (NASA-SP-3012)
electron reactions at 100 kev to 5 Mev, energy losses in, (T), 19: 21423
electron reactions in, at high energies, (T), 19: 41707
element abundances in, at high temperatures, (T), 19: 20762
elementary particle scattering by, optical potentials for, 18: 13098
elementary particle reactions at high energies, diffraction dissociation in, 18: 38137
elementary particle scattering by nuclear, quantum theory of, 19: 5255
energy calculations for dense charged Bose gases, ground-state, 16: 33639
energy difference between normal and superfluid, free-meson lattice model for free, 20: 28213
energy eigenvalues of, calculation by Green's functions, 17: 11357
energy gap and single particle energy in, coupling between, (T), 20: 6311
energy gap in infinite nuclear, 18: 36649
energy gap in nuclear, hard-core potentials in, 17: 34963
energy gap in nuclear, soft-core potentials in, 17: 34964
energy gap in nuclear, 18: 9429
energy gap in nuclear, theory of, 18: 13099
energy gap in nuclear, BCS theory of, 18: 13100
energy levels of, determination from poles of Green's functions, 16: 33622
energy levels of, effects of next-nearest-neighbor distributions on, 17: 15295
energy levels of interacting electron gases in, 19: 1074
energy levels of nuclear, binding energy of ground-state, 17: 26524
energy levels of nuclear, unstable collective modes for ground-state, (T), 19: 33324
energy levels of nuclear, with hard core interaction with neutron excess, (T), 20: 3079
energy levels of systems of bosons, analysis of low-lying, 16: 33711
energy of highly compressed, statistical theory, 16: 1163(T) (UCRL-Trans-722(L))
energy of nuclear, ground-state, 18: 16960
energy release from antimatter in Tunguska meteorite, 20: 9690
entropy at high temperature, effects of electron pair production on, 18: 44841(T)
equation of state at high temperatures and densities, 16: 9300(T) (UCRL-Trans-761(L))
equation of state of, Monte Carlo calculations for hard-sphere interactions, (T), 19: 8007 (NYO-1480-3)
equation of state and thermodynamic properties of, at high pressures and temperatures, 19: 8010 (UCRL-7437)
equation of state of, at supernuclear density, (T), 20: 3016 (NASA-TN-

D-3020)
equation of state at supernuclear density, (T), 20: 15212
equations of state at high pressure and temperature, Thomas-Fermi model for, (T), 19: 30848(R) (UCRL-12473(p.31-63))
evolution of antimatter and, (T), 19: 23250
exchange energy of semi-infinite nuclear, (T), 20: 30395
excitations in nuclear, optical-model description of low-energy, 18: 40582
existence of negative energy and, 19: 23190
fermion energy-loss spectra in, relativistic, 17: 19055
fermion hard-core interactions in low-density, 17: 19327
field theory for, (T), 19: 6578
field theory of, 18: 32664
field theory of, quark, 20: 36068 (IC-66/85)
gamma absorption by, coefficients for, 17: 31307
gamma attenuation by, effects of interfaces on, 17: 35066
gamma backscattering by, effects of surface layers on, 17: 29972
gamma heating of, in and near source regions, (T), 19: 29458
gamma propagation in, investigation using similarity theory, 19: 41958
gamma scattering at 2 to 6 Bev, electron pairs from, (T), 19: 14522 (DESY-64/12)
gravitation equations for space, 20: 44107
gravitational collapse of, in general relativity theory, 20: 34034
gravitational collapse of powdered, oscillatory, 20: 34056
gravitational field of rotating body, Kerr metric in general relativity for, 19: 31111
half life, problems and techniques of determination, 16: 18218
Hartree-Fock state of nuclear, stability of, 19: 21440
heavy-particle cascade in, phenomenological theory for calculation, 16: 13944 (DESY-A2.85)
hyperon (Λ) binding energy in nuclear, 18: 6245
hyperon(Λ) binding energy in nuclear, 18: 40589
interactions of anti-, in atmosphere, (T), 20: 44037
interactions of, with fast neutrons, mechanism of, 17: 12083
interactions of, analysis using thermodynamic Green's functions, (T), 19: 11826 (KFKI-64-2)
interactions with classical gravitational fields, renormalization of, 16: 32198
interactions with radiation, variation-perturbation approach to, 17: 8898
interactions with radiation, elementary processes in, 17: 17156
interactions with electromagnetic waves and particles, Green's functions for, (T), 19: 16263 (USCEC-82-212)
ion diffusion in, heavy, 18: 10637
ion range-energy relations in, (E), 19: 9893 (NAS-NRC-PUB-1133 (p.173-86))
irreversible processes in, 17: 18955
kinetic and scattering properties, relations between, 16: 26440
kinetic theory of, stationary-state, 17: 32766
magnetic field distributions in, computer analysis of, (E), 19: 7838 (UCRL-7880)
magnetic properties of, review, 17: 13174
magnetic properties of, quantum statistical methods for studying, 20: 34864
magnetic resonances in, quantum statistical theory for, 17: 19172
magnetic resonance of, theory of double, 18: 44295
magnetohydrodynamic equations in anisotropic, derivation of, 19: 1066
many-body theory of, Moszkowski and Scott approximation of Brueckner's, 18: 26369
mechanics of, functional averaging method in statistical, 17: 9001
mechanics of, Hilbert-space formulation of classical, 16: 33587
mechanics of superfluid nuclear, statistical, 17: 29604
meson (μ) and (π) absorption and interactions in, (T), 20: 13350
meson (μ) inelastic scattering by nuclear, linear response to, (T), 19: 21393
meson (μ) reactions with, rates for electromagnetic, 18: 40333
meson (π^-) absorption by hydrogenous, (T), 19: 4896 (JINR-P-1816)
meson (π) optical properties in nuclear, low-energy, (T), 20: 22021
meson energy loss straggling in, distribution of, 19: 9894 (NAS-NRC-PUB-1133(p.187-203))
model for nuclear, Fermi gas, 20: 9604
model of finite nuclear, validity of Thomas-Fermi, 20: 2819
motion of, (T), 19: 26951
motion of homogeneous, under gravitation, (T), 19: 20704
muonium chemical reactions with, parameters for, (T), 19: 4052
neutrino gas in superdense, theory of, 17: 31654 (PAN-384/VII)
neutrino motion in superdense, (T), 20: 951 (NP-15517)
neutrino motion in superdense, partial external trajectories of, (T), 20: 19446 (NP-15932)
neutrino reactions at ~500 Mev, 17: 9468
neutron absorption by, shell transmission theory for, 18: 4536 (EANDC-33U(p.161-3))
neutron age and thermalization in, (T), 19: 10221 (GNE/PHYS/64-7)
neutron and photon transport in, theory, (T), 19: 9768 (LAMS-3079)
neutron cross sections of, tables, (E), 19: 8406 (UNC-5090)
neutron detection in, performance of metallic foils for, 19: 826
neutron diffraction by, review of, 17: 5059
neutron diffusion theory and transport theory in, 18: 44713
neutron diffusion in, variational flux-synthesis analysis of, (T), 19: 21638 (CONF-650501-4)
neutron diffusion in, spatial averaging of, (T), 19: 31185 (AP-Note-422)
neutron distribution functions in infinite, in steady state, (T), 19: 8378 (TID-21429)
neutron flux distribution functions in, in cylindrical geometry, 19: 3189 (CRRP-1201)
neutron inelastic scattering by, single-particle effects in, 17: 15095
neutron inelastic scattering by, first-moment calculations of, 18: 40474 (IDO-16977(p.23-43))
neutron moderation in, accuracy of diffusion theory for, (T), 19: 10222 (UCRL-12128)
neutron reactions on, equipment for studying, 17: 15508
neutron resonance absorption by coarse-grained, 17: 31479
neutron resonance effects in, 19: 47542 (ANL-7050, pp 457-70)
neutron s-wave resonances in, (E/T), 19: 45215 (CEA-R-2780)
neutron scattering by, S_n analysis of anisotropic (T), 19: 1536
neutron scattering by, cross sections for inelastic thermal, 19: 47543 (ANL-7050, pp 471-85)
neutron slowing-down in, stochastic analysis of, 17: 13476
neutron slowing-down spectra in discontinuous, 17: 36633
neutron slowing down in hydrogenous, eigenfunction analysis of, (T), 19: 8374 (AE-164)
neutron spectra in homogeneous, computer analysis of, (T), 19: 14468 (RPI-328-18)
neutron thermal diffusion lengths in, iterative calculations of (T), 19: 1534
neutron thermalization in, scattering kernels for, (T), 19: 14467 (PAN-545/IXA)
neutron transmission by, calculation of, 19: 25464
neutron transport in infinite sheets of, 17: 9485
nuclear energy gap in BCS theory, surface effects on, (T), 20: 46682
nuclear reactions in, effects of density and temperature on, 18: 40600
nucleon binding energy in nuclear, 18: 40537
nucleon interactions in superfluid state of nuclear, hamiltonian for strong, 18: 7748
nucleon interactions in nuclear, effective, 18: 42695
nucleon interactions in nuclear, effective, (T), 19: 12564
nucleon interactions in nuclear, three-body, (T), 19: 25527
nucleon interaction boundary condition method for nuclear, 20: 22022
nucleon motion in nuclear, (T), 19: 14545
nucleon potentials in nuclear, soft core, (T), 19: 16934
oscillations and waves in, nonlinear-string model for, 17: 2450
particle absorption by, mathematical analysis of, 17: 15108
particle and quanta scattering by, transport equation solution for anisotropic multiple, (T), 20: 13968
particle interactions with excitations in, photon emission in fast, 17: 37977
particle reactions in, relaxation of nonstationary processes from finite transport velocity of, 20: 39475
particle scattering by, models for many-body, 17: 19101
particle transport in, effects of variations along paths on, (T), 19: 9776 (UCRL-12170)
partition function in, quantum-statistical theory for, 17: 9003
perturbation theory for quantum properties of, 17: 18919
phase states of, at high densities, 18: 7384
phase transformations in, one-dimensional model for shock-induced, (T), 19: 30848(R) (UCRL-12473(p.31-63))
photon absorption by, phonon and photon emission in, (T), 19: 23306
photon absorption by, mathematical analysis of, 17: 15108
photon reactions in, at high energies, (T), 19: 41707
photon reactions with, multiple-boson production in, (T), 19: 20816
physical properties of nuclear, 17: 31393 (CONF-46-6)
positron depolarization in infinite, 18: 36275
positron range-energy relations in, tables, (E), 19: 8004 (NASA-SP-3012)
presence of antimatter in universe, Alfven-Klein hypothesis for, 17: 36384 (ISS-63/30(p.90-100))
production in cosmic explosions, 19: 25137
properties at high density, review, 17: 17650
properties of ground-state nuclear, volume, 17: 22623
properties of ground-state nuclear, surface, 17: 22624
properties of nuclear, uncoupled approximation for, 18: 32834
properties of nuclear, 19: 14308 (BNL-888)
properties of nuclear, off energy shell particle propagators for, (T), 19: 16854 (NP-14792)
properties of nuclear, calculation using boundary-condition model, 20: 30523
properties of nuclear, at high densities, 20: 34592

properties of nuclear, ground-state, (T), 20: 42249
properties of, below nuclear densities, 19: 3254
properties of, in nuclear statistical equilibrium at high densities, (T), 20: 4855
properties with relativistic Fermi energy, 18: 5841(R) (AROD-2800.12)
proton energy loss straggling in, distributions of, 19: 9894 (NAS-NRC-PUB-1133(p.187-203))
proton range-energy relations in, multiple-scattering effects on, (E/T), 19: 9891 (NAS-NRC-PUB-1133(p.69-98))
proton reactions at high energies, process for emission of fast deuterons and very light nuclei in, 17: 21058
proton shielding properties of, calculations of dose, energy, and flux variation factors for, (T), 20: 3250 (NASA-SP-71, pp 493-505)
quantum properties of, having "intermediate" statistics, 17: 633
quantum properties of, exact self-consistent field theory for, 17: 9000
quantum statistical properties of, 17: 2083
quantum statistical properties of, master equations for, 17: 2449
quantum statistical model for evolution to equilibrium in, 17: 14996
quantum statistics of, containing negative-energy particles, 17: 16998
quantum theory in development of, 20: 1045(T)
radiation damage in, cross-section calculations for, 19: 7981 (RISO-84)
radiation effects, introductory survey, 16: 10628
radiation effects on, theory, 17: 16883
radiation effects on, industrial problems posed by, 17: 28946(T) (CEA-tr-A-1308)
radiation effects on, methods for determining, 19: 1021
radiation effects on, review on, 19: 13022
radiation inelastic scattering by time-dependent particle system of, interference in, 20: 23810
radiation reactions with, coherence in models for, (T), 19: 28998
radiation reactions with, pressure broadening of spectral lines from, (T), 20: 21519
radiation transport in, finite difference methods for nonlinear, 20: 6522 (UCRL-12411)
radioinduced damage at low temperatures, facilities for in-pile studies of, (E), 20: 5569 (CONF-650217, pp 108-10)
research on, Stark effect in, 19: 23321
saturation of infinitely extended, and parameters of two-particle interactions, 17: 19517
search for anti-, in cosmic radiation and space, 17: 6915(T)
shock wave interactions with cylindrical cavities in, (T), 19: 20659 (AD-606490)
single-particle energies of superfluid system of nuclear, reference spectrum method of calculating, 17: 38144
sound excitation in nuclear, zero, 18: 24693
space-time properties of, 20: 1042(T)
specific heat of spin systems at negative and positive absolute temperatures, 19: 1172
spectra of disordered, structure in (T), 19: 1183
spectral line widths in, calculation by Green's functions, 17: 11358
spectral representation of Green's function in field theory of, 17: 725
spin wave coherent amplification in, 17: 20722
stability from wave propagation in semi-infinite, 20: 1094
state at high pressures, bibliography, 16: 10678 (UCRL-5926)
statistical mechanics of classical and quantized, 17: 2447
superfluid behavior of, 17: 9574
surface energy of semi-infinite, Hartree-Fock calculations of, (T), 19: 35436
surface properties of, reference-spectrum calculation of, 19: 10359
temperature of nuclear, critical, 17: 24506
tensor of, canonical forms of, (T), 19: 18576
theory of antimatter, 19: 47206
theory of Fermi liquids, with both long- and short-range forces, 16: 33624
theory of Fermi liquids, with both long- and short-range forces, 16: 33625
theory of Fermi liquids for nuclear, 19: 17018
theory of highly compressed, 16: 1169
theory of irreversible processes in, 16: 32206
theory of nearly periodic systems, asymptotic, 16: 32204 (MATT-86)
theory of nuclear, 16: 28316 (NP-11902)
theory of nuclear, 17: 21213
theory of nuclear, two-body correlations in, 20: 42248
theory of, field equations for, 18: 36379
theory of, internal motion in, 18: 11229
theory on anti-, 19: 23449
thermal conductivity of Fermi gases, 16: 32228
thermal radiation transport in, numerical analysis of, (T), 19: 7686 (UCRL-7838)
thermodynamic functions of hard-sphere Fermi gases, near 0°K, 16: 32312
thermodynamic properties of interacting Bose systems, (T), 19: 30848(R) (UCRL-12473(p.31-63))
thermodynamic properties of, research on, 19: 39272(R) (UCRL-12204, pp 27-48)
thermodynamic properties of, research on, (T), 20: 24357(R) (UCRL-14538)
thermodynamic properties at high density and temperature, (T), 20: 34065(T)
thermodynamic properties of, (T), 20: 41513(R) (UCRL-14744, pp 19-36)
transport coefficients for, validity of Kubo formulas for, 17: 31169
transport equations in, quantum theory for (T), 19: 1438
transport of particles and waves in slabs of, spectral theory for, 19: 18559 (ANL-6940)
transport properties of interplanetary, review, 17: 2143
transport properties of, statistical theory for, 17: 6818
transport properties of, quantum-statistical theory for, 17: 9002
transport properties of isotropic, theory, (T), 19: 6382 (ANL-6914)
variational derivation of steady state, 16: 6858
wave propagation in, with nonuniform refractive index, 17: 18985
wave propagation in micro-elastic, plane, 19: 28913 (CNAEM-22)
x ray scattering by amorphous, elimination of Compton components from, 19: 9476 (CONF-640702-3)
x-ray backscattering by, effects of surface layers on, 17: 29972

MATTERHORN PROJECT

see also Stellarators

bibliography on Princeton University Plasma Physics Laboratory reports and publications, 1951 to Nov. 1961, 16: 9499 (MATT-1(3rd Ed.))
developments, October 1 to December 31, 1961, 16: 9500(R) (MATT-Q-17)
research progress on, April 1 to June 30, 1962, 17: 9676(R) (MATT-Q-19)

MCKELVEYITE

composition and occurrence in Green River Formation, Wyoming, 19: 40799

MCR

see Military Compact Reactor

MEA

see Ethanethiol, 2-Amino-

Measurement

see Metrology

MEATS

see also Seafood

analysis for radioinduced aldehydes, 19: 26721
analysis for volatile compounds in irradiated, 20: 39301
carbon-14 content in Norway, 19: 32483
cesium-137 content in caribou, moose, and reindeer, consumed by Alaskan natives, 1962 to 1965, 19: 40780 (BNWL-SA-242)
cesium-137 content of caribou, 19: 44289 (HW-SA-3750)
cesium-137 content in, Finland, 1964, 19: 46587(R) (NYO-3446-3)
cesium-137 content of caribou, effects on radioactivity of diet in Alaska, 20: 10723
cesium-137 content in Alaskan caribou, 20: 23347 (BNWL-SA-572)
cesium-137 content of, in Richland, Washington area, 20: 23298
cesium-137 content in seal, 20: 29053 (NP-15951)
cesium-137 content in Norwegian, 1962 through 1965, 20: 29432
cesium-137 content in caribou and reindeer, Canada, 1965, 20: 33556 (NP-16124)
cesium-137 content in beef, gamma spectrometric measurement of, 20: 35238
cesium-137 content in, method for determining, 20: 35345
cesium-137 content in, importance of monitoring, 20: 37039
cesium-137 content in chicken, 20: 42735
cesium-137 content in reindeer, in Sweden, 20: 42736
cesium-137 content of beef, 1960 through 1962, 18: 10332
Clostridium botulinum incidence in crab, 19: 15958 (CONF-641002 (p.88-93))
consumer acceptance and organoleptic tests on irradiated, 20: 43795
decomposition of carrion, effects of scavenger animals on, 20: 20941 (ORNL-TM-1432)
effects of feeding radiopasteurized, on vitamin metabolism in dogs, 20: 42793
gamma spectra of radiation-processed canned, 20: 7476
iodine-131 losses from fish, effects of cooking on, 20: 6732
phosphorus-32 induced in, by thermal neutron irradiation, 19: 42671
radiation effects on wholesomeness of fish, 19: 32647
radiation effects on salmonellae in, 19: 44557 (NYO-3426-1)
radiation effects on bacterial counts in lobster, 19: 44558(R) (TID-22139)
radiation effects on bacterial counts in scallop, 19: 44558(R) (TID-22139)
radiation effects on bacterial counts in haddock, 19: 44558(R) (TID-22139)
radiation effects on content of free amino acids in beef, γ, 20: 5278
radiation effects on pigments in, 20: 9331 (CONF-651024, pp 88-92)
radiation effects on vitamin B_{12} in, effects of lyophilization on γ, 20: 11185
radiation effects on survival curves of bacteria in crab, γ, 20: 16237

radiation effects on toxoplasma infections in, γ, 20: 19122
radiation effects on organoleptic, chemical, and physical properties of beef at 20 to −196°C, gamma, 20: 29602
radiation effects on heme proteins in, 20: 30999(R) (UCB-34P95-7)
radiation effects on amino acid content of, γ, 20: 31630
radiation effects on stability of fats in, effects of oxygen on, 20: 33351
radiation effects on flavor of beef, review of, 20: 39299
radiation effects on chemical changes in, 20: 39301
radiation effects on microbial flora, organoleptic properties, and storage time of beef and lamb, gamma, 20: 46119
radiation processing of canned ham, effects on bacterial contaminants, 19: 26722
radiation processing of, 19: 26733
radiation processing of canned cured meat products, effects on wholesomeness, 19: 26735
radiation processing of, effects on aldehyde formation, 19: 26721
radiation processing of beef and pork, effects on wholesomeness, 19: 30600(T) (JPRS-29912(p.6-14))
radiation processing of canned beef, effects on wholesomeness, 19: 30615
radiation processing of beef, effects on wholesomeness for rat diets, 19: 36881
radiation processing for extension of storage life, 19: 36883
radiation processing of cooked beef, lamb, pork, and veal, effects on color, 19: 39065
radiation processing of, effects of storage at room temperature on wholesomeness, 19: 46886
radiation processing of, effects of sodium nitrate plus sodium chloride additive on spoilage by *C. botulinum* during refrigerated storage after, 20: 700 (AD-621921)
radiation processing of, effects of fat content, previous cooking, and storage temperature on wholesomeness following, 20: 2203
radiation processing of canned chopped ham, effects on viability of spores of *Clostridium botulinum*, 20: 13134 (AD-625252)
radiation processing of, facility design for, 20: 27374
radioactive contamination of, by fallout, 19: 30401 (CEA-R-2738)
radioactive contamination of beef, from fallout, 19: 32101
radioactivity in caribou, in Alaska, 1964, 20: 10718(R) (BNWL-122, pp 172-5)
radioactivity induced in beef by electron irradiation, 20: 27370 (AD-632360)
radiographic evaluation of live and slaughtered swine, x, 20: 5224
radioinduced chemical changes in, 19: 32642
radioinduced odor in beef, chemical analysis of, 19: 46878 (NP-15455)
radioinduced volatile compounds giving undesirable odors and flavors in, 20: 42973
radiopasteurization of poultry, economic feasibility of salmonellae control by, 19: 44557 (NYO-3426-1)
radiopreservation feasibility in Great Britain, 19: 32636
radiopreservation of, acceptance tests for γ, 20: 14930 (NP-15676)
radiopreservation of, acceptance tests for γ, 20: 14931 (NP-15677)
radiopreservation of, acceptance tests for, 20: 21199
radiopreservation of, use of low temperatures in, 20: 31634
radiopreservation of fish, and resulting effects on microbial assays on refrigerated fillets, 20: 43793
radiopreservation, effects of combining heat treatments with, 19: 32640
radiopreservation, acceptance by military personnel of, 19: 32641
radiosterilization of Salmonella-contaminated, 19: 32647
radiosterilization, Salmonella decontamination by, 19: 32648
radiosterilization, US Army program for, 19: 32653
radiosterilization feasibility, 19: 32653
radiosterilization of, indispensible components of off-flavor in, 20: 7467 (NP-15658)
radiosterilization of crab, bacterial growth after, 20: 14936
radiosterilization of, feasibility of, 20: 41390
sodium-22 content of caribou and reindeer, 19: 44289 (HW-SA-3750)
strontium-90 content in pork, effect of roasting on, 20: 35215
strontium-90 content of, in East Germany from 1961 to 1963, 20: 43538
strontium-90 content in beef, 1960-62, 18: 10332
volatile compounds in irradiated beef, effects of storage at ambient temperatures on, 20: 29589
wholesomeness of irradiated beef fed to rats, 20: 34231
wholesomeness of irradiated chicken and beef, in dog diets, 20: 35232

MECHANICAL BENEFICIATION

equipment for, use of radioisotopes in, 19: 22836
standardization of radiometric separators, 16: 6559

MECHANICAL DRIVES

see also Cams
description of, for producing triangular-wave velocity oscillations for Mössbauer studies, 19: 8404 (TID-21338(p.182-9))
design and operation of, for Mössbauer studies, 20: 21081
design and performance of cam-type, for Mössbauer spectrometers, 20: 21080
design and protection of, for use in vacuum systems, (E), 19: 18136
(UCRL-7830)
design for automatic radioactivity assay of containers, 19: 30589(P)
design for control rods for large graphite reactors, (E), 19: 17204
design for cooling systems of large gas-cooled power reactors, 18: 38268 (A/CONF.28/P/138)
design for Moessbauer spectrometer, (E), 19: 45316
design for package handling in irradiation facilities, 19: 30618(P)
design for pool-type reactor control rods, using watertight electromagnets, 16: 28484(P)
design for positioning fission chambers in MSRE, 18: 28937(R) (ORNL-3578(p.100-21))
design for producing circulatory movement in closed circuits, 19: 24661(P)
design for reactor servicing devices, 16: 28490(P)
design for reactor cooling system pumps, 17: 17414 (HW-SA-2922)
design for shielding doors for accelerators, 19: 23940 (UCRL-11810)
design for sigma motor pump for river samplers, 20: 27247
design of constant-acceleration and constant-velocity, for Mossbauer studies, 17: 13224
design of control-rod, for use through fluid-tight walls, 16: 28503(P)
design of fluid transmissions for, 16: 23800(R) (AD-269399)
design of flywheel drive for reactor cooling systems, (E), 19: 19343 (CEA-R-2517)
design of, for control rods in heterogeneous reactors, 17: 42243(P)
design of, for positioning magnetic beam analyzers, 17: 41202
design of gear sets for multiple film production by vacuum evaporation, 20: 25512 (AERE-R-5097, Paper 5)
design of multiple differential rotary, 18: 5458(P)
design of rack-and-pinion control rod drive, for easy removal, 19: 5416(P)
design of rotary-motion-transmitting device for reactor refueling machine, 17: 40325(P)
design of step-by-step, for reactor control rods, 16: 28477(P)
design of, for rapid occulting and opening of radiation sources, 18: 22213(P)
development of dry-running gears for nuclear power plants, 16: 29078
development of magnetic coupling for, for use in space power transmission systems, 17: 5642(R) (NP-12270)
gear ratios for filament winding machine with three-step transmission system, 19: 19438 (SC-M-65-79)
operation in liquid sodium, 20: 35841(R) (NAA-SR-11900)
pressure seals for reactors, 16: 13189
rotary shaft design with diaphragm seal, 19: 42620(P)
spur gear testing in high-temperature sodium, 20: 46966(R) (NAA-SR-12010)
velocity control in Mössbauer spectrometer, feedback system for, 20: 21079
wear in, tracer technique for measuring pitting, 17: 30190
wear resistance in dry-running, materials and ratings for, 18: 22999

MECHANICAL ENGINEERING

analysis of creep in axisymmetric pressurized copper shells, 20: 39391 (CONF-660629-1)
analysis of deflections and stresses in perforated materials, accuracy of methods for, 17: 24640 (WAPD-BT-28(p.61-75))
analysis of loosely coupled tube sheets, (T), 19: 6020
analysis of the spike phase pulse in two-phase shock tests, 16: 390 (SCTM-316A-60(73))
analysis of threaded joint bellmouthing, 16: 9167 (KAPL-M-JVM-2)
beam vibrations in, effects of water on, 20: 4080 (WAPD-TM-535)
book: *Advanced Bearing Technology*, 18: 13988
book: *Non-Classical Shell Problems*, 19: 24648
book: *Statistical Strength Theory*, 16: 11819(T) (NP-tr-852)
calculation of weight, center-of-gravity, and moment-of-inertia of surfaces of constant lateral cross section, computer program for, 19: 10683 (SCL-DR-64-116)
compensator for leadscrew errors in position transducer, 16: 19147(P)
conference on advanced technology, Univ. of N. Mexico, Nov. 2 and 3, 1962, 17: 30917 (SC-4920(M))
conference on creep, Book (1), 18: 42096
conference on creep, Book (2), 18: 42097
conference on creep, Book (3), 18: 42098
conference on creep, Book (4), 18: 42099
conference on creep, Book (5), 18: 42100
conference on lubrication, Washington, D. C., Oct. 1964, 20: 20834
contamination effects on precision devices, 17: 23458 (ARF-3216-4)
contamination effects on precision devices, 17: 23459(R) (ARF-3216-5)
contour specification in, computer program in, 18: 13372 (SCL-TM-64-26)
design and evaluation of 3-dimensional strain rosettes, 17: 10783 (TID-17773)
design of variable-throw cam, 17: 30658(P)
design optimization in, use of computers in, 16: 20555 (AAEC/E-85)
determination of deflections and stresses in thin cylindrical shells, 16: 7629 (DC-59-7-129)

development of the Positional Tolerance Dimensioning System, 16: 1885 (SCR-431)
disassembly of contaminated parts in AVR Reactor, 18: 31009
drawing dimensioning, positional tolerance method for, 16: 300 (SCR-83A)
drawings, specification of dimensions and tolerances in, 18: 15693 (SC-R-64-105)
elastic body reactions to shocks, spectra for, 17: 21809 (UCRL-7291)
equations of motion for flexible shaft on nonlinear bearings, 18: 3920 (NAA-SR-Memo-8800)
equipment testing, method for pre-test predictions, 16: 10261 (APEX-656)
heat conversion to work, method for direct, 19: 25259(P)
high stress level fatigue theory development, 16: 20805 (ARL-181)
HOT-1 extension to Neumann problem, 20: 4080 (WAPD-TM-535)
machine tool programming, training manual for, 19: 5582 (SCL-DC-64-100 (Vol.I))
machine tool programming, training manual for, 19: 5588 (SCL-DC-64-100(Vol.II))
machine tool programming, reference material for, 19: 5584 (SCL-DC-64-100(Vol.III))
materials problems for elastically reinforced Maxwell bodies, 20: 7219
measurement of system dynamic response, cross correlation techniques for, 18: 5845 (LADC-5876)
notes and specifications issued by Lawrence Radiation Laboratory, index of, 18: 16160 (UCRL-11200(Vol.1))
notes and specifications issued by Lawrence Radiation Laboratory, index of, 19: 32327 (UCRL-11200(Vol.2))
photoelastic instruments for nondestructive stress analyses, 20: 2026 (UCRL-13188)
plane elasticity problems in, numerical solutions for, 16: 29066 (WAPD-256)
problems in, for nuclear power plants, 20: 8432
process start and control procedures, 18: 17357 (SC-DC-64-378)
product design, ground rules for, 17: 18244
program at BNL, July 1963 to July 1964, 19: 24200(R) (BNL-867(p.151-78))
program summary for 1962 at Brookhaven, 17: 12059(R) (BNL-742(p.121-45))
reliability organization, role in design development, 19: 10682 (SC-DC-64-2041)
research programs at BNL, July 1962 to July 1963, 18: 7988(R) (BNL-806(p.125-47))
research progress under U. S. Army auspices, 1961, 16: 20043(R) (NP-11537)
shock spectra for general forcing function, 17: 21809 (UCRL-7291)
solution of a non-axisymmetric surface load problem for circular cylinders, 16: 7828 (DC-58-4-212)
specification guides at HAPO for, 18: 3922 (TID-15245(Rev.))
specification guides at HAPO for, 18: 3923 (TID-15246(Vol.I)(Rev.))
specification guides at HAPO for, 18: 3925 (TID-19753)
strain analysis using moire fringe technique, 20: 1574 (UCRL-13156)
stress in hollow hexagons subjected to external pressure, 16: 9192 (DC-59-4-27)
testing of high-speed gears, 16: 13181 (PWAC-111)
theory of dimensional analysis and model testing, 16: 303(T) (AEC-tr-4850)
tracer applications, survey, 16: 20916
tracer study of critical lubrication areas in machinery, 17: 18252(P)
tracer study of cylinder and piston ring wear, 17: 32226
use of numerical language APT in, 19: 6894 (SCL-R-64-148)

Mechanical Testing
see Materials Testing

MECHANICS
(For studies of the mechanics of specific geometric shapes see also headings of the type: Cylinders, Plates, Rods, Sheets, Shells (Geometry), Spheres, and Tori.)
see also Cylinders
see also Materials Testing
see also Plates
see also Quantum Mechanics
see also Rods
see also Sheets
see also Shells (Geometry)
see also Soil Mechanics
see also Spheres
see also Stress Analysis
see also Structures
see also Tori
see also Wheels
action principle in, variational, (T), 19: 8029
adiabatic invariance for multiple-period equations in (T), 19: 2894
algebraic structure of n-body problem, (T), 19: 41122 (N64-31207)
analysis of ergodic mechanical systems, 17: 2070(T) (UCRL-Trans-874(L))
analysis of forced vibrations in system with viscous friction and Coulomb damping, 16: 4624(T) (SCL-T-389)
analysis of processes in statistical, using Green's functions, (T), 19: 11826 (KFKI-64-2)
analysis of strain energy stored in cylindrical shell from tension wires, 19: 36580 (UCRL-13160(Pt.2))
analysis of tension wire-sphere support structure, 19: 36579 (UCRL-13160(Pt.1))
analysis of three-body problem with two masses equal, 18: 30325
analysis of vibration effects in fluidized-bed calciners, 17: 4368 (IDO-16794)
angular momentum plane in, discontinuities across cuts in complex, 17: 19114
applicability of Schroedinger equation to non-isolated systems, 17: 20602
approaches to equilibrium in dense classical fluids, 16: 13789
approximation of potential energy surfaces, 18: 19488 (TID-20456)
Boltzmann and anti-Boltzmann equation for isolated-system motion, 16: 7836
Boltzmann's equation, derivation of, 18: 24507
book: *Advances in Applied Mechanics. 7.*, 17: 9137
book: *Advances in Applied Mechanics*, Vol. 8, 18: 37814
book: *Electrodynamics of Plasmas Based on Statistical Mechanics, Vol. I, Physical Processes and Mathematical Methods*, 18: 26793
book: *Elements of Hamiltonian Mechanics*, 16: 13836
book: *Classical Dynamics of Particles and Systems*, 20: 7667
book: *Developments in Theoretical and Applied Mechanics*. Vol. 1, 20: 926
book: *Developments in Theoretical and Applied Mechanics*, 20: 45832
book: *Fundamental Problems in Statistical Mechanics*, 16: 20949
book: *Introductory Topics in Theoretical Physics*, 18: 30337
book: *Matrix Mechanics*, 19: 41568
book: *Physics in the Soviet Union*, 16: 14218
book: *Qualitative Methods in the Many-Body Problem*, 16: 9332(T)
book: *Statistical Mechanics of Charged Particles*, 18: 22804
book: *Statistical Mechanics and Dynamics*, 19: 18621
book: *Studies in Statistical Mechanics*. I., 16: 15356
book: *Variational Principles in Dynamics and Quantum Theory*, 17: 9108
calculation of elastic-plastic flow, 18: 2406 (UCRL-7322)
canonical formalism for, 19: 25073
central force problems in statistical, 20: 4488
circulation in relativistic continuum, 19: 11842
cluster expansions in statistical, algebraic structure of, 18: 16412 (CNAEM-14)
cluster formulation of the exact equation for the evolution of a classical many-body system, 17: 38422
cluster-star equations in classical statistical, Möbius formula for inversion of, 19: 39083
cluster-star equations in classical statistical, generating functionals for inversion of, 19: 39084
collision lifetimes in many-body processes, 17: 17030
conference on peaceful uses of atomic energy in, 18: 39720(T) (AEC-tr-6390)
conference on, Karlsruhe, Germany, April 16 to 20, 1963, 18: 33209
conformal transformations for velocities in excess of the velocity of light, 17: 11354
connected-diagram expansion for nonequilibrium systems, 18: 30327
constitutive equations for nonlinear solids in, multiple-time argument material functions with memory in, 19: 969 (UCRL-12039)
construction of invariant scattering amplitudes for arbitrary spin and analytic continuation in total angular momentum, 17: 17035
correlation functionals for particle systems, (T), 19: 14157
coordinates for, complex canonical, 20: 9884
correlation functions in classical statistical, (T), 20: 1082 (COO-720-053)
correlation function in statistical, perturbation method for classical time-dependent pair, 20: 21453
correlation functions in, test field and influence functional methods for multitime, 20: 33971
correlations in evolutionary stochastic point processes, sequent, 18: 36283
coupled systems of linear medium and oscillator, linear decay of, 19: 10144
cylindrical shell deformation under static pressure loadings, 17: 39227
deflection analysis of beams, 17: 26867 (ORNL-TM-557)
derivation of hydrodynamic equations from equations of motion of collective coordinates, 16: 13814
determination of materials behavior from true stress-strain relations, 16: 20806 (NAA-SR-6376)
difference equations of dynamics in hamiltonian form, 19: 41145
differential action principle, 16: 12264
dimensionality of space in, 17: 14987

Dirac formalism in classical, Weyssenhoff model for, 19: 47137
distribution functions in dense classical fluids, evolution, 16: 13790
distribution functions in dense classical fluids, evolution, 16: 13788
distribution of a mutually interacting system of particles, classical, 17: 20634
distribution of charged particles near a charged moving sphere, 16: 9293
Dirac theory of constraints, foliated manifolds in, 20: 33980
distribution functions in statistical, evolution of, 20: 7663
distribution functions for finite-range interactions in statistical, evolution equations for, 20: 7664 (USCEC-83-210)
distribution of the coefficient of coherence for stationary bivariate Gaussian processes, 17: 22082 (SCR-483)
drafting, use of APT geometry program in automatic, 19: 8712(R) (SCL-DC-64-130)
driven classical systems and characteristic functions, 16: 9314
dynamic analysis of lumped-mass systems, using computers, (T), 19: 24213 (SCL-TM-64-110)
dynamic behavior of materials, conference on, 18: 39473
dynamic loading of cylindrical shell, 19: 10691 (SCL-DR-64-113)
dynamic properties of nonlinear string, (T), 19: 48108(T) (ORNL-tr-754)
dynamical systems in, generalized canonical formalism for degenerate, 18: 7353
dynamics of continuous media, perturbation methods for, 18: 44461
dynamics of N-body systems, numerical analysis of, 18: 5851(T) (UCRL-Trans-960(L))
dynamics of nonlinear systems, frequency response characteristics in, 18: 21720 (SC-TM-264-63(15))
dynamics of one-dimensional hard-rod system, (T), 19: 16268
dynamics of rigid cylindrical rotor, analysis of, 18: 6562 (TID-19804)
energy and time as conjugate variables, 17: 20720
energy conservation in relativistic, (T), 19: 12328
energy sharing and ergodicity for nonlinear oscillator systems, 17: 37765
energy sharing and equilibrium for a nonlinear system, 18: 12981
energy state and occupation number fluctuations in, 18: 26411
energy, mass, and momentum in, covariant form of, (T), 20: 9837 (UCRL-14399)
equation in, global master, 18: 28436
equations of motion in nonequilibrium statistical, 19: 44856
equilibrium system, fluctuation-dissipation theorem in classical nonstationary, 18: 26724
exact solutions for one-dimensional n-body problems, 18: 8947
expansion of circular cylindrical tubes under dynamic loads, 17: 4642(T) (UCRL-Trans-876(L))
expansion of universe in Newtonian, (T), 19: 18650
expectation value of physical quantity in disturbed system, 19: 1456
extension of APT computer system to obtain centroids and inertias of surfaces and solids, 17: 32477 (Y-1420)
field theory for classical statistical, one-dimensional oscillator and, 19: 23192
fluctuations of system of anharmonic charged oscillators at negative temperature, Nyquist theorem for, 19: 41537
formalism for collisions of three hard spheres, (T), 19: 8027
formalism for nonequilibrium gas kinetics, 18: 40072
formalism for quantum systems of hard lines, 18: 42477
formulation of classical, treating time as a dynamical variable, 16: 28337
formulation of momentum-space in classical, unified variational, 17: 24130
frequency shift for relativistic oscillator, (T), 19: 18603
fugacity of system of hard-core particles in, lower bound on, 18: 37994
functional averaging method in classical statistical, 17: 9001
gas kinetics in nonequilibrium statistical, 18: 696
gas kinetics in nonequilibrium statistical, 18: 697
gauge invariance in the isobaric model for photoproduction, 17: 13396
gauge transformations and complex space-time for classical fields in, 20: 11373
Gaussian random functions as tool in statistical, 17: 31233
gravitational interactions of 3 bodies, perturbation analysis, 16: 31181
Green function application to Ising ferromagnet model, 17: 9017
Green functions in renormalized theory, nonsymmetric ultraviolet asymptotic expressions for, 17: 20776
Green functions in statistical, 19: 1084
Green's function in, derivation of biharmonic, 17: 6846
Green's functions for finite systems of interacting particles, 18: 42493
Hamiltonian and Lagrangian formalisms in generalized Takahashi transformation, 18: 30631
hamiltonians in classical and quantum, inequivalence of, 19: 32790
identical motion in classical and quantum mechanics, 18: 22788
inelastic continuum theory of dilatating aggregate materials, 19: 18087 (WAPD-TM-421)
infrared divergencies in statistical, of electron plasmas, 17: 21173
interaction matrix element in a shell model, 17: 17217
invariance principles for classical and relavistic point particles in, (T), 19: 47433
invariance properties of extended functional variations in, 16: 33619
invariance properties of extended functional variations in, 16: 33620
invariants, field-theory analogs of, 16: 12020
irreducible representations of SU(3), direct product decomposition in, 17: 19527
Lagrangian formalism in relativistic, 16: 15564
irreversible processes in, (T), 20: 25647
kinetic equation for particle electromagnetic interactions in, anomalous bremsstrahlung in, 20: 36054
Lagrange multiplier problems in, numerical solutions for, (T), 20: 12544 (ORNL-3846)
Lagrange-Euler equations in, (T), 20: 9599 (LA-DC-6559)
lectures on statistical physics, 18: 22582
lever arm problem in, relativistic, (T), 19: 16272
Lie groups in, canonical realizations of, 20: 16939
Liouville equation in, reversibility of, 18: 36104
Liouville theorem in statistical, general forms of, 20: 5830 (CERN-65-38)
Liouville, equation for relativistic motion of charged particles, 18: 42171
Mach's principle, experimental tests, 16: 2639
magnetic resonance and time-dependent temperatures for quantal systems with quasi-equilibrium, 17: 18966
many-body problem in, relativistic equations of motion for, (T), 20: 4766
many-body problem in statistical, variational principles for, 20: 42074
many-body systems in, approach to equilibrium, 18: 22583
many-body systems in classical, eigenfunctions of Liouville operator in, 20: 19280
Markov processes and the H-theorem in, 17: 21203
matrix elements in, invariance hypothesis for hamiltonian, 18: 32026
Mayer's fugacity series for particle systems with two-body interactions, 18: 2431
mixture theories applied to systems of rigid spheres, 16: 19466 (LA-2667)
moment distribution in circular plate with a ring of holes, 16: 31700 (WAPD-T-1145)
momentum conservation equations for variable-mass systems, 16: 29498 (WAPD-T-1344)
motion in, conservation of conditionally periodic, 19: 32668 (JINR-P-2132)
motion in, relativity of uniform rotational, 18: 42487
motion of rigid bodies, analysis of, 18: 44302
motion of unit mass about a slowly varying central force, adiabatic invariance in elliptic, 18: 10634
Newtonian force at long range, inverse square law of, 18: 32661
nonlinear systems analogy to classical, 16: 609
normal products in statistical, 18: 44636
of interacting particles, statistical, 16: 2377
operator representation of Lie algebra in classical, three-dimensional homogeneous rotation group for, 17: 32478
oscillators in, statistics of systems of coupled, 19: 21089
pair distribution function in statistical, Percus-Yevick equation for, 18: 21029
parameters in statistical, power-series expansion for, 20: 17527
particle collisions in relativistic, energy conservation in, 20: 19275
particle dynamics in classical relativistic, spinning, 17: 41778
particle exchange between two initially isolated systems, solution of two Master equations for, 17: 22395
particle interactions in, asymptotic form of structure function for real systems of, 17: 20693
particle interactions in classical relativistic, conservation laws for point-, 20: 15154
partition functions in statistical, analytical method for, 18: 16487(T) (UCRL-Trans-1030(L))
partition functions in classical statistical, 18: 22573
pendulum kinetics in, for gradually shortened suspension, 17: 24081
periodic solutions in restricted problem of three bodies, 17: 13179(T)
periodic solutions in restricted three-body problem, 17: 13184(T)
perturbation method for treating ensemble averages in nonequilibrium statistical, 19: 41155
perturbation theory in classical, 17: 29474
plasmoid existence in relativistic systems, denial of, 17: 16829
Poincare groups in, classical representations of restricted, 17: 34596
potential distribution method in, 18: 8934
principles of celestial, 17: 7674
principles of classical dynamics, 17: 16786 (NYO-10250)
properties of Hilbert-space formulation of classical, 16: 33587
quantization of Dirac Hamiltonian, 19: 25402
quantum mechanics, correlations with classical, (T), 19: 47432
reciprocity relation for strongly coupled systems, validity of Onsager's, 17: 39757
relation to quantum mechanics, Lie group dynamical formalism for, 16: 22805

relativistic dynamics of systems of particles, 18: 40057
relativistic theory of elastic properties, 17: 15003
renormalization in equilibrium statistical, for normal and superfluid systems, (T), 19: 18601
representation theory for, 20: 33972
research programs, Bureau of Standards annual summary, 16: 13835
research programs of U. S. Army on, 1962 summary, 17: 33413(R) (NP-12967)
resolution of Fokker-Planck equation using Campbell theorems, 17: 20674
response of linear damped lumped spring-mass systems, transfer function formalism for transient, 19: 45710 (SC-TM-64-1772)
response of one-degree-of-freedom system to shock pulses, 19: 11308 (NAA-SR-Memo-10591)
response of two-degree-of-freedom system to half-sine-wave ground acceleration, analysis, 19: 7651 (NAA-SR-Memo-10067)
restricted three-body problem with variable masses, equation of motion for, 17: 13186(T)
review of classical and quantum statistical, 19: 23201
role of nuclear, in solving biomedical problems, review, 20: 22840
rotation in slowly dissipating systems, differential, 16: 6851
S matrix singularity at strip boundary, 17: 19146
saturation of infinitely extended nuclear matter in Brueckner theory and parameters of two-particle interactions, relation between, 17: 19517
shock-spectrum analysis of systems of oscillators in, 20: 3631 (SC-DC-65-1723)
solution of Hamilton's motion equations, model for, 18: 690 (RM-3538-PR)
solutions of dynamic equations in, computer programming for, (T), 19: 24912 (NAA-SR-Memo-10692)
solutions to Hamilton-Jacobi equation in, 18: 40056
stability of an infinite system of mass points interacting under a Newtonian force, 17: 16831
statistical, approximations of pair distribution functions in fluids, 16: 26445
statistical, diagrammatic expansion of free energy of Ising model with arbitrary spin and range of interaction, 16: 6862
statistical, for one-dimensional systems with Coulomb forces, 16: 32203 (MATT-108)
statistical formulation using occupational numbers, 16: 3559
statistical, nonequilibrium phenomena of charged particle systems, 16: 2378
statistical, of classical systems, 16: 32234
statistical, path integral in irreversible, 16: 6859
statistics of equally likely quantum systems in, 18: 22803
stochastic Markovian processes, variation principle in, 16: 22527
strength of solids, 19: 22863(R) (AD-606809)
stress analysis of reactor containment structures, 18: 7865(R) (TID-19871)
stress analysis of reactor containment structures, 18: 32980(R) (IITRI-8262-6)
stress analysis of reactor containment structures, 19: 1825(R) (IITRI-578P22-11)
stress analysis of reactor containment structures, 19: 14774(R) (IITRI-578P22-12)
stress distribution around holes in plates loaded in uniaxial tension, 19: 31461(R) (ANL-7010(p.235-87))
stress pulse-trains from multiple reflection at zone of many discontinuities in rods, 16: 33478 (SC-4642(RR))
stress-strain distribution in lap-jointed thin shells, 18: 18355 (UCRL-7304)
stresses in perforated cylindrical-shell, 18: 18453 (IMM-NYU-320)
study of tension wire-sphere support structure in cylindrical shell, 19: 36581 (UCRL-13160(Pt.3))
symmetry in classical, SU(2), 20: 17429 (JINR-P-2529)
symmetry properties in classical and relativistic, 16: 32184
theories and mathematical methods in, reformulation by time-independent techniques, 18: 30101
theories of, space-time in classical, 19: 26950
theory for effect of plastic deformation on elastic behavior of model solids, 16: 12034 (TID-15206)
theory for Lorentz pendulum problem, adiabatic invariance in, 18: 37801
theory for nonequilibrium statistical, information, 18: 42496
theory of accidental degeneracies, contributions to, 17: 13383
theory of adiabatic invariance in, 18: 37800
theory of continuous representation in classical, generalized relation to quantum dynamics, 17: 32763
theory of irreversible processes in, 16: 32206
theory of momentum exchange in elastic scattering of neutral particles by crystals, 18: 21342
theory of nonlinear vibrations, 18: 6935 (SC-TM-284-63(72))
theory of spinors, generalized, 17: 22369
theory of three-body dipole-dipole interaction, use of third virial coefficients in, 18: 153
theory of transport processes, general, 17: 39759
theory of transport processes in, general, 18: 24231
thermodynamic equilibrium statistics, theory of, 17: 41578
thermodynamical functions for normal and superfluid systems in terms of potentials, 17: 20691
Thomas classical spin theory, modern simplified form of, 17: 15296
three-body scattering operator in nonequilibrium statistical, calculation of, 17: 38423
time direction of irreversible physical processes, 16: 14216
transformation of relativistic single-particle hamiltonians, 18: 32656
transport coefficient theory, 18: 2551
transport equation, Fokker-Planck approximation to Boltzmann, 17: 20633
transport equations in quantum statistical, (T), 19: 37220
transport in, equivalence of Boltzmann and Navier-Stokes equations for, (T), 19: 11830 (NYO-1480-7)
transport phenomena in gases at moderate densities, statistical, 17: 16822
transport properties of matter in classical statistical, 17: 6818
two-body problem in geometrodynamics, 17: 22778
two-body correlation functions for lattice gas statistical, integral equations for, 18: 34336
uncertainty relations for particle velocity diminution by interactions, 16: 22792
uniformly accelerated motion and relativity, transformations for, 17: 16798
variable fluctuations in statistical, probability for dynamical, 19: 9788
variation principle for arbitrary operators in, 17: 18946
variational principles in, analogies in neutron diffusion theory, 20: 1136
variational principles of classical, analogies in reactor theory, 20: 3331
variational principles in classical, generalized, 20: 13351
variational principle for quantum and classical, unified, 20: 32302
variational problems in, 17: 8705
vibrations of nonlinear continuous strings in, 17: 2450
von Karman equations for bending of rectangular plates, iterative solutions of, 18: 28089 (IMM-NYU-322)
wall effects in non-equilibrium statistical examination of, 17: 14950(R) (TID-18039)
wave propagation in viscoelastic bars, 16: 13706 (TID-15198)
wave scattering by totally reflecting spheres, scalar plane, (T), 19: 41129
Weyl correspondence between quantum and classical systems, mathematics of, 20: 11876

Mechanisms
see Reaction Mechanisms

Mechlorethamine
see Diethylamine, 2,2'-Dichloro-N-methyl-

Mecholy Bromide
see Ammonium Compounds, Quaternary

MECLIZINE
effects on induction of chromosome aberrations in onion root tips, 20: 35297
protective effects against nausea and vomiting in radiation sickness, 17: 10489

MECONIC ACID
complex formation with uranyl ions, 20: 7081
complexes with uranium, equilibrium constants for, 20: 29096
reactions with uranyl ion, spectra of, 17: 35714

Media
see Culture Media

MEDICAL PERSONNEL
chromosome studies on radiographic, and their families, 20: 20447
determination of radiation exposure in radiology service, use of blood studies for, 20: 38781
effects of laser beams on, prevention of, 20: 26673
experience and training of radiology, effects on dose to patients during fluoroscopy, 20: 43050
hazards of dental radiography, 17: 36077
leukemia incidence in radiologists compared with other specialties, 20: 45250
mongolism incidence in children of, 20: 35196
mortality estimates and availability following thermonuclear explosion, 20: 33583
nursing care of radium-implanted patients, 20: 38751
phosphatase activity in leukocytes of radiological, 20: 5269
pocket chambers for radium ward nursing, design of, 19: 2610
protection from radiation, design of equipment for, 20: 35351
protection of, during operation of microwave equipment, 20: 38622
radiation dose received by radiologists and x-ray technicians in Japan, 1921 to 1965, 20: 6917
radiation dose to dental, during radiography, 20: 5430
radiation dose to gonads of, from therapy of benign tumors in children, 20: 13013

radiation dose to gonads of, in radiographic procedures, 20: 18505
radiation dose to, during diagnostic radiography, x, 20: 22845
radiation effects on life-span of x-ray technicians, 20: 3760
radiation effects on blood coagulation time in, x, 20: 22749
radiation effects on health and fertility of dentists and radiologists, 20: 40615(R) (NYO-901-54, pp 26-8)
radiation effects on diameter and volume of erythrocytes of, from occupational exposure, 20: 40678
radiation effects on aging of radiologists, 20: 45411
radiation exposure records for, 20: 8493 (SZS-7(1965))
radiation hazard to ophthalmological, cobalt-60, 20: 6953
radiation hazards to physiotherapists, during patient radiography, 20: 4203
radiation hazards to radiological, review, 20: 5434
radiation hazards to urologists, during urethrographic examinations, 20: 5459
radiation hazards to veterinary, 20: 6933
radiation hazards to pregnant women employees, 20: 16762
radiation hazards to dental, control of x, 20: 14419
radiation hazards during linear and volumetric radiotherapy, 16: 2081
radiation monitoring of x-ray technicians, 20: 12999 (CEA-R-2746)
radiation monitoring of, using gold-198, 20: 39159
radiation monitoring of radiology, in New Zealand, 20: 43581(R) (NP-16245)
radiation monitoring of, with film badges, 16: 33176
radiation protection measures for, 20: 4199
radiation protection of, 20: 5433
radiation protection of radiography technicians, 20: 5489
radiation protection of, during dental radiography, 20: 6942
radiation protection measures for, 20: 8757
radiation protection of, in Italy, 20: 9208
radiation protection of, during heart radiography, 20: 12757
radiation protection during radiography, 20: 40733 (ISS-66/16)
radiation protection of radiographic, 20: 45993
radiation protection program for radiology, in USSR, 20: 45997
radiation protection for diagnostic x-ray, 20: 45518
radiologic techniques and equipment to reduce x radiation hazard to veterinary, 20: 35677
responsibility of, toward fallout hazards, 18: 18086
role in nuclear war, 17: 37383
role of veterinarian in civilian defense, 20: 33579
training of, in case of nuclear attack on Australian cities, 20: 27218
Medical Research Reactor (MRR)
see Brookhaven Medical Reactor

MEDICAL SUPPLIES

for community fallout shelters, 19: 24753
for handling radiation accident victims, 19: 22638
for shelter occupants, survey of, 18: 12382(AD-411787)
packaging for radiosterilization, standards for, 20: 14942
radiation effects on properties of stored anesthetic agents, 19: 30240
radiation processing of biosynthetic medicaments, use of intense radiation sources in, 19: 26729
radiation processing of, commercial applications, 18: 31987 (CONF-568-1)
radiosterilization, plant designs for, 16: 12856
radiosterilization of surgical materials, 17: 4761
radiosterilization of surgical materials, properties of electrons for, 17: 4762
radiosterilization of adhesive dressings, economics and effectiveness of, 17: 4763
radiosterilization of, gamma facility for, 17: 8505
radiosterilization, 17: 14592
radiosterilization of ophthalmological, 18: 525
radiosterilization of sutures, 18: 8060(P)
radiosterilization, 18: 13549
radiosterilization of sutures, economics of facility for, 18: 13559
radiosterilization of, using Riso linear accelerator, 18: 13560
radiosterilization, 18: 30080
radiosterilization of, design of gamma facility for, 18: 39746(T) (AEC-tr-6390(p.223-38))
radiosterilization of, facilities for, 18: 39774
radiosterilization of, 18: 38801
radiosterilization of, 18: 43996
radiosterilization of, dosage effects on, 19: 7123
radiosterilization of, economic aspects of, 19: 30605
radiosterilization, 19: 20410
radiosterilization of equipment for, environmental influences on, 18: 17389
radiosterilization of equipment in, dose requirements for, 18: 17390
radiosterilization of, 19: 30606
radiosterilization of catgut sutures, effects on properties, 19: 34603
radiosterilization of, comparison of electron accelerators and cobalt-60 plants for, 19: 36877
radiosterilization of, use of electron accelerators in, 19: 39063
radiosterilization of, evaluation, 19: 44559
radiosterilization of, using radioisotopes, 19: 44560
radiosterilization of, evaluation of, 19: 44564
radiosterilization of cotton bacteriological swabs, 19: 46884
radiosterilization, 19: 46890
radiosterilization of surgical sutures, 20: 703
radiosterilization of sutures, unfavorable tissue reactions to, 20: 712
radiosterilization of, 20: 14389
radiosterilization of catgut sutures, 20: 14932
radiosterilization of, conference on, 20: 14940
radiosterilization of, 20: 14943
radiosterilization of prepacked, electrons, 20: 14941
radiosterilization of catgut, beta and gamma, 20: 25451
radiosterilization of, role of chemicals as sensitizers in, 20: 37144
radiosterilization in Canada, 20: 39282 (DP-1066(Vol.1), pp III.3-32)
radiosterilization of surgical cotton and gauzes, 20: 46104(R) (AECL-Pak-RB/10)
radiosterilization of surgical catgut, gamma, 20: 46103(R) (AECL-Pak-RB/3)
radiosterilization of, at Danish accelerator facility, 17: 11812
radiosterilization of, environmental influences on, 18: 17389
radiosterilization of, dose requirements for, 18: 17390
sterilization of surgical materials, conference on, 17: 4760
stockpiling of, for civil defense in Canada, 17: 12069
storage of radioisotopic, design of equipment for, 20: 45849(P)

MEDICINE

(Including clinical medicine.)
see also Epidemiology
see also Hematology
see also Nerology
see also Pharmacology
see also Space Medicine
see also Tracer Techniques (Medicine)
accelerator use in, linear, 19: 14186
action levels in treatment of radiation and radioactivity exposure, 19: 46008
activation analysis applications in forensic, 17: 39006
activation analysis applications in, 17: 39010
activation analysis uses in, 18: 31408
activation analysis in, uses, 20: 22861 (BNL-10130)
activation analysis in, uses of, 20: 35189
activation analysis in dental, use of, 20: 35192
aerospace, problems in, 18: 25044
aspects of, in thermonuclear war, 17: 37381
aspects of, in thermonuclear war, 19: 13130
atmospheric contamination in facility for nuclear, 18: 5158
atmospheric contamination in isotope departments, 18: 5156
beta bremsstrahlung sources in, protective measures for use of, 19: 36185
bibliography of UKAEA publications available to public, 16: 17339 (NP-11504)
bibliography on radioisotopes in, 17: 24831 (AED-C-12-03)
bibliography on radionuclides in oncology, 19: 4018 (AED-C-10-02)
book: *Advances in Biological and Medical Physics*, Volume 9, 18: 29168
book: *Adventures in Radioisotope Research. I and II.*, 16: 17699
book: *Copper and Peroxides in Radiobiology and Medicine*, 19: 1994
book: *Medical Aspects of Radiation Accidents*, 17: 27632
book: *Methods of Animal Experimentation*, 20: 32906
book: *Nuclear Medicine Fundamentals for Veterinarians*, 18: 41014
book: *Nuclear Medicine*, 20: 3860
book: *Progress in Atomic Medicine*, Vol. I., 19: 26211
book: *Progress in Medical Genetics*, Vol. II., 17: 13910
book: *Radiation Biology, Radiation Therapy, Nuclear Medicine, and Cancer Research*, in German, 17: 17702
book: *Radiation Medicine*, 19: 38470(T)
book: *Radioactive Isotopes in Surgery*, in German, 16: 7356
book: *Radioactive Metal Mobilization in Medicine*, 18: 21758(T)
book: *Radioisotopes and Radiation—Recent Advances in Medicine, Agriculture, and Industry*, 18: 43996
book: *X-Ray and Nuclear Physics for Medicine and Biophysics*, 20: 6985
book: *Yearbook of Nuclear Medicine*, Vol. I, 1966, 20: 36690
calcium-47 in, conference on, 19: 6925
cancer research programs, Argonne Cancer Research Hospital, April to Sept, 1962, 17: 24818(R) (ACRH-18)
carbon-14 in, bibliography on, 18: 21759
care in event of nuclear attack in Canada, 17: 12068
care of radiation workers, 18: 39541
civilian defense measures for hospitals, 18: 18093
civilian defense measures in United Kingdom for, 18: 27737
civilian defense measures for, in Great Britain, 18: 27740
civilian defense programs for, 18: 18079

civilian defense procedures for, 18: 18082
civilian defense training program for personnel, Massachusetts, 18: 31810
clinical aspects of radiation, 18: 29490
clinical laboratory procedures, 16: 9741 (AERE-R-3839)
clinical status of residents of Hiroshima and Nagasaki exposed to atomic bomb, 19: 31783 (ABCC-61-62)
computers in, 18: 43151 (ISS-63/50)
conference on chemistry in medicine, 18: 27021
conference on nuclear, Cologne, 1961, 16: 7357
conference on nuclear, 17: 40455
conference on science in the advancement of new states, Rehovoth, Israel, August 1960, German translation, 16: 23361
criteria for physicians in nuclear installations, 18: 8569
data processing and sample handling, systems for, 16: 10232
development of nuclear, in Japan, 19: 12900
development of nuclear, *Technical Progress Review*, Winter 1964–1965, 19: 13824
development of nuclear, and promotion in IAEA, 19: 30059
diagnosis of tuberculosis by silicon content of sputum, 20: 36542
diagnostic tests using radioisotopes for, 18: 31319
diagnostic use of phosphorus-32 in ophthalmology, 17: 23006
dietary factors affecting health in tropical countries, 16: 14406
disaster plan for, 18: 14136
disaster plans for, 18: 14137
dosimetry in radiotherapy, organization of, 20: 35355
educational concepts in nuclear, 16: 23366 (BNL-4931)
effects of thermonuclear warfare on, 18: 14157
electron paramagnetic resonance applications in, 16: 7363
emergency manpower rating system for nuclear accidents, 18: 8585
engineering problems in nuclear, 16: 28696
epidemiology of New Jersey radium cases, 20: 20387(R) (NYO-2181-3)
equipment setup for megavoltage therapy for private practice, 19: 26200
evaluation of fallout effects on people on Rongelap Island after 11 years, 20: 7296 (BNL-9698)
evaluation of index system for recording tissue doses to radiation, 19: 24804
examination of blood picture in x-ray workers, evaluation of, 18: 8571
examination of blood picture of personnel, evaluation of statistical criteria for, 18: 8577
facilities for radiation, effects of erythemal dose data on, design of, 19: 45881
fallout decontamination of incoming patients at remote facilities for, 18: 29183
fallout hazards to building for, 18: 29886
fallout problems for, 18: 25730
fluoroscopy techniques in dental, development of promethium-147 gamma source for use in, 18: 25234 (SGAE-IB/IA-2/1964)
forensic, applications of activation analysis in, 20: 40810(R) (NYO-901-54, pp 20-3)
handling of casualties of thermonuclear explosion, 19: 31831
handling of casualties of thermonuclear explosion, 19: 33872
health problems of shelter occupation, 18: 12382 (AD-411787)
hospital organization for times of disaster and warfare, 17: 27623
hospital planning and maintenance, civilian defense measures for, 18: 22288
image-retaining panel in dental, evaluation of, 18: 33443
industrial, correlation with radiation safety, 19: 227
industrial, effect of tendency to report injuries on accident statistics, 18: 15691 (ORNL-3563)
industrial, practice in beryllium plants, 20: 42756
iodine-131 in, hazards from, 18: 41259
iodine-132 preparation for use in, chromatographic method for, 19: 32251
Italian nuclear personnel evaluation in, 18: 14150
legal aspects in association with atomic energy, 18: 18084
legal control of radiation protection of patients in, possibilities of, 20: 36679
life span and cause of death of American physicians, 19: 45808(R) (NYO-901-36)
life span of radiologists and other medical specialists, 19: 17500
mammalian genetics in, review on, 17: 13912
management of casualties of reactor accident, 19: 19630
management of radiation-contaminated personnel, 19: 22637
medical care in shelters, 19: 12892 (AD-423696)
megavoltage therapy in, evaluation of private installation of equipment for, 19: 26201
military planning for, after nuclear attack, 18: 25729
national fallout shelter program, aspects of, 18: 22294
neutron generator for use in research in, 19: 2(R) (HW-81746(p.2.32-S))
nuclear, and military physicians, 17: 37382
nuclear, basic physics of, 17: 7710
nuclear, criteria for construction of building for research, 17: 7704
nuclear, development of facilities in hospitals in U.S. for, 17: 17668
nuclear energy in, review, 20: 20367
nuclear explosions and, 18: 12395
nuclear instrumentation for use in, 19: 33704
nuclear, pediatrics in, 17: 17674
nuclear techniques in, in Congo, 20: 20373
nuclear, conference on, Tokyo, Nov. 22–23, 1963, 19: 15004
nursing care of patients after radiotherapy, 19: 43908
nursing care of patients with accidental and therapy induced radiation sickness, 19: 45912
nursing care of victims of atomic explosions, organization and techniques of, 17: 19771
nursing techniques in bone marrow transplantation and whole-body irradiation of leukemic patients, 17: 13888
nutritional management of cancer patients after radiotherapy, 19: 43911
occupation radiation injuries to hands, 19: 224
organization and training procedures in, in event of nuclear attack, 17: 8464
organization of control services of, in nuclear installations in U. S., 18: 8573
organization of facilities for nuclear warfare, 19: 19554
organization of facilities for nuclear warfare, 19: 19555
organization of personnel and supplies of, for civilian defense, 17: 17631
personnel control for nuclear, 18: 29893
physical concepts of, 19: 8722 (ISS-64/32)
plants for, breeding experiments on, 18: 13523
precautionary measures in Dutch reactor stations, 19: 9423
preparation of iodine-131-labeled pharmaceuticals for use in, 20: 27027
problems during atomic warfare, 18: 29896
problems in care of casualties from radiological warfare, 18: 19793
problems in, from radiation, 17: 37102
problems in, in atomic energy, 17: 17700
problems in, in radiation exposure to man, 17: 12501
problems of, from nuclear war, 17: 39330
procedures for handling radioisotope-contaminated patients, 18: 18095
procedures for nuclear disaster, 18: 29405
procedures for pathologic psychologic reactions to disaster, 18: 25731
procedures for radiation accidents, 17: 10876
production and separation of iron-52 for use in, 19: 15653
program for nuclear accidents, 18: 31811
program for nuclear warfare, 18: 31814
program of civilian defense, 19: 18212
program of, for nuclear weapon casualties, 18: 5558
protective ointment for gynecological, 18: 13571
psychological criteria in employing radiation workers, 18: 8575
psychotic syndromes in residents of Hiroshima exposed to atomic bomb, 20: 42924
radiation and radioisotopes in, responsibilities of pediatrician using, 18: 138
radiation and radioisotopes in, Russian conference on, 20: 11(T) (AEC-tr-6293)
radiation counters for use in, whole-body, 19: 15295
radiation detectors for, organic-scintillator whole-body, 19: 31692
radiation dosage control in radiography in, 17: 14543
radiation dose monitoring in Germany, 19: 8989
radiation doses used in, 18: 18100
radiation dosimetry in over-exposed personnel, role of, 19: 26621
radiation dosimetry of personnel in accident clinic, 19: 38477
radiation dosimetry of radioisotopes used in, 20: 26713
radiation effects on blood of personnel in, data on, 17: 27620
radiation effects in, bibliography on, 17: 38737 (AED-C-12-04-I)
radiation effects in, bibliography on, 17: 38738 (AED-C-12-04-II)
radiation effects on personnel in, 18: 11770
radiation effects on plants for, x, 18: 13522
radiation effects on biosynthetic, limitation and potentialities of, 19: 115
radiation effects in clinical, as related to anesthesiology, 19: 7045
radiation effects on human cells from clinical and occupational exposures, 19: 42353
radiation exposure to personnel in, techniques for control of, 17: 37384
radiation exposure to personnel in, regulations for, 17: 41075
radiation exposure dose to personnel in, film-badge determination of, 18: 5149
radiation exposure reduction in dental, method for, 18: 31820
radiation exposure problems of forensic, 19: 38495
radiation exposure of dentists, effects on health and fertility, 20: 59(R) (NYO-901-37, pp 31-2)
radiation exposure to populations in, significance of, 20: 36677
radiation exposure in Germany from uses in, percentage of total, 20: 45508
radiation facilities and hygiene in denistry, survey of, 17: 10871
radiation hazards in practice of, review of, 17: 18406
radiation hazards in, review of, 17: 18421
radiation hazards in radiodiagnosis in, 17: 20265
radiation hazards in, 18: 134

radiation hazards, 18: 3626
radiation hazards to infants from diagnostic, evaluation by pediatrician, 18: 17547
radiation hazards from, 18: 31807
radiation hazards to physicians from occupational exposure, 19: 17571
radiation hazards in use of radioisotopes in, 19: 24801
radiation hazards in dental, control of x, 20: 14419
radiation hazards in veterinary, 20: 24949
radiation in, 17: 19743 (TID-18468(p.1-126))
radiation in, 17: 36079
radiation in, 18: 25246
radiation in, and protection problems, 17: 29
radiation in, review on, 17: 17696
radiation in, review, 17: 35361
radiation in, code of practice for, 18: 20244
radiation in, conference on atomic, Bonn, 1964, 18: 35270
radiation in, effects on human genetics of, 19: 226
radiation in, high-energy, 18: 11912
radiation in, population doses from, 18: 11895
radiation in, WHO conference on, 19: 29843
radiation injuries in, legal liability in, 18: 12405
radiation injuries on skin of hands of medical personnel and physicians, 19: 24321
radiation injury problems in, 18: 31281
radiation liability insurance for, 18: 35798
radiation monitoring of personnel in, device for, 20: 36680
radiation physics in, 19: 30056
radiation protection systems and theory in, 16: 2914 (NP-10713)
radiation protection in, aspects of environmental, 16: 33329
radiation protection in, general principles of, 17: 18407
radiation protection measures for, 18: 35404
radiation protection of personnel in, 18: 39016
radiation protection standards for, Florida, 19: 24775
radiation protection procedures in, 19: 43896
radiation protection in radiological, Italian decree on, 19: 44318
radiation protection during intracavitary radiotherapy, design of remote afterloader for, 19: 46111
radiation protection of personnel using radioisotopes, 19: 46080
radiation protection of personnel, 19: 46686
radiation protection in, historical review of, 20: 8737
radiation protection measures for, review of, 20: 9205
radiation protection measures for dental, 20: 20519
radiation protection in the practice of dentistry, x, 20: 38793
radiation sources in, low-energy gamma and x-ray, 20: 4111 (ORNL-IIC-5)
radiation sources for, dose distribution of fast-neutron, 20: 9166(R) (BNWL-36, pp 2.1-58)
radiation sources for use in, preparation of iron-55, 20: 43384
radiation use in dermatological, legal aspects of, 18: 31327
radiation used in, 18: 27157
radiation used in, fundamental principles of, 18: 29553
radiation used in, regulation of, 18: 29905
radiation used in, safety measures for, 18: 29495
radiation uses in British, 19: 15109
radiation uses in, evaluation of types of reactors for, 18: 29126
radiation uses in, standards for, 18: 29894
radiation uses in, economic aspects, 18: 35913
radioactive pharmaceuticals in, developments in, 20: 27000 (CONF-651111)
radiodermatitis of hands of surgeons and radiologists, 19: 33865
radiodiagnosis and radiotherapy in, responsibility of doctor in, 20: 36709
radiodiagnosis in pediatric, method for, 18: 5153
radiodiagnosis in dental, instrument for, 18: 11922
radiodiagnosis in dental, exposure from, 18: 20261
radiodiagnosis in, evaluation of hazards from, 18: 31348
radiodiagnosis using isotopes in ophthalmologic, 18: 13600
radiodiagnostic hazards in pediatric, 18: 22282
radiography in, techniques for improved perception detail in, 17: 22986
radioinduced chromosomal aberrations in persons working in, 17: 40619
radioisotope applications in, review of, 18: 1477
radioisotope applications in, 18: 29491
radioisotope applications in, review, 19: 8731
radioisotope scanning in diagnostic, review, 18: 144
radioisotope scanning in, 18: 5165 (TID-7673)
radioisotope use in, review, 18: 13584
radioisotope use in, instrumentation and methods for, 20: 19091
radioisotope uses in, diagnostic and therapeutic, 16: 27285
radioisotope uses in, review, 17: 27005
radioisotope uses in, 17: 36103
radioisotope uses in, book on laws regulating, in Germany, 18: 9959
radioisotope uses in, protection against hazards from, 18: 37038
radioisotope uses in, in Switzerland, 18: 41889
radioisotope uses in, AEC licensing for, 19: 31690
radioisotope uses in veterinary, in Yugoslavia, 19: 42236
radioisotope uses in gastroenterology, bibliography on, 20: 6924 (AED-C-10-04)
radioisotope uses in, 20: 8786
radioisotope uses in, 20: 23567
radioisotope uses in, 20: 35190
radioisotope uses in veterinary, 20: 42723
radioisotopes for use in, cyclotron production of short-lived, 20: 18515
radioisotopes in, bibliography on, 17: 1 (AERE-READING LIST-10)
radioisotopes in clinical, in China, 16: 28678(T) (JPRS-14829(p.584-93))
radioisotopes in orthopedic, 18: 145
radioisotopes in orthopedic, 18: 146
radioisotopes in, protective measures for using, 18: 20254
radioisotopes in, chemical and radiochemical control of, 19: 853
radioisotopes in, local energy deposition values for, 20: 18958
radioisotopes in, in developing countries, 20: 22525
radioisotopes in, survey of, 20: 31152
radioisotopes used in gynecological, 18: 29903
radiology in dental, survey of hazards from, 20: 20956
radiology in, developments in, 17: 27626
radiology in, hazards, 17: 21941
radiology in hospital, dosimetry of, 17: 12514
radiology in veterinary, 20: 6933
radiology in, teaching manual for, 18: 29552
radiosterilization of glass ampules containing, 17: 32675
radiosterilization in, gamma, 18: 21862
radiosterilization of products in, description and performance of cobalt-60 facility for, 19: 26736
radiosterilization in, facility for, 19: 42776 (AECL-2264)
radiosterilization of products in, design of cobalt-60 facility for, 20: 27386
radiotherapeutic facial and maxillary injuries, plastic surgery for, 18: 11936
radiotherapy in, importance of, 19: 36201
radium sources in, survey of control practices for, 19: 15300
reactor research in, 17: 35211
reactor use in, TRIGA, 18: 36853
recommendation for physician in decontamination of radioactive materials from skin, 19: 19494
record of nuclear energy workers, value of, 18: 8581
regulations governing clinical uses of radioactive drugs, 18: 31831
release of labeled drugs, method for *in vitro* evaluation of, 18: 27022
research activities at Argonne, July–Dec. 1961, 16: 31381(R) (ANL-6535)
research activities at UCRL, Spring, 1962, 16: 32641(R) (UCRL-10211)
research activities at Los Alamos Scientific Lab., July 1963 to July 1964, 18: 43152(R) (LA-3132-MS)
research and development studies under contract with the AEC Division of Biology and Medicine, April 1964, 18: 27015(R) (TID-4203)
research at ORINS Medical Division, 1960, 16: 9838 (ORINS-39)
research in, interference by *Pseudomonas aeruginosa*, 17: 30234
research in nuclear, 20: 36691
research in, uses of reactors in, 20: 10507
research on, review, (E/T), 19: 35876
research on, summaries of, 1966, 20: 22531 (TID-4204)
research program, 16: 11373(R) (AD-259234)
research program at LASL, 1960, 16: 1298(R) (LAMS-2627)
research program at Brookhaven in 1961, 16: 4606(R) (BNL-682)
research program at Julich, 1961-62, 19: 12866(R) (NP-14554)
research program at Julich, 1963, 19: 12867(R) (NP-14555)
research program of Division of Biology and Medicine, AEC, 16: 4008 (TID-13228)
research program of WHO public health practice on nuclear, 19: 25978
research programs at Donner Lab., University of California, 16: 9748(R) (UCRL-9897)
research programs, summary for AEC in 1961, 16: 12824
research programs at BNL on, July 1962 to July 1963, 18: 6586(R) (BNL-806(p.93-122))
research programs on, in Israel, 18: 9752 (IA-900)
research programs on, at LRL in fiscal year 1963, 18: 15729 (UCRL-Pub-48)
research programs on, at LRL in fiscal year 1964, 19: 12886 (UCRL-Pub-49)
research programs in Arab countries on, 19: 31696
research programs on nuclear, 19: 43647(R) (UCLA-12-565)
research programs in, at Juelich Research Center, Germany, 20: 16156
research programs on, at Argonne Cancer Research Hospital, 1965, 20: 18422(R) (ACRH-24)
research programs in India on, 20: 26588(R) (NP-15950)
research programs in India on, 1965–1966, 20: 36539(R) (NP-16171)
research progress in, 16: 21(R) (ACRH-15)

research supported by Division of Biology and Medicine, AEC, 1963, 17: 30226 (TID-4200)
research using high-energy heavy particles, 18: 5
review of nuclear, 20: 14427
review of recent developments in nuclear, 20: 43051
role in handling mass casualties in event of nuclear attack, 17: 17678
role in nuclear industry hygiene, 20: 20955
role in personnel radiation protection of, 18: 29904
role in radiation protection, 19: 26158
role of army medical service in nuclear warfare, 19: 44310
safety hazards of radiological, 20: 20544
scintillation scanning in, conference on, 19: 5739
scintiscanning in, review, 20: 20531
Second International Congress of Neurological Surgery, Washington, D. C., Oct. 1961, 16: 16241
semiannual report on, 18: 21747(R) (UCRL-11184)
semiconductor detector uses in, 19: 11581
shielding facility for personnel in, during decontamination work, 18: 17977(R) (ORNL-TM-793)
solid state track dosimeters for, use with neutrons and high-energy particles, 20: 41262 (BNWL-SA-619)
space flight, 18: 25045
stable isotope uses in, 20: 19120
standards for radiation workers, 18: 8570
strontium-90 use in pterygium surgery, 18: 13601
supervision in nuclear industries in United Kingdom, organization of, 18: 8572
supervision of employees in United Kingdom atomic industries, 16: 9039
supervision of radiation personnel, general principles of, 18: 8574
supervision of radiation-exposed personnel, 18: 29403
supervision of workers in radiation industries, 17: 34170
supervision of workers exposed to radiation, conference on, 18: 8568
survey of genetic damage in offspring of Brazilian physicians exposed to radiation, 19: 36093
therapy of radioactively contaminated wounds, 17: 28640
theses on, in China, Vol. II, 16: 28675(T) (JPRS-14829)
tracer techniques in, development in Hungary, 19: 31966
tracer techniques for diagnostic use, 19: 34052
tracer techniques for diagnostic use, 19: 34099
tracer techniques in veterinary, use of, 20: 3859
training in nuclear medicine in U. S., 18: 29520
treatment for plutonium contamination, 19: 36129
treatment of radiation injuries in man, problems in, 17: 41062
treatment of radiation injuries from atomic explosions, 19: 13116
treatment of thermonuclear casualties, 19: 15803
treatments for radiotherapy complications using, 17: 17924
tropical, use of radioisotopes in studies, 16: 14405
use in treating injuries resulting from radiotherapy, 20: 16319
use of calcium-47 in, review on, 17: 10274
use of gold-198 in, bibliography on, 17: 31814 (KFK-143)
use of gold-198, occupational hazards from, 19: 8988
use of heavy particles in, 19: 26215
use of ionizing radiations in, review, 17: 35391
use of positron emitters and short-lived isotopes in, review on, 19: 26214
use of radiation and radioisotopes in, developments in, 19: 7235
use of radiation in, status of, 17: 17698
use of radiation sources and radioisotopes in, since 1958, review, 18: 37043 (A/CONF.28/P/880)
use of radioactive mineral waters in, 17: 19774
use of radioisotopes in, review on, 17: 17677
use of radioisotopes in, review of, 17: 30233
use of radioisotopes in surgery, 17: 31828
use of radioisotope renogram in internal, 18: 23393
use of radioisotopes in clinical, 19: 13826
use of radioisotopes in, facilities for, 19: 15280
use of radioisotopes in tropical, review on, 19: 34094
use of radioisotopes in diagnostic, review on, 19: 38505
use of short-lived radioisotopes in, review on, 17: 10253
use of short-lived nuclides for research, diagnosis, and therapy, review, 20: 43022
use of strontium-90 in dermatology, methods for radiation protection in, 19: 17701
use of unsealed radioactive materials in, contamination hazards from, 20: 36678
use of whole-body counters, developments in, 19: 26212
use of x-ray spectrometry in, 18: 21998
uses of radioisotopes in diagnosis and therapy, 18: 31354
uses of technetium-99 in, 19: 9551
uses of ultraviolet radiation in, 18: 29537
veterinary, curriculum of, 20: 16761
veterinary, principles and use of radioisotopes in, 20: 38748
x-ray dosimetry in, film pack survey of, 20: 41213

MEDITERRANEAN SEA
see also Adriatic Sea
see also Ligurian Sea
see also Tyrrhenian Sea
bottom layers in, studies on, 20: 41128
cesium-137 and strontium-90 content in, 1963-64, 20: 43540
fallout monitoring, 1961 to 1963, 18: 15758(R) (TID-20347)
fallout monitoring, 1960 to 1963, 18: 15759(R) (TID-20366)
fallout monitoring, 1959, 18: 31752 (BLG-243)
fallout monitoring, 1962 to 1964, 19: 24721
fallout monitoring of, 1963, 20: 41145
fallout monitoring, 1963, 20: 41146
measurements of radioactivity in, 20: 41147
mineral content in eastern, effects of season, temperature, and Nile River flooding on, 20: 43508(R) (NP-16179)
monitoring for beta and gamma activity in plankton in, 19: 30452
nutrient content and dispersion in plants and animals in, 20: 43508(R) (NP-16179)
oceanography of eastern, effects of Nile River floods on, 20: 43508(R) (NP-16179)
oceanography of Israel shelf of, 20: 14731(R) (NP-159861)
oceanography of, effects of Nile River floods on, 20: 14731(R) (NP-159861)
plankton ecology in, 19: 45748(R) (TID-22193)
radioactivity in plankton of, 1961 to 1964, 19: 42641 (TID-22112)
radioactivity of littoral sediments in, gross beta, 19: 2534
radioactivity of plankton from, 1961 to 1963, 18: 15758(R) (TID-20347)
radioactivity of plankton from, 1960 to 1963, 18: 15759(R) (TID-20366)
strontium-90 content in plankton from, 1961 to 1963, 18: 16(R) (TID-19472)
tritium content measurements in natural waters in eastern area of, 19: 7703(R) (TID-21350)
uranium content in sediments of, effects of content of organic materials on, 19: 22585
uranium content of western, 18: 23787
uranium-234/-238 ratio in, 20: 39133

MEG
see Pseudourea, 2-(2-Aminoethyl)-2-Thio-

MEIDA
see Acetic Acid, (2-Mercaptoethylimino)Di-

MEIOSIS
chromosome differentiation during, 19: 36096
cytology of salamander cells during, 19: 2060 (BNL-7596)
effects of ethylenimine and ethyl methanesulfonate on, in peas, 20: 36621
effects of heavy water and hydrostatic pressure on, in starfish oocytes, 20: 30986
effects of suppressible mutations and super-suppressors on Saccharomyces, 20: 40582(R) (ORNL-3922, pp 65-8)
effects of water-d_2 on, in *Tetrahymena pyriformis*, 20: 8532
effects on intragenic recombination in maize, 20: 12678
genetic control of, in mutant peas, 20: 40512
radiation effects on sunflower, gamma, 18: 6678
radiation effects on, in mouse oocytes, 18: 8154
radiation effects on ploidy in mouse spermatocyte, x, 18: 11663
radiation effects on Pinus microsporogenesis, gamma, 18: 13443 (BNL-6991)
radiation effects on oat and wheat, gamma, 18: 17607
radiation effects on *Pinus rigido*, gamma, 19: 43722(R) (TID-22108)
radiation effects on stages of, in Artemia oocytes, x, 20: 5359
radiation effects on, in mealy bugs, 20: 12715
radiation effects on jute, y, 20: 16217 (AECD-AG-7)
radiation effects on male mouse, x, 20: 24934
radiation effects on pea, fast neutron and gamma, 20: 36621
radiation effects on rice chromosomes during, beta, thermal neutron, and x, 20: 40641
radiation effects on *Vicia faba* chromosomes during, x, 20: 42921
radioinduced in asynaptic and male-sterile mutants of peas, 19: 17658
radioinduced mutations in yeasts during, rates of uv and x-ray, 18: 11832
radioinduced mutations in maize during pollen, y, 20: 18335
radiosensitivity, 18: 11758
radiosensitivity effects in female cattle and swine, 19: 36026
radiosensitivity of, in spermatocytes of mice and monkeys, 18: 6672
radiosensitivity of chromosomes in plants during, causes for variations in, 18: 11830
radiosensitivity of *Drosophila melanogaster* eggs during, variations in, 18: 11833
radiosensitivity of, in Trillium, 19: 7124
radiosensitivity of, in yeast, 20: 1664
role in temperature-induced crossing-over frequency in Drosophila, 20: 40625(R) (ORNL-3922, pp 59-64)
water-d_2 effects on Drosophila, 18: 17522

MELAMINE
determination in mock explosive, method for, 20: 14470 (UCRL-7873)
production of carbon-14 labeled, by neutron radiolysis of cyanoguanidine, 16: 7594
production of carbon-14 labeled, in neutron radiolysis of guanidine, 17: 37264
protective effects against radiation injuries in mice, 18: 41269
radiation effects on, in nitrate–nitric acid solution, 17: 20514 (IDO-14598)
MELAMINE, TRIETHYLENE-
aberrant effects on chromosomes, mechanism of, 18: 33271(R) (NIRS-2(p.26-31))
chromosome damage, growth reduction, and mitosis inhibition in *Vicia faba* roots by, 16: 30251
effects on Drosophila spermatozoa, mutagenic, 19: 15131
effects on Drosophila, genetic, 20: 40706
effects on *E. coli* cultures, increased virus-producing cells and other mutants from, 20: 36617
effects on endocrine system of male rat, 17: 23003
effects on enzyme activity in intestine, spleen, and thymus, 16: 3998(R) (NP-11020(p.26-37))
effects on life spans of mice, 17: 33754
effects on lymphoid and myeloid leukemia incidence in mice, 20: 6788 (ORNL-P-1703)
effects on mitosis in rat lens epithelium, 20: 16256
effects on oxygen uptake by normal and leukemic leukocytes, 16: 32819
effects on Paramecium, mutagenic, 19: 31788(R) (ORNL-3768(p.33-57))
effects on *Paramecium aurelia*, effects of streptomycin on recovery from mutagenic, 20: 5417
effects on Paramecium, mutagenic, 20: 40632(R) (ORNL-3922, pp 175-91)
effects on permeability of the blood-brain barrier in rats, 20: 38609
effects on radiosensitivity of tumors, 18: 36964
effects on radiotherapy of retinoblastoma in man, 19: 13146
effects on tumor-bearing mice, effects of radioprotective drugs on, 20: 12719(R) (NP-15668)
mutagenic effects of, in mice, 18: 27007(R) (ORNL-3601(p.83-91))
mutagenic effects on paramecium, 19: 2068(R) (ORNL-3700(p.34-57))
use for treatment of leukemia and polycythemia, 20: 43014(R) (RLO-581-10, pp 33-6)
Melanin
see Pigments
Melanoxetin
see Flavone, 3′,4′,7,8-Tetrahydroxy-
MELLITIC ACID
effects on *Vicia faba* seeds, 16: 1595
preparation of, from phthalic acid and by oxidation of wood charcoal, 16: 7525(T) (AEC-tr-4899)
preparation of, methods for, 16: 4161(T) (AEC-tr-4898)
yields from oxidation of graphite by 90% nitric acid, 18: 31470
MELTING
see also Casting
see also Furnaces
see also Heat of Fusion
degasification mechanism in vacuum, 18: 44119
development of electron-beam techniques for, 17: 3389(R) (USBM-U-978)
electron beam device for vacuum, of refractory materials, 18: 43753
electron beam techniques for metal, 16: 19280
electron beam techniques for, review of, 17: 25761
electron bombardment technique and furnace for horizontal zone, of refractory metals, 16: 19281
electron-bombardment methods of, performance in vacuum, 16: 32045
electron-bombardment methods of, for refractory metals, 16: 32046
electron-bombardment methods and principles of, 16: 31765
electron-beam methods of, 18: 20491
equipment for levitation, of alloys and metals, 20: 25521 (AERE-R-5097, Paper 23)
equipment for, of radioactive or toxic metals, 19: 37022(P)
equipment testing for continuous, 18: 19448(R) (ORNL-TM-757)
equipment using electron beams for, 17: 511 (DMIC-174)
freezing point depression due to anomalous crystal habit and by limitation of crystal size, 18: 25028(T) (ORNL-tr-72)
induction heating in floating zone, 17: 8719
levitation, design and performance of coils for, 17: 21810 (Y-1413)
mass transfer in zone, boundary conditions and equations for, 17: 23874 (UCRL-10433)
methods development for reactor materials, 18: 32119
methods development for reactor materials, 18: 41987
of pure metals, post-melting effect on, 17: 34332(T) (AEC-tr-5960)
of reactive metals, crucibleless vacuum technique for, 18: 580 (UCRL-7388)
of solids in hot supersonic gas flow, 16: 4287(T) (NP-tr-827(p.27-9))
plasma device for metals, oxides, and carbides, 19: 28740 (SGAE-CH-12/1964)
point measurement for refractory metals, 19: 20566(T) (IS-Trans-13)
point measurement for hypostoichiometric urania, 20: 37220
techniques for, development of, 17: 11130
theory, 16: 4291(T) (NP-tr-827(p.48-51))
thermodynamics of cold-mold, 16: 19374(R) (USBM-U-921)
thermodynamics of consumable-electrode arc, 18: 14384(R) (USBM-U-1091)
uses in reactor materials fabrication, 18: 18338
MELTING POINT APPARATUS
description of, for use at 800 to 3000°C, 18: 39943
design using electric conductivity measurements in metals, 17: 8869(T)
Melusine Reactor
see Grenoble Reactors (Melusine)
MEMBRANE FILTERS
alpha detection on, after concentration of radioactive dusts on, 19: 4357
antigen transfer through, 18: 115
design, for air sampling, 16: 10224
development, 19: 348(R) (ORNL-3679(p.117-26))
development for collection of radioactive particles, 17: 34164
development for salt solutions, 19: 23163(R) (ORNL-3650(p.111-86))
efficiency for potassium permanganate and radioactive aerosols, 17: 40960
efficiency of, for removal of radioactive aerosols, 18: 4045
particle burial in, depths of, 18: 10308(R) (UCRL-7571)
penetration by radioactive aerosol, measurement of depth of, 19: 44299 (SZS-2(1965))
performance for collection of particulate materials, 17: 3164 (TID-16988(App.B))
performance in counting megakaryocytes, 20: 5301(R) (UR-668, pp 1-54)
preparation of microporous metallic, from alloys, 17: 30653(P)
preparation of nickel-63-labeled, for assay of aerosols and dusts, 16: 27526
preparation of porous-nickel, 17: 25718(P)
preparation of radioactive nickel, and use in dust measurement techniques, 16: 13408
preparation of, with improved properties, 17: 12191(P)
preparation with graduated pore size from synthetic resins, 16: 16490(P)
pressure losses in beds of molecular sieves, 16: 1728 (AAEC/E-67)
properties of aluminum and lanthanum alginates as, 19: 28262
properties of molecular, for purifying carbon dioxide, 16: 25299 (AAEC/E-86)
recoil atom absorption in deposited aerosol layers, 16: 13495
salt rejection by, method of determining, 19: 15415(R) (ORNL-3714 (Vol.I)(p.87-9))
salt water demineralization by, boundary layer buildup in, 19: 15415(R) (ORNL-3714(Vol.I)(p.87-9))
sorption of krypton and xenon on, at −78 to 25°C and 10^{-2} mm Hg to 1 atm, 19: 17910
surface collection efficiency of large-pore, 17: 29132(R) (UCRL-7254 (p.16-27))
thermal stability of epoxy, at 105 and 145°C, 20: 43067(R) (IDO-14679, pp 6-46)
use for collection of megakaryocytes in bone marrow preparations, 19: 17444 (UR-660)
use for collection of radioactive aerosols, 19: 38896
use in actinide complex separation, 19: 28459(P)
use in gravimetric determinations, errors in, 19: 32059(R) (IDO-14655)
use in reclaiming oils and hydraulic fluids, 20: 45841 (Y-1552)
MEMBRANES
see also Films
biochemical activity of yolk sac, during cell differentiation in chick embryos, 20: 16172(R) (NYO-2194-1)
bioelectric forces involved in material transfer across biological, 19: 43664 (BNL-9337)
biological, calcium and strontium transfer across, 18: 11615
biological, calcium and strontium transfer across, 18: 11617
chloride exchange in gastric mucosa of frogs, tracer study, 19: 35937
depolarization of muscle, induced by x radiation and cesium ions, 17: 17761 (TID-18220)
deposition of polymeric, process for, 17: 30612(P)
development of semipermeable, 20: 29624(R) (TID-22970, pp 257-329)
diffusion of poly(butyl acrylate) across cellophane, tracer study, 16: 23563
diffusion of tracer against concentration gradient through, 19: 44025
effects of naphthoquinone in Streptococcus, on metabolism, 20: 6723(R) (ORNL-3853, pp 175-6)
effects of radiomimetics on permeability of blood-brain barrier, 20: 38609
effects of rare earth metals in contact with dog and rabbit, 20: 25(R) (TID-22294)
excitation of cell, physical mechanisms for, 19: 42212 (NYO-3424-1)
fabrication of corrosion-resistant porous, 18: 4190(P)
fabrication of permeable, of subdivided metallic particles, 19: 46978(P)

fabrication of porous alumina, 18: 41981(T) (AEC-tr-6478)
growth of virus on chick embryo chorioallantoic, 20: 103
ion transport across rabbit duodenum, 20: 14243(R) (TID-22626)
ion transport through biological, isotope effects in, 19: 46898 (HMI-B-44)
ion transport through porous glass, control of, by membrane electric potential, 20: 35478(R) (NYO-3608-2)
isotope diffusion in biological, effects of flux on, 20: 1585
lipid content of sheep erythrocyte, function of, 20: 16160 (UCRL-14739(Pt.2))
material transfer across cell, biological model of, 19: 42199 (BNL-8397)
material transfer across biological, thermodynamics of, 19: 43665 (BNL-9338)
material transfer through biological barriers, theory of, 20: 10454 (BNL-9715)
material transport across biological, 20: 18184(R) (BNL-929, pp 115-25)
metabolism and active transport in biological, tracer studies, 19: 29901(R) (RLO-1754-1)
molecular transport through, of cell nuclei, 18: 17399(R) (ANL-6790 (p.138-44))
permeability of biological, tracer studies of, 17: 25538
permeability of cuticular, to organic compounds, 20: 16146 (COO-588-39)
permeability of erythrocyte, 19: 29847 (ACRH-103(p.48-61))
permeability of, from Nitella, 17: 24844
permeability of lipid, to deuterium oxide and water, 20: 42725
permeability of pulmonary, tracer studies of, 18: 15747 (TID-7689(p.52-4))
permeability of pulmonary, tracer study, 20: 6707
permeability of rabbit erythrocyte to alkali metal ions, tracer study, 18: 17417
permeability of rabbit blood-labyrinth barrier to fluorescein, 18: 29376
permeability of squid axon, to ions, 18: 29
permeability of toad bladder, effects of peptides on, 19: 21817(R) (BNL-867(p.119-50))
permeability of tomato cuticular, to iron and iron chelates, 20: 16147 (COO-888-45)
permeability to chloride and rubidium ions, effects of urea on fruit and leaf cuticular, 20: 14218 (COO-888-44)
permeation of alumina, effects of stresses on, 18: 34056 (UCRL-11355)
phosphate metabolism in erythrocyte, tracer study, 19: 33748
preparation and permaselectivity of zinc phosphate for alkali metal ions, 16: 28857
preparation and properties of porous silver, for ultrafiltration, 18: 19934 (NP-13874)
preparation and properties of polyvinyl alcohol, for use as artificial kidneys, 19: 26380(R) (NYO-3329-2)
preparation of ion-exchange resin, 16: 21995
preparation of ion-exchange, 17: 25109(P)
preparation of ion-permeable water-insoluble, by irradiating sols or dispersion of hydroxyalkyl methylcellulose ethers, 20: 25177(P)
preparation of metallic microporous, 17: 29311(P)
preparation of perm-selective, from graft copolymers, 17: 35861(P)
preparation of porous, from polytetrafluoroethylene powder, 18: 5764(P)
preparation of precipitate, for use in analytical chemistry, 19: 4088
properties for use in filtration, methods for evaluation of, 19: 348(R) (ORNL-3679(p.117-26))
radiation effects on irritation processes in, within the body, 16: 16287
radiation effects on permeability of mesenteric, 16: 30233
radiation effects on regeneration after trauma in intestine, 16: 32744(T) (JPRS-15018(p.83-97))
radiation effects on sodium transport across erythrocyte, reaction mechanisms, 17: 4412
radiation effects on muscle, 17: 15642(R) (TID-18268)
radiation effects on sodium and potassium effluxes in muscle cells, 17: 15641 (TID-18221)
radiation effects on permeability of muscle, 17: 17760 (TID-18219)
radiation effects on permeability of, of nerves, 18: 47(R) (TID-19617)
radiation effects on nuclear, in cells, 18: 11812
radiation effects on permeability of rat blood cell, gamma, 18: 13508
radiation effects on cell, relation to fatty acid properties, 18: 17557
radiation effects on penetrability of nucleoprotein of, 18: 17570
radiation effects on lactic acid dehydrogenase activity in guinea pig oral, x, 18: 17652
radiation effects on biological, ionizing, 18: 25106
radiation effects on tissue characteristics conditioned by, 18: 27090
radiation effects on sodium transport across, in erythrocytes, 18: 29342
radiation effects on ion exchange, gamma, 18: 31653 (COO-770-12)
radiation effects on water permeability of connective tissues in rats, 18: 33277 (STI/DOC/10/28(p.21-38))
radiation effects on formation of plant cell, 18: 33372
radiation effects on permeability of intestinal, tracer study in mice, 18: 38789
radiation effects on pig gastrointestinal, cerium-144 and praseodymium-144, 18: 38775(R) (ORO-624)
radiation effects on mouse intestinal, gamma, 19: 3957
radiation effects on permeability of cell, 19: 7022 (TT-1149)
radiation effects on premeability of Nitella, x, 19: 25958
radiation effects on permeability of cellular, 19: 29896 (EUR-2201.f)
radiation effects on peritoneal, gamma, 19: 29953
radiation effects on permeability of, 19: 31809
radiation effects on permeability of erythrocyte, 19: 33856
radiation effects on, of animal cells, 19: 35964
radiation effects on permeability of connective tissue, in rats, 19: 36019
radiation effects on permeability of frog lysosome, x, 19: 42285
radiation effects on permeability of plant cell, by urea, 19: 45975
radiation effects on animal cell, uv, 19: 45891
radiation effects on electrical potential of frog muscle, γ, 20: 5293(R) (COO-205-55, Paper 2)
radiation effects on permeability of, in plant cells, 20: 5294(R) (COO-205-55, Paper 3)
radiation effects on permeability of monkey erythrocyte, x, 20: 6765
radiation effects on rat intestinal, γ and x, 20: 6858
radiation effects on erythrocyte, in newborn rats, 20: 10589
radiation effects on polymer, used in leak control, 20: 14730 (AWRE-O-10/66)
radiation effects on ionic permeability of muscle cell, 20: 18293 (NP-14898)
radiation effects on permeability of erythrocyte, effects of iodoacetic acid and related compounds on x, 20: 18468
radiation effects on permeability to DNA of cell, x, 20: 22794 (EUR-2769.f)
radiation effects on electric potential of Planorbis nerve cell, x, 20: 22591
radiation effects on rat erythrocyte, protective effects of chemical agents against x, 20: 24943
radiation effects on permeability of blood-brain barrier, x, 20: 38609
radiation effects on microflora of mucous, 20: 38644
radiation effects on properties of nerve, x, 20: 40606 (BMwF-FBK-66-02)
radiation effects on innervation system of dog meninges, 20: 42881
radiation effects on, of lysosomes isolated from rabbit leukocytes, 20: 42975
radiation effects on permeability of Aspergillus cytoplasmic, x, 20: 45338
radioinduced changes in permeability of plant cell, 18: 29289
radioinduced inactivation of ATPase in erythrocyte, use for size estimations, 20: 22584
radioinduced leukoplakia of oral, x, 18: 19624
radioinduced permeability of erythrocyte, effects of cysteamine and sodium cyanide on x, 20: 5342
radioinduced PVA, for use in artificial kidney, 20: 16505 (BNL-949)
radioisotope diffusion through arachnoidal, 18: 43206
radiosensitivity, 17: 40643
radiosensitivity of, of isolated lysosomes, 18: 41100
radiosensitivity of erythrocyte, effects of temperature on, 20: 18454
radiotherapy effects on human mucous, protective effects of trihydroxyethylrutoside against megavoltage, 19: 8977
reactions between chemical agents and ligands of plasma, 17: 13931
stretching method for very thin circular, 16: 19094
structures of ion semi-permeable, 18: 6830
sulfhydryl group functions in, of cells, 18: 4925 (UR-633)
synthesis of artificial kidney, by radiation modification of PVA, 18: 37188 (BNL-874(p.32))
Thorotrast sorption in rabbit synovial, 20: 6733
thyroxine transmission through placental, 18: 1355
transfer rates of radioisotopes across isolated pericardium, 16: 31456
transport across erythrocyte, tracer studies of potassium and sodium, 20: 22564
trauma of animal cell, effects on Coulter electronic cell size distribution, 20: 1636
uranyl ions diffusion across ion exchange, 17: 35799
urea transport across dog intestinal mucosa, tracer study using deuterium oxides of, 18: 31091
use in leak-tight movement transmission through walls, 20: 2005(P)
use of ion-exchange, with electrodialysis in waste processing, 20: 26563
uses of vycor, for separation of neon isotopes, 19: 15977
vibration of L-shaped, method for analysis of, 20: 11206 (TID-22529)

MEMORY DEVICES

bibliography on content-addressable stores, 18: 35920 (AERE-Bib-145)
characteristics of polycrystalline ferroelectric multiremanence elements, 18: 27848 (SC-R-64-122)
circuits of manual entry into, 17: 22079 (HW-71044)
content addressable memories for, statistical behavior of, 19: 32671
defective elements in, corrective codes for, 19: 23164(R) (SU-SEL-64-103)
description of 64-channel analyzer with electrostatic storage in decimal system, 17: 23732
design and circuitry for 256-channel time analyzer, 16: 350(T) (AEC-

tr-4700)
design and construction of 4K word core system, 19: 11657(R) (NYO-1480-2)
design and performance for multichannel analyzers, 19: 22783
design and performance of ferrite-core, 19: 22784
design and performance of multichannel recording system, 19: 26631 (IAE-696)
design for Maniac III, 19: 26747(R) (COO-614-23)
design for multi-channel pulse analyzers, 16: 14085
design for multi-channel pulse analyzers, 17: 382
design for multichannel pulse analyzers, 18: 5655
design for use with amplitude analyzer, 16: 11906
design for use with neutron spectrometers, 16: 27325
design for use with neutron spectrometers, 16: 27324
design for 100-channel pulse analyzer, 20: 39183
design for 2048 channel analyzer, 19: 26656 (IAE-699)
design of address scaler and temporary memory for a transistorized time-of-flight analyzer, 16: 20763
design of analog, using tunnel diodes, 20: 9226 (SC-TM-65-577)
design of analog, with nondestructive readout, 19: 44350 (SC-R-65-959)
design of barrier-grid storage tube, 16: 30647(P)
design of buffer register for multichannel pulse analyzer, 18: 37514 (NP-14189)
design of buffer stores for handling nuclear-experiment data, (E), 19: 11655 (EUR-2160.e)
design of buffer storage system for sonic spark chamber data recording, 19: 36931
design of buffer, using charge-storage tubes, (E), 19: 15855 (CEA-R-2457)
design of electromagnetic analog storage system with nanosecond resolution, 19: 36791
design of ferrite-core, for radiation detection systems, 18: 7045 (JINR-E-1426)
design of ferrite-core matrix for wire spark chamber, 19: 4451 (CERN-64-44)
design of, for pulse analyzers, 17: 30104
design of, for pulse analyzers, 17: 30105
design of high-speed intermediate, 16: 27370
design of intermediate arithmetic, 16: 20768
design of intermediate, for automatic nuclear experiments, 19: 26638
design of linear capacity, 16: 33230
design of linear-selection, for use in pulse analyzers, 17: 41209
design of magnetic, for multi-dimensional selectors, 16: 20774
design of magnetic core memory for restoring information after read-out, 16: 30648(P)
design of magnetic, incorporated in radioisotope scanner, 19: 13795
design of memorizing circuit for long pulses, 16: 20804
design of multi-channel storage device, 17: 23722
design of photographic, for recording and reproducing counts, 17: 39404(P)
design of reactor period meter, 18: 7866(T) (AERE-Trans-969)
design of static, for 100-channel amplitude analyzers, 18: 5664
design of three-state, 19: 21785(P)
design of word-organized cryogenic, 19: 32530(P)
design using delay lines, 16: 33239
development, 17: 23851(R) (TID-18629)
development, 18: 8709(R) (TID-19993)
development, 20: 29499
development, 19: 11657(R) (NYO-1480-2)
development, 19: 26750(R) (NYO-1480-16)
development for Maniac III, 19: 18383(R) (TID-21595)
development for multichannel analyzers, 18: 16340
development for multichannel, multidimensional analyzers, 19: 15865 (NP-14692)
development for multidimensional, multichannel analyzers, 19: 15870 (NP-14716)
development for multichannel analyzers, 19: 18264 (NP-14710)
development for multichannel analyzers, 19: 42708 (AERE-R-4949)
development for Princeton Synchrotron, 20: 7676 (PPAD-567D)
development of analog, with nondestructive readout, 19: 15982 (SC-DC-65-1132)
development of ferroelectric ceramic resonators for, 18: 31051 (SC-R-64-128)
development of magnetic, 18: 30686
development of multiple-level, from quantization of trapped flux in superconductors, 17: 37721
development of superconductive, book, 18: 36438
development of superconductive bridge cells, 20: 16797
development of the cryosar for, 18: 36515
development of thin-film fast magnetic memories, 18: 23862
development of thin-film electrochemical cell for, 18: 27849 (SC-TM-282-63(74))
development of thin magnetic films for, 20: 29709(R) (TID-22970, pp pp 65-119)
matching ferrite operative and permanent, methods for, 18: 24516(T) (JPRS-24633)
model for associative memory, mathematical, 17: 32475 (SCR-641)
multi-parameter recording techniques, data handling by, 16: 14088
nondestructive-read mode for ferrite toroids, 19: 11657(R) (NYO-1480-2)
operation of computer, using light pencil and cathode-ray tube, 20: 5690
operation with defective storage elements, methods for, 19: 39269(R) (SU-SEL-64-133)
PEM, for precision-photographing of data, 17: 26949 (TID-18887)
performance and uses of magnetic, 19: 30498
performance of ferrite-core, in spark chambers, 18: 20371
performance of fourth-type recorder, 18: 43882 (IAE-603)
performance of storage tubes for pulse amplitudes, limiting factors in, 18: 25746 (NAS-NRC-Pub-1184(p.292-5))
properties of, 17: 38595 (CU(PNPL)-227(p.84-9))
properties of cryogenic associative and continuous film, (T), 20: 42108
properties of intermediate, effects of pulsed mode on, (E/T), 20: 2101 (JINR-P-2319)
properties of superconductive, 19: 21193
radiation effects on lithium ferrite cores, fast-neutron, 19: 13868
refrigeration requirements for superconducting continuous-sheet, 20: 46536
storage systems for, development of superconducting thin-film, 18: 26477
storage systems for, development of superconducting cable, 18: 26490
storage systems for nuclear physics, associative, 19: 36787
storage systems for, development of buffer, 19: 36790
storage systems for, survey of, 19: 36930
storage systems for, use of superconducting thin films in, 20: 19720 (CEA-Bib-65)
theory, 18: 23141 (SC-DC-64-433)
theory of superconductive, vortex, 20: 13689
transfer memory for ILLIAC III, information, 18: 3415 (TID-19694)
use for associative storage of multiparameter data, 19: 36789
use in spark detectors, 18: 43960
use of bulk core, to improve time-sharing efficiency of computers, 19: 38295 (CONF-650621-1)
use of cold cathode tubes as address elements and channel stores in multi-channel pulse analyzers, 17: 39384
use of content-addressable store in pulse analysis, 18: 30087 (AERE-M-1411)
use of core, in translator for nuclear physics experiments, 19: 30488 (RT/EL(65-1))
use of ferrite core memories for recording spark locations in wire spark chambers, 17: 14678
use of ferrite, with spark chambers, 17: 16427 (PPAD-461E)
use of storage tubes for high-speed pulse amplitude analysis, 18: 24021
use of storage tubes for display in multiparameter pulse experiments, 18: 25826 (NAS-NRC-Pub-1184(p.322-3))
use with pulse analyzers, 16: 1952(T) (AEC-tr-4701)

MENDELEVIUM
see also Actinides
chemical properties of, 16: 33008
discovery of, review of, 19: 18686
preparation, properties, and separation of, review on, 18: 39180
production, 20: 16543
production in heavy-ion nuclear reactions, review of, 20: 15740
production of, review of methods for, 20: 20796
properties and chemical separation methods of, 17: 15972
properties and separation of, review on, 19: 4161
radiography of, techniques for, 17: 10535 (JINR-P-1118)
separation by partition chromatography in nitric acid–tetrabutyl hypophosphate–tetrabutyl pyrophosphate systems, 19: 540
separation by partition chromatography using perchloric acid–tetrabutyl phosphates, 19: 28250
separation by solvent partition with ammonium citrate, lactate, and 2-methyllactate, 17: 9552
separation from californium and fermium by extraction chromatography using bis(2-ethylhexyl) orthophosphate, 20: 16404
separation from europium by solvent extraction using TBP–nitric acid and TBP–hydrochloric acid systems, 18: 23725
solvent extraction from nitrate solutions by TBP, 16: 29036 (JINR-P-1001)

MENDELEVIUM ISOTOPES
fission barriers and half lives of, spontaneous, (T), 20: 28357
production by neutron reactions with transneptunium elements, (T), 19: 13845 (ANL-6932)
production in fluorine-19 reactions (F-19,xn) with uranium-238, cross sections for, (E), 20: 13889

MENDELEVIUM ISOTOPES Md-250
production in fluorine-19 reactions (F-19,xn) with uranium-238, cross sections for, (E), 20: 13889

MENDELEVIUM ISOTOPES Md-252

production in fluorine-19 reactions (F-19,xn) with uranium-238, cross sections for, (E), 20: 13889
MENDELEVIUM ISOTOPES Md-255
decay properties and production, (E), 19: 47664
MENDELEVIUM ISOTOPES Md-256
chemical properties, 16: 13947 (JINR-P-866)
decay properties and production, (E), 19: 47664
production by neon-22 bombardment of uranium-238, 16: 15626 (JINR-P-874)
production by neon-22 reactions with uranium-238, 16: 13947 (JINR-P-866)
production in neon-22 reactions on uranium-238, 17: 9552
production in neon-22 reactions on uranium-238, 17: 9553
separation by solvent extraction, comparison of hydrochloric and nitric acid systems with TBP, 17: 10735 (JINR-P-1075)
MENDELEVIUM ISOTOPES Md-257
decay properties and production, (E), 19: 47664
MENDELEVIUM ISOTOPES Md-259
production by neutron reactions with various heavy elements, 19: 27504
production in Cyclamen underground thermonuclear explosion, 20: 45766 (LA-DC-8103)
production in neutron reactions with heavy nuclei, 18: 6154 (ANL-6756)
p-MENTHA-6,8-DIEN-2-ONE
radiolysis effects on optical activity of, 18: 5373
MENTHOL
atomic structure of, "electron burning" method of determination of, 20: 29326
radiolysis effects on optical activity of, 18: 5373
MENTHYL ACETATE
radiolysis effects on optical activity of, 18: 5373
MEPROBAMATE
radiation and chemical effects on metabolism of, gamma and x, 17: 35480
Mercamine
see Ethanethiol, 2-Amino-
Mercaptans
see Thiols
MERCAPTO GROUP
content in ascites tumor cells of non-protein bound, effects of cysteamine on, 19: 38464
content in liver and spleen of rats, effects of x radiation and cysteine on, 18: 6706
content in tumor, effects of vitamin K derivatives on, 19: 35908
content of protein, in rat tissues, effects of x radiation, cysteine, and cysteamine on, 18: 6707
determination by amperometric titration, 18: 37205(T) (AEC-tr-6398 (p.403-7))
effects of lipidic peroxides on, in albumin, 18: 33236(T) (ANL-Trans-54)
effects on α-ketoglutarate oxidation by rat-liver homogenates, 20: 20505
effects on distribution of hemoglobin and neutral red in tissues of mice and rats, 18: 17660
effects on DNA synthesis in mouse bone marrow and intestinal epithelium, 20: 31125
effects on fluorescence of europium and terbium dipyridyl complexes, 20: 10842
effects on radiation damage to proteins, 16: 17743
effects on radiation injuries in Ehrlich ascites carcinoma cells, effects of radioprotective agents on, 20: 35328
effects on radiosensitivity of *Escherichia coli*, 18: 33275(R) (NYO-910-2)
effects on radiosensitivity, mechanism for, 19: 2180
effects on uv-induced reactions in 3,4-benzpyrene in protein solutions, 18: 43682
electron spin resonance after irradiation at low doses, detection, 16: 6464
functions of, in cell membrane, 18: 4925 (UR-633)
metabolism in mice of sulfur-35-labeled, 18: 43312
physiological effects, 18: 31287
protective effects of mercazole against lethal radiation effects in mice, 16: 9178
protective effects of sulfanilamide disulfide against enzyme inactivation, 16: 21924
protective effects against radiation damage, reaction mechanisms, 16: 26855
protective effects against radiation injuries, 16: 30285
protective effects against radiation, reaction mechanisms in, 17: 2858
protective effects of, against radiation sickness, review, 17: 14112
protective effects against radiation injury of cells, 17: 30324
protective effects of, against radiation injuries, 17: 38906
protective effects with cysteamine against radiation damage in tumor cells, 18: 1456
protective effects against radiation injuries, 18: 1458
protective effects of, against radiation injuries, 18: 6704
protective effects against radiomimetic poisons and x radiation, 18: 29416
protective effects of, against radiation injuries in embryos of rats and mice, 18: 33423
protective effects against radiation effects in biological systems, review on mechanism of, 18: 35388
protective effects against radiation injuries, 18: 43316
protective effects against radiation injuries, 19: 3999
protective effects against radiation injuries in mice, 19: 8953(R) (NP-14448(p.36-64))
protective effects of, against radiation injuries, 19: 19640
protective effects against radiation injuries, reaction mechanisms for, 19: 29997
protective effects of, against radiation injuries, 19: 33972
radiation chemistry of aqueous solutions of, 18: 11653(R) (UCLA-520 (p.27-42))
radiation effects on levels, in liver proteins, 16: 9858(T)
radiation effects on protein-bound, in testis in rats, 17: 17788
radiation effects on content of, in nucleoproteins of rat liver, 17: 33640(T)
radiation effects on reactivity of, in spleen, 17: 35500
radiation effects on wheat gluten, treatment against x, 18: 3539
radiation effects on content of, in rat tissues, effects of thiols on, 18: 6705
radiation effects on, in skin of rats, 18: 8166
radiation effects on, 18: 31287
radiation effects on content in proteins of cotton seed, gamma and neutron, 18: 37205(T) (AEC-tr-6398(p.403-7))
radiation effects on content of, in cotton seeds, 18: 38944
radiation effects on pig ear, x, 18: 41204
radiation effects on blood levels of, x, 19: 3953
radiation effects on, in wheat gluten, gamma, 19: 17588
radiation effects on content in rat skin and blood serum, ultraviolet, 19: 21929
radiation effects on loss of titratable, in glutamate and lactate dehydrogenase solutions, 19: 25848
radiation effects on activity in blood plasma albumin, uv, 19: 33785(R) (AD-426004)
radiation effects on mouse tissue content of, x, 19: 35952(T) (JPRS-29641(p.44-52))
radiation effects on animal blood levels, 19: 38427
radiation effects on content in rat skin, uv, 20: 93
radiation effects on, in sea urchin eggs, thermal and uv, 20: 12624
radiation effects on content of, in *Serratia marcescens* cells, x, 20: 18448
radiation effects on blood content of, γ and x, 20: 20415
radiation protective effect of compounds containing, 16: 8623
radiation sickness effects on content in blood platelet metabolism, 16: 2918
radioprotective effects on lens of eyes, 17: 4441
radioprotective effects of, reaction mechanisms for, 18: 6680
radioprotective effects of, in plasma albumin solutions, 19: 3886(R) (AD-601083)
radiosensitivity effects in mice, 17: 15842
radiosensitivity effects of, 17: 38895
radiosensitivity effects in *Bacillus cereus*, 18: 11876
radiosensitivity effects of, in bacteria, 20: 1618 (NYO-3319-6)
radiosensitivity effects of ephedrine analogs of, in mice, 20: 3790
radiosensitivity effects in mammalian cells, effects of content on, 20: 14351
radiosensitivity effects in mice, mechanism for, 20: 14351
radiosensitivity effects of endogenous, in mice, x, 20: 18433
radiosensitivity effects of, reaction mechanisms for, 20: 18274
radiosensitivity effects on proteins, uv, 20: 22773(R) (AD-621079)
radiosensitivity effects of, 20: 29039
reactions in cellular proteins with mercurials, 20: 26632
reactions of, with mercury in membrane ligands in yeasts, 17: 13931
reactions with β-hydroxyethyl-2-4-dinitrophenyl disulfide, 20: 18722
reactions with enzymes, 19: 5723
reactivity, method of testing, 16: 31518(R) (TID-16657)
relation to enzyme activity, 17: 2826(R) (TID-17048)
relation to radiosensitivity of amino acids, 17: 2826(R) (TID-17048)
MERCAPTOMERIN
excretion of mercury-203-labeled sodium salt of, in patients in cardiac failure, 17: 10345
excretion rate of mercury-203-labeled, 18: 21794
Mercaptopropylamine
see 2-Propanethiol, 1-Amino-
Merchant Ship Reactor
see Maritime Pressurized Water Reactor
MERCHANT VESSELS
accident analysis for NS *Savannah* power plant, 17: 35135 (BAW-1164

(Vol.VII))
accident analysis for NS *Savannah*, 17: 35136 (BAW-1164(Vol.VIII))
analysis of surface-effect, using nuclear power, 18: 35215
behavior in waves, 16: 8417
book: *Naval Nuclear Power Installations*, 20: 18132
book: *Nuclear Energy Propulsion for Merchant Vessels. 3rd Yearbook of the Research Society for Development of Nuclear Energy Utilization in Shipbuilding and Ship Transport*, in German, 19: 3744
book: *Nuclear Propulsion for Merchant Ships*, 16: 23327
book: *Nuklearna Propulzija* (Nuclear Propulsion), 18: 4839
civil defense use of, as shelters or for evacuation, 18: 1960 (USNRDL-TR-659)
collisions of, effect of angular momentum on, 17: 18242
conference on nuclear ship propulsion with special reference to nuclear safety, Taormina, Italy, Nov. 14 to 18, 1960, 16: 8386
construction rules for nuclear-powered, 18: 7961
cost and operational comparison of conventional and nuclear, 16: 30124
crew training program for NS *Savannah*, 17: 35134 (BAW-1164(Vol.V))
description of first German nuclear-powered, 17: 17579
description of German nuclear (E), 19: 3731
description of German nuclear-powered, 19: 48051
description of proposed nuclear-powered Japanese oceanographic ship, 17: 19653
design and construction of nuclear-powered, as ore freighter, 17: 22865
design, construction, and safety of nuclear, 16: 3298
design, construction, and operation of NS *Savannah*, 18: 7963
design description of N.S. *Savannah*, 16: 7277
design description of NS *Savannah*, 17: 35131 (BAW-1164(Vol.I))
design for easy reactor servicing and re-fueling, 19: 5536(P)
design for easy servicing of reactor, 16: 31315(P)
design having organic moderated reactor, German project, 16: 6229
design of nuclear-powered Alpha II, 17: 2575 (DANATOM-04-62)
design of nuclear-powered tanker, 19: 11316
design of nuclear-powered bulk carrier, 19: 11317
design of nuclear-powered oceanographic research vessel, 19: 11318
design of nuclear-powered, in Japan, 19: 38249
design of nuclear-powered tanker using forced-circulation pressurized-water reactor, 20: 18126 (EUR-2629.i(Vol.1))
design of tanker using direct-cycle boiling reactor, 19: 12832
design of, using pressurized-water power plants, 17: 38560
design specifications of small nuclear experimental, 16: 11296
design using nuclear propulsion, 18: 38566
development of German PWR-powered tanker, 18: 23092
development of nuclear steam generator for, 16: 28530 (GEMP-107)
development of nuclear-propelled tanker, 17: 40370
development of nuclear-powered tankers in Japan, 19: 33626
development of nuclear-powered, in Italy, 19: 33660
development of nuclear-powered, 19: 48114
economic and safety factors of nuclear-powered, comparison with conventional ships, 17: 26876
economic aspects of nuclear oil tankers, 17: 15402 (NP-12554)
economic comparison of conventional and nuclear propelled, 16: 12752 (TID-14557)
economics of nuclear-powered tanker, 19: 45657 (TID-22088)
economics of nuclear, 20: 36511 (CEA-R-3022)
economics of, using Consolidated Nuclear Steam Generator, 19: 12820
electric power system for Lenin icebreaker, 16: 11240(T) (JPRS-12183 (p.35-54))
electric system of NS *Savannah*, 16: 34083
electrical system of NS *Savannah*, 16: 31284
facilities for Lenin icebreaker, 16: 11241(T) (JPRS-12183(p.55-78))
fires on, design of alarm system using radioactive materials for protection against, 18: 7098
gamma shielding for nuclear-powered, use of lead plates for secondary, (E/T), 20: 15932(T) (ORNL-tr-843)
gamma transmission through steel pipes of nuclear powered, 20: 16114
hull construction of nuclear-powered, collision-resisting, 18: 23090
hull model studies on nuclear-powered submarine tanker, 18: 26959 (RTI/ING(63)-4)
monitoring system of *Savannah*, digital, 18: 45077
nuclear design of N. S. *Savannah*, review, 16: 11294
nuclear, mounting of reactor for easy refueling in, 17: 29816(P)
nuclear power in U.S. Merchant Marine, 18: 35203 (NP-14139)
nuclear-powered, boiler for, 16: 34068(R) (GEMP-144)
nuclear-powered, characteristics and problems, 16: 14859
nuclear-powered, classification standards for, 16: 8397
nuclear-powered, control and instrumentation of organic reactor in, 16: 8404
nuclear-powered, construction of collision resisting ship-sides for, 16: 10137
nuclear-powered, comparison of reactors for, 16: 15934
nuclear-powered, control rod drive system specifications for, 17: 42353 (TID-19425)
nuclear-powered, design study for small, 16: 8408
nuclear-powered, design of direct-cycle boiling-water reactor for, 17: 15403 (NP-12555)
nuclear-powered, design feasibility of British, 17: 17632
nuclear-powered, development of ENEA, 17: 37006(R) (NP-13095)
nuclear-powered, effects of reactor scram on maneuverability, 16: 8413
nuclear-powered, effects of oscillation and vibration on reactor design for, 17: 15411 (NP-12564)
nuclear-powered, evaluation of ports for, 16: 8425
nuclear-powered, evaluation of collision-resisting sides, 16: 20573
nuclear-powered, fuel development for *N. S. Savannah*, 16: 28363 (GEAP-3253)
nuclear-powered, fuel irradiation program for Savannah I, 16: 28364(R) (GEAP-3869)
nuclear-powered, hazards analysis and modifications of NS *Savannah* reactor control rod drive system, 17: 26844 (BAW-1249(Vol.II))
nuclear-powered, health physics program for, 16: 9057
nuclear-powered, high-temperature gas-cooled reactors for, 16: 20011
nuclear-powered, hull design for, 17: 15401 (NP-12553)
nuclear-powered, hull structure design for, 17: 15409 (NP-12561)
nuclear-powered, legal problems from operation, 16: 8393
nuclear-powered, maintenance planning for N.S. *Savannah*, 16: 8419
nuclear-powered N.S. *Savannah*, port entry control and safety assessment provisions for, 16: 8400
nuclear-powered, neutron fluxes in shielding of N.S. *Savannah*, 16: 8411
nuclear-powered, optimum maneuverability, 16: 8414
nuclear-powered, operation of reactor, effects of oscillations on, 17: 15406 (NP-12558)
nuclear-powered, operation of, effects of vibrations on, 17: 15407 (NP-12559)
nuclear-powered, operation of, problems in, 17: 15408 (NP-12560)
nuclear-powered, radiation hazards, 16: 6666
nuclear-powered, recommendations and regulations for, 16: 8392
nuclear-powered, regulations governing classification, 16: 8398
nuclear-powered, regulations and rules for, 16: 8399
nuclear-powered, research on collision-resisting construction for, 16: 8418
nuclear-powered, refueling considerations, 16: 8420
nuclear-powered, safety, 16: 8396
nuclear-powered, safety considerations for operation in ports, 16: 8423
nuclear-powered, safety on shore in relation to harbor operation, 16: 8424
nuclear-powered, safety aspects, 16: 9026 (NP-11306)
nuclear-powered, safety system for dispersal of decay heat after reactor shut-down in, 16: 28514(P)
nuclear-powered, safety problems in Fiat Ansaldo study of 50,000-ton tanker, 16: 8401
nuclear-powered, safety measures for, 17: 15404 (NP-12556)
nuclear-powered, safety assessment of NS *Savannah*, 17: 35155 (TID-17885)
nuclear-powered, testing preparations and results for N.S. *Savannah*, 16: 8394
nuclear-powered, theoretical consequences of reactor accidents on N.S. *Savannah*, 16: 8422
nuclear-powered, vapor suppression for reactor container in, 16: 8412
nuclear-powered, waste-disposal problems, 16: 8421
nuclear powered, safety of, 18: 10320
nuclear powered, safety procedures, 19: 14879(T) (JPRS-28656)
nuclear propulsion, safety aspects, 16: 3302
nuclear propulsion, economic aspects, 16: 3949
nuclear propulsion, evaluation of various reactor types for, 16: 8379
nuclear propulsion, economic analysis, 16: 8387
nuclear propulsion, economic studies, 16: 8388
nuclear propulsion, economic studies in Yugoslavia, 16: 8389
nuclear propulsion, activities in Western Europe, 16: 8390
nuclear propulsion, outline of Japanese activities 1955 to 1960, 16: 8391
nuclear propulsion, safety aspects, 16: 8395
nuclear propulsion, effects of direct-cycle operation of boiling-water reactor on safety, 16: 8406
nuclear propulsion, behavior and testing of boiling-water reactors for, 16: 8407
nuclear propulsion systems, comparison, 16: 11283
nuclear propulsion, development in Germany, 16: 11284
nuclear propulsion, comparative study of reactor systems, 16: 11285
nuclear propulsion, Dutch studies, 16: 11287
nuclear propulsion, Norweigen studies, 16: 11288
nuclear propulsion plant design for turbo-tanker of 70,000 tons displacement, 16: 32590
nuclear propulsion, safety of organic-moderated reactors for, 16: 8405
nuclear propulsion of, review of advantages and disadvantages, 17: 10252
nuclear propulsion, use of magnetohydrodynamic generators for, 17: 18243
nuclear propulsion of, design and economic evaluation of, 17: 21326
nuclear propulsion, use of spent plutonium-containing uranium fuel for,

17: 42245(P)
nuclear propulsion system for tanker, design of 20,000-shp, 18: 1289
nuclear propulsion of, review of power plants for, 18: 3309
nuclear propulsion of, prospects for, 18: 4837
nuclear propulsion systems for, 18: 35205
nuclear propulsion for, EURATOM program on, 18: 43066
nuclear propulsion for, economic and safety aspects of, 18: 43070
nuclear propulsion of, 19: 1931
nuclear propulsion of, bibliography on, 19: 12803 (AED-C-22-03)
nuclear propulsion of, status of, 19: 12830
nuclear propulsion for, EURATOM program for, 19: 33658
nuclear propulsion plant for the *Otto Hahn*, 19: 33659
nuclear propulsion of, development of, 19: 42143
nuclear propulsion of, feasibility of, 20: 26523
nuclear propulsion for, economic advantages of, 20: 26524
nuclear propulsion for, cost and performance comparison of conventional power with, 20: 26522
nuclear-powered economic aspects, 19: 19411
nuclear-powered, automatic electric propulsion system drive of ice-breaker *Lenin*, 18: 13324
nuclear-powered, boiling reactor shielding for, (T), 19: 24152
nuclear-powered, containment and installation of German advanced pressurized-water reactor on ore-carrier ship, 18: 38554 (A/CONF.28/P/540)
nuclear-powered, civil responsibility of operators of, 18: 41689
nuclear-powered, cost comparison of, with conventionally powered, 19: 3759
nuclear-powered, collision protection for, 19: 3768
nuclear-powered, classification society requirements for, 20: 26527
nuclear-powered, design of pressurized-water reactor for, 18: 11476
nuclear-powered, development of 27,300-SHP, 18: 13315(R) (GEMP-231)
nuclear-powered, design of reactor for German, 18: 19413
nuclear-powered, design problems for installation of reactor plant, 19: 3765
nuclear-powered, design of integrated pressurized water reactor for, 19: 12821
nuclear-powered, design of natural-circulation pressurized water reactor for, 19: 12822
nuclear-powered, design and economic factors of, 19: 12831
nuclear-powered, development in Germany, 19: 24153
nuclear-powered, development plans and policies for, 19: 24155
nuclear-powered, development in Japan, 19: 33627
nuclear-powered, design of German ore-carrier, 19: 38248
nuclear-powered, design of German, 20: 12463 (CONF-640810, pp 138-55)
nuclear-powered, economics, 18: 33126 (EUR-586.d)
nuclear-powered, economic comparison with conventional ships, 19: 3760
nuclear-powered, economic and legal proplems of insurance for, 19: 3761
nuclear-powered, economics of, (T), 19: 6867
nuclear-powered, Euratom development program on, 19: 21724
nuclear-powered, experiments on repair of damaged, 19: 22628
nuclear-powered, economics and prospects of British, 19: 24154
nuclear-powered, economic comparisons with conventional ships, 19: 42132 (GE-TM-65-3-6)
nuclear-powered, economics of, 20: 12459 (CONF-640810, pp 1-6)
nuclear-powered, feasibility studies on boiling reactors for, 19: 12835
nuclear-powered, hazards of port visits by, 18: 43852
nuclear-powered, hydrodynamic characteristics in collisions, 19: 3769
nuclear-powered, international requirements and safety aspects of, 20: 26526
nuclear-powered, licensing of, 20: 12464 (CONF-640810, pp 156-65)
nuclear-powered, port facilities and requirements for, 20: 26525
nuclear-powered, rules for construction of, 18: 17321 (RTI/ING(63)-5)
nuclear-powered, reactor shielding optimization for, 19: 3770
nuclear-powered, reactor containment vessel leak rate tests on N.S. *Savannah*, 19: 3752
nuclear-powered, reactor safety requirements for, 19: 3766
nuclear-powered, reactor containment vessel design for, 19: 12829
nuclear-powered, research programs on, 19: 23999
nuclear-powered, research on, 20: 12458 (CONF-640810)
nuclear-powered, role of, 20: 12460 (CONF-640810, pp 7-21)
nuclear-powered, safety of waste disposal into water, 18: 15657 (NP-13685)
nuclear-powered, safe containment of reactor for, 19: 3767
nuclear-powered, safety acceptance procedures for, 19: 2564
nuclear-powered, safety acceptance of, standardization of international law for, 19: 2565
nuclear-powered, stopping distances for, 19: 12833
nuclear-powered, servicing facilities and technical support staff for N.S. *Savannah*, 19: 25756
nuclear-powered, status of, 19: 27815
operating manual description for NS *Savannah*, 17: 35132 (BAW-1164 (Vol.III))
operation of N. S. *Savannah*, port evaluation for, 17: 21931 (ORNL-TM-569)
operation of N. S. *Savannah* on first Atlantic voyage, description of, 19: 5532
operation of nuclear icebreaker Lenin, 19: 5535
operation of nuclear-powered, site selection guides to, 19: 12826
operation of N.S. *Savannah*, initial, 18: 1288
operations of N.S. *Savannah*, May 1962 thru March 1963, 18: 33131 (TODD/SML-NSS-6)
operations organization and management for N.S. *Savannah*, 17: 35133 (BAW-1164(Vol.IV))
performance of icebreaker Lenin, 19: 1919
port operation of nuclear-powered, safety analysis for, (T), 19: 12827
power plants for, economics and prospects of nuclear, 18: 9720
power reactors for, effects of ship's motion on kinetics of, 18: 7962
power reactors for, survey of world development of, 19: 33657
propulsion of icebreakers, performance of nuclear systems for, 17: 13788
propulsion of ore-transport, description of nuclear reactors for (E), 19: 3734
propulsion of research-oriented, pressurized-water reactors for (E), 19: 3733
propulsion of, bibliography on nuclear, 18: 38559 (AED-C-22-02)
propulsion of, coupling possibilities of BBC/KRUPP-type reactor for, 19: 3755
propulsion of, design of Dutch NEREUS reactor for, 19: 3746
propulsion of, design of horizontal pressurized-water reactor for, 19: 3748
propulsion of, design of CNSG III reactor for, 19: 3749
propulsion of, design of pressurized-water reactor for, 19: 3750
propulsion of, design of reactor for, 19: 3753
propulsion of, design of 20,000-shp BBC/KRUPP-type reactor for, 19: 3754
propulsion of, design of gas-cooled beryllium oxide-moderated reactor for, 19: 3756
propulsion of, design of FDR pressurized water reactor for, 19: 3762
propulsion of, design of FDR pressurized water reactor for, 19: 3763
propulsion of, development of pressurized-water reactors for, 19: 3745
propulsion of, dynamic processes in boiling reactors for, 19: 3751
propulsion of, economic feasibility of nuclear, 18: 43058 (EUR-586.d (App.))
propulsion of, reactor design for, 19: 33661
propulsion of, reactor development for, 20: 35038
propulsion of, special requirements in design of reactors for, 19: 3764
propulsion systems for, bibliography on, 19: 45647 (AED-C-22-64)
propulsion, development of Vulcain reactor for, 19: 3747
radiation hazards from nuclear-powered, 16: 22489
radiation monitoring at mooring area of Russian atomic icebreaker, Lenin, 16: 2064(T) (AEC-tr-4670)
radiation protection in nuclear-powered, 17: 3255
radiation protection of personnel at nuclear power station of icebreaker *Lenin*, 17: 42365
radioactive aerosols and gases on, monitoring of, 19: 28602
reactor development and economics for, review of, 20: 32854
reactor for, design of Consolidated Nuclear Steam Generator II, 18: 21667 (BAW-1280)
reactor safety in, 18: 35209
reactor startup sequence for, automation of, 20: 18130
safety aspects of N. S. *Savannah*, 18: 43067
safety consideration in N. S. *Savannah*, 16: 11295
safety considerations of nuclear-powered, 19: 12828
safety devices against radiation injuries on nuclear powered, 17: 15485
safety of nuclear-powered, review of 1964 Geneva papers on, 19: 24779
sea-motion acceleration surveys for large, 18: 39406 (RT/ING(64)7)
steam generating plant for, design of, 17: 30656(P)
tour of U.S.S. *Enterprise*, 17: 10106
translations on Lenin icebreaker, 16: 11237(T) (JPRS-12183)
vibration testing of, for determining position for reactor, 17: 15410 (NP-12563)
visit of N.S. *Savannah*, at Copenhagen, 20: 18174(R) (NP-15771)
waste disposal system for Walter F. Perry, 19: 12825

MERCURY
acceleration of plasma of, by electric field gradient, (E), 19: 47714(R) (AD-613307)
activation of, shielding effects during thermal neutron, 18: 6184(T) (SC-T-523)
alkali atomic beam scattering at 7 to 500 ev, cross sections for, 20: 39599
alkali metal scattering by, cross sections and rainbow effect in, (E/T), 20: 2636
analysis and determination, 20: 14500
analysis for mercury-197 and -203, calculation method for, 18: 20059

analytical applications of electrodes of, review on, 16: 16318
behavior in waste solutions, 17: 28581(R) (HW-77299)
behavior of electric arcs in vaporous, 16: 11079(T) (FTD-TT-61-92)
bibliography on technology of liquid, 18: 929 (NP-14434)
bifurcation instability in axial magnetic field, 16: 4610(R) (TID-14435)
binding to erythrocytes, tracer study, 16: 23393
biological effects of exposure to vapor of, in pigeons, 18: 25057 (UR-645)
boiling, 17: 20161 (BNL-756(p.236-61))
boiling and entrainment mechanisms for, 17: 36860(R) (ANL-6648)
boiling heat transfer, pool, 16: 27189(R) (AD-270678)
boiling heat transfer run in agravic apparatus, 19: 9321(R) (AD-606826)
boiling heat transfer and pressure drop, effects of helical flow on forced-flow, 19: 32367 (CONF-640507(p.281-96))
boiling heat transfer, effects of surface and system contaminants on pool, 20: 36987 (NAA-SR-11949)
boiling hexane and water from surface, nucleate, 16: 20617
boiling in agravic fields, 19: 24673 (NP-14953)
boiling in radiantly heated boiler, forced-convection, 18: 31725(R) (SAN-409-5)
boiling kinetics of, nucleate, 18: 6933
boiling of, at accelerations from 1 to 20 g, equipment for studying, 17: 20154 (BNL-756(p.114-25))
boiling of, at 1000 to 1400°F, design of equipment for studying, 17: 20160 (BNL-756(p.228-35))
boiling 2-propanol and water on surfaces of, nucleate, 16: 20618
boiling, surface tension, and wetting of, review on, 20: 29620 (NP-16046)
boundary-layer separation in MHD flow of, magnetic-field effects on, (E/T), 19: 32788(T) (FTD-TT-65-27)
bremsstrahlung reactions (γ,n) at 8 to 16 Mev, spectra from (E), 20: 15723 (MIT-2098-162)
bremsstrahlung reactions (γ,n) with, neutron emission in, (E), 20: 15724 (MIT-2098-224)
bremsstrahlung spectra, 19: 9445 (LA-3130)
bubble entrainment in flow of, 19: 32387 (NP-15051)
catalytic effects on cerium sulfate autoreduction in sulfuric acid solutions, 18: 12086
catalytic effects on labeling hydrocarbons with tritium by photolysis reactions, 18: 31588
catalytic effects on sulfuric acid dissolution of aluminum and SAP, 19: 26474
catalytic effects on dissolution of ceramics, 20: 9088(P)
cavitation damage to materials in, 19: 9623 (NP-14632)
cavitation damage to materials in, (E), 20: 16974 (NP-15889)
cavitation effects on materials in venturi, 18: 3955 (NP-13319)
cavitation effects on steels, tracer study of, 18: 8483 (NP-13517)
cavitation in flow in venturi, detection of, by gamma absorption, 18: 8484 (NP-13518)
cavitation in flowing, void fraction measurements using gamma densitometer, 18: 20167 (NP-13812)
cavitation in flowing, void fraction measurements using gamma densitometer, 18: 20167 (NP-13812)
cavitation number measurements in, effects of argon on, 19: 9330 (NP-14605)
cavitation of iron and steels, 16: 13537
cavitation of iron and steels by liquid, 16: 33434(T) (AEC-tr-5382)
cavitation of stressed stainless steel in, 19: 2725 (NP-14437)
cesium scattering by, velocity dependence of differential cross sections for, 17: 6836
charge exchange with iodine ions near resonance, 18: 34448
charge transfer cross sections for vapor of, resonant, 18: 16708
charged-particle beam interactions with plasma of, 18: 44853 (ML-1214)
condensation, conference on, 16: 14354 (NASA-TN-D-1188)
condensation of saturated vapor in nozzles, theory, 17: 8345
condensation of vapors of, in jet condenser, 19: 4323 (ORNL-3605 (Vol.2)(p.153-97))
condensation of vapors of, in tubes, pressure drop of, 19: 4324 (ORNL-3605(Vol.2)(p.198-234))
condensation of vapors of, 19: 18107 (ANL-6948)
condensation of vapors of liquid, heat transfer during film, 19: 32362 (CONF-640507(p.153-71))
contact angle hysteresis in benzene–water systems, 16: 17881(R) (MITS-47)
containment of boiling, development of loops for, 18: 12627(R) (BNL-823 (p.66-93))
content and distribution in beef heart, 19: 45753 (AE-191)
content in human heart, neutron activation determination of, 18: 33457 (AE-146)
content in teeth after use in dental restorations, 20: 27
cooling rate in magnetic field, equation for, 16: 1775
corrosion effects on titanium, inhibiting effects of dissolved aluminum, nickel, or zirconium on, 19: 44616(R) (ANL-7000, pp 122-37)
corrosive effects on titanium at 371°C, 16: 12649(R) (ANL-6485)
corrosive effects on titanium alloys at 700°F, 16: 16683 (TID-7626 (Pt.I)(p.107-8))
corrosive effects, conference, 16: 16676 (TID-7626(Pt.I))
corrosive effects on carbon steel at 600 to 1400°F, 16: 16677 (TID-7626 (Pt.I)(p.23-34))
corrosive effects of superheated, on loop materials, 16: 20042(R) (BNL-696)
corrosive effects of, on containment materials in aerospace power conversion systems, 16: 29336(R) (AGC-0584-04-3)
corrosive effects of, on cooling system materials for SNAP-II, 16: 32079 (NAA-SR-6306)
corrosive effects on carbon steels and refractory metals at 600 to 1400°F, 17: 2464(R) (BNL-731(p.59-94))
corrosive effects on metal at 900 to 1180°F, 17: 11129
corrosive effects on titanium alloys at high temperatures, 17: 14740 (TID-11295(2nd Ed.))
corrosive effects on Haynes 25 alloy, niobium alloys, and steel at high temperatures, 17: 19726 (BNL-759(p.54-77))
corrosive effects on chromium steels, 17: 31760(R) (MND-P-1175)
corrosive effects on steels, 17: 31761(R) (MND-P-3001)
corrosive effects on steels, 17: 31762(R) (MND-P-3002)
corrosive effects on steels, 17: 31763(R) (MND-P-3003)
corrosive effects, 17: 31798(R) (BNL-782(p.60-91))
corrosive effects on titanium at 538°C, 17: 35078(R) (ANL-6739)
corrosive effects on Haynes 25 Alloy to 1080°F, 17: 36200(R) (NP-13033)
corrosive effects on carbon steel, inhibition by titanium and zirconium, 17: 36233
corrosive effects on titanium at 538°C, effects of magnesium and nickel on, 17: 36861(R) (ANL-6764)
corrosive effects on titanium alloys, effects of inhibitors on, 17: 41333(R) (ANL-6677)
corrosive effects on niobium–zirconium alloy at 315 to 870°C, 18: 4160(R) (BNL-799(p.74-100))
corrosive effects on SNAP-8 materials at high temperatures, 18: 7152
corrosive effects on construction materials, 18: 8455
corrosive effects on insulated electric conductors at 538°C, 18: 10466(R) (AD-404273)
corrosive effects on titanium and titanium alloys, 18: 10492
corrosive effects on titanium at 320 to 454°C, effects of nickel on, 18: 15663(R) (ANL-6808)
corrosive effects of liquid, technical progress review on, 18: 18307
corrosive effects on steels, 18: 18312(T) (CEA-tr-A-1455)
corrosive effects, 18: 21675 (NP-13795)
corrosive effects on Haynes 25 Alloy, tests of separator for products of, 18: 21677 (TID-20552)
corrosive effects on titanium, 18: 21698(R) (ANL-6860)
corrosive effects on titanium, effects of nickel inhibitors on, 18: 25919(R) (ANL-6868(p.190-200))
corrosive effects of, inhibiting effects of titanium and zirconium on, 18: 27892 (NASA-SP-41(p.67-71))
corrosive effects on metals at 600 to 1000°F, 18: 27913
corrosive effects on steel, measurement using tracer techniques, 18: 27336
corrosive effects of liquid, review of, 18: 32082 (A/CONF.28/P/244)
corrosive effects on Croloy 9M at high temperatures, 18: 32086(R) (NASA-CR-54066)
corrosive effects of gaseous, on ceramic-insulated wires, 18: 37304 (APL-TDR-64-42)
corrosive effects of boiling, on niobium–zirconium alloy and tantalum, 18: 41933 (TID-11295(3rd Ed.))
corrosive effects on reactor materials, 18: 41947
corrosive effects on Croloy 9M at high temperatures, 19: 6269(R) (NP-14439)
corrosive effects of boiling, on niobium–zirconium alloy, 19: 7863 (BNL-7642)
corrosive effects on niobium-zirconium alloys, effects of magnesium on, 19: 15991(R) (BNL-841(p.63-101))
corrosive effects on carbon steel, 19: 20493
corrosive effects on tantalum at 650 to 760°C, 19: 23355(R) (BNL-867(p.1-117))
corrosive effects on niobium–zirconium alloys, stress cracking in, 19: 28763
corrosive effects at 350 to 1350°F, 19: 32657(R) (MND-P-3007)
corrosive effects on materials for turboelectric power plants, 19: 36949(R) (BNL-900(p.121-97))
corrosive effects on zirconium nitride, effects of dissolved titanium on, 19: 44616(R) (ANL-7000, pp 122-37)
corrosive effects on aluminum, 19: 48060(R) (IDO-17081, pp 1-47)
corrosive effects on Hastelloy C and tantalum at 150°C, 19: 46428(R) (ORNL-3847)
corrosive effects on alloys and metals, 20: 2264
corrosive effects on type 316 stainless and 9 chromium–1 molybdenum steels at 1250°F, 20: 11214(R) (NASA-CR-54717)

corrosive effects on Croloy 9M at 1074°F, 20: 19189 (N-65-21161)
corrosive effects on high-temperature metals and alloys at 593 to 860°C, 20: 25474(R) (BNL-954, pp 122-67)
corrosive effects on refractory metals and stainless steels at 593 to 703°C, 20: 29646
corrosive effects on titanium at 538°C, effects of additives on, 20: 31669
corrosive effects on Croloy 2¼-molybdenum steel, 20: 33834
corrosive properties at 1075°F, design of loop for testing, 16: 11810(R) (AGC-0584-04-1)
crystallization with thionalid, tracer study of co-, 16: 12961 (USNRDL-TR-551)
crystallographic analysis of solid, 18: 24994(R) (MND-2531-1)
current densities in cesium-seeded plasma of, (E), 20: 39736
density at 234 to 1733°K, 20: 12825 (NYO-2082-1)
detection of vaporous, in vacuum systems, 17: 39223 (UCRL-7399-T)
detection of vapors of, in air, calibration of detector for, 18: 22317 (UCRL-7730)
determination as impurity in and volatilization from tungsten, semi-quantitative spectrographic, 16: 4131 (BM-RI-5903)
determination by atomic absorption spectroscopy, 17: 15857(R) (ORNL-3397(p.57-70))
determination by atomic-absorption spectroscopy, 17: 40716 (TID-7655 (p.379-89))
determination by activation and isotope dilution, substoichiometric, 18: 21997
determination by complex formation with ethylenediamine sulfate and iodine-131, 16: 26925
determination by double activation analysis, 18: 23425
determination by double-activation methods, 19: 13249
determination by flame spectrophotometry, emission sensitivity for, 16: 22028
determination by isotopic exchange with mercury or silver di-n-butyl phosphorothioate extraction system, 18: 6752
determination by isotope exchange, 19: 22818(R) (ORNL-3650(p.221-38))
determination by solvent extraction and spectrophotometry using 1-(2-pyridylazo)-2-naphthol, 16: 139
determination by spectroscopy using high-frequency plasma flames, 18: 10020
determination by thermal-neutron activation methods, sensitivity for, 19: 9071
determination by x-ray fluorescence after paper electrophoretic separation, 17: 1406
determination in aqueous solutions, fabrication of pyrolytic graphite electrode for, 17: 40723
determination in aqueous solutions by gamma-excited x-ray fluorescence, 19: 24477
determination in biological materials, 16: 18823
determination in biological materials, activation, 16: 23403
determination in biological materials by ion exchange and gamma spectrometry, 18: 13660
determination in biological and organic materials, activation, 18: 15971
determination in biological materials, neutron activation analysis for, 19: 2254
determination in biological materials by activation methods, 19: 13229
determination in beneficiation products by neutron absorption, 20: 33183(T) (AEC-tr-6639, pp 114-17)
determination in beneficiation products by beta scattering, 20: 33185(T) (AEC-tr-6639, pp 122-5)
determination in cerium, mass spectrographic, 19: 2232
determination in copper by activation, 19: 40422
determination in conductive tissue of beef heart, activation, 20: 31176
determination in drugs by beta backscattering, 16: 22023
determination in drugs, activation, 19: 4081
determination in drugs, activation, 19: 24400 (KR-91)
determination in enrichment products, activation, 18: 43423
determination in electrolytic cells, radiometric, 20: 2520(R) (IA-920)
determination in galena, radiometric, 18: 31048(R) (COO-689-42)
determination in hair by activation methods for identification of individuals, 19: 17824
determination in human blood, activation analysis method for, 19: 31728
determination in high-purity bismuth by neutron-activation methods, 20: 22887
determination in human heart tissue, activation, 20: 31175
determination in iron meteorites by slow-neutron activation, 20: 43550(R) (NYO-844-67)
determination in minerals by neutron activation, 19: 30424
determination in nitric acid solutions by titration, 18: 13637(R) (ORNL-3537(p.111-18))
determination in ores, activation, 18: 43434
determination in ocean deposits, 20: 43550(R) (NYO-844-67)
determination in presence of ethylenediamine, method for, 16: 25272(R) (TID-16332)
determination in plant materials, isotope dilution method, 16: 28892
determination in pharmaceuticals, method for, 18: 5217
determination in pure uranium compounds by solvent extraction using dithizone, 18: 33509
determination in paint by activation, age estimation of white lead by, 19: 11035
determination in ppm range by d-c arc excitation, spectrochemical, 19: 19827
determination in potato flour, mercury-197 separation in neutron activation, 20: 18595
determination in petroleum, activation, 20: 29139
determination in rice, isotope-dilution method, 17: 29958
determination in rocks, activation, 18: 25307
determination in radioactive glasses, 19: 32059(R) (IDO-14655)
determination in skin tattoo marks, activation, 16: 32924
determination in silicon, activation, 18: 33502
determination in selenium, activation, 18: 39103
determination in solutions, x-ray fluorescence, 19: 5825
determination in sea water by neutron activation methods, 19: 22574
determination in silicates, activation, 20: 26782
determination in seawater, activation, 20: 40834
determination in sagebrush, colorimetric and spectrophotometric, 20: 43067(R) (IDO-14679, pp 6-46)
determination in tobacco leaf and wheat by neutron activation methods, 20: 1755
determination in urine, activation, 16: 12801(R) (IA-685)
determination in urine, chemical procedures for, 18: 13642 (SC-4783(RR))
determination in vanadium, chemico-spectrographic, 18: 13708
determination in water, silver-spark spectrographic, 17: 1381 (IDO-14591)
determination in white lead for age determination of paintings, activation, 19: 5820
determination in wheat, activation, 19: 19771(R) (TEES-2671-4 (Chap.9))
determination in wheat, activation, 20: 1738(R) (GA-4041)
determination in wheat, activation, 20: 1739(R) (GA-4297)
determination in zirconium by activation, 19: 24418
determination of, in biological materials, activation, 17: 19951
determination of submicrogram amounts of, in lithium, lithium hydride, and lithium hydroxide, 19: 34115 (Y-1482)
determination of traces of, by radioisotope methods, 17: 30150
determination of traces of, using oxycellulose, 17: 35656
determination of trace amounts of, by reactor neutron activation methods, 20: 26760
determination of, procedure for, 19: 7274(R) (IDO-14636)
determination of, in radiosensitizers in tissues, neutron activation, 20: 31172 (SGAE-BL-17/1966)
determination of, in high-purity lead by neutron activation analysis, 20: 35412
determination of, using isooctylthioglycolate, 20: 40796(R) (IS-1500 (Sect.C))
determination of, developments in resin spot tests for, 20: 40827
determination of, in whole blood by neutron activation analysis using freezing, 20: 45602
determination of, in water by neutron activation analysis using freezing, 20: 45602
determination using cyclohexanediaminetetraacetic acid, potentiometric, 18: 33507
determination using sulfatoceric acid, titrimetric, 18: 41355
deuteron reactions at 11 Mev, thallium isomers from, 18: 6276
deuteron scattering by, cross sections for, 18: 26560
development of dropping electrode of, 18: 19837(R) (MIT-905-1)
diagnostic tracer use of, for gastrointestinal diseases, 19: 43886
diagnostics of moderate-pressure plasma of, method of detector characteristics for, (E/T), 20: 28533
diffusion in air at 5000°K, 16: 15312(T)
diffusion into zinc, 19: 42459(R) (RPI-1044-7)
dispersion in graphite, optimum pressure and temperature for liquid, 20: 39355 (EUR-2988.f)
dissociation energy of gaseous and heat of vaporization of solid, correlation of, 17: 6095
dissolution of bismuth and tin cylinders in, magnetic boundary layer separation in, 19: 18595
distribution between Dowex-1 × 8 and sodium perchlorate solutions, 16: 12801(R) (IA-685)
distribution between Dowex-1 anion exchanger and halide solutions, 17: 28860
distribution of, between nitric acid and ion-exchange resin, synergistic effects of thorium on, 17: 15948 (LA-2836)
effect on the dissolution of ceramics containing beryllium oxide, catalytic, 20: 2252(P)
effects of inhaled vapor on behavior of pigeons, 16: 25154 (UR-578)
effects of kidney poisoning by, on life span of mice, 17: 31827

effects of plasma of, on thermionic diodes in autonomous discharges, 19: 39435(T) (JPRS-31048)
effects of vapor of, on operation of cartridge heaters in vacuum, 19: 7663 (NAA-SR-Memo-10386)
effects on cesium performance in thermionic diodes, 18: 44502
effects on complexonometric determination of holmium and lanthanum, masking of, 19: 17822
effects on corrosion resistance of beryllium, 19: 22913(P)
effects on decomposition products of cyclobutane, 20: 25125(R) (RRL-2310-174)
effects on determination of lead in cobalt by colorimetric and isotopic dilution methods, 19: 30115
effects on determination of copper in high-purity metals by activation methods, 19: 43973
effects on dissolution of aluminum-base fuels in boiling nitric acid, catalytic, 20: 7214(P)
effects on ductility of brass, 18: 14354(R) (ARF-B215-12)
effects on fluorescence of uranium in sodium carbonate–sodium fluoride melts, 18: 33506
effects on gastrointestinal absorption of copper-64 in rats, 20: 16182
effects on mechanical properties of zinc crystals in presence of radiation, 17: 16749
effects on mechanical properties of irradiated zinc crystals, 17: 29381
effects on mechanical properties of zinc crystals, 18: 10590
effects on neutron-irradiation annealing in gold, 17: 5012
effects on photolysis of propylene and deuterium-labeled propylene, 19: 11193
effects on photosensitized decomposition of cyclobutane, 20: 12884(R) (RRL-2310-171)
effects on radiation effects on mechanical properties of zinc crystals, 19: 23131
effects on radioinduced deformation of zinc single crystals, 17: 16676
effects on spectrophotometric determination of zinc using 1-(2-thiazolylazo)-2-naphthol, 19: 19814
effects on spectrophotometric determination of thorium, 19: 24408
effects on thallium superconducting transition temperature, 18: 21113
electric and thermal conductivities of liquid, correlation over entire liquid range, 19: 44701(R) (TID-22144)
electric arc discharges in, stability of, (E), 19: 21490(R) (TID-21698)
electric arcs in, effects of azimuthal magnetic fields on, 17: 14988
electric arcs in, interactions with 4.4- to 22-kMc electromagnetic waves, 16: 29923
electric arcs in, movement of ball-of-fire and cathode spot during, 16: 26018
electric characteristics of plasma, in thermionic converters, 16: 19625
electric conductivity at 25 to 300°C, 17: 37534
electric conductivity at high temperatures, method for electrodeless determination of, 18: 409 (NAA-SR-8833)
electric conductivity of liquid, temperature dependence of, 19: 16079 (TID-21647)
electric conductivity and thermoelectric power of liquid, (T), 19: 23052
electric conductivity of turbulent plasma of, (E), 20: 15895
electric conductivity of, at 234.28 to 1733°K, 20: 21377
electric conductivity below superconducting transition, temperature effects on surface, (E), 20: 32343
electric conductivity of liquid, 20: 41476
electric conductivity of superheated vapor of, (E), 20: 46320(R) (AD-628187)
electric currents in cylinders of, stability of persistent, 20: 13691
electric dipole moment and KL_I transition in, 20: 9680
electric discharge, ionization coefficients in Townsend-type, 16: 19609
electric discharge, instability in magnetic field, 16: 31166
electric discharge in, ion concentration and spectral broadening in, 17: 9060
electric discharge in vapor of, in diodes, 17: 11441
electric discharge in, dissociative recombination coefficient for, 17: 22711 (AD-283041)
electric discharge in, electron energy distribution in positive column, 17: 36509
electric discharge in, energy exchange between electrons in, 17: 42125
electric discharges in, pressure dependence of parameters of a-c, 18: 7408
electric discharge in, electron–gas temperature differences in positive column of, 18: 13157(T)
electric discharge in, electron distribution function for, 18: 15401
electric discharge in, effects of magnetic field on positive column, 18: 17142
electric discharge in, processes in high-voltage, 18: 18468
electric discharge in, ionization phenomena in, 18: 21476
electric discharge in, Landau damping effects in, 18: 30931
electric discharge in, current limitation in, 18: 42169
electric discharges in, electron free path lengths in, 19: 1743
electric discharge in, double-sheath structure in, (E/T), 19: 14672 (SU-ML-1261)
electric discharge in, longitudinal wave-propagation in, (E), 19: 23891
electric discharges in, electron excitation of uhf oscillations in low-pressure, (E), 20: 38215
electric discharges in, electron excitation of uhf oscillations in low-pressure, (E), 20: 38216
electric double layer in discharge plasma of, thickness of cylindrical, (E), 20: 20086
electric field effects on cylindrical plasma of, secondary resonances from dipolar, 18: 4660
electric power generation with plasma of, 19: 35009(P)
electric power production from jets of ionized vapor in energy conversion device, 16: 19623
electric probe saturation current in plasma of, magnetic field effects on, (E), 19: 14695
electric properties of cesium-seeded plasma of, (E), 20: 39738
electrical effects of surface layers of, on work function of copper in hydrogen, 16: 19608
electrochemical proton discharge on, isotope effects of deuterium, hydrogen, and tritium on, 18: 37118
electrochemical sputtering of graphite by, 17: 20659
electrochemistry of double layer at interface between aqueous solutions and, 18: 8322 (IS-598)
electrochemistry of oxalic acid aqueous solutions on dropping electrodes of, during radiolysis, 19: 15631
electrokinetic effects in liquid, 17: 18797
electrolytic deuterium–hydrogen separation factor at, 18: 32005
electromagnetic and longitudinal wave propagation in plasma column of, dispersion relations for coupled, (E/T), 20: 26243 (IPP-3/33)
electromagnetic wave scattering resonances in plasma of, a-c resonant probe relation to, (T), 20: 12241
electromagnetic wave scattering by electro-acoustic waves in arc column of plasma of, (E), 20: 22232
electromagnetic-wave interactions with oscillations in plasma of, resonant suppression in, (E), 19: 23880
electromagnetic-wave interactions with plasma of, low-frequency resonance excitation in, (E), 19: 23881
electron beam interaction with plasmas of, 17: 4207
electron beam interactions in plasma of, wave propagation in, 18: 1141
electron beam interactions in plasma of, cathode space charge in, 18: 21453
electron beam reactions with plasma of, diagnostics by nonperturbing probe, (E), 19: 47740
electron binding energies in, 18: 37843
electron collision probability in plasma of, 18: 9454 (IPPJ-10)
electron density distributions in plasma of, 18: 21465
electron density in discharge plasma of, uniformity of, 20: 46847
electron density variation along plasma column of, 17: 31609
electron double-elastic scattering by solid, spin polarization from, (E), 20: 19376
electron eigenfunctions for, calculation of one-,(T), 19: 9918
electron elastic scattering at 1 to 2 kev by, polarization in, 17: 25970
electron elastic scattering at 46 and 79 kev, 17: 36694
electron elastic scattering at 204 kev, asymmetry functions and differential cross sections for, 18: 9404
electron elastic scattering at 0.2 to 290 kev, 18: 38113
electron elastic scattering by atomic beams of, electron polarization in, (E), 19: 39392
electron elastic scattering at low energies, polarization effects in, (E), 20: 29937
electron elastic scattering at 180 to 1700 ev, polarization from, (E), 20: 37469
electron energy distribution in discharge plasma of, inert gas effects on, (T), 19: 21579
electron energy levels of, g value of $(6s6p)\ ^3P_1$, 18: 22686
electron energy loss spectra in gaseous, liquid, and solid, 18: 14728
electron energy loss, penetration, and range at 5 to 100 Mev, 19: 9445 (LA-3130)
electron impact excitation in plasma of, resonance absorption from, 20: 30601
electron mobility in high-pressure plasma of, effects of temperature on, 19: 3408
electron Mott scattering by, angular dependence of polarization in, (E), 19: 4848
electron oscillations in plasma of, higher- and sub-harmonics of, 19: 45428
electron reactions with, ionization cross sections for, 18: 2546
electron reactions with, excitation and ionization in, 18: 36167
electron reactions at low energies, bremsstrahlung from, (T), 19: 16409
electron reactions with, cross sections for inelastic, (T), 19: 25178
electron reactions with cathodes of, ion beam production by, 19: 44221 (N64-31088)
electron reactions with, polarization of x radiation from, 20: 7739

electron scattering by atomic, mathematical analysis, 16: 8105(T) (FTD-TT-61-183)
electron scattering at v/c = 0.4 and 0.5, computations, 17: 22660
electron scattering at 87.1 kev, phase shifts for, 17: 24271 (TID-16793)
electron scattering by Coulomb field of, phase shift approximation for, 17: 31417
electron scattering by, 18: 26236
electron scattering at 0.2 to 4 kev, interferences in, 18: 44441
electron scattering at 0.5 to 1.5 kev, polarization in elastic, 19: 1177
electron scattering by, bremsstrahlung from, 19: 746
electron scattering at 9 to 20 ev, spectral line polarization in, (E), 19: 8083
electron scattering by, elastic resonances in, (E), 19: 18702
electron scattering at 100 to 2000 ev, polarization from, (T), 19: 20865
electron scattering by atoms of, at 0.2 to 4.0 kev, (E), 19: 23315
electron scattering by atomic, angular dependence of polarization in Mott, (E), 19: 27108
electron scattering from atomic beams of, polarization in, (E), 19: 44958
electron scattering at 3.5 ev, polarization in, (E), 20: 2615
electron scattering at 3.5 to 45 ev, polarization in, (E), 20: 7733
electron spectra of irradiated, 19: 1956(R) (IDO-16994)
electron tunneling in superconducting films of, analysis of, 18: 28515
electron tunneling in superconducting films of, (E), 19: 8365
electron velocity distributions in mixtures of inert gases and, 18: 28815
electron wakes in plasma of, (E), 19: 8530
electron-beam instability in low-pressure plasma of, counter-streaming, (E), 20: 13951
electronic structures in liquid and solid, 17: 22476
elimination of deposited, from man, effect of therapy on, 19: 13097
emission properties of targets of, 20: 41122
energy level transitions in, Coster-Kronig, (T), 20: 15238 (CONF-233 (Vol.3), pp 398-418)
energy level widths for, K, (T), 20: 15239 (CONF-233(Vol.3), pp 419-39)
energy levels, isotopic shifts in, 16: 26360
energy levels of, spectral line shapes at zero magnetic fields, 19: 17078(R) (TID-21380(p.31-6))
energy levels of, radiative lifetime for, (E), 20: 19360 (UCRL-16441)
erosive effects on turbine blade and nozzle materials at 640°F, 20: 11214(R) (NASA-CR-54717)
erosive effects on metals and alloys at 70 and 500°F, cavitation, 20: 29640 (NP-16048)
exchange currents and kinetics of processes on, design of counting unit for determination of, 18: 1673
excretion of inhaled volatile, by mercury salt-injected rats, 20: 5251(R) (UR-668, pp 123-49)
fabrication of electrodes of, 17: 3264 (ORNL-3344)
flow around insulated bodies, effects of magnetic fields on, 19: 9339
flow at high temperatures, density measurements of cavitating two-phase, 19: 11363
flow in conveying trough with transverse magnetic field, (E/T), 20: 46437
flow in cylindrical cavitating venturi, void fraction distribution and axial pressure profile for two-phase, 20: 33473
flow in magnetic field, Reynolds-number dependence of turbulent, 19: 26509
flow in magnetic field, turbulent velocity pulsations in, (E), 19: 44827
flow in magnetic fields, hydraulics of, (E), 20: 41774
flow in MHD ducts, turbulence at high Hartmann and Reynolds numbers, (E), 20: 41707
flow in rectangular channels, effects of transverse field on MHD, (E), 20: 28070
flow in transverse magnetic field, skin friction coefficients for turbulent, 17: 16229 (NP-12631)
flow of liquid, calculation of two-phase critical, 18: 6921 (ANL-6779)
flow of liquid, Hartmann layer effects in MHD, (E/T), 20: 2831
flow of liquid, in transverse magnetic field, (E), 19: 24683
flow of saturated vapor of, through orifice into vacuum, 17: 23479 (TID-16898)
flow of vaporized, in supersonic nozzles, 17: 37641(R) (AD-290819)
flow of, MHD of oscillating sphere induced, (T), 20: 6161 (NP-15630)
flow of, model calculations of critical, 19: 11346 (COO-926-33)
flow of, radiometric measurement of void fraction in cavitating, 18: 25663
flow stability of two-phase, in parallel-tube condenser against gravity, 19: 4328 (ORNL-3605(Vol.2)(p.293-315))
flow through annuli, eddy conductivities of heat and mass transfer in, 18: 11958(R) (BNL-823(p.20-47))
flow through Venturi tubes, cavitation effects in two-phase, 18: 27673
fluid mechanical properties under two-phase, zero-gravity conditions, 16: 3971 (NAA-SR-6301)
fluorescence yield from L-shell of, following electron-capture decay of thallium-204, 19: 21449
gamma absorption by, (E), 20: 27348
gamma absorption coefficients at 0.511 to 1.2526 Mev, (E/T), 19: 12727
gamma coherent scattering at small angles, 18: 35053
gamma elastic scattering by, 17: 26623
gamma elastic scattering by, 18: 1063
gamma elastic scattering cross sections to 1.33 Mev, (E/T), 19: 45327
gamma resonant scattering by, 17: 29879(R) (IA-822)
gamma scattering at 662 kev, Rayleigh, 18: 26292
gamma scattering by K electrons in, Rayleigh, 17: 15104
gamma scattering by, resonance, 18: 11175 (ANL-6797(p.275-87))
gamma spectra from 14-Mev neutron activation of, determination by, 19: 26241
gamma spectrum for, thermal neutron capture, 17: 38063(R) (IITRI-1193-26)
Hall coefficient of liquid, measurement technique for, 17: 8852
Hall effect measurements, 16: 12231(R) (TID-15135)
heat and momenta transfer in two-phase helical flow, (E/T), 20: 23255(R) (SAN-409-29)
heat capacity of superconducting, at 1.2 to 4.4°K, 17: 35263(R) (UCRL-10706(p.1-110))
heat of absorption on silver, 16: 26009
heat transfer and pressure drop in forced convection boiling of, 17: 18264 (NAA-SR-6309)
heat transfer and laminar flow of, in circular cavity, 19: 13596
heat transfer and pressure drop in forced-flow boiling, models of, 19: 20116(R) (SAN-409-12)
heat transfer by, 18: 17322(R) (TID-19971)
heat transfer by boiling, 18: 10247
heat transfer by bubble boiling of, effects of pressure on, 19: 24682
heat transfer by, equipment development for agravic studies, 17: 20147 (AD-282370)
heat transfer by flowing, effects of magnetic fields on, 19: 46547
heat transfer by, in SNAP systems, 17: 20162 (BNL-756(p.353-79))
heat transfer by liquid, in forced circulation, 20: 4999(R) (ORNL-2599)
heat transfer by, forced-flow boiling, 18: 16177(R) (TID-20133)
heat transfer by, literature review of wetting effects in, 19: 20112 (NAA-SR-Memo-10315)
heat transfer coefficients for, in turbulent flow through rod bundles, 17: 2461(R) (BNL-731(p.18-46))
heat transfer from flowing, 20: 20177(R) (BNL-929, pp 83-105)
heat transfer in, design of apparatus for measuring, 17: 19689(R) (TID-15222)
heat transfer in flow normal to staggered tube bank, 16: 22310
heat transfer in flow through parallel tube bundles, 16: 27203
heat transfer in forced convection of liquid, effects of transverse magnetic field on, 20: 27112
heat transfer in pool boiling of, alloying effects on wetting outside of horizontal tubes used in, 19: 11367
heat transfer in transverse flow around tube bundles, 18: 16175 (NP-13712)
heat transfer of, design of system for measuring, 17: 19691 (TID-16052)
heat transfer of, in circular tubes, 17: 30668
heat transfer of liquid, 17: 282(T) (FTD-TT-61-395(p.121-34))
heat transfer of liquid, in cocurrent-flow, double-pipe, heat exchanger, 20: 27087 (ANL-7056)
heat transfer properties in binary-cycle nuclear power plant, 16: 31303
heat transfer properties of, effects of rubidium additions on, 20: 16972(R) (NASA-CR-54719)
heat transfer research on, 17: 27535 (BNL-801)
heat transfer to copper and steel pipes, 18: 16173 (NP-13656)
heat transfer to, from rods, 17: 31795(R) (BNL-782(p.18-43))
heat transfer to flowing, from rod bundle, 19: 26505
heat transfer to, in in-line flow through bundle of circular rods, 17: 16222 (BNL-6826)
heat transfer to, in auxiliary space nuclear power plants, 17: 20174(R) (TID-17707)
hydrogen evolution at electrodes of, proton tunneling in, 19: 2302
hydrogen ion reactions with, anion production in, 17: 39756
hydromagnetic flow, resistance and flow-profile studies, 16: 12239(T) (FTD-TT-61-281)
hydromagnetic stability in hard-core pinches, 16: 28288
hydromagnetic wave generation by dielectric sphere in spherical shell of, 20: 15581
hyperfine structure transitions in, 18: 42162(R) (TID-20963)
incorporation in styrene polymers using phenyl mercury, 19: 7526
incorporation into polystyrene for use as scintillator, 19: 13406(T) (JPRS-28565)
infrared radiation absorption in superconducting, collective excitations in, 18: 34720
interactions of one-dimensional waves in, with transverse magnetic field, 17: 16784 (NASA-TR-R-161)
iodine ion reactions at 5 to 1250 ev, resonant charge transfer in, 18: 32465
ion drift velocities in, 18: 32473
ion drift velocity in vapor of, 18: 16061
ion exchange behavior in hydrochloric acid–organic solvent media,

18: 39124
ion exchange in concentrated hydrochloric and perchloric acids, distribution coefficients for, 18: 17759
ion exchange paper chromatography of, 18: 17785
ion oscillatory potentials in liquid, (T), 19: 4695
ion reactions with plasma of, two-stream instabilities in, (E), 19: 14716
ion waves on plasma columns of, low-frequency, 18: 28848
ionic nucleation for vaporized, 17: 37641(R) (AD-290819)
ionization by electrons, cross sections and efficiency curve, 16: 1764
ionization by electron bombardment, 17: 21832
ionization by electrons, cross sections for, 18: 20768
ionization by electrons, cross sections for, 18: 20768
ionization by hydrogen ions, 18: 10772
ionization by reactions with potassium ions, electron current from, 19: 7471
ionization cross sections of, calculation of, 18: 16661
ionization in mass spectrometer, formation of multiply charged ions in, 20: 14584(R) (TID-22444)
ionization in MHD duct, excited atom effects on nonequilibrium, (E), 20: 41757
ionization rate in discharge of, microwave determination of, (E/T), 19: 12691
light absorption by atoms of, (E), 19: 18685
lithium ionization in supersonic beam of, (E), 19: 6473
loss from electrolytic cells for caustic soda–chlorine, tracer studies of, 19: 26917(R) (IA-984)
magnetic field enhancement in superconducting tubes of, empirical formula for, (E/T), 20: 13678
magnetohydrodynamic free oscillations in magnetic field, 16: 11093
magnetohydrodynamic flow of, growth rate of Rayleigh-Taylor instabilities in, 19: 37964
magnetohydrodynamic flow of, properties of square-channel, (E), 20: 21807
magnetoplasma resonance in, 17: 16841
maser collision processes in, optical, 18: 32484
mercury ion reactions with vapors of, production of metastable atoms in, 18: 32366
mercury ion reactions with vapors of, production of metastable atoms in, 20: 6003
metabolism in mammals, tracer study, 19: 25844
metabolism in rats, effects of chelating agents on, 18: 27039
metabolism of inhaled vapor in rats, tracer study, 17: 7769
metabolism of inhaled, in rats, 20: 5251(R) (UR-668, pp 123-49)
microwave amplification in plasma of, 20: 20052
microwave emission from plasma of (E/T), 19: 1792
neutron absorption cross sections, 16: 18429
neutron absorption cross sections at 24 kev, (E), 19: 45230
neutron absorption cross section in pitchblende, thermal, 20: 37994
neutron activation in spherical samples of, self-shielding effects in, 18: 6764
neutron capture by, gamma emission in fast, 17: 11659
neutron capture by, resonance fluorescence from, 18: 13063
neutron capture cross sections, 16: 26509
neutron capture cross sections, 18: 9336
neutron capture gamma spectra, 16: 19745(R) (ARF-1193-9)
neutron capture gamma spectrum, 16: 28024(R) (ARF-1193-12)
neutron capture, gamma spectra following, 16: 29750 (ANL-6589)
neutron capture gamma spectra, high-energy, 19: 25468(R) (ARF-1193-17)
neutron elastic and inelastic scattering at 300 to 1500 kev, cross sections for fast, (E), 19: 31215(R) (ANL-7010(p.1-19))
neutron elastic scattering at 0.65 Mev, angular distributions for, 18: 17089
neutron elastic scattering at 0.3 Mev, angular distributions for, 18: 17090
neutron elastic scattering at 0.5 to 0.8 Mev, cross sections for, 18: 26568
neutron elastic scattering at 0.3 to 1.5 Mev, 18: 38155
neutron elastic scattering at 0.3 to 1.5 Mev, differential cross sections for (E), 19: 3381
neutron elastic scattering at 0.3 to 2.2 Mev, angular distributions from, (E), 19: 19095 (WASH-1053)
neutron elastic scattering at 0.8 Mev, angular distributions from, (T), 19: 37884
neutron elastic scattering at 1 Mev, differential cross sections for, (E/T), 20: 9981 (WASH-1064)
neutron elastic scattering at 0.8 Mev, cross sections for, (T), 20: 15770
neutron elastic scattering at 3.2 Mev, (E/T), 20: 46644
neutron inelastic scattering at 14 Mev, 16: 7049
neutron inelastic scattering at 14 Mev, level density and nuclear temperature for fast, 17: 31492
neutron inelastic scattering at 4.0 to 6.5 Mev, energy spectra, 18: 26671
neutron inelastic scattering by, fast, (E/T), 20: 19805(R) (ANL-7110, pp 1-28)
neutron inelastic scattering at 5.8 and 7.5 Mev, gamma spectra from thermal, (E), 20: 22069
neutron inelastic scattering at 14.1 Mev, spectra for, (E), 20: 28268 (FEI-30)
neutron radiative capture cross section at 18 to 300 kev, fast, 17: 21009
neutron radiative capture cross sections at 30 and 65 kev, 18: 34274(R) (NIRS-2(p.3-15))
neutron reactions with, gamma radiation from, 18: 30735(R) (TID-20657)
neutron reactions (n,γ) near 5 Mev, gamma spectra from, (E), 20: 30358(R) (RPI-328-56, pp 1-48)
neutron scattering at 0.4 to 1.2 Mev, cross sections for, 17: 26476
neutron scattering by, cross sections for, 17: 41873 (WASH-1044)
neutron scattering at 14 Mev, nuclear temperature after excitation by, 18: 15235
neutron scattering at 300 to 1500 kev, 18: 21698(R) (ANL-6860)
neutron scattering by, 18: 24625 (WASH-1046)
neutron scattering at 3 to 650 kev, cross sections, phase shifts, and strength functions for, (E), 19: 10319
neutron scattering at 0.3 to 1.5 Mev, cross sections for, (E), 19: 19095 (WASH-1053)
neutron scattering at 0.3 to 1.5 Mev, cross sections for, (E), 19: 19224
neutron scattering by, angular distribution in, 19: 31252
neutron-shielding performance of, 17: 16731(P)
neutron total cross sections at 28.4 Mev, 16: 5969
neutron transmission spectra, isotopic resonance effects, 16: 18428
neutron yield from target of, in electron linear accelerator, 17: 30125
nuclear magnetic resonance in superconducting, 18: 15092
nuclear magnetic resonance in superconducting, spin-orbit coupling effects on Knight shift in, (T), 19: 39727
nuclear magnetic resonance of mercury-199 and mercury-201 in metallic, 19: 43285
nuclear magnetic resonance of liquid, 20: 7744
nuclear quadrupole resonance, 17: 10592 (IS-520)
nucleate pool boiling of, equation for statistical analysis of heat flux in, 16: 30564
Nusselt numbers for liquid, calculation of, 19: 11355
nutritional needs and toxic effects of, in man, 19: 21990
oscillations in hot nonuniform plasma column of, resonance, 18: 1140
oscillations in low-pressure plasma of, electron-beam excitation of uhf, 20: 38214
oscillations in plasma of, from electric current pulse, 18: 21461
oxidation and reduction of indium at electrode of, in sodium perchlorate solutions, 18: 31434(R) (UCRL-11317(p.32-51))
performance as electrode in perchlorate solutions, 18: 19837(R) (MIT-905-1)
performance as lubricant for rotor bearings, 19: 32333 (NYO-3363-1)
performance as propellant in ion engines for space propulsion, 19: 34343 (N64-22453)
performance as reactor coolant, evaluation of, 18: 20192
performance as working fluid in MHD cell, (T), 19: 4875
performance in boiling-liquid-metal heat exchangers for space uses, 18: 29844(R) (SAN-409-1)
performance in dynamic energy conversion systems for space power, 17: 35229
performance in electrohydrodynamic cells for space uses, 17: 9122
performance in electron-bombardment ion engines, 20: 12975
performance in electron-bombardment ion thrustors for space propulsion, durability tests of, 20: 31374
performance in MHD cells, 18: 12875
performance in SNAP-8 power conversion system, 19: 19410(R) (NASA-CR-54219)
performance of cesium seeded plasma of, in magnetohydrodynamic cells, 17: 32817
performance of ionized vapors of, in direct-energy conversion devices, 18: 36249
performance of liquid electrodes of, in electron-bombardment ion thrustors, 19: 13614
pharmacodynamic properties, tracer studies, 16: 1394
photochemical oxidation of, isotopic selectivity in, 17: 23337
photoelectric cross sections of, gamma, (E), 20: 5990
photoelectric cross section of, (E), 20: 11516
photon reactions (γ,n) with, energy spectra from, (E), 20: 42165(R) (MIT-2098-251, pp 16-20)
photonuclear reactions, production of short-lived isomers, 16: 12530
photosensitivity effects on germane and silane systems, formation of volatile hydrides by, 20: 18729(R) (NYO-2007-9)
photosensitized reactions with ethylene, secondary kinetic isotope effects in, 16: 17715
photosensitized reactions with alkyl chlorides, monoisotopic, 18: 39300
physical properties of liquid and vaporous, 17: 19690(R) (TID-15223)
physical properties at 100 to 1000°C, bibliography on, 19: 24993 (Y-889)
physical properties of liquid, 19: 28821
pinch discharge in, stability of linear hard-core, 17: 42099
plasma impedance characteristics, 16: 9536

plasma in, electron and ion oscillations in, (E), 19: 5348
plasma of, diagnostic probe techniques for, 18: 9547
plasma of, harmonic generation and parametric oscillations in, 17: 42148
plasma of, ion density and energy distribution behind charged object in streaming, 17: 19444 (AD-283577)
plasma of, charged-particle currents and temperatures in, 18: 21438
plasma of, cyclotron radiation from electron-beam-generated, 18: 19144
plasma of, double-probe technique for electron velocity distributions in, 18: 19193
plasma of, electroacoustic wave propagation in column of, (E), 19: 31402
plasma of, low-frequency waves in column of, (E), 19: 19309
plasma of, photon emission by atoms of, (E), 19: 41891(T)
plasma of, resonance behavior in slab-condenser systems in, 18: 19168
plasma of, resonance probe diagnostics of, 18: 24771
plasma oscillations near 15 Mc in a dark homogeneous plasma, 16: 19591
polarography of, in acetone solution, 17: 14253
positron annihilation in liquid and solid, photon angular correlation and conduction electron distribution from, 17: 22476
positron annihilation in, angular correlations from, (E), 19: 41285
potassium scattering by, velocity dependence of differential cross sections for, 17: 6836
probe characteristics (pulsed) in vapor, 16: 9537
production of metastable atoms of, by charge exchange, 20: 6003
properties, 16: 19370 (TIM-65)
properties and uses of liquid, review of, 19: 6353
properties as intermediate coolant in sodium–water reactor systems, 19: 21701
properties as reactor coolants, 16: 28545 (TID-7623(p.2-8))
properties as reactor control material, 16: 32120 (TID-16597)
properties as reactor working fluid, 18: 35198 (NAA-SR-8617(Vol.I))
properties as working fluid in Rankine power cycle, 20: 41398
properties at 234 to 1733°K, volumetric, 20: 12825 (NYO-2082-1)
properties for space applications, handbook, 16: 5088 (WADD-TR-61-96)
properties in reactor safety device, 18: 11391(P)
properties of electrodeless-discharge plasma of, 18: 42347 (AI-64-48)
properties of, in two-phase flow with nitrogen, 17: 18257 (ANL-6625)
properties of liquid, as reactor coolant, 16: 23830 (BNL-5377)
properties of plasma sheath of, r-f, 18: 1143
properties of superconducting, (T), 19: 16788
properties of superconducting, electromagnetic, 20: 34441
properties of thin-film electrodes of, for chromatography, 20: 22871(R) (MIT-905-52, pp 42-73)
properties, theory of infrared and optical, 16: 25758 (NP-11675)
properties, thermodynamic and transport, 16: 18932
proton reactions at 0.1 to 0.5 Mev, characteristic x-ray yields from, 16: 33633
proton reactions at 0.05 to 2.9 Bev, induced activity data and cross sections for spallation, (E/T), 20: 32549
pump for, electrodynamic, 19: 44188 (NASA-TN-D-2965)
pumping of, development of thermoelectric pumps for, (E), 19: 20096 (NAA-SR-Memo-10729)
purification of, by countercurrent extraction, 19: 26462 (HW-84509)
purification of, method for, 20: 43069(R) (IDO-14679, pp 51-9)
radiation effects on diffusion of, in zinc, 18: 12740
radiation emission by singly charged-ion plasma of, pressure-temperature region for black-body, (T), 20: 34748
radiative lifetime of excited electronic states in, 20: 31219(R) (UCRL-16658, pp 11-20)
radioinduced emanation from, holdup time of, (E), 20: 6298(R) (PPAD-2137-566)
radiolysis effects on formation of benzene from acetylene, 17: 10698
rare gas reactions with, cross sections for line broadening in, (E), 20: 2637
reactions of excited singlet atoms of, with propane, isobutane, and pentane, 18: 27487
reactions of gaseous, with sodium vapor, luminescence from, 18: 767
reactions of positive hydrogen ions with vaporous, formation of negative hydrogen ions from, (E), 20: 39500
reactions of, with sulfhydryl groups in ligands of plasma membranes, 17: 13931
reactions with gallium, kinetics and mechanisms of, 20: 35477 (NYO-2082-4)
reactions with hydrogen at −195°C, 16: 112
reactions with hydrocarbons, effects of deuterium on quenching cross sections in, 17: 10685
reactions with hydrogen, isotope effects on quenching in, 20: 7075
reactions with magnesium, 19: 22997 (TRG-Report-842)
reactions with Magnox alloy to room temperature in argon, 19: 22997 (TRG-Report-842)
reactions with metal hydrides, review on, 20: 10812 (NAA-SR-Memo-11569)
reactions with nitrosyl fluoride, 17: 3574(R) (NP-12212)
reactions with plutonium hexafluoride, 17: 40421(R) (ANL-6766)
reactions with propane, deuterium isotope effect in, 17: 8060
reactions with sodium in liquid ammonia, intermetallic phase production in, 18: 23149(T) (ANL-Trans-8)
reactions with thallium atoms, cross sections for, 18: 36156
reactions with uranium to 80°C, 19: 22997 (TRG-Report-842)
recovery of spilled, equipment for, 20: 16738(R) (UCRL-14534, pp 41-3)
reduction of zirconium(IV) iodides, 16: 11634
removal of liquid, from melting rods, 20: 33884(R) (SC-CR-66-2029)
resonances in afterglow plasma of, acoustic, 18: 15357
rotation of liquid, in uniform transverse magnetic fields, 19: 23198
scattering length determination using neutron gravity refractometer, coherent, (E), 19: 14481
scattering of atomic beams of lithium-6 and lithium-7 by crossed thermal beam of, quantum effects and cross sections in, 19: 20823
scattering of cesium and potassium by crossed atomic beams of, 16: 29486 (TID-16477)
scattering of electron beams in vaporous discharge, 16: 12227 (TID-14666)
scattering of helium and hydrogen beams by, calculation of differential cross sections, 17: 12849
scattering on beryllium–copper alloys and nickel at 5 to 25 kev, secondary electrons from, 20: 41620 (NIJS-R-471)
selectivity for radiolysis products under gamma irradiation, 18: 37211(T) (AEC-tr-6398(p.462-71))
separation as ferrocyanide on filter paper by precipitation chromatography, 17: 40932
separation by anion exchange in acid-organic solvent media, 18: 23707(R) (TID-20609)
separation by reversed-phase chromatography and solvent extraction using tri-n-octylphosphine sulfide, 19: 19753 (IS-T-3)
separation from acid solutions by solvent extraction using N,N′,N″-trihexylphosphorothioic triamide, 19: 17781(R) (ORNL-3750)
separation from acid chlorides by solvent extraction using amines, 19: 28443(R) (ORNL-3785)
separation from bismuth and lead by solvent extraction using tri-n-octylphosphine sulfide, 19: 19753 (IS-T-3)
separation from calcium by cation exchange, 16: 2978
separation from cadmium and zinc, chromatographic method using ion exchange resin, 19: 2450(T) (ORNL-tr-300)
separation from copper, iron, and zinc by paper precipitation chromatography, 18: 1565
separation from ethanolic hydrochloric acids by ion exchange, 19: 39265(R) (IA-1021)
separation from FTW-65 waste solutions, 18: 19448(R) (ORNL-TM-757)
separation from gallium, indium, and thallium by volatilization, 17: 12296
separation from hydrochloric acid by solvent extraction using tri-n-butylphosphine sulfide, 17: 10754
separation from hydrochloric acid solutions by solvent extraction using 2-ethylhexanol, 19: 36252
separation from hydrochloric and nitric acid solutions by solvent extraction using tri-n-octylphosphine sulfide, 20: 244
separation from liquid lithium nitrate–potassium nitrate eutectic by solvent extraction using polyphenyl mixture, 18: 12255 (IA-864)
separation from lithium chloride in ethanol by ion exchange, 19: 26917(R) (IA-984)
separation from magnesium, niobium, and zirconium, 19: 15332(R) (BNL-841(p.52-62))
separation from metal ionic mixtures, electrochromatographic, 17: 10753
separation from metal mixtures by thin layer chromatography, 20: 36753
separation from nitric acid solutions by solvent extraction using trilaurylamine in toluene, 18: 27615(R) (MITNE-43)
separation from nitric or sulfuric acid solutions, ion exchange selectivity scales for, 19: 9257
separation from nitric acid by solvent extraction using tri-n-octylphosphine sulfide, 20: 244
separation from organic solvents by paper chromatography, 17: 14176
separation from other metals by ion exchange chromatography in tartrate medium, tracer studies of, 19: 7627
separation from other metals by ion exchange, 19: 15692
separation from other products in uranium–radium decay series, 19: 23766
separation from other inorganic ions by paper chromatography, 20: 12939
separation from other elements by ion exchange using triisooctylamine, 20: 43439
separation from perchloric acid solutions by ion exchange materials, 20: 20823
separation from plutonium by ion exchange in nitric acid, 18: 22170 (LA-3040)
separation from Purex waste by passage of solution through copper column, 18: 43091(R) (ORNL-TM-830)
separation from rare earths by ion exchange in isopropyl alcohol,

18: 20104
separation from radioactive waste solutions by amalgamation with aluminum or copper, 18: 24977 (ORNL-TM-827)
separation from rhenium by anion exchange chromatography, 19: 24433
separation from scandium by ion exchange chromatography, 20: 16574
separation from scandium by ion exchange chromatography, 20: 20821
separation from tin by reversed-phase chromatography, 20: 40796(R) (IS-1500(Sect.C))
separation from uranium by ion exchange, 19: 44119
separation from uranium by partition chromatography on silica-gel column, 20: 9073
separation from waste solutions by displacement with copper, 17: 21375 (ORNL-TM-568)
separation from waste solutions during processing, 17: 26932(R) (ORNL-TM-516)
separation from waste solutions, 17: 35618(R) (ORNL-TM-545)
separation of (I) and (II) states by paper chromatography, 17: 1402
separation of, radiochemical and vacuum distillation, 17: 6135
solubilities in aqueous electrolytes, effects of applied potential on, 20: 22871(R) (MIT-905-52, pp 42-73)
solubility in organic solvents at 25°C, 16: 23591
solubility in organic compounds, tracer study of, 20: 3863(R) (IS-1200 (Sect. C))
solubility in organic compounds, tracer studies of, 20: 40796(R) (IS-1500(Sect.C))
solubility in water at 25 to 90°C, activation study, 17: 4451
solvent properties for mercury-203, 17: 394
solvent properties for metals, method of determining, 17: 28906
solvent properties, 17: 31798(R) (BNL-782(p.60-91))
solvent properties for cobalt and titanium at 500 to 700°C, 18: 4160(R) (BNL-799(p.74-100))
solvent properties for chromium, iron, and nickel at 600°C, 18: 14401 (BNL-7553)
solvent properties of liquid, for chromium, iron, and nickel at 600°C, 18: 27886 (NASA-SP-41(p.21-6))
solvent properties for cobalt and titanium, 19: 11293
solvent properties for cobalt and Haynes-25 alloy at high temperatures, 19: 15991(R) (BNL-841(p.63-101))
solvent properties for refractory metals, 20: 20177(R) (BNL-929, pp 83-105)
sorption by arsenic, cadmium, lead, and zinc sulfides, 18: 1614(R) (ORNL-3488(p.65-90))
sorption by cellulose ion exchangers from acetone and ethanol mixtures with hydrochloric acid, 18: 16140
sorption by Dowex-1 anion exchange resin from hydrobromic acid solution, 16: 28936
sorption from hydrochloric acid by cellulose and resin paper ion exchangers, 18: 16139
sorption from nitric acid by ion exchange paper, 19: 24435
sorption of, by lithium chloride cation exchange resin, 17: 15992
sorption of neutron-activated, for specific surface area measurements for solids, 17: 39548(T,R) (EURAEC-646)
sorption on anion exchange papers in hydrobromic and hydrochloric acids and lithium chloride, 18: 25374
sorptive properties for 3-pentanol and 3-pentanone, effects of molecular symmetry on, 20: 12536 (IS-T-66)
space-charge wave attenuation in discharge plasma of, (E/T), 20: 10211
space-charge zone at boundary of arc plasma of, (T), 19: 14675(T) (AI-Trans-71)
spallation of, use in accelerator radiation monitoring, 20: 41276 (UCRL-16769)
sparking potential at 10 to 100 mm-mercury, relation to pressure, 16: 12281
spectra, hyperfine structure of forbidden 2815 Å mercury II line and isotopic displacement constant, 16: 16878
spectra in reaction zone of acetylene air flame, excitation of atomic, 17: 27371(T)
spectra of, coherence effects in Zeeman emission, 18: 5915
spectra of, fine structure of excitation, 18: 762
spectra of, from electron excitation, 18: 759
spectra of, hyperfine structure and isotope shifts in 2537 Å line of, 17: 21101
spectra of, method of measuring excitation function in, 18: 765
spectra of transient chemical species produced by microwave discharges in, absorption, 18: 12097
spectra of water-dissolved, absorbance, 19: 36220(R) (MIT-2098-142)
spectra of, isolated in inert gas matrices at high temperature, 20: 1818 (UCRL-11976)
spectra of, isotope shift of, 19: 34118
spectra of, measurement of transition probabilities in, 20: 2649
spectral line excitation by collisions with hydrogen ions and protons, (E), 19: 41260(T)
spectroscopy of, high-intensity sources for Raman, 17: 12542
sputtering of metals and semiconductors by, yields from, 16: 31727
stability of plasma column of, in longitudinal magnetic field (E), 19: 1774
stability of positive-column plasma of, in constricted column, 18: 44860 (TID-21149)
structure of liquid, 17: 11232
structure of liquid, x-ray diffraction studies of, 18: 14475 (TID-20304)
superconducting critical fields and temperatures for alpha and beta, 17: 41592
superconducting energy-gap function in, 17: 25937
superconducting properties below 1°K, 16: 33596
superconducting properties of filamentary, in glass matrix, 17: 3525
superconducting properties to 0.3°K, (E), 19: 47517
superconducting properties of, 19: 47536
superconducting properties of, effects of λ transition on, 20: 21875
superconducting properties of single-crystal, (E), 20: 34437
superconducting transition temperature in, 16: 15334
superconductivity and uses of, 17: 34451
superconductivity, 17: 41604
superconductivity and supercooling in, surface, 18: 36430
superconductivity in, criteria for, (T), 19: 12448
superconductivity of, 20: 40047
surface properties and volume of, relation between, 17: 41476(T)
surface tension, 16: 1772
surface tension at 20°C, 17: 28828(R) (TID-18951)
surface tension measurement from photographed menisci, 19: 34681 (LA-DC-6514)
surface tension of liquid, relation to critical temperature and surface energy, 16: 25351
surface wave generation in, by time-varying magnetic fields, 17: 12748 (AFOSR-2956)
technetium electrodeposition in, 20: 12809
temperature of plasma of, spectroscopic determination of, 20: 26275
temperature of transient discharge plasma of, determination using Stark broadening, (T), 20: 34736
thermal capacity at 0.35 to 4.2°K, 20: 13692
thermal capacity of superconducting, lattice contribution to, 18: 15081
thermal capacity of normal and superconducting, at 0.35 to 4.2°K, 18: 30675
thermal capacity of normal and superconducting, 19: 43997(R) (UCRL-11889)
thermal capacity of liquid, corresponding states correlation of configurational, 20: 20657 (UCRL-11931)
thermal conductivity in parallel flow through bundles of circular rods, 16: 13245
thermal conductivity near superconducting transition temperature, (E), 19: 8363
thermal conductivity, 20: 4310(R) (ORNL-P-1699)
thermal conductivity of liquid, estimation of, 20: 41477
thermal properties of liquid, 17: 3426(R) (NP-12189)
thermodynamic properties of liquid, Prandtl number at 0 to 700°C for, 20: 31724
thermoelectric potentials at 25 to 500°C, 19: 4656 (ORNL-3605 (Vol.1)(p.116-38))
thermoelectric properties of liquid, 17: 1979
thermophysical properties, 16: 16741
timing device for electrodes of, 17: 40427(R) (NYO-10063(p.1.6))
toxic effects of, effects of chelating agents on, 19: 25844
tracer applications survey, 16: 1359
transition probabilities of forbidden lines of, 18: 14736
transport of heat and momentum in liquid, 17: 288
ultrasonics attenuation in superconducting, 17: 21401(R) (TID-18585)
uptake by *Cladophora fracta*, concentration effects on dynamics of, 19: 25858
uptake by woody plants, regularities in, 19: 6964
use as cathode in electrolytic reduction of uranyl and plutonium(IV) ions, 19: 42474
use as liquid brushes in homopolar generators, 16: 15413
use as threshold detector for fast neutrons, (E), 19: 39007
use in dissolution of aluminum and aluminum–uranium alloy plates, 20: 438 (RT/CHI(65)23)
use in ion propulsion systems, 16: 9717 (NASA-TN-D-1163)
use in Rankine power systems for manned space stations, 19: 10009
use in separation of uranium isotopes by vaporization, 16: 9095(T,P) (AEC-tr-4993)
use in space electric power systems, 18: 36846
use of dropping electrodes of, to study polarographic behavior of rare earth ions in ethanol–lithium chloride solutions, 17: 171
use of electrodes of, in polarographic studies of reduction mechanisms of alcoholic lithium chloride solutions of trivalent lanthanide ions, 17: 4507
uses of electrodes of, in polarographic studies of aquocupric complex in hydrofluoric acid, 17: 15961 (TID-18198)

uses of vapors of, as targets in x-ray tubes, 19: 746
vapor effects on formation of benzene in radiolysis of acetylene at 262°C, 16: 11687(R) (NYO-7986)
vapor flow in single tubes, condensation properties of, 20: 33451 (CONF-651026, pp 553-81)
vapor pressure, 17: 30536
vapor pressure of, 18: 10308(R) (UCRL-7571)
vapor pressure of, correspondence with cesium, potassium, rubidium, and sodium, 18: 16035
vapor pressure over mercury–thorium alloy, 20: 4441
vapor quality, method for measurement of, 20: 27104 (ANL-7100, pp 641-65)
vapor supersaturation during expansion in nozzle, design of experiment on, 20: 481 (NAA-SR-Memo-11194)
vaporization, 18: 3038(R) (ANL-6801)
vaporization lifetimes and behavior of droplets of, on hot surface, 18: 16177(R) (TID-20133)
vaporization lifetimes of droplets of, 19: 20116(R) (SAN-409-12)
vaporization, nonturbulent, 17: 40422(R) (ANL-6784)
vaporization of, effects of liquid level on nonturbulent, 18: 1483(R) (ANL-6687(p.27-85))
vaporization of, mechanisms of nonturbulent, 19: 15662(R) (ANL-6900 (p.45-142))
velocity distribution in turbulent flow of, magnetic-field effect on, (E), 19: 23176
viscosity at 234 to 1733°K, 18: 41373(R) (TID-20951)
viscosity of liquid, kinematic, 19: 44701(R) (TID-22144)
viscosity of liquid, based on atomic parameters, 20: 20656 (UCRL-11930)
viscosity of, relation of atomic mobility to, 17: 4945
volatility of, in radioactive alumina calcine during high-temperature storage, 20: 14207 (IDO-14670)
volumetric properties at 0 to 1733°K, 19: 23046
wave propagation along annular column of plasma of, surface, (E), 20: 30574
wave propagation in plasma of, self-excited surface, 17: 35049
weightless, dynamic behavior of surface of, 18: 5855
wetting Rankine boiler tubes by, effects of surface treatment on, 19: 20111 (NAA-SR-Memo-10224)
wetting zinc surfaces with, effects of microrelief on, 17: 3503
x-ray emission, 17: 12825
x-ray emission by, yield of L-shell, 18: 7732
x-ray emission excited by electrons, relative intensities of L spectrum, 16: 13747
x-ray reactions with vapors of, electricity production in, (E), 19: 47283(T) (BNL-tr-8)
x-ray spectra from mu-mesic atoms of, (E), 20: 38058
x-ray spectra of, Coster-Kronig transition probabilities from, (E), 19: 39410
x-ray-diffraction analysis, 18: 10542(R) (TID-20065)

MERCURY ACETATES

complexes of, composition and formation constant of, 18: 41444

MERCURY, ACETOXYPHENYL-

preparation of mercury-203-labeled, (E), 19: 13409
radiosensitivity effects of, use of activation analysis for determining mechanism of, 20: 31172 (SGAE-BL-17/1966)
radiosensitivity effects of, on *Pseudomonas*, 16: 17509

MERCURY ALKYLS

mercury-203 exchange between, 19: 2289

MERCURY ALLOYS

amalgam decomposition rate in aqueous solutions, electrolytic cell design and method for measuring, 16: 13079(P)
formation of, containing manganese and rare earth metal, 18: 34026 (AD-428771)
preparation of carrier-free silver-110 amalgams, 18: 5207 (SC-DC-3503)
preparation of carrier-free lead-212 amalgams, 18: 5207 (SC-DC-3503)
preparation of, for studies of rare earth–manganese alloys, 18: 34028 (AD-430037)
properties in reactor safety device, 18: 11391(P)
properties of cathode of, for separation of americium and curium-242, 20: 43453
solvent properties of, for samarium and ytterbium, 17: 16157
Al–Hg–Ni, corrosive effects on titanium of mercury-based, 19: 44616(R) (ANL-7000, pp 122-37)
Al–Hg–Zr, corrosive effects on titanium of mercury-based, 19: 44616(R) (ANL-7000, pp 122-37)
alkali metal–Hg, rare earth binding by, 16: 14756
Am–Hg, preparation and properties of, 19: 25001
Ba–Hg, critical temperatures of intermetallic compounds in, 20: 31757
Be–Hg, preparation, 18: 2127(R) (ORNL-3488(p.21-41))
Bi–Hg, ionization processes on, tracer studies of, 17: 35715
Bk–Hg, preparation and properties of, 19: 25001
Ca–Hg, critical temperatures of intermetallic compounds in, 20: 31757
Ca–Hg, properties of intermetallic compounds in, 19: 37081
Cd–Cs–Hg, sorption processes and surface tension of, 17: 41474(T)
Cd–Dy–Hg, phase studies, 20: 11317
Cd–Hg, Ginzburg-Landau parameter in superconducting, (E), 19: 10195
Cd–Hg, superconducting transition temperature of, effect of ordering on, (E), 20: 11914
Cd–Hg, surface superconductivity and supercooling in, 18: 36430
Cd–Hg, surface superconductivity and supercooling in, 19: 16812
Cd–Hg–K, sorption processes and surface tension of, 17: 41474(T)
Ce–Hg, electrolytic separation of cerium from, 18: 35484
Ce–Hg, electrolytic decomposition of, 18: 35484
Ce–Hg, preparation and properties, 17: 14747(T) (AEC-tr-5677)
Cf–Hg, preparation and properties of, 19: 25001
Cm–Hg, preparation and properties of, 19: 25001
Co–Hg, phase studies, 19: 36949(R) (BNL-900(p.121-97))
Cr–Hg, phase studies, 19: 36949(R) (BNL-900(p-121-97))
Dy–Hg, crystal structure of $DyHg_3$, 20: 17060
Dy–Hg, preparation by electrolysis on mercury electrode, 19: 13906
Dy–Hg, structure of DyHg, $DyHg_2$, and $DyHg_3$, 19: 28836
Er–Hg, crystal structure of $ErHg_3$, 20: 17060
Er–Hg, structure of ErHg, $ErHg_2$, and $ErHg_3$, 19: 28836
Eu–Hg, magnetic properties of $EuHg_3$, 20: 17060
Eu–Hg, properties of intermetallic compounds in, 19: 37081
Fe–Hg, phase studies, 19: 36949(R) (BNL-900(p.121-97))
Gd–Hg, crystal structure of $GdHg_3$, 20: 17060
Gd–Hg, preparation and structure of intermetallic compounds of, (E), 19: 4666
Gd–Hg, preparation by electrolysis on mercury electrode, 19: 13906
Hg–Ag, superconducting transistion in gamma phase, 18: 22830
Hg–Ag, uses as electrode in oscillographic determination of rare earths, 20: 38811
Hg–In, superconducting transition temperatures of, 17: 22356
Hg–K, boiling heat transfer and two-phase flow, 19: 4657 (ORNL-3605 (Vol.2)(p.110-31))
Hg–K, calculation of total cross sections as function of velocity, 18: 4347
Hg–K, crystal structure of AB_2-type compound in, 20: 24589(R) (NYO-3560-3)
Hg–K, heat transfer and two-phase flow, 17: 20161 (BNL-756(p.236-61))
Hg–K, liquid-vapor equilibrium diagram, 19: 4657 (ORNL-3605(Vol.2) (p.110-31))
Hg–K, performance in fuel cells, 18: 24354 (ANL-6802(p.49-52))
Hg–K, solvent properties for rare earths, 17: 40939
Hg–K, thermodynamic properties, 20: 21328 (CU-2660-25)
Hg–K, thermodynamic properties at high temperatures, 20: 20651(R) (CU-2660-26)
Hg–K, thermodynamics of, research program on, 19: 24981(R) (CU-2660-16)
Hg–Na, corrosive effects on steels, 18: 18312(T) (CEA-tr-A-1455)
Hg–Na, effects of liquid, on ductility of copper–beryllium alloy, 17: 36220 (AD-287255)
Hg–Na, electric mobility of sodium in liquid, 18: 546 (IP-488)
Hg–Na, nuclear magnetic resonance in, 18: 42036
Hg–Na, solvent properties for rare earths, 17: 40939
Hg–Nb, phase studies, 19: 36949(R) (BNL-900(p.121-97))
Hg–Ni, phase studies, 19: 36949(R) (BNL-900(p.121-97))
Hg–Ni, vapor pressures of intermetallic compounds in, 19: 23091
Hg–Ni–Zr, corrosive effects on titanium of mercury-based, 19: 44616(R) (ANL-7000, pp 122-37)
Hg–Pa, preparation and properties of, 19: 25001
Hg–Pb current-carrying capacity of superconducting, 17: 241 52
Hg–Pt, nuclear magnetic resonance in, 18: 42036
Hg–Pt, vapor pressures of intermetallic compounds in, 19: 23091
Hg–Pu, crystal structure of intermetallic compound Pu_5Hg_{21} in, 20: 37244
Hg–Pu, phase diagram, 17: 4984
Hg–Pu, phase studies and properties of, bibliographic study of, 16: 32115 (KFK-105)
Hg–Pu, preparation and properties of, 19: 25001
Hg–rare earths, crystal structure of intermetallic compounds in, 19: 41040
Hg–rare earth, crystal structure of, CsCl-type intermediate phases in, 20: 31737
Hg–rare earth–transition metal, preparation of rare earth–transition metal alloys by heating, 20: 19185
Hg–Rb, formation and properties of, 20: 11215(R) (NASA-CR-54718)
Hg–Sc, crystal structures of HgSc and Hg_3Sc, 18: 12708
Hg–Sm, preparation and structure of intermetallic compounds of, (E), 19: 4666
Hg–Sm, thermodynamic properties and vapor pressure measurements, 20: 21384
Hg–Sr, properties of intermetallic compounds in, 19: 37081
Hg–Ta, phase studies, 19: 36949(R) (BNL-900(p.121-97))
Hg–Tb, crystal structure of $TbHg_3$, 20: 17060

Hg–Tb, magnetic structure, 18: 39954
Hg–Tb, preparation by electrolysis on mercury electrode, 19: 13906
Hg–Tb, phase studies of, vapor-pressure methods of, 19: 42875
Hg–Th, preparation and properties of, 19: 25001
Hg–Th, preparation and properties of intermetallic compounds in, 20: 4441
Hg–Th, thermodynamic properties of, 18: 44224
Hg–Th, vapor pressure of intermetallic compounds in, 19: 23091
Hg–Th, vapor pressure of mercury over, 20: 4441
Hg–Ti, phase studies, 19: 36949(R) (BNL-900(p.121-97))
Hg–Tl, compound formation in, 18: 34131 (TID-20849)
Hg–Tl, electrode processes on, in perchlorate solution, 17: 32642
Hg–Tl, properties and uses of eutectic, 17: 36204 (TID-17847)
Hg–Tl, superconducting transition temperature of, pressure effect on, (E), 19: 47529
Hg–Tm, crystal structure of $TmHg_3$, 20: 17060
Hg–U, production of, by reduction of chloride, 16: 14810
Hg–U, thermodynamic properties of, 18: 44224
Hg–U, vapor pressure of intermetallic compounds in, 19: 23091
Hg–Y, crystal structure of HgY and Hg_3Y, 18: 12708
Hg–Y, preparation and structure of intermetallic compounds of, (E), 19: 4666
Hg–Y, thermodynamic properties and vapor pressure measurements, 20: 21384
Hg–Y–Zn, phase studies, 20: 11317
Hg–Yb, crystal structure of $YbHg_3$, 20: 17060
Hg–Zn, electro- and radiochemical studies of electrode reactions of, 17: 27398
Hg–Zn, optical maser collision processes in, 18: 32484
Hg–Zn, reaction with protactinium, 20: 45694
Hg–Zr, phase studies, 19: 36949(R) (BNL-900(p.121-97))
Ho–Hg, crystal structure of $HoHg_3$, 20: 17060
Ho–Hg, preparation by electrolysis on mercury electrode, 19: 13906
Ho–Hg, structure of HoHg, $HoHg_2$, and $HoHg_3$, 19: 28836
In–Hg, Brillouin zone effects on superconductivity of, 18: 15086
In–Hg, electrode processes on, in perchlorate solution, 17: 32642
In–Hg, indium-115 NMR in liquid, 20: 20157
In–Hg, lattice thermal conductivity of, 18: 4506
In–Hg, magnetic properties of superconducting, containing iron particles, 20: 11894
In–Hg, superconductivity of, effect of iron particles on, (E), 20: 40024
Li–Hg, solubility of intermetallic compound in, in fused lithium halides, 20: 31959(R) (ANL-7175, pp 184-211)
Li–Hg, solvent properties for rare earths, 17: 40939
Li–Hg, use in removing europium from aqueous electrolytes by extraction and electrolysis, 19: 38753 (LA-DC-7013)
Lu–Hg, crystal structure of $LuHg_3$, 20: 17060
Mg–Hg, corrosive effects on niobium–zirconium alloy at 315 to 870°C, 18: 4160(R) (BNL-799(p.74-100))
Mg–Hg, heat transfer by bubble boiling of, effects of pressure on, 19: 24682
Mg–Hg, superconducting transition temperature of intermetallic compounds in, 20: 31757
Mg–Hg–Ni, corrosive effects on titanium of mercury-based, 19: 44616(R) (ANL-7000, pp 122-37)
Mg–Hg–Zr, corrosive effects on titanium of mercury-based, 19: 44616(R) (ANL-7000, pp 122-37)
Mn–Hg, magnetic structure of, 18: 9317(R) (PR-P-59(p.37-45))
Mn–Hg, magnetic structure of, 19: 9703
Mn–Hg, vapor pressures of intermetallic compounds in, 19: 23091
Mn–Hg–Sm, preparation, 18: 34027 (AD-428772)
Mn–Hg–Y, preparation, 18: 34026 (AD-428771)
Mn–Hg–Y, preparation, 18: 34027 (AD-428772)
Pb–Hg, lead-207 NMR in, 18: 22063
Pb–Hg, lead-207 NMR in, 18: 36035
Pb–Hg, magnetization and resistance transitions of superconducting, (E), 20: 28183
Pb–Hg, preparation and properties of lead-212-containing, 16: 5657 (TID-14423)
Pb–Hg, preparation and properties of carrier-free lead-212-labeled, 19: 15655
Pb–Hg, superconducting transition temperature of, (E), 20: 9934
Pb–Hg, superconducting critical currents and fields in flux-pump fed coils of, (E), 20: 21924
Pb–Hg, use in protective clothing, 19: 18228(P)
Pb–Hg, use in radiation shielding, 17: 5529(P)
Sb–Hg, thermoelectric properties of, (E), 19: 16439(R) (AD-604997)

MERCURY AZIDES

radiolysis of aqueous solutions of, mechanism of, 18: 27494 (TID-19197)

MERCURY BROMIDE COMPLEXES

reactions with bromides in aqueous solutions, 17: 39053
with nitrobenzene, mercury-203 exchange between mercury bromide and, 18: 37559

MERCURY BROMIDES

see also Potassium Mercury Bromides
additive effects on radioinduced vulcanization of rubber, 18: 12144 (PAN-457/XVII)
bromine-82 exchange between, and potassium bromide, 19: 32295
critical temperature, 18: 9792(T) (AI-Trans-29)
electric conductivity at 220 to 930°C, 20: 10272(R) (NAA-SR-9339)
mercury recoil atom reactions, 16: 10084
mercury-203 exchange between nitrobenzylmercurobromide and, 18: 37559
separation from fused salts by solvent extraction using polyphenyls, 19: 39265(R) (IA-1021)
separation from molten salts by solvent extraction, 19: 32295
separation from molten nitrates by solvent extraction using polyphenyls, 20: 2520(R) (IA-920)
separation from water using benzene and polyphenyls, 17: 35253(R) (IA-775)
solubility and structure in organic solvents, 20: 2520(R) (IA-920)
solubility in organic solvents, 18: 9752 (IA-900)
spectra in benzene and water, uv, 19: 39265(R) (IA-1021)
vaporization of, 17: 2956 (UCRL-9840)
$AlBr_3$–$HgBr_2$, phase diagrams, 20: 36787 (YALE-2723(Vol.1))
$PbBr_2$–$HgBr_2$, phase diagrams, 20: 36788 (YALE-2723(Vol.2))

MERCURY CHLORIDE COMPLEXES

polarization in benzene and dioxane solutions, dielectric measurements on, 18: 31487
with adenylic acid oligomers, 20: 1575 (UCRL-16409)
with dioxane, chlorine-35 NQR in, (E), 19: 15544
with propene, decomposition of, separation of primary and secondary isotope effects in, 19: 4183
2,4,6-trioxo-1,3,5-trimethylhexahydrotriazene, crystal structure of, 17: 6792(R) (ISS 62/14)

MERCURY CHLORIDES

corrosive effects on molybdenum and vanadium, stress-, 20: 2254 (BM-RI-6680)
corrosive effects on molybdenum, tungsten, and vanadium at 35, 60, and 100°C, 20: 11230 (BM-RI-6715)
corrosive effects on vanadium-base alloys at low temperatures, 20: 11230 (BM-RI-6715)
critical temperature, 18: 9792(T) (AI-Trans-29)
diffusion in molten, effects of temperature on self-, 19: 26338
effects on exchange of tritium between benzene and nucleosides, catalytic, 19: 28349
effects on gamma-induced polymerization of acrylonitrile in aqueous solution, 18: 29716(T,R) (AEC-tr-6231(p.175-85))
effects on hairs of rats nursed by poisoned mothers, 19: 42246
effects on radioinduced inactivation of β-amylase, 19: 17558
effects on radioinduced vulcanization of rubber, 18: 12144 (PAN-457/XVII)
electric conductivity at 220 to 930°C, 20: 10272(R) (NAA-SR-9339)
enthalpy of vaporization and vapor pressure of molten, to critical point, 20: 18634 (SRIA-106-37)
fixation on anion exchange resin, quantitative, 16: 17640(T) (AEC-tr-5027)
from water using benzene and polyphenyls, 17: 35253(R) (IA-775)
isotopic exchange reactions between phenylmercurichlorides and mercury-203-labeled, kinetics of, 20: 45771
polymerization effects on acrylonitrile in aqueous solution, 16: 30455
positron lifetimes in, 16: 32354
positronium oxidation by, 16: 10859
properties as propellant in colloid-beam thrustor, 19: 13612
radiation effects on oxidation of oxalates by, gamma, 19: 32219
radioinduced reduction of, effects of hydrogen peroxide on, 18: 8424
radioinduced reduction of divalent, effects of pH on, 19: 15585
reactions with lithium and potassium ferrocyanides, 18: 13777
reactions with mercapto group in cellular proteins, 20: 26632
reactions with norborneneboronic esters, neutron absorption measurement of boron-10/boron-11 isotope effects in, 18: 39201
separation by reversed-phase partition chromatography using organophosphorus compounds, 18: 25614
separation from molten salts by solvent extraction, 18: 9752 (IA-900)
separation from molten nitrates by solvent extraction using polyphenyls, 20: 2520(R) (IA-920)
separation from sodium nitrate solutions using polyphenyls, 17: 35253(R) (IA-775)
solubility and structure in organic solvents, 20: 2520(R) (IA-920)
solubility in ethylenediamine-water mixtures, 17: 35622(R) (TID-19359)
solubility in ethylenediamine solutions, 18: 39061(R) (TID-21072)
solubility in organic solvents, 18: 9752 (IA-900)
spectra in argon, krypton, and xenon matrices, infrared, 17: 4497 (UCRL-10451)
spectra of mercury-199 in, nuclear magnetic resonance, 18: 31449
thermal capacity and thermal content at 298.1°K to melting point, 16: 6384 (NAA-SR-6518)

use in colloidal particle generator for electrostatic propulsion, 17: 21838
use of mercury-197-labeled, in renal scintigraphy, 20: 22804
vaporization of, 17: 2956 (UCRL-9840)
CuCl–HgCl, phase diagrams, 20: 36788 (YALE-2723(Vol.2))
$GaCl_3$–HgCl, phase diagram, 19: 5846(T) (ANL-Trans-105)
$HgCl_2$–KCl, phase diagrams, 20: 36788 (YALE-2723(Vol.2))
$HgCl_2$–NaCl, phase diagrams, 20: 36788 (YALE-2723(Vol.2))
$HgCl_2$–TlCl, phase diagrams, 20: 36788 (YALE-2723(Vol.2))
$HgCl_2$–$ZnCl_2$, phase diagrams, 20: 36788 (YALE-2723(Vol.2))
Hg–$HgCl_2$, electric conductivity, 20: 22520(R) (NAA-SR-11805)
Hg–$HgCl_2$, electric conductivity of molten, 20: 35841(R) (NAA-SR-11900)
Hg–$HgCl_2$, electromotive force measurements on, 17: 40815
Hg–$HgCl_2$, electromotive force studies of species in liquid, 18: 11511 (NAA-SR-8881)
Hg–$HgCl_2$, free energy of solution of, 19: 11103
LiCl–$HgCl_2$, phase diagrams, 20: 36788 (YALE-2723(Vol.2))
PbCl–$HgCl_2$, phase diagrams, 20: 36788 (YALE-2723(Vol.2))

MERCURY, CHLOROPHENYL-
preparation of mercury-203-labeled, (E), 19: 13409

MERCURY COMPLEXES
formation, optimum conditions for, 19: 13374
with (ethylenediamine)tetraacetic acid, radioprotective effects of, in mice, 18: 13567
with azide, radioinduced formation of, 18: 27494 (TID-19197)
with cobalt and thiocyanate, solubility behavior of, 18: 17717(R) (TID-20438)
with cupferron, thermal dissociation, 19: 7366
with diacetamide, properties and spectra of, 20: 8494 (TID-22449)
with diethyldithiophosphate, solvent extraction from mineral acids using carbon tetrachloride, 16: 28926(T) (AEC-tr-5202)
with diethylenetriaminepentaacetic acid, formation and stability constants of, 17: 16001
with HEDTA, stability constants, 16: 32054 (IS-304)
with mercaptosuccinic acid and 2,3-dimercaptosuccinic acid, formation and properties of, 18: 8394 (TID-20013)
with propylenediaminetetraacetic acid, stability, 19: 5883

MERCURY COMPOUNDS
chemical effects of igrocin on chromosomes and mitosis in rat sarcomas with and without x radiation, 16: 14556
effects on radiolysis of aqueous azide solutions, 17: 30591
effects on radiolysis of aqueous azide and nitrite solutions, 18: 22155
evaporation of, losses of mercury-203 in, 20: 23027
ionization of dimethylmercury by electron impact, 16: 17708(R) (TID-14812)
isotopic exchange between phenylmercurichloride and mercury-203-labeled mercuric chloride, kinetics of, 20: 45771
organic, isotope exchange in, 16: 3311(T) (AEC-tr-4497(p.30-6))
organic, luminescence quenching effects on diphenylanthracene and p-terphenyl in benzene and cyclohexane solutions, 17: 4564
organic, quenching effects on polyvinyltoluene sciatillators, 18: 12197
organic, reactions with mercapto group in cellular proteins, 20: 26632
radioinduced reduction of, in aqueous nitrite solutions, 17: 35888
use as fixatives for electron microscopy, 18: 23162(R) (ANL-6823 (p.174-7))
use of radioactive organic, in well logging, 18: 5538(P)

MERCURY CYANIDES
crystal structure of $Hg(CN)_2$·KI, 17: 12235
oxidizing effects on uranium compounds in ammonia, 17: 175
reactions of, 20: 3863(R) (IS-1200(Sect.C))
spectra of complexes, infrared, 16: 2937
spectra of, infrared absorption, 16: 2937

MERCURY, DIETHYL-
complex formation with thiocyanate ions, tracer studies of, 19: 32153
radiation effects on, Szilard-Chalmers, 19: 15587

MERCURY, DIMETHYL-
photolysis of deuterated and undeuterated mixtures of, reactions of methyl radicals in, 17: 40869
pyrolysis of, secondary deuterium isotope effect in, 17: 2985
radiolysis in presence of deuterated propane, 17: 28968

MERCURY, DIPHENYL-
neutron activation of, products from, 20: 33336(R) (PRNC-86)
photolysis of, tracer study of phenyl radical to, 17: 2711
quenching effects on liquid scintillators, 16: 21158
radiation effects on, Szilard-Chalmers, 19: 15587
radiation effects on, in benzene and chloroform solutions, 19: 22336
radiolysis, 17: 16062
use in scintillators for gamma energy measurements, 18: 7074

MERCURY FERROCYANIDES
formation and composition of, 18: 13777

MERCURY FLUORIDES
additive effects on radioinduced vulcanization of rubber, 18: 12144 (PAN-457/XVII)
vaporization of, 17: 2956 (UCRL-9840)

MERCURY HALIDES
anion exchange of, constant ionic medium method for, 17: 14207 (IA-782)
enthalpy of formation and stabilization constants of complex, 20: 2520(R) (IA-920)
equilibrium constants and ultraviolet spectra of uncharged mixed, 16: 1748
ion exchange on Dowex-1 resin perchlorate, 17: 29879(R) (IA-822)
molar absorbances, 18: 9752 (IA-900)
neopentyl derivatives of, mercury-199 proton coupling in, PMR spectral studies on, 20: 40908
separation from fused alkali metal nitrates by solvent extraction using polyphenyls, 19: 26917(R) (IA-984)
solubility in organic fluids, 19: 26917(R) (IA-984)
spectra of molecular, electronic, 19: 34148 (UCRL-11979)
thermodynamic properties, 18: 9752 (IA-900)

MERCURY HYDRIDES
properties of diatomic ions of, use of Platt electrostatic model for calculation of, 18: 12074
spectrum, isotope shift in emission, 17: 5109

MERCURY, (2-HYDROXYPROPYL)-
use of mercury-197-labeled, for spleen scanning, 20: 35362

MERCURY IODIDE COMPLEXES
deoxymercuration of, secondary hydrogen isotope effects on, 17: 35860
reactions with iodides in aqueous solutions, 17: 39053

MERCURY IODIDES
critical temperature, 18: 9792(T) (AI-Trans-29)
effects on radioinduced vulcanization of rubber, 18: 12144 (PAN-457/XVII)
electric conductivity at 220 to 930°C, 20: 10272(R) (NAA-SR-9339)
heat of solution in anhydrous ethylenediamine, 16: 5407(R) (TID-14329)
oxidation effects in aluminum, 16: 484(R) (AD-256309)
oxidizing effects on uranium compounds in ammonia, 17: 175
photoluminescence, measurements of absorption spectra and energy distributions in, 16: 22144
separation from molten nitrates by solvent extraction using polyphenyls, 20: 2520(R) (IA-920)
separation from water using benzene and polyphenyls, 17: 35253(R) (IA-775)
solubilities in organic solvents, 19: 39265(R) (IA-1021)
spectra in benzene and water, uv, 19: 39265(R) (IA-1021)
vaporization of, 17: 2956 (UCRL-9840)
AlI_3–HgI_2, phase diagrams, 20: 36787 (YALE-2723(Vol.1))
CdI_2–HgI_2, phase diagrams, 20: 36788 (YALE-2723(Vol.2))
HgI_2–AgCl, phase diagrams, 20: 36787 (YALE-2723(Vol.1))
HgI_2–KI, phase diagrams, 20: 36788 (YALE-2723(Vol.2))

MERCURY, IODOPHENYL-
preparation of mercury-203-labeled, (E), 19: 13409

MERCURY IONS
acceleration, grid tests for rocket propulsion, 16: 12787 (NASA-TN-D-1168)
activity coefficients and potentials of (0-I) and (I-II) couples, effects of hydrogen ion concentration, 16: 22124
catalytic effects on reactions of hydrogen peroxide with uranium(VI) ions, 16: 111
charge exchange in air, cross sections for, 18: 34409
charge exchange with atoms, cross sections for, 17: 8979
chromatography on acetylated filter paper, 16: 6379
crystal sputtering to 800 ev, atom emission and spatial distributions from, 16: 22758
detection using photographic emulsions, 18: 37521
determination of, cerium(IV) oxidimetric, 17: 176
distribution between sodium halide solutions and Dowex-1, effects of halide concentration and molarity on, 17: 35253(R) (IA-775)
effects on aquation of chloropentaaquochromium(III), 20: 3863(R) (IS-1200(Sect. C))
effects on catalase activity of yeast cells, 19: 10764
effects on etching of pyrolytic graphite, 19: 47078 (AD-613643)
effects on gain of electron multiplier tubes, (E), 20: 43659
effects on radioinduced free radical formation in proteins, 20: 31003
effects on radiolysis of naphthalene, 20: 29260
etching effects on pyrolytic graphite, 18: 44112
extraction of beams of, from arc plasma, 20: 28553
formation from neutral metastable mercury atoms, 20: 6003
incorporation into potassium chloride crystals grown from solution, 19: 38696 (MIT-2909-4)
ionization by electrons, cross sections for, 17: 41653
ionization of monovalent, by electrons, cross sections for, 18: 20768
lithium ion scattering by, cross sections for, 18: 9001 (TID-20002)
mobility, 18: 16061
neutralization by electron injection, 18: 19217
nuclear hexadecapole coupling in, second-order quadrupole effect in, 16: 29559 (BNL-6038)

oscillations in discharge plasma, (E/T), 19: 23879
production by electron bombardment, for propulsive use, 17: 21832
production for propulsion systems, development of controlled-growth colloidal source for, 17: 32217
production in low-voltage capillary ion source, 20: 44119
production of beams of, using duoplasmatron source, 18: 39421
production of beams of, using duoplasmatron, 20: 19004
production of multicharged, by hydrogen ion ionization of vapor stream, 18: 10772
production of, r-f source for, 20: 11374
production of, source for, 19: 30862
radioprotective effects in mice, 18: 13567
reactions with aluminum and magnesium, ion emission in, (E), 19: 39374
reactions with iron, molybdenum, niobium, silicon carbide, tantalum, titanium oxide, and vanadium, atom ejection patterns in, 16: 2203(R) (TID-14257)
reactions with mercury vapor, production of metastable atoms in, 18: 32366
reactions with mercury vapor, production of metastable atoms in, 20: 6003
reactions with molybdenum and tungsten surfaces, electron injection in, (E), 19: 41272(T)
recombination at electrodes, 18: 21712(R) (NYO-10065)
separation from silver and thallium ions, electrochromatographic, 16: 5273
solvent extraction from molten nitrate by liquid silicone–TBP at 150°C, 19: 19833 (CEA-R-2628)
sorption by aminodiacetate resin Dowex A-1, 20: 16358
sorption from aqueous solutions by peat, 20: 7002 (INR-609/XIX/D)
sorption from water by peat, 20: 218(R) (STI/DOC/10/42, pp 1-22)
sputtering of bcc metal single crystals by, at up to 800 ev, atom ejection in, 17: 37467
sputtering of copper by, energy distributions from, 18: 7404(R) (NP-13430)
sputtering of copper, molybdenum, nickel, niobium, and tungsten by, 18: 9004
sputtering of graphite, iron, and molybdenum by, 17: 20658
sputtering of metal powders, oxide powders, and steel spheres, yields from, 17: 25870(R) (X62-11400)
sputtering on copper at 80 to 1200 ev, energy distributions from, 18: 22674
sputtering on metals at 10 to 2000 ev, energy spectra and yields from, 18: 20787
sputtering on nickel, adsorption effects on ejection patterns in, (E), 19: 23270
sputtering on single crystals of molybdenum and tungsten, (E), 20: 9676(T)
sputtering ratio for polycrystalline copper, 16: 9114
sputtering reactions with aluminum and Duralumin, particle-energy distributions from, 18: 14625
sputtering reactions on nickel, 18: 20666
toxicity of, in mouse, determination by LD_{50} on thirtieth day of, 17: 17719
voltammetric properties of, on glassy carbon electrode, 19: 13217

MERCURY ISOTOPES
determination in radiation sources, extraction radiometric titration method for, 20: 20567 (UJV-1418/65)
energy levels, (T), 20: 44788
energy levels, interactions, nuclear moments, and transitions in, 17: 24381 (AD-403411)
energy levels of, using intermediate coupling, (T), 19: 25510
exchange in organomercuric compounds, 16: 3311(T) (AEC-tr-4497(pt3 0-6))
excited states in even, first, 16: 12518
gamma reactions on, cross sections for, 19: 12496
gamma spectra of, equipment and methods for measuring, 19: 1956(R) (IDO-16994)
hyperfine structure, 18: 2404(R) (TID-19651)
internal conversion probabilities in, reduced M and N E0, (T), 20: 15771
isomeric transitions, M_4-type, 16: 22985 (NP-11747)
isotope shifts of neutron-deficient, (E), 20: 32517
mass spectra from proton reactions with lead, use of isotope separator for, 20: 19889
nuclear charge distribution in, isomeric and isotopic effects on, (T), 20: 42189
nuclear compressibility, 16: 18531
nuclear properties, rms charge radii and emission-spectra isotope shifts, 16: 26331
production by proton reactions with gold, excitation functions for, 16: 21485
production in gold crystals by transmutation at 85°C, 16: 6814(R) (ORNL-3213(p.45-6))
radioactive, effects on human erythrocyte diameter and volume from occupational exposure to, 20: 40678
separation by electromagnetic methods, 20: 41401(R) (ORNL-4006)
separation by photochemical reaction with water vapor, feasibility of, 19: 20429 (MLM-1214)
separation by photochemical methods, 20: 37164
separation, electromagnetic, 16: 9107
separation of, by photochemical method, 17: 7660(R) (MLM-1137)
separation of, in Orsay separator after formation by proton spallation reactions on gold, 17: 21745
separation of, photochemical methods for, 17: 23824
separation of, improved feed system for electromagnetic, 18: 10438(R) (ORNL-TM-736)
separation of, photochemical, 19: 34607(R) (MLM-1239)
separation of, review of methods for, 19: 11642
separation of, thermodynamic effects in, (E/T), 19: 9568 (NP-14359)
separation, review of methods for, 19: 11639 (CEA-Bib-52)
spectra of, isotopic shifts in emission, 17: 34907
spectra of, isomer and isotope shifts in optical, (T), 20: 42189
spectra of, isotope shifts and hyperfine splittings in, (E), 19: 6724
spectra of, shifts in x-ray, 18: 17064(T)
use in myocardial scanning, 19: 5747

MERCURY ISOTOPES Hg-185
nuclear data, 20: 19882

MERCURY ISOTOPES Hg-186
nuclear data sheets, 20: 44713

MERCURY ISOTOPES Hg-187
nuclear data sheets, 20: 44714

MERCURY ISOTOPES Hg-188
nuclear data sheets, 20: 44715

MERCURY ISOTOPES Hg-189
alpha activity, 17: 19240
energy levels and half life, (E), 20: 6298(R) (PPAD-2137-566)
nuclear data sheets, 20: 44716

MERCURY ISOTOPES Hg-190
alpha activity, 17: 19240
decay, 18: 44784
production in proton reactions on gold, excitation functions, 16: 5964

MERCURY ISOTOPES Hg-191
alpha activity, 17: 19240
production by proton reactions with gold-197 at 2.3 Bev, cross section for, (E), 20: 6298(R) (PPAD-2137-566)
production in proton reactions on gold, excitation functions, 16: 5964

MERCURY ISOTOPES Hg-192
alpha activity, 17: 19240
decay of, excited levels of gold-192 from, 17: 40026
hyperfine structure, 17: 35260(R) (TID-19135)
hyperfine structure and isotope shift of, 20: 32517
isotope and isomer shifts in, 18: 44812
production by proton reactions with gold-197 at 2.3 Bev, cross section for, (E), 20: 6298(R) (PPAD-2137-566)
production in proton reactions on gold, excitation functions, 16: 5964
spectra of, isotope shift in, (E), 20: 1245

MERCURY ISOTOPES Hg-193
alpha activity, 17: 19240
decay, electron spectra, 16: 19772
decay of, gamma spectra from, (E), 20: 6298(R) (PPAD-2137-566)
electron conversion spectra, 18: 34786
energy level lifetime at 39 kev, 16: 7032
energy level schemes, 16: 2513
hyperfine structure, 17: 35260(R) (TID-19135)
hyperfine structure, 18: 2404(R) (TID-19651)
hyperfine structure of isomeric, by Zeeman-level crossings, (E), 19: 8461
hyperfine structure and isotope shift of isomeric, (E), 20: 1245
hyperfine structure and isotope shift, (E), 20: 32517
hyperfine structure and isotope shift of isomeric, (E), 20: 32517
isomeric transitions and decay to gold-193, electron beam spectra from, 16: 28052
isotope and isomer shifts of metastable, 18: 44812
nuclear electric quadrupole moment of metastable, 18: 44812
nuclear magnetic dipole moment of metastable, 18: 44812
nuclear magnetic moment and spin, (E), 19: 5213
nuclear spin of metastable, 18: 44812
production by proton reactions with gold-197 at 2.3 Bev, cross section for, (E), 20: 6298(R) (PPAD-2137-566)
production in proton reactions on gold, excitation functions, 16: 5964
spectra of isomeric, hyperfine structure and isomer shifts from, 17: 28285
spectra of, isotope shifts and hyperfine splittings in, (E), 19: 6724

MERCURY ISOTOPES Hg-194
decay, 18: 32770
decay and half life, 16: 12527
energy levels from thallium-194 decay, negative parity, (E), 20: 30435
fission barrier of compound nucleus, (E/T), 19: 21259(R) (UCRL-11828(p.77-80))

hyperfine structure and isotope shifts in, 16: 19476(R) (TID-15642)
isotope and isomer shifts in, 18: 44812
spectra of, hyperfine structure, isotope shift, and nuclear moments from, 17: 28284
spectra of, hyperfine structure and isotope shifts from, 17: 28285
spectra of, isotope shift in, (E), 20: 1245

MERCURY ISOTOPES Hg-195
decay scheme of metastable, 16: 7032
electron conversion spectra, 18: 34786
energy level schemes, 16: 2513
energy level scheme, 16: 2517
energy levels, mean life of first excited state, 16: 19767
energy levels of, lifetime and gamma transition probability of, 18: 1022 (PAN-428/I)
hyperfine structure and isotope shifts in, 16: 19476(R) (TID-15642)
hyperfine structure, 17: 35260(R) (TID-19135)
hyperfine structure of ground-state and isomeric, by Zeeman-level crossings, (E), 19: 8461
hyperfine structure and isotope shift, (E), 20: 1245
isotope and isomer shifts of ground and metastable states of, 18: 44812
mass of, 16: 3674(T) (CEA-tr-R-1371)
nuclear electric quadrupole moment of metastable, 18: 44812
nuclear magnetic dipole moments of ground and metastable states of, 18: 44812
nuclear magnetic moment and orientation of, 18: 21360
nuclear spin of ground-state and excited, 16: 26331
nuclear spin of ground and metastable states of, 18: 44812
nucleon binding energy, 16: 3674(T) (CEA-tr-R-1371)
production by proton reaction (p,3n), cross section excitation function, and isomerization of, 17: 39993
production by proton reactions with gold-197 at 2.3 Bev, cross section for, (E), 20: 6298(R) (PPAD-2137-566)
production in proton reactions on gold, excitation functions, 16: 5964
separation from gold, rapid carrier-free method for, 16: 8785
separation from other gold irradiation products by volatilization, 16: 3072
separation of neutron-deficient, from gold-197, 20: 43067(R) (IDO-14679, pp 6-46)
spectra of ground-state and isomeric, hyperfine structure, isotope shift, and nuclear moments from, 17: 28284
spectra of ground-state and isomeric, hyperfine structure, isomer and isotope shifts from, 17: 28285

MERCURY ISOTOPES Hg-196
deuteron reactions (d,p) at 15 Mev, isomeric yield ratios for, 20: 16508(R) (NYO-2771-13)
electron (K) conversion coefficient at 426 kev, 16: 17100
energy level structure, (E), 20: 1173
energy levels and gamma spectra, 16: 19787
energy levels from thallium-196 decay, negative-parity, (E), 20: 30435
energy levels of, half life of first-excited, 18: 2942
energy levels of, measurement of lifetime of first excited, 18: 34772 (NP-14184)
energy levels of, doublet of two-phonon, 18: 40561
energy-level transitions from gold-197 (p,2nγ) reactions, anisotropy of conversion electrons from, (E), 20: 46684
mass of, 16: 3674(T) (CEA-tr-R-1371)
neutron capture cross sections, 18: 9336
neutron cross sections for isomer production in, thermal, 17: 18303
neutron cross sections for, thermal, 17: 18303
neutron reactions (n,γ) in, isomeric cross section ratios for, 17: 832
neutron reactions (n,γ), activation cross section for, (E), 20: 16336(R) (NYO-10175)
nucleon binding energy, 16: 3674(T) (CEA-tr-R-1371
production in stars, 16: 12308
spectra of, isotopic shifts in emission, 17: 34907
spectra of, isotope shift in, (E), 20: 1245

MERCURY ISOTOPES Hg-197
beta decay of, energy of electron-capture, (E), 19: 43309
decay of ground-state and isomeric, gold-197 energy levels from, (E), 19: 10326
decay of, gold-197 energy levels from, 19: 23672
decay of, internal bremsstrahlung accompanying electron-capture, (E), 19: 27438 (PAN-532/I-A)
decay of, local energy deposition due to electron-capture and internal conversion, 20: 18958
decay scheme and ground state spin of, 17: 22571(T) (NP-tr-1003)
decay scheme and gamma spectra of ground- and isomeric-state, 18: 18971
decay schemes, 17: 35254(R) (IDO-16898)
determination in biological material by scintillation counting, 19: 32096
diagnostic use for brain tumors, 19: 34006
diagnostic use for localization of brain tumors, 19: 46046
diagnostic use in brain scanning, 18: 17703
diagnostic use in renal diseases, 19: 5756
diagnostic use of, in spleen diseases, 19: 34053
dosimetry of, in nuclear medicine, 20: 26713
electron conversion and gamma correlations in, 17: 22571(T) (NP-tr-1003)
energy from, determination of total, 19: 38878 (ORNL-P-1405)
energy level densities in, effects of spin on, 16: 33853
energy level lifetime at 134 kev, 16: 7032
energy level schemes, 16: 2513
energy level scheme, 16: 2517
energy levels of isomer, hyperfine structure, 16: 2531
gamma dose constants for, 20: 46617
gamma spectra, 17: 17165
half life, (E), 20: 14461(R) (ORNL-3889, pp 48-70)
half life of isomeric, from neutron reactions (n,γ), (E), 20: 16336(R) (NYO-10175)
half life of 134-kev excited state, 16: 2516
half life of, from neutron reactions (n,γ), (E), 20: 16336(R) (NYO-10175)
hyperfine structure of 24-hr isomer, 16: 1055
hyperfine structure, 16: 4610(R) (TID-14435)
hyperfine structure of $^2P_1$ state of, microwave-optical measurement of, 17: 38122
hyperfine structure and isotope shift, (E), 20: 1245
incorporation in bromomercuri-hydroxypropane, 19: 42584
incorporation in bromosulfalein, 20: 16495
incorporation in neohydrin, 20: 43397
isomeric yields from (d,2n) reactions on gold-197, 16: 1025 (NP-9365)
magnetic moments determination by optical pumping, 16: 19476(R) (TID-15642)
mass of, 16: 3674(T) (CEA-tr-R-1371)
neutron reactions (n,2n) at 14.5 Mev, cross section predictions from gold-197 (p,2n) reactions, (T), 20: 36178 (UCRL-14575)
nuclear properties of isomeric, 18: 13626(R) (NYO-10174)
nuclear properties, 19: 46141
nucleon binding energy, 16: 3674(T) (CEA-tr-R-1371)
production by proton reaction (p,n), cross section, excitation function, and isomerization of, 17: 39993
production by proton reactions with gold-197 at 2.3 Bev, cross section for, (E), 20: 6298(R) (PPAD-2137-566)
production in (He-3,t) reactions at 27.5 Mev, ratio of ground- and isomeric-state, 18: 18971
production in (^{3}He,t) reactions at 27.5 Mev, ratio of ground- and isomeric-state (E/T), 18: 18971
production in lithium-6 reactions with gold-197 at 15–40 Mev, excitation functions for ground-state and isomeric, 17: 33038
production of isomeric, in deuteron reactions (d,p) at 15 Mev, 20: 16508(R) (NYO-2771-13)
properties as x-ray source for diagnostic radiography, 19: 46141
properties of, for use in kidney scanning, 18: 8258
properties of, for use in radiography, 19: 7227
properties of, for use in scintigraphy, 20: 33129
scanning of, collimator for, 18: 43956
separation from other products in neutron activation analysis of potato flour for mercury, 20: 18595
standardization of, method for, 20: 43381 (ORNL-P-2433)
uptake by kidneys, effects of pathological conditions on, 19: 15244(T) (ORNL-tr-480)
uptake of chlormerodrin-incorporated, by tumors, 19: 5749
uptake of neohydrin-incorporated, by brain tumors, 19: 26185
use as label for chlormerodrin for evaluation of brain lesions by scanning, 20: 26723
use as label for Neohydrin, in diagnosis of brain tumors, 19: 24384
use as tracer for spleen scintigraphy, 20: 6946
use as tracer for brain tumor localization, 20: 10733
use for diagnosis of brain tumors, 20: 16304
use for diagnosis of kidney diseases, 20: 31148 (CNEA-170)
use for diagnostic scanning of kidneys, liver, and spleen, 17: 35375
use for diagnostic scanning, 20: 45538
use for kidney and spleen scanning and brain tumor localization, 18: 35434
use for kidney function tests, 19: 46130
use for spleen function tests as 1-mercuri-2-hydroxypropane, 20: 35362
use in brain scanning, 20: 40748
use in brain scanning, feasibility of, 19: 34073
use in brain scanning, 19: 22055
use in carcinoma localization by scintillation, 19: 19715
use in kidney function studies, 19: 28168
use in kidney function studies, 19: 28186
use in labeling mercurihydroxypropane for scanning agent, 20: 40777
use in liver scanning, effects of collimator design, photon energy, and radiation dose on, 19: 7239
use in localization of brain tumors, 19: 31973
use in scintiscanning, review, 20: 22828
use in thyroid scanning, 18: 38723

use of bromomercurihydroxypropane-incorporated, for spleen scintigraphy, 20: 22817
use of compounds labeled with, in medicine, 20: 43051
use of mercury chloride-incorporated, in renal scintigraphy, 20: 22804
use of neohydrin-incorporated, in brain scanning, 20: 45528
use of, for labeling organic compounds for use in radiodiagnosis, 20: 26733
use of, in 1-mercuri-2-hydroxypropane for spleen scanning, 19: 15306

MERCURY ISOTOPES Hg-198

electron conversion, 18: 9348
electron transitions in, K-conversion coefficient of 412-kev E2, 18: 2889
energy level at 412 kev, g-factor for, 18: 15245
energy level at 412 kev, half life of, (E), 20: 38031
energy level transition energies of, 18: 44747
energy level transitions in, M1-M2 mixing ratios as test of purity of vibrational, (T), 19: 25503
energy level transitions in, K conversion coefficient for 412-kev, (E), 20: 10001
energy level transitions in, conversion coefficients for E2, (E), 20: 15707 (CONF-233(Vol.2), pp 198-212)
energy level transitions in, conversion coefficients for E2, (E/T), 20: 15708 (CONF-233(Vol.2), pp 213-19)
energy level transitions of, conversion coefficients for E2, (E), 20: 36227
energy level transitions in, conversion coefficients for 412-kev, (E), 20: 36228
energy level transitions of, dynamic contributions to E2 conversion determination from, (E), 20: 36255
energy levels, 16: 5988
energy levels, 16: 17081
energy levels, (E/T), 19: 27451
energy levels, (T), 20: 44788
energy levels from thallium-198 decay, negative-parity, (E), 20: 30435
energy levels of, electric monopole transitions between, 18: 6252
energy levels of, lifetime and nuclear resonance fluorescence of 412-kev, 17: 34975
energy levels of, E0 transition of (2^+) rotational, 18: 28625
energy levels of, conversion coefficients for transition of 412-kev (E), 19: 3297
energy levels of, conversion coefficients for 412-kev, 19: 3252
energy levels of, gamma K conversion coefficients of, (E), 19: 33248 (SGAE-PH-17/1965)
energy levels of, vibration-rotation interactions in, (T), 19: 41818
energy levels of, coincidence measurement of conversion coefficients for, 20: 4843(NP-15456)
energy levels, pressure shifts, and transition wavelengths, 16: 28061
fission barrier of compound, 18: 32746 (UCRL-11213(p.49-63))
gamma reactions (γ,n) in stars, 16: 12308
gamma reactions (γ,n) on, nuclear excited states from, 16: 33853
gamma resonance scattering at 412 kev, 18: 42760
gamma scattering at 412 kev, cross sections for, 17: 34975
gamma spectra, 16: 18428
gamma spectra, 17: 34900
gamma spectra, E-0 transition probabilities, 16: 21445
gamma spectra of, absolute energy of 412-kev line in, 17: 33050
gamma transitions in, angular correlations for, (E), 19: 10353
gamma transitions in, conversion coefficients for, (E), 20: 3038
internal conversion coefficient, 16: 7066
internal conversion coefficients of the E2 transitions, 16: 29798
internal conversion in, transverse polarization of K electrons from, (E), 20: 4900
internal conversion coefficients, 20: 8061
neutron capture by, energy levels from, 18: 9336
neutron reactions (n,γ) at resonance energies, spectra from, (E), 19: 40896
neutron resonance capture by, gamma spectra from, 18: 6256
neutron resonances in, total radiation widths for, 17: 24471
nuclear parameters from angular and polarization correlations in E0 transitions, (T), 20: 46770
nuclear shape parameters for, 18: 11221
photon bunching in discharge lamp containing, spectral profile from, (E), 20: 27629
rotation states of deformed axial symmetry in, 17: 19282
scattering resonances in, interference between, 17: 7109 (NP-12330 (p.147-51))
separation from gold, rapid carrier-free method for, 16: 8785
separation of, from neutron-exposed gold by distillation, 20: 46136
spectra in electric discharge, wavelength shifts as function of temperature, 16: 4637
spectra of, isotopic shifts in emission, 17: 34907
spectra of, vacuum wavelengths from, 17: 25209
spectra of, wavelength of Zeeman filter relative to 2537-Å absorption line of, 18: 4406
spectra of, isotope shift in, (E), 20: 1245
spectral line narrowing by resonance absorption, 16: 22135(T)
spectral line self-absorption properties, 16: 2337
surface oscillations of, 18: 13114
transition in, internal conversion coefficient of 412-kev E2, (E), 19: 16864
transitions in, 412-kev E2, (E), 19: 14580

MERCURY ISOTOPES Hg-199

atomic spectroscopy of, by level-crossing method, 18: 28094(R) (TID-20607)
core isomerism in, (T), 19: 17051
decay of isomeric, conversion coefficients for, (E), 19: 31307
electron conversion spectra, L-Auger, 16: 21359 (TID-15692)
energy level crossings, 18: 26676
energy level lifetime at 158 kev, 16: 7032
energy level lifetimes and transition probabilities of, 158- and 208-kev, (E), 20: 44704
energy level schemes, 16: 2513
energy level spins in, 17: 12802(R) (PR-P-55)
energy level structure from gold-199 beta decay, (E), 20: 30549
energy level transition energies of, 18: 44747
energy level transitions in, retardations in l-allowed M1, (T), 19: 21323
energy level transitions in, conversion electron-gamma correlations in, (E/T), 20: 15699 (CONF-233(Vol.2), pp 117-19)
energy level transitions of, particle parameters for L conversion electrons from, (E), 20: 36253
energy levels, 16: 5988
energy levels at 158 and 208 kev, half life of, 18: 30709 (AFOSR-4867)
energy levels from gold-199 and thallium-199 decay, 17: 825
energy levels in, radiative lifetime of 6^3P_0, 20: 2599
energy levels in, population transfer between hyperfine, 20: 34088
energy levels of, detection of isomeric, 17: 29953
energy levels of, isomer shift in, (T), 20: 28285 (TID-22018)
gamma dose constants for metastable, 20: 46617
gamma reactions (γ,n) in stars, 16: 12308
gamma spectra, 16: 18428
gamma spectra from transitions in, (E), 19: 47576(R) (IDO-17081, pp 49-76)
gamma transition energies of, 18: 14592(R) (PR-P-60)
gyromagnetic ratios of excited, 18: 36575 (NP-14084)
hyperfine structure, 16: 4610(R) (TID-14435)
hyperfine structure, 17: 35260(R) (TID-19135)
hyperfine structure of $^3P_1$ state of, microwave-optical measurement of, 17: 38122
isomeric transitions in, directional correlations of L electrons in, (E/T), 19: 25515
mass of, 16: 3674(T) (CEA-tr-R-1371)
neutron capture by, gamma spectra for thermal, 18: 11195(R) (EANDC(E)-49(L))
neutron capture by, gamma-gamma cascades in thermal, (E), 19: 14561
neutron capture by, γ-γ cascades in thermal, (E), 19: 21292
neutron capture by, analysis of γ-γ cascades from, (E), 20: 13062 (IEA-96)
neutron capture by, (n,γ) at thermal to 175 ev energies, γ-ray spectra from, (E), 20: 46599(R) (RPI-328-68, pp 1-62)
neutron capture cross sections, 18: 9336
neutron capture gamma spectra, level spin assignments from, 16: 14058
neutron capture resonances in, 18: 42622(R) (ANL-6879(p.2-20))
neutron reactions (n,β^-), cross section, 16: 19794
neutron reactions (n,γ) with, partial radiation widths of, 18: 11179 (ANL-6797(p.322-3))
neutron reactions (n,γ) with, polarization correlation, 18: 32277(R) (PR-P-61)
neutron reactions (n,γ) with, linear polarization correlation of, 19: 1053(R) (PR-P-62)
neutron reactions (n,γ) with, energy levels from thermal, (E), 19: 31309
neutron reactions (n,γ) at 0.1 to 8 Mev, spectra from, (E), 19: 35378(R) (EANDC(E)-57(U))
neutron reactions (n,γ) at resonance energies, spectra from, (E), 19: 40896
neutron reactions (n,γ), mercury-200 parity assignments from, 19: 41846
neutron reactions (n,γ) with gamma angular distributions from thermal, (E), 20: 1152 (IFA-RN-21)
neutron resonance capture by, 17: 41527(R) (ANL-6720(p.2-15))
neutron resonance capture gamma spectra of, partial widths for radiative transitions in, 18: 1055
neutron resonance capture by, gamma spectra from, 18: 6256
neutron resonances in, total radiation widths for, 17: 24471
neutron separation energy for, 18: 26576
nuclear magnetic moment of 158-kev $\frac{3}{2}^-$ state, 16: 7105
nuclear magnetic moment of, relative to mercury-201, 18: 6192
nuclear magnetic moment, 18: 21360
nuclear magnetic resonance, Knight and temperature-dependent shifts in, 18: 42036

nuclear magnetic resonance of, Knight shift in, 19: 43285
nucleon binding energy, 16: 3674(T) (CEA-tr-R-1371)
photoactivation of isomeric, cross sections for, 18: 7705
proton coupling in neopentyl derivatives of mercury, PMR spectral studies on, 20: 40908
rare-gas reactions with, hyperfine-level excitation in, (E), 20: 4544
spectra in chloride complexes with mercury, nuclear magnetic resonance, 18: 31449

MERCURY ISOTOPES Hg-200
beta decay scheme, 16: 19794
decay scheme, (E/T), 19: 16852(R) (NP-14647)
decay scheme of, 17: 38018(T) (AEC-tr-5734(p.88-90))
electron conversion (K) coefficient at 368 kev, 16: 4849
electron inelastic scattering at 200 Mev, differential cross sections for, (T), 20: 3124
energy level transitions of, conversion coefficients for E2, (E), 20: 36227
energy levels, 16: 5988
energy levels, 16: 17113
energy levels, 17: 41873 (WASH-1044)
energy levels, 17: 41527(R) (ANL-6720(p.2-15))
energy levels, (E), 19: 12533
energy levels at 1.59 and 2.10 Mev, spins of, 18: 18990
energy levels from mercury-199 (n,γ) reactions, parities of, 19: 41846
energy levels of, properties of high, 19: 26922(R) (PR-P-64)
energy levels of, parity and spin of, (E), 19: 31309
energy levels of, parity and spin of, (E), 20: 1152 (IFA-RN-21)
energy levels of, coincidence measurement of conversion coefficients for, 20: 4843 (NP-15456)
gamma cascades in, six-angle correlations for, 17: 25859(R) (PR-P-56(p.35-42))
gamma reactions (γ,n) in stars, 16: 12308
half life of metastable, 16: 2513
internal conversion coefficient of, K, 17: 2294
mass of, 16: 3674(T) (CEA-tr-R-1371)
neutron capture by, energy levels from, 18: 9336
neutron reactions (n,γ) with, energy levels from thermal, 18: 9388
neutron separation energy for, 18: 26576
nucleon binding energy, 16: 3674(T) (CEA-tr-R-1371)
production in neutron capture by mercury-199, γ-γ cascades from, (E), 19: 21292
production in neutron capture by mercury-199, γ-γ cascades from, (E), 20: 13062 (IEA-96)
spectra of, isotopic shifts in emission, 17: 34907

MERCURY ISOTOPES Hg-201
energy level crossings, 18: 26676
energy level lifetime at 32 kev, 16: 7032
energy level schemes, 16: 2513
energy level spacings and transition probabilities in, 16: 2513
energy levels in, radiative lifetime of 6^3P_0, 20: 2599
Fermi gas coefficient and nuclear temperature, 18: 998 (AD-299005)
gamma reactions (γ,n) in stars, 16: 12308
gamma reactions on, effects of E1 resonances on, 16: 33906
gamma spectra, 16: 18428
isomeric transition in, 92-μsec, 18: 38112
mass of, 16: 3674(T) (CEA-tr-R-1371)
neutron capture cross sections, 18: 9336
neutron capture gamma spectra, level spin assignments from, 16: 14058
neutron capture resonances in, 18: 42622(R) (ANL-6879(p.2-20))
neutron elastic scattering at 1.509 Mev, polarization in, 17: 31410 (TID-19051)
neutron reactions (n,γ) at resonance energies, spectra from, (E), 19: 40896
neutron reactions with, resonances in, (E), 19: 45296
neutron resonance parameters for, 18: 11195(R) (EANDC(E)-49(L))
neutron resonances in, total radiation widths for, 17: 24471
neutron resonances in, degrees of freedom of partial radiation widths for, 18: 1055
neutron separation energy for, 18: 26576
nuclear magnetic moments, 16: 1054
nuclear magnetic moment of, relative to mercury-199, 18: 6192
nuclear magnetic resonance in aligned (E), 19: 1578
nuclear magnetic resonance of, Knight shift in, 19: 43285
nuclear quadrupole relaxation of, on quartz surfaces, 18: 7727
nucleon binding energy, 16: 3674(T) (CEA-tr-R-1371)
photon resonance scattering on, optical orientation of magnetic moment in, 20: 17755(T)
photoproduction of 100-μsec isomer, 16: 31105
proton reactions (p,n) with, gamma spectra from, 19: 1598
rare-gas reactions with, hyperfine-level excitation in, (E), 20: 4544

MERCURY ISOTOPES Hg-202
deuteron and proton elastic scattering by, angular distributions and levels from, (T), 20: 30484
energy levels, (E), 20: 4875
energy levels of, parity and spin for (E), 19: 3327
gamma reactions (γ,n) in stars, 16: 12308
half life of metastable, 16: 2513
neutron capture by, energy levels from, 18: 9336
neutron resonance activation integrals for, 18: 1038
neutron resonance integrals for dilute solutions of, (E), 19: 29260 (TID-21744)
neutron separation energy for, 18: 26576
recoil atom reactions in benzene-mercury bromide systems, 16: 10084
spectra of, isotopic shifts in emission, 17: 34907

MERCURY ISOTOPES Hg-203
beta conversion electron transverse polarization correlation in, 16: 33815
beta decay, internal conversion coefficient at 279 kev, 16: 17075
beta decay of, gravitational effects on rates of, 18: 9369
beta decay of, K-conversion coefficient of 279-kev transition in thallium-203 from, 18: 7735
beta decay of, polarization of conversion electrons in, 17: 13544
beta decay of, polarization of K-conversion electrons following, 18: 6188
beta decay of, transverse polarization of K- and L-conversion electrons following, 17: 19277
beta decay of, transverse polarization of K-conversion electrons following, 17: 38127
beta decay of, β-γ directional and circular polarization correlations in, (E), 20: 30544
beta decay of, circular polarization in, 18: 21317
beta decay of, circular polarization in, 18: 22880
beta decay, polarization of conversion electrons, 16: 26086 (NP-11737)
beta spectra, 20: 8061 (CEA-R-2631)
calibration of, for determining efficiency of thin crystal scintillation detector, 20: 18562(R) (EUR-2640.e)
clearance from feces, kidneys, liver, and lungs, 17: 1242(R) (TID-17178)
containment of sources of, vacuum vessels for, 18: 18334
contamination from diagnostic use of compounds labeled with, 20: 45569
decay of, K/(L + M) conversion ratios in, 17: 31476
decay of, beta-gamma directional correlation in, 18: 18895
decay of, internal conversion coefficients in, 18: 38188
decay of, local energy deposition due to electron-capture and internal conversion, 20: 18958
decay of, peak-to-total ratios for, 18: 18884 (TID-20390)
decay, polarization of internal conversion electrons following beta, 16: 24784 (NP-11622)
detection and measurement of, by 4π-liquid scintillation counting, 19: 11595
diagnostic and therapeutic use, review of various aspects for, 18: 17693
diagnostic use for brain tumors, 19: 15297
diagnostic use for brain tumors, 19: 34006
diagnostic use for localization of brain tumors, 19: 46046
diagnostic use in children, radiation dose from, 18: 39006
diagnostic use of chlormerodrin-incorporated, in brain scanning, 19: 34049
diagnostic use of, in spleen diseases, 19: 34053
diagnostic use of, for brain tumor scanning, 19: 46053
diagnostic uses of, 19: 24391
distribution in fish, 17: 12114
distribution in uremic patients, effects on renal scans of, 18: 33433
distribution of Neohydrin labeled with, in brain tumors, 18: 31320
dosimetry of, in nuclear medicine, 20: 26713
electron spectra at 50 to 300 kev, Auger effects in, 16: 19753 (TID-15684)
elimination from rat kidney, use of BAL for, 19: 12943
energy level crossings in, 18: 42162(R) (TID-20963)
energy level schemes, 16: 2513
energy levels, 17: 35254(R) (IDO-16898)
energy levels of, spin of ground-state, 18: 6188
energy levels of, spin of ground-state, 18: 21317
exchange between labeled mercuric chloride and phenylmercurichloride, kinetics of, 20: 45771
exchange between mercury bromide and nitrobenzylmercurobromide, 18: 37559
exchange between organic mercury compounds, 19: 2289
excretion by rats, 17: 24869
excretion in rats, effects of BAL on, 20: 37025(R) (PG-Report-705)
excretion of injected, effects of BAL in rats, 20: 8571
excretion rate of mercaptomerin labeled with, 18: 21794
gamma dose constants for, 20: 46617
gamma doses from point sources of, sand-scattered, 19: 31429
gamma radiation from, use in moisture determination, 19: 11612
gamma specific emission coefficient, 17: 6431 (CEA-2036)
gamma spectra, 17: 16438
half life, 20: 8076 (NP-15663)
hyperfine structure, 18: 2404(R) (TID-19651)
incorporation in *E. coli*, use for studying oyster self-decontamination,

18: 17441
incorporation in neohydrin, 20: 43397
incorporation in 3-(chloromercuri)-2-methoxypropylurea for medical uses, 19: 46305
internal conversion coefficients of K shell, development of gamma scintillation spectrometry for determination, 16: 21134 (TID-15639)
isomeric transition in, 21-μsec, 18: 38112
localization in brain tumors, diagnostic applications, 17: 5841
localization in tumors of, effects of intra-arterial hydrogen peroxide infusion on, 19: 22053
localization of urea labeled with, in tumors, effects of intraarterial hydrogen peroxide on, 19: 36137
losses in evaporation of mercury compounds, 20: 23027
magnetic moment and spin of, measurement of, 18: 17066
metabolism by aquatic insect larvae in spiked water, 19: 42247(T)
metabolism by rats after repeated vapor inhalation, 19: 3860
properties of, for use in scintigraphy, 20: 33129
radiation doses to ovaries from, estimation of, 20: 6719(R) (ORNL-3849, pp 183-213)
retention in mammals, effect of chelating agents on, 16: 29327 (KFK-76)
separation from animal tissues using complexing agents, 19: 12945
separation from aqueous solutions by exchange on mercury metal, 17: 394
separation from fission products by amalgam exchange, radiochemical, 18: 16148
sorption and distribution in chicks, effects of vitamin D, 17: 23024
sorption by guinea pig skin, disappearance measurements of, 20: 32910
transfer to rat offspring by neohydrin used in tumor diagnosis, 19: 17738
uptake and distribution in blood and tumors in man, mice, and rats, 19: 14960
uptake by aquatic insects, coefficient of accumulation for, 19: 25857
uptake by brain tumors, 18: 1471
uptake by brain, measurement techniques for, 18: 17419
uptake by dog hematomas, 18: 11597
uptake by kidneys as localization technique, 18: 17692
uptake by kidneys, hazards from, 18: 29482
uptake by kidneys, effects of pathological conditions on, 19: 15244(T) (ORNL-tr-480)
uptake by larvae of aquatic insects, 19: 8774
uptake by rabbit tissues *in vitro*, 17: 35430
uptake by tumor tissue in man and rabbits in oxygen environment, 20: 36576
uptake in brain tumors, 16: 16231
uptake of neohydrin-incorporated, by brain tumors, 19: 26185
uptake through excised human and guinea pig skin as chloride, 20: 35202
use as gamma source in well logging, 20: 41165
use as gamma source in radiometric measurement of ore pulp flow rates, 20: 46105 (BM-RI-6855)
use as label for chlormerodrin for evaluation of brain lesions by scanning, 20: 26723
use as label for Neohydrin, in diagnosis of brain tumors, 19: 24384
use as tracer for diagnosis of circulation dyscrasias in brain, 20: 6950
use as tracer for spleen visualization, 20: 8763
use as tracer in brain tumor scanning, 19: 22038
use as tracer in pulp and paper research, 17: 32328
use for diagnosis of brain tumors, 20: 16304
use for diagnosis of kidney diseases, 20: 31148 (CNEA-170)
use for kidney function tests, 19: 46130
use for measurement of blood circulation in brain, 19: 38501
use in brain scanning, feasibility of, 19: 34073
use in brain scanning, 19: 22055
use in brain tumor scanning by collimation, comparison of gallium-68-EDTA scintillation with, 19: 15307
use in brain tumor localization by external scanning, 19: 22076
use in diagnosis of renal tumors by scintillation scanning, 17: 35379
use in diagnosis of brain tumors, 20: 179
use in encephalography for localization of brain tumors, 16: 1453
use in encephalography of brain tumors, 19: 36165
use in gamma encephalography, 19: 38510
use in hematology and radiodiagnosis, 18: 17695
use in kidney function studies, 19: 28168
use in liver scanning, effects of collimator design, photon energy, and radiation dose on, 19: 7239
use in localization of brain tumors, 16: 11393
use in radiodiagnosis of human brain tumors, 19: 15255
use in renal scintiscanning of urologic diseases, 19: 19721
use in scintiscanning, review, 20: 22828
use of compounds labeled with, in medicine, 20: 43051
use of neohydrin-incorporated, for kidney scanning, 20: 22823
use of, for labeling organic compounds for use in radiodiagnosis, 20: 26733
volatilization from rats after injection with chloride salt, 19: 3861

MERCURY ISOTOPES Hg^{-204}
alpha decay energy of, effect of shell structure on, (T), 20: 19848
determination by isotope shift of mercury emission spectra, 19: 34118
fluorescence yields, L-shell, (E), 19: 8454
gamma reactions (γ,n) in stars, 16: 12308
neutron capture cross sections, 18: 9336
neutron separation energy for, 18: 26576
production by monoisotopic photochemical process, estimated costs of, 18: 20429 (HW-71793)
proton reactions (p,4n) with, gamma spectra from, 19: 1598

MERCURY ISOTOPES Hg^{-205}
beta decay parameters of, 17: 2250
energy level schemes, 16: 2513
gamma dose constants for, 20: 46617
gamma spectra, 16: 4751 (JAERI-4019)
gamma spectra, 17: 34966
neutron reactions (n,α) at 14 Mev, nuclear shell effects in cross sections for, 18: 18977

MERCURY ISOTOPES Hg^{-206}
alpha decay energy of, effect of shell structure on, (T), 20: 19848
decay scheme and half life, 19: 23766
half life, 20: 8172
nuclear properties of, 17: 2250
separation from uranium–radium decay products, 20: 8172
yields from uranium–radium decay series, 19: 23766

MERCURY ISOTOPES Hg^{-208}
alpha decay energy of, effect of shell structure on, (T), 20: 19848

MERCURY ISOTOPES Hg^{-210}
alpha decay energy of, effect of shell structure on, (T), 20: 19848

MERCURY ISOTOPES Hg^{-212}
alpha decay energy of, effect of shell structure on, (T), 20: 19848

MERCURY NITRATES
effects on iodine removal from gas streams by nitric acid solutions, 18: 31654 (HW-55735)
effects on radioinduced graft polymerization of acrylamide to polypropene fibers, 18: 29702(T,R) (AEC-tr-6231(p.114-18))
properties as catalyst for reactor fuel reprocessing solutions, 18: 31653(R) (IDO-14635)
radiation effects on electron paramagnetic absorption in, gamma, 18: 3819
reactions with lithium and potassium ferrocyanides, 18: 13777
separation by reversed-phase partition chromatography using organophosphorus compounds, 18: 25614
solubility in aqueous solutions of uranyl nitrate, 16: 18994
spectra in tri-*n*-octylphosphine oxide solutions, infrared, 18: 10075
$HF–Hg(NO_3)_2–HNO_3$, solvent properties for irradiated aluminum–plutonium alloys, 18: 22167 (DP-874)
$Hg(NO_3)_2–HNO_3$, performance for aluminum–plutonium alloy dissolution, 20: 28828 (BNWL-204)
$Hg(NO_3)_2–HNO_3$, solvent properties for SAP, 18: 17938 (RT/CHI(63)-34)
$Hg(NO_3)_2–HNO_3$, solvent properties for aluminum–uranium alloys, 18: 25269(R) (NLCO-905)
$Hg(NO_3)_2–HNO_3$, solvent properties for ATR fuel plates, 19: 24610(R) (IDO-14638)

MERCURY, NITRATOPHENYL-
reactions with benzeneboronic ester, neutron absorption measurement of boron-10/boron-11 isotope effects in, 18: 39201

MERCURY OXALATES
radiation effects on thermal decomposition of, 19: 11813
radiation effects on thermal decomposition of, gamma, sunlight, and x, 20: 36898

MERCURY OXIDES
additive effects on radioinduced vulcanization of rubber, 18: 12144 (PAN-457/XVII)
radiation effects on potential of electrode of, 20: 1932
spectra in low frequency region, infrared, 18: 23549
spectra of, in 300 to 1000 mμ region, reflectance, 17: 15970
Cd–HgO, development for long-life batteries, 19: 17437(R) (UCRL-13141)

MERCURY PERCHLORATES
effects on electron exchange reactions between thallium and uranium in methanol–water solutions, 18: 27418
oxidative effects on tetra-*α*-deuterocyclohexanone, kinetic isotope effects in, 18: 41414
positron lifetimes in, 16: 32354
reactions with dioxane, structure of addition compound formed in, 17: 4452
separation by reversed-phase partition chromatography using organophosphorus compounds, 18: 25614

MERCURY QUADRANGLE (NEV.)
geologic map of, 17: 4728

MERCURY SALTS
protective effects against iodine-131 toxicity in animals, 17: 6005

MERCURY SULFATES

crystal structure of monohydrate of, 18: 31361(R) (UCRL-11213(p.87-138))
crystal structure of monohydrate of, 18: 36902 (UCRL-10969)
Hg–$HgSO_4$, emf measurements vs Ag–Ag_2SO_4 in all-metal cell, 19: 36340 (ORNL-P-814)
$HgSO_4$–H_2SO_4, solvent properties for aluminum tubes, 19: 40655 (RT/(CHI(65)-1)

MERCURY SULFIDES
clearance of mercury-203-labeled, from feces, kidneys, liver, and lungs, 17: 1242(R) (TID-17178)
composition of vaporous, equilibrium, 17: 33905
dissociation energy of, 17: 33906
preparation of single-crystal, 17: 5039(R) (ORNL-3364(p.85-124))
production of single crystals, 17: 34556(R) (ORNL-3480(p.108-14))
production of single-crystal, 19: 346(R) (ORNL-3676(p.167-76))
radiation effects on electric conductivity of thin films of, x, 20: 46961

MERCURY SYSTEMS
amyl alcohol–Hg–$HClO_4$, surface charge density of, dependence on surface excess, 18: 4904 (IS-626)
Ar–Hg, electric discharge in, resonance radiation from, 18: 21464
Ar–Hg, electric discharge in vapor of, excited atom distributions from low-pressure, (E/T), 20: 23887
Ar–Hg, glow discharge initiation in, (E), 20: 3162 (AD-616683)
Ar–Hg, photon emission by atoms in plasma of, (E), 19: 41891(T)
Ar–Hg, r-f resonance measurement of electric conductivity of discharge plasma of, 20: 20088
Cs–Hg, performance in thermionic cells, 18: 36234
He–Hg, calculation of total cross sections as function of velocity, 18: 4347
He–Hg, electric discharge in, 19: 17078(R) (TID-21380(p.31-6))
Hg–$HClO_4$–phenol, surface charge density of, dependence on surface excess, 18: 4904 (IS-626)
Hg–$HgCl_2$, electric conductivity, 20: 22520(R) (NAA-SR-11805)
Hg–$HgCl_2$, electric conductivity of molten, 20: 35841(R) (NAA-SR-11900)
Hg–$HgCl_2$, electromotive force measurements on, 17: 40815
Hg–$HgCl_2$, electromotive force studies of species in liquid, 18: 11511 (NAA-SR-8881)
Hg–$HgCl_2$, free energy of solution of, 19: 11103
Hg–$HgSO_4$, emf measurements vs Ag–Ag_2SO_4 in all-metal cell, 19: 36340 (ORNL-P-814)
Hg–H_3PO_4, reduction of irradiated potassium chloride by, preparation of sulfur-35-labeled sulfuric acid by, 20: 36920
Hg–N, flow characteristics for two-phase, 17: 27535 (BNL-801)
Hg–N, flow of circulating and non-circulating, slip ratios in, 19: 36622
Hg–N, heat transfer in two-phase flow of, 17: 18265 (NAA-SR-8171)
Hg–Ne, electron density and temperature in plasma of, 17: 11883
Hg–Se, performance as indicator electrode, 20: 22871(R) (MIT-905-52, pp 42-73)
H_2–Hg, calculation of total cross sections as function of velocity, 18: 4347
Kr–Hg, optical properties for maser amplification, 17: 26458(R) (ORNL-3425(p.128-30))

MERCURY TELLURIDES
electron effective mass in, plasma reflection methods for determining, 19: 9143

MERCURY THIOCYANATES
radiation damage to crystal lattices of, fission fragment, 17: 34506
solvent extraction in three-phase system using diantipyrilmethane, 18: 13950

MERCURY URANATES
preparation and properties, 18: 20012

Meritectic Reactions
see Phase Studies

MERLIN
see Research Reactors

MESACONIC ACID
radiation chemistry of aqueous solutions, 17: 35902

MESIC ATOMS
(Positively charged nuclei to which negative kaons, pions, or muons are attached in a Bohr-like orbit)
absorption ratios for s-orbitals in deuterium π^-, nonradiative and radiative, 20: 41809
bound states in μH, 18: 26271 (BNL-837(p.277-91))
calculation of the 2p → 1s transition energy in, 17: 9065
capture interactions in mu, 19: 1419 (NP-14404(p.188-201))
capture rates for mesons (μ^-) in helium-3, (T), 19: 6709
capture wave functions in mu-mesic hydrogen molecular ions, 18: 26555(R) (ORNL-3582(p.130))
Coulomb disintegration of, 17: 13549
decay of (μ^-), Goldberger-Treiman relation for, 18: 15304
decay of (μ^-), in carbon tetrachloride, (E), 19: 18746 (AD-423000)
decay of (μ^+), fast chemical reactions based on, (T), 19: 42576
decay of bound muons from K-shell, 16: 21611
decay of (K^-), 17: 11512
decay of (K^-), Auger electron and x ray emission and nuclear absorption in, 17: 26522
decay of K^-, relative probabilities of direct and scattering modes, 16: 21534
decay of lithium-6, helium-6 production in, 18: 17087
decay of mesons (μ^-) in the K shell, 16: 2373
decay of μ^-, of transition metals of the iron group, anomaly in, 17: 6888
decay rate of mesons (μ^-) in, effect of atomic binding on, 17: 774
deuteron reactions with deuterium, yields in, 18: 34617
electromagnetic transition rates in, effects of center-of-mass motion of nucleus on, 17: 41914
electron activation, 16: 7017 (JINR-D-823)
electron emission from, energy and yield of, 18: 11260
elementary particle scattering by, wave functions for, 18: 32412
energy level excitation in heavy, collective, 16: 17151
energy level fluorescence yields of, 20: 31936
energy level shifts in carbon and oxygen (μ)-, 20: 25742
energy level shifts in K, 20: 34601
energy level shifts and line widths of π, (E), 20: 41803(R) (UCRL-16863)
energy level transitions in meson (μ^-), 20: 4825(R) (ANL-7081, pp 81-93)
energy level transitions of $16 \leq Z \leq 24$ μ, 2P-1S, (E), 20: 35996 (JINR-P-2735)
energy levels, 18: 12924
energy levels of (μ^-), hyperfine, 18: 30786
energy levels of (μ^-), quadrupole interaction of 2p doublet, (E), 19: 5169
energy levels of bismuth, lead, and thallium (μ), 2P → 1S transitions in, 17: 41945
energy levels of deformed (μ), resonances in, (T), 20: 17281
energy of 2p-1s transition, 16: 19705
energy-level shifts in hydrogen, from vacuum polarization, (T), 20: 5995
fission by radiationless transitions in plutonium-239, (E), 20: 8068 (JINR-D-2427)
fission of plutonium-239 (μ), by radiationless transitions, (E), 20: 12041
formation by mesons (μ) in hydrogen diffusion chamber, 17: 9473
formation in hydrogenous substances (E), 19: 3237 (JINR-P-1767)
formation of deformed-nucleus, 18: 38167
formation of μ-mesic helium, 17: 33080
formation rates for (μ^-), in neon, 17: 9586
formation rates of ($pp\mu$), ($pd\mu$), and ($dd\mu$), 17: 9404
gamma radiation from nuclei of meson (μ^-), 18: 44797
hyperfine splitting of (μ-ρ), four-fermion V-A weak interactions in, (T), 19: 41410
hyperfine structure of meson (μ), vacuum polarization corrections to, (T), 19: 21395
hyperfine structure of μ-mesic lead, (E), 20: 17268
hyperfine structure of μ-mesic bismuth, E2 and M1, (E), 20: 17792
hyperfine structure of μ, nuclear charge distribution from, (T), 20: 44721
interactions with protons, cloud chamber studies, 16: 7016 (JINR-D-812)
internal conversion between hyperfine states of μ, polarization density matrix in, (T), 19: 21421
ion reactions with hydrogen, meson (μ) exchange in, (E), 20: 7734
magnetic moment of (μ^-), 17: 7213
magnetic moment of mesons (μ^-) in, 17: 31341
magnetic resonance experiments on (μ), 18: 2483
meson (K^-) and (π^-) capture rates in helium, 19: 43356
meson (K^-) and (π^-) moderation and cascade times in levels of helium, (E), 20: 15273
meson (μ^-) capture by helium-3, neutron spectra from, (E), 19: 29254 (NEVIS-128 and Add.)
meson (μ^-) capture by proton pairs in, (E/T), 19: 41753
meson (μ^-) decay in, electron spectra from, (E), 19: 6517 (JINR-P-1778)
meson (μ^-) decay in, nuclear recoil in, (T), 19: 19199
meson (μ^-) exchange between hydrogen and carbon, 18: 34947
meson (μ^-) radiative capture rates in hydrogen molecular ions, (T), 19: 4932
meson (μ^-) transitions in, x rays from, 18: 19044
meson (μ^-) transitions in calcium, isotope effects in x-ray spectra of, 18: 42732
meson (μ) capture by deuterons, neutron spectra from, (T), 19: 41782
meson (μ) capture by helium-3, neutron spectra from, (T), 19: 41783
meson (μ) capture rate in hydrogen, 19: 47227
meson (μ) decay in intermediate-Z, 18: 12964
meson (μ) decay rate in, 19: 23777
meson (μ) depolarization in, of spin-one nuclei, (T), 20: 39616
meson (π^-) energy level transitions in, mass measurements from x-ray spectra from, (E), 19: 33023
meson (π^-) transfer from hydrogen, to heavier atoms, (E), 19: 21281
meson (π) absorption by the nucleus in, calculation of rates of, 18: 15232
meson (π)-nucleus interactions in, interpretation using the optical model, 18: 15203 (NP-13679)
meson (μ) nuclear capture by neon, probability for, 17: 24493

meson (μ) transfer by, probability of, 16: 32453
meson (μ^-) decay in, 16: 24278 (JINR-P-971)
meson (μ^-) decay in, of palladium, titanium, and their hydrides, 16: 26080 (JINR-P-972)
meson (μ^-) decay rates in, theory for, 17: 6968
meson (μ^-) depolarization in, by spin-½ nuclei, 16: 12386
meson (μ^-) magnetic moment in, 16: 13865 (NEVIS-101)
mesonic and radiative capture, Panofsky ratio for, 16: 9369
mesons (μ) transfer in, 16: 26219 (JINR-P-942)
nuclear excitation by muon 2p → 1s transition in, 16: 8185
nuclear polarization, in spherically symmetrical meson states, 16: 4866
nuclear polarization from non-spherical symmetric meson state, 16: 12534
nuclear polarization in, 17: 19367
nuclear quadrupole moment of, vacuum polarization induced by, 17: 36687
nuclear radii for $12 \leq Z \leq 50$ μ, 17: 26578
polarization in (μ), vacuum, (T), 20: 15246 (CONF-233(Vol.3), pp 520-8)
probability of $p\mu$He, 16: 32453
processes in gaseous hydrogen, experimental study, 16: 16884
production and disappearance rates of μ^-, 16: 21174
production and properties of (K^-), 17: 19331
production by meson (μ^-) capture in compounds, (E), 19: 37896
production in deuteron reactions with deuterium mesic atoms, 18: 34617
production in meson (μ^-) capture in liquid hydrogen, rates for, (T), 20: 23899
production mechanisms, 18: 15290
production of (μ^-), (T), 19: 27434 (JINR-P-2063)
production of (μ), 20: 1225
production of carbon, in meson (μ^-) exchange with protons, 18: 34947
production of meson (π^-), in hydrogenous material, (T), 20: 980
production of μ, (T), 20: 28456
production of, probability in gaseous helium-hydrogen mixtures, 17: 20842 (JINR-P-1168)
properties of hydrogen and deuterium, 17: 19245
quantum mechanics of $(p\text{-}\mu\text{-}p)^+$ ion, 18: 32605
reactions involving (μ^+), chemical, (E/T), 19: 29109
reactions of deuterium μ^-, with deuterium and hydrogen, (E), 20: 34109
scattering cross sections of ($p\mu$), by protons, 17: 9404
scattering kinetics, 18: 30722 (JINR-P-1665)
scattering of ($p\mu$), by protons, (E), 20: 2640
spectra of deuterium and hydrogen μ^-, second-order corrections to Lamb shift in, (T), 20: 25741
spectra of meson (μ)–lithium-6, hyperfine structure in, 17: 26298
spectra of μ-mesic hydrogen, nucleon polarization effect in, (T), 19: 6640
spectra of muonic, analysis of (nd–1s) and (nd–2p), 18: 22694
spectra of thallium μ-, effects of shell structure on, 18: 21331
structure of, energy of 2p–1s transition and shell, 17: 19305
survey, 19: 27571
theory for light π^-, 20: 41665
theory of mu, 20: 37479
three-charge problem, application of improved Born-Oppenheimer method, 16: 28322
transition energies in barium–muon, 17: 18982
transitions, non-radiative, 16: 23019
transitions 2P → 1S in heavy, 16: 27819
x-ray deficiency, 16: 12801(R) (IA-685)
x-ray deficiency in carbon, nitrogen, and oxygen μ, 17: 26567
x-ray deficiency in K^-, 17: 26568
x ray emission from calcium (μ), isotopic differences in, 17: 41617
x ray emission from π, bent-crystal spectroscopy of, (E), 19: 4480 (TID-7705(p.240-54))
x ray emission from, isotope effects on energy spectra of, 19: 47582 (NEVIS-129)
x-ray emission from (μ), 2p-1s energies for, 18: 34435
x-ray emission from gold, lead, bismuth, uranium, and tungsten, 2p-1s and 3p-2p energies for, (E/T), 19: 21344
x-ray emission from helium-4, (E), 19: 35494
x-ray emission from (μ^-), isotope effects on K, (E), 20: 11480
x-ray emission from (μ), computer analysis of, 20: 11440(R) (COO-614-34, Sect. IID)
x-ray emission from π, 20: 46580(R) (BMwF-FBK-66-05)
x-ray intensity ratios from bismuth and lead μ, (T), 20: 31945
x-ray spectra from μ, nuclear charge distribution from, 19: 27518
x-ray spectra from (μ^-), nuclear charge distribution from, (T), 20: 17756
x-ray spectra from μ, isotope shifts in, (E), 20: 23888
x-ray spectra from μ, nuclear charge distribution from, 20: 28436
x-ray spectra from K-mesic helium, effects of $\bar{K}$-N interactions on, 20: 29938
x-ray spectra from (μ), (E), 20: 38058
x-ray spectra from μ^-, (E), 20: 42306
x-ray spectra from μ^-, isotope shifts from, (E), 20: 42307
x-ray spectra from μ, (E), 20: 42309
x-ray spectra from μ, (E/T), 20: 42310
x-ray spectra from π, in even-even nuclei, (E), 20: 42311
x-ray spectra from μ, nuclear charge distribution determination from, (E), 20: 42305
x-ray spectra of (μ^-), (E), 19: 5168
x-ray spectra of (π), (E), 20: 21534
x-ray spectra of calcium-40 and -44 and oxygen-14, -16, and -18 μ, (T), 20: 27736
x-ray spectra of gold, electric-quadrupole hyperfine splitting in K, (E), 20: 9667
x-ray spectra of $3 \geq Z \geq 12$ μ and π, (E), 20: 34103
x-ray transitions in μ-mesic tantalum and plutonium-239, 2p–1s, (E), 19: 44962

MESIC MOLECULES
energies and wave functions of $(p\mu p)^+$, (T), 20: 5980 (AD-617522)
energy levels of d-μ-d and p-μ-p, (T), 20: 13630
formation of ($pp\mu$), by proton-mesic atom ($p\mu$) scattering, (E), 20: 2640
meson (μ^-) capture by $(p\mu d)^+$, neutron spectra from, (E), 19: 29254 (NEVIS-128 and Add.)
meson (μ^-) capture by μ-mesic deuterium and hydrogen, (T), 19: 37458(R) (ORNL-3778(p.150-1))
production in meson (μ^-) absorption in liquid hydrogen, (T), 19: 19178
production in meson (μ^-) capture in liquid hydrogen, rates for, (T), 20: 23899
production in reactions of mesic deuterium atoms with deuterons and protons, (E), 19: 45273 (JINR-P-2356)
production of (μ^-), in hydrogen, 18: 38130
production of $dd\mu$ and $pd\mu$, (E), 20: 34109
wave functions for ($p\mu d$), nucleon-deuteron capture cross section from, (T), 20: 11493

Mesidine
see Aniline, 2,4,6-Trimethyl-

MESITYL DISULFIDE
effects on photoreduction of benzophenone in ethers, 20: 7129(R) (NYO-2499-17)

MESITYL OXIDE
formation by disproportionation of 3-methyl-3-penten-2-one in perchloric acid, 20: 16542(R) (TID-22646)
solvent properties for uranium(VI) ions, 19: 2246
solvent properties for zirconium, 19: 36547
solvent properties for uranium, 19: 42445
solvent properties for uranium, 20: 18605
solvent properties for thorium, 20: 35411

MESITYLENE
analysis for nitrogen-13 by fast neutron irradiation, 16: 7494
determination in humidrier liquors by gas chromatography, 20: 26749 (PG-Report-695)
deuterium exchange between, and heavy water, effects of π-complex absorption on transition metals on, 19: 32199
deuterium-hydrogen exchange reactions in, effects of nickel on, 19: 28347
effects as diluent on perchloric and perrhenic acid extractions by tri-dodecylamine, 20: 1747 (UCRL-11616(Rev.))
effects on radiolysis of monoimine of phenanthrene-9,10-quinone, 20: 397
effects on solvent properties for uranium in TBP system, 20: 14655
electronic energy transfer to p-terphenyl, 18: 10620 (AFCRL-63-610)
electronic spectra of, tables, 19: 9156 (IS-450)
hydrogen abstraction from, by methyl radicals, 19: 21760 (NYO-2728-4)
luminescence spectra and quantum yields of pure and cyclohexane solutions of, 19: 21771 (TID-21684)
neutron scattering cross section spectra, 16: 29522 (BNL-5979)
photoionization of, energy spectra of electrons from, 18: 281
preparation of, for measuring natural carbon-14 by scintillation methods, 20: 2062
proton exchange with hydrogen fluoride, 18: 29679
radioinduced electronic energy transfer from, efficiency of nonradiative, gamma and uv, 19: 467
radioinduced oxidation on alumina, alumina–silica system, and silica, 18: 1725(R) (ORNL-3488(p.42-54))
radicinduced oxidation of, adsorbed on alumina, aluminosilicate, and silica gel, 19: 4215
radiolysis of sulfur in, yields in, 18: 27505
solvent effects on gamma-induced polymerization of styrene, 18: 29715(T,R) (AEC-tr-6231(p.170-4))

2-MESITYLENETHIOL
effects on photoreduction of benzophenone in ethers, 20: 7129(R) (NYO-2499-17)

MESON BEAMS
analysis of (μ), for meson (π) contamination, 18: 42410
analysis of 4- to 12-Bev/c meson (π), using gas Cherenkov counter, 19: 44376 (BNL-9466)
attenuation in bubble chambers, 18: 7030 (BNL-7480)

contamination of intense (μ^-), by mesons (π^-), 16: 22889
design and performance of (K), in CERN synchrotron, 17: 23635
design for low meson (π) contamination, 18: 12799 (CERN-63-35)
design of separated K^-, 18: 12811 (TID-7686(p.57-8))
detection and measurement of charged photopion, in Frascati synchrotron, (E), 19: 11864 (LNF-63/82)
detection of secondary, using high-energy photography system, 16: 13346
effects on chromosomes in root meristems, 20: 18190(R) (UCRL-16613)
effects on tumors in mice, biological, 20: 18190(R) (UCRL-16613)
energy transfer from 70-Mev(π^-), to polyethylene, 20: 20525
extraction from synchrocyclotron (E), 19: 1103 (NASA-CR-56934 (p.85-91))
fluxes of Brookhaven Synchrotron and Stanford Linear accelerator, 18: 10697 (SLAC-25(Pt.I)(p.1-18))
focusing and magnetic analysis, apparatus for, 17: 30854 (LNF-63/35)
focusing high-energy, plasma lens for, 17: 19453(R) (LAMS-2874)
focusing of (μ), efficiency of magnetic quadrupole lens for, 20: 23840
focusing of K^+ and π^+, neutrino spectra from magnetic-finger, 19: 30877 (BNL-9062)
focusing of pi, electromagnetic lenses for, 20: 17198 (CONF-650922, pp 650-6)
focusing of, using plasma lens, 19: 20915 (BNL-8967)
identification of mesons (μ) and (π) in mixed beam with electrons by Cherenkov counter, 16: 7705
intensity and quality of CERN-PS external, factors affecting (E/T), 19: 1099 (NASA-CR-56934(p.24-34))
intensity optimization of π, from 300-Bev accelerator, 17: 20590 (UCRL-10022(p.231-3))
measurement, 16: 31838(T) (UCRL-Trans-864)
meson (μ) contamination in meson (π), method for calculating, 19: 44993 (CEA-R-2778)
monitoring of, Cherenkov detector for, 18: 41858
neutrino production in relativistic, spectra of, 18: 12894 (CERN-63-37(p.111-29))
operation of high-energy K^-, 16: 32177(R) (UCRL-10349)
performance of (K^-) and (K^+), at Brookhaven AGS, 17: 23634
polarization, 16: 21262 (CERN-62-8)
production and control, 18: 20703
production and properties of 1-Bev/c K^+, (E), 19: 10017 (NP-14472)
production and transport at Univ. Chicago Synchrotron (T), 19: 1114 (NASA-CR-56934(p.237-63))
production and transport at Univ. Chicago Synchrotron (E), 19: 1115 (NASA-CR-56934(p.264-78))
production and transport of (K^+), 19: 1123 (PPAD-526-D)
production in accelerators, 17: 7391
production in CERN synchrotron, 17: 23638
production in CERN synchrotron at 0.6 to 1.2 Bev/c, (E), 19: 28940 (CERN-65-2)
production in synchrocyclotrons (E), 19: 1117 (NASA-CR-56934 (p.283-9))
production of ($K^\pm$), at Bevatron, 18: 37820 (UCRL-11527)
production of (K^0), regeneration phenomena in, (T), 19: 45034 (NP-15470)
production of (μ), at high energies, 19: 11970
production of (μ), magnetic quadrupole channel for, (T), 19: 11971
production of (μ), in JINR synchrocyclotron, 19: 14173 (JINR-P-1902)
production of (μ), high-intensity channels for, 19: 28955 (LA-DC-6757)
production of, design of 750-Mev linear proton accelerator for, 17: 15325(R) (TID-17766)
production of high-intensity meson (K^-), using CERN PS, 19: 41184
production of K^-, at bevatron, 16: 31946
production of μ, from 300-Bev accelerator, 17: 20574 (UCRL-10022 (p.96-104))
production of μ, from 300-Bev accelerator and use in experiments, 17: 20575 (UCRL-10022(p.105-7))
production of μ, with momentum above 6.5 Bev/c, 17: 15316 (BNL-6823)
production of mu, by electron interactions with lead, 18: 14832
production of μ^-, from CERN synchrocyclotron, 16: 31944
production of π^+, in Cosmotron, 16: 2560 (BNL-5757)
production of polarized pseudovector and vector, 16: 26124
production of, proposed facility for, 18: 8952 (LAMS-3025)
production of separated K^-, optical system for, 18: 40092 (UCRL-11426)
production of, shielding requirements for, 17: 7393
production of 1 Bev (μ), 17: 15313 (BNL-6785)
production of 150 Mev/c, magnetic channel for, 17: 34725 (ISS-63/27)
production of 4 Bev/c K^-, 17: 23631
production of 4- to 16-Bev/c meson (π), in Brookhaven AGS, (E), 19: 32828 (BNL-9213)
production of, review on, 19: 830
production of, systems for, 18: 12810 (TID-7686(p.43-56))
production using high-intensity proton linac, (E), 19: 9808 (TID-21282)
production with sector-focused cyclotron, 17: 7394
production with various accelerators, 17: 7392
production with 700-Mev cyclotron, 17: 7398
profiles of, bubble chamber for studying, 16: 31827 (TID-16668)
pulse duration of 680-Mev synchrocyclotron, increase of, (E), 19: 26972 (JINR-P-1985)
radiation hazards of synchrocyclotron, 19: 41171(T) (N64-33402)
separation at CERN synchrotron, 17: 31551 (CERN-63-12)
separation of (K) and (π), in CERN synchrotron, 19: 11964
separation of (K) and (π), in accelerators, (T), 19: 27038
separation of K and π, 18: 20680 (NIRL/R/49)
separation of (K^+), from charged-particle beams, 18: 2504
separation of mesons (μ) and (π) in, Cherenkov detector for, 17: 37433
separation of, methods for, 18: 37827
separation system design for antiproton and meson (K^-), 19: 30881 (BNL-9129)
separator for $K^\pm$, testing of CERN r-f, (E), 19: 20748
shaping of (μ), electromagnetic lenses for, 19: 23222
shaping of (π), electromagnetic lenses for, 19: 23223
storage ring for 10-Bev, advantages and design of, 17: 21117 (SLAC-5 (p.165-92))
transport system for 0.5 Bev/c pions (E/T), 19: 2928 (UCRL-11086)
trapping of (μ), quadrupole magnetic channel for, 20: 2547 (UR-375-98)
use in radiotherapy of tumors, 19: 40395
use in radiotherapy, feasibility of, 20: 18516
use in therapy, 18: 39042
use of high-LET, for therapy, 20: 18507 (BNL-10009)
viewing external, camera for, 16: 31951 (UCRL-9353)

MESON DECAY

electron spectrum, statistical calculation of, 18: 26384
form factors in, of hyperons, 17: 31382
properties of 3-π, 18: 12937

MESON PAIRS

decay of K^0, (T), 20: 36047
photoproduction cross sections of (μ), nuclear magnetic effects on, (T), 20: 19968
photoproduction of (π), in nuclear coulomb field, 18: 42416
photoproduction of (μ), on protons, (T), 19: 27240
photoproduction of (π), on carbon and hydrogen in Bev range, 19: 45000 (HUX-2752-7)
photoproduction of mu, on carbon, (E), 20: 15306(R) (CEAL-1026)
photoproduction of (π), on protons at 450 to 750 Mev, (E), 20: 27932
photoproduction of (π), on protons at 0.55 to 1.00 Bev, (E), 20: 27933
photoproduction of (μ), on carbon and hydrogen, (E), 20: 27952
photoproduction of (π), at high energies, (E), 20: 27916
photoproduction of (μ), testing quantum electrodynamics by, (E), 20: 27893
photoproduction on protons below 1 Bev, angular distributions and total cross sections for, 20: 4579 (AD-618661)
photoproduction, on carbon of μ, quantum electrodynamics test from, (E), 20: 46373
production in annihilation of polarized electrons and positrons, (T), 19: 43067
production in electron-positron beam interactions, cross sections for, (T), 20: 2753 (JINR-P-2300)
production in meson (π)–nucleon interactions at 12 and 18 Bev/c, 19: 14405 (TID-21409)
production of (μ), by muon-neutrinos, 18: 36344
production of (μ), in neutrino reactions, 18: 40500 (AD-603251)
production of (μ), inelastic nuclear effects on, (T), 20: 27951
production of (π), in meson (π^-)–proton interactions at 18.1 Bev/c, 18: 28360
production of (π), by neutrino reactions with nuclei at 60 Bev, 18: 40642
production of $K^0\bar{K}^0$, interference in 2π decay of, 20: 25787 (JINR-P-2632)
production of μ, in electron-positron annihilation at high energies, (T), 20: 32070
production of μ, in photon reactions with nuclear Coulomb field, 20: 34257
production of pseudoscalar, in antiproton-proton and electron-positron annihilation, (T), 20: 27823
theory of, bound states in, 17: 19068

MESON SHOWERS

altitude dependence of, 17: 13336
analysis of, in accelerator shielding, 18: 7360(R) (ORNL-3499(Vol.II) (p.24-5))
angular distribution of, from 10^{10}–10^{14} ev primaries, 17: 19022
angular distribution of particles in, relation to fire ball motion, 18: 14922
calculations for meson (π^-) reactions with emulsion nuclei at 17 Bev, (T), 20: 38060
calculations of intranuclear, (T), 19: 21239 (LA-3206)
calculations of nucleon-, for accelerator shielding design, 17: 9646 (ORNL-3289)
distributions in jets, theory, 16: 10934
distributions in meson (μ), 18: 42341
distributions in meson–nucleon cascades, (T), 19: 18751 (ORNL-3734)

distributions in (π^0), from cosmic-particle nuclear reactions, 17: 11454
distributions in, produced by 10- to 1000-Bev protons, (T), 19: 10452 (CERN-64-47)
distributions of (μ), near axes of extensive air showers, 17: 19029
distributions of mesons (π) in high-energy, 19: 5127 (INSJ-79)
energy spectra in high-energy nucleon-nucleon interactions, 16: 2419
energy spectra in meson (π)-nucleon, from 2- to 10-Bev primaries, 20: 8079 (ORNL-3855)
equations for, perturbation method for solving, 17: 31281 (ORNL-3467)
four-momentum transfer between fireballs in, 18: 28374
meson (μ) abundance in proton-produced, 17: 3952
meson ($\mu^\pm$) spectra in cosmic, 17: 699
model for, linked heavy-particle, 18: 37928
momentum distribution in, transverse, (T), 19: 18770
momentum spectra at 2 to 200 Bev/c at 7.2 kg/cm^2 depth, 16: 19667
production and properties of high-energy, (T), 19: 41709
production by protons in shielding materials, equations for, 18: 13178 (ORNL-3549)
production by protons in shielding materials, equations for, 18: 13179 (ORNL-3570)
production by proton beams in accelerator shielding, equations for, 19: 35564 (ORNL-P-299)
production in accelerator shielding, 17: 19418 (ORNL-3412)
production in nuclear reactions of 23.5-Bev protons, asymmetry, 16: 8095 (IFA-EM-45)
production in proton reactions with iron at 1 and 3 Bev, (T), 20: 3258
production of meson–nucleon, by 10- and 20-Bev/c protons in steel, (T), 19: 45317
production of narrow, by mesons (μ) underground, 16: 13917
production of nucleon–meson cascade by 200-Bev proton reactions with iron, (T), 19: 41955 (ORNL-TM-1121)
properties of, produced by ultra-high energy interactions, (T), 19: 47400
spectra of mesons (μ) in extensive cosmic, 16: 8081(T) (JPRS-11686)
statistical properties of 2-center jets, 17: 15111
symmetry in 24-Bev proton induced, azimuthal, 17: 20821

Meson Theory
see Nuclear Theory

MESONS
see also Antihyperons
see also Cosmic Mesons
see also Hyperfragments
see also Hyperons
see also Mesons, Resonance
see also Photomesons
see also S Particles

analogy to Cherenkov radiation, 16: 26096
angular distribution of secondary, in high-energy jets (T), 19: 3055
asymptotic behavior of vortex part in pseudoscalar theory, 16: 13864 (JINR-P-888)
Bargmann-Wigner equations for spin-2, 20: 7906
binding energy and mass relationships for, 20: 25791 (PAEC(A)PH-663)
binding forces for two-body pseudoscalar, dynamical calculations on, 20: 30161
book: *Fundamental Particles*, 19: 21072
book: *Meson and Baryon Spectroscopy*, 19: 35177
bootstrap calculations for vector, 18: 34557
bootstrap model for vector, SU(3) symmetry in, 20: 19564
bootstrap theory for, current algebras and symmetries in, 20: 28020
bound state of interacting scalar, (T), 19: 16520
capture by light emulsion nuclei, computer program for kinematics of, 19: 29231 (CERN-65-6)
charge conjugation and parity of U(12) multiplets for, 19: 20974
classification and notation for, 17: 9371
classification and mass, 20: 34164
classification in quark model, (T), 20: 9719(T)
classification in irreducible representations of noncompact groups, 20: 41967
classification in noncompact groups, 20: 41982
classification of positive-parity, using 189-plet of SU(6), (T), 20: 17339 (JINR-E-2557)
classification of, review, 19: 27273
classification scheme for, 17: 22437 (SLAC-13)
composite models for, in SU(6)$_W$, 20: 42034
composite states with baryons, broken U(4) symmetry in, 18: 44587
composition and mass splitting of octets of pseudoscalar and vector, 20: 42007
connection between gauge invariance and mass, 16: 21324
contribution of vector, to nucleon electromagnetic structure, 18: 37927
contribution to three-body forces in tritons, 19: 21075
correspondence theorem for bare, 16: 17041
coupling constants, upper limits for, 16: 28348
coupling constants for spin-2, with two pseudoscalar mesons, 20: 21682
coupling constants and masses for spin-0, current commutators in bootstrap for, 20: 27991
coupling of pseudoscalar and vector octet, (T), 19: 16559
coupling of pseudoscalar and vector, to baryons, (T), 19: 43070(T)
coupling of pseudoscalar triplet, with nucleons, 20: 13611
coupling of pseudoscalar SU(3) octet, (T), 20: 32063
coupling of scalar, (T), 20: 34213
coupling of vector, to baryons, octet, 18: 10932
coupling of vector, octet mixing in, 18: 16793
coupling of vector, to baryons, 18: 37934
coupling of vector, minimal electromagnetic, (T), 19: 6541
coupling of vector, universal, (T), 20: 25880 (IC-66/34)
coupling to baryons, relativistic invariant SU(6) symmetry for, 19: 18840
coupling to baryons in broken SU(6) symmetry, sum rules for, (T), 19: 37583
coupling to baryons, (T), 20: 34220
coupling to baryons, quark model derivation of relations for, 20: 36066 (IC-66/80)
couplings in intrinsically broken U(6) symmetry scheme, (T), 19: 18887
current structure in broken $\bar{U}(12)$ symmetry, matrix element for, 20: 25862
cut-off theories, perturbation expansion convergence in, 16: 18336
cutoff theory perturbation expansion convergence, 16: 21278
decay amplitudes of vector and pseudovector, (T), 19: 27158 (JINR-P-2141)
decay and masses, (T), 20: 34217
decay and production of intermediate vector, of weak interactions, 16: 13897
decay and production of vector, effects on $e^+ e^-$ interactions, 17: 19041 (LNF-63/6)
decay and weak interactions, 16: 18101 (NP-11463(Pt.2)(p.195-211))
decay coupling constants in broken SU$_3$ symmetry, leptonic, (T), 19: 12227
decay modes of, SU(3) representation of currents in leptonic, 18: 14861
decay of heavy, selection rules for, 17: 22437 (SLAC-13)
decay of higher group multiplets of, leptonic isospin in, 17: 24334
decay of positive-parity, SU(6) symmetry for, 20: 25909
decay of pseudoscalar, quark model for leptonic, 20: 27868
decay of pseudoscalar, renormalization of weak vector currents for, 20: 34279
decay of resonance-state, forbidden configurations in many -π, 18: 18664
decay of scalar, current commutation relations for determining coupling constants for, (T), 20: 39852 (INP-480/PL)
decay of scalar, equal-time commutation relations for rates of, 20: 44289
decay of spin 1$^-$, mixing angles for, 20: 30088 (IC-66/50)
decay of spin-0 and -1, forbidden configurations for 3-photon, (T), 20: 11686 (JINR-P-2447)
decay of spin-2, unitary symmetry model for two-body pseudoscalar-meson, (T), 20: 24068
decay of T =0 vector, interpretation of ($K\bar{K}$) resonance as, 17: 9259
decay of vector, from electron pair annihilation processes, 16: 26185
decay of vector in SU(6), amplitudes for, (T), 19: 35066(T)
decay of vector, radiative, 17: 24286
decay of vector, amplitudes for radiative, 19: 39471
decay of vector, algebra of currents for, 20: 19541 (UR-875-121)
decay of vector, conservation of charge-conjugation operator in SU(6) for, (T), 19: 41464
decay of vector, determination by lepton reactions in nuclear Coulomb fields, (T), 19: 35395 (NP-14993)
decay of vector, in SU(3), 18: 14870
decay of vector, in SU(6) symmetry, (T), 20: 7875
decay of vector, into lepton pairs, (T), 20: 13476(T)
decay of vector, radiative, (T), 19: 4994
decay of vector, radiative, (T), 19: 35130
decay of vector, symmetry-breaking two-body photonic, (T), 19: 35046
decay of vector, SU(6) symmetry for radiative, 20: 15472
decay of vector, trilinear couplings forbidden by nonet symmetry in, (T), 19: 45025 (N64-26265)
decay of 1$^+$, unitary symmetry for radiative, (T), 20: 13541 (JINR-P-2419)
decay of 2$^+$, coupling constants for, 20: 27963 (IC-66/37)
decay of, C violation in, (T), 20: 4669
decay of, Cabibbo angle as renormalization effect in, 20: 25883 (IC-66/42)
decay of, covariant field theory calculations of electromagnetic and weak currents for, 20: 44354
decay of, covariant analysis of quark commutators and electromagnetic couplings for, 20: 46358
decay of, CVC in leptonic, 19: 16674
decay of, deformed octet axial vector current for weak leptonic, 20: 37795
decay of, $\Delta S = 1$ leptonic, (T), 20: 11659

decay of, electron-pair production in $\bar{U}(12)$ for, 20: 25926
decay of, leptonic, (T), 19: 39573
decay of, leptonic, 20: 25873
decay of, matrix elements for leptonic, (T), 20: 1055 (JINR-P-2338)
decay of, matrix element relations in SL(6) and $\bar{U}(12)$ for electromagnetic and weak, 20: 25927
decay of, partial widths of electromagnetic and strong, (T), 20: 4674
decay of, partial conservation of tensor current for electromagnetic, (T), 20: 19536 (IC-66/25)
decay of, quark model for electromagnetic, 19: 35064
decay of, relativistic SU(6) invariance for weak semileptonic, (T), 19: 18862
decay of, selection rules for, (T), 19: 16629
decay of, selection rules for leptonic, 20: 19436 (ANL-7130, pp 159-88)
decay of, U(12) symmetry for electron-positron production in, (T), 19: 47308 (JINR-P-2284)
decay of, unitary symmetry in leptonic, 19: 16673
decay of, unitary symmetry for $\Delta Q = 0$ $\Delta S = 1$ ($\pi e^+ e^-$), (T), 19: 47370
decay of, unitary symmetry for, 20: 21708 (CONF-640509(Pt.2), Paper 2)
decay of, unitary symmetry for $\Delta S = -\Delta Q$ leptonic, 20: 32184
decay probabilities, 17: 7022
decay properties of L = 1, 20: 37846
decay rates of, quark model for, 20: 17343 (JINR-P-2524)
decay, spark chamber for observation of rare modes, 16: 20732
decay widths and magnetic moments of vector, in SU_6 theory, 20: 44203
decay, weak currents and broken unitary symmetry in leptonic, 18: 22766
decays of spin-2^+, in quark model, 20: 37780
decays of vector SU(6) symmetry for radiative, 20: 41908
decays of vector, SU(3) and SU(6) symmetries for radiative, 19: 32946 (JINR-P-2089)
decays of vector, U(6) current algebra for, (T), 20: 11750
decays of vector, partially conserved axial-vector current in, (T), 20: 15485
decays of vector, electro-magnetic, (T), 20: 44355
decays of vector, SU(6) algebra of currents for, 20: 44341
decays of, Cabibbo angle for weak, 20: 44354
decays of, SU(3) theory of strong, 20: 44331
decays of, two-angle Cabibbo theory of leptonic, 20: 41987
density matrix of spin-one, positivity conditions for, (T), 20: 21764
detection and measurement, geometric effects on, 16: 20635 (ISS-61/7)
detection and measurement of, design of Cherenkov detector for, 17: 354 (AERE-R-3968)
detection of delayed, equipment for, 17: 22049
detection of hyperstrange, with masses of 640 to 940 Mev, (E), 19: 4954
detection of scalar ($J_\rho = 0^+$), (E/T), 20: 19273(R) (BNL-929, pp 3-43)
detection of secondary, spark chamber for, 17: 23661
diffusion in matter, review, 18: 10636
distribution of, underground charge and mass, 17: 26277
dosimetry of, in transverse shielding of 45-Bev electron accelerator, 17: 15322 (ORNL-3365)
effect of intermediate, on radiative meson (μ) capture, 18: 44580
effect of K-π resonances on meson (K)-nucleon scattering, 16: 22852 (NP-11761)
effects of pseudoscalar massless, 18: 850 (JINR-P-1381)
effects of scalar, on nuclear spin-orbit coupling, (T), 19: 19154
effects of vector, on Y* resonances, 18: 30606
effects of vector, on lepton production by neutrino (ν_μ)-proton interactions, (T), 20: 17504
effects on antinucleon-nucleon and nucleon-nucleon interactions, 17: 37985
eigenfunctions for baryon-meson calculations, 17: 24267 (NYO-9290)
eigenfunctions for reductions of group SU_3, 17: 24268 (NYO-9290A)
electric quadrupole moments of vector, 20: 39835
electrodynamic fields and groups for vector, Yang-Mills, 20: 41929
electrodynamics of spin-one, covariant, 18: 36284
electrodynamics of scalar and vector, renormalizable, 18: 36330
electrodynamics of vector, perturbation theory for, 18: 40338
electromagnetic form factors for, 16: 25896 (LNF-62/37(p.81-8))
electromagnetic form factors, 16: 27971
electromagnetic mass splittings of, in SU(6) symmetry model, (T), 19: 16605
electromagnetic mass differences and form factors of, (T), 19: 16644
electromagnetic moments and leptonic decays of intermediate $W^\pm$, 18: 24464
electromagnetic production and properties of spin-1 charged vector, 16: 18362
electromagnetic properties in SU(3) symmetry, 18: 28329 (TID-20718)
electromagnetic properties of vector, in broken SU(6), (T), 20: 4644 (JINR-P-2299)
electromagnetic properties in broken SU(6) symmetry, (T), 20: 11727(T)
electromagnetic properties of, nonrelativistic quark model for, (T), 20: 13544 (JINR-P-2509)
electromagnetic properties in composite model, 20: 15550
electromagnetic properties in relativistic composite models, (T), 20: 15551
electromagnetic properties of, in static SU(6) model, 20: 24101
electromagnetic properties in SU(6) symmetry, (T), 20: 28034
electromagnetic properties of, composite-particle model for, (T), 20: 30069
electromagnetic properties in non-relativistic quark model, 20: 39835
electromagnetic self-energies and unitary symmetry of neutral vector, 18: 22759
emission in baryon decay, nonvector – vector, 17: 24312
emission in hypernuclei decay, tabulations for, 20: 7800 (TID-22396)
emission in proton interactions in nuclear emulsions at 30.5 Bev, multiple, 19: 45054
emission of vector, by leptons in nuclear Coulomb fields, (T), 19: 35395 (NP-14993)
energy levels in symmetry-breaking SU(2) nonlinear spinor model, 19: 41396
energy levels of hadrons, representation as series of non-compact groups, (T), 19: 32938 (CALT-68-38)
energy levels of, individual-particle approximation of higher-excited, (T), 20: 44220
energy loop of charged vector, Lagrangian field theory for self-, (T), 20: 11749
energy peaks in systems, 16: 6988
energy tensor of, geometrization of, 19: 35197
evidence for new, 17: 22437 (SLAC-13)
exchange amplitude of scalar, strong absorption in, 18: 22755
exchange by nucleons in nuclei, 18: 34915
exchange contributions to nucleon potentials, 16: 10976
exchange currents in light nuclei, 20: 24435
exchange effects on nuclear magnetic moments in three-body nuclei, 19: 25543
exchange in elementary particle interactions, lowest-partial-wave domination of, 16: 22893
exchange in elementary-particle interactions, distorted-wave theory for one-, 20: 17474
exchange in meson(K)-nucleon interactions, S-wave amplitude effects of vector, 17: 24350
exchange in nucleon interactions, pole approximation for, (T), 19: 25263 (IS-987)
exchange in photoproduction of mesons, 18: 26373
exchange in proton interactions, three-body model for, 17: 39924
exchange in scalar particle interactions, 18: 36331
exchange in three-body nuclei, magnetic moment contribution of, 18: 17074
exchange interactions of, products from, (E/T), 20: 20365
exchange of axial vector, in hydrogen, (T), 20: 7852
exchange of axial vector, in hydrogen, (T), 20: 7853
exchange of heavy, in nucleon-nucleon interactions, (T), 20: 11597
exchange of massive and massless, in particle interactions, 18: 30544
exchange of pseudoscalar, scalar, and vector, in nucleon interactions, 18: 34539
exchange of pseudoscalar, in three-body production interactions, (T), 19: 18844
exchange of pseudotensor, pseudovector, and tensor, in nucleon interactions, (T), 19: 29063 (JINR-P-2048)
exchange of spin-zero, test for, 18: 30591
exchange of vector, in meson (K) interactions, 18: 26342
exchange of vector, in meson-baryon interactions, 19: 21018
existence and properties of zero-mass (ξ), (T), 19: 23362 (JINR-P-1993)
existence in high-energy nuclear interactions with isotropic angular distribution of the secondary particles, 17: 2192
existence of I=1 vector, of mass between 750 and 1360 Mev, 18: 14894
existence of L (15 m), 18: 42371 (JINR-P-1750)
existence of neutral at 780 Mev, identity possibilities for mesons (ρ^0) and (ω^0), 16: 6978
existence of ninth pseudoscalar, 18: 32615
existence of two T = 0 vector, 16: 2454
Feynman diagrams for pseudoscalar, majorization of, 18: 34521
field equations for scalar, modified Yukawa potential and Riemannian space-time for, 19: 31264
field equations for scalar, geometrization of, 20: 19553
field equations with scalar, in general relativity, 18: 7584
field interactions with nucleons, magnetic moment addition in, 16: 22877
field theory for neutral scalar, and point sources, 19: 18938
field theory for, self-coupled, 17: 5230
field theory for vector, formulation of renormalizable, 17: 5211
field theory for vector, Stueckelberg formalism for, 18: 42405
field theory for vector, Rainich geometrization of, 20: 17441
field theory for vector, 20: 28010
field theory for weak-vector, interactions in, 18: 26329
field theory for, numerical solution of fixed-source, 19: 8198
field theory for, relativistic quantum, 19: 45131 (JEN-154-DF/1-47)

field theory, non-linear, 16: 2427
field theory of scalar, five-dimensional classical, 19: 41497
field theory of scalar, Hadamard's class of Green functions in regularized $g\phi^4$, 19: 43203
field theory of self-consistent S matrices for scalar, 19: 1261
field theory of vector, degeneracy of physical vacuum in, 20: 44325
field theory, use to describe nuclear forces, 16: 15373
form factors and generalized Poincaré group for, electromagnetic, 19: 20971
form factors for, model for, 19: 37531 (JINR-P-2098)
form factors for, in SL(6,c) symmetry, (T), 20: 11683 (JINR-E-2475)
form factors of hadrons, universality and M(12) invariance for, (T), 19: 33042
form factors of pseudoscalar, sum rules for, 20: 41995
form factors of pseudoscalar and vector, collinear groups SU(3) ⊛ SU(3) ⊛ U(1) and $SU(6)_W$ for electromagnetic, 20: 44394
form factors of, current algebra for studying, (T), 19: 45011 (JINR-E-2294)
form factors of, in U(12) symmetry scheme, (T), 19: 18899
formalism for, intrinsic exclusion principle obedience, 16: 22911
gauge transformations for vector fields, 16: 17018
Green's function in spin-zero meson theory, Lehman weights of, 18: 14821 (UR-875-20)
hypothetical meson (M) and generalization of the Pomeranchuk relations, 17: 5250
interaction amplitudes of vector, Regge behavior of, 19: 39618
interaction mixing of spin-zero, 20: 21746
interaction resonances of, classification of, 17: 750
interaction resonances with baryons, dynamical model analysis of, 18: 7467 (CONF-340-12)
interaction resonances of, review on, 18: 34636
interaction resonances with baryons, dynamical model for $\frac{1}{2}^-$, 18: 37925
interaction resonances with baryons, 18: 42627(R) (ANL-6879(p.88-113))
interaction resonances with baryons, in 70-dimensional representation of SU(6), 18: 44568
interaction resonances with baryons, in static model, 19: 3081
interaction with baryons, relativized SU(6) symmetry for, (T), 19: 35119
interactions at high energies, theoretical problems in, 20: 24116
interactions between protons and neutral scalar, effects of ghost scatterings on, 16: 32319
interactions between nucleons and neutral vector, vector-spinor bootstrap in theory of, 18: 28361
interactions, dispersion relations for, 16: 28006
interactions mediated by intermediate vector ($W^{\pm}$), T-violating, (T), 19: 18859
interactions, model for inelastic, 16: 2463
interactions of baryons and pseudoscalar, total cross sections for, (T), 19: 16614
interactions of, bubble chamber research programs on, 16: 32177(R) (UCRL-10349)
interactions of charged vector, with electromagnetic fields, 17: 744
interactions of charged scalar, with neutral vector mesons, vacuum Regge pole in annihilation, 20: 1081
interactions of degenerate pseudoscalar octet of, with triplet elementary particles, (T), 20: 42029
interactions of equal-mass scalar, N/D equations for amplitude of, (T), 19: 18846
interactions of, exchange of scalar in, Barn amplitudes for, 16: 32265 (AERE-R-4077)
interactions of field of charged scalar, with fixed two-level point source, (T), 19: 45150
interactions of fields of, renormalization theory for, 20: 15453
interactions of heavy, effects of G-parity on, 16: 33764
interactions of, mass relations for resonant and strong, 17: 24357
interactions of massless pseudoscalar, broken symmetry for electromagnetic, 19: 47346
interactions of mesons (ϕ) with vector, T invariance in SU(6) symmetry for, (T), 19: 35140
interactions of multiplet pseudoscalar and vector, self-consistency in, (T), 19: 16564
interactions of neutral vector, with photons, 16: 967
interactions of neutral, Chew-Mandelstam amplitudes for, 16: 29988
interactions of neutral pseudoscalar, with static spin-1 source, (T), 20: 30159
interactions of neutral, model for forward amplitude for, 20: 37805
interactions of pseudoscalar, SU_n symmetry in elastic, 17: 39920
interactions of pseudoscalar, with nucleons, pseudoscalar and vector exchanges in vector meson production from, 18: 9177
interactions of pseudoscalar, with baryons, model for, 18: 14903
interactions of pseudoscalar and vector, bootstrap model for, 18: 18711
interactions of pseudoscalar SU(3) octet, even-signature Regge poles in bootstrap dynamics of, 18: 21042
interactions of pseudoscalar and vector, self-consistent model for strong, 18: 26344
interactions of pseudoscalar, with baryons, vector-meson production in, 18: 28328 (TID-20717)
interactions of pseudoscalar, with nucleons, fermion Regge trajectories for, 18: 34558
interactions of pseudoscalar, with baryons, 18: 34567
interactions of pseudoscalar, resonances in, 18: 36269
interactions of pseudoscalar, effects of "nonsense" channels on, 19: 1267
interactions of pseudoscalar and scalar, bootstrap calculations for, (T), 19: 16586
interactions of pseudoscalar, self-consistent symmetry schemes in V-strap model of, (T), 19: 16640
interactions of pseudovector, classical limit of, (T), 19: 25381
interactions of pseudoscalar, V-strap model for, 19: 43159
interactions of pseudoscalar, with nucleons, unitary symmetry for amplitudes and cross sections of, (T), 19: 43184
interactions of pseudoscalar, with baryons, SU(6) model for cross sections for, 20: 1017
interactions of pseudoscalar and vector, at low energies, (T), 20: 6068
interactions of pseudoscalar, with baryons, isobar parity in, (T), 20: 13474(T)
interactions of pseudoscalar–octet, university principle for, 20: 21752
interactions of pseudoscalar, SU(3) octet-octet, 20: 32011
interactions of pseudoscalar with pseudovector, S-matrix elements in neutral theory for, 20: 32168
interactions of pseudoscalar, P-wave amplitude for, 20: 41837
interactions of scalar, relativistic amplitude singularities in complex angular momentum plane of, 17: 41808
interactions of scalar, theory for scalar, 18: 18721
interactions of scalar fields of, with nucleon fields, 18: 40262
interactions of scalar and vector, sense-nonsense channels in N/D model for, (T), 19: 27231
interactions of scalar, bootstrap for vector mesons from, (T), 19: 43098
interactions of scalar, determinantal method for N/D equations for, (T), 20: 11700
interactions of scalar, many-pole amplitudes and elementarity in two-body, (T), 20: 15490
interactions of scalar neutral, upper bound on coupling constant for, 20: 19569
interactions of separate-singlet vector, relation to neutron electric form factor in U(6), 20: 19572
interactions of single in peripheral collision theory, 16: 5859 (JINR-P-699)
interactions of, spins of resonance, 17: 26330
interactions of spin-0, spin-0-meson bound states from N/D calculations for two-body, 20: 19490
interactions of, strong-coupling treatment of charged scalar theory of, 17: 37987
interactions of T = 2, with nucleons, form factors from off-shell effects in, (T), 19: 45067
interactions of two pseudoscalar-octet, bootstrap and SU(3) assignment of 2^+ mesons from, (T), 19: 41402
interactions of vector fields in particle model, 16: 22904
interactions of vector, effects on meson (π) interactions, 17: 32950
interactions of, vector-meson exchange model for isobar production in, 17: 34788
interactions of vector, self-consistent deviations from unitary symmetry in strong, 17: 41807
interactions of vector, SU(3) model for T = 0 meson resonances in, 18: 4450
interactions of vector, symmetry from bootstrap mechanism, 18: 4461
interactions of vector, symmetry induction in strong, 18: 26327
interactions of vector, with electromagnetic fields, 18: 34545
interactions of vector, resonances in, (T), 19: 12231
interactions of vector, with nucleons, (T), 20: 13479(T)
interactions of vector and scalar, coupling-constant relations for, 20: 13486
interactions of vector, renormalization theory for coupling in, 20: 17465
interactions of vector, cross sections for photon production in, 20: 30057
interactions of zero-mass, Regge poles in, 20: 30163
interactions of, Cabibbo transformation and $\Delta I = \frac{1}{2}$ rule for nonleptonic weak, 18: 30561
interactions of, electron-pair theory of, 18: 40374
interactions of, G_2 symmetry for strong, 18: 36273
interactions of, gauge theory for strong, 19: 1268
interactions of, in lead, anomalous transition effect in, (E), 20: 24023
interactions of, kinematical form factors for relativistic vertex functions in peripheral, (T), 20: 7934
interactions of, model for resonances in, 18: 37933
interactions of, model for broken isotopic symmetry in unified electromagnetic-weak, 20: 34311

interactions of, peratization in weak, 19: 41353
interactions of, PCAC for chiral representation mixing in, 20: 46402
interactions of, quark model for high-energy, 20: 24044
interactions of, resonances and symmetry in strong, 18: 14944
interactions of, relativistic Green's functions from strong coupling of, 20: 13557
interactions of, SU_3 model for strong, 18: 34510 (NP-14146)
interactions of, spin and unitary spin independence in strong, 18: 36347
interactions of, SU_3-invariant field theory for resonances in, 18: 42420
interactions of, SU(6)-invariant theory for couplings in, (T), 19: 21013
interactions of, solution of singular N/D equations for, 20: 6130
interactions of, static characteristics in broken SU(6) for, (T), 20: 25925
interactions of, $SU(6)_w$-symmetric bootstrap model of, 20: 39885
interactions of, with crossed one meson exchange, 18: 37908
interactions with deuterons, inelastic, 16: 2409 (NP-10956)
interactions with deuterons, first- and second-order processes in inelastic, 16: 3623
interactions with baryons, inelastic scattering, 16: 4692 (TID-13955)
interactions with nucleon systems, formalism for, 16: 10823
interactions with mesons and nucleons, dynamical model, 16: 12351
interactions with nucleons, differences in total cross sections at high energies, 16: 12210(R) (ANL-6488)
interactions with deuterons and nucleons, cross sections for, 16: 15575
interactions with nucleons, solution of low equation, 16: 17224
interactions with baryons, multiplet models, 16: 19711
interactions with nucleons, spin structure of high-energy scattering amplitudes, 16: 19713
interactions with mesons and nucleons, three-meson (π) resonance in, 16: 21620
interactions with nucleons at high energies, spin amplitudes in, 16: 26191
interactions with baryons, symmetry schemes for, 16: 27958
interactions with baryons, symmetry schemes for, 16: 27960
interactions with hyperons and nucleons at high energies, cross-section relation to energy resolution in, 16: 27986
interactions with baryons, higher symmetries of, 17: 5224
interactions with baryons and mesons, spinor formalism for, 17: 9221
interactions with baryons and mesons, symmetries in strong, 17: 9277
interactions with baryons and mesons, symmetries in, 17: 13454
interactions with baryons and mesons, Regge asymptotic amplitudes for, 17: 17046
interactions with baryons, analysis of $P_{3/3}$ pseudoscalar amplitudes for, 17: 19046 (TID-18295)
interactions with baryons, resonance effects in pseudoscalar, 17: 20884
interactions with baryons, relative weights of decays in broken symmetry theories for resonance, 17: 26371
interactions with baryons, selection rule for resonant-state, 17: 31328
interactions with baryons, mass formula in octet model for resonance, 17: 34794
interactions with fixed-point particles, theory of relativistic scattering in, 17: 34796
interactions with hyperons, Yukawa-type, 17: 7008
interactions with mesons, asymptotic expression for scattering amplitudes in, 17: 22775
interactions with nucleons, fixed-fermion field theory for, 17: 5210
interactions with nucleons through large angles, Regge fermion poles in, 17: 7034
interactions with nucleons at large angles, amplitudes of, 17: 9415
interactions with nucleons, dispersion relations for, 17: 9455
interactions with nucleons, effects of Regge poles on, 17: 11466 (CERN-62-33)
interactions with nucleons, strong, 17: 11568
interactions with nucleons, theory of radiation damping in, 17: 11916
interactions with nucleons, code for numerical analysis of, 17: 12786(R) (ORNL-3360(p.215-20))
interactions with nucleons, analytic cascade equation for, 17: 12787(R) (ORNL-3360(p.221-4))
interactions with nucleons, physical diagrams for vertex portions of, 17: 16966
interactions with nucleons, Regge trajectories in, 17: 16770(R) (ANL-6666)
interactions with nucleons, algebraic equations for describing, 17: 28142 (JINR-E-1262)
interactions with nucleons, field theory of, 17: 36619
interactions with nucleon two-body systems, ground-state energy of field, 17: 39926
interactions with nucleons, perturbation theory for, 17: 41743 (NP-13127)
interactions with nucleons, statistical theory, 17: 41819
interactions with nucleons, 17: 41533(R) (ANL-6720(p.67-75))
interactions with photons, renormalization of charged spin-1, 17: 19148
interactions with baryons, partially conserved leptonic currents in, 18: 869
interactions with nucleons, energy multiplication in, 18: 2611
interactions with nucleons, static three-body nuclear forces in pseudoscalar, 18: 2599
interactions with baryons, majorization of Feynman diagrams for, 18: 4437
interactions with protons at high energies, model for, 18: 6046
interactions with nucleons, Regge poles in, 18: 6026
interactions with baryons, Clebsch-Gordon coefficients of octet model for strong, 18: 7558
interactions with protons with (baryon resonance + meson) production in SU(3), 18: 10960
interactions with fixed nucleons, theory of, 18: 10967
interactions with baryons, asymptotic cross section relations for, 18: 18638 (JINR-E-1550)
interactions with baryons and mesons, $\frac{3}{2}^+$ resonance in, 18: 22761
interactions with baryons, use of reciprocal bootstrap in SU(3) symmetry in, 18: 24431
interactions with baryons in $U(3) \otimes U(3)$ symmetry, resonance, 18: 24465
interactions with nucleons, phase-shift linearization of differential cross sections for, 18: 24472
interactions with leptons and mesons, field theory for, 18: 26267 (BNL-837(p.237-48))
interactions with baryons, bootstrap calculations for resonances in, 18: 26332
interactions with baryons, baryon-exchange model for inelastic, 18: 26351
interactions with baryons, poles of amplitudes for, 18: 28391
interactions with baryons, octet model for resonance, 18: 32551
interactions with baryons, resonances in, 18: 32563
interactions with nucleons and N*, resonance models for, 18: 32620
interactions with nucleons, asymptotic scattering amplitudes for, 18: 32626
interactions with baryons, unitary symmetry in, 18: 34585
interactions with protons, SU(3) symmetry in, 18: 34586
interactions with nucleons, s-wave, 18: 36289
interactions with nucleons, $\frac{3}{2}$ -baryon production in, 18: 36306
interactions with baryons, SU(3) symmetry in $\frac{3}{2}$ resonances in, 18: 36328
interactions with baryons, model for resonances in, 18: 37932
interactions with baryons, dynamic model for $d_{3/2}$ unitary multiplets of, 18: 40312
interactions with baryons, classification of three-body resonance, 18: 40323
interactions with baryons, model for, 18: 42396
interactions with baryons, resonances in "10*" SU_3 scheme, 18: 42432
interactions with nucleons, asymptotic behavior of Feynman integrals for (T), 19: 1243
interactions with baryons, bootstrap solutions in static models for, (T), 19: 4973
interactions with baryons as test for Born-approximation model of Peierls mechanism, (T), 19: 4984
interactions with conserved currents, gradient-coupling models for, 19: 5033
interactions with heavy particles, vector field, (T), 19: 6526
interactions with baryons, unitary symmetry for, (T), 19: 6559
interactions with baryons, SU(3) invariant, (T), 19: 6561
interactions with strangeness current, in broken-SU(3) field theory, 19: 6576
interactions with nucleons, vertex functions for, (T), 19: 8281
interactions with baryons, SU(3) symmetry in, (T), 19: 12283
interactions with baryons, amplitudes for, (T), 19: 12380
interactions with nucleons, cascade equations for, 19: 17159(R) (ORNL-3714(Vol.II)(p.97-118))
interactions with baryons, static model for couplings in, (T), 19: 16582
interactions with baryons, coupling constants in broken unitary symmetry, (T), 19: 18789
interactions with baryons, $U_3 \otimes U_3$ symmetry for resonances in, (T), 19: 18814
interactions with baryons, mass splitting of resonances in, 19: 18826
interactions with mesons and photons, relativistic SU(6) symmetry for trilinear, (T), 19: 18863
interactions with baryons and mesons, relativistic SU(6) theory for, 19: 21005
interactions with baryons, Johnson-Treiman relations from vector-meson exchange in, 19: 21018
interactions with baryons, M(12) symmetry scheme for, (T), 19: 21024
interactions with baryons, predictions of relativistic SU(6) scheme for, (T), 19: 21025
interactions with baryons, amplitudes in SU(6) scheme for, 19: 21027
interactions with baryons, relativistic invariance and SU_6 symmetry for, (T), 19: 25303
interactions with protons, U(12) symmetry and Johnson-Treiman relations for, (T), 19: 25346

interactions with baryons, minimal bootstrap in, (T), 19: 25353
interactions with baryons, bootstrap solutions in static models for, 19: 27193
interactions with baryons, tests of unitary symmetry in, (T), 19: 26917(R) (IA-984)
interactions with baryons and mesons, bound states in, (T), 19: 29089
interactions with baryons, partial wave amplitude for resonances in, (T), 19: 31001 (CONF-550-96)
interactions with quarks, time reversal in SU(6) and $\bar{U}(12)$ for, 19: 32990
interactions with baryons, Balazs' low-energy approximation for, (T), 19: 33014
interactions with baryons at high energies, polarization in, (T), 19: 33021
interactions with baryons and mesons, C-invariance violation in, (T), 19: 33027
interactions with protons, baryon-resonance and vector-meson formation in, (T), 19: 33065
interactions with baryons, spurion theory for amplitudes of, 19: 35162
interactions with nucleons, asymptotic amplitudes of, (T), 19: 37657
interactions with nucleons, complex angular momentum in, (T), 19: 39518
interactions with baryons in SV_{12} scheme, D/F ratios for vertices of, (T), 19: 39524
interactions with baryons, bootstrap mechanism and symmetries in, 19: 39559
interactions with baryons, long-range forces in, (T), 19: 41421
interactions with baryons, bootstrap model in SU(6) for, 19: 41443
interactions with baryons, second-order perturbation in $\bar{U}(12)$ for, (T), 19: 41444
interactions with baryons, $SU(6)_w$ for amplitudes of, (T), 19: 41462
interactions with baryons, SU(4) symmetry for coupling constants in, 19: 41397
interactions with baryons and mesons, evaluation of crossing matrices for, (T), 19: 41381
interactions with quarks, reciprocal bootstrap mechanism from P-wave, 19: 43092
interactions with baryons, exact bootstrap solutions to Low equation for, 19: 45106
interactions with mesons, sum rules for, (T), 20: 1004
interactions with baryons, testing SU(6) symmetry by, (T), 20: 1006
interactions with baryons, broken W(3) symmetry model for, 20: 1075
interactions with baryons, $SU(6)_w$ scattering relation for S-wave isobar production in, 20: 2788
interactions with baryons and mesons, SU(3) symmetry for hadron-production, 20: 4645 (NP-15599)
interactions with baryons, relativistic SU(6) theory for vertex in, 20: 4677
interactions with nucleons at high energy, sum rule for cross sections of, (T), 20: 4678
interactions with mesons, current commutation relations for, (T), 20: 6077
interactions with baryons, Muskhelishvili method for amplitude of $V-\theta$, 20: 6123
interactions with nucleons at high energy, total cross section differences for, (T), 20: 6082
interactions with baryons, non-compact group representation of, 20: 6102 (IC/65/79)
interactions with baryons, $\bar{U}(12)$ symmetry with SU(3) breaking for, 20: 7920
interactions with baryons, in relativistic generalization of Wigner SU(4) supermultiplet theory, 20: 7931
interactions with baryons, quark model for, (T), 20: 9813
interactions with baryons, bootstraps for, (T), 20: 9831
interactions with baryons, spurion scheme of broken U(L12) symmetry for, 20: 11735
interactions with nucleons, scattering matrix for, (T), 20: 13448 (JINR-E-2521)
interactions with nucleons at high energies, elementary-particle structure from backward-scattering, 20: 13510
interactions with baryons, models for, 20: 13602
interactions with baryons, SU(n) crossing matrices for, (T), 20: 15322
interactions with baryons, $\bar{U}(12)$ symmetry for strong, 20: 15390
interactions with nucleons, peripheral model for, (T), 20: 15419
interactions with nucleons, renormalization theory for, 20: 15453
interactions with nucleons, N/D method for, 20: 15466
interactions with nucleons, classical limit of cross sections for, (T), 20: 15563
interactions with quarks, crossing matrices for, (T), 20: 15322
interactions with mesons, CT invariance for SU(3) amplitudes in octet, (T), 20: 17453
interactions with baryons, symmetry group for coupling in, (T), 20: 17455
interactions with baryons in broken SU(3) symmetry, self-consistent determination of coupling in, 20: 17467
interactions with nucleons, coupling constants for, (T), 20: 19521
interactions with baryons, SU(6) predictions for, 20: 19579
interactions with protons, SU(6W) predictions for spin alignment and forward amplitudes for, 20: 21652
interactions with baryons and photons, parity and spin of particles from polarized, (T), 20: 21715 (JINR-P-2576)
interactions with protons, SU(3) symmetry for three-particle final states in, 20: 21763
interactions with baryons in broken SU(3) in ω-ϕ mixing model, amplitude sum rules for, 20: 24043
interactions with baryons, corrections to the bootstrap pole approximation for, 20: 24128
interactions with baryons, noninvariance groups for, 20: 24148
interactions with octet baryons U_{12} predictions for amplitudes for, 20: 24136
interactions with baryons, coupling-constant relations in SU(6) for, 20: 25924
interactions with baryons, U(3) × U(3) symmetry for, 20: 25812
interactions with baryons in nonlinear spinor theory, coupling constants for, 20: 25816
interactions with baryons at high energies, validity of statistical model for, (T), 20: 25875
interactions with baryons, spin and unitary symmetry theory for relativistic, 20: 27968 (JINR-P-2665)
interactions with baryons, generalized Wigner-Bargmann equations for coupling constants in U(6,6) for, 20: 28021
interactions with baryons at high energies, cross sections for, (T), 20: 28025
interactions with baryons, couplings for, (T), 20: 27863
interactions with nucleons, total cross sections for, 20: 27872
interactions with baryons at low energies, (T), 20: 30070
interactions with baryons, current algebras for, 20: 30006
interactions with baryons, experimental status of baryon-exchange, 20: 32027
interactions with spin-½ baryons in relativistic formulation of SU(6), 20: 32116
interactions with baryons, U(3) × U(3) for amplitudes of collinear, 20: 32131
interactions with baryons, Dashen-Frautschi method for parity-conserving coupling, 20: 32138
interactions with baryons, bootstrap of 70-plet of SU(6) for, 20: 32151
interactions with baryon-antibaryon pairs, N/D method for multi-channel, 20: 32181
interactions with baryons, quark-quark amplitudes and total cross sections for, 20: 34286
interactions with protons, gas target development for, 20: 34152 (JINR-P-2711)
interactions with baryons, coupling constants for, 20: 34259 (IC-66/66)
interactions with baryons, SU(3) symmetry for coupling in, 20: 36060 (CERN-66-19)
interactions with baryons in broken SU(3), renormalization effects on coupling constants for, 20: 37842
interactions with baryons, matrices for modified single-particle exchange model of, 20: 37862
interactions with baryons, bootstrap static model of SU(6) symmetry for, 20: 39813
interactions with baryons, multichannel calculations in static model for, 20: 39887
interactions with baryons at low energies, nonrelativistic SU(6) symmetry for, 20: 39904
interactions with baryons, SU(3) invariant coupling constants for, 20: 41976
interactions with baryons, permutation symmetry in, 20: 41984
interactions with baryons, unitary symmetry for moderately strong, 20: 42013
interactions with baryons, $SU(6)_W$ symmetry scheme for, 20: 42016
interactions with baryons, bootstrap model and SU_6 symmetry for, 20: 41848
interactions with baryons in broken SU(3) symmetry, strong coupling constants for, 20: 41860
interactions with baryons, exchange of even- and odd-parity resonances in, 20: 41880
interactions with equal-mass scalar mesons, renormalization constant Z_1 and vertex function for, 20: 41893
interactions with leptons and photons, covariant field theoretical calculations of currents from, 20: 44353
interactions with quarks, model for, 20: 44365
interactions with electromagnetic fields, energy-momentum tensor for, 20: 44389
interactions with baryons, quark model for coupling constant relations for, 20: 44221
interactions with nucleons, scattering matrix for, 20: 46386
interactions with baryon octet in SU(3), dispersion sum rules for, (T), 20: 46397

invariance for pseudoscalar octet, SU_3, 18: 30587
isobar production in meson (π)–N interactions, 16: 8148
isobaric state production in $\bar{p}$-p interactions, 16: 8153
kinematics of vector, indefinite-metric method for, 18: 14937
magnetic moment of pseudoscalar and vector, Lee commutation relations for, 20: 36038 (N-66-18122)
magnetic moments in SU(3) and SU(6), 20: 36060 (CERN-66-19)
mass breaking in SU(3) symmetry in strong-coupling theory, 20: 32128
mass difference from hyperons, calculation, 16: 27932
mass differences in 0$^-$ and 1$^-$, quark model for electromagnetic, 20: 25918
mass differences of, calculations and theory of, 17: 29558
mass differences of, electromagnetic (T), 19: 3060
mass differences of, quark model for determining electromagnetic, 20: 34302
mass differences of 0$^-$, deformed octet axial vector current for, 20: 37795
mass formula for, 18: 44582
mass formula for, (T), 19: 39584
mass formula for (6,$\bar{6}$) multiplet in U(2) $\otimes$ U(6), 20: 24126
mass formula for pseudoscalar and vector, 18: 37911
mass formula for pseudoscalar, 18: 37924
mass formula for positive-parity, 405 multiplet, 20: 41874
mass formula for SU(3) octet, (T), 20: 24086
mass formula for vector, (T), 19: 6531
mass formula for, (T), 19: 4990
mass formula for, in dynamical symmetry group, (T), 19: 12281
mass formula for, SU(6) intermultiplet, 19: 43139
mass formula for, in covariant spin-unitary-spin scheme, 19: 47352
mass formula for, using SU(6,6) group, 20: 21624 (JINR-P-2606)
mass formulas and SU(3) symmetry for, 18: 30519 (TID-20712)
mass formulas for pseudoscalar and vector, in unitary symmetry, 18: 36299
mass formulas for pseudoscalar and vector, in SU(6) symmetry scheme, 18: 42450
mass formulas for, (T), 19: 12180
mass formulas for SU(6) multiplets of, 19: 31006 (IC/65/46)
mass formulas for pseudoscalar and vector, 19: 33072
mass formulas for vector, in broken symmetries, 19: 35088
mass formulas for baryons and, Gell-Mann-Okubo quark splitting for, (T), 19: 45077
mass formulas for SU(3) multiplets of, 20: 21671
mass formulas for pseudoscalar, in pole approximation in SU(3), 20: 32129
mass formulas for vector, model for, 20: 32130
mass formulas for, squared, 18: 37939
mass formulas for, universal equal-spacing, (T), 19: 18800
mass formulas for, SU(6) collinear subgroups for, 20: 7909
mass formulas for, dynamic quark model for, 20: 37763
mass formulas from SU(12), (T), 20: 2756 (JINR-P-2342)
mass formulas in supermultiplet model for, 20: 13583
mass formulas in SU(3) and SU(6), 20: 36060 (CERN-66-19)
mass formulas in 405 multiplet of SU(6), 20: 39886
mass in covariant SV_{12} scheme, electromagnetic corrections to, (T), 19: 25305
mass levels of pseudoscalar and vector octets, divergence-free composite model of, 17: 24347
mass multiplets of, calculations for, 20: 46412
mass of complex vector, 17: 7519
mass of gauge vector, broken symmetry in, 18: 36349
mass of nonstrange pseudoscalar, generalized Klein-Gordon equation for, 20: 21744
mass of pseudoscalar, (T), 19: 4988
mass of vector, associated with Yang-Mills field theory, 16: 24729
mass of vector, in gauge-invariant theory, 17: 24192
mass of vector, in broken symmetry, 20: 27989
mass of weak-vector, 18: 26329
mass of 1$^+$, current algebra for, 20: 15308 (IC/66/18)
mass of, current-generated algebra for splitting in, 20: 25915
mass of, formulas for, 18: 36311
mass of, quark model for, 20: 17343 (JINR-P-2524)
mass relations for vector, 18: 22751
mass relations for resonances of, empirical, 18: 32607
mass relations for spinless and spin-one, under broken $\bar{W}$, symmetry, (T), 19: 4958
mass relations for, empirical, 19: 20994
mass relations for tensor, in oscillator model, 20: 34191
mass relations for vector, 20: 36031 (ITEF-398)
mass relations with baryons, 18: 9118
mass renormalization in unified field theory, 19: 35024 (JINR-P-2117)
mass shift of, formula for, 18: 37940
mass spectra in bootstrap, current commutators for, 20: 27991
mass spectra in quantum field theory, 17: 15131
mass spectra of, dynamical symmetry for, 20: 30091 (JINR-P-2621)
mass spectrum of, 18: 34603
mass spectrum of, (T), 19: 14380
mass spectrum of, 20: 32203
mass spectrum of, models for, 19: 14348
mass spectrum of, symmetry violations in, (T), 19: 20951
mass splitting of, composite model for, 19: 43169
mass splitting in bootstrap model for pseudoscalar and vector, (T), 19: 16581
mass splitting in $\bar{U}(12)$ for, 20: 34274
mass splitting of pseudoscalar-octet, baryon mass-difference effect on, 19: 41468
mass splitting of vector, under SU(3), 19: 47383
mass splitting of, model of, 20: 9820
mass splitting of, model of, 20: 9821
mass splittings of baryon-meson from symmetry-breaking tadpole diagrams, 18: 20941
mass splittings of, under spontaneous breakdown of SU(3) symmetry, 18: 37929
mass splittings of pseudoscalar, electromagnetic, 18: 40314
mass splittings of, model for, 19: 33024
mass splittings of, dynamical calculations on electromagnetic, 20: 30161
mass sum rules in broken symmetry for, field theory formalism for calculating corrections to, 20: 28011
mass systematics of, equations for, 16: 32336
mass systematics of, (T), 19: 16630
mass tensors for pseudoscalar, unitary covariant equations for, (T), 19: 4917
mass values of scalar, nonlinear spinor theory for, 19: 25376
mass vector for pseudoscalar octet in unitary symmetry, 18: 20939
masses and quark structure of, 20: 42017
masses in self-charge-conjugate multiplets of, (T), 19: 27263
masses of pseudoscalar and vector octet of, relations between, 18: 40309
masses of pseudoscalar, electromagnetic, (T), 20: 17507
masses of pseudoscalar, electromagnetic, 20: 30032
masses of, four-fermion-interaction theory for, 20: 39832
masses of, in SU(6) symmetry, (T), 19: 21030
masses of, regularity in, 18: 32609
mixing of, octet and triplet, 18: 37938
mixing parameters for baryons and vector, calculation of, 20: 4691
model based on SU(3), 18: 14876
model for, as antibaryon-baryon pairs, 17: 19092
model for bound-state, Bethe-Salpeter equation in bootstrap, 20: 44197
model for, derivation of field-theoretical, 17: 31312
model for description of, as bound-state particles, 16: 24722
model for low-lying, double SU(3) symmetry in three-triplet quark, 19: 41406
model for pseudoscalar and vector, extended bootstrap, 18: 7506
model for scalar, mixing, (T), 19: 29087
model for spin-2, in SL(6) symmetry, 20: 11734
model for static charged scalar, with broken charge symmetry, 19: 45072
model for, based on Sp(6), (T), 19: 39568
model for, bound states of quark-antiquark system in, 20: 32147
model for, dynamic, 19: 14352
model for, extension of Fermi–Yang, 18: 22734(R) (NP-13896(p.1-14))
model for, kinetic-energy effects in M(12) in, 19: 27271
model for, oscillator, (T), 19: 16641
model for, supermultiplets in bootstrap, 18: 37917
model for, U_{12} invariance in relativistic quark, 20: 41965
model of nondegenerate vector octet, effects of mass splitting in bootstrap, 18: 2650
model of, binding energy for relativistic degenerate quark, 20: 41978
model of, double octet, 20: 32084
model of, higher unitary symmetry groups for shell, 20: 2781
model of, schematic, 18: 14867
model of, spinor, 20: 13612
models for supermultiplets of, in SU_6 symmetry, (T), 19: 6548
models for, basic Su(3) triplets with integral charge in, 18: 26324
models of resonances of, $N\bar{N}$, $N\bar{\Lambda}$, and $\Lambda\bar{\Lambda}$ bound-state, 18: 22782
momentum spectra of, produced in high-energy interactions, 17: 13122
motion of vector, in Coulomb field, (T), 20: 11668
motion of, electric field strength and Lorentz force for, (T), 20: 37754
motion of, sub-algebras generating relations in Duffin-Kemmer algebra for, (T), 20: 15462
nonexistence of Γ, evidence for, 16: 27953
parity and symmetry of intermediary, 17: 20924
parity as quark-antiquark composites, intrinsic, 19: 23422
parity-SU(3) mixing in octets of, (T), 19: 43151
perturbation theory on scalar, analytic properties of five-point function in, 18: 28271
photoproduction at high energies, (E/T), 19: 45024 (MIT-2098-163)
photoproduction, computer processing of data on, 16: 20635 (ISS-61/7)

photoproduction from protons, program for calculating kinematics of, 17: 20829 (ISS-63/11)
photoproduction of neutral, with mass between 300 and 800 Mev, 16: 25898 (LNF-62/37(p.98-104))
photoproduction of heavy, 16: 25945 (NP-11977(p.129-35))
photoproduction of mass 279.2 Mev, on protons, 17: 16947 (ISS-62/24)
photoproduction of 450-Mev mass, from protons, 17: 20833 (ISS-63/15)
photoproduction of 500-Mev mass, from protons, 17: 20834 (ISS-63/16)
photoproduction of 700-Mev mass, from protons, 17: 20836 (ISS-63/18)
photoproduction of vector, theory, 17: 32913 (TID-7668(Sect.V))
photoproduction of, 17: 32916 (TID-7668(Sect.VIII))
photoproduction of pseudoscalar, unitary symmetry model for, 17: 39879
photoproduction of 300-Mev mass, from protons, 17: 20830 (ISS-63/12)
photoproduction of 350-Mev mass, from protons, 17: 20831 (ISS-63/13)
photoproduction of 400-Mev mass, from protons, 17: 20832 (ISS-63/14)
photoproduction of vector, cross section for, 18: 5989 (JINR-P-1403)
photoproduction of, bibliography of, 18: 19125
photoproduction of 300- to 400-Mev ABC, excitation curve analysis of, 18: 24381 (ISS-64/4)
photoproduction of vector, on nucleons, 18: 34620
photoproduction of spin-1, on nucleons, (T), 20: 4610
photoproduction of vector, spin correlations in, (T), 20: 6076
photoproduction of 0^- and 1^-, on nucleons, U(6W) for collinear, 20: 7904
photoproduction of vector, amplitude for, (T), 20: 11595
photoproduction of, symmetry group for backward and forward, (T), 20: 17455
photoproduction of vector, on protons and mesons (π^+), cross sections for, 20: 17410
photoproduction of vector, on protons, SU(6) symmetry for, 20: 34181
photoproduction of vector, photon dissociation model for, 20: 41863
photoproduction of, vector dominance approximation for, 20: 41869
photoproduction on baryons, unitary symmetry in amplitudes of pair, (T), 19: 33060
photoproduction on protons, $SU(6)_W$ for amplitudes of, (T), 19: 41462
photoproduction on baryons, electromagnetic amplitudes for, 20: 2732
photoproduction on nucleons, SU(6) and SU(6)W for, 20: 6055
photoproduction on nucleons SU(3) ⊗ SU(3) ⊗ U(1) symmetry for amplitudes of coplanar, 20: 7905
photoproduction on nucleons, review of, 20: 9774
photoproduction on nucleons, SU(6) symmetry for, (T), 20: 11581(T)
photoproduction on nucleons, SU(6) sum rules for, (T), 20: 11635
photoproduction on protons, (E), 20: 15306(R) (CEAL-1026)
photoproduction on protons, SU(3) symmetry for, (E/T), 20: 27839
photoproduction on nucleons via spin-J resonance, isobar model for, 20: 27857
photoproduction on protons at 0.5 to 6.0 Bev, (E/T), 20: 27894
photoproduction on protons at high energies, (E), 20: 27895
photoproduction on protons, SU(3) amplitudes for, (E/T), 20: 37773
photoproduction on nucleons, SU(6) symmetry for, (T), 20: 41812
photoproduction on nucleons near threshold, (T), 20: 44211
photoproduction on nucleons, quark model for, 20: 44239
photoproduction on baryon octet in SU(3), dispersion sum rules for, 20: 46397
polarization operator for vector, derivation of covariant, 18: 9186
production and properties of $\eta 2\pi$, 18: 42445
production at accelerator energies and in cosmic radiation, theory, 18: 40365
production at high energy, relativistic kinematics of models for multiple, 19: 27163 (PAN-552/VI)
production at very high energies, elastic diffraction scattering model for multiple, 20: 25907
production by cosmic mesons (μ), 4-momentum transfer in multiple, 18: 22773
production by cosmic nucleon reactions in atmosphere (E), 19: 3002
production by electron-positron annihilation, selection rules for, 20: 25864
production by 24-Bev proton beam incident on heavy concrete, 17: 11489 (ORNL-3367)
production facility for, neutron flux beneath shield of, (T), 20: 3262
production facility for, neutron flux beneath shield of, (T), 20: 20100 (ORNL-TM-1423)
production, fire-ball model for multiple, 16: 26170
production in antinucleon-nucleon annihilation, U(12) symmetry for, (T), 19: 29053 (IC/65/47)
production in antiproton-proton annihilation, (T), 20: 7879
production in antiproton-proton annihilation at rest, coupling constants in SU(3) for two-body, (T), 20: 17377
production in antiproton-nucleon annihilation, (T), 20: 17396
production in collisions of high-energy nuclei in nuclear emulsions, 19: 3348
production in cosmic proton reactions with nuclei, departure from isotropy in, 17: 24254
production in cosmic nucleon interactions, model for multiple, 17: 26268 (PAN-388/VI)
production in cosmic particle interactions in emulsions, 18: 34492
production in cosmic radiation, theory of, 18: 40206
production in electron interactions with positrons, cross sections for, (T), 20: 39802
production in gamma-proton interactions at 0.5 to 4.8 Bev, (E), 19: 4976
production in high-energy nuclear interactions, theory of multiple, 16: 18320 (INSJ-48)
production in high-energy nucleon-nucleon interactions, model for, 16: 22903
production in high-energy interactions, model for multiple, 17: 5399
production in high-energy nuclear-reaction jets, 17: 19159
production in high-energy proton accelerators, dose rates from, (T), 19: 5393
production in high-energy inelastic interactions, transverse momentum distribution of, (T), 20: 2681 (IFA-CR-55)
production in interactions at high energies, peripheral model for, (T), 19: 45037 (TID-21316)
production in meson (K^-)–proton interactions at 3 Bev (E), 19: 1332
production in meson (K^-)–proton interactions at 3 Bev (E), 19: 1333
production in meson (π^-)-neutron interactions at 3.5 Bev/c, cross sections for, (E), 20: 39842
production in meson (π)-neutrino interactions, SU(6) for collinear, 20: 46383
production in neutrino-nucleon interactions, 17: 37970
production in neutrino interactions, unitary spin analysis of, 20: 37751
production in nucleon interaction at 400 to 900 Mev, polarization effect in, 16: 12333 (JINR-P-226)
production in nucleon reactions on heavy emulsion nuclei, above 100 Bev, 16: 32314
production in nuclear reactions, model for multiple, 16: 33736
production in nucleon–nucleus interactions at high energies, 17: 3931 (AFCRL-1089)
production in nucleon-nucleon collisions, model for multiple, 17: 13117
production in nucleon-nucleon collisions, theory of multiple, 17: 13119
production in nucleon-nucleon collisions, multiple, 17: 13120
production in nucleon interactions in heavy cosmic particle reactions in emulsions, 17: 26269 (PAN-398/VI)
production in nucleon interactions at 5 Tev, asymmetry, inelasticity, and multiplicity in, 18: 30515(R) (NP-14096(p.1-4))
production in nucleon-nucleon interactions in emulsions, average multiplicity of, 18: 40189
production in nucleon-nucleon interactions, bremsstrahlung theory for multiple, 20: 6053
production in nuclear reactions with nuclei at high energy, 20: 19458
production in nucleon reactions with accelerator shielding, (T), 20: 24576 (ORNL-TM-951)
production in proton pair annihilation, 17: 5273
production in proton reactions with emulsion nuclei at 26.7 Bev/c, 17: 11611 (AD-277387)
production in proton-antiproton collisions, unitary symmetry model for, 18: 20953
production in proton pair annihilation, amplitudes for, (T), 19: 39527
production in proton interactions with nucleons in emulsions at 20 Bev/c, (E/T), 20: 41829
production in the presence of external electromagnetic field, field theory for pair, 17: 13361
production of (S^0), in intermediate boson pole in meson (K) radiative decay, (T), 20: 2684 (JINR-P-2374)
production of antiproton-proton annihilations, $\bar{U}$ (12) symmetry breaking in two-body, 20: 15346
production of charged vector, by leptons in nuclear Coulomb fields, 16: 23154
production of charged vector, in neutrino-nuclear field interactions, 17: 41741 (LNF-63/44)
production of charged, gauge condition and equal-time commutator for electromagnetic, 20: 37760
production of, in carbon–meson (π^-) interactions at 7 Bev, 16: 33687 (PAN-326/VI)
production of intermediate vector, cross section asymptotic behavior in meson (π^-) inelastic reactions with nuclei for, 17: 41826
production of intermediate vector, in nucleon interactions with mesons (π) and photons, (T), 19: 12262
production of intermediate vector, in annihilation of polarized protons and antiprotons, (T), 20: 7877
production of jets by heavy primary cosmic-ray nuclei, 16: 27890
production of M, in meson (π^-)-proton reactions, 17: 7014
production of many, in relativistic elementary-particle interactions, (T), 19: 41708
production of mass 959-Mev, 18: 22760
production of multiple, in high-energy nuclear collisions, 17: 9441
production of multiple, in collisions with nucleons, 17: 36620
production of neutral scalar, field theory for, 17: 13361

production of neutral, in meson(π^-) reactions with xenon at 9 Bev, 18: 40550
production of neutral, cross sections and mixing angles in quark model for, (T), 20: 37779
production of pseudoscalar and vector, in antiproton–nucleon annihilation, (T), 19: 4970
production of pseudoscalar octet of, in $\frac{1}{2}^+$ baryon resonance decay, (T), 19: 10051
production of pseudoscalar, in electron-positron interactions, 19: 33067
production of pseudoscalar, in electron-positron annihilations, selection rules for, (T), 20: 6040 (NP-15602)
production of two, in proton-antiproton annihilation at rest, 19: 23423
production of vector, as intermediate states in antinucleon-nucleon annihilation, 18: 2619
production of vector, cross sections for, with pseudoscalar and vector exchanges in pseudoscalar meson-nucleon interactions, 18: 9177
production of vector, 18: 16552(R) (UCRL-11132)
production of vector, in pseudoscalar meson–baryon collisions, 18: 28328 (TID-20717)
production of vector, in peripheral model, 18: 32576
production of vector, in baryon-pseudoscalar meson interactions, 18: 34567
production of vector, in meson (π)-nucleon interactions, 18: 34620
production of vector, in electron–electron interactions, (T), 19: 4920
production of vector, in photon-proton interactions, (T), 19: 39621
production of vector, Regge-pole contribution to, 20: 15354
production of vector, in electron interactions with positrons, (T), 20: 30012
production of vector, from meson (π)-nucleon interactions, 20: 46384
production of, accelerator development for, 20: 39534
production of, development of ETH Zurich cyclotron for, 20: 39533
production of, development of negative-hydrogen-ion cyclotron for, 20: 39540
production of, linked heavy-particle model for multiple, 18: 37928
production of, shielding calculations for secondary protons from, 19: 17159(R) (ORNL-3714(Vol.II)(p.97-118))
production of, 800-Mev proton linac for, 20: 44041 (LA-DC-8144)
production, statistical theory of multiple, 16: 10850
production theories for, 17: 19022
properties, 17: 34724 (EFINS-63-33)
properties in SU_3 model having symmetry-breaking interaction, 18: 44546
properties in SU_3 model having symmetry-breaking interaction, 18: 44547
properties in SU(3) symmetry, (T), 20: 15530
properties in SU(6), electromagnetic, (T), 19: 35066(T)
properties of, 19: 47406
properties of, (E/T), 20: 19448 (UCRL-16462)
properties of axial vector, (T), 19: 4938
properties of pseudoscalar 0^-, in symplectic SU_3 model, (T), 19: 4948
properties of pseudoscalar, with $Z_3 = 0$, 20: 25843
properties of resonance, review, 18: 16770
properties of, review of, 18: 4447
properties of scalar and vector, electrodynamic theory for, 19: 20929 (ICTP-64/12)
properties of vector, resonance effects on, 16: 3644
properties of vector, as Regge poles, 17: 17045
properties of vector, field-theoretical models for, 19: 1262
properties of vector, elementarity of, (T), 19: 12214
properties of vector, in bootstrap model, (T), 19: 23409
properties of vector, limitations in bootstrap analysis of, (T), 19: 41373
properties of zero-mass, pseudoscalar paritino, 20: 34162
properties of 1220-Mev ($\pi\omega$) resonance, theoretical, 18: 18684
properties of 2^+ octuplet of, in SU_3 theory, (T), 19: 4945
properties of 2^+ nonet of, in SU(3) theory, 20: 19512
properties of 2^+, 20: 32205
properties of, composite, (T), 19: 41519
properties of, hyper-supermultiplet scheme for, (T), 19: 8175
properties of, Lorentz invariance and SU(6) theory for, 19: 16577
properties of, prediction from quantum theory of symmetric top, 20: 28016
properties of, SU(3) symmetry groups for, 19: 29044 (IC/65/21)
properties of, unified description of space-time and isospace for, (T), 19: 43057
quadrupole moments of vector, anomalous-electric and magnetic-, (T), 20: 44354
quantum numbers for multiparticle systems of, determination of, 18: 845 (JINR-P-1367)
quantum numbers for octet, (T), 19: 4979
quantum numbers for, principle, (T), 19: 16629
quantum numbers for multiplet components of, 19: 41331 (JINR-P-2219)
quantum parameters of, semi-simple groups for invariant, 18: 2601
quark model for, SU(6) symmetry in, (T), 20: 11657
reactions with emulsion nuclei at 1.3 and 1.5 Bev/c, hyperfragments from, 18: 40548
reactions with nuclei, tests of unitary symmetry from, 20: 38009 (BNL-10420)
Regge poles and resonances, 18: 20996
Regge poles in perturbation theory of, 18: 20997
Regge trajectories for vector, (T), 19: 27252
relation of f^0 to B (1.22 Bev), 18: 12954
representation in SU(3) invariant static model, 19: 16670
representation of Vector, bound-state, 18: 9090 (UR-875-11(p.1-26))
representation of vector, using Sp(6) group, 18: 42421
representations for, SU(4), 19: 3095
resonance production in nucleon–nucleon scattering, 18: 10953
resonance states of, SU(4) assignments for (κ), 18: 2664
resonance states of, selection rules and basic-particle descriptions of, 18: 14921
resonance states of, decay of, 18: 14944
resonance states of, determination of quantum numbers for, 18: 14952
resonance states of, in nucleon interactions, 18: 34539
resonance states of, mass equations for, 18: 40279
resonance states of, model for masses of, 18: 40282
resonance states of, level density and mass spectra of, 18: 44558
resonances and threshold mass numerologies in, 16: 17028
resonances in systems of pseudoscalar and vector, SU_3 symmetry for, 18: 44554
resonances of, possible indirect method of measurement of, 18: 30511 (JINR-P-1654)
resonances of, tabulation of properties of, 18: 18674
resonances with baryons in W_3 symmetry, 18: 34553
resonances with baryons, 45-fold $\frac{1}{2}^+$ multiplet of, 18: 34554
resonances with baryons in SU(3) with reciprocal bootstrap, 18: 34556
resonances, spin-parity of, 18: 20998
resonant states of, properties of, 17: 39939
role of vector, in nucleon-nucleon spin-orbit interactions, 17: 11491 (TID-15930)
rotator model for heavy, quasi-molecular, (T), 19: 16663
scalar neutral, evidence for existence of, 16: 32345
scattering by baryons, amplitude relations for, 17: 19526
scattering by nuclei, optical model for elastic, 18: 15303
scattering, Feynman diagram majorization for, 16: 22951
scattering of vector, amplitudes for, 17: 11509
scattering of vector, elementary poles for description of, 17: 34773
search for charged, with rest mass between that of the electron and meson (μ), 17: 31346
search for charged, with mass between electron and meson (μ), 18: 913
search for single-strange, 16: 5876
search for 310-Mev mass neutral, 17: 6792(R) (ISS 62/14)
spectra of peripheral, in fast nucleons, 16: 17016
spin operators for spin-one vector, theory, 19: 1263
structure of, 20: 32082
structure of heavy, electron-pair interpretation, 17: 34750
structure of heavy, molecular, 18: 37982
structure of vector, and multiplets of (T), 19: 1362
structure of, effects in high-energy interactions, 20: 13514
structure of, electron-pair theory of, 18: 40374
structure of, many-fermion nonlocal, (T), 19: 29093
structure of, model for, 20: 25871
structure of, quark, (T), 19: 43068(T)
structure of, SU(3) triplet model for SU(6), 20: 13598
symmetries for systems of, current algebras for, (T), 20: 11748
symmetries for vector, Lie group, (T), 19: 41342
symmetries of noncollinear diagrams and the Johnson-Treiman relations for, 20: 6143
symmetries of, R invariance in group, 18: 20995
symmetry for strongly interacting, fifteenfold way of SU(4), (T), 19: 47328
symmetry for 2^+, bootstrap generalization of $\bar{SW}(3)$, 20: 27851
symmetry for, algebra of current components in approximate, (T), 19: 35137
symmetry for, algebra of current components in, (T), 19: 35138
symmetry for, beyond SU(6), 20: 42030
symmetry for, bootstrap model of supermultiplets in, 19: 35151
symmetry for, covariant extension of SU(6), (T), 19: 39555
symmetry for, generalized Wigner-Bargmann equations for coupling constants in U(6,6), 20: 28021
symmetry for, mass relations in SU(3), (T), 20: 9793 (NYO-3399-44)
symmetry for, mass formula and spectrum from quark-antiquark Reggi trajectory in SU(6), 20: 28013
symmetry for, matrix element of current in, (T), 20: 2753 (JINR-P-2300)
symmetry for, propagator in, (T), 20: 13543 (JINR-P-2474)
symmetry for, relation between Poincare group and exceptional Lie group G(2), 20: 30115
symmetry for, SU(6), 20: 24109
symmetry for, SU(9), 19: 39571
symmetry for, subgroup of SU(8), (T), 20: 6110
symmetry for, triplet hypothesis in, 20: 25870
symmetry for, W-spin and rotation group in, 20: 15467

symmetry group for, Regge trajectories and, 19: 23424
symmetry group for, mass spectra and selection rules in, (T), 19: 41362
symmetry group for classification of, saturation of SU(6), 20: 41968
symmetry in bootstrap model for vector, SU(3), (T), 20: 7897
symmetry of vector, Smushkevich Principle for self-coupling in, 19: 37538 (NYO-3399-36)
symmetry of, SU(9), 19: 37602
symmetry properties in SU(6) and its relativistic extensions, 20: 7795 (JINR-P-2400)
symmetry representations for 2^+, SU(6), 20: 34208
symmetry scheme for hadrons, Sp(3), (T), 19: 39565
systematics of, review on, 18: 37965
theory, 19: 1310
theory for axial and tensor, 20: 17442(T)
theory for axial-vector, 20: 30007
theory for scalar and vector, gauge approximation in dynamic, 20: 15460
theory for vector, currents and sum rules in, 20: 32125
theory for, gauge approximations in non-perturbative mesodynamics, 19: 20928 (ICTP-64/10)
theory of axial vector and scalar, octets in, 18: 36308
theory of charged vector, Lee-Yang, 17: 32959
theory of charged vector, scalar behavior in, 19: 32982
theory of free vector, 19: 20947
theory of intermediate-vector, in interactions with mass breaking asymmetry, 18: 26335
theory of intermediate vector, in high-energy weak interactions (T), 19: 1374
theory of neutral vector, gauge-invariant, 18: 34606
theory of neutral vector, Green's functions for, 18: 44551
theory of neutral vector, formalism of gauge, 20: 15561
theory of neutral vector, mass formulas in, 20: 25865
theory of, nucleon form factors in strong-coupling, 17: 9296
theory of pseudoscalar, effects of almost-conserved currents on, 17: 15136
theory of pseudoscalar and vector, dissymmetries in SU_3 supermultiplets in, 18: 12946
theory of pseudoscalar and vector, symmetry group of vector and axial vector currents in, 18: 40330
theory of pseudoscalar and vector, splitting of spin-unitary spin supermultiplets in, 18: 42451
theory of pseudoscalar, 19: 31129
theory of pseudoscalar and vector, bootstrap algebra for, 20: 6060
theory of scalar, impossibility of bootstrap solutions in, 19: 37589
theory of vector, 18: 862(R) (TID-19590)
theory of vector, relativistic limit of, 18: 14860
theory of vector, angular momentum eigenfunctions in, 18: 42456
theory of vector, with symmetries above SU(3), 19: 1278
theory of vector, many-particle Green functions in, 19: 23389
theory of vector, relativistic covariance of, 19: 29096
theory of vector, Bethe-Salpeter equation for lepton interactions in, 20: 2797
theory of zero-mass pseudoscalar, 18: 36355
theory of, Bethe-Salpeter equation in symmetric, 19: 32950
theory of, commutation relations in pseudoscalar-pseudovector, 20: 41964
theory of, higher symmetry group and three-field model for, 19: 12210
theory of, spin and unitary-spin independence in paraquark model in, (T), 19: 4974
theory of, spurion, 19: 31038
theory of, SU_3 triplets in, 18: 36278
transformations for pseudoscalar and vector, octet–octet, 18: 30584
unitary symmetry model of weak interactions using intermediate vector, 18: 18688
vector, electromagnetic properties of charged, 17: 6961 (UCRL-9889)
vertex function for pseudoscalar and vector, in quantum electrodynamics, 18: 2609
wave equations for vector, in spherically symmetric potential, (T), 20: 15447 (UCRL-14698-T)
wave functions for bound states of, normalization of Bethe-Salpeter, (T), 20: 4671
wave functions in Compton scattering and plane electromagnetic radiation field, 16: 18119 (NP-11463(Pt.3)(p.481-7))
wave functions of vector, use of 10-dimensional beta-formalism in representation of, 17: 29513
wave functions of, space-time symmetry properties of, 20: 44356
wave functions of, Bethe-Salpeter equation for determining properties of, 20: 44357
with interactions with baryons under broken SU(3) symmetry, 18: 36296

MESONS, RESONANCE

(Prior to volume 20 of NSA, *this subject was treated under MESONS and under various headings for mesons.)*
(see also main headings for particles making up the resonance state)

analysis of post- and pre-threshold, (T), 19: 6524
analysis of, (T), 19: 4893 (JINR-P-1788)
angular momentum of, test for, 19: 31060
bootstrap and SU(3) assignment of 2^+, from scattering of two pseudoscalar octets, (T), 19: 14402
bootstrap and SU(3) assignment of $A_2(1310)$, $f^0(1250)$, and $K^*(1415)$ to 2^+ multiplets, 19: 41402
classification in $\bar{U}(12)$ representations, 20: 15496
classification in SU(6) group, 20: 30093 (JINR-P-2701)
classification in D_5 group, 20: 41972
classification of supermultiplets of, dynamical model for, (T), 19: 4967
classification of hypercharge $Y = 2$, in SU(6) theory, 19: 8203
classification of high-spin, 189-plet in SU(6) symmetry for, 19: 27153 (JINR-P-2034)
classification of higher, as kinetic supermultiplets of $\bar{U}(12)$, 20: 15479
classification of positive-parity, using 189-plet of SU(6), (T), 20: 17339 (JINR-E-2557)
classification of positive-parity, in SU(6), 20: 32148
classification of, review, 19: 27273
classification of, supermultiplet for, 20: 6134
classification of, $\bar{W}_3$ symmetry model for, 20: 7887 (JINR-P-2392)
classification of, summary of octet theory of SU(3) for, 20: 25904
conference, 20: 15398
coupling constants for spin-2, with two pseudoscalar mesons, 20: 21682
coupling to nonstrange baryons, (T), 20: 34220
data on, survey of, 19: 37642
decay and spin-parity of A_1 (1080) and A_3 (1310), from meson (π^-)-proton interactions at 2.75 Bev/c, (E), 19: 18849
decay correlations of vector, with baryon resonances, (E), 19: 39542
decay distribution of, effects of ω^0-ρ interference on, 20: 46347 (UCRL-50101)
decay modes of spin-two, partial widths in SU(3) for, (T), 19: 41461
decay modes of, $\bar{U}(12)$ symmetry for forbidden, (T), 19: 33045
decay of $A_2^\pm$, (E), 20: 7847
decay of A_1 and A_2, (E), 20: 11616
decay of A_1 and A_2, charge-parity violation in radiative, (T), 20: 17501
decay of A_2, (T), 19: 25345
decay of A_2 and K^* in U(6,6) symmetry, probabilities for, 20: 46415
decay of A_2, branching ratios for, (E), 19: 41460
decay of $A_2(1320)$ and $K^{**}(1430)$, coupling constants in broken SU(3) for, 20: 24026
decay of $A_2(1310)$ and $K\pi(1430)$, in broken $\bar{U}(12)$, 19: 23435
decay of $\chi(960)$, $\bar{U}(12)$ symmetry for radiative, 20: 17342 (JINR-P-2520)
decay of E(1405) with strangeness and zero isospin, analysis of $KK\pi$, 20: 36048
decay of f^*, KK^* and K_1K_1, (E), 19: 41459
decay of $J_\beta = 2^+$, coupling constant sum rules for, 20: 21640
decay of K^*, (T), 20: 32045
decay of $K^{*\pm}$ and K^{*0}, quark model for electromagnetic, 19: 32993
decay of K^*, (K-2π), (T), 19: 20984
decay of K^*, branching ratios for, (E), 19: 41460
decay of K^*, coupling constants and width for, (T), 20: 7855
decay of K^*, current-algebra prediction of SU(3) violation in, 20: 32035
decay of K^*, test of nonrelativistic quark model in radiative, (T), 20: 1016
decay of K^*, trilinear couplings forbidden by nonet symmetry in, (T), 19: 45025 (N64-26265)
decay of K^*, $\bar{U}(12)$ group for $K\pi$, (T), 19: 18853
decay of K^+_{e4}, (E/T), 19: 25265(R) (UCRL-11776)
decay of K^+, unitary symmetry breaking in, (E/T), 19: 41366
decay of κ (725) and K^* (890), meson (μ) polarization from, (T), 20: 44270
decay of mesons (L), existence of radiative, (T), 19: 20931 (JINR-P-1951)
decay of vector, angular distributions of lepton pairs from, (T), 19: 39451 (CALT-68-43)
decay of vector, test of nonrelativistic quark model in radiative, (T), 20: 1016
decay of vector, $\bar{U}(12)$ group for, (T), 19: 18853
decay of, interference effects in cascade (T), 19: 3077
decay of, interference effects in, (T), 19: 27152 (JINR-P-2027)
decay of, isotopic structure of electromagnetic, (T), 20: 17428 (JINR-P-2498)
decay of, lepton-pair, (E), 19: 18893
decay of, multiparticle, 19: 29075 (UCRL-11971)
decay of, parity and spin analysis in two-step, (T), 20: 4585 (SLAC-42)
decay of, particle and polarization angular distributions in two- and three-body, (T), 20: 21698
decay of, resonance widths and SU(3) symmetry predictions for strong, (E/T), 20: 1025
decay of, resonance widths in, (T), 20: 21713 (JINR-P-2568)
decay of, selection rules for, (T), 19: 16629
decay of, semiclassical theory for, 19: 14362
decay rates of A_2 (1310), f^* (1520), f^0 (1253), and K^* (1400), $\bar{U}$ (12) kinetic supermultiplet scheme for, 20: 7820

decay rates of $\overline{K}^*$ (1400), (E), 20: 9752
decay width and magnetic moment of K*, (T), 20: 44203
decay widths and mass formulas from rank-three Lie groups, (T), 19: 16578
decay widths of K*(1405), current algebra for, 20: 21654
decay widths of K*, (T), 20: 34214
decays of higher, SU(6) × R(3) P-wave 2-quark model for two-body, 19: 43099
decays of, analysis of three-body, (T), 19: 4943
decays of, predictions of static quark model on, 20: 32061
decays of, relative probabalities in U(6,6) for, 20: 46415
detection of B, (E/T), 19: 35181
detection of S-wave, (T), 19: 33003
determination of parameters of K*(888), self-consistent, (T), 19: 18847
dynamic model for, 19: 14352
effects of (K*) on baryon leptonic decays, (T), 19: 10092
effects of K*, on photon-proton interactions, (T), 19: 27234
effects of 2π (400) and (730), on meson (π)-nucleon scattering amplitudes, (T), 20: 17388
electromagnetic properties of K*, in SU_3 symmetry, 19: 35080
electromagnetic properties, (T), 19: 39563
energy levels in symmetry-breaking SU(2) nonlinear spinor model, 19: 41396
exchange of ABC, in meson(π)-proton interactions at high energies, (T), 20: 34224
exchange of ABC, in meson(π)-meson(π) and meson(π)-nucleon interactions, (T), 20: 34225
exchange of K*, in hyperon (Λ)-proton interactions at 0.5 to 3.0 Bev/c, (T), 19: 16544
exchange of 2+, in meson--nucleon and nucleon--nucleon interactions, (T), 20: 19512
existence of $\eta\pi$ and $\pi\pi$, from $\eta\pi\pi$ model of meson (X^0), 20: 15355
existence of unitary multiplets of, 20: 39860 (JINR-P-2790)
interactions of mesons (K*) and mesons (π), energy peaks in, (T), 19: 14335
interactions of neutral vector, with charged scalar mesons, vacuum Regge pole in annihilation, 20: 1081
interactions of S^0 (700) with nucleons, coupling constants for, (T), 20: 9746
interactions with stable particle, strong, (T), 19: 45082
isospin of A_1 and A_2, (E), 20: 15408
isospin, parity, and spin of $\overline{K}^*$ (1400), (E), 20: 9752
lifetime of, Heisenberg uncertainty principle for determining, 20: 31910
mass and isotopic spin of 3π (625), 3π (1000), and K$\pi\pi$ (1175), 19: 32977
mass and Regge trajectories for M^0, (T), 19: 21049
mass and width of K*, self-consistent calculation of, 20: 11669
mass and width of K*(890), (T), 20: 34251
mass calculation, (T), 19: 26917(R) (IA-984)
mass difference ρ^0–ω_8, from meson (π)–nucleon interactions, (T), 19: 41380
mass differences of pseudoscalar and vector octets, self-consistent model for, 19: 8186
mass differences of vector, K^{*+}-K^{*0} and ρ^+-ρ^0 electromagnetic, (T), 19: 47369
mass differences of K* (885), electromagnetic, (T), 20: 30161
mass formula for positive-parity, 405 multiplet, 20: 41874
mass formula for $U_8 \otimes U_8 \otimes O_{3l}$ group for, 20: 44324
mass formula for, in unitary symmetry theory, 19: 33055
mass formula for, in covariant spin-unitary-spin scheme, 19: 47352
mass formula for, empirical, (T), 19: 47384
mass formulas for SU(6) multiplets of, 19: 31006 (IC/65/46)
mass formulas for unitary octet multiplet mixtures of vector, 19: 33065
mass formulas for, (T), 19: 35100
mass formulas for 189 multiplet of SU(6) for, 20: 15478
mass formulas for, universal equal-spacing, (T), 19: 18800
mass formulas in U_4 symmetry, (T), 19: 16545
mass of π-π (T = 0, I = 0) antibound state, bootstrap calculation of, 19: 18900
mass of T = 0, 19: 8145
mass of, quark model for determining, 20: 17443(T)
mass perturbations of, octet enhancement and reciprocal bootstrap for, 20: 4649
mass relations for, (E/T), 19: 25370
mass relations for, linear, 20: 17391
mass relations for J = 2+, in oscillator model, 20: 34191
mass spectra of ϕ-π system, (T), 20: 2741
mass spectrum of, models for, 19: 14348
mass splitting of unitary-octet vector, electromagnetic decays for, (T), 20: 2801
mass systematics of, (T), 19: 16630
masses and quantum numbers of, p-wave multiplet of SU(6) for, (T), 19: 18843
meson (ρ) model in ($\pi\pi$-K$\overline{K}$), 19: 8194
model for A and X^0, (T), 19: 4992
model for $\rho\pi\pi$ vertex, quark, 20: 41876
model for vector, R(n) invariance and pseudoscalar-meson bootstrap, (T), 19: 43098
model for, baryon-antibaryon pair, (T), 19: 8205
model for, composite, 19: 41525
model for, quark, (T), 20: 19531
model for, relativistic composite quark, (T), 20: 11684 (JINR-P-2442)
models for, quark, (T), 20: 21697
models for, quasi-molecular rotator, 19: 41524
models for, quasi-molecular rotator, 20: 15399
models for, vector-meson octet, (T), 19: 12231
models for, with non-unique angular momentum, (T), 19: 16538
parameters of, effects of logarithmic singularities on, (T), 19: 4998
parities and spins of, 19: 43135
parities of, determination of, (T), 19: 16549
parity and spin determinations for, (T), 19: 41447
parity and spin of, method for determining, 20: 15431
parity and spin of A_2 (1300), 20: 32064
parity and spin of K*, 20: 34175
parity and spin of, methods for determining, 20: 34169
parity and spin of A_2, (E), 20: 44178 (UCRL-16881)
photoproduction at 4.8 to 6.0 Bev, (E), 20: 15425
photoproduction of 1$^-$, on nucleons, U(6W) for collinear, 20: 7904
photoproduction of 2π, (E), 20: 27917
photoproduction on baryons, unitary symmetry in amplitudes of pair, (T), 19: 33060
photoproduction on nucleons, review of, 20: 9774
photoproduction on protons at 0.5 to 6.0 Bev, (E/T), 20: 27894
photoproduction on protons at high energies, (E), 20: 27895
photoproduction on protons of X^0 (958), Regge-pole model for, (T), 20: 44204
production, (E/T), 20: 21592 (CERN-65-24(Vol.1), pp 1-44)
production and decay, 19: 23355(R) (BNL-867(p.1-117))
production and decay, (T), 20: 24089
production and decay of, (T), 20: 30085 (CONF-640509(Pt.1), Paper 3)
production and decay of A_1, A_2, and B, in meson (π^-)-proton interactions at 3.2 and 4.2 Bev/c, (E), 20: 44178 (UCRL-16881)
production and properties of, (T), 19: 10015 (JINR-P-1808)
production and properties of, review of, 19: 16510
production and properties of K* (890), 19: 16510
production and properties of, review on, 20: 7868
production and properties of F*, (E/T), 20: 20365
production and properties of A_1 and A_2, from meson (π) interactions with nucleons, (E/T), 20: 30023
production and properties of strange, (E), 20: 34244
production and properties of A_1 and K** (1320), review of, 20: 36044 (UCRL-16744)
production at high energies, singularities in complex j-plane for, 20: 37804
production cross sections of A_2, D, E, and ϕ, in meson (π^-)-proton interactions at 2.0 to 4.0 Bev/c, (E), 20: 41802 (UCRL-16832)
production in antinucleon-nucleon annihilation, (T), 19: 10104
production in antiproton-neutron annihilations at rest, (E), 20: 9785
production in antiproton-proton annihilation at 3.7 Bev/c, cross section for, (E), 20: 15338
production in bremsstrahlung-proton interactions at 0.6 to 5.5 Bev, (E), 19: 44999 (DESY-65/5)
production in deuteron-meson (π^-) interactions at 3.2 Bev/c, (E), 19: 39551
production in meson (K)–meson (π) interactions, (T), 19: 10040
production in meson (π^-)-proton interactions at 3 Bev/c, (E/T), 19: 10084
production in meson (π)–nucleon interactions at 12 and 18 Bev/c, 19: 14405 (TID-21409)
production in meson-nucleon interactions, (T), 19: 35152
production in meson (π^-)-proton interactions at 2.7 Bev/c, (E), 19: 37524 (COO-1428-12)
production in meson (π^-)-proton interactions at 7.5 Bev/c, cross sections for, (E), 19: 41489(T)
production in meson (π) interactions, phase shift analysis for, (T), 20: 2708
production in meson (π^-)-proton interactions at 3.3 and 3.9 Bev/c, (E/T), 20: 6041 (UCRL-11942)
production in meson (π^+)-deuteron interactions at 4.5 Bev/c, (E), 20: 9740
production in meson (π) interactions, Faddeev equations for, (T), 20: 11568 (UCRL-11749)
production in meson ($\pi^\pm$)-proton interactions at 3.65 and 3.70 Bev/c, (E), 20: 13456 (UCRL-16170)
production in meson (K^-)-proton interactions at 700 to 1400 Mev/c, (T), 20: 13460 (UCRL-16274)
production in meson (π^-)-deuteron interactions at 3.2 Bev/c, (E),

20: 15405
production in meson (π^+) interactions with protons at 2.08 Bev/c, cross sections for, (E), 20: 15334
production in meson (K⁻) interactions with protons at 2.24 Bev/c, (E), 20: 17383
production in meson (K⁻)-proton interactions at 1.33 Bev/c, (E), 20: 21615 (COO-1195-52)
production in meson (π^+)-proton interactions via two-meson (π) exchange, (T), 20: 41918
production in proton interactions, mechanism of, 20: 37769
production in quasi-two-body processes, coherent droplet model for, (T), 20: 9750
production in three-body meson (π) interactions, model for relativistic, (T), 20: 11641
production in unstable boson exchange interactions, pole approximation for, 20: 2779
production of (A_1) and (A_2) in meson (π)-proton interactions, (E), 20: 19449 (UR-875-123 and (Add.))
production of ($K^\pm K^\pm \pi^\pm$), in proton pair annihilation, (E), 19: 1355
production of (740), in meson (π^-)–(π^+) interactions, (T), 20: 11555 (DESY-65/13)
production of (962), in meson (π^-)-proton interactions at 3.0 to 5.0 Bev/c, 20: 7848
production of A_2^-, in meson (π^-)-proton interactions at 5.6 and 6 Bev/c, 20: 7847
production of A_1 (1080) in meson (π^+) interactions with protons, (T), 19: 27272
production of A_1 in meson (π^-) reactions with emulsion nuclei at 17 Bev, 19: 43126
production of A_1 and A_2 in antiproton-neutron annihilations at, upper limit for, (E), 20: 9785
production of A_1 and A_2, in meson (π^-)-proton interactions at 5 Bev/c, (E), 20: 25781(R) (COO-1195-56)
production of A_1 and A_2, in meson ($\pi^\pm$)-proton interactions above 2.5 Bev/c, (T), 20: 27825
production of A_1 and A_2, in deuteron-meson (π^-) interactions, (E), 20: 30078
production of A_1 (1090) and A_2 (1310) in deuteron-meson (π^+) interactions at 3.29 Bev/c, (E), 20: 39470(R) (ORNL-3924)
production of A_1 and A_2, in meson (π^-) interactions with protons at 7.0 Bev/c, 20: 39790
production of A_1, E_1(740), and E_2(940) in meson (π^-)-proton interactions at 2.26 Bev/c, 20: 2745
production of A_1(1100), in meson(π^+) interactions with protons at 8 Bev/c, 20: 34198
production of A_2 in meson (π^-)-proton interactions, Regge pole analysis of, (T), 20: 7860
production of A_2 (1286) and R (1675), from meson (π^-)-proton interactions at 7 and 12 Bev/c, (E), 20: 44245
production of A, in meson (π^+)-proton interactions at 4 Bev/c, (E), 19: 25350
production of $\bar{K}^{*0}$(891) in meson (K⁻)-proton interactions at 3 Bev/c, mechanism for, (E), 20: 17380
production of C^0(1215), D^0(1290), and E^0(1410) in proton-antiproton annihilations, (E), 20: 11575
production of E, in relativistic three-body meson (π) interactions, (T), 20: 11640
production of E(1405), in antiproton-proton annihilation, (T), 20: 36048
production of η^* (960), in meson (K⁻)-neutron interactions at 2.24 Bev/c, (E), 20: 39786
production of f*, 20: 19273(R) (BNL-929, pp 3-43)
production of f*, in meson (K⁻)-proton interactions at 4.6 and 5.0 Bev/c, 20: 37730 (BNL-10459)
production of g (1680), in meson (π^-)-proton interactions at 11 Bev/c, (E), 20: 44241
production of I = 0 (1610), from antiproton-proton interactions at 2.7 Bev/c, (E), 20: 7858
production of isoscalar s-wave di-pion, (T), 19: 33029
production of isospin 1 (966), from proton-proton interactions at 3.00 Bev, (E), 20: 44243
production of K*(888), in meson (K⁻)-proton interactions, (E), 19: 16481 (TID-20444)
production of K*(890) and K*(1440) in mesons (K⁻)-proton interactions, (E), 19: 18838
production of K* (1430), in mesons (π^-)–proton interactions at 3.9 and 4.2 Bev/c, (E), 19: 21004
production of K** in meson (K^+)-proton interactions, peripheral, (E/T), 19: 39576
production of K* in deuteron-meson (K^+) interactions at 2.3 Bev/c, 19: 45120
production of K* isobar in meson (K^-)-proton and meson (π^+)-proton interactions, one-particle exchange model for, (T), 20: 7827
production of K*0, in meson (K⁻)-proton interactions at 3.8 Bev/c, (E), 20: 15418
production of K* (1425) in meson ($\pi^\pm$)-proton interactions at 6 Bev/c, 20: 37733 (BNL-10462)
production of K* (890) in meson (π^+) interactions with protons at 8 Bev/c, (E), 20: 37770
production of K* in meson (K⁻)-proton interactions at 1.80 to 1.95 Bev/c, 20: 39838
production of K* (891) in meson (K^+)-proton interactions at 2.7 Bev/c, (E), 20: 41804 (UCRL-17003)
production of K* (1320), from meson (K^+)-proton interactions at 4.6 Bev/c, 20: 44265
production of K*, in meson (K^+)-proton interactions at 3 Bev, (E), 19: 1342
production of K*, in meson (π^+)-proton interactions, (T), 19: 10062
production of K*, symmetry in bootstrap model for, (T), 19: 16627
production of K*, in antiproton-proton annihilation, (E), 19: 20993
production of K*, in meson (K) interactions with mesons (π), (T), 19: 21058
production of K*, joint decay distribution in, (T), 19: 29073 (NP-15070)
production of K*, in antiproton-proton annihilation, (E), 19: 35143
production of K*, in meson (K^+)–proton interactions at 3 Bev/c, (E/T), 19: 45057
production of K*, in meson (K^+)-proton interactions at 3 Bev/c, (E/T), 19: 47356
production of K*, in meson (K^+) interactions with neutrons and protons at 2.3 Bev/c, (E), 20: 1010
production of K*, in meson (K^+)-proton interactions at 0.86 to 1.58 Bev/c, (E), 20: 13462 (UCRL-16370)
production of K*, in meson (K⁻)-proton interactions at 1.80 and 1.95 Bev/c, (E), 20: 15420
production of K*, in meson (K^+)-proton interactions at 2.26 Bev/c, (E/T), 20: 15422
production of K*, in meson (K^+)-proton interactions at 3.6 Bev/c, (E), 20: 15407
production of K*, in meson (K^+)-proton interactions at 4.6 Bev/c, (E), 20: 21629 (UCRL-16332)
production of K*, multi-channel double bootstrap for, (T), 20: 24003 (CALT-68-26)
production of K*, in meson (π^+)-deuteron interactions at 2.5 Bev/c, (E), 20: 25781(R) (COO-1195-56)
production of K*, in meson (K⁻)-proton interactions at 1.455 Bev/c, (E), 20: 31987 (NP-16097)
production of K*, in meson (π^-)-proton interactions at 1.6 to 4.2 Bev/c, (E), 20: 39770 (UCRL-16788)
production of K*, from meson (K̄)-nucleon interactions, (T), 20: 39778
production of K*(890) in mesons (K^+)-proton interactions at 1.45 Bev/c, (E), 19: 25340
production of K*(890) in meson (K^+) interactions with protons at Bev/c, 19: 32988
production of K*(1400) in meson (K^-)-proton interactions at 3 Bev/c, (E), 19: 35133
production of K*(890), in meson (K⁻)-proton interactions at 2.1 to 2.7 Bev/c, (E), 20: 15412
production of K*(890), in meson (K⁻)-proton interactions at 5.5 Bev/c, 20: 15416
production of K*(888), in meson (K⁻)-proton interactions at 1.5 Bev/c, (E/T), 20: 15429
production of K*(891), in meson (K⁻)-proton interactions at 1.45 Bev/c, (E), 20: 30009
production of K*(891), in meson (π^+) and (π^-) interactions with protons at 4 Bev/c, (E), 20: 32029
production of K*(1400) and K**(1320) in meson(K^+) interactions with protons, (E), 20: 34245
production of K*(890), in meson(K^+)-proton interactions at 2.26 Bev/c, (E/T), 20: 34249
production of K*(890) in meson(π^+) interactions with protons at 8 Bev/c, (E), 20: 34197
production of $K\bar{K}\pi$ (1280), (E), 19: 33037
production of $K\bar{K}$ and $K\pi$, in meson (π^+)-proton interactions at 2.35 to 2.90 Bev/c, (E), 19: 41418
production of $K\pi\pi$ (1160), in meson (π^-)-proton interactions at 2.7 Bev/c, (E), 19: 18851
production of K^+K^{+*} (1280) from meson (K^+)-proton interactions at 3.535 Bev/c, 20: 30047
production of $K^0\bar{K}^0$ (1280), in meson (π^-)-nucleon interactions at 2.8 Bev/c, 19: 43048 (NP-15377)
production of K*(888) in meson (K⁻)-proton interactions, isobar diagrams for, (T), 19: 29052 (IC/65/44)
production of κ^0(725) in meson (π^-)-proton interactions, 20: 2715
production of L (1789), in meson (K⁻)-proton interactions at 10 Bev/c, (E), 20: 39788
production of multi-π (959), (E/T), 19: 6564

production of multipion, in meson (π^-) reactions with freon at 16 Bev/c, (E), 20: 37822
production of N*(1238), in meson (π^+)-proton interactions at 2 Bev/c, (E), 20: 11672
production of $N^*_{3,3}$ (1420) pion-nucleon P-wave interactions, Chew-Low model for, 20: 44186
production of neutral A_2 (1300) in deuteron-meson (π^+) interactions at 3.65 Bev/c, (E), 20: 32064
production of non-K*, in proton pair annihilation, 19: 39534
production of ω_{ABC}, in proton-deuteron reactions, 20: 13528
production of πK, in meson (K^+)-nucleon interactions, (E), 19: 10064
production of $\pi^-\pi^0$ (965), in meson (π^-) interactions with protons at 1.7 Bev/c, (E), 20: 44229
production of $\pi^+\pi^-$ (1670) in meson (π^+)-deuteron and meson (π^-)-proton interactions, (E), 19: 39537
production of $\pi^+\pi^-\pi^-$ (1630), in meson (π^-)-proton interactions at 4.7 Bev/c, 20: 30021
production of $\pi\pi$, in meson (π^-)-proton interactions at 6 Bev/c, (E), 20: 37731 (BNL-10460)
production of π-π (720) S-wave, OBE model of N-N scattering for, 20: 7818
production of $\rho\rho$ resonance in antiproton interactions with neutrons, (E/T), 20: 24042
production of S*(1068) in meson (π^-)-proton interactions at 6 Bev/c, (E), 20: 27875
production of S-wave T = 0 $\pi\pi$, in meson (π^-)-proton interactions at 1.7 to 2.5 Bev/c, (E), 19: 45089
production of strangeness +2, (E), 19: 35139
production of strangeness +1, in meson (K^+)-proton interactions at 3.54 Bev/c, 20: 30049
production of T = 2 σ-π, (E/T), 19: 25265(R) (UCRL-11776)
production of T = 0 2π resonance at 720 Mev, (E), 19: 33038
production of 2π(700), in meson (π^-)-proton interactions at 1.52 Bev/c, (E), 19: 35163
production of 2^+, absorption model for, 20: 21644
production of, interference effects in, (T), 19: 27152 (JINR-P-2027)
production of, kinematical form factors for relativistic vertex functions for, (T), 20: 7934
production of, triangle singularities in, (T), 19: 45104
properties and symmetry of f*(1500) and K**(1410), 20: 11552 (CONF-651015-3)
properties in eightfold way symmetry, book on, 19: 6563
properties in SU_4 symmetry, (T), 19: 8171
properties of, 19: 47406
properties of, (E/T), 20: 19533 (BNL-9934)
properties of, (E/T), 20: 19448 (UCRL-16462)
properties of η'*(960) and ϕ(1020), review of, 20: 11552 (CONF-651015-3)
properties of isoscalar $n\rho$ (975), in SU_3 symmetry, (T), 19: 8177
properties of $J = 0^+$, T = ½ Kπ, (T), 19: 18782
properties of K* (890), (T), 19: 12298
properties of K$\bar{K}$(892), (E), 20: 17403
properties of K*, spontaneous mass splitting in bootstrap model for, (T), 19: 18878
properties of K*, self-consistent calculations of, 19: 27143 (JINR-E-2085)
properties of K*, from one- and two-particle exchange forces, (T), 19: 27251
properties of $K\bar{K}$ (1020), (T), 19: 12249
properties of $K^0_1K^{+2}\pi^{-3}$(1410) and m_A(1220), (E/T), 19: 6556
properties of meson (ρ) bound states, (T), 20: 6092
properties of nonstrange meson (f*)(1500), (E), 19: 41459
properties of π, 20: 34170
properties of 1310-Mev K$^-$ K$\bar{K}$p and K$\bar{K}$Kn, (E/T), 19: 25265(R) (UCRL-11776)
properties of 3π (625 and 1000) and 4π (1050), (T), 19: 18756(T) (JPRS-28496(p.32-7))
properties of, data on, 19: 21040
properties of, data tabulation of, 19: 39485 (UCRL-8030(Pt.I) (Mar. '65, ed.))
properties of, dynamical model in, 19: 18873
properties of, dynamical model for, (T), 19: 18876
properties of, effects of extra channels on N/D calculations of, (T), 19: 18754 (UCRL-12344)
properties of, electron-pair model for, (T), 19: 10059
properties of, in $SU(6)_W$, 20: 30048
properties of, maximum likelihood method for determining, 20: 41790 (DESY-66/17)
properties of, prediction from quantum theory of symmetric top, 20: 28016
properties of, review of, 19: 14314 (JINR-P-1887)
properties of, review of, 19: 35068
properties of, review, 19: 45046 (UCRL-16295)
properties of, SU(3) symmetry groups for, 19: 29044 (IC/65/21)
properties of, tables, (E/T), 19: 16642
properties of, 4212+ multiplet of SU(12) for, 19: 23398
properties, determination of, 20: 34174
quantum numbers for, principle, (T), 19: 16629
quantum numbers of, methods for determining, 19: 37651
Regge pole method for, unitarity in, (T), 19: 10035
Regge trajectories for, (T), 20: 34322
Regge trajectory of A_2, from meson (π^-)-proton interactions, (T), 20: 9747
representation of I = 0 states of three-pion, (T), 19: 45042 (UCID-2608)
research on π, 20: 34174
research on, status of, 20: 32089
review, 19: 45056
review on three -and four-pi, 19: 20969
spin and parity determination using helium target, 20: 25807(T)
spin and parity of 1320-Mev A_2 π-ρ, (E/T), 19: 41368
spin determination for, (T), 19: 27264
spin of A_1 and A_2, (E), 20: 30078
spin of K*, analysis of, (E), 19: 1338
spin of, determination of, (T), 19: 14361
spin of, determination of, (T), 19: 14363
stability in broken symmetry, 20: 41994
structure of, based on meson (μ)-meson (π) combinations, (T), 20: 36051
survey on 2π, 20: 24083
symmetries for, lectures on, 20: 34319
symmetries for, relativistic SU(6) supermultiplet, 19: 45112
symmetries for, supermultiplet, 20: 25888 (PUC-937-201)
symmetry classification, (T), 19: 12301
symmetry for H, K^+K^+, and K$\pi\pi$, 20: 2727
symmetry for σ, κ and δ, scalar octet in SU_3, (T), 19: 25345
symmetry for, origin of SU(6), 20: 30117
symmetry for, quark model in SU(18), 20: 28018
symmetry for, 27-supermultiplet in, (T), 19: 41492(T)
symmetry groups and models, (T), 20: 34320
symmetry models for spin-2 SU(6), 20: 6151
symmetry properties in SU(6) and its relativistic extensions, 20: 7795 (JINR-P-2400)
theory for axial and tensor, 20: 17442(T)
theory of (π-κ) (725, 885), (T), 19: 8241
theory of A_1(1072) and K_c(1215), as axial-vector mesons, 20: 30007
theory of scalar Kπ, 19: 16540
theory of 5π, Feynman graphs for, (T), 19: 27268

MESONS (α)

production in N-N and π-N collisions, 17: 5276
production of, theory for, 18: 9197
production of, review of, 18: 12903 (JINR-P-1490)
properties, 20: 34170
properties, (T), 19: 18756(T) (JPRS-28496(p.32-7))
properties of, π-π resonance, 18: 21001

MESONS (B)

decay ($\omega^0 + \pi^0$), 18: 24463
decay of, charge-parity violation in radiative, (T), 20: 17501
decay of, limit on 2π, 18: 30572
decay of, ω-ϕ mixing angle from, (T), 19: 41458
decay of, selection by A invariance, 18: 22758
decay of, unitary symmetry selection rules for, 18: 30556
effects in nucleon-nucleon interactions, (T), 19: 31067
exchange in meson (π)-meson (ω) interactions, (T), 20: 15357
exchange in meson (π)-meson (ω) interactions, 20: 39807
model for, 18: 20958
model for, composite, 19: 41525
model of, N$\bar{N}$ bound-state, 18: 22782
parity and spin, 18: 20957
parity and spin, 18: 32550
production and decay correlations from meson (π^-)-proton interactions, 18: 40246 (UCRL-11443)
production and properties, (E), 19: 37597
production in meson (π) interactions, 18: 36324
production in meson (π^-)-proton interactions at 3.5 Bev/c, 18: 36361
production in meson (π^+)-proton interactions at 4 Bev/c, (E), 19: 25350
production in meson (π^-)--proton interactions at 3.5 Bev/c, (E), 19: 37645
production in meson (π^-)-proton interactions at 2.26 Bev/c, 20: 2745
production in meson (π)-proton interactions above 2.5 Bev/c, (E), 20: 19449 (UR-875-123 and (Add.))
production in meson ($\pi^\pm$)-proton interactions above 2.5 Bev/c, (T), 20: 27825
production of, model for, (E/T), 20: 17402
properties, 18: 22742
properties, 20: 34170
properties of, reciprocal bootstrap model for, (T), 19: 12225
properties, (E/T), 19: 6556
quantum numbers (T), 19: 3065
quantum numbers of, 19: 21066
theory of, SU_3 symmetry in, 18: 44554

MESONS (β)
production of, review of, 18: 12903 (JINR-P-1490)
properties, 20: 34170
properties, (T), 19: 18756(T) (JPRS-28496(p.32-7))
properties of, π-π resonance, 18: 21001
MESONS (C)
properties, 20: 34170
theory of, SU_3 symmetry in, 18: 44554
Mesons (χ)
see Mesons ($K_{\pi 2}$)
MESONS (D)
production in deuteron–meson (π⁻) interactions at 3.7 Bev/c, (E), 19: 37599
production in proton pair annihilations at 1.2 Bev/c, (E), 19: 39535
properties and production, (E/T), 20: 20365
theory of, SU_3 symmetry in, 18: 44554
MESONS (D⁺)
production probability, 16: 18403
search for in meson (K⁺) interactions in propane bubble chamber, 16: 31045
MESONS (δ)
decay of, partial widths of electromagnetic and strong, (T), 20: 4674
production in meson (K⁻)-proton interactions, model for, 18: 42409
MESONS (ε)
decay channels, (T), 19: 33025
production in deuteron-meson (π⁺) interactions at 3.29 Bev/c, (E), 20: 6079
production in meson (π⁻)-proton interactions, (T), 19: 33025
production in nucleon-antinucleon annihilation, selection rules, 16: 24735
properties, (T), 19: 33025
MESONS (η)
branching ratio, (T), 19: 14377
coupling constant of, with nucleon, 18: 24411
coupling with nucleons, constants for, (T), 19: 4986
decay, 17: 39914
decay, 18: 9180
decay, 18: 12914 (TID-7686(p.109-29))
decay, 18: 16552(R) (UCRL-11132)
decay amplitudes and branching ratios for, (E), 19: 31003 (COO-881-43)
decay and photoproduction of, cross sections and branching ratios for, 17: 31364
decay and production in photon interactions with protons, (E), 19: 39620
decay branching ratios and rates and spin determinations, 16: 19709
decay branching ratio for, $(\pi^+ + \pi^- + \gamma/\pi^+ + \pi^- + \pi^0)$, 17: 11552
decay, Dalitz plots and Feynman graphs for 3-pion, 16: 19714
decay into $\pi^0 + \gamma + \gamma$, branching ratio for, (E), 20: 36056
decay, meson (π) distributions from, 17: 19112
decay, meson (π) spectra from, 17: 711 (NEVIS-110)
decay mode, 16: 15591
decay modes and properties, 17: 13440
decay modes for, (T), 20: 44205
decay modes of, branching ratio for Dalitz-pair production and gamma emission in, 18: 7497
decay modes of, resonances in three-meson (π), 18: 9170
decay modes of, 3π, 17: 17027
decay modes of, neutral, 18: 40352
decay modes of, neutral, (E), 20: 15395
decay modes of, 3-π, 18: 28324 (LNF-64/6)
decay of (958) and (549), C-invariance violation in, (E), 19: 47372
decay of, branching ratio for gamma and meson (π), 17: 22427 (LNF-62/99)
decay of, branching ratios and modes for, 17: 29553
decay of, conservation of isotopic spin in, 17: 41838
decay of, electromagnetic, 17: 36577 (JINR-P-1300)
decay of electromagnetic and strong interactions in rare modes of, (T), 19: 41457
decay of, meson (φ) effects on, 17: 41793
decay of, meson (π) emission in, 17: 11553
decay of, products and branching ratios for, 17: 6998
decay of, radiative, 17: 17119 (JINR-P-1164)
decay of, rate of 3-π, 18: 7536
decay of, relation to electromagnetic properties of electrons and mesons (μ), 17: 9406
decay of, research, 17: 21388(R) (LNF-63/11)
decay of, spin-parity effects on branching ratios for 3-π, 17: 3998
decay of, symmetry groups for boson couplings in, 18: 6018
decay of, two-gamma, 17: 17192
decay of, unitary symmetry calculations on, 17: 31368
decay of, unitary symmetry in 3-π, 17: 34770
decay of, (3π), 17: 29502 (UCRL-10492)
decay of, absence of 2π, 18: 14818 (NP-13677)
decay of, boson-pole model for pionic, (T), 19: 6554
decay of, branching ratio for neutral modes of (E), 19: 1327
decay of, branching ratios for, (E), 19: 12194
decay of, branching ratios for, (T), 19: 21059
decay of, branching ratios for neutral modes of, (E), 20: 24050
decay of, branching ratios for, (T), 20: 27865
decay of, branching ratios for, 20: 32055
decay of, C violation in, (E), 20: 15430
decay of, C violation in, (T), 20: 25874
decay of, C violation in $\pi^+\pi^0\pi^-$, (E), 20: 39766 (ORO-3065-10)
decay of, C-nonconserving coupling constants in, (T), 19: 35169
decay of, C-violation in 3π, (T), 19: 39528
decay of, C-violation in, 20: 34153 (ORO-3065-9)
decay of, coupling effects in unitary symmetry, 19: 41335 (NP-15239)
decay of, CP violation in 3π, 20: 44296
decay of, effects of meson (η)-(X^0) mixing on, (T), 19: 31056
decay of, electromagnetic, (T), 19: 14307 (ANL-6942)
decay of, G_1 symmetry in, 18: 24441
decay of, G_2 symmetry in, (E/T), 20: 2520(R) (IA-920)
decay of, matrix elements of 3π, 19: 23454
decay of, meson (σ) hypothesis for, (T), 19: 41518
decay of, model for (3π), 18: 28372
decay of, $\pi^+\pi^-\gamma$, (E), 20: 39771 (UCRL-16923)
decay of, probabilities of weak, 18: 36359
decay of, resonances in 3π, 18: 21021
decay of, search ($\pi^0 e^+ e^-$), (E), 20: 15333
decay of, search for C violation in 3π, (E/T), 20: 41854
decay of, selection by A invariance, 18: 22758
decay of, sigma hypothesis in, 20: 17422
decay of, static quark model for, 20: 44235
decay of, test of C invariance in 3π, (E), 20: 44230
decay of, unitary symmetry in, 18: 14956
decay of, vector interaction constant in, (T), 19: 39589
decay probabilities in unitary symmetry, 18: 14866
decay production, and properties of, 17: 36584 (TID-19343)
decay rate of, determination of two-photon, 17: 9264
decay rate of, two-photon, 17: 19116
decay, relation to meson ($K\pi_3$) decay, 16: 26150
decay scheme, 16: 26138
decay scheme, (E), 19: 25265(R) (UCRL-11776)
decay schemes, perturbation theory, 16: 19712
decay spectra of, 3π, 20: 32010
decay to meson (π^0), unitary symmetry in, 17: 41798
decay, use in analysis of lepton electromagnetic properties, 16: 29707
decay widths of, two-baryon approximation method for determining, 20: 39783
decays of, C-violating interactions in, (T), 20: 11634
decays of, ratio of widths for $\gamma\pi^+\pi^-$ and $\gamma\gamma$, (T), 20: 27873
decays of, weak-interaction, (T), 19: 35156
detection and measurement of, possible method for, 18: 30511 (JINR-P-1654)
effects on meson (π^0) photoproduction on nucleons, 18: 18733
effects on nuclear forces, 20: 15817
effects on nucleon-nucleon interaction amplitudes, 20: 27892
emission in meson (π⁻) interactions with nucleons at 7 Bev, 18: 24391 (JINR-P-1629)
exchange in hyperon (Λ)-nucleon interactions, potentials from, 18: 39274
exchange in hyperon (Λ)-nucleon interaction in hyperfragments, (T), 19: 16541
exchange in hyperon (Λ)-proton interactions at 0.5 to 3.0 Bev/c, (T), 19: 16544
exchange in nucleon interactions at 0 to 400 Mev, effects of, 18: 14954
exchange in nucleon interactions, potentials for, 18: 34539
exchange in nucleon interactions, (T), 19: 18864
exchange in nucleon-nucleon interactions, 20: 41899
exchange of vector, in nucleon-nucleon scattering, 17: 24336
formation in meson (K⁻) interactions with protons, 16: 31048
identification of mesons (η^0) with mesons (ζ^0), 16: 19715
interactions, effects of G-parity on, 16: 33764
interactions of, amplitude parity and radiative effects in, 17: 20882
interactions of, effects on photon-proton scattering, 17: 31311
interactions of, C-violation model for $\rho\eta\pi$ coupling in, 20: 4681
interactions of, resonances in, 18: 36269
interactions with mesons (π), resonance predictions in, 18: 18698
interactions with hyperons (Σ), motion of poles in resonance, 18: 21016
interactions with mesons (π), 1-Bev resonance in, 18: 34572
interactions with mesons (π), resonance effects in, 18: 42445
interactions with mesons (σ), meson (δ) production in, 18: 42409
interactions with mesons (π), properties of resonance, 19: 14314 (JINR-P-1887)
interactions with mesons (K) and (π), symmetry in bootstrap model for, (T), 19: 16627
interactions with nucleons, coupling constants for, (T), 19: 18817

interactions with nucleons, coupling constants for, (T), 19: 29072 (NP-15014)
interactions with baryons, coupling constants for, (T), 19: 31039
interactions with deuterons resonance, (T), 19: 39564
interactions with baryons, (T), 19: 41433
interactions with nucleons, coupling constant for, (T), 20: 9746
interactions with nucleons, (T), 20: 34221
interactions with nucleons from meson (π)-nucleon interaction, (T), 20: 41866
isospin, parity, and spin of, 17: 22437 (SLAC-13)
lifetime, (T), 20: 1005
lifetime of, experimental configuration for measurement of, 18: 10866 (LNF-63/47(p.94-7))
mass formulas in U_s symmetry, (T), 19: 16545
mass measurements of, 20: 7804
mass of, formula for, 18: 9147
mass of, as hyperon (Λ) pair bound state, (T), 19: 8145
mass of, models for, 19: 14348
mass of, nonlinear spinor theory for, 19: 25376
mass, parity, and spin of, 17: 29506
mass relations in octet, 18: 40309
mixing in SU(3), 20: 42005
mixing of, Gell-Mann–Okubo formula for, 20: 25900
mixing with mesons (X^0), (T), 19: 31056
model of, $N\bar{N}$ bound-state, 18: 22782
parity and spin of, 17: 32941
parity, assignment of G-, 16: 33748
photoproduction and decay, 16: 29640 (LNF-62/62)
photoproduction and decay, 17: 9313
photoproduction and decay, 18: 10854 (LNF-63/47(p.1-35))
photoproduction in (γ + p) reactions, 16: 25897 (LNF-62/37(p.89-98))
photoproduction of, ϕ–ω mixing in, 18: 14879
photoproduction on protons, cross section for, 17: 32912 (TID-7668(Sect. IV))
photoproduction on protons, resonance model for, 18: 2614
photoproduction on protons, differential cross section for, 18: 10861 (LNF-63/47(p.71-2))
photoproduction on protons at 740 to 830 Mev, N** effects in, 18: 14960
photoproduction on protons, cross sections for, 18: 24438
photoproduction on protons at 978 and 939 Mev, 18: 28324 (LNF-64/6)
photoproduction on protons, 18: 40352
photoproduction on protons from threshold to 900 Mev, (E), 20: 4578 (AD-618660)
photoproduction on protons at 0.3 to 5.5 Bev, (E/T), 20: 6037 (DESY-65/11)
photoproduction on protons at 0.8 to 1.0 Bev, (E), 20: 9773
photoproduction on nucleons, (T), 20: 13479(T)
photoproduction on protons at 0.3 and 5.5 Bev, (E), 20: 17368
photoproduction on protons at 0.750 to 1.00 Bev, (E), 20: 27915
photoproduction on protons at 0.8 to 1.0 Bev, cross sections for, (E), 20: 36036 (LNF-66/20)
photoproduction on protons, lecture on, (E), 20: 39743 (CALT-68-92)
photoproduction on protons at 0.95 to 1.1 Bev, differential cross sections for, (E), 20: 41889
photoproduction on protons at 0.3 to 5.8 BeV, (E), 20: 46348(T) (SLAC-Trans-44)
production, 17: 9315
production and decay, 17: 9327
production and properties from π^+-d interactions, 16: 26165
production and properties in meson (π^+)-proton interactions, 17: 6997
production and properties, 17: 9316
production and properties in meson (π)-proton interactions, 17: 9328
production and properties, review, 17: 9461
production and properties, 18: 10891
production from antiproton-proton annihilation at rest, rates for, (E), 20: 27846
production from meson (π^-)-nucleon interactions, cross section lower limit determination from, (E), 20: 41910
production in antinucleon annihilation, 17: 20857
production in antiproton-proton interactions (E), 19: 1353
production in antiproton-proton annihilations at rest, (E), 19: 45122
production in antiproton-neutron annihilations at rest, (E), 20: 9785
production in deuteron-meson (π) interactions, 17: 9326
production in deuteron–meson (π^+) interactions (E), 19: 1326
production in deuteron-meson (K^-) interactions at 0.9 to 1.12 Bev/c, (E), 20: 39747 (COO-881-75)
production in meson (π^+) -proton interactions at 3.43 and 3.54 Bev/c, partial cross sections for, 18: 2651
production in meson (K_{e3}) decay, 18: 10973
production in meson (π^-)-proton interactions, 18: 14810 (JINR-P-1506)
production in meson (π^-)–proton interactions at 2 Bev, 18: 14888
production in meson (K^-) interactions with deuterons and neutrons at 765 Mev/c, 18: 16783
production in meson (π^-)-proton interactions at 1.55 to 4.5 Bev/c, 18: 18729
production in meson (π^-)-proton interactions at 4 Bev/c, 18: 36307
production in meson (π^+)-proton interactions at 4 Bev/c, 18: 40285
production in meson (K^-)-proton interactions at 650 to 840 Mev/c, 18: 40225 (BNL-8233)
production in meson(π^+)-proton interactions at 2.35 and 2.90 Bev/c, 18: 44519 (NEVIS-123)
production in meson (π^+)-proton interactions at 1.6 Bev (E), 19: 1347
production in meson (π^-)-proton interactions at 2.75 Bev, (E), 19: 1348
production in meson (π)-nucleon interactions, (T), 19: 8182
production in meson (π^+)-proton interactions, model for, (T), 19: 10065
production in meson (π^+)-proton reactions at 1170 Mev/c, (E), 19: 25265(R) (UCRL-11776)
production in meson (K^-)-proton interactions, (T), 19: 31057
production in meson (π) interactions with nucleons, (E/T), 19: 43114
production in meson (π) interactions with protons, threshold phenomena in, (T), 19: 43120
production in meson (π)-proton interactions at 3 to 18 Bev/c, cross sections for, (E), 19: 43124
production in meson (π)-nucleon interactions, (T), 19: 47401
production in meson (π^-)-proton interactions at 2.26 Bev/c, 20: 2745
production in meson (π^-)-proton interactions at 592 to 1300 Mev, cross sections for, (E/T), 20: 13457 (UCRL-16195)
production in meson (K^-)-proton interactions at 3.8 Bev/c, (E), 20: 15418
production in meson (π^-)-proton charge-exchange interactions, (E), 20: 15380
production in meson (K^-)-proton interactions, cross section and scattering length for, (T), 20: 17376
production in meson (π^-)-proton interactions at 558 to 900 Mev, cross sections for, (E/T), 20: 41871
production in neutrino-nucleon interactions, (T), 19: 25315
production in nucleon-antinucleon annihilation, selection rules, 16: 24735
production in photon-proton interactions, 18: 22552(R) (LAL-1090)
production in proton-proton interactions at 2.85 Bev, 17: 4001
production in proton-proton interactions, 18: 32561
production of second resonant state with protons in photon-proton interactions at low energy, 17: 39918
production of, theory for, 18: 9197
production of, review of, 18: 12903 (JINR-P-1490)
production processes for, phenomenology of, (T), 19: 6523
production with neutrons in meson (π^-)-proton interactions, (E), 20: 2689 (UCRL-16140)
properties, 18: 40347
properties in particle-mixture theory, 16: 32335
properties of, 17: 5259
properties of, 20: 34175
properties of, octet unitary-symmetry model for, 17: 9226
properties of, review of theoretical, 17: 9463
properties of, review of, 17: 24185
properties of, electron-pair model for, (T), 19: 10059
properties of, four-pion models for, (T), 19: 12223
properties of, π-π resonance, 18: 21001
properties of, review of, 19: 16657
properties review, 16: 26158 (UCRL-10167)
quantum-number determinations for, 16: 33765
quantum numbers, 16: 15593
quantum numbers for, 0- + assignment to, 17: 16994
resonance ($\pi^+\pi^-\eta$) at 959 Mev, properties of, 18: 34515 (UCRL-11431)
resonances of, Regge trajectories for unitary symmetry representation of, 19: 3046
review, 18: 34636
role in isosinglet meson series, 17: 41813
scattering of, prediction of interaction symmetry from dispersion relations in, 17: 20905
spin of, calculation from 2-photon decay distributions, 17: 3999
spin of, isotopic, 18: 16783
spin-parity of, 17: 13457

MESONS (η^-)
magnetic moments of, Vigier rotator model for anomalous, 17: 34802

MESONS (η^0)
decay into electron pairs, CP-invariance violation, (E), 19: 37598
decay into three mesons (π), effects of mesons (ρ) on, (T), 19: 4919
decay into two photons, direct measurement of, 17: 19118
decay modes, (E), 20: 1027
decay modes of, 18: 28417
decay modes of, research on, 18: 28325(R) (TID-20702)
decay of, branching ratio and spectra of leptonic, 17: 22428 (LNF-63/16)
decay of, branching ratios, probabilities, and spectra of, 17: 39878
decay of, consequences of G quantum number in, 17: 9340
decay of, radiative branching ratios in, 17: 13456

decay of, branching ratio in (E), 19: 1337
decay of, branching ratios for, (E), 20: 21627 (LNF-66/9)
decay of, branching ratio for $\pi^0 e^+ e^-$, (E), 20: 37767
decay of, C violation in $\pi^+\pi^-\gamma$, (T), 20: 34226
decay of, C-invariance violation in 3π, (E/T), 20: 34230
decay of, C-noninvariant effects in 3π, (T), 19: 41437
decay of, CP violation in, 20: 29988 (ITEF-356)
decay of, $e^+e^-\pi^0$, (E), 20: 15427
decay of, electromagnetic, (T), 19: 12299
decay of, gamma conversion in hydrogen from, (E), 20: 30029
decay of, method for measuring rate of 2γ, (T), 19: 18798
decay of, partial widths of electromagnetic and strong, (T), 20: 4674
decay of, $\pi^+\pi^-\gamma$, (E), 20: 15367
decay quantum numbers, 16: 21318
decay, quantum numbers of, 17: 37982
decay rates of, equal-time commutators for 3π, 20: 32037
decay rates of, vector-meson and ω–ϕ mixing models for 2γ and $\pi\pi\gamma$, (T), 20: 11603
decays of, C and T violation in mixing in leptonic, (T), 20: 4682
emission in Y* decay, 18: 24387 (JINR-P-1615)
exchange in photon interactions with protons, contributions from, 17: 39900
interactions with mesons (K), effects on $K_{\mu 3}$ decays, 17: 16996
interactions with hyperons (Λ), resonance, 18: 24387 (JINR-P-1615)
lifetime calculations, 17: 17184
lifetime of, from bremsstrahlung spectra, 20: 1023
lifetime of, method for determining, 18: 30574
lifetime of, proposal for experimental measurement of, 18: 10870 (LNF-63/47(p.112-14))
magnetic moments of, Vigier rotator model for anomalous, 17: 34802
photoproduction from hydrogen, kinematics for 725 to 1500-Mev, 17: 16946 (ISS-62/15)
photoproduction on protons, 17: 9299
photoproduction on protons, cross sections near threshold for, 18: 4431 (LAL-1077)
photoproduction on protons and neutrons at 1 Bev, 18: 10857 (LNF-63/47(p.58-61))
photoproduction on protons, excitation curve analysis of, 18: 24381 (ISS-64/4)
photoproduction on protons from threshold to 900 Mev, (E), 20: 27914
photoproduction on protons at 0.95 to 1.10 Bev, (E), 20: 27913
production and decay in meson (π^+)-deuteron interactions, 18: 42376 (TID-20762)
production and properties of, review of, 19: 16510
production from meson (π^+)-proton interactions at 2.35 to 2.90 Bev/c, (E), 20: 27844
production in electron-positron interactions, lifetime from, 18: 32532 (LNF-64/15)
production in meson (K^-)-proton interactions near threshold, 17: 13458
production in meson (π^+)-neutron interactions at 1230 Mev/c, 18: 14955
production in meson(π^-)-proton interactions at 10.5 Bev, 18: 30539
production in meson(π^-) reactions with xenon at 9 Bev, 18: 40550
production in meson (π^-)-proton interactions at 500 to 1300 Mev, cross sections for, 18: 42382 (UCRL-11576)
production in meson (π^-)-proton interactions up to 1151 Mev, 18: 44561
production in meson (π^+)-proton interactions at 2.5 Bev/c, (E), 19: 37526 (CU-1932-243)
production in meson (π^-)-proton interactions at 1275 Mev/c, (E), 19: 41507
production in meson (π^-) interactions with protons, Regge pole and SU(3) predictions for, 19: 43147
production in meson (K^-)-proton and meson (π^-)-proton interactions, (T), 19: 41433
production in meson (π^+)-proton interactions at 1.2 Bev/c, (E), 20: 1027
production in meson (π^+)-proton interactions at 2 Bev/c, (E), 20: 11672
production in meson (π) interactions with nucleons, zero-effective-range analysis of, 20: 30033
production in nucleon interactions at high energies, SU(3) for multiple, (T), 20: 17345 (JINR-P-2531)
production in nucleon reactions with nuclei, SU(3) symmetry for multiple, 20: 24380(T)
properties, 20: 34170
properties of, review of, 19: 14314 (JINR-P-1887)
spin, (E/T), 20: 13522
spin of, evidence for 0, 17: 19043 (TID-16260)
structure, 16: 15594

MESONS (η^+)

magnetic moments of, Vigier rotator model for anomalous, 17: 34802

MESONS (f)

decay and isospin, 18: 30572
decay modes of, partial widths in SU(3) for, (T), 19: 41461
exchange in meson–nucleon and nucleon–nucleon interactions, (T), 20: 19512
mass of, formula for, 18: 9147
mass of, as hyperon (Λ) pair bound state, (T), 19: 8145
model for, composite, 19: 41525
model of, $N\bar{N}$ bound-state, 18: 22782
production in meson (π^-)-proton interactions at 2.26 Bev/c, 20: 2745
production in meson (π^+) interactions with protons at 8 Bev/c, cross sections for, (E), 20: 37770
production of, effects of nonresonant d-wave interaction on spin in, 18: 34630
production of, review of, 18: 12903 (JINR-P-1490)
properties of, review of, 19: 16657
role in isosinglet meson series, 17: 41813

MESONS (f^0)

contribution to meson (π)-nucleon scattering, 18: 34611
contribution to proton-proton scattering, 18: 34610
decay, 18: 37922
decay, 20: 27814
decay in broken $\tilde{U}(12)$, 19: 23435
decay into mesons (π^0), 18: 24463
decay of (1253), $\tilde{U}$ (12) kinetic supermultiplet scheme for, 20: 7820
decay of, branching ratio for 2π, (E), 19: 39480 (NP-15247)
decay of, branching ratios for, (E), 19: 41460
decay of, charge-parity violation in radiative, (T), 20: 17501
decay of, mass of axial vector meson (ρ) in 4π, (T), 19: 18834
decay of, parity and spin from $2\pi^0$, 18: 20960
decay of, unitary symmetry model for two-body pseudoscalar-meson, (T), 20: 24068
decay widths of, current algebra for, 20: 21654
detection and measurement of, possible method for, 18: 30511 (JINR-P-1654)
effect on nuclear forces, (T), 19: 14626
effects in nucleon-nucleon interactions, (T), 19: 31067
effects on meson (π)-proton interactions at 2 Bev, 18: 14961
effects on meson (π)-nucleon interactions, (T), 19: 14384
effects on photon–proton scattering, 18: 14862
exchange in meson (π) interactions, parameters for, (T), 20: 4607
existence in $\pi^- + p$ reaction at 6.1 Bev/c, 17: 16965
isotopic spin, 18: 24463
isotopic spin, 18: 24466
isotopic spin of, 17: 39910
mass of, correlations to orbital angular momentum of, 18: 7496
meson (π) scattering near, 17: 29548
Pomeranchuk trajectory for, Regge recurrence of, 19: 25341
production and properties of, 17: 9268
production and properties, (E), 19: 10105
production and properties of, review of, 19: 16510
production in deuteron–meson (π^+) interactions at 6 Bev/c, 18: 30570
production in meson (π)-nucleon interactions at 2 Bev, effects of, 17: 29532
production in meson (π^+)-proton interactions at 3.43 and 3.54 Bev/c, partial cross sections for, 18: 2651
production in meson (π^-)-proton interactions at 3.5 Bev/c, 18: 9200
production in meson (π^+)-proton interactions at 3.5 Bev/c, 18: 14962
production in meson (π^-)-proton interactions at 10 Bev/c, 18: 20960
production in meson(π^-)-proton interactions at 3 Bev/c, sonic spark chamber for study of, 18: 31893 (CERN-64-30(p.251-60))
production in meson (π^-)-proton interactions at 3.5 Bev/c, 18: 36354
production in meson (π^-)-proton interactions at 2.75 Bev/c, 19: 16513
production in meson (π^-)-proton interactions at 3.7 Bev/c, (E), 19: 25385
production in meson (π^+) interactions with deuterons at 3.29 Bev/c, (E), 20: 27814
production in proton–antiproton annihilations at 5.7 Bev/c, (E), 20: 19498
properties, (T), 19: 29103
properties from p-wave amplitudes of meson (π)-meson (π) interactions, (T), 20: 21694
properties of, electron-pair model for, (T), 19: 10059
properties of, field-theoretical, 19: 31241(R) (UCRL-12473(p.1-30))
properties of, review of, 19: 14314 (JINR-P-1887)
relation to mesons (B) (1.22 Bev), 18: 12954
spin, 17: 31318
spin, 18: 9200
spin, 18: 16792
spin, (E), 19: 25385
spin, (E), 20: 34205
spin, (E), 19: 39480 (NP-15247)
spin from meson ($\pi^\pm$)-nucleon interactions, (E), 20: 9730
spin of, from meson (π^-) proton interactions at 10 Bev/c, (E), 20: 41795(R) (MIT-2098-251, pp 21-36)
spin of, measurement, 19: 31004 (CU-1932-240)
theory of, SU_3 symmetry in, 18: 44554

MESONS (K)

abundance of cosmic, electromagnetic cascades for K/π ratio, (T), 19: 12124
angular distribution from proton pair annihilation, 18: 12910 (PAN-450/VII)
beam separator design for, crossed-field, 18: 34365 (BNL-8145)
beams of, characteristics of alternating-gradient synchrotron, 17: 23634
beams of, design and performance of CERN, 17: 23635
bound-state ($\bar{K}NN$) existence, 18: 9151
capture in cobalt-58-silicon fluoride crystals, gamma emission for dealignment and ionic coupling in, 17: 26581
charge symmetry in associated production, 16: 2305(R) (UCRL-9704)
classification of, summary of octet theory of SU(3) for, 20: 25904
coupling in ($\pi\pi$-$K\bar{K}$), meson (ρ) model in, 19: 8194
coupling to baryons, 18: 44566
decay, 18: 44520 (NEVIS-125)
decay amplitude (3π), analytical problems, 16: 18380
decay amplitudes for, $|\Delta I| = \frac{1}{2}$ rule for nonleptonic, 20: 27828
decay amplitudes for, commutation properties of weak hamiltonian for, 20: 34185
decay and production of K* type of, 16: 32294 (UCRL-10232)
decay and properties of, review of theory, 17: 9471
decay and properties of, bibliography on, 17: 9472
decay as test of $\Delta S = \Delta Q$ selection rule, leptonic, 16: 7020 (TID-14474)
decay branching ratios for, leptonic and nonleptonic, 18: 6012
decay, angular correlation in lepton, 16: 22851 (JINR-E-946)
decay, Dalitz plots and Feynman graphs for 3-pion, 16: 19714
decay, effects of intermediate vector bosons on rates of radiative, 16: 27978
decay, form factors for 3-lepton, 16: 8143
decay, phase shift in final-state meson (π) interactions in, (T), 20: 36055
decay, violation of $\Delta Q = \Delta S$ rule in lepton, 16: 22958
decay into three mesons (π), effects of meson resonances on, (T), 19: 4919
decay modes of K*, 17: 41806
decay modes of, resonances in three-meson (π), 18: 9170
decay modes of, form factors in three-lepton, 18: 30605
decay modes of, survey on, 20: 7802 (UCRL-16473)
decay modes, leptonic, 16: 27898 (CTSL-34)
decay ($\mu + \nu + \gamma$), vector boson effects in, 17: 22492
decay of (K_2^0), 2π, 18: 32618
decay of, analysis of three-body leptonic, 17: 39886
decay of, branching ratio for gamma and meson (π), 17: 28190
decay of, intermediate boson theory of leptonic and nonleptonic, 17: 34799
decay of K*, (K-2π), (T), 19: 20984
decay of K*, selection by A invariance, 18: 22758
decay of ($K^\wedge$), meson (π) double- and single-production ratios, 16: 10863
decay of K-π resonance (K*), effects of spin-parity assignments on, 16: 26157
decay of K+, unitary symmetry breaking in, (E/T), 19: 41366
decay of, kinematical tables for two-body, 17: 29495 (CERN-63-20)
decay of (K–π) resonance state, branching ratio and spectra of leptonic, 17: 22428 (LNF-63/16)
decay of (K13), test for six-body Fermi coupling description of strangeness changing weak interactions from, 17: 34804
decay of, model for weak leptonic interactions in, 18: 2621
decay of, review on, 18: 7466 (BNL-7509)
decay of, three-body leptonic, 17: 31338
decay of, (3π), 17: 29502 (UCRL-10492)
decay of, algebra of currents for form factors for three-body leptonic, 20: 34189
decay of, axial vector current in leptonic, 18: 40318
decay of, boson-pole model for pionic, (T), 19: 6554
decay of, bounds on f_-/f_+ for three-body leptonic, 20: 44260
decay of, branching ratios for leptonic, (T), 20: 11658
decay of, breakdown of CP invariance in, (T), 19: 4959
decay of, C violation in, (T), 20: 25874
decay of, charge asymmetry in radiative 2π, (T), 20: 11584(T)
decay of, commutation relations for leptonic, (T), 20: 9772
decay of, contribution to cosmic meson (μ) flux from, (E), 20: 37482
decay of, CP violation in 3-π, (T), 19: 16536
decay of, CP violation and nonlocality in three-body leptonic, (T), 19: 18806
decay of, CP violation in 2π, (T), 19: 43072(T)
decay of, current commutation relations for leptonic, 20: 19479
decay of, current commutation rules and $\Delta T = \frac{1}{2}$ rule in, 20: 21650
decay of, current commutation relations and Cabibbo angles for leptonic, 20: 25819
decay of, current commutation relations in nonleptonic, (T), 20: 25838
decay of, current algebra and $|\Delta I| = \frac{1}{2}$ rule for nonleptonic, 20: 37759
decay of, current-commutator calculation of four-body leptonic, (T), 20: 39815
decay of, dispersion theory model for 3π, 19: 12234
decay of, dynamics and symmetries of nonleptonic, (T), 20: 4676
decay of, effect of final-state strong interactions on probability of (3π), (T), 20: 6086
decay of, effects of weak vector bosons in, 20: 4629
decay of, forbidden transitions in pole models with unitary symmetry, (T), 19: 16584
decay of, form factors for four-body leptonic, (T), 19: 16626
decay of, form factors for three-body leptonic, (T), 20: 27870
decay of, form factors for three-body leptonic, 20: 36028 (IC-66/74)
decay of, four-body leptonic, (T), 19: 39589
decay of, intermediate boson theory of leptonic, 17: 13404
decay of, Lagrangian model for form factors of three-body leptonic, 20: 39796
decay of, lepton pairs in, (T), 20: 25837
decay of, leptonic, 18: 10906
decay of, leptonic, 20: 25873
decay of, matrix elements for leptonic, (T), 20: 6035 (CERN-64-13 (Vol.4), pp 1-49)
decay of, matrix elements for leptonic, 20: 17415
decay of, mechanism for 2π, (T), 19: 12196
decay of, meson (μ) interactions with intermediate weak boson in, (T), 20: 25840
decay of, meson (π) final-state interactions in, 20: 34154(R) (UCR-34P107-33)
decay of, meson (ρ) universality for rate of $\mu\nu$, 20: 44238
decay of, meson (σ) hypothesis for, (T), 19: 41518
decay of, models for, 18: 14803 (ISU-10)
decay of, negative CP-parity of 2π, (T), 20: 13473(T)
decay of, neutrino interactions in, (E), 20: 31986 (NEVIS-148)
decay of, nonleptonic, (T), 20: 15366
decay of, partially conserved axial-vector current hypothesis for non-leptonic, 20: 21666
decay of, phenomenological description of, 20: 21701
decay of, positron momentum spectra from, (E), 20: 27833
decay of, properties of 3-π, 18: 12937
decay of, radiative corrections to electron polarization in, (T), 19: 8169
decay of, resonance effects in, 18: 10849 (JINR-P-1467)
decay of, resonances in 3-π, 18: 21021
decay of, selection rules for nonleptonic, 18: 28380
decay of, sigma hypothesis in, 20: 17422
decay of, SU(3) for 2π, 20: 46374
decay of, SU(3) symmetry for 2π, (E), 20: 1022
decay of, SU(9) composite symmetry model for 2π, 20: 34275
decay of, sum rules for CP-nonconserving, 20: 39812
decay of, symmetry in meson (π), 18: 40327
decay of, symmetry for 2π, (T), 19: 8208
decay of, T violation in meson (μ) polarization in, (T), 20: 19488
decay of, theory of leptonic, 18: 44578
decay of, three-body leptonic, 19: 37664
decay of, time-reversal invariance in, (E/T), 20: 17404
decay of, unitary symmetry in nonleptonic, 18: 10947
decay of, weak interactions in leptonic, 18: 32628
decay of, weak interaction form factors in, 19: 8231
decay of, weak vector bosons in, 18: 32597
decay of, 2π, (T), 20: 15369
decay of, 2π, 18: 42627(R) (ANL-6879(p.88-113))
decay of, 3π, (T), 20: 41900
decay probabilities for K*, in unitary symmetry, 18: 14866
decay radiative modes, leptonic, 16: 6971
decay rate from meson (μ) mass, maximum, 20: 15344
decay rate ratios for, 19: 23455
decay rates, comparison of $e + \nu$ and $\mu + \nu$, 16: 24700 (TID-16108)
decay rates, intermediate-boson model for leptonic, 16: 27974
decay rates of, conserved currents in, 17: 5219
decay review, 17: 9470
decay schemes of K-π resonance state, 16: 3633
decay spectra of, 3π, 20: 32010
decays of, model for $\Delta S/\Delta Q = -1$, 17: 9278
decays of, amplitudes for 2π, 20: 41835
decays of, $\Delta I = \frac{1}{2}$ and $\Delta S = \Delta Q$ rules in weak, 18: 28424
decays of, effective $\Delta I = \frac{1}{2}$ rule in 3π, 20: 41840
decays of, SU(3) symmetry in nonleptonic (T), 19: 3061
decays of, 3π, (T), 20: 4635
detection using emulsions, 19: 44443 (CERN-65-4(Vol.II), pp X61-6)
dispersion relations, interactions, and parities, 16: 10920
dynamical model of K* resonance, 17: 31336
effective-mass distribution in Ξ (K-$\bar{K}$) systems, 17: 5254
effects of vector, on Y* resonances, 18: 30606
electromagnetic properties of, effects of meson (π) resonances on, 17: 37992
electromagnetic self-energies and unitary symmetry of K*, 18: 22759
electromagnetic structure, 16: 4731

energy loss straggling in matter, distributions of, (T), 19: 9894 (NAS-NRC-PUB-1133(p.187-203))
energy losses and ranges in matter, tables, (E), 19: 8005 (NASA-SP-3013)
energy spectra in CERN neutrino experiment, determination of, (E/T), 20: 21604 (CERN-65-32, pp 121-6)
evidence for new, review, 17: 9466
exchange in hyperon (Λ)-nucleon interactions, potentials from, 18: 39274
exchange in hyperon (Λ)-nucleon interaction in hyperfragments, (T), 19: 16541
exchange in hyperon (Λ)-proton interactions at 0.5 to 3.0 Bev/c, (T), 19: 16544
exchange of K* in antiproton-proton interactions with hyperon (Λ) pair production, 18: 7531
existence and spin of (K*), 16: 17048
field equations for multiplets of, transformation invariance in free, 17: 24292
form factors for, meson (ϕ) contribution to, (T), 20: 11598
generation of K* resonance by ρ exchange, 17: 24341
global symmetry in fourth-order perturbation, 16: 22885
identification in bubble chambers at 0.15 to 4.0 Bev/c, 16: 13921
interaction amplitudes, 16: 26083 (JINR-P-1000)
interaction resonance ($K\bar{K}$) at 1020 Mev, interpretation as T = 0 vector meson decay, 17: 9259
interaction resonances (K-$\bar{K}$) of, quantum numbers of 1.02-Bev, 17: 26362
interaction resonance state ($\bar{K}$-N) coupling to (Σ-π), 17: 28136 (BNL-6363)
interaction resonances with mesons (π), 18: 2595 (UCRL-10291)
interaction resonances with mesons (π), boson icosuplet of, 18: 28386
interaction with nucleons, (T), 20: 39840
interaction with protons at 3 to 5 Bev, cross sections, 16: 22373
interactions ($K\bar{K}$) of, meson (ϕ) interpretation in, 18: 26320
interactions (K,$\bar{K}$) of, Schroedinger bootstrap model for meson (ρ) production in, 19: 8187
interactions and production, 18: 22593(R) (SLAC-27)
interactions at high energies, total cross sections for, 17: 9238
interactions at high energy, experimental and theoretical data on elastic, 17: 11507
interactions at high energy, cross section combinations for, 17: 11529
interactions in jet showers, secondary angular distribution and momenta for primary energy of, (T), 19: 47275
interactions of $\bar{K}$ with nucleons, pion-hyperon production and scattering, 16: 4692 (TID-13955)
interactions of (K-$\bar{K}$), resonance, 17: 22474
interactions of $\bar{K}$ with K*, one pion exchange in, 18: 9183
interactions of mesons (K*) with mesons ($\bar{K}$*), SU(3) model for, effects on multichannel Schroedinger equation, 18: 4450
interactions of mesons (K) with nucleons in I = 1 $P_{3/2}$ channel, cross sections for, 18: 7560
interactions of mesons ($\bar{K}$) with hyperons (Σ) in 27-fold representation, dynamics of, 20: 21674
interactions of nucleons with anti-, effects on π-Λ and π-Σ amplitudes, 16: 33772
interactions of, parity in (KΣN), 17: 9384
interactions of, review of properties of strong, 17: 5054
interactions of, resonances in, 17: 7043
interactions of, resonances in, 17: 24186
interactions of, with emulsion nuclei at 0 to 790 Mev, 16: 32267 (AFOSR-1728)
interaction of, with nucleons, formulation by many channel N over D method, 17: 13467
interactions of, bootstrap calculations for, 18: 10935
interactions of, bootstrap solution for, (T), 19: 12232
interactions of, CP violation in weak, (T), 20: 19480
interactions of, inversion expansion with non-Abelian group of parity tripod for strong, (T), 20: 15494
interactions of, meson (ρ) parameters in, 19: 16551
interactions of, resonances in, 18: 36269
interactions of, resonances in, (T), 19: 10015 (JINR-P-1808)
interactions of, research on, (E/T), 20: 15307(R) (COO-1261-22)
interactions with mesons (π), relative Σ-Λ parity, 16: 2436
interactions with nucleons, cross sections, 16: 25877(R) (ANL-6534)
interactions with nucleons, phase shifts for peripheral, 16: 961
interactions with nucleons, relation to antihyperon excited state, 16: 5894
interactions with neutrons and protons, branching ratio of π^-/π^+, 16: 8062 (NP-11232(p.321-6))
interactions with nucleons, meson (μ) mass calculations in, 16: 8107
interactions with mesons (π), resonance effects on decay, 16: 8143
interactions with nucleons, branching ratios, 16: 10835
interactions with baryons, decay regularity of unstable particles formed in, 16: 12332 (JINR-D-824)
interactions with nucleons, isobar mechanism, 16: 13900
interactions with mesons (π), effects on nucleon form factors, 16: 15574
interactions with protons at 3 to 5 Mev, 16: 5491 (JINR-P-782)
interactions with mesons (K), dispersion relations, 16: 15606
interactions with mesons (π), dispersion relations, 16: 15607
interactions with mesons (π), s-wave amplitude for, 16: 17024
interactions with mesons (π), K-π and π-π resonance effects on p-wave, 16: 17025
interactions with mesons (π) at low energies, strangeness violation in, 16: 17048
interactions with emulsion nucleons at 10^{10} to 10^{13} ev, angular distributions, 16: 21308
interactions with nucleons, effects of hyperon parities and meson resonances on scattering, 16: 22852 (NP-11761)
interactions with nucleons, one-meson-exchange domination by lowest partial waves in, 16: 22893
interactions with mesons (π), resonance Regge representation, 16: 22915
interactions with mesons (π), meson (K*) production in, 16: 24734
interactions with particles at high energies, cross sections, 16: 22943
interactions with protons at 1 Bev, elastic, 16: 26071 (JINR-P-817)
interactions with hyperons and nucleons, form factors for, 16: 26089 (NP-11832)
interactions with mesons (π), effects on K_{e3} and $K_{\mu 3}$ decays, 16: 26103
interactions with mesons (π), resonant states at masses 730 and 885 Mev, 16: 26134
interactions with nucleons, S-wave meson ($\bar{K}$)-nucleon scattering amplitudes, 16: 26137
interactions with mesons (π), properties of resonant, 16: 26158 (UCRL-10167)
interactions with nucleons, polarization in, 16: 26191
interactions with nucleons, hyperon-meson (π) resonances in, 16: 29697
interactions with protons, parity in, 16: 32342
interactions with mesons (π), resonance effects in, 16: 33751
interactions with mesons (π), scattering amplitudes for, 16: 33755
interactions with antibaryons and baryons, effects on annihilation processes, 17: 11547
interactions with deuterons at low energy, binding effects and recoil magnitude in impulse approximation for, 17: 39922
interactions with hyperons (Λ) and (Σ), parity in, 17: 9383
interactions with hyperons (Σ), mesons (K) and (π), and nucleons, 17: 28172
interactions with hyperons (Λ), (Σ), and (Ξ) and nucleons, coupling constants for strong, 17: 31373
interactions with hyperons (Ξ) and nucleons, Sawada transformation for multichannel, 17: 34807
interactions with hyperons (Λ) and nucleons, vertex functions for, 17: 34809
interactions with mesons (π), resonances in, 17: 9226
interactions with mesons (π), effects on electromagnetic structure of nucleon, 17: 13464
interactions with mesons (π), decay of resonances in, 17: 13371
interactions with mesons ($\bar{K}$) and (π), resonances in, 17: 15138
interactions with mesons (π), low energy resonances in, 17: 15073 (EFINS-62-5(Rev.))
interactions with mesons (π), spin of resonance, 17: 20949
interactions with mesons(π), parity and spin from decay modes of resonance, 17: 26319
interactions with mesons ($\bar{K}$), quantum numbers for resonance, 17: 26315
interactions with mesons (K) and (π), properties of elastic, 17: 32951
interactions with mesons ($\bar{K}$), physical interpretation of the unphysical region in, 17: 39854
interactions with mesons ($\bar{K}$), coupling constants for generation of mesons (ϕ) from, 17: 39890
interactions with mesons (π) in decays, coupling constant for, 17: 39914
interactions with mesons (π), self-consistency of K* resonance in, 17: 39937
interactions with mesons (π), s-wave phase shifts in, 17: 41753
interactions with mesons (π), resonant state production in, 17: 41812
interactions with nucleons, strange particle production from, 17: 2177
interactions with nucleons, effect of ρ and ω exchanges on, 17: 5246
interactions with nucleons, amplitudes for, 17: 9276
interactions with nucleons, s-wave scattering parameters for, 17: 9383
interactions with nucleons at high energy, total cross sections and Regge poles for, 17: 11493 (TID-16216)
interactions with nucleons, and meson (Yβ) scattering amplitude in, 17: 11514
interactions with nucleons, resonances in, 17: 13367
interactions with nucleons, effects on K^--p interactions, 17: 15133
interactions with nucleons, effects of resonance on, 17: 15117
interactions with nucleons, angular distribution of particles produced near threshold in, 17: 17098

interactions with nucleons at low energies, contributions of mesons (ρ) and (ω) to scattering amplitudes of, 17: 20893
interactions with nucleons, domains of analyticity for, 17: 22504
interactions with nucleons, application of Boundary Condition Model to, 17: 24188
interactions with nucleons, vector meson exchange effects on amplitudes of S-wave, 17: 24350
interactions with nucleons at high energies, double-charge exchange cross sections for, 17: 26326
interactions with nucleons at high energy, 17: 29504 (UCRL-10834)
interactions with nucleons, two-channel formalism for S-wave, 17: 31372
interactions with nucleons, analyticity regions of Feynman integrals in, 17: 31379
interactions with nucleons at low energies, Y_1^* production in, 17: 36605
interactions with protons, review, 17: 9467
interactions with protons at 3 to 19 Bev/c, total cross sections for, 17: 13433
interactions with protons at 2 to 45 Bev, 17: 15081 (NP-12588)
interactions with protons, cross sections and polarizations for, 17: 17003
interactions with protons, fermion Regge poles for asymptotics of, 17: 32933
interactions with mesons (π), theory for p-wave resonance in, 18: 836 (BNL-5569)
interactions with polarized protons, 18: 866 (UCRL-10949)
interactions with mesons (K), contributions to nucleon form factors of intermediate-state, 18: 2671
interactions with mesons (π) at 730 Mev, SU(4) assignments for resonance, 18: 2664
interactions with neutrons and protons, meson (π) production in, 18: 4469
interactions with mesons ($\bar{K}$) and (π), mass correlations to orbital angular momentum in resonance states from, 18: 7496
interactions with hyperons (Λ), Low equation for, 18: 7543
interactions with protons, production of cascade particles in, 18: 9135
interactions with mesons (π), analytical properties of scattering amplitudes for, 18: 9203
interactions with nuclear Coulomb field, meson (ω^0) and (ρ^0) production in, 18: 9169
interactions with mesons (K) and (π), review of resonances in, 18: 12903 (JINR-P-1490)
interactions with nucleons, amplitude for, 18: 12911 (PAN-451/VII)
interactions with mesons (π), resonance production in, 18: 14949
interactions with protons, Regge pole hypothesis in, 18: 14932
interactions with protons, feasibility of using 600- to 1000-Bev accelerators to study elastic, 18: 16749 (BNL-7534(p.83-7))
interactions with mesons (π), quantum numbers for K2π and K3π resonances in, 18: 18661
interactions with mesons (π), model for K$\pi\pi$ resonance in, 18: 18694
interactions with mesons (π), K$\pi\pi$ resonances in, 18: 18696
interactions with mesons ($\bar{K}$), resonance predictions in, 18: 18698
interactions with hyperons (Λ), Ξ^* production in, 18: 18703
interactions with protons, analyticity in complex angular momentum plane for diffraction, 18: 18687
interactions with protons at 2.00 Bev/c, elastic, 18: 20954
interactions with mesons (π), s- and p-wave resonances in, 18: 20977
interactions with hyperons (Ξ) and nucleons, motion of poles in resonance, 18: 21016
interactions with nucleons, S-wave, 18: 21020
interactions with nucleons, hyperon decay in, 18: 22770
interactions with mesons ($\bar{K}$), vector meson exchange in, 18: 26342
interactions with mesons (π), properties of resonance, 18: 28425
interactions with protons, resonance parities and spins from polarized targets in, 18: 30553
interactions with protons, digital data and on-line computer system for, 18: 31871 (CERN-64-30(p.11-20))
interactions with hyperons (Ξ), hyperon (Ω^-) as bound state in, 18: 32604
interactions with deuterons, mesons (π) and nucleons, dispersion relations for, 18: 32629
interactions with mesons (π), 18: 34534
interactions with hyperons (Ξ), hyperon (Ω^-) production in, 18: 34568
interactions with mesons ($\bar{K}$), resonance, 18: 34636
interactions with mesons (π), strangeness-changing currents in resonance, 18: 36261
interactions with mesons (π) and protons, spin-parity test for resonances in, 18: 36281
interactions with nucleons, resonances in, 18: 36285
interactions with protons, parity and spin of resonances in, 18: 36276
interactions with protons, spin of bosons from, 18: 36336
interactions with nucleons, model for strong, 18: 37890
interactions with nucleons, masses of resonances in, 18: 37948
interactions with nucleons, 18: 37987
interactions with deuterons, impulse approximation for elastic, 18: 40274
interactions with nucleons, selection rules and W_3 symmetry for, 18: 40319
interactions with mesons (π), resonance, 18: 42368 (JINR-E-1804)
interactions with neutrons and protons at 6 to 22 Bev/c, total cross sections for, 18: 44515 (BNL-8323)
interactions with protons at 7 Bev/c, elastic-inelastic discrimination in, 18: 44517 (CERN-64-38)
interactions with mesons (K), resonances in, 18: 44530
interactions with mesons (π), resonances in, 18: 44530
interactions with nucleons, secondary diffraction peaks in, 18: 44562
interactions with nucleons, parameters for s-wave, 19: 1274
interactions with nucleons, vector-meson effects in (T), 19: 1293
interactions with distant matter, (T), 19: 4959
interactions with nucleons, A-invariance in, (T), 19: 6543
interactions with nucleons at high energies, models for, (T), 19: 6551
interactions with nucleons, dispersion relations for amplitudes in, 19: 10039
interactions with mesons (π), resonance processes in, (T), 19: 10040
interactions with nucleons, Y_1^* Regge pole in, (T), 19: 10053
interactions with mesons (π), K* (890) in, (T), 19: 12298
interactions with mesons (π), properties of resonance, 19: 14314 (JINR-P-1887)
interactions with mesons (π), energy peaks in, (T), 19: 14335
interactions with mesons (π), scalar resonances in, (T), 19: 16540
interactions with nucleons, total cross sections for, (T), 19: 16615
interactions with baryons, s-wave virtual states in amplitudes for, (T), 19: 16621
interactions with mesons (η) and (π), symmetry in bootstrap model for, (T), 19: 16627
interactions with deuterons, anomalous singularities in elastic, (T), 19: 18779
interactions with mesons (π), resonances in, (T), 19: 18782
interactions with mesons (π), K*(888) in, (T), 19: 18847
interactions with mesons (π), K$\pi\pi$ (1160) resonance in, (E), 19: 18851
interactions with hyperons (Ξ), hyperons (Ω^-) as bound state in, (T), 19: 20970
interactions with mesons (π) at low energies, K* production in, (T), 19: 21058
interactions with nucleons at high energies, Regge trajectories for, (T), 19: 21063
interactions with nucleons at high energies, strange particle production in, (T), 19: 23466
interactions with hyperons (Λ), resonance, (T), 19: 25354
interactions with nucleons at 800 Mev/c, SU(3) invariance in, (T), 19: 25356
interactions with baryons, weak, (T), 19: 25366
interactions with mesons (ρ), coupling constant for, (T), 19: 27281
interactions with baryons, coupling constants for, (T), 19: 31039
interactions with nucleons, microscopic non-causality in, (T), 19: 32949 (LADC-6480)
interactions with nucleons at low energies, s-wave, (T), 19: 35157
interactions with mesons (K) and (π), bootstrap theory for amplitudes of, 19: 35036
interactions with mesons ($\bar{K}$), review on, 19: 37644
interactions with nucleons, resonances in three-particle production, (T), 19: 37649
interactions with deuterons resonance, (T), 19: 39564
interactions with nucleons, peripheral production and decay of K* in, (E/T), 19: 39576
interactions with nucleons at low energies, model for, (T), 19: 39592
interactions with mesons ($\bar{K}$) and (π), resonance production in, (E), 19: 41418
interactions with nucleons at high energies, Regge-pole model for, (T), 19: 41426
interactions with nucleons, resonance effects in, (T), 19: 41506
interactions with nucleons, Regge poles Y_1^* and Y_3^* in scattering amplitude for, (T), 19: 41352
interactions with nucleons, theory of $N_{1/2}^*$ and Y_1^* production in, 19: 43144
interactions with nucleons at high energies, polarization and Regge poles in, (T), 19: 45044 (UCRL-16186)
interactions with mesons (π) at low energy, dispersion relations for, (T), 19: 45085
interactions with nucleons at high energy, absorption model for charge-exchange, (T), 19: 45087
interactions with mesons ($\bar{K}$), nucleon isoscalar form factor from elastic, (T), 19: 47371
interactions with protons, strangeness-conserving axial-vector coupling constant for, 20: 2722
interactions with protons, triangular diagrams for cross sections of, (T), 20: 2741
interactions with nucleons, single and double resonance production in,

(T), 20: 6069
interactions with photons, resonance model for magnetic polarizability from, 20: 6090
interactions with protons, hyperon (Ξ) production in, (E), 20: 6099
interactions with mesons (K) and (π), resonance production in, (E), 20: 11575
interactions with mesons (π), iterative self-consistent solutions for S-wave, 20: 11601
interactions with nucleons, Y_{03}^{*}(1815) production from, (T), 20: 11632
interactions with mesons (π), p- and s-wave phase shifts for, (T), 20: 11648
interactions with mesons (π), meson (K_{e4}) decay for analysis of low-energy s-wave, (T), 20: 11654
interactions with mesons (π), cross section determination for, (T), 20: 13449 (JINR-P-2433)
interactions with nucleons, testing broken M(12) symmetry by vector exchange in, (T), 20: 15421
interactions with nucleons, $\bar{U}(12)$ symmetry for, 20: 15390
interactions with mesons (π) at low energies, sum rules for, 20: 17470
interactions with mesons (π), algebra of currents for, 20: 19541 (UR-875-121)
interactions with nucleons, 2+ meson exchange in, (T), 20: 19512
interactions with mesons (K̄), coupling constants and p-wave amplitudes for, (T), 20: 19520
interactions with nucleons in 27-fold representation, dynamics of, 20: 21674
interactions with nucleons, nucleon–hyperon (Λ)–meson (K) coupling constants from dispersion relations for, 20: 25827
interactions with mesons (π), equivalent-potential calculation of amplitudes in resonance region for, 20: 27854
interactions with nucleons, exact N/D method for phase shifts for, 20: 27855
interactions with nucleons, differential cross sections and structures of, (T), 20: 27874
interactions with protons, Regge cuts in high-energy elastic, (T), 20: 30160
interactions with nucleons, dispersion relations and symmetry groups for, 20: 30018
interactions with nucleons at low energies, N/D methods for s-wave, 20: 32024
interactions with mesons (π), K* resonance in, (T), 20: 34251
interactions with protons, hyperon (Λ) and (Σ) production from, 20: 37756
interactions with protons, kinematic enhancement of resonance production in, 20: 37769
interactions with mesons (K̄), exact bootstrap solution for, 20: 37808
interactions with nucleons, K* production threshold from, (T), 20: 39778
interactions with nucleons, scattering lengths for, (T), 20: 41846
interactions with nucleons, cross sections for, (T), 20: 41898
interactions with mesons (π), one-meson theory for charge distribution from inelastic, 20: 44183
interactions with mesons (π), meson (μ^{+}) polarization from resonances, (T), 20: 44270
interactions with protons at high energies, models for inelastic two-body, 20: 44359
isospin, parity, and spin of, 17: 22437 (SLAC-13)
isospin-½ states of, detection of, 16: 33761
isovector charge, 17: 11542
mass formulas in U_4 symmetry, (T), 19: 16545
mass measurements of, 20: 7804
mass of, models for, 19: 14348
mass relations in octet, 18: 40309
mass relations of K*, in octet, 18: 40309
momentum of, from hyperfragment production by 9-Bev protons in photographic emulsions, 17: 20936
momentum spectra of secondary, transverse, 18: 28344
momentum/velocity ratio of fast, relativity-theory tests by, (E), 20: 1117
pair production and decay, properties of, 16: 32351
pair production in meson interactions (π-π), 18: 34534
pair production in meson (π)-meson (π) interactions at low energies, (T), 20: 39833
pair production in meson (π⁻)-proton interactions at 2.0 to 4.0 Bev/c, (E), 20: 41802 (UCRL-16832)
parities (relative), 16: 10844
parity and spin of K, K̄, K*, and K̄*, 17: 32941
parity of (KΛN) and (KΣN), 17: 9467
parity relative to hyperons (Λ), 17: 22469
photoproduction at high energies, 16: 29680
photoproduction at low energy, 18: 14886
photoproduction at high energies, review on, (T), 20: 15442
photoproduction in hydrogen, 16: 25947 (NP-11977(p.137-9))
photoproduction of, Regge poles in Drell calculations of cross section for, 17: 21110 (SLAC-5(p.20-8))
photoproduction of high-energy, Regge pole hypothesis in, 17: 39888
photoproduction of, resonance model for, 18: 9206
photoproduction of, method of identification of, 19: 41527
photoproduction on nucleons, resonance model for, 16: 31043 (NYO-10133)
photoproduction on nucleons, theoretical review, 16: 32276 (NP-12035)
photoproduction on nucleons, 17: 19107
photoproduction on deuterons, 17: 20564(R) (TID-18442)
photoproduction on nucleons, dispersion relations for, 17: 39857
photoproduction on hydrogen, 18: 10854 (LNF-63/47(p.1-35))
photoproduction on nucleons, resonance model for, 18: 12962
photoproduction on nucleons at high energies, 18: 18735
photoproduction on nucleons at high energies, momentum-transfer distributions in, (T), 19: 47389
photoproduction on nucleons, polarization coefficients for, (T), 20: 17407
photoproduction on deuterons and nucleons, isotopic relations for amplitudes of, (T), 20: 19518
photoproduction with hyperons (Λ) on protons, resonances in, (T), 19: 4936
prediction of, vector theory, 17: 11496 (TID-17742)
production and properties of K* (730 Mev), 18: 9191
production and spin of (K*), total cross sections and angular correlations for, 17: 11487 (NP-12488)
production at Bevatron, 18: 37820 (UCRL-11527)
production by antinucleon annihilation in meson (π)-nucleon and nucleon-nucleon collisions, 17: 16953 (JINR-P-1163)
production by antiproton annihilations in hydrogen, 17: 9376
production by meson (π⁻)-proton interactions, associated, 17: 19131
production by proton reactions with aluminum, beryllium, and iron at 30 Bev, 17: 7259
production by proton-proton interactions at 24.5 Bev/c, cross sections for, 17: 39883
production in antiproton annihilation, conservation laws, 17: 2334
production in antinucleon annihilation and meson (π)-nucleon interactions, cross sections for, 17: 32920
production in antiproton-proton annihilation, 17: 6947 (IA-768)
production in antiproton-proton interactions, 17: 9324
production in antiproton-proton annihilation, statistical model for, 17: 20915
production in antiproton-proton annihilation, (T), 19: 18868
production in antiproton-proton annihilations at rest, (E), 19: 45122
production in antiproton-proton annihilation at 3.7 Bev/c, cross section for, (E), 20: 15338
production in antiproton-proton annihilation at rest, channel branching ratios and invariant mass distributions for, (E), 20: 27845
production in antiproton-annihilation at rest in deuterium, (E), 20: 29992 (UCRL-16717)
production in baryon-nucleon interactions, Regge hypothesis for multiple, 17: 34806
production in deuteron-meson ($\pi^{\pm}$) interactions, systematics of, 17: 9366
production in electron-positron interactions, 16: 25906 (LNF-62/37 (p.166-79))
production in electron-nucleon interactions at high energies, (T), 19: 29080
production in emulsions by cosmic particles, 18: 40623
production in meson (π) interactions with mesons (π), effects of resonances on form factor, 16: 13870 (NYO-10127)
production in meson (π^{-}) interactions with protons, resonances in, 16: 18324(T) (UCRL-Trans-807)
production in meson (π^{-}) interactions with protons at 16 Bev/c, 16: 24737
production in meson (π^{-})-proton interactions at 1.89 and 2.10 Bev/c, cross sections for, 16: 26146
production in meson (π^{-})-nucleus reactions at 2 Bev/c, 17: 2173
production in meson (π^{-})-proton interactions, final-state interactions in, 17: 9256
production in meson ($\pi^{\pm}$)-proton interactions, 17: 9365
production in meson ($\pi^{\pm}$)-proton interactions, 17: 9367
production in meson (K^{-})-proton interactions, 17: 9369
production in meson (π^{-})-proton interactions, 17: 13452
production in meson (π^{-}) reactions with hydrogen at 16 Bev/c, 17: 26323
production in meson (π^{-}) reactions with complex nuclei, 17: 26425 (NP-12886)
production in meson (K)-proton interactions at 2.3 Bev/c, 17: 32898 (BNL-7105)
production in meson (π^{-}) –proton interactions at 7.5 Bev/c, 18: 22722 (JINR-P-1586)
production in meson (π) reactions with beryllium-9, cross sections for, 18: 24587 (JINR-P-1584)
production in meson (π)-nucleon interactions, models for, 18: 26281
production in meson (π)-proton interactions at 1.5 to 2.4 Bev/c, 18: 36255 (UCRL-11360)

production in meson (π) reactions with emulsion nuclei at 4.5 Bev, 18: 38082(T) (AEC-tr-6398(p.153-6))
production in meson (π^-)-proton interactions at 10 Bev/c, 18: 40294
production in meson (π^-)-proton interactions at 10 Bev/c, 18: 40268
production in meson (π^-)-proton interactions at 10 Bev (E), 19: 1401
production in meson (π^-) reactions with carbon, 19: 3032
production in meson (π)–nucleon interactions at 5 Bev/c (T), 19: 3048
production in meson (K^+)–proton interactions at 3 Bev/c, 19: 4941
production in meson (π)-nucleon interactions, pair, (T), 19: 14354
production in meson (π^-) reactions with emulsion nuclei at 7.2 Bev/c, cross sections for, 20: 1224
production in meson (K^+)-proton interactions at 3.52 Bev/c, (E), 20: 39784
production in meson (K)-meson (π) interactions, meson (μ^+) polarization in, (T), 20: 44270
production in neutrino reactions at high energies, 17: 19176
production in neutrino interactions with protons, cross section and form factors for, 17: 22464
production in neutrino-nucleon interactions, single, (T), 19: 23477
production in nuclear collisions up to 5×10^9 Bev, π-K production ratio, 16: 19668
production in nucleon-proton interactions at 14 Bev, 18: 9084 (NP-13484)
production in nucleon-proton interactions at 22 Bev (E/T), 19: 1400
production in p-π interactions at 910 Mev, resonance, 16: 12378
production in proton (p,p) interactions, 17: 24290
production in proton ($\bar{p}$-p) interactions at 3.25 and 3.69 Bev/c, 17: 41736 (BNL-7294)
production in proton pair annihilation, 18: 22750
production in proton–proton interactions, 18: 42447
production in proton-proton interactions at 18.8 Bev (E), 19: 1399
production in proton interactions at 19 and 23 Bev/c, (E), 19: 12221
production in proton interactions with neutrons, high-energy, 19: 33051
production in proton reactions with beryllium and platinum at 2.9 Bev, (E), 20: 39794
production in strong interactions, model of, 18: 36337
production in very high-energy collisions, 17: 9436
production of ($\bar{K}2_\pi N$), 18: 30589
production of ($K\pi\nu$), in proton pair interactions, 18: 40302
production of ($K_1^0K^+\pi^+$), in proton pair annihilation (E), 19: 1355
production of double resonant K*, spin determination in, 17: 7000
production of excited, in N-π^- interactions, 17: 20891
production of, in meson (π)-nucleon interactions at 7 Bev, 17: 22444
production of K* in meson (K_1^0)-proton interactions at 2 Bev/c, 18: 14948
production of K* in meson (π^+)-proton interactions at 2.77 Bev/c, 18: 18702
production of K* in meson (K^+)-deuteron interactions at 2.3 Bev/c, 18: 37885 (UCRL-11465)
production of K*, in pseudoscalar meson interactions, 18: 36269
production of K*, in meson (K^+)-proton interactions at 3 Bev (E), 19: 1342
production of K* in proton–meson (K^-) interactions at 1.15 Bev/c, 16: 18377
production of K* in meson (π^-)-proton interactions, 16: 21289
production of K*, in proton-antiproton annihilations, 17: 9368
production of K', in meson (π^-)-proton interactions, 17: 9370
production of K*, in meson (K^+)-proton interactions at 1.96 Bev/c, 17: 41746 (UCRL-10955)
production of K*, in meson (K^+)–proton interactions at 1.14 Bev/c, 18: 6033
production of K* resonant state at 725 Mev, symmetry breaking by, 17: 41774
production of K* (895) in meson (K^+)-proton interactions at 1.96 Bev/c, 17: 41745 (UCRL-10954)
production of pairs of, in electron-positron interactions, (T), 19: 12209
production of pairs of, in meson (π)–nucleon interactions at 12 and 18 Bev/c, (E), 19: 14405 (TID-21409)
production of pairs of, in π-π P-wave interactions, 20: 41823
production of resonance states, properties of, 17: 29506
production of resonance states in meson (K^+)-proton interactions at 1.96 Bev/c, meson (π) exchange in, 17: 39895
production of ($\Sigma K\pi$) states at 2.1 Bev/c, 17: 13419
production of, review of, 18: 12903 (JINR-P-1490)
production with hyperons (Λ) in meson (π^-)-proton interactions, resonances, 17: 9385
production with mesons (ω^0) in antiproton–proton annihilation, (E/T), 19: 10019 (NP-14497)
properties of (K-$\bar{K}$), review, 18: 10892
properties of, from rotator model of elementary particles, 18: 7517
properties of G_1 multiplets for, decay and electromagnetic, 18: 7537
properties of K* (888), review, 18: 10892
properties of K* (726), review, 18: 10892
properties of K*, calculation from nearby singularities, 18: 10923
properties of K*, calculation of, 18: 44532
properties of K*, review on, 19: 16657
properties of K*888, review, 17: 9466
properties of scalar, spin-zero (K*), 16: 17049
properties of, electron-pair model for, (T), 19: 10059
properties of, model with $Z_3 = 0$ for, 20: 25843
properties of, model for, 19: 16645
properties of, review of, 19: 16657
quantum numbers for states of n, charge and hypercharge, (T), 19: 43088
reactions in emulsions at 790 Mev/c, hyperon (Λ) production in, 17: 10240(R) (NP-12208)
reactions of ($\bar{K}$) with nucleons, bound state effects in meson (K^-) reactions with deuterium and hydrogen, 17: 29535
reactions of K_2 with nuclei, K_1 regeneration and decay in, 18: 40239 (NP-14239)
reactions with liquid hydrogen, energy range graph for, 20: 46601 (UCRL-2426(Vol.2)(1966 Rev.))
reactions with nuclei, hyperfragment production from, (T), 20: 26236
representation of (K*), in Sp(6) group, 18: 42421
resonance (K*) production and decay in meson (K^-)–nucleon interactions, 18: 12936
resonance (K-π) in meson (π^-)-proton interactions, 726-Mev, 18: 20918 (UCRL-10797)
resonance (K*) production in meson (K^+)–proton interactions at 1.96 Bev/c, 18: 5995 (UCRL-11068)
resonance states of, classification of K* in hypercharge space, 18: 6011
resonance states of, theories for production of, 18: 9197
resonance states of, production of M* and Y*, 18: 12903 (JINR-P-1490)
resonance with mesons (π), meson ($\bar{K}^0$) identification as, 16: 4714
resonances of, Regge trajectories for unitary symmetry representation of, 19: 3046
resonances of, review of properties of, 18: 18676
resonant state formation and decay, angular correlations in, 17: 41791
resonant state in meson (K)-meson (π) scattering, 17: 41812
resonant state of ($\bar{K}$-K) system at 1020 Mev, decay scheme of, 17: 9248
resonant state of (K-π) system at 725 Mev, parity and spin of, 17: 41774
scattering by hydrogen at 25 Bev, elastic, (E), 19: 23355(R) (BNL-867(p.1-117))
scattering of, by protons, angular distribution of, 16: 30930(R) (NYO-2669)
scattering of, prediction of interaction symmetry from dispersion relations in, 17: 20905
search for K*, 18: 22749
separation from mesons (π) at high energies, 16: 31883
separation from proton beams in waveguides, 20: 31841
separation of beams of, in accelerators, (T), 19: 27038
spectra from interactions in nuclear emulsion, transverse momentum, 18: 28426
spin assignment for (K*), 17: 2164 (JINR-P-1047)
spin of K*, 17: 9368
spin of (K*), 17: 13442
spin of K*, analysis of (E), 19: 1338
spin of K*, determination by ($\bar{K}$,K*) pair production, 17: 17055
spin of K* resonance, 17: 11542
spin of K*, review, 17: 9467
spin-statistics connection for, 17: 29539
statistics for, test of normal, 18: 28373
stopping by emulsions loaded with carbon, 19: 44398 (CERN-65-4 (Vol.II), pp III12-14)
theory of, quantum, 18: 831 (AD-420626)
wave function renormalization constant of, (T), 20: 9814

MESONS (K^-)

absorption at rest in liquid hydrogen, (E), 19: 29303
absorption by emulsion nuclei at rest, 18: 14797 (AFOSR-4737)
absorption by emulsion nuclei, (E), 19: 23467
absorption by liquid hydrogen, 16: 28000
absorption by nuclei, hyperon effects, 16: 16980 (NP-11592(Vol.I) (p.389-94))
absorption in liquid hydrogen, 16: 24822
absorption in liquid hydrogen, cascade time for, (E), 19: 23764
absorption rate in liquid helium, 19: 43356
beam production system for Bevatron, achromatic, 18: 40092 (UCRL-11426)
capture at rest by nuclei, hyperon production, 16: 9374
capture at rest by light nuclei in emulsions, (E), 20: 42386
capture at rest in emulsion nuclei, hyperfragments from, 19: 5184
capture at rest in nuclear emulsion, hypernuclei from, (E), 20: 34628
capture at rest in nuclear emulsion, hypernuclei from, (E), 20: 34629
capture by atoms, 17: 19331
capture by bromine at 600 Mev/c, hyperons (Λ) production and trapping in, (E), 20: 12092
capture by bromotrifluoromethane, Λ-p effective-mass spectrum and hyperon (Λ) lifetime from, (E), 20: 19485
capture by carbon, nitrogen, oxygen, and silver bromide in emulsions, Auger electron spectra from, 17: 26568

capture by carbon-12, momentum of hyperon (Σ)–meson (π) pairs from, 17: 40074
capture by carbon-12, Y_1^*(1405) production in, (E), 20: 44657 (UCRL-16602)
capture by complex nuclei, nuclear matter distribution and orbit distortion in, 17: 24442
capture by complex nuclei, hyperon resonance production and decay in, 17: 39863
capture by complex nuclei, multi-nucleon, 18: 36615
capture by deuterium and helium nuclei, branching ratios for non-mesic, 18: 44800
capture by deuterium, Y* production in, (T), 20: 11599
capture by deuterons, hyperon (Λ)-nucleon scattering in, 18: 18679
capture by emulsion nuclei at rest, 16: 10919
capture by emulsion nuclei, hyperon (Λ^0) emission in, 16: 10854
capture by emulsion nuclei, use as evidence of Y isobar, 16: 16981 (NP-11592(Vol.I)(p.397-406))
capture by emulsion nuclei at 440 Mev/c, Y_1^* production in, 18: 11244
capture by emulsion nuclei, models for hyperfragment production in, 18: 36652
capture by emulsion nuclei at rest, (T), 19: 5222
capture by emulsion nuclei, production of Y_1^* (1405) in, (E), 20: 6051
capture by emulsion nuclei, meson (π^+) emissions from, 20: 30485
capture by emulsion nuclei, hyperfragment, hyperon, and meson (π) production in, (E), 20: 44657 (UCRL-16602)
capture by helium-4, 18: 36636
capture by helium-4, x-ray emission from, (E), 19: 35494
capture by light nuclei, hyperon (Σ)-meson (π) pair production in, 17: 13411
capture by nuclear emulsions, hyperon (Σ^+) production in, 16: 27952
capture by nuclei, production of hyperfragments, 16: 8067 (NP-11232 (p.360-6))
capture by nuclei, star properties from, 16: 12357
capture by nuclei for nuclear structure measurements, 17: 7232
capture by nuclei, nuclear emulsion study of, 18: 20966
capture by nuclei, hyperfragment production in, (E), 19: 10020 (UCRL-11328(Rev.1))
capture in bromotrifluoromethane, meson (π^+) energy spectrum from, 20: 24326 (AD-626056)
capture in complex nuclei, validity of multi-nucleon process in, 17: 24494
capture in deuterium, hydrogen, and light nuclei, production of Y* in, 17: 20910
capture in emulsions, search for hypernucleus (Σ^- n) in, 16: 2442
capture in emulsions, short-range hyperfragment production in, (E/T), 19: 45342
capture in hydrogen, hyperon mass determinations in, 19: 47302 (CU-1932-246)
capture in liquid helium, de-excitation, (T), 19: 21042
capture in nuclear emulsions, effects of nuclear mass, 16: 26084 (NP-11623)
capture, multi-nucleon, 16: 10906
capture of, multinucleon, 17: 31091(R) (UCRL-10862)
cascade and moderation times in liquid helium, (E), 20: 15273
decay branching ratios, 18: 10921
decay branching ratio of, nonleptonic $\Delta T = \frac{1}{2}$, (T), 19: 10083
decay, intrinsic structure in meson (π) production and interaction in, 16: 13908
decay modes, 16: 10861
decay modes and lifetime, 16: 8065 (NP-11232(p.346-52))
decay modes, evidence of strange particle in, 16: 8056 (NP-11232 (p.259-65))
decay of relativistic, neutrino spectra from, 18: 12894 (CERN-63-37 (p.111-29))
decay of, symmetry violations in leptonic, 18: 7551
decay of, unitary symmetry of weak current structure in, 17: 41781
decay of, branching ratio for, (T), 19: 8231
decay of, effects of CP violation in 3π, (T), 19: 41445
decay of, hyperon (Σ^-) and (Σ^+) production in, (T), 20: 36041 (ORO-2504-90)
decay of, neutrino interactions in, 18: 40280
decay of, neutrino spectra from, (E), 20: 21602 (CERN-65-32, pp 111-14)
decay of, weak interaction theory in SU(3) for 2π, 20: 17379
detection using liquid Cherenkov counters, system for, 19: 34519
interaction cross sections, 16: 13880
interaction of, with emulsion nuclei, properties of hyperfragments produced in, 17: 20864
interactions and reactions, 18: 16552(R) (UCRL-11132)
interactions at high energy, cross section combinations for, 17: 11529
interactions at rest, analysis for hyperon (Σ) and meson (π) spectra, 16: 2305(R) (UCRL-9704)
interactions in lithium-loaded nuclear emulsions at 1.5 Bev/c, hyperfragment production in, 18: 20938
interactions in nuclear emulsions, characteristics and cross section, 16: 8063 (NP-11232(p.327-36))
interactions in nuclear emulsions, analysis of, in flight, 16: 8064 (NP-11232(p.337-45))
interactions in nuclear emulsion, pair production (Σ-π) in, 17: 39907
interactions in nuclear emulsions at 1.5 Bev/c, production of hyperons (Ξ^-) in, 17: 39882
interactions in nuclear emulsions, 18: 9752 (IA-900)
interactions in nuclear emulsions at 800 Mev/c, measurement of short-range hyperfragments from, 18: 24445
interactions in nuclear emulsions at 5 Bev/c, $_{\Lambda}Be^9$ hyperfragment from, (E), 20: 8107
interactions in nuclear emulsion, correlations of meson (π) production and decay chains in, (E), 20: 13487
interactions in nuclear emulsions at 1.5 Bev/c, production and decay properties of hyperfragments from, (E), 20: 41911
interactions of, with protons at 1.05 Bev, 16: 31020 (UCRL-10222)
interactions of, with protons at 1.05 Bev, 16: 32292 (UCRL-10222(Rev.))
interactions of, with protons at 1.22 to 1.51 Bev, 16: 32295 (UCRL-10233)
interactions of, with protons at 1.22 Bev, charge exchange effects in, 16: 32296 (UCRL-10234)
interactions of, with protons at 2.24 Bev, production properties of, 16: 32268 (BNL-6211)
interactions of, with protons at 700 to 1400 Mev, angle, polarization, and range measuring technique for study of, 16: 32299 (UCRL-10249)
interactions of, with protons at 300 to 850 Mev, 16: 32303 (UCRL-10310)
interactions of, with nuclei of ionographic emulsions at 1.5 Bev/c, mesic hyperfragments produced in, 17: 19251
interactions of, with protons at 2.24 Bev, 17: 706 (BNL-6214)
interactions of, SU(6) symmetry for forward amplitudes in, (T), 19: 41515
interactions with alphas, deuterons, and protons, pion-hyperon resonance, 16: 4694 (TID-14137)
interactions with alpha particles and deuterons, resonance production in, 18: 14811 (JINR-P-1508)
interactions with deuterons and nucleons at 630 to 1100 Mev/c, cross sections, 16: 13895
interactions with deuterons and protons, total cross sections at 630 to 1100 Mev, 16: 21360 (UCRL-10125)
interactions with deuterons at 200 Mev, production of hyperons in, 16: 31025 (UCRL-10348)
interactions with deuterons, K^--K^0 mass-difference effects on, 16: 33709
interactions with deuterons, effective-range theory for, 17: 726
interactions with deuterons, capture and transition rates for non-mesic, 17: 13369
interactions with deuterons at 600–850 Mev/c, Y_1^* parity from, 18: 2666
interactions with deuterons and protons at low energies, interaction parameter solutions with Y_1^* (1405 Mev) for, 18: 14858
interactions with deuterons and neutrons at 765 Mev/c, meson (η) production in, 18: 16783
interactions with deuterons, model for, 18: 18633 (AFOSR-3501)
interactions with deuterons at 100 to 150 Mev/c, effects of final-state interactions on cross sections for, 18: 20926
interactions with deuterons and protons, Y_1^* resonance in, 18: 21020
interactions with deuterons and protons at 1.49 to 1.70 Bev/c, Y_1^* resonances in, 18: 26328
interactions with deuterons, amplitudes for elastic, 18: 30555
interactions with deuterons, Y_1^* (1660) parity in (E), 19: 1340
interactions with deuterons, hyperon (Λ) production in, (T), 19: 8173
interactions with deuterons at low energies, cross sections for elastic, (T), 19: 12218
interactions with deuterons, corrections to impulse approximation for, (T), 19: 18786
interactions with deuterons at 2.24 Bev/c, ρ^0 (735) in, (E/T), 19: 18855
interactions with deuterons, hyperon resonances in, (T), 19: 25279
interactions with deuterons and protons at 6 to 22 Bev/c, total cross sections for, (E), 19: 25351
interactions with deuterons at 2.1 Bev/c, (E/T), 19: 25265(R) (UCRL-11776)
interactions with deuterons and protons at 825 to 1100 Mev/c, (E), 19: 25265(R) (UCRL-1176)
interactions with deuterons, hyperon (Λ^0)-(Σ^0) isospin mixing in, (T), 19: 31058
interactions with deuterons at rest, hyperfragment (Σ^-n) production in, (T), 19: 47339
interactions with deuterons at rest, Σ-Λ conversion in, (T), 19: 47358
interactions with deuterons, hyperon (Ξ^-)-neutron resonance production in, 20: 6073
interactions with deuterons below 300 Mev/c, effects of $\bar{K}^0$–K^- and n-p mass differences on, (T), 20: 11630
interactions with deuterons at 670 to 770 Mev/c, Y_1^* (1660) production in, 20: 15397

interactions with deuterons and protons at 1 to 2.4 Bev/c, total cross sections for, (E), 20: 34145 (BNL-10215)
interactions with deuterons at 0.9 to 1.12 Bev/c, Σ-η enhancement in, (E), 20: 39747 (COO-881-75)
interactions with emulsion nuclei at 800 Mev, hyperfragment production, 16: 16976 (NP-11592(Vol.I)(p.363-9))
interactions with hyperons (Λ), compound formation possibilities in, 16: 6932
interactions with hyperons (Ξ^-) and nucleons, resonant states in, (T), 19: 18801
interactions with helium-3 and helium-4 nuclei in mesic atoms, 20: 34601
interactions with mesons (K^+), meson (π) interaction model application to, 16: 5881
interactions with mesons (π^+), coupling constants and cross sections, 16: 9403
interactions with mesons (K^+), 16: 15574
interactions with mesons (K^+), meson (ω) and (ρ) production in, 16: 17043
interactions with mesons (K^+), transitions to mesons (ω) and (ρ) in, 16: 17044
interactions with mesons (K^+), dispersion relations in, 16: 17047
interactions with mesons (π), (K^*) pole contribution to, 16: 17049
interactions with mesons in nuclear emulsions at 800 Mev, 16: 16975 (NP-11592(Vol.I)(p.359-61))
interactions with mesons (K), coupling constants for generation of mesons (ϕ) from, 17: 39890
interactions with mesons (π^-) and protons at 1.51 Bev/c, effective mass distributions from, 17: 41788
interactions with mesons (K^+), cross sections for inelastic, 18: 7532
interactions with mesons (K) and (π), properties of resonance, (E/T), 19: 6556
interactions with mesons (K), nucleon isoscalar form factor from elastic, (T), 19: 47371
interactions with mesons (K), coupling constants and p-wave amplitudes for, (T), 20: 19520
interactions with nucleons and protons at 1.1 Bev/c, 16: 2305(R) (UCRL-9704)
interactions with nucleons, analysis, 16: 4734
interactions with nucleons, 16: 9406
interactions with neutrons, cross sections for, 16: 13880
interactions with nucleons, hyperon (Λ^0) decay asymmetries from, 16: 15556
interactions with nucleons, meson (π)-exchange relations to potential in, 16: 15581
interactions with nucleons, cross-section maxima in, 16: 17043
interactions with neutrons at 765 Mev/c, Λ-π resonance in, 16: 21482
interactions with nucleons, partial-wave dispersion relations in, 16: 21299
interactions with nucleons, resonances from, 16: 26161
interactions with nucleons at low energies, Y* effects on S-wave parameters in, 16: 27949
interactions with nucleons in emulsions at 830 Mev/c, hyperfragment ($A \geq 40$) production in, 16: 27988
interactions with nucleons, p- and s-wave resonances in, 17: 19524
interactions with nucleons, effect of ($\bar{K}$-K) resonance in, 17: 20871
interactions with nucleons in nuclei, dispersion relations for low-energy, 17: 21075
interactions with nucleons in the Mandelstam representation, study of K* Regge trajectory from, 17: 39839
interactions with nucleons, mechanisms for, 17: 39894
interactions with neutrons and protons at 3.5 Bev, final states of $\Xi^- + K^0 + n\pi$ from, 17: 41792
interactions with nucleons in nuclei, Y_0^* production in, 18: 9368
interactions with nucleons at 350 to 450 Mev/c, Y_1^* resonances in, 18: 9143
interactions with nucleons, 18: 862(R) (TID-19590)
interactions with nucleons, Y* (1765 Mev) production in, 18: 10931
interactions with nucleons, resonance (K^*) decay and production in, 18: 12936
interactions with nuclei and nucleons, 18: 15290
interactions with nucleon pairs at 1.13 Bev/c, 18: 22769
interactions with nucleons at high energies, parameters for, 18: 24384 (JINR-P-1577)
interactions with neutrons at 1.15 Bev, resonance ($\Sigma\pi$) production in, 18: 36339
interactions with nucleons, hyperon (Λ) production in, 18: 44522 (UCRL-11432)
interactions with neutrons and protons at 1.15 Bev/c, ($\Sigma\pi$) and ($\Lambda\pi$) resonances in, 18: 44523 (UCRL-11568)
interactions with nucleons at 3.5 Bev (E), 19: 1339
interactions with neutrons at 1.15 Bev/c, Y_0^* production in, (T), 19: 18803
interactions with nucleons at high energies, Regge trajectories in, (T), 19: 23417
interactions with neutrons at 916 Mev/c, Y_1^* resonance from, (E), 19: 25265(R) (UCRL-11776)
interactions with nucleons at 2 to 3 Bev/c, peripheral production and resonance decay in, (T), 19: 35152
interactions with nucleons at low energies, Y* resonance in, (T), 19: 35035
interactions with neutrons and protons at rest, hyperon (Σ^-) production in, (E), 19: 41494
interactions with neutrons, final-state interactions in ($\Lambda\pi^-$), (T), 19: 41405
interactions with nucleons at high energy, sum rule for cross sections of, (T), 20: 4678
interactions with nucleons to 300 Mev/c, effective-range analysis of, (T), 20: 9733
interactions with neutrons at 828 to 1112 Mev/c, Y_1^*(1765) resonance in, (E), 20: 11656
interactions with neutrons and protons at 600 to 850 Mev/c, hyperon (Λ)-meson (π) resonances in, (E), 20: 13522
interactions with nucleons at high energies, resonances in, 20: 15414
interactions with neutrons and protons at high energies, real amplitudes for, (T), 20: 17378
interactions with neutrons at 0.920 to 1.120 Bev/c, Σ-η resonances from, (E), 20: 32103
interactions with nucleons, effective-range parameters for S-wave, 20: 34199
interactions with neutrons at 2.24 Bev/c, η^* (960) production in, (E), 20: 39786
interactions with neutrons at 0.8 to 1.1 Bev/c, Y_1^* resonant amplitudes from, (E), 20: 41886
interactions with nucleons, 17: 19324
interactions with nucleons, 18: 15290
interactions with protons at 1.15 Bev/c, angular momentum and parity, 16: 2461
interactions with protons at 0 to 850 Mev/c, 16: 2305(R) (UCRL-9704)
interactions with protons, resonance states at 1815 Mev, 16: 8127
interactions with protons at 400 Mev/c, angular distributions, 16: 8146
interactions with protons, meson (ω) production, 16: 8152
interactions with protons at about 400 Mev/c, cross-section momentum dependence, 16: 9393
interactions with protons at 1.15 and 2 Bev/c, 16: 9403
interactions with protons up to 20 Mev, total-cross-section relation to isospin independence, 16: 10905
interactions with protons, 16: 10920
interactions with protons at 172 Mev/c, K^-–N bound states in, 16: 10833
interactions with protons at 760 and 850 Mev/c, meson ($K^0_{\pi_3}$) production in, 16: 10887
interactions with protons, angular correlations for, 16: 12354
interactions with protons, hyperon (Ξ^{-*}) production, 16: 12379
interactions with protons in complex nuclei, 16: 12801(R) (IA-685)
interactions with protons at 1.15 Bev/c, hyperon (Σ)-meson (π) resonances from, 16: 4696 (UCRL-9835)
interactions with protons, parity, 16: 10901
interactions with protons, transition matrix for, 16: 17040
interactions with protons at 1.1 to 1.4 Bev/c, 16: 17042
interactions with protons at 1.15 Bev/c, resonance effects, 16: 18377
interactions with protons, effective-range analysis of s-wave, 16: 18373
interactions with protons, hyperon (Σ) production and parity relative to (Λ), 16: 18334
interactions with protons, KΣN parity, 16: 21326
interactions with protons, angular distributions and cross sections, 16: 24701 (UCRL-10126)
interactions with protons at 62 to 172 Mev/c, cross sections, 16: 24704
interactions with protons, hyperon (Σ^+) production in, 16: 26143
interactions with protons at 293 to 513 Mev/c, hyperon production and scattering in, 16: 27914 (UCRL-10175)
interactions with protons and deuterons, branching ratios, 16: 27928
interactions with protons at 75 to 275 Mev/c, 16: 29690 (UCRL-10018)
interactions with protons, Σ/Λ branching ratio of Y_1^* resonance in, 16: 31019 (UCRL-9675)
interactions with protons, meson (η) formation in, 16: 31048
interactions with protons, evidence for T = 0 resonance in $\Sigma\pi$ system from, 16: 32290 (UCRL-9686)
interactions with protons at 1.22 and 1.51 Bev/c, final states from, 16: 32297 (UCRL-10237)
interactions with protons analyticity of amplitudes for, 16: 32315
interactions with protons, resonance effects on, 16: 32334
interactions with protons at 1.2 to 1.6 Bev/c, hyperon (Ξ^-) production in, 17: 721 (UCRL-10236)
interactions with protons below 300 Mev/c, s-wave zero-range parameters for, 18: 883
interactions with protons at 1.22 and 1.51 Bev/c, 18: 2594 (UCRL-10235)
interactions with protons at 7.2 and 9.0 Bev/c and $-t = 0.03$ to 1.1

(Bev/c)², differential cross sections for elastic, 18: 4457
interactions with protons, production of hyperon resonances in, 18: 6000
interactions with protons at high energies, cross sections for elastic, 18: 6011
interactions with protons at high energies, field theory for, 18: 6015
interactions with protons at 1.15 Bev/c, 17: 767
interactions with protons, hyperon (Ξ) resonances from, 17: 3996
interactions with protons at 2.24 and 2.5 Bev/c, meson production in, 17: 5254
interactions with protons at 2.3 and 2.5 Bev/c, hyperon (Ξ^-) production in, 17: 5261
interactions with protons at 1020 Mev, (K-$\bar{K}$) resonance in, 17: 9262
interactions with protons, anomalous threshold effects in, 17: 9269
interactions with protons at 1.47 Bev/c, 17: 9369
interactions with protons, 17: 11487 (NP-12488)
interactions with protons, branching ratios for, 17: 11560
interactions with protons, angular distribution of mesons (π^-) produced in, 17: 11299(R) (ANL-6612)
interactions with protons, resonance effects in, 17: 13458
interactions with protons, resonances in, 17: 15133
interactions with protons, hyperon (Y_1^*) spin from, 17: 17039
interactions with protons, 1.66-Bev Y_1^* from, 17: 17041
interactions with protons at 620 to 850 Mev/c, resonances in, 17: 17042
interactions with protons, p- and s-wave baryon-meson resonances in, 17: 19524
interactions with protons, 17: 20594(R) (UCRL-10572)
interactions with protons at 1150 Mev/c, isobaric model for, 17: 20912
interactions with protons, cross section for four particle final state in, 17: 20939
interactions with protons, test of tenfold assignment of baryon resonances in, 17: 26361
interactions with protons at 1.80 and 1.95 Bev/c, quantum numbers of 1.02-Bev (K-$\bar{K}$) resonance in, 17: 26362
interactions with protons at 2.23 Bev/c, existence and properties of meson (ϕ) in, 17: 26363
interactions with protons, leptonic decay of hyperon (Ξ^-) produced in, 17: 26365
interactions with protons at 1.51 Bev/c, meson (ω) decay and production in, 17: 28159 (UCRL-10723)
interactions with protons, hyperon (Σ) resonances in, 17: 29506
interactions with protons, 17: 31091(R) (UCRL-10862)
interactions with protons, diffraction pattern shrinkage from ω-exchange in, 17: 31370
interactions with protons at 2.23 Bev/c, meson (ϕ) production in, 17: 31270 (BNL-7106)
interactions with protons at 2.7 to 5.2 Bev/c, total cross section for, 17: 32897 (BNL-6962)
interactions with protons at 2.3 Bev/c, resonance production in (Ξ-K-π) final-state, 17: 32898 (BNL-7105)
interactions with protons near 760 Mev/c, $Y_1^*(1660)$ resonance in, 17: 34738 (UCRL-10779)
interactions with protons at 1.80–1.95 Bev/c, (Ξ-π) resonance parity and spin from, 17: 34793
interactions with protons at 5 Bev, Regge pole contributions to cross section of, 17: 34816
interactions with protons at 725 Mev, production of meson (κ) in, 17: 34767
interactions with protons at 250 to 513 Mev/c, elastic and charge-exchange scattering and hyperon production in, 17: 34781
interactions with protons at 2.24 Bev/c, production of resonant states in, 17: 36380 (ISS-63/29(p.1-13))
interactions with protons at 2.5 to 6 Bev/c, total cross sections for, 17: 39844 (BNL-7258)
interactions with protons, meson and baryon exchange diagrams for, 17: 39880
interactions with protons at 1.2 to 1.75 Bev/c, production and properties of mesons (ω) from, 17: 41843
interactions with protons, 17: 40433(R) (NYO-10063(p.71-89))
interactions with protons at 3.5 Bev/c, production of strangeness −3 baryons in, 18: 6027
interactions with protons at 2.24 Bev/c, mesons (ϕ) from, 18: 7463 (BNL-7407)
interactions with protons, resonance production in, 18: 7464 (BNL-7408)
interactions with protons at high energies, exchange of strangeness-carrying trajectories in, 18: 7507
interactions with protons at high energies, effects of Regge trajectories on diffraction peaks in, 18: 7515
interactions with protons at 820 to 1,260 Mev/c, differential cross sections for elastic, 18: 9165
interactions with protons, elastic, 18: 10843 (CONF-122-22)
interactions with protons, forward amplitudes for, 18: 12898 (EFINS-63-72)
interactions with protons at 1.22 Bev/c, 18: 12918 (UCRL-11155)
interactions with protons, coupling constants for resonances in, 18: 14957
interactions with protons at 2.3 Bev/c, resonance production in, 18: 14949
interactions with protons at 2.23 Bev/c, meson (ϕ) production in, 18: 14951
interactions with protons at 1.80 and 1.95 Bev/c, $\Xi^*_{1/2}$ production in, 18: 14953
interactions with protons and carbon nuclei at 300 to 1150 Mev/c, hyperon (Λ^0) production in, 18: 14863
interactions with protons at 5.0 Bev/c, hyperon (Ω^-) production and decay in, 18: 14892
interactions with protons at 1.0 to 1.7 Bev/c, strange-particle resonances in, 18: 14946
interactions with protons at 1.455 Bev/c, resonance (Y_1^{*-}–Y_1^{*+}) mass difference in, 18: 18689
interactions with protons at 1500 Mev/c, $N^*_{3/2}$ and $Y^*_{3/2}$ production in, 18: 18692
interactions with protons at 1.80 and 1.95 Bev/c, hyperon (Ξ^-) production in, 18: 20959
interactions with protons, unitary symmetry model for, 18: 20962
interactions with protons, singularity in, 18: 20903 (JINR-E-1581)
interactions with protons at 1.5 Bev/c, 18: 22749
interactions with protons, meson (ω^0) production in, 18: 22757
interactions with protons, observation of mass 959-Mev mesons in, 18: 22760
interactions with protons, 960-Mev 5π resonance in, 18: 22765
interactions with protons, hyperon (Σ) leptonic decay in, 18: 24402 (TID-19033)
interactions with protons at 1.8 Bev/c, charge exchange in, 18: 26339
interactions with protons, Y_1^* parity and spin from, 18: 26340
interactions with polarized protons, hyperon (Ξ^-) parity and spin from, 18: 26343
interactions with protons at high energies, scaling law for, 18: 28330 (TID-20722)
interactions with protons at 1.455 Bev/c, Y_1^* production in, 18: 28367
interactions with protons, hyperon (Σ^-) and (Σ^0) masses from, 18: 30525 (TID-20769)
interactions with protons at 1.05 to 1.75 Bev/c, hyperon (Λ) production in, 18: 30530 (UCRL-10926)
interactions with protons at 1 to 1.7 Bev/c, 18: 30588
interactions with protons at 1.2 to 1.7 Bev/c, 18: 30589
interactions with protons, production of 1810-Mev S = −2 baryon state in, 18: 30600
interactions with protons at 2.00 Bev/c, charge-exchange cross section for, 18: 30601
interactions with protons at 400 Mev/c, angular distributions for, 18: 32548
interactions with protons at 1.45 Bev/c, $\bar{K}^*$-resonance production in, 18: 32584
interactions with protons, hyperon (Λ) and meson (ω) production in, 18: 32598
interactions with protons at 2.45 and 2.7 Bev/c, $\Lambda\mu^+\mu^-$ and Λe^+e^- production in, 18: 34513 (UCRL-11428)
interactions with protons at 2.4 to 2.7 Bev/c, bubble chamber studies of final-state resonances in, 18: 34515 (UCRL-11430)
interactions with protons at 2.4 to 2.7 Bev/c, production of 959-Mev resonance in, 18: 34515 (UCRL-11431)
interactions with protons at 2.4 to 2.7 Bev/c, (Ξ-π) resonance (1530 Mev) spin and parity from, 18: 34517 (UCRL-11436)
interactions with protons at 1.2 to 1.7 Bev/c, resonances in, 18: 36254 (UCRL-11291)
interactions with protons, unitary symmetry model for resonance production in, 18: 36280
interactions with protons, hyperon (Λ) production at 120 to 400 Mev/c in, 18: 36341
interactions with protons, hyperon (Σ) production in, 18: 36345
interactions with protons at 250 Mev/c, hyperon ($\Sigma^\pm$) production in, 18: 37880 (TID-20952)
interactions with protons, diffracting sphere model for elastic, 18: 37915
interactions with protons at 1150 Mev/c, angular correlations for final-state particles in, 18: 37945
interactions with protons, review of, 18: 40249 (UCRL-11493)
interactions with protons at 2.45 Bev/c, resonances in, 18: 40241 (UCRL-11424(Rev.))
interactions with protons at 2.5 Bev/c, hyperon (Ξ^-) production in, 18: 40242 (UCRL-11427)
interactions with protons at 2.4 and 2.7 Bev/c, production of $\phi \to \mu^+\mu^-$ in, 18: 40243 (UCRL-11428(Rev.))
interactions with protons at 2.4 to 2.7 Bev/c, meson ($\bar{K}^0$) production in charge-exchange, 18: 40244 (UCRL-11429)
interactions with protons at 5 Bev/c, hyperon (Ω^-) production in, 18: 40223 (BNL-8231)
interactions with protons at 650 to 840 Mev/c, cross sections for $\Lambda\eta$

production in, 18: 40225 (BNL-8233)
interactions with protons at 5 Bev/c, hyperon (Ξ^-) production in, 18: 40226 (BNL-8234)
interactions with protons, production and properties of Y* (1660) in, 18: 40224 (BNL-8232)
interactions with protons, meson ($\eta 2\pi$) resonance effects in, 18: 42445
interactions with protons, 960-Mev boson in, 18: 42452
interactions with protons at high momenta, 18: 42365 (JINR-E-1790)
interactions with protons, $\Lambda\pi\pi$ production in, 18: 42370 (JINR-P-1723)
interactions with protons, model for meson (δ) production in, 18: 42409
interactions with protons at 5 Bev/c, hyperons (Ω^-) from, 18: 42424
interactions with protons at 12 to 16 Bev/c and 0.2 to 1.0 $(Bev/c)^2$, 18: 44516 (BNL-8328)
interactions with protons at 60 to 300 Mev/c, cross sections for, 18: 44521 (TID-21205)
interactions with protons at 2.3 to 3.8 Bev/c, meson (X^o) (960 Mev) production in, 18: 44556
interactions with protons at 2.24 to 2.44 Bev/c, 2120-Mev hyperon resonance in, 18: 44592
interactions with protons at 1.455 Bev, charge exchange cross section for (E), 19: 1335
interactions with protons, hyperons (Ω) from (E/T), 19: 1250
interactions with protons at 3 Bev/c, resonances in, 19: 1257
interactions with protons, strange-particle production in, 19: 1266
interactions with protons at 3 Bev (E), 19: 1333
interactions with protons at 700 to 1400 Mev, elastic (E), 19: 1331
interactions with protons at 3 Bev (E), 19: 1332
interactions with protons at 3.5 Bev (E), 19: 1334
interactions with protons at 1.455 Bev, 1660 Mev/c^2 and Y_1^* resonances in (E), 19: 1337
interactions with protons at 1.4 Bev/c, N*(1425) resonances in (E), 19: 3096
interactions with protons at 4.2 Bev/c, hyperon (Ω^-) production in, (E), 19: 4980
interactions with protons at 1 to 3 Bev/c, hyperon final states and resonances in, (E/T), 19: 6564
interactions with protons at high energies, optical models for, (T), 19: 12228
interactions with protons, hyperon (Σ^o), production in, (E), 19: 12235
interactions with protons, $K\bar{K}$ (1020) resonance in, (T), 19: 12249
interactions with protons, resonance (1400) production in, (T), 19: 12303
interactions with protons at 1.34 Bev/c, elastic and total cross sections for, (E), 19: 14323 (TID-20450)
interactions with protons, meson (K^-)–meson ($\bar{K}^o$) mass difference from, (E), 19: 14324 (TID-21438)
interactions with protons at 760 and 850 Mev, Y_1^*(1385) production in, 19: 14396
interactions with protons at 1.34 Bev/c, K* and N* production in, (E), 19: 16481 (TID-20444)
interactions with protons, K* (890) production in, 19: 16510
interactions with protons at 2.45 to 2.70 Bev/c, 1820-Mev resonance in, (E), 19: 16596
interactions with protons below 300 Mev/c, 1405-Mev Y* resonance in, (E), 19: 16597
interactions with protons at 3.5 Bev/c, K*(890) and K*(1400) production in, (E), 19: 18838
interactions with protons at 2.45 to 2.70 Bev/c, Y_1^* (1660) production in, (E), 19: 21017
interactions with protons at 2.24 Bev, hyperon (Ξ) production in, 19: 21065
interactions with protons at 400 Mev, polarization correlation of hyperons (Λ) and hyperons (Σ^o) in, 19: 21071
interactions with protons, SU(6) predictions for amplitudes of, (T), 19: 23432
interactions with protons, SU(6) cross section equalities for, (T), 19: 23433
interactions with protons at high energies, elastic scattering amplitude for, 19: 23381
interactions with protons, relativistic SU(6) model for amplitudes of, 19: 23395
interactions with protons at high energies, equipment for studying, 19: 22862
interactions with protons at 50 to 200 Mev/c, cross sections for, (E), 19: 25343
interactions with protons at 1.03 to 1.09 Bev/c, differential cross sections for, (E/T), 19: 25265(R) (UCRL-11776)
interactions with protons, production of hyperons (Λ) and mesons (π^o) ine, (E), 19: 25265(R) (UCRL-11776)
interactions with protons at 1.2 to 1.7 Bev/c, analysis of events in, (E/T), 19: 25265(R) (UCRL-11776)
interactions with protons at 1.2 to 1.7 Bev/c, cross sections and resonances of, (E/T), 19: 25265(R) (UCRL-11776)
interactions with protons at 2.45 Bev/c, excitation functions and resonances in, (E/T), 19: 25265(R) (UCRL-11776)
interactions with protons at 2.45 to 2.70 Bev/c, angular distributions and cross sections of, (E), 19: 25265(R) (UCRL-11776)
interactions with protons at 700 to 1400 Mev/c, angular distributions from, (E), 19: 25265(R) (UCRL-11776)
interactions with protons at 1.1 to 1.7 Bev/c, hyperons (Ξ) production in, (E), 19: 25265(R) (UCRL-11776)
interactions with protons, meson (ω) production in, (E), 19: 25265(R) (UCRL-11776)
interactions with protons at high energies and low momentum transfers, (T), 19: 27227
interactions with protons at 1.2 to 2.7 Bev/c, hyperon (Ξ^-) production in, (E), 19: 29074 (UCRL-11884)
interactions with protons, isobar diagrams for resonances in, (T), 19: 29052 (IC/65/44)
interactions with protons, Y_0^* (1662) production in, (T), 19: 31057
interactions with protons at 7 to 16 Bev/c, (E/T), 19: 30994 (BNL-8935)
interactions with protons at 812 to 1266 Mev/c, polarization from elastic, (E/T), 19: 31015 (UCRL-11881)
interactions with protons, SU_3 predictions for cross sections for, (T), 19: 32992
interactions with protons at 3 Bev/c, baryon resonance production in, (E), 19: 32996
interactions with protons at 1.2 to 1.8 Bev/c, meson (ω) production in, (E/T), 19: 33044
interactions with protons at 12 to 16 Bev/c, differential cross section for elastic, (E/T), 19: 33050
interactions with protons, Q-value distributions for hyperon (Λ)-meson (π) pairs in, (T), 19: 35070
interactions with protons at 9.50 Bev/c, cross sections for charge-exchange, (E), 19: 35123
interactions with protons at 3 Bev/c, K*(1400) production in, (E), 19: 35133
interactions with protons, phenomenological analysis of, (T), 19: 35170
interactions with protons, resonances in, (E/T), 19: 35181
interactions with protons at 250 Mev/c, charge-exchange, (E), 19: 27165 (TID-21734)
interactions with protons at 940 Mev/c, Y*(1765) resonance in, 19: 37522 (CONF-650410-2)
interactions with protons at low energies, (T), 19: 37592
interactions with protons at 1.22 Bev/c, elastic, 19: 37634
interactions with protons at low energies, charge independence violation in, (T), 19: 37537 (NP-15147)
interactions with protons at low energies, Coulomb-nuclear interference in, (E/T), 19: 39530
interactions with protons, optical model analysis of elastic, (T), 19: 39545
interactions with protons at 2.1 to 2.7 Bev/c, meson (ϕ) production in, (E), 19: 39552
interactions with protons, meson (η^o) production in, (T), 19: 41433
interactions with protons at 4.6 and 5.0 Bev/c, f* (1500) production in, (E), 19: 41459
interactions with protons at high energies, forward amplitudes for, (T), 19: 41376
interactions with protons, baryon resonances from, (T), 19: 41384
interactions with protons, range-energy relations for hyperons (Σ^-) and (Σ^+) from (E), 19: 41369
interactions with protons, energy dependence of diffraction curve for elastic, (T), 19: 43043 (JINR-P-2202)
interactions with protons, hyperon (Ω^-) parity from, (T), 19: 43045 (JINR-P-2258)
interactions with protons at 1.22 to 1.70 Bev/c, charge-exchange, (E/T), 19: 45045 (UCRL-16288)
interactions with protons for hyperon (Ω^-) parity test, 19: 45101
interactions with protons at 2.24 Bev/c, Y_1^*(1660) resonance from, (E), 19: 47300 (BNL-9520)
interactions with protons at 2.1 to 2.7 Bev/c, mesons (η) (958) production in, (E), 19: 47372
interactions with protons, decay-hyperon (Λ^o) polarization in ($\pi^o\Sigma^o$), (T), 20: 1013
interactions with protons, SU(6) model for cross sections for, 20: 1017
interactions with protons at 0.8 to 1.2 Bev/c, Y*(1760) production and properties, (E), 20: 2711
interactions with protons at 6 Bev/c, hyperon (Ω^-) production from, (E), 20: 2717
interactions with protons, meson (ϕ) suppression in, (T), 20: 2719
interactions with protons at 725 to 820 Mev/c, peak in cross sections for, (E), 20: 2724
interactions with protons at 5.0 Bev/c, (E), 20: 4476(R) (IS-1200(Sect.P))
interactions with protons at 2.00 Bev/c, charge exchange in, (E), 20: 4476(R) (IS-1200(Sect.P))
interactions with protons in one-particle-exchange model, Y_1^* (1385) from, 20: 7812

interactions with protons, one-particle-exchange model for K* production in, (T), 20: 7827
interactions with protons at 3 Bev/c, differential cross sections for elastic, (E), 20: 7849
interactions with protons, hyperons (Ξ^-) associated production cross section for, (T), 20: 7859
interactions with protons above 2 Bev, energy dependence of diffraction-curve slope for, (T), 20: 9720(T)
interactions with protons at 9.5 Bev/c, meson (ρ) Regge-pole exchange model for charge-exchange, (T), 20: 9734
interactions with protons, Y* (1385) production in, (E), 20: 9743
interactions with protons at 3 Bev/c, $\bar{K}^*$ production in, (E), 20: 9752
interactions with protons at 9.5 Bev/c, momentum transfer distribution in charge-exchange, (T), 20: 9716
interactions with protons, $J^P = 1/2^+$, Y = 0, I = 0 and 1 octet in strong, (T), 20: 11592
interactions with protons, angular distributions from phase shifts for, (T), 20: 11648
interactions with protons at 900 to 1100 Mev/c, Y*(1765) and Y_3^*(1815) from, (E), 20: 11551 (CONF-650337-3)
interactions with protons, properties of meson resonance produced in, 20: 11552 (CONF-651015-3)
interactions with protons, hyperon (Ω^-) spin-parity from, (T), 20: 11563 (JINR-P-2456)
interactions with protons at 700 to 1400 Mev/c, differential cross sections for elastic, (E), 20: 13460 (UCRL-16274)
interactions with protons, research on, (E), 20: 13463(R) (UCRL-16511, pp 1-53)
interactions with protons at 1.15 Bev/c, Y_1^* production in, (E), 20: 13518
interactions with protons at 2.1 to 2.7 Bev/c, meson (ϕ) production in, (E/T), 20: 15316 (UCRL-16526)
interactions with protons at 2.1 to 2.7 Bev/c, resonance production in, (E), 20: 15412
interactions with protons at 5.5 Bev/c, resonance production in, (E), 20: 15416
interactions with protons at 3.8 Bev/c, resonance production in, (E), 20: 15418
interactions with protons at 1.80 and 1.95 Bev/c, boson exchange in, (E), 20: 15420
interactions with protons, total cross section for, (E/T), 20: 15428
interactions with protons at 1.5 Bev/c, K*(888) and N*(1425) production in, (E/T), 20: 15429
interactions with protons, spin-parity analysis of Ξ^*(1530) from, (E/T), 20: 15464
interactions with protons, U(12) symmetry for, 20: 15390
interactions with protons, cross section and scattering length for hyperon (Λ) and meson (η) production in, (T), 20: 17376
interactions with protons at 2.24 Bev/c, (E), 20: 17383
interactions with protons at 3 Bev/c, mechanism for $\bar{K}^{*0}$(891) yields from, (E), 20: 17380
interactions with protons at 2.10, 2.45, and 2.64 Bev/c, K_δ^*(892) resonances in, (E), 20: 17403
interactions with protons at high energies, resonances from, (E/T), 20: 19273(R) (BNL-929, pp 3-43)
interactions with protons, KNΛ and KNΣ coupling constant ratio from baryon exchange in, (T), 20: 19487
interactions with protons at 1.33 Bev/c, resonance production in, (E), 20: 21615 (COO-1195-52)
interactions with protons at 900 to 990 Mev/c, angular distributions and cross sections for, (E), 20: 21628 (TID-22822)
interactions with protons at high energies, conical function and mean value theorem for amplitude of, 20: 24061
interactions with protons at high energy, review on, 20: 24081
interactions with protons at 2 Bev/c, elastic and charge-exchange, (T), 20: 24082
interactions with protons, unitary symmetry in, (T), 20: 24170
interactions with protons at 4.1 Bev/c, Y* resonance production in, (E), 20: 25781(R) (COO-1195-56)
interactions with protons at 2.63 to 2.70 Bev/c, (E), 20: 25781(R) (COO-1195-56)
interactions with protons at 1.34 Bev/c, two- and three-body final states in, (E), 20: 25781(R) (COO-1195-56)
interactions with protons at 3.46 Bev/c, cross sections for elastic, 20: 27827
interactions with protons up to 300 Mev/c, scattering lengths of, (E/T), 20: 27835
interactions with protons at 1.2 to 1.8 Bev/c, meson (ω) production from, 20: 27842
interactions with protons at 1.2 to 1.8 Bev/c, hyperon (Λ) and meson (ω) production from, (E), 20: 27843
interactions with protons at 1.45 Bev/c, differential cross section for elastic, (E), 20: 27849
interactions with protons, suppression of backward meson (ϕ) production in, (T), 20: 27863
interactions with protons, near forward peaks in charge-exchange, (T), 20: 27871
interactions with protons, forward dispersion relations and coupling constants for, (T), 20: 27886
interactions with protons, properties of hyperons (Ξ^-) and (Ξ^0) from, (E), 20: 30072
interactions with protons at 1.45 Bev/c, K*(891) and N*(1236) production in, (E), 20: 30009
interactions with protons at 5 to 20 Bev/c, meson-exchange model for forward elastic, 20: 30039
interactions with protons at 1.455 Bev/c, K* resonance production in, (E), 20: 31987 (NP-16097)
interactions with protons at 1.05 to 1.7 Bev/c, hyperon (Ξ^0) properties from, (E/T), 20: 31988 (UCRL-11510)
interactions with protons at 1.2 to 2.7 Bev/c, cross sections for, (E/T), 20: 31990 (UCRL-16648)
interactions with protons, decay angular correlation for Y_1^{*-} from, (T), 20: 32052
interactions with protons at high energies, M(12) symmetry for, 20: 32079
interactions with protons at 1.22 to 1.70 Bev/c, Y*(J = 3/2) production in, (E/T), 20: 32068
interactions with protons, experimental status of baryon-exchange, 20: 32027
interactions with protons Y_1^*(1385) and Y_0^*(1660) production in, (E/T), 20: 32034
interactions with protons at 3 Bev/c, baryon exchange in, (E), 20: 34256
interactions with protons at 5.0 Bev/c, $\pi^+\pi^-$(410) enhancement in, (E), 20: 34200
interactions with protons at 2.1 to 2.7 Bev/c, meson(ϕ) production in, (E), 20: 34201
interactions with protons at 1.05 to 1.70 Bev/c, hyperon(Ξ^-) and (Ξ^0) production in, (E), 20: 34206
interactions with protons at 1.00 to 2.45 Bev/c, Y* resonances in, (E), 20: 34231
interactions with protons at 34.0 Bev, kinematic tables for, 20: 36022 (BNL-945)
interactions with protons at 2 Bev/c, differential and total cross sections for, (E), 20: 36042 (TID-23191)
interactions with protons at 2 Bev/c, polarization of Λ^0 in, (E), 20: 36042 (TID-23191)
interactions with protons at 2 Bev/c, K* production in, (E), 20: 36042 (TID-23191)
interactions with protons at 2 Bev/c, angular correlations for, (E), 20: 36042 (TID-23191)
interactions with protons at 2 Bev/c, Y_0^*(1520), Y_1^*(1660) and ρ^0 production in, (E), 20: 36042 (TID-23191)
interactions with protons at 4.6 and 5.0 Bev/c, f* production in, 20: 37730 (BNL-10459)
interactions with protons at high energies, elastic, (E/T), 20: 37796
interactions with protons at 2 to 6 Bev/c, Regge-pole model for cross sections for, (E/T), 20: 39801
interactions with protons, absorptive peripheral model for charge-exchange, 20: 39805
interactions with protons at 1.80 to 1.95 Bev/c, resonance production in, (E), 20: 39838
interactions with protons at 10 Bev/c, meson (L) production in, 20: 39788
interactions with protons at 4.2 Bev/c, strangeness-1 and -2 events in, (E), 20: 41799(R) (ORO-2504-96)
interactions with protons at 0.9 to 1.0 Mev/c, Λ^0, $\Sigma^\pm$, and $\bar{K}^0$ production in, (E), 20: 41799(R) (ORO-2504-96)
interactions with protons, peripheral model for Y* charge-state interference in, 20: 41819
interactions with protons at high energies, branching ratio predictions for, (T), 20: 44237
interactions with protons at 0.8 to 20 BeV/c, model for diffractive and resonant effects in, 20: 46333 (COO-264-343)
interactions with protons, NΛK and NΣK coupling constant estimation from amplitudes of, 20: 46359
interactions with protons at 1.7 to 2.0 BeV/c, differential cross sections for hyperon (Σ^-) and meson (π^+) production in, (E), 20: 46360
interactions with protons at 4.1 and 5.5 BeV/c, differential cross sections for elastic, (E), 20: 46365
interactions with protons, differential elastic cross sections, 16: 21309
interactions, production and properties of, review of data on, 20: 7867
kinetics at 100 kev to 100 Bev, graphs for, 19: 18752 (UCRL-2426(Vol. I) (1965 Rev.))
lifetime relative to mesons (K^+), (E), 20: 41884
magnetic moments of, Vigier rotator model for anomalous, 17: 34802

mass, 17: 31360
mass difference (K^0-K^-), (E), 19: 44998 (CU-1932-247)
mass difference with mesons (K^0), 16: 8054 (NP-11232(p.243-51))
mass difference with mesons, ($\bar{K}^0$), measurements of, (E), 19: 14324 (TID-21438)
mass differences of K^0–K^+ and K^0–K^-, 16: 10931
momentum spectra from proton reactions with aluminum and beryllium at 30 and 33 Bev, 16: 24858
nuclear capture and production in cloud chamber, 16: 1040(T) (JPRS-4956(p.18-22))
parity, (T), 20: 6283 (CERN-64-13(Vol.4), pp 137-86)
parity determination for, 17: 9379
photoproduction at high energies, (E/T), 19: 45024 (MIT-2098-163)
photoproduction at high energies, (E), 20: 15306(R) (CEAL-1026)
photoproduction of, baryon resonances in, (E), 20: 15424
photoproduction on protons at 3.0 to 6.0 Bev, (E), 20: 27920
production by high energy neutrinos, form factors and cross sections for, (T), 19: 8232
production from meson (π^-) reactions with heavy nuclei at 7.2 Bev/c, (E), 20: 28460
production in antiproton-proton interactions, spin of $K^{\wedge-}$, 16: 10851
production in antiproton-proton annihilation at rest, channel branching ratios and invariant mass distributions for, (E), 20: 27845
production in cosmic showers, transverse momentum of, 18: 14770
production in hyperon (Σ^0) decay, 16: 12359
production in meson ($K^+_{\pi 3}$) decay, 16: 6977
production in meson (π)-nucleon interactions, pair, (T), 19: 14354
production in neutrino-nuclear interactions at high energies, 18: 28413
production in proton accelerators, 18: 12912 (TID-7686(p.35-41))
production in proton-proton interactions at 19 and 24 Bev/c, cross sections for, 18: 18678
production in proton reactions with beryllium at 25 Bev, 18: 26165 (BNL-837(p.91-113))
production in proton reactions with beryllium at 12.5 Bev, cross sections for, (E), 19: 21406
production in proton reactions with nuclei at 20 Bev, 19: 41324 (CERN-65-14)
production in proton reactions with beryllium at 12.5 Bev, cross sections for, (E), 20: 21601 (CERN-65-32, pp 109-10)
production of beams of, in CERN synchrotron, (E), 19: 28940 (CERN-65-2)
production of high-intensity beams of, using CERN PS, 19: 41184
production of 4 Bev/c beams of, 17: 23631
properties at 100 kev to 100 Bev, 18: 28331 (UCRL-2426(Vol.I)(1963 Rev.))
reactions ($K^-,\pi^-\Lambda^0$) with helium-4, double-scattering corrections to, (T), 20: 8108
reactions in deuterium, branching ratio ($\Lambda\pi^-p/\Sigma^0\pi^-p$) for, 17: 16981
reactions in emulsions at 435 Mev/c, hyperfragment production in, 16: 15561
reactions in emulsions, nonmesic hyperfragment production, 18: 24654
reactions in nuclear emulsions, 17: 18530 (CERN-63-3(p.315-23))
reactions in nuclear emulsion at 1.5 Bev/c, hyperfragment production in (E), 19: 1668
reactions in nuclear emulsions at 2.3 Bev/c, hyperfragment production in, (E), 19: 37830 (TID-21937)
reactions with bromine and silver at 1.3 and 1.5 Bev/c, 18: 40547
reactions with carbon-12 in emulsion, Y^*_0(1405) production in, 17: 29542
reactions with carbon-12, ($\Sigma\pi$) resonance in, 17: 31294
reactions with carbon-12, hyperon (Σ)–meson (π) resonances from, (T), 19: 8140 (NP-14479)
reactions with complex nuclei, 17: 20594(R) (UCRL-10572)
reactions with deuterium, cross sections for charge-exchange, disintegration and elastic, 17: 28263
reactions with deuterium and hydrogen, ($\bar{K}$-N) bound state for absorption discrepancy in, 17: 29535
reactions with emulsion nuclei, at rest, 16: 5900
reactions with emulsion nuclei at 1.3 and 1.5 Bev/c, production of hyperfragments from, 17: 17191
reactions with emulsion nuclei at 800 Mev/c, hyperfragment ($A \geq 60$) production in, 17: 26555
reactions with emulsion nuclei at 50–300 Mev/c, hyperfragment production, in, 17: 26557
reactions with emulsion nuclei, hyperfragment production from, 17: 34942
reactions with emulsion nuclei at 800 Mev/c, hypernuclei production in, 17: 41917
reactions with emulsion nuclei at 800 Mev/c, production of short-range hyperfragments in, 18: 2755
reactions with emulsion nuclei at 2.3 Bev/c, double-hyperfragment event in, 18: 2656
reactions with emulsion nuclei at 800 Mev/c, hyperfragment production in, 18: 9365
reactions with emulsion nuclei, hyperfragment production in, 18: 11215 (NP-13541)
reactions with emulsion nuclei, mesic atom production in, 18: 11260
reactions with emulsion nuclei, hyperfragments from, 18: 16979
reactions with emulsion nuclei, hyperon (Σ) production in, 18: 24415
reactions with emulsion nuclei at 3.5 Bev/c, hyperfragment production in, 18: 30787
reactions with emulsion nuclei, hyperfragments from, 18: 32807
reactions with emulsion nuclei, ($\Sigma^-\pi$) resonances in, 18: 36266
reactions with emulsion nuclei at 1.5 Bev/c, hyperon (Ξ^-) production in, 18: 38134
reactions with emulsion nuclei at 1.5 Bev/c, hyperon (Ξ^-) production in, 18: 38135
reactions with emulsion nuclei, $^4_\Lambda$He hyperfragment from, 18: 38157
reactions with emulsion nuclei at 800 to 3500 Mev/c, short-range hyperfragments in, 18: 44819
reactions with emulsion nuclei at 3 Bev/c, hyperfragment production in, 18: 44550
reactions with emulsion nuclei, lithium-8 fragments from, 19: 1664
reactions with emulsion nuclei, hyperfragments produced in (E/T), 19: 1665
reactions with emulsion nuclei, hyperfragments from (E), 19: 1666
reactions with emulsion nuclei, hyperfragment production in (E), 19: 1667
reactions with emulsion nuclei, ($\Sigma\pi$) resonance at 1405 Mev in (E), 19: 1344
reactions with emulsion nuclei at 1.5 Bev/c, hyperfragment production in (E), 19: 5143
reactions with emulsion nuclei at 5 Bev/c, hyperfragment production in, (E), 19: 12500
reactions with emulsion nuclei at 0.8 to 3.5 Bev/c, short-range hyperfragment production in, (E), 19: 16967
reactions with emulsion nuclei at rest, hyperon (Σ) and meson (π) production in, (T), 19: 19151
reactions with emulsion nuclei at 3.0 Bev/c, hyperfragment production in, (E), 19: 21429
reactions with emulsion nuclei, hyperfragment production in, (E), 19: 21365
reactions with emulsion nuclei at 0.8 to 3.0 Bev/c, lithium-8 emission in, (E), 19: 21389
reactions with emulsion nuclei at 1.3 and 1.5 Bev/c, hyperfragment and lithium-8 production in, (E), 19: 27444
reactions with emulsion nuclei at 40 to 100 Mev, calculation of spectra from, (T), 19: 26917(R) (IA-984)
reactions with emulsion nuclei at 800 Mev/c, heavy spallation hyperfragments in, (E), 19: 33292
reactions with emulsion nuclei, hyperfragment production in, (E), 19: 35491
reactions with emulsion nuclei, heavy hyperfragments from, (E), 19: 37859
reactions with emulsion nuclei, hyperfragment production in capture, (E/T), 19: 47648
reactions with emulsion nuclei at 1.5 to 3 Bev/c, light charged particle emission in, (E), 19: 47651
reactions with emulsion nuclei at 5 Bev/c, hyperfragment and lithium-8-fragment production in, (E), 20: 3062
reactions with emulsion nuclei, Y^*_0 production in capture, (E), 20: 3064
reactions with emulsion nuclei at 50 to 1500 Mev/c, heavy hypernuclei from, (E), 20: 6294 (NP-15617)
reactions with emulsion nuclei, review on, 20: 11991
reactions with emulsion nuclei at 3.0 and 5.0 Bev/c, hyperfragment production from, (E), 20: 17752
reactions with emulsion nuclei, hyperfragments from, (E), 20: 22161
reactions with emulsion nuclei at 1.5 Bev, Λ-hyperfragment production in, (E), 20: 30448
reactions with emulsion nuclei at 1.5 Bev/c, hyperfragment production and mesic decay from, (E), 20: 32491
reactions with emulsion nuclei at 5.0 Bev/c, lithium-8 emission in, (E), 20: 32469
reactions with emulsion nuclei at 0 to 180 Mev, 18: 14854
reactions with emulsion nuclei at 3 Bev/c, hyperfragment production in, 18: 26290
reactions with heavy emulsion nuclei at 1.3 and 1.5 Bev/c, lithium-8 production in, 18: 36653
reactions with heavy emulsion nuclei at 1.5 to 25 Bev, lithium-8 energy spectra from, (E), 20: 15792
reactions with heavy emulsion nuclei at 1.5 Bev/c, $_\Lambda$He^7 and $_\Lambda$Li^7 production in, 20: 30368
reactions with helium-4, hyperon-meson (π) production and resonances, 16: 5896
reactions with helium-4, Y^*_1 production in, 17: 9373
reactions with helium-4, hyperfragment formation in, 17: 9379
reactions with helium-4, decay modes of $_\Lambda$He^4 and p-wave ratio for $\Lambda \rightarrow n + \pi^0$, 17: 24482

reactions with helium-4, hyperfragments from, 18: 15180 (CERN-64-1 (p.63-74))
reactions with helium-4, hyperfragment production in, 18: 15181 (CERN-64-1(p.75-84))
reactions with helium-4, $_{\Lambda}H^{3}$ lifetime from, 18: 26527 (BNL-837(p.454-6))
reactions with helium at 430 Mev/c, hyperon production in, (E/T), 19: 4901 (ORNL-3717)
reactions with light nuclei, hyperon (Λ) and (Σ) production from, 20: 22033
reactions with lithium-6, hyperfragments from, (E), 19: 26917(R) (IA-984)
reactions with lithium-6, hyperfragments from, (E/T), 19: 39265(R) (IA-1021)
reactions with lithium-6, hyperfragments from, (E), 20: 2520(R) (IA-920)
reactions with matter, dE/dx and range-energy graphs for, 20: 46601 (UCRL-2426(Vol.2)(1966 Rev.))
reactions with matter, range-momentum and dP/dx graphs for, 20: 46342 (UCRL-2426(Vol.4)(1966 Ed.))
reactions with nuclei at 1.15 Bev/c, energy distributions from, 16: 12355
reactions with nuclei at 500 Mev/c, hyperfragment and hyperon production in, 16: 22886
reactions with nuclei in emulsions, $_{\Lambda}Be^{9}$ production in, 16: 26312
reactions with nuclei at 300 Mev/c in emulsions, hyperon (Λ^0) production in, 16: 27947
reactions with nuclei at 500 Mev/c, hyperfragment production in, 17: 24483
reactions with nuclei at 1.455 Bev/c, hyperons ($\bar{\Xi}^0$) and ($\bar{\Xi}^-$) production in, 17: 26334
reactions with nuclei at 800 Mev/c, hyperon (Λ) beta decay branching ratio from, 17: 28192
reactions with nuclei at 800 Mev, heavy spallation hyperfragments from, 18: 9315 (NP-13483)
reactions with nuclei at 1.3 and 1.5 Bev/c hyperon ($\bar{\Xi}$) production in, 18: 18944
reactions with nuclei, nuclear trapping of hyperons (Λ) from, 18: 26623
reactions with nuclei at 1.5 Bev/c, lithium-8 fragments in, 18: 26636
reactions with nuclei, analog hypernuclear states in, (T), 19: 16997
reactions with nuclei, baryons ($\Sigma\pi$) production in, (E), 19: 26917(R) (IA-984)
reactions with nuclei at rest, 19: 47708
reactions with nuclei, baryons Σ-π production in, (E/T), 20: 2520(R) (IA-920)
reactions with nuclear emulsions at 800 Mev/c, computer analysis of, 20: 2520(R) (IA-920)
reactions with nuclei in emulsions at 800 Mev/c, hyperfragment production from, (E), 20: 26102
reactions with nuclei, 17: 19324
reactions with nuclei, 18: 15290
reactions with octafluoropropane at 1 Bev/c, (E), 19: 25265(R) (UCRL-11776)
resonance states of, $\frac{3}{2}^+$ octet for Y_1^*, 18: 32619
scattering by emulsion nuclei, differential cross sections and optical potentials, 16: 12337 (NP-11175)
scattering by emulsion nuclei at 21 Mev, differential and total cross sections for, (E), 19: 35443
scattering by helium, resonance effect in, 18: 26277(R) (ORNL-3582 (p.127-8))
scattering by nuclei at low energies, 16: 4691 (TID-13768)
scattering by nuclei, cross sections for, 16: 33812
separation from antiprotons and mesons (π^-) by electrostatic methods, 16: 13176 (NIRL/R/10)
separation of beams of, system design for, 19: 30881 (BNL-9129)
transport in CERN synchrotron, 17: 18516 (CERN-63-3(p.81-93))
triplet formation with mesons (K^+) and (π), 16: 10902
uses in research on complex nuclear structure, 17: 36641 (CERN-63-28 (p.1-36))

MESONS (K⁰)

angular distribution from meson (π^-) reactions with Freon and xenon at 2.8 Bev, 16: 26189
angular distribution in $K^0N_2^{+,+}$ decay, 18: 22743
anomalous regeneration of mesons (K_1^0) from mesons (K_2^0), 18: 2631
behavior, 16: 18100 (NP-11463(Pt.2)(p.187-94))
beta decay of, $\Delta Q = \Delta S$ rule in, 18: 30564
charge of, non-neutral, 18: 28365
charge symmetry, 18: 9208
charge symmetry of, 16: 32298 (UCRL-10244)
decay, 17: 20594(R) (UCRL-10572)
decay, 17: 31279 (NEVIS-118)
decay, (T), 20: 9771
decay (2π) of, particle-mixture theory for CP invariance in, 20: 2720
decay, (E/T), 19: 25265(R) (UCRL-11776)
decay, analysis of leptonic, 16: 9438(R) (TID-14786)
decay and interactions of, as test of the CPT theorem, 17: 13432
decay and production in meson (π^-)-proton interactions at 775 to 871 Mev, 16: 15592
decay and properties, 17: 19181
decay as test of $\Delta S = \Delta Q$ selection rule, leptonic, 16: 7020 (TID-14474)
decay branching ratios and lifetime, 16: 10931
decay branching ratio of, neutral, 17: 34777
decay, charge-parity conservation in, 16: 10893
decay-component interference effects in, 16: 15578
decay, determination of branching ratio in, 16: 32282 (TID-16550)
decay in mixed ensemble, (T), 19: 47309 (JINR-P-2289)
decay ($K_2^0 \to 2\gamma$) of, violation of $|\Delta I| = \frac{1}{2}$ rule in, 18: 887
decay mechanisms of, (E/T), 19: 23355(R) (BNL-867(p.1-117))
decay mode ($\pi\pi\gamma$), 16: 31040
decay modes, 16: 16956 (NP-11592(Vol.I)(p.241-5))
decay modes, bubble chamber analysis of, 17: 19192
decay modes of K_2^0, (E), 20: 13450 (JINR-P-2488)
decay modes of K_2^0, (E), 20: 19431 (ANL-7130, pp 77-81)
decay modes of K_2^0, 20: 41903
decay modes of, current algebra for 2π, 20: 30015
decay, nonvalidity of $\Delta I = \frac{1}{2}$ and $\Delta S = +\Delta Q$ rules in 3-body, 16: 26151
decay of (K_1^0), spontaneous breakdown of CP symmetry in (2π), (T), 19: 20999
decay of (K_2^0), isotopic spin changes in, (T), 19: 12246
decay of (K_2^0), probabilities for, (T), 19: 16470 (JINR-P-1920)
decay of (K_2^0), CP violation in 2π, (T), 19: 18858
decay of (K_2^0), into two mesons (π) and a photon, (T), 19: 20939 (UR-875-30)
decay of (K_2^0), CP-nonconserving, 19: 39476 (NP-15197)
decay of, charge symmetry in, 17: 5272
decay of, CP invariance and K_1 regeneration in, 17: 6995
decay of, $\Delta I = \frac{1}{2}$ rule and $\Delta S = \Delta Q$ rule in, 17: 9396
decay of K_L and K_S, amplitude interference in 2π, (E), 20: 46368
decay of K^0 and $\bar{K}^0$, violation of CP invariance in, 18: 40329
decay of K_2^0, CP invariance in 3π, (T), 20: 39763 (JINR-P-2850)
decay of K_1^0 and K_2^0, CP-noninvariant interactions in, (T), 19: 27255
decay of K_1^0 and K_2^0, CT invariance in, 19: 41452
decay of K_1^0 and K_2^0, regenerative and relative phases for amplitudes of 2π, (E), 20: 46364
decay of K_2^0, eightfold way symmetry in nonleptonic weak, 18: 10962
decay of K_2^0, CP-nonconserving, (T), 19: 21020
decay of K_2^0, CP violation and regeneration in, (T), 19: 25283
decay of K_2^0, $K^* \to \pi$ weak vertex in nonleptonic, (T), 19: 27254
decay of K_2^0, 2π, (T), 19: 45026 (N64-19243)
decay of K_2^0, SU(9) composite symmetry for 2π, 20: 7885 (IC/65/67)
decay of K_2^0, weak interaction theory for 2π, 20: 17379
decay of K_2^0, 2π, (T), 20: 21675
decay of K_2^0, Cabibbo current theory for parity-violating nonleptonic, 20: 30041
decay of $K^0_{\mu 3}$, evidence of time reversal in 2π, 20: 44193
decay of K_2^0, CP violation in 3π, (E), 20: 46331 (BNL-10606)
decay of K_2^0, 18: 12944
decay of K_2^0, 18: 40303
decay of K_2^0, (E/T), 19: 25265(R) (UCRL-11776)
decay of K_2^0, (T), 20: 4849(R) (UCRL-14360, pp 1-50)
decay of K_2^0, (E), 20: 25781(R) (COO-1195-56)
decay of K_2^0, $\Delta I = \frac{1}{2}$ rule in, 18: 37916
decay of K_2^0, branching ratios for (E), 19: 1317
decay of K_2^0, CP invariance breakdown in, (T), 19: 8199
decay of K_2^0, detection of, (E), 19: 10018 (NP-14487)
decay of K_2^0, rates of three-body, (E), 19: 16616
decay of K_2^0, branching ratios for three-body leptonic, (T), 19: 21060
decay of K_2^0, branching ratios for, (E), 19: 25339
decay of K_2^0, CP invariance breakdown in, (T), 19: 39265(R) (IA-1021)
decay of K_2^0, leptonic, (E), 19: 39474 (JINR-P-2190)
decay of K_2^0, three-body, (E), 19: 39586
decay of K_2^0, time reversal and cosmological effects on, 19: 32961
decay of K_2^0, PC violation through SU_3 transformation for, 19: 32986
decay of K_2^0, CP violation in, 19: 43050 (NP-15395)
decay of K_2^0, mean lifetime from, (E), 19: 43116
decay of K_2^0, CP violation and $\Delta T = \frac{1}{2}$ rule in, (T), 19: 47317(T) (NP-tr-1282)
decay of K_2^0, violation of time reversal invariance in, 20: 918
decay of K_2^0, alternatives to 2π, (T), 20: 2692
decay of K_2^0, statistical irreversibility of 2π, (T), 20: 2699(T)
decay of K_2^0, gravitational effects on, 20: 2865 (JINR-P-2325)
decay of K_2^0, spectra of $\pi\mu\nu$, 20: 4631
decay of K_2^0, method for analysis of, (T), 20: 4583 (JINR-P-2371)
decay of K_2^0, CP nonconservation in 2π, 20: 4626
decay of K_2^0, 3π, (E), 20: 6031 (BNL-9613)
decay of K_2^0, probabilities of 3π, (E), 20: 7871
decay of K_2^0, upper limit for 2π, (E), 20: 9757
decay of K_2^0, relative probability for $e\pi\nu$, (E), 20: 11560 (JINR-P-2449)
decay of K_2^0, 2π, (E/T), 20: 11554 (COO-1195-27)

decay of K_2^0, cosmological and gravitational theories for, 20: 13507
decay of K_2^0, branching ratio for neutral current, (E), 20: 15331
decay of K_2^0, CP noninvariance in 2π, (T), 20: 15446 (UCRL-12380-T)
decay of K_2^0, G_2 symmetry scheme for, 20: 15474
decay of K_2^0, neutral a-particle model for 2π, (T), 20: 15504
decay of K_2^0, meson (μ^+) polarization in, (E), 20: 17424
decay of K_2^0, CP violation in, (E/T), 20: 19428 (ANL-7130, pp 17-28)
decay of K_2^0, CP invariance in 3π, (E/T), 20: 19429 (ANL-7130, pp 59-66)
decay of K_2^0, 3π, (E), 20: 19430 (ANL-7130, pp 67-75)
decay of K_2^0, CP violation in, (T), 20: 19443 (JINR-E-2614)
decay of K_2^0, CP violation in 2π, (T), 20: 19474
decay of K_2^0, 2π, (E), 20: 19507
decay of K_2^0, CP violation in, (T), 20: 19608
decay of K_2^0, CP violation in, (T), 20: 19528
decay of K_2^0, Monte Carlo statistical box for rest-mass configurations for, 20: 24058
decay of K_2^0, Monte Carlo statistical box for laboratory-system configurations and parameters for, 20: 24059
decay of K_2^0, form factors and probabilities for leptonic, (E), 20: 24063
decay of K_2^0, charge asymmetry in $e\pi\nu$, 20: 25781(R) (COO-1195-56)
decay of K_2^0, CP invariance in, (T), 20: 25804(T)
decay of K_2^0, branching ratio and spectra of 3π, (E/T), 20: 25830
decay of K_2^0, random trial method for simulating conditions for recording and identification of, (T), 20: 25844
decay of K_2^0, programs for particle identification from, 20: 25845
decay of K_2^0, coherent regeneration in meson (K^0)-neutrino interactions and CP violation in, (T), 20: 27885
decay of K_2^0, branching ratios for, (E), 20: 27891
decay of K_2^0, probability of 2π, (E), 20: 30056
decay of K_2^0, CP violation in 2π, (E), 20: 30000
decay of K_2^0, test of CP violation in, 20: 32060
decay of K_2^0, CP violation in 2π, (T), 20: 34177
decay of K_2^0, branching ratios for two photon, (E), 20: 34237
decay of K_2^0, paritino CP-invariance mechanism in 2π, (T), 20: 34162
decay of K_2^0, time invariance in, 20: 36043(R) (TID-23206)
decay of K^0, test of time-reversal invariance in leptonic, (E), 20: 44252
decay of K_2^0, CP violation in, (T), 19: 43163
decay of, $K_2^0 \rightarrow 2\gamma$, 18: 863 (TID-19604)
decay of K_2^0, branching ratios and half lives, 16: 16954 (NP-11592 (Vol.I)(p.227-34))
decay of, method for testing time-invariance by, 17: 28414
decay of pair of, (T), 20: 36047
decay of, symmetry violations in leptonic, 18: 7551
decay of, unitary symmetry of weak current structure in, 17: 41781
decay of, amplitudes for 3π, (E/T), 20: 34194
decay of, analysis of CP violation in, 18: 42448
decay of, branching ratio for leptonic and nonleptonic, 18: 20973
decay of, C-violation model for 2π, 20: 4681
decay of, coherent interference in $\pi^+\pi^-$, (E), 20: 39849
decay of, conservation of strangeness changing vector current in leptonic, 17: 15072 (CTSL-38)
decay of, constructive interference between coherently regenerated and CP-nonconserving amplitudes in, (E), 19: 35167
decay of, CP and $|\Delta I| = \frac{1}{2}$ violations in, (T), 19: 41471
decay of, CP invariance and superposition principle in, (T), 19: 4969
decay of, CP invariance and $\Delta S = \Delta Q$ selection rules in leptonic, (E/T), 19: 35110
decay of, CP invariance in 2π, (T), 20: 11608
decay of, CP invariance in 2π, (E), 20: 13495
decay of, CP invariance in, (E/T), 20: 20365
decay of, CP invariance in, (E/T), 20: 21700
decay of, CP invariance in 2π, 20: 24011 (CERN-65-24(Vol.3), pp 87-100)
decay of, CP invariance violation in, 20: 34238
decay of, CP noninvariance in 2π, 20: 31982 (AD-634703)
decay of, CP violation in, 18: 34590
decay of, CP violation in, (T), 19: 12197
decay of, CP violation in, 19: 25336
decay of, CP violation in, (T), 19: 45034 (NP-15470)
decay of, CP violation and regeneration in, (E/T), 20: 1021
decay of, CP violation and superposition principle in 2π, (T), 20: 7831
decay of, CP violation in, (T), 20: 9769
decay of, CP violation, normality, and reciprocity in, (T), 20: 9749
decay of, CP violation amplitude from time-dependent interference effects in 2π, (E), 20: 13496
decay of, CP violation in leptonic, (T), 20: 13515
decay of, CP violation in, (T), 20: 15432
decay of, CP violation in, (T), 20: 15434
decay of, CP violation in 2π, (T), 20: 19461
decay of, CP violation in 2π, 20: 34240
decay of, CP violation in, 20: 34241
decay of, CP violation in 2π, 20: 41849
decay of, CP violation in three-body electron, (E), 20: 44259
decay of, CP-invariance violation in leptonic, 19: 32945 (JINR-P-2083)
decay of, CP-invariance violation in, 20: 19273(R) (BNL-929, pp 3-43)
decay of, CP-violating nonleptonic, (T), 20: 15433
decay of, degenerate SU(4) symmetry for CP violation in 2π, 20: 13625
decay of, $\Delta S = \Delta Q$ conservation in electronic, 18: 26262 (BNL-837(p.54-65))
decay of, $\Delta S = \Delta Q$ rule in leptonic, 18: 32606
decay of, $\Delta S = \Delta Q$ rule in leptonic (E), 19: 1320
decay of, $\Delta S = \Delta Q$ rule in leptonic (E), 19: 1321
decay of, $\Delta S = \Delta Q$ rule, $\Delta I = \frac{1}{2}$ rule, and CP conservation studies of, (E), 19: 37525 (CU-1932-241)
decay of, effects of selection rules and invariance on partial rates for, 18: 34506 (BNL-8094)
decay of, energy dependence of form factors in three-body leptonic, (E), 20: 19432 (ANL-7130, pp 83-90)
decay of, existence of mirror particles from CP violation in 2π, 20: 37806
decay of, form factors for three-body muonic, (E/T), 20: 19433 (ANL-7130, pp 91-105)
decay of, identification by computer analysis, (T), 19: 23360 (JINR-P-1982)
decay of, interference of K_S and K_L in $\pi^+\pi^-$, (E), 20: 30026
decay of, interference between amplitudes in 2π, 20: 37814
decay of, intermediate boson pole with meson (S^0) in radiative, (T), 20: 2684 (JINR-P-2374)
decay of, kinematic tables for, 20: 36022 (BNL-945)
decay of, leptonic, (E/T), 19: 25265(R) (UCRL-11776)
decay of, leptonic, (E), 20: 31991 (UCRL-16771)
decay of, magnetic spectrometer performance for recording 2π, 20: 16814 (ITEF-386)
decay of, meson (μ) polarization in leptonic, (T), 19: 25355
decay of, model for, (T), 19: 16624
decay of, modified V-A interaction and CP invariance for 2π, 20: 13597
decay of, nonleptonic, (T), 20: 15307(R) (COO-1261-22)
decay of, partially conserved currents and CP violation for, (T), 20: 32021
decay of, PC violation in leptonic, (T), 19: 32999
decay of, pole model for nonleptonic, 20: 21688
decay of, radiative (E), 19: 1316
decay of, ratio of K_2^0 to K_1^0 production in, (E), 19: 23355(R) (BNL-867(p.1-117))
decay of, reciprocity principle and CP violation in, 20: 15350
decay of, relative probability of 3π, (E), 20: 11561 (JINR-P-2450)
decay of, review on, 19: 37644
decay of, review on nonleptonic, 19: 37658
decay of, selection rules for nonleptonic, 18: 34628
decay of, selection rules in, (T), 19: 12317
decay of, shadow universe model for, (T), 19: 35127
decay of, shadow universe correlations with neutrino experiment, (T), 20: 6045(T)
decay of, SU(3) model for CP-violating, (T), 19: 41371
decay of, sum rule for amplitudes of 2π, (T), 20: 17369
decay of, test of $\Delta I = \frac{1}{2}$ rule for leptonic, (E), 20: 41799(R) (ORO-2504-96)
decay of, test of $\Delta Q = \Delta S$ rule in neutral leptonic, (E), 20: 46332 (BNL-10609)
decay of, testing of time-reversal invariance by, (E), 20: 11662
decay of, time distribution in, (E), 20: 19435 (ANL-7130, pp 153-7)
decay of, 2π, (T), 20: 7807
decay of, 2π, 20: 46580(R) (BMwF-FBK-66-05)
decay of, 2π, 20: 25787 (JINR-P-2632)
decay properties, 17: 9397
decay rate and lifetime, 17: 9396
decay rate of K_2^0, 2π, (T), 20: 32039
decay rate of long-lived, absolute three-body, (E), 20: 41855
decay rate of, CPT-invariance test and measurement method for, 19: 41413
decay scheme, use in testing $\Delta Q = \Delta S$ selection rule, 16: 16953 (NP-11592(Vol.I)(p.209-15))
decay to $\pi^+ + e^- + \bar{\nu}_e$, weak interaction model for, 17: 34801
decay with $\Delta Q/\Delta S = -1$, 18: 22772
decay, analysis of $\Delta Q = \Delta S$ selection rule in lepton, 16: 27907 (NP-11633)
decays of, branching ratios for 2π, 20: 41872
decays of, CP invariance violation and noninvariant vacuum in, (T), 20: 2698(T)
decays of, CP violation in nonleptonic, 19: 43136
decays of, CP violation in 2π, (T), 20: 30055
decays of, CP violation in radiative, 20: 41905
decays, leptonic, 16: 10812 (CERN-61-30)
detection and identification in bubble chamber experiments, 16: 10813 (CERN-62-2)
detection and measurement of, possible method for, 18: 30511 (JINR-P-

1654)
electric charge of, possibility of nonzero, 19: 1302
electromagnetic form factor, 18: 12958
electromagnetic properties, (T), 20: 7807
existence of $K^{0\prime}$ with 2π decay mode, (T), 19: 43163
interactions, angular distributions in, 16: 15553
interactions of, asymptotic properties of scattering amplitudes in, 18: 2624
interactions of, interference phenomena in, 16: 33693 (TID-16725)
interactions of K_2^0 with protons at low energies, Y_0^* (1405 Mev) production in, 18: 14858
interactions of K_1^0 with protons, K_1^0 regeneration in, 18: 40229 (BNL-8239)
interactions of K_2^0, test of CP violation in, 20: 32060
interactions of K_1^0 with protons, total cross sections for, (E), 20: 41799(R) (ORO-2504-96)
interactions of mesons (K_2^0) with protons, anomalous regeneration of mesons (K_1^0) from, 18: 2631
interactions of mesons (K_2^0) with protons at 300 Mev/c, hyperon-meson (K_1^0) production ratio of, (E), 20: 44250
interactions of, selection rule for weak, 17: 19069
interactions of, SU(6) symmetry for forward amplitudes in, (T), 19: 41515
interactions with mesons (π^0), angular distributions in, 16: 15553
interactions with protons at 200 to 600 Mev, 16: 16955 (NP-11592 (Vol.I)(p.235-9))
interactions with protons, elastic scattering, 16: 21264 (JINR-D-820)
interactions with mesons (K^0), orbital angular momentum in, 16: 26078 (JINR-P-960)
interactions with hyperons (Λ^0) from meson (π^-) reactions with freon and xenon at 2.8 Bev/c, resonances from, 16: 27987
interactions with nucleons, effect of ($\bar{K}$-K) resonance in, 17: 20871
interactions with nucleons, asymptotic properties of scattering amplitudes in, 18: 2624
interactions with mesons ($\bar{K}^0$), cross sections for inelastic, 18: 7532
interactions with protons at 2 Bev/c, resonance production in, 18: 14948
interactions with hyperons (Λ), resonance effects in, 18: 26352
interactions with meson (π^-)-meson (π^+) pairs, resonances in, 18: 40378
interactions with mesons (K) and (π), properties of resonance, (E/T), 19: 6556
interactions with mesons ($\bar{K}^0$), effects of media on, (T), 19: 12258
interactions with protons, relativistic SU(6) model for amplitudes of, 19: 23395
interactions with mesons ($\bar{K}^0$), 1280-Mev resonance in, (E), 19: 37623
interactions with nucleons at high energies, polarization and Regge poles in, (T), 19: 45044 (UCRL-16186)
interactions with hyperons (Λ^0), resonance, (E), 20: 24067
interactions with neutrinos, coherent regeneration and meson (K_1^0) decay in, (T), 20: 27885
interactions with protons at low energies, S-wave scattering length determination from, (E), 20: 44244
interference phenomena in $K^0\bar{K}^0$ systems, 17: 7026
kinetics at 100 kev to 100 Bev, graphs for, 19: 18752 (UCRL-2426(Vol. I) (1965 Rev.))
lifetime, 18: 7470 (JINR-P-1423)
lifetime and mass of K_1 and K_2, 17: 19071
lifetime and properties, 18: 20974
lifetime of K_2^0, 18: 26261 (BNL-837(p.42-52))
lifetime of K_1^0 (E), 19: 3062
lifetime of K_1^0, (E), 20: 34204
lifetime of K_2^0, (E), 20: 39849
lifetime of K_2^0, direct measurement of mean, 17: 13416
lifetime of short-lived, (E), 20: 41855
magnetic moment limits, 16: 15529 (JINR-D-862)
magnetic moments of, Vigier rotator model for anomalous, 17: 34802
magnetic moments, upper limit for, 16: 26182
mass, (E), 19: 44998 (CU-1932-247)
mass and lifetime matrices for (K^0–$\bar{K}^0$), invariance principles for, 20: 21677
mass difference (K_1–K_2), 18: 40239 (NP-14293)
mass difference (K_1^0 – K_2^0) sign in pole approximation model with unitary symmetry, 18: 12953
mass difference (K_1^0 – K_2^0), higher-order effects in, 18: 12965
mass difference (K_1^0-K_2^0), theoretical calculation of, 18: 21007
mass difference (K_1^0–K_2^0), contributions of S-wave T = 0 meson(π)–meson(π) interaction to, 18: 30526 (TID-20771)
mass difference (K_1^0–K_2^0), 18: 30564
mass difference (K_1^0–K_2^0), 18: 34593
mass difference (K_1^0–K_2^0), 18: 42453
mass difference (K_1^0–K_2^0) (T), 19: 3061
mass difference (K_1^0–K_2^0) and K_1^0 regeneration in copper, (E), 19: 43130
mass difference (K_1^0–K_2^0), measurement of, 20: 2748
mass difference (K_1^0–K_2^0), (E), 20: 11661
mass difference (K_S^0–K_L^0), (E), 20: 41922
mass difference (K_L^0–K_S^0), (E), 20: 46368
mass difference (K_1^0–K_2^0), 20: 19437 (ANL-7130, pp 215-30)
mass difference (K_1^0–K_2^0), (T), 20: 21675
mass difference K_1^0–K_2^0, sign of, (E), 20: 39772 (UCRL-17007)
mass difference K_1^0–K_2^0, determination of sign of, 17: 32954
mass difference (K_1^0–K_2^0), sign of, 17: 39847 (UCRL-11018)
mass difference (K_1^0–K_2^0), 18: 2684
mass difference between K-1 and K-2, 18: 26263 (BNL-837(p.74-81))
mass difference K^--$\bar{K}^0$, effects on deuteron-K^- interactions, 16: 33709
mass difference K_1^0-K_2^0, 16: 9438(R) (TID-14786)
mass difference (K_1^0–K_2^0), 16: 31035
mass difference (K_1–K_2), 400-Mev dipion resonance explanation of, 18: 10951
mass difference (K_1–K_2), generation by second order weak interactions, 17: 11522
mass difference $|K_2^0 - K_1^0|$, 16: 6021
mass difference K_2^0–K_1^0, from meson ($K\pi_1$) decay, 18: 36318
mass difference (K^+-K^0), (T), 19: 16556
mass differences of K^0–K^+ and $\bar{K}^0$–K^-, 16: 10931
mass difference of K_1^0, and K_2^0, 16: 6998
mass difference of K_1 and K_2, effect of nonzero charge of K^0 on, 19: 1302
mass difference of (K_2^0-K_1^0), boson-pole term effects on, 17: 9246
mass difference of K_1^0 and K_2^0, method of determining, 17: 19182
mass difference of K_1^0 and K_2^0, 17: 24327
mass difference of K_1^0 and K_2^0, octet dominance model for, (T), 19: 8168
mass difference of mesons (K_1^0) and (K_2^0), (T), 19: 14351
mass difference of K_1^0 and K_2^0, 20: 13495
mass difference of K_1^0 and K_2^0 in S-matrix theory, 20: 32025
mass difference of K_1^0 and K_2^0, measurement of sign of, (E), 20: 41878
mass difference of K_1^0 and K_2^0, current algebra for nonleptonic decay models for, 20: 44266
mass differences with mesons (K^-) and (K^+), 16: 8054 (NP-11232 (p.243-51))
mass differences, 16: 12356
mass differences (K_S^0–K_L^0), 20: 41872
mass differences (K^+–K^0), effects of electromagnetic self-energies, 16: 18321 (NYO-10130)
mass differences, effects on hyperon (Ξ) decay pole approximations, 16: 8151
mass difference (K_1–K_2) in, 17: 13344 (JINR-P-1124)
mass-difference sign for K_1 and K_2, 16: 13907
mass-difference sign of (K_1^0–K_2^0), 17: 29530
mass K_2^0 and K_1^0, difference of, (E), 19: 45099
mass matrix for K^0-$\bar{K}^0$, reciprocity principle for, 20: 15350
mass matrix of K^0–$\bar{K}^0$ system, off-diagonal elements of, 20: 31982 (AD-634703)
mass of K_1^0 and K_2^0, difference in, (T), 19: 18785
mass of K_1^0 and K_2^0, difference in, (E), 20: 24064
mass of K_1^0 and K_2^0, meson (η^0) and, 17: 37982
mass of, CP admixture in, (T), 19: 23442
mass relative to K^+, 20: 30016
mass sign of, comparison with $\bar{K}^0$, 20: 2865 (JINR-P-2325)
masses and gravitational properties of K^0 and $\bar{K}^0$, 16: 18397
pair production by mesons (π^-) in bubble chambers, resonance in, 17: 7039
pairs with antimesons ($\bar{K}^0$), production in proton-meson (π^-) interactions at 7 to 8 Bev/c, 17: 2193
pairs with hyperons (Λ), production in proton-meson (π^-) interactions at 7 to 8 Bev/c, 17: 2193
parity of, intrinsic, 18: 874
parity of, imaginary, (T), 19: 18785
photoproduction on protons, amplitudes for, 18: 18699
photoproduction on protons at 15 Bev, cross sections for, (T), 19: 27245
production amplitudes, resonance with hyperons (Λ^0), 16: 21300
production by meson (π^-)-nucleon interactions, 17: 9360
production by meson (π^-)-proton interactions at 10 Bev/c, 17: 9361
production by meson (K^-)-proton interactions, 17: 9380
production by meson (π^-) interactions with carbon nuclei and protons, 17: 9362
production by proton interactions with mesons (π^-) or nuclei, 16: 10918
production in cosmic nucleon interactions with nuclei at 100 to 500 Bev, cross sections for, 19: 10303
production in cosmic-particle interactions, (E), 20: 23931
production in electron-proton interactions, (T), 20: 27942
production in K^--proton interactions at 293 to 513 Mev/c, 16: 27914 (UCRL-10175)
production in meson (π^-)-proton interactions at 7 to 8 Bev, 16: 26068 (JINR-D-965)
production in meson (π^-)-xenon nucleus reactions, cross sections, 16: 27925
production in meson (π^-) interactions with nucleons, 17: 9282
production in meson (π^-)-proton interactions, resonances in, 17: 9374
production in meson (π^-)-proton interactions, resonance states in, 17: 15076 (JINR-P-1019)

production in meson (π^-)-proton interactions, 17: 19170
production in meson (π^-) reactions with deuterium at 1.23 Bev/c, charge asymmetry of, 17: 22489
production in meson (π^-)-proton interactions, modified K* exchange model for, 17: 31335
production in meson (π^-)-proton interactions at 1170 Mev/c, 17: 34739 (UCRL-10838)
production in meson (π^-)-proton interactions, associated, 17: 34825
production in meson(π^-)-proton interactions, 17: 36568 (BNL-6569)
production in meson (π^-)-nucleon interactions at 11.4 Bev/c, cross sections and angular distributions of, 17: 39864
production in meson (π^-)-nucleon interactions, correlations in, 17: 41765
production in meson (π^-) reactions with carbon at 7 Bev, 18: 13046 (JINR-P-1472)
production in meson (π^-) reactions with carbon at 7 Bev, cross sections for, 18: 28404
production in meson (π^-)-proton interactions at 10 Bev/c, 18: 40267
production in meson (π^-)-nucleon interactions at 6 to 18 Bev/c, (E), 19: 14322 (NP-14637)
production in meson(π^-)-proton interactions at low energies, (T), 19: 37587
production in meson (π^-) reactions with xenon at 9 Bev/c, cross sections for, 19: 39472 (JINR-P-2178)
production in meson (π^-) reactions with xenon at 9 Bev/c, cross sections for, (E), 20: 15841
production in meson (π)-proton interactions, two-resonance model for, (T), 20: 15392
production in meson (π^-)-proton interactions at 900 Mev, (T), 20: 41917
production in neutrino-nuclear interactions at high energies, 18: 28413
production in p–π^- interactions, measurement apparatus, 16: 10213
production of ($K^0\pi^-$p), 18: 30588
production of (K_2^0) in proton reactions with beryllium at 30 Bev, 18: 32618
production of (K_1^0) and (K_2^0) in antiproton-proton interactions, 18: 36306
production of $\overline{K}^*$-resonance in meson (K^-)-proton interactions at 1.45 Bev/c, 18: 32584
production of beams of, regeneration phenomena in, (T), 19: 45034 (NP-15470)
production of K' in (π^- + p) reaction, 16: 8098 (JINR-P-809)
production of K_1^0 in meson (K_2^0) interactions in liquid hydrogen, anomalous, 18: 40229 (BNL-8239)
production of K_2^0, in meson (K_2^0)–proton interactions, (E), 20: 19507
production of K_1 in meson (π^-)-proton interactions at 6 Bev/c, 18: 37875 (BNL-8236)
production of K_1 in antiproton–proton annihilation at 3.69 Bev/c, 18: 40232 (BNL-8242)
production of pairs in propane by mesons (π^-) at 6.1, 11.6 and 18.1 Bev, 16: 16938 (NP-11592(Vol.I)(p.101-10))
production of pairs of, and hyperons (Λ), in meson (π^-)-proton interactions, 17: 9363
production of pairs with hyperons (Λ) in meson (π^-)-nucleon interactions at 6 to 18 Bev/c, correlations in, 17: 41765
production of pairs with antimesons ($\overline{K}^0$) in meson (π^-)-nucleon interactions at 6 to 18 Bev/c, correlations in, 17: 41765
production of Σ^0K^{*0} in meson (π^-)-proton interactions, 18: 9177
production with hyperons(Λ^0), in π-nucleon interactions, 17: 15139
properties at 100 kev to 100 Bev, 18: 28331 (UCRL-2826(Vol.I)(1963 Rev.))
properties of K_1^0 and K_2^0, 18: 40222 (BNL-8230)
reactions with lead at 100 Mev, hyperon production in, 16: 7015 (JINR-D-794)
reactions with lead nuclei at 100 Mev, hyperon production, 16: 17051
regeneration in beryllium, 20: 37814
regeneration in plates, resonance transitions in, (T), 19: 37224(T)
regeneration, mass differences in, 16: 10862
regeneration of K_1, in solid materials, 20: 2748
regeneration of K_1^0, 20: 19437 (ANL-7130, pp 215-30)
regeneration of K_L –K_S in carbon, Regge-pole model for, 20: 37764
regeneration of K-1, in hydrogen, 18: 26264 (BNL-837(p.82-7))
spin-parity of resonance, Adair determination of, 18: 20998
transition (K_1^0-K_2^0) in coulomb field, form factor for, 18: 26319
transitions, form factors for electromagnetic and weak, 16: 2450
transitions, form factors for, 16: 27907 (NP-11633)
transitions of K_2^0 to K_1^0, amplitudes of, 18: 2624

MESONS ($\overline{K}^0$)

absorption cross sections in Ilford G5 emulsion, 18: 30713(R) (AFOSR-4999)
decay, (T), 20: 9771
decay in mixed ensemble, (T), 19: 47309 (JINR-P-2289)
decay of, CP violation in 2π, (T), 19: 23429
decay of, CP violation and interference effects in 2π, (T), 19: 33058
decay of, CP violation, normality, and reciprocity in, (T), 20: 9749
decay of, CP violation in 2π, (T), 20: 19461
decay of, 2π, 20: 25787 (JINR-P-2632)
decay rate of, CPT-invariance test and measurement method for, 19: 41413
interactions of, SU(6) symmetry for forward amplitudes in, (T), 19: 41515
interactions with protons at high energies, exchange of strangeness-carrying trajectories in, 18: 7507
interactions with mesons (K^0), cross sections for inelastic, 18: 7532
interactions with deuterons, resonance production in, 18: 14811 (JINR-P-1508)
interactions with nucleons, assuming Y_0^* Regge particle, 18: 34571
interactions with protons, 960-Mev resonance in, (T), 19: 6539
interactions with mesons (K^0), effects of media on, (T), 19: 12258
interactions with protons, relativistic SU(6) model for amplitudes of, 19: 23395
interactions with mesons (K^0), 1280-Mev resonance in, (E), 19: 37623
interactions with nucleons at high energies, Regge-pole model for, (T), 19: 41426
interactions with nucleons, scattering length for $S_{1/2}$ T = 0, (T), 19: 47365
interactions with nucleons to 300 Mev/c, effective-range analysis of, (T), 20: 9733
mass and lifetime matrices for (K^0–$\overline{K}^0$), invariance principles for, 20: 21677
mass difference with mesons (K^-), measurement of, (E), 19: 14324 (TID-21438)
mass matrix of K^0–$\overline{K}^0$ system, off-diagonal elements of, 20: 31982 (AD-634703)
mass sign of, comparison with $\overline{K}^0$, 20: 2865 (JINR-P-2325)
photoproduction on hyperons (Λ) and (Σ^+), amplitudes for, 18: 18699
production in meson (π^-)-proton interactions at 10 Bev/c, 18: 40267
production in meson (K^-)-proton charge-exchange interactions at 2.4 to 2.7 Bev/c, 18: 40244 (UCRL-11429)
production in meson (K^-)-proton interactions at 0.9 to 1.0 Mev/c, (E), 20: 41799(R) (ORO-2504-96)

MESONS (K^+)

absorption by aluminum, carbon, and copper at 4.75 Bev/c, (E), 19: 21431
charge exchange in hydrogen at 1.12 and 1.45 Bev/c, cross sections for inelastic, 17: 6966
charge symmetry, 18: 9208
charge symmetry of, 16: 32298 (UCRL-10244)
decay, 16: 25920 (NP-11977(p.40-4))
decay, 17: 3985
decay, 17: 20594(R) (UCRL-10572)
decay, 17: 23672
decay ($\pi^+ + \pi^- + \mu^+ + \nu_\mu$) of, emulsion study of, 18: 36342
decay ($\pi^+ + \pi^0 + \gamma$), upper limit for, (E), 20: 11675
decay ($\pi^+ + \pi^- + \gamma$) 20: 15396
decay ($\pi^+ + \pi^- + \gamma$), rate of, 20: 15396
decay ($\pi^0 + e^+ + \nu$), 18: 37889 (UCRL-11553)
decay (31) currents, partial-conservation non-existence in, 16: 15587
decay, 18: 12914 (TID-7686(p.109-29))
decay, 19: 9775(R) (UCRL-11466)
decay and interactions, 18: 16552(R) (UCRL-11132)
decay, branching ratios, 16: 2451
decay branching ratios, 16: 8069 (NP-11232(p.373-9))
decay branching ratios, (E), 20: 32043
decay chains involving mesons (π), directional correlations in, (E), 20: 13487
decay characteristics of, (E), 19: 4890 (AD-606994)
decay correlations, π-π scattering phase shifts from ($\pi\pi e\nu$), (T), 19: 37547 (UCRL-16026)
decay into two mesons (π) and a photon, (T), 19: 20939 (UR-875-30)
decay, intrinsic structure in meson (π) production and interaction in, 16: 13908
decay, meson (π^+) production, 16: 4729
decay mode, (E/T), 19: 25265(R) (UCRL-11776)
decay modes, 16: 27984
decay modes of, branching ratios for (E), 19: 3084
decay modes of, three-body leptonic (E), 19: 3085
decay of, branching ratios and rates for, 16: 33744
decay of, conservation of $\Delta S = \Delta Q$ in ($K^+ \rightarrow \pi^+ + \pi^- + e^+ + \nu$), 18: 9192
decay of, effects of mesons (ω) and (ρ^0) mixtures on spin and parity in, 17: 34800
decay of, evidence for $K^+ \rightarrow \pi^+ + \pi^- + e^+ + \nu$, 17: 6999
decay of, neutrino (ν_μ) mass from meson (μ^+) energy spectra in, 17: 39896
decay of relativistic, neutrino spectra from, 18: 12894 (CERN-63-37 (p.111-29))
decay of, symmetry violations in leptonic, 18: 7551
decay of, unitary symmetry of weak current structure in, 17: 41781
decay of, ($\pi^+\pi^0\gamma$) (E), 19: 3025 (JINR-P-1763)
decay of, amplitudes for 3π, (E/T), 20: 34194
decay of, branching ratio and meson (μ^-) energy spectra in, 18: 20961

decay of, branching ratio for, (T), 19: 8231
decay of, branching ratios for three-body leptonic, (T), 19: 21060
decay of, branching ratios in, (E), 19: 25378
decay of, branching ratio and meson (μ^+) energy spectrum in, (E), 19: 41414
decay of, branching ratio for ($\pi^+\pi^+\pi^-$), (E), 20: 4618
decay of, branching ratios in, (E), 20: 7801 (UCRL-16362)
decay of, branching ratio for two-body leptonic, (E), 20: 19434 (ANL-7130, pp 107-13)
decay of, branching ratios and form factors for, (E), 20: 30075
decay of, branching ratio of $\pi 2$ and $\mu 2$ modes of, 20: 41801 (UCRL-16003)
decay of, bubble chamber study of four-body leptonic, 18: 34519 (UCRL-11549)
decay of, Cabibbo current theory for parity-violating nonleptonic, 20: 30041
decay of, conservation of strangeness changing vector current in leptonic, 17: 15072 (CTSL-38)
decay of, CP violation and neutral lepton current in, (T), 19: 31085
decay of, current-current interaction model for 2π, 20: 32075
decay of, CVC estimate of rate of leptonic, 18: 36252 (TID-19540)
decay of, $\Delta I = \frac{1}{2}$ rule in 3π, (E), 20: 1028
decay of, $\Delta T = \frac{3}{2}$ nonleptonic, 18: 26349
decay of, determination of neutretto mass from, (T), 19: 25329
decay of, effect of final-state strong interactions on probability of (3π), (T), 20: 6086
decay of, effects of selection rules and invariance on partial rates for, 18: 34506 (BNL-8094)
decay of, energy spectra from 3π, 20: 39846
decay of, extrapolation formula for amplitudes of $\pi^+\gamma\gamma$, 20: 44255
decay of, G_2 symmetry scheme for weak, 20: 15474
decay of, intermediate bosons in, 18: 36256
decay of, intermediate boson pole with meson (S^o) in radiative, (T), 20: 2684 (JINR-P-2374)
decay of, isotopic spin changes in, (T), 19: 12246
decay of, kinematic tables for, 20: 36022 (BNL-945)
decay of, leptonic, (T), 19: 45027 (NP-15199)
decay of, leptonic, 18: 26349
decay of, meson (μ) energy spectrum in (E), 19: 1319
decay of, meson (μ^+) energy spectra and polarization from, (E), 19: 25357
decay of, meson (π) spectra and polarization, (E/T), 19: 25265(R) (UCRL-11776)
decay of, neutral leptonic currents in, 18: 36348
decay of, neutrino interactions in, 18: 40280
decay of, neutrino spectra from, (E), 20: 21602 (CERN-65-32, pp 111-14)
decay of, probability ratio for, (T), 19: 21060
decay of, production of spin-1 mesons (π) in, (E), 19: 23446
decay of, radiative corrections to leptonic, (T), 20: 7811
decay of, rare modes in, 20: 2749
decay of, selection rules for leptonic, 20: 19436 (ANL-7130, pp 159-88)
decay of, shadow mesons (π^o) in, (T), 19: 21038
decay of, shadow meson (π^0) in, (E), 19: 37600
decay of, spectra from, (E), 20: 36043(R) (TID-23206)
decay of, SU(3) symmetry for 2π, (E), 20: 1022
decay of, sum rule for amplitudes of 2π, (T), 20: 17369
decay of, tests of time-reversal invariance in, (E), 19: 33030
decay of, theory for radiative, 18: 42404
decay of, three-body leptonic, (T), 19: 16622
decay of, three-body leptonic, (T), 19: 35176
decay of, time-reversal invariance in $\pi^+\pi^0\gamma$, (E/T), 20: 17404
decay of, upper limits for spin-1 particle production in, (E), 20: 13497
decay of, vector and axial-vector Cabibbo angles for leptonic, 20: 34188
decay of, weak interaction theory in SU(3) for 2π, 20: 17379
decay ($\pi^+ + \pi^- + e^+ + \nu$), 17: 31357
decay probability, (E), 20: 4609
decay products, 16: 25945 (NP-11977(p.129-35))
decay products from spectra of, (E), 20: 19273(R) (BNL-929, pp 3-43)
decay spectra, 17: 31091(R) (UCRL-10862)
decay to $\pi^+ + \mu^+ + \mu^-$, branching ratio for, (E), 19: 31059
decays of, parity nonconservation in ($2\pi\gamma$) and ($3\pi\gamma$), (T), 19: 41361
detection and measurement at 3 to 6 Bev/c, Cherenkov counter for, 18: 14276
detection of, equipment for, 20: 15393
detection system for, scintillation, 20: 16826 (PPAD-574E)
detection using liquid Cherenkov counters, system for, 19: 34519
focusing of beams of, neutrino spectra from magnetic-finger, (T), 19: 30877 (BNL-9062)
intensity of cosmic, above 4 Bev, (E), 19: 41294
interaction cross sections, 16: 13880
interactions and nucleons, 18: 15290
interactions at high energy, cross section combinations for, 17: 11529
interactions at very high energies, proposed diffraction-scattering experiment, 17: 20579 (UCRL-10022(p.142-3))
interactions in propane bubble chamber, search for mesons (D^+) in, 16: 31045
interactions of, selection rule for weak, 17: 19069
interactions of, with protons at 0.97, 1.17 and 1.97 Bev, 16: 32291 (UCRL-10221(Rev.))
interactions of, SU(6) symmetry for forward amplitudes in, (T), 19: 41515
interactions with nucleons and protons at 0.8 to 2.9 Bev/c, cross sections, 16: 2305(R) (UCRL-9704)
interactions with deuterons at 52 to 456 Mev, charge-exchange cross sections, 16: 3645
interactions with protons at 120 to 812 Mev/c, 16: 2305(R) (UCRL-9704)
interactions with mesons (K^-), meson (π) interaction model application to, 16: 5881
interactions with deuterons, analysis using two-particle scattering amplitudes, 16: 7019 (NP-11215)
interactions with neutrons, threshold effects in, 16: 8055 (NP-11232 (p.252-7))
interactions with protons up to 20 Mev, total-cross-section relation to isospin independence, 16: 10905
interactions with hyperons (Ξ^{-*}), spin states for (Ξ^{-*}), 16: 12379
interactions with neutrons, cross sections for, 16: 13880
interactions with mesons (K^-), 16: 15574
interactions with nucleons, meson (π)-exchange relations to potential in, 16: 15581
interactions with mesons (K^-), meson (ω) and (ρ) production in, 16: 17043
interactions with mesons (K^-), transitions to mesons (ω) and (ρ) in, 16: 17044
interactions with protons, amplitude studies by dispersion relations, 16: 17047
interactions with mesons (K^-), dispersion relations in, 16: 17047
interactions with nucleons, differential and total cross sections at 0.8 to 2.9 Bev, 16: 16957 (NP-11592(Vol.I)(p.247))
interactions with nucleons at 0.8 to 2.9 Bev/c, cross sections, 16: 19679 (UCRL-10130)
interactions with protons at 0.97 to 1.97 Bev/c, angular distributions and cross sections, 16: 19679 (UCRL-10130)
interactions with nucleons at 50 to 210 Mev, amplitudes for, 16: 21296
interactions with deuterons in I = 0 state, charge-exchange, 16: 24727
interactions with deuterons and protons, meson (π) production in, 16: 33701(UCRL-10225)
interactions with protons at 1.96 Bev/c, resonances in, 16: 33702 (UCRL-10337)
interactions with deuterons and nucleons, amplitudes for, 16: 33708
interactions with protons at 140 to 642 Mev/c, 17: 4002
interactions with protons, production of meson (K^*) resonance in, 17: 7000
interactions with protons, repulsive interaction in elastic, 17: 9261
interactions with deuterons and protons, meson (π) production in, 17: 9377
interactions with protons, analysis of existing information on, 17: 9378
interactions with protons at 1.45 Bev/c, 17: 9380
interactions with protons, total cross sections for, 17: 9382
interactions with protons at 970, 1170, and 1970 Mev/c, elastic, 17: 17015
interactions with protons, 17: 20594(R) (UCRL-10572)
interactions with protons, cross section for four particle final state in, 17: 20939
interactions with nucleons in nuclei, dispersion relations for low-energy, 17: 21075
interactions with protons, polarization of recoil proton from, 17: 22518
interactions with protons at low energies, 17: 24187
interactions with protons, 17: 31091(R) (UCRL-10862)
interactions with protons, proton polarization in, 17: 31091(R) (UCRL-10862)
interactions with protons, diffraction pattern shrinkage from ω-exchange in, 17: 31370
interactions with protons at 910 Mev/c, isobar production in, 17: 34789
interactions with protons at 5 Bev, Regge pole contributions to cross section of, 17: 34816
interactions with protons at 910 Mev/c, recoil proton polarization in, 17: 36586 (UCRL-10813)
interactions with deuterons and protons, total cross sections for, 17: 39844 (BNL-7258)
interactions with protons at 1.96 Bev/c, meson (π) exchange in double resonance production in, 17: 39895
interactions with protons at 1.14 Bev/c, resonances in, 17: 39912
interactions with protons at 1.96 Bev/c, double-resonance production in meson (π) exchange in, 17: 41745 (UCRL-10954)
interactions with protons at 1.96 Bev/c, meson exchange in, 17: 41746 (UCRL-10955)
interactions with protons, cross sections near resonances, 17: 41756

interactions with protons, production of N^*_{33} resonance from, 17: 41785
interactions with protons ($K^+ + p \rightarrow K^0 + \pi^+ + p$) near K* resonances, factorization formula for calculation of inelastic cross sections for, 17: 41754
interactions with nucleons, partial amplitudes for, 18: 856 (PAN-387/VII)
interactions with protons at 6.8 to 14.8 Bev/c and $-t = 0.03$ to 1.1 $(Bev/c)^2$, differential cross sections for elastic, 18: 4457
interactions with protons at 1.96 Bev/c, resonance (K* and N*) production in, 18: 5995 (UCRL-11068)
interactions with protons at high energies, field theory for, 18: 6015
interactions with protons at 1.14 Bev/c, production of K* and N^*_{33} resonances in, 18: 6033
interactions with protons at high energies, effects of Regge trajectories on diffraction peaks in, 18: 7515
interactions with mesons (K^-), cross sections for inelastic, 18: 7532
interactions with neutrons, theory using Feynman diagrams for, 18: 9205
interactions with protons, elastic, 18: 10843 (CONF-122-22)
interactions with protons at 1.3 and 5.0 Bev, particle emission in, 18: 10848 (JINR-P-1462)
interactions with protons, total cross sections for, 18: 10423
interactions with protons, forward amplitudes for, 18: 12898 (EFINS-63-72)
interactions with nucleons at 47.7 to 364 Mev, cross sections and phase shifts for elastic, 18: 12959
interactions with protons at 2.26 Bev/c, K* production in, 18: 14950
interactions with protons at 3 Bev/c, mechanism of ($K^0\pi^+p$) production in, 18: 24449
interactions with deuterons in I = 0 state at low energies, 18: 24457
interactions with protons at 7 to 14 Bev/c, differential cross sections for elastic, 18: 24396(R) (NP-13947)
interactions with protons near $^5/_2$-$^7/_2$ resonance, effective cross sections for, 18: 26288
interactions with protons, isobar production in, 18: 26358
interactions with protons at 910 Mev/c, production of ($K^0 + p + \pi^+$) by, 18: 26381
interactions with protons at high energies, scaling law for, 18: 28330 (TID-20722)
interactions with protons at 910 Mev/c, elastic, 18: 28381
interactions with protons to 450 Mev, 18: 34543
interactions with protons, unitary symmetry model for resonance production in, 18: 36280
interactions with protons at high energies, behavior of diffraction peak in, 18: 36323
interactions with deuterons at 2.3 Bev/c, resonances in peripheral, 18: 37885 (UCRL-11465)
interactions with deuterons below 800 Mev/c, 18: 37955
interactions with protons at 0.85 to 1.5 Bev/c, cross sections for, 18: 42379 (UCRL-11446)
interactions with protons at 3 Bev/c, resonances in, 19: 1257
interactions with protons at 3 Bev (E), 19: 1341
interactions with protons at 3 Bev, mechanisms of (E), 19: 1342
interactions with protons at 7 to 17 Bev/c, single-pole contribution to elastic (T), 19: 3047
interactions with protons at low energy, analysis of elastic (T), 19: 3090
interactions with protons at 1.3 and 5 Bev, multiple particle production in, (T), 19: 4907
interactions with protons at 3 Bev/c, mesons (κ) from, 19: 4941
interactions with mesons (K) and (π), properties of resonance, (E/T), 19: 6556
interactions with nucleons at 900 Mev/c, one meson (π) production in, (E), 19: 10064
interactions with protons at high energies, optical models for, (T), 19: 12228
interactions with protons, Regge exchange mechanism for, (T), 19: 18805
interactions with protons, kinematical effects in peripheral, (T), 19: 20981
interactions with protons, SU(6) predictions for amplitudes of, (T), 19: 23432
interactions with protons at high energies, elastic scattering amplitude for, 19: 23381
interactions with protons, relativistic SU(6) model for amplitudes of, 19: 23395
interactions with protons at high energies, equipment for studying, 19: 22862
interactions with nucleons at high energies, Regge trajectories in, (T), 19: 23417
interactions with protons at 1.45 Bev/c, K*(890) and N*(1220) production in, (E), 19: 25340
interactions with deuterons and protons at 6 to 22 Bev/c, total cross sections for, (E), 19: 25351
interactions with protons at 2.7 Bev/c, cross sections for, (E), 19: 25265(R) (UCRL-11776)
interactions with deuterons at 2.3 Bev/c, analysis of, (E), 19: 25265(R) (UCRL-11776)
interactions with protons at 860 to 1600 Mev/c, cross sections for, (E), 19: 25265(R) (UCRL-11776)
interactions with protons at high energies and low momentum transfers, (T), 19: 27227
interactions with neutrons at 2.3 Bev/c, absorption effects in, (T), 19: 27246
interactions with deuterons at 110 to 230 Mev/c, cross sections for elastic, (T), 19: 27250
interactions with protons, double resonance production in, (T), 19: 29073 (NP-15070)
interactions with deuterons, separable potentials in, (T), 19: 29079
interactions with protons, K-matrix model for peripheral, (T), 19: 31043
interactions with protons at 7 to 15 Bev/c, (E/T), 19: 30994 (BNL-8935)
interactions with protons at Bev/c, K*(890) and N*(1238) production in, 19: 32988
interactions with protons, double resonance production in, (T), 19: 35095
interactions with protons at 3 to 5 Bev/c, production of strangeness +2 meson resonance in, (E), 19: 35139
interactions with nucleons at 2 to 3 Bev/c, peripheral production and resonance decay in, (T), 19: 35152
interactions with mesons (K•), review on, 19: 37644
interactions with protons, peripheral production and decay of K* in, 19: 39576
interactions with protons, mass-spectrum κ singularity in ($K\pi\pi p$), (T), 19: 41417
interactions with protons at 2 Bev/c, (E), 19: 41436
interactions with protons at high energies, forward amplitudes for, (T), 19: 41376
interactions with protons, energy dependence of diffraction curve for elastic, (T), 19: 43043 (JINR-P-2202)
interactions with protons at high energies, resonance production in, (T), 19: 45037 (TID-21316)
interactions with protons at 3 Bev/c, decay distributions and differential cross sections for, (T), 19: 45086
interactions with deuterons at 2.3 Bev/c, coherent K*production in, (E), 19: 45120
interactions with protons at 3 Bev/c, K*N* production in ($KN\pi\pi$), (E/T), 19: 45057
interactions with protons at 3 Bev/c, resonance production in ($K^0p\pi^+$), (E/T), 19: 47356
interactions with neutrons at 2.3 Bev/c, charge-exchange, (E), 20: 1009
interactions with deuterons at 2.3 Bev/c, (E), 20: 1009
interactions with nucleons at high energy, sum rule for cross sections of, (T), 20: 4678
interactions with protons at low energy, inelasticity effects in, (T), 20: 7813
interactions with protons at high energy, Regge-pole exchange model for N* production in, 20: 7814
interactions with protons above 2 Bev, energy dependence of diffraction-curve slope for, (T), 20: 9720(T)
interactions with protons, SU(6) for angular distributions and N*•• production from, (T), 20: 9723(T)
interactions with protons at 0.86 to 1.58 Bev/c, K* and N* resonance production in, (E), 20: 13462 (UCRL-16370)
interactions with protons at 3.6 Bev/c, resonance production in, (E), 20: 15407
interactions with protons at 3.6 Bev/c, (E), 20: 15415
interactions with protons at 2.26 Bev/c, resonance production in, (E/T), 20: 15422
interactions with protons, total cross section for, (E/T), 20: 15428
interactions with protons at 1.96 Bev/c, single-meson (π) production in, (E), 20: 15335
interactions with neutrons and protons at high energies, real amplitudes for, (T), 20: 17378
interactions with protons at 4.6 Bev/c, K* production in, (E), 20: 21629 (UCRL-16332)
interactions with protons at high energies, conical function and mean value theorem for amplitude of, 20: 24061
interactions with protons, unitary symmetry in, (T), 20: 24170
interactions with protons at 3.0 Bev/c, cross sections for elastic, (E/T), 20: 25815
interactions with protons, graphical method for analysis of charge-independent strong, 20: 25821
interactions with protons, forward dispersion relations and coupling constants for, (T), 19: 27886
interactions with protons at 5 to 20 Bev/c, meson-exchange model for forward elastic, 20: 30039
interactions with protons at 3.535 Bev/c, production of K•K•• (1280) from, 20: 30047

interactions with protons at 3.54 Bev/c, production of strangeness +1 resonances from, 20: 30049
interactions with deuterons and protons at 0.9 and 2.4 Bev/c, total cross sections for, (E), 20: 32067
interactions with deuterons and protons at 1 to 2.4 Bev/c, total cross sections for, (E), 20: 34145 (BNL-10215)
interactions with deuterons, mechanisms of, 20: 34253
interactions with protons, K+(1400) and K**(1320) production in, (E), 20: 34245
interactions with protons at 2.26 Bev/c, cross sections and resonances of, (E/T), 20: 34249
interactions with protons at high energies, elastic, (E/T), 20: 37796
interactions with protons at 3.52 Bev/c, meson (κ) production in, (E), 20: 39784
interactions with protons, graphical method for charge independence in strong, 20: 39800
interactions with protons at 2 to 6 Bev/c, Regge-pole model for cross sections for, (E/T), 20: 39801
interactions with protons at 2.7 Bev/c, K* (891), N* (1236), and ω production from, (E), 20: 41804 (UCRL-17003)
interactions with protons at 910 Mev/c, phase-shift analysis of, 20: 41825
interactions with protons at 3.5 Bev/c, existence of K+K- resonance in, (E), 20: 41856
interactions with protons at 2.26 Bev/c, cross sections for Z* baryon production in, (E), 20: 44195
interactions with protons at 3.0 to 5.0 Bev/c, strangeness +2 meson resonance at 1280 Mev production from, (E), 20: 44262
interactions with protons at 4.6 Bev/c, K* (1320) production from, (E), 20: 44265
interactions with protons, test of PCAVC hypothesis for ΔS = 1 currents from, 20: 46353
interactions with protons, NΛK and NΣK coupling constant estimation from amplitudes of, 20: 46359
interactions with deuterons and protons, coupled-channel several-force model for baryon antidecuplet from, (T), 20: 46372
kinetics at 100 kev to 100 Bev, graphs for, 19: 18752 (UCRL-2426(Vol. I) (1965 Rev.))
lifetime relative to mesons (K-), (E), 20: 41884
magnetic moments of, Vigier rotator model for anomalous, 17: 34802
mass determination from xenon bubble chamber data, 16: 31901
mass difference of K0–K+ and K0–K-, 16: 10931
mass difference with mesons (K0), 16: 8054 (NP-11232(p.243-51))
mass differences (K+–K0), effects of electromagnetic self-energies, 16: 18321 (NYO-10130)
mass of, models for, 19: 14348
mass relative to K0, 20: 30016
momentum spectra from proton reactions with aluminum and beryllium at 30 and 33 Bev, 16: 24858
photoproduction, (E), 19: 46643(R) (LAL-1136)
photoproduction at high energies, (E/T), 19: 45024 (MIT-2098-163)
photoproduction at high energies, (E), 20: 15306(R) (CEAL-1026)
photoproduction, experimental and theoretical status, 16: 25946 (NP-11977(p.135-7))
photoproduction from protons at low energies, 17: 13431
photoproduction from complex nuclei, angular and momentum distributions from, (T), 19: 35393 (LNF-65/6)
photoproduction, measurement of cross sections for, 16: 25894 (LNF-62/37(p.72-5))
photoproduction near the threshold, 17: 7051
photoproduction of, baryon resonances in, (E), 20: 15424
photoproduction on protons, cross sections for, 17: 4000
photoproduction on hydrogen, 17: 9364
photoproduction on protons, excitation curve for, 17: 32912 (TID-7668 (Sect.IV))
photoproduction on protons, resonance model for, 17: 41806
photoproduction on protons, review of present experimental and theoretical data on, 18: 10869 (LNF-63/47(p.109-12))
photoproduction on complex nuclei at 1054 Mev, yields from, 18: 13109
photoproduction on protons at 1200 Mev, differential cross sections for, 18: 32602
photoproduction on protons, dispersion relations for, 18: 34536
photoproduction on protons, (T), 19: 14307 (ANL-6942)
photoproduction on protons, (T), 19: 16517
photoproduction on protons at 1160 Mev, angular distribution in, (E), 19: 25377
photoproduction on protons, (E/T), 20: 2735
photoproduction on protons, (E), 20: 11676
photoproduction on protons at 1100–1300 Mev, cross sections for, (E), 20: 15393
photoproduction on protons at 3.4 to 4.0 Bev, cross sections for, (E/T), 20: 17400
photoproduction on protons at 3.4 to 4.0 Bev, cross sections for, (E/T), 20: 24015 (MIT-2098-223)
photoproduction on protons, (E), 20: 27922
photoproduction on protons at 3.0 to 6.0 Bev, (E), 20: 27920
photoproduction on protons, dispersion relations for, (E/T), 20: 27812
photoproduction on protons at 1400 Mev, angular distributions in, (E), 20: 34252
photoproduction on protons at 2.6 to 2.7 Bev, differential cross sections for, (E), 20: 41795(R) (MIT-2098-251, pp 21-36)
photoproduction with hyperons (Λ0) and (Σ0) on protons, 17: 782
polarization, hyperon (Λ0) polarization in, 16: 25895 (LNF-62/37 (p.76-80))
production and decay in atmosphere, 16: 22843
production associated with hyperons (Σ--) in meson (π-)-proton interactions, 19: 14397
production by high energy neutrinos, form factors and cross sections for, (T), 19: 8232
production by proton–meson (π+) interactions at 1170 Mev/c, 16: 31036 (UCRL-10154)
production by proton interactions with mesons (K-) and (π-), 16: 10918
production from meson (π-) reactions with heavy nuclei at 7.2 Bev/c, (E), 20: 28460
production in antiproton-proton interactions, spin of K'+, 16: 10851
production in cosmic showers, transverse momentum of, 18: 14770
production in gamma-proton interactions near threshold, 16: 15480
production in gamma-proton interactions, 17: 22477
production in gamma-proton interactions at 950 to 1050 Mev, 18: 24428
production in hyperon (Σ0) decay, 16: 12359
production in meson (π+) interactions with protons at 1.95 Bev, 16: 32284 (TID-16557)
production in meson (π+) reactions with deuterium at 1.23 Bev/c, charge symmetry of, 17: 22489
production in meson (π+)-proton interactions, 18: 864 (UCRL-10243)
production in meson (π+)-proton interactions, (T), 19: 16557
production in neutrino interactions with protons, cross sections for, 17: 6953 (LNF-62/89)
production in neutrino-nuclear interactions at high energies, 18: 28413
production in neutrino-nucleon interactions, peripheral, (T), 19: 18815
production in photon-proton interactions, quark model for, (T), 20: 17348 (JINR-P-2556)
production in proton-photon reactions at 925 to 1500 Mev, 16: 12330 (ISS-61/14)
production in proton-meson (π) interactions at 1 to 4 Bev, 16: 19704
production in proton reactions with beryllium at 19.2 Bev, 17: 795 (CERN-62-27)
production in proton–proton interactions at 2.85 Bev, 18: 10916
production in proton accelerators, 18: 12912 (TID-7686(p.35-41))
production in proton-proton interactions at 19 and 24 Bev/c, cross sections for, 18: 18678
production in proton reactions with beryllium at 25 Bev, 18: 26165 (BNL-837(p.91-113))
production in proton-proton interactions at 2.40 and 2.85 Bev, (E), 19: 21034
production in proton reactions with beryllium at 12.5 Bev, cross sections for, (E), 19: 21406
production in proton reactions with nuclei at 20 Bev, 19: 41324 (CERN-65-14)
production in proton-proton interactions at 2.40 and 2.85 Bev, (E), 20: 4586 (TID-22315)
production in proton interactions at 2.4 to 2.85 Bev, (E/T), 20: 19273(R) (BNL-929, pp 3-43)
production in proton reactions with beryllium at 12.5 Bev, cross sections for, (E), 20: 21601 (CERN-65-32, pp 109-10)
production of beams of, 19: 1123 (PPAD-526-D)
production of beams of, at 1 Bev/c, (E), 19: 10017 (NP-14472)
production of beams of, in CERN synchrotron, (E), 19: 28940 (CERN-65-2)
properties at 100 kev to 100 Bev, 18: 28331 (UCRL-2426(Vol.I)(1963 Rev.))
ratio to mesons (K + π), 18: 16762 (NP-13694)
reactions with hydrogen at 2.3 Bev/c, 18: 30708(R) (AFOSR-J1446)
reactions with matter, dE/dx and range-energy graphs for, 20: 46601 (UCRL-2426(Vol.2(1966 Rev.))
reactions with nuclei in emulsions at 240 to 300 Mev, 16: 8068 (NP-11232(p.367-72))
reactions with nuclei, 18: 15290
scattering by emulsion nuclei at 320 Mev, optical model analysis of elastic, (T), 19: 27569
scattering by hydrogen at 1.0 to 2.0 Bev/c, 16: 27362
scattering by nuclei at 260 Mev, cross sections for elastic, 16: 27994
scattering by nuclei, cross sections for differential, 16: 29683
separation from charged particle beams, equipment for, 18: 2504
triplet formation with mesons (K-) and (π), 16: 10902

see Mesons (K_{e3})

MESONS (K_{e3})
decay, (E), 19: 39474 (JINR-P-2190)
decay, effects of K-π resonances, 16: 19690
decay, effects of meson (K)-meson (π) resonances, 16: 26103
decay, lepton angular correlations in, 16: 29706
decay model, 16: 15549
decay of, angular distribution of products from, 17: 11484 (NP-12460)
decay of, form factors and spin symmetry for, 17: 2167 (NP-12195)
decay of, form factors in, 17: 6953 (LNF-62/89)
decay of, invalidity of $\Delta Q = \Delta s$ rule in leptonic, 18: 7553
decay of, mixing parameters and $\Delta S = \pm\Delta Q$ amplitudes, 17: 9227
decay of, ratio of K^0_{L3} to K^0_{S3} and K_{e3} to K^0_{S3}, 18: 2673
decay of, branching ratio for (E), 19: 3084
decay of, branching ratio and form factors for, (T), 19: 8232
decay of, coupling for (T), 19: 3085
decay of, current algebra for, (T), 20: 17405
decay of, $\Delta S = \Delta Q$ transition, $\Delta I = ½$, and CP violation in model for strangeness-changing, 20: 27878
decay of, form factors in, (T), 19: 12316
decay of, interactions in leptonic, 17: 19549
decay of, positron momentum spectra and branching ratio for, (E), 20: 27833
decay of, universality in Cabibbo's theory for, (T), 20: 6080
decay, probabilities, 16: 956
decay rate relation to hyperon (Λ) leptonic decay, 16: 22914
decay, theoretical analysis for coupling identification, 16: 6922 (NP-11214)

MESONS (Ke^-_3)
decay, 19: 37664
decay rate and spectra of, radiative corrections to, 20: 15349

MESONS (K^0_{e3})
decay, 18: 12944
decay, 19: 37664
decay, (E), 20: 6095
decay modes, implications of $\Delta Q = -\Delta S$, 16: 13906
decay of (K^0_L), probabilities for, (T), 19: 16470 (JINR-P-1920)
decay of, neutrino production in, 17: 9245
decay of, angular correlations and energy spectra in, (E/T), 19: 16469 (JINR-P-1919)
decay of, CP violation in, (E), 20: 44259
decay of, $\Delta S = \Delta Q$ selection rule in, 19: 1235 (PPAD-521-F)
decay of, $\Delta S/\Delta Q$ rule in, (E/T), 19: 20979
decay of, energy dependence of form factors in, (E), 20: 19432 (ANL-7130, pp 83-90)
decay of, G_2 symmetry scheme for, 20: 15474
decay of, weak interaction model with changing strangeness for, (T), 19: 23459

MESONS (K^+_{e3})
decay, 16: 32301 (UCRL-10277)
decay, 19: 37664
decay, 18: 37889 (UCRL-11553)
decay branching ratio, (E), 20: 32043
decay, form factors, 16: 26135
decay interaction, 16: 4717
decay, lepton energy spectra from, 16: 26160
decay modes, 17: 2170 (UCRL-10205)
decay, electron spectra and polarizations in, 16: 9358 (NP-11263)
decay of, $\Delta I = ½$ amplitudes in, 16: 33751
decay of, electron energy spectrum in, 17: 5275
decay of, angular distribution of products of, 19: 21069
decay of, coupling constants and form factors for, 18: 32630
decay of, energy dependence of form factor from, (E), 20: 46345 (UCRL-17087)
decay of, form factor from, (E), 20: 21658
decay of, G_2 symmetry scheme for, 20: 15474
decay of, meson (π^0) energy spectrum in, (T), 19: 35176
decay of, positron momentum spectra from, (E/T), 20: 7799 (PPAD-571F)
decay of, probability ratio for, (T), 19: 21060
decay of, production of spin-1 mesons (π) in, (E), 19: 23446
decay of, weak interaction model with changing strangeness for, (T), 19: 23459
decay rate and spectra of, radiative corrections to, 20: 15349
decay rate of, form factors for, 17: 22464
positron spectra, 18: 42423

MESONS (K_{e4})
decay, 17: 31091(R) (UCRL-10862)
decay, 18: 16552(R) (UCRL-11132)
decay angular correlations, low-energy π-π phase shifts from, (T), 19: 10086
decay branching ratios of, remarks on, 17: 15126
decay correlations, π-π scattering phase shifts from, (T), 19: 37547 (UCRL-16026)
decay, effects of π-π resonances on, 16: 27963
decay modes of, 17: 11534
decay modes of, analyses of rare, (E), 19: 41446
decay of, validity of $\Delta Q = \Delta s$ rule in leptonic, 18: 7553
decay of, meson (π-π) interactions from, 17: 20935
decay of, test of selection rule for, 17: 31363
decay of, angular correlations and pion phase shifts in, 18: 37882 (UCRL-11437)
decay of, bubble chamber study of, 18: 34519 (UCRL-11549)
decay of, CVC in, 18: 36252 (TID-19540)
decay of, $\Delta S = \Delta Q$ transition, $\Delta I = ½$, and CP violation in model for strangeness-changing, 20: 27878
decay of, isoscalar scalar boson for model of, 19: 43091
decay of, meson (π) final-state interactions in, (T), 19: 39515
decay of, meson (σ) mediation of, 18: 22756
decay of, π-π interaction studies from, (E), 20: 46346 (UCRL-17088)
decay of, s-wave meson (K)-meson (π) interactions in, (T), 20: 11654
decay of, selection rules for leptonic, 20: 19436 (ANL-7130, pp 159-88)
decay of, test of PCAVC hypothesis for $\Delta S = 1$ currents from, 20: 46353
decay of, vector interaction contribution to, 19: 39589
decay of, vector interaction effects in unitary symmetry, 19: 41335 (NP-15239)
decay probabilities of, effect of π-π resonance on, 17: 9190 (JINR-P-1093)
decay rate and spectra, (T), 19: 16592
decay spectra and $KK \to \pi\pi$ amplitudes, 16: 26083 (JINR-P-1000)
decay with $\Delta Q/\Delta S = -1$, 18: 22772

MESONS (K_{e5})
decay mode of, by virtual η-pole approximation, 17: 40066
decay of, angular correlations and energy spectra from, (E), 19: 33066
decay of, intermediate meson (η) production in, 18: 10973

Mesons (K_μ)
see Mesons ($K_{\mu3}$)

MESONS ($K_{\mu2}$)
decay of, branching ratio for (E), 19: 3084
decay of, meson (ρ) universality for rate for, 20: 44238
decay, probabilities, 16: 956
decay rate relation to hyperon (Λ) leptonic decay, 16: 22914

MESONS ($K^-_{\mu3}$)
decay characteristics of, (E), 19: 4890 (AD-606994)
decay of, axial-vector current in, (T), 20: 13508
decay of, branching ratio relative to mesons ($K^\pm_{\pi2}$), 20: 41801 (UCRL-16003)
production in cosmic meson (μ^+) decay, ratio to meson (π^+), 17: 41717

MESONS ($K_{\mu3}$)
branching ratio and meson (μ^+) energy spectrum, (E), 19: 41414
coupling to strangeness-conserving currents, 17: 31365
decay, (E), 19: 39474 (JINR-P-2190)
decay and energy spectra, 19: 9775(R) (UCRL-11466)
decay and polarization, 18: 16552(R) (UCRL-11132)
decay, effects of meson (K)-meson (π) resonances, 16: 26103
decay, lepton angular correlations in, 16: 29706
decay model, 16: 15549
decay of, form factors and spin symmetry for, 17: 2167 (NP-12195)
decay of, mixing parameters and $\Delta S = \pm\Delta Q$ amplitudes, 17: 9227
decay of, branching ratio for (E), 19: 3084
decay of, branching ratio and form factors for, (T), 19: 8232
decay of, coupling constants and form factors in, 18: 36261
decay of, coupling for (T), 19: 3085
decay of, form factors in, 18: 24447
decay of, form factors in, (T), 19: 12316
decay of, form factors for angular distributions of leptons and mesons (π), 19: 39482 (NP-15252)
decay of, form-factor ratio in, (T), 19: 8084
decay of, interactions in leptonic, 17: 19549
decay of, meson (π)-lepton angular correlation in, (T), 19: 41485(T)
decay, theoretical analysis for coupling identification, 16: 6922 (NP-11214)
interactions with mesons (π), possible nonresonant character of ~726-Mev peak in, 18: 40376

MESONS ($K^-_{\mu3}$)
decay, 19: 37664
decay of, form factor ratio in, 18: 28326 (TID-20705)
decay of, meson (μ) energy spectrum and form factors for, (E), 20: 13521
decay rate and spectra of, radiative corrections to, 20: 15349

MESONS ($K^0_{\mu3}$)
decay, 18: 12944
decay, 19: 37664
decay of, form factors for, (E/T), 20: 19433 (ANL-7130, pp 91-105)
decay spectra, (E), 20: 15331
decay spectrum measurement, 20: 4631

MESONS ($K^+_{\mu3}$)

decay, 16: 32301 (UCRL-10277)
decay, (T), 19: 35176
decay, 19: 37664
decay branching ratio, (E), 20: 32043
decay characteristics of, (E), 19: 4890 (AD-606994)
decay form factor ratios, leptonic, 16: 15586
decay, form factors, 16: 26135
decay form factors, 18: 42381 (UCRL-11547)
decay, lepton energy spectra from, 16: 26160
decay modes, 17: 2170 (UCRL-10205)
decay, muon spectra and polarizations in, 16: 9358 (NP-11263)
decay of, $\Delta I = \frac{1}{2}$ amplitudes in, 16: 33751
decay of, branching ratio and meson (μ^-) energy spectra in, 18: 20961
decay of, branching ratio for (E), 19: 1319
decay of, coupling constants and form factors for, 18: 32630
decay of, form factors in, 18: 24447
decay of, form factors in, (T), 19: 27258
decay of, form factors and meson (μ^+) polarization in, (E), 19: 37629
decay of, form factors and branching ratios for, (E), 20: 13459 (UCRL-16253)
decay of, form factor ratio in, 20: 19524
decay of, meson (μ^+) polarization in, 18: 14898
decay of, meson (μ) spectrum from, (E/T), 19: 6542
decay of, meson (μ^+) polarization in, (E), 20: 6075
decay of, meson (μ^+) polarization from, (E), 20: 41799(R) (ORO-2504-96)
decay of, meson (π) energy spectra in, (E), 20: 39846
decay of, production of spin-1 mesons (π) in, (E), 19: 23446
decay of, tests of time-reversal invariance in, (E), 19: 33030
decay parameters, 17: 39886
decay polarization of meson (μ) from, 18: 32611
decay rate and spectra of, radiative corrections to, 20: 15349
decay rate of, form factors for, 17: 22464

MESONS ($K_{\mu 4}$)
decay modes of, 17: 11534
decay of, CVC in, 18: 36252 (TID-19540)
decay of, emulsion study of, 18: 36342
form factors and branching ratio for, (E), 19: 20985

MESONS ($K_{\pi 2}$)
decay, (T), 19: 41420
decay, electromagnetic and weak transition form factors in, 16: 2450
decay into charged-particle pairs, 16: 6987
decay isospin determination, 16: 10888
decay mode, 18: 32613
decay of, current conservation and $\Delta T = \frac{1}{2}$ rule in, 16: 31039
decay of, selection rules for, 18: 4429 (CONF-231-3)
decay of, branching ratio for (E), 19: 3084
decay of, CP violation and superposition principle in 2π, (T), 20: 7831
decay of, isospin structure of, 18: 44573
decay of, matrix elements of, 19: 23454
decay of, partially conserved axial-vector current hypothesis for, 20: 21666
decay of, SU(3) for, 20: 46374
decay of, weak interaction in nonleptonic, 18: 32628
energy and transverse momentum of, in cosmic showers, 17: 13107
exchange in neutrino-nucleon interactions, 16: 22949
interactions with mesons (μ), model, 16: 4728
interactions with hyperons, neutrinos, and nucleons, 16: 4728
interactions with nucleons and V particles in fermion decay models, 17: 26346
interactions with nucleons, Lee model for, 18: 16778
production in cosmic-ray interactions in cloud chambers at height of 1800 mm, 16: 33723
production in cosmic showers, transverse momentum of, 18: 14770
production in meson (ρ) decay, 16: 15585
regeneration in propane bubble chambers, 16: 9362 (UCRL-9606)
Regge poles of, effects in photoproduction of mesons, 18: 26372
role in leptonic nonconservation of strangeness-changing current, 18: 28354
spin assignment, 16: 10903

MESONS ($K^-_{\pi 1}$)
decay, meson (π) resonance production in S-wave, I = 2 isospin state, 16: 26117
decay of, unitary symmetry for 2π, 18: 40313

MESONS ($K^0_{\pi 2}$)
decay, (T), 20: 7807
decay at 10 Bev/c, (E), 19: 18845
decay branching ratios for K^0_1, 17: 19128
decay, CP-invariance consequences in, 16: 6921 (JINR-D-785)
decay $K^0_2 \to 2\pi$, CP-invariant theory for, 18: 42429
decay $K^0_2 \to 2\pi$, CP-invariant theory for, 18: 42433
decay modes, 16: 10899
decay modes and width, 16: 10887
decay of, 18: 34578
decay of (K^0_2), Lagrangian for, 19: 37568
decay of (K^0_2), (T), 19: 16593
decay of, Bose statistics for ($\pi^+ + \pi^-$), (T), 19: 18871
decay of, interference phenomena in radiative, 17: 37969
decay of K^0_2, (E), 19: 18896
decay of K^0_2, 18: 40324
decay of K^0_2, CP invariance in, 18: 42429
decay of K^0_2, model for violation of CP invariance in, (T), 19: 3098
decay of K^0_2, CP invariance in, (T), 19: 16610
decay of K^0_2, effect of galactic field of hypercharges on, (T), 19: 18747 (JINR-D-1925)
decay of K^0_2, T violation in, (T), 19: 18859
decay of K^0_2, Lorentz invariance in, (T), 19: 35225
decay of K^0_2, CP violation in, 19: 39601
decay of K^0_2, CP violation in, (T), 19: 41437
decay of K^0_2, CP conservation in, (E/T), 19: 45055
decay of, selection rules for photon states in, 17: 15116
decay of, Bose statistics for ($\pi^+ + \pi^-$), (T), 19: 18871
decay of, CP invariance in, 18: 42468 (JINR-E-1787)
decay of, CP invariance in, (T), 19: 16619
decay of, CP violation in, 18: 36343
decay of, CP violation in, (T), 19: 20978
decay of, CP violation in, (T), 19: 23429
decay of, CP violation and interference effects in, (T), 19: 33058
decay of, CP violation and $\Delta = \frac{1}{2}$ rule in, (T), 19: 35118
decay of, CP violation in, (T), 19: 47309 (JINR-P-2289)
decay of, CP violation in, 19: 18841
decay of, CP-odd interaction and $|\Delta S| = 2$ in, (T), 19: 43182
decay of, CP-parity in, (T), 19: 43181
decay of, galactic hypercharge field for, (T), 19: 33057
decay of, modified V-A interaction and CP invariance for, 20: 13597
decay of, scalar-pseudoscalar coupling in, (T), 19: 18839
decay of, symmetry for, (T), 19: 43154
decay of, test for particle-mixture theories in, (T), 19: 41454
decay of, test of CP violation and $|\Delta T| = \frac{1}{2}$ rule for radiative, 19: 47351
decay of, U(12) and time-reversal asymmetry in, (T), 19: 27269
decay partial widths, 16: 10898
decay rate, 18: 32564
decay schemes, 16: 13911
decay, analysis of CP-nonconserving, 19: 39457 (CONF-796(Paper 23))
decay, identification of, (T), 19: 23358 (JINR-P-1900)
decay, interference effects in CP-noninvariant, (T), 19: 23357 (JINR-D-1926)
existence of stable, 16: 2449

MESONS ($K^+_{\pi 2}$)
decay branching ratios of, remarks on, 17: 15126
decay branching ratio, (E), 20: 32043
decay, effects of π–π interactions on radiative, 16: 979
decay, meson (π) resonance production in S-wave, I = 2 isospin state, 16: 26117
decay of, 18: 34578
decay of, enhancement of, 17: 24360
decay of, branching ratio relative to mesons ($K^0_{\pi 2}$) for, 20: 41801 (UCRL-16003)
decay of, branching ratios for, (E), 19: 37600
decay of, $|\Delta T| = \frac{1}{2}$ role in, 18: 21012
decay of, octet dominance model for, (T), 19: 8168
decay of, test of CP violation and $|\Delta T| = \frac{1}{2}$ rule for radiative, 19: 47351
decay of, unitary symmetry for, 18: 40313

MESONS ($K_{\pi 3}$)
branching ratios, (E), 19: 20990
decay, 17: 39914
decay amplitudes, analytic properties, 16: 4704
decay, meson (π) spectra from, 17: 711 (NEVIS-110)
decay, model for violation of $|\Delta I| = \frac{1}{2}$ rule in, 17: 16996
decay of, meson (π-π) resonance in, 17: 11528
decay of, meson (π) emission in, 17: 11553
decay of, selection rules for, 18: 4429 (CONF-231-3)
decay of, single-loop four-point diagrams in, 17: 6944 (BNL-5528)
decay of, unitary symmetry in, 17: 34770
decay of, wave function for, 17: 24285
decay of, amplitudes for, (E/T), 20: 34194
decay of, effect of final-state strong interactions on probability of, (T), 20: 6086
decay of, energy spectrum of π^+ in, 18: 32612
decay of, final-state interactions in, 20: 34154(R) (UCR-34P107-33)
decay of, K^0_2–K^0_1 mass difference from, 18: 36318
decay of, model for, 18: 28371
decay of, partially conserved axial-vector current hypothesis for, 20: 21666
decay of, radiative, (T), 20: 6067
decay of, weak interactions in nonleptonic, 18: 32628
decay, p-wave meson interaction effects, 16: 9398

decay probabilities, effects of meson (π) mass difference on, 16: 7001
decay properties, 18: 12937
decay, review of pion-pion interactions in, 16: 8053 (NP-11232 (p.236-42))
decay scheme, (E/T), 19: 25265(R) (UCRL-11776)
decay, vertex diagrams, 16: 2432

MESONS ($K_{\pi 4}$)
decay modes, 16: 10855
decay modes of, 3π, 17: 17027
decay of, interactions in 3π, 18: 36358
decay of, study of low energy (π-π) interaction by, 17: 17007

MESONS ($K^0_{\mu 3}$)
decay ($K^0_2 \rightarrow \pi^+ + \pi^- + \pi^0$) probability for, 17: 41824
decay of K^0_2, 18: 18727
decay of K^0_2, 18: 40277
decay of K^0_2, 18: 42453
decay of K^0_2, final-state interactions in, (T), 19: 18804
decay of K^0_2, branching ratio and meson (π^0) energy spectrum in, (E), 19: 43115
decay of K^0_2, isotopic spin effects in, 17: 19130
decay of, violation of $|\Delta I| = \frac{1}{2}$ rule in, 18: 887
decay of, branching ratios for, (E), 19: 32947 (JINR-P-2090)
decay of, CP violations in, (T), 19: 29086
decay of, possibility of $3\pi^0$, 18: 32627
decay of, probability of, (E), 19: 32942 (JINR-P-2065)
decay of, relative probability of, (E), 20: 11561 (JINR-P-2450)
decay of, relative probability of, 17: 37937 (JINR-P-1332)
decay of, test of CP invariance and $\Delta I = \frac{1}{2}$ rule in, (E/T), 20: 44228
decay of, $3\pi^0$, (E), 19: 12315
decay ($3\pi^0$) of K^0_2, 18: 30576
decay rate of, absolute, 18: 20956

MESONS ($K^+_{\pi 3}$)
decay, 17: 28211
decay, 18: 21018
decay mode, 16: 6977
decay modes of, 17: 17027
decay of, branching ratio and meson (π^-) energy spectrum for three-pi, (E), 19: 16515
decay of, branching ratio for $K^+ \rightarrow 2\pi^+ + \pi^-$, 19: 3087
decay of, branching ratios for 3π, (E), 19: 20990
decay of, evidence for $K^+ \rightarrow \pi^+ + \pi^+ + \pi^- + \gamma$, 17: 11523
decay of, radiative, 17: 11536
decay of, study of low energy (π-π) interaction by, 17: 17007
decay of, analysis of, 18: 21018
decay of, anomalous π^+ decay in, (E), 19: 23440
decay of, branching ratio and meson (π^-) energy spectrum for, (E), 19: 16515
decay of, branching ratios for, (E), 19: 20990
decay of, CP invariance in, (T), 19: 16610
decay of, $\Delta I = \frac{1}{2}$ rule in, (E), 20: 1028
decay of, effects of CP violation in, (T), 19: 41445
decay of, energy spectra for modes of, 19: 39488 (UCRL-16058)
decay of, energy spectra from, (E), 20: 1011
decay of, equations for amplitudes in, 18: 10914
decay of, final-state interactions in, (T), 19: 18804
decay of, interactions in, 18: 36358
decay of, isotopic spin effects in, 17: 19130
decay of, meson (π^+) energy spectrum in (E), 19: 1318
decay, relation to meson (η) decay, 16: 26150

MESONS (κ)
decay of, unitary symmetry selection rules for, 18: 30556
interactions of, resonances in, (T), 19: 10015 (JINR-P-1808)
production in meson (K^+)-proton interactions at 3.6 Bev/c, (E), 20: 15415
production of (725), in meson (π^-)-proton interactions, 20: 2715
properties of, 20: 34175
theory, 18: 30609

MESONS (L)
decay of, existence of radiative, (T), 19: 20931 (JINR-P-1951)
production in meson (K^-)-proton interactions at 10 Bev/c, 20: 39788

MESONS (λ^0)
magnetic moment of, 16: 30930(R) (NYO-2669)

MESONS (μ)
see also Muonium
absorption and interactions in matter, (T), 20: 13350
absorption of polarized, macroscopic-body rotation from, (T), 19: 12314
acceleration in cyclic machines, 17: 38367 (CERN-63-19(p.410-13))
analysis of beams of, for meson (π) contamination, 18: 42410
angular distribution in meson (π) decay, 17: 17019
angular distribution in meson (π) decay at rest in nuclear emulsions, (E), 19: 37593
anomalous magnetic moment, contribution of intermediate vector bosons to, 18: 9156
background in underground low-level gamma-counting laboratory, 19: 20093(R) (ANL-6938(p.194-205))
behavior and properties, 16: 16994 (NP-11592(Vol.II)(p.3-13))
beta decay, (T), 20: 30535
beta decay of, electromagnetic corrections to weak interactions from, 17: 19141
beta decay of, radiative corrections to, 17: 2180
beta decay of, sonic spark chamber measurement of spectrum for, 17: 38608 (CU(PNPL)-227(p.171-2))
bibliography on, 18: 4428 (BNL-809)
biological hazards of, 17: 18392 (TID-7652(p.866-75))
book: ***Fundamental Particles***, 19: 21072
bundle of, in extensive air showers, 17: 20868
capture and decay of, review on, 20: 7806
capture by boron-10, γ-ν correlations for, 18: 28735
capture by calcium-40 and -44, rates for, 16: 21399
capture by calcium-40 and oxygen-16, ratio of normal to radiative, 17: 40084
capture by carbon-12, effects of weak magnetism in, (T), 19: 8492
capture by carbon-12 and oxygen-16, (T), 19: 41766
capture by complex nuclei, hyperfine effects in, 17: 17229
capture by complex nuclei, models for, 17: 19293
capture by complex nuclei, mechanisms of (T), 19: 1419 (NP-14404 (p.188-201))
capture by complex nuclei, correlation functions in, (T), 19: 47656
capture by complex nuclei, coupling constants in, (T), 20: 24382
capture by complex nuclei, effects of giant resonances in, 20: 40151
capture by complex nuclei, (T), 20: 46768
capture by copper, gamma spectra from radiative, (E/T), 19: 10339
capture by deformed nuclei, 18: 38167
capture by deuterons, neutron spectra from, (T), 19: 41782
capture by fluorine-19, hyperfine effect in, 16: 21400
capture by heavy nuclei, theory of, 18: 24658
capture by helium, mesic atoms from, 17: 33080
capture by helium-3, processes for, 18: 21326
capture by helium-3, relativistic rate of, 18: 22909
capture by helium-3, neutron spectra from, (T), 19: 41783
capture by helium, hydrogen, and carbon, intermediate vector boson in, (T), 19: 21420
capture by hydrogen, coupling parameters from radiative (T), 19: 1232 (LNF-64/26)
capture by hydrogen, hyperfine effects in, (T), 19: 8224
capture by hydrogen, (T), 19: 8229
capture by liquid helium, 16: 16943 (NP-11592(Vol.I)(p.141))
capture by lithium-6, effects of hfs of mesic atom on, 17: 26298
capture by lithium-6 and -7, E1 excitation in, (T), 19: 45351
capture by neon mesic atoms, probability for nuclear, 17: 24493
capture by nuclei, Fermi interactions in, 16: 15590
capture by nuclei, neutron emission in, 16: 18486
capture by nuclei, shell-model analysis, 16: 23088
capture by nuclei, (T), 20: 12100
capture by nuclei, Goldberger-Treiman relation for, 18: 15304
capture by nuclei, decay constant for, 18: 40533
capture by nuclei, G-parity violation in, (T), 19: 6648
capture by nuclei, scalar coupling constant in, (T), 19: 8084
capture by nuclei, use in study of nuclear structure, (T), 19: 16852(R) (NP-14647)
capture by nuclei, gamma-neutrino correlation in first-forbidden, (T), 19: 21378
capture by nuclei, decay of collective states excited in, (T), 19: 41769
capture by nuclei, G-parity violation in, (T), 20: 13877
capture by nuclei, review on, 20: 19459
capture by nuclei, probability for, (T), 20: 28456
capture by nuclei, conference on, 20: 42304
capture by nucleons, pseudoscalar coupling magnitude in, 18: 34551
capture by nucleons, form factors in, (T), 19: 12316
capture by oxygen-16, irregular G-parity interaction in, (T), 20: 44767
capture by spin-$\frac{1}{2}$ nuclei, recoil angular distributions in, 18: 28736
capture by 2s-1d nuclei, Nilsson model calculations of rate of, 18: 21277
capture in chemical compounds, 18: 22668 (AD-417241)
capture in chlorine-35 and chlorine-37, shell model calculation of rates for, 17: 7274
capture in complex nuclei, (T), 20: 8062(R) (COO-720-058)
capture in iron and zinc, decay-rate anomaly in, 16: 15690
capture in lead and silver, neutron emission from, 16: 18474
capture in mixed gases, 20: 37741 (JINR-P-2788)
capture in nuclei, coupling constants for, (T), 19: 31227 (NP-15026)
capture, measurement of radiative, 16: 25923 (NP-11977(p.53-4))
capture of, intermediate vector theory in, 17: 41818
capture of, lepton theory of inverse, 17: 5272
capture of, induced pseudoscalar interaction in, 18: 36703
capture of, intermediate-boson effects in radiative, 18: 44580
capture of, nuclear matrix elements in, (T), 19: 5232

capture processes review, 17: 9469
capture rate as function coupling constants, total, 17: 9582
capture rate in, 19: 47227
capture rate in calcium-40, nuclear surface effect on, 17: 15303
capture rates in light nuclei, total, (T), 19: 6681
capture, theory of atomic, 16: 2305(R) (UCRL-9704)
capture transition rates in carbon-12 and oxygen-16, calculation, 18: 32747(R) (UCRL-11213(p.64-86))
Cherenkov light of cosmic neutrino-produced, detection of, 20: 21031 (CERN-65-32, pp 231-40)
collection along channels of magnetic quadrupole lenses from meson (π) decay, 16: 4690 (NP-10773)
collimation of, electromagnetic lenses for, 19: 23222
contamination of meson (π) beam by, 17: 3977
content in meson (π) beams, method for calculating, 19: 44993 (CEA-R-2778)
coupling to heavy vector mesons, asymmetric, 17: 41779
decay ($\mu \rightarrow 3e$) of, higher-order processes in, 18: 12965
decay, asymmetry, 16: 15537
decay, branching ratios, 16: 18330
decay calculations, 16: 10974
decay characteristics and physical properties, 16: 10930
decay constant for bound, neutrino effects on, 18: 40533
decay constant of, effects of meson (W) on, 18: 32535 (NP-14081)
decay $e + \gamma$, 16: 10817 (NP-11301)
decay, even and odd, 16: 992
decay in ambiplasma, energy distribution from, (T), 20: 21684
decay in iron and zinc, 16: 24819
decay in renormalizable vector boson theory, 19: 39489
decay in spark chambers, on-line measurement of electron momenta spectra in, 20: 11553(R) (COO-614-34, Sect. IIC)
decay into leptons without neutrino emission, 16: 3643
decay mediated by a vector boson, radiative corrections to, 18: 21010
decay mode, $e + \gamma$, limits of, 16: 10889
decay mode, $e + \gamma$, limit of, 16: 10890
decay modes of, neutrinoless, 17: 17026
decay modes, U-process probabilities in, 16: 27985
decay ($\mu \rightarrow e + \gamma$), search for, 16: 17056
decay ($\mu \rightarrow e + \gamma$), neutral currents in, 17: 7032
decay $\mu \rightarrow e + \gamma$ and $\mu \rightarrow 3e$, spark detector efficiency for, 17: 41275
decay ($\mu \rightarrow 3e$), neutral currents in, 17: 7032
decay of bound, Cherenkov study, 16: 22870
decay of bound, from K-shell, 16: 21611
decay of bound, in titanium, iron, and lead, 17: 17297
decay of bound, intermediate boson effects on, 16: 15603
decay of bound, in elements of intermediate Z, 18: 12964
decay of, branching ratio for radiative beta, 17: 19095
decay of, coupling constant for, 18: 9361
decay of, intermediate vector bosons in, 18: 9138
decay of, model for weak leptonic interactions in, 18: 2621
decay of, radiative corrections to, 16: 33710
decay of, radiative corrections to, analysis by dispersion and perturbation techniques for, 17: 22520
decay of, rate-determining factor in, 18: 2653
decay of, relativistic three-particle emission in, 17: 32921
decay of, search for 3-e, 17: 9392
decay of, selection rule for, 17: 22468
decay of, strong interaction effects in Feinberg-Pais theory for, 18: 7534
decay of, beta spectra calculation in, (E), 20: 11093(R) (COO-614-34, Sect. IIA)
decay of, coupling constants for, (T), 19: 47378
decay of, CP violation in, (T), 19: 41378
decay of, effects of weak vector bosons in, 20: 4629
decay of, electromagnetic violation of vector current conservation of, 18: 14890
decay of, electron energy spectra from V–A interaction in, 18: 36267
decay of, electron spectra from, 19: 46785
decay of, electron spectra from, (E/T), 20: 19503
decay of, inner bremsstrahlung in, 18: 36319
decay of, integral spectrum and lifetime from, (T), 19: 18784
decay of, intermediate-vector-boson effects in radiative, (T), 19: 4916
decay of, intermediate vector boson in radiative, (T), 19: 10052
decay of, lepton charge in, 18: 26309
decay of, lepton symmetry refraction from, 20: 15448
decay of, model for leptonic, 20: 15360
decay of, modified vector-boson propagator for leptonic, (T), 20: 11588
decay of, neutrino interactions in, 18: 40280
decay of, neutrino mass dependence of electron spectrum in, (T), 19: 31066
decay of, radiative corrections for intermediate vector bosons, 18: 28376
decay of, radiative corrections for, 18: 37951
decay of, radiative corrections to, (T), 19: 8234
decay of, radiative corrections for, 19: 23457
decay of, renormalization of decay constants with intermediate meson (W) in theory of, 18: 32533 (NP-13936)
decay of, review, 18: 10893
decay of, search for $e + \gamma + \gamma$, 19: 32989
decay of, sonic spark chamber-on-line computer system for positron spectrum determinations in, 18: 31872 (CERN-64-30(p.41-8))
decay of, strong interaction effects in peratization theory of, 18: 15308
decay of, strong interaction effects in peratization theory of, 18: 15309
decay of, strong interaction effects in Feinberg-Pais theory for, 18: 20950
decay of, universality of vector-boson-mediated, 18: 30549
decay of, universality of vector-boson-mediated, 18: 30549
decay of, V-A interaction and coupling constants in, (T), 20: 6048
decay of, weak current conservation in, (T), 19: 16671
decay rate of bound influence of intermediate vector boson on, 17: 41817
decay rate of bound, intermediate-boson weak interaction for, (T), 19: 10036
decay rate of bound, 19: 23777
decay schemes, 16: 16950 (NP-11592(Vol.I)(p.191-5))
decay to electron plus gamma ray, phenomenological diagram for, 16: 33678 (AFOSR-1887)
depolarization by weak magnetic fields, 16: 5892
detection and differentiation from electrons and pions in Bev range, 20: 7365 (KFK-342)
detection and measurement of, design of Cherenkov detector for, 17: 3309 (NP-12265)
detection and measurement, 18: 25831
detection and measurement in thick-plate spark chamber (E), 19: 773 (LAL-1114)
detection in nucleon interactions with atmospheric neutrinos, (E), 19: 8149
detection of neutrino-produced, deep underground, 20: 21540 (CERN-65-32, pp 49-56)
detection of, lithium-doped silicon junctions for, 19: 11528
detection of, plastic scintillators for, 19: 42751
detection using flash tubes, computer technique for, 16: 20679
discovery, early work on, 16: 3620
distribution and flux density in extensive air showers at 20 and 40 m underground, 16: 27887
distributions and flux in atmosphere, angular and energy, (T), 19: 20891
distributions near axes of extensive air showers, 17: 19029
dosimetry in Brookhaven AGS, theory of, 18: 12817
dosimetry of, research on, 17: 14525 (BNL-6767)
effects on chromosomes, 19: 2062 (BNL-8462)
effects on maize, mutagenic, 19: 43712 (BNL-9383)
effects on *Zea mays*, RBE for cytogenetic, 19: 5696
electric dipole moments of, in intermediate vector boson theory, 20: 17372
electrodynamics of charged fields with electrons, spontaneous symmetry breakdown in, (T), 19: 4965
electrodynamics of massless, quantum, (T), 19: 6572
electromagnetic properties at small distances, 16: 29707
electromagnetic properties of, methods of studying, 17: 9406
electromagnetic properties, 18: 14914
electron decay, energy spectra of, influence of intermediate vector bosons on, 17: 19161
electron-photon shower production by, at high energies, 17: 7044
electron-pair production by, underground, 18: 28285
emission in decay of meson (K^-)-proton resonances, (E), 19: 18893
emission in hyperon decay, probability for, 18: 36357
emission in meson (π) decay, branching ratio for, 18: 12950
emission in meson (π) decay, radiative corrections to polarization in, (T), 19: 8169
emission in meson (K^+) decay, branching ratios for, (E), 20: 7801 (UCRL-16362)
emission in multiple generation processes at high energies, 16: 27939
emission in neutrino reactions with iron and lead, diffraction mechanism for, 17: 21091
energy from meson ($K^-_{\mu 3}$) decay, (E), 20: 13521
energy loss of ultra-relativistic, in rock and water, (E/T), 19: 41345
energy-loss spectra of relativistic, 17: 19055
energy loss straggling in matter, distributions of, (T), 19: 9894 (NAS-NRC-PUB-1133(p.187-203))
energy losses and ranges in matter, tables, (E), 19: 8005 (NASA-SP-3013)
energy losses in concretes, (T), 20: 3238 (JINR-P-2354)
energy losses in nuclear interactions at high energy, (T), 19: 14334
energy losses of relativistic, in pair production, (T), 19: 31022
energy spectra from neutrino interactions, 20: 34239
energy spectra in CERN neutrino experiment, determination of, (E/T), 20: 21604 (CERN-65-32, pp 121-6)
energy spectra of small bursts at 200 mwe underground, (E), 19: 34915

energy spectrum from meson (K^+) decay (E), 19: 1319
energy-range relation for ultrarelativistic, 18: 32566
escape of neutrino-produced, from atmosphere, 17: 41716
exchange in ion reactions with hydrogen mesic atoms, (E), 20: 7734
field theory for, charge conservation in, 18: 21024
flux at sea level, (E/T), 19: 16525
flux in neutrino shielding, measurement of, 20: 22306 (CERN-65-32, pp 147-52)
fluxes of, in Stanford linear accelerator, 17: 21118 (SLAC-5(p.193-221))
gyromagnetic ratio for, experiment for measuring, 18: 32537 (PPAD-304D)
incorporation in molecules, wavefunctions for, 17: 24361
interactions above 10^{12} ev, model for, (T), 20: 11558 (JINR-E-2496)
interactions and properties, review of theory of, 17: 9471
interactions and properties, bibliography on, 17: 9472
interactions and structure of, review of, 17: 19180
interactions and structure of, survey of, 17: 19184
interactions and structure of, using a cosmic-ray meson (μ) source, 17: 19186
interactions in thick absorbers at high energy, charged-particle showers from, (T), 19: 41354
interactions of high-energy, electron-photon showers from, 19: 41355
interactions of, resonant, 17: 39891
interactions of, structure in weak, 17: 4021
interactions of, electrodynamics of weak, 18: 28740
interactions of, forbidden processes in weak, (T), 19: 8228
interactions of, high-energy, (T), 19: 25362
interactions of, review, 18: 10893
interactions of, weak, 19: 25361
interactions, review of data on electromagnetic and weak, 16: 33722
interactions with nuclear Coulomb field, neutrino pair production in, 16: 1086
interactions with protons, contribution of bremsstrahlung to cross section, 16: 4699
interactions with mesons ($K_{\pi 2}$), model, 16: 4728
interactions with protons, contributions of pion and nucleon currents to radiative, 16: 12437 (NYO-9284)
interactions with nucleons, coupling constants, 16: 12565
interactions with protons, six nucleon form factors, 16: 21325
interactions with protons, differential cross section for, 17: 13391
interactions with protons using beam from 300-Bev accelerator, 17: 20574 (UCRL-10022(p.96-104))
interactions with protons at high momentum transfers, possible information from study of, 17: 20575 (UCRL-10022(p.105-7))
interactions with mesons (μ) as test for mass of, 17: 20851
interactions with protons, assembly for studying, 17: 21117 (SLAC-5 (p.165-92))
interactions with protons, Stanford arrangement for studying elastic, 17: 21118 (SLAC-5(p.193-221))
interactions with protons at the 3/2 resonance in the isobaric model, 17: 26297
interactions with protons, apparatus for studying, 17: 29492 (BNL-7033)
interactions with electromagnetic field, theory of parity-nonconserving, 17: 41799
interactions with electrons, corrections to differential cross sections for, 18: 9142
interactions with neutrinos, theory of, 18: 12890 (CERN-63-37(p.1-20))
interactions with electrons and neutrinos, unitary symmetry in weak, 18: 14940
interactions with electrons, neutrino rest-mass effects in annihilation, 18: 22776
interactions with nucleons, meson (π) production by virtual photons in, 18: 26305
interactions with protons, mesons (π) production and radiative corrections in, 18: 30550
interactions with protons at high momentum transfers, radiative corrections for, 18: 32544
interactions with electrons, depolarization in, 18: 36329
interactions with protons, in isobaric model, 18: 37978
interactions with protons, recoil proton polarization in elastic (T), 19: 1363
interactions with neutrinos, angular and spin correlations in, (T), 19: 5007
interactions with protons, inelastic processes in, (E/T), 19: 6521 (SLAC-25(Pt.II)(p.1-30))
interactions with protons, bremsstrahlung and meson (π) production in, (T), 19: 14321 (NP-14631)
interactions with antineutrinos and neutrinos, polarization in, (T), 19: 14343
interactions with electrons at high energy, (T), 19: 14386
interactions with electrons, pair production in, (T), 19: 18793
interactions with electrons and photons, spontaneous symmetry breakdown in, (T), 19: 23416
interactions with electrons, cross sections for, (T), 19: 29082
interactions with protons, cross sections for, (T), 19: 31045
interactions with photons in meson (η) decay, (T), 19: 41457
interactions with protons at 700 to 1100 Mev/c, cross sections for, (E/T), 20: 4591 (UR-875-108)
interactions with electrons, cross section for, (T), 20: 13484
interactions with neutrinos (ν_μ) at very high energies, (T), 20: 17366(T)
interactions with nucleons, inelastic, (T), 20: 17399
interactions with leptons and nucleons, (E/T), 20: 24260
interactions with protons, computer programs for analyzing, 20: 25778 (BNL-10166)
interactions with intermediate weak bosons, meson (μ) anomalous mass from strong, (T), 20: 25840
interactions with nucleons, inelastic, (T), 20: 30076
interactions with nucleons, cross sections for, (E/T), 20: 29994
interactions with electrons, universality in, (E/T), 20: 31986 (NEVIS-148)
interactions with deuterons, detection of $|\Delta I| = 0$ weak nuclear force from elastic, 20: 32049
ionization loss of relativistic, 19: 25338
lifetime, 18: 28376
lifetime and electromagnetic properties of, review on, 19: 29011
lifetime in intermediate coupling, 17: 760
lifetime of, as test for space-time universal length, (T), 20: 28152
lifetime of, from μ-e symmetry, (T), 19: 12248
lifetime of, method for determining, 18: 42383
magnetic moment, 18: 32674
magnetic moment, (T), 20: 19525
magnetic moment, anomalous, 16: 26115
magnetic moment and mass, 17: 19104
magnetic moment of, anomalous, 16: 26095
magnetic moment of, pionic contributions to, 16: 31042
magnetic moment of, measurement of anomalous, 17: 9403
magnetic moment of, measurement of anomalous, 17: 9473
magnetic moment of, corrections to anomalous, 18: 9127
magnetic moment of, anomalous, (E), 19: 31034
magnetic moment of, dispersion theory for anomalous, 19: 45108
magnetic moment of, anomalous, (T), 20: 21656
magnetic moment of, NMR equipment for measuring, 20: 31817 (CERN-66-15)
magnetic moment of, experiment for measuring anomalous, 20: 41810
magnetic moments, 18: 9104
magnetic moments of, calculation of anomalous, 19: 37635
magnetic moments of, (T), 19: 47378
mass calculations in K–N interactions, 16: 8107
mass difference between electrons and, 17: 15141
mass difference (e-μ), origin of, 17: 39904
mass difference with respect to electrons, 18: 32664
mass differences (β-μ), theory for, 18: 837 (JINR-D-1345)
mass expression for, 17: 9271
mass measurements of, 20: 7804
mass of, charged-meson maximum decay rate from, 20: 15344
mass of, theory for, 18: 26335
mass relations for, empirical, 19: 20994
mass relative to electron, electrodynamic theory for, 18: 7508
mass relative to electrons, calculation using perturbation theory, 20: 13628
mass relative to electrons from spontaneous symmetry breakdown, 20: 21678
mass relative to electrons, (T), 20: 27882
measurement of atmospheric, design of instrument for, 19: 9537
measurement of G/M ratio for, 16: 29661 (UCRL-10107)
model as excited electrons, 16: 21327
models for, description of electromagnetic, (T), 19: 41377
momentum of high-energy, determination using emulsions, 18: 23945
momentum spectra in atmosphere, (E), 19: 16524
neutrino associated with, mass of, 17: 19125
occurrence in extensive cosmic air showers, 18: 12844
pair photoproduction at small angles, asymmetric, 18: 34594
pair production at high energies, inelastic nuclear effects on, (T), 20: 27951
pair production by electrons at 0.75 to 1.30 Bev, cross section for, 18: 30611
pair production in electron-nucleus interactions, 16: 18381
pair production in meson (ω) resonance decay, 17: 11642(R) (TID-17720(p.98-100))
pair production in antiproton-proton annihilation, 17: 24322
pair production in meson (π)-nucleon interactions, 18: 40258
pair production in neutrino reactions, 18: 40500 (AD-603251)
pair production in electron-positron interactions, photon emission in, (T), 19: 29105
pair production in annihilation of polarized protons and antiprotons, (T), 19: 37604(T)
pair production in electron–positron interactions, (T), 19: 37605(T)

pair production in annihilation of polarized electrons and positrons, (T), 19: 43067
pair production in meson (ρ^0), (ω), and (ϕ) decay, branching ratios for, (E), 20: 11673
pair production in strong interactions, 20: 34182
pair production of, spin correlation in, 17: 6952 (LNF-62/75)
pair production of, cross section for, 18: 26564
pair production on carbon by 5-Bev bremsstrahlung beams, (E), 19: 5569(R) (MIT-2098-64)
parity, 16: 21320
penetration through substances, fluctuation losses in, (T), 19: 35509
photoproduction in pairs on carbon, 17: 40433(R) (NYO-10063(p.71-89))
photoproduction in accelerator shielding, (T), 20: 25657 (SLAC-PUB-179)
photoproduction of e-μ pairs on nuclei at high energies, forbidden, 16: 24724
photoproduction of pairs in carbon, 16: 25899 (LNF-62/37(p.105-9))
photoproduction of pairs of, in carbon, 17: 5260
photoproduction of pairs of, in carbon, 17: 9401
photoproduction of pairs of, in carbon, 17: 9473
photoproduction of pairs of, at wide angles, 17: 32916 (TID-7668(Sect. VIII))
photoproduction of pairs of, carbon, 18: 2842 (RT/FI(63)37)
photoproduction of pairs of, 18: 10854 (LNF-63/47(p.1-35))
photoproduction of pairs of, quantum electrodynamic testing by, 18: 10884 (SLAC-25(Pt.I)(p.195-9))
photoproduction of pairs of, wide-angle, 18: 28400
photoproduction of, Regge trajectories in pair, 18: 37981
photoproduction of pairs of, as test for quantum electrodynamics, 18: 40353
photoproduction of pairs of, (T), 19: 31045
photoproduction of wide-angle pairs of, from carbon, (E), 19: 36220(R) (MIT-2098-142)
photoproduction of pairs of, on carbon, (E), 20: 15306(R) (CEAL-1026)
photoproduction of asymmetric pairs of, on carbon and hydrogen, (E), 20: 27952
photoproduction of pairs of, on carbon, quantum electrodynamics test from, (E), 20: 46373
photoproduction on nuclei, experimental set-up measuring, 16: 25931 (NP-11977(p.90-2))
photoproduction on electrons, cross section for pair, 18: 5988 (JINR-P-1402)
photoproduction on nucleons, amplitude of, (T), 20: 2695
polarization at 3860 m above sea level, (E), 20: 36009
polarization in $K^+_{\mu 3}$ decay, 18: 32611
polarization in meson (K^0) leptonic decay, time dependence of, (T), 19: 25355
polarization in mesic atoms of spin-one nuclei, (T), 20: 39616
polarization in neutrino-induced reactions as test for time reversal violation, (T), 20: 13835
polarization of, measurements using Moller scattering in magnetized iron plates of spark chamber, 17: 9193 (LNF-62/61)
production and polarization from neutrino quasielastic scattering by nuclei, 20: 32468
production and transport at Univ. Chicago Synchrotron (T), 19: 1114 (NASA-CR-56934(p.237-63))
production and transport at Univ. Chicago Synchrotron (E), 19: 1115 (NASA-CR-56934(p.264-78))
production at sea-level, from photon-electron cascades, 20: 44160
production by neutrino interactions in Coulomb field, higher order effects, 19: 23475
production by neutrinos, experiment for detecting, 20: 4561 (COO-818-64)
production from cosmic ray reactions with dense matter, differential energy spectra for, (T), 20: 37712
production in antiproton-proton annihilation in ambiplasma, (T), 20: 21684
production in cascades by heavy-particle reactions in matter, 16: 13944 (DESY-A2.85)
production in CERN neutrino spark chamber experiment, 19: 1392
production in cosmic-ray interactions, multiple, (T), 19: 4865
production in crossed electron and electron-positron beams, 17: 37981
production in decay of heavy hypernuclei, (T), 19: 27148 (JINR-P-1998)
production in deep underground interactions of cosmic neutrinos, (E), 19: 43024
production in electromagnetic electron interactions, 17: 7009
production in electron interactions with lead targets, 18: 14832
production in electron-positron interactions, hard photon emission in pair, (T), 19: 16531
production in electron reactions with lead and lithium at 6 to 25 Bev, (E), 20: 41805(T) (SLAC-Trans-46)
production in large plastic scintillators by background neutrals, mechanism and rate of, 20: 21028 (CERN-65-32, pp 65-70)
production in liquid scintillators by cosmic rays, (E), 20: 21029 (CERN-65-32, pp 71-2)
production in Mc^2 cyclotron, 19: 11944
production in meson (π) decay, 16: 10845
production in meson(π) decay, 17: 11471 (JINR-E-1120)
production in neutrino interactions, ratio to electrons, 17: 20933
production in neutrino reactions underground, experimental possibilities for studying, 17: 34764
production in neutrino reactions with nuclei in earth's crust, 17: 41716
production in neutrino interactions with neutrons, differential and total cross sections for, (T), 20: 4611
production in neutrino interactions, polarization measurement of, 20: 30003
production in particle inelastic reactions at 1 to 10 Bev, 16: 5861 (JINR-P-772)
production in photon interactions, (E), 19: 39623
production in proton reactions with beryllium at 30 Bev/c, 20: 34146 (CU-1932-256)
production of beams of, using high-intensity proton linac, (E), 19: 9808 (TID-21282)
production of beams of, magnetic quadrupole channel for, (T), 19: 11971
production of beams of, in JINR synchrocyclotron, 19: 14173 (JINR-P-1902)
production of, by leptons in nuclear Coulomb fields, 17: 22644
production of heavy, in neutrino interactions, 18: 26266 (BNL-837 (p.160-9))
production of high-energy beams of, method for, 18: 18646 (NP-13783)
production of high-energy beams of, 19: 11970
production of high-intensity, channel calculations for, 19: 28955 (LA-DC-6757)
production of pairs in p-$\bar{p}$ annihilation, cross sections, 16: 19697
production of pairs of, by neutrino scattering on nuclei near 1 Bev, 16: 29705
production of pairs of, by electron-positron annihilation, 17: 7031
production of pairs of, by muon-neutrinos, 18: 36344
production of pairs of, in meson (ρ) decay, (E), 20: 9761
production of pairs of, in electron-positron annihilation at high energies, (T), 20: 32070
production of pairs of, in photon reactions with nuclear Coulomb field, 20: 34257
production of pure beams of, 18: 20703
production of stopped, in Brookhaven AGS, 19: 37383
production of very high-energy, by electrons and photons, 17: 29511
production of, cyclotron facility design for, 18: 32319 (TID-20822)
production of, development of high-energy accelerators for, 20: 2560
production of, pair and photo-, 18: 10681(R) (CEAL-1009)
production of, two-virtual-photon exchange in, (T), 19: 12178
production underground from cosmic radiation, 16: 5840 (AD-260876)
production underground by cosmic neutrinos, (E/T), 20: 21542 (CERN-65-32, pp 73-8)
propagation in air, (E), 19: 5569(R) (MIT-2098-64)
properties, 16: 10874
properties, 16: 21272
properties and interactions, review, 18: 42463
properties in self-consistent field theories, 19: 1269
properties of, review of, 18: 7559
properties of, two-neutrino model for, 17: 9273
properties of, CERN synchrotron research on weak and electromagnetic, 18: 20965
properties of, review, 18: 10893
quantum-electrodynamic treatment as Regge poles, 17: 40239
quantum electrodynamics of, dilatationally invariant, 18: 2638
quantum properties of, comparison with those of electrons, 17: 31308
range fluctuations in ground penetration, statistical study of, 18: 28321 (INSJ-70)
range in aluminum and magnesium up to 10^8 Bev, (T), 19: 4897 (LNF-64/38)
range measurements for lead in Bev region, 18: 30230 (CERN-64-31)
reactions (μ,n) with metals, nuclear spin effects on neutron angular distributions from, (E), 20: 36196
reactions in hydrogen, mesic atom formation in, 17: 9473
reactions in nuclear Coulomb fields, polarization effects in intermediate boson production in, 18: 7533
reactions in supernova processes, neutrino emission from, 17: 32880
reactions on nuclei, mesons (π) from, 17: 28341
reactions on thick shields at 10^{13} to 10^{14} ev, showers from, 17: 19173
reactions with aluminum, copper, and lead, electron emission thickness-dependence in, 17: 26546
reactions with copper and lead, electron emission in, (E), 19: 27445
reactions with fluorine-19, spin dependence, 16: 6975
reactions with helium-3 at low temperatures, internal conversion processes, 16: 2547
reactions with helium-3, mass of neutrinos from, 18: 10845 (JINR-P-1454)
reactions with liquid hydrogen, energy range graph for, 20: 46601

(UCRL-2426(Vol.2)(1966 Rev.))
reactions with nuclei, capture, 16: 21609
reactions with nuclei, spin-dependence of capture, 16: 21610
reactions with nuclei as probe of nuclear structure, conference on, 19: 41671 (LADC-6186)
reactions with nuclear Coulomb field, electron pair production in, (T), 19: 41486(T)
reactions with nuclei around 1 Tev, particle distributions from, (T), 19: 41711
reactions with nuclei above 300 Tev, evidence for, (E), 19: 45368
reactions with nuclei, first Born approximation including anapole for, (T), 20: 4612
Regge pole characters of, experiments for testing, 17: 36592
representation in symmetry groups with electrons, 19: 16675
scattering at 3 and 6 Bev, differential cross sections for, 16: 32272 (DESY-A2.88)
scattering by bromotrifluoromethane and propane, cross sections for, (T), 20: 13480
scattering by carbon at 2 Bev/c, comparison with electron scattering at high energies, 16: 3568
scattering by carbon, measurement of elastic and inelastic cross sections for, 18: 28739
scattering by carbon-12 at 1.09 Bev/c, cross sections for, (E/T), 19: 10330
scattering by chlorine-35 and fluorine-19, Coulomb, (T), 20: 21649
scattering by copper nuclei, 17: 15298
scattering by copper and lead at 1.658 Bev/c, 18: 42654
scattering by electrons at 8.12 Bev, 16: 16945 (NP-11592(Vol.I) (p.147-50))
scattering by gold, charge distributions in, 18: 30812
scattering by iron at 2 Bev/c, 16: 2305(R) (UCRL-9704)
scattering by iron, 17: 17228
scattering by lead, anomalous distributions from multiple, 18: 19109
scattering by lead at 0.2 to 1.5 Bev/c, analysis of, 18: 28654
scattering by nuclei, 16: 8060 (NP-11232(p.302-7))
scattering by nuclei, x-ray emission in, 16: 19705
scattering by nuclei, cross section for, 18: 26564
scattering by nuclear matter, linear response to inelastic, (T), 19: 21393
scattering by nuclei at high energies, cross sections for electron pair production from, (T), 20: 27841
scattering by protons, angular distributions from, (E/T), 20: 20365
scattering in nuclear emulsions at 8 Bev, multiple, 18: 34627
scattering in nuclear emulsions at 2.5 and 5.0 Bev/c, distributions from inelastic, (E), 20: 7815
scattering in nuclear emulsions at 5 Bev/c, inelastic, (E), 20: 13526
scattering of fast, by electrons, two-photon exchange corrector for, 17: 37963
selection rule for (e-μ) symmetry, 17: 11478 (LNF-62/97)
separation from mesons (π) in meson beams, Cherenkov detector for, 17: 37433
shielding against, at 200-Bev proton synchrotron, (T), 20: 5945 (UCRL-16464)
shielding for, 18: 26165 (BNL-837(p.91-113))
shielding measurements in heavy concrete, 20: 41534 (DESY-66/18)
shower production by, underground, 16: 13917
spectra of cosmic, at 40 mwe depth, 17: 19028
spin determination of, theory of, 17: 22521
theory, 18: 24469
theory for, radiative reaction and quantum, 18: 28350
transfer from deuteron and proton to carbon and oxygen, 17: 9404
transfer from hydrogen to carbon and oxygen, 16: 32453
transfer from mesic deuterium atoms to carbon and oxygen, (E), 19: 45273 (JINR-P-2356)
transfer from proton to deuteron, rate of, 17: 9404
transfer in mesic atoms, 16: 26219 (JINR-P-942)
transition (2p → 1s) in μ mesic atoms, 16: 8185
transitions in, energy of x rays from 2p-1s, 17: 15147
transport by shielding, calculations of, 17: 22694
transport through thick shields at high energy, 20: 46932(R) (ORNL-3973(Vol.2), pp 71-84)
trapping beams of, quadrupole magnetic channel for, 20: 2547 (UR-375-98)
use in nucleon structure studies, 18: 37969
uses in nuclear structure research, 17: 36646 (CERN-63-28(p.143-71))
wave function for, 18: 12896 (CERN-63-37(p.179-201))
wave functions of molecules containing, theory of Coulomb effects in, 17: 20931
with protons, recoil proton asymmetry in, (T), 19: 1363
x-ray production in metals, 16: 15692

MESONS (μ^-)
absorption by carbon, 17: 41744 (NYO-10561)
absorption in atomic and molecular liquid hydrogen, rates for, (T), 20: 23899
absorption in liquid hydrogen, (T), 19: 19178
beam contamination by (π^-), measurement of, 16: 22889
beta decay parameters, 16: 24725
beta decay, rho value, 16: 24712
beta decay, theory of neutrinoless, 16: 18367
capture and decay rate, 18: 862(R) (TID-19590)
capture by argon and argon–hydrogen gases, spectra from, 20: 39578 (JINR-P-2807)
capture by atoms in compounds, (E), 19: 37896
capture by atoms, effects on electronic spectra, 18: 22694
capture by atoms, x-ray spectra from, (E), 20: 42306
capture by bismuth and lead, x-ray intensity ratios from, (T), 20: 31945
capture by bismuth-209, E2 and M1 hyperfine structure determination from, (E), 20: 42307
capture by calcium, neutron emission in, 16: 5864(T) (UCRL-Trans-759)
capture by calcium, neutron angular distributions at 7 to 23 Mev from, 17: 41935
capture by calcium-40, radiative, 18: 40354
capture by calcium, use for determining nuclear charge distributions, 19: 1626
capture by calcium, gadolinium, oxygen, and tin, isotopic shift of K x-ray transitions in, (E), 20: 11480
capture by calcium, neutron angular distributions from, (E), 20: 15721 (JINR-E-2517)
capture by calcium-40, giant dipole resonance model for radiative, 20: 30451
capture by carbon-12, analysis, 16: 8124
capture by carbon-12, spectra from, 16: 27352
capture by carbon-12, probability of, 17: 5409
capture by carbon-12, partial and total probabilities of, 17: 6986
capture by carbon-12, 17: 11541
capture by carbon-12, photon circular polarization and spectrum from, 17: 26529
capture by carbon-12, giant dipole states in, (T), 19: 35453
capture by carbon-12, boron-12 ground state production probabilities in, 20: 36154 (AD-635312)
capture by chemical compounds, Z-dependence of atomic-capture probability in, 18: 9109
capture by chemical compounds, atomic, 19: 39366 (JINR-P-2185)
capture by chromium and vanadium metals and oxides, K x rays from, (E), 19: 28991 (JINR-P-2039)
capture by chromium isotopes and nickel isotopes, (E), 19: 37897
capture by complex nuclei, gamma spectra from, 18: 6194
capture by complex nuclei, relativistic effects in, (T), 19: 19194
capture by complex nuclei, rates for, (T), 19: 33293
capture by complex nuclei, photon spectra and rates for, (T), 19: 33294
capture by complex nuclei, (E), 20: 42318
capture by copper, search for neutrinoless, 17: 5377
capture by copper, neutrinoless decay modes in, (E), 19: 4966
capture by deformed nuclei, nuclear charge distribution determination from hfs spectra from, (E), 20: 42308
capture by deformed and spherical nuclei, x-ray spectra from, (E), 20: 42309
capture by heavy nuclei, electric-quadrupole hyperfine effects in x-ray spectra of (E), 19: 3369
capture by helium-3, reaction mechanisms, 16: 12550
capture by helium-3, nuclear matrix element from, 16: 21384
capture by helium in hydrogen-helium mixtures, 17: 20842 (JINR-P-1168)
capture by helium-3, 17: 31091(R) (UCRL-10862)
capture by helium-3, angular distributions of tritium from, 18: 6269
capture by helium-3 and -4, relativistic corrections for, 18: 6246
capture by helium-3, partial and total rates for, 18: 9425
capture by helium-3, total rate for, 18: 11281
capture by helium-3, rate of, 18: 21160 (CONF-231-5)
capture by helium-3 and -4 at 100 to 120 Mev/c, rates for, 18: 34776 (UCRL-11004)
capture by helium-4, total rate for, 18: 42715
capture by helium-4, rate of (E), 19: 1661
capture by helium-4, rate of (E), 19: 1662
capture by helium-3, rate of, (E), 19: 10373
capture by helium-3 and -4, rate of, 19: 19198
capture by helium-3, nuclear form factors from, (T), 19: 21236 (JINR-P-1952)
capture by helium-3, pseudoscalar and tensor couplings in radiative, (T), 19: 25504
capture by helium-3, form factors for, (T), 19: 37851
capture by helium-3, probability of, (T), 20: 1189
capture by helium-3, rate for partial, (T), 20: 44194
capture by hydrogen and protons, rates for, 17: 19328
capture by hydrogen, meson (μ)-electron universality in, 17: 33002 (NEVIS-116)
capture by hydrogen, photon circular polarization in, 17: 41834

capture by hydrogen, rates for radiative, 18: 19105
capture by hydrogen, rate for, (T), 19: 5223
capture by lead isotopes, isotope shifts from, (E), 20: 42307
capture by light nuclei, probability of, (T), 19: 27434 (JINR-P-2063)
capture by lithium and oxygen, determination of, 17: 11331(R) (TID-17023)
capture by lithium-6, probability rate for, 18: 17087
capture by lithium-6, hyperfine effects in, 18: 30786
capture by lithium-6, calculation of probability of, 19: 3251
capture by lithium-6 and -7, properties of, (T), 20: 36172 (NP-16190)
capture by manganese atoms, quadrupolar effects on energy levels in, (T), 19: 39368 (NP-15089)
capture by molecules, rates for, 18: 38130
capture by neon nuclei, measurement of disappearance rate in, 18: 2645
capture by neon, probability for, 18: 38130
capture by nuclei, rates, 16: 24826
capture by nuclei, photon angular distributions from, 16: 26236
capture by nuclei, radiative, 17: 9394
capture by nuclei, 17: 36646 (CERN-63-28(p.143-71))
capture by nuclei ($40 \leq Z \leq 70$) at 70 Mev, lifetime and rate of, 17: 40083
capture by nuclei, interaction constants for, 17: 41936
capture by nuclei ($12 \leq Z \leq 50$), x-ray spectra from, 17: 26578
capture by nuclei, calculation of effects of hyperfine structure on, 18: 5992 (NP-13347)
capture by nuclei at 149 Mev/c, x-ray spectra from, (E), 19: 5168
capture by nuclei at 149 Mev/c, transitions in, (E), 19: 5169
capture by nuclei in μ-mesic deuterium and hydrogen molecules, (T), 19: 37458(R) (ORNL-3778(p.150-1))
capture by nuclei, x rays from, 18: 19044
capture by nuclei, photon polarization in, 18: 21310
capture by nuclei, coupling constants in, 18: 26523 (BNL-837(p.292-7))
capture by nuclei, charge symmetry of axial current in radiative, 18: 40554
capture by nuclei, lifetimes and rates of, 18: 40572
capture by nuclei, isotope effects on K x rays from, 19: 47582 (NEVIS-129)
capture by nuclei, elementary-particle model for, 20: 1207
capture by nuclei, x-ray spectra from, (E), 20: 29525 (CONF-660209-9)
capture by nuclei, $\Delta S = 0$ neutron current coupling in, 20: 30141
capture by nuclei, nuclear charge distribution determination from, (E), 20: 42305
capture by nuclei, review of, 20: 42317
capture by nuclei, mass dependence of average neutron emission from, (E/T), 20: 42174
capture by oxygen-16, two-nucleon correlations, 16: 13950 (JINR-P-887)
capture by oxygen-16, rates for, 17: 34960
capture by oxygen-16, neutron emission in, 18: 15196 (JINR-P-1530)
capture by oxygen-16, giant resonance excitation in, 18: 19090
capture by oxygen-16, pseudoscalar coupling constant from, 18: 38131
capture by oxygen-16, partial rates for, 18: 42718
capture by oxygen-16, vector and axial vector matrix elements in, (T), 19: 33309
capture by oxygen-16, pseudoscalar coupling constant from, 19: 47707
capture by oxygen-16, rate of, (E), 20: 6273 (AD-617398)
capture by oxygen-16, breakdown of supermultiplet symmetry in, (T), 20: 24339 (COO-720-060)
capture by oxygen-16, elementary-particle treatment of, 20: 30447
capture by oxygen-16, nitrogen-16 ground state production probabilities in, 20: 36154 (AD-635312)
capture by oxygen-16, coherent antiproton-neutron excitations from, (T), 20: 42279
capture by plutonium-239, radiationless transitions in fission from, (E), 20: 8068 (JINR-D-2427)
capture by plutonium-239, lifetime of, (E), 20: 38114
capture by proton pairs in nuclei, (E/T), 19: 41753
capture by protons in hydrogen, atomic and molecular reactions from, 16: 23081
capture by protons, radiative, 17: 7047
capture by several elements, multiplicity distributions of neutrons emitted in, 18: 40516 (UCRL-11243)
capture by spherical nuclei, (T), 20: 8155
capture by spherical nuclei, (T), 20: 30494
capture by spin-0 nuclei asymmetry in neutron angular distributions from, (E), 19: 45274 (NEVIS-136)
capture by sulfur at high energy, neutron angular distribution from, (E), 20: 46790
capture by sulfur, neutron angular distributions from, (E), 20: 15720 (JINR-E-2516)
capture by thorium-232 and uranium-238, x-ray spectra from, 20: 4825(R) (ANL-7081, pp 81-93)
capture from hydrogen mesic atom by nuclei of other elements, rates for, (E), 19: 35384 (JINR-P-2153)
capture in atomic K shells, angular correlations from, 17: 28215
capture in chemical compounds, (E), 20: 7732
capture in copper, radiative, 17: 29574 (NYO-10562)
capture in heavy materials, neutrino spectra from, 16: 15562
capture in helium-3, rate of, 17: 31529
capture in helium-3, rate of, 18: 4624
capture in iron, detection of, 16: 26142
capture in liquid hydrogen, rates for radiative, (T), 19: 4932
capture in liquid hydrogen, G-parity in rates of, (T), 20: 13505
capture in liquid hydrogen, (E/T), 20: 19374
capture in lithium, transition paths after, 18: 1025 (UCRL-10965)
capture in oxygen 16, pseudoscalar coupling constants from, 19: 43350
capture in solid lithium, transition paths in, (T), 19: 41823
capture, measurement of neutron polarization by, 16: 25922 (NP-11977(p.49-52))
capture of, coupling constants in, 18: 9312 (JINR-E-1457)
capture of helium-3, calculated rates of, (T), 20: 9684
capture of, neutron and nuclear properties from nuclear, 17: 39981 (UCRL-10516)
capture of, nuclear excitation from, 17: 20594(R) (UCRL-10572)
capture of polarized, asymmetry parameter of neutrons and tritons from helium-4, 17: 19338
capture of polarized, by copper, iron, and lead nuclei, neutron angular distributions from, (E), 20: 40096
capture of polarized, by calcium, neutron angular distribution from, (E), 20: 42300
capture of, research on, 17: 21388(R) (LNF-63/11)
capture probabilities in shielding materials, 18: 4081 (CONF-16-15)
capture probability in lithium-6, lithium-6 model testing by, (T), 19: 21368
capture rate and lifetime in various elements, 17: 775
capture rate in ($p\mu p$), 18: 26345
capture rate in helium-4, 17: 9579
capture rate in helium-4, total, 17: 31443
capture rate in helium-3, total, 17: 36656 (JINR-D-1324)
capture rate in hydrogen, 17: 9390
capture rate in hydrogen (liquid), 17: 9391
capture rate in hydrogen (liquid), estimation of, 17: 11480 (LNF-62/109)
capture rate in oxygen-16, 18: 16552(R) (UCRL-11132)
capture rates and lifetimes in beryllium, boron, carbon, lithium, and oxygen, 17: 5324 (NYO-9286)
capture rates in complex nuclei, (E), 20: 28348
capture rates in heavy nuclei, closure approximation for, 20: 30454
capture reactions with helium-3, coupling constants from, (E), 20: 1209
captured of partially polarized, angular distribution and polarization of recoil nuclei in, 17: 17117 (JINR-P-1160)
coupling constant for, pseudoscalar, 18: 11206 (LNF-63/47(p.124-33))
cytogenetic effects on *Zea mays*, 18: 41157
decay, 17: 6962(T) (AEC-tr-5226)
decay, electron polarization in, 16: 26177
decay, electron spectra, 16: 4725
decay from mesonic helium atoms, Michel parameter for, (E), 19: 41480(T)
decay in copper, iron, nickel, and zinc mesic atoms, 16: 24278 (JINR-P-971)
decay in mesic atoms, spin dependence, 16: 974
decay in mesic atoms of palladium, titanium, and their hydrides, 16: 26080 (JINR-P-972)
decay in mesic atoms of transition metals of the iron group, anomaly in, 17: 6888
decay in mesic atoms, nuclear recoil in, (T), 19: 19199
decay modes of, neutrinoless, (E), 19: 4966
decay, neutrino spectra from, 16: 15562
decay of bound, from the K shell, 16: 2373
decay of bound, in carbon tetrachloride, (E), 19: 18746 (AD-423000)
decay of oriented-spin, longitudinal and transverse polarization in, (T), 20: 44272
decay of, branching ratio for leptonic and nonleptonic, 18: 20973
decay of, conserved-vector current theory for, 18: 36262
decay of, divergence-free lepton theory for, 20: 24022
decay of, electron momentum spectra from, 18: 40332
decay of, electron spectra from, (E), 19: 6517 (JINR-P-1778)
decay of, electron momentum spectra in, (E), 19: 39614
decay of, intermediate vector boson for electromagnetic corrections to, (T), 20: 7832
decay of, model for, (T), 19: 16624
decay of, polarization in electron, 17: 36617
decay of, spontaneous symmetry breakdown in, (T), 19: 23416
decay of, universal Fermi interaction and rotational symmetry in leptonic, 17: 19051
decay of, vector boson, 18: 36297
decay of, weak interactions in leptonic, 18: 32628
decay of, weak neutrino current hypothesis for angular asymmetry of, (T),

20: 11578
decay rate of bound, 16: 3624
decay rate of bound, effect of atomic binding on, 17: 774
decay rate relative to mesons (μ^+), effects of non-zero neutrino rest mass on, 17: 31291
decay rates in mesic atoms, theory for, 17: 6968
decay rates of, bound in K-orbit of iron nuclei, 16: 16944 (NP-11592(Vol.I) (p.143-5))
decay spectra, 17: 31091(R) (UCRL-10862)
decay with two kinds of neutrinos, electron spectra in, 18: 24405
depolarization in carbon and liquid argon and helium, (E), 19: 25469 (CAR-882-9)
deuteron fusion catalysis by, 18: 18636 (JINR-D-1551)
disappearance rates in elements, Z-law analysis of, 16: 2305(R) (UCRL-9704)
dosimetry of high-energy, methods for, (T), 20: 4505 (ORNL-P-1738)
effects on deuteron interactions, catalysis, 18: 34617
effects on nuclear reactions in hydrogen and deuterium, catalytic, (E), 20: 34109
emission by mesons (π^-), helicity in, 16: 24747
emission in deuteron reactions with deuterium mesic atoms, 18: 34617
emission in hyperon (Λ) decay, branching ratio for, 18: 12942
emission in meson ($\pi^\pm$) decay, spatial distributions of, 19: 35045
energy level transitions in calcium isotopes, x-ray spectra of, 18: 42732
exchange between hydrogen mesic atoms and carbon, 18: 34947
helicity in meson (π^-) decay, antineutrino helicity from, 18: 28423
interactions of, selection rule for weak, 17: 19069
interactions of 8-Bev polarized, with electrons in magnetized iron, 17: 17017
interactions with nucleons, parity nonconservation in, 16: 5864(T) (UCRL-Trans-759)
interactions with protons, molecular effects, 16: 10892
interactions with nucleons, electron production rates in, 16: 10891
interactions with nucleons, electron emission from, 16: 27365
interactions with protons, cross sections for elastic, 17: 9270
interactions with protons at 1.2 Bev/c, cross section for elastic, 17: 34775
interactions with protons, induced coupling constants in, 17: 34960
interactions with protons, unitary symmetry of weak current structure in, 17: 41781
interactions with electrons, photon contributions to, 18: 11021
interactions with protons in calcium-40, induced pseudoscalar coupling constant from, 18: 26525 (BNL-837(p.315-23))
interactions with protons in hydrogen molecular ions, 18: 26555(R) (ORNL-3582(p.130))
interactions with protons, 18: 26271 (BNL-837(p.277-91))
interactions with deuterons and protons, wave equations for, 18: 28248
interactions with protons, quantum mechanics of $(p\text{-}\mu\text{-}p)^+$, 18: 32605
interactions with protons in calcium-40, radiative, 18: 40354
interactions with mesons (μ^+), resonance (1020 Mev), 18: 40243 (UCRL-11428(Rev.))
interactions with protons, wave functions for $(p\mu p)^+$ molecule in, (T), 19: 5223
interactions with protons at large momentum transfers, 19: 14394
interactions with nucleons at 5 Bev/c meson (π) production in, (E), 19: 21037
interactions with protons at 1.5 to 6.0 Bev/c, high momentum transfer in, (E), 19: 23437
interactions with deuterons, effect of neutron–neutron final state on, (T), 19: 45073
interactions with mesons (μ^-), first Born approximation including anapole for, (T), 20: 4612
interactions with mesons (μ^+), first Born approximation including anapole for, (T), 20: 4612
interactions with electrons and nuclei at 5 to 50 Bev, (E), 20: 6007 (CONF-640919, pp 143-8)
interactions with protons, G-parity in rates of capture, (T), 20: 13505
interactions with protons, calculations using six coupling constants, 20: 13519
interactions with deuterons and protons, quantum mechanics of, 20: 13630
interactions with protons, computer program for capture, 20: 35829(R) (COO-614-45)
interactions with protons in 2s-1d nuclei, (T), 20: 38166
kinetics at 1 kev to 10 Mev, graphs for, 19: 18752 (UCRL-2426(Vol. I) (1965 Rev.))
lifetime, 17: 29497 (NEVIS-114)
lifetime in carbon, composite mean, 16: 10945 (AD-260039)
lifetime in carbon, mean, 16: 10945 (AD-260039)
lifetime in hydrogen (liquid), 17: 9389
magnetic moment in mesic atoms, 16: 13865 (NEVIS-101)
magnetic moment of, bound in field of nucleus, 17: 7213
magnetic moment of, bound in atoms of carbon, magnesium, oxygen, silicon, and sulfur, 17: 31341
magnetic-moment of, anomalous, (E), 20: 44207
mutation induction in staminal hair cells of Tradescantia, comparison with gamma rays, 18: 1406
photoproduction on protons, (T), 19: 27240
polarization by fluorine, phosphorus, and sulfur, 17: 9591
polarization from neutrino (ν_μ)–neutron interactions, (T), 19: 45050
polarization in mesic atoms, effects of nuclear spin, 16: 12386
production by electrons in nuclear Coulomb field, cross sections for, (T), 20: 6089
production by proton pair annihilation, effects of form factors on cross sections for, 20: 44188
production in electron-positron interactions, 17: 9279
production in electron accelerators, (T), 19: 27206
production in electron–neutrino interactions, (T), 20: 19463
production in hyperon (Λ^0) decay, 17: 9265
production in neutrino-nucleon interactions, (T), 19: 25315
production of cosmic, $(\mu^+)/(\mu^-)$ ratio in high-energy, (T), 20: 2702
production of high purity intense beam, 16: 13752
production of meson (μ^-)–meson (μ^+) pairs, in electron–positron interactions, (T), 19: 4942
production of meson (μ^-)-meson (μ^+) pairs in proton-pair annihilation, (T), 20: 2696
production of polarized, in neutrino interactions with nucleons, 18: 9125
properties at 100 kev to 100 Bev, 18: 28331 (UCRL-2426(Vol.I)(1963 Rev.))
properties in mesic atoms, effects on nuclear gamma spectra, 18: 44797
properties of, electron-pair model for, (T), 19: 10059
reactions (μ^-,ν) with helium-3, rates for, (T), 19: 6709
reactions (μ^-,n) with nuclei of different spins, neutron asymmetry from, (E), 20: 24375
reactions in hydrogen (liquid), observations, 16: 9395
reactions in liquid deuterium and hydrogen, fusion, 18: 1070
reactions in nuclear emulsions, cross sections for pair production in, 17: 26299
reactions in nuclear emulsions at 5 Bev/c, (E/T), 19: 23476
reactions ($\mu^-,n\nu$) of polarized, on sulfur nuclei, angular distributions from, 16: 21426
reactions (μ^-,n) with calcium, angular distribution asymmetries from, 16: 27919
reactions (μ^-,ν) with helium-3 at 217 Mev/c, rates of, 16: 28126
reactions (μ^-,ν) with helium-3, measurements of rate of, 17: 17278
reactions on compounds, atomic capture probabilities, 16: 21174
reactions with calcium-40, 18: 11206 (LNF-63/47(p.124-33))
reactions with carbon-12, comparison of experiment and predictions of Universal Fermi Interaction, 16: 24788 (NP-11796)
reactions with carbon-12, rate measurements for, 16: 32398 (NYO-9287)
reactions with carbon-12, coupling constants in capture, (T), 20: 4915
reactions with constituents of chemical compounds, relation to Fermi-Teller Z Law, 17: 2246 (UCRL-10429)
reactions with emulsion nuclei, charged-particle production in capture, 19: 33386
reactions with heavy nuclei, particle emission in, 16: 7100
reactions with helium-3 at 217 Mev/c, measurement of rate, 16: 28027 (JINR-D-988)
reactions with helium-3, probability of formation of tritium and neutrino in, 16: 31124
reactions with helium-3, rate of, 17: 13569
reactions with helium-3, calculation of rates of, 17: 17049
reactions with helium-4, capture rate and neutron and triton spectra for, 17: 24320
reactions with helium-4, branching ratio in decay and, 18: 26524 (BNL-837(p.309-13))
reactions with helium-3, probability of neutrino yield in, (T), 20: 22152
reactions with hydrogen (liquid), neutron spectra from, 16: 15583
reactions with light elements, polarization retention measurements, 16: 8230
reactions with light elements, capture-rate measurements, 16: 8231
reactions with matter, dE/dx and range-energy graphs for, 20: 46601 (UCRL-2426(Vol.2)(1966 Rev.))
reactions with matter, range-momentum and dP/dx graphs for, 20: 46342 (UCRL-2426(Vol.4)(1966 Ed.))
scattering by bromine and silver nuclei, cross sections for elastic, 16: 7117
scattering by carbon at 180 and 240 Mev/c, cross sections for, 16: 33878
scattering by carbon, 17: 9473
scattering by emulsion nuclei at 8 Bev/c, single, (E/T), 19: 16871
scattering by lead, cross sections for Mott, 16: 24747
scattering in emulsions at 8.2 Bev/c, angular distributions, 16: 8123
scattering in nuclear emulsions, elastic, 17: 6988
scattering in nuclear emulsions, elastic, 17: 31383
trajectory in magnetic fields, hodoscope for measuring, 20: 25654 (LNF-65/48)

transfer to helium and neon from deuterons and protons in bubble chambers, 16: 5882
transfer to neon, mesonic molecule formation rates in, 17: 9586

MESONS (μ^0)
decay, existence, and production of boson, 17: 13459

MESONS (μ^+)
beta decay, theory of neutrinoless, 16: 18367
charge exchange in hydrogen, cross section of, 17: 19190
currents of, classification of, 17: 11479 (LNF-62/98)
decay asymmetry in gases, 16: 10958 (NEVIS-99)
decay, electron polarization in, 16: 26177
decay in chemical compounds, reactions from, (T), 19: 42576
decay in longitudinal magnetic field, positron angular distributions for, 18: 36309
decay, measurement of positron polarization from, 18: 9160
decay modes, 16: 8133
decay modes, search for $e^+ + e^- + e^+$, 16: 18333
decay ($\mu^+ \rightarrow e^+ + \gamma$), search for, 18: 9166
decay, neutrino spectra from, 16: 15562
decay of, electron spectrum from, 17: 16991
decay of, search for electron and two positrons in, 17: 9283
decay of, ($e + \gamma$), 18: 26356
decay of, conserved-vector current theory for, 18: 36262
decay of, electron momentum spectra from, 18: 40332
decay of, positron polarization in, 18: 10948
decay of, positron polarization in, 18: 18693
decay of, positron depolarization by bremsstrahlung in, 18: 24435
decay of, positron momentum spectrum in, (E), 19: 21012
decay of, positron momentum spectrum in, (E), 19: 39614
decay of, positron spectra from, (E/T), 20: 34247
decay of, radiative, (E/T), 20: 32104
decay of, radiative, (E/T), 20: 36021
decay of, spontaneous symmetry breakdown in, (T), 19: 23416
decay of, weak neutrino current hypothesis for angular asymmetry of, (T), 20: 11578
decay rate relative to mesons (μ^-), effect of non-zero neutrino rest mass on, 17: 31291
decay schemes, 16: 27352
decay spectra, 17: 31091(R) (UCRL-10862)
decay $\rightarrow e^+ + e^+ + e^-$, 16: 27908 (NP-11634)
depolarization in emulsions in presence of electric field, 16: 31046
depolarization in solids, 17: 7046
distributions from antineutrino reactions on nuclei, angular and energy, (T), 19: 14555
dosimetry of high-energy, methods for, (T), 20: 4505 (ORNL-P-1738)
electric dipole moments, upper limit, 16: 10853
electron decay of, polarization in, 17: 36617
emission by mesons (π^+), helicity in, 16: 24747
emission from κ (725) and K* (890) decay, polarization in, (T), 20: 44270
emission in meson ($K^+_{\mu 3}$) decay, energy spectra for, 18: 20961
emission in meson (π^+) decay in longitudinal magnetic field, angular distributions for, 18: 36309
emission in meson (K+) decay, energy spectra and polarization of, (E), 19: 25357
emission in meson ($\pi^\pm$) decay, spatial distributions of, 19: 35045
energy spectra and polarization in meson (K^+_{e3}) and ($K^+_{\mu 3}$) decays, (T), 19: 35176
energy spectra from meson ($K_{\mu 3}$) decay, (E), 19: 41414
gyromagnetic ratio of, anomalous, 17: 34736 (PPAD-487F)
gyromagnetic ratio of, measurement of anomalous, (E), 20: 21630 (UCRL-16469)
incorporation into organic molecules and radicals, 17: 28342
interactions of, selection rule for weak, 17: 19069
interactions with electrons, probability of absorption, 16: 12339
interactions with electrons, photon contributions to, 18: 11021
interactions with mesons (μ^-), resonance (1020 Mev), 18: 40242 (UCRL-11428(Rev.))
interactions with mesons (μ^-), first Born approximation including anapole for, (T), 20: 4612
interactions with mesons (μ^+), first Born approximation including anapole for, (T), 20: 4612
interactions with electrons and nuclei at 5 to 50 Bev, (E), 20: 6007 (CONF-640919, pp 143-8)
kinetics at 1 kev to 10 Mev, graphs for, 19: 18752 (UCRL-2426(Vol. I) (1965 Rev.))
lifetime, 16: 13894
lifetime in carbon, composite mean, 16: 10945 (AD-260039)
lifetime in hydrogen (liquid), 17: 9389
lifetime of, measurement of, 17: 9388
magnetic moment, 17: 31340
magnetic moment measurement in aqueous solutions, chemical corrections for, 20: 46306
magnetic moment of, g-factor for, 20: 6282 (CERN-64-13(Vol.4), pp 97-136)
magnetic resonance experiments on, 18: 2483
mass, 17: 31340
molecules formed by, 17: 2197
muonium 1s state, hyperfine splitting, 16: 982
photoproduction on protons, pseudoscalar term in, 18: 44526
photoproduction on protons, (T), 19: 27240
polarization for studying chemical-reaction mechanisms, 20: 11377
polarization from antineutrino ($\bar{\nu}_\mu$)–proton interactions, (T), 19: 45050
polarization in decay of mesons ($K^+_{\mu 3}$), (E), 20: 6075
polarization in decay of mesons (K^0_2), (E), 20: 17424
polarization in meson ($K^+_{\mu 3}$) decay, (E), 19: 37629
polarization of, regularities in, 17: 9237
positron decay of, measurement of polarization in, 18: 4610
production by proton pair annihilation, effects of form factors on cross sections for, 20: 44188
production in antineutrino interactions with proton, cross sections for, (T), 20: 2736
production in electron-positron interactions, 17: 9279
production in electron accelerators, (T), 19: 27206
production in electron–neutrino interactions, (T), 20: 19463
production in neutrino interactions with protons at 200 Mev, cross section for, 18: 896
production in proton-proton interactions at 2.0 Bev, (E/T), 19: 41503
production of cosmic, $(\mu^+)/(\mu^-)$ ratio in high-energy, (T), 20: 2702
production of meson (μ^-)–meson (μ^+) pairs, in electron–positron interactions, (T), 19: 4942
production of meson (μ^-)-meson (μ^+) pairs in proton-pair annihilation, (T), 20: 2696
production of polarized, in neutrino interactions with nucleons, 18: 9125
properties at 100 kev to 100 Bev, 18: 28331 (UCRL-2426(Vol.I)(1963 Rev.))
properties of, electron-pair model for, (T), 19: 10059
reactions in organic substances, 16: 32344
reactions in solids, depolarization in, (E), 19: 12167 (NEVIS-124)
reactions in targets, depolarization quenching as function of longitudinal magnetic fields in, (E/T), 19: 45079
reactions with atoms, theory of, 18: 32467
reactions with carbon and hydrogen, ionization losses in, (E), 20: 8070 (JINR-P-2423)
reactions with matter, dE/dx and range-energy graphs for, 20: 46601 (UCRL-2426(Vol.2(1966 Rev.))
reactions with matter, range-momentum and dP/dx graphs for, 20: 46342 (UCRL-2426(Vol.4)(1966 Ed.))
scattering by bromine nuclei, cross sections for elastic, 16: 7117
scattering by lead, cross sections for Mott, 16: 24747
slowdown in targets, depolarization in, (E), 19: 45080
spin precession in muonium compounds, (T), 19: 45278 (NP-15389)
stopping in solids, depolarization and quenching in, (E), 20: 13498
trajectory in magnetic fields, hodoscope for measuring, 20: 25654 (LNF-65/48)

MESONS (ω)
binding in meson (π)-meson (ρ) system, OPE mechanism for, (T), 19: 43078
branching ratio, (T), 19: 14377
contributions to coupled partial-wave-dispersion-relations for nucleon-nucleon scattering, 17: 20918
coupling constant of, with nucleon, 18: 24411
coupling to baryon current, vector-meson dominance and U(6,6) symmetry for, 20: 17457
coupling to nucleon pairs, 17: 13410
coupling with nucleons, constants for, (T), 19: 4986
decay ($\omega \rightarrow \pi^+ + \pi^- + \pi^0$) of, relation to reaction ($\pi^+ + \pi^0 \rightarrow \pi^+ + \omega$), 18: 895
decay, 18: 12914 (TID-7686(p.109-29))
decay, 18: 16552(R) (UCRL-11132)
decay, (E), 19: 25265(R) (UCRL-11776)
decay and production of, bibliography on, 17: 9472
decay and production in meson (π^-)–proton interactions, 18: 14911
decay, branching ratios of four-body, 16: 33748
decay branching ratios for, 17: 41843
decay, effects of spin-parity assignments on, 16: 26157
decay into charged-particle pairs, 16: 6987
decay into mesons (ζ), determination of ζ spin from, 16: 19709
decay into two charged mesons (π), methods for detecting, (T), 19: 41386
decay, isotopic spin nonconservation in, 16: 10903
decay mode ($\omega \rightarrow e^+ + e^-$) of, search for, 18: 18725
decay mode ($\omega \rightarrow 2\pi + \gamma$), 17: 5244
decay modes of, 17: 11499 (UCRL-10089(Rev.))
decay modes of, branching ratios in, 17: 26315
decay modes of, branching ratio for Dalitz-pair production and gamma

emission in, 18: 7497
decay modes of, C-invariance violation in, (E/T), 19: 33044
decay of, conservation of isotopic spin in, 17: 41838
decay of, coupling constants in, 17: 13379
decay of, dispersion relations for radiative, 17: 36615
decay of, dispersion relations in, 18: 5999
decay of, evidence for $\pi^0 + \gamma$, 17: 41786
decay of neutral, branching ratios for lepton pairs in, (E), 19: 23436
decay of, production of lepton pairs in, 17: 11642(R) (TID-17720(p.98-100))
decay of, products and branching ratios for, 17: 6998
decay of, properties of two meson (π), 17: 26376
decay of, symmetry groups for boson couplings in, 18: 6018
decay of, width for 3-π, 18: 7463 (BNL-7407)
decay of, (3π), 17: 29502 (UCRL-10492)
decay of, amplitudes and angular correlations for mesons (π^-), (π^0), and (π^+) from, (E), 20: 27843
decay of, angular correlation functions for, 18: 32598
decay of, angular distributions in, (T), 20: 37807
decay of, as possible test for a strong C violation, (T), 19: 33002
decay of, branching ratios for (E), 19: 1357
decay of, branching ratios for lepton-pair, (E), 20: 11673
decay of, branching fractions and charge conservation for, (E), 20: 27842
decay of, branching ratio for, (E), 20: 41850
decay of, branching ratio for $\pi^+\pi^-\pi^0$, (E), 20: 44176 (LNF-66/31)
decay of, C violation in, (T), 20: 25874
decay of, C-nonconserving coupling constants in, (T), 19: 35169
decay of, coupling constant and width for, (T), 20: 7855
decay of, covariant description of, 19: 16588
decay of, current algebras for, (T), 20: 13491
decay of, electromagnetic interactions in $\bar{U}(12)$ symmetry in, 20: 19568
decay of, G_2 symmetry in, (E/T), 20: 2520(R) (IA-920)
decay of, interference effects in meson (π^-)-proton interactions at 3.25 Bev/c, (T), 19: 33033
decay of, lepton-pair, (E), 19: 18893
decay of, leptonic, (T), 20: 13476(T)
decay of, mass splitting in electromagnetic, (T), 19: 27146 (JINR-P-1974)
decay of, matrix element relations in SL(6) and $\bar{U}(12)$ for electromagnetic and weak, 20: 25927
decay of, meson (ϕ) production in, (T), 20: 41888
decay of, mixing angles for, 20: 30088 (IC-66/50)
decay of, mixing angles for, 20: 32107 (IC-66/48)
decay of, octet dominance model for 2π, (T), 19: 8168
decay of, pi-gamma, (T), 19: 43111
decay of, quark model for electromagnetic, 19: 32993
decay of, quark model for, (T), 19: 35125
decay of, relative rates for leptonic, (T), 20: 27863
decay of, selection by A invariance, 18: 22758
decay of, SU(6) symmetry for radiative, 20: 15472
decay of, SU(6)-invariant theory for couplings in, 19: 21013
decay of, $SU(6)_w$ symmetry for radiative, 20: 30040
decay of, unitary symmetry selection rules for, 18: 30556
decay of, 2π, 18: 14945
decay of, 2π, (T), 19: 25297
decay probabilities in unitary symmetry, 18: 14866
decay properties of, calculation using composite-particle model, (T), 20: 30069
decay rate, (T), 20: 32045
decay rates of, measurement of, 17: 19528
decay schemes, perturbation theory, 16: 19712
decay width of, 17: 31327
decay widths (three-π) of, R-conjugation invariance in strong-interaction, 18: 20949
description in unitary symmetry with (ϕ–ω) mixing, 19: 28912(R) (ANL-6819)
effect of exchanges with mesons (ρ) on KN and $\bar{K}$N interactions, 17: 5246
effects in electron-nucleon interactions, electric and magnetic form factors from, 17: 41800
effects of mixtures with mesons (ρ^0), on weak interaction decays, 17: 34800
effects of $\omega\phi$ mass splitting, on electromagnetic form factors in collinear U(6), 20: 19572
effects of Φ–ω mixing on experimental results, 18: 14879
effects of vector, on Y^* resonances, 18: 30606
effects on mass spectra of meson (π^-), proton interactions at 2.1 Bev/c, 18: 21017
effects on nuclear forces, 20: 15817
effects on nucleon isoscalar structure, 17: 41776
electromagnetic effects of, on charge form factors of protons, 16: 33770
electromagnetic mixing of, with mesons (ρ), 16: 33754
electromagnetic properties in SU_3 symmetry, 19: 35080
emission in meson (β) decay, ω–ϕ mixing angle from, (T), 19: 41458
exchange in alpha particle interactions, effects on potentials in, (T), 19: 25295
exchange in hyperon (Λ)-nucleon interaction in hyperfragments, (T), 19: 16541
exchange in hyperon (Λ)-proton interactions at 0.5 to 3.0 Bev/c, (T), 19: 16544
exchange in meson (K)-nucleon interactions, contributions to the scattering amplitude in, 17: 20893
exchange in meson (π^0) photoproduction on protons, Reggeized, (T), 20: 44240
exchange in nucleon interactions at 0 to 400 Mev, effects of, 18: 14954
exchange in nucleon interactions, potentials for, 18: 34539
exchange in nucleon interactions, (T), 19: 18864
exchange in nucleon-nucleon interactions, 20: 41899
exchange of vector, in nucleon-nucleon scattering, 17: 24336
gamma transition to mesons (ρ^0), 16: 13905
interaction resonances with mesons (π), boson icosuplet of, 18: 28386
interactions in SU(3) model, effects of T = 0 meson resonances on Schroedinger multichannel equation, 18: 4450
interactions of, amplitude parity and radiative effects in, 17: 20882
interactions of, and unitary symmetry, 17: 31367
interactions of, effects on meson (K)–nucleon interactions (T), 19: 1293
interactions of, effects on nucleon form factors, (E/T), 19: 39458 (CONF-796(Paper 24))
interactions of, test of gauge theory of strong (T), 19: 1370
interactions with nucleons, coupling constant for, 16: 26175
interactions with baryons, 17: 36611
interactions with photons, electron and meson (μ) asymmetric coupling in, 17: 41779
interactions with mesons (π), resonance production in, 18: 2651
interactions with mesons (π), bootstrap calculations for, 18: 10935
interactions with mesons (π), interpretation of 1220-Mev resonance in, 18: 10952
interactions with mesons (π), resonance at 1220 Mev from, 18: 10954
interactions with mesons (π), model for resonances in, 18: 18694
interactions with mesons (ρ), resonance predictions in, 18: 18698
interactions with nucleons, double-peripheral model for elastic, 18: 40275
interactions with conserved currents, mixing and renormalization in, 18: 40322
interactions with mesons (π), evidence for resonance (E), 19: 1324
interactions with mesons (π), logarithmic singularities in resonance, (T), 19: 4998
interactions with mesons (π), properties of resonance, (E/T), 19: 6556
interactions with mesons (π), meson (B) and (ρ) production in, (T), 19: 12225
interactions with mesons (π), model for resonances in, (T), 19: 16538
interactions with nucleons, coupling constants for, (T), 19: 19161
interactions with mesons (π) and (ρ), coupling constants for, (T), 19: 18868
interactions with mesons (ϕ) and (ρ), mixing model for, (T), 19: 25297
interactions with mesons (ϕ), SU_3 mass relations for mixing, 19: 35153
interactions with mesons (π), one-trajectory exchange for amplitudes of, (T), 19: 45074
interactions with mesons (π) at low energies, (T), 20: 6068
interactions with nucleons, coupling constant for, (T), 20: 9746
interactions with mesons (π), meson (B) exchange in, (T), 20: 15357
interactions with mesons (ϕ), mixing angles for, (T), 20: 27801 (IC-66/47)
interactions with mesons (π), reciprocal bootstrap of mesons (ρ) and (B) in, 20: 39807
interpretation as meson (ρ-π) bound state, 18: 44574
isospin, parity, and spin of, 17: 22437 (SLAC-13)
lifetime and mass of, (E), 19: 23355(R) (BNL-867(p.1-117))
lifetime, mass, and width (E), 19: 1356
mass and width (E), 19: 1357
mass and width of, 18: 26341
mass degeneracy of, (T), 20: 27989
mass difference ρ^0–ω_8, from meson (π)–nucleon interactions, (T), 19: 41380
mass formula based on model of meson (ϕ) mixing with, unitary-symmetry, 17: 37957
mass formulas from rank-three Lie groups, (T), 19: 16578
mass formulas in U_4 symmetry, (T), 19: 16545
mass of, formula for, 18: 9147
mass of, as hyperon (Λ) pair bound state, (T), 19: 8145
mass, parity, and spin of, 17: 29506
mass spectra of, relation to nuclear forces, 16: 27953
mixing effects for, in degenerate particle systems, 18: 30586
mixing in SU(3), 20: 42005
mixing in unitary octet and unitary singlet with mesons (ϕ), dynamical model of, 18: 2622

mixing in unitary octet and unitary singlet with mesons (φ), (T), 19: 29103
mixing with meson (φ), angle for, 18: 34574
model of, NN̄ bound-state, 18: 22782
parity and spin of, 17: 32941
photoproduction of, photon dissociation model for, 20: 41863
photoproduction on nucleons in the peripheral model, 18: 18635 (DESY-64/1)
photoproduction on nucleons, cross sections and meson exchange in, 18: 26373
photoproduction on nucleons, (T), 19: 41321 (AECD/TP/4)
photoproduction on protons at 0.3 to 5.5 Bev, (E/T), 20: 6037 (DESY-65/11)
photoproduction on nucleons, angular distributions for, (T), 20: 11595
photoproduction on protons at 0.3 and 5.5 Bev, (E), 20: 17368
photoproduction on nucleons, effect of absorption on peripheral, (T), 20: 17414
photoproduction on nucleons, analysis of, (T), 20: 31984 (IC-66/54)
photoproduction on nucleons, asymptotic behavior of cross section for, (T), 20: 37807
polarization of, 18: 9153
prediction of, vector theory, 17: 11496 (TID-17742)
production, 17: 9315
production and decay, 17: 9314
production and decay, 17: 9327
production and decay of, 3-π resonance widths in, 17: 9336
production and decay in meson (π±)-nucleon interactions at 1.7 Bev/c, (E), 20: 15403
production and properties, 16: 8152
production and properties from π⁺-d interactions, 16: 26165
production and properties in meson (π⁺)-proton interactions, 17: 6997
production and properties, 17: 9316
production and properties, review, 17: 9461
production and properties, 18: 10891
production from antiproton-proton annihilation at rest, rates for, (E), 20: 27846
production from meson (π) reactions with nuclear Coulomb fields at high energies, (T), 20: 46385
production in antiproton-proton interactions, ω-N coupling constant from, 16: 26175
production in antinucleon annihilation, 17: 20857
production in antiproton–proton interactions, lifetime, mass, and width from, 18: 2659
production in antiproton–neutron annihilation, 18: 40227 (BNL-8235)
production in antiproton-proton interactions (E), 19: 1353
production in antinucleon-nucleon annihilation, (T), 19: 10104
production in antiproton-proton annihilations at rest, (E), 19: 45122
production in antiproton-proton inelastic interactions at 3.6 Bev/c, (E), 20: 6097
production in antiproton-neutron annihilations at rest, (E), 20: 9785
production in antiproton-proton interactions at 5.7 Bev/c, cross section for, (E), 20: 24033
production in deuteron-meson (π) interactions, 17: 9325
production in deuteron-meson (π) interactions, 17: 9326
production in elementary-particle interactions, 19: 1227 (JINR-P-1741)
production in meson (K⁻)-meson (K⁺) interactions, 16: 17043
production in meson (K⁻)-proton interactions, 17: 9369
production in meson (π⁻)-proton reactions at 3.3 Bev, 17: 34786
production in meson (π⁻)-proton interactions at 3.5 Bev/c, mechanisms for, 18: 894
production in meson (π⁰)–(π⁺) interactions, relation to decay (ω → π⁺ + π⁻ + π⁰), 18: 895
production in meson (π⁺)-proton interactions at 3.43 and 3.54 Bev/c, partial cross sections for, 18: 2651
production in meson (π⁻)-proton interactions at 3.7 Bev/c, 18: 4459
production in meson (π⁻)-proton interactions, 18: 14810 (JINR-P-1506)
production in meson (π⁻)–proton interactions at 2 Bev, 18: 14888
production in meson (π⁻)-proton interactions at 1.7 Bev/c, 18: 14945
production in meson (π⁻)-proton interactions at 4 Bev/c, cross sections for, 18: 16774
production in meson(π)–nucleon interactions, 18: 28328 (TID-20717)
production in meson (K⁻)-proton interactions, analysis of, 18: 32598
production in meson (K⁻)-proton interactions, negative experimental results for, 18: 34513 (UCRL-11428)
production in meson (π⁻)-proton interactions at 2.1 Bev/c, 18: 40377
production in meson (π⁺)-proton interactions at 4 Bev/c, 18: 40285
production in meson (π⁻)-proton interactions at 2.35 and 2.90 Bev/c, 18: 44519 (NEVIS-123)
production in meson (π⁻)-proton interactions at 3.24 Bev (E), 19: 1345
production in meson (π⁻)-nucleon interactions at 6.1 and 18.1 Bev (E), 19: 1398
production in meson (π⁻)-proton interactions at 2.75 Bev, (E), 19: 1348
production in meson (π⁺)-nucleon interactions at 3.25 Bev/c, exchange mechanism for, (E), 19: 23397
production in meson (π⁺)-proton interactions, absorptive effects in, (T), 19: 25328
production in meson (π⁺) interactions with neutrons at 1.7 Bev/c, (E), 19: 41528
production in meson (π⁻)-proton interactions at 3.9 Bev/c, (E), 19: 45121
production in meson (π⁺)-proton interactions at 2.77 Bev/c, (E), 20: 1019
production in meson (π⁻)-proton interactions at 2.26 Bev/c, 20: 2745
production in meson (π)-nucleon interactions, amplitudes for, (T), 20: 4584 (JINR-P-2380)
production in meson (π⁺) interactions with protons, (E), 20: 7823
production in meson (π⁺)-neutron interactions, Regge-pole analysis of, 20: 19510
production in meson (K⁺)-proton interactions at 2.7 Bev/c, (E), 20: 41804 (UCRL-17003)
production in meson (π⁻)-proton interactions at 11 Bev/c, mechanisms for, (E), 20: 44241
production in meson (π)-nucleon interactions, reconstruction of amplitude for, 20: 46384
production in neutrino-nucleon interactions, (T), 19: 25315
production in nucleon-antinucleon annihilation, selection rules, 16: 24735
production in proton-antiproton and proton-meson (π⁻) interactions, 17: 705 (BNL-6181)
production in proton-proton interactions at 2.85 Bev, 17: 4001
production in proton pair annihilation, 17: 9322
production in proton (p̄-p) interactions at 3.25 and 3.69 Bev/c, 17: 41736 (BNL-7294)
production in proton-proton interactions at 4 Bev (E), 19: 1360
production in pseudoscalar meson interactions, 18: 36269
production of neutral, in meson (π⁻)-proton interactions at 3 Bev/c, (E), 19: 23436
production of, theory for, 18: 9197
production of Y₁* in meson (K⁻)-proton interaction, 18: 40241 (UCRL-11424(Rev.))
production of, Regge-pole contribution to, 20: 15354
production of, review of, 18: 12903 (JINR-P-1490)
production of, symmetry in bootstrap model for, (T), 19: 16627
production processes for, phenomenology of, (T), 19: 6523
production via meson (ρ) exchange in meson (π)-nucleon interactions, (T), 19: 35072
properties, 17: 41843
properties, 18: 40347
properties, 20: 34170
properties as massive neutral gauge particle, 19: 20989
properties in particle-mixture theory, 16: 32335
properties of, 20: 34175
properties of, from K⁻ + p → Λ + ω reactions, 18: 9157
properties of, octet unitary-symmetry model for, 17: 9226
properties of, review of theoretical, 17: 9463
properties of, review of, 17: 24185
properties of, role of 2-π resonances in, 17: 741
properties of, electron-pair model for, (T), 19: 10059
properties of, field-theoretical models for, 19: 1262
properties of, nucleon coupling, 18: 21001
properties of, produced by antiproton-proton interaction, 19: 27161 (NEVIS-131)
properties of, review of, 19: 16657
properties of, test for, (T), 19: 39572
properties review, 16: 26158 (UCRL-10167)
quantum numbers, 16: 18349
Regge poles of, effects in photoproduction of mesons, 18: 26372
representation in Sp(6) group, 18: 42421
resonance (πω) of, parity and spin of, 18: 14900
resonance (πω) of, parity and spin of, 18: 14901
resonance (π-ω) at 1220 Mev, properties of meson (B), 18: 18684
review, 18: 34636
role in isosinglet meson series, 17: 41813
role in nucleon core phenomena, 16: 17044
spin and parity, 16: 9381
spin of, harmonic-oscillator model for, 18: 30558
theory of, octet-octet mixing in SU_3, 18: 42406
theory, using 2-pion δ-type potentials, 16: 31032
transitions to mesons (ρ⁰), nonradiative, 16: 6979
unitary spin of, 18: 26323
width of, calculation from elastic unitarity equation, 20: 30077

MESONS (ωρ)

angular distribution in $\omega N_{\frac{1}{2}}^{*++}$ decay, 18: 22743
decay (ω⁰ → π⁰ + γ), (E), 20: 46371
decay branching ratio (π⁺π⁻/π⁺π⁻π⁰), 18: 14865
decay into 2 mesons (π), 18: 22757

decay modes, 16: 10899
decay of, branching ratio in, 17: 19061
decay of, consequences of G quantum number in, 17: 9340
decay of, probabilities of different modes of, 17: 9341
decay of, relation to electromagnetic properties of electrons and mesons (μ), 17: 9406
decay of, angular distributions in, 18: 34622
decay of, angular distributions of electron pairs from, (T), 19: 39451 (CALT-68-43)
decay of, beta, (E), 20: 15406
decay of, branching ratio in (E), 19: 1337
decay of, branching ratio for $e^+ + e^-$, (E), 19: 45102
decay of, C-noninvariant effects in 3π, (T), 19: 41437
decay of, equations for 3π, 18: 18732
decay of, $\pi^0 + \gamma$, (E), 20: 39787
decay of, sonic spark chamber for study of, 18: 31892 (CERN-64-30 (p.229-36))
decay of, SU(6) symmetry for radiative ($\pi^0\gamma$), (T), 19: 18861
decay of, test of nonrelativistic quark model in radiative, (T), 20: 1016
decay of, upper limit to electron-pair, 18: 40304
decay partial widths, 16: 10898
decay partial widths, 16: 15588
decay, possibilities of identity with mesons (ρ^0), 16: 6978
decay quantum numbers, 16: 21318
decay rate, 16: 31037
decay rate of, (2π), (T), 19: 47369
decay rate of, sum rule for, 20: 30036
decay rates and spectra of, ($\pi^+\pi^-\gamma$), (T), 19: 43104
decay schemes, 16: 13911
decay, three-meson (π) resonance disappearance such that nucleon mass $\simeq$ hyperon (Ξ) mass, 16: 4718
decay, use in analysis of lepton electromagnetic properties, 16: 29707
decays of, transition probabilities for, 20: 44354
detection and measurement of, possible method for, 18: 30511 (JINR-P-1654)
electromagnetic self-energies and unitary symmetry, 18: 22759
interactions of, C, T noninvariance in minimal electromagnetic, (T), 20: 4601
interactions with photons, two-field couplings in, 17: 39915
parity and spin of, 20: 34169
photo-production on protons, mechanism of, 20: 39811
photoproduction from hydrogen, attempts at detection, 16: 17065 (CTSL-32)
photoproduction from hydrogen, cross sections for, 17: 6792(R) (ISS 62/14)
photoproduction on protons, computer values of, 16: 24680 (ISS-61/41)
photoproduction on protons, excitation curve analysis of, 18: 24381 (ISS-64/4)
photoproduction on protons at 0.3 to 5.8 BeV, (E), 20: 46348(T) (SLAC-Trans-44)
photoproduction on protons at 1.8 to 5.8 BeV, Regge-pole model for, (E/T), 20: 46367
production and decay in meson (π^-)–proton interactions at 2 Bev, 18: 14888
production and decay in meson (π^+)-deuteron interactions, 18: 42376 (TID-20762)
production and properties in proton pair annihilation, 17: 9321
production and properties in proton pair annihilation, 17: 9324
production and properties of, review of, 19: 16510
production at high energies, mechanisms for, 18: 9169
production from meson (π^+)-proton interactions at 2.35 to 2.90 Bev/c, (E), 20: 27844
production in meson (π^+) reactions with deuterons at 550 Mev, 16: 4716
production in meson (π) interactions (s- and p-wave), 16: 17037
production in meson (π^-)-proton interactions, 17: 9430
production in meson (π^-)–proton interactions, 18: 14865
production in meson (π^+)-neutron interactions at 1230 Mev/c, 18: 14955
production in meson (π)-nucleon interactions, amplitudes and Regge poles for, 18: 34622
production in meson (π^+)-proton interactions at 2.5 Bev/c, (E), 19: 37526 (CU-1932-243)
production in meson (π^+)-proton interactions at 2 Bev/c, (E), 20: 11672
production in meson (π) interactions, Faddeev equations for, (T), 20: 11568 (UCRL-11749)
production with mesons (K) in antiproton–proton annihilation, (E/T), 19: 10019 (NP-14497)
properties of (790), (T), 19: 12300
search for spin-1, in meson (π^0) photoproduction, 16: 9386
spin-parity of, Dalitz determination of, 18: 20998

MESONS (ω^+)
production in proton interactions, theory for, 17: 11465 (BNL-6646)
production of, in proton interactions, theory of, 17: 13438

MESONS (ϕ)
amplitude parity and decay of, theory of, 19: 36220(R) (MIT-2098-142)
branching ratio for, under SU(3) invariance, 18: 44593
classification of, as isoscalar member of vector meson octet, 18: 26320
coupling in (π) reactions, 19: 28912(R) (ANL-6819)
coupling to baryon current, vector-meson dominance and U(6,6) symmetry for, 20: 17457
coupling to nonstrange baryons, (T), 20: 34220
decay, 18: 32664
decay, 19: 33072
decay modes, (E), 20: 34201
decay modes for, (E/T), 20: 15316 (UCRL-16526)
decay of neutral, branching ratios for lepton pairs in, (E), 19: 23436
decay of, as possible test for a strong C violation, (T), 19: 33002
decay of, beta, (E), 20: 15406
decay of, branching ratio of 2π to $\pi + \rho$, 18: 14951
decay of, branching ratios for, (E), 19: 39531
decay of, branching ratios for, (E), 20: 11619
decay of, branching ratios for lepton-pair, (E), 20: 11673
decay of, C violation and S-wave resonances in, (T), 19: 33003
decay of, C violation in, (T), 20: 25874
decay of, C-nonconserving coupling constants in, (T), 19: 35169
decay of, G_3 symmetry in, 18: 24441
decay of, lepton-pair, (E), 19: 18893
decay of, leptonic, (T), 20: 13476(T)
decay of, mass splitting in electromagnetic, (T), 19: 27146 (JINR-P-1974)
decay of, matrix element relations in SL(6) and $\bar{U}(12)$ for electromagnetic and weak, 20: 25927
decay of, mixing angles for, 20: 30088 (IC-66/50)
decay of, mixing angles for, 20: 32107 (IC-66/48)
decay of, quark model for electromagnetic, 19: 32993
decay of, relative rates for leptonic, (T), 20: 27863
decay of, resonance interactions in, 18: 18661
decay of, selection by A invariance, 18: 22758
decay of, selection rules in relativistic SU(6) theory for, 19: 21023
decay of, SU(6) symmetry for radiative ($\pi^0\gamma$), (T), 19: 18861
decay of, SU(6)-invariant theory for couplings in, 19: 21013
decay of, test of nonrelativistic quark model in radiative, (T), 20: 1016
decay of, $\bar{U}(12)$ group for $K\bar{K}$, (T), 19: 18853
decay of, unitary symmetry in, 18: 14956
decay of, unitary symmetry breaking in, (E/T), 19: 41366
decay of, upper limits for C-nonconserving, (E), 19: 39552
decay probabilities in unitary symmetry, 18: 14866
decay rate, (T), 20: 32045
decay rate of, (2π), (T), 19: 47369
decay rates and spectra of, ($\pi^+\pi^-\gamma$), (T), 19: 43104
decay widths (three-π) of, R-conjugation invariance in strong-interaction, 18: 20949
decay widths and mass formulas from rank-three Lie groups, (T), 19: 16578
decays of, widths for K^+K^- and $K_1^0K_2^0$, (T), 20: 27873
description in unitary symmetry with (ϕ–ω) mixing, 19: 28912(R) (ANL-6819)
effects in electron-nucleon interactions, electric and magnetic form factors from, 17: 41800
effects in nucleon-nucleon interactions, (T), 19: 31067
effects of ω-ϕ mass splitting, on electromagnetic form factors in collinear U(6), 20: 19572
effects of Φ–ω mixing on experimental results, 18: 14879
electromagnetic properties in SU_3 symmetry, 19: 35080
electromagnetic self-energies and unitary symmetry, 18: 22759
emission by electrons in nuclear Coulomb field, (T), 19: 35395 (NP-14993)
emission in meson (β) decay, ω–ϕ mixing angle from, (T), 19: 41458
exchange in meson ($K,\bar{K}$) interactions, (T), 19: 8187
exchange in nucleon interactions at 0 to 400 Mev, effects of, 18: 14954
exchange in nucleon interactions, (T), 19: 18864
existence and properties of, 17: 26363
interactions of, and unitary symmetry, 17: 31367
interactions of, C, T noninvariance in minimal electromagnetic, (T), 20: 4601
interactions of, effects on meson (K)–nucleon interactions (T), 19: 1293
interactions of, effects on nucleon form factors, (E/T), 19: 39458 (CONF-796(Paper 24))
interactions with conserved currents, mixing and renormalization in, 18: 40322
interactions with nucleons, coupling constants for, (T), 19: 19161
interactions with mesons (ω), mixing model for, (T), 19: 25297
interactions with vector mesons, T invariance in SU(6) symmetry for, (T), 19: 35140
interactions with mesons (ω), SU_3 mass relations for mixing, 19: 35153
interactions with nucleons, coupling constant for, (T), 20: 9746

interactions with nucleons, coupling constant for, (T), 20: 11598
interactions with mesons (ω), mixing angles for, (T), 20: 27801 (IC-66/47)
lifetime, 17: 29497 (NEVIS-114)
lifetime and mass of, (E), 19: 23355(R) (BNL-867(p.1-117))
mass formula based on model of meson (ω) mixing with, unitary symmetry, 17: 37957
mass formulas for, 18: 44595
mass formulas in U_6 symmetry, (T), 19: 16545
mass of, correlations to orbital angular momentum of, 18: 7496
mass of, formula for, 18: 9147
mass of, as hyperon (Λ) pair bound state, (T), 19: 8145
mass of, calculation of, 20: 13628
mass of, formula for, 18: 16799
mass of, models for, 19: 14348
mass relations in octet, 18: 40309
mixing effects for, in degenerate particle systems, 18: 30586
mixing in SU(3), 20: 42005
mixing in unitary octet and unitary singlet with mesons (ω), dynamical model of, 18: 2622
mixing in unitary octet and unitary singlet with mesons (ω), (T), 19: 29103
mixing with meson (ω), angle for, 18: 34574
model for, composite, 19: 41525
model for, $K\bar{K}$ interactions for dynamical, 20: 19520
model of, $\Lambda\bar{\Lambda}$ bound-state, 18: 22782
parity and spin of, 17: 32941
photoproduction of, photon dissociation model for, 20: 41863
production, (E), 20: 34201
production and decay of, study from meson (K^-)–proton interactions at 2.5 Bev/c, 18: 34514 (UCRL-11430)
production by isoscalar $K\bar{K}$ resonance, coupling constants for, 17: 39890
production from mesons (K^-)-proton and mesons (π)-proton interactions, suppression of, (T), 20: 27863
production in antiproton–proton interactions, mass and width from, 18: 2660
production in antiproton-neutron annihilation, 18: 40227 (BNL-8235)
production in antiproton-proton annihilation, (E), 19: 20993
production in elementary-particle interactions, 19: 1227 (JINR-P-1741)
production in meson (K)-proton interactions at 1.02 Bev, 17: 26362
production in meson (π^+)-proton interactions at 3.43 and 3.54 Bev/c, partial cross sections for, 18: 2651
production in meson (π^-)-proton interactions at 3.7 Bev/c, search for, 18: 4459
production in meson (K^-)-proton interactions at 2.23 Bev/c, 18: 14951
production in meson (π^-)-p interactions, 18: 24396(R) (NP-13947)
production in meson (K) interactions, vector meson exchange in, 18: 26342
production in meson (π)-nucleon interactions, 18: 32664
production in meson (K^-)-proton interactions, negative experimental results for, 18: 34513 (UCRL-11428)
production in meson (K^-)-proton interactions at 2.4 and 2.7 Bev/c, 18: 40243 (UCRL-11428(Rev.))
production in meson (K^-)–proton interactions at 3.5 Bev (E), 19: 1334
production in meson (π^+)-proton interactions at 2.35 to 2.90 Bev/c, isospin from, (E), 19: 41418
production in meson (K^-) interactions with protons, (T), 20: 2719
production in meson (π^+)-proton interactions at 3.65 Bev/c, (E), 20: 7846
production in meson (π^+) interactions with protons at 8 Bev/c, cross sections for, (E), 20: 37770
production in meson (π^-)-proton interactions at 2.0 to 4.0 Bev/c, (E), 20: 41802 (UCRL-16832)
production in pseudoscalar meson interactions, 18: 36269
production of, (E/T), 20: 15316 (UCRL-16526)
production of neutral, in meson (π^-)-proton interactions at 3 Bev/c, (E), 19: 23436
properties, 17: 28154 (NYO-10264)
properties, 17: 31270 (BNL-7106)
properties, 17: 41793
properties, (E/T), 19: 35181
properties as massive neutral gauge particle, 19: 20989
properties of, 18: 7463 (BNL-7407)
properties of, dynamic theory for, 18: 37947
properties of, field-theoretical models for, 19: 1262
properties of, low-energy equivalent-potential approach for, (T), 19: 16576
properties of, produced by antiproton-proton interaction, 19: 27161 (NEVIS-131)
properties of, quantum, 18: 14951
properties of, review of, 19: 14314 (JINR-P-1887)
properties of, review of, 19: 16657
properties of, review of, 20: 11552 (CONF-651015-3)
properties of, spontaneous mass splitting in bootstrap model for, (T), 19: 18878
properties of, test for, (T), 19: 39572
regeneration of, from mesons (ω), (T), 20: 41888
representation in Sp(6) group, 18: 42421
review, 18: 34636
role in isosinglet meson series, 17: 41813
spin and G parity of, (E), 20: 41881
theory of, octet-octet mixing in SU_3, 18: 42406

MESONS (π)
absorption and interactions in matter, (T), 20: 13350
absorption by nuclei, 16: 23134
absorption by nuclei in mesic atoms, calculation of rates of, 18: 15232
absorption by nuclei up to 800 Mev, cross sections for, (T), 20: 32078
absorption cross section per proton in nuclear matter, 17: 22564 (ORNL-3383)
analysis of 4- to 12-Bev/c beams of, using gas Cherenkov counter, 19: 44376 (BNL-9466)
angular correlations for, in antihyperon and hyperon decays, 17: 16984
angular distribution asymmetry of, in proton annihilation, 17: 22471
angular distribution of, from meson (K_{μ_3}) decay, 17: 37969
angular distributions from proton interactions at 9 Bev, 17: 41821
angular distributions in antiproton-proton interactions, 18: 26286
angular distribution in decay of meson (π)-proton isobar, (T), 19: 18766
angular distributions from electron-proton interactions, (T), 20: 9729
angular momentum wave function for systems of, 18: 4440
annihilation in antiproton-proton interactions, three-body, 18: 9137
asymmetry energy dependence in proton pair annihilation, 16: 24730
beam contamination by meson (μ), method for calculating, 19: 44993 (CEA-R-2778)
beam production in synchrocyclotrons (E), 19: 1117 (NASA-CR-56934 (p.283-9))
beta decay, 17: 20594(R) (UCRL-10572)
beta decay branching ratios, 16: 22961
beta decay, conserved vector current theory of, 15: 24691 (JINR-P-968)
beta decay of, branching ratio for, 17: 9386
beta decay of, composite model for axial vector and vector coupling constants in, 17: 39934
biological hazards of, 17: 18392 (TID-7652(p.866-75))
book: *Fundamental Particles*, 19: 21072
book: *Photoproduction and Scattering of Pi-Mesons*, 18: 4464(T)
bound states of, Faddeev-equation reduction for three-particle, 19: 41416
capture by complex nuclei, isobar mechanism for, 17: 26577
capture by light nuclei, two-nucleon emission from, (T), 20: 19843 (UR-875-126, Paper 2)
capture by molybdenum isotopes, x-ray spectra from, (E), 20: 19273(R) (BNL-929, pp 3-43)
capture by nuclei, conference on, 20: 42304
capture by oxygen-16, radiative, (T), 20: 42315
capture, theory of atomic, 16: 2305(R) (UCRL-9704)
charge correlation coefficients for n-body system of, 18: 34530
charge distribution in meson (π)-nucleon systems, (T), 20: 37791
collimation of, electromagnetic lenses for, 19: 23223
contamination of beams of, with mesons (μ), 17: 3977
contribution of one- and two- in nucleon-nucleon scattering, 18: 18656
coupling constant of, with nucleon, 18: 24411
coupling constants, 17: 19139
coupling constants for $N^*_{33}N\pi$ and $NN\pi$, weak, 20: 21655
coupling in ($\pi\pi$-$K\bar{K}$), meson (ρ) model in, 19: 8194
coupling to baryons, 18: 44566
coupling to hyperons (Λ), (T), 19: 18908
coupling to nucleon, resonance of, 19: 36220(R) (MIT-2098-142)
coupling to nucleons, (E), 20: 25781(R) (COO-1195-56)
coupling to Pomeranchuk particle, 17: 13423
decay, 16: 10930
decay along channels of magnetic quadrupole lenses, collection of product, 16: 4690 (NP-10773)
decay amplitude, 18: 14920
decay amplitude of, for pseudoscalar nucleon coupling, 17: 24315
decay at rest, angular distributions from, 18: 7485
decay at rest in nuclear emulsions, meson (μ) angular distribution in, (E), 19: 37593
decay calculations, 16: 10974
decay in a-c and d-c electromagnetic fields, 18: 28411
decay in ambiplasma, energy distribution from, (T), 20: 21684
decay in electromagnetic field, (T), 19: 5003
decay, neutrino-mass analysis in radiative, 17: 19125
decay of, branching ratio for electron-meson (μ), 17: 20851
decay of charged, Goldberger–Treiman relation for, 17: 37955
decay of charged, radiative corrections to, using intermediate vector boson, 17: 34776
decay of charged, spectra of radiative, 16: 26113
decay of K-π resonance (K*), effects of spin-parity assignments on,

16: 26157
decay of, kinematical tables for two-body, 17: 29495 (CERN-63-20)
decay of, leptonic, 18: 9101 (UR-875-11(p.375-89))
decay of, meson(μ) and neutrino production in, 17: 11471 (JINR-E-1120)
decay of, meson (μ) angular distribution in, 17: 17019
decay of, neutrino production in, 18: 2583 (CEA-2259)
decay of π_μ, $\Delta Q/\Delta S = -1$, 18: 22772
decay of (π–K) resonance state, branching ratio and spectra of leptonic, 17: 22428 (LNF-63/16)
decay of, polarization effects in radiative, 17: 7021
decay of, axial vector current in leptonic, 18: 40318
decay of, axial-vector-current contribution to radiative (T), 19: 3070
decay of, beta particles in, 18: 36353
decay of, branching ratio for electron, 18: 22726 (NEVIS-121)
decay of, CP violation in leptonic, (T), 19: 41378
decay of, CP violation in leptonic, (T), 20: 25872
decay of, current commutation relations for leptonic, 20: 19479
decay of, e/μ branching ratio in, 18: 12950
decay of, effects of weak vector bosons in, 20: 4629
decay of, eight-fold symmetry in, (T), 20: 4692
decay of, lepton pairs in, (T), 20: 25837
decay of, leptonic, (T), 20: 9772
decay of, matrix elements for leptonic, 20: 17415
decay of, meson (ρ) universality for rate of $\mu\nu$, 20: 44238
decay of, models for, 18: 14803 (ISU-10)
decay of, neutrino rest-mass effects in, 18: 22776
decay of, neutrino distributions in, (T), 19: 19132
decay of, non-local effects in radiative, (T), 19: 16478 (NP-14850)
decay of, nonoctet currents in leptonic, 20: 24037
decay of, radiative corrections with finite neutrino mass, 18: 37943
decay of, radiative corrections to meson (μ) polarization in, (T), 19: 8169
decay of, radiative corrections to, (T), 19: 8234
decay of, radiative corrections to ($\gamma\mu\nu$), (T), 20: 7811
decay of, review on leptonic, 20: 7806
decay of, theory of leptonic, 18: 44578
decay of, total probability for electron pair production in, (T), 19: 41482(T)
decay of, transverse meson (μ) polarization in, (T), 20: 19488
decay of, weak interactions in leptonic, 18: 32628
decay, parity nonconservation in, 16: 10885
decay rate from meson (μ) mass, maximum, 20: 15344
decay through intermediate vector meson, leptonic, (T), 20: 37781
decays of, static quark model for, 20: 44200
detection and differentiation from electrons and muons in Bev range, 20: 7365 (KFK-342)
detection and discrimination from electrons, 19: 7790 (TID-21338 (p.193-8))
detection and discrimination from electrons at 80 to 340 Mev/c, (E), 19: 46782
detection and measurement in diffusion cloud chambers, 18: 18223
detection and measurement in thick-plate spark chamber (E), 19: 773 (LAL-1114)
detection and measurement of charged photo-, in Frascati synchrotron, (E), 19: 11864 (LNF-63/82)
detection in wide-gap spark chamber, (E), 19: 13799
detection of secondary, spark chamber for, 17: 30875
detection of, lithium-doped silicon junctions for, 19: 11528
determination in meson (μ) beams, 18: 42410
dispersion relations for, Green's function from, 17: 32948
distribution in nucleon clouds, 18: 9146
distributions from $_\Lambda He^5$ decay, 16: 26363
distributions in atmosphere, angular and energy, (T), 19: 20891
dosimetry of beam of, 20: 1621 (UCRL-16387)
dosimetry of high-energy, methods for, (T), 20: 4505 (ORNL-P-1738)
dosimetry of 1- to 5-Bev, 20: 25329
dosimetry, linear energy transfer, and quality factors of, in water, 18: 12817
effects in photodisintegration of deuterons, (E/T), 19: 18903
effects of collective motion of clouds of, on weak interactions, 17: 34800
effects on isoscalar nucleon structure, 18: 9195
effects on maize, mutagenic, 19: 43712 (BNL-9383)
effects on nucleon-nucleon interaction amplitudes, 20: 27892
effects on root meristem cells of *Vicia faba*, biological, 20: 1621 (UCRL-16387)
electro- and photoproduction, theory, 16: 6968
electromagnetic properties of, review, 17: 9465
electromagnetic properties of, effects of meson (π) resonances on, 17: 37992
electromagnetic structure measurement of, from electro- and photoproduction, 16: 29674
electromagnetic structure of charged, analysis using α–w interactions, (T), 19: 41379
electromagnetic structure of, (T), 20: 13878
electroproduction on protons, neutron form factor from, (T), 19: 45065
electroproduction amplitude at finite momentum transfer, 20: 30137
electroproduction on protons, (E), 20: 34246
electroproduction on nucleons in region of N*(1238), (T), 20: 34250
electroproduction of, nucleon electromagnetic form factors from, (T), 20: 36039 (N-66-18134)
electroproduction of, radiative corrections to, 20: 44225
electroproduction on protons at 5 to 6 BeV, (E), 20: 46348(T) (SLAC-Trans-44)
electroproduction on deuterons at 523 MeV, impulse approximation for, (T), 20: 46357
emission by nucleons in nuclear reactions, Cherenkov, (T), 19: 16489
emission by protons moving in magnetic fields, (T), 19: 12267
emission by protons in magnetic fields, (T), 19: 37509(T)
emission in antiproton annihilations in emulsions, energies and numbers for, 17: 31305
emission in cosmic nucleon interactions, asymmetry of, 18: 42399
emission in emulsion jets involving Landau hydrodynamic process, (T), 19: 43073(T)
emission in intermediate boson decay, three-body and four-body, 18: 2665
emission in $_\Lambda H^4$ and $_\Lambda He^4$ decay, final-state interactions in, 20: 32477
emission in meson (π)–proton interactions, 18: 7475(TID-19854)
emission in meson (π^-) interactions with nucleons at 7 Bev, 18: 24391 (JINR-P-1629)
emission in meson (K^-) absorption by emulsion nuclei, (E), 19: 23467
emission in meson ($K_{\mu 3}$) decay, angular correlation in, (T), 19: 41485(T)
emission in meson (K^+) decay, branching ratios for, (E), 20: 7801 (UCRL-16362)
emission in neutrino reactions with iron and lead, diffraction mechanism for, 17: 21091
emission in resonance-state decay, forbidden configurations in, 18: 18664
energy and transverse momentum of, in cosmic showers, 17: 13107
energy distribution from nucleon-nucleon interactions at 100 Bev, 17: 16971
energy loss distributions of 370-Mev, in silicon, (E), 20: 7418
energy loss in hydrogen due to strong interactions, 17: 9287
energy loss straggling in matter, distributions of, (T), 19: 9894 (NAS-NRC-PUB-1133(p.187-203))
energy losses and ranges in matter, tables, (E), 19: 8005 (NASA-SP-3013)
energy spectra from 2-Bev proton bombardment of polyethylene, 16: 14903 (CEA-1810)
energy spectra in CERN neutrino experiment, determination of, (E/T), 20: 21604 (CERN-65-32, pp 121-6)
energy spectrum of charged, from meson (K^-) capture in bromotrifluoromethane, 20: 24326 (AD-626056)
energy transfer in silicon at 0.5 to 1.5 Bev, 18: 20410
energy transferred to, in high-energy nucleon-nucleus collisions, 17: 13336
exchange and production in antiproton-proton interactions at 3 to 4 Bev/c, (T), 19: 27262
exchange between nucleons, static three-body nuclear forces in, 18: 2599
exchange contribution in proton Compton scattering, 16: 2437
exchange contribution to nucleon scattering amplitudes, 17: 9332
exchange contributions in (n-p) and (p-p) scattering at 10 Mev, dispersion relations for, 17: 24349
exchange contributions to hyperons (Λ)-nucleon scattering matrix, 17: 26348
exchange contribution to proton-proton scattering at 52 to 310 Mev, comparison with ALV theory, 18: 9172
exchange contributions to nucleon elastic interactions, Azimov conditions for, 18: 10941
exchange contribution to hyperon (Λ)-nucleon interactions, 18: 28418
exchange contributions to intermediate-range nuclear forces, 18: 42651 (UCRL-7553-T)
exchange contribution in peripheral model of isobar production, (T), 20: 2817
exchange current contributions to form factors of helium-3 and tritium, two-body, 19: 19159
exchange currents in deuteron photodisintegration, dispersion theory, 18: 26375
exchange currents in helium-3 and tritium, (T), 19: 19157
exchange currents in deuterium, helium-3, and tritium, (T), 19: 19158
exchange effects of, on deuteron electromagnetic structure, (T), 20: 11651
exchange in (e-d) interactions, 18: 40325
exchange in antiproton-proton interactions at 3.0 to 3.6 Bev/c, (T), 20: 13494
exchange in deuteron photodisintegration (T), 19: 3091
exchange in deuteron-electron elastic interactions, (T), 19: 10063

exchange in deuteron-electron elastic scattering, (E), 20: 4580 (AD-618662)
exchange in elementary particle inelastic interactions, 18: 10971
exchange in hyperon (Λ) interactions with hyperons (Σ), 16: 2447
exchange in hyperon (Λ)-nucleon and hyperon (Λ) interactions, (T), 19: 10050
exchange in meson (K) interactions with nucleons, relations to potential in, 16: 15581
exchange in meson (K^+) interactions with protons at 1.96 Bev/c, double resonance production in, 17: 39895
exchange in meson (K^+)-proton interactions at 1.96 Bev/c, 17: 41745 (UCRL-10954)
exchange in meson (π)-nucleon interactions, two-body process for, 18: 7549
exchange in meson ($\bar{K}$) interactions with meson (K*), enhancement of, 18: 9183
exchange in meson (π^+)-proton interactions, two-body, (T), 20: 41918
exchange in neutron–proton interactions at 2.04 and 2.85 Bev, 18: 2663
exchange in nuclear reactions with nucleons, potential calculation, 16: 10832
exchange in nucleon interactions, optical model potential from, 17: 38191
exchange in nucleon interactions at 0 to 400 Mev, effects of, 18: 14954
exchange in nucleon-nucleon interactions, 18: 32592
exchange in nucleon interactions, isobar production in, (T), 19: 18780
exchange in nucleon interactions, (T), 19: 18864
exchange in nucleon-nucleon interactions, (T), 19: 29095
exchange in nucleon-nucleon scattering, dispersion theoretic calculation of two-body, 20: 9778
exchange in nucleon-nucleon interactions, correlation effects in, (T), 20: 32073
exchange in particle interactions, non-static effects in single, 16: 26166
exchange in particle elastic interactions, Regge pole method for, 17: 29520
exchange in photon interactions with protons, contributions from, 17: 39900
exchange in photon-nucleon interactions, two-body, (T), 20: 41821
exchange in proton interactions at 142 Mev, 1–π pole for, 16: 27993 (NYO-10035)
exchange model for nucleon-nucleon collisions at high energies, 17: 20866
exchange model (single), tests, 16: 10894
exchange of two-body, in nucleon-nucleon interactions at low energies, (T), 20: 44271
exchange of vector, in nucleon-nucleon scattering, 17: 24336
exchange potential for single, velocity dependence of relativistic, 16: 6959
exchange potentials from nucleon interactions, 16: 18386
exchange potentials from nucleon interactions, 16: 18387
exchange potential in nucleon-nucleon interactions in momentum space, 17: 5271
exchange processes in nucleon-nucleon scattering, resonances in many-pion systems, 16: 8147
existence of heavy unstable, possibility of, 19: 47398
form factor, 16: 4722
form factor effects in peripheral nucleon interactions, 16: 3648
form factor for, Lagrangian models for charge, 20: 39796
form factor of, electromagnetic, (T), 20: 41833
form factors for, linear equations for determining, 16: 26085 (NP-11632)
form factors for, sum rules for electromagnetic, 20: 25782 (DESY-66/8)
form factors for, current algebra for sum rule for, 20: 34148 (IC-66/43)
form factors of charged, 16: 13898
form factors of, asymptotic behavior of, 18: 24471
form factors of, electromagnetic, (E/T), 20: 37812
form factors of, SL (6,C) symmetry for charge, 20: 36030 (IC-66/84)
form factors of, SL (n,C) symmetry for determining charge, 20: 37738 (IC-66/89)
formation of meson (π)-hyperon (Σ) resonant state from 1.15-Bev/c K^--p interactions, 16: 4696 (UCRL-9835)
functions as nucleon components, 16: 15540
identification in bubble chambers at 0.15 to 4.0 Bev/c, 16: 13921
identification in electron background, telescope for, 17: 36146 (CERN-63-25)
interaction amplitudes, integral representation for, 16: 12376
interaction effects in nucleon electromagnetic form factors, 16: 22957
interaction effects in meson (π^+) photoproduction on protons, 18: 37954
interaction in meson (K) decay, final-state, (T), 19: 18804
interaction model application to meson (K) form factor, 16: 5881
interaction of, from $K_{\mu 4}$ decays, (E), 20: 46346 (UCRL-17088)
interaction phase shifts, 16: 15578
interaction resonance effects on nucleon electromagnetic structure, 16: 12380
interaction resonance effects on π–N interactions at low energies, 16: 18335
interaction resonances of, effects in electron pair annihilation, 17: 13384
interaction resonances of, effects in meson (K)-nucleon scattering, 17: 15117
interaction resonances (π-π) at 1250 Mev, Pomeranchuk trajectories for, 17: 26369
interaction resonances with hyperons, property regularities for, 17: 34730 (JINR-P-1290)
interaction resonance (π^+-π^-) in proton pair annihilation, 18: 20894 (BNL-7969)
interaction resonances of, boson icosuplet of, 18: 28386
interaction resonances with mesons (ρ), spin of 1310-Mev, 18: 37913
interaction resonances with mesons (ρ), 1090-Mev, (T), 19: 4992
interaction resonances of, in molecular-rotator model, (T), 19: 16663
interaction resonance with nucleons, form factor of N*, (T), 20: 24014 (DESY-66/4)
interaction theory, 16: 1178
interactions, 18: 16552(R) (UCRL-11132)
interactions, amplitude solutions for P and S waves, 16: 10896
interactions, amplitudes for, 16: 26169
interactions, analysis of inelastic, 16: 983
interactions and properties, research programs, 16: 18124(R) (UCRL-10113)
interactions and production, 18: 22593(R) (SLAC-27)
interactions, angular distributions in, 16: 15553
interactions at high energies, elastic, 16: 2408 (JINR-D-773)
interactions at high energies, strong, 16: 9370
interactions at high energies, double spectral functions for s- and p-wave, 16: 27967
interactions at high energies, amplitudes for, 16: 27975
interactions at high energies, total cross sections for, 17: 9238
interactions at high energy, experimental and theoretical data on elastic, 17: 11507
interactions at high energies, field theory for, 18: 6015
interactions at high energies, amplitudes in, 18: 20983
interactions at high energies, p-wave amplitude for, (T), 19: 12189
interactions at low energies, integral equations for, 16: 10839
interactions at low energies, partial-wave dispersion relations for, 17: 28191
interactions at low energies, amplitudes in, 18: 12951
interactions at low energies, theory of elastic, 18: 26333
interactions at low energies, amplitudes for, (T), 19: 33008
interactions at 1.89 Bev for hyperon production, 16: 16977 (NP-11592 (Vol.I)(p.371-4))
interactions between four, in p-$\bar{p}$ annihilation, 16: 33748
interactions, coincidence measurements in, 16: 17036
interactions, cross sections and resonance energies, 16: 15574
interactions, dispersion relation solutions for, 16: 5884
interactions, dispersion relations in, 16: 17047
interactions, dispersion relation for final-state, 16: 18351
interactions, dispersion relation subtraction constants, 16: 18359
interactions, effects on meson (K^*_{e4}) decay, 16: 27963
interactions, effects on dispersion calculations in scattering theory, 16: 29991
interactions, effects of 2-body potentials on 3-body, 16: 31032
interactions in gamma-meson (ρ) systems, constants for, 17: 7001
interactions in I = 0 state, attractive, 18: 18697
interactions in J = T = 1 resonant state, 16: 27961
interactions in jet showers, secondary angular distribution and momenta for primary energy of, (T), 19: 47275
interactions in meson (π)-nucleon scattering, S-wave dispersion relation in, 17: 32949
interactions in meson (π)-nucleon interactions, effects on invariant amplitude in, 17: 41803
interactions in meson (η) and (K) decay, resonant, 18: 9170
interactions in meson (K^+_{e4}) decay, (T), 19: 39515
interactions in multiple production processes, resonance, 16: 29643 (NP-11605)
interactions in multiple production processes, resonance, 16: 29657 (NP-11978)
interactions in nuclear emulsion, 18: 28426
interactions in nuclei, review of nuclear forces from, 19: 23765
interactions in nuclei and nuclear matter at low energies, nonlocal potentials for, (T), 20: 22021
interactions in S-wave, I = 2 isospin state, resonance in, 16: 26117
interactions, low-energy length of, 17: 17059
interactions, meson (ρ) production in, 16: 24734
interactions, neutron form factors from, 16: 18379
interactions of, amplitude parity and radiative effects in, 17: 20882
interactions of, analyticity and bound states in, 18: 4430 (JINR-E-1400)
interactions of bootstrap method for meson (ρ) production in, 18: 14931
interactions of charged, electromagnetic, 16: 5877

interactions of charged, effects on meson (η) decay, 17: 19112
interactions of, effects on nucleon form factors, 16: 33747
interactions of, effects of Regge poles on, 16: 33776
interactions of, effects of N-$\bar{N}$ intermediate state on, 17: 780
interactions of, effects on meson(π^-)-proton interactions, 17: 15137
interactions of, effects on nucleon potentials, 17: 19124
interactions of, effects on nucleon structure, 17: 20885
interactions of, effects on photon Green's function, 17: 32955
interactions of, electron-pair interpretation, 17: 34750
interactions of, features of low-energy resonance, 17: 741
interactions of high-energy, at large angles, 16: 12391
interactions of, inverse amplitude dispersion relations for inelastic, 17: 742
interactions of, intermediate-vector-meson model for, 17: 32950
interactions of, low momentum transfer in, 17: 39923
interactions of, mass correlations to orbital angular momentum in resonance states from, 18: 7497
interactions of many-body systems of, SU(4) and SU(3) for isotopic structure of, 20: 6150
interactions of meson (K)-produced, intrinsic structure in, 16: 13908
interactions of, mesons (π) and (ρ) production cross sections from, 17: 28189
interactions of, meson (ρ) exchange forces in, 17: 39937
interactions of, model for (π-π) s-wave, 17: 24285
interactions of, particle emission in, 18: 5944 (PAN-454/VI)
interactions of pairs of, effects on p-p phase shifts, 18: 30522(R) (TID-20720(Paper 4))
interactions of, perturbation theory for, 17: 9219
interactions of, phase-parameters for S- and P-wave, 16: 33750
interactions of, possibility of (4-π) resonance, 17: 11499 (UCRL-10089(Rev.))
interactions of, proton annihilation study of, 17: 37940(T) (NP-tr-1056)
interactions of, review of resonances in, 17: 24185
interactions of, Regge pole parameters determination from, 17: 28167
interactions of, resonance properties of, 17: 29506
interactions of, resonances in, 18: 9200
interactions of, scattering lengths and symmetry point amplitudes from boundary condition model for, 17: 26333
interactions of, strip-approximation corrections from inelastic unitarity for, 17: 39901
interactions of, statistical theory of resonance, 17: 41819
interactions of, strip approximation for, 18: 7502
interactions of three, effects on nucleon form factors, 17: 9272
interactions of three, effects of mesons (ρ) on resonances in, 17: 13450
interactions of, theory for resonances in, 17: 17037
interactions of three-body system of, angular momentum wave function for, 17: 34743
interactions of three, meson (A^+) resonance effects in, 18: 42444
interactions of three, 19: 1280
interactions of virtual, with nucleons, (T), 20: 7822
interactions of, with electrons at 16 Bev, 16: 32267 (AFOSR-1728)
interactions of, 3-meson (π) amplitudes for, 16: 33771
interactions of 3, width of, 17: 9336
interactions of, antibound states in, 18: 18695
interactions of, bootstrap calculations for, 18: 10935
interactions of, boundary condition model for strong, 18: 37890
interactions of, bootstrap model for coupling constants of meson (ρ)-exchange, (T), 19: 18797
interactions of, Bethe-Salpeter equation for meson (ρ) exchange in, (T), 19: 25316
interactions of, cross sections for nonresonant, 18: 16774
interactions of, crossing relations and Legendre expansions for, 19: 1264
interactions of, calculation of (T), 19: 1375
interactions of, C-violation model for $\rho\eta\pi$ coupling in, 20: 4681
interactions of, contributions of elastic unitarity to three-body, (T), 20: 30077
interactions of, dispersion relations for, 18: 32629
interactions of, diffraction and scattering effects in, 19: 1270
interactions of, electrodynamics of weak, 18: 28740
interactions of, elastic unitarity conditions in, 18: 32574
interactions of, effects on potential for nucleon three-body interactions, (T), 20: 11650
interactions of, Feynman graphs for meson (ρ) exchange in, (T), 19: 18792
interactions of, from meson (π^-)-proton interactions at 3 and 4 Bev/c, (E), 20: 39769 (UCRL-16655)
interactions of, helicity amplitudes for, 18: 16781
interactions of, isobar model for three-body, 18: 30595
interactions of, inversion expansion with non-Abelian group of parity tripod for, (T), 20: 15494
interactions of, mass distribution in resonance, 18: 20975
interactions of, model for resonance, 18: 24443
interactions of, model for resonances in, 18: 40300
interactions of, modified strip approximation for N/D equation for, 19: 8188
interactions of, meson (η) and (X^0) production in, (T), 19: 12223
interactions of, meson (ρ) parameters in, 19: 16551
interactions of, meson (ρ) Regge pole effects on, (T), 19: 41370
interactions of, models for calculations of three-body, 20: 46401
interactions of, non-resonant, 18: 14959
interactions of, one-pion-exchange model for mesons (ρ^0) and mesons (f^0), (T), 19: 31005 (CU-1932-240)
interactions of, on-shell and off-shell method for T-matrix for, 20: 46392 (UCSD-10P10-9)
interactions of, properties of resonance, 18: 14809 (JINR-P-1494)
interactions of, phase shifts and resonances in (T), 19: 1294
interactions of, properties of mesons (ρ) from, (T), 19: 4926
interactions of, potential in Born approximation for, (T), 19: 18823
interactions of, production amplitudes for, (T), 19: 27223
interactions of, particle pole correlations with Regge poles in spinless two-body, 20: 27860
interactions of, $\pi\pi p$ bootstrap model for, 20: 41867
interactions of, resonance detection in, 18: 12956
interactions of, resonances in, 18: 36269
interactions of, repulsive potentials for resonance, 18: 37947
interactions of, resonance production in, 18: 40347
interactions of, resonances in, (T), 19: 10015 (JINR-P-1808)
interactions of, review of resonances in, 19: 16510
interactions of, strip approximation for, 18: 26331
interactions of, structure of, 18: 30508 (CERN-64-26)
interactions of, slope of Pomeranchuk trajectory for, (T), 20: 4587 (UCRL-11495)
interactions of, strip approximation calculations for meson (ρ) production in, 20: 36045 (UCRL-16874)
interactions, P and S wave solution (coupled) consistency in, 16: 18340
interactions, P-wave resonance in, 16: 3644
interactions, partial-wave, 16: 3649
interactions, partial-wave dispersion relations, 16: 12381
interactions, partial-wave amplitudes for, 16: 15609
interactions, perturbation 2-π approximation for, 16: 26129
interactions ($\pi + N \to 2\pi + N$ and $2\pi + N \to 2\pi + N$) with nucleons, partial-wave s-singularity of production amplitude in fourth-order diagram of, 18: 9188
interactions, range formulas for s- and p-wave, 16: 17037
interactions, Regge poles in relativistic potential, 16: 22912
interactions, relation to nucleon electromagnetic structure, 16: 999
interactions, resonance state for 3π, 16: 8125
interactions, resonances in, 16: 21296
interactions, resonance solutions for, 16: 22899
interactions, resonance properties of, 16: 26118
interactions, scattering lengths for T = 0 and 2, 16: 5908
interactions, two-pion-exchange approximation for, 16: 24723
interactions with antibaryons and baryons, effects on annihilation processes, 17: 11547
interactions with baryons, decay regularity of unstable particles formed in, 16: 12332 (JINR-D-824)
interactions with baryons, isobar mechanism, 16: 13900
interactions with bosons, meson multiple production in, 16: 26170
interactions with baryons, theory of weak, 17: 41809
interactions with baryons, resonance poles in, 18: 24429
interactions with baryons, model for strong, (T), 19: 8150
interactions with baryons, s-wave virtual states in amplitudes for, (T), 19: 16621
interactions with baryons, weak, (T), 19: 25366
interactions with baryons, coupling constants and masses in, (T), 19: 27221
interactions with baryons, coupling constants for, (T), 19: 31039
interactions with baryons, model for isotopic symmetry for, (T), 20: 15454
interactions with bound nucleons at high energies, elastic, (E/T), 20: 19444 (LYCEN-6527)
interactions with baryons, coupling constants for, (T), 20: 19539 (JINR-E-2544)
interactions with bound nucleus at low energies, (T), 20: 42312
interactions with deuterons, dinucleon formalism in adiabatic multiple, 16: 19683
interactions with deuterons, 2-π resonances in, 17: 9325
interactions with deuterons, meson (η) and meson (ω) production in, 17: 9326
interactions with deuterium and hydrogen, strange particle production in, 17: 9466
interactions with deuterons, elastic amplitudes for, 17: 13453
interactions with deuterons, decay asymmetries for charged hyperons (Σ) from, 17: 19042 (NP-12650)
interactions with deuterons at 85 Mev, dispersion theory of elastic,

17: 41751
interactions with deuterons, dispersion theory for elastic, 18: 4436
interactions with deuterons, dispersion relations for, 18: 6008
interactions with deuterons and hyperons (Σ) at high energies, anomalous thresholds in, 18: 7484
interactions with deuterons, cross sections for, 18: 22745
interactions with deuterons, poles of generation amplitudes for, 18: 24470
interactions with deuterons, mesons (π), and nucleons, dispersion relations for, 18: 32629
interactions with deuterons, dispersion methods for elastic, 18: 37957
interactions with deuterons, impulse approximation for elastic, 18: 40274
interactions with deuterons, anomalous singularities in (T), 19: 3057
interactions with deuterons, resonance, (T), 19: 39564
interactions with deuterons, partial wave dispersion relations for disintegration in, 19: 41336 (NP-15335)
interactions with deuterons, p-wave dispersion relations for disintegration, (T), 20: 30074
interactions with deuterons at high energies, charge independence in, (T), 20: 41887
interactions with deuterons, relativistic impulse approximation for elastic, 20: 44210
interactions with emulsion nucleons at 10^{10} to 10^{12} ev, angular distributions, 16: 21308
interactions with electrons, integrals for radiative correction to, 18: 9080 (BNL-7588)
interactions with electrons, radiative corrections to, 18: 34563
interactions with elementary particles, production amplitudes in, (T), 19: 20925 (ICTP-64/3)
interactions with electrons, Mandelstam representation of, (T), 20: 2678 (AD-614843)
interactions with electrons at 16 Bev/c, cross sections for, (E), 20: 6098
interactions with electrons, cross section for, (T), 20: 13484
interactions with elementary particles, Bethe-Salpeter equation for, 20: 25932
interactions with elementary particles, scattering lengths for, (T), 20: 44256
interactions with gamma rays, from meson (π^-)-proton interactions at 338 Mev, (E), 19: 43044 (JINR-P-2255)
interactions with gamma radiation, analysis of 2π production in, (T), 20: 15389
interactions with hyperons, resonance interpretations in, 16: 18356
interactions with hyperons (Λ) and (Σ), dispersion relations, 16: 3642
interactions with hyperons, scattering, 16: 4692 (TID-13955)
interactions with hyperons (Λ), bound state model, 16: 4709
interactions with hyperons (Λ) and (Σ), analysis, 16: 4734
interactions with hyperons (Λ), global-symmetry resonance, 16: 9387
interactions with hyperons (Λ) and (Σ), 16: 9406
interactions with hyperons (Ξ), coupling properties, 16: 12379
interactions with hyperons, resonance state, 16: 17032
interactions with hyperons (Λ) and (Σ), resonances in, 16: 21296
interactions with hyperons (Λ) and (Σ) and mesons (K) and (π), resonance Regge representation in, 16: 22915
interactions with hyperons (Λ), resonance production from, 16: 22917
interactions with hyperons (Λ) and (Σ), S-wave $J = 1/2$ amplitudes, 16: 26111
interactions with hyperons (Λ) and (Σ) and mesons (K), resonances, 16: 26134
interactions with hyperons (Σ), resonance at 1405 Mev, 16: 26137
interactions with hyperons and mesons, properties of resonant, 16: 26158 (UCRL-10167)
interactions with hyperons (Λ) and (Σ), resonances from, 16: 26161
interactions with hyperons (Σ), resonance below meson (K^-)-proton threshold, 16: 27928
interactions with hyperons (Λ) and (Σ), resonance effects in, 16: 32333
interactions with hyperons (Λ), models for resonances in, 16: 33739
interactions with hyperons (Λ) and (Σ), effects of $\bar{K}$-nucleon amplitudes on, 16: 33772
interactions with hyperons and mesons (π), degeneracy with respect to hypercharge and isotopic spin in, 17: 3972
interactions with hyperons (Ξ^*), resonant state at 1.53 Bev in, 17: 3996
interactions with hyperons (Ξ), unitary theory prediction of resonance, 17: 9236
interactions with hyperons, amplitudes for, 17: 9276
interactions with hyperons, resonances in, 17: 9383
interactions with hyperons, spins of resonances, 17: 13413
interactions with hyperons, effects on K^--p interactions, 17: 15133
interactions with hyperons, hyperons (Y^*) from, 17: 16995
interactions with hyperons, coupling constants for, 17: 17025
interactions with hyperons (Λ^0), hyperon (Y_1^*) spin from, 17: 17039
interactions with hyperons (Λ), 1.66-Bev Y_1^* from, 17: 17041
interactions with hyperons (Λ), theory for hyperons (Y_1^*) from, 17: 17043
interactions with hyperons (Λ), parity and spin of Y_1^* from, 17: 17040
interactions with hyperon (Σ), theory for, 17: 20880
interactions with hyperons (Ξ), resonance effects in, 17: 20884
interactions with hyperons (Λ) and (Σ), coupling constants in, 17: 20886
interactions with hyperons, theory of resonance, 17: 20947
interactions with hyperons (Λ), resonances in system of coupled two-particle channels from, 17: 24282
interactions with hyperons/Λ) in hyperon (Ξ) decay, asymmetry parameters from, 17: 26310
interactions with hyperons (Λ), Y_1^* exchange contributions to amplitudes of, 17: 26321
interactions with hyperons (Σ), production of resonance-state, 17: 28136 (BNL-6363)
interactions with hyperons (Σ) and mesons (K) and (π), resonance, 17: 28172
interactions with hyperons (Σ), resonance state, 17: 29542
interactions with hyperons, resonances in, 17: 31646 (NP-12975 (p.82-92))
interactions with hyperons (Λ), (Σ), and (Ξ) and nucleons, coupling constants for strong, 17: 31373
interactions with hyperons (Σ) at 1404 Mev, resonance in, 17: 31294
interactions with hyperons (Σ) in two-channel formalism for S-wave ($\bar{K}$-N) reactions, 17: 31372
interactions with hyperons (Ξ) at 1.530 Bev, parity and spin for resonance, 17: 34793
interactions with hyperons (Λ) and (Σ), Sawada transformation for multichannel, 17: 34807
interactions with hyperons (Λ) and (Σ) and nucleons, vertex functions for, 17: 34809
interactions with hyperons, mesons, and nucleons, mass correlations to orbital angular momentum in resonance states from, 18: 7496
interactions with hyperons (Λ) at low energies, self-consistent S-matrix study of p-wave, 18: 9117
interactions with hyperons (Λ) and (Σ), correspondence of resonances to S-matrix poles in broken-symmetry, 18: 9152
interactions with hyperons (Λ) at low energies, hyperon (Σ) and (Y_1^*) poles in, 18: 9124
interactions with hyperons (Σ), Y_0^* production in, 18: 11244
interactions with hyperons (Ξ) and mesons (K), resonance production in, 18: 14949
interactions with hyperons, resonances in, 18: 21006
interactions with hyperons (Λ) at low energies, analysis of, 18: 21009
interactions with hyperons (Λ) and (Σ), motion of poles in resonance, 18: 21016
interactions with hyperons (Σ), resonance, 18: 26328
interactions with hyperons (Ξ) and nucleons, parity conservation and unitary symmetry in, 18: 28342
interactions with hyperons and mesons (K), properties of resonance, 18: 28425
interactions with hyperons (Λ) and nucleons, CP invariant theory for, 18: 30557
interactions with hyperons (Σ), resonance, 18: 36266
interactions with hyperons (Λ) and (Σ), resonance, 18: 44523 (UCRL-11568)
interactions with hyperons (Λ) and nucleons, effects on Λ--Λ and Λ--N potentials, 18: 44544
interactions with hyperons (Σ), resonance, (E), 19: 1344
interactions with hyperons (Σ), logarithmic singularities in resonance, (T), 19: 4998
interactions with hyperons (Σ), resonances in, (T), 19: 8140 (NP-14479)
interactions with hyperons (Λ), mesons (π), and nucleons, axial-vector current in, (T), 19: 12229
interactions with hyperons (Σ), Σ (1385) in, (T), 19: 12303
interactions with hyperons (Λ), p-wave phase shifts for, (T), 19: 16518
interactions with hyperons (Σ) and nucleons, coupling constants for, (T), 19: 20917 (IC/65/3)
interactions with hyperons (Λ), $\Sigma\Lambda\pi$ coupling constant in, (T), 19: 27225
interactions with hyperons (Σ) and nucleons, coupling in, (T), 19: 27256
interactions, with hyperons, resonances for, 17: 715 (TID-16623)
interactions with hyperons (Σ), dynamics of T = 2 (1415) resonance in, (T), 20: 9731
interactions with hyperons (Λ), partially conserved axial-vector current hypothesis for, 20: 32013
interactions with hyperons, static bootstrap theory and Lie group for, 20: 41862
interactions with leptons, ladder graphs approximation for higher-order weak, (T), 19: 25320
interactions with mesons (K), relative Σ-Λ parity, 16: 2436
interactions with mesons (π), nuclear forces due to, 16: 2439
interactions with mesons (π), low-energy, 16: 4683 (AFOSR-655)
interactions with mesons (π) in mesons ($\kappa\pi_3$) decay, review, 16: 8053 (NP-11232(p.236-42))
interactions with mesons (π) and nucleons, development of models for,

16: 8096 (JINR-D-774)
interactions with mesons (K), resonance effects, 16: 8143
interactions with mesons (π), effect of 3π resonance on 2π resonance, 16: 9388
interactions with mesons (π) and nucleons, strong coupling effects, 16: 10914
interactions with mesons (π), amplitudes and isotopic spin, 16: 12399
interactions with mesons(π) and nucleons, asymptotic behavior of scattering amplitude, 16: 13862 (JINR-D-900)
interactions with mesons (π), effects of resonances on meson (K) form factor, 16: 13870 (NYO-10127)
interactions with mesons (π), bibliography, 16: 13872 (UCRL-9999)
interactions with mesons (π), renormalization in perturbation theory, 16: 13892
interactions with mesons (π), P- and S-wave scattering amplitudes, 16: 15600
interactions with mesons (K), effects on nucleon form factors, 16: 15574
interactions with mesons (π) in 3-π states, integral equations for, 16: 15601
interactions with mesons (K), dispersion relations, 16: 15607
interactions with mesons (K), s-wave amplitude for, 16: 17024
interactions with mesons (π), p-wave resonance effects in K-π scattering, 16: 17024
interactions with mesons (K), K-π and π-π resonance effects on p-wave, 16: 17025
interactions with mesons (π), phase shifts, 16: 16969 (NP-11592(Vol.I) (p.331-5))
interactions with mesons (K) at low energies, strangeness violation in, 16: 17048
interactions with mesons (K), (K*) pole contribution to, 16: 17049
interactions with mesons (π), phenomenological description, 16: 17052
interactions with mesons (π) at high energies, amplitude behavior of elastic, 16: 17053
interactions with mesons (π) at low energies, resonance solutions of equations, 16: 17054
interactions with mesons (π) and nucleons, contributions to nucleon–nucleon potentials, 16: 18382
interactions with mesons (π), renormalization in perturbation theory, 16: 18317 (AD-265526)
interactions with mesons (π) and nucleons, dispersion relations for, 16: 23251
interactions with mesons (π) and protons, cross sections and resonance effects, 16: 22941
interactions with mesons (π) at low energies, higher partial waves in, 16: 22954
interactions with mesons (π), poles in low energy scattering theory, 16: 24912 (AD-270903)
interactions with mesons (K), meson (K*) production in, 16: 24734
interactions with mesons (π^0), resonance properties from, 16: 24744
interactions with mesons (π), resonances in, 16: 26076 (JINR-P-938)
interactions with mesons (π) and nucleons, dispersion relations for, 16: 26077 (JINR-P-949)
interactions with mesons (K), effects on K_{e3} and $K_{\mu 3}$ decays, 16: 26103
interactions with mesons (π), equations for low-energy, 16: 27903 (JINR-E-994)
interactions with mesons (π) and nucleons, Regge poles and scattering amplitudes in, 16: 27915 (UCRL-10254)
interactions with mesons (π) from proton interactions at 9 and 24 Bev, resonances from, 16: 27992
interactions with mesons (π), model for two-pion and three-pion resonances, 16: 29692
interactions with mesons (π), 16: 29694
interactions with mesons (π), effect on nuclear forces, 16: 29695
interactions with mesons (π), cross sections and multiple meson production in, 16: 31024 (UCRL-10340)
interactions with mesons (π), analytical properties of partial amplitudes in l-plane, 16: 31027
interactions with mesons (π) and (ρ), coupling constants for, 16: 32331
interactions with mesons (π) and nucleons, S-wave, 16: 33706
interactions with mesons (K), resonance effects in, 16: 33751
interactions with mesons (K), scattering amplitudes for, 16: 33755
interactions with mesons (π) and nucleons, 17: 768
interactions with mesons (π), prediction of phase shifts from meson (π)–nucleon phase shifts, 17: 769
interactions with mesons (π) at low energies, method of calculation of, 17: 772
interactions with mesons (π), multiple production of mesons (π) in, 17: 2187
interactions with mesons (π) interpretation of ρ and ζ resonances in, 17: 5248
interactions with mesons (π) at low energies, resonances in, 17: 6987
interactions with mesons (π), high-energy behavior in elastic, 17: 7003
interactions with mesons (π), analytic properties of partial amplitudes in, 17: 7028
interactions with mesons (π) and protons, role of vector mesons in elastic, 17: 7045
interactions with mesons (K), resonances in, 17: 9226
interactions with mesons (π) at low energy, Chew-Low analysis of, 17: 9329
interactions with mesons (π) at low energies, 17: 9330
interactions with mesons (π), in meson (π)-nucleon scattering, 17: 9339
interactions with mesons (π), Regge pole application to, 17: 9414
interactions with mesons (π) and nucleons, review of theories of, 17: 9463
interactions with mesons (π) in meson ($K_{\pi 3}$) decay, resonance, 17: 11528
interactions with mesons (π), Regge poles in, 17: 11546
interactions with mesons (π) and nucleons, effects on nucleon form factors, 17: 11559
interactions with mesons (π), effects on meson (π)-nucleon interactions, 17: 11578
interactions with mesons (π) and nucleons, resonances, 17: 13455
interactions with mesons (K), effects on electromagnetic structure of nucleon, 17: 13464
interactions with mesons (K), decay of resonances in, 17: 13371
interactions with mesons (π), effects on low-energy meson (π)-nucleon scattering, 17: 13385
interactions with mesons (π) at 620 Mev, T = 2 particle evidence in, 17: 13406
interactions with mesons (π), off-shell, 17: 13418
interactions with mesons (K) and (π), resonances in, 17: 15138
interactions with mesons (K) low energy resonances in, 17: 15073 (EFINS-62-5(Rev.))
interactions with mesons (π) and nucleons, models for peripheral, 17: 15079 (NP-12566)
interactions with mesons (π), resonance, 17: 16948 (JINR-D-1128)
interactions with mesons (π) at high energies, cross sections for elastic, 17: 16951 (JINR-P-1150)
interactions with mesons (π), amplitudes of, 17: 16966
interactions with mesons (π), review of theory, 17: 16979
interactions with mesons (π), 17: 20594(R) (UCRL-10572)
interactions with mesons (π), meson (K_{e4}) angular correlation analysis of, 17: 20935
interactions with mesons (K), spin of resonance, 17: 20949
interactions with mesons(π), dispersion relations for partial wave amplitudes for, 17: 22423 (JINR-P-1205)
interactions with mesons (π), amplitude for s-wave, 17: 22499
interactions with mesons (π) and nucleons, model for final-state, 17: 22517
interactions with mesons (π) at low energies, S-wave amplitude determination in, 17: 22525
interactions with mesons (π) in $\lambda\phi^4$ theory, 18: 2632
interactions with mesons (ω), resonance production in, 18: 2651
interactions with mesons (K) at 730 Mev, SU(4) assignments for resonance, 18: 2664
interactions with mesons (π) and nucleons, dispersion relation treatment of, 18: 7472 (NP-13451)
interactions with mesons (K), analytical properties of scattering amplitudes for, 18: 9203
interactions with mesons (K), theory for p-wave resonance in, 18: 836 (BNL-5569)
interactions with mesons (π), boundary-condition model for scattering amplitudes of elastic S- and P-state, 18: 10926
interactions with mesons (ω), interpretation of 1220-Mev resonance in, 18: 10952
interactions with mesons (ω), resonance at 1220 Mev from, 18: 10954
interactions with mesons (K) and (π), review of resonances in, 18: 12903 (JINR-P-1490)
interactions with mesons (π), bound state poles in, 18: 14806 (JINR-E-1496)
interactions with mesons (π) with unitary and crossing, 18: 14873
interactions with mesons (K), quantum numbers for K2π and K3π resonances in, 18: 18661
interactions with mesons (K), model for K$\pi\pi$ resonance in, 18: 18694
interactions with mesons (ω), model for resonances in, 18: 18694
interactions with mesons (K), K$\pi\pi$ resonances in, 18: 18696
interactions with mesons (η), resonance predictions in, 18: 18698
interactions with mesons (π), amplitude for, 18: 18642 (JINR-P-1533)
interactions with mesons (K), s- and p-wave resonances in, 18: 20977
interactions with mesons (K), resonance, 18: 21003
interactions with mesons (π), 2-π resonances in, 18: 21021
interactions with mesons (π), K_{e4} decay in, 18: 22756
interactions with mesons (π), meson (ω^0) production in, 18: 22757
interactions with mesons (π) at low energies, resonance width parameter for, 18: 22778
interactions with mesons (π), inverse amplitude solution for low-energy, 18: 24425

interactions with mesons (π) at low energies, threshold behavior of partial amplitudes in, 18: 24413
interactions with mesons (π), amplitudes for s- and p-wave, 18: 26299
interactions with mesons (π) in 3π formation, 18: 26300
interactions with mesons (π), complex angular momentum scattering amplitudes for, 18: 26326
interactions with mesons (ρ), meson (ω) production in, 18: 26341
interactions with mesons (ρ), enhancement at 1 to 1.4 Bev, 18: 26346
interactions with mesons (π), mesons (ρ) in, 18: 28394
interactions with mesons (π) and neutrons, phases from dispersion relations for, 18: 28422
interactions with mesons(π), effects on (K_1^0–K_2^0) mass difference, 18: 30526 (TID-20771)
interactions with mesons(π) in strip approximation, S-matrix theory of ($\rho \to N\bar{N}$) vertex in, 18: 30529 (UCRL-7871-T)
interactions with mesons (π), meson (K) pair production in, 18: 34534
interactions with mesons (K), 18: 34534
interactions with mesons (η), 1-Bev resonance in, 18: 34572
interactions with mesons (π), modified N/D method for, 18: 34573
interactions with mesons (π), 18: 34579
interactions with mesons (ρ), resonance, 18: 34581
interactions with mesons (π), analysis of s-wave, 18: 34595
interactions with mesons (K), strangeness-changing currents in resonance, 18: 36261
interactions with mesons (K), spin-parity test for resonances in, 18: 36281
interactions with mesons (ρ), isoscalar resonances in, 18: 36304
interactions with mesons (π), resonances in, 18: 36324
interactions with mesons (π), mass of antibound state in, 18: 37919
interactions with mesons (ρ) at 1.2 Bev, 18: 38137
interactions with mesons (ρ), production of resonance, 18: 40246 (UCRL-11443)
interactions with mesons (π) at high energies, Regge poles in, 18: 40251 (UCRL-11516)
interactions with meson (K^0)-meson (π^+) pairs, resonances in, 18: 40378
interactions with mesons (π), theory of, 18: 40360
interactions with mesons (κ), possible nonresonant character of ~726-Mev peak in, 18: 40376
interactions with mesons (η), resonance effects in, 18: 42445
interactions with mesons (π), amplitude and singularities in complex l-plane, 18: 42455
interactions with mesons (K), resonance, 18: 42368 (JINR-E-1804)
interactions with mesons (π), meson (A_1) resonances in, 18: 42428
interactions with mesons (ρ), meson (A_1) resonances in, 18: 42428
interactions with mesons (π), resonances in, 18: 44530
interactions with mesons (K), resonances in, 18: 44530
interactions with mesons (π), partial-wave amplitude for, 18: 44548
interactions with mesons (ρ), meson (ω) bound state in, 18: 44574
interactions with meson (π), N/D calculation of meson (ρ) in, 18: 44588
interactions with mesons (π), N/D method for p-wave (T), 19: 1286
interactions with mesons (ω), evidence for resonance (E), 19: 1324
interactions with mesons (π), calculations on (T), 19: 1367
interactions with mesons (π) at high energies, total cross section for (T), 19: 3068
interactions with mesons (π) at high energies, p-wave amplitude for, (T), 19: 4914
interactions with mesons (ρ), logarithmic singularities in resonance, (T), 19: 4998
interactions with mesons (ω), logarithmic singularities in resonance, (T), 19: 4998
interactions with mesons (ω), properties of resonance, (E/T), 19: 6556
interactions with mesons (π), two-pion exchange bootstrap model for mesons (ρ) in, (T), 19: 8163
interactions with mesons (π), strip approximation N/D equation for meson (ρ) exchange in, 19: 8190
interactions with mesons (π), field-theoretical approach to amplitudes in, 19: 8192
interactions with mesons (π), self-consistent calculation of p-wave amplitudes for, 19: 8195
interactions with mesons (π), effects of unstable particles on, 19: 10038
interactions with mesons (K), resonance processes in, (T), 19: 10040
interactions with mesons (π) at low energy, phase shifts for, (T), 19: 10086
interactions with mesons (π) and (ρ), p-wave dispersion relations for, (T), 19: 12220
interactions with mesons (ω), meson (B) and (ρ) production in, (T), 19: 12225
interactions with mesons (π), dispersion theory for, 19: 12293
interactions with mesons (K), K* (890) in, (T), 19: 12298
interactions with mesons (π), ω (790) and ρ (730) resonances in, (T), 19: 12300
interactions with mesons (π), perturbation theory for Regge poles in, 19: 12310
interactions with mesons (η) and (K), properties of resonance, 19: 14314 (JINR-P-1887)
interactions with mesons (K), (K*), (ρ), and (σ), energy peaks in, (T), 19: 14335
interactions with mesons (π), Regge theory for form factor in, 19: 14347
interactions with mesons (π), resonance-meson model from, 19: 14348
interactions with mesons (π), partial-wave amplitude for elastic, (T), 19: 14357
interactions with mesons (ω), model for resonances in, (T), 19: 16538
interactions with mesons (K), scalar resonances in, (T), 19: 16540
interactions with mesons (π) and (ρ), coupling constants for, (T), 19: 16552
interactions with mesons (η) and (K), symmetry in bootstrap model for, (T), 19: 16627
interactions with mesons (π) and nucleons, algebra for describing, (T), 19: 18775
interactions with mesons (K), resonances in, (T), 19: 18782
interactions with mesons (K), K*(888) in, (T), 19: 18847
interactions with mesons (K), $K\pi\nu$ (1160) resonance in, (E), 19: 18851
interactions with mesons (ω) and (ρ), coupling constants for, (T), 19: 18868
interactions with mesons (π), Jacob-Wick method for scattering amplitude in, (T), 19: 21052
interactions with mesons (K) at low energies, K* production in, (T), 19: 21058
interactions with mesons (π), theory of low-energy, 19: 21074
interactions with mesons (π), N/D method for dispersion relations for, 19: 23372
interactions with mesons (π), many body problem for, 19: 23384
interactions with mesons (π), effects on meson (π)-nucleon interaction amplitudes, (T), 19: 25276
interactions with mesons (π), spectra from, (E), 19: 25265(R) (UCRL-11776)
interactions with mesons (π) in cosmic showers at 10^{11} to 10^{14} ev, (T), 19: 27183
interactions with mesons (π) and nucleons, residues of Regge poles in, (T), 19: 27228
interactions with mesons (ρ), modified isobar approximations for, (T), 19: 27243
interactions with mesons (π), fixed-angle method for calculations of p-wave, 19: 29070 (NP-14959)
interactions with mesons (π), strip approximation with Regge poles and bootstrap equations for, 19: 29071 (NP-15010)
interactions with mesons (π), scattering lengths for, (E), 19: 33070
interactions with mesons (π), algebraic equations for, 19: 35050
interactions with mesons (ρ) and nucleons, resonances in, (E/T), 19: 35181
interactions with mesons (K) and (π), bootstrap theory for amplitudes of, 19: 35036
interactions with mesons (π), meson (K_{e4}) decay correlations for phase shifts in, (T), 19: 37547 (UCRL-16026)
interactions with mesons (π) in electromagnetic pair production, (T), 19: 41505
interactions with mesons (ρ), spin-parity of 1320-Mev A_2 resonance in, (E/T), 19: 41368
interactions with mesons (π), partial-wave dispersion relations for mesons (ρ) bootstrap in, 19: 41394
interactions with mesons (π), dynamical calculation of inelasticity in, 19: 41403
interactions with mesons (ρ), OPE mechanism for meson (ω) production in, (T), 19: 43078
interactions with mesons (π), low-energy D-wave phase shifts for, (T), 19: 43090
interactions with mesons (π), N/D method for ρ channel in, 19: 43143
interactions with mesons (K) at low energy, dispersion relations for, (T), 19: 45085
interactions with mesons (π), perturbation theory for p-wave amplitudes in, 19: 45105
interactions with meson (π), dispersion theory for elastic low-energy, 19: 45127
interactions with mesons (π), isotopic structure and unitarity of, 19: 45051
interactions with mesons (π), mesons (ω), and nucleons, one-trajectory exchange for amplitudes of, (T), 19: 45074
interactions with mesons (π), Λ-Λ scattering length from meson (σ) resonance in, (T), 19: 47337
interactions with mesons (π), meson (σ) production in S-wave, (T), 19: 47347
interactions with mesons (ρ), nucleon isoscalar form factor from elastic, (T), 19: 47371
interactions with mesons (π), apparatus for studying, 17: 23656
interactions with mesons (π) and nucleons, application of Boundary

Condition Model to, 17: 24188
interactions with mesons(π), N/D calculation for Pomeranchuk and Regge trajectories for meson (ρ) exchange in, 17: 24319
interactions with mesons(π) in meson(K^+_{e4}) decay, 17: 24360
interactions with mesons (K) and (π), parity and spin from decay modes of resonance, 17: 26319
interactions with mesons (π) and nucleons, amplitudes for, 17: 28212
interactions with mesons(π), p- and s-wave amplitudes for, 17: 31073(R) (ANL-6719)
interactions with mesons (π) and protons, 17: 31091(R) (UCRL-10862)
interactions with mesons (π), unitary upper bound to cross section for, 17: 31359
interactions with mesons (K), properties of elastic, 17: 32951
interactions with mesons(π), asymptotic amplitudes of elastic, 17: 36607
interactions with mesons (π), possibility of experimental study of, 17: 36383 (ISS-63/30(p.55-67))
interactions with mesons (π), numerical solution of equations for, 17: 37932 (JINR-P-1284)
interactions with meson (π), 1250-Mev resonance, 17: 37939 (UCRL-10600)
interactions with mesons (π), effects on meson (π)-nucleon interactions, 17: 37975
interactions with mesons (π), analyticity of partial-wave amplitudes in, 17: 39854
interactions with mesons (K) in decays, coupling constant for, 17: 39914
interactions with mesons (K), self-consistency of K* resonance in, 17: 39937
interactions with mesons (K), s-wave phase shifts in, 17: 41753
interactions with mesons (K), K* production in, 17: 41812
interactions with mesons (π), dispersion relation examination of partial waves for, 17: 41814
interactions with mesons (π), resonance, 17: 41823
interactions with mesons (π), sum rules for, (T), 20: 1004
interactions with mesons (π), strip approximation for meson (ρ) trajectory in, (T), 20: 1012
interactions with mesons (π), field theory for amplitudes of meson (ρ) production in, 20: 1030
interactions with mesons (π) and protons, partially conserved axial vector current in, 20: 1066
interactions with mesons (π), phase shifts to 1.3 Bev for, (T), 20: 2708
interactions with mesons (π), field theory for S and D waves in, (T), 20: 4670
interactions with mesons (π), ρ and f⁰ resonances in, (T), 20: 4607
interactions with mesons (π), dispersion relation for I = 0 scattering length in, 20: 4617
interactions with mesons (π), off-the-mass-shell complete-unitarity equations for, 20: 6044
interactions with mesons (ω) at low energies, (T), 20: 6068
interactions with mesons (π), current commutation relations for, (T), 20: 6077
interactions with mesons (π), OBEC model of N-N scattering for (720) S-wave resonance in, 20: 7818
interactions with mesons (π) and nucleons, dispersion relations for, (T), 20: 7830
interactions with mesons (π), diffraction picture and N/D method for meson (ρ) production in, 20: 7907
interactions with mesons (π), phase shifts and Regge ghosts in, (T), 20: 9765
interactions with mesons (K) and (π), resonance production in, (E), 20: 11575
interactions with mesons (π) and nucleons, ABC anomaly for amplitudes of, (T), 20: 11604
interactions with mesons (π), model analysis for, (T), 20: 11637
interactions with mesons (π), relativistic calculation for three-body, (T), 20: 11639
interactions with mesons (π), resonance from relativistic three-body, (T), 20: 11640
interactions with mesons (π), relativistic spinless resonances in three-body, (T), 20: 11641
interactions with mesons (K), p- and s-wave phase shifts for, (T), 20: 11648
interactions with mesons (π), momentum-space calculation for meson (ρ) exchange in, (T), 20: 11653
interactions with mesons (K), meson (K_{e4}) decay for analysis of low-energy s-wave, (T), 20: 11654
interactions with mesons (π), amplitudes for, (T), 20: 11694
interactions with mesons (π), meson (ωρ) and resonance production in, (T), 20: 11568 (UCRL-11749)
interactions with mesons (K), iterative self-consistent solutions for S-wave, 20: 11601
interactions with mesons (K) and (π), cross section determination for, (T), 20: 13449 (JINR-P-2433)
interactions with mesons (π), two channel generation of mesons (ρ) in amplitude for, (T), 20: 13483
interactions with mesons (π), amplitudes for, (T), 20: 15518
interactions with mesons (π) and nucleons at low energies, dispersion theory of, 20: 15522
interactions with mesons (π), linear integral equations for low-energy, 20: 15351
interactions with mesons (ω), meson (B) exchange in, (T), 20: 15357
interactions with mesons (π), strip approximation for S-wave amplitudes for, (T), 20: 15358
interactions with mesons (π), strip approximation for amplitudes for, (T), 20: 15359
interactions with mesons (π), in meson (π⁻)-proton interactions at 378 Mev, (E), 20: 15368
interactions with mesons (π), analysis of meson (π)-gamma production in, 20: 15389
interactions with mesons (π) and nucleons, inelastic effects on cross sections for elastic, (T), 20: 17419
interactions with mesons (π) and nucleons, dynamical equations for, 20: 17420
interactions with mesons (K) at low energies, sum rules for, 20: 17470
interactions with mesons (π), l-dependence, singularities, and double-spectral function for, (T), 20: 17367
interactions with mesons (K), algebra of currents for, 20: 19541 (UR-875-121)
interactions with mesons (π) and nucleons at low energies, analysis using dispersion relations, (T), 20: 19522
interactions with mesons (π), exponential asymptotic behavior of amplitude for low-energy, (T), 20: 21645
interactions with mesons (π) in T = 0 state, cross sections for $K\bar{K}$ production in S-wave, 20: 21648
interactions with mesons (π), resonance properties of p-wave amplitudes for, (T), 20: 21694
interactions with mesons (π), isovector part of nucleon form factor from amplitudes for, (T), 20: 24056
interactions with mesons (π), resonances in, (T), 20: 24083
interactions with mesons (π), analyticity domain of amplitudes for, 20: 24125
interactions with mesons (π), correlation effect in two-meson (π)-exchange contribution from, (T), 20: 25842
interactions with mesons (π), variational calculation for p-wave, 20: 27819
interactions with mesons (π), analyticity in phase shift analysis of, 20: 27822
interactions with mesons (π), phase shifts and dispersion relations for forward, 20: 30017
interactions with mesons (ρ), sum rules for strong, 20: 30020
interactions with mesons (ρ), elastic unitarity in, (T), 20: 30077
interactions with mesons (π), OPE model for bootstrap for, 20: 30035
interactions with mesons (π), sum rules for, (T), 20: 31999
interactions with mesons (π), meson (ρ) and photon exchange in inelastic, (T), 20: 32011
interactions with mesons (π) in meson (K) decay, final-state, 20: 34154(R) (UCR-34P107-33)
interactions with mesons (K), K* resonance in, (T), 20: 34251
interactions with mesons(π) and nucleons, effects of ABC exchange on, (T), 20: 34225
interactions with mesons (K) and (π), equivalent-potential calculation of amplitudes in resonances region for, 20: 27854
interactions with mesons (π), T = 0, S-wave phase shift in, (T), 20: 36055
interactions with mesons (ω), reciprocal bootstrap of mesons (ρ) and (B) in, 20: 39807
interactions with mesons (π) at low energies, meson (K) pair production in, (T), 20: 39833
interactions with mesons (ρ) Adler-Weisberger sum rules for, 20: 39883
interactions with mesons (π) in meson (π⁻)-proton interactions at 276 Mev, (E), 20: 39779
interactions with mesons (π), P-wave meson (K) pair production cross section in T = 1 state, 20: 41823
interactions with mesons (π) at low energies, S-wave phase shifts for, 20: 41832
interactions with mesons (π), meson (ρ) exchange in, 20: 41837
interactions with mesons (π), analyticity domain of amplitude for, 20: 41841
interactions with mesons (π) from meson (π⁻)-proton interactions at 2.1 Bev/c, (E), 20: 41858
interactions with mesons (π), consistency conditions on strong, 20: 41861
interactions with mesons (π), quark model for ρππ vertex in, 20: 41876
interactions with mesons (K) and (π), one-meson theory for charge distribution from inelastic, 20: 44183
interactions with mesons (π), scattering lengths for, (T), 20: 44256
interactions with mesons (K), meson (μ*) polarization from resonances in,

(T), 20: 44270
interactions with nucleons, calculation of amplitude taking into account π–π interaction, 16: 973
interactions with nucleons, total cross sections, 16: 981
interactions with nucleons, phase shift calculations from one-dimensional representation, 16: 1000
interactions with nucleons to 10 Bev, multiple particle production in, 16: 2413(T) (JPRS-10727)
interactions with nucleons, coupling constant, 16: 3634
interactions with nucleons, dispersion relations, 16: 4707
interactions with nucleons, effective-target-mass model, 16: 4711
interactions with nucleons at 0.2 to 1.4 Bev, resonances, 16: 5879
interactions with nucleons, π-π interaction dominance in, 16: 5880
interactions with nucleons, relation to pion photoproduction on nucleons, 16: 5915
interactions with nucleons, dispersion relations for, 16: 6958
interactions with nucleons at high energies, characteristics, 16: 8052 (NP-11232(p.219-35))
interactions with nucleons, meson (π) production in, 16: 8108
interactions with nucleons at 5 Bev, nucleon structure model, 16: 8138
interactions with nucleons, hyperon and meson isobar production, 16: 8148
interactions with nucleons at Bev energies, isotopic spin relations in hyperon production, 16: 9432 (NP-11280)
interactions with nucleons, general unitarity application, 16: 9383
interactions with nucleons, scattering and single-pion production, 16: 10910
interactions with nucleons, branching ratios, 16: 10835
interactions with nucleons below 1 Bev, multiple meson (π) production in, 16: 10841
interactions with nucleons, partial-wave amplitudes in, 16: 12362
interactions with nucleons, isotopic spin relations, 16: 12382
interactions with nucleons at high energies, inelastic, 16: 12398
interactions with nucleons ($\pi + N \rightarrow N + \pi + \pi$) near threshold, amplitudes and cross sections, 16: 12399
interactions with nucleons, model for hyperon (Λ) production, 16: 12556
interactions with nucleons, chirality conservation, 16: 13891
interactions with nucleons, high-energy inelastic peripheral, 16: 13896
interactions with nucleons, effects of acnodes of Landau curves, 16: 13902
interactions with nucleons, meson (π) production at low energies, 16: 13904
interactions with nucleons, amplitudes in higher-resonance region, 16: 15539
interactions with nucleons, resonance properties, 16: 15551
interactions with nucleons, meson theory for, 16: 15373
interactions with nucleons, coincidence measurements from, 16: 17036
interactions with nucleons, phenomenological description, 16: 17052
interactions with nucleons at high energies, scattering amplitude analysis, 16: 17069 (JINR-D-922)
interactions with nucleons at high energies, nucleon Regge trajectories, from backscattering, 18: 881
interactions with nucleons in the c.m. energy plane, partial-wave dispersion relations for, 18: 886
interactions with nucleons, isotopic symmetry in, bootstrap requirement for, 18: 890
interactions with nucleons, self-consistent calculation of coupling constant in, 18: 912
interactions with nucleons, phase shifts at 0 to 350 Mev, 16: 16988 (NP-11592(Vol.I)(p.461))
interactions with nucleons at 400 to 1500 Mev, mechanisms, 16: 16989 (NP-11592(Vol.I)(p.467-83))
interactions with nucleons at 20 Bev, photon emission in, 16: 17014
interactions with nucleons, phase-space integral for 25-Bev collision, 16: 17020
interactions with nucleons at high energies, cross sections for elastic, 16: 18400
interactions with nucleons at low energies, π–π resonance effects on, 16: 18335
interactions with nucleons at 3 Bev, particle production in, 16: 18353
interactions with nucleons, isobar approximation of production processes in inelastic, 16: 19682
interactions with nucleons at 7.3 Bev, angular distributions, 16: 19692
interactions with nucleons to 100 Bev, effective target masses in, 16: 21271
interactions with nucleons, coupling constant for, 16: 22892
interactions with nucleons, partial-wave dispersion relations for, 16: 22916
interactions with nucleons, π–Λ resonance production from, 16: 22917
interactions with nucleons at high energies, elastic cross sections, 16: 24721
interactions with nucleons, regularization of equations for, 16: 26072 (JINR-P-891)
interactions with nucleons, 16: 26076 (JINR-P-938)
interactions with nucleons, form factors for, 16: 26089 (NP-11832)
interactions with nucleons, coupling constant for, 16: 26105
interactions with nucleons, vertex function in, 16: 26144
interactions with nucleons, complex angular momentum plane singularities in, 16: 26153
interactions with nucleons, amplitude relation to π-π amplitudes, 16: 26169
interactions with nucleons, meson (π) production in, 16: 26174
interactions with nucleons, polarization in, 16: 26191
interactions with nucleons in heavy nuclei, 16: 26340
interactions with nucleons, partial wave dispersion relations for amplitudes in, 16: 27910 (NP-11839)
interactions with nucleons with charge exchange, unsubtracted dispersion relation for, 16: 27946
interactions with nucleons at high energies, spectra from ultrarelativistic, 16: 27951
interactions with nucleons, coupling constants for, 16: 28327
interactions with nucleons below 1 Bev, production amplitudes and unitarity in, 16: 27996
interactions with nucleons, relation to scattering, 16: 29649 (NP-11950 (Vol.I)(p.113-72))
interactions with nucleons, static model for, 16: 29650 (NP-11950(Vol.I) (p.173-207))
interactions with nucleons at 500 to 1500 Mev, 16: 29652 (NP-11950 (Vol.I)(p.261-74))
interactions with nucleons, analyticity properties of scattering amplitudes in, 16: 29654 (NP-11950(Vol.II)(p.275-354))
interactions with nucleons and photons, Mandelstam representation for, 16: 29655 (NP-11950(Vol.II)(p.355-424))
interactions with nucleons, dispersion relations in, 16: 29675
interactions with nucleons, form factors for, 16: 29694
interactions with nucleons, resonances in, 16: 31044
interactions with nucleons at medium energies, amplitudes for, 16: 32313
interactions with nucleons, isobaric model for, 16: 32305
interactions with nucleons at 2 to 20 Bev/c, elastic cross sections, 16: 31047
interactions with nucleons, effects of 2π vector mesons on, 16: 32316
interactions with nucleons, effects of π-π resonances on, 16: 32330
interactions with nucleons and photons, resonance effects on, 16: 32334
interactions with nucleons, strange-particle production in, 16: 33737
interactions with nucleons, cross sections for, 16: 32343
interactions with nucleons, optical model for resonance, 18: 897
interactions with nucleons at 7.5 Bev/c, separation of peripheral and and central collisions in, 18: 2596
interactions with nucleons, relativistically invariant partial-wave analysis of, 18: 2613
interactions with nucleons at low energies, coupling constant and P-wave phase shifts in, 18: 6029
interactions with nucleons at high energies, description by fermion Regge poles, 18: 6040
interactions with nucleons, use in analysis of meson (π) photoproduction, 18: 6044
interactions with nucleons, model for meson (ρ) and N* exchange in, 18: 6028
interactions with nucleons at 3 Bev, information theory for multiple particle production in, 18: 7498
interactions with nucleons, zero momentum-transfer dispersion relations for elastic, 18: 7522
interactions with nucleons, quantum numbers of resonance states in, 18: 7540
interactions with nucleons, ($\frac{1}{2}$,$\frac{1}{2}$) resonance effect and two-pion-exchange process in, 18: 7549
interactions with nucleons in hyperon (Λ) decay, diagonalization for mixture, 18: 7550
interactions with nucleons at 15–600 Mev, interpolative formulas for phase shifts in, 18: 7557
interactions with nucleons, energy-momentum transfers in inelastic, 18: 9113
interactions with nucleons, one-meson (π)-exchange model for, 18: 9114
interactions with nucleons, N* Regge pole and (3,3) phase shifts in, 18: 9168
interactions with nucleons, variational technique for partial-wave dispersion relations for, 18: 9176
interactions with nucleons, interpretations of N_{33} resonance in, 18: 9193
interactions with nuclear Coulomb field, meson (ω^0) and (ρ^0) production in, 18: 9169
interactions with nucleons, forward amplitude zeroes for, 18: 841 (JINR-P-1336)
interactions with nucleons, baryon emission in, 18: 10850 (JINR-P-1469)
interactions with nucleons, zeros in forward amplitude of, 18: 10888
interactions with nucleons, partial amplitudes for, 18: 12911 (PAN-451/VII)

interactions with nucleons, singularities in final-state interactions in, 18: 12941
interactions with nucleons, study of internucleon potentials from, 18: 15291
interactions with nucleons, meson (ρ)-nucleon coupling in, 18: 14801 (CONF-22-32)
interactions with nucleons, crossing relations for helicity amplitudes for, 18: 14825
interactions with nucleons, secondary diffraction peak in elastic, 18: 14896
interactions with nucleons, Regge pole hypothesis in, 18: 14932
interactions with nucleons at 0 to 700 Mev, inelastic effects in, 18: 14939
interactions with nucleons, phenomenological phase shift fit for, 18: 16953(R) (TID-20352)
interactions with nucleons at low energies, ($\frac{3}{2}$, $\frac{3}{2}$) resonances in, 18: 16777
interactions with nucleons at high energies, Regge pole formalism for, 18: 16779
interactions with nucleons at low energies, meson (ρ) effects on, 18: 16781
interactions with nucleons, 556-Mev p_{11} resonance, 18: 16791
interactions with nucleons at high energies, inelastic, 18: 18639 (JINR-P-1524)
interactions with nucleons, isotopic splitting of spin state in, 18: 18690
interactions with nucleons, detection of final state in, 18: 20401
interactions with nucleons, S-wave scattering lengths using N/D method for, 18: 20937
interactions with nucleons, nucleon Regge trajectories from, 18: 20940
interactions with nucleons, coupling constant on Regge trajectory for, 18: 20948
interactions with nucleons at 170 to 600 Mev, model for single meson (π) production in, 18: 20964
interactions with nucleons, Regge poles in, 18: 20988
interactions with nucleons, resonances in, 18: 21004
interactions with nucleons, resonances in, 18: 21005
interactions with nucleons, detection of final state in, 18: 20401
interactions with nucleons at low energies, analysis of, 18: 22727 (NP-13860)
interactions with nucleons, hyperon decay in, 18: 22770
interactions with nucleons at low energies, amplitudes for, 18: 22778
interactions with nucleons, second resonance in elastic, 18: 22779
interactions with nucleons, single-meson exchange in, 18: 24477
interactions with nucleons, coupling constants for, 18: 24423
interactions with nucleons, mechanisms of low-energy, 18: 24474
interactions with nucleons in shell model, constants and coupling in, 18: 24414
interactions with nucleons, production processes in, 18: 26281
interactions with nucleons, models for elastic, 18: 26281
interactions with nucleons at low energies, equations for, 18: 26299
interactions with nucleons, mesons (ρ) in, 18: 26348
interactions with nucleons, resonance effects in, 18: 26352
interactions with nucleons, meson (ω) production in, 18: 28328 (TID-20717)
interactions with nucleons, bootstrap equations for static model of resonance, 18: 28352
interactions with nucleons, diagrams for resonance, 18: 28357
interactions with nucleons, coupling constants for, 18: 28359
interactions with nucleons, meson (ρ) effects on phase shifts in, 18: 28368
interactions with nucleons, field theory model for, 18: 28456
interactions with nucleons below 1 Bev, final-state interaction model for single-meson(π) production in, 18: 30527 (TID-20773)
interactions with nucleons, phase shifts for, 18: 30593
interactions with nucleons, vector meson exchange model for, 18: 30596
interactions with nucleons, Chew-Low's method for $\pi + N \rightarrow N + 2\pi$, 18: 30612
interactions with nucleons, B resonance in, 18: 32550
interactions with nucleons, determination of coupling constant for, 18: 32562
interactions with nucleons, reciprocal bootstrap mechanism in resonance, 18: 32568
interactions with nucleons, one-nucleon exchange in, 18: 32600
interactions with nucleons, bound states in, 18: 32623
interactions with nucleons, meson (ϕ) production in, 18: 32664
interactions with nucleons at low energy, phase shifts for, 18: 32575
interactions with nucleons, relativistic corrections to s- and p-wave, 18: 34507 (JINR-E-1686)
interactions with nucleons, secondary-particle production in, 18: 34509 (NP-14086)
interactions with nucleons, complex singularities in amplitude for, 18: 34524
interactions with nucleons, maximum coupling constant for, 18: 34548
interactions with nucleons below 500 Mev, analysis of, 18: 34604
interactions with nucleons, meson (P^1) contribution to, 18: 34611
interactions with nucleons at low energies, phase shifts in, 18: 34621
interactions with nucleons, mesons (ω^0) and (ρ) production in, 18: 34622
interactions with nucleons, threshold effects for meson (ρ) production in, 18: 36263
interactions with nucleons, model for nonlocal, 18: 36264
interactions with nucleons, amplitude for, 18: 36290
interactions with nucleons, theory for three-body, 18: 36320
interactions with nucleons, model for strong, 18: 37890
interactions with nucleons, strong coupling meson theory for resonances in, 18: 37930
interactions with nucleons at low energies, p-wave resonances in, 18: 37952
interactions with nucleons, meson (π-π) contribution to, 18: 37964
interactions with nucleons, 18: 37977
interactions with nucleons, asymptotic cross sections for, 18: 37983
interactions with nucleons, 18: 37987
interactions with nucleons, decay of N^*, 18: 40258
interactions with nucleons, selection rules and W, symmetry for, 18: 40319
interactions with nucleons, meson (π) production in, 18: 40361
interactions with nucleons at high energies, theory of, 18: 40372
interactions with nucleons, resonance N^* production in, 18: 40240 (UCRL-11423)
interactions with nucleons, criteria for bound state in, 18: 42457
interactions with nucleons above 1 Bev/c, 18: 42366 (JINR-E-1802)
interactions with nucleons at 0 to 700 Mev, phase-shift analysis of, 18: 42378 (UCRL-7846)
interactions with nucleons, phase shifts in, 18: 42408
interactions with nucleons, models for resonances in, 18: 42412
interactions with nucleons, asymptotic parameters for, 18: 42426
interactions with nucleons at 1 to 6 Bev, resonances in, 18: 42430
interactions with nucleons, separation of variables in, 18: 42437
interactions with nucleons, effects of meson (ρ) production on amplitudes for, 18: 42439
interactions with nucleons, theory of, 18: 42627(R) (ANL-6879(p.88-113))
interactions with nucleons, resonance poles in Lee model for, 18: 44557
interactions with nucleons, secondary diffraction peaks in, 18: 44562
interactions with nucleons above 20 Bev, forward amplitudes for, 18: 44599
interactions with nucleons, scattering model for (T), 19: 1379
interactions with nucleons, thresholds for N^*_{33}, resonance in (T), 19: 1236 (UCRL-11622)
interactions with nucleons, phase shift analysis of (E/T), 19: 1369
interactions with nucleons, resonance, (T), 19: 1368
interactions with nucleons at 0.8 to 10 Bev, statistical model calculations for, 19: 3028 (ORNL-3713)
interactions with nucleons, one-virtual-meson one-meson-exchange effects in (T), 19: 3035
interactions with nucleons at 5 Bev/c, meson-exchange study of particle production in (T), 19: 3048
interactions with nucleons, N^* isobar and meson (ρ) effects on (T), 19: 3076
interactions with nucleons, statistical model calculations of distributions from, 19: 4900 (ORNL-3716)
interactions with nucleons at 600 to 900 Mev, (E), 19: 5572(R) (PPAD-525-D)
interactions with nucleons below 1 Bev, (E/T), 19: 4892 (JINR-P-1785)
interactions with nucleons to 1 Bev, (T), 19: 4893 (JINR-P-1788)
interactions with nucleons above 1 Bev, (T), 19: 4895 (JINR-P-1792)
interactions with nucleons, self-consistency in, (T), 19: 4913
interactions with nucleons near 1500 Mev, model for resonance, 19: 4952
interactions with nucleons at high energies, (T), 19: 4956
interactions with nucleons, coupling constants for, (T), 19: 4957
interactions with nucleons to 700 Mev, P_{33} state in, (T), 19: 4961
interactions with nucleons, selection rule for strange particle production in, (T), 19: 4971
interactions with nucleons, phase-shift analyses and dispersion relations for, (T), 19: 4997
interactions with nucleons, local field theory of, (T), 19: 5016 (JINR-P-1793)
interactions with nucleons in nuclei, (T), 19: 6528
interactions with nucleons, A-invariance in, (T), 19: 6543
interactions with nucleons, self-consistent calculations of, (T), 19: 6549
interactions with nucleons, vertex functions for, (T), 19: 6550
interactions with nucleons at high energies, models for, (T), 19: 6551
interactions with nucleous at low energy, un-Reggeized strip approximation for, (T), 19: 8160
interactions with nucleons, meson (η) production in, (T), 19: 8182
interactions with nucleons, ρ-exchange model for N^* production in, (T), 19: 8206
interactions with nucleons, N^*_{11} (1400) production in, (T), 19: 8209

interactions with nucleons, dispersion method for, (T), 19: 8225
interactions with nucleons in Lagrangian field theories, spectral functions for, (T), 19: 8289
interactions with nucleons, distributions from inelastic, (E/T), 19: 10014 (IFA-HE/54)
interactions with nucleons, Lorentz-covariant Low equation for, (T), 19: 10031
interactions with nucleons, Regge pole method for, (T), 19: 10035
interactions with nucleons and photons, form factors from, (T), 19: 12187
interactions with nucleons, 1400-Mev resonance in, (T), 19: 12198
interactions with nucleons, absorption in final-state, (T), 19: 12205
interactions with nucleons at high energies, inelastic peripheral, (T), 19: 12250
interactions with nucleons, polarization effects on single isobar production in, (T), 19: 12262
interactions with nucleons at high energy, Regge poles for backscattering in, (T), 19: 12305
interactions with nucleons at 12 and 18 Bev/c, dibosons from, (E), 19: 14405 (TID-21409)
interactions with nucleons, hard photon emission mechanism for, (T), 19: 14317 (JINR-P-1896)
interactions with nucleons at low energy, resonances in, (T), 19: 14337
interactions with nucleons, meson (K) pair production in, (T), 19: 14354
interactions with nucleons, phase shift analysis of, (T), 19: 16482 (UCRL-11849)
interactions with nucleons, statistical model calculations of, 19: 17159(R) (ORNL-3714(Vol.II)(p.97-118))
interactions with nucleons, small momentum transfer in inelastic, (T), 19: 16487
interactions with nucleons, p-wave dispersion relation for, (T), 19: 16623
interactions with nucleons at high energies, inelastic, (T), 19: 16646
interactions with nucleons, $N_{\frac{5}{2}}^{*}$ production in, (T), 19: 16686
interactions with nucleons at high energies, cross sections and Regge poles for, (T), 19: 18790
interactions with nucleons, coupling constants for, (T), 19: 18817
interactions with nucleons, physical sum rules on real part of amplitude for, (T), 19: 18852
interactions with nucleons at 0 to 800 Mev, energy-dependent phase shift analysis of, (T), 19: 18870
interactions with nucleons at high energies, total cross sections for, (T), 19: 18877
interactions with nucleons, (3,3) partial-wave amplitude in, (T), 19: 18907
interactions with nucleons, dispersion relations for, (T), 19: 18915
interactions with nucleons, parameters for, (T), 19: 20937(R) (TID-21672)
interactions with nucleons, production of massive neutral gauge particle, (T), 19: 20989
interactions with nucleons, position and width of N* (1688) in, (T), 19: 20992
interactions with nucleous, $N_{\frac{3}{2}}^{*}$ resonance in, (T), 19: 21000
interactions with nucleons, phase of forward amplitudes for, (T), 19: 21010
interactions with nucleons, selection rules for final states in, (T), 19: 21023
interactions with nucleons, complex angular momentum in, (T), 19: 21048
interactions with nucleons, Jacob-Wick method for scattering amplitude in, (T), 19: 21052
interactions with nucleons at high energies, Regge trajectories for, (T), 19: 21063
interactions with nucleons, kinematic analysis of, 19: 21076
interactions with nucleons, Regge trajectories in, 19: 21077
interactions with nucleons, numerical solution of integral equation for, 19: 20445
interactions with nucleons, absorptive corrections to one-meson-exchange model for, 19: 23441
interactions with nucleons, OBEC model for phase shift analysis of low-energy, 19: 23460
interactions with nucleons at low energy, vertices in (πN) and ($\bar{N}$D), (T), 19: 23468
interactions with nucleons, quantum numbers of isobars in, (T), 19: 23368
interactions with nucleons, amplitudes of production processes in, (T), 19: 23388
interactions with nucleons at resonance energies, phase shifts in, (T), 19: 23396
interactions with nucleons at 650 Mev, short-range, (T), 19: 23411
interactions with nucleons, effects of meson (π) interactions on amplitudes for, (T), 19: 25276
interactions with nucleons, spin structure of five-point amplitudes in, (T), 19: 25282
interactions with nucleons, meson (π) production in, (T), 19: 25301
interactions with nucleons, effective target mass in, (T), 19: 25308
interactions with nucleons, spin propagators in, (T), 19: 25309
interactions with nucleons at 0 to 350 Mev, phase-shift analysis of, (T), 19: 25352
interactions with nucleons at 300 Mev, design of experiments on elastic, 19: 27159 (LA-3126)
interactions with nucleons, Chew-Low equations and phases in, (T), 19: 27144 (JINR-P-1964)
interactions with nucleons at high energy, pole diagrams for, (T), 19: 27147 (JINR-P-1979)
interactions with nucleons at very high energies, 19: 27182
interactions with nucleons, analytic continuation of amplitudes for, (T), 19: 27212
interactions with nucleons, coupling constants for, (T), 19: 27222
interactions with nucleons, internal symmetries in bootstrap dispersion relations for, (T), 19: 27233
interactions with nucleons, inelastic unitarity contributions to scattering length in, (T), 19: 27238
interactions with nucleons, meson (K) and (ρ) coupling constants from, (T), 19: 27281
interactions with nucleons in nuclei, (T), 19: 29306
interactions with nucleons, coupling constants for, (T), 19: 29072 (NP-15014)
interactions with nucleons, meson (ρ) production in, (T), 19: 29091
interactions with nucleons, coupling constants for, (T), 19: 31041
interactions with nucleons, K-matrix model of peripheral, (T), 19: 31043
interactions with nucleons, peripheral model for meson (ρ) production in, 19: 31002 (CONF-550-97)
interactions with nucleons, meson (π) final-state interactions in, (T), 19: 31008 (LA-3171)
interactions with nucleons, coupling constants for, (T), 19: 31014 (UCRL-7942)
interactions with nucleons, Regge dynamics in, (T), 19: 31016 (UCRL-16115)
interactions with nucleons, microscopic non-causality in, (T), 19: 32949 (LADC-6480)
interactions with nucleons, multichannel approach to high-energy peripheral, (T), 19: 33016
interactions with nucleons, hyperon production in, (T), 19: 33064
interactions with nucleons at 7 to 20 Bev, inelastic, 19: 34909
interactions with nucleons, Monte-Carlo method for inelastic, 19: 35028 (JINR-P-2140)
interactions with nucleons, meson (ω) production via meson (ρ) exchange in, (T), 19: 35072
interactions with nucleons, J = ½, T = ½ phase shifts in, (T), 19: 35091
interactions with nucleons, p-wave amplitude effects on bootstrap calculations of, (T), 19: 35124
interactions with nucleons, three-body forces in, (T), 19: 35145
interactions with nucleons at 2 to 3 Bev/c, peripheral production and resonance decay in, (T), 19: 35152
interactions with nucleons, internal invariance and symmetry groups for, 19: 35039
interactions with nucleons, algebraic equations for, 19: 35050
interactions with nucleons at 300 to 700 Mev, phase-shift analyses of, 19: 37546 (UCRL-12383)
interactions with nucleons at 20 to 340 Mev, phase-shift analysis of elastic, (T), 19: 37584
interactions with nucleons, resonances in three-particle production, (T), 19: 37649
interactions with nucleons at high energy, Regge-pole hypothesis in asymptotic amplitudes for, 19: 39478 (NP-15210)
interactions with nucleons, peripheral production and decay of mesons (ρ) in, (E/T), 19: 39576
interactions with nucleons at high energies, analyses of final-state, (E/T), 19: 39574
interactions with nucleons, reciprocal bootstrap in, (T), 19: 41422
interactions with nucleons at high energies, Regge-pole model for, (T), 19: 41426
interactions with nucleons at low energies, (T), 19: 41498
interactions with nucleons below 1 Bev, single meson (π) production in, (T), 19: 41509
interactions with nucleons at high energies, optical model for backward, (T), 19: 41332 (JINR-P-2220)
interactions with nucleons, effects on nucleon–nucleon interactions at 300 Bev, (T), 19: 41358
interactions with nucleons, one-particle-exchange models for, (T), 19: 41375
interactions with nucleons, meson (ρ^0) and meson (ω_8) effects in, (T), 19: 41380
interactions with nucleons, form factors from, (T), 19: 41385
interactions with nucleons, absorptive corrections and form factors in peripheral model for (Nρ), 19: 41400
interactions with nucleons, SU(3) symmetry for N$\pi\pi$ state in, 19: 43082
interactions with nucleons, meson (η) production in, (E/T), 19: 43114

interactions with nucleons, N/D method for J = 5/2, T = 3/2 phase shifts in, (T), 19: 43081
interactions with nucleons at high energy, nucleon structure in, (T), 19: 43103
interactions with nucleons at high energy, real part of forward scattering amplitude for, (T), 19: 43117
interactions with nucleons, mechanism for T = 1/2 and 3/2 recurrences in, 19: 43137
interactions with nucleons, theory of N$^*_{\frac{3}{2}}$, and Y$^*_1$ production in, 19: 43144
interactions with nucleons at high energies, polarization and Regge poles in, (T), 19: 45044 (UCRL-16186)
interactions with nucleons at high energy, absorption model for charge-exchange, (T), 19: 45087
interactions with nucleons at high energy, multiple production in elastic, (T), 19: 45091
interactions with nucleons below 1 Bev, phase shift analysis of, (T), 19: 45100
interactions with nucleons, form factors from off-shell effects in, (T), 19: 45067
interactions with nucleons, resonance in static, (T), 19: 47298 (AD-613934)
interactions with nuclears, model for P_{11}-state strong, 19: 47350
interactions with nucleons, restriction on forward amplitudes of, (T), 19: 47375
interactions with nucleons, fixed-variable dispersion relations for, (T), 19: 47388
interactions with nucleons, calculation using Regge trajectory, 19: 47395
interactions with nucleons, meson (η) production in, (T), 19: 47401
interactions with nucleons, analysis of data for, 19: 47404
interactions with nucleons, prediction of meson (π)–meson (π) phase shifts from, 17: 769
interactions with nucleons, I = 1/2, J = 1/2 state in, 17: 771
interactions with nucleons, meson (π) production in, 17: 781
interactions with nucleons, dispersion relations for elastic, 17: 2163 (JINR-P-1043)
interactions with nucleons, multiple production of mesons (π) in, 17: 2187
interactions with nucleons, effects on nuclear forces, 17: 2280
interactions with nucleons, resonances in, 17: 5268
interactions with nucleons, production of mesons (α) in, 17: 5276
interactions with nucleons, spin rotation effects in, 17: 6985
interactions with nucleons, dispersion relations in, 17: 7010
interactions with nucleons, effect of π-π interaction on s and p waves of, 17: 7024
interactions with nucleons, interaction constant for, 17: 7027
interactions with nucleons, gauge groups and symmetries of the isospace associated with nonrelativistic rotator, 17: 6970
interactions with nucleons, dispersion-theoretical approach to diffraction, 17: 9202 (PAN-359/VII)
interactions with nucleons, production of slow mesons (π) in, 17: 9289
interactions with nucleons, phase shift calculations for, 17: 9335
interactions with nucleons, γ_5 invariance in, 17: 9338
interactions with nucleons, meson (π-π) interactions in, 17: 9339
interactions with nucleons, analysis of, 17: 9409
interactions with nucleons, Regge pole applications to, 17: 9414
interactions with nucleons, review, 17: 9461
interactions with nucleons, review of data on, 17: 9474
interactions with nucleons, differential cross sections for mesons(π) production by, 17: 11476 (JINR-P-1111)
interactions with nucleons, two-pion exchange terms in, for states T = 0 and T = 1, 17: 11544
interactions with nucleons, Regge poles in, 17: 11546
interactions with nucleons, effects on nucleon properties, 17: 11558
interactions with nucleons, effect of meson (π-π) resonance in, 17: 11578
interactions with nucleons at high energies, target mass in, 17: 13121
interactions with nucleons, review of theories of, 17: 13126
interactions with nucleons, cross sections for antinucleon production in, 17: 13345 (JINR-P-1132)
interactions with nucleons, dispersion relations for, 17: 13377
interactions with nucleons, effects of (π-π) resonances on low-energy, 17: 13385
interactions with nucleons at 25 Bev, elastic-inelastic ratio for, 17: 13389
interactions with nucleons, gauge invariance in isobaric model for, 17: 13396
interactions with nucleons, relativistic effects in low-energy, 17: 15120
interactions with nucleons, resonances in, 17: 15139
interactions with nucleons, calculation of, 17: 17123(R) (TID-18127)
interactions with nucleons, hyperon and meson (K) production in, 17: 16953 (JINR-P-1163)
interactions with nucleons, analyticity and unitarity conditions in, 17: 16955 (NYO-10238)
interactions with nucleons, chirality and structure of, 17: 16989
interactions with nucleons, Regge-pole analysis of, 17: 17038
interactions with nucleons, angular distribution of particles produced near threshold in, 17: 17098
interactions with nucleons, amplitudes for, 17: 19133
interactions with nucleons, theory of J = 3/2, I = 3/2 resonance, 17: 19138
interactions with nucleons, empirical systematics of, 17: 19151
interactions with nucleons, resonance effects on, 17: 19154
interactions with nucleons, distributions from, 17: 19169
interactions with nucleons, model for higher resonances in, 17: 19539
interactions with nucleons, model for large-angle elastic, 17: 19091
interactions with nucleons, dispersion theory of diffraction, 17: 19077
interactions with nucleons, meson (π-π) interaction effects on partial waves of, 17: 20839 (JINR-E-1189)
interactions with nucleons, coupling constants for, 17: 20847 (JINR-P-1207)
interactions with nucleons, effect of S-wave (π-π) interaction on, 17: 20872
interactions with nucleons, effects of π-π interactions on, 17: 20879
interactions with nucleons, coupling constants for, 17: 20883
interactions with nucleons, partial wave dispersion relations for, 17: 20948
interactions with nucleons, asymptotic properties and zeros of forward scattering amplitude in, 17: 20852
interactions with nucleons, cross sectional energy dependence and momentum transfer in, 17: 22435 (NP-12730)
interactions with nucleons at 7 Bev, particle generation in, 17: 22444
interactions with nucleons, forward scattering amplitudes in, 17: 22496
interactions with nucleons, domains of analyticity for, 17: 22504
interactions with nucleons at 2 to 28 Bev, 17: 22505
interactions with nucleons in octet boson–octet fermion model, amplitudes for, 17: 24354
interactions with nucleons, charge independence in, 17: 24514
interactions with nucleons, spinor Regge pole exchange in, 17: 26320
interactions with nucleons, inner Coulomb corrections to phase shifts in, 17: 26324
interactions with nucleons at high energies, fermion Regge pole analysis of cross section and polarization in, 17: 26331
interactions with nucleons, overlapping resonances in final state of, 17: 26353
interactions with nucleons, model for single π production in, 17: 26359
interactions with nucleons, asymptotic relations for cross sections of, 17: 28218
interactions with nucleons, parity and spin of 2190-Mev resonance, 17: 29505 (UCRL-10894)
interactions with nucleons, resonance properties of, 17: 29506
interactions with nucleons, coupling constant for, 17: 29521
interactions with nucleons, energy jets in, 17: 29522
interactions with nucleons in isobar decay, Q values for, 17: 29531
interactions with nucleons at 2 Bev, meson (f^0) effects in, 17: 29532
interactions with nucleons, Regge trajectories in, 17: 29551
interactions with nucleons in the boundary-condition model, inelastic effects on S waves in, 17: 31334
interactions with nucleons, chirality conservation and soft-meson (π) production in, 17: 31353
interactions with nucleons, method for analyzing, 17: 31366
interactions with nucleons, generalization of Minami ambiguity for, 17: 31375
interactions with nucleons, analyticity regions of Feynman integrals in, 17: 31379
interactions with nucleons at 10^{13} ev, effective target mass for, 17: 31380
interactions with nucleons, partial wave amplitudes for, 17: 32899 (CONF-46-80)
interactions with nucleons at ≤ 3 Bev, strange particle production cross sections in, 17: 32920
interactions with nucleons at low energy, S-wave dispersion relation in, 17: 32949
interactions with nucleons, unitarity in, 17: 34726 (ISS-63/34)
interactions with nucleons at low energies, meson (π) production effect in, 17: 34746
interactions with nucleons, resonance-state production effects on polarization in, 17: 34747
interactions with nucleons following proton-proton quasielastic scattering at high energies, 17: 34782
interactions with nucleons, coupling constant for, 17: 34798
interactions with nucleons at intermediate energies, resonance production in, 17: 36571 (EFINS-62-61)
interactions with nucleons, resonances in, 17: 36582 (TID-19336)
interactions with nucleons, meson (π-π) interaction contribution to, 17: 37975
interactions with nucleons, resonances in, 17: 37980

interactions with nucleons, dispersion relations for $\pi + N \to \pi + \pi + N$, 17: 37988
interactions with nucleons, modified phase shift analysis of, 17: 39845 (NP-13114)
interactions with nucleons, formulation of Chew-Low theory for, 17: 41748
interactions with nucleons, 17: 41819
interactions with nucleons in emulsions at 7.5 Bev, inelastic, 17: 41823
interactions with nucleons, fermion Regge poles and polarization phenomena in, 17: 41828
interactions with nucleons, meson (π) interaction effects on invariant amplitude in, 17: 41803
interactions with nucleons, Riemann-Cauchy relations in theory of, 17: 11571
interactions with nucleons at 0 to 20 Bev, data review for, 20: 2725
interactions with nucleons, amplitude of vector meson production in, (T), 20: 4584 (JINR-P-2380)
interactions with nucleons, three-channel N/D equations in pole approximation for, 20: 4593
interactions with nucleons, Dashen-Lee sum rules for intermediate state in, (T), 20: 4598
interactions with nucleons, single and double resonance production in, (T), 20: 6069
interactions with nucleons, calculation of higher resonance energies in, 20: 6096
interactions with nucleons, solutions of Chew-Low equations for, 20: 6106 (JINR-P-2369)
interactions with nucleons in emulsion, intranuclear cascades from, (E/T), 20: 6287 (JINR-P-2373)
interactions with nucleons, analytic continuation of Froissart-Gribov amplitude for, 20: 7817
interactions with nucleons, generated unitarity relations for amplitudes of of multichannel, (T), 20: 7837
interactions with nucleons at low energy, mass of N_{33} from, (T), 20: 7851
interactions with nucleons, generated unitarity relations for amplitudes of multichannel, (T), 20: 7837
interactions with nucleons, sum rule for coupling constant for, (T), 20: 9791 (IC/65/91)
interactions with nucleons, regularization of Chew-Low equations for amplitude of, (T), 20: 9717
interactions with nucleons at high energies, model for elastic and charge-exchange, (T), 20: 9739
interactions with nucleons at 290 to 905 Mev, cross sections for N* production in, (T), 20: 11562 (JINR-P-2454)
interactions with nucleons, self-consistency conditions for πNN-vertex function in, (T), 20: 11576
interactions with nucleons, triangle graphs for three-particle production in, (T), 20: 11596
interactions with nucleons, meson (ϕ)-nucleon coupling in, (T), 20: 11598
interactions with nucleons, Regge poles for, (T), 20: 11647
interactions with nucleons, self-consistent methods for vertex functions for, (T), 20: 11730
interactions with nucleons, N/D calculation with inelastic unitarity for, (T), 20: 11643
interactions with nucleons in Bev range, partial-wave analysis of, (T) 20: 13513
interactions with nucleons up to 500 Mev, quasipotential method for, (T), 20: 13467
interactions with nucleons, phase-space volumes for, (T), 20: 13481
interactions with nucleons, scattering matrix for, (T), 20: 13448 (JINR-E-2521)
interactions with nucleons, amplitudes for, (T), 20: 15312 (MIT-2098-86)
interactions with nucleons, rescattering correction for three-body final-state, 20: 15476
interactions with nucleons, pseudoscalar and scalar, (T), 20: 15325
interactions with nucleons, nucleon mass and coupling constant for, 20: 15352
interactions with nucleons, meson (ρ) exchange in, 20: 15364
interactions with nucleons, review of, 20: 15371
interactions with nucleons, dispersion relations for low-energy, (T), 20: 15385
interactions with nucleons, $\bar{U}(12)$ symmetry for, 20: 15390
interactions with nucleons at 1.68 Bev/c, $Y_0^*(1405)$ and $Y_1^*(1358)$ production in, (E), 20: 15404
interactions with nucleons, high-energy successive field, (T), 20: 17418
interactions with nucleons, coupling constants for, (T), 20: 17336 (AECD/TP-5)
interactions with nucleons, inelastic effects on P_{11} phase shift in, (T), 20: 17355
interactions with nucleons at high energies, optical model for backward, (T), 20: 17373
interactions with nucleons, effect of dipion resonances on amplitude for, (T), 20: 17388
interactions with nucleons, minimal singularity in axiomatic approach to charge-symmetry, (T), 20: 17416
interactions with nucleons, coupled-channel Schroedinger equation model for, 20: 17397
interactions with neutrons at 1.7 Bev/c, products from, (E/T), 19273(R) (BNL-929, pp 3-43)
interactions with nucleons at 300 to 700 Mev, absorption parameters and phase shifts for, (T), 20: 19481
interactions with nucleons, dynamics with invariant collinear vertices, analyticity, and unitarity for low-energy strong, (T), 20: 19491
interactions with nucleons, SU(3) symmetry in bootstrap model for, 20: 19564
interactions with nucleons, absorption model for 2^+-meson production in, 20: 21644
interactions with nucleons, threshold factor in p-wave dispersion relations for, 20: 21667
interactions with nucleons, p-wave amplitudes for off-shell, 20: 21672
interactions with nucleons, mass splittings from, 20: 21758
interactions with nucleons, Lee algebra for isobar-coupling, 20: 21759
interactions with nucleons, Fourier-Bessel representation for helicity amplitudes of, (T), 20: 24031
interactions with nucleons, electromagnetic corrections to low-energy, (T), 20: 24040
interactions with nucleons at high energies, minimum in differential cross sections of, (T), 20: 24048
interactions with nucleons, pole model of resonance production in, (T), 20: 24079
interactions with nucleons, phase-shift analysis of, (E/T), 20: 24087
interactions with nucleons, dispersion analysis of elastic, (E/T), 20: 25785 (JINR-P-2582)
interactions with nucleons, high-energy behavior of charge-exchange forward amplitude for, 20: 25825
interactions with nucleons, multiple meson (π) production in, (T), 20: 25839
interactions with nucleons, parity conservation in, (T), 20: 25841
interactions with nucleons in SU(4) spin-isospin symmetry, 20: 25876
interactions with nucleons, semiclassical peripheral model for, 20: 25877
interactions with nucleons, sum rules of chiral algebra for N*Nπ coupling constants in, 20: 27999
interactions with nucleons at 1 to 10 Bev, phase-space factors for, 20: 27808
interactions with nucleons, resonant amplitudes from elastic and inelastic, (T), 20: 27821
interactions with nucleons, P_{33} amplitude for, (T), 20: 27831
interactions with nucleons below 1 Bev, model for single meson (π) production from, 20: 27861
interactions with nucleons, differential cross sections and structures of, (T), 20: 27874
interactions with nucleons at low energies, dispersion relations for s-wave, (T), 20: 27881
interactions with nucleons, p-wave dispersion relations for, (T), 20: 30073
interactions with nucleons, N/D calculations of p-wave amplitudes for, (T), 20: 30158
interactions with nucleons, amplitudes for, (T), 20: 29986 (CONF-640509(Pt.1), Paper 2)
interactions with nucleons, amplitudes for, 20: 30006
interactions with nucleons, production and properties of mesons A_1 and A_2 from, (E/T), 20: 30023
interactions with nucleons, zero-effective-range analysis for meson (η^0) production in, 20: 30033
interactions with nucleons, inelastic unitarity in eigenstates of total angular momentum for, 20: 32014
interactions with nucleons, boundary condition model for P_{33} resonance in, 20: 32023
interactions with nucleons at high energies, forward dispersion relations for, 20: 32026
interactions with nucleons, asymptotic behavior of amplitudes for elastic, (T), 20: 32032
interactions with nucleons, amplitudes for $N_{\frac{1}{2}}^*$ and $N_{\frac{3}{2}}^*$ production in, (T), 20: 32091
interactions with nucleons, Mandelstam representation and elastic unitarity for amplitudes of, 20: 32095
interactions with nucleons at high energies, ρ Regge residues in charge-exchange, 20: 34154(R) (UCR-34P107-33)
interactions with nucleons at high energies, I = 0 D-wave $\pi\pi$ resonance in, 20: 34154(R) (UCR-34P107-33)
interactions with nucleons, cross sections for quark production in, 20: 34193
interactions with nucleons, Regge-pole model for charge-exchange, 20: 37761

interactions with nucleons, C, P, and T invariances in bootstrap mechanism for, 20: 37794
interactions with nucleons, electromagnetic form factors from, (T), 20: 37801
interactions with nucleons at 500 to 600 Mev, amplitudes for, 20: 37803
interactions with nucleons, Regge dynamics in, (T), 20: 37809
interactions with nucleons, Regge recurrence parity assignments in, (T), 20: 39749 (COO-881-77)
interactions with nucleons, effect of $\pi\pi$-scattering annihilation channels on, 20: 39776(T)
interactions with nucleons, crossing in backward cone and threshold region in, 20: 39798
interactions with nucleons, graphical method for charge independence in strong, 20: 39800
interactions with nucleons, analysis for Λ-K^0 production, (E/T), 20: 39803
interactions with nucleons, sum rule for axial-vector coupling-constant renormalization in, 20: 39814
interactions with nucleons at 290 to 905 Mev, cross sections for N^*_{33} production in, (E/T), 20: 39827
interactions with nucleons, model for, 20: 39839
interactions with nucleons at 300 Mev, phase shift analysis of, (E), 20: 41794 (JINR-E-2860)
interactions with nucleons, modified one-nucleon exchange model for, 20: 41815
interactions with nucleons, Schroedinger theory for static, 20: 41818
interactions with nucleons, scattering lengths for, (T), 20: 41846
interactions with nucleons, consistency conditions on strong, 20: 41861
interactions with nucleons at low energies, modified effective-range approximation for, 20: 41864
interactions with nucleons, meson (η) production and interaction from, (T), 20: 41866
interactions with nucleons, consistency of nucleon-nucleon interaction with, (T), 20: 41873
interactions with nucleons, quark model for $N\frac{3}{2}_3 N\pi$ vertex in, 20: 41876
interactions with nucleons, meson (π)-nucleon and meson (ρ) coupling constants from scattering lengths in, (T), 20: 41885
interactions with nucleons, theory of three particle production in, 20: 41900
interactions with nucleons, review of phase shift analyses for, 20: 41913
interactions with nucleons, P-wave resonances in Chew-Low model for, 20: 44186
interactions with nucleons at high energies, polarization in charge-exchange, (T), 20: 44201
interactions with nucleons at high energies, backward and forward peaks for elastic, (T), 20: 44267
interactions with nucleons, general solution of Chew-Low equations for partial waves in, 20: 44281
interactions with nucleons, reconstruction of reaction amplitude for vector meson production from, 20: 46384
interactions with nucleons, scattering matrix for, 20: 46386
interactions with nucleons, vertex function and Mandelstam representation for, 20: 46354
interactions with nucleons, P_{11} phase shifts for, 20: 46355
interactions with protons at 300 to 600 Mev, pion production cross sections for, 16: 18374
interactions with protons, threshold anomalies, 16: 969
interactions with protons, application of pole method to analysis of, 16: 972
interactions with protons at 960 and 1300 Mev, hyperon (Λ) distribution and polarization in, 16: 2410 (NP-10992)
interactions with protons at 550 to 1020 Mev, differential cross sections for, 16: 6923 (UCRL-9507)
interactions with protons at 1 to 10 Bev, 16: 10912
interactions with protons at 1.5 Bev, meson production in, 16: 10814 (JINR-D-793)
interactions with photons at low energies, (2π, 2γ) vertex, 16: 10865
interactions with protons at 910 Mev, 16: 12378
interactions with protons at high energies, charge exchange and polarization in, 16: 12396
interactions with protons, cross sections of pion production in, 16: 12428 (JINR-D-856)
interactions with photons, meson (π) production amplitudes in, 16: 15559
interactions with protons at 910, 1090, and 1260 Mev, 16: 15636 (TID-15425)
interactions with protons at 1.0, 1.4, and 4.5 Bev, 16: 22934
interactions with particles at high energies, cross sections, 16: 22943
interactions with protons, scattering threshold anomalies, 16: 24690 (JINR-P-966)
interactions with protons at 1 Bev, elastic, 16: 26071 (JINR-P-817)
interactions with protons at 290 to 1500 Mev, 16: 26104
interactions with protons at 2.1 Bev/c, kinematics, 16: 26134
interactions with protons, high-energy, 16: 26159
interactions with protons, determination of π-π resonance cross sections by the Chew-Low extrapolation method, 16: 29687
interactions with protons, resonances in complex diagrams of forward scattering amplitude in, 16: 32274 (NP-12032)
interactions with protons, meson (ζ) production in, 16: 32335
interactions with protons above 1 Bev, models for, 16: 33740
interactions with protons, multiple meson (π) production in, 16: 10816 (NP-11300)
interactions with polarized protons, 18: 866 (UCRL-10949)
interactions with protons at 5 to 20 Bev, Regge-pole representation for, 18: 2661
interactions with protons, models for resonances in, 18: 6002
interactions with protons, bremsstrahlung emission in, 18: 7475 (TID-19854)
interactions with protons at high energies, momentum transfer cut-off in elastic and inelastic, 18: 7519
interactions with protons, resonance effects in, 18: 9199
interactions with protons at 2.0 Bev, multiple meson (π) production in, 18: 9204
interactions with protons at 300 to 700 Mev, resonance (1400 Mev) production in, 18: 12934
interactions with protons at high energies, differential cross sections and comparison with Regge pole theory, 18: 12966
interactions with protons at 4.13 Bev/c, backward scattering in, 18: 14878
interactions with protons, feasibility of using 600- to 1000-Bev accelerators to study elastic, 18: 16749 (BNL-7534(p.83-7))
interactions with protons, resonances in, 18: 18634 (CONF-452-1)
interactions with protons at 7 to 20 Bev, diffraction-scattering, 18: 24392 (JINR-P-1632)
interactions with protons, resonance parities and spins from polarized targets in, 18: 30553
interactions with protons, data on, 18: 22728(R) (NP-13870)
interactions with protons, digital data and on-line computer system for, 18: 31871 (CERN-64-30(p.11-20))
interactions with protons at 1.5 to 2.4 Bev/c, ($\Sigma^0 K^0$), ($\Sigma^- K^+$), and (ΛK^0) production in, 18: 36255 (UCRL-11360)
interactions with protons at 300 to 1300 Mev, 18: 36291
interactions with protons, parity and spin of resonances in, 18: 36276
interactions with protons, spin of bosons from, 18: 36336
interactions with protons, masses of resonance, 18: 40253 (UCRL-11543(Rev.))
interactions with protons at 300 to 1300 Mev, resonances in, 18: 40255 (UCRL-11577)
interactions with protons at 300 to 700 Mev, phase-shift analysis of, 18: 40307
interactions with protons, dispersion relations for, 18: 42384
interactions with protons at 6 to 22 Bev/c, total cross sections for, 18: 44515 (BNL-8323)
interactions with protons at 2 to 10 Bev/c, elastic-inelastic discrimination in, 18: 44517 (CERN-64-38)
interactions with protons at 4.0 Bev/c, cross sections for elastic, 18: 44527
interactions with protons, partial-wave analysis of elastic, 19: 1273
interactions with pions, calculations on (T), 19: 1361
interactions with protons at 3.15 and 4 Bev/c, backward scattering in (T), 19: 3072
interactions with protons at high momentum transfers, (E/T), 19: 4962
interactions with protons, meson (ρ^0) and $N^*_{\frac{3}{2}}$ production in, (T), 19: 4977
interactions with protons, amplitudes for high-energy elastic, (T), 19: 8191
interactions with protons, scattering cross sections in, 19: 9775(R) (UCRL-11466)
interactions with protons at 0.25 to 6.2 Bev, spin dependence of elastic, 19: 9775(R) (UCRL-11466)
interactions with protons, resonances in, (T), 19: 10015 (JINR-P-1808)
interactions with protons at high energies, cross sections for, (T), 19: 10058
interactions with protons at high energies, large momentum transfer processes in, (T), 19: 12211
interactions with protons, Chew-Low method for cross sections for, (T), 19: 12296
interactions with protons at high energy, elastic, (T), 19: 12307
interactions with photons, parameters for, (T), 19: 14317 (JINR-P-1896)
interactions with protons, meson (f^0) effects on, (T), 19: 14384
interactions with protons, polarization effects on, (E), 19: 16478 (NP-14850)
interactions with protons, $\Delta_{\frac{3}{2}}$ resonances in, (T), 19: 16611
interactions with protons at high energies, differential cross sections for elastic, (T), 19: 16631
interactions with protons, single-particle exchange models for, (T), 19: 16579
interactions with photons, induced couplings in, (T), 19: 18811

interactions with protons, kinematical effects in peripheral, (T), 19: 20981
interactions with protons, $K^+ + \Sigma^+$ parity in, (E/T), 19: 25265(R) (UCRL-11776)
interactions with protons at 4.0 Bev/c, cross sections for elastic, 19: 35040
interactions with protons at 780 Mev, angular distributions and cross sections for, 19: 37637
interactions with protons, phase shift and resonance equations for elastic, 19: 39487 (UCRL-14193)
interactions with photons in SU(3) and SU(6), 19: 39470 (JINR-P-2171)
interactions with protons, Regge-pole approximation for forward scattering amplitude in, 19: 43121
interactions with protons at high energies, comparison of photon spectra from, 17: 709 (IFA/EM/47)
interactions with protons, multiple meson (π) production in, 17: 9328
interactions with protons, resonances in, 17: 9337
interactions with protons at 1.5 to 5 Bev/c, elastic, 17: 9429
interactions with protons, isotopic spin independence in, 17: 11561
interactions with photons, γ-3π coupling constant in, 17: 13379
interactions with photons, mechanism for beat production in, 17: 13390
interactions with protons at 310 Mev, phase-shift analysis of, 17: 13437
interactions with protons, strip approximation of diffraction, 17: 15124
interactions with protons at 600 Mev, cross sections for elastic and inelastic, 17: 15128
interactions with protons at 2 to 45 Bev, 17: 15081 (NP-12588)
interactions with protons, cross sections and polarizations for, 17: 17003
interactions with protons, two photon decay of mesons (η^0) from, 17: 19118
interactions with protons at 6 and 18 Bev/c, 17: 19088
interactions with protons, 17: 20594(R) (UCRL-10572)
interactions with protons, nonshrinking diffraction, 17: 20902
interactions with protons, particle tracks from, 17: 23647
interactions with protons at 523, 572 and 689 Mev, phase shifts and proton polarization in elastic, 17: 24275 (UCRL-10629)
interactions with protons, evidence for existence of the f^0 resonance in, 17: 31348
interactions with photons, amplitude for, 17: 32962
interactions with protons at 10 Bev, nonshrinking diffraction peak in, 17: 34765
interactions with protons at high energies, transverse momenta distribution effects on elastic, 17: 34774
interactions with protons, dispersion relation analysis of, 17: 36566(R) (AD-295975)
interactions with protons at 7 Bev, tunnel mechanism for, 17: 40038
interactions with protons at small momentum transfers, model for high-energy, 17: 41796
interactions with protons, 17: 40433(R) (NYO-10063(p.71-89))
interactions, with photons, 17: 22430 (NP-12591(Pt.I))
interactions with protons, polarized hydrogen target for, 20: 4637
interactions with protons at high energies, M(12) invariance and universality for, (T), 20: 6081
interactions with photons, resonance model for magnetic polarizability from, 20: 6090
interactions with protons at high energies, coherent droplet model for boson resonance production in, (T), 20: 9750
interactions with protons, energy dependence of real part of amplitude of, (T), 20: 13503
interactions with protons, sum rule for amplitudes of, (T), 20: 13571
interactions with protons, optical model amplitudes for, 20: 13601
interactions with protons at 450 Mev, (E), 20: 13524
interactions with protons, phase shift analyses of, (T), 20: 15382
interactions with protons at 4 to 12 Bev, elastic, (E), 20: 19273(R) (BNL-929, pp 3-43)
interactions with protons at 1 to 3 Bev/c, proton polarization in elastic, (E/T), 20: 19505
interactions with protons, 2^+ meson exchange in, (T), 20: 19512
interactions with protons at high energies, polarization in, (T), 20: 21653
interactions with protons at high energies, polarization in elastic and charge-exchange, (T), 20: 24032
interactions with photons, contribution to meson (π^-)-proton interactions from, (T), 20: 25851
interactions with protons, suppression of meson (ϕ) production from, (T), 20: 27863
interactions with protons, Regge cuts in high-energy elastic, (T), 20: 30160
interactions with protons, absorptive correction to peripheral model for, 20: 32022
interactions with protons at high energies, amplitudes for large-angle elastic, 20: 32086
interactions with protons at high energies, model for, (T), 20: 34224
interactions with protons, kinematic enhancement of resonance production in, 20: 37769
interactions with protons at 35 and 39 Mev, charge exchange in, (T), 20: 37785
interactions with protons at high energies, review on elastic, (E/T), 20: 39744 (CERN-66-18)
interactions with protons, strongly singular complex potential for high-energy large-angle, (T), 20: 39777
interactions with protons, S-wave $\pi\pi$ scattering length from, (T), 20: 39808
interactions with protons, meson (σ) production in, (E), 20: 39782
interactions with protons at high energies, models for inelastic two-body, 20: 44359
interactions with protons, resonances from, (E), 20: 46344 (UCRL-16968)
interactions with strange particles, 16: 22935
interactions with the nucleus in π-mesic atoms, use of optical model in interpretation of, 18: 15203 (NP-13679)
interactions with virtual nucleons, effects on vertex of, (T), 20: 6054
interactions with Y particles, coupling constants for, (T), 19: 23451
interactions with Y particles, two-channel p-wave, (T), 20: 2694
interpretation as a Regge pole, 18: 7523
interpretation as Regge pole, 18: 9114
ionization reactions with gases, spark chamber studies of, 18: 24473
isospin wave functions for five, in SU_3, 18: 36251 (PAN-475/VII)
kinematics in spark chambers, use of multiple scattering and secondary sparks in determining, (E), 20: 31570
lifetime, measurement of mean, 16: 25901 (LNF-62/37(p.118-38))
magnification of, magnetic lens system for unit, 17: 4159
mass, composite model treatment, 16: 2459
mass difference effects on $K_{\mu 3}$ decay probabilities, 16: 7001
mass difference effects from meson (η) decay, 16: 15593
mass difference ($\pi^- - \pi^0$), determination by neutron time-of-flight measurements, 16: 18322 (UCRL-9951)
mass difference ($\pi^+ - \pi^0$), effects of electromagnetic self-energies, 16: 18321 (NYO-10130)
mass difference ($\pi^- - \pi^0$), 17: 24364
mass differences ($\pi^+ - \pi^0$), (T), 19: 16556
mass differences of, beta decay effects from, 18: 9361
mass distribution of pairs of, from meson (π^-)-proton interactions, 17: 9431
mass distribution in hyperon (Ξ) systems, effective, 17: 5254
mass distributions from meson (η) decay, 16: 15591
mass formulas in U_4 symmetry, (T), 19: 16545
mass from nucleon-nucleon scattering, 16: 24692 (JINR-P-970)
mass measurement from nucleon-nucleon scattering, 17: 7027
mass measurements of, 20: 7804
mass of, nonlinear spinor theory for, 19: 25376
mass of, self-consistent model for, 19: 8186
mass ratio to nucleons, calculation from dispersion relations, 18: 2623
mass relations in octet, 18: 40309
masses of compound, boson and fermion, 17: 24329
model for virtual, nuclear optical, 18: 30821
model for, composite, (T), 20: 34219
model of bipion, 17: 22431 (NP-12591(Pt.II))
model of, $N\bar{N}$ bound-state, 18: 22782
model, composite, 16: 6941
models for, description of electromagnetic, (T), 19: 41377
models of, nucleon-antinucleon and meson (ρ)-meson (π), 20: 9779
momenta of, Castagnoli formula correction from transverse, 17: 13412
momentum of, from hyperfragment production by 9-Bev protons in photographic emulsions, 17: 20936
momentum spectra of secondary, transverse, 18: 28344
momentum/velocity ratio of fast, relativity-theory tests by, (E), 20: 1117
pair production by photons, cross sections for, 16: 6970
pair production in meson (ω) decay, 16: 10903
pair production in emulsions, 16: 25927 (NP-11977(p.66-7))
pair production in annihilation of polarized electrons and positrons, (T), 19: 43067
parameters of low-energy, best fit data, 16: 16987 (NP-11592(Vol.I) (p.459))
parities (relative), 16: 10844
parity and spin of, 17: 32941
phase space integrals for, high-energy behavior of sum of, 20: 13574
photoproduction, 16: 32458(R) (LAL-1035)
photoproduction, (T), 19: 39498
photoproduction, 18: 10681(R) (CEAL-1009)
photoproduction amplitudes, effects of $N\text{-}\bar{N}$ annihilation, 16: 957
photoproduction amplitude for, Regge-Khuric representation for, 18: 37897
photoproduction at high energies, parity conservation in, 16: 25889 (LNF-62/37(p.13-23))
photoproduction at high energies, 16: 29680
photoproduction at 0.300 to 1.5 Bev, meson (ρ) production in pair, (E), 19: 39549
photoproduction at low energies, (T), 20: 15441

photoproduction at high energies, review on, (T), 20: 15442
photoproduction at low energies, (T), 20: 24007 (CERN-65-24(Vol.2), pp 55-66)
photoproduction below 1 Bev, theory of, 18: 28319 (DESY-64/5)
photoproduction from nucleons, amplitude for low-energy, 17: 17274
photoproduction from nuclei, nuclear polarization following, 18: 19009
photoproduction from nucleons at high energy, Regge poles in, 18: 26385
photoproduction from protons at 0.5 to 4.8 Bev (E), 19: 1233 (MIT-2098-79)
photoproduction from protons at 154 to 185 Mev (E), 19: 3088
photoproduction from hydrogen at 530 to 750 Mev, cross sections for, (E), 19: 16852(R) (NP-14647)
photoproduction from deuterium at 544 Mev, cross sections for, (E), 19: 16852(R) (NP-14647)
photoproduction interactions, development of model for, 16: 8096 (JINR-D-774)
photoproduction in helium, anisotropy in distribution from, 16: 25888 (LNF-62/37(p.10-13))
photoproduction in deuterium and hydrogen, 16: 25943 (NP-11977 (p.124-6))
photoproduction in deuterium, hydrogen, and heavy nuclei, 16: 25945 (NP-11977(p.129-35))
photoproduction in liquid deuterium and hydrogen, 16: 29646 (NP-11927)
photoproduction in gamma-proton interactions, double, 17: 41739 (DESY-A-2.103)
photoproduction in nucleons, strip approximation for, 18: 7499
photoproduction in light nuclei, partial transitions in, (T), 19: 33387
photoproduction near threshold, review, 17: 9464
photoproduction of pairs in Coulomb field of nuclei, 16: 18365
photoproduction of pairs of, from deuterium, 16: 29678
photoproduction of pairs of, near threshold, 17: 3984
photoproduction of pairs of, low-mass anomaly in, 17: 5257
photoproduction of pairs of, in hydrogen at 800 to 1200 Mev, 17: 9301
photoproduction of, by electron interactions with protons, 17: 19113
photoproduction of, Regge poles in Drell calculations of cross section for, 17: 21110 (SLAC-5(p.20-8))
photoproduction of pairs of, pion-pion resonance from, 17: 22517
photoproduction of, asymptotic relations for cross sections of, 17: 28218
photoproduction of high-energy, Regge pole hypothesis in, 17: 39888
photoproduction of, higher resonances in, 18: 9082 (LNF-63/66)
photoproduction of pairs of, from protons, 18: 10855 (LNF-63/47(p.50-4))
photoproduction of pairs on protons with one-pion-exchange, 18: 18675
photoproduction of, determination of multipole states in, 18: 32579
photoproduction of, Drell model and off-shell correction in, 18: 32847
photoproduction of, Pomeranchuk theorems and Regge poles in, 18: 42460
photoproduction of pairs of, in nuclear coulomb fields, 18: 42416
photoproduction of, measurements on, 18: 44572
photoproduction of, neutron form factors from, 19: 1372
photoproduction of, dispersion relations in, (T), 19: 8242
photoproduction of, DESY studies of, 19: 23216
photoproduction of, lecture on, 19: 37568
photoproduction of, determination of $\gamma\pi p$ coupling constant from, (E/T), 19: 43162
photoproduction of, meson (ρ) effects in double, (T), 19: 45019 (JINR-P-2286)
photoproduction of di-, in spark chambers, 19: 47303 (DESY-65/7)
photoproduction of pairs of, on protons, 20: 2747
photoproduction of protons, mass shift of meson (ρ^0) in, (T), 20: 9755
photoproduction of, peripheral model formalism and uses for, 20: 24013 (DESY-66/2)
photoproduction of pairs of, on protons at 450 to 750 Mev, (E), 20: 27932
photoproduction of pairs of, on protons at 0.55 to 1.00 Bev, (E), 20: 27933
photoproduction of pairs of, at high energies, (E), 20: 27916
photoproduction of, dispersion relations and $\gamma p\pi$ coupling from, (T), 20: 31996
photoproduction of, determination of $\gamma\pi\omega$ coupling constant from, 20: 32077
photoproduction of, fixed-t dispersion relations for, 20: 41851
photoproduction on nucleons and mesons (π), amplitudes, 16: 5905
photoproduction on nucleons, transition amplitudes, 16: 5915
photoproduction on nucleons, amplitude integral equations for, 16: 18326
photoproduction on nucleons, amplitude integral equations for, 16: 26094
photoproduction on mesons (π) and nucleons, Mandelstam representation for, 16: 29655 (NP-11950(Vol.II)(p.365-424))
photoproduction on hydrogen, polarization of back-scattered nucleons in, 16: 32275 (NP-12034)
photoproduction on hyperons (Λ), 16: 33749
photoproduction on mesons (π), amplitudes, 16: 5905
photoproduction on protons near threshold, calculation of, 17: 9353
photoproduction on protons, 17: 11574
photoproduction on nucleons, isobaric model for analysis of, 17: 13388
photoproduction on deuterons and protons, 17: 15113
photoproduction on nuclei, analysis by N/D method, 17: 17163
photoproduction on nucleons, partial wave dispersion relations for, 17: 20948
photoproduction on helium-4, angular correlations for, 17: 40092
photoproduction on hyperons, dispersion relations for, 17: 39857
photoproduction on nucleons, 17: 41842
photoproduction on nucleons, Regge poles and Mandelstam representation in, 18: 888
photoproduction on deuterons and nucleons at close to threshold energy, 18: 903
photoproduction on mesons (π), determination from meson (π)–nucleon interactions, 18: 6044
photoproduction on nucleons, Regge poles in amplitudes of, 18: 6051
photoproduction on mesons (π), strip approximation for, 18: 7500
photoproduction on nucleons, interaction effects in, 18: 9196
photoproduction on hydrogen, 18: 10854 (LNF-63/47(p.1-35))
photoproduction on complex nuclei, 18: 10854 (LNF-63/47(p.1-35))
photoproduction on nucleons, partial wave analysis of, 18: 16798
photoproduction on nucleons in Regge pole theory, 18: 18680
photoproduction on meson (π), integral equations for, 18: 20921
photoproduction on protons, single, 18: 24380 (DESY-64/3)
photoproduction on nucleons by linearly polarized photons, 18: 26276 (DESY-64/6)
photoproduction on nucleons, 18: 26372
photoproduction on deuterons, polarization from, 18: 30546
photoproduction on protons, analysis by kinematic reconstruction of events, 18: 32731 (ISS-64/5)
photoproduction on nucleons at high energies, meson (ρ) exchange in, 18: 36317
photoproduction on protons, analysis of double and triple, 18: 42415
photoproduction on nucleons, invariant amplitudes for, 18: 44538 (NP-14404(p.140-59))
photoproduction on nuclei, impulse approximation theory for, 19: 1558
photoproduction on nucleons, amplitudes for non-resonant and resonant (E/T), 19: 3049
photoproduction on nuclei and nucleons near threshold, (T), 19: 10097
photoproduction on nucleons, amplitudes for, (T), 19: 12380
photoproduction on nucleons, meson (ρ) effects on, (T), 19: 18813
photoproduction on nucleons at low energy, (T), 19: 23369
photoproduction on nucleons, dispersion relations for, (T), 19: 37541 (UCRL-7953-T)
photoproduction on protons at 0.6 to 5.5 Bev, (E), 19: 44999 (DESY-65/5)
photoproduction on nucleons at high energy, total cross section for, (T), 19: 47353
photoproduction on nucleons at high energies, momentum-transfer distributions in, (T), 19: 47389
photoproduction on protons below 1 Bev, angular distributions and total cross sections for, 20: 4579 (AD-618661)
photoproduction on protons at 0.3 to 5.5 Bev, (E/T), 20: 6037 (DESY-65/11)
photoproduction on nucleons, review of, 20: 9774
photoproduction on nucleons, one-particle exchange theory of, 20: 11572
photoproduction on nucleons, $\gamma\pi p$ interaction in, (T), 20: 13477(T)
photoproduction on protons, E1 and M2 amplitudes in single, (T), 20: 15365
photoproduction on nucleons, dispersion sum rules for, (T), 20: 15503
photoproduction on protons at 0.3 and 5.5 Bev, (E), 20: 17368
photoproduction on nucleons, current algebra for, (T), 20: 17375
photoproduction on nucleons, polarization coefficients for, (T), 20: 17407
photoproduction on nucleons, corrections to static theory for, 20: 19447 (UCRL-14614-T)
photoproduction on deuterons and nucleons, isotopic relations for amplitudes of, (T), 20: 19518
photoproduction on baryons, amplitudes for, (T), 20: 19539 (JINR-E-2544)
photoproduction on deuterons, asymmetry functions for polarized, (E), 20: 21626 (LNF-66/4)
photoproduction on nucleons, charge-dependent corrections in, (T), 20: 24034
photoproduction on protons near second (πN) resonance, (T), 20: 27946
photoproduction on protons, absorption corrections for, (T), 20: 34149 (IC-66/61)
photoproduction on nucleons in region of N*(1238), (T), 20: 34250
photoproduction on nucleons, (T), 20: 36025 (DESY-66/9)
photoproduction on nucleons, (T), 20: 37758
photoproduction on protons, lecture on, (E), 20: 39743 (CALT-68-92)
photoproduction on nucleons, reciprocity relation as test of C and T invariance in, 20: 39810
photoproduction on nucleons, amplitudes for, (T), 20: 41996
photoproduction, parity conservation in, 16: 25944 (NP-11977(p.127-9))
photoproduction, peripheral model interpretation of double, 16: 25887

(LNF-62/37(p.7-9))
photoproduction, peripheral interaction in, 16: 25942 (NP-11977 (p.121-3))
photoproduction, relation to scattering, 16: 29649 (NP-11950(Vol.I) (p.113-72))
physics, theory of low-energy, 16: 16999 (NP-11592(Vol.II)(p.87-102))
polarizabilities of, experimental and theoretical data on electric and magnetic, 16: 33721
polarizability of, neutron-polarizability contribution from, (T), 19: 20949
polarization, electric and magnetic, 16: 5860 (JINR-P-771)
presence in mesons (η^0) and (ζ), 16: 15594
production amplitudes from meson (π)-photon interactions, 16: 15559
production amplitudes for, isospin exchange relations for, (T), 20: 15449
production and absorption of s-wave, in proton-proton interactions, (T), 20: 11642
production and decay of heavy, 16: 26144
production and multiplicities from nucleon interactions with antiprotons, 16: 3711
production and properties in proton pair annihilation, 17: 9320
production and properties of systems of, review, 17: 9461
production anomalies in proton reactions with deuterons, 16: 4710
production by antiproton annihilations in hydrogen, 17: 9376
production by cosmic mesons (μ), 4-momentum transfer in multiple, 18: 22773
production by cosmic nucleon interactions at 100 to 400 Bev, momentum spectra of, (E), 19: 34904
production by electron-proton interactions, 17: 11543
production by electrons on nuclei, radiative corrections to, (T), 19: 41752
production by high-energy electrons, 16: 24707
production by high-energy neutrinos, (E), 19: 29042 (CERN-65-12)
production by high-energy cosmic mesons (μ), multiple, (E/T), 19: 34970
production by linac high-flux meson facility, 18: 44518 (LAMS-3030)
production by meson (π)-proton interactions, cross sections, 16: 12428 (JINR-D-856)
production by meson (π^-) interactions with protons at 4.7 Bev/c in liquid hydrogen bubble chamber, 16: 31005 (BNL-6213)
production by mesons (π), meson (π)–meson (π) interactions from, 17: 20594(R) (UCRL-10572)
production by neutrino-nucleon interactions, amplitudes of, 17: 7023
production by neutron-proton collisions at 1.6 Bev/c, 18: 26376
production by nucleon interactions at 300 Bev, momentum spectra in, (E), 19: 10048
production by polarized virtual photons, (T), 19: 33032
production by primary cosmic nucleons in atmosphere, 18: 34485
production by proton interaction at 24 Bev, 16: 16984 (NP-11592 (Vol.I)(p.433-47))
production by proton interactions with protons at high energies, 16: 33719
production by proton reactions with aluminum, beryllium, and iron at 30 Bev, 17: 7259
production by proton pair annihilation, 17: 9321
production by protons in shielding materials, equations for, 18: 13178 (ORNL-3549)
production by protons in shielding materials, equations for, 18: 13179 (ORNL-3570)
production by proton reactions with emulsion nuclei at 27 Bev, 18: 15311
production by virtual photons in meson (μ)-nucleon interactions, 18: 26305
production by 10-Bev high-intensity FFAG accelerator, 17: 33114 (CONF-125-4)
production cross section for, 17: 15124
production facility using proton linear accelerator, shielding for, 20: 2559
production, Fermi model statistics of multiple, 16: 8108
production from cosmic particle reactions with graphite at high energies, (E), 20: 38110
production from electron and photon interactions with nucleons at 1300 Mev, amplitudes for, (T), 20: 27847
production from meson (K^-) and (K^+) interactions in nuclear emulsions, correlations in, (E), 20: 13487
production from meson (π^-)-proton interactions at 775 Mev, 20: 39780
production from neutrinos, cross section for, high energy increase in, 17: 13350 (JINR-P-1152)
production from neutrino-nucleon interactions, asymmetries in, (T), 20: 21638
production in angular momentum representation, statistics of multiple, (T), 20: 4643 (INR-607/VI/PH)
production in antiproton–proton interactions, 3–π resonance in, 16: 949
production in antiproton-proton interactions, resonances in, 16: 24750 (UCRL-9814)
production in antiproton annihilation on nuclei, 17: 3971
production in antiproton-proton annihilation, 17: 6947 (IA-768)
production in antiproton-proton annihilation, statistical model for, 17: 20915
production in antinucleon annihilation, cross sections for, 17: 32920
production in antiproton-proton interactions at 3 and 3.6 Bev/c, single, 18: 40350
production in antiproton-proton interactions at 7 Bev/c, cross sections for multiple, 18: 44512 (BNL-8312)
production in antiproton-proton interactions at 7 Bev/c, single and multiple, 18: 44514 (BNL-8314)
production in antiproton–proton interactions without annihilation, 19: 1281
production in antiproton-proton annihilation, (T), 19: 18868
production in antiproton-proton annihilation at 7 Bev/c, multiple, (E), 19: 35073
production in antiproton-proton interactions at 7 Bev/c, single, (E), 19: 35073
production in antiproton-proton interactions at 7 Bev/c, multiple, (E), 19: 35074
production in antiproton-proton annihilations at rest, (E), 19: 45122
production in antiproton-proton inelastic interactions at 3.6 Bev/c, (E), 20: 6097
production in antiproton-proton annihilation at 3.7 Bev/c, cross section for, (E), 20: 15338
production in antiproton-neutron interactions in emulsions at 3 Bev/c, (E), 20: 17359
production in antiproton-proton annihilation at 3.3 and 3.7 Bev/c, (E), 20: 17385
production in antineutrino-proton and neutrino-neutron interactions, cross sections for, (E), 20: 19438 (ANL-7130, pp 257-71)
production in antiproton-proton annihilation in ambiplasma, (T), 20: 21684
production in antiproton-proton interactions at 5.7 Bev/c, cross sections for, (E), 20: 24033
production in antiproton-proton annihilation at rest, channel branching ratios and invariant mass distributions for, (E), 20: 27845
production in atmosphere, processes for, 18: 5948
production in baryon-nucleon interactions, Regge hypothesis for multiple, 17: 34806
production in bremsstrahlung-proton reactions (E), 19: 1240
production in cascades by heavy-particle reactions in matter, 16: 13944 (DESY-A2.85)
production in cosmic nucleon interactions, four-momentum transfer in, 18: 42400
production in cosmic nucleon reactions in atmosphere, (E), 19: 27184
production in cosmic meson (μ) reactions with nuclei at high energies, multiple, (E), 19: 35445
production in decay of mesons (η) and mesons (r), 17: 711 (NEVIS-110)
production in deuteron-proton interactions at 670 Mev, resonances in, 16: 13884
production in deuteron interactions with protons at 740 Mev, 17: 719 (UCRL-9599)
production in deuteron-meson (π) interactions, 17: 9325
production in deuteron-proton interactions, cross sections for, (T), 20: 13528
production in electron and neutrino interactions with nucleons, 17: 743
production in electron-nucleon interactions, 17: 19105
production in electron-nucleus reactions, cross section for, 17: 32913 (TID-7668(Sect.V))
production in electron-nucleon interactions at high energies, Regge poles for, 18: 18740
production in electron-nuclear interactions above threshold, 18: 19034
production in electron-proton interactions, 18: 26312
production in electron-proton interactions, in isobaric model, 18: 37978
production in electron-nucleon interaction, 18: 42385
production in electron and neutrino interactions with nucleons, (T), 19: 37631
production in electron scattering by nuclei, (T), 19: 36921
production in electron-proton interactions, (E), 19: 39623
production in electron-proton interactions at 5.2 Bev/c, (E), 19: 47303 (DESY-65/7)
production in electron-nucleon interactions, (T), 20: 27940
production in electron-nucleon interactions, isobar model for, (T), 20: 27941
production in electron-proton interactions at 5.2 Bev/c, (E), 20: 27917
production in emulsions by cosmic particles, 18: 40623
production in e^+–e^- interactions, 3π resonance, 16: 8126
production in galaxies, model for, 20: 41603
production in γ-N and N-π interactions below 1 Bev, 16: 10841
production in γ-p interactions at 550 Mev, 17: 11564
production in gamma-nucleon interactions, 17: 41738 (CTSL-40)
production in high-energy proton-deuteron interactions, 18: 2633
production in high-energy proton–deuteron interactions, 18: 2634

production in high-energy proton–deuteron interactions, 18: 2635
production in high-energy proton–deuteron interactions, 18: 2636
production in high-energy nucleon interactions, angular distribution of secondaries from, 18: 7525
production in high-energy jet showers, 19: 5127 (INSJ-79)
production in high-energy inelastic interactions, transverse momentum distribution of, (T), 20: 2681 (IFA-CR-55)
production in high-energy cascade showers, transverse momentum distribution for, (T), 20: 17371
production in hydrogen-meson (π^-) interactions at 16 Bev/c, 16: 24719
production in hyperon (Σ) decay, 16: 15538
production in hyperon (Λ) and (Σ) decay, self-consistent model for, 16: 26131 (UCRL-9863)
production in linac, 18: 37816 (LNF-64/16)
production in Mc^2 cyclotron, 19: 11944
production in meson (K^-) reactions with helium-4, resonances with hyperons, 16: 5896
production in meson (π^-) interactions with protons at 810,970 and 1100 Mev, cross sections, 16: 6954
production in meson (π^-)-proton interactions at 960 Mev, 16: 9379
production in meson (π^+)-proton interactions at 820, 900, and 1050 Mev, 16: 10828
production in meson (K°) decay, ratios of double and single, 16: 10863
production in meson (ρ) decay, 16: 15585
production in meson (K^-)-proton interactions, 16: 12801(R) (IA-685)
production in meson (K) decay, vertex diagrams, 16: 2432
production in meson (K^-) interactions at rest, 16: 2305(R) (UCRL-9704)
production in meson (η) and (K) 3-pion decay, Dalitz plots, 16: 19714
production in meson (π^-)-proton collisions at 7.2 Bev, cross sections for multiple, 16: 22959
production in meson (π)-proton interactions at 290 to 1500 Mev, 16: 26104
production in meson (π)-proton interactions, 16: 29643 (NP-11605)
production in meson (π)-proton interactions, multiple, 16: 29657 (NP-11978)
production in meson (K^-) interactions with protons, evidence for T = 0 resonance in, 16: 32290 (UCRL-9686)
production in meson (K^-)-proton interactions, amplitudes for, 16: 32315
production in meson (K^+) interactions with deuterons and protons, 16: 33701 (UCRL-10225)
production in meson (π^-)-nucleus reactions at 2 Bev/c, 17: 2173
production in meson (π)-nucleon interactions, 17: 5222
production in meson (π^-)-proton interactions at 7.2 Bev, π-π interactions in multiple, 17: 7035
production in meson (K^-)-proton interactions, 17: 9369
production in meson (π^-)-proton interactions, resonances in, 17: 9374
production in meson (K^+) interactions with deuterons and protons, 17: 9377
production in meson (K^-)-proton interactions, 17: 11560
production in meson (π)-proton interactions, amplitudes in low-energy, 17: 11518
production in meson (π^+)-proton interactions, single, 17: 13392
production in meson (π^-)-proton interactions, 17: 13452
production in meson (π) interactions, cross sections for, 17: 28189
production in meson (μ) reactions on nuclei, 17: 28341
production in meson (π)-proton interactions, 17: 31091(R) (UCRL-10862)
production in meson (π^-)-proton interactions, resonances in, 17: 31287 (TID-19082)
production in meson (π)-nucleon interactions at low energies, effects of, 17: 34746
production in meson (π^-)-proton interactions at 1.59 Bev/c, cross section for, 17: 41771
production in meson (π^+) interactions with protons at 600 Mev, mechanism for single, 17: 41804
production, in meson (π)-nucleon interactions at 7 Bev, 17: 22444
production in meson (π^-)-proton interactions at 905, 960, and 1100 Mev, 18: 889
production in meson (π^-)-proton interactions at 1.97 Bev/c, comparison with theoretical models, 18: 907
production in mesons (K), interactions with neutrons and protons, 18: 4469
production in meson (π)-proton interactions, multiple, 18: 9085 (NP-13532)
production in meson (π)-proton interactions at 2.0 Bev, multiple, 18: 9204
production in meson (π)-nucleon interactions at high energies, Regge pole formalism for, 18: 16779
production in meson (π^+)-proton interactions, multiple, 18: 18743
production in meson (π)-nucleon interactions at 170 to 600 Mev, model for single, 18: 20964
production in meson (π) reactions with beryllium-9, cross sections for, 18: 24587 (JINR-P-1584)
production in meson (μ)–proton interactions, cross sections for, 18: 30550
production in meson (π^-)-proton two-prong events at 3.9 Bev, 18: 40254 (UCRL-11556)
production in meson (π) and proton interactions at 2–25 Bev, review, 18: 40361
production in meson (π^-)-proton interactions at 6 Bev/c, multiple, 18: 40228 (BNL-8237)
production in meson(π^+)-proton interactions at 2.08 Bev/c, 18: 44513 (BNL-8313)
production in mesons(π^+)-proton interactions at 2.35 and 2.90 Bev/c, 18: 44519 (NEVIS-123)
production in meson (π)–proton interactions at 800 and 900 Mev (E/T), 19: 1325
production in meson (π^-)-proton interactions, multiple (E), 19: 1345
production in meson (π^-)-proton interactions at 2.75 Bev, multiple (E), 19: 1348
production in meson (π^-)-nucleon interactions at 6.1 Bev (E), 19: 1397
production in meson (π^-)-nucleon interactions at 6.1 and 18.1 Bev (E), 19: 1398
production in meson (π) –nucleon interactions at 5 Bev/c (T), 19: 3048
production in meson (K^+)-proton interactions at 1.3 and 5 Bev, (T), 19: 4907
production in meson (K^+)-nucleon interactions at 900 Mev/c, (E), 19: 10064
production in meson (μ)-proton interactions, (T), 19: 14321 (NP-14631)
production in meson (μ^-)-proton interactions at 5 Bev/c, 19: 21037
production in meson (μ-) interactions in nuclear emulsion at 5 Bev/c, (E/T), 19: 23476
production in meson (π)-nucleon interactions, (T), 19: 25301
production in meson (π)-nucleon interactions, peripheral model for, 19: 31002 (CONF-550-97)
production in meson (π^-)–nucleon interactions at 7.5 Bev, transverse momentum distribution in, (T), 19: 37611(T)
production in meson (π)-proton interactions, cross sections for, 19: 37637
production in mesons (η), decay, C-violation in, 19: 39528
production in mesons (π)-nucleon interactions below 1 Bev, model for single, (T), 19: 41509
production in meson (π^-) interactions with protons at 16 Bev/c, 19: 43054
production in meson (π^-)-nuclear field interactions at 16.2 Bev/c, coherent trident, (E), 19: 47355
production in meson (π^-) reactions with organic liquids at 6 to 18 Bev/c, (E), 20: 9745
production in meson (π)-proton interactions at 450 Mev, (E), 20: 13524
production in meson (μ) inelastic scattering in nuclear emulsions, (E), 20: 13526
production in meson (π^-)-proton interactions at 350 to 800 Mev, (E), 20: 13527
production in meson (π^-) interactions with protons at 1.89 Bev/c, multiple, (E), 20: 17386
production in meson (π^-) reactions with emulsion nuclei at 3.85 Bev/c, 20: 26085 (JINR-P-2624)
production in meson (π)-nucleon interaction, single, (T), 20: 27861
production in meson (μ)-nucleon interactions, (T), 20: 30076
production in meson (π)-nucleon interactions, (T), 20: 39839
production in meson (K^-) capture by emulsion nuclei, (E), 20: 44657 (UCRL-16602)
production in neutrino–nucleon interactions, cross sections, 16: 12558
production in neutrino-nucleon interactions, 16: 26074 (JINR-P-905)
production in neutrino reactions on nuclei and nucleons, cross sections, 16: 27965
production in neutrino-nucleon interactions at 0 to 5 Bev, 16: 27973
production in neutrino-nuclear interactions, 16: 28002
production in neutrino-nucleon interactions, 17: 11563
production in neutrino interactions with neutrons and protons, relations between cross sections for, 17: 13348 (JINR-P-1141)
production in neutrino reactions at high energies, 17: 19176
production in neutron–proton interactions at 9 Bev, 17: 37442
production in neutrino-nucleon interactions, PC violation in, (T), 19: 10073
production in neutrino reactions with lead, pair, (T), 19: 16530
production in neutrino-nucleon interactions, single, (T), 19: 23477
production in neutrino-nucleon interactions, (T), 19: 25315
production in neutrino-nucleon interactions, (T), 19: 41754
production in neutrino ($\nu\mu$) interactions with nucleons, cross sections for, (T), 19: 43158
production in neutrino-nucleon inelastic interactions, charge radio of, (T), 19: 47377
production in neutrino–nucleon interactions, interpretation of asymmetries in, 20: 19478
production in nucleon interactions, 16: 10910
production in nucleon interactions, 16: 22950
production in nucleon-antinucleon annihilation, selection rules for,

16: 24735
production in nucleon interactions with nucleons, 16: 27940
production in nucleon-nucleon interactions at high energies, semi-phenomenological model for, 17: 6984
production in nucleon-proton interactions at 28 Bev, 17: 41735 (AERI-P/R-7)
production in nucleon interactions, bremsstrahlung mechanism for multiple, 17: 29518
production in nucleon-proton interactions at 14 Bev, 18: 9084 (NP-13484)
production in nucleon interactions at 16 to 2800 Bev, 18: 16775
production in nucleon resonant interactions, 18: 24479
production in nucleon resonances, 18: 28416
production in nuclear reactions, theory of, 18: 40362
production in nucleon interactions, theory of, 18: 40363
production in nucleon-proton interactions at 22 Bev (E/T), 19: 1400
production in nucleon interactions at high energies, SU(3) for multiple, (T), 20: 17345 (JINR-P-2531)
production in nucleon interactions, p-wave analysis of, 20: 19476
production in nucleon-nucleon interactions at 0.8 to 1.4 Bev, 20: 34151 (ISS-66/15)
production in nucleon-nucleon interactions, multiple, (T), 20: 34183
production in particle interactions, multiple, 17: 2187
production in particle decay, forbidden multi-, 17: 16952 (JINR-P-1161)
production in peripheral nucleon-nucleon collisions, 17: 11515
production in photon reactions with deuterium, γ-π-ρ coupling constant from, 17: 31320
production in p-π^+ interactions, 16: 19474(R) (TID-14386)
production in proton-meson (π^-) interactions, 16: 2305(R) (UCRL-9704)
production in proton-nucleus reactions at 23.5 Bev, shower asymmetry, 16: 8095 (IFA-EM-45)
production in proton interactions with protons, 16: 12438 (NYO-9285)
production in proton interactions, multiple, 16: 15571
production in proton–proton interactions at 2.85 Bev, multiple, 16: 18370
production in proton reactions with nuclei, 16: 26089 (NP-11832)
production in proton reactions on helium-3 and tritium, cross sections, 16: 26260
production in proton reactions with nuclei at 9 to 25 Bev, 16: 33837
production in proton-meson (π) interactions at 910 Mev, resonance, 16: 12378
production in proton-meson (π) interactions at 2.8 Bev, 16: 10816 (NP-11300)
production in proton reactions with beryllium at 19.2 Bev, 17: 795 (CERN-62-27)
production in proton-proton interactions at 2.9 Bev, 17: 3983
production in proton pair annihilation, 17: 9322
production in proton (p-p) interactions at 660 Mev, 17: 28140 (JINR-D-1236)
production in proton inelastic scattering by complex nuclei at 27 Bev, angular distributions for, 17: 28304
production in proton interactions at 0.97 Bev, one boson exchange model for single, 17: 34805
production in proton ($\bar{p}$-p) interactions at 3.25 and 3.69 Bev/c, 17: 41736 (BNL-7294)
production, in proton–nucleon interactions at 9 Bev, 17: 22443
production in proton-proton interactions at 657 Mev, phase-shift analysis of, 18: 6042
production in proton interactions,(3,3)-resonances in, 18: 7554
production in proton accelerators, 18: 12912 (TID-7686(p.35-41))
production in proton reactions with emulsion nuclei at 16 to 2800 Bev, 18: 16775
production in proton interactions, 18: 21213 (TID-20440)
production in proton pair annihilation, 18: 22750
production in proton reactions with beryllium at 25 Bev, 18: 26165 (BNL-837(p.91-113))
production in proton–proton interactions at 2 Bev, 18: 34633
production in proton-proton interactions at 25 Bev/c, 18: 44540
production in proton-proton interactions at 4 Bev (E), 19: 1360
production in proton-proton interactions at 18.8 Bev (E), 19: 1399
production in proton interactions at 19 and 23 Bev/c, (E), 19: 12221
production in proton interactions with neutrons, high-energy, 19: 33051
production in proton reactions with emulsion nuclei at 27 Bev, (E), 20: 10095
production in proton-proton interactions at 24 Bev/c, multiple, (E), 20: 32017
production in proton reactions with beryllium at 30 Bev/c, 20: 34146 (CU-1932-256)
production in proton-proton interactions at 655 Mev, (E/T), 20: 37802
production in proton reactions with beryllium and platinum at 2.9 Bev, (E), 20: 39794
production in steady-state universe, selection rules for, 17: 41783
production in strong interactions, model of, 18: 36337
production in very high-energy collisions, 17: 9436
production in very high energy interactions, 17: 15297
production in weak processes, 16: 28001
production in Y_1^* decay, (E), 20: 13518
production of ($\bar{K}2\pi N$), 18: 30589
production of ($K\pi\pi$), in proton pair interactions, 18: 40302
production of beams, 17: 7391
production of beams of, using high-intensity proton linac, (E), 19: 9808 (TID-21282)
production of beams of, in Brookhaven AGS at 4 to 16 Bev/c, (E), 19: 32828 (BNL-9213)
production of charged in proton annihilation, 16: 16961 (NP-11592 (Vol.I)(p.269-75))
production of charged, in meson (K^-) interactions with emulsion nuclei, 18: 14854
production of dipions in proton–meson (π) interactions at 357 Mev, 16: 18371
production of double-charged, in (π^-,p) collisions at 900 Mev, 17: 17028
production of excited, in proton interactions with deuterons, statistical theory calculations, 16: 4685 (CERN-61-27)
production of, in antiproton-proton interactions at 3.25 Bev, 16: 33681 (BNL-6234)
production of multiple, by 2.03 Bev/c mesons (π^-) in hydrogen, 17: 9315
production of multiple, by mesons (π^-) reactions in bubble chambers, 17: 9317
production of multiple, by meson (π^-)-proton collision, 17: 9318
production of multiple, in meson (π)-proton interactions, 17: 9328
production of nucleon-pion, showers in iron by 1- and 3-Bev protons, (T), 20: 5927 (ORNL-P-1733)
production of pairs of, in electron-positron interactions, 17: 32958
production of pairs of, in meson (π)–nucleon interactions at 12 and 18 Bev/c, (E), 19: 14405 (TID-21409)
production of pairs of charged, in meson (ω) decay, (T), 19: 41386
production of pairs of, in meson (π^-) interactions with nucleons at 12 and 18 Bev, (E), 20: 30025
production of, Pomeranchuon exchange as result of Regge poles in multiple, 17: 20917
production of ($\Sigma K\pi$) states at 2.1 Bev/c, 17: 13419
production of single, in antiprotons-proton interactions, 17: 9323
production of single, in nucleon-nucleon interactions, 17: 19110
production of single, in high-energy neutrino interactions, (T), 20: 9784
production of single, in meson (K^+) interactions with protons at 1.96 Bev/c, (E), 20: 15335
production of slow, in meson (π)-nucleon and nucleon-nucleon collisions, 17: 9289
production of slow, in meson (π^-) reactions with emulsion nuclei at 3.8 Bev, 20: 30501
production of spin-1, in meson (K^+) decay, (E), 19: 23446
production of stopped, in Brookhaven AGS, 19: 37383
production of supplementary, in meson (π)–nucleon scattering, 17: 15094
production of T = 0 state, in deuteron–deuteron interactions, (E), 19: 1329
production of three, in antiproton-proton annihilation, 19: 43040 (CU-1932-244)
production of triple, cross section for, 18: 26300
production of, current commutator theory of multiple, 20: 25839
production of, cyclotron facility design for, 18: 32319 (TID-20822)
production of, development of high-energy accelerators for, 20: 2560
production of, dynamics with invariant collinear vertices, analyticity, and unitary for low-energy, (T), 20: 19491
production of, effects of π-N resonances on, (T), 20: 34171
production of, multiple, (T), 20: 36059
production, relation to scattering, 16: 29652 (NP-11950(Vol.I)(p.261-74))
production resonances of antiproton-proton interactions at 1.67 Bev, 16: 26233 (UCRL-10129)
production spectra, 16: 12322
production with bosons in p-$\bar{p}$ annihilation, cross sections, 16: 19697
production with hyperons (Σ) in Y* decay, 17: 13411
production with hyperons (Σ) in meson (K^-) capture by carbon-12, momentum spectra for, 17: 40074
production with $^3/_2$ resonance in isobaric model, 17: 41755
production, coupling constants, and R_4 symmetry predictions, 18: 30610
properties, 16: 21272
properties of G_3 multiplets for, decay and electromagnetic, 18: 7537
properties of, CERN synchrotron research on weak and electromagnetic, 18: 20965
properties of, for use in radiotherapy, 19: 28200
properties of, phenomenological analysis of, (T), 20: 4633
properties of, review of, 19: 16657
properties of, symmetrization postulate for, 18: 40317
range difference ($\pi^- - \pi^+$) in emulsion (E), 19: 3029 (UCRL-11518)
reactions in bubble chambers, meson (K^0) pair production in, 17: 7039
reactions in emulsions at 14 Bev/c, 16: 25927 (NP-11977(p.66-7))
reactions in hydrogen bubble chambers, ionization in, 18: 30033
reactions in nuclear coulomb fields, meson (3π) formation in, 18: 26300

reactions in nuclear emulsion, radii for, 18: 34964
reactions in nuclear emulsions at high energies, ionization losses in, 19: 12622
reactions in nuclear emulsions at 7.5 and 17.5 Bev, charged-particle identification from delta electrons in, (E), 20: 17358
reactions on nuclei, production of meson (π) pairs by peripheral, 16: 32321
reactions with bromine and silver at 17.5 Bev, helium isotope production in, 18: 38102
reactions with bromine and silver at 17 Bev/c, 18: 40551
reactions with bromine and silver at 24 Bev, fast secondaries from (E), 19: 1672
reactions with complex nuclei, data survey for nonelastic, 17: 34883 (ORNL-3455)
reactions with complex nuclei, nuclear research with, 17: 36643 (CERN-63-28(p.47-72))
reactions with complex nuclei, literature survey on, 18: 7690(R) (ORNL-3499(Vol.II)(p.54-6))
reactions with emulsion nuclei at 2 Bev/c, 18: 14797 (AFOSR-4737)
reactions with emulsion nuclei at 4.5 Bev, excited fragments from, 18: 38082(T) (AEC-tr-6398(p.153-6))
reactions with emulsion nuclei at 7.5 Bev, alpha, deuteron, and triton distributions from, (E), 19: 19222
reactions with emulsion nuclei at 5 to 30 Bev/c, particle distributions in, (E), 19: 23693
reactions with emulsion nuclei at 7.5 Bev, production of high-energy fragments in, (E), 20: 17715
reactions with emulsion nuclei at 17.5 Bev, helium particle emission in, (E), 20: 17716
reactions with emulsion nuclei at 17 Bev/c, deuteron and triton production in, (E), 20: 25813
reactions with freon at 16 Bev/c, coherent production of 3π resonances in, (E), 20: 37822
reactions with helium-4, meson (ρ) production in coherent, (T), 20: 22145
reactions with helium-3, decay processes from, 20: 38011 (JINR-P-2805)
reactions with hydrogen at 7 to 8 Bev, antihyperon (Λ) production in, 17: 38154
reactions with light nuclei, double charge exchange in, 20: 22033
reactions with liquid hydrogen at 321 Mev, ionization in, 20: 25392
reactions with liquid hydrogen, energy range graph for, 20: 46601 (UCRL-2426(Vol.2)(1966 Rev.))
reactions with nuclei at 4.15 Bev, mechanism for nuclear evaporation in, 16: 4881
reactions with nuclei, nucleon pair production in, 16: 26089 (NP-11832)
reactions with nuclei, intranuclear cascades from, 17: 22564 (ORNL-3383)
reactions with nuclei, meson (ρ) coherent production in, 18: 44821
reactions with nuclei, three-meson-(π) distributions from, 19: 1280
reactions with nuclei at low energies, charge exchange, (T), 19: 31302
reactions with nuclei as probe of nuclear structure, conference on, 19: 41671 (LADC-6186)
reactions with nuclei below 200 Mev, nuclear structure from, 19: 45339
reactions with nuclei at 2 to 10 Bev, meson (π)-nucleon cascades from, 20: 8079 (ORNL-3855)
reactions with nuclei at low energies, (T), 20: 42312
reactions with nuclear coulomb fields at high energies, meson (ω) production from, (T), 20: 46385
reactions with nuclei at 2 to 10 Bev, calculation of, 19: 17159(R) (ORNL-3714(Vol.II)(p.97-118))
Regge poles of, effects in photoproduction of mesons, 18: 26372
resonance (K-π) in meson (π^-)-proton interactions, 726-Mev, 18: 20918 (UCRL-10797)
resonance ($\Lambda\pi$) production in meson (K^-)-proton interactions at 1.2 to 1.7 Bev/c, 18: 36254 (UCRL-11291)
resonance ($\pi\omega$) of, parity and spin of, 18: 14901
resonance (π-ω) at 1220 Mev, properties of meson (B), 18: 18684
resonance (Ξ-π) at 1530 Mev, parity and spin of, 18: 34517 (UCRL-11436)
resonance effects (Λ–π) on hyperon-nucleon inelastic interactions, 16: 6965
resonance effects on meson (K)-nucleon scattering, 16: 22852 (NP-11761)
resonance mass spectra in gamma-proton interactions, 2π, 18: 26353
resonance of three, 18: 26323
resonance of 5, 960-Mev, 18: 22765
resonance state effects on nucleon isoscalar structure, 17: 41776
resonance states, 16: 16998 (NP-11592(Vol.II)(p.57-85))
resonance states, contribution of 3-π to nucleon isoscalar structure, 16: 9392
resonance states of, mass formula for, 18: 9147
resonance states of, theories for production of, 18: 9197
resonance states of, mass formulas for, 18: 16799
resonance states of, N–N scattering amplitude effects of, 18: 30605
resonance states of, production of four-body, 18: 36361
resonance states of, parity and spin of (X^0) (960 Mev), 18: 44556
resonance states of, mass formulas for, 18: 44595
resonance states, relations between 2-π and 3-π, 16: 9391
resonance with mesons (K), meson ($\overline{K}^0$) identification as, 16: 4714
resonances (ρ–π) in meson (π^+)–proton interactions, 18: 30568
resonances in antihyperon (Λ) decay, vanishing such that nucleon mass $\simeq$ hyperon (Ξ) mass, 16: 4718
resonances of, 18: 10891
resonances of, and nuclear theory, 17: 5262
resonances of 2 and 3, 18: 21001
resonances of 3 at 550 Mev, from meson (π) reactions with deuterons, 16: 4716
resonances of, data on, 19: 37642
resonances of, determination of quantum numbers of, 19: 37651
resonances of, parity and spin of four-meson, 18: 14900
resonances of, production in meson (π^+) –proton interactions (E/T), 19: 3030 (UCRL-11729)
resonances of, production in meson (π)-proton interactions, 19: 3031 (UCRL-11730)
resonances of, quasi-molecular model for, 18: 37982
resonances of, review of properties of, 18: 18676
resonances of, self-coupled fields for, 18: 21002
resonant state energies, empirical regularities in, 16: 18345
resonant state of (K-π) system at 725 Mev, parity and spin of, 17: 41774
resonant state with hyperon (Σ), parity, 16: 21326
resonant state with hyperons, 16: 29697
scattering by alpha particles at 300 Mev, 17: 9223
scattering by bromotrifluoromethane and propane, cross sections for, (T), 20: 13480
scattering by deuterium and hydrogen at 300 Mev, angular distributions and cross sections for, 17: 34812
scattering by helium-3 and tritium, differential cross sections for, (T), 19: 12531
scattering by helium at 500 to 1200 Mev, optical model for cross sections of, (E/T), 20: 8110
scattering by hydrogen at 25 Bev, elastic, (E), 19: 23355(R) (BNL-867(p.1-117))
scattering by light nuclei, high-energy approximation, 18: 34911
scattering by lithium-7, angular momentum coupling and nuclear spins for elastic, 20: 44719
scattering by mesons (π), amplitudes, 16: 16971 (NP-11592(Vol.I)(p.343-6))
scattering by mesons (π), asymptotic behavior, 16: 26069 (JINR-E-943)
scattering by nuclei, optical model potential to the second order, 16: 7074
scattering by nucleons, analysis of low-energy s-wave, 16: 16973 (NP-11592(Vol.I)(p.351-4))
scattering by nucleons, dispersion relations for forward, 16: 16991 (NP-11592(Vol.I)(p.485-6))
scattering by nuclei, double charge exchange in elastic, 18: 15192 (CONF-399-2)
scattering by nuclei, double charge exchange in elastic, 18: 16939 (ANL-6848(p.236-9))
scattering by nuclei at 30 to 150 Mev/c, Coulomb effects in, 18: 28730
scattering by nuclei at 65 to 150 Mev, mechanisms for elastic, 18: 44801
scattering by nuclei at 500 to 1300 Mev, cross sections for, (E), 19: 12529
scattering by nuclei, nucleon correlation effects on quasi-elastic, (T), 20: 15827
scattering by nuclei, optical models for elastic, (T), 20: 42319
scattering constant at 17 Bev/c in emulsions, 18: 28343
scattering in emulsions, multiple, 16: 24702
scattering in nuclear emulsions, multiple, 17: 32931
scattering in nuclear emulsions, 18: 40373
scattering interactions with mesons (π), partial waves effects, 16: 17067 (JINR-D-857)
scattering length for, determination from three-pi decay of mesons (K), 19: 37665
scattering lengths, $\overline{K}N$ and KN energy dependent S-wave, 16: 16974 (NP-11592(Vol.I)(p.355-8))
scattering near meson (f^0) and (ρ) resonances, 17: 29548
scattering of, by mesons (π), amplitude in the l plane of, 16: 28029 (JINR-E-952)
scattering of, by protons, angular distribution of, 16: 30930(R) (NYO-2669)
scattering of cloud, in proton-proton interactions at high energies, 20: 41896
scattering of, measurement of multiple, in energy-loss interactions, 17: 6954 (NP-12259)
scattering of, on mesons (π), effect on nucleon form factor of inelastic, 17: 28198
scattering of, prediction of interaction symmetry from dispersion relations in, 17: 20905

scattering of, resonances in, 17: 5274
scattering on nuclei, electromagnetic form factor from elastic, (T), 20: 13878
separation from antiprotons and mesons (K) at high energies, 16: 31883
separation from mesons (μ) in meson beams, Cherenkov detector for, 17: 37433
separation of beams of, in accelerators, (T), 19: 27038
spectra from interactions in nuclear emulsion, transverse momentum, 18: 28426
spectra from neutron-proton interactions, 16: 22921
spectra in meson ($K^+_{\pi 3}$) decay mode, 16: 6977
spectra of, from meson (η, τ, and τ') decays, 17: 11553
spectrum in hyperon (Λ) and (Σ^+) decay, 16: 10848
spin of, model for, 19: 27166 (UCRL-7523)
statistics of, 18: 34628
statistics of, arguments for Bose–Einstein, 18: 28380
structure, electromagnetic aspects, 16: 16997 (NP-11592(Vol.II)(p.33-55))
structure of, calculation of electromagnetic, 17: 26389
systems of three and four, classification scheme for, 17: 9343
theory, 18: 26667
theory of, as antinucleon-nucleon bound state, 17: 29525
theory of exchange in nucleon–nucleon scattering, 16: 18319 (AFOSR-2117)
theory of, as bound nucleon-antinucleon systems, 20: 39841
theory, proof that pions are elementary particles, 16: 5907
trajectories in magnetic fields, measurement of, 17: 18524 (CERN-63-3(p.211-19))
transport by shielding, calculations of, 17: 22694
triplet formation with mesons (K^-) and (K^+), 16: 10902
use in radiotherapy, 19: 26215
wave function for three relativistic, angular momentum, 17: 13403
wave function renormalization constant of, (T), 20: 9814
wave functions for systems of three free, 16: 19701
wave functions for systems of four free, 16: 21319
wave functions for four free, 17: 9201 (PAN-356/VII)
wave functions for system of three or more, effective angular momentum for, 17: 19053
wave functions for four-body system of, orthonormal, 17: 28162
wave functions for many-body systems of, isotopic spin symmetry in, 17: 28165
wave functions for system of, symmetry properties of, 18: 14826
wave functions for, isospin, 18: 14829
wave functions of n-identical system of, isospin and spin from relative coordinate symmetry in, 17: 24309
wave functions with definite symmetry for, many-body configurational, (T), 20: 15450
wave-function renormalization constant for fields of, using partially conserved axial-vector current, (T), 20: 15402

MESONS (π^-)

absorption and elastic scattering on emulsion nuclei at 5.7 Bev, 16: 16964 (NP-11592(Vol.I)(p.291-4))
absorption and moderation in hydrogen (liquid), 17: 17230
absorption and scattering in nuclear emulsion, at 5.7 Bev/c, small angle, 17: 16980
absorption and slowing-down in liquid deuterium and hydrogen, (E), 19: 6691
absorption at rest by light emulsion nuclei, 18: 16978
absorption by bound hydrogen nuclei, (T), 20: 980
absorption by carbon at 40 to 70 Mev, 17: 38081 (JINR-P-1286)
absorption by carbon, charged particle emission spectra for, 17: 41744 (NYO-10561)
absorption by carbon-12 at rest, (T), 20: 1193
absorption by complex nuclei, 17: 17108 (ISS-62/21)
absorption by complex nuclei, 18: 7339 (ISS-63/40)
absorption by complex nuclei, neutron emission from, 18: 32733 (ISS-64/10)
absorption by copper, lead, and tin, 17: 28139 (ISS-63/28(p.1-11))
absorption by emulsion nuclei, 18: 24582 (AD-439331)
absorption by hydrogen and deuterium, relative rate of, 17: 9517 (UCRL-10417)
absorption by hydrogenous substances, mechanisms for, (T), 19: 4896 (JINR-P-1816)
absorption by light nuclei, products of, (E), 19: 19220
absorption by liquid hydrogen, 16: 28000
absorption by lithium-6, alpha particle spectra from, (T), 19: 25509
absorption by nuclei, nucleon emission from, 17: 19080
absorption by nuclei, with two-nucleon emission, (T), 19: 39932
absorption in carbon, two-nucleon mechanism of, 17: 22507
absorption in freon-propane mixture, cross sections for, 18: 16776
absorption in liquid hydrogen, 16: 24822
absorption in lithium-7, tetraneutron production in, (E), 19: 35460
absorption of bound s-orbit, in heavy nuclei, (T), 19: 33260
absorption rate in liquid helium, 19: 43356
absorption time in hydrogen (liquid), 17: 26561
angular correlations in ($\bar{p}d \to p\pi^-\omega$) interactions, 18: 30533
angular distribution from proton pair annihilation, 18: 12910 (PAN-450/VII)
angular distributions from meson (π^-)–proton inelastic interactions, 18: 30580
angular distribution and energy of cascade, from proton-copper reactions at 1 Bev, (E/T), 19: 17159(R) (ORNL-3714(Vol.II)(p.97-118))
angular distributions from meson (π^-)-proton interactions at 200 to 300 Mev, (E), 19: 33062
attenuation in deuterium and hydrogen (liquid), reaction branching ratios for, 17: 22622
beta decay to mesons (π^0), branching ratios of, (E), 19: 14312 (CU-233)
capture and transfer in hydrogenous media (E), 19: 3237 (JINR-P-1767)
capture at rest by complex nuclei, 17: 34734 (NYO-10278)
capture at rest in hydrogen, Panofsky ratio for, 17: 32947
capture by bound hydrogen, 17: 22600
capture by carbon and oxygen at 80 Mev, helium-8 production in, (E), 20: 40071 (JINR-E-2774)
capture by carbon and oxygen, helium-8 production by, (E), 20: 44770
capture by complex nuclei, neutron spectrum from, 16: 25902 (LNF-62/37(p.138-42))
capture by complex nuclei at 150 Mev/c, neutron emission in, (E), 19: 8437
capture by complex nuclei, radiative, (T), 20: 38064
capture by copper, lead, and tin, 18: 10854 (LNF-63/47(p.1-35))
capture by emulsion nuclei, single charged particle emission in, 17: 11679
capture by emulsion nuclei, neutron energy spectra from, 17: 26543
capture by explosives, thermal initiation theory of spherical hot spots in, 18: 16026
capture by helium-3, nuclear matrix element from, 16: 21384
capture by helium-4, 17: 6979
capture by helium-3, two-nucleon model for, (T), 19: 35490
capture by helium-3, neutron-neutron scattering length from, (T), 19: 45354
capture by helium-3, two-nucleon model for, 20: 26166
capture by helium, de-excitation mechanism for, 18: 19089
capture by hydrogen, internally produced electron pairs from, 16: 21315
capture by hydrogen, in chemical compounds, 17: 7083 (JINR-P-1081)
capture by hydrogen in polythene, probability of, 18: 13044 (JINR-E-1471)
capture by hydrogen nuclei (E), 19: 3086
capture by hydrogen and deuterium, probabilities for fine-structure-level, (T), 20: 17278
capture by light nuclei, formation of protons, deuterons, and tritons from, 17: 17273
capture by light nuclei, yields and energy spectra from, (E/T), 20: 6292 (NP-15601)
capture by nuclei, nuclear structure from two-nucleon emission in, 17: 38175
capture by nuclei, 18: 2585(R) (ISS-63/37)
capture by nuclei, neutron emission spectra in, 18: 7769
capture by nuclei $3 \leq Z \leq 13$, two-nucleon emission from, (E), 20: 19842 (UR-875-126, Paper 1)
capture by nuclei below 300 Mev, gamma and neutron spectra from, (E), 20: 42314
capture by nuclei, neutron spectra from, 18: 19084
capture by nuclei, nucleon correlations from, 18: 34851
capture by nuclei, use in rock age determinations, 18: 43601(R) (TID-21007)
capture by nuclei, radiative, (E), 19: 19149
capture by nuclei, nucleon pair emission from, (T), 19: 47679
capture by nuclei, radiative, (T), 20: 28414
capture by nuclei, angular correlations of particles from, (T), 20: 30504
capture by nuclei, radiative, (T), 20: 42385
capture by nucleons in propane, 18: 24475
capture by protons, neutron emission at 8.9 Mev in, 16: 20683
capture in complex nuclei, 17: 6792(R) (ISS 62/14)
capture in deuterium and hydrogen, branching and Panofsky ratios for, 16: 26232 (UCRL-9884)
capture in flight, radiative, 17: 20594(R) (UCRL-10572)
capture in gaseous helium-3, measurement of cascade time in, 20: 39579 (JINR-P-2838)
capture in liquid helium, cascade time for, 18: 898
capture in liquid helium-4, moderation time for, 18: 901
capture in liquid helium, de-excitation, (T), 19: 21042
capture of, in complex nuclei, 17: 22418 (ISS-62/7)
capture of stopped, by nucleons, 17: 11687
capture on liquid hydrogen and nuclei, radiative, (T), 19: 16964
cascade and moderation times in liquid helium, (E), 20: 15273
cascade showers from 25 Mev to 2 Bev, 18: 7845(R) (ORNL-3499 (Vol.II)(p.27-30))

cascade time in liquid helium, 18: 862(R) (TID-19590)
charge exchange and radiative capture on, (E), 19: 33392
charge exchange on bound hydrogen nuclei, 17: 9307
charge exchange on complex nuclei, 18: 13045 (JINR-P-1470)
charge exchange on hydrogen, detection of chemical bonding by, 20: 20653 (JINR-P-2558)
decay amplitude, ($\mu^- \nu_\mu$), (T), 20: 34181
decay branching ratio $(e^- + \bar{\nu})/(\mu^- + \bar{\nu})$, 18: 24406
decay ($e^- + \nu$) and ($\mu^- + \nu$), effects of e and μ spirality on probabilities of, 17: 28173
decay modes, 16: 8133
decay, neutrino production and properties from, 16: 26147
decay, neutrino spectra from, 16: 15562
decay of accelerated, interactions of neutrinos from, 17: 28151 (NEVIS-111)
decay of relativistic, neutrino spectra from, 18: 12894 (CERN-63-37 (p.111-29))
decay of, symmetry violations in leptonic, 18: 7551
decay of, unitary symmetry of weak current structure in, 17: 41781
decay of, vector form factor in, 17: 32934
decay of, antineutrino and meson (μ^-) helicity from, 18: 28423
decay of, branching ratio for leptonic and nonleptonic, 18: 20973
decay of, kinematic tables for, 20: 36022 (BNL-945)
decay of, neutrino interactions in, 18: 40280
decay of, neutrino spectra from, (E), 20: 21602 (CERN-65-32, pp 111-14)
decay of, spatial distributions in leptonic, 19: 35045
decay ($\pi^+ \to \mu + \nu$), Regge phase shifts in Goldberger-Treiman formula for, 17: 41780
decay probability, $\pi^- \to \pi^0 + e + \bar{\nu}$, 16: 950
decay, probability of β-type, 16: 13861 (JINR-D-844)
decay schemes, 16: 37252
detection and measurement of contamination by, in meson (μ^-) beams, 16: 22889
disperaion in 6-meter synchrotron, angular and energy, 16: 2416
distributions from meson (π^-)-nucleon interactions at 6.8 Bev/c, 18: 40288
distributions from meson (π^-)-proton six-prong interactions at 10 Bev/c, 18: 40293
dosimetry, 18: 37044(R) (UCRL-11387(p.114-26))
dosimetry of, using ionization chambers and lithium fluoride dosimeters, 20: 18516
effects on chromosomes, 19: 2062 (BNL-8462)
effects on γ–γ scattering, (T), 20: 11600
effects on mammals, 18: 15826
effects on mouse lymphoma cells, 20: 42859(R) (UCRL-16246, pp 100-2)
effects on neutron magnetic moment, 17: 24288
effects on tissue, 20: 18185(R) (BNL-929, pp 126-47)
effects on tissues, 18: 37044(R) (UCRL-11387(p.114-26))
effects on *Zea mays*, RBE for cytogenetic, 19: 5696
effects on *Zea mays*, cytogenetic, 18: 41157
electromagnetic structure of, (E), 19: 20935 (NP-14885)
electron separation from beams of, high-energy, (E), 19: 34823
emission from interactions, phenomenological analysis of proton-meson (K^-), (T), 19: 35170
emission in hypernuclei decay, angular correlations for, 18: 28732
emission in mesons (π^-)-nucleon interactions at 4.4 Bev, transverse momentum of, 18: 42395
emission in neutron interactions with protons at 600 Mev, yields of, 18: 10970
energy estimation of, in photographic emulsions by angular distribution of secondary shower particles, 17: 39860
energy loss measurements in silicon at 50 to 365 Mev, (E), 20: 7411
energy spectra from meson ($K_{\mu 3}$) decay, (E), 20: 1011
energy spectra in meson (ϕ^0) and (ω^0) decays, (T), 19: 43104
energy transfer from 70-Mev beams of, to polyethylene, 20: 20525
exchange in neutron-proton reactions, backward peaking in high-energy, 17: 19117
form factors, development of models for, 16: 8096 (JINR-D-774)
form factors, relation to meson ($K^\pm$) form factors for electromagnetic and weak transitions, 16: 2450
interaction cross sections, 16: 13880
interaction lengths and elastic scattering in G5 emulsion at 300 Mev, 16: 21406
interaction resonances with protons, elastic, 18: 37963
interactions at high energy, cross section combinations for, 17: 11529
interactions at 16 and 24 Bev, cross section for strange particle production, 16: 16937 (NP-11592(Vol.I)(p.93-100))
interactions at 17 Bev/c in nuclear emulsions, hyperfragment production in, 16: 27924
interactions at 4.5 Bev, use of Monte Carlo method in interpretation of, 18: 14819 (NP-13680)
interactions in bubble chambers, analysis of events, 16: 29660 (TID-16119)
interactions in bubble chamber, analysis of neutral V-events from, 16: 31008 (CERN-62-21)
interactions in bubble chamber at 6.1 Bev/c, angular and mass distributions from, (E), 20: 7836
interactions in emulsions at 3.5 and 16 Bev, multiple meson (π) production and meson (π^0) lifetime, 16: 2305(R) (UCRL-9704)
interactions in freon at 2.8 Bev/c, meson ($\pi^\pm$) production in, (E), 20: 2739
interactions in hydrogen bubble chamber at Saclay, computer analysis of tracks from, 18: 23887 (PAN-474/VI)
interactions in meson (K) decay, 18: 36358
interactions in nuclear emulsion at 16 Bev, electron pair production in, 17: 29512
interactions of three, analysis of I = 0 states in, (T), 19: 45024 (UCID-2608)
interactions of, with emulsion nuclei at 2 Bev, 16: 32267 (AFOSR-1728)
interactions of, with protons at 1030 to 1140 Mev, charge exchange reactions in, 16: 32289 (TID-16677)
interactions of, with protons at 1.89 to 2.24 Bev, strange-particle resonant states produced in, 16: 32302 (UCRL-10286)
interactions of, with carbon at 7 Bev, 16: 33687 (PAN-326/VI)
interactions of, with xenon nuclei at 8.4 Bev, 16: 33688 (PAN-327/VI)
interactions of, with carbon nuclei at 7 Bev, behavior of heavy particles emitted in, 16: 33689 (PAN-328/VI)
interactions of, with protons at 310 Mev, analysis of phase shifts and recoil-nucleon polarization in, 16: 31021 (UCRL-10253)
interactions of, with carbon at 915 Mev, Monte Carlo calculation of, 17: 28199
interactions of, cross sections for elastic, (E), 19: 10049
interactions of, model for forward amplitude for, 20: 37805
interactions of, SU(6) symmetry for forward amplitudes in, (T), 19: 41515
interactions with protons at 7 Bev, 16: 983
interactions with protons at 8 to 20 Bev/c, total cross sections, 16: 2453
interactions with protons, mesons (π) production in, 16: 2305(R) (UCRL-9704)
interactions with alpha particles at 153 Mev, 16: 22944
interactions with antiprotons, $\bar{N}_3^*$ anti-isobar production in, 17: 7002
interactions with alpha particles, meson (π) form factors from, (T), 19: 41379
interactions with alpha particles at 24 Mev, meson (π) electromagnetic form factor from elastic, (E), 20: 21659
interactions with bound proton at 5.0 Bev, calculation of proportion of forbidden collisions, 16: 18329
interactions with bound nucleons, quasielastic, 16: 22944
interactions with baryons, multiplet structure in strong, 17: 26373
interactions with bound and free protons at 2.8 Bev/c, ratio of, 20: 44177 (NP-16278)
interactions with carbon nucleons, parity conservation in hyperon (Λ^0) production in, 18: 24394 (NEVIS-122)
interactions with deuterons at low energies, p and s wave contributions in, 16: 18344
interactions with deuterons, hyperon (Σ) production in, 17: 9366
interactions with deuterons at 300 Mev, cross section for elastic, 17: 28185
interactions with deuterons and protons, 17: 31091(R) (UCRL-10862)
interactions with deuterons at 142 Mev, 17: 31350
interactions with deuterons at 142 Mev, form-factor approximation in elastic, 17: 31351
interactions with deuterons and protons, total cross sections for, 17: 39844 (BNL-7258)
interactions with deuterons at 330 Mev, cross sections for, 18: 2612
interactions with deuterons at low energy, 18: 4433 (UCRL-10977)
interactions with deuterons and protons, resonances in, 18: 12913 (TID-7686(p.69-107))
interactions with deuterons, energy and angular distributions from, 18: 24451
interactions with deuterons, neutron-neutron scattering length in, 18: 24462
interactions with deuterons, sonic spark chamber for studying photon production in, 18: 31891 (CERN-64-30(p.221-7))
interactions with deuterons at zero-energy, branching ratios and cross sections for, 18: 34634
interactions with deuterons at 420 to 1360 Mev (E), 19: 1328
interactions with deuterons, probability of (2nγ) (E), 19: 3026 (JINR-P-1768)
interactions with deuterons at low energies, (E/T), 19: 10111
interactions with deuterons, neutron-neutron scattering length from, (E), 19: 20995
interactions with deuterons and protons at 6 to 22 Bev/c, total cross sections for, (E), 19: 25351
interactions with deuterons at 3.7 Bev/c, deuteron–meson (π^-) enhancement in, (E), 19: 37599

interactions with deuterons at 3.2 Bev/c, enhancement at 1.0 to 1.4 Bev in, (E), 19: 39551
interactions with deuterons at 3.2 Bev/c, resonance production in, (E), 20: 15405
interactions with deuterons at 3.7 Bev/c, resonances in, (E), 20: 15409
interactions with deuterons, neutron-neutron S-wave scattering length from, (E), 20: 15511
interactions with deuterons, dynamical theory for final-state, 20: 19273(R) (BNL-929, pp 3-43)
interactions with deuterons at high energies, resonances from, (E/T), 20: 19273(R) (BNL-929, pp 3-43)
interactions with deuterons, hyperon (Σ^-)-neutron production and final-state interaction in, (T), 20: 21681
interactions with deuterons and nucleons at 3.7 Bev/c, A_1 and A_2 resonance production in, (E), 20: 30078
interactions with deuterons at 300 Mev, effects of π-N resonance on, (T), 20: 34172
interactions with deuterons and protons, research on, (E), 20: 36043(R) (TID-23206)
interactions with deuterons, nonradiative and radiative absorption ratios for atomic s-orbitals for, (T), 20: 41809
interactions with deuterons, neutron-neutron S-wave scattering length from, (E), 20: 41914
interactions with electrons at 16 Bev/c, 18: 14797 (AFOSR-4737)
interactions with electrons at 16 Bev/c, cross sections for, 18: 30548
interactions with electrons at 21 Bev, meson structure from, (E), 19: 20935 (NP-14885)
interactions with electrons at 4 Bev/c, cross sections for, (E), 19: 35030 (JINR-P-2162)
interactions with electrons at 4 Bev/c, (E), 20: 7873
interactions with gamma radiation, cross sections for, 16: 24695 (NP-11757)
interactions with hyperons (Σ^+), asymptotic relations and invariance properties in, 18: 18700
interactions with hyperons (Λ), resonances in, (E/T), 19: 6518 (JINR-P-1807)
interactions with hyperons (Σ^-), I = 2 resonance in, (T), 19: 18801
interactions with hyperons (Σ^-), T = 2 resonant state in, (T), 19: 18803
interactions with mesons (π^+) at 365 and 430 Mev, cross sections for, 16: 10879
interactions with mesons (π^+), resonance frequency distributions, 16: 15582
interactions with mesons (π^0), amplitudes, 16: 15604
interactions with mesons (π^0), cross section relation to meson (ω^0) decay partial widths, 16: 15588
interactions with mesons (π^-) at 16 Bev, electron-pair production, 16: 16935 (NP-11592(Vol.I)(p.79-83))
interactions with mesons (π^0), resonance production below 765 Mev in, 16: 24748
interactions with mesons (π^0), meson (ρ) properties from, 16: 27983
interactions with mesons (π^+), resonances from, 17: 4003
interactions with mesons (π^+), 17: 5252
interactions with mesons (π^0), cross section for, 17: 31327
interactions with mesons (π^+), cross sections for, 17: 31277 (JINR-P-1260)
interactions with mesons (K^-) at 1.51 Bev/c, effective mass distributions from, 17: 41788
interactions with mesons (π^+), cross section for, 17: 41928
interactions with mesons (π^-) at 1035 to 1325 Mev, test of $|\Delta I| = \frac{1}{2}$ rule in, 18: 4466
interactions with mesons (π^+), cross sections for elastic, 18: 6038
interactions with mesons (π^+), cross sections for inelastic, 18: 7532
interactions with mesons (π^-), cross section for pure I = 2, 18: 10930
interactions with mesons (π^+), meson (ρ^0) domination in Lee model for, 18: 18681
interactions with mesons (π^+) in meson (π^-)-proton interactions at 4 Bev/c, 18: 37886 (UCRL-11468)
interactions with mesons (π^0), kinematics of, (E), 19: 5572(R) (PPAD-525-D)
interactions with mesons (K), properties of resonance, (E/T), 19: 6556
interactions with mesons (π^-) at 3 Bev/c, strange-particle production in, (E/T), 19: 10084
interactions with mesons (π^0), (T), 19: 21000
interactions with mesons (π^+), in deuteron–meson (π^+) interactions at 4.5 Bev, (E), 19: 25388
interactions with mesons (π^+), complex angular momentum and vector mesons in, (T), 19: 43087
interactions with mesons (π^+) and (π^0), phase shifts in elastic, (T), 19: 47357
interactions with mesons (π^+) below 1.3 Bev, phase shifts for elastic, (T), 20: 11555 (DESY-65/13)
interactions with mesons (π^+), annihilation channels in, 20: 39776(T)
interactions with nucleons at 7 to 8 Bev, cross sections, 16: 4689 (JINR-P-765)
interactions with neutrons at 2.8 Bev, cross sections at 10 to 180°, 16: 4724
interactions with nucleons at 7 to 8 Bev, cross sections, 16: 4736
interactions with nucleons at 6.8 Bev, inelastic, 16: 5862 (JINR-P-789)
interactions with nucleons at 7 to 8 Bev, cross sections, 16: 6927(T) (NP-tr-836)
interactions with nucleons at 6.8 Bev, inelastic, 16: 6996
interactions with neutrons, multiple meson (π^0) production, 16: 12548
interactions with neutrons, cross sections for, 16: 13880
interactions with nucleons, coupling strength, 16: 13903
interactions with nucleons, angular distribution, 16: 24682 (JINR-P-868)
interactions with nucleons at 7 Bev, inelastic low-multiplicity, 16: 24715
interactions with nucleons at 7 Bev, inelastic, 16: 24716
interactions with nucleons at 7.5 Bev, inelastic, 16: 24717
interactions with nucleons at 6.8 Bev/c, inelastic, 16: 24718
interactions with nucleons at 7 Bev, properties of mesons (π^0) formed in inelastic, 16: 26081 (JINR-P-974)
interactions with neutrons, meson (π^-) production in, 16: 32353
interactions with nuclei at 4.5 Bev, 17: 5214
interactions with nucleons, meson (K^0) production in, 17: 9282
interactions with neutrons at 2.8 Bev/c, 17: 9317
interactions with nucleons, strange particle correlations in, 17: 9360
interactions with nucleons at large angles, elastic, 17: 9428
interactions with nucleons, peripheral effects in, 17: 9433
interactions with nucleons, "glancing" collisions in, 17: 9434
interactions with nucleons at 7 Bev, inelastic, 17: 9435
interactions with nucleons, mechanisms for gamma production in inelastic, 17: 17192
interactions with neutrons, three-pion resonances obtained from, 17: 17050
interactions with nucleons, effect of ($\bar{K}$-K) resonance in, 17: 20871
interactions with nucleons, production of excited mesons (K) in, 17: 20891
interactions with nucleons at 7 Bev, gamma production in, 17: 20934
interactions with nucleons at 1.89 to 2.36 Mev/c, spin 2 ($\Sigma\pi$) resonant states in, 17: 24335
interactions with nucleons at 7 Bev, peripheral, 17: 28208
interactions with nucleons, parameters of inelastic, 17: 29515
interactions with nucleons, spin-orbit forces in, 17: 29550
interactions with nucleons at 6.8 and 8.0 Bev/c, hyperons (Ξ^-) production in, 17: 32945
interactions with nucleons at 6.8 Bev, inelastic, 17: 34813
interactions with nucleons at 2.66 Bev, inelastic, 17: 38151
interactions with nucleons, meson and baryon exchange diagrams for, 17: 39880
interactions with nucleons at 6, 11, and 18 Bev/c, correlations in strange-particle pairs produced by, 17: 41765
interactions with nucleons, (π-π) resonances in inelastic, 18: 865 (UCRL-10731)
interactions with nucleons at 16.2 Bev/c, separation of central and peripheral, 18: 2616
interactions with nucleons at 7 Bev, peripheral, 18: 6005
interactions with nucleons at low energies, parameters and phase shifts for, 18: 7556
interactions with nucleons at 4.5 Bev, total cross sections for, 18: 10933
interactions with nucleons at 0.3 to 1 Bev, resonance-like effects in, 18: 14959
interactions with nucleons at 6.1 to 18.1 Bev/c, strange particle production in, 18: 16776
interactions with nucleons at 17 Bev/c, 18: 20891 (AD-433625)
interactions with nucleons at 7 Bev, 18: 24391 (JINR-P-1629)
interactions with nucleons at high energies, parameters for, 18: 24384 (JINR-P-1577)
interactions with nucleons, model for resonances in, 18: 32608
interactions with nucleons at 6.8 Bev, inelastic, 18: 32621
interactions with nucleons, vector meson production in, 18: 34620
interactions with nucleons at 7.5 Bev, 18: 40287
interactions with nucleons at 6.8 Bev/c, 18: 40288
interactions with nucleons at 6.8 and 7.5 Bev/c, mesons (π^0) from, 18: 40289
interactions with neutrons at 9 Bev/c, 18: 40290
interactions with nucleons, momentum distributions for, 18: 40373
interactions with nucleons at 4.4 Bev, transverse momentum of mesons (π^-) and (π^+) emitted in, 18: 42395
interactions with nucleons at 6.1 Bev (E), 19: 1397
interactions with nucleons at 6.1 and 18.1 Bev, 3-π production in (E), 19: 1398
interactions with nucleons at 10 Bev, inelastic, (E), 19: 4905
interactions with nucleons in xenon at 9 Bev/c, (E), 19: 8446
interactions with nucleons at high energies, amplitudes and total cross sections for, (T), 19: 10076

interactions with nucleons at 17 Bev, (E), 19: 10108
interactions with nucleons at 6 to 18 Bev/c, strange particle production in, (E), 19: 14322 (NP-14637)
interactions with nucleons at 7.5 Bev, isospin analysis of, (T), 19: 14342
interactions with nucleons at 10 Bev, (E), 19: 14366
interactions with nucleons at 12 and 18 Bev/c, meson (ρ^0) production in, (E/T), 19: 16613
interactions with nucleons at 6.8 Bev/c, angular and momentum distributions in, (E), 19: 21062
interactions with nucleons at 7 Bev/c, proton spectra from inelastic, (T), 19: 25281
interactions with neutrons at 9 Bev/c, quasi-elastic, (E), 19: 37608(T)
interactions with nucleons at 300 to 700 Mev, amplitudes for, (E), 19: 41442
interactions with nucleons at 2.8 Bev/c, $K^0\bar{K}^0$ resonance production in, (E), 19: 43048 (NP-15377)
interactions with neutrons at 1.2 to 4.5 Bev/c, cross sections for backward elastic, (E), 19: 47310 (NP-15376)
interactions with nuclear field at 16.2 Bev/c, coherent production of meson (π) tridents in, (E), 19: 47355
interactions with nucleons at 6.8 Bev/c, meson (π^0) production in inelastic, (E), 19: 35175
interactions with neutrons at 1.4 to 4.0 Bev/c, backward elastic, (E), 20: 2700(T)
interactions with neutrons at 1.38 to 4.05 Bev/c, backward elastic, (E), 20: 2713
interactions with nucleons, phase-shift analysis of, (T), 20: 4849(R) (UCRL-14360, pp 1-50)
interactions with nucleons at high energy, sum rule for cross sections of, (T), 20: 4678
interactions with neutrons in neutron stars, neutrino cooling from, (T), 20: 4532
interactions with nucleons at 4.4 Bev, secondary particles from, (E), 20: 9775
interactions with nucleons, π-π distributions and meson (f^0) from, (E), 20: 9730
interactions with nucleons at low energies, cross sections for scalar, (T), 20: 11574
interactions with nucleons in emulsions at 16.3 Bev, angular distributions from, (E/T), 20: 11602
interactions with nucleons, phase-shift analysis and spin-flip dispersion relations for, (T), 20: 13492
interactions with nucleons in emulsions at 17.2 Bev, mass distributions from, (T), 20: 19472
interactions with nucleons at 6.8 Bev, inelastic, (E/T), 20: 21693
interactions with nucleons at 12 and 18 Bev, meson (ρ^0) and dipion production in, (E), 20: 30025
interactions with neutrons in stars, rates of, (T), 20: 34075
interactions with neutrons, peripheral mechanisms in, (T), 20: 30081
interactions with nucleons at 7 Bev, momentum spectra of secondary particles from, (E/T), 20: 39751 (JINR-E-2738)
interactions with neutrons at 3.5 Bev/c, (E), 20: 39842
interactions with nucleons at 12 and 18 Bev/c, recoil nucleon states from inelastic meson (ρ^0) production in, (E), 20: 41828
interactions with nucleons, cross section lower limit for, (E), 20: 41910
interactions with nucleons, crossing symmetry and spin states for, (T), 20: 46378
interactions with nucleons, resonance production in, 18: 14811 (JINR-P-1508)
interactions with nucleons to 10 Bev, 16: 33752
interactions with nucleons at 16.2 Bev/c, 17: 19086
interactions with photographic emulsions at 4.5 and 17 Bev, angular distribution of secondary shower particles from, 17: 39860
interactions with protons at 550 to 1020 Mev, elastic, 16: 2305(R) (UCRL-9704)
interactions with protons, gamma and neutron production in, 16: 4686 (CERN-61-28)
interactions with protons at 516, 616, 710, 887, and 1085 Mev, 16: 5891
interactions with protons, cross sections, 16: 5909
interactions with protons at 3.4 to 9.2 Bev/c, cross sections, 16: 5928 (JINR-P-805)
interactions with protons at 7 to 8 Bev/c, strange particle production in, 16: 5929 (JINR-P-806)
interactions with protons at 810,970 and 1100 Mev, meson (π) production cross sections, 16: 6954
interactions with protons, absorption and energy dependence in recoil polarization in, 16: 6964
interactions with protons at 224 Mev, cross sections for, 16: 6966
interactions with protons, cross sections for di-pion resonance by Chew-Low methods, 16: 6924 (UCRL-9886)
interactions with protons, cross sections, 16: 6948
interactions with protons at 960 Mev, meson (π^0) production in, 16: 6984
interactions with protons → $\Lambda^0 + K^0$, 16: 8098 (JINR-P-809)
interactions with protons, meson (ω) production, 16: 8152
interactions with protons, Panofsky ratio, 16: 9369
interactions with protons at 960 Mev, meson (π) production, 16: 9379
interactions with protons at 450 to 1650 Mev, total cross sections, 16: 9382
interactions with protons at 1.4 Bev, analysis, 16: 9404
interactions with protons at high energies, cross-section constancy, 16: 10895
interactions with protons at 10 to 20 Bev, total cross sections, 16: 10900
interactions with protons up to 20 Mev, total-cross-section relation to isospin independence, 16: 10905
interactions with protons, strange particle production in, 16: 10918
interactions with protons, measurement apparatus, 16: 10213
interactions with protons at 1.6 Bev/c, cross sections for elastic, 16: 12363
interactions with protons at 1.5 to 3.1 Bev/c, statistical theory treatment, 16: 12423 (CERN-62-6)
interactions with protons, electron pair production cross sections, 16: 13898
interactions with protons at 1.1 Bev, resonances at 575 and 750 Mev in, 16: 15567
interactions with protons at 300 to 1600 Mev, total cross section for neutral processes, 16: 16932 (NP-11592(Vol.I)(p.45-55))
interactions with protons at 6.1, 11.6, and 18.1 Bev, production of K^0 and V^0 pairs, 16: 16938 (NP-11592(Vol.I)(p.101-10))
interactions with protons near 900 Mev, strange particle distributions from, 16: 16952 (NP-11592(Vol.I)(p.203-7))
interactions with protons at 775 to 871 Mev, hyperon (Λ^0) and meson (K^0) production and decay in, 16: 15592
interactions with protons at 128 to 162 Mev, bremsstrahlung production by elastic, 16: 962
interactions with protons at 1.89 Bev, 16: 16958 (NP-11592(Vol.I)(p.249-56))
interactions with protons at 1.6 Bev/c, resonance effects, 16: 16959 (NP-11592(Vol.I)(p.257-64))
interactions with protons at 1.25 Bev, π–σ resonance values, 16: 16960 (NP-11592(Vol.I)(p.265-7))
interactions with protons at 1.6 Bev/c, strange particle distributions from, 16: 16978 (NP-11592(Vol.I)(p.375-83))
interactions with protons at 1 to 5 Bev/c, hyperon production, 16: 16979 (NP-11592(Vol.I)(p.385-8))
interactions with protons at 16 Bev, 16: 16982 (NP-11592(Vol.I)(p.407-17))
interactions with protons at 6 and 18 Bev, 16: 16985 (NP-11592(Vol.I)(p.449-52))
interactions with protons at 6.1 and 18.1 Bev, jet distribution, 16: 16986 (NP-11592(Vol.I)(p.453-7))
interactions with protons at 1.3 Bev, cross sections for, 16: 18361
interactions with protons at 1.1 Bev, single meson (π^0) production, 16: 18369
interactions with protons at 1.44 and 6.80 Bev, bremsstrahlung production, 16: 18376
interactions with protons at 3.4 to 9.2 Bev/c, total cross sections for, 16: 18396
interactions with protons at 340 Mev, cross sections for, 16: 18402
interactions with protons, meson (K)–hyperon resonances in, 16: 18324(T) (UCRL-Trans-807)
interactions with protons, hyperon (Σ) production and parity relative to (Λ), 16: 18334
interactions with protons at 5 Bev, multiple particle production, 16: 19687
interactions with protons at 1 to 4 Bev/c, Y^- production in, 16: 19704
interactions with protons, strange-particle production in, 16: 21289
interactions with protons at 500 to 940 Mev, polarization, 16: 21323
interactions with protons, one-meson-exchange domination by lowest partial waves in, 16: 22893
interactions with protons at 7.2 Bev/c, angular distributions, 16: 22942
interactions with protons at 7.2 Bev, 16: 22959
interactions with protons at 300 to 1600 Mev, total cross sections for, 16: 24677 (CEA-2136)
interactions with protons at 7 to 8 Bev, meson (π^0) production in, 16: 24685 (JINR-P-928)
interactions with protons, final state interactions in strange particle production, 16: 24711
interactions with protons at 16 Bev/c, hyperon (Λ^0) and (Σ) and meson (K) production in, 16: 24737
interactions with protons, 2-π resonances from, 16: 24744
interactions with protons at 775 and 871 Mev, meson (π) resonances below 765 Mev in, 16: 24748
interactions with protons at 170 Mev, direct measurement of cross sections for charge-exchange, 16: 25924 (NP-11977(p.55-7))
interactions with protons at 7 to 8 Bev, 16: 26068 (JINR-D-965)

interactions with protons at 310 Mev, phase shifts and scattering cross sections for, 16: 26093 (UCRL-10252)
interactions with protons, effects of meson (ρ) resonances, 16: 26114
interactions with protons at 16 Bev, cross-section relation to Pomeranchuk-trajectory slope, 16: 26122
interactions with protons to 1.9 Bev, dispersion relations for, 16: 26123
interactions with protons at 20.7 and 31.0 Mev, charge-exchange cross sections for, 16: 26127 (NYO-9545)
interactions with protons at 1.89 and 2.10 Bev/c, meson (K) production cross sections for, 16: 26146
interactions with protons below 1 Bev, meson (ζ) even isotopic spin from, 16: 26152
interactions with protons at 7.2 Bev, differential cross sections for elastic, 16: 26180
interactions with protons at 1.3 Bev, cross sections, 16: 27930
interactions with protons at 1.59 Bev/c, J = T = 1 π-π resonance effects, 16: 27961
interactions with protons at 500 to 940 Mev, polarization in, 16: 27362
interactions with protons, meson (π) multiple production in, 16: 29643 (NP-11605)
interactions with protons, meson (π) multiple production in, 16: 29657 (NP-11978)
interactions with protons at 4.7 Bev/c in liquid hydrogen bubble chamber, multiple meson (π) production in, 16: 31005 (BNL-6213)
interactions with protons, evidence for neutral scalar meson in, 16: 32345
interactions with protons at 2.8 and 7.2 Bev, meson (π^0) production in, 16: 32353
interactions with protons, production of ρ and ω resonances in, 17: 705 (BNL-6181)
interactions with protons at 340 Mev, 17: 2165 (JINR-P-1056)
interactions with protons at 7 to 8 Bev/c, ΛK^0 and $K^0\bar{K}^0$ pair production in, 17: 2193
interactions with protons, hyperon (λ) production and polarization, 17: 3964 (JINR-P-1040)
interactions with protons, mesons (η^0) from, 17: 3999
interactions with protons at 3 Bev/c, π-π resonance in, 17: 4005
interactions with protons, cross sections for, 17: 5222
interactions with protons at high energy, cross sections of, 17: 7013
interactions with protons at 7.2 Bev, π-π interactions in multiple production of mesons (π) in, 17: 7035
interactions with protons at 152 and 226 Mev, elastic, 17: 6977
interactions with protons, one-pion-exchange contributions to, 17: 6980
interactions with protons, meson (M) production in, 17: 7014
interactions with protons at 310 and 377 Mev, cross sections for, 17: 9203 (UCRL-10470)
interactions with protons at 374, 417, and 454 Mev, differential distribution of neutrons from, 17: 9205 (UCRL-10564)
interactions with protons, final-state interactions in ($K\bar{K}N$) production, 17: 9256
interactions with protons at 2 to 5 Bev/c, total cross sections for, 17: 9257
interactions with protons at 3, 4, and 5 Bev/c, elastic, 17: 9258
interactions with protons, cross sections for, 17: 9267
interactions with protons, resonance effects in, 17: 9268
interactions with protons at 240 Mev, π-π resonance in, 17: 9284
interactions with protons, angular distribution in, 17: 9304
interactions with protons, cross section for meson (π^0) production in, 17: 9305
interactions with protons at 1.89 and 2.1 Bev/c, 17: 9314
interactions with protons at 2.03 Bev/c, 17: 9315
interactions with protons at 2.8 Bev/c, 17: 9317
interactions with protons at 7.2 Bev/c, 17: 9318
interactions with protons at 7 to 8 Bev/c, 17: 9319
interactions with protons, anomalies in, 17: 9330
interactions with protons, hyperon (Λ) and meson (K^0) production in, 17: 9362
interactions with protons, production of pairs of hyperons (Λ) and mesons (K^0) in, 17: 9363
interactions with protons, hyperon and meson (K) production in, 17: 9365
interactions with protons, hyperon (Σ) and meson (K) production in, 17: 9367
interactions with protons, strange particle production in, 17: 9370
interactions with protons, 1385-Mev resonance in, 17: 9372
interactions with protons, many-particle resonances in, 17: 9374
interactions with protons, strange particle production in, 17: 9361
interactions with protons, hyperon-meson (K) resonances in, 17: 9385
interactions with protons, elastic charge-exchange cross sections for, 17: 9427
interactions with protons at 10 Bev, 2-prong events produced by, 17: 9430
interactions with protons, mass distribution of ($\pi^+\pi^-$) group in, 17: 9431
interactions with protons, peripheral effects in, 17: 9432
interactions with protons, meson (π-π) amplitudes in low-energy, 17: 11518
interactions with protons, one-pion exchange model in, 17: 11535
interactions with protons in Bev range, model for, 17: 13455
interactions with protons at 4 Bev/c, T = 2 (π-π) resonance production in, 17: 13406
interactions with protons at 95 to 290 Mev, coupling constants for, 17: 13409
interactions with protons at 310 Mev, differential cross section and recoil-proton polarization in elastic, 17: 13436
interactions with protons, exchange mechanism and K* spin assignment in, 17: 13442
interactions with protons, strange particles from, 17: 13452
interactions with protons, meson(π) production from, 17: 15137
interactions with protons at high energies, bubble chamber studies, 17: 15143
interactions with protons, resonances in hyperon (Λ) and meson (K^0) produced by, 17: 15076 (JINR-P-1019)
interactions with protons at 6.1 Bev/c, existence of f^0 particle in, 17: 16965
interactions with protons at 900 Mev, production of double-charged mesons (π) in, 17: 17028
interactions with protons, strange particles from, 17: 19131
interactions with protons at 1.5 to 6 Bev, total cross sections for, 17: 19150
interactions with protons, multiple meson (π) production from, 17: 19168
interactions with protons, strange particles from, 17: 19170
interactions with protons at 276 Mev, cross sections, 17: 19171
interactions with protons at 1 Bev, experimental and theoretical studies of, 17: 19194
interactions with protons, particle production from, 17: 19084
interactions with protons, particle production from, 17: 19085
interactions with protons, mesons (η^0) from, 17: 19043 (TID-16260)
interactions with protons at 11.3 Bev, 17: 20573 (UCRL-10022(p.89-95))
interactions with protons, 17: 20594(R) (UCRL-10572)
interactions with protons at 18 Bev/c, inelastic, 17: 20875
interactions with protons at high energies, charge-exchange and total cross sections for, 17: 20897
interactions with protons, comparison to three Regge pole model for elastic, 17: 20899
interactions with photons, meson (π^0) production in, 17: 20932
interactions with protons, cross section for four particle final state in, 17: 20939
interactions with protons at 7 Bev/c, differential cross sections for elastic, 17: 22466
interactions with protons, (K-$\bar{K}$) resonant states in, 17: 22474
interactions with protons, scattering measurements and phase-shift analysis of, 17: 22523
interactions with protons at 682, 775, and 871 Mev, mass spectra of pions produced in, 17: 22527
interactions with protons, cross sections and systematic behavior in, 17: 24263 (BNL-6934)
interactions with protons at 7 to 8 Bev, antihyperon ($\bar{\Lambda}$) production in, 17: 24264 (JINR-P-1219)
interactions with protons at 365 and 432 Mev, meson (π^+) production in, 17: 24274 (UCRL-10585)
interactions with protons at 6 Bev/c, proton momentum spectra from, 17: 24321
interactions with protons, nucleon isobar contributions to (π-π) scattering from, 17: 24353
interactions with protons, differential cross section for radiative-capture, 17: 24364
interactions with protons at 1.25 and 1.75 Bev/c, mesons (π-π) resonance and total cross sections in, 17: 24277 (UCRL-10703)
interactions with protons at 360–800 Mev, cross sections, Dalitz plots, and mass spectra for, 17: 26339
interactions with protons, test of tenfold assignment of baryon resonances in, 17: 26361
interactions with protons at 7 to 17 Bev/c, Reggeian analysis of differential cross section for elastic, 17: 26364
interactions with protons at 10 Bev/c, diffraction peak shrinkage in elastic, 17: 26368
interactions with protons, theorem on diffraction patterns in, 17: 26375
interactions with protons at 1.7 Bev/c, meson (ω) two-π decay mode from, 17: 26376
interactions with protons, cross section and momentum spectrum of hyperons (Λ) produced in, 17: 28144 (JINR-P-1245)
interactions with protons under 800 Mev, cross sections, Dalitz plots, and mass spectra for, 17: 28158 (UCRL-10720)
interactions with protons at 7 Bev, inelastic two-prong, 17: 28171
interactions with protons at 6.8 Bev/c, inelastic, 17: 28205
interactions with protons at 4.65 Bev/c, meson (π) resonances in, 17: 29491 (BNL-6340)

interactions with protons at 1500 to 2360 Mev/c, analysis for 2190-Mev resonance, 17: 29505 (UCRL-10894)
interactions with protons, hyperon (Σ) resonances in, 17: 29506
interactions with protons in hydrogenous materials, at rest, 17: 29543
interactions with protons at 3 Bev/c, meson (π-π) scattering in, 17: 29548
interactions with protons, analysis of, 17: 31286 (TID-19076)
interactions with protons at 4 Bev/c, existence and spin of meson (f^o) from, 17: 31318
interactions with protons, modified K^* exchange model for ΛK^o production in, 17: 31335
interactions with protons at 31.4 Mev, elastic, 17: 31349
interactions with protons, cross sections and Regge predictions for, 17: 31272 (CONF-22-6)
interactions with protons, charge-exchange cross section for, 17: 31275 (CONF-46-41)
interactions with protons at 210 to 310 Mev, 17: 31277 (JINR-P-1260)
interactions with protons at 1020 Mev/c, hyperon (Λ) production in, 17: 31279 (NEVIS-118)
interactions with protons at 2 Bev/c, angular distributions for, 17: 32906 (NP-12990)
interactions with protons, diffraction scattering curve for, 17: 32911 (TID-7668(Sect.III))
interactions with protons at 1170 Mev/c, strange-particle production in, 17: 34739 (UCRL-10838)
interactions with protons, $K\pi$ resonant state at 726 Mev in, 17: 34766
interactions with protons at 3.3 Bev, meson (π)-meson (π) resonances, 17: 34786
interactions with protons at 5 Bev, Regge pole contributions to cross section of, 17: 34816
interactions with protons, hyperon resonances in, 17: 34824
interactions with protons, neutral strange particles from, 17: 34825
interactions with protons at 2 Bev/c, elastic, 17: 34826
interactions with protons at 11.4 Bev/c, 17: 36568 (BNL-6569)
interactions with protons, hyperon (Λ) production scheme for, 17: 37933 (JINR-P-1297)
interactions with protons at 7 to 17 Bev/c, angular momentum plane fixed cut description of, 17: 37958
interactions with protons at 7 Bev, hyperon (Λ) and (Σ) production cross sections in inelastic, 17: 37980
interactions with protons at 3.5 Bev/c, elastic, 17: 37983
interactions with protons at 1.51, 2.01, and 2.53 Bev/c, cross sections for, 17: 37990
interactions with protons, resonances in, 17: 38151
interactions with protons at 11.4 Bev/c, production cross sections and angular distributions of Λ and K^o particles from inelastic, 17: 39864
interactions with protons, possible Regge-pole behavior in, 17: 39876
interactions with protons, polarization measurements for Regge cuts in, 17: 39897
interactions with protons at 7–8 Bev, two-meson (π) resonances in, 17: 39898
interactions with protons at 2.8 Bev/c, inelastic, 17: 39906
interactions with protons, mesons (f^o) in, 17: 39910
interactions with protons at high energy, diffraction peak shrinking in, 17: 41795
interactions with protons at 3.15–4.95 Bev/c, angular and energy dependence of cross section for elastic, 17: 41801
interactions with protons at 4.13 and 4.95 Bev/c, virtual nucleon exchange in, 17: 41802
interactions with protons, three-Regge-pole model for elastic, 17: 41832
interactions with protons, cross section for π^+-π^- interactions from, 17: 41928
interactions with protons at 1.59 Bev/c, elastic scattering and one-, two-, and three-meson (π) creation cross sections for, 17: 41771
interactions with protons at 1.25 Bev, one-π exchange in, 17: 5251
interactions with protons, cross sections for 2-π resonance in, 17: 9216
interactions with protons at high energies, inelastic cross sections for, 18: 1092
interactions with protons at 16 Bev/c, cross sections for, elastic, 18: 835 (AFOSR-3102)
interactions with protons, asymptotic polarization relations for, 18: 853 (JINR-P-1404)
interactions with protons, strange particle production in, 18: 862(R) (TID-19590)
interactions with protons at 905, 960, and 1100 Mev, single meson (π) production in, 18: 889
interactions with protons at 1.97 Bev/c in liquid-hydrogen bubble chamber, multiple meson (π) production in, 18: 907
interactions with protons at 3.5 Bev/c, 18: 914
interactions with protons at 1.89 to 2.24 Bev/c, 18: 2595 (UCRL-10291)
interactions with protons, 18: 2581 (AD-299108)
interactions with protons at 7 to 20 Bev/c, differential and total cross sections for elastic, 18: 2655
interactions with protons at 6.1 and 18.1 Bev/c, 2- and 4-prong low-momentum-transfer, 18: 4451
interactions with protons at 3.7 Bev/c, meson (ϕ) production in, 18: 4459
interactions with protons, multiple production of particles in, 18: 5993 (NP-13355)
interactions with protons, complex diagram of forward amplitudes in, 18: 6009
interactions with protons at high energies, cross sections for elastic, 18: 6011
interactions with protons at high energies, optical model for, 18: 6014
interactions with protons at high energies, field theory for, 18: 6015
interactions with protons at 210 to 310 Mev, 18: 6038
interactions with protons at high energies, exchange of strangeness-carrying trajectories in, 18: 7507
interactions with protons at high energies, effects of Regge trajectories on diffraction peaks in, 18: 7515
interactions with protons, spark chamber design for polarization measurements in, 18: 8655
interactions with protons, multiple meson (π) production in, 18: 9085 (NP-13532)
interactions with protons, asymmetric meson (ρ^o) decay in, 18: 9086 (TID-20011)
interactions with protons, production of $\Sigma^o K^{*o}$ in, 18: 9177
interactions with protons at 3.5 Bev/c, resonance effect in, 18: 9200
interactions with protons in propane bubble chamber at 600 and 770 Mev, 18: 9209
interactions with protons, elastic, 18: 10843 (CONF-122-22)
interactions with protons, recoil proton spectra in, 18: 10846 (JINR-P-1458)
interactions with protons, partial-wave analysis of ($p + \pi^- \rightarrow K^o + \Lambda^o$), 18: 10924
interactions with protons, one-pion-exchange in, 18: 10930
interactions with protons at 0.5 to 1.5 Bev/c, 18: 10945
interactions with protons, forward amplitudes for, 18: 12898 (EFINS-63-72)
interactions with protons at 4 Bev/c, elastic, 18: 12901 (JINR-P-1481)
interactions with protons, resonances (π-π) in, 18: 12915 (TID-7686 (p.131-4))
interactions with protons, coupling constants for resonances in, 18: 14957
interactions with protons at 2 Bev, meson (f^o) effects on, 18: 14961
interactions with protons at 0.5 to 1.5 Bev/c, γ production in, 18: 14798 (CEA-2306)
interactions with protons at 7.3 Bev/c, meson (π^o) production in, 18: 14802 (IFA-HE/50)
interactions with protons, resonances in, 18: 14810 (JINR-P-1506)
interactions with protons at 4 Bev/c, analyses of two-prong events in, 18: 14855
interactions with protons, Panofsky ratio for pair-producing, 18: 14856
interactions with protons, meson (ω^o) production in, 18: 14865
interactions with protons at 2 Bev/c, multiple meson (π) -production in, 18: 14888
interactions with protons, study of ($\pi^-\pi^+$) system in, 18: 14911
interactions with protons at 300 to 1000 Mev, meson (π) yields in, 18: 14923
interactions with protons at 1.7 Bev/c, meson (ω) production in, 18: 14945
interactions with protons at 1.5 to 2.4 Bev/c, strange-particle resonances in, 18: 14946
interactions with protons at 4 Bev/c, resonance production in, 18: 16774
interactions with protons at 8.5, 12.4, and 18.4 Bev/c, elastic, 18: 16789
interactions with proton, spin of f^o resonances in, 18: 16792
interactions with protons at 3 Bev/c, $K\pi\pi$ resonances in, 18: 18696
interactions with protons, vacuum pole trajectories in, 18: 18741
interactions with protons at 2.8 Bev, 3π resonances in, 18: 18645 (NP-13782)
interactions with protons at 300 to 700 Mev, 18: 18649 (UCRL-11180)
interactions with protons, charge-exchange differential cross section for, 18: 18650 (UCRL-11150)
interactions with protons at 900 Mev/c, N^*_{33} production in, 18: 18692
interactions with protons at 2.8 Bev/c, cross sections for, 18: 18728
interactions with protons at 1.55 to 4.5 Bev/c, charge exchange in, 18: 18729
interactions with protons at 7 to 8 Bev, production of hyperons (Λ) in, 18: 18734
interactions with protons at 1.4 to 3.0 Bev/c, tests of one-pion-exchange model for, 18: 20935
interactions with protons at 10 Bev/c, analyses of 4-prong, 18: 20951
interactions with protons at 10 Bev/c, meson (f^o) production in, 18: 20960
interactions with protons, unitary symmetry model for, 18: 20962
interactions with protons at 170 to 600 Mev, single meson (π)

production in, 18: 20964
interactions with protons at 374, 417, and 454 Mev, neutron differential distributions in inelastic, 18: 21011
interactions with protons at 2.1 Bev/c, meson (ω) and (ρ) interference in, 18: 21017
interactions with protons at 6.8 and 7.5 Bev/c, meson (π^0) production in, 18: 20902 (JINR-E-1557)
interactions with protons to 700 Mev, phenomenological analysis of, 18: 20915 (TID-20490)
interactions with protons, 726-Mev resonance (K-π) in, 18: 20918 (UCRL-10797)
interactions with protons at 7.5 Bev/c, pair production (Λ–K^- and K^0–K^-) in, 18: 22722 (JINR-P-1586)
interactions with protons, cross section for charge-exchange, 18: 22725 (JINR-P-1597)
interactions with protons, meson (ω^0) production in, 18: 22757
interactions with protons at 9 Bev, gamma production in, 18: 24417
interactions with protons at 871 Mev, multiple meson (π) production in, 18: 24418
interactions with protons at high energies, fundamental lengths in, 18: 24436
interactions with protons at 500 to 1000 Mev, cross sections for elastic, 18: 24454
interactions with protons, W-boson production in, 18: 24397 (NP-13954)
interactions with protons at high energies, dispersion relations for, 18: 24386 (JINR-P-1598)
interactions with protons at 7 to 8 Bev/c, hyperon (Λ) resonances in, 18: 24387 (JINR-P-1615)
interactions with protons at 1.5 to 4.2 Bev, π-ρ enhancement in, 18: 26346
interactions with protons, model for inelastic, 18: 26351
interactions with protons at 829 Mev, resonance effects in, 18: 26352
interactions with protons at 310 and 377 Mev, cross sections for ($\pi^- + \pi^0 + p$) production in, 18: 26377
interactions with protons at high energies, scaling law for, 18: 28330 (TID-20722)
interactions with protons at 0.8 to 1.9 Bev, charge exchange in, 18: 28363
interactions with protons at 0.76 to 1.655 Bev, dispersion relations for charge-exchange, 18: 28364
interactions with protons at 604 Mev, 18: 28389
interactions with protons at 18.1 Bev/c, meson (ρ) production in, 18: 28360
interactions with protons at 10 Bev/c, neutron production in, 18: 30517 (PAN-492/VI)
interactions with protons at 683 Mev/c, cross sections for elastic scattering and single-meson (π) production in, 18: 30524 (TID-20750)
interactions with protons at 6, 10.5, and 16 Bev, charge-exchange cross sections for, 18: 30539
interactions with protons, logarithmic singularities in, 18: 30566
interactions with protons at 310 to 454 Mev, inelastic, 18: 30580
interactions with protons, system for detection of unstable particles from, 18: 31873 (CERN-64-30(p.49-56))
interactions with protons at 3 Bev/c, sonic spark chamber-computer system for study of meson (f^0) production in, 18: 31893 (CERN-64-30 (p.251-60))
interactions with protons at 2.4 to 18 Bev/c, resonance in forward-direction charge-exchange, 18: 32614
interactions with protons at 310 Mev, neutron polarization and phase-shift analysis in, 18: 34512 (UCRL-11140)
interactions with protons at 313 and 371 Mev, distribution of neutrons from charge-exchange and inelastic, 18: 34516 (UCRL-11435)
interactions with protons at 7 and 16 Bev/c, quasi-elastic contribution to, 18: 34520
interactions with protons at 10 Bev/c, meson (π^0) production in, 18: 34542
interactions with protons at 285 Mev, final-state (π-π) effects in, 18: 34552
interactions with protons at 2.5 to 5.5 Bev/c, total cross sections for, 18: 34584
interactions with protons, unitary symmetry model for resonance production in, 18: 36280
interactions with protons at 4 Bev/c, meson (η) and (π^0) production in, 18: 36307
interactions with protons at 1030 to 1325 Mev/c, hyperon (Λ) production in, 18: 36338
interactions with protons at 4 Bev/c, cross sections for elastic, 18: 36351
interactions with protons at 3.5 Bev/c, resonance production in, 18: 36354
interactions with protons at 3.5 Bev/c, resonance production in, 18: 36361
interactions with protons at 3.2 and 4.2 Bev/c, baryon and meson resonances in, 18: 37884 (UCRL-11442)
interactions with protons at 6 Bev/c, ($K^+_1 + K^0_1 + n$) production in, 18: 37875 (BNL-8236)
interactions with protons at 4 Bev/c, dipion mass spectrum from, 18: 37886 (UCRL-11468)
interactions with protons, diffracting sphere model for elastic, 18: 37915
interactions with protons at 300 to 700 Mev, 18: 37920
interactions with protons, peripheral processes in, 18: 37970
interactions with protons at 3.2 Bev/c, boson resonances in, 18: 40246 (UCRL-11443)
interactions with protons at 3.7 Bev, 18: 40248 (UCRL-11464)
interactions with protons at 3.9 Bev/c, meson (π) production (two-prong) in, 18: 40254 (UCRL-11556)
interactions with protons at 10 Bev/c, meson (K^0) pair production in, 18: 40267
interactions with protons at 10 Bev/c, K-Y pair production in, 18: 40268
interactions with protons at 4 Bev/c, elastic, 18: 40284
interactions with protons at 9 Bev/c, 18: 40290
interactions with protons at 7 to 8 Bev, hyperon (Λ) production in, 18: 40291
interactions with protons at 10 Bev/c, six-prong, 18: 40293
interactions with protons at 10 Bev/c, strange particles from, 18: 40294
interactions with protons at 10 Bev/c, 18: 40295
interactions with protons at 16 Bev/c, 18: 40296
interactions with protons at 8 to 18 Bev/c, elastic, 18: 40351
interactions with protons at 2.1 Bev/c, resonances in, 18: 40377
interactions with protons at 4.5 Bev, Fermi-Koba statistical theory for inelastic, 18: 40298
interactions with protons at 6 Bev/c, multiple meson (π) production in, 18: 40228 (BNL-8237)
interactions with protons at 3.5 Bev/c, mass distributions for, 18: 40234 (NP-14201)
interactions with protons at 10 Bev/c, model for, 18: 40299
interactions with protons at 17.2 Bev, inelastic two-prong, 18: 40297
interactions with protons at high energies, (π–π) scattering in, 18: 42377(R) (TID-21014)
interactions with protons at 500 to 1300 Mev, meson (η^0) and (π^0) production in, 18: 42382 (UCRL-11576)
interactions with protons at high energies, potentials in diffraction, 18: 42407
interactions with protons at 523 to 689 Mev, polarization in elastic, 18: 42440
interactions with protons at 1.6 Bev/c at low momentum transfer, di-pion resonances in, 18: 44509 (AD-604581)
interactions with protons at 15 to 25 Bev/c and 0.2 to 1.0 $(Bev/c)^2$, 18: 44516 (BNL-8328)
interactions with protons up to 1151 Mev, meson (η^0) production in, 18: 44561
interactions with protons at 4 Bev/c, absorption effects in, 18: 44567
interactions with protons at 7 to 8 Bev/c, 2120-Mev hyperon resonance in, 18: 44592
interactions with protons at 7 Bev, proton spectrum from inelastic, 19: 1228 (JINR-P-1742)
interactions with protons at 800 and 900 Mev, meson (π) production in (E/T), 19: 1325
interactions with protons, total effective cross section for (E), 19: 1328
interactions with protons at 2.75 Bev, multiple meson (π) production in (E), 19: 1348
interactions with protons at 10 Bev, meson (K) production in (E), 19: 1401
interactions with protons at 10 Bev, strange-particle production in (E/T), 19: 1403
interactions with protons near $\Lambda^0 K^0$ threshold (E/T), 19: 1330
interactions with protons at 3.24 Bev, multipion final states in (E), 19: 1345
interactions with protons at 290 to 360 Mev, N^*_{33} isobar production in (E/T), 19: 3024 (JINR-P-1746)
interactions with protons at 4 Bev/c, cross sections for charge-exchange (E), 19: 3027 (JINR-P-1782)
interactions with protons, resonances in (T), 19: 3031 (UCRL-11730)
interactions with protons at 7 to 17 Bev/c, single-pole contribution to elastic (T), 19: 3047
interactions with protons, recoil proton polarization in elastic (E), 19: 3074
interactions with protons at 500 to 1100 Mev, charge exchange in (E), 19: 3097
interactions with protons at 500 to 1000 Mev, (E), 19: 5569(R) (MIT-2098-64)
interactions with protons, angular distribution of mesons (π^0) in, (E), 19: 5569(R) (MIT-2098-64)
interactions with protons at 4 Bev/c, cross sections, (T), 19: 4922
interactions with protons at high energies, (T), 19: 4956
interactions with protons, charge exchange in, (T), 19: 4996
interactions with protons at 3.5 Bev, amplitudes for elastic, (E), 19: 6515 (JINR-E-1813)
interactions with protons, resonances in, (E/T), 19: 6518 (JINR-P-

1807)
interactions with protons at 930 Mev, charge-exchange, (E/T), 19: 6533
interactions with protons, mass spectra from, (E/T), 19: 8138 (JINR-P-1838)
interactions with protons at 365 Mev, polarizations from elastic, (E), 19: 10021 (UCRL-11690)
interactions with protons at 200 to 300 Mev, distributions from, (E), 19: 10016 (JINR-P-1823)
interactions with protons at 17.2 Bev, angular and momentum distributions and cross sections for, 19: 10023
interactions with protons at 2.75 Bev/c, $N_{3,3}^{*++}$ production in, (E), 19: 10049
interactions with protons at 3 Bev, (E), 19: 10105
interactions with protons at high energies, dispersion relations for, (T), 19: 12186
interactions with protons at high energies, optical models for, (T), 19: 12228
interactions with protons at 300 to 700 Mev, cross sections for elastic, (E), 19: 12236
interactions with protons, $K\bar{K}$ (1020) resonance in, (T), 19: 12249
interactions with protons, Chew-Low method for cross sections for, (T), 19: 12296
interactions with protons, hyperon (Λ) momentum distributions in, (T), 19: 14315 (JINR-P-1891)
interactions with protons at 10 to 16 Bev/c, hyperons (Λ) from (τ), 19: 14316 (JINR-P-1892)
interactions with protons at 3 Bev, strange-particle production in, 19: 14393
interactions with protons at 1.13 Bev, 19: 14395
interactions with protons, associated hyperon (Σ^-) and meson (K^+) production in, 19: 14397
interactions with protons, 1250-Mev resonance in, (T), 19: 14626
interactions with protons, polarization effects in, (T), 19: 16480 (NYO-10567)
interactions with protons at 2.01 to 4.95 Bev/c, differential cross sections for, (E), 19: 16477 (NP-14827)
interactions with protons, K* (890) production in, 19: 16510
interactions with protons at 2.75 Bev/c, meson (π) production in, (E), 19: 16513
interactions with protons at high energy, charge exchange in, (T), 19: 16528
interactions with protons at high energy, fireball model for six-prong events in, (T), 19: 18759
intemctions with protons at 4 Bev/c, elastic, (E), 19: 18774
interactions with protons, production of positive strangeness baryon below NK threshold in, (E), 19: 18835
interactions with protons at 1.05 Bev/c, hyperon (Λ^o) magnetic moment from (E), 19: 18848
interactions with protons at 2.75 Bev/c, A_1 (1080) and A_2 (1310) resonances in, (E), 19: 18849
interactions with protons at 2.7 Bev/c, Kπ (1160) resonance in, (E), 19: 18851
interactions with protons, T = 0 scalar di-pion in ($\pi^+\pi^-$n), (T), 19: 20998
interactions with protons at 3.9 and 4.2 Bev/c, K* (1430) production in, 19: 21004
interactions with protons at 6 to 18 Bev/c, charge-exchange cross sections for, (E), 19: 21006
interactions with protons, Regge-pole analysis of charge-exchange, (T), 19: 21007
interactions with protons at 35 Mev, s-wave scattering length for, (E), 19: 21043
interactions with protons, charge exchange in, (E), 19: 23355(R) (BNL-867(p.1-117))
interactions with protons, production of mesons (η) in, (E), 19: 23355(R) (BNL-867(p.1-117))
interactions with protons at 2.5 to 5.5 Mev, cross sections for, (E), 19: 23355(R) (BNL-867(p.1-117))
interactions with protons, SU(6) predictions for amplitudes of, (T), 19: 23432
interactions with protons, SU(6) cross section equalities for, (T), 19: 23433
interactions with protons at 3 Bev/c, neutral vector meson production in, (E), 19: 23436
interactions with protons at 5.9 to 18.2 Bev/c, charge exchange in, (E), 19: 23447
interactions with protons, relativistic SU(6) model for amplitudes of, 19: 23395
interactions with protons at 3.63 Bev/c, differential cross sections for elastic, (E), 19: 23415
interactions with protons at high energies, equipment for studying, 19: 22862
interactions with protons at 2.3 Bev/c, Z* (1370) production in, (E), 19: 25289
interactions with protons at 4 Bev/c, elastic, (E), 19: 25275
interactions with protons, optical analysis of 900-Mev resonance in, (T), 19: 25354
interactions with protons at 3.7 Bev/c, meson (π) two-body resonances in, (E), 19: 25385
interactions with protons at 903 Mev, cross sections for elastic, (E), 19: 25264 (NYO-2262-86)
interactions with protons at 1170 Mev/c, strange particle production in, (E), 19: 25265(R) (UCRL-11776)
interactions with protons at 1030 Mev/c, products of two-pronged events in, (E), 19: 25265(R) (UCRL-11776)
interactions with protons at 1.3 Bev/c, polarization of Σ^o in, (E/T), 19: 25265(R) (UCRL-11776)
interactions with protons at 500 to 1500 Mev, charge exchange in, (E), 19: 25265(R) (UCRL-11776)
interactions with protons at threshold to 1300 Mev, production of mesons (η^o) in, (E), 19: 25265(R) (UCRL-11776)
interactions with protons, charge exchange and radiative capture in, (E), 19: 25265(R) (UCRL-11776)
interactions with protons at 3.9 Bev/c, resonances in, (E), 19: 25265(R) (UCRL-11776)
interactions with protons at 3.7 Bev/c, analysis of, (E), 19: 25265(R) (UCRL-11776)
interactions with protons at 900 Mev, differential cross section for charge exchange, (E), 19: 27167 (UCRL-11333)
interactions with protons at 5.9 and 10.0 Bev/c, absorption model for charge-exchange, (T), 19: 27226
interactions with protons at high energies and low momentum transfers, (T), 19: 27227
interactions with protons at 313 and 371 Mev, angular distributions from charge-exchange, (E), 19: 27259
interactions with protons at 10 Bev/c, star production in, (E), 19: 29059 (INR-597/VI/PH)
interactions with protons, sum rules for scattering amplitude in, (T), 19: 29062 (JINR-P-2020)
interactions with protons near inelastic threshold, recoil polarization in, (T), 19: 29102
interactions with protons, research at University of Toronto, 19: 31025
interactions with protons at 14.8 to 25.3 Bev/c, (E/T), 19: 30994 (BNL-8935)
interactions with protons, data analysis for associated production in, (T), 19: 31013 (UCID-1165(Rev.))
interactions with protons, SU_3 predictions for cross sections for, (T), 19: 32992
interactions with protons at 8 to 12 Bev, forward dispersion relations for, (T), 19: 33000
interactions with protons, Regge pole hypothesis for differential cross sections for, (T), 19: 33022
interactions with protons, meson (ϵ) (730) production in, (T), 19: 33025
interactions with protons, isoscalar s-wave di-pion resonance in, (T), 19: 33029
interactions with protons at 400 to 2000 Mev, total cross sections for, (E), 19: 33031
interactions with protons at 3.25 Bev/c, meson (ω) and (ρ^o) interference in, (T), 19: 33033
interactions with protons at 1.7 to 4.2 Bev/c, resonant states in, (E), 19: 33037
interactions with protons at 2.75 and 3.0 Bev/c, T = 0 2π resonance at 720 Mev in, (E), 19: 33038
interactions with protons at 15 to 26 Bev/c, differential cross section for elastic, (E/T), 19: 33050
interactions with protons at 200 to 300 Mev, angular distributions and cross sections in, (E), 19: 33062
interactions with protons, mass spectra from, (E), 19: 33070
interactions with protons below 1 Bev, cross sections for inelastic, 19: 35033 (UCRL-14202)
interactions with protons at 8.5 to 18.4 Bev/c, differential cross sections for, (E), 19: 35075
interactions with protons at 2.16 Bev/c, final-state enhancement at 1920 Mev in, (T), 19: 35129
interactions with protons at 8 to 14 Bev/c, amplitudes for small-angle elastic, 19: 35161
interactions with protons at 1.52 Bev/c, 2π resonance in, (E), 19: 35163
interactions with protons at 410 and 492 Mev, recoil polarization in, (E), 19: 35164
interactions with protons at 410 and 492 Mev, phase-shift analysis of, (E/T), 19: 35165
interactions with protons at 1 to 2.75 Bev/c, hyperon resonance production in, (E), 19: 35126
interactions with protons at 646 Mev, cross sections for, (E), 19: 37520 (CAR-882-8)
interactions with protons at 1.03 Bev/c, forward differential cross sec-

tion for charge-exchange, (E), 19: 37542 (UCRL-11333(Rev.))
interactions with protons, statistical analysis of, 19: 37543 (UCRL-11408)
interactions with protons at 2.7 Bev/c, strange particle production in, (E), 19: 37524 (COO-1428-12)
interactions with protons at 315 and 371 Mev, angular distributions for, (T), 19: 37544 (UCRL-11548)
interactions with protons at 6 and 10 Bev/c, charge exchange in elastic, (E), 19: 36220(R) (MIT-2098-142)
interactions with protons at 10 Bev/c, dipion mass distribution from, (E), 19: 36220(R) (MIT-2098-142)
interactions with protons at low energies, hyperon(Λ)-meson(K^0) production in, (T), 19: 37587
interactions with protons at 344 Mev, resonance contributions to inelastic, (E/T), 19: 37607(T)
interactions with protons at 3.5 Bev/c, meson (B) production in, (E), 19: 37645
interactions with proton at high energies, data on elastic, 19: 37655
interactions with protons, use of on-line system for detection of mesons (X) in, 19: 36929
interactions with protons at 7 to 17 Bev/c, Regge pole analysis of, (E/T), 19: 39619
interactions with protons at 2.8 Bev/c, angular distribution analysis of, (E), 19: 39480 (NP-15247)
interactions with protons at 8.0 Bev/c, $\pi^+\pi^-$ (1670) production in, (E), 19: 39537
interactions with protons at 1.68 Bev/c, V_0^0 production in, (E), 19: 39553
interactions with protons, determination of nucleon form factors from, (T), 19: 39590
interactions with protons at 3.5 Bev/c, four-prong events in, (E), 19: 39591
interactions with protons, isobar model for hyperon (Λ) production in, (T), 19: 39593
interactions with protons, meson (η^0) production in, (T), 19: 41433
interactions with protons at 1.5 Bev/c, dipion production in, (E), 19: 41441
interactions with protons at 8 and 12 Bev/c, differential cross sections for elastic, (E), 19: 41455
interactions with protons at 7.5 Bev, baryon resonances and strange particle production in, (T), 19: 41488(T)
interactions with protons at 2.0 Bev/c, (E), 19: 41502
interactions with protons at 1275 Mev/c, charge exchange in, (E), 19: 41507
interactions with protons at high energies, forward amplitudes for, (T), 19: 41376
interactions with protons at 7.5 Bev/c, meson resonances and strange particle production in, (E), 19: 41489(T)
interactions with protons at 1275 Mev/c, meson (η^0) and meson (π^0) production in, (E), 19: 41507
interactions with protons at 4 and 8 Bev/c, backward elastic, (E), 19: 41456
interactions with protons at 950 Mev, meson (π^-) and (π^0) production in, (E), 19: 41508
interactions with protons at 1.2 to 1.4 Bev/c, hyperon (Σ^0) polarization from, 19: 43051 (UCRL-16089)
interactions with protons at 3 to 18 Bev/c, cross sections for meson (η) production in, (E), 19: 43124
interactions with protons, energy dependence of diffraction curve for elastic, (T), 19: 43043 (JINR-P-2202)
interactions with protons at 338 Mev, gamma-meson (π^-) final-state interactions in, (E), 19: 43044 (JINR-P-2255)
interactions with protons at 16 Bev/c, multiple meson (π) production in, 19: 43054
interactions with protons at 2.0 Bev/c, exchange mechanisms in (ρ^0n) and (ρ^-p), 19: 43105
interactions with protons, threshold phenomena in meson (η) production in, (T), 19: 43120
interactions with protons, Regge pole and SU(3) predictions for charge-exchange, 19: 43147
interactions with protons at 1030 and 1505 Mev/c, differential cross sections for, (E), 19: 43152
interactions with protons at high energies, statistical model calculations for, 19: 45047 (UCRL-16315)
interactions with protons at 8.5 Bev/c, polarization in elastic, (E), 19: 45081
interactions with protons at 3.9 Bev/c, resonance in $\pi^+\pi^0$p system from, (E), 19: 45121
interactions with protons at 1.7 to 2.5 Bev/c, S-wave final-state $\pi\pi$ in, (E), 19: 45089
interactions with protons, high-energy limits for, 19: 45040 (TPJU-11/65)
interactions with protons at 8 Bev/c, (E), 19: 46643(R) (LAL-1136)
interactions with protons at 2.08 Bev/c, differential cross section and polization for, (E), 19: 47373
interactions with protons at 2.16 Bev/c, single-particle exchange models in, (E), 19: 47403
interactions with protons, SU(6) model for cross sections for, 20: 1017
interactions with protons at 3.7 Bev/c, diffraction scattering effects in, (E), 20: 1008
interactions with protons, mesons (η) and neutrons from, (E), 20: 2689 (UCRL-16140)
interactions with protons, analysis using bubble chambers, (T), 20: 2690(T) (AEC-tr-6591)
interactions with protons, triangular diagrams for cross sections of, (T), 20: 2741
interactions with protons at 2.26 Bev/c, resonances and final states in, 20: 2745
interactions with protons at 7.0 Bev/c, 20: 2746
interactions with protons at 338 Mev, cross sections for, (E), 20: 2682 (JINR-P-2320)
interactions with protons at 1.5 and 1.8 Bev/c, κ^0(725) production from, (E), 20: 2715
interactions with protons at 1.5 to 4.2 Bev/c, analysis of strangeness +1 baryon in, 20: 4589 (UCRL-11754)
interactions with protons at 2.16 Bev, 1920-Mev resonance in, (T), 20: 4849(R) (UCRL-14360, pp 1-50)
interactions with protons at 10 Bev, forward dispersion relations for, (T), 20: 4602
interactions with protons, forward amplitude for, (T), 20: 4603
interactions with protons, Regge poles in optical model for charge-exchange, 20: 4606
interactions with protons at 4 Bev/c, meson (π^0) production in, (E), 20: 4582 (JINR-P-2361)
interactions with protons at 10 Bev/c, analysis of inelastic, (E/T), 20: 6038 (INR-646/VI/PH)
interactions with protons in carbon, hyperon (Λ^0) production in, (E), 20: 6071
interactions with protons, coupling constant and s-wave scattering lengths for elastic, (T), 20: 6083
interactions with protons at 4 Bev/c, cross sections for elastic, (E), 20: 6100
interactions with protons at 3.3 and 3.9 Bev/c, resonances from, (E/T), 20: 6041 (UCRL-11942)
interactions with protons at 2 to 10 Bev, real amplitude for elastic, (E), 20: 7787 (JINR-E-2413)
interactions with protons at 10 to 30 Bev, amplitudes and charge-exchange cross sections for elastic, (E/T), 20: 7793 (JINR-P-2397)
interactions with protons, one-particle-exchange model for K* production in, (T), 20: 7827
interactions with protons, cross sections for N* production in, (T), 20: 7834
interactions with protons at 10 Bev, cross section structure for, (T), 20: 7844
interactions with protons at 5.6 and 6 Bev/c, meson (A_2^-) production from, (E), 20: 7847
interactions with protons at 3.0 to 5.0 Bev/c, boson (962) production from, (E), 20: 7848
interactions with protons at 3.0 to 5.05 Bev/c, meson (ρ^-) production in, (E), 20: 7850
interactions with protons at high energies, single Regge pole analysis for, (T), 20: 7860
interactions with protons at 2.5 to 6.0 Bev/c, differential cross sections for large momentum transfers in, (E), 20: 7863
interactions with protons, mechanism for meson (ρ^-) production in, (E/T), 20: 9758
interactions with protons at 6 Bev/c, A_2(1290) production in, (E), 20: 9763
interactions with protons at 6 to 13 Bev/c, production of M(1675), Γ(66), Q(−1) boson in, (E), 20: 9759
interactions with protons at 2.0 Bev/c, differential cross sections for charge exchange, (E), 20: 9787
interactions with protons above 2 Bev, energy dependence of diffraction-curve slope for, (T), 20: 9720(T)
interactions with protons at high energies, meson (A_2) Regge trajectory from, (T), 20: 9747
interactions with protons at 1.3 to 30 Bev, dispersion calculations for, (T), 20: 9753
interactions with protons, elastic differential cross sections for, (E), 20: 2520(R) (IA-920)
interactions with protons, scalar model for branching ratio of $n\pi$ and $n\gamma$, (T), 20: 11574
interactions with protons, resonance model for low-energy, (T), 20: 11589
interactions with protons, fermion Regge trajectories for, (T), 20: 11590
interactions with protons at high energies, charge-exchange, (E), 20: 11614
interactions with protons at high energies, charge-exchange, (T), 20: 11615

interactions with protons, test for Regge behavior in backward, (T), 20: 11663
interactions with protons at 1.70 to 2.50 Bev/c, charge exchange in, (E/T), 20: 11664
interactions with protons, decay of mesons (ρ^0), (ω), and (ϕ) from, (E), 20: 11673
interactions with protons, forward amplitude for, (T), 20: 11697
interactions with protons at 3.70 Bev/c, resonance production in, (E), 20: 13456 (UCRL-16170)
interactions with protons at 592 to 1300 Mev, cross sections for, (E/T), 20: 13457 (UCRL-16195)
interactions with protons at 500 to 1300 Mev, charge exchange in, (E), 20: 13458 (UCRL-16209)
interactions with protons at high energies, N* (1920) production in, (T), 20: 13454 (UCRL-14100-T(Rev.1))
interactions with protons at 2.01 to 4.95 Bev/c, cross sections and forward dispersion calculations for, (E), 20: 13523
interactions with protons at 1.03 Bev/c, forward differential cross section for elastic, (E), 20: 13525
interactions with protons at 350 to 800 Mev, (E), 20: 13527
interactions with protons, Fubini-Furlan theory for, (T), 20: 13537 (IC/66/8)
interactions with protons at 3.0 and 7.0 Bev, beta decay of vector bosons from, (E), 20: 15406
interactions with protons at 2.7 Bev/c, resonances in, (E/T), 20: 15410
interactions with protons at 600 to 900 Mev, single meson (π) production in, (E/T), 20: 15411
interactions with protons at 1.0 to 1.9 Bev, Y^{*-} production in, (E), 20: 15417
interactions with protons, total cross section for, (E/T), 20: 15428
interactions with protons at 9 to 18 Bev/c, meson (ρ) exchange in, (T), 20: 15364
interactions with protons at 378 Mev, π-π interaction in, (E), 20: 15368
interactions with protons at 875 to 1579 Mev/c, differential cross sections and polarization in elastic, (E), 20: 15372
interactions with protons at 500 to 1150 Mev, charge-exchange, (E), 20: 15374
interactions with protons at 300 to 1000 Mev, N*(1238) production in, (E/T), 20: 15375
interactions with protons at high energies, forward amplitude for charge-exchange, (T), 20: 15376
interactions with protons at 1.72 and 2.07 Bev/c, differential cross sections for elastic, (E), 20: 15377
interactions with protons at 2.0 Bev/c, cross sections for charge-exchange, (E), 20: 15378
interactions with protons at 2.1 to 6.9 Bev/c, resonance effects on total cross sections for, (E/T), 20: 15379
interactions with protons at 5.9 to 18.2 Mev/c, charge-exchange, (E), 20: 15380
interactions with protons at 300 to 700 Mev, isobar production in, (T), 20: 15381
interactions with protons at 9 Bev/c, meson (π^0) multiplicity and photon yields from, (E), 20: 15384
interactions with protons at 240 Mev, phase-shift analysis of elastic, (T), 20: 15388
interactions with protons, $\bar{U}(12)$ symmetry for, 20: 15390
interactions with protons, two-resonance model for hyperon (Λ)-meson (K^0) production in, (T), 20: 15392
interactions with protons, neutral decay modes of mesons (η) from, (E), 20: 15395
interactions with protons at 1.7 Bev/c, meson (ω) and (ρ^0) production and decay in, (E), 20: 15403
interactions with protons in emulsions at 5.5 Bev/c, cross sections for elastic, (E), 20: 17360
interactions with protons at high energies, real amplitudes for, (T), 20: 17378
interactions with protons at 1.5 and 1.8 Bev/c, polarization of hyperons (Σ^0) from, (E), 20: 17382
interactions with protons at 1.89 Bev/c, multiple meson (π) production in, (E), 20: 17386
interactions with protons at 3.2 and 4.2 Bev/c, meson (B) production in, (E/T), 20: 17402
interactions with protons at 24 Bev, forward amplitudes for, (E/T), 20: 19273(R) (BNL-929, pp 3-43)
interactions with protons above 2.5 Bev/c, meson (A_1), (A_2), and (B) production in, (E), 20: 19449 (UR-875-123 and (Add.))
interactions with protons, peripheral model for Y_1^* resonance production in, 20: 19469
interactions with protons, sum rules for real part of forward amplitude for, 20: 19470
interactions with protons above 2.9 Bev, polarization in, (T), 20: 19473
interactions with protons at 2 to 12.4 Bev/c, differential cross sections for elastic, (T), 20: 19483
interactions with protons at 2.01 to 2.08 Bev/c, polarization in elastic, (T), 20: 19484
interactions with protons, $KN\Lambda$ and $KN\Sigma$ coupling constant ratio from baryon exchange in, (T), 20: 19487
interactions with protons at 39 Mev, charge-exchange and elastic, (E), 20: 19515
interactions with protons at 365 Mev, recoil-proton polarization in elastic, (E), 20: 19495
interactions with protons at 5 to 20 Bev, amplitudes for, (T), 20: 21618 (JINR-P-2566)
interactions with protons at high energies, ρ-exchange peripheral model for, 20: 21647
interactions with protons at high energies, conservation laws for, 20: 21657
interactions with protons at 2 to 7 Bev/c, total cross sections for, (E), 20: 21661
interactions with protons, T = 0 S-wave $\pi\pi$ phase shift in, (E), 20: 21685
interactions with protons at 10 Bev/c, angular distributions from charge-exchange, (E), 20: 24028
interactions with protons at 1.59 Bev/c, strange particle production in, (E), 20: 24041
interactions with protons at 1.6 to 5.3 Bev/c, N^* production in, elastic, (E), 20: 24046
interactions with protons at 1.70 to 2.50 Bev/c, N(2190) production in, (E), 20: 24047
interactions with protons at 4 to 8 Bev/c, differential cross sections for, (E), 20: 24053
interactions with protons at high energies, conical function and mean value theorem for amplitude of, 20: 24061
interactions with protons at 2.8 Bev/c, resonances in hyperon (Λ^0)-meson (K^0) system from, (E), 20: 24067
interactions with protons, unitary symmetry in, (T), 20: 24170
interactions with protons, N*(1688) resonance in, (T), 20: 24012 (COO-427-47)
interactions with protons at 5 Bev/c, resonance production in, (E), 20: 25781(R) (COO-1195-56)
interactions with protons at 500 to 700 Mev, meson (π^+) energy distributions from, (E), 20: 25792 (UCRL-16282)
interactions with protons at 700 to 1700 Mev, cross sections and dispersion relations for, (E/T), 20: 25779 (CEA-R-2838)
interactions with protons at 3 to 5 Bev/c, meson (ρ^-) production in, (E), 20: 25811
interactions with protons at 338 Mev, meson (π^0) photoproduction on mesons (π^-) from, (E), 20: 25853
interactions with photons from meson (π^-)-proton interactions at 338 Mev, meson (π^0) production from, (E), 20: 25853
interactions with protons at 338 Mev, cross sections for, (E), 20: 25859
interactions with protons near (3.3) resonance, γ-3π interaction contribution to, (T), 20: 25851
interactions with protons at 10 Bev/c, inelastic, (E/T), 20: 27811
interactions with protons above 2.5 Bev/c, production of A_1, A_2, and B mesons from, (T), 20: 27825
interactions with protons at 6.0 to 10.0 Bev/c, polarization parameter in elastic, (E), 20: 27826
interactions with protons at 10 Bev/c, longitudinal and transverse momenta of secondaries from, (E), 20: 27836
interactions with protons at 2.75 Bev/c, N_{33}^* (1236) and N_{11}^* (1518) production from, (E), 20: 27837
interactions with protons at 8 Bev/c, N^* (2830) production from, (E), 20: 27838
interactions with protons at 2.75 and 3.0 Bev/c, meson (ρ) production from, (E), 20: 27848
interactions with protons, cross sections and Regge recurrences for 180° elastic, (T), 20: 27867
interactions with protons at 6 Bev/c, production of S*(1068) from, (E), 20: 27875
interactions with protons at 340 Mev, cross sections for electromagnetic, (E), 20: 27884
interactions with protons at 1.17 Bev/c, hyperon (Λ^0) and (Σ^0) polarization in, (E), 20: 29987 (COO-1261-4)
interactions with protons at 6.8 Bev/c, criterion for separating products of elastic, (E/T), 20: 30083
interactions with protons at 180 to 500 Mev/c, criterion for separating products of inelastic, (E/T), 20: 30083
interactions with protons at 4.8 Bev/c, differential cross sections for charge-exchange, (E), 20: 29998(T)
interactions with protons at 1.7 Bev/c, differential cross sections for elastic, (E), 20: 30011
interactions with protons at 4.7 Bev/c, production of meson resonance (1630) in, (E), 20: 30021
interactions with protons at 5 to 20 Bev/c, meson-exchange model for forward elastic, 20: 30039

interactions with protons at 1128 to 1326 Mev/c, neutral hyperon production in, (E), 20: 30071
interactions with protons at 1035 to 1170 Mev/c, meson (K^0) production in, (E), 20: 31991 (UCRL-16771)
interactions with protons, experimental status of baryon-exchange, 20: 32027
interactions with protons at 4 Bev/c, cross sections for strange-particle production in, (E), 20: 32029
interactions with protons at high energies, amplitude and nucleon recoil effects on, (T), 20: 32072
interactions with protons at high energies, M(12) symmetry for, 20: 32079
interactions with protons at 1.7 to 2.5 Bev/c, differential cross sections and polarization in elastic, (T), 20: 32087
interactions with protons at 3.0 and 3.5 Bev/c, meson (ρ^-) production from, (E/T), 20: 34254
interactions with protons at 10 Bev/c, $2\pi^0$ mass distribution in, (E), 20: 34205
interactions with protons, meson(η) production in, (T), 20: 34221
interactions with protons from threshold to 1.3 cross sections for Bev, (E), 20: 34229
interactions with protons at high energies, meson(ρ) Regge trajectory in, (T), 20: 34212
interactions with protons at 1.7 Bev/c, meson(ρ) production in, (E), 20: 34234
interactions with protons, near forward peaks in charge-exchange, (T), 20: 27871
interactions with protons at 34.0 Bev, kinematic tables for, 20: 36022 (BNL-945)
interactions with protons at 2.7, 4.2, and 5.0 Bev/c, resonance production in, (E), 20: 36024(R) (COO-1428-16)
interactions with protons, neutral final states formed in, (E), 20: 36040(R) (NYO-2262TB-125)
interactions with protons at 2.8 Bev/c, charge exchange in, (E), 20: 36032 (ITEF-401)
interactions with protons at 6 Bev/c, $\pi\pi$ resonance production in, (E), 20: 37731 (BNL-10460)
interactions with protons at 6 Bev/c, resonance production in, 20: 37732 (BNL-10461)
interactions with protons at 6 Bev/c, K* (1425) production in, (E), 20: 37733 (BNL-10462)
interactions with protons above 4 Bev, Regge shrinkage in, (T), 20: 37742 (UCRL-16293)
interactions with protons at 12 Bev/c, production of charged bosons (1929), (2195), and (2382) in, (E), 20: 37771
interactions with protons at high energies, elastic, (E/T), 20: 37796
interactions with protons at 1.6 to 4.2 Bev/c, strange-particle resonant states from, (E), 20: 39770 (UCRL-16788)
interactions with protons at 3 and 4 Bev/c, π-π final-state interactions from, (E), 20: 39769 (UCRL-16655)
interactions with protons at 7.5 Bev, cross sections for, (E), 20: 39758 (JINR-P-2773)
interactions with protons at 7.5 Bev, angular and momentum distributions from, (E), 20: 39758 (JINR-P-2773)
interactions with protons at 276 Mev, resonant meson (π)-meson (π) interactions in, (E), 20: 39779
interactions with protons at 775 Mev, single meson (π) production from, (E), 20: 39780
interactions with protons at 3.5 Bev/c, elastic differential cross sections for, (E), 20: 39785
interactions with protons at 10 Bev/c, observation of $\omega^0 \to \pi^0 + \gamma$ in, (E), 20: 39787
interactions with protons at 460 Mev, cross sections for elastic and inelastic, (E), 20: 39793
interactions with protons at 2 to 6 Bev/c, Regge-pole model for cross sections for, (E/T), 20: 39801
interactions with protons at 900 Mev, Λ-K^0 production in, (E/T), 20: 39803
interactions with protons, random-phase K-matrix formalism for peripheral, 20: 39804
interactions with protons at 17 Bev, angular correlations for inelastic, (E), 20: 39830
interactions with protons at 900 to 1050 Mev/c, hyperon (Λ^0) production in, 20: 39837
interactions with protons at 7.5 Bev, $N^*_{33}\pi$, N^*_{33}, and ρ^0 production from, (E), 20: 39758 (JINR-P-2773)
interactions with protons at 4 Bev/c, $\Lambda\eta$ resonance production in, (E), 20: 39754 (JINR-E-2858)
interactions with protons at 7.0 Bev/c, meson (A_1) and (A_2) production in, (E), 20: 39790
interactions with protons at 6 to 18 Bev/c, cross sections for elastic charge-exchange, (E), 20: 41795(R) (MIT-2098-251, pp 21-36)
interactions with protons at 10 Bev/c, $2\pi^0$ mass spectra from, (E), 20: 41795(R) (MIT-2098-251, pp 21-36)
interactions with protons at 10 Bev/c, spin of mesons (f^0) from, (E), 20: 41795(R) (MIT-2098-251, pp 21-36)
interactions with protons at 2.0 to 4.0 Bev/c, cross sections for A_2, D, E, and ϕ mesons production in, (E), 20: 41802 (UCRL-16832)
interactions with protons at 2.0 to 4.0 Bev/c, $K\bar{K}$ production in, (E), 20: 41802 (UCRL-16832)
interactions with protons at 300 Mev, recoil polarization from, (E), 20: 41794 (JINR-E-2860)
interactions with protons at 300 to 700 Mev, total cross sections for, (E), 20: 41830
interactions with protons at 875 to 1579 Mev/c, cross sections for elastic, (E), 20: 41857
interactions with protons at 2.1 Bev/c, π-π interactions and N* (1920) production in, (E), 20: 41858
interactions with protons at 2 to 5 Bev, cross section for W boson production in, (T), 20: 41859
interactions with protons at 558 to 900 Mev, cross sections for, (E/T), 20: 41871
interactions with protons at 323 to 900 Mev/c, polarization in, (E), 20: 41890
interactions with protons at 900 Mev, hyperon (Λ) and meson (K^0) production from, (T), 20: 41917
interactions with protons at 3.2 and 4.2 Bev/c, multi-pion final states from, (E), 20: 44178 (UCRL-16881)
interactions with protons at 10 Bev, second correction to phase integral for, (T), 20: 44182
interactions with protons at 7 Bev, one-meson theory for charge distribution from inelastic, 20: 44183
interactions with protons at 1.7 Bev/c, T $\geq$ 1 dipion (965) enhancement in, (E), 20: 44229
interactions with protons at high energies, branching ratio predictions for, (T), 20: 44237
interactions with protons at 11 Bev/c, structures in 4π mass system from, (E), 20: 44241
interactions with protons at 7 and 12 Bev/c, structure within A_2 (1286) and R (1675) from, (E), 20: 44245
interactions with protons, Regge trajectories for minima in differential cross sections for, 20: 44264
interactions with protons at 4 Bev/c, backward elastic, (T), 20: 44267
interactions with protons, ρ^- trajectory contribution to charge-exchange, 20: 44222
interactions with protons at 12 BeV, slope of differential cross section for inelastic, (E), 20: 46361
interactions with protons at 300 MeV, phase shift and recoil proton polarization for elastic, (E), 20: 46366
interactions with protons, ($\pi^- - \pi^0$) mass difference from gamma angular correlation from, (E), 20: 46369
interactions with protons at 500 to 1100 Mev, 16: 16931 (NP-11592 (Vol.I)(p.37-43))
interactions with the Coulomb field of the nucleus at 2.8 Bev/c, production of mesons (π^0) by, 17: 7020
interactions with uncorrelated nucleons in oxygen-16, absorption probability for, (T), 20: 28351
kinetics at 100 kev to 100 Bev, graphs for, 19: 18752 (UCRL-2426(Vol. I) (1965 Rev.))
lifetime, (E), 20: 41891
lifetime in flight, 18: 2585(R) (ISS-63/37)
lifetime in hydrogen, 16: 32453
lifetime of, (E), 20: 24052
lifetime of, on curved and straight path, measurement of, 17: 22418 (ISS-62/7)
lifetime of, relative to mesons (π^+), (E), 20: 39760 (JINR-P-2802)
lifetime relative to mesons (π^+), (E), 20: 41884
magnetic moments of, Vigier rotator model for anomalous, 17: 34802
mass, (E), 20: 13461 (UCRL-16365)
mass determination by neutron time-of-flight measurements, 16: 18322 (UCRL-9951)
mass determination from mesic atom x-ray spectra, (E), 19: 33023
mass difference ($\pi^- - \pi^0$) from meson (π^-) capture by protons, (E), 20: 46369
mass difference with mesons (π^0), 16: 8054 (NP-11232(p.243-51))
mass difference with meson (π^0), 17: 37934 (JINR-P-1309)
mass relative to mesons (π^0), (T), 19: 31021
mass spectrum in meson (ρ^0) decay, 17: 9249
meson (μ^-) emission and helicity from, 16: 24747
meson (ρ^0) production by, at 12 and 17 Bev/c, 17: 9249
momenta and ranges in emulsions, 19: 9775(R) (UCRL-11466)
momentum determination in nuclear emulsions, method for, 19: 44427 (CERN-65-4(Vol.II), pp VIII34-7)
momentum spectra from proton reactions with aluminum and beryllium at 30 and 33 Bev, 16: 24858
photoproduction at 2 to 6 Bev, peripheral effects in, (E), 19: 1387

photoproduction at high energies, (E), 20: 15306(R) (CEAL-1026)
photoproduction from nuclei, 17: 6975
photoproduction from deuterium at 165 to 210 Mev, ratio (π^-/π^+) in, 17: 37959
photoproduction from bismuth-209 by 250-Mev bremsstrahlung, 17: 38136
photoproduction from deuterium at 165 to 200 Mev, cross section ratio to meson (π^+) production, 18: 2649
photoproduction from helium-4 at 180 to 300 Mev peak, (E), 19: 29234 (COO-1195-8)
photoproduction in bremsstrahlung reactions with calcium to 320 Mev, 16: 23127
photoproduction in deuterium, proton angular distribution and energy spectrum from, 17: 20907
photoproduction in hydrogen, proposed study of, 18: 10862 (LNF-63/47 (p.73-4))
photoproduction in hydrogen along with mesons (π^+), 18: 10867 (LNF-63/47(p.98-104))
photoproduction in deuteron-polarized bremsstrahlung interactions (E), 19: 3073
photoproduction in deuterium near threshold, (E), 19: 43188
photoproduction of π^+–π^- pairs on nucleons at 1.05 Bev, parity conservation in, 16: 27981
photoproduction of, from deuterium, differential cross section for, 16: 30930(R) (NYO-2669)
photoproduction of, cross sections for, 18: 10681(R) (CEAL-1009)
photoproduction on protons, partial wave dispersion relations for, 16: 27910 (NP-11839)
photoproduction on boron-11, cross sections for, 16: 33907
photoproduction on deuterium and hydrogen, 17: 878
photoproduction on nuclei, cross sections for, 17: 24443
photoproduction on deuterons close to threshold, 18: 904
photoproduction on carbon at 2.91–4.85 Bev, cross sections and rates for, 18: 2939
photoproduction on beryllium at 2 to 6 Bev, 18: 4455
photoproduction on silicon-29, nuclear polarization in, 18: 6208
photoproduction on nucleons, experiments for, 18: 7514
photoproduction on deuterons, cross sections for, 18: 26317
photoproduction on neutrons at 275 Mev, cross sections for, 18: 40310
photoproduction on helium-3 and tritium, 18: 42707
photoproduction on nitrogen at 1 Bev, 19: 1632
photoproduction on carbon at 3, 4, and 5 Bev, rates of (E), 19: 1669
photoproduction on deuterons, (T), 19: 10097
photoproduction on deuterium at 150 to 200 Mev, (E/T), 19: 10098
photoproduction on deuterons, (E), 19: 16555
photoproduction on nickel-60, cross sections for, (T), 19: 19146
photoproduction on hydrogen, (E), 19: 23625(R) (HUX-2752-1)
photoproduction on protons, differential cross sections for, (T), 19: 27142 (ISS-64/46)
photoproduction on protons, (E), 19: 37554
photoproduction on deuterium at 165 to 210 Mev, angular distributions and cross sections for, (E), 19: 41344
photoproduction on deuterium at 230 Mev, (E), 19: 43039 (COO-1195-34)
photoproduction on carbon and hydrogen in Bev range, (E), 19: 45000 (HUX-2752-7)
photoproduction on protons below 1 Bev, angular distributions and total cross sections for pair, 20: 4579 (AD-618661)
photoproduction on deuterium, yields from, (E), 20: 9782
photoproduction on protons at high energies, (E), 20: 15306(R) (CEAL-1026)
photoproduction on protons at 550 to 1000 Mev, cross sections for, (E), 20: 15332
photoproduction on nucleons, (E), 20: 25781(R) (COO-1195-56)
photoproduction on protons at 2 to 5 Bev, (E), 20: 27918
photoproduction on carbon and hydrogen at high energies, (E), 20: 27919
photoproduction on protons at 0.9 to 1.3 Bev, (E/T), 20: 31983 (CALT-68-71)
photoproduction on protons, (E), 20: 34246
photoproduction on light nuclei, differential cross sections for, (E), 20: 40075 (LNF-66/30)
photoproduction on protons at 0.3 to 5.8 BeV, (E), 20: 46348(T) (SLAC-Trans-44)
photoproduction on protons at 0.9 to 4.0 Bev, cross sections for, 18: 28397
photoproduction with mesons (π^+) on nucleons, angular momentum analysis of, 18: 7495
production and properties of very slow, from 9-Bev proton reactions on nuclei, 17: 9558
production at high energy, (μ^+)/(μ^-) ratio from (π^+)/(π^-) ratio in, (T), 20: 2702
production by hyperon (Σ^-) reactions in nuclear emulsions, 16: 3664 (AFOSR-856)
production by nucleons at 0.5 to 2 Bev, 17: 12784(R) (ORNL-3360(p.199-203))
production by proton-proton reactions at 2.1 and 2.9 Bev, 16: 16933 (NP-11592(Vol.I)(p.57-67))
production by proton-proton interactions at 1 Bev, 17: 5199 (AERE-R-3969)
production from bremsstrahlung reactions with helium below 330 Mev, (E), 20: 41817
production from meson (π^-) reactions with bromine, diffraction dissociation in, (E), 20: 39774
production in antineutrino-proton interactions, cross sections for, 17: 20919
production in antineutrino inelastic reactions with nuclei, cross section asymptotic behavior for, 17: 41826
production in antiproton–proton interactions at 3.6 Bev/c, 18: 22741
production in antineutrino- and neutrino-proton interactions, cross sections for, (T), 19: 29065 (JINR-P-2062)
production in antineutrino interactions with protons at high energy, cross section for, (T), 20: 2733
production in antiproton-proton annihilations at 2.7 Bev/c, (E), 20: 34150 (IS-T-83)
production in bremsstrahlung reactions with deuterium at 320 Mev, 17: 4009
production in deuteron interactions at 3 Bev/c, cross sections for, (E), 19: 32981
production in deuteron-meson (K^-) interactions at rest, (T), 19: 47358
production in electron-positron interactions, cross section for, 18: 20986
production in electron-proton interactions, (E), 20: 27934
production in freon-meson (π^-) interactions at 2.8 Bev/c, (E), 20: 2739
production in hyperon (Σ^0) decay, 16: 12359
production in hyperon (Σ^-)-proton interactions, extrapolation analysis, 16: 19694
production in K^--proton interactions at 293 to 513 Mev/c, 16: 27914 (UCRL-10175)
production in meson (K^+) decay, 16: 4729
production in meson (K^+) decay, 17: 11523
production in meson (K^-)-proton interactions at 1.51 and 1.22 Bev/c, 18: 2594 (UCRL-10235)
production in meson (π^-)–proton interactions at 2 Bev, 18: 14888
production in meson (π^-)-proton interactions at 300 to 1000 Mev, enhancement of, 18: 14923
production in meson (π^-)-proton interactions at 871 Mev, 18: 24418
production in meson(π^-) reactions with xenon at 9 Bev/c, 18: 40549
production in meson (K^-) reactions with emulsion nuclei at rest, (T), 19: 19151
production in meson (K^-)-proton interactions, Q-value distribution for, (T), 19: 35070
production in meson (K^-)-neutron interactions, (T), 19: 41405
production in meson (π^-)-proton interactions at 905 Mev, (E), 19: 41508
production in meson (π^-)-proton interactions at 7.0 Bev/c, 20: 2746
production in neutron-proton interactions at 9 Bev, 16: 4723
production in neutron-proton interactions at 600 Mev, 18: 842 (JINR-P-1334)
production in neutrino-nuclear interactions at high energies, 18: 28413
production in neutron-proton interactions near threshold, (E), 19: 27236
production in neutron-proton interactions at 600 Mev, angular distributions and cross sections for, (E), 20: 11564 (JINR-P-2462)
production in neutron-proton interactions at 600 Mev, (E), 20: 13453 (JINR-P-2511)
production in neutron-proton interactions at 585 Mev, cross sections for, 20: 15310 (JINR-P-2508)
production in neutron-proton interactions at 585 Mev, cross section for, (E), 20: 25809(T)
production in neutron-proton interactions at 600 Mev, (E), 20: 39826
production in neutron-proton interactions at 600 Mev, cross sections for, (E/T), 20: 39834
production in p-$\bar{p}$ annihilation, distributions from, 17: 15134
production in photon–proton interactions, 16: 3646
production in photon-proton interactions, 16: 10857
production in photon reactions with beryllium and hydrogen, 18: 9318 (SLAC-21)
production in photon-proton interactions at 600 to 850 Mev, double, (E), 19: 39519
production in (π^--n) interactions, 16: 32353
production in π^--p interactions, π-π resonance, 17: 4005
production in proton interactions at 2.9 Bev, momentum spectra, 16: 6974
production in proton reactions with nuclei at 450 Mev, 16: 9378
production in proton interactions at 2.0 and 2.85 Bev, 18: 7503
production in proton-proton interactions at 19 and 24 Bev/c, cross sections for, 18: 18678
production in proton interactions at 650 Mev, angular and energy distributions in, 18: 24476
production in proton reactions with beryllium at 12.5 Bev, cross sections for, (E), 19: 21406
production in proton reactions with nuclei at 20 Bev, 19: 41324

(CERN-65-14)
production in proton-proton interactions at 2.0, 2.4, and 2.85 Bev, momentum spectra of, (E), 20: 15336
production in proton–antiproton annihilations at 5.7 Bev/c, (E), 20: 19498
production in proton reactions with beryllium at 12.5 Bev, cross sections for, (E), 20: 21601 (CERN-65-32, pp 109-10)
production in proton interactions with neutrons and protons in nuclear emulsions, charge asymmetry of, (E), 20: 30082
production in proton reactions with beryllium at 600 Mev, cross sections for, (E), 20: 38186
production in proton reactions with carbon at 600 Mev, cross sections for, (E), 20: 38186
production in proton reactions with aluminum at 600 Mev, cross sections for, (E), 20: 38186
production in proton reactions with copper at 600 Mev, cross sections for, (E), 20: 38186
production in proton reactions with silver at 600 Mev, cross sections for, (E), 20: 38186
production in proton reactions with lead at 600 Mev, cross sections for, (E), 20: 38186
production in proton interactions with neutrons at 600 Mev, cross sections (E), 20: 38186
production in reactions of x rays with helium-4, 19: 23809
production of ($K^0\pi^-p$), 18: 30588
production of beam of, for use with liquid hydrogen finger targets, 16: 33698 (TID-16811)
production of beams of, in CERN synchrotron, (E), 19: 28940 (CERN-65-2)
production of resonance ($\Sigma^+\pi^-$), in meson (K^-)-neutron interactions at 1.15 Bev/c, 18: 36339
properties at 100 kev to 100 Bev, 18: 28331 (UCRL-2426(Vol.I)(1963 Rev.))
properties of, electron-pair model for, (T), 19: 10059
properties of, review of physical, 20: 18516
proton interactions at 646 Mev, cross sections for, (E), 20: 34203
range in emulsion, velocity dependence of (E), 19: 3029 (UCRL-11518)
range in nuclear emulsions at 78 and 90 Mev/c, 20: 41826
ranges in emulsions, comparison with mesons (π^+), (E/T), 19: 25265(R) (UCRL-11776)
reaction with hydrogen and polyethylene, charge, exchange ratio in, 16: 26189
reactions (π^-,π^-n) with carbon-12 at 0.45 to 1.9 Bev, excitation function for, 18: 21293
reactions ($\pi^-,n\gamma$) with nuclei, energy spectra from, (E), 19: 21315
reactions (π^-,π^-n) with carbon-12 at 40 to 600 Mev, pole approximation for, (T), 19: 33247 (NP-15048)
reactions (π^-,π^0) on complex nuclei, excitation functions for, (T), 20: 4910
reactions (π^-,π^-pn) with argon-40 at 500 to 1100 Mev, cross sections of, (E), 20: 6298(R) (PPAD-2137-566)
reactions (π^-,n) with carbon-12, boron-11 excitation energy distribution from, (T), 20: 10080
reactions ($\pi^-,2N$) with nuclei, momentum distribution from, (T), 20: 13874
reactions ($\pi^-,2N$) with carbon-12, momentum distribution from, (T), 20: 13874
reactions (π^-,nn) and (π^-,n) with helium-4, nucleon correlations in, (T), 20: 13884
reactions ($\pi^-,2n$) with lithium-6 and -7 at rest, angular distributions and energy spectra from, (E), 20: 15793
reactions (π^-,γ) with complex nuclei, energy spectra and yields from, (E), 20: 15794
reactions (π^-,n) with copper, neutron energy spectra from, (T), 20: 19903
reactions (π^-,π^-p) and (π^-,π^-pn) with argon-40 at 500 to 1100 Mev, excitation functions for, (E), 20: 22125
reactions ($\pi^-,3\pi$) with emulsion nuclei at 17.2 Bev/c, mechanism for coherent, (E/T), 20: 26127
reactions ($\pi^-,2n$) with carbon-12, nitrogen-14, and oxygen-16, energy level excitation in, (E), 20: 38070
reactions ($\pi^-,2n$) with lithium-6, description using various models of the lithium-6 nucleus, (T), 20: 38137
reactions ($\pi^-,2n$) and (π^-,np) with light nuclei, neutron-neutron and neutron-proton pair angular distributions from, (E), 20: 42313
reactions (π^-,π^+4n) with helium-4, (T), 20: 42356
reactions ($\pi^\pm,2N$) with light nuclei, (T), 20: 46789
reactions at 14 to 17 Bev, with non-excited nuclei, 16: 13958 (NP-11422)
reactions at 3.5 Bev/c in nuclear emulsions, helium-8 production in, (E), 20: 44747
reactions in bubble chambers and emulsions, meson (π^0) intensity from, 19: 44439 (CERN-65-4(Vol.II), pp X37-43)
reactions in hydrogen, production of ($\Sigma K\pi$) states in, 17: 13419
reactions in light nuclei, phenomenological analysis of, 20: 41665
reactions in nuclear emulsions, coherent multiple meson (π) production in, 18: 32806
reactions in nuclear emulsion at 17.2 Bev/c, hyperfragment production in (E), 19: 1668
reactions in nuclear emulsions, double charge exchange in, (E), 19: 10243 (JINR-P-1837)
reactions in nuclear emulsions at 50 to 176 Mev, total cross sections for double charge-exchange, (E), 20: 38012 (JINR-P-2806)
reactions in nuclear emulsions at 17 Bev/c, electron pair production from, (E), 20: 41814
reactions in photographic emulsions at 4.5 Bev, emission of lithium-8, beryllium, and boron fragments from, 17: 19354
reactions in xenon bubble chambers at 1.0 to 1.1 Bev, cross sections, 16: 27925
reactions of stopped, with carbon, mechanism of absorption, (E/T), 20: 3123
reactions on emulsion nuclei, Auger electrons from, 17: 13525
reactions on emulsion nuclei, hyperfragments from, 17: 15135
reactions on nuclei, double hyperfragment production, 16: 10921
reactions on nuclei at 2 Bev/c, distributions from, 17: 2173
reactions on xenon at 8.4 Bev/c, mesons (π^0) from, 17: 9551
reactions on xenon nuclei, strange particles from, 17: 28339
reactions (π^-, π^-n) with carbon-12 at 53 to 1610 Mev, cross sections and excitation functions for, 17: 11650 (UCRL-10531)
reactions (π^-,n) on helium-4, branching ratios, 16: 28115
reactions (π^-, π^-n) in carbon-12, excitation function and study of mechanism for, 17: 11648 (UCRL-10312)
reactions (π^-,p) with nuclei in Bev range, cross sections for, 17: 38306
reactions (π^-,π^-n) with carbon-12 at 53 to 1,610 Mev, excitation functions for, 18: 9394
reactions with aluminum-27, copper, and zinc, cross sections and yields for, 17: 11650 (UCRL-10531)
reactions with beryllium, carbon, and lead at 140 Mev, total cross sections for double-charge-exchange, (E), 20: 24479
reactions with bromine and silver in emulsion nuclei at 16 Bev, angular distribution of relativistic particles from, 17: 26462 (PAN-367/VI)
reactions with bromine and silver nuclei at 17 Bev, in nuclear emulsions, (T), 20: 38060
reactions with bromine, diffraction dissociation for meson (ρ^0) production from, (E), 20: 39774
reactions with carbon at 1.3 Bev, hyperon (Λ^0) production and properties from, 16: 12358
reactions with carbon at 915 Mev, angular distributions and cross sections, 16: 15679
reactions with carbon, chloride, fluoride, and xenon at 2.8 Bev, 16: 26190
reactions with carbon and hydrogen at 7-8 Bev, properties of mesons (π^0) produced by, 17: 13347 (JINR-P-1138)
reactions with carbon and nitrogen at 7 Bev, meson (η) radiative decay in, 17: 17119 (JINR-P-1164)
reactions with carbon and lead, meson (π^-) angular distributions for non-elastic, 17: 22564 (ORNL-3383)
reactions with carbon at 69.5 Mev, differential cross section for, 17: 36643 (CERN-63-28(p.47-72))
reactions with carbon at 7 Bev, hyperon (Λ) production in, 17: 38155
reactions with carbon at 17 Bev, meson (π^0) production in, 18: 877
reactions with carbon at 6.1 and 18.1 Bev/c, diffraction dissociation from, 18: 880
reactions with carbon at 2.0 Bev/c, parity conservation in hyperon (Λ^0) production in, 18: 6244
reactions with carbon, intranuclear cascade spectra for, 18: 11200 (JINR-P-1452)
reactions with carbon at 7 Bev, 18: 13046 (JINR-P-1472)
reactions with carbon and nitrogen at 7.5 Bev, 18: 24390 (JINR-P-1624)
reactions with carbon and nitrogen at 7 Bev, 18: 24391 (JINR-P-1629)
reactions with carbon at 7 Bev, hyperon (Λ) and (Σ^0) and meson (K^0) production in, 18: 28404
reactions with carbon, nuclear cascades excited in, 19: 3032
reactions with carbon and fluorine at 17 Bev, (E), 19: 10108
reactions with carbon-12, alpha and triton spectra from, (T), 19: 27476
reactions with carbon nuclei, hyperon (Λ) and meson (K^0) production in, 17: 9362
reactions with carbon-12, resonance production in, 18: 14811 (JINR-P-1508)
reactions with complex nuclei, radiative, 18: 30721 (JINR-P-1663)
reactions with complex nuclei at 25 to 400 Mev, data from inelastic, (E), 20: 44720
reactions with deuterium at 141 Mev, cross sections, 16: 8101 (NYO-9283)
reactions with deuterium at 1.23 Bev/c, meson (K^0) charge symmetry from, 17: 22489
reactions with deuterium, 18: 30708(R) (AFOSR-J1446)

reactions with emulsion nuclei at 4.6 Bev/c, lithium-9 decay in, 17: 28274
reactions with emulsion nuclei at 4.5 Bev, 17: 36663 (TID-19329)
reactions with emulsion nuclei at 7.5 Bev, fragment production in, 18: 11280
reactions with emulsion nuclei, hyperfragments from, 18: 16979
reactions with emulsion nuclei at 16.2 Bev/c, meson (π) multiple production in, 18: 28750
reactions with emulsion nuclei, heavy fragment emission in, 18: 34811
reactions with emulsion nuclei at 4.5 Bev, lithium-8 emission from, 18: 44758
reactions with emulsion nuclei at 4.5 Bev, recoil studies of heavy fragments from (E), 19: 1614
reactions with emulsion nuclei at 17.2 Bev/c, hyperfragment production in (E), 19: 5143
reactions with emulsion nuclei, mass spectrum of charged particles from, (E), 19: 8213
reactions with emulsion nuclei at 3.5 Bev/c, hyperfragment production in, (E), 19: 16966
reactions with emulsion nuclei at 17 Bev/c, secondary particles in, (E), 19: 19148
reactions with emulsion nuclei at rest, (E), 19: 27501
reactions with emulsion nuclei at 68 Mev, proton energy spectra from, (E), 19: 35454
reactions with emulsion nuclei at 17 Bev, production of A_1 resonance in, 19: 43126
reactions with emulsion nuclei at 3.5 Bev/c, hyperfragment production in, (E), 19: 47650
reactions with emulsion nuclei at 7.2 Bev/c, meson (K) production in, (E), 20: 1224
reactions with emulsion nuclei, effective particle mass from diffraction dissociation, (T), 20: 7878
reactions with emulsion nuclei at 16.3 Bev, angular distributions from, (E/T), 20: 11602
reactions with emulsion nuclei at 17.2 Bev/c, cross section for, (E), 20: 13893
reactions with emulsion nuclei at 3.85 Bev/c, meson (π) production in, 20: 26085 (JINR-P-2624)
reactions with emulsion nuclei at 3.8 Bev, slow meson (π) production in, (E), 20: 30501
reactions with emulsion nuclei at 300 Bev, $_{\Lambda}B^{12}$ production in, (E), 20: 32412
reactions with emulsion nuclei at 1.7 Bev/c, proton spectra from, 20: 46932(R) (ORNL-3973(Vol.2)
reactions with emulsion nuclei at 4.2 Bev, meson (π^0) production from, 18: 9110
reactions with freon and xenon at 2.8 Bev/c, K^0–Λ^0 resonances from, 16: 27987
reactions with freon and xenon, mass spectra for, 17: 26425 (NP-12886)
reactions with heavy nuclei of ionographic emulsions at 17-Bev/c, emission of lithium-8 and lithium-9, 16: 29810
reactions with heavy emulsion nuclei, energy spectra for mesons (π^-) from, 17: 22564 (ORNL-3383)
reactions with heavy emulsion nuclei, mesons (π^-) angular distributions for nonelastic, 17: 22564 (ORNL-3383)
reactions with heavy emulsion nuclei, coherent meson (π) production in, (E/T), 19: 37882(T)
reactions with heavy emulsion nuclei at 1.5 to 25 Bev, lithium-8 energy spectra from, (E), 20: 15792
reactions with heavy nuclei at 7.2 Bev/c, meson (K−) and (K+) production cross sections for, (E), 20: 28460
reactions with helium-3, 17: 9308
reactions with helium-3, ratio of gamma to meson (π^0) production in, 17: 22655
reactions with helium-4 at 150 Mev, cross sections, 16: 953
reactions with helium at 153 Mev, angular distributions and cross sections, 16: 24682 (JINR-P-868)
reactions with helium-3, transition radius for hydrogen-3 formation in, 16: 31009 (JINR-E-1012)
reactions with helium-3, resonance production in, 18: 14811 (JINR-P-1508)
reactions with hydrogen at 1140 Mev, bubble chamber analysis, 16: 23850(R) (TID-16074)
reactions with hydrogen at 75 Mev, charge-exchange in, 16: 24689 (JINR-P-948)
reactions with hydrogen at 170 Mev, forward charge-exchange cross section for, 17: 13409
reactions with hydrogen at 16 Bev/c, strange particle production in, 17: 26323
reactions with hydrogen at 16 Bev/c, meson (π) production, 16: 24719
reactions with lead, meson (π^-) spectra for nonelastic, 17: 22564 (ORNL-3383)
reactions with light nuclei at 2.8 Bev, production of hyperons (Λ), 16: 3652
reactions with lithium-6 and -7, hydrogen-4 production in, (E), 19: 15177
reactions with matter, dE/dx and range-energy graphs for, 20: 46601 (UCRL-2426(Vol.2)(1966 Rev.))
reactions with matter, range-momentum and dP/dx graphs for, 20: 46342 (UCRL-2426(Vol.4)(1966 Ed.))
reactions with nuclei at 6 to 17.6 Bev/c, total cross sections for inelastic, 16: 12507
reactions with nuclei at 25 to 300 Mev, 17: 12783(R) (ORNL-3360(p.182-98))
reactions with nuclei in emulsion at 17.2 Bev/c, mesic hyperfragment production in, 17: 29617
reactions with nuclei, calculation of low-energy intranuclear cascades in, 17: 31526
reactions with nuclei, cross section asymptotic behavior for production of intermediate vector mesons in inelastic, 17: 41826
reactions with nuclei at 2.8 Bev/c, meson (π^0) angular distributions from, 17: 41980
reactions with nuclei at 7 Bev/c, particle production in, 18: 24587 (JINR-P-1584)
reactions with nuclei, nucleon emission in (T), 19: 1683
reactions with nuclei at 140 Mev, double charge exchange cross sections for, (E), 19: 43273 (JINR-P-2238)
reactions with nuclei at 120 to 280 Mev, double charge exchange in, (E), 20: 3080
reactions with nuclei, charge exchange in, (E), 20: 37740 (JINR-P-2780)
reactions with nuclei at 16.2 BeV/c, 17: 19086
reactions with nuclei to 10 BeV, 16: 33752
reactions with nuclei at 4.5 Bev, angular distribution of secondary particles in, 16: 2413(T) (JPRS-10727)
reactions with nuclear matter, nuclear emulsion studies, 16: 23850(R) (TID-16074)
reactions with organic liquids at 6 to 18 Bev/c, multi-meson (π) systems from, (E), 20: 9745
reactions with oxygen-16, fission mechanisms in, 16: 18527
reactions with xenon at 2.8 Bev, angular distribution and cross sections for, 16: 24695 (NP-11757)
reactions with xenon, cross sections for, 17: 9347
reactions with xenon, at 8.4 Bev, meson (π^0) production in, 17: 11673
reactions with xenon, meson (π^0) production in, 17: 20932
reactions with xenon at 9 Bev/c, hyperon (Σ^0) production in, 18: 18641 (JINR-P-1529)
reactions with xenon at 9 Bev/c, meson (π^0) production in, 18: 34949
reactions with xenon at 9 Bev/c, meson (π^0) production in, 18: 36305
reactions with xenon at 9 Bev/c, 18: 40549
reactions with xenon at 9 Bev, meson and photon production from, 18: 40550
reactions with xenon at 9 Bev/c, cross sections for meson (π^0) production in, (E), 19: 5250
reactions with xenon at 9 Bev/c, mean-free-path for, (E), 19: 35380 (IFA-CR-51)
reactions with xenon at 9 Bev/c, neutron-proton ratio on nuclear periphery from, (E), 19: 35381 (JINR-P-2097)
reactions with xenon at 9 Bev/c, hyperons (Λ) and mesons (K^0) cross sections from, 19: 39472 (JINR-P-2178)
reactions with xenon at 2.8 Bev/c, meson (π^0) multiple production in, 19: 43279 (NP-15383)
reactions with xenon at 9 Bev/c, cross section for, (E), 19: 47689
reactions with xenon at 9 Bev/c, neutron emission in high four-momentum transfer, (E), 19: 47698
reactions with xenon at 9 Bev/c, hyperon (Λ) and meson (K^0) production in, (E), 20: 15841
reactions with xenon at 9 Bev, secondary angular distributions from, (E), 20: 34519 (JNR-683/VI/PH)
reactions with xenon at 5 and 9 Bev/c, angular, energy, and multiplicity distributions of mesons (π^0) produced in, 20: 39755 (JINR-P-2736)
resonance ($\pi^+\pi^-\eta$) at 959 Mev, properties of, 18: 34515 (UCRL-11431)
resonance ($\pi^+\pi^-$) at 280 to 350 Mev, search for, 18: 34552
scattering by carbon at 2.8 to 6.8 Bev/c, elastic, 16: 2407 (JINR-D-743)
scattering by carbon at 3 and 4 Bev/c, total cross sections for, 17: 9257
scattering by carbon nuclei at 915 Mev, analysis of inelastic, 17: 15300
scattering by carbon, cross sections for nonelastic, 17: 22564 (ORNL-3383)
scattering by carbon at 2.66 Bev, inelastic, 17: 38151
scattering by copper, cross sections for nonelastic, 17: 22564 (ORNL-3383)
scattering by emulsion nuclei at 4.5 Bev, cross sections, 16: 27968
scattering by emulsion particles, cross sections for elastic, 18: 23947
scattering by emulsion nuclei at 4 Bev/c, interference effects between Coulomb and nuclear, (E), 19: 25508

scattering by emulsion nuclei at 7.3 and 17.2 Bev/c, track distortion from spurious, (E), 19: 37787 (IFA-CR-52)
scattering by helium at 153 Mev, 16: 22944
scattering by helium-3, double charge exchange in, (T), 19: 25529
scattering by hydrogen at 6 to 24 Mev, 16: 12433 (NEVIS-102)
scattering by hydrogen at 2.8 Bev, elastic, 16: 23148
scattering by hydrogen at 300 Mev, recoil proton polarization in, 17: 20837 (JINR-D-1202)
scattering by lead, cross sections for nonelastic, 17: 22564 (ORNL-3383)
scattering by nuclei at 960 Mev/c, 16: 19770
scattering by nuclei, 16: 24682 (JINR-P-868)
scattering by nuclei at high energies, inelastic cross sections for, 18: 1092
scattering by nuclear emulsion particles, distributions from, 18: 23949
scattering by nuclei, meson (A_1) production in, 18: 42428
scattering by nuclei at low energies, double-charge-exchange, (T), 19: 41773
scattering by protons, total cross sections at 400 Mev to 1.5 Bev, 16: 29633 (CEA-2092)
scattering by protons at 300 to 700 Mev, elastic, 19: 9775(R) (UCRL-11466)
scattering by tin, cross sections for nonelastic, 17: 22564 (ORNL-3383)
scattering by tritium, differential cross sections for elastic, (T), 20: 10035
scattering in emulsions at 16.2 Bev/c, angular distributions, 16: 8123
scattering in emulsions at 5.7 Mev/c, comparison of experimental and theoretical, 17: 10240(R) (NP-12208)
scattering in emulsions, distortion and noise effects on, 18: 16348
scattering in nuclear emulsions at 17 Bev/c, spurious, 19: 44416 (CERN-65-4(Vol.II), pp VI53-62)
scattering of, on protons at 300 Mev to 9 Bev, calculation of propagation of forbidden collisions in, 17: 16969
scattering on carbon at 5 to 15 Mev, angular distribution in elastic, 16: 26365
scattering on carbon-12 at 7 Bev/c, proton momentum distribution from quasi-elastic, 17: 26463 (PAN-374/VI)
scattering on nuclei at 960 Mev/c, angular distributions for, 17: 41915
separation from antiprotons and mesons (K^-) by electrostatic methods, 16: 13176 (NIRL/R/10)
separation from antiproton beams, deflection system for, 19: 37420
therapeutic use for cancer, 19: 34065
therapeutic use of, evaluation of, 18: 41299
transfer from hydrogen to heavier atoms in ethane and styrene, (E), 19: 21281
use in radiotherapy of tumors, 19: 40395
use in radiotherapy, feasibility of, 20: 3735
use in radiotherapy, 20: 10736

MESONS (π^0)
angular distribution in $\pi^0 N^*_{3/2}$ decay, 18: 22743
angular distribution and energy of cascade, from proton-copper reactions at 1 Bev, (E/T), 19: 17159(R) (ORNL-3714(Vol.II)(p.97-118))
angular distributions from meson (π^+)-proton interactions at 420 to 1070 Mev, (E), 20: 25835
angular distributions from meson (π^+)-proton interactions at 0.5 to 1.46 Bev, (E), 20: 25836
currents of, helicity representation for angular momentum of, 17: 21215
decay, 18: 34574
decay (γe^+e^-) of, ϕ–ω mixing in, 18: 14879
decay and lifetime, 16: 10875
decay and parity, 16: 24749
decay, contributions from baryon anomalous magnetic moments, 16: 13866 (NP-11421)
decay, electromagnetic and weak transition form factors in, 16: 2450
decay, electron-positron pair production from, 16: 10916
decay into electron pairs, 16: 8099 (NEVIS-97)
decay, mean lifetime of, 16: 29691
decay modes, 16: 8133
decay of, 20: 37753
decay of, analysis of cascade, 18: 16761 (NIRL/R/56)
decay of, angular distribution for T-violating 3γ, (T), 19: 32985
decay of, C violation in, (T), 20: 25874
decay of, charge-conjugation invariance in 3γ, (E), 19: 21029
decay of, detection of photons in, 20: 11099 (JINR-P-2436)
decay of, effects of meson (η)-(X^0) mixing on, (T), 19: 31056
decay of, electromagnetic, (T), 19: 14307 (ANL-6942)
decay of, electromagnetic interactions in $\bar{U}(12)$ symmetry in, 20: 19568
decay of, G_3 symmetry in, 18: 24441
decay of, G_2 symmetry in, (E/T), 20: 2520(R) (IA-920)
decay of, Goldberger-Treiman formula for two-gamma, 18: 24434
decay of, induced photon-meson couplings in, (T), 19: 18811
decay of, kinematic tables for, 20: 36022 (BNL-945)
decay of, photon angular distributions from, (E), 20: 26214
decay of, photon energy spectrum for, 18: 857 (PAN-399/VI)
decay of, selection by A invariance, 18: 22758
decay of, spectra in 2γ (T), 19: 3032
decay of, symmetry groups for boson couplings in, 18: 6018
decay of, three-photon, (E), 20: 11587(T)
decay of, velocity of high-energy gamma radiation from, (E), 20: 25800
decay of, 2γ, (T), 20: 22460 (IC-66/28)
decay of, 3γ, (E), 20: 1007
decay of, 3γ, (E), 20: 17340 (JINR-P-2322)
decay of, 3γ, 20: 39757 (JINR-P-2763)
decay ($\pi^0 \to 2\gamma$) of, relation to $\pi^+ \to e^+ + \nu + \gamma$, 17: 24362
decay ($\pi^0 \to 2\gamma$), Regge phase shifts in Goldberger-Treiman formula for, 17: 41780
decay probabilities in unitary symmetry, 18: 14866
decay processes, 17: 37992
decay properties, development of model for, 16: 8096 (JINR-D-774)
decay rate from Compton scattering of protons, 16: 17026
decay rate of, two-photon, 17: 19116
decay rates of, vector-meson dominant and ω–ϕ mixing models for 2γ, (T), 20: 11603
decay widths of, two-baryon approximation method for determining, 20: 39783
decays of, transition probabilities for, 20: 44354
detection and measurement using photon detector, 20: 41320
detection of, bubble-chamber, 17: 21114 (SLAC-5(p.79-89))
detection of, device for, 17: 32915 (TID-7668(Sect.VII))
electromagnetic form factor, 16: 971
electromagnetic structure, symmetry models for, 16: 29699
emission from interactions, phenomenological analysis of proton-meson (K^-), (T), 19: 35170
emission in antiproton-proton annihilation, (T), 19: 14332
emission of shadow, in meson (K^+) decay, (T), 19: 21038
energy and flight direction of, method for measuring, 19: 30566
energy spectra in meson (K^+_{e3}) and ($K^+_{\mu 3}$) decays, (T), 19: 35176
energy transferred to, in cosmic nucleon-nucleon interactions, 17: 13101
energy transmission from nucleon-nucleon collisions in cosmic showers, 16: 27879
existence of second, with rapid electron decay, 18: 20928
gamma emission from, effects of meson energy on gamma speed, (E), 19: 5040
gamma production at 450 and 600 Mev, 17: 7007
interactions with mesons (π^+), differential cross sections for, 16: 6985
interactions with mesons (K^0), angular distributions in, 16: 15553
interactions with mesons (π^+), resonance frequency distributions, 16: 15582
interactions with mesons (π^-) and (π^+), amplitudes, 16: 15604
interactions with mesons (π^-), cross section relation to meson (ω^0) decay partial widths, 16: 15588
interactions with protons, cross sections for, 16: 18370
interactions with mesons (π^-), resonance properties from, 16: 24744
interactions with mesons ($\pi^\pm$), resonance production below 765 Mev in, 16: 24748
interactions with mesons ($\pi^\pm$), meson (ρ) properties from, 16: 27983
interactions with baryons, multiplet structure in strong, 17: 26373
interactions with mesons (π^-), cross section for, 17: 31327
interactions with mesons (π^+), relation to meson (ω) decay, 18: 895
interactions with nucleons, double-peripheral model for elastic, 18: 40275
interactions with mesons (π^-), kinematics of, (E), 19: 5572(R) (PPAD-525-D)
interactions with hyperons (A), Λ (1405) in, (T), 19: 12303
interactions with mesons (π^-), (T), 19: 21000
interactions with mesons (π^0) in meson (π^-)-proton interactions, S-wave T = 0 final-state, (E), 19: 45089
interactions with mesons (π^-), phase shifts in elastic, (T), 19: 47357
interactions with mesons (π^0), analyticity and crossing symmetry for sum rules for, (T), 20: 2709
interactions with protons, charge asymmetry of nuclear forces from, (T), 20: 10043
interactions with mesons (π^+), high-energy limit of total cross section for, (T), 20: 21679
kinetics at 100 kev to 100 Bev, graphs for, 19: 18752 (UCRL-2426(Vol. I) (1965 Rev.))
lifetime, 17: 19106
lifetime, 17: 20594(R) (UCRL-10572)
lifetime, (E), 20: 27925
lifetime (E), 19: 1382
lifetime and photoproduction, 16: 29680
lifetime calculation using relativistic time dilation, 16: 17006 (UCRL-10118)
lifetime measurement using large relativistic time dilation, 18: 906
lifetime of, determination of mean, 17: 19122
lifetime of, mean, 17: 11500 (UCRL-10118(Rev.))
lifetime of, nuclear emulsion techniques for determining, 17: 18531

(CERN-63-3(p.325-37))
lifetime of, peripheral model for determining, 17: 13395
lifetime of, determination of, 18: 17063
lifetime of, inverse decay process for, (E), 19: 45360
lifetime of, mean, (E), 19: 41404
lifetime of, Primakoff effect in photoproduction on lead for, (E), 20: 9732
lifetime of, Williams-Weizsacker covariant method for, (T), 19: 41349
lifetimes of, measurement of mean, (E), 19: 6555
magnetic moments of, Vigier rotator model for anomalous, 17: 34802
mass and momentum measurements on, in bubble chambers, 17: 23704
mass difference (π^+-π^0) in quantum field theory, 19: 1424 (NP-14404 (p.271-99))
mass difference (π^- -π^0) from meson (π^-) capture by protons, (E), 20: 46369
mass difference with mesons ($\pi^\pm$), 17: 37934 (JINR-P-1309)
mass difference with mesons (π^+), theoretical calculation of, 18: 21007
mass differences with mesons ($\pi^\pm$) and ($\pi^\pm$), 16: 8054 (NP-11232(p.243-51))
mass of, difference between mesons(π^+) and, 17: 24326
mass relative to mesons (π^-) and (π^+), (T), 19: 31021
mass spectra of π^0-π^0, from meson (π^-)-proton interactions at 10 Bev/c, (E), 20: 41795(R) (MIT-2098-251, pp 21-36)
momentum distribution of, formulas for determining, (T), 19: 16493
photoproduction, 17: 22418 (ISS-62/7)
photoproduction, 18: 2585(R) (ISS-63/37)
photoproduction and 2-quantum decay, amplitudes for, 16: 31033
photoproduction, at threshold, analysis, 16: 7004
photoproduction at 72 to 84° cms angles, analysis of, (E), 19: 5569(R) (MIT-2098-64)
photoproduction at high energies, (E/T), 19: 45024 (MIT-2098-163)
photoproduction by polarized gamma, 16: 25933 (NP-11977(p.94-6))
photoproduction, differential cross sections for second resonance, 16: 25891 (LNF-62/37(p.34-9))
photoproduction, differential cross sections for, 16: 25890 (LNF-62/37(p.28-34))
photoproduction dispersion relations, contribution from unobserved region, 16: 26073 (JINR-P-904)
photoproduction, energy levels and resonances in, 16: 25939 (NP-11977(p.111-15))
photoproduction from deuterium at 500 Mev, 16: 14017
photoproduction from hydrogen, vector-meson effects on, 17: 5253
photoproduction from hydrogen, design of apparatus for measuring cross sections for, 17: 6792(R) (ISS-62/14)
photoproduction from complex nuclei, 17: 9517 (UCRL-10417)
photoproduction from hydrogen near threshold, 17: 17082
photoproduction from protons at 0.6 to 1.2 Bev, cross sections for, 17: 22490
photoproduction from complex nuclei, 18: 9420
photoproduction from hydrogen at 0°, differential cross section and angular distributions in, 18: 12963
photoproduction from deuterons, cross sections for, (E), 19: 8185
photoproduction from protons at 210 Mev, (E), 19: 8211
photoproduction from hydrogen, polarization of, (E), 20: 13345(R) (NP-15772)
photoproduction in hydrogen at 60° and at 600 to 1100 Mev, 16: 948
photoproduction in complex nuclei, 16: 4706
photoproduction in hydrogen at 600 to 800 Mev, 16: 16926 (NP-11592 (Vol.I)(p.9-15))
photoproduction in hydrogen, cross sections and experimental apparatus for, 16: 25892 (LNF-62/37(p.46-56))
photoproduction in hydrogen, 16: 25936 (NP-11977(p.102-4))
photoproduction in hydrogen, 16: 25937 (NP-11977(p.107-8))
photoproduction in Coulomb field, measurement of Primakoff effect in, 16: 25938 (NP-11977(p.109-10))
photoproduction in deuterium at 500 Mev, coherent, 16: 29674
photoproduction in deuterium and hydrogen, 17: 7036
photoproduction in hydrogen, cross sections for, 17: 21071
photoproduction in aluminum, beryllium, cadmium, copper, and tantalum, cross sections for, 17: 21089
photoproduction in deuterium at 500 Mev, deuteron D wave from, 18: 2657
photoproduction in Coulomb field of nucleus, 18: 10854 (LNF-63/47 (p.1-35))
photoproduction in hydrogen and lead, Primakoff effect in, 18: 10856 (LNF-63/47(p.54-8))
photoproduction in hydrogen by polarized photons (E), 19: 1389
photoproduction on protons, C and T violation in, (T), 20: 32074
photoproduction of, theory, 17: 32913 (TID-7668(Sect.V))
photoproduction of, nuclear size measurement by, 17: 33106
photoproduction of, qualitative analysis of, 17: 39868
photoproduction of, use of polarized gamma rays for, 18: 10863 (LNF-63/47(p.75-82))
photoproduction of, using coherent bremsstrahlung, 18: 10864 (LNF-63/47(p.82-6))
photoproduction of, cross sections for, 18: 10681(R) (CEAL-1009)
photoproduction of, instrument development for, 19: 16852(R) (NP-14647)
photoproduction of, predictions for multipole $E_{\frac{1}{2}}^2$ in, (E/T), 20: 19493
photoproduction of, 20: 37753
photoproduction on helium-4, gamma linear polarization from, 16: 3647
photoproduction on protons, comparison with dispersion theory, 16: 5906
photoproduction on deuterium and hydrogen, 16: 12549
photoproduction on protons, polarization of recoil protons, 16: 21311
photoproduction on protons at small angles, 16: 22940
photoproduction on carbon-12 at 155 Mev, cross sections, 16: 23139
photoproduction on nuclei, Primakoff effect in, 16: 25893 (LNF-62/37 (p.57-71))
photoproduction on protons, partial wave dispersion relations for, 16: 27910 (NP-11839)
photoproduction on nuclei at 170 Mev, models for, 16: 33762
photoproduction on protons, proton polarization in, 17: 2202
photoproduction on hydrogen, cross sections for, 17: 9349
photoproduction on deuterium and hydrogen ratio of cross sections for, 17: 9351
photoproduction on hydrogen at 180 Mev, 17: 9352
photoproduction on deuterons, coherent, 17: 17020
photoproduction on mesons(π^-), 17: 20932
photoproduction on protons at 181 Mev, 17: 28204
photoproduction on protons, 17: 32912 (TID-7668(Sect.IV))
photoproduction on nuclei, distributions from, 17: 33073
photoproduction on protons, Regge pole hypothesis for behavior of cross section for, 17: 34797
photoproduction on hydrogen, contour map of cross sections for, 17: 34980
photoproduction on hydrogen at 290–700 Mev, differential cross sections for, 17: 41805
photoproduction on hydrogen, cross sections for, 17: 40433(R) (NYO-10063(p.71-89))
photoproduction on protons at 550–1050 Mev, in second resonance region, 18: 2615
photoproduction on protons, 18: 7339 (ISS-63/40)
photoproduction on nucleons, experiments for, 18: 7514
photoproduction on protons and neutrons at 1 Bev, 18: 10857 (LNF-63/47(p.58-61))
photoproduction on complex nuclei, theory of Coulomb, 18: 17063
photoproduction on nucleons, amplitudes for, 18: 18699
photoproduction on nucleons, effects of mesons (η) in, 18: 18733
photoproduction on hydrogen, proton polarization from, 18: 22552(R) (LAL-1090)
photoproduction on protons, angular distributions from, 18: 24396(R) (NP-13947)
photoproduction on protons above 800 Mev, models for, 18: 36270
photoproduction on deuterons, impulse approximation for, 18: 40274
photoproduction on protons, polarization in, 18: 42441
photoproduction on protons, 19: 1649
photoproduction on protons, amplitudes for, (T), 19: 6562
photoproduction on deuterons, (T), 19: 10097
photoproduction on deuterons, polarization effects in, (T), 19: 14338
photoproduction on deuterons at 200 to 300 Mev, (E/T), 19: 16475 (LAL-1109)
photoproduction on deuterium in near-threshold energy region, (T), 19: 23390
photoproduction on helium-4 at 1 Bev, (E), 19: 25506
photoproduction on protons, (E/T), 19: 27139 (INSJ-81)
photoproduction on deuterons and protons, angular distributions for, (E), 19: 31000 (CONF-550-93)
photoproduction on protons, cross sections for, (E), 19: 36220(R) (MIT-2098-142)
photoproduction on protons, recoil proton polarization in, (E), 19: 37594
photoproduction on protons near threshold, (T), 19: 37606(T)
photoproduction on hydrogen at 660 to 780 Mev, dynamics of, (T), 19: 43035 (AD-448108)
photoproduction on lead at 1 Bev, lifetime from, 19: 45360
photoproduction on deuterons and protons, detection using emulsions, 19: 44438 (CERN-65-4(Vol.II), pp X33-6)
photoproduction on protons, (E), 19: 46643(R) (LAL-1136)
photoproduction on helium-4, (E), 19: 46643(R) (LAL-1136)
photoproduction on nuclei, (E), 19: 46788
photoproduction on protons at 660 to 800 Mev, angular distributions for, (E), 19: 47368
photoproduction on protons at 500 to 1000 Mev, polarization in, (E), 20: 2679 (AD-618664)
photoproduction on protons, recoil nucleon polarization from, (T), 20: 4627
photoproduction on nuclei, angular distributions from, (E), 20: 4898
photoproduction on deuterium, cross sections for, 20: 6094

photoproduction on helium-4 at 300 Mev, impulse approximation for, (T), 20: 6365
photoproduction on deuterium at 500 to 700 Mev, 20: 7810
photoproduction on nucleons, (T), 20: 13479(T)
photoproduction on deuterium at 500 to 700 Mev, (E), 20: 13345(R) (NP-15772)
photoproduction on helium-4 at 160 to 260 Mev, (E), 20: 26214
photoproduction on mesons (π^-) from meson (π^-)-proton interactions at 338 Mev, (E), 20: 25853
photoproduction on protons at 2.0 to 4.8 Bev, (E), 20: 27923
photoproduction on protons near threshold, (E), 20: 27924
photoproduction on lead, Primakoff effect in coherent, (E), 20: 27925
photoproduction on protons at 400 to 630 Mev, (E), 20: 27928
photoproduction on deuterons at 500 to 700 Mev, elastic, (E), 20: 27929
photoproduction on protons, recoil proton polarization in, (E), 20: 27930
photoproduction on protons at 360 Mev, proton polarization in, (E), 20: 27937
photoproduction on protons, backward anomaly in, (E/T), 20: 27938
photoproduction on helium-4 at 160 to 240 Mev, (E), 20: 27935
photoproduction on deuterons, cross section for elastic, (T), 20: 32041
photoproduction on protons at 250 to 360 Mev, recoil-proton polarization from, (E), 20: 32096
photoproduction on protons at 360 Mev, recoil-proton polarization from, (E), 20: 32097
photoproduction on protons at 600 to 1000 Mev, cross sections for, (E), 20: 32051
photoproduction on deuterons at 220 to 280 Mev, differential cross sections for, (E), 20: 37783
photoproduction on helium-4 near threshold, differential and total cross sections for, (E), 20: 39822
photoproduction on protons, (E), 20: 41798 (MIT-2098-265)
photoproduction on nucleons, isospin amplitudes for S-state, 20: 41906
photoproduction on protons, Reggeized vector meson exchange for, (T), 20: 44240
photoproduction on protons at 1.36 to 3.0 Bev, differential cross section for, (E), 20: 44242
photoproduction on protons at 0.3 to 5.8 Bev, 20: 46348 (SLAC-Trans-44)
photoproduction on protons at 450 to 850 MeV, search for P_{11} resonance and η cusp effect in, (E), 20: 46336 (LNF-66/37)
photoproduction on protons at 0.9 to 4.0 Bev, cross sections for, 18: 28397
photoproduction, polarized gamma, 16: 25934 (NP-11977(p.97-99))
photoproduction, retardation term in low-energy, 16: 15584
photoproduction, recoil proton polarization in, 16: 25941 (NP-11977 (p.120-1))
photoproduction, search for mesons (ω^0) in, 16: 9386
photoproduction, threshold anomalies, 16: 969
production amplitudes in γ-p interactions, 17: 11565
production and decay in meson (π^+)-deuteron interactions, 18: 42376 (TID-20762)
production by charge exchange on bound hydrogen nuclei, 17: 9307
production by cosmic gamma in emulsion chamber, 18: 30438 (INS)-69)
production by electron-proton interactions, (E), 20: 13345(R) (NP-15772)
production by mesons (π^-) at 2.8 Bev/c in the Coulomb field of the nucleus, 17: 7020
production from particle interactions at 8 Bev/c, kinematic properties from multiple, (E), 20: 41910
production in antiproton–proton interactions at 3.6 Bev/c, 18: 22741
production in cosmic-particle reactions on nuclei, 17: 11454
production in cosmic particle reactions with carbon at 5×10^{12} to 10^{13} ev, 18: 36187
production in cosmic showers, 18: 40190
production in cosmic nucleon reactions in graphite and lead, inelasticity coefficients for (E), 19: 3350
production in cosmic particle reactions with nuclei at high energies, (E/T), 19: 27439 (PAN-551/VI)
production in cosmic particle reactions with emulsion nuclei at 5 to 10 Tev, (E), 19: 34910
production in cosmic particle reactions at 3000 to 20,000 Bev, (E), 20: 7786 (INR-650/VI/PH)
production in Coulomb nuclear field, 17: 9347
production in Coulomb nuclear field, review, 17: 9464
production in deuteron-electron interactions, 17: 31337
production in electron-proton interactions at 470 Mev, coincidence measurements of, 18: 32531 (LAL-1111)
production in electron-proton interactions at 470 Mev, 18: 37923
production in electron-proton interactions at 593 Mev, (E), 20: 27911
production in electron-proton interactions at 593 Mev, cross section for, (E/T), 20: 32038
production in extensive cosmic air showers, 18: 12844
production in gamma-nucleus reactions, Primakoff effect in (E), 19: 1670
production in inelastic meson (π^-)-nucleon interactions at 7 Bev, 16: 26081 (JINR-P-974)
production in interactions of cosmic particles with nuclei of air, 19: 3037
production in K^--proton interactions at 293 to 513 Mev/c, 16: 27914 (UCRL-10175)
production in meson (K^+) decay, 16: 4729
production in meson (π^-)-carbon interactions at 17 Bev, 18: 877
production in meson (π^-) interactions with emulsion nuclei at 4.2 Bev, angular distribution and energy spectrum of, 18: 9110
production in meson (π^-)-proton interactions, 18: 10945
production in meson (π^-)-proton interactions at 7.3 Bev/c, 18: 14802 (IFA-HE/50)
production in meson (π^-)–proton interactions at 2 Bev, 18: 14888
production in meson (π^-)-proton interactions at 300 to 1000 Mev, enhancement of, 18: 14923
production in meson (π^-)-proton interactions at 6.8 and 7.5 Bev/c, 18: 20902 (JINR-E-1557)
production in meson (π^-)-proton interactions, cross sections for, 18: 24417
production in meson (π^-)–proton interactions at 10 Bev/c, 18: 34542
production in meson (π^-) reactions with xenon at 9 Bev/c, cross sections for, 18: 34949
production in meson (π^-) reactions with xenon at 9 Bev/c, 18: 36305
production in meson (π^-)-proton interactions at 4 Bev/c, total cross sections for, 18: 36307
production in meson (π^-)-nucleon interactions at 6.8 and 7.5 Bev/c, 18: 40289
production in meson(π^-) reactions with xenon at 9 Bev/c, 18: 40549
production in meson (π^-)-proton interactions at 500 to 1300 Mev, cross sections for, 18: 42382 (UCRL-11576)
production in meson (π^-) reactions with xenon at 9 Bev/c, cross sections for, (E), 19: 5250
production in meson (K^-)-proton interactions, (E), 19: 25265(R) (UCRL-11776)
production in meson (π^-)-nucleon interactions at 6.8 Bev/c, (E), 19: 35175
production in meson (π^-)-proton interactions at 1275 Mev/c, (E), 19: 41507
production in meson (π^-)-proton interactions at 905 Mev, (E), 19: 41508
production in meson (π^-) reactions with xenon at 2.8 Bev/c, multiple, 19: 43279 (NP-15383)
production in meson (π^-) reactions in bubble chambers and emulsions, intensity of, 19: 44439 (CERN-65-4(Vol.II), pp X37-43)
production in meson (π^-) capture in hydrogen and polyethylene, 16: 26190
production in meson (π^-)-proton interactions at 960 Mev, cross sections for, 16: 6984
production in meson (π^-)-proton interactions, 16: 6996
production in meson (π^+)-proton interactions at 1.25 Bev/c, 16: 6985
production in meson (π^+)-proton interactions at 820, 900, and 1050 Mev, resonance with mesons (π^+), 16: 9394
production in meson (π^-)-neutron interactions, 16: 12548
production in meson (π^-)-proton interactions at 1.1 Bev, resonances in, 16: 15567
production in meson (π^-) reactions with xenon at 2.8 Bev, cross sections for, 16: 24695 (NP-11757)
production in meson (π^-) reactions with hydrogen at 75 Mev, 16: 24689 (JINR-P-948)
production in meson (π^+) decay, 17: 9252
production in meson ($\pi^\pm$)-proton reactions, cross sections for, 17: 9305
production in meson (π^-) reactions on xenon at 8.4 Bev/c, 17: 9551
production in meson (π^-)-xenon interactions at 8.4 Bev/c, 17: 11673
production in meson (π^-)–C and meson (π^-)–H interactions at 7-8 Bev, properties of, 17: 13347 (JINR-P-1138)
production in meson (η) decay, unitary symmetry in, 17: 41798
production in meson (π^-) reactions with nuclei at 2.8 Bev/c, angular distributions for, 17: 41980
production in meson (π^-)-proton interactions at 4 Bev/c, 20: 4582 (JINR-P-2361)
production in meson (K^+) decay ($\pi^+ + \pi^0 + \gamma$), upper limit for, (E), 20: 11675
production in meson (π^-)-proton charge-exchange interactions, (E), 20: 15380
production in meson (π^-)-proton interactions at 9 Bev/c, multiplicity of, (E), 20: 15384
production in meson (η) decay, (E), 20: 15395
production in neutrino-nuclear interactions at high energies, 18: 28413
production in neutrino reactions with nuclei at 60 Bev, 18: 40642
production in neutrino-nucleon inelastic interactions, (T), 19: 47377
production in neutron-proton interactions at 600 Mev, cross sections for, (E), 20: 11564 (JINR-P-2462)
production in neutron-proton interactions at 600 Mev, (E), 20: 39826
production in nucleon interactions, angular distributions from, 16: 26082 (JINR-P-981)

production in nuclear Coulomb field, 17: 20932
production in nucleon interactions at high energies, SU(3) for multiple, (T), 20: 17345 (JINR-P-2531)
production in photon-proton interactions, cross sections for, (E), 19: 39620
production in photon-proton interactions, (E), 19: 39623
production in (π^--p) interactions, 16: 32353
production in (π^--p) interactions at 7 to 8 Bev, 16: 24685 (JINR-P-928)
production in π^--p interactions, π-π resonance, 17: 4005
production in proton interactions, single, 16: 5886
production in proton reactions with carbon at 24 Bev, 16: 7099
production in proton interactions at 383 Mev, cross-section measurements, 16: 8134
production in proton interactions at 2 Bev, 16: 15570
production in proton--meson (π^-) interactions at 1.1 Bev, 16: 18369
production in proton-proton interactions at 735 Mev, 17: 2169 (UCRL-10187)
production in proton-proton interactions at 735 Mev, 17: 36608
production in proton interactions at 2.0 and 2.85 Bev, 18: 7503
production in proton interactions at 650 Mev, angular and energy distributions in, 18: 24476
production in proton reactions (p,pπ^0) with complex nuclei at 665 Mev, 18: 42694
production in proton-nucleon interactions, (T), 19: 6536
production in proton-proton interactions at 24 Bev, (E), 19: 35018 (IFA-CR-50)
production in proton-proton interactions at 2.0 Bev, (E/T), 19: 41503
production in proton-proton interactions at 610 Mev, (E), 20: 24030
production in proton-proton interactions at 2.8 Bev/c, (E), 20: 41920
production of, by mesons (π^-)--xenon nuclei interactions at 8.4 Bev, 16: 33688 (PAN-327/VI)
properties, 18: 24390 (JINR-P-1624)
properties at 100 kev to 100 Bev, 18: 28331 (UCRL-2426(Vol.I)(1963 Rev.))
reactions in nuclear emulsions, ionization losses in, 19: 44428 (CERN-65-4(Vol.II), pp IX9-13)
scattering at high energy, ladder model calculations, 17: 13402

MESONS (π^+)

absorption by aluminum, carbon, copper, lead, and tin, at 2.72, 3.70, and 4.75 Bev/c, (E), 19: 21431
absorption by carbon at 40 to 70 Mev, 17: 38081 (JINR-P-1286)
angular distributions from gamma reactions with hydrogen at 187 Mev, 17: 16985
angular distributions from meson (π^-)--proton inelastic interactions, 18: 30580
angular distribution and energy of cascade, from proton-copper reactions at 1 Bev, (E/T), 19: 17159(R) (ORNL-3714(Vol.II)(p.97-118))
angular distributions from meson (π^-)-proton interactions at 200 to 300 Mev, (E), 19: 33062
beta decay, 19: 37663
beta decay, 18: 20905 (JINR-P-1559)
beta decay of, conserved-vector-current theory validity for, 17: 36587 (UCRL-10864)
beta decay of, data recording system for, 18: 14221 (UCRL-10317)
beta decay of, vector current conservation testing by, 18: 36362
beta decay to mesons (π^0), branching ratios of, (E), 19: 14312 (CU-233)
capture by light nuclei, nucleon pair correlations from proton spectra in, 17: 41987
charge exchange by, double, 18: 10851 (JINR-P-1474)
charge exchange on light nuclei, double, 18: 38141
decay, 16: 29683
decay ($\pi^0 + e^+ + \nu$), 18: 26273 (BNL-837(p.344-52))
decay, angular distributions, 16: 10845
decay branching ratio, (E/T), 19: 25265(R) (UCRL-11776)
decay curve of, (E), 20: 46370
decay ($e + \gamma$) of, structure effects in, 17: 9387
decay ($e^+ + \nu$) and ($\mu^+ + \nu$), e and μ spirality effects on probabilities of, 17: 29173
decay in longitudinal magnetic field, meson (μ^+) angular distributions for, 18: 36309
decay into mesons (π^0), 18: 21306
decay ($\mu^+ \rightarrow e^+$), angular distribution of positrons from, 16: 32352
decay, neutrino production and properties from, 16: 26147
decay, neutrino spectra from, 16: 15562
decay of, 20: 37753
decay of accelerated, interactions of neutrinos from, 17: 28151 (NEVIS-111)
decay of, branching ratio for $\pi^0 + e^+ + \nu$, 17: 9229
decay of, branching ratio of $\pi^+ \rightarrow \pi^0 + e^+ + \nu$ process in, 17: 9252
decay of, branching ratio for ($\pi^0 + e^+ + \nu$), 17: 29541
decay of, neutrino (ν_μ) mass from photon energy spectra in, 17: 39896
decay of relativistic, neutrino spectra from, 18: 12894 (CERN-63-37 (p.111-29))
decay of, symmetry violations in leptonic, 18: 7551
decay of, to $e + \nu + \gamma$, 17: 17048
decay of, to $e^+ + \nu + \gamma$, 18: 9150
decay of, unitary symmetry of weak current structure in, 17: 41781
decay of, vector form factor in, 17: 32934
decay of, anomalous, (E), 19: 23440
decay of, axial-vector current in leptonic, (T), 20: 13508
decay of, branching ratio for $\pi^+ \rightarrow \pi^0 + e^+ + \nu$ (E), 19: 3086
decay of, branching ratio for positron, (E), 19: 35149
decay of, conserved-vector current theory for, 18: 36262
decay of, CVC hypothesis for (E/T), 19: 1308
decay of, determination of neutretto mass from, (T), 19: 25329
decay of, intermediate bosons in, 18: 36256
decay of, leptonic, 18: 26349
decay of, meson (π) weak structure from radiative, 18: 30508 (CERN-64-26)
decay of, neutrino interactions in, 18: 40280
decay of, neutrino spectra from, (E), 20: 21602 (CERN-65-32, pp 111-14)
decay of, PT invariant scalar-pseudoscalar coupling in leptonic, (T), 19: 18839
decay of, radiative electronic, (E), 20: 9776
decay of, S-matrix method for radiative correction for, 20: 41865
decay of, spatial distributions in leptonic, 19: 35045
decay of, T invariance in, 20: 29997(T)
decay of, vector and axial-vector Cabibbo angles for leptonic, 20: 34188
decay ($\pi^+ \rightarrow e^+ + \nu + \gamma$) of, relation to $\pi^0 \rightarrow 2\gamma$, 17: 24362
decay ($\pi^+ \rightarrow \mu + \nu$), Regge phase shifts in Goldberger-Treiman formula for, 17: 41780
decay ($\pi^+ \rightarrow \pi^0 + e^+ + \gamma$), experimental measurement of the probability of, 16: 17057
decay ($\pi^+ \rightarrow \pi^0 + e^+ + \nu$), probability for, 17: 22511
decay ($\pi^+ \rightarrow \pi^0 + e^+ + \nu$) of, electromagnetic correction effects on, 17: 31331
decay, probability of β-type, 16: 13861 (JINR-D-844)
decay processes review, 17: 9469
decay schemes, 16: 27352
decay to $\pi^0 + e^+ + \nu_e$, branching ratio for, (E), 19: 31012 (TID-21806)
detection and measurement at 3 to 6 Bev/c, Cherenkov counter for, 18: 14276
detection in intense electron and γ-ray background, equipment for, 18: 39671
detection using bubble chambers, discrimination between protons in, 20: 23484
distributions from meson (π^+)-nucleon interactions at 6.8 Bev/c, 18: 40288
distributions from meson (π^-)-proton six-prong interactions at 10 Bev/c, 18: 40293
effects on γ-γ scattering, (T), 20: 11600
effects on proton magnetic moment, 17: 24288
electromagnetic form factor of, produced by electron--proton reactions, 18: 10868 (LNF-63/47(p.105-8))
electroproduction from deuterium, theory of, 18: 4465
emission from interactions, phenomenological analysis of proton-meson (K^-), (T), 19: 35170
emission in decay of hypernuclei, 20: 30485
emission in $_\Lambda He^4$ decay, 17: 17190
emission in hyperfragment decay, 18: 30787
emission in hypernuclear decays, model for, 18: 42436
emission in mesons (π^-)-nucleon interactions at 4.4 Bev, transverse momentum of, 18: 42395
emission in neutron interactions with protons at 600 Mev, yields of, 18: 10970
emission in proton reactions (p,pπ^+) with copper-65 at 0.49 to 28 Bev, excitation function and recoil properties of, (E), 19: 23751
energy loss measurements in silicon at 50 to 365 Mev, (E), 20: 7411
energy spectra from meson ($K^+_{\pi 3}$) decay, (E), 20: 1011
energy spectra in meson (ϕ^0) and (ω^0) decays, (T), 19: 43104
energy spectrum in $K^+ \rightarrow \pi^+\pi^0\pi^0$ decay, 18: 32612
energy spectrum of, from meson ($K^+_{\pi 3}$) decay (E), 19: 1318
exchange in neutron-proton reactions, backward peaking in high-energy, 17: 19117
exchange in proton interactions at 2.5 Bev/c, effects of single, 17: 26292 (UCRL-10718)
focusing of beams of, neutrino spectra from magnetic-finger, (T), 19: 30877 (BNL-9062)
form factor of, charge, (E/T), 20: 9770
form factors, development of models for, 16: 8096 (JINR-D-774)
form factors, relation to meson ($K^\pm$) form factors for electromagnetic and weak transitions, 16: 2450
intensity of cosmic, above 4 Bev, (E), 19: 41294
interaction cross sections, 16: 13880
interaction resonances with protons, elastic, 18: 37963

interaction with deuterons at 3.29 Bev/c, meson (X^0) production from, (E), 20: 27834
interactions ($\pi^+ d \to \pi^0 pp$) with deuterons at 600 to 900 Mev, 18: 32587
interactions at high-energy, cross section combinations for, 17: 11529
interactions at very high energies, proposed diffraction-scattering experiment, 17: 20579 (UCRL-10022(p.142-3))
interactions at 1170 Mev/c, production of $\Sigma^+ K^+$ by, 16: 31036 (UCRL-10154)
interactions in meson (K) decay, 18: 36358
interactions in meson (π^+)-proton interactions at 2.75 Bev/c, final-state, 19: 25306
interactions in propane bubble chambers, method of identification of, (E), 20: 39211 (JINR-P-2842)
interactions of, model for forward amplitude for, 20: 37805
interactions of, SU(6) symmetry for forward amplitudes in, (T), 19: 41515
interactions with alpha particles, meson (π) form factors from, (T), 19: 41379
interactions with alpha particles at 24 Mev, meson (π) electromagnetic form factor from elastic, (E), 20: 21659
interactions with baryons, multiplet structure in strong, 17: 26373
interactions with carbon-12, resonance production in, 18: 14811 (JINR-P-1508)
interactions with deuterons at 85 to 378 Mev, cross sections for, 16: 10834
interactions with deuterons, three-pion resonances in, 16: 16962 (NP-11592(Vol.I)(p.277-82))
interactions with deuterons at low energies, p and s wave contributions in, 16: 18344
interactions with deuterons, meson (η) and (ω) production and properties from, 16: 26165
interactions with deuterons, meson (ω) and meson (η) production in, 17: 9327
interactions with deuterons, hyperon (Σ) production in, 17: 9366
interactions with deuterons, meson (η^0) properties from, 17: 13457
interactions with deuterons at 300 Mev, cross section for elastic, 17: 28185
interactions with deuterons and protons, total cross sections for, 17: 39844 (BNL-7258)
interactions with deuterons, resonances in, 18: 12913 (TID-7686 (p.69-107))
interactions with deuterons, nucleons, and tritons, resonance production in, 18: 14811 (JINR-P-1508)
interactions with deuterons and neutrons at 1230 Mev/c, meson (η^0) and (ω^0) production in, 18: 14955
interactions with deuterons, meson (f^0) production in, 18: 24463
interactions with deuterons at 6 Bev/c, neutral particle production in, 18: 30570
interactions with deuterons at 0.65 to 1.95 Bev/c, cross sections for, 18: 36302
interactions with deuterons at 4.5 Bev/c, 18: 37922
interactions with deuterons at 1.23 Bev/c, multipion resonances in, 18: 42376 (TID-20762)
interactions with deuterons and nucleons, distribution from, 18: 42418
interactions with deuterons, deuteron polarization in elastic, 18: 44541
interactions with deuterons at 650, 750, and 850 Mev (E), 19: 1326
interactions with deuterons at 420 to 1360 Mev (E), 19: 1328
interactions with deuterons, meson (η) production and decay in, (E), 19: 12194
interactions with deuterons and protons at 6 to 22 Bev/c, total cross sections for, (E), 19: 25351
interactions with deuterons at 4.5 Bev, meson (π^-)–meson (π^+) scattering in, (E), 19: 25388
interactions with deuterons at 6.0 Bev/c, $\pi^+ \pi^-$(1670) production in, (E), 19: 39537
interactions with deuterons at 1.68 Bev/c, Y_0^* production in, (E), 19: 39553
interactions with deuterons, partial wave dispersion relations for disintegration in, 19: 41336 (NP-15335)
interactions with deuterons at 3.29 Bev/c, neutral scalar meson production from, (E), 20: 6079
interactions with deuterons at 6 Bev/c, mechanism for coherent, (T), 20: 7856
interactions with deuterons at 4.5 Bev/c, resonances in, (E), 20: 9740
interactions with deuterons at 4.5 Bev/c, (E), 20: 9741
interactions with deuterons at 2.5 Bev/c, resonance production in, (E), 20: 25781(R) (COO-1195-56)
interactions with deuterons at 3.29 Bev/c, meson (f^0) production in, (E), 20: 27814
interactions with deuterons at 3.65 Bev/c, A_2 (1300) production and properties from, (E), 20: 32064
interactions with deuterons at 300 Mev, effects of π-N resonance on, (T), 20: 34172
interactions with deuterons at 3.29 Bev/c, A_1 (1090) and A_2 (1310) production in, (E), 20: 39470(R) (ORNL-3924)
interactions with deuterons at 1.2 and 2.8 Bev/c, cross section for Z^* baryon production in, 20: 44195
interactions with deuterons, meson (π) resonances of three at 550 Mev, 16: 4716
interactions with hyperons (Σ^-) and nucleons at high energies, double-charge exchange cross sections for, 17: 26326
interactions with hyperons (Λ), resonances in, (E/T), 19: 6518 (JINR-P-1807)
interactions with mesons (π^0), differential cross sections for, 16: 6985
interactions with mesons (K^-), coupling constants and cross sections, 16: 9403
interactions with mesons (π^-) at 365 Mev, cross sections for, 16: 10879
interactions with meson (π^-) and (π^0), resonance frequency distributions, 16: 15582
interactions with mesons (π^0), amplitudes, 16: 15604
interactions with mesons (π^0), meson (ρ) properties from, 16: 27983
interactions with mesons (π^+) and protons at 910, 1090, and 1260 Mev, 16: 32285 (TID-16558)
interactions with mesons (π^-), resonances from, 17: 4003
interactions with mesons ($\pi^\pm$), 17: 5252
interactions with mesons (π^-), cross sections for, 17: 31277 (JINR-P-1260)
interactions with mesons (π^-), cross section for, 17: 41928
interactions with mesons (π^0), relation to meson (ω) decay, 18: 895
interactions with mesons (π^-), cross sections for elastic, 18: 6038
interactions with mesons (π^-), cross sections for inelastic, 18: 7532
interactions with mesons (π^-), meson (ρ^0) domination in Lee model for, 18: 18681
interactions with mesons (π^-) in meson (π^-)-proton interactions at 4 Bev/c, 18: 37886 (UCRL-11468)
interactions with meson (K^0)-meson (π^-) pairs, resonances in, 18: 40378
interactions with mesons (K), properties of resonance, (E/T), 19: 6556
interactions with mesons (π^-), complex angular momentum and vector mesons in, (T), 19: 43087
interactions with mesons (π^-), phase shifts in elastic, (T), 19: 47357
interactions with mesons (π^-) below 1.3 Bev, phase shifts for elastic, (T), 20: 11555 (DESY-65/13)
interactions with mesons (π^0), high-energy limit of total cross section for, (T), 20: 21679
interactions with mesons (π^-), annihilation channels in, 20: 39776(T)
interactions with neutrons, cross sections for, 16: 13880
interactions with nucleons, effect of ($\bar{K}$-K) resonance in, 17: 20871
interactions with nucleons, spin-orbit forces in, 17: 29550
interactions with nucleons, meson and baryon exchange diagrams for, 17: 39880
interactions with nucleons at low energies, parameters and phase shifts for, 18: 7556
interactions with nucleons, isotopic spin of meson (f^0) from, 18: 24466
interactions with nucleons at high energies, parameters for, 18: 24384 (JINR-P-1577)
interactions with nucleons, model for resonances in, 18: 32608
interactions with nucleons, vector meson production in, 18: 34620
interactions with nucleons, double-peripheral model for elastic, 18: 40275
interactions with neutrons at 6 Bev/c, charge-exchange cross sections, (E), 19: 4946
interactions with nucleons at high energies, amplitudes and total cross sections for, (T), 19: 10076
interactions with nucleons at high energies, inelastic, (T), 19: 16646
interactions with nucleons at 3.25 Bev/c, exchange mechanism for (ω) production in, (E), 19: 23397
interactions with nucleons, amplitudes for elastic, (T), 19: 39621
interactions with nucleons at 300 to 700 Mev, amplitudes for, (E), 19: 41442
interactions with neutrons at 1.7 Bev/c, meson (ρ) and (ω) production in, (E), 19: 41528
interactions with nucleons, phase-shift analysis of, (T), 20: 4849(R) (UCRL-14360, pp 1-50)
interactions with nucleons at high energy, sum rule for cross sections of, (T), 20: 4678
interactions with nucleons, π-π distributions and meson (f^0) from, (E), 20: 9730
interactions with nucleons, phase-shift analysis and spin-flip dispersion relations for, (T), 20: 13492
interactions with neutrons at 1.7 Bev/c, meson (ω) and (ρ^0) production and decay in, (E), 20: 15403
interactions with neutrons, Regge-pole analysis of meson (ω) production in, (T), 20: 19510
interactions with nucleons at 3.25 Bev/c, (E), 19: 23397
interactions with protons, threshold effects, 16: 988
interactions with protons at 1.15 Bev/c, associated production, 16: 2440
interactions with protons at 8 to 20 Bev/c, total cross sections,

16: 2453
interactions with protons at 990 Mev, cross sections, 16: 5909
interactions with protons, cross sections for di-pion resonance by Chew-Low method, 16: 6924 (UCRL-9886)
interactions with protons at 1.25 Bev/c, meson (ρ) spin calculations from, 16: 6985
interactions with protons at 120 Mev, analysis of elastic, 16: 8120
interactions with protons at 450 to 1650 Mev, total cross sections, 16: 9382
interactions with protons at 820, 900, and 1050 Mev, meson (π^+) and (π^0) emission and resonance at 575 Mev, 16: 9394
interactions with protons at high energies, cross-section constancy, 16: 10895
interactions with protons up to 20 Mev, total-cross-section relation to isospin independence, 16: 10905
interactions with protons at 820, 900, and 1050 Mev, 16: 10828
interactions with protons, meson (π) production cross sections for, 16: 10879
interactions with protons at 10 to 20 Bev, total cross sections, 16: 10900
interactions with protons at 310 Mev, production cross section for mesons (π), 16: 16929 (NP-11592(Vol.I)(p.25-6))
interactions, with protons at 357 Mev, I = 2 scattering length, 16: 18371
interactions with protons, 16: 19474(R) (TID-14386)
interactions with protons at 310 Mev, cross sections, phase shifts, and polarization in, 16: 19678 (UCRL-10127)
interactions with protons, Heitler-Arnous nonlocal theory, 16: 19686
interactions with protons at 1.0 Bev, angular distributions for elastic, 16: 21293
interactions with protons at 820, 900, and 1050 Mev, angular distributions and cross sections for, 16: 26120
interactions with protons below 1 Bev, meson (ζ) even isotopic spin from, 16: 26152
interactions with protons at 310 Mev, phase shifts and scattering cross sections for, 16: 26093 (UCRL-10252)
interactions with protons near threshold ($\pi^+ + p \rightarrow \Sigma^+ + K^+$), 16: 27998 (UCRL-10025)
interactions with protons at 1035 Mev, creation of Σ^+ hyperon, 16: 29671
interactions with protons at 1.95 Bev, strange particle resonances from, 16: 32284 (TID-16557)
interactions with protons, meson (ζ) production in, 16: 32335
interactions with protons at 500 to 1600 Mev, differential cross sections for, 17: 3969 (UCRL-10378)
interactions with protons at 1090 and 1260 Mev, meson (η) production in, 17: 5259
interactions with protons, pion-pion interactions in, 17: 5279
interactions with protons, resonances in, 17: 6997
interactions with protons, N_α^* isobar production in, 17: 7002
interactions with protons at high energy, cross sections of, 17: 7013
interactions with protons, threshold singularities in total cross sections for $K^+\Sigma^+$ formation, 17: 7033
interactions with protons, one-pion-exchange contributions to, 17: 6980
interactions with protons at 1.25 and 1.75 Bev/c, cross sections for, 17: 9204 (UCRL-10530)
interactions with protons at 3, 4, and 5 Bev/c, elastic, 17: 9258
interactions with protons, cross sections for, 17: 9267
interactions with protons, angular distribution in, 17: 9304
interactions with protons, cross section for meson (π^0) production in, 17: 9305
interactions with protons at 2.35, 2.6, and 2.9 Bev/c, 17: 9316
interactions with protons, hyperon and meson (K) production in, 17: 9365
interactions with protons, hyperon (Σ) and meson (K) production in, 17: 9367
interactions with protons, total cross sections for, 17: 9382
interactions with protons at 180°, elastic cross sections for, 17: 9426
interactions with protons, meson (π-π) amplitudes in low-energy, 17: 11518
interactions with protons, isobaric and (π-σ) models for, 17: 13392
interactions with protons, scattering at 3/3 resonance in isobaric model, 17: 15102
interactions with protons, cross sections for elastic, 17: 19126
interactions with protons at 1.5 to 6 Bev, total cross sections for, 17: 19150
interactions with protons, comparison to three Regge pole model for elastic, 17: 20899
interactions with protons, scattering measurements and phase-shift analysis of, 17: 22523
interactions with protons at high energies, inelastic cross sections for, 18: 1092
interactions with protons at 1050 and 1170 Mev/c, 18: 864 (UCRL-10243)
interactions with protons at 3.5 Bev/c, meson (ω) production mechanisms for, 18: 894
interactions with protons, asymptotic polarization relations for, 18: 853 (JINR-P-1404)
interactions with protons at 3.43 and 3.54 Bev/c, multimeson resonance production in, 18: 2651
interactions with protons at 7 to 20 Bev/c, differential and total cross sections for elastic, 18: 2655
interactions with protons at 1.59 Bev/c, meson (ρ)-isospin current coupling from, 18: 4449
interactions with protons, complex diagram of forward amplitudes in, 18: 6009
interactions with protons at high energies, optical model for, 18: 6014
interactions with protons at high energies, field theory for, 18: 6015
interactions with protons at high energies, exchange of strangeness-carrying trajectories in, 18: 7507
interactions with protons at high energies, effects of Regge trajectories on diffraction peaks in, 18: 7515
interactions with protons, spark chamber design for polarization measurements in, 18: 8655
interactions with protons at 1050 and 1170 Mev/c, 18: 9180
interactions with protons, elastic, 18: 10843 (CONF-122-22)
interactions with protons, total cross sections for, 18: 10423
interactions with polarized protons, 18: 12803 (TID-7685)
interactions with protons, forward amplitudes for, 18: 12898 (EFINS-63-72)
interactions with protons at 3.5 Bev/c, isobars and multipion resonances in, 18: 14962
interactions with protons at 2.35 Bev, meson (f^0) effects on, 18: 14961
interactions with protons at 0.5 to 1.5 Bev/c, γ production in, 18: 14798 (CEA-2306)
interactions with protons at 0.5 to 1.5 Bev/c, cross sections for ($\pi^+p\pi^0$) production in, 18: 14889
interactions with protons, four-meson resonance from, 18: 14900
interactions with protons, parity and spin of ($m\omega$) resonance in, 18: 14901
interactions with protons at 78 Mev, total cross sections for, 18: 14924
interactions with protons at 8.5, 12.4, and 18.4 Bev/c, elastic, 18: 16789
interactions with protons at 3.65 Bev/c, 18: 16790
interactions with protons, asymptotic relations and invariance properties in, 18: 18700
interactions with protons at 2.77 Bev/c, strange-particle production in, 18: 18702
interactions with protons, meson (π) multiple production in, 18: 18743
interactions with protons at 300 to 700 Mev, 18: 18649 (UCRL-11180)
interactions with protons to 700 Mev, phenomenological analysis of, 18: 20915 (TID-20490)
interactions with protons, amplitudes and cross sections for three-particle production in, 18: 22739
interactions with protons, isobar ($\omega N_{3/3}^{3/2,3/2}$) production in, 18: 22743
interactions with protons, meson (ω^0) production in, 18: 22757
interactions with protons, elastic differential cross sections for, 18: 24424
interactions with protons at high energies, fundamental lengths in, 18: 24436
interactions with protons at 600 Mev, branching ratios and cross sections for, 18: 24396(R) (NP-13947)
interactions with protons, W-boson production in, 18: 24397 (NP-13954)
interactions with polarized protons at 250 Mev, polarization parameter for, 18: 24404 (UCRL-11149)
interactions with protons at high energies, dispersion relations for, 18: 24386 (JINR-P-1598)
interactions with protons at 500 to 1600 Mev, cross sections for elastic, 18: 24453
interactions with polarized protons, hyperon (Σ^+) parity and spin from, 18: 26343
interactions with protons, isobar production in, 18: 26358
interactions with protons at high energies, scaling law for, 18: 28330 (TID-20722)
interactions with protons at 4 Bev/c, resonances (ρ–π) in, 18: 30568
interactions with protons at 4 Bev/c, production of 3/3 3/3 isobar in, 18: 30569
interactions with protons at 4 Bev/c, elastic, 18: 30575
interactions with protons at 0.76 to 1.655 Bev, dispersion relations for charge-exchange, 18: 28364
interactions with protons, phenomenological model for, 18: 34533
interactions with protons, meson (π-ρ) resonance in, 18: 34581
interactions with protons at 2.5 to 5.5 Bev/c, total cross sections for, 18: 34584
interactions with protons at 3.54 Bev/c, meson (ρ) exchange mechanism in, 18: 34626
interactions with protons at 3.5 Bev/c, meson (π^+)-meson (π^+) resonance in, 18: 34630
interactions with protons, unitary symmetry model for resonance production in, 18: 36280
interactions with protons at 4 Bev/c, isoscalar $\rho\pi$ resonances in,

18: 36304
interactions with protons at 2.77 Bev/c, final-state interactions in, 18: 37876 (BNL-8248)
interactions with protons, diffracting sphere model for elastic, 18: 37915
interactions with protons at 300 to 700 Mev, 18: 37920
interactions with protons at 3.65 Bev/c, 18: 40247 (UCRL-11445)
interactions with protons at 1.6 Bev/c, angular distributions of elastic, 18: 40269
interactions with protons at 4 Bev/c, 18: 40285
interactions with protons at 8 to 12 Bev/c, elastic, 18: 40351
interactions with protons at 250 Mev, differential cross sections and phase-shift analysis of scattering in, 18: 40252 (UCRL-11537)
interactions with protons at below 4 Bev, cross sections for, 18: 42361 (BNL-8315)
interactions with protons at high energies, potentials in diffraction, 18: 42407
interactions with protons at 523 to 689 Mev, polarization in elastic, 18: 42440
interactions with protons, meson (A^+) resonance effects in, 18: 42444
interactions with protons at 1.39, 1.76, and 2.08 Bev/c, strange-particle production in, 18: 44511 (BNL-8311)
interactions with protons at 2.08 Bev/c, multipion production in, 18: 44513 (BNL-8313)
interactions with protons at 2.35 and 2.90 Bev/c, analysis of two-prong events in, 18: 44519 (NEVIS-123)
interactions with protons at 4 Bev/c, exchange mechanisms in, 18: 44555
interactions with protons at 8 Bev/c, resonance effects in, 19: 1258
interactions with protons at 800 and 900 Mev, meson (π) production in (E/T), 19: 1325
interactions with protons at 1.6 Bev (E), 19: 1347
interactions with protons at 2.75 Bev, single meson production in (E), 19: 1349
interactions with protons at 3.65 Bev/c, resonances in (E/T), 19: 3030 (UCRL-11729)
interactions with protons, resonances in (T), 19: 3031 (UCRL-11730)
interactions with protons at 7 to 17 Bev/c, single-pole contribution to elastic (T), 19: 3047
interactions with protons, recoil proton polarization in elastic (E), 19: 3074
interactions with protons at 240 Mev, phase shift analysis of elastic, (T), 19: 4955
interactions with protons at high energies, (T), 19: 4956
interactions with protons, charge exchange in, (T), 19: 4996
interactions with protons at 500 Mev, (E/T), 19: 6530
interactions with protons at high energies, backward elastic, (T), 19: 8178
interactions with protons at 2.75 Bev/c, $N^{++}_{3/2\,3/2}$ production in, (E), 19: 8179
interactions with protons, one-baryon exchange in, (T), 19: 10062
interactions with protons, model for meson (η) production in, (T), 19: 10065
interactions with protons at high energies, dispersion relations for, (T), 19: 12186
interactions with protons at high energies, optical models for, (T), 19: 12228
interactions with protons, Chew-Low method for cross sections for, (T), 19: 12296
interactions with protons at 1111 to 1265 Mev/c, hyperon (Σ^+) production in, (E), 19: 12162 (COO-1428-7)
interactions with protons, K^* (890) production in, 19: 16510
interactions with protons, hyperon (Σ^+) and meson (K^+) production in, (T), 19: 16557
interactions with protons, resonances in, (T), 19: 16585
interactions with protons at 410 and 492 Mev, phase-shift analyses of, (T), 19: 16618
interactions with polarized protons at 246 Mev, asymmetry in, (E), 19: 16656
interactions with protons at 410 and 492 Mev, recoil proton polarization in, (E), 19: 16617
interactions with protons at 4 Bev/c, exchange mechanisms for N^{*++} production in, (E/T), 19: 18799
interactions with protons, Regge exchange mechanism for, (T), 19: 18805
interactions with protons at 2.5 to 5.5 Mev, cross sections for, (E), 19: 23355(R) (BNL-867(p.1-117))
interactions with protons, SU(6) predictions for amplitudes of, (T), 19: 23432
interactions with protons, SU(6) cross section equalities for, (T), 19: 23433
interactions with protons, relativistic SU(6) model for amplitudes of, 19: 23395
interactions with protons at high energies, equipment for studying, 19: 22862
interactions with protons at 2.75 Bev/c, meson (π^+) final-state interactions in, (E), 19: 25306
interactions with protons, absorptive effects in peripheral production processes in, (T), 19: 25328
interactions with protons at 4 Bev/c, resonance production in, (E), 19: 25350
interactions with protons at 2.5 to 5 Bev/c, cross sections for, (E), 19: 25375
interactions with protons at 1170 Mev/c, strange particle production in, (E), 19: 25265(R) (UCRL-11776)
interactions with protons at 1170 Mev/c, production of mesons (η) in, (E), 19: 25265(R) (UCRL-11776)
interactions with protons at 250-Mev, differential cross section for, (E), 19: 25265(R) (UCRL-11776)
interactions with protons at 3.65 Bev/c, analysis of, (E), 19: 25265(R) (UCRL-11776)
interactions with protons at high energies and low momentum transfers, (T), 19: 27227
interactions with protons, A_1 (1080) production in, (T), 19: 27272
interactions with protons, sum rules for scattering amplitude in, (T), 19: 29062 (JINR-P-2020)
interactions with protons at 3.15 Bev/c at 180°, cross sections for elastic, (E), 19: 29066 (JINR-P-2127)
interactions with protons at 6 to 10 Bev/c, (E/T), 19: 30994 (BNL-8935)
interactions with protons at 8 to 12 Bev, forward dispersion relations for, (T), 19: 33000
interactions with protons, Regge pole hypothesis for differential cross sections for, (T), 19: 33022
interactions with protons at 400 to 2000 Mev, total cross sections for, (E), 19: 33031
interactions with protons at 2.1 to 5.5 Bev/c, spin determination of isospin-½ resonances in, (T), 19: 33043
interactions with protons at 3.2 Bev/c, elastic, (E), 19: 33069
interactions with protons below 1 Bev, cross sections for inelastic, 19: 35033 (UCRL-14202)
interactions with protons at 8.5 to 18.4 Bev/c, differential cross sections for, (E), 19: 35075
interactions with protons at 8 to 14 Bev/c, amplitudes for small-angle elastic, 19: 35161
interactions with protons at 410 and 492 Mev, phase-shift analysis of, (E/T), 19: 35165
interactions with protons at 2.5 Bev/c, resonance production in, (E), 19: 37526 (CU-1932-243)
interactions with protons at 3.7 Bev/c meson (B) production in, (E), 19: 37597
interactions with proton at high energies, data on elastic, 19: 37655
interactions with protons at high energies, cross sections for, (T), 19: 37532 (JINR-P-2126)
interactions with protons, peripheral production and decay of mesons (ρ) and N^* resonance in, (E/T), 19: 39576
interactions with protons at 2.35 to 2.90 Bev/c, resonance production in, (E), 19: 41418
interactions with protons, poles and resonances in, (T), 19: 41427
interactions with protons at 8 and 12 Bev/c, differential cross sections for elastic, (E), 19: 41455
interactions with protons at high energies, forward amplitudes for, (T), 19: 41376
interactions with protons at 4 and 8 Bev/c, backward elastic, (E), 19: 41456
interactions with protons, energy dependence of diffraction curve for elastic, (T), 19: 43043 (JINR-P-2202)
interactions with protons at 1030 and 1505 Mev/c, differential cross sections for, (E), 19: 43152
interactions with protons at high energies, resonance production in, (T), 19: 45037 (TID-21316)
interactions with protons at 1.11 and 1.265 Bev/c, N^{*++} production in, 19: 44997 (COO-1428-14)
interactions with protons at 8 Bev/c, resonance enhancement from, (E), 19: 45103
interactions with protons, high-energy limits for, 19: 45040 (TPJU-11/65)
interactions with protons at 1.45 Bev/c, differential cross section for, (E/T), 19: 47304 (IAE-700)
interactions with protons, cross-sections and systematic behavior in, 17: 24263 (BNL-6934)
interactions with protons at 600 Mev, branching ratios and cross sections for, 17: 28156 (UCRL-10563)
interactions with protons at 7 to 17 Bev/c, differential cross section for, 17: 29552
interactions with protons, 17: 31091(R) (UCRL-10862)
interactions with protons at 1.95 Bev, multi-π resonances from, 17: 31287 (TID-19082)
interactions with protons, Castillejo-Dalitz-Dyson poles and Low equation in, 17: 31292

interactions with protons at 31.4 Mev, elastic, 17: 31349
interactions with protons, real parts of high-energy forward-scattering amplitudes in, 17: 34771
interactions with protons at 5 Bev, Regge pole contributions to cross section of, 17: 34816
interactions with protons at 2 Bev/c, elastic, 17: 34826
interactions with protons at 2.08 Bev/c, resonance production in, 17: 36583 (TID-19342)
interactions with protons, multiple meson(π) production in, 17: 36584 (TID-19343)
interactions with protons near 300 Mev, 17: 37930 (CERN-63-27)
interactions with protons, polarization measurements for Regge cuts in, 17: 39897
interactions with protons at 2.08 Bev/c, strange particle production in, 17: 41737 (CONF-46-102)
interactions with protons at 265 Mev, proton polarization from, 17: 41770
interactions with protons at 2.92 Bev/c, angular and energy dependence of cross section for elastic, 17: 41801
interactions with protons at 600 Mev, single-meson (π)-production mechanism in, 17: 41804
interactions with protons, three-Regge-pole model for elastic, 17: 41832
interactions with protons at 3.65 Bev/c, diffraction scattering effects in, (E), 20: 1008
interactions with protons at 2.77 Bev/c, double resonance production in, (E), 20: 1019
interactions with protons at 1.2 Bev/c, meson (η^0) production in, (E), 20: 1027
interactions with protons, elastic differential cross sections for, (E), 20: 2520(R) (IA-920)
interactions with protons at 4.1 and 4.85 Bev/c, cross sections for elastic, (E), 20: 2683 (JINR-P-2327)
interactions with protons, inelastic S_{31} resonance in, (T), 20: 2716
interactions with protons at 10 Bev, forward dispersion relations for, (T), 20: 4602
interactions with protons, forward amplitude for, (T), 20: 4603
interactions with protons, coupling constant and s-wave scattering lengths for elastic, (T), 20: 6083
interactions with protons at 10 to 30 Bev, amplitudes and charge-exchange cross sections for elastic, (E/T), 20: 7793 (JINR-P-2397)
interactions with protons at high energy, Regge-pole exchange model for N* production in, 20: 7814
interactions with protons, quasi-two-body processes in, (E), 20: 7823
interactions with protons at 10 Bev, cross section structure for, (T), 20: 7844
interactions with protons at 3.65 Bev/c, meson (ϕ) and (X^0) production in, (E), 20: 7846
interactions with protons above 2 Bev, energy dependence of diffraction-curve slope for, (T), 20: 9720(T)
interactions with protons, SU(6) for angular distributions and N^{*++} production from, (T), 20: 9723(T)
interactions with protons at 1.76 and 2.08 Bev/c, cross sections for elastic, (E/T), 20: 9742
interactions with protons at 1090 Mev, N* (1925) parity in model for, (T) 20: 9748
interactions with protons at 8 Bev/c, absorption model for differential cross sections for, (E/T), 20: 9751
interactions with protons at 4 and 8 Bev, absorptive corrections to nucleon exchange term in, (T), 20: 11573
interactions with protons at 2.75 Bev/c, exchange mechanism for $p\pi\pi\pi$, (E/T), 20: 11605
interactions with protons, test for Regge behavior in backward, (T), 20: 11663
interactions with protons at 2 Bev/c, cross sections for inelastic, (E), 20: 11672
interactions with protons, forward amplitude for, (T), 20: 11697
interactions with protons at 8 Bev/c, resonances in, (E), 20: 11616
interactions with protons at 3.65 Bev/c, resonance production in, (E), 20: 13456 (UCRL-16170)
interactions with protons at 4.10 and 4.85 Bev/c, elastic, (E), 20: 13471(T)
interactions with protons, Fubini-Furlan theory for, (T), 20: 13537 (IC/66/8)
interactions with protons, total cross section for, (E/T), 20: 15428
interactions with protons at 4 and 8 Bev, absorption corrections to exchange term for elastic, (T), 20: 15324
interactions with protons at 208 Bev/c, cross sections for elastic scattering and meson production in, (E), 20: 15334
interactions with protons at 781 Mev, cross sections for single- and multiple-pion production in, 20: 15341
interactions with protons, model for high-energy charge-exchange, 20: 15342
interactions with protons at 875 to 1579 Mev/c, differential cross sections and polarization in elastic, (E), 20: 15372
interactions with protons at 410 and 492 Mev, recoil proton polarization in, (E), 20: 15373
interactions with protons at 2.1 to 6.0 Bev/c, resonance effects on total cross sections for, (E/T), 20: 15379
interactions with protons at 300 to 700 Mev, isobar production in, (T), 20: 15381
interactions with protons at 240 Mev, phase-shift analysis of elastic, (T), 20: 15388
interactions with protons, hyperon (Σ^*) production in, (E/T), 20: 15400
interactions with protons, meson (A) and (B) production in, 20: 15408
interactions with protons at 1 to 4 Bev, inelastic, (T), 20: 17344 (JINR-P-2530)
interactions with protons at high energies, real amplitudes for, (T), 20: 17378
interactions with protons at 450 Mev, cross sections for elastic and inelastic, (E), 20: 17384
interactions with photons, cross sections for vector meson production in, 20: 17410
interactions with protons at 180°, spark chamber for recording, 20: 16815 (JINR-P-2506)
interactions with protons at 1.6 Bev/c, meson (ρ^+) and $N^{*+}_{\frac{1}{2}}$ production from, (E), 20: 17374
interactions with protons at 14 Bev, forward amplitudes for, (E/T), 20: 19273(R) (BNL-929, pp 3-43)
interactions with protons above 2.5 Bev/c, meson (A_1), (A_2), and (B) production in, (E), 20: 19449 (UR-875-123 and (Add.))
interactions with protons, sum rules for real part of forward amplitude for, 20: 19470
interactions with protons above 2.9 Bev, polarization in, (T), 20: 19473
interactions with protons at 5 to 20 Bev, amplitudes for, (T), 20: 21618 (JINR-P-2566)
interactions with protons at high energies, conservation laws for, 20: 21657
interactions with protons at 2 to 7 Bev/c, total cross sections for, (E), 20: 21661
interactions with protons at 250 Mev, cross section for elastic, (E/T), 20: 21662
interactions with protons, T = 0 S-wave $\pi\pi$ phase shift in, (E), 20: 21685
interactions with protons at 4 to 8 Bev/c, differential cross sections for, (E), 20: 24053
interactions with protons at high energies, conical function and mean value theorem for amplitude of, 20: 24061
interactions with protons at high energies, absorption effects in single-particle-exchange model for, (T), 20: 24078
interactions with protons, unitary symmetry in, (T), 20: 24170
interactions with protons at 700 to 1700 Mev, cross sections and dispersion relations for, (E/T), 20: 25779 (CEA-R-2838)
interactions with protons at 420 to 1070 Mev, meson (π^0), angular distributions from, (E), 20: 25835
interactions with protons at 0.5 to 1.46 Bev, meson (π^0) angular distributions from, (E), 20: 25836
interactions with protons above 2.5 Bev/c, production of A_1, A_2, and B mesons from, (T), 20: 27825
interactions with protons at 400 to 800 Mev, p-wave analysis of, 20: 27862
interactions with protons at 2.35 to 2.90 Bev/c, meson (η^0), (ω^0), and (ρ^0) and N^{*++} production from, (E), 20: 27844
interactions with protons at 1.840 Bev/c, search for T = $\frac{5}{2}$ isobar in, (E), 20: 30022
interactions with protons at 5 to 20 Bev/c, meson-exchange model for forward elastic, 20: 30039
interactions with protons at 4 Bev/c, cross sections for strange-particle production in, (E), 20: 32029
interactions with protons at high energies, amplitude and nucleon recoil effects on, (T), 20: 32072
interactions with protons at 38 to 307 Mev, resonance formulas for N* (1236) from, (T), 20: 32100
interactions with protons at 4 Bev/c, resonance production cross sections for, (E), 20: 34147 (DESY-66/11)
interactions with protons at 8 Bev/c, A_1(1100) enhancement in, (E), 20: 34198
interactions with protons at 3.23 Bev/c, Y*(1660) production from, (E), 20: 34232
interactions with protons at 4 Bev/c, cross sections for six-prong, (E), 20: 34187
interactions with protons at 8 Bev/c, Y*(1385) and K*(890) production in, (E), 20: 34197
interactions with protons at 6 Bev/c, resonance production in, 20: 37732 (BNL-10461)
interactions with protons at 6 Bev/c, K* (1425) production in, (E), 20: 37733 (BNL-10462)
interactions with protons at 900 Mev, cross sections for, (E), 20: 37744 (UR-875-151)

interactions with protons at 900 Mev, N* (1236) and N* (1518) production in, (E), 20: 37744 (UR-875-151)
interactions with protons at 8 Bev/c, cross sections for strange particle production in, (E), 20: 37770
interactions with protons at high energies, elastic, (E/T), 20: 37796
interactions with protons at 1.95 Bev/c, cross sections for, (E), 20: 39767 (TID-23278)
interactions with protons at 2 to 6 Bev/c, Regge-pole model for cross sections for, (E/T), 20: 39801
interactions with protons, random-phase K-matrix formalism for peripheral, 20: 39804
interactions with protons at 1350 Mev, properties of N* (1920) in, (E), 20: 39845
interactions with protons at 300 to 700 Mev, total cross sections for, (E), 20: 41830
interactions with protons at 8 Bev/c, shadow model for elastic backward peak in, (T), 20: 41839
interactions with protons at 4 and 8 Bev/c, Regge-pole analysis of, 20: 41842
interactions with protons at 875 to 1579 Mev/c, cross sections for elastic, (E), 20: 41857
interactions with protons at 900 to 1580 Mev/c, polarization in, (E), 20: 41890
interactions with protons via two-meson (π) exchange, (T), 20: 41918
interactions with protons at 7 Bev/c, effective mass spectra from, (E), 20: 41919
interactions with protons at high energies, one-Regge-pole exchange model for, 20: 44184
interactions with protons at 8 Bev/c, decay angular distributions of resonances from, (E), 20: 44226
interactions with protons at 0.4 to 4 Bev/c, direct channel Δ_6 resonance model for backward elastic, (T), 20: 44236
interactions with protons at high energies, branching ratio predictions for, (T), 20: 44237
interactions with protons at 2.3 to 4.0 Bev, differential cross sections for, (E), 20: 44248
interactions with protons, Regge trajectories for minima in differential cross sections for, 20: 44264
interactions with protons at 4 Bev/c, backward elastic, (T), 20: 44267
interactions with protons, current algebra computation of scattering amplitudes for, (T), 20: 46338 (NYO-3399-78)
interactions with protons at 2.05 BeV/c, meson (ω^0) production from, (E), 20: 46371
interactions with protons, 17: 20594(R) (UCRL-10572)
interactions with protons at 400 Mev to 1.5 Bev, total cross sections for, 16: 29633 (CEA-2092)
ionization power of, spark chamber measurements of, 18: 41796
kinetics at 100 kev to 100 Bev, graphs for, 19: 18752 (UCRL-2426(Vol. I) (1965 Rev.))
lifetime, (E), 20: 2714
lifetime, (E), 20: 21665
lifetime, (E), 20: 39821
lifetime, (E), 20: 41891
lifetime, (E), 20: 17346 (JINR-P-2534)
lifetime, (E), 20: 19451 (UR-875-126, Paper 3)
lifetime and mass of, 17: 19071
lifetime in circular and rectilinear trajectories, 17: 6792(R) (ISS-62/14)
lifetime in flight, 18: 2585(R) (ISS-63/37)
lifetime of, (E), 20: 24052
lifetime of, on curved and straight path, measurement of, 17: 22418 (ISS-62/7)
lifetime of, relative to mesons (π^-), (E), 20: 39760 (JINR-P-2802)
lifetime relative to mesons (π^-), (E), 20: 41884
magnetic moments of, Vigier rotator model for anomalous, 17: 34802
mass determination from xenon bubble chamber data, 16: 31901
mass difference (π^+-π^0) in quantum field theory, 19: 1424 (NP-14404 (p.271-99))
mass difference with mesons (π^0), 16: 8054 (NP-11232(p.243-51))
mass difference with meson (π^0), 17: 37934 (JINR-P-1309)
mass difference with mesons (π^0), theoretical calculation of, 18: 21007
mass of, difference between mesons(π^0) and, 17: 24326
mass relative to mesons (π^0), (T), 19: 31021
mass spectrum in meson (ρ^0) decay, 17: 9249
meson (μ^+) emission and helicity from, 16: 24747
model for properties of, 19: 16645
momenta and ranges in emulsions, 19: 9775(R) (UCRL-11466)
momentum spectra from proton reactions with aluminum and beryllium at 30 and 33 Bev, 16: 24858
photoproduction at 153.4 to 160.8 Mev, 17: 5287
photoproduction at low energies, 17: 20906
photoproduction at 2 to 6 Bev, peripheral effects in (E), 19: 1387
photoproduction at 60 and 90° cms angles, analysis of, (E), 19: 5569(R) (MIT-2098-64)
photoproduction at high energies, (E/T), 19: 45024 (MIT-2098-163)
photoproduction at high energies, (E), 20: 15306(R) (CEAL-1026)
photoproduction by polarized bremsstrahlung at 227 to 373 Mev, retardation term in, 18: 26382
photoproduction from hydrogen, p,γ,π coupling constant from, 17: 7001
photoproduction from hydrogen near threshold, 17: 17084
photoproduction from protons, 17: 32964
photoproduction from deuterium at 165 to 210 Mev, ratio (π^-/π^+) in, 17: 37959
photoproduction from deuterium at 165 to 200 Mev, cross section ratio to meson (π^-) production, 18: 2649
photoproduction from hydrogen, differential cross sections for, 18: 4625
photoproduction from protons at 170 to 220 Mev, 18: 14853
photoproduction from helium-4 at 180 to 300 Mev peak, (E), 19: 29234 (COO-1195-8)
photoproduction from carbon, (T), 19: 29306
photoproduction ($\gamma + p \rightarrow \pi^+ + n$) at 500 to 900 Mev, differential cross section for, 17: 39875
photoproduction in hydrogen, cross sections at threshold, 16: 13961 (NP-11594)
photoproduction in hydrogen at 154 to 185 Mev, differential cross sections, 16: 13871 (UCRL-9841)
photoproduction in hydrogen at 600 to 800 Mev and angles of 0 to 20° c.m., 16: 16928 (NP-11592(Vol.I)(p.21-4))
photoproduction in bremsstrahlung reactions with calcium to 320 Mev, 16: 23127
photoproduction in hydrogen at 42.4 Mev at laboratory angles between 50 and 170°, 16: 29658 (NP-11992)
photoproduction in hydrogen at 162 to 192 Mev, 16: 8131
photoproduction in helium-4, existence of hydrogen-4 state in, 17: 9581
photoproduction in hydrogen along with mesons (π^-), 18: 10867 (LNF-63/47(p.98-104))
photoproduction in hydrogen, range telescope measurements of cross sections for, 18: 12906 (JÜL-110-HP)
photoproduction in hydrogen, cross sections for, 18: 38186
photoproduction in deuteron-polarized bremsstrahlung interactions (E), 19: 3073
photoproduction in hydrogen at 225-350 Mev, cross sections for, (E), 19: 8218
photoproduction in hydrogen near threshold, (E), 19: 43187
photoproduction of π^+-π^- pairs on nucleons at 1.05 Bev, parity conservation in, 16: 27981
photoproduction of, theory, 17: 32913 (TID-7668(Sect.V))
photoproduction of, qualitative analysis of, 17: 39868
photoproduction of, (T), 19: 39621
photoproduction of, 20: 37753
photoproduction on hydrogen near threshold, 16: 12551
photoproduction on protons, partial wave dispersion relations for, 16: 27910 (NP-11839)
photoproduction on protons at high energies, 16: 29680
photoproduction on boron-11, cross sections for, 16: 33907
photoproduction on deuterium and hydrogen, 17: 878
photoproduction on hydrogen at 200 to 450 Mev, 17: 9348
photoproduction on hydrogen near threshold, 17: 9350
photoproduction on protons, cross section for, 17: 15122
photoproduction on nuclei, cross sections for, 17: 24443
photoproduction on hydrogen, cross sections for, 17: 26641
photoproduction on protons, 17: 32912 (TID-7668(Sect.IV))
photoproduction on protons, Regge pole hypothesis for behavior of cross section for, 17: 34797
photoproduction on hydrogen at 200 to 450 Mev, cross sections for, 17: 34977
photoproduction on hydrogen at 200 to 450 Mev, cross sections for, 17: 34978
photoproduction on hydrogen at 200 to 260 Mev with fixed momentum transfer, 17: 34979
photoproduction on hydrogen, contour map of cross sections for, 17: 34980
photoproduction on hydrogen at 162–225 Mev, angular distributions and cross sections for, 17: 39916
photoproduction on protons at 33.8 Mev, differential cross section for, 18: 2644
photoproduction on carbon at 2.91–4.85 Bev, cross sections and rates for, 18: 2939
photoproduction on beryllium at 2 to 6 Bev, 18: 4455
photoproduction on nucleons, experiments for, 18: 7514
photoproduction on nucleons using polarized gamma radiation, 18: 10865 (LNF-63/47(p.86-9))
photoproduction on hydrogen at constant meson (π^+) energy, ($\gamma\pi p$) coupling in, 18: 18685
photoproduction on protons, analysis of, 18: 26282
photoproduction on deuterons, cross sections for, 18: 26317

photoproduction on protons at 190 to 250 Mev, differential cross sections for, 18: 28370
photoproduction on carbon, effect of 3-3 resonance on, 18: 32829
photoproduction on protons, effect of meson (π) interactions in, 18: 37954
photoproduction on protons at 275 Mev, cross sections for, 18: 40310
photoproduction on protons at 157.3 to 182.6 Mev, cross sections for, 18: 39671
photoproduction on helium-3 and tritium, 18: 42707
photoproduction on nitrogen at 1 Bev, 19: 1632
photoproduction on carbon at 3, 4, and 5 Bev, rates of (E), 19: 1669
photoproduction on hydrogen near threshold (E), 19: 1383
photoproduction on hydrogen at 175 to 230 Mev, 19: 1580
photoproduction on carbon, (E/T), 19: 6529
photoproduction on protons, amplitudes for, (T), 19: 6562
photoproduction on deuterons, (T), 19: 10097
photoproduction on deuterium at 150 to 200 Mev, (E/T), 19: 10098
photoproduction on protons, (T), 19: 14307 (ANL-6942)
photoproduction on deuterons, (E), 19: 16555
photoproduction on carbon, effects of 3-3 resonance on, (E), 19: 16852(R) (NP-14647)
photoproduction on hydrogen, (E), 19: 23625(R) (HUX-2752-1)
photoproduction on oxygen-16 at 240 Mev, cross sections for, (E), 19: 27566
photoproduction on protons, neutron coincidence study of, (E), 19: 27141 (ISS-64/41)
photoproduction on protons, differential cross sections for, (T), 19: 27142 (ISS-64/46)
photoproduction on protons at 300 to 600 Mev, cross sections for zero-angle, (E), 19: 37535 (LAL-1139)
photoproduction on protons, (E), 19: 37554
photoproduction on protons near threshold, cross sections for, (E), 19: 39461 (COO-1195-35)
photoproduction on protons near first resonance, (E), 19: 39597
photoproduction on protons at .6 to 1.2 Bev, angular distributions of, 19: 41323 (CALT-68-42)
photoproduction on deuterium at 165 to 210 Mev, angular distributions and cross sections for, (E), 19: 41344
photoproduction on deuterium at 230 Mev, (E), 19: 43039 (COO-1195-34)
photoproduction on carbon and hydrogen in Bev range, (E), 19: 45000 (HUX-2752-7)
photoproduction on protons, (E), 19: 46643(R) (LAL-1136)
photoproduction on helium-4, (E), 20: 1210
photoproduction on protons at 1 Bev, 20: 2718
photoproduction on protons at 165 to 230 Mev, amplitudes and cross sections for, (E/T), 20: 2737
photoproduction on protons below 1 Bev, angular distributions and total cross sections for pair, 20: 4579 (AD-618661)
photoproduction on deuterium, yields from, (E), 20: 9782
photoproduction on helium-3 at 180 to 260 Mev, cross sections for, (E), 20: 12046
photoproduction on protons at high energies, (E), 20: 15306(R) (CEAL-1026)
photoproduction on protons at 550 to 1000 Mev, cross sections for, (E), 20: 15332
photoproduction on protons at 225 to 350 Mev, (E), 20: 15340
photoproduction on protons at 3.4 to 4.0 Bev, cross sections for, (E/T), 20: 17400
photoproduction on nucleons by polarized bremsstrahlung at 475 to 750 Mev, (E), 20: 21660
photoproduction on protons at 475 to 750 Mev, asymmetry in polarized, (E/T), 20: 21589 (AD-626683)
photoproduction on protons at 3.4 to 4.0 Bev, cross sections for, (E/T), 20: 24015 (MIT-2098-223)
photoproduction on nucleons, time-reversal invariance in, (T), 20: 24039
photoproduction on protons at 2.0 to 4.8 Bev, (E), 20: 27923
photoproduction on protons using coherent bremsstrahlung, asymmetry ratios for, (E), 20: 27926
photoproduction on protons at 300 to 600 Mev, (E), 20: 27927
photoproduction on protons at 0.6 to 1.2 Bev, (E), 20: 27931
photoproduction on protons, testing T invariance by, (T), 20: 27939
photoproduction on protons, near first (πN) resonance, angular distribution for, (T), 20: 27945
photoproduction on helium-3, nuclear form factors from, (E), 20: 28444
photoproduction on protons at 2 to 5 Bev, (E), 20: 27918
photoproduction on carbon and hydrogen at high energies, (E), 20: 27919
photoproduction on protons at 600 to 840 Mev, (E), 20: 34184
photoproduction on protons, (E), 20: 34246
photoproduction on light nuclei, differential cross sections for, (E), 20: 40075 (LNF-66/30)
photoproduction on protons at 2.6 to 2.7 Bev, differential cross sections for, (E), 20: 41795(R) (MIT-2098-251, pp 21-36)
photoproduction on protons at high energies, absorption correction in, 20: 41844
photoproduction on protons at 0.3 to 5.8 BeV, (E), 20: 46348(T) (SLAC-Trans-44)
photoproduction with polarized photons, 16: 25935 (NP-11977(p.99-100))
photoproduction with mesons (π^-) on nucleons, angular momentum analysis of, 18: 7495
polarization in condensed media, (T), 19: 25277
positron emission probabilities, 16: 21321
production and decay in atmosphere, 16: 22843
production and properties of very slow, from 9-Bev proton reactions on nuclei, 17: 9558
production and transverse momentum distributions in proton-proton interactions at 11.6 to 22.9 Bev/c, (E/T), 20: 1031
production as particle beam in Cosmotron, design of parallel plate velocity spectrometer for, 16: 2560 (BNL-5757)
production at high energy, $(\mu^+)/(\mu^-)$ ratio from $(\pi^+)/(\pi^-)$ ratio in, (T), 20: 2702
production by meson (K^+)-proton interactions, 17: 9380
production by nucleons at 0.5 to 2 Bev, 17: 12784(R) (ORNL-3360(p.199-203))
production by polarized bremsstrahlung, 17: 5291
production by proton-proton reactions at 2.1 and 2.9 Bev, 16: 16933 (NP-11592(Vol.I)(p.57-67))
production by proton-proton interactions at 1 Bev, 17: 5199 (AERE-R-3969)
production from bremsstrahlung reactions with hydrogen and helium below 330 Mev, (E), 20: 41817
production from meson (π^-) reactions with bromine, diffraction dissociation in, (E), 20: 39774
production in antiproton–proton interactions at 3.6 Bev/c, 18: 22741
production in antineutrino- and neutrino-proton interactions, cross sections for, (T), 19: 29065 (JINR-P-2062)
production in antiproton-proton annihilations at 2.7 Bev/c, (E), 20: 34150 (IS-T-83)
production in bremsstrahlung reactions with deuterium at 320 Mev, 17: 4009
production in Brookhaven Alternating-Gradient Synchrotron, 16: 33912 (BNL-6212)
production in cosmic meson (μ^+) decay, ratio to meson ($K_{\mu 2}$), 17: 41717
production in decay of hypernuclei, mechanisms and rates for, (T), 19: 5186
production in deuteron interactions at 3 Bev/c, cross sections for, (E), 19: 32981
production in electron-positron interactions, cross section for, 18: 20986
production in electron-proton interactions, (E), 20: 9770
production in electron-proton interactions, (E), 20: 27934
production in electron-proton interactions, (E), 20: 27910
production in freon-meson (π^-) interactions at 2.8 Bev/c, (E), 20: 2733
production in gamma reactions with protons at 185 Mev, angular distributions, 16: 9396
production in gamma interactions with protons at 165 Mev, 16: 32263 (59-RL-2326E)
production in gamma interactions with protons at 230 Mev, cross sections for, 19: 47393
production in helium-3 (γ,π^+) reactions, cross sections for, (E), 20: 13896
production in hyperon (Σ^0) decay, 16: 12359
production in hyperon-proton interactions $\Lambda + p \rightarrow \Sigma^- + p + \pi^+$, 18: 9163
production in interactions of mesons (K^+) with protons at 910 Mev/c, 18: 26381
production in $_{\Lambda}He^4$ decay, 16: 12360
production in $_{\Lambda}He^4$ decay, 16: 26307
production in meson (K^+) decay, 16: 4729
production in meson (π^+)-proton interactions at 820, 900, and 1050 Mev, resonance with mesons (π^0), 16: 9394
production in meson (K^+) decay, 17: 11523
production in meson (π^-) interactions with protons at 365 and 432 Mev, 17: 24274 (UCRL-10585)
production in meson (K^-)-proton interactions at 1.51 and 1.22 Bev/c, 18: 2594 (UCRL-10235)
production in meson (π^-)–proton interactions at 2 Bev, 18: 14888
production in meson (π^-)-proton interactions at 300 to 1000 Mev, enhancement of, 18: 14923
production in meson (π^-)-proton interactions at 871 Mev, 18: 24418
production in meson (K^-)-proton interactions at 1150 Mev/c, angular correlations for, 18: 37945
production in meson (K^-) reactions with emulsion nuclei at rest, (T), 19: 19151
production in meson (K^-)-proton interactions, Q-value distribution for, (T), 19: 35070
production in meson (K^-)-nucleus reactions, 19: 47708
production in meson (K^+) decay ($\pi^+ + \pi^0 + \gamma$), upper limit for, (E), 20: 11675
production in meson (π^-)-proton interactions at 500 to 700 Mev, energy

distributions for, (E), 20: 25792 (UCRL-16282)
production in meson (K^-)-proton interactions at 1.7 to 2.0 BeV/c, differential cross sections for, (E), 20: 46360
production in neutrino-proton interactions, cross sections for, 17: 20919
production in neutrino inelastic reactions with nuclei, cross section asymptotic behavior for, 17: 41826
production in neutron-proton interactions at 600 Mev, 18: 842 (JINR-P-1334)
production in neutrino-nuclear interactions at high energies, 18: 28413
production in neutrino reactions with nuclei at 60 Bev, 18: 40642
production in neutrino-nucleon interactions, peripheral, (T), 19: 18815
production in neutrino-nucleon inelastic interactions, (T), 19: 47377
production in neutrino interactions with protons at high energy, cross section for, 20: 2733
production in neutron-proton interactions at 600 Mev, angular distributions and cross sections for, (E), 20: 11564 (JINR-P-2462)
production in neutron-proton interactions at 600 Mev, (E), 20: 13453 (JINR-P-2511)
production in neutron-proton interactions at 585 Mev, cross sections for, (E), 20: 15310 (JINR-P-2508)
production in neutron-proton interactions at 585 Mev, cross section for, (E), 20: 25809(T)
production in neutron-proton interactions at 600 Mev, (E), 20: 39826
production in neutron-proton interactions at 600 Mev, cross sections for, (E/T), 20: 39834
production in nucleus-proton collisions above 20 Bev, 16: 990
production in nucleon-proton interactions, parity non-conserving contribution, 16: 12369
production in p-$\bar{p}$ annihilation, distributions from, 17: 15134
production in p-p interactions, 18: 9161
production in photon–proton interactions, 16: 3646
production in photon-proton interactions, 16: 10857
production in photon reactions with beryllium and hydrogen, 18: 9318 (SLAC-21)
production in photon-proton interactions, quark model for, (T), 20: 17348 (JINR-P-2556)
production in π^--p interactions, π-π resonance, 17: 4005
production in polarized nucleon-nucleon interactions at 600 Mev, (E/T), 20: 7791 (JINR-P-2382)
production in proton interactions, single, 16: 5886
production in proton interactions at 2.9 Bev, momentum spectra, 16: 6974
production in proton reactions with nuclei at 450 Mev, 16: 9378
production in proton interactions at 2 Bev, 16: 15570
production in proton interactions at 405 Mev, 16: 27991
production in proton interactions at 2.1 to 8.9 Bev/c, differential cross sections for, 18: 6019
production in proton interactions at 2.0 and 2.85 Bev, 18: 7503
production in proton-proton interactions at 19 and 24 Bev/c, cross sections for, 18: 18678
production in proton interactions at 650 Mev, angular and energy distributions in, 18: 24476
production in proton-proton interactions at 990 Mev, 18: 37910
production in proton-nucleon interactions, (T), 19: 6536
production in proton reactions with beryllium at 12.5 Bev, cross sections for, (E), 19: 21406
production in proton reactions with nuclei at 20 Bev, 19: 41324 (CERN-65-14)
production in proton-proton interactions at 655 Mev, cross sections for, (T), 20: 13470
production in proton-proton interactions at 2.80 Bev/c, single, (T), 20: 15423
production in proton-proton interactions at 2.0, 2.4, and 2.85 Bev, momentum spectra of, (E), 20: 15336
production in proton–antiproton annihilations at 5.7 Bev/c, (E), 20: 19498
production in proton reactions with beryllium at 12.5 Bev, cross sections for, (E), 20: 21601 (CERN-65-32, pp 109-10)
production in proton interactions with neutrons and protons in nuclear emulsions, charge asymmetry of, (E), 20: 30082
production in proton reactions with beryllium at 600 Mev, cross sections for, (E), 20: 38186
production in proton reactions with carbon at 600 Mev, cross sections for, (E), 20: 38186
production in proton reactions with aluminum at 600 Mev, cross sections for, (E), 20: 38186
production in proton reactions with copper at 600 Mev, cross sections for, (E), 20: 38186
production in proton reactions with silver at 600 Mev, cross sections for, (E), 20: 38186
production in proton reactions with lead at 600 Mev, cross sections for, (E), 20: 38186
production in proton interactions with protons at 600 Mev, cross sections for, (E), 20: 38186
production of beams of, in CERN synchrotron, (E), 19: 28940 (CERN-65-2)
production of resonance ($\Sigma^-\pi^+$), in meson (K^-)-neutron interactions at 1.15 Bev/c, 18: 36339
production of separated beams of 2 Bev/c, 19: 46643(R) (LAL-1136)
production of slow, in proton reactions with emulsion nuclei at 9 Bev, (E), 20: 30370
properties at 100 kev to 100 Bev, 18: 28331 (UCRL-2426(Vol.I)(1963 Rev.))
properties of, electron-pair model for, (T), 19: 10059
proton reactions (P,π) at 310 Mev, 16: 16930 (NP-11592(Vol.I)(p.27-35))
proton scattering at 820 and 900 Mev, 16: 16931 (NP-11592(Vol.I) (p.37-43))
range in emulsion, velocity dependence of (E), 19: 3029 (UCRL-11518)
range in nuclear emulsions at 78 and 90 Mev/c, 20: 41826
ranges in emulsions, comparison with mesons (π^-), (E/T), 19: 25265(R) (UCRL-11776)
reactions (π^+,2p) with light nuclei at 106 Mev, two-hole states in, (E), 19: 25513
reactions (π^+,2p) with nitrogen-14 at 80 Mev, angular distribution and cross sections for, (E), 19: 33385
reactions (π^+,π^-) with nuclei, model for, 19: 47660
reactions (π^+,2p) with lithium-6 at 30-Mev, excited states from, (E), 20: 19912
reactions (π^+,2p) with carbon-12, nitrogen-14, and oxygen-16, energy excitation in, (E), 20: 38070
reactions (π^+,2N) with light nuclei, (T), 20: 46789
reactions in emulsions at 1.86 Bev/c, 16: 10252
reactions in nuclear emulsions, double charge exchange in, (E), 19: 10243 (JINR-P-1837)
reactions (π^+,p) with nuclei at 1.4 to 4.0 Bev/c, cross sections, 16: 9467
reactions (π^+,p) with nuclei in Bev range, cross sections for, 17: 38306
reactions (π^+,2p) with lithium-6 at 100 Mev, proton correlations from, 17: 38176
reactions (π^+,3α) with carbon-12 at 80 Mev, 17: 7288
reactions with aluminum, beryllium, and lead at 80 Mev, total cross sections for double-charge-exchange, (E), 20: 24479
reactions with beryllium-9 and lithium-7, double-charge-exchange cross sections for, (T), 20: 15813
reactions with carbon and lithium, energy spectra of nonelastic meson (π^+) from, 17: 22564 (ORNL-3383)
reactions with carbon and lead, meson (π^+) angular distributions from, 17: 22564 (ORNL-3383)
reactions with carbon at 80 Mev, analysis of, 18: 15298
reactions with carbon, nitrogen, and oxygen at 80 Mev, cross sections for, (E), 19: 21279
reactions with carbon and hydrogen, ionization losses in, (E), 20: 8070 (JINR-P-2423)
reactions with complex nuclei at 442 Mev, cross sections for, 16: 18502
reactions with complex nuclei at 25 to 400 Mev, data from inelastic, (E), 20: 44720
reactions with deuterium at 1.23 Bev/c, meson (K^+) charge symmetry from, 17: 22489
reactions with deuterium, 18: 30708(R) (AFOSR-J1446)
reactions with lead at 15 Bev/c, meson (ρ) production in, (E), 20: 11618
reactions with matter, dE/dx and range-energy graphs for, 20: 46601 (UCRL-2426(Vol.2(1966 Rev.))
reactions with matter, range-momentum and dP/dx graphs for, 20: 46342 (UCRL-2426(Vol.4)(1966 Ed.))
reactions with nitrogen, quasi-deuteron formation in, 17: 40433(R) (NYO-10063(p.71-89))
reactions with nuclei at 25 to 300 Mev, 17: 12783(R) (ORNL-3360(p.182-98))
reactions with nuclei, calculation of low-energy intranuclear cascades in, 17: 31526
reactions with nuclei, nucleon emission in (T), 19: 1683
reactions with nuclei at low energies, charge-exchange, (T), 19: 31302
reactions with nuclei at 80 Mev, double charge exchange cross sections for, (E), 19: 43273 (JINR-P-2238)
reactions with nuclei, double-charge-exchange cross sections for, (T), 20: 15813
reactions with oxygen-16 at 80 Mev, alpha production in disintegration, (E), 19: 12617
reactions with spark chamber gases at 600 Mev/c, ionization power in, 19: 18315
reactions with vanadium-51 and zirconium-90 at 220 to 320 Mev/c, double charge exchange in, (E), 20: 42316
resonance (π^+p) at 1922 Mev, production in proton-proton peripheral collisions, 18: 20927
resonance ($\pi^+\pi^-\eta$) at 959 Mev, properties of, 18: 34515 (UCRL-11431)
resonance ($\pi^+\pi^-$) at 280 to 350 Mev, search for, 18: 34552
scattering by calcium-48 at 210 Mev, excitation of analog states in

double-charge-exchange, 19: 33311
scattering by carbon and oxygen at 87 Mev, angular distributions, 16: 24720
scattering by carbon, cross sections for nonelastic, 17: 22564 (ORNL-3383)
scattering by carbon at 78 Mev, total cross sections for, 18: 14924
scattering by carbon-12 at 3 Bev, cross sections for inelastic, (T), 20: 19823 (JINR-P-2431)
scattering by emulsion nuclei at 4 Bev/c, interference effects between Coulomb and nuclear, (E), 19: 25508
scattering by helium-3, differential cross sections for elastic, (T), 20: 10035
scattering by helium-4 at 100 to 160 Mev/c, phase shift analysis for elastic, (E), 20: 42320
scattering by helium-4 at 1000 to 160 Mev/c, inelastic, (E), 20: 42321
scattering by hydrogen at 3.7 to 25 Mev, cross sections for, 17: 9302
scattering by lead, cross sections for nonelastic, 17: 22564 (ORNL-3383)
scattering by lithium, cross section for nonelastic, 17: 22564 (ORNL-3383)
scattering by nuclei at low energies, double-charge-exchange, (T), 19: 41773
scattering by oxygen-18, double charge exchange in, (T), 19: 25529
slowing down of, by electrons in dense plasma and metal, 17: 17268
yields from bremsstrahlung reactions with helium and hydrogen, absolute, 20: 41816

MESONS (ρ^-)
mass formulas for, 18: 44595
mass of, formula for, 18: 16799

MESONS (ρ)
amplitudes for, self-consistent calculation of p-wave, 19: 8195
angular distributions in antiproton-proton interactions, 18: 26286
bootstrap calculation for, 18: 28394
bound states in systems of, (T), 20: 6092
branching ratio, (T), 19: 14377
classification of, SL(2C) unitary representation for, 19: 32940 (IC/65/56)
contributions to coupled partial-wave-dispersion-relations for nucleon-nucleon scattering, 17: 20918
coupling constant of, with nucleon, 18: 24411
coupling constants with the $\bar{K}K$ and N^*N currents, 17: 41785
coupling to baryon current, vector-meson dominance and U(6,6) symmetry for, 20: 17457
coupling to isospin current, universality hypothesis of, 17: 9342
coupling to isospin current, universality hypothesis of, 18: 4449
coupling with nucleons, constants for, (T), 19: 4986
decay, 17: 36584 (TID-19343)
decay, (E), 20: 11616
decay, 18: 12914 (TID-7686(p.109-29))
decay angular distribution from meson (π^+)-proton interactions at 8 Bev/c, (E), 20: 44226
decay, branching ratios of four-body, 16: 33748
decay, effects of spin-parity assignments on, 16: 26157
decay into meson (μ) pairs, 20: 7862
decay into meson (η), determination of η spin from, 16: 19709
decay mode $\eta + \pi$, 16: 15585
decay mode of, peripheral model for determining, 17: 13395
decay modes of, 17: 11499 (UCRL-10089(Rev.))
decay modes of, branching ratios in, 17: 26315
decay modes of, branching ratio for Dalitz-pair production and gamma emission in, 18: 7497
decay of, consequences of G quantum number in, 17: 9340
decay of, coupling constants in, 17: 13379
decay of, inner bremsstrahlung from, 18: 7526
decay of neutral, branching ratios for lepton pairs in, (E), 19: 23436
decay of, 4-π mode of, 17: 9248
decay of, analysis of $\pi\gamma$, (T), 20: 15389
decay of, as possible test for a strong C violation, (T), 19: 33002
decay of, C violation in, (T), 20: 25874
decay of, charge asymmetry in radiative 2π, (T), 20: 11584(T)
decay of, current-algebra prediction of SU(3) violation in 2π, 20: 32035
decay of, leptonic, (E), 20: 27893
decay of, mass splitting in electromagnetic, (T), 19: 27146 (JINR-P-1974)
decay of, matrix element relations in SL(6) and $\bar{U}(12)$ for electromagnetic and weak, 20: 25927
decay of, meson (μ) pair production in, (E), 20: 9761
decay of, partial width for $\pi\gamma$, (E), 20: 11618
decay of, radiative, 18: 37953
decay of, radiative, (T), 20: 13477(T)
decay of, relative rates for leptonic, (T), 20: 27863
decay of, selection by A invariance, 18: 22758
decay of, SU(6)-invariant theory for couplings in, 19: 21013
decay of, $SU(6)_w$ symmetry for radiative, 20: 30040
decay of, test of nonrelativistic quark model in radiative, (T), 20: 1016
decay of, trilinear couplings forbidden by nonet symmetry in, (T), 19: 45025 (N64-26265)
decay of, $\bar{U}(12)$ group for 2π, (T), 19: 18853
decay of, unitary symmetry selection rules for, 18: 30556
decay of, unitary symmetry breaking in, (E/T), 19: 41366
decay of, upper limit for partial width for meson (π) and photon production from, (E), 20: 46363
decay probabilities in unitary symmetry, 18: 14866
decay rate, (T), 20: 32045
decay schemes, 16: 13911
decay to π and γ in SU(3) and SU(6), 19: 39470 (JINR-P-2171)
decay, use in analysis of lepton electromagnetic properties, 16: 29707
decay width, (T), 20: 34214
effect of exchanges with mesons (ω) on KN and $\bar{K}N$ interactions, 17: 5246
effects in double photoproduction of mesons (π), (T), 19: 45019 (JINR-P-2286)
effects in electron-nucleon interactions, electric and magnetic form factors from, 17: 41800
effects in neutron–proton charge-exchange interactions at 2.04 and 2.85 Bev, 18: 2662
effects on baryon leptonic decays, (T), 19: 10092
effects on mass spectra of meson (π^-)-proton interactions at 2.1 Bev/c, 18: 21017
effects on meson (π)-nucleon interactions at low energies, 18: 16781
effects on meson (π)–nucleon scattering phase shifts, 18: 28368
effects on nuclear form factors, 17: 22494
effects on nuclear beta decay, (T), 19: 17006
effects on nuclear forces, 20: 15817
effects on nucleon isoscalar structure, 17: 41776
effects on three-meson-(π) decay of mesons (η^0), (T), 19: 4919
effects on Y^* resonances, 18: 30606
electromagnetic mixing of, with mesons (ω), 16: 33754
exchange contribution in peripheral model of isobar production, (T), 20: 2817
exchange effects in meson (π) photoproduction on nucleons, (T), 19: 18813
exchange effects of, on deuteron electromagnetic structure, (T), 20: 11651
exchange forces in meson (π) interactions, 17: 39937
exchange in (π-κ) resonance interactions, (T), 19: 8241
exchange in antiproton-proton and proton-proton interactions, (T), 20: 32065
exchange in deuteron-electron interactions, (E), 19: 41453
exchange in isobar production model, ρ-photon analogy in, 18: 24456
exchange in meson (K)-nucleon interations, contributions to the scattering amplitude in, 17: 20893
exchange in meson(π-π) scattering, N/D calculation of Pomeranchuk and Regge trajectories for, 17: 24319
exchange in meson (π)–nucleon interactions, model for, 18: 6028
exchange in meson (π^+) production from p-p interactions, 18: 9161
exchange in meson (π) interactions, bootstrap calculations for, 18: 10935
exchange in meson (π^+)-proton interactions at 3.54 Bev/c, mechanism of, 18: 34626
exchange in meson (π) photoproduction on nuclei, 18: 36317
exchange in meson (π^+)-proton interactions at 2.75 Bev, (E), 19: 8179
exchange in meson (K,$\bar{K}$) interactions, (T), 19: 8187
exchange in meson (π-π) interactions, strip approximation N/D equation for, 19: 8190
exchange in meson (π)-nucleon interactions, N^* production in, (T), 19: 8206
exchange in meson (π) interactions, Feynman graphs for, (T), 19: 18792
exchange in meson (π) interactions, bootstrap model for coupling constants in, (T), 19: 18797
exchange in meson (ω) production in, 19: 23397
exchange in meson (π) interactions, Bethe-Salpeter equation for, (T), 19: 25316
exchange in meson (π)-nucleon interactions, (T), 19: 35072
exchange in meson (π) interactions, parameters for, (T), 20: 4607
exchange in meson (K^-)-proton interactions, (T), 20: 9734
exchange in meson (π)-meson (π) interactions, momentum-space calculation for, (T), 20: 11653
exchange in meson (π)-nucleon interactions, (T), 20: 15364
exchange in meson (π) interactions, OPE model for bootstrap for, 20: 30035
exchange in meson (π)-meson (π) elastic interactions, (T), 20: 32011
exchange in meson (π)-meson (ω) interactions, 20: 39807
exchange in meson (π)-nucleon interactions, coupling constant for, 20: 41885
exchange in meson (π^+)-proton interactions at high energies, one-Regge-pole exchange model for, 20: 44184

exchange in neutron–proton interactions at 2.04 and 2.85 Bev, 18: 2663
exchange in nucleon interactions at 0 to 400 Mev, effects of, 18: 14954
exchange in nucleon interactions, isobar production in, (T), 19: 18780
exchange in nucleon interactions, (T), 19: 18864
exchange in nucleon-nucleon interactions, 20: 41899
exchange in photon-nucleon interactions, (T), 20: 41821
exchange in $\pi p \to \omega N^{++}_{3/2}$, 18: 22743
exchange of, generation of K* resonance by, 17: 24341
exchange of vector, in nucleon-nucleon scattering, 17: 24336
formation in proton–pion interactions at 820, 900, and 1050 Mev, 16: 10828
half-width, mass, and total cross section for, 17: 39923
interaction resonances with mesons (π), boson icosuplet of, 18: 28386
interaction resonances with mesons (π), spin of 1310-Mev, 18: 37913
interaction resonances with mesons (π), 1090-Mev, (T), 19: 4992
interactions in gamma-meson (π) systems, constants for, 17: 7001
interactions in SU(3) model, effects of T = 0 meson resonances on Schroedinger multichannel equation, 18: 4450
interactions of, amplitude parity and radiative effects in, 17: 20882
interactions of, Regge trajectory and high-energy charge exchange in, 17: 34787
interactions of, C-violation model for $\rho\gamma\pi$ coupling in, 20: 4681
interactions of, effects on meson (K)–nucleon interactions (T), 19: 1293
interactions of, effects on meson (π)–meson (π) interactions (T), 19: 1294
interactions of, effects on nucleon form factors, (E/T), 19: 39458 (CONF-796(Paper 24))
interactions of, effects on meson (π)–nucleon interactions, (T), 19: 41375
interactions of, Regge-pole parameters for, (T), 19: 41370
interactions with nucleons, coupling constant, 16: 8138
interactions with nucleons, coupling strength, 16: 13903
interactions with mesons (π^-) and protons, resonant, 16: 26114
interactions with nucleons, resonances in, 16: 31044
interactions with mesons (π) and nucleons, coupling constants for, 16: 32331
interactions with mesons (π), effects on 3-meson (π) scattering, 16: 33771
interactions with mesons (π), 3-pion resonance effects in, 17: 13450
interactions with photons, electron and meson (μ) asymmetric coupling in, 17: 41779
interactions with nucleons, electric coupling constant for, 18: 2663
interactions with nucleons, resonance, 18: 14801 (CONF-22-32)
interactions with mesons (ω), resonance predictions in, 18: 18698
interactions with mesons (π), meson (ω) production in, 18: 26341
interactions with mesons (π), enhancement at 1 to 1.4 Bev, 18: 26346
interactions with mesons (π), resonance, 18: 34581
interactions with mesons (π), isoscalar resonances in, 18: 36304
interactions with mesons (π) at 1.2 Bev, 18: 38137
interactions with mesons (π), production of resonance, 18: 40246 (UCRL-11443)
interactions with conserved currents, mixing and renormalization in, 18: 40322
interactions with mesons (π), meson (A_1) resonances in, 18: 42428
interactions with mesons (π), meson (ω) bound state in, 18: 44574
interactions with mesons (π), logarithmic singularities in resonance, (T), 19: 4998
interactions with mesons (π), p-wave dispersion relations for, (T), 19: 12220
interactions with mesons (π), energy peaks in, (T), 19: 14335
interactions with mesons (π) coupling constants for, (T), 19: 16552
interactions with mesons (ω) and (π), coupling constants for, 19: 18868
interactions with mesons (ω), mixing model for, (T), 19: 25297
interactions with mesons (π), modified isobar approximation for, (T), 19: 27243
interactions with mesons (K), coupling constants for, (T), 19: 27281
interactions with mesons (π), resonances in, (E/T), 19: 35181
interactions with mesons (π), spin-parity of 1320-Mev A_2 resonance in, (E/T), 19: 41368
interactions with mesons (π), OPE mechanism for meson (ω) production in, (T), 19: 43078
interactions with mesons (π), nucleon isoscalar form factor from elastic, (T), 19: 47371
interactions with nucleons, coupling constant for, (T), 20: 9746
interactions with mesons (π), elastic unitarity in, (T), 20: 30077
interactions with mesons (π), sum rules for strong, 20: 30020
interactions with mesons (π), Adler-Weisberger sum rules for, 20: 39883
interpretation of, in meson (π)–meson (π) scattering, 17: 5248
isospin, parity, and spin of, 17: 22437 (SLAC-13)
mass and width of, (T), 20: 27819
mass and width of, N/D calculation of, 18: 44588
mass and width of, from interaction singularities, (T), 20: 21668
mass and width of, from meson (π) interactions, 20: 41837
mass and width of, $\omega\pi$ bootstrap model for, 20: 41867
mass degeneracy of, (T), 20: 27989
mass differences of, electromagnetic, (T), 20: 30161
mass formulas from rank-three Lie groups, (T), 19: 16578
mass formulas in U_4 symmetry, (T), 19: 16545
mass of, and Yang-Mills field, 17: 9448
mass of, correlations to orbital angular momentum of, 18: 7496
mass of, calculation of, 20: 13628
mass of, models for, 19: 14348
mass, parity, and spin of, 17: 29506
mass relations in octet, 18: 40309
mass splitting of, electromagnetic, (T), 20: 32011
masses of compound, boson, 17: 24329
meson (π) scattering near, 17: 29548
model for, two-pion exchange in bootstrap, (T), 19: 8163
model of, $N\bar{N}$ bound-state, 18: 22782
model of, strip approximation for $\pi\pi$-$K\bar{K}$ coupling, 19: 8194
parameters of, Balazs-type bootstrap model for, 19: 10085
parity and spin of, 17: 32941
photoproduction in carbon at 4.85 Bev, (E), 20: 7862
photoproduction of, Regge poles in Drell calculations of cross section for, 17: 21110 (SLAC-5(p.20-8))
photoproduction of pairs of, testing quantum electrodynamics by, (E), 20: 27893
photoproduction of, photon dissociation model for, 20: 41863
photoproduction on nucleons in the peripheral model, 18: 18635 (DESY-64/1)
photoproduction on nucleons, cross sections and meson exchange in, 18: 26373
photoproduction on aluminum, beryllium, carbon, copper, and hydrogen, cross sections for, (E), 19: 23625(R) (HUX-2752-1)
photoproduction on nucleons, (T), 19: 41321 (AECD/TP/4)
photoproduction on protons at 0.3 to 5.5 Bev, (E/T), 20: 6037 (DESY-65/11)
photoproduction on protons at 0.3 and 5.5 Bev, (E), 20: 17368
photoproduction on nucleons, effect of absorption on peripheral, (T), 20: 17414
photoproduction on nucleons, analysis of, (T), 20: 31984 (IC-66/54)
prediction of, vector theory, 17: 11496 (TID-17742)
production, 17: 9315
production and decay, 17: 9327
production and properties in meson (π^+)-proton interactions, 17: 5279
production and properties in meson (π^+)-proton interactions, 17: 6997
production and properties, 17: 9316
production and properties in proton pair annihilation, 17: 9320
production and properties in proton pair annihilation, 17: 9321
production and properties, review, 17: 9461
production and properties, 18: 10891
production and properties of, review of, 19: 16510
production at 1.89 and 2.1 Bev/c, 17: 9314
production by one- and two-particle exchange forces, two-channel, (T), 20: 13483
production from antiproton-proton annihilation at rest, rates for, (E), 20: 27846
production from meson (π^-)-proton interactions at 2.75 to 3.0 Bev/c, (E), 20: 27848
production in antiproton-proton interactions, 16: 24750 (UCRL-9814)
production in antiproton-proton annihilation, statistical model for, 17: 20915
production in antiproton-proton interactions (E), 19: 1353
production in antinucleon–nucleon annihilation, (T), 19: 10104
production in antiproton-proton annihilation, (E), 19: 20993
production in antiproton-proton annihilations at rest, (E), 19: 45122
production in antiproton-neutron annihilations at rest, (E), 20: 9785
production in antiproton-proton interactions at 5.7 Bev/c, cross section for, (E), 20: 24033
production in antiproton interactions with deuterons, 20: 37813
production in deuteron-meson (π) interactions, 17: 9325
production in elementary-particle interactions, 19: 1227 (JINR-P-1741)
production in meson (π) interactions (s- and p-wave), 16: 17037
production in meson (K^-)-meson (K^+) interactions, 16: 17043
production in meson (π) interactions, 16: 24734
production in meson (π^-)-proton interactions at 7 to 8 Bev/c, 17: 9319
production in meson (π^-)-proton interactions, 17: 9431
production in meson (π) interactions, cross sections for, 17: 28189
production in meson (π)-proton interactions at 4.65 Bev/c, 17: 29491 (BNL-6340)
production in meson (π^-)-proton reactions at 3.3 Bev, 17: 34786
production in meson (π^+)-proton interactions at 3.5 Bev/c, 18: 14962
production in meson (π^-)-proton interactions, 18: 14810 (JINR-P-1506)
production in meson (π) interactions, bootstrap method for, 18: 14931
production in meson (π)-nucleon interactions, 18: 20988
production in meson (π) interactions, strip approximation for, 18: 26331
production in meson (π^-)–proton interactions at 18.1 Bev/c, cross sections for, 18: 28360

production in meson(π)–meson(π) interactions, S-matrix theory with strip approximation for amplitudes of, 18: 30529 (UCRL-7871-T)
production in meson (π)-nucleon interactions, amplitudes and Regge poles for, 18: 34622
production in meson (π)-nucleon interactions, threshold effects in, 18: 36263
production in meson (π) interactions, 18: 36324
production in meson (π^+)-proton interactions at 4 Bev/c, 18: 40285
production in meson (π)-nucleon interactions, amplitudes for, 18: 42439
production in meson (π) reactions with nuclei, coherent, 18: 44821
production in meson (π^+)-proton interactions at 2.35 and 2.90 Bev/c, 18: 44519 (NEVIS-123)
production in meson (π)–meson (π) interactions, 19: 1264
production in meson (π^+)-proton interactions at 1.6 Bev (E), 19: 1347
production in meson (π)–meson (π) interactions, calculations on (T), 19: 1361
production in meson (π^-)-nucleon interactions at 6.1 and 18.1 Bev (E), 19: 1398
production in meson (π)-nucleon interactions, effects of (T), 19: 3076
production in meson (π) interactions, field theoretical approach to, 19: 8192
production in meson (π^-)-proton interactions at 3 Bev, (E), 19: 10105
production in meson (π^+) interactions with protons, (T), 19: 27272
production in meson (π)–nucleon interactions, (T), 19: 29091
production in meson (π)-nucleon interactions, peripheral model for, 19: 31002 (CONF-550-97)
production in meson (π)-nucleon interactions, analyses of, (E/T), 19: 39574
production in meson (π) interactions with nucleons, peripheral, (E/T), 19: 39576
production in meson (π^-) interactions with protons at 1.5 Bev/c, (E), 19: 41441
production in meson (π^+) interactions with neutrons at 1.7 Bev/c, (E), 19: 41528
production in meson (π)–nucleon interactions, absorptive corrections and form factors in peripheral model for, 19: 41400
production in meson (π)–meson (π) interactions, partial-wave dispersion relations for bootstrap, 19: 41394
production in meson (π^-)-proton interactions, (E), 19: 47403
production in meson (π)-meson (π) interactions, strip approximation for trajectory of, (T), 20: 1012
production in meson (π)-meson (π) interactions, field theory for amplitudes of, 20: 1030
production in meson (π^-)-proton interactions at 2.26 Bev/c, 20: 2745
production in meson (π) interactions, phase shift analysis for, (T), 20: 2708
production in meson (π)-nucleon interactions, amplitudes for, (T), 20: 4584 (JINR-P-2380)
production in meson (π)-meson (π) interactions, diffraction picture and N/D method for, 20: 7907
production in meson (π) coherent reactions with helium-4, (T), 20: 22145
production in meson (π)-meson (π) interactions, variational calculation for, 20: 27819
production in meson(π^-)-proton interactions at 1.7 Bev/c, (E), 20: 34234
production in meson (π) interactions, strip approximation for, 20: 36045 (UCRL-16874)
production in meson (π)-nucleon interactions, reconstruction of amplitude for, 20: 46384
production in neutrino-nucleon interactions, (T), 19: 25315
production in nucleon-antinucleon annihilation, selection rules for, 16: 24735
production in p-p interactions, resonance with mesons (π), 16: 8152
production in peripheral collisions, 17: 29502 (UCRL-10492)
production in photon reactions with deuterium, γ-π-ρ coupling constant from, 17: 31320
production in π-σ interactions meson (π) form factor from, (T), 19: 14347
production in proton-antiproton and proton-meson (π^-) interactions, 17: 705 (BNL-6181)
production in proton pair annihilation, 17: 9322
production in proton ($\bar{p}$-p) interactions at 3.25 and 3.69 Bev/c, 17: 41736 (BNL-7294)
production in proton-proton interactions at 1.5, 2.5, and 2.9 Bev, (E), 19: 41523
production in pseudoscalar meson interactions, 18: 36269
production of axial vector, in meson (f^0) decay, (T), 19: 18834
production of neutral, in meson (π^-)-proton interactions at 3 Bev/c, (E), 19: 23436
production of, Pomeranchuon exchange as result of Regge poles in multiple, 17: 20917
production of $\rho\rho$ resonance in antiproton interactions with neutrons, (E/T), 20: 24042
production of, theory for, 18: 9197
production of Y_1^* in meson (K^-)-proton interaction, 18: 40241 (UCRL-11424(Rev.))
production of, analysis using OPE model, (T), 20: 24083
production of, electromagnetic, (E), 19: 46643(R) (LAL-1136)
production of, multi-channel double bootstrap for, (T), 20: 24003 (CALT-68-26)
production of, Regge-pole contribution to, 20: 15354
production of, symmetry in bootstrap model for, (T), 19: 16627
production processes for, phenomenology of, (T), 19: 6523
properties, 18: 40347
properties, 20: 34170
properties, effects on nucleon electromagnetic structure, 16: 8144
properties from meson (π) -nucleon interactions, peripheral model for, 18: 26348
properties from p-wave amplitudes of meson (π)-meson (π) interactions, (T), 20: 21694
properties in coupled $\pi\pi$-$K\bar{K}$ problem, determination of, (T), 19: 16551
properties in particle-mixture theory, 16: 32335
properties, measurements of, 16: 27983
properties of, effects on nucleon isovector form factors on, 17: 41790
properties of G_0 multiplets for, decay and electromagnetic, 18: 7537
properties of, octet unitary-symmetry model for, 17: 9226
properties of, review of, 17: 24185
properties of, role of 2-π resonances in, 17: 741
properties of, composite meson (π) model for, (T), 19: 23384
properties of, dynamic theory for, 18: 37947
properties of, electron-pair model for, (T), 19: 10059
properties of, low-energy equivalent-potential approach for, (T), 19: 16576
properties of, reciprocal bootstrap model for, (T), 19: 12225
properties of, review of, 19: 14314 (JINR-P-1887)
properties of, review of, 19: 16657
properties of, single-channel calculations of, 19: 27241
properties of, spontaneous mass splitting in bootstrap model for, (T), 19: 18878
properties of, 2π resonance, 18: 21001
properties review, 16: 26158 (UCRL-10167)
Regge poles of, effects in photoproduction of mesons, 18: 26372
Regge trajectories for, calculation using strip approximation, (T), 19: 10103
Regge trajectory in meson(π^-)-proton interactions at high energies, (T), 20: 34212
Regge trajectory of, effect of threshold singularity on, 17: 9250
representation as a composite of two composite mesons (π), (T), 19: 4926
representation in Sp(6) group, 18: 42421
resonances (ρ–π) in meson (π^+)–proton interactions, 18: 30568
review, 18: 34636
role in nucleon core phenomena, 16: 17044
scattering amplitude effects of, N–N, 18: 30605
spin, 16: 22942
spin calculations, 16: 6985
theory, using 2-pion δ-type potentials, 16: 31032
trajectories of, bootstrap calculations of, 20: 39927
trajectories of, in high-energy scattering, 18: 12945
trajectory in meson (π^-)-proton interactions at high energy, (T), 19: 16528
trajectory of, calculation, 17: 28145 (JINR-P-1246)
width of, from $\pi\pi$ elastic interaction phase shifts, (T), 20: 11555 (DESY-65/13)

MESONS (ρ^-)

decay of, radiative, 17: 26337
decay of, quark model for electromagnetic, 19: 32993
decay of, upper limit for 4π, (E), 20: 7850
mass relative to (ρ^0), (T), 19: 33061
mass relative to meson (ρ^0), field-theoretical sum rules for calculating, 20: 41824
production in meson (π^-)-nucleon interactions at 3.3 Bev/c, 18: 865 (UCRL-10731)
production in meson (π^-)-proton interactions at 2.8 Bev/c, 18: 18728
production in meson (π^-)-proton interactions at 4 Bev/c, absorption effects in, 18: 44567
production in meson (π^-)-proton interactions at 3.7 Bev/c, (E), 19: 25385
production in meson (π^-)-proton interactions at 3.0 to 5.05 Bev/c, (E), 20: 7850
production in meson (π^-)-proton interactions, mechanism for, (E/T), 20: 9758
production in mesons (π^-)-proton interactions at 3 to 5 Bev/c, (E), 20: 25811
production in meson (π^-)-proton interactions at 3.0 and 3.5 Bev/c, mechanism for, (E/T), 20: 34254
production mechanism in meson (π^-)-proton interactions at 2.0 Bev/c, 19: 43105

production of, review of, 18: 12903 (JINR-P-1490)
properties of (730), (T), 19: 12300

MESONS (ρ⁰)
alignment of, one-pion-exchange model for, (T), 19: 31004 (CU-1932-240)
decay amplitude, ($\mu^+\mu^-$), 20: 34181
decay angular distributions for photoproduced, strong absorption model for, 20: 37768
decay of, forward-backward asymmetry in, 18: 9086 (TID-20011)
decay of, properties of two meson (π), 17: 26376
decay of, radiative, 17: 26337
decay of, symmetry groups for boson couplings in, 18: 6018
decay of, angular distributions of electron pairs from, (T), 19: 39451 (CALT-68-43)
decay of, asymmetries in two-meson (π), (E/T), 19: 4949
decay of, beta, (E), 20: 15406
decay of, branching ratios for lepton-pair, (E), 20: 11673
decay of, C-nonconserving coupling constants in, (T), 19: 35169
decay of, interference effects in meson (π^-)-proton interactions at 3.25 Bev/c, (T), 19: 33033
decay of, Lee model with cut-off for 2π mode of, 18: 18681
decay of, leptonic, (T), 20: 13476(T)
decay of, quark model for electromagnetic, 19: 32993
decay of, SU(6) symmetry for radiative ($\pi^0\gamma$), (T), 19: 18861
decay of, T = 0 scalar di-pion in, (T), 19: 20998
decay of, test of nonrelativistic quark model in radiative, (T), 20: 1016
decay partial widths, 16: 10898
decay, possibilities of identity with mesons (ω^0), 16: 6978
effects of mixtures with mesons (ω), on weak interaction decays, 17: 34800
electromagnetic properties in SU_3 symmetry, 19: 35080
electromagnetic self-energies and unitary symmetry, 18: 22759
existence and decay, 17: 19191
interactions of, C, T noninvariance in minimal electromagnetic, (T), 20: 4601
interactions with nucleons, isovector form factors for, 16: 12367
interactions with photons, two-field couplings in, 17: 39915
interactions with nucleons, double-peripheral model for elastic, 18: 40275
interactions with nucleons, total cross section for, (T), 20: 19506
mass difference with resonance meson (ω_8), in meson (π)–nucleon interactions, (T), 19: 41380
mass difference, ρ^+-ρ^0, (T), 19: 47369
mass of, 17: 19071
mass relative to ($\rho^\pm$), (T), 19: 33061
mass relative to mesons (ρ^0), field-theoretical sum rules for calculating, 20: 41824
mass spectra of, relation to nuclear forces, 16: 27953
mass spectrum structure in, peak-broadening effect on, 19: 45092
mixing effects for, in degenerate particle systems, 18: 30586
photo-production on protons, mechanism of, 20: 39811
photoproduction at 4.8 to 6.0 Bev, (E), 20: 15425
photoproduction at high energies, (E), 20: 27916
photoproduction from protons at 0.5 to 4.8 Bev (E), 19: 1233 (MIT-2098-79)
photoproduction of protons, mass shift in, (T), 20: 9755
photoproduction on protons, excitation curve analysis of, 18: 24381 (ISS-64/4)
photoproduction on protons, 18: 44563
photoproduction on aluminum, carbon, copper, and hydrogen in Bev range, (E), 19: 45000 (HUX-2752-7)
photoproduction on protons, 20: 2747
photoproduction on nuclei, (T), 20: 19506
photoproduction on protons, absorption effects in peripheral, (T), 20: 27944
photoproduction on protons, SU(6) symmetry for, 20: 34181
photoproduction on protons at 1.5 to 6.0 Bev, cross sections for, (E/T), 20: 37766
photoproduction on protons at 0.3 to 5.8 BeV, (E), 20: 46348(T) (SLAC-Trans-44)
production and decay in meson (π^+)-deuteron interactions, 18: 42376 (TID-20762)
production and decay in meson ($\pi^\pm$)-nucleon interactions at 1.7 Bev/c, (E), 20: 15403
production at high energies, mechanisms for, 18: 9169
production by mesons (π^-) at 12 and 17 Bev/c, 17: 9249
production from meson (π) pair photoproduction, 19: 39549
production from meson (π^+)-proton interactions at 2.35 to 2.90 Bev/c, (E), 20: 27844
production from meson (π^-) reactions with bromine, diffraction dissociation in, (E), 20: 39774
production in bremsstrahlung reactions with protons at threshold to 6 Bev, (E), 20: 30030
production in deuteron-meson (K^-) interactions at 2.24 Bev/c, (E/T), 19: 18855
production in final-state meson (π) interactions in meson (K) decay, phase shift studies for, (T), 20: 36055
production in meson (ω) gamma emission, 16: 13905
production in meson (π^-)-proton interactions, 16: 22959
production in meson (π^-)-proton interactions, 17: 9430
production in meson (π^-)-nucleon interactions at 3.3 Bev/c, 18: 865 (UCRL-10731)
production in meson (π^+)-proton interactions at 3.43 and 3.54 Bev/c, partial cross sections for, 18: 2651
production in meson (π^-)-proton interactions at 3.5 Bev/c, 18: 9200
production in meson (π^-)-proton interactions at 4 Bev/c, cross sections for, 18: 16774
production in meson (π^+)-proton reactions at 3.65 Bev/c, 18: 16790
production in meson (π^-)-proton interactions at 3.5 Bev/c, 18: 36354
production in meson(π^-)-proton interactions at 1.6 Bev/c, 18: 44509 (AD-604581)
production in meson (π^-)-proton interactions at 2.75 Bev, (E), 19: 1348
production in meson (π^-)-nucleon interactions at 12 and 18 Bev/c, (E/T), 19: 16613
production in meson (π^-)-proton interactions at 3.7 Bev/c, (E), 19: 25385
production in meson (π^+)-proton interactions at 2.5 Bev/c, (E), 19: 37526 (CU-1932-243)
production in meson (π^+)-proton interactions at 2.77 Bev/c, (E), 20: 1019
production in meson (π^-)-proton interactions at 7.0 Bev/c, 20: 2746
production in meson (π^-)-proton interactions at 6 Bev/c, (E), 20: 9763
production in meson (π^+)-proton interactions at 2.75 Bev/c, (E/T), 20: 11605
production in meson (π^+)-proton interactions at 2 Bev/c, (E), 20: 11672
production in meson (π^-) interactions with nucleons at 12 and 18 Bev, (E), 20: 30025
production in meson (π^-)-proton interactions at 7.5 Bev, (E), 20: 39758 (JINR-P-2773)
production in meson (π^-) interactions with protons at 7.0 Bev/c, (E), 20: 39790
production in meson (π^-) interactions with nucleons at 12 and 18 Bev/c, recoil nucleon states from inelastic, (E), 20: 41828
production in nucleon interactions, 16: 10910
production in p-π interactions at 1.25 Bev, 17: 5251
production in photon-proton, interactions at high energy, (T), 19: 4977
production in photon-proton interactions via two-meson (π) exchange, (T), 20: 41918
production in proton–antiproton interactions, evidence from final-state correlations, 18: 14881
production in proton–antiproton annihilations at 5.7 Bev/c, (E), 20: 19498
production mechanism in meson (π^-)-proton interactions at 2.0 Bev/c, 19: 43105
production of, review of, 18: 12903 (JINR-P-1490)
properties of (730), (T), 19: 12300
transitions to mesons (ω), nonradiative, 16: 6979

MESONS (ρ^+)
decay of, radiative, 17: 26337
decay of, detection of radiative, (E), 19: 6514 (CEA-R-2525)
decay of, quark model for electromagnetic, 19: 32993
decay width and magnetic moment of, (T), 20: 44203
electromagnetic properties in SU_3 symmetry, 19: 35080
mass difference, ρ^+-ρ^0, (T), 19: 47369
mass relative to (ρ^0), (T), 19: 33061
mass relative to meson (ρ^0), field-theoretical sum rules for calculating 20: 41824
production in meson (π^-)-proton interactions at 2.75 Bev (E), 19: 1349
production in meson (π^+)-proton interactions at 2.75 Bev/c, 19: 25306
production in meson (π^+)-proton interactions at 4 Bev/c, (E), 19: 25350
production in meson (π^+)–proton interactions at 8 Bev/c, (E), 19: 45103
production in meson (π^+)-proton interactions at 2 Bev/c, (E), 20: 11672
production in meson (π^+)-proton interactions at 1.6 Bev/c, cross sections for, (E), 20: 17374
production of, review of, 18: 12903 (JINR-P-1490)
properties of (730), (T), 19: 12300

MESONS (σ)
exchange in alpha particle interactions, effects on potentials in, (T), 19: 25295
exchange in nucleon interactions, (T), 19: 18864
interactions with mesons (η), meson (δ) production in, 18: 42409
interactions with mesons (π), energy peaks in, (T), 19: 14335
production in meson decays, (T), 19: 41518
production in meson (π)-meson (π) interactions, Λ-Λ scattering length from, (T), 19: 47337
production in meson (π)-proton interactions, (E), 20: 39782
production in S-wave meson (π)-meson (π) scattering, (T), 19: 47347

role in decay of mesons (η), (K), and (X°), (T), 20: 17422
MESONS (σ^0)
decay of, probabilities of different modes of, 17: 9341
effects on three-meson-(π) decay of mesons (η^0) and (K), (T), 19: 4919
existence of heavy pseudoscalar, 16: 12388
production in antinucleon annihilation, 17: 20857
Mesons (τ)
see Mesons ($K_{\pi 3}$)
Mesons (θ)
see Mesons ($K_{\pi 2}$)
Mesons (W)
see Bosons
MESONS (X)
decay, 17: 5276
decay modes and quantum numbers, 18: 34592
decay modes, $\eta\pi\pi$, 18: 30602
decay of (950), SU(6) symmetry for radiative, (T), 19: 18861
decay of, branching ratios for, (E), 19: 39531
decay of, radiative, (T), 19: 16550
decay of, $SU(6)_w$ symmetry for radiative, 20: 30040
mass of, as hyperon (A) pair bound state, (T), 19: 8145
mixing in SU(3), 20: 42005
production in meson (π^-) interactions with protons, design of experiment using on-line computer for, 19: 36929
production of, review of, 18: 12903 (JINR-P-1490)
properties in symplectic SU_3 model, (T), 19: 4948
properties of X° (960), four-pion models for, (T), 19: 12223
properties of, π-π resonance, 18: 21001
MESONS (X°)
decay of, C violation in, (T), 20: 25874
decay of, C violation in $\pi^+\pi^-\gamma$, (T), 20: 34226
decay of, C-nonconserving coupling constants in, (T), 19: 35169
decay of, effects of meson (η)-(X°) mixing on, (T), 19: 31056
decay of, meson (σ) hypothesis for, (T), 19: 41518
decay of, sigma hypothesis in, 20: 17422
decay scheme, (E/T), 20: 19273(R) (BNL-929, pp 3-43)
decays of, C and T violation in mixing in leptonic, (T), 20: 4682
decays of, C-violating interactions in, (T), 20: 11634
mixing with mesons (η), (T), 19: 31056
model of, $\eta\pi\pi$, 20: 15344
photoproduction on protons, Regge-pole model for, (T), 20: 44204
production, (E/T), 19: 23355(R) (BNL-867(p.1-117))
production in deuteron-meson (π^+) interactions at 3.29 Bev/c, (E), 20: 27834
production in meson (π^+)-proton interactions at 3.65 Bev/c, (E), 20: 7846
production in meson (K-)-neutron interactions at 2.24 Bev/c, (E), 20: 39786
properties, (T), 19: 25265(R) (UCRL-11776)
properties and production, (E/T), 20: 20365
properties of, review of, 20: 11552 (CONF-651015-3)
MESONS (ζ)
decay and properties, 16: 15595
evidence for, reinterpretation of, 17: 13426
identification of mesons (η^0) with mesons (ζ^0), 16: 19715
interactions, effects of G-parity on, 16: 33764
interpretation of, in meson (π)–meson (π) scattering, 17: 5248
mass formulas in U_6 symmetry, (T), 19: 16545
mass, parity, and spin of, 17: 29506
photoproduction and decay, 16: 29640 (LNF-62/62)
photoproduction and decay, 17: 9313
production and properties in proton pair annihilation, 17: 9321
production in antinucleon annihilation, 17: 20857
production in meson (π) interactions with protons below 1 Bev, 16: 26152
production in meson (π) interactions in protons, search for, 17: 40433(R) (NYO-10063(p.71-89))
production in nucleon-antinucleon annihilation, selection rules, 16: 24735
production of, theory for, 18: 9197
properties in particle-mixture theory, 16: 32335
properties of, octet unitary-symmetry model for, 17: 9226
properties of, review of theoretical, 17: 9463
properties of, electron-pair model for, (T), 19: 10059
properties of, π-π resonances, 18: 21001
quantum-number determinations for, 16: 33765
quantum numbers, intrinsic, 16: 32320
role in electromagnetic nonconservation of vector current, 18: 28354
spin, 17: 28153 (NP-12904)
structure, 16: 15594
MESONS (ζ^0)
decay partial widths, 16: 10898
photoproduction on protons, 17: 16987
spin determinations, 16: 19709
MESOSPHERE
charged-particle content in, (E), 20: 44463
charged-particle density in, measurement of, 19: 29150
electron precipitation at subauroral latitudes, effects of relativistic, (E), 20: 6201
radio wave absorption in polar, detection of, 18: 28466
temperature and wind structure of, review of mechanisms for, 20: 33505
Mesotrons
see Mesons
METABOLIC DISEASES
see also Diabetes
calcium, tracer studies, 19: 31701(R) (COO-587-2)
diagnosis of Wilson's disease, 18: 35280 (TID-7678(p.581-606))
diagnosis of, involving iron, tracer methods using whole-body counting, 18: 35425 (TID-7678(p.537-63))
diagnosis of, use of carbon-14 as tracer for, 18: 35409 (TID-7678 (p.107-33))
dysproteinemia, prevention in mice by use of steroid anabolicum, 20: 45495
effects of acromegaly, on glucose kinetics in man, 19: 31707(R) (UCRL-11833(p.50-72))
effects on calcium kinetics in cancer patients, 19: 45757(R) (NYO-910-23, pp 183-92)
etiology of cystinuria, 19: 10696 (TID-20342)
pathology of necrotizing encephalomyelopathy, familial occurrence of, 19: 42219 (TID-21177)
plasma protein metabolism in patients with, tracer study, 20: 10570
radiodiagnosis of, 19: 31992
radiodiagnosis of, 19: 13136
radiodiagnosis of bone, 19: 34027
radiodiagnosis of bone, using strontium-85, 19: 34035
radiodiagnosis of calcium, 19: 34055
radiodiagnosis of, involving fatty acid absorption, 19: 12916
radiodiagnosis of, involving parathyroid insufficiency, 19: 17403 (BNL-7961)
radiodiagnosis of, isotope dilution method for, 19: 22049
radiation effects on growth hormone levels in patients with acromegaly, heavy particles, 19: 31797(R) (UCRL-11833(p.73-9))
radiodiagnosis of diabetes, 18: 35424 (TID-7678(p.47)-95))
radiodiagnosis of liver, 18: 35423 (TID-7678(p.433-43))
radiodiagnosis of bone, by radiation transmission through finger bone, 19: 31929(R) (ACRH-23(p.10-20))
radiotherapy of, effects of, on hormone level, 19: 42287
radiodiagnosis of, involving vitamin B_{12}, 19: 34056
radiodiagnosis of, involving calcium, 19: 46138
radiodiagnosis of, involving proteins, 19: 46142
radiodiagnosis of megaloblastic anemias, 19: 32041
radiodiagnosis of, use of carbon-14 as substrate tracer in, 19: 31776
radiodiagnosis of, use of whole-body counting for, 20: 6988
radiodiagnosis of, use of whole-body counting for, 20: 6990
radiodiagnosis of, use of whole-body counting for, 20: 6991
radiodiagnosis of, use of whole-body counting for, 20: 6992
radiodiagnosis of, use of whole-body counting for, 20: 6993
radiodiagnosis of, use of whole-body counting for, 20: 6994
radiodiagnosis of, use of whole-body counting for, 20: 6995
radioinduced hypothyroidism in dogs, x, 20: 40698
radioinduced pituitary ablation for treatment of acromegaly, 20: 12748
radiotherapy of acromegaly, heavy particle, 20: 3828
review of phenylketonuria, 19: 10695 (TID-20274)
therapy of acromegaly, use of radioinduced pituitary ablation in, 20: 12753
vitamin B_{12} requirements of patients with pernicious anemia, tracer study of, 18: 35279 (TID-7678(p.497-518))
METABOLISM
see also Animal Metabolism
see also Basal Metabolism
see also Circadian Clock
see also Mineral Metabolism
see also Plant Metabolism
alkaline earth metal effects on bovine, 18: 17459
analog computer studies of metabolic pool size and turnover, 17: 23015
analysis of sulfurated urinary metabolites, 18: 36941
analysis of, computer analysis of data from tracer, 19: 46055
basal, effects of iodine-131 therapy for diabetes-hyperthyroidism, 20: 40790
bibliography on calcium and strontium, in animals and man, 17: 5747
biological model for theoretical studies of, 18: 11653(R) (UCLA-520 (p.27-42))
bone mineralization studies in fetal chickens, 20: 40558
book: *Clinical Aspects of Iodine Metabolism*, 18: 41295
book: *Ionizing Radiation and Metabolism*, 17: 27192
book: *Mineral Metabolism*, 19: 63
book: *Physiological-Biochemical Effects of Nuclear Radiation on Plants*,

19: 17659
calcium and strontium, in algae, 20: 40524(R) (TID-23271)
chromium-51, in clams, 20: 40575
correlation with resistance to tuberculosis in rabbits, 16: 20068
data acquisition, reduction, and analysis in, automatic systems for 19: 25822 (LA-DC-6794)
data analysis, electronic processing, 17: 31815 (LADC-5627)
data on, computer program for reduction of scintillation counting, 20: 6718 (LA-3298)
determination of skeletal, methods for, 20: 5237(R) (UR-668, pp 55-109)
deuterium oxide effects on rat, 18: 33250
diurnal rate variation in rat bone and cartilage, 19: 19472(R) (ANL-6938(p.179-93))
double label experiments on thyroid with technetium-99m and iodine-125, 20: 40547
during chloroplast-formation in Euglena, 18: 23126 (BNL-805(p.89-108))
during pregnancy, effects of progesterone, 16: 8533
dynamics of, in open biological systems, 18: 19537
effect of metabolic state on radiosensitivity of Drosophila, 17: 28710
effects of AET on carbon dioxide and oxygen, in dogs, 19: 14968
effects of age on iodine-131-labeled triolein, in man, 20: 42782
effects of age on, in human cells in culture, 20: 8675
effects of anti-metabolic drugs on thyroid, 20: 38785
effects of cystamine on yeast-cell, 20: 18372
effects of cysteamine and cysteine on gas exchange, 17: 4437
effects of heat-treated and γ-irradiated meals on swine, 20: 41394
effects of inhibition of, on labeled carbon dioxide evolution from tissue cultures, 19: 33738(R) (N64-22756)
effects of injected radioisotopes, 16: 21911(R) (COO-225(p.109-21))
effects of leukemia on, in children, 20: 10545
effects of, on radiosensitivity of animals, 17: 27047
effects of pethidine on, in rats with radiation sickness, 19: 19481
effects of pituitary hormones on, 20: 3809
effects of rare earths and yttrium on, in bacteria, fungi, molds, and yeasts, 20: 16191
effects of simulated altitude on rat iodine, 20: 42745(R) (UCRL-16246, pp 126-37)
effects on cesium-137 and zinc-65 uptake and retention in algae, 20: 8582
effects on plant uptake of divalent cations, 20: 16174(R) (RLO-1547-3)
effects on radioinduced dominant lethality in Drosophila oocytes, 18: 19622
effects on radiosensitivity of organs and animals, 18: 6700
effects on radiosensitivity of rats, 19: 154
effects on radiosensitivity of tumors in rats, 19: 10855
effects on radiosensitivity of rats, 20: 12703
energy flow at population level in nature, tracer studies, 17: 33588
gastroenterologic, tracer studies, bibliography on, 20: 6924 (AED-C-10-04)
genetic factors affecting, in mice, 19: 29849(R) (ANL-6971(p.1-28))
glycolytic reaction rates in anaerobic *E. coli*, calculation from data treated with analog computer, 20: 6728 (TID-22369)
human radon, effects of silicosis on, 19: 31732
hyper-, effects on radiosensitivity of sarcomas, 17: 35542
in tracer studies of animal, 20: 3685
inhibitors for cultured bacteria and yeast, for use in Gulliver program, 19: 33739(R) (N64-22793)
insect, technical problems of radioisotope measurement in, 16: 16120
interspecies comparisons in mammalian cesium and potassium, 20: 42768
kinetics of, 18: 11622
kinetics of calcium-47, in goats, 20: 42739(R) (COO-1339-3)
kinetics of strontium, in man, 18: 20235 (NP-13868)
localizing events in HeLaS$_3$ cell, method of, 17: 35484
mammalian rare earth and ruthenium, 18: 1366
mathematical model for cerium-144, in animals, 20: 38571
mathematical treatment of processes, review of methods used in tracer studies, 16: 1362
measurement in isopods, comparison of methods for, 20: 12610
measurement *in vivo* by external counting of iodine-131-labeled albumin as a function of iodine labeling intensity, 20: 28871(R) (EUR-2636.f,i)
measurement of cesium-137, in cattle and sheep, 20: 42739(R) (COO-1339-3)
measurement of double-labels in, methods for, 19: 30122
measurement of long-term calcium, in human bones using radioisotope tracers and whole-body counters, 20: 42764
measurement of rat calcium, automatic sample and data processing methods for, 19: 31782
measurements of bone, triple tracer method for calcium, phosphorus, and strontium, 19: 31780
metal, in human brain, relation to degenerative diseases, 17: 35419
model for calcium, 18: 11678
models for, of phosphatides and proteins, 20: 3658(R) (EUR-2414.f,i)
mycobacterial phosphate and sulfate, tracer techniques for studying, 19: 31745
of aldosterone in man, 18: 19543
of alkaline earths, calculation of, (T), 19: 6985
of barium-133 and calcium-45 by embryonic chick and rat bone, 18: 15803
of blood plasma proteins, tracer studies of, 18: 35278 (TID-7678 (p.445-72))
of calcium and strontium in beef cattle, 18: 38775(R) (ORO-624)
of calcium in men, tracer studies, 17: 33510 (TID-18990)
of calcium in osteoporosis patients, tracer study using calcium-47, 19: 6997
of calcium in rachitic infants, effects of vitamin D on, 19: 7002
of calcium in rats, effects of age on, 18: 3469
of calcium in thyroid patients, calcium-47 tracer study of, 19: 6996
of calcium in tumor patients, effects of prednisone on, 19: 3870
of calcium-45 by patients with renal stones, 19: 27923
of calcium-47 in mean, whole-body counters for measuring, 19: 15295
of calcium-47 in thyroid patients, 19: 6990
of calcium-47 in tumor patients, 19: 7257
of calcium, disturbances in, 19: 65
of calcium, dynamics and function, 19: 64
of calcium, model for, 19: 6983
of calcium, use of saliva in studies of, 19: 6926
of carbohydrates in Saccharomyces, enzyme reactions in, 18: 41138
of carbohydrates in sapwood of *Populus deltoides*, 19: 17463
of carbohydrates, radiospirometric methods, 16: 8501
of carbohydrates, tracer study, 17: 30231
of certain chemicals in rats, effect of radioinduced liver enzyme defect on, 18: 5000(R) (NP-13281(p.1-24))
of cesium-132 and -137 in pregnant women through partus, activity transfer to children in, 19: 25893
of cesium-137 by marine fish, 19: 59
of cesium-137 in man, 19: 25894
of cobalt-60 in rabbits and rats, 18: 4996(T)
of cobalt-60 in chickens, 18: 17425
of copper, effects of molybdenum in rats, 19: 21823
of diiodosalicylic acids and sodium iodide in cattle, tracer study, 18: 38775(R) (ORO-624)
of Dipterex in normal and resistant flies, 16: 16116
of dog body water, tracer study using deuterium, 18: 19530
of ethanol, tracer study, 17: 30258
of fission products in mammals, research program at Hanford Lab., 1956 to 1964, 19: 12893(R) (HW-83613)
of fluorine-18, in dogs, 20: 40554
of glucose, role in radiation injury, 19: 19538
of insoluble radioisotopes in man, 18: 11589
of internal radioisotopes, symposium on, 18: 11890
of iodine in thyroid, effects of age in mice, 19: 25865
of iodine-131 and phosphorus-32 in antlering and growing deer, 17: 35408(T) (AEC-tr-5631)
of iodine-131, effects of thyroid gland steady state function on, 16: 25105
of iron, tracer studies, 16: 14411
of lipids in rat lung tissue, tracer study of, 18: 41038(R) (HW-80500 (p.134-7))
of marine microorganisms, tracer study of, 19: 25839(R) (NYO-1918-100)
of marine organisms collected in Ligurian Sea, 18: 21761(R) (RT/BIO(63)-8)
of minerals, tracer technique using calcium-48 for studying, 19: 6984
of minerals, tracer studies, 19: 31992
of nucleic acids, effects of radiation, 16: 26846
of nucleic acids, tracer study, 16: 28692
of nucleic acids, genetic control mechanisms for, 18: 36866 (BNL-7213)
of nucleotides, radiation effects, 16: 9859(T)
of phosphorus, tracer study of, 18: 38
of plasma proteins in liver, 18: 35423 (TID-7678(p.433-43))
of plutonium-239, 18: 13415 (CEA-2381)
of prostaglandin E_2 in guinea pig lungs, 19: 25860
of proteins, tracer studies, 16: 14407
of radioisotopes, 19: 29871
of radioisotopes in animals, 19: 38357(T)
of radiometals, survey, 18: 22
of radionuclides in beagles, 18: 23184(R) (ANL-6823(p.44-75))
of radionuclides in man, 19: 21817(R) (BNL-867(p.119-50))
of radionuclides, in man, 18: 43321 (ORNL-P-350)
of radiosulfate, in normal and irradiated mouse embryos, 20: 42765
of radium-228 and thorium-228 in rats, 19: 2014
of RNA by mouse leukemic cells, 19: 31677(R) (ORNL-3768(p.119-30))
of scandium-47 and calcium-47 in rat bones, 20: 40545
of skeletal bones, study, 16: 1433(R) (TID-14099)
of sodium in man, tracer study, 18: 38754
of strontium in bones of animals, 18: 1348

of strontium-85 in mice and rats, effects of age on, 19: 2038
of strontium-85 in dogs, effects of age on, 19: 2039
of strontium-90 by marine algae, 19: 14997
of strontium-90 in human bone, 18: 21
of strontium-90 in man, theoretical analysis of, 18: 38738
of strontium-90 in dogs, rabbits, and rats, effects of magnesium sulfate on, 19: 42254
of strontium, effects of magnesium on, 18: 41063
of strontium, review, 19: 66
of sulfur-35 in rats, effects of methionine sulfoximine and x radiation on, 17: 21437
of tritiated polyester in digestive mucous membrane in rat, 16: 25110 (CEA-2155)
of tritium-labeled thymidine incorporated into desoxyribonucleic acid, 16: 16098
of tryptophan, 19: 14901 (BNL-7942)
of tryptophan in man, 19: 21817(R) (BNL-867(p.119-50))
of vinca alkaloids by rats, 18: 15790
of vitamin D by rats, 17: 38710
of zinc-65 in rabbits, 18: 43190
of 1-(4-dimethylaminobenzylidene)indene in rats, 20: 40632(R) (ORNL-3922, pp 175-91)
of 3-hydroxyanthranilic acid in man, tracer studies of, 19: 21817(R) (BNL-867(p.119-50))
oxidative phosphorylation mechanism for, 18: 21775(R) (UCRL-11215(p. 13-14))
pathways in embryonic development, 16: 5133(R) (TID-14432)
pathways of, in embryonic development, tracer studies, 20: 16172(R) (NYO-2194-1)
periodicity in bone, tracer study, 17: 25595(R) (ANL-6646(p.110-12))
pharmacological and toxicological effects of niobium chloride, 16: 2876 (UCLA-491)
pharmacological and toxicological effects of gadolinium and samarium chlorides, 16: 2877 (UCLA-492)
photoreactivation of prototrophic, in uv-induced mutants of *E. coli*, 20: 38669
properties of antimetabolites for use in Gulliver program, 19: 33738(R) (N64-22756)
radiation and chemical effects on meprobamate, in rats, 17: 35480
radiation and hydrogen peroxide effects on Ascite tumor cell, effects of light and thionine on, 18: 17413
radiation dose effects on thyroid, x, 20: 43029
radiation effects on respiratory, whole-body exposure, 16: 4044
radiation effects, in liver, 16: 6296(T) (JPRS-11322(p.86-99))
radiation effects on acid-base equilibrium, 16: 6308(T) (JPRS-11322 (p.316-36))
radiation effects, 16: 14499
radiation effects in algae, 16: 14521
radiation effects on dehydro-ascorbic acid, in rabbit, 16: 14582
radiation effects on tryptophan, in rabbit, 16: 14584
radiation effects on tryptophan, after adrenal and testicle exposure in mice, 16: 14570
radiation effects, continuous whole-body gamma, 16: 1550
radiation effects on, in tumor cells, 16: 12902
radiation effects, rate of nervous system in, 16: 20192
radiation effects on, in lactic-acid bacteria, 17: 1235 (NP-12155)
radiation effects on oxidative, in fats, 17: 5821
radiation effects on rate, 17: 14031
radiation effects in liver mitochondria, whole-body exposure, 17: 15570
radiation effects on intestinal, 17: 21592
radiation effects on cellular, 17: 27108
radiation effects on, effects of dose rate in rats, 17: 27143
radiation effects on rat, effects of nutritional condition on, 17: 31838
radiation effects from injected plutonium-239 on, in bone, 17: 31926
radiation effects on sodium, radiotherapy, 17: 33696
radiation effects on abdominal fat, 17: 37130
radiation effects on riboflavin, in rats, x, 17: 37028(T) (JPRS-21171 (Del,)(p.24-31))
radiation effects on nuclein, in rat skeletal muscle, 17: 37068(T) (JPRS-20997)
radiation effects on phosphorus, in mouse strain L cells, gamma, 17: 37090
radiation effects on, of calcium-45, selenium-75, and sulfur-35, 17: 38742(R) (NYO-10602)
radiation effects on glucose, in guinea pigs, x, 17: 38771
radiation effects on, in mammals, 17: 38896
radiation effects on rabbit albumin, gamma, 18: 94
radiation effects on erythrocyte, in man, 18: 1419
radiation effects on bone, x, 18: 3535
radiation effects on, in heart of guinea pigs, 18: 3554
radiation effects on protein, effects of dianabol on, 18: 3595
radiation effects on wheat leaf phosphorus, gamma, 18: 5116
radiation effects on rat liver carbohydrate, gamma, 18: 5127(T)
radiation effects on rabbit carbohydrate-phosphorus, gamma, 18: 5128(T)
radiation effects on, in liver of mice, 18: 5002(R) (NP-13281(p.92-103))
radiation effects on, in rat thyroid, 18: 9880
radiation effects on, in rat skin, 18: 11741
radiation effects on metabolite, 18: 11749
radiation effects on rat sulfur, tracer study of, x, 18: 13420
radiation effects on rat liver phosphate, x, 18: 17422
radiation effects on cellular, 18: 17523
radiation effects on lipid, in human bone marrow and leukocytes, 18: 19552(R) (NYO-2769-1)
radiation effects on *E. coli* DNA, x, 18: 19641
radiation effects on rabbit palmitic acid, x, 18: 19665
radiation effects on mouse and rat serum protein, x, 18: 19590
radiation effects on mouse blood cell and hematopoietic, x, 18: 19730
radiation effects on mouse carbohydrate, effects on phagocytosis in hematopoietic system, 18: 19734
radiation effects on bis(2-guanidoethyl) disulfide and 2-mercaptoethylguanidine, in mice, 18: 19772
radiation effects on rat liver, x, 18: 23233(R) (ANL-6823(p.157-60))
radiation effects on bull spermatozoa, gamma, 18: 23297
radiation effects on sperm, gamma, 18: 23334
radiation effects on, in ascites tumor cells, x, 18: 27087
radiation effects on oxidative phosphorylation in mitochondria, 18: 27147
radiation effects on, in carrot tissues, 18: 30074(R) (TID-20703)
radiation effects on mouse Ehrlich ascite tumor cell energy, x, 18: 29332
radiation effects on *E. coli* nucleic acid, x, 18: 29252
radiation effects on rat glucose, infusion method using carbon-14-labeled glucose for, gamma, 18: 29291
radiation effects on plant, gamma, 18: 31136
radiation effects on, in intestinal mucosa of guinea pigs, 18: 31162
radiation effects on plant, ionizing, 18: 31231
radiation effects on, in isolated erythrocytes, 18: 31244
radiation effects on sodium, by fish, 18: 33272(R) (NIRS-2(p.31-42))
radiation effects on mouse liver histidine, gamma, 18: 33359
radiation effects on rat blood protein, x, 18: 33362
radiation effects on mercaptopropylamine, in mice, 18: 33373
radiation effects on thyroid, after administration of therapeutic dose of iodine-131, 18: 35319 (TID-7678(p.413-32))
radiation effects on iron-59, 18: 35353
radiation effects on, of calcium by teeth and skeleton, role of denervation in x, 18: 37003
radiation effects on chick selenium-75, gamma, 18: 38882
radiation effects on iodine-131-labeled insulin, x, 18: 38885
radiation effects on bird cerium-144, 18: 38775(R) (ORO-624)
radiation effects on, in lungs of rabbits, 18: 38968
radiation effects on nucleoside incorporation into RNA, tracer study of, 18: 41103
radiation effects on, in tumor-bearing rats, effects of thiamine on, 18: 41133
radiation effects on rat thymine, x, 18: 41139
radiation effects on, in rat tissues, 18: 41173
radiation effects on, in Chlamydomonas, 18: 43217 (COO-1117-6)
radiation effects on rat phosphorylation, gamma, 18: 43244
radiation effects in man, whole-body, 19: 12952 (DASA-1422)
radiation effects on goldfish sodium, gamma, 19: 105
radiation effects on rat gas, x, 19: 150
radiation effects on, in mouse bone marrow chimeras, 19: 2079 (ORNL-P-656)
radiation effects on, in rats, 19: 2093
radiation effects on human protein, 19: 2123
radiation effects on, in rats, 19: 3895(R) (ORO-625(p.103-8))
radiation effects on oxidative phosphorylation, in ascitic fluid of tumor-bearing mice, x, 19: 3899
radiation effects on, 19: 3973
radiation effects on swine calcium-45 and strontium-89, 19: 5699
radiation effects on, calculation by two-compartment model having age variables, 19: 6949(R) (ORNL-3697(p.193-8))
radiation effects on mouse gastrointestinal tract, protective effects of AET against, 19: 7198
radiation effects on adenosinephosphoric acid, in rats, 19: 8933
radiation effects on, in animal cells in culture, 19: 10784(R) (NYO-2564-1)
radiation effects on, in biological systems, 19: 12932
radiation effects on iron, 19: 13035
radiation effects on, in rat liver, 19: 13054
radiation effects on gas, in rats, protective effects of methandrostenolone against x, 19: 13115
radiation effects on protein, in rabbit kidney and liver, 19: 15116
radiation effects on RNA, in Ehrlich ascite and thymocyte nuclei, x, 19: 15063
radiation effects on, in microorganisms, 19: 17496(T) (JPRS-28405

(p.1-32))
radiation effects on lipid, in germinating and maturing cotton seed, 19: 17519(T)
radiation effects on total, in mice and rats, 19: 17649
radiation effects on, in rabbit cornea, 19: 19552
radiation effects on lipid, in newborn and weanling rat brain, 19: 19610
radiation effects on, in animal cells, 19: 19613
radiation effects on lactate, pyruvate, hydroxbutyrate, and acetate, in mice, 19: 21949
radiation effects on, 19: 21971
radiation effects on regenerating liver cell, 19: 21983
radiation effects on liver glucose, short wave, 19: 26008
radiation effects on cholesterol, in rat muscle and spleen, 19: 26017
radiation effects on potato, x, 19: 25934
radiation effects on guinea pig liver, effects of ATP on x, 19: 28112(T) (FTD-TT-64-1163)
radiation effects on, protective effects of serotonin against, 19: 28125
radiation effects on, in frog skin, 19: 29901(R) (RLO-1754-1)
radiation effects on, in animal cells, 19: 29917
radiation effects on mouse oxygen and nitrogen, protective effects of bone marrow against x, 19: 31905(R) (ORNL-3768(p.99-108))
radiation effects on sunflower seed, relation of growth to, 19: 33894
radiation effects on glycogen, in rat brain and liver, 19: 36063
radiation effects on, 19: 36101(T) (JPRS-29788, pp 31-41)
radiation effects on pyrocatechol, in macacus monkeys, 19: 40373
radiation effects on human and rat, use in exposure diagnosis, 19: 43852
radiation effects on, in connective tissue cells, 19: 45895
radiation effects on lipid, in pigeons, 20: 110
radiation effects on, 20: 5308
radiation effects on oxidative phosphorylation in rat thymus and spleen, 20: 5341
radiation effects on bacterial, γ, 20: 5346
radiation effects on animal lens, effects of age on x, 20: 5333
radiation effects on, in human cells in culture, x, 20: 8675
radiation effects on skin, in man, uv, 20: 8678
radiation effects on gas, protective effects of methylandrostenolone in rats against x, 20: 14392
radiation effects on rat, neutron and x, 20: 14368
radiation effects on yeast-cell, β, 20: 18372
radiation effects on animal-cell, effects of dose-modifying chemical compounds on, 20: 18444
radiation effects on carbohydrate-phosphorus, in cardiac and skeletal muscles in animals, γ, 20: 32956
radiation effects on, in guinea pig and rat retina, x, 20: 36630
radiation effects on, in Ascites tumor cells, x, 20: 38599 (TID-22968)
radiation effects on, in rats, x, 20: 38600(R) (TID-23034)
radiation effects on animal, 20: 38544
radiation effects on, of dairy cows, calcium-45 and radium-226, 20: 38552
radiation effects on, in soil organisms, gamma, 20: 40637(R) (ORO-2754-7)
radiation effects on human, from iodine therapy, 20: 40659
radiation effects on protein, in animals, 20: 40602 (AD-624934)
radiation effects on DNA, in mammalian cells *in vitro*, x, 20: 42777
radiation effects on epiphysis and metaphysis of bones, x, 20: 42785
radiation effects on nitrogen, in frog liver, gamma, 20: 42787
radiation effects on rat thymidine, x, 20: 42806
radiation effects on oxygen consumption and phosphate esterification by mitochondria from rat liver, x, 20: 45430
radiation effects on nitrogen balance following therapy, x, 20: 45447
radiation effects on, effects of bone marrow transplants on, 20: 45485
radiation effects on diurnal variation in, of mice, gamma, 20: 45310
radiation sickness effects on, pathology of, 19: 30433(T)
radioinduced inheritable deficiencies of, in animal cells in culture, 18: 41072 (CONF-534-3)
radioinduced reversion from auxotrophic, in *E. coli*, uv, 18: 31172
radioinduced reversions in *E. coli* from auxotrophic, stability of uv, 18: 31173
radioisotope, 19: 29879
radioisotope tracers for study of, 18: 3659
radiosensitivity effects on rats, 18: 33365
radiosensitivity of rats with increased, 20: 42959
radiotherapeutic and prednisone effects on tumor, 18: 9904
radiotherapy of thyrotoxicosis, iodine-131, 19: 46082
rat protein, effects of irradiated potatoes in diet on, 20: 40576
rate of animal, double tracer technique for measurement of, 20: 18211(R) (UCLA-12-576, pp 89-111)
rate of, role in radioprotective action, 17: 15794
rates of, use of stable isotopes and activation analysis for measurement of, 20: 45318
relation to radiation injury recovery rate, 16: 17542
research activities at Pacific Northwest Laboratory on, 19: 33714 (BNWL-C-43)
research on protein, criteria for, 20: 10563
research programs at BNL on, July 1962 to July 1963, 18: 6586(R) (BNL-806(p.93-122))
role in mutation processes, 17: 7699
serum protein, in rats, effects of carbon tetrachloride, radiation, and venous bleeding on, 20: 28954
strontium-90 in man as function of age, model for estimating, 20: 6724 (ORNL-P-1830)
succinic oxidase, in *Mycobacterium phlei*, 20: 40571
technetium-95 and technetium-96, in man, 20: 45297
theory of alkaline earth, use of barium-133 retention in rats for testing Marshall's, 20: 40565
thermodynamics of material transfer across biological membranes, 19: 43665 (BNL-9338)
trace elements in human, activation analysis for, 20: 38847
tracer studies, 16: 16162
tracer studies, data analysis by electronic processing, 17: 31815 (LADC-5627)
tracer studies, evaluation of kinetic data, 17: 5726
tracer studies of antimetabolites, 16: 1415
tracer studies of substrate oxidation, diagnostic applications in man, 18: 35409 (TID-7678(p.107-33))
tracer studies of, 19: 15319
tracer studies of, 19: 31776
tracer studies of, mathematical data analysis of, 18: 35277 (TID-7678 (p.55-79))
tracer studies of, in man, 18: 41021 (BNL-857)
tracer studies of, in health and disease, 19: 15006
tracer studies using iron-59, calcium-47, and carbon-11, 16: 16160
tracer studies using carbon-14, 19: 24239 (BNL-8031)
tracer study, use of carbon-14 in, 16: 7367
tracer techniques in, 18: 36926(T) (AEC-tr-6398(p.49-58))
tracer techniques for studies of, 19: 31749
tracer techniques in, measurement methods for, 19: 36848
tracer techniques for research on, nitrogen-15, 20: 10560
use as indicator of radiation effects, 19: 43753
use in studying, of digital printout system for whole-body scanners, 18: 20346
use of iodine-131 and technetium-99m in study of thyroid, 20: 40555
use of radioisotopes for studies on, methods for, 19: 6977
use of radioisotopes in studies of, bibliography on, 20: 6727 (TID-3515(Suppl.1))

METABOLISM CAGES
design and cost of air conditioned, 19: 43644(R) (UCD-472-112)
design and operation for cricket study, 19: 6931(R) (ORNL-3697(p.65-84))
design for animal movement and position monitoring in, 20: 30960(R) (BNWL-235-4, pp 22-5)
design for individual mice, 17: 30227 (TID-19053)
design for radioisotope treatment of dogs, 17: 38633(R) (UCD-108 (p.1-9))
design of rat, 19: 43728(R) (UCLA-12-565, pp 59-64)
design of rat, for determinations of *in vivo* thyroid uptake, 20: 45306
design of, for aerospace environmental studies in man, 19: 21812 (AEDC-TDR-63-256)
design of, for small rodents, 20: 35230
for mice, radiation source avoidance during chronic exposure, 19: 7019 (LADC-6168)
for plants grown in carbon-14 atmosphere, 19: 10771
gas concentration measurements for, 19: 33692(R) (NYO-1397-1)

METABORIC ACID
spectra of vapor of, infrared, 17: 6045(R) (RAD-SR-62-251)

Metacil
see Uracil,6-Methyl-

METACINNABARITES
crystal structure of, neutron and x-ray diffraction studies of, 19: 7364

Metal Amides
see Amides

Metal Borides
see Borides

Metal Carbides
see Carbides

Metal Carbonyls
see Carbonyls

Metal Chelates
see Chelates

Metal Chlorides
see Chlorides

METAL COATINGS
(Uses, characteristics, and preparation including metal spraying, vacuum vaporization, and chemical deposition.)
see also Coatings
see also Plating

anodized, spectral reflectance, effect of variables in anodizing process, 16: 8434 (ASD-TR-61-147)
applications in weapon systems and metals processing, 16: 502 (WAL-TR-371.1/1)
bibliography on, 18: 14376 (SB-409(Suppl.1))
bonding of ceramic, nondestructive evaluation methods for, 16: 29311 (ARF-1213-2)
bonding strength of vapor-deposited, tensile tester for measuring, 20: 11063 (RFP-672)
book: *Physics of Metal Coatings*, 20: 43880
compatibility with fissionable materials, 17: 29255 (ZFK-WF-13)
corrosion by boric acid–potassium hydroxide solutions, 18: 30133 (WCAP-3737)
corrosion inhibition on magnesium alloys, 16: 10454(R) (NP-11312)
deposition by plasma jet spraying, 17: 517 (NOTS-TP-2616)
deposition by thermal decomposition of gases and vapors, bibliography, 17: 1818 (UCRL-6997)
deposition by vacuum distillation of metals, 16: 10143(P)
deposition of high-melting, plasma-jet-gun for, 20: 2251(P)
deposition of, by chloride and fluoride reduction, 20: 39354 (BMwF-FBK-66-09)
deposition of, method for vapor, 19: 30699(T,P) (AD-611421)
deposition on aggregated reactor fuel particles, 19: 40994(P)
deposition on ceramics using gas discharge, 18: 44061 (SC-R-64-1330)
deposition on spheres, 16: 3481 (WAL-TR-375/1)
deposition on uranium and uranium dioxide particles, 16: 26479 (TID-7622(p.98-107))
deposition on uranium by electroplating, 16: 30760
development for protection of materials at high temperatures, 20: 37192
evaluation of platinum-group, on tungsten, 18: 14440
preparation of three-component, with composition varying with position on the substrate, by vacuum vaporization, 20: 7502 (UCRL-16393)
production with sorbed gas, 16: 5706(P)
properties and cleaning methods for, 20: 43599
properties of coatings of, for protection of refractory metals, 20: 33825
radiation effects on, for spacecraft, 20: 2428 (NASA-SP-55, pp 365-79)
research on, for French reactor fuels, 19: 23034
thickness distribution of evaporated, effects of crucible shape on, 20: 16151 (RFP-647)
thickness measurement of, by x-ray spectroscopy, 17: 30113
thickness measurement using x-ray fluorescence, 20: 37151

METAL COMPACTS

fabrication and properties of non-metallic fibrous reinforced, 16: 2184 (NP-10952)
mechanical properties of, of tungsten fibers in copper matrix, 20: 884
packing efficiency of, equations for, 20: 11260
preparation of high-density refractory, 17: 37500(P)
production of fiber-reinforced, 20: 760
sintering of dense, continuous, 16: 21002(P)

METAL COMPLEXES

atom clusters in, bonding in, 17: 28826 (NYO-10551)
determination in organic phase following solvent extractions, feasibility of polarography for, 18: 13628(R) (ORNL-3537(p.1-17))
determination in two-phase systems, methods for, 17: 7939 (AERE-R-4187)
electron exchange reactions in solution, calculations of rates of, 19: 32119 (BNL-9171)
electron-transfer reactions in solution, mechanisms of, 18: 33521 (BNL-8081)
equilibrium distribution data for inorganic-ligand, 19: 4104 (ORNL-3620)
formation by sulfoxides, 20: 20360(R) (PRNC-73)
formation constants and classification of, by spectrophotometric methods, 19: 26365
formation in aqueous solutions, 20: 18449
formation, stability constants in stepwise, 16: 4125(T) (AAEC/Trans-7)
ligand substitution in, review of, 17: 25229
photochemistry of, review on, 17: 8196
radioinduced destruction of porphyrin, in oil solutions, 18: 5405(P)
relaxation effects, in aqueous solutions of hydrated metal ions, 16: 180
role in reactions of radioprotective compounds, 20: 18449
solid state reactions and synthesis, 16: 21010(R) (AD-264878)
spectra of hexafluoroacetylacetone, infrared, 17: 18035
stability constants by electrometric methods, 16: 1729 (AAEC/E-72)
stability constants of successive, calculation, 17: 7998 (NP-12391)
stability constants of coordination, kinetic methods for measurement of, 17: 25106
stereoisomerism in eight-coordination of, 17: 18029
structure of transition, tetradentate ligands in, 19: 32048(R) (NP-15073)
substitution reaction mechanisms, 16: 1667
with amines, structure of, 19: 17430(R) (TID-21412)
with arsenazo III, formation mechanism of, 17: 6007
with benzoylpivaloylmethane and dipivaloylmethane, preparation and properties of, 17: 14258
with chloride in fused chlorides, crystal field spectra, 17: 25228
with N,N-dimethylacetamide, properties of, 17: 18032
with olefins, synthesis of, 19: 32048(R) (NP-15073)
with oxy acids, chemical technology of, 17: 15918
with tributyl phosphate and trioctyl phosphine oxide, infrared spectra of, 18: 255 (IS-595)

METAL COMPOUNDS

see also Alkali Metal Compounds
see also Intermetallic Compounds
see also Organic Compounds Metallo-
analysis of powders of, for water by vacuum distillation, 17: 5963 (PG-Report-350)
bibliography on ternary group V and VI, 16: 13005 (NP-11598)
gamma cross sections for, tables, 16: 29824
neutron cross sections for, tables, 16: 29824
preparation of doubly labeled, for use in industry and medicine, 18: 39758(T) (AEC-tr-6390(p.545-52))
properties, research progress at Lawrence Radiation Lab. on chemical and physical, 16: 24175(R) (UCRL-10119)
radiation effects, bibliography on, 16: 24233 (57GL77)
radioinduced phase transformations in, 18: 12748
reactions with amidinothiourea and amidinourea, 17: 14127
separation of sparingly soluble rare-, effects of ultrasonic vibrations on, 18: 39390
solubilities in N-methylacetamide at 40°C, 17: 12318
spectra of volatile inorganic, 17: 4445 (IS-500(Sect.C))
superconductivity in, rules for, 18: 6101 (AD-402708)
thermodynamic properties of, method for estimation of, 16: 31586 (UCRL-10397)
vaporization of ternary gaseous species of, review of, 17: 25227

METAL COUPLES

growth of intermetallic layer in, effects of pressure, 16: 3431 (SEP-258)
heat transfer at interfaces of, theoretical study of directional effects in, 16: 27216 (UCRL-9885(Rev.))
preparation by ion plating, 19: 7879
thermal resistance of contacts, methods of surface analysis for prediction, 16: 16476(R) (NYO-9457)
ceramic/metal, many-particle method for tunneling in, (T), 19: 18931

METAL CRYSTALS

binding energy of, theory of, 17: 29357
defect clusters in irradiated, 16: 13649
defect structure of, field ion microscopy of, 17: 35772
defects in irradiated, properties of, 16: 13648
deformation, review of alloying and temperature effects, 16: 9243
dislocation theory for, 18: 3432 (UCRL-10455)
electron spiral spin polarization in conduction bands of, 17: 9053
glide elements for hexagonal, determination by asterisms in Laue photographs, 16: 12139
glide elements for hexagonal, determination by asterisms in Laue photographs, 16: 21045(T) (AEC-tr-5138)
growth of, modes of operation of electron-beam floating-zone melting furnace for, 18: 8739
lattice dynamics of, theory for, 18: 26142
microstructure of face-centered cubic, effects of quenching and radiation on, 17: 18089
neutron scattering by, effects of conduction electron-phonon interactions on, 17: 2216
neutron scattering by low-impurity, oscillation frequency and resonance location from slow, (E), 20: 22320
orientation and positioning of single, device for, 17: 12543
oxide film growth on, homogeneous field approximation of kinetics of, 17: 36229 (TID-17856)
preparation and properties of ultra-thin-layered, 16: 21010(R) (AD-264878)
preparation and testing, 17: 32575(R) (TID-19181)
preparation of single, 16: 30722 (NYO-10554)
properties of binary, concentration effects on, 17: 4955
radiation damage in, equipment and methods for measuring, 16: 33516 (NAA-SR-Memo-7428)
radiation effects on contact melting results, 16: 25868
radiation effects on structure of, studies with field ion microscope, 16: 31378
radiation effects on face centered cubic, 16: 33551
radiation effects on structure, 17: 2028
radiation effects on plastic behavior of, beta, gamma, and neutron, 17: 37576
screw-spin structures in, magnetization properties of, 17: 13173
tensile properties of single, apparatus for measurement of, 16: 25769(T) (SCL-T-434)
theory of kink bands in deformed, 18: 42026(T) (ORNL-tr-296)
ultrasonic wave attenuation in, 18: 34454

Metal Fluoride Complexes

see Fluoride Complexes

METAL-FOIL DETECTORS

see also Plastic-Film Detectors

analysis of, radiochemical, 19: 7274(R) (IDO-14636)
calibration and use for neutron measurements, 16: 19074 (NARF-62-4T)
calibration of indium, 16: 15026 (TID-15398)
calibration of threshold, 19: 7205(R) (ORNL-3697(p.159-64))
calibration of threshold neutron detection system, 19: 7786 (NDL-TM-16)
corrections for flux perturbations in water, 16: 3848(R) (ORNL-3193 (p.78-94))
corrections for neutron flux depression in water, 16: 3843(R) (ORNL-3193(p.52-5))
counting data system design, 16: 11852 (IDO-16715)
counting facility for, 19: 31460(R) (ANL-7010(p.179-233))
design and performance of beryllium foil monitor for proton beams, 16: 19131
design and performance for neutron flux distribution measurements, 16: 25562 (NP-11705)
design and performance, 16: 31940
design for neutron flux determinations, above uranium-238 threshold, 20: 25440(P)
design of fast neutron, 18: 33978(P)
design of gold, for neutron-source calibration, 19: 15877
design of secondary-emission, for monitoring electron-linac beams, 19: 833
development for fission fragments, 20: 14852 (CEA-R-2862)
development for neutron dosimetry, 17: 3207 (HW-SA-2785)
development for neutron fluxes, 18: 43114(R) (NP-14236)
development for plutonium subcritical experiment program, 19: 29506(R) (GEAP-4845)
development of neutron, using normal and depleted uranium, 19: 20340
lifetime of, in neutron flux detectors, mathematical analysis of, 16: 30574 (HW-71142)
neutron activation perturbation, thermal, 16: 24363
neutron activation, effects of self-shielding and thickness on, 16: 24364
neutron activation integrals for, computer program for, 18: 23871 (ANL-6822)
neutron cut-off energy for, 20: 25413
neutron dosimetry using, 18: 33979(P)
neutron flux depression by, in reactors, 16: 6128
neutron flux depression by, Monte Carlo calculation of, 16: 24362
neutron flux perturbation by, thermal, 17: 34298
neutron resonance integrals and self-shielding factors for, 17: 17106 (DP-817)
performance as neutron dosimeters, effects of orientation to neutron source, 17: 3237 (Y-1405)
performance for absolute thermal neutron flux measurements, 19: 32567
performance for determining leakage spectra from reactors, 17: 34275
performance for neutron flux measurements, 17: 30871
performance for neutron monitoring, 17: 34276
performance for neutron dosimetry, 18: 38727
performance for neutron dosimetry, 18: 38728
performance for neutron dosimetry, 18: 38732
performance for neutron counting, effects of flux anisotropies on, 19: 826
performance for neutron beam dosimetry, 19: 775 (MITNE-47)
performance for neutron spectrum and dose measurements, nuclear cross sections for, 19: 31316
performance for neutron dosimetry, 19: 31930 (NYO-3267-2)
performance for neutrons in fast reactors, (T), 20: 8346 (EUR-2532.e)
performance for thermal neutron radiography, 19: 22018 (BNL-8165)
performance for xenon stability determinations in reactors, 20: 30843
performance of aluminum and gold foils in, for neutrons, 19: 8376(R) (GA-5176)
performance of cadmium-covered indium foils for neutron counting (E), 19: 825
performance of catcher-foil, for measuring power distributions in critical assemblies, (E), 19: 27753 (PWAC-453)
performance of fission, for neutrons above 6 Mev, 19: 15861 (NDL-TR-46)
performance of gilded-foil monitor in linear accelerators, 17: 23629
performance of Hurst Threshold Detector using enriched-uranium foil for neutron dose measurements, 17: 23747 (TID-18647)
performance of nickel and titanium, for neutron integral flux measurements, 19: 26671(T) (CEA-tr-A-1822)
performance of non-1/v probes in measurements of very hard thermal neutron spectra, 19: 31201 (ZfK-RN-25)
properties of, for heavy ions, 17: 11008 (TID-16174)
review, 17: 8625
sample changer design for, with punched tape-controlled sequencing, 17: 23600 (LADC-5476)
sample changing systems for use with, design of automatic, 20: 14846 (AECL-2517)
self-shielding factor in foil stacks, 16: 3855(R) (ORNL-3193(p.123-8))
threshold, parameter evaluation for, 17: 26038
use for fast neutrons at AB Atomenergi, Sweden, 17: 41117
use for measuring angular distribution of neutron flux, technique for, 17: 3789
use for neutron detection, evaluation of factors affecting, 17: 26236
use for neutron flux measurements, thermal disadvantage factors for, 20: 34904 (CONF-660606-3)
use for neutron spectra measurements in reactors and shield (E/T), 19: 3771 (AE-155)
use for nondestructive determination of burnup in nuclear fuel, 20: 11004
use in calibration of proportional counters, 16: 3956 (NP-11107)
use in calibration of thermal neutron area monitor, 16: 11971(R) (JAERI-5003(p.209-14))
use in calibration of neutron sources, 16: 13934
use in measuring fast reactor neutron spectra, 16: 7694
use in neutron age measurements, 16: 1008
use in reactors for neutron spectra measurements, 17: 31669 (AAEC/TM-191)
use of dysprosium foils for neutron flux measurements in reactors, 16: 31844
use of gold as, for absolute neutron flux measurements, 18: 23876 (KFK-180)
use of resonance, for neutron flux spectra measurements, 17: 32418
use of titanium as, for fast-neutron flux measurements, 17: 34299

Metal Halide Complexes
see Halide Complexes

METAL HALIDES

see also Alkali Metal Halides

bibliography on absorption spectra of, 17: 21669 (UCRL-7238)
phase studies of groups I and II in binary systems with plutonium halides, 16: 15185 (LA-2661)
radiation effects on, review of, 20: 46944
reactions of niobium and tantalum with acetonitrile, 19: 9604(R) (IS-900(Sect.M))
reactions with magnesium cyclopentadienide, 20: 35493
solvent extraction of trivalent, effects of strong acids, 16: 14378(R) (NYO-2302)
synthesis of niobium and tantalum polynuclear, 19: 9604(R) (IS-900 (Sect.M))
vapor pressures, bibliography on, 17: 14202 (BM-IC-8147)
vaporization of, 17: 2956 (UCRL-9840)

Metal Hydrides
see Hydrides

Metal Hydroxides
see Hydroxides

Metal Ions
see Ions

Metal–Metal Oxide Systems
see Cermets

Metal Nitrides
see Nitrides

Metal–Organic Compounds
see Organic Compounds, Metallo-

Metal Oxides
see Oxides

Metal Oxychlorides
see Oxychlorides

Metal Plates
see Plates

METAL POWDERS

analysis for oxygen by neutron activation methods, 20: 26774
analysis of, for water by vacuum distillation, 17: 5963 (PG-Report-350)
compacting and pelleting by ultrasonic techniques, 16: 5687(R) (NYO-9584)
compacting in various shapes for electrodes, design of apparatus for, 17: 14793 (UCRL-6932)
compacting into tubes, use of opposing magnetic fields in coaxial conductor for, 18: 39868
electron thermionic emission from charged spherical, 16: 2329
electrorefining, 17: 8270(P)
fabrication for nuclear reactor applications, evaluation of methods for, 17: 1862
fabrication of, by pressing, development of theory for, 17: 6603(T) (JPRS-16573)
fabrication of, method for, 18: 34117(P)
hot extrusion of, review, 19: 20518 (NMI-TJ-29)
humidity effects on flow of refractory, 17: 3480 (LAMS-2773)
porosity of, effects of cyclic sintering on, 18: 18337
preparation by reduction of metal compound, continuous, 16: 17789(P)
pressing of, for plate and sheet fabrication, 20: 29679
production of extremely fine, 16: 27585(P)
rolling of refractory, 17: 3480 (LAMS-2773)
sintering of, engineering drawings of induction furnace for, 19: 18442

use of heavy, in radiation-attenuating films, 19: 44670(P)
x-ray absorption analysis of, instrument for automatic continuous, 20: 37152

METAL SPRAYING
combustion powder and rod and plasma flames in, 16: 16703
development of, for refractory materials, 17: 410 (DMIC-175)
equipment and procedure for, plasma, 20: 5837 (NLCO-966)
method for preparation of beta sources, 16: 5387
plasma jet method for, for forming alloy coatings, 17: 517 (NOTS-TP-2616)

METAL SYSTEMS
free energies of interaction of metal-metallic salt systems, 18: 24996(R) (NAA-SR-8888(Sect.VI))
gas–liquid equilibrium data for, computer program for integration of Gibbs–Duhem equation for, 20: 4375 (IS-1241)
fused salt–metal, review of, 17: 33872 (ORNL-3391)

METALLIC FILMS
see also Coatings
see also Metal Coatings
see also Metallic Foils
analysis of ferromagnetic, for cobalt, iron, and nickel, activation, 20: 14489
bonding to solid-state devices, methods for, 19: 20520 (SC-DC-65-1256)
charged-particle reactions with, plasmon excitation by, (T), 20: 28656
damage by fission fragments, 19: 36949(R) (BNL-900(p.121-97))
damage by fission fragments, 20: 20183
density of thin aluminum, proton-produced x rays for determining surface, 20: 17051
deposition of cobalt, method for vacuum, 19: 34664
deposition of, on ceramic materials, 16: 29324(T,P) (SCL-T-432)
deposition of radioactive, electrolytic cell for, 19: 852
deposition of thin, by radiation decomposition of molecules, 16: 22213
deposition of thin, vacuum system shutter arrangement for, 17: 33149(R) (NBS-7919)
deposition of thin, tracer study of vacuum, 18: 16386 (TID-7688(p.40-3))
deposition of thin, by ion plating, 19: 7879
deposition of tungsten, for uniform thermionic emission, 19: 30703
design and performance of thin superconducting cryotron, 20: 13048
development of high-temperature, 17: 8873
electromagnetic radiation emission, calculation of peaks at plasma frequency, 16: 9327
electron beam reactions, light spectra from, 16: 1942(R) (ORNL-3189 (p.155-66))
electron interaction effects from superimposed magnetic and superconducting, (E), 20: 11918
electron ranges in thin, 20: 29952
electron scattering by, uses for analysis of electron plasma frequencies in metals, (T), 20: 1326 (ORNL-P-1600)
electron tunneling between aluminum and lead-thulium, effects of magnetic fields on, 19: 12865(R) (NAA-SR-10501)
electron tunneling in lead–thallium, effects of magnetic fields on, 19: 27735(R) (NAA-SR-10850)
electron tunneling excitation spectra in laminates of normal and superconducting, (T), 20: 15653
fabrication of porous, 16: 10449(P)
fission fragment track production in thin, effects of conductivity and thickness on, 19: 14261
growth and nucleation by sputtering in glow discharge environment, 17: 36464
growth of evaporated and sputtered, (E), 20: 39587
interactions with fast electrons, plasma resonance effects in, 17: 2074
ion energy losses in, light, 17: 25984
ion penetration coefficient for partially mobile, 19: 16448(R) (TID-21380(p.85-111))
light absorption, theory, 16: 3484(T) (UCRL-Trans-728(L))
magnetic properties of very thin, 16: 24142 (AD-270673)
magnetic properties of superconducting, 17: 11399
mechanical properties of thin, review, 18: 20515 (CONF-356-11)
microwave absorption in, on normal and superconducting tin, (T), 20: 30290
Moessbauer effect in thin, Debye-Waller factor for, 20: 44137
plastic deformation of thin gold, by Talysurf stylus, 19: 38916 (SC-DC-65-1589)
preparation, 16: 6703
preparation and properties of thin, ultra-high-vacuum system for, 18: 24225
preparation of thin unsupported, 17: 411 (IA-633)
preparation of 100 to 1000A, 16: 1157
production from separated isotopes by cathodic sputtering, chamber design for, 16: 16433
properties of normal and superconducting, 17: 5140
properties of superconducting, in magnetic fields, (T), 20: 9937
radiation effects on physical properties, gamma, 16: 565 (AD-255465)
radiation effects of fission fragment bombardment, 16: 33406
radiation effects on, ion bombardment studies of, 17: 446
radiation effects on superconductivity of niobium stannide, (E), 19: 1023
radiation effects of neutrons on niobium stannide, (E), 19: 1506
radiation effects on evaporated, fission-fragment, 19: 26889
radiation effects on thin, fission-fragment, 20: 33947
sorptive properties for gases in vacuum, research program, 17: 11193(R) (TID-17635)
superconducting critical fields in thin, angular dependence of upper, (T), 20: 13681
superconducting critical fields for plane, in longitudinal magnetic fields, (T), 20: 28191
superconducting energy gaps of binary, (E), 20: 34425
superconducting phase transitions in, hysteresis of, 17: 13146
superconducting transitions in, 17: 36443 (NP-13089)
superconducting transitions in tubular niobium stannide (E), 19: 1513
superconducting transitions in niobium stannide, (E), 19: 1510
superconducting, hysteresis in magnetic transitions in, (E/T), 19: 5097
superconductivity of superimposed, 16: 27656
superconductivity of thin bridges in, magnetic field effects on, 18: 42566
superconductivity in copper, on superconducting indium–lead alloys in magnetic fields, (E), 20: 1124
superconductivity of aluminum and tungsten, 20: 25474(R) (BNL-954, pp 122-67)
thermoelectric power of thin, 17: 6700(T) (UCRL-Trans-892(L))
thickness measurement of, design of radiometric beta gage for, 18: 25751
thickness measurements on, by scattering of accelerated alpha particles, 20: 36719
track formation in thin, by electron beams, 19: 38950
tritium sorption on, 20: 23358 (CONF-640413, pp 40-52)
use as seals in vacuum uv spectroscopy systems, 18: 29864
x-ray specular reflection from thin, interference structure in, 18: 704

METALLIC FILTERS
brazing of sintered stainless steel, to stainless steel flanges for use at 1300°F, 20: 786 (ORNL-TM-1252)
calcine removal from porous, upstream-downstream overpressure during blow-back, 18: 27279(R) (HW-80284(p.4.1-23))
cleaning of porous, in fluidized beds, 20: 10810 (JEN-153-DMa/I-19)
cleaning of, use of ejector nozzle for, 20: 14645
design of, for use in production of monoenergetic x-ray beams, 16: 29100 (HASL-129)
development for sodium purification, 19: 15662(R) (ANL-6900(p.45-142))
development of metal-ceramic, for organic coolants, 19: 35628
fabrication of strontium, for x-ray absorption, 20: 5692
performance in carbon removal from sodium, 17: 18220 (NAA-SR-Memo-8239)
processing of tubular, for securing to support element, 18: 7193(P)
testing for volatility separation processes, 20: 7192(R) (K-1649)

METALLIC FOAMS
preparation by bonding hollow metal spheres, 16: 3481 (WAL-TR-375/1)
preparation of, for aerospace uses, 19: 37141

METALLIC FOILS
see also Metallic Films
beta reactions with thin, bremsstrahlung energy spectra from, (E), 19: 23950
changer for 100 neutron flux measuring, tape-controlled sequence, 17: 14633
charged-particle reactions with, gamma spectra from, 16: 26314
crystallographic analysis of, 18: 24994(R) (MND-2531-1)
defects in, study by electron microscopy, 18: 12561 (UCRL-11009)
electron absorption anomalies in, experiment and theory, 16: 29577
electron energy dissipation in, ionization chamber measurements of, 20: 23133
electron microscopy of thin, 17: 25789
electron reactions with, gamma spectra from, 16: 26315
electron secondary emission from thin, (E), 20: 13103
fabrication of thin self-supporting, by rolling, 20: 25520 (AERE-R-5097, Paper 22)
fission-fragment reactions with, secondary electron production in, 20: 17168
heat transfer in porous air-cooled aluminum, using radiant heat source, 20: 18875
implosion of, for magnetic flux compression, (E), 20: 44031
impurity distributions in, measurement using two-dimensional activation analysis, 20: 33230
laser-beam reactions with, plasma ion energies from, 20: 44932
neutron flux measurements using, effects of inter-foil interactions on, 16: 30939
neutron resonance absorption by adjacent cadmium and indium, 19: 825
performance of neutron-sensitive, in pocket ion chambers, 20: 11119
performance of superconducting niobium stannide ribbon in electromagnets, (E), 19: 571
performance of vapor-deposited gold, as lubricants in vacuum, 20: 27516

pinch discharge on, plasma production in Z, 18: 21537
plasma oscillations in, 16: 12285
preparation, electrolytic, 16: 9218(T) (AEC-tr-4999)
preparation for electron microscopy, electrolytic, 16: 18081(R) (EURAEC-180)
preparation of isotopic, by rolling, 20: 25519 (AERE-R-5097, Paper 21)
properties as thermal insulation, 16: 11835
properties of, effects of temperature and time on low-pressure, 20: 41440(R) (ALO-3632-4)
radioinduced atomic displacement near threshold in single-crystal, electron, 20: 27618
superconductivity degradation in niobium stannide, (E), 19: 1515
thickness gage design for, 20: 46024
thickness measurement by beta and x-ray fluorescence, 16: 29117(T) (AEC-tr-5097)
thickness of, soft x rays for measuring, 17: 41222
use as window for electric discharge device, 20: 13052(P)
use of high-atomic-number, in plastic scintillators for gamma detection, 20: 11165(P)

METALLOGRAPHY

acid saw for cutting single crystals, 19: 31634 (NYO-3029-2)
applications of electron microprobe to chemical analysis, 19: 13199 (LA-3157)
book: *Metals Reference Book.*, Vol. I and II, 3rd edition, 18: 32080
book: *Stereometric Metallography*, 16: 4454(T) (NP-tr-823(Pts. I & II))
book: *Theoretical Metallography*, translated from German, 16: 480(T) (AEC-tr-4500)
camera for remote, motor-driven roll-film, 19: 46711 (BNWL-SA-161)
camera for, use of 35 mm, 19: 46928 (NMI-4998, pp 14-19)
cell description for examination of irradiated fuel elements, 19: 13572
conference, 19: 46936 (NMI-5025(Pt.I))
conference on, at Armour Research Foundation, Jan. 14–15, 1959, 17: 6524 (TID-7625)
conference on, ORNL, April 20–22, 1965, 20: 16945 (ORNL-TM-1161)
cutting uranium-base ceramic crystals, electrolytic jet machining method for, 20: 11216 (PEL-79)
defect analysis by transmission electron microscopy, (E), 20: 7582 (UCRL-16271)
design of remote metallography cell, 20: 2247
development of techniques for irradiated materials, 16: 388 (ANL-6316)
development of techniques for remote, 16: 3120
development of vibratory polisher for remote use on irradiated specimens, 16: 30511 (DP-764)
developments at Brookhaven, 17: 31798(R) (BNL-782(p.60-91))
dislocation etching of deformed molybdenum, equipment and methods for, 20: 39432
electrolytic polishing uses in, 18: 24107(T) (SC-T-64-903)
electropolishing method for rare-earth metals, 19: 7854 (IS-1036)
equipment and procedures for, for radioactive materials, 20: 9403
equipment and techniques for remote, 16: 650
equipment and technique for, development for specialized uses, 16: 30169(R) (ORNL-3313(p.133-78))
equipment and techniques used at ORNL, 20: 4309(R) (ORNL-3870, pp 300-4)
equipment design for, 20: 39340
equipment for, electronic probe microanalyzer with linear scan device, 18: 543 (CEA-2291)
equipment for, engineering drawings for remotely controlled, 17: 30646
equipment for, of plutonium, 20: 7576 (RFP-543)
etchants for Inconel 600 and X-750, 19: 42838 (AECL-2271)
etching by ion bombardment, methods of, 18: 2284(T)
etching by monoenergetic ion bombardment, 17: 32505
etching methods for zirconium dislocations, 20: 37227
etching of radioactive metals by positive ion sputtering, 16: 30526(P)
etching technique for plutonium, electrolytic swab, 20: 751 (RFP-543)
etching using alternating current method, 19: 44601 (LA-DC-6407)
facilities and methods for transuranium, (E), 19: 22969 (DPSPU-65-30-18)
facilities design for radioactive materials, 16: 663
facilities for plutonium study, design of, 20: 46143(R) (HW-66081)
facilities for, description of portable, 19: 46935 (NMI-4999, pp 129-36)
facility design for radioactive materials, 18: 12303(P)
identification of sigma phase in austenitic stainless steel, 19: 32723 (AECL-2234)
identification of inclusions in uranium by color, 20: 33881 (NLCO-977)
impregnation techniques for radioactive specimens, 19: 2498
inversion of pole figures for materials having orthorhombic symmetry, method for, 18: 22489 (NLCO-903)
methods at high temperatures, 19: 47000 (NMI-4996, pp 8-18)
methods for color microphotography, 19: 46931 (NMI-4999, pp 26-9)
methods in, microprobe, 19: 2841
methods in, survey of modern, 19: 9665 (UCRL-11067)
microphotometer for measuring grain reflectance, 19: 13994(R) (NLCO-940(p.8.1-4))
mounting of irradiated specimens, remote, 16: 7850
of intermetallic-high-melting metals, 19: 39214
of powder materials, 17: 29251 (LADC-5785)
optical microscopic techniques for electron probe analysis, 19: 40951 (NBL-6290)
particle number and size analysis and measurement, 17: 29256(T) (AEC-tr-5833)
polishing cloth for, evaluation of commercial, 19: 46923 (NMI-4997, pp 36-44)
potting compound for specimen mounting, 19: 28739 (RFP-545)
preparation of irradiated specimens by vacuum impregnation, 19: 6264
preparation procedures for ceramic, cermet, and metallic specimens, 19: 46937 (NMI-5025(Pt.I), pp 1-25)
radiation effects on crystal structure, 17: 2028
radioactive materials preparation for, engineering drawings of cave for, 19: 24927
remote-control equipment for, 16: 3133
replica preparation from irradiated fuels, device for primary, 19: 16207 (AECL-2138)
replica technique using polyvinyl chloride for high-burnup reactor fuels, 18: 7132 (WAPD-T-1595)
replication of irradiated samples using silicone rubbers, 19: 47091 (NMI-4999, pp 69-77)
replication using silicone rubber and epoxy resin, 19: 46932 (NMI-4999, pp 60-8)
sample coating in, apparatus for, 18: 41953(P)
sample mounting, curing properties of polyester resins for, 18: 4895 (ANL-6712)
sample mounting in epoxy resins using multiple cavity molds, 19: 46927 (NMI-4998, pp 1-5)
sample mounting in epoxy resin using a radio-frequency furnace, accelerated, 20: 16947 (ORNL-TM-1161, pp 98-102)
sample mounting in, effects of curing stresses in epoxy resins on, 20: 43906 (ORNL-P-2361)
sample mounting resins for irradiated specimens, evaluation of, 20: 16948 (ORNL-TM-1161, pp 103-11)
sample polishing by vibratory polisher, 17: 37458 (IS-662)
sample preparation by electrolytic polishing, 16: 29321(T) (AEC-tr-5247)
sample preparation in, 19: 40964(P)
sample preparation, description of remote grinder for, 19: 46507 (NMI-4997, pp 157-62)
sample preparation procedures, vibratory grinding and polishing, 19: 46939 (NMI-5025(Pt.I), pp 135-219)
sample preparation for irradiated materials, 19: 47089 (NMI-4999, pp 30-50)
sample preparation for irradiated material, 19: 47085 (NMI-4997, pp 134-56)
sample preparation by vibratory polishing, techniques for hot-cell, 19: 47086 (NMI-4997, pp 184-8)
sample preparation techniques for irradiated specimens in, for electron microscope studies, 20: 17128 (ORNL-TM-1161, pp 194-207)
sample preparation for, using electrical-discharge machining, design and operation of equipment for, 20: 16951 (ORNL-TM-1161, pp 159-81)
sample preparation of urania containing metallic inclusions for, 20: 16953 (ORNL-TM-1161, pp 249-66)
sample preparation for high-magnification examination of ceramic materials, 20: 16954 (ORNL-TM-1161, pp 267-71)
sample preparation in, vibratory grinding and polishing method and fixture for, 20: 19176 (ANL-6975)
sample preparation, procedures and standards for uranium, 20: 19180 (NLCO-954)
section preparation by thermal etching in vacuum, 17: 29259
specimen wafering technique for transmission electron microscopy, 19: 14907 (HW-SA-3353)
surface passivation on reactive metals, 16: 20970(P)
surface replication for hot-cell applications, development of methods for, 16: 657
technique for determining micro structures, using digital computer, 17: 18724
technique for determination of pole figures in Zircaloy-2 and of basal pole figures in hcp metals, 19: 34687 (ORNL-P-1266)
technique for rapid preparation of uranium surfaces for, attack-polish, 18: 32049 (NLCO-911)
techniques for chemically active and radioactive materials, replication, 19: 46951 (NMI-4996, pp 19-20)
techniques for evaluating coated-particle reactor fuels, 18: 27864 (ORNL-3577)
techniques for preparation of irradiated materials, 19: 30659
techniques for quantitative studies of dispersed second-phase particles in dilutely alloyed uranium, 18: 32045 (HW-SA-3579)
techniques for quantitative studies of precipitate particles in dilutely alloyed uranium, 19: 30643 (BNWL-30)
techniques for study of irradiated materials, 18: 12731 (TRG-Report-

611(p.1-3))
techniques in, review on, 19: 4599
thermal etching of plutonium and uranium alloys and systems, 17: 41423 (CEA-2314)
use of electron microscopy for studies of defects in crystals, 18: 12561 (UCRL-11009)
use of storage oscilloscope with scanning electron probe, 16: 10239
use of transmission electron microscopy in examination of bcc metals and alloys, 19: 44610 (TIM-943)
use to study phase equilibria in plutonium alloys, 19: 16073 (MLM-1163 (p.L-1-14))
uses for microstructural studies of cast uranium, 19: 47007 (NMI-5025 (Pt.I), pp 127-51)
uses in evaluating coated fuel particles, 18: 30199
uses in nondestructive testing methods, 19: 46556 (NMI-4997, pp 1-21)
uses of color film in, 20: 16949 (ORNL-TM-1161, pp 112-29)
uses of image-splitting eyepiece in, 20: 16952 (ORNL-TM-1161, pp 182-91)
uses of microphotometers in, 20: 16950 (ORNL-TM-1161, pp 132-45)
visual standards for estimating recrystallization, inclusions, and stringers in uranium, 18: 34047 (NLCO-910)
x-ray diffraction analysis in, conference on, 20: 15943 (RL-REA-2595)

METALLURGICAL EQUIPMENT
see also Metallurgy
see also Mineral Dressing
autoclaves for stress corrosion cracking experiments, 19: 24932(R) (COO-1319-12)
catalog of, 16: 30515 (TID-4100(1st Rev. Index 2))
cathodic etcher design and operation, 17: 3386 (TID-14534)
control of, using isotopes and radiations, 20: 43789
description of 50,000 and 150,000 psi hydrostatic compacting systems, 19: 28778 (UCRL-7841)
design for extrusion bonding of metals, 19: 28775 (CRE-1195)
design for hot pressing, symposium on, 20: 37179
design for preparing pure powders of air-sensitive alloys, 18: 30120(T) (ANL-Trans-37)
design for purification of metals by electron bombardment, 16: 18014 (AD-263880)
design for rectangular plate-bending analysis, 19: 46555 (KAPL-M-6493)
design for splatcooling, 19: 34654(R) (NMI-1263)
design of bending device for stress corrosion studies, 19: 26766(R) (EURAEC-1309)
design of orienting device for metal single crystals, 17: 12543
design of stirrer-vibrator for recovering entrapped plutonium from casting skulls and turnings, 18: 18289 (LADC-6023)
development for magnetic-pulse process, 20: 40490 (Y-1483)
development for testing high-temperature alloys, 18: 16424(R) (GEMP-270A)
development of, for use in shielded cells, 17: 22090 (CEA-2256)
extrusion apparatus for diffusionless bonding, 19: 28774 (CRE-1139)
extrusion of die design, hydrostatic pressure, 19: 30688 (CEA-R-2750)
furnace using low density inert gas flush, 18: 16425(R) (NP-13741)
hot press design for glove boxes and manipulator cells, 20: 14666 (ORNL-P-1946)
InFab facility for processing and fabrication of reactive metals, 19: 30705
magnetic balance for magnetic saturation measurements, 18: 8033(T) (AEC-tr-6165)
press design for plutonium pressure transformation studies, 19: 22987(R) (NUMEC-3428-6)
press design, hydrostatic, 20: 6692(P)

Metallurgical Processes
see Mineral Dressing

METALLURGY
see also Electrometallurgy
see also Hydrometallurgy
see also Lyometallurgy
see also Powder Metallurgy
see also Tracer Techniques (Metallurgy)
analysis of heterogeneous equilibrium in ternary alloys, 16: 29322(T) (AEC-tr-5248)
analysis of mechanical hysteresis in lattices, 20: 33859(R) (AD-634128)
apparatus for study of martensitic transformations, 17: 1960(T,R) (EURAEC-343)
autoradiographic techniques used in, 18: 30121(T) (NP-tr-1150)
Bauschinger effect and its practical applications, 18: 4935(T) (SC-T-524)
bibliography, 16: 6721 (NP-11206)
bibliography of UKAEA publications available to public, 16: 17339 (NP-11504)
bibliography on all-metal sandwiches, 16: 20957 (NP-11677)
bibliography on DMIC selected accessions, 17: 39464 (NP-13122)
bibliography on effects of weld-pool agitation on properties and characteristics of welds, 17: 32533 (AD-409795)
bibliography on high-energy-rate metal working, 17: 505 (AD-272693)
bibliography on information resources, 16: 15141
bibliography on Japanese developments in, 16: 21868 (SB-477)
bibliography on Soviet scientific and technical literature, Vol. I, 16: 7340 (XDC-60-4-2)
binary alloys and systems, 16: 17967(R) (USBM-U-887)
book: *Aviation Physical Metallurgy*, 17: 39474(T) (FTD-TT-62-1678)
book: *Diffusion of Metals: Exchange Reactions*, 16: 15128(T) (AEC-tr-4506)
book: *Energetics in Metallurgical Phenomena*. Vol. I, 19: 41075
book: *Engineering Physical Metallurgy*, 19: 34634(T)
book: *Extraction and Metallurgy of Uranium, Thorium, and Beryllium*, 19: 919
book: *International Conference on Beryllium Metallurgy*, Grenoble, May 17–20, 1965, 20: 41416
book: *Investigation of Heat-Resistant Alloys*, 17: 41370(T) (NP-tr-1066)
book: *Joint Plastic Deformation of Dissimilar Bodies*, 19: 32707(T) (JPRS-29696)
book: *Lithium; Its Chemistry and Technology*, 16: 30373(T) (AEC-tr-4940)
book: *Mechanical Behavior of Materials at Elevated Temperatures*, 16: 2260
book: *Metallurgy and Fuels*. Vol. IV, 16: 19268
book: *Metallurgy in Nuclear Power Technology*, 17: 23887
book: *Metallurgy of Rare Metals*, 20: 46147(T) (NASA-TT-F-359)
book: *Metals Reference Book.*, Vol. I and II, 3rd edition, 18: 32080
book: *New Physical and Chemical Properties of Metals of Very High Purity*, 19: 36968
book: *Nickel and Its Alloys (Vol. I)*, 18: 10462(T) (OTS-63-11098 (Vol.I))
book: *Niobium and Tantalum*, 17: 36331
book: *Physical and Process Metallurgy and Physicochemical Research Methods*, 17: 8866(T)
book: *Plutonium 1960*, 16: 4458
book: *Problems in Physics of Metals and Metal Studies*, 16: 29334
book: *Properties of Grain Boundaries*, 16: 19414
book: *Purer Metals. Lectures Delivered at the Institution of Metallurgists Refresher Course, 1961*, 18: 8740
book: *Radioactive Tracers in Physical Metallurgy*, 18: 5741(T)
book: *Radioisotopic Instruments in Metallurgy*, 20: 29598
book: *Solid State Diffusion in Metals and Alloys*, 18: 20536(T) (AEC-tr-6313)
book: *Strength of Sintered Materials and Alloys at Room and High Temperatures*, 17: 34468
book: *The Action of Lubricants in Pressure Working of Metals*, 16: 10489(T) (NP-tr-821)
book: *The Chemistry, Purification and Metallurgy of Plutonium*, 20: 35383 (MUC-JCW-223(Books 1 and 2))
book: *The Encyclopedia of X Rays and Gamma Rays*, 18: 8043
book: *Toughness and Brittleness in Metals*, 16: 19413
book: *Uranium*, 18: 27876
book: *Uranium Metallurgy. Vol. I. Uranium Process Metallurgy*, 16: 33386
book: *Uranium Metallurgy. Vol. I. Uranium Process Metallurgy*, 17: 6539
book: *Vanadium, Niobium, Tantalum. The Metallurgy of the Pure Metals and Their Alloys*, in German, 18: 25906
chemical reactions of metals in formation of intermetallic compounds and solid solutions, 16: 25702(T) (AEC-tr-5182)
conference on advanced technology, Univ. of N. Mexico, Nov. 2 and 3, 1962, 17: 30917 (SC-4920(M))
conference on behavior of sheet materials, New York, August 16 to 19, 1960, 16: 6696 (NP-11199)
conference on cold working, recovery, and recrystallization, Gif-sur-Yvette, France, June 27 and 28, 1963, 18: 39834
conference on corrosion, Brookhaven National Lab., May 23 to 25, 1962, 16: 20975 (BNL-728)
conference on materials research in Canada, Vancouver, B. C., June 7 and 8, 1960, 16: 7888 (NP-11196)
conference on physical, of titanium and its alloys, 20: 2359(T) (NASA-TT-F-338)
conference on relation between atomic defects and macroscopic properties, Saclay, France, July 6 and 7, 1962, 18: 30126
conference on stress corrosion, delayed failures, and fatigue corrosion, 20: 14998
conference on vacuum techniques, 16: 2124
conference on vacuum, 17: 25756
conference on vacuum, 18: 41951
consolidation and fabrication of refractory sheet, panel discussion on, 16: 7863 (MAB-179-M)
development and research at Lawrence Radiation Laboratory in, 17: 35262(R) (UCRL-10706)

development of hot-pressing techniques, 16: 497 (NAA-SR-6441)
development of structural materials for nuclear weapons, 19: 26753 (AD-610502)
developments, US-EURATOM joint research program, 16: 14382
developments at Brookhaven, 17: 31798(R) (BNL-782(p.60-91))
developments in high-temperature, 20: 29623(R) (TID-22970, pp 121-256)
developments in reactor fuel elements, review on, 18: 36797
dislocation break-away and motion theory, 16: 15124 (NP-11462)
dislocation network analysis, 16: 19348(R) (EURAEC-239)
dislocation theory in engineering, 17: 27810 (UCRL-10788)
dislocations and ductility in metals and alloys, theory of, 17: 39603
effects on iodine-131 deposition in urban districts in Japan, 20: 29479
electron beam uses in, 19: 20466
electron microprobe uses in, 18: 22429(T) (TRG-Inf-Ser-382)
electron microscopy in, use of high-voltage, 19: 20548 (CONF-640204 (p.35-43))
fabrication and phase studies on alloys, 20: 2350(R) (USBM-RC-1205)
fabrication by explosive forming, bibliography on, 17: 8752 (AD-270900)
fabrication by high-energy-rate forming, bibliography on, 18: 15672 (HW-80934)
fabrication characteristics and mechanical properties of reactor materials, 16: 4511 (GA-2235)
fabrication of metal sheets by explosive forming, 18: 11552(P)
facility for radioactive material, 19: 44163 (BNL-9502)
gammagraphy applications in, 18: 14315
handbook on electron fractography, 19: 34625 (AD-612912)
handbook on properties of magnesium, nickel, and titanium alloys, 18: 10535 (N63-18835)
heat for processes in, from power reactors, 19: 38686(P)
hot laboratory design, construction, and operation in JAERI, 16: 7641
internal friction measurements, formation and diffusion of kinks as process of dislocation movement in, 16: 29320(T) (AEC-tr-5107)
laboratory for, Riso, 17: 11121
lectures on point defects in metals, 18: 8788 (BNL-7623)
manual on practice of, for laymen after nuclear attack, 19: 46918 (IITRI-B6018-1)
measurement of depth of defects by replication techniques, 20: 14966 (RFP-673)
measurement of metal purity by damping techniques, 17: 23881(T) (NP-tr-1011)
mechanical properties of two-phase dispersion-strengthened crystalline materials, 17: 27882
metal production by pressure decomposition and pressure reduction, 17: 22097 (NP-12722)
metalworking using electron-beam techniques, 17: 30921 (SC-4920(M) (p.73-6))
metalworking, ad hoc committee report on, 19: 20507(R) (MAB-206-M)
methods in high-purity, 19: 18408
microstructural examination in, evaluation of, 20: 11275 (ORNL-TM-1338)
neutron activation analysis uses in, for preparation and study of high-purity materials, 19: 36258
of pure metals, translations of Russian articles on, 18: 10458(T) (JPRS-22697)
performance of pyro-, for processing spent nuclear fuels, (E), 19: 34286
physical, effects of quantum mechanical concepts on, 18: 34066
plasma jet uses in, 20: 1277 (TID-22136)
pole figure inversion for orthorhombic symmetry, 17: 23868 (NLCO-862)
preparation of photomicrograms of crystalline material, 16: 30513 (HW-SA-2081)
production of styli for removal of microscopic inclusions, 17: 6201 (ANL-FGF-300)
properties of, research on, (E/T), 19: 38027(R) (ORNL-3841)
radiation damage to crystal lattices, 16: 30896 (BNL-5179)
radiation effects on processes in, review, 20: 46223 (BNL-10543)
radioisotope uses in, literature survey, 16: 9067(R) (ARF-1194-7)
radioisotope uses in Yugoslavia, survey of, 17: 36093(T) (JPRS-20805)
radioisotope uses in Soviet bloc countries, 19: 4559(T) (ORNL-tr-387)
radioisotope uses in, 19: 20417
radioisotope uses in, 20: 19128
radioisotope uses in, 20: 23567
radioisotopes in, 20: 706
radioisotopes in, in USSR, 17: 10888
radioisotopes in, in Japan, 17: 30045
reaction of hydrogen with solutes in metals, 17: 24003
relation to superconductivity, 18: 6124
research and development programs at Materials Control, Wright-Patterson AFB, 16: 1292 (WADC-TR-53-373(Suppl.7))
research and development on, 17: 6532 (WADC-TR-53-373(Suppl.9))
research at BNWL, 20: 27407(R) (BNWL-207)
research at Chalk River National Laboratories, review, 19: 25782 (AECL-1580)
research at IFA, 19: 40287(R) (NP-15188)
research facilities for, Casaccia, Italy, 20: 36540
research in progress under Army Research Office, 20: 40485(R) (AD-636091)
research on, review of, 17: 3390(R) (WADC-TR-53-373(Suppl.8))
research on, in CEA, 20: 10471(R) (NP-15720)
research program on reactor technology, 18: 27859 (KAPL-2000-21)
research programs, summary for AEC in 1961, 16: 12825
research programs progress on, 17: 16527(R) (USBM-U-1001)
research programs in, AEC, 17: 19744 (TID-18468(p.127-244))
research programs on rolling, 17: 27759 (MAB-139-M(R3))
research programs of U. S. Army on, 1962 summary, 17: 33413(R) (NP-12967)
research programs on, Seibersdorf Reactor Center, 1962, 18: 6560(R) (SGAE-1963/1B)
research programs at BNL on, July 1962 to July 1963, 18: 7987(R) (BNL-806(p.3-90))
research programs on, in Denmark, 18: 7996(R) (NP-13476)
research programs in, summaries of USAEC, 18: 9766 (TID-4005(Pt.1, 7th Ed.))
research programs at UCRL on, 18: 32148(R) (UCRL-11317(p.79-130))
research programs in, summaries of USAEC, 19: 8713 (TID-4005(Pt.1, 8th Ed.))
research programs on, in Denmark, 19: 12868(R) (NP-14628)
research programs on, at Karlsruhe Nuclear Research Centre, 19: 17442
research programs on, 19: 30647(R) (HW-84573)
research programs at BNL, 1964, 19: 38077(R) (BNL-900)
research programs at Battelle-Northwest, 20: 744(R) (BNWL-120)
research programs on, at Risö nuclear research center, Denmark, 20: 3646
research programs at Ames Laboratory, July 1964–June 1965, 20: 5213(R) (IS-1200)
research programs at ORNL on, 20: 4300(R) (ORNL-3870)
research programs on, 20: 9375(R) (BNWL-166)
research programs in, summaries of USAEC, 20: 13182 (TID-4005(Pt.1, 9th Ed.))
research programs on, for production of pure metals, 20: 20365
research programs on, at University of Illinois, 20: 23583(R) (COO-1198-358)
research programs at Chalk River on, 20: 45234 (AECL-2460)
research progress under U. S. Army auspices, 1961, 16: 20043(R) (NP-11537)
research progress at Argonne National Lab., October to December 1961, 16: 20296(R) (ANL-6477)
research progress at Ames Laboratory, 16: 24108 (IS-351)
research progress at Hanford, Oct. to Dec. 1962, 17: 16741(R) (HW-76228)
research progress during Jan. 1963 at Nuclear Materials, Inc., 17: 18760 (NMI-2114)
research progress on, 1963 AEC, 18: 11550
review of electron-beam welding techniques, 17: 29296 (PB-181458)
review of flat rolling theory, 18: 3403 (LADC-5694)
review of metal physics relations with modern technology, 16: 27567(T) (JPRS-13977)
review of metallic reactor fuel, 18: 34130 (TID-8540(p.331-410))
review of progress in sintering, 17: 11090 (IS-460)
role of arc-plasma in, 19: 916
role of surface tension in, conference on, 17: 41472(T)
rupture of metals resulting from interaction of dislocations, 17: 18779(T) (TRG-Inf-Ser-6)
solvent extraction systems in, inorganic chemistry of, 18: 3905
stacking fault energy, ordering, and stress corrosion in austenitic alloys, 17: 36206 (UCRL-10712)
surface phenomena in melts, 18: 32078
survey of hot-forming methods, 19: 6279
temperature distribution in a rod during contactless zone recrystallization, 17: 29299(T) (AEC-tr-5884)
theory of heat-resisting alloys, 17: 8867(T)
thermal protection of materials for hypersonic and space flight, use of mass transfer cooling for, 16: 3477 (WADD-TR-59-366(Pt.III))
translation of selected Russian articles on casting, production, and refining of high-temperature alloys, 18: 22462(T) (JPRS-22336)
translations of Russian studies on, 19: 44614 (JPRS-24761)
use of electron beam techniques in, bibliography on, 20: 25476 (CEA-Bib-43)
use of mass action law in, for determining equilibrium between liquid metals and slags, 16: 28928(T) (AEC-tr-5268)
use of radioautography in, 16: 6684 (ANL-6412)
use of ultrahigh vacuum systems in, design considerations, 18: 31744 (UCRL-7914)
uses of electron-bombardment furnaces in, 19: 39109
vacuum techniques in, 16: 20967
vacuum techniques for, review, 19: 16003 (UCRL-7562)
vacuum use of plasma electron beam in, 18: 41952

METALS

(See also specific metals.)
see also Alkali Metals
see also Alkaline Earth Metals
see also Alloys
see also Building Materials
see also Electromagnetic Pumps
see also Metal Powders
see also Platinum Metals
see also Porous Metals
see also Pumps (Liquid Metal)
see also Rare Earths
see also Reactor Materials
abstracts on technology of liquid, 16: 33373 (LM/TAB-20)
abundances in high-velocity A stars, ratio to hydrogen, 16: 16896
abundances in stars, two-color diagram for, (T), 20: 19347
acceleration of milligram mass, magnetic field compression techniques for, 20: 41084
acoustic wave absorption by, 17: 5118
acoustic wave propagation in, nuclear spin resonance in, 20: 45023
activity coefficients of dilute binary solutions of liquid, 17: 32633
adhesion to ceramics, theory for, 20: 27401(R) (AD-632362)
age-hardening of, theories and mechanisms of, 18: 24154(T) (RSIC-174)
amplitude-dependent internal friction of refractory, effects of temperature on, 17: 18744 (GA-3367)
analysis by activation methods, 19: 19796
analysis by mass spectroscopy, detectors and ion sources for, 16: 30352
analysis by spark-source mass spectrometry, 20: 31202
analysis by spectroscopy of x rays produced by beta particles, 17: 5982(T) (CEA-tr-X-461)
analysis for boron, carbon, nitrogen, and oxygen, activation, 17: 39003
analysis for boron, fluorine, nitrogen, and oxygen, activation, 20: 38840
analysis for carbon traces, improvement of combustion-conductometric method for, 19: 293 (NASA-TN-D-2153)
analysis for carbon, nitrogen, and oxygen by helium-3 activation, 19: 46174 (LA-DC-7319)
analysis for cerium sulfide inclusions, 19: 26275
analysis for elements using 2-Mev charged particles, 20: 43097
analysis for gases, vacuum fusion, 18: 33491
analysis for gases, emission spectrographic, 19: 13233
analysis for gases, equipment and methods for spectral-isotopic, 20: 1793
analysis for hydrogen by micro-platinum bath vacuum fusion method, 17: 5967 (PG-Report-381)
analysis for hydrogen, nitrogen, and oxygen by manometric techniques using inert-gas fusion, 17: 30466 (CONF-14-13)
analysis for hydrogen and oxygen, spectrographic, 18: 8289(T) (AEC-tr-6266)
analysis for hydrogen, gravimetric, 18: 33538
analysis for hydrogen, nitrogen, and oxygen, methods for, 20: 3863(R) (IS-1200(Sect. C))
analysis for hydrogen and oxygen, equipment and method for activation, 20: 20602
analysis for impurities, activation methods for, 16: 3325(T) (AEC-tr-4497(p.169-78))
analysis for impurities, activation, 17: 33853
analysis for interstitial impurities, 18: 1489(R) (IS-700(Sect.C))
analysis for nitrides and oxides by high-temperature fluorination, 16: 23638 (TID-7629(p.295-307))
analysis for nitrogen, design of modified Kjeldahl apparatus for, 16: 8682 (TID-11411)
analysis for nitrogen by micro-platinum bath vacuum fusion method, 17: 5967 (PG-Report-381)
analysis for nitrogen and oxygen by carrier-gas fusion extraction, 20: 40796(R) (IS-1500(Sect.C))
analysis for oxide in liquid, apparatus for, 17: 16409(P)
analysis for oxygen, fast-neutron activation, 16: 26914
analysis for oxygen, bibliography on, 17: 1378 (CEA-Bib-23)
analysis for oxygen by micro-platinum bath vacuum fusion method, 17: 5967 (PG-Report-381)
analysis for oxygen by neutron activation, 17: 30116
analysis for oxygen, comparison of neutron-activation and vacuum-fusion, 18: 15951(R) (GA-4855)
analysis for oxygen, activation, 18: 19886
analysis for oxygen, mass spectrographic, 19: 5781
analysis for oxygen, spectral-isotopic, 19: 9065(T) (FTD-MT-64-64 (p.69-74))
analysis for oxygen by emission spectrometry, development of master analytical curve for, 19: 15397
analysis for oxygen by radioactivation, 19: 17826
analysis for oxygen by activation methods, elimination of container effects in, 19: 22115
analysis for oxygen by neutron activation, apparatus for, 19: 26249
analysis for oxygen, activation, 19: 43928 (EUR-2290.f)
analysis for oxygen, comparison of activation and vacuum fusion methods for, 20: 8831 (NP-15634)
analysis for oxygen by neutron activation methods, 20: 26765
analysis for rare earths, thorium, and uranium by ion exchange, review on, 20: 3888 (TID-22402)
analysis for surface oxygen by neutron activation methods, 19: 24410
analysis for tantalum and tungsten by neutron activation, 20: 3863(R) (IS-1200(Sect. C))
analysis for trace elements, spectrographic, 17: 2929
analysis for trace elements in, activation, 17: 35663
analysis for trace carbon, fluorine, and oxygen, activation, 19: 5817
analysis for trace elements by mass spectrometry using isotope dilution, 19: 15405
analysis for uranium, extraction-spectrophotometric, 20: 43067(R) (IDO-14679, pp 6-46)
analysis for uranium, extraction-spectrophotometric, 20: 43071 (IDO-14679, pp 75-191)
analysis of, for heat of combustion and oxide composition in burning, methods for, 17: 15933
analysis of, for impurities, ignition techniques for, 17: 15933
analysis of liquid, for impurities using resistivity meter, 17: 6382 (APDA-149)
analysis of liquid, for oxygen, 17: 27731 (NASA-TM-X-884)
analysis of liquid, for oxide particles, apparatus for, 20: 45619(P)
analysis of perturbations in, 16: 12219(R) (NP-11304)
analysis of pure, review of spectrochemical, 16: 9940 (BM-IC-8039)
analysis of surfaces of, for contaminants by rinse method, 19: 5775 (RFP-419)
analysis of surfaces of, for carbon, nitrogen, and oxygen, deuteron-activation, 20: 33238
analysis of, by beta backscattering methods, 20: 29110
analysis of, using charged-particle inelastic scattering at high energy, 20: 36732
analysis, use of radioisotopes in development and evaluation of methods for, 16: 3334(T) (AEC-tr-4497(p.243-50))
analysis using electron microprobes, 18: 22429(T) (TRG-Inf-Ser-382)
annealing after heavy-particle bombardment, liquid nitrogen cryostat for temperature control in, 18: 9278
annealing effects on bubble coalescence and diffusion in, containing radioinduced gases, 18: 42130
annealing model for quenched, 18: 33180 (COO-1198-178)
annealing of point defects in, theory of, 17: 1922 (BNL-6322)
anode polarization curves, method for obtaining, 16: 8727(T) (AEC-tr-5005)
atom reactions with, 17: 41534(R) (ANL-6720(p.77-89))
atomic potentials and separations in, 18: 42071
atomic structure, 17: 10664
atomic structure and properties of liquid, review of, 20: 29755
atomic structure of, use of field-ion microscopy in determining, 17: 30922 (SC-4920(M)(p.77-9))
atomic vibrations and melting process in, calculation of, 18: 25990
atomic volume, density, and thermal expansion of liquid, gamma absorption measurements of, 20: 27559
availability of high-purity, American, 18: 2164 (ISC-1029(Rev.))
band structure of hexagonal close-packed, 16: 27673
band structure, study by cyclotron resonance methods, 16: 15444
bibliography, 16: 6721 (NP-11206)
bibliography, 16: 12106 (NP-11374)
bibliography, 17: 6518 (NP-12288)
bibliography, 17: 11100 (NP-12493)
bibliography, Defense Metals Information Center selected accessions, 16: 5717 (NP-11166)
bibliography of DMIC selected accessions on, 18: 550 (NP-13276)
bibliography of DMIC selected accessions on, 18: 12537 (AD-426732)
bibliography of DMIC selected accessions on, 18: 18278 (AD-433095)
bibliography of selected accessions at Defense Metals Information Center, 18: 4169 (NP-13393)
bibliography on, 16: 27559 (NP-11963)
bibliography on, 16: 27560 (NP-11964)
bibliography on, 17: 36201 (NP-13043)
bibliography on boiling technology, 16: 25522 (ASD-TR-61-594)
bibliography on composites, 17: 32482 (AD-408618)
bibliography on defense, 17: 16523 (NP-12632)
bibliography on defense, 17: 30915 (NP-12974)
bibliography on dispersion-strengthened, 19: 6260 (RISO-48(Suppl.1))
bibliography on DMIC selected accessions, 17: 39464 (NP-13122)
bibliography on high-strength and light, 16: 18037 (NP-11502)
bibliography on high-purity, 20: 39328 (AD-624997)
bibliography on information resources, 16: 15141
bibliography on light and refractory, 16: 2187 (NP-10973)
bibliography on light and refractory, 16: 24111 (NP-11825)
bibliography on light and refractory, 16: 30721 (NP-12081)
bibliography on light and refractory, 17: 23869 (NP-12789)

bibliography on liquid, 17: 34326 (LM/TAB-22)
bibliography on liquid, 18: 20444 (AD-417111)
bibliography on liquid, 20: 27415 (TRG-Inf.Ser.-312)
bibliography on properties at high temperatures, 19: 30741 (NP-15045)
bibliography on refractory, 16: 16727 (NP-11553)
bibliography on refractory, 18: 32076
bibliography on technology of liquid, 16: 10532 (LM/TAB-19)
bibliography on technology of liquid, Sept. 1962 to Feb. 1963, 17: 16519 (LM-TAB-21)
bibliography on technology of liquid, 18: 2172 (TID-3544(Rev.1))
bibliography on technology of liquid, 19: 929 (NP-14434)
binding energy and mechanisms of, theory of, 19: 34188
boiling and condensation of liquid, 17: 3426(R) (NP-12189)
boiling and condensation of liquid, 18: 20174 (TID-7694(p.37-41))
boiling and entrainment, mechanisms of, 17: 14116(R) (ANL-6596 (p.29-118))
boiling and entrainment of, mechanism of, 19: 15662(R) (ANL-6900(p.45-142))
boiling and entrainment mechanisms of, 20: 5594(R) (ANL-6925, pp 21-(ANL-6925, pp 21-106)
boiling and entrainment of, mechanisms of, 20: 20802(R) (ANL-7055, pp 21-98)
boiling heat transfer, pool, 16: 27189(R) (AD-270678)
boiling heat transfer of liquid, research program on, 19: 9321(R) (AD-606826)
boiling heat transfer studies on liquid, 19: 24673 (NP-14953)
boiling heat transfer in high-acceleration fields, research program on, 19: 40741(R) (SAN-409-23)
boiling heat transfer by liquid, 20: 18870(R) (SAN-409-28)
boiling mechanisms in liquid, 17: 1359(R) (ANL-6569)
boiling of liquid, review of superheat requirements in, 19: 4315 (ORNL-3605(Vol.1)(p.310-33))
boiling of liquid, heat exchange models for, 19: 32393
boiling of liquid, under forced convection, 20: 16608(T) (ANL-Trans-257)
boiling phenomena in forced- and natural-circulation loops, 17: 37335 (ORNL-TM-618)
boiling 2-propanol and water on surfaces of, nucleate, 16: 20618
boiling, analysis of liquid superheat for nucleate, 19: 13576 (ANL-6980)
Boltzmann equation for, in inhomogeneous electric fields, 17: 25971
bombardment by gaseous ions, color production in, 17: 24061 (UCRL-9845(Rev.))
bond formation in, 19: 5848
bond mechanisms of, in relation to structure, 17: 6686 (UCRL-10012)
bonding dissimilar, co-extrusion, 18: 25953
bonding refractory, by diffusion methods, 17: 37487(R) (AD-295919)
bonding to ceramics using copper–silver–titanium braze wire, 16: 501 (SCTM-215-61(11))
bonding to ceramic materials, development of techniques and theories for, 16: 2198(R) (RADC-TR-60-236)
bonding to ceramic materials, 18: 41928(R) (NASA-CR-54089)
bonding to ceramics, methods for, 19: 24916(R) (GEMP-334A)
bonding to ceramics, development of metalizing paint for, 20: 27401(R) (AD-632362)
bonding to glass, 19: 43997(R) (UCRL-11889)
bonding to glass, theory of, 17: 41362 (UCRL-10611)
bonding to graphite, performance of gold–molybdenum–nickel alloy for, 20: 31683(R) (ORNL-3936, pp 95-121)
bonding to polymers, use of radiation in, 18: 39778(P)
bonding to porcelain, effects of pretreatment and surface roughness on, 18: 16457(T) (AI-Trans-41)
bonding, gas-pressure, 17: 3379(R) (BMI-1596(Del.))
bonding, methods for cold, 16: 5681(R) (BMI-X-185)
book: *An Atlas of Models of Crystal Surfaces*, 19: 41072
book: *Aspects of the Theory of Heat Resistance of Metals and Alloys*, 17: 549(T) (OTS-60-51083)
book: *Atomic and Ionic Impact Phenomena on Metal Surfaces*, 19: 35601
book: *Atomic Migration in Crystals*, 19: 18718
book: *Coatings of High-Temperature Materials*, 20: 33809
book: *Constitution Diagrams of Metal Systems*, Vol. VI, 18: 24180
book: *Constitution Diagrams of Metal Systems*, Vol. VII, 18: 24181
book: *Corrosion and Protection of Metal Construction Materials*, 16: 24129
book: *Corrosion of Metals and Alloys*, 18: 16446
book: *Corrosion Resistance of Metals and Alloys, Second Edition*, 18: 22451
book: *Corrosion. Vol. I. Corrosion of Metals and Alloys*, 19: 7868
book: *Corrosion. Vol. II. Corrosion Control*, 19: 7869
book: *Data Book on Physical Properties of Materials*, 20: 41442 (CNLM-2393)
book: *Defects and Failures in Pressure Vessels and Piping*, 20: 7506
book: *Effect of Radiation on Metals and Other High-Melting Materials*, 18: 20601
book: *Effects of Radiation on Materials and Components*, 18: 37783
book: *Electron Radiation Damage in Semiconductors and Metals*, 20: 41508
book: *Elevated-Temperature Testing of Metals*, 20: 7245(T)
book: *Energetics in Metallurgical Phenomena*. Vol. I, 19: 41075
book: *Fundamental Phenomena in the Material Sciences*. Vol. I, 19: 37147
book: *High-Temperature Oxidation of Metals and Alloys*, in Russian, 19: 13930
book: *Intercrystalline Corrosion and Corrosion of Metals Under Stress*, 16: 13539(T)
book: *Investigation of Liquid and Solid-State Metals*, 19: 34732
book: *Irradiation Effects in Cladding and Structural Materials*, 19: 41107
book: *Liquid Metal in An Electromagnetic Field*, 18: 42166(T) (JPRS-26459)
book: *Liquid Metals*, 18: 10247
book: *Materials of Reactor Construction with Special Consideration of Metals*, in German, 16: 33385
book: *Mechanical Behavior of Materials at Elevated Temperatures*, 16: 2260
book: *Metal Failure*, Chapter V, 16: 10548(T) (FTD-TT-61-285)
book: *Metals Handbook. Vol. 1. Properties and Selection of Metals*, 17: 585
book: *Metals Reference Book.*, Vol. I and II., 3rd edition, 18: 32080
book: *Mineralogy and Geochemistry of Rare Elements in Cherry Mountains (Urals)*, in Russian, 19: 20190
book: *New Physical and Chemical Properties of Metals of Very High Purity*, 19: 36968
book: *New Types of Metal Powders*, 19: 30814
book: *Optical Properties and Electronic Structure of Metals and Alloys*, 20: 39339
book: *Phase Transformations in Metals and Alloys*, in Russian, 20: 33933
book: *Physical and Process Metallurgy and Physicochemical Research Methods*, 17: 8866(T)
book: *Plasticity and Creep of Metals*, 16: 562
book: *Point Defects in Metals*, 18: 20568
book: *Preferred Orientation in Wrought and Annealed Metals*, 20: 15099
book: *Problems in Metal Physics and Metallography*, 17: 16540
book: *Problems in Metal Physics and Metallography*, 18: 16432
book: *Processes of Creep and Fatigue in Metals*, 17: 31013
book: *Purer Metals. Lectures Delivered at the Institution of Metallurgists Refresher Course, 1961*, 18: 8740
book: *Radioactive Metal Mobilization in Medicine*, 18: 21758(T)
book: *Rare Elements and Rare Earths in Technology*, 20: 4451
book: *Rare Metal Extraction by Chemical Engineering Techniques*, 18: 13952
book: *Rare Metals*. Vol. I. *Beryllium, Boron, Cesium, Gallium, Germanium, and Hafnium*, in German, 18: 25905
book: *Rare Metals*. Vol. III, in German, 18: 35950
book: *Rare Metals*. Vol. II. In German, 18: 35949
book: *Reactor Materials. Part I. Metallic Materials*, in German, 19: 13907
book: *Selected Values of Thermodynamic Properties of Metals and Alloys*, 18: 32205
book: *Separation of Heavy Metals*, 16: 8822
book: *Solid State Physics*, Vol. 16, 19: 14065
book: *Spectral Analysis of Pure Metals and Alloys*, 17: 1413
book: *Strength and Structure of Engineering Materials*, 20: 33932
book: *Superconductivity of Metals and Alloys*, 20: 19773(T)
book: *Surface Phenomena in Metals and Alloys*, 16: 29434
book: *The Influence of Temperature on the Mechanical Properties of Metals and Alloys*, 17: 16725
book: *Thermal Radiative Properties*, 19: 41074
book: *Toughness and Brittleness in Metals*, 16: 19413
book: *Wave Mechanics of Crystalline Solids*, 16: 15350
book: *X-Ray Diffraction Analysis of Raw Materials*, 20: 36386
borides of, method for production of, 19: 30664(P)
boron distribution in, determination by neutron activation, 16: 7890 (NP-11196(p.34-41))
brazing alloy and method for, 19: 10714(P)
brazing and soldering, 17: 4917(T)
brazing in vacuum, 16: 27572
brazing of graphite to, feasibility of, 17: 32547
brazing of reactive, torch for, 16: 16492(P)
brazing to alumina and sapphires, 20: 24490(R) (AD-624927)
brazing to ceramics, 18: 44499(R) (MND-2812-4)
brazing to graphite, alloy for, 17: 12653(P)
brazing to graphite, 19: 34629(R) (ORNL-3812(p.63-86))
brittle failure in, uncertainty in Robertson test for, 19: 42627 (EURAEC-1406)
brittle fracture in body-centered cubic, relation with twinning, 17: 39530 (EURAEC-650)
bromine-82 localization in aqueous solutions of, beta/gamma ratio

measurements for determining, 20: 39336
bubble growth in superheated liquid, kinetics of, 20: 33459 (ORNL-TM-1413)
bulk modulus of 33 pure, effects of temperature, 16: 22640
carburization, 19: 24975(P)
casting equipment and process for, 19: 26800(P)
casting of reactive, crucibleless vacuum technique for, 18: 580 (UCRL-7388)
casting radioactive or toxic, equipment for, 19: 37022(P)
casting radioactive and toxic, 18: 22467
cavitation damage in refractory materials by liquid, 17: 39489(R) (NP-13116)
cavitation damage in liquid sodium, 20: 2243
cavitation damage in liquid, at high temperatures, 20: 33835
cesium ionization on surfaces of porous refractory, 20: 31776
charged particle energy losses in, 18: 10765 (CONF-381-2)
charged-particle reactions with, transition radiation from relativistic, (E/T), 20: 13788(T) (ORNL-tr-1062)
charged-particle stopping powers in, low-temperature method for measuring, 19: 35565 (RISO-93)
chemical activities of components in liquid, by electromotive-force measurements in oxygen-concentration cells, 17: 22213
chemical properties of metal-salt systems at high temperatures, 17: 4249(R) (NAA-SR-7400(Sect.VII))
chemical reactions with borides, carbides, nitrides, and oxides, review on high-temperature, 20: 39331(T) (UCRL-Trans-10044)
chemical reactions of molten, with refractory materials, 20: 39429
chemisorption of gases by, 18: 25033(T) (SC-T-64-901)
cleaning and coating cylindrical, apparatus for electrolytic, 17: 41374(P)
cleaning of surfaces of nuclear, comparison of solvents for, 19: 6008 (RFP-469)
cleanness of degreased, tracer techniques for evaluation, 16: 13436(T) (AEC-tr-4492(p.123-6))
coating for, fabrication of vitreous insulating, 20: 15131(P)
coating for, preparation of refractory, 20: 14974(P)
coating of, equipment for electrolytic, 18: 41491(P)
coating with beryllide by electrolysis in fused bath, 16: 18008(P)
coating with beryllides by electrolytic deposition, 19: 34668(P)
coating with boride by electrolysis in fused bath, 16: 18009(P)
coating with boron by electrolysis, 16: 7623(P)
coating with ceramic materials, review of methods for, 20: 27460
coating with refractory materials, use of arc plasma in, 19: 18406
coating with refractory metals by electroplating methods, 19: 42827
coating with silicide by electrolysis in fused bath, 16: 18010(P)
coating with silicides, 19: 11711
coating with titanium esters and polymers, 17: 3436(P)
coating with uranium oxide by electrolytic deposition in sodium fluoride, 18: 23557
coating with uranium oxide by electrolysis, effects of electrolyte on, 20: 18691
coating with zirconium carbide by electrophoresis at 19 to 20 mv, 20: 17004
coating with zirconium, sheath, 19: 24973(P)
combustion in fluorine, assessment of methods for, 19: 15408(R) (ANL-6900(p.221-31))
combustion of, 17: 8800 (CAL-86-P)
combustion of, temperature of flame during, 19: 38583(R) (SC-DC-65-1480)
compaction by gas pressures, method for isostatic, 19: 941
compatibility with graphite, review of, 17: 3413
compatibility with cesium to 1400°C, 17: 24029(R) (AD-286324)
compatibility with cesium vapor at 500, 800, and 1200°F, 17: 36227 (NASA-TN-D-1739)
compatibility with liquid and gaseous cesium at temperatures up to 1000°C, 17: 39488 (LAMS-2948)
compatibility with ceramics for use in reactors, 20: 26875
compressibility at high pressures, 17: 3494 (UCRL-6696-T)
condensation at high temperatures, 16: 16685 (TID-7626(Pt.I)(p.111-14))
condensation of liquid, velocity distribution of vapor flow in, 18: 39451
condensation of liquid, in tubes, 19: 28502 (PWA-2530)
condensation of vapors of, review of theory of, 19: 18107 (ANL-6948)
condensation of vapors of liquid, heat transfer during film, 19: 32362 (CONF-640507(p.153-71))
condensation to liquid, electromagnetic rate control of, 20: 29974(R) (ANL-7190, pp 167-75)
conduction electron coupling to acoustic waves in, effects of presence of longitudinal magnetic field on, 17: 36487
conduction electron density-to-mass ratio in, tables of effective, 17: 37659(R) (TID-19325)
conductivity electron scattering by impurity centers in, mechanisms of momentum transfer in, 18: 24167
conference on application of high pressure in metal-deformation processing, Bureau of Naval Weapons, BMI, Columbus, Ohio, Oct. 3, 1963, 18: 24099 (DMIC-199)
conference on corrosion of, New York, March 11–15, 1963, 20: 21276
conference on electronic and atomic structure of metallic solid solutions, 19: 16185
conference on high-temperature heat transfer of liquid, 19: 4310 (ORNL-3605(Vol.1))
conference on high-temperature heat transfer of liquid, 19: 4318 (ORNL-3605(Vol.2))
conference on high-strength, 20: 817 (CONF-710)
conference on lattice defects in quenched, ANL, Argonne, Illinois, June 15 to 17, 1964, 19: 37148
conference on liquid–metal heat-transfer technology, BNL, Upton, New York, May 17 and 18, 1962, 17: 20148 (BNL-756)
conference on materials in space technology, London, Nov. 22, 1961, 18: 44081
conference on rare metals, 16: 3513
consolidation and fabrication of refractory sheet, panel discussion on, 16: 7863 (MAB-179-M)
containment of boiling, properties of tantalum for, 19: 21690(R) (LA-3244)
contamination of, radioactive process for detection of, 20: 9215(P)
content in brain, effects of Huntington's chores on, 18: 29235
content in meteorites, 20: 42064
content in stellar G dwarfs, ratio to hydrogen, 17: 24199
control and testing, gamma spectroscopic, 18: 25676
convection (free) heat transfer in laminar boundary-layer flow, magnetic field effects on, 16: 7667
correlation between the electron gas bulk modulus and the shear elastic constants of monovalent, 16: 29427
corrosion and oxidation at high temperatures, conference, Norway, May 1960, 16: 4494 (NP-11056)
corrosion and oxidation of, development of impedance methods for measuring, 17: 22115(T,R) (EURAEC-559(Pt.2))
corrosion and oxidation, review of Euratom/US studies of, 19: 931 (TID-21221(p.87-109))
corrosion and protection of, book on, 19: 34649
corrosion and wear of, engineering drawings of system using tracer techniques for determining, 17: 32380
corrosion by alkali metals at high temperatures, review, 16: 25714 (DMIC-169)
corrosion by aqueous solutions, kinetics, 16: 4498 (NP-11056(p.41-62))
corrosion by aqueous media, review, 17: 3431
corrosion by barium vapor, 18: 44497(R) (MND-2812-2)
corrosion by bismuth and tin at 700 to 1000°C, 20: 46963(R) (ANL-7132)
corrosion by fused salts, 16: 5312(R) (TID-14370)
corrosion by gases, volumetric apparatus for determining kinetics of, 18: 35953 (BM-RI-6359)
corrosion by gases, classification of phenomena in, 19: 20486
corrosion by high-temperature gases, electrical process for protection against, 18: 24092(P)
corrosion by humid air, measurement, 16: 12054(T) (AEC-tr-5009)
corrosion by liquid metals, mechanisms, 16: 22155
corrosion by liquid alkali metals, mechanisms of, 17: 36228 (ORNL-3424)
corrosion by liquid metals, effects of polarization on, 18: 21698(R) (ANL-6860)
corrosion by liquid metals, surface energy phenomena in, 18: 27899 (NASA-SP-41(p.109-25))
corrosion by metals (liquid), thermoelectric potential effect on, 17: 3421 (BNL-5574)
corrosion by organic vapors in restricted spaces, 16: 4506
corrosion by potassium at 1500 to 2200°F, development of apparatus and techniques for studying, 16: 27586 (AI-Memo-6416)
corrosion by pure or contaminated humid air, 16: 9157(T) (AEC-tr-5008)
corrosion by pure water, research programs on, 19: 37008
corrosion by sodium, effects of carbon on, 20: 20802(R) (ANL-7055, pp 21-98)
corrosion cracking in, mechanisms of transgranular stress-, 20: 779
corrosion cracking of, circulating autoclave for studies of stress, 20: 33814 (COO-1319-40)
corrosion in radiation environment, effects of radioinduced oxidation and reduction products on, 17: 30940
corrosion of amphoteric, cathodic protection from, 17: 14772 (TID-17913)
corrosion of, bibliography on, 17: 4904 (LAMS-2779)
corrosion of, by uranium(VI) fluoride, 17: 20423
corrosion of, coating with epoxy resin for protection against, 17: 3088 (UCRL-9828)
corrosion of electrolytic-cell, by sodium hydroxide, 19: 28420(R) (NP-14825)
corrosion of, review of present state of knowledge on, 17: 20421
corrosion of stressed, effects of protective films, 16: 12053(T) (AEC-tr-5007)
corrosion of, used in nuclear reactors, 18: 2182(T) (CEA-tr-X-517)

corrosion of, bibliography on, 18: 22447 (SB-401(Suppl.1))
corrosion of, measurement of, by beta backscattering and x-ray induction methods, 20: 19196
corrosion of, methods of studying, 19: 32048(R) (NP-15073)
corrosion of, method for measuring intensity of, 20: 31682 (NP-16003)
corrosion rate measurement, electrochemical, 16: 22559
corrosion rates in flowing sodium, loop geometry effects on, 20: 2295
corrosion studies on, at National Chemical Laboratory, England, 17: 30932
corrosion test for liquid, 20: 41064(R) (IS-1500(Sect.E))
corrosion, unusual oxidation states in, 16: 32082 (TID-6408)
corrosive effects of liquid, thermoelectric potential effect on, 17: 3421 (BNL-5574)
corrosive effects of liquid, gravity reflux capsule for measuring, 17: 8748
corrosive effects of liquid, mechanisms of, 17: 19726 (BNL-759(p.54-77))
corrosive effects of liquid, in reactor coolant loops, 18: 22997
corrosive effects of liquid, conference on, 18: 27885 (NASA-SP-41)
corrosive effects of liquid, solubility aspects of, 18: 27886 (NASA-SP-41(p.21-6))
corrosive effects of liquid, chemical processes in, 18: 27887 (NASA-SP-41(p.27-33))
corrosive effects of liquid, diffusion-controlled processes in, 18: 27888 (NASA-SP-41(p.35-43))
corrosive effects of liquid, solution-controlled processes in, 18: 27889 (NASA-SP-41(p.45-7))
corrosive effects of liquid, heterometallic problems in, 18: 27893 (NASA-SP-41(p.73-4))
corrosive effects of vapors of, survey, 18: 27895 (NASA-SP-41(p.83-6))
corrosive effects of liquid, downstream effect in, 18: 28797 (NASA-SP-41 (p.91-5))
corrosive effects of liquid, mechanism of embrittlement in, 18: 27898 (NASA-SP-41(p.97-9))
corrosive effects of liquid, review of, 18: 32082 (A/CONF.28/P/244)
corrosive effects of liquid, on reactor materials, (E), 19: 33628
corrosive effects of liquid, on materials in Rankine cycle power plants, 19: 46955 (NP-15431)
corrosive effects of liquid, model for, 20: 33833
cratering and vaporization by hyper-velocity impact, 16: 22611
creep cavities, methods for metallographic examination of intergranular, 16: 25790
creep, construction and evaluation of dynamic creep test machine, 16: 8971 (AGN-3059)
creep-fatigue properties, review of combined, 16: 27668
creep in, equations for analysis of first-stage, 20: 7499(R) (GEMP-53A)
creep in, mathematical procedure for determining mechanisms of, 18: 25974 (EURAEC-1037)
creep properties at high temperatures, effects of hydrogen on, 18: 4254(R) (ORNL-3470(p.89-93))
creep properties of, effects of hydrogen on, 18: 44050(R) (ORNL-3670 (p.116-21))
creep property measurements on, mathematical system for extrapolation of, 20: 5880(R) (EURAEC-1310)
creep-rupture properties, 17: 39531(R) (EURAEC-689)
creep-rupture properties, 17: 39534(R) (EURAEC-791)
creep-rupture properties, 18: 14535(R) (EURAEC-878)
critical constants and temperature ranges of liquid, 16: 11632
crystal deformations in, analysis of double kink, (T), 19: 47011 (ORNL-3862)
crystal lattice defects in fcc, theoretical study of, 19: 44739(R) (ANL-7000, pp 233-77)
crystal lattice defects in, 17: 6669 (NP-12295)
crystal lattice distortions in, effects of, on x ray scattering, 19: 2803 19: 2803 (NYO-2994-2)
crystal lattice dynamics of, model for, (T), 19: 16128
crystal lattice dynamics of, axially symmetric model for, 17: 430
crystal lattice dynamics of, (T), 19: 14078
crystal lattice measurements on, methods for, 19: 4667
crystal lattice vibrations in, theory on, 18: 8919(R) (PR-P-59(p.65-78))
crystal lattice vibrations in, review of, 20: 34807 (BNL-940, pp 29-43)
crystal lattice vibrations in, review, (T), 20: 40344
crystal structure of, derivation of dispersion relation in, 16: 26644(R) (NP-11755)
crystal structure of, basic studies of, 16: 30170(R) (ORNL-3313(p.179-208))
crystal structure of fcc, relations with glissile and prismatic dislocations, 17: 540 (UCRL-10427)
crystal structure of, lattice vibration frequency distribution in, 17: 13143
crystal structure of intermetallic compounds, review, 17: 25822
crystal structure lattice constant determinations for, design of x-ray goniometer for, 18: 27765
crystal structure and Fermi surfaces of, 18: 36155(R) (TID-20873)
crystal structure of, theory of defects in, 19: 11763
crystal structure of, quenched-in lattice defects in, 19: 11764
crystal structure and magnetic properties of, neutron diffraction studies of, 19: 25029
crystal structure, 19: 46984(R) (AD-612275)
crystal structure of, effects of fabrication on, 20: 17158(R) (ORNL-3900, pp 82-149)
crystal structure of, analysis using inelastic scattering of thermal neutrons, 20: 20170
crystal structure of plastically deformed, research on, 20: 28607(R) (NYO-2471-21)
crystal structure and growth kinetics of undercooled, 20: 29623(R) (TID-22970, pp 121-256)
crystal structure of, electron irradiation experiments at low temperatures for determining, 20: 32319
crystal structure of transition, review of, 20: 34805 (BNL-940, pp 8-15)
crystallographic dislocations in, dynamics of, 18: 34122(R) (GA-4900)
current rectification processes at semiconductor contacts with, 20: 29569
cutting and J grooving of, efficiency of oxyacetylene blowpipe for gas, 20: 35860(R) (EURAEC-1651)
cutting of, electron-beam techniques in, 17: 30921 (SC-4920(M)(p.73-6))
cutting, tracer studies of deterioration of tools in, 16: 13433(T) (AEC-tr-4492(p.104-11))
cyclotron resonance of simple, Doppler-shifted, 18: 22571
cyclotron resonance in, 18: 40084
data processing on radiation effects on, 17: 3539 (HW-SA-2805)
decontamination and descaling of, development of solution for, 20: 21238 (NP-15928)
decontamination by ultrasonics, 18: 16250
decontamination in water using ultrasonics, 17: 29145
decontamination of, using ultrasonics, 17: 32304
decontamination of, electrolytic surface, 18: 32069
decontamination testing of highly contaminated, 16: 13179 (ORNL-2811)
decontamination using ultrasonics and cleaning solutions, 20: 43623
defects, effects of size and chemical interactions, 17: 16694
defects in fcc, method for studying point, 18: 30289
defects in, annealing observation, and production of point, 20: 39386 (CEA-R-2905)
defects in, gamma radiometric measurement of, 20: 4114(T) (AD-621784)
defects in, methods for studying point, 18: 30283
defects in, observation of, 18: 30281
defects in, research on point, 20: 19273(R) (BNL-929, pp 3-43)
defects in, study by electron microscopy, 20: 17158(R) (ORNL-3900, pp 82-149)
deficiency of heavy, in Population II halo stars, 18: 8983
deformation and rupture mechanisms of, determination by activation energies, 20: 41445(R) (EURAEC-1622)
deformation by shock loading, 18: 18338
deformation by shock waves in explosive forming, 18: 34208
deformation characteristics, 20: 46183(R) (AD-630427)
deformation during fabrication into tubes, study using radioactive inserts, 16: 16055
deformation during rolling, tracer study using phosphorus-32, 16: 33462
deformation during hot working, structural changes in plastic, 19: 14003(T) (ORNL-tr-461)
deformation energy measurement in, liquid-gas calorimeter for, 17: 27663
deformation in hexagonal compact, mechanisms of, 20: 21330 (EUR-2621.f)
deformation of bcc, energy of formation of double kink in dislocation in low-temperature, 18: 44145(R) (ORNL-3670(p.11-16))
deformation of bcc, electron microscopic studies of, 18: 44146(R) (ORNL-3670(p.17-20))
deformation of, calorimeter for measuring energy during, 20: 4384(R) (ORNL-3870, pp 7-14)
deformation of, effects of inclusions on plastic, 20: 15055(R) (NYO-2394-19)
deformation of, interface friction in hot, 19: 46981(R) (AD-611821)
deformation processing of, research program on, 18: 25952
deformation processing characteristics, review, 19: 13937 (DMIC-208 (Vol.I))
deformation resistance of strengthened, 16: 21069
deformation, response to high velocity, 16: 19277
deformation, role of point defects in plastic, 16: 25764 (TID-16222)
deformation twinning in fcc crystals of, review of, 18: 599 (CONF-276-1)
deformation twinning in, conference on, 19: 41076
deformation twins in, factors influencing shape of, 18: 31057 (UCRL-11451)
densities of, 16: 21041(R) (TID-15663)
density and energy of plasma of, produced between damped h-f accelerators, (E), 20: 28515
density measurements of liquid, development of apparatus for, 16: 22594(R) (TID-15836)

density measurement at high temperature, activation method for, 20: 25481
density of liquid, temperature dependence of, review, 18: 14511
deposition by electroplating for radiation targets, 20: 25516 (AERE-R-5097, Paper 13)
deposition by flame spraying, 18: 20134(R) (ORNL-TM-792)
deposition by levitation evaporation in vacuum, system for, 19: 16007
deposition from metal halide vapor dissociation, 16: 24178(R) (WAL-TR-766-3/1-3)
deposition of vaporous, on carbon microspheres, 20: 35880(P)
deposition of, for buildup to desired shapes, 19: 6286
deposition on electrodes in fused salts, mechanisms of, 19: 30067(R) (ORNL-3789(p.56-98))
deposition on solid electrodes by voltammetry, 20: 14453(R) (ORNL-3889, pp 12-14)
deposition on textiles by spraying, 19: 28608(P)
design of level indicators for molten, 20: 41233(R) (ORNL-3875, pp 101-24)
deterioration by friction, material transfer in, 16: 13420(T) (AEC-tr-4492(p.35-6))
determination by activation, method for avoiding correction for chemical yield in, 20: 5494 (AEET-217)
determination in liquid, plans for ultrasonic, 20: 20802(R) (ANL-7055, pp 21-98)
determination in methanol–mineral acid media using azo dyes, spectrophotometric, 20: 14469(R) (TID-22650)
determination in ores, beta radiation method for, 17: 27283
determination in ores by rapid radiometric methods, 19: 5793
determination in reactor waters, trace polarographic, 19: 11030
determination in uranium, heavy water, and water using atomic absorption spectroscopy, 19: 46166 (DP-980)
determination of rare, book, 19: 22151
determination of traces of, by neutron activation followed by ion-exchange and solvent-extraction processes, 18: 13652
determination of traces of, activation or isotope dilution, 18: 19852 (UJV-992/63)
determination of trace amounts of, in isolated cell nuclei, 18: 41051
determination of trace amounts of, x-ray-fluorescence, 20: 8846
determination of, in tissue samples, by activation analysis, 18: 43184(R) (MIT-952-1(p.150-62))
determination trace amounts in cells, electron microscopic, 20: 16160 (UCRL-14739(Pt.2))
development and properties of liquid, for use as working fluid in aerospace systems, 16: 10410 (ASD-TR-61-322(p.339-55))
development as thermal coatings in space uses, 18: 43114(R) (NP-14236)
development at Hanford, Jan. to March 1962, 16: 32539(R) (HW-73915)
development for energy-conversion systems, survey, 16: 10422 (ASD-TR-61-322(p.615-35))
development for space applications, 16: 6244 (NP-11177)
development of dispersed phase systems of, for nuclear applications, 17: 1854
development of ductile high-strength, review, 18: 44158 (UCRL-11588)
development of ferrous and non-ferrous, for nuclear technological uses, 17: 4973
development of fibrous structures from, for use to 2000°F, 16: 10426 (ASD-TR-61-322(p.711-37))
development of high-strength, for naval structures, 19: 20462(R) (NRL-6258)
development of ultrahigh-strength, by nucleation of precipitates, 17: 35264(R) (UCRL-10706(p.111-203))
developments in extraction of, at National Chemical Laboratory, England, 17: 30932
developments in high-temperature, 16: 27641(T) (FTD-TT-62-503)
developments in research on, bibliography on, 20: 14506 (CRDL-SP-5-7)
diamagnetic shielding of nuclei by conduction electrons, 16: 21215
diamagnetic shielding of nuclei in, 17: 681
dielectric penetrability, plasmic theory, 16: 9331
diffusion activation energies for materials in refractory, 18: 2179(R) (GEMP-28A)
diffusion activation energies for, thermal expansion coefficient dependence of self-, 19: 43476
diffusion and coalescence of bubbles in, theory of, 20: 15132 (ANL-7079)
diffusion and precipitation of rare gases in, 16: 30852
diffusion and production of rare gases in, 16: 7890 (NP-11196(p.34-41))
diffusion and solubility of gases in, bibliography on, 19: 2730 (SC-R-1322)
diffusion by exchange reactions, 16: 15128(T) (AEC-tr-4506)
diffusion coefficients of liquid, 20: 41064(R) (IS-1500(Sect.E))
diffusion in bcc, 18: 44151(R) (ORNL-3670(p.129-31))
diffusion in bcc and fcc, self-, 20: 21230 (AEET-233)
diffusion in bcc, theory for interstitial, 19: 31457
diffusion in fcc, surface, 19: 6302 (NYO-2994-3)
diffusion in high-melting powder compacts of, by low-melting liquid metals, 20: 43822
diffusion in liquid, theory, 18: 30109 (CONF-524-9)
diffusion in, measurement by absorption of alpha-recoil radiation, 17: 33942
diffusion in pure, bibliography on tracer self-, 19: 28812 (ORNL-3795)
diffusion in pyrolytic graphite, mechanism of, 20: 46202
diffusion in, analysis of surface and volume, 19: 6304 (NYO-2994-3(App.C))
diffusion in, bibliography on, 20: 35842 (ORNL-3795(Pts.1 and 2) (Suppl.))
diffusion in, book, 18: 20536(T) (AEC-tr-6313)
diffusion in, thermodynamic analysis of, 20: 23736
diffusion in, uses of thermodynamics of irreversible processes for analysis of solid-state, 20: 23737
diffusion of fission products in nonfuel, review on, 20: 27484 (GA-6542)
diffusion of gas bubbles in, effects of temperature gradient on, 19: 14031
diffusion of high-temperature, methods of predicting, 19: 23996(R) (ORNL-3650(p.1-110))
diffusion of hydrogen in, effects of oxidation, 16: 10516 (DC-60-3-35)
diffusion of hydrogen through, review, 19: 39165 (NAA-SR-10462)
diffusion of hydrogen in, mechanism of, 20: 1324(R) (EURAEC-1428)
diffusion of interstitials in bcc, 19: 23114
diffusion of ions in, tracer study, 16: 15049
diffusion of krypton-85 in, 18: 37566(R) (NYO-2757-3)
diffusion of liquid, 20: 31166(R) (UCRL-16658, pp 89-92)
diffusion of low-solubility materials in, 17: 30152
diffusion of solutes in, bibliography on, 20: 4383 (ORNL-3795(Pt.2))
diffusion of sulfur in high-melting, 19: 2812
diffusion of tracer solutes in, activation energies and frequency factors for, 20: 4383 (ORNL-3795(Pt.2))
diffusion of tritium in, research on, 20: 17892(R) (ORNL-3908, pp 149-53)
diffusion rates in, lattice energy effects on, 16: 13597
diffusion rates near free surfaces, 16: 16045
diffusion saturation of, seminar on, 17: 12694
diffusion of gases in, bibliography, 16: 14688 (NP-11440)
dimensional instability, review, 18: 34121 (DMIC-Memo-189)
disintegration by re-entry processes, 18: 33130(R) (SC-DC-64-1061)
dislocation anchoring during kink band formation in plastically deformed crystals of, 19: 9672(T) (ORNL-tr-385)
dislocation climb in, efficiency of, 20: 11274 (NYO-3504-2)
dislocation loops in quenched fcc, electron microscopic analysis, 19: 41026 (UCRL-16024)
dislocation mobility in fcc, below 1°K, (E), 19: 37114
dislocation motion in, size distribution of obstacles to, 20: 17980(T) (ANL-Trans-274)
dislocation movements in, formation and diffusion of kinks as process, 16: 29320(T) (AEC-tr-5107)
dislocation multiplication mechanisms in, 16: 33482 (UCRL-10200)
dislocation on {110} planes in bcc, dissociation of, 20: 33918
dislocation reactions and hardening in body-centered cubic, 20: 43923
dislocation velocities in single crystals of, machine for measuring, 18: 13375 (TID-20172)
dislocations in fcc and hcp, constriction energy of dissociated, 20: 31714(R) (UCRL-16658, pp 99-103)
dislocations in, origin and multiplication of, 17: 25785 (UCRL-10714)
dislocations in strained f.c.c., experimental verification of theories of, 17: 27842
dislocations with condensed impurity atmospheres, effects of temperature, 16: 15124 (NP-11462)
dispersion-strengthened, bibliography on, 17: 6677 (RISO-48)
dispersion-strengthened, bibliography on, 20: 11278 (RISO-48(Suppl.2))
dissolution by nitric acid, electrolytic, 16: 13138
dissolution in acids, valency of ions formed during anodic, 16: 3401
dissolution in molten salts, 17: 1420 (TID-14906)
dissolution of, methods for high-rate anodic, 20: 31220(R) (UCRL-16658, pp 39-72)
distillation for vacuum deposition, 16: 10143(P)
distillation of liquid, bibliography on high-vacuum, 18: 32047 (IS-799)
distillation of liquid, surface concentration changes in, 20: 4077(R) (IS-1200(Sect. E))
distillation of liquid, flash, 20: 41064(R) (IS-1500(Sect.E))
distillation of, diffusion coefficients for, 19: 9281(R) (IS-900(Sect.E))
distillation of, tracer study of vacuum, 18: 16386 (TID-7688(p.40-3))
distribution and excretion of biologically important trace, effects of chelates on, 20: 14256
distribution between alkyl amines and nitric acid, 17: 18209
distribution of carbon and oxygen in, determination by helium-3 activation, 20: 2227
distributions of, in estuarine environment, 17: 7684(R) (NYO-8103)
ductile-brittle transition temperature, development of methods for determining, 16: 18029(R) (EURAEC-225)
ductility, 19: 25028
ductility of, theory of, 17: 39603

ductility of, effects of liquid metals on, 18: 14354(R) (ARF-B215-12)
effects as interstitial and substitutional solutes on tensile properties of molybdenum, niobium, tantalum, and tungsten, 18: 34203
effects of flowing, on fuel elements, 19: 44181(R) (APDA-174, pp 56-60)
effects of heavy, on radiation damage in polymers, 17: 32700(P)
effects of ions of, on protein synthesis systems, 20: 16160 (UCRL-14739(Pt.2))
effects of liquid, on reactor building materials, 20: 31682 (NP-16003)
effects of precious, on solubility and drip temperature of fission products in Purex process wastes, 20: 12517(R) (BNWL-170)
elastic constants of, superconducting transition effects on, (T), 19: 16772
elastic moduli at room temperature to 1800°F, graphs, 16: 12115 (WADD-TR-60-438)
elasticity of, methods of measuring modulus of, 17: 4934(T) (AEC-tr-5534)
electric conduction of metal-insulator sandwich, (E/T), 20: 2405
electric conductivity of, effects of lattice vacancies on, 17: 11231
electric conductivity of, effects of defect pairs on, 17: 16695
electric conductivity, effects of vacancy-impurity pairs on, 17: 27776 (BNL-6358)
electric conductivity and relaxation time of electron-phonon model of, frequency-dependent, 17: 34606
electric conductivity of liquid monovalent, theory, 17: 37522
electric conductivity of liquid, measurement with compensation for temperature changes, 17: 37476(P)
electric conductivity at low temperatures, 18: 9281
electric conductivity and Hall constant of liquid, in pseudopotential, 18: 22494 (TID-19959(Rev.))
electric conductivity of, electron-phonon interactions in, 18: 24557
electric conductivity theory, 18: 28757(R) (AFOSR-5119)
electric conductivity measurement in liquid, design of temperature-compensated inductive device for, 19: 2594(P)
electric conductivity and permeability of, engineering drawings of instrument for, 19: 11491
electric conductivity and thermoelectric power of liquid, (T), 19: 23052
electric conductivity and Meissner effect in weak magnetic fields, (T), 19: 37738
electric conductivity of thin films of, with unlike surfaces, 19: 45479 (TID-21301)
electric conductivity of high temperatures, (T), 20: 25577(T) (LA-tr-66-22)
electric conductivity of, many-body effects of electron scattering on, (T), 20: 36365
electric conductivity of, model for nonmagnetic impurity-containing, 20: 39395 (IAE-1028)
electric conductivities of liquid, effects of Z on, 20: 41476
electric contacts between normal and superconducting, joule heating in, 17: 12830
electric field gradient in, sign of conduction electron contribution to, 18: 14633
electric properties of, calculation from neutron scattering data, 18: 36028
electrical properties of polyvalent liquid, theory, 16: 29423
electrical properties of monovalent liquid, 16: 2240
electrochemical reactions of, isotope separation factors in hydrogen evolution by slow discharge from, 18: 29645
electroforming of, survey of, 19: 30697 (RSIC-210)
electrolysis of liquid, measuring methods and theory of, 18: 1607 (IP-603)
electromagnetic field interaction with electrons in, 17: 5458
electromagnetic wave diffraction by, oblique, 18: 14928
electromagnetic wave diffraction, 18: 14929
electromagnetic wave propagation in, in magnetic fields, 18: 28160
electromagnetic wave absorption in magnetic fields, relaxation in, 18: 28178
electromagnetic wave propagation in, at low temperature, (T), 19: 23875
electromagnetic wave propagation in, effect of Fermi fluid interactions on, (T), 19: 23981
electromagnetic wave propagation in, (T), 20: 15941 (NP-15698)
electromagnetic wave propagation in, (T), 20: 44993 (NYO-2150-19)
electromagnetic-wave scattering by velocity fluctuations in, (T), 20: 28523
electromagnetic, plasma, and spin wave interactions in antiferromagnetic, coupling of, 20: 43982
electron and hole diffusion in, energetic, 17: 9045
electron beam focusing in, by magnetic fields, (E), 19: 42939(T)
electron beam reactions with, plasma production from melting in, 18: 24798
electron beam reactions with, physical aspects of penetrations from, 20: 40347
electron bombardment of, theory of spectra from, 18: 18562
electron conduction dynamics in, lectures on, 17: 13195
electron density and momentum distribution calculations for, 17: 3374(R) (ARL-230)
electron distribution functions in anisotropic, Boltzmann equations, 16: 21211
electron distributions in, wave-field theory for, 16: 33643
electron distributions in normal and superconducting, 17: 22291(T) (NP-tr-1000)
electron emission from, by helium and hydrogen collisions, secondary, 17: 11397
electron emission from, secondary, 17: 22218(R) (GA-4164)
electron emission from, kinetics of ion induced, 17: 25985
electron emission by abraded surfaces of, decay of, 18: 11302 (NP-13526)
electron emission from surfaces of, in strong electromagnetic fields, (T), 19: 32813
electron emission from, in cesium-fluorine vapors, (T), 20: 17334
electron emission from alkali earth-surrounded, models for, (T), 20: 37431(R) (INDEC-SR-7, pp 3.76-111)
electron emission models for, with adsorbed monolayers, 20: 39641
electron emission from cathodes of, method for calculating, 20: 46321 (AWRE-O-50/66)
electron energy levels, 18: 44290(R) (ORNL-3670(p.54-5))
electron energy levels in, exchange-coupled to localized spin, 20: 32085
electron energy loss in, hot, 16: 19462(R) (AD-268422)
electron energy losses in normal, at impurities, (T), 19: 28925
electron enhancement around positive point charges in, 16: 21201
electron Fermi energy in, sample size dependence of free, 17: 24093
electron gas at high temperatures in, perturbative effects, 16: 21217
electron gas interactions in, one-particle properties of inhomogeneous, 20: 28651
electron indirect exchange in, thermodynamic theory of, 17: 37705
electron inelastic scattering by impurities in, 17: 4011
electron interactions in, correlation using density matrix, 16: 22741
electron interactions on surfaces of, 17: 25988
electron interaction in, collective theory for free, 20: 15987
electron interband tunneling in, Bloch, 18: 38001
electron interband transport in, quantum theory of, 20: 30735(R) (TID-22970, pp 331-73)
electron levels in, virtual bound, 18: 8805(T) (AI-Trans-64-1)
electron microscopic examination of bcc, absorption contrast effect in, 18: 12675
electron momentum distribution in, 16: 18137 (AD-264847)
electron pairs in, quasi-bound, 18: 44170
electron penetration from high-power-density beams, mechanisms of, 18: 28127
electron penetration, (E/T), 20: 7659(R) (ORNL-3849, pp 101-50)
electron-phonon interactions in, cyclotron resonance from, 17: 41637
electron–phonon interactions in, failure of quasiparticle picture of, 18: 2450
electron plasma oscillations in, random phase approximation for magnetization-density-wave, (T), 20: 24608
electron plasma resonances in, analysis using photon scattering, (T), 20: 1326 (ORNL-P-1600)
electron polarization in, theory of conduction, 20: 30735(R) (TID-22970, pp 331-73)
electron production in, secondary, 17: 3569 (ASD-TDR-62-707)
electron quantization in, in magnetic fields, 17: 2110
electron range in, 16: 21197
electron reactions with vacuum-contained, transition radiation from, (E/T), 20: 5008(T) (ORNL-tr-872)
electron resonances in, 16: 32244
electron scattering by liquid, pseudopotential calculation of, 16: 27820
electron scattering by localized moments in, conduction, 17: 11367
electron scattering by, at 6–40 kev, radiation spectra from, (E), 20: 5017
electron scattering in, cross section for free, (T), 20: 12284
electron scattering by, effects of nonmagnetic impurities on, 20: 39395 (IAE-1028)
electron spin resonance in, minimum entropy production in conduction band, 20: 8289
electron spin susceptibility in, (T), 19: 23989
electron structure of, method for studying, 19: 41068
electron systems in, Fermi statistics of two-dimensional free-, 18: 42167
electron theory of, 18: 8789 (CONF-356-7)
electron transport in, Boltzmann relaxation equation for, 18: 18580
electron transport through thin films of, 20: 19097 (N-65-17886)
electron transport in, Boltzmann relaxation equation for (T), 18: 18580
electron tunneling in metal–insulator–superconductor sandwiches, 18: 15095
electron tunneling into normal, from superconducting films, electron interference effects in, (E/T), 20: 17621
electron tunneling conductance in junctions of superconductors and normal, zero-bias anomalies in, 20: 32714
electron wave functions in, effects of point defects on, 17: 18905

(TID-16660)
electron work functions of, effects of gas immersion on zero-field, 18: 30481 (NASA-TN-D-2357)
electron work function for, a-c method for measuring, 20: 13025 (IPP-2/37)
electron-beam penetration through, mechanism of, 19: 39417
electron-electron interactions in, effects of Coulomb, (T), 19: 18476
electron-energy changes due to point defects in, expression for, 18: 12783
electron-gas interactions in, one-particle Green's function for, 19: 39658
electron-phonon interactions in, transport theory for, 18: 18712
electron-phonon interaction in, (T), 19: 11863
electron-phonon interactions in, (T), 19: 18599
electron-phonon interactions in, in magnetic fields, effects on electron mass, (T), 20: 15939 (AD-620189)
electron-phonon interactions in, strong, (T), 20: 30312
electron-phonon systems in, frequency-dependent relaxation time of, 18: 10793
electron--phonon systems in normal and superconducting, coupled, 18: 15124
electronic band structure, low-temperature study, 16: 12082 (AFOSR-2041)
electronic bonding strength theory for, 20: 31219(R) (UCRL-16658, pp 11-20)
electronic density in, impurity effects on, (T), 19: 4745(T) (ANL-Trans-131)
electronic properties of liquid, 18: 10564
electronic properties of liquid, 18: 20628 (NP-13844)
electronic structures, relation to de Haas-van Alphen effect, 16: 12272
electronic structure of liquid, 16: 20439
electronic structure of liquid, tight-binding approximation, 16: 12150
electronic structure in nontransition, 18: 20548
electronic structure and physical properties of, quantum mechanical concepts for predicting, 18: 34066
electronic structure, 19: 11763
electronic structure of, 20: 46966(R) (NAA-SR-12010)
electroosmosis in liquid, mechanism of, (T), 20: 11289(T) (IS-Trans-26)
electrostatic potential of spheres of, in interplanetary space, 16: 26050
electrotransport in liquid and solid, review of theory of, 18: 2256
embrittlement by hydrogen, review, 16: 9244
embrittlement by liquid metals, mechanism of, 18: 27898 (NASA-SP-41 (p.97-9))
emission current in magnetic fields, 18: 10762 (AFOSR-4759)
emissivities at 500 to 1100°C, device design for measuring total hemispherical, 16: 17969
emissivity at high temperatures, apparatus for determining integral, 18: 12670
emissivity of coated, in vacuum, 18: 27968(R) (PWA-2309)
emulsion of gas and liquid, for MHD generators, (T), 20: 39678
energy of, calculation from electronic structure, 18: 30163 (62RL-3145(M))
energy spectra in vicinity of superconductor contact with, 17: 20726
engineering problems in installations for liquid, 18: 14008(T) (AEC-tr-6352)
enthalpy, free heat content, and work function of, relations among, 17: 10658
entrainment in boiling, mechanism of, 18: 43359(R) (ANL-6800(p.43-196))
entropy and Seebeck coefficient changes in mixing of liquid, 17: 6044 (NP-12311)
equation-of-state of, at low temperature, 17: 2941 (IS-359)
equation of state near critical point, 18: 39886 (AWRE-O-36/64)
equations for systems of normal and superconducting, solution of Ginzburg-Landau, 19: 23585
erosion by high-velocity glass spheres, mechanism of, 19: 33701(R) (TID-21897)
etching of, design and operation of vacuum cathodic instrument for, 20: 25477 (NLCO-971)
evaluation for low-temperature design applications, 20: 40051
evaporation of films of, device for monitoring, 20: 14819 (RFP-602)
extrusion at elevated temperatures, hydraulic, 16: 2152(T) (NP-tr-755)
extrusion of easily oxidizing, design of press for, 17: 36273(P)
extrusion of, method and apparatus for, 19: 46975(P)
extrusion through non-metallic dies, equipment for, 20: 29693(P)
extrusion, review of theories of, 19: 6273 (AAEC/E-129)
fabrication and properties of extruded, review, 19: 881(R) (AD-600363)
fabrication by deformation processing, research programs on, 19: 16029 (DMIC-209)
fabrication by explosive forming, optimization of strain rate conditions in, 16: 3427(R) (NP-11124)
fabrication by explosive forming, 20: 5867
fabrication by high-intensity arc process, 17: 36208
fabrication by high-energy-rate forming, bibliography on, 18: 15672 (HW-80934)
fabrication by rolling, research programs on, 17: 27759 (MAB-139-M(R3))
fabrication of, by high-velocity working, bibliography on, 17: 22128 (DMIC-179)
fabrication of conical shapes by explosive forming, drawing and gathering, 16: 29351 (CARDE-TM-280/59)
fabrication of cubical shapes of, procedure for, 19: 13951(R) (RMI-1)
fabrication of honeycomb panels of, by explosive forming, 19: 11711
fabrication of plates of, by explosive forming, 18: 11552(P)
fabrication of pure, by zone-melting process, 20: 23715
fabrication of refractory, development of optimum methods for primary, 16: 4518 (WADD-TR-60-418(Pt.II))
fabrication of, techniques for, 18: 25955
fabrication processes for, review of, 20: 27446(R) (MAB-206-M(3))
fatigue crack formation in, mechanism of, 17: 1923 (BNL-6338)
fatigue, factors in thermal, 16: 13618
fatigue of, effects of aerospace environments on, 17: 29262
fatigue of, energy criterion for, (T), 20: 27521
fatigue, review of low-cycle, 16: 24172 (SSC-137)
fatigue, theory of high stress level, 16: 20805 (ARL-181)
fatigue under cyclic plastic strain at high temperatures, (T), 19: 23110
fatigue, nondestructive evaluation of, 19: 39151 (AFOSR-65-0981)
Fermi level of, shift in magnetic field, 17: 34544(R) (ORNL-3480(p.8-10))
Fermi surface of, relativistic effects in, 19: 40076 (IS-1172)
Fermi surface studies at low temperatures, 16: 5815
Fermi surfaces of, effects of Coulomb interactions on, 18: 14636
fermion pairing in, second-kind coherent, 18: 26426
fixation of rare gases by electric discharge method, 16: 19252
flanged joints in systems for liquid, 16: 1894
flaw detection by gamma spectroscopy, 16: 3291(T) (JPRS-9706(p.79-80))
flaw detection, use of Hall effect for, 16: 19149 (NP-11650)
flow and heat transfer technology of liquid, 16: 12831
flow instabilities in magnetic fields, 17: 4681
flow of liquid through parallel plates, effects of magnetic field, 16: 27218
flow of liquid, friction factor measurement in MHD, 18: 28094(R) (TID-20607)
flow of liquid, friction measurement in MHD, 19: 23172
flow of liquid, gravitational stability in MHD, 20: 34133
flow of liquid, in magnetic fields between coaxial cylinders, 19: 592
flow of liquid, in liquid-metal-lubricated journal bearings, 20: 4078(R) (SWRI-1228-67)
flow of, void fraction detection in, 20: 41111
flowmeter for liquid, ultrasonic, 20: 41225(R) (NYO-3622-4)
forming by explosions, bibliography, 16: 10498
forming by magnetic-pulse process, 20: 40490 (Y-1483)
forming of, methods for, 19: 6286
forming of, survey of methods for, 20: 46183(R) (AD-630427)
forming, review of developments in, 16: 13553
forming, stereophotographic study of explosive, 16: 32100 (NOTS-TP-2698)
fracture, electron microscopic techniques for studying, 17: 11083 (DMIC-Memo-161)
fracture of body-centered cubic, role of twinning in, 17: 463
fracture of, inclusion mechanism of ductile, 17: 36303 (TID-17914)
fracture of polycrystalline, method for measuring, 18: 18348 (IITRI-B183-16)
fracture strength in pressure vessels, physical bases for brittle, 16: 31704
fracture toughness testing, effects of geometry on, 20: 12555 (WAPD-T-1828)
fracture toughness of, double cantilever beam testing method for, 20: 12972 (BNWL-168)
freezing point of, effects of electric fields on, 20: 4297(R) (IS-1200 (Sect.M))
friction and wear studies at 70 to 1600°F, 16: 22584 (DC-61-2-4)
friction and wear of low-melting, 17: 3497 (WADC-TR-59-603(Pt.III))
friction and wear in liquid sodium, 17: 14727(R) (BMI-1600(Del.))
friction coefficients with carbon, ceramics, metals, and metals with dry lubricants *in vacuo*, 20: 7571 (NAA-SR-9644)
gamma absorption pressure dependence, 16: 7083
gamma reactions at 1.02 Mev, electromagnetic effects from, 19: 41956 (SC-R-65-933)
gamma reactions with, quantum efficiency for, (T), 20: 9695(R) (EGG-1183-2043)
gas desorption from, electron-beam, 19: 25099(R) (SLAC-34)
gas desorption from surfaces of, by electron bombardment, 18: 43779(R) (ORNL-3670(p.262-5))
gas desorption from, effects of photons on, 19: 5974
grain boundary embrittlement, segregation, and sliding, 16: 19424
grain boundary migration in, review on, 20: 3626 (ORNL-P-1722)
grain-boundary sliding in, 17: 464

grain reflectance measurement in, description of microphotometer for, 19: 13994(R) (NLCO-940(p.8.1-4))
granulation process for, 19: 36971(P)
Hall constants of liquid, theory for, 18: 9000 (TID-19959)
Hall effect in, apparatus for measurement of, 19: 42217 (SC-RR-65-325)
halogenation and oxidation of, development of equipment and methods for, 18: 41366(R) (EURAEC-1129)
handbook on aerospace structural ferrous, 18: 32132 (ASD-TDR-63-741 (Vol.I)(Suppl.I))
handbook on aerospace structural nonferrous, 18: 32133 (ASD-TDR-63-741(Vol.II)(Suppl.I))
hardness of moving, radiation-reflection method for determination of, 20: 13054(P)
heat capacities, 16: 21041(R) (TID-15663)
heat exchanger design for liquid, 19: 34335(P)
heat flow at interfaces of dissimilar, 17: 3117 (UCRL-9885)
heat formation of monomers and dimers, mass spectrometry, 16: 15294
heat of vaporization at melting point, relation of energy and surface tension to, 18: 35530
heat resistance, effects of structural stability on, 16: 534(T) (NP-tr-790)
heat transfer and charge losses in MHD flow of liquid, 19: 26502
heat transfer aspects of liquid, for space systems, 18: 14047
heat transfer by boiling of liquid, design of apparatus for studying, 17: 20172(R) (NP-12699)
heat transfer by free convection, apparatus design using thermosyphon principle for study of, 16: 5474
heat transfer by liquid, review, 16: 31802
heat transfer by liquid, development of equipment for studying, 17: 20157 (BNL-756(p.155-80))
heat transfer by liquid, development of equipment for studying, 17: 20162 (BNL-756(p.262-75))
heat transfer by liquid, design of loop for studying, 17: 20165 (BNL-756 (p.292-3))
heat transfer by liquid, 17: 20162 (BNL-756(p.353-79))
heat transfer by liquid, development of equipment for studying boiling, 17: 20147 (AD-282370)
heat transfer by liquid, review of forced-convection, 18: 12318 (TRG-Report-546)
heat transfer by liquid, to pipes, 18: 16174 (NP-13660)
heat transfer by liquid, research on forced-convection, 19: 36216(R) (BNL-900(p.29-72))
heat transfer by liquid, 20: 27114
heat transfer by liquid, 20: 29381
heat transfer by, research on, 17: 27535 (BNL-801)
heat transfer coefficients of liquid, 16: 23352(R) (BNL-705)
heat transfer coefficients of liquid, eddy diffusivity effect in, 17: 20170 (BNL-756(p.386-98))
heat transfer during film condensation of vapors from liquid, 18: 23768 (MIT-2995-1)
heat transfer during vertical upflow of liquid, nucleate boiling effects in single-phase, 19: 46528 (ANL-7038)
heat transfer from submerged ribbon to water, 16: 27213
heat transfer from elliptical rods to flowing liquid, analysis, 18: 39425 (BNL-7390)
heat transfer from boiling, kinetics of, 20: 24971(R) (BNL-954, pp 50-83)
heat transfer in boiling liquid, 18: 14033 (RTD-TDR-63-4130)
heat transfer in boiling liquid, review of, 20: 10999
heat transfer in convective flow of liquid, boiling, 17: 40972 (BNL-7319)
heat transfer in flow through parallel tube bundles, 16: 27203
heat transfer in flowing, 16: 10155(T) (FTD-TT-62-57)
heat transfer in liquid, eddy transport in, 17: 8320 (BNL-6046)
heat transfer in liquid, generalization of data for, 17: 8333
heat transfer in liquid, natural-convection, 18: 1483(R) (ANL-6687 (p.27-85))
heat transfer in liquid, 18: 3038(R) (ANL-6801)
heat transfer in liquid, review, 18: 31715 (A/CONF.28/P/225)
heat transfer in liquid, review of, 18: 39439 (WCAP-4402)
heat transfer in liquid, high-temperature, 19: 4311 (ORNL-3605(Vol.1) (p.139-70))
heat transfer in quenching, 16: 29084(R) (AROD-1540.6)
heat transfer in region of thermal stabilization during turbulent flow, 16: 33135
heat transfer of liquid, 16: 20042(R) (BNL-696)
heat transfer of liquid, in tube bank, comparison of experiment and theory on, 16: 22310
heat transfer of liquid, development of facility for study of, 16: 24651
heat transfer of liquid, in pipes, 16: 27156 (AD-269792)
heat transfer of liquid, bibliography, 16: 13203 (CNLM-1802-16))
heat transfer of liquid, contact thermal resistance problem in, 16: 1913
heat transfer of liquid, in two-phase flow, effects of liquid fraction on, 17: 18265 (NAA-SR-8171)
heat transfer of liquid, survey of, 18: 1879
heat transfer of liquid, in co-current flow double-pipe heat exchangers, 18: 39457
heat transfer phenomena in strong magnetic fields, (T), 19: 16179
heat transfer properties of liquid, 18: 6424
heat transfer system using, development and testing, 17: 22953 (TID-18474)
heat transfer to flowing liquid, through annuli, 17: 39236 (BNL-6692)
heat transfer to liquid, in rectangular channels, 16: 29092(T) (FTD-TT-62-714)
heat transfer to liquid, in flow through annuli, 17: 2461(R) (BNL-731 (p.18-46))
heat transfer to liquid, in concentric annuli, 17: 3105 (BNL-5615)
heat transfer to liquid, in flow through a pipeline, 17: 21885
heat transfer to liquid, 17: 31795(R) (BNL-782(p.18-43))
heat transfer to liquid, in cross-flow through rod bundles, 18: 20185
heat transfer to liquid, flowing between parallel plates, (T), 19: 6078
heat transfer to liquid, flowing turbulently through annuli, (T), 19: 6079
heat transfer to liquid, flowing past spheres and elliptical-rod bundles, 19: 13578 (BNL-7664-R)
heat transfer to liquid, flowing turbulently in eccentric annuli, 19: 20123
heat transfer to liquid, flowing turbulently in eccentric annuli, 19: 22500
heat transfer to turbulently flowing liquid, annulus eccentricity effects on, 20: 16612
heat transfer under turbulent conditions in liquid, 17: 25417
heating by electron bombardment, 16: 26065 (AFCRL-975)
heating by ion bombardment, apparatus for study of, 18: 28109
heating liquid, space-borne thermionic generators for, 18: 24370(R) (PWA-2337)
heating loop for, emitter temperature distribution in electron, 18: 20183 (TID-18835)
heating of liquid, by electron bombardment for boiling studies, 18: 33731 (ANL-6869)
heating of, design of furnace for oxidation-free, 20: 479(P)
heats of fusion of, high-temperature calorimeter for measuring, 20: 4297(R) (IS-1200(Sect.M))
hydrogen evolution from, mechanism of electrolytic, 18: 35575
hydromagnetic flow, resistance and flow-profile studies, 16: 12239(T) (FTD-TT-61-281)
hyperfine structure of, core-electron contribution to, 18: 20749
ignition and oxidation, kinetics study, 16: 11501(R) (ANL-6413)
impurity distributions in foils of, measurement using two-dimensional activation analysis, 20: 33230
impurity effects on electric conductivity in, 16: 10575
impurity effects on electronic states in, Green's functions for, 18: 40045 (BNL-7350)
impurity shielding, calculation using perturbation theory, 16: 2336
injection of liquid, in MHD generators, (T), 20: 39669
injection with rare gases by electric discharge, 18: 28116
inspection of, methods of gamma defectoscopy for, 17: 1629
inspection techniques, radiographic, 16: 10270
inspection using Lamb waves, 19: 10715(P)
inspection with 8-Mev linear accelerator, 16: 10271
interactions between grain boundaries and impurities, review, 16: 19425
interactions in, many-body theory for, 19: 18597
interactions of charged particles with stratified metal–dielectric media, electromagnetic radiation from, 16: 33741
interactions with atomic particles, book on, 18: 10769(T) (AEC-tr-6089)
interfaces of liquid, with gases and liquid salts, determination of, 20: 33408 (ANL-7153)
intergranular fragility, mechanisms, 16: 19416
internal defect measurements using infrared inspection, 16: 23973 (ANL-6515(p.163-86))
internal friction due to point defects, 16: 12032 (TID-15068)
internal friction of body-centered-cubic, effects of cold work, 16: 22587 (GA-3076)
internal friction of, design of apparatus for measuring, 17: 20404 (NP-12682)
internal friction and Young's modulus of, design of apparatus for measurement of, 20: 17013 (INR-632/XIV/PS)
internal friction of, effects of lattice bonding forces and defect mobility on, 20: 27508
ion beam reactions with, secondary electron emission from, (E), 20: 31645(R) (AD-627094)
ion bombardment at 10 to 150 kev, cathodic pulverization and secondary emission, 18: 28106
ion bombardments, 16: 7891 (NP-11196(p.43-61))
ion emission from cesiated surfaces of, at room temperature, (E/T), 20: 17267
ion formation and emission at hot surfaces of, 17: 8079
ion pairing interactions in normal, (T), 20: 17008 (CEA-R-2820)
ion reactions at 30 to 300 ev, electron production in, 18: 10797
ion reactions, color production in, 16: 12183 (UCRL-9845)
ion reactions with surfaces of, erosion effects on, 18: 747(T) (NP-tr-1068)
ion reactions with, range theory for heavy, 18: 2527

ion reactions with surfaces of, Auger neutralization in, (E/T), 19: 37219
ion reactions with monocrystalline surfaces of, electron emission in high-energy, (T), 19: 39405
ion reactions with single crystals of, secondary electron emission in, (E), 20: 23874(R) (ANL-7108, pp 43-56)
ion reactions with surfaces of, microbalance for measurement of forces from, 20: 23422 (N-65-33177)
ion reactions with, coefficient of surface ionization of secondary ions from, 20: 31913
ion reactions with, 17: 41534(R) (ANL-6720(p.77-89))
ion scattering by surfaces of, 20: 29499
ion sputtering on, neutral particle energies from, 20: 44139
ionization by electron beam reactions, cross sections for, 18: 766
ionization cross sections of atoms of, measurement by electron impact, (E), 19: 41276
ionization-equilibrium equation of state for liquid, 17: 3586
ionization of, electric-field effects on surface, (T), 19: 32767
iron-57 impurities in nonmagnetic, Mössbauer spectra of, 20: 28606 (LA-DC-7561)
isotope abundance ratios of, selected-area mass spectrometric analysis of, 19: 44354
isotope effects on ion exchange in liquid, 17: 23339
isotope electromigration in, 17: 23340
joining by diffusion, literature survey, 19: 36996 (CEA-Bib-44)
joining, conference, 17: 6627
joining dissimilar, metallurgical factors in, 16: 27610
joining dissimilar, chemical and physical problems in, 19: 46968(T) (AEC-tr-6615)
joining to aluminum silicate glass, techniques for, 19: 44337(R) (AD-425708)
joining to ceramic materials in seals for thermionic converters, research program on, 17: 34369(R) (RBESO-3404-3)
joining to ceramics, development of seals for, 18: 29928(R) (NP-13979)
joining to ceramics, mechanisms and methods of, 18: 39864
joining to ceramics for use in vacuum systems, 19: 22526
joining to ceramics using pressure at high temperatures, 20: 5866
joining to ceramic materials, review of methods for, 20: 27458
joining to refractory metal carbide, 16: 9182(P)
kinetic equations for electrons and phonons in, 17: 36845
laser-beam reactions with, energy and intensity of ions from, (E), 20: 11463
lattice defects in, electron microscopy of, 20: 20365
level indicator for liquid, design of, 20: 1367
level indicators for liquid, design of ultrasonic, 18: 33830(R) (NYO-10556)
level indicators for liquid, testing ultrasonic, 20: 13031(R) (NYO-2910-13)
level measurements of liquid, engineering drawings of ΔP manometer for, 19: 4292
levels of liquid, engineering drawings of equipment for measuring, 20: 634
levitation of, electromagnetic, 19: 38315 (UCRL-16073)
levitation of, review of electromagnetic, 18: 34057 (UCRL-11411)
liquid boiling, under forced convection, 20: 38415
liquid, review on technology of, 18: 597 (BNL-825)
liquid-vapor equilibrium in, measurement of, 20: 4077(R) (IS-1200 (Sect. E))
loop formation in bcc, interstitial, (T), 19: 41056
lubricating properties of liquid, 18: 594(R) (ASD-TDR-63-134)
lubrication behavior of liquid, 16: 6708 (ASD-TR-61-459)
lubricity of liquid, magnetohydrodynamic analysis of, 16: 20570
lubricity of liquid, in journal bearings, 20: 5613 (SWRI-1228-8-16)
lubricity of liquid, in coupled rotor-bearings, 20: 10973 (TID-21992)
machining, electronic techniques for, 17: 6598 (SCTM-39-62(25))
machining of, by sputtering through mask of contamination, 19: 39136
machining of, graphs of running time vs. radius generation in, 20: 43847 (BDX-613-85)
machining, use of electron beams in, 17: 511 (DMIC-174)
magnetic and thermal properties, effects of electron interactions, 16: 16713 (AROD-431:44)
magnetic breakdown in, (T), 19: 9701
magnetic coupling in ferromagnetic and nonmagnetic, long-range spin-density, (T), 19: 20690
magnetic field diffusion in, Joule heating effects on, 20: 41087
magnetic field effects on complex permeability and conductivity of, 19: 22998 (UCRL-11251)
magnetic flux permeability and tunneling in superimposed layers of superconductors and, in magnetic fields, (T), 19: 39700
magnetic interactions of magnetic ions imbedded in, 18: 42076
magnetic moments of dilute iron impurities in, from Mössbauer effect studies, 18: 40047 (LA-DC-6463)
magnetic properties of, survey, (T), 19: 40074 (CONF-796(Paper 3))
magnetic properties of, research using Mössbauer effect, 20: 26385
magnetic susceptibility of, 18: 26393
magnetic transitions in, detection devices for, 17: 39382(T,R) (EURAEC-700)
magnetohydrodynamics of liquid, book, 18: 42166(T) (JPRS-26459)
magnetohydrodynamics of liquid, bibliography on, 19: 5265 (JUL-Bibl-6)
magnetohydrodynamics of liquid, developments in, 19: 23353
magnetohydrodynamic properties of liquid, (T), 20: 11771(T) (NP-tr-1346)
magnetohydrodynamic flow of one-dimensional conducting liquid, in channels, (T), 20: 25954
magnetohydrodynamic flow resistance of liquid, in circular channels section, 20: 30183
magnetoresistance measurements using high pulsed fields, 20: 42526
magnetoresistivity at low temperatures, (T), 20: 22333
mass transfer in zone melting of, boundary conditions and equations for, 17: 23874 (UCRL-10433)
mechanical properties at low pressures, 16: 13564 (AFOSR-2139)
mechanical properties at high temperatures, high-rotational-speed techniques for studying, 16: 24166 (NP-11854)
mechanical properties of, bibliography on effects of strain rate on, 16: 33479 (TID-16734)
mechanical properties and structure of, relation between, 18: 37725
mechanical properties at high temperature and under neutron radiation, 18: 37752 (A/CONF.28/P/460)
mechanical properties at low temperatures, review of, 20: 883
mechanical properties for high-temperature uses, 20: 15129
mechanical properties of, use of computer for storage, interpretation, and recovery of data on, 20: 21354 (TRG-Report-1160)
mechanical requirements and properties of nonferrous, for use at high temperatures, 16: 27683
mechanical weakness during phase transformations, quantitative theory, 16: 24202
melting by electron beams, review of, 17: 25761
melting for purification of, design of electron-beam furnace for, 16: 31764
melting in levitation coils, 17: 21810 (Y-1413)
melting of pure, post-melting effect on, 17: 34332(T) (AEC-tr-5960)
melting of reactive, crucibleless vacuum technique for, 18: 580 (UCRL-7388)
melting of refractory, design of vacuum electron beam device for, 18: 43753
melting of, design of electron bombardment evaporator for, 18: 41986
melting of, plasma device for, 19: 28740 (SGAE-CH-12/1964)
melting of, use of laser beam for, 20: 9105
melting parameters and self-diffusion of cubic, empirical correlation of, 18: 25994
melting point measurement for refractory, method for, 19: 20566(T) (IS-Trans-13)
melting points and viscosity activation energy of liquid, relation between, 16: 18899
melting points of polymorphic, methods for calculation of, 17: 23975
melting radioactive and toxic, furnace for, 18: 22467
melting radioactive or toxic, equipment for, 19: 37022(P)
melting utilizing electron-beam furnace with multiple guns, 16: 31765
metallochemistry of intermetallic compounds and solid solutions, 16: 25702(T) (AEC-tr-5182)
metallographic techniques for radioactive, 19: 2498
metallography of high-melting, 19: 39214
metallography of irradiated, design of hot cell for, 18: 674
metallography of types for use above 2500°C, 16: 30803 (TID-11432)
metallography of, thermal cycling effects on, 17: 27755
microwave surface impedance of, with periodic electric conductivity, 18: 34656
mining of, cancer mortality from, 18: 33813
mixing and transport in liquid, convective, 19: 9604(R) (IS-900(Sect.M))
molecular beam interactions with surfaces of, energy exchange in, (E), 19: 41275
molecular structure, 20: 6551
morphology of interface between liquid and solid, 18: 16005(R) (TID-20354)
Mössbauer effect in, uses of, 20: 20162
neutron activation, neutron shielding effects in thermal, 18: 6184(T) (SC-T-523)
neutron coherent scattering in liquid, Kohn anomaly in slow, (T), 20: 2948
neutron inelastic scattering by polycrystalline, cold, 17: 15247 (AERE-R-4101)
neutron scattering in, atom motion analysis from, 16: 32375
neutron scattering by, analysis of slow, (T), 19: 43263
neutron scattering by liquid, review on, (E), 20: 19799
neutron scattering by conduction electrons and impurities in, polarization effects on, 20: 26377(T)
neutron scattering by, Fermi surface determination from, (T), 20: 34835
neutron scattering by electrons in, cross sections for, (T), 20: 44135
nuclear ferromagnetic state in, stability of, 18: 5868
nuclear magnetic fields of oriented nuclei of IB, in ferromagnetic hosts,

18: 31361(R) (UCRL-11213(p.87-138))
nuclear magnetic line shapes in polycrystalline, 19: 9767(R) (IS-900(Sect.P))
nuclear magnetic resonance in, review, 16: 9469
nuclear magnetic resonance, 17: 32569 (CONF-54-1)
nuclear magnetic resonance in ferromagnetic alloys and metals, (T), 19: 5886
nuclear magnetic resonance line shapes in powder of, Knight shift in, 19: 7429
nuclear magnetic resonance in, 20: 28619
nuclear magnetic resonance in magnetic, (E), 20: 46509(R) (COO-1569-1)
nuclear spin-lattice relaxation time in, failure of quasiparticle picture of, 18: 2450
nuclear spin relaxation in, electron interaction effects on, 17: 23992
optical properties, determination of, 16: 3484(T) (UCRL-Trans-728(L))
ordering in, with one-dimensional lattice, 18: 40456
outgassing, 17: 14943(R) (NYO-9812)
overstress in, use of acoustic emission for detection of, 20: 11001 (BNWL-SA-438)
oxidation and ignition kinetics, 16: 2923(R) (ANL-6379)
oxidation and ignition kinetics, 16: 20300(R) (ANL-6477(p.168-203))
oxidation by aqueous acids, electrochemical surface behavior in, 19: 24935(R) (EURAEC-1295)
oxidation by carbon dioxide, tracer studies of carbon deposition in, 18: 41961
oxidation kinetics of, parabolic growth law for, 18: 27908
oxidation mechanisms and rates, 17: 468
oxidation of phosphided refractory, 19: 9604(R) (IS-900(Sect.M))
oxidation of, review, 17: 25732
oxidation of, theory taking into account space charge, 17: 23892 (TID-16858)
oxidation of, use of xenon-125 in studies of anodic, 17: 32532
oxidation of, design of apparatus for measuring weight changes in, 18: 20480
oxidation protection during melting and heat treatments, development of lithium-gas generator for, 18: 25933
oxidation rate constants for, computer program for, 20: 43172 (NAA-SR-Memo-11966)
oxidation-reduction states, determination by use of hydroquisone–krypton-85 clathrates, 16: 20324(R) (TID-15661)
oxide films on, measurement using polarized light, 17: 39026(R) (TID-19485)
particle reactions with surface of, on space vehicles, (E/T), 19: 25149
passivation of, for use in Marcoule reactors, 19: 26771
penetration resistance of high-strength, equipment and methods for testing, 20: 14702 (Y-1490)
performance and selection of, for use in space vehicles, 20: 16944 (NASA-SP-3025)
performance as melting-point temperature sensors up to 6000°F, (E), 19: 30489 (SC-DC-65-1237)
performance as reactor housing, 20: 10272(R) (NAA-SR-9339)
performance in MHD cycles for commercial power systems, 19: 25254
performance in two-phase liquid–vapor MHD generators, (E/T), 19: 14289 (CONF-640701-113)
performance of liquid, in MHD cells, 18: 36227(R) (AD-603235)
performance of liquid, in space nuclear power plants, 19: 1923 (ANL-6857)
performance of liquid, in MHD cells, 20: 4573
performance of liquid, in MHD power cycles, (T), 20: 9694 (ANL-6954)
performance of liquid, as reactor coolant, 20: 30910
permeability to hydrogen, 18: 39903 (NAA-SR-Memo-9844)
phase diagrams, method of investigating and expressing, 16: 30822
phase studies on, x-ray diffraction method for, 17: 39265
phase studies on, liquid-solid transitions in, (T), 19: 46233 (CEA-R-2752)
phase transformations in, analysis of martensitic, 18: 24994(R) (MND-2531-1)
phase transformations in hcp, relation of c/a ratio and elastic moduli temperature dependence with, 19: 44676(R) (ANL-7000, pp 176-82)
phase transformation mechanisms, 20: 4297(R) (IS-1200(Sect.M))
phonon and spin-wave spectra, images of electronic Fermi surface in, 16: 15190 (NP-11468)
phonon dispersion curves for, (T), 19: 14077
phonon spectra, images of Fermi surface in, 16: 9289 (NP-11315)
phonon spectra in, measurement of critical points of, 18: 15096
photoelectric effect on, gamma, 17: 25860(R) (PR-P-56(p.43-67))
photoelectric effect in, theory, (T), 19: 8015(T) (UCRL-Trans-1120(L))
photoelectric effect in, model for analysis of, (T), 20: 29916 (ORNL-TM-1458)
photoelectron emission, energy distribution, 16: 9313
photoelectron emission by, theory of, 17: 16797(T) (UCRL-Trans-907(L))
photon absorption by, effects of impurity scattering centers on, 17: 39307(R) (ORNL-3492(p.119-33))
physical chemistry, 17: 27755
physical properties of oriented polycrystalline, 17: 32631
physical properties of liquid, review, 18: 20516 (EUR-599.d)
physical properties of liquid, review of, 19: 28821
physical properties of, equipment and methods for measuring, 20: 14719
physiology of trace, study by activation and isotopic methods, 20: 18185(R) (BNL-929, pp 126-47)
pitting by wear, tracer studies, 17: 41371
plasma and spin wave interactions in, 20: 26392
plasma model, quantum theory of transverse acoustic oscillations, 16: 19525
plasma properties near plates of, (T), 19: 5337
plastic deformation of polycrystalline, review of technology on, 17: 11196 (UCRL-10152)
plastic deformation and sintering of, 19: 37147
plastic deformation of, theory of, 20: 11331
plastic deformation of fcc, cross-slip mechanisms in, 20: 31713(R) (UCRL-16658, pp 93-8)
plastic flow of polycrystalline, determination by hardness, 20: 37230
plastic flow of, crack propagation in, 19: 22863(R) (AD-606809)
point defect clustering in irradiated and quenched, effects of annealing on, 18: 26069(R) (ANL-6868(p.373-417))
point defects in, lectures on, 18: 8788 (BNL-7623)
point defects in, metallurgy of, 16: 30788 (IS-268)
Poisson's ratio and sound velocities in pure, 17: 8859
polarization in high-susceptibility, long range, 18: 28149
polarization in nonferromagnetic, long-range spin, (T), 19: 20689
pole figures in hcp, metallographic technique for determination of basal, 19: 34687 (ORNL-P-1266)
pole figures of hexagonal, use of polarized-light microscope in determining, 17: 23966(R) (TID-18637)
polishing of, preparation of samples for electrolytic, 20: 23595(P)
polishing of, tracer studies of surface processes in, 18: 27935
positron annihilation in, 17: 4010
positron annihilation rates in, semi-empirical correlation of, 17: 6960 (UCRL-9793)
positron annihilation in, 17: 11539
positron annihilation in, polarization effects in (T), 19: 2904
positron annihilation in, 3-quantum, (E/T), 19: 39546
positron annihilation in, many-body theory of, 19: 41159
positron annihilation in, theory of, 19: 43127
positron annihilation in, theory of, 19: 43128
positron annihilation rates in, 19: 43157
positron annihilation in, (E/T), 19: 47217 (AD-613582)
positron annihilation in, (T), 20: 19499
positron annihilation in, analysis of, (T), 20: 29991 (ORNL-TM-1443)
positron annihilation in, review of, 20: 37820
positron annihilation in, ladder correction to static dielectric constant for, 20: 44247
positron effective mass in, 20: 27864
positron thermalization in, (E), 20: 11660
positronium formation in, (T), 19: 23421
preferred orientation and thermal expansion in hexagonal, x-ray method for measuring, 20: 9504 (WAPD-TM-472)
preparation and properties, 16: 24108 (IS-351)
preparation and purification of refractory, by vacuum electron-bombardment methods, 16: 32045
preparation and purification of refractory, by electron-bombardment methods, 16: 32046
preparation and purification of less-common, 17: 25714
preparation by fusion electrolysis, device for introducing gases in salt melt for, 19: 22956(P)
preparation of alloy samples, design of arc melting furnace for, 16: 20989 (ASD-TN-61-32)
preparation of, by pressure leaching, precipitation, and reduction, 17: 22097 (NP-12722)
preparation of chemically reactive, review of, 17: 32504
preparation of high-purity, 16: 30722 (NYO-10554)
preparation of high-melting, vacuum techniques for, 19: 11686
preparation of pure, review of progress on, 20: 17158(R) (ORNL-3900, pp 82-149)
preparation of radioactive, for oxygen determination, cathodic etching method for, 20: 40817 (UCRL-14959)
preparation of strain-free tensile specimens of, by electron-beam zone melting, 18: 30161
preparation of thin foils of, for electron metallography, 19: 44610 (TIM-943)
preparation of ultrafine particles of, equipment for, 19: 26795
preparation of, radiochemical, 17: 199
preparation, properties, and uses of hard compounds of refractory, 16: 25768(T) (NASA-TT-F-102)
preparation, properties, and uses of high-purity, survey of, 19: 18405
pressure bonding of, grain growth across bond interface in, 17: 40423(R)

(BMI-1639(Del.))
pressure drop in in-pile loops, calculation for PW-19, 16: 13212 (TIM-483)
pressure effects, bibliography and data on high-, 16: 24115
pressure gage for liquid, design of, 19: 28613
pressure measurements in liquid, thermionic and variable impedance systems for, 20: 23246
processing of, waste monitoring and disposal in, 17: 25717
production by electrochemonuclear processes, 20: 36506 (BNL-959)
production by vacuum metallurgy, 16: 20967
production from halides, 17: 27220(P)
production in contracting gaseous spheres, (T), 20: 19345
production in interstellar medium, (T), 19: 18661
production of heavy, by chlorination of oxides, 17: 27490
production of high-purity, methods for, 20: 20365
production of pure refractory, from ore, 16: 17772(P)
production of pure refractory, from ore, 16: 17773(P)
production of pure refractory, from ore, 16: 17774(P)
properties and structure of liquid, review, 16: 19377(T) (AEC-tr-4879)
properties and structures of, relation between, 17: 18818
properties and structure correlations of, review of, 17: 30987(T) (AEC-tr-5873)
properties and structure, 17: 35264(R) (UCRL-10706(p.111-203))
properties and structure of, pressure effects on, 19: 46983 (AD-612159)
properties and uses of liquid, 19: 6353
properties and uses of corrosion resistant, review on, 19: 37105
properties and uses of sintered, 20: 25532
properties as cladding and structural materials in reactors, 18: 32072
properties as cladding and structural materials in reactors, 18: 41947
properties at high temperature, bibliography on, 20: 19216 (NP-15388)
properties at high temperatures, 17: 6669 (NP-12295)
properties for construction of high-temperature ionization chambers, 18: 25776 (AEEW-M-381)
properties for radiation shielding, 17: 36213
properties for use in thermionic converters, 17: 3464 (ARA-1029)
properties for use in space vehicles, 20: 4312
properties, handbook, 17: 426
properties in carbon dioxide at high temperatures, 16: 19372 (TRG-Report-267)
properties in space uses, survey, 16: 30826
properties in space, 16: 30726
properties measurement on liquid, conference on uses of high-temperature instrumentation for, 20: 27226 (ANL-7100)
properties of ceramic-coated, 20: 27460
properties of, effects of minor constituents on, 17: 41441
properties of, effects of impurities on, 17: 41442
properties of electron gas in lattice of positive charges, 18: 43455
properties of liquid, 16: 7891 (NP-11196(p.43-61))
properties of liquid, as working fluid in space power plants, 18: 15602
properties of liquid, for use as reactor coolant, 18: 31002
properties of liquid, as reactor working fluids, 18: 35198 (NAA-SR-8617 (Vol.I))
properties of liquid, for use in magnetohydrodynamic cells, (T), 19: 9992
properties of liquid, for use as reactor coolant, review of, 19: 22885
properties of liquid, review of engineering, 20: 486
properties of liquid, as bearing lubricants, instrument for measurement of, 20: 27129 (ANL-7100, pp 291-306)
properties of liquid, as high-temperature lubricants, 20: 31720(T) (AD-629415)
properties of liquid, in MHD generator cycles, 20: 39726
properties of porous, for use as isolation traps in vacuum systems, 19: 46573 (UCRL-12393-T)
properties of reactor pressure vessel, 18: 34181
properties of refractory, summary of, 17: 11119(T) (JPRS-17322)
properties of superconducting, data on, 19: 21187
properties of, effects of electron structure on mechanical and physical, 19: 11746
properties of, effects of electron-phonon interactions on, (T), 19: 40073 (CONF-796(Paper 1))
properties of, effects of low temperature on, 20: 4417
properties of, effects of space environment on, 16: 2786 (JPL-TR-32-150)
properties of, research on, (E/T), 19: 38027(R) (ORNL-3841)
property requirements of non-ferrous, for nuclear power projects, 18: 18376
protection by oxide films, 19: 23163(R) (ORNL-3650(p.111-86))
proton reactions at 160 Mev, proton production in, (E), 19: 17160(R) (ORNL-3714(Vol.II)(p.119-33))
proton reactions with, single bi-particle elastic collisions in, 19: 23290
proton reactions with, radioactivity from, (E/T), 20: 3263
pulverization by fast deuterium ions, 16: 4650
pump design for liquid, 18: 1856
pump development for liquid, 19: 38781(R) (N64-25903)
pump operation and performance for liquid, electromagnetic, 17: 4643
pumping liquid, development of electromagnetic pumps for, 18: 1855
pumps for liquid, development and testing seals for, 19: 40718 (TIM-909)
purification by electron-beam melting, 18: 20491
purification by electrotransport, survey on, 20: 41412(R) (IS-1500 (Sect. M))
purification by ion-exchange chromatography, 17: 229 (IS-377)
purification by melting techniques, 18: 16153
purification by melting techniques, 18: 41583
purification by vacuum distillation, study of process variables in, 18: 41935 (UCRL-7387)
purification of, by chemical processes, survey of, 17: 6515 (IS-394)
purification of reactive, by electrolysis, 16: 20969(P)
purification processes for high-purity, 19: 7625
purification studies, impurity transport in intense thermal gradient, 16: 22530 (ARF-3133-23)
purification using electron-bombardment furnaces, 19: 39109
purity of, measurement by damping techniques, 17: 23881(T) (NP-tr-1011)
purity requirements for, for use in reactor cores, 18: 26034
quenching in liquid helium II, 18: 11115
quenching liquid, technique for rapid, 16: 27564 (TID-16379)
radiation and environmental effects in space, 18: 34235
radiation damage by fission events in, model, 16: 10618 (NAA-SR-6642)
radiation damage in, variation of parameters of, 16: 29460
radiation damage in, 17: 8878 (BNL-6051)
radiation damage in, theory, 18: 14537(R) (HW-79766(p.4.1-76))
radiation damage in fcc crystals of, computer programs for binary collision model of, 18: 18410 (AD-416313)
radiation damage in bcc, 18: 30286
radiation damage in, mechanisms of, 19: 24916(R) (GEMP-334A)
radiation damage in hcp, review, 19: 37162 (BNWL-SA-236)
radiation damage in bcc, theoretical studies of neutron, 20: 9378(R) (GEMP-54A)
radiation damage mechanisms, 19: 1009
radiation damage, review, 16: 22691
radiation damage studies, equipment and techniques used in, 16: 16795
radiation damage studies on, thermal effects in, (T), 19: 34737 (AD-612810)
radiation damage to, 18: 30251
radiation damage to, annealing of, 19: 11807
radiation effects on surface reactions, 16: 2263 (GA-2229)
radiation effects on precipitate particles in, 16: 7890 (NP-11196(p.34-41))
radiation effects on high-temperature alloys, 16: 9195(R) (GEMP-7A)
radiation effects of neutrons on creep rates, theory, 16: 9256 (FXM-3389)
radiation effects of fast neutrons on creep rupture, 16: 9257 (FXM-3932)
radiation effects of high-energy particles, surface, 16: 12195
radiation effects on, conference, 16: 13647
radiation effects at cryogenic temperatures, 16: 15982
radiation effects, point defect cluster behavior, 16: 9271
radiation effects in engineering uses, 16: 16625
radiation effects on surface properties, development of apparatus and techniques for determining, 16: 19435 (GA-563)
radiation effects, displacement-spike formation mechanisms, 16: 21106
radiation effects on high-temperature alloys, 16: 22532(R) (GEMP-11A)
radiation effects, bibliography on, 16: 24233 (57GL77)
radiation effects on nonfissionable, bibliography on neutron, 16: 24269 (STI/PUB/21/6)
radiation effects on mechanical properties, tables, 16: 29457
radiation effects on high-temperature alloys, 16: 29314(R) (GEMP-13A)
radiation effects at cryogenic temperatures, development of equipment for determining, 16: 30909(R) (NP-12004)
radiation effects at surface of, 16: 31371
radiation effects on diffusion rates in, 16: 31374 (BNL-4663)
radiation effects, 16: 33522 (REIC-24)
radiation effects on creep rates in fcc, fast neutron, 16: 33536
radiation effects on electric resistance, method for measuring, 16: 7942 (AEC-tr-4679)
radiation effects on face-centered-cubic, role of dynamic crowdions in, 17: 438
radiation effects on, theory of, 17: 458
radiation effects on, in nuclear engineering applications, 17: 1830
radiation effects at 4°K, 17: 5038(R) (ORNL-3364(p.57-84))
radiation effects on electric resistance of, 17: 6732 (62-GC-207)
radiation effects on, 17: 6733 (62-GC-209)
radiation effects on, 17: 6768
radiation effects on, in space, 17: 8910
radiation effects, 17: 11129
radiation effects on, review, 17: 13201
radiation effects on atomic displacements in, 17: 14900 (TID-17964)

radiation effects on, tolerance limits for space, 17: 22241
radiation effects at 4.2°K, design of cryostat for electron, 17: 28091
radiation effects on, review of, 17: 30919 (SC-4920(M)(p.41-62))
radiation effects on magnetic and mechanical properties of, 17: 32683
radiation effects on bcc, 17: 31798(R) (BNL-782(p.60-91))
radiation effects on wear of surface layers of, deuteron, electronic, and ionic, 17: 36366
radiation effects on, 18: 658 (REIC-32)
radiation effects on, at cryogenic temperatures, development of equipment for studying, 18: 2296(R) (NP-13163)
radiation effects on, mechanisms for annealing and producing, 18: 2322
radiation effects on, information storage and retrieval system for, 18: 7335
radiation effects on corrosion properties of, 18: 8900
radiation effects on corrosion, 18: 8902
radiation effects of neutron on mechanical properties, estimations of doses from, 18: 10585
radiation effects on mechanical properties and structure, 18: 14396
radiation effects on transmutation and crystal structure of, 18: 17909
radiation effects on displacement cascades and electric conductivity of, 18: 18441
radiation effects on, BMI Abstracts, March 1964, 18: 22533 (REIC-ACCESS-73)
radiation effects of neutrons on high-temperature creep of, 18: 28039(R) (EURAEC-1020)
radiation effects on corrosion by liquid, 18: 28046 (NASA-SP-41(p.101-4))
radiation effects on electric conductivity, use for measuring neutron doses, 18: 30247
radiation effects on hardness of fcc, neutron, 18: 30285
radiation effects on diffusion in, 18: 30287
radiation effects on dislocation effects in, 18: 30288
radiation effects on, at low temperatures, 18: 30284
radiation effects on residual resistivity of, theory of displacement cascades in, 18: 32223 (IFA-FT-51)
radiation effects on electric conductivity of, theoretical corrections to measurements of electron, 18: 36039 (AFCRL-64-2)
radiation effects on mechanical properties of fcc crystalline, neutron, 18: 37754 (A/CONF.28/P/471)
radiation effects on structural, review on, 18: 37786
radiation effects on interstitials and vacancies in, 18: 39993 (EUR-1643.e(p.246-53))
radiation effects on noble, bibliography, 18: 40009 (UCRL-7810)
radiation effects on, in space applications, 18: 44274
radiation effects on, in space environment, 18: 44275
radiation effects on creep of, equipment for in-reactor tests of, 18: 43778(P)
radiation effects on properties of, 19: 1010
radiation effects on, review on, 19: 1027
radiation effects on mechanical properties of, data tabulations on, 19: 4714 (HW-81334(Pt.2))
radiation effects on long-term mechanical properties of stressed, research program on neutron, 19: 11777(R) (EURAEC-1243)
radiation effects on, computer study of, 19: 12865(R) (NAA-SR-10501)
radiation effects on long-term mechanical properties at high temperatures of, research program on, 19: 11778(R) (EURAEC-1268)
radiation effects on electric conductivity of, (T), 19: 11797
radiation effects on non-fissionable, 19: 11807
radiation effects on brittleness of, review, 19: 11809
radiation effects on, theory for swelling in, 19: 11679
radiation effects on electric conductivity of, role of interstitial and vacancy cascades in, 19: 14093
radiation effects, 19: 15994(R) (HW-84281)
radiation effects on bcc, neutron, 19: 23355(R) (BNL-867(p.1-117))
radiation effects on structure and physico-chemical reactivity, 19: 23140
radiation effects on displacement of atoms in, 19: 23147
radiation effects on, 19: 25046(R) (HW-83615)
radiation effects on catalytic activity in conversion of cyclohexane, 19: 26417
radiation effects in, computer program for simulation of, 19: 30823 (GEMP-356)
radiation effects on, in electron microscopy, 19: 36490
radiation effects on diffusion in, 19: 37172 (ORNL-P-1397)
radiation effects on, defect structure and saturation from, 19: 41102
radiation effects on mechanical properties of, displacement spike density model for neutron, 19: 44599(R) (GEMP-50A)
radiation effects on tensile properties of, design of equipment for measuring, 19: 46712 (BNWL-SA-169)
radiation effects on microstructure, use of silicon rubber for replication of, 19: 47091 (NMI-4999, pp 69-77)
radiation effects on, compilation of projects on, 20: 2433 (REIC-Memo-27)
radiation effects on hardness of bcc, neutron, 20: 2457
radiation effects on, ASTM symposium on, 20: 2470
radiation effects on mechanical properties, 20: 2471
radiation effects on, review of, 20: 4464
radiation effects on creep at high temperatures, 20: 4299(R) (ORNL-2711)
radiation effects on, specimen holder for investigating deuteron, 20: 11410
radiation effects on body-centered cubic, 20: 20177(R) (BNL-929, pp 83-105)
radiation effects on dislocation damping and elastic constants of, review of, 20: 33948
radiation effects on, review of neutron, 20: 29819
radiation effects on, annealing of electron, 20: 35841(R) (NAA-SR-11900)
radiation effects on creep of, extrapolation method for neutron, 20: 41495(R) (EURAEC-1621)
radiation effects on rate-controlling mechanism for slip in body-centered-cubic, neutron, 20: 43998 (ORNL-3993)
radiation effects on physical properties of, 20: 46966(R) (NAA-SR-12010)
radiation effects on, in integrated MOS circuit, 20: 46097(R) (AD-63044)
radiation effects on, review of, 20: 46098
radiation enhanced diffusion in, effects of correlated defects in gamma-, 20: 17131
radiation hardening, 16: 30895 (BNL-5120)
radiative lifetimes of excited states in gaseous, 20: 31219(R) (UCRL-16658, pp 11-20)
radioactivity of chondritic, measurement of cosmic-ray-induced, 16: 915
radiographic detection of flaws in ingots of, gamma, 20: 43870
radiographic studies of, 19: 9348(T) (FTD-MT-63-261)
radiography of heavy, thermal-neutron, 18: 4240 (CONF-356-1)
radioinduced annealing of point defects in, mechanisms of, 17: 37597
radioinduced defects in, model for recovery from, 20: 45040
radioinduced defects in, ultrasonic measurement of nonlinearity parameters of, 20: 46943 (ORNL-TM-1573)
radioinduced dislocation loops, factors affecting size, 16: 22671
radioinduced dislocations in, formation and annealing of, 17: 432
radioinduced hardening of bcc, neutron, 20: 20183
radioinduced helium bubble formation in, neutron, 20: 25623
radioinduced interstitials and vacancies in, distribution function for, 18: 14566
radioinduced internal energy in, design of equipment for measuring, 20: 25629(P)
radioinduced length changes of, dilatometer for measuring, 19: 6372
radioinduced light emission by, cross sections for electron, 19: 21792(R) (ORNL-3650(p.187-219))
radioinduced multiple thermal points in, 16: 27701
radioinduced phase transformations in, 18: 12748
radioinduced polymer layer formation on, mechanism of initial, 18: 1758
radioinduced relaxation of stresses in, 18: 42120(T) (AEC-tr-6474)
radioinduced thermal points in, 16: 10626
rare gas bubbles in, contrast effects in transmission electron microscopy of, 19: 9594 (CEA-R-2431)
reactions of heavy, with alkylphosphoric acids to form polymers, 17: 21664 (AERE-R-4281)
reactions of liquid, with liquid salts, 17: 14212(R) (NYO-10535)
reactions of, with glass at interfaces, mechanisms of, 20: 31719(R) (UCRL-16658, pp 155-69)
reactions with gases at high temperatures, 19: 2761
reactions with gases, computer program for calculating weight gains in, 20: 43898 (NAA-SR-Memo-11967)
reactions with liquid fluorides, 19: 23163(R) (ORNL-3650(p.111-86))
reactions with metal chlorides, thermodynamics of, 18: 1602 (CONF-117-11)
reactions with molten lithium fluoride–potassium fluoride–sodium fluoride eutectic at 1000°K, 19: 9096 (ORNL-P-403)
reactions with polyacrolein, effects of pH and temperature on, 18: 23542
reactions with rare earth borates and oxides at high temperatures, 17: 14740 (TID-11295(2nd Ed.))
reactions with water, 16: 2923(R) (ANL-6379)
reactions with water, 16: 12843
reactions with water, reactor safety studies, 16: 20300(R) (ANL-6477 (p.168-203))
reactions with water, theory of, 18: 27432
reactions with water, development of methods for study of, 18: 44922(R) (ANL-6800(p.326-402))
reactions with water in reactor environment, TREAT studies of, 19: 25765
reactions with water in reactors, (E), 19: 35624
reactions with water at high temperatures, 20: 20183
reactions with water, analysis in LOFT meltdown, (T), 20: 26518(R) (IDO-17145)
reactions with water during reactor meltdown, hydrogen combustion in, 20: 28685(R) (BMI-X-10163)
recrystallization, behavior of impurities at grain boundaries during,

17: 560
reduction of niobium and tantalum chlorides, fluorides, and oxides, methods for, 17: 35950
refining of reactor, electrolytic cell design for, 20: 29373(P)
reflectivity of, microphotometer for measuring, 20: 16950 (ORNL-TM-1161, pp 132-45)
refractory, fabrication and properties of, 17: 3380 (ERR-FW-049)
reinforcement with ultra-high strength aluminum oxide fibers, 16: 10499 (AD-267891)
removal by electrochemical methods, effects on mechanical properties, 19: 28776 (DMIC-213)
Report of National Chemical Laboratory 1963, 18: 43365
research and development on, 17: 6532 (WADC-TR-53-373(Suppl.9))
research and development programs on, opportunities, roadblocks, and problems in, 20: 13185 (TID-22424)
research on control of solidification in, 20: 29623(R) (TID-22970, pp 121-256)
research on, review of, 17: 3390(R) (WADC-TR-53-373(Suppl.8))
research program on, 19: 43997(R) (UCRL-11889)
research programs on reactor-associated, 16: 30165(R) (ORNL-3313)
research programs on liquid, in France and Great Britain, 17: 27731 (NASA-TM-X-884)
research programs on liquid, in France and Great Britain, 17: 29250 (GEST-2012)
research programs of U. S. Army on, 1962 summary, 17: 33413(R) (NP-12967)
research programs on high-temperature liquid, review of, 20: 743 (BNL-939)
review of status and future potential of, for defense, 18: 8718 (DMIC-Memo-183)
review of technology of liquid, 17: 18671 (BNL-788)
review on liquid, 17: 14759
reviews of high-temperature technology of liquid, 18: 8714 (BNL-836)
reviews of high-temperature technology of liquid, 19: 14896 (BNL-896)
reviews of high-temperature technology of liquid, 19: 26754 (BNL-920)
reviews of high-temperature technology of liquid, 20: 25475 (BNL-980)
role of trace, in physiology and pathology of man, 18: 23199 (BNL-828)
rupture of, effects of interactions of dislocations on, 17: 18779(T) (TRG-Inf-Ser-6)
sample preparation for electron microscopy of, by electrodeposition, 18: 41941
scattering of hydrogen on surfaces of, ion production from, 20: 42460
scattering processes in, compared to insulators, 17: 31381
sealing of, to dielectrics, 17: 6676(R) (RADC-TDR-62-401)
sealing to ceramic materials, manual of techniques for, 17: 34367 (NP-13027)
self-diffusion coefficients of liquid, determination using radioisotopes, 16: 27657
self-diffusion in, effects of plastic deformation on, 16: 29385 (TID-16372)
self-diffusion, method of predicting atomic mobility for, 16: 25816
self-diffusion in, prediction of activation energies for, 18: 14478 (UCRL-10581)
separation by cation exchange, 17: 10733 (IS-466)
separation by ion exchange using hydrochloric acid as eluant, 16: 22274
separation by paper chromatography using glyoxal-bis-(2-hydroxyanil), 18: 31670
separation by solvent extraction using dialkylphosphoric acids, mechanism of, 17: 6197
separation by solvent extraction using liquid stearic acid, 17: 21789
separation by solvent extraction using amines, review of, 18: 356
separation by solvent extraction, chemical and physical principles of, 18: 39088
separation by solvent extraction using mixtures of organic reagents, review on, 19: 7293
separation by solvent extraction, use of electric fields in, 19: 28458(P)
separation from acid solutions of lithium chloride by solvent extraction using amines, 20: 9049(R) (ORNL-3830, pp 193-221)
separation from americium, multi-channel ion exchange process for, 20: 43183 (RL-SEP-729(Rev.))
separation from animal tissues using complexing agents, 19: 12945
separation from aqueous solutions by solvent extraction using thenoyl trifluoracetone, antisynergism in, 17: 3071 (TID-14891)
separation from aqueous solutions by solvent extraction using dibutyl phosphorothioic acid, 17: 27408
separation from aqueous sulfate solutions, electrolytic, 18: 3917(P)
separation from beryllium by ion exchange and using EDTA, 16: 135(T) (NP-tr-797)
separation from chloride, fluoride, and nitrate solutions by solvent extraction using amines, 17: 39185(R) (ORNL-3452(p.168-88))
separation from hydrochloric and sulfuric acid by solvent extraction using O,O'-dialkyl phosphorodithioic acid, 16: 29040
separation from hydrochloric and nitric acid solutions by solvent extraction using tri-n-octylphosphine sulfide, 20: 244
separation from ores by ion exchange, 16: 7622(P)
separation from organic solvents by paper chromatography, 17: 14176
separation from petroleum, use of reactor irradiation in, 19: 22393(P)
separation from perchloric acid solutions by cation exchange, 19: 28280(P)
separation from rare earths by anion exchange, 20: 4067
separation from solutions by foam distillation, 16: 30510(P)
separation from solutions by chelate formation using polyamidoxime, 17: 25375(P)
separation from solutions by chelate formation using polyamidoxime, 17: 25376(P)
separation from solutions by foam, studies of factors of, 18: 17939 (TID-20461)
separation from solutions by solvent extraction using trialkylphosphoric triamides, 20: 14461(R) (ORNL-3889, pp 48-70)
separation from uranium by fixation of acetate on anion-exchange resins, 20: 41030 (CEA-R-2994)
separation of di-, tri-, and tetravalent, by solvent extraction, synergism in, 17: 6050 (TID-15323)
separation of impurities from, using thionalide, 16: 18835
separation of ions of, in fused salts by electrophoresis on glass fiber paper, 16: 20550
separation of liquid from fused salt, countercurrent extractor for, 16: 827
separation of liquid, by flash distillation, 18: 1834(R) (IS-700(Sect.E))
separation of liquid, by flash distillation, 19: 9281(R) (IS-900(Sect.E))
separation of nonferrous, by liquid-liquid extraction, review on, 20: 41047
separation of trace, from uranium by chromatography, 20: 14461(R) (ORNL-3889, pp 48-70)
separation of, from inorganic ions, reversed-phase partition chromatographic, 20: 45582
sheet-rolling, development of techniques for, 16: 3420 (DMIC-161)
shock-wave studies in, review of very high-pressure, 18: 20454 (LADC-5561)
sintering of, size sensitivity of two-particle model for, 17: 1839
sintering reactions with transition metal carbides and nitrides, formation of complex compounds by, 20: 25539
slip mechanisms in single crystals of hexagonal close-packed, survey of, 18: 44156 (UCRL-11418)
solidification of, effects of electric fields on, 20: 41412(R) (IS-1500 (Sect. M))
solubility, effects of ionization potential of atoms on mutual, 16: 24181(T) (AEC-tr-5177)
solubility of refractory, in mercury, 20: 20177(R) (BNL-929, pp 83-105)
solute segregation during dendritic growth, 16: 7891 (NP-11196(p.43-61))
solutes in, reactions with hydrogen, 17: 24003
solvent distribution in ammonium thiocyanate–methanol–water systems, distribution coefficients for, 19: 40447
solvent extraction with organophosphorus compounds, chemistry, 16: 11795
solvent extraction of, review of, 17: 18197
solvent extraction by acetylacetone, benzoylacetone, and dibenzoylmethane, 17: 20103
solvent extraction of salts of, using amines, 17: 4626 (HW-SA-2797)
solvent partition in hydrohalic acid–organic diluent–tridodecylamine system, 19: 46180 (UCRL-16254)
solvent properties for hydrogen, radiation target cans for studying, 16: 27697(T) (AEC-tr-5170)
solvent properties of, for gases, high-temperature technique for determining terminal, 20: 31250
sorption and self-diffusion on, tracer studies of, 18: 16479 (TID-7689 (p.86-9))
sorption as fillers in resins, chemi-, 16: 2190(R) (NP-10983)
sorption by zirconium phosphate and tungstate gels, effects of dehydration on, 19: 7622
sorption from sulfuric acid solutions by anion exchange materials, 20: 40822
sorption properties for radioisotopes, 20: 45670
sorptive properties for impurities in helium, 16: 12833
sorptive properties for protactinium, 16: 16388
sorptive properties for protactinium, 16: 26964(T) (AEC-tr-5253)
sorptive properties for gases, 17: 2061(R) (TID-16592)
sorptive properties for radioisotopes, 17: 4374(R) (MLM-1129)
sorptive properties for gases, research program on, 17: 36452(R) (TID-19303)
sorptive properties for barium-140, effects of impurities on, 18: 19468(R) (MLM-1176)
sorptive properties for gases, review of techniques in studies on, 18: 33454
sorptive properties for cesium, plutonium, and protactinium, 19: 32311
sorptive properties for ionic radioisotopes, review on, 20: 7003 (INR-634/V/C)

sorptive properties for gases, method for measuring, 20: 21351(R) (SRIA-425-8)
sorptive properties for helium, 20: 22520(R) (NAA-SR-11805)
sound wave reactions in magnetic fields, nonextremal Fermi-surface orbits from resonances in, 18: 32070
spalling of plates of, effects of geometry on, 20: 27434 (SC-RR-66-134)
spalling of, stress effects on time-dependent, 18: 30182
specific heat and static paramagnetic spin susceptibility of, effects of electron interactions on, 16: 33493
specific heat at low temperatures, continuous warming method of measuring, (E), 20: 30734(R) (TID-22970, pp 1-63)
specific heat of superconducting, at transition point, (T), 20: 17612(T)
specific heats of, effects of electron interactions on, 17: 571
specification guides at HAPO for, 18: 3925 (TID-19753)
spectra, equipment and methods for standardization of thermal emittance measurements, 16: 19375 (WADC-TR-59-510(Pt.III))
spectra of heavy, effects of polyethylene coating on potassium bromide windows for infrared, 20: 40805(R) (MLM-1325, pp 63-70)
spectra of neutral, atomic beam measurement of absolute oscillator strengths of lines in, 18: 9008
spreading of liquid, on solid metallic surfaces, 17: 3503
sputtering by bombardment with rare-gas ions, yields at low energies, 16: 21116 (AD-267458(Pt.V))
sputtering by ion beams, breakdown as function of angle of incidence in, 17: 16818
sputtering by mercury and rare gas ions, yields from, 16: 31727
sputtering by noble gas ions, 18: 20745
sputtering by rare gases at 5 to 65 kev, 16: 31726
sputtering mechanisms for high-energy ions, 18: 18296 (ZFK-WF-6)
sputtering processes on, theoretical model of, 16: 31728
sputtering rates, 17: 32770
sputtering, threshold effects in mechanical collision theory, 16: 22749
sputtering yields from rare-gas ion bombardments, 16: 21114(R) (AD-267458)
sputtering, secondary emission mechanism, (T), 20: 46298
stability of liquid, accelerated in magnetic fields, 19: 3019
stability of work-hardened fcc, parameters of, 20: 31713(R) (UCRL-16658, pp 93-8)
stacking fault tetrahedra stability in quenched cubic surface-centered, 16: 19381(T) (UCRL-Trans-824)
stacking faults in, method for determination of types of, 17: 39602
Stark effect in, 19: 23321
stored-energy in release, calorimetric measurement of, 17: 20556 (GA-2732)
strain inhomogeneities in, 18: 7294(R) (HW-77954(p.4.19-77))
strength, of crystalline properties and grain substructure, 16: 3499
strength of polycrystalline, factors affecting high-temperature, 16: 12085 (ARL-101)
strength of structural, review, 18: 33199 (UCRL-10811)
strength of whiskers, 16: 3500
strengthening by irradiation, 20: 11366
structural analysis, use of radioautography in, 16: 529(T) (AEC-tr-4505)
structural properties of, effects of thermal cycling on, 18: 22510
structure of liquid, research program on x-ray studies of, 17: 37464(R) (TID-19394)
structure of molten, review of x-ray diffraction studies of, 19: 26812 (CEA-Bib-54)
structure of, neutron radiography of internal, 17: 1984
structure of, conduction electron-core scattering in, 19: 959(R) (ORNL-3676(p.9-11))
structure of, relations with electronic energy states, 19: 10675(R) (NAA-SR-9999)
structure surfaces of, 17: 34550(R) (ORNL-3480(p.49-56))
superconducting critical temperatures of, pressure effects on, 18: 15091
superconducting properties in one-dimensional systems of, monovalent model for, (T), 20: 9904(T)
superconducting transition temperature and energy gap function of superposed films of, 18: 2762
superconductivity in, theory of, 17: 17076
superconductivity in bismuth-type, effects of electron excitation interactions on, 17: 41652
superconductivity of, effects of electron-phonon interactions on, 18: 9272
superconductivity in, theory of, 18: 34694
superconductivity of, research program on, 18: 44147(R) (ORNL-3670 (p.21-2))
superconductivity in, with p- and d-wave pairing, (T), 19: 19028
superconductivity in, effect of ion core on, (T), 19: 23559
superconductivity of, effects of communal entropy of crystal structure on, (T), 20: 19734
superconductivity, two-fluid model of, 20: 40037
supercooling in, mechanism of, 19: 9604(R) (IS-900(Sect.M))
surface analysis for films by proton elastic scattering, (E), 19: 40962
surface cleaning by ion bombardment, literature survey, 19: 4596
(RFP-433)
surface diffusion coefficients of, determination by tracer techniques, 17: 1946(R) (TID-16980)
surface energy in ultrahigh vacuum, use of nuclear transformation in measuring, 19: 24471
surface finish, effects of electrochemical metal removal methods on, 19: 28776 (DMIC-213)
surface friction of clean, in sodium (liquid), 17: 2080
surface ionization of, effects of adsorbed-atom migration on, (T), 19: 27109
surface junctions of, contact points at, (E), 19: 28748
surface layer removal by vibratory polishing, 20: 7504
surface phenomena in melts of, 18: 32078
surface physics of, use of field emission microscopy in study of, 20: 32742
surface preparation, 18: 10655
surface properties and volume of, relation between, 17: 41476(T)
surface temperature fluctuations during nucleate boiling of water, measurement, 16: 5469
surface tension measurement by pendant drop method in liquid, tables for, 19: 34682 (LA-DC-6515)
surface tension of liquid, relation to critical temperature and surface energy, 16: 25351
surface tension of liquid, calculation of, from thermal conductivity, 16: 5726(T) (AEC-tr-4937)
surface tension of liquid, expression as function of temperature for, 17: 6708
surface tension of, conference on, 17: 41472(T)
surface tension of liquid, review on measurement of, 19: 47064
technology of high-temperature liquid, review, 17: 27535 (BNL-801)
technology of high-temperature liquid, 17: 36192 (BNL-814)
technology of high-temperature liquid, 18: 18282 (BNL-844)
technology of high-temperature liquid, review, 18: 24064
technology of high-temperature liquid, review, 18: 35927 (BNL-866)
technology of high-temperature liquid, review, 18: 35928 (BNL-875)
technology of high-temperature liquid, review, 19: 13872 (BNL-892)
technology of high-temperature liquid, review, 19: 18389 (BNL-905)
technology of high-temperature liquid, review, 19: 36950(R) (BNL-928)
technology of high-temperature liquid, review, 20: 7494(R) (BNL-953)
technology of high-temperature liquid, review, 20: 14958 (BNL-972)
technology of high-temperature liquid, review, 20: 39330 (BNL-962)
technology of liquid, review, 17: 16535
technology of liquid, review on, 18: 40771
technology of liquid, review on, 20: 4330(T) (ORNL-tr-854)
technology review on high-temperature liquid, 20: 43808 (BNL-991)
temperature measurement by induction method, 18: 12416 (HW-79621)
tensile properties of body-centered-cubic, theory of, 17: 27730(R) (HW-77052)
tensile properties of, review on, 20: 4399 (UCRL-16301)
tensor properties of oriented, 19: 892 (DP-927)
testing methods for heat-resisting, 20: 46207
testing of sheets of, electromagnetic pulse method for, 19: 28523(P)
testing thin sheets of, using Lamb waves, 18: 35208
theory for helicon dispersion relations in, (T), 19: 4760
theory of binding in, 20: 4476(R) (IS-1200(Sect.P))
theory of liquid analysis of Morse potential in, 16: 9213(R) (TID-14690)
theory of localized states in, impurity pairs in many-body, 18: 24170
theory of, neutral pseudo-atoms in, 18: 25897
thermal conductivity at low temperature, theory, 16: 15352
thermal conductivity of surfaces in contact, method of prediction, 16: 27244
thermal conductivity coefficients of liquid, effects of ratio of eddy diffusivities for heat and momentum, 16: 13260
thermal conductivity of surface-contacting, 17: 22276 (NYO-9459)
thermal conductivity of, effects of crystal imperfections on, 17: 35773
thermal conductivity of surface contacting, 18: 42038
thermal conductivity of liquid, classification of temperature dependence of, 19: 30747 (TID-21737)
thermal conductivity of high-temperature, (T), 20: 25577(T) (LA-tr-66-22)
thermal decomposition of steam on, 18: 26824(R) (ANL-6885)
thermal expansion of, theory for, 18: 44219
thermal expansion coefficients of oriented, prediction from growth index method, 19: 951 (DP-904(p.117-23))
thermal insulation uses, in stacks with refractory materials, 16: 27689(P)
thermal properties of, quantum field theory for, 17: 16806
thermal properties at high temperatures, measurements of, 17: 30833
thermal properties at ambient temperature, data tabulation of, 20: 2343 (SC-TM-65-242)
thermal resistance, 16: 3482(T) (FTD-TT-61-160)
thermionic cell collectors of liquid, analysis of, 17: 27987
thermionic emission, calculation of periodic deviations from Schottky effect in, 16: 25954 (TID-16225)

thermionic work functions of cesium-coated surfaces of, method for measuring, 20: 19422 (N-65-26628)
thermodynamic properties of, at high temperatures, 17: 6043 (NP-12310)
thermodynamic properties of liquid, 18: 10543(R) (TID-20117)
thermodynamic properties at high pressures and temperatures, 19: 40459 (NP-15324)
thermodynamic stability of, in relation to structure, 17: 6686 (UCRL-10012)
thermodynamics of liquid, plasma theory of, 18: 18374
thermodynamics of high-strength, 19: 2731 (UCRL-11470)
thermodynamics of interfaces of, with glass, 19: 36344 (UCRL-11816)
thermodynamics of mass transport in, 19: 38678
thermodynamics of interfaces with glass, 19: 40464 (UCRL-11816(Rev.))
thermoelectric properties measurements for liquid, methods development for, 17: 36860(R) (ANL-6648)
thermoelectric stability in PBRE, 18: 23099(R) (ORNL-3591(p.156-9))
thermomagnetic phenomena in strong magnetic fields, (T), 19: 16178
thermomagnetic wave propagation in, (T), 19: 11849
thermophysical and transport properties of high-temperature energy-storage, survey of, 19: 35002 (TID-7687(Suppl.))
thermophysical properties in composite structures, 16: 2204 (WADC-TR-58-476(Vol.IV)(Rev.))
thermopower factor of, 17: 41523 (AFCRL-62-1047)
thickness measurement using Lamb waves, ultrasonic method for, 18: 11551(P)
thickness measurements of, by fast-neutron defectoscopy, 20: 25454
thickness of coatings of, device for measuring, 18: 7021(P)
thickness of evaporated layers of, measurement of, 20: 25341 (AERE-R-5097, Paper 25)
thickness of, use of gamma absorption and backscattering for measuring, 20: 23558
thinning down by ionic bombardment in preparation of transparent samples for electron microscopy, 18: 28110
time-to-rupture tests of, analysis, 19: 47081 (EURAEC-1432)
titration of ionic, potentiometric, 19: 9046(R) (IS-900(Sect.C))
toxicology of radioactive, 18: 22
transactions of American Society for Metals, 16: 2245
transport effects in, research on, 20: 2519(R) (AD-615152)
transport of heat and momentum in liquid, 17: 288
transport processes in magnetic fields, quantum theory for, 19: 23978
transport theory for electron-phonon gas, quantum, 19: 1434
tunneling characteristics of contacts of superconductors and normal, (T), 20: 2910
tunneling junctions with superconductors, asymmetries in, 19: 7952
ultrasonic attenuation in, effect of coulomb interaction on, 18: 26408
ultrasonic attenuation in, fluid-dynamic approximations for, 19: 915
ultrasonic attenuation in longitudinal magnetic fields, giant quantum oscillations in, (T), 19: 9794
ultrasonic energy effects, bibliography, 16: 19250 (TID-15414)
ultrasonic extinction in, effects of drift motion of carriers on, 17: 4982
ultrasonic wave attenuation at low temperatures in, effects of transverse magnetic fields on, 17: 36487
ultrasonic wave propagation in strong magnetic field, attenuation oscillations and velocity of, 20: 34862
use in MHD conversion systems of two-phase liquid, 20: 41734
use in space environments, considerations for, 16: 2790 (NP-10947)
use of fluid, in magnetohydrodynamic power generation, (T), 19: 9978
use of liquid, in heavy-particle electrostatic rockets, 18: 4351
use of liquid in MHD generators, 18: 22710(R) (NP-13881)
use of liquid, in vortex magnetohydrodynamic cells, 18: 7462
use of liquid, as bearing lubricants, 18: 13990
use of liquid, as reactor coolants, 18: 38348
use of liquid, in MHD generators, 18: 18616 (ASD-TDR-63-700)
use of liquid, in two-fluid magnetohydrodynamic system, 19: 14303(P)
use of liquid, in d-c MHD generators, 19: 47292
use of liquid, in SNAP cooling and power cycles, 20: 20303
use of liquid, in thermionic cells, 20: 31969
vacancies in quenched fcc, review of, 19: 4648 (CONF-615-5)
vacancy annealing in, theory, 18: 30282
vacancy clustering during quenching in fcc, 19: 44739(R) (ANL-7000, pp 233-77)
vacancy migration to sinks during quenching, theory, 18: 33179 (COO-1198-176)
vapor pressure of, isotope methods for determination, 17: 36100
vapor pressure of liquid, measurement by carrier gas method, 17: 37519(T) (AEC-tr-5983)
vapor pressures of, 20: 331
vapor, thermodynamic properties of "perfect", (T), 20: 42045
vaporization from cylindrical cells, calculation of rates of, 19: 46943(T) (FTD-TT-65-611)
viscosity as a function of temperature, 16: 12147
viscosity measurements of liquid, torsional oscillation method for, 16: 16343(T) (NASA-TT-F-88)
viscosity of liquid, relation between activation energy and melting point in, 17: 23988
viscosity of liquid, activation energy of, 17: 28828(R) (TID-18951)
viscosity of liquid, equation for determining, 20: 20656 (UCRL-11930)
void fraction measurement in boiling liquid, x-ray technique for, 20: 27095 (ANL-7100, pp 195-215)
wave absorption in magnetic field, acoustic and electromagnetic, 18: 36507
wear in carbon dioxide at high temperatures, 16: 29079
weight determination of large masses of liquid, using radioisotopes, 17: 25400(P)
weldability of, review of, 17: 11166 (HW-SA-2527)
welding by vertical ascending method, stress distributions from, 18: 35973(T,R) (EURAEC-1023)
welding of reactive, problems, 16: 10488(T) (FTD-TT-61-251)
welding of reactive, design of apparatus for controlled atmosphere, 17: 23900 (KR-38)
welding of, residual stresses caused by upward vertical, 18: 8779(T,R) (EURAEC-820)
welding of, thermal cycling calculations for, 18: 8776(T,R) (EURAEC-433)
welding of, electron-beam techniques in, 17: 30921 (SC-4920(M)(p.73-6))
welding specification guides at HAPO for, 18: 4215 (TID-15247(Rev.))
welding to ceramics, graphite, and metals in SNAP reactor environment at 700 to 1300°F, self-, 20: 7570 (NAA-SR-9643)
welding, use of electron beams in, 17: 511 (DMIC-174)
wetting behavior of molten salts on, 18: 22011(R) (ORNL-3591(p.38-58))
wetting behavior of, sonic effects on, 19: 32048(R) (NP-15073)
wetting of dispersed fuel particles by, 16: 15812(P)
wetting properties of liquid, apparatus for measuring, 19: 9281(R) (IS-900(Sect.E))
wetting surfaces of refractory oxides, methods for controlling degree of, 17: 41473(T)
work function relation to thermal desorption rate, (T), 19: 16181
work functions in cesium, methods for measuring, 19: 16182
work functions of refractory, coated with cesium, 18: 30176 (TID-7687(p.117-31))
work functions of, effects in silicon diodes, 19: 28662
work hardening of bcc, literature survey, 18: 12622 (ASD-TDR-62-354 (Pt.II))
work softening of, Bauschinger effect in cold, 18: 4935(T) (SC-T-524)
x-ray scattering by liquid, computer program for analysis of, 18: 609 (TID-19548)
x-ray diffraction analysis of liquid, high-temperature furnace for, 19: 22882
x-ray emission band spectra of, alloying effects on, (E/T), 19: 16205
x-ray scattering in, measurement and theory of, 19: 38524
air–iron–metal, magnetic field calculations in planar geometries of, 19: 9774 (UCRL-7784)
fused salt–metal, mass transfer and mixing in columns of, 16: 20042(R) (BNL-696)
gas–metal, phase studies of ideal, comparison with niobium–nitrogen system, 16: 33492
NH_3–metal, kinetics and structure of solutions of, 20: 31218(R) (UCRL-16658, pp 1-9)

METAMICT MINERALS
occurrence and properties of niobium–uranium, in Powhatan County, Virginia, 19: 44279

METAPHOSPHATES
effects on strontium-89 metabolism in mice, 19: 2019
hexa-, effects on yttrium-91 metabolism by mice, 19: 3865
performance of silver-activated glasses of, for neutron dosimetry, 20: 5713 (AD-623384)
protective effects of cyclic tri- and tetra-, against lethal effects of x rays, 16: 4069

METAPHOSPHORIC ACID
effects of, on radiolysis of ascorbic acid, mechanism of, 17: 1546
esters of, structure and mechanism of hydrolysis of $[PO_2(C_2H_5)]_n$, 18: 17718(R) (UCRL-11046(p.152-8))

METASTASES
detection of bone, by strontium-85 scanning, 20: 40794
effects of radiotherapy, surgery, and other treatments on growth of tumor, 20: 40745(R) (NYO-901-54, pp 29-47)
evaluation of radiotherapy for bone, 20: 43038
growth rates in patients with different types of primary tumors, 20: 43033
localization of pelvic, of genital cancers, tracer method for, 20: 12751
pain from bone, phosphorus-32 radiotherapy of, 19: 36164
radiation effects on rat sensitivity to pulmonary, following lymph node irradiation, x, 20: 3718
radiation effects on, following therapy for breast cancer, 20: 40793
radiodiagnosis in bones using calcium-45 and strontium-85, 19: 45729(R) (NYO-910-23, pp 1-111)

radiodiagnosis of bone, using strontium-85, 20: 18513
radiodiagnosis of bone, using calcium-47 or strontium-85, 20: 20404
radiodiagnosis of, using iodine-131-labeled fibrinogen, 20: 28871(R) (EUR-2636.f,i)
radiography of liver, using Thorotrast, 20: 5465
radioinduction of, model for, 20: 42963
radiosensitivity in neoplastic, biological factors affecting, 19: 45920
radiosensitivity of epithelial tumor, biological factors affecting, 19: 45921
radiotherapy of breast, using pituitary ablation by gold-198, 20: 22816
radiotherapy of cutaneous, arising from internal neoplasms, 20: 43039
radiotherapy of gynecological, using gold-198 particle implants, 20: 8809
radiotherapy of lymph node, evaluation of supervoltage, 20: 205
radiotherapy of lymph node, use of lymphography in, 20: 22806
radiotherapy of nasopharynx and parotid, in skull base, 20: 45562
radiotherapy of orbital, gamma, 20: 22829
radiotherapy of sacral, effects on embryo of gamma, 20: 22702
radiotherapy of skeletal, protective, 19: 42361
radiotherapy of, method for, 20: 3842
radiotherapy using sulfur-35-labeled triethylenethiophosphoramide, 20: 45534
therapy of nervous system, chemical and radiation, 19: 36055

METEORITES

age and thermal history of, 18: 35709
age determination by rhenium–osmium method, 17: 30733
age determination from argon-39 and chlorine-36 contents, 17: 30745
age determination from carbon-14 contents, 17: 30746
age determination from long-lived nuclides, 18: 20221
age determination of amphoteric, 19: 41225
age determinations of, review of methods for, 17: 12475
age estimation, 16: 27442
age estimation, 20: 16715
age estimation by rhenium–osmium method, 16: 10751
age estimation by rubidium–strontium method, 16: 31969
age estimation for iron, by potassium-40/potassium-41 method, 18: 26198
age estimation for, review on (E/T), 19: 1141
age estimation for iron, (E), 19: 28537
age estimation from potassium isotopic composition, 17: 30744
age estimation of iron, determined by ratio of potassium-40 to argon-40, 16: 25614 (JPL-TR-32-147)
age estimation of Farmington, based on ratio of carbon-14 to argon-39 and aluminum-26 to argon-39, 18: 2518
age estimation of chondrites and chondrules, rubidium–strontium, 20: 529
age estimation of Barwell, potassium–argon, 20: 34052
age estimation of, methods for, 18: 22262(T) (JPRS-24435(p.46-63))
age estimation of, by strontium–rubidium method, 20: 12992
age estimation of, methods for, 20: 20365
age estimation, radiometric, 16: 24007
age estimations for, cosmic ray exposure and helium–thorium–uranium, 20: 956
age estimations from potassium isotope abundance, 16: 10750
age estimations of Cold Bokkeveld and Farmington, analysis for cosmic-ray-produced aluminum-26, 16: 33661
age, nature, and origin of, 17: 20815 (BNL-779)
age of, and time of formation, 17: 12476(T)
age of Bjurbole, separated phase study of, 18: 4383(R) (NYO-10517 (p.119-20))
age of carbonaceous, rubidium-87/strontium-86 estimation of, 20: 45916(R) (MIT-1381-12)
age of, fine structure constant from, 17: 9298
age of Sikhote Alin, from potassium-argon ratio, 17: 36005 (BNL-6451)
age of stony, rubidium–strontium, 18: 4382(R) (NYO-10517(p.7-15))
age of stony, rubidium-87/strontium-86 estimation of, 20: 45916(R) (MIT-1381-12)
age, composition, and origin of, review of, 19: 14223
age, composition, and histories of, 20: 18556(R) (BNL-929, pp 66-82)
age, origin, and rare-gas loss of, (E), 20: 5979
ages by rhenium/osmium determination, 16: 16040
ages of Estherville, Haraija, Juvinas, Shergotty, and Stannern, 20: 41162
ages of, potassium–argon method, 17: 3925
ages of, argon–potassium, helium-4–thorium, and uranium methods for estimating, 20: 15193 (NP-15654)
ages of, from rare gas contents, 18: 35708
ages of, radiometric estimation of, 18: 26189
aluminum-26 and manganese-53 content and radiation ages of iron, (E), 20: 41614
aluminum-26 content in Pribram, cosmic ray exposure flux from, (E), 20: 7688
aluminum-26 content of iron, 17: 30743
aluminum-26 content, 18: 10757
aluminum-26 production in chondrites by cosmic radiation, 18: 12365
analysis by activation and gamma spectrometry, 18: 31402
analysis by activation, computer program for gamma spectra analysis in, 19: 18387
analysis by activation methods, 20: 35987
analysis for aluminum-26 and sodium-22, γ–γ coincidence, 16: 6887
analysis for aluminum-26 and beryllium-10, 17: 4717
analysis for aluminum-26 and sodium-22, radiometric, 17: 10839
analysis for aluminum-26, beryllium-10, and chlorine-36, 18: 20221
analysis for aluminum in chondritic, activation, 18: 27327
analysis for antimony, activation, 20: 43080 (ORO-2670-15)
analysis for argon isotope ratios, 16: 24668
analysis for argon, helium, and neon content and isotopic composition, 20: 15193 (NP-15654)
analysis for barium, bismuth, palladium, silver, and uranium, 17: 25445
analysis for beryllium, fluorometric, 17: 4698
analysis for bismuth, mercury, and thallium by slow neutron activation, 20: 43550(R) (NYO-844-67)
analysis for bromine by activation, 19: 26253
analysis for bromine and zinc, activation, 19: 42451
analysis for bromine, activation, 20: 40811 (ORO-2670-13)
analysis for calcium-48/calcium ratio, activation, 18: 8529
analysis for cesium and rubidium, activation and mass spectrometric, 18: 15976
analysis for chlorine by activation, 19: 26254
analysis for cobalt, activation, 20: 2055
analysis for cosmic-ray-induced carbon-14 and chlorine-36, 16: 23984 (NYO-8922)
analysis for cosmic-ray-induced nuclides, mass spectrographic and radiochemical, 17: 29480 (NASA-TN-D-1844)
analysis for cosmogenic iodine-129, 18: 43601(R) (TID-21007)
analysis for elements, activation, 19: 7349
analysis for gold, activation, 20: 7033
analysis for gold, iridium, and platinum by thermal neutron activation, 20: 40835
analysis for hafnium and zirconium in iron and stone, activation, 16: 17896
analysis for hafnium and zirconium, neutron activation, 17: 31986 (TID-19179)
analysis for hafnium and zirconium, activation, 19: 4078
analysis for hafnium by neutron activation, 17: 13270
analysis for hafnium by neutron activation, 18: 32339
analysis for indium by activation, cellulose acetate–dithizone columns for, 16: 16319
analysis for indium, selenium, and tellurium, neutron activation, 20: 23859
analysis for iodine, tellurium, and uranium, neutron activation, 16: 25623
analysis for iridium, tantalum, and tungsten, activation, 17: 38999
analysis for iron using Mössbauer effect, 19: 9076
analysis for krypton isotopic composition, 18: 40106
analysis for krypton and xenon isotopes for indication of fission, neutron capture, and spallation anomalies, (E/T), 20: 11424 (NP-15629)
analysis for lead by alpha activation, 17: 2903 (BNL-5628)
analysis for lead by neutron activation methods, 19: 36303
analysis for lead by fast-neutron activation, 20: 43550(R) (NYO-844-67)
analysis for lead, and uranium, activation, 20: 42062
analysis for long-lived nuclides, 17: 696
analysis for oxygen and silicon simultaneously, activation, 18: 11984
analysis for oxygen by fast-neutron activation, 19: 30125
analysis for oxygen and silicon, fast-neutron activation, 19: 43927 (CONF-650405-16)
analysis for oxygen and silicon, activation, 20: 22875 (ORO-2670-10)
analysis for radioactivity produced by cosmic-rays in Bogou iron, non-destructive, 18: 27707
analysis for rare-earth and yttrium abundance, activation, 16: 20841
analysis for rhenium by neutron activation, 19: 28264
analysis for rubidium and uranium, isotope dilution, 18: 1547
analysis for scandium by neutron activation methods, 19: 36254
analysis for silicon by activation, 19: 26250
analysis for tungsten, activation, 17: 1636
analysis for zirconium by neutron activation, 18: 32339
analysis for zirconium by neutron activation, 17: 13270
analysis of achondrites and chondrites for rare earths, 18: 14708
analysis of achondritic, for thorium and uranium, 18: 24286
analysis of achondritic, for uranium and thorium, 19: 27051
analysis of, activation, 17: 26205
analysis of, activation, 17: 26206
analysis of, activation, 17: 33851
analysis of Aroos and Sikhote-Alin, for radioactive constituents, 17: 12452 (LA-2765)
analysis of bronzite chondrites, for rare gases, (E), 20: 5975
analysis of Bruderheim chondritic, for radioactive constituents, 16: 917
analysis of Bruderheim chondritic, for xenon isotopes, 16: 415
analysis of Bruderheim, for argon-39 and tritium, 16: 916
analysis of Canyon Diablo, mass spectrometric and metallographic, 20: 17238

analysis of chondritic, for thorium and uranium, 18: 24285
analysis of dark and light, for barium, cerium, europium, phosphorus, scandium, and uranium by neutron activation methods, 20: 26788
analysis of, for chemical and physical properties, 17: 37912
analysis of, for helium and neon, 17: 14518
analysis of, for tritium, 17: 5947(R) (AFCRL-62-295)
analysis of iron, for lead isotopes, 18: 5897 (JPL-TR-32-371)
analysis of iron-type, for zinc, activation, 18: 39098
analysis of iron, for manganese-54, spectrometric, 18: 15985
analysis of iron, for molybdenum isotopes, 18: 44350
analysis of iron, for argon, helium, and neon isotopes, (E), 20: 5977
analysis of iron, for gallium and germanium simultaneously, by neutron activation, 20: 38825
analysis of iron, for calcium and lithium, 20: 7701
analysis of iron, for gallium, 20: 530
analysis of, neutron capture, 17: 26419(R) (ARF-1193-23)
analysis of Pesyanoe, for rare gases and sulfides, spectrographic and x-ray diffraction, 16: 17893
analysis of Sikhote-Alin, 16: 29627
analysis of stone, for cosmogenic radionuclides, 18: 43601(R) (TID-21007)
analysis of Tunguska event, 16: 16032(T) (JPRS-13480)
analysis of, cosmic-ray variation determination by, 18: 20815 (BNL-7948)
analysis of, cosmic-ray and solar-wind data from, (E), 19: 34963
analysis, radiochemical, 16: 8760(R) (TID-14830)
anomalies in, use in study of early chronology of solar system, 16: 30989 (NASA-TN-D-1465)
anti-matter content of Tunguska, of 1908, 19: 30929
argon abundances and isotopic compositions of iron and stone, 16: 19168
argon content, 17: 25466
argon content and isotopic composition in Sikhote-Alin, 16: 22412(T) (AEC-tr-5119)
argon isotope content of, bibliography on, 17: 6270(R) (NYO-10325)
argon isotope diffusion in iron and stone, 18: 5486
argon isotopes in Kapoeta and Staroe Pesjanoe, 16: 27445
argon-37 content in chondritic, 16: 16080
argon-38 and -39 contents of iron, estimation of cosmic-ray exposure ages from, 20: 21505
argon-39 content of Bruderheim, 16: 27444
atomic abundances in chondrites, review of data on, 18: 14059
barium isotope abundance in stony, 16: 7983
beryllium content ratio to sun, 17: 24202
beryllium-10 content of iron, 17: 30743
book: *Earth Science and Meteorites*, 18: 12343
boron isotopic abundances in, 17: 5097
boron isotopic abundances in, 17: 36553
bromine isotopic composition in, 19: 26253
cadmium content in, 18: 5899
calcium and lithium production in iron, from cosmic radiation, (E), 20: 37603
calcium isotope content of, bibliography on, 17: 6270(R) (NYO-10325)
calcium isotopic contents of, 18: 3980(R) (NYO-10517(p.3-5))
calcium-40 and -46 ratio in Homestead and Pasamonte, 18: 27708
carbon isotopic abundance in minerals of Orgueil chondrite, 17: 18310
carbon-14 content in, terrestrial age estimations from, 16: 19170
carbon-14 content in iron and stone, age estimations from, 16: 20828
carbon-14 content of Henbury and Richardton, 16: 9018
cerium isotope abundance in stony, 16: 7983
characteristics of Bondoc, 17: 10838
charged particle fossil tracks in minerals of Vaca Muerta, 19: 25140
chlorine-36 content in iron, 17: 30743
chlorine-36 production by neutron capture in, 18: 44358
chondritic earth model, evaluation of, 18: 22662
chromium isotope content in iron, cosmic-ray produced enrichment of, 20: 25697
chromium isotope occurrence in, 17: 6257 (IS-438)
chromium isotopic content in, (E), 19: 44907
cobalt in ablation products of iron, 19: 30910
collection of micro-, with sounding rocket, 17: 8916 (AFCRL-1049)
composition, 18: 42283
composition and classification of, 20: 42064
composition of, in relation to early history of solar system, 17: 6902 (EFINS-62-50)
composition of Murray, 17: 17652(R) (UCRL-10634)
composition of, lead, thorium, and uranium ratios in, 18: 44357
composition of, radiometric determination of, 18: 22656
composition of, role of uranium photofission in, 20: 7703
compositional and petrological relations in, 18: 34398
conference on, Arizona State Univ., Mar. 1961, 16: 9015
copper-63 and -65 abundance ratio in, 19: 11398
cosmic particle reactions with, cross sections for radioisotope production in, (E/T), 19: 10267
cosmic proton reactions in, argon-39/chlorine-36 ratios from, 17: 9165 (BNL-5909)
cosmic proton reactions with, Monte Carlo calculation of radionuclide production in, 20: 22035
cosmic radiation reactions in, production of radioisotopes by, 16: 1808(R) (TID-12849)
cosmic radiation reactions on, review of, 17: 5060
cosmic-ray-exposure history of, 17: 22406 (TID-18600)
cosmic-ray exposure ages of iron, from argon-39 and chlorine-36 abundances, 17: 40988 (AFCRL-62-1092)
cosmic-ray exposure ages of eight iron, by potassium isotope method, 18: 8972 (NP-13493)
cosmic-ray exposure ages of 47 stony, from helium and neon isotopic abundances, 18: 8974 (NP-13495)
cosmic ray exposure ages of, 18: 22656
Cosmic-ray-induced argon-37, -39 ratio in recently fallen, 17: 11448 (BNL-6545)
cosmic ray interaction effects in, estimation of half lives of isotopes from, 19: 12054
cosmic-ray effects on graphite in, age estimation from, 18: 40175
cosmic-ray exposure ages of dated-fall iron, (E), 19: 9864
cosmic-ray exposure ages of iron, (E), 19: 20760
cosmic-ray reactions with iron, magnesium, silicon, and sulfur in stony, production of helium-3 and neon-21 by, 18: 20204
cosmic-ray reactions with, determination of exposure ages and radiation intensities from, 19: 23355(R) (BNL-867(p.1-117))
cosmic-ray reactions in, argon-39 and chlorine-36 production, 20: 21508
cosmic-ray spallation reactions with iron, chromium isotopes from, (E), 20: 7747 (NP-15591)
dating by analysis of charged particle tracks resulting from spontaneous uranium fission, 19: 39038
description and radioactivity analysis of Ehole (Angola), 16: 20842
detection at impact, instrument development for, 16: 27725 (AD-269126)
diffusion of tritium in stone, 20: 17247
Dirac monopoles in, search for, 18: 16552(R) (UCRL-11132)
dissolution of iron, in sulfuric acid, 20: 43550(R) (NYO-844-67)
distribution of rare earths in, 16: 25648(R) (GA-2782(Rev.))
distribution of rare earth in, 17: 10821(R) (GA-2985)
distribution toward Mars, 18: 2409(T) (FTD-TT-63-968)
dust production by micro-, on lunar surface, 16: 21132 (NP-11652)
effect of micro-, on space vehicles, 16: 30916
effects on space vehicles, estimates of magnitude and nature of, 20: 2036 (AD-618030)
element abundances in, 19: 37428(R) (N64-32896)
element abundances in Bjurböle, 20: 4526
element abundances in, 20: 23868
element abundances in, review on, 18: 26201
element abundances in chondritic, 18: 8267 (CONF-151-4)
element abundances in chondritic, (E), 19: 28536
energy release from impact of Tunguska, antimatter annihilation theory for, 20: 9690
europium isotope content, 17: 25468
explosion effects of, review of Soviet research on, 19: 32786 (AD-610054)
fluorine content in stone, 19: 4351
fluorine-19 content in, ratio to oxygen-18, 18: 4384
formation and ages of, potassium-40 abundance for determination of, (E), 20: 19341
formation of Bruderheim, hypotheses concerning, 20: 7716
free radical occurrence in carbonaceous matter of, electron paramagnetic resonance determination of, 18: 32341
frequency, mass, and impact data, 16: 20233
gadolinium isotope content, 17: 25468
gallium content in chondritic, 19: 44900
gamma activity in Granes stone, 19: 40788
gas content of, solar wind source for primordial, 20: 5976
geochemical studies of achondrites, 17: 37361
geology of Argentine craters from, 17: 37361
germanium isotope content in, 17: 30720
glass crystallization in, 16: 1275(R) (NP-10832)
gold content, 19: 23242
hafnium–zirconium fractionation with terrestrial rocks, 17: 1637
halogen abundance and inter-relations in, 20: 44077
heavy-element isotopic abundances in, 18: 34400
helium abundances and isotopic compositions of iron and stone, 16: 19168
helium content and isotopic composition in Sikhhote-Alin, 16: 22412(T) (AEC-tr-5119)
helium content and isotopic ratio in iron, 18: 20205
helium contents and isotopic compositions of 22 iron, 18: 8973 (NP-13494)

helium distribution in surfaces and inner grain boundaries of, microprobe detection technique, 20: 25696
helium isotope abundance in iron, 16: 4652
helium isotope diffusion in iron and stone, 18: 5486
helium isotope diffusion losses in stony, 18: 8975 (NP-13496)
helium isotopes in Kapoeta and Staroe Pesjanoe, 16: 27445
helium-3 and -4 content in, 17: 41685
helium-3 production rates in stony, by cosmic rays, 18: 8976 (NP-13497)
helium-4 diffusion from stony, activation energy, 17: 29100
hydrocarbon mass spectra as evidence of extraterrestrial life, criticism, 17: 8393
hydrogen diffusion from alpha- and gamma-iron, 18: 16210
impact effects of micro-, accelerator for simulating, 20: 37340(P)
iodine-xenon formation intervals for, (E), 20: 4526
iodine-129 in, origin of extinct, 20: 29891
iridium abundance, 17: 3181
iridium content, 19: 23242
iridium content in stone, from activation analysis, 16: 27443
iridium distribution in, 16: 417
iron-60 content in Odessa, cosmic-ray produced, 19: 16345
isotope content of iron, cosmic-ray produced stable, 17: 3177
isotope distributions in, 19: 14214
isotope production in, by cosmic rays, 20: 7690
isotopes produced by cosmic rays in, review of, 17: 4693
isotopic abundances in, 16: 13841
isotopic abundances of rare earths in, 17: 30690
isotopic composition and spallation reactions in iron, 16: 6886
isotopic composition and content of, helium and neon, 20: 956
isotopic composition of xenon from calcium-poor achondritic, (E), 20: 39984
isotopic composition of achondritic, cosmic-ray-produced xenon, (E), 20: 44079
isotopic compositions of, review on, 18: 26201
isotopic displacements in, significance for early history of planetary system, 17: 4702
krypton and xenon content in chondrules and minerals of Bruderheim, 20: 11430
krypton content, 17: 25466
krypton isotope abundances in, fission, neutron capture and spallation anomalies in, 20: 31875
lead in Devil's Canyon, primary, 16: 9004
lead isotope ratios in carbonaceous, 16: 19166
lead isotope ratios in, age estimation from, 20: 12991
lead isotopic content in, 18: 22654
life-like forms in, conference at New York City, April 30–May 1, 1962 on, 17: 38652
lithium content in stone, 19: 4362
lithium content ratio to sun, 17: 24202
lithium isotope abundance in, ratio to terrestrial rocks, 17: 23524
lithium isotopic content of Bjurbole and Bruderheim, 20: 39102
lithium isotopic composition of Bruderheim and Bjurbole, 20: 42061
lithium-6 content in ratio with lithium-7 in stone, 19: 4362
lithium-6 to lithium-7 ratio in Holbrook, 20: 7266
luminescence of stony, proton-excited, 18: 20072
manganese-53 content of, half life calculation from, 19: 47627
measurements by rockets and satellites, 16: 10400 (ASD-TR-61-322 (p.1-7))
microstructure of Orgueil carbonaceous, 20: 27696
molybdenum isotope abundance anomalies in, 16: 10711
molybdenum isotope and zirconium abundances in iron and stone, 18: 5901
molybdenum isotope content, 17: 25468
morphology of organized elements in carbonaceous chondrites, 17: 38654
neon abundances and isotopic compositions in iron and stone, 16: 19168
neon content, 17: 25466
neon content and isotopic ratio in iron, 18: 20205
neon content and isotopic composition in Sikhote-Alin, 16: 22412(T) (AEC-tr-5119)
neon contents and isotopic compositions of 22 iron, 18: 8973 (NP-13494)
neon isotope abundance in iron, 16: 4652
neon isotope diffusion in iron and stone, 18: 5486
neon isotope diffusion losses in stony, 18: 8975 (NP-13496)
neon isotopes in Kapoeta and Staroe Pesjanoe, 16: 27445
neon-21 production rates in stony, 18: 8976 (NP-13497)
neutron capture and spallation reactions on, chlorine-36 production by, 19: 30937
neutron flux encountered by chondrite, calculation, 16: 6891
neutron production and reactions in, 17: 15008
nickel in ablation products of iron, 19: 30910 (EUR-1819.e(p.59-61))
nuclear reactions in, krypton and xenon isotopic content as indicators of, (E/T), 20: 11424 (NP-15629)
nucleosynthesis model for heavy elements, 17: 8402
origin, 18: 14069
origin and properties of, review of, 20: 2590
origin of bronzite chondrites, lunar, 20: 21507
origin of Canyon Diablo No. 2 and No. 3, cosmogenic rare gas analysis of, 18: 44342 (COO-382-48)
origin of carbonaceous chondrites, review of clues to, 17: 38655
origin of chondritic, erosion and radiation ages for, (T), 20: 34043
origin of gas-rich, evidence for, 18: 28203
origin of, theory of, 17: 34689
origin of, chemical evidence relative to, 20: 19346
origin of, evidence of moon, 19: 23253
origin of, Monte Carlo analysis of, 18: 34396
osmium content in stony, 18: 24292
osmium isotope abundance in, 17: 19001 (TID-16599)
oxidation of Urey-Craig, 18: 34397
oxygen-16 and oxygen-18 abundances in minerals in stony, 19: 599 (CONF-759-1)
oxygen-16 and oxygen-18 abundance in chondritic, 19: 600 (CONF-759-2)
oxygen-16/-18 ratio in, measurement of, 20: 45915(R) (CALT-427-14)
particle tracks in, fossil, 20: 7375
platinum abundance in, 17: 3181
platinum content in, 19: 23242
plutonium-244 fission tracks in, solar system history from, 19: 32863
potassium content in amphoterite chondrites, (E), 20: 5979
potassium content of stony, 17: 30688
potassium-40 abundance in, variations in, (E), 20: 19341
potassium-40 content, 18: 10757
potassium-40 distribution in, 16: 918
production of gas-rich, (T), 20: 4526
properties of Bruderheim chondritic, 16: 414
properties of organized elements in carbonaceous chondrites, 17: 38656
properties of, book on, 19: 1162
protection of space vehicles against, 17: 36988 (SY-5394-R(Vol.II))
proton bombardment of, production of cosmogenic nuclides by, 17: 5336
proton cross section measurements for iron and stone, 17: 28943(R) (TID-18961)
proton radiation effects at 30 kev on, luminescence emission, 20: 44035
proton reactions at 1-Bev, nuclear cascades from, 17: 18391 (TID-7652(p.852-65))
proton reactions at 1 to 3 Bev with chondritic, distributions from, (E), 20: 3015 (NASA-SP-71, pp 357-62)
proton reactions at 1 to 3 Bev, cascades in, (E), 20: 12262 (BNL-8721)
proton reactions with, rare gas and tritium production in, 18: 15189 (CERN-64-12)
proton reactions with nuclei in, 20: 11377
quark content in iron, (E), 20: 34236
radiation ages by cosmic-ray activation analysis, 16: 16039
radiation effects on, review on cosmic, 18: 8993
radiation exposure ages of iron and stone, analysis by sputtering experiments, 16: 29530
radiation exposure ages of classes of, distribution in, 17: 25430 (NP-12807)
radiation exposure ages of, from helium-3/tritium ratio in, 18: 5966
radiation exposure ages of, from rare gas isotopic content, 19: 47194
radioactivities, argon-37, argon-39, and tritium, 17: 4708
radioactivity and composition of, 18: 28228
radioactivity from gamma emitters of Bogou iron, 20: 16674
radioactivity in Bondoc, cosmogenic, 19: 32884
radioactivity induced by cosmic radiation in Bogou, 19: 12045
radioactivity measurements in iron and stone, cosmogenic, 17: 28943(R) (TID-18961)
radioactivity measurements in Bogou and Bondoc Achondrite, cosmogenic, 17: 28943(R) (TID-18961)
radioactivity of Bogou, 18: 10756
radioactivity of iron, gamma scintillation spectrometric study of, 18: 2516
radioactivity of stony, gamma scintillation spectrometric study of, 18: 2515
radioactivity of, measurement of, 18: 22656
radioactivity of, analysis of gamma, 18: 42282
radioactivity of, presence of extinct, 17: 5167
radiochemical analysis of rock, cosmic-ray variations from, 20: 23961
radioinduced luminescence of enstatite, proton, 18: 36148
radioinduced luminescence of stony, proton and ultraviolet, 20: 46283
radioinduced particle tracks in, cosmic, (E), 19: 14209
radioisotope production by cosmic rays, review, 17: 3192
radioisotope production rates in iron, 16: 9017
radionuclides in iron, depth distribution of, 18: 43601(R) (TID-21007)
radionuclides in stone, 19: 8052 (NYO-8924)
rare earth abundance in, 16: 13380
rare earth abundance and distribution in, 20: 23278
rare earth abundance and isotope ratio in, 18: 10753

rare earth content in, 19: 36648
rare earth content, review on, 19: 13620
rare earths abundance in, comparison with earth's crust, 20: 17233
rare gas abundances in iron, 16: 19652
rare gas abundance and isotopic composition of, 20: 31876
rare gas concentrations in stone, 16: 29586
rare gas concentration in Pantar chondrite, 16: 29587
rare gas content and isotopic ratios in Bruderheim chondrite, 19: 9859
rare gas content in Pantar chondrite, 16: 12309
rare gas content in Renazzo chondrite, 18: 34390
rare gas content in amphoteric, (E), 19: 41225
rare gas content in Khor Temiki, (E), 19: 44906
rare gas content in silicates from Estherville Mesosiderite, heavy, 20: 31859
rare gas content of, radiogenic, spallogenic, and primordial, 18: 26197
rare gas contents in iron, 16: 9016
rare gas contents in, primordial, 19: 37450
rare gas contents and isotopic abundances in Achilles, LaLande, and Peace River, 20: 16672
rare gas contents in, evidence for paired falls from, 20: 16673
rare gas diffusion from stony, 18: 20206
rare gas isotope abundances in pantar, 16: 19167
rare gas isotope contents and age estimation of minerals from Indarch, (E), 19: 9863
rare gas isotope content and distribution in pyroxene and feldspar of Khor Temiki, 20: 25695
rare gas isotope distribution in, 16: 17892
rare gas isotopes in stony, 17: 30688
rare gas isotopic content in, 18: 20726
rare gas isotopic contents in mineral fractions of Indarch, 18: 35714 (BNL-7329)
rare gas occurrence in chondrite Tabor, primordial, 16: 23999
rare gas occurrence in, primordial, 16: 23998
rare earth abundances in, 17: 8406
rare earth content of iron, 17: 10148
rare-earth content of, isotope abundances of, 17: 12465
rare earth content of, 17: 19405
rare earth content in, variation in, 17: 25435
rare earth fractionation in, 17: 34689
rare earths content in, 17: 30719
rare-gas isotopic abundances in, 17: 24235
rare gases in Fayetteville, 18: 18033
rare-gas content in, 18: 12345
rare-gas isotopic abundances in Fayetteville, 19: 9882
rare-gas isotopic content of stone, 19: 25141
reactions with cosmic rays, analysis of simulated, 17: 28943(R) (TID-18961)
rhenium content in stony, 18: 24292
rubidium-87, strontium-86, and strontium-87 contents, 20: 9157
ruthenium isotope abundance in, 17: 19001 (TID-16599)
ruthenium isotopic composition in iron, 17: 6289
samarium content in, 17: 25468
scandium abundance and isotope ratio in, 18: 10753
scandium content, review on, 19: 13620
shielding against micro-, requirements for thermionic converter-space radiators, 18: 12852(R) (AD-409570)
silver content in Canyon Diablo, isotopic composition of, (E), 20: 31861
silver isotopic composition in iron, 16: 20829
silver isotopic content of Canyon Diablo, 20: 39102
silver isotopic content in, 17: 25468
silver-107 and -109 content in, ratio of, 18: 10755
size of stony, pre-atmospheric, 19: 30937
sodium-22 content in Pribram, cosmic ray exposure flux from, (E), 20: 7688
sodium-22 production in chondrites by cosmic radiation, 18: 12365
soil and plant samples from Tungus crash of 1908, 16: 1343
sorptive properties for argon, shock-wave effects on, 18: 18031
sorptive properties for argon, shock-wave effects on, 18: 18032
sputtering by noble gas ions at 20 kev, erosion rates for, 18: 22655
strontium isotope abundances, 16: 31969
strontium isotope content of, bibliography on, 17: 6270(R) (NYO-10325)
strontium-87/86 ratio in, 19: 30426
studies of Orgueil chondrite for substances of biological origin, 17: 38676
sulfur content and isotopic abundances in, 20: 29893
sulfur isotope abundance in, 17: 23523
sulfur isotope content of, (E), 19: 38847
sulfur isotope content in, 20: 18909
sulfur isotope ratios in, 16: 2028
sulfur isotopes distribution in, comparison of Abee and Bruderheim with others, 16: 416
sulfur isotopic abundances in standard, 17: 20230
sulfur-32/-34 ratio in troilite from, 18: 42281
sulfur-32/-34 ratio in Canyon Diablo, 17: 28615
sulfur-33 and -36 in iron, cosmic-ray-produced, 19: 47195
sulfur-34 to sulfur-32 ratio in Orgueil, 19: 39351
tantalum content, 19: 14207
tantalum distribution in, 16: 417
thermal history of Bruderheim, from argon-40 and potassium distributions, 20: 34041
thermoluminescent properties, 20: 37359
thorium content, 18: 34401
trace element contents of, comparison with earth, (E), 19: 9858
tritium content in iron and stone, 16: 20827
tritium content in, relation of tritium diffusion in iron to, 18: 1897
tritium content in chondrites, (E), 20: 34040
tritium content in chondritic, 16: 16080
tritium content in Bruderheim, 16: 27444
tritium content of iron, 17: 14495
tritium diffusion from alpha- and gamma-iron, 18: 16210
tritium retention in iron, 18: 1896
tungsten distribution in, 16: 417
Tungus, search for radioactivity increase in vegetation in region of, negative results, 17: 22310
uranium concentration in achondrites, chondrites, and stone, 16: 402(T) (NP-tr-805)
uranium content and distributions in Vaca Muerta, 19: 25140
uranium content of Sikhote-Alin, relation to lead method, 16: 4380
uranium contents, 18: 34401
uranium distribution in, 20: 16684
uranium isotope abundance in, 17: 19001 (TID-16599)
use for studies of cosmic-ray spectra, 20: 23960
use in establishing intensity variations of cosmic radiation in last million years, 16: 24672
use to measure solar-system cosmic ray flux, by induced activity, 16: 16038
vanadium-50 distribution in, 16: 918
xenon content, 17: 25466
xenon isotope abundance in, histories from, 17: 23528
xenon isotope abundances in, anomaly patterns in, 19: 47213
xenon isotope abundances in Pasamonte, fission-produced, 20: 29892
xenon isotope abundances in, fission, neutron capture, and spallation anomalies in, 20: 31875
xenon isotope content in Pasamonte, anomalies from, 20: 17239
xenon isotopic abundance anomalies in, 18: 34399
xenon isotopic composition in, 20: 25715
xenon isotopic ratios in Bruderheim, 17: 8990
xenon-129 distribution in, origin of excess in Abee, 16: 418
xenon-isotope content of Pasamonte, fissiogenic, 19: 16344
xenon-124, -126, and -128 in, cosmic-ray production of, 20: 7694
xenon-129 production in, mechanisms for, 20: 5978
xenon-129 transport in, mechanism of, 20: 18901
yttrium abundance and isotopic ratio in, 18: 10753
yttrium abundance in, review on, 19: 13620
zirconium content and ratio with hafnium in, 19: 4350
zirconium content of, role in nucleosynthetic theories, (E/T), 19: 9857

METEOROIDS

density, 18: 37837
density distributions in interplanetary space, 18: 28223
detection, distributions, and properties of micro- (E/T), 19: 2947
distribution and properties of, relevant to SNAP 8 reactor and shield design, 17: 22950 (NAA-SR-8127)
effects of penetration rate on propulsion system weights, 17: 32210
effects on materials in space vehicles, 20: 7649
effects on space vehicles, simulation of, 18: 20707
effects on spacecraft, 17: 36559
flux in space, thin film measurements of, 18: 42280
fluxes in space, 19: 44893 (NASA-CR-294)
properties between 300 and 22,000 miles in space, 18: 12996 (RTD-TDR-63-1050)
protection of manned Van-Allen-belt space vehicles against, (T), 19: 11315

METEOROLOGICAL INSTRUMENTS

(See also specific instruments.)
see also Anemometers
apparatus using radioactive probes for atmospheric potential gradient measurements, 16: 17886
descriptions, 18: 9255 (AWRE-O-68/63)
descriptions, 18: 9256 (AWRE-O-69/63)
design for determining coordinates and power of nuclear explosions, 18: 14584
design for rain scavenging studies, 16: 22438 (TID-7632(p.74-97))
design of bi-directional wind vane for atmospheric particle diffusion measurements, 16: 5614
design of constant-temperature wind component meter, 20: 516 (TID-

22278)
design of nuclear/weather cloud indicator, 17: 23615 (USASRDL-TR-2272)
design of remote recording annular vane assembly, 17: 25470(P)
design of wind recording system, 20: 29502
development at HAPO, 19: 13703(R) (HW-83606)
development for air pollution control, capabilities of, 17: 34142 (BNL-7022)
development for measuring shock waves in atmosphere, 16: 5107 (SCR-163)
development for prediction of rain-out, 16: 8984(R) (AD-263069)
development of continuous-recording, for near-ground use, 18: 43114(R) (NP-14236)
development of strontium-90-fueled telemetry package for remote use, 17: 18898 (MND-SR-2428)
performance for measuring atmospheric turbulence, 16: 25611 (BNL-718)
review of, used at Hanford, 18: 32260 (HW-62455)
use in field study of accidental chemical detonation of nuclear weapons, 19: 4403 (SC-DC-64-1572)

METEOROLOGY

see also Atmosphere
see also Stack Disposal
see also Tracer Techniques (Meteorology)
aerospace studies, 19: 44771 (BNL-914, pp 44-50)
air diffusion, pollution, and transport studies, survey of Weather Bureau, 18: 14581 (TID-7677(p.348-67))
air flow patterns over western Europe in Nov. 1962, 20: 23315
air movements in clear air and in clouds, tracer study of, 17: 8411
air trajectories from Cape Thompson, Alaska, during summer 1960, 19: 24212 (PNE-477)
analysis of data from Parr, South Carolina, 20: 14732 (CVNA-172)
atmosphere stability at Italian stations, 20: 515 (RT/PROT(65)17)
atmospheric advection models in, 19: 10705 (UCRL-7822)
atmospheric circulation, continental and global tracer studies, 17: 3159 (TID-16988(Paper 2))
atmospheric deposition problems, 19: 44247 (BNL-914, pp 139-40)
atmospheric diffusion conditions in U. S., 18: 14583
atmospheric diffusion considerations in reactor siting, 18: 37791 (A/CONF.28/P/714)
atmospheric diffusion and deposition of particles over flat terrain, 18: 42145
atmospheric diffusion studies in Canada, 19: 44790 (BNL-914, pp 149-50)
atmospheric diffusion from ground sources, data on, 19: 44792 (BNL-914, pp 153-5)
atmospheric dispersion parameters at reactor sites by smoke plume ratio method, 18: 40040 (CONF-337-41)
atmospheric dispersion in, summary of diffusion experiments for prediction of, 19: 44789 (BNL-914, pp 146-8)
atmospheric dispersion in urban areas, 19: 44791 (BNL-914, pp 151-2)
atmospheric movements, tracer studies on large-scale, 18: 34255
atmospheric release and movement of radioactive materials, research in U. S. on, 20: 33558 (ORNL-NSIC-10)
atmospheric studies using vertical proton beams, 19: 31461(R) (ANL-7010(p.235-87))
atmospheric tracer techniques for diffusion studies using phosphorescence–fluorescence analysis, 17: 20193 (HW-70892)
atmospheric transport in tropopause, 16: 7764
atmospheric transport and dilution of radioisotopes, methods of measuring, 16: 29241 (TID-7627(p.475-93))
atmospheric turbulence, 18: 45161 (BNL-7328)
atmospheric turbulence, low-level, 19: 44793 (BNL-914, pp 156-7)
bivariate normal model for atmospheric diffusion from elevated sources, 19: 1034(R) (HW-81746(p.1.29-36))
book: *Aerosols. Physical Chemistry and Applications*, 19: 38321
book: *Air Chemistry and Radioactivity*, 18: 28086
book: *Problems of Nuclear Meteorology*, 17: 25455
book: *Problems of Nuclear Meteorology*, 18: 10603(T) (AEC-tr-6128)
charged particle beams in, 18: 22546 (CONF-173-4)
circulation of the stratosphere, 16: 4374 (TID-13093)
circulation processes in the upper atmosphere, 17: 23498(R) (GCA-TR-63-3-G)
circulation processes and mixing mechanisms in the upper atmosphere, 18: 31050(R) (SC-DC-64-764)
climatic and hydrologic factors affecting distribution of strontium-90 in soil, 16: 3239 (AFOSR-1623)
climatological observations at Tonopah Test Range, 18: 13371 (SC-TM-354-63(72))
communication problems in micro-, 19: 44797 (BNL-914, pp 173-4)
computer analysis of data on Montgomery stream functions and thermodynamics, 20: 5645(R) (COO-1340-2, pp 122-45)
conditions for diffusion and deposition of small particles in atmosphere, 16: 29242 (TID-7627(p.494-506))
conference on AEC activities in, 19: 44761 (BNL-914)
conference on Air Cleaning, BNL, Upton, New York, October 10 to 12, 1961, 16: 29214 (TID-7627)
conference on meteorological aspects of atmospheric radioactivity, Geneva, 1964, 20: 23307
conference on use of radioisotopes in, 20: 16636
consistency of atmospheric diffusion measurements, 19: 2886
contribution of meteorological data in interpretation of fall-out measurement, 16: 22449 (TID-7632(p.256-70))
criteria for rapid transport of nuclear debris from stratosphere to troposphere, 20: 5649(R) (COO-1340-2, pp 54-83)
data and measurements for 1961, summary, 17: 35253(R) (IA-775)
data collection and recording system for studies in, automatic, 19: 1041(R) (HW-81746(p.5.6-10))
data for Oak Ridge, 10-year history, 17: 16264 (ORO-199)
data from IGY and IGC, catalog of, 18: 42522
data handling and computer system for mesoscale application, 16: 22441 (TID-7632(p.136-44))
data recording system for, 20: 9167(R) (BNWL-36, pp 5.1-102)
data recording system for meteorological studies at reactor sites, design of automatic, 20: 16710
definition of extreme desert environments with microclimatological measurements, 16: 20821 (SC-4853(RR))
description of studies in, at Ispra in 1963, 18: 30296(R) (EUR-1617.i)
determination of Pleistocene climatic curves by isotope geochemistry, 20: 43557
determination of vertical turbulent flows of heat, moisture and momenta by gradient measurements, 18: 22547(T) (ANL-Trans-12)
diffusion and deposition of air-borne materials, tracer study, 17: 1174(R) (HW-70050(p.12-30))
diffusion and rainout of stratospheric radioisotopes, seasonal model studies of, 20: 45888(R) (NYO-3654-1)
diffusion climatology studies, 19: 44771 (BNL-914, pp 44-50)
diffusion experiments, 19: 44796 (BNL-914, pp 163-72)
diffusion studies at Cape Canaveral and Vandenberg Air Force Base, fluorescent tracer techniques and field procedures for, 16: 33276 (HW-SA-2723)
diffusion tests in, elevated line source, 19: 44779 (BNL-914, pp 93-4)
dispersion in meso-scale, studies, 19: 44784 (BNL-914, pp 110-12)
distribution ranges of natural radioactivity in aerosols of northern Alps, 16: 27462
dynamics of transport of fallout by atmospheric precipitation, 18: 37456
effects of atmospheric precipitation on the radioactivity of the atmospheric surface layer, 18: 10609(T) (AEC-tr-6128(p.199-214))
effects of atmospheric variables on radon-222 contents and flux in soils, 18: 35737
effects of climate on ground waste disposal at shallow depth, 18: 17347
effects of climate on iodine-131 uptake by sagebrush, 20: 28883
effects of climatic regimes on particle diffusion and transport in the atmosphere, 18: 2389(R) (HW-77609(Sect.1))
effects of convective storm activity on deposition of fallout strontium-90, 20: 23285 (HNS-58)
effects of local winds on fallout deposition, 18: 37365(R) (AD-600447)
effects of meteorological conditions on precipitation of fall-out, 16: 14996 (NSEC-48)
effects of meteorological conditions on ground-level fall-out concentrations, 16: 22448 (TID-7632(p.242-55))
effects of meteorological conditions on fallout concentrations in ground-level precipitation, 17: 14481(R) (TID-17518)
effects of meteorological conditions on radioactivity in rain water, 17: 36014
effects of meteorological conditions on deposition of fallout by precipitation, 17: 37349 (NSEC-98)
effects of meteorological factors on radioactive fallout in convective shower precipitation, 17: 39267(R) (HNS-24)
effects of meteorological conditions on fallout transport in atmosphere, 18: 10273 (AD-403276)
effects of meteorological conditions on fallout transport and deposition, 18: 37381
effects of meteorological factors on beta activity at ground level, 18: 41664
effects of meteorological conditions on sources of iodine-131 content in pasteurized milk, 18: 42150
effects of meteorological conditions on atmospheric diffusion, 19: 1044
effects of meteorological conditions on radioactivity in atmosphere, 19: 4407
effects of meteorological conditions on gamma activity from argon-41 in atmosphere, 19: 14118
effects of meteorological conditions on iodine-131 deposition pattern after acute release to atmosphere, 19: 22014 (HW-SA-3338)
effects of meteorological conditions on sampling of fallout, 20: 16656
effects of meteorological conditions on radioactivity in atmosphere over oceans, 20: 16699
effects of meteorological factors on global distribution of fallout,

20: 23309
effects of meteorological processes on particle deposition and transport, 20: 23311
effects of nuclear explosions on weather, 18: 27714
effects of nuclear detonations on, 20: 43510 (RM-4989-TAB)
effects of precipitation and temperature on plant communities, 20: 10510 (BNL-9835)
effects of pressure and temperature changes on cosmic-ray intensity data, 18: 34466(T) (NASA-TT-F-126(p.194-214))
effects of ragweed pollen dispersion, 20: 45235 (BNL-957)
effects of thermonuclear warfare on, 18: 23822 (HI-303-RR/A-IV)
effects of topography on surface winds at Lucas Heights, 18: 40039 (AAEC/TM-244)
effects of vertical turbulent diffusion on subsidence of a heterogeneous aerosol from the atmosphere, 18: 10612(T) (AEC-tr-6128(p.248-67))
effects of weather conditions on radon content in air, 16: 2869(R) (ANL-6398(p.86-95))
effects of weather conditions on fallout deposition, 17: 20215
effects of weather conditions on dispersion of wind-borne particles, 18: 28081 (AHSB(RP)-R-42)
effects of weather on distance travelled by sheep on winter range, 19: 35870 (ORNL-P-1340)
effects of wind and precipitation on fallout dispersion, · 20: 41133(R) (SC-CR-66-2030)
effects of wind conditions on accuracy of fall-out predictions, 16: 22440 (TID-7632(p.122-35))
effects of wind variability on deposition of stack particles on ground, 18: 33801 (HW-80204)
effects of wind-driven currents on eddy viscosity at various ocean depths and structure of wind waves, 18: 25013 (TID-20612)
effects on cesium-137 uptake by Alaskan animals and natives, 20: 12983
effects on climate, 20: 43505(R) (COO-689-60, App.A-5)
effects on deposition of methyl iodide on grass, · 20: 41192(R) (IDO-12053
effects on diffusion of effluents from elevated source in atmosphere, equations for, 20: 23334 (AAEC-TM-307)
effects on disease incidence, 19: 12897
effects on dry-fallout, 19: 11817
effects on fallout diffusion in troposphere, 18: 27709
effects on fallout dispersion in atmosphere, 19: 24713
effects on fallout deposition in Japan, 19: 28550
effects on fallout distribution in convective rainstorms, 19: 36651 (COO-1199-6)
effects on fallout transport, 20: 523
effects on fallout distribution, 20: 527
effects on fallout deposition, 20: 5678
effects on fallout, 20: 18198
effects on iodine-131 uptake by frog thyroid, 18: 31099
effects on iodine-131 deposition on forage plants, 20: 18941(R) (IDO-12047)
effects on iodine-131 and -133 dispersion from 100-meter stack, 20: 45948 (BNL-10527)
effects on particulate rainout from nuclear device cloud, 20: 39107 (UCRL-14700)
effects on radioactivity of airborne dusts, 18: 43814
effects on radioactive particles after radiation accident, 19: 46693
effects on radiological decontamination, 18: 22310
effluent flow around buildings, 20: 562 (CONF-650407, pp 455-9)
ellipsoidal wind distributions, 18: 14574(R) (ANL-6769(p.181-96))
factor affecting radioactive pollution of atmosphere, 17: 14484
factors affecting transfer of fission products from stratosphere to troposphere, 16: 4417
factors affecting strontium-90 fallout in precipitation, 17: 3664
factors affecting particle diffusion and transport in atmosphere, 17: 10848(R) (HW-73337(p.1-28))
factors affecting radon concentration in the air above the Atlantic Ocean, 17: 14498
factors affecting prediction of movements of ocean waters, 18: 4924(R) (TID-19779)
factors affecting sampling of radioactive aerosols, 19: 11820
factors governing prelaunch of aerospace nuclear systems, 18: 8908 (SC-DC-3553(p.209-18))
factors in, affecting atmospheric pollution, 17: 36004 (BNL-784)
fallout distribution from weapon tests, effects of fog and rain on, 18: 14085
fallout in rain, role of nucleation by radioactive particles in, 20: 23281
fallout perturbations by local sea breezes, 20: 16661(R) (ECOM-00392-F)
fallout rates, 19: 44255 (RT/PROT(65)-10)
fallout transport from Nevada to southeastern U.S., 18: 14077
fallout transport from Nevada to southeastern U.S., 18: 14078
fallout transport from Nevada to southeastern U.S., 18: 14079
fluorescent tracer material content in air, instrument for determining, 19: 1040(R) (HW-81746(p.5.1-5))
forecasting dispersion from a ground source, 18: 8907 (HW-SA-3192)
formulas for calculating the turbulent diffusion of a contaminant settling from a point source, 18: 10610(T) (AEC-tr-6128(p.215-30))
formulas for calculating plume rise from stacks, 19: 20653(R) (ANL-6938(p.209-41))
German Weather Service annual report, 20: 37009
Green Glow program measurements of atmospheric diffusion, 18: 40043
Green Glow Program data, 19: 1033(R) (HW-81746(p.1.1-19))
hailstone formation in, isotopic analysis of, 19: 14119
harmonic analysis of scalar fields in, (T), 19: 10701 (UCRL-7617-T)
hurricane air mixing calculations, based on tritium content of air, 20: 519
hurricane energy input calculations, based on tritium content of rain water, 20: 519
instrumentation for, developments in, 20: 9165(R) (BNWL-36, pp 1.1-84)
investigations in, before reactor startup, 17: 4694
iodine-131 dispersion after stack release, 19: 624 (IDO-12035)
ionized column for research in, use of electron or proton beams for producing, 18: 14576(R) (ANL-6769(p.220-9))
isentropic analysis, computer program for calculating parameters in, 19: 12884 (TID-21609)
isentropic stream functions and trajectories, computer analysis of radiosonde data on, · 20: 41188(R) (BNWL-235-1)
jet stream behavior over U. S., 20: 5644(R) (COO-1340-2, pp 110-21)
Lagrangian autocorrelation functions for turbulent circulation in the atmosphere, 18: 12761 (ANL-6794)
luminosity curves of high aurorae, 16: 8088
manual of, for reactor safety analysis, 20: 42584
measurements at Casaccia, Italy, in 1963, 19: 16245(R) (RT/PROT(64)-19)
measurements at Casaccia, Italy, 1964, 20: 16635 (RT/PROT(65)-40)
measurements at Risø, Denmark, 17: 25431 (RISÖ-39)
measurements during IGY, survey, 16: 16817
measurements during IGY and IGC in, Italian and world, 19: 44819
measurements in, data processing system for, 19: 47109 (RISO-99)
measurements in, translated articles on, 19: 6379(T) (JPRS-26742)
measurements on, at Risoe, 1962 through 1964, 20: 27145 (RISO-121)
mechanisms of capture and precipitation of atmospheric contamination, 18: 10607(T) (AEC-tr-6128(p.139-82))
methods of studying reactor-site, by smoke plume photography and tower data, 19: 13647
microclimatological study of Chariot site, 19: 24211 (PNE-474)
microclimatology of Ogotoruk Valley, Alaska, 19: 25809 (PNE-475)
microclimatology of Ogotoruk Valley, Alaska, 19: 25810 (PNE-476)
microclimatology of Ogotoruk Valley, Alaska, 19: 25811 (PNE-478)
model of oceans in Northern Hemisphere, 20: 4153(R) (UCRL-14360, pp 73-85)
models for hemispheric weather prediction, comparison of grid and spectral, (T), 19: 31136(R) (UCRL-12473(p.64-71))
models for particle diffusion over long distances, 20: 18988(R) (ORNL-929, pp 58-66)
natural pollutant-removal processes in the atmosphere, 17: 37364 (HW-SA-3144)
nuclear explosion effects, 18: 16546 (AWRE-O-87/63)
observations by Japanese Atomic Energy Research Institute, 17: 17624(R) (JAERI-5006)
of Solway Firth area of North East Irish Sea, 18: 14580 (PG-Report-551)
of the Republic of Mexico, relation of fallout to, 18: 8909
of Tonopah Test Range at Nevada Test Site, 1963, 18: 29154 (SC-TM-64-576)
of upper atmosphere, effects on wind velocity, 16: 27418 (NP-11961)
of Willow Run, Mich., Sept., 1961, 16: 22438 (TID-7632(p.74-97))
operations and servicing of radiological-meteorological telemetering systems, instruction manual for, (E), 19: 27845 (HW-83854)
parameters for fallout prediction, 19: 9364 (AD-420825)
particle collection efficiency of raindrops in lower atmosphere, 18: 24212 (HW-SA-3167)
particle distribution in atmosphere, dual tracers for determining, 19: 1038(R) (HW-81746(p.3.68-76))
particle fallout and dispersion below 30 km in the atmosphere, 19: 6378 (SC-DC-64-1463)
particle sampling in air stream, subisokinetic, 19: 1039(R) (HW-81746(p.4.63-6))
particle transport in atmosphere, tracer study, 16: 16584
performance of radio-telemetering system for data accumulation on, 20: 41188(R) (BNWL-235-1)
phenomena in underwater nuclear explosions in Crossroads and Teapot Operations, 20: 1979 (AD-614814)
polar-region heating by cosmic radiation and temperature effects, 17: 14505

precipitation and throughfall relations in mixed mesophytic plant community, 19: 25832 (TID-21827)
predictions in, for Salmon Event, 20: 5667 (VUF-1020)
problems in determining particle size distribution from explosions and fires, 18: 10616
problems in forecasting fallout from nuclear explosions over sea areas, 19: 24719
problems in meso-scale, fundamental, 19: 44782 (BNL-914, pp 103-6)
problems in, meso-scale and mean transport, 19: 44781 (BNL-914, pp 99-102)
processes in iodine-131 transport, 18: 8910
program at Air Force Cambridge Research Laboratories, 19: 44776 (BNL-914, pp 75-84)
program at Argonne, 19: 44763 (BNL-914, pp 4-13)
program at Brookhaven, 19: 44762 (BNL-914, pp 1-3)
program at Dugway Proving Ground, 19: 44778 (BNL-914, pp 91-2)
program at Hanford, 19: 44767 (BNL-914, pp 24-6)
program at Nevada Test Site, 19: 44774 (BNL-914, pp 65-8)
program for reactor sites, 20: 12333
program in Oak Ridge, Tennessee, 19: 44765 (BNL-914, pp 18-19)
program of U. S. Public Health Service, 19: 44775 (BNL-914, pp 69-74)
program of U. S. Weather Bureau, 19: 44770 (BNL-914, pp 33-43)
quantitative determination of point and areal precipitation by radar echo measurements, 18: 12760(R) (AD-412528)
radiation data for, interpretation of satellite, 20: 30221(T) (NASA-TT-F-389, pp 741-57)
radiation dose from passage of radioactive cloud, numerical method of determination, 16: 8987 (FZM-2029)
radioactive aerosol behavior in atmosphere, 18: 42143 (CEA-R-2347)
radioactive-waste-disposal studies in, (E), 19: 35858
radioactivity distribution in convective rainstorms, (E), 19: 18154
radioactivity in atmosphere over Lithuania, USSR, effects of air temperature, cyclone conditions, and cloud passage on, 20: 23280
radioisotope content in clouds, 17: 29094(T) (AEC-tr-5891)
radioisotope vertical distribution in clouds, 17: 29093(T) (AEC-tr-5871)
radiotelemetry system for Hanford studies in, 19: 1042(R) (HW-81746 (p.5.10-16))
radon distribution in lower atmosphere and, 18: 24213
rain scavenging of particulates, 18: 14579 (HW-79382)
rain scavenging of atmospheric particulate matter, 20: 41130(R) (COO-1407-10)
reactor site selection considerations in, 19: 13646
relation of convective shower activity to rate of strontium-90 deposition in precipitation, 19: 619(R) (HNS-50)
relation of precipitation to fallout, 19: 22561
relation of stratospheric mass variations and fallout content of surface air, 18: 7337
relation to air pollution control, 17: 10843 (BNL-6538)
relations of local atmospheric conditions and topography with Kiwi-induced fallout deposition, 17: 29128 (UCLA-513)
research at National Reactor Testing Station on, 19: 44773 (BNL-914, pp 57-64)
research in, for nuclear industry, 19: 44780 (BNL-914, pp 95-8)
research planned during IQSY, 19: 16761
research problems concerned with snow, ice, and glaciers, use of deuterium content for dating, 18: 36071
research program for International Years of Quiet Sun, 18: 44360
research program on atmospheric boundary layer, 19: 44777 (BNL-914, pp 85-90)
research programs, Bureau of Standards annual summary, 16: 13835
research programs at BNL on, July 1962 to July 1963, 18: 7987(R) (BNL-806(p.3-90))
research programs on, Hanford, 1963, 19: 1(R) (HW-81746)
research programs on, NASA Semiannual Report to Congress, Jan. 1 to June 30, 1964, 19: 19453
research, review, 16: 4370 (ONR-9(Vol.3))
reviews of synoptic climatology for 1945–58, 18: 43110 (HW-67944)
role in management of airborne radioactive wastes, 16: 5614
role of turbulent wind scattering in atmospheric turbulent diffusion, 18: 10611(T) (AEC-tr-6128(p.231-47))
silver iodide smoke studies of waste gas diffusion from stack disposal, 19: 14117
small particle diffusion in non-uniform atmosphere, 16: 33275 (GCA-TR-62-1-G)
soil climatology observation program, 18: 14577(R) (ANL-6769(p.230-9))
soil temperature and weather conditions, 16: 10272 (ANL-6470)
source configuration effects on downwind concentrations, 19: 44786 (BNL-914, pp 116-18)
stratosphere sampling, design and development of air ejector particle sampler for, 19: 720(R) (COO-401-105)
stratospheric wind temperature and isobaric height conditions during IGY, 18: 20619 (TID-20511)
strontium-90 deposition in Pacific cyclonic storm, 17: 39266 (HNS-17)
strontium-90 content in precipitation from convective activity and extratropical cyclones, 19: 1032 (HNS-55)
strontium-90 transport from stratosphere to ground by intense convective storms, 19: 22560
studies of equatorial stratosphere above Hyderabad, India, 17: 39269 (TID-19483)
summary of NRTS activities in 1960, 16: 4395(R) (IDO-12019)
support in radiation monitoring at National Reactor Testing Station after nuclear accident of Jan. 1961, 16: 29182 (IDO-19310)
survey of nuclear meteorology problems, 16: 15004(T) (JPRS-13335)
survey of nuclear meteorology problems, 16: 7753
Sutton's turbulence index from wind profiles at Lucas Heights in Australia, 18: 40038 (AAEC/TM-243)
temperature profiles, problems in, 19: 44795 (BNL-914, pp 161-2)
tetroons in meso-scale, 19: 44783 (BNL-914, pp 107-9)
thunderstorm forecasting method, 16: 27418 (NP-11961)
transport theory for, radiative transfer for, (T), 20: 33977
tropopause-level cyclogenesis, effects of, on fallout transport from stratosphere, 20: 5650(R) (COO-1340-2, pp 84-109)
turbulence at Douglas Point, Ontario, (E), 19: 18170
turbulence characteristics near ground in micro-, dimensional analysis, 19: 44772 (BNL-914, pp 81-4)
turbulence structure in micro-, 19: 44798 (BNL-914, pp 175-7)
use in predicting dispersion of radioactive gases released near ground level, 18: 4017 (HW-SA-3176)
use in prediction of early fall-out transport, 16: 22441 (TID-7632 (p.136-44)
use in reactor safety evaluation, 19: 44270 (BNL-914, pp 178-9)
use of deuterium concentration measurements in study of, 17: 23503
use of particulate nuclear bomb debris as tracer material in, 20: 2044 (NDRE-51)
use of radar in rainfall measurements, 17: 3141 (AD-273451)
use of weather radar in fall-out prediction, 16: 4366(R) (AD-257178)
uses of hydrodynamic-theory computer code in, (E), 19: 34624
uses of natural atmospheric radioisotopes in studies in, 18: 10604(T) (AEC-tr-6128(p.1-51))
waterdrop evaporation, computer program for, 19: 41110 (BNWL-74)
weather and surface radiation prediction for SEDAN, 17: 24746 (PNE-201F)
weather effects on sodium distribution in atmosphere and on beaches, 20: 4148 (AD-623515)
weather observations for SHOAL explosion, 18: 44281 (VUF-1008)
weather predictions for Project Gnome, 16: 18715 (PNE-126P)
weather prediction, comparison of grid and spectral methods for numerical, 19: 14928 (UCRL-7865-T(Rev.I))
weather prediction, 20: 4153(R) (UCRL-14360, pp 73-85)
weather prediction from atmospheric electric conductivity measurements, 20: 29402
wind analysis using digital computers, (T), 19: 17427 (SC-TM-8-62(51))
wind distributions at 100,000 to 300,000 ft, 16: 10277 (SC-4482(RR))
wind effects on diffusion of radioactive gases from nuclear power plants, 19: 18555
wind fluctuations and velocity at Risö, Denmark, 17: 12454 (RISO-45)
wind predictions for National Reactor Testing Station, 20: 41129
wind profile in lowest 400 feet of the atmosphere, 16: 14995(R) (BNL-697)
wind profile law evaluation, 18: 14575(R) (ANL-6769(p.197-219))
wind profiles, review, 19: 44794 (BNL-914, pp 158-60)
wind tunnel studies of effects of wind eddies on stack performance, 18: 22545 (AEEW-R-227)
wind turbulence in, analog-computer analysis of, (E), 19: 13859 (HW-84448-10)
wind velocity, effects on atmospheric particle diffusion, 16: 11948 (AFCRL-468)
wind velocity profiles in, method for measuring, 20: 25280
zonal two-dimensional weather code ZAM, (T), 19: 31136(R) (UCRL-12473(p.64-71))

METEORS

see also Meteorites
antimatter nature of micro-, from showers, (E/T), 20: 29895
book: *Space Physics and Radio Astronomy*. (E/T), 19: 2943
composition of, mass spectral analysis of ions for determining, 17: 18307(T)
conference on, 18: 20710 (AFCRL-62-497)
cosmic proton reactions with, processes in, 18: 28228
explosion of Tunguska, anti-matter, 20: 41607
isotope production in, by cosmic rays, 20: 7690
penetration experiments in Explorers XIII and XVI, 18: 741
properties of, book on, 19: 1162
protection of space vehicles against, for interplanetary missions, 17: 31782
radio-wave reflection from trails of, polarization phenomena in, (E), 19: 41223

reactions with atmosphere, radiation emission in, 18: 36145
shielding of space vehicles from, magnetic, 18: 26107 (ERR-FW-210)
simulation of, design of microparticle accelerator for, 18: 2456
simulation of micro-, in linear accelerators, 19: 37339

METERS
see also Altimeters
see also Anemometers
see also Barometers
see also Bolometers
see also Calorimeters
see also Colorimeters
see also Coulometers
see also Densitometers
see also Dilatometers
see also Dynamometers
see also Electric Meters
see also Electrometers
see also Extensometers
see also Flowmeters
see also Fluorimeters
see also Fluxmeters
see also Frequency Meters
see also Gages
see also Galvanometers
see also Goniometers
see also Hygrometers
see also Interferometers
see also Magnetometers
see also Manometers
see also Nephelometers
see also Ohmmeters
see also Penetrameters
see also pH Meters
see also Photometers
see also Potentiometers
see also Pyrometers
see also Quantometers
see also Radiometers
see also Rate Meters
see also Reflectometers
see also Refractometers
see also Rotameters
see also Seismometers
see also Spectrometers
see also Tachometers
see also Thermometers
see also Viscometers
see also Voltmeters
design and performance of moisture-density, for soil measurements, 20: 33537
design for measuring nuclear-explosion yield, 20: 37061
design for remote measurements in radiation environment, (E), 19: 40714 (EUR-2421.d)
design of radiometric quality, for hydrogen, 20: 32347
design of solvent purity, for measuring soluble residue content in volatile cleaning solvents, 20: 25323 (SC-R-66-865)
development of torsion pendulum for recording internal friction, 19: 9751
performance of radiometric, scale linearity in, 20: 14836

METHACROLEIN
radioinduced polymerization, 17: 40902(P)

METHACRYLAMIDE
aryl-, radioinduced polymerization in solid state, 17: 27448
electron spin resonance spectra of irradiated, effects of hydrogen sulfide and nitrogen oxide on, 16: 8781
N-octadecyl-, synthesis, 18: 272(R) (TID-19484)
polymerization induced by irradiation and heat treatment, 18: 23652(T,R) (AEC-tr-6316(p.587-97))
radioinduced free radicals, 17: 3047
radioinduced graft polymerization on vinyl alcohol polymers, 19: 26423
radioinduced polymerization of, in solid state, effects of oxygen on, 17: 8130 (PAN-307/XVII)
radioinduced polymerization in solid state, 17: 27448
radioinduced polymerization with acrylamide, 19: 500
radioinduced polymerization with acrylamide in solid state, 19: 28400
radioinduced polymerization of, to yield foamed plastics, 20: 38981(P)
radioinduced reactions with gases, 18: 23650(T,R) (AEC-tr-6316(p.567-72))

METHACRYLAMIDE POLYMERS
radioinduced free radicals, 17: 3047
radioinduced reactions with gases, 18: 23650(T,R) (AEC-tr-6316 (p.567-72))
viscosity of, 17: 6129 (PAN-308/XVII)

METHACRYLIC ACID
ester (di-) with triethylene glycol, radioinduced gelation of, fast-neutron, 20: 20720 (AD-630891)
radiation effects on solid, uv, 19: 26411
radioinduced block and graft polymerization of dispersions of, with acrylonitrile, 16: 17726
radioinduced crosslinking with polymers, 17: 8135(R) (RAI-311)
radioinduced graft polymerization of styrene mixtures on polypropylene, comparison of accelerator and isotopic initiation, 16: 13083(R) (NYO-9420)
radioinduced graft polymerization on polyethylene fibers, 16: 24265
radioinduced graft polymerization with polyethylene in benzene and methanol solutions, 17: 4608
radioinduced graft polymerization with polyethylene by mutual graft technique, 17: 8181
radioinduced graft polymerization with polyethylene films, 17: 8182
radioinduced grafting with styrene on polyethylene, 19: 13832
radioinduced polymerization of crystalline, 16: 1734 (TID-14087)
radioinduced polymerization in solid states, 16: 18965
radioinduced polymerization in methanol solution, 18: 17881
radioinduced polymerization of menthol esters of, mechanism of polymerization of, 18: 33674
radioinduced polymerization with allylamine, 19: 24576
radioinduced polymerization, 20: 18794
radioinduced polymerization with isocyanic acid at low temperatures, 20: 20747
radioinduced polymerization of, to yield foamed plastics, 20: 38981(P)
radioinduced solid-state polymerization of barium salt of, electron spin resonance study of, 18: 272(R) (TID-19484)
radiolysis at −40 to 10°C, ESR spectra of yields in uv, 20: 1916
methacrylic acid–styrene, radioinduced graft polymerization onto poly (vinyl alcohol), 18: 27547

METHACRYLIC ACID, ALKALI METAL SALTS
radioinduced polymerization, 16: 1809 (TID-14086)
radioinduced polymerization, 16: 18964
radioinduced polymerization of, mechanism of, 17: 21747

METHACRYLIC ACID, ALKYL ESTER POLYMERS
radiation effects on free radical concentration, 16: 17966(R) (BMI-1541 (Del.))
radioinduced polymerization of, gamma, 19: 28379

METHACRYLIC ACID, ALLYL ESTERS
effects on radioinduced crosslinking of polymers, 18: 8407 (RAI-329)
effects on radioinduced crosslinking of polyisobutylene, 18: 33652
radioinduced crosslinking to polyethylene, 17: 8193
allyl methacrylate–methanol–H_2O, effects on radioinduced crosslinking of nylon 66 and poly (vinyl alcohol), 20: 1909

METHACRYLIC ACID, BUTYL ESTER POLYMERS
radioinduced reactions in, electron spin resonance studies of, 18: 27592
radiolysis of, 17: 22237
radiolysis of isomeric, production of free radicals in, 17: 16070
radiolysis of, mechanism of gas formation process in electron, 18: 327
radiolysis of, diffusion and penetrability coefficients of gases formed in, 19: 11182
radiolysis of, mechanism and spectra of free radical formation in, 19: 11196
use in combination with carbon as coating for reactor gas circuits, 19: 35651(P)

METHACRYLIC ACID, DODECYL ESTER
radioinduced polymerization of liquid and solid, effect of mineral oil on, 20: 36875

METHACRYLIC ACID, 2,3-EPOXYPROPYL ESTER
radiation effects of pre-irradiation on polymerization of, on polypropylene or polyvinyl chloride, 19: 42532

METHACRYLIC ACID, ESTERS
cetyl-, polymerization of, 17: 16059
cetyl, radioinduced polymerization in liquid and solid states, 19: 489
effects on adhesive properties of polyethylene, 20: 4029
effects on radioinduced crosslinking of polymers, 17: 4584 (TID-7643 (p.245-58))
radiation effects on copolymerization with polyethylene, 16: 445(R) (NYO-9988)
radiation effects on mixtures with polyethylene, 16: 13084(R) (NYO-9830)
radio- and thermal-induced gelation of allyl, 16: 14774 (TID-14855)
radioinduced cross linking with, 18: 27531
radioinduced gelation of glycol, 16: 14774 (TID-14855)
radioinduced gelation in polymer systems, effects of dose rate on, 16: 27036(R) (RAI-307)
radioinduced graft polymerization with polyethylene, effects of hexane on, 17: 4583 (TID-7643(p.233-44))
radioinduced graft polymerization on polyvinyl alcohol, gamma, 18: 23583(T,R) (AEC-tr-6316(p.76-8))
radioinduced graft copolymerization with butadiene and polyvinyl chloride, gamma, 18: 31644(P)

radioinduced polymerization, 16: 19274
radioinduced polymerization of cetyl, in liquid and solid states, 18: 12216
radioinduced polymerization of cetyl, at 60 to −195°C, kinetics of, 19: 38699
radioinduced polymerization of, gamma, 20: 4029
radioinduced polymerization of, in organic solvents, mechanism and rate of, 20: 23159
radioinduced polymerization of emulsions of, gamma, 20: 43374
radioinduced polymerization of, with polyethylene, kinetics of, 20: 45745
triethylene glycol di-, radioinduced polymerization in inhibitors, effects of temperature on, 18: 31569 (TID-20812)
triethylene glycol di-, effects of additives on G-values in radioinduced polymerization of, 17: 37254 (TID-19381)

METHACRYLIC ACID, ETHYL ESTER POLYMERS
proton polarization in neutron-irradiated, 17: 20011
radioinduced block and graft polymerization of dispersions of, with acrylonitrile, 16: 17726
radioinduced reactions in, electron spin resonance studies of, 18: 27592

METHACRYLIC ACID, METHYL ESTER
complexes with boron fluoride, radioinduced polymerization of, 18: 12230
effects as scavenger on gamma radiolysis of Hydyne and RP-1 rocket fuels, 20: 25118 (AD-632461)
effects on acid photolysis of oxalic acid, 20: 45613
effects on hydrogen yields from radiolysis of hydrogen sulfide, 20: 4017
effects on isomerization of stilbene in gamma radiolysis of benzene and cyclohexane, 20: 40961
effects on radioluminescence of styrene, 20: 4001
effects on radiolysis of cyclohexylamine and *N,N*-dimethylcyclohexylamine, 19: 13469
effects on radiolysis of methylhydrazine, 19: 30237 (USNRDL-TR-843)
effects on radiolysis of diethylenetriamine, dimethylhydrazine, and their mixtures, 20: 357 (USNRDL-TR-896)
europium β-diketone chelate spectra in, 18: 25462
graft polymerization of, on cellulose acetate, ceric ion, preirradiation, and radiation methods for, 17: 31809
impregnation of wood by, methods for, 20: 33335 (ORO-2945-4)
polymerization, 17: 25685(R) (BMI-1624(Del.))
polymerization of, graft, 17: 6511(R) (BMI-1593(Del.))
polymerization of, with methyl chloroacrylate, tracer studies of, 20: 23201
polymerization of, at various pH's, use of molybdenyl, uranyl, and vandyl, salts as photosensitizers in, 20: 38934
polymerization with toluene, 17: 35251(R) (BMI-1632(Del.))
polymerization with teflon induced by electric discharge, 17: 40863
polymerization with pre-irradiated cotton fibers, 19: 44094
production by low-temperature radioinduced polymerization of isopropylamine, 18: 23591(T,R) (AEC-tr-6316(p.129-30))
properties of radioinduced graft polymerized polyvinyl alcohol fibers on, 16: 19443
purification, 17: 25685(R) (BMI-1624(Del.))
radiation chemistry of, effects of oxygen, nitric oxide, and carbon dioxide on, 18: 1777
radiation effects on, cosmic, 17: 32693
radiation effects on, hardening against, 19: 9547
radiation effects on polymers with styrene in benzene, effects of oxygen on, 19: 15581
radiation effects on polymerization of emulsions of, gamma, 20: 23212 (AERE-R-3420)
radiation grafting with vinyl alcohol polymers, mechanical properties after, 19: 11180
radiation stability, 19: 15571(R) (TID-21385)
radioinduced anionic polymerization in amine solvents, 18: 29714(T,R) (AEC-tr-6231(p.163-9))
radioinduced copolymerization, anionic and cationic mechanisms, 16: 209(T) (AEC-tr-4470(p.1-7))
radioinduced copolymerization to styrene in ethyl chloride, gamma, 16: 25458
radioinduced copolymerization with α-methylstyrene, 17: 29938
radioinduced copolymerization with formaldehyde, 17: 30139
radioinduced copolymers with ethylene, properties of, 17: 37276
radioinduced crosslinking, localized neutron, 16: 11772
radioinduced curing of, in mixtures with polyesters, electron, 20: 35819
radioinduced emulsion polymerization with styrene, 17: 40876
radioinduced emulsion polymerization of, 19: 30236(R) (TID-21683)
radioinduced gel formation in, for chemical dosimetry, 16: 29135
radioinduced gelation, 16: 14774 (TID-14855)
radioinduced graft polymerization on polyethylene in benzoyl peroxide–dimethylaniline, 16: 11714
radioinduced graft polymerization with polyvinyl alcohol, 16: 229
radioinduced graft polymerization on cellulose, 16: 22180
radioinduced graft polymerization on polyvinyl alcohol films, 16: 22190
radioinduced graft polymerization on polyethylene, effects of slight chlorination, 16: 22185
radioinduced grafting to polyethylene oxide, 17: 18108(R) (TID-18126)
radioinduced graft polymerization on wool, 17: 27900
radioinduced graft polymerization on polystyrene, 17: 28987
radioinduced graft polymerization to PVA, gamma, 17: 30049
radioinduced graft polymerization of, on nylon 6, properties of product in, 17: 30200
radioinduced graft polymerization to polyvinyl alcohol, effects of ferrous ions on, 17: 33985
radioinduced graft polymerization to beryllium, magnesium, and zinc oxide powder surfaces, 18: 320
radioinduced graft polymerization to fibrous materials, technique for, 18: 6869
radioinduced grafting on polypropylenes of different structures, 18: 12225
radioinduced grafting on cellulose, effects of water swelling on, 18: 12163
radioinduced graft polymerization on polyoxymethylene, 18: 23607(T,R) (AEC-tr-6316(p.223-5))
radioinduced graft polymerization on cotton and rayon, gamma, 18: 23658(T,R) (AEC-tr-6316(p.650-9))
radioinduced graft polymerization with capron and ethylene and propene polymers in gaseous phase, 18: 27535
radioinduced graft polymerization to cellulose pulp, 18: 29697(T,R) (AEC-tr-6231(p.79-90))
radioinduced graft polymerization to polyvinyl alcohol, 18: 29698(T,R) (AEC-tr-6231(p.91-101))
radioinduced graft polymerization to rayon, 18: 29699(T,R) (AEC-tr-6231(p.102-4))
radioinduced graft polymerization to polypropene fibers, 18: 29702(T,R) (AEC-tr-6231(p.114-18))
radioinduced graft polymerization on chlorinated polyethylene, 18: 29726(T,R) (AEC-tr-6231(p.233-8))
radioinduced grafting on polypropylene, 19: 494
radioinduced graft polymerization on polyethylene, 19: 9204
radioinduced graft polymerization of, mechanism and spectra of, 19: 36468
radioinduced grafting to chloroethylene polymers, 19: 38739(P)
radioinduced graft polymerization with polyethylene and polyvinyl chloride, 19: 44083
radioinduced graft polymerization onto polystyrene, 18: 20096(P)
radioinduced graft polymerization with polypropylene, properties of product formed by γ, 20: 23127
radioinduced graft polymerization on cellulose, 20: 25176(P)
radioinduced graft polymerization of, on fibrous cotton and nylon, gamma, 20: 35822
radioinduced graft polymerization to cotton cellulose, properties of products formed by gamma, 20: 40995
radioinduced polymerization reactions, effects of mono-functional additives on, 16: 8789
radioinduced polymerization reactions, effects of mono- and difunctional additives on, 16: 8790
radioinduced polymerization, effects of polyvinyl acetate, 16: 22195
radioinduced polymerization on polyvinyl alcohol film from aqueous solution, 16: 22234
radioinduced polymerization, effects of amine, 16: 22191
radioinduced polymerization for Plexiglas production, 16: 24064
radioinduced polymerization with acrylonitrile, 16: 23739
radioinduced polymerization at low temperatures, 16: 29012
radioinduced polymerization of, aspects of post-effect in, 16: 31641(R) (TID-16608)
radioinduced polymerization of, in solid state, 17: 4578 (TID-7643(p.136-49))
radioinduced polymerization in wood, 17: 4589 (TID-7643(p.335-44))
radioinduced polymerization in aqueous emulsions, 17: 4596
radioinduced polymerization with acrylonitrile, 17: 28989
radioinduced polymerization of, for production of shaped articles, 17: 40905(P)
radioinduced polymerization, 17: 40867
radioinduced polymerization of, effects of additives and dose rate on, 18: 297
radioinduced polymerization with nylon and natural silk, 18: 319
radioinduced polymerization of, effects of zinc oxide on, 18: 10167
radioinduced polymerization in presence of organic additives, yields of free radicals in, 18: 10171
radioinduced polymerization of, effects of magnesium oxide on, 18: 12171
radioinduced polymerization of, effects of LET in, 18: 12198
radioinduced polymerization in liquid and solid states, 18: 12215
radioinduced polymerization of, post-effect studies of mechanisms of, 18: 12149(R) (TID-20072)
radioinduced polymerization with styrene in glass, gamma, 18: 12168

radioinduced polymerization with ethylene at 20°C and up to 680 atm, 18: 13900
radioinduced polymerization in wood, 18: 13906
radioinduced polymerization in wood, 18: 17889
radioinduced polymerization of liquid and solid, effects of temperature on, 18: 22159
radioinduced polymerization with acrylonitrile and styrene on alumina base, gamma, 18: 23594(T,R) (AEC-tr-6316(p.137-44))
radioinduced polymerization with β-propiolactone, 18: 23604(T,R) (AEC-tr-6316(p.190-4))
radioinduced polymerization with formaldehyde, kinetics of, 18: 25492(T) (AEC-tr-6372(p.213-22))
radioinduced polymerization with acrylonitrile, 18: 25535(T) (AEC-tr-6372(p.603-12))
radioinduced polymerization with acrylonitrile at −78 to 50°C, 18: 27530
radioinduced polymerization with ethylene, gamma, 18: 29691 (BNL-8056)
radioinduced polymerization at low temperature, 18: 29710(T,R) (AEC-tr-6231(p.143-9))
radioinduced polymerization with styrene, kinetics, 18: 29717(T,R) (AEC-tr-6231(p.186-90))
radioinduced polymerization in ethyl acetate and polyvinyl acetate, 18: 29721(T,R) (AEC-tr-6231(p.205-11))
radioinduced polymerization effects on glass transition temperature of, 18: 31590
radioinduced polymerization of, effects of linear energy transfer on, 18: 31638
radioinduced polymerization, 18: 35924 (BMI-1678)
radioinduced polymerization with styrene at −78°C, gamma, 18: 37216(T) (AEC-tr-6398(p.529-37))
radioinduced polymerization of, kinetics of, 19: 2399
radioinduced polymerization of, in solid mixtures with paraffin oil, mechanism and free radical yields in, 19: 4211
radioinduced polymerization with acryloanitrile, effects of magnesium oxide additive on, 19: 11183
radioinduced polymerization in acetone–benzene, 19: 15579
radioinduced polymerization with styrene, effects of γ-alumina on, 19: 18000
radioinduced polymerization of, effects of electric fields on, 19: 26426
radioinduced polymerization in wood, gamma, 19: 30234 (ORO-628)
radioinduced polymerization at low temperatures, rates of, 19: 36484
radioinduced polymerization with isobutylene and ethylene–propylene rubber, 20: 367
radioinduced polymerization with formaldehyde, effects of dichloromethane and ethyl ether on, 20: 1914
radioinduced polymerization on polyethylene, 20: 3996
radioinduced polymerization with styrene, 20: 4001
radioinduced polymerization of, in presence of zinc oxide, 20: 7128(R) (NYO-2206-1)
radioinduced polymerization with styrene in presence of zinc oxide, 20: 7128(R) (NYO-2206-1)
radioinduced polymerization of, effects of mineral fillers on gamma, 20: 20778
radioinduced polymerization of, in organic solvents and paraffin, mechanisms and rates of, 20: 23159
radioinduced polymerization of, in wood, effects on dimensional stability, 20: 23110
radioinduced polymerization with styrene, pulsed-electron, 20: 23123
radioinduced polymerization of, with polystyrene at −78°C, gamma, 20: 26939
radioinduced polymerization with lignin, gamma, 20: 29288
radioinduced polymerization of, in wood, gamma, 20: 33335 (ORO-2945-4)
radioinduced reactions with iron carbonyls, 20: 33381
radiolysis of mixtures of, with paraffin oil, reactions of free radicals formed in, 19: 40580
radiolysis of, mechanism and spectra of free radical formation in, 19: 11196
radiolysis with amines, formation of amine cation radicals in, 17: 10687
radiolysis with amines, formation of cation radicals in, 18: 27604
scavenging effects on hydrogen yields in radiolysis of liquid cyclohexane, 18: 35610
use of dyed, for dosimetry of vacuum envelopes in Nimrod proton synchrotron, 20: 31832
acrylonitrile–methyl methacrylate, radioinduced graft polymerization to cotton fabric, properties of products formed in gamma, 20: 40953
methyl methacrylate–polystyrene, radioinduced polymerization effects on transition temperature of, 18: 31590
methyl methacrylate–styrene, radioinduced graft polymerization onto poly (vinyl alcohol), 18: 27547
methyl methacrylate–vinyl acetate, radioinduced graft polymerization onto poly (vinyl alcohol), 18: 27547
methyl methacrylate–styrene, radioinduced polymerization of, in organic halogen solvents, mechanism of, 20: 23159
methyl methacrylate–wood, radioinduced polymerization of, economics and properties of products from, 20: 39287 (KLX-1876)
methyl methacrylate–styrene, radioinduced graft polymerization to cotton fabric, properties of products formed in gamma, 20: 40953

METHACRYLIC ACID, METHYL ESTER POLYMERS

beta radiation absorbed dose, 16: 4201
cavitation damage to, in mercury and water, 18: 3955 (NP-13319)
cavitation damage of plexiglas in mercury and water, 19: 9623 (NP-14632)
Cherenkov light absorption in lucite, (E), 20: 19021 (CALT-68-53)
crosslinking degree of high-conversion methylene dimethacrylate copolymer, 16: 24196
decontamination of surface of, by chemical reagents, 19: 4419
design of Lucite light pipes for gamma cameras, thickness optimization for, (T), 20: 11079
dielectric constant and losses, 17: 40424(R) (BMI-1642(Del.))
dielectric properties of radio-polymerized effects of fabrication and thickness on, 18: 2157(R) (BMI-1644(Del.))
diffusion of oxygen in, 16: 24195
electromotive force in irradiated, kinetics, 16: 4204
electron dose distribution in, three-dimensional, 20: 21470 (PB-181506, pp 116-29)
electron penetration depths, at 631 kev to 13.8 Mev, LET variations with, 20: 13969
electron scattering at 280 to 1750 kev by, depolarization in (E), 19: 2977
erosion of plexiglass, by mercury and water at 70°F, cavitation, 20: 29640 (NP-16048)
explosions in Plexiglas, seismic wave production in, 19: 13561(R) (AD-439079)
fabrication into light pipes for organic scintillators, 19: 15873(R) (ORNL-3714(Vol.II)(p.134-46))
fabrication of light pipe using adiabatic collection, 18: 25785 (NAS-NRC-Pub-1184(p.46-7))
fission fragment tracks in films of, 18: 2428
fracture of Plexiglas, effects of polyaxial stresses on, 17: 39537(R) (IITRI-B6012-2)
free radical recombination in condensed phase, 16: 5252
gamma absorption by, effective atomic numbers for, 19: 40069
gamma radiation effects on, induced electric conductivity, 20: 44997
gamma scattering by, detection of Rayleigh, 17: 13252
gamma transmission in Plexiglas, (E), 19: 14728 (APEX-581)
grafting vinyl pyrrolidone to radiation-peroxidized, 18: 2157(R) (BMI-1644 (Del.))
luminescent properties of ultraviolet absorbing and transmitting, 17: 16418 (BNL-6865)
mechanical properties of wood impregnated with, 19: 2416
moderating properties in plutonium assemblies, 16: 2701
neutron cross sections, 16: 8289 (DC-59-9-124)
neutron diffusion anisotropy in media with empty channels, thermal, 18: 21141
neutron diffusion coefficients in media with empty channels, anisotropy of, 18: 33036
neutron moderation by, at 20, 77, and 300°K, (E), 20: 11944
neutron reactions in, cross sections and spatial distributions, 16: 17059
neutron reactions in, cross section and spatial distribution for, 16: 22971(T) (JPRS-13609)
neutron reflector savings in polystyrene-plutonium (IV) oxide arrays, 18: 22850(R) (HW-80020(p.31-7))
neutron removal cross sections, 17: 21202
neutron resonance absorption integral of, (E), 20: 14008(R) (ANL-7122, pp 42-69)
neutron scattering by, geometrical optimization for cold, 20: 34470 (EUR-2953.e)
neutron shielding efficiency of, measurement of, 19: 35572
neutron transmission in Plexiglas, (E), 19: 14728 (APEX-581)
performance as radiation scatterer in high-dose detector, 20: 25415
performance of Lucite, for gamma dosimetry, 20: 35738 (BNL-985)
performance of Plexiglas as moderator-reflector for plutonia–polystyrene critical experiments, (E), 19: 38127(R) (HW-84608(p.77-9))
peroxidation-grafting with vinyl pyrrolidone, evaluation of radiation-induced, 17: 35251(R) (BMI-1632(Del.))
plastic deformation of beams of, 17: 26867 (ORNL-TM-557)
Poisson's ratio measurements in Plexiglas, 19: 26823 (TID-21843)
polymerization of pre-irradiated, with vinyl pyrrolidone, 17: 4580 (TID-7643(p.185-98))
polymerization with acrylonitrile, effects of pre-irradiation, 16: 20502
positronium formation and annihilation in, effects of temperature on, 20: 9783
preparation, 17: 25685(R) (BMI-1624(Del.))
preparation and properties, 17: 35251(R) (BMI-1632(Del.))
preparation and properties of tritiated, 20: 25185
preparation of carbon-14-labeled, for use as beta source, 18: 6863

preparation of gold-198-labeled aerosol particles of, 19: 3848
preparation of kryptonated, by diffusion, 20: 18570(R) (NYO-2757-5)
production of Plexiglas by radiopolymerization, 16: 24064
production of radioactive monodisperse, using spinning disk generator, 19: 4124
properties as gamma dosimeter in 2 to 3 MRad range, 19: 13436
properties of plexiglas as nuclear poison, 17: 232 (RFP-265)
properties of plexiglas for use as radiation dosimeter, 19: 4497
proton reactions at 1-Bev, nuclear cascades from, 17: 18391 (TID-7652(p.852-65))
proton reactions at 1 to 3 Bev, distributions from, (E), 20: 3015 (NASA-SP-71, pp 357-62)
proton reactions at 1 Bev, cascades in, (E), 20: 12262 (BNL-8721)
quenching effects of, molecular structure relation to, 19: 11185
radiation behavior of, effects of pigments on, 18: 24199(T,R) (AEC-tr-6316(p.359-67))
radiation damage in, protective effects of organic additives against x and gamma, 20: 4036
radiation damage, protective effects of organic additives against gamma, 19: 15646
radiation effects of alpha particles on physical properties, 16: 1834
radiation effects, mechanisms, 16: 1813(T) (AEC-tr-4709)
radiation effects on free radical formation, 16: 4450(R) (BMI-1546(Del.))
radiation effects on mechanical properties, 16: 11750(R) (TID-15191)
radiation effects on free radical concentration, 16: 17966(R) (BMI-1541 (Del.))
radiation effects on viscosity of α-methylstyrene copolymer, 16: 22186
radiation effects on electron paramagnetic resonance spectra of free radicals in, gamma, 16: 27049
radiation effects on, gamma and ultraviolet, 16: 29462
radiation effects on, gamma, 16: 33537
radiation effects on aerosols of, 17: 3026(R) (TID-17250)
radiation effects on specific heat, 17: 12331
radiation effects, 17: 13876(R) (BMI-1603(Del.))
radiation effects on color change in spectra of dyed, 17: 22259
radiation effects on EPR spectrum of, gamma, 17: 35913
radiation effects on properties of coatings, 17: 36362
radiation effects on transient-current decay in insulators of, gamma, 18: 18428
radiation effects on electric conductivity of, electron and gamma, 18: 24203
radiation effects on, temperature effect in Lichtenberg image in electron, 18: 30241(T,R) (AEC-tr-6231(p.44-7))
radiation effects on dye-containing, gamma, 18: 37201(T) (AEC-tr-6398(p.366-8))
radiation effects on optical density of, electron, 18: 41801
radiation effects on oxygen sorption by, 19: 11197
radiation effects to 180°C, comparison of uv data with gamma, 19: 13435
radiation effects on dielectric constant and dissipation factor of, in vacuum, 19: 13444
radiation effects on thermoelectric charge displacement in, 19: 22328
radiation effects on electric conductivity of, gamma, 19: 32779
radiation effects on, ESR spectra of radicals formed in, 19: 36485
radiation effects on physical properties of, 19: 39231 (COO-1224-8)
radiation effects on free radical density, gamma and x, 19: 38706
radiation effects on, dose determination from, 19: 46367
radiation effects on, protective effects of aromatic additives against, 19: 46321 (AD-611779)
radiation effects on elasticity of hardened, 20: 406
radiation effects on, role of LET in gamma and helium-4/lithium-7, 20: 20764
radiation effects on inter- and intramolecular energy transport in, electron, 20: 33387
radiation effects on viscosity of, 20: 45737
radiation exposure to compact, measurement of electron energy distributions in, 19: 15057
radioactive contamination build-up on, from dilute solutions of plutonium, 19: 2747 (NP-14343(Discussion, Session II))
radioinduced copolymerization with vinyl pyrrolidone, 16: 4450(R) (BMI-1546(Del.))
radioinduced copolymerization with styrene, 16: 29010
radioinduced copolymerization with polystyrene, 16: 29011
radioinduced copolymerization with polyvinyl acetate, 17: 29923
radioinduced crosslinking, localized neutron, 16: 23720(T) (AEC-tr-5144)
radioinduced cross-linking in, 18: 12250(P)
radioinduced cross-linking with polystyrene and teflon, localized neutron, 20: 23087(T) (AEC-tr-6466/1, pp 238-41)
radioinduced decomposition of solid, scavenger reactions of diphenyl-picryl hydrozyl in, 16: 30454
radioinduced defects in, electron spin resonance studies of decay, 17: 16060
radioinduced defects in dyed, decay spectra of, 18: 8412
radioinduced degradation in acetone–benzene, 19: 15580
radioinduced discharge figures in, electron, 17: 34496
radioinduced electric charges in lucite, use in gamma dosimetry, 19: 42719 (TID-22087)
radioinduced electric discharge figures in, electron, 20: 21440
radioinduced film formation from, on glass and quartz, 17: 32695
radioinduced free radical site formation in, effects of structure, 16: 2093(R) (BMI-X-179)
radioinduced free radicals in Perspex, effects of oxygen, 16: 13111
radioinduced free radicals, thermal decomposition, 16: 23743
radioinduced free radicals in, reactions with diphenylpicrylhydrazyl, 17: 27215
radioinduced free radicals in, electron spin resonance studies of, 17: 30132
radioinduced free radicals in, singlets in electron spin resonance spectra produced at high doses, 18: 23616(T,R) (AEC-tr-6316(p.306-9))
radioinduced free radicals in, output saturation in electron spin resonance spectra of, 18: 23617(T,R) (AEC-tr-6316(p.310-13))
radioinduced free radicals in, concentration of, 18: 23618(T,R) (AEC-tr-6316(p.314-21))
radioinduced free radicals in, electron spin resonance spectra, 18: 29735(T,R) (AEC-tr-6231(p.292-309))
radioinduced free radicals in, reactions with sulfur dioxide, 18: 29747(T,R) (AEC-tr-6231(p.439-50))
radioinduced free radicals in, electron spin resonance of, 19: 13479
radioinduced free radicals in, electron spin resonance studies of, 19: 15573 (UJV-1138/64)
radioinduced gel formation in, effects of triallyl cyanurate on electron and gamma, 18: 3856
radioinduced graft polymerization to vinyl pyrrolidone, 17: 23864(R) (BMI-1619(Del.))
radioinduced graft polymerization to vinyl pyrrolidone, 17: 25685(R) (BMI-1624(Del.))
radioinduced graft polymerization of vinyl pyrrolidone on, 17: 26944(R) (BMI-1630(Del.))
radioinduced graft polymerization of vinyl acetate on, 17: 27449
radioinduced graft polymerization of vinyl pyrrolidone on, 17: 40424(R) (BMI-1642(Del.))
radioinduced graft polymerization of vinyl pyrrolidone on, effects of irradiation temperature on, 18: 7985(R) (BMI-1650(Del.))
radioinduced grafting with vinyl pyrrolidone, 18: 13904
radioinduced graft copolymerization with styrene, 18: 22130
radioinduced graft polymerization, study of factors in, 19: 7536 (BMI-1695)
radioinduced oxidation of, effects of styrene groups on peroxide production in, 18: 31609
radioinduced peroxidation and grafting to vinyl pyrrolidone, 17: 40423(R) (BMI-1639(Del.))
radioinduced peroxidation, 18: 13904
radioinduced peroxidation graft polymerization of, 18: 15664(R) (BMI-1655(Del.))
radioinduced polymerization with woods, properties of products of, 18: 37190 (BNL-874(p.37-8))
radioinduced polymerization of, with acrylonitrile and styrene, gamma, 20: 26939
radioinduced production of shaped articles of, process for, 17: 40905(P)
radioinduced production of Lichtenberg Figures in, by 6-Mev electrons, 20: 14607
radioinduced racemization of isotactic, electron, 19: 36488
radioinduced reactions in, electron spin resonance studies of, 18: 27592
radioinduced reactions with polystyrene, 19: 10675(R) (NAA-SR-9999)
radioinduced sulfonation, 18: 29726(T,R) (AEC-tr-6231(p.233-8))
radioinduced welding with aluminum, method for neutron, 18: 325
radioinduced, effects of acetone–benzene mixture on, 19: 15579
radiolysis, 17: 22237
radiolysis, 17: 32176
radiolysis of copolymer with polystyrene, formation of peroxides in, 17: 27475
radiolysis of, effects of dose and oxygen on peroxide formation in, 17: 27475
radiolysis of, diffusion and penetrability coefficients of gases formed in, 19: 11182
radiolysis of, effects of uv and visible light on free radicals in, 18: 43681
radiolysis of, effects of linear energy transfer in, 19: 429(R) (ORNL-3679 (p.39-48))
radiolysis of, mechanism and spectra of free radical formation in, 19: 11196
radiolysis of, protective effects of aromatic amines on, 16: 27063
reactions of free radicals at low temperature in irradiated, 16: 5237
reactions with muonium, (E), 20: 29247
reactions with nitrogen dioxide and nitric oxide, ESR spectra of,

19: 22355
reactor criticality effects of reflectors of, 18: 6523(R) (ORNL-3499 (Vol.I)(p.81-5))
refractive index of lucite at 0.86A, 16: 3574
shock wave research on, review, 20: 7960 (LA-DC-7462)
sorptive properties for ionic radioisotopes in aqueous solutions, effects of acidity on, 20: 7003 (INR-634/V/C)
stress analysis of thick-walled vessel of, comparison of experimental and numerical, 19: 22503 (GAMD-5503)
thermal degradation of, with divinylbenzene, mechanism of, 20: 38930 (TID-23264)
use for radiation dosimetry, 20: 46084
use in gamma dose measurements, 20: 2165
use in model of concrete pressure vessel, 19: 28469 (GAMD-6027)
use in radiation dosimetry, 20: 46085
use in scintillation detectors for slow neutrons, 19: 13790
use of colored, in radiation dosimetry, 18: 39610 (AERE-R-3360)
use of vaseline on, for fallout collection, 18: 43821
uses in nuclear technology, 19: 18101
uses in preparation of kryptonates, 20: 1862
x-ray absorption in Grenz region, dosage determination in, 19: 24784
x-ray scattering on isotactic and syndiotactic, in solution, (T), 19: 6391

METHACRYLIC ACID POLYMERS
crystal structure of barium methacrylate dihydrate, 17: 3027(R) (TID-17273)
gels of, activity coefficients in sodium chloride, 19: 36463(R) (TID-22060)
phase equilibria in polymer-monomer-solvent systems, 16: 445(R) (NYO-9988)
properties for use as ion exchanger, 19: 36556
properties of radioinduced, 16: 18965
properties of, effects of chain transition on physicochemical, 20: 18794
radiation effects on aqueous solutions, 16: 22234
radiation effects, 17: 12323 (BMI-1610)
radiation effects on aerosols of, x, 20: 4015
radioinduced cross-linking in aqueous solutions, 17: 1545
radioinduced electron paramagnet resonance spectra, gamma dose effects on, 16: 13099
radioinduced gel formation in, for chemical dosimetry, 16: 29135
radioinduced graft polymerization on synthetic fibers, 18: 8419
radioinduced polymerization with woods, properties of products of, 18: 37190 (BNL-874(p.37-8))
radioinduced reactions in, electron spin resonance studies of, 18: 27592
radiolysis of, ESR spectra of free radicals produced by, 19: 17976
solution properties, effects of tacticity on, 18: 25463

METHACRYLONITRILE
radiation effects on cyanide group inversion in, 19: 46326 (CNAEM-28)
radiation stability, 19: 15571(R) (TID-21385)
radioinduced polymerization of, 17: 29911
radioinduced polymers, stereoregularity of, 17: 33963
radioinduced polymerization of liquid, gamma, 19: 46336 (TID-22236)
radioinduced polymerization of emulsions of, gamma, 20: 43374

Methallyl Chloride
see Propene, 3-Chloro-2-methyl-

Methanal
see Formaldehyde

Methandriol
see Androstenone, Hydroxymethyl-

METHANDROSTENOLONE
effects on protein and nucleic acid content in irradiated rats, 20: 8735
radiosensitivity effects in rats, mechanism for, 20: 8735
sensitivity effects of, on gas metabolism in rats, 19: 13115

METHANE
alpha energy loss and ionization in, 16: 6931
alpha reactions with, mean ionization energy for, 18: 6862
alpha stopping power of, 5-Mev, 20: 2147
alpha-particle molecular stopping cross section at 300 keV to 5 MeV, 20: 46300
analysis for carbon-13 by NMR spectrometry, 19: 30630(R) (MLM-1245)
analysis for carbon-13 enrichment, 19: 34607(R) (MLM-1239)
analysis for carbon-13 by NMR, 20: 3879(R) (MLM-1266)
analysis for impurities by infrared spectrometry, 20: 20553(R) (MLM-1142)
analysis for tritium in chromatographic flow mixture with helium, proportional counter, 16: 17594
analysis of atmospheric, for tritium, 17: 5947(R) (AFCRL-62-295)
anharmonicity constants of isotopically substituted, 17: 4546(T)
atom inelastic reactions with gaseous, dissociative ionization in metastable, 18: 32487
bismuth-212 transport in carrier gas of, 20: 427
boiling data for, nucleate and film, 20: 36993
bond amplitudes in, effects of deuterium on, 19: 13322
bond dissociation energies and ionization potentials of, calculation of, 18: 43489
bond rupture from tritium beta decay in, recoil energy for, 19: 42574
carbon deposition from, in fluidized bed at 1900 to 2400°C, (E), 20: 43930
carbon exchange with sorbed methane in molybdenum films, 16: 23576
carbon-13 coupling constants with protons in, 16: 7976
carbon-11 recoil reactions with, in presence of oxygen, 19: 4173 (BNL-8621)
carbon-13 concentration in, by thermal diffusion, 20: 20806(R) (MLM-1274)
carbon-13 enrichment in, using thermal diffusion column, 18: 19466(R) (MLM-1170)
carbon-13 enrichment in, efficiency of thermal diffusion column for, 18: 19467(R) (MLM-1175)
carbon-13 enrichment in, by thermal diffusion, 18: 45173(R) (MLM-1203)
carbon-13 enrichment in, by thermal diffusion, 19: 30629(R) (MLM-1238)
carbon-13 enrichment in, by thermal diffusion, 19: 34607(R) (MLM-1239)
carbon-13 enrichment in, by thermal diffusion, 20: 20553(R) (MLM-1142)
carbon-13 equilibria with carbon dioxide, use in determining underground temperatures, 19: 28420(R) (NP-14825)
chemical shift of gases from, in nuclear magnetic resonance spectra, 16: 1758
chlorination of labeled, kinetic isotope effects in, 16: 22093
chromatographic behavior of, effects of deuterium on, 19: 40672
collisions with metastable argon and helium, 18: 9042
collisions with metastable neon, inelastic, (E), 19: 16378
concentration of carbon-13-enriched, methods for, 20: 14444(R) (MLM-1268)
content in natural gases, 18: 12366
content in upper atmosphere, from rocket soundings, 18: 37794(T) (NASA-TT-F-141(p.1-21))
conversion of carbon-13-enriched, to barium carbonate, 18: 45173(R) (MLM-1203)
conversion to carbon by pyrolysis, 18: 35246(R) (MLM-1196)
conversion to higher hydrocarbons, chemonuclear reactor design for, 19: 5401(P)
corrosive effects on Hastelloy X and Haynes 25 alloy, 19: 40961
corrosive effects on superalloys at high temperatures, 19: 46946 (BNWL-100)
critical and inversion temperatures, 17: 30460
crystal lattice dynamics of solid, in alpha, beta, and gamma phases, (E/T), 19: 45239
crystal vibrations and rotational motions in solid, 17: 20977
decomposition and synthesis in vacuum systems, 19: 31332(R) (ORNL-3789(p.334-40))
decomposition by electron impact, kinetic energy in, 18: 22107
decomposition by electron impact, kinetic energy distribution in, 19: 28912(R) (ANL-6819)
decomposition, deposition of pyrolytic carbon in graphite by, 16: 7870
decomposition in graphite pores, 16: 6773
decomposition in hydrogen plasma jets, acetylene production by, (T), 20: 3197
decomposition of, carbon deposition in fluidized beds from, 20: 9447
decomposition, kinetics of unimolecular, 18: 31550 (NP-14122)
desorption from molybdenum surface at 80 to 115°K, 18: 27696
detection and measurement using ionization detectors, 16: 28875(T) (AEC-tr-5287)
determination as impurity in ultrapure gases, mass spectrometric, 20: 29083(R) (UCRL-14767)
determination in air using kryptonates, 18: 33450(R) (NYO-2757-4)
determination in argon in gas chromatography, electron drift velocity detector for, 18: 33476
determination in air using beta sources, instrument for, 20: 37150
determination in geothermal bores, fumaroles, and pools in New Zealand, mass spectrometric, 16: 16581
determination in helium coolant in Dragon Reactor, evaluation of methods for, 19: 22155
determination in helium at reduced sample pressures by gas chromatography, 20: 1751
determination in klystrons during operation and life-testing, 16: 31757
determination in metals, vacuum fusion, 18: 33491
determination in mines by activation, equipment for, 20: 23527 (CONF-651206)
determination in purified helium, use of chromatography and radioactive ionization detector for, 18: 31397
determination in pure helium, chromatograph for, 19: 28220 (BNWL-12)
determination in reactor blanket gas, design of continuously operating gas chromatogram for, 20: 43157
determination in small gas samples, chromatographic, 19: 36227 (AWRE-O-22/65)
determination in vented gases from underground nuclear explosion, apparatus for, 19: 19776 (UCRL-12169)
determination of deuterated, in reactor helium, chromatographic, 16: 31541 (DP-754)

determination of deuterated in normal, by infrared spectrometry, 19: 46157(R) (MLM-1254)
determination of isotopic molecular weight, 16: 2997(T) (NP-tr-808)
determination of, in products of biphenyl pyrolysis, chromatographic, 17: 19941 (ORNL-TM-523)
determination of, factors affecting continuous on line, 20: 1734 (EG-Report-36)
determination, use of beta ionization detector in chromatographic, 19: 40415(T) (CEA-tr-R-1839)
deuterium exchange, effects of tritium, 16: 26997
deuterium exchange with hydrogen in, xenon radiosensitized, 17: 8161
deuterium exchange with hydrogen in, over palladium–ruthenium alloys at 90 to 170°C, 20: 5557
deuterium exchange reactions with hydrogen in, catalytic effects of palladium alloys on, 20: 14542
deuterium exchange with hydrogen in, catalytic effects of gold–palladium alloy on, 20: 16457
deuterium exchange with hydrogen of, over platinum–rhodium alloys, 20: 23048
deuteron nuclear quadrupole coupling constant in deuterated, 20: 40894
deuteron spin-lattice relaxation in deuterated and normal, at 1.2 to 90°K, 20: 28188
diffusion coefficients in carbon tetrachloride, 18: 19963
diffusion from stored, solid plutonium residues, vacuum-drying effects on, 20: 4364 (AERE-M-1644)
diffusion in tissue-simulating plastics, 18: 13716(R) (ANL-6769(p.21-9))
dipole moment of, effects of isotopic substitution on, 18: 6816
effects on carbon dioxide–graphite reactions at 960 to 1200°C, 20: 10859
effects on electron spin resonance signal of activated charcoal, 19: 36332 (IFA-IS-31(1965))
effects on helium bivalent ion yields in cyclotron sources, impurity, 17: 31222
effects on neon performance in spark chambers, 18: 14210 (JINR-P-1498)
effects on oxidation of graphite by vacuum ultraviolet irradiated carbon dioxide, 20: 29733
effects on pyrolytic decomposition of biphenyl and terphenyls, 17: 35847
effects on quenching in irradiated argon, 18: 37850
effects on radioinduced luminescence of argon in electric field, 19: 9185
effects on radioinduced reactions between carbon dioxide and graphite, 19: 11161 (AERE-R-4817)
effects on radioinduced reactions between carbon dioxide and graphite, 19: 11162 (AERE-R-4819)
effects on radioinduced carbon dioxide-graphite reactions, (E), 19: 19953 (AERE-R-4201)
effects on radioinduced oxidation of graphite in carbon dioxide, oxygen effects on, 20: 1895 (AERE-R-4988)
effects on reactions of photolyzed carbon dioxide with graphite, 20: 23097
electric discharge in, radiation from, 16: 33654
electric discharge in, secondary ionization in, 18: 20137
electric discharge in, electron avalanches in, 18: 21490
electric properties of combustion products of, (E), 20: 41731
electron beam fragmentation, mass spectra from, 16: 10062
electron diffusion in, at low energies, 16: 24325
electron diffusion energy in, 19: 14266
electron drift velocities in, 18: 18233
electron impact ionization coefficient in gases of, (E), 19: 26953
electron inelastic scattering by, energy distribution and total cross sections for, 20: 335
electron reactions with deuterated and natural, appearance potentials for ions produced in, 18: 28134
electron reactions with, cross sections for dissociative ionization in, 19: 27078
electron reactions with, ionization cross sections for, (E/T), 20: 5989
electron scattering by, excitation mechanisms in 0 to 15 ev, 18: 1781
electron scattering by, inelastic 390 v, 18: 14836
electron spin resonance studies of gamma-irradiated, at 4 and 77°K, 16: 5239
electron wave function for molecules of, one-center, 17: 27366
electronic energy, 16: 16357
energy transfer with excited argon atoms, cross sections for, 18: 39213
evaporation of labeled-, separation coefficients of carbon-12 and -14 in equilibrium, 20: 43093(T) (BNL-tr-84)
exchange reactions with deuterium on platinum, ruthenium, and their alloys, catalytic, 18: 16034
excitation of, relations with incident electron energies, 18: 11512(R) (NARF-63-9p)
flow rates and partial pressures in pyrolytic carbon coating deposition, 19: 2785
formation from graphite and hydrogen at 1900 to 2300°C, effects of helium additions on, 17: 34328(R) (NP-12991)
formation in Fischer-Tropsch synthesis, mechanism, 16: 31598
formation in graphite reactions with hydrogen at 360 to 800°C, 18: 223
formation in radiolysis of polyoxymethylene at low temperature, mechanism of, 18: 25514(T) (AEC-tr-6372(p.437-43))
formation in rare gas sensitized radiolysis of labeled propane, 17: 4601
formation in reactions between rare earth dicarbides and water, 20: 17048
formation of, in gamma radiolysis of 2-butyne, mechanism of, 17: 20054 (ASD-TDR-63-65)
formation of tritiated, during copper ore mining using nuclear devices, 20: 45570(R) (ORNL-3945, pp 189-94)
fragmentation and ionization of, method for direct observation of, 19: 24505
gamma and fast neutron heating in moderators of, for cold neutron production, (T), 20: 36152
heat capacity of deuterated, 18: 15681 (LADC-5738)
heat of adsorption of, 18: 31743(R) (ORNL-3652(p.132-45))
heat of desorption, 17: 33159(R) (ORNL-3472(p.107-18))
heat of formation, 17: 27322 (UCRL-7301-T)
heat of vaporization of, calculation from rigid-sphere equation of state, 18: 224
heats of vaporization of carbon-12- and -14-labeled, 20: 43093(T) (BNL-tr-84)
helium atom reactions with, electron kinetic energy from ionization in, (E), 20: 29927
helium ion stopping cross sections at 40 to 200 kev, (E), 19: 27541
hydrogen abstraction from, by hot tritium atoms, theoretical treatment of, 20: 43408
hydrogen atom and proton reactions with gaseous, emission spectra from, 17: 41641(T)
hydrogen bonding in, effects of substitutions on, 17: 8110
hydrogen exchange with tritium, mechanism, 17: 12251
hydrogen ion reactions at 10 to 50 kev, equilibrium fractions in, (E), 19: 14243
hydrogen ion reactions with molecular, at 1 to 55 kev, particle production cross sections for, 20: 29919 (UCRL-14214)
hydrogen ion reaction at 20 to 120 kev, ionization cross sections for, 20: 31909
intermolecular forces in, isotopic effects on second virial coefficient, 16: 22132
ion energy loss in, below 10 Mev/amu, 17: 671
ion reactions with, 17: 41534(R) (ANL-6720(p.77-89))
ionization by alpha particles, impurity and temperature effects on energy of, 18: 18467
ionization by alpha particles and electrons, cross sections and mass spectra for, (E), 20: 44122
ionization by electron impact, ion-molecule reactions following, 17: 200
ionization by electron impact, cross section for, 17: 8113
ionization by electron impact at energies up tp 500 ev, cross sections for dissociative, 19: 14127 (FSU-2690-14(Paper 1))
ionization by excited noble gas atoms, 19: 9943
ionization by fission products in proportional detector, (E), 19: 20376
ionization by kev electrons and Mev helium ions and protons, mass spectrometric comparison of, 18: 18567
ionization by metastable helium ions, relative cross sections for, 19: 6479
ionization by x radiation, energy expenditure in, 16: 29585
ionization by x rays at high energies, spectra of, 18: 41506(R) (ML-TDR-64-169)
ionization cross section for, electron-impact, 19: 38630
ionization energy in, measurement of effective, 20: 43193
ionization of deuterated and normal, isotope effect in, 17: 30592
ionization of deuterated, by metastable rare gas atoms, isotope effects in, 18: 39215
ionization of, appearance potential measurements on secondary ions produced by, 18: 33569
ionization of, by electrons at 0.6 to 20 kev, cross sections for, (E/T), 20: 31906
ionization potential of, method of calculating, 19: 22208
ionization potential of, (E), 20: 351
isotope effects on zero-point energy, calculation of, 17: 19938
isotopic composition of atmospheric, from 1948 to 1960, 16: 4381
isotopic exchange with deuterium and tritium, 20: 3980
isotopic exchange with deuterium in shock tubes at 1440 to 1755°K, 20: 35498
labeling of, with tritium in electric discharge fields, 20: 45776
labeling with tritium, mass spectrometric study of mechanisms in, 17: 6781(R) (ANL-6603(p.57-73))
lead-212 transport in carrier gas of, 20: 427
lithium-6 reactions at 0.6 to 3.75 Mev, molecular stopping power for, (E), 19: 23297
magnetic resonance in solid, 16: 13183(R) (TID-15140)
mass difference with oxygen, (E), 19: 28336
mass spectra, 17: 7655(R) (ANL-6600)
mass spectra of, 17: 6791 (IS-424)

mass spectra of, at −150 to +200°C, 17: 38984
mass spectra of, intramolecular deuterium isotope effects on, 18: 1721
meson (K⁻) capture in, meson (π^0) energy spectrum from, 20: 24326 (AD-626056)
methane ion reactions with molecular deuterated, dissociation in charge-exchange, (E), 19: 23258
methane rearrangement collisions at high energies, 18: 16676
model for liquid, 19: 19095 (WASH-1053)
molecular motion in liquid, neutron scattering analysis of, 16: 32236
molecular properties of, in infrared vibrational range, (T), 20: 8496 (UCRL-16265)
molecular size and shape of CH_4^+, calculation of, 20: 5006(R) (ORNL-3870, pp 50-5)
molecule scattering by, cross sections for inelastic, 19: 14265
neutron cross sections for, computer program calculation of, 19: 35379 (IDO-17087)
neutron inelastic scattering in, cold, 16: 32379
neutron inelastic scattering in liquid, total cross sections for thermal, 16: 32368
neutron inelastic scattering by, partial differential cross sections for, 17: 36669 (WASH-1042)
neutron inelastic scattering by liquid, at 0.009 to 0.17 ev, 18: 4512 (GA-4292)
neutron inelastic scattering by liquid, cold, 18: 13030(R) (GA-4434)
neutron inelastic scattering by, first-moment calculations of, 18: 40474 (IDO-16977(p.23-43))
neutron inelastic scattering by, dynamic processes in slow, 20: 40338
neutron moderating properties at 20 to 150°K, 16: 29716
neutron partial differential scattering cross sections for, reduced slow, 16: 28026 (IDO-16699(Rev.))
neutron reactions at 0 to 0.306 ev, Krieger-Nelkin method for calculating differential scattering cross sections, 16: 2482 (IDO-16692)
neutron reactions (n,2n) in, effects of carbon-11 production on yields in, 17: 37270
neutron scattering, inelastic, 16: 3661
neutron scattering at 0.015 and 0.0252 ev by gaseous, rotational level effects, 16: 7087
neutron scattering at 0.07 ev, angular distributions from, 16: 18424
neutron scattering by liquid, energy distribution at low energies, 16: 19743
neutron scattering by, effect of interference scattering on, 16: 29718
neutron scattering by, thermal, 16: 33787
neutron scattering by, 17: 4330(R) (IDO-16781)
neutron scattering by liquid, cluster model for, 17: 22967(R) (IDO-16857)
neutron scattering cross sections, comparison of calculated and experimental differential, 17: 26540
neutron scattering cross sections, 17: 4036
neutron scattering cross sections for liquid, 17: 15216 (NP-12502)
neutron scattering by, calculated and experimental results, 17: 15168 (BNL-719(Vol.I)(p.172-202))
neutron scattering at −148°C, 17: 17623(R) (IDO-16827)
neutron scattering by solid, energy distributions from, 17: 20977
neutron scattering by, 17: 38026(T) (AEC-tr-5734(p.119-39))
neutron scattering from liquid, thermal, 17: 4333(R) (IDO-16805(p.7-35))
neutron scattering by rotating states in, 18: 24299 (NP-13930(p.56-7))
neutron scattering by, cross sections for slow, 18: 32715 (KFKI-64-3)
neutron scattering by, cross sections for slow, 18: 40474 (IDO-16977 (p.23-43))
neutron scattering by deuterated, cross sections for slow, 18: 40474 (IDO-16977(p.23-43))
neutron scattering by gaseous, excitation in, 18: 40574
neutron scattering by deuterated, thermal (T), 19: 1639
neutron scattering in, contribution of molecular rotation to inelastic, 19: 1540
neutron scattering by gaseous, liquid, and solid, relations with free rotation theory, 19: 1956(R) (IDO-16994)
neutron scattering by, spin correlation effects on (T), 19: 3377
neutron scattering by gaseous, liquid, and solid, inelastic slow, 19: 8076
neutron scattering cross sections for, spin correlation effects on, (T), 19: 23737
neutron scattering by liquid, model of, 19: 29228(R) (AEET/NP/10)
neutron scattering by, distributions from cold, (E), 19: 45237
neutron scattering by, calculation methods for, (E/T), 19: 47576(R) (IDO-17081, pp 49-76)
neutron scattering by liquid, use of Langevin equation of Brownian motion for analysis of cold and slow, 20: 313
neutron scattering by liquid, model of, 20: 26396(R) (IDO-17140)
neutron scattering by, effects of molecular rotation on differential cross sections for, 20: 25740
neutron scattering by gaseous and solid deuterated, (E), 20: 30360 (WASH-1068)
neutron scattering by liquid, Langevin equation of Brownian motion for analyzing, 20: 33255 (BNL-940, pp 149-54)
neutron scattering at 0 to 156 Mev by deuterated, intramolecular coherent, (E), 20: 38000
neutron scattering by gaseous, calculation of, (T), 20: 38004
neutron scattering by solid, effects on molecular rotation from, (T), 20: 40323
neutron scattering by, effect of nuclear spin correlations on, 20: 42144
neutron scattering by gaseous, cold, (T), 20: 44599
neutron scattering by deuterated liquid cold, (E), 20: 46571
neutron thermalization, 16: 18449
neutron total cross sections of solid, cold, 18: 17081
nuclear magnetic resonance of, deuterium isotope effects on, 19: 11152
nuclear spin coupling constants in, molecular orbital theory for, 18: 44773
nuclear spin coupling constants in, effects of excitation energies on, (T), 20: 44126
nuclear spin relaxation in liquid and solid, isotope effects in, (E), 19: 32191
nuclear spin relaxation in liquid, intermolecular contribution to, 20: 36828
oxidation by copper oxide, effects of carbon-14 on, 20: 29187
oxidation in presence of nickel–chrome–palladium catalyst, 16: 17617(R) (ORNL-TM-122)
oxidation induced by fission fragments, 19: 5946 (TID-21382)
oxidation of, in flow through copper-oxide beds, 17: 39196(R) (ORNL-3452(p.229-32))
oxidizing effects on graphite in helium, 16: 12833
oxygen ion reactions at 15 to 50 kev in, equilibrium fractions for, (E), 19: 18687
performance in proportional counters, effects of oxygen on, 20: 33641
performance of particle-seeded, as rocket-reactor coolant, (E), 19: 24149 (NASA-CR-212)
phase transitions in solid deuterated, theory of, 16: 33597
photochemistry of deuterated and natural, 18: 25561
photochlorination of, deuterium isotope effects on, 17: 17958
photochlorination of deuterated, kinetic isotope effects in, 18: 10129
photoionization of, mass spectrometric studies of deuterium effects on, 19: 26370
photolysis at 20.4°K, tracer studies of effects of rare gases on, 19: 7558
photolysis by vacuum ultraviolet, mechanism, 16: 29006
photolysis of mixtures of deuterated and undeuterated, effects of pressure on, 18: 17897
photolysis of mixtures of deuterated and normal, hydrogen isotope distribution in, 17: 40875
plasma properties of, for use in electro-thermal engines, 17: 9674 (ASD-TDR-62-451)
polarizability of liquid, corrections for zero-field many-body, 17: 4526
positron annihilation rates in, 18: 4454
preparation from water for tritium counting, 18: 16075
preparation of high-purity, for use in radiation detectors, 19: 46319
pressure losses in beds of molecular sieves, 16: 1728 (AAEC/E-67)
production by gas discharge and radioinduced cracking of butane, 20: 20740
production by hydrolysis of rare earth and yttrium carbides in mineral acids and water, 18: 39221
production by hydrolysis of uranium di- and monocarbides in nitric and sulfuric acids and water, 18: 39222
production by neutron radiolysis of cyanoguanidine, 16: 7594
production during hydrolysis of thorium uranium carbides, 20: 29159
production for carbon-14 dating, 20: 20917
production in argon-sensitized radiolysis by liquid propane, 20: 43368
production in hydrolysis of scandium carbide, 20: 26890
production in pentane-radiolysis, effects of mineral powders, 16: 3323(T) (AEC-tr-4497(p.162-6))
production in pyrolysis of toluene using deuterium and hydrogen carrier gases, 18: 39204
production in radioinduced oxidation of methanol, effects of dose rate on, 20: 38942 (UJV-1457)
production of, in radiolysis of labeled gaseous isobutane, effects of inert gases on, 17: 12338
production of tritium-labeled, in methane-tritium reactions, 19: 28363 (UCRL-16009)
properties as Cherenkov counter gas, 17: 18591 (BNL-6889)
properties for use in gas flow counters, 19: 7791
protective effects against radiation injury to bean seedlings, 16: 32866
proton magnetic relaxation in, temperature dependence of, 17: 21703
proton magnetic resonance in deuterated and normal, 19: 13380
proton reactions (p,pn) in, effects of carbon-11 production on yields in, 17: 37270
proton spin-lattice relaxation in deuterated, 19: 30224
proton spin-lattice relaxation in deuterated and normal, at 1.2 to 90°K, 20: 28188

proton stopping cross sections at 40 to 250 kev, 17: 31211
proton stopping cross sections at 40 to 250 kev, 18: 4617
purification using cascaded hot-wire columns, 17: 33412(R) (MLM-1146)
pyrolysis for carbon deposition on uranium carbide particles, 20: 13215(R) (ORNL-3885, pp 3-86)
pyrolysis on graphite at 2000°C, 17: 34328(R) (NP-12991)
radiation chemistry, 18: 13899
radiation effects on deuterium exchange with hydrogen on deuterated silica gel, 16: 22221
radiation effects of fission products on, at 165 and 300°C, 17: 1527 (TID-17046)
radiation effects of gamma rays on deuterated, in solid rare-gas matrix, 17: 3051
radiation effects on reactions with ammonia, 17: 10704
radiation effects on properties as dosimeter, 17: 35253(R) (IA-775)
radiation effects on, validity of Born approximation for molecular fragmentation in electron and proton, 18: 43629
radiation effects on conductivity of halogen derivatives of, in diethyl ether, 19: 30278
radiation effects on desorption of graphite surfaces in, 20: 17114 (AERE-R-5163)
radiation effects on, in krypton at 4.2°K, ESR of free radicals from gamma, 20: 40968
radioactivity content ratio of carbon-12/carbon-13 in, in natural gases in Italy, 19: 22577
radioinduced chlorination, 19: 24586
radioinduced decomposition of deuterated and natural, in solid matrices, 18: 29783
radioinduced deuterium exchange reactions in gaseous, mechanism of tritium, 20: 20719 (AD-624657)
radioinduced dimerization, reaction mechanisms in, 17: 39163(P)
radioinduced exchange with deuterium, recombination rate constants for xenon sensitized, 18: 12190
radioinduced free radicals of, in krypton, 20: 36909
radioinduced halogenation of, 19: 35615(R) (NP-15037)
radioinduced ionization of, electron dosimetry by, 18: 29764
radioinduced isotopic exchange with deuterium, 19: 28385
radioinduced oxidation on alumina, alumina–silica system, and silica, 18: 1725(R) (ORNL-3488(p.42-54))
radioinduced oxidation of, mechanism of fast-electron, 18: 41512(T) (ORNL-tr-226)
radioinduced oxidation of, adsorbed on alumina, aluminosilicate, and silica gel, 19: 4215
radioinduced oxidation of, fission-fragment and gamma, 19: 9169(R) (NYO-2915-1)
radioinduced oxidation, effects of rare gases on, 19: 15571(R) (TID-21385)
radioinduced reactions with alkenes, 16: 17750(P)
radioinduced reactions with ammonia and nitrogen, yields in, 17: 29012
radioinduced reactions with graphite in presence of other gases, 18: 13835 (HW-78948)
radioinduced reactions with Teflon, electron spin resonance studies of, 18: 23648(T,R) (AEC-tr-6316(p.534-7))
radiolysis at low dosages, mechanisms and products of, 19: 429(R) (ORNL-3679(p.39-48))
radiolysis at various dosages, yields of acetylene from electron and gamma, 20: 38951
radiolysis at 20.4 and 77°K, tracer studies of effects of rare gases on, 19: 7558
radiolysis by deuterons at 2 Mev, chemistry of nitrogen-13-labeled products from, 16: 13108
radiolysis by fast electrons, 18: 41511(T) (ORNL-tr-224)
radiolysis by fission products, 16: 24589
radiolysis by fission fragments and gamma rays, effects of hydrocarbon additions on, 19: 5947 (TID-21383)
radiolysis, electron spin resonance of free radicals produced in gamma, 16: 7600
radiolysis in gaseous phase, effects of intensity, pressure, and temperature on, 16: 16419
radiolysis in liquid argon at −183°C, 19: 11169(R) (RRL-152)
radiolysis in presence of ammonia and hydrogen by 5-Mev electrons, 16: 5117(R) (UCRL-9900)
radiolysis in presence of xenon, 16: 20524(P)
radiolysis in presence of oxygen, yields from, 18: 25465 (AERE-R-4581)
radiolysis, ionic mechanism, 17: 200
radiolysis, mechanisms, 16: 253
radiolysis of aqueous solutions of, reactions of hydrated electron in, 18: 25579
radiolysis of deuterated and normal, sensitized by argon, krypton, and xenon, 20: 379
radiolysis of, effects of nitric oxide and oxygen on ionic reactions in, 18: 6858
radiolysis of, electron spin resonance spectra of radicals produced by, 18: 288
radiolysis of, formation of products of, in reactor, 17: 27479
radiolysis of, formation of acetylene and ethylene in, 17: 39160
radiolysis of, formation and destruction of aerosols in, 18: 311
radiolysis of gaseous, production of high molecular weight products in 4-Mev electron, 16: 5386
radiolysis of gaseous, mechanism and mass spectra, 16: 14798
radiolysis of gaseous, 17: 23382(R) (RRL-109)
radiolysis of gaseous, reactions in, 17: 34005
radiolysis of hydrogen in deuterated, proton transfer reactions of H_3^+ in, 18: 33639
radiolysis of labeled, by electron bombardment, identification of products from, 16: 20495
radiolysis of liquid, effects of propene on gamma, 20: 1898(R) (RRL-2310-164)
radiolysis of, mechanism of, 17: 28966
radiolysis of, mechanism of, 18: 1756
radiolysis of mixture with propane, carbon-14-labeled compound yields in, 16: 7597
radiolysis of mixtures of deuterated and undeuterated, effects of pressure on, 18: 17897
radiolysis of mixtures of deuterated and normal, hydrogen isotopic distributions in, 17: 40875
radiolysis of solid, formation of viscous polymeric oil in, at 77°K, 18: 23697
radiolysis of, effects of argon, oxygen, and xenon on products from, 19: 479
radiolysis of, effects of temperature on hydrogen yields in, 20: 381
radiolysis of, evaluation of ionic reactions in, 19: 7556
radiolysis of, fission-fragment and gamma, 19: 9169(R) (NYO-2915-1)
radiolysis of, intermediate yields in, 20: 3982(R) (AGN-8156)
radiolysis of, yields of acetylene from, 19: 46366
radiolysis with low energy electrons, composition of condensable products in, 16: 10075
radiolysis, ethylene yields in electron, 18: 27527
radiolysis, product yields in, 19: 28375
radioinduced polymerization of solid, positive ion chemistry in, 20: 29314
radiosensitivity effects on *Drosophila virilis* oocytes, 17: 7886
radiosensitivity effects on animal and plant cells, 18: 38977
radon-219 and radon-220 decay in, properties of recoils from, 20: 29325
Raman effect and resonant four-photon interactions in, laser-stimulated, 18: 7344
reaction with fission recoil bromine, separation from uranium target by, 20: 46762
reactions in mass spectrometer, ion-molecule, 18: 8400
reactions in plasma jets, 20: 17959
reactions of deuterated and normal mixtures of, in mass spectrometer, 18: 8400
reactions of deuterated, with hot hydrogen atoms, 18: 25597
reactions of ions of, with gases, mass spectrometry of dissociation in, 18: 220
reactions of, with ions, atom and charge transfer in, 20: 31224
reactions with bromine-80 recoil atoms, radioactivity in organic yields in deuterated and normal, 19: 40618
reactions with carbon-black surface, hydrogen-isotope effect on, 17: 20050
reactions with CF_3 radicals, deuterium isotope effects on, 17: 1439
reactions with copper oxide, 16: 14690(R) (ORNL-TM-121)
reactions with copper oxide in helium, 16: 21994(R) (ORNL-TM-150)
reactions with deuterium and tritium ions, spectral studies on, 20: 18657
reactions with excited iodine-128 ions, effects of gaseous additives on, 16: 10061
reactions with excited hydrogen atoms, energy losses in, 18: 29766
reactions with excited helium, 19: 19937
reactions with fission-recoil radioiodine, 17: 29010
reactions with fission recoils, 19: 46330 (NP-15370)
reactions with fission-recoil bromine, 20: 45747
reactions with free radicals in irradiated polytetrafluoroethylene, 16: 3042
reactions with graphite at 1600°K and high pressure, 17: 18004 (LADC-5453)
reactions with graphite, constants for (6-exp) potential in, 17: 29442
reactions with Hastelloy X and Haynes 25 alloy at 2050°F, 19: 34745(R) (HW-84384(p.8.1-5))
reactions with Haynes 25 and Hastelloy-x at 1121°C, 19: 16017(R) (HW-84281(p.5.6-25))
reactions with helium induced by electron impact, 17: 18045
reactions with hot deuterium atoms, 18: 25597
reactions with hydrogen ions, potential energy curves for, 16: 18198
reactions with hydrogen from plasma torch, kinetics and thermodynamics, 16: 20391
reactions with hydrogen at 3 to 10 ev, energy losses in, 18: 31539

reactions with iodine-125 formed by electron capture in xenon-125, 19: 13449
reactions with lead by flash-heating, species formed in, 16: 18902
reactions with liquid sodium, 19: 32279(R) (ANL-7020(p.3-99))
reactions with methylene, mechanism, 17: 184
reactions with methoxy radicals, rate constants for hydrogen abstraction from, 20: 23025
reactions with niobium at low pressures and high temperatures, 20: 5181(R) (ORNL-3029)
reactions with nitrogen, kinetics and mechanisms of, 19: 26382(R) (RPI-321-1)
reactions with protons and tritons at 0.8 to 3.75 Mev mass spectra of, 19: 13496
reactions with rare gas ions in metastable states, fragmentation and ionization in, 19: 17874
reactions with rare gas ions at 2 to 200 ev, 19: 22319
reactions with recoil tritium atoms, isotope effects on hydrogen displacement in, 16: 9934
reactions with recoil tritium atoms in presence of butane, 16: 28947
reactions with recoil tritium atoms in presence of deuterium, 17: 30573
reactions with recoil tritium, isotope effects in abstraction, 17: 18098
reactions with recoil halogen atoms, 18: 20041 (MMPP-167-6)
reactions with recoil fluorine-18, mechanism of gaseous, 19: 13485
reactions with recoil tritium, kinetic isotope effects in, 19: 40615
reactions with recoil carbon-11 atoms, mechanism and products of, 20: 5570 (JUL-228-RC)
reactions with recoil tritium, 20: 9031
reactions with sodium at 190 to 385°C, 19: 17176(R) (ANL-6965(p.1-41))
reactions with sulfur dioxide, sulfur-35 activity in, 16: 28982 (UCRL-10360)
reactions with tritium, kinetics of exchange, 18: 41527
reactions with tritium, production of labeled methane and ethane in, 19: 28363 (UCRL-16009)
reactions with tritiated water, chromatography and scintillation spectra of products from, 20: 14455(R) (ORNL-3889, pp 25-32)
reactions with uranium hydride, 16: 4986(R) (NYO-2687)
reactions with uranium to prepare uranium carbide, 16: 24168(R) (NYO-2694)
reactions with uranium hexafluoride in presence of hydrogen at low pressure and high temperature, 17: 35619 (ORNL-TM-669)
reactions with uranium hexafluoride in plasma jet, 18: 29605 (ORNL-TM-872)
reactions with xenon, mass-spectrometric studies of, 17: 38988
refractive index at 1 atmosphere and 0°C, 16: 8897 (AERE-R-3867)
rotation of molecules in solid, (E), 19: 32189
scattering of molecular beams of, by silver single crystals, (E), 20: 44121
self-diffusion of liquid, 16: 13183(R) (TID-15140)
separation by molecular weights, in thermal columns, 17: 12579
separation by thermal diffusion, 18: 45175(R) (MLM-1209)
separation by thermal diffusion, 19: 14911(R) (MLM-1216)
separation from carbon-13 by thermal diffusion, 19: 24611(R) (MLM-1227)
separation from carbon monoxide and hydrogen by selective oxidation, isotope effects in, 20: 29187
separation from gas-cooled reactor helium coolants, 16: 29240 (TID-7627 (p.461-74))
separation from helium, 18: 1608 (JAERI-4025)
separation from other atmospheric gases, chromatographic, 18: 29799 (CEA-2361)
separation of carbon-13-enriched, by thermal diffusion cascade, 18: 29146(R) (MLM-1192)
separation of carbon-13-enriched, by thermal diffusion, 19: 13201(R) (MLM-1217)
separation of carbon-13-enriched, by sweep diffusion, 19: 42794 (K-OA-1360)
separation of carbon-13-enriched, by thermal diffusion, 20: 35827(R) (MLM-1299, pp 22-33)
separation of deuterated, by gas chromatography, 19: 40672
separation of normal and deuterated, by gas chromatography, 20: 12930
separation of nuclear spin species by preferential adsorption, 16: 7812(R) (TID-14658)
solubility in Santowax-OMI, 20: 20708 (AEET-213)
sorption and decomposition on iridium films at 27 and 100°C, 17: 40842
sorption by carbon black, deuterium isotope effects on, 16: 30946
sorption by graphitized carbon black, isotherms for, 16: 31536
sorption by graphite, two-dimensional second virial coefficients of deuterated and normal, (E), 19: 42487
sorption by Mylar windows in flow-gas proportional detector, 18: 22343 (RSA-39)
sorption by titanium films in getter pumping of vacuum systems, 16: 3098 (ORNL-3217)
sorption by vapor-deposited titanium films at 10°C, 16: 9511(R) (ORNL-3239(p.85-95))
sorption by vapor-deposited titanium films, 18: 14591 (ORNL-3481)
sorption by zeolite at 21°C, 16: 31719 (UCRL-6396)
sorption of labeled and unlabeled, by graphitized carbon black, 16: 10030
sorption on chromatographic columns, isotope effects of deuterium or tritium on, 19: 5863
sound absorption by deuterated, at 26°C, 18: 40052 (TID-21037)
sound absorption in, effect of deuteration on, 17: 28923 (TID-18976)
sound absorption in deuterated, 19: 8716 (TID-21414)
spectra, fine structure and rotational lines of $2\nu_3$ band in, 16: 22175
spectra of bideuterated, analysis of infrared, 17: 13128
spectra of deuterated, experimental and theoretical comparison of absolute intensities of infrared, 16: 18230(T)
spectra of deuterated and normal, theory of vibration-rotation interactions in, 16: 32979
spectra of deuterated and normal, in argon, krypton, and xenon, infrared, 17: 33951
spectra of deuterium-labeled at 4430 to 4550 cm^{-1}, infrared, 16: 25345
spectra of ionic deuterated, isotope effects on metastable transitions in mass, 19: 4137
spectra of labeled and unlabeled, vibration-rotation interactions in overtone levels of, 17: 1445
spectra of molecular fragmentation in, design of pulsed ion source for, 19: 15474
spectra of normal and tetradeuterated, Raman, 17: 25236
spectra of ν_3 fundamental of liquid and solid deuterated and normal, infrared absorption, 18: 8401
spectra of tritiated, isotope effects in, 18: 3801
spectra of, isotope effects on C–H vibrational transition probability in, 20: 18639
spectra with rare gas solids at 4.2 and 20.4°K, transition of C_2 molecule, 16: 5258
spectrum of monodeuterated, Raman, 16: 18900
spectrum of monodeuterated, infrared, 17: 30578
storage of liquid, high-pressure cryogenic vessels for, 18: 44699
thermal capacity of liquid, at boiling point, 18: 19929 (CONF-417-20)
thermal conductivity and viscosity of liquid, at critical point, 17: 25849 (LADC-5791)
thermal conductivity of compressed, at 0 to 300°C and 1 to 500 kg/cm^2, 19: 16254(T) (LA-tr-65-4)
thermal conductivity of liquid, 20: 19614 (N-65-17283)
thermal diffusion of carbon-13 in, 18: 21707(R) (MLM-1177)
thermal diffusion of carbon-13 in, 18: 21708(R) (MLM-1178)
thermal diffusion of carbon-13 in, 18: 21709(R) (MLM-1179)
thermal diffusion of, for separation of carbon isotopes, 19: 2694 (K-OA-899)
thermal diffusion of, column behavior calculations for total reflux operation in, 19: 2696 (K-OA-1173)
thermal diffusion of carbon-13-labeled, enrichment in, 20: 11194
thermal diffusion factors for carbon-labeled systems of, with methane as function of temperature, 20: 25034 (IFA-IS-35)
thermal diffusion factors for carbon- and deuterium-labeled systems of, with methane as function of temperature, 20: 25034 (IFA-IS-35)
thermal stability, 18: 1277(R) (TID-19574)
thermodynamic and transport properties of liquid, 16: 18932
thermodynamic properties of liquid and solid, 17: 33910
thermodynamic properties of deuterated, in liquid and solid states, 17: 33910
transport properties, 16: 3553
transport properties in pure gaseous and liquid, 16: 18933
tritium content in atmospheric, origin of, 16: 7763
tritium content in atmospheric, 18: 12363
tritium content of atmospheric, over Australia, Singapore, and United Kingdom, 1957 to 1959, 16: 16079
tritium content of atmospheric, amount and distribution of, 17: 30694
tritium content of atmospheric, origin of artificial, 17: 30695
tritium decay in tetratritiated, products from, 20: 33398
tritium exchange with water, 20: 469(R) (ORNL-TM-1275)
tritium reactions with, at 3 ev, 20: 29265
use as carrier in plasmochemistry, 20: 38314
use in flow counters for beta preparations, 18: 35857
uses in proportional counters for detection of thermal neutrons, 18: 41798
vapor pressure of liquid, up to critical point, 18: 3722 (UCRL-7167)
vapor pressure of, isotope effects on, 20: 18556(R) (BNL-929, pp 66-82)
vapor pressure up to critical point, 18: 41374 (UCRL-7167(Rev.I))
vapor pressures in isotopic systems of, 17: 23334
vibrational relaxation times in, effects of deuteron substitution on, 17: 12286
vibrations of trapped, in β-quinol clathrates, localized, 20: 41651
viscosity at 223 to 423°K, 18: 27404
viscosity of deuterated and normal liquid, at 90 to 115°K, 17: 6094
viscosity of deuterated and normal gaseous, 18: 39167 (TID-21064)

volume of normal and deuterium-substituted liquid, molar, (E), 19: 36443
x-ray attenuation by, coefficients for soft, 17: 22433 (NP-12661)
yield in radiolysis of methanol in absence and presence of oxygen, mechanisms, 16: 222
yield in radiolysis of 2,2,4-trimethylpentane, 16: 3048
yields from ethanol radiolysis, ionization detector for determining, 20: 7381
yields from gamma radiolysis of polypropylene, effects of nitrous oxide on, 20: 18770
yields from gamma radiolysis of alkaline solutions of nitrous oxide in aliphatic alcohols, 20: 26937
yields from gamma radiolysis of poly(ethylene terephthalate), 20: 26968
yields from gamma radiolysis of frozen carbon tetrachloride–methanol solutions, 20: 29305
yields from gas-phase radiolysis of cyclobutane, 20: 12894
yields from irradiation of polyethylene terephthalate, 20: 43378
yields from radiolysis of ethyl ether, deuterium effects on, 19: 22317
yields from radiolysis of butane, effects of density on, 19: 30245
yields from radiolysis of mono-, di-, and trimethylamine, 19: 30246
yields from radiolysis of methanol, 19: 38716
yields from radiolysis of ethylene, 19: 46361
yields from radiolysis of benzene–dioxane mixtures, 19: 46363
yields from radiolysis of iodomethane in cyclohexene, tracer studies of, 20: 18771
yields from radiolysis of methanol vapor, effects of scavengers on, 20: 20776
yields from reactions of recoil carbon-14 with ammonia, 20: 7145
yields from recoil tritium reactions with alkenes, 16: 11748
yields in carbon-11 recoil reactions with hydrocarbons, 19: 20018
yields in electron radiolysis of, liquid pentane, 18: 43619
yields in gamma radiolysis of, methylcyclohexane, 16: 16417
yields in gamma radiolysis of methylcyclohexane, effects of benzene on, 16: 16418
yields in gamma radiolysis of squalane at –196 to 350°C, 18: 25551
yields in gamma radiation decomposition of potassium sodium tartrates, mass spectra of, 19: 15599
yields in gamma radiolysis of liquid cyclopentane, 19: 38712
yields in gamma radiolysis of deaerated methanol, effects of sulfuric acid on, 20: 14579(R) (NYO-2383-15)
yields in gamma radiolysis of carbon monoxide–water vapor mixture, 20: 25122 (HW-SA-3440)
yields in gamma radiolysis of Hydyne and PR-1 rocket fuels, 20: 25118 (AD-632461)
yields in gamma radiolysis of carbon dioxide–hydrogen mixture, 20: 26922 (BNWL-SA-591)
yields in gamma radiolysis of nitroalkanes, 20: 33362
yields in gamma radiolysis of liquid 2-propanol, effects of benzophenone and naphthalene additions on, 20: 41006
yields in hydrolysis of as-cast uranium carbides, 18: 10065
yields in hydrolysis of irradiated uranium monocarbide, 18: 13853
yields in hydrolysis of thorium carbide at 25 to 99°C, 19: 24513
yields in photolysis of gaseous 1,3-dioxolane, 20: 25125(R) (RRL-2310-174)
yields in radiolysis of ethanol in presence of organic solutes, mechanisms, 16: 221
yields in radiolysis of methanol vapor, 16: 10087
yields in radiolysis of benzene–methanol systems, 16: 239
yields in radiolysis of butane, effects of field strength on, 17: 39162
yields in radiolysis of 2,2,4-trimethylpentane, 18: 5386
yields in radiolysis of acetone in aqueous solutions, acidity effects on, 18: 25582
yields in radiolysis of benzene–ethanol, 18: 25545
yields in radiolysis of acetaldehyde–cyclohexene, effects of benzene and cyclohexane on, 18: 27569
yields in radiolysis of acrylamide–propionamide solid solutions, 18: 35613
yields in radiolysis of methylhydrazine, 19: 30237 (USNRDL-TR-843)
yields in radiolysis of liquid tetramethylsilane, 20: 18729(R) (NYO-2007-9)
yields in radiolysis of hydrocarbons at high temperatures, 20: 23083(T) (AEC-tr-6466/1, pp 197-202)
yields in radiolysis of ethyltoluene isomers, effects of dose, scavenger, and temperature on, 20: 43359
yields in recoil reactions of carbon-11 in liquid hydrocarbons, 20: 1896 (IS-T-23)
yields in x radiolysis of ethyl mercaptan, 20: 43320
yields of deuterated, from radiolysis of methanol–perdeuterobenzene solutions, 20: 26938
yields of deuterated, in hydrolysis of aluminum, thorium, and uranium carbides in heavy water, 20: 40905
yields of deuterated, in radioinduced exchange between deuterium and methane, 18: 12190
yields of labeled, in exchange reactions between deuterium or heavy water water and hydrocarbons, 18: 13802
yields of labeled, in beta decay in doubly tritiated ethane, 19: 42575
yields of triply tritiated, from tritium decay in tetratritiated methane, 20: 33398
yields of tritiated, in exchange reactions between methane and tritium, 18: 41527
yields of, from radiolysis of benzene–isopropanol–benzophenone mixtures, 20: 1931
air–methane, combustion of beryllium in flame system of, 20: 2341 (SC-DC-65-1637)
Ar–CH_4, ionization by alpha particles, slow component in, 17: 16849
Ar–CH_4, radiolysis of gaseous, production of high molecular weight products in 4-Mev electron, 16: 5386
Ar–methane, alpha ionization, 17: 24052 (ORNL-3422)
Ar–methane, analysis for radioactive contaminants by scintillation counting, 19: 28717(R) (MLM-1221)
Ar–methane, distribution in nonequilibrium plasma of, 20: 17959
Ar–methane, electron ionization loss at 20 to 150 Mev in, 20: 44232
Ar–methane, ion pair production in, 19: 13473
Ar–methane, ionization energy in, measurement of effective, 20: 43193
Ar–methane, performance as proportional counter gas, 18: 25831
Ar–methane–NO, positron annihilation rates in gases of, (E), 19: 35172
Ar–methane, radiolysis of gaseous, hydrocarbon and hydrogen yields from charge and energy transfer in electron, 20: 23167
Ar–methane, specific ionization by curium-244 and uranium-235 fission fragments, 18: 33895
butane–methane, thermal diffusion factors in liquid, calculated, 19: 16257 (MLM-1163(p.C-1-7))
CO_2–CO–methane, effects of oxygen on radioinduced oxidation of graphite in, 20: 1895 (AERE-R-4988)
CO_2–CO–methane, radiation effects on desorption of graphite surfaces in, 20: 17114 (AERE-R-5163)
CO_2–methane, radiolysis in static and circulating-flow systems, electron and gamma, 19: 15562 (AERE-R-4838)
CO_2–methane, radiolysis of carbon-14-labeled, production of labeled molecules in gamma, 19: 17954 (EUR-2203.f)
CO_2–methane, radiolysis of, formaldehyde yields in, 20: 3981 (AERE-R-5051)
CO_2–methane, radiolysis of carbon-14-labeled, 20: 8978 (AERE-M-1663)
deuterium–methane, collision energy loss in reactions with recoil hydrogen atoms, 18: 3835
ethylene–methane–N, radiolysis of, 19: 46324(R) (AGN-8132)
ethylene–methane–NO, radiolysis of, 19: 46324(R) (AGN-8132)
graphite–H–CH_4, radiation effects on, reactor, 19: 13421(R) (HW-81984(p.6.1-14))
graphite–H–CH_4, radiation effects on, gamma, 19: 13421(R) (HW-81984(p.6.1-14))
H–CH_4–O, reactions with beryllium, 17: 26113
HCl–methane, formation of polymeric yields in reactions with carbon-14 and sulfur-35 recoil atoms, 19: 40628
HCl–methane, neutron reactions (n,p) with gaseous, 19: 13495
He–H–CH_4, analysis for helium-4 by mass spectrography, 17: 7960 (SCTM-14-62(14))
He–methane, electron drift velocity, 18: 12445 (BNL-7656)
He–methane, electron drift velocities in, 18: 18233
^{3}He–methane–Ne, performance in proportional counters for thermal neutrons, 18: 30058
He–methane, reactions with graphite, effects of water on, 20: 23774(R) (ORNL-3913, pp 75-109)
He-3–methane–Ne, performance as filling in thermal neutron detectors, 19: 44373(R) (ANL-6877, pp 15-20)
HF–methane, radiolysis yields in, 19: 46324(R) (AGN-8132)
H–methane, phase equilibria in gas–solid, at low temperatures, 16: 32248
H–methane, reactions with uranium hexafluoride, kinetics of, 20: 35479 (ORNL-TM-1454)
Kr–methane, ionization appearance potential measurements on secondary ions produced by, 18: 33569
methane–Ne, cosmic mesons (μ) energy loss rate in, 17: 29489
methane–Xe, counting plateau characteristics, 18: 13357(R) (MLM-1148)
methane–N, electron avalanche in discharges in, 18: 21491
methane–N, electron drift velocity and mean energy in, determination of, 19: 47124(T) (SLAC-Trans-19)
methane–oxygen, electron scattering by neutral atoms of slightly ionized, cross sections for, 18: 16702
methane–N, fission fragment effects on, effects of nitric oxide and temperature on, 20: 23071(R) (AGN-8169)
methane–PH_3, formation of phosphorus-32-labeled products in thermal neutron irradiation of gaseous, 19: 5962
methane–O, oxidation induced by fission fragments in, 19: 40611
methane–Ne, performance in spark chambers, 19: 22750
methane–N, phosphorescence of, 18: 37856
methane–O, radiation effects on production of methyl hydroperoxide in,

20: 248
methane–Na_2SiF_6, radiolysis yields in, 19: 46324(R) (AGN-8132)
methane–SiF_4, radiolysis yields in, 19: 46324(R) (AGN-8132)
methane–N, radiolysis of, 19: 46324(R) (AGN-8132)
methane–N, radiolysis in fissiochemical loop, 19: 46324(R) (AGN-8132)
methane–N, radiolysis of, products from fission-fragment, 20: 3982(R) (AGN-8156)
methane–N, radiolysis of, products from electron, 20: 3982(R) (AGN-8156)
methane–Xe, radiolysis of gaseous, hydrocarbon and hydrogen yields from charge and energy transfer in electron, 20: 23167
methane–water vapor, rate of tritium-exchange reactions with hydrogen in, 20: 14662(R) (ORNL-TM-1394)
methane–O, reactions with recoil carbon-11 atoms, 20: 5570 (JUL-228-RC)
methane–N, spectra of ion molecule reactions in deuterated, 20: 23071(R) (AGN-8169)
methane–Ne-20, thermal diffusion in, (E/T), 19: 28292
methane–Ne-22, thermal diffusion in, (E/T), 19: 28292
methane–Ne, thermal diffusion in deuterated, (E/T), 19: 28292
methane–propane, tritium decay in tetratritiated methane in, products from, 20: 33398
methane–HTO, tritium exchange with hydrogen in, 20: 23236(R) (ORNL-TM-1496)
methane–H_2O, tritium exchange in, 20: 41067(R) (ORNL-TM-1582)
methane–O, yields in electron and gamma radiolysis of, 19: 28359 (AERE-R-4871)
NH_3–methane–H_2O, formation of cyanamide and dicyanamide in radiolysis of, 19: 9217
NH_3–methane, radiolysis yields in, 19: 46324(R) (AGN-8132)
Methane, Bis (Dicyclohexylphosphinyl)-
see Phosphine Oxide, Methylenebis[Dicyclohexyl-
METHANE, BROMO-
beta decay of bromine-82-labeled, production of fragmented ions in, 17: 39123
bromine-82 beta decay in, fragment ion abundance in, 17: 26451(R) (ORNL-3425(p.96-8))
chemistry of nitrogen-13 recoils produced by carbon-12 (d,n) reactions in, 16: 11759
deuterium exchange with hydrogen in, effects of vibrational excitation on, 20: 7077
effect on excited electron emission into argon, (E), 19: 9173
effects of soil treatment with, on uptake of iodine-131 by pine trees, 17: 15735
effects on hydrogen yields in electron radiolysis of methanol vapor, 19: 11210
effects on radiolysis of methanol vapor, 19: 46395
effects on soils, sterilization, 20: 40637(R) (ORO-2754-7)
effects on yields from radiolysis of methanol vapor, 20: 20776
ionization by x rays at high energies, spectra of, 18: 41506(R) (ML-TDR-64-169)
isomeric transition, distribution of positively charged fragments from, 16: 6474
labeling with deuterium, 19: 5935
molecular structure of, deuterium effects on bond lengths in, 19: 11151
neutron activation and radiolysis, failure to bond rupture and nuclear recoil in, 16: 11721
production in bromine-82 recoil reaction with acetic acid, 17: 20085
radiolysis of solid, energy migration in gamma, 19: 13440
reactions of, with tritium, mechanism of, 17: 20064
reactions with bromine-80 recoil atoms, radioactivity of organic yields in, 19: 40618
reactions with electrons in organic glasses, yields of free radicals from, 20: 5577
reactions with recoil halogen atoms, 18: 20041 (MMPP-167-6)
soil sterilization by, 18: 35908
solubility in heavy and light water, initial state and transition state isotope effects, 16: 11617
solubility in heavy and light water, role of initial state structure in, 19: 13294
transport properties, 16: 3553
use of bromine-82-labeled, in leak detection in gas mains, 19: 9552 (EUR-1645.f)
yields in radioinduced oxidation of isobutane using hydrobromic acid catalyst, 20: 12883 (ORO-634)
METHANE, BROMOCHLORO-
fragmentation by isomeric transition of 4.4-hr bromine-80, 16: 6474
fragmentation pattern from β^-, γ-decay in bromine-82-labeled, 16: 6474
METHANE, BROMODIFLUORO-
meson (μ) and (π) scattering cross sections of, (T), 20: 13480
METHANE, BROMOTRICHLORO-
effects on radiolysis of polyisobutene at 4 Mev, 18: 20066
molecular fragments from dissociation by nuclear decay of bromine-82 and bromine-80m, charge states of, 16: 18958
neutron activation and radiolysis, failure to bond rupture and nuclear recoil in, 16: 11721
neutron capture and phase transitions in, 18: 39315
photolysis, radiolysis, and exchange with bromine in gaseous and liquid phases, 16: 10072
radiation effects at −190 to 180°C, 17: 14314 (TID-17939)
radiation effects on bromine-80 and -82 retentions in, isomeric transition reaction in, 19: 38715
radioinduced reaction of, with butadiene, products in, 17: 30596
radioinduced reactions of, with 2,3-dimethylbutadiene and isoprene, products in, 17: 30597
radioinduced reactions with ethylene, 20: 23113
radiolysis of, free-radical scavenging by anthracene and its homologs in, 19: 478
spectra of, in irradiated 3-methylpentane glasses, 18: 13859
yields in radiolysis of dibromodichloromethane, 16: 30451 (TID-16579)
METHANE, BROMOTRIFLUORO-
charged-particle ionization loss in, density effects on, (T), 20: 28642
meson (K−) capture by, Λ-p effective-mass spectrum and hyperon (Λ) lifetime from, (E), 20: 19485
neutrino interactions in, 18: 26265 (BNL-837(p.114-36))
neutron activation and radiolysis, failure to bond rupture and nuclear recoil in, 16: 11721
radiolysis of, effects of temperature on yields of products in gamma, 20: 40948(R) (COO-578-3-32)
radiolysis of, mechanism and yields of products in gamma, 20: 40948(R) (COO-578-3-32)
reactions with bromine-80 recoil atoms, radioactivity of organic yields in, 19: 40618
reactions with recoil halogen atoms, 18: 20041 (MMPP-167-6)
refractive index and dispersion for Cherenkov counters (E), 19: 2268 (ANL-6916)
yields in gamma radiolysis of carbon tetrachloride in presence of bromine, 20: 40948(R) (COO-578-3-32)
benzene–bromotrifluoromethane, radiolysis of, mechanism and yields of products in gamma, 20: 40948(R) (COO-578-3-32)
bromotrifluoromethane–propane, meson (π^-) reactions at 6 to 18 Bev/c, multi-meson (π) systems from, (E), 20: 9745
$CBrF_3$–propane, meson (π^-) absorption in, cross section for, 18: 16776
METHANE, CHLORO-
chemistry of nitrogen-13 recoils produced by carbon-12 (d,n) reactions in, 16: 11759
effect on excited electron emission into argon, (E), 19: 9173
electron drift velocities in, at low energy, 19: 46393
electron reactions with, ionization cross sections for, (E/T), 20: 5989
energy level density of, vibrational, 17: 27367
energy transfer in vibrational collisions of, catalytic effects of ammonia and deuterated ammonia on, 17: 20040
heat of vaporization of, calculation from rigid-sphere equation of state, 18: 224
ionization by x rays at high energies, spectra of, 18: 41506(R) (ML-TDR-64-169)
ionization potential of, method of calculating, 19: 22208
molecular spectra, 16: 15365
molecular structure of, deuterium effects on bond lengths in, 19: 11151
neutron capture by chlorine-37 in, chemically bound chlorine-38 from, 18: 20041 (MMPP-167-6)
neutron reactions (n,p) with gaseous, sulfur-35-labeled products in, 19: 13495
nuclear quadrupole resonance frequencies, in gaseous and solid states, 16: 7537
quenching effects on fluorescence of liquid scintillators, 19: 11186
radiolysis of, in benzene solution of, ionic mechanism of, 16: 33035
radiolysis of solid, by charged particle bombardment, 16: 17708(R) (TID-14812)
reactions of, with tritium, mechanism of, 17: 20064
reactions with bromine-80 recoil atoms, radioactivity in organic yields in, 19: 40618
reactions with chlorine-38 recoil atoms, stereochemistry in, 19: 40625
reactions with iodine, energy transfer processes in, 19: 25157
reactions with recoil tritium, yields in, 18: 17893
reactions with recoil halogen atoms, 18: 20041 (MMPP-167-6)
solubility in heavy and light water, initial state and transition state isotope effects, 16: 11617
solubility in heavy and light water, role of initial state structure in, 19: 13294
transport properties, 16: 3553
vibrational energy transfer, isotope effects on catalytic properties of water for, 17: 3644
yields of tritiated, in recoil tritium reactions with methyl chloride, 18: 17893
bromoethane–chloromethane, neutron reactions with bromine-81 in, yields of bromine-82-labeled compounds from, 19: 22370

chloromethane–cyclohexane, radiolysis of, mechanism of transfer mechanism in, 20: 40957
METHANE, CHLORODIFLUORO-
boiling flow oscillations, research program on, 19: 28499(R) (GEAP-4844)
heat transfer and void formation in two-phase flow of, 20: 12962(R) (GEAP-4959)
heat transfer in two-phase flows of, 18: 37346(R) (GEAP-4631)
heat transfer properties of, in two-phase flows, 18: 27653(R) (GEAP-4577)
heat transfer properties of Refrigerant-22 in two-phase flows, 19: 7680(R) (GEAP-4733)
neutron capture by chlorine-37 in, chemically bound chlorine-38 from, 18: 20041 (MMPP-167-6)
properties of, for use in peripheral compressor, 19: 11337
radiosensitivity effects on animal and plant cells, 18: 38977
refractive index and dispersion for Cherenkov counters (E), 19: 2268 (ANL-6916)
surface tension of mixtures with lubricants, 18: 8025(T) (AEC-tr-6241)
METHANE, CHLORODIPHENYL-
chlorine-36 exchange between lithium chloride and, 19: 4129
chlorine-36 exchange between tetraethyl ammonium chloride and, 19: 4130
solvolysis of, isotope effects on kinetics of, 19: 5868
spectra of, infrared and Raman, 20: 16498
substituted, deuterium isotope rate effects on solvolysis in acetone–water and ethanol–water mixtures, 20: 336
METHANE, CHLOROFLUORO-
dehydrohalogenation by tritium recoil reactions to form monochlorocarbene, 19: 22315
METHANE, CHLOROTRIFLUORO-
density of, measurement by gamma scattering, (E), 20: 6694(R) (MIT-952-2)
effects on graphite oxidation by air, (E), 20: 43839
effects on radioinduced ionic polymerization of styrene, 20: 23138
electric conductivity of liquid, (E), 19: 31169 (LA-DC-7026)
heat transfer properties of Refrigerant-22 in two-phase flows, 19: 44185(R) (GEAP-4910)
meson (μ^+) depolarization quenching in, as function of longitudinal magnetic field, (E/T), 19: 45079
meson (μ^+) depolarization in targets of, (E), 19: 45080
neutron capture by chlorine-37 in, chemically bound chlorine-38 from, 18: 20041 (MMPP-167-6)
properties as Cherenkov counter gas, 17: 18591 (BNL-6889)
proton spin-lattice relaxation in mixture with hydrogen, 16: 18887
radiolysis of, mechanism and yields of products in gamma, 20: 40948(R) (COO-578-3-32)
radiolysis of, yields in, 18: 37181 (BNL-874(p.12-13))
radiosensitivity effects on animal and plant cells, 18: 38977
reactions with plutonium and uranium hexafluorides, 20: 445
refractive index at 1 atmosphere and 0°C, 16: 8897 (AERE-R-3867)
refractive index and dispersion for Cherenkov counters (E), 19: 2268 (ANL-6916)
use in proportional detectors for neutron flux measurements, 18: 31943
yields in gamma radiolysis of carbon tetrachloride in presence of chlorine, 20: 40948(R) (COO-578-3-32)
Ar–chlorotrifluoromethane, distribution ratio in vortex flow, 20: 20293 (JPL-TR-32-808)
$CClF_3$–C_3H_4, radioinduced polymerization, 17: 25342
chlorotrifluoromethane–H, distribution ratio in vortex flow, 20: 20293 (JPL-TR-32-808)
chlorotrifluoromethane–N, distribution ratio in vortex flow, 20: 20293 (JPL-TR-32-808)
chlorotrifluoromethane–H, vortex flow in gaseous, 19: 40236 (LA-3229, pp 237-50)
METHANE, CHLOROTRIPHENYL-
ionization of, carbon isotope effects on S_N1 and S_N2 reactions in, 17: 20020
ionization of, effects of carbon-13 on, 19: 13411
methanolysis in benzene, isotope effects on, 19: 5569(R) (MIT-2098-64)
reactions with benzene, mechanisms of, 20: 23044(R) (MIT-905-52, pp 74-94)
Methane, Diantipyrinyl-
see Antipyrine, 4,4'-Methylenedi-
METHANE, DIAZO-
deuterium exchange with hydrogen in, effects of vibrational excitation on, 20: 7077
effects on reactions of photolyzed carbon dioxide with graphite, 20: 23097
pyrolysis of, ionization of methylene radical from, 17: 1517
reactions with carbon dioxide, mechanism and products of, 16: 31531 (UCRL-10352)
spectra of deuterium- and nitrogen-15-labeled, infrared, 18: 12130
spectra of deuterium- and nitrogen-15-labeled solid, vibrational assignment of infrared, 18: 12131
METHANE, DIAZODIPHENYL-
reactions with molecular acids, isotope effects on, 19: 7529
spectrum of ground-state triplet in, paramagnetic resonance, 17: 4532
Methane, Dibenzoyl-
see 1,3-Propanedione, 1,3-Diphenyl-
METHANE, DIBROMO-
analysis for carbon-14 by oxygen flask method, 18: 11992
neutron activation and radiolysis, failure to bond rupture and nuclear recoil in, 16: 11721
radiolysis in mixture with ethylene, yields in, 18: 27571
benzene–dibromomethane, yields from neutron reactions with bromine-81 in, 18: 43680
METHANE, DIBROMOCHLORO-
neutron activation and radiolysis, failure to bond rupture and nuclear recoil in, 16: 11721
photolysis of, chlorine and deuterium isotope effects on absorption spectra of chloromethylene radical from, 20: 23096
METHANE, DIBROMODICHLORO-
radioinduced exchange with bromine, 16: 30451 (TID-16579)
radiolysis, bromine and organic yields in, 16: 30451 (TID-16579)
METHANE, DIBROMODIFLUORO-
neutron activation and radiolysis, failure to bond rupture and nuclear recoil in, 16: 11721
yields in gamma radiolysis of bromotrifluoromethane, mechanism of, 20: 40948(R) (COO-578-3-32)
METHANE, DICHLORO-
analysis for carbon-14 by oxygen flask method, 18: 11992
analytical use for photometric determination of boron in uranium tetrafluoride, 17: 27307
dehydrohalogenation by tritium recoil reactions to form monochlorocarbene, 19: 22315
effects on gamma-induced polymerization of styrene at −78°C, 20: 43308
effects on polymerization of styrene, 20: 43339
effects on radioinduced polymerization of butadiene, 17: 4575 (TID-7643(p.109-17))
effects on radioinduced post polymerization of trioxane, 18: 27532
effects on radioinduced polymerization of cyclopentadiene, 19: 9193
effects on radioinduced polymerization of vinyl butyrate, 19: 46389
effects on radioinduced polymerization of isobutylene, 20: 409
effects on radioinduced polymerization of liquid and solid acetylene, 20: 1913
effects on radioinduced polymerization of formaldehyde, 20: 1914
effects on radioinduced polymerization of formaldehyde with acrylonitrile, isobutene, methyl methacrylate, and styrenes, 20: 1914
effects on radioinduced ionic polymerization of styrene, 20: 23138
effects on radioinduced polymerization of isobutene with styrene at −78°C, 20: 23139
effects on radioinduced ionic polymerization of styrene, 20: 23141
effects on radioinduced polymerization of styrene with formaldehyde, 20: 40973
effects on rate of radioinduced polymerization of butadiene, isobutylene, and isoprene, 20: 23159
force constants and vibration frequencies of labeled and unlabeled, infrared spectra, 16: 13054
force constants of deuterated from normal, method for adjusting vibrational, 19: 7396
heat transfer coefficients, nucleate boiling, 19: 7688
ionization potential of, method of calculating, 19: 22208
labeling with carbon-14, 20: 18708
neutron capture by chlorine-37 in, chemically bound chlorine-38 from, 18: 20041 (MMPP-167-6)
oxidation in solution by ultrasonic waves, effects of oxygen and inert gases, 16: 14474(T) (JPRS-12465(p.43-62))
radioinduced polymerization with dimethylketene, products and reactivity of, 18: 25494(T) (AEC-tr-6372(p.237-46))
radioinduced polymerization of, with ethylene, yields of 1-chloroalkanes and 1,1-dichloroalkanes from, 19: 46370
radioinduced polymerization of fluoral in, at low temperatures, 20: 20718(R) (AD-623307)
radioinduced reactions with cycloalkenes, gamma, 19: 38695 (KFK-317)
radioinduced reactions with ethylene, gamma, 20: 20757
radiolysis, 16: 22183
radiolysis in mixture with ethylene, yields in, 18: 27571
reactions of recoil chlorine-38 in, chemical effects from, 19: 459
reactions of, with tritium, mechanism of, 17: 20064
reactions with bromine-80 recoil atoms, radioactivity in organic yields in, 19: 40618
reactions with recoil halogen atoms, 18: 20041 (MMPP-167-6)
solvent properties for molybdenum–pyridine–pyrocatechol complex, 18: 13706
spectra of deuterated and undeuterated, Raman, 17: 25277

transport properties, 16: 3553
yields in gamma radiolysis of chloroform, 20: 33380
dichloromethane–cyclohexane, radiolysis of, mechanism of transfer mechanism in, 20: 40957

METHANE, DICHLORODIFLUORO-
boiling burnout data for clusters of reactor fuel rods cooled by, 20: 35615 (AEEW-R-468)
boiling burnout in heated tubes, effects of film flow rate on, 19: 36606 (AEEW-R-430)
boiling burnout in upward flow through uniformly and non-uniformly heated tubes, forced-convection, 19: 46527 (AEEW-R-426)
boiling heat transfer scaling laws in tubes of, forced-convection, 19: 32345 (AEEW-R-363)
bubble formation in superheated, by recoils from alpha emitters, 16: 19495
detection and measurement of gaseous, by surface ionization, 16: 30569 (ANL-6579)
determination in SRE gallery gas, methods for, 17: 19625 (NAA-SR-Memo-8041)
determination using labeled sodium chlorite-clathrates, effects of moisture on, 18: 17866(R) (NYO-2766)
diffusion in latex and neoprene, 18: 25315 (AWRE-O-56/57)
effects on graphite oxidation rate, reduction, 18: 29044(R) (HW-79280(p.6.1-16))
effects on graphite oxidation by air, (E), 20: 43839
effects on radioinduced polymerization of isobutylene, 20: 409
flow transients and heat-driven pressure in supercritical thermodynamic region of, 19: 13595
heat transfer in boiling, electroconvection effects on, 16: 25533
heat transfer parameters of channel flows of, 19: 590
ionization of uranium on heated tungsten in atmosphere of, 16: 30938
ionization potential of, method of calculating, 19: 22208
meson (π^-) reactions in liquid, meson (K^o) pair production in, 17: 7039
molecule scattering by, cross sections for inelastic, 19: 14265
positron annihilation rate and collision complex in, 18: 3762
radiolysis of cyclohexane solutions of, yields of hydrochloric acid in, 18: 1757
radiosensitivity effects on animal and plant cells, 18: 38977
reactions in SRE gallery-gases, hazard of, 17: 19625 (NAA-SR-Memo-8041)
reactions with plutonium and uranium hexafluorides, 20: 445
refractive index and dispersion for Cherenkov counters (E), 19: 2268 (ANL-6916)
surface tension of mixtures with lubricants, 18: 8025(T) (AEC-tr-6241)
use for detecting leaks in activated carbon beds, 18: 18011(R) (DP-870)
use in binary cycle for nuclear power production, economic analysis of, 17: 33351
use in gas Cherenkov counter, 20: 21071
use in proportional detectors for neutron flux measurements, 18: 31943
yields in gamma radiolysis of chlorotrifluoromethane, mechanism of, 20: 40948(R) (COO-578-3-32)

METHANE, DICHLOROFLUORO-
heat transfer coefficient, 17: 20178
nuclear spin relaxation in, relaxation mechanisms in, 17: 12254
proton magnetic double resonance in, method for measuring, 18: 27409
radiolysis of cyclohexane solutions of, yields of hydrochloric acid in, 18: 1757

METHANE, DIFLUORO-
effects on iodine-128 reaction with methane, 16: 10061
ionization potential of, method of calculating, 19: 22208
nuclear magnetic resonance spectra of, collision-narrowing theory of, 19: 38629
reactions of, with tritium, mechanism of, 17: 20064
reactions with bromine-80 recoil atoms, radioactivity of organic yields in, 19: 40618
reactions with recoil halogen atoms, 18: 20041 (MMPP-167-6)
reactions with recoil tritium, 20: 9031

METHANE, DIIODO-
neutron activation and radiolysis, failure to bond rupture and nuclear recoil in, 16: 11721
properties for oxide particle suspension in centrifuges, 20: 36933
radioinduced ESR spectra in, at 77°K, 20: 14597
reactions with muonium, (E), 20: 29247
reactions with pyrrole to form pyridine, 17: 10669(T) (NP-tr-942)

Methane, Dimethoxy-
see Methylal

METHANE, DIPHENYL-
analysis for trace contaminants, activation, 19: 2241
hydrogen abstraction from, by methyl radicals, 19: 21760 (NYO-2728-4)
neutron diffusion in, temperature dependence of thermal, 20: 26065(T) (AECL-2330, pp 251-4)
preparation and spectra of deuterated, 20: 16498
radiation effects on dihydroxydiphenylmethanes, 16: 569 (NP-10756)
radiation effects on single-crystal, ESR studies of, 19: 26396
radiation effects on carbon tetrachloride polycrystalline solutions of, spectra of resonance charge transfer in, 20: 18752
radiolysis, 19: 477
radiolysis of sulfur in, yields in, 18: 27505
radiolysis of, effects of type of radiation on, (E), 19: 40591
radiolysis of, EPR studies of yields of stabilized charges in low-temperature, 20: 40962
radiolysis of, G-values of products in, (E), 19: 40370
spectra of, infrared and Raman, 20: 16498
biphenyl–diphenylmethane, analysis for impurities by activation methods, 19: 24451
biphenyl–diphenylmethane, heat transfer properties and radiation stability of, for use in reactor loops, 20: 20792
biphenyl–diphenylmethane, radiolysis, 19: 477

Methane, Dipivaloyl-
see 3,5-Heptanedione, 2,2,4,4-Tetramethyl-

METHANE, FLUORO-
complexes with boron fluoride, isotopic exchange of boron-10 in gaseous boron fluoride system and stability of, 18: 43492
fluorine-18 positron decay in, fragment ion abundance in, 17: 26451(R) (ORNL-3425(p.96-8))
ionization potential of, method of calculating, 19: 22208
molecular dipole moments of deuterated and normal, 20: 3958
molecular force constants and normal coordinates of normal and deuterated, calculation of, 16: 26884
nuclear magnetic resonance spectra of, collision-narrowing theory of, 19: 38629
positron decay of fluorine-18-labeled, production of fragmented ions in, 17: 39123
reactions of, with tritium, mechanism of, 17: 20064
reactions of, with tritium, isotopes effects in deuterated and protonated, 17: 20065
reactions with recoil tritium, helium-4 moderator effects on, 19: 13441
reactions with recoil tritium, 20: 9031
solubility in heavy and light water, initial state and transition state isotope effects, 16: 11617
solubility in heavy and light water, role of initial state structure in, 19: 13294

METHANE, HALO-
nuclear spin coupling constants in, effects of excitation energies on, (T), 20: 44126
reactions with recoil tritium, inertial effects of substituents on hot atom capture, 16: 4195
spectra, deuterium isotope effects on band intensities in infrared, 19: 17930(T)

METHANE, IODO-
adsorption on charcoal under humid conditions, 20: 41202 (UCRL-14990)
analysis for beta activity, 19: 525
analysis for carbon-14 by oxygen flask method, 18: 11992
behavior of iodine-131-labeled, in Containment Mockup Facility, 19: 34409 (ORNL-P-1324)
chemical properties, 19: 19340 (ORNL-NSIC-4)
decay of radioactive iodine in, charge and fragment spectra from, 16: 23003(R) (ORNL-3268(p.88-90))
decomposition following decay of iodine-131 in, 16: 22215
deposition on grass of atmospheric, tracer study, 20: 41192(R) (IDO-12053)
detection in elemental radioiodine, mass spectrometric, 19: 7276 (ORNL-TM-1009)
determination in aerosols, mass spectrometric, 19: 22096(R) (ORNL-3776 (p.3-17))
determination in radioactive aerosols, chromatographic, 19: 22096(R) (ORNL-3776(p.3-17))
effect on excited electron emission into argon, (E), 19: 9173
effects of carbon-14-labeled, on radiolysis of 1,4-cyclohexadiene, 19: 15601
effects on gamma radiolysis of aqueous solutions of ammonium iron (II) sulfate, 20: 25167
effects on hydrogen yields in radiolysis of liquid hydrocarbons, 18: 20057
effects on iodine-128 reaction with methane, 16: 10061
effects on radioinduced polymerization of butadiene, 17: 4575 (TID-7643(p.109-17))
effects on radiolysis of polyisobutene at 4 Mev, 18: 20056
effects on radiolysis of methanol, 19: 28376
electric conductivity of aluminum, gallium, and indium iodides in, 18: 23449 (PAN-491/V)
electron reactions with, ion excess kinetic energy from, 19: 42506
exchange reactions with sodium iodide in ethanol and methanol, 19: 11296
exchange reactions of radioiodine between ethyl iodide and, radio-

chromatography equipment for studies on, 20: 41019
focusing of molecules of, by electric six-pole field, 18: 43138 (WIS-TCI-63G)
formation under reactor accident conditions, chemical equilibrium studies of, 20: 43166 (BMI-1781)
iodine exchange with iodine atoms in gaseous phase, 16: 23588
iodine exchange with iodine, photolyzed, 18: 25597
iodine isotope exchange with iodoethane at 92.4°C, mechanisms of, 20: 26852
iodine-131 activity in, produced by bond rupture of tellurium-131-labeled dibenzyl telluride, 16: 11760
iodine-131 exchange with silver iodide, effects of surface structure on, 20: 5544
iodine-131 exchange between, and iodide ions, kinetic studies of, 20: 29207
iodine-131 exchange between, and molecular iodine in nitrobenzene, 20: 33143(R) (COO-733-13)
iodine-131 exchange between, and iodide ions, 20: 40939
ionization by kev electrons and Mev helium ions and protons, mass spectrometric comparison of, 18: 18567
ionization by x rays at high energies, spectra of, 18: 41506(R) (ML-TDR-64-169)
isotope exchange with metal iodides, effects of electron donors on, 17: 39060
labeling by fission-product iodine, selectivity effects in, 20: 2520(R) (IA-920)
labeling with iodine by fission recoil, 17: 29879(R) (IA-822)
metabolism in man of inhaled or ingested, tracer study, 20: 41192(R) (IDO-12053)
metabolism of inhaled, 19: 40800(R) (AERE-PR/HPM-7)
molecular beam scattering by potassium, angular distributions of elastic and reactive, 18: 39219
molecular fragments from dissociation by nuclear decay of iodine-125, formation of, 17: 33993
molecule scattering at thermal energies, total cross sections for, 18: 33407 (UCRL-11071)
neutron activation and radiolysis, failure to bond rupture and nuclear recoil in, 16: 11721
neutron reactions (n,2n) with, chemical effects of, 20: 9007
neutron scattering by, cross sections for thermal, 19: 30158
nuclear magnetic resonance spin-lattice relaxation times in, deuteron and proton, 20: 12839
photo-oxidation of, effects of deuterium oxide and hydrobromic acid on, 18: 25587
photolysis of deuterated and nondeuterated gaseous, reactions of hot methyl radicals in, 18: 37231
photolysis of mixtures of, with diethyl ketone, reactions between atomic iodine and ethyl radical in, 17: 12336
photolysis, molecular beam determination of energy partition in, 18: 31570 (UCRL-11359)
preparation by reactions of methane with iodine-125 formed by electron capture in xenon-125, 19: 13449
preparation of iodine-labeled, by fission recoil method, 19: 11144
preparation of iodine isotope-labeled, effects of diluent gases on, 19: 39265(R) (IA-1021)
preparation of labeled, 20: 4185(R) (ORNL-3843, pp 169-234)
properties as bubble chamber liquid, 16: 31906
properties as bubble chamber fluid, 17: 12572
radiation chemistry of liquid, helium ion beam irradiation, 16: 33050
radiation effects of neutrons, behavior of recoiling iodine atoms, 16: 6484
radiation effects on benzene solutions of, hot and thermal yields in, 17: 18132
radiation effects on, recoil-energy spectra and relative abundances of ions produced from x, 20: 33354
radiation reactions with, iodine-128 extraction yield from gamma and neutron, 17: 27456
radioinduced decomposition of iodine-130-labeled, 17: 28964
radioinduced decomposition of, distribution and energies of fragments from, 19: 46161(R) (ORNL-3832, pp 116-50)
radiolysis in iodine–pentane solutions, 17: 12333
radiolysis in olefin glasses, spectral studies on uv, 18: 25588
radiolysis in pentane solutions, Auger electron reaction hypothesis on (n,γ), 17: 37268
radiolysis in presence of deuterated propane, 17: 28968
radiolysis of, in benzene solution, ionic mechanism of, 16: 33035
radiolysis of solid, by charged particle bombardment, 16: 17708(R) (TID-14812)
radiolysis of solutions of, with ethyl iodide, yields from, 17: 1526(R) (RRL-90)
radiolysis of, use of charged plates in collecting products from neutron, 20: 43367
reactions with alkali metals, distributions from, 17: 8970
reactions with chemically impregnated charcoal, 20: 4185(R) (ORNL-3843, pp 169-234)
reactions with dodecane and sodium bisulfite, 19: 40402 (BMI-X-10137)
reactions with electrons in organic glasses, yields of free radicals from, 20: 5577
reactions with ethyl malonate, side reactions in, 19: 13408
reactions with fission-product iodine, factors effecting, 19: 26917(R) (IA-984)
reactions with iodine-126, hot atom substitution, 18: 27593
reactions with iodide and water, calculated carbon-13 and deuterium isotope effects in, 18: 33612 (BNL-8066)
reactions with iodine-126, hot atom, 19: 11175
reactions with iodine recoil atoms above 10 ev, excitation function and yields in, 20: 43291 (IA-1096)
reactions with potassium in crossed molecular beams, 18: 213 (UCRL-10848)
reactions with potassium crossed beams, scattering in, 18: 33564
reactions with recoil halogen atoms, 18: 20041 (MMPP-167-6)
reactions with recoil iodide, selectivity of labeling in, 19: 20020 (IA-907)
reactions with tertiary amines, secondary deuterium isotope effects in, 19: 13407
release and sorption in HFIR maximum credible accident, 20: 3586 (ORNL-TM-1291)
removal from air by activated charcoals, 20: 280 (CONF-650407, pp 869-84)
removal from air using foams, 20: 43585 (ORNL-TM-1589)
removal from air–steam mixtures by steam suppression system, 20: 576 (CONF-650407, pp 776-804)
removal from air–steam systems by activated charcoals, 20: 45049 (ORNL-P-2431)
removal from collectors, method for testing off-gas air-cleaning systems for efficiency in, 20: 27210(R) (UCRL-14680)
removal from gases by sorption on charcoals, 20: 279 (CONF-650407, pp 852-68)
retention in atmosphere, efficiency of Whatman Type ACG/B filter paper for, 20: 16719 (AEEW-M-568)
scattering by molecules at thermal energies, total cross sections for, 18: 34407 (UCRL-11071)
scattering of molecular beams of, 17: 35263(R) (UCRL-10706(p.1-110))
separation from air by activated charcoal filters, 20: 20940(R) (ORNL-3915)
separation from gases by sorption by activated carbon, 20: 23376(R) (ORNL-391, pp 133-46)
solubility in heavy and light water, initial state and transition state isotope effects, 16: 11617
solubility in heavy and light water, role of initial state structure in, 19: 13294
solvolysis in water, isotope effects of deuterium on, 18: 27367
solvolysis of, effects of carbon-13 and deuterium on, 20: 40939
sorption by activated charcoal, effects of moisture and temperature on, 19: 22163(R) (ORNL-3776(p.43-6))
sorption by activated charcoal, effects of humidity and temperature on, 20: 4086(R) (ORNL-3843, pp 137-67)
sorption by charcoal, effects of humidity and temperature on, 20: 4184(R) (ORNL-3843, pp 71-135)
sorption by coconut charcoal, factors affecting, 20: 4185(R) (ORNL-3843, pp 169-234)
sorption of vapors of, coating development for, 20: 45045(R) (BMI-X-10173)
spectra of deuterated, analysis of vibration-rotation, 17: 37243
spectra of deuterated and normal, energy constant calculation from, 19: 11066
synthesis of iodine-labeled, 16: 23559
synthesis of iodine-labeled, selectivity effects in recoil, 18: 12123 (IA-906)
use in preparation of carbon-13 and -14 foils, 20: 25029 (AERE-R-5097, Paper 19)
x-ray decomposition due to inner shell vacancies in, 19: 430 (ORNL-P-591)
yields in reactions of fission-recoil iodine with gases, 19: 46330 (NP-15370)
cyclohexane–iodomethane, radiolysis of, iodine production in, 17: 3041
cyclohexene–iodomethane, radiolysis of, tracer studies of yields from, 20: 18771
cyclohexane–iodomethane, radiolysis of, methyl radical yields in, 20: 38941(R) (RRL-2310-182)
iodoethane–iodomethane, radiolysis of, 17: 37252 (RRL-118)
iodomethane–SiH_4, preparation of volatile hydrides by mercury sensitized photolysis of, 20: 18729(R) (NYO-2007-9)
iodomethane–1-iodopropane, radiolysis of, 17: 37252 (RRL-118)

METHANE, NITRO-
complexes with uranyl perchlorate, preparation of, 20: 10825

detonation in DUGOUT row-charge experiment, 19: 26486 (PNE-609F)
detonation initiation of, by shock interactions at discontinuities, 19: 42207 (LA-DC-6994)
detonation of, air-blast wave measurements on, 20: 43461 (PNE-607F)
detonation of, one-dimensional time-dependent reaction zone in, (T), 19: 42203 (LA-3297)
detonation wave interactions in condensed, 19: 42205 (LA-DC-6990)
detonation wave structure, 18: 43112 (LADC-6180)
electric conductivity profiles of explosion products of, 18: 43113 (LADC-6181)
electric conductivity of detonation products of, 19: 40284 (LA-DC-6993)
electrochemical reduction of, effects of dielectric constant of organic solvent on, 20: 18636(R) (TID-22725)
electron elastic scattering at 295°K, cross sections, 16: 33844
electron transfer reactions with negative ions, 16: 6471
initiation of liquid, electric transducer studies, 19: 43631 (LA-DC-6995)
nuclear magnetic resonance in electric fields, 19: 25071(R) (TID-21667)
photolysis of liquid and vaporous, yields from uv, 20: 14613
photolysis of, effects of copper and zinc oxides on, 20: 8988
radiation effects on free radical induction in solid solutions of, EPR spectra of gamma, 20: 23103
radioinduced free radical formation in, electron paramagnetic resonance study of, 19: 40579
radiolysis in presence of deuterated propane, 17: 28968
radiolysis of liquid and vaporous, yields from gamma, 20: 14613
radiolysis of, mechanisms of gamma, 20: 8988
radiolysis of, reactions of hydrated electrons in pulse, 20: 20735
radiolysis of, yields in gamma, 20: 33362
shock interaction with void in, analysis of, 18: 27656 (LA-3077)
shock interaction with discontinuities in, theoretical study, 19: 36218 (LA-3235)
shock interactions in corners filled by, hydrodynamics of, (E/T), 20: 21784 (LA-3450)
solvent properties for cerium, 17: 40934
solvent properties for cerium, 18: 23727
solvent properties for ammonium and cesium iodides, 19: 541
use in Dugout cratering experiment, 19: 28474 (PNE-600F)

Methane, Oxo-
see Formaldehyde

Methane, Tetrabromo-
see Carbon Tetrabromide

Methane, Tetrachloro-
see Carbon Tetrachloride

Methane, Tetrafluoro-
see Carbon Tetrafluoride

Methane, Tetraiodo-
see Carbon Tetraiodide

METHANE, TETRANITRO-
analysis of, 16: 30682(R) (UCRL-6936)
radioinduced hydrolysis, 18: 276(T) (PA-TM-1029)
radiolysis at 77°K, EPR spectra of free radicals produced by gamma, 20: 23104
radiolysis of deaerated and oxygenated solutions of, extinction coefficients and rate constants of pulse, 19: 11195
radiolysis of, reactions of hydrated electrons in pulse, 20: 20735
reactions with hydrated electrons produced in gamma radiolysis of water, 18: 37219

METHANE, TETRAPHENYL-
radiation effects on carbon tetrachloride polycrystalline solutions of, spectra of resonance charge transfer in, 20: 18752
scintillation quenching by organometallics in, 18: 12197

Methane, Tribromo-
see Bromoform

METHANE, TRIBROMOCHLORO-
yields in radiolysis of dibromodichloromethane, 16: 30451 (TID-16579)

Methane, Trichloro-
see Chloroform

METHANE, TRICHLOROFLUORO-
boiling flow oscillations in, 19: 15717 (NASA-CR-164)
boiling on horizontal plate, film, 16: 16508
combustion of Freon-11, Hopcalite-catalyzed, 18: 40988(R) (NRL-6053)
effects on gamma-induced polymerization of styrene at −78°C, 20: 43308
flow in high-pressure loops, two-phase, 20: 29375(R) (ANL-7190, pp 193-200)
flow in vertical, rectangular conduit, two-phase, 20: 31340 (ANL-7093)
flow of saturated, through apertures and short tubes, 17: 18258 (ANL-6667)
flow of, heat transfer in two-phase, 18: 20171 (TID-7694(p.18-23))
heat transfer by, forced-flow boiling, 18: 16177(R) (TID-20133)
heat transfer coefficient, 17: 20178
heat transfer in forced-flow boiling, 19: 20116(R) (SAN-409-12)
meson (μ^+) depolarization quenching in, as function of longitudinal magnetic field, (E/T), 19: 45079
meson (μ^+) depolarization in targets of, (E), 19: 45080
neutron capture by chlorine-37 in, chemically bound chlorine-38 from, 18: 20041 (MMPP-167-6)
radioinduced cavitation in, nucleation by ultrasonic neutron, 17: 23409
radioinduced cavitation in, nucleation by ultrasonic nuclear-recoil, 18: 32265 (CERN-64-30(p.313-14))
radiolysis of cyclohexane solutions of, yields of hydrochloric acid in, 18: 1757
radiolysis of Freon-11, 17: 25304
reactions with plutonium and uranium hexafluorides, 20: 445
spectra of, in irradiated 3-methylpentane glasses, 18: 13859
use in proportional detectors for neutron flux measurements, 18: 31943
vaporization lifetimes of droplets of, 19: 20116(R) (SAN-409-12)

Methane, Trifluoro-
see Fluoroform

METHANE, TRIFLUOROIODO-
effects on iodine-128 reaction with methane, 16: 10061
neutron activation and radiolysis, failure to bond rupture and nuclear recoil in, 16: 11721
reactions with recoil halogen atoms, 18: 20041 (MMPP-167-6)

Methane, Triiodo-
see Iodoform

Methane, Trinitro-
see Nitroform

METHANE, TRIPHENYL-
activity coefficient in benzene, organic-phase, 19: 28443(R) (ORNL-3785)
determination in polyphenyls by chromatography, thermal conductivity, and flame ionization, 20: 16341
effects on radiolysis of 2-propanol, 19: 13423 (KFK-243)
hydrogen abstraction from, by methyl radicals, 19: 21760 (NYO-2728-4)
radiation effects on luminescence of, beta and photon, 16: 30481
trisulfonated, proteolysis and hydrolysis constants for several, 17: 1176(R) (HW-70050(p.78-142))
use as a radical scavenger reagent to minimize radiation effects on TBP, 19: 46406(P)
anthraquinone–polyphenyl–triphenylmethane, properties of, as reactor coolant-moderator, 20: 35566(P)
polyphenyl–pyrene–triphenylmethane, properties of, as reactor coolant-moderator, 20: 35566(P)

METHANE, TRIPHENYL-, DERIVATIVES
analytical use of eriochrome cyanine R for microdetermination of beryllium by ring oven technique, 16: 12969
properties of, in polystyrene as chemical dosimeters, 19: 46369
thermal decomposition of, isotope effects on, 19: 5569(R) (MIT-2098-64)
uses for radiation dosimetry, 20: 16521

METHANE, TRIS(HYDROXYMETHYLAMINO)-
effects on deuterium exchange with hydrogen-bonded N–H groups in *N*-methylacetamide in aqueous solutions, 20: 354
radiosensitivity effects in cats, 20: 12724
solvent properties of solutions of, for carbon dioxide, 18: 1492(R) (TID-19592(Sect.VII))

METHANE, TRIS(TRIFLUOROMETHYL)-
exchange between deuterium and hydrogen in methanol–sodium methoxide system, formation of perfluorocarbanions in, 18: 25451

METHANES, HALO-
ionization potentials, calculated, 19: 46161(R) (ORNL-3832, pp 116-50)
recoil atoms in bromine-isotope-containing, isotope effects and secondary reactions in (n,γ) processes, 16: 23723(T) (AEC-tr-5151)
recoil atoms in bromine-isotope-containing, isotope effects and secondary reactions in (n,γ) processes, 16: 6483
structure, 19: 32048(R) (NP-15073)

METHANESULFINIC ACID
hydroxy-, reactions with uranyl nitrate in nitric or perchloric acid solution, kinetics, 19: 24480 (CNAEM-23)

METHANESULFONIC ACID
effects on chlorophyll and morphological mutations in pea varieties, 20: 36624
effects on red clover, morphological and mutagenic, 20: 5491
effects on seeds or seedlings of *Zea mays*, mutagenic, 20: 1656
heat of solution of sodium salt of, in heavy and light water, 20: 1825
hydrolysis of various esters of, inverse gamma-deuterium isotope effects in, 18: 39179

METHANESULFONIC ACID, BUTYL ESTER
effects on cytology and physiology of *Triticum durum* and *T. monococcum*, 19: 43653
mutagenic effects on barley, comparison of x radiation and, 18: 3543

METHANESULFONIC ACID, 1,4-DIMETHYLTETRAMETHYLENE ESTER
effects on leukemia cells, cytotoxic, 20: 3736

METHANESULFONIC ACID, ETHYL ESTER
chemical and physical properties and mutagenic action on barley seeds, 20: 40717
effects of, on life span of mice, 17: 40649

effects on, 20: 40513
effects on algae, patterns of expressions of mutagenic, 20: 16294
effects on *Arabidopsis thaliana*, genetic, 20: 40710
effects on barley, genetic, 20: 40712
effects on chlorophyll mutation frequency, meiosis, and mitosis in peas, 20: 36621
effects on Drosophila genes, mutagenic, 20: 40625(R) (ORNL-3922, pp 59-64)
effects on durum and bread wheats, first generation, 16: 1599
effects on genetic variability in *durum* wheat, 19: 42267
effects on maize seeds, mutagenic, 20: 45361 (TID-22622)
effects on maize, genetic, 20: 8664
effects on maize, genetic, 20: 18334
effects on maize, genetic, 20: 40708
effects on mitosis in Pisum, 20: 24890
effects on morphology of seedlings of *Vicia sativa* and *Vicia villosa* exposed as seeds, 17: 38692
effects on mutations in maize, 20: 18184(R) (BNL-929, pp 115-25)
effects on mutations in X_1 and X_2 *Vicia faba* L., 17: 28648
effects on Neurospora, mutagenic, 20: 40632(R) (ORNL-3922, pp 175-91)
effects on pea seeds, 20: 81
effects on potatoes, 18: 31170
effects on seedling development in Vicia spp. for fodder, 17: 38691
effects on seeds of *Lakota durum*, biological and mutagenic, 20: 33064
effects on wheat, mutagenic, 19: 3888 (EUR-1829.f)
frequency of chlorophyll mutations induced in wheat seeds by, 17: 38689
frequency of mutations induced in maize seeds by, 17: 38690
genetic effects in Habrobracon, 16: 31406
genetic effects in *Escherichia coli*, 17: 38789
genetic effects of, in wheat, 18: 23320
genetic effects of, in castorbean seeds, 18: 25180
genetic effects of, in barley seeds, 18: 25182
genetic effects on oats, 18: 3579
labeling with tritium to prepare labeled cells, 19: 43651
mutagenic effects on barley, 16: 17469
mutagenic effects on plants, 16: 20208
mutagenic effects in neurospora, 17: 35453(R) (TID-19287)
mutagenic effects on barley, comparison of x radiation and, 18: 3543
mutagenic effects on plants, comparison with gamma radiation, 18: 31126 (EUR-1610.f)
mutagenic effects on wheat, 19: 2161
mutagenic effects in pea plants, 19: 8728
mutagenic effects in barley, 19: 87
mutagenic effects of, in *Vicia sativa*, 20: 45476
mutagenic effects on Drosophila gonads, 19: 31789(R) (ORNL-3768 (p.58-63))
preparation and properties of tritium-labeled, 20: 36916
preparation from ethyl iodide and silver methanesulfonate, 20: 10809 (EUR-2531.f)
protective effects of, against mutagenic effects of radiation in barley seeds, 19: 36122
radiomimetic effects on barley and *Vicia faba* chromosomes, 18: 13568
synergistic effects of, with x radiation on genetic effects in barley, 17: 5861

METHANESULFONIC ACID, ISOPROPYL ESTER
mutagenic effects on barley, comparison of x radiation and, 18: 3543
preparation and properties of tritium-labeled, 20: 36916

METHANEDISULFONIC ACID, 2-METHOXYETHYL ESTER
effects on cytology and physiology of *Triticum durum* and *T. monococcum*, 19: 43653

METHANESULFONIC ACID, METHYL ESTER
effects of, in *Bacillus subtilis*, 20: 1624
effects on Kurloff bodies in guinea pig lymphocytes, 20: 22690
mutagenic effects on barley, comparison of x radiation and, 18: 3543
preparation, 20: 14576(R) (ORNL-3889, pp 73-7)
preparation and properties of tritium-labeled, 20: 36916

METHANESULFONIC ACID, PROPYL ESTER
hydrolysis of, inverse gamma-deuterium isotope effects in, 18: 39179
mutagenic effects on barley, comparison of x radiation and, 18: 3543

METHANESULFONIC ACID, TETRAMETHYLENE ESTER
effects of, on chromosomes of bone marrow cells, 20: 22582
effects on cytology and physiology of *Triticum durum* and *T. monococcum*, 19: 43653
effects on leukemia induction in mice, 16: 6272
effects on lymphoid and myeloid leukemia incidence in mice, 20: 6788 (ORNL-P-1703)
effects on mitosis in rat lens epithelium, 20: 16256
effects on neutron-induced chromosome aberrations in barley and *Vicia faba* seeds, 20: 31136
effects on rat lifespan, 18: 41246
effects on secondary disease after bone marrow transfusions, 17: 22994
effects on *vicia faba* seeds combined with radiometric compounds and x rays, 16: 1595
effects with radiotherapy on chronic myeloses, 19: 13170
lethal administration in inbred rats, effects of bone marrow transfusions on survival from, 16: 17368
sensitivity of *Vicia faba* bean roots to, 17: 21503
therapeutic use for radioinduced leukemia in man, 18: 43275
toxic effects in mice, 17: 113
toxic effects in rats, effects of treatment with ribonucleic acid, 17: 113

METHANETHIOL
analysis of carbon-14- and sulfur-35-labeled, method for, 16: 11710
neutron reactions (n,γ) on sulfur-34 in, chemical effects in, 17: 23386 (UCRL-10360(Rev.))
neutron scattering cross sections, verification of Krieger and Nelkin theory, 16: 7160
neutron scattering in gaseous and liquid, total cross sections for thermal, 16: 32368
neutron scattering cross sections for gaseous and liquid, total, (E), 20: 325
radiolysis of aqueous solutions of, effects of pH on gamma, 19: 7545
reactions with sulfur-35, 16: 28982 (UCRL-10360)
yields of sulfur-35-labeled, in neutron reactions (n,p) with ethyl and methyl chlorides, 19: 13495

1,6-METHANOCYCLODECAPENTAENE
electron spin resonance spectra of, deuterium effects on, 20: 7122

Methanoic Acid
see Formic Acid

METHANOL
amine complexes of, carbon-13 and oxygen-18 exchange with carbon dioxide, 20: 9364(R) (NYO-755-2, Paper 4)
analysis for active hydrogen by NMR spectroscopy, 18: 33475
analysis for water using krypton-85, 18: 37566(R) (NYO-2757-3)
analysis for water using kryptonated calcium carbide, 19: 36267
analysis of, for water using krypton-85, 17: 27639(R) (TID-18881)
boiling of, transition from discrete-bubble to merging-bubble regime in nucleate, 18: 39459
boiling on horizontal plates, liquid-vapor interactions in, 17: 37343
bubble motion in, 16: 6535
Cannizzaro reactions in, mechanism, 16: 16087
chemistry of nitrogen-13 recoils produced by carbon-12 (d,n) reactions in, 16: 11759
complexes with uranyl perchlorate, preparation of, 20: 10825
content in frozen cherries, effects of storage time on, 19: 13837
determination by xenon trioxide oxidation, titrimetric, 20: 20579
determination of, method for, 19: 46324(R) (AGN-8132)
deuterium nuclear relaxation in labeled, 18: 39265
deuterium-hydrogen exchange between chlorophyll and, location of, 18: 16042(T)
distillation for carbon-13 concentration, molecular, 17: 23840
distillation of, carbon-13 separation in molecular, 18: 4147
effects of aqueous solutions of, on sorption europium and yttrium by cation exchanger, 19: 40664
effects on acid depletion in Tramex feed solution, 20: 45792(R) (ORNL-3945, pp 129-40)
effects on chromatographic separation of rare earths from acid solutions, 17: 20109
effects on electrolytic precipitation of nickel alloys, 18: 26057
effects on electrochemical reduction of aliphatic nitro compounds, 20: 18636(R) (TID-22725)
effects on energy transfer in liquid scintillators under beta and uv irradiation, 19: 24578
effects on formation of nitrate radicals in pulse radiolysis of nitrate solutions, 20: 43321
effects on gamma radiation effects on aliphatic or aromatic ketones, ESR studies on, 20: 43313
effects on gamma radiation effects on biphenyl, spectral studies on, 20: 43314
effects on gamma-irradiated polyvinyl acetate, 16: 18950
effects on gamma-irradiated methyl vinyl ether polymers, 16: 18772
effects on hydrogen abstraction by trifluoromethyl radicals in photolysis of hexafluoroazomethane, 20: 45709
effects on ion exchange of uranium and other elements in system with organic acids, 18: 25305
effects on ion exchange separation of rare earths using α-hydroxyisobutyric acid, 19: 40663
effects on ion exchange separation of europium and yttrium, 19: 40666
effects on ion exchange behavior of hafnium, molybdenum, niobium, tantalum, titanium, and zirconium, 20: 7039
effects on paramagnetic defects in gamma-irradiated high-surface-area silica, ESR studies of, 20: 27608
effects on phophatase activity in chloroplasts, 17: 4380(R) (UCRL-10479)
effects on phosphorus-31 chemical shifts in triphenylphosphine oxide, 19: 2296
effects on polymerization of polyvinyl chloride to vinyl monomers,

20: 23004
effects on praseodymium ion exchange between aqueous acid solutions and resins, 16: 25354
effects on radical yields from radiolysis of alkaline aqueous solutions, 19: 26447
effects on radioinduced graft polymerization, 17: 4583 (TID-7643(p.233-44))
effects on radioinduced graft polymerization, 17: 16041(R) (NCSC-2477-10)
effects on radioinduced redox processes in iron–oxygen–sulfuric acid–water, 18: 13877
effects on radioinduced graft polymerization of styrene on polyvinyl alcohol, 18: 23581(T,R) (AEC-tr-6316(p.66-9))
effects on radioinduced graft polymerization of styrene on polyvinyl alcohol, 18: 23582(T,R) (AEC-tr-6316(p.70-5))
effects on radioinduced graft polymerization of styrene on celluloses, 18: 25474(T) (AEC-tr-6372(p.83-8))
effects on radioinduced graft polymerization of acrylonitrile and styrene on viscose rayon, 18: 25476(T) (AEC-tr-6372(p.97-102))
effects on radioinduced post polymerization of trioxane, 18: 27532
effects on radioinduced polymerization modification of acrylonitrile, 18: 33650
effects on radioinduced grafting of styrene to vinyl alcohol polymers, 19: 11181
effects on radioinduced carbon dioxide-graphite reactions, (E), 19: 19953 (AERE-R-4201)
effects on radioinduced grafting of vinyl monomers to wool, 20: 7154
effects on radioinduced rayon to styrene graft polymerization, 20: 16528
effects on radioinduced graft polymerization of polypropene to acrylonitrile, 2-methyl-5-vinylpyridine, and styrene, 18: 25505(T) (AEC-tr-6372(p.363-9))
effects on radioinduced graft polymerization of cotton cellulose and rayon on polystyrene, 17: 31808
effects on radioinduced graft polymerization of styrene to viscose rayon yarn, 17: 32676
effects on radioinduced graft polymerization of polyvinyl alcohol to styrene, 17: 33986
effects on radiolysis of alkaline, aqueous solutions of potassium ferricyanide, 17: 39159
effects on radiolysis of water vapor at 116°C, 17: 39148
effects on radiolysis of lithium chloride solutions containing hydrochloric acid, 19: 17983
effects on radiolysis of *p*-nitrosodimethylaniline, 19: 32216
effects on reactions of hydroxyl radicals with iodide ions in pulse radiolysis, 19: 26444
effects on sorption of calcium and strontium by cation exchangers, 19: 18061
effects on sorption of europium and yttrium on ion exchangers, tracer studies of, 19: 40665
effects on spectra of neodymium complexes, 20: 14560
effects on Tramex extraction process, 18: 13917(R) (ORNL-3558(p.7-55))
effects on *trans-cis* isomerization of stilbene in solutions of, 20: 14579(R) (NYO-2383-15)
effects on uranium adsorption on Dowex-1, 16: 10109
effects on yields in radiolysis of *α*- and *p*-toluenethiol, 18: 25549
effects on yields in radiolysis of deuterated sodium formate aqueous solutions containing nitrous oxide, 18: 31602
efficiency of, with toluene for carbon-14 dating by liquid scintillation counting, 20: 18935
electric conductivities of cesium and lithium chlorides in, 18: 206 (NYO-10695)
electric conductivity of anhydrous uranyl nitrate in, 18: 25394
electron reactions at 10 to 16 ev, ionization potentials from, 18: 31538
electron reactions with, ion excess kinetic energy from, 19: 42506
electron spin resonance spectra of labeled, 16: 10051(R) (TID-15003)
electron spin resonance spectra of, 20: 42433
equilibrium and standard free energy constants for alkali metals in, 18: 8362
europium ion fluorescence in, deuterium effects on, 19: 32157
exchange between solvated cations and solvent, 17: 12258
exchange between solvated cations and solvent, 19: 11105
exchange in dilute solutions of neptunium ions, NMR spectra of, 20: 26838
film boiling on submerged heating surfaces in, analysis of, 17: 1610(T) (AEC-tr-5517)
formation by radiolysis of propanediol in air and nitrogen, 17: 27424
heat of mixing with water, deuterium isotope effects on, 17: 28876
heat of vaporization of, calculation from rigid-sphere equation of state, 18: 224
heat transfer coefficient, 17: 20178
heat transfer coefficients, nucleate boiling, 19: 7688
heat transfer in, during forced-convection film-boiling flow, 17: 287
iodine-131 exchange between, and iodinated platinum foil, 20: 33143(R) (COO-733-13)
ionization by excited noble gas atoms, 19: 9943
ionization potentials of, 17: 19935
labeling with deuterium, 19: 7532
labeling with oxygen-17 and -18, 20: 16547
metabolism in mice, effects of catalase activity on, 20: 42837(R) (ANL-7136, pp 124-40)
neutron inelastic scattering in, cold, 16: 32381
neutron inelastic scattering by, dynamic processes in slow, 20: 40338
neutron moderating properties at 20 to 150°K, 16: 29716
neutron reactions at 0.025 to 0.4 ev, total cross sections for, (E), 20: 40069(R) (EANDC(E)-66(U))
neutron scattering by, cold, 16: 31873
neutron scattering, studies using spinning sample method, 16: 7158
neutron scattering cross sections for gaseous and liquid, total, (E), 20: 325
neutron scattering by, spectra for, (T), 20: 26348 (NP-16010, pp 102-39)
neutron spectra in cooled, thermal, (E), 20: 2945
nuclear magnetic resonance of sorbed, on thorium oxide, temperature dependence of, 18: 20632 (TID-18689)
nuclear magnetic resonance of adsorbed, on thorium oxide, 18: 27426
nuclear magnetic resonance spin-lattice relaxation times in, deuteron and proton, 20: 12839
oxidation by peroxydisulfate ions, 18: 39166(R) (TID-21041)
oxidation by peroxydisulfate ions in aqueous solution, kinetics of, 20: 1571(R) (TID-22186)
oxidation of, mechanisms of electrochemical, 17: 4886(R) (AD-275610)
photolysis in presence of acetone, mechanism of, 17: 28977
photolysis of aqueous solutions of, mechanism yields in uv, 18: 43634
photolysis of, electron spin resonance spectra of free radicals trapped at 77°K in, 17: 14330
photolysis of, mechanism of free radical formation in, 19: 24554
piezo-optic coefficients and refractive index, 20: 4484
polymerization effects on monomeric and polymeric materials, 16: 6437 (NYO-2530)
polymerization effects in methacrylic acid grafting to polyethylene, 17: 4608
positronium lifetime in, effects of oxygen on, 19: 7402
preparation from carbon monoxide and hydrogen, deuterium effects on, 19: 15557
preparation of deuterated, isotope effects in, 19: 13413
properties for polarographic reduction of organic compounds, 20: 18636(R) (TID-22725)
proton-transfer ion-molecule reactions in, tracer studies of, 18: 29638
quenching effects on carbon-14 and tritium counting by liquid scintillators, 18: 29682
quenching effects on liquid salicylic acid phosphor in scintillation counting, 20: 22866 (CONF-651214-1)
radiation effects on decomposition with zinc oxide, 16: 20516
radiation effects on hydrogen abstraction from deuterated, isotope effects in, 19: 4216
radiation effects on anodic oxidation of, 19: 5970
radiation effects on, at 77°K, electron spin resonance of radicals from, 19: 9240
radiation effects of recoils from thermal neutron-boron-10 reactions on deuterated, 19: 36514
radiation effects on reactions with hydroxyl ions, 19: 44090
radiation effects on decomposition of, in presence of catalysts, 19: 46329 (EUR-2455.e)
radiation effects on, spectral studies on gamma, 20: 14579(R) (NYO-2383-15)
radiation effects on glassy solutions of, spectral studies on effects of hydrocarbon solutes on gamma, 20: 43314
radioinduced carboxylation, 20: 8992
radioinduced carboxylation to glycolic acid, kinetic studies of gamma, 20: 23180
radioinduced carboxylation of, in aqueous solutions, yields of glycolic acid from gamma, 20: 31278
radioinduced catalytic conversion of, on silica gel, 20: 29278
radioinduced color centers in, EPR spectra of trapped electrons and radicals in, 19: 4212
radioinduced free radicals in, 16: 10051(R) (TID-15003)
radioinduced free radicals in, EPR spectrum of, 18: 10148
radioinduced graft polymerization effects on methyl methacrylate and polyvinyl alcohol, 16: 229
radioinduced graft polymerization effects on styrene and polyethylene, 16: 5384
radioinduced oxidation, 19: 32221
radioinduced oxidation of, yields of formaldehyde in, 20: 4011
radioinduced oxidation of, effects of dose rate on yields in, 20: 38942 (UJV-1457)

radioinduced oxidation of, yields in, 20: 41004
radioinduced polymerization with β-propiolactone, 18: 23605(T,R) (AEC-tr-6316(p.201-7))
radioinduced reactions with perchloroethylene, 17: 29903
radioinduced reactions with 1,2-dichlorotetrafluorocyclobutene and 1,2-dichlorohexafluorocyclopentene, 19: 38708
radioinduced reactions with ethylene at high pressure and temperature, beta, 20: 355(R) (NYO-2978-42)
radioinduced telomerization with ethylene, yields from beta, 20: 20724(R) (NYO-2978-44)
radioinduced telomerization with tetrafluoroethylene, gamma, 20: 23084(T) (AEC-tr-6466/1, pp 203-10)
radiolysis at 77 to 293°K, mechanism of, 19: 28377
radiolysis by alpha and lithium-7 recoils from boron-10-neutron reactions, linear energy transfer in, 19: 4224
radiolysis by deuterons at 2 Mev, chemistry of nitrogen-13-labeled products from, 16: 13108
radiolysis by gamma radiation and recoil nuclei, products of, 18: 13840(R) (TID-20203)
radiolysis by gammas and recoils, effects of oxygen on, 18: 33618 (CONF-322-14)
radiolysis by pulsed electron beams, production and reactivity of solvated electrons in, 17: 39097 (CONF-224-2)
radiolysis by pulsed electron beams, properties of solvated electron in, 18: 31592
radiolysis, correlation of ionic yields with mass spectral data on, 16: 30461
radiolysis, effects of carbon dioxide on hydrogen yields in, 16: 1827
radiolysis, effects on yields, 16: 4197
radiolysis, effects of ultraviolet and visible light on yields, 16: 6455
radiolysis in arene solutions, lifetimes of aromatic anions in pulse, 18: 39318
radiolysis in liquid and solid states and in presence of oxygen, mechanisms, 16: 222
radiolysis in presence of deuterated propane, 17: 28968
radiolysis, isotope effects of deuterium and tritium in, 16: 16086
radiolysis of acid and neutral solutions, effects of bicarbonate on hydrogen yields in, 16: 11717
radiolysis of aerated, effects of water, 17: 201
radiolysis of aerated, deaerated, and oxygenated, 17: 14315(R) (TID-18027)
radiolysis of aerated, effects of sulfuric acid and water on hydrogen peroxide yield from gamma, 19: 13425(R) (NYO-2383-12)
radiolysis of aerated, effects of sulfuric acid on formaldehyde and hydrogen peroxide yields in, 20: 14579(R) (NYO-2383-15)
radiolysis of aqueous solutions of, reactions of hydrated electron in, 18: 25579
radiolysis of aqueous solutions of, 18: 31563 (AD-429919)
radiolysis of aqueous solutions of, mechanism of yields in electron, 18: 43634
radiolysis of, comparison of boron-10(n,α) lithium-7 recoil reactions and gamma radiation in, 18: 1746
radiolysis of deaerated, effects of sulfuric acid on yields in gamma, 20: 14579(R) (NYO-2383-15)
radiolysis of d_4-labeled, reaction mechanisms, 16: 17741
radiolysis of, effects of additives, 16: 32137 (ARL-91)
radiolysis of, effects of additions of aromatic hydrocarbons and nitrogen oxides on, 17: 12322 (ARL-90)
radiolysis of frozen carbon tetrachloride solutions of, formation of stabilized radicals in, 20: 10879
radiolysis of glassy and liquid, spectra of electron pulse and gamma, 18: 43662
radiolysis of isotopically substituted, electron spin resonance studies of, 16: 8777
radiolysis of labeled and unlabeled vapor, effects of benzene on yields, 16: 10087
radiolysis of labeled and unlabeled, ion-molecule reactions in, 18: 277
radiolysis of liquid, effects of cesium, potassium, and rare earth salts on yields in, 17: 10699
radiolysis of liquid, effect of nitrous oxide on gamma, 19: 36466
radiolysis of low temperature glassy, visible, uv, and ESR spectra from gamma, 19: 32235
radiolysis of solid, by charged particle bombardment, 16: 17708(R) (TID-14812)
radiolysis of vaporous, effects of methyl bromide, nitrous oxide, and propene on hydrogen yields in, 19: 11210
radiolysis of vaporous, scavenging effects of carbon tetrachloride, bromomethane, and oxygen on, 19: 46395
radiolysis of vapors of, effects of scavengers on hydrogen yields from gamma, 20: 20776
radiolysis of, absorption spectra of solvated electron in, 19: 7559
radiolysis of, analysis of liquid-phase products in, 18: 27602
radiolysis of, effects of nitrous oxide environment on, 18: 10139(R) (AD-403358)
radiolysis of, effects of cobalt, copper, and nickel ions on gamma, 19: 9216
radiolysis of, effects of carbon tetrachloride, ferric chloride, iodine, and potassium iodide on, 19: 28376
radiolysis of, effects of water on yields of hydrogen peroxide from, 20: 5581
radiolysis of, effects of catalysts on yields from, 20: 18744
radiolysis of, ethylene glycol and formaldehyde synthesis in, 18: 13871
radiolysis of, free radical yields in gamma, 18: 25538
radiolysis of, free-radical scavenging by anthracene and its homologs in, 19: 478
radiolysis of, hydrogen yields from gamma, 20: 7150
radiolysis of, linear energy transfer effects on yields from, 18: 29779
radiolysis of, production of high-kinetic-energy fragment ions in electron, 18: 43615
radiolysis of, product yields from gamma, 19: 38716
radiolysis of, quasi-equilibrium theory calculations of yields from gas-phase, 20: 40959
radiolysis of, radical captor properties of disaphthofuranoxyl and DPPH in, 18: 43607
radiolysis of, reactions of reducing species in, 19: 15640
radiolysis of, reactivity of electrons produced in gamma, 20: 20750
radiolysis of, vapor chromatographic determination of products of gamma, 19: 13425(R) (NYO-2383-12)
radiolysis of, yields of hydrogen in, 20: 36861 (UJV-1553)
radiosensitivity effects on animal and plant cells, 18: 38977
radiosensitivity effects on *E. coli*, 19: 26059
reactions of deuterated, with hot methyl radicals in photolysis of deuterated and nondeuterated methyl iodide, 18: 37231
reactions of ionized and molecular, cross sections for, 17: 31219
reactions of nucleophilic reagents in, 16: 14378(R) (NYO-2302)
reactions of, with metal carbides, 17: 1363(T) (AEC-tr-5515)
reactions with anhydrous praseodymium and neodymium chlorides to form alcoholates, 20: 316
reactions with beryllium oxyacetates, 16: 30427
reactions with chlorides, methoxide complex formation equilibrium in, 19: 11075
reactions with hydroxyl radicals from irradiated benzoic acid solutions, 19: 32224
reactions with metal complexes, isotopic dilution studies on, 17: 2948(R) (TID-17216)
reactions with muonium, (E), 20: 29247
reactions with rare gas ions in metastable states, fragmentation and ionization in, 19: 17874
reactions with recoil tritium atoms, 17: 1552
reactions with sodium borohydrides, effects of sodium carbonate and methoxide on, 16: 13043
reactions with tetracyanoethylene and polyacrylonitrile under high pressure, addition, 19: 36457 (NYO-3185-1)
reactions with tritium recoil atoms with and without benzene and cyclohexane, energy transfer in, 19: 40622
reactions with trideuteromethyl radicals, deuterium and hydrogen atom abstraction from, 20: 23025
reactions with yttrium oxides, infrared spectroscopy studies of, 20: 26917
scavenging effects on electron and hydrogen yields in irradiated aqueous solutions, 17: 4602
self-diffusion coefficient at 25°C, 17: 17953(R) (TID-18448)
solvation of charge groups in, substituent effects on chemical equilibria and rate in, 18: 33613
solvent properties for polymer-monomer systems, 16: 445(R) (NYO-9988)
solvent properties for cerium(III) chlorides, 16: 11630
solvent properties for neodymium and praseodymium chlorides, 17: 28916
solvent properties for elements, 17: 32194(R) (TID-19068)
solvent properties for strontium-90 and yttrium-90, 17: 35893
solvent properties for carbon dioxide, 18: 1492(R) (TID-19592 (Sect.VII))
solvent properties for coal-tar pitch binders for graphite, 19: 13875(R) (GA-4022(Pt.1))
solvent properties for rare earth oxides in the presence of ammonia, 20: 20686
sorption by barium sulfate (labeled and unlabeled), 17: 14277
sorption by thorium dioxide, 18: 41469
sorption by uncorroded and corroded uranium, 20: 1805 (AWRE-0-69/65)
sorption of vapors by potassium sulfate containing sulfur-35, 16: 27099
spectra of deuterated, between 2 and 15 μ, absorption, 18: 1715
spectra of uranium tetrachloride in, absorption, 18: 19935 (TID-18814)
synthesis from carbon dioxide and moisture in air using mobile nuclear power system, 20: 12877 (BNL-955)
synthesis using mobile power reactor, for liquid-fuel use, 19: 29689
synthesis using nuclear power in mobile energy depot system, 19: 276

(BNL-8489)
synthesis using nuclear power, for use in mobile energy depot system, 19: 13195 (BNL-8808)
thermodynamic properties of ions in, at 25 to 45°C, 18: 4918(R) (TID-19727)
thermodynamic properties of, in water and heavy water, 19: 46318
transport properties, 16: 3553
uranyl nitrate hexahydrate dissociation and electric conductivity in, 16: 2945
use for regeneration of ion exchange resins, 20: 7200
uses as medium for drifting lithium into germanium, (E), 20: 5702
uses in paper electrochromatographic separation of barium and strontium, 18: 41573
vibrations of trapped, in β-quinol clathrates, localized, 20: 41651
yields in electron and gamma radiolysis of methane–oxygen system, 19: 28359 (AERE-R-4871)
yields in gamma radiolysis of carbon monoxide–water vapor mixture, 20: 25122 (HW-SA-3440)
acetic acid–methanol, deuterium exchange between, and azulene, 20: 29245
acetonitrile–methanol, effects on ESR spectra of oxygen-17-labeled benzoquinone, 20: 43224
allyl methacrylate–methanol–H_2O, effects on radioinduced crosslinking of nylon 66 and poly (vinyl alcohol), 20: 1909
Al_2O_3–CH_3OH, analysis for cerium, photometric, 17: 25146
benzene–methanol, diffusion in air at 35°C, 19: 34147 (UCRL-9987 (Rev.2))
benzene–methanol, radiation effects on, at 77°K, ESR and tracer studies of x, 20: 12890
benzene–methanol, radiolysis of deuterated and normal, hydrogen and methane yields in, 16: 239
benzene–methanol, radiolysis of, radical scavenging in, 19: 4204
benzene–methanol, radiolysis of, free-radical scavenging in, 20: 16530
benzene–methanol, radiolysis of, effects of deuterium on yields from, 20: 26938
butyl acetate–methanol, solvent properties of, for rare earths in paper chromatographic separation, 20: 43452
carbon tetrachloride–methanol, radiolysis of frozen, free radical formation in gamma, 20: 29305
CCl_4–methanol, diffusion in, 18: 15712(R) (TID-20260)
CCl_4–methanol, diffusion in air at 35°C, 19: 34147 (UCRL-9987(Rev.2))
CCl_4–methanol, mechanism of chemical processes in reactions with chlorine-38 recoil atoms, 19: 40623
CCl_4–methanol, solvent effects on gamma-irradiated polyvinyl acetate, 16: 18950
cyclohexane–methanol, interface in critical fluids of, reflectivity of diffuse, 19: 19952
cyclohexane–methanol-d, vapor pressure, 18: 16066 (NP-13736)
ethyl ether–methanol, solvent properties of, for rare earths in paper chromatographic separation, 20: 43452
GeH_4–methanol, preparation of volatile hydrides by mercury sensitized photolysis of, 20: 18729(R) (NYO-2007-9)
HBr–methanol–H_2O, effects on ion exchange of metals, 19: 30085(R) (TID-21853)
HCl–methanol, effects on ion exchange behavior of rare earths, thorium, and uranium, 18: 39124
HCl–methanol, effects on titanium and zirconium, corrosive, 20: 14988
HCl–methanol, radiolysis products from, analysis of, 20: 14581(R) (ORNL-3889, pp 14-16)
HCl–methanol, solvent properties of, for zirconium, 16: 13126 (IDO-14573)
HCl–methanol, spectrophotometric analysis for metals, 20: 14469(R) (TID-22650)
HCl–methanol, use in cation exchange of alkaline earth elements, 18: 17958
$LiNO_3$–methanol–HNO_3, use as solvent in ion-exchange separation of rare earths, 20: 4067
methanol–H_2O, activity coefficients of salts in, rule for calculation of, 16: 16375
methanol–2-propanol, carbon-13 exchange between monoethanolamine and, 20: 39320(R) (MLM-1311)
methanol–H_2O, diffusion of potassium chloride in, 18: 15712(R) (TID-20260)
methanol–H_2O, dissociation constants for acetylacetone and metal acetylacetonates in, 19: 26295 (TID-21811)
methanol–$HClO_4$–H_2O, electron exchange reactions between thallium and uranium in, 18: 27418
methanol–H_2O, equilibrium and standard free energy constants for alkali metals in, 18: 8362
methanol–methyl borate, neutron transmission in, at low energies, angular distribution in, 16: 3877(R) (ORNL-3193(p.278-87))
methanol–sodium methoxide, perfluorocarbanion formation in deuterium–hydrogen exchange in monohydrofluorocarbons in, 18: 25451
methanol–NaI, properties for oxide particle suspension in centrifuges, 20: 36933
methanol–$AgNO_3$, radioinduced free silver atoms in solid solutions of, EPR of x, (E), 20: 15975(T)
methanol–Ag_2SO_4, radioinduced free silver atoms in solid solutions of, EPR of x, (E), 20: 15975(T)
methanol–AgF, radioinduced free silver atoms in solid solutions of, EPR of x, (E), 20: 15975(T)
methanol–$AgClO_4$, radioinduced free silver atoms in solid solutions of, EPR of x, (E), 20: 15975(T)
methanol–$NaNO_3$, radiolysis of oxygen-saturated, 18: 12147(R) (RRL-127)
methanol–$NaNO_3$, radiolysis of aerated, deaerated, and oxygenated aqueous, 18: 22117(R) (RRL-133)
methanol–$NaNO_3$, radiolysis of aqueous solutions of, 18: 43641
methanol–naphthalene, radiolysis yields in, 19: 46324(R) (AGN-8132)
methanol–pyridine, radiolysis of, yields of hydrogen from gamma, 20: 18736
methanol–H_2O, radiolysis of, yields of hydrogen from gamma, 20: 18736
methanol–NO–H_2O, radiolysis of, nitrous oxide yields from, 20: 23168
methanol–H_2O, solvent effects of, on acetylacetone equilibrium constants with copper perchlorate, 16: 13013(R) (TID-15227(p.3-32))
methanol–H_2O, solvent effects of, on stability constants of copper acetylacetonates, 16: 13015(R) (TID-15227(p.65-79))
methanol–H_2O, solvent effects of, on gamma-irradiated polyvinyl acetate, 16: 18950
methanol–HNO_3, solvent properties of, for rare earths, scandium, and yttrium, 16: 25280 (TID-15598)
methanol–KOH, solvent properties for tissues, 20: 1767
methanol–methyl acetate, solvent properties of, for rare earth in paper chromatographic separation, 20: 43452
methanol–HNO_3, spectrophotometric analysis for metals, 20: 14469(R) (TID-22650)
methanol–nitrogen oxides, synthesis of glycol from, radiochemical, 18: 33629
methanol–H_2O, thermodynamic properties of acetylacetone in, 16: 13014(R) (TID-15227(p.33-64))
methanol–HNO_3, use as eluant in separation of americium and curium by anion exchange, 20: 439(T) (ORNL-tr-893)
methanol–H_2O, use in paper chromatography of compounds labeled with iodine-125 and iodine-131, 20: 5515
methanol–$HClO_4$, use in universal electropolishing method, 19: 36954 (IS-1184)
NH_4SCN–methanol–H_2O, distribution coefficients of metals in, 19: 40447
2,5-diphenyloxazole–methanol–naphthalene–2,2'-p-phenylenebis-5-phenyloxazole, properties of, for counting blood glucose, 18: 13659
Methanol, Benzoyl-
see Acetophenone, 2-Hydroxy-
Methanol, Diphenyl-
see Benzhydrol
METHEMOGLOBINEMIA
radiation effects on rat, protective effects of aminopropiophenones against, 19: 7215
radioinduced in rabbits, effects of radioprotective compounds on, 19: 26021
METHIONAL
effects on flavor of irradiated beef, 20: 39299
METHIONINE
carbon-14 uptake by, in algae proteins during photosynthesis, 19: 24244
complexes with chlorophyllin and metal ions, radiosensitivity effects in mice of, gamma, 20: 1692
complexes with lanthanum, stability of, 19: 36421
complexes with uranium, polarography and zone electrophoresis studies on, 20: 43229
determination of, in rabbit urine, design of photometer for, 17: 30214
determination of sulfur-35-labeled, in intestine, 16: 14445
effects of absence of, on viability of uv-irradiated *E. coli*, 20: 38562
effects of methyl-carbon-14-labeled, on oviposition of crickets, 16: 4070
effects of, on calcium-45 uptake and retention by chicks, 17: 21449
effects of thiophosphamide on uptake of sulfur-35-labeled, by blood serum, 18: 23247(T) (JPRS-24164(p.1-8))
effects of, on incidence of hemorrhagic disease and growth rate in rats fed irradiated beef, 18: 11633(R) (NP-13574)
effects on amino acid and protein restoration in irradiated guinea pigs, rabbits, and rats, 18: 9911
effects on growth and sporulation of *Bacillus cereus* mutants, 17: 40550(R) (TID-19486)
effects on hemorrhage in rats, 17: 16364(R) (NP-12602)
effects on hemorrhage in rats, 19: 103
effects on hemorrhages induced by irradiated beef in diet of rats, 19: 36881

effects on survival of whole-body irradiated mice on protein diet, 17: 35613
formation during electron irradiation of primitive Earth atmosphere, tracer studies of, 20: 42726
hydrolysis by hydrochloric acid in tritiated water, hydrogen exchange in free and protein combined, 19: 9243
ionization potential, 20: 3863(R) (IS-1200(Sect. C))
L-seleno-, metabolism of selenium-75-labeled, by animals, 20: 26633
labeling with sulfur-35 by biosynthesis in *E. coli* from labeled sulfates, 18: 43584
labeling with tritium following radiolysis of ribonuclease, 20: 18749
lability of, in lipid-protein reaction systems, 20: 14587
metabolism by calcified tissues during acute radiation sickness, tracer studies, 16: 32860
metabolism by *Micrococcus radiodurans*, 18: 41067
metabolism by Neurospora, 17: 33463(R) (ANL-6723(p.149-52))
metabolism, effects of physical activity, 16: 34
metabolism in blood serum of dogs, tracer study on, 20: 5249(R) (COO-119-232, pp 203-18)
metabolism in mice, tracer study, 19: 32067
metabolism in mice, tracer study, 20: 3661 (NP-15594)
metabolism of sulfur-35-labeled, by irradiated rabbit bone marrow and spleen, 17: 15843
metabolism of sulfur-35 labeled, in mice with Ehrlich's ascitic carcinoma, 20: 42728
photolysis of, transformation of amino acids in uv, 18: 23204(T) (JPRS-24164(p.19-42))
preparation of carbon-14-labeled DL-, method for, 20: 23196 (CEA-R-2989)
preparation of high purity sulfur-35-labeled, method for, 19: 24597
preparation of sulfur-35-labeled, by reactions with sulfur-35 recoil atoms, 19: 40619
protective effects against radioinduced inactivation in urease, 16: 1530
protective effects against nitrogen mustard induced inactivation in urease, 16: 1531
protective effects against radiation injuries and nitrogen mustard in *E. coli*, 16: 16297
protective effects against radiation injuries in mice, 16: 25253
protective effects of sulfur-35-labeled, against whole-body x irradiation in rats, 17: 12148
protective effects of, on hemagglutinin and infectivity of influenza virus, 17: 15668
protective effects against radiation damage in other amino acids, 18: 11623(R) (AD-407411)
protective effects against uv radiation in *Hansenula wingei*, 18: 43303
radiation chemistry of, and derivatives, 18: 25573
radiation chemistry of, uv and x, 20: 18791
radiation effects on electron spin resonance spectra, 17: 1529
radiation effects on, in absence of fats and fatty acids, 17: 14341
radiation effects on, in ovomucoid, protective effects of AET against, 17: 38769
radiation effects on ESR spectra of, uv and x, 18: 22149
radiation effects on rat tissue uptake of carbon-14-labeled, x, 18: 23293
radiation effects on metabolism of, in rabbits, 18: 25198
radiation effects on uptake of sulfur-35-labeled, by serum protein fractions in rats, 18: 27172
radiation effects on content of, in kidneys and liver of mice, 19: 7149
radiation effects on uptake of sulfur-35-labeled, by rabbit marrow and spleen proteins, 19: 19604
radiation effects on metabolism of sulfur-35-labeled, in healing wounds in rats, 19: 33900
radiation effects on intestinal sorption in rats, 19: 43728(R) (UCLA-12-565, pp 59-64)
radiation effects on content in proteins, gamma, 20: 50
radiation effects on, ESR studies of effects of molecular structure on, 20: 25132
radioinduced synthesis of sulfur-35-labeled, 20: 20786
radioinduced thermoluminescence in, 17: 27427
radiolysis in reactors, 20: 20786
radiolysis of, chromotographic analysis, 18: 41552
radiolysis of, formation of α-amino butyric acid in, 17: 25331
radiolysis of, in aqueous solution, γ, 20: 38582
radioprotective activity in *E. coli*, method of determining, 17: 35409
radiosensitivity effects of, in *E. coli* and Streptomyces, 17: 38770
radiosensitivity effects of, on fatty infiltration of mouse liver, 17: 40586
reaction kinetics of, in biological transmethylation, 18: 25061
S-methyl-, synthesis in *Escherichia coli*, 17: 33465(R) (ANL-6723(p.165-73))
S-adenosyl-, reaction kinetics in biological transmethylation, 18: 25061
synthesis by cell-free extracts of *Escherichia coli*, 18: 17398(R) (ANL-6790(p.122-5))
synthesis in liver, effects of whole-body irradiation, 16: 14512
synthesis in Saccharomyces, 18: 23193(R) (ANL-6823(p.128-40))
synthesis in yeast, enzyme reactions for, 20: 42737(R) (ANL-7136, pp 231-42)
synthesis of tritium-labeled, 18: 10119(T) (NP-tr-1093)
therapeutic use of, in mice fed irradiated beef, 18: 524
use of labeled, in analysis of urinary metabolites, 18: 36941
use of selenium-75-incorporated seleno-, in scanning for parathyroid tumors, 20: 22810
use of selenium-75-labeled, in pancreatic diagnosis, 20: 22828
use of sulfur-35-labeled in study of horny tissue formation, 16: 14399
vapor pressure, 18: 15678 (IS-790)

METHIONINE, *N*-ACETYL-
conversion of carbon-14-labeled DL- to L-, by enzymatic resolution, 20: 23196 (CEA-R-2989)
radioinduced free radicals, 16: 29002
radioinduced free radicals in, electron spin resonance studies of, 18: 8439

METHIONINE, S-ADENOSYL-
alkaline hydrolysis of, in tritiated water, 17: 33467(R) (ANL-6723 (p.178-80))
hydrolysis of, tracer studies of mechanism in alkaline solutions, 16: 23729
metabolism, 16: 31393(R) (ANL-6535(p.84-9))
metabolism by Neurospora, 17: 33463(R) (ANL-6723(p.149-52))
reaction kinetics of, in biological transmethylation, 18: 25061

METHIONINE, SELENO-
determination of selenium-75-labeled, in intestine, 16: 14445
selenium-75 incorporation in, biosynthetic, 20: 3661 (NP-15594)
use of selenium-75-labeled, in parathyroid diagnosis, 18: 43341
use of selenium-75-labeled, for diagnosis of parathyroid or pancreas tumors, 19: 34054
use of selenium-75-labeled, in parathyroid scanning, 19: 5744
use of selenium-75-labeled, in pancreas scanning, 19: 5746
use of selenium-75-labeled, for pancreatic scanning, 19: 36194
use of selenium-75-labeled, in radiodiagnosis of pancreatic diseases, 18: 23392
uses of selenium-75-labeled, in pancreatic scanning, 18: 38723

METHIONINESULFOXIMINE
effect on urinary excretion of phosphorus and desoxyribose in rats, 17: 27037
effects of, on liver and spleen in rats, 17: 17712
effects on adenine nucleotide content in rat blood and liver, 20: 14270
effects on distribution of potassium in rat tissues, tracer study, 17: 15687
effects on glucose metabolism in rats, tracer study, 20: 3678
effects on iron-59 metabolism in rats, 20: 40561
effects on sulfur-35 uptake and distribution by rat tissues, 17: 21437
effects on urinary excretion of ammonia and phosphates in rats, 20: 14270

Methotrexate
see Amethopterin

METHOXY GROUP
activity in labeled and unlabeled methoxyamine, 19: 13415
reactions of free radicals of, with methane, hydrogen abstraction in, 20: 23025

METHOXYAMINE
activities of amino and methoxy groups in labeled and unlabeled, 19: 13415
effects on deuterium exchange with hydrogen bonded N–H groups in *N*-methylacetamide in aqueous solutions, 20: 354
hydrogen abstraction from labeled and unlabeled, isotope effect on, 19: 13415

Methyl Acetates
see Acetic Acid, Methyl Ester

Methyl Acrylate
see Acrylic Acid, Methyl Ester

Methyl Alcohol
see Methanol

Methyl Benzoate
see Benzoic Acid, Methyl Ester

METHYL BORATES
efficiency of, with toluene for carbon-14 dating by liquid scintillation counting, 20: 18935
molecular structure and infrared spectra of, isotope effects on, 19: 40470
vapor pressure of, isotope effects on, 17: 2701
methanol–methyl borate, neutron transmission in, at low energies, angular distribution in, 16: 3877(R) (ORNL-3193(p.278-87))

Methyl Bromide
see Methane, Bromo-

Methyl Chloride
see Methane, Chloro-

Methyl Cyanide
see Acetonitrile

METHYL ETHER
electron drift velocities in, at low energy, 19: 46393
exchange of boron trifluoride between, and ethyl ether, 18: 2127(R) (ORNL-3488(p.21-41))
hydrogen bonding in deuterium chloride mixtures, isotope effects on infrared spectra from, 19: 17946
radiolysis of solid, by charged particle bombardment, 16: 17708(R) (TID-14812)
reactions of deuterated, with hot methyl radicals in photolysis of deuterated and nondeuterated methyl iodide, 18: 37231
reactions with pentafluorides of niobium and tantalum, adduct formation in, 19: 17895
reactions with recoil tritium atoms, effects of scavengers on radioactivity in yields from, 16: 11746
transport properties, 16: 3553
yields from radiolysis of methanol, 19: 38716
BF_3–methyl ether, boron isotope exchange between boron fluoride and, 16: 30703
BF_3–methyl ether, boron isotopic exchange thermodynamics of, 19: 46899(R) (ORNL-3832, pp 33-49)
BF_3–methyl ether, boron-10 exchange in, 16: 12839
BF_3–methyl ether, spectra, isotope effects on infrared, 16: 20445
BF_3–methyl ether, spectra of, Raman, 18: 2127(R) (ORNL-3488(p.21-41))
$HO–(CH_3)_3O$, isotope enrichment in distillation of, 17: 2683
METHYL GROUP
see also Trichloromethyl Groups
analysis of, for carbon-14 and tritium, 20: 18600
coupling constants for fluoro-, labeled, and unlabeled, isotopic acid vibrational effects in, 16: 14726
deuterium isotope effects in fluorine-substituted and normal, addition reactions, 17: 8159
deuterium uptake by C-19 angular, in 17-ketosteroids, 18: 22106
effects on chemical equilibrium and rate of solvation of charge groups in aromatic compounds, 18: 33613
effects on radiation stability of polystyrene, 19: 24577
electron spin resonance of, in irradiated DNA and thymine, 19: 24575
meson (π^-) capture in (E), 19: 3086
metabolism of N and S, review, 16: 1372
preparation of deuterated, attached to oxygen, 19: 20034
proton hyperfine spectra of radicals containing, 17: 8084
proton spin densities in, 18: 33548
radiation effects on addition to aromatic compounds, 19: 482
reaction kinetics of, in biological transmethylation, 18: 25061
reactions with tritium-labeled heptane, isotope effects in, 16: 30406
rotation in free radical of irradiated alanine crystals, electron spin resonance study, 16: 18959
rotational dynamics of, 18: 24625 (WASH-1046)
rotational freedom in methylbenzenes, 16: 29522 (BNL-5979)
spectra of tritium in, high resolution NMR, 18: 27517
spectra vibrational amplitude constants of, deuterium isotope effects of, 19: 30217
Methyl Hexyl Ketone
see 2-Octanone
METHYL HYDROPEROXIDE
radioinduced in methane–oxygen mixture, iodometric analysis of mixture with hydrogen peroxide, 20: 248
reactions with potassium iodide in mixture with hydrogen peroxide, iodometric analysis of, 20: 248
Methyl Iodide
see Methane, Iodo-
Methyl Isobutyl Carbinol
see 2-Pentanol, 4-Methyl-
Methyl Isobutyl Ketone
see 2-Pentanone, 4-Methyl-
METHYL ISOCYANIDE
isomerization of, unimolecular, 17: 25107
synthesis, 18: 10118 (ORNL-TM-777)
thermal isomerization of deuterated, kinetic isotope effects in, 17: 33959
thermal isomerization of deuterated, fall-off and inverse isotope effects in, 19: 13313
Methyl Methacrylate
see Methacrylic Acid, Methyl Ester
METHYL NITRITES
reactions with cyclohexanone in acid ethereal solution, preparation of 2,6-dioximinocyclohexanone by, 20: 25109 (ORNL-TM-1510)
METHYL ORANGE
radiation effects, 18: 13841(R) (TID-20295)
radiolysis in alcohol and water, 17: 16043(R) (TID-18094)
radiolysis in polyvinyl alcohol, alpha and gamma, 19: 32237
radiolysis of, as spectrophotometric dosimeter at 500 to 5000 rad, 17: 41279
sensitivity for use as indicator in titration of molybdenum(V) with cerium sulfate, 19: 15396
METHYL PEROXIDE
reactions with potassium iodide in mixture with hydrogen peroxide, iodometric analysis of, 20: 248
METHYL RADICALS *(Free Radicals)*
abstraction of deuterium and hydrogen from methylamine by, isotope effects in, 19: 30226
abstraction reactions of, deuterium isotope effects in, 18: 16071
electron spin resonance of transient, 17: 23383 (RRL-112)
exchange reactions with deuterium at 200 to 350°C, kinetics, 16: 13076
formation in irradiated methyltrideuteriomethylphenylcarbinyl hypochlorite, deuterium isotope effects and transition state in, 18: 16086
formation in methyltrideuteriomethylphenylcarbinyl hypochloride decomposition, secondary isotope effects in, 18: 39203
formation of, in radiolysis of hydrocarbons, radioiodine scavenging studies of, 17: 18107 (RRL-87)
hydrogen abstraction reactions with aromatic compounds, 19: 21760 (NYO-2728-4)
hydrogen abstraction by, from ammonia, hydrazine, and methylamine, isotope effects on, 20: 20713
ionization potential of, 17: 41534(R) (ANL-6720(p.77-89))
production by radiolysis of aromatic hydrocarbons, 19: 5943(R) (RRL-147)
production in liquid hydrocarbons by carbon-12 (n,2n) reactions, 18: 27528
production of carbon-13-labeled, in hydrogenous materials, 16: 25419(R) (RRL-84)
production of neutral and positive, in interstellar space, 16: 27863
production of trideutero-, from hexadeuteroacetone photolysis, 20: 23025
reaction kinetics of, in biological transmethylation, 18: 25061
reactions of hot, with added compounds in photolysis of deuterated and nondeuterated methyl iodide, 18: 37231
reactions of trideutero-, with methanol and trideuteromethanol abstraction of deuterium and hydrogen atoms from, 20: 23025
reactions with ammonia, trideuteroammonia, and hydrazine, hydrogen bond dissociation in, 18: 29688
reactions with deuterium sulfide to abstract deuterium atom, 19: 26367
reactions with dimethylmercury during photolysis, 17: 40869
reactions with hydrocarbons, effects of structure and medium, 16: 25335
reactions with hydroxy hydrogen of tertiary butyl alcohol, role of hydrogen bond in, 16: 26986
reactions with labeled nitric oxide, preparation of *cis*- and *trans*-dimers of nitrosomethane by, 16: 11725
reactions with lead for lead isotope abundance determination by gas-source mass spectrometry, 19: 18151
reactions with saturated hydrocarbons, 16: 11595
recombination rate constant for, in radioinduced exchange reaction between deuterium and methane, 18: 12190
relaxation in methanol in presence of neptunium ions, NMR spectra of, 20: 26838
scavenging of deuterated, by nitric oxide at low temperature, 17: 27337
shape calculation, 17: 2901
spectra of carbon-13-labeled deuterated and normal, ESR, 20: 38941(R) (RRL-2310-182)
trifluoro-, abstraction of deuterium and hydrogen from hexafluoroacetone by, isotope effects in, 20: 45709
use of carbon-14-labeled, as radiolysis scavenger for hydrocarbons, 19: 19985
yield from gamma radiolysis of hexane–silica gel systems, 20: 16511
yields from gamma radiolysis of nitromethane at 77°K, EPR studies of, 19: 40579
yields from radiolysis of ethylene, 19: 46361
yields from radiolysis and photolysis of acetonitrile at 77°K, 20: 35551
yields in radiolysis of ethylene–methane–nitrogen, 19: 46324(R) (AGN-8132)
yields in radiolysis of cyclohexane–iodomethane, 20: 38941(R) (RRL-2310-182)
METHYL RED
analytical use as indicator for ammonia and nitrate in ores, 16: 18815 (PG-Report-225)
color change induced in, by unknown x-agent, 17: 27452
dissociation of, calculation of equilibrium constants of, 18: 31422 (HW-SA-3505)
sensitivity for use as indicator in titration of molybdenum(V) with cerium sulfate, 19: 15396
solubility of, in heavy water, isotope effects on role of hydrogen bonds in, 20: 43287
METHYL SELENIDES
BF_3–dimethyl selenide, boron isotopic exchange reactions of, 19: 46899(R) (ORNL-3832, pp 33-49)
METHYL SULFATES
t-butylmethylphenylsulfonium, preparation and nuclear properties, 18: 19837(R) (MIT-905-1)
METHYL SULFIDES

complexes with niobium and tantalum pentahalides, compositions and properties, 16: 11629
electron reactions on, radical ion production from, 18: 6870
heat of formation and ionization constants of, electron impact studies of, 17: 35761
reactions with pentafluorides of niobium and tantalum, adduct formation in, 19: 17895
sorption by, nickel catalysts, mechanism of, 16: 31597
sulfur-35 exchange reactions between liquid hydrogen sulfide and, effect of acidity on rate of, 20: 27007
yields of sulfur-35-labeled, in neutron reactions (n,p) with ethyl and methyl chlorides, 19: 13495
BF_3–methyl sulfide, boron isotopic exchange thermodynamics of, 19: 46899(R) (ORNL-3832, pp 33-49)

METHYL SULFOXIDE
complex formation reactions with thorium and zirconyl perchlorates, 19: 13339
complexes with molybdenum chlorides, 19: 43990 (MIT-1965-15)
complexes with plutonium, thorium, and uranium, spectra and susceptibility of, 20: 25077
complexes with rare earth chlorides, preparation and composition of, 20: 25051
complexes with uranyl perchlorate, bonding in, 19: 4126
complexes with uranyl nitrate, preparation and properties of, 19: 34156
complexes with uranium and thorium tetrahalides, preparation and properties of, 20: 33293
effects of bone marrow preserved with, on radioinduced lesions in dogs, 20: 10706
effects of cupferron and, on frequency of radioinduced chromosome aberrations in Tradescantia, 20: 29028
effects on ESR spectra of oxygen-17-labeled benzoquinone, 20: 43234
effects on fluorescence yield of rare earth complexes, 19: 7551
effects on frequency of radioinduced chromosome aberrations in Tradescantia, 20: 29028
effects on isotopic exchange between iron(II) and iron(III), 19: 17882
effects on oxygen effect in irradiated barley seed, 20: 5298(R) (RLO-353-4)
effects on radioinduced graft polymerization of celluloses on styrene, 18: 25474(T) (AEC-tr-6372(p.83-8))
effects on radioinduced polymerization of acrylonitrile and styrene on viscose rayon, 18: 25476(T) (AEC-tr-6372(p.97-102))
effects on radioinduced graft polymerization of styrene on amylose, 19: 9205
effects on scintillation efficiencies of toluene phosphors, 20: 9278
effects on *Tribolium castaneum*, 20: 35260
effects on Wolff-Kishner reactions of hydrazones, 20: 20360(R) (PRNC-73)
effects on yeasts, 20: 18206(R) (N-65-16815)
exchange of deuterium and tritium between toluene and, solvent polarity effects on, 19: 36447
iron isotope exchange between iron(II) and iron(III) in, 20: 14571
nuclear magnetic resonance spin-lattice relaxation times in, deuteron and proton, 20: 12839
physiological effects of, in mice and cats, 18: 13563(R) (TID-20236)
preparation of deuterated, 19: 36264
preservation of autologous bone marrow in, 17: 1346
properties of solutions of inorganic salts in, 20: 293 (UCRL-16330)
properties of, for use as solvent in measuring scintillation mixtures, 20: 16355
protective effects against radiation injuries in Pseudomonas, 17: 108
protective effects against radiation injuries in mice, synergistic effects of 2-aminoethylisothiourea or cysteamine, 17: 111
protective effects against radiation injuries in mice, synergistic effects of aminoethylisothiuronium, 17: 1337
protective effects against radiation injuries in bacteria, 17: 1350
protective effects against radiation injuries in mice, 17: 19922
protective effects against radiation injuries in mice, 17: 21589
protective effects in Serratia against x radiation, 18: 19785
protective effects against radiation injuries in mice, effects of solvent on, 18: 19797
protective effects against radiation in mammals, 18: 29400
protective effects of, against radiation injuries in mice, 19: 22019(R) (UCLA-12-541(p.51-91))
protective effects of, against radiation injuries in mice, 19: 30014 (ACRH-103(p.121-42))
protective effects against radiation injuries in mouse spleen, 19: 31901(R) (NP-15072(p.71-81))
protective effects of AET mixtures against gamma radiation, 19: 43883(R) (UCLA-12-565, pp 65-85)
protective effects of, against radiation injuries in mice, 19: 43859(R) (NP-15310, pp 1-13)
quenching effects on liquid salicylic acid phosphor in scintillation counting, 20: 22866 (CONF-651214-1)
radiation effects on viscosity of solutions of polyvinyl alcohol in, 18: 29740(T,R) (AEC-tr-6231(p.339-41))
radiosensitivity effects of, in *E. coli*, 18: 126
radiosensitivity effects on catalase, x, 19: 33970
radiosensitivity effects on catalase, 20: 18449
radiosensitivity effects of, relation between cellular anoxia and, 20: 31122
radiosensitivity effects on *Tribolium castaneum*, x, 20: 35260
reactions with niobium and tantalum pentabromides and -chlorides, properties and spectra of products in, 18: 25398
reactions with thorium, titanium, and zirconium perchlorates, 19: 7419
solvent properties, 20: 31220(R) (UCRL-16658, pp 39-72)
use for low-temperature preservation of mouse lymphocytes, 18: 8048 (USNRDL-TR-689)
use in bone marrow preservation, 20: 8727
use in liquid scintillation counting, 20: 9278
use in polarographic studies of uranium salts, 20: 36745

Methyl Yellow
see Aniline, N,N-Dimethyl-p-Phenylazo-

METHYLAL
radiolysis, 20: 20758
radiolysis of, 19: 26428
spectra, effects of deuterium substitution on infrared, 16: 20447
use in proportional detectors for ultra-soft x radiation, 20: 7433

METHYLAMINE
abstraction of deuterium and hydrogen by methyl radicals from, isotope effects in, 19: 30226
bond lengths in, deuterium isotope effects on, 19: 22251
carbon-11 recoil reactions in, mechanisms and yields of, 20: 33329 (BNL-9408)
carbon-14 exchange with ethane, radioinduced, 16: 11702 (TID-15083)
charge transfer collisions with positive ions, mass spectra of products from, 19: 46262
complexes with niobic acid, infrared spectra and thermal studies on, 18: 17804
dissociation by electron bombardment, mass spectra from, 18: 23608(T,R) (AEC-tr-6316(p.232-7))
dissociation constant of alpha-deuterated, potentiometric and spectrophotometric determination of, 17: 15990
dissociation, intramolecular rearrangements, and ionization of deuterated and normal, by electron bombardment in mass spectrometer, 20: 38887
distillation of, with carbon dioxide, isotope effects in, 17: 10521
electron spin resonance spectra splitting of cesium and rubidium in, 17: 31120
hydrogen abstraction by methyl radicals from, isotope effects on, 20: 20713
hydrogen isotope exchange with fluorene and indene, 19: 13362
isotopic exchange of hydrogen, 16: 30309
molecular structure of, deuterium effects on, 19: 11150
neutron scattering total cross sections for liquid, thermal, 16: 28016
nitrogen isotopic exchange with cation exchanger, 19: 22840 (IS-1059)
photolysis, 17: 25099
preparation of carbon-14-labeled hydrochloride of, 17: 10517 (PAN-336/XIII)
production of carbon-14-labeled, by neutron radiolysis of cyanoguanidine, 16: 7594
protective effects against x radiation in mice, 16: 14459(R) (NP-11359 (p.35-75))
radiation effects on carboxylation of, effects of acidity and dose on gamma, 20: 33368
radiation effects on, reactions of recoiling carbon-11 in, 20: 38964
radioinduced carboxylation of, yields in, 20: 20732 (SGAE-CH-21/1965)
radiolysis, 20: 7145
radiolysis, 18: 13841(R) (TID-20295)
radiolysis in presence of deuterated propane, 17: 28968
radiolysis of gaseous, gamma, 18: 12248
radiolysis of solid, by charged particle bombardment, 16: 17708(R) (TID-14812)
radiolysis of, analysis of yields in, 19: 46324(R) (AGN-8132)
radiolysis of, effects of pressure and radiation intensity on yields from gas-phase, 19: 30246
radiolysis of, reactions of hydrogen atoms from gamma, 20: 26932
radiolysis products of, 17: 16043(R) (TID-18094)
reactions with niobium and tantalum pentabromides and niobium pentachloride, 16: 12945
reactions with recoil carbon-11 atoms, mechanism and products of, 20: 5570 (JUL-228-RC)
separation from amines and amino acids by thin-layer chromatography-ionophoresis and ionophoresis, 18: 19854(T) (SC-T-64-49)
spectra of hydrated electron in aqueous solutions of, 17: 1436
spectral effects on ESR of lithium and potassium, 18: 22042
yields from reactions of recoil carbon-14 with ammonia, 20: 7145
yields in gamma radiolysis of glycine, 18: 35596

yields in gamma radiolysis of choline chloride in aqueous solutions, 19: 17969
yields in radiolysis of aqueous glycine, 18: 25584
yields in x radiolysis of dimethylhydrazine, 18: 35589 (NASA-TN-D-2452)
yields of carbon-14-labeled, in thermal neutron reactions with nitrogen-14 in hydrazine sulfate, 18: 43636
yields of, in uv-radioinduced oxidation of dimethylthymine in aqueous solutions, 20: 23158
ethane–methylamine, radiation chemistry, 18: 13841(R) (TID-20295)
n-hexane–methylamine, vapor pressure of, deuterium isotope effects on, 20: 12879
Methylamine, Bis(2-chloroethyl)-
see Diethylamine, 2,2'-Dichloro-N-methyl-
METHYLAMINES, FLUORO-
synthesis in nitrogen plasma jets, (E), 19: 24532
METHYLENE
addition to 2-butene, deuterium isotope effects, 17: 18099
chloro-, preparation by gas-phase decomposition of dihalomethane by tritium recoil reactions, 19: 22315
cyano-, paramagnetic resonance of triplet-ground-state, 19: 32048(R) (NP-15073)
gamma and fast neutron heating in moderators of, for cold neutron production, (T), 20: 36152
incorporation in carbon–hydrogen bonds of cyclohexane and cyclopropane, deuterium isotope effects on, 19: 26372
insertion in irradiated propane, phase dependence of carbon-11 recoil products for, 17: 27415 (BNL-6354)
insertion in saturated hydrocarbons for carbon-14 labeling, 19: 32258
ionization potential of, from diazomethane pyrolysis, 17: 1517
mass difference with nitrogen, (E), 19: 28336
neutron scattering at 2 to 14 Mev, total cross sections for, (E), 20: 8062(R) (COO-720-058)
neutron scattering spectra from, Monte Carlo analysis of time-of-flight, 17: 41868 (TID-18080)
neutron spectra in, 20: 36428 (GA-7072)
polymerization using ruthenium oxide catalysts, 18: 5365
radioinduced reactions with benzene and cyclohexane, isotope effects in, 18: 35620
reactions with *cis*-2-butene, isotope effects, 18: 27486
reactions with hydrogen and methane, mechanism, 17: 184
shape calculation, 17: 2901
spectra of tritium in, high resolution NMR, 18: 27517
spin state of labeled, 19: 23355(R) (BNL-867(p.1-117))
CH_2–W–U, critical mass calculations for enriched, 18: 36221 (LAMS-1969)
METHYLENE BLUE
complexes with beryllium, rare earths, thorium, and uranium, preparation and stability of colored, 18: 27366
effects of, on phosphorus-32 uptake by phosphatides in guinea pig brain slices, 17: 23044
effects on radioinduced chromosome aberrations in barley and *Vicia faba*, 19: 38462
effects on radioinduced oxidation of ergosterol, 20: 20738
effects with light on inactivation of *E. coli* phages T4, protective effects of spermine against, 20: 33096
electric charging of aerosols of, at 0.001 to 1.0 atm measurement of, (E/T), 20: 8811(R) (COO-1248-4)
leukobase, radiolysis in organic solvents, 18: 304
preparation of pure leuco-, 18: 41496 (PAN-523/XVII)
production of aerosols of, design of spinning-disk generator for, 19: 4287
protective effects against lethality by sodium nitrite, 16: 4001(R) (NP-11020(p.78-81))
protective effects against radiation injuries and nitrogen mustard in *E. coli*, 16: 16297
protective effects against radiation in embryo intestine and testis, 16: 20186
protective effects against radiation damage in chicken embryos, 19: 36104
radiation effects on sorption of, by barium sulfate, 16: 27099
radiation effects on sorption of, by barium sulfate, 18: 332
radiation effects on color of glycerol or water solutions of, 18: 16081
radiation effects on, protective effects of amino and sulfur compounds against, 18: 43310
radiation effects on, gamma and x-ray, 19: 30249
radiation oxidation and reduction mechanism, electron paramagnetic resonance study, 16: 14783
radioinduced bleaching in aqueous solutions, effects of phenol concentration, 16: 23768
radioinduced bleaching of, in presence of aromatic carboxylic acids and esters, 17: 12350
radioinduced bleaching of, in presence of sulfuric acid, 18: 3844
radioinduced oxidation of, sensitization of gamma, 18: 37208(T) (AEC-tr-6398(p.434-43))
radioinduced reactions in aqueous solutions, effects of aeration, deaeration, ethanol, hydrogen, and sodium benzoate on, 17: 4592 (TID-14927)
radiolysis in organic solvents, oxidation and reduction reactions in, 18: 304
radiolysis in polyvinyl alcohol, alpha and gamma, 19: 32237
radiolysis of aqueous solutions of, with and without formate ions, 20: 10925
radiolysis of, in glycerol solution, 19: 20016
radioprotective effects in conjunction with aminothiazol and dinitrophenol, 16: 6357
radiosensitivity effects of, in *E. coli* and Streptomyces, 17: 38770
radiosensitivity effects in chick embryos, 18: 17637
radiosynthesis, 16: 23708 (CEA-1991)
reactions with cerium sulfates, stability constants of complexes formed in, 19: 22243
sensitizing effects on photoinactivation of trypsin, 18: 8115 (TID-20001)
sensitizing effects on photoinactivation of trypsin, 19: 7586
sorption by siliceous minerals, tracer and transmittance studies of, 18: 16193 (TID-7689(p.85-6))
sorption of, particle size determination using, 17: 15938 (AEET/CD/5)
sorption on radioactive barium sulfate, 17: 20083
therapeutic use of sulfur-35-labeled, 19: 13134 (NP-14426)
methylene blue–uranin, particle deposition and reentrainment in long vertical tubes, 20: 39103(R) (BNWL-235-3, pp 51-69)
methylene blue–uranin, use of solutions of, in aerosol generators, 20: 39103(R) (BNWL-235-3, pp 51-69)
Methylene Oxide, Tetra-, Polymers
see Furan, Tetrahydro-, Polymers
METHYLENE SULFIDE POLYMERS
preparation by radioinduced polymerization of trithiane, 18: 17901
radioinduced from trithiane, orientation of twinned, 20: 353
radioinduced polymerization of trithiane to, orientation and structure of polymer crystals of, 19: 452
METHYLENIMINE
radiolysis, 20: 7145
yields from reactions of recoil carbon-14 with ammonia, 20: 7145
METHYLIDYNE
production by reactions of carbon-11 with hydrogen, 20: 18716
reactions with ethylene, 20: 18716
spectrum in polar aurorae, 19: 16740
17-Methyltestosterone
see Androstenone, Hydroxymethyl-
METHYLTHYMOL BLUE
analytical properties for lanthanum and yttrium, 18: 3688
analytical use for determination of thorium in presence of uranium, 19: 36312
analytical use in determination of rare earths, 20: 252
analytical uses for determination of yttrium, 20: 8860
analytical uses in determination of cerium, lanthanum, and yttrium, 19: 17840
analytical uses in determination of thorium, 19: 22121
analytical uses in determination of fluorides by titration using uranium, 20: 5520
complex with hafnium and zirconium, 17: 19960
reaction of, with thorium ions, 19: 36312
use for selective detection of niobium in hydrogen peroxide, 16: 12983
uses of, for photometric determination of ytterbium, 20: 45581
Methythyrine
see Imidazole-2-Thiol, 1-Methyl-
METRAZOLE
effects of, on radiation injury in central nervous system in mice, 17: 10263
preparation of tritium-labeled, 20: 35571
METROLOGY
apparatus functions for low-accuracy measurements, unfolding of, (T), 20: 13038
at high temperatures, 19: 2741
calibration of Mangiagalli for biradial coordinates, 18: 30097 (TID-20751)
effects of measurement process on knowledge obtained in, (T), 19: 8026
effects on wave function superposition principle in quantum theory, 18: 36397
electron microscopic study of plastic deformation of thin gold films by Talysurf stylus, 19: 38916 (SC-DC-65-1589)
equipment and methods for, conference on, 19: 46732
equipment and methods for, in machining to submicron tolerances, 20: 46146 (Y-KE-204(Rev.))
equipment for automatic, conference on, 19: 20303
gravitational effects in, 18: 32665
machine gaging philosophy on instrumentation, 20: 3627 (RFP-670)
positional measurement of curved surfaces, alpha angle adjuster for,

19: 17425 (RFP-480)
prediction of subsequent measurements from partial information in quantum mechanics, 18: 21051
quantum, gauge invariance in, 19: 16708
quantum, morality of, 20: 26021
resolution corrections in, error propagation in, (T), 20: 13040
response relations in, minimum bias designs for exponential, (T), 20: 13167 (ORNL-3873)
signal analysis in noise background using data accumulation, (T), 20: 5695
standard calibration in, effects of temperature variations on, 19: 15698(T) (UCRL-Trans-1145(L))
survey of measuring instruments for quality control, 19: 8694 (BDX-613-57)
temperature effects on gaging in machining, 20: 39009 (UCRL-14944)
theory for quantum, 20: 13664
theory for space-time regions, equivalence of states in, 18: 15005
theory of quantum, 18: 15004
theory of quantum micro- and macromeasurements in, 18: 36371
theory of quantum-mechanical, 18: 14974
theory of quantum, for microsystems, 19: 31130
theory of, time symmetry in quantum, 18: 26417
tolerance charts in industrial process control, 19: 4275 (RFP-432)
use in nondestructive testing of fuel rods, 20: 4123
use in nondestructive testing of irradiated fuel materials, 20: 4124
use of dimensional, for nondestructive fuel element testing, 20: 6632(T) (AEC-tr-6628)
use of electromagnetic waves in, theory of, 19: 16500
wave packet variances in quantum, relations between (T), 19: 3116

MEXICO

(See also headings of the form Mexico (Puebla))
atomic energy in, educational, protective, and research programs for, 19: 35875
beryl occurrence in northeastern, 17: 24780
education program in nuclear sciences in, 17: 24815
fall-out monitoring, Feb. 1959 to Oct. 1961, 16: 25674
fallout monitoring in, relation to meteorology, 18: 8909
fallout monitoring, 1961 to 1963, 18: 27699 (A/AC.82/G/L-931)
fallout studies in, 18: 12350
geochemistry and radioactivity of curative waters in Lourdes Spa, San Luis Potosi, Mexico, 19: 40835
geological survey results in, 18: 31048(R) (COO-689-42)
nuclear engineering training in, 17: 24816
nuclear power plant site evaluation in, 17: 19662
pitchblende occurrence in tertiary volcanic rocks in Granaditas Area, Sonora, 17: 24781
radiation hazards in, from medical radiography, 20: 24948
radiation monitoring of atmosphere in, 19: 42677
radiation monitoring in, 1962, 20: 9155
radioactive minerals in, geological and mining explorations of, 17: 24779
radioisotope importation and use in, 17: 24791
radiological monitoring of atmosphere over Mexico City for lead-212 as a measure of radioactive contamination, 17: 27628
reactor safety code, 16: 22484
reactor site selection in Valley of Mexico basin in, 17: 24765
research reactor site studies in, 17: 19683
strontium-90 content of milk in, 1963 to 1965, 20: 40854

MEXICO (NUEVO LEON)
radiation monitoring of atmosphere at Monterrey in 1959, 16: 5568

MEXICO (PUEBLA)
radiation monitoring of atmosphere at Puebla in 1959, 16: 5568

MEXICO (SONORA)
lead uranyl tellurite occurrence in Moctezuma, 20: 4173

MEXICO (ZACATECAS)
geology and mineralogy of Providencia area in, 20: 18631 (NYO-2266-1)

MGCR
see Maritime Gas Cooled Reactor

MH-1
see Army Reactors (MH-1)

MICA
see also Biotites
see also Lepidolites
see also Muscovites
age determination by argon–potassium method, 16: 10287
age estimation by potassium-argon isotopic measurements, 16: 27477
age estimation by potassium-argon measurements in Norwegian basement, 16: 27478
age estimation by uranium fission track analysis in, 18: 10271
age estimation from charged particle track in, 17: 34132
age estimation of phlogopites, in Aldanian deposits, Russia, 19: 46596
age estimation of, by argon–potassium method, in Ontario, Canada, 20: 18929
age estimation of, by rubidium–strontium method, 20: 20891
age of, estimation by argon-potassium method, 20: 43503(R) (COO-689-60, App.A-3)
alpha range in, 5-Mev, 20: 2147
analysis for rubidium and strontium by emission spectrography, 18: 13651
argon-40 content in, upper limit for excess, 20: 23295
argon/potassium ratios in Alpine Fault, age estimations from, 16: 13379
beta recoil of bismuth-212 and -214 from, 16: 26009
cesium-137 sorption by, successive desorption method for calculating, 20: 20618
coating thickness of gold on, use of proton beam scattering for measuring, 20: 21246
crystal properties of cesium–iron, 18: 4171(R) (ORNL-3470(p.3-5))
crystal properties of $RbFe_4^{+2}(Si_3,Fe^{+3})O_{10}(OH)_2$, 18: 3714(R) (ORNL-3470(p.41-4))
dating by uranium fission traces, 18: 27716
desorption of carbon-14-labeled carbon dioxide and helium from, rate of, 20: 10464 (COO-920-5)
development as coating for thermoelectric materials, 17: 23861(R) (AD-282505)
effects of uranium fission tracks on, electron microscopy of, 19: 37187
elastic properties, 16: 2202 (TID-14231)
electron diffraction scattering by thin foils of, analyzing system for, 18: 20670
europium sulfide epitaxial growth on crystals of, 19: 11079
fission fragment track distribution in, 19: 9512
fission product traces in, uranium, 18: 27716
fission product tracks in, neutron detection by, 18: 35861
fission product tracks in, formation and stability of, (E), 19: 20674
fixation of fission product solutions in, 16: 16027(T) (NP-tr-874)
formation of extremely small holes in, using fission fragments, 17: 25991
fossil tracks of charged particles in, characteristics of, 17: 34132
heavy particle track production in, 17: 8630
ion tracks in, registration mechanisms of heavy, 20: 5755
neutron reflections from crystal of, time-of-flight spectrum, 19: 7765 (IDO-17029)
nuclear fission in, dating by, 18: 12371
particle tracks in, visibility under electron microscope, 16: 33404
performance as cold neutron monochromator, 20: 21949
performance as heavy ion detector, 20: 5756
performance for slow neutron dosimetry, 19: 44385 (CERN-65-4(Vol.II), pp 112-19)
performance of sandwiches of, as detectors of high-energy fission, (E), 20: 652 (INR-647/1-A,VI/PH)
performance of sandwiches of, for fission fragment track registration, 20: 13099
performance of sheets of, as detectors for high-energy proton-induced nuclear fission, (E), 19: 7782 (CERN-64-49)
preparation of sandwiches of, for registering fission events, 20: 13099
properties as detector in high-energy proton reactions, 20: 29551
properties as radiation detector, 16: 13334
properties as x-ray fluorescence analyzer, 18: 12022
properties for neutron dosimetry, 17: 29205
properties for use as particle track detector, 19: 11589
proton channeling in foils of, at 3.55 Mev, (E), 20: 40324
proton reactions at 3 Bev, heavy-particle tracks in, 18: 44766
proton spallation at 3 Bev in, tracks from, 16: 13334
radiation effects on electric conductivity, 16: 22659
radiation effects on phase transformations in, fission-fragment, 16: 29454
radiation effects on thin single crystals of, air- and argon-ion, 16: 33403
radiation effects on photoconductivity of reconstituted, 17: 27893 (TID-18843)
radiation effects on capacitance and dielectric properties of, in critical assemblies, 18: 2381
radiation effects on, 18: 12752
radiation effects on capacitors of, gamma and neutron, 18: 12412 (AFCRL-63-753)
radiation effects on dielectric properties of paper of, effects of silicones on, 20: 1897 (NASA-TN-D-3032)
radiation effects on current induction in capacitor of, electron beam, fast neutron, and gamma, 20: 21151 (IBM-66-825-1944)
radiation effects on dielectrics of, gamma, neutron, and proton, 20: 23764(R) (AD-626474)
radioinduced transient conductivity in, 17: 41520
reactions with Magnox alloy to 500°C in argon, 19: 22997 (TRG-Report-842)
rubidium/strontium ratios in Alpine Fault, age estimations from, 16: 13379
sorptive properties for uranium, 18: 17943
sorptive properties for cesium-137, 20: 20696
sorptive properties for fission products in waste solutions, 20: 29332 (ORNL-P-1811)
sorptive properties for aluminum, 16: 26009

sputtering of, by krypton ions at 4 to 30 kev, cathode coefficient for, 17: 16817
thermal desorption energies for bismuth and lead, 16: 26009
thickness of, in end-window counters, use of alpha particles for measuring, 20: 14826
use for detecting charged particles, 20: 21060
use for fission detection at high temperatures, 20: 39208 (JINR-P-2705)
use in detection of fission fragments, efficiency for, 18: 5630 (JINR-P-1433)
use in detection of neutrons by fission-track production, 18: 29048(R) (HW-80284(p.6.1-10))
use in neutron dosimeters based on fission fragment damage principle, 20: 35740 (BNWL-SA-516)
x-ray-diffraction properties above 10 Å, 18: 2097
x-ray fluorescence line tables for mica-48 crystals, 18: 27361 (Y-1470-F)
x-ray reflections from, relative intensities of higher order, 19: 26627 (CALT-221-7)
x-ray-fluorescence tables for mica-80, 18: 30316 (Y-1470-G)

MICE

acceleration tolerance of, effects of radioprotective agents on, 20: 43004
activation of carbon-12, nitrogen-14, and oxygen-16 in, by protons, 18: 15828
adoptive transfer of sensitivity to allogenic or xenogenic skin grafts in irradiated, 18: 33388
age estimation of, 19: 21811(R) (UCLA-12-541(p.101-30))
aging, effects of somatic mutations, 17: 28750
aging in ICR, effects of microbial flora on, 20: 40502(R) (ORNL-3922, pp 115-27)
aging of, biological factors affecting, 19: 29889(R) (ANL-6971(p.90-116))
aging of, effects of ancestral radiation exposure on, 18: 15808(R) (LAMS-3034(p.116-23))
air blast effects on, as function of ambient pressure, 20: 32904
alcohol metabolism in, effects of catalase activity on, 20: 42837(R) (ANL-7136, pp 124-40)
allometric relation between radiosulfate metabolism and weight changes in embryos, 20: 42765
altitude effects on, 17: 35286(T) (FTD-MT-62-78(p.564-75))
aminoethylisothiuronium metabolism in tumors and normal tissues of, 19: 24370
amyloid metabolism in, effects of iodine-131 and thiouracils on, 19: 27959
analysis for phosphorus-32 in tissues in, by deuteron activation and radioautography, 17: 21620
anemia in, effects of gamma-irradiated schistosome infections on, 20: 20446
anemia in, protective effects of erythropoietin against chemical and radioinduced, 19: 26110
anemias in, effects of genes on, 20: 14290(R) (NYO-1800-12)
antibody formation in radiation chimeras, 17: 21531
antibody levels in circulating blood of, effects of deuteration on, 20: 28988
antibody production in, morphologic changes in spleen lymphatic tissue during, 20: 40632(R) (ORNL-3922, pp 175-91)
antibody titers in, effects of Schistosoma egg purification on, 20: 14304
antibody-antigen reactions to *Schistosoma mansoni* cercariae, 20: 20360(R) (PRNC-73)
antibody-forming potential in, effects of age on secondary, 20: 40626(R) (ORNL-3922, pp 80-3)
antigen development in embryos, transplantation immunity, 16: 21917 (USNRDL-TR-556)
antigenic specificity of chemically induced sarcomas in, 18: 29318
antigenicity of cell-free tumor extracts from, 20: 45483
antitoxin responses in thymectomized, 18: 4898 (BNL-6910)
arsenic-74 uptake by tissues in tumor-bearing, from inorganic and organic compounds, 19: 6968
audiogenic convulsive seizures and low-level irradiation, 16: 23499
autoradiography of, whole-body, 18: 4971
autoradiography of iodine-125 distribution in thyroid gland of, 19: 45783
autoradiography of erythropoietic cells, 20: 40675
bacteremia in x-irradiated, factors affecting, 20: 8721
barium-140 uptake by melanomas in, 18: 3489(R) (COO-228(p.127-31))
behavior response to gamma radiation, 20: 40519 (NP-16259)
benzimidazole distribution in tissues of, tracer study, 20: 22544 (CEA-R-2899)
beryllium-7 metabolism by, biological half life for, 18: 43177(R) (LA-3132-MS(p.59-65))
biological characteristics of populations of, effects of sex-linked mutants on, 20: 42837(R) (ANL-7136, pp 124-40)
blood catalase screening technique for, 19: 6913(R) (ANL-6906(p.65-9))
blood cell populations in germ free, effects of age on, 19: 31677(R) (ORNL-3768(p.119-30))
blood cell production in, effects of DNA biosynthesis on, 19: 42245
blood circulation in liver of, use of colloidal chromic phosphate for measuring, 20: 26594
blood picture in, effects of extracorporeal irradiation of blood on, 17: 35341(R) (UCLA-515(p.75-80))
blood picture in irradiated, after serial transplantation of bone marrow in, 17: 40631
blood picture in irradiated, origin of hemic cells in, 18: 11757
blood picture in, effects of age and sex on, 20: 30970 (COO-1170-5)
blood plasma from irradiated, effects on tumors of, 19: 31814
blood platelet production and destruction in, 18: 19470 (NYO-2138-1)
bone formation in, effects of aminoacetonitrile and estrogen on, 19: 19471(R) (ANL-6938(p.162-78))
bone marrow aspiration technique for use in, 18: 33223
bone marrow cell migration in, 19: 43836
bone marrow chromosomes in leukemic, 19: 21792(R) (ORNL-3650(p.187-(p.187-219))
bone marrow from, effects of freeze-storage techniques on, 17: 35615
bone marrow grafts in, effect of genetic factors on reactions to, 19: 26109(R) (ORINS-49(p.40-62))
bone marrow grafts in, effects of hybridization on sex-associated, resistance to, 19: 31677(R) (ORNL-3768(p.119-30))
bone marrow mitotic cycles in, autoradiographic studies of, 17: 35422
bone marrow of, methods for preserving, 20: 8529
bone marrow therapy in lethally irradiated, heterologous, homologous, and isologous, 16: 18799
bone marrow transplantations in irradiated, effects on hematopoietic system in, 16: 26671(T) (JPRS-14767(p.22-34))
bone marrow transplantation in irradiated and normal, effects of, on lymphatic tissues, 17: 14084
bone marrow transplantation in irradiated, compatibility factors in acceptance of rat, 17: 19877
bone marrow transplantation in irradiated, effects of irradiation of donor cells on survival and chromosome aberrations in recipients following, 18: 25201
bone marrow transplants in, genetic study using iodine-131 of, 18: 29396
bone marrow transplantation in irradiated, storage effects on selective elimination of immunologically competent cells in, 19: 15233
bone marrow transplants in hybrid, effects of genetic constitution on growth of parental, 19: 24226 (ORNL-P-1111)
bone marrow transplant therapy of leukemia in, 20: 8793
bone metabolism in, effects of injected blood components on, 19: 21832
bone tumors induced by strontium-90, 16: 31477 (A/AC.82/G/L.785)
bone tumors induced by strontium-90, 16: 31478 (A/AC.82/G/L.790)
bone tumors induced by plutonium-239 in, 19: 45808(R) (NYO-901-36)
boron metabolism in, 19: 24245
brain lesions induced by goldthioglucose in, 19: 35879
brain weight and learning behavior of, effects of genetic factors on, 20: 42833(R) (ANL-7136, pp 16-46)
breeding and reproduction of pathogen-free, 20: 6907(R) (EUR-2511.e)
bremsstrahlung from injected strontium-85 plus strontium-90 in, whole-body measurements of, 18: 29196(R) (COO-119-229(p.170-85))
cadmium metabolism in, tracer study of, 19: 6947 (BNL-7745)
cadmium-109 uptake and distribution by organs in, 18: 3457
cage design for individual, 17: 30227 (TID-19053)
caging effects on mortality of x-irradiated, 18: 5003(R) (NP-13281(p.104-14))
calcium-47 uptake and distribution in, effects of age on, 17: 35435
calcium-45 retention in, effects of tetracycline on, 18: 23220
cancer cell mutation in, antimutagenic effects of streptomycin, 17: 2793
carcinogenesis in, effects of hormonal changes on, 17: 24830(R) (ACRH-18(p.155-60))
carcinogenesis, metabolic factors in spontaneous, tracer study, 17: 23014
carcinogenic effects of soft x rays on, 17: 15823
carcinogenic effects of fast neutrons and x radiation in, 18: 21828 (USNRDL-TR-713)
carcinogenic effects of urethan in, 19: 35986
carcinogenicity of methylcholanthrene in, effect of vitamin E, 17: 28668(R) (ACRH-19(p.54-6))
carcinostatic effects of nitrogen mustard derivative of 6-mercaptopurine on tumors of, 18: 1323 (TID-19670)
care, feeding, and pathological conditions for Brookhaven colonies, 17: 13881 (BNL-6744)
care of, 18: 43153(R) (LA-3132-MS(p.103-8))
care of colonies of, 19: 197
care of colonies of, 19: 3828
care of experimental, design of facilities for, 20: 3 (LF-23)
care of experimental, 20: 6784(R) (ORNL-3853, pp 118-27)
care of laboratory, 19: 29830(R) (ANL-6971(p.159-65))
care of laboratory, program for, 20: 42699(R) (ANL-7136, pp 94-108)
care of, in laboratory colonies, 19: 6911(R) (ANL-6906(p.27-40))
care on Japtan Island for Operation Greenhouse, 16: 12805 (WT-2)
catalase activity in 19 strains of, 17: 33474(R) (ANL-6723(p.208-10))
catalase content of, effects of injection of exogenous catalase on,

19: 6939(R) (ANL-6906(p.73-4))
catalase distribution in tumor cells of, 18: 38758
catalase reduction in erythrocytes of, 18: 23186(R) (ANL-6823(p.86-90))
catalase-inhibition by 5-mercapto-1,2,3,4-tetrazole in, 18: 23187(R) (ANL-6823(p.91-8))
cataract development in, from wounds after x irradiation, 16: 20200
cataract induction in frogs and mice after x irradiation, 16: 20200
cataract induction in, by 4-(*p*-dimethylaminostyryl)quinoline, 18: 3585
cell generative cycle in neoplastic mammary gland of, 18: 21701 (BNL-7925)
cell proliferation and life span of, effects of starvation on, 20: 42840(R) (ANL-7136, pp 164-90)
cell proliferation and life span of, effects of rapidly growing tumors on, 20: 42840(R) (ANL-7136, pp 164-90)
cerium-144 effects on fertility of female and male, 16: 32823
cerium-144 distribution after intravenous injection in, effects of sex on, 18: 19545
cerium-144 excretion, effects of DTPA on, 18: 33417
cerium-144 metabolism after inhalation as aerosol, 18: 19544
cerium-144 removal from, using TTHA chelates, 20: 10556
cesium metabolism in, comparison with other mammals, 20: 42768
cesium-137 excretion by, effects of chemicals on, 17: 30019
cesium-137 genetic effects in, injected, 17: 14054
cesium-137 retention, 16: 1320(R) (LAMS-2627(p.175-82))
cesium-137 distribution in tissues of, after chronic exposure, 18: 15766(R) (LAMS-3034(p.41-8))
cesium-137 effects on, protective effects of chemicals against, 18: 17647
cesium-137 excretion by, effects of exercise on, 18: 15765(R) (LAMS-3034(p.34-40))
cesium-137 excretion by, effects of environmental temperatures on, 17: 37042 (LADC-5554)
cesium-137 metabolism in, effects of environmental temperature on, 19: 29867
cesium-137 metabolism in, effects of metabolic rate and temperature on, 20: 18203(R) (LA-3432, pp 21-55)
chemotherapy of Ehrlich carcinoma and sarcoma 180 by radioprotective drugs and alkylating agents, 20: 40664
chromium phosphate colloid distribution in, tracer studies of, 20: 1598
chromium uptake, effects of x irradiation and serotonin, tracer study, 17: 30312
chromosomal aberrations in cornea of, induced by tissue extracts from x-irradiated donors, 20: 28959
chromosome aberrations in, effects of age on, 18: 41094(R) (TID-21156)
chromosome anomalies in leukemic and pre-leukemic cells in, 17: 40632
chromosome anomalies in, with spontaneous or virus-induced leukemia, 17: 40633
chromosome cytology of, review on, 17: 24835
chromosome number in bone marrow of normal and leukemic, 18: 15744(R) (LAMS-3034(p.307-11))
chromosome pattern of, 20: 18286 (EUR-2462.1)
chromosome sampling methods for, 19: 27948(R) (TID-21862)
chronic irradiation of, dosimetry of fast neutron source for, 20: 40504(R) (ORNL-3922, pp 146-60)
congenital deformity induced by radiation and radiomimetic treatments, 17: 17764(R) (TID-18338)
content of RNA in spleen of, effects of immune reactions on, 20: 6780(R) (ORNL-3853, pp 93-7)
copper metabolism in adult and young, 16: 28719
crystalline lens protein of, separation of, by zonal ultracentrifugation, 20: 6698(R) (ORNL-3853, pp 141-2)
crystalline structure of lens of, 20: 6697(R) (ORNL-3853, pp 78-87)
cystamine uptake by thymus cells of, *in vivo* and *in vitro*, 20: 10708
cystine metabolism in, 20: 3661 (NP-15594)
cytology of splenomegaly in embryos of, 18: 27065(R) (ORNL-3601 (p.98-104))
desoxyribonucleic acid thermal denaturation in irradiated and leukemic, by trichloratriethylamine, 17: 21539
desoxyribonucleic acid synthesis in various cell types in, 18: 27034(T) (ANL-Trans-31)
desoxyribonucleic acid synthesis in mammary gland of, effects of ovarian hormones, 19: 24240 (BNL-8053)
deuteration following ingestion of deuterium oxide, 17: 1208
deuterium intoxication in, cellular effects of, 18: 36930
deuterium uptake by, pathologic anatomy of, 18: 15800
development of leukemia in lethally irradiated, effects of protection using cells from high-leukemia-incidence strain, 18: 21912
diets for breeding, 19: 43654
dissemination of metastases from strontium-90 induced osteosarcoma, 16: 31476 (A/AC.82/G/L.788)
distribution and chemical forms of 2-mercaptoethylguanidine and bis(2-guanidoethyl)disulfide in, after oral administration, 17: 40509
distribution and chemical forms of diethyldithiocarbamate and tetraethylthiuram disulfide in relation to radioprotection in, 20: 26703
distribution and nature of AET in mammary-tumor-bearing, 17: 14022
distribution of cerium-144 in, demonstrated by whole-body autoradiography, 18: 27037
distribution of promethium-147 in, demonstrated by whole-body autoradiography, 18: 27037
distribution of sulfur-35-labeled mustard gas in, 18: 4971
distribution of 2-mercaptoethylguanine in leukemic, 18: 8202
DNA synthesis in X-autosome translocations in, 19: 31788(R) (ORNL-3768(p.33-57))
DNA synthesis inhibition by AET and cysteamine in, 18: 19524
DNA-ase activity in urine of, 19: 28005
dysprosium oxide accumulation in lungs of, 18: 41062
edema in, radiometric analysis of 5-hydroxytryptamine-induced, using iodine-131, 18: 31268
effect of hematoporphyrin on radiosensitivity of rhabdomyosarcoma, 20: 40657
effect of radiomimetic substances on, effects of homologous or heterologous tissue transplants on, 20: 22784
effect of 5-methoxytryptamine and cystamine on myelogram of irradiated, 20: 42938
effects of AET on survival of irradiated tumor-bearing, 18: 43336
effects of AET, glutathione, and serotonin mixture on lysosome morphology in stem cells in, 20: 30964
effects of alkylating agents on lymphoid and myeloid leukemia incidence in, 20: 6788 (ORNL-P-1703)
effects of ancestral irradiation of, on morphology of bone marrow chromosomes, 18: 15812(R) (LAMS-3034(p.303-6))
effects of *Bacillus subtilis* preparations on radiosensitivity of, 20: 36673
effects of bacterial infection on skin homograft survival in, 18: 19511
effects of carbon tetrachloride poisoning on enzyme activity in, 19: 33770
effects of carbon tetrachloride on, carcinogenic, 20: 14373
effects of cesium-137 chronic ingestion on life span and reproduction of, 20: 38551
effects of colchicine and x radiation on intestinal mucosa in, comparison of, 20: 31082
effects of combined radiation and actinomycin D therapy on tumors, 20: 40762
effects of combined irradiation and surgical incisions on mortality of mice and rats, 20: 45498
effects of corticosteroids on immune reactions in, 20: 6893
effects of cortisone on amniotic fluid content in, 19: 17592
effects of cosmic-irradiated virulent tubercle bacilli on, 19: 99
effects of cosmic-irradiated tubercle bacilli on, 19: 100
effects of cystamine and serotonin on, pharmacological, 20: 38713
effects of cysteine and β-mercaptoethylamine on sorptive properties of irradiated tissues in, 16: 30258
effects of diet containing irradiated food on growth, life span, and tumor incidence in, 17: 41179(R) (NP-13181)
effects of diet containing irradiated beef on life span and reproductive performance of, 17: 40483(R) (NP-13169)
effects of diet containing radiation-processed foods on weight life-span, and tumor incidence in, 17: 40443(R) (NP-13182)
effects of diet on survival of dystrophic, 19: 3943
effects of dose-time factors on radiotherapy of skin damage, 20: 40764
effects of embryonic irradiation on adult life expectancy and pathology, 16: 25177(R) (TID-16129)
effects of epithelial cell graft on thymectomized, 19: 43883(R) (UCLA-12-565, pp 65-85)
effects of erythropoietin on erythropoiesis in, 19: 25983
effects of erythropoietin administration in, on stem-cell populations, 20: 42713(R) (UCRL-16246, pp 107-18)
effects of erythropoietin on erythropoiesis in transfused, 20: 45479
effects of estradiol on immune system and lymphatic tissue in adult and newborn, 20: 40577
effects of europium chloride on, pharmacology and toxicology of, 19: 31731
effects of free-radical-reaction inhibitors on leukemia in, 20: 8726
effects of free-radical-reaction inhibitors on radiation sickness in, 20: 8726
effects of gamma ray or proton irradiation on, following acceleration, 20: 42985
effects of heavy water on reproductive ability of, 19: 22287(R) (UCRL-11948)
effects of immune reactions on reticulo-endothelial function in, 20: 18190(R) (UCRL-16613)
effects of ingested deuterium oxide on sterility of, 20: 10550
effects of ingested deuterium on, pathological, 20: 30975
effects of injected ribonucleic acid or yeast autolysate on infections in irradiated, 16: 14574
effects of injected tryptamine on hemorrhagic syndrome in irradiated, 17: 25054
effects of injected x irradiated cystamine-treated ascitic cell and

normal tissue homogenates on mitotic activity in, 20: 5412
effects of injected tritium oxide on, pathological, 20: 38568
effects of injected sheep bone marrow in irradiated, 18: 43324
effects of irradiated foods in diet on carcinogenicity, 16: 32726(R) (NP-12089)
effects of irradiation of graft site on transplanted unirradiated tumors in, x, 18: 19695
effects of irradiated liver fluke cysts on fascioliasis immunity in, 19: 12901
effects of irradiated diet on, histopathological, 19: 15009 (AMRNL-279)
effects of irradiated spleen cells on immune response in, 19: 17538
effects of irradiated *Schistosoma japonicum* cercariae in, immunizing, 19: 43848
effects of irradiated *Schistosoma japonicum* cercariae on, 20: 12545(R) (PAEC(A)AR651)
effects of irradiated bacon lipids on, 17: 8499
effects of low barometric pressure on, protective effects of indolylalkyl- and mercaptoalkylamines against, 19: 27944
effects of MEA on formation of radioinduced peroxides in, 18: 6709
effects of merophan on tumor growth in, effects of thiols on, 20: 8517
effects of microbial antigens in radiation sensitized, 17: 30422
effects of muscular dystrophy on iodine-131 metabolism in, 19: 29717
effects of nitrogen mustards on, protective effects of mycelium-derived nucleotides against toxic, 20: 18452
effects of nitrogen mustard on, effects of thioglycollic acid derivatives on toxic, 20: 18474
effects of ozone on myocardial cell nuclei in, 18: 33334
effects of parabiosis on blood circulation, 16: 17372
effects of parabiosis on blood circulation, 16: 17373
effects of plutonium-239 in, pathological, 20: 60(R) (NYO-901-37, pp 33-68)
effects of prednisolone on distribution of mycobacterial vaccine in, 20: 10655
effects of pretreating newborn, on subsequent Rous sarcoma challenge, 20: 6825
effects of radiation sickness on alveolar macrophages and phagocytosis in, protective effects of zymozan against, 20: 35341
effects of radiation-processed fruits on, 20: 37156
effects of radiomimetic substances in, late somatic, 19: 10814
effects of radiomimetic substances on tumor-bearing, effects of drugs on, 20: 12717(R) (NP-15666)
effects of radiomimetic agents on tumor-bearing, effects of radioprotective drugs on, 20: 12718(R) (NP-15667)
effects of radiomimetic agents on tumors in, effects of drugs on, 20: 12719(R) (NP-15668)
effects of radiomimetic substances on tumors in, effects of radioprotective compounds on, 20: 18475
effects of radioprotective agents on alkylating agents in, 17: 35414
effects of radioprotective drugs on distribution of hemoglobin and neutral red in tissues of, 18: 17660
effects of radioprotective compounds on oxygen tension in, 18: 31295
effects of radioprotective compounds on, delayed toxic, 20: 18488
effects of ribonuclease and deoxyribonuclease on development of Ehrlich's ascitic carcinoma, 20: 42728
effects of shock and stress on survival of, effects of 19-nor-testosterone phenylpropionate on, 20: 38610
effects of space flight conditions on hematopoietic system, 17: 17772(T) (JPRS-18395(p.123-35))
effects of space flight conditions on, physiological, 20: 22623(T) (UCRL-Trans-1232)
effects of stress on reticulo-endothelial activity in, 20: 6700(R) (ORNL-3853, pp 183-207)
effects of stress on organic peroxide production, 17: 67
effects of radiomimetic substances on, late somatic, 17: 24971
effects of strontium-90 chronic ingestion on life span and reproduction of, 20: 38551
effects of sulfhydryl compounds on DNA synthesis in, tracer study, 20: 31125
effects of thio-TEPA on bone marrow in, protective effects of isogenic bone marrow infusion against, 19: 3840
effects of thiopentobarbital on oxygen tension in, 20: 38738
effects of thymectomy on neoplasm development in, exposed to polyoma virus, 19: 17450
effects of thymus on immune response to homografts in irradiated, bone-marrow infused, 18: 113
effects of thymus on tolerance response in, 20: 10632
effects of transplanted hematopoietic tissue on phosphatase activity in spleen and liver in, 17: 35314(R) (HW-76000(p.161-6))
effects of ultraviolet-irradiated linolenic acid extract on skin of, 19: 38366
effects of uranium poisoning on phosphatase activity in kidney of, 20: 8600
effects of uranyl nitrate in, toxic, 19: 33769
effects of uranyl nitrate poisoning on enzyme activity in, 19: 33770
effects of urethan on marrow and thymus injury in irradiated and non-irradiated mice, 19: 6919
effects of urethan on leukemia induction in, effects of thymectomy and thymus implantation on, 20: 35327
effects of uv irradiated benzopyrene on, carcinogenic, 19: 13114
effects of x rays in combination with acceleration and/or velocity on genetics in, 20: 42986
effects of 4-(*p*-dimethylaminostyryl)quinoline injections on liver of, 18: 8204
effects of 6-purinethiol on immune reactions to pneumococcal polysaccharides in, x, 20: 8716
effects on gonads, phosphorus-32, 17: 1247
efficiency of preserved bone marrow transplants in stimulating blood formation in, 20: 36546
electromagnetic wave effects on internal and sexual organs in, 17: 17833
electrophoresis of liver cell subfractions from, 19: 10698 (TID-20372)
elimination of cerium-144, iodine-131, thallium-204, zinc-65, and isotope mixtures by, effects of DTPA, pectin, and zirconium phosphate on, 20: 38733
enteric flora of, effects on infections during radiation sickness, 19: 31904(R) (NYO-2628-1)
enzyme activity in kidney of, after uranyl nitrate intoxication on, 18: 23213
epithelial cell distribution in, tracer study, 19: 31674(R) (ORNL-3768 (p.64-9))
erythrocyte catalase levels in, attempts at reduction of, 17: 33475(R) (ANL-6723(p.211-14))
erythrocyte chimerism and acquired immunologic tolerance in neonatal, 19: 43657
erythrocyte esterase content of, genetic factors affecting, 20: 6775(R) (ORNL-3853, pp 36-49)
erythropoiesis and lymphocytopoiesis in, role of splenic reticular cells in, 20: 12681
erythropoiesis in, effects of anoxia, 19: 31700(R) (ACRH-23(p.33-9))
erythropoiesis in, iron-59 tracer technique for measuring, 20: 8530
erythropoiesis in, tracer study, 20: 18304
erythropoiesis maintenance in marrow cultures from, 19: 45740
erythropoietic activity of spleen in lethally irradiated, effects of injected bone marrow on, 20: 18295(R) (UCLA-12-576, pp 27-56)
etiology of leukemia in, 20: 45367
etiology of Proteus bacteremia in irradiated, 18: 9867
etiology of Pseudomonas bacteremia in irradiated, 18: 9868
europium isotope effects on, 19: 39265(R) (IA-1021)
europium-152, -153, and -154 transfer to offspring during pregnancy and lactation, 20: 26618
excretion of iron salts, 16: 23871
fate of tumor cells injected into portal system, 17: 26974
fertility of artificially and normally ovulated, 18: 1325(R) (UCRL-10934)
fission neutron dosimetry in phantom, 20: 41268(R) (NYO-2740-3, pp 5-165)
foreign spleen reaction in, duration of donor sensitization to, 19: 31677(R) (ORNL-3768(p.119-30))
fractionation of bone marrow from, 18: 27211(R) (TID-20695)
gadolinium oxide accumulation in lungs of, 18: 41062
gamma counting of internally deposited radioisotopes in, whole-body, 18: 35838 (LF-14)
gamma dosimetry in phantom, 20: 41268(R) (NYO-2740-3, pp 5-165)
gamma exposure, lethal effects of, 17: 35597 (LADC-5549)
gamma lethal dosage determinations for, 17: 37138 (LADC-5747)
gastrointestinal transit time in, for ceramic spheres containing manganese-54 or uranium carbide particles, 20: 42740 (LA-DC-7764)
genetic effects of radiomimetic agents on fertility in, 18: 23177
genetic effects on hybrid antigenicity in, methods for demonstrating, 19: 31905(R) (ORNL-3768(p.99-108))
genetic factors causing anemia in, 19: 14934 (NYO-1800-2)
genetic factors in hereditary anemia in, 18: 13450(R) (TID-20205)
genetic factors in hereditary anemia in, 18: 13455(R) (TID-20231)
genetic factors in, 18: 27007(R) (ORNL-3601(p.83-91))
genetic factors involved in mosaicism in, 18: 29166 (ORNL-P-70)
genetic factors in, 19: 2072(R) (ORNL-3700(p.83-8))
genetics of oligosyndactylism and serum esterase patterns in, 19: 31788(R) (ORNL-3768(p.33-57))
glucose metabolism, tracer studies, 16: 11448(R) (ANL-6464(p.97-9))
glucose uptake by hypothalamus of, tracer study, 20: 10541
glutamine metabolism in, 19: 10745
glycoprotein content in liver and spleen of radiation chimera, with secondary disease after bone marrow transplants, 20: 45487
gold uptake by hypothalamus of, tracer study, 20: 10541
gold-198 distribution in skeletal tissue and synovia of, autoradiographic determination of, 17: 19759
grafting of spleen and thymus tissue in, runt disease induction by, 18: 38718

growth kinetics of epithelial and spindle cell tumors in, using autoradiography and tritiated thymidine, 19: 43698
growth of irradiated transplanted tumor cells in, 19: 36095
growth of transplanted tumors in, effects of feeding irradiated coliform bacilli on, 17: 4408
handling procedures for control of *P. aeruginosa* in radiobiological labs, 17: 30235
heart function in, effects of magnetic fields on, 19: 5598(R) (NYO-3291-1)
heart lesions induced in, by diet, etiology of, 17: 40484 (NP-13172)
hematology of White Oak Lake area, 19: 6931(R) (ORNL-3697(p.65-84))
hematopoiesis in, 19: 31699(R) (ACRH-23(p.21-32))
hematopoietic organs of, effects of acceleration and vibration on, 20: 33010
hematopoietic recovery in lethally irradiated, 20: 45322(R) (UCLA-12-595, pp 6-28)
hematopoietic stem cell reproduction in spleens of irradiated, 19: 7118
hematopoietic tissue distribution in, 19: 28066
hemoglobin amino acid structure of, 20: 6775(R) (ORNL-3853, pp 36-49)
hereditary anemia, etiology, 16: 9747(R) (TID-14999)
holmium-166 distribution in, 18: 31087
homograft immunity in γ-irradiated, effects of methotrexate on, 20: 29035
homograft tolerance induction in sublethally irradiated chimeras, 17: 38749 (USNRDL-TR-668)
homotransplantation antigens in hemopoietic tissues of, 17: 30246
housing of, 17: 7746(P)
humoral immunity of, effects of irradiated cercariae of *Schistosoma mansoni* on, 19: 7121
hybrid spleen cells of, induced immunological tolerance in parental strain, 20: 40651
hypobaric oxygen respiration in, design of exposure chamber for, 20: 5228(R) (AD-623599, pp 28-36)
immune reactions in, role of hematopoietic system in, 18: 15705 (TID-20107)
immune reactions in spleen of, effects of age on, 18: 27065(R) (ORNL-3601(p.98-104))
immune reactions in, 19: 2003 (ORNL-3700(p.89-94))
immune reactions in radiation chimeras, role of thymus, 19: 17504
immune reactions in radiation chimeras, role of thymus, 19: 17505
immune reactions in inbred, 19: 26109(R) (ORINS-49(p.40-62))
immune reactions in, 19: 29883 (ACRH-103(p.1-27))
immune reactions in, 19: 29838
immune reactions in, effects of antigen dose and number on primary, 19: 31676(R) (ORNL-3768(p.112-18))
immune reactions in hemocytoblasts of, morphological effects of, 19: 31905(R) (ORNL-3768(p.99-108))
immune reactions in cultured spleen from irradiated, treated with rat bone marrow, 20: 5397
immune reactions in, effects of Thorotrast on, 20: 10617
immune reactions of, to injected spleen homogenates, 18: 43116 (ORNL-P-274)
immune reactions of transplanted spleen cells in irradiated, 19: 3905
immune reactions to injected hematopoietic tissue in irradiated, 17: 5802
immune reactions to tritiated antigens in, 18: 11573(R) (TID-20106)
immune reactions to bone marrow transplants in, 19: 8785 (EUR-1607.e)
immune reactions to transplanted antigen-stimulated human lymph node and spleen cells, 19: 17446
immune reactions to gamma-irradiated *Brucella melitensis* vaccine, 19: 22019(R) (UCLA-12-541(p.51-91))
immune reactions to bone marrow grafts in, 19: 22075
immune reactions to liver flukes in, 19: 21962
immune reactions to bone marrow grafts, 19: 25909 (ORNL-P-1211)
immune reactions to spleen transplants in, 19: 25885
immune reactions to *Pastuerella tularensis* vaccine from irradiated bacteria, 19: 25971
immune reactions to bone marrow grafts in, effects of steroids on, 19: 33728
immune reactions to injected bone marrow in irradiated, 19: 42349(R) (NP-15345)
immune reactions to injected bone marrow in irradiated, 19: 42350(R) (NP-15346)
immune reactions to injected fetal liver in, effects of folic acid antagonist on, 19: 42351(R) (NP-15347)
immune reactions to Brucella vaccine prepared from irradiated bacteria, 19: 45868
immune reactions to virus-induced transplanted leukemias in, 20: 3694
immune reactions to injected bone marrow in, 20: 6784(R) (ORNL-3853, pp 118-27)
immune reactions to antigens in, effects of age on, 20: 16159(R) (ORNL-3900, pp 150-81)
immune reactions to irradiated Schistosoma cercariae, 20: 42947
immune response of, to gamma-irradiated tubercle bacilli, 18: 15824
immune response of thymic grafts in irradiated, 18: 41147
immune response to injected spleen cells in irradiated, 18: 9831(R) (AD-403109)
immune response to transplanted tumors in, following x-radiation cure of previously transplanted tumors, 20: 40643
immunity in irradiated and urethan-treated, role of thymus in recovery of, 17: 10412
immunity in, effects of actinomycin on, 19: 31678(R) (ORNL-3768 (p.137-45))
immunity in, effects of fetal liver and thymus on, 20: 8718
immunity to myxofibrosarcomas after serial passage in, 20: 40502(R) (ORNL-3922, pp 115-27)
immunity to *Schistosoma mansoni* in, effects of injections of irradiated cercariae on, 17: 28733
immunity to sequentially administered antigens in, antinomycin effects on, 19: 31681(R) (ORNL-3768(p.164-76))
immunity to transplanted leukemia viruses in, 20: 40502(R) (ORNL-3922, pp 115-27)
immunization by irradiated Sarcoma I ascites tumor, 16: 25108
immunization of, against *Schistosoma japonicum* by inoculation with irradiated larvae, 18: 15890
immunological characteristics of radiation chimeras in, 20: 35302
immunological competence of cells in, 20: 8530
immunological reactions to skin homografts, 17: 15758
immunological tolerance to skin homografts, effects of irradiation and injection of donor-type spleen cells, 17: 96
immunological tolerance in radiation chimeras, 17: 15759
immunoresistant sarcoma cells in, 20: 10634
incorporation of tritium labeled amino acids into cell nuclei of, 17: 31887
induced by desoxyribonucleic acid and virus in, 19: 22019(R) (UCLA-12-541(p.51-91))
infection with irradiated Schistosoma cercariae, 18: 5113
infection with mousepox, effects of deuterium oxide on, 17: 10285
infection with *Pseudomonas aeruginosa*, method for detection of, 16: 31388(R) (ANL-6535(p.28-32))
infections in, control measures for, 19: 30013 (ACRH-103(p.104-20))
infectivity of Gross and Rauscher leukemia viruses and their nucleic acids, 20: 45511(R) (UCLA-12-595, pp 33-66)
inflammatory cells in, origin and fate of, 16: 17400
ingestion of irradiated *E. coli* by, effects on carcinomas, 18: 6
inhalation of carbon-14-labeled carbon dioxide by, design of nonrecirculating apparatus for, 18: 38772
inhalation of neodymium oxide aerosol by, 20: 1593 (COO-1170-4)
inoculation of, with influenza virus, aerosol, 20: 6700(R) (ORNL-3853, pp 183-207)
intestinal bacteria of, effects of diet on, 19: 29889(R) (ANL-6971 (p.90-116))
intestinal histamine content in, effects of radioprotective sulfur compounds on, 18: 38770
intestine homogenates from irradiated, effects on tumors of, 19: 31813
iodine isotope uptake by vibrissal hairs of, 19: 19479
iodine metabolism, tracer study, 17: 15588 (LADC-5209)
iodine metabolism by thyroid, effects of age, 19: 25865
iodine-131 concentration by submaxillary glands, effects of sex, 17: 1202
iodine-131 concentration by submaxillary glands, effects of sex, 17: 1203
iodine-131 retention and excretion, 16: 1321(R) (LAMS-2627(p.183-9))
iodine-125 distribution in thyroidal colloids of, 18: 38767
iodine-125 localization in thyroid gland of, 18: 17450
iodine-125 metabolism in thyroid gland of, 19: 44
iodine-131 and propylthiouracil response in, effects of age on, 18: 17434
iodine-131 distribution in tissues of, effects of carnitine on, 18: 11562
iodine-131 distribution in, whole-body autoradiographic study of, 18: 27035
iodine-131 effects on thyroid gland of, pathological, 20: 62(R) (NYO-901-37, pp 74-9)
iodine-131 metabolism by thyroid gland of, effects of thiocyanates on, 19: 12929
iodine-131 metabolism in, 19: 33771
iodine-131 metabolism in, effects of thiouracil diet on, 19: 38350
iodine-131 retention in, specificity of inhibitor reduction of, 19: 25888
iodine-131 uptake by thyroids during estrus cycle in, 18: 11605
iodine-131 uptake by blood plasma, liver, muscles, renal organs, and skin of, 18: 33251
iodine-131 uptake by submaxillary glands of, 18: 38766
iodine-131 uptake by salivary glands of, effects of thyroidectomy on, 18: 43191
iodine-131 uptake and elimination from thyroid of, effects of potassium iodide and thiouracil on, 20: 38734
iodine-131 uptake by melanomas in, 18: 3489(R) (COO-228(p.127-31))
iron-59 uptake by spleens of, determination of marrow transplant efficiency using, 18: 31090
iron-59 uptake by skin of, from bath water, 20: 28892
irradiation facility for, design of remote-control, 17: 37034

kidney lesions induced by uranyl nitrate in, microstructural, 18: 23214
labeling sperm of, with tritium, 20: 26593
lens development as cause of malformations of anterior optic segment in, born from x-ray exposed females, 19: 171
leukemia in, cell-free transmission of chemical and radioinduced, 17: 40599
leukemia in, treatment with cerebrospinal axis x irradiation combined with chemotherapy, 18: 29476
leukemia in, variations in virus-induced, 18: 38824
leukemia incidence in, effects of thymus, lymph system, and desoxyribonucleic acid on, 17: 35340(R) (UCLA-515(p.55-73))
leukemia incidence in, effects of x radiation and radiomimetic substances on, 17: 40630
leukemia induced by cell-free extract, 17: 77
leukemia induction in, effects of x radiation and leukemogenic agent extracts on, 17: 22985
leukemia induction in, by tissue homogenates or cell-free extracts from irradiated mice plus urethan, 17: 40629
leukemia induction in, by irradiated virus-containing tissue extracts, 19: 7047
leukemia induction in, role of desoxyribonucleic acid, radiation, thymus, and viruses in, 19: 22019(R) (UCLA-12-541(p.51-91))
leukemia induction in, growth and properties of cells from, 19: 43883(R) (UCLA-12-565, pp 65-85)
leukemia transplantation in, 19: 33876
leukemia treatment in, use of whole-body x irradiation and bone marrow transplants for, 20: 1700
leukemia treatment in, use of whole-body x irradiation and hematopoietic tissue transplants for, 20: 1701
leukemic treatment in, using nitrogen mustard and radioprotective compounds, 19: 8962
leukemogenesis in newborn, effects of bone marrow injections on urethan-induced, 20: 18191
leukemogenesis in newborn, effects of thymectomy and subsequent thymus implantation on urethan-induced, 20: 18192
leukocyte colony formation in spleen of, effects of bovine-leukopoiesis-stimulating factor on, 20: 42708(R) (TID-22931)
leukocyte count, strain differences, 17: 7837
life span of, 19: 45809(R) (NYO-1979-12)
life span of irradiated, effects of chemical radioprotective compounds, 17: 23085(R) (NP-12760(p.77-91))
life span of 21 inbred strains of, 18: 41094(R) (TID-21156)
life-span of tumor-bearing, effects of tissue homogenates from irradiated rabbits on, 19: 7132
lipid content in livers of, effects of tissue hydration on, 20: 14268
liver enzyme release in, effects of endotoxin tolerance, cortisone, and Thorotrast on, 18: 4956
liver response to syngenic and xenogenic tissue transplants, 20: 10505(R) (BNWL-122, pp 146-9)
longevity in, agents effecting, 17: 33754
lutetium-177 distribution and dose calculations in, 18: 35
lymphomas in, antigenic characteristics of virus-induced, 20: 28873
malignancy in, effects of tumor grafts on, 20: 24829(R) (NEIC-RR-17)
mammary tumors in, treatment with bone marrow transplants, 20: 22534
manganese-54 uptake in female, 18: 20
manganese-52 metabolism in, 18: 17452
manganese-52 uptake by, effects of age on, 18: 17453
manganese-54 excretion by, effects of temperature on, 18: 43173(R) (LA-3132-MS(p.32-6))
manganese-54 metabolism in, 18: 15767(R) (LAMS-3034(p.49-52))
manganese-54 metabolism in, 18: 43172(R) (LA-3132-MS(p.25-31))
manganese-54 metabolism in, 20: 36554 (LA-DC-7305)
marrow transplants in, factors affecting survival of, 19: 31905(R) (ORNL-3768(p.99-108))
mercaptopropylamine distribution and elimination in, carbon-14-labeled-, 18: 33373
metabolic disturbances in irradiated, given bone marrow transplants, 19: 2079 (ORNL-P-656)
metabolic patterns during spontaneous carcinogenesis, 16: 8527(R) (ACRH-16(p.54-61))
metabolism in, effects of cystamine on, 20: 18240
metabolism of AET in, 20: 24830
metabolism of aminoethylisothiuronium in, 19: 12914 (SGAE-BL-6/1964)
metabolism of aminoethylisothiuronium in irradiated, normal, and tumor-bearing, 19: 43867
metabolism of ascites tumors in, effects of x radiation and alkylhydrogen peroxides on, 18: 29515
metabolism of calcium, phosphorus, and strontium in bones of, triple tracer method for, 19: 31780
metabolism of carbon-14-labeled methyl palmitate in reticulo-endothelial system in, 20: 14241 (TID-21437)
metabolism of cysteamine in, 19: 12914 (SGAE-BL-6/1964)
metabolism of desoxyribonucleic acid in, tracer study using tritiated thymidine, 19: 38336 (TID-21106)
metabolism of injected gold in brain of, tracer study, 19: 33760
metabolism of iodine-131 in, effects of strain, 16: 31460
metabolism of iodine-125 in thyroid gland in, autoradiography of, 17: 35423
metabolism of iodine in, effects of chlorpromazine, tracer study, 20: 3677
metabolism of iodine, thyroxine, and triiodothyronine in, autoradiography of, 20: 36570
metabolism of manganese-54 by tissues of, retention functions for, 20: 45296
metabolism of methionine in, tracer study, 20: 3661 (NP-15594)
metabolism of normal and tumor-bearing, GED and MEG, 20: 8585
metabolism of promethium-147 in, after inhalation of chloride aerosols, 20: 6747
metabolism of selenium-75-labeled-L-selenomethionine by, 20: 26633
metabolism of strontium-85, -89, and -90 in live, design of radiation detectors for measuring, 20: 36556
metabolism of sulfur-35-labeled mercapto group in, 18: 43312
metabolism of tritiated thymidine to produce labeled desoxyribonucleic acid, 18: 43569
metabolism of tritium-labeled thymidine in, 20: 42738(R) (ANL-7136, pp 255-65)
metabolism of zinc-65, effects of whole-body irradiation, 16: 42
metabolism of zinc-65, effects of whole-body irradiation, 16: 5209
metabolism of 2-mercaptoethylguanine in, tracer study of, 19: 8966
metabolism of, genetic factors, 19: 29849(R) (ANL-6971(p.1-28))
methionine metabolism in, tracer study, 19: 32067
methionine metabolism in, 20: 3661 (NP-15594)
mitosis in duodenal crypt cells of germ-free, tracer study, 19: 2032
mitosis in skin of, effects of strain on induced, 17: 28755
morphology of brown fat tissues in, effects of age on, 20: 6696(R) (ORNL-3853, pp 66-77)
mortality in short-duration overpressures, 16: 20864(R) (DASA-1242)
mortality in, effects of injections of irradiated Ehrlich ascites tumors on, 18: 13555
muramidase activity in kidneys of, 19: 31906(R) (ORNL-3768(p.179-80))
mutants of, breeding of acatalasemic and hypocatalasemic, 20: 42837(R) (ANL-7136, pp 124-40)
mutation frequency in, spontaneous, 19: 31791(R) (ORNL-3768(p.89-93))
mutation processes in, 19: 21807
mutations in house, natural, 18: 19483(R) (TID-20391)
mutations induced by DNA in, methods for testing, 20: 40627(R) (ORNL-3922, pp 84-8)
mutations of Ehrlich ascites tumors of, isolation of ploidy, 19: 10725
mutations of, rate for sex-linked recessive lethals in, 18: 17466(R) (ANL-6790(p.84-6))
myeloid leukemia virus of, reproduction and growth of, in tissue culture, 18: 4929(T) (AEC-tr-6161)
myeloid leukemia virus in, action and properties of, 18: 4928(T) (AEC-tr-6160)
neodymium oxide inhalation by, pathogenetic study of, 18: 25078
neoplastic lesions in mammary glands of, chemically induced, 20: 20502
nervous system of, effects of curare alkaloids on, 19: 31777
neutron dose linear energy transfer in phantoms simulating, 18: 38725
neutron dosimetry in, 18: 38732
neutron lethal dosage determinations for, fast, 17: 33487(R) (NP-13010(p.66-73))
neutron reactions in soft tissues of, effects of element composition on kerma, 20: 3708 (CEA-R-2833)
neutron relative biological effectiveness in, from deuteron reactions with tritium, 18: 31148
nitrogen balance in normal and irradiated, 18: 27209(R) (ORNL-3601(p.116-27))
nitrogen mustard effects on, protective effects of AET against, 18: 11881
non-H-2, isoantigen in, characterization of, 19: 31788(R) (ORNL-3768 (p.33-57))
nucleic acid and radiation effects on chromosomes aberrations in, comparison, 18: 33309
nucleic acid metabolism in tumor cells from, effects of tritium on, 18: 23215
of bis(2-guanidoethyl)disulfide chemical nature and distribution in, 17: 23066
ossification in, effects of estrogen on endochondral, 20: 22853(R) (ANL-7060)
oxidation-reduction in tissues of, 18: 19680
oxygen consumption in, effects of 2,4-dinitrophenol on, 19: 13099
oxygen level in brain of, effects of amino and sulfur compounds on, 18: 9930
ozone effects on x-irradiated erythrocytes in, 18: 19538
p-aminopropiophenone metabolism and excretion by, 17: 33486(R) (NP-13010(p.55-65))

parasite infestations in, effects of treatment with organic phosphates, 18: 27209(R) (ORNL-3601(p.116-27))
parasitic infections of, 20: 42854(R) (TID-23127)
parental isoantigens in hybrid, 18: 43224 (ORNL-P-346)
particle passage into diaphragmatic lymphatics from peritoneal cavity of, role of endothelial cells in, 20: 16
pathological effects of injected strontium-90, 16: 21953
pathological effects of injected strontium-90, 16: 31479 (A/AC.82/G/L.789)
pathological effects of strontium-90 in, 16: 32692 (TID-16796)
pathological effects of space flight on internal organs, 17: 17773(T) (JPRS-18395(p.136-47))
pathological effects of 2-aminothiazolidine-4-carboxylic acid alone or with bone marrow in irradiated, 18: 11845(R) (NP-13555(p.84-95))
pathological effects of injected radium-226 in, 18: 17464(R) (ANL-6790 (p.26-30))
pathological effects of inhaled radon in, 18: 17480 (UR-624)
pathological effects of injected plutonium in, effects of DTPA treatment on, 18: 17631(R) (ANL-6790(p.87-91))
pathological effects of subcutaneous rare earth metal implants in, 19: 38334 (COO-1170-1)
pathological effects of inhaled gadolinium oxide in, 19: 42242 (COO-1170-6)
pathological effects of cortisone in, effects of age on, 19: 45808(R) (NYO-901-36)
performance capacity of, effects of adrenalectomy on, 19: 45823(T) (JPRS-31933, pp 1-5)
phagocytic activity of reticulo-endothelial system in, effects of lipids on, 18: 8208
pharmacological effects of thiuronium compounds on blood pressure, gut, and respiration in, 17: 1349
pharmacological effects on tumors in, of sulfhydryl-containing boron hydrides, 20: 38745(R) (NYO-3267-3)
phosphatase activity in kidney and liver of, 18: 13421
phosphatide metabolism in liver of, effects of carbon tetrachloride on, tracer study, 19: 8744
phosphorus-32 uptake by phospholipids in liver and spleen in irradiated and normal, 17: 4419
phosphorus-32 removal from bones of, by ionic phosphate, 20: 8575
phosphorus-32-labeled colloid distribution in, 20: 8908
photoperiodism effects on mitosis in cartilage of, 19: 1992
physiological effects of AET in, 18: 13563(R) (TID-20236)
physiological effects of dimethyl sulfoxide in, 18: 13563(R) (TID-20236)
physiological effects of injected glucose oxidase in, 19: 6940(R) (ANL-6906(p.81-4))
physiology of appetite inhibition and obesity in, tracer study, 20: 10541
physiology of immune reactions, serum albumins, and esterase in, 19: 2068(R) (ORNL-3700(p.34-57))
physiology of thymus tissues in, 20: 18509(R) (UCLA-12-576, pp 61-80)
pituitary hormones in, effects of iodine-131 and goitrogens on, 19: 45808(R) (NYO-901-36)
placental transfer of calcium and fluoride in, tracer study, 19: 35897
plasma enzyme levels in, during Riley virus infection, 20: 45252
plutonium carcinogenicity and metabolism in, 20: 42997(R) (ANL-7136, pp 191-204)
plutonium distribution in bone and reticuloendothelial tissues of, 20: 42997(R) (ANL-7136, pp 191-204)
plutonium injection, mortality and tumor incidence after, 16: 11443(R) (ANL-6464(p.82-4))
plutonium metabolism in blood plasma and tissues in, effects of desferrioxamine B-methanesulfonate on, 19: 8769
plutonium metabolism in, 19: 12926
plutonium poisoning in, effects of diethylenetriaminepentaacetic acid on, 19: 6941(R) (ANL-6906(p.90-1))
plutonium poisoning in, therapeutic measures for, 19: 29994(R) (ANL-6971(p.206-14))
plutonium uptake by bones and liver of, protective effects of diethylene-triaminepentaacetic acid against, 18: 23350(R) (ANL-6823(p.105-8))
plutonium-239 distribution in, autoradiography of injected, 17: 10260
plutonium-239 effects on bones of, carcinogenic, 20: 40745(R) (NYO-901-54, pp 29-47)
plutonium-239 removal from, using calcium salt and pentaethyl ester of carboxymethyliminobis(ethylenenitrilo)tetraacetic acid, 18: 23369
pneumonia incidence in laboratory, 20: 12545(R) (PAEC(A)AR651)
polonium removal from, effects of lagochiline on, 18: 33412
polonium-210 distribution and excretion by, 19: 2052
polycythemia induction in, by confinement in silicone rubber cages, 20: 40718(R) (ORNL-3922, pp 99-105)
polycythemic, effects of testosterone on erythropoiesis in, 19: 14952(R) (ACRH-22(p.48-52))
potassium metabolism in, comparison with other mammals, 20: 42768
praseodymium-143 metabolism and distribution in, following injections, 19: 6979
praseodymium-143 metabolism after inhalation as aerosol, 18: 19544
procaine activity in, effects of deuterium oxide on, 17: 33519
production of acatalasemic, requirements for, 18: 43208
promethium-147 distribution in tissues of, 20: 8579
promethium-147 distribution in tissues in, after intraperitoneal and intravenous injection, 20: 35236
promethium-147 metabolism in, effects of [(carboxymethylimino)bis-(ethylenenitrilo)]tetraacetic acid on, 20: 35235
protection against lethal effects of x rays by inorganic condensed phosphates, 16: 4069
protection against radiation injury, effects of AET and 5-HT on, 17: 35340(R) (UCLA-515(p.55-73))
protection against radiation injuries in, evaluation of 23 chemical compounds for, 18: 23354(R) (NP-13918(p.58-74))
protection against radiation injuries in, evaluation of chemical compounds for, 18: 23355(R) (NP-13918(p.75-98))
protection against chemical carcinogen in, with bone marrow injection, 18: 27008(R) (ORNL-3601(p.146-51))
protection against whole-body radiation, chemical, 16: 25252 (TID-16160)
protection from post-irradiation leukemia transplantation by radio-immunization, 16: 1312(R) (LAMS-2627(p.117-20))
protective effects of serotonin antagonist against radiation injuries in, 18: 110
protein synthesis in bones of, tracer study of, 19: 2001 (BNL-8471)
Pseudomonas aeruginosa in, occurrence of, 17: 35380
pulmonary absorption and retention of inhaled cerium-144 particles in, effects of sodium phosphate aerosols on, 18: 29371
purification of histocompatibility antigens, 16: 26859
radiation absorption by bone marrow in, relative biological effectiveness of gamma and x, 16: 17517
radiation and alkylating agent effects on immunologic disorders in, hypothesis on, 19: 17507
radiation and chemical effects on treatment of chronic homologous disease in, 19: 9042
radiation and chemical effects on genetic properties of strain L cells of, 19: 12996
radiation and cytostatics effects on desoxyribopolynucleotides in tissues of, 18: 11687
radiation and fasting effects on plasma lipids in, 20: 3604
radiation and hydrogen peroxide effects on tumor development in, 19: 15027
radiation and hyperimmune liquid effects on immunity transfer to sarcoma I homografts in newborn, 19: 17574
radiation and radiomimetic-substance effects on age-specific death rates in, gamma, 17: 33756
radiation and surgical effects on tumor recurrence in, injected with irradiated cells, 17: 28734
radiation and tetanus effects on, protective effects of bone marrow cells against, 17: 38802
radiation and thymectomy effects on response to tumor transplants of, 19: 21896
radiation and transplantation effects on antibody formation in, 17: 30399
radiation and urethane effects on virus-induced leukemogenesis in, 18: 36988
radiation and urethan effects on leukemia development in, transmissible factor in, 19: 7025
radiation and vibration effects on bone marrow cells of, 19: 17494(T) (FTD-TT-64-1316(p.205-16))
radiation chimera of, effects on skin grafts, 17: 33675
radiation chimeras, lysozyme activity of kidneys, 17: 31919
radiation chimeras, leukemia incidence and life span of homologous, 17: 40680
radiation chimeras in two closely related strains of, stability of, 18: 8057
radiation chimeras, amino acid metabolism in, 18: 13390(R) (ORINS-43)
radiation chimeras of, immune reactions to skin grafts and specificity of gamma globulins in allogenic, 18: 17411 (USNRDL-TR-709)
radiation chimeras in, effects of fetal thymus cell transplantation on, 18: 19766
radiation chimeras from hamsters in, 18: 31191
radiation chimeras, immune reactions in, 19: 10797
radiation chimeras, effects of irradiation of incompatible donors on survival of, 19: 13063
radiation chimeras in, role of lymph system in hematopoietic recovery in, 19: 15218
radiation chimeras in, effects of bone marrow and spleen cells on colony-forming units in, 19: 17679
radiation chimeras, abnormal immune mechanism in allogenic, 19: 36074
radiation chimeras in, immunologic role of thymus in, 19: 38451
radiation chimeras in, mortality from secondary disease in, 19: 45910
radiation chimeras of, effects of bone marrow transplants on, 20: 6907(R) (EUR-2511.e)
radiation chimeras, investigation of eosinophil origin in, 20: 32972

radiation chimeras, nitrogen balance in, 20: 38636
radiation chimeras in, effects of antigen excess on immunological tolerance of, 20: 42730
radiation chimeras, effects of bone marrow injections on immune reactions and metabolism in, 20: 42854(R) (TID-23127)
radiation-conditioned behavior, effects of habituation to laboratory and radiation procedures, 16: 16266
radiation contamination of milk of lactating, effects on growth of suckling young and mammary glands, 19: 6963
radiation damage, reliability of sex-ratio method for estimating, 16: 5218 (A/AC.82/G/L.671)
radiation dosage determinations, 16: 11466 (USNRDL-TR-550)
radiation dosage determinations, lethal, 16: 21898 (AF-SAM-61-5)
radiation dosage determinations, effect of dose rate on lethal, 16: 21971
radiation dosage schedules for, model for lethal, 18: 11646 (TID-13635)
radiation dose effects on recurrent tumor, x, 20: 43035
radiation dose measurements for, lethal, 18: 25165
radiation dose rate effects and significance in survival time curves, 16: 4405 (UCLA-455)
radiation dose-rate and fractionation effects on mutations in, 18: 3569
radiation dose to gonads of, beta, 18: 23185(R) (ANL-6823(p.76-80))
radiation dose to mammary tumors of, methods for determination of, 19: 26077
radiation dose, effects of dose rate on lethal, 17: 80
radiation dosimetry in, phantom depth dose studies of, gamma and neutron, 20: 5286 (CONF-650616-16)
radiation effects from acute and chronic neutron and gamma exposure of, 18: 17568
radiation effects from high-energy protons on reproductive capacity of male, effects of chemical protective agents against, 18: 6694
radiation effects from internally deposited beta particles on gastrointestinal tract in, 18: 105
radiation effects from polonium-210 on spermatogenesis in testes of, 20: 31063
radiation effects on, 17: 25030
radiation effects on, 19: 45990
radiation effect on life span of, inhaled plutonium-239, 17: 35307(R) (HW-76000(p.115-17)
radiation effects and lethal dosage determinations for, fission-neutron, 17: 37138 (LADC-5747)
radiation effects combined with lipoxidase on mortality of, 17: 17921
radiation effects combined with antibiotics on leukemia in, therapeutic, 17: 23223
radiation effects combined with actinomycin D on skin and tumors on, therapeutic, 17: 28741
radiation effects combined with silicon dioxide on liver of, alpha, 18: 41156
radiation effects combined with spleen injections on blood system and organs in, 19: 8833
radiation effects combined with splenectomy and thymectomy on skin homotransplantation in, 19: 29982
radiation effects combined with spleen cells and thymus grafts on graft tolerance in, 19: 29983
radiation effects combined with bone marrow and thymectomy on skin grafting in, 19: 29984
radiation effects combined with acceleration or vibrations on mitosis in marrow cells of, x, 20: 18439
radiation effects combined with urethan on tumor-resistant strain, x, 20: 42873
radiation effects, damage sequence in brain, 16: 23481
radiation effects, effects of diet, 16: 14464(R) (NP-11359(p.106-23))
radiation effects, efficiency of radioprotective agents as function of oxygen inhaled and in tissues, 16: 30229
radiation effects, genetic, 19: 28076
radiation effects, genetic, 19: 33957
radiation effects, genetic, 17: 14036
radiation effects, genetic, 17: 20270
radiation effects, genetic, 17: 28682(R) (TID-18992)
radiation effects, hematological factors, 16: 23(R) (TID-13432)
radiation effects, high-energy-proton, 18: 13448(R) (ORNL-TM-720)
radiation effects in, similarity to aging of, 16: 17501
radiation effects in fetus after male exposure, protective effects of S-β-aminoethylisothiuronium against, 16: 25211
radiation effects in, protective effects of hypoxia against x, 17: 30346
radiation effects in, protective effects of chemical protective compounds on, 18: 5138(R) (NP-13281(p.115-23))
radiation effects in progeny of, after gonad exposure, 18: 6621(R) (UCSF-23)
radiation effects in, genetic, 18: 6673
radiation effects in, genetic, 18: 6672
radiation effects in cerebellum of, 18: 15830
radiation effects in, fractional-dose, 18: 17624
radiation effects in, lethal, 18: 23245 (UR-654)
radiation effects in, 18: 27068(R) (ORNL-3601(p.128-45))
radiation effects in, genetic, 18: 27007(R) (ORNL-3601(p.83-91))
radiation effects in, RBE effects of fast neutrons for late somatic, 18: 41232
radiation effects in, genetic, 19: 5681
radiation effects in, late somatic, 19: 10814
radiation effects in, electron beam, 19: 12965
radiation effects in, hematological, 19: 27955
radiation effects in, lethal, 19: 45982
radiation effects in, protective effects of chelated complexes against gamma, 20: 1692
radiation effects in, mechanism for leukemogenic, x, 20: 3696
radiation effects in producing lymphomatoses of thymic origin in various strains of, x, 20: 36613
radiation effects in, mathematical model of lethal, 17: 35601(R) (TID-19324)
radiation effects, lethal, 18: 8101 (BNL-7603)
radiation effects of bacterial endotoxin sensitivity in, 18: 33370
radiation effects of chronic, low-dose gamma exposure, 17: 15686
radiation effects of daily doses, effects of liver shielding, 16: 14462(R) (NP-11359(p.86-96))
radiation effects of fast neutrons and x rays on gonads of, 17: 31891
radiation effects of fractionated x-ray doses on embryonic development in, 18: 19719
radiation effects of heavy charged particles on skin of, 18: 15827
radiation effects of implanted cobalt-60 pellets in, biological, 20: 58(R) (NYO-901-37, pp 14-30)
radiation effects of mutation rates in, x, 20: 20461
radiation effects of thyroid cells in, protective effects of anoxia against, 20: 10710
radiation effects of whole-body doses on mitotic activity of shielded cornea, indirect, 17: 30392
radiation effects on aging and behavior, 16: 16269
radiation effects on acute mortality in female, backscatter and beam direction, 16: 17495
radiation effects on ability to withstand cold stress, 16: 17502
radiation effects on antibody formation by spleen cells in, 16: 20274
radiation effects on antibody-forming cells, 16: 20273
radiation effects on adrenal glands and hormones, 16: 30297
radiation effects on age specific mortality rate of female, effects of estrogen on, 17: 1301
radiation effects on aging in, 17: 4418
radiation effects on active and passive immunity to bone marrow transplantations in, 17: 5916
radiation effects on antibody formation, 17: 10255(R) (TID-17648)
radiation effects on ascites tumors and testis in, fast neutron and x-ray, 17: 12143
radiation effects on antibody responses to influenza virus in, 17: 14043
radiation effects on aging in, 17: 15726
radiation effects on antibody cell response to antigens in radiochimeras in, 17: 17871
radiation effects on aging of, whole-body, 17: 19815
radiation effects on amyloidosis development in, injected with casein, 17: 25046
radiation effects on amino acid content in tissues of, 17: 30377
radiation effects on activity of proteolytic enzymes in spleen in, 17: 33631
radiation effects on activity of skin tyrosinase in, gamma, 17: 37095
radiation effects on anesthetized, x, 18: 3545
radiation effects on amino acid content in blood of, x, 18: 11718
radiation effects on anlage of anterior limbs of embryos of, cultivated *in vitro*, gamma, 18: 13538
radiation effects on adrenal morphology and function in, local and whole-body exposure, 18: 17627
radiation effects on aging and kidney function in, x, 18: 23291
radiation effects on audiogenic seizure in, gamma, 18: 25206
radiation effects on amino acid decarboxylase activity in liver and spleen, 18: 31195
radiation effects on adrenal glands of, gamma, 18: 33367
radiation effects on autotransplants of mammary adenocarcinomas in mouse, 19: 7041
radiation effects on amino acid content in kidneys and liver of, whole-body, 19: 7149
radiation effects on adrenal cortex mitoses in, comparison of detoxified snake venom effects with, 19: 8814
radiation effects on acid deoxyribonuclease activity in spleen and thymus in, 19: 10895
radiation effects on anaerobic glycolysis in spleens of, x, 19: 13070
radiation effects on antibody formation in spleen cells in recipient, 19: 17546
radiation effects on amniotic fluid content in, 19: 17592
radiation effects on ability to withstand critical acceleration, proton, 19: 21936

radiation effects on antibody formation in, 19: 24301
radiation effects on acid deoxyribonuclease activity in spleen and thymus of, whole-body x-ray, 19: 24345
radiation effects on anemia development in splenectomized, injected with spleen cells, 19: 25986
radiation effects on antitumor factors in, 19: 31813
radiation effects on antitumor factors in, 19: 31814
radiation effects on AET distribution in organs of, factors affecting, 19: 33977
radiation effects on antibody production by transferred spleen cells in, 19: 45986
radiation effects on alkaline phosphatase production in bones of, 19: 45729(R) (NYO-910-23, pp 1-111)
radiation effects on antibody formation in, injected with sheep erythrocytes, 20: 1661
radiation effects on amino acid excretion in urine of, β, 20: 10582
radiation effects on antibodies in, gamma, 20: 12631 (CEA-R-2776)
radiation effects on activity of lipolytic enzymes in, x, 20: 14279
radiation effects on acid and alkaline phosphatases in tibiae of, x, 20: 32943
radiation effects on acetyl coenzyme A content in liver in, whole-body, 20: 33024
radiation effects on adrenal, spleen, and testes weights in, neutron and x, 20: 33068
radiation effects on antibody production in, x, 20: 40626(R) (ORNL-3922, pp 80-3)
radiation effects on adaptation to incompatible bone marrow, 16: 20282
radiation effects on audiogenic seizures, low-level gamma, 16: 32801
radiation effects on brain, histochemical studies, 16: 16276
radiation effects on blood picture and organ weight in, fractionated-dose, 17: 7819
radiation effects on blood vessels in conjunction with high-fat diets, 17: 13974(R) (NP-12484(p.63-93))
radiation effects on blood picture, effects of bone marrow injections, 17: 13985(R) (TID-18018)
radiation effects on behavior, focal deuteron exposure of central nervous system, 17: 13963 (BNL-6186)
radiation effects on breeding characteristics, 17: 15629 (LADC-5278)
radiation effects on bone marrow in, protective effects of DNA against, 17: 17902
radiation effects on blood pressure in, effects of epinephrine and norepinephrine on, 17: 19828
radiation effects on bone marrow and gonads of, protective effects of cysteamine against, 17: 19913
radiation effects on bone marrow and spleen in, cosmic, 17: 27198
radiation effects on breeding characteristics, long-term, 17: 27101
radiation effects on bone marrow of, proton, 17: 30366
radiation effects on bone marrow cells in, proton, 17: 31942
radiation effects on blood picture in isogenic chimeras of, 17: 40657
radiation effects on bactericidal activity of fixed phagocytes in liver and spleen in, effects of injected ribonucleic acid on, 18: 109
radiation effects on brains of, cosmic, 18: 5056
radiation effects on brains of, cosmic, 18: 5056
radiation effects on bone marrow in, effects of DNA, 18: 11714
radiation effects on bone marrow in, effects of hypothermia on, 18: 11856
radiation effects on breeding characteristics of, after exposure for 15 generations, 18: 15809(R) (LAMS-3034(p.124-8))
radiation effects on bone homograft antigenicity, electron, 18: 17529
radiation effects on body temperature in, x, 18: 17550
radiation effects on body weight of, comparison of x rays, gamma rays, and fast neutrons, 18: 17560
radiation effects on bone marrow and spleen cell of, analysis of clones from, 18: 17635(R) (TID-20443)
radiation effects on bone marrow in, regenerating effects of 6-azauridine on, 18: 17638
radiation effects on bone marrow stem cell kinetics in fasted, 18: 19636
radiation effects on blood serum metabolism in, x, 18: 19590
radiation effects on bone marrow repopulation in, x, 18: 19592
radiation effects on blood cell and hematopoietic system metabolism in, x, 18: 19730
radiation effects on bone marrow and spleen of, protective effects of homologous cells against, 18: 19767
radiation effects on bis(2-guanidoethyl) disulfide and 2-mercaptoethylguanidine distribution and metabolism in, x, 18: 19772
radiation effects on behavior of, chronic, early exposure, 18: 25190
radiation effects on blood serum proteins in, 18: 27158
radiation effects on blood protein content in, 18: 29276(T)
radiation effects on bacterial immunity in, 18: 31181
radiation effects on bone marrow transplants in, x, 18: 31207
radiation effects on bone composition in, 18: 33276(R) (NYO-910-7)
radiation effects on blood picture and survival of, effects of hormones on, 18: 33416
radiation effects on bacteriophage in, 18: 36970
radiation effects on body temperature of, 18: 38817(T)
radiation effects on breeding characteristics, x, 18: 43220(R) (LA-3132-MS(p.109-41))
radiation effects on blood picture and blood chemistry, x, 18: 43220(R) (LA-3132-MS(p.109-41))
radiation effects on bone marrow in, 18: 43282
radiation effects on bone marrow of, effects of low-frequency vibration on, 19: 2103
radiation effects on BCG activity in, 19: 2125
radiation effects on blood serum proteins in, 19: 8908
radiation effects on brain development in embryos, 19: 10794
radiation effects on breast tumors and myeloma in, potentiation effects of 5-iododeoxyuridine on, 19: 10921
radiation effects on brain and nervous system in, 19: 13058
radiation effects on brain of deuteron-beam, 19: 13018
radiation effects on bone marrow in, hypothermia effects on, 19: 17520
radiation effects on brain and skeleton of, *in utero* gamma and x-ray, 19: 17646
radiation effects on blood picture in, 19: 21889
radiation effects on blood picture in conventional and germfree, whole-body, 19: 19619
radiation effects on bone marrow and lymph cell grafts in, effects of chemical agents on, 19: 28123
radiation effects on blood picture in, 19: 29884 (ACRH-103(p.37-47))
radiation effects on bone marrow from, effects of incubation temperature on x, 19: 31905(R) (ORNL-3768(p.99-108))
radiation effects on bone marrow cells in, 19: 33911
radiation effects on *B. breslau* virulence in, x, 19: 33950
radiation effects on blood vessels in, pathological, 19: 36023
radiation effects on bone-injection-protected, effects of plethora on, 19: 43682(R) (UCLA-12-565, pp 33-57)
radiation effects on bone marrow of, protective effects of pyridoxal-5-phosphate, aminoethylisothiuronium, and homocysteinethiolactone against, 19: 46028
radiation effects on bone marrow, x, 20: 5320
radiation effects on biochemical properties of tissue homogenates from, γ, 20: 10577
radiation effects on blood picture and bone marrow in, β, 20: 10641
radiation effects on bacterial population in intestine of, β, 20: 10642
radiation effects on blood cells, globulins, and proteins in, fractionated-dose x, 20: 16224 (CEA-R-2848)
radiation effects on body and renal weight in nephrectomized, x, 20: 16282
radiation effects on blood formation in, protective effects of mucopolysaccharides against x, 20: 20510
radiation effects on body weight and tumor incidence in mice irradiated embryonically or fetally, x, 20: 22724
radiation effects on butyric and glutamic acid content in brain of, γ, 20: 22747
radiation effects on bone marrow in, immuno-electrophoretic technique for determining x, 20: 24913
radiation effects on blood serum proteins in, x, 20: 28899
radiation effects on bone marrow cells in, factors affecting recovery from x, 20: 40634 (ORNL-P-2312)
radiation effects on blood cell counts in fast neutron, 20: 40502(R) (ORNL-3922, pp 115-27)
radiation effects on behavior of, neutron, 20: 42833(R) (ANL-7136, pp 16-46)
radiation effects on blood and liver enzyme activity in, with secondary syndrome after bone marrow grafting, 20: 45486
radiation effects on chromosomal aberrations in, 16: 11461(R) (TID-15047)
radiation effects on chromosomes in tumor cells with chloramphenicol post treatment, 16: 17540
radiation effects on Candida albican infection in, 16: 17483
radiation effects on cycle and oestrus, evaluation of methods for determining, 16: 20288
radiation effects on, combined with antimitotic and bone marrow grafts, 16: 26872
radiation effects on cell cultures, continuous low level gamma, 16: 28780
radiation effects on calcium-45 storage by bones of, 17: 4425
radiation effects on central nervous system in, injected with stimulants, 17: 10263
radiation effects on chromium-51 uptake by, protective effects of serotonin against, 17: 14021
radiation effects on cytoplasm of distal tubule cells of kidneys in, 17: 15713
radiation effects on catabolism of hexobarbital in, whole-body, 17: 17716
radiation effects on course of homologous disease, whole-body exposure, 17: 17889
radiation effects on cleft palate development in embryo of, 17: 21482

radiation effects on chromosomal patterns in normal and leukemic, 17: 23118
radiation effects on cell elements in bone marrow and spleen in, 17: 23131
radiation effects on course of influenza virus infections in, 17: 27123
radiation effects on, continuous, 17: 27148
radiation effects on co-enzyme A content in, x, 17: 38837
radiation effects on crypt cell survival in, x, 18: 1389
radiation effects on cytology and histology of thymus gland in, 18: 3557
radiation effects on cell morphology and weight of spleen in, 18: 3493 (TID-18352)
radiation effects on central nervous system in, protective effects of drugs against, 18: 5014
radiation effects on cell division in corneal epithelium in, 18: 8142(T)
radiation effects on catalase activity in liver of, 18: 9890
radiation effects on course of tuberculosis in, cosmic, 18: 11793
radiation effects on cells of Ehrlich's ascitic carcinoma in, radioautographic studies of, 18: 13482
radiation effects on chromosomes and male sterility in, x, 18: 15893
radiation effects on carbohydrate metabolism in, 18: 17628
radiation effects on corneal mitosis in, partial and whole-body exposure, 18: 17629
radiation effects on carcinomas in, effects of heavy metal drugs on, gamma, 18: 17645
radiation effects on cell regeneration in, 18: 19553(R) (TID-20513)
radiation effects on corneal and intestinal epithelium in, 18: 19689
radiation effects on corneal epithelium in, proton, 18: 23303
radiation effects on cell growth in gonads of, 18: 27106
radiation effects on collagen from, factors affecting x, 18: 27118
radiation effects on chromosomes of, protective effects of AET against, 18: 31299
radiation effects on composition of liver lipids in, gamma, 18: 33360
radiation effects on central M-choline reactive system in, gamma, 18: 33368
radiation effects on carcinoma immunity in, x, 18: 35357
radiation effects on chromosomes in, protective effects of streptomycin against whole-body, 19: 196
radiation effects on course of tuberculosis in, effects of light and shielding on cosmic, 19: 98
radiation effects on colony-forming cells among spleen colonies in, 19: 120
radiation effects on cerebral cortex in, 19: 170
radiation effects on catalase and FAD activities and growth in, gamma, 19: 7152
radiation effects on Crockers sarcomas in, effects of AET and cysteamine on, 19: 8969
radiation effects on circulating stem cells in, partial body, 19: 10853
radiation effects on chromosomes in, aberrant, fast neutrons, gamma, and x, 19: 10879
radiation effects on cornea and lens of eyes in newborn, pathogenesis of *in utero*, 19: 13032
radiation effects on course of encephalitis in, 19: 15025
radiation effects on chromosome breakage in corneal epithelium in, 19: 17612
radiation effects on cytology and histology of thymus of, whole-body, 19: 17693
radiation effects on cell distribution changes in bone marrow of, electronic particle counting of, 19: 21940
radiation effects on calcium metabolism in bones of, influence of age, 19: 21975
radiation effects on content of gamma globulin in, effects of thymectomy followed by isologous restoration on, 19: 24280
radiation effects on conventional and germ-free, lethal, 19: 25908 (ORNL-P-81)
radiation effects on cells of, x, 19: 26154
radiation effects on chromosome aberrations and mitosis in bone marrow in, 19: 28083
radiation effects on course of leprosy in, 19: 28017
radiation effects on cartilage development in, 19: 29968
radiation effects on colony formation in tissue cultures of cells of, 19: 35997
radiation effects on content of glutamic-pyruvic transaminase and glutamic-oxalacetic transaminase in blood serum of, 19: 36012
radiation effects on corneal epithelium in, protons, 19: 36088
radiation effects on cell cycle duration in tail tissues of embryonic, gamma, 19: 38405
radiation effects on cell nuclei in, 19: 45992
radiation effects on creatine excretion by, use as damage indicator, 19: 45864
radiation effects on content of phosphatase in intestinal cells of, 20: 6839
radiation effects on corneal epithelia in, 126-Mev proton, 20: 10608(T) (NASA-TT-F-353, pp 142-50)
radiation effects on cell survival in sarcomas of, effects of oxygen inhalation on x, 20: 12725
radiation effects on chromosomes in Perognathus, chronic-exposure, 20: 12666
radiation effects on chromosomes in, distant-irradiation, 20: 18356
radiation effects on cellular reproduction in, survival curve analysis of y, 20: 18370
radiation effects on cells in peritoneal cavity of, morphological x, 20: 18285 (AD-630103)
radiation effects on chromosomes of, β, 20: 18286 (EUR-2462.1)
radiation effects on carcinoma transplants in, effects of inhaled carbon dioxide on, 20: 22802
radiation effects on cellular infiltrates of liver tissues in, x, 20: 22639
radiation effects on chromosomes in bone marrow in, x, 20: 22649
radiation effects on catecholamine metabolism in, 20: 28940
radiation effects on cell population kinetics in intestine in, double-labeling autoradiography of gamma, 20: 33035
radiation effects on cytokinetics and regulation of progenitor cells in bone marrow in, methods for assaying, 20: 36594
radiation effects on collagen in skin of, uv, 20: 36595
radiation effects on colony formation by transplanted bone marrow cells in spleen of, 20: 38708(R) (IAEA-3173-5)
radiation effects on cataractogenesis in embryos of, x, 20: 40619(R)
radiation effects on carcinogenesis induced by dimethylbenzanthracene in skin of, beta and x, 20: 42969
radiation effects on central nervous system of, effects of chloral and strychnine on strontium-90, 19: 17578
radiation effects on development of embryonic lung in, 16: 26832
radiation effects on desoxyribonucleoprotein in spleen in, 17: 15706
radiation effects on distribution of strontium-90 and yttrium-90 in tissues, 17: 19848
radiation effects on DNA synthesis in tissue cultures of embryos of, infected with polyoma virus, 17: 24924
radiation effects on development of transplanted oocytes, 17: 27117
radiation effects on DNA synthesis in duodenum and spleen of, 17: 28728
radiation effects on development of hyperostosis and ovarian tumors in, 17: 28747
radiation effects on drug toxicity in, x, 18: 11882
radiation effects on desoxyribonucleotide content in blood of, 18: 11710
radiation effects on desoxyribonucleic acid content of spleen in, gamma, 18: 11759
radiation effects on disease immunity in, x, 18: 13467
radiation effects on developing hematopoietic system in embryos of, 18: 17625
radiation effects on deoxyribopolynucleotide content in hematopoietic and lymphatic tissues in, 18: 19630
radiation effects on desoxyribonucleic acid synthesis in *in vitro* spleen of, 18: 25186
radiation effects on DNA synthesis in spleen, gamma, 18: 27130
radiation effects on desoxyribonucleic acid synthesis in tumors in, 18: 35339
radiation effects on DNA synthesis and mitosis in antigen-injected, x, 18: 36986
radiation effects on donor cell antigens in, x, 18: 38853
radiation effects on duration of mitosis in corneal epithelium of, 18: 41165
radiation effects on desoxyribonucleic acid synthesis in spleen and intestine of, 18: 41169
radiation effects on desoxyribonuclease content of liver and spleen of, 19: 13059
radiation effects on development of runt disease in intestine of, 19: 15108
radiation effects on DNA structure and pycnotic cells in bone marrow and thymus of, 19: 15048
radiation effects on dry mass distribution changes in bone marrow of, 19: 15055
radiation effects on DNA synthesis in antibody-forming cells in, effects of antigen injection on, 19: 15102
radiation effects on DNA synthesis during s-phase in L-strain cells of, 19: 17548
radiation effects on DNA-ase activity in urine of, x, 19: 28005
radiation effects on desoxyribonucleic acid metabolism in thyroid gland of, 19: 29900 (NYO-901-33)
radiation effects on deoxyribopolynucleotides in tissues of, x, 19: 29933
radiation effects on DNA and phosphate metabolism in small intestines of, fasting effects on, 19: 42314
radiation effects on, dose-rate dependence of early, 17: 4421
radiation effects on desoxyribonucleotide content in bone marrow, spleen, and thymus of, β and γ, 20: 10633
radiation effects on distribution of mycobacterial vaccine in, 20: 10655
radiation effects on developing embryos of, x, 20: 12650

radiation effects on developing fetuses of, pathological x, 20: 12650
radiation effects on developing fetuses of, pathological neutron and x, 20: 12683
radiation effects on decarboxylase activity for aromatic amino acids and protein content of liver of, 20: 12782
radiation effects on DNA synthesis in embryonic cells from, x, 20: 18265
radiation effects on DNA synthesis in ascites tumor cells from, x, 20: 18266
radiation effects on dehydrogenase and transaminase activity in spleens of, 20: 18280
radiation effects on DNA content and weight of kidneys of, effects of unilateral nephrectomy on x, 20: 22726
radiation effects on development of embryos of, 20: 22614(R) (NIRS-4, pp 28-34)
radiation effects on DNA synthesis in uterine epithelium of, x, 20: 31088
radiation effects on DPN metabolism in tumor cells transplanted into, x, 20: 35259
radiation effects on DBA/2J strain, gamma, 20: 40687
radiation effects on development of, exposed *in utero*, x, 20: 40619(R) (NYO-2740-3, pp 216-57)
radiation effects on diurnal variations in activity and metabolism, gamma, 20: 45310
radiation effects on embryonic, 16: 48(R) (TID-12787)
radiation effects on erythropoiesis in pregnant, 16: 20190
radiation effects on eyes in developing embryos in pregnant, 16: 25215
radiation effects on, electron, gamma, and x, 17: 1328
radiation effects on embryonal development, 17: 5897
radiation effects on eye pigmentation in young, 17: 7847
radiation effects on, effects of protein diet on, 17: 14055
radiation effects on, effects of lipoxidase and olive oil on, 17: 15813
radiation effects on, effects of anesthetics on, 17: 17784
radiation effects on epilation in, protective effects of chemicals against, 17: 17818
radiation effects on embryonic, whole-body preimplantation, 17: 17911
radiation effects on, effects of vitamin E on, 17: 23123
radiation effects on, effects of natural and purified diets on, 17: 23181
radiation effects on embryonic development, x, 17: 33672
radiation effects on, effects of protein diet on survival, 17: 35613
radiation effects on enzymes in thymus nuclei, whole-body, 17: 40573
radiation effects on enzyme activity in heart, liver, and kidney of, after whole-body exposure, 18: 3555
radiation effects on endocrine cells in, 18: 3490(R) (COO-228(p.143-68))
radiation effects on estrus cycle, 18: 8185
radiation effects on embryos of, x, 18: 11672
radiation effects on energetic balance in, 18: 11704
radiation effects on enhanced antitoxin response in, 18: 15856
radiation effects on embryos of, x, 18: 15891
radiation effects on energy metabolism in Ehrlich ascites tumor cells of, x, 18: 29332
radiation effects on Ehrlich tumor immunity in, x, 18: 31155
radiation effects on embryos of, effects on post-natal physiological processes and adult pathology, 18: 33280(R) (TID-20831)
radiation effects on embryo cytokinetics, x, 18: 35329
radiation effects on establishment of bone marrow grafts in, 18: 38856
radiation effects on erythropoiesis in, 18: 38870
radiation effects on endogenous respiration in tumor cells from, 18: 38892
radiation effects on epithelium of, protective effects of vitamin A against x, 18: 43309
radiation effects on erythropoietic activity in, protective effects of fresh and frozen bone marrow against, 19: 192
radiation effects on enzyme activity in, 19: 2075(R) (ORNL-3700(p.101-11))
radiation effects on endogenous respiration in spleens of, x, 19: 13070
radiation effects on electrolyte transport in spleens of, x, 19: 13070
radiation effects on enzyme activity in liver of, 19: 21858(R) (NP-14779 (p.1-14))
radiation effects on enzyme activity in, gamma, 19: 21860(R) (NP-14779 (p.89-98))
radiation effects on evolution of encephalitis in tick virus infected, beta and gamma, 19: 24265
radiation effects on erythrocytes in, ultraviolet, 19: 25913
radiation effects on erythropoiesis in, 19: 25983
radiation effects on erythropoiesis in, effects of postirradiation temperature on x, 19: 31905(R) (ORNL-3768(p.99-108))
radiation effects on embryo and fetus of, maternal, 19: 31964
radiation effects on enzyme activity and cell growth in thymus of, 19: 31801 (USNRDL-TR-840)
radiation effects on erythroid clone formation in polycythemia, bone marrow effects on, 19: 36079
radiation effects on erythrocyte size in, 19: 38363
radiation effects on Ehrlich ascites tumors in, at various times following inoculation, 19: 38402
radiation effects on embryonic, seasonal effects on low dose whole-body, 19: 42298
radiation effects on embryonic lethality of, from paternal spermatozoa exposure, 19: 42303
radiation effects on ear of, skin recovery processes in, 19: 45987
radiation effects on embryos of, pathological, 19: 45852
radiation effects on Ehrlich ascites cells in, comparison of radiomimetics with x, 20: 118
radiation effects on embryos of, pathological, 20: 6892
radiation effects on enzyme activity in starved, 20: 8612
radiation effects on electrophoretic patterns of serum proteins of, β, 20: 10581
radiation effects on etiology of bacteremia in, 20: 12704
radiation effects on embryos of, delayed pathological x, 20: 14315
radiation effects on estrus cycle in, *in utero*-exposure x, 20: 18403
radiation effects on embryos of, teratologic, 20: 18404
radiation effects on eyes of, x, 20: 18185(R) (BNL-929, pp 126-47)
radiation effects on erythropoiesis in, y, 20: 18289(R) (LA-3432, pp 56-101)
radiation effects on embryonic mortality and sex-chromosome loss in, effects of exposure during cleavage on x, 20: 33008
radiation effects on embryos of, dose dependence of x, 20: 33027
radiation effects on epilation of skin of, protective effects of blood serum against, 20: 33081
radiation effects on embryos of, lethal, RBE of neutrons and x, 20: 40618(R) (NYO-2740-3, pp 166-215)
radiation effects on embryos, 20: 40649
radiation effects on fertility, deformities, postnatal and infant mortality, and sex ratio, 16: 20220
radiation effects on fertility of male, after embryonic exposure, 16: 28756(T) (JPRS-14833)
radiation effects on frequency of lymphosarcomas in, 17: 2844
radiation effects on function and structure of villus epithelium in, 17: 4420
radiation effects on fertility in male, 17: 7854
radiation effects on fertility of, effects of olive oil on, 17: 12154
radiation effects on fertility of female, exposed during infancy, 17: 23178
radiation effects on fertility of, 17: 25039
radiation effects on female genital glands and fetuses of, 17: 30394
radiation effects on fertility in female, 17: 33755
radiation effects on fatty acid and glucose metabolism in, x, 17: 35512
radiation effects on, from daily lifetime exposure, 17: 35599 (TID-17479)
radiation effects on fungus infections in, x, 17: 38809
radiation effects on *Fasciola hepatica* in liver of, 18: 1411
radiation effects on fetuses of, x, 18: 11739
radiation effects on fertility of male, pre- and post-natal, 18: 11665
radiation effects on fibroblasts of, protective effects of chemical agents against, 18: 11875
radiation effects on forecasting recovery from lymph tissue in, 18: 11707
radiation effects on fibroblasts in, protective effects of cysteamine against, 18: 17639
radiation effects on fertility of male, protection against, using serotonin, 18: 19711
radiation effects on fertility of, x, 18: 23325
radiation effects on functioning of vestibular nerve in, in presence of vibrations, 18: 31213
radiation effects on fitness of populations of, 18: 35348
radiation effects on fitness and skeletal variation in, 19: 7091
radiation effects on fine structure of liver and spleen of, gamma and x-ray, 19: 7170
radiation effects on function and structure of mitochondria in liver of, 19: 10863
radiation effects on fractionation of spleen-colony-forming cells from bone marrow in, 19: 19617
radiation effects on female, cytogenesis of bone marrow cell grafts in, 19: 26142
radiation effects on fertility in, 19: 31791(R) (ORNL-3768(p.89-93))
radiation effects on, fast-neutron, 17: 10358 (BNL-6575)
radiation effects on fetuses of, protective effects of splenectomy against, 20: 18436
radiation effects on fertility of, chronic low-level y, 20: 18211(R) (UCLA-12-576, pp 89-111)
radiation effects on fetal, 20: 22681
radiation effects on fine structure of Paneth cells in, x, 20: 31083
radiation effects on germinal cells in, long-term gamma, 17: 7856
radiation effects on glomerular lesions in kidneys in, pathogenesis of whole-body, 17: 10433
radiation effects on glomerulus and proximal tubule of kidneys in, 17: 15712
radiation effects on glycolysis, oxygen uptake, and protein synthesis in hepatoma cells in, 17: 23151

radiation effects on, genetic, 17: 27098
radiation effects on growth and osteogenesis, 17: 28774
radiation effects on gonads and developing embryos in, 17: 38905
radiation effects on gastrointestinal tract in, protective effects of AET against, 17: 38908
radiation effects on growth of injected Ehrlich ascites tumors in, 17: 40640
radiation effects on glioma growth in, x, 18: 17690
radiation effects on glycogen content of splenic leukocytes in, when used with antigens, x, 18: 19741
radiation effects on growth of hematopoietic cells in, 18: 27003(R) (ORNL-3601(p.27-46))
radiation effects on growth of, neutron and x, 18: 31198
radiation effects on growth and transplantability in tumors of, thermal-neutron, 18: 41225
radiation effects on genetics in populations of, x, 18: 43220(R) (LA-3132-MS(p.109-41))
radiation effects on growth of transplanted sarcoma in, 19: 124
radiation effects on growth of transplanted cells in, 19: 125
radiation effects on germ cells in, whole-body, 19: 168
radiation effects on growth of tumor cells in, disseminated at surgery, 19: 243
radiation effects on germ-free, x, 19: 2135
radiation effects on growth of transplanted tumor cells in, 19: 5660
radiation effects on giant cells in bone marrow of, dose relation to, 19: 5676
radiation effects on gonads of progeny of female, 19: 7032
radiation effects on genetics of, research on, 19: 7130
radiation effects on gonads of, protective effects of serotonin against, 19: 7196
radiation effects on gastrointestinal tract in, protective effects of AET against, 19: 7198
radiation effects on gamma aminobutyric and glutamic acid contents in brain tissue in, 19: 8921
radiation effects on giant nuclei formation in tumors of, 19: 8939
radiation effects on granulocytopoiesis in, 19: 10865
radiation effects on growth of transplanted tumors in, 19: 12975
radiation effects on growth and senescence of primary antibody-forming potential in spleen of, 19: 15104
radiation effects on growth and regression of bone marrow grafts in hybrid, 19: 17655
radiation effects on growth of bone marrow grafts in, 19: 25909 (ORNL-P-1211)
radiation effects on growth of, gamma and neutron, 19: 31833
radiation effects on growth of transplanted tumors in, synergistic effects of cruzine, 19: 38428
radiation effects on growth of transplanted tumors in, 19: 38387
radiation effects on granulocyte and lymphocyte counts in, protective effects of MEA against, 19: 43876
radiation effects on growth of transplanted sarcoma in, 19: 43763
radiation effects on growth of tumor transplants in, 19: 45858
radiation effects on growth of bone marrow transplants in, effects of arabinofuranosylcytosine on, 20: 1687
radiation effects on growth of tumor transplants in, x, 20: 3751
radiation effects on germ-free, lethal, 20: 3778
radiation effects on growth of thymus transplants in kidneys of, x, 20: 5376
radiation effects on growth of infused bone marrow cells in, 20: 6775(R) (ORNL-3853, pp 36-49)
radiation effects on γM antibody response in, x, 20: 6863
radiation effects on germfree, x, 20: 6907(R) (EUR-2511.e)
radiation effects on growth of bone marrow transplants in spleen of, neutron and x, 20: 8710
radiation effects on growth in newborn, effects of dose and strain on, 20: 10673
radiation effects on growth of cellular transplants in, genetic effects on x, 20: 18304
radiation effects on growth of transplanted tumors in, x, 20: 18460
radiation effects on growth of hematopoietic tissue transplants in, γ, 20: 22735
radiation effects on graft-versus-host reaction in, x, 20: 24887
radiation effects on growth and development of, continuous low-dose gamma, 20: 31074
radiation effects on growth of transplanted hematopoietic cells in, x, 20: 38592 (ORNL-P-2158)
radiation effects on growth of transplanted lymphoma cells is, effects of anoxia on, 20: 38699
radiation effects on growth of cells from experimental fibrosarcoma, x, 20: 42888
radiation effects on growth and reproduction of, cesium-137 and strontium-90, 17: 33633
radiation effects on hair, 16: 5214
radiation effects on heterologous and homologous red blood cells in, 16: 17487
radiation effects on histologic structure of hair follicles, effects of castration, 17: 1249
radiation effects on hematopoietic system in, single, whole-body, 17: 4398
radiation effects on hematopoietic organs and hypophysis in, 17: 5872
radiation effects on hematopoietic system, protective effects of allogenic bone marrow grafts against, 17: 14027
radiation effects on hair growth on, effects of cortisone on, 17: 15822
radiation effects on hematopoietic cells in, microcinematography method for determination of, 17: 21542
radiation effects on hematopoiesis in, protective effects of injected amino acids against, 18: 130
radiation effects on hematopoiesis in bone marrow and spleen of, 18: 107
radiation effects on homologous bone marrow treated, effects of amethopterin on, 18: 17641
radiation effects on hind limb circulatory system, x, 18: 19640
radiation effects on hematopoietic cells of, repair of gamma, 18: 19761
radiation effects on histology and saline-soluble DNA content in spleen of, 18: 23257
radiation effects on histidine decomposition in livers of, gamma, 18: 33359
radiation effects on hematopoietic tissue transplants in, x, 18: 37009
radiation effects on hair regrowth in, fast neutron and gamma, 18: 41140
radiation effects on hematopoietic tissues in, 18: 43226 (ORNL-P-394)
radiation effects on hematopoietic system of, effects of toxin on, 18: 43315
radiation effects on hypothermic, protective effects of MEA against x, 19: 3994
radiation effects on hematopoietic tissue in spleen of, 19: 5648
radiation effects on hair of, 19: 5658
radiation effects on host-parasite relationships of Schistosoma in, 19: 8944
radiation effects on histone synthesis in tumors of, by inhibition of DNA replication, 19: 15052
radiation effects on host-cell interactions of hemopoietic grafts in, 19: 19615
radiation effects on hypoxiated, protective effects of second homologous bone marrow grafts against, 19: 26144
radiation effects on histology of organs in, protective effects of homologous bone marrow against, 19: 26145
radiation effects on hematopoiesis in, effects of tumor growth on, 19: 28049
radiation effects on hematopoiesis in plasma and spleen of, x, 19: 29935
radiation effects on hematopoietic colonies in spleens of, x, 19: 31852
radiation effects on hematopoietic system in normal and cancer-bearing, 19: 36020
radiation effects on hair of, local and whole-body, x, 19: 43833
radiation effects on hair follicles and skin on, elongate microbeam, 17: 23154
radiation effects on homograft tolerance in, with and without urethan, 17: 24993
radiation effects on hematopoietic system in, 17: 40628
radiation effects on heart, kidneys, and liver of, pathological, 20: 102
radiation effects on healing of skin wounds of, effects of radioprotective compounds on x, 20: 6878
radiation effects on health and life-span of, exposed as embryos, x, 20: 6785(R) (ORNL-3853, pp 128-40)
radiation effects on hematopoietic tissues in, γ and protons, 20: 18364
radiation effects on head of, pathological γ, 20: 18376
radiation effects on hematopoietic organs of, gamma and proton, 20: 33010
radiation effects on hematopoiesis in, effects of transplanted bone marrow cells in, 20: 35289
radiation effects on heritable histocompatibility changes in, hypothesis on x, 20: 35309
radiation effects on hybrid, grafted with skin from parents, 20: 40651
radiation effects on hematology of, x, 20: 42831 (AD-635600)
radiation effects on hematopoietic system of, comparison with dogs, 20: 45366 (UCSF-10P2-14)
radiation effects on immune responses, 16: 20267
radiation effects on immunity to *Trichinella spiralis*, 16: 21935
radiation effects on intercapillary glomerulosclerosis development in kidneys, gamma, 16: 23453
radiation effects on immune reactions to skin grafts in, 18: 115
radiation effects on, injected with fetal liver, bone marrow, or isogenic spleen, 18: 5035
radiation effects on iron-59 metabolism during, erythropoiesis in, 18: 15833
radiation effects on immune response of hyperimmune spleen cells in, 18: 15855
radiation effects on immunological tolerance in, x, 18: 25157
radiation effects on immune reactions to virus infection in, effects of

stress on, 18: 29243 (TID-20774)
radiation effects on incorporation of iron-59 in erythrocytes in, protective effects of cysteamine, histamine, serotonin, and splenectomy against, 18: 29423
radiation effects on immune reactions in, 18: 31183
radiation effects on intestine of, protective effects of sodium nitrate against, 18: 31304
radiation effects on immune reactions of tumor cells in, 18: 35326(T) (JPRS-25464(p.22-30))
radiation effects on immune response in, 18: 35303(R) (AD-438541)
radiation effects on influenza in, x, 18: 38805
radiation effects on immune reactions in, 18: 38957
radiation effects on immune reactions of chimeras in, 18: 41146
radiation effects on intestine of, fast-neutron, 18: 41226
radiation effects on immune reactions to injected hematopoietic tissues in, 18: 41258(R) (TID-20989)
radiation effects on infective capacity of *Schistosoma mansoni* cercariae in, 19: 126
radiation effects on immunogenesis in, protective effects of chemical agents against x, 19: 2177
radiation effects on immune reactions in, 19: 2075(R) (ORNL-3700 (p.101-11))
radiation effects on immune reactions of, 19: 3905
radiation effects on intestinal mucosa of, gamma, 19: 3957
radiation effects on immune reactions in, 19: 5642
radiation effects on immune reactions in, effects of novocaine on, 19: 5643(T)
radiation effects on *in vitro* or *in vivo* oocyte survival in, 19: 8861
radiation effects on immune response in thymectomized, protective effects of thymus grafts against, 19: 8978
radiation effects on immune reactions in, 19: 8838
radiation effects on inhibition of antitumoral immunity in, protective effects of cystamine against, 19: 8961
radiation effects on intestinal mucosa of, 19: 10832
radiation effects on immune reactions to allogenic hematopoietic cell grafts in, 19: 10915
radiation effects on immune reactions in, 19: 13012
radiation effects on immune reactions in, 19: 13014
radiation effects on immune reactions to Rickettsial infections in, 19: 13015
radiation effects on iodine metabolism and thyroid function in, x, 19: 13081
radiation effects on immune responses of spleen cells in thymectomized, 19: 15217
radiation effects on immune reactions in, 19: 17503
radiation effects on immune reactions in, 19: 17506
radiation effects on iron-59 uptake by, sex differences in, 19: 17652
radiation effects on immune reactions to bone marrow transplants in, 19: 22011
radiation effects on immune reactions to bone marrow transplants in, 19: 21961
radiation effects on intestinal mucosa in germfree, whole-body, 19: 25997
radiation effects on immune reactions to skin grafts, 19: 28093
radiation effects on immune reactions to injected spleen cells in, effects on liver, 19: 27967
radiation effects on immunity and intoxication in parabiotic, x, 19: 28006
radiation effects on immune reactions to skin grafts by sensitized, 19: 28032
radiation effects on immune reactions in, 19: 29883 (ACRH-103(p.1-27))
radiation effects on immune reactions in, 19: 29896 (EUR-2201.f)
radiation effects on immune reactions in germ-free, 19: 29939
radiation effects on immunological tolerance to skin grafts after cell transfer in, 19: 29985
radiation effects on immune reactions in, 19: 31907(R) (TID-21799)
radiation effects on induced cancer at high altitudes and sea level, cosmic, 19: 33927
radiation effects on induction of viral leukemia in, 19: 33793
radiation effects on immune reactions in, 19: 33805
radiation effects on immune reactions to homografts in, 19: 33807
radiation effects on immune reactions in, effects of thymectomy and parabiosis on, 19: 33855
radiation effects on immune reactions in adult and neonatal, 19: 33859
radiation effects on immune reactions to spleen cell transplants in, 19: 36029
radiation effects on immune reactions to homografts in, 19: 36037
radiation effects on immune reactions to injected hematopoietic tissues in, 19: 36100(R) (NP-15170)
radiation effects on immunity against tumor tissue in, 19: 42292
radiation effects on immune reactions in, effects of thymus, 19: 42338
radiation effects on immune reactions in, 19: 45806 (AD-621543)
radiation effects on immune reactions to transplanted ultraviolet-induced sarcomas, 19: 45827
radiation effects on immune reactions in, 19: 45858
radiation effects on immune reactions in, 19: 45903
radiation effects on iron metabolism in, 17: 5913(T)
radiation effects on iodine-131 and phosphorus-32 uptake by liver fragments in, gamma, 17: 7876
radiation effects on immunity to *Trichinella spiralis* infection in, 17: 10424
radiation effects on incidence and latent period of leukemia in, 17: 15724
radiation effects on intestinal epithelium in, 17: 15746
radiation effects on incidence of mammary and ovarian tumors in, 17: 17819
radiation effects on immune mechanisms in, 17: 17866
radiation effects on immunity in, protective effects of combined vaccines against, 17: 19826
radiation effects on immune reactions to transplanted tumors, 17: 19867
radiation effects on intercapillary glomerulosclerosis in young, 17: 17862
radiation effects on immunobiological reactions in, 17: 23222
radiation effects on immunity to *Schistosoma mansoni cercariae* in, 17: 24992
radiation effects on iron-59 uptake by organs in, 17: 30386
radiation effects on intensity of second fluorescence of lymphocytes in, 17: 31952
radiation effects on immune reactions in, 20: 1632
radiation effects on immune reactions of, to injected allogenic and syngenic bone marrow, 20: 1660
radiation effects on immune reactions to rat tissue transplants in, 20: 10505(R) (BNWL-122, pp 146-9)
radiation effects on immune reactions in injected thymocytes and lymph node cells in, 20: 3777
radiation effects on immune reactions in thymectomized, 20: 5408 (USNRDL-TR-920)
radiation effects on immune reactions in, 20: 5413
radiation effects on incidence of urethan-induced tumors in lungs of, γ, 20: 5328
radiation effects on immune reactions to marrow transplants in, methods for assaying x, 20: 5372
radiation effects on isograft resistance to Rous sarcomas in, x, 20: 6825
radiation effects on immune reactions of, to skin grafts, 20: 6883
radiation effects on immune reactions to bone marrow transplants in, effects of previous transfusions, 20: 6886
radiation effects on immune reactions in, x, 20: 6893
radiation effects on immune reactions to pneumococcal polysaccharides in, x, 20: 8716
radiation effects on immunity in, β, 20: 10580
radiation effects on immune reactions in, γ, 20: 10632
radiation effects on immune reactions to allogenic skin grafts, effects of isogenic grafts on, 20: 12656
radiation effects on intestinal epithelium of, lethal whole-body x, 20: 16223 (BNL-8952)
radiation effects on intracellular organelles in, x, 20: 20413
radiation effects on immune reactions to injected bone marrow and lymph cells in, x, 20: 20472
radiation effects on immunity to uv-irradiated ascites tumor cells transplanted into, x, 20: 20484
radiation effects on intraperitoneal cavity tumor cells in, intracellular enzyme oxidation-reduction state changes from x, 20: 22708
radiation effects on iron-59 uptake by bone marrow and spleen in intact and splenectomized, 20: 22610 (AD-632049)
radiation effects on immune reactions in, x, 20: 22615(R) (NIRS-4, pp 34-58)
radiation effects on immune reactions in, 20: 24918
radiation effects on iron-59 uptake by erythrocytes in, following head exposure, 20: 24849
radiation effects on immune reactions to bone marrow transplants in, 20: 29006
radiation effects on intact thymus in, effects of hypoxia on fast-neutron, 20: 32982
radiation effects on iron-59 clearance in blood plasma in, effects of cysteamine, histamine, and serotonin on, 20: 35338
radiation effects on interactions of Polyoma virus with cells of, 20: 38702
radiation effects on immune system and lymphatic tissue in estradiol-injected, effects of marrow transplants on x, 20: 40577
radiation effects on intra- and extra-cellular potassium content in, x, 20: 45444
radiation effects on immune reactions to skin grafts in, 20: 45473
radiation effects on immune reactions in, effects of injected lymph node cells on, 20: 45482
radiation effects on immune reactions in, effects of cell-free extracts on, antigenic, 20: 45483
radiation effects on immune response to bone marrow grafts, x, 20: 45484
radiation effects on inheritance of susceptibility to pentobarbital of, γ

and neutron, 20: 45374
radiation effects on kidneys undergoing compensatory hyperplasia, 16: 11465 (USNRDL-TR-532(Rev.))
radiation effects on kidney morphology of, during early post-natal life, 18: 55
radiation effects on kidney function in, 19: 38409
radiation effects on kidneys of, exposed at birth, pathological x, 20: 22733
radiation effects on kidney tissues and renal clearance rates in, neutron and x, 20: 36608
radiation effects on kidneys of, pathological, local x, 20: 45382
radiation effects on life span of descendants of irradiated, 16: 1310(R) (LAMS-2627(p.103-9))
radiation effects on life span, 16: 1313(R) (LAMS-2627(p.121-3))
radiation effects on life span of progeny, 16: 11432(R) (ANL-6464(p.15))
radiation effects on life span, five-generation exposure, 16: 17503
radiation effects on life span, 16: 18764(R) (NP-11660(p.67-75))
radiation effects on, large-dose gamma, 16: 32825
radiation effects on lymphocytic choriomeningitis in, 16: 20271
radiation effects on lymphocytic choriomeningitis in, 16: 20272
radiation effects on life span of, chronic fast neutron exposure, 16: 26658(R) (NP-11966(p.36-42))
radiation effects on life span of first and second generation offspring after exposure of male, 16: 31472 (LADC-5323)
radiation effects on life span of, whole-body gamma and x, 16: 31382(R) (ANL-6535(p.5-12))
radiation effects on liver mitochondria in, x, 18: 1429
radiation effects on long-term aging of skin on, 18: 3574
radiation effects on lethality in pulsed gamma and neutron, 18: 8178
radiation effects on life span of, low-level neutron, 18: 11632(R) (NP-13555(p.107-17))
radiation effects on life span of, fractionated, 18: 11666
radiation effects on life span of, comparative effects of x rays, gamma rays, and fast neutrons, 18: 17559
radiation effects on liver catalase activity in, x, 18: 17600
radiation effects on lymphoid regeneration in, effects of thymus on x, 18: 19546
radiation effects on lymph node plasmacytic reaction in, x, 18: 19557(T) (JPRS-23956(p.18-26))
radiation effects on lethality in, fission neutron *vs.* gamma, 18: 19576
radiation effects on liver regeneration in, brief and prolonged, 18: 25122
radiation effects on lymph tissue and serum-γ-globulin in, as affected by microflora, 18: 27122
radiation effects on life span of, protective effects of callicrein and callicrein-inactivator against, 18: 27234
radiation effects on lymphatic choriomeningitis in, x, 18: 29462
radiation effects on life span, radiosensitivity, and productivity of, chronic long-term exposure, 18: 31128 (LADC-6472)
radiation effects on liver cell nuclei in, x, 18: 33350
radiation effects on life span of, effects of age on, 18: 38887
radiation effects on liver and spleen of, gamma, 18: 41201
radiation effects on leukocytes of, x, 18: 41206
radiation effects on life span of, 18: 41094(R) (TID-21156)
radiation effects on life span of, after 15 generations of exposure, 18: 43220(R) (LA-3132-MS(p.109-41))
radiation effects on life span of, from continuous exposure, 18: 43259
radiation effects on lysozyme content of tissues of, 19: 2113
radiation effects on life span, calculation of, 19: 7207(R) (ORNL-3697 (p.199-202))
radiation effects on life spans of, 19: 7089
radiation effects on life span of, 19: 8790(R) (NP-14448(p.116-31))
radiation effects on lung metastase development in tarred, 19: 8834
radiation effects on lung metastasis development in tarred, 19: 8834
radiation effects on Listeria susceptibility in, gamma, 19: 10878
radiation effects on life spans of, protective effects of vitamin A against, 19: 10911
radiation effects on lethality in, protective effects of cyclobutane derivatives against, 19: 10922
radiation effects on life span of, high-energy gamma and x rays, 19: 13005
radiation effects on life-expectancy of erythrocytes in tumor-bearing, 19: 17513
radiation effects on life span, 19: 22019(R) (UCLA-12-541(p.51-91))
radiation effects on lymphocytes in, 19: 21883
radiation effects on latency of *Coxiella burnetii* infections in, 19: 24269
radiation effects on leukopenia production in, dose duration effects in local, 19: 24343
radiation effects on lethality in, modifying effects of microwaves on, 19: 24375
radiation effects on lethality in, protective effects of sodium nitrate against, 19: 24376
radiation effects on liver mitochondria in, 19: 26033
radiation effects on lethal anaphylactic shock suppression in, whole-body, 19: 26050
radiation effects on life span of, 19: 28076
radiation effects on limb development in embryos of, x, 19: 28003(T)
radiation effects on life-span of, low-level gamma, 19: 28069
radiation effects on liver of, cytological, 19: 29964
radiation effects on life spans in, fast-neutron, 19: 31677(R) (ORNL-3768(p.119-30))
radiation effects on lens in, 35-Mev proton, 19: 31793(R) (ORNL-3768 (p.109-11))
radiation effects on lethality in, fractionated, 19: 33895
radiation effects on levels of cholinesterases, mercapto groups, and peroxides in tissues of, x, 19: 35952(T) (JPRS-29641(p.44-52))
radiation effects on life spans of progeny of irradiated male, protective effects of cysteamine against x, 19: 42366
radiation effects on lens opacity in, proton, 19: 43721(R) (ORNL-TM-1217)
radiation effects on life spans in, effects of genetic damage on, 19: 45969
radiation effects on lactic dehydrogenase activity in blood plasma in, 19: 45844
radiation effects on life span of, chronic post-exposure, 19: 21966
radiation effects on lungs of embryonic, developed *in vitro*, 17: 1272
radiation effects on, lethal gamma, 17: 5863
radiation effects on lymph system of, x, 17: 10406
radiation effects on life span, 17: 13972(R) (NP-12484(p.45-53))
radiation effects on leukemia and secondary syndrome in, effects of bone marrow transfusions on, 17: 14011
radiation effects on leukemic, protective effects of bone marrow and chemical agents against, 17: 14019
radiation effects on liver in, protective effects of 2-methylpiperazine dithioformate against, 17: 15809
radiation effects on longevity and total body weight, 17: 17920
radiation effects on life span of, protective effects of pantothenic acid against, 17: 28740
radiation effects on, lethal, 17: 33449(R) (ANL-6723(p.41-3))
radiation effects on leukocyte recovery in, dose-response characteristics of, 17: 40677
radiation effects on life span of, 17: 40649
radiation effects on life span of, 17: 40654
radiation effects on life span of, 17: 40650
radiation effects on liver fatty infiltration in, protective effects of lipotropic substances on x, 17: 40586
radiation effects on liver size in, treated with bone marrow, 17: 35508
radiation effects on life span of, effects of genotype on, 20: 3711(R) (NYO-3314-2)
radiation effects on life span of, computer program for evaluation of, 20: 5300 (UCLA-12-573)
radiation effects on lymph nodes in, effects of serum injection on recovery from x, 20: 6809
radiation effects on lens of, proton, 20: 6783(R) (ORNL-3853, pp 105-10)
radiation effects on life-span of germ-free, effects of diet and mouse strain on, 20: 6785(R) (ORNL-3853, pp 128-40)
radiation effects on leukemia incidence in, x, 20: 6788 (ORNL-P-1703)
radiation effects on lymphoma cultures from, continuous-exposure γ, 20: 8670
radiation effects on lyophilized liver of, effects of cysteine and oxygen on radicals from x, (E), 20: 8688
radiation effects on lymphoid repopulation in, x, 20: 8717
radiation effects on lipid content in liver of, x, 20: 14268
radiation effects on leukemic cells from, γ, 20: 14367
radiation effects on leukemic, combined with cyclophosphamide and hyperbaric oxygen, x, 20: 16262
radiation effects on litter size in, gamma and neutron, 20: 20453
radiation effects on leukemia cells in, x, 20: 22642
radiation effects on life span of, x, 20: 26684
radiation effects on lymphocytes in blood and peritoneal cavity in, x, 20: 26651 (AD-632282)
radiation effects on leukemia incidence, life span, and mutation induction in, review on low-dose x, 20: 36652
radiation effects on life spans in, effects of age at exposure on x, 20: 40633 (ORNL-P-2287)
radiation effects on lymphoma cells incubated with phytohemaglutinin in, x, 20: 40588
radiation effects on lymphoma cells from, negative pion, 20: 42859(R) (UCRL-16246, pp 100-2)
radiation effects on leukemia induction in, x, 20: 42867
radiation effects on lymphocyte content and morphology of thymus of infant, x, 20: 42880
radiation effects on leukemic, phosphorus-32, 20: 43045
radiation effects on liver and spleen of, pathological, whole-body x, 20: 45434
radiation effects on lifespans of, continuous x, 20: 45443

radiation effects on manganese-54 metabolism, 16: 9882
radiation effects on mitochondria in liver, *in vitro*, 16: 17485
radiation effects on metabolism of sulfanilamide in liver of, 18: 5002(R) (NP-13281(p.92-103))
radiation effects on male, ecology of natural populations from, 18: 8113 (TID-19982)
radiation effects on mitotic activity in contact irradiation after pretreatment with carcinogen and tumor enhancer, 18: 8186
radiation effects on mitosis in, gamma, 18: 19609(T)
radiation effects on mitosis in, gamma, 18: 19610(T)
radiation effects on mitosis in malignant and nonmalignant epidermal hyperplasia in, 18: 19704
radiation effects on mortality of, effects of age on spleen cell transfusions for, x, 18: 19727
radiation effects on microstructure of duodenum cells of, x, 18: 23266
radiation effects on mutations in, protective effects of AET and cysteine against x, 18: 27217
radiation effects on malignant cells of, protective effects of photoreactivation against uv, 18: 29428
radiation effects on MPA metabolism, 18: 33373
radiation effects on mortality, uv, 18: 37006
radiation effects on mitosis in corneal epithelium of, 18: 38948
radiation effects on mutagenesis in spermatozoa of, protective effects of AET against x, 18: 38987
radiation effects on mitosis in bone marrow cells of, effects of vibration on, 18: 41182
radiation effects on monoaminoxydase in, 18: 41202
radiation effects on mitosis and ploidy in embryos of, strontium-90, 18: 41096
radiation effects on mortality, protection from gamma and proton, 18: 41243(T) (FTD-TT-64-892(p.217-31))
radiation effects on marrow transplants in, 18: 43262
radiation effects on mouse spermatogonial genes, gamma and x, 19: 5652
radiation effects on metabolism in, 19: 5665
radiation effects on mitotic activity in corneal epithelium of, x, 19: 10813
radiation effects on marrow cell transplants in, protective effects of ribosemononucleotides against gamma, 19: 13098
radiation effects on mammary gland development in pregnant, 19: 17617
radiation effects on metabolism in, 19: 21949
radiation effects on morphology of liver cells in, fast neutron, 19: 28081
radiation effects on mitosis in bone marrow of, gamma, 19: 29922(T)
radiation effects on mitosis in, femoral marrow of, x, 19: 29936
radiation effects on migration of medullary hematopoietic cells in, 19: 31871
radiation effects on morphology of peritoneal leukocytes in, 19: 31802 (USNRDL-TR-841)
radiation effects on mitotic activity of corneal epithelium, 19: 33825(T)
radiation effects on metabolism of urethan in, 19: 35986
radiation effects on mortality of, effects of histocompatibility of bone marrow on, 19: 36120
radiation effects on mortality from *Pseudomonas aeruginosa* in, protective effects of antibiotics against, 19: 36121
radiation effects on mitochondria function and structure in liver of, 19: 38424
radiation effects on mammary gland activity in, 19: 40353(T) (FTD-TT-65-48, pp 16–17)
radiation effects on metabolism of desoxyribonucleic acid in tumor cells of, tracer study, 19: 45936
radiation effects on mineral metabolism in, x, 19: 45729(R) (NYO-910-23, pp 1-111)
radiation effects on, mathematical expression for, 17: 7875
radiation effects on mortality in, infected with *Trichinella spiralis*, 17: 10431
radiation effects on metaphase/prophase ratio in, 17: 10411
radiation effects on morphology of liver in, 17: 15817(T)
radiation effects on mortality of, fission spectrum neutron and pulsed gamma, 17: 19811 (USNRDL-TR-627)
radiation effects on, mechanism of protective effects of cysteamine against, 17: 19876
radiation effects on metabolism, 17: 21528
radiation effects on mucin production by glands, 17: 23103
radiation effects on mitotic activity of male, whole-body, 17: 30335
radiation effects on muscles in, protective effects of cysteamine against, 17: 31967
radiation effects on mitotic activity in corneal epithelium of, 17: 35459(T) (JPRS-20735)
radiation effects on morphology and blood picture of thymus in, 17: 35467
radiation effects on mitosis of transplanted antibody-containing cells in, x, 17: 35519
radiation effects on mutation in, 17: 38806
radiation effects on mitosis in cornea of, x, 20: 5421
radiation effects on myocardium in, β, 20: 10643
radiation effects on metabolism in spleen of, effects of injected bone marrow on x, 20: 22797
radiation effects on mast cells in skin of, uv, 20: 28937
radiation effects on mitotic response of thymus-derived cells to sheep erythrocytes and skin grafts in, x, 20: 35339
radiation effects on mitotic cycle of duodenal crypt cells of, γ, 20: 45425
radiation effects on metabolism in, effects of bone marrow transplants on, 20: 45485
radiation effects on mortality, reproduction, and tumor tolerance in, 18: 23210
radiation effects on nervous system, 16: 16283
radiation effects on nucleic acid metabolism in, gamma and x, 16: 25212
radiation effects on nucleic acid metabolism in, protective effects of AET and MEA against, 16: 25255
radiation effects on nucleic acid synthesis in tumors in, synergistic effects of radiomimetic drugs on, 18: 25166
radiation effects on nucleic acid synthesis in tumors in, synergistic effects of radiomimetic drug on, 18: 25173
radiation effects on nucleic acid content and hematopoietic activity in spleen of, 18: 27192
radiation effects on nitrogen content of, effects of bone marrow injections on, 19: 138
radiation effects on nuclear ATP synthesis in, x, 19: 26062
radiation effects on neonatal and prenatal mortalities in, by fetal or maternal exposure, 19: 43760
radiation effects on neuromuscular system in, gamma, 17: 40615
radiation effects on normal and tumorous tissues of, effects of RNA on x, 20: 14401
radiation effects on nervous system of, γ, 20: 18376
radiation effects on nitrogen distribution in bone marrow-treated, x, 20: 20407 (ORNL-P-1118)
radiation effects on organ weight in, 18: 31199
radiation effects on organs of, protective effects of drugs against x, 18: 36966
radiation effects on omentectomized and splenectomized, time dependence of x, 18: 41205
radiation effects on oxidative properties of tissue of, effects of β-amino ethyl sulfate on, 18: 41167
radiation effects on oxidative phosphorylation in ascitic fluid from tumor-bearing, x, 19: 3899
radiation effects on ovaries in, direct, partial, and whole-body, 19: 15029
radiation effects on oocytes in, effects of time on mutagenic fission-neutron, 19: 31791(R) (ORNL-3768(p.89-93))
radiation effects on oocytes in, 19: 31791(R) (ORNL-3768(p.89-93))
radiation effects on oocytes in, beta, 19: 45831
radiation effects on osteogenesis in long bones of embryos of, 19: 45872
radiation effects on oxygen consumption, 17: 1291
radiation effects on ovaries in, local and whole-body, 17: 12169
radiation effects on oocyte maturation in ovaries in, 17: 15816(T)
radiation effects on ovaries in, 17: 21473
radiation effects on oxidative enzyme systems in gonads of, γ and x, 20: 31090
radiation effects on oxidative activity of tissues, x and ultraviolet, 20: 40642
radiation effects on organic peroxide production in, x, 17: 67
radiation effects on physiological regeneration of epithelial cells in cornea, 16: 1479(T) (JPRS-10170(p.158-77))
radiation effects on, protective effects of aminoethylisothiourea against, 16: 23517
radiation effects on population genetics, gonad exposure, 16: 25182(R) (TID-16323)
radiation effects on, protective effects of nitrous oxide against whole-body, 16: 28842
radiation effects on, protection against, 16: 28851
radiation effects on, protective effects of AET-Thiogel A against lethal, 16: 31386(R) (ANL-6535(p.19-20))
radiation effects on, protective effects of hesperidin against whole-body, 16: 32852
radiation effects on, protective effects of magnetic field pre-treatment against, 18: 1453
radiation effects on protein catabolism in, protective effects of dianabol against x, 18: 3595
radiation effects on, protective effects of catalase against x, 18: 5026
radiation effects on phosphorus-32 uptake by DNA in, x, 18: 5049
radiation effects on, protective effects of EDTA and serotonin against external and internal, 18: 6701
radiation effects on, protective effects of ascorbic acid and polyphenols against, 18: 8221
radiation effects on, protective effects of cystamine and mercamine against, 18: 8206
radiation effects on productivity of, x, 18: 11734

radiation effects on ploidy of spermatocytes in, x, 18: 11663
radiation effects on physiology of testis in, 18: 17588
radiation effects on production of adrenal hormones in, 18: 17628
radiation effects on parotitis virus reproduction in, x, 18: 19556(T) (JPRS-23956(p.9-17))
radiation effects on peritoneal cell transplants in, 18: 19591
radiation effects on postnatal development of cerebellum in, 18: 23284
radiation effects on polyovulated egg developments in eggs of, 18: 29287
radiation effects on productivity of, x, 18: 29300
radiation effects on production of bacteriophage-neutralizing antibody by, x, 18: 29301
radiation effects on population fitness of, 18: 35345
radiation effects on permeability of intestinal membranes of, tracer study, 18: 38789
radiation effects on peritoneal cavity cells in, 18: 41104
radiation effects on physiological response to stress, x, 18: 43220(R) (LA-3132-MS(p.109-41))
radiation effects on physiological capacitance, x, 18: 43220(R) (LA-3132-MS(p.109-41))
radiation effects on progeny survival in, protective effects of chemical agents against x, 19: 2179
radiation effects on physical reactivity of, in space, (E), 19: 3898(T) (FTD-TT-64-1077(p.234-46))
radiation effects on phosphorylase activity of muscles in, 19: 7146
radiation effects on pneumonia development in influenza virus inoculated, sparing, 19: 8899
radiation effects on persistence of leukemia in, x, 19: 21985
radiation effects on piliary system of, protective effects of chemicals against x, 19: 26124
radiation effects on phagocyte activity in, x, 19: 31676(R) (ORNL-3768(p.112-18))
radiation effects on Pseudomonas pathogenicity in, x, 19: 31905(R) (ORNL-3768(p.99-108))
radiation effects on phosphatase activity in, 19: 31870
radiation effects on protein metabolism in, 19: 31891
radiation effects on proliferative capacity of ascites tumor cells in, alpha, proton, and x, 19: 31798(R) (UCRL-11833(p.80-94))
radiation effects on performance capacity of, 19: 45823(T) (JPRS-31933, pp 1-5)
radiation effects on pneumococcal infection in, time factors in, 17: 4413
radiation effects on prolan stimulation of ovaries, 17: 5817
radiation effects on, protection against electron, 17: 12175
radiation effects on, protection against, using cyanides, 17: 13976(R) (NP-12484(p.116-33))
radiation effects on, protective effects of spleen cell injection or splenectomy on, 17: 15811
radiation effects on, protective effects of chemicals against, 17: 15826
radiation effects on, protective effects of dialyzed and whole spleen homogenates against lethal, 17: 15812
radiation effects on, protective effects of *N*-2-mercaptoethylpiperazine against, 17: 17857
radiation effects on, protective effects of drugs against proton, 17: 21590
radiation effects on, protective effects of injections of organs from irradiated animals against, 17: 21583
radiation effects on phosphorus-32 uptake by DNA in mammary adenocarcinoma in, 17: 23183
radiation effects on phosphorus-32 uptake by DNA in mammary adenocarcinoma in, local and whole-body, 17: 23184
radiation effects on progeny of male, 17: 25038
radiation effects on, protective effects of sodium cyanide against, 17: 28677 (TID-17148)
radiation effects on, protective effects of human blood serum on, 17: 28742
radiation effects on production of anti-influenza antibodies in, 17: 30387
radiation effects on, protective effects of *S*-ethylisothiuronium against, 17: 31948
radiation effects on, protective effects of drugs against, 17: 31966
radiation effects on plasma lactic dehydrogenase activity in, 17: 33632
radiation effects on, protective effects of cysteamine and reserpine against x, 17: 35470
radiation effects on, protective effects of ethyl palmitate against, 17: 35471
radiation effects on phagocytic mechanisms of antibacterial defense in, x, 17: 35520
radiation effects on, protective effects of chemicals against x, 17: 37067(T) (JPRS-20964)
radiation effects on Pseudomonas infection of, 17: 37082
radiation effects on, protective effects of chemicals against, 17: 38900
radiation effects on, protective effects of cysteine against x, 17: 40583
radiation effects on phagocytic activity of intestinal cells of, 20: 6839
radiation effects on postnatal survival in, following prenatal exposure, 20: 6860
radiation effects on polycythemic, protective effects of cloned marrow cells against, 20: 8723(R) (TID-22503)
radiation effects on Pseudomonas susceptibility in, x, 20: 10669
radiation effects on pigments in hair of, protective effects of melanogenetic substrates against x, 20: 18502
radiation effects on protein metabolism in, x, 20: 22607
radiation effects on properties of blood serum proteins in, 20: 26650
radiation effects on phagocytosis and immunity mechanism in, x, 20: 33011
radiation effects on postnatal activity and excretion by, neonatal whole-body x, 20: 33036
radiation effects on populations of, whole-body x, 20: 38590(R) (NYO-1979-13)
radiation effects on reproductive capacity of tumor cells, dose-response relation for neutron and x, 16: 17496
radiation effects on reproductive capacity of tumor cells, modification by pharmacological agents, 16: 17497
radiation effects on rearrangement of chromosomes in corneal cells of, following adrenalectomy, 18: 1395
radiation effects on reaction to foreign spleen, 18: 6625
radiation effects on reproductive rate of, 18: 9831(R) (AD-403109)
radiation effects on retina of, x, 18: 17540
radiation effects on reproduction in, gamma, 18: 23326
radiation effects on reproduction in, gamma, 18: 23328
radiation effects on reproduction in, 18: 23329
radiation effects on response of spleen to virus infection in, 18: 25223
radiation effects on reproductive fitness of populations of, 18: 35346
radiation effects on reproduction and growth of, 18: 35303(R) (AD-438541)
radiation effects on resistance to influenza virus infection in, 18: 41179
radiation effects on reproduction of, 19: 3901
radiation effects on reproduction in, x, 19: 5701
radiation effects on resistance of, to *Schistosoma mansoni*, 19: 7063
radiation effects on reproductive capacity of, 19: 7083
radiation effects on reproduction of, 19: 7085
radiation effects on reproduction of, 19: 7092
radiation effects on rabbit blast cells cultured in, 19: 7098
radiation effects on reproduction genetics in female, spermatogonial, 19: 7117
radiation effects on radiation chimeras, 19: 21943
radiation effects on reproductive behavior in, chronic low-dose gamma, 19: 25957
radiation effects on response to allogenic skin grafts, effects of mercaptopurine and bromodeoxyuridine on, 19: 26027
radiation effects on reproductive capacity in female, strain differences in, 19: 31791(R) (ORNL-3768(p.89-93))
radiation effects on regeneration of thymus grafts in, 19: 42340
radiation effects on response to antigen, 17: 7802 (TID-17650)
radiation effects on reductase activity of liver, 17: 13968(R) (NP-12484 (p.1-14))
radiation effects on reproduction, chronic exposure, 17: 21467 (TID-18549)
radiation effects on resistance to urethan-induced tumors, 17: 33666
radiation effects on reactivity of sulfhydryl groups in spleen of, 17: 35500
radiation effects on retina in newborn, x, 20: 117
radiation effects on retinal development in embryos of, x, 20: 3725
radiation effects on reproductive ability of female, small fractionated doses of x, 20: 6880
radiation effects on reticulo-endothelial function of, x, 20: 14374
radiation effects on resistance to dengue virus in, gamma and x, 20: 20360(R) (PRNC-73)
radiation effects on reproduction of, x, 20: 22611 (CEA-R-2874)
radiation effects on reproduction of, internal cesium-137, 20: 22692
radiation effects on resistance to Ehrlich ascites tumors of, 20: 29017
radiation effects on response to immunotherapy of leukemic, effects of methylhydrazine on, 20: 38794
radiation effects on recovery of erythropoietin-responsive erythrocytes in plethoric or spleen-shielded, x, 20: 45479
radiation effects on survival of albino, effects of dietary deficiencies on, 16: 20130 (NP-11741)
radiation effects on survival of isografted hearts, 16: 21936
radiation effects on spermatogonia of, 16: 31487
radiation effects on skin of, proton, 18: 1372 (BNL-7359)
radiation effects on sub-cellular structure and ATPase activity in tumors of, x, 18: 3534
radiation effects on Schistosoma cercariae in, gamma, 18: 4986
radiation effects on sulfur-35 distribution in blood, kidneys, and liver in, 18: 9900
radiation effects on sheep erythrocyte immunity in, continuous gamma, 18: 19623
radiation effects on stem cells in, effects of erythropoietin on, 18: 19635

radiation effects on splenic uptake of iron-59 by, x, 18: 19594
radiation effects on splenic proteolysis in, x, 18: 19744
radiation effects on survival of, protective effects of cysteamine against x, 18: 19788
radiation effects on survival and tumorigenesis in, gamma and neutron, 18: 23230(R) (ANL-6823(p.15-19))
radiation effects on susceptibility to virus infections of, 18: 23248(T) (JPRS-24696)
radiation effects on survival of, factors affecting, 18: 23347
radiation effects on spleen proliferation by transplanted marrow cells in, 18: 25189
radiation effects on spleen cell transplants in, x, 18: 27120
radiation effects on skin homografts in thymectomized, 18: 31234
radiation effects on skin grafting in, effects of prior newborn liver injection on x, 18: 31237
radiation effects on sorption in brain and kidneys of, fission-product, 18: 33358
radiation effects on splenic amino acid content in, 18: 37004
radiation effects on spleens of, after foreign cell injection, 18: 38863
radiation effects on secondary disease in chimeras in, protective effects of thymectomy against, 18: 38988
radiation effects on spermatogenesis in, protective effects of AET against, 19: 206
radiation effects on survival of, protective effects of chemicals against x, 19: 2181
radiation effects on survival of, fractionated-dose x, 19: 2081 (USNRDL-TR-784)
radiation effects on sulfur-35 uptake by knee joints of, x, 19: 2090
radiation effects on splenic stem cell release in, effects of thigh-shielding on, 19: 2129
radiation effects on stem cell pool in transplanted marrow of, x, 19: 3942
radiation effects on survival of dystrophic, iodine-131, 19: 3943
radiation effects on successive generations of populations of, 19: 7116
radiation effects on survival of, with skin lesions, 19: 7148
radiation effects on survival of skin grafts in, effects of 6-mercaptopurine and 5-bromodeoxyuridine on, 19: 8909
radiation effects on survival of, effects of methyl cellulose on whole-body, 19: 8920
radiation effects on sterility of female, irradiated at birth to 2 months, 19: 8816
radiation effects on steroid synthesis by testes, 19: 10783(R) (COO-119-231(p.76-84))
radiation effects on stunting of, exposed *in utero*, 19: 10796
radiation effects on survival of, protective effects of ribosemono-nucleotides against gamma, 19: 13098
radiation effects on survival of, lifetime gamma, 19: 15180
radiation effects on species of wild, gamma, 19: 15186
radiation effects on survival time of conventional and germ-free, x, 19: 17587
radiation effects on sulfur-35 uptake by soft tissues in hind limb of, 19: 21887
radiation effects on skin of, ultraviolet, 19: 21930
radiation effects on skin of, dosimetry of fractionated, 19: 28153
radiation effects on stem cells of, x, 19: 28066
radiation effects on spermatogenesis in, 19: 29968
radiation effects on secondary antibody-forming potential of spleen cells in, recovery from x, 19: 31676(R) (ORNL-3768(p.112-18))
radiation effects on stem cells in bone marrow of, x, 19: 31677(R) (ORNL-3768(p.119-30))
radiation effects on splenic and thymic weight in, x, 19: 31670(R) (NIRS-3(p.19-56))
radiation effects on *Salmonella typhimurium* immunity in, gamma, 19: 33946
radiation effects on susceptibility to bacterial toxins, protective effects of cortisone against, 19: 33975
radiation effects on susceptibility to bacterial toxins in, protective effects of cortisone against, 19: 33975
radiation effects on serum proteins in, following rat-to-mouse chimera transplants, 19: 38404
radiation effects on spleen weight in, genetic factors, 19: 54956
radiation effects on skin of, effects of dose-fractionation on electron, 19: 45885
radiation effects on seminiferous epithelium, whole-body exposure, 17: 1269
radiation effects on survival rate and weight loss, comparison of neutrons and x rays, 17: 2886
radiation effects on spread of tick-borne encephalitis in lymphatic system in, 17: 5786
radiation effects on survival of dormice in hibernating and waking state, 17: 7827
radiation effects on spleen and thymus of, from localized abdominal irradiation, 17: 12123 (BNL-6586)
radiation effects on stem cell compartment in, *in vivo*, 17: 15725
radiation effects on serum protein synthesis in mouse/rat chimeras, 17: 19843
radiation effects on sterility of, cause of, 17: 19910
radiation effects on spermatogenesis in, 17: 21472
radiation effects on spermatogenetic epithelium in, 17: 25051
radiation effects on spermatogenic line in, effects of AET on, 17: 28726
radiation effects on sulfur-35 distribution in blood, kidneys, and liver, 17: 33649
radiation effects on survival, protective effects of homologous bone marrow against, 17: 35454(R) (TID-19291)
radiation effects on secondary response to tetanus toxoid in, x, 17: 35530
radiation effects on survival of, protective effects of allogenic and isogenic bone marrow on, 17: 35600(R) (TID-19293)
radiation effects on secondary tetanus antitoxin responses in, 17: 38740 (BNL-6709)
radiation effects on sarcomatous, protective effects of testosterone on x, 17: 38823
radiation effects on sexual cells of male, fast-neutron, 17: 33668
radiation effects on spermatogenesis in, x, 20: 65(R) (TID-22174)
radiation effects on survival in, gammas, 20: 105
radiation effects on survival of transplanted tumors in, x, 20: 3751
radiation effects on spermatogenesis in, living on radioactive soils, 20: 5387
radiation effects on skeletal development of embryos of, x, 20: 5395
radiation effects on skeletal development in embryos of, x, 20: 5316
radiation effects on skeletal development of embryos of, x, 20: 5326
radiation effects on skeletal development in embryos of, x, 20: 5327
radiation effects on skeletal development in embryos of, x, 20: 5337
radiation effects on syngeneic bone marrow transplants in, x, 20: 6824
radiation effects on survival in carcinomatous, x, 20: 6852
radiation effects on skeletal development of embryos, x, 20: 6891
radiation effects on survival in virus-infected, x, 20: 8677
radiation effects on survival in transplanted, x, 20: 8718
radiation effects on serum transaminase activity in, x, 20: 12545(R) (PAEC(A)AR651)
radiation effects on spleen in, cytological x, 20: 12681
radiation effects on survival in, electrolytic balance as predictor of x, 20: 14266
radiation effects on survival of 5-bromo-deoxycytidine-treated bone marrow cells in, fast-neutron and x, 20: 14333
radiation effects on Schistosoma infectivity in, γ, 20: 14304
radiation effects on succinic dehydrogenase activity in, uv, 20: 16196
radiation effects on sensitivity to antigen-antibody complex in, 20: 18282
radiation effects on survival in, protective effects of 5-BUdR, MEA, and combined 5-BUdR and MEA against x, 20: 18498
radiation effects on skin of urethan-tested, x, 20: 20476
radiation effects on spermatogenesis and testicular development in, effects of age at irradiation on x, 20: 20499
radiation effects on survival of, protective effects of organophosphorus derivatives against x, 20: 20515
radiation effects on Salmonella antigenicity in allogeneic and syngeneic bone marrow chimeras in, x, 20: 22573 (ORNL-P-1316)
radiation effects on subcellular structure in brain of, proton, 20: 22710
radiation effects on skin graft immune reactions in, x, 20: 22741
radiation effects on spleen of, cytological x, 20: 22614(R) (NIRS-4, pp 28-34)
radiation effects on submandibular glands in, gamma, 20: 22684
radiation effects on serum proteins in, proton, 20: 24853 (CERN/HER/AP-1-66)
radiation effects on serotonin content in blood of, x, 20: 24884
radiation effects on survival of, effects of dose rate on electron and x, 20: 24923
radiation effects on skin graft survival in, x, 20: 24930
radiation effects on spermatogenesis in, x, 20: 24934
radiation effects on synthesis of blood plasma proteins induced by injected lymphoid cells in, 20: 28926 (AD-633469)
radiation effects on survival of, depth-dose factor in 120-Mev proton, 20: 28972
radiation effects on skin in, protection by, against effects of 7,12-dimethylbenzanthracene, 20: 28973
radiation effects on skin epithelial cells, dose-response relations for x, 20: 28990
radiation effects on susceptibility of newborn, to congenital anomalies, x, 20: 31066
radiation effects on survival of synchronized L cells in, uv, 20: 31084
radiation effects on submicroscopic structures of liver cells in, x, 20: 33041
radiation effects on spermatogonia of, β and x, 20: 22632
radiation effects on serum proteins in, x, 20: 35316
radiation effects on skin pigments, use in studying affinity of melanin for chloroquine, uv, 20: 36564
radiation effects on survival of, effects of 19-nor-testosterone phenyl-

propionate on x, 20: 38610
radiation effects on sex chromosomes in, x, 20: 40627(R) (ORNL-3922, pp 84-8)
radiation effects on survival of, protective effects of AET or glutathione combined with bone marrow transplants against x, 20: 40719(R) (ORNL-3922, pp 136)
radiation effects on sarcoma immunity in CBA, x, 20: 42890
radiation effects on skin of, comparison of electron, neutron, and x, 20: 45426
radiation effects on structure of RNA extracted from brain of, 20: 45345
radiation effects on stem cell regeneration in, transfused with syngeneic bone marrow, x, 20: 45348 (AD-637782)
radiation effects on skeletal system in progeny of female, exposed prior to mating, 20: 45399
radiation effects on susceptibility to leprosy bacillus, following thymectomy, whole-body x, 20: 45408
radiation effects on sulfur-35, 17: 35515
radiation effects on skin phospholipids in, uv, 17: 37074
radiation effects on tritium incorporation in brain and liver, 16: 20221
radiation effects on tumor metastasis in, 16: 20268
radiation effects on tissues of, fractionated and protracted fast neutron, 16: 26656(R) (NP-11966(p.1-26))
radiation effects on tibia in living, 16: 26740(R) (TID-16395)
radiation effects on thermoregulation in, x, 18: 1428
radiation effects on thrombocyte count in, protective effects of ultraviolet against x, 18: 3537
radiation effects on tumors in, 18: 5009(R) (UCRL-11033(p.139-51))
radiation effects on thrombocytes of, 18: 11745
radiation effects on tuberculosis in, altitude dependence of cosmic, 18: 15882
radiation effects on tubercle bacilli virulence in, cosmic, 18: 15884
radiation effects on thymus of, effects of, on immunity and lymphopoiesis, 18: 17498
radiation effects on thrombocyte count in, protective effects of ultraviolet radiation against, x, 18: 17648
radiation effects on transplantation antigens in, x, 18: 19589
radiation effects on tissue cells of, wavelength-dependent, 18: 19757
radiation effects on tumor-bearing, protective effects of chemicals against, 18: 19774
radiation effects on tumor growth and metastases development from transplanted tumors in, 18: 25162
radiation effects on tumor growth in, direct and indirect, 18: 29535
radiation effects on testicular zinc-65 uptake in, x, 18: 33270(R) (NIRS-2(p.23-6))
radiation effects on typhoid immunity in, gamma, 18: 33369
radiation effects on tumor cells of, protective effects of drugs against gamma, 18: 35389
radiation effects on testes of, neutron, 18: 41230
radiation effects on taurine excretion in splenectomized, 18: 41240
radiation effects on tumor cell growth in, beta, 19: 149
radiation effects on tumors in, protective effects of AET against, 19: 7179
radiation effects on tumors in, protective effects of chemical compounds against, 19: 7180
radiation effects on testes of, RBE of electron, gamma, and x-ray, 19: 10860
radiation effects on tuberculosis in, effects of altitude, daylight, and sex on, 19: 13065
radiation effects on transplanted tumors in, method for assessing, 19: 13090
radiation effects on thiamine metabolism in, mechanism of, 19: 15054
radiation effects on thymus tumors in, absence of synergistic effects of local and whole-body, 19: 17556
radiation effects on tumors of, preoperative fractionated, 19: 17632
radiation effects on total metabolism in, whole-body, 19: 17649
radiation effects on thymidine uptake by DNA in, four-factor model for analysis of, 19: 24337
radiation effects on teratology in, seasonal effects in, 19: 29947
radiation effects on tumor growth in, synergistic effects of ultrasound on, 19: 29972
radiation effects on tumorigenic, x, 19: 31817
radiation effects on tumor development in hairless, effects of 7,12-dimethylbenz[a]anthracene on uv, 19: 31843
radiation effects on transplanted leukemia in, 19: 33876
radiation effects on toxicity of 64 drugs for, 19: 33780
radiation effects on transfer and maintenance of adoptive immunologic tolerance to Shigella antigens in, 19: 36078
radiation effects on tetanus antitoxin formation in, after immunization with tetanus toxin, 19: 42302
radiation effects on thymus weight in, genetic factors, 19: 45956
radiation effects on testicles of sexually mature, during embryonic development, 17: 53
radiation effects on *Trichinella spiralis*, immunity in, 17: 15654
radiation effects on toxicity of plant substances on, 17: 15678
radiation effects on tolerance to skin grafts, 17: 15760
radiation effects on testes of, fractionated and single dose, 17: 19911
radiation effects on take of skin grafts, 17: 21468 (USNRDL-TR-628)
radiation effects on tolerance to toxic material, 17: 23116
radiation effects on tritium content in organs and skin of, 17: 27181
radiation effects on tumor cells in, evaluation of radioprotectants by, 17: 35575
radiation effects on testicular development in embryos of, 17: 37066(T) (JPRS-20960)
radiation effects on the thymus of, gamma, 17: 38835
radiation effects on thymus lymphatic tissue regeneration in, x, 17: 40584
radiation effects on testes in, effects of actinomycin on x, 20: 6865
radiation effects on transplanted tumors in, x, 20: 8662
radiation effects on toxicity of amphetamine in, x, 20: 18380
radiation effects on transplanted tumors in, electron and x, 20: 18396
radiation effects on thymus cytology in, 20: 22697
radiation effects on tritiated thymidine uptake by brain in, γ, 20: 22688
radiation effects on tularemia bacteria and infection in, x, 20: 26701
radiation effects on thiamine metabolism in, x, 20: 29003
radiation effects on thymus cells in, methods for evaluating, 20: 29008
radiation effects on tumor beds in, x, 20: 31073
radiation effects on testes of, x, 20: 33069
radiation effects on transplantable brain tumors in, protective effects of AET and iododeoxyuridine against proton and x, 20: 33090
radiation effects on thymus in, regeneration processes following whole-body x, 20: 35262
radiation effects on thymus of, metabolic, whole-body x, 20: 38606
radiation effects on tumors in, combined vincaleucoblastine, x, 20: 38613
radiation effects on taurine excretion in, effects of AET and cysteine on, whole-body x, 20: 38717
radiation effects on tumor transplants in, x, 20: 42889
radiation effects on toxicity of various drugs in, 20: 45448
radiation effects on tissues and tumors of hematopoietic system, effects of cytostatic drug on, 20: 45494
radiation effects on urinary excretion of oxalic acid, 16: 21962
radiation effects on uv-induced thrombopoiesis in, x, 18: 11744
radiation effects on urethan induced leukemia and lung tumor incidence in, fractionated and regional x-ray, 19: 7069
radiation effects on ultrastructure in fibroblasts of, electron, 19: 26065
radiation effects on ultrastructure of duodenal crypts in, 19: 33896
radiation effects on urethan-stimulated proliferation of lung cells in, tracer studies using tritiated thymidine, 17: 38821
radiation effects on ultrastructure of gastric fundus glands of, whole-body, 20: 111
radiation effects on urinary excretion of desoxycytidine by, γ, 20: 6871
radiation effects on urinary excretion of potassium and sodium in, fractionated x, 20: 6889
radiation effects on urethan-induced tumors in, effects of dose on x, 20: 10671
radiation effects on urinary excretion of taurine and urea in, effects of open skin wounds on, 20: 35248
radiation effects on viability of first generation, 16: 26785
radiation effects on vitamin B_{12} content in kidneys and liver of, gamma and x, 18: 19743
radiation effects on vestibular apparatus of, x, 19: 3969
radiation effects on various strains of, tumorigenic uv, 19: 36031
radiation effects on vertebral malformation in embryos of, *in utero*, 19: 42279
radiation effects on virulence of tumor grafted in successive generations of, 19: 43762
radiation effects on viability of *Schistosoma mansoni* cercariae in, γ, 20: 5313
radiation effects on wound healing in, 18: 23273
radiation effects on white blood cell count and tumor development in, small dose, 19: 7042
radiation effects on wound healing time in, x, 20: 12684
radiation effects on young embryos of, 19: 36007
radiation effects on zinc-65 metabolism by livers of, x, 18: 19531
radiation effects on zinc-65 uptake of testes in, x, 17: 33725
radiation effects on, 10 generation exposure, 17: 19840
radiation effects on 5-hydroxytryptamine content in small intestine in, 17: 15705
radiation effects on, 19: 2076(R) (ORNL-3700(p.113-26))
radiation effects on, 19: 25911 (TID-21727)
radiation effects on, acute gamma, 18: 11766
radiation effects on, as affected by dose rate, 18: 41220
radiation effects on, amyloidosis in chimeras and relation to lymphoid hypoplasia in whole-body, 19: 19650
radiation effects on, after exposure of 35 generations, 20: 18289(R) (LA-3432, pp 56-101)

radiation effects on, β, 20: 18353
radiation effects on, biological, 20: 22615(R) (NIRS-4, pp 34-58)
radiation effects on, biological, 20: 38627
radiation effects on, biological, effects of environmental oxygen on γ, 20: 38642
radiation effects on, biological, x, 20: 38648
radiation effects on, combined silicon dioxide and alpha, 19: 43831
radiation effects on, carcinogenic x, 20: 22697
radiation effects on, during simulated space flight, gamma, 20: 18443
radiation effects on, effects of bone marrow injections and influenza virus on x, 18: 9917
radiation effects on, effects of S-phosphorylated thiols on x, 18: 11851
radiation effects on, effects of cysteamine on x, 18: 11852
radiation effects on, effects of dose intensity on gamma, 18: 21883
radiation effects on, effects of procaine on, 18: 23384
radiation effects on, effects of bleeding on, x, 18: 25116
radiation effects on, effects of dose rate and irradiation time on, 18: 27084
radiation effects on, effects of bone marrow and spleen cell transplants on, 18: 33320
radiation effects on, effects of AET on, 18: 33407
radiation effects on, electron and proton, 18: 38928
radiation effects on, effects of splenectomy on, 18: 41198
radiation effects on, effects of sodium pentobarbital on response to x, 19: 205
radiation effects on, effects of metabolic products on whole-body, 19: 7195
radiation effects on, effects of splenectomy on whole-body, 19: 8906
radiation effects on, effects of sex on protective effects of AET against, 19: 8957
radiation effects on, effects of allogenic chimeric bone marrow on re-population of lymphatic tissue in, 19: 19646
radiation effects on, effects of blood transfusions on subsequent marrow transplants in, 19: 19653
radiation effects on, evaluation of drugs for protection against, 19: 26129
radiation effects on, effects of phytohemagglutinin on lymphoid noduli formation in, 19: 25984
radiation effects on, effects of dose fractionation on fast-neutron, 20: 3728
radiation effects on, effects of estradiol and estriol on x, 20: 6864
radiation effects on, effects of pyridine-deficient diet on, 20: 8671
radiation effects on, effects of age and dose fractionation on x, 20: 8691
radiation effects on, effects of adrenal hormones on x, 20: 18437
radiation effects on, effective residual dose for γ, 20: 18289(R) (LA-3432, pp 56-101)
radiation effects on, effects of mechlorethamine on, 20: 22775
radiation effects on, effects of sulfurated mineral water on, 20: 22775
radiation effects on, effects of mechlorethamine combined with sulfurated mineral water on, 20: 22775
radiation effects on, effects of homologous or heterologous tissue transplants on, 20: 22784
radiation effects on, effects of fractionated doses on protective effects of AET against, 20: 22788
radiation effects on, effects of oral cystamine on gamma, 20: 36666
radiation effects on, effects of AET and hypoxia on recovery from x, 20: 42988
radiation effects on, fast-neutron, 18: 41221
radiation effects on, fission-neutron, 18: 41224
radiation effects on, fast neutron, 19: 21817(R) (BNL-867(p.119-50))
radiation effects on, fission-neutron, γ, proton, and x, 20: 33055
radiation effects on, fast-neutron and gamma, 18: 11760
radiation effects on, gamma, 18: 41134
radiation effects on, genetic, 19: 7090
radiation effects on, gamma, 19: 43662(R) (UCLA-12-565, pp 97-128)
radiation effects on, gamma and proton, 19: 45821(T) (JPRS-31547, pp 1-5)
radiation effects on, genetic, 19: 45809(R) (NYO-1979-12)
radiation effects on, genetic, 20: 1622 (WT-820)
radiation effects on, genetic, 20: 3711(R) (NYO-3314-2)
radiation effects on, genetic, 20: 6781(R) (ORNL-3853, pp 98-101)
radiation effects on, genetic x, 20: 28957
radiation effects on, genetic x, 20: 31048
radiation effects on, γ and proton, 20: 31100
radiation effects on, γ and proton, 20: 31102
radiation effects on, genetic, fast neutron and γ, 20: 38647
radiation effects on, γ, neutron, and x, 20: 42833(R) (ANL-7136, pp 16-46)
radiation effects on, genetic, 18: 15810(R) (LAMS-3034(p.129-32))
radiation effects on, *in vitro* studies of lymphoid recovery following, 20: 42984
radiation effects on, lethal, 18: 43233 (UR-649)
radiation effects on, LET for, 19: 43721(R) (ORNL-TM-1217)
radiation effects on, late somatic x, 20: 20441 (ORNL-P-1173)
radiation effects on, lethal neutron, 20: 42934
radiation effects on, late somatic, 17: 24971
radiation effects on, methods for assay of bone marrow transplantation potential in, 19: 15229
radiation effects on, model for β, 20: 10640
radiation effects on, mechanism for protective effects of lymphoid and myeloid cell transplants against x, 20: 40727
radiation effects on, neutron, 18: 38732
radiation effects on, neutron, 18: 38933
radiation effects on, number and type of cells required for protection against, 19: 26135
radiation effects on, protective effects of trithiocarbonates of guanidine derivatives against, 18: 11866
radiation effects on, protective effects of sodium γ-hydroxybutyrate against, 18: 13565
radiation effects on, protective effects of clones against, 18: 17635(R) (TID-20443)
radiation effects on, protective effects of preserved bone marrow against lethal, 18: 17640
radiation effects on, protective effects of human platelets against, x, 18: 17649
radiation effects on, protective effects of ozone against, x, 18: 17654
radiation effects on, protective effects of iodoacetic acid against, 18: 17664
radiation effects on, protective effects of cysteamine against x, 18: 19775
radiation effects on, protective effects of fresh vs. stored bone marrow, 18: 19777
radiation effects on, protective effects of 2-(2-aminoethyl)-2-thiopseudourea and bone marrow against, 18: 19796
radiation effects on, protective effects of antioxidants against, 18: 19797
radiation effects on, protective effects of radiation-resistant whole bacterial cells against, 18: 19808
radiation effects on, protective effects of bone marrow against x, 18: 19770
radiation effects on, protective effects of frozen and stored bone marrow against x, 18: 19805
radiation effects on, proton and x, 18: 21827(R) (UCRL-11184(p.128-35))
radiation effects on, protective effects of chemical agents against gamma, 18: 21917
radiation effects on, protection against, using chlorotrianise, 18: 23371
radiation effects on, protective effects of antibiotics against, 18: 23380
radiation effects on, protective effects of diethylenetriaminepentaacetic acid against, from plutonium, 18: 23351(R) (ANL-6823(p.114-15))
radiation effects on, protective effects of ethyl palmitate against, x, 18: 25216
radiation effects on, protective effects of olive oil against, 18: 25231
radiation effects on, protective effects of low temperature against x, 18: 29387
radiation effects on, protective effects of chemical agents against, 18: 31273
radiation effects on, protective effects of AET against, 18: 31301
radiation effects on, protective effects of indolylalkylamines against, 18: 31302
radiation effects on, protective effects of thiophosphates against, 18: 31306
radiation effects on, protective effects of thiazolidines against, 18: 31307
radiation effects on, protective effects of sex hormones against gamma, 18: 31292
radiation effects on, protective effects of 3-amino-1,2-propanedithiol and its derivatives against gamma, 18: 31298
radiation effects on, proton, 18: 33286(T) (UCRL-Trans-1068)
radiation effects on, protection against x, 18: 33406
radiation effects on, protective effects of histamine against x, 18: 33414
radiation effects on, protective effects of bone marrow transplants and estradiol against x, 18: 35390
radiation effects on, protective effects of bone marrow and chemicals against x, 18: 37024
radiation effects on, protective effects of folic acid against, 18: 37026
radiation effects on, protective effects of gallates against x, 18: 38978
radiation effects on, protective effects of cysteamine and histamine against x, 18: 41247
radiation effects on, protective effects of castration against x, 18: 41248
radiation effects on, protective effects of protoporphyrins against, 18: 41250
radiation effects on, protective effects of chemicals against x, 18: 41253
radiation effects on, protective effects of psychotropic drugs against, 18: 43300
radiation effects on, protective effects of AET, glutathione, and serotonin against whole-body, 19: 199
radiation effects on, protective effects of pyridoxal-5-phosphate against whole-body, 19: 200
radiation effects on, protective effects of histamine against x, 19: 207

radiation effects on, protective effects of AET pretreatment on bone marrow transplantation immunity in, 19: 3988
radiation effects on, protective effects of cloned bone marrow and spleen cells against, 19: 8979
radiation effects on, protective effects of bone marrow and spleen cell transplantation against midlethal, 19: 17675
radiation effects on, protective effects of thiazoline derivatives against, 19: 17689
radiation effects on, protective effects of zinc complexes with MEG against, 19: 17911
radiation effects on, protective effects of AET or MEA with serotonine against lethal, 19: 19627
radiation effects on, protective effects of frozen bone marrow grafts against, 19: 19645
radiation effects on, protective effects of allogenic marrow inoculation against, 19: 19648
radiation effects on, protective effects of Pyrexal against, 19: 28115
radiation effects on, protective effects of antigens and polysaccharides against, 19: 28122
radiation effects on, protective effects of D- and L-cysteine against x, 19: 31906(R) (ORNL-3768(p.179-80))
radiation effects on, protective effects of hybrid bone marrow transplants against gamma, 19: 31911
radiation effects on, protective effects of hematopoietic transplants against gamma and x, 19: 33979
radiation effects on, protective effects of spleen cell induced immunological unresponsiveness against, 19: 38454
radiation effects on, protective effects of cobalt–chlorophyll and glucuronic acid against whole-body, 19: 38456
radiation effects on, protective effects of orotic acid against, x, 19: 38458
radiation effects on, protective effects of hematoporphyrin against x, 19: 42354
radiation effects on, protective effects of plasma properdin levels against x, 19: 42355
radiation effects on, protective effects of DNA against, 19: 42358
radiation effects on, protective effects of nitrogenous heterocyclics against x, 19: 43863
radiation effects on, protective effects of *p*-aminopropiophenone and MEA against proton and x-ray, 19: 43873
radiation effects on, protective effects of *p*-aminopropiophenone against whole-body proton, 19: 43874
radiation effects on, protective effects of hematoporphyrins against x, 19: 43862
radiation effects on, protective effects of erythropoiesis-stimulating preparation against, 19: 43872
radiation effects on, protective effects of 1-phenyl-1-acetylthio-2-nitroethane and -propane against, 19: 43868
radiation effects on, protective effects of sodium cysteinethiosulfonate against, 19: 46006
radiation effects on, protective effects of AET, glutathione, and serotonin against, 19: 46016
radiation effects on, protective effects of bone marrow transplants against, 20: 133
radiation effects on, protective effects of bone marrow grafts against lethal, 20: 138
radiation effects on, protective effects of heparin against, 20: 10705
radiation effects on, protective effects of splenic marrow transplants against, 20: 10713
radiation effects on, protective effects of MEA against, 20: 10714
radiation effects on, protective effects of chemicals against gamma, 20: 3792
radiation effects on, protective effects of bone marrow cells against x, 20: 6908(R) (NYO-2862-1)
radiation effects on, protective effects of cysteamine and hypoxia against electron, 20: 8731
radiation effects on, protective effects of bone marrow against y, 20: 8738
radiation effects on, protective effects of preserved bone marrow against, 20: 8529
radiation effects on, protective effects of bone marrow therapy against, 20: 12720(R) (TID-22466)
radiation effects on, protective effects of sodium hyposulfite against x, 20: 14393
radiation effects on, protective effects of 1,3,4-oxadiazolium salts and *s*-triazole derivatives against, 20: 16490(R) (TID-22681)
radiation effects on, protective effects of sulfur compounds against, 20: 16297(R) (EUR-2548.f)
radiation effects on, protective effects of 5-methoxytryptamine against x, 20: 18430
radiation effects on, protective effects of endogenous sulfhydryl groups against x, 20: 18431
radiation effects on, protective effects of endogenous sulfhydryl compounds against x, 20: 18433
radiation effects on, protective effects of chemical agents against y and proton, 20: 18440
radiation effects on, protective effects of psychotropic drugs against x, 20: 18501
radiation effects on, protective effects of antioxidant inhibitors against x, 20: 20506
radiation effects on, protective effects of drugs against x, 20: 20513
radiation effects on, protective effects of cultured fetal liver cells against, 20: 22787
radiation effects on, protective effects of fresh fetal liver cells against, 20: 24942
radiation effects on, protective effects of preserved homologous bone marrow against gamma, 20: 29033
radiation effects on, protective effects of preserved homologous fetal liver against gamma, 20: 29034
radiation effects on, protective effects of AET combined with bone marrow transplants against, y, 20: 29036
radiation effects on, protective effects of AET and bone marrow against, 20: 33073
radiation effects on, protective effects of antiserum, chimeric donor transplants, and preimmunization against gamma, 20: 33074
radiation effects on, protective effects of *Bacillus subtilis* preparations against x, 20: 36673
radiation effects on, protective effects of aminothiols and their derivatives against, 20: 38724
radiation effects on, protective effects of bone marrow against x, 20: 40718(R) (ORNL-3922, pp 99-105)
radiation effects on, protective effects of transplants of parental tissue against x, 20: 40718(R) (ORNL-3922, pp 99-105)
radiation effects on, protective effects of nibufin on x, 20: 40724
radiation effects on, protective effects of vaccines, thiophosphates, and AET against y and x, 20: 42992
radiation effects on, protective effects of bone marrow treated with cortisone or nitrogen mustard against, 20: 42995
radiation effects on, protective effects of indolyl- and mercapto-alkylamines against y and proton, 20: 43002
radiation effects on, protective effects of apilac and cystamine against x, 20: 43009
radiation effects on, protected by various agents post-irradiation, 20: 45492
radiation effects on, repair mechanisms in AET-protected, 18: 31300
radiation effects on, recovery from gamma, 18: 33377
radiation effects on, repopulating potential of frozen and normal bone marrow in, 19: 191
radiation effects on, relative biological effectiveness of gamma, 19: 7172
radiation effects on, RBE of 595-Mev high-energy proton, 19: 13041
radiation effects on, review on recovery from, 20: 12631 (CEA-R-2776)
radiation effects on, role of bone marrow cells in immune reactions in, 20: 12716 (AD-626682)
radiation effects on, role of adrenal and pituitary glands in, 20: 16232(T) (JPRS-34120)
radiation effects on, RBE for 15-Mev x, 20: 31072
radiation effects on, RBE for 35-Mev electron, 20: 42974
radiation effects on, synergistic effects of vibration with, 20: 28968
radiation effects on, therapeutic effects of stimulants against x, 18: 43313
radiation effects on, use of nicotinic acid derivatives to treat, 18: 23365
radiation effects on, use of testis weight for evaluation of x, 20: 42841(R) (ANL-7136, pp 266-89)
radiation effects on, x, 18: 38859
radiation effects on, 10-kev x, 20: 20475
radiation effects on, 2.2-Bev proton, 20: 8616 (BNL-9703)
radiation effects on, 2.2-Bev proton, 20: 18185(R) (BNL-929, pp 126-47)
radiation effects on, 2.0-Bev proton, 18: 1371 (BNL-7343)
radiation effects on, 20-generation analysis of, 17: 31853 (LADC-5618)
radiation effects with open skin wound on mortality of, whole-body, 19: 17645
radiation effects with spleen cell transplants on polyvalent tolerance in adult and newborn, 19: 38376
radiation effects, fractionated exposure, 17: 7804 (USNRDL-TR-595)
radiation effects, pathological, 20: 60(R) (NYO-901-37, pp 33-68)
radiation effects, protective effects of chemicals, 16: 14459(R) (NP-11359(p.35-75))
radiation effects, protective effects of sodium nitrite, 16: 14460(R) (NP-11359(p.76-80))
radiation effects, protective effects of spleen cells against, 16: 20263
radiation effects, protective effects of drug-amino acid mixtures against, 16: 28838
radiation effects repair processes in bone marrow in, 17: 23156
radiation effects therapy using marrow infusion, 18: 43317
radiation effects therapy in, factors in homologous spleen, 17: 14106
radiation fractionation effects on, gamma and neutrons, 18: 3494 (TID-

18386)
radiation hazards to skin of, uv, 20: 32970
radiation injuries, dose-mortality relations for toxic and protective effects of chemical agents, 16: 18760(R) (NP-11660(p.1-15))
radiation injuries, evaluation of toxicity and radioprotective effects of 60 compounds, 16: 18761(R) (NP-11660(p.16-41))
radiation injuries in, protective effects of chemical agents against, 16: 25253
radiation injuries, protective effects of pharmacological and toxicological compounds against, 16: 26662(R) (NP-11966(p.79-94))
radiation injuries to gastrointestinal tract of, protective effects of MEA and p-aminopropiophenone against, 16: 26665(R) (NP-11966(p.128-30))
radiation injuries, protection by various agents using oxygen effect, 16: 30305
radiation injuries, beneficial effects of shielding nonhomopoietic organs on restoration of hematopoiesis in, 16: 30308
radiation injuries in, protective effects of acylated derivatives of MEA against, 17: 5924
radiation injuries in, effects of dithiocarbamates against, 17: 10428
radiation injuries in, effects of foreign spleen cells on blood and tissue changes in, 17: 10434
radiation injuries in, effects of isologous bone marrow and leukemoid leukocyte injections on, 17: 10283
radiation injuries, protective effects of aminoethylisothiuronium, 17: 13991(T) (JPRS-17819(p.25-31))
radiation injuries, correlation of systemic and hematological recovery, 17: 15804 (USNRDL-TR-606)
radiation injuries in, protective effects of shielded spleen implants against, 17: 17785
radiation injuries in, toxic effects of procaine on, 17: 23217
radiation injuries, effects of various protective treatments, 17: 23086(R) (NP-12760(p.92-102))
radiation injuries, age and sex factors, 17: 23174
radiation injuries in, therapy of, using sodium sulfite, 17: 33485(R) (NP-13010(p.49-54))
radiation injuries in, protective effects of β-mercaptoethylamine against, 17: 33489(R) (NP-13010(p.81-106))
radiation injuries in, protective effects of β-mercaptoethylamine and p-aminopropiophenone against, 17: 33490(R) (NP-13010(p.107-26))
radiation injuries in, protective effects of bone marrow, spleen, and thymus transplants against, 17: 38893
radiation injuries in, protective effects of bone marrow transplantation against, 17: 38894
radiation injuries of skin of, effects of continued hair plucking on recovery from, 17: 40653
radiation injuries in, evaluation of 54 chemical compounds for protective effects against, 18: 5137(R) (NP-13281(p.70-91))
radiation injuries in bone marrow in, protective effects of alanine and proline against, 18: 6699
radiation injuries in, protective effects of 2-aminoethanethiol and pyrimidine derivatives against, 18: 6710
radiation injuries to, protective effects of aqueous spleen extract against, 18: 8205
radiation injuries in infantile, treatment using desoxyribonucleic acid injections, 18: 8207
radiation injuries in, protective effects of lipids on, 18: 8208
radiation injuries in, kinetics of fractionated or split dose, 18: 8215
radiation injuries to, effects of treatment with desoxynucleotide derivatives on, 18: 11899
radiation injuries in, protective effects of AET, 18: 11846(R) (NP-13555(p.96-106))
radiation injuries in, effects of pre-treatment with MEA or PAPP on, 18: 11847(R) (NP-13555(p.118-30))
radiation injuries in, protective effects of AET against, 18: 11846(R) (NP-13555(p.96-106))
radiation injuries in, kinetics of protracted, split, and fractionated dose for acute mortality, 18: 17463(R) (ANL-6790(p.21-5))
radiation injuries in, effects of splenectomy on lethal, 18: 17556
radiation injuries to, protective effects of MEG against, 18: 17655
radiation injuries to, protective effects of MEG against fast neutrons and x rays, 18: 17656
radiation injuries in, protective and restorative effects of cysteine, 18: 17657
radiation injuries of, protective effects of thiazolidinecarboxylic acid derivatives on, 18: 17670
radiation injuries in, protection against using sodium nitrate, 18: 23356(R) (NP-13918(p.99-106))
radiation injuries in, protective effects of p-aminopropiophenone against, 18: 23357(R) (NP-13918(p.107-15))
radiation injuries in, protective effects of amino compounds combined with thiols, 18: 23385
radiation injuries in, protection against, using sodium nitrate, 18: 23356(R) (NP-13918(p.99-106))
radiation injuries in, protective effects of injected lipids against, 18: 25217
radiation injuries to, protection against, by olive oil, 18: 27226
radiation injuries in, protective effects of glutathione alone and combined with AET, 18: 27210(R) (ORNL-3601(p.187))
radiation injuries in, protective effects of ethyl palmitate and plant oils against, 18: 27214
radiation injuries in, protective effects of cysteine on, 18: 29420
radiation injuries of, protective effects of cysteamine, reaction mechanisms of, 18: 29425
radiation injuries in, protective effects of standard radioprotective agents against late effects of, 18: 31259(R) (AD-427279)
radiation injuries in, protective effects of 2,3-dimercaptosuccinic acid against, 18: 31271
radiation injuries in, protective effects of phosphates and ethylenediaminetetraacetic acid against, 18: 31276
radiation injuries in, protective effects of cysteamine derivatives and nitrogen mustards against, 18: 31278
radiation injuries of, protective effects of amines against, 18: 33277 (STI/DOC/10/28(p.21-38))
radiation injuries in, protection against, using previously aspirated bone marrow, 18: 33223
radiation injuries in, effects of conditioning irradiation on recovery from lethal, 18: 35365
radiation injuries in, protective effects of anoxia and serotonin on, 18: 35398(R) (NP-14210(p.48-54))
radiation injuries in, protective effects of cyclobutane derivatives against, 18: 35399(R) (NP-14210(p.55-80))
radiation injuries in, protective effects of p-aminopropiophenone against, 18: 35400(R) (NP-14210(p.90-104))
radiation injuries in, protective effects of AET and PAPP against, 18: 36951(R) (TID-20979)
radiation injuries of testis in, protective effects of AET on, 18: 38888
radiation injuries in, kinetics of accumulation of, 18: 38891
radiation injuries in, protective effects of cystamine on, 18: 39022
radiation injuries of liver of, effects of dose rate on regeneration time, 18: 41106(T)
radiation injuries in, protective effects of melamine against, 18: 41269
radiation injuries of corneal epithelium in, use as test system for evaluation of radioprotective compounds, 18: 41270
radiation injuries of, protective effects of injected paraffin oil in, 18: 43327
radiation injuries in, protective effects of bone marrow injections on, 19: 193
radiation injuries of, protective effects of vitamin B_{12} on, 19: 190
radiation injuries in, protective effects of vegetable oils on, 19: 208
radiation injuries in, protective effects of anabolic hormone on, 19: 209
radiation injuries in, effects of bone marrow injections, 19: 213
radiation injuries of, effects of bone marrow transplants on, 19: 2156
radiation injuries in, protective effects of AET and glutathione on, 19: 2164(R) (ORNL-3700(p.155-6))
radiation injuries of, protective effects of injections of bone marrow or fetal liver against, 19: 2169
radiation injuries of, protective effects of cysteinethiosulfonate on, 19: 3986
radiation injuries in, protective effects of streptomycin on, 19: 4000
radiation injuries of, effects of foreign bone-marrow cells on, 19: 5722
radiation injuries of, protective effects of triazoles against, 19: 7176(R) (ANL-6906(p.78-80))
radiation injuries of bone in, effects of hormone activity on, 19: 7134
radiation injuries of, protective effects of hypoxia and cysteamine on, 19: 7191
radiation injuries to, effects of thymus on, 19: 7193
radiation injuries in, evaluation of protective effects of chemicals on, 19: 8953(R) (NP-14448(p.36-64))
radiation injuries in, evaluation of protective effects of chemicals on, 19: 8954(R) (NP-14448(p.65-97))
radiation injuries in, protective effects of sodium nitrate on, 19: 8955(R) (NP-14448(p.108-15))
radiation injuries in, protective effects of 2-mercaptoethylguanine, 19: 8966
radiation injuries in, protective effects of serotonin on, 19: 8968
radiation injuries in, protective effects of bone marrow injections on, 19: 8974
radiation injuries in, protective effects of injections of cloned bone marrow cells against, 19: 10898(R) (TID-21613)
radiation injuries in, protective effects of psychotropic drugs against, 19: 10897 (SGAE-BL-7/1964)
radiation injuries in, protective effects of sodium cysteine thiosulfate against, 19: 10899
radiation injuries in, protective effects of 36 mineral anions against, 19: 10903
radiation injuries in, protective effects of injections of blood plasma or

bone marrow from irradiated donors against, 19: 10914
radiation injuries of, protective effects of transfused allogenic bone marrow against, 19: 10919
radiation injuries in, effects of 2,4-dinitrophenol on, 19: 13099
radiation injuries of skin of, effects of temperature on ultraviolet-induced, 19: 17510
radiation injuries in, protective effects of aminoethylisothiourea and serotonin in, 19: 19635
radiation injuries in, protective effects of prochlorperazine against, 19: 19631
radiation injuries in, protective effects of prochlorperazine against, 19: 19632
radiation injuries in, protective effects of methyl sulfoxide, 19: 22019(R) (UCLA-12-541(p.51-91))
radiation injuries, protective effects of β-2,4,5-trichlorophenoxyethanol, 19: 22007
radiation injuries, protective effects of bacterial toxins, 19: 22010
radiation injuries, protective effects of anoxia, 19: 22011
radiation injuries, protection against, evaluation of 35 chemical compounds for, 19: 21993(R) (NP-14779(p.29-44))
radiation injuries, protection against, evaluation of 6 chemical compounds for, 19: 21994(R) (NP-14779(p.45-63))
radiation injuries, protective effects of 3,5-demethyl-1-dimethyl carbamyl pyrazole, 19: 21998
radiation injuries to hematological system, effects of post-irradiation bleeding on, 19: 21890
radiation injuries, protective effects of 2-mercaptoethylguanine, 19: 24373
radiation injuries of, protective effects of injected hematopoietic cells of, 19: 29995 (TID-21871)
radiation injuries in, protective effects of injected bone marrow, 19: 30013 (ACRH-103(p.104-20))
radiation injuries, protective effects of mercaptobenzothiazole, 19: 30003
radiation injuries of, protective effects of injected hematopoietic cells, 19: 31907(R) (TID-21799)
radiation injuries, protective effects of hyperbaric oxygen, 19: 31903(R) (NP-15072(p.88-102))
radiation injuries, protective effects of cysteamine and cystamine, 19: 31910
radiation injuries, protective effects of bone marrow in normal and germ-free, 19: 31917
radiation injuries to, effects of injections of bone marrow and spleen cells on, 19: 31918
radiation injuries in, protective effects of serotonin, 19: 31921
radiation injuries in, protective effects of cytidine and uridine monophosphates, 19: 31922
radiation injuries, protective effects of fifty compounds, computer analysis, 19: 31900(R) (NP-15072(p.37-70))
radiation injuries, protective effects of aminoethylisothiuronium, dimethylsulfoxide, and p-aminopropiophenone, 19: 31901(R) (NP-15072(p.71-81))
radiation injuries, protective effects of p-aminopropiophenone, 19: 31902(R) (NP-15072(p.82-7))
radiation injuries in, effects of methylcellulose on, 19: 31847
radiation injuries in, protective effects of injected nucleotides, 19: 33967
radiation injuries in, protective effects of organophosphorus compounds in, 19: 33962
radiation injuries, protective effects of bone marrow injections and reticulo-endothelian stimulation, 19: 36056
radiation injuries, protective effects of injected hematopoietic tissues, 19: 36100(R) (NP-15170)
radiation injuries, protective effects of ethanol, glucose, and propylene glycol, 19: 36107
radiation injuries in, effects of hypothermia on protective effects of chemicals, 19: 36108
radiation injuries, effects of chemical radioprotective compounds, 19: 38452
radiation injuries, protective effects of morphine, 19: 38453
radiation injuries, protective effects of 2-mercaptobenzothiazole, 19: 38466
radiation injuries, protective effects of anoxia against, 19: 38450 (USNRDL-TR-851)
radiation injuries, protective effects of aminoethylisothiuronium against, 19: 38450 (USNRDL-TR-851)
radiation injuries in, protective effects of aminoethylisothiuronium combined with bone marrow injections against, 19: 42349(R) (NP-15345)
radiation injuries in, protective effects of bone marrow injections against, 19: 42350(R) (NP-15346)
radiation injuries in, protective effects of fetal liver transplants against, 19: 42351(R) (NP-15347)
radiation injuries in, protective effects of Mycobacterium emulsion against, 19: 42373
radiation injuries in, protective effects of tryptamine against, 19: 43864
radiation injuries, protective effects of injected nucleic acid precursors, 19: 43866
radiation injuries in, pathology and recovery, 19: 43771
radiation injuries and recovery in, after exposure to fractionated doses, 19: 43792
radiation injuries, protective effects of dimethyl sulfoxide against, 19: 43859(R) (NP-15310, pp 1-13)
radiation injuries of, protective effects of chlorotrianisene against, 19: 46029
radiation injuries in, protective effects of injected bovine liver homogenates against, 19: 46024
radiation injuries, protective effects of sodium cysteinethiosulfonate against, 20: 130
radiation injuries of sarcomas in, protective effects of cysteinethiosulfonate against, 20: 131
radiation injuries in, recovery kinetics for, 20: 1685
radiation injuries of, induced by high-energy protons and alpha particles, 20: 1614 (NASA-SP-71, pp 97-103)
radiation injuries of, protective effects of bone marrow injections in germ-free, 20: 3788
radiation injuries in, effects of mercapto analogs of ephedrine on, 20: 3790
radiation injuries in, protective effects of AET against γ, 20: 5410
radiation injuries in, protective effects of 2-aminothiazoline salts against γ, 20: 5410
radiation injuries in, protective effects of mercaptoethylamine against, 20: 5407(R) (AD-623599, pp 37-44)
radiation injuries of, evaluation of protective effects of 60 compounds on, 20: 6919
radiation injuries of, protective effects of bone marrow injections against, 20: 6784(R) (ORNL-3853, pp 118-27)
radiation injuries in, protective effects of injected bone marrow against, 20: 6909(R) (ORNL-3853, pp 116-17)
radiation injuries of, evaluation of protective effects of fourteen compounds on, 20: 8725
radiation injuries of, protective effects of anoxia against, effects of age, 20: 10707
radiation injuries in, protective effects of polysaccharide prepared from yeast cultures against, 20: 10703
radiation injuries of, protective effects of anoxia against, effects of age on, 20: 10707
radiation injuries in, protective effects of cystamine against, 20: 10708
radiation injuries of, effects of drugs affecting central nervous system on, 20: 18459
radiation injuries in, effects of quinoxaline-di-N-oxide on, 20: 18465
radiation injuries to, protective effects of chemical compounds against low-dose, 20: 18473
radiation injuries of, protective effects of thioglycollic acid derivatives against, 20: 18474
radiation injuries of, effects of cysteamine and prochlorperazine on, 20: 18491
radiation injuries of, effects of bacterial toxins on, 20: 18496
radiation injuries to, effects of bleeding on proliferative activity of bone marrow cells after x, 20: 20452
radiation injuries to tissues in, effects of bone marrow therapy on, 20: 31108
radiation injuries of, use of cadaver bone marrow for treatment of, 20: 31135
radiation injuries in liver and tumor tissues in, protective effects of cystine, glutathione, and MEA against gamma, 20: 31141
radiation injuries of, effects of cysteamine on, 20: 33085
radiation injuries in, protective effects of indolylalkylamines against, 20: 38725
radiation injuries in, protective effects of chemical agents against, 20: 38726
radiation injuries to hearts of, x, 20: 40648
radiation injuries to oral tissues in, following subcutaneous injection of radionuclides, 20: 42967
radiation injuries in, protective effects of isologous bone marrow injections against proton, 20: 42981
radiation injuries in, protective effects of locally administered cysteamine against, 20: 42983
radiation injuries in, protected by iproniazid or serotonin, x, 20: 42991
radiation injury diagnosis using hematopoietic changes, 20: 22705
radiation injury kinetics in, 19: 7012(R) (ANL-6906(p.7-18))
radiation injury of hematopoietic system, effects of injected peritoneal cells, 17: 13995
radiation injury of hematopoietic system in, effects of age on recovery from, 18: 1422
radiation injury, protective effects of 5-oxytryptamine derivatives, 16: 30310
radiation injury recovery rate and its relation to life expectation, 16: 4110(R) (TID-13911)

radiation injury repair rate, 17: 23232
radiation injury recovery kinetics of, measurement of, 17: 40660 (TID-18174)
radiation injury to, effects of 43 chemicals on, 17: 13975(R) (NP-12484 (p.94-115))
radiation injury to Ehrlich carcinoma cells in, protective action of cysteamine and cystamine against, 17: 33671
radiation injury to chromosomes of testes in, protection against, using streptomycin, 18: 23359(T) (JPRS-24593(p.120-5))
radiation lethality in, effects of propyl gallate and tocopherols on, 17: 4442
radiation lethalite in, pyromellitic acid protection against, 17: 14105
radiation lethality in, synchrotron dose for, 17: 22690
radiation lethality in, 157-Mev proton, 17: 22691
radiation lethality in, kinetics of, 17: 33455(R) (ANL-6723(p.67-72))
radiation lethality in, combined fast-neutron and gamma or x-ray, 20: 45256
radiation lethality in, effect of dose rate on proton and x, 17: 38886 (UCRL-11014)
radiation lethality in, proton and x, 18: 43 (CONF-250-3)
radiation lethality in, reaction mechanisms of proton and x, 18: 5004(R) (UCRL-11033(p.12-18))
radiation lethality in, 660-Mev proton, 17: 17779(T) (JINR-18395 (p.363-8))
radiation protection by peritoneal fluid injection in, 17: 30378
radiation protective effect of morphine in, 17: 30424
radiation protection effects of polyanions in, 17: 30428
radiation protection of hematopoiesis by hormones in, 17: 31941
radiation protective effect of spleen extract in, 17: 33758
radiation protection of intestinal and hematopoietic systems in, chemical, 17: 33762
radiation protection using anesthetics, 17: 40654
radiation protection of embryos of, 18: 33423
radiation protection and recovery in endotoxin-treated, 20: 40732 (AD-636209)
radiation sensitivity, protective effects of complex amine oxides against, 16: 31519
radiation sensitivity of, effects of hypoxia on, 18: 21892
radiation sickness in, pathology of acute, 16: 28848
radiation sickness and tumor transplants, protective effects of dextran, 16: 30306
radiation sickness, protective effects of bacterial antigens, 16: 30307
radiation sickness, effects of organophosphorus compounds on, 17: 183(T) (JPRS-15432(p.983-9))
radiation sickness, protection against, using phytolipopolysaccharides and vinylbutyl ether polymer, 17: 2880
radiation sickness, protection against, using mercaptoethylguanidine, 17: 2888
radiation sickness in, protection against, using 2-(2-aminoethyl)-2-thiopseudourea, 17: 2887
radiation sickness in, protective effects of Tanderil against, 17: 10472
radiation sickness of, protection against, using p-aminopropiophenone and 2-mercaptoethylamine, 17: 13977(R) (NP-12484(p.134-58))
radiation sickness of, effects of accelerations at moment of irradiation on acute, 17: 14091(T) (JPRS-17202(p.7-9))
radiation sickness of, protection against, using 2-aminoethanethiol, 17: 14094(T) (JPRS-17222(p.22-31))
radiation sickness in, effects of Caucasian yam tinctures on proteins during, 17: 14097(T) (JPRS-17872(p.9-13))
radiation sickness in, protective effects of properdin against, 17: 14103
radiation sickness, protective effects of vegetable oils against, 17: 14111
radiation sickness of, effects of appendectomies, chemicals, and splenectomies on resistance to, 17: 15754
radiation sickness prophylaxis and therapy in, 17: 15841
radiation sickness of, biometrical studies of, 17: 15846
radiation sickness of, protection against, using cysteamine, 17: 17937
radiation sickness of, effects of lowering tissue level of serotonin on, 17: 17938
radiation sickness in, protective effects of Librium against, 17: 27189
radiation sickness in, protective effects of ozone against, 17: 28772
radiation sickness in, protective effects of antibiotics and chlorinated drinking water against, 17: 28773
radiation sickness, protective effects of diethyl stilbestrol propionate against, 17: 30457
radiation sickness of, protective effects of β-mercaptoethylamine against, 17: 33759
radiation sickness of, reduction of protective effect of cysteamine against, 17: 40670
radiation sickness of, effects of sex hormones on, 18: 3584(T) (JPRS-22000)
radiation sickness in, effects of lipopoly- and polysaccharides on properdin content during, 18: 8226
radiation sickness effects on sensitivity to typhoid endotoxin in, 18: 8216
radiation sickness in, protective effects of pethidine and thiopental against, 18: 9924
radiation sickness in, effects of manganese and zinc complexes on, 18: 9931
radiation sickness in, protective effects of peat substances against, 18: 17666
radiation sickness in, effects of influenza virus vaccine and bone marrow injections on, 18: 23366
radiation sickness in, protective effects of gallates against, 18: 31133(T) (JPRS-25274)
radiation sickness of, nucleated cell depletion in bone marrow in, 18: 33351
radiation sickness induced by injected polonium-210 in, therapy of, 19: 218(T) (JPRS-26542(p.6-10))
radiation sickness in, protective effects of phenol and procaine against, 19: 8960
radiation sickness in, protective effects of sympatheticomimetic substances against, 19: 17696
radiation sickness in, effects of homologous gamma globulin on, 19: 24311
radiation sickness in, control of intestinal infections during, 19: 31904(R) (NYO-2628-1)
radiation sickness in, effects of preserved isologous bone marrow on, 19: 33964
radiation sickness in, protective effects of rutin against, 19: 46030
radiation sickness in, mechanism of death from, 20: 38666
radiation sickness in, protective effects of procaine against, 20: 38727
radiation sickness in, gamma and x, 20: 40694
radiation source avoidance by, γ, 20: 20495
radiation source recognition by, during chronic gamma exposure, 19: 7019 (LADC-6168)
radiation theory of tumors in, production of hydrogen sulfide in tumor during, 16: 32873
radiation tolerance, application of probit method to study, 16: 6329
radiation tolerance acquired by, by transfer of tolerant state, 17: 19769
radiation used with vaccination in, effects on lymph nodes and spleen, 18: 19740
radiation xenogenic chimeras of, immune reactions in, 18: 41079(R) (HW-80500(p.124-6))
radiation, space flight, and vibration effects on serotonin content in blood of, 19: 15095
radio- and chemotherapy of leukemia in, 18: 41283
radio- and urethane-induced pulmonary adenomas, x, 20: 42891
radio- and viral-induced lymphomas in, *in vitro* reactions of lymphocytes in, 20: 35268
radio- or chemically-induced leukopenia and lymphopenia in, effects of pertussis vaccine on x, 20: 22685
radioactivity of lymphocytes and macrophages of, after injections of tritiated tetanus toxin, 17: 17888
radioactivity of, effects of AET on γ, 20: 18509(R) (UCLA-12-576, pp 61-80)
radioactivity retained following injection of iodine-131-labeled 5-iodo-2'-deoxyuridine in, 19: 6931(R) (ORNL-3697(p.65-84))
radiocontamination of, toxicity of chelates used for therapy of, 18: 29225
radiodiagnosis of tumors in, by detection of bremsstrahlung from injected phosphorus-32, 19: 10957
radiodiagnosis of brain tumors in, use of copper-64 complexes for, 19: 26206
radioinduced aging, reaction mechanisms, 17: 7788 (BNL-6165)
radioinduced alcohol aversion in, whole-body, 18: 17606
radioinduced and hydrocarbon-induced tumors in, 18: 23349
radioinduced and spontaneous leukemia in, antigenic properties of, 17: 40671
radioinduced and spontaneous aging of, 17: 40651
radioinduced and spontaneous leukemia incidence in germ-free, 19: 2076(R) (ORNL-3700(p.113-26))
radioinduced and spontaneous leukemia in, factors affecting, 20: 22738
radioinduced anomalies in, following prenatal exposure, 20: 22756
radioinduced anti-infection resistance in, protective effects of cysteine against, 16: 25258
radioinduced bone tumors in, 16: 31389(R) (ANL-6535(p.33-5))
radioinduced bone sarcomas in, beta and x, 18: 23231(R) (ANL-6823 (p.20-43))
radioinduced bone tumors by strontium-90 in, protective effects of zirconium citrate against, 19: 17677
radioinduced brain lesions in, deuteron, 17: 40606
radioinduced cancer in, mechanisms for, 20: 6851
radioinduced carcinogenesis in, effects of benzopyrene on, 19: 13114
radioinduced cataracts in, 18: 8105(R) (NYO-2740-1(p.81-154))
radioinduced cataracts in, induced by embryonic and fetal exposure of,

18: 29344
radioinduced changes in amino acid metabolism in, protective effects of splenectomy against, 18: 27233
radioinduced chimeras in, two-step transplantation therapy for, 17: 4432
radioinduced chimeras in, effects of spleen cell injections on, 20: 22789
radioinduced chromosome aberrations in bone marrow cells, effects of dose rate, 17: 28700 (USNRDL-TR-644)
radioinduced chromosome aberrations in liver of, acute chronic gamma neutron, 18: 3479 (BNL-7353)
radioinduced chromosome aberrations in, 18: 11697
radioinduced chromosomal aberrations in, method for radiation detection and dosimetry, 18: 19643
radioinduced chromosomal abnormalities in, x, 18: 19583
radioinduced chromosomal aberrations in tumors of, protective effects of Serotonin and Mexamine against, 18: 31305
radioinduced chromosome aberrations in liver cells of, 18: 35372
radioinduced chromosome aberrations in, at Nevada Test Site, 19: 27948(R) (TID-21862)
radioinduced chromosome aberrations in liver of, gamma and proton, 19: 28084
radioinduced chromosome aberrations in, from incorporated tritiated thymidine, 19: 29929
radioinduced chromosomal aberrations in, effects of age on x, 19: 43729(T) (BNL-tr-12)
radioinduced chromosomal aberrations in, x, 20: 65(R) (TID-22174)
radioinduced chromosomal aberrations in cultures of fibroblasts of, effects of culture density on x, 20: 3691
radioinduced chromosome aberrations in fibroblasts of embryonic, exposed at different phases of mitotic cycle, 20: 35271
radioinduced congenital deformity in, effects of anoxia and fasting on, 18: 8117(R) (TID-20029)
radioinduced corneal tumors in, ultraviolet, 19: 13016
radioinduced damage to bone marrow of, splenic mechanisms for regulation of blood cell populations following strontium-89, 20: 45424
radioinduced depletion of nucleated cells in bone marrow, spleen, and thymus of young, y, 20: 14365
radioinduced dominant mutation effects on skeleton of, frequency of, 19: 24290
radioinduced dominant lethal mutations in spermatogonia in, 19: 38394
radioinduced dominant lethals in spermatozoa of, effects of dose on x, 20: 18351
radioinduced drop in catalase activity of blood of, protective effects of triethylenetetramine on, 16: 32855
radioinduced effects on corneal epithelium of, gamma and neutron, 17: 30359
radioinduced epilation in, protective effects of macromolecules against x, 17: 35472
radioinduced epilation in, protective effects of heparinized rabbit serum against x, 20: 24915
radioinduced erythema in, effects of histamine and histidine on uv, 20: 6798
radioinduced eye defects in embryos and fetuses of, x, 18: 11753
radioinduced eye opacities in, 19: 34098
radioinduced fatality, effect of ultraviolet radiation, 16: 9866
radioinduced fatality, effects of dose output, 16: 9805
radioinduced formation of organic peroxy compounds in tissues of, x, 20: 38660
radioinduced Friend's disease in, after splenic irradiation, x, 18: 29284
radioinduced gastrointestinal lesions in aged conventional and germfree, 20: 45359 (ORNL-P-2407)
radioinduced genetic effects in progeny of, 19: 42347
radioinduced glomerulosclerosis in, effects of AET, age, exposure, and shielding on, 19: 42368
radioinduced granulocytopenia, 17: 17757 (TID-16572)
radioinduced hair dysplasia, protective effects of cysteamine, 17: 27174
radioinduced histocompatibility mutations in, x, 20: 6828
radioinduced immunizing property of tubercle bacilli in, cosmic, 18: 15883
radioinduced inhibition of phosphatase activity in liver and brain tissues, 17: 40596
radioinduced injury to bone marrow of, erythrocyte repopulation following y, 20: 45429
radioinduced lamellar cataract in, effects of age on, 17: 14080
radioinduced lens opacities in, RBE for fast neutron, 19: 26004
radioinduced lens opacity in, method for recording, 20: 75
radioinduced lethality in, mercaptoethylamine dosage as function for dose reduction factor for, 16: 26664(R) (NP-11966(p.123-7))
radioinduced lethal factors in, effects of mercaptoethylamine on, 17: 7855
radioinduced lethal mutations in, 18: 1442
radioinduced leukemia in, 16: 1514
radioinduced leukemia in, 17: 14018
radioinduced leukemia, effects of single and repeated irradiation, 17: 19837
radioinduced leukemia in, antigenic properties of, 17: 40672
radioinduced leukemia in, effects of thymic tissue grafts on, 18: 6684
radioinduced leukemia in, radiation effects on susceptibility to transmission by cell-free extracts, 18: 8147
radioinduced leukemia in, x, 18: 11795
radioinduced leukemia in urethan-treated, protective effects of bone marrow against, x, 18: 15899
radioinduced leukemia in, effects of filtrate injection from, 18: 17561
radioinduced leukemia in, effects of estrogen and tissue transplants on, x, 18: 17658
radioinduced leukemia in black, resistance to, 18: 19663
radioinduced leukemia in, effects of ACTH on, 18: 21921
radioinduced leukemia in, effects of treatment with ACTH on, 18: 25226
radioinduced leukemia in, protection against, using sheep spleen, 18: 27222
radioinduced leukemia in, x, 18: 333111
radioinduced leukemia in, 18: 35267(R) (UCLA-12-529(p.49-62))
radioinduced leukemia in germ-free, x, 18: 36962
radioinduced leukemia in, 18: 41073 (COO-1038-4)
radioinduced leukemia in germfree, x, 18: 41158
radioinduced leukemia in, effects of age at exposure on, 19: 2092
radioinduced leukemia in, 19: 7122
radioinduced leukemia in, phosphorus-32, 19: 3919
radioinduced leukemia in, transfer by cell-free filtrate, 19: 10856
radioinduced leukemia in germ-free, 19: 10871
radioinduced leukemia in, x, 19: 12997
radioinduced leukemia in, metabolic factors, 19: 13064
radioinduced leukemia in, effects of croton oil on, 19: 15092
radioinduced leukemia in, protective effects of ACTH against, 19: 17692
radioinduced leukemia in, 19: 24274
radioinduced leukemia in, 19: 24275
radioinduced leukemia in, etiology of virus in, 19: 27954
radioinduced leukemia in, role of virus in, 19: 28055
radioinduced leukemia in, effects of injected leukemic tissues on, 19: 33824
radioinduced leukemia in, 19: 38372
radioinduced leukemia in, effects on chromosomal aberrations of x, 19: 45911
radioinduced leukemia in, 19: 45808(R) (NYO-901-36)
radioinduced leukemia in, effects of genotype on x, 20: 3765
radioinduced leukemia in, etiology and pathology of, 20: 5309
radioinduced leukemia in, effects of age, dose, and sex on, 20: 5367
radioinduced leukemia in, neutron and x, 20: 6901
radioinduced leukemia in, after tritium injection, 20: 10623
radioinduced leukemia in, effects of hematopoietic tissue transplants on incidence of, 20: 12647
radioinduced leukemia transmission in, effects of viruses on, 20: 16159(R) (ORNL-3900, pp 150-81)
radioinduced leukemogenesis in C57BL, mechanism for, 20: 18317
radioinduced leukemia in germfree, x, 20: 18371
radioinduced leukemia in, effects of injected parental bone marrow or spleen cells on, 20: 31127
radioinduced leukemia in, effects of urethane on transmission of, through thymus and bone marrow centrifugates, 20: 33005
radioinduced leukemia in, etiology of, 20: 33016
radioinduced leukemia in, effects of acridine orange on x, 20: 33080
radioinduced leukemia in, effects of thymectomy and thymus implantation on, 20: 35327
radioinduced leukemia in, effects of AET and endotoxin on, 20: 38715
radioinduced leukemia in, protective effects of 5-methoxytryptamine and propamine against, 20: 38722
radioinduced leukemia and thymic lymphoma in, effects on thymic cell ultrastructure, 20: 42882
radioinduced leukemia, effects of grafting cells from different strains, 20: 42893
radioinduced leukemia in, isolation of virus from cell-free filtrates, y, 20: 45288(R) (SAN-322-4)
radioinduced lung tumors, 17: 10476
radioinduced lung adenomas in, effects of gamma dose on frequency of, 17: 33664
radioinduced lung tumors in, effects of urethan on incidence of, 20: 1606 (AD-623079)
radioinduced lung tumors in, effects of urethane on, 20: 33022
radioinduced lymphoid leukemia in, plasma lactic dehydrogenase activity in, 18: 23256
radioinduced lymphomas in, gamma, 18: 38809
radioinduced lymphosarcomas in, etiology of x, 20: 18359
radioinduced lymphoid leukemia in, following low-dose exposure of successive generations, x, 20: 22646
radioinduced lymphoid leukemia in, lactic dehydrogenase activity and characteristics from, 20: 33051
radioinduced malformations in embryos, 17: 17870

radioinduced mouth lesions, 17: 22976(R) (AD-286799)
radioinduced mutagenesis in, 19: 21792(R) (ORNL-3650(p.187-219))
radioinduced mutations, role of dose rate, 16: 7453
radioinduced mutations from tritiated thymidine, 16: 9881
radioinduced mutations, effects of fractionated dose, 17: 1314
radioinduced mutations, 17: 19874
radioinduced mutations in natural populations of, 17: 30398
radioinduced mutations of, reaction to skin grafts in, 18: 6621(R) (UCSF-23)
radioinduced mutations in germ cells of, effects of dose rate and fractionation on, 18: 11837
radioinduced mutations of, after male exposure, 18: 43295
radioinduced mutations in, 19: 2072(R) (ORNL-3700(p.83-8))
radioinduced mutations in spermatogonia of, x, 19: 5651
radioinduced mutations of, screening for low blood catalase content in, 19: 7014(R) (ANL-6906(p.75-7))
radioinduced mutations in spermatogonia of, x, 19: 15132
radioinduced mutations in, 19: 28062
radioinduced mutations in male, superlethal, 19: 38393
radioinduced mutations in spermatogonia of, effects of dose, dose rate, and radiation quality on, 19: 43788
radioinduced mutations in, effects of dose rate on, 19: 43789
radioinduced mutations in, effects of time between irradiation and conception on frequency of fission-neutron, 20: 18368
radioinduced mutations in, effects of radioprotective compounds on, 20: 24882
radioinduced mutations in spermatogonia of, effects of dose on frequency of x, 20: 40627(R) (ORNL-3922, pp 84-8)
radioinduced myeloid leukemia in, 18: 6623(T) (AEC-tr-6234)
radioinduced myeloid leukemia in, physical factors affecting gamma, fast neutron, x, 18: 19577
radioinduced myeloid leukemia in, virus effects on x, 18: 19578
radioinduced neoplasms in hematopoietic organs in, dose rate relation to, 18: 9854
radioinduced neoplastic lesions in mammary glands of, x, 20: 20502
radioinduced nondisjunction, chromosome losses, and deficiencies in, sensitivity of, 18: 3571
radioinduced ovarian tumors in, effects of age and racial stock, 17: 17823
radioinduced peroxides in, 19: 5666
radioinduced pituitary tumors in, 19: 27959
radioinduced pituitary tumors in, after iodine-131-thyroidectomy, effects of chlorpromazine on, 20: 12657
radioinduced protein loss into gastrointestinal tract in, dose effects on neutron and x, 20: 32933
radioinduced resistance to grafted tumors in, x, 18: 5012
radioinduced sarcomas in, 19: 28045
radioinduced sarcomas in, growth of transplants of, 20: 22631
radioinduced skeletal malformations in fetuses of, 19: 21927
radioinduced skeletal malformations in fetuses of, 19: 21928
radioinduced skin lesions on, healing effects of triglyceride ointment on, 17: 21585
radioinduced skin tumors in, 18: 25081 (AHSB(RP)R-39(p.21-9))
radioinduced skin lesions in, role of adipose tissue in repair of x, 20: 28946
radioinduced sterility in, protective effects of drugs and refrigeration against, 18: 8106(R) (NYO-2740-1(p.155-98))
radioinduced sterility in, following fetal and suckling exposure, gamma, 19: 33796
radioinduced sterility in, x, 20: 65(R) (TID-22174)
radioinduced sterilization in female, genetic control of x, 20: 40627(R) (ORNL-3922, pp 84-8)
radioinduced tanning of skin, ultraviolet, 18: 31174
radioinduced thymic lymphomas, 20: 42892
radioinduced tolerance to skin grafts in, x, 18: 43293
radioinduced translocations in spermatogonia in, 19: 38396
radioinduced tumors in, cosmic, 18: 1430
radioinduced tumors in tails of, comparison of fractionated electrons and x-rays, 18: 13553
radioinduced tumors in, 18: 41092(R) (TID-21125)
radioinduced tumors in, 19: 19594
radioinduced tumors in, reaction mechanisms, 19: 29887(R) (ANL-6971 (p.47-58))
radioinduced tumors in lungs of, 19: 29910
radioinduced tumors in, effects of injected cholesterol on, 19: 29915
radioinduced tumors in, co-carcinogenic effects of chemicals and viruses on, 19: 31678(R) (ORNL-3768(p.137-45))
radioinduced tumors in, antigenic adaptation in transplantable, 19: 45873
radioinduced tumors in, 19: 45808(R) (NYO-901-36)
radioinduced tumors of, after injections of radioactive thymidine, 20: 66 (TID-22292)
radioinduced tumors in, x, 20: 14373
radioinduced tumors in, from external β exposure, 20: 42840(R) (ANL-7136, pp 164-90)
radioinduced tumorigenesis in, 20: 45419
radioinduced tumors in, fast-neutron and γ, 20: 45417
radioinduced ulcers in, actihaemyl treatment of x, 18: 38984
radioinduced ultrastructural lesions in duodenal crypts in, x, 20: 33007
radioisotope determination in, design of whole-body counter for, 18: 43934(R) (LA-3132-MS(p.76-83))
radioisotope transport in blood of, 16: 31464
radiomimetic effects of ferrous chelates, 16: 32677
radioprotection by imidazole derivatives in, 17: 30429
radioprotection of, comparison with yeast cells, 17: 30423
radioprotective activity of imidazole derivatives in, 20: 42979
radioprotective and toxic effects of p-aminopropiophenone in, 16: 26663(R) (NP-11966(p.95-122))
radioprotective compound evaluation in, 18: 11843(R) (NP-13555 (p.46-63))
radioprotective compound evaluation in, 18: 11844(R) (NP-13555 (p.64-83))
radioprotective compound screening in, 18: 37030(R) (AD-600228)
radioprotective effects of liver, spleen, and bone marrow cells in, 16: 20160
radioprotective effects of cultured bone marrow cells of, 18: 1450
radioprotective effects of various compounds in, 18: 13567
radioprotective effects of bone marrow and spleen preserved with PVP in, 18: 19778
radioprotective effects of mixed bacterial toxins and anthramycin, liver and spleen studies, 20: 40736
radioprotective effects of sulfur and thiol compounds on, reaction mechanisms of, 20: 42998(R) (EUR-2992.f)
radioresistant sarcoma cells in, 20: 10634
radiosensitivities of lymphoma cells, 16: 4067
radiosensitivity, 16: 30285
radiosensitivity, age factor in, 16: 7429
radiosensitivity and growth of tumors in, effects of triiodothyronine on, 18: 38876
radiosensitivity and growth of tumors in, effects of L-triiodothyronine on, 18: 38877
radiosensitivity alteration by drinking sulfurated mineral water, 20: 38709
radiosensitivity, effects of genetic factors, 16: 9844(R) (TID-15002)
radiosensitivity, effects of conditioning dose, 16: 11466 (USNRDL-TR-550)
radiosensitivity, effects of hypothermy and oxygen tension, 16: 30289
radiosensitivity, effects of partial-body shielding, 16: 21899(R) (AFSWP-920)
radiosensitivity, effects of ferrous chelates on, 16: 32677
radiosensitivity, effects of age and previous radiation exposure, 16: 32732(R) (TID-16776)
radiosensitivity, effects of previous exposure to fission neutrons of gamma radiation, 17: 5776 (TID-14698)
radiosensitivity, effects of ancestral radiation exposure, 17: 5777 (TID-15181)
radiosensitivity, effects of various variables, 17: 5671(R) (LAMS-2780 (p.85-129))
radiosensitivity, effects of sex, 17: 12124 (TID-15508)
radiosensitivity, effects of age on, 17: 25034
radiosensitivity, effects of age on, 17: 25041
radiosensitivity, effects of thyroid function, 17: 27173
radiosensitivity effects of pyrimidine derivatives on tumors in, 18: 38905
radiosensitivity effects of bacterial toxins on conventional and germ-free, 19: 15228
radiosensitivity effects of amines in, 20: 18454
radiosensitivity effects of ozone on, 20: 18454
radiosensitivity effects of methandrostandiol in, 20: 18477
radiosensitivity effects of 2-methyl-1,4-naphthalenediol bis(disodium phosphate) on ascites tumor cells in, mechanism of, 20: 33082
radiosensitivity effects of glycine on, 20: 38714
radiosensitivity effects of thiopentobarbital on, 20: 38738
radiosensitivity, genetic factors, 16: 4047
radiosensitivity in BaLB and C57B, comparison of, 19: 33832
radiosensitivity of inbred strains, 16: 14529
radiosensitivity of unfertilized eggs, 16: 17524
radiosensitivity of oöcytes, 16: 17488
radiosensitivity of female, as function of age, 16: 17500
radiosensitivity of, effects of sodium cyanide on, 16: 31391(R) (ANL-6535(p.55-7))
radiosensitivity of leukocytes, 16: 32681
radiosensitivity of nervous system, 16: 32793
radiosensitivity of offspring of, injected with cerium-144, 16: 32823
radiosensitivity of, sex differences in, 16: 32857
radiosensitivity of blood cells in, 17: 4405
radiosensitivity of spermatogonia in, relation of cell cycle stage to, 17: 4415

radiosensitivity of, under mild hypothermia, 17: 10438
radiosensitivity of spermatogenesis, 17: 15637(R) (TID-18135)
radiosensitivity of gonads of, gamma and x-ray, 17: 17912
radiosensitivity of female and male, 17: 19909
radiosensitivity of intestine, 17: 23076 (BNL-6929)
radiosensitivity of pure albino, 17: 27182
radiosensitivity of mammary tumor cells in, effects of membrane system and mitochondria on, 17: 27135
radiosensitivity of rapidly dividing cells in, 17: 27138
radiosensitivity of cells in, molecular nature of, 17: 27140
radiosensitivity of, infected with pseudomonas, 17: 30236
radiosensitivity of, effects of dose rate and fractionation on, 17: 30459
radiosensitivity of embryos and fetuses of, 17: 30400(R) (TID-19041)
radiosensitivity of marrow cells in, 17: 33624
radiosensitivity of lymph node cells of, x, 17: 33728
radiosensitivity of heat-treated tumors in, 17: 35355
radiosensitivity of Ehrlich tumors in, protected with chemicals, 17: 35479
radiosensitivity of erythropoiesis in, genetic effects on, 17: 35600(R) (TID-19293)
radiosensitivity of tumors of, in presense of oxygen, 17: 37114
radiosensitivity of transplanted leukemic cells in, 17: 37081
radiosensitivity of spinal cord cells in, 17: 40545 (BNL-7284)
radiosensitivity of, cyclic variations in x, 17: 40621
radiosensitivity of hematopoietic system of newborn, 18: 131
radiosensitivity of eye lens in, 18: 1375 (BNL-7371)
radiosensitivity of germfree and conventional, 18: 1426
radiosensitivity of genetic structure of cells of, 18: 5041
radiosensitivity of, effects of immunization to tuberculosis on, 18: 6693
radiosensitivity of ovaries in developing, 18: 8165
radiosensitivity of bone marrow and lymph nodes in, 18: 9837(T) (JPRS-22778)
radiosensitivity of DNA in spleen and thymus of, 18: 11703
radiosensitivity of bone marrow in, criterion for prediction of, 18: 11697
radiosensitivity of bone marrow in, effects of age on, 18: 11700
radiosensitivity of, exposed in center of cobalt-60 source, 18: 11848(R) (UCLA-520(p.53-74))
radiosensitivity of, effects of oxygen partial pressure on, 18: 11859
radiosensitivity of, protective effects of thiol group against, 18: 11860
radiosensitivity of, inert gas and nitrous oxide effects on, 18: 11878
radiosensitivity of tumors induced by methylcholanthrene in, 18: 11699
radiosensitivity of, genetic factors in, 18: 13455(R) (TID-20231)
radiosensitivity of, effects of age on, 18: 15807(R) (LAMS-3034(p.112-15))
radiosensitivity of ovaries in, 18: 17622
radiosensitivity of gonads of, to single and repeated exposure to x radiation and fast neutrons, 18: 17623
radiosensitivity of, effects of strain on, 18: 17630
radiosensitivity of, index for, 18: 19680
radiosensitivity of, effects of cystamine on, 18: 19800
radiosensitivity of, effects of strain on, 18: 23251(T) (JPRS-24803)
radiosensitivity of, circadian rhythmicity of, 18: 29362
radiosensitivity of, effects of stress on, 18: 29374
radiosensitivity of, effects of analgesics on, 18: 29374
radiosensitivity of sarcomas in, immunological method for increasing, 18: 29483
radiosensitivity of intestinal crypt cells in, 18: 29421
radiosensitivity of, effects of thyroxine on, 18: 29349
radiosensitivity of, effects of Endoxan on, 18: 29350
radiosensitivity of, effects of sex and age on, 18: 29256
radiosensitivity of splenectomized, 18: 31285
radiosensitivity of, genetic factors affecting, 18: 33281(R) (TID-20844)
radiosensitivity of, prediction by urine potassium–sodium ratios, 18: 33321
radiosensitivity of fetal liver in, 18: 33344
radiosensitivity of skin of, effects of anoxia on, 18: 33408
radiosensitivity of, effects of temperature on, 18: 35337
radiosensitivity of Peroganthus, 18: 35362
radiosensitivity of, effects of genotype on, 18: 35369
radiosensitivity of tissues in, effects of liver shielding on, 18: 35316(R) (NP-14210(p.81-9))
radiosensitivity of epithelium in cornea and intestine of, 18: 38951
radiosensitivity of corneal epithelium of, 18: 38948
radiosensitivity of, effects of adrenal gland removal and radioprotective compounds on, 18: 41272
radiosensitivity of, from irradiated sires, 18: 43220(R) (LA-3132-MS (p.109-41))
radiosensitivity of hematopoietic system in, 19: 68(R) (AD-600960)
radiosensitivity of, effects of age on, 19: 106
radiosensitivity of, determination by sodium/potassium ratio in urine after irradiation, 19: 2132
radiosensitivity of cancer cells in, 19: 4039
radiosensitivity of intestinal epithelium of, 19: 5707
radiosensitivity of, effects of electrolyte balance on, 19: 5712
radiosensitivity of isologous and spontaneous tumor transplants in, 19: 7040
radiosensitivity of Ehrlich ascites carcinoma cells in, effects of phenol compounds on, 19: 7177
radiosensitivity of Ehrlich tumors in, effects of 4-methyluracil and 5-oxymethyl-4-methyluracil on, 19: 7178
radiosensitivity of allogenic skin graft response in, sensitized with Freund's adjuvant and spleen cells, 19: 8928
radiosensitivity of, effects of microwave exposure on, 19: 10785 (RADC-TDR-63-352)
radiosensitivity of, effects of Chondron, Marcobin, Marinamycin, and Pydoxal on, 19: 10912
radiosensitivity of tumors of, effects of radioprotective compounds on, 19: 10805
radiosensitivity of lymph and spleen cells of, 19: 13012
radiosensitivity of cells from, 19: 13061
radiosensitivity of bone marrow cells in, age effects on, 19: 15189
radiosensitivity of embryonic cells of, in culture, 19: 17609
radiosensitivity of hemopoietic colony-forming cells after transplantation in, 19: 17601
radiosensitivity of, effects of female and male gonadal hormones on, 19: 17680
radiosensitivity of intestines of, comparison with other species, 19: 21954
radiosensitivity of crossed strains of, effect of albino gene on, 19: 21955
radiosensitivity of transplanted tumors in, 19: 21957
radiosensitivity of, factors affecting, 19: 21984
radiosensitivity of mammary carcinomas of, cellular, 19: 26076
radiosensitivity of tumors in, protective effects of chemicals against, 19: 26116
radiosensitivity of bovine gamma globulin in, effects of bovine serum albumin on, 19: 26130
radiosensitivity of tumor-bearing, effects of cytosine, thymine, and uracil on, 19: 26149
radiosensitivity of, effects of oxygen pressure on, 19: 25919
radiosensitivity of, effects of injected acetone and urethane on, 19: 25938
radiosensitivity of lymphocytes in peripheral blood from, 19: 25945
radiosensitivity of bone marrow of, 19: 29889(R) (ANL-6971(p.90-116))
radiosensitivity of liver and intestinal cells of, 19: 29889(R) (ANL-6971 (p.90-116))
radiosensitivity of, genetic factors affecting, 19: 29891(R) (ANL-6971 (p.120-32))
radiosensitivity of sarcomas in, 19: 29928
radiosensitivity of, cyclic influences on, 19: 29938
radiosensitivity of developing fetuses of, 19: 31787(R) (NYO-2740-2)
radiosensitivity of transplanted carcinoma cells in, 19: 31960
radiosensitivity of populations of, age effects on, 19: 33892
radiosensitivity of transplanted lymphoma cells in, assay of, 19: 33897
radiosensitivity of, effects of strain on, 19: 33881
radiosensitivity of nervous system in, effects of biological stress on, 19: 42334
radiosensitivity of, effects of hematoporphyrin on, 19: 43748
radiosensitivity of, effects of mouse strain, 19: 43792
radiosensitivity of tumor implants in, effects of oxygen on, 19: 46003
radiosensitivity of autochthonous radioinduced lymphosarcomas in, single- and split-dose, 19: 54977
radiosensitivity of genotype S1/S1 anemic, cellular basis of hemopoietic defect in, 19: 45856
radiosensitivity of, genetic factors in, 19: 45857
radiosensitivity of cells of thymus gland of, 19: 45871
radiosensitivity of, effects of oxygen on, 19: 21995(R) (NP-14779(p.64-9))
radiosensitivity of, effects of oxygen on, 19: 21996(R) (NP-14779(p.70-88))
radiosensitivity of hematopoietic cells of liver of embryos of, 20: 96
radiosensitivity of bone marrow cells in adult, 20: 96
radiosensitivity of, effects of dietary content of pyridoxine on, 20: 1646
radiosensitivity of transplanted tumors in, effects of inhalation of 5% carbon dioxide and 95% oxygen on, 20: 1683
radiosensitivity of fibrosarcoma cell line in, 20: 5362
radiosensitivity of, effects of circadian rhythmicity on x, 20: 5336
radiosensitivity of, effects of drug stimulation of central nervous system on x, 20: 12685
radiosensitivity of placenta of, x, 20: 12650
radiosensitivity of sperm of, effects of streptomycin on, 20: 14404
radiosensitivity of, effects of tissue sulfhydryl ratios on, 20: 14351
radiosensitivity of cultured cells of, effects of serum and temperature on, 20: 16298
radiosensitivity of, effects of aspartic acid and Solcoseryl on, 20: 16302
radiosensitivity of, effects of bacterial toxins on, 20: 18425
radiosensitivity of antibody response in, 20: 18185(R) (BNL-929, pp 126-47)

radiosensitivity of, effects of colchicine derivatives and urethane on x, 20: 18467
radiosensitivity of, effects of nitrated procainamide derivatives on, 20: 18478
radiosensitivity of, effects of organophosphorus compounds on, 20: 18482
radiosensitivity of, effects of dithiosuccinic acid on, 20: 18483
radiosensitivity of, effects of cyclic analogs of AET on, 20: 18484
radiosensitivity of, effects of pantothenic acid on, 20: 18486
radiosensitivity of, effects of mixed radioprotective compounds on, 20: 18488
radiosensitivity of, effects of 5,7-dihydroxyisoflavone compounds on, 20: 18489
radiosensitivity of, effects of 4-hydroxybutyrate compounds on, 20: 18490
radiosensitivity of, effects of AET and DNA on, 20: 18492
radiosensitivity of, effects of heterologous spleen extraction, 20: 18493
radiosensitivity of, neutron and x, 20: 18548
radiosensitivity of, effects of oxygen environment on, 20: 20430(R) (AD-629311, pp 26-32)
radiosensitivity of, effects of age on, 20: 20494
radiosensitivity of, effects of β-mercaptoethylamine on, 20: 20511
radiosensitivity of, effects of bacterial toxins on, 20: 20512
radiosensitivity of, effects of polyhydroxyl alcohols on, 20: 20520
radiosensitivity of brain of, effects of AET and potassium cyanide on, 20: 20521
radiosensitivity of, relation of oxygen consumption by tissues to, 20: 22712
radiosensitivity of, effects of actinomycin and 5-fluorouracil on, 20: 22785
radiosensitivity of, effects of serotonin and age on, 20: 22791
radiosensitivity of hematopoietic stem cells in, x, 20: 22640
radiosensitivity of germ-free, effect of diet and strain on x, 20: 22730
radiosensitivity of, effects of chemicals on, 20: 26712
radiosensitivity of catalases in, effects of glycine on, 20: 26702
radiosensitivity of, effects of time of day on x, 20: 28938
radiosensitivity of, effects of hormones on, 20: 28978
radiosensitivity of, effects of removal of endocrine glands on, 20: 28978
radiosensitivity of, effects of porphyrins on, 20: 29042
radiosensitivity of intestinal crypt cells of, x, 20: 31128
radiosensitivity of bone marrow cells in, 20: 31071
radiosensitivity of L-strain cells of, effects of 5-bromodeoxyuridine on gamma, 20: 33033
radiosensitivity of immunologically competent cells in graft-versus-host reaction in, before and after antigenic contact, 20: 33083
radiosensitivity of tumors of, effects of uracil on x, 20: 40668
radiosensitivity of spermatogenic epithelium of, γ and x, 20: 42942
radiosensitivity of tumors in, as affected by diurnal variations of exposure, x, 20: 43048
radiosensitivity of, relation between local and general, 20: 45446
radiosensitivity of, effects of sulfurated mineral waters on, 20: 45490
radiosensitivity, protective effects of phencyclidine against, 16: 31522
radiosensitivity, strain differences, 17: 7837
radiosensitivity, strain differences, 17: 17758 (TID-16650)
radiosensitivity to x rays, 16: 1486(T) (JPRS-10170(p.279-312))
radiosensitivity to gamma rays, effects of age, 16: 1311(R) (LAMS-2627(p.110-16))
radiosensitivity to x rays, 16: 4009(R) (UCSF-21)
radiosensitivity to repeated monthly doses of gamma radiation, protective effects of 2-aminoethanethiol against, 16: 31520
radiosensitivity, therapeutic effects of spleen transplants from irradiated donors, 16: 32842
radiotherapeutic effects of 3,4-dihydroxyphenylalanine on, 17: 28616
radiotherapy and chemotherapy of sarcomas in, synergistic effects in, 19: 10963
radiotherapy and surgery of cervical carcinomas in, 19: 31933
radiotherapy effects combined with Actiheamyl in sarcomas in, histology, 19: 46123
radiotherapy for malignant tumors in, effects of dose fractionation on, 18: 3654
radiotherapy of cancer in, effects of chemical radiation protectors on x-ray, 20: 31142
radiotherapy of implanted ascites hepatoma in, 20: 45516
radiotherapy of leukemia in, effects of allogeneic lymphoid cell transplants on, 20: 45552
radiotherapy of leukemia in, 17: 35362
radiotherapy of melanoma in, using radium-226, 18: 29435(R) (COO-119-229(p.74-9))
radiotherapy of sarcomas in, effects of nicotinic acid on, 19: 13113
radiotherapy of spleen and thymus of, synergistic effects of Mitomycin C and Endoxan in, 20: 31131
radiotherapy of tumors in, effects of heat on, 17: 35363
radiotherapy of tumors in, dose fractionation effects on, 17: 40618
radiotherapy of tumors and leukemia in, effects of 2-mercaptoethylguanine on, 18: 8201
radiotherapy of tumors in, effects of pre-operative, 18: 9950
radiotherapy of tumors in, effects of preoperative, 18: 29454
radiotherapy of tumors in, 19: 22075
radiotherapy of tumors in, effects of preoperative exposure, 19: 28149
radium and radon retention in, after injection of radium-226, 17: 35424
radium retention after ingestion, 17: 23036 (TID-16185)
radium-224 and -226 uptake by melanomas in, 18: 3489(R) (COO-228 (p.127-31))
radium-226 metabolism in, 19: 21815(R) (ANL-6839(p.40-62))
rare earth toxicity in, 20: 30970 (COO-1170-5)
rat erythrocyte immunity in, determination using lactic and dehydrogenase activity, 19: 31681(R) (ORNL-3768(p.164-76))
Rauscher leukemia virus in, cytopathologic effects of, 19: 31677(R) (ORNL-3768(p.119-30))
reactions of humoral H-2 antibodies in irradiated and normal embryonic and newborn, 17: 21519
recognition and avoidance of radiation by, effects of dose rate, 16: 32793
recognition response to gamma radiation by, 18: 15811(R) (LAMS-3034 (p.133-40))
reproduction of, tracer study using tritium-labeled sperm, 20: 26593
resistance to γ-irradiated cercariae, 20: 8591
resistance to leukemia tumor growth, effects of irradiated tumor cells, 16: 31410
resistance to spleen grafts in, effects of hybridization on, 19: 31677(R) (ORNL-3768(p.119-30))
respiration in, effects of cysteamine, 19: 38469
respiration in, effects of aminoethylisothiourea, 19: 38469
response to antigens, suppression by anti-tumor agents, 17: 15584
response to rat skin graft of irradiated adult, effects of thymus on, 17: 40662 (USNRDL-TR-661)
retention of chronically administered cesium-137, 16: 9825
retention of strontium by, effects of thyroid hormones on, 20: 22853(R) (ANL-7060)
reticulo-endothelial metabolism in, effects of cysteine on, 18: 29420
reticuloendothelium stem cell response to erythropoietin in, 17: 24819(R) (ACRH-18(p.13-20))
ribonuclease uptake by kidneys in, tracer study following intravenous injection, 20: 10453 (BNL-8683)
Riley virus levels in blood of, following RES interference, 20: 45253
RNA metabolism in leukemic cells of, 19: 31677(R) (ORNL-3768(p.119-30))
ruthenium distribution in tissues of whole male and pregnant female, tracer study, 17: 7752
ruthenium-106 retention and excretion, 16: 1326(R) (LAMS-2627(p.213-18))
ruthenium-106 excretion by, effects of temperature on, 18: 43173(R) (LA-3132-MS(p.32-6))
ruthenium-106 metabolism in, 18: 43171(R) (LA-3132-MS(p.19-24))
selection for radiation resistance, 17: 15680
selenium metabolism, 17: 12111
selenium-75 metabolism in, 18: 17426
selenium-75 uptake by milk of, 18: 17426
sensitivity of normal hematopoietic and transplanted lymphoma colony-forming cells to tritiated thymidine, 19: 31730
serotonin content of blood of, effects of space flight on, 17: 35284(T) (FTD-MT-62-78(p.358-69))
serum hemagglutinin formation in heterologous radiation chimeras, 17: 40441 (HW-SA-2867)
shock wave lethality, 17: 22977(R) (DASA-1325)
skeletal abnormalities in offspring of irradiated, 17: 7841
skin graft tolerance of C3H and CBA, 18: 1367
skin grafts, genetic factors affecting take, 17: 15585
skin homograft survival in irradiated, effects of A-methopterin on, 16: 26874
skin tumor incidence in, receiving 9,10-dimethyl-1,2-benzanthracene and gamma or x irradiation, 16: 17492
skin tumors in, induced by x radiation and chemical carcinogens, 17: 40638
sodium xenate injections in, metabolic and toxicologic effects of, 18: 4993
sodium-22 uptake and distribution in organs and tissues in, kinetics of, 17: 21429
species specificity of reannealed DNA of, 20: 42757
spleen cell transplantations in, models for study of immune reactions in, 17: 13915
sterility of male, effects of deuterium oxide on, 18: 1325(R) (UCRL-10934)
storage of immunologically competent and myeloid cells from, 18: 21760
strontium excretion by, mechanisms for, 18: 27051
strontium isotope excretion by, effects of various chemicals on,

20: 8564
strontium metabolism in bones of, effects of age and diet on, 20: 35237
strontium-85 body burdens in, effects of sodium salicylates on, 20: 18229
strontium-85 deposition in embryos of, 19: 14953 (BNL-7859)
strontium-85 elimination in, agents affecting, 17: 38707
strontium-85 elution from bones of, by chelating agents and salts, 19: 43706
strontium-85 metabolism in, effects of environmental temperature on, 18: 15770(R) (LAMS-3034(p.65-72))
strontium-85 metabolism in, effects of age on, 19: 2038
strontium-85 metabolism and excretion in, 19: 21828
strontium-85 retention by, effects of thyroid hormones on, 20: 42769
strontium-85 retention in, effects of tetracycline on, 18: 23220
strontium-85 transfer through placenta in, 20: 14244
strontium-89 and -90 removal from skeleton of compounds for, 19: 29999
strontium-89 metabolism after liquid aerosol inhalation by, effects of hexametaphosphate on, 19: 2019
strontium-90 content in, effects of zirconium citrate treatment on, 18: 35288
strontium-90 distribution in tissues, 16: 21880
strontium-90 excretion by, effects of various salts on, 20: 8563
strontium-90 excretion by, effects of chelating agents on, 20: 8561
strontium-90 excretion by, effects of tetracycline on, 20: 8562
strontium-90 excretion from, effects of inorganic salts, chelates, and antibiotics on, 20: 32922
strontium-90 excretion in, effects of aluminum citrate on, 17: 5744
strontium-90 genetic effects in, injected, 17: 14054
strontium-90 genetic effects in, 17: 33713
strontium-90-induced bone tumors in, 18: 6630
strontium-90-induced bone tumors in, effects of bacterial infection on incidence of, 20: 5373
strontium-90 metabolism in, after intraperitoneal or subcutaneous injection, 20: 18225
strontium-90 radiotoxicity in, control by strontium-enriched diet, 20: 45497
strontium-90 retention by, effects of tetracycline on, 18: 35275 (LADC-5996)
strontium-90 retention in, effects of dietary levels of phosphorus on, 17: 38715
strontium-90 sorption by skeleton in, 17: 13956
strontium-90 toxicity in, effects of strain on, 19: 24252
strontium-90 uptake and retention in strontium-90-induced osteosarcomas in, 16: 26691
sulfur distribution in tissues, tracer study, 16: 28708
sulfur-35 content in blood of, after intravenous or intraperitoneal injection, 19: 27942
sulfur-35 uptake by vibrissal hairs of, 19: 19479
sulfur-35-labeled MEG distribution in, 18: 43311
survival and cell growth in germ-free, 18: 27068(R) (ORNL-3601 (p.128-45))
survival curves of, following total body irradiation, 20: 40767
survival of irradiated, effects of homologous bone marrow injection on, 17: 25050
susceptibility to Trypanosome infections of, 19: 21991
swelling properties of mitochondria in liver and tumor in, 19: 35881
synthesis of DNA in alveolar cells of mammary glands in, effects of 17-β-estradiol and progesterone on, 19: 6924
terbium-160 distribution in, 18: 31087
tetanus toxin distribution in immunized and non-immunized, after injection, 16: 17408
therapeutic effect of a steroid anabolicum after whole-body irradiation, 20: 45495
therapy of virus-induced leukemia in, using deuterium, 18: 29484
therapy of virus-induced leukemia in, effects of whole-body irradiation and hematopoietic tissue transplants, 20: 45550
thermal stability of DNA of, 20: 42757
thorotrast-induced reticuloendothelial blockage in, effects on virus infection, 18: 17618
thymectomy effects on immunological tolerance in, 18: 25157
thymic cell populations in, effects of bone marrow injections on, 20: 6824
thymic lymphoma induced by radiation, pathogenesis studies, 20: 40677
thymidine re-utilization from dead tumor cells in, tracer studies of, 18: 11601
thymidine uptake by tumor tissue in, autoradiography of tritiated, 19: 27912 (TID-19014)
thymidine uptake by DNA in, effects of AET, glutathione, and serotonin on, 19: 46016
thymidine uptake by adrenal DNA in, tracer study, 20: 26616
thyroid function in, effects of thyroid hormones on, 18: 43196
thyroid metabolism studies, 20: 40547
thyroid physiology in, effects of chlordiazepoxide on, 18: 15788
thyroid uptake of iodine-131 in, 18: 29274
thyroxine deiodination by pyridoxal phosphate–vanadium complex in, 17: 13922 (IA-748)
tissue cultures in, dialysis method for maintaining *in vivo* marrow and spleen, 19: 31905(R) (ORNL-3768(p.99-108)
tissue transplant growth in, genetic factors affecting, 20: 6785(R) (ORNL-3853, pp 128-40)
tolerance of, to explosive decompression, effects of x radiation and oxygen atmosphere on, 18: 11624 (AD-407916)
toxic effects of beryllium chloride on, protective effects of aminoalkyl-phosphinic acids against, 19: 12924
toxic effects of carbon tetrachloride in, 20: 10548
toxic effects of inhaled plutonium-239, 17: 10323
toxic effects of injected glucose oxidase in, 17: 33473(R) (ANL-6723 (p.205-7))
toxic effects of lutetium chloride in, 19: 5619
toxic effects of niobium pentachloride and potassium niobate on, 19: 45768
toxic effects of plutonium, polonium, and radium on, after single injection, 19: 2056
toxic effects of *p*-aminopropiophenone in, 19: 8742(R) (NP-14448 (p.132-9))
toxic effects of rare earth compounds, 17: 7756
toxic effects of rare earth nitrates in, 17: 40489 (SAM-TDR-63-38)
toxic effects of sulfur-35 on blood of, 19: 17473
toxic effects of sulfur-35 in, 19: 29855(T) (JPRS-29411(p.1-7))
toxic effects of tritiated thymidine on bone marrow transplants in, 16: 17507
toxic effects of tritiated thymidine on, 17: 23067
toxic effects of ultraviolet-irradiated linoleic acid in, 19: 4007
toxic effects of uranyl nitrate in, 19: 33769
toxic effects of uranyl nitrate in, 20: 3670
toxic effects of uranyl nitrate in, 20: 10548
toxic effects of water-t_2 on, 19: 25881
toxic effects of 2-mercaptoethylamine or *p*-aminopropiophenone in diet of normal and irradiated, 18: 23358(R) (NP-13918(p.116-28))
toxicity of plutonium in, 17: 10317
toxicity of rare earth nitrates and oxides in, 18: 17458
toxicity of TTHA chelates in, 20: 10556
transmission of maternal erythrocytes across placenta, radiation effects, 16: 20066
transmission of radioinduced leukemia by cell-free filtrate in, 18: 6653
transmission of serum albumin from mother to fetus, radiation effects, 16: 20067
transplantation of leukemia in, 17: 82
transplantation of bone marrow and spleen cells in irradiated, repopulation during serial, 17: 23130
transplantation of bone marrow in spherocytic, model system for, 17: 38909
transplantation of spleen cells in irradiated, protection from killing effect of, 19: 19651
transplantation of ascites lymphoma cells from, 20: 3750
transport of nucleic acids and proteins through cellular membranes in, 17: 24868
trisomy in, 19: 5681
tritiated thymidine uptake by testes of, dose-effect measurement in, 18: 25069
tritium uptake from thymidine by proteins in tissues in, 20: 35216
trypsin digestion of injured lymph node cells from chimeras of, 18: 41011(R) (HW-80500(p.129-31))
tumor cell growth in, chemical and radioactive agents for inhibition of local and systemic, 17: 19770
tumor growth after implantation in, effects of nicotinamide on, 17: 33476(R) (ANL-6723(p.215))
tumor growth in, effects of x-irradiated cell injections on, 17: 5824
tumor growth in irradiated, inhibitory effects of spleen cells on, 18: 43307
tumor growth in, effects of fatty acids from liver of irradiated rabbits on, 18: 23208
tumor growth in, effects of irradiated fatty acids on, 19: 29963
tumor incidence in, effects of irradiated diet on, 19: 25887
tumor induction by strontium-90 injections, 16: 23464 (UAC-4763)
tumor induction by methylcholanthrene in, effects of cosmic electrons and photons on, 18: 17605
tumor induction by 3,4-benzopyrene in, immunological properties of, 19: 12895
tumor induction in, by x radiation and chemical carcinogens, 17: 40637
tumor induction in pituitary grafts in radiothyroidectomized, 18: 4955
tumor induction with tritiated thymidine, 16: 4066
tumor therapy, complications induced by virus, 17: 17660
tumor transplantation in, radiation effects on donor tumor, 18: 29522
tumor transplants in, effects of injection of irradiated cells on growth of, 19: 21897
tumor ultrastructure in, 18: 21732(T) (ANL-Trans-7)

tumorigenic effects of drugs and radiation in, 18: 31192
tumorigenic effects of dried cells in, 18: 36938
tumors in, classification by type, 17: 40443(R) (NP-13182)
tumors in, effects of drugs on transplanted, 20: 8662
tumors induced by injections of thymidine labeled with tritium or carbon-14, 16: 31498
tumors induced by chemicals in, 19: 45808(R) (NYO-901-36)
tumors radioinduced in female, reverse response of thyrotropic property to gonadotropic activity in, 16: 26778
uptake and distribution of thorium dioxide in organs in, 20: 35223
uptake by organs in, effects of, 17: 19777
uptake of iodine-131-labeled IUdR by recipient, 19: 3872
uptake of iodine-125-labeled beef insulin by kidneys and liver in, 20: 35229
use of carcinoma and sarcoma cells of, for testing cancerostatic therapeutic agents, 20: 40550
use of iodine-131-labeled colloidal albumin as scanning agent, 20: 40777
use of sodium gallate prophylaxis and therapy of radiation sickness in, 20: 38728
vaccine effects on immunity of, formaldehyde and radiosterilized, 17: 17701
vaginal epithelia in, autoradiographic studies of, 20: 40502(R) (ORNL-3922, pp 115-27)
virus-induced leukemia in, 18: 35267(R) (UCLA-12-529(p.49-62))
virus-induced leukemia in, 18: 41073 (COO-1038-4)
water turnover in, tracer study of climatic effects on, 19: 2017
weight of tumor-bearing, effects of endogenous hydrogen peroxide on, 20: 42840(R) (ANL-7136, pp 164-90)
whole-body radiosutograms, 16: 31476(A/AC.82/G/L.788)
wound healing in, effects of immune reactions on, 18: 8119 (USNRDL-TR-683)
x-irradiated, bone marrow cell proliferation after bleeding of, 20: 40722
x-ray-induced leukemia, protection against, 20: 40658
ytterbium-169 distribution in, 18: 31087
yttrium-90 injections in sarcomas in, distribution in organs from colloidal, 17: 30213
yttrium-91 uptake by, 17: 21460
yttrium-91 distribution in, whole-body autoradiographic study of, 20: 22550
yttrium-91 metabolism by, effects of hexametaphosphate aerosols on, 19: 3865
yttrium-91 metabolism after inhalation as aerosol, 18: 19544
yttrium-91 removal from, using TTHA chelates, 20: 10556
zinc metabolism and pathway in, 16: 8489
zinc metabolism in, tracer study of, 19: 6947 (BNL-7745)
zinc-65 metabolism in, effects of environment on, 19: 35904
zinc-65 uptake by Ehrlich ascites carcinomas in, effects of antimony complexes on, 19: 33783
zirconium-95 metabolism in, 18: 15768(R) (LAMS-3034(p.53-8))
2-mercaptoethylguanidine chemical nature and distribution in, 17: 23066
2-mercaptopropylamine metabolism in, tracer study, 20: 28888
5-iodo-2′-deoxyuridine distribution in, iodine-125-labeled, 19: 31738

MICHIGAN
climatology of Willow Run, 16: 15002 (TID-15367)
environs monitoring of Enrico Fermi Atomic Power Plant in, 17: 23561
fallout monitoring, 1959 to 1963, 17: 34145 (CONF-66-6)
fallout monitoring in surface dusts in, Nov. 1962 to March 1963, 19: 4366
radiology in, survey of dental, 20: 20956
reactor environmental surveillance program in, 19: 22556

MICHIGAN, LAKE
radioactivity, 18: 4006
strontium-90 content in waters and land areas surrounding, 20: 41131(R) (HASL-172)

MICHIGAN BASIN
geology and hydrology of, for potential use for radioactive waste disposal, 19: 14894 (SAN-413-2)

MICHIGAN RESEARCH REACTOR
control rod deformation in, 18: 3377
control rod deformation in, analysis of causes of, 18: 4882
control rods, design, 16: 16000 (MMPP-110-3)
core modification for enhanced thermal neutron beams for neutron spectrometers, 20: 10432
development and operation of, 17: 6132(R) (TID-17272)
neutron beam intensity measurements on, 19: 25768
neutron lifetimes in, measurements of prompt, 17: 1069
neutron spectra in, 19: 849(R) (FDL-TDR-64-30)
power level measurements in, calorimetric method for, 20: 12514
power measurements in, absolute, 19: 43605
reactivity void coefficient, 16: 18629
reflector design modification and performance for, 20: 16128
reflector modifications, 19: 43616

MICROANALYSIS
absorption corrections for electron-probe x-ray, tables, 19: 294 (NLCO-914)
absorption correction tables for electron-probe, 19: 26231 (NLCO-944)
activation methods of, application of ion-exchange resins in, 20: 45618
applications of electron-probe, 19: 13199 (LA-3157)
bibliography and review on inorganic, 16: 14638
bibliography on electron-probe, 18: 40986 (NP-14292)
book: *Instrument and Chemical Analysis Aspects of Electron Microanalysis and Macroanalysis*, 20: 29119
chemical and isotopic, using secondary ion emission, (E/T), 19: 10989
chopped-beam method for trace analysis using electron probe, 20: 225 (CONF-650810-2)
computational methods in electron-probe x-ray, 17: 40741
conference on electron-probe, of nuclear materials, 19: 30074 (EUR-1819.e)
correction factors for electron penetration in x-ray, 19: 19746 (CEA-R-2728)
correction formulas for quantitative electron-probe, 19: 9058 (EUR-2156.e)
corrections for electron-probe, theoretical, 19: 15349 (NLCO-929)
corrections for quantitative microprobe, evaluation of absorption and fluorescence, 20: 7009 (NLCO-960)
detection threshold and limit calculations for electron-probe, 19: 30077 (EUR-1819.e(p.27-36))
developments in electron probe, review on, 20: 22885
electron microprobe for, development of, 20: 29083(R) (UCRL-14767)
electron-probe scanning for light elements in metals, 19: 30075 (EUR-1819.e(p.1-14))
equipment and method for uranium recovered from magnesium fluoride slag, 18: 43380(R) (NLCO-920(p.13-17))
equipment and methods for environmental samples, 20: 26600(R) (NP-16002, Paper 4)
equipment for, electron probe-x-ray diffractometer, 17: 33855(P)
equipment for electron-probe, for highly radioactive samples, 20: 224 (CNLM-6352)
equipment for light-element, 18: 15986
fluorescence corrections for microprobe analysis, tables, 19: 295 (NLCO-917)
method of, using secondary ion emission, 20: 31200
neutron activation in, 17: 30038
of semiconductors, activation, 20: 22879(T) (AEC-tr-6466/1, pp 260-7)
optical microscopic techniques for electron-probe, 19: 40951 (NBL-6290)
performance of electron-probe, 18: 17760
physical basis of electron-probe x-ray, 17: 40740
procedures for quantitative microprobe, comparison of, 20: 7012 (NLCO-969)
properties of electron-probe, 18: 17744
properties of electron probe, 19: 19747 (CONF-650214-1)
technique for electron-probe, for studying oxidation of chromium–iron–nickel alloys in steam, 19: 17774 (GEAP-4490)
use of cathodoluminescence as ancillary technique to, 18: 43379(R) (NLCO-920(p.7-12))
use of electron-probe, to study phase equilibria, 19: 15348 (MLM-1163 (p.K-1-10))
use of electron-probe, in studies of beryllium structure, 19: 30732 (EUR-1819.e(p.49-58))
use of electron-probe, in studies of plutonium distribution in plutonium–uranium ceramic materials, 19: 30078 (EUR-1819.e(p.171-85))
use of electron-probe, 19: 32055(R) (ANL-7020(p.231-7))
use of electron-probe, to determine light elements in alloys, diffusion couples, and carbides, 19: 40412 (TIM-924)
use of electron-probe, for segregation studies in oxides, 20: 38469 (ANL-7120, pp 400-9)
use of nuclear reactions in, 18: 13625 (LAL-1053)
use of x-ray, in studies of high-temperature coated fuel particles, 19: 30733 (EUR-1819.e(p.63-89))
x-ray emission in electron-probe, dependence on accelerating voltage, 19: 11042
x-ray emission in electron probe, of alloys and metals, 20: 20593

Microbalances
see Balances

Microclines
see Feldspars

Micrography
see Photomicrography

MICROLITES
analysis for niobium and tantalum by ion exchange, 16: 16312

MICROORGANISMS
see also Algae
see also Bacteria
see also Fungi
see also Protozoa
see also Rotifers

see also Viruses
see also Yeasts
B. coli flora changes during radiation sickness, 16: 5172(T) (JPRS-11242(p.110-14))
biological activity and nature of scrapie agent, 20: 18314
biological effects of space flight, 17: 17774(T) (JPRS-18395(p.148-55))
biological effects of deuterium in, 18: 31081
book: *Problems of Radiation Genetics*, 19: 42348(T)
cellular fine structure of, 20: 42701(R) (ANL-7136, pp 205-30)
changes in intestinal, in irradiated rats, 17: 27074
content in marine ecosystem, 20: 16175(R) (RT/BIO(65)-1)
content in radiopasteurized crab and flounder, 18: 37570(R) (TID-19585(p.108-44))
control in irradiated foods of, legislation on, 20: 41389
control of, in radioinduced pasteurization of foods, 17: 30053
criteria for handling infectious agents in laboratories, 19: 31635 (ORNL-TM-1162)
culture and physiology of *Tetrahymena pyriformis*, *Astasia longa*, *Escherichia coli*, and bacteriophage T4, 18: 27009(R) (ORNL-3601 (p.152-72))
desoxyribonucleic acid synthesis in *Stentor coeruleus*, cytoplasmic control of, 20: 18295(R) (UCLA-12-576, pp 27-56)
detection and study of, development of radioisotopic methods for extraterrestrial bodies, 17: 12080(R) (N62-11554)
detection in extraterrestrial environments, 20: 18187(R) (N-65-16497)
detection in jet fuel, tracer method for, 19: 39061 (ADR-09-08a-63.1)
detection in water of, radiometric method for, 18: 29181
detection on Mars, radiobiochemical probe for, 16: 34135
detection on Mars, probe for, 17: 2633
detection on other planets, 17: 3661
determination of, on crab meat, 17: 33618(R) (TID-17557)
effectiveness as biological warfare agents, 16: 28655(R) (JPRS-14284)
effects of nuclear war on soil, 20: 45962 (RM-4827-TAB)
effects of water-t_2 on growth of Rickettsiae in eggs, 16: 17390
effects of water-d_2 on growth in, 20: 3651
effects of, on decomposition of vascular hydrophytes in aquatic ecosystems, 20: 12543(R) (NYO-3018-12)
effects on aging in ICR mice, 20: 40502(R) (ORNL-3922, pp 115-27)
effects on decomposition of swine carrion, 20: 20941 (ORNL-TM-1432)
extraterrestrial, collection and growth, equipment, 16: 18733 (NP-11678)
fission product accumulation by, in water supply reservoirs, 18: 29911
genetic variations in natural and irradiated, 17: 28674(R) (NP-12940)
growth and reproduction of *Tetrahymena pyriformis*, 16: 7353
growth chamber for, design of, 19: 29886(R) (ANL-6971(p.29-46))
growth in heavy water in reactor cooling systems, 16: 32531 (AAEC/E-90)
growth in radioactive sludge, 19: 24196
growth in radioactive sludge, 19: 24197
growth of, development of synthetic culture medium for, 17: 7684(R) (NYO-8103)
growth of, on irradiated starch and amylose–acrylamide copolymers, 20: 20767
hydrocarbon and organic compound metabolism by, 16: 1431 (ORO-469)
hypoxanthine production by, radiation enhancement of, 18: 10177(P)
incidence and virulence of *Chondrococcus columnaris* in Columbia River, 1960 and 1961, 16: 25145(R) (HW-72500(p.151-5))
incidence and virulence of columnaris, in Columbia River, 17: 35326(R) (HW-76000(p.223-6))
incorporation of radioisotopes by, 19: 46409
isolation of mycoplasmas from human leukemic bone marrow, direct agar, 19: 17451
light effects on, 19: 17664
lysis of *H. aegyptius*, effects of hyaluronidase on, 17: 6792(R) (ISS 62/14)
marine, metabolism of fission products, 16: 22455 (TID-7632(p.348-59))
metabolism and primary productivity of benthic, 18: 45192(R) (TID-21157)
metabolism of marine, tracer studies of, 19: 25839(R) (NYO-1918-100)
metabolism of S-adenosylmethionine and S-adenosylhomocysteine in, 16: 31393(R) (ANL-6535(p.84-9))
metabolism, tracer studies, 16: 1408
morphology of, problems of environmental control on, 17: 38652
morphology, growth, and survival of, in irradiated soils, 18: 15885
mutations, role of peroxides, 17: 24984
nucleocytoplasmic interactions during oral structure differentiation in *Stentor coeruleus*, 18: 11653(R) (UCLA-520(p.27-42))
origin of DNA in cytoplasmic organelles of, tracer study, 20: 42701(R) (ANL-7136, pp 205-30)
photochemical reactions of nucleic acids in, 19: 42212 (NYO-3424-1)
photoprotection from ultraviolet damage, 17: 2859
photosynthesis in, effects of vitamin B_{12} on, 18: 19486(R) (TID-20433)
preparation of labeled *Coxiella burnetii*, 17: 7697
radiation control of crop pests, 16: 30190(T) (AEC-tr-5142)
radiation control of, 19: 74 (PDL-42277)
radiation control of, in eggs, 20: 9351
radiation control of growth on fish, 20: 43775
radiation control of growth of, on sea foods, 20: 43774
radiation effects on reproduction of Hemophilus influenzae, 16: 1307(R) (LAMS-2627(p.82-93))
radiation effects in foods, 16: 10356 (AECL-1329(p.17-24))
radiation effects on enzyme activity, 16: 9862
radiation effects on, application to crop protection, 16: 16110
radiation effects on reproduction of rotifers, 16: 30184(R) (ANL-6474 (p.52-7))
radiation effects on *B. sal.*, lethal, 16: 14567
radiation effects on morphology of *B. sal.*, 16: 14568
radiation effects on number in soil samples, 17: 1298
radiation effects on, review of, 17: 8504
radiation effects on nuclear structures of cells in, 17: 19916
radiation effects on, 17: 24937
radiation effects on, effects of ambient environment on, 17: 24939
radiation effects on filament formation in, 17: 27136
radiation effects on activity of, synergistic effects of halogenophenols on, 17: 30215
radiation effects on soil, 17: 30334
radiation effects, biological, 17: 33562
radiation effects on, 17: 41074
radiation effects on clam content of, gamma, 18: 521
radiation effects on potato susceptibility to phytopathogenic, 18: 13495
radiation effects on spore *A. aureofaciens* with and without water, 18: 17514
radiation effects on fruit and vegetable, gamma, 18: 17524
radiation effects on, review, 18: 17536
radiation effects on *Pseudomonas aeroginosa*, effects of humidity and inositol on uv, 18: 17551
radiation effects on *Serratia marcescens*, effects of humidity and inositol on x ray, 18: 17551
radiation effects on populations of, in Dover sole, 18: 21817 (TID-7684 (p.64-8))
radiation effects on wheat straw use by rumen, gamma, 18: 21849
radiation effects on, environmental factors affecting, 18: 21903
radiation effects on, gamma, 18: 21910
radiation effects on mouse serum-γ-globulin and lymph tissue as affected by, 18: 27122
radiation effects on, beta, 18: 41193
radiation effects on genetic recombination in, x, 19: 3945
radiation effects on susceptibility of plants to, 19: 10828
radiation effects on *Trypanosoma brucei*, biological, 19: 21991
radiation effects on *Prorocentrum micans*, genetic, 19: 31867
radiation effects on fruit pathogenic, gamma, 19: 39265(R) (IA-1021)
radiation effects on infectiousness and motility of *Treponema pallidum*, 19: 38380
radiation effects on, in ionizing field, 20: 6710
radiation effects from inhaled strontium-90 on spirochetal population in dogs, 20: 8638(R) (LF-28, pp 250-6)
radiation effects on immune reaction to *Treponema pallidum*, γ, 20: 14308
radiation effects on, in fish, 20: 21200
radiation effects on populations of, in fish, gamma, 20: 29583(R) (TID-22515)
radiation effects on, in fruit juices, 20: 37156
radiation effects on genetic mutations in, tritium, 20: 38624
radiation effects on food-borne, review, 20: 41388
radiation effects on, in proteinaceous food, 20: 41390
radiation effects on, in beef and lamb, gamma, 20: 46119
radiation effects on, contaminating sunflower seed, gamma, 20: 45416
radiation effects on food-spoilage, on berries and fruits, gamma, 20: 43782
radiation effects, genetic, 19: 21981
radiation inactivation of, hypothesis on dose effects in, 18: 11667
radiation injuries, reaction mechanisms, 16: 30263
radiation pasteurization of shrimp, effects of gamma, 18: 21810 (TID-7684(p.28-31))
radiation resistance, 16: 24043
radiation resistance of, review of, 17: 24936
radioactivity of Lake Maggiore, 1952 to 1961, 19: 11391(R) (NP-14658)
radioactivity transfer by marine, by detritus, 19: 21825
radiobiological research on, statistical method for analyzing population interactions in, 20: 6706
radioinduced chromosomal aberrations and lethals in *Aspergillus nidulans*, 16: 21983
radioinduced division block in protists, research program on recovery from, 16: 8541(R) (TID-14809)
radioinduced inactivation of, additive effects of chemical agents on, 17: 30027
radioinduced mutations in, mechanism of ultraviolet, 17: 19915
radioinduced mutations in, ultraviolet, 18: 19650
radioinduced mutations in, 19: 10719 (AECL-2107)

radioinduced mutations, 19: 21922
radioinduced sensitization of, in food, 20: 5816
radioinduced suppression of cell-division in, recovery mechanisms, 19: 21856 (COO-878-15)
radioisotope distribution in fresh-water, 17: 34137
radioisotope uptake by marine, 16: 14998(R) (NYO-8100)
radioisotope uptake by, 17: 33562
radiosensitivity, effects of irradiated medium, 16: 17439(T) (JPRS-12921(p.1-11))
radiosensitivity of, causing food spoilage, 16: 9086
radiosensitivity of the ciliate, *Spathidium spathula*, 16: 21954
radiosensitivity of cysts of *Tillina magna*, 16: 26827
radiosensitivity of food-spoilage, 17: 16374
radiosensitivity of, isolated from irradiated flounder, 17: 25514 (TID-7657(p.59-61))
radiosensitivity of, effects of dose rate on, 17: 24938
radiosensitivity of, effects of postirradiation growth medium and temperature on, 17: 24941
radiosensitivity of the ciliate *Spathidium spathula*, 17: 33619(R) (TID-19153)
radiosensitivity of mitosis in, effects of stage in reproduction on, in *Oedogonium cardiacum*, 17: 38795
radiosensitivity of *Astasia longa*, effects of cell division on, 18: 27009(R) (ORNL-3601(p.152-72))
radiosensitivity of *Spathidium spathula*, ultraviolet, 18: 35321(R) (TID-20937)
radiosensitivity of, factors affecting, 19: 19590
radiosensitivity of scrapie agent, use in size estimations, 20: 18314
radiosensitivity of *Micrococcus radiodurans*, effects of pigments on, 20: 29016
radiosterilization effects with storage on microbial flora in dover sole fillets, 19: 46882
recommendations of FAO/WHO/IAEA on radiosterilization of, in food, 20: 43786
regeneration of irradiated monocellular, effects of energy metabolism on, 17: 31890
responses of test, research on, 20: 18187(R) (N-65-16497)
review articles on, 18: 21753
ribonucleic acid and ribosome molecular properties and thermostability in thermophilic, 17: 6792(R) (ISS 62/14)
ribonucleic acid synthesis in, 19: 29846 (ACRH-103(p.28-36))
role in breakdown of leaf litter and humus formation in forests, 19: 1960 (ORNL-P-517)
role in breakdown of leaf litter and humus formation in forests, 19: 1961 (ORNL-P-586)
role in digestion of fatty acids in sheep rumen, 18: 15708 (TID-20218)
role in formation and decomposition of organic compounds in soil, 20: 42795
ruthenium transport by, in surface waters, 18: 1340 (TID-19529)
scavenging of sorbed material from mineral particles by, tracer study, 17: 31830 (TID-19127)
selenium-75 uptake and retention by, 19: 6962
sensitivity to antibiotics in intestine, strontium-90 effects on seasonal fluctuations in, 16: 16210
sterilization, bibliography, 17: 31765 (N63-16122)
sulfur isotope fractionation, 17: 20234
survival curves of, effects on radiation dosimetry of, 20: 14814
synchronous growth of several strains, 17: 5674(R) (LAMS-2780(p.211-45))
synthesis of desoxyribonucleic acid in *M. lysodeickticus*, 16: 8529

Microradiography
see Radiography

MICROSCOPES
see also Electron Microscopes
see also Field Emission Microscopes
see also Particle Microscopes
adaptation of toolmaker's, for remote operation, 19: 36590 (WAPD-T-1690)
conversion of optical, to microphotometer for measuring grain reflectance in metals, 19: 13994(R) (NLCO-940(p.8.1-4))
description of hot-stage, for studying plutonium, 19: 20546 (CEA-R-2726)
design and operation of reflecting, for high temperature use, 17: 6406 (TID-13148)
design and performance of high-temperature, for observing radiometallic samples, 16: 23839 (CEA-2082)
design and performance of vibrating mirror flying spot microscope, 17: 12132(R) (TID-17840)
design and performance of surface ionization, 17: 36134
design and performance of semi-automatic, for particle track measurements in nuclear emulsions, 20: 23477
design for examination of metal surfaces immersed in liquid helium, 20: 19732
design for measuring particle lengths in nuclear emulsions, 19: 39000
design for nuclear emulsion measurements, 16: 299 (PAN-238/VI)
design for radioactive specimen examination, 16: 3177(P)
design of automatic following, for analysis of nuclear emulsion tracks, 20: 27287
design of camera-microscope with tissue culture chamber and phase contrast optics, 20: 32963 (AD-627686, pp 455-64)
design of digitized, for analysis of particle tracks, 18: 20295
design of, for use at ultrahigh temperatures, 17: 40704 (TID-7655(p.135-46))
design of phase-contrast uv microbeam, with television equipment, 19: 45891
design of television, for automatic blood cell scanning, 16: 25568 (NYO-9644)
design of ultraviolet, 19: 12962(R) (TID-21611)
design of vibrating mirror flying spot, 19: 10787(R) (TID-21581)
design using multiple radiation sources, 18: 22329(P)
development of high-vacuum, hot-stage, for use with plutonium, 20: 7576 (RFP-543)
development of particle-track analyzing, 19: 25265(R) (UCRL-11776)
development of thermionic-emission, 17: 25687(R) (GA-4173)
development of vibrating mirror flying-spot, 16: 8539 (TID-14541)
device for measuring lengths under, 16: 4251 (PAN-241/VI)
drive design for, automatic, 16: 6600
electrostatic immersion objective of, translation of papers on, 18: 6567(T) (AI-Trans-11)
electrostatic immersion objective for, development of high-resolving-power, 18: 6569(T) (AI-Trans-11(Paper 2))
electrostatic immersion objective of, focusing curve of flat-electrode, 18: 6570(T) (AI-Trans-11(Paper 3))
hot stage design for metallographic, 19: 47000 (NMI-4996, pp 8-16)
image brightness intensifiers for, development of, 18: 33221
operation of ultrasonic, principles for, 17: 6792(R) (ISS 62/14)
performance for particle track analysis in emulsion, 18: 23941
performance of digitized-travel, for particle track analysis in emulsions, 18: 23940
performance of image-splitting eyepieces in, in metallographic applications, 20: 16952 (ORNL-TM-1161, pp 182-91)
performance of KSM-1, for nuclear track measurements, 17: 18565
resolution of immersion objective of thermoelectric emission-type, 18: 6568(T) (AI-Trans-11(Paper 1))
stage design for scanning of emulsion plates, engineering drawings, 17: 21857
use for cloud chamber track photographs, semiautomatic device for, 19: 40888
use of polarized-light, for determining pole figure of hexagonal metal, 17: 23966(R) (TID-18637)
use of remote-control stereo zoom, for viewing and photographing radioactive materials, 19: 9314 (WAPD-T-1689)
use with glove boxes, arrangement for, 19: 6063(P)

MICROSCOPY
see also Electron Microscopy
see also Field Emission Microscopy
see also Photomicrography
see also X-Ray Microscopy
automatic data recording systems for, 20: 6901
automation of, of nuclear emulsions, 17: 18525 (CERN-63-3(p.221-4))
Cintel flying spot, 17: 6529 (TID-7625(p.52-62))
data recording system for histological sections, 20: 6785(R) (ORNL-3853, pp 128-40)
design and performance of vibrating mirror flying spot microscope, 17: 12132(R) (TID-17840)
determination of tritium-labeled cells in tissue sections, autoradiographic method for, 18: 11566
development for analysis of inorganic materials, 16: 25275(T) (AEC-tr-5194)
development of television microscope scanner for blood cell identification and imaging, 16: 3096 (NYO-9645)
development of ultraviolet, for biochemical and cytological studies, 20: 42702(R) (ANL-7136, pp 243-55)
effectiveness of luminescence–microscopic methods for revealing radiation injuries, 16: 1534
equipment for nuclear emulsion, survey of, 17: 18523 (CERN-63-3 (p.199-209))
field-ion, use in determining atomic structure of metals, 17: 30922 (SC-4920(M)(p.77-9))
fluorescence, device for phase contrast in, 19: 38923(T) (UCRL-Trans-1228)
fluorescence, use in observations on bone marrow during radiotherapy, 18: 33399
histone preparation for, 20: 22709
luminescent, sample preparation for, 18: 27179
mammalian leukocyte preparation for, 18: 15682 (LADC-5746)
methods for membrane radiation injuries, 19: 45891

methods for, review, 16: 25275(T) (AEC-tr-5194)
optical techniques for electron-probe analysis, 19: 40951 (NBL-6290)
preparation of photomicrograms of crystalline material, 16: 30513 (HW-SA-2081)
preparation of root cells for, 20: 45386
replica technique using polyvinyl chloride for high-burnup reactor fuels, 18: 7132 (WAPD-T-1595)
sample preparation for luminescent, 18: 13458(T) (JPRS-22915)
sample preparation of monkey blood, 18: 15738(R) (LAMS-3034(p.227-34))
sample preparation for demonstration of lipid component of arteries, 18: 17373(R) (UCRL-Trans-1033)
sample preparation for, of bone, 19: 6914(R) (ANL-6906(p.117-25))
sample preparation of mammalian tissues by supravital staining of wet drop samples, 19: 35964
sample preparation of ceramic materials for high-magnification optical, 20: 16954 (ORNL-TM-1161, pp 267-71)
ultraviolet microbeam irradiation of living cells and tissues, 17: 14035
use of flying-spot, for detecting uv-absorbency of cultured cells during interphase, 20: 20473
use of polarization, in muscle contraction studies, 20: 16259
use of polarized-light in measuring basal-pole orientation in zirconium, 20: 37266

MICROSOMES
association of alkaline metal and alkaline earth cations with, in dog kidney cells, 20: 35224
binding site for messenger RNA in *Escherichia coli*, tracer study, 20: 1592 (BNL-7903)
biochemistry in regenerating liver, 19: 31681(R) (ORNL-3768(p.164-76))
calcium-45 content in shell gland mucosa cells, 20: 40551
catalase activity in mouse tumor cell, 18: 38758
chemical dissection of rat liver, method for, 20: 16160 (UCRL-14739 (Pt.2))
dissociation of reticulocyte, 20: 5264
effects of actinomycin on synchronized Tetrahymena, 19: 31679(R) (ORNL-3768(p.146-8))
effects of radioprotectants on enzyme systems of rat hepatic, 17: 35415
electrophoresis of, 20: 18205(R) (LA-3432, pp 178-262)
enzymatic decarboxylation of fatty acids in rat brain, tracer study of, 17: 35337(R) (UCLA-515(p.15-31))
function of ribosomes in Clostridium, 20: 40503(R) (ORNL-3922, pp 137-45)
function of, electron microscopic analysis of, 20: 16160 (UCRL-14739 (Pt.2))
metabolic activity of, 20: 6721(R) (ORNL-3853, pp 161-9)
microscopy of isolated, from rat liver, 20: 6721(R) (ORNL-3853, pp 161-9)
production in antibody-forming cells, tracer study using carbon-14 of, 20: 40626(R) (ORNL-3922, pp 80-3)
properties of subunits of reticulocyte, 20: 5264
radiation effects on L-ascorbic acid synthesis in rat liver, x, 19: 10803
radiation effects on synthesis of enzymes in hepatic, x, 20: 5282(R) (AD-623599, pp 1-15)
radiation effects on synthesis of enzymes in hepatic, x, 20: 5283(R) (AD-623599, pp 16-27)
radiation effects on protein synthesis in spinach chloroplast, uv, 20: 22590
radiation effects on uptake of heat-killed sulfur-35-labeled mycobacterial vaccines by rat spleen, x, 20: 42907
radiation effects on *Escherichia coli*, β and x, 20: 45463
radioinduced inactivation of isolated *Escherichia coli*, γ, 20: 14363
radiosensitivity effects on *E. coli*, 19: 31790(R) (ORNL-3768(p.85-8))
role in immune reactions in rat spleen, 20: 6721(R) (ORNL-3853, pp 161-9)
role in protein synthesis, 20: 40503(R) (ORNL-3922, pp 137-45)
synthesis in bacteria, 20: 42702(R) (ANL-7136, pp 243-55)
synthesis in rat liver, 20: 6700(R) (ORNL-3853, pp 183-207)

Microstructure
see Grain Structure

Microtron
(An electron cyclotron)
see Cyclotrons

Microwave Discharge Detectors
see Spark Chambers

MICROWAVE EQUIPMENT
see also Cavity Resonators
see also Electron Tubes
see also Masers
see also Microwave Oscillators
see also Microwave Spectrometers
admittances of waveguides radiating into plasma layers, mutual and self, (T), 19: 33401 (AD-611202)
amplification in traveling-wave devices, using cyclotron resonance effects, 16: 30619
assembly procedures for klystrons, 18: 2501(R) (TID-19422(Suppl.II))
attenuation in spiral waveguides, 18: 20315
beam amplitudes in traveling-wave tubes, 18: 31851
book: *Electromagnetic Waveguides and Cavities, Physics and Technology*, Vol. 5, translation from German, 16: 29077(T) (AEC-tr-3926)
book: *Electromagnetic Slow Wave Systems*, 18: 31860
book: *Methods of Experimental Physics. II. Electronic Methods*, 18: 29963
characteristics of beam-plasma waveguides, (T), 19: 16255 (ML-1146)
charged particle deflection by iris-loaded waveguides, (T), 19: 14125 (BNL-8663)
charged particle energy losses in waveguides, 16: 28250
charged particle emission from open end of waveguide, generation of electromagnetic radiation in, 18: 42389
charged-particle emission from semi-infinite waveguides, (T), 20: 29828
charged-particle motion in semi-infinite round waveguide, radiation field from, (T), 19: 23484
charged-particle radiation emission in, 18: 26150
Cherenkov emission by charged particles in circular waveguide filled with gyrotropic ferrite, (T), 20: 2550
Cherenkov radiation from charged particles in waveguides with laminated dielectric, 19: 33100
Cherenkov radiation from electron beams in waveguides, traveling wave nature of, 20: 39501
circuit network representation of $\pi/2$ mode accelerating waveguide system, (T), 19: 28933 (BNL-8914)
conference, 19: 12285
conference on microwave tubes, 19: 36795
data handling and chart recording for resonance wavemeter, 18: 41727(T) (SLAC-Trans-9)
deflector properties of iris-loaded waveguides, R/Q measurements of (E/T), 19: 2921 (BNL-8544)
delay system for plasma waveguides, consisting of plasma rod surrounded by helix, 17: 22290(T) (JPRS-18823(p.322-35))
description and performance of frequency-separating, for multifrequency u-h-f plasma probing, (E/T), 20: 28529
description of high-speed phase shifter with varactor diodes, 20: 9232
description of probe for electromagnetic wave-plasma interactions, 20: 8217
design and operation of 6-Bc series-tuned f-m discriminator for demodulation of fast-risetime telemetry, 18: 20285 (SCL-DR-64-13)
design and performance of coaxial reflectometric, 16: 14918 (SCTM-10-62(24))
design and performance of millimeter wavelength oscillator, 17: 23607 (ML-918)
design and performance of klystron, 18: 821(R) (RADC-TDR-62-464(Vol.3))
design and performance of detectors and mixers using superconducting tunnel diodes, 18: 41710(R) (AL-TDR-64-46)
design and performance of frequency discriminator for plasma diagnostics, 19: 19253 (NP-14725)
design and performance of, for charged particle track measurement, 20: 37043
design and performance of cavity Q sampler for plasma diagnostics, 20: 38307
design and testing, 17: 17317(R) (SLAC-8)
design and testing of mm-wave beam-plasma amplifier, (E), 19: 13705 (RADC-TDR-64-207)
design for electron linear accelerators, 19: 16312
design for electron density determinations in weakly ionized plasma, 19: 31408
design for irradiation of biological and biochemical systems, 16: 11377(R) (AD-259234(p.31-46))
design for microwave angular deflection measurements, 16: 12603(R) (AD-261667)
design for microwave propagation in plasma, 19: 23895
design for moisture determination in solids, 16: 8704
design for phase measurements in plasmas, 16: 12600(R) (AD-261663)
design for phase-shift detection, 18: 44852 (MATT-273)
design for plasma heating, 18: 13137(R) (ORNL-3564(p.28-43))
design for plasma, 18: 15418(P)
design for plasma diagnostics, 18: 21368 (AFCRL-63-161)
design for plasma diagnostics, 19: 1793
design for plasma diagnostics, 19: 1794
design for plasma electron-density diagnostics, (E/T), 19: 5285(T) (AEC-tr-6518(p.118-25))
design for plasma electron density measurements, 19: 41854 (MATT-369)
design for plasma diagnostics, nonuniform, 19: 41855 (NP-15142)
design for plasma density measurements, 20: 38338(P)
design for plasma diagnostics, 20: 41120
design for study of rapidly varying plasma parameters, 17: 4173 (NP-12230)

design of bridge apparatus for determination of electron density in nitrogen plasma, 19: 8544
design of cavity for fast wave plasma cyclotron amplifier, 17: 27650(R) (AD-297382)
design of Cherenkov radiator for production of millimeter and submillimeter waves, 16: 4254 (WADD-TN-61-1)
design of discharge cavity operating at 2450 Mc/sec, 19: 15842
design of electron beam harmonic wave generator, 18: 10360(P)
design of frequency control system for optimizing x-ray output of microwave linear electron accelerator, 16: 23952
design of Fresnel zone lenses for microwave focusing, (E/T), 19: 28920 (UCRL-7785-T)
design of generation of millimeter waves from cyclotron excitation of trapped electrons, 18: 39590
design of interferometer for plasma density fluctuations, 18: 11339
design of interferometer using electron phase inverter, (E/T), 19: 4433(T) (AEC-tr-6518(p.74-81))
design of linear selective circuitry for plasma phase-shift diagnostics, (T), 19: 4434(T) (AEC-tr-6518(p.82-90))
design of millimeter single-side-band generators, 18: 14161 (MATT-167)
design of mixers using superconducting tunnel diodes, 18: 33824(R) (AD-428788)
design of panoramic wavemeter, 18: 41726(T) (SLAC-Trans-8)
design of phase meter for plasma diagnostics, 18: 30919
design of plasma-beam signal generator, 19: 32532(P)
design of probe for electron-density measurements in shock tubes, 20: 38305
design of r-f beam separator for Brookhaven AGS, (E), 20: 2532 (BNL-9505)
design of semiconductor amplifier, electromagnetic oscillation theory for, 20: 30677
design of stub tuner for impedance matching between cables and cavity in helium cryostat, 17: 14436
design of waveguide for increasing efficiency of electron linear accelerators, 17: 890
design of waveguides with diaphragms, 17: 22282(T) (JPRS-18823)
design of waveguide with collinear termination for linear accelerators, 20: 41583(P)
design of X-band interferometer for electron density measurements in plasma positive column, 17: 26686
design of 8-MH_z ultrasonic waveguide, 17: 6792(R) (ISS 62/14)
development, 16: 3535(R) (NP-11112)
development, 18: 685(R) (MDL-Q1)
development for Brookhaven AGS beam separator, 20: 4493 (BNL-9642)
development for in-core measurement of dynamic reactor response, (E), 19: 12846
development for linear accelerators, 20: 5965(P)
development for measuring neutron fluxes, 19: 34425(R) (HW-84384 (p.7.1-27))
development for measuring magnetic fields, (E/T), 20: 28495(R) (MATT-Q-22, pp 321-85)
development for neutron flux monitoring, 19: 22660(R) (HW-83298(p.7.1-30))
development for neutron flux monitoring in reactors, 19: 35703(R) (BNWL-38)
development for phase measurements in plasma, 16: 12601(R) (AD-261665)
development for plasma diagnostics, 17: 19465(R) (UCRL-10607)
development for Stanford linear accelerator, 17: 29643(R) (SLAC-16)
development for Stanford Linear Accelerator, 17: 35000(R) (SLAC-10)
development for Stanford linear accelerator, 17: 42015(R) (SLAC-18)
development for Stanford linear accelerator, 18: 8958(R) (SLAC-23)
development for Stanford linear accelerator, 18: 22593(R) (SLAC-27)
development for Stanford Linear Accelerator, 20: 13366(R) (SLAC-53)
development of accelerator waveguides, (E/T), 19: 14171 (CERN-64-43)
development of directional coupler in oversize waveguide, 16: 20671
development of electron-beam and solid-state, 18: 29925(R) (MDL-Q3)
development of ferrites for, 20: 29709(R) (TID-22970, pp 65-119)
development of high-power cyclotron resonance switch, 19: 46708(R) (AD-611560)
development of infrared and optical masers, 16: 19476(R) (TID-15642)
development of infrared and optical, 16: 30172(R) (TID-16489)
development of ion chamber for detection and measurement of gamma rays, 16: 7675 (ASD-TR-61-32)
development of iris-loaded guide configuration for accelerator traveling waves, 17: 7322 (BNL-6511(p.171-3))
development of klystrons, 17: 9647(R) (TID-17021)
development of klystrons, 17: 11798(R) (TID-17221)
development of klystrons, 17: 24517 (DESY-A-2.97)
development of lenses for plasma diagnostics, 20: 3169 (NASA-CR-319)
development of loaded waveguides for linear accelerators, 19: 12034
development of optical maser program, 16: 21129(R) (NP-11640)
development of optical masers, 16: 23002(R) (ORNL-3268(p.84-7))
development of rectangular plasma package, (E), 19: 25555 (RADC-TDR-64-244)
development of reflection probe for plasma electron densities, 18: 32922
development of tubes, 18: 1124(R) (ML-894)
development of waveguide, for cyclic accelerators, (E), 19: 9812
development of waveguides, for accelerators, 20: 17209(R) (LA-3479)
development of, using superconducting point contacts, 20: 31482
development, review, 17: 20647
dispersion equations for rectangular septate waveguide, (T), 19: 37235
dispersion of iris-loaded cylindrical waveguides, 17: 18567
electromagnetic deflecting modes in iris-loaded waveguides, 17: 39396
electromagnetic field distribution in plasma waveguides, (T), 19: 31400
electromagnetic wave confinement by plasma waveguides, 17: 11828 (AFCRL-62-63)
electromagnetic wave propagation in cylindrical waveguide containing inhomogeneous plasma, 17: 11843
electromagnetic wave propagation in waveguides, analysis of, 18: 20623 (JINR-P-1565)
electromagnetic wave propagation in plasma wave guides, (T), 19: 27625(T) (UCRL-Trans-1170(L))
electromagnetic wave dispersion in rectangular waveguides, (E/T), 19: 27030
electromagnetic wave propagation in plasma in waveguide, 19: 37974
electromagnetic wave-plasma interactions in, amplification in, (E/T), 19: 47219 (AD-614253)
electromagnetic wave emission by electron beams in ring waveguide, 20: 1001
electromagnetic wave reflection coefficients in plasma waveguides, 20: 46904
electromagnetic-wave propagation in plasma-filled waveguide, (T), 19: 23870
electromagnetic-wave emission from open end of semi-infinite plane waveguide, (T), 19: 32820
electromagnetic-wave propagation in dielectric-layer circular waveguides, (T), 19: 46743
electromagnetic-wave propagation in waveguides, (E/T), 20: 13370
electron beam focusing in, theory of, 18: 39603
electron beam interactions with, production of electromagnetic radiation by, 17: 26388
electron beam interactions with plasma-filled waveguides, 20: 13925(R) (TID-22419, pp 99-147)
electron beam oscillations in traveling-wave tubes, 20: 919
electron-gun characteristics in crossed-field, model for, 16: 30618
electron interactions in uniformly loaded waveguides, Cherenkov radiation from, (T), 20: 17485
electron redistribution in plasma waveguide in strong electromagnetic field, (T), 20: 24564
electron-beam pulsing in waveguides, (T), 19: 27042
energy absorption in electron cyclotron resonance isolator, (T), 19: 25555 (RADC-TDR-64-244)
energy mechanisms in plasma waveguides, 16: 5832
extraction of microwave power from plasma, (E/T), 19: 10397 (RADC-TDR-64-174)
feasibility of wide-band multi-channel telemetry system, 19: 27889 (UCRL-13132)
field calculation in plasma waveguides, 19: 38005
field distributions in plasma waveguides, 18: 26778
frequency-mixer, design using superconductors, 16: 3527 (AFCRL-75)
frequency of antenna inside magnetoplasma-filled parallel-plate waveguide, (E), 20: 2096 (AD-617928)
frequency stabilization system for K-band reflex klystron oscillator, 16: 337(R) (NP-10868)
frequency stabilizer for klystron generator, 16: 11853 (IFA-RS-15)
hydromagnetic wave propagation in liquid-filled waveguides, (E/T), 19: 4758
hydromagnetic wave propagation in plasma-filled waveguides, 20: 10167
hydromagnetic wave scattering by open end of semi-infinite plasma waveguide, 20: 12207
hydromagnetic wave propagation in magnetoplasma waveguide, viscous effects on, (T), 20: 15925
interactions of electron beams with plasma in waveguides, (T), 19: 12641 (RLE-TR-423)
interferometer for plasma diagnostics, design and performance of, 17: 42062
interferometer for plasma diagnostics, dual-frequency phase-shift, 18: 19211
klystron development for Stanford Linear Accelerator, 17: 39381(R) (TID-19482)
klystron development and testing, 19: 25099(R) (SLAC-34)
klystron sweeping arrangement, 17: 27650(R) (AD-297382)
magnetic field structure in waveguide filled with plasma, 17: 29694
magnetic-field-plane bifurcation in waveguide filled with anisotropic plasma, (T), 20: 6481

magnetohydrodynamic waveguides, experiments with liquid metal, 19: 39270(R) (TID-21894)
magnetohydrodynamic waveguide excitation by coaxial waveguide, 20: 12208
microwave propagation in plasma waveguide, 18: 21444
microwave propagation in plasma-filled waveguide, 18: 44858 (RADC-TDR-64-117)
microwave propagation in plasma-filled waveguides, 19: 21536
mode coupling in, 18: 15711(R) (TID-20256)
mode identification in iris-loaded waveguide of a r-f particle separator, 17: 13609 (BNL-6726)
nuclear resonance "maser" frequency dependence on equipment parameters, 18: 37479(T) (AEC-tr-6398(p.314-21))
operation in standing-wave linacs, normal-mode analysis of, (T), 20: 929 (BNL-9514)
operation of, analysis of deflecting mode in synchrotron waveguides, 17: 11783 (BNL-6670)
operation of, in accelerator acoustic filters and resonators, 17: 2338 (MURA-644)
oscillations in unloaded waveguides, backward-wave, 17: 23607 (ML-918)
oscillations of open resonators and wave guides with plane mirrors, 18: 20313
oscillations of open resonators with cylindrical mirrors, 18: 20314
particle dynamics in waveguide separators, 20: 31841
performance of ferrite in, high-power effects in, 17: 18972
performance of, for gas discharge duplexers, 17: 6403(R) (RADC-TDR-62-254)
performance of gas-discharge duplexers, effects of magnetic fields on, (E), 19: 42678 (AD-609658)
performance of hydromagnetic waveguides, 18: 28094(R) (TID-20607)
performance of, in measurements of electron density of transient plasma, 18: 6357
performance of iris-loaded waveguides as charged-particle accelerator-beam deflectors, (E), 19: 14169 (BNL-8782)
performance of low-loss plasma waveguides, 18: 32944
performance of magnetic undulator generation system, 16: 13330
performance of multimode cylindrical, 19: 39269(R) (SU-SEL-64-133)
performance of short-circuited waveguide as EPR sensor for stabilizing magnetic fields, 20: 31813
performance of tapered waveguides as plasma analogs, (E), 19: 8496 (AD-606981)
performance of traveling-wave pumps for accelerating plasma, 16: 16014
performance of waveguides, factors affecting, 19: 26915(R) (AD-609133)
performance of 3-Gc circular guides, for charged-particle-beam separations, 18: 20925
performance of, frequency and power increases in, 18: 15356
periodic waveguide propagating circuits, dispersion properties of, 17: 22664 (ML-915)
phase length measurements for, accurate, 20: 35965 (SLAC-PUB-181)
phase shifter for, varactor diodes utilization in, 19: 40297 (UCRL-7753)
plasma acceleration in waveguide by electromagnetic field, 18: 44862(T) (UCRL-Trans-1077(L))
plasma acceleration by microwave reflection in, 20: 8211
plasma characteristics in resonance isolator in rectangular waveguide, 18: 34977(R) (RADC-TDR-64-94)
plasma coupling to waveguides, impedance in, 19: 23852
plasma diagnostic using multiple-probe, 18: 1167
plasma diagnostics with multiple-probe, 17: 5448
plasma-filled waveguides, cold three-fluid model for hydromagnetic wave propagation, 18: 9510
plasma instrumentation with, 16: 18566
plasma oscillation modes in anisotropic guides and resonators, (T), 19: 10383 (AL-TDR-64-157)
plasma oscillation modes in circular waveguides, (E), 19: 47743
plasma perturbation in disk-loaded wave-guide, (E), 20: 3219
plasma production in pulsed cavities, 17: 15037
plasma uses in, 18: 10342 (RADC-TDR-63-54)
power flow in plasma-filled waveguides, (T), 20: 38239
power generation by crossed-field amplifier and klystron amplifier in magnetohydrodynamic generator, 18: 821(R) (RADC-TDR-62-464(Vol.3))
production in galaxy, origin of, 20: 37362
propagation characteristics of bidirectional waveguides, 16: 29954
propagation characteristics of plasma-filled waveguides, 16: 31155
propagation constants for waveguides, 17: 24547
propagation constants of quasi-TE_{11} modes in cylindrical waveguides, (E), 20: 44903
properties of Alfvén cylindrical waveguides, terminal, (T), 20: 17522
properties of cavity chain as amplifier, 16: 337(R) (NP-10868)
properties of disc-loaded waveguides, 17: 11798(R) (TID-17221)
properties of disc-loaded deflecting waveguides, (T), 20: 5934 (CERN-65-37)
properties of grid-loaded structures, 17: 11798(R) (TID-17221)
properties of plasma cathode, 16: 337(R) (NP-10868)
properties of synchrotron waveguides, 18: 14672 (CERN-64-10)
protection of patients and personnel during operation of medical, 20: 38622
radiation effects on operating characteristics of ferrite duplexing devices and wave guides, 17: 41499(R) (NP-13159)
radiation effects of high-speed secondary electrons on performance of a helix-type traveling-wave tube, 18: 482
radiation effects on traveling-wave tubes, pulsed, 18: 4296(R) (AD-423158)
radiation from plasma-filled waveguides, 18: 44847 (AFCRL-64-279)
radiation hazards and protection during operation, 17: 31911
reflection coefficient of septate waveguide of linear accelerator, (E), 19: 32849
reflection coefficients in plasma-filled waveguides, method for determining, 19: 45401 (NP-15196)
research on electron-beam tubes, 19: 27586 (AD-428606)
research on klystrons, 17: 17317(R) (SLAC-8)
research progress on, 17: 38616(R) (MDL-Q2)
resonances of plasma-filled cavity, 19: 3400 (UCRL-12053)
shower development and heating in the waveguide structure by 800-Mev electron beam, 17: 11794 (SLAC-3)
sonic regions and temporal instabilities in traveling-wave amplifiers, 16: 5776(R) (NP-11141)
space harmonic analysis for maximum deflection of iris-loaded waveguides, 17: 24516 (BNL-6974)
study of tubular plasma coupler, 19: 25552 (AL-TDR-64-155)
superconducting cavities, field emission in, 19: 23557
surface-wave production in waveguides, 16: 14915(R) (NP-11265)
testing tube windows for klystrons for linac, 18: 44322 (SLAC-PUB-49)
theory of M-type transverse interaction tube, 18: 30898(T) (JPRS-25168)
theory of multistream, nonlinear, 18: 22977
theory of plane traveling-tube, nonlinear, 18: 22324
theory of plasma waveguide, nonlinear, 17: 33185
theory of plasma waveguide, nonlinear, 18: 14697
theory of waveguides, use of longitudinal fields in, 17: 8950 (UCRL-6731)
use for determination of plasma velocities, 18: 6308 (NP-13362)
use in atomic collision process studies, 17: 35019 (AD-411955)
use in neutron flux monitor, 18: 8606(R) (HW-78388(p.7.1-10))
use in neutron flux monitor, 18: 27750(R) (HW-79280(p.7.1-22))
use in plasma diagnostics, 17: 33439
use in plasma electron-density measurement, 18: 32925
use in remote surveillance, 20: 41224 (EGG-1183-2078)
use of diaphragmed waveguides, as deflector of h-f separator, 20: 13362 (JINR-P-2503)
use of iris-loaded waveguide with periodic structure in linear particle accelerator, 19: 23233(P)
use of iris-loaded waveguides for extending electron beam duration, 20: 5964(P)
use of open waveguide in plasma diagnostics, (E), 20: 41717
use of waveguides for excitation of accelerator resonance cavity, 16: 23160 (MURA-637)
wave group velocity and damping in septate waveguide of linear accelerator, (T), 19: 32848
wave modes in coaxial circuits in, 19: 26915(R) (AD-609133)
wave motion in plasma-filled waveguides, 18: 30869 (AD-428783)
wave phase velocity and resonant frequency in iris waveguide of linear accelerator, (T), 19: 32846
wave propagation between dielectric media without reflection in, 18: 682 (LADC-5635)
wave propagation in isotropic plasma waveguide, 16: 13825
wave propagation in, 17: 17388
wave propagation in focusing waveguides, 17: 34638
wave propagation in magnetoplasma-filled waveguides, two-fluid analysis of, 18: 2423
wave propagation in plasma waveguides, 18: 28866
wave propagation in plasma waveguide, nonlinear, 18: 44897
wave propagation in plasma waveguides, dispersion equation for asymmetric, 20: 34757
wave splitting in plasma-filled waveguides, (T), 20: 19300 (N-65-23065)
waveguide admittance for radiation into plasma layers, (E/T), 20: 2098 (AD-618398)
waveguide all-metal vacuum gate valve, design of, 20: 949(P)
waveguide analog of tunneling through quantum potential barriers, 20: 37929
waveguide behavior in, correlation with elementary particle behavior, 19: 47319
waveguide bunchers for linear accelerator, similarity of, 17: 24554
waveguide characteristics of magneto-ionic ducts, 18: 30878(R) (AFCRL-64-219)
waveguide characteristics for non-homogeneous media, 19: 26915(R) (AD-609133)

waveguide coupling seal for, 20: 645(P)
waveguide design for traveling-field linear accelerator, 20: 31851(P)
waveguide development, 19: 5271(R) (TID-21252)
waveguide development and testing, 19: 25099(R) (SLAC-34)
waveguide development for proton linacs, 20: 2538 (LA-DC-7281)
waveguide excitation by steadily moving charged filament, (T), 19: 16292
waveguide fabrication using diffusion techniques, 18: 22629 (TID-7691 (p.456-8))
waveguide fabrication for electron linac, demountable method for, 18: 22630 (TID-7691(p.459-62))
waveguide fabrication and measurement for linear accelerators, methods for disk-loaded, 19: 26981 (MURA-714(p.75-83))
waveguide for radiofrequency particle separator, properties of, 18: 5886 (CERN-63-33)
waveguide performance for proton linacs, crossbar and slotted iris, 20: 27645 (KFK-403)
waveguide resonator design for separation of elementary particles, 16: 4891(P)
waveguide space harmonics in linear accelerators, coefficients for iris-loaded, (E), 20: 11393 (NP-15715)
waveguide structures for proton linac, 18: 22602 (TID-7691(p.104-30))
waveguide structures for proton linac, shunt impedances of, 18: 22603 (TID-7691(p.131-52))
waveguide-taper design, procedure for, 17: 24520 (LADC-5474)
waveguides for accelerators, deflecting mode in circular iris-loaded, (E/T), 19: 28938 (CEA-R-2745)
waveguides for iris-loaded linac, effects of errors in repetitive, 18: 22606 (TID-7691(p.190-5))
waveguides for linear accelerators, resonance method for adjusting circular-iris, 20: 5955
waveguides for π-mode standing-wave acceleration, bandwidth, tank flatness, and shunt impedance of iris-loaded, 18: 22604 (TID-7691 (p.153-70))
waveguides for proton linacs, feasibility of traveling-mode, 18: 22607 (TID-7691(p.196-203))
waveguides for 200-Mc standing-wave linacs, design data for, 18: 22608 (TID-7691(p.204-20))
waveguides, reactions of radiation of moving charge in, 16: 27753(T) (JPRS-14515(p.259-71))
waveguides with anisotropic magnetodielectric medium, dispersion equation for spiral, 18: 2460
waves in Brillouin-focused electron-beam waveguide, 17: 21401(R) (TID-18585)
window development for high-power klystrons, radiofrequency, 18: 2500(R) (TID-19422)

MICROWAVE OSCILLATORS

development, 17: 607(T) (JPRS-15740)
development for ion cyclotron experiments, 18: 9458(R) (NP-13515)
operating characteristics and Q-factors of, method for determining, 17: 31090 (SCTM-71-57(14))
power amplifier design using parallel klystrons and flywheel, 16: 20662
radiation effects on voltage-tunable magnetron, pulsed, 18: 4296(R) (AD-423158)
stability of electron beams in cylindrical-geometry, (T), 19: 11469 (AD-609638)
use of superconducting tunnel diodes as, 18: 41710(R) (AL-TDR-64-46)
x radiation production by, in radar installations, 19: 46673

MICROWAVE SPECTROMETERS

see also Radiofrequency Spectrometers

coupling to diaphragm-type waveguides, method description, 16: 26389(T) (FTD-TT-61-242(p.147-50))
description of, for free-radical studies, 20: 15272
design and performance, 16: 30622
design and performance of nuclear magnetic resonance, review, 17: 10929
design for observation of perturbations in rotational energy levels, 18: 29640
design for study of irradiated substances, 17: 29178
design of electron-spin-resonance, using ammonia maser as pre-amplifier, 17: 34215
design of high-temperature, 18: 22022 (UCRL-11229)
design of high-temperature absorption, 17: 25852(R) (NP-12877)
design of nuclear magnetic resonance, 16: 11918
design of wide-band, for noise from magnetoplasmas, 18: 28897
design with amplitude modulation, methods for, 20: 31490
design with co-axially fed cavity, 17: 36439 (NP-13020(p.460-5))
development, 20: 23527 (CONF-651206)
instrumentation for, development of, 20: 2106 (UJV-1346/65)
magnetic field calibrator for EPR, 20: 43720
modification of, for quantitative intensity measurements, 19: 802
performance for time-resolved electron density measurement in plasma afterglows, 20: 20054
performance in measurement of accelerator waveguide phase velocity, comparison of circuit types, 16: 26387(T) (FTD-TT-61-242(p.134-46))
performance of single sample spin generator nuclear magnetic resonance type, 16: 8940
sensitivity of, maser technique for improving, 17: 36442(R) (NP-13084)

MICROWAVE SPECTROSCOPY

see also Microwave Spectrometers

bibliography and review on spectrometry, 16: 14705
book: *Quantum Radiofrequency Physics*, 20: 925(T)
development, 16: 7634(R) (TID-13000)
development, 16: 13177(R) (NP-11413)
development, 17: 6801(R) (TID-17303)
development of, 16: 30172(R) (TID-16489)
developments at Columbia Radiation Laboratory, 17: 36442(R) (NP-13084)
developments at M.I.T. electronics lab., 16: 4610(R) (TID-14435)
developments at M.I.T. electronics lab, 16: 19476(R) (TID-15642)
developments in, 16: 3535(R) (NP-11112)
methods for submillimeter wavelength, 18: 27438
methods of millimeter-wave molecular-beam, 18: 19990
research on, 17: 21401(R) (TID-18585)
research programs at MIT on, 17: 35260(R) (TID-19135)
research programs on, 20: 14227(R) (TID-22419)
spin resonance line shapes in, effect of probes on, 19: 20839
use in neutron flux measurements in reactor, 18: 18861(P)
use in plasma diagnostics, 18: 15405
uses in biology and medicine, 16: 7363
uses of electron spin resonance, in inorganic and organic chemistry, 16: 9970

MICROWAVES

see also Radar

absorption and emission in plasma, resonance, 18: 28806
absorption and emission spectra in atmosphere, water vapor effects in, 18: 42162(R) (TID-20963)
absorption and thermal energy transfer in plasma, 18: 30871 (AFCRL-63-199(Vol.1))
absorption at electron cyclotron resonance in slightly ionized gases, 16: 5810
absorption at electron cyclotron resonance in slightly ionized gases, 16: 5811
absorption at electron cyclotron resonance in slightly ionized gases, 16: 5812
absorption by carbon dioxide, 17: 36442(R) (NP-13084)
absorption by carbon dioxide, (E), 19: 14230(R) (AD-608160)
absorption by cylindrical plasma, effects of polarization on, 18: 6330
absorption by metal films on tin at low temperatures, (T), 20: 30290
absorption by plasma, 17: 4175 (RADC-TDR-62-87)
absorption by plasma, 17: 11836 (RADC-TDR-62-186)
absorption by plasma electrons, effects of cyclotron resonance on, 17: 31627
absorption by plasma at electron cyclotron resonance, plasma acceleration by, (E), 19: 34346
absorption by plasma, (E/T), 19: 35539
absorption by plasma in magnetic fields, resonances in, (E/T), 19: 35540
absorption by plasma, analysis of, (E/T), 20: 4943 (MATT-379)
absorption by plasma in magnetic fields, (T), 20: 22209
absorption by plasma, in cavity resonator, negative, (T), 20: 30587
absorption by rare-earth metals at 10 to 290°K, (E), 20: 24650
absorption by superconducting films, effects of magnetic fields on, 19: 10210
absorption by superconducting aluminum, effects of magnetic field on, (E), 19: 14450
absorption by superconducting aluminum, effects of magnetic field on, (E), 19: 14456
absorption coefficient and conductivity in plasma, 17: 24572
absorption from and emission by plasma in magnetic fields, 16: 26418
absorption in afterglow plasma, electron-density correlation with resonance, (E), 19: 23877
absorption in cold plasma, negative, (T), 19: 43425
absorption in copper–tin and gold–tin superconductors, proximity effects in, (E), 20: 30289
absorption in magnetoplasma, near electron cyclotron resonance, 20: 42439
absorption in moving striations in glow discharge, 18: 36092
absorption in plasma, electron hybrid-resonance heating by, (E), 19: 23876
absorption in rare earth metals, 19: 34715
absorption in strontium titanates above phase transition, 16: 15324
absorption in strontium titanates, 16: 15325
absorption in superconducting films, magnetic field dependence of, 18: 40452
absorption in superconducting aluminum, frequency and temperature dependence of, (E), 20: 15658

absorption in weakly ionized xenon plasma in magnetic fields, (E), 20: 3204
amplification, 18: 24516(T) (JPRS-24633)
amplification by charged-particle interaction with magnetic field, 18: 18454 (NP-13778)
amplification by electron beam interactions with plasma, 16: 19842 (ML-833)
amplification by electron beam-plasma interactions, 17: 36773
amplification by electron beam-plasma interactions in millimeter region, 18: 22978
amplification by electron beam-plasma coherent scattering, 18: 38203 (AD-600542)
amplification by electron beam interactions with plasma, 18: 40684
amplification by electron beam-plasma interactions, gap coupling in, (E/T), 19: 34423(R), (AD-612538)
amplification by electron beam-plasma interactions, 20: 30718
amplification by plasma interactions with modulated electron beams, 16: 29947
amplification by power-saturated resonant media, 17: 22350
amplification by superconducting films, 18: 16879
amplification by xenon plasma in magnetic field, (E), 19: 31370
amplification in beam-plasma interactions, 18: 28762 (RADC-TDR-63-465(Vol.1))
amplification in cesium and mercury plasmas, 20: 20052
amplification in electron beam reactions with plasma, 18: 42818
amplification in electron beam interactions with cesium plasma, (E), 19: 40036
amplification in plasma, 18: 28767 (RADC-TDR-63-477)
amplification in superconducting films, (T), 19: 25450
amplification of, in traveling-wave devices using cyclotron resonance effects, 16: 30619
amplification using superconducting films, 18: 34714
amplification using superconducting films, 20: 26027
amplification using electron beam interactions with plasma, (E), 20: 46923
amplifier development for, 16: 31884
attenuation by rocket exhaust plasma, 20: 41120
attenuation by shock waves at Mach 8 to 12, time dependence of, 18: 16565
attenuation by shock waves in air, 18: 19227
attenuation by shock waves in argon and neon, 20: 4934 (AD-619093)
behavior in cyclotron masers, 16: 15719(R) (LAMS-2682)
bibliography on research at Duke Microwave Laboratory, 1953 to 1962, 16: 12223(R) (NP-11428)
biological effects on man and higher animals, 16: 32727 (NP-12127)
biological effects, synergistic effects of ionizing radiation in dogs, 17: 2823 (RADC-TDR-62-102)
biological effects on response to ionizing radiation in dogs, 17: 19814
biological hazards from, 19: 85
book: *Plasma Diagnostics with Microwaves*, 19: 19322
cataract induction by, 17: 17863
characteristics, at wavelengths of 0.1 to 3 mm, 16: 5834
characteristics, development of methods of solving Maxwell's equations for, 16: 3377 (AD-257024)
conductivity of bounded plasma, 16: 5813
coupling to shock-produced plasma, 17: 21164
detection and measurement using superconducting sandwiches, 18: 41875
detection and measurement of, selective receiver for, 20: 32626
detection and measurement of, design and performance of plasma device for, 20: 37119
detection by electron tunneling between superconductors, 18: 41710(R) (AL-TDR-64-46)
detection of centimeter, in gas discharge plasma, 19: 41876
detection of, theory of operation of equipment for, 18: 4673
detection system for, design of rotatable, 17: 26673 (SIT-P84)
development of high-level, for plasma production, 16: 14140 (NP-11583)
diagnostic use for shock tube ionization phenomena, 18: 32919
diagnostic use for determining plasma electron densities, 18: 32922
diagnostic use for transient plasma properties, 18: 36748
diagnostic use for plasma, measurement of shaped probing beams in (E/T), 19: 1793
diagnostic use for plasmoids, (E), 19: 6780
diagnostic use for magnetoactive plasma, (E), 19: 6782
diagnostic use for self-quenching cylindrical discharges at low pressures, (E/T), 19: 11822 (AFCRL-63-343)
diagnostic use for plasma, (E/T), 19: 14673 (USCEC-103-101)
diagnostic use for plasma density measurements, (E), 19: 17129
diagnostic use for ionization afterglow plasma, (E), 19: 19313
diagnostic use for plasma parameters, (E), 19: 23835(T) (AEC-tr-6527(p.437-46))
diagnostic use for plasma electron density, 19: 31323(R) (AD-610846)
diagnostic use for magnetoplasma helical instabilities, 19: 31362
diagnostic use for shock-produced plasma, 19: 33458
diagnostic use for plasma electron density, 19: 35535
diagnostic use for plasma electron density variations, 19: 35536
diagnostic use for in-core neutron flux measurements, 19: 36806 (BNWL-SA-163)
diagnostic use for plasma jet electron densities, (E), 19: 37946 (UTIAS-108)
diagnostic use for plasma density spatial distribution, (E/T), 19: 39965 (NP-15203)
diagnostic use for thermally ionized alkali plasmas, (E), 19: 39980
diagnostic use for plasma, open waveguide method for, (E), 20: 41717
diagnostic use for plasma research, 16: 31142 (UCRL-5721)
diagnostic use in plasma electron density determinations, 19: 33451
dielectric breakdown in gases by, hydrodynamic effects in, 17: 37837
diffraction by wide slit in anisotropic plasma, 20: 28507
discharge production by, striated, 16: 8268
discharges produced by, formative processes in argon-neon mixtures from pulsed, 17: 24133
discrimination of u-h-f, plasma diagnostics using waveguide, (T), 20: 28528
dispersion in helical slow wave structures, 16: 337(R) (NP-10868)
dispersion in rectangular septate waveguide, equations for, (T), 19: 37235
dispersion in rifled waveguides, 16: 378
dispersion in spiral waveguides with anisotropic magnetodielectric medium, equations for, 18: 2460
effect on tunneling in superconducting junctions, (E), 19: 23582
effects of combined, and x radiation on hematologic response of dogs, 20: 40650
effects of, on electroencephalographs of workers, 17: 17787
effects of, on organs and skin of x-irradiated guinea pigs, 17: 21545
effects on abdominal organs in rabbits, 17: 17858
effects on animals, 20: 5302(R) (UR-668, pp 161-6)
effects on critical supercurrents in constricted tin films, (E), 20: 32328
effects on directional electron emission in electric discharge, 17: 36792(T)
effects on dogs, synergistic effects of x radiation on, 19: 8857
effects on eyes, 16: 21914(R) (RADC-TN-61-226)
effects on gaseous magnetoplasma, helical instability, (E/T), 20: 6446 (AD-617696)
effects on hydrogen optical transitions, (T), 19: 8086
effects on Josephson currents in superconducting tunneling, 17: 34614
effects on Josephson currents in superconductors, 18: 4502
effects on Josephson superconducting junctions, induced d-c voltages from, (E), 20: 21882
effects on man, 19: 28014
effects on man and experimental animals, thermal, 20: 16235
effects on man, maximum safe exposure criteria for, 19: 46706
effects on man, pathological, 20: 38622
effects on plasma afterglow in magnetic mirror (E), 19: 3401 (UCRL-12057-T)
effects on protein in blood serum of man and rabbits, 20: 42876
effects on superconducting tin, switching speed and nonlinear, 17: 28045
effects on tumors, synergistic, 19: 4019
effects on x radiation sensitivity of mice, 19: 10785 (RADC-TDR-63-352)
effects on yeast alcohol dehydrogenase, 16: 11377(R) (AD-259234 (p.31-46))
electron cyclotron heating in DCX-1 using, 18: 13135(R) (ORNL-3564 (p.1-13))
electron density profile measurements in plasma using, 18: 22948 (PIBMRI-1056-62)
electron relativistic electrodynamics and technology, 16: 6869
electron spin resonance transition saturation by, nuclear polarization by, 18: 11294
emission by atmospheric oxygen, 18: 2404(R) (TID-19651)
emission by cold plasma at cyclotron frequencies, 17: 7435(T) (AEC-tr-5564)
emission by cylindrical plasma, 18: 34986
emission by discharges in cold-cathode ion pumps, 17: 25981
emission by discharges in magnetic fields, 18: 22963
emission by excited particles in resonator with coupled modes, spontaneous, (T), 20: 2527
emission by hot-cathode-discharge plasma, 17: 7452
emission by hydrogen plasma formed by electrodeless induction discharge, 18: 21394
emission by hydroxyl ions in space, spectra of, (T), 19: 4806
emission by infinite plasma, thermal, 17: 2386
emission by Penning discharge in helium, spectra, 16: 19581
emission by plasma in magnetic field, anomalous, 17: 22718 (IPPJ-6)
emission by plasma in magnetic field, structured, 18: 9455 (IPPJ-13)
emission by plasma at cyclotron resonances, 18: 9488
emission by plasma, radiometer for measuring, 18: 19138(T) (CEA-tr-A-1464)
emission by plasma column, resonance structure of, 18: 24786

emission by plasma in magnetic field, 18: 28897
emission by plasma, anomalous cyclotron, 18: 36713 (IPPJ-25)
emission by plasma, at electron-cyclotron harmonic frequencies, (T), 19: 21477 (MATT-290)
emission by plasma near electron cyclotron harmonics, (E), 19: 23882
emission by plasma at electron cyclotron frequency harmonics, (T), 20: 13903 (CLM-R51)
emission by sun, 18: 12827
emission by sun, determination of coronal electron density from, 17: 13280(T)
emission by superconducting bridges, 20: 31482
emission by turbulent plasma, 18: 19127 (CLM-R35)
emission by turbulent plasma, 18: 26730
emission from atmospheric oxygen, measurement of, 19: 39270(R) (TID-21894)
emission from cylindrical plasma, 18: 22962
emission from dense unstable plasma in pulsed magnetic mirror field, (E), 19: 29391 (GA-6330)
emission from electron-beam-generated mercury plasma, 18: 19144
emission from electron-beam-generated helium plasma at cyclotron harmonics, 18: 19145
emission from fully ionized plasma, (E), 19: 31386
emission from hot plasma, radiometer sensors for, (E/T), 19: 5286(T) (AEC-tr-6518(p.126-36))
emission from ionized plasma, (E/T), 20: 28493(R) (MATT-Q-22, pp 113-214)
emission from Josephson junctions, (E/T), 19: 41614
emission from Josephson tunnel junctions, 20: 40028
emission from magnetic mirror plasma, properties of, (E), 20: 30645
emission from neon plasma, 17: 4194
emission from non-Maxwellian plasmas, 17: 7469
emission from PIG reflex discharge plasma, (E), 20: 20082
emission from planet Mercury, 17: 6907
emission from plasma, review, 16: 4933
emission from plasmas, electron temperature from, 17: 26586
emission from plasma in magnetic field, harmonics in, 18: 17147
emission from plasma in magnetic field, harmonics in, 18: 17148
emission from plasma, cyclotron-resonance, 18: 28874
emission from plasma oscillations at upper hybrid frequency, 18: 36737
emission from plasma, at electron cyclotron frequencies, 19: 1767
emission from plasma (E/T), 19: 1792
emission from plasma in cavity resonator, electron-temperature diagnostics from, (E/T), 19: 5287(T) (AEC-tr-6518(p.137-45))
emission from plasma at cyclotron harmonics, (E), 19: 5266(R) (NP-14385)
emission from plasma in strong electric fields, mechanisms of, (E), 19: 23904
emission from plasma at electron cyclotron harmonics, (T), 19: 27661
emission from plasma, coherent, (E), 19: 43448
emission from plasma in magnetic mirrors, (E), 19: 45388 (GA-6432)
emission from plasma, review of nonthermal and thermal, 20: 12256
emission from plasma, properties of, (T), 20: 15870 (CEA-R-2881)
emission from plasma column, structure in, (E/T), 20: 15893
emission from positive column arc discharge at cyclotron harmonics, 18: 26691 (IPPJ-23)
emission from radars, 20: 9188
emission from rare-gas discharges, resonance in, 18: 24772
emission from solar corona, source of, 17: 6906
emission from solar flares, 18: 44388
emission from solar flares, 18: 44389
emission from solar activity centers at 9.4 kMc, 18: 44393
emission from solar flares, models for, 19: 44931
emission from stationary inhomogeneous plasma, (E/T), 20: 42457
emission from sun, associated cosmic-ray increases, 17: 12912
emission from Venus, 17: 9154
emission from Zeta plasma, 19: 39953 (CLM-R-40)
emission in plasma discharges, high-power, 20: 46918
emission in solar flares, (E), 19: 37443
Faraday rotation in plasma in magnetic field, (E), 20: 24512 (N-66-15979)
focusing of, design of Fresnel zone lenses for, (E/T), 19: 28920 (UCRL-7785-T)
frequency multiplier for, 18: 5842 (ASD-TDR-62-720)
generation and amplification by fast-wave interactions, 16: 337(R) (NP-10868)
generation and transmission, basic research, 16: 13694(R) (ML-877)
generation by electron beam oscillations, 16: 27849
generation by electron-beam–plasma interactions, (E), 19: 11468 (AD-604088)
generation by magnetic undulator system, 16: 13330
generation, dynamic pinch for optical pumping in, 16: 4907(R) (UCRL-9777)
generation, elastic deformation method of mode control in, 16: 4610(R) (TID-14435)
generation from magnetohydrodynamic cells, device for, 17: 36447
(RADC-TDR-62-464(Vol.2))
generation in cold-cathode Penning discharges, 18: 32293
generation, properties of masers for, 16: 5834
generation, studies of maser systems, 16: 13713(T) (JPRS-12754)
generation, theory of masers, 16: 14915(R) (NP-11265)
generation, use of optical masers to accelerate electrons, 16: 9484
harmonic generation by, in plasma, (T), 19: 21517
harmonics generation in plasma, current density of second, 16: 14157
hazards from, at radar stations, 20: 27221
hazards of, health, 17: 18449
interaction with plasma boundary, 17: 2385
interactions in cyclotron-wave devices, parameters of, 19: 26915(R) (AD-609133)
interactions in magneto-plasma, electron cyclotron resonance absorption of energy from gyro-, 17: 33215
interactions in magnetoplasma, energy absorption in, (E), 19: 37905 (AD-426186)
interactions in oxygen plasma in magnetic fields, (E), 19: 29409
interactions in plasma, 16: 18552(R) (AD-265113)
interactions in plasma, electron density and transitional velocity from, 18: 2995
interactions in plasma, 18: 30880 (AROD-3420.8)
interactions of, with plasma, analysis of, 16: 32469 (62-RL-3011E)
interactions with plasma, power transfer to plasma from, 16: 4894 (D1-82-0007)
interactions with solid state materials, 16: 5776(R) (NP-11141)
interactions with plasma, magnetic effects, 16: 9538
interactions with ionized gas downstream of a shock wave, 16: 12234(R) (USCEC-75-3)
interactions with plasma, 16: 17178 (ML-793)
interactions with plasma, resonance effects, 16: 26419
interactions with arc-type plasma at 4.4 to 22 kMc, resonance effects, 16: 29923
interactions with plasma, 16: 29951
interactions with plasma, analysis in Born approximation, 16: 31151
interactions with exploding wires, 17: 5480
interactions with nonuniform plasma sheaths, 17: 15030
interactions with shock-generated plasma, diagnostic uses of, 17: 15031
interactions with shock-produced plasma, 17: 21165
interactions with electron beams, power measurement from reflection in, 17: 37409
interactions with plasma, electron collision frequency, density, and diffusion and recombination coefficients from interferometer measurements of, 17: 40198
interactions with plasma, nonsteady effects in, 18: 1131 (R63SD78)
interactions with inhomogeneous plasma, 18: 3027
interactions with gaseous plasma in magnetic field, 18: 4674
interactions with accelerated plasma, multidimensional nonlinear, 18: 22981
interactions with bounded gyroelectric plasma, 18: 22930 (AFOSR-64-0803)
interactions with plasma slab in waveguide, 18: 22949 (RADC-TDR-63-240)
interactions with atmosphere and surface of Venus, 18: 28094(R) (TID-20607)
interactions with plasma, gyro-, 18: 28839
interactions with plasma, energy transfer in, 18: 28841
interactions with plasma sheath adjacent to conducting wall, 18: 28888
interactions with cryogenic afterglow plasma, 18: 35015
interactions with classical plasma, crossed-beam modulation in, 18: 42784 (AD-439831)
interactions with superconductors, two-fluid model for, 19: 1498
interactions with gyroelectric plasma, magnetic-field effects on, (T), 19: 10415
interactions with plasma, (E/T), 19: 10436
interactions with shock-produced plasma, (E), 19: 12640 (R63SD91)
interactions with Puffatron plasma, excitation from, (E), 19: 21491 (UCRL-12057(Rev.I))
interactions with cathode fall and negative glow in glow discharges, (E/T), 19: 27650
interactions with plasma slabs, effect of, 19: 27618 (RADC-TDR-64-272)
interactions with inhomogeneous anisotropic plasma column in magnetic field, (T), 19: 31337 (USCEC-82-218)
interactions with cylindrical plasma, (E), 19: 37960
interactions with inhomogeneous anisotropic plasma column, in axial magnetic field, (T), 19: 39994
interactions with plasma, harmonic generation by, (E), 19: 45420
interactions with plasma in gas discharges and semiconductors, (E/T), 20: 3157 (AD-614654)
interactions with plasma, (T), 20: 8263
interactions with plasma, helical instability from, (E/T), 20: 13959
interactions with energetic free electrons at cyclotron resonance, quantum

mechanical properties of, 20: 19462
interactions with plasma in mirror-type magnetic fields, (E), 20: 22216
interactions with plasma, induced ionization wave propagation by, 20: 36313
interactions with magnetoplasma space-charge waves, (E), 20: 38202 (NP-16236)
interactions with plasma, reflection and transmission coefficients for, (T), 20: 40252
interactions with nonhomogeneous cylindrical plasma, refraction of, (T), 20: 44981
interactions with plasma, density determination from, (E), 20: 44982
interactions with plasma, diagnostics from, (E), 20: 44983
interactions with positive column plasma, near second harmonic, 20: 46819(R) (NP-16293)
measurement of geomagnetic, 19: 32048(R) (NP-15073)
measurements on precursor afterglow in shock tube, 17: 7422 (AWRE-O-11/62)
origin of 7.3-cm background, (T), 20: 46287
origin of 7.3-cm cosmic background, 20: 46288
performance for plasma diagnostics, effects of space-charge waves on, 17: 15034
performance for plasma diagnostics, (E), 19: 12636 (IPPJ-29)
phase changes in, system for measuring, (E), 19: 10392(R) (MATT-Q-21)
phase shifts in plasma, null method of measuring, 19: 45412 (UCRL-7978)
phase shifts in plasma, null method of measuring, 20: 10206
phase shifts of three superimposed beams, interferometer for measuring, 20: 42408 (IPP-2/49)
phase variations of, measurement of, 18: 44852 (MATT-273)
plasma acceleration by nonuniform uhf field, (E), 19: 33500
plasma acceleration by reflection of, 20: 8211
plasma acceleration by reflection of, 20: 8212
plasma density measurement with, 17: 24047(R) (NP-12792)
plasma diagnostics using, 17: 968
plasma diagnostics using, 17: 38616(R) (MDL-Q2)
plasma diagnostics with, 17: 15342 (AD-275762)
plasma diagnostics with, 17: 24567(T) (AERE-Trans-925)
plasma diagnostics with, space-charge interactions in, 18: 1168
plasma diagnostics using, for electrodeless discharge, 18: 15413
plasma diagnostics using, focusing in, 18: 19161
plasma diagnostics in millimeter and submillimeter region, 18: 19208
plasma diagnostics using, 18: 21368 (AFCRL-63-161)
plasma diagnostics using Fabry-Perot resonators, (E/T), 19: 12704
plasma diagnostics using, (E/T), 19: 12705
plasma diagnostics using, (E), 19: 17098
plasma heating by, (E), 19: 25561
plasma studies using cavities, 16: 4915
plasma velocity measurements using, methods for, 18: 28887
polarization of, from galactic radio sources, 18: 36130
power generation in beam-plasma interactions, 18: 28764 (RADC-TDR-63-465(Vol.1)(Paper 2))
power measurements using in-line calorimeters, 16: 24868 (TID-16053)
production and amplification in plasma, 20: 29499
production by Cherenkov radiation, 16: 937 (AD-256271)
production by drifting plasma, 18: 2404(R) (TID-19651)
production by electron beam interaction with dielectrics, 18: 689(R) (RADC-TDR-62-524)
production by electron-beam Cherenkov interactions in ferrites, 18: 30414
production by energy conversion in plasma, (E/T), 19: 47717 (AD-614285)
production by field emission cathode in superconducting cavity, harmonics in, (E), 20: 9894
production by injection of free electrons into high magnetic fields, (E), 19: 20684
production in electron beam-plasma reaction, 18: 13142 (RADC-TDR-63-135)
production in rare earth films, from magneto-elastic effect, (E), 20: 24643
production of harmonic, in ionized gases, (E), 19: 8033
production of submillimeter, linear electron accelerator for, 19: 34802 (AD-610190)
production of, apparatus for, 19: 34463(P)
production of, development of Cherenkov generator for, 20: 33976
production of, using Josephson-type superconducting tunnel junctions, 20: 28212
propagation along plasma magnetic field of circularly-polarized millimeter, 18: 28853
propagation along plasma column in argon discharge, (E), 19: 25562
propagation by coaxial plasma–conducting helix systems, 16: 29920
propagation from 100-kev electron bunches in circular orbit, (E), 19: 29111(R) (AD-611161)
propagation from 100-kev electron bunches in circular orbit, calculations for, (T), 19: 29113(R) (AD-611161(App.II))
propagation in afterglow plasmas and magnetoplasmas, 17: 11834(R) (NP-12367)
propagation in argon plasma, resonance from, (E), 20: 4935 (AFCRL-65-556)
propagation in bidirectional waveguides, 16: 29954
propagation in circular waveguides filled with anisotropic dielectric, properties of, 19: 42680 (JINR-P-2274)
propagation in compressible plasma gaps, properties of, 20: 22163 (AD-621034)
propagation in cylindrical beam-plasma systems in longitudinal magnetic fields, (T), 20: 8227
propagation in decaying plasma, interferometric diagnostics from (E/T), 19: 1714 (NP-14398)
propagation in decaying plasma, particle distributions from, (T), 19: 5281(T) (AEC-tr-6518(p.91-8))
propagation in diaphragmed waveguides, complex constants for, (T), 20: 13363 (JINR-P-2507)
propagation in dielectric-layer circular waveguides, 19: 46743
propagation in germanium crystals, frequency multiplication by hot electrons in, 17: 37723
propagation in hollow cylinders, equations for, (T), 19: 16253 (HW-SA-3320)
propagation in hot plasma waveguides with infinite magnetostatic fields, (T), 19: 21536
propagation in lithium at conduction-electron resonant frequency, 18: 28150
propagation in magneto-ionic ducts, 18: 30878(R) (AFCRL-64-219)
propagation in magnetoplasma, 17: 40187
propagation in magnetoplasma, near electron cyclotron resonance, 20: 42439
propagation in multimode waveguides, 19: 39269(R) (SU-SEL-64-133)
propagation in nonhomogeneous media, optical-ray, (T), 19: 26915(R) (AD-609133)
propagation in nonuniform plasma column, (T), 20: 24557
propagation in overdense magnetoplasma, 18: 28791
propagation in overdense plasma along magnetic field, 17: 2410
propagation in plasma, 17: 18903 (RADC-TDR-62-264)
propagation in plasma along magnetic field, effects of electron random motion, 16: 14153
propagation in plasma at subcritical frequencies, in magnetic field, 16: 15736
propagation in plasma-filled waveguides, 16: 31155
propagation in plasma waveguide, 18: 44858 (RADC-TDR-64-117)
propagation in plasma above electron density cut-off, longitudinal (E/T), 19: 1715 (NP-14402)
propagation in plasma discharge, from sheath rotation instability, 17: 38380
propagation in plasma, interferometric circuit for phase-shift measurement in (E/T), 19: 4433(T) (AEC-tr-6518(p.74-81))
propagation in plasma, phase-modulation circuitry for, (T), 19: 4434(T) (AEC-tr-6518(p.82-90))
propagation in plasma, electron-density diagnostics from, (E/T), 19: 5285(T) (AEC-tr-6518(p.118-25))
propagation in plasma pinch, phase-shift analysis of electron density from, 19: 5280(T) (AEC-tr-6518(p.65-73))
propagation in plasma with sheared magnetic field, (T), 19: 8523
propagation in plasma, (E), 19: 10392(R) (MATT-Q-21)
propagation in plasma, (T), 19: 17103
propagation in plasma in Stellarator (C), (E/T), 19: 19298
propagation in plasma, waveguide cell for, 19: 23895
propagation in plasma, cyclotron resonance echoes from, (E), 19: 33474
propagation in plasma, magnetoionic, (E/T), 19: 35515(R) (AD-608478)
propagation in plasma, transient, (T), 19: 40034
propagation in plasma columns, resonances from, 19: 43409 (IPPJ-34)
propagation in pure air plasma, 20: 32667
propagation in shock plasma, 18: 11297 (AD-407885)
propagation in warm magnetoplasma, (T), 19: 40027
propagation of, in plasma, 16: 33930 (R62SD8)
propagation of Pi-2 micropulsations through ionosphere, phase velocities for, (T), 19: 45181
propagation through a plasma, bibliography, 16: 12614 (NP-11414)
propagation through a plasma in a magnetic field, 17: 11862
propagation through thick lithium films, resonant, 18: 28151
protective effects against radioinduced lethality in mice, 19: 24375
reactions in thermally ionized plasma, solutions for, 18: 7812
reactions with deuterium, electron ionization frequency for, 18: 21510
reactions with gases, spectra of decay afterglow from, 19: 32048(R) (NP-15073)
reactions with isotropic collisionless plasma, transient phenomena in, (T), 19: 40035
reactions with molecular gases, spectral line shapes in, 18: 44303
reactions with plasma, 17: 17371
reactions with plasma column, high frequency resonances from, 17: 26673

(SIT-P84)
reactions with plasma behind shock waves, 17: 35027 (R63SD60)
reactions with plasma, amplification in, (T), 19: 14653 (AFCRL-64-445)
reactions with plasma, heating in, (E/T), 20: 28493(R) (MATT-Q-22, pp 113-214)
reactions with superconducting bismuth–indium alloys, surface impedance of, 18: 9276
reactions with superconductors of second kind, surface impedance in, 18: 34705
reactions with toroidal plasma discharges, heating in, (E/T), 20: 28492(R) (MATT-Q-22, pp 1-111)
reactions with uranium carbide crystals at 300°K, elastic constants from, 17: 37528
reflection and transmission in plane plasma layers, 16: 19859
reflection and transmission by bounded plasma slab, (T), 19: 23893
reflection and transmission by thin superconducting films, 20: 19772
reflection by dense plasma, diagnostics from, 18: 19209
reflection by magnetoplasma, resonances in, 17: 35043
reflection by plasmas with exponential electron distribution, coefficients and phase-shift angles for, 17: 24562 (R62SD47)
reflection by plasma, characteristics of, 18: 4658
reflection by plasma, 18: 9458(R) (NP-13515)
reflection by plasma, 18: 30910
reflection by plasma column surface, diameter diagnostics from, (E/T), 19: 5282(T) (AEC-tr-6518(p.99-106))
reflection by plasma, diagnostics using, 19: 27615 (NBS-TN-256)
reflection by plasma density gradients, 19: 29414
reflection by plasma, ray-theory interpretation of, 20: 44898
reflection by shock-produced plasmas, 18: 1130 (R63SD77)
reflection by uniform dense plasmas, 17: 5451
reflection from anisotropic plasma, diagnostics by, 18: 9460 (NP-13530)
reflection from anisotropic plasma surface, (E/T), 19: 21513
reflection from flat earth, pulse distortion in, 18: 7999 (SC-DC-3567)
reflection from hydrogen plasma, (E), 19: 47795
reflection from surface of anisotropic hydrogen plasma, magneto-Kerr effect from, (E), 20: 28565
reflection in plasma-filled waveguides, 19: 45401 (NP-15196)
reflection of, apparatus for measurement of, 18: 4658
reflection of, plasma density distribution measurement by, 18: 9461 (NP-13531)
reflection of, diagnostics of shock-produced plasma by, (E), 19: 39997
refraction by plasma in magnetic mirrors, (T), 19: 5334
refraction in cylindrical plasma, plasma density from, (E/T), 20: 30700
research programs, summary for microwave research institute, 16: 28255(R) (NP-11787)
research programs of U. S. Army on, 1962 summary, 17: 33413(R) (NP-12967)
resonances in hot plasma column, theory of, 17: 31584
scattering by argon plasma jets, resonances from, (E), 20: 34756
scattering by collective plasma density fluctuations, 18: 15711(R) (TID-20256)
scattering by column of ionized gas, 16: 3770 (ZPh-096)
scattering by conducting spheres, amplitude, 16: 943
scattering by cylindrical plasma, 17: 40155 (ARL-63-159)
scattering by large-amplitude ion waves in cesium plasma, (E), 20: 28564
scattering by linearly varying surface impedance, 16: 5776(R) (NP-11141)
scattering by magneto plasma waves, (E), 19: 40033
scattering by plasmas, reflection coefficient for, 17: 22743
scattering by plasma frequency resonance peak, 17: 36440(R) (NP-13061)
scattering by plasma, incoherent, 18: 1129 (NP-13274(p.37-9))
scattering by plasma column, collision frequency and electron density from, 18: 9548
scattering by plasma column, resonances in, 18: 26763
scattering by plasma columns, resonant oscillations in, 18: 28895
scattering by plasma column in rectangular waveguides, 18: 40659 (IPPJ-27)
scattering by plasma, from acoustic-ion-plasma-wave instability, (E/T), 19: 47776
scattering by plasma, electron density determination by, 20: 17876 (IPP-1/37)
scattering by plasma, magneto-Kerr effect in, (E/T), 20: 20014 (NP-15938)
scattering by plasma for electron density determination, 20: 20022
scattering by plasma oscillations, Raman, (E), 20: 24547(T)
scattering by positive plasma column, (T), 19: 25608
scattering by turbulent helium plasma in magnetic fields, (E), 20: 20039
scattering by turbulent plasma, (E/T), 20: 30658
scattering by underdense cylindrical helium plasma, phase-shift analysis for, (T), 20: 15894
scattering by unstable plasma waves, 17: 4205
scattering by unstable electron oscillations in plasma, incoherent, (E), 20: 32622
scattering from moving density fluctuations in plasma, (E), 19: 14689
scattering from multiple spheres, 16: 2294 (AFOSR-1186)
scattering from positive plasma column, (E), 19: 23921
scattering from resonant plasma oscillations, incoherent, (E), 19: 45436
scattering from underdense cylindrical plasma, (E), 20: 38254
scattering of, plasma diagnostics by, 18: 1111 (ARL-63-151(p.275-93))
scattering on plasma cylindrical column at 1.5 Bc, resonance of surface waves in, 17: 38388
scattering on plasma, electron density distributions from, 18: 9478
scattering on small-diameter plasma columns, 18: 11317
spectrum in solar radiation, review of, 19: 20785
transmission along boundary of dielectric columns in cylindrical metallic waveguide by magnetic ring current, 16: 12616 (PIBMRI-857-60)
transmission by argon and nitrogen plasmas, 17: 33439
transmission by Penning discharge helium plasma, 18: 6302(R) (LAMS-3004)
transmission by plasma, absorption and refraction in, 17: 21131 (CLM-R-27)
transmission by plasma cylinder, 18: 21372 (CLM-R-34)
transmission by plasma, (T), 19: 23897
transmission by plasma in magnetic fields, (T), 20: 12258
transmission by turbulent plasma, coefficient for, (T), 20: 22230
transmission in plasma, suitability for estimating electric conductivity, 16: 3963 (AFOSR-1468)
transmission in plasma-filled waveguides in E_{01} mode, 16: 24893
transmission in thin films of tin superconductors, nonlinear electrodynamics study using, (E), 20: 28199
transmission of, electron density measurement by, 18: 2985(R) (UCRL-10852)
transmission, relativistic equations for waveguides, 16: 13713(T) (JPRS-12754)
transmission through plasma, effects of electron density fluctuations, 16: 19604
transmission through ionized layer around re-entry body, 16: 33946
transmission through thin superconducting films, 18: 15115
tunneling effects in superconductors, (E), 19: 12437
use for diagnostics of shock propagation in gases, 20: 22182 (IPP-3/35)
use for plasma analysis, sources of error in, 16: 33949
use for plasma column diagnostics, beam width of antenna systems in, (E), 20: 12192
use for plasma density measurements, (T), 20: 4971
use for plasma diagnostics of free-space, 18: 28842
use for plasma diagnostics, cross-polarized backscatter in, (T), 19: 45424
use for plasma diagnostics, free space method for, (E), 19: 47755
use for plasma diagnostics, effects of dielectric walls on, (T), 20: 24533
use for plasma diagnostics, 20: 24493 (AD-627267)
use for plasma electron density measurements, (E), 19: 45429
use for plasma electron density measurements, (E), 20: 17510 (IPP-3/25)
use for plasma electron density determination, 20: 42419(T) (AD-636608)
use for studies of superconductivity (E), 19: 1511
use in determining electron densities in shock-wave-produced plasmas, 17: 21153
use in determining electron densities in plasmas by phase shifts, 17: 42083
use in determining electron temperatures in afterglow plasmas, 18: 9551
use in determining electron energy decay in afterglow plasma at 4°K, 18: 9552
use in diagnostics of plasma flows, 18: 19210
use in examination of small bores in metal surfaces, 19: 4341 (ACF-3)
use in in-core measurement of neutron fluxes, (E/T), 19: 13702(R) (HW-81984(p.7.1-26))
use in measurement of steady and fluctuating number densities in plasma, 17: 38389
use in measurement of plasma ionization rates, 20: 12169 (JUL-322-PP)
use in measuring electron diffusion in ionized gases, 19: 25071(R) (TID-21667)
use in plasma diagnostic studies, developments in, 18: 685(R) (MDL-Q1)
use in plasma diagnostics, system for, 18: 15323 (AFCRL-63-155)
use in plasma diagnostics, 18: 17143
use in plasma diagnostics, 18: 35020
use in plasma diagnostics, controlled mode technique for, 18: 35041
use in plasma diagnostics, 19: 34995(R) (AD-612901)
use in plasma diagnostics, 20: 8243
use in plasma diagnostics, 20: 15882(R) (NP-15868)
use in plasma diagnostics, method of, 20: 20012 (N-65-27813)
use in plasma electron density determination, 18: 42813
use in plasma electron density determination, 19: 33459
use in plasma frequency diagnostics, bridge for, 20: 12249
use in plasma noise measurements, 20: 4991
use in probing ionized gas flows, 16: 12615 (NP-11433)

use in shock wave diagnostics, 18: 19228
use in shock wave diagnostics, 20: 4934 (AD-619093)
use in studies of pulsed glow discharges, 16: 33956
use in studies of electrically driven shock waves in nonionized gases and gaseous plasmas, 17: 36482
use in studies of kinetic plasmas, 19: 10435
use of angularly scattered, in diagnostics of cylindrical plasma, 18: 26798
use of focused beams of, in plasma diagnostics, (E/T), 20: 17881 (N-65-19804)
use to determine ionization rate in mercury discharge, (E/T), 19: 12691
use to measure shock propagation in plasma, (E), 19: 14692
uses for plasma diagnostics, 18: 29925(R) (MDL-Q3)
uses for plasma diagnostics, (E), 19: 10384 (CEA-R-2427)
uses in plasma diagnostics, 18: 11306 (USCEC-96-101)
uses in studies of gas-detonation plasmas, 18: 26765

MILITARY COMPACT REACTOR

fuel development for, 18: 29047(R) (HW-80284(p.3.1-9))
fuel temperatures and thermal performance, computer programs for, 19: 14831(R) (HW-81984(p.3.1-14))
shielding calculations for, test of Monte Carlo code for, 18: 15425 (UNC-5072)
shielding for, design and testing of, (E/T), 20: 6626 (UNC-5118)
shielding for, design and testing of, 20: 38506 (NDA-2143-7)
shielding for, design and testing of, 20: 38507 (NDA-Memo-2143-11)
shielding for, gamma production and transport in, (E/T), 19: 45575 (GMAD-3078-23)

MILITARY FACILITIES

design and construction for atomic weapon tests, 16: 12806 (WT-60(REF)Pt.I)
design and construction for atomic weapon tests, 16: 12807 (WT-60(REF)Pt.II)
design and construction for atomic weapon tests, 16: 12808 (WT-60(REF)Pt.III)
development and economics of nuclear power plants, (E), 19: 10575 (WL-TDR-64-25)
protective structures, design fundamentals, 17: 30634 (NP-12961)
survey of dental x-ray units in U. S. Navy, 17: 20268

MILITARY PERSONNEL

see also Aviation Personnel
acceptance of food radiopreservation, 19: 32641
beta dosage accumulated by, factor influencing skin lesions from, 16: 17930
cesium-137 content of, whole-body liquid-scintillation measurement of, 19: 28600
feeding, uses of radiation-processed food in, 16: 4007 (ORO-SP-174)
gamma activity of, from nuclear submarine, 18: 10299 (AD-401763)
medical aspects of planning by, 17: 37381
medical care for Soviet, review, 16: 14388(T) (JPRS-12169)
medical services for, after nuclear attack, 18: 25729
nuclear warfare casualty collection program for, 18: 31814
physicians and nuclear medicine, 17: 37382
protection against thermal effects of nuclear weapons, 16: 1 (AD-254980)
protection from atomic explosions, properties of localities for, 16: 33337
protection from fallout, decay-curve estimates for, 19: 20223
protection of, during chemical and radiological warfare, 18: 1961(T) (FTD-TT-63-585)
radiation effects on striking power, 18: 11797
radiation effects on vision in, 18: 29323
radiation effects on behavior in, 18: 29324
radiation effects on, dose and time factors after nuclear-explosion, 20: 14287 (AD-626996)
radiation monitoring and protection guide for, 17: 317
radiation processing of foods for, 16: 9085
radiation protection of, aboard space vehicles, (T), 20: 2656 (NASA-SP-71, pp 265-86)
radiation protection of, medical facilities at San Piero for, 20: 18963
radiobiology research by, at Bethesda Naval Medical Center, 18: 29184
radiological hygiene program for, 18: 29898
reliability in controlling nuclear weapons, 19: 10712
role of Canadian Army in civil defense, 17: 12067
shelters for, design of dual-use, 18: 20197 (NAVDOCKS-P-310)
survey for radiation exposure by gamma spectrometric examination of raw urine samples, 17: 2789(R) (ORNL-3347(p.142-54))
survival from nuclear attack, 16: 5616
thermal effects of nuclear explosions on aircrews, 18: 29884
training of, for disaster casualty control, 17: 18429
water supplies for, removal of radioactive contamination, 16: 9044
water supplies for, removal of radioactive contamination, 16: 9061

MILK

acidophilous with lactose, protective effects against radiation injuries in rats, 18: 15903
acidophilus, protective effects against radiation injury in guinea pigs, 17: 27082
acidophilus, protective effects against radiation injury in guinea pigs, 17: 27083
analysis for alkaline and alkaline earth metals, 18: 43719
analysis for calcium and strontium by flame photometry using plasma jets, 19: 43924 (AERE-R-4990)
analysis for cesium and strontium, 16: 14449(R) (TID-14780)
analysis for cesium-137 by beta counting, 17: 10551
analysis for cesium-137, losses in ashing process in, 18: 11993
analysis for cesium-137, iodine-131, strontium-89, and strontium-90 in samples collected in Canada, 1963, 18: 12386 (NP-13599)
analysis for cesium-137, iodine-131, strontium-89, and strontium-90, 19: 13232
analysis for cesium-137 by radiochemical methods, 19: 15399
analysis for cesium-137, rapid method for, 19: 19805
analysis for cesium-137, radiochemical, 19: 28420(R) (NP-14825)
analysis for cesium-137, chromium-51, and potassium-40, source of error in gamma spectroscopic, 19: 32596
analysis for cesium-137 by ion exchange and gamma spectroscopy, 20: 16342
analysis for fall-out radioactivity, 1962, 16: 30693
analysis for fallout radioactivity, radiochemical, 18: 8281 (NYO-4700
analysis for fallout fission products, 1963, 18: 6944(R) (HASL-142) (Rev.))
analysis for fallout fission products, 1961, 1962, and 1963, 18: 18048
analysis for fallout, Apr.–Oct. 1963, 18: 37458
analysis for fallout fission products, 1964, 19: 7712
analysis for fallout fission products in European, 1962, 19: 18143 (EUR-1838.d.f.i.n)
analysis for fallout in bovine, gamma spectrometric, 19: 32101
analysis for fission products in pasteurized, 1963, 18: 12398
analysis for iodine-131 in United Kingdom, 16: 2085
analysis for iodine-131 content of bulk samples, radiometric, 16: 16594 (AEEW-R-138)
analysis for iodine-131 and strontium-90 in Great Britain, 1961, 16: 33304(R) (ARCRL-7)
analysis for iodine-131, radiometric, 17: 2789(R) (ORNL-3347(p.142-54))
analysis for iodine-131 by anion exchange, spectrometric, 17: 10554
analysis for iodine-131, strontium-89, and strontium-90, radiochemical, 17: 21453
analysis for iodine-131, radiochemical, 17: 21454
analysis for iodine-131, cesium-137, and barium-140, spectroscopic, 17: 21456
analysis for iodine-131, after anion exchange separation, 17: 33828
analysis for iodine-131, method for, 18: 15959 (SCPRI(S)-94)
analysis for iodine-131, radiochemical, 18: 17762
analysis for iodine-131, using scintillating organic anion exchange resin, 18: 25259 (NYO-10405)
analysis for iodine-131, method for, 18: 41346
analysis for iodine-131, rapid radiochemical method for, 19: 7314
analysis for iodine-131, radiochemical, 19: 18153
analysis for iodine-131, quality control procedures for, 19: 22124
analysis for iodine-131 in picocurie concentration, method of, 19: 26257
analysis for iodine, isotope dilution, 19: 27921
analysis for iodine-131, radiochemical, 19: 38560
analysis for iodine-131, by ion exchange and beta or gamma counting, 20: 35404
analysis for iodine-131, strontium-89, and strontium-90, 20: 40809 (NP-16235)
analysis for iodine-131, method for, 20: 40852
analysis for radioactivity of, samples collected in northern Europe, 1961 and 1962, 16: 25167(R) (NP-11884)
analysis for radioactivity, 16: 30694
analysis for radioactivity, 1962, 16: 33308(R) (HASL-131)
analysis for radioactivity, 1961, 17: 1677
analysis for radioisotopes, techniques for, 17: 25113 (DPSPU-63-30-6)
analysis for radioactivity, samples collected in West Germany, 1962 and 1963, 17: 30287(R) (NP-12977)
analysis for radionuclides, 18: 3696
analysis for radioactivity in France, 18: 16204(R) (SCPRI(RM)-XII-1963)
analysis for radiocesium using fluoboric acid, 18: 27349
analysis for radioisotope traces, gamma spectrometric, 18: 33485
analysis for radionuclides, 18: 39059 (NP-14260)
analysis for radionuclides, laboratory and methods for, 19: 11454
analysis for radionuclides, methods for, 19: 10999
analysis for radioactive contamination, gamma spectrometric, 19: 17792(T) (UCRL-Trans-1188(L))
analysis for radioisotopes, methods for, 20: 16369
analysis for radioisotopes, 20: 45264(R) (UCLA-12-595, pp 72-89)
analysis for selenium, activation, 19: 19771(R) (TEES-2671-4(Chap.9))
analysis for sodium-22, radiochemical, 19: 42433
analysis for stable strontium, 17: 38640(R) (UCD-108(p.66-74))
analysis for stable strontium, activation, 20: 25003

analysis for strontium-90, radiometric, 16: 14654
analysis for strontium isotopes, 16: 18818 (TID-15415)
analysis for strontium-90, 16: 19204
analysis for strontium by gel filtration, 16: 23654
analysis for strontium, atomic-absorption spectrophotometric, 16: 26913
analysis for strontium-90 by ion exchange, 16: 28889 (HW-SA-2011)
analysis for strontium-90, radiochemical, 17: 1176(R) (HW-70050(p.78-142))
analysis for strontium-90, rapid method for, 17: 17977(T) (JPRS-18632)
analysis for strontium-90, radiochemical, 17: 21439
analysis for strontium-89 and strontium-90, radiochemical, 17: 21455
analysis for strontium-90, samples collected in 1962, 17: 27592(R) (HASL-138)
analysis for strontium-90 and yttrium-90, 17: 38920 (IEA-60)
analysis for strontium by x-ray fluorescence, 17: 38962
analysis for strontium-89, strontium-90, and iodine-131 in samples collected in U. S. and Canada, 1961 and 1962, 18: 461
analysis for strontium-90 by ion exchange, 18: 11990
analysis for strontium-90, radiochemical, 18: 35472
analysis for strontium-89 and -90, method for, 18: 39087
analysis for strontium-90, ion exchange, 18: 41343
analysis for strontium-90 using TTA, 19: 4083
analysis for strontium-90, solvent extraction method for, 19: 9077
analysis for strontium-89 and -90, radiochemical, 19: 19739 (AERE-AM-101)
analysis for strontium-90 by ion exchange, method for, 19: 32102
analysis for strontium by neutron activation, 19: 36250
analysis for strontium-90, 19: 38556
analysis for strontium-90, 20: 20938 (NP-15921)
analysis for strontium-89 and -90, method for, 20: 24980 (SZS-2(1966))
analysis for strontium-90, 20: 40854
analysis for trace elements by reactor neutron activation methods, 20: 26760
analysis for uranium, absorptiometric, 16: 23607 (PG-Report-187)
analysis for uranium, colorimetric, 17: 4473
analysis for vanadium, activation, 18: 1585
analysis for vanadium in powdered, activation, 18: 10028
analysis for yttrium-90, 19: 38856
analysis of dried, for strontium-90, 16: 22459 (TID-7632(p.415-24))
analysis of, for iodine-131, gamma spectrometric, 17: 36020 (AECL-1797)
analysis of, for strontium-89, strontium-90, and iodine-131 in samples collected in U. S., 1963, 17: 41079
analysis of human, for cesium-137 from fallout, 17: 14561
analysis of miniature swine, for availability of strontium-90 and calcium to offspring during lactation, 17: 19796
analysis of, for cesium-137 and strontium-90 by beta-counting after chemical separation, 20: 43532
barium-140 content in German, Sept.–Nov. 1961, 17: 34166
barium-140 content in German, Sept. 1961–Jan. 1962, 17: 34172
beta activity of, in Italy, 1962, 18: 18040 (BIO/03/63)
cadmium secretion in, of sheep, 19: 8739 (HW-SA-3746)
cadmium-115 secretion in sheep, 20: 10527(R) (BNWL-122, pp 94-8)
calcium content in beagle, 17: 38638(R) (UCD-108(p.45-51))
calcium content of Holstein and Jersey, seasonal variations in, 16: 27503
calcium transfer to, 18: 11621
calcium-45 uptake by rabbit and rat, 19: 8766
carbon-14 content in, following atmospheric atomic explosions, (E), 19: 24709
carbon-14 content in Norway, 19: 32483
carbon-14 uptake by components in, after intravenous injection in lactating goats, 18: 13438
cesium transfer to milk products, 16: 33331
cesium-136 content in, in England after 1961 nuclear weapons tests, 16: 13402
cesium-137 content in, in Finland, 1959, 16: 9037
cesium-137 content in Argentina, 1961, 16: 20856 (A/AC.82/G/L.746)
cesium-137 content in powdered, in U. S., 16: 22462 (TID-7632(p.477-516))
cesium-137 content in, in United States, 1957 to 1960, 16: 1327(R) (LAMS-2627(p.220-2))
cesium-137 content of dried, vegetation zone relation to, 17: 5752 (HW-SA-2337)
cesium-137 content of, effects of precipitation on, 17: 14494
cesium-137 content in, in Norway, 18: 1361
cesium-137 content in, 1957 to 1961, 18: 8063(T) (AEC-tr-6049(p.258-70))
cesium-134 and -137 content in, relation of content in man to, 19: 20225
cesium-134 separation from, by ion exchange, 19: 7710
cesium-137 and potassium contents in Finnish, 20: 35397 (SFL-A2)
cesium-137 and strontium-90 content in Israeli, 20: 2520(R) (IA-920)
cesium-137 and strontium-90 content of Canadian, 20: 41198 (NP-16192)
cesium-137 contamination in, uptake by man of, 20: 18220
cesium-137 content of, in southern Finland, 1961 to 1964, 18: 25687 (NP-13981)
cesium-137 content of, in Italy, 1963, 19: 7711
cesium-137 content in U. S., 1963 and 1964, 19: 18160
cesium-137 content of, effects of cattle feeding practices on, 19: 22553
cesium-137 content of, in Sweden, 1958 to 1964, 19: 22558
cesium-137 content in U. S., 1964, 19: 22562
cesium-137 content in Japanese and U. S., 1963, 19: 22625
cesium-137 content in powdered, produced in U. S., 1923 to 1936 and 1946 to 1961, 19: 24787
cesium-137 content of, from Norway, 1964, 19: 26533 (NYO-3364-1)
cesium-137 content in milk in Norway, correlation with precipitation, 19: 26534 (NYO-3364-4)
cesium-137 content in German, 19: 26606
cesium-137 content in, near Ispra, Italy, 19: 28546
cesium-137 content in, uptake by butter and cheese of, 19: 28592
cesium-137 content in, effects of cattle feeding practices, 19: 27932
cesium-137 content in New Zealand, 19: 35892 (NP-15082)
cesium-137 content in Norway, 1962 to 1965, 19: 36653 (NYO-3364-5)
cesium-137 content in, effects of diet on, 19: 36666
cesium-137 content in, Japan, 1964, 19: 42639 (NP-15278)
cesium-137 content in, in Switzerland, 1963, 19: 44269
cesium-137 content in Australian, 1963, 19: 44309
cesium-137 content of, effects of diet of cows on, 19: 45780
cesium-137 content of, 19: 46612
cesium-137 content of Australian, 1964, 19: 46660
cesium-137 content in Canadian, 1965, 20: 596 (NP-15542)
cesium-137 content of Canadian, 1965, 20: 597 (NP-15563)
cesium-137 content of, in Germany, 20: 524
cesium-137 content in, Italy, 1963, 20: 2046 (BIO/04/64)
cesium-137 content of, Italy, 1964, 20: 2047 (EUR-2509.e)
cesium-137 content in Toronto, 20: 5671
cesium-137 content in, factors affecting, 20: 8586
cesium-137 content in German, effects of precipitation on, 20: 11017
cesium-137 content in cow and human, 1959 to 1961, 20: 13012
cesium-137 content of, in Norway, 20: 14739 (TID-22655)
cesium-137 content in powdered, in Japan, 1962 and 1963, 20: 16755
cesium-137 content of, in Richland, Washington area, 20: 23298
cesium-137 content in, long-term prediction of, 20: 23299
cesium-137 content in Canadian, 1960 to 1964, 20: 23390
cesium-137 content in Colorado, May 1965, 20: 29429
cesium-137 content in Norwegian, 1962 through 1965, 20: 29432
cesium-137 content in Norwegian, 1960 through 1964, 20: 31465
cesium-137 content in Australian, 1965, 20: 33564
cesium-137 content in, effects of processing on, 20: 33595
cesium-137 content in, by deposition from fallout on forage, 20: 37036
cesium-137 content in Canadian, April 1965, 20: 41209
cesium-137 content in Chicago, Ill., 1965, 20: 43512(R) (ANL-7136, pp 315-27)
cesium-137 content in Japanese, November 1962 to September 1963, 20: 43520
cesium-137 content in, Bombay, 1964 to 1965, 20: 43532
cesium-137 content in powdered, in Japan, 20: 45887 (NP-16290)
cesium-137 content in Icelandic, 1958 to 1964, 20: 45908
cesium-137 content in Great Britain, 1962, 20: 45909
cesium-137 content in Norwegian, March 1962 to 1966, 20: 41132 (NYO-3364-20)
cesium-137 content in German, Sept.–Nov. 1961, 17: 34166
cesium-137 content in German, Sept. 1961–Jan. 1962, 17: 34172
cesium-137 content in, in Finland, Sept. 1962–Aug. 1963, 18: 139
cesium-137 content in, in Australia, Europe, India, UK, and U. S., 16: 10321
cesium-137 content in Japanese, 16: 26688(T) (AEC-tr-4642)
cesium-137 content in, in Netherlands, 1959–60, 16: 9837
cesium-137 content in, in Great Britain, 1960, 16: 5620
cesium-137 content in powdered, in Japan, 17: 21938
cesium-137 content in, near nuclear power plants in England, 18: 6775
cesium-137 content in Italian, 1961, 17: 27591 (EUR-223.1)
cesium-137 content in, from Australia, Europe, India, and U. S., 18: 10282
cesium-137 content in Italian, 18: 18098
cesium-137 content in UK, 18: 22252
cesium-137 content in Hungarian, 18: 29220
cesium-137 content in, in Finland, 1961–62, 19: 7741
cesium-137 content in Japanese, 19: 15755 (NP-14797)
cesium-137 content in Canadian, 1964, 19: 20161 (NP-14869)
cesium-137 content in, 19: 34365(R) (HASL-161)
cesium-137 content in, effects of diet on, 19: 45772
cesium-137 content of, in German Federal Republic, 1956–62, 19: 5602
cesium-137 content in Japanese, Nov. 1961–Oct. 1962, 19: 7707
cesium-137 content in, in New Zealand, July–Sept. 1964, 19: 9371(R) (NP-14618)

cesium-137 distribution in, 16: 17909 (AERE-M-985)
cesium-137 removal from, effectiveness of ion-exchange resins, 19: 34371
cesium-137 transfer from fallout to, 20: 45264(R) (UCLA-12-595, pp 72-89)
cesium-137, potassium-40, radium-226, and strontium-90 contents in, in Australia, 20: 156
consumption in Nashville, Tennessee, relation to cesium-137 body burdens, 18: 16232 (TID-18603)
consumption in U. S., 1962, effects on radionuclide intake, 20: 29474
consumption of cow's and goat's, by human populations, 20: 14243(R) (TID-22626)
consumption of, in Canada, 17: 41026 (NP-13193)
consumption of, effects on strontium-90 deposition in body, 18: 11595
consumption of, effects on cesium-137 body burdens of school boys in Oslo, Norway, 19: 6980
contamination by beta sources in lactating mice, effects on mammary glands and growth of suckling young, 19: 6963
contamination by fall-out after nuclear attack, radiation hazards from, 16: 24014 (NP-11715)
contamination by fallout, protection from harmful effects of, 17: 6338
contamination by fallout, methods for reducing, 17: 35441
contamination by fallout, hazards and control of, 18: 443 (NP-13278)
contamination by fallout, effects of, 18: 6980
contamination by iodine-131, hazards to man from, 18: 8241
contamination by strontium-90 from fallout, 17: 7773 (NYO-9934(Vol. I))
contamination by strontium, mechanism in goats, 19: 8759
contamination from fallout, health implications of, 17: 15619
contamination in U. S. by fallout iodine-131, July 1962, 17: 3246
contamination of, by fallout, hazards to man from, 17: 12503
contamination of, by iodine-131, effects on iodine uptake by thyroid gland of, 17: 15605
contamination of, by iodine-131 and strontium-90 from fallout, 17: 17747
contamination through exposed cattle or contaminated pastures, 16: 20124
content of cesium-137, iodine-131, strontium-89, and strontium-90 in U. S., 1965, 20: 38743
decontamination by electrodialysis, equipment and method for, 20: 1972(P)
decontamination by electrodialysis, pilot plant study of, 20: 12997 (AD-626210)
decontamination for human consumption, methods for, 18: 6980
decontamination of strontium-90 from, 17: 27606
decontamination of, ion-exchange process for iodine removal in, 18: 41273(P)
decontamination of, review on equipment and procedures for, 20: 3872 (EUR-2507.d)
dietary importance as a calcium source for young children, 20: 39157
effects on calcium–strontium discrimination in bones and gastrointestinal tract in rats, 17: 35425
electrodialysis of, effects on removal of radioisotopes, 18: 12257 (NP-13620)
evaporation for gamma pulse-height analysis, equipment for, 20: 16741(R) (UCRL-14534, pp 54-6)
fall-out monitoring, 16: 441
fallout contamination in United Kingdom of, 18: 27706
fallout contamination in France of, 19: 32488
fallout contamination in Japan, 1961 to 1964, 19: 44268
fallout contamination at Argonne, New York, and New Zealand, 20: 521(R) (HASL-164)
fallout content in, effects of soil-plant transport on cesium-137 and strontium-90, 20: 20926(R) (ARCRL-14)
fallout fission product contamination of, mathematical analysis of, 18: 6973 (NP-13432)
fallout fission product contamination of, 18: 38993 (HW-SA-3693)
fallout in, data on, 18: 22257
fallout monitoring, radiological health data, July 1962, 16: 28739
fallout monitoring in samples collected in 1962, 17: 21954
fallout monitoring, 1961 and 1962, 17: 21955
fallout monitoring in, measurements at Ispra, Italy, 1960 to 1962, 17: 33530 (EUR-294.i)
fallout monitoring in California, April through June 1963, 18: 10330
fallout monitoring in U. S. and Canada, 1963, 18: 10329
fallout monitoring in samples of, 1963, 18: 14090
fallout monitoring in, 1963, 18: 18041(R) (HASL-144)
fallout monitoring in Swedish, 1962, 18: 23790 (NP-13828)
fallout monitoring in Canada, 1964, 18: 31788 (NP-14052)
fallout monitoring in, 18: 31816
fallout monitoring in Polish, 1959 through 1961, 18: 39507
fallout monitoring in U. S. and Canada, 1964, 19: 637
fallout monitoring in Canada, 1964, 19: 9368 (NP-14459)
fallout monitoring in Canada, 19: 15817
fallout monitoring in, in England, 19: 24783
fallout monitoring in Canada, 1965, 19: 30440 (NP-15064)
fallout monitoring of Canadian, October 1965, 20: 14737 (NP-15853, pp 8-20)
fallout monitoring in, Canada, March 1966, 20: 33556 (NP-16124)
fallout products in, distribution of, 18: 23800
fallout radioactivity in samples collected from 1960 through 1962, 17: 18454
fallout radioactivity in samples collected in 1962, 17: 18455
fallout radioactivity in samples collected in 1961 and 1962, 17: 18456
fallout radioactivity in samples of, collected in 1963, 18: 4047
fallout uptake by, in England, 18: 20208 (AERE-R-4415)
fission product content in Iowa, 18: 14138
fission product content in United Kingdom, 18: 22308
fission product content in, of lactating cows, effects of calcium on, 16: 26717
formation, conversion of plasma calcium and phosphorus in, 17: 5722
iodine content in cow, trace study, 20: 3674
iodine content in, seasonal variations in, 19: 27922
iodine content of, bound and exchangeable, 19: 45782
iodine excretion in, tracer studies of, 19: 5611
iodine-125 and -131 in, uptake by abomasum, feces, plasma, thyroid, and urine of, 19: 45782
iodine-127 content in Swedish dairy, effects on thyroidal uptake of iodine-131 from fallout, 17: 36040
iodine-131 contamination of, after stock release, 17: 32284 (DPSPU-63-30-26B)
iodine-131 content in Egypt, 1956 to 1957, 16: 20125
iodine-131 content in Italy, Oct. to Dec. 1961, 16: 20127
iodine-131 content in Italian cities from Nov. 29 to Dec. 31, 1961, 16: 24024
iodine-131 content in, in New Zealand, 17: 4690(R) (DXRL-F5)
iodine-131 content in, effects of pasture and stored feed consumption by cows on, 17: 6356
iodine-131 content in, in United Kingdom, Oct. 1961, 17: 12119
iodine-131 content in Buenos Aires in summer of 1962, 17: 18314 (A/AC.82/G/L-808)
iodine-131 content estimated from results of *in vivo* measurements of radioactivity of thyroid gland, 17: 21440
iodine-131 content in, effects of stable iodide feedings on, 17: 28650
iodine-131 content in, in Utah from 1962 fallout, 17: 31848
iodine-131 content of, in Nevada, effects of 1962 nuclear explosions on, 17: 34182
iodine-131 content of samples of, collected in Canada, 1961, 17: 36020 (AECL-1797)
iodine-131 content, 17: 39314(R) (ORNL-3492(p.194-206))
iodine-131 content of, after 1962 Pacific weapons tests, 18: 1938 (AEET/AM/35)
iodine-131 content of, from cattle grazing on forage contaminated by fallout fission products, 18: 1945 (CEA-2323)
iodine-131 content of, in Japan, 18: 3615
iodine-131 content of, 50 to 400 miles from nuclear explosion, 18: 3598 (TID-19266)
iodine-131 content of U. S., 1960 through April 1963, 18: 8236
iodine-131 content of New York City, variabilities of 1962, 18: 8239
iodine-131 content of Hanford area, Jan. 1961–April 1963, 18: 8069
iodine-131 content of, at Brookhaven National Lab., 18: 8070
iodine-131 content of, effects of feed and pasture environment on, 18: 8071
iodine-131 content of, after oral administration to cattle, 18: 8086
iodine-131 content in, effects of meteorological processes on, 18: 8910
iodine-131 deposition from, in thyroid gland, 17: 31849
iodine-131 excretion in, effects of mild hyperthyroidism in cattle on, 17: 5721
iodine-131 fallout content in U. S., after May 1962 underground nuclear explosion in Nevada, 18: 8528
iodine-131 levels in U.S., 1961, 16: 17943
iodine-131 transport in, methods for preventing, 18: 8240
iodine-131 and -133 content in, as a result of nuclear explosions, calculations for, 18: 22246 (UCRL-7716)
iodine-131 and -133 content in, following uptake by cows from hay, 20: 43576 (CONF-660621-7)
iodine-131 and iodine-133 content in, from cows feeding on fallout-contaminated pasture, mathematical estimation of, 19: 31711 (UCRL-14146)
iodine-131 contamination of, by fallout, 18: 9938
iodine-131 contamination of, after accidental release, 18: 17672(T) (HW-tr-67)
iodine-131 contamination of, by ingestion of contaminated food, 18: 22281(T) (NP-tr-1136)
iodine-131 contamination of, 18: 39558
iodine-131 contamination of, after stack release, 19: 624 (IDO-12035)
iodine-131 contamination of, 19: 5725 (UR-653)
iodine-131 contamination of, by acute release to atmosphere, 19: 22014

(HW-SA-3338)
iodine-131 contamination of, in reactor accidents, 19: 24769
iodine-131 contamination in Italian, radiation dose to children's thyroid from, 20: 18962
iodine-131 content in Italian, 1962 and 1963, 18: 10333
iodine-131 content in, from cows after long-term ingestion, 18: 11559(R) (TID-19977)
iodine-131 content of, after ingestion of contaminated grass, 18: 13404 (TID-7677(p.392-400))
iodine-131 content of, fallout, 18: 18099
iodine-131 content of, effects of atmospheric radioactivity and rainfall on, 18: 23819 (CEA-R-2409)
iodine-131 content of, in France, 1962 and 1963, 18: 23819 (CEA-R-2409)
iodine-131 content in, 18: 37454
iodine-131 content in pasteurized, meteorological evaluation of sources of, 18: 42150
iodine-131 content of, effects of dietary level of stable iodine of dairy cattle on, 18: 41023(R) (HW-80500(p.19-23))
iodine-131 content in, effect of land fertilization on, 18: 43871
iodine-131 content of, effects of atmospheric contamination on, 18: 43873
iodine-131 content in U. S., 1962, 19: 11450
iodine-131 content of, after fallout contamination of pasture, 19: 30403 (TID-21764)
iodine-131 content in, effects of diet of cows and goats on, 19: 31750
iodine-131 content of, mathematical analysis, 19: 31751
iodine-131 content in, effects of contamination of pasture and dietary factors on, 20: 598 (NP-15568)
iodine-131 content of, in Germany, 20: 524
iodine-131 content of, in Kansas and Missouri, 1962, 20: 5648(R) (COO-1340-2, pp 1-53)
iodine-131 content in, anion exchange resins for determining, 20: 9153
iodine-131 content in German, effects of precipitation on, 20: 11017
iodine-131 content of, effects of dietary content of radioactive and stable iodine on, 20: 10530(R) (BNWL-122, pp 113-17)
iodine-131 content of, assessment of, 20: 14243(R) (TID-22626)
iodine-131 content in Japan, 1964, 20: 16730 (NP-15882)
iodine-131 content in, following accidents at nuclear facilities, 20: 18983
iodine-131 content in, effects of forage contamination on, 20: 18941(R) (IDO-12047)
iodine-131 content in fresh, ion exchange studies on, 20: 22543 (CEA-R-2897)
iodine-131 content in cow's, feeding and management systems affecting, 20: 22556
iodine-131 content in Colorado, May 1945, from Chinese nuclear test, 20: 29429
iodine-131 content in French, 1961 to 1963, 20: 31456
iodine-131 content in, use in nuclear accident monitoring, 20: 33577
iodine-131 content in, effects of processing on, 20: 33595
iodine-131 content in Great Britain, 1962, 20: 45909
iodine-131 content in German, Sept.–Nov. 1961, 17: 34166
iodine-131 content of, in German Federal Republic, 1956–62, 19: 5602
iodine-131 content in, ORNL measurements of, 1962, 17: 39294(R) (ORNL-3490)
iodine-131 content in, factors influencing, 18: 3604
iodine-131 content of, fallout, 18: 18110
iodine-131 content of cow's, 18: 23829
iodine-131 content in, 18: 29205
iodine-131 content in German, Sept. 1961–Jan. 1962, 17: 34172
iodine-131 content in UK, 18: 22253
iodine-131 content in Italian, 1961, 17: 27591 (EUR-223.1)
iodine-131 content in, in Finland, Sept. 1962 to Aug. 1963, 18: 139
iodine-131 determination in fresh, methods for, 19: 31672(R) (NIRS-3(p.65-77))
iodine-131 levels in Australian, 18: 31097
iodine-131 levels in, after Chinese nuclear explosion, 20: 43608
iodine-131 removal from, effect of evaporation and powdering processes on, 18: 14146
iodine-131 removal from, by moving bed ion exchange columns, 19: 40697(P)
iodine-131 secretion in cow, after single dose, 19: 19477
iodine-131 secretion in human, 19: 36141
iodine-131 secretion in sheep, 20: 10517(R) (BNWL-122, pp 52-4)
iodine-131 separation from, ion exchange, 19: 11395
iodine-131 separation from, field use of ion exchange cartridges for, 20: 10722
iodine-131 separation by ion exchange and gamma counting, 19: 28252
iodine-131 uptake and distribution in dairy cattle, long term studies on, 18: 11592
iodine-131 uptake by dairy cow, 18: 17437
iodine-131 uptake from blood plasma in cattle by, effects of milk secretion and yield on, 19: 6966
iodine-131 uptake by, of miniature goat, before and after parturition, 20: 8549 (HW-SA-3603)
iodine-131 uptake from, by human thyroid gland, 20: 10530(R) (BNWL-122, pp 113-17)
iodine-132 uptake by, of lactating sheep, 18: 8085
lanthanum-140 content in, in Germany Sept. 1961-Jan. 1962, 17: 34172
measurements of strontium-90 and cesium-137 activity in Great Britain, 20: 41186 (ARCRL-15)
mercury-203–neohydrin transfer to unweaned rats by, 19: 17738
monitoring for cesium-137, iodine-131, and strontium-89 and -90 in, from fallout, 18: 16229 (NP-13760)
monitoring for fallout radioactivity, 1963, 17: 18322(R) (HASL-135)
monitoring for iodine-131 from Nov. 1961 to Feb. 1962 in France, 17: 14526 (CEA-2223)
monitoring for radioactivity in U. S., Nov. 1961, 16: 2089
monitoring for radioactivity, method for, 16: 17937
monitoring for radioactivity, 1961, 16: 27510
monitoring, 1961, 16: 20906
monitoring, 1961 and 1962, 16: 20907
plutonium-239 uptake from cow, 18: 29206
potassium content of, regional and seasonal variations in, 20: 43597
potassium distribution in, 16: 17909 (AERE-M-985)
potassium-140 content in, in Australia, Europe, India, United Kingdom, and United States, 16: 10321
preservation by thimerosal for radioactivity monitoring, 19: 26593
processing, control of dry materials content in, 16: 13452(T) (AEC-tr-4492(p.217-20))
processing for alkaline and alkaline earth separation by ion exchange, 18: 43719
processing for barium-140, cesium-134, and strontium-85 separation, ion exchange method for, 16: 17935
processing for calcium and strontium separation by liquid ion exchange, 18: 1514
processing for cesium and strontium removal by ion exchange, 16: 10352
processing for cesium-134, iodine-131, and strontium-85 separation by ion exchange, 19: 11397
processing for iodine-131 and strontium-90 removal, 18: 3894
processing for iodine-131 and strontium-85 removal by ion exchange, 19: 11396
processing for radionuclide removal, 18: 3895
processing for strontium-85 removal, effects of acidification on, 18: 39539
processing for strontium-85 separation, 19: 26467(R) (TID-21796)
processing for strontium-85 removal using tricalcium phosphate, effects of, 20: 33580
processing plants for removal of radioisotopes by electrodialysis, cost factors for, 18: 12257 (NP-13620)
production by sheep, tracer study, 20: 10517(R) (BNWL-122, pp 52-4)
production in virgin heifers after estrogen stimulation, 18: 45163 (CONF-707-2)
protective effects of dietary, against radiation injuries in dog, 16: 16294
protein sediments in, sulfur-35 determination of, 18: 38756
radiation dose in, from fallout, 1963, 18: 31771
radiation effects on bacteria in, 16: 23455
radiation effects on alkaline phosphatase activity in cow's, 16: 26806 (AERE-R-3363)
radiation effects on nutritive properties as medium for Lactobacilli, 16: 29286
radiation effects of iodine-131 in, on infant thyroids, 16: 30691
radiation effects on properties of, 17: 30216
radiation effects on flavor of fats in, 18: 15848
radiation effects on growth of *Lactobacillus lactis* in, 18: 36978
radiation effects on production in cattle of, gamma, 18: 38775(R) (ORO-624)
radiation effects on production of, by dairy cows, 19: 43800
radiation effects on synthesis of, gamma and x, 20: 22594
radiation effects on fat from, γ, 20: 33382
radiation monitoring, 19: 42677
radiation monitoring at Argonne, Jan.-June 1965, 19: 44300 (TID-22171)
radiation monitoring of Swiss, 1963, 20: 7273
radiation monitoring for Salmon Event, 20: 16743 (VUF-1021)
radiation monitoring of, near Canadian reactors, 20: 7311 (NP-15642, pp 33-45)
radiation processing of evaporated, effects on wholesomeness, 16: 8459(R) (NP-11260)
radiation processing of evaporated, effects on wholesomeness, 18: 11639 (NP-13580)
radiation processing of evaporated, effects on wholesomeness, 19: 30615
radioactive contamination by fall-out iodine-131, 16: 28738
radioactive contamination of, from fallout, 17: 17745
radioactive contamination of Rumanian, 19: 640

radioactive contamination of, by radiation accident, 19: 46694
radioactive contamination of, near CANDU and WNRE sites, 20: 14738 (NP-15853, pp 21-33)
radioactive contamination of, control measures for, 20: 16754
radioactive contamination in, survey, 20: 18976
radioactive contamination of, methods for removing, 20: 18976
radioactive contamination of, by gaseous discharges from atomic energy plants, 17: 39283 (AHSB(RP)R-26)
radioactive, removal from surfaces, 16: 20071
radioactivity, 16: 9064
radioactivity, 19: 28597
radioactivity after nuclear accidents, 20: 18969
radioactivity content in, in Italy Jan.–June 1962, 17: 36024 (BIO/26/62)
radioactivity content of, from fallout in West Germany, 20: 40570
radioactivity content of, from fallout in West Germany, 20: 43626
radioactivity due to fallout, 1964, 18: 31784(R) (HASL-146)
radioactivity due to fallout in, 1964 and 1965, 19: 20154(R) (HASL-158)
radioactivity due to fallout in, monitoring in Great Britain, 19: 33991
radioactivity due to fallout in Canadian, Nov. 1965, 20: 20883 (NP-15914)
radioactivity due to fallout in Canadian, Dec. 1965, 20: 20938 (NP-15921)
radioactivity due to fallout in Canadian, 1964, 20: 20938 (NP-15921)
radioactivity from cesium-137 and strontium-90 in, New Zealand, April–June 1965, 20: 5664(R) (NP-15639)
radioactivity from cesium-137 and strontium-90 in Faeroe Islands, 1964, 20: 7320 (RISO-108)
radioactivity from cesium-137 and strontium-89 and -90 in Canada, Sept. 1965, 20: 9176 (NP-15763, pp 13-25)
radioactivity from cesium-137 and strontium-90 in Canada, Sept. 1965, 20: 9177 (NP-15763, pp 26-38)
radioactivity from cesium-137 and strontium-90, in Japan, 1964, 20: 16731 (NP-15883)
radioactivity from iodine-131 and strontium-90 in, at Chapelcross, Annan, Scotland, 20: 23407
radioactivity from cesium-137 and strontium-90 in fallout in Canadian, Feb. 1966, 20: 27203 (NP-16041, pp 3-13)
radioactivity from cesium-137 and strontium-90 in fallout in vicinity of Canadian reactors, Feb. 1966, 20: 27204 (NP-16041, pp 14-24)
radioactivity from cesium-137 and strontium-90 in New Zealand, 1965, 20: 31446(R) (NP-16015)
radioactivity in Ankara, Turkey, Nov. 1961 to Feb. 1964, 19: 11392(R) (NP-14683)
radioactivity in British, July to December 1964, 20: 45947 (ARCRL-13)
radioactivity in, data on, 17: 20262
radioactivity in East Tennessee, 1963, 18: 37442(R) (ORNL-3665)
radioactivity in Israel, cesium-137 and strontium-90, 19: 26917(R) (IA-984)
radioactivity in Japan before and after second Chinese nuclear test, 20: 25321 (NP-16036)
radioactivity in Milan, November and December 1961, 16: 24023
radioactivity in samples collected in U.S., 1962, 17: 14571
radioactivity in samples collected in U.S., 1962, 17: 14572
radioactivity in U. S. and Canadian, July 1964, cesium-137 and strontium-90, 19: 18159
radioactivity in 1958, 1959, and 1960 at Ispra, 16: 4983 (NP-10731 (p.129-44))
radioactivity in, 1961 and 1962, 16: 14447(R) (HASL-122)
radioactivity in, Sept. 1964, 19: 22554
radioactivity in, 1965, 20: 18914
radioactivity in, 1965, 20: 18915
radioactivity in, 1965, 20: 18918
radioactivity in, Jan. to July, 1965, 20: 18972
radioactivity in, and milk products, 20: 29464
radioactivity in, 1965 fallout, 20: 29428
radioactivity measurements in New Zealand, 20: 40521(R) (NP-16270)
radioactivity monitoring in Italy, 19: 42637 (BIO/32/63)
radioactivity of Arctic, effects of fallout fission products on, 18: 25055 (NP-13985)
radioactivity of Belgian, 1963, 19: 46632(R) (A/AC.82/G/L.987)
radioactivity of cesium-137, strontium-89, and strontium-90, Aug. 1964, 19: 22552
radioactivity of Canadian and U. S., 1964, 19: 22557
radioactivity of Canadian, Feb. 1965, 19: 34366 (NP-15079(p.17-27))
radioactivity of Canadian, June 1965, 19: 44251 (NP-15519, pp 23-51)
radioactivity of effects of atmospheric transport of fallout on, 19: 38857
radioactivity of, from natural potassium, 17: 29148
radioactivity of German, 1962, 19: 38858
radioactivity of Italian, network for monitoring, 19: 30467
radioactivity of Israeli, cesium-137 and strontium-90, 19: 32434
radioactivity of Italian, effects of strontium-89 and strontium-90 content on, 1962 and 1963, 20: 9150
radioactivity of samples collected in U. S., 1964, 18: 41644(R) (HASL-149)
radioactivity of U. S., 1957 to 1963, 19: 22551
radioactivity of Utah, cesium-137 and ruthenium-103 and -106, 19: 46675
radioactivity of, in Great Britain, 1962, 18: 15735(R) (ARCRL-10)
radioactivity of, German Federal Republic, Sept. 1961 to Sept. 1962, 18: 19809
radioactivity of, from fallout in India, 1962 and 1963, 18: 23789 (AEET/AM/39)
radioactivity of, caused by fallout strontium-90 and iodine-131, 18: 25727
radioactivity of, in Canada, March 1965, 20: 7305 (NP-15641, pp 9-21)
radioactivity of, in Canada, August 1965, 20: 7310 (NP-15642, pp 20-32)
radioactivity of, in Hanford area, Wash., Jan. to June 1965, 20: 7297 (BNWL-165)
radioactivity of, near Osaka, Japan, Sept. 1961–March 1962, 20: 7274
radioactivity of, AERE monitoring of cesium-137, iodine-131, and strontium-90, 20: 14784(R) (AERE-R-5015)
radioactivity of, in Savannah River Plant area, July through Dec. 1965, 20: 27195(R) (DPST-66-30-1)
radioactivity of, near Canadian reactor installations, March 1966, 20: 33556 (NP-16124)
radioactivity of, effects of environmental cesium-137, iodine-131, and strontium-90 on, 20: 39157
radioactivity of, analytical model for iodine-131, 20: 41192(R) (IDO-12053)
radioactivity uptake by, in farm animals from fallout, 19: 25886
radioiodine excretion in goat, 18: 31105
radioiodine uptake by man from, method for predicting, 20: 30980
radioiodine uptake by man from, use of countermeasures in predicting, 20: 30981
radioisotope levels in, 17: 5751(R) (HASL-132)
radioisotope transfer from mother to progeny through rat, 18: 13432
radiological monitoring near Nevada Test Site, 16: 9030 (TID-14776)
radiological monitoring, 1961, 16: 20905
radiological monitoring in November 1962 in France, 17: 14537 (SCPRI(M)62-11)
radiological monitoring in Dec. 1962 in France, 17: 14538 (SCPRI(RM)-62-12)
radiological monitoring, 18: 41648 (NP-14254)
radiological monitoring after Shoal nuclear explosion, 19: 697 (VUF-1009)
radionuclide contamination of human, in Boston and Chicago, 19: 28601
radionuclide content of, 18: 3605
radionuclide content of, effects of farming practices on, 18: 3624
radionuclide contents in, 19: 9365(R) (HASL-155)
radionuclide content in Boston of, 19: 28599
radionuclide content in Amsterdam, 1960 to 1963, 20: 20949
radionuclide content in, dietary intake estimates for, 20: 43573 (CONF-765-13)
radionuclide levels in, measure for moderating, 20: 18985
radionuclide levels in, effects of plasma levels on, 16: 25121(R) (HW-72500(p.44-9))
radionuclide transfer kinetics from plasma to, in sheep, 17: 35304(R) (HW-76000(p.98-108))
radionuclides in Italian, detection and measurement, 20: 20950
radiosterilization effects on flavor, 16: 22498(R) (NP-11725)
radiosterilization of evaporated, dietary effects on dogs, 16: 32006(R) (NP-12066)
radiosterilization, 19: 11629
radiosterilization effects on coliform bacteria in raw, 19: 13825
radium content in, near uranium mines and processing plants, 17: 41140
radium-226 content in French, 20: 16752
radium-226 content in French, 20: 16753
rubidium-87 content in powdered, produced in U. S., 1923 to 1936 and 1946 to 1961, 19: 24787
sampling in France for control of radioactive contamination, 20: 33567
sampling of, and preparation for radiochemical analysis, 18: 8519(T) (AEC-tr-6049(p.1-10))
sampling of, in New Zealand, 17: 5750(R) (DXRL-F6)
secretion of dietary calcium-45 and strontium-89 in cow and goat, 16: 8505
selenium-75 uptake by ewe and mouse, 18: 17426
separation of barium-140, strontium-89, and strontium-90 from ashes of, 20: 40858
separation of iodine-131 from, by ion exchange, 17: 14383
separation of iodine-131 from, by ion exchange, 20: 23223
separation of manganese from solutions of ashes of, by solvent extraction, 20: 10950
separation of strontium-90 from, 16: 27504
separation of strontium-90 from, ion-exchange process for pilot plant, 17: 18423
separation of strontium-90 from, method for, 17: 27038
separation of strontium isotopes from, in absorption column, 18: 6976(R) (TID-19893)

separation of strontium isotopes from, ion exchange, 19: 34415
separation of strontium and cesium from, 20: 1975(P)
separation of strontium-85, -89, and -90 from, using calcium phosphate precipitation method, 20: 16382
separation of yttrium from, by solvent extraction using TBP, 17: 17977(T) (JPRS-18632)
sodium-22 content of, Italian, 1961–64, 19: 42433
sodium-22 content in, relation of content in man to, 19: 20225
sodium-22 uptake from fallout, 20: 16678
strontium content in breast and bottled, effects on babies, 17: 5730
strontium dietary availability from, tracer study, 16: 20899
strontium removal from, cation exchange process for, 17: 8469
strontium removal from, ion exchange, 17: 27223(P)
strontium secretion in, 19: 66
strontium transfer to, 18: 11621
strontium transfer to milk products, 16: 33331
strontium uptake by breast-fed babies from, 18: 29219
strontium uptake from, relative to cereals, 16: 14453
strontium-85 and strontium-90 removal from, ion exchange method for, 18: 17952
strontium-85 and strontium-89 excretion in goat, effects of dietary calcium and strontium on, 20: 40568
strontium-85 content of, after parenteral administration to cows, 19: 36733
strontium-85 removal from, ion-exchange resins for, 18: 13925
strontium-85 removal from, effectiveness of ion-exchange resins, 19: 34371
strontium-89 and -90 transfer to cheese and whey from, 18: 22299
strontium-89 and -90 content in, in Germany, Sept.-Nov. 1961, 17: 34166
strontium-89 and -90 content in, around nuclear power plants in England, 18: 6775
strontium-89 and -90 content in Japanese, Nov. 1961 to Oct. 1962, 19: 7707
strontium-89 and -90 content of cow's, 18: 23829
strontium-89 and -90 content in breast and cow's, 17: 21943
strontium-89 and strontium-90 uptake by, age effects on, 18: 18045
strontium-89 and strontium-90 content in, in Finland, 1960 through 1965, 20: 41134 (SFL-A3)
strontium-89 content in U. S., 1962, 19: 11450
strontium-89 content in U. S., 1963 and 1964, 19: 18160
strontium-89 content of, in Germany, 20: 524
strontium-89 content in, effects of diet of cattle on, 20: 4162
strontium-89 content in German, effects of precipitation on, 20: 11017
strontium-89 separation from, by ion exchange, 19: 7710
strontium-89 uptake by rabbit and rat, 19: 8766
strontium-90 activity in, in Potsdam, 1963, 19: 15805
strontium-90 activity in, Potsdam, Germany, 1964, 20: 35680
strontium-90 and cesium-137 content in samples of, collected in Germany between 1955 and 1961, 18: 31770
strontium-90 concentration in, of Palermo in November and December 1961, 17: 13958
strontium-90 contamination in bovine, human, and soybean, 17: 29143
strontium-90 contamination of, protective measures against, 18: 12402
strontium-90 contamination of, methods for removing, 20: 43537
strontium-90 content, from fallout, 18: 31760
strontium-90 content in, effects of deposition rate and soil level concentration, 16: 429 (TID-13945)
strontium-90 content in, in relation to other foods in Germany, 16: 19202
strontium-90 content in, due to fall-out, Canada, Jan.–March 1962, 16: 25616(R) (NP-11914)
strontium-90 content in, from ingested strontium-90, 16: 25112(R) (HW-72500(p.1-12))
strontium-90 content in New Zealand, 16: 29181 (DXRL-F4)
strontium-90 content in bulk, in Amsterdam, Holland, 1960-61, 16: 33336
strontium-90 content in, in Poland, 1959, 16: 6626(T) (GAT-Z-5022)
strontium-90 content in, in Finland, 1959, 16: 9036
strontium-90 content in, in pregnant cows, 16: 9909
strontium-90 content in, in Fiji Islands and New Zealand, 17: 4690(R) (DXRL-F5)
strontium-90 content in, in United Kingdom, 1960, 17: 6363
strontium-90 content in, in New Zealand, 17: 5750(R) (DXRL-F6)
strontium-90 content in dried, in Austria, 1960–61, 17: 18432
strontium-90 content in, in great Britain, correlation with deposition rates, 17: 23073
strontium-90 content in Germany, 18: 3629
strontium-90 content in Great Britain, 18: 5151
strontium-90 content in Western Germany, 18: 5152
strontium-90 content in, 1957 to 1961, 18: 8063(T) (AEC-tr-6049(p.258-70))
strontium-90 content in, in selected cities of U. S., 1962 and 1963, 18: 12399
strontium-90 content in U. S., 1963, 18: 12401
strontium-90 content in, in West Germany, 1960, 18: 27029
strontium-90 content in samples of, collected in Mexico, August 1961 to July 1963, 18: 27699 (A/AC.82/G/L-931)
strontium-90 content in, effects of calcium content of forage grass on, 18: 38774(R) (EUR-1881.e)
strontium-90 content in, Australia, 1962, 18: 39493
strontium-90 content in, effect of land fertilization on, 18: 43871
strontium-90 content in Thailand, 18: 45094(R) (THAI-AEC-2)
strontium-90 content in U. S., 1962, 19: 11450
strontium-90 content in New Zealand, from fallout, 19: 13682
strontium-90 content in London, 19: 14991
strontium-90 content of Brazilian, 19: 15786 (NP-14627)
strontium-90 content in U. S., 1963 and 1964, 19: 18160
strontium-90 content in, in Czechoslovakia, 19: 18203
strontium-90 content in dried, in Czechoslovakia, 1957 to 1963, 19: 18204
strontium-90 content of, in Sweden, 1963, 19: 22558
strontium-90 content in U. S., 1964, 19: 22562
strontium-90 content of, in Czechoslovakia, 19: 24704
strontium-90 content of, 17: 36041
strontium-90 content of, 18: 3625
strontium-90 content of, effects of dietary calcium content on, 18: 11559(R) (TID-19977)
strontium-90 content of, effects of processing on, 17: 17711(T) (JPRS-18492(p.26-33))
strontium-90 content of Finnish, 18: 22254
strontium-90 content of, in Italy, 17: 36073
strontium-90 content of, in Italy, 1963, 19: 7711
strontium-90 content of, in USSR during 1960-1962, 19: 13667 (NP-14696)
strontium-90 content of, uptake by infants' bones, 18: 15796
strontium-90 content of, relation to fallout and rainfall in Potsdam, 18: 31188
strontium-90 content in powdered, produced in U. S., 1923 to 1936 and 1946 to 1961, 19: 24787
strontium-90 content in powdered, in Uruguay, 1960 and 1962, 19: 26586
strontium-90 content in, near Ispra, Italy, 19: 28546
strontium-90 content in New Zealand, 19: 35892 (NP-15082)
strontium-90 content in German, 19: 38876 (NP-14927)
strontium-90 content of, after chronic ingestion by milk cows, 19: 40332
strontium-90 content in, effects of dietary calcium consumed by cows, 19: 40341
strontium-90 content in, Japan, 1964, 19: 42639 (NP-15278)
strontium-90 content of Indian, 1959 to 1964, 19: 44244 (AEET/AM/40)
strontium-90 content in, 1959 to 1962, 19: 45749
strontium-90 content in Canadian, 1965, 20: 596 (NP-15542)
strontium-90 content of, in Germany, 20: 524
strontium-90 content of Canadian, 1965, 20: 597 (NP-15563)
strontium-90 content in, Italy, 1963, 20: 2046 (BIO/04/64)
strontium-90 content of, Italy, 1964, 20: 2047 (EUR-2509.e)
strontium-90 content in, effects of diet of cattle on, 20: 4162
strontium-90 content of, from Mandan-Minot region of North Dakota, 20: 5678
strontium-90 content in Mexican, 1962, 20: 9155
strontium-90 content in German, effects of precipitation on, 20: 11017
strontium-90 content in cow and human, 1959 to 1961, 20: 13012
strontium-90 content in U. S., 1965, 20: 16662(R) (HASL-165)
strontium-90 content in powdered, in Japan, 1962 and 1963, 20: 16755
strontium-90 content in Californian, 1960 to 1963, 20: 18968
strontium-90 content in, effects of diet of cattle on, 20: 20882(R) (HASL-171)
strontium-90 content in, long-term predictions of, 20: 23299
strontium-90 content in Canadian, 1960 to 1964, 20: 23390
strontium-90 content in, effects of dietary calcium on, 20: 29459
strontium-90 content in Norwegian, 1960-64, 20: 31465
strontium-90 content in, Oak Ridge environs, 1965, 20: 33557(R) (ORNL-3969)
strontium-90 content in, effects of processing on, 20: 33595
strontium-90 content in, measurement of, by yttrium-90 before equilibrium, slide-rule method for, 20: 35352
strontium-90 content of, in Germany, 1962 through 1964, 20: 36674
strontium-90 content in Canadian, April 1965, 20: 41209
strontium-90 content of global samples, 1965 and 1966, 20: 41131(R) (HASL-172)
strontium-90 content of, in Mexico, 1963 to 1965, 20: 40854
strontium-90 content in, in Japan, 1963–64, 20: 43610
strontium-90 content of, in Belo Horizonte, Brazil, 20: 42999 (NP-15934)
strontium-90 content in Japanese, November 1962 to September 1963, 20: 43520
strontium-90 content of, in Bombay, 1964 to 1965, 20: 43532
strontium-90 content in, 1958 to 1964, 20: 45886 (NP-16262)
strontium-90 content in powdered, in Japan, 20: 45887 (NP-16290)
strontium-90 content in Icelandic, 1958 to 1964, 20: 45908
strontium-90 content in Great Britain, 1962, 20: 45909
strontium-90 content in Holstein's and Jersey's, seasonal variations in,

16: 27503
strontium-90 content in beagle, 17: 38638(R) (UCD-108(p.45-51))
strontium-90 content in, in Japan, 16: 26688(T) (AEC-tr-4642)
strontium-90 content in, in United Kingdom, 18: 22252
strontium-90 content in, in Great Britain, 1969, 16: 5620
strontium-90 content in powdered, in Japan, 17: 21938
strontium-90 content in, from Australia, Europe, India, and U. S., 18: 10282
strontium-90 content in Hungarian, 18: 29220
strontium-90 content in Japanese, 19: 15755 (NP-14797)
strontium-90 content in Canadian, 1964, 19: 20161 (NP-14869)
strontium-90 content in, 19: 34365(R) (HASL-161)
strontium-90 content in, effects of various foodstuffs on, 19: 45772
strontium-90 contents of, German Federal Republic, 1956 to 1962, 19: 5602
strontium-90 content, effects of grass contamination, 17: 10352
strontium-90 content in New Zealand, July to Sept. 1964, 19: 9371(R) (NP-14618)
strontium-90 content in lactating cows', effects of calcium on, 16: 26717
strontium-90 contents in, measurements at ORNL, 1962, 17: 39294(R) (ORNL-3490)
strontium-90 contents of, factors affecting, 18: 3604
strontium-90 content from fallout, 18: 18110
strontium-90 content in, from fallout in United Kingdom, 18: 22253
strontium-90 content in, 18: 29205
strontium-90 content in, in Finland, 1961–62, 19: 7741
strontium-90 content of Italian, 18: 18098
strontium-90 distribution and uptake in Japanese, 20: 7269
strontium-90 excretion in cow's, effects of calcium uptake on, 18: 43170(R) (EUR-1882.e(p.31-6))
strontium-90 in, effects of physico-chemical state on rat uptake of, 20: 18224
strontium-90 in, in Rhodesia, 17: 34163
strontium-90 in, uptake by butter and cheese of, 19: 28592
strontium-90 level in, effects of calcium diet on, 16: 9910
strontium-90 levels in, in Netherlands, 1959 and 1960, 16: 9837
strontium-90 levels in, in Italy, 1961, 17: 27591 (EUR-223.i)
strontium-90 levels in human, in Toronto, Canada, 16: 9041
strontium-90 levels in, mathematical model of effects of transport mechanisms on, 17: 6353
strontium-90 removal, 17: 25302
strontium-90 removal by ion exchange process, 16: 22279
strontium-90 removal from, ion exchange method for, 19: 34289(P)
strontium-90 removal from, ion exchange process, 17: 8458
strontium-90 removal from, by moving bed ion exchange columns, 19: 40697(P)
strontium-90 secretion in cows, effects of dietary calcium on, 20: 8565
strontium-90 separation from, ion exchange process for, 20: 45826(P)
strontium-90 transfer by, after chronic ingestion by female dogs, 19: 40327
strontium-90 transfer in, to nursing calves, 19: 40329
strontium-90 transfer in, to nursing calves, 19: 40330
strontium-90 transfer through, to young rats, 20: 35
strontium-90 transfer from mother to baby monkeys by, 20: 28896
strontium-90 uptake by infant bones from, 18: 17432
supplies, problems associated with possible nuclear reactor accidents, 16: 9060
tellurium-132 uptake by lactating sheep, 18: 8085
tritium uptake by cattle, 19: 43694
uptake of radioactivity in, by thyroid in children following nuclear weapons test in Nevada, 20: 43590 (UCRL-14707)
uranium content in, of lactating dogs following U_3O_8 administration, 20: 35222
use of injected, as antigen in dogs and guinea pigs, 19: 33963(T)
zinc secretion in, of sheep, 19: 8739 (HW-SA-3746)
zinc-65 secretion in sheep, 20: 10527(R) (BNWL-122, pp 94-8)

Milky Way
see Galaxies

Millimeter Waves
see Microwaves

Milling
see Crushing

Millipore Filters
see Membrane Filters

MILLSTONE POINT POWER REACTOR
control systems for, design and performance of, 20: 36485 (NP-16147 (Vol.2))
design and analysis of, 20: 36484 (NP-16147(Vol.1))
design of, engineering drawings for, 20: 36485 (NP-16147(Vol.2))

Milne's Problem for Neutron Transport
see Neutrons

MINE MOUNTAIN QUADRANGLE (NEV.)
geologic map of, 17: 4722

MINERAL BENEFICIATION
analysis of products of, for copper by neutron activation, 20: 33177(T) (AEC-tr-6639, pp 82-5)
analysis of products of, by slow-neutron absorption, 20: 33183(T) (AEC-tr-6639, pp 114-17)
analysis of products of, by x-ray fluorescence excited by alpha particles, 20: 33184(T) (AEC-tr-6639, pp 118-21)
analysis of products of, by beta scattering, 20: 33185(T) (AEC-tr-6639, pp 122-5)
analysis of solutions from, for silver by neutron activation, 20: 33179(T) (AEC-tr-6639, pp 92-6)
analysis of solutions from, for tungsten by gamma absorption, 20: 33186(T) (AEC-tr-6639, pp 126-30)
methods of, for pegmatitic uranium ores, 18: 4013

MINERAL DEPOSITS
(This heading may be modified by location in the form Mineral Deposits (N. Mex.).)
see also Beryllium Deposits
see also Coal Deposits
see also Granite Deposits
see also Limestone Deposits
see also Manganese Deposits
see also Minerals
see also Pegmatite Deposits
see also Phosphate Deposits
see also Placer Deposits
see also Sandstone Deposits
see also Sedimentary Deposits
see also Shale Deposits
see also Thorium Deposits
see also Uranium Deposits
age estimations, in Romania, 17: 14483
age of Uralian, alpha-lead, 16: 2032
analysis of sandstone, at Mas Alary, Herault, France, 19: 9390
analysis of, in South Atlantic floor, 18: 43794
analysis of, pulsed-neutron equipment for, 20: 43163(P)
genesis of, using sulfur isotopic ratios in studying, 20: 41151
isotopic analysis of, in Middle Europe, 19: 13644
prospecting, exploration, and working methods, 16: 16043
prospecting, exploration, and working methods for, 16: 33279(T) (AEC-tr-5404)
uranium content in, determination of, by analysis of sulfides, 20: 26779
zoning in Argentina, Chile, Peru, and western United States, hydrothermal, 17: 34116 (CONF-123-1)
zoning of, hydrothermal, 17: 34116 (CONF-123-1)

MINERAL DEPOSITS (UTAH)
geochemical survey, 16: 27437

MINERAL DRESSING
see also Mineral Beneficiation
research programs at MIT on, 19: 9362(R) (MITS-52)
waste monitoring and disposal, 17: 25717

MINERAL METABOLISM
book: *Mineral Metabolism*, 19: 63
control of, in corn, genetic, 18: 3454(R) (TID-19786)
effects of beta particles from injected phosphorus-32 on, in rats, 17: 31925
effects of nerve supply on, in rat bones, tracer study, 20: 5370
effects of vitamin D_3, in rats, 19: 38347
in aquatic plants, 19: 10681(R) (NYO-3018-7)
in trees, effect of vegetative cycle on, 17: 40514 (CEA-2317)
measurement in bones, 20: 3803 (ORNL-IIC-5, pp 257-76)
mechanisms of, in marine animals, 20: 26549(R) (NP-15915)
radiation effects on bone tissue processes, 16: 5175(T) (JPRS-11242 (p.126-34))
radiation effects on rabbit and rat, 18: 11790
radiation effects on mouse, x, 19: 45729(R) (NYO-910-23, pp 1-111)
radiation effects on, in rat bones, tracer study, 20: 5370
radiation effects on, in adult dog bones, 20: 6896
radiation effects on rat skeletal, tracer study of x, 20: 10587
radiation effects on rat, tracer study of y, 20: 16187
strontium-85 and -90 uptake by osteosarcomas, 18: 11578

Mineral Oil
see Petroleum

MINERAL RESOURCES
see also Thorium Reserves
see also Uranium Reserves

MINERAL UPTAKE
by bone, cartilage, and teeth, reaction mechanisms, tracer study, 16: 31445
by bone, cartilage, and teeth, reaction mechanisms, tracer study, 16: 31446

Mineral Wool

see Glass Wool

MINERALOGY
see also Crystallography
see also Geology
see also Minerals
see also Tracer Techniques (Mineralogy)
bibliography of UKAEA publications available to public, 16: 17339 (NP-11504)
book: *Mineralogy and Geochemistry of Rare Elements in Cherry Mountains (Urals)*, in Russian, 19: 20190
engineering problems in, 16: 30790(R) (MITS-48)
geologic studies on, in western United States, 20: 18942(R) (NYO-1669-11)
research programs at MIT on, 19: 9362(R) (MITS-52)
research techniques in, 16: 17881(R) (MITS-47)
research techniques in, 20: 7282(R) (NYO-10334)
uraniferous mineralizations of Brugeaud Mine, Limousine, France, secondary, 20: 23332

MINERALS
(See also specific minerals and classes of minerals identified by specific metals.)
see also Eulytites
see also Metamict Minerals
see also Radioactive Minerals
age and thermal history of, 18: 35709
age determination, analysis of error in absolute, 16: 10288
age determination, radiometric, 16: 27421(R) (TID-16348)
age determination, review of isotopic methods, 16: 29200
age determination by helium method, 17: 30734
age determination by radioactive halos in, evaluation of, 19: 46616(T) (ORNL-tr-768)
age determination by potassium–argon content, 20: 37016
age determinations in pyroxene, effects of excessive argon content, 16: 29203
age determinations from lead, 17: 20205
age determinations in Northern Rhodesia, review of, 18: 43793
age estimation by strontium–rubidium method, 17: 34122
age estimation by argon-potassium method, effects of metamorphoses on, 17: 40992
age estimation from lead–uranium isotope ratios in, interpretation of calculations of, 19: 649
age estimation methods for, radiometric, 18: 31048(R) (COO-689-42)
age estimation of holocene deposits by radiocarbon and stratigraphic methods, 16: 29198
age estimation of, effects of escape of radioactive gases on, 17: 10829
age estimation of, theoretical and technical aspects of rubidium–strontium geochronology for, 17: 12462
age estimation of, lead-207 to uranium-235 ratio for, 17: 23529
age estimation of, comparison of potassium–argon and rubidium–strontium methods, 17: 30741
age estimation of volcanic, at Marysvale, Utah, 17: 40989 (BNL-5555)
age estimation of, data compilation for, 18: 1900
age estimation of uranium-containing, by comparison of fission product tracks, 18: 27718
age estimation of glassy, by fission track evidence, 18: 31773
age estimation of, methods for, 18: 22262(T) (JPRS-24435(p.46-63))
age estimation of, by potassium–argon and rubidium–strontium methods in Norwegian eclogites, 20: 20891
age estimation of, in Arizona, 20: 43503(R) (COO-689-60, App.A-3)
age measurements on British Guiana dolerite, isotopic method, 17: 23537
age of, in eastern Congo Republic, 17: 8394
age of, use of uranium-235 in estimating, 16: 1808(R) (TID-12849)
ages in eclogitic and granulitic xenoliths, argon-potassium, (E), 19: 4384
ages of vein, from Rwanda-Urundi, 17: 32268
analyses of, strontium contamination in, 18: 19888
analysis by alpha radioluminescence, 16: 7505
analysis by beta-induced x-ray fluorescence, 18: 27322
analysis by gamma spectrometry, geologic, 19: 4385
analysis by neutron capture gamma spectra measurements, 18: 43433
analysis by neutron activation and gamma spectroscopy, 19: 30424
analysis by x-ray fluorescence spectrometry, 16: 32922(T) (CEA-tr-A-1032)
analysis by x-ray fluorescent spectrometry, multielement calibration in, 17: 15893
analysis for alkali metals, method for, 17: 27243(T) (AEC-tr-5822)
analysis for alkaline-earth metals, chromatographic and spectrophotometric, 17: 40745
analysis for alpha emitters using reticulated slides, 16: 31965
analysis for aluminum, activation, 16: 31560
analysis for argon and helium for age estimations, 16: 16577 (TID-14861(Vols.I&II))
analysis for argon-40, design of mass spectrometer for, 19: 4444
analysis for argon-37 by activation, 19: 26255
analysis for argon-40, use of nitrogen-15 as internal standard in, 19: 43960
analysis for argon-40 using isotopic dilution method, 20: 33213
analysis for boron by neutron bombardment, equipment for, 19: 4080
analysis for bromine, activation, 19: 2223
analysis for calcium-48/calcium ratio, activation, 18: 8529
analysis for cesium, flame photometric, 18: 8295
analysis for cesium, lithium, and rubidium, spectroscopic, 18: 19853(T) (CEA-tr-R-1711)
analysis for cesium by neutron activation, 20: 33180(T) (AEC-tr-6639, pp 97-102)
analysis for gold and silver, activation, 19: 39265(R) (IA-1021)
analysis for gold by neutron activation methods, 20: 26785
analysis for gold, iridium, and platinum by thermal neutron activation, 20: 40835
analysis for hafnium and zirconium, activation, 19: 4078
analysis for iridium and selenium by activation methods, 19: 22148
analysis for iron(II) in presence of uranium(IV), 17: 23277
analysis for isotopic composition of strontium in limestone, carbonatites, and strontium minerals, 17: 25446
analysis for lanthanum and samarium by neutron activation followed by gamma spectrometry, 18: 43430
analysis for lanthanum and yttrium using Alizarin Red S, photometric, 19: 13258
analysis for manganese, activation, 18: 21991
analysis for niobium, tantalum, titanium, and tungsten by precipitation from homogeneous solution, 19: 7321
analysis for niobium, radiometric-spectrophotometric, 19: 43943
analysis for niobium and tantalum simultaneously, activation, 20: 16336(R) (NYO-10175)
analysis for oligoelements by combination of neutron activation and paper chromatography, 16: 27436
analysis for oxygen, activation, 18: 1523
analysis for polonium-210 and lead-212, radiochemical, 17: 27252
analysis for potassium, thorium, and uranium, gamma spectrometric techniques for, 18: 35888
analysis for radium-228 and thorium-228, radiochemical, 18: 27300
analysis for radium, thorium, and uranium, equipment for radiometric, 18: 29578
analysis for rare earths, spectrographic, 17: 6008
analysis for rare earth traces, 17: 7973
analysis for rare earths, thorium, and uranium by ion exchange, review on, 20: 3888 (TID-22402)
analysis for rare earths, activation, 20: 22950
analysis for rare earths, spectrometric, 20: 29134
analysis for rare earths by neutron activation, 20: 33178(T) (AEC-tr-6639, pp 86-91)
analysis for rubidium, activation, 20: 20560 (EUR-2753.f)
analysis for scandium, spectrophotometric, 17: 33829
analysis for scandium, colorimetric, 19: 9091
analysis for scandium, activation, 20: 22886
analysis for silicon oxide by isotope dilution, 18: 1528
analysis for silver, spectrochemical, 19: 39265(R) (IA-1021)
analysis for silver, activation, 20: 20574
analysis for strontium, flame photometric, 16: 400(T) (CEA-tr-R-1382)
analysis for tantalum by neutron activation, 20: 33181(T) (AEC-tr-6639, pp 103-7)
analysis for thorium with Solochromate Fast Red, spectrophotometric, 16: 2973
analysis for thorium and uranium, spectrographic, 17: 35637
analysis for thorium, photometric, 18: 13705
analysis for thorium, fluorometric, 18: 17723 (IDO-12034)
analysis for thorium by neutron activation methods, 20: 26805
analysis for trace elements, spectrographic, 17: 2929
analysis for trace elements by activation, use of paper chromatography and computers in, 19: 7338
analysis for uranium, fission, 17: 10555
analysis for uranium, method for, 17: 28795 (AEET/ANAL/5)
analysis for uranium by paper chromatography, 17: 28799 (AEET/ANAL/10)
analysis for uranium using Arsenazo III, photometric, 20: 36774
analysis for zinc by neutron activation methods, 19: 7283
analysis for zinc-68/zinc-64 ratio, activation, 18: 27299
analysis of carnallites for carbon and oxygen isotopes, 16: 22029
analysis of sulfide, for palladium and platinum, by neutron activation methods, 19: 9081
analysis of, use of paper chromatography in, 20: 35389 (CEA-R-2791)
analysis, spectrographic, 16: 28911
analysis, activation using 14.5-Mev neutrons, 19: 36243(R) (X64-17610)
argon isotope content of, bibliography on, 17: 6270(R) (NYO-10325)
bibliography on ternary, and compounds, 16: 13005 (NP-11598)
book: *Mineral Metabolism*, 19: 63

book: *Mineral Tables (Hand Specimen Properties of 1500 Minerals)*, 20: 39100
book: *Minerals for the Chemical and Allied Industries*, 16: 7765
book: *New Data on Rare Element Mineralogy*, 17: 18312(T)
book: *Radiogenic Argon in Minerals and Rock*, 17: 32278
book: *X-Ray Diffraction Analysis of Raw Materials*, 20: 36386
boron isotopic abundances in, 17: 36553
calcium isotope content of, bibliography on, 17: 6270(R) (NYO-10325)
charge compensation effects on cation site preferences in complex oxides, 17: 28889
charge trapping centers in, use of thermoluminescence for measuring, 20: 45913 (BNL-10545)
charged particle tracks in, identification after chemical etching, 19: 39038
chlorine-36 oxidation states in neutron-irradiated, 16: 25443
content in human bone, use of iodine-125 for measuring, 18: 31406
content in human vertebrae, effects on crushing strength, 20: 45247(R) (COO-119-234, pp 211-26)
content in lungs during chronic berylliosis, 17: 28647
content of excess argon-40 in, 20: 43506(R) (COO-689-60, App.A-6)
cosmic radiation spallation in, track methods for observing, 16: 13334
crystal algebra of chalcopyrite and stannite, 16: 4610(R) (TID-14435)
crystal structure of, data on, 17: 20406 (TEI-830)
cycling of, in ecosystem on site contaminated by radioactive wastes, 18: 10 (TID-19618(p.5-37))
cycling of, in regional ecosystems, 18: 11 (TID-19618(p.38-112))
density measurements on, by gamma absorption and scattering, 19: 42651
detection and measurement of marine, nuclear techniques for, 20: 23527 (CONF-651206)
determination in bones, radiographic method, 17: 19794
determination in bones, gamma-attenuation, 17: 40752
determination in bone, nondestructive radiographic densitometric, 19: 4077
determination in biological materials, fluorescence, 19: 45729(R) (NYO-910-23, pp 1-111)
determination in rocks by x-ray-induced phosphorescence, 19: 13650
deuterium content of crystallization water of saline, 19: 44240
diffusion of argon and helium from, determination of activation energy spectra in, 17: 10830
diffusion of argon in, 17: 10831
diffusion of argon-40 from perthite, activation energy, 17: 29099
diffusion of ions in chabazite, self-, 17: 20029
diffusion of radioactive gases from, spectra of, 17: 3171
distributions in Atlantic sediments, 18: 33790
distributions in fresh-water systems, heterogeneous equilibria in, 17: 40522 (TID-7664(p.61-70))
effects as fillers on radioinduced polymerization of methyl methacrylate and styrene, 20: 20778
effects on soil volume weight determination by gamma scattering, 19: 26566
effects on strontium-90 uptake from soils by plants, 20: 26613
fission fragment damage to, plutonium particle size analysis by, 20: 27189 (BNWL-SA-26)
fission product tracks in, formation and stability of, (E), 19: 20674
fixation properties for strontium, 16: 16019 (CEA-2114)
formation of, effects of beryllium concentration and migration on, 17: 21919
gamma spectra of neutron-irradiated, 20: 33161(T) (AEC-tr-6639, pp 13-17)
geological dating of, chemical etching of fission fragment tracks, 19: 4380
hafnium–zirconium ratio in, 16: 25631
heating *in situ* with radioactive materials, process for, 20: 30950(P)
hydrogen bonding in, effects of cation substitution on, 20: 7057
identification and metamorphism by gamma attenuation, 19: 11407
ion-exchange properties of, for purifying radioactive liquids discharged to ground, 17: 29872
ion exchange properties of, for alkali and alkaline earth metals, 20: 38858 (BNWL-235-3, pp 23-51)
ion exchange study of clay, 18: 16200
isotope ratios in, mass spectrographic determination of lead, thorium, and uranium, 19: 32091
lead-uranium ages in, effects of lead losses on discordant, 18: 1895
metabolism in human lumbar vertebrae, effects of age and sex on, 20: 45280(R) (COO-119-234, pp 191-210)
metabolism in rabbit bones, effects of cortisol on, 20: 45246(R) (COO-119-234, pp 120-79)
mining undersea, 20: 45927
neutron emission by, 18: 16209
oxidation rate of uranium-234 and uranium-238 in, 20: 38894
paramagnetic interrelations in, 17: 3173
particle tracks in, fossil, 20: 7375
phase diagrams of binary systems of, entropy of melting of, 20: 16711(R) (MIT-1381-13)
properties of, from vicinity of Brookhaven National Lab., Upton, N. Y., 18: 1909
prospecting for, neutron activation methods for, 20: 31434
prospecting for, uses of radioisotopes in, 18: 39721(T) (AEC-tr-6390 (p.1-3))
prospecting for, use of neutron activation analysis in, 20: 33169(T) (AEC-tr-6639, pp 50-4)
radiation effects on surface wettability, gamma, 16: 12201
radiation effects on color of pearl, 17: 27901
radiation effects on chlorine-36 oxidation states in, 18: 35579
radiation effects on physiology of content of, in developing guinea pig brain, 19: 19534
radiation processing by flotation method, 19: 46453
radioactive halos in cassiterite and yttrofluorite, measurements of, 19: 46592(T) (ORNL-tr-701)
radioactive halos in, review, 19: 46593(T) (ORNL-tr-755)
radioactivity distribution in Alno alkaline area, 19: 30406
radioinduced coloration in, with and without pleochroic halos, 19: 46625(T) (ORNL-tr-757)
rare earth abundances in, 17: 8406
rare earth abundance and distribution in, 20: 23278
rare earth distribution, 17: 16278
rare-earth contents of, from batholith of Southern California, (E), 19: 38848
recovery of, use of underground explosions in, 20: 43463 (UCRL-14756)
rubidium-85/87 ratios in 27, 17: 20211
separation from rhenium by anion exchange, 19: 13220
separation from rocky formations by underground explosions and leaching of fissures, 16: 15013(P)
separation of alkaline earths, rare earths, thorium, and uranium from, by ion exchange, 20: 14469(R) (TID-22650)
separation of argon-40 from, determination of activation energy for use in, 19: 20166
shock-induced transitions in, from Gnome explosion, 19: 281 (PNE-112F(Pt.III))
sorption of cesium, ruthenium, and strontium from waste solutions by, 16: 2801 (ORNL-3189(p.27-42))
sorption of cesium from, 18: 19448(R) (ORNL-TM-757)
sorption of methylene blue by siliceous, tracer and transmittance studies of, 18: 16193 (TID-7689(p.85-6))
sorptive properties for phosphorus-32, 16: 22267 (HW-71583)
sorptive properties for radioisotopes in water, 16: 25035 (HW-69225)
sorptive properties for cesium and strontium, 17: 39270 (UCRL-13074)
sorptive properties for strontium-90 in ground waters, 19: 46602
sorptive properties for cesium, review of selective, 20: 1555
sorptive properties for cesium, 20: 22541(T)
spectra of, effects of temperature on infrared, 17: 33880
strontium isotope content of, bibliography on, 17: 6270(R) (NYO-10325)
strontium–rubidium ages of, from rocks of Kasai basement in Congo, 17: 32269
sulfur isotopic abundances in Australian and New Zealand, 17: 20232
testing for separation of strontium from waste solutions, 17: 26932(R) (ORNL-TM-516)
thermonuclear activities in natural terrestrial, 17: 4716
ultrasonic attenuation in, effects of structure on, 20: 43500(R) (COO-689-60)
uranium content in, delayed-neutron determination of, 20: 27181
uranium distribution in, 20: 16684
x-ray absorption and fluorescence analysis of, instruments for automatic continuous, 20: 37152

MINING

air analysis for radon in uranium mines, 17: 28805
atmospheric radioactivity in uranium, 20: 14747
book: *Safety Problems in Uranium Mines*, 17: 8483
book: *Uranium Mining Chemistry*, 17: 20223
cancer incidence in miners of Colorado Plateau, 19: 4015
cancer mortality attributable to uranium, 18: 20256
cancer mortality in personnel, 18: 33813
caving method using nuclear explosions, 19: 46472 (UCRL-14201)
concentrations of uranium and radium-226 in uranium mine waters, 17: 40912
control of radioactive contaminants found in air of radium and uranium mines, 18: 31812
determination of origin of mine gases by isotopic constitution of carbon and nitrogen, 18: 5530
dust activity measurement in uranium, methods for, 18: 18126
dust analysis for polonium, radium, and uranium in uranium mines, methods for, 18: 41361
dust hazard prevention in nuclear materials, 18: 20270
environmental studies in uranium, 18: 18116
epidemiology of uranium, 18: 18117
equipment and excavations for, on Nevada Test Site, 20: 14754 (NVO-38-1)

equipment for, 18: 4112
evaluation of commercial undersea, 20: 45927
evaluation of nuclear explosions for use in, 16: 5110 (UCRL-6636)
evaluation of, using nuclear explosives, 19: 13565
feasibility of nuclear, 19: 11322 (UCRL-13104)
gamma monitoring in uranium, in Japan, 20: 25284
hazards in coal and uranium, 18: 3609
health and safety in uranium, 18: 18115
health and safety measures in uranium, in France, 19: 9411
health of uranium miners in Yugoslavia, 17: 41167
health regulations for uranium, 18: 18124
health standards and enforcement methods in Australian mines, 17: 41157
hydrogeological studies in, tracer techniques for, 17: 8403
hygiene measures for radioactive ore, 20: 9197
industrial hygiene in rare metal ore mines, 17: 27603(T) (JPRS-19866)
installations for thorium and uranium, in Euratom countries, 19: 29470 (EUR-2271.f)
lead-210 content in bones, hair, and lymph nodes in persons in uranium, 19: 34412
light sources for use in, use of beta-emitting radioisotopes in, 20: 704
lung cancer frequency from fluorspar, 18: 29460
lung cancer incidence in uranium, 19: 44314
lung carcinoma incidence related to fluorspar, 18: 43842
measurement of radon concentrations in uranium mines, 17: 41146
measurements in air in mines, use of alpha sources for, 19: 706
medical considerations for employment of workers in uranium mines, 17: 41166
medical examinations for French uranium miners, 17: 41164
methods for broken rock from nuclear explosions, 18: 33710
methods of, uranium, 19: 46629
methods of, using light from nuclear reactors, 19: 21710
monitoring methods for atmosphere for uranium, 20: 43594(T) (AEC-tr-6763)
monitoring uranium mine for bismuth-214, radon, and uranium, 19: 4416
mortality patterns among uranium miners, 17: 41150
nuclear energy in, 16: 11368(T) (UCRL-Trans-768(L))
nuclear explosion uses in, 19: 9297
nuclear explosion applications in, underground, 20: 33438
nuclear explosion uses for overburden stripping in, 20: 35603 (CONF-660114-1)
nuclear explosion uses for, 20: 36975
nuclear explosion in, evaluation of, 18: 23751 (UCRL-7350)
nuclear explosive applications in, 19: 36588 (UCRL-14197-T)
nuclear explosives in, 19: 13562
nuclear-physical methods in, review, 16: 16043
nuclear-physical methods in, review, 16: 33279(T) (AEC-tr-5404)
operations in the Nevada area, effects of Sedan event on, 17: 19729 (PNE-204F)
personnel protection from radon decay products in, efficiency of polymeric fiber filters for, 18: 4028
pillar strength in heated salt mines, 19: 8675(R) (ORNL-3697(p.19-31))
pillar-model tests in salt mines, 20: 18897 (ORNL-P-2006)
preventive maintenance in, bibliography on, 20: 1976 (VDDIT-94)
procedures used at Los Ratones mine in Spain, 20: 45934
protective measures in French uranium mines, 17: 41143
radiation hazard from radon and dusts in uranium mines, 17: 41148
radiation-hazard measurements in Spanish mines, 17: 41162
radiation hazards in, of uranium, 16: 16592 (AEET/HP/SM-4)
radiation hazards in, of uranium, 17: 20276
radiation hazards in uranium, 17: 27617
radiation hazards in, of thorium, 17: 41145
radiation hazards in, protection from, 18: 4035
radiation hazards in uranium, 18: 18119
radiation hazards in, from sorption of bismuth-214, lead-214, and polonium-218 on walls from turbulent air stream, 18: 41690
radiation hazards to lungs of personnel in uranium mines, 19: 4014
radiation hazards to lungs of personnel in rare metal, 19: 8984
radiation hazards to immunity in workers in uranium, 19: 8985
radiation hazards in uranium, diagnostic tests for external and internal, 19: 8986
radiation hazards to hematopoietic system of workers in uranium, 19: 8987
radiation hazards in uranium, protection from, 19: 11455
radiation hazards from radon in uranium, in South Africa, 19: 11460
radiation hazards in uranium, 19: 24800
radiation hygiene in uranium, 17: 4747
radiation monitoring practices, 16: 3282(T) (JPRS-9706(p.21-7))
radiation monitoring of dust in uranium mines, 17: 41144
radiation monitoring in French uranium mines, 17: 41141
radiation monitoring of dust in Japanese uranium mines, 18: 35800
radiation protection in uranium, 17: 14556
radiation protection measures for uranium, in the Congo, 18: 18120
radiation protection in uranium, in Japan, 19: 9421
radiation protection measures for uranium, in France, 19: 24800
radioactive pollution control in uranium, 20: 31457
radioactivity in Czechoslovakian coal and metal ore mines, natural, 18: 43860
radioactivity measurements of air in uranium, 18: 18127
radioinduced sterility from radium and uranium, 18: 29429
radioisotope uses in, literature survey, 16: 9067(R) (ARF-1194-7)
radiological health and safety in uranium mines in Japan, 17: 41139
radiological health and safety in nuclear materials, conference on, Vienna 1963, 18: 18114
radiological health and safety in, of nuclear materials, 18: 20267
radon and daughters in, measurement of, 18: 20268
radon content in Yugoslav uranium mine, 19: 4414
radon dose measurement methods for uranium, 18: 18125
radon hazards in uranium, removal of, 18: 3769
radon hazards of underground, effects of air overpressures on, 20: 6694(R) (MIT-952-2)
radon hazards of uranium, 20: 43617
radon monitoring in uranium, method for, 20: 27213
safety regulations in uranium mines, 17: 41165
safety review on nuclear materials, 18: 43851
silicosis incidence in personnel in, 16: 33328
stimulation of natural gas reservoirs, Gasbuggy experiment on nuclear, 20: 470 (PNE-1000)
use of nuclear explosives in, 17: 40991
use of nuclear explosives for caving, 18: 35676 (TID-7695(p.371-84))
use of nuclear explosives in, 19: 2474
use of nuclear explosives to break copper ore deposits, 19: 40706 (ORNL-TM-1191)
use of nuclear explosions in, 20: 469(R) (ORNL-TM-1275)
use of nuclear explosives in, 20: 14665
use of underground nuclear explosions for, 19: 4277 (UCRL-7350 (Rev.1))
uses of atomic and chemical explosions in excavations, 17: 27504 (EUR-7.f)
ventilation in uranium, for radon and daughter control, 18: 20269

MINING EQUIPMENT
automation, use of radioisotopes in, 16: 13444(T) (AEC-tr-4492(p.170-2))
control of, use of gamma radiation in automatic, 18: 12516
control of, using isotopes and radiations, 20: 43789
design for measuring thickness of coal seam by radiation scattering, 16: 17859(P)
design for obtaining samples from bore holes, 17: 36018(P)

MINKS
histology of ear of normal and congenitally deaf white, 20: 14214 (BNL-8564)

MINNESOTA
bovine leukemia incidence in, 19: 17406 (CONF-640807-1)
fallout monitoring, 1959, 17: 10352
feldspar and zircon ages in northeastern, 20: 4169
iodine-131 content in cow's milk in, 20: 22556

Minometer
see Radiation Detection Instruments (Ion Current Type)

MINOR (Switzerland)
see Exponential Piles

MIRRORS
see also Magnetic Mirrors
aberrations in large-aperture spherical, correction of, (E), 19: 30382(T) (UCRL-Trans-1219(L))
calibration of rigid solar-collector, 17: 9131
characteristics of solar, summary, 17: 9121
design of turbine-driven, engineering drawings of, 19: 20308
development for stellar x rays, 19: 14224
neutron reflection from magnetized cobalt, polarization from, 17: 32977
neutron reflection from cobalt, 18: 11157
neutron scattering on cobalt, polarization in thermal, 18: 30703
neutron total reflection from metallic, 17: 4033
neutron total reflection by cobalt, (E), 19: 21201(T) (KFK-tr-164)
performance with photovoltaic cells in space, 17: 9125
performance with solar-thermionic cells for space uses, 17: 9126
polarization of thermal neutron beams by magnetized iron-chromium, 17: 18537 (KR-37)
radiation effects on coatings of dielectric, protective effects of nitrobenzene immersion on pulsed laser, 20: 31787
solar energy collection by conic-section, for thermionic cells, 17: 9129
solar energy collection by, for thermionic generators, 17: 9130
use of beryllium, in streak cameras, 18: 29957
uses with observation windows for nuclear reaction chambers, 19: 1831(P)
x-ray beam reflection from surface of, anomalous, (E), 19: 6408

MISCH METAL
analysis for cerium, iron, and lanthanum, x-ray spectral, 20: 25018
determination in cast steels, spectrophotometric, 16: 17602

effects on hot-working properties of electron-beam-melted molybdenum, 20: 23720
effects on properties of cast austenite chromium–nickel steel, 19: 22879(T) (JPRS-28849(p.319-25))
interactions with rare earth chlorides in the presence of oxygen, 16: 5362(T)
mechanical properties of magnesium-containing, at 100 to 300°C, 17: 1920 (BM-RI-6078)
separation from fused-salt baths by electrowinning, 16: 478 (BM-RI-5868)
Mg–misch metal–Zn, plastic anisotropy of ZE10A sheet, 19: 39149 (AD-425880)

MISSILES

see also Crater Missiles
see also Guided Missiles
accelerator for small high-velocity, 18: 25636
aerodynamic heating of, traveling at supersonic velocities through compressible fluid, 19: 35874 (UCRL-7807)
behavior of secondary, in blast waves, 19: 11312(R) (TID-21444)
bibliography on power for, 17: 4349 (AD-273676)
bibliography on power for, 17: 4350 (AD-273677)
bibliography on power for, 17: 4351 (AD-273678)
blast effects on axisymmetric supersonic, transient base pressure study of, (E/T), 19: 36574 (SC-TM-65-218)
containment, from runaway reactors, 16: 12844
containment of, from runaway reactors, 18: 9565 (SRIA-43)
design of, for study of dynamic behavior of surface of liquids during weightlessness, 18: 5855
detection by tracking stations near trajectories, (E), 19: 21767 (SC-TN-65-44)
determining heating of, problems pertaining to aerodynamic, 17: 8371
effects of, from nuclear explosions, traumatic, 20: 2083 (CEX-65.4)
flight through blast wave, axi-symmetric base pressure analysis of, 17: 32730 (TID-19116)
flight through blast wave, transient base pressure study of axi-symmetric supersonic, 19: 8008 (SC-DC-64-1595)
flight through blast wave, transient base pressure from, 20: 9850
impact of cylindrical, effects on ground, 18: 25001(R) (SC-DC-64-459)
interactions with electromagnetic fields in atmosphere, (T), 20: 4730 (SC-DC-65-1797)
materials development for, powder metallurgy techniques in, 17: 1864
nose tips for, shear-spinning process for fabricating molybdenum, 20: 25508 (AD-631423)
penetration of particulate material, 20: 45240 (SC-RR-66-376)
penetrative effects on steel plates in runaway reactor, 18: 3042 (SRIA-113)
performance, 20: 27072
power supply for, design of simplified radioactive, 17: 28578(P)
production of secondary, by blast waves in Plumbbob, 18: 1836 (WT-1468)
radiation effects on firing circuits of, transient-gamma, 18: 29926(R) (NAVWEPS-8177)
radiofrequency blackout on re-entry of atmosphere, 16: 28620 (NP-11924)
radiography using linear electron accelerator, 17: 18287
recovery systems for payloads of Hawk sounding rockets, 20: 8491 (SC-RR-65-470)
response to impulsive mechanical and thermal loadings, (T), 20: 24683
safety on test ranges for, diffusion studies for, 18: 14578 (HW-78435 (Vol.I))
scoring system for, using radiation sources, 20: 39190(P)
testing of, conference on nondestructive, 17: 34114
tracking at low altitudes, using gamma rays, 19: 15848
trajectories of blast-induced structural fragments, 19: 9402 (AD-422319)
trajectories of structural fragments produced by nuclear weapons, analysis, 20: 3610 (AD-622333)
trauma induced by blast-energized debris, 17: 18320(R) (DASA-1341)
velocity, displacement, and acceleration with time of blast-energized debris, 17: 17622(R) (DASA-1336)
vibration data, system for airborne analysis, 16: 7688 (SCTM-230-61(81))
vibrations in, analysis of nonstationary, 18: 4910 (SC-DC-2049)
water entry impact shock on blunt-nosed, 18: 45188 (SC-TM-64-987)

MISSISSIPPI

(See also headings of the form Mississippi (Lamar Co.))
crustal structure in southern, seismic measurements for determining, 20: 36965
radiation protection in, program for, 20: 14807
radiation protection program in, 20: 45980
x-ray equipment evaluation in, 18: 22303

MISSISSIPPI (LAMAR CO.)

environs monitoring for Salmon Event, 20: 16743 (VUF-1021)

MISSISSIPPI RIVER VALLEY

lead and sulfur isotopic abundances in galenas, 16: 29195

MISSOURI

see also St. Louis
fallout monitoring at Kansas City, 1962, 20: 5648(R) (COO-1340-2, pp 1-53)
fallout monitoring, 1963, 20: 5649(R) (COO-1340-2, pp 54-83)
lead isotope ratios in galenas of, 20: 45882
seismic data from BILLIKEN calibration explosion in southeast, 19: 20171 (AFCRL-64-659)

MIT RESEARCH REACTOR

design and use, 17: 10141
development, 19: 42007 (MIT-2344-3)
development of in-pile loop for, 16: 30147(R) (TID-15978)
equipment for transferring irradiated solutions from, pneumatic, 19: 21741
experimental facilities, 16: 6903 (NYO-9658)
fast neutron dosimetry in, using calorimeter and threshold detectors, 20: 20723(R) (MIT-334-33)
neutron leakage in, spectra of, 18: 19439
neutron spectrum, thermal, 16: 3960
operating costs, 16: 24491
process system requirements and hazard analysis for 5-Mw operation, 18: 1301 (MIT-NE-23)
safety of, technical specifications for, 20: 24792 (MITNE-62)

Mites

see Arachnids

Miticides

see Insecticides

MITOCHONDRIA

association of alkali metal and alkaline earth cations with, in dog kidney cells, 20: 35224
barium content in rat kidney, effects of vitamin D on, 20: 8559
calcium content in rat kidney, effects of vitamin D on, 20: 8559
calcium uptake by rat liner, 19: 14971 (p.95-7))
calcium uptake by, in liver and kidney of rats, 17: 35303(R) (HW-76000
calcium-45 content in shell gland mucosa cells, 20: 40551
carcinogenicity, photodynamic effects of polycyclic hydrocarbons on, 16: 17361(R) (TID-14387)
catalase activity in mouse tumor cell, 18: 38758
catheptic activity in beef heart, effects of TRITON-X-100 and x rays, 16: 1466(R) (TID-13639)
cerium-144 metabolism in liver, effects of DTPA on, 19: 21822
cholesterol and sodium octanoate oxidation by rat liver, effects of water-d_2 on, 20: 18217
contraction and swelling of rat liver, effect of strontium on, 19: 43688
desoxyribonucleic acid occurrence and properties in, in *Neurospora crassa*, 18: 43209
DNA content in Tetrahymena, tracer study, 19: 31675(R) (ORNL-3768 (p.70-84))
effects of cytochrome C on oxidative phosphorylation in, isolated from spleen of irradiated animals, 20: 45500
effects of disulfides and thiols on, biochemical, 20: 18453
effects of fatty acid extracted from liver of irradiated rats on, 17: 30327
effects of steroids in the presence of light on, 17: 7798(R) (TID-17544)
effects on manganese distribution in tissues, 18: 21763 (BNL-7940)
effects on radiosensitivity of mammary tumor cells in mice, 17: 27135
electron microscopy of, sample preparation for, 19: 10699 (TID-20374)
electrophoresis of mouse liver, 19: 10698 (TID-20372)
energy-coupling in rat liver, tracer study using calcium-45 and strontium-85, 19: 25846
enzyme activity and electron transport system, 16: 2872 (TID-14283)
fatty acid content of rat, effects of lipid content in diet on, 18: 11642(R) (NP-13583)
formation of, in lymphocytes in culture, 19: 25824 (ORNL-P-67)
function in mouse skin, effects of chemical carcinogens on, 17: 40638
functional tests in Amphiuma liver, 20: 8573
identification of unit of, by electron microscopy, 16: 8538(R) (TID-14201)
iron metabolism in rat liver, 19: 21820(R) (UCLA-12-541(p.25-44))
luminescence of, from biochemical reactions, 20: 36547
magnesium content in rat kidney, effects of vitamin D on, 20: 8559
metabolic processes in rat liver, effects of cystamine and cysteamine in, 19: 35907
metabolism of calcium and strontium by, tracer study, 17: 1225
metabolism of cations in, 19: 31725
metabolism of proteins of, in rat tissues, 19: 6942(R) (ANL-6906(p.93-100))
metabolism, radioisotopic studies, 16: 1407
morphology and nature of inclusions, 16: 28670(R) (UCLA-507)
morphology and oxidative phosphorylation of kidney and liver, in mice injected with irradiated serum, 18: 11612
morphology and physiology, 17: 13986(R) (UCLA-510)
oxidative phosphorylation after freezing and vacuum drying, 16: 1467(R) (TID-14093)

oxidative phosphorylation by corn seedlings root and shoot, temperature effects on, 19: 6920
oxygen metabolism in rat, effects of cystamine on, 19: 45777
performance and structure in liver, effects of fatty metamorphosis, 16: 8466(T) (AEC-tr-4628)
phosphate metabolism by, 17: 33466(R) (ANL-6723(p.174-7))
phosphohistidine labeling in, rate of phosphorus-32, 18: 31114
phospholipid synthesis in liver, effect of oxidative phosphorylation inhibitors, 17: 23002
phosphorus-32 effects on, in lymphocytes in lymph nodes, spleen, and thymus in rabbits, 16: 4050
properties in radiosensitive tumor cells, 16: 26753
protective effects against radiation damage in glutamic dehydrogenase, 16: 23456
protein synthesis in isolated glycerinated, 20: 22613(R) (NIRS-4, pp 21-8)
radiation effects on permeability, 16: 1556
radiation effects on phosphorylation and red spectrum photomorphogenesis, 16: 1583
radiation effects, in bone marrow cells in rats, 16: 4097
radiation effects of lethal and compatible doses of x radiation, 16: 4104
radiation effects of red and far-red light on phosphorylative activity, 18: 41160
radiation effects on liver, 16: 8602
radiation effects on liver, 16: 11450(R) (ANL-6464(p.114-15))
radiation effects on oxidative phosphorylation, 16: 17450(T)
radiation effects on enzyme systems in mouse, *in vitro*, 16: 17485
radiation effects on enzyme activity, 16: 28749(R) (TID-16446)
radiation effects on enzyme activity, 16: 28750(R) (TID-16447)
radiation effects on oxidative phosphorylation uncoupling in rabbit and rat tissues, whole-body gamma and x, 16: 28774
radiation effects on cerebral, 16: 28805
radiation effects on respiration and phosphorylation in isolated, from radiosensitive organs, 17: 1246
radiation effects on lipid composition in rat liver, 17: 5772 (TID-13322)
radiation effects on oxidative phosphorylation in isolated liver, in rats, 17: 5784
radiation effects on lipid levels in liver, , 17: 12125 (TID-15755)
radiation effects on oxidative phosphorylation in, effects of dinitrophenol on, 17: 12137
radiation effects on oxidative phosphorylation in liver, whole-body exposure, 17: 15570
radiation effects on oxidative phosphorylation of, in kidney and liver in rats, 17: 17890
radiation effects on stability of cytochrome c and lipids in thymus, in animals, 17: 23111
radiation effects on activity of adenosinetriphosphatase and cathepsin C in, 17: 24925
radiation effects on phospholipids in, in rat liver, 17: 28705
radiation effects on phospholipid content of liver, whole-body exposure, 17: 28681(R) (TID-18980)
radiation effects on ultraviolet fluorescence of, x, 17: 37093
radiation effects on rat zona fasciculata, x, 17: 38774
radiation effects on rat liver, x, 17: 38775
radiation effects on KB tumor cell, x, 17: 38817
radiation effects on lipids in, of rat liver, 17: 38744(R) (TID-19410)
radiation effects on function of, in mouse skin, 17: 40638
radiation effects on rat liver cell, x, 17: 40582
radiation effects on mouse liver, x, 18: 1429
radiation effects on ATPase activity in mouse tumor, x, 18: 3534
radiation effects on desoxyribonuclease activity of, from liver and spleen of rats, 18: 8124(T) (JPRS-22613(Del.)(p.12-28))
radiation effects on phosphate esterification and hydrolysis in rat spleen, 18: 8176
radiation effects on formation of lipid oxidation products in rat liver, 18: 9892
radiation effects on rat liver, electron microscopy of, 18: 9895
radiation effects, 18: 11811
radiation effects on enzyme activity of beef heart, 18: 13451(R) (TID-20207)
radiation effects on enzyme activity and phosphate metabolism in rat spleen, 18: 17467(R) (ANL-6790(p.145-9))
radiation effects on membranes of, isolated from rat liver, 18: 17570
radiation effects on rat liver, x, 18: 17602
radiation effects on L-cell, x, 18: 19783
radiation effects on oxidative phosphorylation in rat liver, x, 18: 23233(R) (ANL-6823(p.157-60))
radiation effects on oxidative phosphorylation in, protective effects of cysteamine and AET against, 18: 27227
radiation effects on oxidative phosphorylation in, 18: 27147
radiation effects on phosphate metabolism in, ultraviolet, 18: 29222
radiation effects on contraction of glycerinated, gamma, 18: 33270(R) (NIRS-2(p.23-6))
radiation effects on inclusions in chicken heart and liver, x, 18: 36974
radiation effects on respiratory control and adenosinetriphosphatase activity of liver, x, 18: 36958(T) (JPRS-25741(p.87-94))
radiation effects on enzymes in rat kidney and liver, 18: 38839
radiation effects on respiration in, of rat liver, 18: 38858
radiation effects on metabolism of, in nervous system of mammals, 18: 38952
radiation effects on oxidative phosphorylation in, of rat liver cells, 19: 7016(R) (ANL-6906(p.110-12))
radiation effects on human skin, beta and x, 19: 8902
radiation effects on oxidative phosphorylation in rats, protective effects of cytochrome C against, 19: 8935
radiation effects on enzyme release from, x, 19: 8818
radiation effects function and structure of mouse liver, whole-body, 19: 10863
radiation effects on rat liver, x, 19: 15193
radiation effects on enzymes activity in rabbit, 19: 15216
radiation effects on rat liver, x, 19: 15098
radiation effects on oxidative phosphorylation processes in rat liver, whole-body, 19: 17627
radiation effects on oxidative phosphorylation in rat liver, effects of insulin and other compounds on, 19: 17669
radiation effects on oxidative phosphorylation in rat, protective effects of polyanions and spleen extracts against, 19: 17673
radiation effects on activity of ATPase in rat heart, liver, and spleen, 19: 21869
radiation effects on function and structure of, in mouse liver, 19: 26033
radiation effects on mouse, cytological x, 19: 26154
radiation effects on distribution, morphology, or number in rat cells, 19: 35951 (UR-666)
radiation effects on function and structure of, in mouse liver, 19: 38424
radiation effects on content in rat liver, x, 19: 42262
radiation effects on chick embryo, protective effects of cysteamine against x, 19: 42357
radiation effects on enzymes in beef heart muscle, x, 20: 63(R) (STI/DOC/10/42, pp 45-55)
radiation effects on lipids of, isolated from rabbit liver, y, 20: 5379
radiation effects on contractive ability of, 20: 10678
radiation effects on mouse spleen, x, 20: 12681
radiation effects on phospholipids in rabbit liver, y, 20: 14278
radiation effects on dehydrogenase activity in rat liver, y, 20: 14284
radiation effects on enzyme activity in, from rat liver, spleen, and thymus, x, 20: 14376
radiation effects on ultrastructure of, 20: 14335
radiation effects on $NADH_2$ oxidation in suspensions of cattle heart, x, 20: 20496
radiation effects on metabolism in, of dog brain, x, 20: 6817
radiation effects on enzyme activity in fruit, 20: 9339 (CONF-651024, pp 115-16)
radiation effects on enzyme activity in mouse liver, effects of starvation on, 20: 8612
radiation effects on mouse brain, proton, 20: 22710
radiation effects on cytochrome c content of, x, 20: 22586
radiation effects on enzyme activity in, y, 20: 22613(R) (NIRS-4, pp 21-8)
radiation effects on chicken heart myoblast, x, 20: 24936
radiation effects on rat liver, y, 20: 26656(R) (NYO-3361-6)
radiation effects on RNA content in rat liver, 20: 26642
radiation effects on rat liver, x, 20: 26675
radiation effects on uncoupling of oxidation and phosphorylation in, of green plants, x, 20: 28947(T)
radiation effects on guinea pig, x, 20: 28976
radiation effects on content in pear tissues, y, 20: 31633
radiation effects on, in duodenal crypt epithelium of mice, x, 20: 33007
radiation effects on oxidative phosphorylation in chicken embryo, x, 20: 33042
radiation effects on rat liver, biochemical and morphological, x, 20: 38639
radiation effects on number in lutein cells of rat ovary, x, 20: 40672
radiation effects on adensosine triphosphatase activity in rat liver, x, 20: 40695
radiation effects on ribonucleoproteins of, gamma and x, 20: 42866
radiation effects on uptake of heat-killed sulfur-35-labeled mycobacterial vaccines by rat spleen, x, 20: 42907
radiation effects on phosphorylative capacity of rat liver, x, 20: 45430
radioinduced autolytic decomposition of proteins in rat liver, x, 20: 45339
radioinduced changes in size and form of, in irradiated bone sarcoma cells, 17: 30367
radioinduced changes in, x, 20: 5301(R) (UR-668, pp 1-54)
radioinduced decrease of phosphorus/oxygen ratio in rabbit, by acetone fraction of liver lipids, 20: 42825
radioinduced effects on permeability of membrane of, in nerves and

connective tissue, 17: 30368
radioinduced effects on oxidative phosphorylation and optical density of, in rat liver, x, 17: 30354
radioinduced inactivation of enzymes from, gamma, 19: 10881
radioinduced lesions in rat thymus, electron transfer chain, 18: 17503
radioinduced swelling and degeneration in retinal cells of rabbit, x, 20: 42958
radiosensitivity of oxidation-reduction reactions, 16: 6299(T) (JPRS-11322(p.142-61))
radiosensitivity of rat liver, 16: 32797
radiosensitivity of enzymes in, in rat liver, 17: 7853
radiosensitivity of enzyme systems in thymus, 17: 27086
radiosensitivity of visual receptors in, uv, 18: 11776
radiosensitivity of, in Paramecium, ultraviolet, 18: 31241
radiosensitivity of rat tumor, effects of AET and MEA on, 19: 7181
radiosensitivity of oxidative phosphorylation in rat liver, effects of hormones on, 19: 13118
respiration in, 18: 35265(R) (UCLA-12-529(p.23-40))
respiration in rat, effects of AET on, 20: 20505
respiration in rat liver and spleen, effects of cystamine on, 20: 30984
respiration of rat liver, effects of β-hydroxybutyrate, metal ions, and succinate on, 19: 14972
role in radioisotope accumulation by higher animals, 20: 16160 (UCRL-14739(Pt.2))
strontium cation uptake by rat liver, 20: 24842
strontium content in rat kidney, effects of vitamin D on, 20: 8559
strontium uptake by rat liver, mechanism and requirements of, 19: 14970
strontium uptake by, in kidney and liver of rats, 17: 35303(R) (HW-76000(p.95-7))
strontium uptake by rat liver, 19: 14971
strontium uptake by rat liver, effects of β-hydroxybutyrate, metal ions, and succinate on, 19: 14972
structural changes in lymphocytes in radiation injuries, 16: 30302
swelling properties of mouse liver and tumor, 19: 35881
synthesis of proteins by hepatic and kidney, tracer study, 20: 5254
toxic effects of rare earths on adenosine triphosphate metabolism in, 17: 13928
ultraviolet effects on enzyme activity in liver, 17: 30313
vacuolization in thymic cell, in mice suffering from radioinduced leukemia or thymic lymphoma, 20: 42882
zinc content in rat kidney, effects of vitamin D on, 20: 8559

MITOMYCINS

effect on damage induced by alkylating agents, 20: 40664
effect on radiotherapy of thymic and splenic tumors in mice, 20: 31131
effects of mitomycin C combined with gamma radiation on cancer, bone marrow transplants for hematopoietic injuries from, 20: 40726
effects on antibody synthesis in spleen cells, 16: 28784
effects on chromosomal DNA in human cells as related to mutagenicity, 19: 33829
effects on DNA priming activity, 18: 43169(R) (AD-439063)
effects on Drosophila, mutagenic, 19: 28011
effects on *E. coli* mitosis, 19: 31790(R) (ORNL-3768(p.85-8))
effects on *E. coli* and relationship to thymineless death, 20: 45341
effects on enzyme susceptibility of DNA, 19: 12980
effects on frequency of chromosome aberrations radioinduced in *Trillium kamtschaticum*, 18: 8198
effects on genetic properties of mouse strain L cells, 19: 12996
effects on growth of L cells in tissue culture, synergistic effects of gamma radiation, 19: 13033
effects on radiation damage in cultured mouse fibroblasts, 19: 46018
effects on radioinduced chromosome aberrations in plant cells, 20: 71
effects on RNA synthesis in derivatives of *E. coli*, 19: 38381
effects on tumor-bearing mice, effects of radioprotective drugs on, 20: 12719(R) (NP-15668)
effects on uptake of zinc-65 by Ehrlich ascites cells *in vitro*, 20: 42775
effects on yeasts, genetic, 20: 8663
isolation of tritium labeled, 18: 43169(R) (AD-439063)
radiation effects combined with, on HeLa cells, 16: 14527
radiosensitivity effects on leukopenia in rabbits, 20: 29055

MITOSIS

see also Chromosomes
see also Genetics
see also Meiosis
activity in mouse tissue cultures, effects of x-irradiated feeder layers on, 20: 12654
biological model, 16: 25135(R) (HW-72500(p.104-8))
chromosome differentiation during, 19: 36096
cycle in *Pisum* root meristem cells, use of colchicine and tritiated thymidine for measuring, 19: 14979
cytology of Paramecium, 18: 23163(R) (ANL-6823(p.178-88))
deuterium effects on hydrostatic pressure sensitivity in sea urchin, 19: 27929
effects of AET on, in rat bone marrow, 20: 143
effects of agmatine on, in irradiated cell cultures, 16: 26799
effects of calcium on, in irradiated cell cultures, 16: 26800
effects of cell cycle of, on radiosensitivity of, 18: 29355
effects of chemicals on, in hepatomas in rats, 16: 14560
effects of chemotherapeutic agent on HeLa and L cell, 18: 43306
effects of chloramphenicol on *E. coli*, 20: 40630(R) (ORNL-3922, pp 106-8)
effects of colchicine on Pisum, 18: 13413 (BNL-7317)
effects of Decortilen on, in HeLa cells in culture, 20: 14375
effects of deuterium oxide on, in sea urchin eggs, effects of pressure and temperature on, 20: 32917
effects of ethyl methanesulfonate on pea, 20: 24890
effects of ethylenimine and ethyl methanesulfonate on, in peas, 20: 36621
effects of gold-198 on, in Yoshida ascites tumors in rats, 19: 13045
effects of growth on gamma-irradiated culture media on human leukocyte, 20: 45331
effects of growth-regulators on plant, 19: 10730
effects of heavy water on, in onion roots, 19: 21924
effects of hormones and cytolytic factors on, in irradiated organisms, 16: 30278
effects of irradiated liver transplants on rat, 20: 6704
effects of magnetic field on, in cells in tissue culture, 18: 19495(T) (UCRL-Trans-1027(L))
effects of MEA on, in tumor cells, 20: 12680
effects of mitomycin C on *E. coli*, 19: 31790(R) (ORNL-3768(p.85-8))
effects of mitomycin on mitotic recombination in yeast, 20: 8663
effects of myleran and TEM on, in rat lens epithelium, 20: 16256
effects of photoperiodism on mouse cartilage, 19: 1992
effects of protein and RNA synthesis on plant cell control of, 18: 23124 (BNL-805(p.59-72))
effects of RNA-synthesis inhibitors on root cell, 20: 6776(R) (ORNL-3853, pp 50-3)
effects of stage of, on radiosensitivity of cells in tissue culture, 18: 41181
effects of stage of, on radiosensitivity of cells, 20: 16292
effects of tritium oxide on, in chick embryo skeletal muscle tissue, 16: 31480
effects of variability of, on cell multiplication, 18: 26982(R) (NYO-2462-1)
effects of water-d_2 on, 20: 3651
effects of water-d_2 on, in *Tetrahymena pyriformis*, 20: 8532
effects of 2-aminopurine and 5-bromouracil alone or in combination with x rays on, in barley and onion roots, 20: 45400
effects on desoxyribonucleic acid metabolism in human blood cells during leukemia, tracer study, 20: 20 (EUR-2451.e)
effects on liver cells, relation between death and division after irradiation, 16: 9861
effects on nucleic acid synthesis in mammalian cells in culture, 20: 18204(R) (LA-3432, pp 130-77)
effects on protein synthesis in mammalian cells in culture, 20: 18204(R) (LA-3432, pp 130-77)
effects on radiosensitivity of cells, tracer study, 17: 1286
effects on radiosensitivity of chromosomes in pea seedlings, 18: 35308 (BNL-7316)
effects on radiosensitivity of the insect *Rhodnius prolixus*, 19: 94
effects on radiosensitivity of animal cells, 19: 43790
effects on radiosensitivity of chromosomes in leukocytes in tissue culture, 20: 88
electron microscopy study of, in *Pelomyxa illinoisensis*, 17: 35335 (TID-17851)
frequency in hamster cells after pulse-labeling with thymidine, 20: 40686
frequency in tumors, correlation with growth rate, 20: 43033
genetic information transfer during, role of histones in, 18: 43156(R) (LA-3132-MS(p.218-23))
hamster-cell, effects of oxygen tension on, 19: 26153
in bone marrow cells of mice, autoradiographic studies of, 17: 35422
in bone marrow cells, 18: 19509
in duodenal crypt cells of germ-free mice, tracer study, 19: 2031
in germinating seeds in *Zea mays*, 17: 35272 (BNL-6547)
in irradiated bone marrow, stimulation by cell-free spleen extract, 16: 6358
in mammalian cells in culture, synchronization of, 19: 17454 (LA-DC-6384)
in root meristem cells, effects of sucrose content on, 19: 6946 (BNL-7725)
in sea urchin eggs, effects of deuterium oxide and hydrostatic pressure on, 19: 35996
in sperm of mealy bug, 18: 65
in synchronized cultures of mammalian cells, actinomycin effects on role of nucleic acid synthesis in, 18: 43155(R) (LA-3132-MS(p.208-12))
in transferred lymphoid cells, relation to antibody production, 17: 38808
in tumor cells, effects on radiosensitivity, 18: 8152

induced in mouse skin, effects of strain on, 17: 28755
inhibition by irradiated media, 16: 20204
inhibition, effects of irradiation, 16: 6326
inhibition in RCP cell strain by nitrogen mustard, 20: 5323
inhibition induced in *Vicia faba* roots by triethylenemelamine and x radiation, 16: 30251
luminescence production in, 20: 36547
metabolism of DNA during, in hamster cells, tracer study of, 20: 6775(R) (ORNL-3853, pp 36-49)
nuclear protein migration during, 18: 1354
nucleoprotein turnover during, tracer study, 18: 19518 (BNL-7007)
of blast cells from rabbits cultured in irradiated mice, 19: 7098
of hamster cells in culture, electron microscopic studies of chromosomes during metaphase, 18: 25008 (TID-19032)
phases in transplanted Yoshida sarcomas, effects of fatty acid extracts from irradiated rabbits on, 16: 25228
photosynthetic activity during Euglena, 18: 21721 (TID-18753)
protein synthesis in tumor cells during, tracer study of, 17: 33472(R) (ANL-6723(p.203-4))
radiation effects on activity of cell population at exponential growth stage, 16: 1487(T) (JPRS-10170(p.313-34))
radiation effects on time of division in Yoshida sarcoma cells, 16: 4078
radiation effects on nucleolus of grasshopper embryo, ultraviolet, 16: 1622
radiation effects combined with prednisolone on, in MTK sarcomas, 16: 8603
radiation effects combined with maleic acid on, in MTK sarcomas in mice, 16: 8604
radiation effects in carcinoma and onion root cells, protection effects of synkavite on, 16: 14555
radiation effects combined with igrocin on, in rat sarcomas, 16: 14556
radiation effects combined with citric acid on, in rat sarcoma, 16: 14557
radiation effects and effects of cystamine, of corneal epithelium and of duodenal crypts, 16: 21940
radiation effects, energy dependence of, 16: 20212
radiation effects on, in Yoshida ascites sarcomas in rats, 16: 25220
radiation effects, 16: 26760
radiation effects, 16: 26761
radiation effects, 16: 26763
radiation effects in cestodes, 16: 26791
radiation effects on phosphate metabolism during, 16: 30276
radiation effects, 16: 30278
radiation effects on, in leaves, 16: 30279
radiation effects combined with the sodium salt of arsphenamine on, in MTK sarcomas, 16: 8594
radiation effects on, of kidney cells cultured *in vivo*, 17: 21501
radiation effects on, induced in guinea pig skin by chrysarolin, erucic acid, and estrogen, 17: 21502
radiation effects on activity of, in rat lens epithelium, 17: 21485
radiation effects in HeLa cells in culture, 17: 21493
radiation effects in root meristems, genetic, 17: 23146
radiation effects on stimulating activity of, in blood serum in hepatectomized rats, 17: 24922
radiation effects, 17: 27108
radiation effects on, gamma, 17: 28766
radiation effects on activity in male mice, whole-body, 17: 30335
radiation effects on shielded cornea in mice, indirect, 17: 30392
radiation effects on daily periodicity of, in corneas of mice, 17: 30403
radiation effects on, 17: 31935
radiation effects on, in duodenal crypt cells, 17: 33735
radiation effects on, in grasshopper neuroblasts, x, 17: 33729
radiation effects on rate of, in mouse corneal epithelium, 17: 35459(T) (JPRS-20735)
radiation effects on, in rat lens epithelium, x, 17: 35497
radiation effects on transplanted antibody-containing cell, x, 17: 35519
radiation effects on human amnion cell, gamma, 17: 35574
radiation effects on, in mammalian cells in tissue culture, 17: 37079
radiation effects on, in tumor cells, 17: 38834
radiation effects on, in rat bone marrow, protective effects of *N*-phenyl-2-thiophenecarboxamidine against, x, 17: 38889
radiation effects on synthesis of desoxyribonucleic acid during, in *Physarum polycephalum*, 17: 57
radiation effects on duration in mouse epidermis, tracer study, 17: 59
radiation effects in bone marrow, 17: 1290
radiation effects on rate in animal cells, 17: 2831 (TID-17198)
radiation effects, 17: 5876
radiation effects on metaphase/prophase ratio in man and mice, 17: 10411
radiation effects on, in rat skin, 17: 15694
radiation effects on, in crystalline lens in rabbits, 17: 15818(T)
radiation effects on maize root meristem, x, 18: 5016
radiation effects on F_1 pepper, x, 18: 5040
radiation effects on human, beta, 18: 5193
radiation effects on sunflower, gamma, 18: 6678
radiation effects on, in Ehrlich ascites tumor cells, 18: 8182
radiation effects on, in corneal epithelium in mice, 18: 8142(T)
radiation effects on, in mice in contact irradiation after pretreatment with carcinogen and tumor enhancer, 18: 8186
radiation effects on, in sea urchin eggs, 18: 9835 (UCRL-10979)
radiation effects on, in HeLa tumor cells, 18: 9898
radiation effects on fibroblast, x, 18: 11723
radiation effects on chromosome and nucleoli ultrastructure in rat, x, 18: 11772
radiation effects on, in Ehrlich ascites tumor cells, 18: 11800
radiation effects on *Pisum sativum* root meristem, x, 18: 13531
radiation effects on, in cells of rat small intestine of rats, 18: 17462(R) (ANL-6790(p.8-10))
radiation effects on, in rat liver cells, 18: 17583
radiation effects on HeLa cell, x, 18: 17599
radiation effects on corneal, in mice, partial and whole-body exposure, 18: 17629
radiation effects on, protective effects of Synkavite against, x, 18: 17687
radiation effects on mouse, gamma, 18: 19609(T)
radiation effects on mouse, gamma, 18: 19610(T)
radiation effects on, in epidermal hyperplasia in mice, 18: 19704
radiation effects on frog, x, 18: 19781(T)
radiation effects on, in cornea and intestinal epithelia, 18: 19689
radiation effects on root meristem, x, 18: 21806 (BNL-805(p.46-58))
radiation effects on bean seed, gamma, 18: 23252(T) (ORNL-tr-84)
radiation effects on *Aedes aegypti*, x, 18: 23262
radiation effects on mouse kidney, x, 18: 23291
radiation effects on rat, x, 18: 25101
radiation effects on onion root, x, 18: 29399
radiation effects on, in root tips, 18: 29237 (BNL-8004)
radiation effects on *E. coli*, x, 18: 29252
radiation effects on, 18: 29307
radiation effects on, in cells in tissue culture, 18: 31154
radiation effects on pea root, x, 18: 31222
radiation effects on telophase of, microbeams, 18: 33271(R) (NIRS-2(p.26-31))
radiation effects on, in antigen-injected mice, x, 18: 36986
radiation effects on somatic, moderate-dose, 18: 38796
radiation effects on, in corneal epithelium, 18: 38948
radiation effects on, in bone marrow cells, 18: 38949
radiation effects on, in bone marrow cells of mice, effects of vibration on, 18: 41182
radiation effects on, in *Chlamydomonas reinhardi*, 18: 41074 (COO-1117-9)
radiation effects on mouse embryo, strontium-90, 18: 41096
radiation effects on, in thymocytes in tissue culture, effects of media salinity on, 18: 41109
radiation effects on *Protemnodon bicolor*, 18: 41120
radiation effects on mammalian, fast-neutrons, 18: 41229
radiation effects on duration of, in mouse corneal epithelium, 18: 41165
radiation effects on, in Chlamydomonas, 18: 43217 (COO-1117-6)
radiation effects on HeLa and L cell, x, 18: 43306
radiation effects on rat liver, whole-body, 19: 82
radiation effects on, in soybeans, 19: 96
radiation effects on Tradescantia, beta, 19: 2117
radiation effects on human fibroblast, gamma, 19: 3962
radiation effects on daily rhythm of, in root tips of *Vicia faba*, 19: 8878
radiation effects on mouse adrenal cortex, comparison of detoxified snake venom effects with, 19: 8814
radiation effects on duration of, in corneal epithelium in fasting rats, 19: 8832(T)
radiation effects on, in *Helianthus annuus* and *Vicia faba* root tips, 19: 8839
radiation effects on, in monkey kidney cells, 19: 8841
radiation effects on mouse corneal, x, 19: 10813
radiation effects on disassembly of organelles in, microbeam, 19: 10896
radiation effects on cells in, uv, 19: 10787(R) (TID-21581)
radiation effects on *E. coli*, effects of pantoyl lactone on, uv, 19: 10836
radiation effects on rate of, in animal cells in tissue culture, 19: 13073
radiation effects on, in plant cells, 19: 15012 (BNL-7898)
radiation effects on Eranthis, recovery from x, 19: 15145
radiation effects on yeast, effects on lifespan of inhibitory uv, 19: 15169
radiation effects on, in rat bone marrow, 19: 15190
radiation effects on, in cornea of *Axaloti* and *Triton punctatus* larvae, 19: 15044
radiation effects of spleen exposure on, in rabbits, 19: 15056
radiation effects on frequency of multipolar anaphases in KB human cell, 19: 15074
radiation effects on pollen-tube, in flowers, 19: 17525
radiation effects on production of dihaploid plants in *Solanum tuberosum*, 19: 17657

radiation effects on, in regenerating rat liver cells, 19: 19510(T) (JPRS-29250(p.27-32))
radiation effects on suppression of, in cytoplasmic structures and nucleus of *Tradescantia paludosa*, 19: 19579
radiation effects on, in animal cells, 19: 19613
radiation effects on, in animal cells, 19: 19614
radiation effects on, in microorganisms, 19: 21856 (COO-878-15)
radiation effects on, in onion roots, 19: 21924
radiation effects on, in regenerating rat liver, 19: 21892
radiation effects on Tradescantia, aberrant gamma and x, 19: 24328
radiation effects on *Vicia faba*, x, 19: 24336
radiation effects on HeLa cell, x, 19: 26069
radiation effects on Chinese hamster and L-cell, x, 19: 25961
radiation effects on trypsinated HeLa cell, x, 19: 25960
radiation effects on mouse bone marrow, gamma and proton, 19: 28083
radiation effects on human leukocyte, beta, 19: 27993
radiation effects on human kidney cell, tracer study of x, 19: 28001
radiation effects on, in animal cells, 19: 29917
radiation effects on mouse bone marrow, gamma, 19: 29922(T)
radiation effects on mouse marrow, x, 19: 29936
radiation effects on, in tissue cultures, 19: 29968
radiation effects on wheat, effects of gibberellic acid on gamma, 19: 31795(R) (ORNL-3768(p.181-6))
radiation effects on, in *Vicia faba*, 19: 31878
radiation effects on, in *Perophora viridis*, 19: 33939
radiation effects on diurnal rhythym of, in mouse corneal epithelium, 19: 33825(T)
radiation effects on, in gonocytes in testes of rats, 19: 38369
radiation effects on duration in mouse embryos, gamma, 19: 38405
radiation effects on Tradescantia, synergistic infrared and x, 19: 38416
radiation effects on Planaria, dose effects on regenerating capacity in, 19: 40366
radiation effects on Trillium, x, 19: 42291
radiation effects on, in animal cells, 19: 43758
radiation effects on, in brain of rat embryos, 19: 43768
radiation effects on, in bone marrow cells in mice, tracer study, 19: 43792
radiation effects on Tribulus root, y, 19: 43855
radiation effects on rat bone marrow, integral dose effects on, 19: 43733
radiation effects on, in proliferating cellular systems, 19: 45923
radiation effects on, in intestinal cells of rats, 19: 45926
radiation effects on, in animal cells in tissue culture, 19: 45867
radiation effects on, in rat liver cells, 20: 95
radiation effects on, in animal cells in tissue culture, x, 20: 1617(R) (NP-15149)
radiation effects on, in L-strain cells, uv, 20: 1625
radiation effects on, in animal cells, 20: 3764
radiation effects on, in plant cells, 20: 3764
radiation effects on rate in mouse cornea of, effects of ganglionic blocking drugs and head shielding on, 20: 5421
radiation effects on Chilomonas, photoreactivation of uv, 20: 6823
radiation effects on in cultured cells, uv and x, 20: 8666
radiation effects on, in HeLa cells in culture, 20: 14375
radiation effects on animal, x, 20: 14397
radiation effects on, low-dose, 20: 16160 (UCRL-14739(Pt.2))
radiation effects on *E. coli*, repair of x, 20: 16200
radiation effects on jute, y, 20: 16217 (AECD-AG-7)
radiation effects on, in rat lens epithelium, 20: 16256
radiation effects on, in *Vicia faba* seeds, effects of infrared radiation on x, 20: 16278
radiation effects on rat marrow, protective effects of sodium against x, 20: 18326
radiation effects on, in spermatogenesis of *Drosophila melanogaster*, 20: 18354
radiation effects on animal cells during interphase, x, 20: 18430
radiation effects on mouse, protective effects of intestinal shielding against x, 20: 18432
radiation effects on turtle, gamma, 20: 18291(R) (N-65-17058)
radiation effects on, in regenerating rat liver, x, 20: 18457
radiation effects on *Proteus mirabilis*, effects of dose on uv, 20: 22758
radiation effects on root and terminal bud meristem cell, in peas, fast neutron and gamma, 20: 24890
radiation effects on rat kidney, x, 20: 24909
radiation effects on chicken heart myoblast, x, 20: 24936
radiation effects on, in root tips of Haplopappus, 20: 26666
radiation effects on HeLa cell, gamma, 20: 31008
radiation effects on, in *Vicia faba* root meristem, comparison with effects of DNA, 20: 32976
radiation effects on, during cleavage in mice, x, 20: 33008
radiation effects on, in Chinese hamster cells *in vitro*, uv, 20: 33070
radiation effects on nucleolus, uv, 20: 36592
radiation effects on pea, fast neutron and gamma, 20: 36621
radiation effects on *Pisum sativum* root tip cell, thermal neutron, 20: 36644
radiation effects on, in Tradescantia cells, microbeam uv, 20: 38614
radiation effects on, in rat bone marrow cells, gamma, 20: 38663
radiation effects on, in rat thymus, x, 20: 38720
radiation effects on *E. coli*, factors affecting, 20: 40630(R) (ORNL-3922, pp 106-8)
radiation effects on human leukocyte, uv, 20: 40581(R) (ORNL-3922, pp 50-1)
radiation effects in human blood cells, 20: 40665
radiation effects on rat spermatogonial, following exposure at birth, x, 20: 40682
radiation effects in rats on male germ cell, following exposure at birth, x, 20: 40683
radiation effects on DNA synthesis during, in chick fibroblasts and myoblasts, x, 20: 40587
radiation effects on, in mouse lymphoma cells, negative pion, 20: 42859(R) (UCRL-16246, pp 100-2)
radiation effects on, in erythroblasts of man, chronic low-level exposure, 20: 42884
radiation effects on *Vicia faba* chromosomes during, comparison with exposure during meiosis, 20: 42921
radiation effects on diurnal variations in frequency of, in root tips of Pinus seedlings, gamma, 20: 42953
radiation effects on bacterial, kinetics of incorporated tritium and phosphorus-32, 20: 45421
radiation effects on, in mammalian cells, steady state population studies, 20: 45366 (UCSF-10P2-14)
radiation effects on, in Saccharomyces, 20: 16255
radiation effects on, in hepatomas in rats, 16: 14560
radiation injuries to cellular, resulting from incorporation of carbon 14- or tritium-labeled thymidine, 20: 45396
radioinduced block recovery in protists, 16: 8541(R) (TID-14809)
radioinduced changes in, in plant cells, 19: 5632(T) (ANL-Trans-114)
radioinduced chromosome aberrations in rat liver during, effects of hypothermia on, 17: 38748 (USNRDL-TR-666)
radioinduced chromosome aberrations during, in *Vicia faba*, 18: 45178 (ORNL-P-483)
radioinduced crossing-over in dividing cells in *Ustilago maydis*, uv, 19: 24288
radioinduced delay in dog erythroblast, x, 18: 15874
radioinduced delay of, in sea urchin eggs, mechanisms for x, 20: 6861
radioinduced effects on, in corneal epithelium of mice, gamma and neutron, 17: 30359
radioinduced formation of antimitotic substances, 16: 1493(T) (JPRS-10170(p.418-22))
radioinduced inhibition of, 17: 37090
radioinduced inhibition of, in wheat, gamma, 18: 17488
radioinduced inhibition of, in RCP cell strain, x, 20: 5323
radioinduced mutations in yeasts during, rates of uv and x-ray, 18: 11832
radioinduced recombination in *Aspergillus nidulans*, uv, 18: 43252
radioinduced recombination in heterozygous Saccharomyces, mechanism of uv and x, 20: 33053
radioinduced reversion in, giant cell production by x, 20: 18325
radioinduced, use in estimating dose distribution in sarcomas and tumors, 19: 42336
radiomimetic action of radiation-processed fruit juices on, in germinating seeds, 17: 23141
radioprotective effects of AET on, in mice, 17: 31942
radiosensitivity effects in pea seedlings, gamma, 18: 1417
radiosensitivity effects of state of, on nucleic acid synthesis in cells in culture, uv, 20: 6816
radiosensitivity effects in mouse leukemia cells, 20: 22710
radiosensitivity effects of length of, in plant cells, 20: 22728
radiosensitivity effects of stage of, in hematopoietic tissue transplants in mice, 20: 22735
radiosensitivity effects of, on animal cells in culture, y, 20: 3737
radiosensitivity in developing sperm, 16: 25192
radiosensitivity in rats after partial hepatectomy, 18: 11857
radiosensitivity in grasshopper neuroblasts, effects of tonicity on, 19: 13119
radiosensitivity of human cells during, 17: 23164
radiosensitivity of cells during, 17: 25026
radiosensitivity of cells in various phases, 17: 27152
radiosensitivity of chromosomes in different phases, 17: 27168
radiosensitivity of 4 stages in, 17: 27138
radiosensitivity of human cells at various stages of, 17: 30358
radiosensitivity of *Tradescantia paludosa* microspores during, changes in, 17: 31937
radiosensitivity of, in *Saccharomyces cerevisiae*, 17: 33653
radiosensitivity of, during reproductive stages in *Oedogonium cardiacum*, 17: 38795

radiosensitivity of, effects of ploidy on, 17: 38879
radiosensitivity of, in mouse spinal cells, 17: 40545 (BNL-7284)
radiosensitivity of stages of, in Habrobracon eggs, x, 18: 3568
radiosensitivity of, in bone marrow and lymph nodes from guinea pigs, hamsters, mice, and rats, 18: 9837(T) (JPRS-22778)
radiosensitivity of chromosomes in plants during, causes for variations in, 18: 11830
radiosensitivity of, in root tips, 18: 27003(R) (ORNL-3601(p.27-46))
radiosensitivity of various stages in HeLa cell, x, 18: 29306
radiosensitivity of, in corneal and intestinal epithelium of mice, 18: 38951
radiosensitivity of, in mouse corneal epithelium, 18: 41270
radiosensitivity of, in *Macrozamia communis*, 19: 5693
radiosensitivity of, in tumor cells in rats, 19: 7081
radiosensitivity of L-strain mouse cell, effects of 5-bromodeoxyuridine on gamma, 20: 33033
radiosensitivity of, effects of ploidy in plant cells, 20: 8697
radiosensitivity of, in mice, 20: 22785
radiosensitivity of, in yeast, 20: 1664
rate in thymus gland during regeneration after radiation injury, 16: 32746(T) (JPRS-15018(p.107-18))
regeneration by irradiated extract injections, 17: 12117
stimulation in lymphoid tissue by factor from blood serum of irradiated lymphopenic rats, 16: 30240
synchronization in Chinese hamster cell, use of 5-aminouracil for, 19: 31788(R) (ORNL-3768(p.33-57))
time intervals of epithelial and spindle cell mouse tumor, using autoradiography and tritiated thymidine, 19: 43698
time sequence of, in bone marrow cells of dogs, tracer study of, 18: 36870 (BNL-7260)
water-d_2 effects on Drosophila, 18: 17522

MIXED SPECTRUM CRITICAL ASSEMBLY
activation measurements in, neutron Doppler, 19: 45572(R) (GEAP-4755)
activation measurements of Doppler effect in uranium-235 and uranium-238 in, 20: 38430 (ANL-7120, pp 616-24)
core flooding in, effects of superheat, (T), 19: 5488 (SAN-8003 (p.163-89))
criticality studies, thermal-core, 19: 3629 (GEAP-4620)
criticality studies, (E), 19: 5488 (SAN-8003(p.163-89))
design, 18: 19367 (GEAP-4320)
design of, 17: 21243 (TID-7658(p.101-12))
neutron spectra in, fast and thermal, 20: 3402
operation and physics experiments in, 18: 45020(R) (GEAP-4619)
operation of MSSCEF, 20: 3471(R) (GEAP-4861)
performance of, 19: 29670
physics experiments for superheat reactor in, 19: 38178(R) (GEAP-4790)
power distributions in (E), 19: 3573
power distributions in fast and thermal regions of, 19: 45572(R) (GEAP-4755)
reactivity effects of hydrogenous material in (E), 19: 3573
reactivity of, effects of flooding and poisons on, 19: 45572(R) (GEAP-4755)
reactivity of, effects of flooding and poisons on, 20: 38439 (ANL-7120, pp 826-36)
reactivity of, flood safety study for, 19: 29521
shutdown of, excursion-limiting fuse for, 19: 21617
startup and operation of, 19: 3545

MIXER-SETTLERS
behavior of nitric acid and uranium in, in Eurochemic extraction flowsheet No. 3, 18: 1795 (NP-13272)
contamination barrier for pulsed, design of, 19: 36569(P)
design, 16: 1873(P)
design, 17: 23453(P)
design and operation of single-stage continuous-box, for conversion of low-grade uranium residues to Winlo feed, 17: 23425(R) (NLCO-870)
design and performance for extraction experiments, 17: 27501
design and performance of air-pulsed laboratory, 19: 11263 (ORNL-TM-896)
design for use in removing TBP from aqueous streams, 16: 20534(R) (IDO-14574)
design of critically safe, for processing concentrated solutions of fissionable materials, 18: 3879 (NP-13287)
design of high-capacity, general, 17: 10786
design of in-line, for liquid conveyance through ports, 17: 29065(P)
design of pulsed, with contamination barrier, 16: 27179(P)
design of pulverizer-, for solid molten salt fuel samples, 17: 2779
design of series for processing finely divided reactor fuels, 19: 44127(P)
design of 16-stage, engineering drawings for, 18: 5430
design of, epoxy casting techniques for, 18: 17977(R) (ORNL-TM-793)
design parameters of, for the Amex process, 17: 21775 (ORNL-3381)
design without moving mechanical parts in contact with liquid, 18: 16158(P)
development, 16: 21994(R) (ORNL-TM-150)
development, 17: 8246 (NP-12395)
development and testing for production of thoria microspheres, 20: 20808(R) (ORNL-3916)
development and uses, review, 16: 23793
development and uses, review, 16: 30498(T) (AEC-tr-5327)
discharge apparatus for, use of radioisotopes for control of, 19: 858
efficiency for solvent extraction of fission products, 20: 9050(R) (ORNL-3830, pp 222-7)
electric field in, 17: 4797(P)
evaluation of small modified CEN, for use in Acid Thorex and Purex processes, 19: 44117 (ORNL-TM-1256)
extraction performance, model of, 19: 9281(R) (IS-900(Sect.E))
extraction performance in Purex process, 20: 7209
hydraulic properties of horizontal and vertical, 18: 3935
interface level measurement in, ultrasonic apparatus for remote, 17: 246(P)
liquid-liquid separation by gravity-induced settling in, effects of induced coalescence on, 18: 23708 (UCRL-11182)
mixing of liquid phases in, apparatus for, 18: 25628(P)
operation of, dispersion band formation in, 16: 29027(R) (NLCO-855)
optimization of two-stage chemical, 18: 20156
performance for solvent extraction processes, 16: 284
performance in Thorex Process, 20: 18823 (DP-1022)
performance of air-pulsed, 18: 17935(R) (ORNL-TM-532)
performance of lab-scale, in separation of fission products, plutonium, and uranium, 16: 13158
performance of single-stage, for cesium recovery from Purex 1WW waste, 19: 28444(R) (ORNL-TM-1094)
review of critically safe, 19: 13529 (NP-14593)
steady-state of, prediction of approach to, 20: 1953 (IS-T-34)
testing for pyrochemical fuel processing, 20: 20802(R) (ANL-7055, pp 21-98)
testing of small, for solvent extraction flowsheet development, 19: 2205(R) (ORNL-TM-936)
uranium determination in, equipment for continuous colorimetric, 19: 2217 (NP-14343(p.IIe1-12))

MIXERS
book: *The Optimal Design of Chemical Reactors. A Study in Dynamic Programming*, 16: 13507
design, 18: 8440
design and construction of air-water, for use in fog-cooling studies, 16: 17794 (EURAEC-49)
design for uranium ore leaching, 19: 4259
design of fluidized-bed, 19: 24222(P)
design of remote-control, for blending thorium dioxide–uranium dioxide powders, 20: 14668 (ORNL-TM-1397)
effectiveness of turbine, methods of measurement, 16: 302(T) (AEC-tr-4846)
efficiency in mixing powders, 16: 25512(T) (NP-tr-887)
heat and mass transfer performance of turbine contactor, 18: 10179 (DP-847)
operation of, effects of physical properties of powders on optimal conditions for, 16: 32959(T) (NP-tr-922)
performance of ribbon-type, comparison with rotary-type, 16: 25514(T) (NP-tr-889)
pneumatic spillway operating under vacuum for, 19: 2439 (NP-14343 (p.Id1-4))
transients in packed tubular chemical, models for computation of, 19: 19734 (UCRL-11757)

MIXING
see also Stirring Apparatus
agitation in gas-liquid and liquid-liquid systems, power requirements, 18: 31362(R) (UCRL-11213(p.154-61))
control of liquid blending process with imprecise feedback information, proportional, 18: 27281 (UCRL-11295)
control of, use of radioisotopes in, 18: 14318
effects of properties on solution, 19: 5896
efficiency of 1000-m^3 silo for cement, tracer studies of, 18: 25871 (SGAE-IB/IA-1/1964)
efficiency of, use of radioisotopes in evaluating, 19: 24454
fluids in small-diameter tanks by recirculation, (E/T), 20: 24811 (Y-1531)
frequency response of aqueous systems in, tracer studies of, 18: 16001 (TID-7689(p.126-8))
in pressurized-water loop, research program on, 19: 7679(R) (EURAEC-1200)
in turbulent chemical flow reactor, 19: 27886 (UCRL-7759-T)
longitudinal dispersion in packed columns, 18: 31362(R) (UCRL-11213 (p.154-61))
measurements on, of enriched uranium-235 fluid in cylindrical storage tanks, 20: 25198 (Y-1502)
of gas–liquid systems, power requirements for, 18: 1835 (UCRL-10996)

of immiscible liquids in baffled cylindrical tanks, 18: 41307 (UCRL-9787 (Rev.))
suspension of solids in liquids by impellers, correlation studies, 19: 1970 (TID-21230)
suspension of solids in liquids in tanks by impellers, 19: 36576 (TID-22073)
suspension of solids in liquids by impellers, effects of particle shape on, 19: 36577 (TID-22074)
suspension of solids in liquids by fan turbine impellers, study of conditions for, 19: 36578 (TID-22075)
ML-1 Reactors
see Army Reactors (ML-1)
MLPA (Monolaurylphosphoric Acid)
see Phosphoric Acid, Diethyloctyl Ester
MMA
see Methacrylic Acid, Methyl Ester
MOAB DISTRICT (UTAH)
geology of mineralogical changes in uranium deposit sediments in, 18: 20228
Mobile High Power Plant-1
see Army Reactors (MH-1)
MOCTEZUMITE
occurrence in Moctezuma, Sonora, Mexico, 20: 4173
Moderator Control Reactor
see Spectral Shift Control Reactor
Moderators (Reactor)
see Reactor Moderators
Modifiers
see Pulse Modifiers
Modulation
see Frequency Modulation
Modulation Receivers
see Frequency Modulation Receivers
Moessbauer Effect
see Mossbauer Effect
MOHAWK RIVER
radioactive contamination in, 19: 46646(R) (PHS-999-RH-13)
MOJAVE DESERT (CALIF.)
hafnium content and hafnium–zirconium ratio in zircon from, 18: 39483
rodents in, life spans of, 20: 45264(R) (UCLA-12-595, pp 72-89)
MOLDING MATERIALS
see also Plastics
analysis of thermosetting diallyl phthalate powders for *tert*-butyl perbenzoate, 19: 40285 (MLM-1284)
evaluation of diallyl phthalate powders as, 19: 16030 (MLM-1163 (p.G.1-7))
evaluation of thermosetting plastic powders using capillary extrusion rheometer, 18: 40983 (MLM-1211)
extrusion of diallyl phthalate powder, rheometer evaluation of changes in, 19: 14911(R) (MLM-1216)
radiation modification of dyeability of synthetic fibers, 17: 20302(P)
temperature effects on RTV-20, 19: 42215 (RFP-625)
MOLDS
(See also as heading by the material of the mold; in the biological sense see Fungi)
see also Dies
defects in polyvinyl chloride plastisol, effects of moisture on, 20: 18179 (Y-1508)
design and testing of, for static casting of uranium tubes, 19: 13945(R) (NLCO-940(p.3.1-8))
design for casting plutonium, 16: 8860(P)
design for multiple casting of uranium alloys, 19: 42824(R) (NLCO-955, pp 5.1-16)
design of, for coating multiple elements, 18: 5766(P)
design of plate casting, 18: 27921(R) (NMI-1129)
design principles for plastic potting shells, 19: 21764 (SC-DR-64-2135)
development of expendable graphite-base, for casting reactive metals, 18: 39854 (BM-RI-6509)
fabrication of beryllium–copper, methods for, 19: 20519 (NP-14879)
heat transfer of cold, used for vacuum arc-melting, 17: 34330(R) (USBM-U-1057)
properties of electro-graphite for braze-ring, 16: 13169 (CNLM-1730)
radiation effects on, in egg noodles, gamma, 20: 27378
MOLECULAR BEAMS
see also Ion Beams
analysis of, construction and calibration of deflecting magnets for, 17: 14953 (UCRL-10526)
attenuation in point-particle systems, 18: 42308
behavior of cesium, minimization of transient, 17: 21401(R) (TID-18585)
bibliography on production of 1–1000 ev, 1950–1962, 17: 12760 (NP-12500)
chemical reactions in crossed, 19: 402
chemical reactions in crossed, kinetics studies using, (E/T), 19: 32052
collimation of high-intensity, (E), 19: 18694
collision mechanics between crossed Maxwellian, 16: 3552
collisions in, inelastic, 16: 5086(R) (NP-11057)
concentrations in, theory, 17: 12850
condensation embryos in expanding, 18: 37855
construction and performance of generator with oscillations of crossed, (E), 19: 9933
deceleration of large-dipole-moment, electrodynamic method of, (T), 19: 41200
deceleration system for, development of, 18: 42162(R) (TID-20963)
detection and measurement of neutral, equipment for, 16: 31865
detection and measurement of, design of instrument using electron bombardment and mass filter for, 17: 16466
detection and measurement of, instrument using electron collision ionization for, 17: 30840
detection and measurement, design and performance of mass filter detector for, 17: 35263(R) (UCRL-10706(p.1-110))
detection and production of neutral, 17: 30851 (EUR-CEA-FC-197)
detection of weak alkali, by ionization on hot tungsten, 18: 16555 (UCRL-Trans-1031)
detection of, by electron bombardment method, 20: 31492
detection of, electron bombardment ionizer for, 20: 21066
detection of, field-ionization detector for, 20: 21089
detection of, Kingdon cage for, 18: 41859
detector for, design and operation of electron-bombardment, 20: 31488
development of high-intensity, shock-tube driven, 16: 3531 (CAL-RM-1396-A-1)
development of low-temperature helium, 19: 25071(R) (TID-21667)
electric resonance and velocity selection in, 16: 21129(R) (NP-11640)
energy transfer from, method for measuring, 19: 23195
equipment design for high-resolution, 17: 9141
equipment for aerodynamically accelerated, design of, 19: 30378(R) (SR-4-5)
equipment for gas-solid reactions, 17: 6520(R) (NP-12373)
focusing of symmetric-top, by electric six-pole field, 18: 43138 (WIS-TCI-63G)
focusing of, alternate-gradient technique for, 20: 44120
injection and trapping in mirror fields, use of r-f field for high-energy, 20: 30580
intensity distribution of, design of mass spectrometer for determining, 20: 43658
interactions with molecules, distributions from inelastic, (T), 19: 8066 (UCRL-11135)
interactions with metallic surfaces, energy exchange in, (E), 19: 41275
ion reactions with molecules in, charge and momentum exchange in, 18: 40153
ionization and acceleration of condensed, 16: 4651
ionization with plasma ion source, 16: 26020
isotope separation in, efficiency of choppers for, 18: 39783
isotope separation in free jet, effect of nozzle-exit size on, 20: 25471
kinetics in vacuum, 16: 22815
magnetic moment measurements using multiple, system for, 19: 6714
mean free path of molecules in, 16: 871
modulation of, design of vibrating reed ultrahigh vacuum beam chopper for, 18: 7010
momentum transfer against heated metals at normal incidence, 16: 13692 (HE-150-182)
nuclear magnetic resonance of, collision-narrowing theory of, 19: 38629
oscillations of crossed, frequency stability of, (T), 19: 9930
oscillations of crossed, frequency and energy dependence of, (E), 19: 9931
oscillations of crossed, frequency stability of, (T), 19: 9932
production, 17: 1800
production and properties of, 19: 26925(T) (JPRS-29075)
production and properties of, conference on, 20: 28090
production by nozzles, shock wave effects on, 18: 40158
production by nozzle sources, 18: 40159
production by nozzle sources, properties of, 18: 40160
production, design of generator using deuterated ammonia for, 16: 594(T) (NP-tr-788(p.10-15))
production in high vacua by jets, 17: 16796(T) (AEC-tr-5695)
production of argon, using gaseous mixtures, 18: 12836
production of argon and nitrogen, method for, (E), 19: 6446
production of continuum-source, survey of methods for, 19: 32887
production of crossed, equipment for, 18: 36177
production of crossed, apparatus for, 19: 30378(R) (SR-4-5)
production of dense thin, 17: 20800(P)
production of gaseous cesium, source for, 17: 1605(P)
production of helium and nitrogen, 20: 4479(R) (TID-22179, pp 1-83)
production of high-intensity, three-fluid model for analysis of skimmer for, 17: 28042
production of high-intensity, with energies over 1 ev, 18: 2554

production of hydrogen, ion source for, 20: 6000
production of noble-gas, for detection devices, 19: 28717(R) (MLM-1221)
production of pulsed, with nozzles, 18: 4346
production of, using nozzle, avoidance of compression shocks in, 17: 15006
production of, using nozzle with gaseous mixtures, determination of enrichment in, 18: 7355
production of 0- to 2-kev, design of source for, 16: 30615
production of, apparatus design considerations for, 20: 29918 (UCRL-11670)
production of, engineering drawings of baffle of oil diffusion pump in, 18: 12331
production of, equipment for, 18: 10359
production of, optimum design of equipment for, 20: 41250
production using cylindrical tubes, (T), 20: 17279
reactions in, 18: 1491(R) (ORNL-3488(p.102-22))
reactions in, 19: 280(R) (ORNL-3679(p.94-116))
reactions in crossed, distributions from, 17: 8970
reactions in crossed, apparatus for analysis of, 18: 10112
reactions in crossed, stripping mechanism in, 18: 31480
reactions in crossed alkali-halogen, 19: 46161(R) (ORNL-3832, pp 116-50)
reactions of crossed, equipment for measuring energy dependence of cross sections in, 18: 8408(R) (TID-20006)
reactions of crossed hydrobromic acid and potassium, velocity distribution of potassium bromide produced in, 18: 43139 (WIS-TCI-65G)
reactions of crossed, apparatus for studies of, 19: 13282 (UCRL-11605)
reactions of crossed, velocity selector for studying, 19: 34891
reactions of crossed, apparatus for study of, 20: 37478
reactions of crossed, mass spectrometer for studies on, 20: 43288(R) (CALT-532-1)
reactions with gases at high energies, forces in, 16: 26041
reactions with ion beams, calculation of total cross section from angular measurements in, 19: 27080
reactions with ion beams at low energies, absolute cross sections for charge transfer, (E), 20: 19670
reactions with revolving surfaces, 18: 40154
research on heavy, in propulsion, 17: 16872
research programs on, 16: 30172(R) (TID-16489)
review of studies involving, 19: 41143
scattering at high velocities, total elastic cross sections, 17: 12841
scattering at thermal energies, review on elastic, 18: 18589
scattering by gases, cross sections for, 19: 14265
scattering by surfaces, decrease of frictional resistance in, 18: 40155
scattering by surfaces, normal momentum transfer in, 18: 40156
scattering cross section measurements in, resolution in, 18: 10777
scattering during thermal diffusion, computer program for calculating, 20: 39321(R) (MLM-1312)
scattering, equipment and methods for analyzing, 17: 35263(R) (UCRL-10706(p.1-110))
scattering in, effects of source pressure on, 19: 30629(R) (MLM-1238)
scattering of argon and helium, from lithium fluoride cleavage plane, 17: 6794 (K-1498)
scattering of, comparison of approximations of total elastic cross sections for, 17: 29439
scattering of deuterium and helium, by platinum surfaces, 17: 34650
scattering of, interaction potential in thermal-energy, 17: 39716(R) (CONF-186-3)
scattering of, computer program for calculating classical deflection function for, 20: 13415 (ORNL-3881)
scattering of, cross sections for nonadiabatic elastic, (T), 19: 6454
scattering of, determination of intermolecular potential parameters from, 18: 35580
scattering of, electric deflection analysis of rotational excitation of products in, (E), 19: 42485
scattering of, measurement methods for, 19: 36889(R) (MLM-1250)
scattering of, measurement methods for, 20: 20807(R) (MLM-1287)
scattering of, quantum-mechanical calculations of differential cross sections in small-angle, 18: 20736
scattering of, use of, in intermolecular force studies, (E/T), 20: 30734(R) (TID-22970, pp 1-63)
scattering phase shifts from differential cross sections, determination of, 18: 4337
scattering phase shifts for, calculation of intermolecular potential parameters from, 18: 4338
scattering, relation of intermolecular potentials to, 18: 4347
scattering, semiclassical equivalence relation calculation of phase shift, 16: 15298
scattering, use of Lennard-Jones potential in calculating cross sections, 17: 12849
scattering, validity of WKB approximation of elastic, 17: 12848
separation of particles of given magnetic substate from, using congruent inhomogeneous electric and magnetic fields, 18: 4361(P)
source design and performance for nitrogen, 16: 7714
source for, design of electric resonance, 17: 25852(R) (NP-12877)
spectroscopy of alkali fluoride, millimeter-wave, (E), 19: 27089
stability, frequency-standard studies, 16: 19476(R) (TID-15642)
transmission in cylindrical tube with wall sorption, probability for, (T), 20: 28061
transmission properties, equipment design for measurement of, 16: 9506(R) (ORNL-3239(p.16-46))
use for tandem accelerator neutral beam injectors, 19: 9819
use in studies of high-temperature molecules, 19: 36345 (UCRL-11927)
use to study reaction dynamics, instrumentation for crossed, 20: 44109 (CALT-532-3)
uses in chemistry, 18: 10058
uses in physical chemistry, 19: 23163(R) (ORNL-3650(p.111-86))
uses in spectroscopy, review on, 19: 23311
uses of hydrogen, for plasma density measurements, 18: 15377
uses of, in studies of high-temperature molecules, 20: 31219(R) (UCRL-16658, pp 11-20)
velocity dispersion of square-modulated Maxwellian, 18: 42310
velocity distribution in, time-of-flight measurement of atom, 18: 16653(T) (UCRL-Trans-1032)
velocity selection for, design and testing of apparatus for, 17: 25579

MOLECULAR FILMS
preparation of thin inorganic, electrolytic, 17: 1451
use as standard beta sources, 20: 16143 (AD-620276)

Molecular Filters
see Membrane Filters

Molecular Forces
see Intermolecular Forces

Molecular Moments
see Moments

MOLECULAR PROPERTIES
book: *Symmetry. An Introduction to Group Theory and Its Applications*, 18: 39803
chemical, determination by quantum theory, 16: 15364
electron energy levels in atoms and molecules, 18: 4396 (D1-82-0302)
force field constants for octahedral XY_6-type molecules, vibrational analyses of, 17: 25174
force field parameters from isotope effects in phase equilibria, 18: 25373
ionization by electron of labeled and nonlabeled, review on isotope effects in, 18: 35519
measurement of the rotational and vibrational freedom of hydrogen atoms in molecules using slow neutrons, 17: 21607
modification of Rydberg-Klein-Rees method for obtaining potential curves for doublet states, 16: 13700 (NP-11429)
research programs on, 1964 Army Dept. summary, 19: 32048(R) (NP-15073)
spectral studies of resonance, using infrared lasers, 20: 30734(R) (TID-22970, pp 1-63)
stability of molecules in the Thomas-Fermi theory, 17: 11419

MOLECULAR REARRANGEMENTS
mechanism of alkyl-group, 19: 32048(R) (NP-15073)
radioinduced *cis* ⇌ *trans* transformation, 16: 5390

MOLECULAR STRUCTURE
analysis of, computer methods for, 18: 24296(R) (AD-417517)
bond length measurement by electron diffraction, 17: 27358
book: *Physical Methods for Determining Molecular Geometry*, 19: 40530
book: *The Molecular Designing of Materials and Devices*, 20: 6551
book: *The Structure of Atoms and Molecules*, 20: 11512(T)
cell theory for hard particles, 20: 4708(R) (UCRL-14360, pp 50-73)
conference, 20: 12320
conference on electronic and atomic structure of metallic solid solutions, 19: 16185
correlation energy in two-pi-electron system, 17: 31115
determination by dielectric relaxation times, 19: 32048(R) (NP-15073)
determination by high-resolution electron microscopes, 18: 25749(R) (ORNL-3582(p.40-1))
determination by isotopic substitution, 19: 7426
determination by spectroscopic effective moments on inertia, effects of vibration-rotation perturbations on, 17: 35263(R) (UCRL-10706 (p.1-110))
determination from electron diffraction photographs, 19: 24531
determination of, from rotational spectra, 16: 32906 (UCRL-10377)
determination of, for biological molecules using neutron-diffraction analysis, 20: 40632(R) (ORNL-3922, pp 175-91)
diatomic forces and force constants in, equations for, 20: 2650
electron energy levels in atoms and molecules, 18: 4396 (D1-82-0302)
electronic wave patterns for, 19: 13383
electrostatic energy matrices of f^7 configuration, 16: 16356
elucidation by isotope labeling and mass spectrometry, 19: 7534
expansion of free energy of Ising model with arbitrary spin and range of

interaction, diagrammatic, 16: 6862
force field constants for octahedral XY_6-type molecules, vibrational analyses of, 17: 25174
force field parameters from isotope effects in phase equilibria, 18: 25373
many-body interactions in, 16: 15321
nuclear magnetic resonance studies of, 18: 31435(R) (UCRL-11317 (p.52-78))
orbital density comparisons in, 20: 5524 (ANL-7076)
orbital theory, 18: 22022 (UCRL-11229)
orbital theory for nitrogen–fluorine and oxygen–fluorine systems, 19: 32048(R) (NP-15073)
orbital theory prediction of hydrogen exchange in chlorophyll, 19: 9159
orbitals in nonsaturated compounds, computer program for calculations, 16: 20359 (NP-11530)
radiation effects on, of DNA, 18: 17566
reduced matrix element of an irreducible spherical tensor operator for, derivation of, 20: 1329
relation to isotope effects on vapor pressure, 17: 23332
research program on, 19: 28281(R) (AD-607838)
research program summary for M.I.T., 16: 588(R) (NP-10932)
research programs of U. S. Army on, 1962 summary, 17: 33413(R) (NP-12967)
review of diatomic, 19: 47265
separated-electron-pair model, 19: 15487
study by neutron diffusion, 18: 13714 (AD-415804)
theory, evaluation of multicenter integrals in, 16: 12219(R) (NP-11304)
use in crystal structure determination, review on, 20: 5212 (BNL-930)
use of Mössbauer effect in studies on, 18: 41433
uses of one-center self-consistent-field models for ir vibration analyses, (T), 20: 8496 (UCRL-16265)
valence electron approximations in, 19: 46284

MOLECULAR WEIGHTS
computation from ultracentrifugal data by Archibald method, computer program for, 19: 30065 (LA-3291)
determination by double labeling of molecule with carbon-14 and tritium, 18: 43532
determination in organic reactor coolants, cryoscopic method for, 19: 44045 (JEN-151-DQ/I-52)
determination in organic reactor coolants, cryoscopic method for, 19: 44046 (JEN-152-DQ/I-53)
determination in polyglucin, 20: 12722(T) (JPRS-33766)
determination of blood factor VIII and factor IX, using electron irradiation, 18: 29233
determination of isotopic, 16: 2997(T) (NP-tr-808)
determination of, using magnetically suspended ultracentrifuge, 17: 20134
determination of, using NMR, technique for, 20: 26747 (LA-DC-7143)
effects on free radical formation in x-irradiated DNA, 20: 420
effects on radioprotective properties of heterologous and homologous DNA in mice, 19: 46013
radiation effects on deoxyribonucleohistone, 20: 18789
use in determining trace quantities of radioiodine compounds, 19: 11015
use in separating products of gamma-induced RNA-ase inactivation, 20: 24870
use in separating products of gamma-induced ribonuclease A inactivation, 20: 24870

MOLECULES
see also Carbon Molecules
see also Mesic Molecules
adsorption on target surfaces, 17: 629
airglow emission from, in upper atmosphere, 19: 25432
angular correlation diagrams for AH_3-type, 18: 27384
angular momentum and polarization of, in structural continua, 18: 2455
appearance potentials for doubly charged ionic, in ionization by 70-kev electrons, 19: 20807(R) (UCRL-11828(p.201-4))
atom rearrangement in collisions, 18: 44467
atomic mixing coefficients in, 16: 12278
atomic positions in vibrating polyatomic, calculation of, 17: 31117
bibliography on hindered internal rotation in, 17: 14124 (UCRL-10404)
binding energy in statistical theory, 19: 44936 (TID-21692)
binding energy of homonuclear diatomic, chemical, 20: 3863(R) (IS-1200 (Sect. C))
binding of diatomic, perturbation method for homopolar, 18: 7419
Boltzmann equation for rigid nonspherical, 17: 29430
Boltzmann equation for gases of rigid, theorem for linearized, 18: 2543
bond dissociation energies of polyatomic, correlation, 19: 26291(R) (NYO-7240)
bond length measurement by electron diffraction, 17: 27358
bond oscillations in vibrating, secondary isotope effects on, 19: 13322
book: *Advances in Atomic and Molecular Physics*, 19: 39415
book: *Atomic and Molecular Processes*, 16: 26024
book: *Atoms, Molecules, and Nuclei*, 17: 41658
book: *Atoms, Molecules and Quanta*, Vol. I, 19: 34894
book: *Atoms, Molecules and Quanta*, Vol. II, 19: 34895
book: *The Structure of Atoms and Molecules*, 20: 11512(T)
calculations of polyatomic, quantum mechanical, 20: 3863(R) (IS-1200 (Sect. C))
calibration of labeled, procedures and instrumentation used by CNEA in, 17: 10677 (NP-12235)
charged particle reactions with, energy transfers in, 16: 26039
charged-particle inelastic scattering by, (T), 20: 17306
chemical binding in, 18: 15675 (IS-530)
chemical binding in homonuclear diatomic, energies of atomic and molecular orbitals in, 18: 41431
chemical bonding in, quantum N-particle calculations for, (T), 19: 5019(T) (ANL-Trans-123)
chemical bonds in, analysis of, by absorption spectra, 16: 21221
chemical bonds in, quantum-mechanical theory of, 17: 12283
collective states in small, 18: 44464
collision cross sections for, effects of quadrupole-induced dipole and dipole-induced quadrupole interactions on, 19: 13319
collision theory for, two-term approximation in, 18: 2552
collisions of, under accidental resonance conditions, energy exchange in, 18: 752
collisions of, bibliography on, 19: 47258
collisions of, conference on inelastic, 18: 30409
collisions of, directory of international workers on, 20: 1563 (ORNL-AMPIC-2)
collisions of, vibrational transition in, 18: 24320
collisions with molecules, asymmetry effects in, (T), 19: 37222
combination coefficients of, with ions in air, 16: 29576
condensation and equilibria in solar nebula and cool stellar atmosphere, (T), 19: 39352
condensation with ions in radioinduced polymerization of ethylene at −196°C, 16: 6459
conference on preparing and storing marked molecules, Brussels, Nov. 13 to 16, 1963, 18: 43529
conference on spectral line shape and molecular interactions, summary, 16: 2296 (K-1495)
conference on structure of electronically excited, 18: 28242
configurational instability due to electronic degeneracy in, theory of Jahn-Teller-type, 17: 31210
containment of quantum magnetic dipoles by magnetic bottle, 17: 25992
content in upper atmosphere, 18: 7616
coupling scheme for, in ligand field theory, 20: 29205
data tabulations of bond dissociation energies, electron affinities, and ionization potentials of, 17: 23301 (NASA-TN-D-1791)
deceleration of, apparatus for, 19: 25071(R) (TID-21667)
density in plasma, measurement technique for, 19: 37936(R) (NP-15135)
deposition on surfaces, adsorption probability measurements, 16: 19479 (UCRL-6772)
deposition on target surfaces, 17: 629
descent through upper atmosphere, 16: 13772
detection and measurement of neutral, using scintillation detectors, (E), 19: 44499
determination of absorptive, in light beam, from dispersion electron measurement, (E), 20: 25724(T) (ORNL-tr-1144)
diamagnetic susceptibility and nuclear magnetic shielding in, theory of, 17: 36437 (NP-13020(p.451-3))
diffusion in solid organic compounds, tracer studies of, 20: 18673
diffusion of, parameters affecting Knudsen, 20: 37307 (LA-3509)
dissociation and energy-transfer in, effects of electronic coupling on, 17: 6151
dissociation and ionization of, statistical models for, 18: 26204
dissociation and recombination in, diffusion theory of nonequilibrium, 19: 42488
dissociation by electron and ion bombardment, 17: 8157
dissociation by electron-ion collisional recombination, 19: 45450
dissociation by ionization, theory of, 19: 19937
dissociation energy computations of diatomic, without exact wave functions, 17: 30541
dissociation energies and ionization potentials of diatomic, compilation of, 18: 2525
dissociation of diatomic, mechanism, 16: 6467
dissociation of diatomic, in inert gases, 16: 9558 (NP-11225)
dissociation of diatomic gaseous, classical adiabatic approach to, 16: 11625
dissociation of diatomic, diffusion properties, 16: 13771
dissociation of diatomic, theory of neutron, 16: 27039(T) (AEC-tr-5152)
dissociation of diatomic, effects of anharmonicities on, 17: 8044
dissociation of diatomic, mean first-passage times for, 17: 12840
dissociation of diatomic, impulsive collision model for, 17: 31193
dissociation of gaseous, in electric discharges, 18: 36720 (RADC-TDR-63-275)
dissociation of, statistical theory of kinetic energy of fragmentation in,

18: 29765
dissociation processes in electronically excited, 17: 40686
dissociation processes in electronically excited, model for, 19: 9228
dissociation rates in thermal plasmas of polyatomic, collision-induced, 18: 15415
dissociation, fragmentation, and ionization of gases of, mass spectrometric studies of, 20: 4215(R) (ANL-7081, pp 134-49)
distribution and motion of interstellar, 20: 23854
distribution functions for (T), 19: 2976
distribution function for system of hard spheres, radial, 20: 4708(R) (UCRL-14360, pp 50-73)
distribution function for system of neutral, evolution equation for double, 20: 24194
distribution of isotopic, kinetics of isotope effects in, 20: 1866
dynamics in liquids, cold neutron studies of, 18: 7403 (BNL-7414)
effects of d-hybridization in pi bonds, 17: 2137
effects of heavy ions on, 18: 19571
eigenvectors of slightly asymmetric rotator, perturbation theory calculations of, 19: 13345
electric conductivity and magnetic resonance in gases of, variation principle for, 18: 2712
electro-optical properties of, determination by spectroscopy, 17: 12203
electro-optical parameters from infrared band intensities of isotopic, 19: 25169(T)
electromagnetic field equations for, Maxwell, (T), 19: 30955
electromagnetic oscillations in resonance system of two-level, (T), 19: 28928
electromagnetic radiation reactions with, variation-perturbation approach to, 17: 36683
electromagnetic-wave reactions with, ionization by, (T), 20: 17284
electron binding by, coefficients and cross sections for, 16: 26030
electron capture by, theory of dissociative attachment in, 17: 6862
electron capture by gaseous, mechanism of, 19: 9229
electron capture by, (E/T), 20: 18557 (ORNL-TM-1409)
electron collisions with, in plasma, 17: 21129 (CEA-2224)
electron collision cross sections for, design of electron spectrometer for measurement of inelastic, 18: 14839
electron correlation energy in, theory of many-, 16: 12258
electron coupling in, Born-Oppenheimer approximation of energy shifts due to (T), 19: 2974
electron coupling in, (T), 19: 10273
electron density change during nuclear vibration, 16: 18865
electron diffusion coefficient in neutral, 16: 22830
electron dissociative capture by, resonance, (T), 19: 19899
electron elastic collisions with, in homogeneous weakly ionized plasma, (T), 20: 15888(T) (SC-T-65-775)
electron elastic scattering, 16: 26033
electron emission by excited, origin of secondary, 19: 32048(R) (NP-15073)
electron energies in diatomic, automatic computation of, 17: 27360
electron energy levels of diatomic, wave functions and energy eigenvalues of molecular orbitals for small internuclear separations, 16: 29574
electron energy levels in, calculation of, 18: 4396 (D1-82-0302)
electron energy levels of polar, in inert-gas crystals, 18: 29606(R) (RTD-TDR-63-4110)
electron energy level calculations, 18: 44289(R) (ORNL-3670(p.31-5))
electron energy levels of diatomic, in electric field, calculation of, 18: 44427 (UCRL-11665)
electron energy levels of, field theory of rotational, 19: 3111 (AD-601193)
electron energy levels in polyatomic, multiple-scattering model for, (T), 20: 39618
electron energy transfer from solids to, 19: 1029
electron excitation of few-center, calculations for slow, 16: 32168 (AD-272156)
electron excitation at low energies (E), 19: 1191
electron impact excitation cross section for vibrational states of polyatomic, effects of vibrational mixing of first-order electronic wave function on, 18: 20760
electron impact on organic, energetic fragment ion production in, 17: 23387 (UCRL-10687)
electron interaction energies in diatomic, 20: 40796(R) (IS-1500(Sect.C))
electron ionization cross sections of diatomic, review of data on, 20: 9674
electron orbitals in, one- and three-dimensional models for free, (T), 19: 29807 (IS-1119)
electron orbitals in united atom model, (T), 19: 39372
electron orbitals in, spin hamiltonian for nonorthogonal, (T), 19: 47254
electron orbitals of homonuclear diatomic, at small internuclear separations, 19: 47265
electron paramagnetic resonance of, hyperfine and Zeeman anisotropy in, 17: 18904 (TID-14713)
electron reactions, excitation and ionization from, 16: 26035
electron reactions, excitation and ionization cross sections for, 16: 26036
electron reactions, mass spectra calculations by critical slope method, 16: 25320 (TID-16157)
electron reactions with, review of inelastic, 18: 32424
electron reactions with, at low energies, 19: 21792(R) (ORNL-3650 (p.187-219))
electron reactions with, classical calculation of cross sections for inelastic, (T), 19: 44947
electron reactions with, cross sections for inelastic, (T), 19: 23267
electron reactions with, selection rules for excitation in, 19: 23276
electron reactions with diatomic, dissociation in, (T), 19: 34892
electron reactions at low energies, vibration excitation from, (T), 20: 15256
electron reactions with, cross sections for, (T), 20: 27722
electron reactions at low energies, processes in, 17: 39812
electron reactions with, review of, 19: 44950
electron reactions with, review on, 19: 32906
electron reactions with, validity of Born approximation for fragmentation in, 18: 43629
electron scattering by diatomic, dissociation-product angular-distribution anisotropies, 16: 6981
electron scattering by, effects of negative-ion states on theory of, 17: 7076 (BNL-5801)
electron scattering by polar, diffusion cross section for, 17: 31150
electron scattering by, theoretical development of, 17: 37197
electron scattering by, effects of compound negative ion states in, 18: 34303
electron scattering at low energy, (T), 19: 30954
electron scattering by, momentum transfer cross-section theorem for, 19: 32891
electron scattering by polar, cross sections for low-energy, (T), 20: 973
electron scattering at low energies by homonuclear diatomic, method for prediction of, (T), 20: 11495
electron scattering by, resonances in, (T), 20: 17289
electron scattering at low energies by polarizable and polar gas, 20: 25735
electron scattering by, diffraction patterns from, (T), 20: 34118
electron scattering by diatomic, theory of resonances in, 20: 41657
electron scattering by diatomic, (E/T), 19: 6439 (AFCRL-63-697)
electron shell electrostatic potential in diatomic (T), 19: 1178(T)
electron shell electrostatic potential at nuclei in diatomic, (T), 19: 20836(T)
electron spin resonance spectroscopy, 19: 366
electron structure and wave functions for, 17: 2058(R) (NP-12207)
electron structure of, variation of orbital exponents in theory of, 17: 8056
electron structure of, superconducting theory for, (T), 19: 47230
electron transfer to positive ions from, 17: 34646
electron transitions in diatomic, methods for calculating spectral absorption coefficients of, 20: 1803 (AD-619266)
electron transitions in, many-body theory for probability of, 20: 15275
electron wave function calculations for diatomic, use of diatomic orbitals in, 17: 32721 (NYO-10423)
electron wave functions in (E/T), 19: 2967
electronic energies of diatomic, Thomas-Fermi calculations of, 17: 29438
electronic energy and isotope effects in, 16: 16357
electronic spectra of, theory of solvent effects on, 19: 13383
electronic structure and properties, 19: 13383
electronic symmetry in polar diatomic, electric-deflection determination of, (E), 19: 42493
electronic transitions in, equipment for detecting forbidden, 18: 8408(R) (TID-20006)
energy flow in classical, intramolecular, 18: 8408(R) (TID-20006)
energy levels in, pseudopotential calculation of, 16: 27820
energy levels in perturbation theory, energy eigenvalues of, (T), 19: 37685
energy levels of, 20: 29931(T)
energy levels of diatomic, vibrational, (T), 19: 47215 (AD-613375)
energy levels of nine-valence-electron diatomic, spectral studies of low-lying, 19: 34148 (UCRL-11979)
energy levels of polyatomic, crossed-beam studies of, 17: 33944
energy levels of, electron excitation of vibrational, 18: 32371
energy levels of, independent particle model for metastable, 18: 32444
energy levels of, virtual-state, (T), 20: 11439 (BNL-8800)
energy levels of, dynamical Jahn-Teller effect with strong coupling, (T), 20: 33306
energy levels of, electron correlations for, 20: 41630
energy of diatomic, curves for potential, (E/T), 20: 7659(R) (ORNL-3849, pp 101-50)
energy transfer in interactions in solutions, 16: 15280(T) (AEC-tr-5067)
energy transfer in, 19: 32825
energy transfer in systems of complex, 20: 7067

energy transfer mechanisms for, 17: 40686
equation of state for systems with steep repulsive potentials, quantum corrections to, 19: 37476
exchange reactions with atoms, collision dynamics of, 20: 312
exchange with atoms, model for isotope effects in, 18: 12080
excitation and ionization of, slow electron detection by, 18: 41550
excitation behind shock waves, 16: 12305
excitation by electron impact, rotational, (T), 19: 4852
excitation by electrons, cross section for vibrational, 20: 44125
excitation delocalization and transfer, (T), 19: 22159 (FSU-2690-18)
excitation energy transfer mechanisms for, 17: 40685
excitation energy of, from slowing down of charged particles in gas, 19: 30965
excitation of, gauge invariance of g-tensor in, 17: 13171
excitation of homonuclear, cross sections for rotational electron-impact, 17: 25863 (R63SD43)
excitation resonance transfer among, S-matrix theory for, 20: 27759
excited states of linear chains containing impurity, low, 18: 1493
exciton model for molecular aggregates, 17: 40685
exciton states in, coupled with nuclear vibrations, 18: 14733
exciton states of, in solid rare gases, 17: 41638
exciton states of, in helical polynucleotides, 17: 40846
exciton theory of, by second quantization, 17: 40687
exciton wave-packet radiation in, in crystals, (T), 19: 40088
flow field of free, over moving circular plate, 18: 33742
flow of free, on concave cylindrical surface, heat transfer, 17: 8356
flow of free, relativistic theory of, 20: 2841
flow of gases of, computer program for analysis of, 20: 20855 (CLM-R-54)
fluid transport mechanisms in hard-sphere systems, 20: 4708(R) (UCRL-14360, pp 50-73)
force constants of hexacarbonyls, 17: 5108
force constants of, theory of, 17: 18938
formation and observation of μ^+ mesic organic, 17: 28342
formation by fission fragment reactions, mechanism of, 19: 11223
formation of quark, (T), 20: 46335 (JINR-P-2871)
friction constant in liquids, use of isotope separation data for calculation of, 18: 34308
fundamental constants, effects of change in electronic state on, 17: 14973
gamma scattering by resting, momentum transfer in, (T), 19: 8240
ground states of high-temperature, determination of, by molecular beam fluorescence, 20: 31219(R) (UCRL-16658, pp 11-20)
heavy-particle scattering by diatomic, 16: 21122 (AFCRL-1062-II)
hyperfine structure of, core-electron contribution to, 18: 20749
inertia defects in ethylene-type, calculation of, 19: 13343
integrals in diatomic, coulomb and exchange, 20: 3863(R) (IS-1200 (Sect. C))
inter-electron coordinates in atomic wavefunctions for, mathematical generalizations of, 18: 30412
interactions between, electronically polarizable continuum model of, 17: 34580
interactions between diatomic, rotational and vibrational transitions from, 18: 18588
interactions in dielectric medium, equation of motion for, (T), 19: 26943
interactions in gases, mixed pair correlation functions for, 18: 26133
interactions in ground-state, three-body systems with Coulomb, 18: 36171
interactions in plasma, processes in, (E), 19: 19229 (AD-274249)
interactions in Rydberg states of diatomic, rotation-electronic (T), 19: 2969
interactions of electronic and nuclear motion in, time-dependent theory of, 18: 40126
interactions of, distributions from inelastic, (T), 19: 8066 (UCRL-11135)
interactions through long-range forces, dynamics of, 17: 22270 (LADC-5771)
interactions with atoms and molecules at high energies, potential for neutral, 16: 10769
interactions with atoms and molecules in molecular structure, 16: 15321
interactions with atoms, theory of, 17: 34632
interactions with molecules, cross sections for vibrational transitions in, 18: 24322
interactions with molecules, distorted-wave method in inelastic, 18: 24323
interactions with resonant cavity of electromagnetic field, quantum electrodynamics of, 18: 26399
interactions with molecules, atom switching in, 20: 33256 (CONF-660320-2)
internal rotation in, relations with structure, 19: 9046(R) (IS-900(Sect.C))
ion reactions at low energies, processes in, 17: 39812
ion reactions with, ion cyclotron resonance spectrometer for analyzing, 19: 18245
ion reactions with, energy transfer in, 20: 18556(R) (BNL-929, pp 66-82)
ion reactions with polar, capture cross sections for, 20: 34080 (N-66-16939)
ion reactions with, review of, 19: 44950
ionization by action of high-intensity light in magnetic trap, 18: 22972
ionization by electron impact, isotope and molecular-structure effects on, 17: 35747
ionization by electrons or photons, evaluation of studies on, 18: 35520
ionization by electrons, effects of competitive decomposition processes on efficiency curves for, 18: 41406
ionization cross sections and partial vapor pressures of, use of evaporation isotherms and mass spectroscopy in determining, 17: 33891
ionization in collision, (E), 19: 14264
ionization in comets, processes for, 18: 8998(T)
ionization of gaseous, colloquim on chemical physics of, Liège, Oct. 1963, 18: 35517
ionization of, isotope effects, nature of, and yields in, 17: 30593
ionization of polyatomic, diabatic effect on electron-impact, 18: 16692
ionization of simple gaseous, by electron impact, studies, 19: 14126 (FSU-2690-14)
ionization of, effects of Rydberg electron in auto-, 20: 36819
ionization of, isotope effects on electron-impact, 20: 22853(R) (ANL-7060)
ionization of, isotope effects on photo-, 20: 22853(R) (ANL-7060)
ionization potentials of, effects of substitution on, 17: 35669 (AD-295124)
ionization potentials of, mass spectrometer measurement of, 18: 25345
isotope effect in organic, 17: 27411
isotope effects on, calculation of initial and transitional state vibration frequencies for determination of, 18: 19951
isotope effects on dipole moments of linear YXY', 18: 33597
isotope exchange of, effects of separation factor on properties of, 19: 46408(T) (ORNL-tr-770)
isotopic abundance determination from emission spectra of, 17: 32023
isotopic separation of homo- and heteronuclear diatomic, by adsorption at low temperatures, 17: 23807
Jahn-Teller effect in, energy values of, 19: 39265(R) (IA-1021)
kinetic theory of loaded spheres, 17: 29431
kinetics of many-body systems of, statistical mechanics for, 18: 42477
kinetics of polyatomic, hamiltonian for, 19: 23488
labeling with radioisotopes, rules for formulas and nomenclature following, 19: 19736
localized self-consistent-field orbitals in, theory of, 20: 3863(R) (IS-1200(Sect. C))
luminescence properties in liquids, 18: 25562
magnetic moments of, 20: 37750
magnetic properties of, calculation of, 19: 32048(R) (NP-15073)
magnetic relaxation in liquids, effects of shapes on, 17: 18077
magnetic susceptibility of diatomic, method for calculation of, 17: 31109
many electron theory of, and reactions with molecules, 18: 43456
mass-radius relation at low temperatures, 16: 27866
mean free path in a molecular beam, 16: 871
mesic (μ^-), formation rates in hydrogen, 17: 9586
microwave reactions with gases of, spectral line shapes in, 18: 44303
models for, self-consistent-field, 19: 32888
molecular orbital studies of diatomic, 17: 31122
moment equations for gaseous di-, 17: 12845
motion in compounds, study by neutron transmission, (E/T), 20: 19273(R) (BNL-929, pp 3-43)
motion in condensed phases, isotope and vapor pressure effects of, 19: 23355(R) (BNL-867(p.1-117))
motion in liquids, Van Hove functions for, 18: 29666
motion in liquids, models for, 19: 23738
motion of, in solids, review of NMR studies of, 20: 18672
motions in condensed matter, slow neutron studies of, 19: 40455 (BNL-9297)
neutron cross sections of, tabulations, (E), 20: 3018 (NYO-72-27)
neutron differential scattering cross sections of gaseous, calculation of, (T), 20: 3135
neutron elastic and quasielastic scattering by, cross sections for, (T), 20: 26076
neutron inelastic scattering by, first-moment calculations of, 18: 40474 (IDO-16977(p.23-43))
neutron resonance absorption and scattering by, cross sections for, (T), 20: 6266
neutron scattering, 16: 10981
neutron scattering cross sections of free, 16: 33684 (NP-12134)
neutron scattering by gaseous, thermal, 16: 33787
neutron scattering cross sections for, classical selfcorrelation for thermal, 17: 19236
neutron scattering by, cross sections, 17: 19379
neutron scattering by rotating, cross sections for thermal, 17: 22545
neutron scattering by complex, thermal, 18: 2805

neutron scattering by rotating states in, 18: 24299 (NP-13930(p.56-7))
neutron scattering by, cross sections for slow, 18: 32715 (KFKI-64-3)
neutron scattering by, modification of Krieger-Nelkin approximation for thermal, (T), 19: 5120
neutron scattering by free, low-energy, (T), 19: 33212
neutron scattering by, kinetic equations for thermal, (T), 19: 35366
neutron scattering cross sections for OH, calculation of differential, 17: 26540
neutron scattering by, thermal, 17: 36629 (PAN-255)
neutron scattering by nonspherical, 17: 36669 (WASH-1042)
neutron scattering by, at chemical bond energies, 17: 38036(T) (AEC-tr-5734(p.213-17))
neutron scattering on gases of, mass tensor approximation for thermal, 17: 39963
neutron scattering by, thermal, (T), 20: 19800
neutron scattering by, review on, (E), 20: 19801
neutron scattering by, mass-tensor approximation for slow, 20: 28253
neutron scattering by, nuclear spin correlation effects on, (T), 20: 34814 (BNL-940, pp 169-72)
neutron scattering by linear, thermal, (T), 20: 38002
neutron scattering by, effects of nuclear spin correlations on, (T), 20: 38004
neutron scattering by, effect of nuclear spin correlations on, 20: 42144
neutron scattering by nonspherical, in fluids, (T), 19: 16382
nuclear interactions in, 17: 19237
nuclear magnetic dipole-dipole relaxation in, 19: 16381
nuclear magnetic relaxation of 3-spin asymmetric, in liquids, 16: 22790
nuclear magnetic relaxation and resonance in liquids, 17: 822
nuclear magnetic relaxation of spin-½ nuclei in spherical, dipole interactions in, 17: 26584
nuclear magnetic resonance of, role of multiple quantum transitions in, 18: 13081
nuclear magnetic relaxation of many-spin system of, (T), 20: 20116
nuclear magnetic resonance spectra of, performance of INDOR technique for, 20: 42529
nuclear magnetic shielding in linear, 16: 22096
nuclear magnetic shielding in, neighbor anisotropy effect on, 17: 36436 (NP-13020(p.448-50))
nuclear quadrupole coupling constant in polar, 17: 30545(T)
nuclear quadrupole coupling constant in polyatomic, 19: 11086
nuclear spin relaxation for linear, in dilute gases, (T), 20: 11784
nuclear spin-spin coupling in, 17: 36435 (NP-13020(p.423-41))
nuclear spin-spin interactions in, variational calculation of coupled, 16: 7976
nuclear transformations in, chemical and physical effects in, 19: 9230
optical excitation of biological, 20: 30974
orbitals in, contour diagrams for localized, 20: 40796(R) (IS-1500 (Sect.C))
orbitals of, constant- and minimum-energy orthogonalization of, 19: 14249
oscillations in system of two-level, in radiation field, (T), 19: 29009
oscillations of tetragonal, in fcc crystals, 20: 15940 (JUL-292-RW)
pair distribution function in gases, properties of, 20: 7959 (ANL-7063)
particle scattering by polyatomic, models for, 17: 19101
perturbation theory calculations for, virial theorem inclusion in, 19: 14252
perturbation theory for symmetrical, field form of, 20: 2607
perturbation theory for symmetrical, field form of, 20: 2608
photochemistry of polyatomic, 19: 32048(R) (NP-15073)
photodissociation of polyatomic, molecular beam determination of energy partition in, 18: 31570 (UCRL-11359)
photoionization, 16: 26027
photoionization in electromagnetic field, analysis of, (E/T), 20: 27721(T) (NP-tr-1380)
photoionization of, equipment for measuring, 19: 19955(R) (ANL-6938 (p.21-2))
photon absorption by, phonon and photon emission in, (T), 19: 23306
photon propagation in system of resonant, (T), 19: 32812
photon reactions with, excitation and ionization by multi-, 19: 47234
physical chemistry of macro-, 20: 18184(R) (BNL-929, pp 115-25)
polarizability and shielding factor for, perturbation theory calculation of dipole, 20: 4537 (NP-15576)
polarizability and shielding factor for, perturbation theory calculation of quadrupole, 20: 4538 (NP-15577)
polarization of imperfect-gas, statistical theory of, 18: 42163 (UCRL-11595)
positron reactions with, resonance annihilation in, (T), 19: 8081
positron reactions with, resonant annihilation in, (T), 19: 14271
potential curves for BeH^+ and CH^+ ions, 16: 29520
potential energy curves of diatomic, 16: 12277
potential energy curves from band-spectral data, 16: 13700 (NP-11429)
potential-energy functions of diatomic, method of calculating, 17: 39055
potential energy functions for, determination from spectral data, 20: 31949
potential energy of diatomic, determination methods for, 19: 32048 (NP-15073)
potential energy surface-crossing transitions, 16: 6835
potential functions for, 18: 42313
potential of systems of ions and dipolar, classical theory, 16: 26019
precession of spinning, in nonuniform magnetic field, 18: 9239
preparation of labeled, review on methods for, 19: 28423
preparation of labeled, survey of SORIN, 20: 18804 (SORIN-34)
preparation of tritium-labeled, bibliography on, 19: 30300 (IFA/CO/29)
production in atom recombination on surfaces, energy transfer in, 18: 40157
production of meson (μ), in hydrogen, 17: 33003 (NEVIS-117)
properties, four-dimensional electron density function for calculating, 16: 19497
properties of heavy, for ion thrustor propellant, 18: 12284 (NASA-TN-D-1185)
properties of isotopic condensed systems of, theory for, 18: 28264
properties of macro-, electric and magnetic, 16: 11586(T) (JPRS-12342)
properties of, research on, 19: 41967(R) (MIT-QPR-57)
properties of, unified treatment of integrals for quantum calculations of chemical and physical, 19: 8255
proton chemical shifts for, electron density relation to, 18: 29676
proton reactions with, review on, 19: 32906
proton reactions with, validity of Born approximation for fragmentation in, 18: 43629
proton scattering by diatomic, (E/T), 19: 6439 (AFCRL-63-697)
proton transfer between, by hydrogen bond formation, 19: 22183
proton transfer to positive ions, 17: 34646
quantum mechanics of, research on, 17: 22278(R) (TID-18543)
quantum mechanical three-body problem applied to nonlinear triatomic, 18: 36172
quantum mechanics description of, density matrix behavior at Coulomb singularities of Schroedinger equation for, 18: 15003
quantum statistics of, with internal rotator, 17: 11343
quantum theory and wave functions, 19: 1436
quantum theory of, group theory in, 18: 26438
radiation absorption and transformation by, density matrix equations for monochromatic, 17: 34760(T)
radiation damage, initial actions, 16: 8571
radiation damage to, partial, 17: 27114
radiation decomposition of, 17: 14314 (TID-17939)
radiation effects on reaction mechanisms, use of metal ions as protective agents, 16: 9932
radiation effects on macro-, mechanism of uv, 18: 11690
radiation effects on macro-, 18: 11767
radiation effects on, in biological systems, 18: 25105
radiation effects on, excitation processes in, 18: 37198(T) (AEC-tr-6398(p.252-7))
radiation effects on *E. coli* macro-, chemical repair of x, 19: 10917
radiation effects on biological, 19: 26058
radiation effects on diffusion of, 19: 45922
radiation effects on, distribution of energy in, 20: 14595
radiation effects on biological, 20: 16160 (UCRL-14739(Pt.2))
radiation effects on, 20: 16160 (UCRL-14739(Pt.2))
radiation effects on collagen, uv, 20: 18252
radiation effects on, in mixtures, partition of absorbed energy from charged-particle, 20: 33392
radiation scattering by, stimulated-resonance Raman, (T), 20: 23902
radiative emission of, spectra of nonequilibrium, 20: 23903
radioinduced changes in, in desoxyribonucleic acid, 16: 26836
radioinduced dissociation of, laser-beam, 18: 35632
radioinduced ionization of, mechanisms of, 20: 22853(R) (ANL-7060)
radiolysis of gaseous, ion yields and dose partition in, 20: 18754
radiosensitivity of, in biological systems, effects of environment on, 18: 1433
reaction kinetics and mechanisms at high temperatures, 17: 27538(R) (NP-12767)
reaction mechanisms of protein macro-, with radiomimetic and radioprotective compounds, 20: 5423
reactions, electron spin exchange in, 16: 25986
reactions in gases, eigenfunctions of Boltzmann operator for, 18: 34331
reactions in gases, principle of detailed balancing in, (T), 19: 8019
reactions in mixtures of, statistical mechanics of, 19: 41130
reactions in optical masers, resonant excitation transfer in, 18: 32491
reactions in planetary and stellar atmospheres, 17: 16886
reactions of, analysis in coincidence mass spectrometers, 17: 29935
reactions of diatomic, wave functions for atomic, 18: 32412
reactions of gaseous with positive ions at 3×10^{-3} to 10^{3} ev, 16: 6473
reactions of gaseous with cations at 3×10^{-3} to 10^{3} ev, 16: 14777(T) (CEA-tr-R-1461)
reactions of gaseous, with positive ions at 3×10^{-2} to 10^{3} ev, 16: 23725(T) (AEC-tr-5155)
reactions of polyatomic, with electrons, 20: 16159(R) (ORNL-3900,

pp 150-81)
reactions of, bibliography on, 20: 15248 (ORNL-AMPIC-3)
reactions of, quantum corrections to transport collision integrals for, 20: 34078 (N-65-32048)
reactions of, quantum corrections to transport collision integrals for, 20: 34079 (N-65-32195)
reactions of, vibrational energy transfer probabilities for, 18: 32490
reactions, reliability of Hellmann-Feynman theorem for approximate charge densities in, 16: 25970
reactions with atoms and molecules, ionization in, 16: 26042
reactions with atoms, calculations of resonance behavior of cross sections for, 17: 37878
reactions with atoms, vibrational energy transfer in, 18: 20776
reactions with atoms, vibrational relaxation in, 18: 22678
reactions with atoms, asymmetry effects in, 18: 36164
reactions with atoms, asymmetry effects in, 18: 36165
reactions with atoms and molecules, compilation of cross sections for, 18: 36718 (ORNL-3113(Rev.))
reactions with atoms, combined electric-dipole and magnetic-dipole EPR spectra of gaseous, 19: 11108
reactions with atoms, effects of double-impact collision on dissociation rate in, 19: 36414
reactions with electronically excited species and free radicals in gases, 18: 22928(R) (AD-435879)
reactions with electrons, effects of long- and short-range forces on, (E/T), 20: 7659(R) (ORNL-3849, pp 101-50)
reactions with hydrated electrons, review on, 20: 5525 (IA-1041)
reactions with ions in high electron-affinity gases, 16: 6471
reactions with ions, design of drift tube-mass spectrometer for studying, 16: 8952
reactions with ions, excitation and ionization cross sections for, 16: 26036
reactions with ions, charge transfer and electron detachment in, 16: 26042
reactions with ions in gases, 17: 8095
reactions with ions in mass spectrometer, velocity-dependence of cross sections for, 17: 12187
reactions with ions, distributions, 17: 12829
reactions with ions, cross sections for, 17: 31219
reactions with ions, cross sections for, 17: 36538
reactions with ions, mass spectrometer for studies of, 17: 38989
reactions with ions, method for determining mechanism of electron-induced, 17: 40853 (TID-18176)
reactions with ions, use of mass spectrometer in studies of, 18: 21703 (CONF-296-4)
reactions with ions in afterglow plasma, 18: 36078 (AFCRL-64-107)
reactions with ions in beams, charge and momentum exchange in, 18: 40153
reactions with ions, effects of polarization energy on, 19: 13323
reactions with ions at atmospheric pressure, evidence for chain, 19: 28385
reactions with ions, role in ionosphere formation of, 19: 30191
reactions with ions at 100 ev to 25 kev, mechanisms in, 19: 32048(R) (NP-15073)
reactions with ions, energy effects on cross sections for dissociation in, (E), 19: 44948
reactions with ions in ethylene, mass spectrometry of, 19: 46161(R) (ORNL-3832, pp 116-50)
reactions with ions, ion-cyclotron double resonance in, 20: 38902
reactions with molecules, sensitized fluorescence theory for, 20: 27754
reactions with molecules, device for studying forces of, 20: 44145
reactions with moving unequal-mass particles, energy transfer in, (T), 20: 37447
reactions with muonium, 20: 17297
reactions with solid surfaces, 20: 29624(R) (TID-22970, pp 257-329)
research programs on physics of, 20: 41511(R) (RLO-1388-501)
research using Mössbauer effect, 20: 34630
role in radiation injuries of biological systems, 20: 18274
rotation and vibration levels in triatomic, coordinate system for theory of, 19: 16696
rotational and vibrational freedom of hydrogen atoms in, from neutron cross-section measurements, 17: 21607
rotational excitation of ionized, by slow electrons, 18: 783
rotational states of polar, in rare gas crystals, 16: 16330 (AD-264708)
rotations in gases, neutron scattering measurements of, 20: 25740
rotations of, determination by cold neutron scattering by liquids and solids, 18: 43658
scattering by atoms, cross sections and transition probabilities in, 18: 10779
scattering by gases, cross sections for, 19: 14265
scattering by metal surfaces, book, 19: 35601
scattering by solids, transition probabilities for, (T), 20: 2594 (N64-23208)
scattering by surfaces, misalignment effects in, 18: 8914 (K-1584)
scattering by, theory of resonance, 18: 44571
scattering cross section measurements on, determination of Lennard-Jones parameters from total, 18: 22046
scattering in linear lattice systems, time-dependent, (T), 19: 47255
scattering of atoms by diatomic, 17: 35263(R) (UCRL-10706(p.1-110))
scattering of chemically reactive, 17: 35263(R) (UCRL-10706(p.1-110))
scattering of chemically reactive, cross sections for elastic, 18: 32482
scattering of, quantum effects in elastic, 18: 30616 (COO-1328-7)
scattering of, quantum scattering theory of, 18: 42323
scattering of, R-matrix theory for elastic and reactive, (T), 20: 17259
scattering of, wave packets in quantum theory for, 19: 21092
Schroedinger equation for, one-electron solution to, 18: 34422
Schroedinger equation for, Monte Carlo evaluation of integrals in, 18: 34423
Schroedinger equation for, ground state energies in, 18: 34424
separation of isotopic constituents in, electrolytic, 17: 33876(T) (CEA-tr-A-1303)
separation of isotopic, gas chromatography method for, 18: 12240
sorption of isotopic hydrogen, theory of, 18: 28502
sound propagation in gases of, disturbances in, 18: 26135
spectra, allowed transitions and probabilities for, 16: 26026
spectra at low pressure and high temperature, Stark and Zeeman components of microwave, (T), 19: 37235
spectra, forbidden transitions in, 16: 26025
spectra in systems of, two-photon absorption, (T), 19: 47236
spectra lines from ion excited, rotational structure of, 20: 37471
spectra, molecular beam electric resonance apparatus for studying hyperfine structure, 16: 29481(R) (NP-11989)
spectra of axially symmetric, analysis of vibration-rotation, 17: 37243
spectra of charged diatomic, intensities of rotational and vibrational, 16: 10005
spectra of di- and polyatomic, review, 16: 15365
spectra of diatomic, electronic, 18: 31432(R) (UCRL-11317(p.15-17))
spectra of dissolved free-radical, hyperfine structure of, 19: 5903
spectra of, isotopic shifts in, 17: 27396
spectra of isotopic polar, equations for infrared band intensities for sets of, 19: 17930(T)
spectra of isotopically disordered linear chain, integrated, (T), 19: 47256
spectra of, lattice combination bands in, 17: 8057
spectra of linear triatomic, Renner effect in, 20: 31943
spectra of polyatomic, infrared, 19: 32048(R) (NP-15073)
spectra of tetrahedral XY_4, calculation of mean amplitudes of vibration and related quantities from, 18: 17788
spectra of vibrational modes of, in crystals, (T), 19: 45492
spectra of, fine structure of rotational, (T), 19: 9932
spectra of, isotope effects on vibrational transition probabilities in, 20: 18639
spectra, polarization of emission, 16: 4738(T)
spectral fragmentation patterns and vibrational isotope shifts in, correlation between, 19: 4139
spectroscopy of, neutron, 20: 11377
spin conversions in, NMR observation of, 18: 29616
spin coupling in, nuclear, 19: 5153
spin couplings of, Heitler-London method of calculation of, 17: 11420
spin Hamiltonian coupling constants for, 19: 14251
spin orientation by resonance radiation in cosmic space, 20: 7697(T)
spin relaxation theory for, in gases, 18: 29633
spin-rotation nuclear resonance relaxation effect for large, 17: 8075
sputtering of gold by atmospheric, rates for, 18: 40151
sputtering on surfaces, re-emission law for, 18: 40152
stability of, in Thomas-Fermi theory, 17: 11419
structural peculiarities of biological macro-, in radiobiology phenomena, 17: 17832
structure and properties of diatomic, computational techniques, 16: 7834 (NYO-9490)
structures of simple polyatomic electronically excited, 18: 27383
superexcited states, 16: 30480
temperature in acetylene–air flames, (E), 19: 41922
temperature in gas flow, electron excitation for, 18: 39446
temperatures in stellar atmospheres, (T), 20: 23845
thermal dissociation in shock wave, (T), 19: 29010
thermodynamic functions of, Coriolis interaction correction to, 18: 15681 (LADC-5738)
thermodynamic properties of globular, at 5 to 350°K, 16: 2928 (TID-14259)
thermodynamics of isotopic, Bigeleisen series expansion for, 20: 7101
topology of electronic potential energy surfaces of degenerate electronic states, 17: 12269
topology of electronic potential energy surfaces of non-degenerate electronic states, 17: 12270
transport cross sections for, quantum corrections to, 18: 34650
transport processes, analysis by moment method techniques, 16: 15379

transport through nuclear membranes in animal cells, 18: 17399(R) (ANL-6790(p.138-44))
vapor pressure of diatomic, vibrational spectroscopy and isotope effect on, 20: 10831
vibration-rotation interaction factors for diatomic, calculation, 18: 32280 (UCRL-10644)
vibration–rotation energies of, perturbation theory for calculation of higher order corrections for, 19: 13344
vibrational force field of polyatomic, 16: 24300
vibrational-frequency sum rule for isotopic, 16: 14747
vibrational frequencies sum rule for symmetrical isotopic, modified, 17: 31113
vibrational frequencies of perturbed and substituted, exact isotope rule for, 18: 12073
vibrational frequencies and intensities of polyatomic, method for theoretical calculation of, 19: 7397
vibrational frequencies of isotopically substituted, relations between, 20: 23001
vibrational potential constants of bent xy_2, third-order, 20: 14559
vibrational relaxations at high temperatures, mechanisms for, 16: 19469 (NP-11613)
vibrational spectra of, group theory for, 19: 11855
vibrational zero-point energy calculations for, perturbation methods for, 17: 35674 (BNL-6551)
vibronic states of dimers, 17: 40688
viscosity of, correlation function for hard-sphere, 18: 25362
wave equation for, solution by configuration interaction method using spin-operator process, 18: 22791
wave equation solution for diatomic, iterative method for, 17: 29421
wave functions for, intra-atomic correlation correction method for elimination of atomic errors in, 17: 40252
wave functions for diatomic, nonadiabatic theory for, 17: 40253
wave functions for homonuclear diatomic, (T), 19: 9883 (ANL-6931)
wave functions for, two-center Coulomb integrals for, (T), 19: 36336 (N64–33904)
wave functions for, in momentum space, (T), 19: 39660
wave functions of diatomic, calculation from potential energies, 16: 27841
wave functions of diatomic, effects of vibration-rotation interaction on, 17: 31110
wave functions of diatomic, quasiclassical calculations of, (T), 19: 6441 (JINR-P-1779)
wave functions of, time-dependent perturbation theory of Hartree-Fock, 18: 34426
wave functions of, program for solution of 2-dimensional Schroedinger, 19: 32051
wave theory of diatomic, relative partial, 17: 36473
wavefunctions for nuclear fusion and vibrations in meson (μ), 17: 24361
wavefunctions of two-electron homonuclear diatomic, (T), 19: 9907
wavefunctions of, cluster expansions and unitary group for incorporating many-body effects in, 19: 23486
weight determinations of desoxyribonucleic acid, in bacteriophages, 19: 35885
x-ray analysis of large biological, 18: 10655
x-ray scattering by helical, 19: 14270
x-ray scattering by non-spherical, in fluids, (T), 19: 16382
yields of excited, from radiolysis of hydrocarbons, 19: 28373
zero-point energies of isotopic homologs and isomers, formula for, 17: 19937

MOLLUSKS

age estimation in marine Pleistocene deposits in Palos Verdes Hills, Calif., from thorium-230 to uranium-234 ratio, 19: 22563
age estimation of, from raised marine terraces by thorium-230/uranium-234 method, 20: 18925 (NYO-3450-1, pp 1-27)
analysis for chromium, isotope dilution, 19: 5831
analysis for magnesium and strontium contents in Mytilus shells, ecological effects on, 19: 26251
analysis for radioactivity in, collected in Italy during 1960, 16: 22428 (CNI-58)
analysis for trace elements, activation, 18: 9818 (EUR-474.e)
analysis for zinc-65 and phosphorus-32 by radiochemical techniques, 19: 46218
analysis of clams for carbonyl compounds, 20: 9334 (CONF-651024, pp 99-100)
analysis of Connecticut, for zinc-65, 1961 to 1963, 18: 6598(R) (TID-19922)
analysis of magnesium content, activation, 17: 26963 (EUR-128.i)
analysis of shells of, for thorium, activation, 18: 43405
barium uptake by, mechanism of, 19: 6971
biological studies on, use of photography in, 19: 12899
cadmium content, 16: 32690(R) (TID-16635)
calcium content in Clinch and Tennessee River, 16: 23410 (ORNL-TM-270)
calcium uptake by aquatic, 17: 35416
calcium uptake by, mechanism of, 19: 6971
carbon-14/carbon-12 ratio in shells of living clams and snails, 17: 34136
carbon-13 content in ratio with carbon-12 in, 18: 36932
carbon-13 content in fresh-water and marine, 19: 4363
carbon-14 content in river, relation of soil humus content to, 18: 12341
carbonate formation in shell of *Strombus gigas*, 18: 19520(R) (TID-20499)
cerium-144 content, Ibaraki, Japan, 16: 5623
cerium-144 uptake by, 18: 3448
cesium-134 uptake by, 18: 29216
cesium-137 absorption by Mytilus, 20: 42770
cesium-137 content in, effects on radioactivity levels of food chain, 19: 17453(T) (JPRS-28560)
cesium-137 uptake by, 18: 4959
cesium-137 uptake by Potamopyrgus, 18: 3463
chromium distribution in, 20: 36552
chromium-51 uptake by clam, chemical and physical factors affecting, 20: 40575
cobalt-60, manganese-54, and zinc-65 content in Columbia River estuary, 20: 40523(R) (RLO-1750-8(Vol.1))
control of, preparation of methyl carbamate pesticide for, 19: 38748
copper content, 16: 32690(R) (TID-16635)
decontamination of oyster, tracer studies using bacteria, 18: 17441
decontamination of, radioactive, 18: 29907
decontamination of Mediterranean, 19: 4425
diet of, used for food by man, 17: 14539(R) (TID-17907)
electron reactions with nonpolar and polar, thermal, 20: 5985 (ORNL-TM-1262)
environmental factors affecting distribution in Bogue Sound area, North Carolina, 17: 31817(R) (TID-19122)
excretion of foreign particles by, tracer study in Bullia, 19: 43695
fission product metabolism by marine, 18: 21780(T) (JPRS-24227)
fission product metabolism by marine, 19: 25780
fission product metabolism in, 19: 24759
fission product metabolism by, 19: 24809
fission product metabolism by marine, 20: 26549(R) (NP-15915)
fission product metabolism, 16: 22456 (TID-7632(p.360-71))
isotope uptake by Bay of Venice, cobalt, manganese-54, ruthenium-106, and zinc-65, 20: 20386(R) (NP-15916)
isotopic abundance in shells of marine, effects of time on, 18: 6943
isotopic composition of shells of, in Lake Managua, Nicaragua, 18: 12340
manganese and manganese-54 distributions in tissues of Lake Maggiore, 19: 45788
manganese content in Lake Maggiore, activation determination of, 19: 45788
manganese-54 content in Lake Maggiore, Italy, 20: 16185
manganese-54 content in freshwater clams, 20: 29462
manganese-54 content in, relation of age to, 17: 31847
manganese-54 determination in Unio, 19: 2058
manganese-54 metabolism in fresh-water, 20: 16160 (UCRL-14739(Pt.2))
manganese-54 uptake, 19: 10762
manganese-54 uptake by marine and terrestrial, 20: 24844
marine, metabolism of fission products, 16: 19210
metabolism of strontium-90 by *Nerita forskali*, 20: 3659(R) (NP-15156)
myocardia of, effects of inorganic ions on, 19: 14942
oxygen-18 content in fresh-water and marine, 19: 4363
paleotemperature analysis of fossil shells, 18: 33784
permeability of axon membrane of, to ions, 18: 29
potassium uptake by, 18: 4959
potassium-42 uptake by Potamopyrgus, 18: 3463
radiation effects on storage life of soft-shelled clams, 16: 22501(R) (NYO-9575)
radiation effects on mussel gills, protective effects of benzimidazoles against ultraviolet, 17: 15674(T)
radiation effects on enzyme systems in, 18: 27062(R) (NYO-1680-1)
radiation effects on shell color, gamma and neutron, 19: 2863
radiation effects on life span of embryonic, beta, 19: 26025
radiation effects on content of carbonyl compounds in, 20: 9334 (CONF-651024, pp 99-100)
radiation effects on wholesomeness of clams, in rat diet, γ, 20: 9330 (CONF-651024, pp 85-7)
radiation effects on coliform contamination in *Venerupis semidecussata*, gamma, 20: 22753
radiation effects on electrophysiological parameters in nerve cells of *Planorbis corneus*, x, 20: 22591
radiation effects on *Physa acuta*, following exposure at various stages of life cycle, x, 20: 40700
radiation injuries in mussels, 20: 139
radiation pasteurization of, gamma, 18: 520
radiation pasteurization of, gamma, 18: 521
radiation processing of shucked soft-shelled clams, effects on storage life

of refrigerated, 17: 8491 (NYO-10412)
radiation processing of, effects on refrigerated storage life and wholesomeness, 18: 11647 (TID-18285)
radiation processing of clams, effects on wholesomeness, 18: 41091(R) (TID-21116)
radiation processing of, to increase storage life, 18: 41113
radiation processing of clams, effects on refrigerated storage life, 19: 8845
radiation processing of clams, effects on amino acid and vitamin content, 19: 8846
radiation processing of oysters, effects on storage life, 19: 20407(R) (ORO-626)
radiation processing of king crab meat, effects on wholesomeness, 19: 26730
radiation processing of, effects on wholesomeness, 19: 32626(R) (NYO-3461-1)
radiation processing of crab, effects on refrigerated storage life, 19: 34599
radiation processing of clams, effects on wholesomeness, 20: 9332 (CONF-651024, pp 93-4)
radiation processing of clams, effects on flavor and odor, 20: 9334 (CONF-651024, pp 99-100)
radioactive contamination of, 18: 29907
radioactive contamination of, 19: 20230
radioactivity from cobalt-60 and silver-110m in coastal and oceanic, 19: 30410
radioactivity in, from Thames River, Conn., 1960 and 1961, 17: 33555
radioactivity in Neman River, Soviet Union, 1961, 18: 10279(T) (JPRS-22702(Del.))
radioactivity in, from fallout in Baltic Bay of Tvären, 1957 to 1963, 19: 22532 (AE-171)
radioactivity of Lake Maggiore, 1961, 19: 10731(R) (NP-14669)
radioactivity of Lake Maggiore, 1952 to 1961, 19: 11391(R) (NP-14658)
radioinduced muscle inactivation in, combined with polarization microscopy for contraction studies, uv, 20: 16259
radioisotope accumulation by ocean-dwelling, 20: 40546
radioisotope content in, near Columbia River mouth, 17: 24866
radioisotope content in, ecological implications of, 19: 43663
radioisotope uptake by, in Clinch River, 17: 40529 (TID-7664(p.193-207))
radioisotope uptake from lake sediments by *Viviparus ater*, 19: 1996
radioisotopes in, chemical properties of, 20: 33502
radionuclide content in, from California waters, 19: 38895
radionuclide distribution in, from coastal and offshore waters of Oregon and Washington, 19: 27910 (UWFL-86)
radionuclide metabolism by marine, 19: 43669(R) (NP-15159)
radionuclide uptake by clams, from water in pond, 18: 25079
RNA synthesis in embryos of, 19: 31675(R) (ORNL-3768(p.70-84))
rubidium-86 exchange in hearts of, effects of corticosterones on, 18: 31093
ruthenium-106 uptake by organs and tissues in mussels, 19: 25882
shell dating of, radiocarbon method for, 17: 34135
sodium-22 uptake by, in reservoir, 19: 35926
strontium and strontium-90 content in Clinch and Tennessee River clams, 16: 23410 (ORNL-TM-270)
strontium content in shells of 1000 to 2000 year old, 20: 6711(R) (ORNL-3849, pp 43-100)
strontium deposits in shells of, as related to morphology, 19: 2059
strontium uptake by, mechanisms of, 19: 6971
strontium uptake by aquatic, 17: 35416
strontium-90 content in clam shells, 16: 21889
strontium-90 uptake by, effects of strontium and calcium content of water, 17: 33566
strontium-90 absorption by Mytilus, 20: 42770
strontium-90 content of, from Pacific Ocean in vicinity of Japan, 1959 through 1961, 18: 23792 (WP/37)
strontium-90 content in, 1965, 19: 45748(R) (TID-22193)
strontium-90 content of, effects on radiation levels of food chain, 19: 17453(T) (JPRS-28560)
strontium-90 uptake and release from, kinetics of, 18: 36917 (A/CONF.28/P/811)
strontium-90 uptake by, 18: 36918
strontium-90 uptake and release in *Nerito forskali* Recluz in seawater, 20: 218(R) (STI/DOC/10/42, pp 1-22)
strontium-90 uptake by marine, correlation with buildup factor, 20: 18215
thorium dioxide permeability of Schwann-cell-layer in squid, 18: 38744
thorium isotopic composition in, in Molodova, Ukraine, 17: 21917
uptake of radioisotopes by marine, 20: 40528
uptake of radioisotopes by, factors affecting, 20: 40578
uptake of sediment-sorbed radioisotopes by, in marine environment, 17: 33561
uptake of trace elements by Indian Ocean, use as biological indicator, 20: 40572
uranium isotopic composition in, in Molodova, Ukraine, 17: 21917
zinc content, 16: 32690(R) (TID-16635)
zinc metabolism in limpets, 18: 6598(R) (TID-19922)
zinc metabolism of, in Thames River, Conn., 17: 35407(R) (TID-19332)
zinc uptake by soft, from silts, 18: 45176 (NYO-10544(Rev.))
zinc-65 content of, from Thames River, Conn., 1960 and 1961, 17: 33558
zinc-65 content in tissues of, along Pacific coast of the United States, 20: 27159
zinc-65 metabolism in fresh-water, 20: 16160 (UCRL-14739(Pt.2))
zinc-65 uptake by, from radioactive wastes in fresh water, 20: 18157 (BNWL-SA-466)

MOLLY-G (White Sands)
see Critical Assemblies

Molten Metal Extraction Processes
see High Temperature Separation Processes

MOLTEN SALT REACTOR EXPERIMENT
see also Power Reactors
accidents during filling, analysis, 20: 40412 (ORNL-TM-497)
chemical basis for, 19: 10564(R) (ORNL-3708(p.214-51))
chemical behavior of flush salt-fuel salt mixtures in, 17: 25061(R) (ORNL-3417(p.17-40))
component development, 19: 10560(R) (ORNL-3708(p.167-90))
component development, 19: 35772(R) (ORNL-3812(p.27-53))
component development, 20: 8399(R) (ORNL-3872)
component development for, 20: 32802(R) (ORNL-3936, pp 53-81)
component positioning for, optical tooling for, 18: 17977(R) (ORNL-TM-793)
components and materials for, data on, 18: 7937
components, compatibility with fuels, 16: 17555(R) (ORNL-3262 (p.19-26))
components development and testing, 20: 18020(R) (ORNL-3900, pp 2-81)
computer programming for, 20: 41232(R) (ORNL-3875, pp 75-90)
control and instrumentation, 19: 10558(R) (ORNL-3708(p.115-46))
control and instrumentation, 20: 8399(R) (ORNL-3872)
control by boron trifluoride poisoning, 16: 12682
control of, computer for, 19: 45585 (ORNL-P-1502)
control rod design for, 18: 28937(R) (ORNL-3578(p.100-21))
control rod reactivity calculations for, xenon-135 effects on, 20: 32803(R) (ORNL-3936, pp 82-92)
control system modes in, 19: 43502(R) (ORNL-3782, pp 102-14)
coolant and fuel density measurements for, 20: 8399(R) (ORNL-3872)
coolant and fuel for, voltammetric properties of, 19: 17781(R) (ORNL-3750)
coolant and fuel for, production of, 19: 31608(R) (ORNL-3789(p.99-109))
coolant and fuel pump tanks for, strain-fatigue and thermal-stress analyses of, 16: 34075 (ORNL-TM-78)
coolant and fuel preparation for, 18: 22172(R) (ORNL-3591(p.59-64))
coolant and fuel production for, 19: 10566(R) (ORNL-3708(p.288-303))
coolant chemistry of, 20: 32804(R) (ORNL-3936, pp 122-71)
coolant loops of, corrosion studies on, 20: 8399(R) (ORNL-3872)
coolant preparation and properties for, 19: 3786
cooling system of, thermal stresses in, 19: 45587 (ORNL-P-1504)
core of, development of graphite for, 19: 10570(R) (ORNL-3708(p.373-89))
criticality studies, 19: 45586 (ORNL-P-1503)
criticality studies, 20: 8399(R) (ORNL-3872)
criticality studies on, 20: 3505
data analysis and collection system for, 19: 42688(R) (ORNL-3782, pp 74-83)
data collection and analysis for, 20: 41232(R) (ORNL-3875, pp 75-90)
data-handling system for, criteria and specifications for, 17: 14611(R) (ORNL-3378(p.37-43))
description, 17: 40384
description of, review, (E), 19: 43553
design, 16: 801
design, 18: 35152 (ORNL-TM-732)
design and construction, 19: 10556(R) (ORNL-3708(p.22-82))
design and development, 16: 11260
design and development of, 17: 7562(R) (ORNL-3369)
design and development, Feb.-July 1963, 18: 7968(R) (ORNL-3529 (p.3-67))
design and development, 19: 35770(R) (ORNL-3812)
design and fabrication of, 18: 29122(R) (ORNL-3578(p.96-9))
design and fabrication, 18: 35221(R) (ORNL-3626(p.3-58))
design and nuclear characteristics of, 18: 9650 (ORNL-TM-730)
design and operation, 16: 11168
design characteristics, 20: 36442
design, components development, and engineering analysis, 16: 9665(R) (ORNL-3215)
design data sheet revisions, 18: 29056 (ORNL-TM-871)
design, development, and engineering analysis, 17: 26765(R) (ORNL-3419)
design of, revisions of data sheets for, 17: 33375 (ORNL-TM-638)

design of, survey, (E), 19: 14887 (ORNL-TM-728)
design, development, and operation, 19: 35771(R) (ORNL-3812(p.5-26))
development, 16: 25023(R) (ORNL-3282)
development, 16: 31311
development, 18: 33080 (A/CONF.28/P/212)
development and fabrication of, 19: 23996(R) (ORNL-3650(p.1-110))
development and operation, 16: 18634
development mission, 19: 10555(R) (ORNL-3708(p.3-21))
development objectives, 19: 10554(R) (ORNL-3708(p.1-3))
development of, 16: 30166(R) (ORNL-3313(p.1-18))
development of, chemical, 19: 10567(R) (ORNL-3708(p.304-20))
development, Feb.-July 1964, 19: 10553(R) (ORNL-3708)
emergency and safety procedures for, (E), 19: 31611 (ORNL-TM-909)
fabrication and installation, 19: 29793
fuel analysis for, methods of, 18: 13632(R) (ORNL-3537(p.47-57))
fuel analysis for, development of methods of, 19: 10568(R) (ORNL-3708(p.320-30))
fuel analysis for, methods of, 19: 17781(R) (ORNL-3750)
fuel analysis for, methods development for, 20: 32804(R) (ORNL-3936, pp 122-71)
fuel analysis of, development of methods for, 20: 8399(R) (ORNL-3872)
fuel analysis, methods for, 20: 14454(R) (ORNL-3889, pp 17-24)
fuel and structural materials compatibility, capsule irradiation test on, 18: 24907 (ORNL-TM-870)
fuel circulation in, pump design for, 20: 14164
fuel development, 18: 1660
fuel for, chemical reactions and properties of, 18: 22011(R) (ORNL-3591(p.38-58))
fuel for, processing for uranium tetrafluoride recovery by distillation, 19: 30067(R) (ORNL-3789(p.56-98))
fuel for, rare earth separation from, 19: 30149(R) (ORNL-3789(p.3-35))
fuel irradiation experiments in, krypton and xenon release in, 17: 34481 (CONF-126-8)
fuel irradiation testing, 18: 22111(R) (ORNL-3591(p.16-37))
fuel level and temperature in, ultrasonic instrumentation for measuring, 19: 19390(R) (NYO-2910-8)
fuel level indication in, design of ultrasonic sensing probe for, 18: 18136(R) (NYO-2910-2)
fuel level indication in, development of ultrasonic sensing probe for, 18: 31842(R) (NYO-2910-4)
fuel level indication in, design of ultrasonic sensing probe for, 18: 31843(R) (NYO-2910-3)
fuel preparation and properties for, 19: 3786
fuel processing by atomization, 16: 11503(R) (ORNL-TM-34)
fuel processing facility design and development for, 19: 10562(R) (ORNL-3708(p.201-5))
fuel processing for, equipment flowsheet for, 19: 4255(R) (ORNL-3627 (p.267-8))
fuel processing for, 20: 16582
fuel processing plant, description and operation of, 19: 24612 (ORNL-TM-907)
fuel processing system status, 19: 35774(R) (ORNL-3812(p.169-73))
fuel processing, review, 19: 34284
fuel production for, facility design and operation for, 17: 25063(R) (ORNL-3417(p.51-60))
fuel pump back diffusion in, determination for fission gas of, 16: 28392 (TID-7631(p.76-84))
fuel pump development and water tests, 16: 13180 (ORNL-TM-79)
fuel reprocessing facility for, continuous moisture analyzer for gases containing hydrogen fluoride in, 20: 20581
fuel samples for, pre-analysis homogenization procedures for, 16: 30021 (ORNL-TM-291)
fuel sampling for analysis, apparatus for, 19: 44168 (ORNL-P-1532)
fuel solutions for, development of, 17: 25060(R) (ORNL-3417(p.3-16))
fuel storage and drain tank critical factors, 18: 43081 (ORNL-TM-759)
fuel storage tank of, ultrasonic level probe for, 20: 8399(R) (ORNL-3872)
fuels for, preparation and loading of, 20: 22856(R) (ORNL-3913, pp 1-51)
fuels of, vapor pressure of, 20: 8399(R) (ORNL-3872)
hazards analysis, 18: 35152 (ORNL-TM-732)
heat exchanger fabrication, 18: 44055(R) (ORNL-3670(p.216-24))
heat exchanger fabrication for, 19: 2477
heat exchanger for, design and fabrication of, 18: 10512
heat exchanger tube bundle fabrication, 18: 4214 (ORNL-3500)
heat exchanger tube plugging for pressure drop reduction, 19: 12844 (ORNL-TM-1023)
heating-system design and operation for, 1200°F, 19: 29794
instrument design, 16: 11863(R) (ORNL-3191(p.66-88))
instrument development status of, 19: 42691(R) (ORNL-3782, pp 140-3)
instrument development for, 19: 43503(R) (ORNL-3782, pp 115-39)
instrumentation development for, 17: 14614(R) (ORNL-3378(p.63-79))
instrumentation development for, 20: 42581(R) (ORNL-3875, pp 125-50)
instrumentation for, modular, 20: 28849
kinetics analysis, computer program for, 16: 17239 (ORNL-TM-203)
kinetics of, computer analysis program for, 16: 26619 (ORNL-TM-203 (Add.))
maintenance equipment for, remote, 17: 2769
maintenance of, remote, 17: 3719
maintenance of, remote, 19: 10561(R) (ORNL-3708(p.190-200))
materials corrosion testing for, 20: 31683(R) (ORNL-3936, pp 95-121)
materials development and testing for, 18: 7129(R) (ORNL-3529(p.71-143))
materials development for, 18: 44055(R) (ORNL-3670(p.216-24))
materials fabrication and testing for, 19: 34629(R) (ORNL-3812 (p.63-86))
materials for, 19: 2844
materials for, mechanical properties of INOR-8 heats used as, 19: 16078 (ORNL-TM-1017)
materials for, metallurgy of, 19: 10569(R) (ORNL-3708(p.330-72))
materials for, metallurgy of, 20: 8399(R) (ORNL-3872)
materials for, production and properties of, 18: 34050(R) (ORNL-3626 (p.59-164))
materials for, radiation effects on compatibility of, 19: 10565(R) (ORNL-3708(p.252-87))
materials for, status of, 18: 26937
materials problems in, 18: 22996
metallurgical test rig for, on-line digital control of, 20: 42581(R) (ORNL-3875, pp 125-50)
neutron losses in, delayed, 20: 18048 (ORNL-P-1967)
neutron sources in unirradiated fuel, inherent, 17: 36875 (ORNL-TM-611)
nuclear characteristics, 19: 10557(R) (ORNL-3708(p.83-114))
operating safety limits for, (E), 19: 31610 (ORNL-TM-733)
operation and maintenance of, 20: 32801(R) (ORNL-3936, pp 7-52)
operation and performance, 20: 47015 (ORNL-P-2397)
operation at steady power, effective contributions of delayed neutrons during, 17: 4337 (ORNL-TM-380)
operation, core temperatures during steady-state, 17: 15500 (ORNL-TM-378)
operation of, Mar.–Aug. 65, 20: 8399(R) (ORNL-3872)
operation of, neutron-source safety requirements in, 18: 43082 (ORNL-TM-935)
operation of, personnel training simulators for, 20: 30934 (ORNL-TM-1445)
operation plans for, 19: 10563(R) (ORNL-3708(p.205-13))
operation safety limits of, 19: 40189 (ORNL-TM-733(Rev.))
operator training simulator for, 20: 42581(R) (ORNL-3875, pp 125-50)
piping for, fabrication of brazed joints in, 18: 2212
production of fluoride mixtures for, 16: 17556(R) (ORNL-3262(p.27-30))
pump design and development, 19: 10559(R) (ORNL-3708(p.147-67))
pump development for, 20: 8399(R) (ORNL-3872)
radiation and contamination monitoring systems, 19: 27782 (ORNL-TM-1127)
radiation effects on fuels in, 18: 32215 (A/CONF.28/P/241)
reactivity accidents, analysis of conceivable, 16: 24988 (ORNL-TM-251)
safety, chemical aspects, 16: 17557(R) (ORNL-3262(p.31-4))
safety features of, 17: 1038 (IDO-16791(p.293-6))
salt level indicators for, design and installation of, (E), 19: 24175(R) (NYO-2910-9)
shutdown photoneutron sources in, 18: 43082 (ORNL-TM-935)
solvent for, chemistry and thermodynamics of beryllium fluoride–lithium fluoride as, 19: 38582 (ORNL-P-1428)
stability analysis, 19: 35773(R) (ORNL-3812(p.54-60))
stability analysis of, 20: 8463 (ORNL-TM-1070)
stability analysis and dynamic testing programs for, 20: 42581(R) (ORNL-3875, pp 125-50)
steam generator-superheater design for, 17: 8373
stresses of cast metal in, 17: 32573 (ORNL-TM-607)
temperature-kinetic behavior in, mathematical analysis of, 17: 1152 (ORNL-TM-379)
thermocouple scanner system for, engineering drawings of, 19: 6836
use of on-line digital computer in data analysis for, 20: 3591
valves, development of frozen-seal type, 16: 10133 (ORNL-TM-128)

MOLTEN SALT REACTORS
see also Molten Salt Reactor Experiment
breeding behavior of MOSEL-II, with external lead cooling, 20: 28752 (JUL-321-RG)
characteristics of homogeneous and quasi-homogeneous, catalog, 20: 6554 (ANL-7092)
chemical basis for, 19: 10564(R) (ORNL-3708(p.214-51))
control using boron trifluoride poisoning, 16: 12682
coolants and fuels for MOSEL, properties of molten fluorides for use as, 20: 4376 (JUL-268-RG)
core structure of, design of, 20: 1423
cost evaluation of 1000-Mwe converter, 18: 30997 (SL-1954)
description of mercury-boiling fast, 20: 36474 (INR-706/C)
design, 20: 10349(P)
design and economics of power-breeder, 19: 45588 (ORNL-TM-1060)

design of fast-breeder, 20: 16037
design of liquid metal-cooled power breeder, 20: 35098(P)
design of liquid-metal-cooled fast-breeder, 20: 16036
design of power-breeder, 20: 18088 (INR-669/C)
design of power, using potassium-steam binary vapor cycle, 20: 24737 (ORNL-P-2052)
design of 1000-Mw(e) power breeder, 20: 45116 (ORNL-3996)
design principles for, 18: 38352
design, development, and principles, 20: 36442
development, 18: 35064(R) (ORNL-3626)
development, 19: 10567(R) (ORNL-3708(p.304-20))
development, 18: 35064(R) (ORNL-3626)
development, 19: 10555(R) (ORNL-3708(p.3-21))
development and economics of epithermal thorium breeder, 20: 45155
development of, chemical, 19: 10567(R) (ORNL-3708(p.304-20))
evaluation of Molten-salt Epithermal Reactor, 18: 38343 (A/CONF.28/P/538)
feasibility of power-breeder, 17: 40384
fuel analysis for, development of methods of, 19: 10568(R) (ORNL-3708(p.320-30))
fuel and fertile stream reprocessing for breeder, design study of continuous fluorination-distillation plant for, 20: 43422 (ORNL-3791)
fuel cycle for, evaluation of thorium, 20: 14126 (JUL-276-RG)
fuel development for power breeders, 20: 12407 (NEIC-RR-13)
fuel economics for breeding in, 20: 8400 (ORNL-P-1784)
fuel processing cost study for Molten-Salt Converter Reactor, 17: 39201(R) (ORNL-3452(p.240-51))
fuel processing for breeder-type, flowsheet for, 20: 12928(R) (ORNL-3868)
fuel processing methods for thorium–uranium fueled, 20: 9055(R) (ORNL-3830, pp 299-305)
fuel radiolysis in, 18: 34050(R) (ORNL-3626(p.59-164))
heat transfer and power density in MOSEL, (T), 20: 14128 (JUL-296-RG)
neutron cross sections for MOSEL, tabulations of, 20: 14062 (JUL-214-RG)
neutron spectra in power-breeder, 20: 14127 (JUL-291-RG)
neutron spectra in power-breeder, using beryllium fluoride and sodium fluoride, 20: 14129 (JUL-315-RG)
operation of thorium-fueled, economic and technical aspects of, 19: 38186 (ORNL-TM-1145)
performance of breeder-power, 20: 3498
structural materials for, 16: 630
thermodynamic problems of MOSEL, 20: 8319

MOLYBDATE COMPLEXES
complexes with zirconium, properties, 17: 35825
with ferrocyanide, ion exchange properties and crystal structure, 19: 18068
with zirconium properties, 17: 35825

MOLYBDATE IONS
effects on colorimetric determination of uranyl ions using Schiff base, 19: 24421
effects on quantitative separation of niobium and tantalum, 19: 24437
exchange on iron hydroxide, 19: 13525 (KFK-216)
sorption on anion exchange papers in hydrobromic and hydrochloric acids and lithium chloride, 18: 25374
spectra of aqueous, Raman, 18: 1613(R) (ORNL-3488(p-18-20))

MOLYBDATES
see also Ammonium Molybdates
see also Barium Molybdates
see also Calcium Molybdates
see also Cobalt Molybdates
see also Erbium Molybdates
see also Fluomolybdates
see also Holmium Molybdates
see also Lead Molybdates
see also Lithium Molybdates
see also Magnesium Molybdates
see also Nickel Molybdates
see also Phosphomolybdates
see also Potassium Molybdates
see also Rare-Earth Germanium Molybdates
see also Samarium Molybdates
see also Sodium Molybdates
see also Strontium Molybdates
see also Thorium Molybdates
see also Uranium Molybdates
see also Uranyl Molybdates
see also Yttrium Molybdates
see also Zirconium Molybdates
determination in molten salts by potentiometric acid-base titrations, 19: 42436
effects on complexometric titration of zirconium, 18: 41336
effects on complexometric determination of zirconium using stilbazogall II, 19: 30138
effects on copper metabolism, 16: 25151(R) (TID-16073)
fluorescent emission intensity of europium and terbium ions in scheelites, 17: 627
heats of formation of, equation for estimation and correlation of, 20: 35482 (UCRL-16865)
hydrolysis, 18: 1614(R) (ORNL-3488(p.65-90))
luminescence of, mechanisms of, 17: 22275 (NP-12725)
magnetic properties of divalent transition metal, 19: 7430
phase studies of systems with potassium and sodium chlorides and tungstates, 16: 17623(T) (AEC-tr-4456(p.225-30))
reactions with cerium(III), electrometric studies, 17: 15997
reactions with lanthanum nitrate, 17: 8022
reactions with lanthanum, amperometric studies on, 18: 19901
sorptive properties of ferrocyanide molybdate for cesium from acid waste solutions, 19: 7613 (BLG-267)
spectra of europium and terbium ions in, intensities of emission, 17: 6837
thermodynamic properties, 18: 17780 (SC-RR-64-67)

MOLYBDENITES
age determination by rhenium–osmium method, 17: 30733
age of, rhenium method for determining, 17: 27566(T) (AEC-tr-5858)
analysis for rhenium by neutron activation, 19: 28264
analysis for rhenium by neutron activation methods, 20: 38802
availability of, review of, 17: 29253 (NRC-7129)
crystal cleavage of, in ultrahigh vacuum, 20: 21366
effects of uranium fission tracks on, electron microscopy of, 19: 37187
mining of low-grade ore body using nuclear explosives, evaluation, 19: 13565
radiation effects on crystals of, fission-fragment, 17: 24022
sputtering by ion bombardment, layer structure damage in, 17: 35796

MOLYBDENUM
abrasion of, friction, wear, and work-hardening during, 18: 18363
abundance in solar atmosphere, 16: 29599 (AFOSR-3024)
alloying characteristics with rare earths, 18: 41924(R) (IITRI-578P19-13)
alloying effects on oxidation of niobium–zirconium alloys in air and steam, 16: 32078 (AERE-R-4134)
alloying effects on high-temperature properties of uranium alloys, 16: 2246
alloying effects on chromium steel, 16: 3503
alloying effects on cobalt–tungsten carbide systems, 16: 6741
alloying effects on properties of niobium, 16: 7897 (WADC-TR-57-344 (Pt.V))
alloying effects on temper embrittlement of chromium–nickel steel, 16: 7887 (NP-11168)
alloying effects on stainless steel corrosion, 16: 13536
alloying effects on beryllium binary systems, 16: 13593(T) (CEA-tr-X-259)
alloying effects on air-casting and properties of chromium–nickel alloys, 16: 15216
alloying effects on alpha phase nuclei in beta uranium, 16: 4576
alloying effects on creep properties of niobium–zirconium alloy, 16: 16772(P)
alloying effects on cobalt–tungsten alloys, 16: 22617
alloying effects on physical metallurgy of cobalt alloys, 16: 29312 (DMIC-171)
alloying effects on uranium alloys, 16: 33477(R) (NMI-7253)
alloying effects on zirconium alloy corrosion, 17: 6581
alloying effects on iron–nickel–ruthenium–tungsten alloys, 17: 14806(R) (ARF-2158-18)
alloying effects on iron–nickel–tungsten alloys, 17: 14806(R) (ARF-2158-18)
alloying effects on iron–nickel–tungsten alloys, 17: 14826(R) (LAR-14)
alloying effects on iron–nickel–tungsten alloys, 17: 14827(R) (LAR-17)
alloying effects on cobalt–nickel–tungsten alloys, 17: 14827(R) (LAR-17)
alloying effects on iron–nickel–tungsten alloys, 17: 14825(R) (LAR-12)
alloying effects on titanium, 17: 16580(P)
alloying effects of, on uranium diffusion in zirconium, 17: 18821
alloying effects of, on corrosion of iron- and nickel-base alloys, 17: 20412 (HW-76952)
alloying effects of, on oxidation of niobium alloys, 17: 22122
alloying effects on iron self-diffusion, 17: 22177
alloying effects on corrosion of zirconium by steam and water, 17: 23889(R) (ARF-B198-39)
alloying effects on mechanical properties of solid-solution-strengthened niobium alloys, 17: 24001
alloying effects on mechanical properties of vanadium, 17: 25771 (ASD-TDR-62-667)
alloying effects on corrosion resistance of nickel, tungsten, and zirconium alloys, 17: 34352
alloying effects on corrosion resistance of niobium to steam at 540°C, 17: 36221 (BMI-1636)

alloying effects on hardness of chromium, 17: 37548
alloying effects on corrosion of zirconium alloys in steam and water, 17: 37495(T) (TRG-Inf-Ser-100)
alloying effects on ductility and electric conductivity of hardened steel, 17: 39545(T,R) (EURAEC-599)
alloying effects on uranium, 17: 39623
alloying effects on uranium, effects of quenching temperature on, 17: 39627
alloying effects on aluminum–zirconium alloys at 800 to 1000°C, 17: 39657
alloying effects on grain-refinement and alpha to beta transformation in uranium, 17: 41468
alloying effects on corrosion of zirconium by steam, 18: 7134 (AERE-R-4458)
alloying effects on magnetic, mechanical, and oxidation properties of aluminum–iron alloys, 18: 7226
alloying effects on corrosion resistance of zirconium in carbon dioxide, 18: 12576 (GEAP-4089(Vol.I)(Paper 3))
alloying effects on oxidation of niobium–zirconium alloy at 500 and 1000°, 18: 14413(T) (FTD-TT-63-1020)
alloying effects on grain size of uranium, 18: 16509
alloying effects on physical properties of iron–nickel alloys, 18: 24159
alloying effects on iron–nickel alloys, 18: 24161
alloying effects on niobium oxidation, 18: 25936
alloying effects on electric conductivity, hardness, and structure of niobium, 18: 25999
alloying effects on oxidation of plutonium–uranium alloys, 18: 26893(R) (ANL-6868(p.11-108))
alloying effects on high-temperature properties of niobium–tantalum base alloys, 19: 37151(P)
alpha reactions at 24 Mev, isomer production in, (E), 20: 46717
analysis and determination, 20: 14500
analysis for aluminum, iron, magnesium, and silicon, spectrographic, 19: 30143
analysis for boron traces, spectrophotometric, 19: 4064 (RTD-TDR-63-4082)
analysis for carbon, hydrogen, nitrogen, and oxygen, review of methods for, 16: 12995
analysis for carbon, hydrogen, iron, nitrogen, and oxygen, review of methods for, 18: 33516
analysis for carbon, method for, 19: 30142
analysis for copper, iron, nickel, titanium, and zirconium, classical methods for, 18: 19921
analysis for hydrogen, nitrogen, and oxygen, vacuum fusion, 18: 33491
analysis for hydrogen, combustion-gravimetric, 19: 19758 (LA-3225)
analysis for impurities and alloying elements, methods survey, 16: 5267 (MAB-178-M)
analysis for impurities, methods of spectrochemical, 16: 22038
analysis for impurities, spectrographic, 18: 17766
analysis for impurities, review of methods for, 18: 33515
analysis for iron traces, spectrophotometric, 17: 7984
analysis for nickel in high-purity, spectrophotometric, 17: 38959
analysis for nitrogen and oxygen by d-c carbon-arc, gas chromatographic technique, 19: 9069
analysis for nitrogen, isotope-dilution method for, 19: 40444
analysis for oxygen by heat extraction, 16: 7515
analysis for oxygen, comparison of inert gas-fusion and vacuum extraction methods for, 16: 28872 (TID-11794)
analysis for oxygen, vacuum-fusion, 16: 30332 (WAL-TR-823/5)
analysis for oxygen, comparison of fast neutron activation and vacuum fusion methods for, 18: 43419
analysis for oxygen, activation, 20: 16331 (GA-6568)
analysis for rhenium by anion exchange, 19: 13220
analysis for tantalum by ion exchange in hydrofluoric–nitric acid mixtures, 18: 35455
analysis for titanium and zirconium by ion exchange, 20: 3896
analysis for trace amounts of nickel, photometric, 19: 19799
analysis for trace elements by atomic absorption spectrophotometry, 20: 43154
analysis for zirconium by solvent extraction using cupferron, 17: 6012
analysis of high-purity, for copper, spectrophotometric, 17: 25140
analysis of, mass spectrographic, 16: 33515(R) (GEAP-4053-2)
analysis for oxygen, method for, 20: 29108
analytical chemistry review, 16: 32947
annealing in the presence of beryllium vapors, chemical reactions in diffusion, 18: 27388
annealing of neutron radiation effects on electric conductivity of, 16: 27700(T) (AEC-tr-5263)
annealing of, tracer studies of grain boundary migration in, 20: 19251
arc initiation in toroidal hydrogen discharge, effects of impurity gases, 17: 16538
arcing characteristics, surface impurity effects on, 16: 2582 (AERE-R-3805)
argon atom and ion bombardment of, secondary emission in, 16: 21156
argon ion reactions with crystals of, at 50 kev, focused collision sequences in, 17: 22336
argon-ion reactions with, Auger-electron emission in, (E), 19: 41272(T)
argon-ion reactions with, nuclear temperature from, (E), 20: 13885
argon-40 reactions with, neutron and gamma spectra from (E), 19: 3236 (JINR-P-1765)
Auger spectrum, 17: 16810
behavior of rolled single crystals of, 18: 44131 (BM-RI-6539)
bibliography on, 17: 6521 (NP-12417)
bibliography on, 18: 32076
bibliography on, 20: 753 (SB-415(Suppl. 1))
bibliography on, Defense Metals Information Center selected accessions, January 1963, 17: 14739 (NP-12525)
bibliography on, DMIC selected accessions, Sept. 1962, 17: 419 (NP-12170)
bibliography on, DMIC accessions, May 1963, 17: 29246 (AD-407822)
bibliography on metallurgical properties, 16: 15164 (AGARDograph-50)
bibliography on preparation, fabrication, and uses of, 18: 34151
bonding and brazing methods for, 16: 22564 (DMIC-Memo-153)
bonding by ceramic adhesives, 17: 25750
bonding by gas-pressure at high temperature, 16: 13555
bonding of plasma-sprayed tungsten on hot, 18: 39875
bonding of, controlling factors in diffusion, 19: 24964
bonding to alumina, 17: 25691(R) (RBESO-3404-2)
bonding to alumina, 18: 4179 (RTD-TDR-63-4109)
bonding to alumina, 18: 42348 (GEST-2035)
bonding to alumina ceramics using manganese glass, 18: 41931 (SC-R-64-1331)
bonding to cobalt, iron, nickel, palladium, or platinum, method of measuring quality of, 20: 8503(P)
bonding to glass, techniques for fusion, 16: 17781(T) (SCL-T-417)
bonding to itself and other refractory metals by solid-state diffusion methods, 19: 16050(P)
bonding to refractory metals, temperature requirements for solid-state diffusion, 17: 25688(R) (GEMP-177A)
bonding to stainless steel by extrusion, 18: 27937
bonding to tungsten by extrusion, 18: 27937
bonding to uranium carbide and iron–uranium carbide cermets, 20: 9468
book: *Behavior and Properties of Refractory Metals*, 19: 14066
book: *Critical Review of the Analytical Methods of the Titanium, Vanadium, and Chromium Transition Element Groups*, 18: 3702
book: *Tungsten and Molybdenum*, 17: 31014(T)
boron-11 reactions with, neutron and gamma spectra from (E), 19: 3236 (JINR-P-1765)
brazing alloys for, development of, 20: 5867
brazing developments for, 18: 549(R) (NP-13241)
brazing, exothermic, 17: 27760(R) (NP-12901)
brazing in vacuum by r-f induction, 17: 25765
brazing properties, review, 16: 10424 (ASD-TR-61-332(p.661-76))
brazing to carbide cermets, 18: 44049(R) (ORNL-3670(p.77-111))
brazing to graphite, 16: 19322
brazing to graphite, 17: 4912(R) (ORNL-TM-413)
brazing to graphite, 17: 23915 (TID-7620(Pt.I)(p.144-54))
brazing to molybdenum coating on alumina-coated niobium, 17: 36983(R) (AD-290068)
brazing to molybdenum-coated materials, 17: 42401(R) (AD-296862)
brazing to TZM molybdenum alloy, brazing alloy development for, 20: 5866
brazing with stainless steel, 17: 31763(R) (MND-P-3003)
bremsstrahlung reactions (γ,p) at 24 Mev, direct photoeffect and evaporation contributions in, 17: 38209
bremsstrahlung reactions with, heating effects of, (T), 20: 12166 (CONF-651126-1)
bremsstrahlung spectra, 19: 9445 (LA-3130)
brittle fracture and twinning in crystals of, relation of, 17: 25772 (ASD-TDR-63-360)
brittle fracture of, relationship to twinning, 18: 32131 (ASD-TDR-63-360 (Pt.II))
brittle fracture of electron-beam-melted, 19: 26849
brittle-ductile transition temperature in, method for determining, 20: 29757
brittle-fracture stresses and yield in polycrystalline, effects of temperature on, 18: 32184
brittleness testing, 17: 30974 (LAMS-2906)
bulk modulus, Debye temperature, and elastic constant of crystals of, 17: 22189
carbide precipitation on internal and external surfaces of, on annealing, 19: 23085
carbon deposition on surfaces of, 20: 35893(R) (ORNL-3951, pp 84-134)
carburization in presence of graphite and MSRE fuel salt, in-pile, 18: 44055(R) (ORNL-3670(p.216-24))
casting, 17: 4910(R) (MAB-139-M(C7))

casting, melting, and properties of, 17: 16532
catalytic effects on hydrocracking of polyphenyls, 17: 28434 (IDO-16858)
catalytic properties of filaments of, for hydrogen–deuterium exchange, 19: 29812(R) (SRIA-425-4)
cavitation damage, correlation with mechanical properties, 19: 2714 (AD-606050)
cesium film behavior on electrodes of, 17: 32827
cesium ion bombardment, secondary ion emission in, 16: 16881
cesium ion reactions with, excited cesium atom emission from, 20: 23896(T)
cesium ion scattering at 20 to 260 eV, angular regularities in, 19: 16405(T)
cesium ion scattering by, energies of, 17: 17257
cesium ion scattering by, spectra from, 17: 5154(T)
cesium ionization by diffusion through, 16: 884
cesium ionization on, efficiency of, 17: 32825
cesium ionization on surfaces of, 20: 31776
cesium-ion sorption on, 18: 26233(T)
charged particle reactions with, cross sections for, 17: 34886 (UCRL-10783)
chemical regeneration of, in thermionic cells, 17: 27968
chlorination at 400 to 1530°K, kinetics of, 20: 7086
chlorination of, kinetics, 19: 42454 (BM-RI-6649)
cladding, 17: 7571 (TID-17402)
cleaning and polishing, chemical, 18: 12860(R) (NP-13591)
cleavage cracks in single-crystal, method for producing, 20: 21245
cleavage fracture in cast, 18: 36011
coalescence of alpha, with cubic nitrides, 18: 14510
coating by aluminum-base alloys, method for, 20: 43962
coating by zirconium from vapor of iodides, 17: 32507
coating development for, 16: 2174(R) (ER-11462-2)
coating developments for, 18: 541(R) (AD-419549)
coating for protection at high temperatures, 17: 1867(P)
coating for protection at high temperatures, pack cementation process for, 19: 2722 (ML-TDR-64-55)
coating of, by anodic treatment and vapor deposition, 16: 25701 (WADD-TR-61-64)
coating of, effects of, on compression and high-temperature damage and oxidation, 17: 32526
coating of sheet, development of protective, 16: 27603 (MAB-181-M)
coating of sintered, by aluminizing and siliconizing, 20: 37204
coating of, review of techniques for protective, 19: 4605
coating sintered, by electroplating in aqueous electrolytes, 18: 44117
coating techniques for, review of, 18: 7270
coating with aluminum, aluminum alloys, beryllium, and beryllium alloys, 16: 527 (SCNC-326)
coating with boron, properties of boride layers formed in, 18: 6824
coating with ceramics, radiometric method for measuring thickness, 16: 503(T) (CEA-tr-R-1394)
coating with chromium–nickel for oxidation protection at 1100°C, 16: 9149 (ARDE(MX)-89/60)
coating with chromium–nickel and chromium–nickel–cobalt alloys for oxidation protection, 16: 30840
coating with chromium-nickel, stainless steel and zirconium at 1200°C, 17: 22147
coating with chromium–rhenium and rhenium by electrolytic deposition, bonding in, 20: 4404(T) (JPRS-32773)
coating with copper–silicon eutectic for oxidation protection, 20: 11236
coating with disilicides, 18: 34209
coating with germanium by vapor-phase deposition, 19: 16036
coating with glass, diffusion of cobalt in, 16: 5663
coating with molybdenum silicide, effects of diffusion kinetics on, 19: 22943
coating with oxidation-resistant materials by flame spraying, 17: 31763(R) (MND-P-3003)
coating with rhenium by electrolysis, optimum conditions for, 19: 20529
coating with rhenium, electrolytic, 20: 11260
coating with silicides for oxidation protection, studies, 19: 7848(R) (ASD-TDR-63-753(Pt.II))
coating with silicides, 19: 40998(P)
coating with tungsten, 17: 36300(R) (NP-13070)
coating with tungsten, 18: 12860(R) (NP-13591)
coating with zirconium, effects of iodine circulation rate, pressure, and temperature on, 17: 39555
coatings, development of oxidation-resistant, 16: 6705 (AD-261006)
coatings for, 16: 24148(R) (ASD-TR-61-676)
coatings for, development of oxidation-resistant, 16: 2173 (DMIC-Memo-137)
coatings for, development of high-temperature gas resistant, 16: 27595
coatings for, for high-temperature uses, 16: 27687
coatings for, bibliography and review of high-temperature protective, 20: 7516 (OTR-131)
coatings of, compatibility with alumina at high temperatures, 20: 43927
coatings on, lifetime and performance of molybdenum silicide, 20: 5910
compatibility and encapsulation with neodymium, promethium, and samarium oxides, 20: 11267 (BNWL-SA-488)
compatibility of coatings of, with plutonium, thorium, and uranium, 17: 8843
compatibility of coating of, with uranium carbide–zirconium carbide thermionic diode at 1800 to 2500°C, 20: 29820
compatibility with niobium beryllide at 2500°F, 17: 532 (GEMP-105)
compatibility with lead telluride at 600 to 700°C, 17: 23927 (WCAP-1703)
compatibility with bismuth germanium telluride and lead telluride at 500 to 700°C, 17: 23971 (WCAP-1868)
compatibility with uranium dioxide at 1800 and 1900°C, 17: 26944(R) (BMI-1630(Del.))
compatibility with oxide mixtures of aluminum, beryllium, calcium, and magnesium at high temperatures, 17: 41354 (NP-13158)
compatibility with uranium carbide and uranium carbide–uranium sulfide at 1150°C, 17: 40422(R) (ANL-6784)
compatibility with plutonium nitride at 1430°C, 17: 40423(R) (BMI-1639(Del.))
compatibility with plutonium nitride and thorium–uranium carbide, 18: 7985(R) (BMI-1650(Del.))
compatibility with uranium dioxide, 18: 7985(R) (BMI-1650(Del.))
compatibility with plutonium nitrides, 18: 13354(R) (BMI-1657(Del.))
compatibility with uranium dioxide in cesium and vacuum to 1900°C, 18: 12857(R) (GESR-2017)
compatibility with alumina, beryllia, thoria, and yttria in cesium vapor, 18: 12857(R) (GESR-2017)
compatibility with uranium dioxide at 1800°C in vacuum, 18: 15488(R) (GESR-2006)
compatibility with uranium dioxide at 1800°C, 18: 15489(R) (GESR-2007)
compatibility with thorium and uranium borides and carbides, 18: 20450(R) (BMI-1661(Del.))
compatibility with uranium nitride, 18: 20450(R) (BMI-1661(Del.))
compatibility with fissium–plutonium–uranium alloys at 550 to 650°C, 18: 26893(R) (ANL-6868(p.11-108))
compatibility with beryllium–thorium–uranium alloy, 18: 34034(R) (BMI-1672(Del.))
compatibility with graphite–nitrogen environment at 1000 and 1200°C, 19: 40966 (BNWL-92)
compatibility with uranium carbide–zirconium carbide system at 2000°C, 20: 4335
compatibility with plutonium-uranium carbides, 20: 6600(R) (ANL-7105, pp 1-35)
compatibility with urania, 20: 11224
compatibility with cesium at 550°C, 20: 13203
compatibility with alumina, beryllia, magnesia, and boron nitride, 20: 17022 (N-65-18933)
compatibility with uranium carbide and uranium carbide–10 uranium sulfide at 1150°C, 20: 9556
compatibility with uranium phosphides at high temperatures, 20: 23640(R) (ANL-7176, pp 45-72)
compatibility with solid solution uranium carbide–zirconium carbide at high temperatures, 20: 27490 (LA-DC-6901)
compatibility with plutonium carbides at 1200 to 1400°C, 20: 29820
compatibility with cesium vapor at 1800°C, 20: 31669
compatibility with plutonium and uranium nitrides, 20: 35834(R) (BMI-1767)
compatibility with cadmium and indium tantalates, (E), 19: 17202
conference on refractory metals, Oslo, Norway, June 23 to 26, 1963, 18: 34068
conference on, University of Sheffield, Sept. 1960, 16: 25708
conglomeration of powders of, in reduction of molybdenum dioxide with hydrogen, 18: 30124
contact frictional behavior in liquid sodium, 16: 22605
contamination by residual gases in vacuum systems, 18: 14355 (CONF-373-7)
contamination by residual gases in high vacuum, 18: 39826 (ORNL-3674)
contamination in high vacua at 578 to 1202°C, analysis of, 18: 4255(R) (ORNL-3470(p.98-125))
content and distribution in beef heart, 19: 45753 (AE-191)
content in African pitchblende, estimation of induced fission vs spontaneous fission from, 20: 37994
content in high-purity depleted uranium metal, 19: 24481 (GAT-T-1141)
content in human brain, 17: 35419
content in human heart, neutron activation determination of, 18: 33457 (AE-146)
content in mammalian cells, effects of cell cycle stage on, 20: 18204(R) (LA-3432, pp 130-77)
content in organs and tissues of humans outside continental U. S., 19: 21831
content in red-colored Paleozoic deposits in Northern Tien Shan,

20: 14780(T) (AEC-tr-6579)
content in river waters, 17: 30687
content in rocks from North Tien Shan Mountains, U.S.S.R., 20: 33544
content in standard rocks G-1 and W-1, 16: 20830
contrast effect in, absorption, 17: 23954 (LADC-5478)
corrosion, 20: 27538
corrosion by alkali metals, 18: 37634 (A/CONF.28/P/343)
corrosion by ammonium hydroxide, sodium hydroxide, and sodium hypochlorite at 35 and 60°C, 20: 11230 (BM-RI-6715)
corrosion by bismuth–uranium solutions, 17: 14765 (BNL-736)
corrosion by bismuth and tin, 20: 2275
corrosion by cesium at 1600 to 2500°F, 16: 16684 (TID-7626(Pt.I) (p.109-10))
corrosion by cesium at high temperatures, design of capsules for testing, 17: 3426(R) (NP-12189)
corrosion by cesium, 17: 21835
corrosion by cesium at 1000°C, 18: 42348 (GEST-2035)
corrosion by cesium vapors, 19: 11682
corrosion by cesium at 400°C, 20: 4337
corrosion by cesium at 400°C, 20: 11227
corrosion by chloride solutions at 35, 60, and 100°C, 20: 11230 (BM-RI-6715)
corrosion by flowing steam at 1100 to 1700°C, 19: 26774
corrosion by formic, hydrochloric, and oxalic acids at 35°C, galvanic, 20: 11230 (BM-RI-6715)
corrosion by gaseous and liquid cesium, 17: 30944
corrosion by lead (liquid) at high temperatures, 17: 7606(R) (ORNL-1515)
corrosion by liquid cerium at 800 to 1200°C, 16: 16693
corrosion by liquid lead, 17: 31762(R) (MND-P-3002)
corrosion by liquid lead, 17: 31763(R) (MND-P-3003)
corrosion by liquid rubidium, 18: 3298(R) (ORNL-2221(Pts.1-5)(Del.))
corrosion by liquid cesium, role of oxygen in, 18: 16447
corrosion by liquid lithium, 18: 36751 (ANL-6912)
corrosion by liquid potassium, sodium, and potassium–sodium alloy, 19: 34643
corrosion by lithium and lithium hydride, 16: 25718 (NP-11952)
corrosion by lithium at 1500 to 1900°F, 17: 6570 (ORNL-2674)
corrosion by lithium at 2000 to 3000°F, 18: 14420
corrosion by lithium hydrides at 1165 to 1600°F, 18: 24085(R) (NASA-CR-54053)
corrosion by lithium at 1200°C, 19: 35605(R) (ANL-7045(p.24-48))
corrosion by lithium at high temperatures, effects of nitrogen on, 19: 40112(R) (ANL-7046(p.36-66))
corrosion by lithium at 1000°C, 19: 44616(R) (ANL-7000, pp 122-37)
corrosion by lithium at 1200°C, 20: 3321(R) (ANL-7082, pp 29-53)
corrosion by mercury at high temperatures, 18: 7152
corrosion by mercury at 593 to 703°C, 20: 29646
corrosion by molten tin, static, 19: 32924(R) (ANL-7020(p.198-225))
corrosion by molten chlorides, electrochemical, 19: 39122
corrosion by nitric acid at 35°C, galvanic, 20: 11230 (BM-RI-6715)
corrosion by oxygen at 1000°C, 19: 34745(R) (HW-84384(p.8.1-5))
corrosion by polyphenyls at 330 to 400°C, 16: 22547
corrosion by sea water, sodium chloride, and sodium hydroxide, galvanic, 20: 11230 (BM-RI-6715)
corrosion by sodium at 760 to 1315°C, 18: 4160(R) (BNL-799(p.74-100))
corrosion by sodium at 1200°F, 18: 20472 (NAA-SR-Memo-9340)
corrosion by tin at 1000°C, 20: 6024(R) (ANL-6925(p.235-47))
corrosion by Wood's metal at 500°F, 19: 32657(R) (MND-P-3007)
corrosion by zinc and magnesium–uranium–zinc alloy, effects of molten chlorides on, 20: 2266
corrosion cracking by inorganic and organic acids and inorganic salt solutions, stress-, 20: 2254 (BM-RI-6680)
corrosion, effects of surface saturation with silicon, 16: 25721(T) (FTD-TT-61-31(p.60-9))
corrosion of, by liquid tin at 630 and 800°C, 17: 18704
corrosion of, book, 18: 22451
corrosion of, by acids and bases, crevice, galvanic, and spray, 20: 11230 (BM-RI-6715)
corrosion of, review, 19: 7868
corrosion protection of uranium by flame-sprayed deposits, 19: 13922
corrosion protection of, by chromium coatings topped by nickel coatings, 19: 32700
corrosion resistance of, summary of data on, 17: 18708
corrosion resistance, review, 17: 20420
corrosion resistance of, effects of alloying and coating on, 18: 34084
corrosion resistance and strength at high temperatures, 18: 44201
corrosion resistance to mercury at 900°F, 20: 2264
crack propagation and strength, 16: 19335 (ASD-TR-61-207)
crack-propagation resistance, 18: 5769 (AD-290278)
creep activation energy of, 18: 41921(R) (GEMP-37A)
creep and rupture of, numerical methods for analysis of, 20: 15041 (GEMP-397)
creep and stress-rupture properties in argon and hydrogen at 2200°C, 17: 26168
creep and stress-rupture properties in hydrogen at 2000 and 2200°C, 18: 7121(R) (GEMP-29A)
creep and stress-rupture properties at 2600°C, 18: 12543(R) (GEMP-31A)
creep and stress-rupture in argon and hydrogen at 1200 to 2400°C, 18: 16424(R) (GEMP-270A)
creep and stress-rupture of, in hydrogen, 18: 30111(R) (GEMP-35A)
creep and stress-rupture properties of arc-cast, at 1600 to 3000°C, 20: 27485(R) (GEMP-400A, pp 21-61)
creep and tensile properties at high temperatures, 20: 4999(R) (ORNL-2599)
creep mechanisms in, 20: 13249(R) (GEMP-55A, pp 29-53)
creep properties at 2200°C, 17: 34398 (CONF-39-43)
creep properties at 1800 and 2200°C, 19: 37030(R) (GEMP-47A, pp 27-84)
creep properties at 1600 to 2200°C of arc-cast, 19: 44598(R) (GEMP-49A)
creep properties of arc-cast at 2200°C, 20: 29710 (TID-22986)
creep rupture at 1600°C, effects of annealing at 1600 to 2400°C on, 20: 13249(R) (GEMP-55A, pp 29-53)
creep-rupture testing at high temperatures, 17: 25688(R) (GEMP-177A)
creep-rupture properties at high temperatures, 20: 17011 (CONF-651025-14)
creep-rupture properties at 1600°C of, comparison of, with other refractory metals and alloys, 20: 27485(R) (GEMP-400A, pp 21-61)
critical magnetic fields in superconducting, down to 0.12°K, 17: 6857
critical shear stress of crystals of, temperature dependence of, 18: 12709
critical surface temperature relations with cesium ion current, 16: 24280 (NASA-TN-D-1307)
crystal deformations in, internal friction from, 18: 26041(T)
crystal dislocations in, internal friction from, 18: 20559
crystal growth in mixture with molybdenum nitride, 19: 23040
crystal lattice dynamics of, 18: 9317(R) (PR-P-59(p.37-45))
crystal lattice dynamics of, Krebs's model for, 20: 17081
crystal lattice vacancies in quenched, 18: 42033
crystal lattice vibrations in, inelastic neutron scattering measurements of, 20: 42573
crystal structure, 16: 3479 (WADD-TR-61-181)
crystal structure, effects of deformation and heat treatment, 16: 30838
crystal structure, 17: 3500(T) (JPRS-16059)
crystal structure and grain growth at high temperatures, effects of cesium vapor on, 17: 25779(R) (NP-12891)
crystal structure, 17: 32565 (ASD-TR-61-181(Pt.III))
crystal structure and grain growth at high temperatures, effects of cesium vapor on, 17: 36300(R) (NP-13070)
crystal structure and grain growth at high temperatures, effects of cesium vapor and vacuum on, 18: 12860(R) (NP-13591)
crystal structure distortions in deformation testing, 18: 32176
crystal structure of platinum-coated wires of, effects of heat treatment on, 18: 32190
crystal structure of, effects of strain on, 18: 41921(R) (GEMP-37A)
crystal structure, 19: 1053(R) (PR-P-62)
crystal structure of rolled-sheet, 19: 7960
crystal structure of, plastic deformation effects on, 19: 16097
crystal structure lattice dynamics at 296°K, neutron spectrometric studies of, 19: 16138
crystal structure of, dislocation subboundaries in, 19: 20602
crystal structure dislocations in, electrolytic etching studies of, 19: 26855
crystal structure of deformed, dislocations in, 19: 37110
crystal structure of, 19: 43480
crystal structure of single-crystal, effects of plastic deformation on, 20: 11227
crystal structure of, effects of macroetching on, 20: 23729
crystal structure and gas saturation in, effects of vacuum rolling on, 20: 23744
crystal structure of, determination by phonon dispersion, 20: 37273
crystallization diagrams for sintered and wrought, 20: 9524
crystallization of, during soldering and welding, 20: 13267(T) (AD-624909)
crystallization of, effect of lanthanum and yttrium on, 20: 35905
crystallization of, effects of metal additives on, 20: 35930
decomposition voltage potential in fluorides at 500°C, 19: 17781(R) (ORNL-3750)
deformability, effects of deoxidation using lanthanum on, 19: 22929(T) (JPRS-28849(p.179-83))
deformation and annealing of, changes in x-ray reflections during, 19: 16142(T)
deformation and microhardness, 16: 12155
deformation and recovery of, dislocation substructures in, 16: 30809 (UCRL-9593)
deformation at high temperatures, 18: 12606(T) (JPRS-23121(p.6-12))
deformation at low and moderate temperatures, 17: 11223

deformation behavior at low and moderate temperatures, 16: 29420
deformation mechanisms in, thermally activated, 19: 34741(R) (BNWL-79(p.3.1-22))
deformation of crystalline, effects of annealing on, 19: 952(R) (GA-5620)
deformation of recrystallized polycrystalline and single-crystal, 20: 29758
deformation of single crystals of, translations on, 19: 18470(T) (FTD-TT-64-371)
deformation of single crystals of, orientation effects in, 19: 23086
deformation of single-crystal, as function of strain rate at 300°K, 20: 23667
deformation of, dislocation configurations from, 19: 6343
deformation of, effects of strain rate on, 20: 11227 pp 3.1-22)
deformation properties of single-crystal, 20: 745(R) (BNWL-120,
deformation structures in zone-melted single crystals of, 18: 36027
deformation, thermally activated, 17: 27879
deformation, recrystallization, and welding of single crystals of, effects of orientation on, 19: 39139
degasification in vacuum heating, 18: 30214
density changes in cold-worked, effects of annealing on, 18: 27934
density of compacts of, effects of pressure and lattice polygonization on, 19: 22939
density of compacts of, 17: 27829
deposition and structure of metal films on, 17: 29333(T) (NP-tr-1032)
deposition by electrolytic methods, 20: 35870
deposition from carbonyl decomposition, temperature effects on, 20: 41468
deposition from fused salt mixtures, electro-, 20: 11260
deposition method for, thermochemical, 19: 44640 (ORNL-P-1446-1)
deposition of, by electrophoresis, 16: 30369 (TID-11153)
deposition of coatings of, on alumina-coated niobium by plasma spraying, 17: 42401(R) (AD-296862)
deposition of coatings of, on container walls for obtaining ultrahigh vacuum by vaporization, 16: 1895
deposition of coatings of, on plutonium dioxide–uranium dioxide systems, 16: 12735(R) (EURAEC-80)
deposition of coatings of, on uranium dioxide particles, 17: 1857
deposition of coatings of, on uranium dioxide by fluidized bed technique, vapor-phase, 17: 34389
deposition of coatings of, by chloride reduction using hydrogen, 20: 39354 (BMwF-FBK-66-09)
deposition of films of, by vacuum evaporation, 18: 8930
deposition of films of, on oxidized silicon wafers, using electron-bombardment vacuum evaporation, 19: 36394
deposition of silicon on, protective effects of electrolytic, 19: 22908
deposition of, thermochemical, 20: 4342(R) (ORNL-3870, pp 85-101)
deposition on alumina, 18: 42348 (GEST-2035)
deposition on aluminum oxide powder, method of, 19: 11704
deposition on aluminum oxide, method for, 19: 28804(P)
deposition on ceramic powders by chloride and oxide processes, evaluation of, 19: 40986
deposition on other metals by electroplating methods, 19: 42827
deposition on refractory metal–nonmetal powders by chloride and oxide processes, 20: 29631
deposition on rhodium by electroplating, 17: 25691(R) (RBESO-3404-2)
deposition on uranium dioxide particles, 19: 44596 (EURAEC-1392)
descaling treatment, 16: 3440(P)
desorption energy of silver on, tracer study, 17: 36474
desorption from, at low pressure and temperature, 17: 33159(R) (ORNL-3472(p.107-18))
desorption of argon, carbon monoxide, hydrogen, and methane from, 18: 27696
desorption of carbon monoxide and oxygen from, by electrons at 0 to 300 ev, 18: 20641
determination as impurity in and volatilization from tungsten, semi-quantitative spectrographic, 16: 4131 (BM-RI-5903)
determination as pyridine–pyrocatechol complex, 18: 13706
determination as trace in standard rocks G-1 and W-1, spectrographic, 16: 20831
determination as trace impurity in uranium, 18: 29591
determination as trace impurity in plutonium–thorium–uranium and thorium–uranium alloys, 19: 17798
determination by activation, substoichiometric, 18: 21997
determination by charged-particle reactions at 2 Mev, 20: 43097
determination by extraction of oxine complexes, spectrophotometric, 16: 14616(R) (NBL-177)
determination by ion exchange using tiron, 18: 173
determination by neutron activation, 20: 35390 (CEA-R-2965)
determination by thermal-neutron activation methods, sensitivity for, 19: 9071
determination by titration using cerium sulfate, 19: 15396
determination in artificial graphite, 18: 9584
determination in alloys using vacuum cup electrode, spectrographic, 19: 22103 (TIM-904)
determination in automobile lubricants, activation, 20: 14439(R) (GA-5556)
determination in biological materials, activation, 16: 23403
determination in borides, carbides, nitrides, and silicides, titrimetric, 17: 12217
determination in biological materials by ion exchange and gamma spectrometry, 18: 13660
determination in boron, x-ray-fluorescence, 18: 29564(R) (NBL-210 (p.41-7))
determination in biological tissues, activation, 19: 15333 (AE-168)
determination in biological materials by neutron activation analysis, 20: 7046
determination in carbide mixtures containing uranium, x-ray fluorescence spectrographic, 18: 1499 (CONF-285-3)
determination in cadmium sulfide and lithium fluoride crystals, amperometric, 18: 13699
determination in cerium and erbium, mass spectrographic, 19: 2232
determination in chromium-nickel alloy, use of fluorescent x-ray instrument for, 19: 13221
determination in copper by activation, 19: 40422
determination in cermets of, and plutonium carbide–uranium carbides, 20: 8873
determination in conductive tissue of beef heart, activation, 20: 31176
determination in dissolver solutions, spectrochemical, 16: 5266 (DP-648)
determination in diabase W-1 and granite G-1, spectrographic, 16: 17895
determination in diabase and granite by spark source mass spectrography, 19: 11406
determination in europium oxide, spectrographic, 17: 2931
determination in fissium–uranium alloys, fluorescent x-ray spectrometric, 17: 27255
determination in fissium–uranium alloys, spectrochemical, 18: 43367 (ANL-6913)
determination in fission product and irradiated fuel solutions by controlled-potential coulometry, 20: 10758 (EUR-2618.f)
determination in fission product solutions, method for, 20: 40803 (KFK-387)
determination in germanium oxides, activation, 17: 38932
determination in heteropoly acid, 17: 1475
determination in hydrochloric and nitric acids and hydrogen peroxide, activation, 18: 31390
determination in high-alloy steels, rapid method for, 19: 17844
determination in hair and wool, activation, 19: 46192
determination in high-purity tantalum by spectrography using d-c arc method, 20: 20608
determination in human heart tissue, activation, 20: 31175
determination in iron and steel alloys, x-ray spectrochemical, 17: 5997
determination in iron, activation, 19: 10980 (EURAEC-1273)
determination in irradiated uranium dioxide, 20: 10787
determination in legumes, activation, 19: 17810
determination in lanthanum oxide, spectrographic, 20: 22895
determination in metallic uranium, colorimetric, 17: 14153(T) (CEA-tr-X-455)
determination in molybdenum–uranium alloys, polarographic, 17: 38939
determination in molybdenum–uranium alloys, gravimetric, 18: 19846 (LA-3058)
determination in MSRE fuel salts, 18: 34050(R) (ORNL-3626(p.59-164))
determination in molybdenum silicides, 19: 10996
determination in minerals by neutron activation, 19: 30424
determination in molybdenum–uranium alloys, volumetric, 19: 36240 (TRG-Report-961)
determination in multielement mixtures by x-ray fluorescence methods, 20: 20644
determination in minerals and rocks using paper chromatography, 20: 35389 (CEA-R-2791)
determination in nickel, 16: 11567
determination in natural water, quantitative spectrographic, 16: 17597
determination in niobium by radioactivation analysis, 16: 23633 (TID-7629(p.239-44))
determination in niobium and its alloys, 16: 25294
determination in nickel steel and electro-etch residues, activation, 17: 5984
determination in niobium alloys, evaluation of method for, 18: 1520
determination in nucleic acids, activation, 18: 19892
determination in niobium alloys, polarographic, 19: 19781
determination in niobium and tantalum by activation, 19: 24416
determination in niobium or niobium oxide by d-c arc excitation, photometric, 19: 26268
determination in niobium or niobium oxide by fusion and d-c arc excitation, photometric, 19: 26269
determination in ores by x-ray fluorescence, 16: 9967

determination in organic reactor coolants, spectrographic, 18: 184
determination in ores, activation, 18: 13626(R) (NYO-10174)
determination in plants, activation, 16: 14667
determination in plutonium using dithiol, spectrophotometric, 16: 23620 (TID-7629(p.62-8))
determination in polyphenyls by activation analysis, 17: 38945
determination in petroleum and its products, activation, 18: 15968
determination in presence of uranium, x-ray-fluorescence spectrographic, 18: 35449 (LADC-5930)
determination in prerence of uranium by x-ray fluorescence spectrometry, 18: 39077
determination in presence of 71 elements, spectrographic, 18: 43420
determination in pure water by extraction photometry, 19: 15388
determination in powdered samples by spectrochemical methods, 19: 22120
determination in plutonium fluorides and peroxides, review on spectrographic, 20: 14464 (RFP-599)
determination in plutonium by carrier distillation methods, spectrographic, 20: 40814 (RFP-664)
determination in powder samples by spectrographic methods, semiquantitative, 20: 43104
determination in reactor materials using 8-quinolinol, spectrophotometric, 16: 16314
determination in rare earths at 1 to 1000 ppm level, 17: 1377 (BM-RI-6097)
determination in reactor-grade uranium dioxide, activation, 19: 5827
determination in silicate rocks, activation, 16: 1712
determination in still by extraction with 6,7-dihydroxy-2,4-diphenylbenzopyrylium chloride, photometric, 16: 1717
determination in Santowax OMP by spectrographic methods, 17: 7959 (RT/CHI(62)13)
determination in sea water by quantitative solvent extraction and spectrography, 19: 28253
determination in silicon dioxide by activation and ion exchange chromatography, 17: 19979
determination in steel, activation, 18: 8265 (AE-128)
determination in silicon, activation, 19: 2240
determination in sodium uranate, spectrochemical, 19: 15367
determination in soil, activation, 18: 21994
determination in solids by spark source mass spectrometry, quantitative, 19: 13247
determination in solutions by x-ray fluorescence analysis, in presence of uranium, 19: 26271
determination in stainless steel microspheres, activation, 17: 27253
determination in sodium loop transfer samples, methods for, 20: 12766 (GEAP-4178)
determination in solutions, x-ray-fluorescence, 20: 14497
determination in silicon, activation, 18: 33502
determination in silicon dioxide, activation, 20: 20635
determination in steels by x-ray fluorescence methods, 20: 20642
determination in silicates, activation, 20: 26782
determination in superconductor materials, activation, 18: 31389
determination in tantalum by d-c arc method, spectrographic, 18: 19894
determination in tissue, after neutron activation, 17: 31813 (AERE-R-4309)
determination in trace amounts in uranium and uranium compounds, 18: 25272 (VDDIT-90)
determination in tungsten, spectrophotometric, 18: 25281
determination in tantalum by anion exchange in hydrofluoric–nitric acid mixtures, 18: 35455
determination in tungsten, spectrophotometric, 19: 314
determination in tungsten, activation, 19: 11023
determination in uranium alloys using hollow cathode tube, 16: 11542
determination in uranium dioxide for burnup calculations, 16: 23626 (TID-7629(p.152-65))
determination in uranium compounds by reversed-phase partition chromatography, 16: 23636 (TID-7629(p.276-84))
determination in uranium base alloys, photometric, 16: 26928
determination in uranium tetrafluoride, spectrographic, 17: 1391 (TID-17030)
determination in uranium(IV-VI) oxide by carrier distillation excitation, effects of graphite electrode grade on, 17: 10538 (TID-16295)
determination in uranium using Xylenol Orange, 17: 40757
determination in uranium tetrafluoride, spectrographic, 18: 170 (RT/CHI(63)-21)
determination in uranium using 8-quinolinol, spectrophotometric, 18: 1530
determination in uranium-233-labeled uranium dioxide, spectrographic, 18: 9980
determination in uranium, methods for, 18: 9991
determination in uranium alloys, photometric, 18: 19845 (JAERI-1053)
determination in uranium hexafluoride, colorimetric, 18: 29563(R) (NBL-210(p.29-33))
determination in uranium compounds and uranyl nitrate solutions, absorptiometric, 18: 35452 (PG-Report-572)
determination in uranium alloy by isotope dilution, use of neutron activation in, 19: 5816
determination in uranium and its compounds and alloys, methods for, 19: 19823
determination in uranium tetrafluoride, spectrographic, 20: 14473
determination in uranium by carrier distillation, spectrographic, 20: 18563 (EUR-2647.f)
determination in uranium trioxide by emission spectrography, 20: 40802 (HW-65402(Rev.1))
determination in water, silver-spark spectrographic, 17: 1381 (IDO-14591)
determination in zirconium, polarographic, 16: 18820
determination in zirconium by activation, 19: 24418
determination in Zircaloy-2, spectrographic, 20: 29113
determination of, design of quantometer for x-ray, 17: 40751
determination of hexavalent, spectrophotometric, 17: 7965(T) (CEA-tr-R-1638)
determination of, in presence of alkali metals, chemical spectrographic, 17: 15923
determination of, in uranium–molybdenum alloys, gravimetric, 17: 15882 (PG-Report-418)
determination of, in residues by iron flux method, spectrographic, 17: 19942 (PG-Report-157)
determination of pentavalent, using 8-hydroxyquinoline-5-sulfonic acid, photometric, 16: 12994
determination of, procedure for radiochemical, 16: 28871 (LA-1721(2nd Ed.)(Rev.))
determination of ratio with uranium in hexafluoride mixtures, spectrometric, 16: 25313 (K-1433)
determination of, radiation effects on spectrophotometric, 17: 15856(R) (ORNL-3397(p.54-6))
determination of traces in marine organisms, activation, 17: 4468
determination of traces of, in uranium carbides, 19: 4061 (PG-Report-516)
determination of traces of, in tungsten, using anion exchange column, 19: 28217(R) (AD-608074)
determination of trace amounts of, in uranium, spectrophotometric, 19: 36281
determination of trace amounts in uranium compounds, activation, 20: 1784
determination of trace amounts of, in iron, activation, 20: 14471
determination of trace amounts of, in beryllium by spectrography, 20: 16352
determination of trace amounts of, by reactor neutron activation methods, 20: 26760
determination of trace amounts of, in tungsten by atomic absorption spectrophotometry, 20: 43154
determination of, use of azo dye in spectrophotometric, 17: 35945
determination of 10^{-9}-g samples of, activation method for, 17: 32026
determination of, photometric, 18: 10016
determination of, tracer techniques for, 18: 33483
determination of, review on methods for, 19: 22108
determination of, comparison of colorimetric and x-ray fluorescence methods for, 19: 30124
determination of, in steel, use of beta source in x-ray spectroanalysis for, 20: 22961
determination of, by neutron activation methods, 20: 29078(R) (AD-633252)
determination of, developments in resin spot tests for, 20: 40827
determination of, in water by neutron activation analysis using freezing, 20: 45602
determination of, by neutron activation analysis, linear equation for, 20: 45603
determination simultaneously with uranium or vanadium, potentiometric, 17: 38961
determination using ammonium diethanoldithiocarbamate, spectrophotometric, 18: 185
determination using thioglycolic acid, spectrophotometric, 18: 17764
determination using 1-mercaptopropionic and *p*-phenetidide-1-mercaptopropionic acids, photometric, 18: 19914
determination using tiron, photometric, 18: 27345
determination using sulfatoceric acid, titrimetric, 18: 41355
determination using 5,5′-thiodisalicylic acid, spectrophotometric, 19: 19823
deuterium exchange with hydrogen on films of, steady-state, 20: 21351(R) (SRIA-425-8)
deuterium ion reactions at 29 and 50 kev, sputtering from, 20: 39581(R) (ORNL-3989, pp 134)
deuterium–hydrogen exchange on, at 25 to 800°C, 20: 36818
deuteron elastic scattering at 15 Mev, strong absorption model analysis of, 18: 42708
deuteron inelastic scattering at 15 Mev, energy spectra from, (E), 20: 13872

deuteron reactions with, 18: 2985(R) (UCRL-10852)
deuteron scattering, angular distributions, 16: 29881(R) (ORNL-1383)
deuteron sputtering at 30 kev, yields from, 20: 17892(R) (ORNL-3908, pp 149-53)
development of coatings of, for thermal production, 17: 410 (DMIC-175)
development of ductile, 19: 37041(R) (NP-15174)
diffusion and permeation coefficients for hydrogen in, 20: 14976 (AWRE-O-16/66)
diffusion and position energies of interstitial impurities in, (T), 20: 28679
diffusion at 1850 to 2350°C in, tracer studies of self, 19: 16200
diffusion at 2155 to 2540°C in, self-, 19: 6322
diffusion from irradiated uranium, effects of burnup and irradiation level on, 16: 25841 (HW-72321)
diffusion in barrier materials at 1700 and 1800°C, 17: 1918 (ASD-TDR-62-432)
diffusion in chromium–iron alloy at 1000 to 1200°C, 18: 10522(R) (BMI-X-10072)
diffusion in chromium and nickel as function of temperature, 20: 2357(T) (AERE-Trans-1032)
diffusion in gamma cerium, electro-, 19: 34722
diffusion in gamma-cerium, gamma-uranium, and epsilon-plutonium, electro-, 20: 23734
diffusion in molten silicates, 19: 36649 (AD-614997)
diffusion in molybdenum–zirconium alloys, self-, 17: 32593
diffusion in molybdenum–tungsten alloys, tracer studies of, 19: 26852
diffusion in molybdenum carbides at 900 to 1600°C, tracer studies of activation energies and coefficients in, 19: 32744
diffusion in molybdenum disulfide, inter-, 20: 5846
diffusion in molybdenum–tungsten alloys at 1500 to 2400°C, tracer studies of, 20: 17101
diffusion in niobium, 16: 2194(R) (NP-11060)
diffusion in titanium, 17: 33859 (ARF-2208-16)
diffusion in titanium at 900 to 1650°C, 17: 34454
diffusion in titanium at 905 to 1210°C, inter-, 20: 17111
diffusion in uranium carbides and (uranium–zirconium) carbides, 18: 35929(R) (GA-4769(Pt.I))
diffusion in, self-, 20: 11227
diffusion into liquid iron at 1923°K, 18: 26010
diffusion of atoms in bcc, activation energy for interstitial, (T), 19: 40086
diffusion of beryllium in, 20: 5846
diffusion of boron and carbon in, conditions for, 18: 20540
diffusion of boron and carbon in, 18: 36001
diffusion of boron and carbon in surface of, 20: 11228
diffusion of carbon in film-coated wire of, 19: 16131
diffusion of cesium through membranes of, surface ionization following, (E), 19: 6449
diffusion of cobalt and niobium at 1850 to 2350°C in, tracer studies of, 19: 16200
diffusion of cobalt-60 in, effects of argon environment on, 19: 30792
diffusion of cobalt and niobium in, coefficient for, 20: 11227
diffusion of cobalt-57 in, mechanism for, (E), 20: 28662
diffusion of hydrogen in, at high temperatures, 16: 8713 (NEPA-1841)
diffusion of nitrogen and oxygen in, activation energies and coefficients of, 19: 9682
diffusion of oxygen at 1500 to 1800°C, 19: 39072(R) (NP-15187)
diffusion of oxygen in, at high temperatures, 19: 44979(R) (NP-15419)
diffusion of potassium in monocrystalline and polycrystalline, at 800 to 1500°C, tracer studies of, 20: 33908
diffusion of rhenium, tantalum, tungsten, and vanadium in, 16: 2194(R) (NP-11060)
diffusion of rhenium in, at 1700 to 2100°C, tracer studies of, 20: 15127
diffusion of sulfur in, 19: 2812
diffusion of titanium in, gamma attenuation analysis of, 19: 988
diffusion of tungsten in, at 1700 to 2100°C, 20: 15126
diffusion of uranium in, 19: 28852
diffusion of uranium in, temperature dependence of, 20: 11290
diffusion penetration by plutonium-uranium alloys, 16: 28555 (TID-7623 (p.105-21))
diffusion rate of oxygen in, at 1500 to 1800°C, 19: 39070(R) (GEST-2046)
diffusion, tracer study, 16: 18049
dislocation etch-pits on crystalline surface of, 18: 36030
dislocation loops in zone-melted, prismatic, (E), 19: 4693
dislocation loops in quenched, 20: 5851
dislocation mechanisms in single-crystal, 20: 15946 (UCRL-16643)
dislocation mechanisms of single-crystal, 20: 31714(R) (UCRL-16658, pp 99-103)
dislocation motion in single-crystal, induced by electrolytic etching, 18: 34150
dislocation multiplication in polycrystalline, effect of strain rate on, (E), 20: 3286
dislocation on {110} planes in bcc, dissociation of, 20: 33918
dislocation parameters for, 20: 17033
dislocation-relaxation spectra of cold-worked, 16: 25807 (GA-1745)
dislocation structures, 18: 26063
dislocation structure in fatigue-deformed single crystals of, electron microscopic studies, 19: 30726 (ARL-65-11)
dislocation structure in, effects of cold working on, 19: 41015 (MIL-TDR-64-282)
dislocation structures in annealed and deformed sheets of, 20: 5846
dislocations in crystalline, effects of annealing on, 20: 33859(R) (AD-634128)
dislocations in primary slip systems of crystals of, dynamical behavior of, 17: 37526
dissociation energy of gaseous and heat of vaporization of solid, correlation of, 17: 6095
distribution coefficient in hydrochloric acid and ion exchange resins, 16: 7503
distribution coefficient between fused bismuth and fused salt eutectic, 17: 21683
distribution, metabolism, and transfer, tracer studies, 16: 1400
distribution of, in neutron-irradiated plutonium dioxide suspensions, 20: 41009 (AERE-R-3268)
drawing into wire, effects of lubrication on shear stresses of, 19: 16032(T) (AEC-tr-6541)
ductile properties of tubing of, 18: 22511
ductile-to-brittle transition temperature of sheet of, effects of recrystallization and welding on, 19: 41016 (N64-30997)
ductile-to-brittle transition in, effects of grain size and temperature on, 20: 11227
ductility, 20: 11227
ductility and fine grain structure of, effects of boron on, 19: 2819
ductility and weldability of, purification treatment for improvement of, 20: 27443(R) (GEMP-400A, pp 109-33)
ductility of arc-melted, 19: 25046(R) (HW-83615)
ductility of electron-beam-melted, 18: 30212
ductility of electron-beam-melted, effects of carbon, titanium, or zirconium additions on, 20: 29783
ductility of, effects of liquid cesium on, 18: 14354(R) (ARF-B215-12)
ductility of, effects of purity on, 18: 32176
ductility of, effects of solid-solution hardening at grain boundaries on, 19: 23078
ductility of, effects on additives on, 19: 37041(R) (NP-15174)
ductility of, effects of boron on, 20: 5851
ductility of, effects of rhenium on, 20: 23681
ductility of, effects of boron additions on, 20: 29675
ductility of, mechanism controlling, 20: 5851
effect on properties of low-alloy steels for reactor pressure vessels, 20: 39444(P)
effect on thermoelectric properties of tantalum, 19: 30812
effects of alloy additions of, on mechanical properties of niobium, 20: 11302
effects of alloying additions of, on thermal stability of $TiAl_3$, 20: 11335
effects of alloying additions of, on corrosion resistance of type 430 stainless steel, 20: 16975 (NP-15900)
effects of dietary, on zinc-65 uptake by rat tissues, 19: 35915
effects of dietary, on iodine-131 uptake and retention by rabbit thyroid, 19: 43689
effects of dietary, on response to radiation stress in rats, 17: 35317(R) (HW-76000(p.178-82))
effects of foils of, on carbon exchange between methane and sorbed methane, 16: 23576
effects of nitrogen mustard on content of, in spleen in rats, 17: 40547(R) (NYO-10569)
effects of, on stress release of chromium–iron–nickel alloys, 16: 30842
effects of, on superconducting properties of vanadium silicides, 16: 30821
effects of, on thoria compacts, 16: 30777 (ANL-6529)
effects on aluminum–copper–iron–tin–titanium–vanadium alloys, 18: 35944(R) (WAL-TR-401/303-4)
effects on coatability of niobium, 20: 43827 (GTR-19)
effects on colorimetric determination of vanadium in uranium compounds, 20: 12802
effects on complexometric titration of zirconium, 18: 41336
effects on copper metabolism in rats, 19: 21823
effects on corrosion resistance of zirconium, 18: 41972(P)
effects on corrosion of steels by liquid sodium at 450, 600, and 750°C, 19: 4629
effects on corrosion resistance of chromium–cobalt–tungsten alloys, 19: 18415
effects on corrosion resistance of stainless steel in acidic solutions, 20: 4325 (TB-58)
effects on corrosion, stability, and strength of niobium, 20: 43905 (ORNL-3212)
effects on coulometric titration of uranium(VI) in aqueous solutions of

sodium fluoride, 19: 15357
effects on creep and thermal cycling resistance of uranium, 18: 42104(P)
effects on creep and thermal cycling resistance of uranium, 18: 41487(P)
effects on creep and thermal cycling resistance of uranium, 18: 41488(P)
effects on crystal structure of alpha-iron, 20: 13317
effects on crystal structure and properties of thoria-tungsten cermets, 20: 37185
effects on deformation and flow of polycrystalline uranium, 19: 4675
effects on deformation of uranium, 19: 16206(P)
effects on determination of uranium in sulfuric acid solutions, 16: 1700 (CNI-90)
effects on determination of plutonium using Arsenazo III and its analogs, 20: 45614
effects on diffusion of niobium, 17: 23876(R) (USBM-U-1031)
effects on ductility of iodide chromium, 18: 32189
effects on fabrication and mechanical properties of niobium–tantalum–titanium–vanadium alloy sheet, 19: 20552(R) (IITRI-B6021-6)
effects on fabricability of titanium–vanadium alloys, 19: 44587(R) (ANL-7000, pp 3-63)
effects on fluorescence of uranium in sodium carbonate–sodium fluoride melts, 18: 33506
effects on fracture mechanisms in beryllium single crystals, 20: 23714
effects on grain size of uranium, 19: 23047
effects on grain size and transformations in alpha-uranium and uranium alloys at 720 to 800°C, 20: 31666
effects on grain size of tungsten, 20: 39400 (NASA-TN-D-3531)
effects on growth and nitrogen fixation in Nostoc, 18: 33237
effects on high-temperature properties of aluminum–iron–silicon–uranium systems, 19: 40958
effects on hot-cracking susceptibility of Monel, 19: 30751 (WERL-8844-8)
effects on internal friction of uranium at 77 to 360°K, 19: 26863
effects on ion exchange between alumina and tellurium, 19: 15332(R) (BNL-841(p.52-62))
effects on isotopic exchange between cyclobutane and deuterium, 20: 304
effects on magnetic moments of iron–nickel alloys, neutron-diffraction analysis of, 18: 27990
effects on mechanical properties of thorium–uranium alloys, 18: 18304
effects on mechanical properties of niobium, 19: 11734
effects on mechanical properties of niobium alloys prepared by electron-beam melting, 19: 30768
effects on mechanical properties of sintered zirconium diboride, 19: 46907 (AD-456724)
effects on mechanical properties of aluminum–copper–iron–tin–titanium–vanadium alloys, 19: 46985 (AD-613651)
effects on microstructure of tungsten–thoria dispersion-hardened alloys, 20: 31781
effects on oxidation of niobium in air at 1000 to 1200°C, 19: 11693
effects on oxidation of graphite, 19: 22911
effects on oxidation resistance of silicon carbide at high temperatures, 19: 36993(P)
effects on oxidation resistance and strength of chromium–magnesia composites, 19: 41022(R) (NP-15292)
effects on oxygen overvoltage and proton diffusion in nickel oxide, 18: 27457
effects on phase transformations in steel, 18: 24152(T,R) (EURAEC-1001)
effects on photometric determination of cerium in cast iron and steels, 20: 43143
effects on plutonium purification by ion exchange in nitric acid, 18: 13965
effects on polarographic determination of uranium, 16: 2982
effects on preparation of uranium carbide by carbothermic reduction of oxide, 20: 33841 (NAA-SR-10624)
effects on properties of niobium–titanium–vanadium alloys, 18: 22418(R) (IITRI-B6021-1)
effects on properties of uranium carbide dispersions in chromium or iron, 18: 42106(P)
effects on properties of heat-resistant nickel alloys, 18: 44222
effects on properties of zirconium alloys, 19: 36990(P)
effects on properties of tantalum, 19: 41067
effects on properties of chromium–nickel alloys, 20: 25587
effects on properties of graphite, with and without copper and silver infiltration, 20: 29764
effects on properties of boron steel, 20: 39426
effects on properties of beryllium–nickel alloys, 20: 46208
effects on radiation growth and swelling of uranium, 18: 37736 (A/CONF.28/P/145)
effects on radioinduced swelling of clad uranium fuel tubes in pressurized heavy-water reactor, 19: 37163 (CONF-650904-3)
effects on radioinduced cavitational swelling of uranium, 19: 37164 (CONF-650904-4)
effects on radioinduced swelling in uranium irradiated at 400 to 500°C, 20: 31666
effects on radioinduced swelling in uranium, 20: 37303
effects on sintering of zirconium boride, 19: 26794
effects on spectrophotometric determination of aluminum, 19: 13226
effects on spectrophotometric determination of thorium, 19: 24408
effects on spectrophotometric determination of uranium using 3-benzyl-4,5-dihydroxycoumarin, 20: 24991
effects on strength of thorium at high temperatures, 19: 20560 (ORNL-3777)
effects on stress-rupture behavior of chromium–cobalt–nickel alloys, 18: 44165
effects on superconducting transition temperature of vanadium silicide, 19: 39196
effects on swelling of neutron-irradiated beta-phase uranium, 16: 7935 (NMI-1249)
effects on tantalum–tungsten alloys, 18: 34059(R) (WANL-PR(Q)-003)
effects on tensile properties of tantalum, 18: 42010 (ASD-TR-61-203 (Pt.III))
effects on thermal properties of thoria–urania systems, 16: 7924 (ANL-6397)
effects on thermal expansion of niobium, 18: 22516
effects on uranium hardness transition temperature, 16: 33989(R) (SRO-72)
effects on yield stress of nickel, 18: 44145(R) (ORNL-3670(p.11-16))
effects on zirconium alloys for use in reactors, 20: 9560(P)
effects on zirconium alloys for use in nuclear reactors, 20: 9561(P)
efficiency as emitter for thermionic converter, 17: 20604
elasticity and texture of, 17: 23872(R) (TID-18626)
electric and galvanomagnetic properties of, effects of temperature on, 20: 7620
electric conductivity of pure monocrystalline, temperature effects on, 18: 26007
electric conductivity of evaporated films of, effects of hydrogen and oxygen on, 19: 13296
electric conductivity and temperature coefficient at –196 to 100°C, 19: 26834
electric conductivity at 0 to 2300°C, 20: 821 (GE-TM-65-10-1)
electric conductivity at 0 to 2000°C, 20: 2223(R) (GEMP-51A)
electric conductivity and structure of thin films of sputtered, 20: 21394
electric discharge effects on, arcing in, 18: 26806
electric discharge explosion of wires of, MHD instabilities in, 20: 39010
electrochemical machining of, effects of friction, surface finish, and tool erosion on, 17: 34386
electrocladding and electroforming of, process for, 18: 14439
electrode development for thermionic cells, 18: 20865
electrodeposition in organic solvents, 18: 13602 (BM-RI-6303)
electrodeposition from molten electrolytes, 18: 25316 (BM-RI-6444)
electrodeposition from fused fluoride bath, 19: 11711
electrodeposition from molten fluorides, 19: 16034
electrolytic polishing and etching, 19: 13971
electromagnetic wave absorption and electron reactions on, elastic wave generation in, 17: 37732
electron backscattering coefficients for, empirical equations of, 19: 37794 (NASA-TN-D-2909)
electron binding energies of, measurements for, 17: 18924
electron bombardment at low energies, secondary electron distributions, 16: 8019
electron ejection from, by argon ions and neutral atoms, potential and kinetic, 17: 13158
electron emission in cesium and cesium fluoride vapors, 16: 22759
electron emission from a clean surface of, by bombardment with low-energy noble gas ions, 17: 6855
electron emission from cesiated recrystallized and tungsten-coated, 18: 12860(R) (NP-13591)
electron emission by, in cesium atmosphere, 18: 21367(R) (AD-429133)
electron emission by pyrographite layers on, 18: 29928(R) (NP-13979)
electron emission from surfaces of, thermionic, 19: 46571 (HRL-5249-S)
electron emission by electrodes of, effects of cesium and cesium fluoride on, 16: 30926 (LADC-5230)
electron emission from surfaces of, by positive and negative ion bombardment, (E), 20: 2628
electron emission in MHD generators from electrodes of, (E), 20: 39736
electron emission from filaments of, surface micropatch effects on, 20: 39642
electron energy loss, penetration, and range at 5 to 100 Mev, 19: 9445 (LA-3130)
electron energy losses at 150 to 250 ev, (T), 19: 19335
electron ranges in thin films of, 20: 29952
electron reactions at 70 Mev with thin foils of, secondary emission from, 19: 37463
electron reactions with atomic, screening effects on bremsstrahlung and pair production in, (T), 19: 39389

electron scattering by cesium-coated, parameters for 0.05 to 5.0 ev, 18: 10834
electron scattering at 0.6 to 1.8 Mev, backscatter and secondary emission in, (E), 19: 29441 (NASA-TN-D-2782)
electron secondary emission coefficient, 16: 12276
electron secondary emission from thin foils of, (E), 20: 13103
electron work function of, after cold deformation in high vacuum, 18: 5754
electron work functions for thermionic cathodes of, effects of cesium fluorides on, 20: 4572 (EUR-2283.d)
electronegativity, 18: 13797
electronic specific heats and magnetic susceptibility of, variation with temperature, 18: 8837
electronic structure of, De Haas-Van Alphen studies of, 17: 8077
electronic structure, 18: 2401(R) (IS-700(Sect.P))
electronic structure, physical properties, and alloying properties, 18: 34202
electrowinning from minerals and natural compounds, method for, 19: 910
electrowinning of, effects of repetitive electrolysis on, 20: 45622 (BM-RI-6834)
embrittlement at 200 to 1500°C, 20: 25593
emission behavior, current-field characteristics of, 17: 21989
emissivity, 17: 31009
emissivity, 18: 12669
emissivity at high temperatures, apparatus for determining integral, 18: 12670
emissivity at 1600 to 3100°K and 0.4 to 4 μ wavelength, 17: 30832
emissivity of coated, in vacuum, 18: 24138(R) (PWA-2206(Vol.I))
emissivity of coated, in vacuum, 18: 24139(R) (PWA-2206(Vol.II))
emissivity of coated, in vacuum, 18: 24140(R) (PWA-2206(Vol.III))
emissivity of sandblasted coatings of, to 2200°F, 16: 30800(R) (PWA-1877)
emissivity of sandblasted coatings of, to 2000°F, 16: 30801(R) (PWA-1878)
emittance properties of disilicide oxidation-protective coatings on, 19: 13869(R) (ASD-TDR-63-269)
energy level transitions in, Coster-Kronig, (T), 20: 15238 (CONF-233 (Vol.3), pp 398-418)
energy level widths for, K, (T), 20: 15239 (CONF-233(Vol.3), pp 419-39)
energy levels, isotopic shifts in, 16: 26360
engineering properties of, data tabulation on, 18: 10526 (DMIC-190)
enthalpy and heat capacity at 0 to 2500°C, 17: 3515
enthalpy and heat capacity at 1100 to 2540°K, 16: 2214(T) (NP-tr-754)
enthalpy and heat capacity at 700 to 2337°C, 16: 15212
enthalpy and specific heat at high temperatures, 19: 2852
etch pits at dislocations in, direct observation of, 20: 43966
etch-pit studies of arc-cast, 20: 13249(R) (GEMP-55A, pp 29-53)
etching dislocations on oriented single-crystal faces of, 20: 866
etching of dislocations in deformed, equipment for electrolytic, 20: 39432
evaporation and condensation of, design of electron beam device for, 18: 43753
evaporation from irradiated uranium dioxide at 750 to 1600°C, 20: 17102
evaporation in cesium vapor, 17: 3463(R) (AD-276411)
evaporation in cesium-filled thermionic cells, 17: 27967
evaporation in vacuum at 2063 to 3203°K, effects of pressure on, 20: 36834
evaporation of, in cesium vapor, 16: 32169(R) (AD-272849)
evaporation of, from irradiated uranium(IV-VI) oxides at 900 to 1500°C in flowing hydrogen, nitrogen, or oxygen, 20: 29211
explosibility of powders of, 19: 36698 (BM-RI-6516)
explosion of wires of, in nitrogen, x-ray analysis of aerosol composition and size produced by, 18: 41381
extrusion as clad in uranium carbide fuel elements, 19: 24952 (NMI-2523)
extrusion at high energy rates, 18: 8769 (LADC-5763)
extrusion by hydrostatic methods, 19: 18436
extrusion by hydrostatic methods, 19: 44651
extrusion into tube shells, 18: 44049(R) (ORNL-3670(p.77-111))
extrusion of alloy-clad billets of, 20: 4299(R) (ORNL-2711)
extrusion of complex shapes of, 18: 7170
extrusion of tube blanks, 17: 40422(R) (ANL-6784)
extrusion of, factors affecting, 18: 14443
extrusion, two-temperature technique, 16: 10534(R) (NMI-2102)
fabrication, 18: 3038(R) (ANL-6801)
fabrication and properties, 16: 19396
fabrication and properties as refractory material, 16: 19404
fabrication and properties review, 16: 29328
fabrication and properties of, review of, 17: 29253 (NRC-7129)
fabrication and properties, 17: 34330(R) (USBM-U-1057)
fabrication and properties for process equipment in aerospace, cryogenics, and nuclear engineering, 17: 39556
fabrication and properties for use as superconductors, 18: 34179
fabrication and properties of, handbook on, 20: 5874 (AGARDograph-94)
fabrication by arc melting, electron-beam melting, and powder metallurgy methods, 18: 34102
fabrication by electroforming, 19: 42827
fabrication by explosive forming, effects of 0.5% titanium, 16: 20994(R) (NP-11621)
fabrication by extrusion, 16: 9141(R) (NMI-2101)
fabrication by extrusion at 3200 to 3400°F with reduction ratio of 19:1, 17: 507(R) (ASD-TR-7-785(VII))
fabrication by plasmic powdering, 20: 7540
fabrication for impaction testing of particulate materials, 19: 39125(R) (BNWL-91)
fabrication of bodies of, by flame- and arc-plasma-spraying, 19: 36994 (AMRA-TR-64-50)
fabrication of compacts of, 16: 5714 (NEPA-1050)
fabrication of powders into crucible susceptors, 16: 25704
fabrication of sheet, by rolling, 16: 33456(R) (NP-12119)
fabrication of sheets of electrowon, procedure for, 20: 23643 (BM-RI-6771)
fabrication of tubular, 16: 28647(R) (ORNL-2340(Pts.1-5))
fabrication of tube shells of, by extrusion, 18: 4255(R) (ORNL-3470 (p.98-125))
fabrication of, mechanical tests to evaluate, 18: 34101
fabrication of, review of primary working operations for, 18: 34104
fabrication techniques for, control of grain growth by, 17: 11295(R) (AD-277713)
fabrication, ore processing, properties, and uses of, 18: 35949
fabrication, oxidation, and properties of, 18: 35986 (ERR-FW-049A)
fabrication, properties, and uses of, review on, 18: 34178
fatigue of, effects of air, nitrogen, and water vapor on, 19: 44730
fatigue of, effect of crystal structure on, 20: 4443
Fermi surface of single crystals of, (E/T), 19: 42003
Fermi surface of, magnetoacoustic studies, 19: 23987
Fermi surface of, by augmented-plane-wave method, 19: 35596
Fermi surface parameters for, (E), 20: 22337
Fermi surface properties of de Haas-van Alphen effect in, 19: 9767(R) (IS-900(Sect.P))
Fermi surfaces calculations for, 20: 4476(R) (IS-1200(Sect.P))
fission product bombardment, annealing of point defect clusters formed by, 18: 32245
fixation in phosphate glass, process for, 19: 5566(P)
flow forming of, for rocket engine techniques, 18: 34109
fluorescence yields in proportional and scintillation detectors, 18: 3796
forging characteristics, 16: 9162 (DMIC-Memo-143)
forging of, studies of plasticity in, 17: 18721(T) (FTD-TT-62-1789)
forging of, comparison of arc-cast, pressed, and sintered billets for, 20: 29683
fracture and initial yielding in notched sheet, 19: 37088
fracture of, at −78 to 300°C, 19: 16160
fracture of, at 78 to 298°K, role of twinning in, 20: 35925
fracture of, by thermal stress, effects of dislocation interactions on, 20: 33891
fracture of, crack initiation sites in, 18: 44195
fracture properties of recrystallized and wrought stress-relieved, 20: 11227
gamma attenuation coefficients at 0.01 to 100 Mev, 20: 36350
gamma coherent scattering at small angles, 18: 35053
gamma reactions on, effects of E1 resonances on, 16: 33906
gamma scattering by, spectra of resonant, (E), 19: 39265(R) (IA-1021)
gamma spectra from 14-Mev neutron activation, determination by, 19: 26241
gamma transmission in slabs of, (E), 19: 14728 (APEX-581)
gas gettering and hydrogen adsorption rate at liquid nitrogen temperatures, 16: 10546 (UCRL-6652)
grain boundaries of, effects of evaporating silver and dielectrics on, 17: 36285 (AERI-P/R-2)
grain boundary cracking in, twin-induced, 18: 32165
grain boundary grooving in, mechanisms of, 20: 31672
grain boundary inclusions of electron-beam-melted, 19: 26850
grain boundary structure in, internal friction studies of, 20: 15128
grain growth at 1800°K, effects of cesium vapor on, 17: 12589(R) (NP-12543)
handbook, 17: 16549
hardening of, dispersion methods of, 19: 28843
hardness, 16: 21080
hardness, 17: 11093(R) (NMI-2112)
hardness, 17: 11094(R) (NMI-2113)
hardness and recrystallization at high temperatures, 17: 27760(R) (NP-12901)
hardness and strengths at 1000 to 2000°C, relation between, 19: 37120
hardness and tensile properties, 16: 20955(R) (NMI-2105)
hardness and ultimate strength of, relation between, 19: 23065
hardness and Young's modulus of, at 20 to 2700°C, 17: 14881
hardness at high temperatures, long-time, 18: 39986

hardness at 20 to 2500°C, 16: 32132
hardness of annealed and strain-hardened, at 20 to 2500°C, 18: 16518(T)
hardness of, effects of aluminum, chromium, or nickel alloying additions on, 20: 31741
heat of sublimation and vaporization of solid, 17: 6093
heat of vaporization, 17: 10240(R) (NP-12208)
helium and hydrogen ion attenuation at 0.1 to 500 Mev, tables for, 20: 41619 (CEA-R-3042)
helium ion energy-range relations in, 18: 14726 (UCRL-10647)
helium-3 reactions (He-3,n) at 19 to 25 Mev, angular distributions and cross sections for, (E), 20: 22132
hot rolling of, under low partial pressures of oxygen, 20: 46173
hot-working properties of electron-beam-melted, effects of alloying additions on, 20: 23720
hydrogen atom reactions with surface of, dissociation and recombination in, 19: 28995
hydrogen ion reactions at 1 to 30 kev, electron emission in, 17: 24173
hydrogen sorption by, in glow discharges, 20: 22857(R) (ORNL-3913, pp 111-32)
hydrogen–deuterium exchange on films of, 20: 916(R) (SRIA-425-6)
impact testing of, high-velocity, 20: 33490 (CONF-651026, pp 737-68)
impregnation with beryllium, diffusion, 20: 27455
inflammability of powdered, at 180 to 1100°C, 18: 44211
interdiffusion in rhodium and tungsten at 1700°C, 16: 9207(R) (NP-11348)
interference in amine extraction of uranium, use of oxidizer to prevent, 19: 4266(P)
internal friction, effects of purity, 17: 14740 (TID-11295(2nd Ed.))
internal friction peaks in single-crystal, effects of interstitial movement on, 18: 28033
internal friction in, effects of annealing on, 19: 9723
internal friction of annealed and deformed, 20: 5846
internal friction in deformed, 20: 19250
internal friction of, effects of bonding forces in lattice and defect mobility on, 20: 27508
ion bombardment, secondary ion emission during, 16: 16880
ion emission coefficient in positive ion bombardment, 16: 595(T) (NP-tr-792)
ion exchange behavior of alumina, 18: 12521(R) (BNL-823(p.57-65))
ion exchange in concentrated hydrochloric and perchloric acids, distribution coefficients for, 18: 17759
ion ranges in, determination from collection experiments, 17: 6820
ion reactions at 0 to 1400°C, secondary-ion and sputtering yields, 16: 19568
ion reactions at 2 to 15 kev, ejected electron energy distribution from argon and helium, (E), 20: 31939
ion reactions at 5 to 12 Mev, neutron spectra from, (E), 19: 41810(T)
ion rocket accelerator grid of, lifetime of, 17: 24043 (NASA-TN-D-1657)
ion scattering at 0.4 to 4 kev, secondary electron emission in alkali, (E), 19: 14236(T) (ORNL-tr-467)
ion scattering by, yields from, 18: 9005
ionization by laser beam, energy spectra of, (E), 20: 27728
iron impurities in, paramagnetism of, 16: 25999
iron-57 Mössbauer effect in, localized magnetic moments from, 19: 18511
iron-57 Mössbauer effect in, Debye-Waller factor for, (E), 20: 28662
iron-57 Mössbauer spectra in, 20: 30766
isotopic composition of natural, 18: 31767
isotopic compositions of naturally occurring, variations in, 19: 44242
joining by brazing and welding, 17: 6631
joining to alumina in ceramic-to-metal seals for high-temperature use, 17: 34369(R) (RBESO-3404-3)
joining to tungsten, brazing materials for, 20: 21312
krypton ion range in cathode of, in glow discharge, 18: 36091
lattice-defect observation in, using field-emission microscopes, 16: 2241
lattice defects in single-crystal, effects of annealing on, 20: 41434
lattice parameter and length recovery after fast-neutron irradiation, 19: 34741(R) (BNWL-79(p.3.1-22))
light reactions with, electrons, ions, and neutral atoms from laser-induced, 17: 18923
Lilienfeld emission from, 18: 10796
machining of, optimum conditions for turning, 19: 30696 (RDB(C)TM-278)
machining procedures for, 20: 43864 (Y-1550)
machining properties, 16: 4528 (DMIC-Memo-134)
machining studies on TZM, 16: 10469(R) (ASD-TR-7-532a(V))
machining, processing, and welding, 20: 27538
magnetic moment of, effect of iron impurities on, 17: 18827
magnetostriction in pure monocrystalline, 19: 39199
mass transfer from emitter to collector in thermionic diodes, 17: 27964
mechanical properties, 16: 3479 (WADD-TR-61-181)
mechanical properties at high temperatures, 16: 10509 (DC-56-3-115)
mechanical properties, determination of brittle-ductile transition temperature and high-temperature strain aging, 16: 12080(R) (AD-259795)
mechanical properties and preparation, 17: 14818 (DRI-2039)
mechanical properties, 17: 32565 (ASD-TR-61-181(Pt.III))
mechanical properties of arc-cast and sintered, effects of argon and hydrogen at high temperatures on, 17: 41341(R) (GEMP-27A(p.9-24))
mechanical properties, 18: 7292(R) (HW-77954(p.4.1-12))
mechanical properties of electroclad and electroformed, 18: 14439
mechanical properties of high-purity, effects of temperature and strain rate on, 18: 14366(R) (HW-79766(p.3.1-64))
mechanical properties of consumable-electrode vacuum-furnace produced, 18: 18397
mechanical properties of, effects of trace elements on, 18: 34206
mechanical properties of, polygonization effects on, 18: 37722
mechanical properties at −196 to 2800°C, temperature effects on, 18: 42065
mechanical properties of, effects of heat treatment on, 19: 7959
mechanical properties of, effects of hydrogen at 2200°C on, 19: 18390(R) (GEMP-43A)
mechanical properties and recrystallization of, effects of carbon, titanium, and zirconium on, 19: 37138
mechanical properties of, effects of hot plastic deformation on, 20: 4403(T) (JPRS-32317)
mechanical properties and structure of, effects of hot rolling in air, argon, and vacuum on, 20: 11249
mechanical properties of, effects of interstitial impurities on, 20: 23641(R) (AROD-4074:2)
mechanical properties of electrowon, 20: 23643 (BM-RI-6771)
mechanical properties of, effects of production processes on, 20: 33770(R) (GEMP-59A)
mechanical relaxation measurements, 16: 12092(R) (GA-2848)
melting of, effects of additives, arc current, and electrode density on vacuum-arc, 18: 24070 (RTD-TDR-63-4089)
melting of, electron-beam, 20: 29674
melting of, performance of plasma electron beam source for, 18: 41952
melting of, properties of boron, carbon, and titanium hydride as deoxidizers during arc-, 20: 29675
melting point measurement by black-body method, 19: 20566(T) (IS-Trans-13)
melting point of, effects of gas impurities on, 20: 17094
melting temperature of, equations for calculating, 18: 25990
mercury-ion reactions with, Auger-electron injection in, (E), 19: 41272(T)
meson (μ^-) capture by, x rays from, 18: 19044
meson (μ^-) capture at 149 Mev/c, x-ray spectra from, (E), 19: 5168
meson (μ^-) capture by, probability for, (T), 20: 28456
meson (μ) capture, Fermi interactions in, 16: 15590
meson (μ) scattering, x-ray emission in, 16: 19705
meson (μ^-) capture by, x-ray spectra from, 17: 26578
metabolism in cattle and swine, tracer study, 19: 12928
metabolism of, in rats, 18: 3407(R) (NYO-10710)
metallurgical properties, 16: 15164 (AGARDograph-50)
metallurgy of, bibliography on, 17: 36203 (TID-3572)
metallurgy of powders of, 16: 3425 (LAMS-2612)
metallurgy of, book on, 20: 46147(T) (NASA-TT-F-359)
microstrain in, from 5 to 298°K, 18: 42094
microstructure of evaporated films of, 19: 40463(R) (SRIA-425-5)
microstructure of, effects of sintering on, 19: 47054
microstructure of, effects of melting method on inclusions in, 20: 41467
negative ion emission, after positive ion bombardment, 18: 28121
neon atom and ion bombardment, electron spectra from, 18: 24318
neon-22 reactions with, neutron and gamma spectra from (E), 19: 3236 (JINR-P-1765)
neutron absorption cross sections, 16: 18429
neutron absorption cross sections at 24 kev, (E), 19: 45230
neutron absorption cross section in pitchblende, thermal, 20: 37994
neutron average total cross sections at 11 to 101 kev, (E/T), 19: 8457
neutron capture by, at 0 to 50 kev, cross sections for, 17: 41883
neutron capture by, use of lead spectrometer for studying, 18: 24608 (NP-13930(p.110-11))
neutron capture by, 18: 40630
neutron capture cross sections at 0.3 to 10 Mev, 16: 1032(T) (AEC-tr-4685)
neutron capture cross sections at high energies, 16: 11501(R) (ANL-6413)
neutron capture cross sections, 16: 26509
neutron capture cross sections at 30 kev, 17: 26521
neutron capture cross sections, 18: 12294
neutron capture cross sections, energy dependence of, 18: 15562
neutron capture cross section of, energy dependence of radiative (E/T), 19: 3391
neutron capture cross sections at 0.025 to 20 kev, (E), 19: 35378(R) (EANDC(E)-57(U))
neutron capture gamma spectra, low-energy, 19: 25468(R) (ARF-1193-17)

neutron capture resonance integrals, (E), 20: 40146
neutron cross sections, library of 40-group BPG and spectral "B" codes, 16: 12422 (BAW-158)
neutron cross sections, 16: 33579 (GA-2911)
neutron cross sections for, nine and sixteen group, 17: 22789 (GEMP-173)
neutron cross sections for, fast, 17: 28245 (KFK-120)
neutron cross sections and nuclear data for, 18: 7680 (KFK-120(Pt.III))
neutron cross sections for, from 0.414 ev to 5.5 Mev, 19: 45244 (AEEW-M-472)
neutron cross sections for, 9- and 16-group, 20: 4829 (GEMP-173(Suppl.1))
neutron cross sections for, 20: 4830 (GEMP-384)
neutron cross sections for, 20: 14062 (JUL-214-RG)
neutron differential scattering cross sections at 14 Mev, 16: 1072
neutron Doppler coefficients for, fast, (E/T), 19: 29199
neutron elastic scattering at $\theta = 0°$, 16: 4741(R) (TID-14157)
neutron elastic scattering cross section at 14 Mev, 17: 5393
neutron elastic scattering by, 17: 17094 (TID-18277)
neutron elastic scattering at 0.275 to 0.85 Mev, nonlocal optical model analysis of, 18: 6241
neutron elastic scattering anisotropy in, 18: 15139 (NAA-SR-Memo-9023)
neutron elastic scattering at 3.7 Mev, angular distributions and polarization of, 18: 15222
neutron elastic scattering at 3.25 Mev, polarization in, 18: 19103
neutron elastic scattering at 400 kev, cross section for, 18: 38074(T) (AEC-tr-6398(p.64-9))
neutron elastic scattering at 0.3 to 1.5 Mev, differential cross sections for (E), 19: 3381
neutron elastic scattering at 300, 500 and 800, (E), 19: 17017
neutron elastic scattering at 0.3 to 1.5 Mev, angular distributions from, (E), 19: 19095 (WASH-1053)
neutron elastic scattering at 0.2 to 2.0 Mev, compound, (T), 19: 19190
neutron elastic scattering at 0.8 Mev, angular distributions from, (T), 19: 37884
neutron elastic scattering at 1 Mev, differential cross sections for, (E/T), 20: 9981 (WASH-1064)
neutron elastic scattering at 0.8 Mev, cross sections for, (T), 20: 15770
neutron elastic scattering at 3.2 Mev, (E/T), 20: 46644
neutron inelastic collision cross sections, 16: 10984
neutron inelastic collision cross sections, 16: 29793(T) (FTD-TT-62-953)
neutron inelastic scattering by, collective nuclear energy levels from fast, 17: 848
neutron inelastic scattering cross sections at 9.6 to 12.2 Mev, 17: 5393
neutron inelastic scattering at 14 Mev, level density and nuclear temperature for fast, 17: 31492
neutron interaction threshold values for fission spectrum, 16: 7036
neutron microscopic cross sections for, 17: 41866 (NAA-SR-Memo-8904)
neutron radiative capture cross sections at 30 and 65 kev, 18: 34274(R) (NIRS-2(p.3-15))
neutron reactions at 3.7 Mev, cross-section measurements, 16: 8224
neutron reactions at 0.1 to 100 Mev, total cross sections for, 16: 11021
neutron reactions at 0.05 to 1.00 Mev, capture cross sections, 16: 29744
neutron reactions at high energies, table of radioisotopes produced in, 17: 794 (CERN-62-22)
neutron reactions (n,p) in, cross sections for, 17: 9592
neutron reactions with, gamma production in, 18: 21169 (GEMP-278)
neutron reactions (n,γ) with, effective cross sections for, (E), 19: 16958
neutron reactions (n,n′γ) at 0.3 to 2.6 Mev, excitation cross sections for, (E/T), 19: 31284
neutron reactions with, production of technetium in, 19: 36305
neutron reactions (n,n′γ) with, cross section for, 19: 45263 (JAERI-1078)
neutron reactions (n,2n) at 14 Mev, use in fusion-reactor blankets, 19: 47721 (LA-3385)
neutron resonance absorption integrals for, (E), 20: 15691 (CEA-R-2840)
neutron scattering at 1 Mev, 16: 3662
neutron scattering, polarization effects, 16: 4792
neutron scattering angular distribution, 16: 12419 (ANL-5567(Rev.))
neutron scattering resonance cross sections for, fast, 16: 24387
neutron scattering at 2.5 Mev, inelastic cross sections, 16: 29741
neutron scattering at 0.4 to 1.2 Mev, cross sections for, 17: 26476
neutron scattering at 1 Mev, nonlocal model analysis of, 17: 41873 (WASH-1044)
neutron scattering by, cross sections for, 17: 41873 (WASH-1044)
neutron scattering at 0.275 and 0.85 Mev, optical model analysis of, 18: 7676 (CONF-340-3)
neutron scattering at 0.4 to 1.2 Mev, cross sections for, 18: 9331
neutron scattering at 14 Mev, nuclear temperature after excitation by, 18: 15235
neutron scattering by, optical model analysis of, 18: 24625 (WASH-1046)
neutron scattering at 0.275 to 0.850 Mev, 18: 42623(R) (ANL-6879 (p.21-34))
neutron scattering at 6 Mev, angular distributions for, (E), 19: 5171
neutron scattering at 3 to 650 kev, cross sections, phase shifts, and strength functions for, (E), 19: 10319
neutron scattering by, angular distribution in, 19: 31252
neutron total cross sections at 28.4 Mev, 16: 5969
neutron total cross sections at 10 to 1000 ev, 16: 25877(R) (ANL-6534)
neutron total cross section of, fast, 17: 20982 (HW-SA-2875)
neutron total cross sections at 10 to 100 kev, 18: 4525 (BNL-7349)
neutron transmission resonances, parameters, 16: 28056
neutron transmission by, 17: 41527(R) (ANL-6720(p.2-15))
neutron transmission in slabs of, (E), 19: 14728 (APEX-581)
neutron transport properties at 0.3 to 2.7 Mev, 17: 787(T) (AEC-tr-5413)
nitrogen ion reactions, Coulomb excitation of energy levels in, 16: 33826
nitrogen ion sputtering reactions at 0 to 8 kev, 16: 587 (NASA-TR-R-105)
nitrogen reactions at 1.47 Mev, alpha and proton angular distributions and energy spectra from, 17: 38293
noble-gas-ion reactions on, secondary electrons from, 17: 16836
nuclear spin relaxation in metallic, (E), 20: 17998
oxidation at high temperatures, 20: 41421
oxidation at 1000 to 1725°C, kinetics, 16: 27588 (ASD-TDR-62-203(Pt.I))
oxidation at 1000 to 1540°C, alloying effects of hafnium and yttrium, 17: 8739 (AD-277355)
oxidation at 1000 to 1600°C, kinetics of, 18: 10493
oxidation at 1000 to 1500°K, 18: 27400
oxidation at 1500 to 2600°K, mass spectrometric study, 17: 33945
oxidation at 20 to 400°C, 16: 27684
oxidation at 550 to 1700°C, 18: 32072
oxidation by air and oxygen at high temperatures, 17: 31761(R) (MND-P-3001)
oxidation by air and gas mixtures, kinetics of, 18: 34083
oxidation by air at 800°C, effects of phosphiding treatment on, 19: 6268 (IS-854)
oxidation by air at 1000°C, effects of pressure on, 19: 16017(R) (HW-84281(p.5.6-25))
oxidation by air at 800°C, effects of phosphide coatings on, 20: 5851
oxidation by low-pressure oxygen at 1000°C, 19: 13883(R) (HW-81984 (p.9.1-6))
oxidation by potassium hydroxide and by sulfuric acid, passivation mechanisms in, 20: 37184
oxidation by steam at 1100 to 1700°C, 20: 31669
oxidation, development of coatings and techniques for protection against, 16: 10406 (ASD-TR-61-322(p.101-18))
oxidation in air, effects of pressure on, 18: 44037(R) (HW-82651 (p.5.1-33))
oxidation kinetics, 16: 32974
oxidation kinetics at 1400 to 2000°K, 17: 30961 (ASD-TDR-62-204(Pt.II))
oxidation kinetics at 1300 to 2400°C, 19: 40961
oxidation mechanisms of, 19: 32048(R) (NP-15073)
oxidation of, at volatile trioxide temperatures, 20: 35850 (N-66-17887)
oxidation of, at 1380 to 2470°C, 19: 34646
oxidation of, effects of iridium coatings on, 20: 33818(R) (N-66-12875)
oxidation of, effects of coatings on, 20: 33825
oxidation of, protective effects of molybdenum disilicide coatings against, 18: 12586
oxidation of, protective effects of silicon coating against, 19: 22908
oxidation protection, thermal resistance studies of coatings for, 16: 30841
oxidation protection of, by ceramic coatings, 20: 7528
oxidation rates of, effects of dissociation of molecular oxygen on, 20: 5846
oxidation resistance of, development of coatings for improving, 18: 10491
oxidation studies, 16: 28379(R) (ORNL-3302(p.232-79))
oxygen removal from, by contact with gas mixture, 19: 36972(P)
particle waves and phonon fission in crystals of, 18: 27874
performance as adsorption cesium reservoirs, 20: 41680(R) (NYO-3642-2)
performance as collector in thermionic generators, (E), 19: 18739(R) (NP-14830)
performance as collector in a thermionic converter, 19: 39431(R) (AD-608554)
performance as collector in thermionic generators, 19: 43028(R) (AD-609966)
performance as collector electrode for thermionic cells, 20: 11540(R) (AD-626444)
performance as electrodes in ion engines in spacecraft, 18: 23740(R) (NP-13899)
performance as electrodes in low-temperature thermionic cells, 18: 36230(R) (NP-14101)
performance as electrodes in barium-filled thermionic cells, 18: 44498(R) (MND-2812-3)
performance as electrodes in barium-filled thermionic cells, 18: 44496(R) (MND-2812)
performance as electrodes in barium-filled thermionic cells, 18: 44497(R) (MND-2812-2)

performance as electrode in thermionic cells, facility for testing, (E), 19: 18741 (TE-41-65)
performance as emitter in thermionic cell (E), 19: 1206 (AERE-R-4715)
performance as emitter in cesium diodes, digital computer program for analysis of, 20: 9700
performance as fuel cladding in fast reactors, 18: 24952(R) (ANL-6880(p.6-48))
performance as reflector in fast rocket reactors, 19: 29769
performance as seed material for gas coolant in rocket reactors, (E), 19: 24149 (NASA-CR-212)
performance as thermionic emitter, 18: 20872
performance compatibility with fission heat source in thermionic cells, 18: 20876
performance in cesium diodes, effects of cesium fluoride on, (E), 19: 6497
performance in neon glow discharge, effect of active gas additives on, 18: 21456
performance in thermionic cells, 18: 26933
performance in thermionic cells, effects of additives on, 18: 24350(R) (AD-418276)
performance of alkaline earth-coated electrodes of, 17: 20664
performance of cesium-coated, as thermionic emitter, 18: 38392 (A/CONF.28/P/44)
performance of electrodes of, in contact ion engines, 19: 13613
performance of electrodes of, in thermionic cells, 17: 22265 (ASD-TDR-63-183)
performance of electrodes of, in vapor-filled thermionic converters, 17: 34654
performance of monocrystalline, as thermionic emitter, (E), 19: 9962 (AFCRL-64-410)
performance of pelletized, for control of radiant heat transfer in nuclear rockets, (E), 19: 24148 (NASA-CR-210)
performance of perforated electrodes of, as ion sources, 18: 24366 (ASD-TDR-63-750)
polarization of uranium and uranyl chlorides in potassium chloride–sodium chloride melts on, 18: 22065
permeability to hydrogen in thermionic cells, 18: 36224(R) (AD-434908)
permeability to hydrogen, 20: 39098(R) (WERL-2823-21)
permeation by hydrogen and nitrogen at high temperatures, 17: 14928 (ASD-TDR-62-324)
phase studies at high temperatures, 17: 29353
phase transition in alloyed and unalloyed, effects of interstitials on ductile-to-brittle, 16: 25751 (DMIC-Memo-155)
photodesorption of carbon monoxide from, efficiency and mechanism of, 19: 7408
photoelectric Schottky deviations for single-crystal, 18: 42326
photon reactions with, proton angular distributions and yields at >8 Mev, 17: 28265
physical properties, 16: 15209
physical properties of, effects of alloying additions and chemical reactions on, 18: 34205
plasma accelerator electrodes of, mass losses by pulsed, (E), 19: 17082
plastic deformation of single crystals of, 18: 18408
plastic deformation of single-crystal, mechanism of direct-shear, 18: 20563
plastic deformation of single crystals of, slip planes in, 19: 18471(T) (FTD-TT-64-371(p.1-20))
plastic deformation of, mechanisms of, 19: 40961
plastic deformation of, use of stress relaxation in studying, 20: 33891
plastic strain in, use of stress relaxation technique for studying, 19: 2810
polarization during electrolysis in fused salts containing cerium trichloride, 20: 14562
polarization of cathodes of, in electrolysis of chloride melts containing uranium, 19: 32128(T) (NP-tr-1236(p.12-20))
polygonization in rod of, creep-rupture-tested at 2200°C, 19: 37030(R) (GEMP-47A, pp 27-84)
polygonization of, effects on elastic limit, microhardness, microstructure, and recrystallization of, 17: 36317
positron lifetime in, 16: 3626
potassium ion scattering at 20 to 260 eV, angular regularities in, 19: 16405(T)
potassium-ion thermionic emission from, at 30 to 1100°C, 19: 39197
powder metallurgy, status of, 16: 24110(R) (MAB-139-M(C4))
powder metallurgy of, 19: 2774
powder production by atomization in plasma jet, 19: 37012
powders of, arrangement in lines-of-force pattern by electric fields, 18: 5848 (SC-TM-40-59(51))
precipitation using cinchonin, 17: 39073
preparation and ductility of, scavenged using yttrium, 16: 25696(R) (DRI-2010)
preparation and properties, review, 16: 29419
preparation and properties of single crystals of, 18: 10460(T) (JPRS-22697(p.39-45))
preparation and properties of foams of, for aerospace uses, 19: 37141
preparation and properties of single crystals of, 20: 41481
preparation by reduction of oxides using hydrogen–water vapor mixtures, design of gas flow apparatus for studying, 18: 31444
preparation by zinc reduction of molybdenum halides, 20: 9405(P)
preparation for electron microscopy, 18: 7298(R) (HW-78962(p.3.1-14))
preparation of beta-phase, 20: 31717(R) (UCRL-16658, pp 143-9)
preparation of crystals of, by electron beam melting, 18: 27871(T)
preparation of fine-powdered, 19: 7859
preparation of fine powders of, by flame reduction of fluorides, 19: 15997 (K-L-6020)
preparation of high purity by magnesium reduction of molybdenum trioxide, 16: 10429 (BM-RI-5934)
preparation of high-purity, 20: 31741
preparation of pure, 20: 819(R) (GA-6413)
preparation of pyrolytic, 18: 4173(R) (ORNL-3470(p.75-88))
preparation of single crystals of, by arc-zone melting, 18: 18339
preparation of single crystals of, by electron-beam zone melting, 18: 22463(T) (JPRS-22336(p.6-9))
preparation of single crystals of, by electron-beam floating-zone melting, 18: 34061(T) (FTD-TT-64-350)
preparation of single crystal, 19: 9604(R) (IS-900(Sect.M))
preparation of single-crystal, by floating-zone methods, 20: 33859(R) (AD-634128)
preparation of single crystals of, using electron-beam zone refining, 20: 41434
preparation of spherical particles of, by plasma jet atomization, 20: 11219
preparation of thin films of, by jet-polishing and electro-polishing, 20: 27464
preparation of, vacuum techniques for, 19: 11686
preparation, properties and uses of, chemical process monograph on, 19: 18407
pressing and sintering of powdered, properties of billets formed by, 18: 39873(T)
pressing and sintering of powdered, 19: 22939
pressing and sintering properties of powders of, 20: 43867
pressing of powdered at 700 to 1200°C and 5000, 15,000, and 30,000 psi, hot-, 20: 9452
production and properties of low-carbon unalloyed, arc-cast, evaluation of, 20: 29756
production by reduction of oxide, gas recycle system for, 19: 911
production by reduction of oxide, fluidized-bed reactor for, 19: 912
production of high-quality sheet, panel summary on, 20: 39357 (MAB-212A-M)
production of large-surface-area powders, 19: 30658
production of powders of, from ammonium molybdate or molybdenum oxide, 18: 39873(T)
production with defect free surfaces by electropolishing, 19: 37013
properties, 16: 3460 (NP-11108)
properties, 16: 19398
properties and reactions at elevated temperatures, 16: 4527 (DMIC-160)
properties and structure of, effects of yttrium on, 17: 8811 (NP-12481)
properties and use of, in non-nuclear industries, 18: 44072
properties and uses in nuclear energy applications, 19: 7861
properties and uses of, review of, 19: 36966
properties and uses of, review on, 20: 2307 (AD-613023)
properties as brazing material, 19: 24916(R) (GEMP-334A)
properties as capacitance temperature sensors, 17: 29712(R) (GEMP-77)
properties as carbon-diffusion barrier for hafnia thermocouple insulators at 2450°C, 20: 7499(R) (GEMP-53A)
properties as catalyst for hydrocracking reclaimed high boiler, 16: 9978(R) (TID-14949)
properties as die insert, 17: 14788(R) (NMI-9700.6)
properties as emitter in thermionic converters, 17: 20607
properties as fuel element cladding, 18: 15563
properties as high-temperature coating, 20: 29650
properties as radiation target when incorporated into nuclear emulsion, 16: 16967 (NP-11592(Vol.I)(p.307-25))
properties as thermionic cell emitter, 17: 24030(R) (AD-286693)
properties at high temperatures, 17: 34409(R) (NMI-1253)
properties at high temperatures for use as heating element, 19: 4699
properties at high temperatures, 20: 4418
properties at 1250 to 4000°K, electric and thermal, 17: 30833
properties at 4000 to 6000°F, mechanical and physical, 16: 24162 (NP-11654)
properties for aerospace uses, 19: 47068
properties for capping Mo-3 alloy ingots to prevent cracks, 20: 37219
properties for exothermic brazing, 17: 16608(R) (NP-12615)
properties for high-temperature thermocouples, 17: 29170(R) (ASD-TDR-63-233)
properties for high-temperature brazing, 19: 11669(R) (GEMP-41A)

properties for use as reactor material, 16: 4994
properties for use at high temperatures, 18: 34201
properties for use as fuel cladding material, 19: 11679
properties for use as oxidation-resistant coating for uranium, 19: 13925
properties for use in uncooled nuclear rocket nozzles, 19: 36641
properties in nitric acid solutions, 16: 25311 (IG-Memo-466)
properties of arc-plasma and flame-sprayed coatings of, 17: 31086(R) (NP-12988)
properties of compacts of, effects of compaction pressure and sintering temperatures on, 16: 3424 (LA-2621)
properties of electron beam melted, 16: 19280
properties of electron multiplier resistance-strip of, 19: 41124(R) (NP-15108)
properties of flash-welded, 16: 4537 (NP-11127)
properties of, for use in thermionic reactors, 17: 5577 (GA-3523)
properties of, for formation of transition metal pseudosilicides, 17: 18668(R) (AFOSR-2647)
properties of, mechanical and structural, 17: 3499 (WADD-TR-61-181 (Pt.II))
properties of porous, for cesium ionization, 20: 31388
properties of sheet, 18: 573(R) (AD-422116)
properties of single-crystal, relations between, 20: 5851
properties of sintered, using argon, hydrogen, and vacuum environments, 18: 41930(R) (NP-14294)
properties of sprayed bodies of, effects of sintering on, 19: 36994 (AMRA-TR-64-50)
properties of thorium oxide- and yttrium oxide-coated electrodes of, 17: 25810
properties of, at 2000°C, for use in thermionic converters, 20: 29729
properties of, effects of dispersed phases of various borides, oxides, and nitrides on, 19: 26853
properties of, effects of annealing medium and temperature on, 20: 41482
properties of, effects of sodium coolant on, 20: 46995
properties of, effects of protective coatings on, 19: 47061
properties of, mechanical and physical, 20: 27538
properties of, physicochemical, mechanical, and radiation stability, 19: 26818 (NAA-SR-8617(Vol.III))
properties of, review on, 18: 34180
properties, review, 16: 33495
properties, review, 17: 12596
protection against oxidation, silicon carbide coatings for, 20: 37189
protection at high temperatures, coatings for, 19: 2762
proton bombardment of, production of niobium-88 by, 18: 36593
proton elastic scattering at 57 Mev, angular distributions and polarizations, 16: 23056
proton elastic scattering at 17.8 Mev, polarization in, (E/T), 19: 14599
proton nonelastic scattering cross sections at 10 Mev, 17: 13581
proton reactions at 0.1 to 0.5 Mev, characteristic x-ray yields from, 16: 33633
proton reactions at 0.05 to 2.9 Bev, induced activity data and cross sections for spallation, (E/T), 20: 32549
proton scattering at 1.5 Mev, x-ray emission from, 18: 14664
proton spallation at 660-Mev, 16: 22924
purification by electron-bombardment zone-melting methods, 16: 32046
purification by electron-beam melting, 19: 26849
purification by electron-beam melting, 20: 5181(R) (ORNL-3029)
purification by wet hydrogen, 20: 7499(R) (GEMP-53A)
purification by zirconium hydride exchange reaction, 20: 27476(R) (BNWL-207, pp 3.14-16)
purification methods for, 20: 33770(R) (GEMP-59A)
purification of, 19: 37041(R) (NP-15174)
purification of electrodeposited, by arc-melting, 18: 25316 (BM-RI-6444)
purification of, radiochemical method for, 20: 8838 (UCRL-14258)
radiation and temperature effects on mechanical and physical properties of, 17: 16760
radiation damage, 16: 29460
radiation damage and recovery, point defects in neutron, 16: 24258
radiation damage in, production and recovery of electron-induced, 16: 27719
radiation damage in, effects of carbon on neutron, 18: 2294 (HW-SA-2953)
radiation damage in, effects of carbon on 10^{20} nvt neutron, 19: 42901 (BNWL-SA-151)
radiation damage in crystals of, basic mechanism study of, 16: 13643 (TID-14667)
radiation damage in, isothermal recovery of fast-neutron, 20: 9378(R) (GEMP-54A)
radiation damage mechanisms in, neutron, 20: 9566(R) (BNWL-166, pp 3.15-23)
radiation damage recovery processes in carbon-doped, fast-neutron, 19: 34741(R) (BNWL-79(p.3.1-22))
radiation damage to, annealing of, 18: 7290(R) (HW-77954(p.3.1-20))
radiation damage, x-ray-diffraction studies, 16: 2265 (HW-SA-47)
radiation effects and isochronal annealing data at 4°K, 16: 6810(R) (ORNL-3213(p.15-23))
radiation effects on corrosion by chemicals, 16: 17976(R) (EURAEC-94)
radiation effects on brittle-ductile transition, neutron, 16: 21068
radiation effects on electric conductivity of, annealing neutron, 16: 22706
radiation effects, 16: 26467(R) (HW-73100)
radiation effects on relaxation of elastic stresses in, neutron, 16: 27699(T) (AEC-tr-5257)
radiation effects of fission fragment bombardment, 16: 33407
radiation effects of neutrons on embrittlement of, 16: 33557
radiation effects on electric conductivity, neutron, 16: 578(T) (SCL-T-371)
radiation effects on electric conductivity at 20 to 135°C, 16: 7942(T) (AEC-tr-4679)
radiation effects on electric resistance of, 17: 6732 (62-GC-207)
radiation effects, 17: 8877 (AFCRL-62-316)
radiation effects, 17: 11129
radiation effects on K absorption spectrum, neutron, 17: 14319
radiation effects, 17: 22093(R) (GEMP-21A)
radiation effects on electric conductivity of, isochronal recovery curves for, 17: 22248
radiation effects on, hardening in stage III recovery from neutron, 17: 27922
radiation effects on properties and structure of, 17: 27730(R) (HW-77052)
radiation effects on mechanical properties of, at high temperatures, 17: 41342(R) (GEMP-27A(p.25-48))
radiation effects on properties and structure of, role of carbon impurities in, 17: 41519
radiation effects on content of, in spleen in rats, 17: 40547(R) (NYO-10569)
radiation effects on carbon-containing foils of, neutron, 18: 2314
radiation effects on, mechanisms for annealing and producing, 18: 2322
radiation effects on, effects of carbon on, 18: 7290(R) (HW-77954(p.3.1-20))
radiation effects on, neutron, 18: 7298(R) (HW-78962(p.3.1-14))
radiation effects on creep-rupture properties and electric conductivity of, 18: 12543(R) (GEMP-31A)
radiation effects on mechanical properties of, 18: 16526 (NP-13663)
radiation effects on interstitial loops in, 18: 16536
radiation effects on electric and mechanical properties of, 18: 16424(R) (GEMP-270A)
radiation effects on mechanical properties of, review, 18: 20456 (ORNL-3593)
radiation effects on, stage III recovery from neutron, 18: 20596
radiation effects on thermal control coatings of, in nuclear spacecraft, 18: 20603
radiation effects on hardness and thermoelectromotive force of, neutron, 18: 28066
radiation effects on hardness and oxidation of, by water at 50°C, 18: 32043(R) (HW-81269(p.4.1-64))
radiation effects on crystalline, 18: 32042(R) (HW-81269(p.3.1-38))
radiation effects on, in fluoride salt baths, 18: 34050(R) (ORNL-3626 (p.59-164))
radiation effects on, recovery from neutron, 18: 34221
radiation effects on mechanical and thermal properties of, 18: 41921(R) (GEMP-37A)
radiation effects on electric resistivity of, annealing of neutron, 18: 41933 (TID-11295(3rd Ed.))
radiation effects on elastic modulus of, neutron, 18: 44240(T) (AEC-tr-6475)
radiation effects on crystalline, 18: 44035(R) (HW-82651(p.3.1-59))
radiation effects on structure of, neutron, 19: 997(R) (NYO-2994-1)
radiation effects on, neutron, 19: 4719(T) (AEC-tr-6227/2(p.63-72))
radiation effects on, 19: 10675(R) (NAA-SR-9999)
radiation effects on compatibility with graphite and molten fluorides, 19: 10565(R) (ORNL-3708(p.252-87))
radiation effects on mechanical properties of, neutron, 19: 11669(R) (GEMP-41A)
radiation effects on, neutron, 19: 16209(R) (HW-84281(p.3.1-16))
radiation effects on mechanical properties of, 19: 18390(R) (GEMP-43A)
radiation effects on, annealing of neutron, 19: 20634
radiation effects on structure of, neutron, 19: 23132
radiation effects on reactions with fueled graphite, 19: 24922(R) (ORNL-3731(p.1-110))
radiation effects on fuel rod jackets of, 19: 26876 (ANL-6750)
radiation effects annealing, stored-energy release in, 19: 27709(R) (GA-5734)
radiation effects on creep-rupture properties of, fast neutron, 19: 28887
radiation effects on slip lines in single-crystal, fast neutron, 19: 30822 (BNWL-44)

radiation effects on, in fused salts, 19: 30825(R) (ORNL-3689(p.36-55))
radiation effects on, neutron, 19: 30648(R) (HW-84573(p.3.1-74))
radiation effects on structure of, neutron, 19: 37195
radiation effects on, anelastic after-effects from electron, (E), 19: 39247
radiation effects on stored energy release in, fast neutron, 19: 40961
radiation effects on hot hardness of, fast neutron, 19: 44598(R) (GEMP-49A)
radiation effects of 38-Mev alpha particles and 85-kev protons on, foils of, 16: 27716 (AERE-M-991)
radiation effects on crystal structure in foils of, neutron, 16: 27717
radiation effects on dislocation channeling in, effects of prestrain on fast neutron, 20: 745(R) (BNWL-120, pp 3.1-22)
radiation effects on structure of, combined effect of carbon impurity atoms on neutron, 20: 895
radiation effects on hardness of, neutron, 20: 2457
radiation effects on, annealing of, at 60 to 1200°C, 20: 2476
radiation effects on hardening and embrittlement of bcc, 20: 2472
radiation effects on properties of, combined impurity and neutron, 20: 5851
radiation effects on creep-rupture of, fast neutron, 20: 5851
radiation effects on microhardness of, effects of test temperature on fast-neutron, 20: 9378(R) (GEMP-54A)
radiation effects on x-ray low-angle scattering properties of, combined carbon and fast-neutron, 20: 9565(R) (BNWL-166, pp 3.10-14)
radiation effects on microstructure of, neutron, 20: 11227
radiation effects on crystal structure of, neutron, 20: 15136 (RL-REA-2595, pp 51-62)
radiation effects on tensile properties of, effects of annealing on neutron, 20: 27582(R) (GEMP-400A, pp 63-98)
radiation effects on hot-hardness of, effects of test temperature on fast-neutron, 20: 27582(R) (GEMP-400A, pp 63-98)
radiation effects on tensile properties of, neutron, 20: 27571(R) (BNWL-207, pp 4.1-3)
radiation effects on mechanical properties of, fission fragment and neutron, 20: 29820
radiation effects on, for use as sensor material, 20: 29486(R) (NASA-CR-54964)
radiation effects on lattice parameter of, neutron, 20: 31669
radiation effects on, at 11 to 7°K, electron, 20: 41499
radiation from promethium-147 beta-excited, 20: 3882 (ORNL-IIC-5, pp 51-71)
radiation heating deposition rates in, cross sections for, 17: 36347(R) (NARF-62-18P)
radioinduced defects, annealing, 16: 22693
radioinduced defects in foils of, 18: 14366(R) (HW-79766(p.3.1-64))
radioinduced defects in, effects of prestrain on fast-neutron, 20: 17132
radioinduced dislocation loops in, interactions during annealing, (E), 19: 37182
radioinduced hardening of, relative importance of grain boundaries and sub-grain boundaries in, 17: 2027
radioinduced hardness in, effects of annealing and temperature on fast neutron, 19: 37165(R) (GEMP-47A, pp 85-99)
radioinduced heating of, gamma, 18: 10346(R) (X64-11113)
radioinduced interstitial loops in, neutron, 19: 20636
radioinduced lattice defects in, x-ray diffraction study of, 17: 37602
radioinduced lattice defects in, electron microscopic observations of, 19: 11812
radioinduced production of helium and hydrogen in, neutron, 19: 26901
radioinduced relaxation of elastic stresses in, 17: 455
radioinduced swelling in, effects of carbon on fast neutron, 20: 745(R) (BNWL-120, pp 3.1-22)
rare-gas ion reactions at 1 to 10 kev, secondary-electron emission in, (E), 19: 39404
reactions in gaseous mixtures, combustion, 20: 29641(R) (SC-DC-65-1691)
reactions of, with uranium ceramics at 1200 to 2000°C, 16: 33468 (GA-3124)
reactions of, with aluminum, silicon, and zirconium chlorides in hydrogen, 17: 21681
reactions with argon, mercury, and neon ions, atom ejection patterns in sputtering by, 16: 2203(R) (TID-14257)
reactions with beryllium, copper, stainless steel, and niobium alloys to 760°C *in vacuo*, 19: 44606 (PWAC-483)
reactions with beryllium to 700°C in carbon dioxide and *in vacuo*, 19: 22997 (TRG-Report-842)
reactions with boron nitrides at high temperatures, 19: 44220 (N64-31011)
reactions with borides, carbides, and nitrides at 900 to 2200°C, 20: 25578(T) (N-65-35787)
reactions with carbon dioxide, 16: 2993 (NP-10967)
reactions with carbides at 1000 to 2100°C and oxides at 1600 to 2100°C, 16: 4555(T) (FTD-TT-61-74)
reactions with carbon dioxide to 600°C, 19: 22997 (TRG-Report-842)
reactions with cesium ions, secondary electron emission in, (E), 19: 6471
reactions with cesium vapor at high temperatures, 19: 9628
reactions with combustion gas species in launch pad abort environments, 20: 19192 (SC-DR-65-1918)
reactions with fast neutrons, helium and hydrogen production in type 347 stainless steel in, 20: 7490(R) (BMI-1745, Sect.A)
reactions with fission–plutonium–uranium alloys at 750°C, 19: 44587(R) (ANL-7000, pp 3-63)
reactions with hafnium and magnesium oxides at 2450°C, 19: 44598(R) (GEMP-49A)
reactions with ions, mechanisms and secondary ion emission coefficients, 16: 1036(T) (AEC-tr-4695)
reactions with low-melting metals, 20: 4077(R) (IS-1200(Sect. E))
reactions with magnesium, 19: 22997 (TRG-Report-842)
reactions with metal oxides at high temperatures, 19: 44685 (CONF-650908-5)
reactions with metals to 2600°C in different atmospheres, 19: 22997 (TRG-Report-842)
reactions with molten uranium dioxide, compatibility in, 19: 28852
reactions with plutonium oxide during sintering, 17: 14209 (LA-2828)
reactions with plutonium nitride, 18: 34032(R) (BMI-1668(Del.))
reactions with plutonium carbide–uranium carbide, 20: 9438
reactions with samarium boride, 19: 15502
reactions with silica, interfacial, 16: 31595
reactions with silicon in vacuum, temperature effects in, 18: 37626
reactions with sodium oxides at 400°C, 17: 35251(R) (BMI-1632(Del.))
reactions with sodium sulfide to form molybdenum sulfide, 18: 20001
reactions with sodium at 2100 to 2400°C, 19: 39090(R) (ANL-7046(p.78-82))
reactions with steam, reactor safety studies of, 18: 33678(R) (ANL-6875)
reactions with steam at high temperatures, 18: 44922(R) (ANL-6800 (p.326-402))
reactions with steam at high temperatures, kinetics of, 19: 32447(R) (ANL-7020(p.175-97)) pp 187-233)
reactions with refractory metal borides, carbides, nitrides, and oxides, 20: 14989
reactions with sodium, high-temperature, 20: 15033(R) (ANL-7152, pp 87-96)
reactions with sodium at high temperatures, 20: 20925(R) (ANL-7055, pp 177-212)
reactions with steam at 1100 to 1700°C, 20: 6552(R) (ANL-6925,
reactions with titanium carbide, 19: 18521(T)
reactions with titanium nitride, 20: 7097
reactions with tritium atoms at 50 to 100 kev, research on, 20: 22857(R) (ORNL-3913, pp 111-32)
reactions with uranium di- and monocarbides and nitride at 1000°C, 16: 30829
reactions with uranium-bearing reactor fuels, 17: 27961
reactions with uranium monocarbide at 1000 to 2400°C, 18: 8795 (HW-72031)
reactions with uranium in alloy with niobium and zirconium, 18: 34174
reactions with uranium to 1300°C, 19: 22997 (TRG-Report-842)
reactions with uranium dioxide at high temperatures, 19: 44593 (CONF-650908-4)
reactions with uranium carbide–zirconium carbide solid solutions at high temperatures, compatibility in, 20: 2332 (LA-3307)
reactions with uranium carbides, thermodynamic calculation of, 20: 9432
reactions with water at 1100 to 1700°C, 20: 5846
reactions with 1-mercaptopropionic acid derivatives, 18: 19914
reactivity with carbides, graphite, refractory metals, and uranium compounds, 16: 5714 (NEPA-1050)
reactor criticality effects, 18: 30963
reactor criticality effects per atom, (E), 19: 42077 (ANL-7014)
recrystallization behavior, 16: 3445 (ASD-TR-61-193)
recrystallization temperature, effects of heating rate on, 16: 6737
reduction by hydrofluoric acid for titration, 18: 5245
refining by electron beam melting, 18: 27875
refining of, zone, 20: 11218
refractive index of gaseous, (E/T), 20: 5879 (D-910092-6)
reinforcing effects on properties of strontium zirconates for use at high temperatures, 17: 34471
relaxation effect, 19: 16053(R) (AD-424622)
relaxation peaks at 100 to 300°K, 16: 33505
review of status and future potential of, for defense, 18: 8718 (DMIC-Memo-183)
rolling and recrystallization textures of single crystals of, cold, 19: 9718
rolling, effects of media and temperature on friction in, 17: 30953
rubidium ion bombardment, secondary ion emission in, 16: 16881
rubidium ion scattering by, spectra from, 17: 5154(T)
rubidium ion scattering by, energies, 17: 17257

rubidium ion scattering at 20 to 260 ev, angular regularities in, 19: 16405(T)
seals for, preparation of devitrified glass, 20: 46181(P)
self-diffusion in, tracer studies of, 18: 18307
separation by anion exchange in mixed aqueous and non-aqueous systems, 19: 2243
separation from acid solutions by extraction using amine–ether in hydrocarbon diluent, 20: 12941(P)
separation from aliphatic alcohol-nitric acid solutions by anion exchange, 17: 32194(R) (TID-19068)
separation from alcohol-nitric acid solutions by ion exchange, 17: 35945
separation from antimony, tantalum, and tin by ion exchange chromatography on chloride form resin, 20: 20635
separation from aqueous solutions by cellulose, lignin, oxycellulose, and wood, 16: 20090
separation from berkelium by solvent extraction, 19: 22112
separation from beryllium by ion-exchange chromatography, 17: 3075(T) (AWRE/Trans/33)
separation from bones and teeth by solvent extraction using chloroform–cupferron, 18: 1518
separation from carrier-free niobium, method for, 20: 262
separation from chloride solutions by solvent extraction using amines, 18: 1799(R) (ORNL-3496)
separation from cobalt, iron, and nickel by thin-layer chromatography, 19: 9266
separation from fission products by solvent extraction using TBP and TOPO, 17: 243
separation from fission products in nitric acid by solvent extraction using alkyl phosphoric acids, 19: 8679
separation from fission product solutions by ion exchange, 20: 29357
separation from hydrochloric acid solutions by solvent extraction using acetylacetone, 18: 31389
separation from hydrochloric acid solutions by solvent extraction using 2-ethylhexanol, 19: 36252
separation from iron, steel, and tungsten by reversed-phase chromatography using hydrochloric and sulfuric acids, 18: 25280
separation from low grade ores, reductive chlorination process for, 20: 4072(P)
separation from metallic mixture by ion exchange chromatography, 17: 5991
separation from metal solutions by anion exchange in ammonium and hydrogen chlorides and fluorides, 18: 17941
separation from molybdenum–tungsten compounds, method for, 19: 9274
separation from neodymium by ion exchange and solvent extraction, 18: 24856(R) (GEAP-4430)
separation from niobium and zirconium by carrier precipitation, 17: 2242 (TID-16949)
separation from nitrate solutions using alkyl amines, 17: 3873
separation from niobium using 4-phenyldaphnetin, 19: 2233
separation from nitric or sulfuric acid solutions, ion exchange selectivity scales for, 19: 9257
separation from nitric acid solutions by solvent extraction, 19: 24632(P)
separation from niobium by solvent extraction using tetra-n-butyl-ammonium bromide, 20: 12933
separation from niobium, tantalum, and tungsten by solvent extraction using methyl isobutyl ketone, 20: 40796(R) (IS-1500(Sect.C))
separation from other metals by ion exchange chromatography in tartrate medium, tracer studies of, 19: 7627
separation from other metal ions by ion exchange, 19: 40658
separation from other inorganic ions by paper chromatography, 20: 12939
separation from other elements by ion exchange using triisooctylamine, 20: 43439
separation from plutonium by anion exchange, 17: 4629
separation from plutonium by ion exchange, 20: 35585 (EURAEC-1639)
separation from rhenium by evaporation with sulfuric acid, 16: 14673
separation from rhenium by ion exchange in ammonium thiocyanate–hydrochloric acid solution, 18: 27301
separation from rhenium using amyl acetate, 20: 1965
separation from rhenium in aqueous solutions by extraction using quaternary ammonium compound, 20: 25223(P)
separation from ruthenium and technetium by solvent extraction using triphenylguanidine, 16: 27138
separation from scandium by ion exchange chromatography, 20: 20821
separation from solutions by solvent extraction, review of methods for, 19: 13543
separation from solutions of irradiated uranium-235, methods for, 19: 36217(R) (IDO-14656)
separation from solutions formed by dissolution of molydenum–uranium fuel alloys, 20: 4070(P)
separation from sulfate solutions by solvent extraction using tri-n-octylamine, 20: 14653
separation from technetium by solvent extraction using acetone, 16: 30336
separation from technetium-99, 17: 28994
separation from technetium by solvent extraction using diethyl ether, methyl isobutyl ketone, and trioctylamine, 18: 17960
separation from tellurium by solvent extraction using TBP, 18: 22184
separation from technetium, 19: 19820
separation from technetium by sorption on iron oxide, 20: 16552
separation from technetium by sorption by charcoal or coal, 20: 18830
separation from technetium by solvent extraction using acetophenone and cyclohexanone, 20: 44817
separation from thorium using liquid-metal extraction, 17: 28465 (TID-7650(p.436-53))
separation from tin by reversed-phase chromatography, 20: 40796(R) (IS-1500(Sect.C))
separation from tungsten, methods for, 17: 27401
separation from tungsten, 18: 12264
separation from tungstic anhydride, method for, 19: 30660
separation from uranium concentrates, 16: 4208(R) (NLCO-800)
separation from uranium by oxidation-reduction in fused salts, 16: 10100 (IS-286)
separation from uranium by electrolysis in fused salts, 16: 29043
separation from uranium ores by alkaline and sulfuric acid leaching, 17: 39167
separation from uranium ore concentrates, 18: 5431(P)
separation from uranium by cation exchange chromatography, 19: 13245
separation from uranium by ion exchange, 19: 32285
separation from uranium by partition chromatography on silica-gel column, 20: 9073
separation from uranium fission products by precipitation using α-benzoin oxime and diethyl ether, 20: 44815
separation from vanadium and zirconium by zone melting, 18: 8456
separation from zirconium by solvent extraction using ethyl acetate, 18: 1808
separation from zirconium in nitric acid solutions, 19: 38778(P)
separation of diphenylguanidinium salts of, by solvent extraction using tiron, 18: 27345
separation of, from iron by ion exchange chromatography, 17: 18184(T) (UCRL-Trans-898(L))
separation of, from boron, method for, 17: 17999
separation of, from bauxite by direct electrolysis and precipitation, economics of, 17: 32065
separation of interstitial impurities from, technique for, 20: 23641(R) (AROD-4074:2)
separation of, radiochemical, 17: 27264
separation of rare earths from, by solvent extraction using butyric acid, 20: 45612
separation of scandium from, by ion exchange chromatography, 19: 533
separation of technetium-99 from irradiated, 17: 8125 (JAERI-1036)
separation of uranium from aqueous solutions of, by solvent extraction using alkylamines, 17: 40916(P)
separation of uranium values from waste solutions of, 19: 36567(P)
separation of (V) and (VI) states by paper chromatography, 17: 1402
separation of, from other fission products by fractional electrolytic dissolution, 20: 35589 (NP-16170)
separation of, from other fission products, by extraction into acetylacetene, 20: 38824
separation processes for, tracer studies of, 17: 21774 (NP-12726)
shear stress of single crystals of, temperature dependence of critical, 20: 4445
shock wave interactions with, thermodynamic parameters from mirror-image approximation for particle velocity and pressure in, 17: 37676
siliconizing by vapor deposition, mechanism of, 19: 47073
sintering by induction heating, 18: 44111
sintering of compacts of, at 1700°C in liquid oxide phase, 16: 4520
sintering of, diffusion mechanism for nickel-activated, 19: 11706
sintering procedure for, 20: 11253
soldering to lanthanum boride, 17: 2959(T) (AEC-tr-5264)
solubility in alpha-iron at 600 to 900°C, 20: 13317
solubility in aluminum, microhardness studies on, 20: 21362(T) (SC-T-66-0723)
solubility in bismuth (liquid) at 482 to 1010°C, 16: 6716 (NEPA-1221)
solubility in bismuth at 300 to 700°C, 16: 24216
solubility in cesium, 19: 11682
solubility in liquid zinc, 20: 22966 (ANL-7083)
solubility in lithium (liquid) at 482 to 1010°C, 16: 6718 (NEPA-1465)
solubility in lithium at 1200 to 1700°F, 19: 36980 (PWAC-355)
solubility in lithium and potassium, effects of carbon, nitrogen, and oxygen on, 20: 7579 (TIM-850)
solubility in plutonium at 700 to 1000°C, 20: 40868 (LA-3523)
solubility in pure potassium at 1000°C, 19: 40946(R) (AI-65-93)
solubility in rubidium at 1000 to 2000°F, 17: 16634 (AGN-8063)
solubility in zinc (liquid), 16: 544
solvent extraction from hydrobromic acid systems, 16: 17769
solvent extraction of, from nitric acid solutions, evaluation of solvents

for, 16: 33515(R) (GEAP-4053-2)
solvent properties for sulfur at 1100°C, 18: 27452
solvent properties for carbon at high temperatures, 20: 31669
solvent properties for hydrogen, 20: 14976 (AWRE-0-16/66)
sorption by cellulose ion exchangers from acetone and ethanol mixtures with hydrochloric acid, 18: 16140
sorption from hydrochloric acid by cellulose and resin paper ion exchangers, 18: 16139
sorption from nitric acid by ion exchange paper, 19: 24435
sorption of deuterium and hydrogen by evaporated, 16: 1895
sorption of hydrogen and oxygen on evaporated films of, 19: 13296
sorption of nitrogen on films of, sticking probability determination in, 19: 32131
sorption of rare gases by, in ion bombardment, 16: 31731
sorption on silicates from oxygen, 19: 36649 (AD-614997)
sorptive properties for residual gases, 16: 4907(R) (UCRL-9777)
sorptive properties of films of, for nitrogen, 18: 2405(R) (TID-19665)
sorptive properties of films of, for xenon, 18: 18021(R) (TID-20411)
sorptive properties for nitrogen in ultrahigh vacuum and constant pressure, 18: 22002 (CONF-209-26)
sorptive properties for nitrogen, 18: 44200
sorptive properties for deuterium and hydrogen in ultrahigh vacuum, 19: 903(R) (SRIA-128)
sorptive properties of films of, for nitrogen and xenon at −195 and −185°C, 19: 11052(R) (SRIA-135)
sorptive properties for deuterium, nitrogen, and xenon, mechanism of, 19: 26822 (TID-20853)
sorptive properties of films of, for nitrogen and xenon, 19: 29812(R) (SRIA-425-4)
sorptive properties of evaporated films of, for nitrogen and xenon, 19: 40463(R) (SRIA-425-5)
sorptive properties for deuterium, hydrogen, and deuterium–hydrogen mixtures at room temperature, 19: 40463(R) (SRIA-425-5)
sorptive properties of foils of, for nitrogen, 17: 35706(R) (TID-19307)
sorptive properties of foils of, for krypton and xenon, relation of surface area to, 17: 39589
sorptive properties for deuterium, 20: 8887(R) (SRIA-425-7)
sorptive properties for krypton and xenon, 20: 31242
sorptive properties for krypton and xenon, 20: 916(R) (SRIA-425-6)
sorptive properties for oxygen, (E), 20: 11322
sorptive properties for deuterium, nitrogen, and rare gases, kinetics of, 20: 21351(R) (SRIA-425-8)
sorptive properties of evaporated films of, for krypton and xenon, 20: 21387
sorptive properties of evaporated films of, for carbon monoxide at 0°C, 20: 21388
sorptive properties of evaporated films of, for carbon dioxide at room temperature, 20: 21389
sorptive properties for gold atoms, 16: 19552
sorptive-desorptive properties for hydrogen at 300 to 1000°K, 18: 22043
spallation by protons at 340 Mev, separation of technetium from products from, 20: 18843
spark patterns produced by grinding of, 18: 19493(T) (SC-T-64-47)
specific heat at 1300 to 2500°K, determination of vacancy formation by, 18: 42080(T)
specific heat of crystals of, 16: 15222
specifications for sheet rolled, 16: 24160 (MAB-184-M)
spectra in reaction zone of acetylene air flame, excitation of atomic, 17: 27371(T)
spectra of, arc, 18: 6358
spectra of, effects of temperature on absorption, 17: 5996
spectra of, electric discharge, 17: 34642
spectra of, flame, 17: 19990 (IS-517)
spectra of, low energy neutron-capture gamma, 17: 15943(R) (ARF-1193-20)
spectra of, effects of impurities on M-emission band of, 18: 39197
spectra of, for uv reflectance, 18: 29651
spectra of, isotopic shift in K-series x-ray, (E), 20: 2641
spectra of, Ohlin structure near limit of continuous x-ray, (E), 19: 44940
spectral emissivity at high temperatures, 17: 41363 (WADD-TR-60-646 (Pt.II))
spectral emittance of coated and uncoated, at 800 to 5000°F, 16: 18939
spheroidization of powders of, by induction-coupled plasma torch method, 16: 5698
sputtering at 50 to 600 ev by rare gas ions, 17: 8931(R) (NP-12389)
sputtering by argon and neon ions, glow discharges, 16: 19563
sputtering by argon ions, full-plane threshold energies for, 17: 37743
sputtering by argon, angular dependence of ion-electron emission in, (E), 19: 6475
sputtering by argon at 2 to 10 kev, yields at high temperatures from, (E), 19: 23299
sputtering by argon ions at 100 to 900 ev, of atoms in, (E), 19: 25177
sputtering by argon ions at 1.5 to 30 kev, yields from, (E), 20: 4546
sputtering by cesium at 2–5 kv, 17: 21830
sputtering by cesium ions, 18: 40168
sputtering by cesium ions, (E/T), 19: 6477
sputtering by helium ions at 600 ev, yield curves for, 17: 25870(R) (X62-11400)
sputtering by hydrogen ions, yields from, 18: 8926
sputtering by mercury ions, 17: 20658
sputtering by mercury ions at 10 ev, energy distribution from, 18: 9004
sputtering by noble-gas ions at 0.1 to 1 kev, yields, 16: 19566
sputtering by noble-gas ions at 100 to 600 ev, yields from, 16: 22753
sputtering by xenon ions at 1.5 to 30 kev, yields from, (E), 20: 4546
sputtering of crystals of, by argon, mercury, neon, and xenon ions at low energies, atom ejection in, 17: 37467
sputtering of electrodes of, in high-pressure discharges, erosion from, 17: 24086
sputtering of powders of, by mercury ions, yields from, 17: 25870(R) (X62-11400)
sputtering of single crystals of, by mercury ions, (E), 20: 9676(T)
strain rates, 16: 9172(R) (NP-11351)
strain-aging behavior in crystals of, effects of annealing and impurities on, 16: 24146 (ASD-TDR-62-11)
strength at high temperatures, effects of alloying on, 20: 43969
strength of, methods of improving, 17: 29316 (DMIC-182)
stress analysis of single-crystal, orientation effects on yield, 20: 33917
stress recovery of, effects of carbon and tungsten on flow, 20: 4409
stress relaxation prior to yield point in, 20: 5851
stress relaxation in polycrystalline, at 90 to 298°K, 20: 23672
stress-rupture and creep properties at 2200 and 2400°C, 17: 34399 (CONF-94-4)
stress-rupture of, at 2200°C, in hydrogen, 16: 32034(R) (GEMP-15A)
stress rupture of arc-cast, summary, 17: 36194(R) (GEMP-25A)
stress-rupture properties at 2200°C in argon and hydrogen, 17: 11087(R) (GEMP-19A)
stress-rupture properties at 2200°C, 17: 34398 (CONF-39-43)
stress-rupture properties of diffusion-bonded joints, 17: 36243 (CONF-53-8)
stress-rupture testing of, in argon and hydrogen at 2200°C, 17: 3381(R) (GEMP-17A)
stress-rupture testing of, in argon and hydrogen at 2200°C, 17: 22093(R) (GEMP-21A)
stress-rupture testing at 2200°C , 17: 29320(R) (GEMP-23A)
stress-rupture and creep properties, 18: 41933 (TID-11295(3rd Ed.))
stress-rupture at 2200°C in hydrogen, 19: 24916(R) (GEMP-334A)
stress-rupture properties at high temperatures, 19: 37146
stress-rupture properties, 19: 40961
structural properties at 1000 to 2600°F, 16: 10510 (DC-57-3-19)
structure of arc-cast, creep tested at 2200°C, 20: 27485(R) (GEMP-400A, pp 21-61)
substructure of cold-rolled, 19: 13948(R) (NP-14675)
superconducting critical fields and temperatures for, 17: 41592
superconducting isotope effect in, 17: 11375
superconducting properties, (E), 20: 8031
superconducting properties of, effects of λ transition on, 20: 21875
superconductivity of, energy gap and critical field in, 17: 6877
superconductivity of, 18: 15084
superconductivity in films of, (E), 19: 37867
superconductivity of, 20: 40047
surface friction of clean, in sodium (liquid), 17: 2080
surface migration of, field emission methods for, (E), 19: 11756(T)
surface properties of, studies by mass spectrometry, 17: 6634 (AFOSR-2273)
surface structure of cesiated crystals of, effects of temperature and time on, 17: 12589(R) (NP-12543)
surface structures of clean and oxygen-covered, low-energy electron-diffraction study of, 20: 22319
surface tension and solid surface energy of, effects of alloying additions of rhenium on, 20: 31773
surface tension at melting point, 17: 39612
surface tension of, measurement by electron bombardment heating, 17: 37538
surface tension of, 18: 27994
surface tension of, measurement by pendant drop method, 19: 47065
tensile and notch-tensile properties of, effects of metallurgical structure and of titanium on, 19: 16158
tensile ductility transition in, 18: 39914(R) (WADD-TR-61-181(Pt.IV))
tensile properties at 0 to 2200°C, 17: 1863
tensile properties of electron-beam-refined arc-cast, additive effects of carbon on high-temperature, 17: 30962(R) (ASD-TDR-63-238)
tensile properties, 18: 7298(R) (HW-78962(p.3.1-14))
tensile properties, 18: 18307
tensile properties of polycrystalline, under ultrahigh vacuum, 18: 18362
tensile properties at high temperatures, 18: 22512

tensile properties of, effects of hydrostatic pressure on, 18: 30183
tensile properties after flow-stress recovery, 18: 34194
tensile properties of, effects of interstitial and substitutional solutes on, 18: 34203
tensile properties of, effects of interaction of interstitial solute and substructure on, 18: 34204
tensile properties of, effects of explosive forming on, 18: 34208
tensile properties of, method of testing, 18: 34210
tensile properties of recrystallized, 19: 13948(R) (NP-14675)
tensile properties at 243, 293, and 373°K, 19: 16147
tensile properties of, effects of dislocation density on, 19: 16161
tensile properties of, grain size and temperature effects on, 19: 20594
tensile properties of, effects of sintering on, 19: 47054
tensile properties of electron-beam-refined arc-cast crystals of, additive effects of carbon on high-temperature, 17: 30962(R) (ASD-TDR-63-238)
tensile properties of electron-beam melted, arc-melted, and sintered wires, 20: 858
tensile properties of, effects of exposure to cesium at 1200°C on, 20: 11227
tensile properties of, effects of working reduction, stress-relief annealing, and grain size on, 20: 11227
tensile properties of, effects of purification on, 20: 27476(R) (BNWL-207, pp 3.14-16)
tensile testing of, dislocation motion in, 20: 27548
tensile-ductility transition in, mechanism of, 19: 40961
testing for use as cladding of fissium–plutonium–uranium alloy fuel, 18: 10572 (CONF-373-2)
testing for use in shaft seals for potassium space power plants, 20: 2242
testing for use in thermionic collector electrodes,, 20: 23992(R) (AD-626593)
testing tubes of, nondestructive, 18: 4255(R) (ORNL-3470(p.98-125))
thermal absorbance, emittance, and reflectance, 16: 9193 (DMIC-Memo-141)
thermal capacity and total emittance at 1250 to 2350°K, 19: 23049
thermal capacity of, from 1288 to 2015°K, 17: 23976
thermal capacity of, Krebs's model for lattice contributions to, 20: 17081
thermal conductivity of, at 2100 to 2400°K, 16: 31813 (ASD-TR-61-528)
thermal conductivity of, at 200 to 2500°C, 16: 33146 (ASD-TDR-62-348)
thermal conductivity, 17: 18818
thermal conductivity at 300 to 900°C, 17: 39719(R) (MND-2945-3)
thermal conductivity and emissivity at 1000 to 2000°C, 18: 27959 (ML-TDR-64-59)
thermal conductivity at high temperatures, (E), 19: 20576
thermal conductivity of superconducting thermal switches of, at 0.3 to 2°K, (E), 19: 23584
thermal conductivity at 900 to 1975°C, 20: 821 (GE-TM-65-10-1)
thermal conductivity at 900 to 2000°C, 20: 2223(R) (GEMP-51A)
thermal conductivity of, effects of diffusion mobility of lattice defects on, 20: 7617
thermal conductivity at 1500 to 2200°K, effects of grain size on, 20: 7626
thermal conductivity at 900 to 2000°C, 20: 27485(R) (GEMP-400A, pp 21-61)
thermal conductivity at high temperatures, 20: 43977
thermal diffusivity at 1900 to 2500°K, 18: 36029
thermal dissociation of hydrogen on catalyst of, at 1200 to 2500°K, 18: 22044
thermal expansion at 800 to 2000°C, 18: 32198
thermal expansion to 2000°C, 18: 34190
thermal expansion at 1.5 to 12°K, 18: 37716
thermal expansion at 480 to 530°C, 18: 42037
thermal expansion to 2000°C, 19: 4678(T)
thermal expansion to 2500°C, 19: 41009 (GEMP-375)
thermal expansion coefficient of, x-ray determination of, 19: 47023(T) (LA-tr-65-20)
thermal expansion of, at 25 to 2500°C, 20: 27552
thermal properties of, data compilation, 17: 8801 (DMIC-177(Vol.2))
thermal properties up to 2500°C, enthalpy and thermal expansion, 19: 16071 (GE-TM-64-2-8)
thermal properties for use as temperature sensor, 19: 38090(R) (GEMP-88)
thermal radiation properties of uncoated, 16: 32039(R) (PWA-1863)
thermal radiation properties of, effects of various coatings on, 16: 32039(R) (PWA-1863)
thermal radiation spectral emittance, temperature effects, 17: 41563 (WADD-TR-60-370(Pt.III))
thermal radiative properties, 17: 6650 (DMIC-177(Vol.I))
thermal strain measurements in tubes of, during transient heating by plasma, 19: 34692 (UCRL-13147(Pt.2))
thermionic emission properties, 17: 20622
thermionic emission properties, 17: 20624
thermionic emission from crystalline, in cesium, potassium, and rubidium vapors, 18: 12794
thermionic emission characteristics for use in cesium thermionic converter, 18: 14792
thermionic emission from vapor-deposited, 18: 14616
thermionic emission from surfaces of, molecular, 19: 32768
thermionic emission by capillary electrodes of, electron-ion, 17: 39710 (ASD-TDR-63-865)
thermionic work function of polycrystalline electrodes of, in cesium vapor, 19: 29029(R) (AD-607528)
thermodynamic properties of, bibliography on, 17: 27793 (NP-12938)
thermodynamic properties of normal and superconducting, (E), 19: 8362
thermodynamic properties of normal and superconducting, (E), 19: 27381
thermodynamic properties, 20: 10816(T) (NASA-TT-F-285)
thermodynamic properties at high temperatures and pressures, 20: 19217 (NP-15933)
thermoelectric effects on strontium titanate to 1100°C, 16: 4422(R) (MND-2584)
thermoelectric emission and work function of, in cesium vapor, (E), 19: 6447
thermoelectric potentials at 25 to 900°C, 19: 4656 (ORNL-3605(Vol.1) (p.116-38))
thermoelectric properties of, effects of aluminum, beryllium, magnesium, and zirconium oxides on, 18: 622
thermoelectric properties, 18: 30493 (TID-7687(p.247-93))
thermoelectric properties at 1000 to 2000°C, (E), 19: 40859
thermoelectric stability of thermocouples of, at 1000 to 2000°C, 19: 22986 (NRL-6231)
thermophysical properties, 18: 34207
thermophysical properties at 1300 to 3000°K, (E), 20: 41762
toxic properties of, review of, 18: 13423
toxicology, comparison of compounds and pure metal dusts, 16: 9827
tracer applications survey, 16: 1359
transition temperature in recrystallized, tensile-ductility, 20: 11227
uptake by tomato plants, competitive effects of tungsten, 16: 17367
use as barrier in bonding uranium, zirconium, and their alloys to ferrous metals, 18: 25962(P)
use as cathodes for getter ion pumps, 20: 16789
use as emitter in low-voltage-arc thermionic power converter, 17: 24031(R) (AD-286711)
use as scavengers for radioactive particles, 16: 19184 (TID-15305)
use for electroless and electrolytic coating of bearings and dies, review of, 19: 4604
use in separation of uranium isotopes by vaporization, 16: 9095(T,P) (AEC-tr-4993)
use in tungsten to tungsten diffusion bonding, 20: 25553(P)
use of electrically heated, for melting rocks, 19: 24205 (LA-3243)
use of electrodes of, in cesium vapor thermionic cells, 17: 14925(T) (AD-278817)
use of, in nuclear rockets, 17: 8710 (TID-16315(Del.))
uses in nuclear technology, 17: 12679
uses in thermonuclear reactors, 20: 6452 (AD-619669)
vacancies in, entropy and heat of formation, 20: 22972 (TID-22851)
vapor pressure, 20: 331
vapor pressure at 2140 to 2535°K, 18: 27997
vapor pressure of, design of thermobalance for measuring, 20: 13029 (LA-3423)
vaporization of, under vacuum and forced convection conditions, (T), 20: 831 (UCRL-14274)
volatilization in fluid-bed fluoride volatility process, 19: 32280(R) (ANL-7020(p.100-49))
volatilization in water vapor, hydrogen, and argon mixtures, 19: 32161
wear properties of plasma-arc-deposited coatings of, 20: 21319(AD-621064)
wear resistance of electroslag welding cell of, in molten fluxes, 18: 44168
welding, 17: 36271
welding and properties of welded, 16: 4516 (NP-11126)
welding by electron beams, 17: 25763
welding by solid-state methods, 19: 22937
welding by tungsten inert gas process, effects of hydrogen, nitrogen, and oxygen, 17: 34382
welding by TIG techniques, effects of parameters on welds in, 18: 573(R) (AD-422116)
welding, development of flash techniques for, 16: 4537 (NP-11127)
welding, electron beam techniques, 16: 9158 (ASD-TR-61-461)
welding of, electron-beam, 18: 4220
welding of, equipment and properties for electron-beam, 17: 34378
welding of, evaluation of electron-beam, 16: 31763
welding of, review of, 17: 29301
welding of, effects of purification treatments on, 20: 13251(R) (GEMP-55A, pp 57-82)
welding of, electron-beam, 20: 15012
welding of, equipment and procedures for, 19: 9629(R) (AD-608818)
welding of, feasibility of vacuum-diffusion, 19: 22946(T)

welding of, method for spot-, 18: 18333
welding of, properties of product formed by electron-beam, 20: 23623
welding properties, 16: 10486 (TID-14971)
welding properties, review, 16: 10424 (ASD-TR-61-332(p.661-76))
welding to alumina, electron-beam, 17: 25691(R) (RBESO-3404-2)
welding to carbides by vacuum diffusion, 19: 22931(T) (JPRS-29550)
welding to molybdenum, electron beam, 19: 23347(R) (NYO-3429-2)
welding to molybdenum, titanium, and tungsten carbides, diffusion, 20: 7545
welding to stainless steel, explosive techniques for, 16: 3419 (ASD-TR-61-124)
welding to stainless steel, 20: 21309
welding to tungsten by electron beams, 17: 25763
welding, ultrasonic, 16: 4515 (NP-11054)
welding, ultrasonic, 16: 24130(R) (AD-271377)
wetting by liquid sodium, effects of time and temperature on, 19: 17897
wetting by liquid aluminum oxide, 20: 23685
work function, 17: 27970
work function, 18: 30491 (TID-7687(p.214-19))
work function, effects of metallic films on, 16: 9231
work function in cesium–hydrogen atmosphere, (E), 19: 37097
work function of, reduction of, 17: 27972
work function of, effects of cesium fluoride vapor on, 20: 15297 (CONF-640921, pp 101-9)
x-ray emission from, isolation of components of Kα, 18: 8627
x-ray emission lines, 17: 1760
x-ray emission lines of, widths of K, 17: 18925
x-ray emission spectra of, L and K, (E), 20: 41350
x-ray scattering at small angles by neutron-irradiated, 20: 27569(R) (BNWL-207, pp 3.7-13)
x-ray scattering by, elimination of Compton component in, (E), 19: 9929
x-ray spectra of, precision redetermination of wavelength of $K\alpha_1$ line in, 18: 34341
x-ray spectra of, performance of spectroanalyzer with promethium-147 beta source for K, 20: 11133
x-ray spectra of, emission bands in, 20: 27730
xenon ion reactions with, sputtering in, 17: 39709 (ARL-63-125)
xenon-131 ranges in, at 5 to 30 kev, 18: 20672
yield stress of, correlation of thermal component of, 17: 18793
yields from radiolysis of molybdenum phthalocyanine, 20: 36886
Young's modulus of, as function of temperature, 18: 39970

MOLYBDENUM ALLOY COUPLES

Mo/Mo–Re, calibration of thermocouples of, pressure effects on, 20: 43636 (UCRL-14993)
Mo/Mo–W, densification of sintered tungsten–molybdenum powder compact, Kirkendall-effect in, 20: 16994
Mo–Nb/Re–W, thermoelectric potential at 200 to 1800°C, 19: 37031(R) (GEMP-47A, pp 101-6)
Mo–Nb/Re–W, thermoelectric potential to 1800°C, 19: 44598(R) (GEMP-49A)
Mo–Ni/Ti, solid state bonding of, 18: 24112
Mo–Os/Re–W, thermoelectric potential at 200 to 1800°C, 19: 37031(R) (GEMP-47A, pp 101-6)
Mo–Os–Ru/Re–W, thermoelectric properties at 100 to 1400°C, 20: 2223(R) (GEMP-51A)
Mo–Re/Re, development of thermocouples of, 18: 24937 (APEX-917)
Mo–Re/Re, stability of thermocouples of, (E), 19: 40859
Mo–Re/Re, thermoelectric stability at 1000 to 2000°C, 19: 22986 (NRL-6231)
Mo–Re/Re–W, stability of thermocouples of, (E), 19: 40859
Mo–Re/Re–W, thermoelectric stability at 1000 to 2000°C, 19: 22986 (NRL-6231)
Mo–Re–W/Mo–Re–W, thermoelectric output of, 19: 24916(R) (GEMP-334A)
Mo–Ru/Re–W, thermoelectric potential at 200 to 1800°C, 19: 37031(R) (GEMP-47A, pp 101-6)
Mo–Ti/Ti, solid state bonding of, 18: 24112

MOLYBDENUM ALLOYS

see also A-286 Alloy
see also Croloy
see also Durimet 20
see also Hastelloy C
see also Hastelloy F
see also Hastelloy X
see also Haynes Stellite No. 21
see also INOR-8
see also Ni-O-Nel
see also René-41
see also René-62
see also Waspaloy

analysis for copper, iron, nickel, titanium, and zirconium, classical methods for, 18: 19921
analysis for hafnium, titanium, and zirconium by ion exchange, 20: 7039
analysis for niobium using xylenol orange, photometric, 17: 30496
analysis for niobium and tantalum, photometric method for, 19: 40442
analysis for titanium and zirconium, plasma arc technique for spectrochemical, 18: 25268 (ML-TDR-64-36)
availability, fabrication, and properties of refractory sheet, 19: 9617
bibliography on, 18: 32076
bibliography on, 20: 753 (SB-415(Suppl. 1))
bibliography on phase diagrams of, 17: 18689
bonding to alumina, 17: 25691(R) (RBESO-3404-2)
bonding to themselves or other refractory metal alloys, 19: 16050(P)
book: *Less-Common Alloys of Molybdenum*, 17: 25716
brazing developments for, 18: 549(R) (NP-13241)
brazing, equipment and methods for, 18: 27938
brittleness testing, 17: 30974 (LAMS-2906)
casting of, effects of titanium and zirconium on, 16: 33368(R) (ASD-TDR-62-508)
cavitation damage resistance in lithium to 2000°F, design of rotating disk test unit for determining, 17: 39552
coating and fabrication of, methods for, 18: 14444
coating developments for, 18: 541(R) (AD-419549)
coating for protection at high temperatures, pack cementation process for, 19: 2722 (ML-TDR-64-55)
coating of, review of techniques for protective, 19: 4605
coating techniques for, review of, 18: 7270
coatings for, development of oxidation-resistant, 16: 2173 (DMIC-Memo-137)
coatings for, problems of protective, 20: 43877
coatings on, lifetime and performance of molybdenum silicide, 20: 5910
composition, crystal structure, and phases of precipitates in, 16: 22582 (ASD-TDR-62-7)
conference on refractory metals, Oslo, Norway, June 23 to 26, 1963, 18: 34068
corrosion, 20: 27538
corrosion by inorganic and organic acids at 35, 60, and 100°C, 20: 11230 (BM-RI-6715)
corrosion by potassium at high temperature, 16: 16680 (TID-7626(Pt.I) (p.69-86))
corrosion by sodium at 1200°F, 18: 20472 (NAA-SR-Memo-9340)
corrosion of, by rubidium at 1000 to 2000°F, effects of titanium on, 17: 16634 (AGN-8063)
corrosion resistance of, summary of data on, 17: 18708
corrosion resistance, review, 17: 20420
corrosion resistance and strength at high temperatures, 18: 44201
corrosion studies, 18: 14396
crack-propagation resistance of TZM, 18: 5769 (AD-290278)
creep-rupture of TZM, in hydrogen at 2000 to 2200°C, 18: 16424(R) (GEMP-270A)
creep-rupture properties at 560 to 650°C, 19: 18390(R) (GEMP-43A)
crystal growth by recrystallization, methods for, 18: 4223
deposition by electrolytic methods, from aqueous solutions, 20: 35870
design for hardness and strength at high temperatures, 18: 4295(P)
development for high-temperature reactor applications, 18: 2226(R) (NMI-1258)
development for high-temperature applications, review, 18: 34069
development, properties, and uses as engineering materials in aerospace vehicles, 16: 10409 (ASD-TR-61-322(p.307-36))
end milling of U-500, 17: 6614
engineering properties of, data tabulation on, 18: 10526 (DMIC-190)
extrusion, 16: 3445 (ASD-TR-61-193)
extrusion, 16: 25729(R) (ASD-TR-7-785(VI))
extrusion, 17: 6589 (ASD-TDR-62-670)
extrusion, 19: 11711
extrusion of, factors affecting, 18: 14443
fabrication and properties as refractory material, 16: 19404
fabrication and properties of, review of, 17: 29253 (NRC-7129)
fabrication and properties for process equipment in aerospace, cryogenics, and nuclear engineering, 17: 39556
fabrication and properties of, 18: 7264
fabrication and properties for use as superconductors, 18: 34179
fabrication and properties of, handbook on, 20: 5874 (AGARDograph-94)
fabrication for high temperature uses, development of techniques for, 16: 10427 (ASD-TR-61-322(p.817-32))
fabrication of sheets of, 19: 34651(R) (AD-612490)
fabrication of TZM, 17: 1888(R) (ASC-TR-7-786(I))
fabrication of, mechanical tests to evaluate, 18: 34101
flow forming of, for rocket engine techniques, 18: 34109
forging, 17: 6589 (ASD-TDR-62-670)
machining characteristics, 17: 34358(R) (ASD-TDR-63-581)
machining characteristics of, 19: 4637
machining studies, 16: 20990(R) (ASD-TR-7-532a(VI))
machining, processing, and welding, 20: 27538
mechanical properties, 16: 3445 (ASD-TR-61-193)
mechanical properties, 17: 6517 (MAB-188-M)
mechanical properties of, review, 18: 20456 (ORNL-3593)

mechanical properties of, effects of strain softening on, 18: 24119 (AD-425148)
mechanical properties of, effects of heat treatment on, 19: 7959
metallurgical properties, 16: 15164 (AGARDograph-50)
microstructure of, effects of melting method on inclusions in, 20: 41467
oxidation by oxygen, effects of pressure and temperature on, 19: 23124(R) (HW-83298(p.8.1-4))
oxidation in air, effects of pressure on TZM, 18: 44037(R) (HW-82651 (p.5.1-33))
oxidation of platinum-clad, at 1200 and 1400°C, 18: 12652(R) (NP-13593)
oxidation protection of, development of coatings for, 18: 30190
oxidation resistance of bare and coated, 16: 4548 (WADC-TR-59-744 (Vol.VII))
oxidation resistance of, alloying effects of hafnium and yttrium on, 17: 20411 (AD-282638)
phase diagrams of binary and ternary, 17: 27778 (DMIC-183)
preparation and properties, 17: 11224
preparation of fine-grained alpha-phase, 19: 24930(P)
preparation of TZM, 17: 15385(R) (ANL-6683)
production in electric arc furnace, fabrication of consumable electrodes for, 18: 8741(P)
properties, 16: 3460 (NP-11108)
properties and liquid-phase sintering techniques for, 16: 24145 (ANL-6268)
properties and use of, in non-nuclear industries, 18: 44072
properties and uses of, review of, 19: 36966
properties and uses of, review on, 20: 2307 (AD-613023)
properties as cladding and structural materials in reactors, 18: 41947
properties at high temperatures, methods for improving, 16: 12152
properties at high temperatures, mechanical and tensile, 17: 12657(R) (AD-277910)
properties for aerospace uses, 19: 47068
properties for structural use in gas-cooled reactors, 16: 19993 (NYO-9793)
properties of, review, 17: 1826
properties of welded sheaths, sheets, and tubes of, 18: 7172
properties of, mechanical and physical, 20: 27538
properties of, research on fundamental, 19: 23163(R) (ORNL-3650(p.111-86))
properties of, review on, 18: 34180
radiation effects on electric and mechanical properties of, neutron, 19: 24916(R) (GEMP-334A)
reactions with nitrogen at 900°C, 19: 24064(R) (ANL-6997)
reactivity with carbides, graphite, refractory metals, and uranium compounds, 16: 5714 (NEPA-1050)
sheet bending of, methods and problems of, 18: 34107
sheet rolling of, 17: 6517 (MAB-188-M)
specifications for sheet rolled, 16: 24160 (MAB-184-M)
structural properties at 1000 to 2600°F, 16: 10510 (DC-57-3-19)
structure and tensile properties of, additive effects of carbon, titanium, and zirconium on, 18: 27978
survey of, for nuclear energy applications, 19: 7861
tensile properties, 16: 22586 (DMIC-Memo-150)
tensile properties of recrystallized and stress-relieved, 17: 1915(R) (AD-274206)
thermal properties of, data compilation, 17: 8801 (DMIC-177(Vol.2))
thermal radiative properties, 17: 6650 (DMIC-177(Vol.I))
thermoelectric properties of sintered, for use as thermocouples at high temperatures, 19: 47019(T) (AD-619334)
use for electroless and electrolytic coating of bearings and dies, review of, 19: 4604
welding, 17: 36271
welding metallurgy, 16: 13556
welding of, electron beam, 18: 34092
welding of, embrittlement in, 18: 34108
welding properties, review, 16: 10424 (ASD-TR-61-322(p.661-76))
welding properties, review, 16: 10424 (ASD-TR-61-322(p.661-76))
welding sheaths, sheets, and tubes of, techniques for, 18: 7172
welding sheet, electron beam, 16: 4517 (NP-11128)
welding to ceramics, graphite, and metals in SNAP reactor environment at 700 to 1300°F, self-, 20: 7570 (NAA-SR-9643)
welding, ultrasonic, 16: 24130(R) (AD-271377)
Al–Be–Mo–Zr, corrosion resistance and mechanical properties, 16: 30891(P)
Al–Be–Mo–Zr, development of high-strength corrosion-resistant, 18: 22434(P)
Al–Co–Mo, reduction of scaling of, 20: 25611(P)
Al–Cr–Co–Fe–Mo–Ni–Ti, joining of Udimet 500 and 700, by mechanical fastening, 20: 29667 (RSIC-509)
Al–Cr–Co–Fe–Mo–Ni–Ti, mechanical properties at high temperatures, 17: 14811 (ASD-TDR-61-529)
Al–Cr–Co–Fe–Mo–Ni–Ti, mechanical properties of, at 70 to 2000°F, 17: 18758 (NAA-SR-Memo-8052)
Al–Cr–Co–Fe–Mo–Ni–Ti, mechanical properties at 1500°F, 17: 22852(R) (GA-2696)
Al–Cr–Co–Fe–Mo–Ni–Ti, stress-rupture properties of Udimet 700, at high temperatures and strain rates, 20: 11265 (AD-626375)
Al–Cr–Co–Fe–Mo–Ni–Ti, surface treatments for Udimet 500 and 700, coating and mechanical, 20: 29706 (NASA-TM-X-53448)
Al–Cr–Co–Mo–Ni–Ti, corrosion of Udimet 500 by lithium fluoride in cyclic high-temperature environment, 20: 4326 (TRW-ER-6561)
Al–Cr–Co–Mo–Ni–Ti, fabrication and properties of atomized, extruded, and sintered Udimet 700, 18: 10449(R) (IITRI-B247-12)
Al–Cr–Co–Mo–Ni–Ti, fabrication of Udimet 700, by extrusion, 18: 18329(R) (ASD-TDR-7-945(IV))
Al–Cr–Co–Mo–Ni–Ti, joining of M-252, by mechanical fastening, 20: 29667 (RSIC-509)
Al–Cr–Co–Mo–Ni–Ti, properties of Udimet 700, as extrusion liner for use at 1900 to 3600°F, 18: 18329(R) (ASD-TDR-7-945(IV))
Al–Cr–Co–Mo–Ni–Ti, strength, effects of severe stress and thermal histories, 16: 21023 (ASD-TR-61-194)
Al–Cr–Co–Mo–Ni–Ti, surface treatments for Astroloy, coating and mechanical, 20: 29706 (NASA-TM-X-53448)
Al–Cr–Co–Mo–Ni–Ti–V–Zr, surface treatments for IN-100, coating and mechanical, 20: 29706 (NASA-TM-X-53448)
Al–Cr–Co–Mo–Ni–Ti, tensile properties, statistical evaluation, 16: 3448 (ASD-TR-61-516)
Al–Cr–Co–Mo–Ni–Ti, thermal radiation properties of, 17: 542 (WADD-TR-60-370(Pt.II))
Al–Cr–Cu–Fe–Mo–Sn–Ti–V, fabrication and properties, 18: 22424(R) (WAL-TR-401/303-2)
Al–Cr–Cu–Fe–Mo–Sn–Ti–V–Zr, fabrication and properties, 18: 22424(R) (WAL-TR-401/303-2)
Al–Cr–Fe–Mo–Nb–Ti, brazing of René 62 T-joints, 18: 44103(R) (ORNL-3670(p.259-61))
Al–Cr–Fe–Mo–Ni–Nb–Ti–W, corrosion by carbon dioxide, helium, nitrogen, and steam of PRDL-102, 20: 9408 (BNWL-154)
Al–Cr–Fe–Mo–Ni–Nb, fabrication and properties of atomized, extruded, and sintered Inco 713C, 18: 10449(R) (IITRI-B247-12)
Al–Cr–Fe–Mo–Ni–Nb–Ti, corrosion and mechanical properties of Inconel 713C as gas turbine material, 16: 32114 (IDO-28591)
Al–Cr–Fe–Mo–Ni, fabrication and properties of atomized, extruded, and sintered PH15–7Mo, 18: 10449(R) (IITRI-B247-12)
Al–Cr–Fe–Mo–Ni–Ti, heat treatment effects on welded, 16: 7842 (DC-59-10-174)
Al–Cr–Fe–Mo–Ni–Ti–W, joining of D-979, by mechanical fastening, 20: 29667 (RSIC-509)
Al–Cr–Fe–Mo–Nb–Zr, machining characteristics, 17: 14778(R) (ASD-TR-7-532a(IX))
Al–Cr–Fe–Mo–Ni, mechanical properties at high temperatures, 17: 14811 (ASD-TDR-61-529)
Al–Cr–Fe–Mo–Ni–Ti, mechanical properties at 1100 to 1200°F, 17: 22852(R) (GA-2696)
Al–Cr–Fe–Mo–Nb–Ti, mechanical properties at 1100 to 1500°F, 17: 22852(R) (GA-2696)
Al–Cr–Fe–Mo–Ti, mechanical properties and heat resistance, 19: 39193
Al–Cr–Fe–Mo–Ni–Nb–Ti, mechanical properties of René-62, 19: 24081(R) (GNEC-361)
Al–Cr–Fe–Mo–Ni–Ti, mechanical properties and microstructure of, effects of heat treatments and molybdenum content on, 20: 23721
Al–Cr–Fe–Mo–Ni–Nb–Ti, oxidation of Inconel 718 by water vapor in helium at 1700°F, 19: 30820 (BNWL-23)
Al–Cr–Fe–Mo–Ni–Ti, properties of, for use at 1600 to 2100°F, 16: 13575 (DC-60-1-55)
Al–Cr–Fe–Mo–Nb–Zr, properties, 17: 1997(P)
Al–Cr–Fe–Mo–Ti, properties of, effects of high-temperature thermo-mechanical treatment on, 20: 43961
Al–Cr–Fe–Mo–Ni–Ti, radiation effects on, 18: 7292(R) (HW-77954 (p.4.1-12))
Al–Cr–Fe–Mo–Ni–Nb–Ti, radiation effects on Inconel 718, 18: 7292(R) (HW-77954(p.4.1-12))
Al–Cr–Fe–Mo–Ni–Nb–Ti, radiation effects on mechanical properties of Inconel 718, neutron, 19: 30820 (BNWL-23)
Al–Cr–Fe–Mo–Ni–Ti, radiation effects on tensile properties of Nimonic PE16, thermal-neutron, 20: 31669
Al–Cr–Fe–Mo–Ni, tensile properties, 17: 16640 (DMIC-Memo-164)
Al–Cr–Fe–Mo–Ni–Nb–Ti, thermal response and microstructure of Inconel 718 at 1200 and 1400°F, 19: 39158 (GEAP-4751)
Al–Cr–Mo, gravimetric analysis for zirconium using *p*-iodoamygdalic acid, 18: 17749
Al–Cr–Mo–Ni–Ti, development of Udimet 700, for use in extrusion billet liners, 18: 39859 (IITRI-B244-18)
Al–Cr–Mo–Ni, fabrication of vertical-rib sandwich panels of, by roll-welding, 20: 25509(R) (AD-632831)
Al–Cr–Mo–Ni–Nb–Ti–W, phase diagrams, 20: 9533
Al–Cr–Mo–Ti, corrosion by sulfuric acid, effects of thermal treatment on,

16: 12062
Al–Fe–Mo, magnetic properties of, effects of heat treatment on, 19: 9717
Al–Fe–Mo–Ti, engineering and mechanical properties at varying concentrations, 19: 23089
Al–Fe–Mo–Ti, machining characteristics, 17: 14778(R) (ASD-TR-7-532a(IX))
Al–Fe–Mo–Ti, phase stability in, 17: 1968
Al–Fe–Mo–Ti–V, properties of aged, 20: 4360(R) (AD-619399)
Al–Fe–Mo–U, preparation and properties as reactor fuel, 19: 16008(P)
Al–Hf–Mo, phase studies on intermetallic compounds in, 20: 17075
Al–Mo, crystal structure of intermetallic phase $Al_{12}Mo$ in, 18: 8810
Al–Mo, crystal structure of intermetallic phase Al_4Mo in, 18: 32161
Al–Mo, crystallization of intermetallic compounds in, effects of casting temperature on, 20: 27554
Al–Mo, empirical formula determination of $Al_{12}Mo$ by activation, 18: 8811
Al–Mo, fabrication and production of stoichiometric, 19: 42831
Al–Mo, formation of intermetallic compound, on sintered molybdenum, 20: 37204
Al–Mo, phase diagrams, 17: 3429
Al–Mo, phase diagram, 18: 20549
Al–Mo, phase studies, 16: 549
Al–Mo, phase studies, 17: 6729
Al–Mo, phase studies, 20: 5846
Al–Mo, properties of, for use in coating space vehicle components, 16: 15203 (WCLT-TM-59-104)
Al–Mo, properties of intermetallic compound, 20: 37260
Al–Mo, solubility of Mo_3Al in Nb_3Sn at 1300 to 1600°C, 18: 4271
Al–Mo–Nb–U, preparation and properties as reactor fuel, 19: 26873(P)
Al–Mo–Sn–Ti–V–Zr, beta transus temperature of, 19: 20462(R) (NRL-6258)
Al–Mo–Sn–Ti–V, beta transus temperature of, 19: 20462(R) (NRL-6258)
Al–Mo–Sn–Ti–V, corrosion by sodium chloride, effects of stress on, 20: 33858(R) (AD-634094)
Al–Mo–Sn–Ti–V–Zr, corrosion by sodium chloride, effects of stress on, 20: 33858(R) (AD-634094)
Al–Mo–Sn–Ti–V, fracture modes in surfaces of, 20: 9485 (AD-623567)
Al–Mo–Sn–Ti–V, fracture toughness properties of titanium-base, effects of heat treatments on, 20: 11273(R) (NRL-6364)
Al–Mo–Sn–Ti–Zr, mechanical properties of, effects of heat treatments on, 19: 41052
Al–Mo–Sn–Ti–V, mechanical properties of titanium-base, 20: 33858(R) (AD-634094)
Al–Mo–Sn–Zr, carburization by uranium carbide, 18: 10537 (NAA-SR-Memo-9015)
Al–Mo–Sn–Zr, compatibility of 3Z1 with uranium carbide fuels in sodium, 18: 35957 (NAA-SR-7502)
Al–Mo–Sn–Zr, corrosion by terphenyls, 16: 22551
Al–Mo–Sn–Zr, corrosion by sodium, 18: 25937
Al–Mo–Sn–Zr, effects of hydrogenation on delayed failure susceptibility of, 18: 18406
Al–Mo–Sn–Zr, fabrication and welding of alloy 3Z1, 16: 5685 (NAA-SR-6431)
Al–Mo–Sn–Zr, fatigue due to hydrogen embrittlement, 17: 526(R) (ARF-2230-12)
Al–Mo–Sn–Zr, fatigue, effects of applied stress and hydrogen sorption on static, 16: 25746(R) (ARF-2230-9)
Al–Mo–Sn–Zr, properties as claddings for uranium carbide fuels, 17: 16650 (NAA-SR-7696)
Al–Mo–Sn–Zr, thermal conductivity of 3ZI, 18: 12650 (NAA-SR-Memo-9334)
Al–Mo–Ti, beta transus temperature of, 19: 20462(R) (NRL-6258)
Al–Mo–Ti, corrosion by mercury, 18: 10492
Al–Mo–Ti, corrosion by sodium chloride, effects of stress on, 20: 33858(R) (AD-634094)
Al–Mo–Ti, fracture toughness of weldments of titanium-base, effects of heat treatments on, 20: 11273(R) (NRL-6364)
Al–Mo–Ti, fracture toughness of plasmarc welds in titanium-base, 20: 11273(R) (NRL-6364)
Al–Mo–Ti, fracture toughness of titanium-base, effects of composition and heat treatments on, 20: 11273(R) (NRL-6364)
Al–Mo–Ti, mechanical properties of titanium-base, effects of aging and annealing on, 20: 33858(R) (AD-634094)
Al–Mo–Ti, transformation behavior in, during cooling, 17: 16721
Al–Mo–Ti–V, annealing, 17: 3367 (AD-275092)
Al–Mo–Ti–V, corrosion by mercury, 18: 10492
Al–Mo–Ti–V, corrosion cracking of, mechanisms for stress, 19: 44621 (CONF-651006-1)
Al–Mo–Ti–V, corrosion cracking by salts at 550 to 600°F, stress-, 20: 11227
Al–Mo–Ti–V, corrosion by sodium chloride, effects of annealing on, 20: 33858(R) (AD-634094)
Al–Mo–Ti–V, creep properties of, effects of sheet processing variables on, 16: 21009(R) (AD-264815)
Al–Mo–Ti–V, fabrication characteristics of, 19: 16024 (AD-425058)
Al–Mo–Ti–V, fatigue studies, 19: 30740 (NASA-CR-246)
Al–Mo–Ti–V, fracture modes in surfaces of, 20: 9485 (AD-623567)
Al–Mo–Ti–V, mechanical properties of sheet and welds, 16: 2142(R) (AD-256167)
Al–Mo–Ti–V, mechanical properties, 17: 3468 (ASD-TR-62-7-675)
Al–Mo–Ti–V, mechanical properties of weldments, 17: 14886
Al–Mo–Ti–V, mechanical properties of diffusion-bonded plates of, 19: 20462(R) (NRL-6258)
Al–Mo–Ti–V, mechanical properties of solution-annealed and aged T-19, 19: 20462(R) (NRL-6258)
Al–Mo–Ti–V, mechanical properties of titanium-base, 20: 33858(R) (AD-634094)
Al–Mo–Ti–V, phase studies, 18: 42090
Al–Mo–Ti–V, phase studies, 20: 5851
Al–Mo–Ti–V, properties of rolled sheet, 16: 19294 (AD-267448)
Al–Mo–Ti–V, properties, 17: 3367 (AD-275092)
Al–Mo–Ti–V, properties at −400 to 100°F, 19: 26803(R) (AD-611165)
Al–Mo–Ti–V, radiation effects on, fast-neutron, 19: 6364(R) (NP-14443)
Al–Mo–Ti–V, radiation effects on tensile properties of, irradiated at 30°R, fast-neutron, 20: 27589(R) (NASA-CR-54881)
Al–Mo–Ti–V, rolling, 17: 3367 (AD-275092)
Al–Mo–Ti–V, rolling, 17: 3468 (ASD-TR-62-7-675)
Al–Mo–Ti–V, rolling of, component distribution in, 16: 2143(R) (AD-256168)
Al–Mo–Ti–V, strip processing, 17: 3468 (ASD-TR-62-7-675)
Al–Mo–Ti–V, tensile properties, 17: 3468 (ASD-TR-62-7-675)
Al–Mo–Ti–V, tensile properties at 30 and 540°R, 17: 25776(R) (NP-12812)
Al–Mo–Ti–V, tensile properties, 19: 6364(R) (NP-14443)
Al–Mo–Ti–V, thermal stability of, effects of composition on, 20: 11336
Al–Mo–Ti–V, welding characteristics, 16: 4510 (DMIC-Memo-140)
Al–Mo–Ti–Zr, beta transus temperature of, 19: 20462(R) (NRL-6258)
Al–Mo–Ti–Zr, corrosion by sodium chloride, effects of stress on, 20: 33858(R) (AD-634094)
Al–Mo–U, deformation resistance of, at high temperature, 19: 16206(P)
Al–Mo–U, grain size of end-quenched, 19: 23047
Al–Mo–U, grain structure of, effects of accelerated cooling rate at 75 to 300°C/min on, 19: 30712(P)
Al–Mo–U, measurement and tests on, preirradiation data on Piqua fuel specimens, 17: 14736 (NAA-SR-Memo-7839)
Al–Mo–U, mechanical properties at high temperatures, 17: 8875(P)
Al–Mo–U, metallurgical properties, 18: 37677 (A/CONF.28/P/701)
Al–Mo–U, microstructure and phases of heat-treated, 18: 42051
Al–Mo–U, preparation and properties as reactor fuel, 19: 34637(P)
Al–Mo–Zr, properties of, alloying effects of beryllium on, 16: 30891(P)
Al–Mo–Zr, welding of, in various atmospheres, 17: 509 (CW-R&DL-29)
Au–Mo–Ni, performance for bonding graphite to metals, 20: 31683(R) (ORNL-3936, pp 95-121)
Au–Mo–Ni, properties as brazing alloy, 17: 12653(P)
Be–Co–Mo, oxidation, strength, and ductility at high temperatures, 20: 25611(P)
Be–Mo, analysis of, x-ray absorption, identification of $MoBe_{22}$ using, 18: 14525
Be–Mo, crystal structure of $MoBe_{22}$, 17: 25818(T)
Be–Mo, crystal structure of $MoBe_{22}$, 18: 7246(T)
Be–Mo, crystal structure of MoB_{12} and MoB_{22}, 18: 34149
Be–Mo, diffusion and phase studies, 18: 26013
Be–Mo, fabrication and properties of arc-cast, 18: 32107 (NP-14128)
Be–Mo, high temperature oxidation resistance of intermetallic compounds in, 18: 27912
Be–Mo, intermetallic compounds in, properties of, for use in aerospace technology, 20: 29770
Be–Mo, mechanical and physical properties of intermetallic compounds in, 19: 7942
Be–Mo, oxidation resistance of intermetallic compounds in, at 1000 to 2000°F, 19: 7943
Be–Mo, oxidation in air at 800 to 2200°F, 20: 43886(R) (BBC-111)
Be–Mo, properties of intermetallic compounds in, 16: 10517 (DC-60-4-80)
Be–Mo, thermal conductivities of, at 300 to 1000°C, 16: 19393
Bi–Mo, superconductivity, 20: 44554
Bi–Mo–Zr, corrosion resistance and mechanical properties, 17: 37535
Co–Fe–Mo–Ni, properties of Maraging Steel for use in space electric power systems, 20: 4379 (NASA-CR-54091)
Co–Mo, atomic radii and interatomic distances in intermetallic compounds in, 18: 28029
Co–Mo, effects of additives on high-temperature properties of eutectic, 20: 17108
Co–Mo, mechanical properties and microstructure of, effects of small additions of selected elements on, 20: 27550
Co–Mo, physical and metallurgical properties of, 20: 25611(P)
Co–Mo, recrystallization variables of flat rolled, 20: 2313 (AD-619208)

Co–Mo, structure of sigma phase Co_xMo_x, 17: 27818
Co–Mo–Nb, yield strength and ductility at high temperatures, 20: 25611(P)
Co–Mo–Ni, mechanical properties of welded plates of, 19: 11718 (AD-604052)
Co–Mo–Ni, strength of laminated, 17: 23970(R) (WAL-TR-766.2/3-3)
Co–Mo–Ni–Ti, fabrication of vertical-rib sandwich panels of, by roll-welding, 20: 25509(R) (AD-632831)
Co–Mo–Pt, catalytic effects on hydrocracking of polyphenyls, 17: 28434 (IDO-16858)
Co–Mo–Ta, yield strength and ductility at high temperatures, 20: 25611(P)
Cr–Co–Cu–Mo–Ni–W, corrosion resistance to strong acids, 19: 18415
Cr–Co–Fe–Mo–Ni, corrosion and mechanical properties of Multimet Alloy N-155 as gas turbine material, 16: 32114 (IDO-28591)
Cr–Co–Fe–Mn–Mo, corrosion by mercury at high temperatures, 18: 7152
Cr–Co–Fe–Mo–Ni, corrosion by superheated steam at 1050 and 1150°F, 19: 2853
Cr–Co–Fe–Mn–Mo–Ni–W, corrosion of Raonel, by coal gasification products at high temperatures, 19: 42127(R) (TID-22009)
Cr–Co–Fe–Mn–Mo–Ni, corrosion of Vitallium, by boiling hydrofluoric acid–nitric acid solutions, 20: 37169(R) (BMI-1774)
Cr–Co–Fe–Mn–Mo–Ni–Ti, corrosion of Hanford 22, by boiling hydrofluoric acid–nitric acid solutions, 20: 37169(R) (BMI-1774)
Cr–Co–Fe–Mo–Ni, corrosion of Haynes 21, by boiling hydrofluoric acid–nitric acid solutions, 20: 37169(R) (BMI-1774)
Cr–Co–Fe–Mn–Mo–Ni–Ti, corrosion of Hanford 23 and 24, by boiling hydrofluoric acid–nitric acid solutions, 20: 37169(R) (BMI-1774)
Cr–Co–Fe–Mn–Mo–Ni–W, mechanical properties at high temperatures, 17: 14811 (ASD-TDR-61-529)
Cr–Co–Fe–Mo–Ni–W, mechanical properties of, at 70 to 2000°F, 17: 18758 (NAA-SR-Memo-8052)
Cr–Co–Fe–Mo–Ni, welding characteristics, 16: 4510 (DMIC-Memo-140)
Cr–Co–Mo, atomic radii and interatomic distances in intermetallic compounds in, 18: 28029
Cr–Co–Mo, corrosion by mercury at high temperatures, 18: 7152
Cr–Co–Mo–Ni, drilling of hardened Astroloy, 17: 6617
Cr–Co–Mo–Ni–W, erosion by mercury vapor at 640°F of Stellite 6B, 20: 11214(R) (NASA-CR-54717)
Cr–Co–Mo–Ni, fabrication and properties of thoria-dispersion-strengthened, 18: 18277(R) (AD-432420)
Cr–Co–Mo–Ni–Ti, machining, 16: 3417(R) (ASD-TR-7-532a(IV))
Cr–Co–Mo–Ni, mechanical properties of, effect of rhenium admixture on, 16: 24200
Cr–Co–Mo–Ni, mechanical properties of S-1, to 1800°F, 17: 29070(R) (NP-12934)
Cr–Co–Mo–Ni–W, oxidation by air at 1600°F of Stellite 6B, 20: 11215(R) (NASA-CR-54718)
Cr–Co–Mo–Ni, tensile properties of Udimet 500, effects of thoria additions on, 18: 592(R) (AD-421756)
Cr–Co–Mo–Ni–W, testing for bearing parts in liquid sodium, 20: 22520(R) (NAA-SR-11805)
Cr–Cu–Fe–Mo–Ni, corrosion and metallurgical changes in, caused by steam at 1200 to 1500°F, 16: 24126
Cr–Cu–Fe–Mo–Ni–Ti, corrosion of, by reactor fuel dissolver solutions, 17: 6566 (HW-SA-2307)
Cr–Cu–Fe–Mo–Ni, corrosion by boiling magnesium chloride, 18: 4796(R) (GEAP-4153)
Cr–Cu–Fe–Mo–Ni–Ti, corrosion and fabrication properties for use as nuclear fuel reprocessing plant dissolver, 18: 25996
Cr–Cu–Fe–Mn–Mo–Ni–Ti, corrosion of Hanford 21, by boiling hydrofluoric acid–nitric acid solutions, 20: 37169(R) (BMI-1774)
Cr–Cu–Fe–Mo–Ni, descaling by sodium carbonate–sodium hydroxide solutions, 18: 22441 (HW-79048)
Cr–Cu–Fe–Mo–Ni, effects of ammonium fluoride–formic acid–nitric acid anodic solutions against corrosion of, 18: 35959
Cr–Cu–Fe–Mo–Ni, performance of Ni–O–Nel 825 in nuclear superheater environment, 18: 24886(R) (GEAP-4565)
Cr–Cu–Fe–Ni–Mo, corrosion by boiling magnesium chloride, 18: 4796(R) (GEAP-4153)
Cr–Cu–Fe–Nb–Mo–Ni, corrosion of Illium R, by boiling hydrofluoric acid–nitric acid solutions, 20: 37169(R) (BMI-1774)
Cr–Fe–Mn–Mo–Ni–W, corrosion and metallurgical changes in, caused by steam at 1200 to 1500°F, 16: 24126
Cr–Fe–Mn–Mo–Ni–Ti, corrosion of Hanford 20, by boiling hydrofluoric acid–nitric acid solutions, 20: 37169(R) (BMI-1774)
Cr–Fe–Mn–Mo–Ni–Ti, corrosion of Hanford 17, by boiling hydrofluoric acid–nitric acid solutions, 20: 37169(R) (BMI-1774)
Cr–Fe–Mn–Mo–Ni, specification for type 355 plate, sheet, and strip for irradiation testing, 17: 41347 (HW-75208)
Cr–Fe–Mo, machining studies on D6AC, 16: 10469(R) (ASD-TR-7-532a (V))
Cr–Fe–Mo, machining characteristics, 17: 14778(R) (ASD-TR-7-532a (IX))
Cr–Fe–Mo, magnetic hyperfine field and electric quadrupole coupling in, (E), 20: 28657
Cr–Fe–Mo, oxidation of chromized, at 1900 to 2200°F, 16: 10451 (DC-60-6-125)
Cr–Fe–Mo, phase studies, 20: 17093
Cr–Fe–Mo, strain aging of, 20: 15063 (UCRL-16585)
Cr–Fe–Mo–Ni, compatibility with niobium beryllide at 2000°F, 17: 532 (GEMP-105)
Cr–Fe–Mo–Ni, corrosion of, by acid, 16: 12057
Cr–Fe–Mo–Ni, corrosion of, by fluorides (liquid), 16: 630
Cr–Fe–Mo–Ni, corrosion of, by hydrofluoric acid in volatility pilot plant, 16: 20538 (ORNL-TM-186)
Cr–Fe–Mo–Ni, corrosion of, by water in pressurized water reactors, 16: 7855
Cr–Fe–Mo–Ni–Ti, corrosion and mechanical properties of Inconel 901 as gas turbine material, 16: 32114 (IDO-28591)
Cr–Fe–Mo–Ni, corrosion by aqueous chlorides at 500 to 550°F, 17: 500(R) (KAPL-2000-19(p.IV.1-IV.11))
Cr–Fe–Mo–Ni, corrosion by molten fluorides at 500°C, 17: 29279 (BMI-X-227)
Cr–Fe–Mo–Ni–Nb, corrosion by boiling magnesium chloride, 18: 4796(R) (GEAP-4153)
Cr–Fe–Mo–Ni, corrosion of Hastelloy X-280, by helium–water system at 1700, 1900, and 2100°F, 20: 5846
Cr–Fe–Mo–Ni, corrosion by carbon dioxide, helium, nitrogen, and steam of Hastelloy X-280, 20: 9408 (BNWL-154)
Cr–Fe–Mo–Ni, corrosion by water vapor at 815, 930, and 1038°C of Hastelloy X-280, 20: 9409 (BNWL-155)
Cr–Fe–Mo–Ni, corrosion of Hymu-80 by potassium chloride–uranium trichloride eutectic at 900°C, 20: 21261 (LA-3476)
Cr–Fe–Mo–Ni, corrosion by molten fluoride salts, 16: 32080 (ORNL-TM-328)
Cr–Fe–Mo–Ni, creep and stress-rupture properties in air, liquid metal, and salt at 1350 to 1650°F, 16: 13588 (TIM-287)
Cr–Fe–Mo–Ni, creep of irradiated, at 1600°, 16: 28642(R) (BMI-1581 (Del.))
Cr–Fe–Mo–Ni–Nb–W, descaling by sodium carbonate–sodium hydroxide solutions, 18: 22441 (HW-79048)
Cr–Fe–Mo–Ni, effects of ammonium fluoride–formic acid–nitric acid anodic solutions against corrosion of, 18: 35959
Cr–Fe–Mo–Ni, evaporation at 2050°F of Hastelloy X-280, effects of oxide film on, 20: 9410(R) (BNWL-166, pp 5.1-3)
Cr–Fe–Mo–Ni, mechanical properties of Inconel 713C, 16: 15153(R) (ASD-TR-7-886(IV))
Cr–Fe–Mo–Ni, mechanical properties at high temperatures, 17: 14811 (ASD-TDR-61-529)
Cr–Fe–Mo–Ni–Ti, oxidation of V-57, induced by cyclic strain at high temperatures, 18: 18311 (62RL3190M)
Cr–Fe–Mo–Ni–Ti–W, oxidation of M-308, induced by cyclic strain at high temperatures, 18: 18311 (62RL3190M)
Cr–Fe–Mo–Ni, oxidation of Hastelloy X-280 by helium–steam at 1700°F, 18: 32043(R) (HW-81269(p.4.1-64))
Cr–Fe–Mo–Ni–Nb, oxidation of Inconel 625 by water vapor in helium at 1700°F, 19: 30820 (BNWL-23)
Cr–Fe–Mo–Ni, oxidation at 2050°F of Hastelloy X-280, 20: 5851
Cr–Fe–Mo–Ni–W, properties of, mechanical and physical, 20: 33861 (BAW-237)
Cr–Fe–Mo–Ni, radiation effects on mechanical properties of, fast neutron, 16: 572 (REIC-20)
Cr–Fe–Mo–Ni, radiation effects on mechanical properties, 17: 18852 (BNL-6249)
Cr–Fe–Mo–Ni–Nb, radiation effects on Inconel 625, 18: 7292(R) (HW-77954(p.4.1-12))
Cr–Fe–Mo–Ni–Ti, radiation effects on Nimonic, in-pile, 18: 28075
Cr–Fe–Mo–Ni, radiation effects on mechanical properties of Hastelloy X-280 at 280°C, 18: 32043(R) (HW-81269(p.4.1-64))
Cr–Fe–Mo–Ni–Nb, radiation effects on mechanical properties of Inconel 625, neutron, 19: 30820 (BNWL-23)
Cr–Fe–Mo–Ni, radiation effects on mechanical properties of Hastelloy X-280, fast-neutron, 20: 9408 (BNWL-154)
Cr–Fe–Mo–Ni, radiation effects on tensile properties of Hastelloy X-280, neutron, 20: 23769 (BNWL-202)
Cr–Fe–Mo–Ni–W, radiation effects on mechanical properties of Hastelloy X-280, fast-neutron, 20: 31669
Cr–Fe–Mo–Ni, stress-corrosion cracking by boiler water at 500°F and sea water at 550°F, 17: 27749 (KAPL-M-CC-3)
Cr–Fe–Mo–Ni–Ti, tensile and crack-propagation properties of, at 75 to 1500°F, 16: 12081(R) (AD-260547)
Cr–Fe–Mo–Ni, tensile properties of, for use as forging die at 2400°F, 16: 27623(R) (ARF-2220-15)
Cr–Fe–Mo–Ni, tensile properties, 17: 16640 (DMIC-Memo-164)
Cr–Fe–Mo–Ni, tensile properties at room temperature, 19: 30667(R)

(COO-1319-24)
Cr–Fe–Mo–Ni–Nb–W, tensile properties of IN-102, 19: 39156(R) (CEND-532)
Cr–Fe–Mo–Ni–Nb, thermal response and microstructure of Inconel 625 at 1200 and 1400°F, 19: 39158 (GEAP-4751)
Cr–Fe–Mo–Ni–Nb–W, welding properties of Inco IN-102, 20: 4306(R) (ORNL-3870, pp 194-213)
Cr–Fe–Mo–Pu, mechanical properties of, 17: 6511(R) (BMI-1593(Del.))
Cr–Fe–Mo–V, erosion by mercury vapor at 640°F of Lapelloy, 20: 11214(R) (NASA-CR-54717)
Cr–Fe–Mo–V, mechanical and thermophysical properties of H-11, at 80 to 1600°F, 18: 41928(R) (NASA-CR-54089)
Cr–Fe–Mo–V, properties of H-11 Steel for use in space electric power systems, 20: 4379 (NASA-CR-54091)
Cr–Mn–Mo–Ni, properties for use in liquid-hydrogen bubble chamber, 19: 42808
Cr–Mo, corrosion of, by mercury, 16: 29336(R) (AGC-0584-04-3)
Cr–Mo, fabrication and mechanical properties, 18: 43062(R) (NASA-CR-54111)
Cr–Mo, hardness at 400 to 1080°C, effects of molybdenum content on, 19: 30754(T) (FTD-TT-64-1297)
Cr–Mo, phase diagrams, 18: 25998
Cr–Mo, phase studies based on thermochemical data, 18: 33603
Cr–Mo, plastic deformation, effect of molybdenum content on, 19: 30754(T) (FTD-TT-64-1297)
Cr–Mo, preparation, fabrication, mechanical properties, and oxidation resistance, 18: 16423(R) (GEMP-197)
Cr–Mo, production by electrolysis, 19: 18440
Cr–Mo, properties of, at high temperatures, 16: 30779 (BMI-1277)
Cr–Mo, thermal expansion of, 20: 43964
Cr–Mo, thermodynamic properties, 16: 13636
Cr–Mo, welding, 17: 23919 (TID-7620(Pt.I)(p.193-205))
Cr–Mo, wetting effects of alloying elements on outside of, 19: 11367
Cr–Mo–Nb, corrosion by steam at 1000°F, 17: 493(R) (BMI-X-10003)
Cr–Mo–Nb, mechanical properties and oxidation rate, 19: 32754
Cr–Mo–Nb, oxidation at 800 to 1200°C, 18: 34080
Cr–Mo–Nb, phase diagrams at 1000 to 1550°C, 20: 33936
Cr–Mo–Nb, phase studies, 16: 3493
Cr–Mo–Nb, phase studies, 16: 12157
Cr–Mo–Nb, phase studies, 18: 30187
Cr–Mo–Nb, phase studies at 1000 to 2000°C, 18: 44180
Cr–Mo–Nb, properties and structure at high temperatures, 18: 26012
Cr–Mo–Nb, properties, 19: 26848
Cr–Mo–Nb–Ta, composition having superior high-temperature strength, 18: 25917(P)
Cr–Mo–Nb–Ti, corrosion by steam at 1000°F, 17: 23890(R) (BMI-X-10040)
Cr–Mo–Nb–Ti–V, corrosion by steam at 1000°F, 17: 23890(R) (BMI-X-10040)
Cr–Mo–Nb–Ti–V, corrosion by steam at 540 and 650°C, 18: 8747(R) (BMI-X-10071)
Cr–Mo–Nb–Ti–V, corrosion by steam at 540 and 650°C, 18: 22415(R) (BMI-X-10082)
Cr–Mo–Nb–Ti–Zr, mechanical and oxidation properties of, at high temperatures, 16: 27691(P)
Cr–Mo–Nb–U, preparation and properties as reactor fuel, 19: 26873(P)
Cr–Mo–Ni, compatibility with plutonium and uranium carbides, 20: 30790(R) (ANL-7204, pp 1-31)
Cr–Mo–Ni, corrosion of, by acid, 16: 12057
Cr–Mo–Ni, corrosion of Incoloy and Timken 16-25-6, by sodium at 1200°F, 18: 20472 (NAA-SR-Memo-9340)
Cr–Mo–Ni, corrosion by acids at 800 to 2375°F, effects of heat treatments and microstructure on, 20: 21277
Cr–Mo–Ni, crystal structure of, neutron diffraction studies of atom ordering in, 19: 9676
Cr–Mo–Ni, effect of ferrite content on strength of, 17: 23924 (TID-7620(Pt.I)(p.243-50))
Cr–Mo–Ni, intercrystalline corrosion by hydrochloric acid, 17: 34356
Cr–Mo–Ni, oxidation of, causes of catastrophic, 16: 4500 (ORNL-TM-51)
Cr–Mo–Ni, phase studies, 16: 19412
Cr–Mo–Ni, phase studies at 500 to 1200°C, 20: 27556
Cr–Mo–Ni, thermal properties of, at high temperatures, 16: 4551 (WADD-TR-60-904)
Cr–Mo–Ni–Nb, corrosion and oxidation resistance in fused salts, 18: 41968(P)
Cr–Mo–Ni–Nb–W, creep-rupture properties, 17: 39531(R) (EURAEC-689)
Cr–Mo–Ni–Nb–Ti–W, melting temperatures in, effects of chromium and nickel content on, 16: 19411
Cr–Mo–Ni–Nb–Ti–W, melting temperatures in, effects of chromium and nickel content on, 16: 32127(T) (JPRS-14484)
Cr–Mo–Ni–Ta, corrosion and oxidation resistance in fused salts, 18: 41968(P)
Cr–Mo–Ni–V, corrosion and oxidation resistance in fused salts, 18: 41968(P)
Cr–Mo–Ni–W, corrosion and oxidation resistance in fused salts, 18: 41968(P)
Cr–Mo–Ru, ductility of, effects of molybdenum and ruthenium content on, 19: 37030(R) (GEMP-47A, pp 27-84)
Cr–Mo–Ta, composition having superior high-temperature strength, 18: 25917(P)
Cr–Mo–Ti, phase conversions and properties of, 20: 43970
Cr–Mo–U, corrosion and hardness, 17: 39641
Cr–Mo–U, grain structure after beta treatment, 17: 23957(R) (NMI-7247)
Cr–Mo–U, hardness at 20 to 600°C, 17: 23957(R) (NMI-7247)
Cr–Mo–U, microstructure and phases of heat-treated, 18: 42051
Cr–Mo–U, phase studies, 16: 30876
Cr–Mo–U, preparation and properties as reactor fuel, 19: 26875(P)
Cr–Mo–U, radiation effects on, 16: 15122(R) (NMI-2103)
Cr–Mo–U, radiation effects on gamma-quenched, 16: 4450(R) (BMI-1546 (Del.))
Cr–Mo–U, radiation effects on dimensional stability of, 16: 9141(R) (NMI-2101)
Cr–Mo–U, radiation effects on, 17: 14894 (NMI-1255)
Cr–Mo–W, friction and wear properties of, effects of sodium on, 20: 7588
Cr–Mo–W, solid solution in, 16: 18073
Cr–Mo–Zr, corrosion by pressurized water and workability of, 18: 20461
Cr–Mo–Zr, heat treatment effects on mechanical properties and microstructure of, 18: 20461
Cr–Mo–Zr, oxidation and mechanical properties, 17: 32621
Cu–Mo, electrodeposition, optimal conditions for, 20: 41487
Cu–Mo–stainless steel, vacuum pressure braze cladding of, 18: 7177
Cu–Mo–Zr, analysis for boron by direct absorptiometric method, 17: 5965 (PG-Report-362)
Cu–Mo–Zr, corrosion by steam at 280 to 500°C and 15 to 800 lb/in.², 17: 12619
Cu–Mo–Zr, corrosion resistance and mechanical properties of, effects of bismuth and niobium on, 17: 37535
Cu–Mo–Zr, corrosion by superheated steam at 500°C, hydrogen uptake from, 17: 41368(T,R) (EURAEC-784)
Cu–Mo–Zr, corrosion by superheated steam at 500°C, hydrogen uptake from, 18: 14386(T,R) (EURAEC-822)
Cu–Mo–Zr, corrosion and hydridation by steam and water, 18: 30134(T,R) (EURAEC-955)
Cu–Mo–Zr, corrosion by steam, effects of heat treatments on copper-base and zirconium-base, 20: 39347 (NP-16239)
Cu–Mo–Zr, effects of transformation reactions on properties of, 17: 14835 (NP-12520)
Cu–Mo–Zr, mechanical properties of, effects of hydrogen content on, 18: 14386(T,R) (EURAEC-822)
Cu–Mo–Zr, oxidation by carbon dioxide up to 600°C, 18: 30192
Cu–Mo–Zr, oxidation by steam, oxide films from, 19: 2763 (AECL-1999)
Cu–Mo–Zr, oxidation resistance of, in carbon dioxide at 600 and 700°C, 20: 5860
Cu–Mo–Zr, properties of compositions being used in reactors, 17: 23995
Cu–Mo–Zr, reactions with carbon dioxide to 500°C, 19: 22997 (TRG-Report-842)
Cu–Mo–Zr, reactions with beryllium to 600°C *in vacuo*, 19: 22997 (TRG-Report-842)
Cu–Mo–Zr, reactions with Magnox alloy to 500°C in carbon dioxide–carbon monoxide, 19: 22997 (TRG-Report-842)
Fe–Mn–Mo, crystal structure of, neutron diffraction studies of atom ordering in, 19: 9676
Fe–Mo, analysis of cast, for impurities, 18: 2157(R) (BMI-1644(Del.))
Fe–Mo, casting, 17: 13876(R) (BMI-1603(Del.))
Fe–Mo, crystal structure of, effects of molybdenum content on, 19: 47029
Fe–Mo, deposition of coatings of, by plasma jet spraying, 17: 517 (NOTS-TP-2616)
Fe–Mo, diffusion rates of hydrogen through 10-mil-thick, at 350 to 800°C, 18: 2569(R) (ANL-6687(p.188-203))
Fe–Mo, diffusion into liquid iron at 1923°K, 18: 26010
Fe–Mo, electric conductivity of, at low temperatures, 17: 20489
Fe–Mo, electron interaction effects in films of, superimposed on superconducting lead films, (E), 20: 11918
Fe–Mo, fabrication, 17: 22966(R) (BMI-1614(Del.))
Fe–Mo, fabrication of compacts of, 17: 15532(R) (BMI-1607(Del.))
Fe–Mo, formation of intermetallic compound of, in steels, 20: 35899(T) (AI-Trans-208)
Fe–Mo, iron-57 gamma absorption in, s-electron density from isomer shifts in spectra of, 17: 37777
Fe–Mo, magnetic moments in, determination of, using Moessbauer effect, 20: 26819 (NML-64-2)
Fe–Mo, magnetization at 295°K, saturation, 19: 44678(R) (ANL-7000, pp 186-200)
Fe–Mo, mass transfers in, under constant electric field, 16: 27639(T)

(AERE-Trans-889)
Fe–Mo, phase diagram, 16: 30332 (WAL-TR-823/5)
Fe–Mo, radiation effects on relaxation of elastic stresses in bent ferromolybdenum plates, neutron, 16: 22704
Fe–Mo, strain aging of, 20: 15063 (UCRL-16585)
Fe–Mo, strain-aging effects on, 20: 31716(R) (UCRL-16658, pp 121-32)
Fe–Mo, structure, 17: 22177
Fe–Mo, thermal expansion of solid solutions of, anomalies in, 17: 11238
Fe–Mo, thermodynamic properties of oxygen in liquid, 19: 37071
Fe–Mo, vacancy formation in, 18: 24160
Fe–Mo–Nb, electric conductivity at 1.5 to 77°K, 18: 34183
Fe–Mo–Nb, magnetization, magnetoresistance, and resiativity of, 19: 7955
Fe–Mo–Ni, brazing to molybdenum, 17: 42401(R) (AD-296862)
Fe–Mo–Ni, corrosion of, by chloride solutions, 16: 23528(R) (ORNL-3290)
Fe–Mo–Ni, corrosion of, by molten fluoride salts, 16: 20974 (BMI-X-198)
Fe–Mo–Ni, corrosion of, under hydrofluorination conditions during dissolution of Zircaloy-2, 16: 5665 (BMI-X-184)
Fe–Mo–Ni, corrosion by fluorine and hydrofluoric acid, 17: 8740 (BMI-X-213)
Fe–Mo–Ni, corrosion by hydrofluoric acid, 17: 25720 (BMI-X-234)
Fe–Mo–Ni, corrosion by molten fluorides at 500°C, 17: 29279 (BMI-X-227)
Fe–Mo–Ni, corrosion by molten fluoride mixture at 650°C, 17: 34345 (BMI-X-247)
Fe–Mo–Ni, corrosion by molten fluoride mixture in hydrofluorinator at 500°C, 17: 36222 (BMI-X-253)
Fe–Mo–Ni, corrosion of Hy–Mu-80, by fluoride salt melts at 500 to 650°C, 17: 35251(R) (BMI-1632(Del.))
Fe–Mo–Ni, corrosion of Alloy 79-4, by dissolution-fluorination cycles during volatility single vessel studies, 17: 37292(R) (ORNL-TM-586)
Fe–Mo–Ni, corrosion in hydrofluorination processing of reactor fuels, 17: 39179(R) (ORNL-3452(p.26-50))
Fe–Mo–Ni, corrosion by liquid fluoride salts, 18: 2178 (BMI-X-260)
Fe–Mo–Ni, corrosion by potassium fluoride–zirconium fluoride under hydrofluorination conditions at 600°C, 18: 7985(R) (BMI-1650(Del.))
Fe–Mo–Ni, corrosion by fluorides in Fluoride Volatility Process, 18: 17351(R) (BMI-1659(Del.))
Fe–Mo–Ni, corrosion by fused salt fluoride volatility media, 18: 35641(R) (ORNL-TM-785)
Fe–Mo–Ni, corrosion by fluoride volatility process fused salts, 19: 2716(R) (BMI-1681(Del.))
Fe–Mo–Ni, corrosion of HyMu-80, by aluminum fluoride–potassium fluoride–uranium fluoride–zirconium fluoride system at 600°C, 19: 13871(R) (BMI-1691(Del.))
Fe–Mo–Ni, corrosion by metallic fluorides, effects of hydrogen fluoride on, 19: 18421(R) (BMI-1697(Del.))
Fe–Mo–Ni, diffusion of hydrogen in, effects of glass and oxide coatings on, 16: 2179 (NAA-SR-6109)
Fe–Mo–Ni, effects of ammonium fluoride–formic acid–nitric acid anodic solutions against corrosion of, 18: 35959
Fe–Mo–Ni, magnetic properties of thin film of, uniaxial anisotropic behavior, in, 16: 26644(R) (NP-11755)
Fe–Mo–Ni, magnetization directions in cold-worked, effects of mechanical and thermal history on, 18: 12678
Fe–Mo–Ni, neutron scattering by, cross sections for magnetic, 18: 27990
Fe–Mo–Ni, preparation and magnetic properties of films of, 18: 12676
Fe–Mo–Ni, magnetic properties of cube-textured sheets of, 18: 12677
Fe–Mo–Ni, radiation effects on corrosion of, by aqueous chlorides, 16: 14772 (ORNL-3265)
Fe–Mo–Ni, radiation effects on magnetic properties of, 17: 32692
Fe–Mo–Ni, radiation effects on magnetic properties of, proton, 17: 37701
Fe–Mo–Ni, radiation effects on magnetic properties of polycrystalline, electron, 18: 12744
Fe–Mo–Ni, radiation effects on domain orientation and magnetism of molybdenum Permalloy, 19: 23158
Fe–Mo–Ni, radiation effects on, uniaxial anisotropy from low-temperature magnetic anneal of electron, (E), 20: 23789
Fe–Mo–Ni, radioinduced magnetic annealing effects in, 19: 4722
Fe–Mo–Ni–Ru–W, properties at 1400 to 2000°F, 17: 14808(R) (ARF-2158-24)
Fe–Mo–Ni–Ti–W, joining to alumina ceramics by soldering, 19: 11699 (IPP-4/15)
Fe–Mo–Ni–V, effects of ammonium fluoride–formic acid–nitric acid anodic solutions against corrosion of, 18: 35959
Fe–Mo–Ni–W, coatings for, 17: 6563 (DC-61-7-6)
Fe–Mo–Re, electric conductivity at 1.5 to 77°K, 18: 34183
Fe–Mo–Ti, magnetic properties of, 17: 32651
Fe–Mo–U, microstructure and phases of heat-treated, 18: 42051
Fe–Mo–U, phase studies, 17: 536 (NP-12128)
Fe–Mo–Zr, oxidation and mechanical properties, 17: 32621
Fe–Mo–Zr, oxidation by steam at 900°F, 18: 2162(R) (IITRI-B198-46)
Fe–Mo–Zr, phase studies, 17: 22209
Gd–Mo, mechanical properties, effects of sintering, 17: 3389(R) (USBM-U-978)
Gd–Mo, phase studies of, 20: 41465
Ge–Mo, crystal structure of $MoGe_2$ and $MoGe_{1-7}$, 19: 28837
Ge–Mo, effects of Nb_3Sn on crystal structure of $GeMo_3$ in, 18: 12705
Ge–Mo, phase studies of intermetallic compound in, 19: 16036
Ge–Mo, production of Mo_3Ge by hot-pressing, 20: 21247
Ge–Mo, shear modulus and sound velocity of, 18: 24174
Hf–Mo, aging kinetics of, at 1300 to 1500°K, 20: 41466
Hf–Mo, analysis of oxidation and hafnium diffusion in, 18: 35980(R) (AD-437500)
Hf–Mo, fabrication of, by extrusion, 16: 9141(R) (NMI-2101)
Hf–Mo, free energies of formation of Laves phases in, 16: 13636
Hf–Mo, hardness, 17: 11094(R) (NMI-2113)
Hf–Mo, hardness at 1000 to 1200°C, 17: 25689(R) (NMI-2115)
Hf–Mo, mechanical properties of extruded, at high temperatures, 16: 29375(R) (NMI-2106)
Hf–Mo, oxidation resistance, 17: 34344(R) (AD-287429)
Hf–Mo, oxidation, 17: 39524(R) (AD-296987)
Hf–Mo, preparation, 16: 5656(R) (NMI-2099)
Hf–Mo, properties at high temperatures, 17: 34409(R) (NMI-1253)
Hf–Mo, properties at high temperatures, 20: 4418
Hf–Mo, structure of intermetallic compound $HfMo_2$ in, 16: 2253
Hf–Mo–Nb–W, mechanical properties, 19: 23039
Hf–Mo–Re, hardness at 1000 to 1200°C, 17: 25689(R) (NMI-2115)
Hf–Mo–Re, phase diagrams, 16: 29376(R) (NMI-9237)
Hf–Mo–Re, phase diagram, 17: 34409(R) (NMI-1253)
Hf–Mo–Re, phase studies, 16: 21036(R) (NMI-9235)
Hf–Mo–Re, phase studies of, 17: 18792
Hf–Mo–Re, properties at high temperatures, 18: 2226(R) (NMI-1258)
Hf–Mo–Ta, fabrication and properties, 16: 514(R) (AD-255012)
Hf–Mo–Ta, mechanical properties, 17: 31010
Hf–Mo–V, forgeability and tensile strength, 17: 25771 (ASD-TDR-62-667)
Hf–Mo–W, extrusion and properties of, 19: 18419(R) (AD-424207)
Ho–Mo–Zr, magnetic properties of, 17: 32651
Ir–Mo, crystal structure and phase studies of $Mo_{21.5}Ir_{8.3}$, 19: 6308
Ir–Mo, crystal structure of ordered intermediate phases, 19: 28817
Ir–Mo, isotope effect in superconducting, 18: 36492
Ir–Mo, phase diagrams, 18: 25985 (WADD-TR-60-132(Pt.III))
Ir–Mo, phase studies, 16: 27627(R) (NMI-9243)
Ir–Mo, phase studies, 17: 6668(R) (NMI-9246)
Ir–Mo, phase studies, 17: 12588(R) (NMI-9249)
Ir–Mo, phase studies, 20: 11309
Ir–Mo, superconducting isotope effect in, 17: 11375
Ir–Mo, superconductivity of, isotope effects on, 17: 34617
Ir–Mo, superconductivity of, order-disorder effects on, (E), 19: 39689
Mn–Mo, magnetic susceptibility and specific heat of superconducting binary complex phases of, 18: 37715
Mn–Mo, radiation effects on A302B at 450 to 480°F, 20: 37289
Mn–Mo–Ti, stability of beta phase, effects of aluminum on, 20: 9512
Mo–Nb, analysis for niobium, 17: 30500
Mo–Nb, coating development of, for high-temperature applications in air, 16: 10415 (ASD-TR-61-322(p.482-502))
Mo–Nb, compatibility with sodium at 650°C, 17: 41333(R) (ANL-6677)
Mo–Nb, corrosion of, by steam and water, 16: 29346
Mo–Nb, corrosion by flowing sodium at 650°C, 17: 37001(R) (ANL-6780)
Mo–Nb, corrosion by sodium at 650°C, 17: 36861(R) (ANL-6764)
Mo–Nb, corrosion by steam at 1000°F, 17: 23890(R) (BMI-X-10040)
Mo–Nb, corrosion of, by fluorine-containing fluids, 17: 8750(P)
Mo–Nb, corrosion by potassium at 1500 to 1800°F, 18: 5728 (ASD-TDR-63-270(Pt.II))
Mo–Nb, corrosion by sodium at 650°C, 18: 15663(R) (ANL-6808)
Mo–Nb, corrosion by potassium vapor at 1500 to 1800°F, 18: 18282 (BNL-844)
Mo–Nb, corrosion by sodium at 650°C, 18: 26893(R) (ANL-6868(p.11-108))
Mo–Nb, corrosion by hydrochloric, phosphoric, and sulfuric acids, effects of alloy composition on, 20: 14997
Mo–Nb, creep strength of, effects of composition on, 20: 11302
Mo–Nb, crystal lattice vibrations in, inelastic neutron scattering measurements of, 20: 42573
Mo–Nb, crystal structure of, phonons in disordered, (E), 20: 5911
Mo–Nb, crystal structure and electric conductivity of, 20: 29766
Mo–Nb, crystal structure of, determination by phonon dispersion, 20: 37273
Mo–Nb, diffusion in bcc, 19: 23112
Mo–Nb, electric and mechanical properties, 18: 24158
Mo–Nb, electric conductivity at 300°K, effects of 1% iron solute on, 18: 12688
Mo–Nb, electric conductivity at 1.5 to 77°K, 18: 34183
Mo–Nb, electronic specific heat and magnetic susceptibility of, variation with temperature, 18: 8837

Mo–Nb, electronic structure of, at superconducting critical temperatures, 20: 31747
Mo–Nb, extrusion, 19: 20500 (AFML-TR-64-387)
Mo–Nb, fabrication and properties of extruded and rolled, 18: 5727(R) (AD-294579)
Mo–Nb, fabrication and properties, 18: 26893(R) (ANL-6868(p.11-108))
Mo–Nb, forging characteristics, 16: 9162 (DMIC-Memo-143)
Mo–Nb, hardness, 20: 15073
Mo–Nb, hardness of, at 20 to 2000°C, effects of molybdenum content on, 16: 30839
Mo–Nb, hydrogen affinity of, 18: 24165
Mo–Nb, iron magnetic moment in, discontinuous, (E), 19: 38031
Mo–Nb, Knight shift of niobium-93 in, 17: 16709
Mo–Nb, magnetic susceptibility and hydrogen affinity, 17: 3523
Mo–Nb, mass transport by sodium; 18: 15563
Mo–Nb, mechanical properties of, effects of composition on, 17: 24001
Mo–Nb, mechanical properties at 1100 and 1300°C, 19: 11734
Mo–Nb, mechanical properties of, effects of composition on, 20: 11288(T) (AD-622477)
Mo–Nb, mechanical and thermal properties of niobium-base, 20: 43940
Mo–Nb, metallurgy of, bibliography on, 17: 36203 (TID-3572)
Mo–Nb, microstructures, 19: 44610 (TIM-943)
Mo–Nb, neutron inelastic scattering by, Kohn effect from, (E), 20: 34805 (BNL-940, pp 8-15)
Mo–Nb, niobium-93 nuclear magnetic relaxation in, (E), 19: 41989
Mo–Nb, oxidation kinetics and mechanism of, 18: 34078
Mo–Nb, oxidation at 1000 to 1200°C, 18: 34079
Mo–Nb, oxidation, 18: 37627
Mo–Nb, oxidation at 400 to 1200°C, 18: 41960
Mo–Nb, oxidation in air at 1000 to 1200°C, 19: 11693
Mo–Nb, oxidation of coated, by air at high temperatures, 19: 27768(R) (SCNC-308)
Mo–Nb, oxidation by oxygen at 400 to 1200°C, 20: 5851
Mo–Nb, oxidation by air at 1000 to 1200°C, effects of composition on, 20: 11227
Mo–Nb, oxidation rate of, at 1100°C, 20: 23614
Mo–Nb, paramagnetic susceptibility, 16: 10576
Mo–Nb, preparation of vacuum-arc-cast, 16: 18016(R) (AD-265129)
Mo–Nb, preparation and properties of single crystals of, 20: 41481
Mo–Nb, preparation by electron-bombardment zone-melting methods, 16: 32046
Mo–Nb, properties of wrought, 17: 6672 (NP-12383)
Mo–Nb, properties of welded, 17: 11242
Mo–Nb, recrystallization temperature and strength of, effects of molybdenum content on, 20: 7618
Mo–Nb, self-diffusion of niobium in, 20: 35907
Mo–Nb, solid-state bonding of, 18: 24112
Mo–Nb, solvent properties of, for oxygen at 1000°C, 16: 13611
Mo–Nb, strength of, effects of carbon additions on, 17: 6672 (NP-12383)
Mo–Nb, superconductivity of, below 1°K, 16: 615
Mo–Nb, superconductivity below 20 millidegrees in, 17: 31217
Mo–Nb, superconductivity of, 18: 15084
Mo–Nb, superconductivity of, 18: 15085
Mo–Nb, superconductivity of, measurement of heat capacity to test theory of, 18: 36486
Mo–Nb, superconductivity of, 18: 36487
Mo–Nb, superconductivity, 20: 40047
Mo–Nb, superconducting transition temperature of 75Nb–25Mo, pressure effects on, 20: 44568
Mo–Nb, thermal capacity of solid solutions of, at low temperatures, 19: 4703
Mo–Nb, thermal expansion coefficient determination by x-ray method, 19: 47023(T) (LA-tr-65-20)
Mo–Nb, thermal expansion of, 20: 43964
Mo–Nb, thermodynamic properties, 16: 13636
Mo–Nb, yield strength of, effects of oxygen on, 17: 18811
Mo–Nb–Pt–U, corrosion resistance in water, 19: 20497(P)
Mo–Nb–Pt–U, properties for use as reactor fuel, 19: 20497(P)
Mo–Nb–Ru–Ti–V, oxidation of siliconized, at 2200°F, 17: 23942(R) (ARF-B6001-3)
Mo–Nb–Ru–Ti–V, oxidation life at 2200°F of siliconized, static, 17: 35997(R) (IITRE-B6001-5)
Mo–Nb–Ta, corrosion of, by fluorine-containing fluids, 17: 8750(P)
Mo–Nb–Ta, fabrication and properties, 16: 514(R) (AD-255012)
Mo–Nb–Ta, mechanical properties of, effects of composition on, 17: 24001
Mo–Nb–Ta, mechanical properties at high temperatures, 19: 34734
Mo–Nb–Ta, properties of wrought, 17: 6672 (NP-12383)
Mo–Nb–Ta, tensile properties at 3000°F, 18: 12562(R) (X63-12299)
Mo–Nb–Ta–W, cavitation damage of Cb-132M in liquid sodium to 1500°F, 20: 46154 (NASA-CR-72035)
Mo–Nb–Ta–W, corrosion of, by fluorine-containing fluids, 17: 8750(P)
Mo–Nb–Ta–W, creep slip of solution-hardened, at 980 to 1370°C, 19: 47049
Mo–Nb–Ta–W–Zr, creep tests on NB132M at 3200°F, 20: 5885(R) (NAS-CR-54773)
Mo–Nb–Ta–W, deformation mechanisms in solution-hardened niobium-base, 20: 17082
Mo–Nb–Ta–W, electric conductivity of Cb-132, at 80 to 400°K, 20: 23749
Mo–Nb–Ta–W, mechanical properties of, effects of composition on, 17: 24001
Mo–Nb–Ta–W, mechanical properties, 18: 18307
Mo–Nb–Ta–W, mechanical properties of solution-hardened, strain-aging studies of, 19: 7935
Mo–Nb–Ta–W, mechanical properties at 77 to 423°K, 19: 34724
Mo–Nb–Ta–W, properties as hollow turbine vanes, 20: 16963
Mo–Nb–Ta–W, strain aging of solution-hardened, 20: 5851
Mo–Nb–Ta–W, tensile properties, 17: 27812(R) (WADD-TR-61-134(Pt.II))
Mo–Nb–Ta–W, tensile properties at 3000°F, 18: 12562(R) (X63-12299)
Mo–Nb–Ta–W, tensile properties at 3000°F, 19: 16156
Mo–Nb–Ta–W, thermal expansion of Cb-132, at 80 to 400°K, 20: 23749
Mo–Nb–Ta–W, vacuum arc furnace design for melting of, 18: 44071
Mo–Nb–Ti, coating evaluation for D-31, 19: 9607 (ML-TDR-64-70)
Mo–Nb–Ti, coating of D-31 with silicides for oxidation protection, evaluation, 19: 7876(R) (ML-TDR-64-71)
Mo–Nb–Ti, coating of, for oxidation protection at 2300°F, 19: 20483 (SCNC-318)
Mo–Nb–Ti, coating with aluminum–tin-base alloys for protection against oxidation, 17: 39465 (SCNC-328(Del.))
Mo–Nb–Ti, coatings for, for high-temperature uses, 16: 27687
Mo–Nb–Ti, corrosion resistance, 16: 10464
Mo–Nb–Ti, corrosion by steam at 1000°F, 17: 493(R) (BMI-X-10003)
Mo–Nb–Ti, corrosion by steam at 1000°F, 17: 23890(R) (BMI-X-10040)
Mo–Nb–Ti, corrosion by potassium at 1500 to 1800°F, 18: 5728 (ASD-TDR-63-270(Pt.II))
Mo–Nb–Ti, corrosion by sodium at 650°C, 18: 15663(R) (ANL-6808)
Mo–Nb–Ti, corrosion by potassium vapor at 1500 to 1800°F, 18: 18282 (BNL-844)
Mo–Nb–Ti, corrosion by sodium at 650°C, 18: 26893(R) (ANL-6868 (p.11-108))
Mo–Nb–Ti, elastic properties and shear modulus of annealed and quenched, 18: 35999
Mo–Nb–Ti, evaluation of protective coatings for, 20: 29651
Mo–Nb–Ti, extrusion properties, 16: 12065(R) (AMC-TR-7-775(V))
Mo–Nb–Ti, fabrication and structure, 16: 10470 (ASD-TR-7-784(VI))
Mo–Nb–Ti, fabrication of rolled sheet, 17: 6597(R) (DMIC-176)
Mo–Nb–Ti, fabrication by vacuum rolling, 17: 36270
Mo–Nb–Ti, fabrication and properties, 18: 26893(R) (ANL-6868(p.11-108))
Mo–Nb–Ti, fabrication, oxidation, and properties of, 18: 35986 (ERR-FW-049A)
Mo–Nb–Ti, forging characteristics, 16: 9162 (DMIC-Memo-143)
Mo–Nb–Ti, machining, 16: 3417(R) (ASD-TR-7-532a(IV))
Mo–Nb–Ti, machining studies on pressed, sintered, and arc-cast, 16: 30742(R) (ASD-TR-7-532a(VII))
Mo–Nb–Ti, mechanical and thermal properties of niobium-base, 20: 43940
Mo–Nb–Ti, oxidation at 1000 to 1200°C, 18: 34079
Mo–Nb–Ti, oxidation of coated, by air at high temperatures, 19: 27768(R) (SCNC-308)
Mo–Nb–Ti, oxidation at 500 to 1200°C, 19: 36981
Mo–Nb–Ti, oxidation protection by aluminum–tin coatings with chromium and titanium additions, 20: 7580 (TIM-945)
Mo–Nb–Ti, properties of coated, at high temperatures, 16: 9189 (ASD-TR-61-66(Pt.II))
Mo–Nb–Ti, properties of arc-melted, 19: 27768(R) (SCNC-308)
Mo–Nb–Ti, specifications for machining, 18: 12609
Mo–Nb–Ti, thermal absorbance, emittance, and reflectance of, 16: 9193 (DMIC-Memo-141)
Mo–Nb–Ti, welding, 16: 30741 (ASD-TDR-62-292)
Mo–Nb–Ti, welding of D-31, ultrasonic, 17: 36240(R) (AD-290604)
Mo–Nb–Ti, welding of, ultrasonic, 19: 16025 (AD-425218)
Mo–Nb–Ti, x-ray diffraction of nonmetallic phases chemically extracted from, 19: 7973
Mo–Nb–Ti–U–Zr, ductility of uranium-base, effects of aging, forging, and rolling on, 20: 43883 (AD-637777)
Mo–Nb–Ti–U–Zr, mechanical properties for possible structural use, 19: 9651 (AMRA-TR-64-28)
Mo–Nb–Ti–U–Zr, mechanical properties of high-strength uranium-base, 20: 39440(P)
Mo–Nb–Ti–U–Zr, transformation diagram and kinetics of, 17: 25769(R) (AMRA-CR-63-02/1(F))
Mo–Nb–Ti–V, coating for oxidation protection, 19: 20459(R) (IITRI-B6019-6)
Mo–Nb–Ti–V, corrosion by steam at 1000°F, 17: 23890(R) (BMI-X-10040)
Mo–Nb–Ti–V, elastic properties and shear modulus of annealed and

quenched, 18: 35999
Mo–Nb–Ti–V, mechanical properties of low-ruthenium content, at 2000°F, 16: 33444(R) (ARF-2231-6)
Mo–Nb–Ti–V, mechanical properties of, at high temperatures, effects of molybdenum, tantalum, and tungsten additions on, 16: 33444(R) (ARF-2231-6)
Mo–Nb–Ti–V, phase studies, 19: 7967
Mo–Nb–Ti–V, preparation and properties, 16: 22577(R) (ARF-2231-4)
Mo–Nb–Ti–W, forging characteristics, 16: 9162 (DMIC-Memo-143)
Mo–Nb–Ti–W–Zr, forging characteristics, 16: 9162 (DMIC-Memo-143)
Mo–Nb–Ti–Zr, analysis using vacuum cup electrode, 19: 22103 (TIM-904)
Mo–Nb–Ti–Zr, coating with aluminum–tin-base alloys for protection against oxidation, 17: 39465 (SCNC-328(Del.))
Mo–Nb–Ti–Zr, corrosion by lithium at 1600°F, 19: 36980 (PWAC-355)
Mo–Nb–Ti–Zr, creep properties of niobium-modified TZM, 20: 29705(R) (NAS-CR-54973)
Mo–Nb–Ti–Zr, fabrication and properties of cast and extruded, 18: 12536(R) (AD-412904)
Mo–Nb–Ti–Zr, fabrication and properties of extruded and rolled, 18: 22412(R) (AD-422106)
Mo–Nb–U, corrosion by water at 650°F, alloying effects of platinum on, 18: 16449(P)
Mo–Nb–U, isothermal transformations of gamma-phase, 19: 40958
Mo–Nb–U, microstructure and phases of heat-treated, 18: 42051
Mo–Nb–U, nonmetallic inclusions in, 16: 30874
Mo–Nb–U, phase boundaries at 675, 700, and 720°C, 18: 5801
Mo–Nb–U, phase diagrams, 16: 30868
Mo–Nb–U, phase studies and properties of, at 450 and 500°C, 16: 30871
Mo–Nb–U, phase studies and properties of, at 500°C, 16: 30867
Mo–Nb–U, phase studies and properties of, at 500 to 560°C, 16: 30869
Mo–Nb–U, phase studies of, at 575 to 1200°C, 16: 30870
Mo–Nb–U, phase studies, 18: 18387
Mo–Nb–U, phase studies, 17: 39631
Mo–Nb–U, production of fine-grained, 19: 30663(P)
Mo–Nb–U, transformation of gamma phase of, isothermal, 19: 7910 (UCRL-7824)
Mo–Nb–U–Zr, alloying effects of chromium and vanadium on aging and stability of, 17: 39644
Mo–Nb–U–Zr, mechanical properties, 17: 39643
Mo–Nb–U–Zr, mechanical properties of gamma-phase uranium-base, 20: 15060 (UCRL-7771)
Mo–Nb–U–Zr, nonmetallic inclusions in, 16: 30874
Mo–Nb–U–Zr, phase structure of, at 800 and 1000°C, 16: 30872
Mo–Nb–U–Zr, phase studies below 800°C, 17: 39633
Mo–Nb–U–Zr, phase transformation in, at 430 to 550°C, 16: 30873
Mo–Nb–V, corrosion of, by steam and water, 16: 29346
Mo–Nb–V, corrosion by steam at 1000°F, 17: 493(R) (BMI-X-10003)
Mo–Nb–V, ductility, strength, and weldability of, 18: 14448
Mo–Nb–V, fabricability, strength, and weldability, 20: 29763
Mo–Nb–V, mechanical properties of, effects of composition on, 17: 24001
Mo–Nb–V, preparation and properties, 16: 22577(R) (ARF-2231-4)
Mo–Nb–V, properties, 17: 34419(R) (WADC-TR-57-344(Pt.VII))
Mo–Nb–V–Zr, bend ductility of B-66, effects of argon atmosphere contamination on, 19: 9592(R) (ASD-8-170(IV))
Mo–Nb–V–Zr, bonding of B-66, method for diffusion, 20: 5867
Mo–Nb–V–Zr, casting and testing of B-66 ingots, 18: 571(R) (AD-297246)
Mo–Nb–V–Zr, coating evaluation for B-66, oxidation-resistant, 19: 36945 (AD-610867)
Mo–Nb–V–Zr, coating of B-66, with chromium–silicon–titanium systems and silicides, 18: 14373(R) (NP-13498)
Mo–Nb–V–Zr, coatings for B-66 foils, development of high-temperature oxidation-resistant, 18: 30118(R) (RTD-TDR-63-4006(Pt.I))
Mo–Nb–V–Zr, coatings on B-66, properties of oxidation-resistant, 19: 26801(R) (AD-607530)
Mo–Nb–V–Zr, compatibility of rocket nozzles of, with hydrogen, 20: 19228
Mo–Nb–V–Zr, composition, crystal structure, and phases of precipitates in, 16: 22582 (ASD-TDR-62-7)
Mo–Nb–V–Zr, contamination of B-66 by rolling in argon atmosphere, 19: 9592(R) (ASD-8-170(IV))
Mo–Nb–V–Zr, corrosion protection by silicide coatings, 19: 11682
Mo–Nb–V–Zr, corrosion by cesium and lithium above 2500°F, 19: 28766
Mo–Nb–V–Zr, corrosion of B-66, by lithium, effects of oxygen on, 20: 4301(R) (ORNL-3870, pp 102-35)
Mo–Nb–V–Zr, corrosion by cesium vapor and liquid lithium at 2500 to 3400°F of B-66, 20: 5851
Mo–Nb–V–Zr, corrosion by refluxing potassium at 1800 to 2400°F, 20: 25485 (NASA-TN-D-3429)
Mo–Nb–V–Zr, creep-rupture properties of B-66, temperature dependence, 18: 44049(R) (ORNL-3670(p.77-111))
Mo–Nb–V–Zr, creep-rupture properties of, 20: 2336 (ORNL-P-1634)
Mo–Nb–V–Zr, ductility transition temperature of B-66, effects of protective coatings and welding on, 20: 27466
Mo–Nb–V–Zr, ductility, strength, and weldability of, 18: 14448
Mo–Nb–V–Zr, evaporation tests of B-66 in high vacuum, 18: 44049(R) (ORNL-3670(p.77-111))
Mo–Nb–V–Zr, evaporation losses of B-66, at 1200 to 1500°C in high vacuum, 19: 37043 (ORNL-P-1394)
Mo–Nb–V–Zr, evaporation losses in high vacuum of B-66, 20: 4301(R) (ORNL-3870, pp 102-35)
Mo–Nb–V–Zr, extrusion, 17: 3445(R) (NP-12225)
Mo–Nb–V–Zr, extrusion of tubing from, optimization studies, 17: 11140(R) (AMC-TR-7-775(VII))
Mo–Nb–V–Zr, extrusion of tubes of, 17: 23895(R) (AD-403514)
Mo–Nb–V–Zr, extrusion of, program outline for, 17: 25749(R) (WANL-PR-(N)-001)
Mo–Nb–V–Zr, extrusion by Dynapak process of B-66, 19: 30686(R) (AD-608945)
Mo–Nb–V–Zr, fabrication of rolled sheets of B-66, 18: 12591(R) (AD-409960)
Mo–Nb–V–Zr, fabrication of B-66, by rolling, 18: 12593(R) (AD-411155)
Mo–Nb–V–Zr, fabrication and mechanical properties of B-66, 18: 18292(R) (N63-20341)
Mo–Nb–V–Zr, fabrication of B-66, by extrusion and forging, 18: 20484(R) (AD-418992)
Mo–Nb–V–Zr, fabrication of B-66, by extrusion, 18: 20487(R) (WANL-PR-(N)-002)
Mo–Nb–V–Zr, fabrication and properties of coated B-66, 18: 24068(R) (NP-13955)
Mo–Nb–V–Zr, fabrication of extruded B-66, 18: 24093(R) (AD-424593)
Mo–Nb–V–Zr, fabrication and properties of B-66 tubing, 18: 27924(R) (WANL-PR-(N)-004)
Mo–Nb–V–Zr, fabrication of B-66, by rolling, 18: 30106(R) (AD-430773)
Mo–Nb–V–Zr, fabrication B-66 into sheets, 18: 30146(R) (AD-414497)
Mo–Nb–V–Zr, fabrication of B-66 tubing, 18: 41933 (TID-11295(3rd Ed.))
Mo–Nb–V–Zr, fabrication by forging and by extrusion, 19: 11711
Mo–Nb–V–Zr, fabrication and properties of B-66 sheet, 19: 20499(R) (AD-606291)
Mo–Nb–V–Zr, fabrication and properties of B-66 foil, 19: 24945 (ASD-TDR-63-829(Pt.I))
Mo–Nb–V–Zr, fabrication and properties of B-66 strip and foil, 19: 24946 (ASD-TDR-63-829(Pt.II))
Mo–Nb–V–Zr, fabrication of tubing of B-66, 20: 16998
Mo–Nb–V–Zr, joining of foils of B-66, for honeycomb panel fabrication, 18: 37661 (ASD-TDR-63-799(Pt.I))
Mo–Nb–V–Zr, mechanical properties of Pfaudler silicide and TRW chromium–silicon–titanium-coated B-66, in air at 70 to 2600°F, 18: 20523(R) (NP-13811)
Mo–Nb–V–Zr, mechanical properties of B-66, 19: 13978 (AMRA-TR-64-16)
Mo–Nb–V–Zr, oxidation and mechanical properties of coated B-66, 17: 39525(R) (AD-416459)
Mo–Nb–V–Zr, oxidation protection of B-66 by chromium–silicon–titanium coatings at 2000 to 2700°C, 18: 30127 (ASD-TDR-62-934(Pt.II))
Mo–Nb–V–Zr, properties of B66 sheet, 18: 573(R) (AD-422116)
Mo–Nb–V–Zr, properties as space reactor fuel cladding, 18: 9713 (CONF-375-3)
Mo–Nb–V–Zr, properties of coated B-66, to 2600°F, 18: 14373(R) (NP-13498)
Mo–Nb–V–Zr, properties of B-66, to 2600°F, 18: 14353(R) (AD-408310)
Mo–Nb–V–Zr, properties of B-66 foils at high temperatures, effects of coatings on mechanical and thermophysical, 18: 34128 (RTD-TDR-63-4068)
Mo–Nb–V–Zr, properties of welds in B-66, 19: 40989
Mo–Nb–V–Zr, reactions with cesium at 3400°F, metallographic specimen preparation of B-66, 19: 46954 (NMI-5025(Pt.I), pp 39-58)
Mo–Nb–V–Zr, reactions with uranium carbide, nitride, and dioxide, metallographic specimen preparation of B-66, 19: 46954 (NMI-5025 (Pt.I), pp 39-58)
Mo–Nb–V–Zr, rolling of foils of B-66, 19: 7871(R) (AD-422001)
Mo–Nb–V–Zr, stress-rupture properties of B-66, 19: 40961
Mo–Nb–V–Zr, tensile properties of welded plates of B-66, 20: 4301(R) (ORNL-3870, pp 102-35)
Mo–Nb–V–Zr, tensile properties of B-66, effects of welds on, 20: 29712(R((WANL-PR-(P)-009)
Mo–Nb–V–Zr, tensile strength of B-66, at 1100 to 1400°C, 17: 30950(R) (NMI-2117)
Mo–Nb–V–Zr, tests of B-66 tubing, nondestructive, 19: 13950 (ORNL-TM-990)
Mo–Nb–V–Zr, thermal properties, 18: 7201 (ASD-TDR-63-597)
Mo–Nb–V–Zr, thermal properties to melting point, 20: 878
Mo–Nb–V–Zr, weld bend tests of B-66, 19: 13955(R) (WANL-PR-(P)-005)
Mo–Nb–V–Zr, weld stability in B-66, 20: 5866
Mo–Nb–V–Zr, weld structural stability in, 18: 22459(R) (NP-13816)

Mo–Nb–V–Zr, weldability of B-66, 17: 39498 (DMIC-Memo-169)
Mo–Nb–V–Zr, weldability of B-66 sheet, 18: 44049(R) (ORNL-3670 (p.77-111))
Mo–Nb–V–Zr, weldability study of B-66, 19: 24957(R) (WANL-PR(P)-006)
Mo–Nb–V–Zr, weldability studies of B-66, 19: 46966(R) (WANL-PR(P)-007)
Mo–Nb–V–Zr, weldability evaluation of, 20: 39366
Mo–Nb–V–Zr, welding of B66, effects of parameters in T1G welds in, 18: 573(R) (AD-422116)
Mo–Nb–V–Zr, welding of B-66, power force programmed ultrasonic, 18: 12594 (AD-427997)
Mo–Nb–V–Zr, welding of B-66, tungsten-arc, 18: 34058(R) (WANL-PR(P)-003)
Mo–Nb–V–Zr, welding of B-66, equipment and procedures for, 19: 9629(R) (AD-608818)
Mo–Nb–V–Zr, welding paramete.s for B-66, electron-beam, 20: 5867
Mo–Nb–V–Zr, welding properties of B-66, 20: 27466
Mo–Nb–V–Zr, welds in B-66, thermal stability of, 20: 27467
Mo–Nb–W, consolidation from elemental powders by hot pressing and annealing, 18: 41982
Mo–Nb–W, corrosion of, by fluorine-containing fluids, 17: 8750(P)
Mo–Nb–W, creep strength of, effects of composition on, 20: 11302
Mo–Nb–W, extrusion, 17: 6592 (ASD-TDR-62-781)
Mo–Nb–W, extrusion and properties of, 19: 18419(R) (AD-424207)
Mo–Nb–W, extrusion, 19: 20500 (AFML-TR-64-387)
Mo–Nb–W, fabrication and tensile properties at high temperatures, 18: 12562(R) (X63-12299)
Mo–Nb–W, fabrication of, effects on mechanical properties, 18: 20485 (ASD-TDR-62-670(Pt.II))
Mo–Nb–W, factors affecting vacuum-arc melting of, 18: 24070 (RTD-TDR-63-4089)
Mo–Nb–W, mechanical properties of, effects of composition on, 17: 24001
Mo–Nb–W, melting, 17: 6592 (ASD-TDR-62-781)
Mo–Nb–W, phase studies and properties of, 16: 22618
Mo–Nb–W, workability, 17: 6592 (ASD-TDR-62-781)
Mo–Nb–W–V, mechanical properties of, effects of composition on, 17: 24001
Mo–Nb–W–Zr, composition, crystal structure, and phases of precipitates in, 16: 22582 (ASD-TDR-62-7)
Mo–Nb–W–Zr, creep testing of F-48, at 2200°F, 17: 35251(R) (BMI-1632(Del.))
Mo–Nb–W–Zr, fabrication and structure, 16: 10470 (ASD-TR-7-784(VI))
Mo–Nb–W–Zr, fabrication and properties of rolled sheet, 17: 6597(R) (DMIC-176)
Mo–Nb–W–Zr, fabrication by vacuum rolling, 17: 36270
Mo–Nb–W–Zr, forging characteristics, 16: 9162 (DMIC-Memo-143)
Mo–Nb–W–Zr, friction and wear of, at high temperatures and in vacuum, 16: 5708 (ASD-TR-61-301)
Mo–Nb–W–Zr, hardness of niobium-base, effects of composition on hot-, 20: 31669
Mo–Nb–W–Zr, homogenization kinetics of sintered, 18: 26047
Mo–Nb–W–Zr, mechanical properties, 17: 14727(R) (BMI-1600(Del.))
Mo–Nb–W–Zr, mechanical properties of warm-extruded and rolled, 17: 32567 (BMI-X-249)
Mo–Nb–W–Zr, mechanical and oxidation properties of F-48, 17: 34415 (UCRL-6187(Rev.))
Mo–Nb–W–Zr, mechanical properties, 18: 18307
Mo–Nb–W–Zr, mechanical properties at 1999 to 1600°C, 19: 23043
Mo–Nb–W–Zr, mechanical properties, 19: 28833
Mo–Nb–W–Zr, mechanical properties of niobium-base, effects of composition on, 20: 7599
Mo–Nb–W–Zr, phase studies, 19: 7968
Mo–Nb–W–Zr, properties of coated, at high temperatures, 16: 9189 (ASD-TR-61-66(Pt.II))
Mo–Nb–W–Zr, properties of F-48, as journal bearing material, 17: 25382 (ASD-TR-61-705)
Mo–Nb–W–Zr, shear strength of F-48 fasteners at room temperature and 1600°F, 17: 36281 (AD-295526)
Mo–Nb–W–Zr, tensile properties, 17: 3378(R) (BMI-1583(Del.))
Mo–Nb–W–Zr, tensile properties, 17: 27878
Mo–Nb–W–Zr, tensile strength of F-48, at 1100 to 1500°C, 17: 30950(R) (NMI-2117)
Mo–Nb–W–Zr, welding, 16: 30741 (ASD-TDR-62-292)
Mo–Nb–Zr, corrosion of, by steam and water, 16: 29346
Mo–Nb–Zr, corrosion resistance and mechanical properties, 17: 37535
Mo–Nb–Zr, oxidation by steam at 900°F, 18: 2162(R) (IITRI-B198-46)
Mo–Nb–Zr, oxidation in air, composition of scale formed during, 18: 10477(T) (JPRS-22697(p.27-38))
Mo–Nb–Zr, phase diagram, 18: 8809(T) (JPRS-22593)
Mo–Nb–Zr, phase studies, 18: 625
Mo–Nb–Zr, phase studies on, 18: 16494
Mo–Nb–Zr, phase studies and properties, 18: 26056
Mo–Nb–Zr, phase studies of, isothermal sections at 1200°C in, 20: 41464
Mo–Nb–Zr, phase transformation kinetics, 16: 15166 (ARF-2198-21)
Mo–Ni, analysis of, for oxygen by sulfur monochloride method, 16: 14631(T) (UCRL-Trans-801(L))
Mo–Ni, atomic radii and interatomic distances in intermetallic compounds in, 18: 28029
Mo–Ni, atomic structure of, short-range order and size-effect coefficients for, (E), 20: 4421
Mo–Ni, brazing and welding, 18: 3298(R) (ORNL-2221(Pts.1-5)(Del.))
Mo–Ni, corrosion of, by acid, 16: 12057
Mo–Ni, corrosion by molten fluorides, 18: 3298(R) (ORNL-2221(Pts.1-5)(Del.))
Mo–Ni, corrosion in solvent extraction processes, 18: 8761
Mo–Ni, corrosion resistance and hardening mechanism of, 18: 18322
Mo–Ni, corrosion and oxidation resistance in fused salts, 18: 41968(P)
Mo–Ni, creep-rupture properties, 18: 3298(R) (ORNL-2221(Pts.1-5)(Del.))
Mo–Ni, crystal structure of, x-ray studies of short-range order of, 19: 25041
Mo–Ni, crystal structure stacking faults in, effects of rolling textures on, 19: 44723
Mo–Ni, phase studies at 500 to 1200°C, 20: 27556
Mo–Ni, development of, for ANP program, 16: 28646(R) (ORNL-2274 (Pts.1-5))
Mo–Ni, development of, for ANP program, 16: 28647(R) (ORNL-2340 (Pts.1-5))
Mo–Ni, development, 18: 3298(R) (ORNL-2221(Pts.1-5)(Del.))
Mo–Ni, diffusion in, effects of crystal deformation on, 16: 25831
Mo–Ni, electric conductivity of, effects of crystal structure on, 20: 41457(R) (ORO-3291-3)
Mo–Ni, fabrication by sintering, 18: 30145(R) (AD-401528)
Mo–Ni, intercrystalline corrosion by hydrochloric acid, 17: 34356
Mo–Ni, phase diagram, 18: 44194
Mo–Ni, short-range order in, x-ray diffuse-scattering determination of, (E), 20: 11325
Mo–Ni, specific heats of, methods of measuring, 20: 41457 (ORO-3291-3)
Mo–Ni, structure of, short-range order in atomic, 19: 28815(T) (ORNL-tr-632)
Mo–Ni, thermal capacity data and order-disorder reactions in, 20: 37278
Mo–Ni, thermal properties of, at high temperatures, 16: 4551 (WADD-TR-60-904)
Mo–Ni–Nb–Ta–Ti, corrosion resistance and ductility of, 19: 34735(P)
Mo–Ni–Pt–Ru–W, properties at 1400 to 2000°F, 17: 14808(R) (ARF-2158-24)
Mo–Ni–Ru–W, properties at high temperatures, 17: 14807(R) (ARF-2158-21)
Mo–Ni–Ti–W, joining to alumina ceramics by soldering, 19: 11699 (IPP-4/15)
Mo–Ni–W, mechanical properties, effects of aging temperature and molybdenum and tungsten content on, 20: 5851
Mo–Ni–Zr, corrosion by pressurized water and workability of, 18: 20461
Mo–Ni–Zr, heat treatment effects on mechanical properties and microstructure of, 18: 20461
Mo–Ni–Zr, oxidation and mechanical properties, 17: 32621
Mo–Os, crystal structure and phase studies of $Mo_{1-x}Os_{1+x}$, 19: 6308
Mo–Os, hardness, 17: 11094(R) (NMI-2113)
Mo–Os, hardness at 1000 to 1200°C, 17: 25689(R) (NMI-2115)
Mo–Os, magnetic susceptibility and specific heat of superconducting binary complex phases of, 18: 37715
Mo–Os, phase diagrams, 16: 29376(R) (NMI-9237)
Mo–Os, phase diagram, 17: 34409(R) (NMI-1253)
Mo–Os, phase studies, 16: 21036(R) (NMI-9235)
Mo–Os, properties at high temperatures, 18: 2226(R) (NMI-1258)
Mo–Os–W, phase diagrams, 18: 25985 (WADD-TR-60-132(Pt.III))
Mo–Os–W, phase diagrams at 1600, 2000, and 2375°C, 19: 41048
Mo–Os–W, phase studies, 16: 27627(R) (NMI-9243)
Mo–Os–W, phase studies, 17: 6668(R) (NMI-9246)
Mo–Os–W, phase studies, 17: 12588(R) (NMI-9249)
Mo–Pd, crystal structure of intermetallic compounds in, 19: 987
Mo–Pd, crystal structure and electric conductivity of, 20: 29766
Mo–Pd, electric conductivity and Hall constant of, 17: 580
Mo–Pd, equilibrium in, 18: 12694
Mo–Pd, equilibrium diagram of, 18: 36016
Mo–Pd, magnetic properties at 90 to 1100°F, 20: 7585(T) (ANL-Trans-251)
Mo–Pd, phase studies, 19: 11682
Mo–Pd–Re, properties as brazing material, 19: 24916(R) (GEMP-334A)
Mo–Pt, crystal structure of intermetallic compounds in, 19: 987
Mo–Pt, crystal structure of equiatomic intermetallic compound in, 19: 24994
Mo–Pt, crystallographic parameters, 17: 18822

Mo–Pt, phase diagram, 16: 30332 (WAL-TR-823/5)
Mo–Pt, phase studies, 16: 24185(T) (AERE-Trans-884)
Mo–Pt, phase studies, 18: 32190
Mo–Pt, superconductivity transition temperature of $Mo_3(Mo_{0.4}Pt_{0.6})$, 20: 7597
Mo–Pt, thermoelectric properties, 18: 14177
Mo–Pu, phase diagram, 17: 16567
Mo–Pu, phase diagram, 18: 7220(R) (JPRS-22599)
Mo–Pu, phase diagrams of, 18: 16493
Mo–Pu, phase studies and properties of, bibliographic study of, 16: 32115 (KFK-105)
Mo–Pu–U, analysis for plutonium, review of method for, 20: 10797
Mo–Pu–U, burnup in fast reactors, 18: 17290(T) (AEC-tr-6359)
Mo–Pu–U, burnup testing, 18: 19392
Mo–Pu–U, casting procedures for, 19: 40978 (ANL-6955)
Mo–Pu–U, combustion of, effects of fabrication on, 19: 17174(R) (ANL-6900(p.232-303))
Mo–Pu–U, corrosion by air, 19: 2753
Mo–Pu–U, corrosion in air, 19: 11679
Mo–Pu–U, corrosion by air at room temperature, 19: 44587(R) (ANL-7000, pp 3-63)
Mo–Pu–U, development and fabrication for ZPPR and ZPR-VI fuels, 20: 3320(R) (ANL-7082, pp 1-28)
Mo–Pu–U, development for SEFOR fuels, 20: 38531 (GEAP-5133)
Mo–Pu–U, fabrication and radiation behavior of, 17: 19561 (HW-75007 (Paper 4))
Mo–Pu–U, fabrication and properties for use as fuel element in Rapsodie, 18: 17290(T) (AEC-tr-6359)
Mo–Pu–U, fabrication and properties for use in zero-power reactors, 18: 44925(R) (ANL-6923(p.14-45))
Mo–Pu–U, fabrication of clad, specifications for, 19: 17176(R) (ANL-6965(p.1-41))
Mo–Pu–U, fabrication for ZPR fuel elements, 20: 16060(R) (ANL-7152, pp 1-49)
Mo–Pu–U, ignition of, effects of molybdenum content on, 20: 5843
Mo–Pu–U, ignition temperatures in dry and wet air, 18: 15426(R) (ANL-6810)
Mo–Pu–U, ignition temperatures in air, 18: 15663(R) (ANL-6808)
Mo–Pu–U, oxidation by air at 24°C, 18: 15663(R) (ANL-6808)
Mo–Pu–U, performance as zero-power reactor fuel, 18: 24952(R) (ANL-6880(p.6-48))
Mo–Pu–U, performance as zero-power-reactor fuel, 18: 36751 (ANL-6912)
Mo–Pu–U, performance in fast breeder reactor (E/T), 19: 3613 (CEA-R-2450)
Mo–Pu–U, phase studies, 18: 26893(R) (ANL-6868(p.11-108))
Mo–Pu–U, phase transformations in, at 350 to 500°C, 16: 25786
Mo–Pu–U, preparation and properties, 18: 37601 (A/CONF.28/P/58)
Mo–Pu–U, properties of, as reactor fuel for Rapsodie, 16: 4482
Mo–Pu–U, properties as reactor fuel, 17: 8763
Mo–Pu–U, properties for use in RAPSODIE, 17: 19570 (HW-75007 (Paper 15))
Mo–Pu–U, properties as zero-power reactor fuels, 18: 26824(R) (ANL-6885)
Mo–Pu–U, properties, 19: 4647 (CEA-R-2531)
Mo–Pu–U, properties of cast, 19: 44587(R) (ANL-7000, pp 3-63)
Mo–Pu–U, properties of, compressive, thermal expansion, and tensile, 20: 5843
Mo–Pu–U, radiation effects on, 16: 32135 (ANL-6429)
Mo–Pu–U, radiation effects on, 17: 16572
Mo–Pu–U, radiation effects on, 18: 2369
Mo–Pu–U, radiation stability, 18: 17290(T) (AEC-tr-6359)
Mo–Pu–U, radiation effects on dimensions of, in-pile, 18: 37736 (A/CONF.28/P/145)
Mo–Pu–U, reactions of, with stainless steel as canning material, 16: 4484
Mo–rare earth, preparation, 17: 8795(P)
Mo–Re, a-c conductivity of superconducting, 17: 41541 (BSD-TDR-63-147)
Mo–Re, analysis for rhenium by anion exchange, 19: 13220
Mo–Re, bonding to refractory metals, temperature requirements for solid-state diffusion, 17: 25688(R) (GEMP-177A)
Mo–Re, brittle fracture and twinning in, relation of, 17: 25772 (ASD-TDR-63-360)
Mo–Re, compatibility with oxide mixtures of aluminum, beryllium, calcium, and magnesium at high temperatures, 17: 41354 (NP-13158)
Mo–Re, compatibility and encapsulation with neodymium, promethium, and samarium oxides, 20: 11267 (BNWL-SA-488)
Mo–Re, corrosion by lithium at high temperatures, 20: 2269
Mo–Re, corrosion by bismuth and tin, 20: 2275
Mo–Re, corrosion by bismuth and tin at 1000°C, (E), 20: 21566(R) (ANL-7055, pp 213-29)
Mo–Re, creep and stress-rupture properties at 1600°C, 19: 40961
Mo–Re, creep-rupture testing at high temperatures, 17: 25688(R) (GEMP-177A)
Mo–Re, creep-rupture properties at high temperatures, 18: 7121(R) (GEMP-29A)
Mo–Re, creep-rupture properties at high temperatures, 20: 17011 (CONF-651025-14)
Mo–Re, creep-rupture properties at 1600°C of, comparison of, with other refractory metals and alloys, 20: 27485(R) (GEMP-400A, pp 21-61)
Mo–Re, crystal structure, 16: 16705 (62-GC-206)
Mo–Re, development for nuclear rocket nozzles, 19: 40254
Mo–Re, development, 20: 2223(R) (GEMP-51A)
Mo–Re, dislocation twinning in, mechanism, 18: 26063
Mo–Re, dislocation structures in annealed and deformed sheets of, 20: 5846
Mo–Re, dislocation pile-ups in, 20: 23681
Mo–Re, ductility and crystal structure of, deformation testing of, 18: 32176
Mo–Re, ductility, phase studies, and properties of, 20: 2323 (GEMP-314)
Mo–Re, elastic properties of, determination by ultrasonics, 19: 40112(R) (ANL-7046(p.36-66))
Mo–Re, electric and thermal conductivities at low temperature in magnetic field, 19: 6297 (ML-TDR-64-176)
Mo–Re, electric and thermal conductivity of superconducting, 20: 4361 (AD-619719)
Mo–Re, electric and thermal conductivity of superconducting, critical field measurements from, (E), 20: 13686
Mo–Re, electric conductivity at 300°K, effects of 1% iron solute on, 18: 12688
Mo–Re, electric conductivity of nonideal superconducting, a-c, 18: 18836
Mo–Re, electric conductivity at 1.5 to 77°K, 18: 34183
Mo–Re, electrical properties, 17: 8810 (NP-12451)
Mo–Re, fabrication by powder metallurgy, 17: 8728
Mo–Re, fabrication, properties, testing, and uses of superconducting of, 19: 16110
Mo–Re, fabrication of sheets of high-purity, 19: 24955(R) (USBM-RC-1157)
Mo–Re, fabrication, properties, and uses of, 20: 29768
Mo–Re, grain boundary structure in, internal friction studies of, 20: 15128
Mo–Re, grain boundary grooving in, mechanisms of, 20: 31672
Mo–Re, hardness, 17: 11094(R) (NMI-2113)
Mo–Re, hardness and tensile properties, 16: 20955(R) (NMI-2105)
Mo–Re, hardness at 1000 to 1200°C, 17: 25689(R) (NMI-2115)
Mo–Re, hydrogen affinity of, 18: 24165
Mo–Re, internal friction in deformed crystals of, 18: 26041(T)
Mo–Re, internal friction of annealed and deformed, 20: 5846
Mo–Re, internal friction in deformed, 20: 19250
Mo–Re, longitudinal critical currents in cold-drawn superconducting, 17: 14961
Mo–Re, longitudinal critical electric currents in, 17: 34549(R) (ORNL-3480(p.41-5))
Mo–Re, magnetic and resistive transitions of, 18: 11131
Mo–Re, magnetic properties of superconducting, effects of temperature on critical field, 16: 15467
Mo–Re, magnetic susceptibility and hydrogen affinity, 17: 3523
Mo–Re, magnetic susceptibility and specific heat of superconducting binary complex phases of, 18: 37715
Mo–Re, magnetic susceptibility, 19: 7888 (AD-607799)
Mo–Re, maximum critical field of superconductors of, 17: 8959
Mo–Re, mechanical properties, 17: 8729
Mo–Re, mechanical properties and microstructure of, 17: 22176
Mo–Re, mechanical properties of sintered, effects of argon and hydrogen at high temperatures on, 17: 41341(R) (GEMP-27A(p.9-24))
Mo–Re, mechanical properties at 1600°C in hydrogen, 19: 11669(R) (GEMP-41A)
Mo–Re, performance as superconducting solenoids, (E), 19: 10189 (RLE-TR-427)
Mo–Re, performance of superconducting for linac resonant cavities, 19: 27012 (MURA-714(p.540-4))
Mo–Re, phase diagram, 17: 8727
Mo–Re, phase precipitation in, sigma, 18: 44162
Mo–Re, plastic properties at room temperature, 20: 35906
Mo–Re, preparation, 16: 10534(R) (NMI-2102)
Mo–Re, properties of electron-beam-melted, 16: 19280
Mo–Re, properties as superconducting magnets, 17: 24053(R) (ORNL-3432)
Mo–Re, properties for high-temperature thermocouples, 17: 29170(R) (ASD-TDR-63-233)
Mo–Re, properties as superconducting magnet, 17: 32712 (LNF-63/26)
Mo–Re, properties at high temperatures, 17: 34409(R) (NMI-1253)
Mo–Re, properties for thermocouples, 18: 4292
Mo–Re, properties for use in electron tubes, 19: 4698

Mo–Re, properties of sigma-phase precipitates in, 20: 5851
Mo–Re, properties of porous, for cesium ionization, 20: 31388
Mo–Re, purification process variables, 19: 44598(R) (GEMP-49A)
Mo–Re, purification by wet hydrogen, 20: 7499(R) (GEMP-53A)
Mo–Re, purification methods for, 20: 33770(R) (GEMP-59A)
Mo–Re, radiation effects on sigma phase structure of, 19: 37051
Mo–Re, radiation effects on tensile properties of, effects of annealing temperature on fast-neutron, 20: 27409(R) (GEMP-58A)
Mo–Re, radiation effects on hot-hardness of, effects of test temperature on fast-neutron, 20: 27582(R) (GEMP-400A, pp 63-98)
Mo–Re, reactions with beryllium, hafnium, and magnesium oxides at 2450°C, 19: 44598(R) (GEMP-49A)
Mo–Re, relation between structure anisotropy and superconducting anisotropy in, 17: 20493
Mo–Re, segregation in, 17: 8810 (NP-12451)
Mo–Re, slip and cleavage planes in, 19: 37035(R) (N64-29195)
Mo–Re, stress-rupture and creep properties at 2200°C, 17: 34399 (CONF-94-4)
Mo–Re, stress-rupture and creep properties, 18: 41933 (TID-11295 (3rd Ed.))
Mo–Re, stress-rupture at 1600°C in hydrogen, 19: 24916(R) (GEMP-334A)
Mo–Re, stress-rupture properties at high temperatures, 19: 37146
Mo–Re, stress-rupture at 2200°C in hydrogen, 16: 32034(R) (GEMP-15A)
Mo–Re, superconducting, critical fields in bulk and wire form, 16: 15427
Mo–Re, superconductivity, 16: 16830
Mo–Re, superconductive properties and technical applications of, 17: 16705
Mo–Re, superconductivity, 17: 34438
Mo–Re, superconductivity and uses of Mo_3Re, 17: 34451
Mo–Re, superconductivity, 17: 41604
Mo–Re, superconducting transitions in, 18: 15071
Mo–Re, superconductivity of, 18: 15084
Mo–Re, superconducting properties of, (E/T), 20: 2890 (AFML-TR-65-154)
Mo–Re, superconductivity, 20: 40047
Mo–Re, superconducting transition temperature of 90Mo–10Re, pressure effects on, 20: 44568
Mo–Re, surface tension and solid surface energy of, 20: 31773
Mo–Re, tensile properties of high-purity, 19: 24955(R) (USBM-RC-1157)
Mo–Re, thermal capacity of solid solutions of, at low temperatures, 19: 4703
Mo–Re, thermal expansion to 2500°C, 19: 41009 (GEMP-375)
Mo–Re, thermal expansion of, at 25 to 2500°C, 20: 27552
Mo–Re, thermal properties up to 2500°C, enthalpy and thermal expansion, 19: 16071 (GE-TM-64-2-8)
Mo–Re, thermoelectric properties at 1000 to 2000°C, (E), 19: 40859
Mo–Re, twin formation in, kinetics of, 18: 32131 (ASD-TDR-63-360(Pt.II))
Mo–Re, twinning in, 17: 8810 (NP-12451)
Mo–Re, twinning of, transmission electron microscopic studies of, 18: 32164
Mo–Re–Ta, fabrication and properties, 16: 514(R) (AD-255012)
Mo–Re–W, bend testing at high temperatures, 18: 7121(R) (GEMP-29A)
Mo–Re–W, creep and stress rupture at 1600 to 2000°C in hydrogen, 19: 24916(R) (GEMP-334A)
Mo–Re–W, creep at 1600 and 2200°C, 20: 2223(R) (GEMP-51A)
Mo–Re–W, creep properties of, effects of molybdenum and rhenium content on, 19: 37030(R) (GEMP-47A, pp 27-84)
Mo–Re–W, creep-rupture properties, effects of composition on, 19: 44598(R) (GEMP-49A)
Mo–Re–W, creep-rupture properties of, effects of composition on, 20: 27485(R) (GEMP-400A, pp 21-61)
Mo–Re–W, creep-rupture properties at 1600°C of, comparison of, with other refractory metals and alloys, 20: 27485(R) (GEMP-400A, pp 21-61)
Mo–Re–W, development of molybdenum-base and tungsten-base alloys of, 20: 7499(R) (GEMP-53A)
Mo–Re–W, ductility and melting points of sintered, 19: 20584
Mo–Re–W, ductility of, effects of annealing temperature on bend, 19: 37030(R) (GEMP-47A, pp 27-84)
Mo–Re–W, ductility of, effects of composition on, 20: 2223(R) (GEMP-51A)
Mo–Re–W, ductility and hardness of, effects of composition and heat treatments to 2400°C on, 20: 7499(R) (GEMP-53A)
Mo–Re–W, fabrication and mechanical properties, 19: 894(R) (GEMP-39A)
Mo–Re–W, fabrication of, effects on properties, 19: 11669(R) (GEMP-41A)
Mo–Re–W, fabrication of, methods development for, 19: 18390(R) (GEMP-43A)
Mo–Re–W, fabrication of seamless tubing of, procedures for, 19: 44598(R) (GEMP-49A)
Mo–Re–W, fabrication and properties of, 20: 2354(R) (USBM-RC-1205, pp 15-19)
Mo–Re–W, fabrication of thin-walled tubing of, 20: 5867
Mo–Re–W, fabrication process development, 20: 7499(R) (GEMP-53A)
Mo–Re–W, fabrication process development, 20: 13251(R) (GEMP-55A, pp 57-82)
Mo–Re–W, fabrication of rods of, by extrusion and sintering, 20: 16989(R) (COO-1518-2)
Mo–Re–W, fabrication into sheet, plate, and rods, process development for, 20: 27443(R) (GEMP-400A, pp 109-33)
Mo–Re–W, fabrication and purification methods for, 20: 33770(R) (GEMP-59A)
Mo–Re–W, fabrication of tubing of, by extrusion or thermochemical deposition, 20: 33845 (ORNL-P-2203)
Mo–Re–W, fission product release, 19: 44599(R) (GEMP-50A)
Mo–Re–W, mechanical properties at high temperatures and phase studies, 17: 41341(R) (GEMP-27A(p.9-24))
Mo–Re–W, mechanical properties of, effects of composition on, 18: 16424(R) (GEMP-270A)
Mo–Re–W, mechanical properties of, effects of heat treatments on, 19: 18390(R) (GEMP-43A)
Mo–Re–W, mechanical properties at high temperatures and melting of, 19: 24916(R) (GEMP-334A)
Mo–Re–W, mechanical properties of, at high temperatures, effects of hydrogen on, 20: 33770(R) (GEMP-59A)
Mo–Re–W, nuclear reactions in, thermal-neutron, 20: 27582(R) (GEMP-400A, pp 63-98)
Mo–Re–W, phase diagram at 1000°C, 17: 8727
Mo–Re–W, phase diagrams for transmutation studies, electron-concentration, 20: 13251(R) (GEMP-55A, pp 57-82)
Mo–Re–W, phase studies, 19: 24916(R) (GEMP-334A)
Mo–Re–W, precipitation of sigma-phase in, effects of composition and temperature on, 20: 7499(R) (GEMP-53A)
Mo–Re–W, production of high-purity, 19: 24916(R) (GEMP-334A)
Mo–Re–W, production of sleeves of, process development for, 20: 25479(R) (USBM-RC-1232)
Mo–Re–W, properties, 19: 40961
Mo–Re–W, properties as carbon-diffusion-barrier for hafnia thermocouple insulators at 2450°C, 20: 7499(R) (GEMP-53A)
Mo–Re–W, recovery of scrap, methods for, 20: 41429(R) (USBM-RC-1249)
Mo–Re–W, sectioning of, method for submicron, 20: 2321(R) (GEMP-52A, pp 43-5)
Mo–Re–W, stress-rupture properties, 19: 40961
Mo–Re–W, tensile properties at 25 and 1600°C, 20: 7499(R) (GEMP-53A)
Mo–Re–W, thermoelectric properties, 19: 894(R) (GEMP-39A)
Mo–Re–W, weld integrity of, effects of carbon and oxygen on, 20: 13251(R) (GEMP-55A, pp 57-82)
Mo–Rh, equilibrium diagram of, 18: 36016
Mo–Rh, phase studies, 20: 11309
Mo–Rh–Ti, superconductivity, 18: 21112
Mo–Ru, analysis of, for ruthenium, 16: 31554
Mo–Ru, enhanced superconductivity in plasma-jet sprayed, 18: 37625
Mo–Ru, equilibrium diagram of, 18: 36016
Mo–Ru, fabrication and properties, 17: 1865
Mo–Ru, magnetic susceptibility and specific heat of superconducting binary complex phases of, 18: 37715
Mo–Ru–U, mictrostructure and phases of heat-treated, 18: 42051
Mo–Sc, phase studies, 18: 12623 (ASD-TDR-63-204)
Mo–Sc, phase studies of solid solution formation in, 19: 41050
Mo–Sn, crystal structure of $MoSn_{1-5}$, 19: 28837
Mo–Sn, preparation and crystal structure of Mo_3Sn, 19: 7936
Mo–Sn–U, fission effects on, reduction of swelling in, 18: 24996(R) (NAA-SR-8888(Sect.VI))
Mo–Sn–Zr, corrosion by steam and water, 17: 39659
Mo–Ta, corrosion of, by fluorine-containing fluids, 17: 8750(P)
Mo–Ta, crystal structure of electron-beam zone-refined, 20: 21364
Mo–Ta, electric conductivity of, effects of composition on, 20: 11227
Mo–Ta, electric conductivity of single-crystal, specific, 20: 17083
Mo–Ta, fabrication and properties, 17: 29312(R) (ASD-TDR-62-594(Pt.II))
Mo–Ta, fabrication and properties at high temperatures, 18: 7178
Mo–Ta, fabrication and tensile properties at high temperatures, 18: 12562(R) (X63-12299)
Mo–Ta, mechanical properties, 17: 31010
Mo–Ta, mechanical properties of single-crystal, 20: 11227
Mo–Ta, mechanical properties of single-crystal, 20: 21364
Mo–Ta, preparation of, by electron-bombardment zone-melting methods, 16: 32046
Mo–Ta, properties of wrought, 17: 6672 (NP-12383)
Mo–Ta, properties, electrical and mechanical, 19: 16082 (UCRL-11752)
Mo–Ta, properties of single-crystal, electric and mechanical, 20: 31715(R) (UCRL-16658, pp 105-20)
Mo–Ta, tensile properties at high temperatures, 17: 30962(R) (ASD-TDR-63-238)
Mo–Ta, thermal expansion of, 20: 43964
Mo–Ta–V, mechanical properties, 17: 31010

Mo–Ta–V, phase diagram, 19: 41036
Mo–Ta–W, availability, properties, and uses of, 20: 29760
Mo–Ta–W, corrosion of, by fluorine-containing fluids, 17: 8750(P)
Mo–Ta–W, fabrication and properties of, alloying effects of carbon, hafnium, rhenium, and zirconium on, 17: 29312(R) (ASD-TDR-62-594(Pt.II))
Mo–Ta–W, fabrication and mechanical properties of sheet of, 19: 11700 (ML-TDR-64-63)
Mo–Ta–W, fabrication of tantalum-base, process development for, 20: 11260
Mo–Ta–W, mechanical properties, 17: 3465 (ASD-TDR-62-594)
Mo–Ta–W, mechanical properties, 17: 31010
Mo–Ta–W, properties of, data tabulations of mechanical, metallurgical, and physical, 18: 5774 (DMIC-189)
Mo–Ta–W, tensile properties at 3000°F, 18: 12562(R) (X63-12299)
Mo–Tc, crystalline-phase and superconducting properties of, 17: 11363
Mo–Tc, magnetic susceptibility, 18: 12680
Mo–Tc, phase studies on, 17: 11220
Mo–Tc, phase studies by x-ray diffraction, 17: 36308
Mo–Tc, superconducting, transition temperature maxima in, 16: 22632
Mo–Tc, superconductivity, 17: 41604
Mo–Th, corrosion by water at 120 to 260°C, 19: 22889 (ANL-7006)
Mo–Th, phase diagrams, 17: 6659 (IS-442)
Mo–Th–U, mechanical properties and phase studies at high temperatures, 17: 12660 (ATL-A-128)
Mo–Th–Zr, properties and structure of, 18: 37670 (A/CONF.28/P/337)
Mo–Ti, aging kinetics of, at 1300 to 1500°K, 20: 41466
Mo–Ti, atomic arrangements in solid solutions in, 16: 25772 (NYO-7062)
Mo–Ti, axial load fatigue tests on, 18: 18282 (BNL-844)
Mo–Ti, bonding to foils of nickel, niobium, tantalum, and titanium by vacuum hot-pressing, 20: 5866
Mo–Ti, brittle-ductile transition temperature and high-temperature strain aging in, 16: 12080(R) (AD-259795)
Mo–Ti, cavitation damage in bismuth–lead alloy at 500°F, 19: 24938 (NP-15024)
Mo–Ti, cavitation in bismuth–lead alloy at 500 and 1500°F, ultrasonic-induced, 19: 39116 (NP-15263)
Mo–Ti, cavitation damage in bismuth–lead alloy at 500 and 1500°F, 20: 771 (NP-15558)
Mo–Ti, cavitation damage in mercury and water, 20: 16974 (NP-15889)
Mo–Ti, cavitation damage in liquid, at high temperatures, 20: 33835
Mo–Ti, coating evaluation for, 19: 9607 (ML-TDR-64-70)
Mo–Ti, coating with silicide for oxidation protection at high temperatures, 19: 7877 (ML-TDR-64-74)
Mo–Ti, coating with silicides, 19: 40998(P)
Mo–Ti, coating with silicon by fluidized-bed process, 20: 29630
Mo–Ti, compatibility with cesium at 2500°F, 18: 22444(R) (MSAR-63-126)
Mo–Ti, composition, crystal structure, and phases of precipitates in, 16: 22582 (ASD-TDR-62-7)
Mo–Ti, corrosion of, by potassium at 1000 to 1800°F, 16: 16679 (TID-7626(Pt.I)(p.63-8))
Mo–Ti, corrosion by boiling cesium, 19: 13913(R) (AFML-TR-64-327)
Mo–Ti, corrosion by lithium at 1500°F, 19: 36980 (PWAC-355)
Mo–Ti, crack-propagation resistance, 18: 5769 (AD-290278)
Mo–Ti, creep properties of, effects of nitriding on, 17: 41461
Mo–Ti, creep-rupture properties at 1500 and 1800°F, effects of helium, potassium, and vacuum on, 17: 35223(R) (SY-5396-R5)
Mo–Ti, creep-rupture properties at 1500 to 2000°F, effects of helium, potassium, and vacuum on, 18: 5728 (ASD-TDR-63-270(Pt.II))
Mo–Ti, creep rupture at 1500 to 2000°F, 18: 18282 (BNL-844)
Mo–Ti, creep rupture and fatigue evaluation of, 18: 29103(R) (APS-5071-R)
Mo–Ti, creep strength at 2300 to 3000°F, short-time, 20: 46182 (AD-630070)
Mo–Ti, creep tests on TZC and TZM at 3200°F, 20: 5885(R) (NAS-CR-54773)
Mo–Ti, critical current density of superconducting, in transverse field of 30 kgauss, 18: 6128
Mo–Ti, critical field for superconducting, temperature dependence of lower, (E/T), 19: 19031
Mo–Ti, critical field and magnetization of superconducting, Pauli spin and spin-orbit effects on, (E), 20: 37951
Mo–Ti, development for use in TORY IIA components, 17: 15472 (UCRL-7183)
Mo–Ti, diffusion of silicide coatings in, at 2500°C, 18: 39824 (NASA-TN-D-2039)
Mo–Ti, diffusion in bcc, 19: 23112
Mo–Ti, ductile-to-brittle transition temperature of sheet of, effects of recrystallization and welding on, 19: 41016 (N64-30997)
Mo–Ti, ductility transition temperature, effects of flexing on, 19: 9644(R) (AD-603067)
Mo–Ti, ductility of, effect of strain softening on, 19: 30722(R) (AD-608146)
Mo–Ti, effects of surface treatments on ductility measurements on, 19: 30722(R) (AD-608146)
Mo–Ti, effects of protective coatings on oxidation and properties of, 19: 47061
Mo–Ti, emissivity measurements at 800 to 5000°K, 18: 20566
Mo–Ti, erosion by water of rotating disks of, 19: 44625 (TIM-894)
Mo–Ti, erosion by mercury vapor at 640°F, 20: 11214(R) (NASA-CR-54717)
Mo–Ti, erosion by mercury, water, and bismuth–lead alloy, cavitation, 20: 29640 (NP-16048)
Mo–Ti, extrusion of, at 3200°F, 16: 12067(R) (ASD-TR-7-785(V))
Mo–Ti, extrusion of TM into tube shells, 18: 44049(R) (ORNL-3670 (p.77-111))
Mo–Ti, fabrication of rolled sheet, 17: 6597(R) (DMIC-176)
Mo–Ti, fabrication for grain growth control, 17: 11295(R) (AD-277713)
Mo–Ti, fabrication, oxidation, and properties of, 18: 35986 (ERR-FW-049A)
Mo–Ti, factors affecting vacuum-arc melting of, 18: 24070 (RTD-TDR-63-4089)
Mo–Ti, fatigue in helium, potassium, and vacuum at 1500 and 2000°F, 18: 6516 (SY-5396-R6)
Mo–Ti, forging characteristics, 16: 9162 (DMIC-Memo-143)
Mo–Ti, friction and wear of, at high temperatures and in vacuum, 16: 5708 (ASD-TR-61-301)
Mo–Ti, grain structure of ω-phase, 16: 6731
Mo–Ti, hardening of powdered, by internal oxidation, 16: 10539 (NP-11402)
Mo–Ti, hardness of dispersion-hardened, 17: 20480
Mo–Ti, joining to aluminum oxides by reaction pressing, 18: 44078
Mo–Ti, local order in, x-ray diffuse scattering studies of, 17: 36289 (ASD-TDR-63-567(Pt.1))
Mo–Ti, machining studies, 16: 10469(R) (ASD-TR-7-532a(V))
Mo–Ti, machining, 20: 15014
Mo–Ti, magnetization of high-field superconducting type-II, mixed state paramagnetism in, (E), 20: 8018
Mo–Ti, mechanical properties, 16: 3445 (ASD-TR-61-193)
Mo–Ti, mechanical properties, 16: 33455(R) (NP-12097)
Mo–Ti, mechanical properties of, effects of potassium vapor at 2000°F on, 17: 12036(R) (SY-5396-R3)
Mo–Ti, mechanical properties and preparation, 17: 14818 (DRI-2039)
Mo–Ti, mechanical properties of, effects of high-temperature potassium on, 17: 30939(R) (SY-5396-R4)
Mo–Ti, mechanical properties of, strain-softening effects on, 18: 24119 (AD-425148)
Mo–Ti, mechanical properties, 19: 13978 (AMRA-TR-64-16)
Mo–Ti, mechanical and wear properties, 19: 29732(R) (APS-5152-R2)
Mo–Ti, melting of, effects of composition on electron-beam, 20: 29674
Mo–Ti, microstructures, 19: 44610 (TIM-943)
Mo–Ti, nondestructive testing of tubes of, 18: 4255(R) (ORNL-3470 (p.98-125))
Mo–Ti, oxidation of, at 20 to 400°C, 16: 27684
Mo–Ti, oxidation of silicide-coated sheet of, by air at 2500°C, 18: 39825 (NASA-TN-D-2040)
Mo–Ti, performance as filament for titanium sublimation in getter ion pumps, evaporation rates for, 20: 27515
Mo–Ti, polygonization effects on elastic limit, microhardness, microstructure, and recrystallization, 17: 36317
Mo–Ti, polygonization effects on mechanical properties of, 18: 37722
Mo–Ti, preparation and properties of single crystals of, 20: 41481
Mo–Ti, properties of rolled sheet of, 19: 18447(R) (AD-423981)
Mo–Ti, properties at high temperatures, 20: 4418
Mo–Ti, quality control of, effects of melting procedures on, 16: 33455(R) (NP-12097)
Mo–Ti, radiation effects on bend properties of, neutron, 18: 32226 (ORNL-TM-880)
Mo–Ti, radiation effects on ductility of, fast-neutron, 18: 44049(R) (ORNL-3670(p.77-111))
Mo–Ti, shear strength of fasteners of, at room temperature and 1600°F, 17: 36281 (AD-295526)
Mo–Ti, solid-state bonding of, 18: 24112
Mo–Ti, solubility in cesium at 2500°F, 19: 13913(R) (AFML-TR-64-327)
Mo–Ti, sorptive properties for hydrogen, 17: 22206
Mo–Ti, specific heat, 20: 35841(R) (NAA-SR-11900)
Mo–Ti, spectral emissivity of Chromalloy W-2-coated, 17: 41363 (WADD-TR-60-646(Pt.II))
Mo–Ti, strain softening by flexing of sheet of, 19: 7887(R) (AD-421621)
Mo–Ti, strain softening effects on properties of, 20: 2311 (AD-618925)
Mo–Ti, strength of, effects of carbon additions on, 17: 6672 (NP-12383)
Mo–Ti, strength of, effects of boron additions on, 17: 6672 (NP-12383)
Mo–Ti, stress-rupture properties at 1090 to 1315°C, 18: 4255(R) (ORNL-3470(p.98-125))

Mo–Ti, superconducting properties of, 17: 8973
Mo–Ti, superconducting transitions in high magnetic fields, 17: 25938
Mo–Ti, superconductivity of, 18: 15084
Mo–Ti, superconducting transition temperature, effects of phase transformation on, 18: 42050(T) (AI-Trans-49)
Mo–Ti, superconducting properties, 18: 44681
Mo–Ti, superconductivity and phase transformations, 19: 7965
Mo–Ti, superconducting transition anomalies in, (E), 19: 10214
Mo–Ti, tensile properties at high temperatures, effects of nitriding on, 17: 23989
Mo–Ti, tensile properties, 17: 27878
Mo–Ti, tensile properties of, effects of working reduction, stress-relief annealing, and grain size on, 20: 11227
Mo–Ti, thermal absorbance, emittance, and reflectance, 16: 9193 (DMIC-Memo-141)
Mo–Ti, thermal properties of, at 500 to 5000°F, 17: 16636 (ASD-TDR-62-765)
Mo–Ti, transformation characteristics during continuous cooling, 18: 20545
Mo–Ti, use as reinforcing media in refractory ceramic coatings on N-155 superalloy, 19: 9608 (ML-TDR-64-81)
Mo–Ti, welding, effects of various parameters for ultrasonic, 16: 20987(R) (AD-266249)
Mo–Ti, welding of, ultrasonic, 16: 19295 (ASD-TR-7-888(1))
Mo–Ti, welding of, power-force programmed ultrasonic, 18: 12594 (AD-427997)
Mo–Ti, welding of, ultrasonic, 19: 16025 (AD-425218)
Mo–Ti, welding, use of power-force programming in ultrasonic, 19: 13933(R) (AD-422935)
Mo–Ti–U, corrosion cracking in air, stress-, 20: 11224
Mo–Ti–U, metallurgical properties of, fabrication effects on, 17: 22101 (WAL-TR-420.5/1)
Mo–Ti–U, stress cracking of gamma-phase, 19: 30749 (UCRL-14132)
Mo–Ti–U, tensile properties, 19: 30749 (UCRL-14132)
Mo–Ti–U, transformation diagram and kinetics of, 17: 25769(R) (AMRA-CR-63-02/1(F))
Mo–Ti–U, transformation kinetics of, isothermal, 18: 18405
Mo–Ti–V, aging characteristics and phase studies of, 16: 6743
Mo–Ti–V, corrosion by sodium at 650°C, 19: 31462(R) (ANL-7028)
Mo–Ti–V, corrosion by sodium at 650°C, effects of oxygen on, 19: 35604(R) (ANL-7045(p.1-23))
Mo–Ti–V, creep and tensile properties of, at 1800°F, 16: 6747
Mo–Ti–V, development of refractory, for use in oxygen-contaminated sodium systems, (E), 20: 14007(R) (ANL-7122, pp 1-41)
Mo–Ti–V, elastic properties and shear modulus of annealed and quenched, 18: 35999
Mo–Ti–V, elastic properties, 20: 6556(R) (ANL-7105, pp 36-58)
Mo–Ti–V, fabrication for fuel-coating tests, 19: 14765(R) (ANL-6977)
Mo–Ti–V, properties as fuel cladding, 19: 24064(R) (ANL-6997)
Mo–Ti–Zr, analysis for titanium and zirconium by ion exchange, 20: 3896
Mo–Ti–Zr, analysis for alloying elements and impurities, comparison of results from 25 laboratories on TZM, 20: 18567 (MAB-217-M)
Mo–Ti–Zr, analysis using vacuum cup electrode, 19: 22103 (TIM-904)
Mo–Ti–Zr, bend ductility of TZM, effects of argon atmosphere contamination on, 19: 9592(R) (ASD-8-170(IV))
Mo–Ti–Zr, bend-transition temperature in TZM, 19: 24976(R) (AD-612759)
Mo–Ti–Zr, bonding of TZM, method for diffusion, 20: 5867
Mo–Ti–Zr, brazing developments for, 18: 549(R) (NP-13241)
Mo–Ti–Zr, brazing molybdenum to TZM, brazing alloy development for, 20: 5866
Mo–Ti–Zr, brazing of TZM, exothermic, 17: 27760(R) (NP-12901)
Mo–Ti–Zr, brazing techniques for TZM, 19: 30690(R) (ML-TDR-64-270)
Mo–Ti–Zr, brazing tungsten carbide–cobalt cermet to TZM, use of boron–nickel–silicon for, 20: 4307(R) (ORNL-3870, pp 238-42)
Mo–Ti–Zr, brittle-ductile transition temperature and high-temperature strain aging in, 16: 12080(R) (AD-259795)
Mo–Ti–Zr, cavitation damage to TZM, in liquid sodium, 20: 2243
Mo–Ti–Zr, cavitation damage of TZM in liquid sodium to 1500°F, 20: 46154 (NASA-CR-72035)
Mo–Ti–Zr, coating evaluation for TZM, oxidation-resistant, 19: 36945 (AD-610867)
Mo–Ti–Zr, coating of TZM, with platinum and platinum–rhodium alloy, 18: 20445(R) (AD-434441)
Mo–Ti–Zr, coating of TZM, with palladium–platinum alloy and platinum, 18: 34029(R) (AD-601740)
Mo–Ti–Zr, coating of TZM for oxidation protection at high temperatures, 19: 7845(R) (AD-608135)
Mo–Ti–Zr, coating of TZM for oxidation, 19: 36957(R) (NP-15113)
Mo–Ti–Zr, coating with silicides, 19: 40998(P)
Mo–Ti–Zr, coatings for TZM foils, development of high-temperature oxidation-resistant, 18: 30118(R) (RTD-TDR-63-4006(Pt.I))
Mo–Ti–Zr, compatibility of TZM, with niobium–zirconium alloy in flowing zirconium, 20: 2238
Mo–Ti–Zr, compatibility of TZM, with niobium–1 zirconium alloy in refluxing potassium at 2000°F, 20: 13192(R) (NASA-CR-54843)
Mo–Ti–Zr, compatibility of TZM, with alumina, beryllia, magnesia, and boron nitride, 20: 17022 (N-65-18933)
Mo–Ti–Zr, compression properties at room-temperature of TZM, 19: 24976(R) (AD-612759)
Mo–Ti–Zr, contamination by residual gases in vacuum systems, 18: 14355 (CONF-373-7)
Mo–Ti–Zr, contamination of TZM by residual gases in high vacuum, 18: 39826 (ORNL-3674)
Mo–Ti–Zr, contamination of TZM by rolling in argon atmosphere, 19: 9592(R) (ASD-8-170(IV))
Mo–Ti–Zr, corrosion of platinum- and platinum–rhodium-clad TZM, by air at 2550°F, 18: 20445(R) (AD-434441)
Mo–Ti–Zr, corrosion by potassium at 2000 to 2200°F, 18: 24091
Mo–Ti–Zr, corrosion by potassium vapor, design of test capsule for, 19: 20473(R) (NASA-CR-54629)
Mo–Ti–Zr, corrosion of TZM by boiling potassium, 19: 34640 (CNLM-6246)
Mo–Ti–Zr, corrosion by cesium and lithium above 2500°F, 19: 28766
Mo–Ti–Zr, corrosion of TZM, by potassium at high temperatures, 20: 2271
Mo–Ti–Zr, corrosion of TZM, by potassium, 20: 4301(R) (ORNL-3870, pp 102-35)
Mo–Ti–Zr, corrosion by cesium vapor and liquid lithium at 2500 to 3400°F of TZM, 20: 5851
Mo–Ti–Zr, corrosion by potassium at 1010°C of TZM, 20: 7518 (PWAC-501)
Mo–Ti–Zr, corrosion of TZM, by sodium at high temperatures, 20: 25474(R) (BNL-954, pp 122-67)
Mo–Ti–Zr, corrosion of TZM, by potassium at 1600°F, 20: 27432(R) (NASA-CR-54892)
Mo–Ti–Zr, corrosion by hydrochloric, phosphoric, and sulfuric acids at high temperatures, 20: 46158
Mo–Ti–Zr, creep and stress-rupture properties of TZM, in hydrogen at 2000 and 2200°C, 18: 7121(R) (GEMP-29A)
Mo–Ti–Zr, creep of TZM at 2000 and 2130°F, long-time, 19: 18459(R) (NASA-CR-54287)
Mo–Ti–Zr, creep properties in ultra-high vacuum of TZM, long-time, 19: 37039(R) (NASA-CR-54393)
Mo–Ti–Zr, creep properties of TZM, 20: 4301(R) (ORNL-3870, pp 102-35)
Mo–Ti–Zr, creep properties of TZM, 20: 29705(R) (NAS-CR-54973)
Mo–Ti–Zr, creep rupture and fatigue evaluation of TZM, 18: 29103(R) (APS-5071-R)
Mo–Ti–Zr, creep tests on TZC and TZM at high temperatures, 20: 21346(R) (NASA-CR-54895)
Mo–Ti–Zr, dislocation structure in, effects of cold working on, 19: 41015 (MIL-TDR-64-282)
Mo–Ti–Zr, elongation tests and fabrication studies of TZM sheet, 19: 13949(R) (NP-14768)
Mo–Ti–Zr, erosion by sodium at 400, 1000, and 1500°F of TZM, 20: 769(R) (NASA-CR-54459)
Mo–Ti–Zr, erosion by mercury vapor at 640°F of TZM, 20: 11214(R) (NASA-CR-54717)
Mo–Ti–Zr, extrusion of, at 2300 to 2700°F, process evaluation for, 16: 12066(R) (ASD-TR-7-785(IV))
Mo–Ti–Zr, extrusion of tubes of TZM, 17: 41333(R) (ANL-6677)
Mo–Ti–Zr, extrusion of TZM into tube shells, 18: 44049(R) (ORNL-3670(p.77-111))
Mo–Ti–Zr, extrusion of TZM at room temperature, hydrostatic, 19: 6277 (ML-TDR-64-205)
Mo–Ti–Zr, extrusion of TZM into T-sections, 19: 7874(R) (ASD-TDR-7-911(V))
Mo–Ti–Zr, extrusion of complex shapes of TZM, using ceramic dies, 19: 9636(R) (NMI-9700-24)
Mo–Ti–Zr, extrusion of thin H-sections of TZM, 19: 13952(R) (RTD-TR-8-112(Vol.IV))
Mo–Ti–Zr, extrusion of thin H-sections of TZM, 19: 18431(R) (RTD-TR-8-112(V))
Mo–Ti–Zr, extrusion by Dynapak process of TZM, 19: 30686(R) (AD-608945)
Mo–Ti–Zr, extrusion of TZM, process for, 20: 5867
Mo–Ti–Zr, fabrication of rolled sheet, 17: 6597(R) (DMIC-176)
Mo–Ti–Zr, fabrication by vacuum rolling, 17: 36270
Mo–Ti–Zr, fabrication of honeycomb structures of, 17: 36271
Mo–Ti–Zr, fabrication and properties of extruded and rolled, 18: 5727(R) (AD-294579)
Mo–Ti–Zr, fabrication and properties of extruded and sintered TZM, 18: 10449(R) (IITRI-B247-12)
Mo–Ti–Zr, fabrication and testing of brazed honeycomb sandwich panels

of TZM, 18: 10494 (AD-427700(p.245-80))
Mo–Ti–Zr, fabrication by extrusion, 18: 12601(R) (RTD-TR-8-112)
Mo–Ti–Zr, fabrication and properties of cast and extruded, 18: 12536(R) (AD-412904)
Mo–Ti–Zr, fabrication of TZM, by extrusion, 18: 18329(R) (ASD-TDR-7-945(IV))
Mo–Ti–Zr, fabrication and properties of extruded and rolled, 18: 22412(R) (AD-422106)
Mo–Ti–Zr, fabrication and properties of forged TZM, 18: 22414(R) (ASD-TR-7-756(X))
Mo–Ti–Zr, fabrication, oxidation, and properties of, 18: 35986 (ERR-FW-049A)
Mo–Ti–Zr, fabrication and properties of forged TZM, 19: 6240(R) (ASD-8-170(V))
Mo–Ti–Zr, fabrication of TZM powder compacts, 19: 7874(R) (ASD-TDR-7-911(V))
Mo–Ti–Zr, fabrication of TZM into thin H-sections by extrusion and drawing, process development for, 19: 7878(R) (RTD-TR-8-112(I))
Mo–Ti–Zr, fabrication and properties, 19: 11676
Mo–Ti–Zr, fabrication of honeycombed-sandwich panels from TZM, 20: 7541
Mo–Ti–Zr, fabrication of missile nose tips of TZM by shear spinning, 20: 25508 (AD-631423)
Mo–Ti–Zr, factors affecting vacuum-arc melting of, 18: 24070 (RTD-TDR-63-4089)
Mo–Ti–Zr, fasteners for use to 3000°F, 19: 32702(R) (AD-609653)
Mo–Ti–Zr, fatigue behavior at high temperatures in ultrahigh vacuum, 20: 824(R) (NASA-CR-54458)
Mo–Ti–Zr, fatigue in sodium at 1000 and 1500°F of TZM, high-frequency, 20: 769(R) (NASA-CR-54459)
Mo–Ti–Zr, fatigue properties at 982°C of stress-relieved TZM, notched, 20: 7572(R) (NASA-CR-54775)
Mo–Ti–Zr, fatigue properties of TZM, at high temperatures, 20: 31710(R) (NASA-CR-54983)
Mo–Ti–Zr, fatigue tests on TZC and TZM at high temperatures, 20: 21347(R) (NASA-CR-54916)
Mo–Ti–Zr, fatigue testing of TZM in liquid sodium at 1000 and 1500°F, high-frequency, 20: 46154 (NASA-CR-72035)
Mo–Ti–Zr, forging of, studies of plasticity in, 17: 18721(T) (FTD-TT-62-1789)
Mo–Ti–Zr, forging of TZM at 2400°F, 18: 44097 (ML-TDR-64-228)
Mo–Ti–Zr, hardness and recrystallization of TZM, at high temperatures, 17: 27760(R) (NP-12901)
Mo–Ti–Zr, joining of, by fiber metal resistance brazing, 16: 20988 (ARF-2232-2)
Mo–Ti–Zr, joining of foils of TZM, for honeycomb panel fabrication, 18: 37661 (ASD-TDR-63-799(Pt.I))
Mo–Ti–Zr, machining, 16: 3417(R) (ASD-TR-7-532a(IV))
Mo–Ti–Zr, machining of TZM, 20: 15014
Mo–Ti–Zr, mechanical properties, 16: 3445 (ASD-TR-61-193)
Mo–Ti–Zr, mechanical properties, 16: 33455(R) (NP-12097)
Mo–Ti–Zr, mechanical properties of TZM, effects of high temperatures and potassium on, 19: 2794 (APL-TDR-64-116(Pt.I))
Mo–Ti–Zr, mechanical properties of TZM at room temperature, 19: 6277 (ML-TDR-64-205)
Mo–Ti–Zr, mechanical and wear properties of TZM, 19: 29732(R) (APS-5152-R2)
Mo–Ti–Zr, mechanical properties of TZM, effects of carbon content on, 19: 41002 (APS-5157-R)
Mo–Ti–Zr, mechanical properties of TZM, effects of forging schedule and ingot processing on, 19: 41002 (APS-5157-R)
Mo–Ti–Zr, mechanical properties at 25 to 3500°F, 20: 21322 (AMRA-TR-65-25)
Mo–Ti–Zr, oxidation tests of coated TZM bolts and nuts, 19: 7844(R) (AD-602500)
Mo–Ti–Zr, oxidation by air at 1000°C, effects of pressure on, 19: 16017(R) (HW-84281(p.5.6-25))
Mo–Ti–Zr, oxidation by oxygen, effects of pressure and temperature on 19: 23124(R) (HW-83298(p.8.1-4))
Mo–Ti–Zr, performance as fuel cladding in fast reactors, 18: 24952(R) (ANL-6880(p.6-48))
Mo–Ti–Zr, performance as coating on fast reactor fuel elements, 18: 26824(R) (ANL-6885)
Mo–Ti–Zr, phase diagrams, 18: 25985 (WADD-TR-60-132(Pt.III))
Mo–Ti–Zr, phase studies, 16: 27627(R) (NMI-9243)
Mo–Ti–Zr, phase studies, 17: 6668(R) (NMI-9246)
Mo–Ti–Zr, phase studies of, isothermal sections at 1200°C in, 20: 41464
Mo–Ti–Zr, physical properties of TZM sheets, 18: 30165(R) (AD-431114)
Mo–Ti–Zr, physical properties of sheets of TZM, 19: 945(R) (AD-600281)
Mo–Ti–Zr, polygonization effects on elastic limit, microhardness, microstructure, and recrystallization of, 17: 36317
Mo–Ti–Zr, polygonization effects on mechanical properties of, 18: 37722
Mo–Ti–Zr, powder metallurgy, 17: 6668(R) (NMI-9246)
Mo–Ti–Zr, preparation by arc-melting, 16: 16724(R) (NMI-9238)
Mo–Ti–Zr, preparation of vacuum-arc-cast, 16: 18016(R) (AD-265129)
Mo–Ti–Zr, preparation of homogeneous, 17: 12588(R) (NMI-9249)
Mo–Ti–Zr, production and properties of sheets of, 20: 29756
Mo–Ti–Zr, properties of TZM sheet, 18: 573(R) (AD-422116)
Mo–Ti–Zr, properties of TZM foils at high temperatures, effects of coatings on mechanical and thermophysical, 18: 34128 (RTD-TDR-63-4068)
Mo–Ti–Zr, properties of TZM rolled sheet, 19: 18447(R) (AD-423981)
Mo–Ti–Zr, properties of TZM as cladding material for SNAP hydride reactors, 19: 39166 (NAA-SR-Memo-11149)
Mo–Ti–Zr, radiation effects on hardness and oxidation of, by water at 50°C, 18: 32043(R) (HW-81259(p.4.1-64))
Mo–Ti–Zr, radiation effects on mechanical properties of, neutron, 19: 11669(R) (GEMP-41A)
Mo–Ti–Zr, radiation effects on mechanical properties of, 19: 18390(R) (GEMP-43A)
Mo–Ti–Zr, radiation effects on electric and mechanical properties of, neutron, 19: 24916(R) (GEMP-334A)
Mo–Ti–Zr, radiation effects on creep-rupture of TZM, fast-neutron, 20: 9378(R) (GEMP-54A)
Mo–Ti–Zr, radiation effects on tensile properties of TZM, neutron, 20: 27571(R) (BNWL-207, pp 4.1-3)
Mo–Ti–Zr, radiation effects on creep-rupture properties of TZM, fast-neutron, 20: 27582(R) (GEMP-400A, pp 63-98)
Mo–Ti–Zr, radiation effects on hot-hardness of, effects of test temperature on fast-neutron, 20: 27582(R) (GEMP-400A, pp 63-98)
Mo–Ti–Zr, reactions with cesium at 3400°F, metallographic specimen preparation of TZM, 19: 46954 (NMI-5025(Pt.I), pp 39-58)
Mo–Ti–Zr, reactions with uranium carbide, nitride, and dioxide, metallographic specimen preparation of TZM, 19: 46954 (NMI-5025 (Pt.I), pp 39-58)
Mo–Ti–Zr, reactions with niobium–1 zirconium alloy at 2000°F in refluxing potassium, TZM, 20: 9423(R) (NASA-CR-54735)
Mo–Ti–Zr, specifications of TZM, for use in corrosion test loop fabrication, 20: 21293 (R-66SD3007)
Mo–Ti–Zr, strain softening by flexing of TZM sheet, 19: 7887(R) (AD-421621)
Mo–Ti–Zr, strength of, effects of carbon additions on, 17: 6672 (NP-12383)
Mo–Ti–Zr, stress-rupture properties at high temperatures, 19: 37146
Mo–Ti–Zr, stress-rupture at 2000°F of TZM, 20: 31669
Mo–Ti–Zr, substructure of cold-rolled TZM, 19: 13948(R) (NP-14675)
Mo–Ti–Zr, tensile properties at room temperature, 18: 18380
Mo–Ti–Zr, tensile properties of TZM at room temperature and 650°C, 18: 35060(R) (ANL-6904)
Mo–Ti–Zr, tensile properties of recrystallized TZM, 19: 13948(R) (NP-14675)
Mo–Ti–Zr, tensile properties of TZM sheet, 19: 20542(R) (AD-606310)
Mo–Ti–Zr, tensile properties at 1200 and 2000°F of TZM, 19: 24976(R) (AD-612759)
Mo–Ti–Zr, tensile properties of TZM, statistical analysis of variations in, 19: 26802(R) (AD-610564)
Mo–Ti–Zr, tensile properties of, effects of disilicide coatings on, 20: 27549
Mo–Ti–Zr, tensile properties of TZM, effects of brittle coatings on, 20: 37276
Mo–Ti–Zr, testing of TZM, for use in liquid-metal turbine blades and nozzles, 20: 2240
Mo–Ti–Zr, thermal properties, 18: 7201 (ASD-TDR-63-597)
Mo–Ti–Zr, thermal properties to melting point, 20: 878
Mo–Ti–Zr, welding of TZM, effects of parameters on T1G welds in, 18: 573(R) (AD-422116)
Mo–Ti–Zr, welding of brazed joints of, electron-beam, 18: 32123
Mo–Ti–Zr, welding of TZM, equipment and procedures for, 19: 9629(R) (AD-608818)
Mo–Ti–Zr, yield strength of TZM, effects of boiling potassium exposure on, 19: 34640 (CNLM-6246)
Mo–U, analysis for impurities, visual, 17: 6528 (TID-7625(p.45-51))
Mo–U, analysis for molybdenum, gravimetric, 17: 15882 (PG-Report-418)
Mo–U, analysis for molybdenum, gravimetric, 18: 19846 (LA-3058)
Mo–U, analysis for molybdenum, volumetric, 19: 36240 (TRG-Report-961)
Mo–U, analysis for carbon, coulometric, 20: 38796 (CEA-R-2968)
Mo–U, analysis of, for iron, absorptiometric, 16: 12957 (PG-Report-272)
Mo–U, annealing of quenched, reaction mechanisms in, 17: 6716
Mo–U, bibliography on, 17: 3377 (AWRE/LIB/BIB/6)
Mo–U, bonding of, to niobium diffusion barrier for aluminum-clad fuel elements, 17: 18716 (NAA-SR-7973)
Mo–U, burnup capability of fuels of, 20: 8398(R) (NAA-SR-11450, Sect. 6)
Mo–U, burnup of, irradiation studies of, 16: 808

Mo–U, casting and melting of highly reactive, 18: 44119
Mo–U, casting of, testing of products from, 20: 29803
Mo–U, casting tubes of, 20: 27453
Mo–U, casting, drawing, and rolling, effects on properties of, 19: 28779(T) (AEC-tr-6519)
Mo–U, cesium-137 removal in processing of, 18: 37252 (A/CONF.28/P/100)
Mo–U, characteristics and performance in gas-cooled graphite-moderated reactors, 18: 15496(T) (AEC-tr-6329)
Mo–U, chill effects on cast plates of, 19: 4636
Mo–U, coating with nickel to prevent stress-corrosion cracking in air, electrolytic, 20: 5867
Mo–U, combustion of, effects of coating and moisture on, 19: 17174(R) (ANL-6900(p.232-303))
Mo–U, combustion kinetics of, 20: 43612
Mo–U, corrosion of, during long-term storage, effects of coatings on, 16: 25713 (BMI-1563)
Mo–U, corrosion, 17: 39640
Mo–U, corrosion by water at 650°F, alloying effects of platinum on, 18: 16449(P)
Mo–U, corrosion and reaction rates in chloride volatility processing of, 18: 39386
Mo–U, corrosion cracking in air, stress-, 20: 11224
Mo–U, corrosion by biphenyl, 20: 25491(T) (AECL-2330, pp 179-95)
Mo–U, creep, 18: 18304
Mo–U, creep during temperature cycling, effects of microstructure on, 20: 23700
Mo–U, creep of, at 550 and 600°C, 16: 30167 (ORNL-3313(p.19-64))
Mo–U, critical behavior of enriched, unreflected, unmoderated assembly of, superprompt, 16: 24540
Mo–U, criticality studies, 16: 765
Mo–U, criticality studies, 16: 24419
Mo–U, crystal structure of tempered, effects of carbon on, 20: 11292
Mo–U, decomposition of gamma solid solution in, mechanism of, 16: 30831
Mo–U, decomposition of gamma-phase in, 17: 41459
Mo–U, deformation resistance of, effects of temperature and strain rate on, 18: 42012 (AWRE-O-66/64)
Mo–U, deformation and flow of polycrystalline, 19: 4675
Mo–U, deformation resistance of, at high temperatures, 19: 16206(P)
Mo–U, deformation resistance at high temperatures, 20: 9379(R) (NAA-SR-11650, Sect.4)
Mo–U, detection of metastable phase in, 18: 18385
Mo–U, diffusion of uranium in, mechanism of, 16: 2223
Mo–U, dissolution of, by ferric nitrate–nitric acid solution and nitric acid, 16: 13135
Mo–U, dissolution of irradiated, equipment and techniques for, 18: 25610 (SGAE-CH-4/1964)
Mo–U, dissolution of Zr-clad, by hydrofluoric acid, chemical analysis of solutions from, 16: 5266 (DP-648)
Mo–U, dissolution using nitric acid, equipment and procedures for, 20: 4048(R) (NP-15406)
Mo–U, economics as reactor breeding blanket in spherical and paste form, 18: 38533 (APDA-160)
Mo–U, effects of forming method on mechanical properties and microstructure of, 19: 30800
Mo–U, elastic modulus of, effects of heat treatments on, 19: 41023 (NP-15334)
Mo–U, electric and thermal conductivity of, 18: 34143
Mo–U, electron microscope studies of thin films of, 17: 6712
Mo–U, electronic probe microanalyzer study of surface of, 18: 543 (CEA-2291)
Mo–U, etching and anodic attack on gamma phases in, use of sulfates and sulfites for, 19: 14038
Mo–U, etching by ion bombardment, 18: 2284(T)
Mo–U, evaluation as HNPF fuel, 18: 24892(R) (NAA-SR-8888(Sect.II))
Mo–U, evidence of late grain boundaries in, 17: 27855
Mo–U, exponential measurements in lattices of, with uranium carbide, 16: 24984 (NAA-SR-Memo-7134)
Mo–U, extrusion of, for irradiation testing, 16: 30086(R) (NMI-7250)
Mo–U, extrusion and rolling, 17: 40422(R) (ANL-6784)
Mo–U, fabrication and properties, 16: 25735(R) (NMI-7251)
Mo–U, fabrication into long and thin plates by casting, 16: 496 (NAA-SR-6227)
Mo–U, fabrication and testing, 17: 11096(R) (NMI-7256)
Mo–U, fabrication, 17: 19720 (ANL-6698)
Mo–U, fabrication, 17: 30949 (NAA-SR-8412)
Mo–U, fabrication by extrusion and rolling, 17: 35078(R) (ANL-6739)
Mo–U, fabrication by extrusion and multicavity-mold vacuum casting, 17: 35079(R) (ANL-6749)
Mo–U, fabrication of aluminum-, SAP-, and zirconium-clad, 17: 36249 (NAA-SR-Memo-8161)
Mo–U, fabrication by swaging of powders, 17: 36301 (ORNL-TM-455)
Mo–U, fabrication and properties, 18: 557
Mo–U, fabrication and properties, 18: 26893(R) (ANL-6868(p.11-108))
Mo–U, fabrication into small balls, 18: 41978 (NP-14348)
Mo–U, fabrication, 19: 11711
Mo–U, fabrication into massive enriched core components for Super Kukla, safety in, 19: 46967 (Y-KB-62)
Mo–U, fabrication of, by melting and vacuum casting, 20: 27463
Mo–U, fatigue tests on compression and tension of, 18: 36021
Mo–U, formation of oriented oxide films on gamma-phase, 17: 16536
Mo–U, γ–γ' transformation mechanism in, 17: 32605
Mo–U, grain size of end-quenched, 19: 23047
Mo–U, grain structure of, effects of accelerated cooling rate at 75 to 300°C/min on, 19: 30712(P)
Mo–U, growth of alpha and beta phases in, 18: 2247
Mo–U, hardness of cast, to 600°C, 18: 5735(R) (NMI-2122)
Mo–U, hardness to 600°C, 16: 33477(R) (NMI-7253)
Mo–U, hardness to 600°C, 17: 41352(R) (NMI-1259)
Mo–U, heat treatment, 17: 32619
Mo–U, heat treatment, 19: 1025
Mo–U, hydridation and swaging of dispersed, 17: 14749(T,R) (EURAEC-408)
Mo–U, hydridation of, kinetics, 20: 2222 (EURAEC-1390)
Mo–U, ignition and oxidation of nickel-plated and unclad, by air to 925°C, 18: 15426(R) (ANL-6810)
Mo–U, induction melting and casting of, vacuum, 19: 32674 (AD-610003)
Mo–U, inspection of irradiated OMRE fuel elements of, 20: 10272(R) (NAA-SR-9339)
Mo–U, irradiation growth of, 18: 32246
Mo–U, isothermal transformations of gamma-phase, 19: 40958
Mo–U, kinetics of isothermal decomposition of gamma phase, 17: 39566
Mo–U, mechanical properties of, at high temperatures, alloying effects on, 16: 2246
Mo–U, mechanical properties of, for use as reactor fuel alloy, 16: 15237(P)
Mo–U, mechanical and physical properties of, 17: 476
Mo–U, mechanical properties at high temperatures, 17: 8875(P)
Mo–U, mechanical properties of, 17: 39636
Mo–U, mechanical properties and phase studies, 17: 39637
Mo–U, mechanical properties and phase studies, 17: 39628
Mo–U, mechanical properties, 17: 39634
Mo–U, mechanical properties, 19: 11679
Mo–U, mechanical properties under dynamic tensile loads, 19: 24990 (UCRL-12357(Rev.I))
Mo–U, mechanical properties, dynamic tensile, 19: 37046 (UCRL-12357)
Mo–U, mechanical properties of, effects of strain rate on, 20: 11284 (UCRL-14599)
Mo–U, mechanical properties of, effects of dynamic tensile loads on, 20: 11224
Mo–U, mechanical properties for use in prompt-burst reactor, 20: 13287
Mo–U, mechanical properties of gamma-phase uranium-base, 20: 15060 (UCRL-7771)
Mo–U, mechanical properties and structure of, effects of heat treatments on, 20: 17014 (INR-645/XIV/PS)
Mo–U, mechanical properties and dimensional stability of, 20: 27463
Mo–U, mechanical properties, 20: 29803
Mo–U, mechanical properties, metallography, and structure of, 20: 29775
Mo–U, mechanical properties of, under dynamic tensile loads, 20: 33902
Mo–U, media for dissolution of, 18: 26903
Mo–U, meltdown studies of irradiated Zr-clad, 16: 24642
Mo–U, metallography, 17: 27790 (NAA-SR-Memo-8408)
Mo–U, metallographic examination of carbide particles in, 18: 6884(R) (NP-13412)
Mo–U, metallurgical properties of, fabrication effects on, 17: 22101 (WAL-TR-420.5/1)
Mo–U, metallurgical properties, 18: 37677 (A/CONF.28/P/701)
Mo–U, microstructure characteristics, 16: 25785
Mo–U, microstructure of, effects of carbon on, 20: 15070
Mo–U, microstructure of uranium-rich, effects of heat treatments on, 20: 21372
Mo–U, morphology after $\gamma \rightarrow \beta + \gamma \rightarrow \alpha + \gamma$ transformation, effect of γ grain shape on, 17: 23979
Mo–U, morphology of alpha-pseudo-grains of, 18: 37706
Mo–U, nonmetallic inclusions in, 16: 30874
Mo–U, oxidation of, by carbon dioxide and helium, 16: 12694
Mo–U, oxidation of, by nitric acid, electrolytic, 16: 17759 (DP-647)
Mo–U, oxidation by moist air at 300 to 700°C, 18: 19456(R) (ANL-6840)
Mo–U, paramagnetic susceptibilities of, at 100 to 300°K, 16: 12149
Mo–U, performance as reactor fuel, 18: 3250
Mo–U, performance as HNPF fuel, 19: 12865(R) (NAA-SR-10501)
Mo–U, performance as Hallam Reactor fuel, 19: 27735(R) (NAA-SR-10850)
Mo–U, performance in HNPF, 19: 40286(R) (NAA-SR-11200)

Mo–U, phase deformation in, mechanism of alpha- and gamma-, 18: 26027
Mo–U, phase diagrams of, metastable phases in, 20: 23717
Mo–U, phase formation in gamma-gamma prime transformation in, transient alpha, 17: 1987
Mo–U, phase stability limits of, at 550°C, gamma, 16: 4530 (NAA-SR-6125)
Mo–U, phase structure, 18: 37675 (A/CONF.28/P/506)
Mo–U, phase studies, 16: 2158
Mo–U, phase studies, 16: 30861
Mo–U, phase studies, 16: 30876
Mo–U, phase studies and properties of, effects of heat treatment on, 16: 7900(T) (AEC-tr-4468)
Mo–U, phase studies and properties of, at 450 and 500°C, 16: 30871
Mo–U, phase studies and properties of, at 600 to 1200°C, 16: 30859
Mo–U, phase studies of, below 600°C, 16: 30860
Mo–U, phase studies, 17: 536 (NP-12128)
Mo–U, phase studies, 17: 29255 (ZFK-WF-13)
Mo–U, phase studies, 17: 39624
Mo–U, phase studies of uranium-base, 20: 39388 (CEA-R-2956)
Mo–U, phase transformations in, kinetics of gamma to gamma prime, 16: 4532 (NAA-SR-6617)
Mo–U, phase transformations in, metastable, 16: 32108 (AERE-M/R-2840)
Mo–U, phase transformations, 17: 8812 (RT/MET(62) 4)
Mo–U, phase transformation, 17: 14740 (TID-11295(2nd Ed.))
Mo–U, phase transformation, 17: 32619
Mo–U, phase transformation (β–α'), 17: 39626
Mo–U, phase transformations at 500 to 640°C, 18: 12697
Mo–U, phase transformations, 18: 14477 (UCRL-7595)
Mo–U, phase transformations in, 18: 24124 (CEA-2341)
Mo–U, phase transformations, gamma-beta and gamma-alpha, 19: 42841 (CEA-R-2763)
Mo–U, phase transformations in, effects of lattice orientation on, 20: 39389 (CEA-R-2973)
Mo–U, polarization of, effects of sodium borate and sodium citrate on, 19: 7914
Mo–U, polarographic analysis for molybdenum, 17: 38939
Mo–U, post irradiation annealing effects on density changes in, 17: 39571
Mo–U, preparation of specimens of, for reactor irradiation, 16: 9140 (CNEN-98)
Mo–U, preparation of tubular, for HWCTR test irradiation, 16: 30085(R) (NMI-7249)
Mo–U, preparation of uranium-rich, by coreduction, 16: 29331
Mo–U, preparation and use as reactor fuel in foamy state, 17: 41478(P)
Mo–U, preparation for use as reactor fuel, 18: 7192(P)
Mo–U, preparation and fabrication, 18: 12617(P)
Mo–U, preparation, 18: 41487(P)
Mo–U, preparation and properties, 18: 41488(P)
Mo–U, preparation of powders of, 20: 2222 (EURAEC-1390)
Mo–U, processing for uranium recovery, 18: 3914(P)
Mo–U, processing by fluidized-bed method, 18: 13976
Mo–U, processing by volatilization, 18: 37280 (A/CONF.28/P/771)
Mo–U, processing of irradiated, headend process for, 18: 39370 (NP-10416)
Mo–U, processing of irradiated, 19: 18066
Mo–U, processing reactor fuels of, 20: 4070(P)
Mo–U, production of, for use as reactor fuel, cost reduction in, 16: 7264
Mo–U, production of tubes of, 19: 9630 (CEA-R-2579)
Mo–U, properties of cast, 16: 34065(R) (DP-775)
Mo–U, properties as reactor fuel, 18: 3259
Mo–U, properties as reactor fuel, 18: 2347
Mo–U, properties for use as fuel element in gas-graphite reactors, 18: 4818
Mo–U, properties as reactor fuel, 18: 34130 (TID-8540(p.331-410))
Mo–U, properties as reactor fuel, 18: 42024 (UJV-926/63)
Mo–U, properties for use as fuel material, 19: 9652 (CEA-R-2568)
Mo–U, properties, 19: 41023 (NP-15334)
Mo–U, properties evaluation of Zr alloy-clad, by irradiation testing, 16: 13579 (NMI-7212)
Mo–U, properties as fuel material, 20: 25614(P)
Mo–U, radiation effects on particles of, in liquid potassium–sodium alloys, 16: 27715
Mo–U, radiation effects on crystalline structure of, 16: 29443(R) (AEC-tr-5325)
Mo–U, radiation effects on, at 300 to 1200°F, 17: 33510 (BMI-APDA-660)
Mo–U, radiation effects, 17: 3379(R) (BMI-1596(Del.))
Mo–U, radiation effects, 17: 3378(R) (BMI-1583(Del.))
Mo–U, radiation effects, 17: 7563(R) (PRDC-TR-59)
Mo–U, radiation effects on, 17: 477
Mo–U, radiation effects on stability, 17: 14727(R) (BMI-1600(Del.))
Mo–U, radiation effects on dimensional stability of, 18: 2368
Mo–U, radiation effects on swelling, neutron, 18: 37733 (A/CONF.28/P/62)
Mo–U, radiation effects on, 18: 37744 (A/CONF.28/P/338b)
Mo–U, radiation effects on, neutron, 18: 37757 (A/CONF.28/P/735)
Mo–U, radiation effects on, 19: 1025
Mo–U, radiation effects on, 19: 2874
Mo–U, radiation effects on aluminum-clad, 19: 10675(R) (NAA-SR-9999)
Mo–U, radiation stability, 19: 11792
Mo–U, radiation and fission fragment effects on, 19: 11810
Mo–U, radiation effects on, at high burnup levels and low fission rates, 19: 14087 (NAA-SR-8955)
Mo–U, radiation effects on high-temperature corrosion of, 19: 18540 (SC-RR-65-28)
Mo–U, radiation effects on, at 260 to 600°C, 19: 26900
Mo–U, radiation effects on fuel elements of, 19: 41090 (NAA-SR-11121)
Mo–U, radiation effects on Zr alloy-clad, at 300 to 1200°F, 16: 33510 (BMI-APDA-660)
Mo–U, radiation effects on corrosion rate of, by carbon dioxide and nitrogen, reactor, 20: 11224
Mo–U, radiation effects on uranium-rich, neutron, 20: 21436
Mo–U, radiation effects on microstructure of, reactor, 20: 23793
Mo–U, radiation effects on dimensional changes in tubular fuel elements of, exposed in HWCTR, 20: 25615 (DP-1019)
Mo–U, radiation effects on stainless steel-clad fuel elements of, 20: 31666
Mo–U, radioinduced relaxation of elastic stresses in, 17: 455
Mo–U, radioinduced swelling of, effects of finely dispersed phases on, 18: 5814 (CONF-331-2)
Mo–U, radioinduced swelling of, neutron, 18: 8870 (NAA-SR-6262)
Mo–U, radioinduced relaxation of stresses in, 18: 42120(T) (AEC-tr-6474)
Mo–U, radioinduced swelling of, effects of silicon and tin additives on, 18: 41933 (TID-11295(3rd Ed.))
Mo–U, radioinduced fission product swelling of, reducing effects of finely dispersed phases on, 19: 14097
Mo–U, radioinduced swelling, phase reversion, and intergranular cracking of, 19: 14088 (NAA-SR-8956)
Mo–U, radioinduced swelling in clad tubular, 19: 46917(R) (DP-975)
Mo–U, radioinduced swelling in, reactor, 20: 5848
Mo–U, radioinduced swelling of Zircaloy-clad, at 500°C, 20: 37302
Mo–U, reactions with hydrogen chloride- and hydrogen fluoride-oxygen mixtures, 17: 14379(T) (AEC-tr-5652)
Mo–U, reactions with hydrogen halides, 17: 27403(P)
Mo–U, reactions with Magnox alloy to 475°C in argon, 19: 22997 (TRG-Report-842)
Mo–U, reactions of irradiated, in TREAT excursions, 19: 31530(R) (ANL-7010(p.77-177))
Mo–U, self-diffusion coefficients of gamma-phase uranium in, 16: 29416
Mo–U, separation of uranium from, 16: 263(P)
Mo–U, separation of uranium from, 17: 18198
Mo–U, separation of uranium from, by volatilization of molybdenum as oxychloride, 18: 43728(P)
Mo–U, separation of uranium from, by fused salt electrolysis, 19: 46448
Mo–U, spectrographic analysis for aluminum, 18: 35451 (PG-Report-390)
Mo–U, spectrophotometric analysis for uranium, 19: 19759 (LA-3226)
Mo–U, stress corrosion cracking, 17: 32518 (Y-1417)
Mo–U, stress-cracking of, 19: 16080 (UCRL-7767)
Mo–U, superconducting transitions in high magnetic fields, 17: 25938
Mo–U, tensile properties of quenched, 18: 26026
Mo–U, thermal cycling effects on dimensional stability of, 16: 9657(R) (NAA-SR-1109)
Mo–U, thermal cycling behavior and thermal stability, 18: 598 (CEA-2289)
Mo–U, thermal stability, 18: 15564
Mo–U, transformation kinetics of, at 500 to 550°C, 16: 30167 (ORNL-3313(p.19-64))
Mo–U, transformation diagram and kinetics of, 17: 25769(R) (AMRA-CR-63-02/1(F))
Mo–U, transformation kinetics of, isothermal, 18: 18405
Mo–U, transformation of gamma phase of, isothermal, 19: 7910 (UCRL-7824)
Mo–U, use as reactor fuels, burnup and cost studies for, 17: 16521 (NAA-SR-Memo-2974)
Mo–U, use in the preparation of uranium compounds, 20: 1885(P)
Mo–U, x-ray-diffraction pattern of irradiated, 18: 10347(T) (JPRS-22697 (p.146-62))
Mo–U–V, properties and structure, 17: 6725
Mo–U–Zr, isothermal transformations of gamma-phase, effects of zirconium on, 19: 40958
Mo–U–Zr, mechanical properties, 17: 39643
Mo–U–Zr, phase diagrams and properties of, at 1000 to 625°C, 16: 30865
Mo–U–Zr, phase studies and structure of, at 500, 575, and 600°C, 16: 30866
Mo–V, creep and tensile properties of, at 1800°F, 16: 6747
Mo–V, fabrication and properties, 18: 26893(R) (ANL-6868(p.11-108))

Mo–V, properties as brazing material, 19: 24916(R) (GEMP-334A)
Mo–V, thermal expansion of, 20: 43964
Mo–V–Zr, oxidation by steam at 900°F, 18: 2162(R) (IITRI-B198-46)
Mo–W, casting methods for, 18: 25954
Mo–W, corrosion of, by aqua regia and nitric acid–oxalic acid solutions, 16: 17987
Mo–W, corrosion of, by lithium and lithium hydride, 16: 25718 (NP-11952)
Mo–W, corrosion of, by halide flux systems, 16: 28641(R) (ANL-6543)
Mo–W, corrosion under skull reclamation conditions, 17: 14116(R) (ANL-6596(p.29-118))
Mo–W, corrosion by halide salt–metal systems at 800°C, 17: 36860(R) (ANL-6648)
Mo–W, corrosion by lithium chloride–magnesium chloride–magnesium fluoride–zinc chloride solution, 17: 40421(R) (ANL-6766)
Mo–W, corrosion by liquid halides at 1000°C, 18: 17921(R) (ANL-6725 (p.31-88))
Mo–W, corrosion by zinc–molten halide system, 18: 33678(R) (ANL-6875)
Mo–W, corrosion by argon–nitrogen at 900°C, 19: 32279(R) (ANL-7020(p.3-99))
Mo–W, corrosion by cesium and lithium above 2500°F, 19: 28766
Mo–W, corrosion by lithium at 1200°C, 20: 3321(R) (ANL-7082, pp 29-53)
Mo–W, corrosion by zinc and magnesium–uranium–zinc alloy, effects of molten chlorides on, 20: 2266
Mo–W, corrosion by bismuth and tin, 20: 2275
Mo–W, corrosion by liquid lithium and cesium vapor at 2500 to 3400°F, 20: 5851
Mo–W, corrosion by argon–nitrogen mixtures at 900°C, 20: 20802(R) (ANL-7055, pp 21-98)
Mo–W, corrosion by bismuth and tin at 1000°C, (E), 20: 21566(R) (ANL-7055, pp 213-29)
Mo–W, crystal structure, 18: 36031
Mo–W, deoxidation, 17: 6672 (NP-12383)
Mo–W, diffusion in uranium carbide, 17: 25687(R) (GA-4173)
Mo–W, diffusion of molybdenum and tungsten in, tracer studies of, 19: 26852
Mo–W, diffusion of molybdenum and tungsten in, at 1500 to 2400°C, tracer studies of, 20: 17101
Mo–W, ductility and melting points of sintered, 19: 20584
Mo–W, electric transport in, for wide composition ratio and temperature range, 20: 15116(T)
Mo–W, electron transfer in, electronic structure determination from, (E), 20: 24598
Mo–W, extrusion, 16: 3445 (ASD-TR-61-193)
Mo–W, extrusion, 16: 29349(R) (ASD-TR-7-793(IV))
Mo–W, extrusion, 17: 6589 (ASD-TDR-62-670)
Mo–W, extrusion of complex shapes of, 18: 44096(R) (ML-TDR-64-217)
Mo–W, extrusion, 19: 20500 (AFML-TR-64-387)
Mo–W, fabrication and extrusion of ingots of, 16: 2148(R) (NP-11044)
Mo–W, fabrication and properties of extruded and rolled, 18: 5727(R) (AD-294579)
Mo–W, fabrication and properties of extruded and forged, 18: 20447(R) (ASD-TR-7-797(IX))
Mo–W, factors affecting vacuum-arc melting of, 18: 24070 (RTD-TDR-63-4089)
Mo–W, forging, 17: 6589 (ASD-TDR-62-670)
Mo–W, forging characteristics, 16: 9162 (DMIC-Memo-143)
Mo–W, forging of, studies of plasticity in, 17: 18721(T) (FTD-TT-62-1789)
Mo–W, mechanical properties of, effects of carbon, titanium, and zirconium on, 17: 33368(R) (ASD-TDR-62-508)
Mo–W, mechanical properties of wrought, 17: 6672 (NP-12383)
Mo–W, mechanical and physical properties of cast, 18: 25954
Mo–W, mechanical properties of Oremet HPC, 20: 15069
Mo–W, melting, 17: 6672 (NP-12383)
Mo–W, order measurement of, by x-ray scattering, 16: 18053
Mo–W, performance compatibility with thermionic cell fission heat source, 18: 20874
Mo–W, performance as cladding for carbide thermionic emitters, 18: 35929(R) (GA-4769(Pt.I))
Mo–W, phase studies based on thermochemical data, 18: 33603
Mo–W, phase studies, 19: 41035
Mo–W, preparation of, by electron-bombardment zone-melting methods, 16: 32046
Mo–W, preparation of fine powders of, by flame reduction of fluorides, 19: 15997 (K-L-6020)
Mo–W, preparation of thin films of, for transmission electron microscopy, 20: 27464
Mo–W, preparation and properties of single crystals of, 20: 41481
Mo–W, production of large-surface-area powders, 19: 30658
Mo–W, properties for high-temperature thermocouples, 17: 29170(R) (ASD-TDR-63-233)
Mo–W, properties for ultrahigh temperature thermocouples, 17: 30822
Mo–W, properties for thermocouples, 18: 4292
Mo–W, properties in high-temperature argon-nitrogen, 19: 14765(R) (ANL-6977)
Mo–W, reactions with cesium at 3400°F, metallographic specimen preparation of, 19: 46954 (NMI-5025(Pt.I), pp 39-58)
Mo–W, reactions with uranium carbide, 19: 11679
Mo–W, reactions with uranium carbide, nitride, and dioxide, metallographic specimen preparation of, 19: 46954 (NMI-5025(Pt.I), pp 39-58)
Mo–W, rupture properties of cold-worked, stress-, 20: 7616
Mo–W, stress recovery of, flow, 20: 4409
Mo–W, tensile properties at 3000°F, 18: 12562(R) (X63-12299)
Mo–W, use in tungsten to tungsten diffusion bonding, 20: 25553(P)
Mo–W, use of, for containment capsules in SNAP, 16: 7326(R) (MND-P-3014-III)
Mo–W, welding characteristics, 16: 4510 (DMIC-Memo-140)
Mo–W–Zr, extrusion of, comparison of high-velocity and conventional, 17: 1889 (ASD-TDR-62-506)
Mo–W–Zr, extrusion and properties of, 19: 18419(R) (AD-424207)
Mo–W–Zr, fabrication and properties of extruded and rolled, 18: 5727(R) (AD-294579)
Mo–W–Zr, fabrication and properties of cast and extruded, 18: 12536(R) (AD-412904)
Mo–W–Zr, fabrication and properties of extruded and rolled, 18: 22412(R) (AD-422106)
Mo–W–Zr, phase diagram, 19: 37090
Mo–W–Zr, phase studies and properties of W_2Zr–Mo_2Zr phase in, 19: 6350
Mo–W–Zr, phase studies, 19: 41035
Mo–Y, mechanical properties and preparation, 17: 14818 (DRI-2039)
Mo–Y, oxidation at high temperatures, effects of yttrium content on, 20: 41421
Mo–Y, phase studies, 18: 12623 (ASD-TDR-63-204)
Mo–Y, phase studies of solid solution formation in, 19: 41050
Mo–Zn, impurity behavior at grain boundaries during recrystallization, 17: 560
Mo–Zr, aging kinetics of, at 1300 to 1500°K, 20: 41466
Mo–Zr, annealing of, tracer studies of grain boundary migration in, 20: 19251
Mo–Zr, beta phase stabilization in, 17: 11213
Mo–Zr, corrosion of, by potassium at 1000 to 1800°F, 16: 16679 (TID-7626(Pt-I)(p.63-8))
Mo–Zr, corrosion by steam and water, 17: 39659
Mo–Zr, corrosion by hydrochloric, phosphoric, and sulfuric acids at high temperatures, 20: 46158
Mo–Zr, critical current density of superconducting, in transverse field of 30 kgauss, 18: 6128
Mo–Zr, diffusion in bcc, 19: 23112
Mo–Zr, electronic properties, 18: 44150(R) (ORNL-3670(p.44-53))
Mo–Zr, free energies of formation of Laves phases in, 16: 13636
Mo–Zr, grain boundary structure in, internal friction studies of, 20: 15128
Mo–Zr, hardness of dispersion-hardened, 17: 20480
Mo–Zr, internal friction in deformed crystals of, 18: 26041(T)
Mo–Zr, internal friction of annealed and deformed, 20: 5846
Mo–Zr, internal friction in deformed, 20: 19250
Mo–Zr, mechanical properties, 16: 3445 (ASD-TR-61-193)
Mo–Zr, melting of, effects of composition on electron-beam, 20: 29674
Mo–Zr, on creep properties of, effects of nitriding, 17: 41461
Mo–Zr, oxidation by carbon dioxide up to 600°C, 18: 30192
Mo–Zr, oxidation in carbon dioxide and carbon monoxide at 500 to 900°C, 19: 24942
Mo–Zr, phase studies, 19: 41035
Mo–Zr, phase studies, 20: 35924
Mo–Zr, polygonization effects on elastic limit, microhardness, microstructure, and recrystallization of, 17: 36317
Mo–Zr, polygonization effects on mechanical properties of, 18: 37722
Mo–Zr, properties at low temperatures, 20: 3920(R) (ORNL-3870, pp 27-37)
Mo–Zr, properties at high temperatures, 20: 4418
Mo–Zr, reactions with hydrogen, thermochemical and structural aspects of, 20: 27436
Mo–Zr, reactions with hydrogen and nitrogen, 20: 29632
Mo–Zr, resistance to scaling at elevated temperatures, 19: 32770(P)
Mo–Zr, self-diffusion of molybdenum in, 17: 32593
Mo–Zr, strength of, effects of carbon additions on, 17: 6672 (NP-12383)
Mo–Zr, strength of, effects of boron additions on, 17: 6672 (NP-12383)
Mo–Zr, superconducting transition temperature of, (E), 20: 8021
Mo–Zr, tensile properties at high temperatures, effects of nitriding on, 17: 23989
Mo–Zr, transformation kinetics, 18: 44052(R) (ORNL-3670(p.147-59))
Mo–Zr, use as brazing alloys for refractory metals, 18: 7956(R) (GA-3992(Pt.I))
Sb–Mo, crystal structure of Mo_3Sb_7, 19: 28837

Sb–Mo, crystal structure of intermetallic compounds in, 19: 39209
Sb–Mo–Zr, oxidation by steam at 900°F, 18: 2162(R) (IITRI-B198-46)

MOLYBDENUM ARSENIDES
crystal structure, 19: 7945
crystal structure, 19: 9101
crystal structure of $MoAs_2$ and $Mo_{0.4}As_2$, 19: 28837
crystal structure of Mo_2As_3, 20: 43187

MOLYBDENUM BORIDES
abrasive properties, 20: 15109
bibliography on phase relations of, 17: 30913 (NP-12972)
bibliography on phase relations of, 18: 10518 (AD-410526)
bonding in nuclear magnetic resonance analysis of, 17: 8081
boron-11 quadrupole resonance in, 17: 3511
chemical and phase composition studies on, 18: 28037
chemical bonding and electric conductivity of, 20: 16439
crystal structure, 17: 3500(T) (JPRS-16059)
effects on thermoelectric properties of MCC 50, 19: 12129(R) (ASD-TDR-62-896(Pt.II))
electric properties of, effects of non-metallic atoms on, 17: 8854
emissivity of coatings of, to 2000°F, 16: 30801(R) (PWA-1878)
fabrication and properties of MHD cell electrodes of, 19: 6495
hot pressing of high density, apparatus for, 16: 19267
melting temperature, evaluation for space technology, 18: 16521
phase studies of molybdenum-rich, 20: 5850
preparation, 19: 15502
preparation and properties of crucibles of, 16: 9219(T) (CEA-tr-R-1440)
preparation and purification, 19: 46941 (NP-15514(Vol.3))
preparation by carbon reduction of boric oxide and molybdenum oxide, 20: 18702
preparation of, effects of pressure, temperature, and time on, 18: 28037
preparation, properties, and aerospace applications, 19: 37142
properties as brazing material, 19: 24916(R) (GEMP-334A)
reactions with copper and nickel mattes, slags, molten salts, and refractory metals, 20: 14989
reactions with graphite to 2200°C, 19: 38654
reactions with molten metals at 400 to 1500°C, 19: 37112
structural characteristics, 16: 7913
superconducting properties, 16: 22631
superconducting transition temperatures of, 18: 36493
thermodynamic properties at 300 to 1200°K, 16: 25401
MoB–MoC, superconducting properties, 18: 34283 (UCRL-11390)

MOLYBDENUM BROMIDES
preparation and properties, 17: 10590 (IS-487)
separation from ethyl ether by solvent extraction using adiponitrile, ethanolamine, and formamide, 17: 40933
solubility and molecular weight of, in liquid bromine, 20: 40796(R) (IS-1500(Sect.C))
spectra of complex, in aqueous hydrobromic acid, 17: 23438 (TID-18604)
thermodynamic properties, 18: 2163(R) (IS-700(Sect.M))
thermodynamic properties, 20: 10816(T) (NASA-TT-F-285)

MOLYBDENUM BRONZES
preparation, properties, and structure of, phases with potassium, rubidium, and sodium, 20: 43213

MOLYBDENUM CARBIDES
abrasive properties, 20: 15109
analysis for carbon using electron microprobe, 19: 43966
analysis for oxygen by heat extraction, 16: 7515
bibliography on phase relations of, 17: 30913 (NP-12972)
bibliography on phase relations of, 18: 10518 (AD-410526)
bibliography on properties, 17: 27809 (UCRL-7284)
brittle fracture and twinning in, relation of, 17: 25772 (ASD-TDR-63-360)
coating of, with graphite, development of production scale procedure for, 17: 33279
crystal structure and thermodynamic properties, 16: 13590(T) (AEC-tr-5000)
crystal structure of divalent, 16: 19364(R) (NP-11699)
crystal structure of, veining substructure in, 20: 23696
deposition on carbon bodies, 16: 13527(P)
diffusion of carbon and molybdenum in, at 900 to 1600°C, tracer studies of, 19: 32744
dislocations in single-crystal, effects of structure on, 20: 37247
effects of films of, on thermal radiation properties of molybdenum, 16: 32039(R) (PWA-1863)
effects on graphite microstructure, 20: 2318(R) (GA-5915(Pt.1))
effects on molybdenum single crystals, 20: 33859(R) (AD-634128)
effects on radiation resistance and mechanical properties of plutonium or uranium carbides, 18: 44230(P)
elastic properties of stoichiometric, 20: 39430
electric conductivity of, at high temperatures, 17: 8856
electric conductivity at high temperatures, 18: 28012(T)
electric properties of, effects of non-metallic atoms on, 17: 8854
electrowinning from minerals and natural compounds, method for, 19: 910
emissivity at 800 to 5000°K, relation of structure to, 18: 20566
entropy of formation at 298°K, 18: 19974
fabrication by hot-pressing, 20: 31699
figure of merit and atomic characteristics, 19: 2284
formation as inclusions in molybdenum and molybdenum alloys, 20: 41467
free energy of formation of MoC and Mo_2C to 5000°F, 16: 22582 (ASD-TDR-62-7)
free energy of formation, 16: 28963
friction between surfaces of, at high temperatures in vacuum, argon, helium, and nitrogen atmospheres, 19: 28826
friction between surfaces of, at high-temperatures in vacuum, 19: 28827
hot pressing of high density, apparatus for, 16: 19267
hot pressing of powders, 17: 11170(T) (AEC-tr-5604)
inflammability of powdered, at 180 to 1100°C, 18: 44211
melting point, 17: 11201(T) (AEC-tr-5598)
melting temperature, evaluation for space technology, 18: 16521
oxidation of, at 1000 to 2000°K, kinetics of, 17: 21665(R) (ASD-TDR-62-203(Pt.II))
performance in focus electrodes in cesium-contact ion thrustors, 20: 31383
phase studies by differential thermal analysis, 20: 9525
plasticity and strength at 20 to 2500°C, 16: 27679
precipitation on internal and external surfaces of molybdenum on annealing, 19: 23085
preparation in fluidized beds, 20: 9397
preparation of high-purity, using cobalt or iron-nickel alloy bath, 19: 42828
preparation of high-purity, auxiliary metal bath for, 20: 27452
preparation of spherical particles of, procedure and apparatus for, 20: 14971(P)
preparation, properties, and aerospace applications, 19: 37142
production and properties of, 18: 7262
production of close-packed, at high pressures, 16: 4550 (WADD-TR-60-893)
production of graphite-coated particles of, by fluidized bed process, 17: 11174
properties of, at 2000°C, for use in thermionic converters, 20: 29729
reactions with copper and nickel mattes, slags, molten salts, and refractory metals, 20: 14989
reactions with graphite at 1800 to 2200°C, contact, 18: 30208
reactions with magnesium and zirconium oxides at 1800 to 2000°C, 18: 43463
reactions with molten metals at 400 to 1500°C, 19: 37112
reactions with molybdenum, niobium, tantalum, and tungsten at 900 to 2200°C, 20: 25578(T) (N-65-35787)
review, 18: 39899 (LA-2942)
sintering reactions with metals, formation of complex compounds by, 20: 25539
spectral emittance at 800 to 5000°F, 16: 18939
stability in acids, alkalis, and oxidizers, 16: 2952
stability in acids, alkalis, and oxidizers, 16: 11583(T) (AEC-tr-5040)
stability in gases, 16: 29421
stabilization by vanadium, 17: 22195
strength of powdered, at 20 to 2800°C, 18: 39984
structure and tensile properties of, additive effects of titanium and zirconium on, 18: 27978
superconducting critical temperature of, correlation with valence electrons, (E), 20: 21911
superconducting properties, 19: 20572
superconducting transition, effects of structure on, 18: 34283 (UCRL-11390)
superconducting transition temperature of, structure effects in, (E/T), 19: 23565
superconducting transition temperature of, 20: 17607
superconductivity of, high-field, (E), 19: 25449
superconductivity, (E), 19: 37739
superconductivity, 19: 43997(R) (UCRL-11889)
tensile properties at 475 to 650°C, 17: 30962(R) (ASD-TDR-63-238)
thermal expansion at temperatures up to 2000°C, 17: 12688
thermal properties to 5000°F, 16: 18938
thermal properties of, at 500 to 5000°F, 17: 16636 (ASD-TDR-62-765)
thermionic emission properties of, microstructure effects on, 17: 37532
thermionic emission from cesiated surfaces of, (E), 20: 21584
thermodynamic properties, 17: 3470 (BMI-1601)
thermodynamic properties of, tables of, 17: 40777(R) (RAD-SR-63-183)
thermodynamic properties, 20: 10816(T) (NASA-TT-F-285)
thermodynamic stability of, review of data on, 19: 23064
use of, in nuclear rockets, 17: 8710 (TID-16315(Del.))
welding to high-melting metals by vacuum diffusion, 19: 22931(T) (JPRS-29550)
welding to titanium and tungsten carbides and molybdenum and tungsten metals, diffusion, 20: 7545

wetting by liquid cobalt, copper, iron, and nickel, 20: 1837
graphite–MoC, fabrication of dispersions of, by hot-working, 20: 21306
graphite–Mo_2C, fabrication and properties of hot-pressed composites of, 20: 31688 (NASA-CR-507)
graphite–MoC, fabrication and physical properties of, 20: 39367
graphite–MoC, properties and structure of hot-pressed, 20: 5089(R) (GA-6181)
Hf–MoC–Ta, preparation and properties of dispersion-hardened, 20: 39441(P)
MoB–MoC, superconducting properties, 18: 34283 (UCRL-11390)
MoC–NbC, use of, in nuclear rockets, 17: 8710 (TID-16315(Del.))
MoC–NbN, superconducting properties, 20: 17589 (CONF-650922, pp 541-9)
MoC–Ta–Zr, preparation and properties of dispersion-hardened, 20: 39441(P)
MoC–UC, crystal structure of $UMoC_2$, 17: 40773 (LADC-5656)
MoC–UC, free energy of formation of, 16: 25833
MoC–UC, performance as thermionic emitters, 18: 35929(R) (GA-4769(Pt.I))
MoC–UC, thermionic emission constants of, 17: 16783 (LADC-5128)
MoC–UC, thermodynamic properties, 18: 2222 (LADC-5907)
MoC–UC, use of, in nuclear rockets, 17: 8710 (TID-16315(Del.))
MoC–UC–ZrC, analysis for molybdenum and zirconium by x-ray fluorescence spectrometry, 18: 39077
MoC–UC–ZrC, x-ray-fluorescence spectrographic analysis for molybdenum and zirconium, 18: 35449 (LADC-5830)
MoC–VC, high-field superconductivity of, (E), 19: 25449

MOLYBDENUM CARBONYLS

azulene-, crystal structure, 20: 40796(R) (IS-1500(Sect.C))
complexes with cyclic phosphite esters, 20: 1561 (IS-T-31)
decomposition in ion source of mass spectrometer, mechanism of, 20: 14584(R) (TID-22444)
force constants for hexa-, from infrared spectra, 17: 14288
heat of formation, ionization potentials, and fragmentation schemes of, 19: 13304
labeling with molybdenum-99 by uranium fission in presence of chromium carbonyl, 18: 43696
preparation of labeled, utilization of uranium fission in, 16: 6463
proton magnetic resonances of, 17: 15962 (TID-18199)
pyrolysis of, oxycarbides from, 18: 31501
thermal decomposition of, properties of deposits from, 20: 41468

MOLYBDENUM CHLORIDES

complexes with dimethylformamide and methyl sulfoxide, 19: 43990 (MIT-1965-15)
complexes with tetramethylammonium salt, bonding in, 19: 19841 (MIT-1965-18)
reduction for coating deposition using hydrogen, 20: 39354 (BMwF-FBK-66-09)
separation by reversed-phase partition chromatography using organophosphorus compounds, 18: 25614
separation from ethyl ether by solvent extraction using adiponitrile, ethanolamine, and formamide, 17: 40933
superconductivity of cubic modification of, 20: 2346 (UCRL-11471)
synthesis of anhydrous, 17: 30553
thermodynamic properties of, in molten alkali metal chlorides, 20: 1882
thermodynamic properties, 20: 10816(T) (NASA-TT-F-285)
Fe–Mo_2C, growth and orientation of carbide precipitates in ferrite 20: 29726

MOLYBDENUM COMPLEXES

formation and properties of, in oxalic acid–sulfuric acid systems, 20: 7039
magnetic susceptibility and spectra, 19: 19892
separation of cerium-, using ethyl acetoacetate and ketones, 18: 10202
stereochemistry of discrete eight-coordination in, 17: 18029
thiocyanatopentacarbonyl, preparation and properties, 19: 7412
with α-carboxy-β-methyltropolone, composition of, spectrophotometric studies of, 20: 29179
with carbamic acid, synthesis, 16: 6425
with cesium oxychloride, chemistry of, 19: 13328
with diantipyrilmethane and thiocyanate, formation and structure, 18: 10016
with diethyldithiophosphate, solvent extraction from mineral acids using carbon tetrachloride, 16: 28926(T) (AEC-tr-5202)
with diethylenetriaminepenta- and triethylenetetraminehexaacetic acids, preparation, properties, and structure, 16: 11610
with germanium and pyridine or 8-quinolinol, properties for use as thin-layer chromatograms, 19: 20069
with myricetin, composition and stability of, 20: 20674
with niobium, formation and reduction, 16: 16315
with phosphoroniobium, formation and structure of, 17: 1469
with pyridine–pyrocatechol, determination of, 18: 13706
with thiocyanate, solvent extraction in three-phase system using diantipyrilmethane, 18: 13950
with thiourea, preparation and stability of, 18: 13785
with 2,2′-bipyridine-1,1′-dioxide, preparation and properties of, 20: 25067

MOLYBDENUM COMPOUNDS

analysis for impurities, spectrographic, 18: 17766
atom clusters in complex, bonding in, 17: 28826 (NYO-10551)
bibliography on, 20: 753 (SB-415(Suppl. 1))
catalytic effects on reduction of tellurate with tin, 16: 14673
crystallography of, with perovskite-like structure, 19: 25014
cyclopentadienyl, covalent radii and length of metal-metal bonds in, 19: 17922
organic, beta decay in, 19: 13486
toxicology, comparison of compounds and pure metal dusts, 16: 9827
use as photosensitizer for polymerization of methyl methacrylate at various pH's, 20: 38934
with molybdenum and tungsten bronzes, preparation, properties, and structure of, 20: 43213

MOLYBDENUM COUPLES

Mo/Mo–Re, calibration of thermocouples of, pressure effects on, 20: 43636 (UCRL-14993)
Mo/Mo–W, densification of sintered tungsten–molybdenum powder compact, Kirkendall-effect in, 20: 16994
Mo/Nb, fabrication and performance as thermocouple at high temperature, 19: 22927 (TIM-888)
Mo/Nb, interdiffusion in, 18: 42031
Mo/Nb, performance to 2300°F, 19: 44348 (PWAC-473)
Mo/Ni/Nb/stainless steel, diffusion in bimetallic tubing of, with molybdenum and nickel diffusion barriers, inter-, 20: 11215(R) (NASA-CR-54718)
Mo/Ni/Nb–Zr/stainless steel, diffusion in bimetallic tubing of, with molybdenum and nickel diffusion barriers, inter-, 20: 11215(R) (NASA-CR-54718)
Mo/Ni/stainless steel/Ta, diffusion in bimetallic tubing of, with molybdenum and nickel diffusion barriers, inter-, 20: 11215(R) (NASA-CR-54718)
Mo/Re, performance as thermocouples to 3200°F, 16: 13277 (DC-57-8-150)
Mo/Re–W, fabrication and performance as thermocouple at high temperature, 19: 22927 (TIM-888)
Mo/Re–W, properties as thermocouple, 18: 14164 (PWAC-422)
Mo/Re–W, stability of clad, at 2000°F for 10,000 hr, 19: 18237 (PWAC-454)
Mo/Re–W, stability of thermocouples of, (E), 19: 40859
Mo/Re–W, thermoelectric stability at 1000 to 2000°C, 19: 22986 (NRL-6231)
Mo/Re–W, thermoelectric potential at 200 to 1800°C, 19: 37031(R) (GEMP-47A, pp 101-6)
Mo/U, diffusion coefficients and Kirkendall effect in, 17: 32578(T) (AEC-tr-5932)
Mo/UO_2, uranium diffusion rate at 1600 to 1800°C, 19: 39070(R) (GEST-2046)
Mo–W, calibration and performance, 16: 22597 (WADD-TR-60-924)
Mo/W, stability of thermocouples of, (E), 19: 40859
Mo/W, thermoelectric stability at 1000 to 2000°C, 19: 22986 (NRL-6231)

MOLYBDENUM FLUORIDES

complexes with sodium fluoride, dissociation pressures of, 18: 43362 (ORNL-P-321)
complexes with sodium fluorides, preparation and dissociation pressures of, 19: 2292
complexes with sodium fluoride, preparation, 20: 22987
corrosive effects on nickel and nickel alloys at 500°C, (E), 20: 14008(R) (ANL-7122, pp 42-69)
fluorine-19 NMR and spin-lattice relaxation in, 20: 40892
molecular force constants of hexavalent, calculation of, 17: 25174
molecular force constants of MoF_6, 20: 26865
molecular structure of, mean-square amplitudes of interatomic distances in hexavalent, 18: 1639
molecular structure of, mean amplitudes of vibration at 0 and 298°K in, 20: 38897
physical properties, 16: 16464
preparation and purification, 16: 17621(T) (AEC-tr-4456(p.14-17))
reactions of hexavalent, with nitrosyl chloride, nitrosyl fluoride, and nitryl fluoride, 18: 5272
reactions with liquid and gaseous dinitrogen tetroxide, 17: 1417 (GAT-T-970)
reactions with nitrogen oxides, 16: 4156 (GAT-T-552(Rev.1))
reactions with nitrogen oxides, 16: 25339 (GAT-T-969)
reactions with nitrogen dioxide, 17: 7993 (GAT-T-971)
reactions with nitrosyl fluoride, 17: 7993 (GAT-T-971)
reactions with nitryl fluoride, 17: 7993 (GAT-T-971)
reactions with nitrosyl chloride, 17: 7993 (GAT-T-971)
reactions with uranium hexafluoride, 20: 36803
reduction to metal powder by hydrogen–fluorine flame, 19: 15997

(K-L-6020)
separation from uranium hexafluoride, 19: 13553(P)
spectra, infrared and Raman, 16: 22118
spectra of, vibrational, 17: 7655(R) (ANL-6600)
thermodynamic properties, 16: 7957(R) (TID-14392)
thermodynamic properties at 50 to 1600°K for ideal gaseous state at one atmosphere pressure, 16: 26979
thermodynamic properties, 20: 10816(T) (NASA-TT-F-285)
thermodynamic properties at 4 to 350°K, 20: 18669
valence force constants of, (T), 19: 14245
MoF_6–UF_6 analysis of, for molybdenum to uranium ratio, spectrometric, 16: 25313 (K-1433)
MoF_6–UF_6, phase studies, 19: 23991(R) (ANL-7003)
MoF_6–UF_6, phase studies, 20: 20803(R) (ANL-7055, pp 99-162)

MOLYBDENUM HALIDES
reduction to molybdenum using zinc, 20: 9405(P)
vaporization, 19: 9604(R) (IS-900(Sect.M))

MOLYBDENUM IODIDES
thermodynamic properties, 20: 10816(T) (NASA-TT-F-285)

MOLYBDENUM IONS
coordination chemistry of quadrivalent and tervalent, 19: 19892
determination of hexavalent, gravimetric, 18: 37084
effects of pentavalent, on deuteron and proton relaxation times in aqueous solutions, 20: 38893
effects on cobalt determination in steel, 20: 43145
effects on copper determination, 20: 36726
electron spin resonance in calcium tungstates, (E), 19: 8464
energy spectra of, produced by laser-beam ionization, (E), 20: 27728
hyperfine structure of, core polarization effects on, (T), 20: 23875 (BNL-10040)
paramagnetic resonance of pentavalent, in molybdenum oxide, 16: 30967
production of beams of, in magnetron gas discharges, 18: 7417
production of, for mass spectrometry, thermal techniques for, 20: 31226
reactions with graphite at 30 kev, x-ray diffraction studies of products from, 16: 33804
reduction by lead–sodium alloy in acid solution, 19: 17867
separation from titanium using vanillin, 19: 333

MOLYBDENUM ISOTOPES
abundance anomalies in meteorites, 16: 10711
abundances in iron and stone meteorites, 18: 5901
binding energies and energy levels, (T), 19: 6661
book: *Radioactive Molybdenum Isotopes*, in Russian, 20: 16917
content in meteorites, 17: 25468
determination in irradiated fuels for burnup calculations, 16: 23627 (TID-7629(p.166-76))
determination in irradiated uranium-235, 20: 5493(R) (ANL-6925, pp 253-4)
determination of stable, in iron meteorites, 18: 44350
deuteron reactions (d,p) and (d,t) with, nuclear structure studies from, 18: 32877
diffusion in chromium–iron alloy at 600 to 1200°C, 18: 22477(R) (BMI-X-10081)
energy levels, Coulomb excitation, 16: 15658
energy levels, interactions, nuclear moments, and transitions in, 17: 24381 (AD-403411)
energy levels of, isobaric analogue, 19: 14640
excited states in even, first, 16: 12518
gamma emission by, radiative widths for, (E), 19: 23626 (JINR-P-1995)
gamma reactions on, cross sections for, 19: 12496
isomeric transitions, M_4-type, 16: 22985 (NP-11747)
masses and neutron separation energies of even-A, 17: 38102
neutron binding energies in, 18: 32881
neutron resonance integrals for, 17: 22566 (TID-18590)
nuclear masses and binding energies, 16: 1066
nucleon interactions in, effective, (T), 20: 6337
photon reactions (γ,n), threshold energy for, (E), 19: 21287
proton reactions (p,n) and (p,p) with, isobaric analog states from, (E), 20: 12078
proton reactions (p,α) and (p,2n) at 11.2 Mev, cross sections for, 17: 40056
separation of, Aston band effects on mass-spectrometric, 18: 18267
separation, operational efficiency of calutrons for, 18: 27811(R) (ORNL-TM-198)

MOLYBDENUM ISOTOPES Mo-88
decay and half life of, 18: 36594
preparation by niobium-93 (p,xn) reactions, half life of, 18: 36594

MOLYBDENUM ISOTOPES Mo-89
decay and half life of, 18: 36594
preparation by molybdenum (p,pxn) reactions, 18: 36594

MOLYBDENUM ISOTOPES Mo-90
beta decay of, lifetime of 24-sec isomer of niobium-90 from, 20: 3088
beta decay of, very low energy isomer in, (E), 20: 36265
decay of, conversion-electron spectra from, (E), 20: 15751
decay of, conversion electron and positron spectra from, (E), 20: 30388
decay of, gamma transitions in, (E), 19: 21258(R) (UCRL-11828 (p.67-71))
decay of, low energy isomer in, (E), 20: 1159 (UCRL-16306)
decay scheme, (E), 20: 24358(R) (UCRL-16580, pp 1-93)

MOLYBDENUM ISOTOPES Mo-91
beta decay half life (E), 19: 3295
decay of, niobium-91 levels from, (E), 20: 24364
deuteron reactions (d,p) at 13.6 Mev, angular distributions from, 17: 24414
energy level densities in, effects of spin on, 16: 33853
gamma spectra, 18: 1050
gamma spectra, (E), 19: 16840(R) (IDO-17050)
isomeric yield ratio from molybdenum-92 (γ,n) reactions to 70 Mev, (E), 19: 43299
production in gamma reactions (γ,n) at 20.5 Mev, 16: 18512
production of isomeric, in neutron reactions (n,2n) with molybdenum-92, (E), 19: 39790

MOLYBDENUM ISOTOPES Mo-92
alpha reactions (α,p) at 20 Mev, spectra of, 18: 28645
alpha reactions (α,α′n), (α,α′2n), (α,α′pn), (α,n), (α,2n), (α,3n), (α,p), (α,pn), (α,p2n), and (α,p3n), excitation functions for, 18: 28746
alpha reactions (α,α′n), (α,α′2n), (α,α′pn), (α,n), (α,2n), (α,3n), (α,p), (α,pn), (α,p2n), and (α,p3n), angular momentum effects on nucleus decay, 18: 28746
alpha reactions (α,n) and (α,p) at 7 to 29 Mev, excitation functions for, (E), 19: 27531
alpha reactions (α,n) with, conversion-electron spectra from, (E), 19: 33388
alpha reactions (α,n) with, conversion electron spectra from, (E), 20: 13881
alpha reactions at energies up to 40 Mev, excitation functions, 16: 3671(R) (TID-14241)
bremsstrahlung reactions (γ,p) at 24 Mev, direct photoeffect and evaporation contributions in, 17: 38209
bremsstrahlung reactions (γ,n) to 70 Mev, isomeric yield ratio in, (E), 19: 43299
content in natural molybdenum, synthesis processes for, 18: 31767
deuteron reactions (d,p) on, angular distribution of protons from, 17: 17258
deuteron reactions (d,p) at 13.6 Mev, angular distributions from, 17: 24414
deuteron reactions (d,t) at 20 Mev, angular distributions and energy spectra from, 17: 38177
deuteron reactions (d,p) with, spectra from, 19: 21394
deuteron reactions (d,n), cross sections for isomer production in, 19: 25476(R) (TID-21525)
deuteron reactions (d,n) at 15 Mev, isomeric yield ratios for, 20: 16508(R) (NYO-2771-13)
energy level transitions in, probability for E2, (T), 19: 10311
energy levels, 18: 22898
energy levels from $(g_{9/2})^2$ configuration, (T), 19: 47617
energy levels of, 17: 38002(T) (AEC-tr-5734(p.20-4))
energy levels of, Coulomb excitation of first, 17: 9601
energy levels of, configuration of two-particle isomeric, 18: 28614
energy levels of, shell model, 18: 30795
energy levels of, half life of, 18: 32797
energy levels of, shell model analysis of, (T), 19: 37824(R) (ORNL-3800(p.50-7))
energy levels with soft core potential, (T), 19: 45311
energy levels, configuration mixing, and proton-neutron interaction in, (T), 19: 23678
gamma reactions at 20.1 to 21.2 Mev, activation cross sections, 16: 4755 (TID-13492)
gamma reactions (γ,n) at 20.5 Mev, cross sections, 16: 18512
gamma reactions (γ,n) on, nuclear excited states from, 16: 33853
gamma scattering by, resonance, 18: 11175 (ANL-6797(p.275-87))
helium-3 reactions (He-3,α), (He-3,αn), (He-3,d), and (He-3,p) at 18 Mev, cross sections for, (E), 19: 43391
neon-20 and -22 reactions with, delayed proton emitters from, (E), 20: 17687 (JINR-P-2514)
neon-20 reactions at 100 Mev, delayed proton emission in, (E), 20: 11964 (JINR-E-2464)
neon-20 reactions (Ne-20,xn) with, cross sections for production of tellurium isotopes in, (E), 20: 46774
neutron capture and total cross sections at 7 to 15,000 ev, 17: 22657
neutron capture cross section, 17: 36669 (WASH-1042)
neutron radiative capture cross sections, (T), 19: 19106
neutron reactions at 14.6 Mev, mechanisms and shell effects, 16: 12487
neutron reactions (n,p), separation energies for, 17: 2242 (TID-16949)
neutron reactions [(n,d) + (n,np) + (n,pα)] at 14.8 Mev, cross section limit, product half life, and Q value for, 17: 2242 (TID-16949)
neutron reactions (n,p) at 14.8 Mev, cross sections for, 17: 2242 (TID-

16949)
neutron reactions (n,2n) at 14.8 Mev, cross sections for, 17: 2242 (TID-16949)
neutron reactions (n,α) at 14.8 Mev, cross sections and product half-life for, 17: 2242 (TID-16949)
neutron reactions (n,αγ), (n,αn), (n,np), (n,2p), (n,pγ), and (n,pn) at 14.8 Mev, cross sections for, 17: 2242 (TID-16949)
neutron reactions (n,p), cross sections for, 17: 7101 (NP-12330(p.97-103))
neutron reactions (n,2n) at 14.1 Mev, cross sections for, 17: 15299
neutron reactions (n,p) and (n,α) at 14.7 Mev, total activation cross sections for, 17: 19261
neutron reactions (n,α), preparation of zirconium-89 by, in reactor, 17: 24508
neutron reactions (n,p), preparation of niobium-92 by, in reactor, 17: 24508
neutron reactions (n,p) with, cross sections for fast, 17: 31056
neutron reactions (n,2n) with, cross sections for positron production in, 18: 13061
neutron reactions (n,α) at 15 Mev, energy spectra of, 18: 36597
neutron reactions (n,2n) at 14 Mev, shell effects in, (T), 19: 12536
neutron reactions (n,2n) with, excitation function for, (E), 19: 32279
neutron reactions (n,2n) at 14.8 Mev, isomer production in, (E), 19: 39790
neutron reactions (n,2n) at 3 Mev above threshold, cross section for, (E), 20: 46614
neutron reactions (n,2n) at 13.56 to 14.7 Mev, excitation functions for, (E), 20: 46614
neutron reactions (n,2n) at 14.6 Mev, cross section for, (E), 20: 46614
neutron strength functions, (T), 19: 25497
neutron strength functions of, calculation of, 20: 38038
oxygen-16 reactions with, coulomb excitation in, 18: 24620(R) (ORNL-TM-874)
photodisintegration of, cross sections for, 18: 44793
photon reactions (γ,n), threshold energy for, (E), 19: 21287
production in stars, 16: 12308
proton reactions (p,p), fine structure near isobaric analog resonances in, 20: 4923
proton reactions (p,n) and (p,p) with, isobaric analog states from, (E), 20: 12078
proton reactions (p,pγ) at 10 Mev, energy level structure from, (E), 20: 32471
proton reactions (p,γ) with, gamma decay of analog resonances in, (E) 20: 42331
proton scattering by, isobaric resonances in, 18: 42750
proton scattering by, isobaric spin analog resonances in, (T), 19: 6723
separation by gaseous diffusion, economics and rate of, 19: 22855 (ORNL-TM-1047(p.127-36))

MOLYBDENUM ISOTOPES Mo-93

core isomerism in, (T), 19: 17051
decay, 18: 26595
decay of, fluorescent yield of niobium L-shell from electron capture, 18: 7732
decay of, semiconductor detection of, 18: 23990
electron transitions in isomeric, total conversion coefficient of 0.265-Mev, 18: 7737
energy level spacings, 16: 6018
energy level spins in, 18: 22893
energy levels, 16: 18488
energy levels, (E), 19: 43391
energy levels at 5.3 and 5.6 Mev, fine structure of, 18: 42750
energy levels of, configuration of three-particle isomeric, 18: 28614
energy levels of, shell model analysis of, (T), 19: 37824(R) (ORNL-3800(p.50-7))
energy levels, configuration mixing, and proton-neutron interaction in, (T), 19: 23678
energy-level density and transitions, (E), 20: 42331
gamma dose constants for metastable, 20: 46617
internal conversion spectra of isomeric, (E), 20: 15751
isomeric states in, transition probabilities in nuclear core, 18: 28597
preparation and isolation of carrier-free, 18: 33665
production in niobium-93 decay, mass discrepancies from, 16: 26287 (IS-408)
production, methods evaluation for, 18: 27811(R) (ORNL-TM-198)
production, separation, and uses of, 20: 16917
separation of neutron-deficient, from zirconium-92, 20: 43067(R) (IDO-14679, pp 6-46)
spins and parities of ground and first excited states in, 17: 17258

MOLYBDENUM ISOTOPES Mo-94

abundance in naturally occurring molybdenum, 19: 44242
alpha reactions (α,p2n), angular momentum effects on nucleus decay, 18: 28746
alpha reactions (α,p2n), excitation functions for, 18: 28746
beta feeding of 1.57-Mev state in, from decay of niobium-94m, 17: 4330(R) (IDO-16781)
content in natural molybdenum, synthesis processes for, 18: 31767
decay of 1.57-Mev state of, 17: 7257
deuteron reactions (d,p) on, angular distribution of protons from, 17: 17258
deuteron reactions (d,2n) with, technetium-94 production in, 17: 24460
deuteron reactions (d,t) at 20 Mev, angular distributions and energy spectra from, 17: 38177
energy level transitions in, M1-M2 mixing ratios as test of purity of vibrational, (T), 19: 25503
energy levels, 16: 23073
energy levels and transition probabilities of second 2^+ states, 16: 23142
energy levels and gamma spectra, 16: 24837
energy levels of, 17: 38002(T) (AEC-tr-5734(p.20-4))
energy levels of, shell model analysis of, (T), 19: 37824(R) (ORNL-3800(p.50-7))
energy levels, (E), 19: 5231
gamma spectra from Coulomb excitation of, (E), 19: 37817(R) (ORNL-3778(p.116-19))
gamma transition at 871.1 kev following Coulomb excitation, (E), 20: 3043
neon-20 reactions at 100 Mev, delayed proton emission in, (E), 20: 11964 (JINR-E-2464)
neon-20 reactions with, delayed proton emitters from, (E), 20: 17687 (JINR-P-2514)
neutron capture and total cross sections at 7 to 15,000 ev, 17: 22657
neutron radiative capture cross sections, (T), 19: 19106
neutron reactions (n,p), separation energies for, 17: 2242 (TID-16949)
neutron reactions (n,p) at 14.8 Mev, cross sections and product half life for, 17: 2242 (TID-16949)
neutron reactions (n,α) at 15 Mev, energy spectra of, 18: 36597
neutron strength functions, (T), 19: 25497
neutron strength functions of, calculation of, 20: 38038
oscillations and transition probabilities, 18: 18921
photon reactions (γ,n), threshold energy for, (E), 19: 21287
production in stars, 16: 12308
proton reactions (p,n) and (p,p) with, isobaric analog states from, (E), 20: 12078
proton reactions (p,d) and (p,n) at 11.2 Mev, cross sections for, 17: 29586
proton reactions (p,α), (p,d), and (p,n) at 11.2 Mev, cross sections for, 17: 40056
separation by gaseous diffusion, economics and rate of, 19: 22855 (ORNL-TM-1047(p.127-36))

MOLYBDENUM ISOTOPES Mo-95

abundance in naturally occurring molybdenum, 19: 44242
content in natural molybdenum, synthesis processes for, 18: 31767
Coulomb excitation by nitrogen ions, (E), 19: 16895
deuteron reactions (d,p) on, angular distribution of protons from, 17: 17258
deuteron reactions (d,p) at 13.6 Mev, angular distributions from, 17: 24414
deuteron reactions (d,t) at 20 Mev, angular distributions and energy spectra from, 17: 38177
energy level lifetime, (E), 20: 7449
energy level spacings, 16: 6018
energy levels, 16: 18488
energy levels, (E), 19: 29290
energy levels of, lifetime of 768-kev, (E), 19: 23781
energy levels of, parity and spin of, 19: 47605
energy levels of, lifetime of, (E), 20: 1175
energy levels of, g-factor of 204-kev, (E), 20: 10012
gamma-gamma directional correlations in, 17: 4101
hyperfine structure, (E), 19: 8464
neutron capture and total cross sections at 7 to 15,000 ev, 17: 22657
neutron capture by, gamma spectra of p- and s-wave resonances in, 17: 34951
neutron capture cross sections at 10^3 to 10^5 ev, 16: 26518
neutron capture gamma spectra, level spin assignments from, 16: 14058
neutron capture resonances in, 18: 42622(R) (ANL-6879(p.2-20))
neutron radiative capture cross sections, (T), 19: 19106
neutron reactions (n,p), separation energies for, 17: 2242 (TID-16949)
neutron reactions (n,γ) in, gamma spectra from resonances in, 17: 6776(R) (ANL-6603(p.1-8))
neutron reactions (n,p), cross sections for, 17: 7101 (NP-12330(p.97-103))
neutron reactions (n,γ) with, spin and parity values for first and second excited levels in, 17: 13519
neutron reactions (n,p) with, cross sections for fast, 17: 31056
neutron reactions (n,α) at 15 Mev, energy spectra of, 18: 36597
neutron resonance capture, observation of p-wave, 16: 33886
neutron resonance capture in, gamma spectra from, 17: 41527(R) (ANL-6720(p.2-15))
neutron resonances in, 17: 22568 (WASH-1041)

neutron resonances at 45.1 and 161.0 ev, radiation widths of, (E), 20: 3133
nuclear moments of, E2 and M1, (E), 20: 17998
nuclear quadrupole moment, (E), 19: 8478
nuclear spin relaxation in molybdenum metal, (E), 20: 17998
proton reactions (p,n) and (p,p) with, isobaric analog states from, (E), 20: 12078
spins and parities of ground and first excited states in, 17: 17258

MOLYBDENUM ISOTOPES Mo-96
abundance in naturally occurring molybdenum, 19: 44242
alpha scattering by, 17: 40436(R) (NYO-10063(p.105-15))
content in natural molybdenum, synthesis processes for, 18: 31767
deuteron elastic scattering at 15 Mev, optical model for, 19: 14604
deuteron reactions (d,p) on, angular distribution of protons from, 17: 17258
deuteron reactions (d,p) at 13.6 Mev, angular distributions from, 17: 24414
deuteron reactions (d,t) at 20 Mev, angular distributions and energy spectra from, 17: 38177
deuteron reactions (d,p) at 12 Mev, molybdenum-97 energy levels from, (E), 20: 46747
energy level scheme, 17: 41961
energy level spacings, 16: 6018
energy level structure, 16: 14030
energy levels and transition probabilities of second 2^+ states, 16: 23142
energy levels and gamma spectra, 16: 33886
energy levels and gamma spectra of, 17: 9545
energy levels and gamma spectra of, from niobium-96 decay, (E), 19: 45341
energy levels at 2.73 Mev, spin of, 19: 29228(R) (AEET/NP/10)
energy levels of, vibrational, (T), 19: 5248
energy levels of, multipolarity and spin-parity of, (E), 19: 17057
Fermi gas coefficient and nuclear temperature, 18: 998 (AD-299005)
gamma spectra from Coulomb excitation of, (E), 19: 37817(R) (ORNL-3778 (p.116-19))
gamma transition at 778.5 kev following Coulomb excitation, (E), 20: 3043
neutron capture and total cross sections at 7 to 15,000 ev, 17: 22657
neutron elastic scattering at 1.509 Mev, polarization in, 17: 31410 (TID-19051)
neutron inelastic scattering at 6 Mev, compound-nucleus and direct reactions in, 17: 38207
neutron radiative capture cross sections, (T), 19: 19106
neutron reactions at 14.6 Mev, mechanisms and shell effects, 16: 12487
neutron reactions (n,p) at 14.8 Mev, cross sections and product half life for, 17: 2242 (TID-16949)
neutron reactions (n,p), cross sections for, 17: 7101 (NP-12330(p.97-103))
neutron reactions (n,α) at 15 Mev, energy spectra of, 18: 36597
neutron resonance at 132.6 ev, radiation width of, (E), 20: 3133
neutron strength functions, (T), 19: 25497
neutron strength functions of, calculation of, 20: 38038
nuclear parameters from angular and polarization correlations in E0 transitions, (T), 20: 46770
proton reactions (p,n) and (p,p) with, isobaric analog states from, (E), 20: 12078
proton reactions at 1.8 Bev, isobaric yield distributions in, 18: 7761
proton reactions (p,γ) in stars, 16: 12308
spins and parities of ground and first excited states in, 17: 17258
x-ray spectra of, K_α muonic, (E), 19: 17001
x-ray spectra of, muon-capture-induced, (E), 20: 19273(R) (BNL-929, pp 3-43)

MOLYBDENUM ISOTOPES Mo-97
abundance in naturally occurring molybdenum, 19: 44242
burnup calculations for, in reactor fuels, 20: 16061(R) (BAW-296)
content in natural molybdenum, synthesis processes for, 18: 31767
Coulomb excitation by nitrogen ions, (E), 19: 16895
deuteron reactions (d,p), proton angular distributions from, 17: 21084
deuteron reactions (d,t) at 20 Mev, angular distributions and energy spectra from, 17: 38177
energy level spacings, 16: 6018
energy levels from molybdenum-96 (d,p) reactions at 12 Mev, (E), 20: 46747
energy levels of, lifetime of 665-kev, (E), 19: 23781
hyperfine structure, (E), 19: 8464
magnetic moment, (T), 20: 3118
neutron capture and total cross sections at 7 to 15,000 ev, 17: 22657
neutron radiative capture cross sections, (T), 19: 19106
neutron reactions at 14.6 Mev, mechanisms and shell effects, 16: 12487
neutron reactions (n,p), separation energies for, 17: 2242 (TID-16949)
neutron resonance at 71.6 ev, radiation width of, (E), 20: 3133
nuclear moments of, E2 and M1, (E), 20: 17998
nuclear quadrupole moment, (E), 19: 8478
nuclear spin relaxation in molybdenum metal, (E), 20: 17998
photodisintegration of, cross sections for, 18: 44793
photon reactions (y,n), threshold energy for, (E), 19: 21287
proton reactions (p,n) and (p,p) with, isobaric analog states from, (E), 20: 12078
separation from neutron-deficient technetium-96m, 20: 43067(R) (IDO-14679, pp 6-46)
spins and parities of ground and first excited states in, 17: 17258

MOLYBDENUM ISOTOPES Mo-98
abundance in naturally occurring molybdenum, 19: 44242
alpha reactions (α,n) and (α,2n) with, conversion-electron spectra from, (E), 19: 33388
alpha reactions (α,n) with, conversion electron spectra from, (E), 20: 13881
burnup calculations for, in reactor fuels, 20: 16061(R) (BAW-296)
content in natural molybdenum, synthesis processes for, 18: 31767
deuteron reactions (d,t) at 20 Mev, angular distributions and energy spectra from, 17: 38177
energy level spacings, 16: 6018
energy levels, (E), 20: 12152
energy levels and transition probabilities of second 2^+ states, 16: 23142
energy levels from niobium-98 decay, (E), 20: 36201
energy levels of, 17: 38002(T) (AEC-tr-5734(p.20-4))
gamma spectra from Coulomb excitation of, (E), 19: 37817(R) (ORNL-3778(p.116-19))
gamma transition at 786.8 kev following Coulomb excitation, (E), 20: 3043
neutron capture and total cross sections at 7 to 15,000 ev, 17: 22657
neutron capture by, at 0 to 50 kev, cross sections for, 17: 41883
neutron capture cross section, 16: 10991
neutron capture cross sections, 16: 20302(R) (ANL-6477(p.217-23))
neutron capture cross section of, at 0.2 to 2.0 ev, 16: 28641(R) (ANL-6543)
neutron capture cross sections, 17: 2222 (JINR-P-1010)
neutron capture cross section of, energy dependence of radiative (E/T), 19: 3391
neutron radiative capture cross sections, (T), 19: 19106
neutron reactions at 14.6 Mev, mechanisms and shell effects, 16: 12487
neutron reactions (n,p) at 14.8 Mev, cross sections and product half life for, 17: 2242 (TID-16949)
neutron reactions (n,γ) with, production of carrier-free technetium-99m by, 18: 20071
neutron reactions (n,α) at 15 Mev, energy spectra of, 18: 36597
neutron reactions (n,γ) at 0.4 to 3 Mev, cross sections for, (E), 20: 6556(R) (ANL-7105, pp 36-58)
neutron reactions (n,γ) at 10 kev to 3 Mev, cross sections for, (E), 20: 32370(R) (ANL-7175, pp 212-16)
neutron reactions (n,p) at 14.8 Mev, cross sections for, (E), 20: 36201
neutron resonance cross sections of, determination of, by boron absorption technique, 16: 28036 (TID-16059)
neutron resonance integral, 17: 11979(R) (DP-805)
neutron resonance integrals and self-shielding factors for detector foils of, 17: 17106 (DP-817)
neutron resonance at 12.15 ev, radiation width of, (E), 20: 3133
neutron strength functions, (T), 19: 25497
nuclear structure of, subshell closure in, 18: 40506 (IS-878)
photodisintegration of, cross sections for, 18: 44793
proton reactions (p,n) and (p,p) with, isobaric analog states from, (E), 20: 12078
proton reactions (p,γ) in stars, 16: 12308
x-ray spectra of, K_α muonic, (E), 19: 17001
x-ray spectra of, muon-capture-induced, (E), 20: 19273(R) (BNL-929, pp 3-43)

MOLYBDENUM ISOTOPES Mo-99
analytical uses, 18: 33483
beta decay of, branching ratios for, (E), 19: 16957
beta decay of, levels from, (E), 19: 19143
beta decay scheme, (E), 19: 16949
chemical effects on specific surface of molybdenum disulfide, 18: 23696
content in air from Chinese detonations in 1964, 20: 8980(R) (BNWL-36, pp 3.1-122)
content in atmosphere from underground nuclear explosion, effects of filtering on, 20: 45833 (UCRL-14778)
content in fallout particles, 20: 2053
content in fallout from Chinese nuclear test of May 14, 1965, 20: 33530
content in fallout and precipitation near Leningrad, 20: 16704
content in ocean fish, effects of content in sea water on, 20: 11054
content in rain water, Fayetteville, Arkansas, Oct. 1964, 20: 16663 (TID-21470)
content in stratospheric and tropospheric air filter samples collected in 1961 and 1962, 19: 9755 (HASL-153)
content in stratosphere, 19: 20657(R) (DASA-1309)
content in stratospheric and tropospheric samples in Project Star Dust, 1963, 20: 16727(R) (HASL-168)
decay of, correction factors for, 17: 24384 (AERE-R-4237)

decay of, gamma branching in, 18: 13636(R) (ORNL-3537(p.71-105))
decay of, gamma branching spectra in, 19: 22818(R) (ORNL-3650(p.221-38))
decay of, production of 6.06-hr technetium-99 in, 18: 32001
decay of, production of technetium-99m in, 19: 17781(R) (ORNL-3750)
decay scheme, 18: 28722
determination by autoradiographic measurement of half life using ring oven methods, 20: 18584
determination in fission products, 16: 11507 (AERE-AM-88)
determination in fallout particles, gamma spectrometric, 19: 17821
determination in fission product mixtures for calculating uranium-235 abundance in uranium, 20: 31189
determination in mixed fission products, 16: 2988
determination in radiation source mixture with lanthanum-140, from decay data, 17: 10547
determination in reactor effluents, methods for, 17: 35627(R) (AFSWC-TDR-62-146)
determination in rain water, method for, 17: 38952
determination in sea water, methods for, 20: 1749 (USNRDL-TR-912)
determination of, radiochemical, 18: 17729 (PG-Report-564)
determination of, gamma spectrometric, 19: 32545 (CEA-R-2461)
differentiation from technetium-99 in rabbits, effects on gamma counting rate of, 20: 18213
diffusion in irradiated fuel element cladding alloys and materials at 600 to 1200°C, 20: 21232 (BMI-1763)
diffusion in, self-, 17: 27868
diffusion in uranium dioxide single crystals, 19: 38034
distribution and volatility in air-burst debris, 20: 9184 (USNRDL-TR-933)
distribution from nuclear excavation in basalt, 20: 613
effects of radiation from, on surface of molybdenum oxide, (E), 20: 44026(T)
energy level spacings, 16: 6018
fission yield of, 17: 22608
fractionation in surface bursts, correlation of data on, 20: 27211 (USNRDL-TR-991)
gamma dose constants for, 20: 46617
gamma spectra, 17: 34966
incorporation in molybdenum carbonyl by uranium fission in presence of chromium carbonyl, 18: 43696
metabolism in domestic animals, 18: 11645(R) (ORO-614)
metabolism in normal and deficient cows, 19: 6954
metabolism in rats, 19: 40319
metabolism in sheep and swine, 19: 45759(R) (ORO-631, pp 77-82)
metabolism in sheep and swine, 20: 32907(R) (ORO-648, pp 62-70)
physical properties of, 19: 46139
placental permeability studies using, review of, 18: 1345
preparation by Szilard-Chalmers reactions in 8-hydroxyquinolinates, 16: 8763(T) (CEA-tr-X-425)
preparation of carrier-poor, by sublimation from neutron target, 20: 27013
production and use of, 17: 6171
production facilities for, 19: 36452(R) (BNL-900(p.105-20))
production in atmosphere by neutron activation of airborne dust, inhalation hazard from, 19: 26589
production in reactors, 17: 3022 (BNL-6407)
production of, techniques for, 18: 41892 (BNL-864)
production, separation, and uses of, 20: 16917
properties and uses of, produced at Brookhaven, 19: 22853 (ORNL-TM-1047(p.113-16))
ranges of thermal-fission, in aluminum, (E/T), 20: 24351(R) (MIT-905-52, pp 1-41)
ranges of uranium-235 fission-recoil, in aluminum, 17: 36651 (EFINS-62-71)
ranges of uranium-238 proton fission-recoil, in aluminum, 17: 36651 (EFINS-62-71)
sensitivity for activation analysis using beta-gamma-gamma sum-coincidence gamma spectrometer, 20: 16335(R) (NBS-TN-276)
separation from fission products by ion exchange, 18: 5427
separation from fission products, chromatographic, 19: 23998(R) (TID-21733)
separation from impurities by anion exchange chromatography, 16: 10991
separation from irradiated uranium by ring-oven technique, 18: 41326
separation from metastable technetium-99 by sorption on ferric oxide, 20: 5591 (SGAE-CH-18/1965)
separation from neutron-irradiated uranium by fractionated sorption on aluminum oxide, 16: 20544
separation from neutron-irradiated biological materials, use of Szilard-Chalmers effect in, 20: 18583
separation from technetium-99 by anion exchange, 19: 13525 (KFK-216)
separation from technetium-99 by milking, equipment and process for, 20: 1730 (BNL-9601)
separation from technetium-99m by ion exchange on hydrous zirconium oxide in nitric acid, 20: 20566 (ORNL-TM-1468)
separation from technetium-99m sorbed on aluminum oxide using physiologic solution, 20: 38997 (NIJS-R-483)
separation from uranium-238 fission products, determination of fission-rate ratio of uranium-238-to-uranium-235 from, 18: 26249
separation from uranium and fission products, chromatographic, 18: 29557 (KR-83)
separation from yttrium-90 in food by solvent extraction using di-(2-ethylhexyl) phosphoric acid, 19: 15386
separation method for, 20: 46102(R) (ORNL-4013)
separation of metastable technetium-99 from, design of eluting generator for, 20: 27068
sorption in rat gastrointestinal tract, effects of segmental ligation on, 19: 33768
tracer uses for vaporization of molybdenum in vacuo, 20: 36834
uptake and excretion in man, 18: 21800
uptake by eggs and tissues of chickens following intramuscular and oral administration, 18: 38775(R) (ORO-624)
uptake by liver, differential, 17: 33498
use as gamma source in radiometric measurement of ore pulp flow rates, 20: 46105 (BM-RI-6855)
use as source of technetium-99, for medical uses, 20: 38986
use for diagnosis of liver diseases, 20: 174
use for studies of flow characteristics and mixing properties in systems, 18: 37628
use in liver scanning, 19: 46139
yield from neutron fission of uranium-235, 16: 21347 (AWRE-0-58/61)
yields from helium ion-induced fission of lead-207 at 41.1 to 26.3 Mev, 20: 37996
yields from neutron fission of plutonium-239, uranium-235, and uranium-238, 16: 1037(T) (AEC-tr-4696)
yields from neutron fission of thorium-232, 18: 9311 (IS-558)
yields from photofission of uranium by 650-Mev bremsstrahlung, 20: 22040
yields from spontaneous fission of uranium-238, equilibrium-ratio calculations of, 20: 44815
yields from thorium-232 fission, (E), 20: 17860
yields from 14.7-Mev neutron-induced fission of uranium-238, 19: 19135
yields in helium-4 fission of thorium-232, 17: 826
yields in neutron fission of uranium at 14.7 Mev, 18: 44835
yields in neutron fission to natural thorium at 14.7 Mev, 18: 44836
yields in plutonium-239 fission in resonance region, (E), 20: 17858
yields in proton fission of uranium-238 at 7.1, 9.4, and 12.0 Mev, 20: 37995
yields in thermal neutron fission of plutonium-239, 19: 16873

MOLYBDENUM ISOTOPES Mo-100

abundance in naturally occurring molybdenum, 19: 44242
alpha reactions (α,α'n), (α,α'p), (α,n), and (α,p), excitation functions for, 18: 28746
alpha reactions (α,α'n), (α,α'p), (α,n), and (α,p), angular momentum effects on nucleus decay, 18: 28746
alpha reactions (α,n) at 7 to 29 Mev, excitation functions for, (E), 19: 27531
alpha reactions (α,n) at energies up to 23 Mev, excitation functions, 16: 3671(R) (TID-14241)
bremsstrahlung reactions (γ,p) at 24 Mev, direct photoeffect and evaporation contributions in, 17: 38209
burnup calculations for, in reactor fuels, 20: 16061(R) (BAW-296)
content in natural molybdenum, synthesis processes for, 18: 31767
energy level strength functions for, 16: 26518
energy levels and transition probabilities of second 2^+ states, 16: 23142
energy levels of, 17: 38002(T) (AEC-tr-5734(p.20-4))
gamma spectra from Coulomb excitation of, (E), 19: 37817(R) (ORNL-3778(p.116-19))
gamma transition at 535.5 kev following Coulomb excitation, (E), 20: 3043
neutron capture and total cross sections at 7 to 15,000 ev, 17: 22657
neutron capture by, at 0 to 50 kev, cross sections for, 17: 41883
neutron capture by, cross sections for radiative, (E/T), 19: 10263
neutron capture cross sections at 30 to 2100 kev, 16: 2501(T) (AEC-tr-4680)
neutron capture cross sections, 17: 2222 (JINR-P-1010)
neutron capture cross section of, energy dependence of radiative (E/T), 19: 3391
neutron capture, rate measurements, 16: 17233 (CRRP-985-D)
neutron radiative capture cross sections, (T), 19: 19106
neutron reactions (n,2n) at 14.8 Mev, cross sections for, 16: 7072
neutron reactions at 14.6 Mev, mechanisms and shell effects, 16: 12487
neutron reactions (n,γ) at fission energies, 16: 18429
neutron reactions (n,α) at 15 Mev, energy spectra of, 18: 36597
neutron reactions (n,2n) at 14 Mev, shell effects in, (T), 19: 12536
neutron reactions (n,γ) with, 20: 44817
neutron resonance cross sections of, determination of, by boron absorption technique, 16: 28036 (TID-16059)
neutron resonance integrals and self-shielding factors for detector foils of, 17: 17106 (DP-817)

neutron strength functions, (T), 19: 25497
nuclear shape parameters for, 18: 11221
oscillations and transition probabilities, 18: 18921
photodisintegration of, cross sections for, 18: 44793
photon reactions (γ,n), threshold energy for, (E), 19: 21287
proton radiative capture by, 18: 14590(R) (NIRL/R/60)
proton reactions (p,n) and (p,p) with, isobaric analog states from, (E), 20: 12078
proton reactions (p,γ) in stars, 16: 12308
proton reactions (p,α), (p,d), and (p,2p) at 11.2 Mev, cross sections for, 17: 29586

MOLYBDENUM ISOTOPES Mo-101
beta decay of, gamma spectra from, (E), 20: 34611
decay schemes for, 20: 44817
determination in mixed fission products, 16: 2988
energy level spacings, 16: 6018
gamma dose constants for, 20: 46617
gamma spectra, 17: 34966
gamma spectra, 18: 1050
gamma spectra resolution of, in presence of technetium-101, 20: 45603
preparation and properties of, for use as neutron sources, 18: 16379
use for studies of flow characteristics and mixing properties in systems, 18: 37628

MOLYBDENUM ISOTOPES Mo-102
determination in mixed fission products, 16: 2988

MOLYBDENUM ISOTOPES Mo-103
decay and half life, 17: 29629
half life, 19: 39892

MOLYBDENUM ISOTOPES Mo-104
half life, 16: 31085
production by uranium-235 fission, decay and half life of, 18: 32769

MOLYBDENUM ISOTOPES Mo-105
detection in fission products, 16: 31085
detection in fission products, 16: 31086
half life, 16: 31086
half life, 19: 39892

MOLYBDENUM NITRIDES
analysis for nitrogen by reactions with chlorine and measurement of nitrogen released, 19: 17800
electric properties of, effects of non-metallic atoms on, 17: 8854
electron band structure, 20: 23427(R) (UCRL-16580, pp 219-50)
electron structure and physical properties of crystals of, 17: 27875
molybdenum epitaxy with, 19: 23040
preparation and properties of, 19: 18472(T) (JPRS-28739)
preparation of single-crystal, 20: 18556(R) (BNL-929, pp 66-82)
preparation, properties, and uses of, review on, 16: 27640(T) (FTD-TT-62-430)
review, 18: 39899 (LA-2942)
sintering of, electron density in phase lattices and optimal conditions for, 17: 27767
spectra of, isotope shifts in, (E), 20: 965
thermal conductivity, effects of electronic and crystalline structure, 16: 24208
thermodynamic properties, 20: 10816(T) (NASA-TT-F-285)

MOLYBDENUM ORES
book: *Geology of Commercial Uranium–Molybdenum Ore Deposits*, 20: 45937
processing by reductive chlorination, 20: 4072(P)

MOLYBDENUM OXIDES
see also Lithium Scandium Molybdenum Oxides
analytical uses as standard in rubidium determination in cesium by x-ray fluorescence spectroscopy, 19: 46186
catalytic effects on recombination of gases in thorium oxide slurries, 16: 25407(P)
catalytic effects on hydrocracking of polyphenyls, 17: 28434 (IDO-16858)
catalytic effects on decomposition of tritium-labeled compounds, 19: 7491
corrosion by biphenyl, 20: 25491(T) (AECL-2330, pp 179-95)
dehydration to 600°C for neutron transmission measurements, 20: 3914 (AERE-M-1654)
dust mixtures of, with silicon dioxide, effects on lungs in rats of, 16: 27499
effects on lubricating properties of ceramic-bonded calcium fluoride coatings, 19: 18395 (NASA-TN-D-2688)
effects on production of boron nitride by reaction of boron oxide with nitrogen or ammonia, catalytic, 19: 36430(P)
effects on sintering behavior of urania powders, 20: 37202
electric conductivity of, effects of structure on, 19: 42858
electric properties of, negative-resistance effect in, (E), 19: 16132
electron band structure, 20: 23427(R) (UCRL-16580, pp 219-50)
evaporation, effects of radioactivity content, 16: 9452
exchange reactions with oxygen-18, mechanism of, 18: 33545
fission fragment damage in, 19: 23163(R) (ORNL-3650(p.111-86))
free energy of formation, 16: 28963
free energy of formation of tetravalent, 17: 23367
free energy of formation at 1100°F, 17: 32571(R) (MSAR-63-105)
growth of scheelite single-crystal $Li_{0.5}Dy_{0.5}MoO_4$, $Na_{0.5}Pr_{0.5}MoO_4$, $Na_{0.5}Tm_{0.5}MoO_4$, $Sr_{0.9}Eu_{0.1}MoO_4$, and $Sr_{0.9}Gd_{0.1}MoO_4$, 19: 26304
growth of single crystals of, (E), 20: 32697
helium atom interactions at 0.5 to 2 kev, physical mechanisms, 16: 27777
molecular shrinkage effects and vibration mean amplitudes for MoO_2 and MoO_3, (T), 20: 31233
oxidation of, mechanism of, 20: 13198
phase studies, 16: 30823
phase studies at 600 to 1700°C, 19: 34727
polarographic behavior in molten borax, 16: 17770
preparation and properties of monocrystalline, 18: 25893(R) (ANL-6868 (p.355-72))
preparation and properties of thin films, 18: 30189
preparation of crystalline, 16: 17582(R) (ORNL-3262(p.187-94))
preparation of spherical particles of, procedure and apparatus for, 20: 14971(P)
preparation of thin films of, 20: 5846
production of ionic, from heating molybdenum surfaces, 19: 32768
radiation effects of molybdenum-99 on surface, 16: 580
radiation effects of fission fragment bombardment, 16: 33409
radiation effects on, 29-Mev helium-3 ion, 18: 37778
radiation effects of incorporated molybdenum-99 on surface of, (E), 20: 44026(T)
radiation effects on photosensitivity of single crystals of, gamma, neutron, and x, 20: 46235
radioinduced defects in, fission fragment, 17: 37604
radioinduced dislocation formation, 16: 29463
reactions in ammonium fluoride and hydrofluoric acid solutions, 19: 19913
reactions with boric oxide and carbon to prepare molybdenum boride, 20: 18702
reactions with fluorine, 20: 5595(R) (ANL-6925, pp 107-64)
reactions with fused potassium nitrate at 350°C, 19: 42436
reactions with liquid sodium, composition and properties of products in, 19: 44021
reactions with niobium and titanium oxides, 20: 26864
reactions with oxygen, equilibrium oxygen pressures produced in, 20: 277 (AERE-R-4942)
reactions with rare earth oxides at 1200°C, 16: 13003(R) (NP-11299)
reduction by hydrogen, molybdenum-powder conglomeration in, 18: 30124
reduction by hydrogen–water vapor mixtures, design of gas flow apparatus for studying, 18: 31444
reduction by magnesium in bombs to high-purity molybdenum, 16: 10429 (BM-RI-5934)
reduction from tri- to dioxide by hydrogen at 350 to 600°C, 19: 25002
reduction in molten electrolytes and electrodeposition of molybdenum from, 18: 25316 (BM-RI-6444)
reduction of dioxide to metal by hydrogen at 600 to 850°C, 19: 25002
reduction to metal by hydrogen, design of gas recycle system for, 19: 911
reduction to metal using hydrogen development of fluidized-bed reactor for, 19: 912
separation of technetium-99m from irradiated, by solvent extraction using triisooctylamine, 19: 42595 (NIJS-R-450)
solubility in borax at 760 to 900°C, 20: 3951
solubility in nitric acid, nitric acid–ferric nitrate, nitric acid–uranyl nitrate, and water systems, 16: 168
sorptive properties for chloride and potassium ions, effects of pH on, 20: 14651
spectra in low frequency region, infrared, 18: 23549
spectra of, isotope shifts in, (E), 20: 965
stability in gases, 16: 29421
structure of, high-resolution electron microscopy of, 19: 960(R) (ORNL-3676(p.32-4))
testing for use in shaft seals for potassium space power plants, 20: 2242
thermal decomposition of, mass spectrometry of gases from, 19: 5890
thermodynamic properties, 20: 1880
thermodynamic properties at 0 to 1200°K, 20: 7115
thermodynamic properties, 20: 10816(T) (NASA-TT-F-285)
uptake of vapors of, by oxides, isopiestic study, 19: 26296 (USNRDL-TR-823)
use of films of, for detection of energetic hydrogen ions, 17: 6409 (UCRL-6793)
Al–MoO_3, ignition tests on, in contact with electrically pulsed bridge-wires, 20: 26820(R) (SC-CR-66-2019)
Al_2O_3–CoO–MoO_3, catalytic properties for benzene synthesis from acetylene, for radiocarbon dating, 19: 19944 (ORINS-50)

Al_2O_3–Mo_2O_3, radiation effects on spectra of catalysts of, effects of hydrocarbon sorption on, 17: 22258
CdO–MoO_3, melting point of $CdMoO_4$, (E), 19: 17202
Eu_2O_3–MoO_3, fabrication and properties testing, 18: 4177(R) (ORNL-3470(p.221-6))
Ga_2O_3–MoO_3–Sm_2O_3, crystal growth in, composition diagrams for, 19: 17902
Gd_2O_3–MoO_3–Na_2O, crystal growth in, composition diagrams for, 19: 17902
$H_4Fe(CN)_6$–Mo_2O_3, ion exchange properties for fission products, 18: 31400
Li_2MoO_4–MoO_3, density and electric conductivity of molten, 19: 24528
Li_2MoO_4–MoO_3, temperature effects on density and electric conductivity of, 18: 23486
Li_2MoO_4–MoO_3, use as flux in growth of beryllium oxide single crystals, 18: 22417 (CONF-281-46)
MnO_2–MoO_3, properties as metalizing paint for metal-to-ceramic seals, 20: 27401(R) (AD-632362)
Mo–MoO_2, reactions with oxygen, equilibrium oxygen pressures produced in, 20: 277 (AERE-R-4942)
MoO_3–K_2MoO_4, density and electric conductivity of molten, 19: 24528
MoO_3–K_2MoO_4, temperature effects on density and electric conductivity of, 18: 23486
MoO_2–MoO_3–UO_2, phase studies, 20: 2384
MoO_3–Nb_2O_5, crystal structure of complex compounds in, 19: 25037
MoO_3–Nb_2O_5, double oxide formation and composition in, after sintering, 18: 12057
MoO_3–Nb_2O_5, phase studies, 19: 41049
MoO_3–NiO, radiation effects on catalytic activity in hydrodesulfurization of hydrocarbons, 17: 16117(P)
MoO_3–Ta_2O_5, crystal structure of complex compounds in, 19: 25037
MoO_3–UO_2, reduction of, by carbon, 16: 18613(R) (EURAEC-22)
MoO_3–UO_2–UO_3, phase studies at 750°C, 20: 29798
MoO_2–VO_2, phase studies, 19: 42859
$Pb_3Nb_2O_7$–MoO_3, electric properties, 17: 14801(R) (AD-278452)

MOLYBDENUM OXYCHLORIDES
preparation and properties of oxidetetrachloride, 18: 23465

MOLYBDENUM OXYFLUORIDES
physical properties, 16: 16464
structure of ions of, 18: 27393

MOLYBDENUM PHOSPHIDES
phase studies of, using mass spectrometry, 20: 31723
properties, 19: 2802 (NYO-2541-1)
superconductivity of, (E), 20: 9901
vaporization, 18: 8800(R) (TID-19990(Paper 3))
vaporization behavior, 18: 3430 (TID-19737)

MOLYBDENUM SELENIDES
intercalation of strongly electropositive metals in, 19: 46265
preparation and properties of single crystals of, 16: 31611
thermoelectric properties of doped, 18: 37115 (ANL-6856)

MOLYBDENUM SILICIDES
analysis for molybdenum and silicon, 19: 10996
behavior and stability at 1700 to 2000°C, 18: 16499
bibliography on phase relations of, 17: 30913 (NP-12972)
bibliography on phase relations of, 18: 10518 (AD-410526)
coating of, effects of, on oxidation resistance of graphite, 20: 29773
coating on refractory metals, cementation processes for, 18: 34091
decomposition of divalent, into Mo_5Si_3 at 1700 to 2000°C, 18: 16499
degradation in, effects of stoichiometry and temperature effects on pest, 18: 42055
deposition on molybdenum–titanium alloy for oxidation protection, 19: 7877 (ML-TDR-64-74)
development and testing for use at 2500°F, 16: 18044 (WADD-TR-60-889)
development of coatings of, for tantalum alloy and metal protection, 16: 24148(R) (ASD-TR-61-676)
effects of films of, on thermal radiation properties of molybdenum, 16: 32039(R) (PWA-1863)
effects on thermoelectric properties of MCC 50, 19: 12129(R) (ASD-TDR-62-896(Pt.II))
electron emission from surfaces of, thermionic, 19: 46571 (HRL-5249-S)
electron emission at high temperatures, 19: 4743(R) (NP-14444)
electron structure and physical properties of crystals of, 17: 27875
evaporation rate and vapor pressure at 1100 to 2000°C, 16: 2208(T) (AEC-tr-4865)
fabrication by slip casting, 20: 31697
formation on molybdenum surface, effects of diffusion kinetics on, 19: 22943
formation on sintered molybdenum, protective effects of, 20: 37204
hardness and surface friction of, effects of temperature on, 20: 29771
heat of formation, 17: 2959(T) (AEC-tr-5264)
heats of formation, 16: 20394
ion emission at high temperatures, 19: 4743(R) (NP-14444)
joining to aluminum oxides by reaction pressing, method for, 18: 44078
lubricity of Molykote X-107 and Z, for journal bearings, 17: 25382 (ASD-TR-61-705)
magnetic susceptibility, 18: 20541
oxidation at reduced pressures, effects of additives on, 20: 41424
oxidation at 1500 to 1800°C, kinetics of, 20: 13195
oxidation at 450 to 650°C, 20: 31669
oxidation kinetics, 20: 4077(R) (IS-1200(Sect. E))
oxidation kinetics of, in air at 500 to 1000°C, 20: 13198
oxidation of, at 1300 to 2100°K, kinetics of, 17: 21665(R) (ASD-TDR-62-203(Pt.II))
oxidation at 1100 to 1700°C and oxygen pressures of 10^{-7} to 1 atm, 19: 26775
oxidation at 1300 to 2000°K and 2 to 20 torr, 19: 28760
oxidation at 1400 to 1700°C, 18: 25928
oxidation at 450 to 650°C, 19: 30683
oxidation kinetics, 18: 1834(R) (IS-700(Sect.E))
oxidation protection properties of, 19: 40961
oxidation resistance of, role of silica in, 18: 44091
oxidation tests of Kanthal at 1400 to 1650°C, 19: 9624 (SCNC-270)
performance as coating on molybdenum and molybdenum alloys, 20: 5910
performance as electrode in contact ion engines, 19: 13613
performance in focus electrodes in cesium-contact ion thrustors, 20: 31383
performance of coatings of, on Pebble Bed Reactor fuel, 16: 9663 (NYO-9064)
production by vacuum-siliciding, temperature effects in, 18: 37626
properties as die support, 17: 14788(R) (NMI-9700.6)
properties as high-temperature coating, 20: 29650
properties as magnetohydrodynamic electrodes, 18: 7458 (PWA-2125)
protective effects against oxidation of molybdenum, additive effects of chromium and iron on, 18: 12586
protective effects as coating on molybdenum and molybdenum–titanium alloy, 19: 47061
reactions with beryllium, 18: 34149
reactions with copper and nickel mattes and molten salts, 20: 14989
reactions with molten metals at 400 to 1500°C, 19: 37112
shear modulus and sound velocity of, 18: 24174
sintering conditions, 17: 22142
space-environment effects on coatings of, 17: 36333
spectral emittance at 800 to 5000°F, 16: 18939
stability in gases, 16: 29421
thermal expansion of, mean coefficient of, 18: 24173
thermal properties at high temperatures, 16: 4551 (WADD-TR-60-904)
thermionic emission from cesiated surfaces of, (E), 20: 21584
thermodynamic properties at 0 to 1200°K, 20: 7115
thermoelectric properties, 17: 8855
B_4C–$MoSi_2$–ZrB_2, development of composite of, 20: 9391
BCN–$MoSi_2$, preparation and properties, 20: 29169
BN–$MoSi_2$–ZrB_2, mechanical properties of composites of, 20: 5845
BN–$MoSi_2$–ZrB_2, tensile properties at 70 to 3500°F, 18: 30170 (CONF-553-1)
$CrSi_2$–$MoSi_2$–WSi_2, phase studies, 20: 27542
Mo–$MoSi_2$, kinetics of formation of intermediate silicides in, 19: 16145
$MoSi_2$–H_2O, zeta potential, 18: 18294(R) (NP-13758)
$MoSi_2$–$NbSi_2$–WSi_2, phase studies, 20: 27542
$MoSi_2$–$ReSi_2$, phase studies, 20: 27542
$MoSi_2$–$ReSi_2$–WSi_2, phase studies, 20: 27542
$MoSi_2$–SiC, oxidation tests at 1400 and 1500°C, 19: 9624 (SCNC-270)
$MoSi_2$–SiC–TiC, oxidation tests at 1400 to 1650°C, 19: 9624 (SCNC-270)
$MoSi_2$–SiC–ZrC, oxidation tests at 1400 and 1500°C, 19: 9624 (SCNC-270)
$MoSi_2$–$TaSi_2$–WSi_2, phase studies, 20: 27542
$MoSi_2$–TiC, oxidation tests at 1400°C, 19: 9624 (SCNC-270)
$MoSi_2$–$TiSi_2$–WSi_2, phase studies, 20: 27542
$MoSi_2$–WSi_2–VSi_2, phase studies, 20: 27542
$MoSi_2$–ZrB_2, emittance testing of coatings of, 19: 18465(R) (PWA-2518)
$MoSi_2$–ZrB_2, oxidation of, in argon–carbon dioxide mixtures at 2250°C, 17: 6520(R) (NP-12313)
$MoSi_2$–ZrB_2, oxidation and thermodynamic properties at high temperatures, 18: 35939(R) (NP-14192)
MoSi–ZrB, oxidation of, kinetics of, 20: 7527
$MoSi_2$–ZrB_2, preparation and properties of oxidation-resistant, 16: 9223
$MoSi_2$–ZrB_2, preparation and properties of, 19: 37121
$MoSi_2$–ZrB_2, properties of Boride Z, 17: 12692
$MoSi_2$–ZrB_2, tensile properties of pressed and sintered, at 70 to 3650°F, 18: 7217(R) (TID-19877)
$MoSi_2$–ZrB_2, tensile properties at 70 to 3650°F, 19: 7909 (TID-21430)
$MoSi_2$–ZrB_2, tensile properties at 70 to 3650°F, 19: 26823 (TID-21843)
$MoSi_2$–ZrC, oxidation tests at 1400 and 1500°C, 19: 9624 (SCNC-270)

MOLYBDENUM STEEL
brittle fracture behavior of, temperature effects on, 17: 23972(T,R) (EURAEC-521)

corrosion by carbon dioxide at 460 to 525°C, 17: 1869 (AAEC/E-97)
corrosion by carbon dioxide at 450 to 825°C, 18: 16444
corrosion by mercury, 18: 21675 (NP-13795)
corrosion by steam and water at 100 to 600°C, 17: 23894
crack propagation and strength, 16: 19335 (ASD-TR-61-207)
creep-rupture properties, 17: 39531(R) (EURAEC-689)
ductility of, effects of hydrogen on, 18: 24153(T,R) (EURAEC-1002)
fatigue under cyclic plastic strain at high temperatures, 19: 23110
flame cutting of 200-mm-thick sheets of, 17: 23928(T) (EURAEC-511)
physical properties of, effects of high-temperature sodium on, 17: 18756(R) (MSAR-63-47)
preparation, and properties, and uses of cast, 18: 14529
properties of, review of methods of improving, 19: 18523
radiation effects at 60 to 400°C, 17: 24014(T,R) (EURAEC-530)
radiation effects on SA 212 B, 20: 30788(R) (ANL-7190, pp 176-88)
radiation effects on fatigue of A302B, neutron, 20: 39406 (WAPD-T-1864)
radiation embrittlement, effects of dispersed second phase on fast neutron, 20: 5846
reactions with carbon dioxide to 565°C, 19: 22997 (TRG-Report-842)
reactions with uranium dioxide to 800°C, 19: 22997 (TRG-Report-842)
rupture strength of chromium, in helium at 1000 and 1200°F, 17: 4980
stress-relieving practices for, 17: 23925 (TID-7620(Pt.I)(p.251-7))
welding of plates of, deformation and temperatures in electroslag, 17: 23929(T) (EURAEC-593)
B–C–Cr–Mn–Mo–Ni–Nb–V, precipitation of niobium carbide in, 18: 37726
B–Cr–Mo–Ni, fabrication and properties, 18: 15565
B–Mo, properties of, for pressure vessels, 16: 19384
B–Mo, radiation effects on pressure vessels of, fast-neutron, 20: 21228 (AE-221)
C–Cr–Co–Mn–Mo–Ni, mechanical properties of welded, 19: 22863(R) (AD-606809)
C–Cr–Mn–Mo–Ni, mechanical properties of welded, 19: 22863(R) (AD-606809)
C–Cr–Mn–Mo–Ni–Si, strength and toughness of dynamically strain-aged, 20: 7584 (UCRL-16363)
C–Cr–Mn–Mo–Ni–Si–V, strength and toughness of dynamically strain-aged, 20: 7584 (UCRL-16363)
C–Cr–Mo–Ni–Nb, mechanical properties, effects of low-temperature tempering on, 19: 9647 (AD-604876)
C–Cr–Mo–Ni, mechanical properties, effects of low-temperature tempering on, 19: 9647 (AD-604876)
C–Cr–Mo–Ni–V, mechanical properties, effects of composition variations on, 19: 9645 (AD-604867)
C–Cr–Mo–Ni–V, mechanical properties, effects of low-temperature tempering on, 19: 9647 (AD-604876)
Co–Mo–Ni, mechanical properties of, effects of strain rate on, 20: 11284 (UCRL-14599)
Co–Mo–Ni, properties of Mar-aging, 16: 24153 (DMIC-Memo-156)
Co–Mo–Ni, tensile properties of strain-aged, 20: 31716(R) (UCRL-16658, pp 121-32)
Cr–Mn–Mo–Ni, development of high-strength weldable low-alloy, 20: 27481(R) (EURAEC-1419 and App.)
Cr–Mn–Mo–Ni, ductility of low-alloy, effects of alloying additions on, 20: 27481(R) (EURAEC-1419 and App.)
Cr–Mn–Mo–Ni, welding of very thick plates of, process development for, 20: 23621(R) (EURAEC-1548)
Cr–Mn–Mo–V, reactions with carbon dioxide to 400°C, 19: 22997 (TRG-Report-842)
Cr–Mo, bonding to type 316 stainless steel, 17: 36200(R) (NP-13033)
Cr–Mo, brittleness in, during time-to-rupture tests, theory of notch-, 20: 25563 (EURAEC-1350)
Cr–Mo, carburization, 18: 32144(R) (MSAR-64-75)
Cr–Mo, carburization of, by carbon-saturated sodium at 1200°F, 19: 901(R) (MSAR-64-102)
Cr–Mo, carburization by carbon-rich sodium at 1200°F, 20: 9413 (CONF-650620, pp 1-17)
Cr–Mo, carburization by high-carbon sodium at 1200°F, 20: 11235 (COO-65-194)
Cr–Mo, compatibility with plutonium carbide–uranium carbide, 18: 8729 (UNC-5074)
Cr–Mo, compatibility with plutonium carbide–uranium carbide, 19: 24923(R) (UNC-5081)
Cr–Mo, compatibility of Croloy 2¼ in sodium-heated boiler containing type 316 stainless steel, 19: 44133(R) (BAW-1280-31)
Cr–Mo, compatibility with boron carbide of AISI 4130, 20: 11226
Cr–Mo, corrosion of, by carbon dioxide, effects of additives on, 16: 22556
Cr–Mo, corrosion of, by carbon dioxide, effects of additives on, 16: 29344(T) (AEC-tr-5303)
Cr–Mo, corrosion of, by sodium, 16: 28558 (TID-7623(p.135-48))
Cr–Mo, corrosion by bismuth–uranium solutions, 17: 14765 (BNL-736)
Cr–Mo, corrosion and mass transfer by sodium at 1000 to 1200°F, 17: 29280 (GEAP-3726)
Cr–Mo, corrosion by air, helium, and sodium at 1100°F, 17: 29281(R) (MSAR-63-57)
Cr–Mo, corrosion by sodium, test run data on, 17: 37479 (GEAP-4181)
Cr–Mo, corrosion by sodium at 1100°F, 18: 564(R) (MSAR-63-142)
Cr–Mo, corrosion by liquid sodium in test loop, 18: 4195 (GEAP-4182)
Cr–Mo, corrosion by sodium at high temperatures, 18: 10472(R) (MSAR-64-6)
Cr–Mo, corrosion by flowing sodium, test run data on, 18: 12575 (GEAP-3726(Vol.3))
Cr–Mo, corrosion by sodium at 500 to 600°C, 18: 25937
Cr–Mo, corrosion by air, helium, and sodium at high temperatures, 18: 30131(R) (MSAR-64-65)
Cr–Mo, corrosion by flowing sodium, 18: 34073(R) (GEAP-4438)
Cr–Mo, corrosion by liquid sodium at 1100°F in air, helium, and oxygen, 18: 35988 (MSAR-64-81)
Cr–Mo, corrosion by nitrogen and sodium, development of loops and techniques for studying, 18: 35955(R) (MSAR-60-34)
Cr–Mo, corrosion by air, helium, and liquid sodium, 18: 35956(R) (MSAR-64-93)
Cr–Mo, corrosion of Croloy 2¼ by fused alloy–salt mixtures, 18: 36751 (ANL-6912)
Cr–Mo, corrosion by sodium (liquid), 18: 38467 (A/CONF.28/P/537)
Cr–Mo, corrosion of Croloy 2¼, by sodium at 1250°F, 19: 568(R) (TID-20894)
Cr–Mo, corrosion of Croloy 2¼, by sodium hydroxide in sodium and water to 1200°F, 19: 566(R) (BAW-1280-16)
Cr–Mo, corrosion of Croloy 2¼, by sodium hydroxide in sodium and water to 1200°F, 19: 565(R) (BAW-1280-15)
Cr–Mo, corrosion by sodium with high carbon content at 1200°F, 19: 6298(R) (MSAR-64-126)
Cr–Mo, corrosion of Croloy 2¼ by sodium–sodium hydroxide at 900°F, 19: 7676(R) (BAW-1280-20)
Cr–Mo, corrosion by flowing sodium, test run data on, 19: 7866 (GEAP-4437)
Cr–Mo, corrosion by sodium, (E), 19: 13916 (SAN-8002(p.189-209))
Cr–Mo, corrosion by sodium–water reaction products, 19: 13582 (SAN-8002(p.231-57))
Cr–Mo, corrosion of Croloy 2¼ by sodium at 980°F, decarburization in, 19: 15712(R) (BAW-1280-18)
Cr–Mo, corrosion of Croloy 2¼ in sodium-heated steam generator after 4000 hr, 19: 20107(R) (BAW-1280-22)
Cr–Mo, corrosion by sodium in test loops, 19: 22894 (GEAP-4183)
Cr–Mo, corrosion of Croloy 2-¼ by cadmium–magnesium–uranium–zinc/chloride flux at 600 and 650°C, 19: 32279(R) (ANL-7020(p.3-99))
Cr–Mo, corrosion by mercury at high temperature, 19: 36949(R) (BNL-900(p.121-97))
Cr–Mo, corrosion of Croloy 2¼ by sodium hydroxide solutions at 0 to 900°F, 19: 38803(R) (BAW-1280-26)
Cr–Mo, corrosion of Croloy 2¼ by sodium hydroxide solutions at high temperatures, 19: 46530(R) (BAW-1280-27)
Cr–Mo, corrosion of Croloy 2¼ by sodium–water reaction products, 19: 46478(R) (BAW-1280-25)
Cr–Mo, corrosion and mass transfer in flowing sodium, 20: 9414 (CONF-650620, pp 18-35)
Cr–Mo, corrosion by flowing sodium at 1000 to 1200°F, equation for, 20: 11227
Cr–Mo, corrosion by mercury vapor at 1250°F, 20: 11214(R) (NASA-CR-54717)
Cr–Mo, corrosion by sodium at 700°F, 20: 14979 (GEAP-4835)
Cr–Mo, corrosion by mercury, corrosion loop testing of, 20: 16972(R) (NASA-CR-54719)
Cr–Mo, corrosion by sodium, 20: 23601(R) (GEAP-4837)
Cr–Mo, corrosion of Croloy 2¼, by lead at 1100°F, 20: 23603 (ORNL-TM-1437)
Cr–Mo, corrosion by mercury at high temperatures, 20: 25474(R) (BNL-954, pp 122-67)
Cr–Mo, corrosion by boiling water reactor coolants, effects of ammonia on suppression of, 20: 26920 (AECL-2562)
Cr–Mo, corrosion of Croloy 2¼, by mercury, 20: 33834
Cr–Mo, corrosion and mass transfer in flowing sodium, 20: 39345 (GEAP-4831)
Cr–Mo, corrosion by sodium in loops, statistical analysis of data on, 20: 43826 (GEAP-4830)
Cr–Mo, corrosive effects of sodium on mechanical properties, 19: 22896(R) (MSAR-65-47)
Cr–Mo, crack growth in, effects of pressure and temperature on fatigue, 20: 46981(R) (GEAP-5147)
Cr–Mo, creep and fatigue properties, effects of air, helium, and sodium on, 18: 8754 (MSAR-63-168)
Cr–Mo, creep at 1325°F, effects of welding on, 20: 11215(R) (NASA-CR-54718)
Cr–Mo, creep rupture properties of weldments of, 17: 3520

Cr–Mo, creep-rupture properties of carbonized, effects of air, helium, and sodium at 1100°F on, 17: 34406(R) (MSAR-63-117)
Cr–Mo, creep-rupture properties, 17: 39531(R) (EURAEC-689)
Cr–Mo, creep-rupture properties of carbonized, effects of air, helium, and sodium at 1100°F on, 18: 4201(R) (TID-19756)
Cr–Mo, creep-rupture properties of carbonized, effects of air, helium, and sodium at 1100 and 1200°F on, 18: 8755(R) (MSAR-63-174)
Cr–Mo, creep rupture of, effects of aging at 1100°F, 20: 2258(R) (MSAR-65-149)
Cr–Mo, creep-rupture properties in air, helium, and high- and low-oxide sodium at 1100°F, 18: 18315(R) (MSAR-64-30)
Cr–Mo, creep-rupture properties, 19: 7899(R) (EURAEC-1112)
Cr–Mo, decarburization by exposure to sodium at 1100°F, 19: 4623(R) (MSAR-63-6)
Cr–Mo, decarburization of Croloy 2¼ by sodium at 980°F, 19: 7676(R) (BAW-1280-20)
Cr–Mo, development for high-temperature sodium service, 18: 4167 (NAA-SR-7544)
Cr–Mo, diffusion of, in uranium carbide at 820°C, 16: 6686(R) (NDA-2162-5)
Cr–Mo, diffusion in type 316 stainless steel, 17: 36200(R) (NP-13033)
Cr–Mo, effects of hydrogen on embrittlement of irradiated pressure vessels of, 19: 47098
Cr–Mo, electroslag welding of thick, 19: 9634(R) (EURAEC-1166)
Cr–Mo, fatigue of type 4130, energy criterion for, (T), 20: 27521
Cr–Mo, fatigue properties, 19: 24670 (NAA-SR-9827)
Cr–Mo, fatigue tests of Croloy 2¼, 19: 7889(R) (ATL-A-143)
Cr–Mo, fission product deposition on, from gas streams, 18: 7926(R) (GA-3307)
Cr–Mo, hardness of welded, effects of heat treatments on, 20: 11215(R) (NASA-CR-54718)
Cr–Mo, hydrogen embrittlement in high pressure water, 18: 37702
Cr–Mo, impact strength of, relation to carbon content, 19: 6298(R) (MSAR-64-126)
Cr–Mo, joining of, to Zircaloy-2 in NPR tube-to-nozzle fabrication, 16: 32096 (HW-72086)
Cr–Mo, mechanical properties of, effects of sodium (liquid) on, 17: 3425(R) (MSAR-62-126)
Cr–Mo, mechanical and physical properties of, effects of molten sodium on, 17: 14768(R) (MSAR-63-33)
Cr–Mo, mechanical properties at 1100 to 1200°F, effects of air, helium, and sodium on, 17: 29252(R) (MSAR-63-91)
Cr–Mo, mechanical properties of, effects of 1200°F sodium on, 17: 39538(R) (MSAR-63-125)
Cr–Mo, mechanical properties of, effects of sodium and contaminants on, 18: 12582(R) (MSAR-64-14)
Cr–Mo, mechanical properties of, effects of sodium and contaminants on, 18: 22445(R) (MSAR-64-45)
Cr–Mo, mechanical properties of, effects of sodium and contaminants at 1200°F on, 19: 928(R) (MSAR-64-112)
Cr–Mo, mechanical properties, 19: 3621(R) (GA-3830)
Cr–Mo, mechanical properties, effects of 1100°F sodium on, 19: 4621(R) (MSAR-62-142)
Cr–Mo, mechanical properties of, effects of 1100°F sodium on, 19: 4622(R) (MSAR-62-159)
Cr–Mo, mechanical properties of, effects of 1100°F sodium on, 19: 4623(R) (MSAR-63-6)
Cr–Mo, mechanical properties in 1100°F sodium, research program on, 19: 11726(R) (MSAR-65-05)
Cr–Mo, mechanical properties of, effects of exposure to high- and low-oxygen sodium on, 20: 11227
Cr–Mo, mechanical properties of, effects of air, helium, and sodium at 1100°F on, 20: 43897 (MSAR-66-174)
Cr–Mo, oxidation of, by carbon dioxide, 16: 2131 (AAEC/E-71)
Cr–Mo, oxidation resistance of Croloy 2-¼ at 600°C, 19: 32279(R) (ANL-7020(p.3-99))
Cr–Mo, oxidation by oxygen-rich sodium at 1200°F, 20: 9413 (CONF-650620, pp 1-17)
Cr–Mo, performance in Sodium Test Facility, 18: 15567
Cr–Mo, performance in very thick pressure vessels, 18: 40772
Cr–Mo, physical properties of, effects of sodium at 1100 to 1200°F on, 17: 534(R) (MSAR-62-63)
Cr–Mo, physical properties of, effects of 1200°F sodium on, 17: 18754(R) (MSAR-62-77)
Cr–Mo, physical properties of, effects of 1200°F sodium on, 17: 18755(R) (MSAR-62-92)
Cr–Mo, physical properties of, effects of 1200°F sodium on, 17: 18752(R) (MSAR-62-41)
Cr–Mo, physical properties of, effects of 1200°F sodium on, 17: 18753(R) (MSAR-62-50)
Cr–Mo, physical properties of carbonized, effects of air, helium, and sodium at 1100°F on, 17: 32571(R) (MSAR-63-105)
Cr–Mo, physical properties of, effects of 1200°F sodium on, 18: 7149(R) (MSAR-62-12)
Cr–Mo, physical properties of, effects of 1200°F sodium on, 19: 4624(R) (MSAR-63-75)
Cr–Mo, physical properties in air, helium, and sodium, (E), 19: 13998 (SAN-8002(p.210-30))
Cr–Mo, properties as fast reactor material, 18: 15566
Cr–Mo, properties, 20: 13186 (TRG-Report-840)
Cr–Mo, properties of, effects of potassium–sodium environment on, 20: 16972(R) (NASA-CR-54719)
Cr–Mo, radiation effects at high temperatures, neutron, 17: 31060
Cr–Mo, radiation effects on deformation characteristics and structure of, neutron, 17: 31065
Cr–Mo, radiation effects on Charpy impact and tensile properties of, 18: 40018
Cr–Mo, radiation effects on corrosion of AISI 4130, by Santowax OM at 500 to 700°F, fast-neutron, 20: 5846
Cr–Mo, reactions with carbon dioxide to 400°C, 19: 22997 (TRG-Report-842)
Cr–Mo, reactions with plutonium uranium carbide and uranium monocarbide at 820°C, 20: 27416(R) (UNC-5134(Vol.1))
Cr–Mo, rupture tests, extrapolation to long times, 19: 11777(R) (EURAEC-1243)
Cr–Mo, tensile properties at 70°F, effects of helium at 1100°F on, 18: 32144(R) (MSAR-64-75)
Cr–Mo, tensile properties of, effects of welding on, 20: 11214(R) (NASA-CR-54717)
Cr–Mo, thermal stress fatigue tests of Croloy 2¼, 19: 13980(R) (ATL-A-144)
Cr–Mo, welding and notch impact strength of joints of, 19: 13940(R) (EURAEC-1242)
Cr–Mo, welding of thick, by electroslag techniques, 18: 25945(T,R) (EURAEC-1039)
Cr–Mo, welding of, automatic inert gas tungsten arc, 20: 11246
Cr–Mo, welding procedures for, electro-slag, 20: 2281(R) (EURAEC-1408)
Cr–Mo, welding to stainless steel, 19: 4592(R) (MSAR-61-114)
Cr–Mo, welding to type 316 stainless steel, weld-filler metal for, 20: 11214(R) (NASA-CR-54717)
Cr–Mo, wetting by bismuth–lead eutectic, 20: 7564 (IS-T-56)
Cr–Mo–Ni, corrosion by mercury and sodium amalgam at 200 to 500°C, 18: 18312(T) (CEA-tr-A-1455)
Cr–Mo–Ni, extrusion of type 4340, Dynapak, 19: 30686(R) (AD-608945)
Cr–Mo–Ni, fabrication and properties of reactor pressure vessel of, 18: 27926
Cr–Mo–Ni, fatigue of type 4130, energy criterion for, (T), 20: 27521
Cr–Mo–Ni, formation of Fe_2Mo in, 20: 35899(T) (AI-Trans-208)
Cr–Mo–Ni, fracture toughness properties of 12% maraging, 20: 11273(R) (NRL-6364)
Cr–Mo–Ni, hardness of welded type 4340, effects of heat treatments on, 20: 11215(R) (NASA-CR-54718)
Cr–Mo–Ni, oxidation of, causes of catastrophic, 16: 4500 (ORNL-TM-51)
Cr–Mo–Ni, performance in very thick pressure vessels, 18: 40772
Cr–Mo–Ni, phase transformations in martensitic, 18: 39917(T,R) (EURAEC-1120)
Cr–Mo–Ni, properties of Super-Elso, 19: 41008 (EURAEC-1407)
Cr–Mo–Ni, properties of Super-Elso, effects of heat treatments on, 20: 41447(R) (EURAEC-1669)
Cr–Mo–Ni, protection and rupture potentials in sodium bicarbonate–sodium chloride solutions at 40 and 80°C, 17: 25728(T) (EURAEC-677)
Cr–Mo–Ni, radiation effects on, surveillance tests on, 17: 31062
Cr–Mo–Ni, radiation effects on, neutron, 18: 40829 (EURAEC-1175)
Cr–Mo–Ni, radiation effects on ductility of, neutron, 19: 9735(R) (NRL-Memo-1424)
Cr–Mo–Ni, radiation effects on notch ductility of, neutron, 19: 11781(R) (NRL-Memo-1556)
Cr–Mo–Ni, radiation hardening in low-alloy, effects of irradiation temperature on fast-neutron, 20: 11342 (EURAEC-1502)
Cr–Mo–Ni, radioinduced embrittlement of, neutron, 20: 27610
Cr–Mo–Ni, tempering behavior of pressure-vessel, 19: 26817 (KAPL-3092)
Cr–Mo–Ni, transformation temperatures in Super Elso, effects of heating rate on, 20: 21331(R) (EURAEC-1569)
Cr–Mo–Ni, weld embrittlement in joints in, effects of time at high temperatures on, 20: 21393
Cr–Mo–Ni, welding techniques for HY-80, 20: 11261
Cr–Mo–Ni–Nb–V, development as HY-180/210 steel, 20: 5851
Cr–Mo–Ni–V, development, 19: 20462(R) (NRL-6258)
Cr–Mo–Ni–V, fatigue crack propagation in, effects of air or salt water environment on, 20: 11273(R) (NRL-6364)
Cr–Mo–Ni–V, mechanical properties, effects of carbon on, 19: 9646 (AD-604872)
Cr–Mo–Ni–V, mechanical properties of, effects of processing on, 20: 33858(R) (AD-634094)
Cr–Mo–Ti, corrosion by sodium, test run data on, 17: 37479 (GEAP-

4181)
Cr–Mo–Ti, corrosion by liquid sodium in test loop, 18: 4195 (GEAP-4182)
Cr–Mo–Ti, corrosion by flowing sodium, test run data on, 18: 12575 (GEAP-3726(Vol.3))
Cr–Mo–Ti, corrosion by flowing sodium, test run data on, 19: 7866 (GEAP-4437)
Cr–Mo–Ti, corrosion by sodium, (E), 19: 13916 (SAN-8002(p.189-209))
Cr–Mo–Ti, corrosion by sodium in test loops, 19: 22894 (GEAP-4183)
Cr–Mo–Ti, corrosion and mass transfer in flowing sodium, 20: 9414 (CONF-650620, pp 18-35)
Cr–Mo–Ti, corrosion by flowing sodium at 1000 to 1200°F, equation for, 20: 11227
Cr–Mo–Ti, corrosion by sodium, 20: 23601(R) (GEAP-4837)
Cr–Mo–Ti, corrosion and mass transfer in flowing sodium, 20: 39345 (GEAP-4831)
Cr–Mo–Ti, corrosion by sodium in loops, statistical analysis of data on, 20: 43826 (GEAP-4830)
Cr–Mo–V, creep of, enthalpy and entropy of activation of, 18: 25974 (EURAEC-1037)
Cr–Mo–V, creep-rupture properties of, 17: 3521
Cr–Mo–V, creep-rupture properties, 17: 39531(R) (EURAEC-689)
Cr–Mo–V, effects of cerium on impurities, mechanical properties, and oxidation of, 17: 27859
Cr–Mo–V, friction coefficients with metals and metals with dry lubricants of H-11 Tool, *in vacuo*, 20: 7571 (NAA-SR-9644)
Cr–Mo–V, radiation effects on relaxation of elastic stresses in bent plates of, neutron, 16: 22704
Cr–Mo–V, radiation effects of neutrons on high-temperature creep, 18: 28039(R) (EURAEC-1020)
Cr–Mo–V, rupture mechanisms of, determination by time-to-rupture tests, 20: 41445(R) (EURAEC-1622)
Mn–Mo, addition of metallic aluminum and aluminum nitride to, for improved mechanical properties, 19: 41085(P)
Mn–Mo, brittle fracture of welded plates of, 17: 39469(T) (EURAEC-602)
Mn–Mo, embrittlement during stress-relief annealing after welding, 17: 12638
Mn–Mo, embrittlement by stress-relief annealing after welding operations, 18: 8807(T) (EURAEC-431)
Mn–Mo, embrittlement by plastic fatigue of A302B, 20: 15039 (EURAEC-1475)
Mn–Mo, embrittlement by plastic deformations at 20 to 400°C, 20: 23718
Mn–Mo, fatigue strength of A302B, effects of weld defects on, 20: 15059(R) (SWRI-1228-1-20)
Mn–Mo, fracture toughness of ASTM A302 B, 20: 10487 (WERL-8844-9)
Mn–Mo, heat treatment to improve notch toughness of, 20: 23724
Mn–Mo, mechanical properties of weld in, 17: 39512(T) (EURAEC-667)
Mn–Mo, mechanical properties of electroslag welds in, effects of oxidation on, 18: 8731(T) (EURAEC-510)
Mn–Mo, mechanical properties of A302-B, effects of cold-working and heat treatments on, 20: 19205(R) (GA-6923)
Mn–Mo, mechanical properties of ASTM A302B, effects of fabrication on, 20: 27449 (SWRI-1228-4-17)
Mn–Mo, properties of 200 mm thick plate, effects of sample position on, 19: 42846(R) (EURAEC-1399)
Mn–Mo, properties of type 302B, effects of fabrication and heating on, 20: 41451(R) (GA-7101)
Mn–Mo, radiation effects on embrittlement of, 16: 33569
Mn–Mo, radiation effects on embrittlement of, neutron, 16: 22700
Mn–Mo, radiation effects on embrittlement and hardening of neutron, 17: 31063
Mn–Mo, radiation effects on tensile properties of, effects of irradiation temperature on fast neutron, 18: 8877(T) (EURAEC-816)
Mn–Mo, radiation effects on mechanical properties of, fast-neutron, 18: 30263
Mn–Mo, radiation effects on embrittlement of, 18: 37749 (A/CONF.28/P/420)
Mn–Mo, radiation effects on deformation properties of A302B, neutron, 20: 2436 (WERL-8844-4)
Mn–Mo, radiation effects on mechanical properties of A302B and AMMO2, fast-neutron, 20: 5846
Mn–Mo, radiation hardening of A302B, effects of irradiation temperature on fast-neutron, 20: 11342 (EURAEC-1502)
Mn–Mo, radiation effects on impact strength of A-302B, combined stress and fast neutron, 20: 11227
Mn–Mo, radiation effects on mechanical properties of SA302B, fast-neutron, 20: 19178(R) (IDO-17154)
Mn–Mo, radiation effects on pressure vessels of, fast-neutron, 20: 21228 (AE-221)
Mn–Mo, radioinduced embrittlement of, neutron, 20: 27610
Mn–Mo, specification for A302 Grade B plate specimens for irradiation testing, 17: 41344 (HW-74939)
Mn–Mo, tempering behavior of pressure-vessel, 19: 26817 (KAPL-3092)
Mn–Mo, tensile properties of 200-mm-thick plate, effects of heat treatment and cooling rate on, 20: 33909
Mn–Mo, thermal stress fatigue of A-302B, 20: 11227
Mn–Mo, weld bead deposition on sheet specimens of, for bending tests, 17: 41390(T,R) (EURAEC-768)
Mn–Mo, weld bead deposition and properties on sheet specimens of, 18: 32115(T,R) (EURAEC-1018)
Mn–Mo, weld zone fracture toughness of A302B, 20: 9488(R) (BNWL-166, pp 4.8-11)
Mn–Mo, welding of, inspection and testing of sheets for, 17: 520(T,R) (EURAEC-351)
Mn–Mo, welding of thick plates of, by submerged-arc techniques, 19: 11691(R) (EURAEC-1221)
Mn–Mo, welding procedures for A302B, electro-slag, 20: 2281(R) (EURAEC-1408)
Mn–Mo, welding techniques for pressure-vessel, 18: 23074
Mn–Mo, welding thick plates of LMS2V, cracking and hardness changes from, 20: 15000 (EURAEC-1517)
Mn–Mo–Ni, stress rupture properties at 500 and 600°C of stainless-clad, 18: 10567
Mn–Mo–Ni–Nb, radiation effects on mechanical properties of low-alloy, neutron, 20: 19258 (UJV-1470/65)
Mn–Mo–Ni–V, welding procedures for, electro-slag, 20: 2281(R) (EURAEC-1408)
Mn–Mo–V, properties of Ammo, variations in samples of, 20: 41447(R) (EURAEC-1669)
Mn–Mo–V, transformation curves for continuous cooling of, from 1100°C, 20: 46184 (EURAEC-1677)
Mo–Ni–V, fracture toughness, 18: 44138 (KAPL-3031)
Mo–Ni–V, fracture toughness, 19: 24984 (KAPL-3088)
Mo–Ni–V, fracture toughness tests on specimens of, of different sizes, 20: 27479 (CONF-660406-1)

MOLYBDENUM SULFIDES

analysis for rhenium, activation, 18: 13676
bibliography on properties and uses as lubricant, 16: 24167 (NP-11899)
development as solid lubricant, 17: 7606(R) (ORNL-1515)
development for use as solid lubricant, 16: 4554(T) (FTD-TT-61-58)
diffusion in molybdenum, inter-, 20: 5846
effects of, as filler on tensile strength of irradiated butadiene–styrene elastomers, 18: 27594
effects on radiation resistance of nitrile elastomers, 16: 30903 (HW-66977)
electron attenuation and diffraction by, 17: 620
emissivity at 800 to 5000°K, relation of structure to, 18: 20566
exchange reactions between deuterium and hydrogen or hydrogen sulfide on, catalytic, 16: 14751
fission fragment damage to crystalline, from collimated beam, 18: 7327
friction on copper surfaces in ultrahigh vacuum, 20: 21366
intercalation of strongly electropositive metals in, 19: 46265
lubricity, 18: 23742 (TID-7690(p.106-20))
preparation from molybdenum and sodium sulfide, 18: 20001
properties as lubricant between ceramic/ceramic and metal/metal couples *in vacuo*, 20: 7571 (NAA-SR-9644)
properties for use as dry lubricant for bearings in dry helium atmosphere in reactors, 18: 21575
radiation effects of fission fragment bombardment, 16: 33409
radiation effects on spectra of catalysts of, effects of hydrocarbon sorption on, 17: 22258
radioinduced damage to lattices of, fission-fragment, 18: 32253
radioinduced dislocation formation, 16: 29463
reactions with samarium and ytterbium, preparation of intercalation compounds by, 20: 20648 (AD-621029)
sputtering by air and argon ions, (E), 20: 21529
surface area measurements by isotopic exchange method, 16: 13056
surface area of, effects of radiation from sulfur-35 or molybdenum-99 on, 18: 23696
thermal decomposition in vacuum, 20: 7068
thermal expansion, 20: 23005
thermodynamic properties, 20: 10816(T) (NASA-TT-F-285)
vapor pressure variation of sulfur with composition in, at 1100°C, 18: 27452
welding to ceramics, graphite, and metals in SNAP reactor environment at 700 to 1300°F, self-, 20: 7570 (NAA-SR-9643)
B_2O_3–PbS–MoS_2, radiation effects on properties as solid-film lubricants, 17: 36347(R) (NARF-62-18P)
B_2O_3–PbS–MoS_2, radiation effects on wear life of solid-film lubricants of, 19: 23121
B_2O_3–PbS–MoS_2, radiation effects on lubricant wear properties of solid films, 19: 44095
graphite–MoS_2–Na_2SiO_3, radiation effects on solid-film lubricants of, 19: 23121
graphite–MoS_2–$NaSiO_3$, radiation effects on lubricant wear properties of solid films, 19: 44095

graphite–MoS_2–Na_2SiO_3–H_2O, radiation effects on properties as solid-film lubricants, 17: 36347(R) (NARF-62-18P)
MoS_2–UO_2SO_4–H_2O, phase studies at 200 to 360°C, 19: 17868
PbS–MoS_2, frictional properties of coatings of, 17: 8818 (UCRL-13052)

MOLYBDENUM SYSTEMS

bibliography on phase diagrams of, 17: 18689
bonding to alumina, 17: 25691(R) (RBESO-3404-2)
book: *Less-Common Alloys of Molybdenum*, 17: 25716
preparation and properties as paint, 18: 35923(R) (AD-602215)
Al–Al_2O_3–Cr–Fe–Mo, preparation and evaluation of dispersion-strengthened, 19: 18400(R) (TID-21663)
Al–B–C–Cr–Mo–Ni–Ta–W–Zr, corrosion and properties of TAZ-8A, 20: 46166 (NASA-TN-D-3597)
Al–C–Cr–Co–Mo–Ni–Ti, extrusion of Udimet 700 into T-sections, 19: 7874(R) (ASD-TDR-7-911(V))
Al–C–Cr–Co–Mo–Ni–Ti, gas contents of atomized powder compacts of Inco-713C and Udimet 700, 19: 7874(R) (ASD-TDR-7-911(V))
Al–C–Cr–Mo–Ni–Ti–W, sorptive properties for zirconium, tracer studies of, 20: 35912
Al–C–Mo, crystal structure and phase studies, 18: 12706
Al–C–Mo, crystal structure and phase studies of superconducting, 18: 32149(R) (UCRL-11317(p.131-49))
Al–C–Mo, high-field superconductivity of Mo_3Al_2C, (E), 19: 25449
Al–C–Mo, lattice parameters of filled β-manganese structure phases in, 19: 37109
Al–C–Mo, phase studies of sintered, 19: 4688
Al–C–Mo, superconductivity of Mo_3Al_2C, 18: 32702
Al–C–Mo, superconducting transition of Mo_3Al_2C, 18: 34283 (UCRL-11390)
Al–C–Mo, superconductivity, 19: 43997(R) (UCRL-11889)
Al–C–Mo, superconductivity of Mo_3Al_2C, 20: 6228
Al–C–Mo, superconductivity of Mo_3Al_2C in, 20: 32312(R) (UCRL-16658, pp 133-43)
Al–C–Mo–Ni–Si–U–Zr, preparation and fabrication as refractory fuel material, 18: 34071(P)
Al–Cr–Fe–Mn–Mo–Ni–Si, machining characteristics, 17: 14778(R) (ASD-TR-7-532a(IX))
Al–Cr–Mo–Si, phase studies, 18: 12704
Al–Fe–Mo–Si–U, radioinduced swelling in, resistance to, 19: 47103
Al–Fe–Mo–Si–U, thermal expansion rates for, 20: 33880 (NLCO-946, pp 103-6)
Al–Mo–Si, crystal structure and phase studies on, 18: 12704
Al–Mo–Si, oxidation kinetics at 800 to 1200°C, 20: 7530
Al–Mo–Si–U, deformation resistance of, at high temperatures, 19: 16206(P)
Al_2O_3–Cr–Mo–TiO_2, friction and wear at high temperatures and in vacuum, 16: 5708 (ASD-TR-61-301)
Al_2O_3–Cr–Mo–TiO_2, properties of LT-1B, as journal bearing material, 17: 25382 (ASD-TR-61-705)
Al_2O_3–Cr–Mo, wear characteristics, 16: 30518
Al_2O_3–Mo, brazing to niobium using vanadium braze, 18: 44496(R) (MND-2812)
Al_2O_3–Mo, preparation and properties of multilayer cermet, 18: 42348 (GEST-2035)
Al_2O_3–Mo, pressing, equipment and techniques for hot-, 16: 5699
As–Mo, crystal structure of compounds in, 19: 39209
B–C–Mo, phase studies, 17: 18733 (AD-278041L)
B–C–Mo, preparation and phase studies, 17: 29370
B–Cu–Mo, crystal structure, 20: 14532
Be–BeO–Mo, thermal conductivities at 300 to 1000°C, 16: 19393
Be–Mo–Si, compounds in, properties of, for use in aerospace technology, 20: 29770
Be–Mo–Si, properties for high-temperature applications, 17: 543 (WADD-TR-60-889(Pt.II))
BeO–Mo, use in dielectric thermometers, 17: 36868(R) (GEMP-78)
B–Fe–Mo, crystal structure, 20: 14532
B–Fe–Mo, phase studies at 1000°C, 20: 27540
B–Mo, phase diagrams, 19: 6348
B–Mo, preparation, properties, and uses of, review on, 16: 27640(T) (FTD-TT-62-430)
B–Mo–Nb–Ti, mechanical and thermal properties of niobium-base systems, 20: 43940
B–Mo–Nb–Ti–Zr, mechanical and thermal properties of niobium-base, 20: 43940
B–Mo–Ni, crystal structure and phase diagrams, 18: 22502
B–Mo–Ni, phase composition and properties of, 20: 43973
B–Mo–Si, diffusion reactions in boron chloride–hydrogen–silicon chloride, 18: 34146
BN–Mo, stability and strength at 1650 to 2210°C, 19: 26853
C–Al–Mo, phase studies of sintered, 19: 4688
C–Ce–Mo, phase studies, 19: 16130
C–Cr–Co–Fe–Mn–Mo–Ni–W, corrosion by mercury at high temperatures, 18: 7152
C–Cr–Co–Mo–W–Y, oxidation resistance of, at high temperatures, 19: 37155(P)
C–Cr–Fe–Mn–Mo–Si, corrosion of Croloy 1¼ and 5Si by liquid bismuth alloys, 18: 4193 (BNL-811)
C–Cr–Fe–Mn–Mo–Si, corrosion of Croloy 1¼ by liquid lead alloys, 18: 4193 (BNL-811)
C–Cr–Fe–Mn–Mo, corrosion of Croloy 2¼ by liquid lead alloys, 18: 4193 (BNL-811)
C–Cr–Fe–Mn–Mo, corrosion of Croloy 2¼ and 9M by liquid bismuth alloys, 18: 4193 (BNL-811)
C–Cr–Fe–Mn–Mo, corrosion of 2¼ Croloy by steam and chloride salt at high temperatures, 18: 4161 (GEAP-4351)
C–Cr–Fe–Mn–Mo–Si–Ti, corrosion of 5 Croloy Ti by steam and chloride salt at high temperatures, 18: 4161 (GEAP-4351)
C–Cr–Fe–Mo, corrosion of Croloy ½ by liquid bismuth alloys, 18: 4193 (BNL-811)
C–Cr–Fe–Mo–Ni–Nb–Ta–W–V, production of corrosion and oxidation resistant, 18: 12618(P)
C–Cr–Fe–Mo–Ni, reinforcement of graphite by, 19: 39114(P)
C–Cr–Mo, phase studies, 20: 15111
C–Cr–Mo, phase studies and thermodynamics of, for use at high temperatures, 20: 29774
CeO_2–HfO_2–MgO–Mo, composites of, process development for macrolaminate particle, 19: 36958(R) (NP-15139)
CeO_2–HfO_2–MgO–Mo, development of macrolaminate particle composite materials of, 19: 13894(R) (NP-14677)
CeO_2–HfO_2–MgO–Mo, preparation and properties as macrolaminate particle composites, 18: 35923(R) (AD-602215)
CeO_2–HfO_2–MgO–Mo, preparation and properties of laminated sheets of, 18: 41930(R) (NP-14294)
CeO_2–HfO_2–MgO–Mo, preparation and properties of macrolaminate particle composites of, 19: 20558(R) (NP-14888)
C–Fe–Mo–Ni, corrosion of HyMu 80 by potassium fluoride–zirconium fluoride under hydrofluorination conditions at 600°C, 18: 7985(R) (BMI-1650(Del.))
C–Fe–Mo–Ni, corrosion of HyMu 80 by liquid fluoride salt at 500°C in presence of fluorine and hydrofluoric acid, 18: 10468 (BMI-X-269)
C–Fe–Mo–Ni, corrosion of HyMu-80 by fluoride melt at 650°C during hydrofluorination of stainless steel and Zircaloy-2, 18: 30128 (BMI-X-288)
C–Fe–Mo–Ni, corrosion of HyMu-80 in fluoride volatility process, 18: 34034(R) (BMI-1672(Del.))
C–Fe–Mo–Ni, corrosion of HyMu 80 in molten-salt fluoride-volatility process for spent aluminum-base fuels, 18: 43717 (ORNL-P-391)
C–Fe–Mo–Ni, corrosion of HyMu 80 by molten salt under fluorination and hydrofluorination conditions, 19: 2744 (BMI-X-315)
C–Fe–Mo–Ni, corrosion of HyMu 80 by liquid aluminum fluoride–potassium fluoride–zirconium fluoride under fluorination conditions at 600°C, 19: 6267 (BMI-X-316)
C–Ge–Mo, crystal structure and phase studies on, 18: 10561
C–Ge–Mo, preparation and structure of T_5M_3X type compound in, 19: 30788
C–Hf–Mo, superconducting transition temperature of $Mo_{0.95}Hf_{0.05}C_{0.75}$, 20: 17607
C–Hf–Mo–N–Re–Ta–W–Zr, creep properties at 2400°F, 19: 18401(R) (WANL-PR(Q)-005)
C–Hf–Mo–N–Re–Ta–W–Zr, development of dispersion-strengthened tantalum-base, 20: 21240(R) (WANL-PR-(Q)-006)
C–Hf–Mo–N–Re–Ta–W–Zr, effects of heat treatment on hardness of, 19: 18401(R) (WANL-PR(Q)-005)
C–Hf–Mo–N–Ta–W–Zr, effects of heat treatment on hardness of, 19: 18401(R) (WANL-PR(Q)-005)
C–Hf–Mo–V, fabrication of, cracking in, 17: 41427(R) (IITRI-B231-9)
C–Mo, phase diagram, 19: 24977 (AFML-TR-65-2(Pt.I, Vol.I))
C–Mo, phase studies at high pressures, 16: 13508(R) (AD-262812)
C–Mo, phase studies at high temperatures, 19: 30791
C–Mo, phase studies, stabilities, and thermodynamics of, at high temperatures, 20: 29774
C–Mo, preparation, properties, and uses of, review on, 16: 27640(T) (FTD-TT-62-430)
C–Mo, radiation effects on, neutron, 19: 30648(R) (HW-84573(p.3.1-74))
C–Mo, superconductivity, 17: 41604
C–Mo, tensile properties at 475 to 650°C, 17: 30962(R) (ASD-TDR-63-238)
C–Mo–Nb, phase studies of, at 1500 and 1900°C, 16: 13590(T) (AEC-tr-5000)
C–Mo–Nb, phase studies and thermodynamics of, for use at high temperatures, 20: 29774
C–Mo–Nb, phase transformations in, thermodynamics of, 17: 22205
C–Mo–Nb, phase transformations in, thermodynamics of, 18: 44161(T) (AERE-Trans-1009)
C–Mo–Nb–Ta–Ti–W–Zr, creep properties at 1800 to 2200°F of Cb132M, 20: 2333(R) (NASA-CR-54457)

C–Mo–Nb–Ta–W–Zr, erosion by sodium at 400, 1000, and 1500°F of Cb-132M, 20: 769(R) (NASA-CR-54459)
C–Mo–Nb–Ta–W–Zr, extrusion parameters for Cb-132M, 20: 21263(R) (NASA-CR-54911)
C–Mo–Nb–Ta–W–Zr, preparation and specifications for corrosion loop testing, 20: 4380 (NASA-CR-54761)
C–Mo–Nb–Ta–Zr, thermal-mechanical processing of a precipitation-hardenable, dispersion-hardened, 20: 21250
C–Mo–Nb–Ti–Zr, bend and tensile ductility properties of, 20: 21410
C–Mo–Nb–Ti–Zr, corrosion of PWC-533 by boiling potassium, 19: 34640 (CNLM-6246)
C–Mo–Nb–Ti–W, corrosion of tungsten-base Grade 7178, by potassium at 1600°F, 20: 27432(R) (NASA-CR-54892)
C–Mo–Nb–Ti–Zr, extrusion, heat treatment, and rolling of, 19: 32720(R) (AD-609815)
C–Mo–Nb–Ti–Zr, mechanical and metallurgical properties, 19: 32720(R) (AD-609815)
C–Mo–Nb–Ti–Zr, preparation and properties of castings of, 19: 32720(R) (AD-609815)
C–Mo–Nb–Ti–Zr, yield strength of PWC-533, effects of boiling potassium exposure on, 19: 34640 (CNLM-6246)
C–Mo–Nb–W–Zr, corrosion by potassium at 2000 to 2200°F, 18: 24091
C–Mo–Nb–W–Zr, evaluation of protective coatings for, 20: 29651
C–Mo–Nb–W–Zr, thermal properties, 18: 7201 (ASD-TDR-63-597)
C–Mo–Nb–W–Zr, thermal properties to melting point, 20: 878
C–Mo–Nb–Zr, heat treatment of, 20: 14972(P)
C–Mo–O, thermodynamic equilibrium diagrams for, Pourbaix-Ellingham, 19: 30810
C–Mo–Pu, fabrication, properties, and structure of, 20: 46156
C–Mo–Si, superconducting transition temperature of $Mo_{4.8}Si_3C_{0.6}$, 20: 17607
C–Mo–Si, phase studies of $Mo_{4.8}Si_3C_{0.6}$ in, 20: 7587
C–Mo–Ta, phase studies and thermodynamics of, for use at high temperatures, 20: 29774
C–Mo–Th, phase equilibria at 900 to 1600°C in, 17: 39586
C–Mo–Th, phase studies on arc-melted, pressure-sintered, and vacuum-annealed, 17: 32616
C–Mo–Ti, fabrication and properties of arc-cast, 18: 32107 (NP-14128)
C–Mo–Ti, phase studies, 16: 22582 (ASD-TDR-62-7)
C–Mo–Ti, phase studies, 16: 3505
C–Mo–Ti–Zr, crack formation in Mo-3 alloy ingots, effects of molybdenum capping on, 20: 37219
C–Mo–Ti–Zr, creep properties in ultra-high vacuum of TZC, long-time, 19: 37039(R) (NASA-CR-54393)
C–Mo–Ti–Zr, creep properties at 1800 to 2200°F of TZC, 20: 2333(R) (NASA-CR-54457)
C–Mo–Ti–Zr, creep properties of TZC, 20: 29705(R) (NAS-CR-54973)
C–Mo–Ti–Zr, creep testing, fabrication, and properties of, 20: 9501 (UCRL-14437)
C–Mo–Ti–Zr, dispersed phase studies in Mo-TZC, 18: 20512 (ASD-TDR-62-7(Pt.II))
C–Mo–Ti–Zr, dispersion-hardening characteristics in, 18: 27979
C–Mo–Ti–Zr, extrusion of, cast and wrought, evaluation of, 16: 3418(R) (ASD-TR-7-785)
C–Mo–Ti–Zr, extrusion of molybdenum-TZC, 19: 20500 (AFML-TR-64-387)
C–Mo–Ti–Zr, extrusion parameters for TZC, 20: 21263 (NASA-CR-54911)
C–Mo–Ti–Zr, extrusion, heat treatment, and rolling of, 19: 32720(R) (AD-609815)
C–Mo–Ti–Zr, fabrication and properties of arc-cast, 18: 32107 (NP-14128)
C–Mo–Ti–Zr, fabrication and properties of TZC, 20: 43830(R) (NASA-CR-72029)
C–Mo–Ti–Zr, fatigue properties at 1093°C of annealed TZC, notched, 20: 7572(R) (NASA-CR-54775)
C–Mo–Ti–Zr, fatigue properties of TZC, at high temperatures, 20: 31710(R) (NASA-CR-54983)
C–Mo–Ti–Zr, mechanical and metallurgical properties, 19: 32720(R) (AD-609815)
C–Mo–Ti–Zr, mechanical properties at high temperatures, 19: 44674(R) (ANL-7000, pp 69-83)
C–Mo–Ti–Zr, microstructure and tensile properties of, effects of composition, heat treatment, and processing on, 20: 5846
C–Mo–Ti–Zr, preparation and properties of castings of, 19: 32720(R) (AD-609815)
C–Mo–Ti–Zr, preparation and specifications for corrosion loop testing, 20: 4380 (NASA-CR-54761)
C–Mo–Ti–Zr, properties at high temperatures, 20: 29756
C–Mo–Ti–Zr, radiation effects on mechanical and thermal properties of, 18: 41921(R) (GEMP-37A)
C–Mo–Ti–Zr, reduction of gross ingot defects in vacuum arc-melted, 19: 7885
C–Mo–Ti–Zr, stress-rupture properties of TZC, at high temperatures and strain rates, 20: 11265 (AD-626375)
C–Mo–U, corrosion by air, 20: 46156
C–Mo–U, fabrication, properties, and structure of, 20: 46156
C–Mo–U, mechanical properties at 30 to 600°C, 17: 14844 (SCNC-269)
C–Mo–U, metallurgical properties, 16: 24150 (CNEN-113)
C–Mo–U, phase diagram, 18: 41933 (TID-11295(3rd Ed.))
C–Mo–U, phase diagram, 20: 9552
C–Mo–U, phase equilibria at 900 to 1600°C in, 17: 39586
C–Mo–U, phase equilibria in, 18: 14499
C–Mo–U, phase studies on arc-melted, pressure-sintered, and vacuum-annealed, 17: 32616
C–Mo–U, phase studies, 18: 39892 (BMI-1685)
C–Mo–U, phase studies, 20: 5843
C–Mo–U, thermionic emission at low pressures, 17: 41338(R) (GA-4391)
C–Mo–U–Zr, preparation and properties, 19: 36949(R) (BNL-900(p.121-97))
C–Mo–V, phase studies and structure of, 17: 1958(T) (AEC-tr-5459)
C–Mo–V, phase studies, 17: 22195
C–Mo–V, phase studies and thermodynamics of, for use at high temperatures, 20: 29774
C–Mo–V, phase transformations in, thermodynamics of, 17: 22205
C–Mo–V, phase transformations in, thermodynamics of, 18: 44161(T) (AERE-Trans-1009)
C–Mo–V, superconductivity, 19: 43997(R) (UCRL-11889)
C–Mo–W, phase transformations in, thermodynamics of, 18: 44161(T) (AERE-Trans-1009)
C–Mo–W, preparation of vacuum-arc-cast, 16: 18016(R) (AD-265129)
C–Mo–W–U, phase studies, 19: 27735(R) (NAA-SR-10850)
C–Mo–W–Y, corrosion by hydrochloric, phosphoric, and sulfuric acids at high temperatures, 20: 46158
C–Mo–W–Zr, extrusion, heat treatment, and rolling of, 19: 32720(R) (AD-609815)
C–Mo–W–Zr, mechanical properties and preparation, 17: 22150(R) (AD-281728)
C–Mo–W–Zr, mechanical and metallurgical properties, 19: 32720(R) (AD-609815)
C–Mo–W–Zr, preparation and properties of castings of, 19: 32720(P) (AD-609815)
C–Mo–W–Zr, thermal properties, 18: 7201 (ASD-TDR-63-597)
C–Mo–W–Zr, thermal properties to melting point, 20: 878
C–Mo–Zr, fabrication and properties of arc-cast, 18: 32107 (NP-14128)
C–Mo–Zr, phase studies of, 17: 23991
C–Mo–Zr, phase studies, 19: 23066
C–Mo–Zr, phase studies, 20: 31669
Co–Mo–S, catalytic effects on deuterium labeling of hydrocarbons, 18: 13802
Co–Mo–Si, oxidation, strength, and ductility at high temperatures, 20: 25611(P)
Cr–Fe–Mn–Mo–Ni–Si, corrosion and metallurgical changes in, caused by steam at 1200 to 1500°F, 16: 24126
Cr–Fe–Mn–Mo–Si, corrosion of Sicromo by cesium, 17: 30944
Cr–Mo–Si, corrosion by mercury at 600 to 1000°F, 18: 27913
Cr–Mo–Si, deposition on niobium alloys B-66 and D-43, 18: 14373(R) (NP-13498)
Cr–Mo–Si, deposition on niobium alloys B-66, FS-85, and X-110, 18: 14353(R) (AD-408310)
Cr–Mo–Si, deposition of coatings of, on and evaluation for FS-85 alloy in air to 2600°F, 17: 36188(R) (AD-289857)
Cr–Mo–Si, oxidation resistance properties as coatings for niobium alloys, 17: 16633(R) (AD-296341)
Cr–Mo–Si, phase studies and thermal properties, 19: 26861
Cr–Mo–Si, properties as anti-oxidation coatings for niobium alloys, 17: 14802(R) (AD-278727)
Cr–Mo–Si, properties as coating for B-66 and D-43 alloys, 18: 20523(R) (NP-13811)
Cr–Mo–Si, properties of, for use as protective coating on niobium and its alloys, 20: 29651
Cr–Mo–UO_2, radiation effects on stainless steel-clad, 17: 11254 (BMI-1608)
Cs–CsF–Mo, properties as thermionic emitter, 17: 27973
Fe–Mo–N, preparation of kryptonates of Moly-Perma-Foil by diffusion, 20: 18570(R) (NYO-2757-5)
Fe–Mo–Ni–Si, corrosion of, by lithium fluoride–sodium fluoride–zirconium fluoride systems at 500°C, 16: 4502 (TID-13691)
Gd_2O_3–Mo, fabrication, 17: 23876(R) (USBM-U-1031)
GdO–Mo, fabrication and properties, 17: 34330(R) (USBM-U-1057)
Gd_2O_3–Mo, preparation, 16: 19374(R) (USBM-U-921)
graphite–Mo, properties of, effects of graphite source material on, 20: 33876(R) (N-66-17087)
HfC–Mo, phase diagram, 20: 31729
HfC–Mo, solidus at 2350°C, 19: 44612(R) (USBM-RC-1199)
HfN–Mo, stability and strength at 1650 to 2210°C, 19: 26853

HfO_2–Mo, preparation and properties as laminate, 18: 35923(R) (AD-602215)
LaB_6–Mo, stability and strength at 1650 to 2210°C, 19: 26853
La–Mo–O–Ti, crystal structure of $LaTi_{1.5}Mo_{0.5}O_6$ in, 20: 26863
Li–Mo–O, equilibrium distribution of oxygen in, at 500 to 800°C, 18: 4253(R) (ORNL-3470(p.63-6))
MgO–Mo, stability and strength at 1650 to 2210°C, 19: 26853
Mo–MoO_2, reactions with oxygen, equilibrium oxygen pressures produced in, 20: 277 (AERE-R-4942)
Mo–$MoSi_2$, kinetics of formation of intermediate silicides in, 19: 16145
Mo–N, superconductivity, 17: 41604
Mo–Nb–N–Zr, heat treatment of, 20: 14972(P)
Mo–Nb–O–Zr, heat treatment of, 20: 14972(P)
Mo–Nb–Si, phase diagram and properties of, 20: 23683
Mo–Nb–Si, phase studies and properties of, 19: 39194
Mo–Ni–NbC–TiC, friction coefficients with alumina and solar glass of K-162B Kentanium, *in vacuo*, 20: 7571 (NAA-SR-9644)
Mo–Ni–NbC–TiC, friction coefficients with alumina with molybdenum disulfide coatings of K-162B Kentanium, *in vacuo*, 20: 7571 (NAA-SR-9644)
Mo–Ni–NbC–TiC, self-welding to ceramics, graphite, and metals in SNAP reactor environment at 700 to 1300°F, 20: 7570 (NAA-SR-9643)
Mo–Ni–NbC–TaC–TiC, thermal expansion at 68 to 1800°F, 18: 20513 (CNLM-4234)
Mo–Ni–ThO_2, compaction of powdered, methods for, 20: 33842 (NASA-TN-D-3511)
Mo–Ni–ThO_2, development and properties of dispersion-strengthened, 20: 31669
Mo–Ni–ThO_2, oxidation and properties of composite effects of high temperatures on, 20: 43845(R) (AD-637573)
Mo–Ni–ThO_2, preparation and tensile properties, 19: 26854
Mo–Ni–TiC, oxidation of, by air at 600 to 1300°C, effects of molybdenum content on, 20: 29653
Mo–Ni–TiC, phase studies and sintering of, 19: 9685
Mo–N–Re–Ta–W–Zr, effects of heat treatment on hardness of, 19: 18401(R) (WANL-PR(Q)-005)
Mo–O, phase diagrams, 20: 1880
Mo–O–K, equilibrium distribution of oxygen in, at 500 to 800°C, 18: 4253(R) (ORNL-3470(p.63-6))
Mo–O–Na, equilibrium distribution of oxygen in, at 500 to 800°C, 18: 4253(R) (ORNL-3470(p.63-6))
Mo–O–Ti–Zr, phase studies, 16: 25826
Mo–O–V, reduction by hydrogen at 400 to 800°C, 19: 28823
Mo–PuC, fabrication, 18: 12643(R) (HW-76303(p.2.1-35))
Mo–PuC, fabrication of cermets, 18: 29001(R) (HW-79280(p.5.1-25))
Mo–PuC, preparation and fuel-matrix interactions in, 18: 22484 (HW-SA-3131)
Mo–PuC–UC, analysis for carbon, molybdenum, nitrogen, plutonium, and uranium in cermets of, 20: 8873
Mo–PuC–UC, analysis for plutonium, review of methods for, 20: 10797
Mo–PuO_2, preparation and properties of sintered, effects of type 302B stainless steel additions on, 18: 547 (LAMS-2898)
Mo–PuO_2, properties of fabricated, effects of compaction pressure and sintering temperatures on, 16: 3424 (LA-2621)
Mo–Si, diffusion reactions at 1250°C, 18: 26001
Mo–Si, effects of Nb_3Sn on crystal structure of Mo_3Si in, 18: 12705
Mo–Si, effects on wetting of graphite at high temperatures, 20: 29764
Mo–Si, electronic structure of compounds in, 19: 16177
Mo–Si, heats of dissociation, 17: 4933 (WADD-TR-60-463(Pt.II))
Mo–Si, oxidation of, at 1000 to 1725°C, kinetics of, 16: 27588 (ASD-TDR-62-203(Pt.1))
Mo–Si, preparation, properties, and uses of, review on, 16: 27640(T) (FTD-TT-62-430)
Mo–Si–U, fission effects on, reduction of swelling in, 18: 24996(R) (NAA-SR-8888(Sect.VI))
Mo–Si–U, hot hardness and microstructure, 19: 32734 (NMI-7075)
Mo–Si–U, hot hardness and microstructure of, effects of quenching temperature on, 20: 31666
Mo–Si–U, preparation and crystal structure of compounds in, 19: 19871
Mo–Si–U, structure of $U_4Mo_4Si_3$, 18: 12716
Mo–Si–U, thermal expansion rates for, 20: 33880 (NLCO-946, pp 103-6)
Mo–Si–V, phase studies and properties, 16: 30849
Mo–Si–W, deposition on D-14 niobium alloy, 18: 34052 (RTD-TDR-63-4063)
Mo–Si–W, phase studies, 17: 18733 (AD-278041L)
Mo–TaB_2, stability and strength at 1650 to 2210°C, 19: 26853
Mo–Te–Zr, oxidation by steam at 900°F, 18: 2162(R) (IITRI-B198-46)
Mo–ThO_2, preparation and thermionic evaluation, 17: 4886(R) (AD-275610)
Mo–ThO_2, stability and strength at 1650 to 2210°C, 19: 26853
Mo–TiB_2, preparation and properties of crucibles of, 16: 9219(T) (CEA-tr-R-1440)
Mo–TiC, corrosion of refractory-metal-bonded, by potassium at 1600°F, 20: 27432(R) (NASA-CR-54892)
Mo–TiC, phase diagram, 19: 18521(T)
Mo–TiN, preparation and properties, 19: 42881
Mo–Ti–Zr, creep at 1800 to 2200°F of TZM, 20: 2333(R) (NASA-CR-54457)
Mo–UC, properties as thermionic cell emitters, 17: 27962
Mo–UC, properties of cermets of, physicochemical, mechanical, and radiation stability, 19: 26818 (NAA-SR-8617(Vol.III))
Mo–UC, radioinduced swelling in dispersions of, 19: 10675(R) (NAA-SR-9999)
Mo–UN, fabrication by pneumatic impaction, 17: 36197(R) (HW-76301 (Paper 2))
Mo–UN, irradiation at 2000°C in-pile of molybdenum-clad, 18: 29001(R) (HW-79280(p.5.1-25))
Mo–UN, properties of cermets of, physicochemical, mechanical, and radiation stability, 19: 26818 (NAA-SR-8617(Vol.III))
Mo–UN, radiation effects on molybdenum-clad, 18: 12724(R) (HW-76303 (p.4.1-43))
Mo–UN, radiation effects, 19: 11679
Mo–UO_2, chemical reactions of tungsten coated at 1800°C, 20: 39383 (BMwF-FBK-66-08)
Mo–UO_2, chlorination, 20: 10961
Mo–UO_2, compacting into tubes, use of opposing magnetic fields in coaxial conductor for, 18: 39868
Mo–UO_2, creep properties, 16: 29381 (TID-11173)
Mo–UO_2, deposition of, by electrophoresis, 16: 30369 (TID-11153)
Mo–UO_2, development for fast reactor fuel, 20: 45100
Mo–UO_2, diffusion of uranium dioxide from, at 1700 to 2500°C, 19: 41043
Mo–UO_2, diffusion and reactions in, 20: 339
Mo–UO_2, dissolution of, 18: 13972
Mo–UO_2, dissolution in nitric acid, (E), 20: 10384(T,R) (EURFNR-3F)
Mo–UO_2, electric conductivity, 17: 26944(R) (BMI-1630(Del.))
Mo–UO_2, electric conductivity, thermal conductivity, and tensile properties, 19: 14032
Mo–UO_2, electric conductivity at 25 to 1300°C, effects of composition and fabrication process on, 20: 29699 (CONF-650674-1)
Mo–UO_2, electric conductivity of cermet, effects of microstructure on, 20: 41478
Mo–UO_2, fabrication and properties, 16: 29335
Mo–UO_2, fabrication and testing of, for fuel pellets for thermionic converters, 17: 22272(R) (MND-2945-2)
Mo–UO_2, fabrication and testing, 17: 22966(R) (BMI-1614(Del.))
Mo–UO_2, fabrication by magnetic field compaction, 19: 11679
Mo–UO_2, irradiation at 2000°C in-pile of molybdenum-clad, 18: 29001(R) (HW-79280(p.5.1-25))
Mo–UO_2, mechanical and thermal properties, 17: 35251(R) (BMI-1632 (Del.))
Mo–UO_2, performance as reactor fuel, 18: 3134(R) (GEAP-4094)
Mo–UO_2, performance in thermionic diodes, 18: 30497 (TID-7687(p.360-83))
Mo–UO_2, preparation, 18: 5351(P)
Mo–UO_2, preparation, 18: 17351(R) (BMI-1659(Del.))
Mo–UO_2, preparation and properties of, 18: 42047
Mo–UO_2, preparation by cold pressing and sintering, 19: 13961
Mo–UO_2, preparation and phase studies, 19: 13962
Mo–UO_2, properties at high temperatures, 17: 15532(R) (BMI-1607(Del.))
Mo–UO_2, properties of cermets of, physicochemical, mechanical, and radiation stability, 19: 26818 (NAA-SR-8617(Vol.III))
Mo–UO_2, radiation effects on stability of, 16: 4450(R) (BMI-1546(Del.))
Mo–UO_2, radiation effects on molybdenum-clad, 18: 12724(R) (HW-76303 (p.4.1-43))
Mo–UO_2, radiation effects, 19: 14032
Mo–UO_2, sintering at 1500 to 1800°C on, 18: 36020
Mo–UO_2, tensile properties, 17: 38428 (ANL-6656)
Mo–UO_2, thermal conductivity, 17: 26944(R) (BMI-1630(Del.))
Mo–UO_2, thermal conductivity at 20 to 800°C, 17: 39719(R) (MND-2945-3)
Mo–UO_2, thermal conductivity of fuel rods of, effects of molybdenum additions on, 19: 45573 (GEAP-4902)
Mo–UO_2, use as thermionic fuel material, 18: 12858(R) (MND-2945-4)
Mo–UP, compatibility, 20: 15032(R) (ANL-7152, pp 50-72)
Mo–U–UC, fabrication as fuel material for Fermi Fast Breeder Reactor, process developments for, 17: 28531 (ORNL-3437)
Mo–U–UO_2, fabrication as fuel material for Fermi Fast Breeder Reactor, process developments for, 17: 28531 (ORNL-3437)
Mo–Y_2O_3, phase studies, 17: 39717 (GEST-2021)
Mo–Y_2O_3, stability and strength at 1650 to 2210°C, 19: 26853
Mo–ZrB_2, sintering of, effects of composition on, 20: 31698
Mo–ZrB_2, stability and strength at 1650 to 2210°C, 19: 26853
Mo–ZrN, stability and strength at 1650 to 2210°C, 19: 26853
Mo–ZrO_2, stability and strength at 1650 to 2210°C, 19: 26853
Mo–ZrO_2, structure of dispersion-hardened, effects of sintering process on, 20: 17109

MOLYBDENUM TELLURIDES
preparation and properties of single crystals of, 16: 31611
thermoelectric properties of doped, 18: 37115 (ANL-6856)
MOLYBDENUM ZINC OXIDES
crystal structure, 20: 43919
Molybdophosphates
see Ammonium Phosphomolybdates
MOMENTS
see also Data Tabulations
see also Electric Moments
see also Magnetic Moments
see also Nuclear Electric Moments
see also Nuclear Magnetic Moments
determination of nuclear, using optical double resonance, 20: 1237
measurement of nuclear quadrupole, using Coulomb excitation, 20: 21991 (BNL-948, pp 1005-44)
Monazite Sands
see Monazites
MONAZITES
see also Black Sands
see also Thorium Ores
see also Uranium Ores
age estimation by complete lead method, 16: 27458
age estimation by the xenon method, 17: 34128
age estimation, in Dominion Reef conglomerates, 16: 13377
age estimation of, by lead–thorium method, 20: 43134
age of, estimation from lead, thorium, and uranium contents, 19: 42652
age of, in Japanese granites, 20: 43556
age of, in Sweden, 20: 39125
analysis for cerium using potassium dichromates, potentiometric, 18: 25308
analysis for cerium and lanthanum, activation, 20: 24994
analysis for dysprosium and scandium, activation and spectrometric, 16: 2975
analysis for europium and ytterbium, polarographic, 20: 22913
analysis for lead, radium, and thorium, 16: 20325(T) (NP-tr-895)
analysis for radium-228, 20: 26808
analysis for rare earths, thorium, and uranium, 16: 20343
analysis for rare earths and thorium, 18: 19885
analysis for rare earths, thorium, and uranium, 19: 13227
analysis for rare earths in black and yellow, by ion exchange chromatography, 20: 35424
analysis for scandium, activation, 20: 16383
analysis for thorium and uranium, radiometric, 16: 11565
analysis for thorium, amperometric, 16: 11538
analysis for thorium, 17: 6021
analysis for thorium, fluorescent x-ray spectrometric, 18: 1595
analysis for thorium, amperometric, 18: 13693
analysis for thorium, x-ray-fluorescence, 18: 21971
analysis for thorium dioxide in Taiwan, by gamma scintillation spectrometry, 18: 21977
analysis for thorium, 19: 17823
analysis for thorium by titration with sodium fluoride, 19: 43970
analysis for thorium by titration using fluoride ions, 20: 3905
analysis for thorium and uranium, 20: 14491
analysis for thorium, photometric, 17: 35665
analysis for uranium using dibenzoylmethane, spectrophotometric, 17: 40742
analysis for uranium, double column method for, 18: 21974
analysis for uranium, fluorometric, 19: 30085(R) (TID-21853)
analysis for uranium by ion exchange separation and fluorimetry, 19: 46223
analysis of concentrates of, for thorium, 20: 8861
analysis of, ion exchange chromatography for separation of cerium and thorium in, 19: 7643
analysis scheme using ion exchange, 17: 19959
chlorination and separation of thorium chloride, 16: 1844
crystal structure of, effects of calcium, thorium, and rare earth contents on, 20: 4174
decomposition using pyrophosphoric acid, 17: 10556
diffusion of lead isotopes in, differentials in, 19: 9571
effects on *Phaseolus vulgaris*, 20: 18237
gamma spectra of, performance of germanium detectors for determining, 20: 29079 (AERE-M-1736)
leaching thorium from, acid, 16: 31670
mining in India, status of, 20: 36539(R) (NP-16171)
processing by electromagnetic separation and decomposition, production of rare earth salts in, 20: 23220
processing for rare-earth extraction using TBP, 19: 11279
processing for thorium separation, effects of phosphate on ion-exchange and solvent extraction, 18: 1806
processing for thorium separation by solvent extraction, 19: 18071
processing for uranium recovery, new UAR technology for, 18: 37404 (A/CONF.28/P/454)
processing of, determination of radium-228 in wastes from, 20: 43442
processing of, rare earth separation from, 19: 38859
properties for use with leak oxide and silicate as neutron-trapping material, 19: 23941
radiation from, effects on rats of, 19: 2131
radioactivity equilibrium between radium, thorium, and uranium in, in Ukraine, 19: 20189
radioactivity of foods grown on Brazilian, 20: 12988
radioactivity of, in Ceylon, Egypt, and India, 20: 35648
radioecological studies in Brazil, 20: 40522(R) (NYO-3273-7)
reduction by carbon at high temperature, 19: 18064
separation of cerium, rare earths, and thorium from, 18: 3916(P)
separation of rare earths from, by ion exchange, 17: 30626
separation of rare earths from, by solvent extraction using TBP, 19: 9281(R) (IS-900(Sect.E))
separation of rare earths and thorium from, 19: 17823
separation of thorium from, by solvent extraction with amine, 17: 8226
separation of thorium from, by ion exchange, effects of phosphate ions on, 19: 34270
sorption of sodium tridecylate by, tracer studies of oxygen effects, 16: 27655
structural relation to uranium content, 16: 6632
thorium and uranium content in, in Brazil, 20: 45259 (NYO-2577-3)
thorium content of, in Spokane Co., Wash., 18: 18060
thorium extraction from, acid process for, 18: 37410 (A/CONF.28/P/521)
thorium recovery from, health physics measures for, 18: 18121
uptake and elimination of radioactive dusts of, from rat lungs, 19: 17484
uranium content in, in Taiwan, 19: 36665
uranium oxide content in, in Spokane County, Wash., 18: 18060
uses in preparation of protactinium sources, 19: 24618
xenon isotope abundances in, from pegmatite, 17: 29101
MONEL
alpha scattering by, at 5.3 Mev, 19: 18690
brazing criteria for, 17: 11163 (DMIC-181)
cavitation damage, correlation with mechanical properties, 19: 2714 (AD-606050)
corrosion by air, carbon oxides, hydrogen sulfide, and sulfur dioxide to 1200°C, 18: 39844
corrosion by ammonium fluoride–formic acid–nitric acid solutions, anodic protection against, 18: 35959
corrosion by anisole–boron trifluoride, evaluation of, 20: 19135(R) (K-C-718)
corrosion by aqueous solutions, galvanic, 18: 41959 (WCAP-1844)
corrosion by boiling niobium pentafluoride, 17: 26944(R) (BMI-1630 (Del.))
corrosion by fluoride volatility process atmospheres, 20: 7192(R) (K-1649)
corrosion by hydrofluoric acid processing solution, 17: 1564(R) (IDO-14593)
corrosion by hydrofluoric acid–nitrogen oxide systems, 17: 2461(R) (BNL-731(p.18-46))
corrosion by hydrofluoric acid solutions, 17: 39494
corrosion by hydrofluoric acid–nitrogen dioxide solutions and nitrosyl chlorides, 18: 3671(R) (BNL-799(p.26-54))
corrosion by hydrofluoric acid–nitrogen dioxide systems, 18: 11958(R) (BNL-823(p.20-47))
corrosion by hydrofluoric acid fuel-dissolver solutions, 18: 17929(R) (IDO-14616)
corrosion by hydrofluoric acid–nitrogen oxide solutions, 19: 15331(R) (BNL-841(p.18-42))
corrosion by hydrofluoric acid–nitrogen oxide, 19: 36216(R) (BNL-900(p.29-72))
corrosion by hydrofluoric acid-nitrogen oxide solutions, 20: 20177(R) (BNL-929, pp 83-105)
corrosion by liquid potassium, sodium, and potassium–sodium alloy, 19: 34643
corrosion by uranium hexafluoride up to 1000°C, 18: 20469 (CEA-2385)
corrosion in solvent extraction processes, 18: 8761
corrosion in zirconium dissolver product solutions at 100°C, 17: 30582(R) (IDO-14611)
corrosion of, by hydrofluoric acid, 16: 20535(R) (IDO-14583)
corrosion of, by hydrofluoric acid–hydrogen peroxide mixtures, 16: 20534(R) (IDO-14574)
corrosion of, by hydrofluoric acid solutions, 16: 20042(R) (BNL-696)
corrosion of, by niobium pentafluoride, 17: 22111 (BMI-X-229)
corrosion of, by water and vapor at 450°F, 16: 5668 (MND-E-2655)
corrosion of, effect of Teflon on, 17: 24639 (WAPD-BT-28(p.53-9))
corrosion of welded, by fixed wastes at 200 to 500°C, 18: 19448(R) (ORNL-TM-757)
ductility of, at −269°C, 20: 21416
effects of decontaminating and descaling solution on metal loss on, 20: 21238 (NP-15928)

effects on boiling heat transfer of pressurized saturated water from outside surfaces of tubes, 19: 28503 (SROO-260-6)
electron scattering by cesium-coated, parameters for 0.05 to 5.0 ev, 18: 10834
gamma absorption by, effective atomic numbers for, 19: 40069
hot-cracking susceptibility of, effects of additives on, 19: 30751 (WERL-8844-8)
joining by brazing, soldering, or welding, 20: 29666 (RSIC-484)
machining properties of, 20: 29665 (RSIC-482)
mechanical properties at 70 to 2000°F, 17: 18758 (NAA-SR-Memo-8052)
mechanical properties at cryogenic temperatures, 19: 47013 (PB-171809(Rev.)(Suppl.2))
performance of K-, as melting-point temperature sensors up to 6000°F, 19: 30489 (SC-DC-65-1237)
properties at −400 to 100°F, 18: 42020 (PB-171809(Rev.))
properties of, for use in hydrofluoric acid dissolver construction, 17: 8242 (IDO-14594)
radiation effects on tensile properties at 30°R, fast neutron, 19: 14086(R) (N65-13446)
radiation effects on tensile properties of, at 30°R, 20: 23772(R) (N-65-13446)
radiation effects on tensile properties of, irradiated at 30°R, fast-neutron, 20: 27589(R) (NASA-CR-54881)
surface treatments for types 400 and K-500, coating and mechanical, 20: 29706 (NASA-TM-X-53448)
tensile properties at 30 and 540°R, 17: 25776(R) (NP-12812)
thermal conductivity at low heat fluxes, 17: 38551(R) (SRO-93)
thermal stresses in cladding of, during thermal cycling of reactor fuel, 16: 18031 (GAMD-1172)
welded joints of, effects of multiple repairs and 400°F interpass temperature on, 19: 34655 (NP-15134)
welding criteria for, 17: 11163 (DMIC-181)
welding to Inconel, method for, 18: 35093
welding 2-inch pipes of, parameters for tungsten arc, 19: 22928 (WERL-8844-7)

Monitoring
see Radiation Monitoring

Monitron
see Radiation Detection Instruments (Ion Current Type)

MONKEYS
age estimation of rhesus, by skeletal growth, 17: 7926
anesthetic for, use of phencyclidine hydrochloride as, 20: 18289(R) (LA-3432, pp 56-101)
atherosclerosis development in, effects of chondroitin sulfate on, 20: 18295(R) (UCLA-12-576, pp 27-56)
behavior response to gamma radiation, 20: 40519 (NP-16259)
beryllium poisoning in, effects of aurintricarboxylic acid on, 19: 33757
blood picture and immune reactions of Tamarinus, 19: 26109(R) (ORINS-49(p.40-62))
blood picture of *Macaca mulatta* and *M. speciosa*, 18: 15773 (LAMS-3034(p.96-102))
body water volume and turnover in *Macaca mulatta* and *M. speciosa*, 18: 15772(R) (LAMS-3034(p.76-80))
bone marrow from, effects of freeze-storage techniques on, 17: 35615
brain tumor radiotherapy in, using proton beam Bragg peak, 18: 3668
calcium metabolism in teeth of, tracer study, 19: 24249
calcium transport in placenta of, 19: 31742
calcium-45 uptake by bones and teeth in, 17: 27039
calcium-45 transport in placenta of, 19: 31742
calcium-47 transport in placenta of, 19: 31742
care and feeding of, 19: 29831 (CEA-R-2714)
care and handling of rhesus, 17: 7928
care of, 18: 43153(R) (LA-3132-MS(p.103-8))
care of laboratory colonies of, 19: 8785 (EUR-1607.e)
cesium-137 retention, 16: 1320(R) (LAMS-2627(p.175-82))
characteristics and care of chimpanzees, 17: 7927
chromosome analysis of blood cells of *Macaca mulatta and M. speciosa*, 18: 15738(R) (LAMS-3034(p.227-34))
dermatosis in, pathology of systemic, 17: 7930
development of immunity in rhesus fetuses, 17: 7925
effects of aging on behavior of, 20: 8695
effects of Aspergillus toxins on, 18: 4917 (TID-18382)
effects of bone marrow grafts on secondary disease in, methods for modification of, 19: 19647
effects of diet containing irradiated foods on, 17: 40485(R) (NP-13174)
effects of diet for, containing irradiated peaches and oranges, 20: 35233
effects of focal-head irradiation on performance, 16: 26808
effects of irradiated peaches and oranges in diet of, 18: 11635 (NP-13576)
effects of irradiated Schistosoma cercariae on, 19: 15201
effects of irradiated cercariae on immunization of rhesus, against *Schistosoma japonicum*, 19: 36045
effects of nitrogen mustard on, effects of thioglycollic acid derivatives on toxic, 20: 18474
effects of Schistosoma infection on blood serum of, 19: 8937
effects of thorium oxide on sensitivity to toxin, 17: 31918
effects of vitamin K-deficiency, 16: 33344(R) (NP-12093)
erythropoiesis in, stimulation by erythropoietin of nonprimate origin, 18: 36923(R) (UCRL-11387(p.91-5))
evaluation of *Tamarinus nigricollis* as a laboratory primate, 17: 7929
excretion of tritium-labeled normorphine by, fecal and urinary, 17: 15601
function of transplanted bone marrow in irradiated, 17: 7920
hematological effects of small doses of gamma radiation in, 16: 31504
hematopoietic chimerism in the marmoset, *Tamarinus nigricollis*, 19: 21798
hematopoietic function in, effects of injected bone marrow cells on restoration of, 19: 8785 (EUR-1607.e)
immune reaction to normal and irradiated Schistosoma cercaria, 20: 24917
immune reactions to Schistosoma cercariae, 19: 8937
immune reactions to irradiated tendon grafts in, 19: 45965
immunization by irradiated *Schistosoma masoni* cercariae, 16: 20202
immunization of, against *Schistosoma japonicum* by inoculation with irradiated larvae, 18: 15890
infection with irradiated Schistosoma cercariae, 18: 5113
iodine metabolism, tracer study, 17: 15588 (LADC-5209)
iodine-131 retention and excretion, 16: 1323(R) (LAMS-2627(p.194-7))
iodine-131 content of thyroid lymph, 18: 17440
iodine-131 metabolism by, species difference in *M. mulatta* and *M. speciosa*, 18: 43179(R) (LA-3132-MS(p.84-92))
iodine-131 metabolism in baboons, effects of gonadotropic hormone, 19: 33749
iodine-131 uptake in respiratory tract and thyroid of, 19: 45776
kidney function tests of renal transplants in, using Neohydrin labeled with mercury-197 or mercury-203 and external counting, 19: 28168
laser photocoagulation of retina of eyes of, 20: 45370
learning performance of, effects of radiation exposure and sex on, 18: 9866
leukocyte morphology, effects of sex, bone marrow transplants, and x radiation, 17: 19820
manganese-54 metabolism in, 18: 43172(R) (LA-3132-MS(p.25-31))
manganese-54 metabolism in, 20: 36554 (LA-DC-7305)
metabolism of manganese-54 by tissues of, retention functions for, 20: 45296
oxidative enzyme levels in tissues of, effects of temperature on, 19: 43632 (LA-DC-7135)
placental transfer of calcium-45 in pregnant, 18: 11848(R) (UCLA-520(p.53-74))
protection against lethal irradiation by cysteine and 2-(2-aminoethyl)-2-thiopseudourea, 16: 17539
protection against radiation injuries, effectiveness of bone marrow transfusion, 17: 7918
protection against radiation injuries, effectiveness of homologous and autologous bone marrow transfusions, 17: 7919
protection against radiation injuries, effectiveness of bone marrow transfusions, 17: 7921
proton depth-dose measurements in phantom, 20: 31467
proton dosimetry in *Macaca mulatta*, 20: 31096
radiation and age effects on response to training of, 18: 15850
radiation-conditioned behavior, effects of habituation to laboratory and radiation procedures, 16: 16266
radiation death in chemically protected, pathology of, 16: 1624(AF-SAM-61-102)
radiation dosage to, determination of, by monitoring dental gold restorations, 17: 19849
radiation dose measurements in, exposed to reactor pulse environment, 20: 25378 (AFRRI-SR-66-3)
radiation dosimetry in *Macaca mulatta*, proton, 20: 28928 (CONF-651109, pp 417-25)
radiation effects on behavioral changes, 16: 16267
radiation effects on central nervous system, 16: 16277
radiation effects on poliovirus yield in cultured kidney cells from rhesus, 16: 20201
radiation effects on nervous system, delayed effects, 16: 23483
radiation effects on development of Morgan's toxinfection in, 16: 30244
radiation effects on hemopoiesis in *Macaca mulatta*, 17: 1234 (AF-SAM-62-51)
radiation effects on visual acuity in, proton, 17: 1320
radiation effects on endogenous bacterial invasion of tissues in *Macaca mulatta*, 17: 2824 (SAM-TDR-62-77)
radiation effects on measles infection and immunity in, 17: 4401
radiation effects on central nervous system in, whole-body, 17: 12176
radiation effects on central nervous system, 17: 13984(R) (TID-18003)
radiation effects on performance of, acute, 17: 18372 (TID-7652(p.343-74))
radiation effects on reactivity of cerebral cortex in, 17: 17908
radiation effects on performance of repetitious work by, 17: 19852

radiation effects on bone marrow and gonads of, protective effects of cysteamine against, 17: 19913
radiation effects on immunity to intestinal infections in, 17: 24953
radiation effects on chromosomal rearrangement in spermatogenesis in, 17: 31950
radiation effects on blood picture in, 17: 33452(R) (ANL-6723(p.61-2))
radiation effects on heart cell nuclei size in, x, 17: 38833
radiation effects on glucose metabolism in *Macaca mulatta*, 17: 38885 (SAM-TDR-63-40)
radiation effects on carbohydrate metabolism in Rhesus, 17: 40663(T) (FTD-TT-63-641)
radiation effects on behavior aging in, x, 18: 81
radiation effects on learning in, female versus male, 18: 1399
radiation effects on antibody formation in, 18: 1404
radiation effects on gas gangrene immunization in, gamma, 18: 3530
radiation effects on genetics of, review of, 18: 3538
radiation effects on chromosomes aberrations in spermatogenesis in, 18: 5108
radiation effects of mixed gamma and neutrons on hematopoietic system and life span of *Macaca mulatta*, 18: 6616 (SAM-TDR-63-55)
radiation effects in, genetic, 18: 6673
radiation effects in, genetic, 18: 6672
radiation effects on brain of, 18: 8102 (BNL-7620)
radiation effects on kidney cells from, in tissue culture, 18: 8150
radiation effects on sorbed tritoxoid vaccinated, protective effects of revaccination against gas gangrene and, 18: 8191
radiation effects on, proton, 18: 11658
radiation effects on immune reactions in *Tamarinus nigricallis*, 18: 13390(R) (ORINS-43)
radiation effects on lipid metabolism in, 18: 13419(R) (TID-20242)
radiation effects on learning behavior of, effects of sex on, 18: 13500
radiation effects on behavior of, x, 18: 13501
radiation effects on monkey social, x, 18: 13503
radiation effects on response to stimulus of, 18: 15849
radiation effects on response to stimulus of, 18: 15851
radiation effects on response to stimulus of, 18: 15852
radiation effects on learning performance in, 18: 15853
radiation effects on rectal and skin temperature of, dose relation to, 18: 17544
radiation effects on responses of, x, 18: 19586
radiation effects on enzymes in kidney tissue cultures of, 18: 21861
radiation effects on chromosome aberrations in spermatogenesis of *Macaca mulatta* at 5 to 400 r, gamma, 18: 23317
radiation effects on testes of, gamma, 18: 23330
radiation effects on central nervous system, 18: 29382
radiation effects on conditioned behavior of, in massive and acute doses, 18: 35310 (NP-14043)
radiation effects on spermatogenesis in, x, 18: 36999
radiation effects on 17-ketosteroid secretion by, 18: 38867
radiation effects on testes cytology in, x, 18: 38898
radiation effects on eyes of, proton, 18: 38929
radiation effects on adrenal function in rhesus, 18: 43281
radiation effects on spermatocytes and spermatogonia in *Macaca mulatta*, 18: 43290
radiation effects on tumor development in, gamma and x-ray, 19: 7033
radiation effects on pathology of fetuses of, exposed *in utero*, 19: 8811
radiation effects on reproduction of kidney cells in, 19: 8841
radiation effects on granulocytopoiesis in, 19: 10865
radiation effects on chromatids and chromosomes in bone marrow, 19: 17608
radiation effects on sarcoma development in mouth of, 19: 17599
radiation effects on effectiveness of tetanus vaccination in, 19: 19608
radiation effects of simulated space situation on blood cells in, gamma and proton, 19: 19616
radiation effects on acid levels and peripheral blood fractions in brain of, 19: 26020
radiation effects of Bragg peak of proton beam on brain of, 19: 26210
radiation effects on behavior of, fast neutrons, 19: 28029
radiation effects on learning behavior of rhesus, fast neutron, 19: 28030
radiation effects in *Macaca mulatta*, whole-body x, 19: 28072
radiation effects on brain thalamus, 19: 30013 (ACRH-103(p.104-20))
radiation effects on Rhesus, protective effects of bone marrow transplants against, x, 19: 31915
radiation effects on gas gangrene immunity in, gamma, 19: 33945
radiation effects on response to food stimulus of, 19: 33857
radiation effects on hemopoiesis in, recovery from gamma, 19: 36043
radiation effects on pyrocatechol content in tissues of Macacus, 19: 40373
radiation effects on skin of, beta, 19: 42258 (LA-3365)
radiation effects on learning ability of rhesus, 19: 43805
radiation effects on learning ability of rhesus, 19: 43806
radiation effects on food satiation in rhesus, 19: 43807
radiation effects on performance tests requiring visual discrimination, by *Macaca mulatta*, 19: 45803
radiation effects on behavior of, sex factors in, 19: 45898
radiation effects on response to stimulus-position conditions in female rhesus, 19: 45899
radiation effects on learning by rhesus, 19: 45900
radiation effects on learning behavior of Rhesus, sex factors in, 20: 92
radiation effects on, protective effects of cysteine-AET against, 20: 140
radiation effects on immune reactions in, 20: 1631
radiation effects on retinal development in embryos of, x, 20: 3725
radiation effects on development and eruption of teeth in, x, 20: 3743
radiation effects on enzyme levels in blood of, γ, proton, and x, 20: 3692
radiation effects on visual discrimination in, effects of age on x, 20: 3721
radiation effects on immune reactions of man to kidney transplants from baboons, x, 20: 6813
radiation effects on membrane permeability of erythrocytes in, x, 20: 6765
radiation effects on behavior of, x, 20: 8695
radiation effects on, protective effects of bone marrow against, 20: 8727
radiation effects on behavior in, γ, neutron, and x, 20: 14286 (AD-625837)
radiation effects on blood picture and survival in, whole-body x, 20: 14302
radiation effects on conditioned and avoidance behavior of, γ, 20: 18283 (AD-611869, pp 375-89)
radiation effects on cardiovascular system in *Macaca mulatta*, γ, 20: 20488
radiation effects on neuromuscular competence and response to stimuli in, massive pulsed-dose reactor, 20: 24872 (AFRRI-SR-66-2)
radiation effects on properties of blood serum proteins in, 20: 26650
radiation effects on *Macaca mulatta*, whole-body proton, 20: 28931 (CONF-651109, pp 624-35)
radiation effects on, pathological γ, 20: 28986
radiation effects on blood pressure of *Macaca mulatta*, γ and proton, 20: 31104
radiation effects on enzyme activity in serum and tissues of *Macaca mulatta*, γ and proton, 20: 31105
radiation effects on spermatocytes of, pathological γ and x, 20: 31117
radiation effects on *Macaca mulatta*, pathological proton, 20: 31097
radiation effects on *Macaca mulatta*, pathological proton, 20: 31098
radiation effects on *Macaca mulatta*, pathological proton, 20: 31099
radiation effects on *Macaca mulatta*, pathological proton and x, 20: 31101
radiation effects on *Macaca mulatta*, pathological proton and x, 20: 31103
radiation effects on *Macaca mulatta*, proton, 20: 31106
radiation effects on embryo cell tissue cultures of, protective effects of serotonin and thiourea against x, 20: 31121
radiation effects on work performance of, chronic γ and neutron, 20: 32962 (AD-627686, pp 423-33)
radiation effects with bone marrow transplants on hematology and pathology in, whole-body x, 20: 33071
radiation effects on retinal blood vessels of, laser, 20: 35258
radiation effects on rhesus, psychological testing of fast-neutron, 20: 35281
radiation effects on serum proteins in, gamma, 20: 35316
radiation effects on cerebral cortex of, x, 20: 36656
radiation effects on response-perseveration learning set for nonrewarded cues in male, fast-neutron, 20: 36638
radiation effects on social distractibility behavior of female, γ and neutron, 20: 36639
radiation effects on buccal flora of, γ, 20: 38667
radiation effects on, localized vs. whole-body γ and x, 20: 40694
radiation effects on eye tissues of, γ, 20: 40646
radiation effects on, dynamics of lethal x, 20: 42934
radiation effects on, effects of antibiotics, blood platelets, and bone marrow on mortality in, 20: 42980
radiation effects on development of, exposed *in utero*, x, 20: 40619(R) (NYO-2740-3, pp 216-57)
radiation injuries, protection afforded by combined chemical prophylaxis and therapy, 17: 15633 (SAM-TDR-62-103)
radiation injuries, treatment with autologous bone marrow, 17: 15821
radiation injuries in, effects of treatment with antibiotics and vaccine on, 18: 27223
radiation injuries in, protective effects of mercaptopyridoxine against, after acute and chronic exposure, 18: 31313
radiation injuries in, pathology of proton-induced, 19: 24260(R) (NASA-CR-53780)
radiation injuries in, protective effects of AET and PAPP against, 18: 36951(R) (TID-20979)
radiation injuries in, protective effects of injected bone marrow against, 18: 36951(R) (TID-20979)
radiation injuries, protective effects of bone marrow transplants,

19: 26114
radiation injuries of central nervous system of, 19: 8797(T) (JPRS-27289)
radiation injuries of, protective effects of fetal hematopoietic grafts against, 20: 6907(R) (EUR-2511.e)
radiation sickness, effects of chemotherapy on, 16: 26875
radiation sickness of, effects of, on maturation and proliferation of bone marrow in, 17: 10495
radiation sickness in, protective effects of serotonin against, 17: 25053
radiation sickness prophylaxis in, using 5-methoxytryptamine, 17: 30425
radiation sickness in, effects of BCG on, 18: 41244
radiation sickness in, effects on reproduction, 16: 23522
radiation source avoidance by, γ, 20: 20495
radiation, space flight, and vibration effects on serotonin content in blood of, 19: 15095
radiodiagnosis in brain of, safety of radioalbumin aggregates for, 20: 3832
radioinduced granulocytopenia, 17: 17757 (TID-16572)
radioinduced infection with pox virus, 16: 31521
radioinduced lesions in cerebral cortex of, physiology of alpha, 19: 26081
radioinduced lesions in cerebral cortex of, therapy for, 19: 36034
radioinduced leukemia in *Macaca mulatta*, 19: 28074
radioinduced osteonecrosis in jaws of, effects of dose fractionation on x, 20: 3742
radiosensitivity of reproductive cells in, 16: 28832
radiosensitivity of hematopoietic system in Rhesus, tracer study, 17: 54
radiosensitivity of hematopoietic system in Rhesus, 17: 55
radiosensitivity of hematopoietic system in Rhesus, 17: 56
radiosensitivity of chimpanzees, 17: 13981 (TID-17837)
radiosensitivity of gonads of, gamma and x-ray, 17: 17912
radiosensitivity of fetuses of, 18: 8106(R) (NYO-2740-1(p.155-98))
radiosensitivity of, effects of female and male gonadal hormones on, 19: 17680
radiosensitivity of developing fetuses of, 19: 31787(R) (NYO-2740-2)
radiosensitivity of chromosomes in leukocytes in, 20: 5304(T) (JPRS-32985, pp 45-50)
radiotherapy of, method for yttrium-90, 18: 3638
rare earth toxicity in, 20: 30970 (COO-1170-5)
respiration of radioactive aerosol by, measurement of, 20: 26624
response to thalamic lesions in, 19: 31660(R) (ACRH-23(p.40-57))
sarcoma induced by Rous sarcoma virus in, 19: 21806
screening of radioprotective compounds in, 18: 37031(R) (AD-600229)
sodium-22 metabolism by *Macaca mulatta* and *Macaca speciosa*, 18: 43179(R) (LA-3132-MS(p.84-92))
species specificity of reannealed DNA of, 20: 42757
strontium-90 uptake and retention by bone in, 16: 28660
strontium-90 content and distribution in skeletons of, after intravenous and oral administration, 20: 28896
suitability of *Tomarinus nigricollis* for radiation studies, 16: 30212(R) (ORINS-41)
thymidine distribution in tissues of *Oedipomidas oedipus*, 20: 22569
tissue cultures of leukocytes, 17: 5676 (SAM-TDR-62-99)
tooth extraction techniques for, 20: 18289(R) (LA-3432, pp 56-101)
toxic effects of mercaptoethylamine in, 18: 37031(R) (AD-600229)
tumor induction in, by chemicals and cobalt-59 and silver-110, 17: 35465
uranium carbide microsphere gastrointestinal passage by, 19: 42258 (LA-3365)
vaccination against Schistosoma using irradiated cercariae, 19: 8937
yttrium-90 distribution in, injected intravenously with yttrium chloride, 17: 38729
zinc-65 metabolism in, 20: 35214

MONOCHLOROETHYL GROUPS
reactions of, with trichloromethyl group, disproportionation and recombination in, 17: 12337

MONOCHROMATORS
see also Neutron Monochromators
see also X-Ray Monochromators
calibration for photomultiplier tubes, 20: 9221 (INR-642/XVIII/PP)
calibration of vacuum-ultraviolet, for absolute radiation intensities, 18: 481
construction of gamma, 18: 37508 (BNL-874(p.19-20))
counting rate and resolution of Compton gamma, (T), 19: 28619
design and performance of grating, 17: 40718 (TID-7655(p.400-13))
design and performance of filter-lens, for fast electrons, 20: 23443
design and theory of gamma, 20: 16505 (BNL-949)
design for charged-particle beams, 20: 9623(P)
design modification for use in instrument for observation of time-dependent spectral line profiles, 17: 8537 (UCRL-9843(Rev.))
design of bent-crystal gamma, 16: 29146
design of Fabry-Perot ultraviolet, for nebula electron density determination, 19: 9867
design of gamma, 20: 20177(R) (BNL-929, pp 83-105)
design of gamma, 20: 25180(R) (BNL-954, pp 84-113)
design of high intensity uv, 20: 19011
design of high-resolution Echelle, 20: 44920
design of u-v, 20: 27234
design of ultra-high vacuum ultraviolet, 16: 31759
design of 10- to 20-Mev photon, 16: 13699 (NP-11426)
development and performance of time-of-flight electron beam, 19: 7540(R) (ORNL-3697(p.144-52))
development for electron beam spectroscopy, 20: 9284
development of electron, using modified Wien filter, 17: 10939
development of electron, using resonance scattering in helium, 18: 5592
development of electron, 20: 15235(R) (AD-620289)
development of gamma, 19: 36451(R) (BNL-900(p.73-104))
development of improved electron, for excitation potential determinations, 19: 25155
review on photon, 20: 14841
spectral line splitter for, for plasma profile measurements, 18: 22950 (RISO-74)
use for energy level measurements, 19: 41828
wavelength modulation of spectral, Doppler shift detection by, 17: 25548 (MATT-162)

Monopoles
see Magnetic Monopoles

MONOSACCHARIDES
see also Arabinose
see also Fructose
see also Galactose
see also Glucose
see also Hexoses
see also Inositol
see also Lyxose
see also Mannose
see also Pentoses
see also Rhamnose
see also Ribose
see also Talose
see also Xylose
determination, radiochromatographic, 16: 1702 (PAN-237/X)
mass spectra of methylated, 17: 35856
mass spectra of methylated, 17: 10557
radiation effects on, electron-, gamma-, neutron-, and x-, 16: 31669
radioinduced free radicals, 16: 13113
radioinduced polymerization, 16: 27103(P)

MONROE QUADRANGLE (UTAH)
geology, 16: 3256

MONTANA
(See also headings of the form Montana (Ravalli Co.))
geologic datings in Jardine-Crevasse Mountain area in, rubidium–strontium method for, 20: 16711(R) (MIT-1381-13)
geological dating in southwest, potassium–argon and rubidium–strontium, 20: 41163
geology of Powder River Basin, 17: 3155 (TEI-823)
strontium-86 to strontium-87 ratios in carbonate veins and vein-dikes in Rocky Boy Stock, 20: 12980
strontium-90 uptake by wheat in, 18: 13403 (HW-SA-2977)
zoning of mineral deposits in, hydrothermal, 17: 34116 (CONF-123-1)

MONTANA (RAVALLI CO.)
mineralogy and paragenesis of carbonatic niobium–rare earth deposits, 16: 5559
strontium-86 to strontium-87 ratios in carbonate veins and vein-dikes in, 20: 12980

MONTE CARLO METHOD
see also Mathematics
see also Statistics
see also Stochastic Methods
accuracy comparison with known solution, 16: 25690 (RM-3184-PR)
adaptation to analysis of gamma ray attenuation in shielding materials, 17: 36347(R) (NARF-62-18P)
adaptation to gamma absorption by crystal detectors, 16: 4617(R) (NP-11098(p.38-45))
backward, for reversing stochastic processes, 16: 9138 (UCRL-6649)
bibliography, 16: 4445 (UCRL-6581)
bibliography on, 18: 41909 (UCRL-7823)
book: *Methods in Computational Physics*, 18: 30336
calculating neutron penetration through straight cylindrical ducts, 16: 3657 (NARF-61-33T)
calculation of charged-particle diffusion and penetration, 18: 30941
calculation of criticality by, 16: 12842
calculation of efficiencies and photofractions of scintillation detectors, 17: 32416
calculation of gamma scintillation counter response, 18: 30063
calculation of neutron spectra for radiation damage experiments,

16: 22817
calculation of neutron production in heavy elements, 19: 26922(R) (PR-P-64)
calculation of neutron reflection from concrete slab, 20: 13742
calculation of pulse-height response of scintillation detectors to gamma radiation by, 16: 5497 (ORNL-3169)
calculation of recoil spectra induced by fast neutron spectra in emulsions, 16: 5528
calculation of reflection and transmission of scattered gamma radiations from concrete, 16: 21693 (NP-11819)
calculations for particle transport, computer code for direction selection from uniform azimuthal distribution, 16: 15100 (CDRP-182-102)
calculations of ranges of energetic atoms in solids, 18: 28111
comparison with phase-space integral for meson (π)-nucleon collisions, 16: 17020
computer code for, MOCA-2, 17: 26017
computer program for, CEP, 18: 24377 (AEEW-M-442)
computer program for evaporation calculations in high-energy nuclear reactions, 19: 37835(R) (TID-22024)
computer program for, general purpose, 19: 46905(R) (IDO-17081, pp 125-35)
confidence limits from, normality test for, (T), 19: 32672
derivation for neutron scattering by thin plates, 16: 29715
development for analysis of electron-induced photon showers, 17: 12792(R) (ORNL-3360(p.248-56))
development for atom ranges in crystals using Thomas-Fermi potential, 18: 32367
development for temperature coefficients in fast reactors, 17: 35116
equations for, basic, 18: 16410 (CERN-64-13(Vol.I)(p.169-72))
estimators for calculation of scattered flux of particles in sphere or slab (T), 19: 1527 (ORNL-TM-974)
evaluation of, for reactor calculations, 18: 44979
for analysis of laminar gamma shielding, 18: 15423 (NP-13626)
for calculating fast neutron attenuation and thermalization in water, 20: 30340
for calculation of plasma radial distribution functions, (T), 19: 23848
for changes in thermal neutron absorption, use of correlated sampling in (T), 19: 3217
for computing slowing down probability in infinite homogeneous mediums, 16: 8305 (DC-58-8-64)
for criticality of interacting systems of complex geometry, 20: 16034
for diffusion of hydrogen in thermosphere, 18: 7604
for dose estimation from gamma sources, 20: 6719(R) (ORNL-3849, pp 183-213)
for electron-photon cascade shower structure, (T), 20: 15938
for energy and spatial interference among resonance nuclides (T), 19: 3570
for grain coordinates for artificial construction of particle tracks, 19: 20325 (UCRL-11624)
for meson (K_2^0) decays, with statistical box for rest-mass configurations, 20: 24058
for meson (K_2^0) decays, with statistical box for laboratory system configurations and parameters, 20: 24059
for neutron scattering from cylinders, 19: 35349 (ORNL-TM-1156)
for neutron slowing down in thin plates of hydrogenous materials, 19: 45216 (CEA-R-2804)
for neutron slowing-down moments in aluminum–water systems, (T), 20: 8040 (NAA-SR-Memo-11239)
for neutron transport problems, 20: 8044 (UCRL-7630(Suppl.I))
for neutron transport problems, 20: 40460(R) (IDO-17191)
for pair distribution functions in classical electron gases, (T), 19: 30848(R) (UCRL-12473(p.31-63))
for reactivity of bare enriched uranium metal assemblies (E/T), 19: 3561
formalism for electron transport in metals, 18: 28010
formalism for gamma transmission through cylindrical and spherical shields, 18: 35052
intranuclear cascade calculations by, statistical fluctuations in, 18: 13056 (ORNL-TM-771)
intranuclear cascade calculations by, fluctuations in, 19: 17159(R) (ORNL-3714(Vol.II)(p.97-118))
matrix inversion by, 18: 36883 (HW-SA-3193)
maximum in ideogram of Gaussian distribution, 18: 10446 (JINR-P-1460)
meteorite origin analysis by, 18: 34396
neutron attenuation at high energies, 16: 14076
neutron backscattering by plane and spherical reflectors, 18: 16896 (NP-13720)
neutron cross section library for codes FMC-N, 18-0, and 18-1, 20: 4830 (GEMP-384)
neutron density calculations by, spatial-distribution functions for, 18: 34745
neutron diffusion formulas, 16: 2466 (AAEC/E-66)
neutron distribution from, analytic expressions for, 17: 39949 (NP-13117)
neutron distribution functions by, analytic expressions for, 19: 10240
neutron flux distribution in subcritical sphere with central point source, (T), 19: 40162
neutron scattering cross sections of nuclei, multiple scatter corrections for fast, 16: 9454
neutron transmission by slab of liquid, fission, 18: 13029 (D2-4643-2)
neutron transport in, selection of scattering angle from anisotropic distributions in, (T), 19: 10232
neutron transport in, selection of scattering angle from anisotropic distributions in, (T), 19: 10233
particle penetration calculations with, transport equation transformation for, 18: 12909 (NP-13627)
performance for calculating neutron albedo from concretes, 20: 6519(R) (ORNL-3858(Vol.1), pp 20-41)
performance for fitting experimental data to theoretical curves, 20: 6286 (ISS-65/10)
principles and use for calculating collision probabilities, 20: 9800
program for multivertex event generation for high-energy physics, 20: 9824
random number generation for, methods of, 18: 2144 (IDO-16921)
random number generator for ZRA-1 computer, 20: 7484 (ZFK-TPH-14)
review, 18: 16409 (CERN-64-13(Vol.I)(p.147-67))
sample correlation techniques in, (T), 19: 10223 (WAPD-T-1734)
sampling and scoring in solution of radiation transport equation, 16: 29665(R) (UNC-5014(Vol.A))
sampling, generalization of quota, 17: 25681
scintillation detector responses to neutrons and photons, (T), 19: 9495 (UCRL-12150)
shielding calculations using, exponential transformation for, 20: 15937
theory, for particle transport problems, 17: 4882
theory of, for reactor transport problems, 18: 42608 (TID-7050(p.1441-61))
use for analysis of neutrons from small atomic explosions, 17: 19198 (LA-2390(Suppl.))
use for analysis of radiation absorption by rigid spheres, 18: 6409
use for analysis of nucleon interactions at 3×10^{13} ev, 18: 12948
use for analysis of equation of state of hard-sphere systems, (T), 19: 8007 (NYO-1480-3)
use for analysis of neutron transmission through ducts, (E/T), 19: 23939 (NP-14882)
use for analysis of electron–photon cascades in lead by 6-Bev primaries, 20: 8272 (DESY-65/6)
use for analysis of uranium-235–enriched fast critical assemblies, 20: 18057
use for analyzing x-ray distributions from electron reactions on solids, 17: 37871
use for buckling calculations in uranium-water lattices, 19: 47954 (BNWL-127)
use for calculating neutron absorption in square lattices, 16: 21715 (BAW-154)
use for calculating energy-dependent multiple neutron scattering in thin plates, 17: 11595 (TID-15571)
use for calculating meson-nucleon cascade distributions from 10- to 1000-Bev protons, (T), 19: 10452 (CERN-64-47)
use for calculating infinite multiplication factors for homogeneous media, (T), 19: 31499 (BNWL-3)
use for calculating neutron dose rates in shelter entranceways, 19: 38017 (NP-15094)
use for calculating source-to-detector geometry, 20: 41316
use for comparison of source arrangement for simulation of gamma radiation environment from fallout, 20: 23345 (AFRRI-CR-65-2)
use for cosmic particle cascades analysis, 20: 21545 (MIT-2098-227)
use for design of fast-neutron shielding, (T), 19: 12725 (WAPD-TM-481)
use for determining error magnitudes for height and radius extrapolations for cylindrical reactor, 18: 21550 (EUR-1624.e)
use for determining efficiency of neutron scintillation detectors, 19: 24848
use for electron transport properties in a low-density ionized gas, 20: 42413 (NASA-TN-D-2959)
use for energy-response calculations of fast-neutron dosimeters, 17: 34306
use for gamma and neutron transmission in slab geometries, 19: 14732(R) (TO-B-63-83)
use for gamma and neutron shielding calculations, (T), 19: 19331 (RRA-T44)
use for gamma and neutron transport calculations, 19: 43463 (TIM-941)
use for gamma transport analysis in finite shielding slabs, 18: 4684 (NRL-5981)
use for gamma transmission through slabs, (T), 19: 14733 (WAPD-BT-31(p.43-9))
use for integration of Schroedinger equation, (T), 20: 7998
use for intra-nuclear cascade calculations, 20: 36157(R) (CU-1019-51)
use for multiplication factor calculations, 20: 45076 (K-DP-1637)
use for neutron albedo calculations for concrete, 19: 43462 (ORNL-TM-

1205)
use for neutron distributions in water, first- and last-flight expectation values for, 19: 27395 (ORNL-RSIC-3)
use for neutron Doppler effect calculations for fast reactors, 20: 38423 (ANL-7120, pp 462-77)
use for neutron fission coefficient calculations, 20: 32778
use for neutron multiple scattering, 20: 26062 (CEA-R-2971)
use for neutron penetration problems, useful techniques and their effectiveness, 16: 24605
use for neutron resonance escape calculations, superposition principle in (T), 19: 3551
use for neutron resonance escape calculations, 19: 40153 (IA-1001)
use for neutron transport calculations, 19: 16818 (ORNL-3622)
use for nucleon cascades in aluminum at 30 to 400 Mev, 20: 8274 (LNF-65/30)
use for particle track construction in emulsions, 19: 44433 (CERN-65-4 (Vol.II), pp IX44-7)
use for photon transport calculations, 19: 41957 (UCRL-14165)
use for prompt neutron emission calculations, 19: 16848 (MIT-905-30)
use for prompt neutron decay analysis, 19: 42039(R) (BNWL-95, pp 36-9)
use for reactor perturbation calculations, 20: 20196 (AEEW-M-581)
use for selecting experimental conditions for (e,e' p) reactions on nuclei, 18: 32732 (ISS-64/8)
use in analysis of void gap effects, 16: 8304 (DC-58-5-97)
use in analysis of gamma heating of reactors, 16: 8306 (DC-59-3-119)
use in analysis of Argus bomb debris, 17: 24033 (AFSWC-TDR-62-127 (Vol.II))
use in analysis of neutron scattering, 18: 982 (NAA-SR-Memo-9060)
use in analysis of gamma transport from distributed sources in laminated shields, 18: 22859
use in analysis of four-momentum transfer in jets, 18: 40208
use in analysis of neutron collimator efficiency, (T), 19: 29187
use in analysis of shielding effectiveness of compartmented structures, 20: 3275
use in analysis of gamma and neutron transport in complex geometry, 20: 3348
use in analysis of neutron transmission by finite water slabs, 20: 4999(R) (ORNL-2599)
use in analysis of gamma streaming through ducts, 20: 15929 (AD-627890)
use in analyzing gamma scattering from cylinders, 20: 5181(R) (ORNL-3029)
use in analyzing photon emission in photon reactions with atoms, 20: 4949(R) (UCRL-14360, pp 85-94)
use in calculating secondary gamma dose from nuclear weapon explosion, 18: 34285 (WL-TDR-64-46(Vol.I))
use in calculating Doppler effects in fast reactors, 19: 26917(R) (IA-984)
use in calculating gamma heating in shields, 20: 4999(R) (ORNL-2599)
use in calculating gamma response functions of cesium iodide and sodium iodide crystals, 20: 5181(R) (ORNL-3029)
use in calculating neutron angular distributions from shielding, 20: 5181(R) (ORNL-3029)
use in calculating fast-neutron dose rates in cylindrical compartment, 20: 4299(R) (ORNL-2711)
use in calculating radionuclide production in proton reactions with iron at 400 Mev, 20: 22035
use in calculation of neutron spectra and buildup factors in conical configurations, 16: 31218 (NASA-TN-D-1434)
use in calculation of resonance integral of Calder Hall Reactors, 16: 32532 (AEEW-M-217)
use in calculation of radiation scattering in multibend ducts, 17: 21201 (NARF-62-13T)
use in calculations of equation of state of 12 and 48 hard circles, 17: 31083 (LA-2827)
use in calculation of Doppler effect in reactor fuel elements, 17: 38510
use in calculation of deep neutron penetration in shields, 18: 15424 (NP-13719)
use in calculation of electron-photon cascades, 18: 21322
use in calculation of nucleon emission in nucleon-stimulated decay of hyperfragments, 18: 40334
use in calculation of yields from kinetic theory of hot atom reactions, 18: 39346
use in calculation of dose rates behind iron barriers, 18: 40737 (TO-B-64-49)
use in calculation of intranuclear cascades, (T), 19: 21239 (LA-3206)
use in calculation of deep gamma penetrations, 20: 5181(R) (ORNL-3029)
use in calculation of intranuclear cascades, 20: 18556(R) (BNL-929, pp 66-82)
use in calculation of thermal-neutron fluxes, computer programs for, 20: 19786 (WAPD-T-1835(Rev.))
use in calculation of gamma self-absorption and scattering by cylindrical gamma sources, 20: 33404
use in calculation of neutron resonance absorption integral of thorium-232, (T), 20: 34626
use in computer programs for criticality calculations, 20: 35686
use in critical-size calculations for neutron systems, 17: 11462 (UCRL-6707)
use in determination of correlated quantities from empirical data, 16: 30713 (TID-11268)
use in determination of radiation penetration into enclosure shields in fallout field, 20: 41201 (RRA-T55 and Summary)
use in determining critical mass of plutonium, (E), 19: 25246(R) (HW-84369(p.53-4))
use in dose distribution calculations in telecobalt therapy, 20: 22832
use in efficiency calculations for gamma scintillation detectors, 20: 14897
use in electron beam noise calculations, 18: 42250
use in evaluation of integrals in molecular Schroedinger equation, 18: 34423
use in experiments on gas reaction kinetics, 19: 28288 (LADC-6439)
use in fast critical assembly calculations, 18: 5972(R) (ORNL-3499 (Vol.I)(p.77-81))
use in gamma propagation near air-ground interface, 17: 6955 (RM-3399-PR)
use in gamma transport calculations, 18: 22987
use in gamma transport calculations, 19: 38023
use in heat-transfer calculations for a rarefied gas, 17: 4680
use in hyperon (Λ) binding energy calculations, 20: 22161
use in interpreting meson (π^-) interactions at 4.5 Bev, 18: 14819 (NP-13680)
use in meson-shower analysis, 19: 47400
use in moderated neutron source spectra calculation, 18: 10308(R) (UCRL-7571)
use in neutron migration calculations, 16: 2469 (UCRL-5918-T)
use in neutron penetration problems, geometry for, 17: 26393 (LAMS-2856)
use in neutron resonance absorption calculations, 20: 18046 (BNL-9644)
use in neutron transport calculations, energy-independent biasing functions for, 20: 2985
use in neutron well logging calculations, 20: 12994
use in neutron production in proton reactions with heavy nuclei at 0.3 to 1.0 Bev, 18: 34961
use in neutron resonance escape probability calculations, 19: 47970
use in neutron scattering calculations, 19: 15981(R) (ORNL-3714 (Vol.I)(p.70-7))
use in neutron thermalization calculations, 18: 42602 (TID-7050(p.379-409))
use in neutron transport calculations, 18: 42592 (TID-7050(p.125-37))
use in neutron transport calculations, 19: 1956(R) (IDO-16994)
use in neutron transport calculations, 19: 47545 (KFK-297)
use in neutron transport calculations, computer program for, 19: 47546 (KFK-298)
use in nonlinear radiation transport calculations, 18: 30705
use in one-component plasma analysis, 20: 12181 (UCRL-14467-T)
use in optimization of plutonium distribution in reactor fuels, 20: 3456
use in polaron energy calculations, 18: 21737(T) (UCRL-Trans-1040(L))
use in proton migration calculations, 19: 45462 (NP-15163)
use in radiation shielding calculations, 17: 24602
use in random matrix diagonalization, 17: 32480
use in reactivity calculations, 18: 7922 (CONF-360-7)
use in reactor calculations, 16: 19946
use in reactor calculations, multigroup transport theory for, 18: 21601
use in reactor eigenvalue calculations, 18: 24818 (WAPD-T-1649)
use in reactor shielding calculation, test of, 18: 15425 (UNC-5072)
use in rocket reactor analysis, 19: 35841
use in sampling technique for multi-phonon processes in neutron thermalization, 16: 9353 (AE-62)
use in shielding and transport calculations, 20: 46930(R) (ORNL-3973(Vol.1), pp 52-9)
use in simulation of gamma well logging for oil well prospecting, 20: 27174
use in solving gamma transport problems, 18: 20932
use in solving the Schroedinger equation, 18: 22800
use in study of one-component plasma, 20: 44910
use in well logging, 20: 4168
use of, in calculation of reactor neutron spectra, 16: 34060 (AERE-R-4080)
use of, in calculation of cascades for incident particles at 50 Mev to 2 Bev, 17: 12784(R) (ORNL-3360(p.199-203))
use of, in determination of neutron diffusion in hexagonal lattices, 16: 33677 (AAEC/TM-123)
use of, in quantum statistics, 16: 29307(R) (TID-16302)
use with superposition principle for calculating neutron resonance escape probabilities, (T), 19: 14472 (WAPD-T-1718)
uses for analysis of deep penetrations of neutrons into shielding,

18: 28914
uses for analysis of intranuclear cascades, (E/T), 20: 6287 (JINR-P-2373)
uses for calculation of backscattering of gamma radiation by air, 18: 40741
uses for studies of neutron doses behind shielding, 18: 28538
uses in calculation of photo fractions of thallium-activated sodium iodide scintillation detectors for collimated gamma rays, 18: 29978 (KFK-188)
uses in calculation of gamma transmission by matter, 18: 39750(T) (AEC-tr-6390(p.279-89))
uses in GEM code for criticality studies, 19: 47949 (ANL-7050, pp 657-79)
uses in reduction of Compton distribution in gamma scintillation spectrograms, 18: 39647
uses in TIMOC code for calculating reactor parameters, 19: 47919 (ANL-7050, pp 581-92)
weight function in conditional, optimum choice of, 17: 3818
MONTEZUMA CANYON AREA (UTAH)
uranium–vanadium deposits in, diffusion characteristics, 16: 17891
MONTICELLO DISTRICT (UTAH)
environs monitoring, 20: 16729 (IDO-12049)
MONTMORILLONITES
see also Bentonites
acidity and structure of, relation between, 17: 34138
adsorption of zinc-65 on, in salt-marsh ecosystems, 20: 40573
adsorptive properties of Japanese acid clay for cesium, 17: 2899
bonding to water, NMR study of, 18: 16031
cesium displacement and sorption by, effects of salt solutions on, 17: 39072
hydrogen bonding in hydrogen, 19: 612
ion exchange capacity and selectivity, 16: 2809(R) (ORNL-TM-49)
ion exchange isotherms and free energy changes of cesium–sodium, cesium–strontium, and sodium–strontium systems on, 20: 27042
ion exchange properties, effects of heating, 16: 25048 (TID-7628(p.179-86))
ion exchange properties of calcined, for radioactive ions, 17: 27218
ion exchange properties of natural and thermally altered, for barium and cesium, 17: 35621 (TID-17798)
ion exchange properties for barium, cesium, and sodium, thermodynamics of, 17: 37299
ion exchange properties of calcined, for cesium, 17: 40943
ion exchange properties of, 19: 19794
ion exchange properties for cesium, sodium, and strontium, 20: 38858 (BNWL-235-3, pp 23-51)
phosphorus-32 adsorption on, in salt-marsh ecosystems, 20: 40573
preparation and properties of acidic, as cation exchange material, 17: 28778 (CISE-96)
properties of Niigata, for strontium-90 removal, 17: 30074
radioinduced polymerization of acrylonitrile in occlusion compounds of, 18: 31619
radiolysis effects on pentane, 16: 3323(T) (AEC-tr-4497(p.162-6))
reactions with waste-solution ions, thermodynamics of, 17: 19704 (TID-7644(p.13-28))
sorptive properties for cesium and strontium, 16: 2808(R) (ORNL-TM-15)
sorptive properties for cesium and strontium, effects of aluminum and iron hydroxides and potassium on, 18: 17344
sorptive properties for water in electrolytes, 18: 17820
sorptive properties for uranium, 18: 17943
sorptive properties for strontium, 19: 7617(R) (ORNL-3697(p.49-53))
sorptive properties of calcium and potassium, for cesium, cobalt, and rubidium, 19: 7514
sorptive properties for cesium-137, 19: 7638
sorptive properties for strontium-89, 19: 10659(R) (EURAEC-703)
sorptive properties for cesium and barium, 19: 36561
sorptive properties for cesium, role of exchangeable magnesium and potassium in, 19: 43964
sorptive properties for uranyl ions, 20: 8830(R) (LF-28, pp 40-3)
sorptive properties for cesium, 20: 12873
sorptive properties for manganese-54 and zinc-65 in sea water, 20: 18576(R) (TID-22660)
sorptive properties for fission products in waste solutions, 20: 29332 (ORNL-P-1811)
sorptive properties for cesium, 20: 43455
sorptive properties for phosphoric ions, 16: 25305 (CEA-1650)
sorptive properties of Japanese acid clay for cesium, 17: 2899
use as Szilard-Chalmers medium for production of cobalt-60 and barium-139, 19: 18039 (IITRI-578P15-12)
MONUMENT NO. 1 MINE (ARIZ.)
mapping of Monument No. 1-Mitten No. 2 Mine, Monument Valley, Navajo County, 16: 4384
MOON
altitude measurements on, using radiation sources and detectors, 20: 14817 (N65-20421)
analysis by neutron-gamma inelastic scattering technique, 16: 6371 (UCRL-6487)
analysis by neutron activation, 16: 33194
analysis of, radiometric, 17: 35250(R) (TID-19135)
analysis of surface of, activation, 17: 3660
analysis of surface of, use of computers in remote, 17: 15888(R) (TID-18257)
analysis of surface of, instrumentation for radiometric, 17: 16894
analysis of surface of, activation, 17: 26206
analysis of surface of, from albedo radiation, 18: 7399
analysis of surface of, system for remote activation, 18: 9973(R) (TID-19999)
analysis of surface activation, 19: 10983(R) (TEES-2671-3)
analysis of surface of, development of automatic activation method for, 19: 36243(R) (X64-17610)
analysis of surface of, by remote neutron techniques, 20: 22931
analysis of surface of, neutron activation methods for, 20: 29140
analysis of surface of, combination neutron technique for, 20: 31211
analysis of, equipment for, 16: 19058 (AD-263521)
analysis, gamma-neutron spectrometer for, 16: 16532
atmosphere and exploration, 16: 25094
atmosphere density of, effects of solar wind on, 18: 18546
atmosphere of, effect of solar wind on, 18: 6100
atmosphere of, origin of, 20: 23870
atmosphere, properties, 16: 26049
bases on, nuclear power plant design for manned, 18: 36811(R) (WANL-PR(S)001-A)
book: *Handbook of Geophysics and Space Environments*, 20: 25997
brightness of, correlation to solar wind, 20: 41604
composition and internal constitution, 16: 29608
composition of, neutron devices for studying, 17: 33845
composition of surface of, neutron capture gamma analysis for, 17: 26419(R) (ARF-1193-23)
composition, probable internal, 17: 4378
cosmic radiation scattering on, effective temperature from, 18: 44487
cosmic-ray-induced gamma radiation at surface of, 17: 26207
cosmic-ray intensity variations on, 19: 47273
development of, theory of, 18: 42291
effect on equatorial spread-F, 18: 24535
effect on geomagnetic storms, 17: 16285
effects on cosmic radiation, variations, 18: 12843
effects on cosmic-ray intensity variations, 18: 30464(T) (NASA-TT-F-127(p.387-90))
effects on electron density distribution in ionospheric F2 layer, 18: 40419
effects on electromagnetic activity correlated with naphthalene test, 20: 37891
effects on frequency of geomagnetic storms, (T), 19: 6591
effects on geomagnetic activity, 18: 34677
effects on geomagnetic activity, (E/T), 19: 6592
effects on geomagnetic field fF_2 and H, 20: 1109
effects on geomagnetic activity variations, (E/T), 20: 39982
effects on ionospheric sporadic ionization in magnetic equatorial regions of earth, 17: 23515
effects on tidal oscillations in F layer of ionosphere, 18: 24533
electric power systems for use on, status of radioisotope-fueled, 20: 19132 (N-65-24571)
electron excitation of x rays on surface of, from solar-geomagnetic cavity tail, 20: 17246
electrostatic screening by photoelectron clouds, 16: 18695 (AFOSR-1399)
elemental constituents, determination by nuclear experiments, 16: 11339 (UCRL-5916)
exploration of, conference on, 17: 26250
exploration of, power supplies for vehicles for, 18: 22579
gamma radiation from, effect of cosmic radiation and radioisotope decay on, 20: 46286
gamma surveying of, purposes of, 18: 5529
geomagnetic effects, 17: 34688
gravitational effects on ionospheric F2 layer, 18: 44654
heat transfer from internal radiogenic heating and melting of, calculations on, 19: 27049
hydrogen atmosphere, 16: 27857
hydrogen atmosphere, 16: 27858 (CRSR-118)
interaction of magnetohydrodynamic wake of, with solar wind, (E/T), 19: 16343
luminescence from crater Kepler on, evaluation of, 18: 26195
luminescence of laboratory simulation of, 19: 34832 (AFCRL-64-749)
luminescence of, mechanisms of, 18: 7400
luminescence of, mechanism for, (E), 20: 28623
luminescence of, solar flare excitation of, 18: 10758
magnetic field of, parameters for, 17: 32879
magnetic field of, measurement of, 18: 5959
magnetic field of, shielding of lunar surface from solar wind by, (T),

19: 9865
magnetic field production by solar plasma wind, laboratory simulation of, 20: 21502
magnetic fields, 16: 27860(T) (JPRS-13505)
magnetic field of, review on, 18: 2513(T) (FTD-TT-63-968(p.89-171))
magnetic fields of, measurement, 19: 43226
magnetic fields of, from trapped solar plasma stream, 20: 19328 (NP-15939)
magnetic storms on, 18: 30395
magnetohydrodynamic wake of, observation using IMP-1, 20: 17235(T)
magnetosphere of, detection of, 18: 40423
materials on, alpha-scattering analyses of, 19: 44901
meteorite origin and, 19: 23253
meteorites from, bronzite chondrite, 20: 21507
neutron albedo on surface of, from cosmic radiation, 17: 34715
nuclear power plant on, conversion systems for, 20: 1516
nuclear power plant for manned base on, communications and command for, 20: 24746
organic matter on, observability of indigenous, 20: 31854
origin of, review of theories on, 20: 35986 (UCSD-34P43-5)
position relation to cosmic-neutron diurnal variations, 16: 6889
power plants for lunar-exploration bases, nuclear-thermionic, 18: 28311
power plants for manned base on, design of SNAP-8, 19: 10631
power supplies for base on, development of SNAP-50/SPUR, 20: 3553
probe design for, subsurface geophysical, 16: 20659
properties of, book on, 19: 1162
properties of, conference on, 20: 7717
properties of, from radio and radar studies, 18: 32356
proton reactions with surface, luminescence from, 20: 44035
radar reflection from, 19: 35229(R) (AD-612484)
radiation brightness temperature at 4 mm, 18: 26192
radiation doses at surface, 16: 17329
radio emission, 18: 14594(T) (JPRS-23436)
radio emission at 50 cm from, 18: 24516(T) (JPRS-24633)
radio emission from, measurement of, 17: 607(T) (JPRS-15740)
radioactive dating of surface, apparatus for, 17: 8280 (N62-11797)
radioactivity of surface of, from diffusion of radon and thoron, 20: 27714
radioinduced luminescence on, by solar protons, 18: 28281
relation to geomagnetic storms, 17: 31251
satellite orbits about, general relativity tests by precession of, (T), 20: 11883
solar and thermal radiation from, 16: 32252 (NASA-TN-D-1360)
solar and thermal radiation from, 16: 32253 (NASA-TN-D-1361)
solar plasma flow around, (T), 19: 4813
solar proton-induced hydroxyl formation on surface of, simulation by bombarding glass, 20: 46491
solar radiation sintering of dusts on, 20: 7695
solar storm and wind bombardment of surface of, sputtering rates from, 17: 25870(R) (X62-11400)
solar-wind bombardment of, surface modifications from, 18: 5906
solar-wind contributions to atmosphere, 16: 18285
solar wind effects on photometric properties, 19: 44896
solar wind interactions with, lunar magnetosphere from, (T), 20: 31899
solar wind interactions with, effects of interplanetary magnetic fields on, 20: 34006 (N-66-10681)
solar wind reactions with, (E/T), 19: 8060
solar wind reactions with, bibliography on, 20: 35985 (NASA-SP-7026)
space flight to, (T), 19: 34857
space vehicle motion under influence of earth and, (T), 19: 41205 (N64-31725)
sputtering by solar wind, rate of material loss by, 17: 41694
steam power system evaluation for base on, 19: 3611 (ASTRA-G-39.2)
surface analysis using neutron activation analysis, 20: 46932(R) (ORNL-3973(Vol.2), pp 71-84)
surface characteristics, estimation from explosion crater analysis, 16: 409
surface damage from cosmic radiation and micrometeorites, 16: 21132 (NP-11652)
surface density, 17: 22282(T) (JPRS-18823)
surface properties of, review (E/T), 19: 2946
surface properties, chemical flare study of, (T), 20: 39469 (LA-3453)
tail in solar wind, (E/T), 19: 6432
temperature variations during eclipses, measurement using lunar radio emission, (E), 19: 41222
tidal effects of, in ionosphere, 18: 6097
tidal effects on equatorial geomagnetic field, separation of semidiurnal, 17: 23511
tidal effects on equatorial electrojet current of earth, 17: 23514
wake of, structure of, (E), 20: 31900
water extraction from, feasibility of nuclear versus solar power for, 19: 34360 (AD-608225)
water extraction from rock of, feasibility of using nuclear explosives for, 18: 10213 (UCRL-7515)
x rays from, research program on fluorescent, 19: 43017 (AD-501274)
x-ray generation by, theories on detection of, 20: 2666

8-MOP
see Psoralen, 8-Methoxy-

MORIN
analytical use in spectrophotometric determination of uranium in water, 16: 17592(T) (CEA-tr-R-1569)
analytical use in determination of thorium by fluorometric techniques, 16: 22026
analytical uses for photometric determination of niobium and tantalum, 18: 31411
analytical uses in determination of beryllium, 17: 35641
complexes with beryllium, rare earths, thorium, and uranium, preparation and stability of colored, 18: 27366
complexes with rare earths, 17: 8018
complexes with thorium, dissociation of, use of absorption and excitation spectra to determine, 18: 39272
reaction with gallium and indium, molar extinction coefficients and instability constants for, 16: 18838
reactions with beryllium, fluorometric studies of products from, 19: 17799
use in photocolorimetric determination of zirconium in magnesium alloys, 16: 149

MOROCCO
uranium resources in, 20: 28868

MORPHINES
see also Normorphine
effects of, on scybala production in irradiated rabbits, 17: 30389
effects on radiosensitivity of mice, 19: 42334
hydrogen bonding in crystalline, 19: 32048(R) (NP-15073)
nitrogen-15 content in, significance of excess, 17: 23043
preparation of tritium-labeled, 17: 15602
production by *Papaver somniferum* plants, effects of gamma exposure of seed on, 19: 25951
protective effects of heroin against radiation in protozoa, 16: 30309
protective effects against radioinduced changes in reactivity of sulfhydryl groups in spleens of mice, 17: 35500
protective effects against radiation injuries in mice, 19: 38453
protective effects of, against radiation injuries in rats, 19: 46021
radioactivity distribution in, from biosynthesis with labeled carbon dioxide, 16: 1665
radiosensitivity effects on erythrocytes, 16: 1475(T) (JPRS-10170 (p.90-110))
radiosensitivity effect of, in mice, 17: 30424
radiosensitivity effects in mice, 20: 18459
radiosensitivity effects on mice, x, 20: 20513
synthesis from codeine and thebaine in *Papaver orientale* and *P. somniferum*, 16: 32
transformation of tritium-labeled, to normorphine, 17: 15602

MORPHOLINE
complexes with europium benzoylacetonate, ligand field spectra of, 18: 33565
genetic effects on *Drosophila melanogaster*, 18: 27097
ionization by electron impact, 16: 17708(R) (TID-14812)
reactions with polyacrylonitrile under high pressure, addition, 19: 36457 (NYO-3185-1)
3-methyl-2-phenyl-, effects on stomachs of patients during radiotherapy, 20: 33110

MORPHOLOGY
effect on uranium content of zircons, 20: 43565
effects on strontium deposits in clam shells, 19: 2059
radiation effects on Quercus, gamma, 18: 1368 (BNL-6893)
radiation effects on, of excised frog muscle, 18: 17569
radiation effects on, of rat bone marrow cells in tissue culture, 18: 17587
radiation effects on rat-organ, gamma, 18: 41207
radiation effects on, in colchicine-treated Pinus, gamma, 19: 10829
radiation effects on sea urchin, ultraviolet, 19: 45840
radiation effects on fine structure of ovarian cells, x, 20: 40672
radiation effects on fish embryo and prelarvae, 20: 40527
radiation effects on ectoderm and endoderm of coelenterates, regeneration studies, x, 20: 45383
radiosensitivity effects of cellular, x, 19: 26154
thyroid, changes induced by iodine-131, 20: 40647

MORRISON FORMATION (COLO.)
localization of uranium–vanadium deposits by sedimentation, 17: 1647

MORRISON FORMATION (UTAH)
localization of uranium–vanadium deposits by sedimentation, 17: 1647

MORTARS
see also Cements
age estimation using carbon-14, 19: 40795
tests of Freyssinet, for traction machine, 18: 378(T) (EURAEC-440)

MOSEL (Molten Salt Epithermal Reactor-Germany)
see Molten Salt Reactors

MOSQUITOES

blood ingestion by *Aedes aegypti*, tracer study, 20: 33020
control of populations of *Culex fatigans* by release of irradiated males, 19: 43796
control of, using radiation-sterilized males, 18: 25047
DDT metabolism by larval, 19: 10778
dispersion and life-span, tracer study, 16: 14420
distribution in Hawaii of Culex, 20: 5240
ecology of *Rhodnius prolixus* in Venezuela, tracer studies of, 17: 24809
effects of irradiated egg rafts on *C. fatigans*, 16: 32773
effects of phosphorus-32 on fertility of *Aedes aegypti*, 19: 25939
labeling of larvae and adults with phosphorus-32, 17: 10423
labeling with phosphorus-32, 18: 3440(T) (JPRS-22186)
life history of *Anopheles stephensi*, tracer study, 17: 20287
mating behavior of, tracer studies of, 19: 12907
phosphorus-32 uptake by, effects of, on development and growth of larvae of, 17: 19823
phosphorus-32 incorporation in, 20: 5240
phosphorus-32 labeling of, in investigation of flight range, gonotrophic cycle length, and mortality rate, 20: 35195
population control by release of radiosterilized males, 19: 21964
production of radiosterilized male, 20: 35287
radiation control of malaria vector, 18: 23168(R) (STI/DOC/10/25(p.99-111))
radiation control of malaria mosquito (*Anopheles quadrimaculatus*) populations, 19: 45960
radiation effects on development of *Plasmodium gallinaceum* in *Aedes aegypti*, 16: 28782
radiation effects on fertility of *A. egypti*, 16: 32772
radiation effects on genetics of *Rhodnius prolixus*, 17: 24809
radiation effects on blood-fed *Aedes aegypti*, 18: 79
radiation effects on Dirofilaria development in, gamma, 18: 13527
radiation effects on cytogenetics in *Aedes aegypti*, x, 18: 23262
radiation effects on population dynamics of *Aëdes aegypti*, x, 20: 10692
radiation effects on populations of *Aedes aegypti*, x, 20: 12668
radiation effects on respiration in eggs of Bombyx, x, 20: 18301
radiation effects on pupal mortality and reproductive capacity in *Culex fatigans*, gamma and x, 20: 24904
radiation effects on fecundity of *Aedes aegypti*, β, 20: 33020
radioinduced mutations in adult male, 17: 10385
radioinduced mutations in *Aedes aegypti*, gamma, 19: 88
radioinduced sex-linked mutation of, 18: 5067
radiosensitivity, 16: 14425
radiosensitivity of selected strain of *Aedes aegypti*, 20: 33032
radiosterilization of, gamma, 16: 26843
radiosterilization effects on mating ability of *Aedes Aegypti* L., 17: 28743
radiosterilization of Anopheles, gamma, 18: 19654
radiosterilization of male, effects on population density, 19: 24315

MÖSSBAUER EFFECT

absorber for iron-57, 20: 22158
absorber thickness optimization for, 20: 6336
absorption areas in, for thick absorbers, (T), 20: 28631
absorption spectra shift, kinetic parameters of electron shell excited states from, (T), 20: 10238(T)
analogy to optical phenomena in solids, 18: 14648
analysis at high pressures, methods for, (E), 19: 21231 (COO-1198-255)
analysis of, uses of superconducting magnets in, (E), 19: 14507 (BNL-8745)
analysis using terminology of high-energy elementary-particle physics, (T), 19: 14500 (ANL-6878(p.481-504))
angular correlation in, 17: 38074 (JINR-P-1231(p.115-17))
anisotropy in tin monocrystal, 17: 38077 (JINR-P-1231(p.167-72))
anisotropy of, in β-tin single crystals, 17: 2123
bibliography on, 20: 12277 (PAEC(A)IN-656)
bibliography on isotopes exhibiting, through Aug. 1, 1963, 18: 14650
book: *Mossbauer Effect and Its Application in Chemistry*, 18: 33604(T)
book: *Mossbauer Effect: Principles and Applications*, 19: 16293
book: *The Mössbauer Effect*, 16: 24655
book: *The Mössbauer Effect and Its Applications in the Study of Internal Fields*. (E/T), 19: 1658
characteristics, 18: 12159
characteristics of, in organic tin compounds, 16: 32442
characteristics of, in thin films, 17: 29592
cobalt-57 preparation for experiments on, 18: 29781
coherence and interference effects in, 17: 13223
conference of methodology, 20: 22156
conference on, 18: 14639
conference on detection and properties of, 17: 13221
contour of the Mössbauer line taking into account local vibrations, 17: 41642
cryostats for measurement of, at liquid helium temperatures, (E), 20: 3093
crystal recoil in, average value theorem for, (T), 20: 1162(T) (AD-619487)
crystal structure effects on, (T), 19: 43266
data acquisition system for, 20: 15973
data index on, 20: 3146
data on, 18: 32302
Debye-temperature dependences in, in β-tin polycrystals, 18: 7356
Debye-Waller factors in, tables for computing, 17: 19214 (AI-6699)
detection and measurement in iron-57, temperature effects on, 17: 13229
detection and measurement in iron-57, in alloys and compounds, 17: 13230
detection and measurement of small shifts in, 17: 13248
detection and measurement in tin-119 in tin oxides, 17: 19369
detection and measurements of, problems in, 17: 38066 (JINR-P-1231 (p.7-16))
detection and measurements in tungsten-182, 17: 38067 (JINR-P-1231 (p.48-51))
detection and measurements in tin-119 and praseodymium-141, 17: 38069 (JINR-P-1231(p.55-63))
detection and measurement in tin-119, 17: 37432
detection and measurement, 17: 38065 (JINR-P-1231)
detection and measurement, (E/T), 20: 9977 (TID-22403)
detection in beta-gamma cascade to ground state of nickel-61, 17: 13238
detection in crystalline and vitreous ferric chloride, 18: 16036
detection in dicyclopentadienyliron compounds, 17: 13233
detection in heme proteins and iron porphyrins, 19: 423
detection in higher excited states, coincidence method for, 18: 30791
detection in stainless steel, from iron-57, 17: 13252
detection in terbium-159, 17: 38070 (JINR-P-1231(p.64-5))
detection of dynamic orientation of cobalt-57 using, (T), 19: 14649
detection of, in seignettoelectric ionic crystals, 17: 38071 (JINR-P-1231(p.107-11))
detection of, cam-driven constant-acceleration spectrometer for, 20: 21080
detection of, design and performance of automatic spectrometer for, 19: 46831
detection of, spectrometer for, 18: 37540
detection of, spectrometer for, 19: 39032
detection of, spectrometer for, 20: 16872
detection of, spectrometer for, 20: 19050
determination in graphite at 20 to 470°C, 17: 13234
determination of electrostatic, gravitational, and pressure shifts in, 17: 13248
development, properties, and uses, 16: 15648
diffraction in nuclear resonant scattering, 18: 34929
discovery and fundamental properties of, 16: 30976
dispersion, nuclear polarizability, and reflection near phononless absorption line, 18: 42759(T)
drive systems for studying, design and operation of constant-velocity, 20: 21081
dynamical motion and gamma cross section of isolated impurities in crystals, 17: 31179
dynamics of, in liquids and solids, 17: 15229
effects of line broadening of source and absorber on, 17: 24140
effects of twinning on, in tin oxides, 20: 16335(R) (NBS-TN-276)
effects on magnetic hyperfine splitting in polycrystalline materials, (T), 20: 12299
electron spin relaxation effects on, (T), 20: 18009
electron spin-relaxation effects on, in ferric ammonium sulfate, (T), 20: 8298
energy emission in, temperature dependence of, (T), 20: 5004 (IAE-927)
equations for recoilless, 17: 38073 (JINR-P-1231(p.113-14))
equipment design for study of, 18: 41838
equipment drives for, design of constant-acceleration and constant-velocity, 17: 13224
equipment for, design of high-velocity drive for, 17: 27665
equipment for studies of, electromechanical drive system for, 20: 21079
equipment for studying, electromagnetic velocity drive system for, 20: 31590
experimental studies of, using Compton-scattered radiation, 17: 33034
experiments using, 19: 39795
for impurity nucleus in a crystal, 17: 16868
for impurity nucleus in Bravais crystal, 18: 10632
frequency modulation effects in, for constant relative velocities, 17: 13227
frequency-shift detection and measurement in, 17: 13226
gamma angular and energy distributions of, (T), 20: 24631
gamma emission and scattering in solid subjected to periodic vibrations, 17: 13597(T)
gamma line intensities in, pressure effects on, 18: 44749
gamma polarization observation in, 16: 28163
gamma-ray magneto-optical rotation in, 18: 9133
gamma recoilless fractions in, determination of, (T), 19: 10354

gamma relaxation narrowing in, (T), 20: 20153
gamma resonance absorption by impurity nuclei in crystals, 17: 6854
gravitational effects on, (T), 19: 43359
hyperfine structure of, in rare earth oxides, 17: 13244
hyperfine structure of, in tin and ferromagnetic tin alloys, 17: 13245
hyperfine structure of trivalent iron-57, in corundum, 18: 27434
hyperfine structure splitting in magnetic materials, (T), 19: 43384
in alkali metal iodides, 19: 28321
in aqueous metal salts, 19: 39265(R) (IA-1021)
in beta tin, properties of, (E), 20: 10235(T)
in biological materials, 19: 40306
in biotite, 17: 14993
in bone crystals and cesium-133, 20: 22853(R) (ANL-7060)
in cobalt-57, effects of heating on, (E), 20: 45033
in crystal impurity atoms, (T), 19: 43493
in crystals, effects of lattice defects on, 17: 35776
in diatomic lattices, 19: 23768
in dysprosium-161, effects of high pressures on, 18: 21214 (UCRL-10630(Rev.))
in germanium–iron alloys, 19: 16123
in gold alloys, correlation with electric conductivity, 18: 26534(R) (ORNL-3582(p.16-17))
in gold-197, solid-state and nuclear results from, 17: 7234
in iodine-127 compounds, (E), 20: 46304
in iodine-127 in ferromagnetic chromium iodide for, (E), 19: 45491
in iodine-129 complexes, 19: 39265(R) (IA-1021)
in iron at very high pressures, 18: 36661
in iron at 4 to 1300°K, 17: 3626
in iron at 4 to 1300°K, 17: 6778(R) (ANL-6603(p.20-46))
in iron compounds, quadrupole coupling-isomeric shift relation in, (E/T), 19: 16267
in iron dithiocarbamates, relaxation studies by, (E), 19: 38653
in iron ions in sodium chloride crystals, vacancy-impurity associated state of, 17: 31200
in iron-57 in cobalt spinel, 18: 688 (PAN-269)
in iron-57 in iron sulfides, 18: 4357
in iron-containing biochemicals, 19: 24585
in iron-57, 19: 2893(T) (JPRS-27049(p.79-83))
in iron-57 spectra in pyridine complexes, 20: 26862
in iron-57, from iron-56 (d,p) reactions at 1.8 Mev, (E), 19: 41793
in iron-57, source matrix effects on, (E), 19: 23814
in isomeric tin-119 de-excitation in tin compounds, 19: 13518
in liquids, effect of diffusion broadening on, 18: 1650
in naturally occurring iron, 18: 43601(R) (TID-21007)
in neptunium-237, review of applications of, 19: 27416 (CONF-650425-1)
in one- and two-dimensional crystals, (T), 20: 12283
in organic iron and tin compounds, 19: 38576 (CONF-650425-2)
in organic tin halides, 19: 7564
in organo-tin compounds, effects of intermolecular bonding on, 19: 38577 (CONF-650425-3)
in organo-tin compounds, determination of isomer shift and quadrupole splitting of, 19: 24545
in organotin compounds, effects of gamma radiation on resonance spectra line shape in, 17: 9063
in osmium-186 137-kev level, quadrupole interaction for, (E), 20: 12301
in paramagnetic materials, hyperfine structure of lines in, 18: 6286
in rare earth intermetallic compounds, review, 20: 42570
in rare gases, review on, 20: 26384
in recoilless resonance absorption of 14.4-kev gammas from iron-57, (E), 19: 6654
in steel, plastic deformation effects on, 18: 25903(T)
in systems with local degrees of freedom, 18: 36682
in terbium-159 isomeric state width of 58-kev resonance from, (E), 20: 12303
in thin films, temperature dependence of, 19: 44847
in thulium compounds, effects of thulium-169 on, 19: 9767(R) (IS-900(Sect.P))
in tin compounds, 17: 8971
in tin compounds, explanation in terms of the valence state of the tin atom, 18: 14662
in tin compounds, chemical aspects of, 20: 26380
in tin single crystals, anisotropy of, (E), 20: 10237(T)
in tin-119m oxides, 17: 30584(R) (TID-18955)
in tin-114 in yttrium iron garnet lattice, (T), 19: 35423
in tin-119 impurity in barium titanate, phase transition effects on probability of, (E), 20: 10236(T)
in tin-119 super-exchange induction of nuclear magnetic fields from, 19: 35424(T)
in tin-120, anisotropy of, (E), 20: 4932
in transition metal silicides, 20: 40300
in transition-metal complexes, bonding effects on, 20: 25088
in unsymmetrical organic tin compounds containing electron-donor substituents, 19: 2378
in uranium dioxide single crystals, 18: 18477
in xenon compounds, 18: 10034 (CONF-303-15)
in xenon-129, use in production of xenon compounds by beta decay in iodine-129, 19: 13519
in ytterbium-171, properties of, (E), 19: 14521 (CONF-640606-18)
index of data on, 18: 12790
instrumentation for, at low temperatures, 19: 40863
intensity and temperature shift in nonideal crystals, (T), 19: 41997(T)
interference with Rayleigh scattering, 17: 9232
interference with Rayleigh scattering, 17: 13251
iron-57 spectra in copper–manganese alloys, (E), 19: 39212
isomer shift and quadrupole splitting of, for iron-57 iron compounds, 17: 38145
isomer shifts in, 18: 31361(R) (UCRL-11213(p.87-138))
isomer shifts in, calibration by incorporation of nuclides in rare-gas matrices, 17: 13255
isomer shifts in, for tin-119 in tin alloys and compounds, 17: 13256
isomer shifts in ferroin-type iron(II) complexes, 18: 4902 (CONF-303-8)
isomer shifts in rare earths, 20: 26383
isomer shifts in, theory, 17: 13254
isomer shifts in, applications and interpretations of, 18: 14640
isomer shifts of 81-kev gamma transition in cesium-133, (E), 20: 26195
isomeric shift of iron-57 due to pressure, 16: 33651
kinetics of induced, in infinite crystals, 17: 33084
lattice dynamical aspects of, 18: 14647
line broadening and transmission in, 16: 26225 (NP-11913)
line broadening in tin oxide, tin-119, 19: 27493
line broadening of Gaussian spectra from, 18: 21315
mathematical characteristics of, 17: 13222
measurement device for, design of, 20: 16866
measurement in cesium-133, 20: 42239
measurement in dysprosium-160 and -161, in dysprosium ferrites, 17: 13242
measurement in dysprosium-161 in dysprosium, 17: 13243
measurement in ferrocenes, 17: 30584(R) (TID-18955)
measurement in hemin at 80°K, using iron-57, 17: 13262
measurement in iron-57, in ferrous compounds, 17: 13240
measurement in iron impurities in beryllium, using iron-57, 17: 13258
measurement in iron carbonyl and dicyclopentadienyl compounds, 17: 13259
measurement in iron diffused in pyrolytic graphite, 17: 13261
measurement in iron diffused in semiconductors, using iron-57, 17: 13263
measurement in iron-57 in fused quartz and pyrex glass, 17: 13264
measurement in iron(II) tetrazole compounds, 17: 30584(R) (TID-18955)
measurement in iron carbonyl derivatives of cyclooctatetraene, 17: 30584(R) (TID-18955)
measurement in iron-57 bound in crystals, 17: 39787
measurement in iron-57, from Coulomb excitation, (E), 19: 33338
measurement in iron-57, internal conversion coefficients from, (E), 19: 33319
measurement in iron complexes and covalent iron compounds, crystal lattice effects on, 20: 3927(T) (AERE-Trans-1026)
measurement in nickel-61, using Coulomb excitation, (E), 19: 33337
measurement in platinum-195, (E), 19: 5569(R) (MIT-2098-64)
measurement in samarium-149, 17: 38068 (JINR-P-1231(p.52-4))
measurement in tin compounds, 20: 41637
measurement in tungsten-182 by γ-γ coincidences, 19: 35411
measurement of absolute fraction of self-absorption effects on, (E/T), 20: 17990
measurement of, design and performance of constant-velocity-drive spectrometer for, 17: 17954(R) (TID-18450)
measurement of, design of servomechanism for constant-velocity drive spectrometer for, 18: 5671
measurement of, equipment for, 16: 27314
measurement of, equipment for, 17: 36176
measurement of hyperfine interactions in Laves phases in iron alloys using, 19: 4683
measurement of iron-57, in metal-oxide matrices, 17: 13235
measurement of iron-57, absorbers and sources for, 18: 29656
measurement of iron-57, in powdered ferric oxide, (E), 19: 5187
measurement of iron-57, in cobalt sulfate, 20: 40311
measurement of isomer shift for chromium and copper absorbers, 17: 30584(R) (TID-18955)
measurement of Mössbauer gamma fraction, errors in, (T), 19: 35427
measurement of partial isotope shifts for R_3As, R_3Sb, and R_3P ligands, 17: 30584(R) (TID-18955)
measurement of recoilless fraction in, technique for, 20: 12326
measurement of, backscattering technique for, (T), 19: 41845
measurement of, constant speed drive for, 20: 11073
measurement of, design equipment for, 18: 41766 (IAE-599)
measurement of, design and performance of hydraulic constant-velocity transducer for, 19: 34449
measurement of, design of vacuum cryostat and furnace for, (E),

19: 40858
measurement of, design of cryostat for, 19: 46748
measurement of, design of high pressure spectrometer for, 20: 43732
measurement of, Doppler drive for, 18: 31970
measurement of, Doppler modulation system for, 20: 25359
measurement of, Doppler spectrometer for, 20: 25425
measurement of, drive and waveform generator for, 18: 43962
measurement of, equipment for, 19: 46826
measurement of, following alpha decay, effects of recoil stopping times on, 20: 22037
measurement of, mechanical driving unit for, 20: 22050
measurement of, scattering techniques for, (E), 19: 40922
measurement of, spectrometer for, 18: 14220 (UCRL-7043)
measurement of, spectrometer for, 19: 15917
measurement of, spectrometer errors in, 19: 18292
measurement of, spectrometer for, 20: 2113
measurement of, spectrometer and technique for, 20: 3145
measurement of, spectrometer for, 20: 7440
measurement of, spectrometer for, 20: 21069
measurement of, spectrometer for, 20: 37056
measurement of, spectrometer for, 20: 39250(P)
measurement of, technique for, 18: 30771
measurement of, technique for, (E), 20: 1250
measurement of, techniques in, 20: 1166
measurement of, techniques for, 20: 26196
measurement of, using opaque absorbers, 20: 22157
measurement of, velocity spectrometer for, 18: 10417
measurement of, velocity spectrometer for, 18: 33834 (RT/EL(63)-15)
measurement of, velocity drive for, 19: 2580
measurement of, velocity calibration of spectrometers for, 20: 5786
measurement using crystal spectrometers, (E), 19: 4479 (TID-7705 (p.214-30))
measurement using multiscaler mode of pulse-height analyzer, 19: 20327(R) (UCRL-11828(p.221-2))
measurement using Doppler effect, cosine effect in, 20: 16335(R) (NBS-TN-276)
measurement using scattering geometry, 20: 26194
measurements of, design of device for, 18: 6160 (NP-13326)
measurements of, use of water-cooled solenoids in spectrometer for, 19: 41848
method for interpreting spectrum areas in, 18: 8928
model for, relaxation effects in, 18: 10633
near crystal surfaces, 17: 21056
nuclear energy level charge distributions from isomer shift in, (T), 19: 35456
nuclear hyperfine interactions in rare earth salts, general aspects of, 18: 7338 (CONF-303-13)
nuclear orientation effects on, in beta–gamma decay, 18: 4528 (CONF-303-9)
nuclear resonance fluorescence studies of rare earths, 18: 14642
observation of nuclear Zeeman effect in gold-197 using, 17: 20998 (UCRL-10649)
occurrence of, tabulation of actual and probable, (T), 20: 9977 (TID-22403)
of iridium-193 in cobalt, iron, and nickel, (E), 19: 21255(R) (UCRL-11828(p.57-8))
of iron-57 in ferrocene derivatives, 17: 29420
of iron-57 in beryllium, copper, platinum, and tungsten, 18: 12785
of iron-57 in iron compounds, (E), 19: 6395
on absorption of 77-kev gamma radiation from gold-197 in metallic gold, 17: 34973
on gamma absorption spectra of ferric oxyhydroxide, 19: 15494
on gamma emission by iron-57 in gold lattices, effects of temperature on, 18: 22923
on iron-57 in stainless steel, effects of pressure on, 20: 32684(R) (UCRL-16658, pp 21-38)
on iron-57 spectra in ferrocene, 19: 11087
on tin-119 in a vanadium matrix, 18: 5881
optical analog of, local-mode resonance, (E/T), 20: 24610
phase-modulation methods in, 17: 13260
phonon annihilation and creation effects on, 17: 11658
polarization of reflected photons in, 18: 26535(R) (ORNL-3582(p.20-3))
preparation of cobalt-57 source on chromium backing for studies on, 18: 35916
pressure cell for studying, 20: 20850
pressure effects on, 17: 17130 (UCRL-10630)
pressure effects on, 17: 36501
pressure effects on, 18: 35573
principles, 17: 41583
probability of, in degenerate systems and possibility of creating such systems, 17: 9066
properties and uses of, 17: 5404
properties and uses of, in spectroscopy, 20: 46301
properties of, for tin-119 in stannate lattices, 17: 32107
properties of krypton for studies on, 18: 5341
properties of, bibliography on, 20: 13974 (STI/PUB/21/16)
properties of, in passing through phase transitions, 18: 44750
properties of, review, 20: 37464
radiation coupling in, (T), 19: 27576
radiation damage effects on tin-119, in magnesium–tin oxide crystals, 20: 3065
reflection at small angles in, method for total, 17: 13253
relaxation effects in, from impurity nuclei, 18: 10633
research, 20: 4826(R) (ANL-7081, pp 121-7)
research, 20: 6302(R) (TID-22384)
research on, at ANL, 17: 41531(R) (ANL-6720(p.48-58))
review, 17: 14967
review, 18: 22914
review, 18: 34298
scattering amplitude for multipole mixtures in, 20: 42240
scattering experiments in europium-153, osmium-186, osmium-188, and praseodymium-141, (E), 19: 6638 (NP-14541)
scattering function in, intermediate, 17: 22475
significance in chemistry, 18: 1626
similarity to Shpol'skii effect, 17: 30546(T)
source preparation for study of, 17: 30584(R) (TID-18955)
source preparation for, cobalt-57, 18: 22561
source preparation for, cobalt-57, 18: 31498
spectra display on pulse-height analyzer, production of linear, 18: 32281(R) (UCRL-11213(p.139-53))
spectra, Doppler broadening, 16: 22931
spectra from, Doppler broadening, 16: 22931
spectra from isotropic polycrystalline sources, asymmetric quadrupole lines in, (T), 19: 16284
spectra from, computer analysis and calculation of, (T), 19: 41724
spectra from, effects of pressures to 150 kbar on, 18: 35994 (UCRL-10899)
spectra in cobalt oxides, Auger aftereffects from, 20: 39603
spectra in crystals, two peaks of quadrupole splitting in, 17: 16013
spectra in crystals, lattice anharmonic vibration effects on intensity of, 18: 2459
spectra in crystals, effect of nuclear quadrupole interaction on, 20: 12314
spectra in inorganic tin compounds, interpretation of, in terms of oxidation state, 18: 27411
spectra in iron proteins, 20: 32929
spectra in iron–platinum alloys, (E), 19: 36220(R) (MIT-2098-142)
spectra in, isomer shifts in quadrupole, 17: 38075 (JINR-P-1231(p.121-32))
spectra in potassium chloride as evidence for impurity ion-vacancy association, 16: 33623
spectra in simple cubic crystals, detection of localized mode vibrational, 17: 27375
spectra in solids, nuclear magnetic interaction effects on, (T), 19: 33525
spectra of, difference in peaks in quadrupole splitting, 17: 21080
spectra of, in diene and dienyl carbonyl complexes, 17: 33895
spectra of iron(III) and cobalt(III) acetylacetonates, 16: 32191
spectra of iron-57 in ferrocene derivatives, effects of substituents on, 18: 22050
spectra of iron-57 in ferrichrome and ferrichrome A, 19: 21270(R) (UCRL-11828(p.214-16))
spectra of nuclei with fluctuating hyperfine magnetic fields, (T), 20: 40152
spectra of organo-tin compounds, 20: 26381
spectra of tin-bearing boroörganic compounds, 20: 26382
spectra of, anharmonism effects on line intensity in, 18: 19123
spectra of, computer programs for analyzing, 19: 11719 (AD-609315)
spectra of, computer programs for, 20: 22159
spectra of, effects of local phonon damping on, (T), 19: 19201
spectra of, effects of geometry and velocity fluctuations on, 19: 25533
spectra of, effects of nuclear polarization on, (T), 19: 42001
spectra of, effects of electric quadrupole and magnetic interactions on, (E/T), 20: 10260(T)
spectra of, hyperfine structure, 20: 39615(T)
spectra of, in iron-57 at surface of η aluminum oxide, 18: 17823
spectra of, in iron compounds, 18: 17871
spectra of, in strontium ferrates, 19: 7516
spectra of, optical shift in, (T), 20: 10238(T)
spectra of, properties of sodium nitroprusside for use as standard in, 20: 16335(R) (NBS-TN-276)
spectral intensity of, alpha-decay effects on, (T), 19: 18699
spectral line broadening and shifting in ferromagnetics by nuclear magnetic field, 18: 42631 (IAE-609)
spectral line deformation and shifts of, time correlation function technique for, 18: 40637
spectral line shape associated with spread of electric field intensity

gradient, 18: 15297(T)
spectral line thermal broadening, 19: 4157
spectral lines of dibutyldichlorotin, quadrupole splitting of, 20: 26350 (STI-DOC-10/50)
spectral position and width in, lattice-oscillation anharmonicity effect on, (T), 19: 21422
spectral structure of, in paramagnetic rare earths, 17: 13241
spectroscopy of, design of drives for, (E), 19: 45316
spectroscopy of, design and performance of wide range vacuum thermostat for, 20: 41253
spectroscopy of, self-modulation method for, 20: 28638
spectrum of, exact formula for elastic and inelastic, 18: 749
standard reference material for studies of iron and iron compounds, 20: 25597
standards for chemical applications of, review, 20: 20684
sum rule for, formulation of, 18: 30828
sum rules and energy spectra in, 16: 19759
surface effects in the second-order Doppler shift of, 16: 30962
survey on Mössbauer spectroscopy, 20: 34556
temperature dependence of, in crystal, 17: 38079 (JINR-P-1231(p.181-3))
temperature effects on, second-order, 17: 13231
temperature effects on iron-57, in copper and iron, 17: 13232
temperature effects on, for tin-119 in tin below 77°K, 17: 13247
temperature effects on, theory, 17: 38072 (JINR-P-1231(p.112))
temperature shift in, effects of anharmonicity on, 17: 39794(T)
theory, 18: 2439
theory, 18: 14646
theory, 20: 18015
theory, (T), 19: 12479 (AFCRL-64-840)
theory and detection, 18: 10660
theory and experimental use, 20: 28471
theory and use of, 17: 38139
theory for, 20: 8290
theory for thin films, Debye-Waller factor for, 20: 44137
theory of, on impurity nuclei in solids, 17: 28340
theory of, multipole mixtures in, 18: 36667
thermal broadening of spectral lines of, in solids, 17: 659
thermal-shift measurements, theory of atom dynamics in solids for analysis of, 20: 28660
time dependence of resonance fluoresence from identical nuclei, 18: 24228
transducer design for studies of, constant-acceleration, 17: 8295
transducers for studies of, electric-to-velocity, 17: 13225
ultrasonic splitting of the absorption line in tin-119 oxide, 17: 6889
use at high pressure for solid-state studies, 19: 38025 (COO-1198-266)
use for analysis of gravitational red shift, 18: 40113
use for crystal structure analysis, 18: 43462
use for detection of relativistic Doppler shift, 17: 17208
use for determination of g-factor of excited nuclear levels, possibility of, 17: 40008
use for determining gyromagnetic ratio of nuclear excited states, (E), 19: 41791
use for determining low-spin iron in metmyoglobin, 20: 22552
use for determining behavior of iron-57 impurities in noamagnetic metals, 20: 28606 (LA-DC-7561)
use for determining replacement probabilities for energetic primary atoms in crystals, (T), 19: 35495
use for magnetic moments of iron–nonmagnetic metal alloys, 20: 26819 (NML-64-2)
use for measurements of relative velocity, 17: 36125
use for measuring Debye temperature in iron-57, 16: 27810
use for measuring isomer and nuclear-multipole spectral effects on powdered crystals, 19: 39876
use for nuclear and solid-state studies of iodine-129 compounds, 18: 26111 (NP-13990)
use for nuclear orientation production diagnostics, (T), 19: 47615
use for studies of internal magnetic fields, review, 17: 13200
use for studies of ordering in iron–nickel alloys, 17: 36478
use for study of iron ions in sodium chloride crystals, 17: 31199
use for studying hemoglobin and iron-containing biological compounds, 19: 40305
use for thermometry below 4°K, 17: 13246
use for time dilation experiments, 19: 20699
use in accelerometers for inertial navigation, 17: 36106 (AD-286924)
use in acoustical measurements, 17: 3673
use in analysis of electron spin-lattice relaxation, 18: 44426 (UCRL-11538)
use in analytical chemistry and geochemistry, 20: 11377
use in checking relativity theory, 17: 31665
use in chemical analysis, review on developments for, 20: 22884
use in chemistry and solid-state physics, 18: 19998
use in crystal study of jarosite-group iron sulfates, 18: 30311 (PAN-301)
use in detection of localized vibrational modes in crystals, 18: 37860
use in determination of crystal lattice properties, 17: 13228
use in determination of relativistic time dilation, 17: 13249
use in determination of relativistic gravitational effects, 17: 13250
use in determination of crystal lattice properties, 17: 41603
use in determining lifetime of trivalent iron ions in ionic solids, 19: 26393
use in determining electronic shielding by closed shells in thulium compounds, 19: 40528
use in ether drift experiment, 18: 8936
use in gamma circular polarization analysis, 17: 34936
use in geochemistry, equipment for, 20: 43550(R) (NYO-844-67)
use in isomer shift correlation with residual electrical resistance of gold alloys, 17: 26453(R) (ORNL-3425(p.103-11))
use in lattice dynamics studies, 19: 43494
use in magnetic studies of rare earths, 18: 14644
use in measurement of tin-119 nuclear parameters, 17: 13257
use in measurement of magnetic moments, 17: 40435(R) (NYO-10063 (p.99-104))
use in measurement of hyperfine interactions in rare earth ferrates, 18: 22087
use in measurement of nuclear moments, 18: 30854
use in measurement of electric charge distribution in alloys, (E/T), 20: 17158(R) (ORNL-3900, pp 82-149)
use in measurement of hyperfine field distribution, (T), 20: 42571
use in measuring nuclear electric-field gradient, (E), 20: 3299
use in metallographic studies, 19: 4599
use in metallurgy problems, 18: 4246(R) (ORNL-3470(p.16-19))
use in molecular structure studies on iron complexes, 18: 41433
use in molecular structure studies, review, 20: 20684
use in narrow-angle multiple-scattering measurements for inhomogeneous materials at 14.4 kev, (E), 20: 19904
use in nondestructive testing, 18: 10255
use in nondestructive testing, 18: 10256
use in nondestructive testing, 18: 12326
use in nuclear physics, 20: 6293 (NP-15603)
use in physics, review of advances in, 20: 22327
use in relativistic time dilatation measurements, 17: 29447
use in relativity theory for frequency shift measurements, 18: 10671
use in relativity theory testing, (E), 20: 2880
use in research on magnetism of alloys, intermetallic compounds, and metals, 20: 26385
use in research on hyperfine structure, (T), 20: 26193
use in sensing motion, 20: 41224 (EGG-1183-2078)
use in studies of chemical structure, 20: 26885
use in studies of atoms, molecules, and nuclei, 20: 34630
use in study of bonding in iron compounds, 20: 1874
use in study of effective magnetic field in spinel-type ferrites, 19: 38026 (INP-407/PL)
use in study of magnetic moments of iron impurities in metals, 18: 40047 (LA-DC-6463)
use in study of magnetic properties of rare earth single crystals, 20: 12316
use in study of nuclear spectral line shapes, 18: 28609
use in studying antiferromagnetic to ferromagnetic transition in iron–rhodium alloys, 18: 30198
use in studying hyperfine interactions in the ground state and 21.7-kev state of europium-151 in europium iron garnet, 17: 38121
use in studying magnetism of dilute alloys, 18: 14645
use in surface studies, 19: 40078 (NP-15111)
use in the study of solids, review of, 18: 10646
use in tin solid solution and iron–tin alloy studies, 20: 12315
use in tracer techniques, 20: 25184
use of, review of, 18: 2419
use to detect dynamically oriented cobalt-57, (T), 19: 16994
use to determine magnetic hyperfine fields in iron alloys, 18: 39952
use to determine quadrupole moment of iodine-127 excited state, (E), 19: 5212
use to distinguish elastically and inelastically scattered components at Bragg diffraction peaks, 18: 8935
use to measure the magnetic field oscillation amplitude in superconductors, 18: 15046
uses for determination of iron in meteorites, 19: 9076
uses for measuring hfs of iron in rhodium alloys, 18: 25982(R) (ORNL-3582(p.18-19))
uses in biochemistry and chemistry of iron compounds, 20: 25089
uses in biology, nuclear physics and solid-state physics, 18: 43151 (ISS-63/50)
uses in chemical bonding studies, 19: 13478
uses in chemical research, 20: 23198
uses in chemistry, review, 17: 38076 (JINR-P-1231(p.133-65))
uses in chemistry, 18: 12159
uses in chemistry, 18: 43602
uses in chemistry, 20: 25188

uses in measurement and control technology, 19: 13831
uses in metallurgy, 20: 17158(R) (ORNL-3900, pp 82-149)
uses in physics research, review of, 18: 40054(T) (ORNL-tr-221)
uses in solid state physics, (E/T), 20: 17158(R) (ORNL-3900, pp 82-149)
uses in studies of chemical properties, (E), 19: 30238 (WERL-2989-1)
uses in studies of chemical and physical properties, 20: 17989
uses in studies of metals, 20: 20162
uses in studying electronic configurations and structures of chemical compounds, 19: 22369
uses of, at low temperature, 17: 5065
uses of isomeric shift in, to determine ionic character of absorber, 19: 15531
uses of Lamb-Moessbauer, for analyzing magnetic systems, (T), 19: 43484
uses of, review, 18: 10638
velocity drive for, using amplifier with negative output impedance, 19: 31268
velocity drive linearization by shape correction, 20: 41238
velocity drive systems for studying, 19: 8404 (TID-21338(p.182-9))
velocity drives for studying, triangle and square wave generators for, 20: 14827

Moessbauer Spectrometers
see Gamma Spectrometers

Mosses
see Liverworts

MOTION-PICTURE FILMS
use in cinefluorography, 18: 11943

Motor Vehicles
see Vehicles

MOTORS
see also Laboratory Equipment
see also Liquid Metal Brushes
see also Rocket Motors
bibliography on, 20: 7223 (TID-22477)
control circuit design modifications for three-phase linear induction, 17: 29712(R) (GEMP-77)
control of electric, design of relay for, 16: 10168 (DC-57-1-103)
control of induction, design of circuits for, 17: 24626(R) (GEMP-76)
control of synchronous, in neutron choppers, 20: 11177 (UJV-1388/65)
design and operation of synchronous reluctance, for telecontrol of control rods, 17: 9868
design and performance of three-phase superconducting, 18: 22322
design and uses of superconducting d-c, (T), 19: 12432
design of control, for servomechanisms, 18: 478 (NP-13201)
design of drive unit for traveling crane bridge in EBR-II fuel cycle facility, 19: 9301 (ANL-6966)
design of electric, for use at high temperatures in radioactive atmosphere, 19: 46516(P)
design of high-temperature air, 16: 13172 (DC-58-1-89)
design of pneumatic-nutator, for actuating reactor control drums, (E), 20: 14029 (NASA-CR-54788)
design of three-phase induction, with superconductive bearings, 19: 45196
development of hot-gas powered torque, using solid propellant, 18: 27643 (UCRL-13082(Rev.I))
development of pneumatic nutator actuator, for drum control of reactor, 19: 10469(R) (NASA-CR-54204)
development of pneumatic-nutator, for actuating reactor control drums, (E), 19: 21615(R) (NASA-CR-54282)
development of servo-type air in, 16: 23267 (DC-61-6-17)
drive design for, torque reversing, 18: 30374
drive systems for machining of round parts, 19: 46461 (RFP-562)
drive transmission for rotary members, 16: 21751(P)
energy conversion characteristics of brushless d-c, 18: 34498 (UCRL-11334)
fluid, for reactor control rod drive, 17: 4317
heat transfer characteristics of magnetohydrodynamic, 18: 2490
operating experience of Calder Hall gas-circulator, 16: 34092
operation of stepping, control circuit for, 18: 25654(P)
power amplifier design for d-c servo-, 19: 42685(R) (ORNL-3782, pp 24-8)
power control of double-acting steam type, 16: 25539 (AD-269391)
power losses in liquid between rotor and stator of induction, MHD and EM, (E/T), 19: 20119
radial force and torque in collapsible-rotor canned reluctance-type, method of calculating, 16: 33996 (WAPD-BT-26(p.19-37))
radiation effects on materials for construction of electric, 16: 7925 (DC-55-11-11)
radiation effects on performance of d-c torquer, 17: 30795(R) (AD-258338)
radiation effects on performance of, in telemetry electronics, 18: 33839 (RTD-TDR-63-4287(Vol.II))
radiation effects on insulated statorettes, 19: 25049 (NP-15022(Vol.II))
speed control circuit for, using feedback system, 20: 11073
speed control using silicon-controlled rectifier, 18: 29826 (UCRL-7358-T)
stators for electric, development of glass-coated, 20: 29366(R) (TID-22970, pp 375-91)
step positioning of synchro, transformer apparatus for, 16: 10145(P)
switch-off, high voltage surges at, 16: 27164(T) (IG-Inf-Ser-9)
use with fuel cells, in propulsion of ordnance land vehicles, 16: 3983 (DOFL-TR-777)

Moulage
see Biological Models

MOUND LAB., MIAMISBURG, OHIO
conference on research at, 19: 17412 (MLM-1163)
environs monitoring, 1961, 16: 30693
environs monitoring, Jan. to June 1963, 17: 41032(R) (TID-19492)
environs monitoring, 1962, 18: 461
environs monitoring, 1964, 18: 43803(R) (MLM-1210)
environs monitoring, July through Dec. 1963, 19: 18165
environs monitoring, 1964, 19: 30439 (MLM-1241)
environs monitoring, Jan. through June, 1965, 20: 595(R) (MLM-1275)
environs monitoring, July through Dec., 1964, 20: 18972
isotope separation and purification in 1963, stable gaseous, 19: 34607(R) (MLM-1239)
monitoring of environs, 1961, 17: 18393(R) (TID-18316)
monitoring of environs, 1961, 17: 18394(R) (TID-18317)
monitoring of environs, 1962, 17: 18395(R) (TID-18318)

MOUNT EVEREST
tritium accumulation in glaciers and high-altitude climatology in ice of, 19: 44262

MOUNT PEALE QUADRANGLE (COLO.–UTAH)
geologic map of 2NW Quadrangle, San Juan County, Utah, 16: 3257

MOUTH
analysis of tissue of, for trace elements, after neutron activation, 19: 43634 (NYO-3481-6)
book: *Radiation Protection and Dentistry*, 17: 3254
cancer radiotherapy, 16: 17530
cancer radiotherapy, dosage definitions and measurements in, 18: 9948
cell population kinetics of epithelium, tracer study in monkeys, 20: 22569
development of osteomyelitis of jaws after radiotherapy of oral tumors, 18: 15860
gingival ulceration induced by radium-226, radium-228, or thorium-228, 17: 10296(R) (COO-226(p.35-49))
malignancies of, treatment with radiation and surgery, 20: 45561
osteomyelitis of mandible induced by radiotherapy of lesions of, surgical treatment of, 19: 33837
radiation effects on mucous membrane, 16: 16213
radiation effects on, role of humoral factors in, 16: 32861
radiation effects on oral tissues in hamsters, whole-body exposure, 17: 1308
radiation effects on cleft palate development in, in mouse embryos, 17: 21482
radiation effects on rat, x, 17: 38755
radiation effects on enzyme activity of, in persons exposed to atomic bomb, late, 18: 101
radiation effects on, whole-body, 18: 15843
radiation effects on dog, from gold-198 injection into tongue, 18: 17444
radiation effects on membranes of human, x, 18: 19624
radiation effects dental trauma in rat, phosphorus-32 tracer study of, 19: 8903
radiation effects on sarcoma development in monkey, 19: 17599
radiation effects on carcinoma cells from, x, 19: 43802
radiation effects on development of, in mouse embryos, x, 20: 5326
radiation effects on osseous development of, in mouse embryos, x, 20: 5327
radiation effects on development of, in mouse embryos, x, 20: 5337
radiation effects from inhaled strontium-90 on spirochetal population in dog, 20: 8638(R) (LF-28, pp 250-6)
radiation effects on, following facial therapy, γ and x, 20: 14324
radiation effects on, antibiotic therapy of, 20: 22778
radiation effects on, following oral radiotherapy, review, 20: 22650
radiation effects on, following γ therapy for oral cancer, 20: 24961
radiation effects on flora of dogs and monkeys, γ, 20: 38667
radiation effects on jaws and teeth of weanling rabbits, x, 20: 45354(R) (COO-119-234, pp 227-50)
radiation effects on palate and tongue in rat, following head-only exposure, x, 20: 45350 (AD-640158)
radiation effects on, 16: 21973
radiation injuries induced by dental radiography, 19: 28092
radiation injuries of bones of, 19: 31942
radiation injuries to, in experimental animals following subcutaneous injection of radionuclides, 20: 42967
radiation injury of bones of, after radiotherapy, 19: 34021

radiation protection of, during dental radiography, 20: 6942
radiography of, hazards from, 20: 3846
radiography of, Panoramix method for, 20: 40795
radiography of, use of iodine-125 as x-ray source for, 19: 42377 (NYO-3481-1)
radioinduced infections in, 20: 18308
radioinduced lesions in mice, 17: 22976(R) (AD-286799)
radioinduced lesions of, in hamsters, effects of antibiotics on, 19: 36092
radioinduced necrosis in, 17: 37135
radioinduced necrotic ulcers in hamster, effects of antibiotics, bone marrow, and cysteamine on, 18: 43302
radioinduced periodontal lesions in mice, dietary factors, 17: 1295
radioinduced stomatitis in human, following oral cancer therapy, gamma, 20: 22716
radionecrosis of soft tissues of, role of alveolectomy in prevention of, 17: 17673
radiosensitivity of, 19: 13074
radiosensitivity of, 19: 15214
radiosensitivity of mucosa of, 20: 3744
radiosensitivity of, 20: 18308
radiotherapy effects, 16: 1538
radiotherapy for cancer of, osteoradionecrosis from, 18: 15921
radiotherapy of cancer, development and treatment of necrosis resulting from, 16: 9814
radiotherapy of carcinomas of, device for holding radium capsules in, 17: 17675
radiotherapy of cancer of, indications for, 17: 28621
radiotherapy of cancer of, 18: 31353
radiotherapy of carcinomas in, effects on Synkavit on, 18: 43355
radiotherapy of cancer of, 19: 9029
radiotherapy of cancers of, 19: 17729
radiotherapy of cancer of, 19: 31975
radiotherapy of cancer of, surgical repair of lesions resulting from, 19: 34010
radiotherapy of carcinomas of, late pathological effects, 19: 34024
radiotherapy of cancer of, 19: 42387
radiotherapy of cancers of, 19: 43903
radiotherapy of cancers of, evaluation, 20: 175
radiotherapy of cancer in, measures for preventing injuries from, 20: 3813
radiotherapy of cancer in, intra-oral prostheses for beam localization in, 20: 6956
radiotherapy of cancers of, effects on cytology, x, 20: 7850
radiotherapy of cancer of, effects on recovery from subsequent surgery of, 20: 12653
radiotherapy of cancers of, electron, gamma and x, 20: 22818
radiotherapy of palatine arch carcinomas in, x, 20: 14416
radiotherapy of, technique for, 18: 3636
radiotherapy of tumors in, prevention and treatment of sores from, 18: 11931
radiotherapy of tumors of tongue using injected colloidal gold-198, 19: 10964
radiotherapy of tumors of, 19: 43912
radiotherapy of tumors of, 19: 46066
radiotherapy of tumors of, effects on taste sensitivity, x, 20: 8789
radiotherapy of tumors of, late pathological effects, 20: 18523
radiotherapy of tumors in, mandibular osteoradionecrosis following, 20: 22682

MOZAMBIQUE
mining and prospecting of nuclear raw materials in, 18: 37408 (A/CONF.28/P/501)

MPA
see 2-Propanethiol, 1-Amino-

MRR
see Brookhaven Medical Reactor

MSRE
see Molten Salt Reactor Experiment

MTR
see Materials Testing Reactor

MUCIC ACID
complex formation with thorium, 16: 8745
complexes with uranyl nitrates, chemical structure of, 19: 30183
compound formation with samarium, gadolinium, and erbium, 19: 44028
reactions with dysprosium, 20: 43140
uses in determination of ytterbium, 20: 14490

Muconic Acid
see 2,4-Hexadienedioic Acid

MUCOPROTEINS
radiation effects on production in glands of rodents, 17: 23103
radiation effects on ovomucoid, protective effects of AET against, 17: 38769
radiation effects on properties of, in cartilage, 18: 6620(R) (TID-19929)
radiation effects on, in rat connective tissue, 18: 33277 (STI/DOC/10/28(p.21-38))
radiation effects on content of, in working personnel, 19: 15070
radiation effects on synthesis of, in rat intestine, x, 20: 10600 (BNWL-122, pp 131-4)
radiation effects on metabolism in mouse spleen, effects of bone marrow injections on x, 20: 22797
radiation effects on excretion in rats, x, 20: 42960
separation and purification of, method for, 18: 23188(R) (ANL-6823 (p.102-4))

MUCOSA
calcium distribution in avian shell gland, 20: 40551
characteristics of rat gastrointestinal, during alkaline earth absorption, 19: 8775
enzyme activity in sheep intestinal, 20: 32907(R) (ORO-648, pp 62-70)
iodine-131 content in cervical, tracer study of, 19: 8754
mucopolysaccharide content in intestinal, in cattle, sheep, and swine, 20: 32907(R) (ORO-648, pp 62-70)
physiology of intestinal, in rats, 20: 78
radiation and/or thermal trauma effects on intestinal, in rats, 20: 12630 (BNL-8383)
radiation effects on enzyme activity of intestinal, 16: 1553
radiation effects on oral, 16: 16213
radiation effects on acid secretion by parenchymal cells of gastric, 17: 14039
radiation effects on rectal, after telecobalt gamma therapy of pelvis, 18: 43288
radiation effects on intestinal, of mice, 19: 10832
radiation effects on intestinal, in germfree mice, 19: 25997
radiation effects on oral, following facial tumor therapy, 19: 36040
radiation effects on phospholipase activity in intestinal, of rats, 19: 45820(R) (TID-22227)
radiation effects on laryngeal, pathological, 20: 166(T) (N64-20943, pp 1–8)
radiation effects on intestinal, after uterine cancer therapy, gamma, 20: 12700
radiation effects on intestinal, after abdominal therapy, x, 20: 14339
radiation effects on, of exteriorized rat intestine, x, 20: 14364
radiation effects on hamster oral, laser, 20: 22717
radiation effects on intestinal, effects of dose fractionation on γ, 20: 22811
radiation effects on bladder and rectal, following treatment of uterine cancer, x, 20: 45540
radiation effects on intestinal, x, 20: 45351 (BNL-10534)
radiosensitivity of rabbit jaw, effects of castration and testosterone, 16: 32774
radiosensitivity of rat head, 19: 36097
radiosensitivity of intestinal, 19: 45929
radiosensitivity of rectal, in rats, 19: 45918
radiosensitivity of, protective effects of rutin derivative, 20: 3840
radiosensitivity of oral, 20: 3744
radiosensitivity of intestinal, 20: 3821
radiosensitivity of gastric, γ, 20: 43019
radiotherapy of cancer of oral, indications for, 17: 28621
radium-224 content in rat, after intravenous injection, 19: 40315
sodium effect on electric potential in gastric, 17: 15645 (USNRDL-TR-608)
sulfur metabolism in nasal, of guinea pigs, tracer study of, 19: 5626

MULLITES
crystallization and sintering of, effects of beryllium, calcium, and magnesium oxides on, 19: 13973
diffusion of helium in, at 25 to 1000°C, effects of tensile stress on, 17: 29329 (UCRL-10755)
effects on reactions between outgassed graphite and steam at 1000°C, 19: 26348
properties as induction furnace coil lining material, petrographic analysis of, 18: 43381(R) (NLCO-920(p.25-9))
thermal conductivity of, for use above 3000°F, 18: 16520
vaporization of, to 2300°C, 20: 13265(T) (AD-623208)

MULTIPLE SCLEROSIS
gamma globulin transfer between cerebrospinal fluid and plasma in, tracer study of, 19: 43666 (BNL-9406)
geographic distribution, 16: 23479
geomagnetic latitude effects on occurrence of, 18: 5111
immune reaction as a possible mechanism in etiology of, 20: 40643
radiation effects as possible etiology of, cosmic, 20: 40639

MULTIPLICATION FACTOR
analysis of subcritical, neutron-noise, 18: 23015 (TID-7662(p.1-26))
approximate iterative methods applied to "non-separable" multiplying systems in basic symmetry, 17: 15070
book: *Introductory Nuclear Reactor Theory*, 17: 33266
calculation for bare cylinders, 17: 5198 (HASL-124)
calculation for enriched uranium assemblies, Monte Carlo techniques for, 20: 45076 (K-DP-1637)
calculation for fast reactor with heterogeneity effects, 19: 3580

calculation for fast breeder reactors, comparison of methods, 20: 38421 (ANL-7120, pp 440-8)
calculation for fissile units, computer program for, 20: 40375 (DP-1031)
calculation for heterogeneous assemblies, computer program for, 18: 23014 (ORNL-TM-838)
calculation for natural-uranium heavy-water reactors, 18: 6458
calculation for one-dimensional multiregion reactors, 17: 28495
calculation for plutonium cores, computer methods for, 19: 14788(R) (HW-81984(p.10.1-15))
calculation for plutonia-urania critical experiments, 19: 31521(R) (WCAP-3385-3)
calculation for small fast assemblies, computer program for, 20: 8350 (RT/FTMA(65)5)
calculation for spherical uranium-fueled assemblies, 20: 22383(T) (AEC-tr-6693)
calculation for uniform water-moderated lattices, 19: 42054
calculation for water-moderated aluminum–plutonium and plutonium
calculation of, critical equation in three-group diffusion approximation, 17: 15432
calculation of Doppler coefficient, development of basis for, 19: 10675(R) (NAA-SR-9999)
calculation of Doppler coefficient of reactivity, basis for, 19: 40286(R) (NAA-SR-11200)
calculation of effective, for interacting assemblies of fissionable materials, 20: 35685
calculation of excess, computer program for, 19: 14791 (KAPL-M-6431)
calculation of, for ZPR III assemblies of various compositions using ANL cross-section Set 635, 16: 29630 (ANL-6570)
calculation of, for small heavy water lattices with high enrichment, 18: 6450
calculation of, MOCA-2 code for, 17: 26017
calculation of negative, for subcritical reactors, 19: 29575(P)
calculation of reactivity of central air gap in a bare reactor, 16: 26540
calculation of reactivity for bare homogeneous thermal reactor during fuel burnup, 17: 29729
calculation of reactor eigenvalues using Monte Carlo method, 18: 24818 (WAPD-T-1649)
calculation of small-amplitude auto-oscillations in reactors, 18: 24850 (NP-13963)
calculation of, computer code for, 19: 29510 (KAPL-M-6408)
calculation of, computer programs for, 20: 6581 (CEA-R-2872)
calculation of, effect of cross section uncertainties on, 20: 46964(R) (BNWL-284)
calculation of, formulas for, 18: 17285
calculation of, methods for, (E/T), 20: 11929 (CEA-R-2849)
calculation of, methods for, 20: 24714
calculation of, multifactor and multigroup techniques for, 19: 10658
calculation of, resonance absorption concepts for, (T), 20: 8352
calculation of, two-dimensional S_N perturbation theory for, 19: 29567
calculation of, using reactor-statics methods, (T), 20: 3367 (BNWL-156)
calculation using Monte Carlo method, computer programs for, 20: 35686
calculation using discrete transfer matrix, 20: 40060
calculations in two and three dimensions, EQUIPOISE program for few-group, 16: 18412
calculations of infinite, for homogeneous fuel mixtures, (T), 19: 31499 (BNWL-3)
changes in, computer program for calculation of, 20: 3366 (ANL-7052)
changes of, effects on circulating-water reactors, 20: 38449
compensation for excess, in intermediate reactors, 18: 38342 (A/CONF. 28/P/375)
computer program for zero-power reactor transfer function amplitudes and phase shifts, 18: 30945 (HW-80957)
control in reactors, elements for, 19: 35690(P)
control rod movement effects on, in fast reactors, 16: 23287
critical size and reactivity calculations, validity of the transport approximation, 16: 26539
decay-constant measurements at different bucklings in a uranium–water sub-critical assembly, 17: 42238
definition for off-critical reactors, 19: 31495(R) (ANL-7010(p.21-76))
derivation in cylindrical symmetry, 18: 17282(T) (CEA-tr-X-319)
determination during and after shutdown, 18: 38319 (A/CONF.28/P/686)
determination for thermally fissionable isotopes, techniques for, 20: 26081 (IDO-17173)
determination from Monte Carlo calculations, 16: 24434
determination from characteristics of xenon poisoning, 18: 38662
determination in light-water-moderated assemblies, 17: 15422
determination in light-water lattices by boron-poisoning methods, (T) 19: 10478 (CEA-R-2489)
determination of excess, computer program for, 19: 17218 (KAPL-M-6162)
determination of impulse response and transfer functions for, (E/T), 20: 8362
determination of, machine generation of cross sections and parameters for, 17: 4053 (KAPL-M-BM-2)
determination of, pulsed source techniques for, (T), 19: 40151 (EIR-79)
determination of, modulated and pulsed experiments for, (T), 20: 13723
determination of, experimental and theoretical, 16: 10804 (ANL-6487)
determination using noise and pulsed-neutron measurements, 19: 27756
determination using pulsed neutron source methods, (T), 20: 14075
dioxide–uranium dioxide lattices, 20: 20200(R) (ANL-7110, pp 29-98)
Doppler coefficient measurement, methods for, 19: 27735(R) (NAA-SR-10850)
dynamic reactivity effect in compressible fissile media, 18: 42345
dynamics of, in compressible fissile media, 18: 23027 (TID-7662 (p.447-90))
effect of epithermal fission on, (E/T), 20: 30841
effects of fuel configurations on, 19: 8602(R) (ORNL-3691(p.89-98))
effects of holes and voids on, (T), 20: 5064
effects of hydrogen on reactivity, 16: 26544
effects of linear increase of, on reactor response, 17: 1046 (NP-12158)
effects of parameter variation in Doppler effect calculations, 18: 11378
effects of small fuel displacements on, 17: 12765(R) (ORNL-3360 (p.12-16))
eigenvalue matrix solution to N-component neutron interaction problems in arrays of neutron emitters, 17: 11458 (HW-75887)
evaluation in critical and subcritical assemblies, 16: 24353
evaluation in critical and subcritical assemblies, 16: 24354
evaluation of two-region reactor parameters by random noise measurements, 18: 15436
evolution in power reactors, effects of burnup on, 18: 38398 (A/CONF.28/P/77)
experimental determination of β^{eff}/l, 18: 17284
experimental results on large dilute fast critical systems with metallic and ceramic fuels, 16: 26524
fast fission factors in slightly enriched light water-moderated slab lattices, 18: 35117
fission products effects, uncertainties in predicted, 16: 21814 (KAPL-M-ECH-8)
flow-void feedback effects in BWR, 18: 23021 (TID-7662(p.189-226))
fluctuations in boiling-water reactors, minimization of, 17: 12008
fluctuations in, method for measuring, 18: 11404
geometrical factors for reactivity calculations, 18: 42949
kinetic equations for, stable numerical solutions of, 18: 28964
mathematical functions related to Doppler coefficients, 17: 1044 (NDA-2014-162)
measurement, 18: 15471 (GA-4838)
measurement by pulsed-neutron technique (T), 19: 3558
measurement, design of reactivity monitor for reactor startup, 16: 24546
measurement experience at Brookhaven, 17: 42226
measurement for an infinite medium, method for, 20: 45078 (MIT-2344-6)
measurement for borated aluminum-plutonium-polyethylene systems, 20: 6578(R) (BNWL-149, pp 45-7)
measurement for borated aluminum-polyethylene-uranium and aluminum-plutonium-polyethylene systems, 20: 6577(R) (BNWL-149, pp 22-35)
measurement for fertile and fissile isotopes, methods of, 19: 40286(R) (NAA-SR-11200)
measurement for gas-cooled graphite-moderated reactors, 18: 1270
measurement for light water-moderated reactors, analog system, 18: 42917 (CEA-R-2513)
measurement for poisoned infinite lattices of enriched uranium and heavy water, 19: 42046(R) (MIT-2344-3, pp 109-14)
measurement for samples in ARMF, computer program for data analysis for, 19: 6837 (IDO-17026)
measurement for subcritical cylinders of enriched uranium, 20: 34941
measurement for thermally fissionable isotopes, (E), 20: 44626 (CONF-660303, pp 919-32)
measurement in control rods and reactor startup, design of meter for, 18: 44935
measurement in critical and subcritical assemblies, review of, 17: 22796 (MITNE-25)
measurement in heavy water-natural uranium dioxide lattices, errors in, 16: 32556
measurement in plutonium-fueled heavy-water reactor, 18: 40834 (HW-80253)
measurement in power reactors, neutron detection probabilities for, 18: 9705
measurement in reactors, system for, 20: 18032
measurement in subcritical reactors, design of potentiometer with reference voltage for, 17: 42286(P)
measurement in subcritical systems, source-jerk theory for, 19: 25687(R) (ORNL-3731(p.239-51))
measurement in unreflected oralloy assemblies, 18: 40212 (LA-1209)
measurement near delayed critical by pulsed-source method, 19: 29562
measurement of conversion ratio, resonance escape, and fast fission as student experiments, 17: 26235

measurement of control rod transfer functions using pulse analyzers and cross-correlation, 18: 25813 (NAS-NRC-Pub-1184(p.207-9))
measurement of Doppler coefficient, 18: 24816(R) (NAA-SR-8888 (Sect.IV))
measurement of Doppler coefficient in fast spectra, 19: 12865(R) (NAA-SR-10501)
measurement of eta and other nuclear properties of uranium-233 and uranium-235, 16: 12326
measurement of eta for uranium-233, uranium-235, and plutonium-239, 16: 12501
measurement of, in a water-moderated uranium dioxide lattice, 17: 24656
measurement of, in epithermal lattices, 18: 3352
measurement of K_{∞} and thermal utilization in heavy-water-moderated and -cooled lattices of 19-rod clusters of UO_2, 17: 3739
measurement of low, square-wave neutron-pulse response (E/T), 19: 3772 (CEA-R-2377)
measurement of low, square-wave methods for (T), 19: 3506 (CEA-R-2229)
measurement of low, (E/T), 19: 12752
measurement of negative, 17: 26085
measurement of negative reactivity using neutron fluctuation spectral density, 17: 40275 (ORNL-TM-690)
measurement of negative, use of spectral density of neutron fluctuations for, 18: 35074 (TID-7679(p.171-81))
measurement of parameters of subcritical heavy water assembly, 16: 11170
measurement of small changes in, precision limitations in, 18: 3046
measurement of space-dependent, of absorption and fission, 19: 3523
measurement of subcritical reactivity by source-jerk method, 17: 9882
measurement of subcritical, using h-f sine-wave modulated neutron source, (T), 19: 14785 (AEEW-R-398)
measurement of test sample, in critical assemblies, 18: 3353
measurement of $_{98}\rho$ and δ^{98} by chemical separation of neptunium-239 and molybdenum-99 from uranium and fission products, 18: 26249
measurement of, definition of sensitivity for, 19: 29554
measurement of, experiment for static, 18: 30949 (NYO-9077)
measurement of, instrumentation for, 19: 46716(R) (IDO-17081, pp 77-123)
measurement of, pseudo-random impulse response method for, 20: 26440
measurement of, pulsed-source methods in, 18: 42940 (TID-7050 (p.1319-57))
measurement of, using small sample, 18: 15467 (CONF-187-108)
measurement on-line in power-reactor core, meter for, 19: 5481 (NAA-SR-10186)
measurement, performance of d-c period meters, 16: 8899 (CEA-2075)
measurement using pulsed-neutron methods, 18: 28981
measurement using pseudo-random source excitation (T), 19: 3507 (CEA-R-2230)
measurement using pulsed-neutron methods, 19: 6125 (HW-80913)
measurements of negative, methods for, 19: 33570
meter for, error in digital reactor period, (T), 19: 12739
neutron spectra effects on thermal utilization, 16: 12414
neutron statistical behavior in multiplying media, 16: 24775
Nordheim equation for, derivation from diffusion equation, 17: 29564 (CNAM-7)
of arrays of cylinders, computer program for calculating, 18: 42920 (K-DP-36)
of arrays of spheres, computer program for calculating, 18: 42921 (K-DP-46)
of plutonium-fueled lattices, effects of plutonium-240 on temperature dependence of, 17: 37003(R) (HW-78118)
of polyethylene-moderated aluminum–uranium lattices, effects of boron-10 on, 19: 25685(R) (HW-84369(p.25-33))
optimization for natural uranium–graphite reactors, 20: 20217
physics of, in water-type reactors, 17: 5585
reactivity and reaction rate calculations for mixed graphite lattices, 17: 29705 (AEEW-R-288)
reactivity calculations and experimental correlations for light-water-moderated reactors, 17: 42234
reactivity coefficient calculation by perturbation theory, 16: 26543
reactivity coefficient of sodium in large fast reactors, temperature, 19: 17214 (CEA-R-2555)
reactivity concept and its application to kinetic measurements, 17: 26816
reactivity effects of expulsion of moderating water, 16: 28438
reactivity effects due to variations in nuclear parameters in a thermal power reactor, 17: 33307 (EUR-281.e)
reactivity, measurement of dynamic temperature coefficients by forced oscillations in coolant flow, 16: 24542
reactivity measurement in subcritical reactors, 17: 26801
reactivity measurement in highly subcritical range by digital cross-correlation technique, 17: 28444 (NP-12910)
reactivity measurements in exponential piles by pulsed-neutron-source method, 17: 42232
reactivity measurement in sub-critical region, integration method for, 18: 44985
reactivity measurement by a pulsed-source method, 19: 1842
reactivity of subcritical assemblies, 17: 31697
reactivity of subcritical assemblies, determination by statistical methods, 17: 42207
reactivity of subcritical assemblies, 18: 21607
reactivity transients in, limitations of inhour formula for, 18: 4744 (WAPD-T-1627)
reactivity, complex eigenvalues in diffusion calculations of, 18: 28965
relation between effective and infinite, in reflected medium, 16: 33987 (NP-12059)
relations with prompt neutron lifetime in diffusion theory, 19: 31495(R) (ANL-7010(p.21-76))
sensitivity to cross section uncertainties for thermal systems, (T), 20: 26423 (BNWL-SA-614)
solution of the kinetic equation in periodic reactivity changes, 17: 26817
spatial dependence of, measurement of, 19: 17227
stability of, in boiling-water reactors, 18: 3134(R) (GEAP-4094)
stability of, in power reactors, 17: 4324
stability of, in reactors with negative-feedback control, 17: 12004
statistical theory of neutron chain reactions, 17: 7059
statistical theory of neutron chain reactions, 17: 7060
statistical theory of neutron chain reactions, 17: 7061
temperature coefficient of, in homogeneous medium, (T), 19: 8604
temperature dependence of infinite, in graphite-uranium lattices, (E), 19: 17229
temperature effects on, 17: 29724 (RM-3089-PR)
temperature effects on, zero-power measurements of, 18: 38313 (A/CONF.28/P/649)
theory, 19: 8605
theory, 20: 32779
theory of delayed supercritical excursions to measure Doppler coefficients of fast reactors, 17: 33242 (KFK-153)
theory of heterogeneous and homogeneous exponential experiments involving a single fuel element, 18: 19317
thermal utilization factor, theoretical calculations, 16: 2688(T) (AEC-tr-4677)
variation of long-term reactivity for different types of fuel cycles, 17: 28426 (EUR-129.f)
variations due to burnup, 18: 36795 (UJV-1008/63)
variations in boiling water reactors, minimization of mean square value of, 18: 26924(R) (EURAEC-1065)
variations of, reactivity feedback analyses of, 18: 42933 (TID-7050(p.877-955))
void coefficients, theoretical calculations, 16: 3875(R) (ORNL-3193 (p.258-60))
xenon oscillation effects on, 17: 31699
xenon poisoning effects on reactivity coefficients, 16: 2696

MUONIUM

see also Mesons (μ)
antimuonium-muonium conversion in, electromagnetically induced, (T), 19: 23407
chemical properties of, methods for studying, 20: 29177
decay of, meson (μ^+) depolarization in, (T), 19: 25277
discovery, preparation, and properties, 17: 28163
formation and properties of bi-, in electron-positron collisions, 16: 7000
formation in solids, from meson (μ^+) stopping, (E/T), 20: 13498
hyperfine splitting in gases, 16: 10958 (NEVIS-99)
hyperfine splitting of, four-fermion V-A weak interactions in, (T), 19: 41410
hyperfine structure, 16: 10885
hyperfine structure splitting in, 17: 9402
hyperfine structure splitting in, 17: 9473
hyperfine structure interval for, 18: 34921
hyperfine structure, 18: 38181
hyperfine structure interval of ground-state, review on, 19: 29011
hyperfine structure of, second-order quantum electrodynamic corrections for S-state, (T), 20: 37445
hyperfine structure of, review of, 20: 41661
magnetic resonance experiments on, 18: 2483
production in photon resonance interactions, (T), 19: 12266
production in polarized meson (μ^+) reactions with targets with longitudinal magnetic field, (E/T), 19: 45079
properties of types one and two, 16: 992
properties of, chemical and physical, 20: 11377
properties of, review of, 20: 24060
reactions of, chemical, (E/T), 19: 29109
reactions with atoms, theory of, 18: 32467
reactions with atoms and molecules, 20: 17297
reactions with atoms and molecules, review of, 20: 41661
reactions with ethylene, nitrous oxide, and oxygen, cross sections for, 20: 29177
reactions with matter, parameters for chemical, (T), 19: 4052
reactions with organic molecules, μ^+ mesic molecules from, 17: 28342

reactions with organic compounds and mixtures, (E), 20: 29247
spin precession in compounds with, (T), 19: 45278 (NP-15389)
spin precession in quartz, in magnetic field, (E), 20: 17361(T)
Muons
see Mesons (μ)
MURA Accelerator
see FFAG Accelerators
MUREXIDE
analytical uses for complexometric determination of thorium, 18: 193
MUSCLE RELAXANTS
biochemical effects of malt extract as, 16: 26666(T) (JPRS-13555)
effects on calcium metabolism in guinea pig muscles, tracer study of, 19: 8748
radiation effects on physiological response of rabbits to, 19: 43871
MUSCLES
activity of guinea pig intestine, effects of radioprotective compounds on, 19: 46005(T) (JPRS-31933, pp 6-12)
analysis for alpha activity in normal human, spectroscopic, 16: 17433
analysis for estrogen in, of broilers fed 3,4-dianisyl-2-*t*-3-hexene, use of tritium for, 17: 27050
analysis for magnesium, activation, 18: 39054 (AE-151)
analysis for uranium content, 17: 33512
analysis of electrolytes of, neutron activation, 17: 37051
analysis of tissues from, for tritium, combustion procedure in liquid scintillation counting for, 20: 20570
analysis of, by activation methods, Szilard-Chalmers effect in, 20: 18583
analysis of, for carbon-14 and tritium by scintillation counting, combustion method for, 20: 36721
blood circulation in normal and with venous stasis, double tracer study of, 18: 38755
blood circulation in, tracer studies of, 19: 10751
blood flow in, tracer techniques for measurement of, 18: 35413 (TID-7678(p.189-212))
bromine content in human, 16: 20098
bromine-82 resorption by rabbit, 17: 30266
cadmium-109 uptake and distribution in, in mice, 18: 3457
calcium content in brown trout, 18: 16243
calcium content of guinea pig, tracer study, 19: 33772
calcium content of guinea pig, tracer study, 19: 33773
calcium metabolism in guinea pig, tracer study of effects of drugs on, 19: 8748
calcium metabolism during contracture of, tracer study of effects of thiocyanates on, 20: 35220
calcium-45 distribution in rat, effects of age on, 18: 33
calcium-45 uptake and release by frog ventricular, effects of nicotine on, 18: 1347
calcium-45 deposition in cow and goat, dietary, 16: 8505
calcium-45 distribution in, 16: 8488
calcium-45 exchange between blood and, in hyperparathyroid and normal rats, 19: 6953
calcium-45 uptake by frog sartorius, effects of potassium concentration on, 19: 35912
calcium-47 uptake by rat, 20: 40557
capillary circulation in, of dogs, 19: 31689
cesium content in human, 17: 15603
cesium content of, isotopic dilution determination of, 19: 25833
cesium uptake by sartorius, in frogs, 17: 19797
cesium-137 content in, in human body in Tokyo, Dec. 1961 to Nov. 1962, 18: 4983
cesium-137 levels in Japan, 16: 4388 (A/AC.82/G/L.691)
cesium-137 uptake by human breast, 18: 3614
cesium-133 and -137 contents in, in animals and man, 18: 21790
cesium-134 metabolism in rat, effects of aldosterone on, 19: 31733
cesium-134 uptake by dog, 17: 35428
cesium-137 content in human, in Japan, 1960 to 1962, 18: 13428
cesium-137 content of human, 18: 31316
cesium-137 content in human, 19: 25895
cesium-137 content in, at various times after endoperitoneal and oral administration, 19: 29872
cesium-137 content in guinea pig, following injection by different routes, 20: 33
cesium-137 content in deer, factors affecting, 20: 12984
cesium-137 content in bull, fallout, 19: 20215
cesium-137 uptake by rat, cesium chloride and steroid effects on, 18: 17443
cesium-137 uptake by rat, 18: 17442
cesium-137 uptake from fallout by, 18: 33427
cesium-137 uptake by rat, after exposure to chloride and nitrate aerosol solutions, 19: 3858
cesium-137 uptake and distribution in rat, 19: 21835
chlorine-36-labeled 6-chlorocoumarin distribution in rabbit, 18: 12026
cobalt-60 uptake by rat, effects of complexing agents on, 19: 5620
composition of swine, estimated by radiography of knuckle, 20: 5224
content of cesium-137 in, 20: 7335
contraction of frog heart, tracer study, 19: 33725
contraction of guinea pig, effects of calcium and potassium on, 19: 25843
contraction of smooth visceral, role of calcium, tracer study, 17: 1206
contraction of, effects of anions on, 19: 14937
contraction of, effects of barium, calcium, magnesium, and strontium on, in rabbit aorta, 19: 25851
contraction of, effects of strontium on, 19: 33725
contraction of, effects of cations on, 19: 33725
contraction of, Grotthuss mechanism in, 20: 340
contraction of, in goldfish intestine, effects of drugs on, 18: 33198 (UCLA-12-528)
deuterium–hydrogen exchange in proteins of, 20: 349
development of, in zebrafish embryos, 18: 17381(R) (ANL-6790 (p.194-204))
diseases of, effects of whole-body potassium content on, incidence of muscular dystrophy and myotonia atrophica, 20: 6989
dye uptake by frog sartorius, effects of heavy water on neutral red, 20: 5317
dystrophy of, effects on iodine-131 metabolism in mice, 19: 27917
effects of calcium, strontium, and magnesium on the inotropic action of fluoride in rat ventricle, 20: 36567
effects of cysteine and β-mercaptoethylamine on sorptive properties of irradiated, 16: 30258
effects of deuterium on action potential of excised fibers of, 19: 2012
effects of layers of, on sorption of electromagnetic energy in man, 20: 45439
effects of radiation sickness on renewal intensity and specific radioactivities of proteins in rabbit, 20: 36600
effects of rat, on deiodination of rose bengal *in vitro*, 19: 25872
effects of water-d_2 on isometric contraction, 16: 32754
enzyme activity of heart, 18: 15707 (TID-20144)
excitation-contraction coupling in frog, chemical effects and role of action potential in, 19: 45736
fiber development in grasshopper embryos, electron-microscope studies, 17: 7655(R) (ANL-6600)
fluorine-18 distribution in, 16: 8488
gamma dosimetry in, model for, 20: 24967
insulin binding to striated, 20: 18185(R) (BNL-929, pp 126-47)
iodine-131 absorption by, effects of trauma on, 20: 6742
iodine-131 metabolism in mouse, effects of thiouracil diet on, 19: 38350
iodine-131 resorption from, effects of blood volume on, 19: 17489
iodine-131 uptake by, in animals and chickens, 18: 33251
iodine-131 uptake and distribution in rat, from labeled etabrine, 19: 14988
iodine-131 uptake by chick, age and dose effects on, 19: 43704
iron content in human, 16: 20098
isotope effects of deuterium on lactate dehydrogenase of rabbit, 18: 41053
magnesium-28 uptake by, in magnesium-deficient rats, 18: 29204
magnesium-28 uptake by magnesium-deficient rat, 19: 27933
manganese-52 uptake by mouse, 18: 17452
membrane depolarization induced by x radiation and cesium ions, 17: 17761 (TID-18220)
mercury-203 uptake by rabbit, 17: 35430
mercury-203 uptake by rat, after repeated vapor inhalation, 19: 3860
microscopy of heart, 20: 10631
morphology, effects of storage in Ringer solution, 17: 17759 (TID-18218)
necrosis of rat, effects on taurine excretion, 18: 27145
neutron total cross sections, 16: 3722
niobium-95 distribution in rabbit, 19: 27939
oxidative enzyme levels in monkey, effects of temperature on, 19: 43632 (LA-DC-7135)
paresis induced by proton irradiation of peripheral nerves, 17: 1252
phantom preparation for depth dose measurement, 16: 17370
phosphorus-32 uptake by, in scorpion, 17: 35431
phosphorus-32 content in rat, following epiphysiolysis and pseudo-epiphysiolysis, 20: 45316
phosphorus-32 uptake and excretion by chicken, 19: 8765
physiology of movement of, 19: 42212 (NYO-3424-1)
physiology, tracer studies, 16: 1404
plutonium content in dogs', 16: 26719
plutonium-239 deposition in inhaled, 16: 8504
polonium-210 distribution and metabolism by dog, man, mouse, rabbit, and rat, comparison of, 19: 2052
polonium-210 uptake by rat, after single gavage or intravenous dose, 19: 2043
polonium-210 uptake and distribution by rat, long-term, 19: 2045
polonium-210 uptake and distribution by rat, comparison of multiple and single dose effects on, 19: 2046
potassium content of, in sheep, 17: 30268
potassium content in human, 17: 15603

potassium contents in animal and human, 18: 21790
potassium-42 uptake *in vitro* by, 18: 8093
protein synthesis in heart, 19: 29846 (ACRH-103(p.28-36))
radiation and hypothermia effects on dehydrogenase activity in rat, 17: 37097
radiation damage reaction of, with mechanical trauma, biochemical analysis of, 16: 20166
radiation dose calculations for, x-ray, 19: 10959
radiation effects on heart, in dogs, 16: 4080
radiation effects on quantity of porphyrin bodies, in guinea pigs, 16: 4082
radiation effects on electrical processes in, 16: 9900
radiation effects on dye sorptive properties of tissue, 16: 11470(T) (JPRS-12829(p.1-6))
radiation effects on presynaptic failure of neuromuscular transmissions, 16: 16258
radiation effects on electric properties of frog, 16: 16181(T) (JPRS-13154(p.8-15))
radiation effects on skeletal and heart electrophysiological parameters, 16: 17473
radiation effects on regeneration after trauma, 16: 32743(T) (JPRS-15018(p.73-82))
radiation effects on carbohydrate-phosphorus exchange in, 16: 32808
radiation effects on electrical and mechanical activity, whole-body, 16: 14510
radiation effects on quantity of porphyrin bodies in guinea pig, 16: 4082
radiation effects on collagen levels, local exposure, 17: 1265
radiation effects on glutathione content in, in rabbits with and without implanted sarcoma, 17: 7877
radiation effects on prepyriform electrical activity in, in rats, whole-body, 17: 10373
radiation effects on skeletal, 17: 14056
radiation effects on cell membrane, 17: 15642(R) (TID-18268)
radiation effects from high-level exposure on morphology and metabolism, 17: 15641 (TID-18221)
radiation effects on membrane permeability, 17: 17760 (TID-18219)
radiation effects on oxygen consumption *in vitro*, 17: 17762 (TID-18222)
radiation effects on calcium metabolism in, in rabbits, 17: 19790 (TID-18422)
radiation effects on electrolyte balance, whole-body exposure, 17: 21566
radiation effects on respiration in rat, formula for analysis of dose dependence in, 17: 23177
radiation effects on electric properties of, in rats, 17: 24961
radiation effects on amino acid content in mouse, 17: 30377
radiation effects on mouse, protective effects of cysteamine against, 17: 31967
radiation effects on Annelid, x, 17: 33626
radiation effects on nuclein metabolism of rat skeletal, x, 17: 37068(T) (JPRS-20997)
radiation effects on Staphylococcus growth in chicken, gamma and particles, 17: 39364
radiation effects on electric and electrochemical properties of, 17: 40542
radiation effects on mouse, gamma, 17: 40615
radiation effects on, 14-Mev neutron, 17: 2860
radiation effects on adenosinephosphoric acid levels in rat, x, 18: 3521
radiation effects on glycogen content of, 18: 6655
radiation effects on cholesterol metabolism in guinea pig, protective effects of pellagra preventive and vitamin B_1 against, 18: 9928
radiation effects on enzymes in guinea pig, x, 18: 17494
radiation effects on morphology of excised frog, 18: 17569
radiation effects on regeneration of mouse, after trauma, 18: 19553(R) (TID-20513)
radiation effects on extracellular space in, 18: 19718
radiation effects on proteolysis in rat skeletal, gamma, 18: 19745
radiation effects on rabbit, fluid flow method for detection of, 18: 25134
radiation effects on catabolism and anabolism in, x, 18: 29380
radiation effects on cellular ultrastructure in guinea pig heart, x, 18: 29336
radiation effects on enzyme activity of heart, in guinea pigs, 18: 29267
radiation effects on dehydrogenase and glutathione levels in guinea pig, 18: 31246
radiation effects on cholesterol in, in guinea pigs, 18: 31247
radiation effects on enzyme activity in rat, x, 18: 35327(T) (JPRS-25630)
radiation effects on responses to activity in, of dogs, 18: 36952(R) (TID-20979(Add.))
radiation effects on manganese content in, beta and x, 18: 38872
radiation effects on regeneration after trauma of, in rats, 18: 38972
radiation effects on enzymes of cod, neutrons, 18: 41888
radiation effects on response of dogs, to induced contraction, 18: 41217
radiation effects on cells of frog, x, 18: 43234
radiation effects on creatine in rat, x, 19: 5705
radiation effects on phosphorylase activity of, in mice and rabbits, 19: 7146
radiation effects on proteinic nitrogen and potassium content in rat, 19: 7157
radiation effects on cholesterol content of rat, 19: 8885
radiation effects on regeneration of skeletal rat, fractionated, 19: 8925
radiation effects on oxygen tension in mouse, 19: 17564
radiation effects on susceptibility to Coxsackie B1 virus in neonatal rat skeletal, 19: 17594
radiation effects on ATP content in rat, 19: 17626
radiation effects on reduced glutathione behavior in rat heart, 19: 17650
radiation effects on, 19: 19551
radiation effects on acid and alkaline phosphatase and esterase activity in guinea pig skeletal, 19: 19574
radiation effects on content of adenosinetriphosphoric acid and inorganic phosphorus in cardiac and skeletal, of rats, 19: 21868(T) (JPRS-29183(p.10-16))
radiation effects on resting potentials of frog, 19: 24362
radiation effects on cholesterol metabolism in rat, 19: 26017
radiation effects on rest potential of frog leg, effects of external media on, 19: 25954
radiation effects on sarcomere structure in rabbit, uv, 19: 28021
radiation effects on, morphology of, 19: 33954
radiation effects on sarcosomes of housefly flight, 19: 42345
radiation effects on propylhydroperoxide reduction by filtrates of rat, 20: 54
radiation effects on content of free amino acids in beef, γ, 20: 5278
radiation effects on activity of, γ, 20: 5375
radiation effects on mechanical properties of excised frog and rat, γ, 20: 5292(R) (COO-205-55, Paper 1)
radiation effects on electrical properties of excised frog, γ, 20: 5293(R) (COO-205-55, Paper 2)
radiation effects on activity of alanine–2-oxoglutarate and aspartate–2-oxoglutarate-aminotransferase in rat, x, 20: 10593
radiation effects on mouse myocardial, β, 20: 10643
radiation effects on transplanted Yoshida sarcoma cells in rat, tracer study, 20: 16188
radiation effects on physiology of, γ and x, 20: 18293 (NP-14898)
radiation effects on excised diaphragm-nerve preparations, 20: 18293 (NP-14898)
radiation effects on contraction of, effects of ion content and fluxes on, 20: 18293 (NP-14898)
radiation effects on neuromuscular competence and response to stimuli in monkeys, massive pulsed-dose reactor, 20: 24872 (AFRRI-SR-66-2)
radiation effects on striated rabbit, x, 20: 24883
radiation effects on solubilization of cholinesterase from plaice, by bacteria, 20: 28933
radiation effects on carbohydrate-phosphorus metabolism in cardiac and skeletal, γ, 20: 32956
radiation effects on uptake of carbon-14-labeled acetate by proteins in rabbit, 20: 36574
radiation effects on aminotransferase activities in rat skeletal, neutron, 20: 36601
radiation effects on content and metabolism of phosphoproteins in denerved and intact rabbit, x, 20: 36602
radiation effects on electrical parameters of skeletal, α, 20: 38776
radiation effects on phospholipid metabolism, gamma, 20: 42796
radiation effects on heart, in frogs and rabbits, 20: 42877
radiation effects on electric conductivity in rat abdominis, gastrocnemius, and rectus, gamma, 20: 42929
radiation injuries after large doses of x radiation, 16: 12890
radiation injuries, protective effects of transplanted pulverized tissue, 16: 30230
radiation injuries to, from therapy of neoplasms in early childhood, 17: 4400
radiation injuries of, in children treated for hemangiomas by radium, 20: 38787
radiation injuries of rat, biochemical effects of, 18: 31131(R) (RRA-T42)
radioinduced autolysis in rat abdominis, gastrocnemius, and rectus, gamma, 20: 42929
radioinduced changes after radiotherapy of Wilms's tumor, 16: 32814
radioinduced free radicals in tissues of rabbit, ESR of gamma and x, 19: 45947
radioinduced inactivation of, combined with polarization microscopy for contraction studies, uv, 20: 16259
radioinduced inflammations of, Padutin therapy of, 20: 45356 (EUR-2752.e)
radiosensitivity in worms, 16: 30283
radiosensitivity of myosin in, 16: 6300(T) (JPRS-11322(p.162-79))
radiotherapy of myositis in, electromyographic changes from, 20: 35354
radiotoxins released by, 18: 19653
relaxation after ATP-induced contraction in rabbit psoas, effects of deuterium oxide on, 20: 18228

response to deformation in smooth, 19: 25071(R) (TID-21667)
rubidium content in, in man, 17: 15603
rubidium uptake by sartorius, in frogs, 17: 19797
rubidium-86 distribution in dog, myocardial scanning, 16: 7393
rubidium-86 uptake by dog, 17: 35428
sodium components and exchange, tracer study, 16: 1441
sodium-24 clearance from human gastrocnemius, 19: 8770
sodium-24 resorption rate from rabbit, with ligated vena femoralis, 18: 9830
sodium-24 resorption by rabbit, 17: 30266
sorption of injected cerium from, 16: 4022(T) (NP-tr-825)
stretch reflex in, model for, 18: 2404(R) (TID-19651)
strontium and strontium-90 concentrations in brown trout, 18: 16243
strontium-89 deposition in cow and goat, dietary, 16: 8505
strontium-90 content in bull, fallout, 19: 20215
synthesis of nuclei acid in rat diaphragm, effects of corticosteroids, tracer study, 16: 28802
thorium distribution in rat, after single inhalation of thorium chloride and citrate aerosols, 17: 23042
toxic effects of uranyl nitrate on rat myocardium, 19: 14980
tritium-labeled-albumin penetration in toad, space accessible to, 19: 35918
uptake and distribution of phosphorus-32 and strontium-89 given in trachea, 16: 4026
uptake of neutral red by frog sartorius, effects of heavy water on, 20: 5317
uptake of phosphorus-32-labeled Endoxan and thio-TEPA by rat, 20: 45315
uptake of tritium-labeled prostaglandin E_1 by rat, 19: 6965
use of myographic signals for control functions, study of feasibility of, 19: 46459 (CONF-640508, pp 100-57)
xenon equilibrium distribution and uptake by, in dog, 16: 7389
yttrium-90 localization in rabbit, injected, 17: 21405
zinc content in human, 16: 20098
zinc distribution and turnover in, in rats, tracer study, 17: 10275
zinc-65 uptake and distribution in, of sheep, 16: 28712 (HW-SA-2338)
zinc-65 metabolism in rabbit, 18: 43190
zinc-65 uptake and retention by rat, 18: 36933
zinc-65 uptake and distribution in human, 19: 17480
zinc-65 uptake and distribution in normal and tumorous, in man, 19: 43699
zinc-65 uptake by chicken, dietary effects on, 19: 14962
zinc-65 uptake by rat, effects of dietary copper, molybdenum, and zinc on, 19: 35915
zirconium-95 distribution in rabbit, after intravenous injection, 19: 27939
fats—muscles, determination of fractional composition by x-ray beam attenuation measurements, 20: 3885 (ORNL-IIC-5, pp 277-89)

MUSCOVITES

age determination of Blue Ridge and Piedmont, by rubidium–strontium method, 16: 19165
age estimation of Surinam, using isotopic ratio measurements, 20: 33535
argon-40 activation energy in, 19: 20166
etching of monocrystalline, thermal stability of uranium fission products in chemical, 20: 40889
fission fragment tracks in, characteristics of, 18: 10411
radiation effects on electric conductivity, 16: 22659
radiation effects on crystal structure of, fission-product, 19: 28378
rubidium-85/87 ratios in, 17: 20211
sorptive properties for strontium, 19: 7617(R) (ORNL-3697(p.49-53))
sorptive properties for cesium, 20: 22541(T)
uranium fission fragment tracks in, 19: 22584
uranium-235 and -238 fission track measurement in, 20: 35661
uranium-235 fission tracks in, angular distribution and ranges of, 20: 35662

MUSTARD GAS

distribution of sulfur-35-labeled, in mice, 18: 4971
effects on oxygen consumption by embryonic chick intestine, protective effects of cystamine against, 20: 24937
reactions with proteins, protective effects of AET compounds against, 19: 35895
synthesis of sulfur-35-labeled, 19: 32188 (UJV-1118/64)
toxic effects on *E. coli*, recovery from lethal, 19: 19485

Mustards

see Nitrogen Mustards

Mutagenic Agents

see Mutagens

MUTAGENS

see also Mutations

chemical, genetic effects in man, 19: 36085
effects of actinomycin, 8-azoguanine, and 5-fluorouracil deoxyriboside in *Vicia faba*, 20: 6776(R) (ORNL-3853, pp 50-3)
effects of alkylating sulfonates on barley, biological, 20: 40717
effects of chemical, on *Schizosaccharomyces pombe*, genetic, 20: 1654
effects of chemical, on DNA synthesis in plants, 20: 38589(R) (EUR-2761.f)
effects of chemical, on *Escherichia coli*, 20: 38620
effects of chemical, on autogenic development of mutations in *Arabidopsis thaliana*, 20: 40709
effects of chemical, in Neurospora, 20: 40510(R) (TID-23137)
effects of chemical, on genetics of oats, 20: 10645
effects of EMS on barley seeds, 20: 22679
effects of ethyl methanesulfonate, on pea seeds, 20: 81
effects of sixteen chemical, on chromosome aberration induction in plants, 20: 40714
effects of uv light, triethylene melamine, and hydrogen peroxide on the proportion of virus-producing cells and other mutants in cultures of *E. coli*, 20: 36617
effects of various chemical, on plants, 20: 38589(R) (EUR-2761.f)
effects of 2-chloroethyltrimethylammonium chloride on plant growth, 19: 45817(R) (ORO-631, pp 145-71)
effects on DNA in *E. coli*, 20: 38620
effects on DNA of chemical, 20: 38542(T) (UCRL-Trans-10029)
effects on human cells in tissue culture, 19: 43844
effects on induction of chromosome aberrations in onion root tips, 20: 35297
effects on peas, 19: 43734
radiation effects on reaction mechanisms of hydroxylamine, uv, 20: 38574(R) (NYO-3449-1)
reactions to chemical, 20: 12564

MUTATIONS

analysis of, in 15 generations of Habrobracon, 17: 38746(R) (TID-19432)
antibiotic-resistant and virus-carrying, of *Bacillus megatherium*, 16: 32643(R) (UCRL-10211(p.9-15))
bacterial, effects of deuterium-containing media on, 16: 26675
bacteriophage-induced, of *Escherichia coli*, 18: 9812
biochemical analysis of x-radioinduced barley, 20: 45335
book: *Ionizing Radiation in Biology*, 20: 45257
breeding by, role of mutagen specificity in, 20: 32898
characteristics of *Bacillus cereus*, 17: 40550(R) (TID-19486)
characterization of Neurospora leaky and nonleaky, effects of carbon dioxide on, 20: 40624(R) (ORNL-3922, pp 52-8)
chemical induction in Ehrlich ascites and onions by arginine and cystine, 19: 26119
chemically induced, reaction mechanisms, 16: 31511
chemically induced in plants, 18: 1439
chemically induced, in maize and tomatoes, 18: 3496(R) (TID-19724)
chemically induced in barley, 18: 25182
chemically induced in rice by diethyl sulfate, 18: 38936
chemically induced in insects, 18: 43225 (ORNL-P-388)
chemically induced in barley, 19: 87
chemically induced in wheat, 19: 2161
chemically induced in yeast, 19: 2002(R) (ORNL-3700(p.63-8))
chemically induced in sugar beets, 19: 3927
chemically induced in tobacco plants, 19: 7153
chemically induced in pea plants, 19: 7043
chemically induced in plants, 19: 8728
chemically induced by diethyl sulfate in barley, 19: 8776
chemically induced in *Escherichia coli*, 19: 10839
chemically induced in *Zea mays*, 19: 15010 (BNL-7815)
chemically induced, of *Escherichia coli*, 19: 29891(R) (ANL-6971 (p.120-32))
chemically induced in Drosophila, 19: 31789(R) (ORNL-3768(p.58-63))
chemically induced in Drosophila, 19: 31888
chemically induced in Paramecium, 19: 31788(R) (ORNL-3768(p.33-57))
chemically induced in human populations, 19: 36085
chemically induced in peas, 19: 35962
chemically induced, for screw-worm fly, 19: 45950
chemically induced in *Salmonella typhimurium*, genetic analysis of pyrimidine, 19: 45878
chemically induced, of peas, 20: 81
chemically induced, of wheat, 20: 1655
chemically induced, of *Zea mays*, 20: 1656
chemically induced by ethylenimine in Chlorella, 20: 3716(T) (JPRS-31514, pp 65-76)
chemically induced in peas, 20: 5238
chemically induced in presoaked Arabidopsis seeds, 20: 5357
chemically induced in Saccharomyces, for radioresistance, 20: 5360
chemically induced in red clover, 20: 5491
chemically induced in oats, use in crop improvement, 20: 10645
classification in Saccharomyces, 20: 40582(R) (ORNL-3922, pp 65-8)
comparison of chemical and radioinduced, in *Schizosaccharomyces pombe*, 19: 26035
comparison of chemically and radioinduced, in *Act. antibioticus*, 19: 26023
comparison of radio- and chemically-induced, in barley, 18: 11732
complementation and recombination in pyrimidine-3 heteroalleles of

Neurospora crassa, 16: 12858
complementation and recombination in Neurospora, 18: 13394
conference on radioinduced mutagenesis, Erwin–Baur Memorial Lectures, II, German Academy of Science at Berlin, June 6 to 10, 1961, 17: 40552
conference on somatic, 18: 21904
detection in first generation plants of *Arabidopsis thalia* grown from mutagen-treated seed, 20: 40513
detection in plants, methods for, 19: 45737
developmental effects of euploid and near-euploid, on Drosophila, 16: 26789
developmental effects of, in *Drosophila melanogaster*, 18: 7
E. coli T5 resistance, absence of segregation in light-induced, 19: 10870
effectiveness in phage kappa, 17: 35383
effects of arginine, cysteamine, and cysteine on, in carcinomas and plants, 19: 17481
effects of chemicals and radiations on, in *Pisum sativum*, 20: 35269
effects of chemisterilants on *Neurospora crassa*, 18: 15868
effects of desiccation in, 18: 36938
effects of ethylenimine on *Drosophila melanogaster*, comparison of x rays with, 19: 14944
effects of ethylenimine and radiations on variability induction in gibberellin-producing strains of *F. moniliforme*, 20: 32991
effects of ethylenimine and ethyl methanesulfonate on chlorophyll, in peas, 20: 36621
effects of ethylenimine and methanesulfonic acid on chlorophyll and morphological, in pea varieties, 20: 36624
effects of extragenic factors on, in maize, 16: 31509
effects of heavy water on *Escherichia coli*, 19: 42234
effects of incorporated carbon-14 on, in *Drosophila melanogaster*, 19: 38400
effects of incorporated carbon-14, phosphorus-32, and sulfur-35 on, in adenine-dependent yeast, 20: 33000
effects of incorporated phosphorus-32 on, in adenine-dependent diploid yeast, 20: 32999
effects of irradiated DNA on, in *Drosophila melanogaster*, 19: 38413
effects of phosphorus-32 on development of, in cotton plants, 19: 19580
effects of sex-linked, on biological characteristics of mouse population, 20: 42837(R) (ANL-7136, pp 124-40)
effects of somatic, on aging, 18: 23165 (BNL-854)
effects of storage on Drosophila spermatozoa, 18: 33273(R) (NIRS-2(p.42-8))
effects of subcritical temperatures and ultraviolet radiation on, in yeasts, 17: 37088
effects of various mutagens in increasing proportion of virus-producing cells and other *E. coli*, 20: 36617
effects of water-d_2 on replication of western equine encephalitis virus, 20: 39
effects on enzymes and proteins, 20: 38542(T) (UCRL-Trans-10029)
effects on origin of radioinduced tumors, hypothesis of, 19: 17555
effects on radioinduced aging in Campanularia and Drosophila, 18: 27119
effects on ultraviolet and proflavine resistance in *E. coli*, 18: 15844
extrachromosomal, induced in yeast by ultraviolet radiation, 16: 16222
formation of, role of metabolic processes in, 17: 7699
frequency in BaLB and C57B mice, use in determining genetic radiosensitivity of, 19: 33832
frequency of chemical and radioinduced, in wheat seeds, 17: 38689
frequency of chemical and radioinduced, in maize seeds, 17: 38690
genetic analysis of chemically and ultraviolet induced, of *Schizosaccharomyces pombe*, 20: 1654
genetic code for messenger ribonucleic acid for induction of, 19: 40296 (TID-21856)
genetic codes in, 18: 15805
genetic effects on direction and frequency of radioinduced, affecting cell division in yeast, 16: 7435
genetic factors in *Neurospora crassa*, 17: 19764
genetic factors in animal and plant, 20: 26655(R) (NP-15975)
genetic studies of, 19: 21809
human load of, 19: 43642(R) (NYO-2280-8)
in *Arabidopsis thaliana*, induction by x radiation and chemical mutagens, 17: 33502
in *Aspergillus fumigatus*, 17: 26978
in bacteria, effects of natural radiation, 16: 8609
in bacteria induced by ultraviolet radiation, modification by basic dyes, 16: 7448
in barley seeds, 16: 7413 (BNL-675(p.128-57))
in carcinogenesis, inherited and somatic, 16: 25106
in cells, effects of irradiated DNA on, 17: 40564
in *D. melanogaster* males, effects of carbon-14- and tritium-labeled DNA precursors on, 17: 10401
in Drosophila, effects of asynapsis, 16: 16203
in Drosophila populations, 17: 26977
in *Escherichia coli*, galactose, 17: 26980
in Habrobracon, induced by ethyl methanesulfonate and nitrogen mustard, 16: 31406
in irradiated and nonirradiated maize, variations in polygenic, 16: 28766 (RT/BIO(62)49)
in maize, analysis, 17: 28765
in man, 19: 28062
in man, radiation dose necessary to double natural rate, 16: 8550(T) (JPRS-11901)
in mice, rate of natural, 18: 19483(R) (TID-20391)
in microorganisms, effects of peroxides, 17: 24984
in mycobacterium, effects of atom decay and beta radiation on, 16: 7434
in oats grown from irradiated seed, 16: 1515
in *Pinaceae* induced by chemicals and radiation, 17: 19804 (BNL-6896)
in plants, applications in plant breeding programs, 16: 31513
in plants, applications in plant breeding programs, 18: 1439
in plants, induction and use in crop improvement, 16: 31508
in potatoes, anatomic and genetic response of somatic, to x radiation, 17: 33721
in *Salmonella typhimurium*, 18: 4
incidence of x-radioinduced chlorophyll, in diploid and polyploid wheat species, 20: 45395
induced by acridine mustard, molecular moiety causing, 19: 31788(R) (ORNL-3768(p.33-57))
induced by alkylating sulfonates in barley, 20: 40717
induced by chemicals in *Bacillus subtilis*, 20: 26688
induced by chemicals in Neurospora, 20: 40510(R) (TID-23137)
induced by chemicals, in Drosophila, 20: 40706
induced by chemicals in plants, effects of exogenous factors on, 20: 40709
induced by EDTA in Drosophila, 20: 40707
induced by ethyl methanesulfonate in plants, 20: 40710
induced by ethyl methanesulfonate in barley, use for hybridization breeding, 20: 40712
induced by exogenous desoxyribonucleic acid in Drosophila, 19: 38408
induced by irradiated DNA in Drosophila, 19: 10910
induced by irradiated food, in Drosophila, 20: 8665
induced by nitrogen mustard in Drosophila, 16: 28680
induced by nitrosomethylurea in Anacystis pigments, 20: 28958
induced by radiation and other environmental agents, discussion, 18: 35383
induced by space flight, in Drosophila, 17: 35279(T) (FTD-MT-62-78 (p.303-24))
induced by space flight, in Drosophila, 17: 35280(T) (FTD-MT-62-78 (p.324-9))
induced by space flight in fungi and higher plants, 17: 35281(T) (FTD-MT-62-78(p.329-44))
induced by sulfonate in maize, 19: 19527
induced by triethylenemelamine during mitosis in Paramecium, 20: 40632(R) (ORNL-3922, pp 175-91)
induced by ultraviolet radiation in *Escherichia coli*, 16: 31512
induced by ultraviolet light in fungi, 17: 17697
induced by wild-type recombinants in *Salmonella typhimurium*, 17: 1196
induced in algae, delayed and persistent expression of, 20: 16294
induced in barley by chemicals, neutrons, and x radiation, viable, 16: 17469
induced in barley by methanesulfonates and x radiation, comparison of, 18: 3543
induced in barley by diethyl sulfate and radiation, 20: 14384
induced in barley by chemical agents and gamma radiation, 20: 22656
induced in barley and wheat by chemical agents, 20: 22658
induced in barley by EMS, 20: 22679
induced in Drosophila, by tritiated thymidine, 18: 17521
induced in Drosophila by water-d_2, 19: 2015(T)
induced in Drosophila 2nd chromosomes by DNA feeding, 19: 45876
induced in Drosophila by aromatic compounds, 20: 22667
induced in *E. coli* by dyes and light, 19: 31670(R) (NIRS-3(p.19-56))
induced in *E. coli* by water-d_2 for phage resistance, 20: 31033(R) (NASA-CR-59196)
induced in *E. coli* by tritium decay, 20: 31033(R) (NASA-CR-59196)
induced in maize, comparisons of radiation- and chemical-, 20: 45361 (TID-22622)
induced in mice by DNA, methods for testing, 20: 40627(R) (ORNL-3922, pp 84-8)
induced in neurospora by ethylmethyl sulfonate and nitrous acid, mechanism of, 17: 35453(R) (TID-19287)
induced in Neurospora by methanesulfonate, 20: 40632(R) (ORNL-3922, pp 175-91)
induced in Neurospora by diethyl- and dimethylnitrosamine, 20: 40632(R) (ORNL-3922, pp 175-91)
induced in peas by oxygen and x rays, comparison of, 19: 35960

induced in peas by oxygen and x rays, segregation in, 19: 35961
induced in peas by ethylenimine, frequency and spectra of, 20: 22657
induced in phage by ultraviolet reactivation, 20: 24899
induced in rice by ethylenimine, 19: 7140
induction by chemicals, review, 16: 14480(T) (JPRS-13373(p.94-119))
induction by chemicals in maize, reaction mechanisms of, 20: 40708
induction by diethyl sulfate and gamma radiation in seeds, 16: 1580
induction by dinitrophenol in *Vicia faba*, 20: 42913
induction by nitrogen mustard in mice, 16: 5207
induction by nitrous acid and ultraviolet in Aspergillus, 17: 31893
induction by phosphorus-32, review on, 18: 35332
induction by x radiation or nitrogen mustard in Drosophila, 17: 27099
induction in bacteria by ultraviolet light, reaction mechanisms, 16: 7449
induction in bacteriophages, molecular mechanisms for, 20: 38542(T) (UCRL-Trans-10029)
induction in barley seeds by gamma rays, sulfates, and sulfonates, 16: 1588
induction in crop plants, applications in plant breeding programs, 16: 31515
induction in Drosophila by irradiated DNA and food, 20: 6848
induction in Drosophila by irradiated DNA, 20: 6849
induction in Drosophila by irradiated food, 20: 6850
induction in endosperm and seedlings of maize by diepoxybutane and x irradiation, 16: 1602
induction in *Escherichia coli*, synergistic effects of caffeine and ultraviolet radiation, 17: 1294
induction in *Hemophilus influenzae*, 16: 25152(R) (TID-16075)
induction in *Lakon durum* by alkylating chemicals, 20: 33064
induction in *Neurospora crassa*, spectra of allelic complementation and leakiness in chemical, spontaneous, and radiation, 19: 8862
induction in plants by extracts from irradiated plants, 16: 6318(T) (JPRS-11322(p.463-7))
induction in polyploids by seed irradiation, effects of diplontic selection on frequency and spectrum, 17: 1592
induction in rice seeds by chemicals and radiation, 16: 1608
induction in *Schizosaccharomyces pombe* by *N*-nitroso-*N*-methyl-*N'*-nitroguanidine, *N*-nitroso-*N*-methylurethane, nitrous acid, and uv light, 19: 42266
induction in vegetatively propagated plants by natural selection and irradiation, 16: 31514
induction of chlorophyll, in *Vicia sativa*, by chemical mutagens and x rays, 20: 45476
induction of *E. coli*, role of DNA in, 20: 42838(R) (ANL-7136, pp 140-54)
induction of isoleucine- and valine-requiring, in *E. coli*, 19: 15083
isolation by cycloserine, 19: 31790(R) (ORNL-3768(p.85-8))
isolation of ploidy, of Ehrlich ascites tumors of mice, 19: 10725
isolation of Pseudomonas, 20: 26682
mechanism for uv-induced, in *E. coli*, 20: 42918
mechanisms for, in Neurospora, 18: 35262(R) (TID-20914)
mechanisms for, review of chemical, radiation, and spontaneous, 19: 184
natural and artificially induced, in maize, 18: 3499 (TID-19787)
natural and induced, review on, 17: 19912
nonchromosomal genetic system for, in algae, 19: 42212 (NYO-3424-1)
occurrence in unirradiated ovicell chromosomes of Drosophila fertilized by irradiated male gametes, 16: 1490(T) (JPRS-10170(p.373-86))
of bacteriophage T_4, radiosensitivity and thymine dimerization in, 18: 38812
of Drosophila, 18: 27018(R) (TID-20714)
of *E. coli* radiosensitivity gene, 18: 15846.
of *Escherichia coli*, induced by ethylmethanesulfonate or ultraviolet radiation, 17: 38789
of *Escherichia coli*, filamentous forms, 19: 33852
of kappa in *Paramecium aurelia*, 19: 19464
of mice, rate for sex-linked recessive lethals in, 18: 17466(R) (ANL-6790(p.84-6))
of *Micrococcus radiodurans*, radiosensitivity of, 19: 24324
of *Neurospora crassa*, 19: 21772(R) (TID-21709)
of Neurospora, enzymatic and antigenic properties of proteins in, 19: 2002(R) (ORNL-3700(p.63-8))
of *Ophiostoma multiannulatum*, genetic influence on the back-mutation rate, 17: 1191
of *Paramecium aurelia*, 17: 26979
of sorghum induced by gamma radiation or colchicine, 18: 25130
of wheat induced by gamma radiation or ethyleneimine, 18: 17594
photoreversal of uv-induced, in *E. coli*, 20: 42812
plastid development and chlorophyll production in Chlorella, 18: 23196(R) (ANL-6823(p.161-4))
processes for production of, in mice, 19: 21807
processes in natural and radioinduced, limitation of action of, 16: 4103
production by radiomimetic agents in T2 coliphage, 17: 33717
production in *Drosophila melanogaster* by *N*-nitroso-*N*-methylurethan, *N*-nitrosomorpholine, and x rays, 18: 27097
production in *Escherichia coli* by *N*-nitroso-*N*-methylurethan and x rays, 18: 27098
production of asporogenic, by *Bacillus cereus* and *B. subtilis*, 20: 1582(R) (NYO-2038-2)
properties of spontaneous actinophage C52, 20: 32899
proton tunneling effects on, 19: 42235
radiation and chemical effects on frequency of, in dormant rice seed, 19: 8855
radiation and chemical effects on, in *B. subtilis* isolated DNA, 19: 19542
radiation and chemical effects on *E. coli*, mechanism of, 19: 33912
radiation and formaldehyde effects on Drosophila, x, 18: 11728
radiation dose-rate and fractionation effects on, in mice, 18: 3569
radiation effects on mutability of polygenes, 16: 4032(R) (TID-13959)
radiation effects on, in *Neurospora crassa*, 16: 16191
radiation effects on, in *Neurospora crassa* exposed to nitrogen mustard, 17: 10455
radiation effects on *Neurospora crassa*, visible and x-ray, 17: 15652
radiation effects on, in man, 17: 15665
radiation effects on, biophysics of, 17: 15701
radiation effects on, in man, 17: 19908
radiation effects on occurrence of sex-linked, recessive, lethal, in Drosophila, 17: 19914
radiation effects on spectra of butterfly somatic, effects of temperature on, 17: 23206
radiation effects on *Drosophila* sperm frequency of, effects of cyanide and dose rate on, 17: 24901
radiation effects on, in X_1 and X_3 *Vicia faba* L., chemical and, 17: 28648
radiation effects on rate of, in Drosophila sperm, 17: 31895
radiation effects on occurrence frequency of, 17: 31936
radiation effects on rate of, 17: 38806
radiation effects on frequency and type of wheat seed, ultraviolet and x-ray, 17: 40588
radiation effects on yeast, mechanism for x, 18: 5054
radiation effects on *Nicotiana tabacum*, thermal-neutron, 18: 9852
radiation effects combined with methylated purines on synergism in *E. coli*, uv and x, 18: 9863
radiation effects on Ophiostoma, effects of oxygen on uv, 18: 9918
radiation effects on sorghum, x, 18: 13534
radiation effects on, in rats, 18: 25215(T) (AEC-tr-6227/1(p.25-44))
radiation effects on frequency of recessive lethal, in *Drosophila melanogaster*, combined x and ultraviolet, 18: 29272
radiation effects on frequency patterns of Drosophila, x, 19: 109
radiation effects combined with chemicals on, of rice seed, 19: 8854
radiation effects on genetic increase of, in Drosophila populations and plants, 19: 15113
radiation effects on reversion of yeast, uv, 19: 15127
radiation effects on, in female and male *Drosophila melanogaster* mature sperm, 19: 15085
radiation effects on animal mature sperm, RBE of fast neutron, gamma, proton, and x-ray, 19: 17607
radiation effects combined with formaldehyde or hydroxylamine on induction of inverse, in *E. coli*, 19: 17613
radiation effects on, in rye grass seed, 19: 17527
radiation effects on *Chlorella vulgaris*, protective effects of chemicals against, 19: 17688
radiation effects on, in maize, 19: 17569
radiation effects on chlorella, 19: 28080
radiation effects on somatic, in tulip bulb flowers, 19: 31859
radiation effects on, in tulips, 19: 31877
radiation effects on wheat, fast neutron and gamma, 19: 36061
radiation effects on bacteriophage, gamma and x, 20: 80
radiation effects on reversion of white-ivory, in Drosophila, x, 20: 10693
radiation effects on, in *D. melanogaster* gonads, 20: 12637 (TID-21466)
radiation effects on frequency of, in inseminated and virgin Drosophila females, x, 20: 12663
radiation effects on plants, 20: 20360(R) (PRNC-73)
radiation effects on rate of mouse specific locus, x, 20: 20461
radiation effects combined with 1,4-bisdiazoacetylbutane on Chlorella, uv, 20: 24900
radiation effects on rates of, at specific *Autosomal loci* in Drosophila, 20: 31108
radiation effects on Triticum, fast and fission neutron and gamma, 20: 31080
radiation effects with formaldehyde or hydroxylamine on *E. coli* back, uv, 20: 32992
radiation effects with streptomycin on frequency of, in Chlorella, x, 20: 32993
radiation effects on bacteriophage yield of virulent, direct and indirect gamma, 20: 32996
radiation effects on *Dahlbominus fuscipennis* eye color, 14-Mev neutron and gamma, 20: 33023
radiation effects on, in Sippe 50 of *Antirrhinum majus*, x, 20: 33052
radiation effects on dry *Arabidopsis thaliana* seed, gamma and heavy particle, 20: 35298

radiation effects on *Trifolium subterraneum*, second cycle x, 20: 35300
radiation effects of frequency of, in hydrated wild-type tomato pollen, x, 20: 35299
radiation effects on peas chlorophyll, fast neutron and gamma, 20: 36621
radiation effects on barley chlorophyll, effects of partial reparation on, 20: 36622
radiation effects on chlorophyll and morphological, in pea varieties, gamma, 20: 36624
radiation effects on embryonic wheat, gamma, 20: 36650
radiation effects on peas chlorophyll, fast neutron and gamma, 20: 36621
radiation effects in causing chlorophyll, in rice, mechanisms for, 20: 40641
radiation response in *Drosophila melanogaster*, gamma, 17: 31894
radio- and mutagen-induced in *Vicia faba*, x, 18: 33303
radioinduced, 16: 19211
radioinduced, 17: 13989(T) (JPRS-17819(p.1-14))
radioinduced, 19: 21922
radioinduced, 19: 33938
radioinduced, 19: 33838
radioinduced, 19: 43823
radioinduced, 20: 28864(R) (NP-15976)
radioinduced Anacystis pigment, uv and x, 20: 28958
radioinduced and chemically induced in the moth Ephestia, reaction mechanisms in, 17: 31856(R) (TID-19166)
radioinduced and chemically induced in *Escherichia coli*, effects of growth factors on, 17: 33458(R) (ANL-6723(p.138-9))
radioinduced and chemically induced, in durum wheat, 18: 23320
radioinduced and chemically induced, in oats, 18: 25184
radioinduced and chemically induced in Drosophila, 19: 2069(R) (ORNL-3700(p.58-62))
radioinduced and spontaneous, in rhizobial plants, 17: 15649
radioinduced and spontaneous, in hamster lung cells in tissue culture, 18: 17468(R) (ANL-6790(p.156-60))
radioinduced and spontaneous, in Drosophila, 18: 27004(R) (ORNL-3601(p.47-59))
radioinduced and spontaneous, in mice, 19: 29891(R) (ANL-6971 (p.120-32))
radioinduced antibiotic-resistant, of *Staphylococcus aureus*, 19: 19531
radioinduced antibiotic-resistant, of *Staphylococcus aureus*, 19: 19532
radioinduced Aspergillus, gamma, 18: 13509
radioinduced barley, x, 20: 12714
radioinduced biochemical, of duckweed, 17: 37063(R) (NYO-10616)
radioinduced biochemical, in Arabidopsis, 20: 42900
radioinduced, book 16: 32827
radioinduced by irradiation of males, in Drosophila, 16: 25192
radioinduced by medical diagnosis, 18: 39007
radioinduced by strontium-90 in *Chlorella algae*, 18: 36946 (A/CONF.28/P/386)
radioinduced by tritium in mice, 16: 9881
radioinduced carcinogenesis model using multistage somatic, 18: 41108
radioinduced Chlorella, uv, 20: 8648
radioinduced chromosomal, effects of hypothermia in mice on x, 20: 12693
radioinduced, chronic vs. acute gamma, 18: 3570
radioinduced compact, of apple trees, 19: 35985
radioinduced crop, in Japan, 18: 13484
radioinduced *Digitalis lanata EHRH* following seed exposure, 19: 43746
radioinduced dominant, effects on mouse skeleton, 19: 24290
radioinduced dominant lethal, in mouse spermatogonia, 19: 38394
radioinduced dominant lethal, in mouse spermatozoa, effects of dose on x, 20: 18351
radioinduced, dose for doubling frequency of, 17: 38875
radioinduced Drosophila, x, 19: 15130
radioinduced *E. coli*, photoreactivation of uv, 19: 31788(R) (ORNL-3768(p.33-57))
radioinduced, economic significance and genetic basis, 16: 8542(R) (TID-14829)
radioinduced, effects of dose rate, 16: 58
radioinduced, effects of AET, 16: 4094
radioinduced, effects of meiotic stage and species, 17: 19874
radioinduced, effects of dose rate and exposure time on, 17: 25019
radioinduced, effect on viability, in Drosophila, 17: 28748
radioinduced, effects of dose fractionation on x, 17: 38766
radioinduced, effects of heat following irradiation on frequency of, 17: 38876
radioinduced, effects of DNA molecule alterations in, 17: 40554
radioinduced extrachromosomal factor, in yeast, 20: 8628 (COO-1249-3)
radioinduced eye color, in male progeny of irradiated Dahlbominus females, γ, 20: 12691
radioinduced for histocompatibility in mice, x, 20: 6828
radioinduced, for solid stem in Triticum, 18: 3520
radioinduced, for wheat rust resistance, neutrons and x, 17: 39362
radioinduced, gamma, thermal neutron, x, 17: 30055
radioinduced, genetic variability in maize and wheat, 16: 32735(R) (TID-16979)
radioinduced histidine-dependent, biochemical and genetic analysis of *Staphylococcus aureus* for, 19: 42256
radioinduced host-range, in T2 bacteriophage, gamma, 18: 33297
radioinduced in actinophages, mechanisms for uv, 19: 15124
radioinduced in *Actinomyces coelicolor*, coelicomycin production in uv, 19: 17570
radioinduced in *Acer negundo*, 19: 45865
radioinduced in Actinomyces for tetracycline production, gamma, 20: 24935
radioinduced in AD-3 region of *Neurospora crassa* kinetics of, 19: 15153
radioinduced in *Aedes aegypti*, gamma, 19: 88
radioinduced in agricultural plants, 18: 13453(R) (TID-20220)
radioinduced in alfalfa, morphology of single-leaf, 17: 21499
radioinduced in algae, 19: 45842
radioinduced, in animals, relation of dose to, 17: 38848
radioinduced in animals and plants, 17: 40553
radioinduced in animal cells in culture, 19: 25941
radioinduced in animal cells in tissue culture, 19: 42317
radioinduced in animals, review, 19: 45973
radioinduced in animals and plants, fast neutron, 20: 1622 (WT-820)
radioinduced in apple trees, fast neutron and γ, 20: 38692
radioinduced, in Arabidopsis, 17: 35590
radioinduced in *Arabidopsis thaliana*, 19: 19548
radioinduced in Arabidopsis, x, 19: 28010
radioinduced in *Arachis hypogea*, review, 19: 43779
radioinduced in Arabidopsis seeds, x, 20: 5357
radioinduced in *Arachis hypogaea* peanuts, 20: 16247
radioinduced in *Aspergillus terreus*, 17: 14009
radioinduced in Aspergillus, 17: 15679
radioinduced in *Aspergillus nidulans*, 18: 71
radioinduced in Aspergillus, environmental modification of frequencies of, 18: 19724
radioinduced in asparagus, 18: 33323
radioinduced in *Aspergillus oryzae*, uv, 18: 43287
radioinduced in *Ascobolus immersus*, uv and x, 19: 111
radioinduced in Aspergillus, characterization of uv, 20: 3755(T)
radioinduced in Aspergillus, uv, 20: 3756(T)
radioinduced in Aspergillus, uv, 20: 26680
radioinduced in *B. subtilis* and transforming DNA, uv, 20: 24860
radioinduced in bacteria with greater radioresistance, 16: 10361 (AECL-1329(p.48-55); AECL-1208)
radioinduced in barley seedlings, 16: 1572
radioinduced in barley seeds, 16: 28775
radioinduced in barley, 17: 2835(R) (TID-17307)
radioinduced, in barley seeds, scoring of, 17: 33720
radioinduced in barley, 18: 8112(R) (TID-19964)
radioinduced in *Bacillus subtilis*, ultraviolet, 18: 9878
radioinduced in bacteria, uv and x, 18: 17486
radioinduced in *Bacillus subtilis*, ultraviolet, 18: 19753
radioinduced in barley, 18: 25176
radioinduced in barley, 18: 25182
radioinduced in bacteria, beta, 18: 27121
radioinduced in barley, effects of development stage on, 18: 38834
radioinduced in barley, gamma, 19: 87
radioinduced in bacteriophage, uv, 19: 2110
radioinduced in barley seedlings, characteristics of, 19: 8856
radioinduced in barley pollen grains, strontium-90, 19: 10761
radioinduced in bacteriophage T4, theory of marker stimulation of crossing over of, 19: 15086
radioinduced in bacteriophage, ultraviolet, 19: 21901
radioinduced in bacteriophage, 19: 24264(T) (JPRS-29606)
radioinduced in bacteriophage, 19: 28098
radioinduced in bacteriophage, 19: 28099
radioinduced in barley seeds, gamma, 19: 27996
radioinduced in bacteria, 19: 31807
radioinduced in barley, 19: 36122
radioinduced in barley seed, protective effects of aminoethylisothiuronium against, 19: 36105
radioinduced in barley, γ, 20: 8696
radioinduced in bacteria, effects of spermine on rate of uv, 20: 8687
radioinduced in barley, effects of ethylenimine on γ, 20: 14334
radioinduced in barley seed, x, 20: 18411
radioinduced in barley, use in plant breeding programs of x, 20: 18418
radioinduced in bacteriophage, uv and x, 20: 22765
radioinduced in bacteriophage, uv and x, 20: 22767
radioinduced in barley and wheat, fast-neutron and gamma, 20: 22658
radioinduced in barley, x, 20: 22679
radioinduced in bacteriophage, uv and x, 20: 22766
radioinduced in *Bacillus subtilis*, uv, 20: 26688
radioinduced in barley, oats, and wheat, γ and neutron, 20: 28960
radioinduced in bacteriophage, uv, 20: 28969

radioinduced in barley and rice seeds, *y* and x, 20: 31050
radioinduced in bacteriophage T4, uv, 20: 36636
radioinduced in barley, effects of dose fractionation on x, 20: 40701
radioinduced in barley, selection in first generation plants, x, 20: 40711
radioinduced in barley, use for hybridization breeding, 20: 40712
radioinduced in barley, x, 20: 40717
radioinduced in barley, x, 20: 45464
radioinduced in barley seeds, uv, 17: 35539
radioinduced in bees, 18: 13447(R) (NYO-2315-1)
radioinduced in bean plants, 18: 27017(R) (TID-20708(p.42-51))
radioinduced in beans, use in plant breeding program, 19: 33786(R) (NYO-2043-108(p.33-43))
radioinduced in beans and soybeans, *y*, 20: 6797(T) (JPRS-33170, pp 240-8)
radioinduced in beans and soybeans, use in plant breeding programs, 20: 18419
radioinduced in beans by gamma radiation, 20: 42850(R) (NYO-2043-130)
radioinduced in blue-green algae, ultraviolet, 20: 35256
radioinduced in blue-green algae, uv, 20: 35257
radioinduced in bread wheat, frequency and spectrum of beta, neutron, and x, 18: 9853
radioinduced in bud-grafts of fruit trees by internal irradiation, 16: 1604
radioinduced in buckwheat, 18: 41189
radioinduced in buckwheat, gamma, 20: 22665
radioinduced in cabbage seed by gamma and x rays, 17: 35527
radioinduced in carnations, gamma, 18: 33302
radioinduced in carnations, gamma, 19: 24330
radioinduced in cereals, flowers, and fruits for breeding, 19: 7147
radioinduced in chrysanthemums, 16: 9851(T) (NP-tr-848)
radioinduced in *Chlamydomonas reinhardi* by ultraviolet light, 16: 20203
radioinduced in *Chondrococcus columnaris*, 17: 5769 (HW-SA-2540)
radioinduced in chrysanthemum, 17: 23112
radioinduced in *Chironomus tentans*, 17: 33585
radioinduced in *Chironomus tentans* population exposed to chronic low-level radiation environment, 18: 8108 (ORNL-3531)
radioinduced in *Chlorella vulgaris*, 18: 17581
radioinduced in chrysanthemum, x, 19: 5646
radioinduced in chrysanthemum, x, 19: 5653
radioinduced in chickens, 19: 7087
radioinduced in *Chrysanthemum carinatum*, 19: 17534
radioinduced in *Cholera vibrio*, streptomycin resistance of hard and soft x-ray, 19: 17547
radioinduced in Chlorella, x, 20: 3716(T) (JPRS-31514, pp 65-76)
radioinduced in Chlorella, uv, 20: 3716(T) (JPRS-31514, pp 65-76)
radioinduced in Chlorella, beta and x, 20: 22674
radioinduced in Chlorella, y, 20: 38605
radioinduced in Cicer, 18: 21869
radioinduced in *Cl. perfringens*, 19: 38445
radioinduced in *Cl. perfringens*, 19: 38446
radioinduced in Collinsia, 16: 21944
radioinduced in coffee plants, 17: 15565
radioinduced in cotton, tobacco, and wheat, evaluation of use in breeding of macro- and micro-, 17: 38688
radioinduced in cotton seed, 18: 33313
radioinduced in cotton, 18: 41116
radioinduced in cosmos plants, 18: 41117
radioinduced in *Cosmos bipinnatus*, gamma and x, 19: 21912
radioinduced in cotton plant, *y*, 20: 6794(T) (JPRS-33170, pp 217-25)
radioinduced in *Corchorus olitorius*, 20: 18385
radioinduced in cotton, beta, 20: 22664
radioinduced in cotton, 20: 24897
radioinduced in cotton species *Gossypium barbadense*, gamma and thermal neutron, 20: 36623
radioinduced in *Crotalaria intermedia*, 18: 36994
radioinduced in cultivated rise, 19: 17533
radioinduced in cytosine–guanine in DNA, mechanism of, 18: 21872
radioinduced in *Cyathodium tuberosum*, x, 19: 45901
radioinduced in dallisgrass, 18: 8193
radioinduced in Datura, 18: 13523
radioinduced in Dahlbominus oogonia, gamma and x-ray, 19: 38392
radioinduced in Delphinium, 17: 19763
radioinduced in different wheat varieties, phylogenetics of, 19: 26047
radioinduced in dormant rice seeds, 16: 30253
radioinduced in Drosophila, effects of cytochrome c oxidase on, 16: 9870
radioinduced in Drosophila, 16: 11427 (A/AC.82/G/L.734)
radioinduced in *Drosophila melanogaster*, 16: 12883(R) (TID-15001)
radioinduced in Drosophila, 16: 14515
radioinduced in Drosophila, spermatogonia and spermatozoa, 16: 1527
radioinduced in Drosophila, effects on rate at specific autosomal loci, 16: 1465(R) (TID-13638)
radioinduced in *Drosophila melanogaster*, 16: 1489(T) (JPRS-10170 (p.361-72))
radioinduced in Drosophila, 16: 16201
radioinduced in Drosophila, 16: 16202
radioinduced in Drosophila, 16: 16204
radioinduced in Drosophila, 16: 20175
radioinduced in Drosophila, 16: 20176
radioinduced in Drosophila, 16: 21942
radioinduced in Drosophila, 16: 21945
radioinduced in Drosophila, doubling dose for, 16: 25210
radioinduced in Drosophila, 16: 26737(R) (TID-16026)
radioinduced in Drosophila, 16: 28680
radioinduced in Drosophila, 16: 28746(R) (TID-16428)
radioinduced in Drosophila, 16: 28789
radioinduced in Drosophila, 16: 7455
radioinduced in Drosophila, 17: 74
radioinduced in Drosophila, 17: 1236(R) (TID-17000)
radioinduced in Drosophila, 17: 1237(R) (TID-17001)
radioinduced in Drosophila, 17: 1238(R) (TID-17002)
radioinduced in Drosophila, 17: 1239(R) (TID-17003)
radioinduced in Drosophila oocytes, effects of gases on lethal, 17: 7886
radioinduced in Drosophila, 17: 15681
radioinduced in Drosophila, 17: 19838
radioinduced in Drosophila, beta, 18: 74
radioinduced in Drosophila, protective effects of 2,4-dinitrophenol against, 18: 3594
radioinduced in Drosophila, effects of AET on rate of, 18: 3597
radioinduced, in Drosophila, 18: 5118
radioinduced in Drosophila, 18: 6618(R) (TID-19899)
radioinduced in Drosophila, silkworms, Salmonella, wheat, and rice, 18: 8046(R) (NP-13507)
radioinduced in Drosophila, 18: 8156
radioinduced in Drosophila spermatogonia, dose-frequency response of, 18: 9860
radioinduced in Drosophila, review of x, 18: 11733
radioinduced in *Drosophila melanogaster*, effects of anoxia on fast neutron, gamma, and x-ray, 18: 11831
radioinduced in Drosophila germ cells, effects of fractionation and intensity on gamma, 18: 11838
radioinduced in *Drosophila melanogaster*, affects of chloramphenicol, penicillin, and streptomycin on, 18: 11886
radioinduced in Drosophila germ cells, effects of chloramphenicol, dinitrophenol, nitrogen, oxygen, and ribonuclease on, 18: 11887
radioinduced in Drosophila, 18: 17520
radioinduced in Drosophila, dose-rate effects on, 18: 19646
radioinduced in Drosophila, effects of, on viability of populations, 18: 27135
radioinduced in Drosophila, 18: 27136
radioinduced in Drosophila, effects of arginine on, 18: 33371
radioinduced in Drosophila and *E. coli*, protective effects of AET, cysteine, and serotonin against, 18: 35401
radioinduced in *Drosophila melanogaster* by small doses, 18: 36946 (A/CONF.28/P/386)
radioinduced in Drosophila, protective effects of sulfhydryls against x, 18: 36987
radioinduced in *Drosophila melanogaster* during space flight, 18: 41129
radioinduced in Drosophila, uv, 18: 43256
radioinduced in Drosophila, x, 19: 8848
radioinduced in Drosophila, 19: 10790(R) (TID-21601)
radioinduced in Drosophila, 19: 10791(R) (TID-21608)
radioinduced in Drosophila, 19: 10840
radioinduced in Drosophila, 19: 10841
radioinduced in Drosophila, 19: 10842
radioinduced in Drosophila, 19: 10843
radioinduced in Drosophila, 19: 10822
radioinduced in Drosophila, 19: 12998
radioinduced in Drosophila, 19: 12999
radioinduced in Drosophila spermatozoa, gamma, 19: 15131
radioinduced in *Drosophila melanogaster*, effects of actinomycin D on frequency of, 19: 15084
radioinduced in Drosophila, comparison of external gamma and internal carbon-14, 19: 17606
radioinduced in Drosophila, *Escherichia coli*, and mice, 19: 21792(R) (ORNL-3650(p.187-219))
radioinduced in Drosophila, 19: 21862(R) (NP-14937(p.93-116))
radioinduced in Drosophila, 19: 21989
radioinduced in Drosophila, 19: 28103
radioinduced in Drosophila, 19: 28062
radioinduced in Drosophila, 19: 31888
radioinduced in Drosophila, x., 19: 31670(R) (NIRS-3(p.19-56))
radioinduced in Drosophila, 19: 36003
radioinduced in Drosophila oogonia, gamma, 19: 43724 (TID-22160)
radioinduced in Drosophila, effects of dose rate on, 19: 43785
radioinduced in Drosophila, 19: 43787
radioinduced in Drosophila, 19: 45949
radioinduced in Drosophila 2nd chromosomes, x, 19: 45876

radioinduced in Drosophila, 17: 21514
radioinduced in Drosophila by space flight, lethal, 17: 21549
radioinduced in Drosophila, effect of maternal nutrition, 17: 27102
radioinduced, in Drosophila, 17: 28683(R) (TID-19003)
radioinduced in Drosophila, effects of oxygen and metabolic state, 17: 28710
radioinduced in Drosophila, 17: 28599(R) (TID-18979)
radioinduced in *Drosophila melanogaster*, 17: 30397
radioinduced, in Drosophila reared on irradiated medium, 17: 33747
radioinduced in *Drosophila melanogaster*, protective effects of cysteine against, 17: 35526
radioinduced in Drosophila, modifications of x, 17: 35567
radioinduced, in Drosophila, 17: 38788
radioinduced in Drosophila, effects of sulfhydryl compounds on, 20: 1619(R) (TID-22293)
radioinduced in Drosophila, effects of high temperature on x, 20: 3713(T) (JPRS-31514, pp 29-43)
radioinduced in Drosophila, effects of genotype on x, 20: 3715(T) (JPRS-31514, pp 59-64)
radioinduced in Drosophila, x, 20: 5338
radioinduced in Drosophila, x, 20: 5358
radioinduced in Drosophila, 20: 5301(R) (UR-668, pp 1-54)
radioinduced in Drosophila, effects of argon and oxygen on, 20: 6898
radioinduced in Drosophila, effects of sex on, 20: 16229(R) (NYO-1472-1)
radioinduced in Drosophila, β, γ, and x, 20: 18332
radioinduced in Drosophila, 20: 18333
radioinduced in Drosophila sperm, x, 20: 18336
radioinduced in Drosophila, x, 20: 22653
radioinduced in Drosophila spermatocytes, effects of temperature on x, 20: 22662
radioinduced in Drosophila, gamma, 20: 22667
radioinduced in Drosophila, x, 20: 22761
radioinduced in Drosophila, effects of dose on x, 20: 24893
radioinduced in Drosophila, x, 20: 26681
radioinduced in Drosophila, x, 20: 26683
radioinduced in Drosophila, 20: 28955
radioinduced in Drosophila, x, 20: 28956
radioinduced in Drosophila, x, 20: 31036(R) (SAN-529-3)
radioinduced in Drosophila, x, 20: 31047
radioinduced in Drosophila, x, 20: 31049
radioinduced in Drosophila males, effects of AET and N_2 treatment on x, 20: 33072
radioinduced in Drosophila sperm cells and spermatids, protective effects of 2,4-dinitrophenol against gamma, 20: 33079
radioinduced in Drosophila, x, 20: 38596(R) (SAN-590-1)
radioinduced in Drosophila, fast neutron, 20: 38645
radioinduced in Drosophila, x, 20: 38646
radioinduced in Drosophila, x, 20: 38650
radioinduced in *Drosophila melanogaster*, mechanisms of x, 20: 38607
radioinduced in Drosophila, x, 20: 40622(R) (NYO-3096-8)
radioinduced in Drosophila, x, 20: 40706
radioinduced in Drosophila, effects of EDTA on x, 20: 40707
radioinduced in Durum wheat, 16: 25195 (CNEN-126)
radioinduced in Durum wheat, 16: 25196 (CNEN-120)
radioinduced in *E. coli*, analysis, 16: 28788
radioinduced in *E. coli*, protective effects of chemicals against, 18: 126
radioinduced in *E. coli*, effects of AET on, 17: 40597
radioinduced in *E. coli*, blockage of DNA synthesis and photochemical modification in uv, 18: 11835
radioinduced in *E. coli*, dark repair of uv, 18: 11836
radioinduced in *E. coli*, locus of genes of, 18: 21839
radioinduced in *E. coli*, segregation of, 18: 35355
radioinduced in *E. coli*, tritium, 18: 38813
radioinduced in *E. coli*, dark repair and photoreversal to prototrophy in uv, 19: 7115
radioinduced in *E. coli*, temperature effects on x, 19: 15125
radioinduced in *E. coli*, tritium, 19: 15126
radioinduced in *E. coli*, uv and x-ray, 19: 15188
radioinduced in *E. coli*, effects of chemicals on uv, 19: 26061
radioinduced in *E. coli*, protective effects of chloride ions against gamma, 19: 26126
radioinduced in *E. coli*, relation between B and filament forming K-12, 19: 25979
radioinduced in *E. coli* phage ϕX174, x, 19: 42289
radioinduced in *E. coli*, RBE for neutron-induced reversions, 20: 29002
radioinduced in *E. coli*, genetics and physiology of uv, 20: 40629(R) (ORNL-3922, pp 94-8)
radioinduced in Ecballium, fast-neutron, 20: 8690
radioinduced in Einkorn wheat, 19: 2152
radioinduced in Einkorn wheat seeds, beta, fast neutron, gamma, and thermal neutron, 20: 20497
radioinduced in Emericellopsis, methods for assaying uv, 20: 16238
radioinduced in Ephestia, effects of developmental stage on spectra of x, 20: 42970
radioinduced in *Escherichia coli*, 16: 30274
radioinduced in *Escherichia coli*, 18: 17582
radioinduced in *Escherichia coli*, 19: 5672
radioinduced in *Escherichia coli*, 19: 7015(R) (ANL-6906(p.85-6))
radioinduced in *Escherichia coli*, 19: 8836
radioinduced in *Escherichia coli*, uv, 19: 10839
radioinduced in *Escherichia coli*, 19: 43751(T)
radioinduced in *Escherichia coli*, 19: 43794
radioinduced in *Escherichia coli*, 19: 43795
radioinduced in *Escherichia coli*, 19: 43804
radioinduced in *Escherichia coli*, 17: 10364(R) (TID-17690)
radioinduced in *Escherichia coli*, gene locus for uv, 20: 3758
radioinduced in *Escherichia coli*, gene locus for uv, 20: 3757
radioinduced in *Escherichia coli*, β, 20: 5350
radioinduced in *Escherichia coli*, photosensitivity of uv, 20: 22769
radioinduced in *Escherichia coli*, uv and x, 20: 26678
radioinduced in *Escherichia coli*, effects of temperature on uv, 20: 26679
radioinduced in extracellular *E. coli* phages, uv, 20: 22666
radioinduced in female Drosophila, effects of x ray voltage and high temperature on, 20: 3714(T) (JPRS-31514, pp 44-58)
radioinduced in fodder peas, 19: 42268
radioinduced in food-borne microorganisms, 20: 41388
radioinduced in fruit trees, 19: 2160
radioinduced in fruits, gamma, 19: 3888 (EUR-1829.f)
radioinduced in fungi, ultraviolet, 19: 24313
radioinduced in fungi, 19: 33884
radioinduced in *Funaria hygrometrica* plants, x, 20: 3781
radioinduced in gametes, maximum permissible dose from x, 20: 107
radioinduced in germ cells in mice, effects of dose rate and fractionation on, 18: 11837
radioinduced in germ cells of silkworms, effects of sex on gamma, 18: 11839
radioinduced in grasshoppers and Drosophila, 18: 9831(R) (AD-403109)
radioinduced in groundnut, 18: 21868
radioinduced in grain, effects of post-irradiation soaking and temperature changes on gamma, 20: 22779
radioinduced in Habrobracon, 16: 30237
radioinduced in hair cells of *Tradescantia occidentalis* by 650-kev neutrons and 250 kvp x rays, RBE of, 18: 1409
radioinduced in hamster cells in tissue culture, 18: 17469(R) (ANL-6790 (p.161-70))
radioinduced in Habrobracon oocytes, 17: 21513
radioinduced in herbaceous plants, 18: 43298
radioinduced in heterozygous Drosophila population, method for determining, 20: 22675
radioinduced in heterochromatinic region of *D. melanogaster*, effects of development temperature on lethal x, 20: 35272
radioinduced in Hirsutum, frequency and sites of, 18: 38775(R) (ORO-624)
radioinduced in homozygote and isogenic Saccharomyces yeast strains, ploidy effects on, 18: 33394
radioinduced in human populations, 19: 36085
radioinduced in human populations, detection, 20: 22644
radioinduced in hybrid corn, 18: 1440
radioinduced in *Hymenolepis diminuta*, review on behavior and structure of, 18: 9841
radioinduced in *Impatiens balsamina*, 16: 18789
radioinduced in insects, 18: 43225 (ORNL-P-388)
radioinduced in insects, 19: 33799
radioinduced in insects, 20: 6711(R) (ORNL-3849, pp 43-100)
radioinduced in jute plants, 16: 17480
radioinduced in jute plants, *Corchorus olitorius* and *Corchorus capsularis*, 19: 116
radioinduced in jute plants, *Corchorus olitorius* and *Corchorus capsularis*, 19: 165
radioinduced in jute, γ, 20: 16217 (AECD-AG-7)
radioinduced in jute, cytogenetic study of x, 20: 22686
radioinduced in jute plants, γ, 20: 31027 (AECD/AG-14)
radioinduced in jute, gamma, 20: 40681
radioinduced in Kappa phages, recovery from, 20: 24859
radioinduced in larvae of silkworms, 19: 43786
radioinduced in lambda phage, reactivation of uv, 20: 24899
radioinduced in *Lakota durum*, x, 20: 33064
radioinduced in leeches, 16: 28764
radioinduced in lespedeza, 16: 31488
radioinduced, in leaf plastids of *Arabidopsis thaliana*, 17: 35589
radioinduced in Luzula, frequency of x, 19: 3929
radioinduced in Lupinus, review, 19: 43776
radioinduced in Lupinus, protective effects of moisture against x, 19: 45847
radioinduced in mammals, 16: 1486(T) (JPRS-10170(p.279-312))
radioinduced in male insects, role in control of populations, 16: 16129

radioinduced in male germ cells at specific loci in Drosophila, 16: 28747(R) (TID-16429)
radioinduced in male germ cells at specific loci in Drosophila, 16: 28748(R) (TID-16430)
radioinduced in maize seedlings, effects of temperature on somatic, 16: 28765 (RT/BIO(62)44)
radioinduced in maize, 16: 28828
radioinduced in *Marchantia polymorpha* liverwort, nutritionally deficient, 16: 31497
radioinduced in mammals, effects of environment on, 18: 1442
radioinduced, in maize and tomatoes, 18: 3496(R) (TID-19724)
radioinduced in *Marchantia polymorpha*, nutritionally deficient, 18: 9847
radioinduced in man, 18: 22297
radioinduced in man, cosmic, 18: 21900
radioinduced in maize and wheat, 18: 33279(R) (TID-20823)
radioinduced in maize, 18: 36967
radioinduced in man, 18: 38818
radioinduced in male Drosophila, effects of radiation dose on, 18: 41183
radioinduced in male Drosophila, 19: 3940
radioinduced in maize, 19: 19527
radioinduced in maize, 19: 21918
radioinduced in mammals, 19: 33957
radioinduced in man, 19: 36093
radioinduced in male Drosophila, effects of sperm maturity on frequency of, 19: 38390
radioinduced in male mice, superlethal, 19: 38393
radioinduced in maize, meson, neutron, proton, and x, 19: 43712 (BNL-9383)
radioinduced in man, 19: 43914
radioinduced in man, 19: 45967
radioinduced in maize and wheat, 17: 2834(R) (TID-17287)
radioinduced in maize, 17: 7880
radioinduced in man by radiodiagnosis, 17: 8439
radioinduced in maize, 17: 15626 (BNL-6027)
radioinduced in male *Drosophila* using carbon-14- and tritium-labeled adenine, cytidine, and thymidine, 17: 21500
radioinduced in maize, 17: 28711
radioinduced in maize seedling by seed exposure, rate of artificial, 17: 38694
radioinduced in male *D. melanogaster* germ cells, effects of age on, 20: 12636 (TID-21459)
radioinduced in maize, x, 20: 12678
radioinduced in mammals, neutron, 20: 16159(R) (ORNL-3900, pp 150-81)
radioinduced in maize pollen mother cells, y, 20: 18335
radioinduced in maize endosperm, frequency of y, light, and uv, 20: 18392
radioinduced in maize, gamma and neutron, 20: 22661
radioinduced in maize, fast-neutron and x, 20: 31092
radioinduced in maize, 20: 38617
radioinduced in maize, reaction mechanisms of x, 20: 40708
radioinduced in man, 20: 40662
radioinduced in meal moth at low doses, somatic, 16: 20281
radioinduced in mealy bug, 18: 68
radioinduced in mealy bug, 18: 67
radioinduced in *Medicago sativa L.*, cytogenetics of, 17: 10398
radioinduced in *Medicago sativa L.*, morphology of, 17: 10399
radioinduced in medicinal plants, y, 20: 16290
radioinduced in mice, 16: 5207
radioinduced in mice, 18: 11760
radioinduced in microorganisms, ultraviolet, 18: 19650
radioinduced in mice, 18: 27007(R) (ORNL-3601(p.83-91))
radioinduced in mice, 18: 33281(R) (TID-20844)
radioinduced in mice, neutron, 18: 38933
radioinduced in mice after male exposure, 18: 43295
radioinduced in mice, 19: 2072(R) (ORNL-3700(p.83-8))
radioinduced in mice, screening for low blood catalase in, 19: 7014(R) (ANL-6906(p.75-7))
radioinduced in mice, 19: 7083
radioinduced in mice, 19: 7090
radioinduced in microorganisms, 19: 10719 (AECL-2107)
radioinduced in microorganisms, 19: 21981
radioinduced in mice, 19: 28076
radioinduced in mice progeny, 19: 42347
radioinduced in mice, effects of dose, dose rate, and radiation quality on, 19: 43788
radioinduced in mice, effects of dose rate on, 19: 43789
radioinduced in mice, effects of dose fractionation, 17: 1314
radioinduced in mice, 17: 5673(R) (LAMS-2780(p.181-210))
radioinduced in mice, 17: 14036
radioinduced in mice, 17: 15629 (LADC-5278)
radioinduced in mice, 17: 20270
radioinduced in microorganisms, mechanism of, 17: 19915
radioinduced in microorganisms, 17: 25024
radioinduced in mice, search for sex-linked lethals, 17: 27098
radioinduced in mice, 17: 38905
radioinduced in mice, effects of time between irradiation and conception on frequency of fission-neutron, 20: 18368
radioinduced in mice, effects of mixture of radioprotective compounds on, 20: 24882
radioinduced in mice, x, 20: 28957
radioinduced in mice, x, 20: 31048
radioinduced in mice, fast neutron and y, 20: 38647
radioinduced in Mormoniella, 18: 73
radioinduced in mouse sperm, protective effects of AET against x, 18: 38987
radioinduced in mouse spermatogonia, x, 19: 5651
radioinduced in mouse sperm, x, 19: 15132
radioinduced in Mormoniella, x, 19: 31674(R) (ORNL-3768(p.64-9))
radioinduced in mouse oocytes, effects of time on fission-neutron, 19: 31791(R) (ORNL-3768(p.89-93))
radioinduced in Mormoniella males, frequency of dominant lethal, x, 20: 20464
radioinduced in mouse and rats, review of, 20: 36652
radioinduced in mouse spermatogonia, effects of dose on frequency of x, 20: 40627(R) (ORNL-3922, pp 84-8)
radioinduced in mycobacteria, correlation of pigment formation and virulence in, 19: 28039
radioinduced in *Mycobacterium smegmatis*, effects of external exposure to sulfur-35 on, 19: 43816
radioinduced, in natural populations of vertebrates, 17: 30398
radioinduced in Neurospora, 16: 31491
radioinduced in Neurospora, uv, 18: 19621
radioinduced in Neurospora, genetic analysis of, 18: 29292
radioinduced in Neurospora, 19: 2068(R) (ORNL-370(•p.34-57))
radioinduced in Neurospora, 19: 2078 (ORNL-P-652)
radioinduced in Neurospora, x, 19: 2111
radioinduced in Neurospora, allelic complimentation from uv and x, 19: 15081
radioinduced in Neurospora, biochemistry and genetics and uv and x, 19: 15082
radioinduced in *Neurospora crassa*, physiological and structural relations within TD locus in, 19: 17517
radioinduced in Neurospora, functional inactivation of x, 19: 31788(R) (ORNL-3768(p.33-57))
radioinduced in Neurospora, protective effects of anoxia against x, 19: 42363
radioinduced in Neurospora, protective effects of MEA against x, 19: 42364
radioinduced in Neurospora, stability of uv, 20: 6708
radioinduced in Neurospora, genetic analysis of, 20: 6777(R) (ORNL-3853, pp 54-61)
radioinduced in Neurospora, uv, 20: 18196
radioinduced in Neurospora, uv and x, 20: 31012
radioinduced in Neurospora, complementation between nonallelic, x, 20: 40624(R) (ORNL-3922, pp 52-8)
radioinduced in Neurospora, photoreactivation of uv, 20: 40624(R) (ORNL-3922, pp 52-8)
radioinduced in Neurospora, x, 20: 42926
radioinduced in Neurospora, y, 20: 45248(R) (NYO-2043-129)
radioinduced in oats, 18: 25181
radioinduced in oats, effects of ploidy on thermal neutron, 19: 38419
radioinduced in oats, 17: 24898 (TID-18794)
radioinduced in oats, effects of phosphorus on rate of, 17: 37091
radioinduced in oat seeds, 20: 1665
radioinduced in oats, use in crop improvement, 20: 10645
radioinduced in oats, neutron, 20: 18417
radioinduced in oats, frequency of somatic, 20: 31078
radioinduced in oats, 20: 45369
radioinduced in *Oenothera berteriana* by seed exposure, trisomic plants in descendents of diploid, 19: 33943
radioinduced in *Oenothera flavens* by phosphorus-32 and sulfur-35, 17: 23207
radioinduced in *Oenothera berteriana*, 20: 22762
radioinduced in *Oenothera hookeri*, x, 20: 22763
radioinduced in *Oenothera berteriana*, x, 20: 22770
radioinduced in oocytes in *Artemia salina*, 16: 26771
radioinduced in organisms, effects of, 20: 106
radioinduced in pathogenic plant organisms, 18: 21843
radioinduced in Paramecium, 18: 27003(R) (ORNL-3601(p.27-46))
radioinduced in Paramecium, effects of dose rate on, 18: 43229 (ORNL-P-472)
radioinduced in *Paramecium aurelia*, distribution of chromosomal strands to, 19: 7114
radioinduced in Paramecium, x, 19: 31788(R) (ORNL-3768(p.33-57))
radioinduced in *Paspalum dilatatum*, 17: 7831
radioinduced in *Paspalum dilatatum*, 17: 7832

radioinduced in paramecium, reaction mechanisms, 17: 7842
radioinduced in paramecium, 17: 19784
radioinduced in paramecium, 17: 21515
radioinduced in Paramecium, temperature-sensitive x, 20: 18348
radioinduced in Paramecium, conditions affecting yield of temperature-sensitive x, 20: 18349
radioinduced in peas, genetic problems of breeding by, 16: 1605
radioinduced in peas by neutrons, time of flowering, 16: 1593
radioinduced in pea plants, 19: 7043
radioinduced in peanut plants, use in breeding programs, 19: 15020 (TID-20442)
radioinduced in peas, fast-neutron and x, 19: 35962
radioinduced in peas, 19: 43732
radioinduced in peas, 19: 43734
radioinduced in peas, 20: 81
radioinduced in peas, x, 20: 5238
radioinduced in peas, economic importance and inheritance of y, 20: 22673
radioinduced in peas, factors affecting x, 20: 22676
radioinduced in *Penicillium expansum*, uv, 20: 22680
radioinduced in peas, frequency and spectra of gamma, 20: 22657
radioinduced in *Pellicularia filamentosa*, gamma and uv, 20: 35293
radioinduced in peas, y and fast neutron, 20: 36634
radioinduced in peanuts, resistance to virus disease, y, 20: 36647
radioinduced in Phaseolus for chlorophyll, x, 18: 23263
radioinduced in *Phaseolus vulgaris*, y, 20: 12709
radioinduced in *Phaseolus vulgaris*, y, 20: 12710
radioinduced in phage ϕX174, uv, 20: 20463
radioinduced in phage κ of *Serratia marcescens*, uv, 20: 38670
radioinduced in *Pisum sativum*, 18: 17617
radioinduced in *Pisum sativum*, 19: 5686
radioinduced in *Pisum sativum*, 19: 25992
radioinduced in *Pisum sativum*, 19: 25993
radioinduced in *Pisum sativum*, 19: 29897 (EUR-2218.e)
radioinduced in *Pisum sativum*, effects of mutant gene penetrance on, x, 20: 6773 (EUR-2510.d)
radioinduced in *Pisum sativum*, x, 20: 8660
radioinduced in plants, 16: 9078
radioinduced in plants, use in plant breeding programs, 16: 9082
radioinduced in plants, 16: 15046(R) (TID-15341)
radioinduced in plants, 16: 18784
radioinduced in plants, comparison of effects of pollen and somatic, 16: 18786
radioinduced in plants, role in improvement of agricultural crops, 16: 23469
radioinduced in plants, role in improvement of agricultural crops, 16: 23369
radioinduced in plants, 16: 28740 (BNL-5039)
radioinduced in plants, role in crop improvement, 16: 28741 (BNL-5089)
radioinduced in plants, 16: 31516
radioinduced in plants, 16: 31510 (BNL-5381)
radioinduced in plants, 18: 64
radioinduced in plants, 18: 1320(R) (NP-13315)
radioinduced in plants, 18: 1439
radioinduced in plants, 18: 21908
radioinduced in plants, 18: 25133
radioinduced in planaria, chronic x, 18: 31249
radioinduced in plants, 18: 33213 (ST1/DOC/10/28(p.79-103))
radioinduced in plants, 18: 38774(R) (EUR-1881.e)
radioinduced in plants, neutron, 18: 38935
radioinduced in plants, 18: 43218(R) (EUR-1882.e(p.7-26))
radioinduced in plants, 19: 3896(R) (ORO-625(p.109-29))
radioinduced in plants, 19: 3982
radioinduced in plants, quantitative analysis of, 19: 5670
radioinduced in plants, facility for studying, 19: 5678
radioinduced in plants, use in plant breeding programs, 19: 5683
radioinduced in plants, 19: 12992
radioinduced in plants, 19: 12961(R) (TID-21604)
radioinduced in plants, value in plant breeding programs, 19: 15013 (CONF-551-3)
radioinduced in plants, 19: 21855 (BNL-8892)
radioinduced in plants, 19: 21861(R) (NP-14937(p.116-25))
radioinduced in plants, 19: 25994
radioinduced in plants, 19: 27971
radioinduced in plants and trees, 19: 33955
radioinduced in plants, 19: 33956
radioinduced in plants, 19: 33827
radioinduced in plants, agricultural importance of, 19: 38327
radioinduced in plants, 17: 15541(R) (ORO-598)
radioinduced in plants, 17: 15563
radioinduced in plants, limiting factors in usefulness for breeding purposes, 17: 17809
radioinduced in plants, 17: 19748 (BLG-167)
radioinduced in plants, use of probability theory in calculating frequency of, 17: 23205
radioinduced in plants, 17: 28678(R) (TID-18936)
radioinduced in plants, 17: 31816(R) (ORO-605)
radioinduced, in plants, 17: 33541
radioinduced in plants, technique for, 17: 37078
radioinduced in plants, 17: 38746(R) (TID-19432)
radioinduced in plant cells, 20: 71
radioinduced in plants, applications of, in breeding programs, 20: 3710(R) (EUR-2493.e)
radioinduced in plants, review of agricultural use of y, 20: 16225 (EUR-2715.f)
radioinduced in plants, x, 20: 29018
radioinduced in plants, effects of exogenous factors on, 20: 40709
radioinduced in plants, x, 20: 40710
radioinduced in plants, genetic structure demonstrated after, 17: 27100
radioinduced in pneumococci and streptococci for streptomycin resistance, uv, 20: 6835
radioinduced in potatoes, 16: 20177
radioinduced in potato eye sprouts, gamma, 18: 17616
radioinduced in potatoes, gamma, 19: 19518
radioinduced in potato plants, gamma, thermal neutron, and x-ray, 19: 42318
radioinduced in *Poa pratensis*, agricultural significance of x, 19: 43778
radioinduced in potatoes, 20: 6796(T) (JPRS-33170, pp 233-9)
radioinduced in potatoes following tuber exposure, fast neutron, gamma, and x, 20: 24898
radioinduced in potatoes, gamma, 20: 32990
radioinduced in poliovirus, x, 20: 42966
radioinduced in populations of Hiroshima and Nagasaki, 20: 45406
radioinduced in *Prorocentrum micans*, ultraviolet, 19: 31867
radioinduced in *Prunus avium* cherries, 20: 16244
radioinduced, in Quercus seed, gamma, 18: 3477 (BNL-6892)
radioinduced in rats by monazite sand, 19: 2131
radioinduced in rats, 19: 7084
radioinduced in rats, 19: 10719 (AECL-2107)
radioinduced in rats, x, 20: 38619
radioinduced in region of X chromosome in *D. melanogaster* DNA, 19: 45879
radioinduced in red clover, Ultuna, 19: 45882
radioinduced in red clover, x, 20: 5491
radioinduced in rhizobium, 16: 7427
radioinduced in rice by phosphorus-32, short-culm, 16: 1615
radioinduced in rice, 16: 1618
radioinduced in rice, 16: 32010
radioinduced in rice, thermal neutron and x-ray, 16: 32764
radioinduced in rice, analysis of reciprocal translocations in, 16: 32765
radioinduced in rice grains, 16: 32766
radioinduced in rice, neutron, 18: 21867
radioinduced in rice, 18: 36995
radioinduced in rice by mixed neutrons and gamma radiation, 18: 38934
radioinduced in rice, thermal neutron, 18: 38936
radioinduced in rice by seed exposure, 19: 2118
radioinduced in rice, gamma and x, 19: 7140
radioinduced in rice and wheat, 19: 21917
radioinduced in rice, 19: 43781
radioinduced in rice, 17: 14010
radioinduced in rice, 17: 15564
radioinduced in rice, 17: 15566
radioinduced in rice, 17: 24893 (TID-18672)
radioinduced in rice, x, 20: 5393
radioinduced in rice, characterization of y, neutron, and x, 20: 8652
radioinduced in rice, y, 20: 8693
radioinduced in rice, x, 20: 18414
radioinduced in rice, use in plant breeding programs, 20: 18416
radioinduced in rice, y, 20: 18417
radioinduced in rice, beta, thermal neutron, or x, 20: 40640
radioinduced in rye, 17: 19841
radioinduced in *Saccharomyces cerevisiae*, allelic mapping of, 18: 11794
radioinduced in Saccharomyces, effects on protein synthesis of, 18: 29286
radioinduced in Saccharomyces, ultraviolet, 18: 41138
radioinduced in Saccharomyces, gene control of pigmentation in specific lysine requirement in, 19: 8729
radioinduced in Salmonella, uv, 19: 10844
radioinduced in sand oats, dose rate effects on, 19: 15172
radioinduced in *Sarcina lutea*, 19: 26041
radioinduced in *Salmonella typhimurium*, genetic analysis of, 19: 45878
radioinduced in Saccharomyces, 17: 19839
radioinduced in *Saccharomyces* yeast strain, rates of, 17: 23204
radioinduced in *Saccharomyces pombe*, 17: 40569

radioinduced in Saccharomyces, x, 20: 3717(T) (JPRS-31514, pp 77-91)
radioinduced in Saccharomyces, uv, 20: 3717(T) (JPRS-31514, pp 77-91)
radioinduced in Saccharomyces, β, uv, and x, 20: 5360
radioinduced in Saccharomyces, genetic analysis of, 20: 12655
radioinduced in Saccharomyces, 20: 18405
radioinduced in *Salmonella typhimurium*, uv, 20: 28977
radioinduced in Schizosaccharomyces, uv, 19: 110
radioinduced in seed, gamma source for, 18: 29189
radioinduced in *Serratia marcescens*, effects of cold, dryness, and treatment with biochemicals on, 17: 40565
radioinduced in sex chromosomes following prenatal exposure, 20: 22756
radioinduced in seeds, factors affecting beta, 20: 45432
radioinduced in silkworms, effects of fractionated vs. single dose on, x, 18: 31143
radioinduced in six-rowed barley in X_1 and X_2 generations, 19: 10826
radioinduced in silkworms, 19: 21915
radioinduced in silkworms, 19: 21916
radioinduced in silkworms, 19: 21862(R) (NP-14937(p.93-116))
radioinduced in silkworms, 19: 43784
radioinduced in silkworms, 19: 43786
radioinduced in silkworms, 19: 43787
radioinduced in silkworm larvae, 19: 43783
radioinduced in silkworm gonial cells, fission neutron and gamma, 19: 45883
radioinduced in silkworms, RBE of fast neutron and x, 20: 38626
radioinduced in soybeans, 16: 8572
radioinduced in *Sordaria brevicollis*, ultraviolet, 19: 19547
radioinduced in *Sordaria brevicollis*, uv, 20: 3783
radioinduced in soybeans by thermal neutrons, 20: 45358(R) (NP-16208)
radioinduced in soybeans, by thermal neutrons and x rays, 20: 45388
radioinduced in spermatogonia and spermatozoa of *Drosophila melanogaster*, 16: 20197
radioinduced in spinach, 17: 15682
radioinduced in staminal hair cells of Tradescantia, RBE of gamma and mesons (μ^-), 18: 1406
radioinduced in *Streptomyces citreus*, antibiotic properties of, 19: 45991
radioinduced in *Streptomyces citreus*, gamma and uv, 20: 124
radioinduced in summer barley, combined and single beta and x-ray, 19: 17582
radioinduced in sweet potatoes, 16: 20178
radioinduced in sweet potatoes, review, 19: 43777
radioinduced in synchronous populations of *Streptococcus faecalis*, chromosome mapping by, 20: 36635
radioinduced in *Tetrahymena pyriformis*, 16: 7353
radioinduced in the grain beetle, *Tribolium castaneum*, 19: 7021 (TID-20082)
radioinduced in tomatoes, 16: 25197 (CNEN-119)
radioinduced in tobacco plants, 19: 7153
radioinduced in tomatoes, 19: 8858
radioinduced in tomatoes by gamma radiation, comparison with ethylenimine-induced, 17: 5892
radioinduced in tomato plants, 17: 17765(R) (TID-18414)
radioinduced in tomato seeds, effects of temperature and oxygen during storage on, 20: 1638
radioinduced in tomato pollen, factors affecting frequency of y, 20: 18393
radioinduced in tomatoes, economic value of gamma, 20: 22659
radioinduced in tomatoes for somatic ploidy, x, 20: 22663
radioinduced in tomatoes, somatic conversion in x, 20: 40713
radioinduced in *Trifolium repens*, effects of dose fractionation on, 18: 1441
radioinduced in Triticum wheat, 18: 17484(T) (OTS-62-11755/4(p.17-28))
radioinduced in Trillium, 19: 7124
radioinduced in Trillium, 19: 8866
radioinduced in Trillium, 19: 8867
radioinduced in Tradescantia, 19: 25976
radioinduced in *Tribolium confusum*, 19: 33928
radioinduced in Tradescantia by neutrons, 19: 40800(R) (AERE-PR/HPM-7)
radioinduced in Tradescantia, 20: 8698
radioinduced in tulips, gamma, 18: 21907
radioinduced in tulips, 19: 33929
radioinduced in tulip buds, mechanism of, 17: 30223
radioinduced in two-rowed barley, gamma and x-ray, 19: 8915
radioinduced in T4 bacteriophage in *E. coli*, 16: 18783
radioinduced in Ustilago, uv, 20: 12694
radioinduced in *Vicia faba*, 18: 29293
radioinduced in *Vicia faba*, 19: 21950
radioinduced in *Vigna sinensis*, neutron and x, 20: 14341
radioinduced in Vicia, x, 20: 16276
radioinduced in *Vicia faba*, effects of DNP on recovery from fast-neutron and gamma, 20: 22670
radioinduced in wasps, 20: 3733
radioinduced in wheat plants, 16: 6315(T) (JPRS-11322(p.429-46))
radioinduced in wheat, 16: 23454
radioinduced in wheat and oats, 16: 26811
radioinduced in wheat seed, 16: 28790
radioinduced in wheat by incorporated tritium, 18: 1424
radioinduced in wheat for disease resistance, gamma, 18: 31224
radioinduced in wheat, fast-neutron, 18: 33374
radioinduced in wheat and maize, 18: 38777(R) (TID-21068)
radioinduced in wheat species, 18: 41115
radioinduced in wheat, effects of boron on gamma and thermal neutron, 19: 2153
radioinduced in wheat, x, 19: 2154
radioinduced in wheat, gamma, 19: 2155
radioinduced in wheat, neutron and x, 19: 2161
radioinduced in wheat, 19: 21913
radioinduced in wheat, 19: 24261(R) (TID-21649)
radioinduced in wheat, 19: 36077
radioinduced in wheat, 19: 42260 (TID-22115)
radioinduced in wheat, 19: 43781
radioinduced in wheat, 17: 15731
radioinduced in wheat by internal phosphorus-32, 17: 17843
radioinduced in wheat, maize, and tobacco, 17: 24894(R) (TID-18673)
radioinduced in wheat, 17: 28713
radioinduced in wheat, 17: 28714
radioinduced in wheat, 17: 28715
radioinduced in wheat, x, 20: 5403
radioinduced in wheat, y, 20: 6795(T) (JPRS-33170, pp 226-32)
radioinduced in wheat, effects of ploidy on, 20: 6897
radioinduced in wheat, classification of chlorophyll, 20: 12632(R) (EUR-2546.f)
radioinduced in wheat, y and x, 20: 16285
radioinduced in wheat, x, 20: 16286
radioinduced in wheat seeds, x, 20: 20501
radioinduced in wheat seed, effects of dose rate on beta, gamma, and fast-neutron, 20: 22743
radioinduced in wheat, effects on gluten content and quality, 20: 22672
radioinduced in wheat, fast neutron and gamma, 20: 36620
radioinduced in wheat, x, 20: 42846 (IAEA-2466-13)
radioinduced in wheat, thermal neutron, 20: 45392
radioinduced in winter paddy, beta, 18: 43291
radioinduced in winter wheat, 19: 17621
radioinduced in xanthine dehydrogenase in Drosophila, effects on activity, 18: 25208
radioinduced in yeast, effects of dose rate and mitotic state on, 18: 1438
radioinduced in yeasts during meiosis and mitosis, rates of uv and x-ray, 18: 11832
radioinduced in yeast, 18: 17479 (UCRL-11191)
radioinduced in yeast, 18: 36955(R) (UCRL-11387(p.35-53))
radioinduced in yeast, gamma and neutron, 19: 2091
radioinduced in yeasts, complementation of, uv, 19: 8847
radioinduced in yeast, 19: 21920
radioinduced in yeast, 19: 25912 (UCRL-8268)
radioinduced in yeast, 19: 36002
radioinduced in yeast, 17: 5809
radioinduced in yeast, effects of environment on, 17: 17842
radioinduced in yeast, 20: 1663
radioinduced in yeast, mutagen specificity among reversions of uv, 20: 6830
radioinduced in yeast, heavy-ion, 20: 6859
radioinduced in yeast, antibiotic production by, 20: 10695
radioinduced in yeast, uv, 20: 14327
radioinduced in yeast, genetic studies of uv and x, 20: 18190(R) (UCRL-16613)
radioinduced in yeasts, photoreactivation of uv, 20: 22783
radioinduced in yeast, 20: 26661(T) (ORNL-tr-1234)
radioinduced in yeast, uv and x, 20: 45364 (UCRL-16851)
radioinduced in *Zea mays*, 19: 15010 (BNL-7815)
radioinduced lethal, in *E. coli*, electrons and ultraviolet, 18: 1414
radioinduced lethal allele, in Saccharomyces, 18: 5063
radioinduced lethal, in *Tribolium castaneum*, fast-neutron and x, 20: 11184(R) (BNWL-122, pp 137-9)
radioinduced lethal, in honeybee gametes, x, 20: 38631
radioinduced maize, acute vs. chronic gamma, 18: 11731
radioinduced maize, effects of dose on y, 20: 8692
radioinduced micro-, in barley, x, 20: 35320
radioinduced mutations in, 19: 28062
radioinduced mutations of, 19: 45853
radioinduced mutations of *Oenothera berteriana*, 20: 22764
radioinduced, of *Escherichia coli*, 18: 8105(R) (NYO-2740-1(p.81-154))
radioinduced, of tomato plants, 18: 8111 (TID-19942)
radioinduced phage induction in *Serratia marcescens*, uv, 19: 43847

radioinduced Pisum chlorophyll, x, 18: 41155
radioinduced plant, applications in plant breeding programs, 18: 1373 (BNL-7360)
radioinduced plant statistical, method for selecting, 19: 42284
radioinduced plasma and plastid, in leaves, 19: 29988
radioinduced polygenic, mathematical analysis of, 18: 9865
radioinduced polygenic, in R_2 generation of *Nicotiana tabacum*, 17: 38693
radioinduced polygenic, in *Drosophila melanogaster*, x, 20: 18415
radioinduced prototrophic *E. coli*, action spectra for photoreactivation of uv, 20: 38669
radioinduced R-locus deleterious, in Mormoniella, 16: 9871
radioinduced rate of, in Japan, 18: 17555
radioinduced, reaction mechanisms, 16: 8610
radioinduced, reaction mechanisms, 17: 5875
radioinduced recessive lethals in paramecium, 16: 7451
radioinduced recessive lethal, uv and x, 18: 27095
radioinduced recessive lethal, in Drosophila second chromosomes, 20: 42922
radioinduced reversion of transition, in *E. coli*, 19: 7052
radioinduced reversions in *E. coli* mutant, effects of native wild DNA on, 17: 24917
radioinduced revertants in *Neurospora crassa*, uv, 20: 6829
radioinduced reversions in Neurospora, uv, 20: 20462
radioinduced, review of research of significance to man, 17: 92
radioinduced, review of, 17: 40555
radioinduced rice recessive, x, 19: 10825
radioinduced, role of dose rate, 16: 7453
radioinduced, role of DNA denaturation in, 18: 6691
radioinduced Saccharomyces cytoplasmic, effects on reactivation, 18: 15819(T) (UCRL-Trans-1029)
radioinduced sex-linked recessive lethal, in *Sciara coprophilia*, 16: 20138
radioinduced sex-linked, of mosquitoes, 18: 5067
radioinduced sex-linked recessive lethal, in Drosophila, 17: 21516
radioinduced silkworm, frequency of β and γ, 20: 12692
radioinduced somatic, in moth wing scales, 18: 41090 (TID-21097)
radioinduced somatic, relation to chronic diseases, 19: 43749
radioinduced somatic, carcinogenesis of, 19: 43754
radioinduced somatic, in plants, 19: 45817(R) (ORO-631, pp 145-71)
radioinduced somatic mosaic, in heterozygous Drosophila females, x, 20: 22655
radioinduced somatic, in trees, γ, 20: 18421
radioinduced somatic crossing over in *D. melanogaster*, effects of age on location of, 20: 36619
radioinduced somatic, in carnations, gamma, 20: 45474
radioinduced, summary of repair phenomena and differential sensitivity in, 18: 1446
radioinduced supervital, in Arabidopsis, 16: 21943
radioinduced, use of interchanges involving A and B chromosomes in maize, 16: 1597
radioinduced wheat, use in breeding program, 20: 18322
radioinduced with tretamine in reproductive system of screw-worm flies, dose effects in, 19: 24289
radioinduced yeast prototrophic, effects of ploidy on gamma and uv, 19: 3963
radioinduced, compared with other mutagens, 18: 21887
radioinduced, effects on fitness of *D. pseudoobscura*, 19: 24292
radioinduced, effects on eye color in Mormoniella, x, 20: 40669
radioinduced, etiology of human, 20: 3779
radioinduced, for jute crinkled leaf, x, 18: 17519
radioinduced, for immunity, 19: 32631
radioinduced, for plant improvement, 20: 8656
radioinduced, in *Arabidopsis thaliana*, 19: 21914
radioinduced, in bacteria and yeast, 19: 10789(R) (TID-21591)
radioinduced, in barley, 19: 45819(R) (TID-22176)
radioinduced, in barley, x, 20: 3782
radioinduced, in cotton, 18: 25129
radioinduced, in *Corynebacterium fascians*, uv, 20: 3723
radioinduced, in *Crotolaria intermedia*, x, 20: 3759
radioinduced, in cotton, gamma and thermal neutron, 20: 42899
radioinduced, in Drosophila, 18: 29295
radioinduced, in Drosophila, 19: 21973
radioinduced, in Drosophila population, 20: 1642
radioinduced, in Drosophila, 20: 1644
radioinduced, in ethionine-resistant Saccharomyces, 18: 31071
radioinduced, in *E. coli* for metabolic reversion, 18: 31172
radioinduced, in *Escherichia coli*, uv, 20: 6775(R) (ORNL-3853, pp 36-49)
radioinduced, in five varieties of winter wheat, gamma, 20: 42897
radioinduced, in insects, 19: 10719 (AECL-2107)
radioinduced, in L cells in tissue culture, 18: 29343
radioinduced, in maize, wheat, and tomatoes, 18: 11649 (TID-20031)
radioinduced, in mice, protective effects of AET and cysteine against 18: 27217
radioinduced, in *Mycobacterium smegmatis* by transmutation of incorporated sulfur-35, 19: 43816
radioinduced, in mice, 19: 45809(R) (NYO-1979-12)
radioinduced, in maize, x, 20: 1656
radioinduced, in mice, 20: 6781(R) (ORNL-3853, pp 98-101)
radioinduced, in mice, x, 20: 38590(R) (NYO-1979-13)
radioinduced, in *Oenothera berteriana*, 18: 11676
radioinduced, in peanuts, x, 18: 25132
radioinduced, in *Phaseolus mungo*, x, 18: 33324
radioinduced, in plants, 19: 45884
radioinduced, in *Paramecium aurelia*, 20: 6775(R) (ORNL-3853, pp 36-49)
radioinduced, in peanuts, 20: 40636(R) (ORO-1747-12)
radioinduced, in *Sorghum arundinaceum*, 18: 25131
radioinduced, in Saccharomyces, effects of dose rate and ploidy on uv, 18: 27096
radioinduced, in seedlings of *Haplopappus gracilis*, 18: 29246 (TID-20784)
radioinduced, in Saccharomyces, 18: 29294
radioinduced, in sugar beets, 19: 12957 (SGAE-BL-10/1964)
radioinduced, in *Trifolium subterraneum*, neutron and x, 20: 8704
radioinduced, in unisexual wasp Devorgilla, 20: 1643
radioinduced, in wheat, 20: 3762
radioinduced, of grass, 18: 25177
radioinduced, of *Streptococcus lactis*, ultraviolet, 19: 25980
radioinduced, of screw-worm fly, 19: 45950
radioinduced, of wheat, 20: 1655
radioinduced, possible effects of tautomerism in cytosine–guanine bonding on, 20: 40589
radioinduced, reaction mechanisms for, 19: 77(T) (JPRS-26532)
radioinduced, reaction mechanisms for, 19: 2157
radioinduced, reaction mechanisms for, uv, 17: 40575
radioinduced, relation to dose, 18: 17490
radioinduced, role of cytidylic acid in, 19: 32212
radioinduced, theoretical bases for methods of producing, 19: 38420
radioinduced, use in field crop breeding programs, 20: 18420
radioinduced, usefulness of, 19: 29911
radioinducted in T2 phage by carbon-14 decay, 20: 24891
radiosensitivity in barley and wheat, effects of polyploidy on, 16: 12933
radiosensitivity of transforming DNA in pneumococci, uv, 19: 15087
radiosensitivity of *Bacillus subtilis*, 19: 33851
radiosensitivity of *Escherichia coli*, 19: 43794
radiosensitivity of *Escherichia coli*, uv, 19: 45948
radiosensitivity of *Paramecium* production of, relation of repair to, 17: 38854
radiosensitivity of cytoplasmic, *Aspergillus nidulans*, uv, 20: 36629
radiosensitivity of *E. coli*, uv, 20: 38620
radiosensitivity of radioinduced *E. coli*, uv and x, 20: 38621
rate in man, 19: 43642(R) (NYO-2280-8)
rate in *Vicia faba*, effects of sodium gallate on, 18: 11591
rate of radioinduced, in swine, 20: 45362(R) (TID-23311)
rates in first and later formed sprouts in barley seeds, radiation effects on, 16: 1578
rates of, mathematical analysis of, 18: 9811
relation to chemical and radiation effects on chromosomal DNA, 19: 33829
reversions of autotropic, during growth of yeast and Tetrahymena, 20: 6696(R) (ORNL-3853, pp 66-77)
role in aging of gametic and somatic, 17: 33748
role in evolution of human populations, 20: 8511 (NYO-2260-6)
role in mammalian aging, review on, 20: 6771 (BNL-9653)
role of, in carcinogenesis, 18: 19505 (BNL-7912)
sex-linked lethal, in *Drosophila*, 20: 40515
somatic, effects on aging process, 17: 28750
somatic, in tropical plants, radiosensitivity to, 18: 31243
somatic, role in neoplasm induction, 19: 33806
specificity, nonrandomness, and differential effect of induced, 16: 31517
spontaneous, frequency in mice, 19: 31791(R) (ORNL-3768(p.89-93))
spontaneous Habrobracon, frequencies of, 19: 31793(R) (ORNL-3768 (p.109-11))
suppressor, for the isoleucine locus in Saccharomyces, 17: 31821
use in plant breeding programs, 19: 5683
use of A-B translocations in studies of, in maize, 18: 19513
use of *E. coli*, for studies in germfree mice, 20: 40629(R) (ORNL-3922, pp 94-8)
use of plant, review, 19: 43656
use of radio- and chemically induced, in Neurospora, 20: 18347
viability effects of newly induced second chromosome, in flies, 16: 5159 (TID-14463)

Mylar
see Terephthalic Acid, Ethylene Polymer Esters

Myleran
see Methanesulfonic Acid, Tetramethylene Ester
Myleran, Dimethyl-
see Methanesulfonic Acid, 1,4-Dimethyltetramethylene Ester
MYOGLOBIN
radiation chemistry of, 20: 9331 (CONF-651024, pp 88-92)
radiation effects on single crystals of, x-ray, 16: 30260
x-ray scattering cross sections for, 18: 20035
MYOSINS
properties of heavy meromyosin, oxygen-18 exchange reactions, 17: 23047
radiation effects and heat effects, 16: 14509
radiation effects on ATPase activity of, x, 18: 23258
radiation effects on, protective effects of ATP against γ, 20: 18259
radiation effects on proteolytic activity, 16: 1473(T) (JPRS-10170 (p.38-68))
radiation effects on rabbit tropomyosin, gamma, 17: 16379
reactions with β-hydroxyethyl-2,4-dinitrophenyl disulfide, 20: 18722
synthesis in cultured heart cells, 19: 43681(R) (UCLA-12-565, pp 17-31)
MYRISTIC ACID
determination in commercial coconut oils, gas chromatographic, 20: 14463 (PAEC(D)CH-652)
etching of lithium fluoride crystals by, adsorption-locking and Rebinder effect in, 16: 20437
methyl ester, radiation effects on peroxide accumulation in, 19: 15603
separation from lauric and stearic acids by reversed-phase chromatography using polymerized cellulose, 18: 16145
uses as inhibitor of total reflections of thermal neutrons, 17: 13477
MZFR (SIEMENS REACTOR)
auxiliary installations for, design of, 19: 42168
building construction and pressure vessel installation for, 19: 42177
cable bushings for, 19: 25766
construction, 20: 5138
construction of, 19: 42176
containment of, 19: 42167
control of, 16: 11165
coolant and moderator circuits of, construction of, 19: 42164
coolant heat and flow testing in, loops for, 20: 47039
coolant pumps for, 19: 42174
description, 20: 26545
description and uses of, 20: 10428
description of, 19: 42160
design and construction of, 16: 16002
design and fabrication principles for, 19: 42162
design of 50-Mw(e), 17: 26800
design of, for economic optimum, 19: 42161
development of, 19: 42158
economics and utilization of, 19: 42159
experimental facilities of, 19: 42179
fuel element design for, 19: 43598
fuel element testing for, in NRX, 19: 42185
fuel elements for, 17: 12027
fuel elements for, design, construction, and testing of, 19: 42165
fuel rod fabrication for, 19: 42175
instrumentation and controls for, 19: 42170
loading equipment for, 19: 42166
pressure vessel for, design, construction, and installation of, 19: 42163
pressure vessel for, fabrication of, 19: 42172
reactivity measurements in, zero-energy, 19: 42186
reactivity of, zero-power experiment for, 19: 42178
reactivity parameters of fueled-nonmoderated, zero-energy experiment for determining, 20: 47079
reactivity states in, zero-energy experiment for determining, 20: 47080
steam generator for, construction of, 19: 42173
steam generator for MZFR, construction of, 19: 42173
steam power installation for, 19: 42169
steam power installation for MZFR, 19: 42169
structural design of, 19: 42171
structural design of MZFR, 19: 42171
zero-energy experiment for, 19: 43599

DEPOSITORIES OF USAEC REPORTS

In Countries Other than the U.S.

ARGENTINA
Buenos Aires, Comisión Nacional de Energía Atómica
AUSTRALIA
Canberra, Australian National Library
Sutherland, New South Wales, Australian Atomic Energy Commission
AUSTRIA
Vienna, Zentral Bibliothek der Physikalischen Institute der Universität
BELGIUM
Mol-Donk, Centre d'Etude de l'Energie Nucleaire
BOLIVIA
La Paz, Comisión Nacional de Energiá Nuclear
BRAZIL
Rio de Janeiro, Instituto Brasileiro de Bibliografia e Documentacao
São Paulo, Instituto de Energia Atomica, Cidade Universitaria São Paulo
BURMA
Rangoon, Union of Burma Applied Research Institute, Atomic Energy Center Library
CANADA
Hamilton, McMaster University
Ottawa, National Research Council Library
Vancouver, University of British Columbia
CHILE
Santiago, Departamento de Fisica, Universidad de Chile
CHINA
Hsinchu, Taiwan, Free China, National Tsing Hua University
COLOMBIA
Bogota, Instituto De Asuntos Nucleares
COSTA RICA
San Pedro, University of Costa Rica Library
DENMARK
Risö, Danish Atomic Energy Commission
ECUADOR
Quito, Escuela Politécnica Nacional
EL SALVADOR
San Salvador, Universidad de El Salvador, Biblioteca de Energia Nuclear
FINLAND
Helsinki, Teknillisen Korkeakoulun Kirjasto
FRANCE
Gif-sur-Yvette, Centre d'Etudes Nucléaires de Saclay
Paris, Académie des Sciences
GERMANY
Berlin, Hahn-Meitner-Institut für Kernforschung Berlin
Frankfurt/Main, Gmelin-Institut
Munich, Technische Hochschule, Bibliothek
GHANA
Accra, University College of Ghana
GREECE
Athens, Nuclear Research Center "Democritus"
GUATEMALA
Guatemala, Comisión Nacional de Energía Nuclear
INDIA
Bombay, Department of Atomic Energy
INDONESIA
Djogjakarta, Java, Science Faculty Gadjah Mada University
IRAN
Tehran, Tehran University Nuclear Centre
IRAQ
Baghdad, Iraqi Atomic Energy Commission
IRELAND
Dublin, University College
ISRAEL
Rehovoth, Israel Atomic Energy Commission
ITALY
Rome, Centro di Studi Nucleari della Casaccia
Rome, Comitato Nazionale per l'Energia Nucleare
JAPAN
Tokyo, National Diet Library
KOREA
Seoul, Office of Atomic Energy
LEBANON
Beirut, Lebanese National Council for Scientific Research
LUXEMBOURG
Luxembourg, Ministry of Transport and Electricity
MALAYSIA
Kuala Lumpur, University of Malaysia
MEXICO
Mexico, D.F., Comisión Nacional de Energía Nuclear
NETHERLANDS
The Hague, Reactor Centrum Nederland
NEW ZEALAND
Lower Hutt, Institute of Nuclear Sciences
NIGERIA
Ibadan, University of Ibadan
NORWAY
Lillestrom, Institutt för Atomenergi
PAKISTAN
Islamabad, Pakistan Institute of Nuclear Science and Technology
PERU
Lima, Junta de Control de Energia Atomica
PHILIPPINE REPUBLIC
Manila, Philippine Atomic Energy Commission
POLAND
Warsaw, Biura Pelnomocnika Rzadu do Spraw Wykorzystania Energii Jadrowej
PORTUGAL
Sacavem, Junta de Energía Nuclear
REPUBLIC OF SOUTH AFRICA
Pretoria, Atomic Energy Board Library
REPUBLIC OF THE CONGO
Leopoldville, Université Lovanium
SPAIN
Madrid, Junta de Energía Nuclear, Biblioteca Documentación y Publicaciones, Ciudad Universitaria
SWEDEN
Nyköping, Aktiebolaget Atomenergi
SWITZERLAND
Zürich, Eidgenössische Technische Hochschule, Bibliothek
THAILAND
Bangkok, Office of the Thai Atomic Energy Commission, Department of Science
TURKEY
Ankara, Turkish Atomic Energy Commission, Atomic Energy Library
UNITED ARAB REPUBLIC
Cairo, Atomic Energy Commission
UNITED KINGDOM
Birmingham, Central Library
Boston Spa, National Lending Library for Science and Technology
Kingston upon Hull, Central Library
Liverpool, Central Library
London, Central Library, Acton
London, National Reference Library
London, Science Museum Library, South Kensington
Manchester, Central Library
Newcastle upon Tyne, Central Library
Nottingham, Central Library
Sheffield, Central Library
URUGUAY
Montevideo, Comision Nacional de Energia Atomica
VENEZUELA
Caracas, Instituto Venezolano de Investigaciones Científicas
VIET-NAM
Saigon, Atomic Energy Office
YUGOSLAVIA
Belgrade, Federal Commission for Nuclear Energy

In International Agencies

AUSTRIA
Vienna, International Atomic Energy Agency
BELGIUM
Brussels, La Bibliotheque EURATOM
FRANCE
Paris, European Nuclear Energy Agency, O.E.C.D.
ITALY
Ispra, EURATOM Research Center
SWITZERLAND
Geneva, United Nations Library

UNITED STATES
GOVERNMENT PRINTING OFFICE
DIVISION OF PUBLIC DOCUMENTS
WASHINGTON, D.C. 20402

OFFICIAL BUSINESS

POSTAGE AND FEES PAID
U.S. GOVERNMENT PRINTING OFFICE

TECHNICAL PROGRESS REVIEWS

The Division of Technical Information, U. S. Atomic Energy Commission, also publishes the Technical Progress Reviews, a series of four quarterly journals on nuclear technology. These journals, compiled by specialists and recognized authorities, summarize, evaluate, and reference the progress of development in four important fields.

Isotopes and Radiation Technology P. S. Baker, A. F. Rupp, and associates, Oak Ridge National Laboratory. Reviews AEC-sponsored projects and related significant worldwide developments in radioisotopes and radiation technology.

Nuclear Safety Wm. B. Cottrell, W. H. Jordan, J. P. Blakely, and associates, Nuclear Safety Information Center, Oak Ridge National Laboratory. Covers topics relevant to the analysis and control of hazards associated with nuclear reactors and with operations involving fissionable materials and the products of nuclear fission.

Power Reactor Technology Argonne National Laboratory. Reviews research, development, design practices, and operating experiences associated with power reactors, including aerospace applications.

Reactor Materials E. M. Simons and associates, Battelle Memorial Institute. Covers the properties, behavior, and fabrication processes of materials used in nuclear reactors and associated equipment.

Availability

SUBSCRIPTION RATE: The Technical Progress Reviews may be purchased from the Superintendent of Documents, U. S. Government Printing Office, Washington, D. C. 20402. *Nuclear Safety* at $3.00 per year for each subscription or $1.00 per issue; each of the other journals at $2.50 per year or $0.70 per issue.

POSTAGE: Postpaid within the United States, Canada, Mexico, and all Central and South American countries except Argentina, Brazil, Guyana, French Guiana, Surinam, and British Honduras. For these Central and South American countries and all other countries, add $0.75 for each annual subscription or $0.20 for a single issue.

REMITTANCE: Payment should be by check, money order, or document coupons and MUST accompany order. Remittances from foreign countries should be made by international money order or draft on an American bank payable to the Superintendent of Documents or by UNESCO book coupons.